NASA
Reference
Publication
1111

September 1985

High-Density Digital Recording

NASA

NASA Reference Publication 1111

September 1985

High-Density Digital Recording

Ford Kalil, *Editor*
NASA Office of Space Tracking and Data Systems
Washington, D.C.

Al Buschman, *Assistant Editor*
Naval Intelligence Support Center
Suitland, Md.

In association with
Tape Head Interface Committee, Inc.

NASA

National Aeronautics
and Space Administration

Scientific and Technical Information Branch

List of Contributors

Anthony Bucher, *Odetics Incorporated*
Al Buschman, *Naval Intelligence Support Center*
David Christofar, *Spin Physics*
L. C. Csengery, *Lockheed Electronics Company, Incorporated*
Datatape, Incorporated, Technical Staff
Martin Davidson, *The Johns Hopkins University Applied Physics Laboratory*
Richard E. DeFrancesco, *Naval Air Development Center*
Neal Glover, *Data Systems Technology*
Headwear Advisory Committee, *Tape Head Interface Committee*
  Don Ballman, *Chairman*
Paul Heffner, *NASA Goddard Space Flight Center*
H. F. Hinteregger, *Haystack Observatory*
John M. Howard, *Thorn EMI Technology Incorporated*
Ford Kalil, *NASA Headquarters*
James Kelly, *Ampex Corporation*
W. D. Kessler, *Fairchild Weston Systems, Incorporated*
E. L. Law, *Pacific Missile Test Center*
Leighton Meeks, *Honeywell, Inc.*
Roger Mersing, *Ampex Corporation*
John Montgomery, *Martin Marietta Corporation*
Geoffrey C. Nottley, *Thorn EMI Technology Incorporated*
R. S. Reynolds, *Sandia Laboratories*
David Ricards, *Spin Physics*
Walter Shaffer, *Ampex Corporation*
R. A. Schultz, *Illinois Institute of Technology Research Institute*
James H. Stein, *Fairchild Weston Systems, Incorporated*
Edward R. Wuori, *Vertimag Systems Corporation*
M. A. Zoeller, *Datatape, Incorporated*

Library of Congress Cataloging in Publication Data
Main entry under title:

High-density digital recording.

(NASA reference publication ; 1111)
Continues: Magnetic tape recording for the eighties / Ford Kalil, editor.

Includes index.
1. Magnetic recorders and recording. 2. Error-correcting codes (Information theory) 3. Optical storage devices. I. Kalil, Ford, 1925- . II. Buschman, Al. III. Series.
TK7881.6.H52 1985 621.389'324 85-8926

For sale by the Superintendent of Documents, U.S. Government Printing Office, Washington, D.C. 20402

Preface

The first chapter, "High-Density Digital Magnetic Recording—A User's Perspective," by Richard E. DeFrancesco, Technical Director, Antisubmarine Warfare Tape Recorder Steering Group, Department of the Navy, gives the reader an excellent history, background, and perspective of high-density digital recording from a user's viewpoint. Although the user in that case is an antisubmarine warfare user, the information is relevant to all users and hence is used in this text as the first chapter in lieu of a more general introduction. Chapters 6 to 9 are also user oriented.

Other chapters in this book give the latest, off-the-shelf, state of the art in high-density digital recording (HDDR), including not only the magnetic technology but the optical and bit error correction technologies as well. There are also chapters on magnetic recording/reproducing heads and magnetic tapes for space-flight use.

This text should be of interest and useful to all who have a need to record, keep/store, transmit, read out, analyze, reuse, and play back data/information of all types and categories. The advent of the information explosion, the more prolific use of computers requiring digital information, and the inherent advantages of digital information have stimulated the development of HDDR techniques, including techniques for bit error correction and recovery. This text covers these topics thoroughly and is a very useful guide, perhaps an essential reference, for any user or potential user, including individuals as well as organizations—students, technicians, engineers, scientists, educators, libraries, colleges and universities, laboratories, Government, military, and industry.

This text is a sequel to *Magnetic Tape Recording for the Eighties,* NASA Reference Publication 1075, April 1982. Both were prepared as activities of the Tape Head Interface Committee (THIC), a professional society that cohosts its meetings with the American National Standards Institute (ANSI) and the Range Commanders Council (RCC), formerly the Inter-Range Instrumentation Group (IRIG).

Ford Kalil
NASA Headquarters

Contents

Chapter		Page
1	HIGH-DENSITY DIGITAL MAGNETIC RECORDING—A USER'S PERSPECTIVE *Richard E. DeFrancesco*	1
2	A METHOD TO DETECT AND CORRECT ERRORS IN A STREAM OF DIGITAL DATA ENCODED IN MILLER CODE *L. C. Csengery*	13
3	INTRODUCTION TO ERROR DETECTION AND CORRECTION TECHNIQUES *Neal Glover*	25
4	HIGH-DENSITY MAGNETIC RECORDING HEADS: OPTIMIZATION THEORY *David Ricards and David Christofar*	43
5	PERPENDICULAR RECORDING *Edward R. Wuori*	57
6	SERIAL HIGH-DENSITY DIGITAL RECORDING USING A WIDEBAND ANALOG INTER-RANGE INSTRUMENTATION GROUP RECORDER/REPRODUCER *E. L. Law*	67
7	BIT ERROR RATE PERFORMANCE OF IMAGE PROCESSING FACILITY HIGH-DENSITY TAPE RECORDERS *Paul Heffner*	93
8	THE DENSITY UPGRADE: MARK III A (A FUTURE IMPROVEMENT OF THE MARK III VERY LOW BASEBAND INTERFEROMETRY SYSTEM) *H. F. Hinteregger*	103
9	MODULAR HIGH-DENSITY RECORDING SYSTEM USING AN ALTERNATING DISPARITY BLOCK CODING SCHEME *Martin Davidson*	109
10	MILLER SQUARED CODING *James Kelly*	127
11	PARALLEL MODE HIGH-DENSITY DIGITAL RECORDING: TECHNICAL FUNDAMENTALS *Technical Staff, Datatape, Incorporated*	143
12	THE APPLICATION OF 3-POSITION MODULATION CODING TO LONGITUDINAL INSTRUMENTATION TAPE RECORDING *John M. Howard*	195

Chapter		Page
13	THE HONEYWELL HD-96 HIGH-DENSITY DIGITAL TAPE RECORD/REPRODUCE SYSTEM .... *Leighton Meeks*	215
14	THE DEVELOPMENT OF A HIGH-PERFORMANCE HIGH-DENSITY DIGITAL RECORDING ERROR CORRECTION SYSTEM .... *James H. Stein and W. D. Kessler*	231
15	ERROR CORRECTION FOR HIGH-DENSITY DIGITAL TAPE RECORDERS .... *John Montgomery*	247
	Appendix A—PULSE-CODE-MODULATED TAPES FOR HIGH-DENSITY DIGITAL RECORDING REQUIREMENTS .... *Walter Shaffer*	255
	Appendix B—TESTING MAGNETIC TAPE FOR HIGH-DENSITY DIGITAL RECORDING SYSTEMS .... *R. A. Schultz*	257
	Appendix C—INCREASING HEAD LIFE	271
	Section 1—EXTENDED-LIFE INSTRUMENTATION HEADS *David Christofar*	271
	Section 2—WEAR CHARACTERISTICS OF ULTRASIL™ VERSUS ALFESIL INSTRUMENTATION HEADS .... *Roger Mersing*	274
	Section 3—LONG-LIFE INSTRUMENTATION HEAD .... *Anthony Bucher*	278
	Appendix D—HIGH-DENSITY DIGITAL RECORDING (HDDR) USERS SUBCOMMITTEE EVALUATION OF PARALLEL HDDR SYSTEMS .... *R. S. Reynolds, Chairman*	281
	Appendix E—CARE AND HANDLING OF MAGNETIC TAPE HEADS .... *The Headwear Advisory Committee of the Tape Head Interface Committee*	293
	Appendix F—ACRONYMS	297
	Appendix G—GLOSSARY	299
	INDEX	307

CHAPTER 1

High-Density Digital Magnetic Recording – A User's Perspective

Richard E. DeFrancesco
Department of the Navy

HISTORY

To understand high-density digital recording (HDDR) in the Navy, one needs to appreciate the nature of naval recording and its history in the past decade. Fundamentally, there are many navies in the U.S. Navy. From a recording point of view, there are distinct communities comprised of members who share common functions and tape exchange requirements. However, these communities have stronger recording links to non-Navy affiliates than other Navy-only users. The reason is common function or mission. The Navy groupings fall into the security community, missile and space community, test instrumentation community, and the anti-submarine warfare (ASW) community. Each community can be characterized as having a central controlling influence and a set of standards that govern its recording. This chapter discusses the ASW community, which I have been serving for 16 years.

As the name suggests, the ASW community has a dedicated purpose – to protect the United States from the danger of a submerged threat. Not too many years ago the Navy was perceived as having many independent forces engaged in the same interest; many indeed, but interdependent. Everyone knew the merits of having good communication systems, but few understood that recorded sensor data interchange was also a powerful means of communication. In 1971 a bold step was taken by the Chief of Naval Operations in the formation of an ASW Tape Recorder Steering Group. Its purpose is to discover the root of recording problems plaguing the fleet; find solutions; and recommend changes in policy, practices, and planning to avoid future recurrences. This Steering Group, which carries the banner for the ASW recording community, is intent on eliminating recording weaknesses that have hampered the Navy in fulfilling its mission. Figure 1-1 gives an overview of the community network.

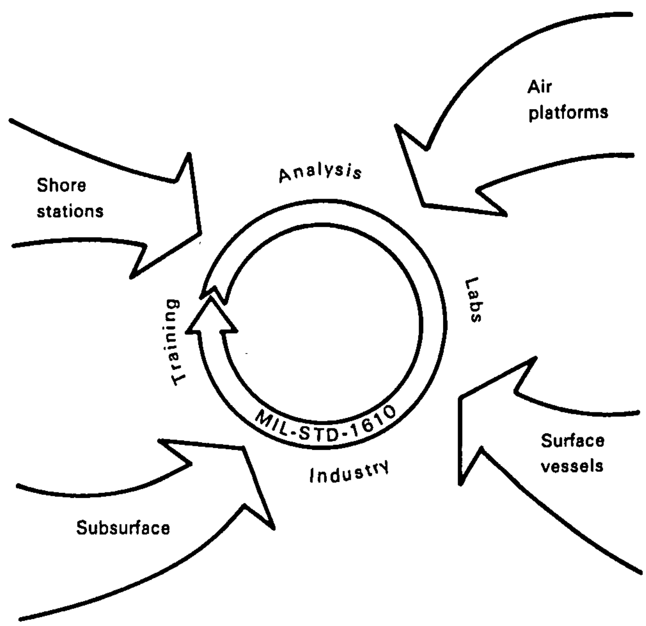

Figure 1-1.—Navy communities' recording interface.

The principal difficulties encountered in the early seventies were –

(1) Noncompatibility of recording equipment
(2) Improper use of existing recording technology for ASW applications
(3) Poor specification and test methods to assure good system performance
(4) Misunderstandings of the role of the recorder
(5) Lack of concern over selection and care of the tape media
(6) Nonstandard recorded tape format
(7) Lack of a mechanism to regulate existing recorders or bring about changes in a way that would preserve stability and avoid costly assets in the user's network

The manner in which we dealt with these deficiencies has set the style for the future, especially with regard to the introduction and use of HDDR. I will review these seven areas to show the basis for our current posture in ASW recording.

By noncompatibility of recording equipment I mean that no two types of sensor data recorders were even similar, even though they did the same job. Having so many different recorders has created a nightmare in logistics, training, publications, and other nonglamorous, expensive, yet important, aspects of ownership. The recorders received very little attention during the procurement of major systems, especially aircraft systems. Recorders were viewed as an accessory—much like a radio in an automobile's dashboard. Our systems were completely manual in the mid-sixties. We renovated the old systems to the point of upheaval. Now our ASW systems are thoroughly computer integrated, yet until very recently sensor data recording has been virtually ignored by the designers of the systems.

With the advent of HDDR, the options for data management and systems interface with the computers are abundant, but so are the challenges to cost-effective use. Recall that the purpose of recording does not lie in data management finesse, but in helping to ascertain the location and intent of submarines.

All too often we lose sight of the realities of the fleet environment: harsh weather, constant vibration, limited spare parts, varying degrees of personal motivation, inadequate experience with high-technology equipment, minimal funds for essentials (let alone nonessentials), and high stress in performing a military role on demand. The result of these experiences has been to strive for true hardware standardization in the operating fleet.

We own over $100 million in hardware that we cannot afford to discard. That would be too easy. We had to use every innovation to fix what we have and to upgrade and modernize along the way; that means some recorders would survive and others would not. To the industry at large we have had to take the position that we must use what we have all the way from intermediate-band FM to high-density digital unless something new solves a real recording problem and is worth the logistics impact.

Most people, when confronted with such a nightmare, would like to start over with a clean slate. Unfortunately, we were compelled to work with what was there; we could not bury the mistakes. This has led to the recurring notion that new, high-technology gadgets are the answer. Indeed, they offer promise, but the designers never come to grips with the easy recording devices with their simple systems hookup. In reviewing the merits of our existing recorders, we found that they were intrinsically more capable than was obvious due to poor man/machine considerations, operating conditions, and needless deviations from prevailing industry (Inter-Range Instrumentation Group[1] (IRIG)) practices. I say needless because the recorder designer strove to meet the specifications, which, unfortunately, did not accurately define the parameters associated with ASW excellence. The specifications were an extension of existing parameters, only tougher. We at the Naval Air Development Center found that the whole foundation for ASW data recording specifications was missing. We had a strong suspicion that with some changes to the existing equipment the machines could be made more useful. The optimism has endured; however, a bitter lesson was learned. It takes many years to fix a low-priority piece of equipment. The maxim is, "Do it right the first time, there may not be a second chance."

We have endeavored to develop meaningful specifications and irrefutable, repeatable test procedures. This brought to the surface many controversies. For example, we greatly value low spectral flutter sidebands and low noise floor/artifacts even if we trade for higher time base error, cumulative flutter, and broadband signal-to-noise ratio (SNR). The reasons stem from the nature of the sensor data and the signal processing used to enhance it.

Two significant aspects of our recording practices are crossplay and speedup during replay. Because the recording operation consumes many hours or even days, we want a time-compressed reconstruction, or we will never get an answer. Crossplay refers to playback on a device different in design and manufacturer than the recorder. All of these factors have forced us to take a view of recording hardware different from the bulk of the industry's customers.

We had to develop special fast-Fourier-transform-based (FFT) measurement techniques to allow for quick amplitude and phase response measurements for many channels over many speeds. We developed a technique for measurement of servo bandwidth using a pseudorandom noise (PRN) source as opposed to sweeping with a fixed sinusoid. This is a more accurate stimulus for the servo in predicting its performance and in adjusting its gain. We measure the noise floor with and without a data tone pair in the passband for combined SNR/linearity test. We measure the recorder system response, amplitude, and phase with tape moving using a PRN correlation technique followed by an FFT. Admittedly, the equipment required is not trivial but neither are the system applications or the value of the data. I will return to equipment attributes in the next section of this chapter.

In the past much of the trouble associated with the recorder has come not from an inadequate technology

[1] Now Range Commanders Council.

but from human ignorance in how to specify, procure, and use recorders. Even more, the role of the recorder has been misunderstood. It is an on-board historian. It contains a journal of events in raw form, which will provide reconstruction of a mission. In times of peace its role is more vital and should be more obvious. It supplies a measurement of crew proficiency and tactics effectiveness. It allows for collection of information about new events, both natural and manmade. It is the source of real data to feed a network of trainers and emulators. It provides proof that the weapons system could do its job if necessary. All too often, the worth of a device is judged by its esoteric or obscure attributes, its cost, and its mystical appearance. I. M. Brown, the Chairman of our Tape Recorder Steering Group, said most eloquently that we have a multimillion dollar aircraft connected to a multimillion dollar support center by a $100 roll of tape. Think of recorders as data links using tape as their medium of propagation.

Tape used to be bought from the cheapest source of supply because it had to be paid for out of the basic operating fund. Over the years the fleet users realized that they were hurting themselves. They initiated tape awareness, handling, and care programs. This has evolved into a large-scale effort that, we hope, will culminate in central procurement and commodity management. In this way we will avoid the need for special and uncontrolled tapes in standard applications. We will also have a mechanism to adopt the "right" digital tape. It is a matter of record that we believe in standards. The same is true with tape, for which we have been using the General Service Administration (GSA) standards. We will build on these in the future.

The most severe problem was the complete lack of a format standard for tape interchange. Our community did not make the best use of IRIG 106. We found that even if we had, what we really needed was absolute standardization. We generated MIL-STD-1610, an outgrowth of IRIG 106, but more restrictive. It has taken since 1974 to see widespread use of this analog format standard. Our challenge is to augment it for digital recording without fracturing the stability that has been achieved and also to keep the analog standard from becoming an anchor to progress.

We are still struggling with item (7) because recorders are a low priority with weapons system acquisition managers, yet are funded by them. We are trying to change the focus so that the mission support centers that really define the specific recording requirements take an active role in furnishing the hardware for the aircraft. I will take a few liberties to show that aircraft applications are different from those in surface vessels, shore stations, and submarines. All are different enough to warrant separate treatment but with a view toward standardization.

We have aircraft that range from smooth passenger types to shakers like helicopters, but from the standpoint of temperature and humidity, they are all bad. Some aircraft have to endure the shock and rigors of repeated carrier launches and landings. Oddly enough, some aircraft applications are similar to those of a submarine, while others are like those of a destroyer. The aircraft carrier application is similar to that of a shore station in allowable size, but not in environment and vibration. Shore station environments are most like laboratory or industrial sites except for logistics, maintenance, and crew skill. We cannot call for factory-authorized field service except in special circumstances.

All of our work is directed at making improvements within the complex framework of limited dollars and options as well as in harmony with the time scale of the host system itself. Figure 1-2 shows how we envision the application of MIL-STD-1610.

HARDWARE ATTRIBUTES

The machines are high-quality, high-unit-cost devices intended to work in the harsh environments of the operating fleet. We do not have many systems that have poor parametric peformance. Oddly enough, they might not "work" or they may be despised, but the reasons are rarely SNR, flutter, skew, or dropouts. In almost every case the recorders have had to meet tight signal bandwidth, distortion, and SNR specifications. This translates into equipment with a high intrinsic quality. Some pieces of equipment, however, have suffered from poor tape handling and the necessity of loading them in the dark, unpowered, with only poorly located threading diagrams as a guide.

Electronically, the equipment is excellent. The packaging is modular, which allows for ease of maintenance and growth. However, growth is very cumbersome because it affects the highly controlled documentation: manuals, provisioning for spare parts, drawings, and so on. Mechanically, the packages are sound and able to endure the tests, but they do show signs of leading a rough life at sea. In other words, they work well until they break, then they may not recover easily. Every platform's case is different, so generalizations beyond these are difficult to form.

Hardware attributes are best perceived from how they have to perform. The recorders rarely are required to play their own tapes back, yet all are required to have a very capable data recording monitor. This requires a full set of replay heads and a few full channels of reproduce. Our most modern sensor data recorders are truly fine analog devices by any measure. The reproducers are required to replay or crossplay source tapes, to copy tapes at high speed, and to deliver high-quality data to high-powered analyzers. We have

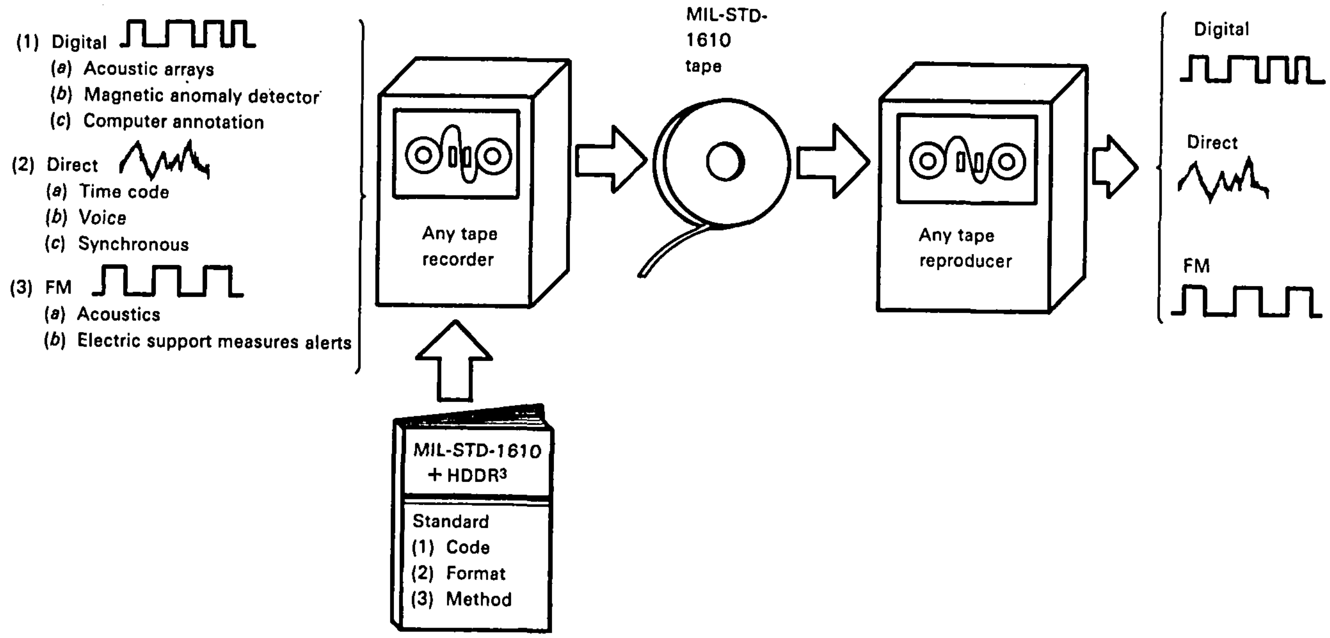

Figure 1–2.—MIL–STD–1610 usage.

pushed electromechanical servos to practical limits, but all fall short of requirements at high speeds. We developed an all-digital time base corrector to satisify this need, but, until recently, technology has not been available to implement the high clock rates in miniature packages. Figure 1–3 gives the concept of the time base corrector. Time base correction is not flutter compensation by subtraction or discriminator pulse-width compensation; it is time domain variable length delay applied to reproduced FM carrier prior to detection and filtering.

When we implemented our first serial HDDR system, we made use of the fact that, to the recorder, the flux transitions were similar to those in wideband group II FM, and that we had high carrier to noise ratio, hence, high SNR (30 dB direct) for self-clocking digital streams.

We have a base of hardware that demands to be fixed and improved, or we will go broke replacing it; however, we are vigilant toward the emerging requirement that can only be filled with a truly new technique; e.g., optical or laser-magnetic. Our recorders cost about $100,000 (in round numbers) each now. We can buy a few more at that price but cannot afford to switch to one that costs half as much because the total ownership cost impact, even for that model, would be $10 million in a typical aircraft or ship.

I may have given harsh indictments against some of

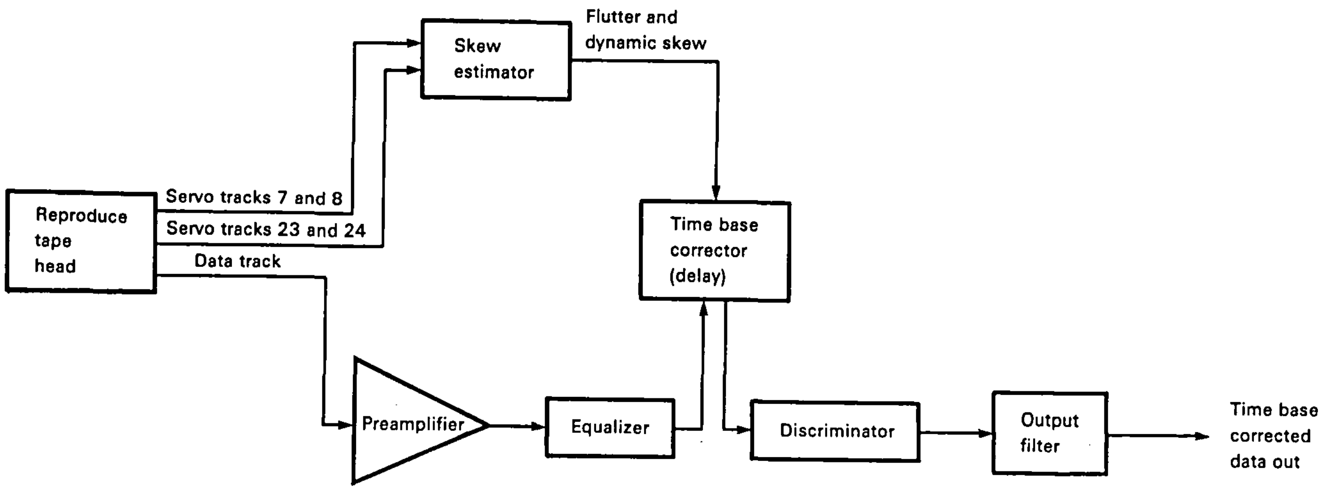

Figure 1–3.—Time base correction.

our equipment, but in all fairness the equipment has to operate in truly miserable environments. We all know that magnetic tape has limited operating temperature and humidity ranges, yet we have to operate the equipment from 0° to 125° F in different locations during the year. We can hardly afford what we have already, so tightening the specifications would drive the tape cost beyond our price range.

In dealing with the problems associated with crossplay, we came to understand that beyond the obvious physical alignment requirements there were definite electronic subtleties that needed to be addressed. One of the most famous is covered in Avner Levy's note (ref. 1-1) on amplitude and phase errors due to record head gap length differences when measured using a reference reproducer. For us this was the tip of the iceberg. We found that in wideband group II FM systems, bias-recorded FM yielded significantly lower second harmonic distortion than nonbias recording; amplitude and phase equalizer settings were significantly different for each type of recording as well. This meant that we had to require, in MIL-STD-1610, the use of bias. (Not unreasonable considering the need for direct channels for voice and time code recording.) We also found that the servo bandwidth had to be wider than the flutter spectrum of the source recorder and that there could be no high amplitude rates at any reproduce servo resonance points or the servo would oscillate. In HDDR we found that when using analog-type phase-locked loops, the bandwidth in the decoder had to be wide enough to correct for the flutter bandwidth of the source recorder. All analog phase-locked loops have a natural 12-dB/octave gain characteristic, and, hence, do not correct all flutter frequencies with the same amount. For this reason, we prefer an all-digital phase-locked loops design. Our experience has been that an all-digital time base corrector, implemented without any analog circuits, is inevitably more capable.

DATA INTERMIX

A significant factor in all ASW recordings is that all forms of recording, direct, FM, and HDDR, are often present on the same tape simultaneously. If information density is the real issue, then analog always wins over digital because analog has full amplitude freedom. Digital recording conventionally has two binary values. If fidelity alone is the issue, one could digitize the signal to any desired number of bits as frequently as technology will allow. From a recording point of view, digitizing analog data results in a requirement of 20 bits/cycle of bandwidth nominally (8 bits quantization × 2.5 sampling factor) or a record speed five times higher than the equivalent wideband group II FM system, hence, five times more tape. This leads us to be careful in jumping on the "everything is going digital" bandwagon.

There are applications in which digital sensor recording is a natural; for example, when the signals are already digital and conversion back to analog would deteriorate quality below acceptable limits, when amplitude and phase requirements cannot be satisfied by analog means, or when the number of channels far exceeds the number of tape tracks available.

With the application of time base correction, analog FM record channels can be made very well, almost the equal of a digital channel, with the further advantage that the recorder does not have to be modified. It could mechanically degrade yet still be electronically corrected during replay, and it uses no more channels or tape.

As a result, I recommend to system and hardware designers a match of recording techniques to the sensor and intended processing concepts.

The operational value of the tape recorder is and should be independent of the techniques used. As a corollary, recording techniques that are barely stable can only hurt, and our operators should not be burdened with the subtleties of recording, just its use.

Before I leave this topic, I would like to share a basic belief that has helped many of us grapple with the mysteries of recording; that is, all recording is fundamentally analog. Figure 1-4 shows our understanding of the mostly analog parameters that form the HDDR model.

I hasten to add that we are avid students of Finn Jorgensen, who has contributed immensely to our understanding of the recorder/reproducer process both practically and mathematically. His impulse model is the most enlightening contribution to this subject in years.

TAPE ISSUES

Tape is like a battery, a rechargeable one. Take care of it and it lasts a long time. Many people view tape as an expendable item. In a sense, it has been. We have seen less than two good passes of a roll of tape on certain recorders. Unfortunately, tape is so expensive for the fleet user to replace, he will try to reuse a bad roll. "Bad" does not mean a high dropout count, but wrinkled tape. (See figs. 1-5 and 1-6 for examples.) We insist that tape is a resource, although inevitably consumable, in the tough naval environment.

We are launching a widespread effort to build awareness of proper tape handling and care. This includes all the basics about cleanliness, wrapping, sealing, degaussing, shipping, and storage; however, achieving conformance is difficult. We simply do not have laboratory technicians in today's Navy. The work of building systems is increased by the need for their use by relatively unskilled operators.

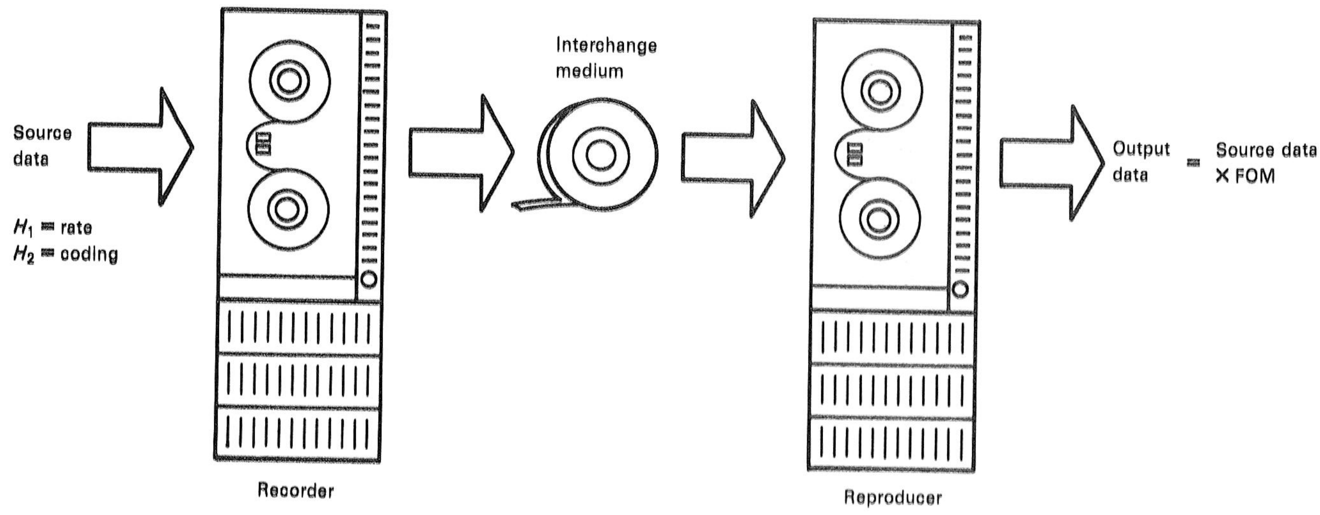

Variables:

k_1 = bias
k_2 = drive
k_3 = head gap length
k_4 = frequency bandwidth
l_1 = skew
l_2 = flutter
l_3 = alignment
l_4 = tracking
l_5 = speed change
m_1 = oxide coercivity
m_2 = oxide remanence
m_3 = oxide switching field distribution
m_4 = handling
m_5 = channel capacity
m_6 = viscoelasticity
m_7 = physical parameters
m_8 = environment (temperature/humidity)
p_1 = gap λ
p_2 = head inductance
p_3 = servo
p_4 = alignment
p_5 = tracking
p_6 = speedup
p_7 = SNR
p_8 = wrap angle
p_9 = azimuth
p_{10} = tension
q_1 = amplitude equalization
q_2 = phase equalization
q_3 = coding
q_4 = clock rate
q_5 = detector loop bandwidth
q_6 = lock range
q_7 = data format
q_8 = error corrector

Figure 1–4.—HDDMR parametric model. (FOM = bit error rate required for interoperability via data exchange $= f(k, l, m, p, q)$.)

There was a time when we had every kind of tape in the inventory that you could imagine. Our fleet would look for "freebies" and obtain tapes unsuitable for the intended application. We have sought to limit the authorized tape to only GSA E-2 oxide as a means of easing the situation. In general, that has worked because the tapes move faster and to more places than before. I should not overlook the fact that we have not, in general, procured the tape from a central place. In fact, until recently we have not used even central wisdom to guide the procurement of tape, which is done by hundreds of independent supply clerks. We have promulgated the ease of buying tape under the GSA schedule in an attempt to let human nature take the simplest way out.

An intimate part of the tape acquisition process is the specification. In general, the specification used by GSA, W-T-001553, has been a foundation document for all our tape activities. The only areas in which we perceive a need for additional controls have been tape slitting aberrations, especially cyclic patterns of width variations; dynamic thickness (cyclic) variations; and backcoating "traction." The whole topic of dropouts is large. We seek additional knowledge as well.

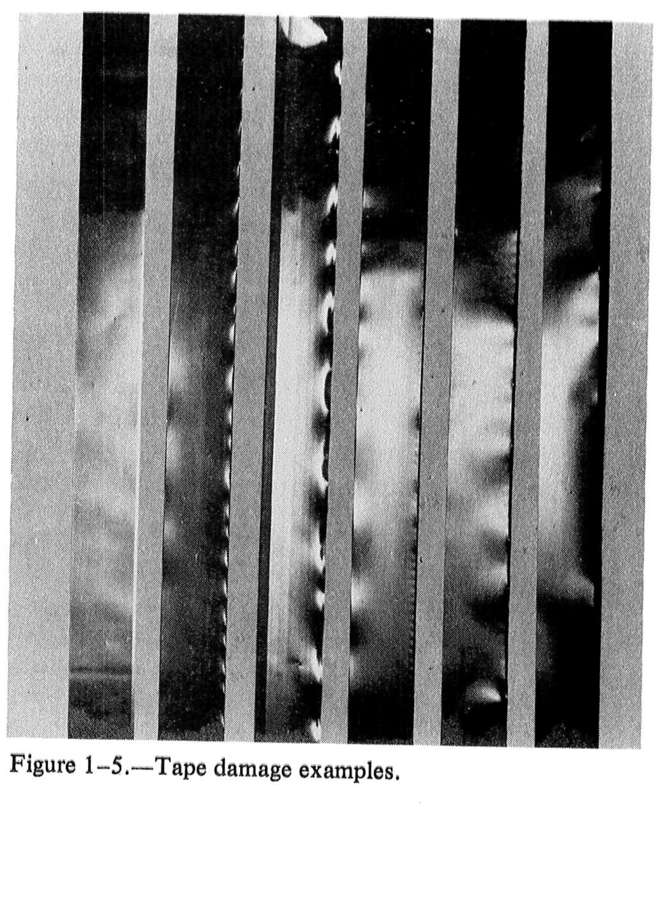

Figure 1–5.—Tape damage examples.

Figure 1–6.—Reel with damaged tape.

With the dramatic changes taking place in GSA's handling of tape procurement, the Navy is examining its needs very closely and is proposing to buy the tape centrally and, hopefully, establish a commodity manager who would set up a pipeline for reconditioning/refurbishing tapes and rejecting the poor ones. Other recording communities have done excellent work and will serve as a model for our venture. We are preparing to settle on specification values and initial procurement practices.

We have seen the value of cleaning tape operationally. New tape has become so clean that there is no trace visually of debris on the tissue rollers. Our experience with precision packing and winding has been even more fascinating. Empirically we have found that we can repack a scatter-wound reel of tape and keep it from being destroyed on several of our noncoplanar tape drives. These drives have many posts and rollers and inevitably put a twist on the tape to change levels as the tape moves from the lower to the upper reels. Many of these machines scatter the tape during fast wind and rewind modes. In the past, the operator did not realize he was being had when he rewound the tape and then tried to replay a portion. The transports were well behaved if you gave them a good wind. If you gave them even their own scattered wind they would chew the tapes up, usually by curling or rolling the edges over. For this reason we discourage rewinding before shipment. Let the lab-type reproducer do that just prior to replay. We established some guidelines for packing, settling, and reuse. These are just guides that were promulgated out of a sense of urgency because we were desperate to improve the "two-pass" life of tape. There have been some positive results. I believe our lower limit is now 12 passes, with 50 a distinct possibility. We look forward to the time when we can tame the wild transports. If we are to get the best yield from HDDR, we absolutely must have transports that handle the tape with finesse.

OPERATIONAL APPLICATIONS/ EXPERIENCE

Hardware

In our hall of fame we have many magnificent entries. Some had horrible reputations and have begun the journey toward excellence. The first is the RD–420, figure 1–7, made currently by Precision Echo. It is descended from a long line of workhorse tape recorders that date back to the PI–214 made by Precision Instruments. The RD–420 is a recorder that was designed to airborne military specifications but procured with only minimal ruggedization requirements in an attempt to keep the cost low for what was perceived to be an interim system, LAMPS MK–I AN/SQR–17. The Navy did not actually control the development and procurement of the recorder. A prime contractor decided what it needed for a destroyer application. Unfortunately, the LAMPS MK–I systems had to endure much longer than planned in the mid-seventies; therefore, we had to modify them. With the advent of the latest modifications they work magnificently. In 1975 a need arose to incorporate into the RD–420 35 more channels of information on the remaining 7 tracks. Several multiplexing schemes were considered, but the stringent amplitude, phase, and time coherence requirements of the signals eliminated all but a digital approach.

The first full-scale fleet venture into HDDR had begun. We worked closely with the prime contractor, but in all honesty we just did not know all the problems.

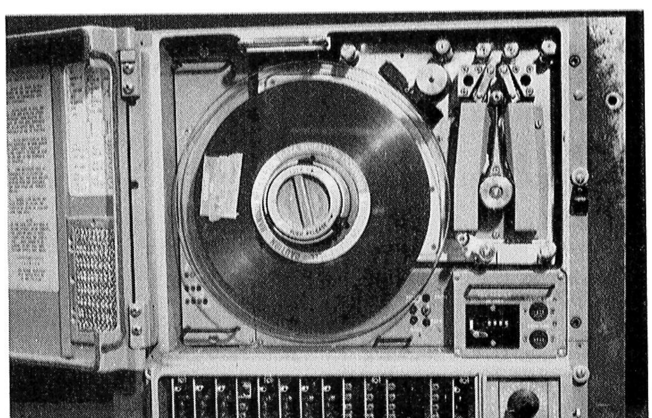

Figure 1–7.—RD–420A.

Initially everything worked very poorly. We found that the good analog machine had short noise spikes that drove the digital logic wild. The heads were fine for FM, but the 27-kbpi delay modulation, mark (DM−M), required very good high-end response. Only the heads from one vendor had the needed performance beyond the analog specifications. As it turned out, the RD-420 did not have a direct record/reproduce specification because there were no wideband direct channels as such. We tried to use the implicit direct performance. There was also a 200-kHz artifact in the system that fed a spurious signal into the bit synchronizing signal centered at 199.7 kbps. In addition, the bit synchronizer was primitive, yielding only 10^{-4} bit error rate (BER). The "A" suffix in the RD-420A designates a modification, which in this case refers to the addition of the digital record capability and the multiplex voice subcarriers. The track assignments of the RD-420A are as follows:

Tape Track	*Data Type*
1	Digital (time-multiplexed acoustic data serially encoded in Miller code (26.6 kbpi/7½ ips)) tactical towed array sonar (TACTAS) acoustics
3	Digital (time-multiplexed acoustic data serially encoded in Miller code (26.6 kbpi/7½ ips)) tactical towed array sonar (TACTAS) acoustics
5	Digital (time-multiplexed acoustic data serially encoded in Miller code (26.6 kbpi/7½ ips)) tactical towed array sonar (TACTAS) acoustics
7	Direct servo
9	Digital (time-multiplexed acoustic data serially encoded in Miller code (26.6 kbpi/7½ ips)) tactical towed array sonar (TACTAS) acoustics
11	Digital (time-multiplexed acoustic data serially encoded in Miller code (26.6 kbpi/7½ ips)) tactical towed array sonar (TACTAS) acoustics
13	Digital (time-multiplexed acoustic data serially encoded in Miller code (26.6 kbpi/7½ ips)) tactical towed array sonar (TACTAS) acoustics
15	Digital (time-multiplexed acoustic data serially encoded in Miller code (26.6 kbpi/7½ ips)) tactical towed array sonar (TACTAS) acoustics
17	Analog (IRIG wideband group II) LAMPS MK-I acoustics
19	Analog (IRIG wideband group II) LAMPS MK-I acoustics
21	Analog (IRIG wideband group II) LAMPS MK-I acoustics
23	Direct servo
25	Analog (IRIG wideband group II) LAMPS MK-I acoustics
27	IRIG B time code; TACTAS Track Beam Audio plus three channels of voice (direct time code plus four IRIG FM subcarriers: 5B, 7B, 9B, and 11B)

The two servo tracks are in accordance with MIL-STD-1610, which allows for flutter and dynamic skew correction of analog signals. Because the high-density digital recordings are self-clocking and contain block markers, all flutter and skew are removed in the process of synchronizing and reformatting. This recorder format is unusual in that the seven digital tracks are taken as an ensemble. Each track is treated as an independent serial stream, then after buffering the words, which are serial along the track, the words are loaded into registers for each of the 35 data channels, which are then converted back to analog for the AN/SQR-18A system to process. There is no error-detect/correct scheme in this system although there could have beeen if we raised the overhead and chip count. At the time we started this program we needed a BER of 10^{-6} to guarantee that data would not be corrupted after replay on another type machine, copied, and then replayed on the original type machine. The prime contractor went back to the drawing board, hired a consultant, and produced a bit synchronizer that yielded 10^{-7} when playing the same pseudorandom sequence that gave only 10^{-4} a year before.

This program forced us to examine many little known aspects of recording. We had to explore using DM−M in regions where few had confidence it would work well. We have used Miller/DM−M routinely to about 30 kbpi (user data) and experimentally to 40 kbpi with an uncorrected BER of 2×10^{-6}. The key has been the quality of the bit synchronizer. We were fortunate to have experimental access to eight or more different designs.

Another most significant and very contemporary aspect of HDDR that we have explored is that of duplicating tapes—more specifically, "counterfeiting" or "cloning" the tapes in a manner so that they can be replayed on the source recorder faithfully. This allows us to make training tapes for the operating fleet. We determined that to make the copies work, the magnetic imprint on tape needed to closely resemble that from the original recording. We achieved this by reducing by several decibels the bias from the optimum wideband II FM setting and raising the record level significantly. This will markedly change the shape of the recording transition zone to achieve the desired end result.

Another frequently used recorder in our world is the AN/AQH-4(V)2, figure 1-8, also made by Precision Echo. Its track format is as follows:

Tape track	*Data type*
1	Direct (voice recording from the aircraft intercom system)
2	FM
3	FM
4	FM
5	FM
6	FM
7	High-density digital
8	Direct (servo reference)
9	FM
10	FM
11	FM
12	FM
13	High-density digital
14	FM
15	High-density digital
16	FM
17	High-density digital
18	FM
19	High-density digital
20	FM
21	High-density digital
22	FM
23	High-density digital
24	Direct (servo reference)
25	High-density digital
26	FM
27	Direct (time code)
28	FM

In this case the digital version was made for the Royal Australian Air Force in cooperation with the Data Recording Laboratory at the Naval Air Development Center. We had the pleasure of guiding the development of this first airborne ASW HDTR application in the P-3C aircraft even before we in the U.S. Navy would take advantage of the technology. As in the case of the RD-420A, the experiences we gained were invaluable though painful. The lesson learned by the Navy, which I personally stress any chance I get, is to let the recording industry do the job it does best. When a prime contractor starts meddling or redesigning parts of a recorder, hold on for a rough ride. We have paid the price in a dozen cases.

The recording technique used here is very similar to that used in the RD-420A, Miller/DM–M coding. Independent but this time asynchronous clocks drive each serial high-density digital channel to 30 kbpi (user data). This system is operational and successful using GSA E-2 type oxide, which is currently Ampex 795 tape, with a BER of 10^{-6}. These two systems have formed the benchmarks for our serial high-density digital standard now operating with success. Again in the case of the Royal Australian Air Force, the bit synchronizer made the difference. The replay machine is not principally the AN/AQH-4(V)2 but a Honeywell Model 96 specially equipped with remote switchable bit rate bit synchronizers. These use analog-based phase-locked loop circuits whose locking bandwidth needed to be widened to accept the flutter of the digital stream of the airborne recorder.

Our third recorder in this category is the AN/AQH-5(V)XD, figure 1-9. We had a legendary, successful flight test of this 1969 style recorder in 1981. Emerson Electric augmented the recorder to have 28 tracks of record and reproduce per MIL-STD-1610. They repackaged the card cage very neatly and we flew it, the one and only model on an SH-3H helicopter at sea in a controlled exercise. It performed flawlessly. In this case we had serial HDDR tracks for computer data and

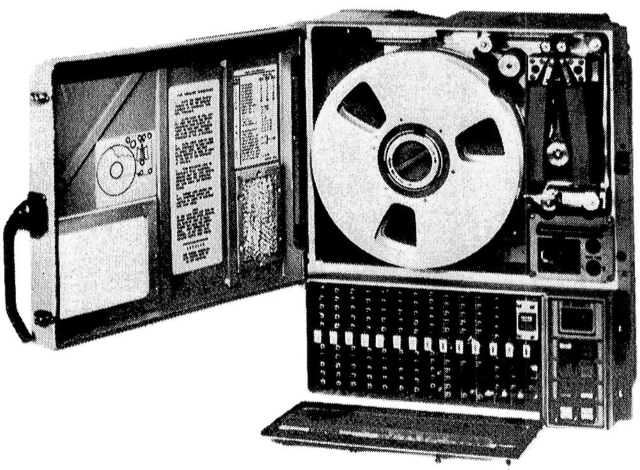

Figure 1-8.—AN/AQH-4(V)2D.

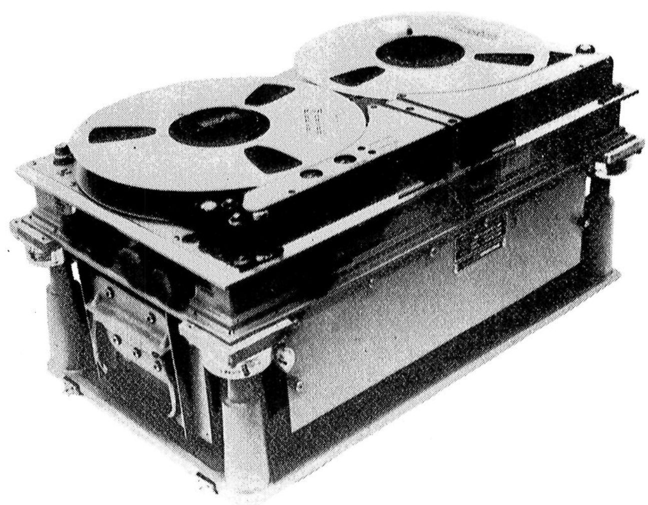

Figure 1-9.—AN/AQH-5(V)XD.

display video. We still have some software knots to take out, but the recorder worked superbly. The replay was on a representative aircraft carrier reproducer suite, AN/USH-31(V), built by Honeywell as a derivative of its Model 96.

The proposed track assignments for the AN/AQH-5(V)XD are as follows:

Tape track	*Data type*
1	Direct (voice recording from the aircraft intercom system)
2	Digital
3	Digital annotation
4	Not assigned (growth)
5	FM
6	FM
7	Direct (servo)
8	Direct (servo)
9	FM
10	FM
11	FM
12	FM
13	FM
14	FM
15	FM
16	FM
17	FM
18	FM
19	FM
20	FM
21	FM
22	FM
23	Servo
24	Direct (servo reference)
25	Direct (servo reference)
26	FM
27	Direct (time code)
28	Not assigned (growth)

The coding scheme was again Miller/DM – M at 27 kbpi (user bits). The most novel accomplishment in this recorder effort was found in the system interface unit built by Diagnostic Retrieval Systems, Inc. They captured the display video with an array of analog-to-digital converters and sorted through the known-to-be empty display *x-y* data positions to reduce the 10-mbps throughput rate to 200 kbps. On replay, they reformatted the single serial stream into analog drive signals to exercise an *x-y* display that gave a flicker-free replica of what the operator saw in the air. So powerful a tool has this system been, that it has been used as instrumentation to back up flight tests of other systems. Again the total system is a hybrid of analog and digital. In the parallel recording format, as it is conventionally understood, we have used with instant unparalleled success a variation of the AN/USH-31(V) known as the AN/USH-31(V)3, figure 1–10. Its format is as follows:

Tape track	*Data type*
1	Unpopulated (auxiliary)
3	Error correction
5	Digital data 9
7	Digital data 7
9	Digital data 5
11	Digital data 3
13	Digital data 1
15	Digital data 11
17	Digital data 2
19	Digital data 4
21	Digital data 6
23	Digital data 8
25	Digital data 10
27	Digital data 12

In the parallel format we were looking for fleet hardware commonality with existing USH-31(V) systems as well as a system that would have the flexibility of packing densities and a wide range of easily selectable bit rates. What we got was that and more – a BER of 10^{-10} with one correction track using Ampex 799 tape. Our fleet need in the specific application was 10^{-8} with Ampex 795, E-2 oxide. The hardware has very sensitive bit synchronizers capable of reading through deep dropouts. This device in various configurations has

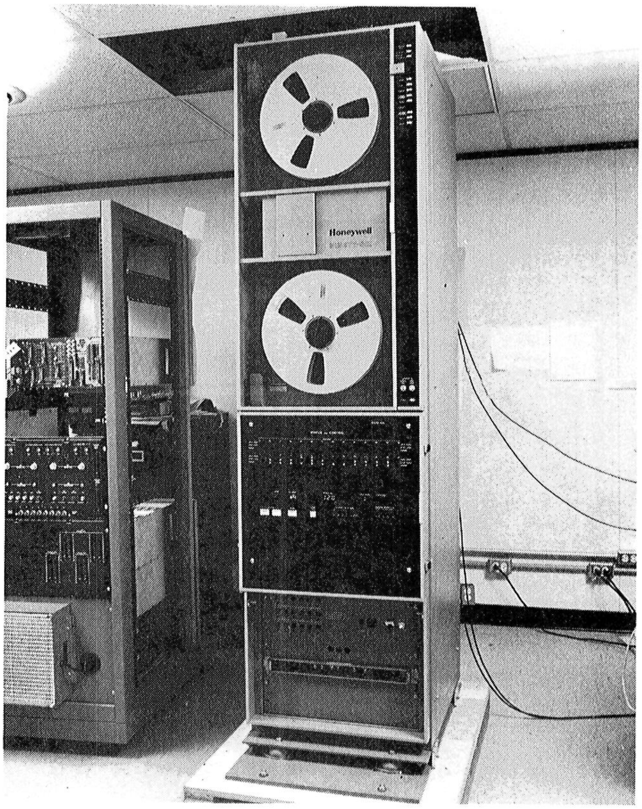

Figure 1–10.—AN/USH-31(V)3.

spread in similar applications throughout the ASW community and has also become a benchmark for our future parallel HDDR standard. The track configuration of the USH-31(V)3 series, when it is configured for 28 tracks, is compatible with 14-track in-line versions on 28-track spacing. This is an essential requirement of ASW Navy recorded data interchange.

The last recorder is our newest, the AN/USH-32, figure 1-11. It is the first fully Navy-owned MIL-STD-1610 recorder. It is being groomed for a broad range of high reliability and severe shipboard applications—both analog and digital. It is currently made by Bell and Howell, who did a magnificent job; it exceeded its specifications in many very important performance areas. Because it is a descendant of all Bell & Howell's fine work in the M-14 and AN/USH-24(V) series, it has the intrinsic ability to record both serial and parallel high-density digital data. Our challenge will be to arrive at a standard format between this and already existing ASW parallel recording schemes.

Tape

I must now turn to the tape and its performance at the systems level. Early in our digital explorations we found that tape was much better than that for which it was given credit. In the last 7 years, our problems have rarely been with tape. The quality control has been excellent

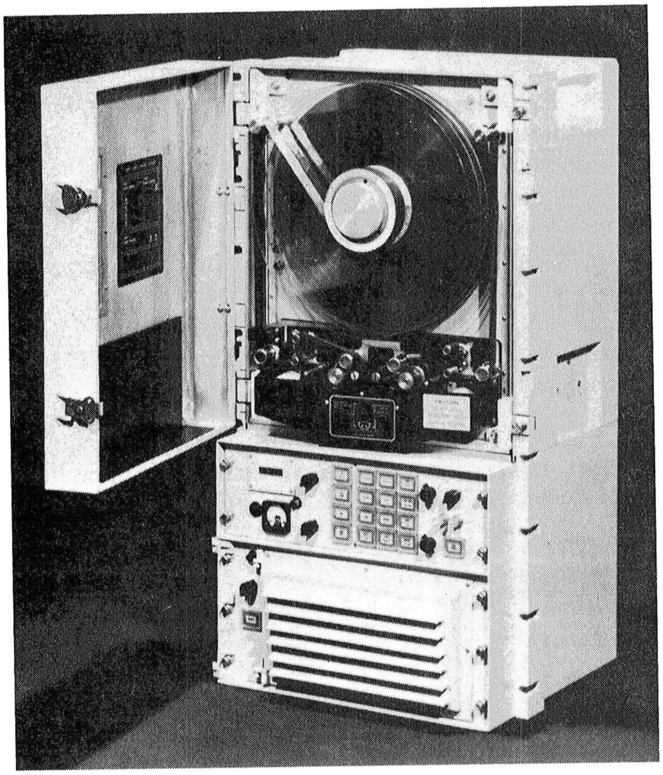

Figure 1-11.—AN/USH-32.

in the conventional areas. We do, on the other hand, have a great appetite for quality. The same tape gave results from 10^{-4} to 10^{-7} BER, depending on the intrinsic quality, not size or cost, of the bit synchronizer. We have also noted that there is a definite relationship between FM analog broadband SNR and randomly distributed dropouts. In practice, 35-dB FM SNR is roughly equivalent to 10^{-6} BER. The tape has been blamed for what we believe is the below par performance of rudimentary hardware. This also will drive some recorder system designers to use more loops of correction than minimally necessary. We also believe, based on observations, that there is very little performance difference (<20 percent) between coding schemes, that the real difference in system performance (10^{-4} to 10^{-7} serial, 10^{-8} to 10^{-10} parallel) results from the hardware design and its ability to deal with the actual characteristics of tape.

In the future we will need track densities double and quadruple what we now have as well as higher flux densities. Based on the recent work done by industry, I am confident that it can be done, with the right encouragement and stimulation by the customer.

Before I leave the topic of tape, there are two other areas worthy of comment—dropouts and certification. A dropout is meaningful only when it hurts the data. In FM recordings a single dropout serves to raise the noise level. In digital recordings the dropout can cause an implied increase in the noise level if the data represented a signal, or it could be a false command or an error in a paycheck of arbitrarily large magnitude. We have not independently embarked on the pursuit of the size of dropout ϵ that we can ignore as insignificant. We expect to do so after learning more from the abundance of work taking place already. We do need to quantify the tape amplitude characteristics to predict initial performance and to measure change during the life of the tape. Our initial departure will be to devise a method, perhaps a fixed (dc) field to highlight any errors.

With regard to certification, because different systems have different sensitivities, screening the tape to fixed thresholds is very limiting. We believe that an independent profile of amplitude versus length, perhaps quantized to many levels screenable by a computer sort, is a better and more objective method.

We have been experimenting confidently with monitors of data signals after recording without elaborate data analysis techniques. Figure 1-12 depicts the block diagram of our first scheme. We are examining the amplitude of the FM carrier or the bit stream in the case of the high-density digital channel. This method has limitations, admittedly, but it is an "in situ" technique. We recommended the use of a preamble and an interspersed synchronization pattern that can be used for a calculation on the run.

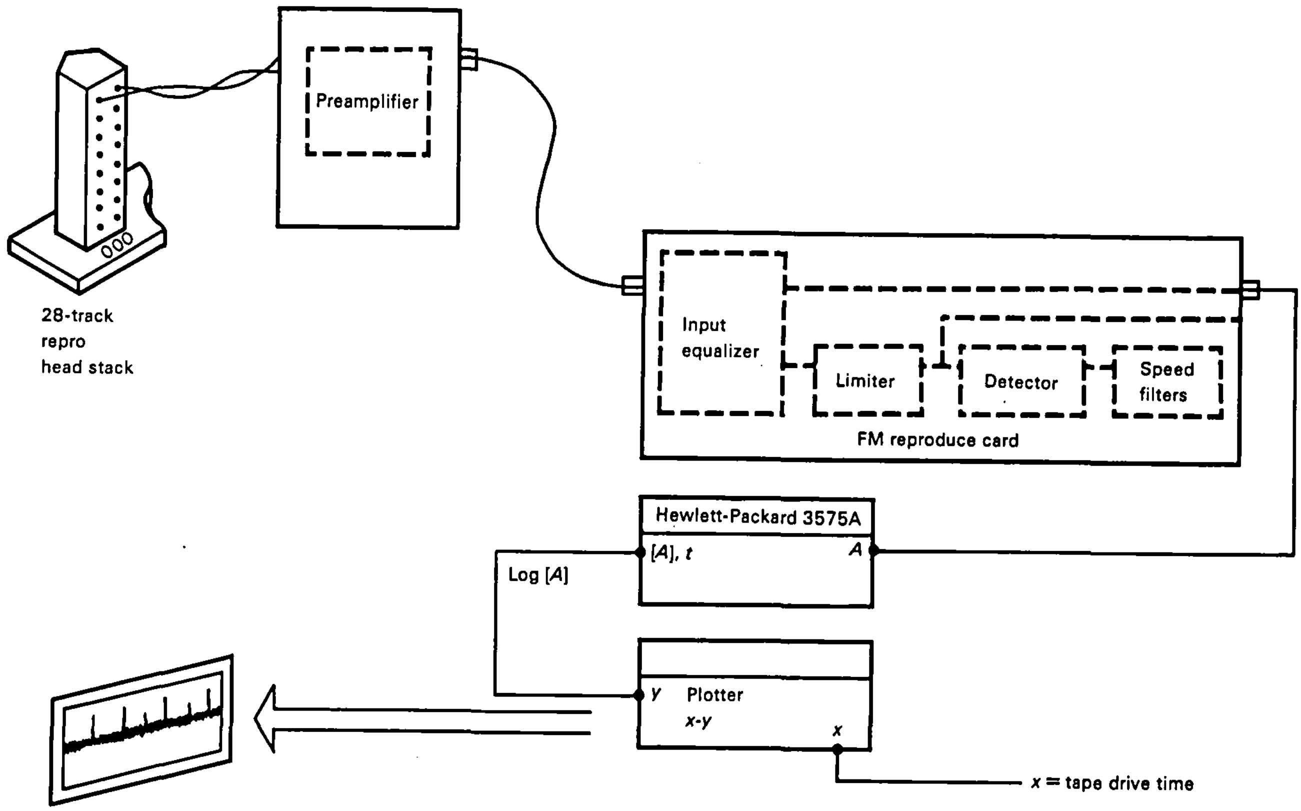

Figure 1–12.—Data signal monitoring.

USER'S REQUIREMENTS

Our fleet wants dependable, easy-to-use common hardware. It wants self-threading and magazine load equipment that does not destroy the tape and digital recorders that are no more difficult to use than analog recorders. It expects better diagnostics and fault isolation (built-in test equipment) in digital than in analog recorders. The fleet wants performance with readily available tape, preferably the same as that being used now for MIL-STD-1610 systems, which admittedly exceed E-2 minimum specifications.

The requirements are not great in number, but they present a real challenge.

SUMMARY

I have attempted to give insight into our world of ASW recording. Because there are so many decision-makers in the loop, we are subject to many constraints and complications in finding a path to bring about change. This leads me to give some opinions:

(1) Do it right the first time.

(2) Know what you want and insist on it.

(3) Trace specifications to real requirements and sound judgments.

(4) Use the techniques that make sense.

(5) Value the recorder and the tape for the costly data, not the hardware glamour.

(6) Select standard systems that work throughout the community.

(7) Give the industry clear requirements, not wishes.

REFERENCE

1-1. Levy, Avner: *Machine-to-Machine Compatibility in Wideband Recording.* Instrumentation Technical Information No. 10, Ampex Corp., 1980.

BIBLIOGRAPHY

Jorgensen, F.: *The Complete Handbook of Magnetic Recording.* Tab Books, Inc., Blue Ridge Summit, Pa., 1980.

CHAPTER 2

A Method to Detect and Correct Errors in a Stream of Digital Data Encoded in Miller Code

L. C. Csengery
Lockheed Electronics Company, Incorporated

The performance goal for any data storage or transmission system is to produce error-free data. Because of imperfections of the media or the mechanisms used, this goal can only be approximated; the data received from such a system will contain errors. It is possible to improve the performance of such systems by correcting some of these errors. A prerequisite to error correction is error detection. In the past, error detection has been accomplished by adding to the data information that would make certain characteristics of the data predictable. This predictability then would make an examination of the data useful, and deviations from the predicted characteristic will indicate errors. Typical examples of information added to data for error detection are parity bits and cyclic redundancy check (CRC) characters. All such techniques reduce the efficiency of the system because, in addition to the actual data, the error detection information must also be stored or transmitted. In general, none of these techniques will detect all errors, but the number of errors detected will increase when more error detecting information (overhead) is added to the data. However, because all the overhead information must also be stored or transmitted, system efficiency decreases as more overhead is included in the data.

This chapter presents a method that will detect errors in a stream of digital data that is encoded in Miller (or Wood) code. This method will detect errors without the need to add error detecting information to the data stream.

The addition of a parity channel to a multichannel parallel data stream will result in a system with error correcting capabilities.

OVERVIEW OF DIGITAL RECORDING CONCEPTS

Data transmission and data storage systems are in use in such a wide variety of applications that such systems influence everyone's life to a significant degree. All such systems have some characteristics in common: they receive data inputs, they provide data outputs, and the output data must correspond to the data received.

The vast majority of the data stored or transmitted is generated by or for computers; and most current computers are digital, consequently, almost all such data are also digital. Even such traditionally analog information as music has been recorded in digital form with excellent fidelity. Digital data are in the form of a series of digits, these having only two possible values: "0," or "1." Such data are often called binary data. One element, or digit, is called a bit (*bi*nary digi*t*).

One of the principal shortcomings of a digital data storage or transmission system is the presence of errors in the output data. No system exists that is completely free of this problem. This problem may be an insidious one because a system that operates well, producing very few errors, is often regarded by its users as infallible.

In any event, the user of such a system needs to know the expected reliability of the data that he receives from his system. The measure of this data reliability is the bit error rate (BER), customarily expressed as the ratio between the number of errors e and the number of bits N that contain these errors:

$$\text{BER} = \frac{e}{N} \qquad (2\text{-}1)$$

Equation (2-1) is applicable for both expected and observed errors.

This chapter primarily addresses data storage systems, in particular, magnetic tape recorder/reproducer (MTRR) systems, but some of the concepts are equally applicable to other data storage and data transmisssion systems.

The output of a digital MTRR typically consists of a stream of digital bits that ideally is identical to the stream of digital bits that was originally presented to the MTRR for storage.

The principal sources of errors in the data from an MTRR are the tape and the drive mechanism. Imperfections in the tape cause dropouts; i.e., inaccurate signal reproduction resulting from discontinuities of the magnetic coating of the tape or insufficient head-to-tape contact either during the record or the reproduction process. Imperfections of the mechanism cause variations in the tape speed. These result in time distortions in the signal, prohibiting accurate recovery of the data. In addition, the imperfections of tape and mechanism combined cause lateral movements of the tape, resulting in further degradation of the reproduction signal.

Obviously, errors can also result from shortcomings of the electronics that are used to manipulate the data, but these errors are generally less frequent than those from the aforementioned causes.

Recognizing that it is not possible to manufacture a consistently error-free MTRR, engineers have spent a considerable effort to analyze the characteristics of these errors. Naturally, if methods could be developed that would operate on the MTRR output and correct the errors in the data, such methods would, together with an imperfect MTRR, result in a perfect storage system.

Although a definitive method to correct all errors cannot be devised, due to the random nature of the data, a plethora of error-correcting techniques have been developed. While none of these is perfect, they are certainly able to enchance the data reliability of MTRR's. The BER of a system with error correction can be orders of magnitude better than the BER of a system without that feature, both using an identical MTRR.

All known error-correcting methods have to include some way of detecting errors—an error must be identified before it can be corrected. Accordingly, any discussion of errors in a digital data stream will have two topics: error detection and error correction.

Historically, error detection has always been examined before error correction. This is not surprising, detection being easier and also a necessary prerequisite for correction.

Binary data streams are by nature a chain of bits in which the value of each is either "1" or "0." The sequences are essentially random; therefore, the probability of either value is 0.5 for each individual bit. Consequently, observation of such a data stream cannot and will not offer any clue as to the value of any particular bit. Conversely, if any such bit would be known to be in error, the correct value of it would be immediately known.

The value of any particular bit cannot be predicted and no particular data pattern can be predicted because of the inherent randomness of the data. The earliest error-detecting techniques developed consisted of *adding* information to the data such that some characteristic of the data pattern would be predictable. Such predictability could then be used to detect errors. For example, one of the earliest ideas was to break up the data into groups of bits, sometimes referred to as words, count the number of "1" bits in each word, then add one more bit to each word such that the number of "1" bits in each enlarged word be always odd. When a data stream so augmented would be checked for errors, the predictable characteristic would be the odd number of "1" bits in each word, called the odd parity of each word. Obviously, each word that did not have odd parity was in error. This scheme is not perfect, because a word with two bits in error would appear correct; furthermore, it is not possible to isolate the bit that is in error, only the word that contains the bad bit. Data parity is, however, a valuable tool, because in many applications it is useful to know whether errors are or are not present. The election of odd parity is arbitrary; even parity works the same way, but odd parity has advantages that will be shown later.

In systems that record and reproduce data in several parallel channels, there is the possibility of improving the effectiveness of error detection using data parity. Such data can be augmented two ways. Let us consider eight parallel channels of data as an example. In each channel, n bits can be enlarged with a parity bit to create words of $n + 1$ bits with known parity; in addition, a ninth channel can be added; this channel would contain bits generated to maintain odd parity across the channels; i.e., the first bit in each channel would constitute a lateral "word," and the first bit in the ninth channel would be generated by looking at the bits of this lateral or vertical "word" and assuring that the nine bits have odd parity. The second bit in the ninth channel would be generated from the second bit of each channel, and so on.

When data encoded in this manner are decoded, the combination of the in-channel parity information, or longitudinal parity, with the across-channels parity information, or vertical parity, can identify a single bit error in such a way that it can be corrected and can detect multiple errors that otherwise would escape detection.

There are many other schemes to detect errors, but all have one characteristic in common: Bits are added to the data to generate a predictable pattern, and the errors are detected as violations of the pattern that is predicted. The added bits are referred to as overhead, and, in general, the amount of the overhead will increase as more complex error detection techniques are employed. To analyze the performance of different techniques, the overhead is usually expressed in percent of the actual data; e.g., a parity bit added to each eight-bit word will result in

$$\text{OH} = \frac{\text{Added bits}}{\text{Data bits}} \tag{2-2}$$

$$= \frac{1}{8}$$

$$= 12.5 \text{ percent}$$

Increased overhead increases the bandwidth required to process the data.

To evaluate the performance of a data storage system, certain concepts must be defined: frequency, bandwidth, signal-to-noise ratio (SNR), and density.

Frequency is an inherent characteristic of any data stream; it is a measure of how often bits occur in the stream. Theoretically it would be possible to transmit or store data where the bits occur at random time intervals; however, this study will be limited to data streams in which the bits follow at a constant rate:

$$f = \frac{1}{t} \qquad (2\text{–}3)$$

where f is the frequency in hertz and t is the time in seconds between each successive bit.

Bandwidth is a characteristic of any system; it is the difference between the minimum and maximum frequencies that the particular system can handle. Bandwidth is also a characteristic of the data stream because it is dependent on the coding scheme and the bit frequency; for a given code and bit frequency, the bandwidth of the data is a frequency band from f_1 to f_2, where f_1 is the lowest and f_2 the highest frequency that must be transmitted or stored to assure correct processing of the data. In general, f_1 and f_2 are the lowest and highest frequencies that are present in the signal that represents the data.

SNR is a characteristic of the signal that represents the data stream. Any such signal is composed of the actual data (the ideal voltage waveform representing the data) and noise, which is superimposed on the ideal waveform. Noise is defined as any electrical signal that is not part of the ideal waveform; it can originate from a variety of sources, but if the amplitude of these unwanted signals approaches that of the actual data, the data will be no longer detectable.

Density, or packing density, is a concept related only to data storage systems. It is a measure of the quantity of data that is stored in the storage medium. Two types of density figures are used for magnetic tape: (1) the surface density, which is the number of bits stored per unit of surface, expressed in bits per square inch, and (2) the track density (for longitudinal recording), which is the number of bits stored in a track per unit length, customarily given in bits per inch.

The design of storage systems is oriented toward maximum possible density, because for a given length of tape that may be contained in a tape unit, the highest density allows the maximum number of bits to be stored. There are technological limits to the maximum density that it is practical to obtain.

The performance of a data storage system is measured essentially in terms of three main parameters:

(1) Data capacity; i.e., number of bits that can be stored

(2) Data rate; i.e., the frequency or speed with which the data can be recorded and/or retrieved

(3) Data reliability; i.e., probability of retrieving the data accurately

Data capacity is expressed in bits, data rate is expressed in bits per second, and data reliability is expressed in predicted error rate, BER. See equation (2–1).

The design of tape recorders is also influenced by other factors such as size, weight, and power consumption. These, however, fall outside the scope of the present discussion.

Review of High-Density Codes

As mentioned earlier, there are technological limits of bit density on tape. This statement assumes that bits are stored on tape in a particular way. There are, however, many ways to store bits of data on tape. The storage of digital data bits on a magnetic medium, such as tape, has been the subject of extensive research and analysis, but, basically, all such techniques rely on the ability of the medium to be magnetized and to remain magnetized for extended periods of time.

Because this study deals with the storage of binary data, the magnetization must be such that two clearly detectable states are created. Essentially, the requirement is that an electrical signal received by the recorder be imparted to the medium such that upon reproduction, the original signal is recoverable. The electrical signal must then be encoded to contain the data, and the method of encoding is also important.

The reproduction process of a tape unit consists of passing the previously magnetized tape in front of a transducer commonly called the reproduce head. This head will respond only to changes in magnetization on tape. Because we are only interested in binary digital data, we can expect that the optimum output signal from the head is obtained when sharp changes in magnetization occur. The sharper the change in magnetization, the larger the amplitude of the head output signal. As we have already seen, this head signal will contain noise in addition to the data. If the amplitude of the noise approaches that of the data, recovery of the data will be impossible. Accordingly, the highest data amplitude possible is desirable. This means that transitions from one magnetic state to an opposite one will give the best signal to interpret.

The data, then, should be encoded in the form of

transitions from one distinct level to another; such a signal, when used to magnetize the tape during the record process, will produce the optimum reproduce signal for data detection.

We can now return to the first statement of this section: There are technological limits of bit density on tape. This statement can be restated as follows: There are technological limits of transition density on tape. It is then up to the coding scheme to minimize the number of signal transitions needed to store a bit. There are several coding schemes to accomplish this. The most important of these methods will be reviewed.

Digital bit encoding was being done before magnetic storage devices existed. The first such code was simply to generate a signal that had a positive pulse to indicate a "1" bit and a negative pulse to indicate a "0" bit. Between these pulses, the value of the signal returned to zero, thus the name of this coding scheme: return to zero, or RZ. This code has obvious disadvantages:

(1) It contains three voltage levels.

(2) There are two transitions for each bit. (See fig. 2-1(*b*).)

A second type of RZ coding evolved consisting of a signal that had a pulse for each "1" and nothing for each "0" bit. (See fig. 2-1(*c*).) This method no longer required three voltage levels, but it still needed two transitions for each "1" bit. Another difference between the two schemes is that the timing of the first is clear, a pulse for each bit, whereas the timing of the second is undefined. The absence of pulses for "0" bits makes the signal impossible to decode without some timing reference to determine the number of "0" bits between any two "1" bits. This difference is commonly referred to by calling the signal shown in figure 2-1(*a*) self-clocking and the signal in figure 2-1(*b*) non-self-clocking. This distinction will be made in the discussion of all other codes.

The advent of magnetic tape recorders as digital storage devices started the development of new methods to encode digital data into an electrical signal. These new codes evolved as engineers attempted to tailor them to the characteristics of the magnetic recording/reproducing process.

It was soon discovered that there is no inherent requirement to have two transitions per bit. This gave rise to the nonreturn-to-zero (NRZ) codes. The two most important versions of these are NRZ−L, shown in figure 2-1(*d*), and NRZ−M, shown in figure 2-1(*e*). NRZ−L consists of a transition between any two bits that are different, thus the signal level for "1" bits is opposite of the level for "0" bits. NRZ−M consists of a transition for each "1" and no transition for any "0" bit. The significant difference between NRZ−L and NRZ−M in magnetic recording/reproducing is that only transitions of the signal are detected by the reproduce head, not the level of the signal; therefore, one missed transition in NRZ−L will invert every succeeding bit, creating a string of errors, whereas one missed transition in NRZ−M will create only one error, the "1" bit corresponding to the missed transition. What all NRZ codes have in common is that they need at most one transition per bit, and none of them are self-clocking. The requirement for a timing reference, commonly called a clock, to decode any NRZ signal is a definite drawback for all NRZ methods. NRZ, however, is used extensively because encoding and decoding are very simple. Several methods were invented to add clocking information. All of these consist of adding transitions not otherwise required to transmit data. All such added transitions are generally referred to as "overhead." In general, NRZ−M has been used extensively in magnetic tape systems in which several channels of data are recorded in several parallel tracks. In such systems only one additional track is required to add the clock, so that for an eight-track system, the addition of a ninth track results in only 12.5 percent overhead.

As mentioned earlier, odd parity is more advantageous than even parity. In the strict sense, this is only true for NRZ codes. When the ninth track is used as a vertical parity track with odd parity, there will always be at least one "1" bit in each vertical or lateral word. The clock can therefore be extracted by connecting the output of each track to a oneshot to generate a pulse for each transition. If the outputs of all these oneshots are connected as inputs to an OR gate, the output of the OR gate will be a pulse for each lateral word on tape; i.e., for each bit in each track, providing a clock. In this way, for 12.5 percent overhead added to eight parallel tracks, both clock and simple error detection are generated.

The clock extracting method described loses reliability as the density increases because of missed transitions and, more significantly, tape skew. Skew tends to prevent the pulses from the same lateral word from appearing simultaneously at the input of the OR gate, resulting in clocking errors.

The evolution of the computers that used these magnetic storage devices imposed requirements for ever increasing data rates. The increasing data rates required increased packing densities on tape. This led to the development of the next family of codes, the biphase, or Biϕ, codes. These codes are constructed in such a manner that each and every bit has at least one signal transition associated with it. The two significant codes of this family are Biϕ−L (fig. 2-1 (*f*)), and Biϕ−M (fig. 2-1 (*g*)). The latter is also known as HDDR™. HDDR™ is a registered trademark of Lockheed Electronics Company, Incorporated.

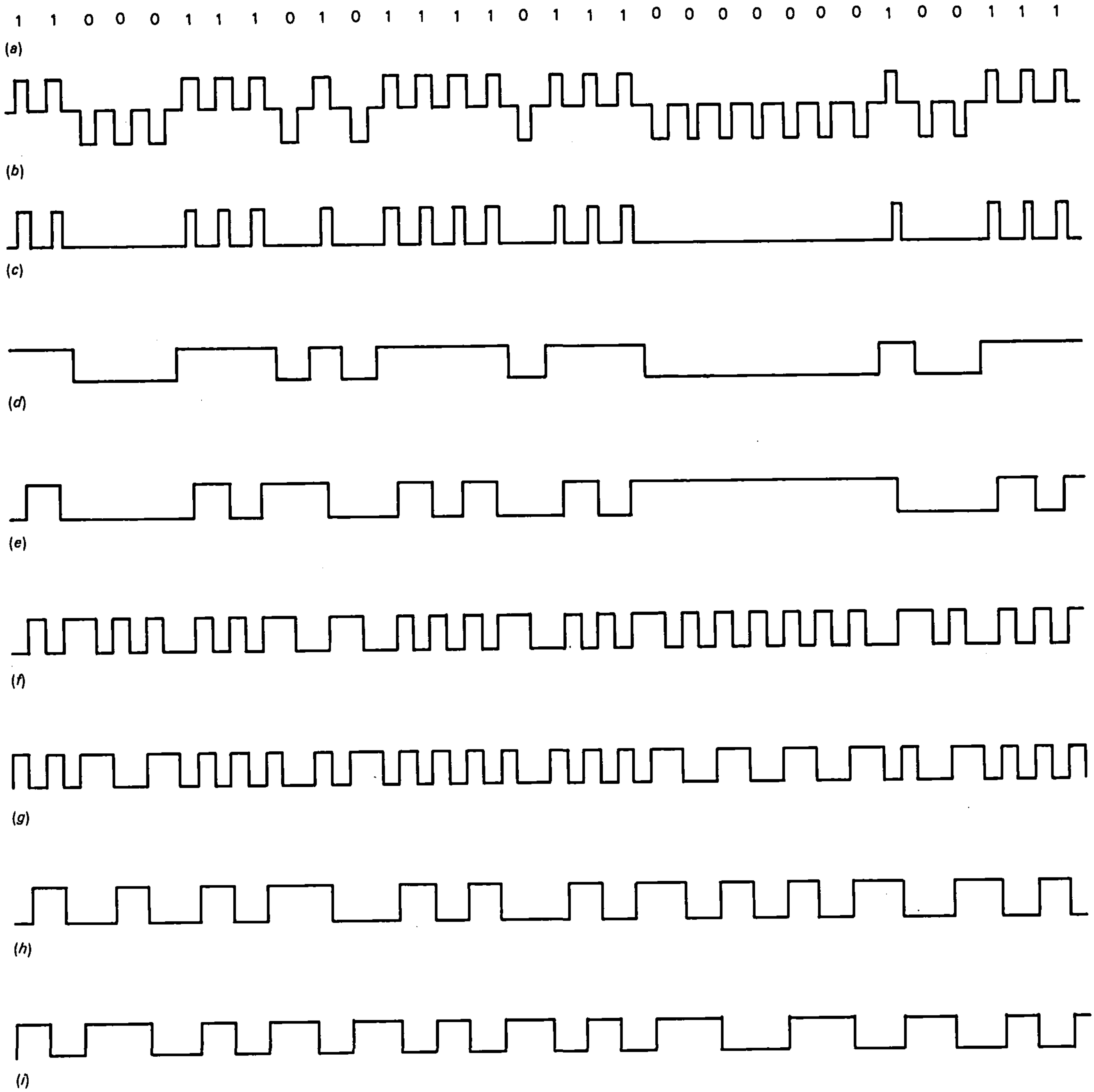

Figure 2-1.—High-density codes. (*a*) Data pattern. (*b*) RZ, bipolar. (*c*) RZ. (*d*) NRZ—L. (*e*) NRZ—M. (*f*) Biϕ—L. (*g*) Biϕ—M. (*h*) Miller. (*i*) HDDR™ II.

All biphase codes are self-clocking, but need up to two transitions per bit. They are used extensively because they have no clocking overhead. As the density requirements increased, the bandwidth required to process biphase data increased and limited further density increases.

New coding schemes were developed to reduce the bandwidth requirements. These codes are called double density codes because they allow doubling the bit density for the same bandwidth. Two significant double density codes are Miller (fig. 2-1(*h*)) and HDDR™II (fig. 2-1(*i*)). Miller code is also known as Wood code and delay modulation code.

All these codes need a maximum of one transition per bit, and although neither is directly self-clocking in that neither has transitions for every bit like the biphase codes, their structure does allow extraction of the clock signal from the data due to the fact that the spacing of

transitions can only be 1-, 1½-, or 2-bit cells. A bit cell is defined as a time period whose length is exactly the time between any two adjacent bits; e.g., for a 2-Mbps data stream, one data bit is stored every 5μs; the bit cells are, therefore, 0.5μs, or 500 ns, long. Because double density codes have a variable transition spacing, for certain data patterns the reproduce signal can have an increasing dc voltage content. Figure 2-2(*a*) shows such a pattern, figure 2-2(*b*) shows its signal encoded in Miller code, and figure 2-2(*c*) shows the resulting reproduce signal. To eliminate this dc content, the Miller squared or M^2 code was introduced by Ampex (ref. 2-1). Figure 2-2(*d*) shows the same pattern encoded in the M^2 code, and figure 2-2(*e*) shows that the resulting signal no longer has an increasing dc voltage content.

In addition to the double density codes, NRZ is also being used for high-density recording. Several modifications to the basic NRZ code have been devised to eliminate the main shortcoming of NRZ; that is, the inability of decoding long strings of "0" bits reliably. Several methods have been developed and are in use:

(1) Enhanced NRZ (E-NRZ)
(2) Randomized NRZ (R-NRZ)
(3) Group coding (GCR)

E-NRZ consists of breaking up the data into groups of *n* bits and inserting one extra bit after each group. Two methods are E-NRZ_p and E-NRZ_c. In E-NRZ_p the added bit is such that the $(n + 1)$ bit word always has odd parity; in E-NRZ_c the added bit is simply a complement of the bit that it follows. There are other E-NRZ methods, but the idea is similar. All E-NRZ methods include overhead bits and, therefore, the bandwidth required to process all such codes is increased.

R-NRZ consists of adding a pseudorandom word of $2^{11} - 1$ bit length to each $2^{11} - 1$ bits of the data. The idea is that long strings of "0" bits will be broken up by this process; however, a random data pattern has the same probability of containing a string of K zeros before "randomizing" as after; R-NRZ, therefore, is only advantageous if either the data are not entirely random, in that it tends to have long strings of "1" and "0" bits more often than a truly random bit sequence, or if there are security considerations.

GCR consists of taking groups of *n* bits and encoding each in a group of $n + m$ bits, usually using a lookup table. The best known application of GCR is the 4/5 code of IBM in which $n = 4$ and $m = 1$. In this code the 16-bit configurations that 4 bits can take are encoded in 16 five-bit groups according to a lookup table; the 5-bit groups are selected such that each has at least two "1" bits; and no more than two "0" bits are allowed together. The resulting bit stream is recorded in NRZ form. This code limits the length of a string of "0" bits

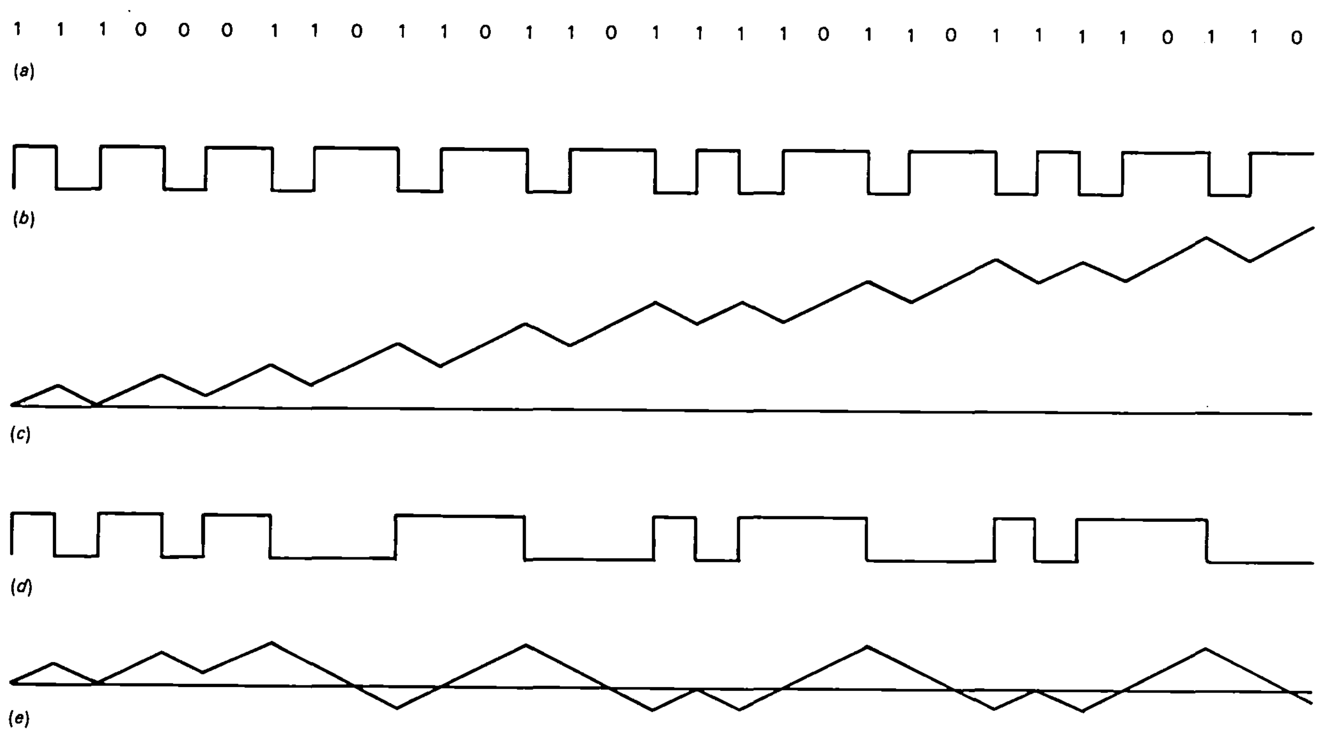

Figure 2-2.—(*a*) Data pattern with increasing dc voltage content. (*b*) Coding of (*a*) in Miller code. (*c*) Reproduce signal of (*b*). (*d*) Coding of (*a*) in Miller^2 code. (*e*) Resulting reproduce signal using (*d*).

to two, but it requires 25 percent overhead, with its corresponding increase in required bandwidth.

From all the codes mentioned, only HDDR™II, Miller, M², E-NRZ, and R-NRZ have been used to any extent for in-track packing densities above 10 000 bpi. Considering that Miller is used in all recent IBM disk drives and, until recently, was used in all Ampex longitudinal high-density tape systems, it can be safely stated that Miller is one of the most popular codes (ref. 2-2).

PROPERTIES OF DIGITAL DATA STREAMS

All digital data streams except the RZ method requiring three levels (a theoretical method not actually in use in any magnetic equipment) consist of a succession of transitions between two levels. Accordingly, the properties of data streams can be defined in terms of those of a succession of these transitions. Some general properties include the following:

(1) For most codes, a random data pattern results in a random sequence of transitions.

(2) For the same code, the spacing between transitions decreases when the data frequency increases.

(3) The detection of transitions becomes more and more difficult as the spacing between them decreases.

(4) Transitions are more difficult to detect when the signal contains noise; the difficulty increases as the noise increases.

(5) Increasing difficulty in detecting transitions increases the probability of erroneous detection; i.e., data errors.

Due to the impact of noise on the ability to accurately detect data, it is important to be able to predict the noise that will be part of the signal. The probability of errors can be expressed as a function of the signal-to-noise ratio (SNR). The influence of the SNR on error rates is illustrated in figure 2-3 (ref. 2-3). In addition to the common noise sources, such as amplifier noise, power supply noise, and radiofrequency interference pickup, the effects of imperfections of the medium and mechanisms will have unwanted effects on the signal, such as flutter that will act like noise.

An increased data rate accentuates the influence of tape and mechanism imperfections; therefore, SNR decreases, and the probability of errors increases. It is, therefore, very desirable to hold the overhead data to a minimum; clearly, increasing the overhead will allow the data rate for the same data capacity to be increased. Some codes, however, do inherently require the addition of overhead.

Several studies have been performed comparing Miller code to some of the other codes in use (refs. 2-4 to 2-6). The Miller and HDDR™II codes were assigned the number 1.00. The numbers associated with the other codes indicate the comparative efficiency of the codes; e.g., if a certain storage system can store data encoded in HDDR™II or Miller at 25 000 bps, then the same system using E-NRZ (adding a "1" bit after each group of seven bits in an NRZ data stream) could store data at

$$0.85 \times 25\,000 = 21\,250 \text{ bps}$$

and achieve similar data reliability. The results of these studies are shown in table 2-1.

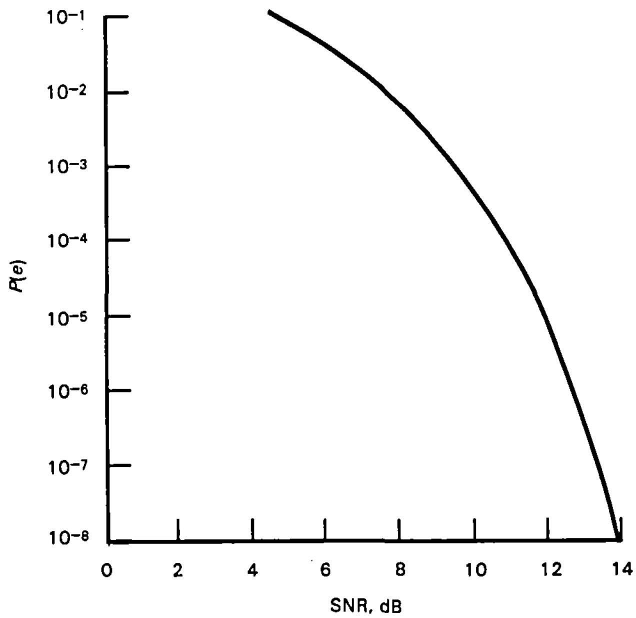

Figure 2-3.—$P(e)$ as a function of SNR. BER = $P(e)$.

Only group coding methods exceed the performance of HDDR™II and Miller. The reason for this is that although all group coding schemes have inherent overhead, the transitions in them always occur either between bit cells or at bit cell centers, never both. In HDDR™II and Miller transitions occur both between bit cells and at bit cell centers, although never for the same bit. (See fig. 2-1.)

Table 2-1. – *Comparison of Efficiency of Selected Data Codes*

Code	Efficiency
Miller or HDDR™ II	1.00
GCR	1.08
3PM	1.02
Miller²	.95
E-NRZ	.85
R-NRZ	.99

ERROR DETECTION

The reliability of any data storage or transmission system can be improved through error correction, and the principal requirement for error correction is the ability to detect the errors.

All known error-detecting schemes rely on information added to the data stream to detect errors. The addition of a parity bit after each group of bits has been already discussed. Another method is CRC. The CRC method typically adds a 16-bit CRC word to each block of 240 bits; the overhead is approximately 7 percent, less than a longitudinal parity bit each 8-bit word, which results in 12.5 percent overhead. Generally speaking, most simple error-detecting schemes add approximately 10 percent overhead to the data.

Using HDDR™II or Miller code, an error-detecting method is available that does not require the addition of any overhead. Observing the transition pattern in figures 2-1(*h*) and (*i*), it becomes apparent that the pattern is composed of periods between transitions that are either 1, 1½, or 2 times the bit cell period. For decoding such a pattern, it is convenient to derive a clock that has twice the data frequency. Figure 2-4(*a*) repeats the pattern of figure 2-1(*h*); figure 2-4(*b*) shows the double frequency clock. Inspection of figure 2-4 shows that the transitions occur, in terms of the clock signal in figure 2-4(*b*), two, three, and four clock periods from each other. A signal in HDDR™II or Miller can be described, then, as a succession of "two's," "three's," and "four's," in terms of the double frequency clock. The common characteristic of both HDDR™II and Miller is that "two's" and "three's" occur two different ways and can be interpreted in either of two ways. (See fig. 2-5.) However, a "four" has a unique interpretation in each code. (See fig. 2-5.)

Accordingly, to decode a string of transitions encoded in either HDDR™II or Miller, a "four" must be found. This does not present a major problem, because high-density recording schemes do break the data into portions of 250 to 500 bits, called frames, and insert some known sequence of transitions, called synchronization words, between frames.

This is required because all schemes risk the loss of a complete string of data if synchronization between data and clock is lost. Systems using HDDR™II and Miller must use synchronization words that contain "four's," this assures proper decoding. The decoder must have a means to detect "four's." One circuit for this could consist of a four-bit shift register; when the data are clocked through such a register using a double frequency clock, a "four" will cause all four outputs of the register to be in the same state.

There exists another characteristic in both HDDR™ II and Miller. The number of "three's" between any two "four's" must be even. This is a predictable characteristic of any string of transitions corresponding to a digital data stream encoded in HDDR™II or Miller code. Any predictable characteristic of a random data stream can be used for error detection. Analysis shows that the decoding of any between-transition time erroneously will violate this pattern; e.g., a "two" changed to a "three" or a "three" into a "two" will add or subtract one "three" from the correct number as will a "three" read as a "four." Accordingly, if a single bit memory is added to the decoder, the parity of "three's" can be counted. The detector must contain some means of detecting "four's" to properly phase the data. This inherent characteristic of "three's" parity of the HDDR™ II and Miller codes presents the system designer with the most economical error detection method possible: no overhead is required for error detection.

The same method is applicable to data encoded in M², because the M² decoder first converts the M² data into Miller coded data, which can then be checked for errors just as if M² had never been used.

Referring to table 2-1 and considering that all simple in-channel error detection schemes require approximately 10 percent overhead, table 2-2 can be constructed. It is clear that with error correction added, HDDR™II or Miller are the most efficient codes. In addition, system reliability is improved because the codes requiring overhead for error detecting also require that the corresponding systems include the necessary circuits to generate and insert the error-detecting overhead into the data stream and to remove this overhead before the

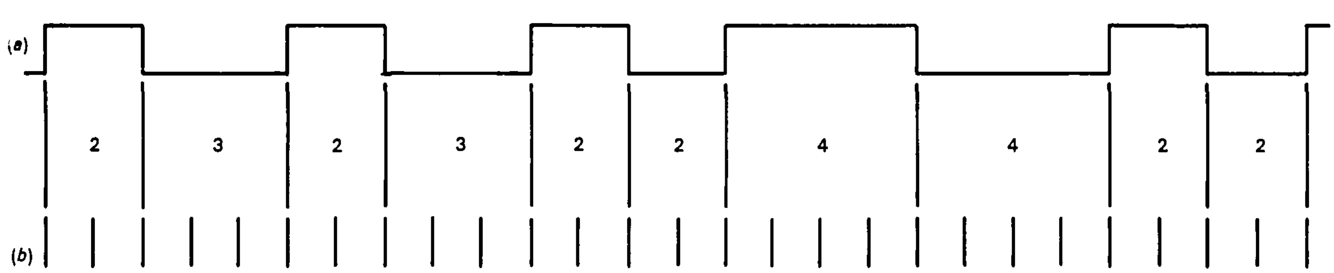

Figure 2-4.—(*a*) Miller code of figure 2-1 (*h*). (*b*) Double frequency clock of (*a*).

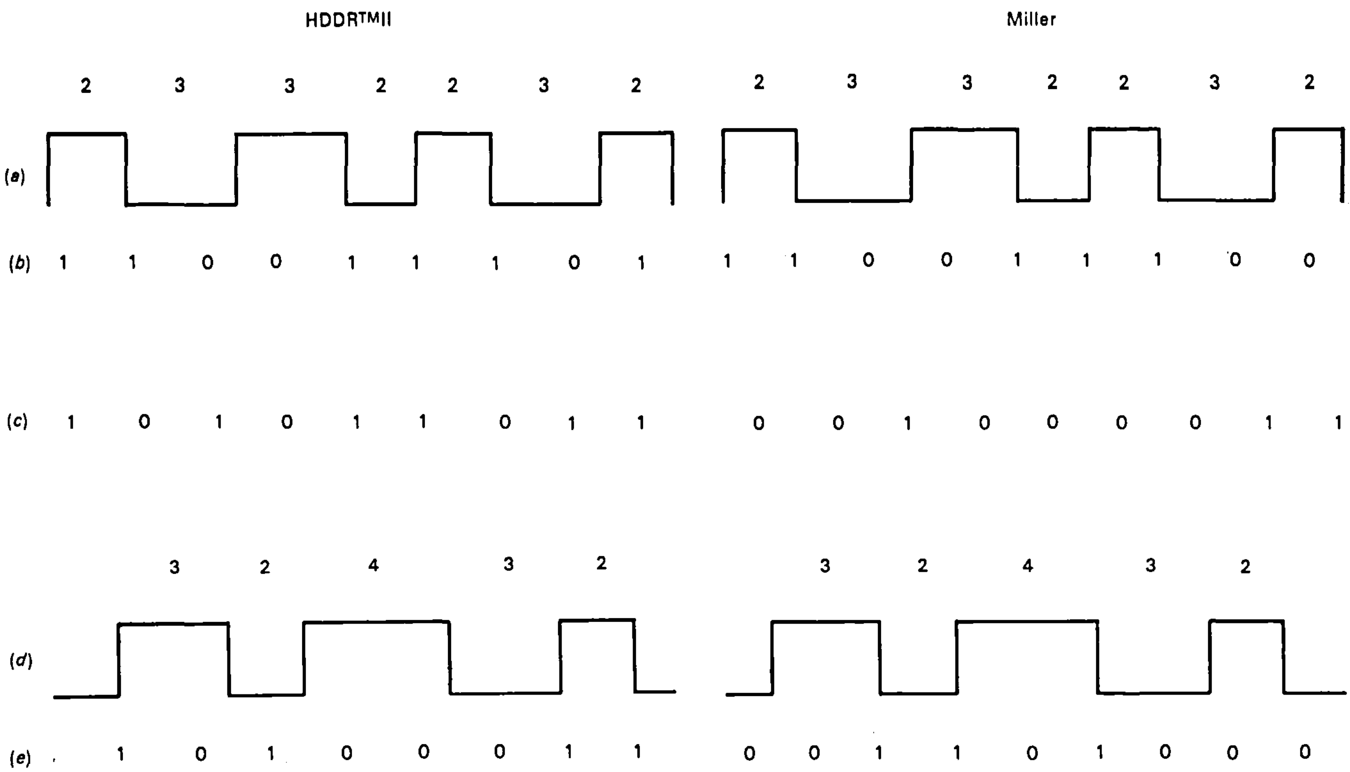

Figure 2–5.—(*a*) Pulse train of only "two's" and "three's." (*b*) One decoding of (*a*). (*c*) Another decoding of (*a*). (*d*) Pulse train containing a "four." (*e*) A unique decoding of (*d*).

Table 2-2. – *Comparison of Efficiency of Selected Data Codes With and Without Error Correction*

Code	Without error detection	With error detection
Miller and HDDR™II	1.00	1.00
GCR	1.08	.97
3PM	1.02	.92
E-NRZ*	.85	.85
R-NRZ	.99	.90

*E-NRZ can be coded in such a way that the enhancing bit is a parity bit, thus it would not require any further overhead.

reproduced and corrected data are presented to the system output interface.

ERROR CORRECTION

An in-channel error detection method used in a multichannel tape recorder lends itself to a simple error-correcting technique. The addition of a parity track to a multitrack recording format is well known in the industry. In fact, there are existing integrated circuits that generate the information to be recorded in such a parity track, such as the 54LS280. Assuming that such a parity track has been added to eight tracks of data, as an example, and that the HDDR™II or Miller decoder develops an error signal for each track, in-channel error detection can be expanded to detect dropouts that cause between-transition times that exceed two bit cells (the typical error caused by tape imperfections or loose particles on tape). As a result, a channel error can be either a "three's" parity error or a lack of transitions for more than two bit cells. Considering a nine-channel parallel system, one of the nine tracks being parity, the location of the error within the channel is not even important. Typically, such systems record data in 400- to 500-bit frames per channel and insert synchronization words periodically between such frames. These systems generally contain buffers to eliminate skew and bit-to-bit jitter. The output of these buffers can be processed through a network similar to that shown in figure 2-6. As shown there, the input consists of the parallel data and the error signal for each channel A through I (parity channel included). The output of the network is nine channels of data, corrected as necessary, provided that no more than one channel was found with error(s).

The synchronization word would reset the error signal so that in any 400- to 500-bit frame, depending on the system, error(s) would be corrected, provided that in

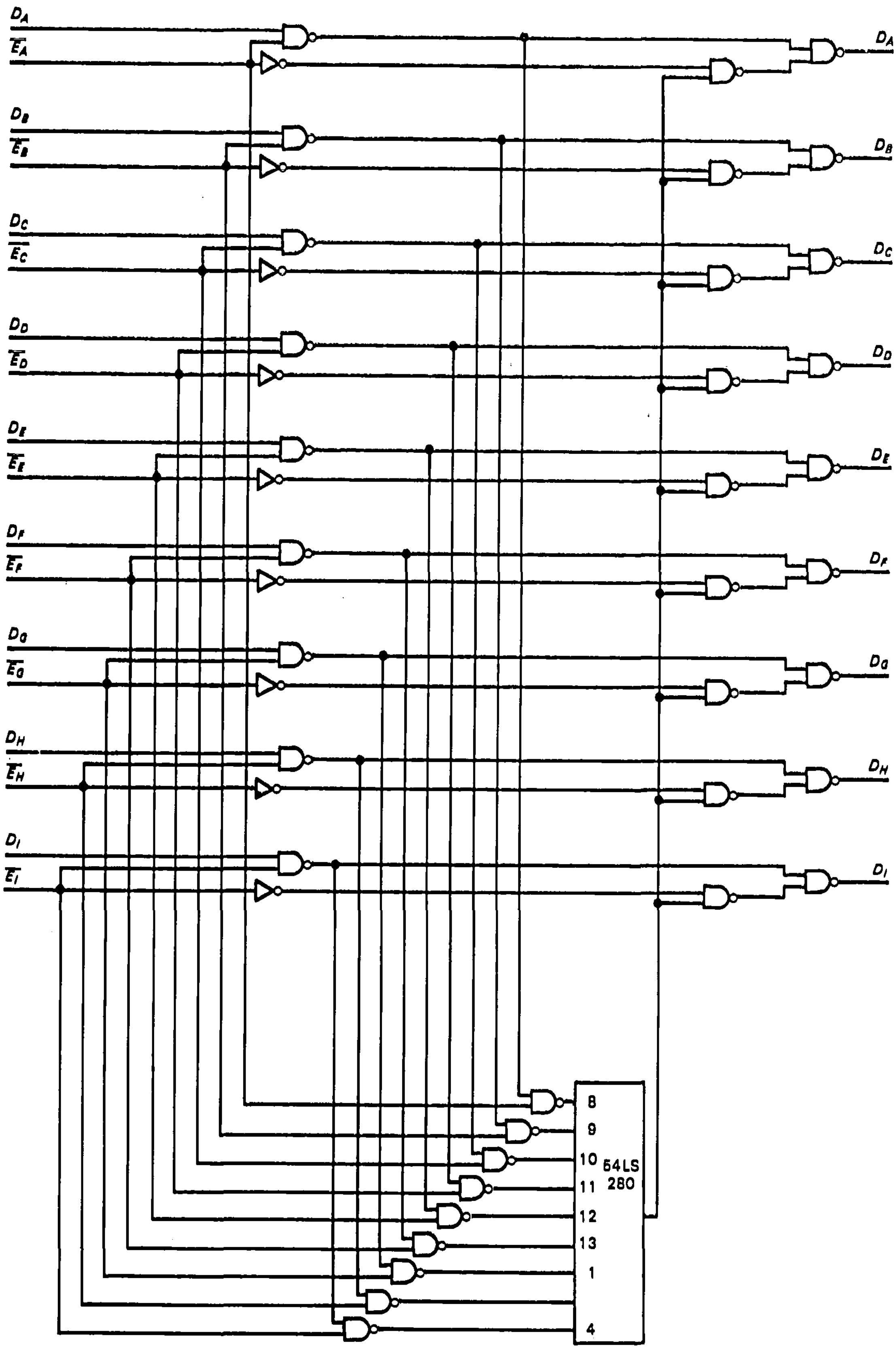

Figure 2-6.—Error correction network.

each frame only one channel is in error. The error correction provided by such a system requires very little additional hardware, and the data reliability should increase by 1 to 1½ orders of magnitude.

CONCLUSION

The use of the described error-detecting method increases the efficiency of HDDR™II, Miller, or M^2 codes by approximately 10 percent and, combined with error correction using only an added parity track, improves the data reliability by at least an order of magnitude. The hardware required for error correction is simple and readily available; therefore, the impact on system reliability and complexity is kept to a minimum.

REFERENCES

2-1. Miller, J. W.: U.S. Patent 4,027,335. May 31, 1977.

2-2. Mackintosh, N. J.: "The Choice of a Recording Code." *Radio Electron. Eng.* 50(4): 177–193, Apr. 1980.

2-3. Norris, K. A.: *A Technique for High Density Digital Magnetic Recording.* Leach Corp., 1971.

2-4. Tamura, Takashi; Tsutsumi, M.; Aoi, H.; Matsuishi, H.; Nakagoshi, K.; Kawano, S.; and Makata, M.: "A Coding Method in Digital Magnetic Recording." *IEEE Trans. Magn.* 8(3): 612–614, Sept. 1972.

2-5. King, D. A.: "Comparison of PCM Codes for Direct Recording." *Int. Telemetering Conf. Proc.*, Los Angeles, Sept. 1976, pp. 526-540.

2-6. Huber, W. D.: Maximization of Lineal Recording Density." *IEEE Trans. Magn.* 13(5): 1208–1210, Sept. 1977.

CHAPTER 3

Introduction to Error Detection and Correction Techniques*

Neal Glover
Data Systems Technology

INTRODUCTION TO ERROR CORRECTION

Parity

A vector, word, or data stream is said to have odd parity if the number of "1" bits it contains is odd; otherwise, the vector, word, or data stream is said to have even parity.

Parity may be determined with combinational or sequential logic. The parity of two bits may be determined with an XOR gate (fig. 3-1). Parity across a nibble (part of a byte) may be determined with a parity tree (fig. 3-2). Parity of a bit stream may be determined by a single shift register stage and an XOR gate (fig. 3-3). The shift register is assumed to be initialized to zero.

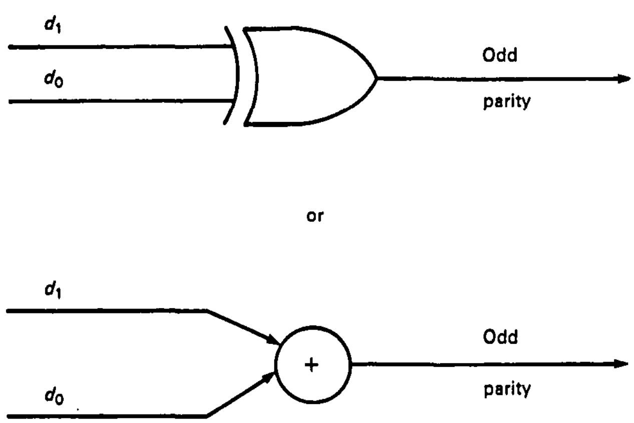

Figure 3-1.—Using XOR gate to determine parity of two bits.

Editor's note: The original submission to the editors for this chapter was a copy of *Practical Error Correction Design for Engineers* by Neal Glover (ref. 3-1). Mr. Glover did not have time to rewrite the material in a chapter format for this publication; however, the editors felt the material was very important for digital recording and agreed to condense some areas of the original publication for insertion as a chapter here.

Linear Sequential Circuit Fundamentals

Linear sequential circuits (LSC) are constructed with three building blocks: modulo 2 addition (XOR gates), memory circuits (latches), and constant multipliers (figs. 3-4 to 3-6). Any connection is permissible as long as a single arrow is mated to a single arrow of another

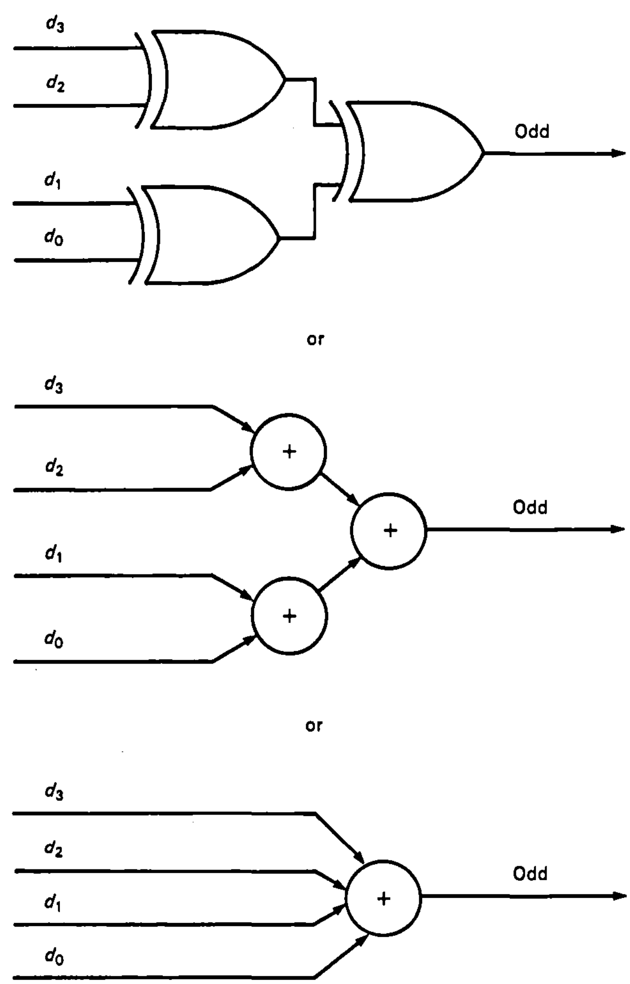

Figure 3-2.—Using a parity tree.

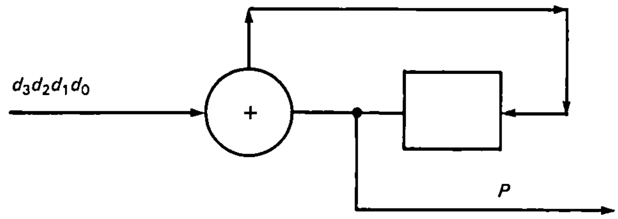

Figure 3-3.—Using shift register and XOR gate to determine parity of a bit stream. The highest numbered bit is always transmitted and received first. $P = d_3 \oplus d_2 \oplus d_1 \oplus d_0$ or $P = d_3 + d_2 + d_1 + d_0$; the $\oplus$ is understood to mean XOR.

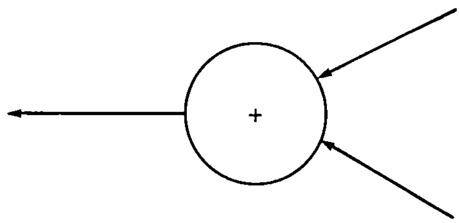

Figure 3-4.—Modulo 2 addition (XOR gates): single output; no restriction on the number of inputs.

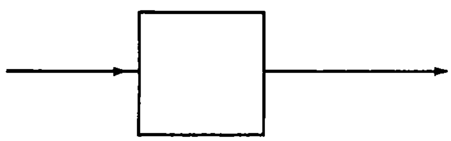

Figure 3-5.—Memory circuits (latches): single input, single output.

block, keeping the same direction of flow. The output of a modulo 2 adder at any time is the modulo 2 sum of the inputs at that time. Latches are clocked by a synchronous clock. The output of a latch at any time is the binary value that appeared on its input 1 time unit earlier. At this point in this discussion, the constant multiplier a will be either 1 or 0. If the constant multiplier is 1, a connection exists. No connection exists for a constant multiplier of 0. The form of LSC shown in figure 3-7 is also called a linear shift register (LSR).

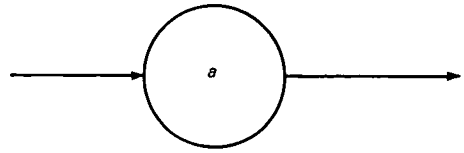

Figure 3-6.—Constant multipliers: single input, single output.

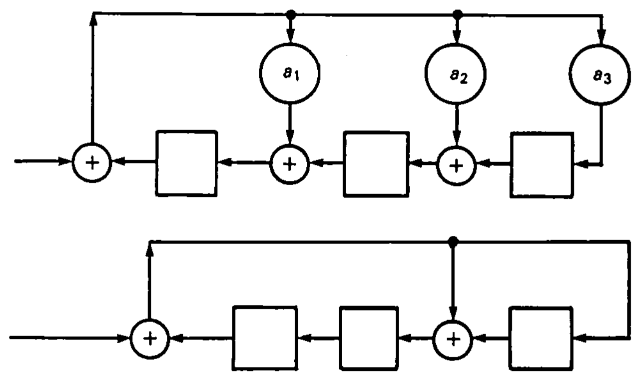

Figure 3-7.—Examples of two equivalent linear sequential circuits where $a_1 = 0$, $a_2 = 1$, and $a_3 = 1$.

The circuits shown in figures 3-8 and 3-9 determine parity across groups of data stream bits. In figure 3-8 each bit is included in only one parity check. The contribution of each data bit to the final shift register state is as follows:

Data bit	Contribution $P_2P_1P_0$
d_6	100
d_5	010
d_4	001
d_3	101
d_2	111
d_1	110
d_0	011

Each data bit affects a unique combination of parity checks. The contributions to the final shift register state

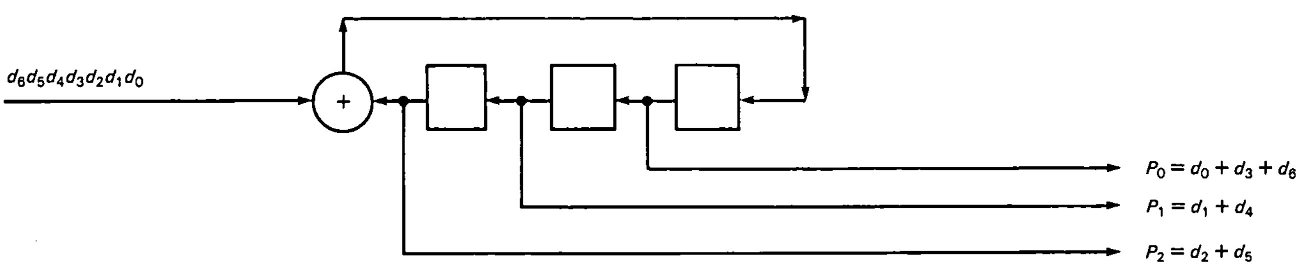

Figure 3-8.—Circuit for determining parity across groups of data stream bits.

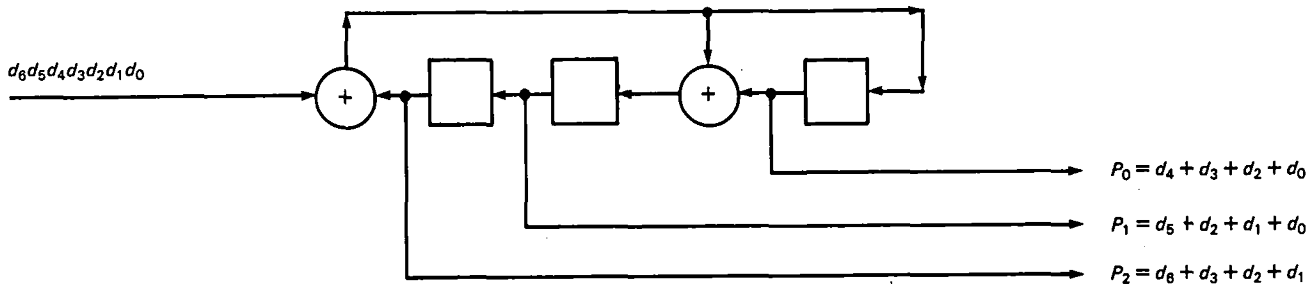

Figure 3–9.—Alternative circuit for determining parity across groups of data stream bits.

made by several strings of data bits are as follows:

String	Contribution $P_2P_1P_0$
d_6,d_4	101
d_3,d_2,d_0	001
d_4,d_0	010

Because the circuit is linear, the contribution to the final shift register state by each string is the XOR sum of contributions from individual bits of the string:

$$f(x + y) = f(x) + f(y)$$

The parity function P is linear; therefore,

$$P(x + y) = P(x) + P(y)$$

Circuits of this type are the basis of many error correction systems.

Single-Bit Error Correction

This section introduces single-bit error correction using a code that is intuitive and simple.

A syndrome is a vector providing symptoms of an error or errors. Some codes use a single syndrome while other codes use multiple syndromes. A syndrome vector is generated by taking the XOR sum of a set of parity checks generated on receive and a set of parity checks generated on transmit.

Consider the two-dimensional parity check code defined as follows (fig. 3–10):

(1) Check-bit generation

$$P_0 = d_0 + d_4 + d_8 + d_{12}$$
$$P_1 = d_1 + d_5 + d_9 + d_{13}$$
$$P_2 = d_2 + d_6 + d_{10} + d_{14}$$
$$P_3 = d_3 + d_7 + d_{11} + d_{15}$$
$$P_4 = d_{12} + d_{13} + d_{14} + d_{15}$$
$$P_5 = d_8 + d_9 + d_{10} + d_{11}$$
$$P_6 = d_4 + d_5 + d_6 + d_7$$
$$P_7 = d_0 + d_1 + d_2 + d_3$$

(2) Syndrome generation

$$S_0 = d_0 + d_4 + d_8 + d_{12} + P_0$$
$$S_1 = d_1 + d_5 + d_9 + d_{13} + P_1$$

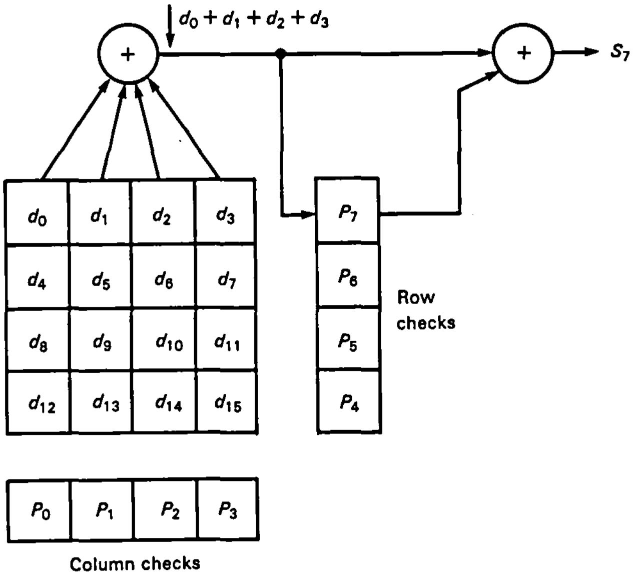

Figure 3–10.—One of the eight check/syndrome circuits required for the parity check code defined in text.

$$S_2 = d_2 + d_6 + d_{10} + d_{14} + P_2$$
$$S_3 = d_3 + d_7 + d_{11} + d_{15} + P_3$$
$$S_4 = d_{12} + d_{13} + d_{14} + d_{15} + P_4$$
$$S_5 = d_8 + d_9 + d_{10} + d_{11} + P_5$$
$$S_6 = d_4 + d_5 + d_6 + d_7 + P_6$$
$$S_7 = d_0 + d_1 + d_2 + d_3 + P_7$$

On write, each row check bit and each column check bit is selected to make the parity of its row or column even. The data bits and the parity bits together are called a code word.

On read, row syndrome bits are generated by checking parity across each row, including the row check bit. Column syndrome bits are generated in a similar fashion. For this code, syndrome bits can be viewed as the XOR differences between read checks and write checks. All syndrome bits are "0" when there is no error.

When a single-bit error occurs, one row and one column will have inverted syndrome bits (odd parity). The bit in error is at the intersection of this row and column.

The circuit in figure 3-10 shows the logic necessary for generating the write check bit and the syndrome bit for one row. For parallel decoding, this logic is required for each row and column. In addition, 16 AND gates are required for detecting the intersections of inverted row and column syndrome bits and 16 XOR gates are required for inverting data bits. The correction circuit for one particular data bit is shown in figure 3-11. Two data bits in error will cause either two rows, two columns, or both to have inverted syndrome bits (odd parity). This condition can be trapped to give the code detection capability for double-bit errors in data.

All single check-bit errors are detected, but not all double check-bit errors. One row and one column check bits in error will result in miscorrection (false correction). If an overall check bit across data is added, the code is capable of detecting all double-bit errors in data and check bits. This includes the case in which one data bit and one parity bit are in error. The overall check bit can be generated by forming parity across all row or all column check bits. With the overall check bit added, all double-bit errors are detectable but uncorrectable.

Miscorrection occurs when three bits are in error on three corners of a rectangle (fig. 3-12).

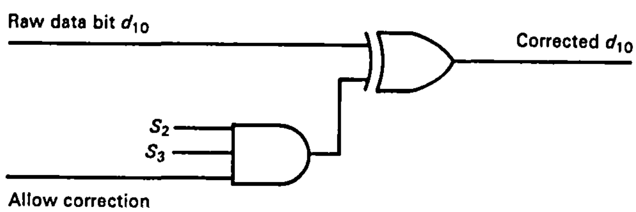

Figure 3-11.—Correction circuit for a data bit.

The three errors X in the figure cause the decoder to respond as if there were a single-bit error at location *M*.

Miscorrection does not result for all combinations of three bits in error, only those in which there are errors on three corners of a rectangle. Miscorrection probability for three-bit errors is the ratio of three-bit error combinations that result in miscorrection to all possible three-bit error combinations.

Misdetection (error condition not detected at all) occurs when four bits are in error on the corners of a rectangle (fig. 3-13). This error condition leaves all syndrome bits "0."

Misdetection does not result for all combinations of four bits in error, only those where there are errors on four corners of a rectangle. Misdetection probability for four-bit errors is the ratio of four-bit error combinations that result in misdetection to all possible four-bit error combinations.

Accomplishing Multiplication With Shifts, Adds, and Subtracts

Many eight-bit processors do not have a multiply instruction. This discussion describes techniques to minimize the complexity of multiplying a variable by a constant when such processors are used. These techniques provide another alternative for accomplishing the multiplications required in solving the Chinese remainder problem, based on the Chinese remainder theorem (ref. 3-2).

On an eight-bit processor, any shift that is a multiple of eight bits can be accomplished with register moves; therefore, multiplying by a power of 2 that is a multiple of 8 can be accomplished by register moves. Any string of "1" bits in a binary value can be represented by the power of 2 that is just greater than the highest power of

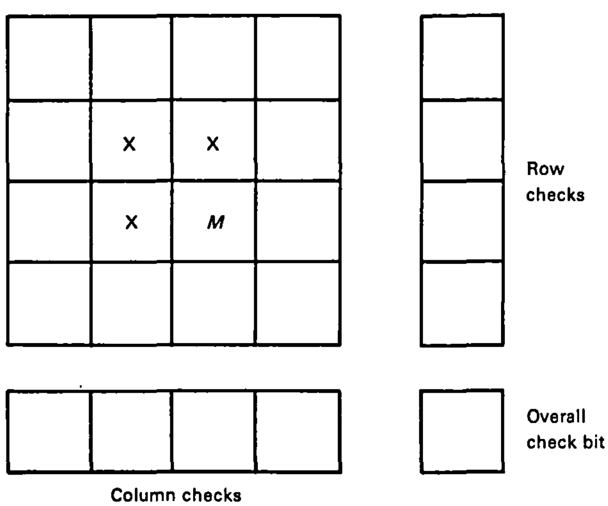

Figure 3-12.—Example of miscorrection.

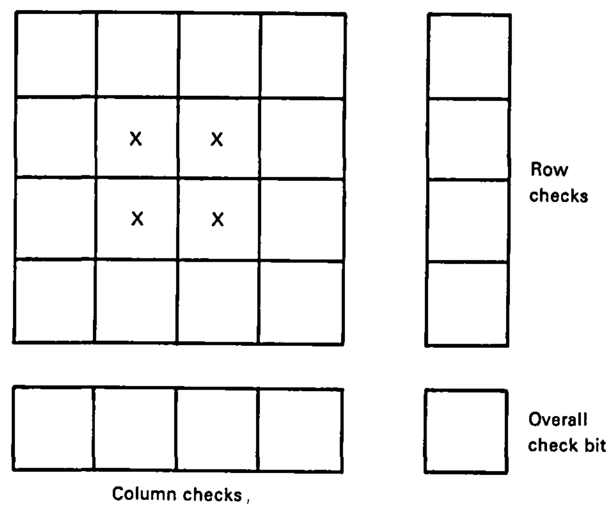

Figure 3-13.—Example of misdetection.

2 in the string minus the lowest power of 2 in the string. These results can be used to minimize the complexity of multiplying a variable by a constant using register moves, shifts, adds, and subtracts.

In all examples, X is less than 256. The results are shown in a form where register moves and shifts are identifiable. In example 4, only two unique shift operations are required, even though the original constant contains nine powers of 2. This particular example is from the Chinese remainder problem when moduli 255 and 127 are used.

Example 1

$$\begin{aligned} Y &= 257 * X \\ &= (2^8 + 1) * X \\ &= 2^8 * X + X \end{aligned}$$

Example 2

$$\begin{aligned} Y &= 255 * X \\ &= (2^8 - 1) * X \\ &= 2^8 * X - X \end{aligned}$$

Example 3

$$\begin{aligned} Y &= 992 * X \\ &= (2^9 + 2^8 + 2^7 + 2^6 + 2^5) * X \\ &= (2^{10} - 2^5) * X \\ &= 2^{10} * X - 2^5 * X \end{aligned}$$

Example 4

$$\begin{aligned} Y &= 32131 * X \\ &= (2^{14} + 2^{13} + 2^{12} + 2^{11} + 2^{10} + 2^8 + \\ &\quad 2^7 + 2^1 + 2^0) * X \\ &= (2^{15} - 2^9 - 2^7 + 2^1 + 2^0) * X \\ &= 2^{15} * X - 2^9 * X + 2^7 * X + \\ &\quad 2^1 * X + 2^0 * X \\ &= 2^8 * (2^7 * X) - (2^7 * X) - \\ &\quad 2^8 * (2^1 * X) + (2^1 * X) + X \end{aligned}$$

DETECTION FUNDAMENTALS

Polynomial Shift Registers

The shift register form in figure 3-14 is used frequently for error detection and correction. This circuit multiplies by X^m and divides by $g(x)$, where m is the polynomial degree and also the shift register length and $g(x)$ is the generator polynomial of the code. In figure 3-14, m is 3 and $g(x)$ is $X^3 + X + 1$. Two properties of this form of shift register are discussed in the following paragraphs.

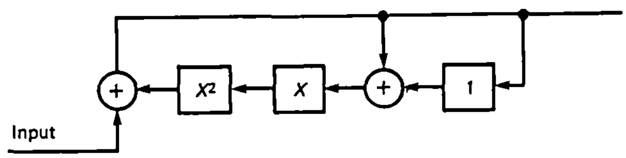

Figure 3-14.—A shift register form used frequently for error detection and correction.

Property 1

If the shift register is receiving data bits, the last m data bits (in this case three) must match the shift register content for the final shift register state to be zero. This is because a difference between the data bit and the high-order shift register stage causes the low-order stage to be set to one again.

Assume an all-"0" bit data record. If an error burst is to leave the shift register in its zero state, the last m bits of the burst must match the shift register contents.

Property 2

Assume the shift register is zero. Receiving a burst of bits of length m bits or less has the same effect as placing the shift register at the state represented by the burst of bits.

When reading an all-"0" bit data record, an error burst of length m bits or less sets the shift register to a state on its sequence that is b (burst length) shifts away from the state representing the error burst.

Selecting Check Bits

The following paragraphs describe intuitively how check bits must be selected so that on read, the received polynomial $R(x)$ leaves the shift register at zero.

Assume a shift register configuration that premultiplies by X^m and divides by $g(x)$. From property 1, it is clear that in order for the check bits to leave the shift register at zero, the check bits must match the shift register contents immediately after the data part of the received polynomial has been processed. For this to be true, the contents of the shift register after processing all write data bits must be written for check bits.

Euclidean Division Algorithm

If $g(x)$ and $D(x)$ are polynomials with coefficients in a field F, and $g(x)$ is not 0, there exist polynomials $Q(x)$ and $r(x)$ with coefficients in F such that

$$D(x) = Q(x) * g(x) + r(x) \qquad (3\text{-}1)$$

where

$D(x)$ = data polynomial
$Q(x)$ = quotient polynomial
$g(x)$ = generator polynomial
$r(x)$ = remainder polynomial

and either $r(x) = 0$ or the degree of $r(x)$ is less than the degree of $g(x)$. The Euclidean division algorithm provides a formal method for determining how check bits should be selected.

Rearranging equation (3-1) gives

$$\frac{D(x) + r(x)}{g(x)} = Q(x)$$

This shows that to make the data polynomial divisible by $g(x)$, $r(x)$ must be XOR'd to $D(x)$, but this would modify the last m bits of the data polynomial. Modifying the data polynomial has disadvantages. A better method of determining the check bits must be found.

Instead of dividing the data polynomial $D(x)$ by the generator polynomial $g(x)$, first premultiply $D(x)$ by X^m and divide by $g(x)$. Then,

$$\frac{X^m * D(x)}{g(x)} = Q(x) + \frac{r(x)}{g(x)}$$

and

$$\frac{X^m * D(x) + r(x)}{g(x)} = Q(x)$$

This shows that if $r(x)$ is XOR'd with the data polynomial premultiplied by X^m, the resulting polynomial will be divisible by $g(x)$. This is equivalent to appending $r(x)$ to the end of the original data polynomial. The original data polynomial is not modified when check bits are added with this method.

Symbology

The following symbology will be employed for frequently used polynomials:

$D(x)$ = data polynomial
$C(x)$ = check polynomial
$T(x)$ = transmit polynomial
$E(x)$ = error polynomial
$R(x)$ = receive polynomial

These polynomials are related by

$$T(x) = X^m * D(x) + C(x)$$

and

$$R(x) = T(x) + E(x)$$

For a number of information and check symbols,

k = Number of information symbols
m = Number of check symbols
n = Number of information plus check symbols (record length is the number of data plus the number of check symbols)

The efficiency of a code will be given by

$$R = \frac{k}{n}$$

where R is called the rate or code rate.

Appending Redundancy

The Euclidean division algorithm shows that to cause a data record to be divisible by the generator polynomial, the remainder after dividing $X^m * D(x)$ by $g(x)$ must be appended to the data record. This can be accomplished with the form of internal XOR shift register circuit shown in figure 3-15. This particular example premultiplies by X^3 and divides by $X^3 + X + 1$.

At check-bit time the multiplexer switches from write data to check bits, the gate is disabled, and check bits are shifted out of the shift register. The external XOR shift register circuit in figure 3-16 performs the same function. It writes the same check bits for a given data record.

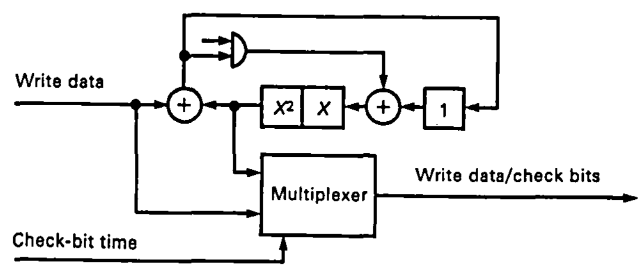

Figure 3-15.—Internal XOR shift register circuit.

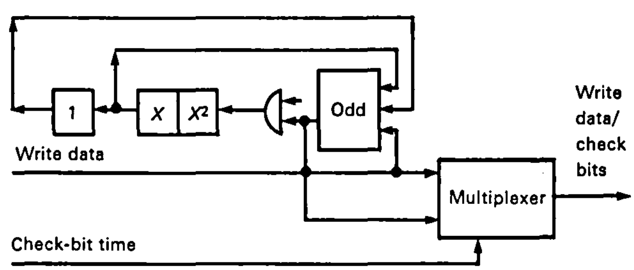

Figure 3-16.—External XOR shift register circuit.

Single-Burst Detection Span for an Error Detection Code

The single-burst detection span for a detection-only code is equal to the shift register length. Assume a shift register configuration that premultiplies by X^m and divides by $g(x)$, and assume the shift register to be initialized to zero and an all "0" bit data record. The only "1" bits will be from an error burst. The first bit of the burst sets certain shift register bits to "1," including the low-order bit.

To set the shift register to zero, the next m error burst bits must match the shift register contents. Therefore, for an error burst to set the shift register to zero, it must be longer than the length of the shift register.

To consider the same development using polynomial mathematics, it must be shown that the length of an error burst required to leave the shift register at zero is greater than m bits. For an error burst to leave the shift register at zero, it must be divisible by the generator polynomial. It must be shown that to be divisible by the polynomial, a burst must be greater than m bits in length.

Let $b(x)$ be an error burst of length m or fewer bits and let the exponent of the first term of $b(x)$ with a nonzero coefficient be the exponent of X^j. Then,

$$b(x) = X^j * b_0(X)$$

The terms X^j and $g(x)$ are relatively prime. If $g(x)$ is to divide $b(x)$, it must divide $b_0(X)$. This is impossible because $g(x)$ has a greater degree than $b_0(x)$. If $b_0(x)$ is a burst of length m or fewer bits, it is a polynomial of degree $(m - 1)$ at most, and is clearly not divisible by $g(x)$, which has degree m.

Theorems for Error Detection Codes

Theorem 1

All single-bit errors will be detected by any code the generator polynomial of which has more than one term. The simplest example is the code generated by the polynomial $(x + 1)$.

Theorem 2

All cases of an odd number of bits in error will be detected by a code whose generator polynomial has $X^c + 1$, $(c > 0)$ as a factor. The check bit generated by $X + 1$ is simply an overall parity check. All polynomials of the form $X^c + 1$ are divisible by $X + 1$. Therefore, any code whose generator polynomial has a factor of the form $X^c + 1$ includes an overall parity check.

Theorem 3

A code will detect all single- and double-bit errors if the record length (including check bits) is no greater than the period of the generator polynomial.

Theorem 4

A code will detect all single-, double-, and triple-bit errors if its generator polynomial is of the form $(X^c + 1)P(x)$ and the record length (including check bits) is no greater than the period of the generator polynomial.

Theorem 5

A code generated by a polynomial of degree m detects all single-burst errors of length no greater than m. (A burst of length b is defined as any error pattern for which the number of bits between and including the first and last bits in error is b.)

Theorem 6

A code with a generator polynomial $(X^c + 1)p(x)$ has a guaranteed double-burst detection capability provided the record length (including check bits) is no greater than the period of the generator polynomial. It will detect any combination of double bursts when the length of the shorter burst is no greater than z (degree of $p(x)$) and the sum of the burst lengths is no greater than $c + 1$. This theorem allows selection of a code by structure for accomplishing double-burst detection. Codes that do double-burst detection can also be selected by a computer evaluation of random polynomials.

Theorem 7

The fraction of error bursts b greater than m that go undetected is $1/2^m$ if $b > m + 1$ or $1/2^{m-1}$ if $b = m + 1$. The fraction of all possible error bursts that go undetected is called misdetection probability P_{md}. It is given by

$$P_{md} = \frac{1}{2^m}$$

This assumes all errors possible and equally probable. If some particular error bursts are more likely to occur than others, then misdetection probability becomes polynomial sensitive.

CORRECTION FUNDAMENTALS

This section introduces single-bit and single-burst error correction from the viewpoint of shift register sequences. The examples given use very short records and a small number of check bits; however, the techniques

apply to longer records and a greater number of check bits as well.

Single-Bit Error Correction

The circuit shown in figure 3-17 can be used to correct a single-bit error in a seven-bit record (four data bits and three check bits). Data bits are numbered d_3 through d_0. Check bits are numbered P_2 through P_0. Data and check bits are transmitted and received in the following order:

$$d_4\ d_3\ d_2\ d_1\ d_0\ P_2\ P_1\ P_0$$

Both the encode and decode shift registers premultiply by X^m and divide by $g(x)$, where m is 3 and $g(x)$ is $X^3 + X + 1$.

For encoding, the shift register is cleared. Data bits d_3, d_2, d_1, and d_0 are processed. As the data bits are processed, they are also written to the media or channel. After data bits are processed, the gate is disabled and the multiplexer is switched from data bits to the high-order shift register stage. The shift register contents are then written to the media or channel as check bits.

Decoding (fig. 3-18) takes place in two cycles: the buffer load cycle and the buffer unload cycle. A syndrome is generated by the shift register circuit as the buffer is loaded. Correction takes place as the buffer is unloaded. The shift register is cleared just prior to the buffer load cycle.

How Correction Works

Because $g(x)$ is primitive (polynomial with period $2^m - 1$, where m is the degree of the polynomial), it has two sequences: the zero sequence of length one and a sequence of length seven (fig. 3-19). Assume an all-"0" bits data record and data bit d_1 in error. The contents of the decode shift register during buffer load would be as shown in table 3-1. Notice that after the error is processed, the shift register clocks through its sequence until the end of the record is reached. The final shift register state for this example is 001. This is the syndrome.

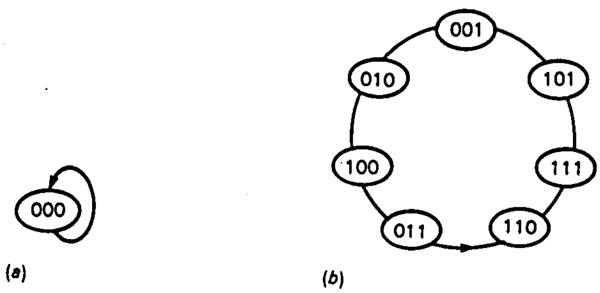

Figure 3-19.—The two sequences of $g(x)$. (*a*) Zero sequence. (*b*) Sequence of length seven.

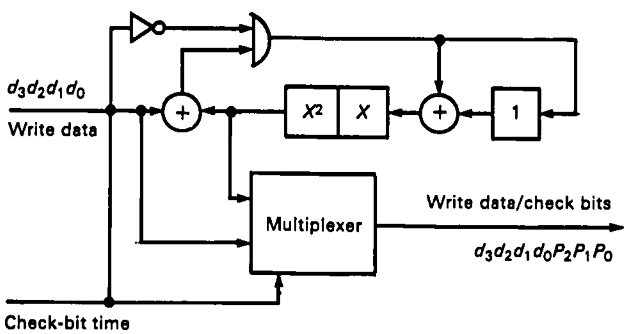

Figure 3-17.—Encoding circuit.

Table 3-1.—*Shift Register Contents for All-"0"-Bit Record and* d_1 *in Error*

Clock number	Error bits	Shift register contents
–	–	000
d_3	–	000
d_2	–	000
d_1	1	011
d_0	–	110
P_2	–	111
P_1	–	101
P_0	–	001

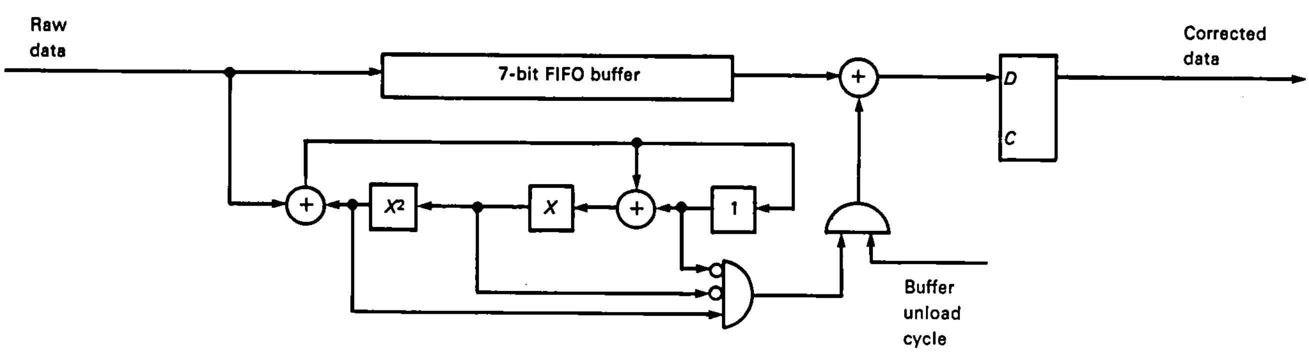

Figure 3-18.—Decoding circuit. (FIFO = first in, first out.)

The syndrome remains in the shift register as the buffer unload cycle begins. The shift register is clocked as data bits are unloaded from the buffer. As each clock occurs, the shift register clocks through its sequence. Simultaneously, the gate monitors the shift register contents for the 100 state. Correction takes place on the next clock after the 100 state is detected.

The shift register contents during the buffer unload cycle is shown in table 3-2.

During the buffer load cycle, because the data record is all "0" bits, the shift register remains all "0" bits until the error bit d_1 is clocked. (See fig. 3-20.) The shift register is then set to the 011 state. As each new clock occurs, the shift register advances along its sequence. There is an advance for d_0, P_2, P_1, and P_0. After the P_0 clock, the shift register is at state 001. This is the syndrome for the assumed error.

When the error bit occurs, it has the same effect on the shift register as loading the shift register with 100 and clocking once. Regardless of where the error occurs, the first nonzero state of the shift register is 011.

Error displacement from the end of the record is the number of states between the 100 state and the syndrome. It is determined by the number of times the shift register is clocked between the error occurrence and the end of record.

Consider what happens on the shift register sequence during the buffer unload cycle. (See fig. 3-21.) The number of states between the syndrome and 100 state represents the error displacement from the front of the record. To determine when to correct, it is sufficient to monitor the shift register for state 100. Correction occurs on the next clock after this state is detected.

Consider the case when the data are not all "0" bits. The check bits would have been selected on write such that when the record (data plus check bits) is read without error, a syndrome of zero results. When an error occurs, the operation differs from the all-"0" bit data case, only while the syndrome is being generated. A given error results in the same syndrome, regardless of data content because the code is linear. Once a syndrome is computed, the operation is the same as previously described for the all-"0" bit data case. This code is a single-error correcting Hamming code. It can be implemented with combinatorial logic as well as sequential logic.

Table 3-2.—*Shift Register Contents During Buffer Unload Cycle*

Clock number	Shift register contents
—	001
d_3	010
d_2	[a]100
d_1	[b]011
d_0	110
P_2	111
P_1	101
P_0	001

[a]The gate enables after this clock because the 100 state is detected.
[b]Correction takes place on this clock.

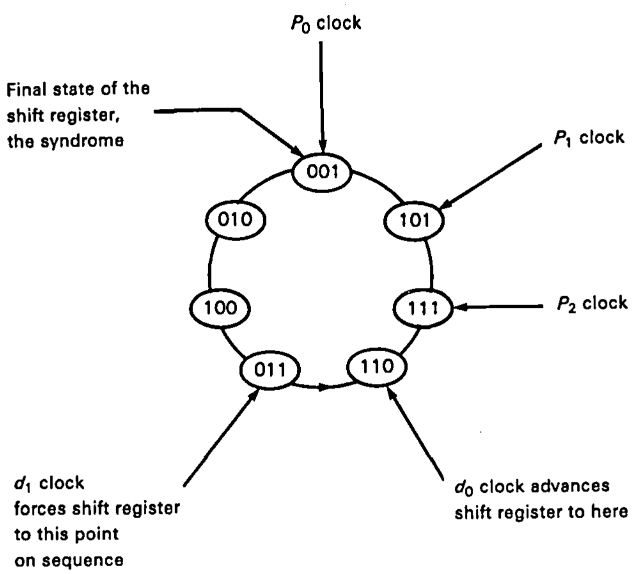

Figure 3-20.—Shift register sequence during buffer load cycle.

Single-Bit Error Correction and Double-Bit Error Detection

If an $X + 1$ factor is combined with the polynomial of the previous example, the resulting polynomial

$$\begin{aligned} g(x) &= (X + 1)(X^3 + X + 1) \\ &= X^4 + X^3 + X^2 + 1 \end{aligned}$$

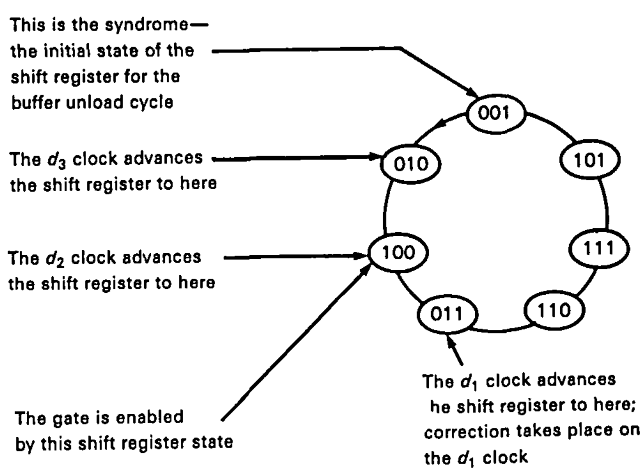

Figure 3-21.—Shift register sequence during buffer unload cycle.

can be used to correct single-bit errors and detect double-bit errors on seven-bit records (three data bits and four check bits). Double-bit errors are detected regardless of the separation between the two error bits.

The polynomial $g(x)$ has four sequences: two sequences of length seven and two sequences of length one. (See fig. 3-22.) If a single-bit error occurs, the syndrome will be on sequence A. If a double-bit error occurs, the syndrome will be on sequence B. This gives the code the ability to detect double errors.

The circuit in figure 3-23 could be used for decoding. Encoding would be performed with a shift register circuit premultiplying by X^m and dividing by $g(x)$.

Gate A detects the 1000 state on the clock prior to the clock that corrects the error. Gate B blocks the shift register feedback on the clock following detection of the 1000 state. This causes the shift register to be cleared.

If a double-bit error occurs, the syndrome is on sequence B. The shift register follows sequence B as it is clocked during the buffer unload cycle. Because the 1000 state is not on this sequence, gate A will not enable, and correction will not take place. Because correction does not occur, the shift register remains nonzero. If the shift register is nonzero at the end of the buffer unload cycle, a double error is assumed.

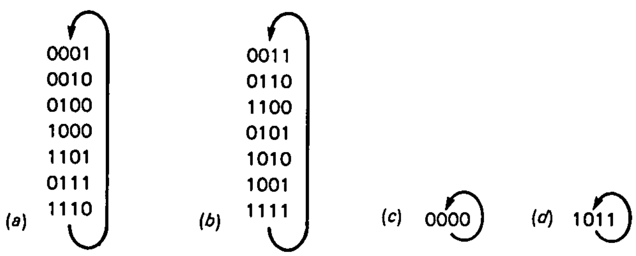

Figure 3-22.—Sequences of $g(x)$. (*a*) Sequence A. (*b*) Sequence B. (*c*) Sequence C. (*d*) Sequence D.

If three bit errors occur, the syndrome will be on sequence A. During the buffer unload cycle, the shift register state 1000 is detected, and a data bit is invented. This is miscorrection because the bit invented is not one of the bits in error.

This code corrects a single-bit error. It detects all occurrences of an even number of bits in error. When more than one bit is in error and the total number of bits in error is odd, miscorrection results.

This code is a single-error correcting, double-error detecting Hamming code. It can be implemented with combinatorial logic, as well as with sequential logic.

Burst Length 2 Correction

The polynomial of the previous example can also be used for burst length 2 correction. The circuit is identical except that AND gate A detects 1X00.

If a burst of length 1 occurs, the syndrome will be on sequence A. Gate A enables on state 1000. If a burst of length 2 occurs, the syndrome will be on sequence B. Gate A enables on state 1100. When the shift register is clocked from the 1100 state, it goes to 1000, due to the action of gate B. Gate A remains enabled. On the next clock, the shift register is cleared due to the action of gate B. Gate A is enabled for two consecutive clock times, and, therefore, two adjacent bits are corrected.

Correction of Longer Bursts

The concepts discussed in the preceding section can be extended to correction of longer bursts as well. To construct such a code, select a polynomial, irreducible or composite, meeting the following requirements:

(1) Each correctable burst must be on a separate sequence.

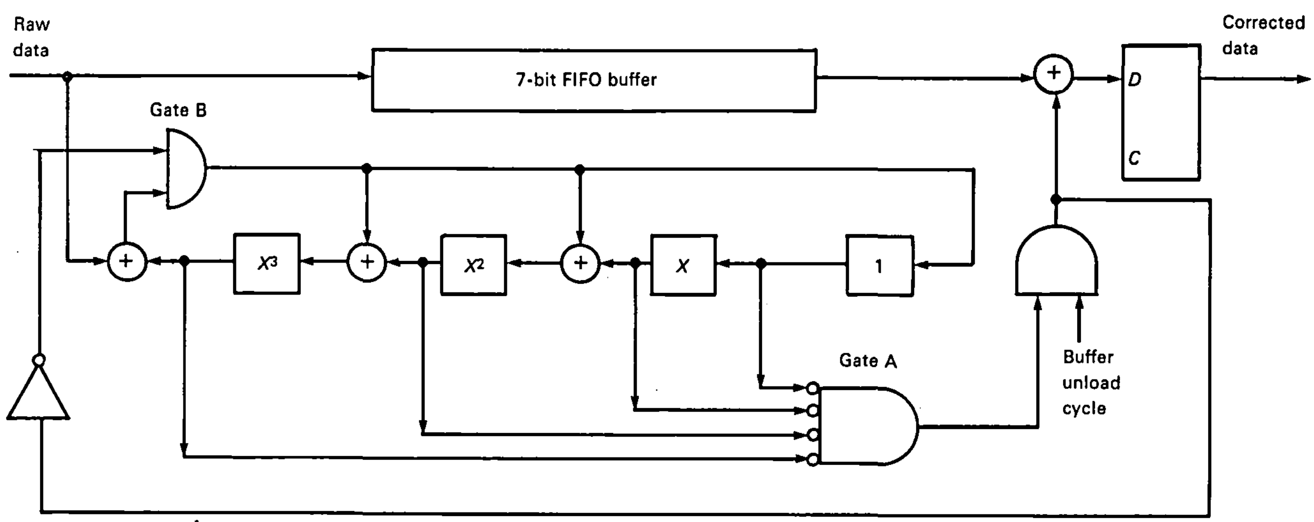

Figure 3-23.—Decoding circuit.

(2) The lengths must be equal for sequences containing correctable bursts.
(3) The sequence length must be equal to or greater than the record length for sequences containing a correcting burst.
(4) Any burst that is to be guaranteed detectable must not be on a sequence containing a correctable burst.

Requirement (2) is not necessary if the correction step is to be performed with the reciprocal polynomial (reverse clocking).

Assume a polynomial with multiple sequences. Assume that the bursts 1, 11, 101, and 111 are all on separate sequences of equal length. There may be other sequences as well. (See fig. 3-24.)

The code has at least the following capability. Its correction span can be selected to be one, two, or three bits, and its detection span is guaranteed to be at least three.

Primitive polynomials can also be used for burst correction. In this case the polynomial requirements are as follows:

(1) The polynomial period must be equal to or greater than the record length.
(2) Correctable bursts must be separated from each other on the sequence by a number of states equal to or greater than the record length in bits.
(3) Any burst that is to be guaranteed detectable must be separated from correctable bursts by a number of states equal to or greater than the record length in bits.

It is also possible to state more general requirements for a burst-correcting code:

(1) If more than one correctable burst is on a given sequence, these bursts must be separated by a number of states equal to or greater than the record length in bits.
(2) If one or more bursts that are to be guaranteed detectable are on a sequence with one or more correctable bursts, they must be separated from each correctable burst by a number of states equal to or greater than the record length in bits.
(3) The length must be equal for sequences containing correctable bursts.

Requirement (3) is not necessary if the correction step is performed with the reciprocal polynomial (reverse clocking). Any polynomial satisfying either of the two previous sets of requirements would satisfy the more general requirements. Many other polynomials would meet the general requirements as well.

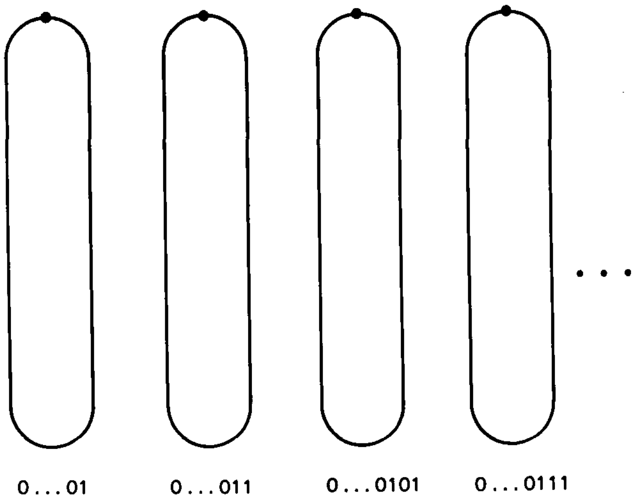

Figure 3-24.—Example of requirement (2).

PATTERN SENSITIVITY

When selecting a code for a particular application, it is important to consider pattern sensitivity. Some error detecting and error correcting codes are more likely to misdetect or miscorrect on certain classes of error patterns than others. This is called pattern sensitivity. If these classes of errors are also the most likely to occur, then protection provided by these codes may not be as good as expected. In this section several examples of pattern sensitivity are discussed. The codes named in this section are presented in detail in the original publication (ref. 3-1).

Error Detection Codes

Some error detection codes have pattern sensitivity. The polynomial for the circuit in figure 3-25 is $(X^{16} + 1)$. Of all possible error bursts, this circuit will fail to detect 1 out of 65 536. Any degree 16 polynomial would have the same misdetection probability for all possible error bursts. However, this circuit has a pattern sensitivity. It will fail to detect 1 out of every 16 possible error patterns, consisting of 2 bits in error, separated by more than 16 bits.

To understand the pattern sensitivity, consider reading a data record that is all "0" bits except for 2 bits in error, 16 bits apart. The shift register will be all "0's" until the first error bit arrives. After arrival of the first error bit, the shift register will contain 0 . . . 01. After receiving the 15 "0's" separating the error bits, the shift register will contain 10 . . . 0. After receiving the second error bit, the shift register will again contain all

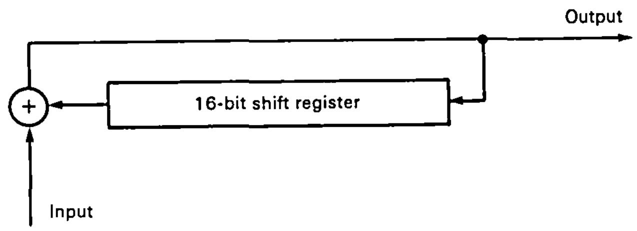

Figure 3-25.—Circuit defining an error detection code with pattern sensitivity.

"0's" due to the cancellation of the high-order bit by the second error bit.

This circuit is 4000 times more likely to fail to detect an error pattern consisting of 2 bits in error, separated by more than 16 bits, than it is to fail to detect a pattern consisting of many random bits in error.

The pattern sensitivity of this circuit is obvious. Nevertheless, it was implemented by a large computer manufacturer on the 2314 magnetic disk device in the mid 1960's. After the product was in the field, additional checking was installed to correct the problem.

Error Correction Codes

The Fire code is used for single-burst correction. Many Fire codes have a high pattern sensitivity for short double bursts. (See the section entitled "Data Accuracy" for a discussion of Fire code pattern sensitivity.)

Many interleaved error correcting codes have a pattern sensitivity for multiple short bursts. The 3370 code is such a code. It uses a single-symbol error correcting, double-symbol error detecting Reed-Solomon code interleaved to depth 3. Symbols are 1 byte wide. Its miscorrection probability is 2.2×10^{-16} for all possible error bursts; however, the miscorrection probability is 2.6×10^{-3} for all possible errors exceeding code guarantees and affecting a single interleave.

Other Forms

Many codes are sensitive to the error patterns caused by circuit or power supply failures. For example, if the line supplying data bits to a magnetic disk error correction circuit fails, the failure may not be detected by these circuits. One way to protect against this form of pattern sensitivity is to make sure nonzero check bytes are guaranteed for an all "0" bit data record.

A semiconductor memory error correction circuit may not detect the error when a word of all "0" bits (data and check bits) is erroneously read from memory, due to a circuit or power supply failure. Again, a solution is to cause nonzero check bytes to be generated for an all "0" bit data record.

DATA ACCURACY[1]

Data accuracy is one of the most important considerations in error correction system design. The following discussion on data accuracy is concerned primarily with magnetic disks; however, the concepts are extendable to many other error correction applications.

Most users of disk subsystems consider data accuracy even more important than data recoverability. Nevertheless, many disk subsystem designers are unaware of the factors determining data accuracy.

Polynomial Selection

In disk subsystems, the error correction polynomial has a significant influence on data accuracy. Fire code polynomials, for example, have been widely used on disk controllers, yet they provide less accuracy than carefully selected computer-generated codes.

Many disk controller manufacturers have employed one of the following Fire code polynomials:

$$(X^{21} + 1)(X^{11} + X^{2} + 1)$$

or

$$(X^{21} + 1)(X^{11} + X^{9} + 1)$$

The natural period of each polynomial is 42 987. Burst correction and detection spans are both 11 bits for record lengths, including check bits, no greater than the natural period. These codes are frequently used to correct 11-bit bursts on record lengths of 512 bytes.

When used for correction of 11-bit bursts on a 512-byte record, these codes miscorrect 10 percent of all possible double bursts in which each burst is a single bit in error. With the same correction span and record length, the miscorrection probability for all possible error bursts is 1 in 1000. The short double burst, with each burst a single bit in error, has a miscorrection probability two orders of magnitude greater.

Such codes have a high miscorrection probability on other short double bursts as well. Double bursts are not as common as single bursts; however, due to error clustering, they occur frequently enough to be a problem.

The data accuracy provided by these Fire codes for all possible error bursts is comparable to that provided by a 10-bit cyclic redundancy check (CRC) code. The data accuracy for all possible double-bit errors is comparable to the data accuracy provided by a three- or four-bit CRC code.

Fire codes are defined by generator polynomials of the form

$$\begin{aligned} g(x) &= c(x)p(x) \\ &= (X^{c} + 1)p(x) \end{aligned}$$

where $p(x)$ is any irreducible polynomial of degree z and period e and e does not divide c. The period of the generator polynomial $g(x)$ is the least common multiple of c and e. For record lengths (including check bits) not exceeding the period of $g(x)$, these codes are guaranteed

[1]This discussion is excerpted with permission from the October 1982 issue of *Computer Design.*

to correct single bursts of length b bits and detect single bursts of length d bits ($d \geq b$) provided $z \geq b$ and $c \geq d + b - 1$.

The composite form of the generator polynomial $g(x)$ is used for encoding. Decoding can be performed with a shift register implementing the composite generator polynomial $g(x)$ or by two shift registers implementing the factors of the generator polynomial $c(x)$ and $p(x)$. Code performance is the same in either case.

The $p(x)$ factor of the Fire code generator polynomial carries error displacement information. The $c(x)$ factor carries error pattern information. It is this factor that is responsible for the pattern sensitivity of the Fire code. To understand the pattern sensitivity, it is assumed that decoding is performed with shift registers implementing the individual factors of the generator polynomial. For a particular error burst to result in miscorrection, it must leave in the $c(x)$ shift register a pattern that qualifies as a correctable error pattern. A high percent of short double bursts do exactly that. For example, two bits in error $c + 1$ bits apart would leave the same pattern in the $c(x)$ shift register as an error burst of length 2. The same would be true of two bits in error separated by any multiple of $c + 1$ bits.

If $p(x)$ has more redundancy than required by the Fire code formulas, the excess redundancy reduces the miscorrection probability for short double bursts, as well as the miscorrection probability for all possible error bursts.

The overall miscorrection probability P_{mc} for a Fire code (assuming all errors possible and equally probable) is given by

$$P_{mc} \approx \frac{n * 2^{b-1}}{2^m} \qquad (3\text{-}2)$$

where

n = record length in bits including check bits
b = guaranteed single-burst correction span in bits
m = total number of check bits

For many Fire codes, the miscorrection probability for double bursts where each burst is a single bit in error (assuming all errors of this type are possible and equally probable) is given by

$$P_{mc,db} \approx \frac{2 * n * (b - 1)}{c^2 * (2^z - 1)} \qquad (3\text{-}3)$$

where

c = degree of the $c(x)$ factor of the Fire code polynomial
z = degree of the $p(x)$ factor of the Fire code polynomial

This equation is unique to the Fire code. It is applicable only when the product of $P_{mc,db}$ and the number of possible double-bit errors is much greater than 1. When this is not true, a computer search should be used to determine $P_{mc,db}$.

The ratio of $P_{mc,db}$ to P_{mc} provides a measure of pattern sensitivity for one particular double burst (each burst being a single bit in error). The Fire code is sensitive to other short double bursts as well.

Properly selected computer-generated codes do not exhibit the pattern sensitivity of Fire codes. In fact, it is possible to select computer-generated codes that have a guaranteed double-burst detection span. The miscorrecting patterns of these codes are more random than those of Fire codes, and they are selected by testing a large number of random polynomials of a particular degree. Provided the specifications are within certain bounds, some polynomials will satisfy them.

There are equations that predict the number of polynomials one must evaluate to meet a particular specification. In some cases, thousands of computer-generated polynomials must be evaluated to find a polynomial with unique characteristics. For a computer-generated code, correction and detection spans are determined by computer evaluation. Overall miscorrection probability is given by equation (3-2). To increase data accuracy, many disk controller manufacturers are switching from Fire codes to computer-generated codes.

Error Recovery Strategy

Error recovery strategies also have a significant influence on data accuracy. A strategy that requires data to be reread before attempting correction provides more accurate data than a strategy requiring the use of correction before rereading.

An equation for data inaccuracy is as follows:

$$P_{ued} \approx P_e * P_c * P_{mc} \qquad (3\text{-}4)$$

where

P_{ued} = probability of undetected erroneous data: ratio of undetected erroneous data occurrences to total bits transferred; a measure of data inaccuracy
P_e = raw burst error rate: ratio of raw burst error occurrences to total bits transferred
P_c = catastrophic probability: probability that a given error occurrence exceeds the guaranteed capabilities of a code
P_{mc} = miscorrection probability: probability that a given error occurrence, exceeding the guaranteed capabilities of a code, will result in mis-

correction, assuming all errors are possible and equally probable.

It is desirable to keep P_{ued} as low as possible. P_e, P_c, or P_{mc} must be reduced to reduce P_{ued}. (See eq. (3-4).) P_{mc} can be reduced by decreasing the record length and/or the correction span, or by increasing the number of check bits. P_c can be reduced by increasing the guaranteed capabilities of the code, or by reducing the percent of error bursts that exceeds the guaranteed code capabilities. P_e can be reduced by using reread. Most disk products exhibit soft burst error rates several orders of magnitude higher than hard burst error rates. Rereading before attempting correction makes P_e (in eq. (3-4)) the hard burst error rate instead of the soft burst error rate, reducing P_{ued} by several orders of magnitude. Rereading before attempting correction provides additional improvement in P_{ued} due to the different distributions of long error bursts and multiple error bursts in hard and soft errors.

Another strategy that reduces P_{ued} is to reread until an error disappears, or until there has been an identical syndrome for the last two reads. Correction should be attempted only after a consistent syndrome has been received.

Design Parameters

For data accuracy, a low miscorrection probability is desirable. Miscorrection probability can be reduced by decreasing the record length and/or correction span, or by increasing the number of check bits.

For most Winchester media, a five-bit correction span is adequate. A longer correction span is needed if the drive uses a read/write modulation method that maps a single encoded bit in error into several decoded bits in error, such as group coded recording and run-length limited codes.

For most cases, 32 check bits are adequate for sectored Winchester disks, provided that the polynomial is selected carefully, record lengths are short, correction span is low, correction is used only on hard errors, and the occurrence rate for hard errors exceeding the guaranteed capability of the code is low.

Some disk controller developers are using 40-, 48-, and 56-bit codes for their new designs. Using more check bits increases data accuracy and provides flexibility for correction-span changes when the product is enhanced. More check bits will also allow other strategies to be considered, such as on-the-fly correction.

Disk controller developers are also implementing redundant sector techniques and Reed-Solomon codes. Redundant sector techniques allow very long bursts to be corrected. Reed-Solomon codes allow multiple bursts to be corrected.

Error Correction Code Circuit Implementation

Cyclic codes provide very poor protection when frame synchronization is lost; that is, when synchronization occurs early or late by one or more bits. One protection from this type of error is to initialize the shift register to a nonzero value. The same initialization constant must be used on read and write. Another method is to invert check bits on write and read. Each method gives the error correction code (ECC) circuit another important feature—nonzero check bits are written for an all "0" bit data record. This allows certain logic failures to be detected before inaccurate data are transferred.

Some ECC circuit failures still can result in transferring inaccurate data. If the probability of ECC logic failure contributes significantly to the probability of transferring inaccurate data, some form of self-checking must be included.

Defect Strategy

All defects should have alternate sectors assigned, either by the drive manufacturer or subsystem manufacturer, before the disk subsystem is shipped to the end user.

There are problems with a philosophy that leaves defects to be corrected by ECC on each read, instead of assigning alternate sectors. First, if correction before reread is used, a higher level of miscorrection results. This is because a soft error in a sector with a defect results in a double burst. Once a double burst occurs that exceeds the double-burst detection span, miscorrection is possible. In the second case, if reread before correction is used, revolutions will be lost each time a defective sector is read.

Error Rates

Disk drive error rates also significantly influence data accuracy. If errors exceeding the guaranteed capability of the code never occurred, inaccurate data would never be transferred. When a data separator is part of the controller, its design affects error rate and therefore data accuracy. While most drive manufacturers provide recommended data separator designs, there are also well qualifed consultants who specialize in this area.

Specifying Data Accuracy

P_{ued} is a measure of data inaccuracy. Sophisticated developers of disk subsystems are now targeting 10^{-15} or less for P_{ued}. Even when P_e and P_c are high, one can still achieve any arbitrarily low value of P_{ued} by carefully selecting the correction span, record length, and number of check bits. (See eqs. (3-2) and (3-4).)

Summary of Data Accuracy Considerations

When designing error correction for a disk controller, keep data accuracy high by using the following techniques:

(1) Use a computer-generated code to avoid pattern sensitivity.
(2) Reread before attempting error correction.
(3) Use the lowest possible correction span meeting the requirements of supported drives.
(4) Insure that the ECC circuit provides adequate protection from synchronization framing errors.
(5) Design the ECC circuit to generate nonzero check bits for an all "0" bit data record.
(6) Include self-checking if it is required to meet the specification for P_{ued}.
(7) Use a manufacturer recommended data separator or get assistance from a consultant who specializes in this area.
(8) Assign alternate sectors for known defects.
(9) Establish a target for P_{ued}. Determine P_e and P_c by the manufacturer specification, measurement, and estimation. Select the number of check bits to meet the target for P_{ued}.

In computing P_{ued}, derate P_e and P_c to account for error clustering and marginal drives.

TESTING ERROR CONTROL SYSTEMS

This section is concerned primarily with diagnostic capability for storage device applications; however, the techniques described are adaptable to semiconductor memory, communications, and other applications.

Microdiagnostics

There are several approaches for implementing diagnostics for storage device error correction circuits. Two approaches are discussed here. The first approach requires the implementation of "read long" and "write long" commands in the controller.

The "read long" command is identical to the normal read command except that check bytes are read as if they were data bytes. The "write long" command is identical to the normal write command except that check bytes to be written are supplied, not generated. They are supplied immediately behind the data bytes.

The "read long" command is used to read a known defect-free data record and its check bytes. A simulated error condition is XOR'd into the record. The modified data record plus check bytes are written back to the storage device using the "write long" command. On read back, using the normal read command, an ECC error should be detected and the correction routines should generate the correct response for the error condition simulated. The test should be repeated for several simulated error conditions, correctable and uncorrectable.

It is often desirable to reserve one or more diagnostic records for the testing of error correction functions. It is important for any diagnostic routines testing these functions to first verify that the diagnostic record is error free.

In some cases, hardware computes syndromes but is not involved in the correction algorithm. The correction algorithm is totally contained in software. In this case, it is easy to get a breakdown between hardware and software failures by testing the software first. Syndromes for which proper responses have been recorded are supplied to the software.

Using the second diagnostic approach, the hardware is designed so that, under diagnostic control, data records can be written with the check bytes forced to zero. A data record is selected that would normally cause all check bytes to be zero. Simulated error conditions are XOR'd into this record. The record is then written to the storage device under diagnostic control, and check bytes are forced to zero. On normal read back of this record, an error should be detected and the proper responses generated.

These techniques apply to error control systems employing very complex codes as well as those employing simple codes and to the interleaved Reed-Solomon code as well as the Fire code.

Host Software Diagnostics

Host testing of error correction functions can be accomplished by implementing at the host software level either of the diagnostic approaches discussed in the preceding section.

If the controller corrects data before it is transferred to the host, the host diagnostic software must check that the simulated error condition is corrected in the test record. The entire test record must be checked to verify that the error is corrected and that correct data are not altered. Alternatively, the controller could have a diagnostic status or sense command that transfers error pattern(s) and displacement(s) to the host for checking; however, this is not as protective as checking corrected data.

Verifying an ECC Implementation

Error correction implementations should be carefully verified to avoid incorrect operation and the transfer of undetected erroneous data under subtle circumstances. This verification should be performed at the host software level using host level diagnostic commands.

Forcing Correctable Error Conditions

The "read long" command is used to read a known error-free data record and its check bytes. A simulated error condition that is guaranteed to be correctable is XOR'd into this record. Data record plus check bytes are written back to the storage device using the "write long" command. The record just written is read back using the normal read command. Controller correction of the simulated error condition should be verified. These procedures should be repeated using many random guaranteed-correctable error conditions.

Some nonrandom error conditions should be forced as well. A set of error conditions that is known to test all paths of the error-correction implementation should be selected.

Forcing Detectable Error Conditions

The test defined in the preceding section should be repeated by substituting simulated error conditions that exceed guaranteed correction capability but not guaranteed detection capability. An uncorrectable error should be detected for each simulated error condition.

Forcing Errors That Exceed Detection Capability

The test defined in the section entitled "Forcing Correctable Error Conditions" is repeated by substituting simulated error conditions that far exceed both the guaranteed correction and guaranteed detection capabilities. The number of correctable and uncorrectable errors reported by the error-correction implementation are counted. The ratio of counts should be approximately equal to the miscorrection probability of the code. This procedure is repeated for error conditions known to have a higher miscorrection probability.

Error Logging

For implementations where the data are actually corrected by the controller, it may be desirable to include an error-logging capability within the controller. A minimum error-logging capability would count the errors recovered by reread and the errors recovered by error correction. Logging requires the controller to have a method of signaling the host when the counters overflow and a command for offloading counts to the host.

A more sophisticated error log would also store information useful for the following:

(1) Reassigning areas of media for repeated errors

(2) Retiring media when the number of reassignments exceeds a threshold

(3) Isolating devices writing marginal media, which may require that the physical address of the writing device be part of each record written

(4) Isolating hardware failure

It may be desirable to reserve space for error logging on each storage device.

Self-Checking

Hardware

Hardware self-checking can limit the amount of undetected erroneous data transferred when error correction circuits fail. Self-checking should be added to

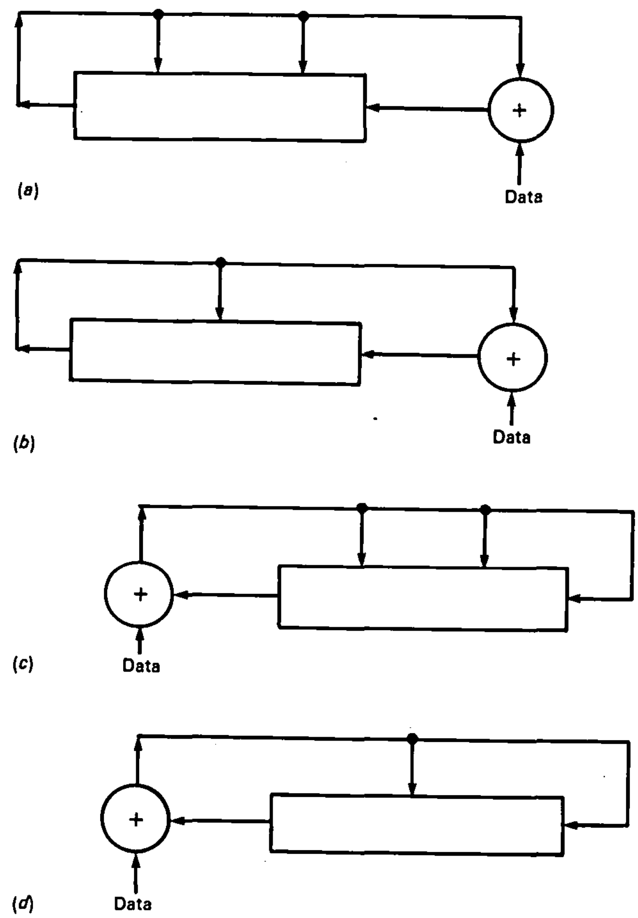

Figure 3–26.—Selected shift register configurations. (*a*) Divide by $g(x)$; odd number of feedbacks; the parity of the shift register will flip each time when the data bit is "1." (*b*) Divide by $g(x)$; even number of feedbacks; the parity of the shift register will flip when a "1" is shifted out of the shift register or (exclusive) if the data bit is "1." (*c*) Multiply by X^m and divide by $g(x)$; odd number of feedbacks; the parity of the shift register will flip when the data bit is "1." (*d*) Multiply by X^m and divide by $g(x)$; even number of feedbacks; the parity of the shift register will flip if a "1" is shifted out of the shift register.

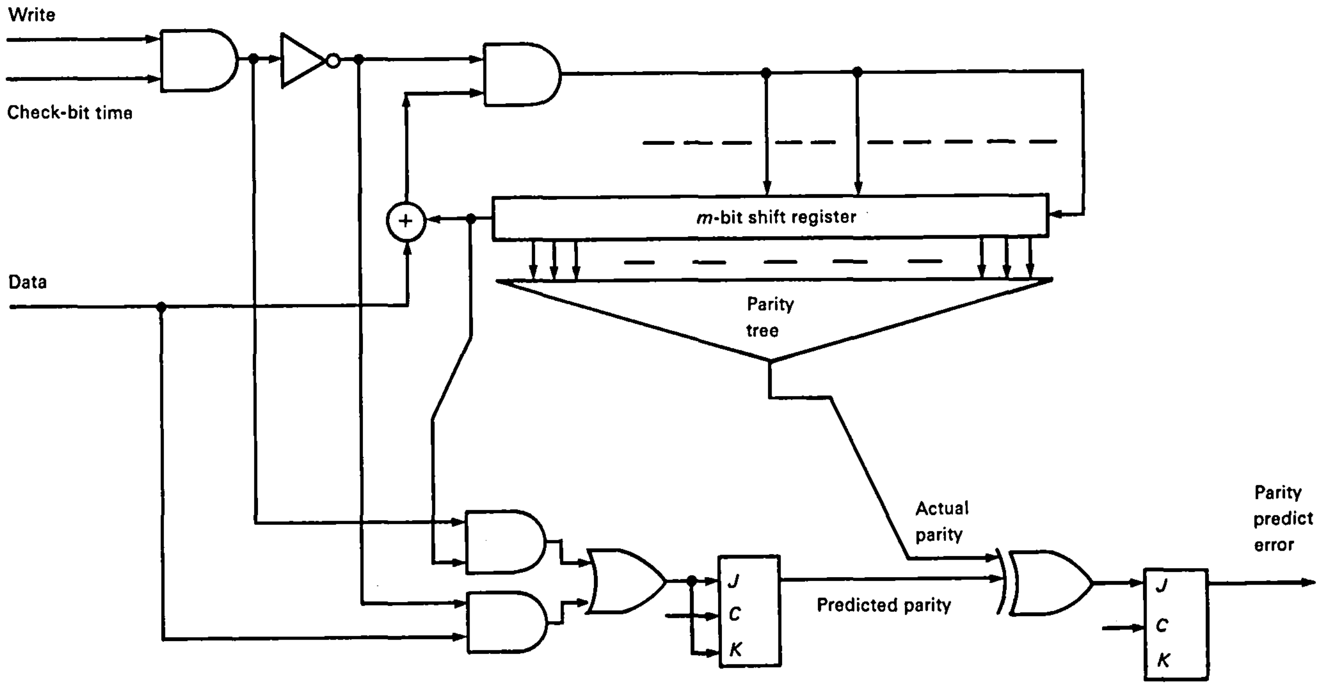

Figure 3-27.—Parity predict circuit.

the design if the probability of error correction circuit failure contributes significantly to the probability of transferring undetected erroneous data. One self-checking method duplicates the error correction circuits and, on read, verifies that the error latches for both circuits agree. No circuits from the two sets of error correction hardware share the same integrated circuit package. This concept can be extended by having separate sources and/or paths for clocks, power, and ground.

Another self-checking method is called parity predict. It is used for the self-checking of shift registers that are part of an error correction implementation. On each clock, new parity for each shift register is predicted. The actual parity of each shift register is continuously monitored and is compared to the predicted parity at each clock. If a difference is found, a hardware check flag is set. Figure 3-26 defines when parity is predicted to change for four shift register configurations.

An m-bit shift register circuit using parity predict for self-checking is shown in figure 3-27. An odd number of feedbacks and premultiplication by X^m is assumed. It is also assumed that the feedbacks are disabled during write check-bit time but not during read check-bit time. While writing data bits, reading data bits, and reading check bits, parity of the shift register is predicted to change for each data bit that is "1." While writing check bits, parity is predicted to change for each "1" that is shifted out of the shift register.

Another technique that aids the detection of error correction hardware failures is to design the circuits so that nonzero check bytes result when the data are all "0's".

Microcode and/or Software

Periodic microcode and/or software checking is another approach that can be used to limit the amount of undetected erroneous data transferred in case of an error correction circuit failure. Diagnostic microcode or software could be run on a subsystem powerup and during idle times. These routines would force ECC errors and check for proper detection and correction. In some cases, this approach is the only form of self-checking incorporated in an implementation, even though it is not as protective as self-checking hardware. In other cases, this approach is used to supplement self-checking hardware.

REFERENCES

3-1. Glover, Neal: *Practical Error Correction Design for Engineers.* Data Systems Technology Corp., Broomfield, Colo., Oct. 1982.

3-2. Niven, I.; and Zuckerman, H. S. *An Introduction to the Theory of Numbers.* John Wiley & Sons, Inc., New York, 1960.

CHAPTER 4

High-Density Magnetic Recording Heads: Optimization Theory

David Ricards and David Christofar
Spin Physics

This chapter outlines the important dimensions and parameters of high-density heads and discusses why each is important and how they are related. Among factors discussed are head to media contact; record gap size; media coercivity and remanence; record demagnetization fields; record and reproduce gap edge saturation in ferrite, metal, metal in gap, and thin film heads; and head wear. Gap edge straightness is discussed. Magnetoresistive read heads are described. Vertical recording and pole type heads are discussed. Principal sources of head noise are outlined.

To achieve good high-density performance, the heads and media must be in intimate contact. The record gap must be as small as possible, but gap edge saturation must be avoided. In thin film heads, yoke saturation must be avoided. This is made more difficult because high density media have high coercivity. The reproduce gap must be small enough to avoid gap loss but must be large enough that adequate signal is obtained with a gap depth providing adequate head life. Gap edges must be as straight and parallel as possible.

Vertical recording media give improved high-density performance because the demagnetization fields aid rather than oppose the record fields. Vertical pole heads work well in record but not in reproduce mode because of a tradeoff in gap loss and efficiency. Ring-type heads offer superior reproduce performance with vertical media.

Magnetoresistive reproduce heads offer much higher signal levels than inductive heads, but the advantage becomes smaller as media speed increases.

Primary head noise sources are resistance noise of the reproduce head, amplifier current noise that varies with net head impedance and amplifier voltage noise. The goal in a properly designed system is to make the sum of these noises smaller than the media noise.

This chapter amplifies the preceding statements and provides a semiquantitative basis for making design optimization tradeoffs.

RECORDING PROCESS

In high-density recording, nearly all of the reproduce signal comes from the surface of the medium. If Bl is the bit length, 90 percent comes from the top $0.74Bl$ of the surface. At 100 kbpi, $Bl = 0.25\ \mu m$ so $0.74Bl = 0.19\ \mu m$. Because it is not practical to coat conventional media in such layers, high-density data are recorded on the surface of the media only.

If a signal field H is applied and removed, neglecting demagnetization fields, the medium is magnetized according to the curve in figure 4-1, where $4\pi M_r$ is the remanence.

H_1 and H_2 define the boundaries of the record field range, and the 50 percent field is generally close to the media coercivity H_c. Standard record head and record field contours are shown in figure 4-2. The cross-hatched region is where recording takes place and is called the record zone. The depth of recording y_m is the height of the $H = H_c$ contour.

The deep gap field H_g is related to the record current i_r and the number of turns on the record head N by the expression

$$H_g = E\,\frac{4\pi N i_r}{10g} \tag{4-1}$$

where E is the head efficiency and H_g is in oersteds, and i_r in amperes, and g in centimeters. E represents that fraction of the magnetomotive force Ni_r that appears across the gap. (It is also the fraction of the tape flux passing through the coils during reproduce.) McKnight (ref. 4-1) gives a good review of detailed efficiency calculations for standard heads. Neglecting "air leakage," E is given approximately by

$$E = \frac{R_g}{R_g + R_c} \tag{4-2}$$

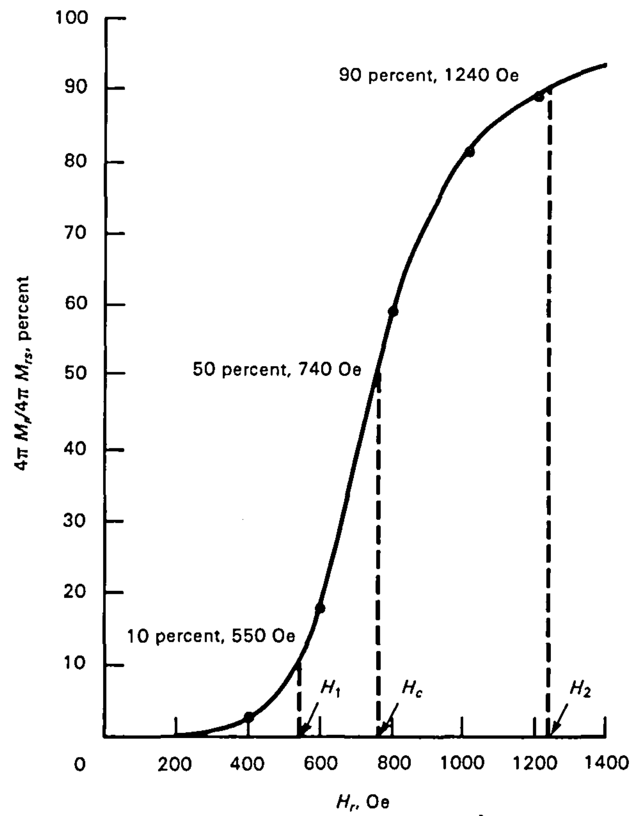

Figure 4-1.—Remanence versus record field H_r($H_c = 750$ Oe; $4\pi M_r = 1600$ G).

where R_g is the gap reluctance given by

$$R_g = \frac{g}{Tl} \tag{4-3}$$

where T is the trackwidth and l is the gap depth. The core reluctance R_c is given by

$$R_c + \frac{C}{\mu \bar{A}} \tag{4-4}$$

where μ is the core permeability, C is the circumference of the core, and A represents the average cross-sectional area of the core. Care must be taken to be sure that the fabrication process does not reduce the permeability of the head core material by inducing strain. Reduction of a factor of 5 is not uncommon.

At high density, when the bit length approaches half the record zone length $L/2$, the high H_c fraction of the particles in the medium are recorded "positive" and the low H_c fraction are recorded "negative," as shown in figure 4-3.

This results in cancellation and, therefore, a low recorded signal. This is called subsequent cycle erasure.

When the head/tape separation d increases, L, at the surface of the medium, increases, giving more erasure at high density. Bertram (ref. 4-2) has shown that for standard high-density media having $4\pi M_{rs}/H_c$ ratios $\cong$ 3, the record separation loss is given by $-44d/\lambda$ dB, where λ is the fundamental wavelength or twice the bit

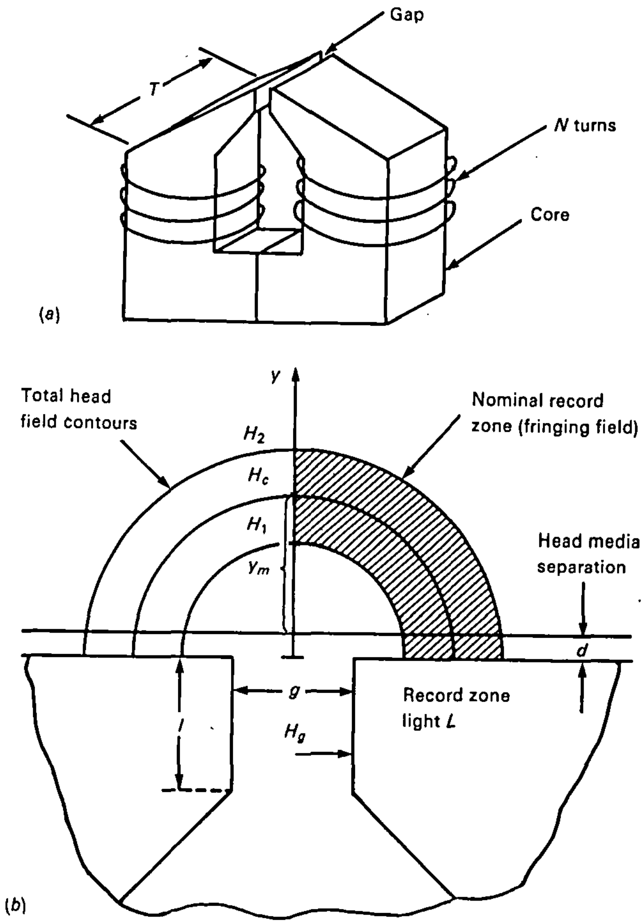

Figure 4-2.—(a) Magnetic head. (b) Cross section of record gap and head field contours. (H_g = deep gap field.)

length Bl. This expression is a conservative estimate of the loss caused by a momentary loss of contact (such as that due to a speck of dirt on the medium) because the record current was increased to partially compensate for the loss of contact. If H_c is increased, this loss factor becomes smaller.

The reproduce separation loss is the familiar $-55d/\lambda$ dB (ref. 4-3), so the net separation loss is about

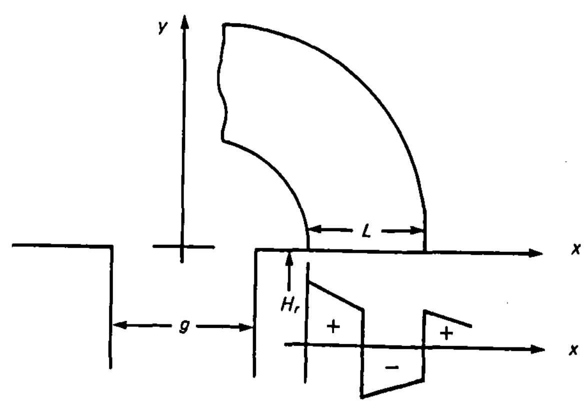

Figure 4-3.—High-density record field versus distance compared with a long record zone length (subsequent cycle erasure).

$-99d/\lambda$. If d is $\lambda/10$, the signal loss is 9.9 dB, or about a factor of 3. If the recording density is 100 kfci, $\lambda/10 = 0.05$ μm or about 250 air molecules lined up in a row. The importance of good head to media contact cannot be overemphasized.

The standard approach to achieving a narrow record zone is to use a small record gap. It has been shown that for any bit length less than the media thickness, when the head and media are in good contact, the maximum recordable signal increases as the record gap is reduced and reaches a maximum when saturation occurs at the gap corner (ref. 4-4). Figure 4-4 shows the maximum unbiased RMS signal versus frequency at a constant tape speed of 19.1 cm/s for three metal-tipped record heads having gaps of 1.9, 0.86, and 0.25 μm. The heads have ferrite cores and "glued on" Sendust pole tips. The same reproduce head having a gap of 0.25 μm was used for each curve. The media was an acicular Co-doped γFe_2O_3 tape with $4\pi M_{rs} \cong 1500$ G and $H_c \cong 860$ Oe. The record current was optimized at each frequency. The highest frequency of 300 kHz corresponds to 80-kfci digital density. The very small 0.25-μm gap head records 10 dB, or a factor of 3, more 80-kfci signal than does the 1.9-μm gap head.

Smaller gap record heads also give less record phase shift because the record zone has less curvature; therefore, the recording occurs closer to the gap. For applications such as disk storage devices in which no erasure takes place, but old data are simply overwritten, Lemke (ref. 4-5) has shown that excellent overwrite of 30 dB can be obtained using 0.25-μm record gaps at a density of 80 kfci.

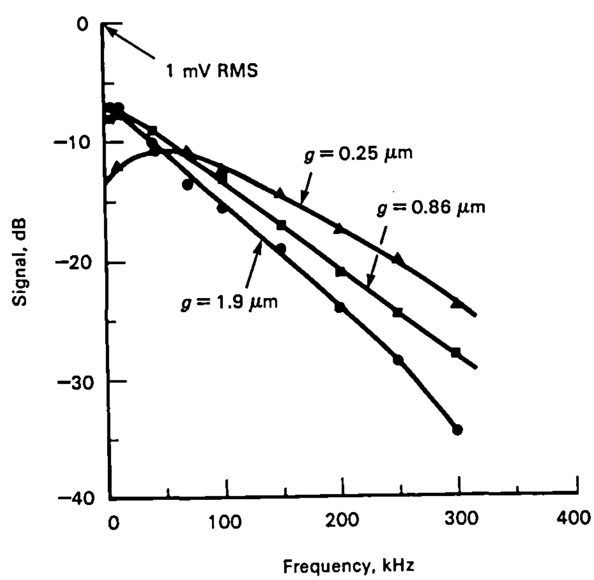

Figure 4-4.—Record performance at band edge of three different record gaps. (Tape speed = 19.1 cm/s; trackwidth = 250 μm; reproduce gap = 0.25 μm; reproduce turns = 198; H_c = 860 Oe; and B_r = 1500 G.)

Making the record gap small is not the complete picture, however. In addition to the head fields acting on the medium, there are also the demagnetization fields arising from the medium itself. In conventional media these fields tend to oppose the head record fields and thus smear out or increase the length of the record zone, thus reducing recorded signal. It also leads to nonlinear bit shift in which the location of a recorded transition is influenced by the preceding bit or string of bits.

The demagnetization fields are limited to $4\pi M_{rs}$, while the record fields are proportional to H_c. Increasing H_c requires a porportional increase in the record fields; the demagnetization fields then have less effect on the record zone, which allows more signal to be recorded.

GAP CORNER SATURATION

Unfortunately, making record gaps smaller and coercivity higher, in an effort to achieve more signal at high density, requires higher gap fields to do the recording. In typical high permeability ferrites, like MnZn ferrite, when the gap field exceeds about half the saturation flux density $4\pi M_s$, the corners of the gap become saturated. This causes the record zone to become longer, and loss of signal results; therefore, gap edge saturation sets a lower limit on the record gap length.

Equation (4-5) relates the gap field H_g required to record maximum level signals of wavelength λ on a medium of coercivity H_c using a head of gap g where λ and g are in micrometers and the fields are in oersteds (good head to media contact is assumed):

$$H_g \cong \left(\frac{1.7}{g^{0.33}} + \frac{0.8\lambda}{g^{0.78}} \right) H_c \qquad (4\text{-}5)$$

This field is very nearly the same as the bias field in ac bias recording, so the conclusions apply there as well as in unbiased recording.

This expression was derived using record currents and other data obtained in generating the curves in figure 4-4 and similar curves using tapes of different H_c.

The apparent maximum in the g = 0.25-μm curve at about 70 kHz in figure 4-4 is due to saturation in the Sendust pole tips of the record head. The saturation flux density of Sendust is about 9500 G, and equation (4-5) gives H_g = 7800 Oe for λ = 2.73 μm, g = 0.25 μm, and H_c = 860 Oe. This gap field is 82 percent of saturation and causes gap edge saturation.

Equation 4-5 can be used to determine whether a head design will suffer from saturation effects. For ferrites, if H_g is much larger than about 0.5 ($4\pi M_s$), saturation is occurring and a larger gap or a higher $4\pi M_s$ head material should be used.

For systems in which the record head must also serve as the reproduce head, the maximum gap is limited to

no more than about $\lambda/2.5$, because of the gap loss term,

$$\frac{\sin(1.14\pi g/\lambda)}{1.14\pi g/\lambda}$$

(See ref. 4-6.) Even for $g = \lambda/2.5$, the band edge signal loss is 3 dB. Using $g = \lambda/2.5$ in equation (4-5) yields

$$H_g \cong \left(\frac{2.3}{\lambda^{0.33}} + 1.63\,\lambda^{0.22}\right)H_c \qquad (4\text{-}6)$$

For densities of 50 to 100 kfci, λ is 1 to 0.5 μm, and over that range the term in parentheses in equation (4-6) is nearly constant and equal to 4, hence

$$H_g \cong 4H_c \qquad (4\text{-}7)$$

If the record/reproduce head is ferrite, then

$$H_g \leq \frac{4\pi M_s}{2}$$

and the result is that a coercivity of more than

$$H_c \cong \frac{4\pi M_s}{8}$$

should not be used. The saturation flux density for MnZn ferrite is generally about 5000 G, so the maximum media coercivity one can safely use with a ferrite record/reproduce head is about 5000/8 $\cong$ 625 Oe.

If the head is Sendust tipped, a gap field up to about $H_g \cong 0.8(4\pi M_s)$ can be used because the metal has a more rapid approach to saturation than does ferrite. Because $4\pi M_s \cong 9500$ G, equation (4-7) gives $H_c \lesssim 1900$ Oe, which is higher than that of any high-density medium yet reported.

SATURATION AND EDDY CURRENTS IN METAL HEADS

Although small gap Sendust heads can record on very high coercivity media, at high frequencies, the flux is confined to the surface of the head by eddy currents in the conductive metal. This causes the gap field to be shifted in phase relative to the record current by various amounts, depending on frequency (ref. 4-1). In addition, because of saturation in the "skin" of the head, the efficiency in equation (4-1) and, hence, H_g, can become much smaller as the record frequency is increased. For example, experiments at various tape speeds indicate that the efficiency of the 0.25-μm gap-tipped heads used in generating figure 4-4 decreases from 48 percent at 10 kHz to only about 9 percent at 10 MHz. If a constant record current is used in these or other metal heads while recording digital data, long strings of zeros (low frequencies) will be severely overrecorded, which causes peak shift and resultant errors.

METAL IN GAP HEAD

Figure 4-5 shows a new type of Sendust-ferrite composite head in which the Sendust is sputter deposited on the gap faces of an otherwise all ferrite head, thus the name metal in gap (MIG). (See ref. 4-4). Because the Sendust film and the ferrite core are magnetically in series, H_g is limited to the $4\pi M_s$ of the ferrite, which is about 5000 G. Because the Sendust $4\pi M_s = 9500$ G, the gap edges do not saturate at this gap field, and the maximum gap field for the MIG is $H_g = 5000$ Oe. Using equation (4-3) we see that an $H_c = 1250$ Oe can be used with an MIG record/reproduce head without saturation being a problem.

THIN FILM RECORD HEADS

A simple one-turn thin film head is shown in figure 4-6. Multiple turn heads have also been made (ref. 4-7). The poles are typically sputter deposited or electroplated 81 percent nickel and 19 percent iron having a permeability of about 2500 and a $4\pi M_s$ of 10^4 G. The structure is fabricated photolithographically. Integrated circuits are made in a similar way. The composition of 81/19 NiFe is important because there the magnetostric-

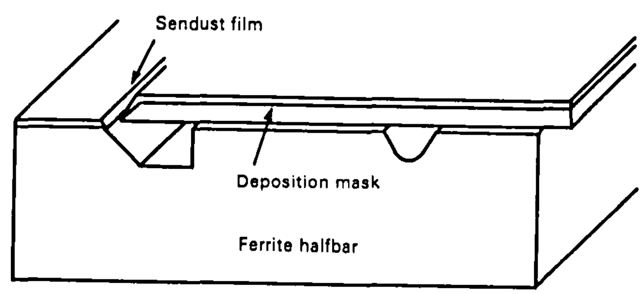

(a)

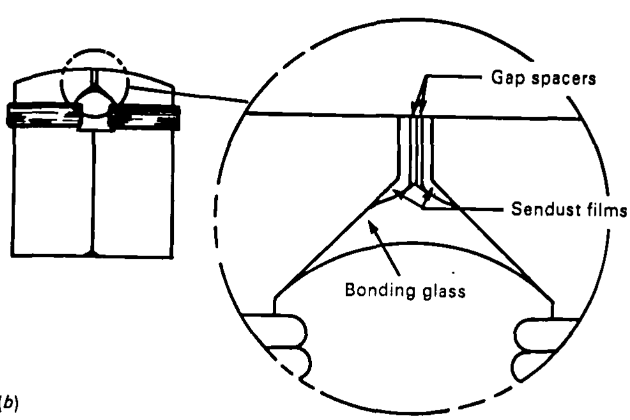

(b)

Figure 4-5.—Construction of MIG head. (a) Deposition geometry. (b) Finished head.

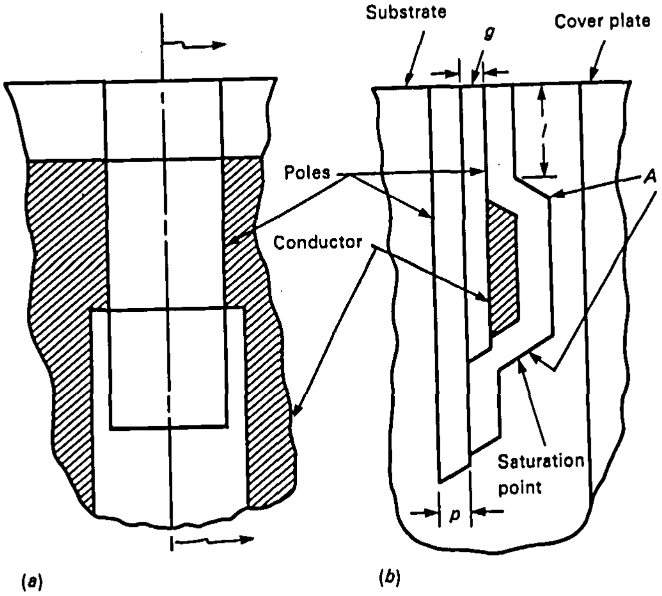

Figure 4-6.—Single-turn thin film head. $B_{max} \simeq 10\,000$ G. (*a*) Top view. (*b*) Cross section.

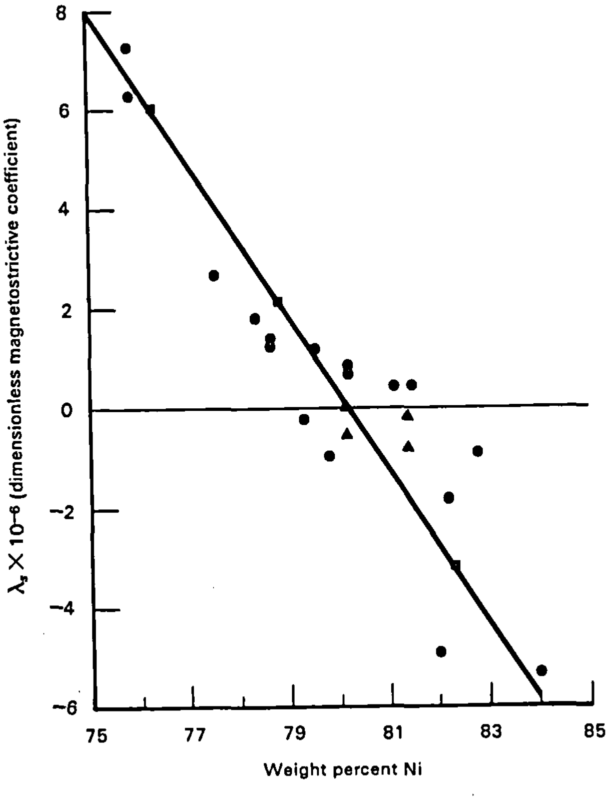

Figure 4-7.—Magnetostriction versus composition for NiFe (ref. 4-8).

tion constant is zero. Figure 4-7 shows the magnetostriction constant plotted versus composition. When films are deposited at an oblique angle, as occurs at the "shoulders" at points *A* in figure 4-6(*b*), the films are invariably strained to some degree. If λ is not very small, this strain can reduce the effective permeability of the shoulders by a factor of 5 or 10, and hence drastically reduce the head efficiency.

The pole thickness p for high-density recording is typically about 4 μm. This thickness is about the maximum that can be processed conveniently, by photoresist and ion mill etching, at the 3-μm line resolution required for high-track density multitrack heads. Track densities of up to about 500 tpi on two interleaved stacks can be made this way. The gap depth l is determined by the wear rate of the substrate and the expected life of the head. The gap depth needs to be as small as possible because the ratio p/l determines the maximum H_g that can be generated.

At low gap fields (and in reproduce) the efficiency of this sort of head is generally high when $p \cong l$ (refs. 4-9 and 4-10). However, when the gap flux (per unit track width) $H_g \cdot l$ approaches the pole layer saturation flux $4\pi M_s \cdot p$, the core saturates in the region noted in figure 4-6(*b*), and no further gap field increase occurs. The saturation gap field is as follows:

$$H_{g,\max} = 4\pi M_s \frac{p}{l} \tag{4-8}$$

Figure 4-8 shows a sketch of the gap field versus record current i_r for $g = 0.25$ μm.

Figure 4-9 shows a sketch of the 80-kfci signal recorded by a 0.25-μm gap single-turn record head having two gap depths, plotted versus record current in decibels. Also plotted is the corresponding curve for a Sendust-tipped head, which does not saturate in this current range. The curves in figure 4-8 have been shifted horizontally to compensate for differences in low field efficiency. As may be seen, the $p = 3$ μm, $l = 3$ μm

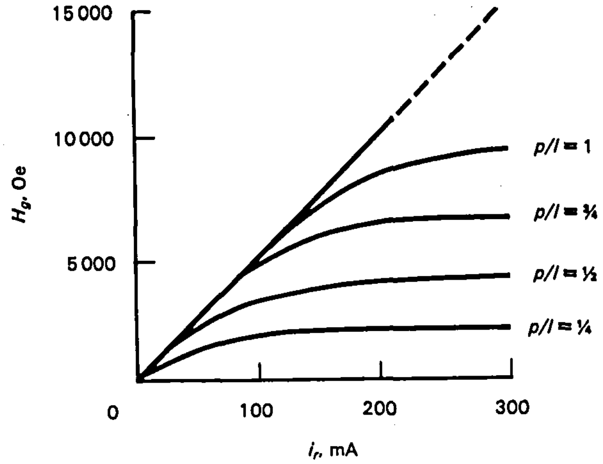

Figure 4-8.—H_g versus i_r for single-turn record head with $g = 0.25$ μm and various p/l values.

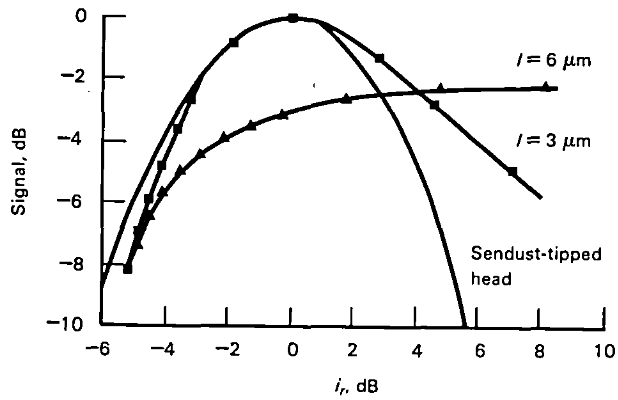

Figure 4–9.—80 kfci or $\lambda = 0.635$-μm signal level versus record current for a single-turn record head. ($p = 3\ \mu$m; $g = 0.3\ \mu$m; $H_c = 860$ Oe; $B_r = 1500$ G.)

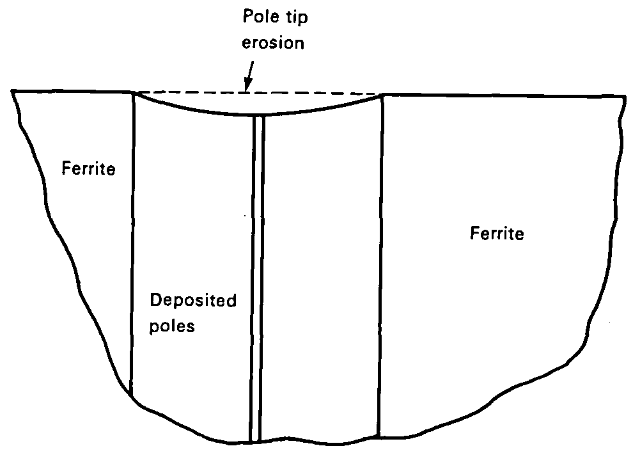

Figure 4–10.—MIG head showing pole tip erosion.

head does succeed in "saturating" the tape while the $l = 6\ \mu$m head does not. Zero decibels is 180 mA peak to peak for the $l = 3\ \mu$m curve.

If a MnZn ferrite substrate is used, the bottom pole can be eliminated. If the top deposited pole is downstream of the gap, the partial saturation of the ferrite gap corner is of little concern because it is so far from the record zone.

Head Wear

Because of the stringent requirement for minimum head-to-medium spacing, the head-to-medium pressures may need to be high, which increases wear rate. As the gap is reduced, gap depth is also reduced to maintain head efficiency. Head life is, therefore, reduced.

Fortunately, thin film and MIG head materials such as ferrite and sapphire are much more resistant to wear than Sendust and permalloy used in conventional heads. Sapphire and ferrite wear rates are about 5 to 10 times lower in comparable conditions.

An important problem with MIG heads running in contact is that the softer metal layers tend to erode due to differential wear, as shown in figure 4–10. Because so little metal is exposed, the undercut is only about 0.05 μm, but at a recording density of 100 kfci, even this tiny amount gives about a 4.5-dB record and 5.5-dB reproduce separation loss. Efforts to solve this problem are in progress.

RECORD HEADS FOR THIN FILM MEDIA

Equation (4-5) relating H_g, λ, g, and H_c was obtained from data generated using thick particulate coated media. If deposited thin film media in which the media thickness is comparable to the record gap are being recorded, equation (4-5) does not hold and ferrite heads can be used with much higher H_c values than 625 Oe. In this case it is assumed that $H = H_c$ at the back of the medium as sketched in figure 4-11. The field is written in terms of the Karlqvist approximation (ref. 4-11):

$$H_x = \frac{H_g}{\pi}(A_1 - A_2) \tag{4-9}$$

and

$$H_y = \frac{H_g}{\pi}\ln\frac{R_2}{R_1} \tag{4-10}$$

where the angles and distances are defined in figure 4-12. These expressions were used to sketch the field contours in figure 4-2 where $H = |\bar{H}| = \sqrt{H_x^2 + H_y^2}$. Defining y_m to be the height of the $H = H_c$ contour at the back of the medium,

$$\frac{y_m}{g} = \left(2\tan\frac{\pi H_c}{2H_g}\right)^{-1}$$

$$\cong \frac{1}{2.95}\frac{H_g}{H_c} - 0.15 \tag{4-11}$$

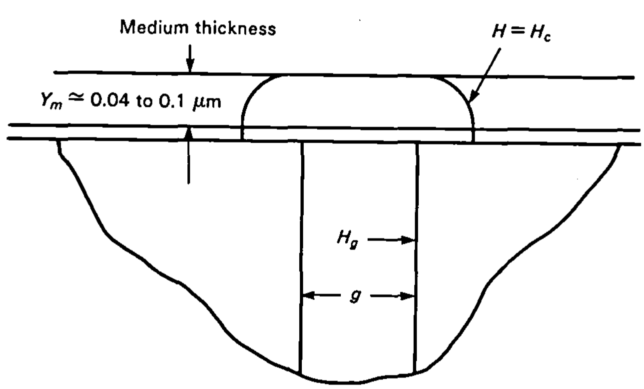

Figure 4–11.—Record contour for thin film media.

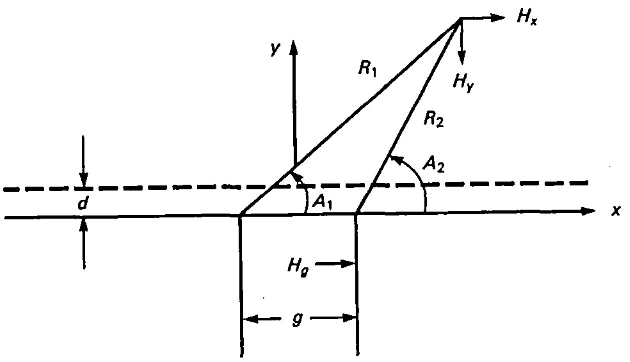

Figure 4–12.—Angle and distance for equations (4–9) and (4–10).

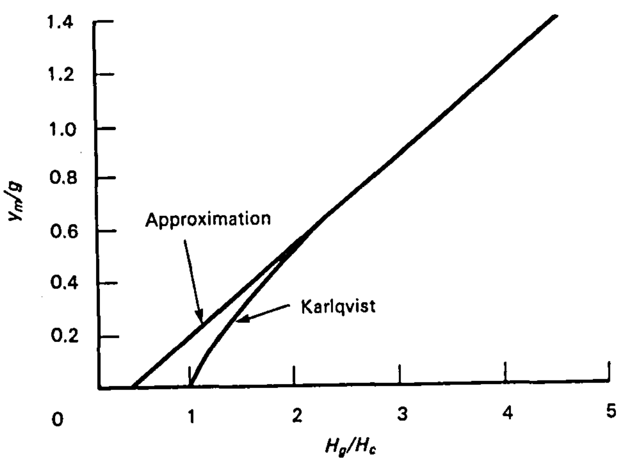

Figure 4–13.—Plot of y_m/g versus H_g/H_c.

The exact expression and approximation are plotted in figure 4–13. The approximation is good for $y_m/g \geq 0.4$.

Solving equation (4–11) for H_c and saying $H_g \leq 4\pi I_s/2 = 2500$ Oe for the ferrite head material gives

$$H_c \leq \frac{847}{y_m/g + 0.15} \tag{4–12}$$

If $y_m/g = 0.5$, equation (4–12) gives $H_c \leq 1300$ Oe for the maximum H_c that can be used with a ferrite head when the layer is very thin. This is much larger than the 625 Oe upper bound determined previously for thick media.

Vertical Recording Heads[1]

In vertically oriented media such as sputter-deposited CoCr (ref. 4–12), the demagnetization fields coming from the previously recorded bit aid the record field in recording the next bit, rather than opposing it as in conventional media. This results in a narrower record zone, hence a larger high-density signal and less nonlinear bit shift. Conventional ring record heads work well with vertical media because at the surface of the media where most of the high-density signal resides, the record field is vertical. However, improved record performance is obtained with vertical pole heads, as shown in figure 4–14, when recording on two-layer vertical media (ref. 4–12).

Toda (ref. 4–13) has compared the record capability of the head shown in figure 4–14(c) having a pole thickness T_m of 1.2 μm, to a ferrite ring head having a gap of 0.16 μm. Both were tested on a two-layer CoCr medium. The pole head recorded up to 7.6 dB more signal than the ring head, and the ring head pulses were very asymmetric. This indicates that significant horizontal moment as well as vertical was recorded by the ring head, which complicates reproduction. Pole heads seem better than ring heads for recording on two-layer vertical media. However, when recording on single-layer vertical media, very high current levels are required with pole heads because demagnetization fields in the pole tip are very high. Magnetomotive forces $i_r N$ of 30 ampere-turns are common for the single layer while only 2 ampere-turns are needed for the two-layer medium, because of the "keepering" provided by the NiFe layer.

Okuwaki (ref. 4–14) has shown that $D50$ densities (where the signal is down 50 percent) of 70 kfci can be recorded successfully on single-layer CoCr media with very little distortion using ring heads.

REPRODUCE

The output voltage of an inductive reproduce head is given by

$$S = -10^{-8} N \frac{d\phi}{dt} \tag{4–13}$$

where S is in volts, N is the number of turns, and ϕ is the flux in the head in Maxwells (or electromagnetic units or gauss-centimeters squared in the centimeter-gram-second system). The head flux ϕ is determined by the reciprocity principle (ref. 4–6):

$$\phi = \int \bar{M}_r \cdot \bar{H}\, dv \tag{4–14}$$

where M_r is the recorded remanence in the medium and H is the field above the read head generated by a unit "test current" in the reproduce windings. For a ring head, $\bar{H}$ is given by equations (4–9) and (4–10) and in the context is called the "read head sensitivity function." Equation (4–14) can be broken down into horizontal

[1]See chapter 5 of this book entitled "Perpendicular Recording."

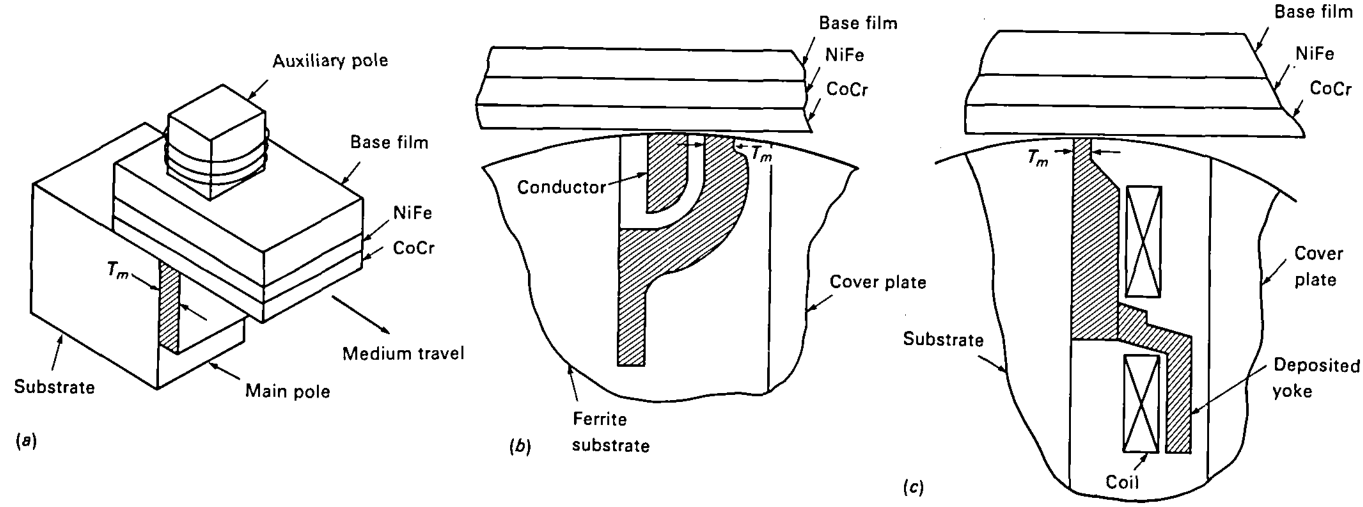

Figure 4–14.—Vertical pole heads. (*a*) Auxiliary vertical pole head. (*b*) Cross section of single-turn one-sided vertical pole head. (*c*) Cross section of one-sided single-pole head.

and vertical components as

$$\phi = \int M_{rx} H_x \, dv + \int M_{ry} H_y \, dv \qquad (4\text{–}15)$$

If $M_{rx} = M_{ry}$, the two terms in equation (4–15) are equal except for a 90° phase shift, hence equal horizontal and vertical magnetizations produce the same read signal.

We can get a rough idea of the expected signal amplitude S if we make the crude approximation that the medium is sinusoidally magnetized at the 50 percent remanence level; i.e.,

$$M_{rx} = \frac{M_{rs}}{2} \sin \frac{2\pi}{\lambda} x \qquad (4\text{–}16)$$

to a depth y_m and is unmagnetized beyond that. Equation (4–15) can then be easily integrated to give the simple expression

$$S = A f_1(\lambda) \, f_2(\lambda) \, f_3(\lambda) \qquad (4\text{–}17)$$

where

$$A = 10^{-8} ENTv 4\pi M_{rs} \qquad (4\text{–}18)$$

$$f_1(\lambda) = e^{-(2\pi+5)d/\lambda}$$

$$f_2(\lambda) = (1 - e^{2\pi y_m/\lambda})$$

$$f_3(\lambda) = \frac{\sin(1.14\pi g/\lambda)}{1.14\pi g/\lambda}$$

The first part of the exponent in $f_1(\lambda)$, $-2\pi d/\lambda$, gives the $-55d/\lambda$ dB reproduce separation loss. The second part, $-5d/\lambda$, gives the $-44d/\lambda$ dB record separation loss, both discussed earlier. The $f_2(\lambda)$ term is the thickness loss term and gives a 6-dB per octave increase at long wavelengths and shows that 90 percent of the signal comes from the top λ/e of the layer. Hence little is gained by making $y_m > \lambda/e$. The remaining term is the gap loss. It is unity at long wavelengths and zero when $\lambda = 1.14g$, having subsequent "bumps" as the wavelength is further reduced (ref. 4–6). E in equation (4–18) is the reproduce head efficiency given by equation (4–2), or more accurately by equations in reference 4–1. N is the number of turns on the reproduce head, T is the trackwidth in centimeters, v is the media velocity in centimeters per second, and $4\pi M_{rs}$ is the saturation remanence flux density in gauss; i.e., 100 percent in figure 4–10.

Figure 4–15 shows a response curve obtained using the 0.25-μm gap record head, 0.25-μm reproduce head, and tape used to obtain the data shown in figure 4–4. The recording was unbiased sine wave, with the record current held constant and set to maximize the 300 kHz or $\lambda = 0.635$-μm signal. Using a record gap $g = 0.25$ μm and $\lambda = 0.635$ μm in equation (4–5) gives $H_g H_c \cong 4.2$. Using this in equation (4–11) gives $y_m/g \cong 1.27$ or $y_m \cong 0.32$ μm. $4\pi M_{rs}$ for the tape used was 1500 G, the reproduce turns were $N = 198$, the track width was $T = 0.025$ cm, and the tape speed was $v = 19.1$ cm/s. The reproduce gap was also 0.25 μm. A reasonable upper bound on the reproduce head efficiency was $E \cong 0.65$, and a head/tape separation of $d = 0.1$ μm was estimated. Using these values in equations (4–17) and (4–18) gives the HP-85 computer drawn curve in figure 4–15. The program is also shown. The fit is about 5 dB low, which is not bad considering the gross approximations made. The shape is about right.

In digital recording one records "square waves." Figure 4–16 shows the data from figure 4–15 and a

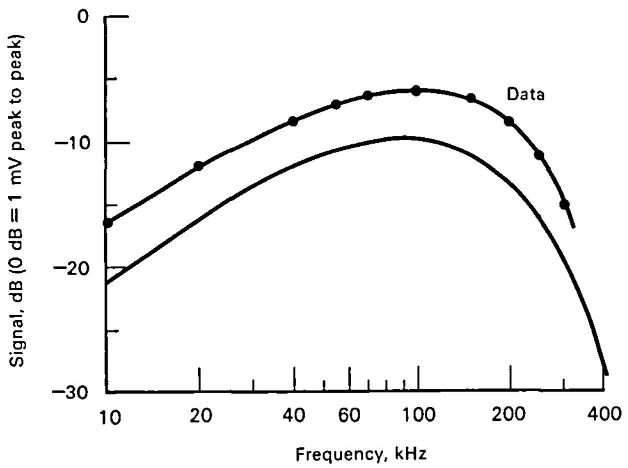


```
10 PLOTTER IS 705
20 SCALE 4,6,-35,0
30 D=.1*10^-4
40 E=.65
50 V=19.1
60 N=198
70 B=1500
80 T=.025
90 Y=.32*10^-4
100 G=.25*10^-4
110 A=10^-8*E*N*T*V*B
120 FOR Q=4 TO 5.7 STEP .1
130 F=10^Q
140 L=V/F
150 Z=A*EXP(-(2*PI+5)*D/L)*(1-EX
    P(-2*PI*Y/L))*SIN(1.14*PI*G/
    L)/(1.14*PI*G/L)
160 PLOT Q,20*LGT(ABS(Z))+60
170 NEXT Q
180 END
```

Figure 4–15.—Sine wave response curve and computer fit. (Tape: $H_c = 760$ Oe; $B_r = 1600$; isomax.)

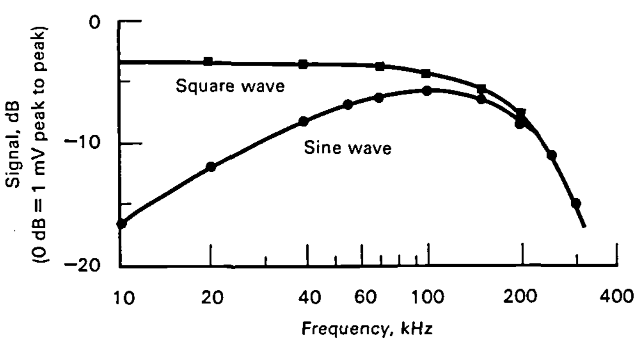

Figure 4–16.—Comparison of sine wave and square wave recording. Record and reproduce heads are Sendust tipped. (Record head: $T = 250$ μm; $g = 0.25$ μm. Reproduce head: $T = 250$ μm; $g = 0.25$ μm; $N = 198$. Tape (isomax): $H_c = 760$ Oe; $B_r = 1600$ G; speed = 19.1 cm/s.)

square-wave response curve done at the same time. At short wavelengths the higher odd harmonics that make up the square wave do not come through the record/reproduce process, so the sine and square wave signals are the same.

GAP EDGE STRAIGHTNESS

Gap edge straightness is very important at high density. If the gap edges are not straight and parallel, various parts of the recorded track produce signals that are out of phase, which then tend to cancel when combined in the reproduce windings. Mallinson (ref. 4–15) has shown that if σ represents the "average" gap edge deviation from straightness, the gap irregularity loss can be written as

$$\text{Gap irregularity loss} \simeq 338 \left(\frac{\sigma}{\lambda}\right)^2 \text{ dB} \quad (4\text{–}19)$$

Hence, if $\sigma = 0.1\lambda$, the signal loss is about 3.4 dB. If $\lambda = 0.5$ μm (100 kfci), $\sigma = 0.05$ μm: 250 air molecules in a row.

The loss in equation (4–19) is calculated for a negligibly small gap. If the signal is investigated in the region of the "first gap null," $\lambda = 1.14g$, the gap null is washed out when the gap edges are not straight. Figure 4–17 shows a 250-μm trackwidth polycrystalline Sendust pole tip reproduce head compared with a 36-μm trackwidth single crystal ferrite read head. A single 0.3-μm gap record head was used, and the current was set to maximize the 300-kHz or 80-kfci signal for both curves. The ferrite head curve was shifted vertically to compensate for trackwidth, turns, and core efficiency differences so as to make the long wavelength signals equal.

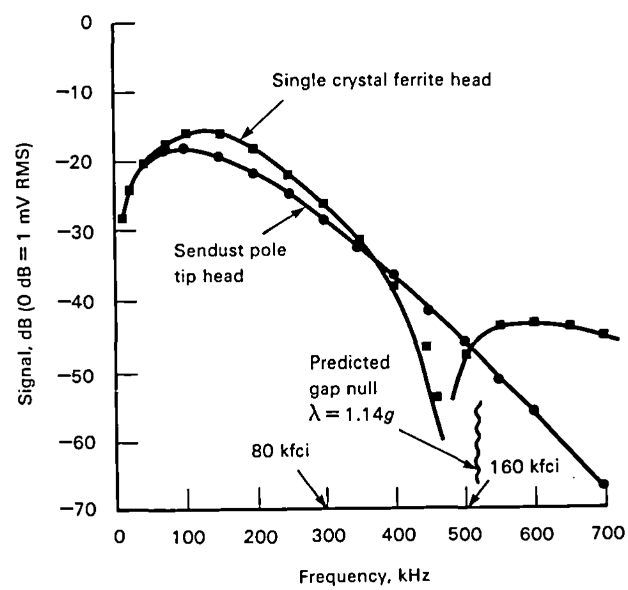

Figure 4–17.—Response curve showing gap null behavior. (Single crystal ferrite head: $T = 36$ μm; shifted upward 32 dB. Sendust pole tip head: $T = 250$ μm; $N = 200$. Both gaps are nominal: 0.3 μm. Tape (isomax): $H_c = 760$ Oe; $B_r = 1600$ G; speed = 19.1 cm/s.)

The gap null of the Sendust head is washed out because of gap edge irregularity, which causes the gap length to change across the trackwidth. The 3- to 4-dB signal advantage of the ferrite head in the mid band from 100 to 300 kHz is due to its lower gap irregularity loss from equation (4–19).

From 400 to 500 kHz the output of the Sendust tip head is higher than the single crystal head, but this is misleading because there is phase distortion in the Sendust head over this range. An examination of equation 4–17 shows that there is an abrupt phase shift of 180° at the gap null. Because the null of the Sendust head is smeared out, its phase shift is also smeared out. Hence, although the signal of the Sendust head is higher from 400 to 500 kHz, its signal phase is changing in a completely unpredictable and unusable way over this range.

The null smearing shown by the Sendust head is typical of polycrystalline head materials. Apparently the slightly different lapping rates of the randomly oriented crystals causes a very slight "orange peel" or roughness of the gap surfaces. The single crystal ferrite does not have this problem.

VERTICAL POLE HEADS IN REPRODUCE

The vertical heads shown in figure 4–14 work well in recording on vertical media, but in reproduce they suffer from "gap nulls" caused by the thickness of the main pole T_m. Figure 4–18 shows a typical example where $T_m = 1.1\ \mu m$.

This head is not usable beyond about 40 kfci. If T_m is reduced, to move the gap nulls out to higher density, the record function suffers, apparently because of pole tip saturation (ref. 4-13).

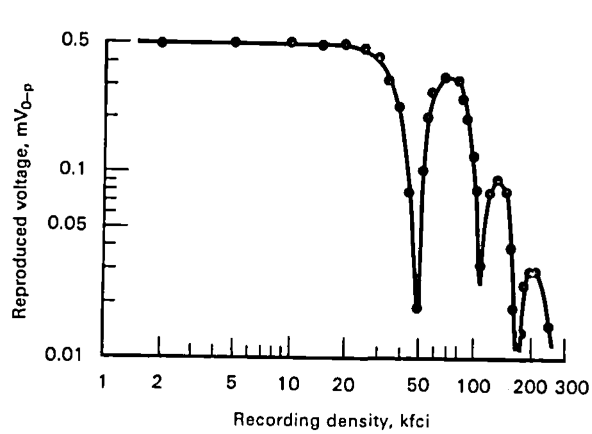

Figure 4–18.—Vertical pole head—record/reproduce. (T_m = 1.1 μm; W_t = 300 μm; N = 50; L = 10 μH; speed = 2 m/s; 0–p = 0 to peak.)

MAGNETORESISTIVE READ HEADS

Magnetoresistive heads generally use a 200- to 500-Å-thick single domain layer of 81/19 permalloy, the resistivity of which changes in response to rotation of the film magnetization vector according to the expression (ref. 4–16)

$$\rho = \rho_0 + \Delta\rho \cos^2 \theta \qquad (4\text{–}20)$$

where θ is the angle between the current and the magnetization of the film. ρ_0 is the isotropic resistivity and $\Delta\rho$ is the magnetoresistivity. The deposition takes place in a magnetic field that gives rise to an internal anisotropy field $\mathbf{H}_k$. This field exerts a torque on the magnetization, which acts to keep $\theta = 0$, the so-called "easy axis." $\mathbf{H}_k$ is about 3 to 10 Oe.

The sensor carries a constant sense current i_s, and the field from the recorded medium rotates the moment, changing the resistance, which varies the voltage across the magnetoresistive element, producing a signal.

Figure 4–19 shows a diagram of a magnetoresistive element. Figure 4–20 is a graph of $(\rho - \rho_0)/\rho_0$ versus applied field H. The "skirts" of the curve are the result

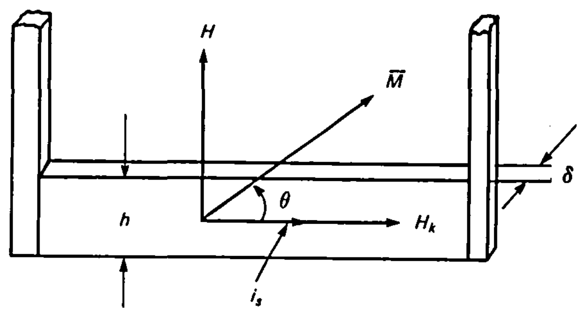

Figure 4–19.—Magnetoresistive element.

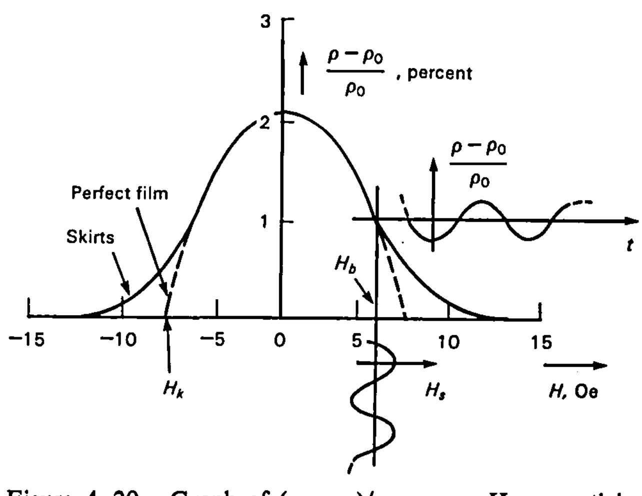

Figure 4–20.—Graph of $(\rho - \rho_0)/\rho_0$ versus H, magnetizing strength. (H_s = saturation magnetizing strength.)

of minor local deviations in the direction and magnitude of the anisotropy field $\mathbf{H}_k$, called "dispersion," and also the result of any demagnetizing fields $\mathbf{H}_d$ that may exist. The dashed curve in figure 4-20 shows how a "perfect" film would behave. The element is subjected to a constant bias field $\mathbf{H}_b$ to move the signal field to the inflection point in the curve so as to get maximum signal and minimum second harmonic distortion. This generally corresponds to $\theta \simeq 45°$. Standard signal in/out versus time sketches are also shown in figure 4-20.

The resistivity ρ_0 of permalloy is about 20 to 25 $\mu\Omega$ cm depending on thickness. $\Delta\rho$ is about 0.55 $\mu\Omega$ cm, so $\Delta\rho/\rho_0 \cong 2.5$ percent. When the element is deposited on a high thermal conductivity substrate, such as silicon or sapphire, current densities of $j \cong 10^7$ A/cm^2 can be handled. This corresponds to an internal electric field of $E = j\rho \cong 200$ V/cm. For an element length of 50 μm (2 mils), the applied voltage V is a nominal 1 V. Because the peak-to-peak $\Delta\rho/\rho_0$ is 2.5 percent, the maximum signal $S \cong V\,\Delta\rho/\rho_0 \cong 25$ mV. The nonlinearities shown in figure 4-20 limit the usable signal to about half this, or approximately 10 mV for a 50-μm element length.

Magnetoresistive heads are typically classified in terms of how the bias field $\mathbf{H}_b$ is applied. Perhaps a dozen different bias techniques have been reported, including external fields, adjacent hard and soft magnetic layers, shunt current in adjacent and nonmagnetic layers, asymmetric placement of the sensor element in a magnetic gap, rotation of the current by "barber pole" conductor layers placed on the sensor layer, paired sensors each current biasing the other, and "canted easy axis" (ref. 4-17). Bias has also been accomplished by "exchange coupling" between the magnetoresistive element and an adjacent antiferromagnetic layer (ref. 4-8).

Discussion of all these techniques is beyond the scope of this chapter, but the simplest head due to Hunt (ref. 4-18) is instructive. Figure 4-21 is a sketch of the Hunt head. It responds to the vertical field above the media averaged over the element height h. The height must be more than approximately 4 or 5 μm because of wear considerations. As a result, it detects approaching digital transitions before they are under the sensor. The isolated pulse shape is as shown in figure 4-22. The full width at half maximum $PW_{50} \cong h$ for small head–medium separation. As a result, the signal spectrum covers a very large range as shown by figure 4-23, where spectra for several elements are shown. The peak-to-band-edge signal ratio, even for the $h = 9$-μm head, is about 40 dB for a 2-μm-band-edge wavelength.

This signal is relatively free of amplitude or phase nonlinearity, and, hence, in principle, should be equalizable. However, people have not wanted to equalize this much signal range, so they put shields on either side of the magnetoresistive element (ref. 4-19).

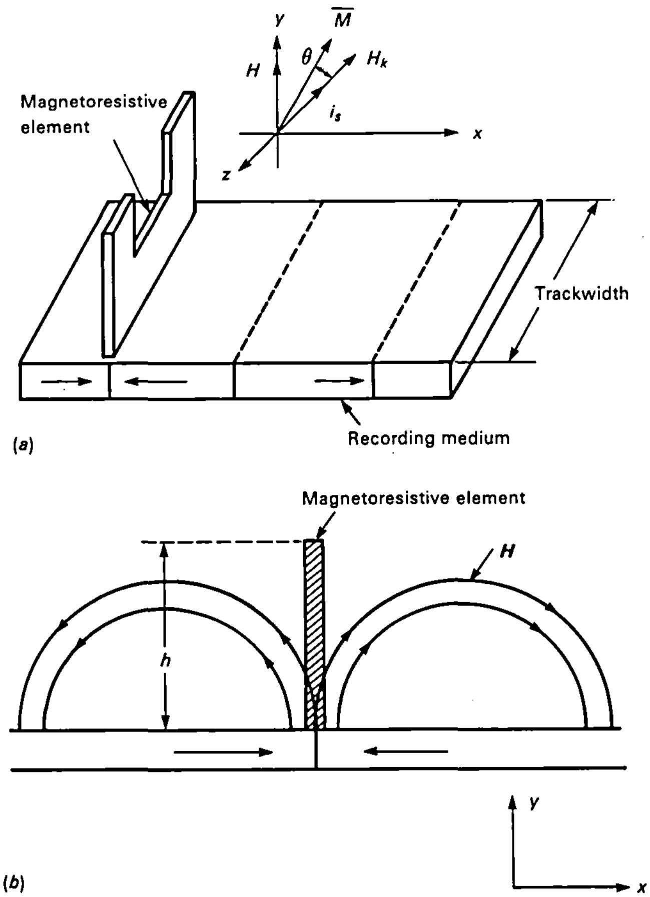

Figure 4-21.—Hunt vertical magnetoresistive element. (*a*) Diagram. (*b*) Cross section.

This has the result of greatly reducing the long wavelength signal and reducing the short wavelength signal a lesser amount so the peak-to-band-edge ratio is smaller. Putting on the shields also creates a gap null at $\lambda \cong g$, where g is the sensor to shield spacing (ref. 4-20).

The short wavelength loss of signal caused by the use of shields can be a serious problem if the electronic noise, which stays the same, causes the signal-to-noise ratio to decrease.

Another type of magnetoresistive head is called a "yoke" magnetoresistive head (fig. 4-24). Here the flux is collected by the yoke structure and conducted to the magnetoresistive element, which is some distance removed from the media.

Magnetoresistive heads have more signal than inductive heads at low media speeds. This is illustrated in figure 4-25 where yoke magnetoresistive signal is plotted versus $1/\lambda$. Also plotted is the output of a 200-turn inductive head, similar to that used in generating figures 4-15 and 4-16, at various tape speeds. As the tape speed increases, the signal advantage enjoyed by the magnetoresistive head decreases.

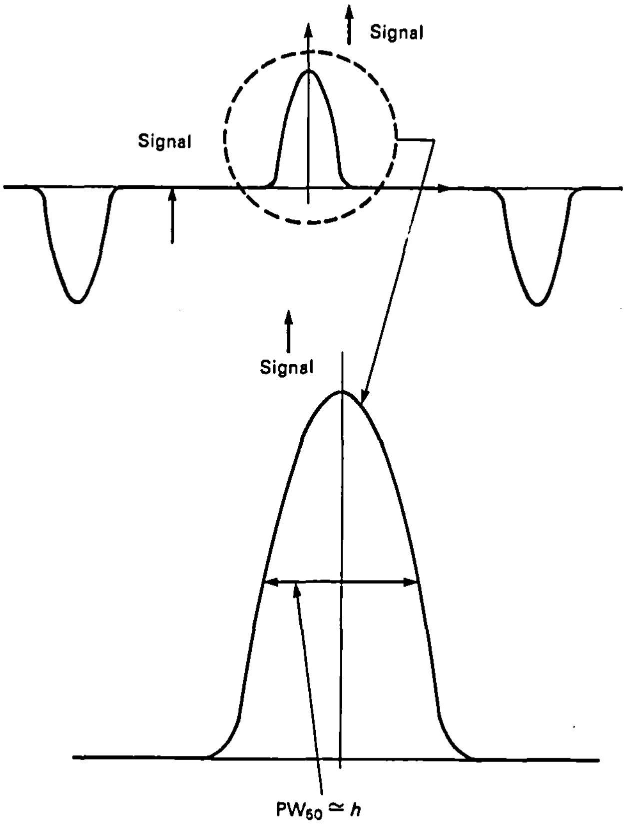

Figure 4-22.—Hunt head isolated pulse shape.

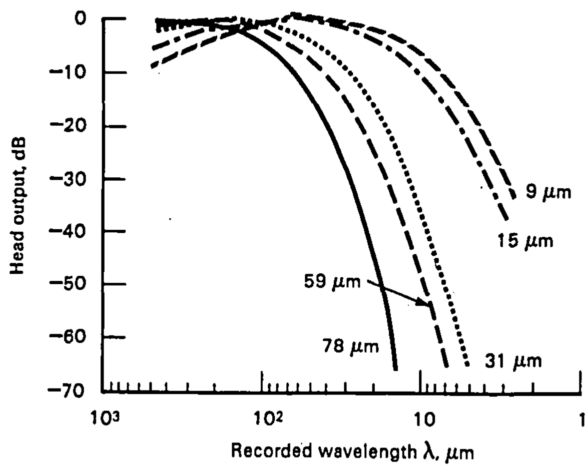

Figure 4-23.—Fundamental frequency responses of unshielded, optimally biased magnetoresistive heads for five different element heights. (0 dB is taken as the peak response for each head height.)

Another magnetoresistive head is the "over-biased Hunt head" of Uchida (ref. 4-21). The demagnetization fields are greatest at the edges of the sensor element. A bias field about four times larger than required for optimum signal is applied, saturating the center of the element and causing the edge of the element in contact with

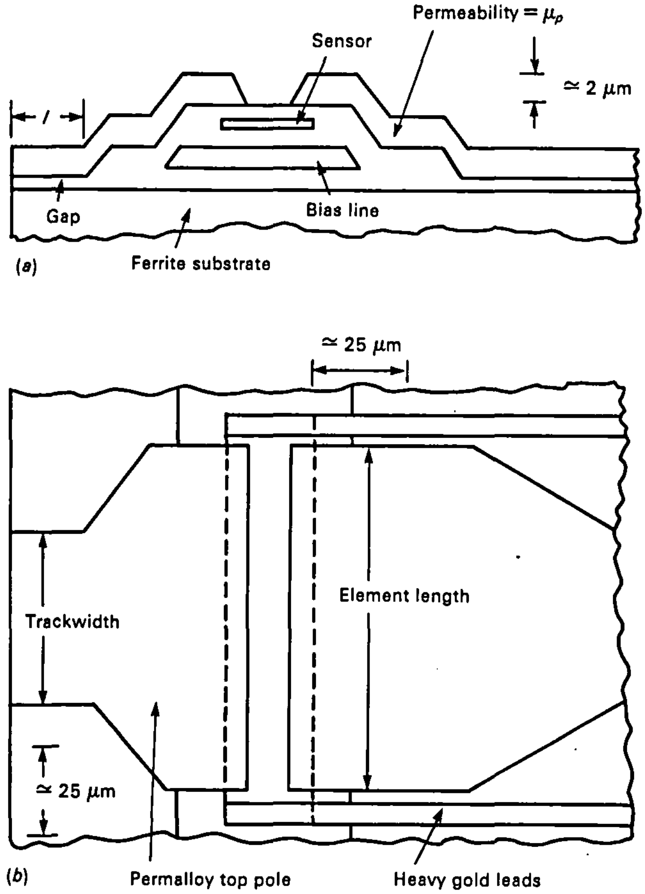

Figure 4-24.—Yoke magnetoresistive head. (*a*) Cross section. (*b*) Top view.

the medium to be optimally biased. This reduces the short wavelength signal somewhat but reduces the long wavelength signal much more, hence giving "improved resolution" and a smaller peak-to-band-edge ratio, which is easier to equalize.

Magnetoresistive read heads have been combined with inductive thin film record heads to form a complete read/write structure (ref. 4-22).

HEAD NOISE

There are many sources of noise in magnetic recording, including record and reproduce crosstalk, signal modulation noise, overwrite, flutter and wow, and dropouts. The minimum tape noise is bulk erased noise, which is easy to measure. The goal of the head designer is to cause the head noise to be less than the bulk erased noise so that it does not affect the signal-to-noise ratio.

The primary sources of inductive head noise are amplifier voltage noise E_V, amplifier current noise E_c, and head resistance noise E_r. E_V and E_c for a good wide-band 40-dB gain amplifier are given by

$$E_V \cong 1 \times 10^{-9} (B)^{1/2} \qquad (4\text{-}21)$$

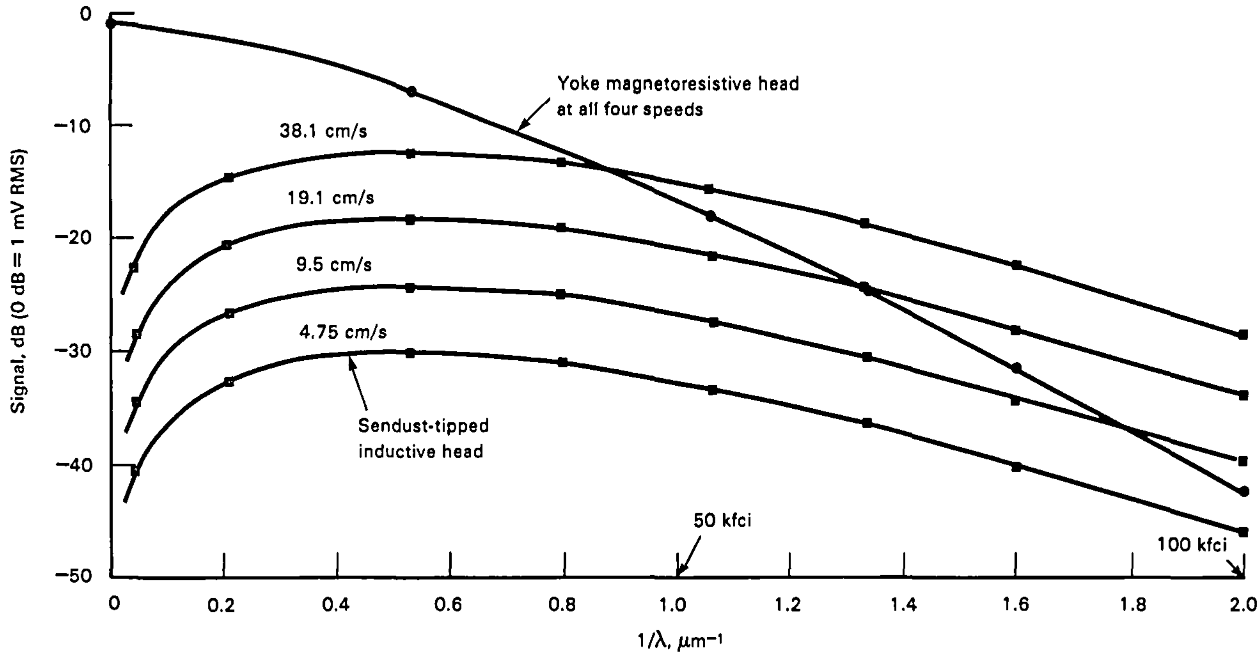

Figure 4–25.—Yoke and Sendust-tipped inductive heads compared. (Trackwidth = 250 μm; both heads have $g \simeq 0.3$ μm; $N = 200$ for Sendust-tipped heads.)

and

$$E_c \cong 1 \times 10^{-12} (B)^{1/2} Z \qquad (4\text{–}22)$$

E_r is given by

$$E_r \cong (4KTBR)^{1/2} = 1.29 \times 10^{-10} (BR)^{1/2} \qquad (4\text{–}23)$$

where B is the frequency bandwidth of concern in hertz, Z is the magnitude of the complex head impedance, K is Boltzmann's constant $K = 1.38 \times 10^{-23}$ J/K, T is the absolute temperature $T \simeq 300$ K, and R is the real part of Z.

Figure 4–26 shows the tape-stopped electronic noise spectrum for the Isomax tape and 200-turn head. The bandwidth used was $B = 3100$ Hz. Vector impedance measurements were made of the head, giving Z and R versus frequency. E_V, E_c, and E_r were computed from equations (4–21) through (4–23). The inductance was about 745 μH, and the dc resistance was 16 Ω. These results were also plotted in figure 4–26. The total expected electronic noise E_e was computed as follows:

$$E_e = (E_V^2 + E_c^2 + E_r^2)^{1/2} \qquad (4\text{–}24)$$

E_e is also plotted in figure 4–26 and is seen to agree very well with the tape-stopped noise except at low frequency where electronic pickup may be occurring. E_r increases with frequency primarily because of eddy current resistance in the conductive Sendust pole tips. Finally, the bulk-erased tape running noise is also plotted in figure 4–26. As may be seen, this head and tape make up a tape-noise limited system, but with only 4 to 5 dB to spare.

Figure 4–27 shows the slot, signal-to-noise ratio for this Sendust-tipped head and Isomax tape at 19.1-cm/s tape speed. The record current was set to maximize the 80-kfci signal.

In single crystal ferrite heads magnetostriction noise can be a problem. The choice of crystal orientation in the head is a compromise between permeability, wear rate, and magnetostriction noise. The composition of the ferrite is chosen to minimize the magnetostriction constant, but a zero value is difficult to achieve at high saturation flux density.

Magnetoresistive heads generate thermal noise. The temperature coefficient of resistance is about 0.28 percent per degree celsius so a 4°C temperature change gives a noise spike equal to the maximum signal of 1 percent. At 10^7 A/cm^2 the sensor may be 10 to 40° C hotter than room temperature, and the moving medium serves as a heat sink. Intermittent contact between head and medium caused by poor medium surface smoothness or dust particles causes thermal noise spikes as the element temperature goes up momentarily.

Magnetostriction can also be a problem with magnetoresistive heads. For these reasons it is best to use a substrate like sapphire, which is very hard and has a high thermal conductivity, to minimize stress and temperature increase in the element.

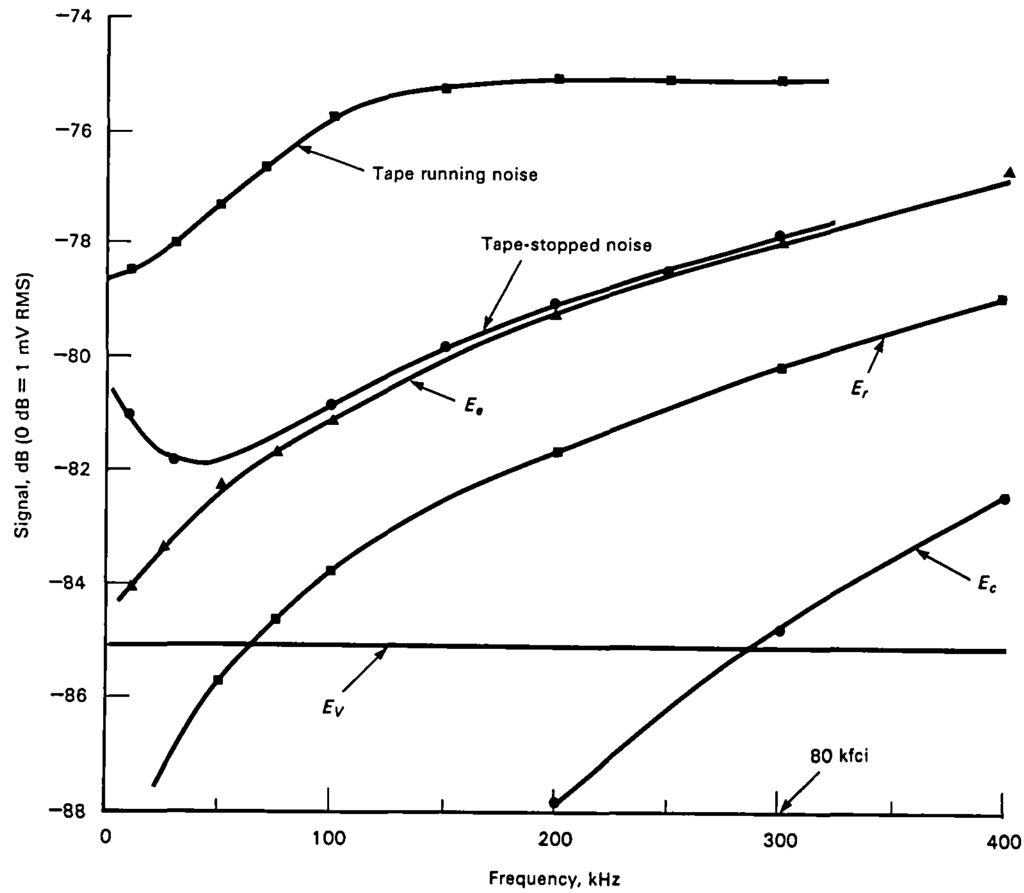

Figure 4–26.—Inductive head noise spectra. (Tape speed = 19.1 cm/s; BW = 3100 Hz.)

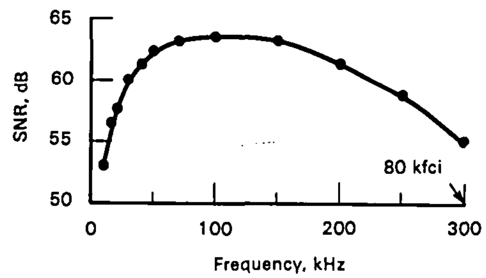

Figure 4–27.—RMS to RMS, 3.1-kHz slot, signal-to-noise ratio for a Sendust-tipped head. (Tape (isomax): $H_c = 760$ Oe; $B_r = 1600$ G; speed = 19.1 cm/s.)

Several other techniques have been developed to solve these problems. See references 4-16 and 4-17.

REFERENCES

4-1. McKnight, J.: *Audio Eng. Soc.* **27**(3): 106, Mar. 1979.
4-2. Bertram H.: *IEEE Trans. Magn.* **18**(6): 1206, Nov. 1982.
4-3. Wallace, R.: *Bell Tech. J.* 1145, Oct. 1951.
4-4. Jeffers, F.: *IEEE Trans. Magn.* **18**(6): 1146, Nov. 1982.
4-5. Lemke, J.: *IEEE Trans. Magn.* **15**(6): 1561, 1979.
4-6. Westmijze, W.: *Philips Res. Rept.* **8**: 148, 1953.
4-7. Wakabayashi, N.: *IEEE Trans. Magn.* **18**(6): 1140, Nov. 1982.
4-8. Tsang, C.: *Appl. Phys.* **52**(3): 2471, Mar. 1981.
4-9. Jones, R.: *IEEE Trans. Magn.* **14**: 509, 1978.
4-10. Kanai, K.: *IEEE Trans. Magn.* **15**: 1130, 1979.
4-11. Karlqvist, O.: *Trans. Res. Inst. Tech. Sweden* **86**: 3, Oct. 1954.
4-12. Iwasaki, N.: *IEEE Trans. Magn.* **18**(6): 1110, Nov. 1982.
4-13. Toda, J.: *IEEE Trans. Magn.* **18**(6): 1164, Nov. 1982.
4-14. Okuwaki, T.: *J. Appl. Phys.* **53**(3): 2588, Mar. 1982.
4-15. Mallinson, J.: *IEEE Trans. Magn.*, 71, Mar. 1969.
4-16. Thompson, D.: *IEEE Trans. Magn.* **11**(4): 1039, 1975.
4-17. Jeffers, F.: *IEEE Trans. Magn.* **15**(6): 1625, Nov. 1979.
4-18. Hunt, R.: *IEEE Trans. Magn.* **7**(7), 1971. U.S. Patent 3,493,694.
4-19. Davies, A.: *IEEE Trans. Magn.* **11**(6): 1689, Nov. 1975.
4-20. Potter, R.: *IEEE Trans Magn.* **10**: 502, 1974.
4-21. Uchida, H.: *IEEE Trans. Magn.* **10**: 502, 1974.
4-22. Bajorek C.: *Amer. Inst. Phys. Conf. Proc.* **24**: 548, 1975.

CHAPTER 5
Perpendicular Recording

Edward R. Wuori
Vertimag Systems Corporation

Perpendicular magnetic recording (refs. 5-1 to 5-5) has recently been recognized as a promising method of achieving ultrahigh-density recording. This promise has caused a great deal of interest because of the very large potential market, the present disk drive market being billions of dollars per year. If perpendicular recording can achieve reliable systems with 10 times its current capacity as is promised, it will have a large impact on the digital recording marketplace.

The present status is that perpendicular recording has been demonstrated in a number of laboratories around the world and systems are being designed for commercial manufacture and these drives will apparently be available for field trials soon from more than one company. Perpendicular recording will certainly get its chance at a place in this market; it will be interesting to see if it lives up to its promise. It will also be interesting to see how fast the present longitudinal recording technology can evolve as this forms the basic competition for any new technology such as perpendicular recording. The promise of greatly increased capacity systems using perpendicular recording means the use of new recording materials such as cobalt-chromium (CoCr) perpendicular films will be pursued by many people around the world.

Perpendicular recording received its biggest input from Professor Iwasaki and his laboratory staff at Tohoku University in Sendai, Japan. Their work in the early 1970's and their discovery of vertically oriented CoCr films together with the new head geometries initiated the high level of interest in perpendicular recording. The rate of work was slow at first but by 1979 other researchers at such organizations as the University of Minnesota and IBM had verified Iwasaki's observations. Now many universities and companies, especially in Japan, have established significant technical programs in perpendicular recording, including Vertimag Systems Corp., IBM, Lanx Corp., Toshiba, Anelva, Sony, Hitachi, Fujitsu, Teijin, NEC, and TDK. In addition to work on CoCr metal films by sputtering, other

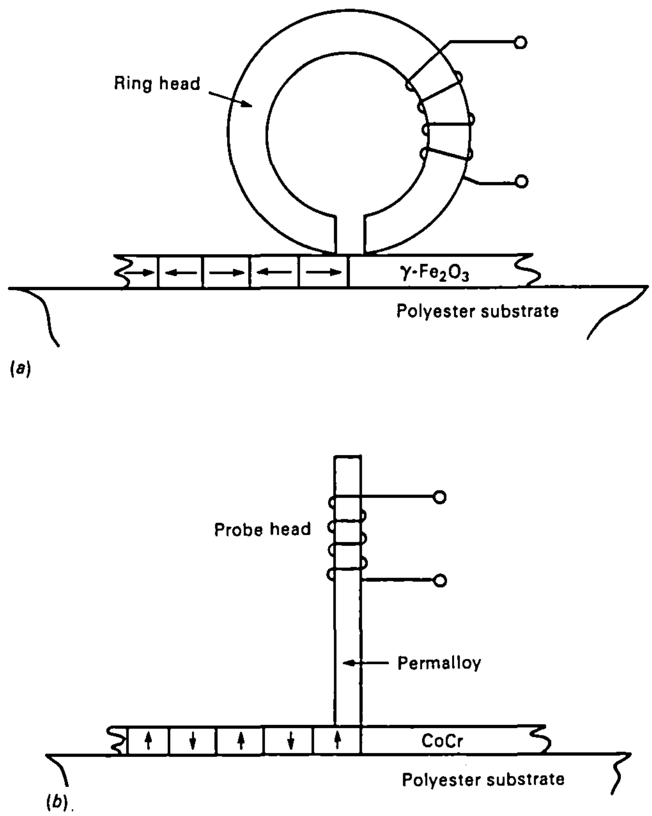

Figure 5-1.—Comparison of longitudinal and perpendicular structures. (*a*) Longitudinal structure. (*b*) Perpendicular structure.

materials and fabrication techniques are being investigated, such as oriented particulates and barium ferrite particles, and *e*-beam and wet chemical plating processes. Perpendicular recording is moving in many directions to make the materials as producible as possible.

Figure 5-1 shows a simplified comparison of the structures presently used in conventional "longitudinal" recording, which uses a ring head (drawn schematically), and that used in the perpendicular recording

technique, which uses a probe head (drawn schematically only to illustrate the principle; many styles of perpendicular heads have been proposed).

In the longitudinal recording case, the recording process is driven by the fringing fields produced by the gap in the ring head as the recording media moves by the head. Every time the write current in the head changes sign, the magnetization reverses direction. Due to the properties of the recording media, the magnetization is constrained to be primarily in the plane of the film (although at high recording densities there may be significant vertical components also). Because the field emanating from the gap of the head has cylindrical symmetry and the field drops off as the inverse of the distance from the gap, the recorded pattern has only finite depth into the media and at high recording densities often does not record through the media. The depth of recording is half the recorded bit length.

In the case of perpendicular recording, a thin shim of permeable material is placed in contact with the recording media. This shim is excited by the write current to produce magnetic flux emanating from the tip that goes through the media in primarily the perpendicular direction. In the case of CoCr, the crystalline anisotropy is large enough to overcome the demagnetizing effects of the surface poles and the material can retain permanent magnetization in this direction. This is distinctly different from longitudinal recording in which the demagnetizing fields caused by the surface poles prevent effective magnetizing in the perpendicular direction. That perpendicular recording can be accomplished is due primarily to the discovery of a material, CoCr, that has this suitable property (perpendicularly oriented crystalline anisotropy large enough to overcome demagnetizing). The sketch is, of course, oversimplified and several improvements are immediately evident that should improve the magnetic performance. Several things can be done to make the head better, and these are discussed in the section on heads. For the media, the magnetic reluctance for recording can be reduced considerably by adding a second layer of permeable material, such as permalloy, under the CoCr recording layer. Although some people are working with single-layer CoCr recording systems, this chapter concentrates on the double layer scheme of CoCr on a layer of permalloy.

ADVANTAGES OF PERPENDICULAR RECORDING

The primary driving force to using perpendicular recording is the potential for reliable high-density digital recording, as mentioned already. There are, however, several apparent attributes to perpendicular recording that appear to be making its realization easier.

In longitudinal recording, for a long time the trends have been to go toward thinner media with higher coercivities. This allows higher recording densities because both of these parameters tend to overcome the inherent self-demagnetizing of the recorded patterns that are inherent in longitudinal recording. The magnetization reversal region in longitudinal recording cannot be infinitesimally small because the shorter the transition length, the higher the pattern-generated demagnetizing fields in the media, which prevent transitions shorter than some limit. Increasing the coercivity reduces the limit but causes recording problems, such as pole tip saturation effects in the heads (although improvements are being made continually). Decreasing recording layer thickness allows higher densities while keeping the aspect ratio of the recorded cell the same. In addition, if thinner layers are used, which can be as small as 1 or 2 μm, wear and defects are much more of a problem and are the current limiting factors for particulate media.

In perpendicular recording, these limitations seem to be relaxed somewhat. The recorded pattern-induced demagnetization actually goes to zero as the recording density goes to infinity. Higher density is better, in terms of demagnetization. Figure 5–2 shows a comparison of the magnetization transition for the two cases. For perpendicular media, fields from adjacent bits actually reinforce each other and have a self-sharpening effect on the transition region. In principle, the width could be zero, but, in actuality, it is limited by the grain size of the film. The transition width can be as small as one grain, and this is what determines the maximum recording density. In the case of CoCr, the grain size is a column that goes all the way through the film and has a diameter of about 50nm, implying a maximum density of about 500 000 fci. Densities of 400 000 fci have been observed in the laboratory under special conditions (ref. 5–6). Another benefit of the columnar grain structure of the CoCr films is that the recording layer records all the way through (using a probe style head) so that thinner layers are not needed from the recording point of view. In addition, pole tip saturation effects are absent in the probe style head structures used in perpendicular recording because the actual flux path goes straight through the media with no corner saturation effects. This allows the use of higher coercivity medias if desired, although increased coercivity does not seem to be necessary, at least up to 50 000 to 100 000 fci. Coercivities of 400 or 500 Oe appear to be sufficient in the laboratory.

Some effects in longitudinal recording have roughly the same effect in perpendicular recording; for example, spacing losses. Perpendicular recording suffers about 55-dB signal loss when the separation/wavelength ratio is equal to 1, the same as in longitudinal recording.

Perpendicular recording seems to relax the need for

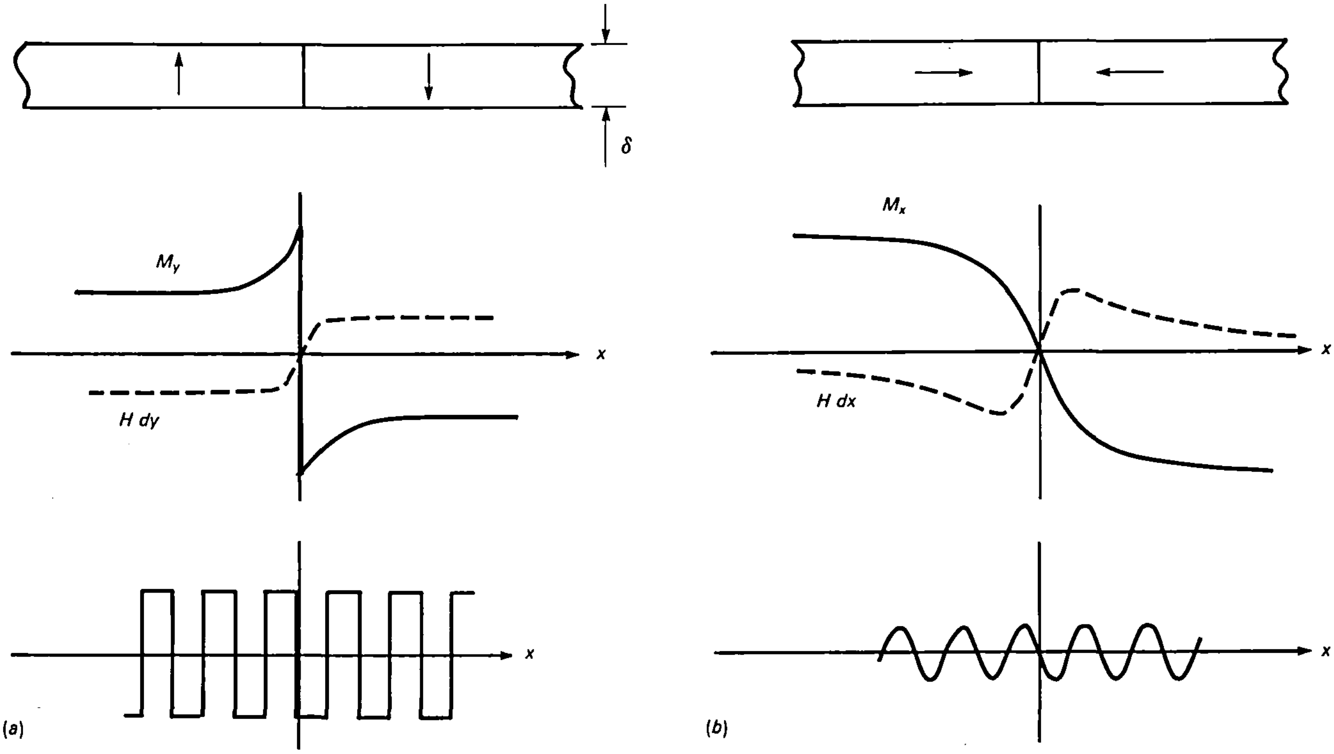

Figure 5–2.—Comparison of the magnetization transition regions for the perpendicular and longitudinal recorded cases. (*a*) Perpendicular recording. (*b*) Longitudinal recording.

thinner films, allowing high-density recording with less of a problem with wear and defects because thicker films can be made with higher quality. Because higher coercivity can be used in these structures (even though the need is not apparent from recording data), more flexibility is available for recording system optimization. Finally, self-demagnetization effects on transition widths do not appear to be a limiting factor for perpendicular recording. Perpendicular recording appears to offer some distinct advantages.

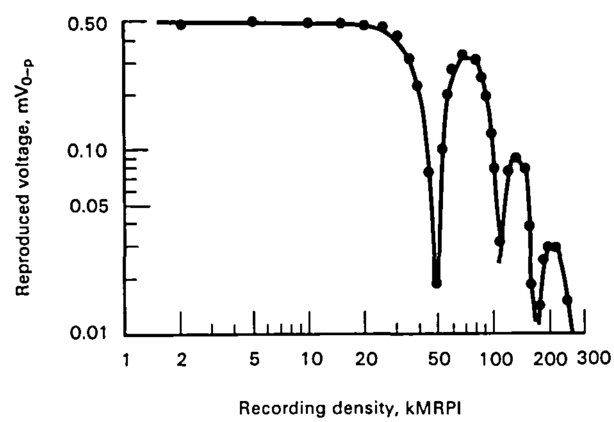

Figure 5–3.—Typical frequency response for perpendicular recording (reproduced from work of Iwasaki's laboratory, ref. 5–7). (Shim dimension $T_m = 1.1$ μm; film thickness $W_t = 300$ μm; number of turns $N = 50$ turns; inductance $L = 10$ μH; speed = 2 m/s; 0–p = 0 to peak; and kMRPI = thousand magnetization reversals per inch.)

RECORDING PERFORMANCE

Figure 5-3 shows typical recording performance as reported by Iwasaki (ref. 5-7). These particular data show results for a shim dimension of 1.1 μm. The response has approximately a sin x/x form and shows several peaks. Nulls occur when a flux transition approaches the shim just as a previous transition leaves. Cancellation occurs when there are exactly two transitions under the head. Nulls in head output voltage occur whenever there is an even number of transitions under the head, and peak output occurs when there are an odd number of transitions. Observing that the signal-to-noise ratio is large even on higher order peaks in the response, it is speculated that data could be recovered there if a way could be found to account for the odd order that the bits are recovered (compared to the way they were written). This response is different from that of longitudinal systems in which the response curve drops off and does not usually show higher order peaks. The frequency response characteristics of perpendicular recording show high signal-to-noise ratios and higher order peaks with usable response to very high densities.

Figure 5-4 shows the dipulse response characteristic for a perpendicular head and media. The dipulse is assumed to be two transitions written on a dc erased media. The distance between these two transitions is varied, and the head output waveform examined. The distance between these two pulses is measured (distance between peaks), converted to an equivalent distance in micrometers, and compared to the known distance of the written transitions: The transition separation as measured electrically from the head is compared to the actual transition separation as written. In figure 5-4 when the transitions are far apart, the written and read-back separations agree perfectly and so result in the 45° slope on the log-log plot. When the written separation approaches the shim dimension, the read-back pulse separation approaches a constant value equal to the record shim dimension. No matter how closely spaced the written transitions are, the read-back separation remains at the shim dimension. This response is almost entirely a geometric effect and is also a good description of peak shift phenomenon in perpendicular recording. Because the ideal response should be a line with 45° slope on this figure, deviations from it must be a measure of peak shift, and because this peak shift appears to be geometric in origin, it must be read-induced peak shift. This figure indicates that there is very little peak shift for densities up to transition separations equal to the shim dimension, and beyond this the peak shift is almost entirely read induced with almost no write-induced peak shifts. For comparison, typical peak

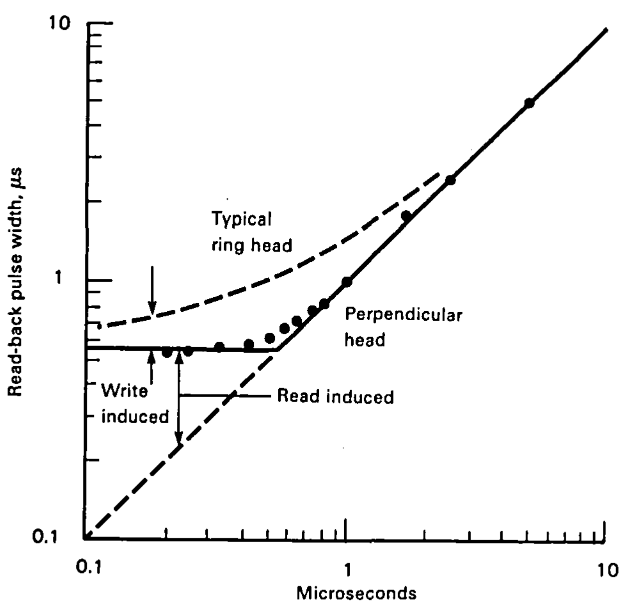

Figure 5-4.—Typical dipulse response (two transitions in a field of no transitions, dc erased; 0.55-µm shim; 1.0 m/s surface velocity).

shift for a ring head on oxide media is indicated by the dashed line on the figure. The distance between this curve and the geometric part of the peak shift is taken to be write-induced peak shift. Based on this type of data, read- and write-induced peak shift can be identified. It appears that in the case of perpendicular recording, peak shift is almost entirely read induced with very little write-induced peak shift.

HEAD STRUCTURES

A variety of head structures have been proposed for use with perpendicular recording media. These include auxiliary pole structures (as proposed by Iwasaki), probe style structures, ring heads, and combination structures. Figure 5-5 illustrates the general features of some of the types of heads that have been proposed. Each has its own advantages and disadvantages.

Iwasaki has had success with his auxiliary pole concept. In terms of recording performance, it has worked extremely well. It presents no head saturation effects in recording. In its simplest form, it is very easy to make. The drawbacks to this head structure are as follows:

(1) Apparatus is required on both sides of the recording media. This puts constraints on the thickness of the media substrate as the auxiliary pole is required to be within perhaps 100 µm of the recording layer. In a tape or floppy disk application this is no problem, but there are difficulties in rigid disk applications.

(2) In applications requiring tunnel erase capability, such as floppy disks, the fabrication becomes difficult; in other applications that require both tunnel erase capability and two-sided recording, the construction becomes very difficult. In applications that require recording on both sides but no tunnel erase (for example, where track following servo is used), this is a very reasonable construction. So, although the recording performance of this head is very good, use of this head structure depends heavily on the application requirements.

Various probe-style heads have been proposed. Figure 5-5 illustrates a typical construction. These heads can be designed to perform well. They make use of the permalloy underlayer as part of the magnetic structure of the head so that no apparatus is required on the opposite side (except for a pressure pad, of course, in some applications such as floppy disk). The construction allows inclusion of tunnel erase and two-sided recording. It fits in a standard floppy disk button. The drawback of this style structure is that the magnetic design is more difficult. Head saturation effects become more important. Probe-style heads can be made to work well in applications that demand certain features.

Ring heads of standard construction have been used on perpendicular media with good results. Ring heads

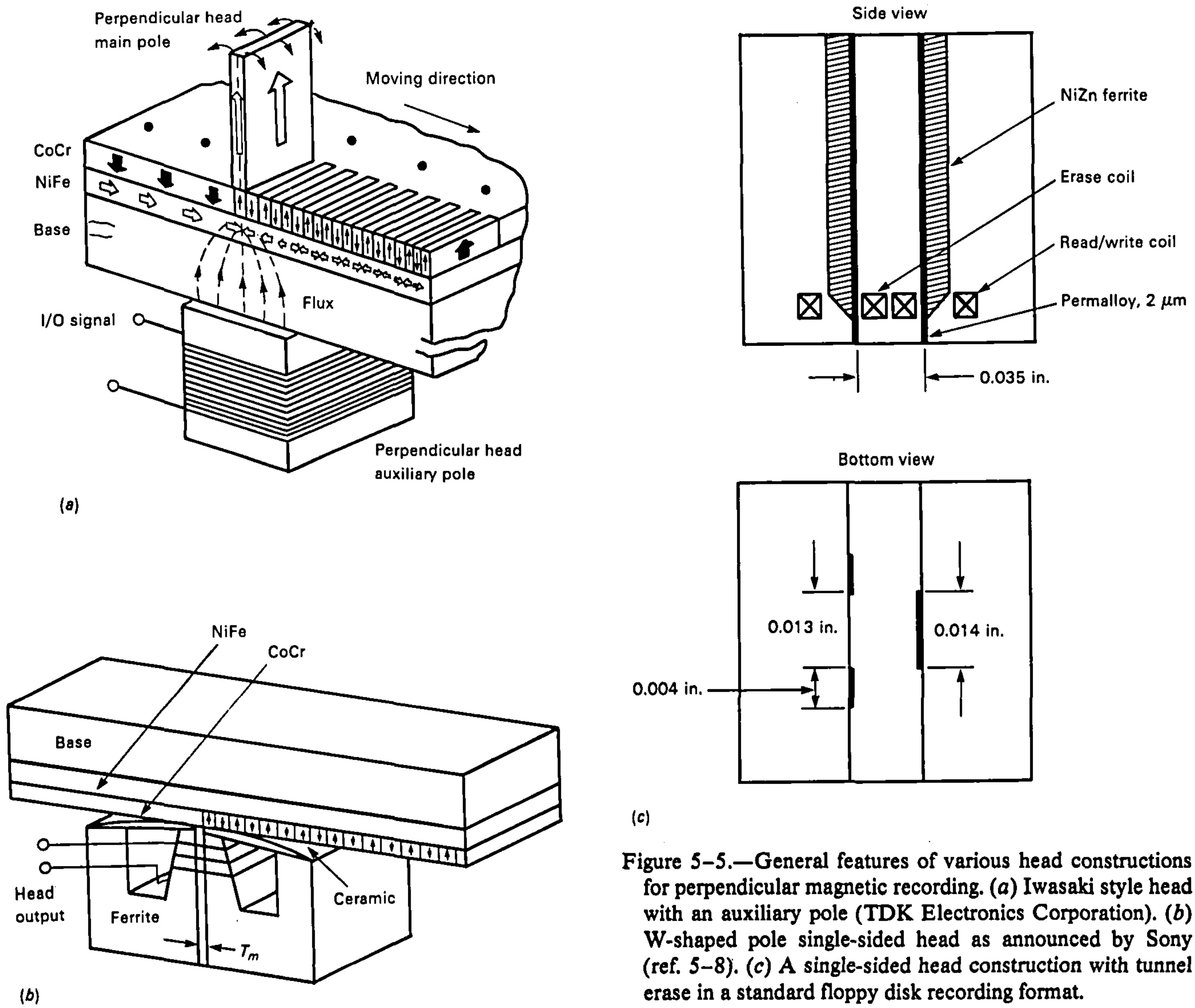

Figure 5–5.—General features of various head constructions for perpendicular magnetic recording. (*a*) Iwasaki style head with an auxiliary pole (TDK Electronics Corporation). (*b*) W-shaped pole single-sided head as announced by Sony (ref. 5–8). (*c*) A single-sided head construction with tunnel erase in a standard floppy disk recording format.

can be used on both single-layer CoCr and on double-layer media. Recording results using ring heads have been reported with D50's as high as 70 kfci; using separate read and write gaps, D50's of over 100 kfci have been reported. The drawbacks to use of ring heads in perpendicular recording are as follows:

(1) Media of higher quality and better orientation are required for good performance.

(2) Ring heads are reported to be more sensitive to separation losses, especially during the write process, with total write loss plus read loss of 400 dB at separation/wavelength ratios of 1. This is much worse than with longitudinal recording (95 dB) or perpendicular recording with a shim-style head (95 dB).

(3) Reports have been heard that the ring heads do not record all the way through the perpendicular media, although the problems this will cause are not known. So ring heads can probably be used in contact recording schemes up to at least intermediate densities of 50 000 fci, but for applications that are sensitive to spacing losses (such as rigid disk), use of ring heads and perpendicular media may be difficult.

Composite head structures have been proposed also. All sorts of combinations are possible using probe style heads, ring heads, and magnetoresistive heads. Most work has concentrated on probe write/ring read and ring write (wide gap)/ring read (narrow gap). The idea is to combine heads that perform individual functions best. For example, probe heads write on perpendicular media the best while ring heads have higher flux gathering efficiency; therefore, a combination probe write/ring read head may perform better than either head individually. The only drawback to this approach is the added complexity. Excellent recording results have been

reported in the literature using composite heads of various types.

In summary, a wide variety of head structures are possible. The choice of a particular head is strongly dependent on the particular application.

MEDIA

As mentioned earlier, this chapter assumes perpendicular media in the double layer construction. Figure 5-6 shows a diagram of this construction and typical dimensions for the various layers. The metal layers are at present sputtered onto a polyethylene terephthalate (PET) substrate using any of the cathodic sputtering techniques such as radio frequency, dc, or dc magnetron. The primary problem is keeping the substrate cool during the deposition process to prevent damaging it. The PET is plated on both sides with layers of permalloy and CoCr. Typically, each layer is 0.5 μm thick. Although not considered here, the single layer construction used by some people simply omits the permalloy layer.

The important layer is, of course, the CoCr layer as it is the one that does the actual recording. To be a good layer for perpendicular recording, it must have a high degree of perpendicular crystalline anisotropy to overcome the demagnetizing effects of the surface poles. Typical values for the anisotropy energy for CoCr films with about 15 percent Cr are in the range of 1.5×10^6 erg/cc. The physical character of the film is that of a columnar microstructure where columns are formed through the film thickness with a diameter of about 50 nm. This is about the size needed (based on theory) for single domain particles. Based on X-ray diffraction studies, the columns are taken to be approximately single crystals of the *hcp* phase with their *c* axes oriented perpendicular to the film plane. The origin of the coercivity appears to be crystalline anisotropy. The physical cause of the columnar microstructure is not completely clear but may be due to gas-induced shadowing effects as described by Thornton (ref. 5-9) or self-shadowing effects that take place during the sputtering formation of the films. There may also be some Cr segregation to the column boundaries. The net effect is that the columns act as though they are magnetically separated with a high degree of perpendicular orientation.

Figure 5-7 shows a fracture cross section of a typical film showing the columnar formation. Figure 5-8 shows a Lorentz micrograph of a section of a CoCr film (ref. 5-10), which displays the single domain character of the film.

The following sections discuss anticipated manufacturing techniques for the manufacture of the perpendicular recording media. These sections draw heavily on a talk given by Johnson (ref. 5-11).

FLEXIBLE DISK FABRICATED BY SPUTTERING

Sputtering is a century old technology, but its use for the commercial manufacture of magnetic media is in its infancy. In fact, while there are a number of groups actively working on the commercialization of sputtering,

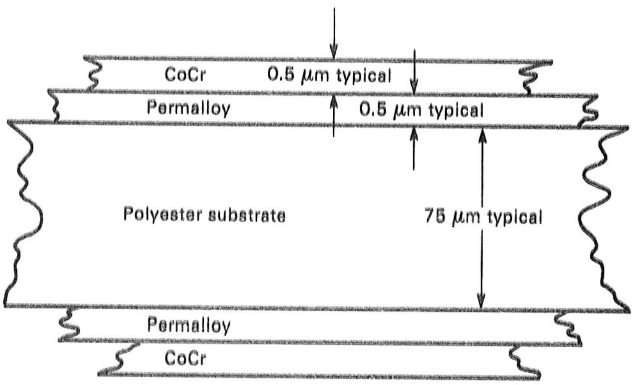

Figure 5-6.—Diagram of a typical perpendicular media construction.

Figure 5-7.—Scanning electron microscope photograph of media fracture cross section (30 kV anode voltage in the electron microscope).

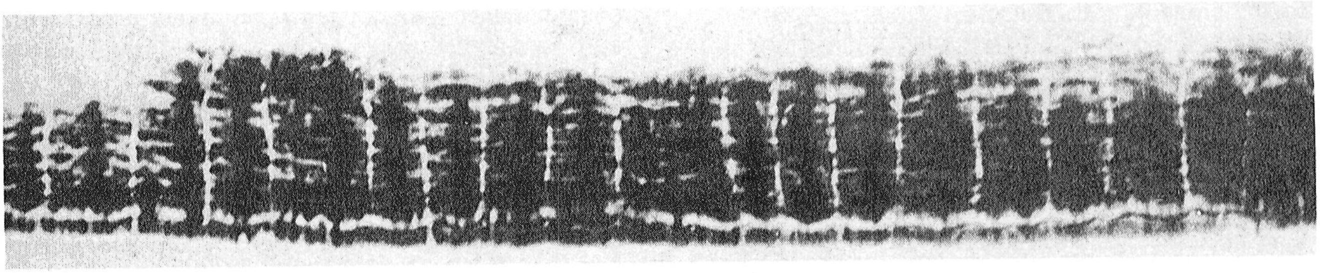

Figure 5–8.—Lorentz electron photomicrograph of a CoCr film. This photo was provided by Ouchi from Professor Iwasaki's laboratory at Tohoku University, Sendai, Japan (ref. 5–10).

especially for the coating of perpendicularly oriented CoCr films, no products are yet available in the marketplace. Thus, this paper will by necessity limit itself to the problems that are expected in the commercialization of sputtering, and plans to overcome them.

With the exception of Anelva Corporation, sputtered magnetic media has only been fabricated in the laboratory on a batch processing basis. In batch processing, a typical semiconductor sputtering system is modified to handle flexible substrates. This requires some sort of a carrier to maintain uniform tension on the substrate, and generally some modifications to the cathode structure of the sputtering machine to handle the magnetic target materials.

PET has normally been the substrate of choice, although polyimides and polyamide/polyimide copolymers have been used by others. We have limited ourselves to PET because it can be obtained with sufficient surface smoothness on both sides. Because of the relatively low glass transition temperature of PET films (approximately 80° C), sputtering has to be carried out at low rates and in a configuration to limit overheating. These heat transfer problems are greatly diminished when sputtering CoCr magnetic films onto rigid aluminum substrates that can be intimately thermally coupled to a cooling platen. The PET substrate heating problem requires a solution before the use of sputtered magnetic films will be financially viable.

For a number of reasons, PET film produced for the magnetic recording industry is unsatisfactory for magnetic media sputtering. Most manufacturers supply PET film with slip agents. A typical slip agent is ultrafine silica that is dusted on the film's surface to facilitate the winding and unwinding of the film. Figure 5-9 shows a typical PET film with silica. If some sort of slip agent is not used, the van der Waal's forces between the ultrasmooth surfaces of the films cause great difficulty in the winding of the film by the manufacturer, and its unwinding by the users. Clearly, slip agents are unacceptable because the sputtered films simply follow the contour of the film surface and reproduce the silica as bumps.

During the manufacture of PET films, there is a spectrum of polymer molecular weights. The lower molecular weights, oligimers, migrate to the surface of the film when the film is heated, thus distorting the surface. Figure 5-10 shows a typical oligimer eruption on the surface of a typical PET film. Oligimer migration cannot be controlled totally, but the manufacturer of the film can reduce the percent of oligimers. He can also produce what is known as "tight" film, which has a high density that inhibits the migration of the lower molecular weight components to the surface. In the sputtering process, the effect of oligimers can be controlled by reducing the maximum temperature to which the film is exposed and the time of exposure.

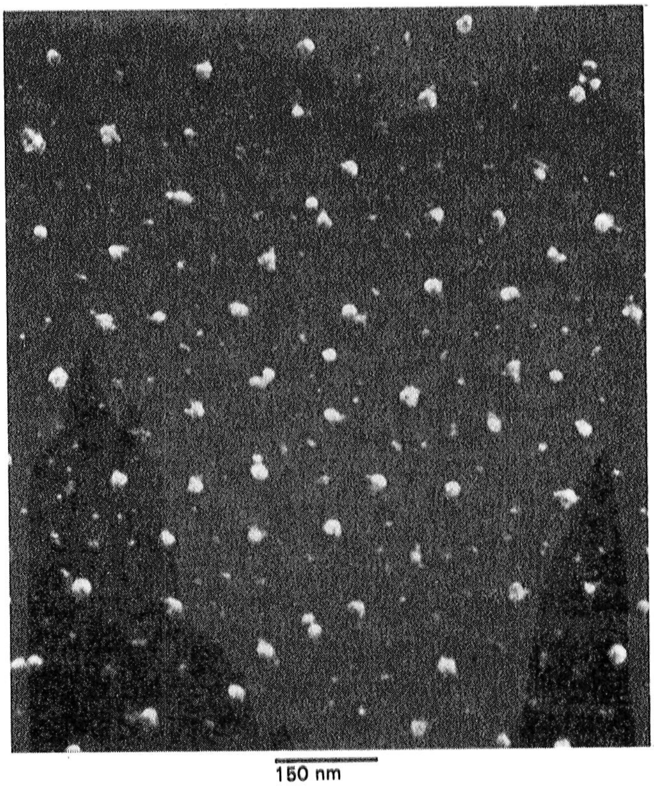

Figure 5–9.—Scanning electron photograph of a polyester film that has a surface treatment (Slip Coat; 25 kV anode voltage in the electron microscope).

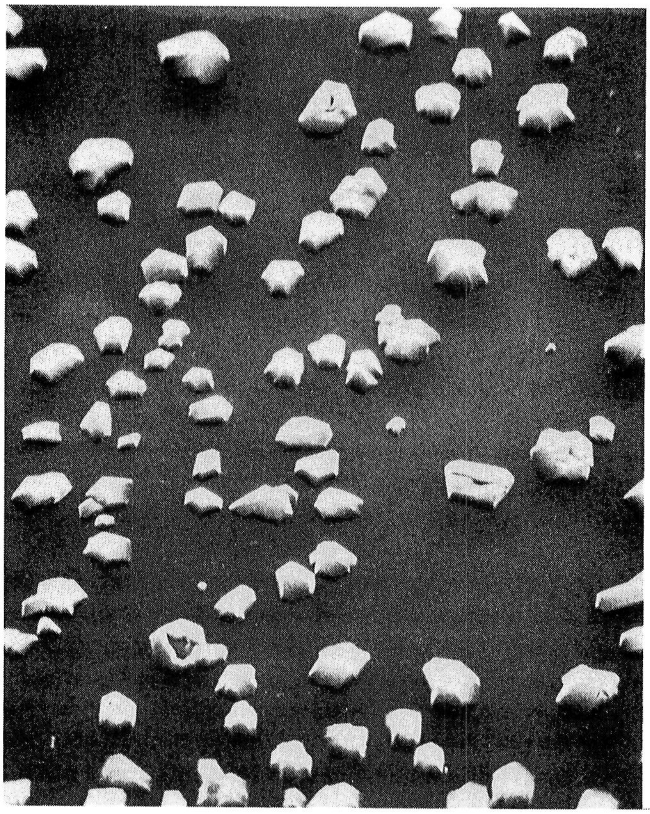

Figure 5–10.—Typical oligimer eruptions on a polyester film surface after heating 1 h at 150° C (25 kV anode voltage in the electron microscope; magnification factor is 100).

PET films are biaxially stretched during manufacture. During this process, a significant amount of electrostatic charge is "built in" the film, sometimes amounting to as much as 200 esu/cm^2. This is considerably above the breakdown of air, and thus requires PET web handling to be equipped with corona discharge equipment. This volume electrostatic charge stored in the PET film attracts oppositely charged ions as "keeper" ions until the surface charge is below the breakdown of air, or about 300 esu/cm^2. Because the internal charge is not completely neutralized by "keeper" ions, dust particles are attracted from a wide area. Thus, PET films to be used for sputtering must be manufactured and hermetically sealed in a clean room environment by the vendor, and subsequently opened by the user in a clean room environment. We have seen a dust particle suddenly appear on the surface of the film being observed under a microscope. When this dust particle was removed with a pair of tweezers, another one would shortly thereafter deposit itself in exactly the same location. From this we conclude that the volume electrostatic charge is highly localized.

The conclusions are that PET films for sputtering must be of extraordinary smoothness (less than 1 μm rms surface variation) on both sides, the film must have a low oligimer content, must be "tight," and finally, must be handled under clean room conditions from manufacture to use.

Targets of magnetic materials present a number of problems when used for magnetron sputtering. Magnetron sputtering is only one of a number of techniques that provide the possibility of high deposition rates. High deposition rates require high plasma current resulting in the generation of large amounts of heat. Only a tiny fraction (less than 1 percent) of the energy that goes into the sputtering process is actually used to transmit materials from the target to the substrate. All of the remaining energy is dissipated in heat, with about 85 percent being absorbed by the target itself and 15 percent being in the form of radiation and in secondary electrons. Because the sputtering rate is limited by the heating of the substrate, high rates require that the substrate be protected from thermal radiation and from the secondary electrons. To achieve the latter, a magnet is placed below and in the neighborhood of the target so that the secondary electrons spiral around in the vicinity of the target and aid the plasma rather than flying off in all directions, impinging on the substrate. Also, secondary electron shields are used to reduce substrate heating. Fortunately, the use of magnetic target materials severely constrains the use of magnetron sputtering because the targets "short circuit" the magnetic flux from the magnets.

There have been a number of suggestions to help overcome this, including slotted targets, laminated targets, and opposed targets, but in all of them the magnetic targets themselves significantly alter the magnetic field of pattern. In addition, magnetron sputtering is a low target utilization technique. The magnetic fields constrain the plasma to form a "race track" around the surface of the target, and it is from these race track areas that the sputtering occurs. Target use rarely exceeds 40 percent. Considerable work is being done in the area of sputtering target technology to improve target use; increase plasma power and, therefore, sputtering rate; and to reduce the thermal transfer to the substrate. The ultimate limiting factor is the power dissipation into the target itself, and most researchers agree that this cannot exceed about 20 W/cm^2 without the danger of severe target distortion and consequent water leaks.

Sputtering for magnetic CoCr films takes place at an argon pressure range from 1 to 20 mT. The mean free path of argon ions at 1 mT is about 10 cm, and at 20 mT about 0.5 cm; thus argon pressure is important to the process.

The background pressure is also important. It is normally monitored with a residual gas analyzer. We have found the background pressure should not exceed 1.0×10^{-6} torr.

Although no one has put into use a fully operational, commercial sputtering system, we have designed and are now building such a system (figure 5-11). This production sputtering system has the following characteristics:

(1) Mechanical/electrical

Size, m. . . . . .15 by 3 by 4 (high)
Weight, tons. 35
Connected power, kVA 1200
Cooling water, m^3/hr. . 50

(2) Substrate

Material . . . . Polyethylene terephthalate (PET)
Surface smoothness, μ in. (rms). 1
Thickness, μm. . . . . . . .50 to 75
Web size, m. . . . . .2000 maximum length by 1.20 width
Web tension, N. 1000
Web speed, m/min. . . .0.25

(3) Coating

Method . . . . .dc magnetron sputtering
Cathodes . . . . 4 per side (2 permalloy, 2 CoCr)
Thickness, μm. . . . . . . .0.5 per layer
Layers . . . . .2 each side
Sputtering rate, A/min 6000

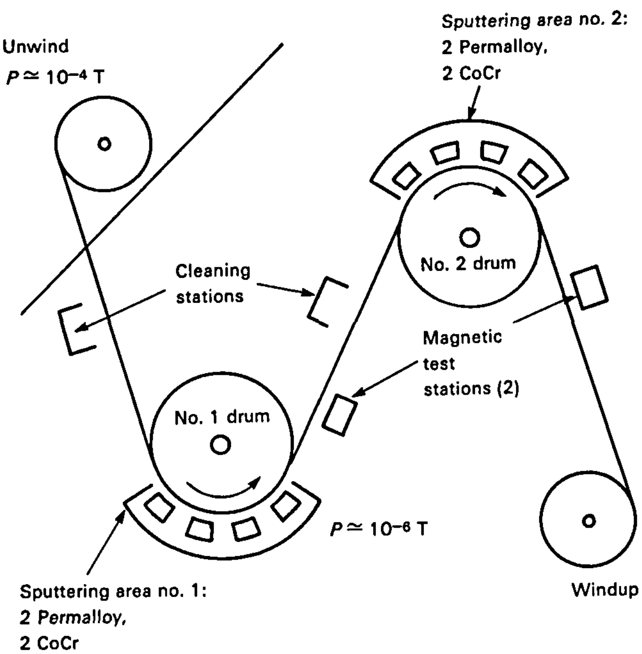

Figure 5–11.—Schematic diagram of a production sputtering roll coating system.

(4) Vacuum

Pumpdown time from loading, hr. 8
Pressure in unwind chamber, T. . . . . 10^{-3}
Background pressure in sputter chamber, T. . 10^{-5}
Sputtering gas. . . . . . . .Argon

The system sputter coats a 48-in.-wide web of PET on both sides with a layer of permalloy followed by a layer of CoCr. The capacity of the machine is 2 km of 50 μm thick PET. When fully operational this machine will be capable of producing more than 3 million 5¼-in. floppy disks per year. The machine will be located in a class 100 clean room to minimize the effects of airborne contamination and will be equipped with numerous in-process measuring devices, to check the quality of all four magnetic films as they are made. The machine should be operational approximately 50 percent of the time, the other 50 percent being required to change cathodes and targets, load PET film, unload coated film, and to perform general maintenance and cleanup.

The building of such an enormous vacuum chamber has a number of pitfalls. First of all, to obtain the ultimate vacuum required, the chamber has to be made entirely of stainless steel. In addition, the builder must eliminate all possible trapped volumes within the machine—this means porting all bolts and venting all holes on the inside of the chamber.

In addition, great care must be taken in the structure of the support for the web handling rollers so that there is no structural displacement occurring when the system is under vacuum. A solution to this problem is to support the bearing plates independently of the walls of the vacuum vessel itself.

In general, all web guide rollers should be tendency driven. This means that the roller axle is supported on ball bearings and the outside race is driven somewhat faster than the fastest web speed. Considerable care must be taken in web handling to avoid slippage of the PET web because if slippage should occur, a scoring of the film is almost certain to occur, making the media at the point of slippage unacceptable. Media tension through the system should be in the neighborhood of 50 to 100 N to provide intimate contact between the cooling drums and the substrate itself.

After sputtering, the rolls are removed from the vacuum chamber and punched into 5¼ in. floppy disks. These blanks are then tested on an automatic testing machine where they are sorted into groups by quality and placed into special floppy disk envelopes. Only at this time are they removed from the clean room environment for final testing, packaging, boxing, and shipment.

CONCLUSIONS

Some of the more important factors to be considered in a design of production web sputtering are the following:

(1) PET film carries a large amount of water on its surface, and this water must be removed before the web enters the sputtering chamber. Normally this is done by means of Meissner traps located close to the unwind station.

(2) The system described requires approximately 1.2 MW of connected power; this much power may not be available at any given location.

(3) The input power must be dissipated, requiring extensive heat exchangers and a cooling tower.

(4) Means must be provided to handle both the uncoated and coated webs of PET under clean room conditions.

(5) Because of their relatively high cost and constant use, consideration should be given to in-house fabrication of targets and cathodes.

(6) Because of the large number of process variables and relatively long coating time involved per roll, the entire system should be under computer control and real-time process monitoring.

The approximate manufacturing cost of a 5¼-in. floppy disk by this system, excluding machine depreciation, site preparation, and testing, is $2.74 per disk. Clearly, for a storage media with 10 times the capacity of standard floppy disks, this is a most reasonable cost.

REFERENCES

5-1. Iwasaki, S.; and Nakamura, Y.: *IEEE Trans. Magn.* **13**(5): 1272-1277, Sept. 1977.

5-2. Iwasaki, S.; and Ouchi, K.: *IEEE Trans. Magn.* **14** (5): 849-851, Sept. 1978.

5-3. Iwasaki, S.; Nakamura, Y.; and Ouchi, K.: *IEEE Trans. Magn.* **15**(6): 1456-1458, Nov. 1979.

5-4. Iwasaki, S.: *IEEE Trans. Magn.* **16**(1): 71-76, Sept. 1980.

5-5. Potter, R. I.; and Beardsley, I. A.: *IEEE Trans. Magn.* **16**(5): 967-972, Sept. 1980.

5-6. Fujiwara, T.; and Yamamori, K.: *Proc. 1982 Symp. Perpendicular Magn. Recording,* Tohoku Univ., Sendai, Japan, Mar. 11-12, 1982, p. 57.

5-7. Iwasaki, S.: *Proc. 1982 Symp. Perpendicular Magn. Recording,* Tohoku Univ., Sendai, Japan, Mar. 11-12, 1982, p. 1.

5-8. *Nikkei Electronics,* Apr. 25, 1983.

5-9. Thornton, J. A.: *J. Vac. Sci. Technol.* **12**(4): 830, July/Aug. 1975.

5-10. Ouchi, K.; and Iwasaki, S.: *IEEE Trans. Magn.* **18**(6):1110, Nov. 1982.

5-11. Johnson, C.: *Symp. Magn. Media Manufacturing Methods,* Magnetic Media Information Services, Honolulu, May 25-28, 1983.

CHAPTER 6

Serial High-Density Digital Recording Using a Wideband Analog Inter-Range Instrumentation Group Recorder/Reproducer*

E. L. Law
Pacific Missile Test Center

The purpose of this study was to determine the performance characteristics of several pulse code modulation (PCM) codes when used to store telemetry data on a Range Commanders Council (RCC) wideband analog magnetic tape recorder/reproducer.

The storage technique studied is called high-density digital recording (HDDR). Basically, HDDR is a recording technique by which digital signals are recorded directly onto magnetic tape. The information presented in this chapter is limited to serial recording using ac bias and tape track widths of 50 mils.The important properties of recorder/reproducers, magnetic tape, PCM bit synchronizers and PCM codes are presented. A discussion of the RCC serial HDDR standard and candidate RCC test methods is also included.

This study was conducted under AIRTASK A6306302-054D-8W06040000, Range Instrumentation Development and Test, Work Unit A6302D-02, Range Telemetry Support. The purpose of this AIRTASK was to provide technical support to the Telemetry Group of the Range Commanders Council.

TAPE RECORDER/REPRODUCER PARAMETERS

All recorder/reproducers used in this study were RCC wideband analog machines with 50-mil trackwidths and ac bias. The effects of bias level, bandwidth (amplitude equalization), reproduce level, record level, crossplay between machines, tape speed, signal-to-noise ratio (SNR), and tape dropouts were studied (ref. 6–1). The method of determining the effect of each parameter was to set all other parameters to their nominal value and record sections of tape with a variety of packing densities for each of the settings of that parameter. This was done for biphase, level (Biϕ-L); delay modulation (DM; also known as Miller code and modified frequency modulation); non-return-to-zero, level (NRZ-L); and randomized NRZ-L (R-NRZ-L). The tape was then reproduced and the "best" setting of each parameter was defined to be the setting that yielded the highest packing density with a bit error rate (BER) of 10^{-6} or less. These tests were performed at tape speeds of 30 and 120 ips. All tests were performed using the same reel of tape to eliminate tape as a parameter. Limited experiments with other tapes yielded essentially the same results. The test configuration is shown in figure 6–1. Test methods are described in appendix 6–A.

Bias Level

The bias was adjusted by recording and reproducing an upper-band-edge signal and increasing the bias level until the reproduced output decreased by 2 dB from defined as the 0-dB bias level point. The +2-dB bias level point was achieved by further increasing the bias until the reproduced output decreased by 2 dB from the maximum. Other bias levels were obtained by use of this same technique. The reproduce section equalizers were readjusted for each bias level to obtain the flattest possible frequency response characteristic. The frequency response was always within ±3 dB from 400 Hz to the −3-dB bandwidth frequency (±1 dB over most of this range).

The effects of bias level variations on maximum bit packing density are illustrated in figures 6–2 and 6–3. Figure 6–2 presents results for a 2.0-MHz bandwidth (−3 dB) at 120 ips. The maximum bit packing density for all three codes occurred at a +2-dB bias level (Biϕ-L has essentially the same performance at 0- and +2-dB

*Now the Range Commanders Council.

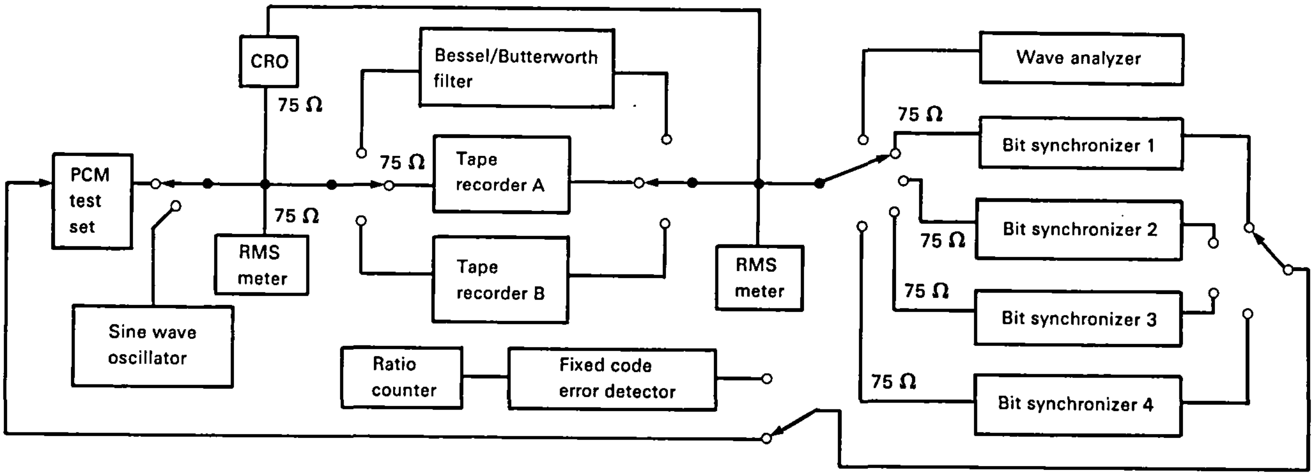

Figure 6-1.—Test configuration. (CRO = cathode ray oscilloscope.)

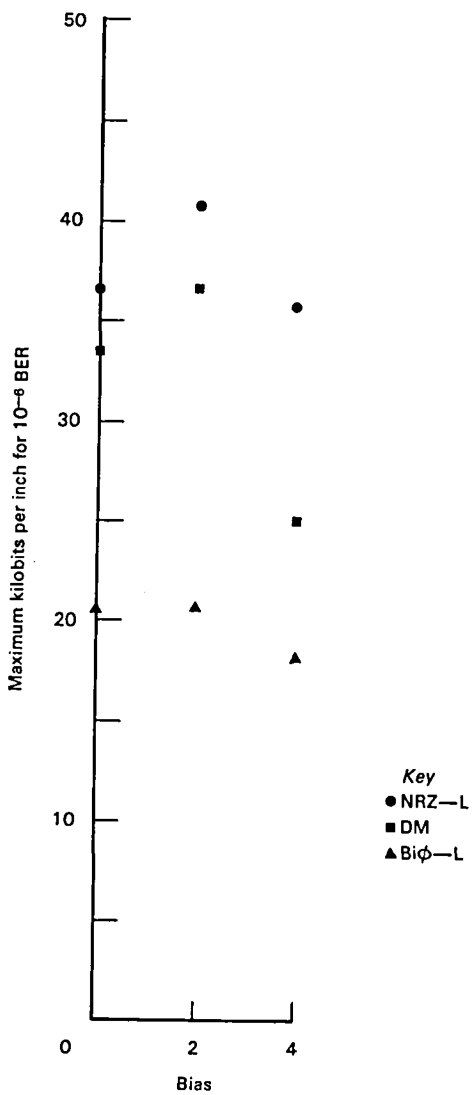

Figure 6-2.—Effect of bias level variations on maximum bit packing density at 120 ips.

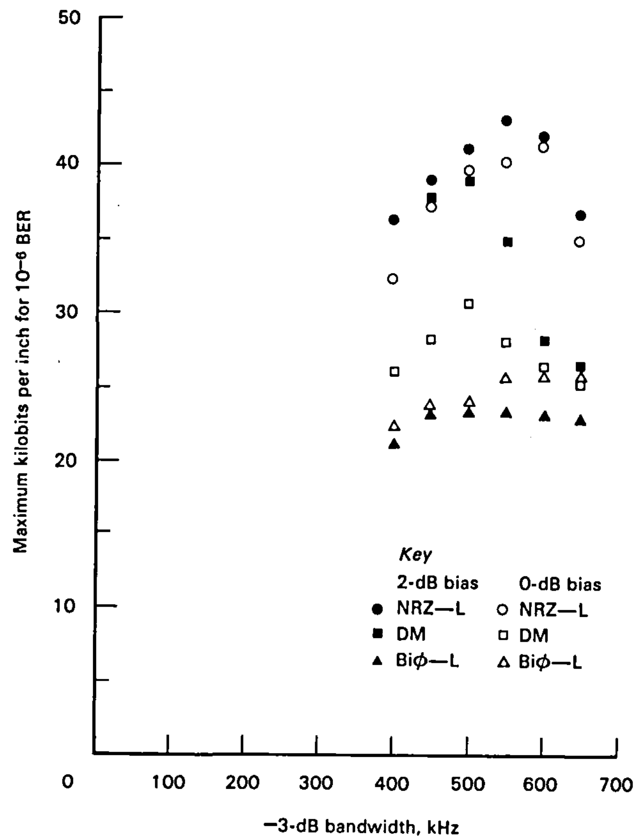

Figure 6-3.—Effect of bias level and bandwidth variations on maximum bit packing density at 30 ips.

bias levels). Figure 6-3 presents results from various bandwidths at 30 ips. The maximum packing density for NRZ-L and DM occurred at a +2-dB bias level; however, the maximum packing density for Biφ-L occurred at a 0-dB level (the performance at +2 dB was almost as good).

Bandwidth (Reproduce Equalizer)

The recorder/reproducer bandwidth was varied by adjusting the reproduce equalizer. The bandwidth (−3 dB) was varied from 400 to 650 kHz at 30 ips and from 1500 to 2750 kHz at 120 ips. The frequency response from 400 Hz to the −3 dB frequency was always within ±3 dB of the response at 50 kHz (30 ips) or 200 kHz (120 ips). It should be noted that varying the −3-dB signal bandwidth in this manner has a large effect on the noise spectrum near the upper band edge.

The effect of varying the recorder/reproducer bandwidth on maximum bit packing density is shown in figures 6-3 and 6-4. It should be emphasized that the recorder/reproducers used in this study did not have an adjustment for optimizing phase equalization. Therefore, these results include the effects of both amplitude and phase equalization changes.

Figure 6-3 shows that with a 0-dB bias level at 30 ips, both NRZ-L and Biϕ-L had the highest bit packing density when the bandwidth was increased by 20 percent. The best NRZ-L packing density occurred with a +2-dB bias level and a 10 percent increase in bandwidth. The best DM performance occurred with the nominal 500-kHz bandwidth. Figure 6-4 shows that both NRZ-L and DM had their highest packing density when the bandwidth was at the nominal value (2.0 MHz at 120 ips) for a +2-dB bias level. The Biϕ-L packing density was slightly higher when the bandwidth was reduced 25 percent than it was at the nominal bandwidth.

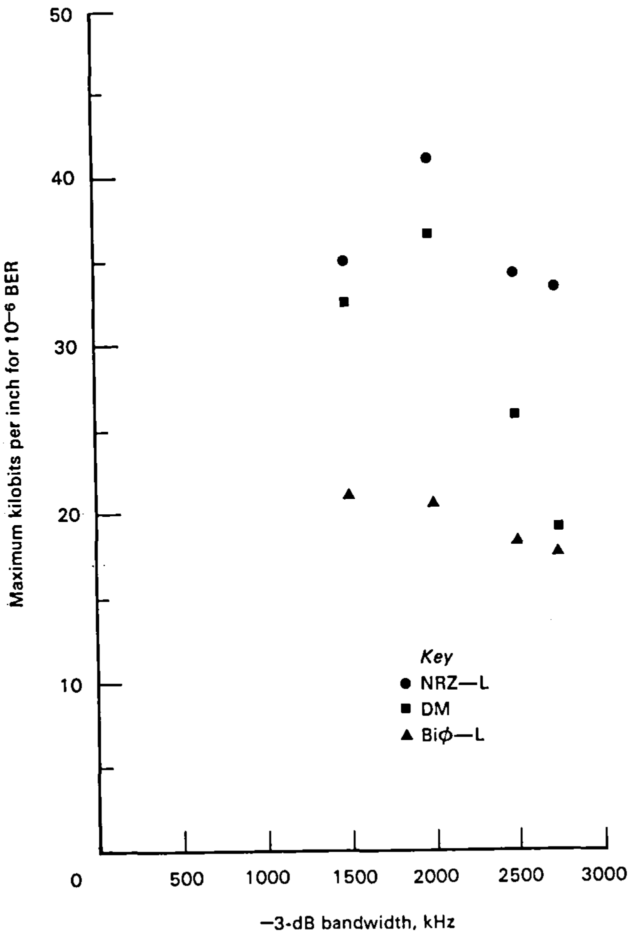

Figure 6-4.—Effect of varying the recorder/reproducer bandwidth on maximum bit packing density at 120 ips. (+2 dB bias.)

Reproduce Level

The reproduce level had no significant effect on the maximum bit packing density for reproduce levels between 0.5 and 2.0 V_{RMS}. Above 2.0 V_{RMS} the reproduce amplifier went into saturation, and the maximum bit packing density was reduced.

Record Level

For this test, the recorder/reproducer output was adjusted for 1 percent third harmonic distortion with a 1-V_{RMS} record level at a frequency equal to 10 percent of the frequency at the upper band edge. The results for NRZ-L at 30 ips and +2-dB bias are shown in figure 6-5. The best packing densities were achieved at record

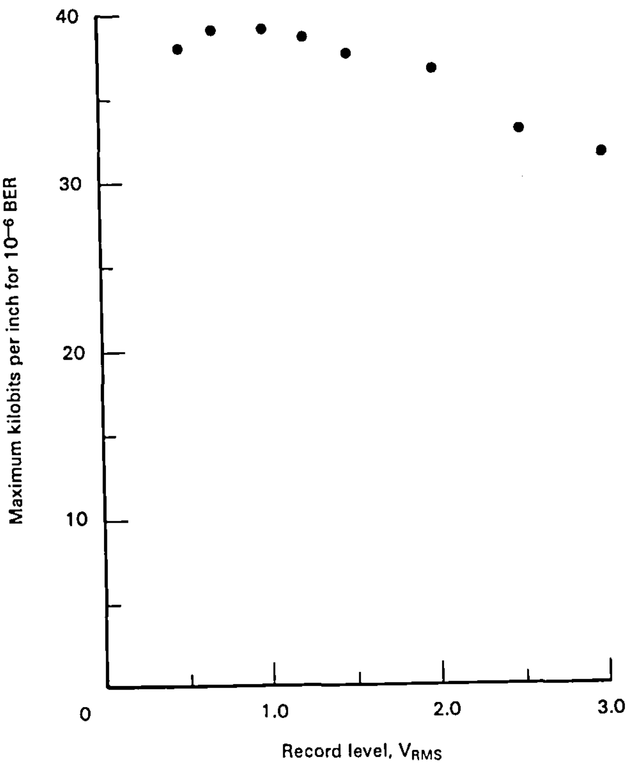

Figure 6-5.—Effect of record level on maximum bit packing density for NRZ—L at 30 ips and +2 dB bias. (One percent third harmonic distortion at 1 V_{RMS} record level.)

levels of 0.7 and 1.0 V_{RMS}. Higher record levels caused a decrease in maximum bit packing density because of additional distortion and intersymbol interference. The sine wave third harmonic distortion was 2.5 percent at a record level of 1.25 V_{RMS} and 9 percent at 2.0 V_{RMS}. The results with DM and Biϕ-L were very similar to the NRZ-L results. Table 6-1 shows the increase in BER as the record level is increased.

Crossplay

The crossplay tests were conducted by recording data at several bit packing densities on each of two recorder/reproducers for each code. These data were then reproduced on each recorder/reproducer, and the bit error rates were measured. The maximum bit packing density that yielded a BER of 10^{-6} or less for each combination of recorder/reproducer and code is presented in figure 6-6. The SNR of recorder/reproducer A was 34 dB, and the SNR of recorder/reproducer B was 28 dB. Both recorder/reproducers were set up to nominal conditions, and the only adjustment was to optimize azimuth. Recorder A had a record gap length of 90 μin., while recorder B had a record gap length of 140 μin. The reproduce gap length of both reproduce systems was 30 μin. The best combination was to record and reproduce using machine A. The worst combination was to record using A and reproduce with B. The standard condition for the bias, bandwidth, record level, reproduce level, and bit synchronizer tests was to both record and reproduce using machine A.

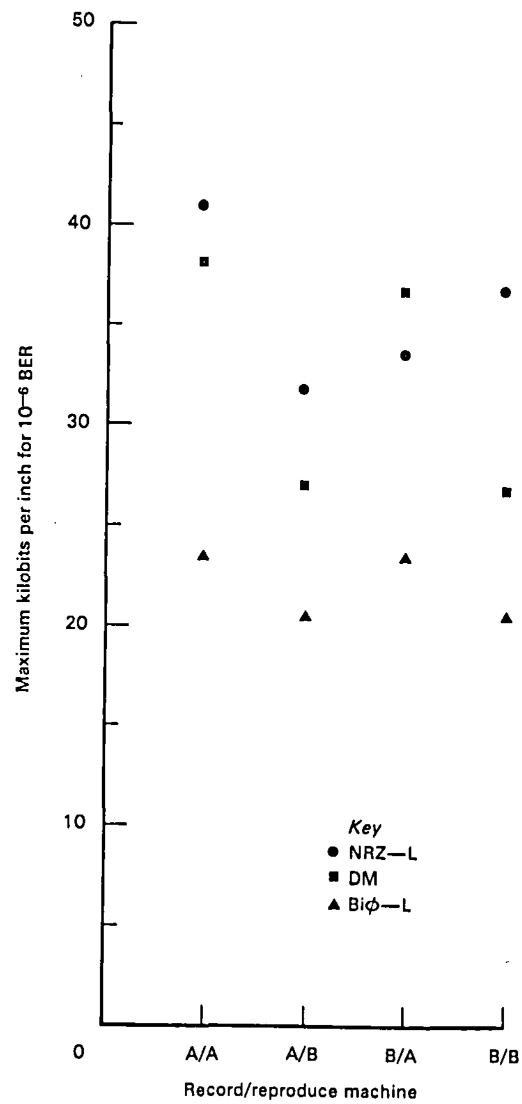

Figure 6-6.—Maximum bit packing density yielding a BER of 10^{-6} during crossplay between two recorder/reproducers.

Tape Speed

The maximum bit packing densities for a BER of 10^{-6} at tape speeds of 30 and 120 ips are presented in figure 6-7. The maximum bit packing density for both NRZ-L and DM was approximately 5 percent lower at 120 than at 30 ips. The maximum bit packing density for Biϕ-L was nearly 12 percent lower at 120 than at 30 ips.

Signal-to-Noise Ratio

One of the important performance factors for the evaluation of PCM codes for HDDR is the SNR required to give a specified BER at a specified bit packing density (refs. 6-2 and 6-3). The bit packing density versus SNR performance for a BER of 10^{-6} and a tape speed of 30 ips is shown in figure 6-8 for NRZ-L, Miller, and Biϕ-L codes. The test pattern used was a 2047 bit pseudorandom sequence. The SNR was calibrated using the following procedure:

(1) A step attenuator with 1-dB resolution was inserted between the PCM test set and tape recorder A. (See fig. 6-1.)

(2) The PCM bit rate was set to 100 kbps, and the PCM signal was recorded and reproduced. The true RMS signal level at the output of the reproduce amplifier was measured for attenuator settings of 0, 3, 6, and 9 dB. A check was made to verify that a 3-dB change in input level produced a 3-dB change in output level.

Table 6-1.—*Bit Error Rate (× 10^{-6}) Versus Record Level*

Code	Kilobits per inch	Record level V_{RMS} 0.5	1.0	1.25	2.0
NRZ–L	41	1	1	10	5 000
DM	38	1	1	10	60
Biϕ–L	23	1	1	100	10 000

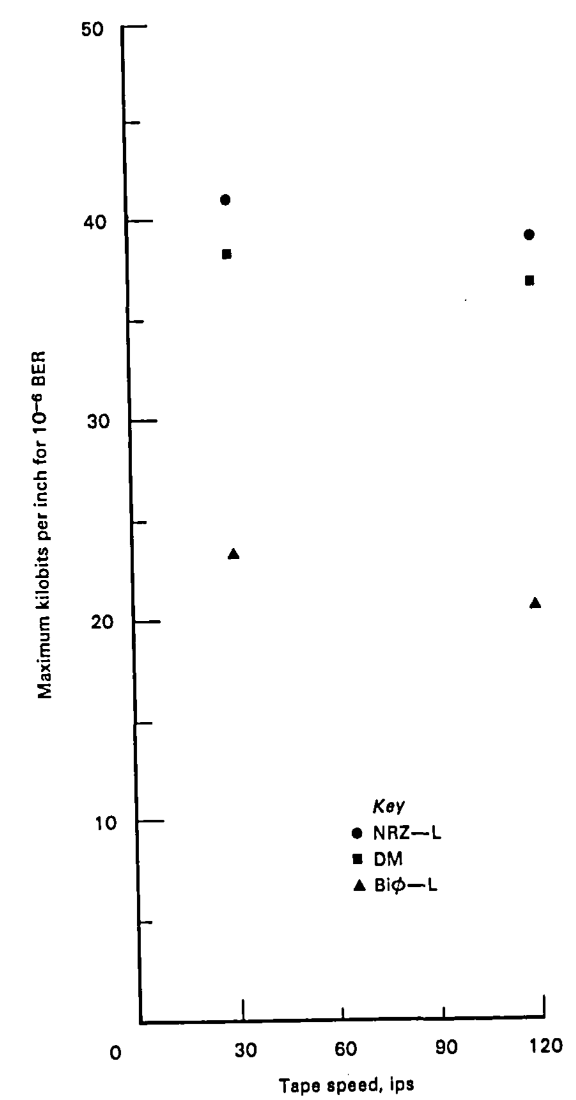

Figure 6–7.—Maximum bit packing densities for a BER of 10^{-6} at tape speeds of 30 and 120 ips.

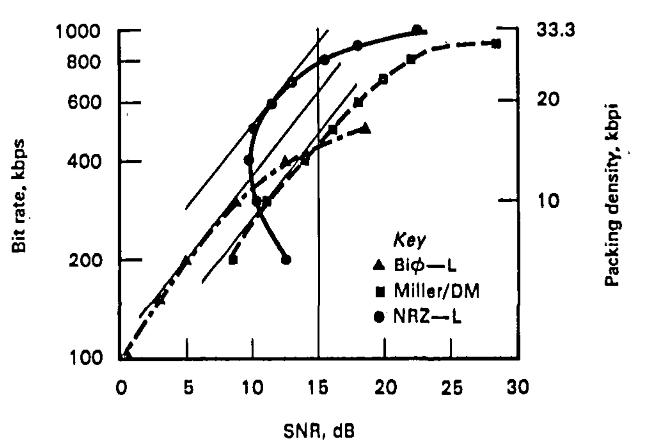

Figure 6–8.—Bit rate and bit packing density versus SNR performance for a BER of 10^{-6} and a tape speed of 30 ips.

(3) The PCM signal was removed from the recorder input. The input to the recorder was then terminated in its characteristic impedance, and the true RMS value of the output noise was measured while simultaneously recording and reproducing. The measurement bandwidth was 3 to 500 kHz.

(4) The ratio of the signal level with 0 dB of attenuation to the noise level was defined to be the reference SNR.

For each bit rate and code, the attenuator setting was varied until the BER was approximately 10^{-6}. The SNR was calculated by subtracting the attenuator setting from the reference SNR value. The reproduce level was maintained within 2 dB of 1 V_{RMS} by adjusting the gain of the reproduce amplifier. This was done to eliminate the effects of widely varying levels into the bit synchronizer. All tests were performed on sections of tape that had no apparent dropouts.

The NRZ-L data in figure 6–8 show that an SNR of 18 dB is required for a packing density of 30 kbpi, 11.5 dB for 20 kbpi, and 10.5 dB for 10 kbpi. As the packing density is increased above 20 kbpi, the slope of the packing density versus SNR data starts to decrease. This is caused by the band-limiting of the signal, which reduces the signal energy into the bit detector. As the reproduce bit rate is reduced below 400 kbps, the slope of the bit rate versus the SNR curve changes sign. This occurs because the reproduce system acts like a high-pass filter with a −3-dB frequency of approximately 400 Hz. As the NRZ-L bit rate is reduced, the maximum time between transitions is increased, and the amount of energy at frequencies below 400 Hz is also increased. This causes an increase in the baseline wander that the dc restorer in the bit synchronizer must track. Because it is difficult to track the baseline wander perfectly, especially at low SNR, the SNR at the bit synchronizer input must be increased to maintain a constant BER. The exact characteristics of the curve in the high packing density and low reproduce bit rate regions depend on the recorder/reproducer, tape, equalization, and bit synchronizer used. However, the results for other equivalent systems should be similar to the results presented in figure 6–8.

The Miller and Biφ-L data in figure 6–8 show band-limiting effects similar to those of NRZ-L. NRZ-L required a lower SNR than Miller above 300 kbps (10 kbpi), but Miller performed better below 300 kbps. Biφ-L performed better than Miller below 450 kbps (15 kbpi), but rapidly degraded due to band-limiting effects above 15 kbpi.

Tests were also conducted with R-NRZ-L, DM, and odd-parity NRZ-L using 16-bit worst-case patterns (ref. 6-2) and with NRZ-L, R-NRZ-L, and DM using repeated 6-bit ramps (refs. 6-2 and 6-4). These tests were conducted using a four-pole Bessel bandpass filter

with a 0.4 to 500-kHz bandwidth and spectrally conditioned noise to simulate the tape recorder/reproducer.

The test results with the 16-bit worst-case patterns and the 6-bit ramps are shown in figures 6–9 and 6–10, respectively. R-NRZ-L performed the best at all bit rates tested. Because the R-NRZ-L bit stream characteristics are similar to those of a pseudorandom NRZ-L bit stream, the R-NRZ-L data would also demonstrate the effects of baseline wander at low reproduce bit rates.

Tape Dropouts

Tape dropouts are defined as reductions in the output level of a recorder/reproducer when a constant-level input signal is recorded. The duration and depth of the dropout determine the effect on data quality. Tape dropouts are caused by either defects in the magnetic material of the tape or an increase in separation between the tape and the magnetic heads. Tape dropouts are the primary cause of bit errors in a properly set up HDDR system. The quantity, duration, and depth of tape dropouts are a function of such factors as the magnetic tape used, the trackwidth, the type of recorder/reproducer used, the tape tension, and the amount of debris on the tape (refs. 6-5 and 6-6).

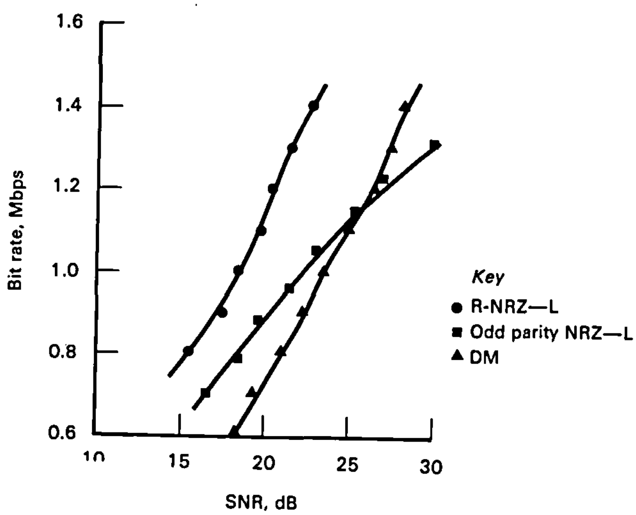

Figure 6–9.—Bit rate versus SNR for 10^{-6} BER, repeated 16-bit worst-case patterns.

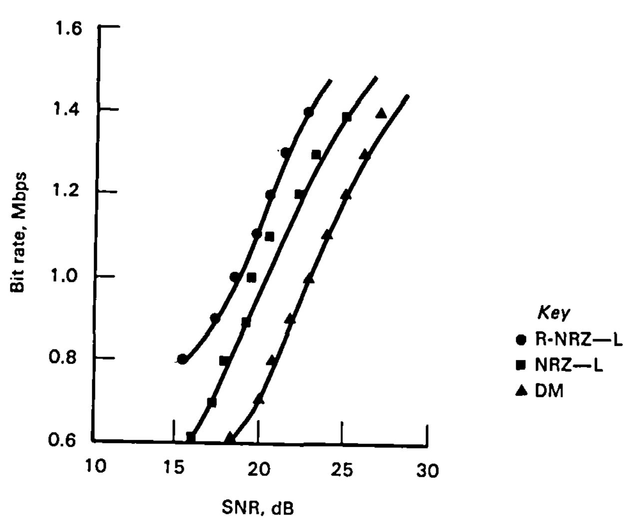

Figure 6–10.—Bit rate versus SNR for 10^{-6} BER, repeated 6-bit ramp.

Dropout tests were conducted on several tapes by monitoring the clock slips and bit errors versus tape footage. A sample of the test results is presented in table 6–2. These tests were conducted on a seven-track recorder/reproducer set up to the standard conditions defined in this chapter. The recorder used a vacuum chamber tape tension system and had 50-mil-wide tracks. The bit packing density was 25 kbpi at a tape speed of 120 ips. The test pattern used was a 2047-bit pseudorandom NRZ-L sequence. The tests were conducted using 8000 ft of Ampex 786 wide-band instrumentation magnetic tape; therefore 2.4 × 10^9 bits were recorded on each track. The first run on track 1 was performed with degaussed, virgin tape. The number of clock slips and bit errors on the first run was much larger than on a later run on the same track. This was due to the cleaning and polishing of the tape as it passed over the heads. It should also be noted that the dropouts were much less frequent and less severe on the center tracks than on the edge tracks. The reduction in dropouts after the first tape pass and the smaller number of dropouts on the center tracks were observed with all tapes tested. This supports the "rule-of-thumb" that critical data should be recorded on the center tracks of a recorder and also indicates that virgin tape should not be used for critical recordings. The bit error rates on the center tracks of "polished" wide-band instrumentation tapes were typically 10^{-7} or better for test condi-

Table 6–2.—*Bit Errors and Clock Slips for Various Tracks of a Recorder/Reproducer*[a]

Track	Clock slips	Error bursts[b]	Total errors[b]
1[c]	7	78	945
1	2	17	122
2	2	4	179
3	0	2	4
4	0	1	1

[a]Test conditions: 120 ips; 25 kbpi; 50-mil trackwidth; 2047-bit pseudorandom NRZ–L sequence; 8000 ft of Ampex 786 tape; 2.4 × 10^9 bits.

[b]Total errors and error bursts do not include errors during bursts with clock slips.

[c]First run.

tions similar to those listed earlier. Bit error rates will be higher for systems with narrower trackwidths or higher bit packing densities.

Clock slips occurred when the tape dropout was severe enough to deprive the bit synchronizer of the transitions required to maintain synchronization for a time interval long enough for the recovered clock of the bit synchronizer to depart from the actual data rate by one or more bits. The time interval required for this to occur is a function of the loop bandwidth of the bit synchronizer and the difference in frequency between the "free-running" bit synchronizer clock rate and the actual data rate.

PULSE CODE MODULATION BIT SYNCHRONIZER

Tests were conducted to determine the variations in maximum bit packing density when four different bit synchronizers were used to reconstruct the data from the recorder/reproducers. Only two manufacturers were represented and the bit synchronizers were not all different models. The test results are presented in figure 6-11. Bit synchronizer 1 had the best performance for all codes and was used for all other tests. Bit synchronizer 3 did not work for DM, and bit synchronizer 4 performed very poorly for DM. A modification can be made to bit synchronizer 4 to improve its performance to the level of bit synchronizer 1. This modification has a negative effect on performance in the presence of baseline wander. If DM is being used in a band-limited channel and very poor results are achieved, it is recommended that the bit synchronizer manufacturer be contacted to determine if a modification is needed.

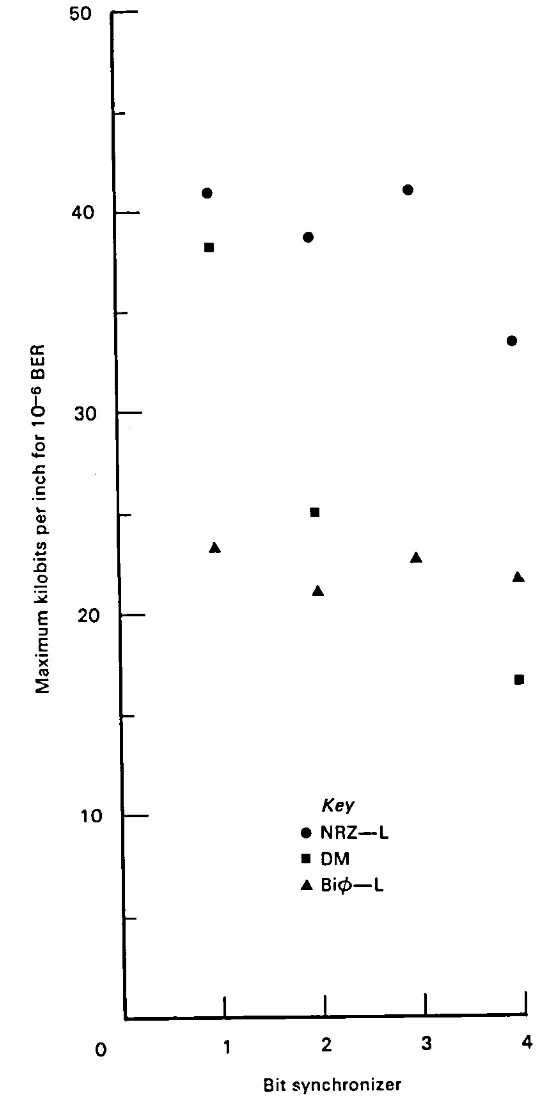

Figure 6–11.—Maximum bit packing densities for four different bit synchronizers.

PULSE CODE MODULATION CODE PROPERTIES

There has been much discussion over the past few years about the advantages and disadvantages of various codes for HDDR. The relevant properties of the codes included in this study will be discussed in the following sections. Plots of the spectrums of NRZ-L, R-NRZ-L, Biϕ-L, DM, and M^2 for various input patterns are contained in appendix 6–B. All codes discussed in this chapter are bilevel codes.

NRZ-L Properties

NRZ-L is a code wherein a "1" is represented by one level and a "0" by the other level (ref. 6-7). This is illustrated in figure 6-12. Because the symbols for a "1" and a "0" can be characterized as being the opposites of each other, the NRZ-L symbols are antipodal. Therefore, the bit error rate in a wide-band binary symmetric channel with additive white gaussian noise is optimum. However, the HDDR system is band limited at both low and high frequencies, has intersymbol interference, has noise that is not white, and a BER that is largely determined by the depth and duration of the tape dropouts encountered. The NRZ-L code is not well suited to HDDR because of the lack of dc response in the reproduction process and the possibility that a very large percent of the signal energy may be at dc.

Because the NRZ-L code has desirable SNR and high-frequency response characteristics, several variations have been proposed to minimize the undesirable characteristic of NRZ-L. The mark and space versions of NRZ (NRZ-M and NRZ-S) provide a simple alternative to NRZ-L (ref. 6-7). These codes are polarity insensitive because the information is contained in the

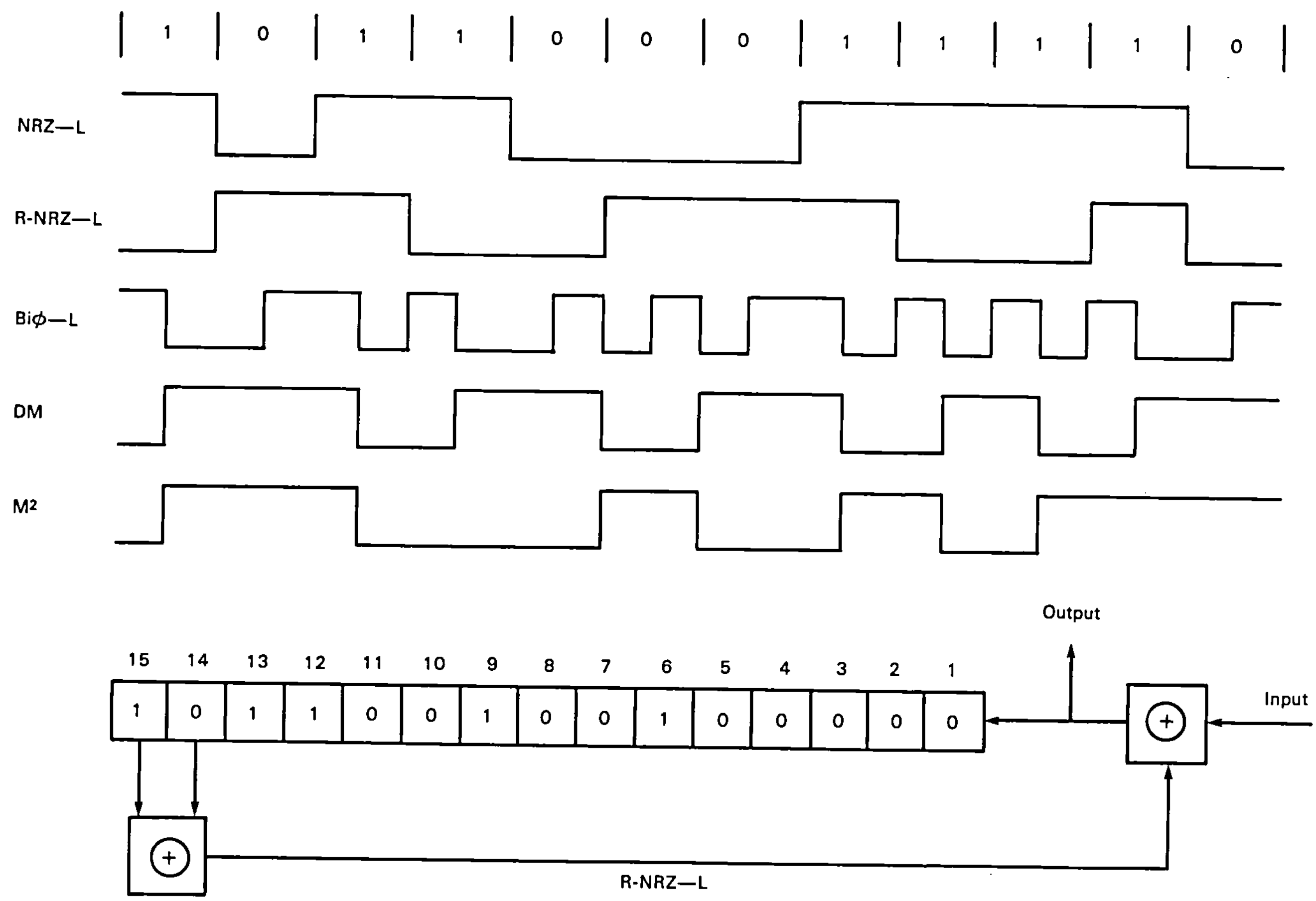

Figure 6–12.—PCM code waveforms.

transitions rather than the levels. These codes do not provide any general improvement in transition density or low-frequency reduction compared with NRZ-L. They do have the disadvantage that each isolated bit error causes two errors in the decoded data. NRZ-M and NRZ-S are not recommended as general purpose HDDR codes.

Another alternative to ordinary NRZ-L is block coding (ref. 6–8). A popular example is the (6,8) block code. The input is grouped into 6-bit blocks. Each 6-bit block is encoded into an 8-bit sequence that contains four "1's" and four "0's". Because 70 such 8-bit sequences exist, all 64 possible 6-bit input blocks can be uniquely encoded and decoded. The (6,8) block code is dc-free and has at least two transitions every 8 bits. This code also provides the capability for detection of all 8-bit blocks that contain an odd number of bit errors and some 8-bit blocks that contain an even number of bit errors. The main disadvantage of this code is the high overhead rate. The encoded bit sequence would have to be recorded at a bit packing density of 33.3 kbpi to produce a data packing density of 25 kbpi. Other disadvantages of this code include the relative complexity of the encoding and decoding schemes.

Another commonly used block code is the (7,8) code. This code is usually generated by grouping the data in blocks of 7 bits and adding an 8th bit such that the encoded 8-bit block contains an odd number of "1's" (odd parity). This technique is sometimes coupled with the inversion of certain of the 7 input bits (ref. 6–9). This coding technique insures that the maximum time between transitions will be no greater than 14 bits. It also reduces the maximum possible dc content to 75 percent of the total energy. The (7,8) code does not perform as well as the (6,8) code in two areas; however, it requires only an encoded bit packing density of 28.6 kbpi to achieve a data packing density of 25 kbpi. The odd-parity (7,8) code has the capability to detect any odd number of bit errors occurring in the 8-bit block.

All block codes require the decoder to determine the location of the block boundaries before the data can be properly decoded. This can be accomplished either by inserting synchronization words into the data stream or by searching a long string of bits for the block boundary locations. Once the block boundaries are located, their position will not change unless a clock slip occurs. Therefore, these codes can be used to detect clock slips (unless a multiple of eight clocks was slipped), and in

some cases the proper number of bits may be added or deleted to eliminate the effect of the clock slip. However, clock slips are usually associated with a large burst of bit errors, and the addition or deletion of the correct number of bits does nothing to alleviate the effect of these errors. It can prevent the loss of "good" data that are misinterpreted because the data bits will be assigned the wrong value until proper data (frame) synchronization is achieved by restoring the bits to their correct positions within the data frame.

R-NRZ–L Properties

Randomized NRZ-L is a coding technique by which the input data are modified to have properties similar to random data. One method of accomplishing this is shown in figure 6-13. The input NRZ-L data are modulo-2 summed with the modulo-2 sum of the output of the 14th and 15th stages of a shift register, where the input to the shift register is the randomized NRZ-L data. The decoder for this randomizing technique is shown in figure 6-14. A sample R-NRZ–L waveform is shown in figure 6-12. The shift register contents at the start of the sequence were "101100100100000." This sequence was chosen by flipping a coin (the first bit in the sequence is in register 15). With a different choice of initial contents of the shift register, the R-NRZ-L bit stream could have been any combination from 12 "0's" to 12 "1's". In general, the R-NRZ-L encoder converts any input bit sequence into an output bit sequence with properties approximating those of random data.

Figure 6-15 shows the results of randomizing a pseudorandom bit sequence. The pseudorandom input sequence was generated using a 15-stage pseudorandom generator with the modulo-2 sum of the 14th and 15th stages tied to the input to the first stage. The initial contents of the shift register were the same as shown for the shift register of figure 6-12. The initial contents of the randomizer shift register were identical to the contents of the pseudorandom generator shift register. The data in figure 6-15 show that the randomized bit sequence is dominated by "0's" for the first 180 bits (125 "0's" and only 55 "1's"). The next 1020 bits consisted of approximately 52 percent "0's" and 48 percent "1's". The longest sequence without a transition was 19 bits. Figure 6-15 illustrates that if the input of the randomizer is a pseudorandom sequence that is generated using a register that is in the same configuration as the randomizer register, the randomized data are temporarily nonrandom. However, the overall effect is not a catastrophic loss of transitions. The sequence shown in figure 6-15 will create no problems if the bit detector includes a "good" dc restorer and the reproduce bit rate is 200 kbps or higher.

The 15-stage R-NRZ-L encoder will generate a maximal length pseudorandom sequence of $2^{15} - 1$ (32,767) bits if the input data consist only of "0's" and there is at least a single "1" in the shift register. A maximal length pseudorandom sequence is also generated when the input data consist only of "1's" and the shift register contains at least a single "0." However, if the shift register contains all "0's" at the moment that the input bit stream is all "0's" the R-NRZ-L output bit stream will also be all "0's". The converse is also true; when the shift register is filled with "1's" and the input bit stream is all "1's" the R-NRZ-L output bit stream will contain only "1's." In

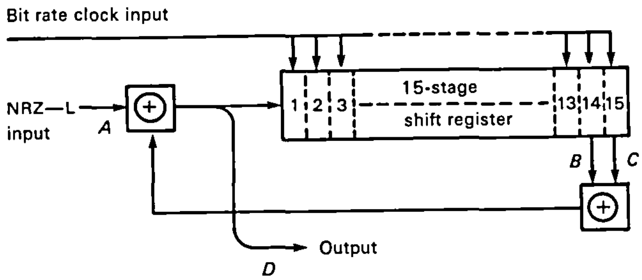

Boolean expression: $D = A + B + C$

Figure 6-13.—Randomizer block diagram.

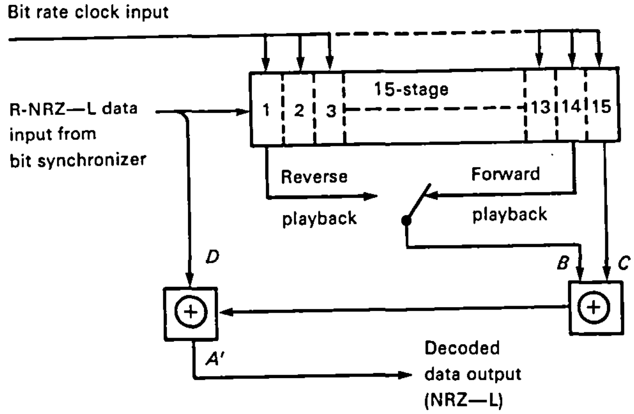

Boolean expression:
with input data A into randomizer,
errorfree R-NRZ—L data, $D = A \oplus B \oplus C$

$$
\begin{aligned}
A' &= D \oplus B \oplus C \\
&= A \oplus B \oplus C \oplus B \oplus C \\
&= A \oplus B \oplus B \oplus C \oplus C
\end{aligned}
$$

but

$$
\begin{aligned}
B \oplus B &= 0 \\
C \oplus C &= 0
\end{aligned}
$$

Therefore,

$$A' = A \oplus 0 \oplus 0 = A$$

Figure 6-14.—Randomized NRZ—L decoder block diagram.

```
RANDOMIZED BIT SEQUENCE (60 BITS/LINE)                          ONES
101100100100000000000000000001011110110100000000000000000100      14
100101100100000000000000001011011001111010000000000001001101      19
111100100100000000001011110100011101101000000000010010010010      22
110101100100000010110110110011000111101000001001101101111111      31
101100100100010111101101000001011110110101001001011001000100      28
100101100001101110011110101011011001110011101111110010000110      33
111101111010100011101000111010001010010000101101001011010010      30
100011010010011011001100110001011100110111111111111111111010      37
010111110100000000000000001001100100010010000000000001011111      19
101010110100000000000100100001000001100100000000010110100101      18
000111110100000001001100110001011000100100000101111111110100      27
111010110100010001000000100111010001100101011010000010111010      26
010111110000110010001001010011001000110011111010101100011111      31
101011111100010000111011000010001000011010100011010111001010      28
010100111000010111000101110000000111011001001011010010110000      26
011010111101100110011001110001110001001011111111111111110110      38
110101100100000000000101101101100011110000000000010011011011      25
101100100100000010101111011010101111011010000010010010110000      26
100101100100010110110011100010110011110101001101111101101001      33
111100100001111010001011001110001110100110010010100111110110      32
```

Figure 6–15.—Randomized pseudorandom sequence.

these two cases, the contents of the shift register do not change, and the output data are not randomized. However, the randomizer is not permanently locked up in this state because a change in the input data will again produce a randomized output. In general, if the input bit stream contains runs of X bits without a transition, with a probability of occurrence of $p(X)$, the output will contain runs having a length of up to $(X + 15)$ bits, with a probability of $2^{-15}p(X)$ of having a run length of $X + 15$ bits. Therefore, the output can contain long runs of bits without a transition, but the probability of occurrence is low.

The spectrum resulting from randomizing a repeated ramp is shown in appendix 6–B. The spectrum of the repeated ramp consists of a few discrete spectral lines, while the randomized ramp has a spectrum resembling the NRZ-L spectrums with pseudorandom data.

Tests were conducted to determine the effects of varying the length of the randomizing register. As the register length is made shorter, the probability that the register will be filled with "1's" when a run of "1's" appears at the input or "0's" when a run of "0's" appears at the input is increased by a factor of 2 for each stage that is removed from the register. Tests were conducted with registers of length 5, 7, 9, 11, 15, 17, and 20 (all feedback tapes were for maximal length sequences). Registers of length 5 and 7 performed very poorly with repeated ramps. Registers of length 9 and 11 performed somewhat worse than registers of length 15, 17, or 20. No differences were observed in the performance of the registers of length 15, 17, and 20. One disadvantage of the longer registers is that the length of an error burst (number of bits between the first and last errors in a burst) in the derandomized data is always greater than the length of the input error burst by a number of bits equal to the shift register length. Thus, long shift registers have the undesirable property of spreading the errors over more data words. Therefore, it appears that 15 is a good choice for the length of the randomizing register.

The R-NRZ-L decoding system has an error multiplication factor of 3 for isolated bit errors (separated from adjacent bit errors by at least 15 bits). An isolated bit error introduced after randomization will produce three errors in the output data, the original bit in error plus two additional errors 14 and 15 bits later. In addition, a burst of errors occurring after the data have been randomized will produce a burst of errors in the derandomized output. The number of errors in the output depends on the distribution of errors in the burst and can be greater than, equal to, or less than the number of errors at the input to the derandomizer. Errors introduced before randomization are unaffected by either the randomizer or the derandomizer. The reverse decoder has the same bit error multiplication properties as the forward decoder. An error multiplication of 3 is approximately equivalent to an SNR penalty of 0.5 dB at a BER of 10^{-6}. The SNR penalty approaches 0 dB if most bit errors occur during long bursts.

The R-NRZ-L decoder is self-synchronizing and does

not require overhead bits for serial HDDR. However, 15 consecutive error-free bits must be loaded into the shift register before the output data will be valid. A bit slip will cause the decoder to lose synchronization, and 15 consecutive error-free data bits must again be loaded into the shift register before the output data are valid. The decoded output data, even though correct, will contain the bit slip, causing a shift in the data with respect to the frame synchronization pattern. Therefore, frame synchronization must be reacquired before the output provides meaningful data. The basic R-NRZ-L code has no inherent properties for detecting either bit errors or bit slips. Parity bits could be added to the data before or after randomization. It is the author's opinion that in most cases it is preferable to add the parity bits at the data source rather than at the recording site. If the parity bits are added at the data source, the data quality of the entire communications link can be monitored rather than just the quality of the record/reproduce process. Another technique for estimating the data quality is to monitor the bit errors occurring in the data frame synchronization word. The decision on whether to use parity should be determined by the data analysis requirements rather than by the recording techniques. (This assumes serial recording on 50-mil trackwidths. The dropout characteristics for narrower trackwidths may modify this recommendation.)

The R-NRZ-L data can be bit synchronized and signal conditioned using existing bit synchronizers with the input code selector set to NRZ-L. The bit synchronizer should contain a "good" dc restorer (a dc restorer is required for acceptable results at reproduce bit rates below 1 Mbps). R-NRZ-L is a reliable code for reproduce bit rates above 200 kbps. At lower reproduce bit rates, special low-frequency restoration circuitry is required for reliable operation. The maximum recommended bit packing density for this code is 25 kbpi (ref. 6-7) for recorder/reproducers with a bandwidth of 1 MHz at 60 ips. The maximum recommended bit packing density for recorder/reproducers with a bandwidth of 750 kHz at 60 ips is 18.75 kbpi. In other words, the maximum recommended bit rate is 1.5 times the recorder/reproducer bandwidth.

Another technique for randomizing a data stream is illustrated in figure 6-16. This technique requires the insertion of a synchronization word periodically to synchronize the pseudorandom sequence in the decoder (see figure 6-17) to the sequence in the encoder. The synchronization word is not randomized because the pseudorandom sequence at the input to the EXCLUSIVE OR gate is zero during the synchronization word. This can either be accomplished by proper manipulation of a shift register generator or by the use of a read-only memory. This technique can also be combined with parity.

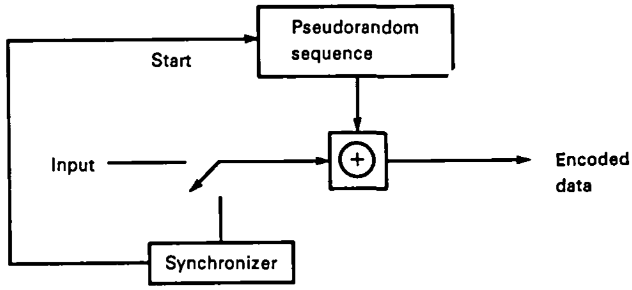

Figure 6–16.—Pseudorandom noise-modulated NRZ—L encoder.

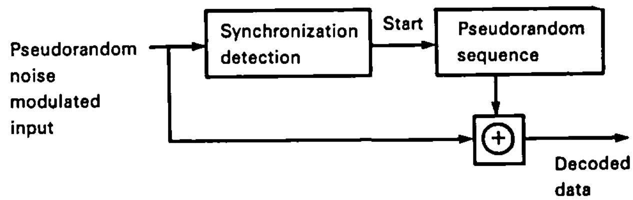

Figure 6–17.—Pseudorandom noise-modulated NRZ—L decoder.

This technique does not have error multiplication and can detect clock slips using the synchronization detection circuitry (of course, all other systems with synchronization words can also do this). This technique has the disadvantage (for serial HDDR) that synchronization words must be inserted, thus reducing the data bit packing density. This also requires the generation of new clock frequencies to insert the synchronization words without deleting data and to remove the synchronization words at the decoder output. A synchronizaton detector is also required. This technique is normally used only for parallel HDDR because synchronization words are required for deskewing, and these same words can also be used for data synchronization. Therefore, no extra overhead is required for parallel HDDR. In general, the properties of this code are similar to those of the self-synchronizing R-NRZ-L code. One other difference is that long runs without a transition are generated whenever the input data sequence is the same as or the complement of the pseudorandom sequence. Therefore, the probability of generating N bits without a transition is $2^{-(N-1)}$. Also, the desired characteristics of the pseudorandom generator are different from those for self-synchronizing R-NRZ-L, and 15 may not be a good register length for this application (shorter register lengths may work equally well). This code is not recommended for serial HDDR because of the added complexity when compared with the self-synchronizing R-NRZ-L code. However, the pseudorandom NRZ-L modulated code is very competitive for parallel HDDR.

Biϕ-L Properties

The Biϕ-L code (ref. 6–7) is illustrated in figure 6–12. This code can be generated by modulo-2 adding NRZ-L data and a bit rate clock with the rising transition in the middle of the bit period. The symbols for a "1" and a "0" are antipodal, and each symbol has a mean value of "0"; therefore, the Biϕ-L code has no dc content and good bit error rate properties. The main disadvantage of the Biϕ-L code is the large amount of high-frequency energy. (See app. 6–B for spectra.) This limits the maximum recommended bit packing density to approximately 15 kbpi, with recorder/reproducers having a 1-MHz bandwidth at a 60 ips, or, alternatively, limits the maximum recommended bit rate to 90 percent of the recorder/reproducer system bandwidth. The data in figure 6–8 show that Biϕ-L performs better than NRZ-L for reproduce bit rates below 300 kbps at a tape speed of 30 ips. Biϕ-L appears to be the best code whenever the bit rate is less than 60 percent of the recorder/reproducer system bandwidth and is also highly recommended whenever the bit rate is between 60 and 90 percent of the system bandwidth.

DM and M^2 Properties

Delay modulation (DM) and Miller-squared (M^2) were both invented by the Ampex Corp. The DM encoding rule is as follows: transitions occur in the middle of all "1's" and between all "0's" (ref. 6–7). This is illustrated in figure 6–12. The maximum time between transitions is two bit periods, and this maximum occurs only for a 101 sequence. The 101 sequence is required to synchronize the DM decoder properly. The maximum dc content of DM is 1/3 and results from repeated 101 sequences.

The M^2 encoding rule is as follows (ref. 6–10):

(1) The bit stream is broken into three types of sequences:

- (*a*) Any number of consecutive "1's"
- (*b*) Two "0's" separated by either no "1's" or an odd number of ones (00, 010, 01110)
- (*c*) One "0" followed by an even number of "1's" (terminated by a "0" not counted as part of the sequence) (011, 01111)

(2) Types (*a*) and (*b*) sequences are encoded the same as DM

(3) Type (*c*) sequences are encoded the same as DM except the transition corresponding to the final "1" is inhibited.

Each of these sequences has no dc content after encoding, and, therefore, M^2 is a dc-free code. A typical M^2 sequence is shown in figure 6–12. The maximum time between transitions is three bit periods, and synchronization can be achieved by using the transition-free intervals of 2, 2½, or 3 bit periods. Both DM and M^2 require a clock at twice the bit rate to detect the symbols. DM and M^2 have been shown (ref. 6–11) to require approximately 3.2-dB higher SNR than NRZ-L or Biϕ-L to achieve a 10^{-6} BER with non-band-limited signals and additive white gaussian noise. The data in figure 6–8 show that DM required a 6-dB higher SNR than NRZ-L at 16.7 kbpi, a 6.5-dB higher SNR than NRZ-L at 25 kbpi, and a 10-dB higher SNR than NRZ-L at 30 kbpi to achieve a BER of 10^{-6}. This additional degradation is mainly due to three effects: the fast rolloff of the recorder/reproducer frequency response above 500 kHz, the nonconstant group delay of the recorder/reproducer, and the chromatic noise spectrum. All these factors seem to degrade DM more than NRZ-L. However, when the reproduce bit rate was reduced to 200 kbps, DM required a 4-dB lower SNR than NRZ-L for a 10^{-6} BER. The best code at 200 kbps and 30 ips was Biϕ-L, which required a 3.5-dB lower SNR than DM. These values will vary, depending on the recorder/reproducer and bit synchronizer used; the alignment of the recorder/reproducer; and, in some cases, the test pattern used. The performance of M^2 is similar to the performance of DM if a good dc restorer is used for M^2. Figure 6–18 presents eye patterns for R-NRZ-L at 25 kbpi and M^2 at 20 kbpi. The tape speed was 7½ ips, and the test pattern was a 6-bit ramp with each 6-bit word repeated 256 times before the binary value of the word was increased by one. These eye patterns were photographed by applying the raw reproduce bit stream to the vertical input of an oscilloscope and the recovered bit rate clock to the external synchronization input. Even though the R-NRZ-L reproduce bit rate is only 187.5 kbps (200 kbps is the minimum recommended reproduce bit rate) and the R-NRZ-L packing density is 25 percent higher than the M^2 packing density, the R-NRZ-L eye opening is higher and wider than the M^2 eye opening. The R-NRZ-L data quality was also better than the M^2 data quality under these conditions.

The power spectra of NRZ-L, DM, and M^2 are shown in figure 6–19 for pseudorandom data. The total power of all three signals is the same and is equal to 0 dB. The spectrum analyzer bandpass filter bandwidth was equal to 1/128 times the bit rate for all three signals. This figure shows that the power spectrum of M^2 is greater than that of DM for frequencies between approximately 4 and 28 percent of the bit rate. M^2 has less energy at frequencies below approximately 4 percent of the bit rate and also has a lower spectral peak at approximately 28 percent of the bit rate. The spectral density of NRZ-L is greater than that of M^2 at frequencies less than 25 percent of the bit rate, but is less than M^2 for most other frequencies (exceptions exist near 60 percent of the bit

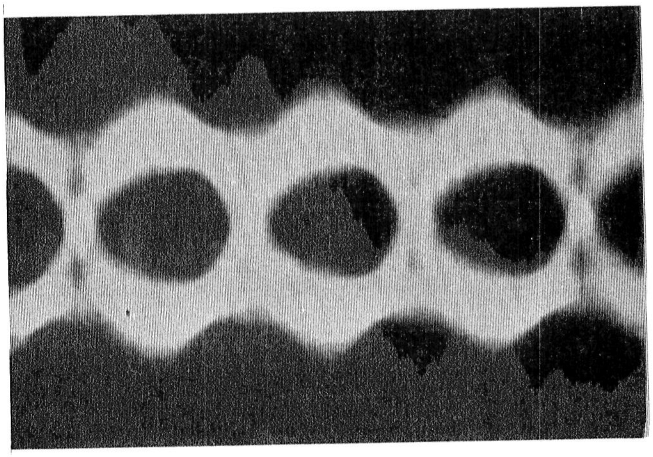

(a)

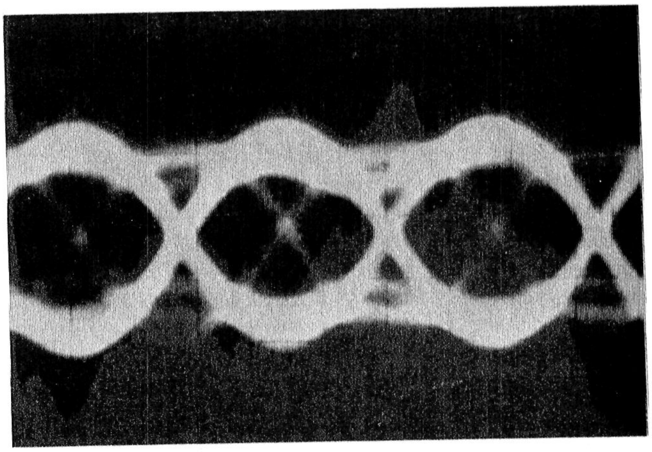

(b)

Figure 6–18.—Eye patterns. (Tape speed: 7½ ips; test pattern: 6-bit ramp with each 6-bit word repeated 256 times). (a) R-NRZ—L at 25 kbpi. (b) M^2 at 20 kpbi.

rate, 140 percent of the bit rate, etc.). It is difficult to relate the power spectrum of a code to performance in a band-limited environment because of other factors such as group delay (phase linearity) sensitivity and criticality of certain frequencies (ref. 6–11). In fact, certain spectrally compact codes may actually require more bandwidth for acceptable error rate performance than codes with "wider" power spectrums (ref. 6–12). Figures 6–20 and 6–21 present the power spectra of pseudorandom NRZ-L and DM data at the output of a recorder/reproducer as well as the noise spectra at the recorder/reproducer output. The bit rate was 1 Mbps at a tape speed of 30 ips. The NRZ-L data were error-free and the DM data had a BER of approximately 5×10^{-6}.

The DM and M^2 codes are not recommended as standard codes for serial HDDR using RCC standard recorder/reproducer systems because (1) Biφ-L performs better than DM and M^2 at bit packing densities below approximately 15 kbpi, (2) R-NRZ-L performs

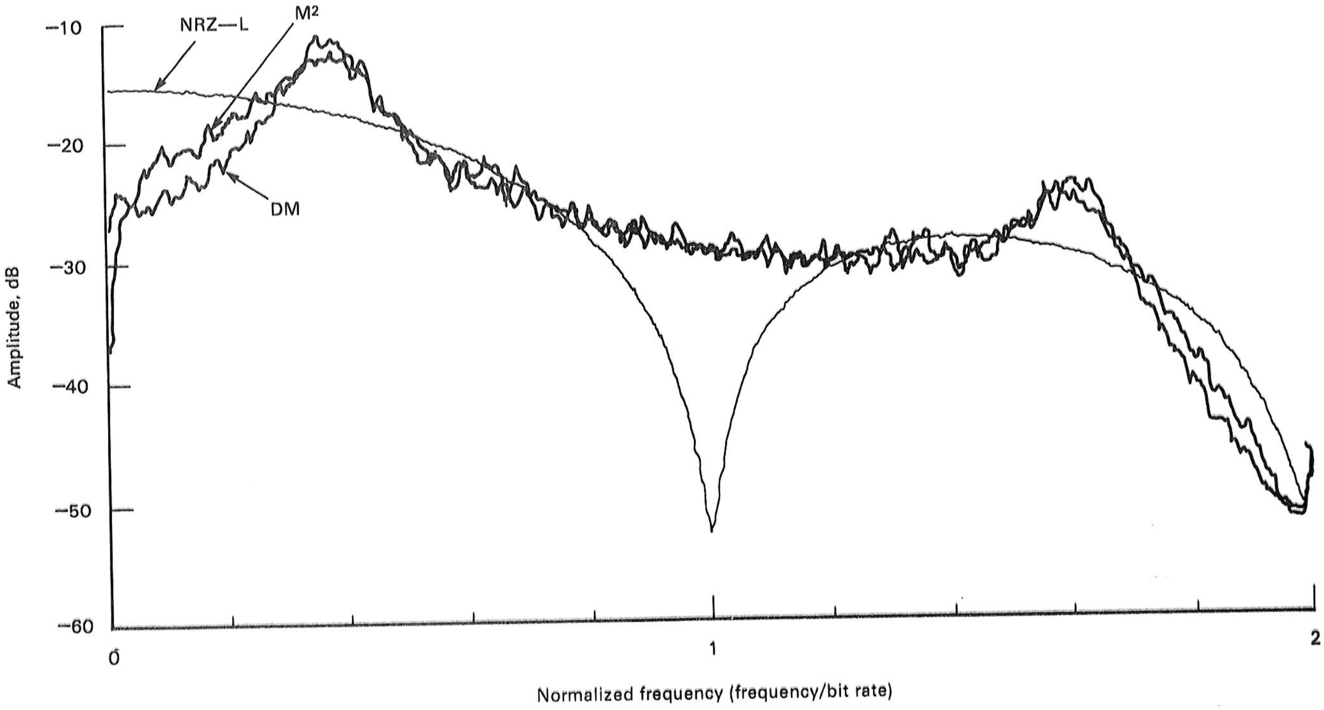

Figure 6–19.—Power spectra of NRZ—L, DM, and M^2 for pseudorandom data.

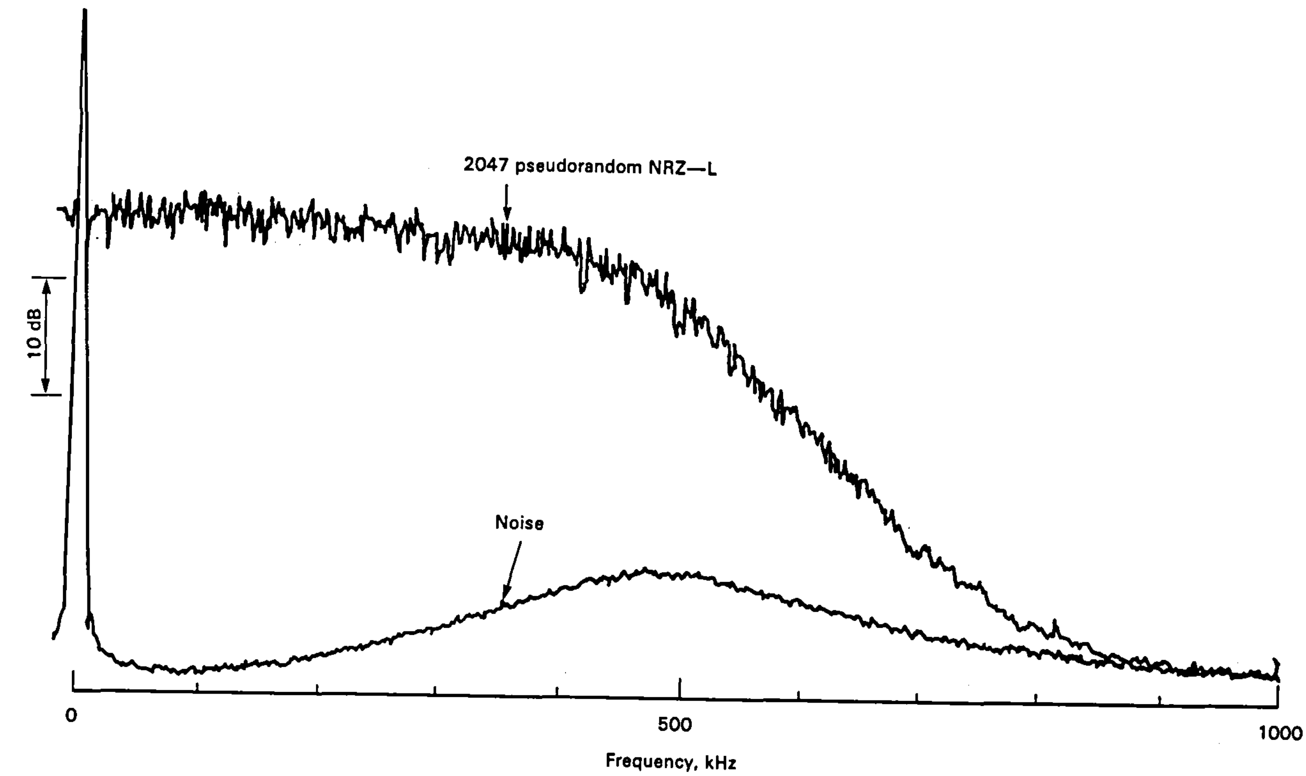

Figure 6–20.—Power spectra of pseudorandum NRZ—L data and noise at the output of a recorder/reproducer. (30 ips; 1 Mbps.)

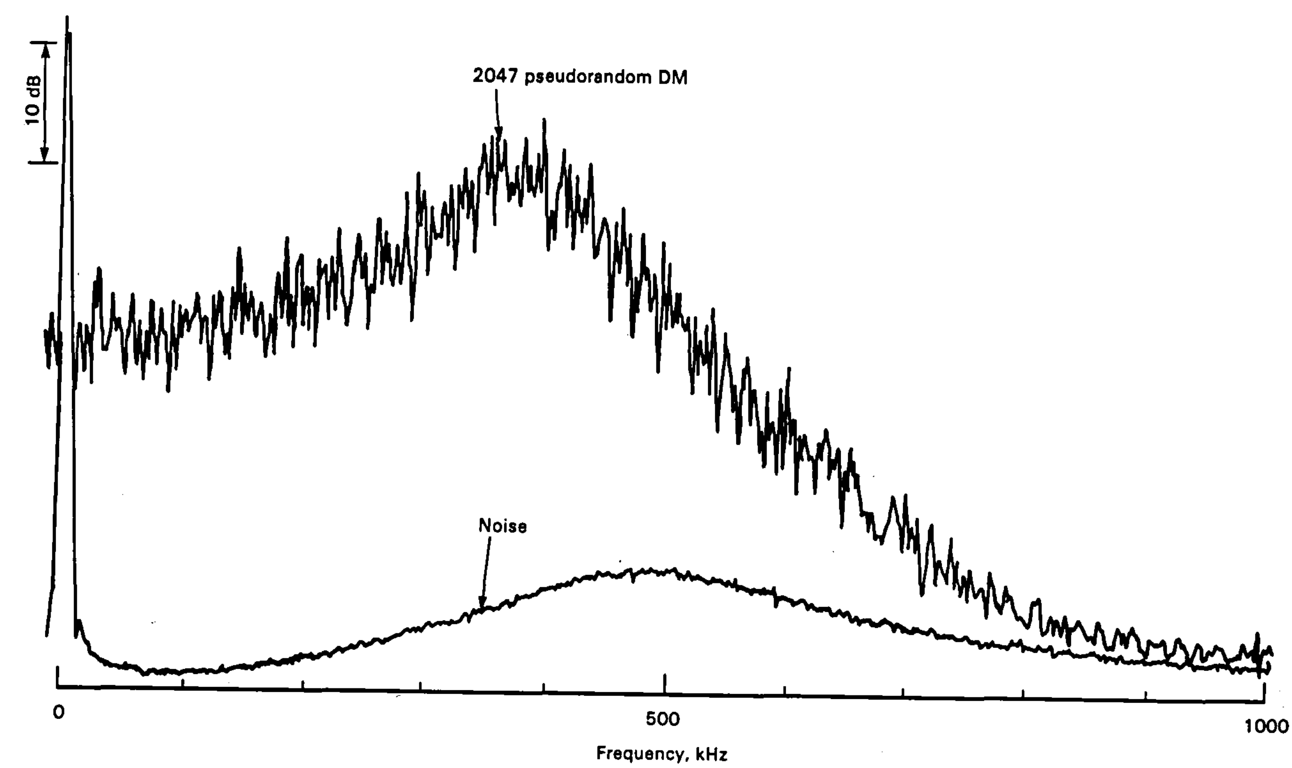

Figure 6–21.—Power spectra of pseudorandom DM data and noise at the output of a recorder/reproducer. (30 ips; 1 Mbps.)

better at bit packing densities above 15 kbpi when the reproduce tape speed is 15 ips or faster. DM or M^2 may be the best code at playback tape speeds of 7½ ips or lower and bit packing densities between 15 and 20 kbpi unless an excellent dc restorer is available for R-NRZ-L. However, the required wideband SNR is greater than 15 dB for these cases.

Other Codes

Many other codes have been proposed for use in HDDR systems. Some of these codes are the Hedeman codes (refs. 6–11 and 6–13; H-1, H-2, and H-3), the 3PM code (ref. 6–14) and the Quadra-Phase code (ref. 6–15). These codes were not included in this study and are mentioned only as additional information for the interested reader.

IRIG SERIAL HDDR STANDARD

One of the major objectives of this study was to develop a serial HDDR standard for inclusion in the *Telemetry Standards* (RCC Document 106–80 (ref. 6–7)). This serial HDDR standard had to be compatible with current RCC wideband recorder/reproducers and also had to provide reliable high-quality data (BER of 10^{-6} or better) when tapes were exchanged between organizations. These guidelines led to the serial HDDR standard that is contained in the 1980 edition of the *Telemetry Standards.* The recorder/reproducer is set up to normal IRIG parameters (bias, bandwidth, etc.), and the nominal record level is 1 V_{RMS}. The recommended codes are Biϕ-L for bit packing densities up to 15 kbpi and R-NRZ-L for bit packing densities up to 25 kbpi. These bit packing densities are for recorder/reproducers that have a 1-MHz bandwidth at 60 ips. A further restriction on R-NRZ-L is that the reproduced bit rate must be at least 200 kbps. The complete standard is contained in reference 6–7. The codes were selected based on the results contained in references 6–1 to 6–3 and 6–16. It was determined that if good performance was to be achieved in an operational environment without excessive "tweaking," the technique selected must provide a BER of 10^{-6} at a wideband SNR of 15 dB or less. This value was based on test results with various combinations of recorder/reproducers, codes, and tapes. The data presented in figure 6–9 give the following bit packing densities at 15-dB SNR (10^{-6} BER): NRZ-L, 26.5 kbpi, Biϕ-L 15 kbpi, and DM 15 kbpi. The bit packing density for R-NRZ-L is approximately 94 percent of the NRZ-L value (0.5-dB SNR penalty) and is, therefore, approximately 25 kbpi. Because Biϕ-L performs better than DM at all bit packing densities below 15 kbpi, Biϕ-L was selected for the standard instead of DM.

The addition of serial HDDR, 240 ips tape speed, and the new predetection carrier series (2.4 MHz at 240 ips) increases the maximum serial bit rate capability from approximately 1 Mbps (ref. 6–17) to 6 Mbps for R-NRZ-L, 3.6 Mbps for Biϕ-L, and 2.4 Mbps for predetection NRZ-L.

PARALLEL HDDR

Parallel HDDR was not included in this study. The results contained in this chapter may not apply to parallel HDDR systems because many current parallel HDDR systems use nonbias recording and narrow head gaps and trackwidths. Parallel HDDR also requires the addition of synchronization words on each track of data to allow the reproduce electronics to compensate for the effects of tape skew.

ERROR DETECTION AND CORRECTION

Error detection and correction were not included in this study. BER's with 50-mil trackwidths, the maximum recommended bit packing densities, and good quality wideband instrumentation tape were typically 10^{-7} or better. Typical telemetry BER requirements are in the range of 10^{-5} to 10^{-6}. Therefore, no error detection and/or correction is necessary in the recorder/reproducer system to achieve the required data quality. Error detection and correction are required if BER's of better than 10^{-7} are specified. Error detection and correction may be required on systems with higher bit packing densities or narrower trackwidths.

CONCLUSIONS

The conclusions reached after analyzing the information collected during this study are as follows:

(1) The standard RCC conditions for analog recording with bias are also nearly optimum for serial HDDR with bias when a wideband RCC recorder/reproducer is used.

(2) The best codes for serial HDDR when using wideband IRIG analog recorder/reproducers are Biϕ-L and R-NRZ-L. The maximum reliable bit packing density for Biϕ-L is 15 kbpi. The maximum reliable bit packing density for R-NRZ-L is 25 kbpi. The minimum reliable reproduce bit rate for R-NRZ-L is 200 kbps. Fifteen appears to be a good choice of shift register length for the R-NRZ-L randomizer.

(3) BER's of 10^{-6} or better are easily achieved when good quality wide-band instrumentation tape, 50-mil trackwidths, and the maximum recommended bit packing densities are used.

(4) Tape dropouts are the main cause of bit errors in serial HDDR when the standard RCC conditions are

used. The effect of tape dropouts can be minimized by avoiding edge tracks and using "broken-in" (polished) tape.

(5) All the codes studied will provide acceptable results for serial HDDR, but the margin for system degradation will not be as large as the margin for the two recommended codes. Therefore, adding additional codes to the serial HDDR standard will merely increase the cost and complexity of the recorder/reproducer and associated electronics without supplying any significant advantages.

(6) The codes selected for serial HDDR use on wideband RCC analog recorder/reproducers are not necessarily the best codes for use in parallel HDDR systems or non-RCC systems.

RECOMMENDATIONS

(1) The recommended codes for serial high-density digital recording with RCC analog recorder/reproducers are Biϕ-L and R-NRZ-L.

(2) The maximum recommended bit packing densities are 15 kbpi for Biϕ-L and 25 kbpi for R-NRZ-L.

(3) The minimum recommended reproduce bit rate with R-NRZ-L is 200 kbps. Bit synchronizers used for recovering R-NRZ-L data should contain dc restoration circuitry.

(4) Critical data should be recorded on the center tracks of the recorder/reproducer to minimize the effects of tape dropouts.

ACKNOWLEDGMENT

The author wishes to express his gratitude to the following individuals and groups, who made important contributions to this study. D. A. King (now with Cooper Medical Devices Corp., San Leandro, Calif.), was in charge of the study during its early phases. He designed and conducted the early laboratory experiments, and his diligent, dedicated efforts were critical to this study. D. H. Rilling designed the special test circuitry that was needed during the study and also participated in the testing. F. R. Hartzler and D. R. Hust provided technical assistance in the area of recorder/reproducers. G. H. Schulze (formerly Bell & Howell, currently Ampex Corp.) provided many constructive comments on the measurement techniques used and on the presentation of results. Ampex Corp. and EMR Telemetry provided hardware for the evaluation of coding techniques. The members of the Recorder/Reproducer Committee of the Telemetry Group of the Range Commanders Council and the members of the Instrumentation Tape Standards Committee (X3B6) of the American National Standards Institute provided many valuable suggestions during the course of this study.

REFERENCES

6-1. King, D. A.: "Comparison of PCM Codes for Direct Recording." Vol. XII, *Int. Telemetering Conf. Proc.*, Instrum. Soc. Amer., Pittsburgh, 1976, pp. 526-540.

6-2. Law, E. L.: "Experimental Comparison of Pulse Code Modulation Codes for Magnetic Recording." Vol. XIII, *Int. Telemetering Conf. Proc.*, Instrum. Soc. Amer., Pittsburgh, 1977, pp. 239-250.

6-3. Law, E. L.; and Hedeman, W. R., Jr.: *Optimum Digital Data Storage on Magnetic Tape.* TP-80-03, Pacific Missile Test Center, Dec. 1979.

6-4. Spitzer, C. F.; Jensen, T. A.; and Utschig, J. M.: *Study, Tests, and Evaluation for Wideband High-Density Data Acquisition (WHIDDA).* Final Report (Wright-Patterson Air Force Base AFAL-TR-76-115), Ampex Corp., Redwood City, CA., Jan. 1977.

6-5. Meeks, Leighton: *Characterization of Instrumentation Tape Signal Dropouts for Appropriate Error Correction Strategies in High Density Digital Recording Systems.* Honeywell, n.d.

6-6. Schoeck, K. O.; and Kobylecky, G. M.: "Correlation of Tape Dropouts With Data Quality." Vol. XV, *Int. Telemetering Conf. Proc.*, Instrum. Soc. Amer., Pittsburgh, 1979, pp. 101-106.

6-7. Secretariat, Range Commanders Council. *Telemetry Standards.* IRIG 106-80, White Sands Missile Range, N. Mex., Sept. 1980.

6-8. Davidson, M.; Haase, S. F.; Machamer, J. L.; and Wallman, L. H.: "High Density Magnetic Recording Using Digital Block Codes of Low Disparity." *IEEE Trans. Magn.* **12:** 584-586, Sept. 1976.

6-9. Severt, R. H.: "Encoding Schemes Support High Density Digital Data Recording." *Computer Design,* pp. 181-190, May 1980.

6-10. Felix, M.: *Definition of Miller Squared Code.* Doc. No. X3B6/214, American National Standards Institute, Jan. 12, 1977.

6-11. Costello, D. J.; Peach, L. C.; LoCicero, J. L.; and Wright, C. D.: *An Evaluation of Hedeman H-2 and H-3 Codes for Data Transmission and High Density Digital Recording.* Final Report (Project E6444), Illinois Institute of Technology Research Institute, July 1979.

6-12. Pelchat, M. G.; and Geist, J. M.: "Surprising Properties of Two-Level 'Bandwidth Compaction' Codes." *IEEE Trans. Commun.* 23(9): 878-883, Sept. 1975.

6-13. Hedeman, W. R., Jr.: *Baseband Recording of Digital Data.* Document No. X3B6/386, American National Standards Committee, Aug. 10, 1978.

6-14. Jacoby, G. V.: "A New Look-Ahead Code for Increased Data Density." *IEEE Trans. Magn.* **13**(5) 1202-1204, Sept. 1977.

6-15. Bixby, J. A.; and Ketchman, R. A.: *Q. P., An Improved Code for High Density Digital Recording.* Spin Physics, Inc., San Diego, Calif., n.d.

6-16. Law, E. L.: "Serial High Density Digital Recording Using an Analog Magnetic Tape Recorder/Reproducer." Vol. XIV, *Int. Telemetering Conf. Proc.*, Instrum. Soc. Amer., Pittsburgh, 1978, pp. 547-552.

6-17. Inter-range Instrumentation Group: *Telemetry Standards.* IRIG 106-77, Range Commanders Council, White Sands Missile Range, N. Mex., May 1977.

APPENDIX 6-A: TEST METHODS

Magnetic Tape

Sine Wave Test

Record and reproduce a sine wave with a specified wavelength. Detect this sine wave with a full wave rectifier. A dropout is counted if the output level falls below the nominal level by a specified amount for a specified length of time.

PCM Test

Record and reproduce a pseudorandom Biϕ-L stream at a bit packing density of 15 kbpi, or a pseudorandom NRZ-L bit stream at a bit packing density of 25 kbpi. Apply the reproduced bit stream to a PCM bit synchronizer and a bit error detector. (See fig. 6-22.) Measure the total bit errors and clock slips in a specified number of bits.

Analog Tape Recorder/Reproducers

Record and reproduce a Biϕ-L bit stream at a bit packing density of 15 kbpi. Apply the reproduced output to a PCM bit synchronizer and bit error detector. (See fig. 6-22.) Attentuate the input to the recorder until the nominal bit error rate is approximately 10^{-6}. Record the difference (in decibels) between the nominal record level (1 V_{RMS}) and the input level for 10^{-6} BER.

Repeat steps in preceding paragraph for 25 kbpi R-NRZ-L and 200 kbps R-NRZ-L. (If an R-NRZ-L encoder/decoder is not available, a 2047-bit pseudorandom NRZ-L sequence at a BER of 3.3×10^{-7} can be used instead of R-NRZ-L.) **NOTE:** The results of this test are a function of the PCM bit synchronizer and magnetic tape used as well as the recorder/reproducer.

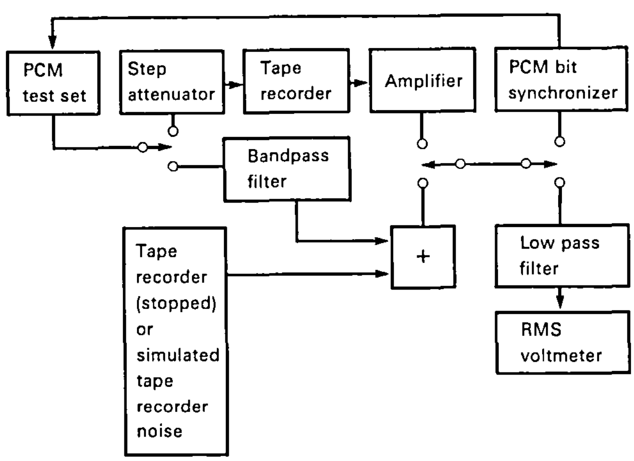

Figure 6-22.—Test configuration.

PCM Bit Synchronizers

With recorder/reproducer—See preceding section entitled "Analog Tape Recorder/Reproducers."

With simulated recorder/reproducer—Simulate a recorder/reproducer by using a linear phase bandpass filter plus spectrally conditioned gaussian noise. (See fig. 6-22.) The spectrally conditioned noise can be simulated using a white noise source plus a simple resistance-inductance-capacitance filter network or by using the output of a recorder/reproducer in the stopped mode. The step attenuator is varied until the BER is 10^{-6} for each bit rate and code to be tested. The minimum test rates and codes are as follows: (1) 15 kbpi, Biϕ-L, (2) 25 kbpi, R-NRZ-L, (3) 200 kbps, R-NRZ-L. The wide-band SNR is measured with a low pass filter set to the tape recorder upper band edge frequency and a true RMS voltmeter. The wide-band SNR for a 10^{-6} BER should be less than 15 dB for the three combinations of bit rates and codes.

APPENDIX 6-B: PLOTS OF POWER SPECTRA OF PCM CODES

The spectra in figures 6-23 through 6-40 were measured using an EMR 1510 spectrum analyzer. This spectrum analyzer performs a 1024-point discrete Fourier transform on the input data. A rectangular weighting window was used, and the plots are the result of averaging 256 spectra. The total power in the PCM bit sequence is equal to 0 dB for all figures. The equivalent noise power bandwidth of the spectrum analyzer was equal to 1/250 times the maximum frequency listed on each plot.

The spectra of two different bit sequences are presented. Figures 6-23 through 6-26 and 6-32 through 6-35 present spectra for 2047-bit pseudorandom sequences. Figures 6-27 through 6-31 and 6-36 through 6-40 present spectra for a repeated 6-bit ramp with each 6-bit word repeated 64 times before the value of the word is incremented by one. The spectra for R-NRZ-L with the repeated 6-bit ramp (figs. 6-28 and 6-37) are essentially identical to the NRZ-L spectra with the pseudorandom sequence (figs. 6-23 and 6-32, respectively.

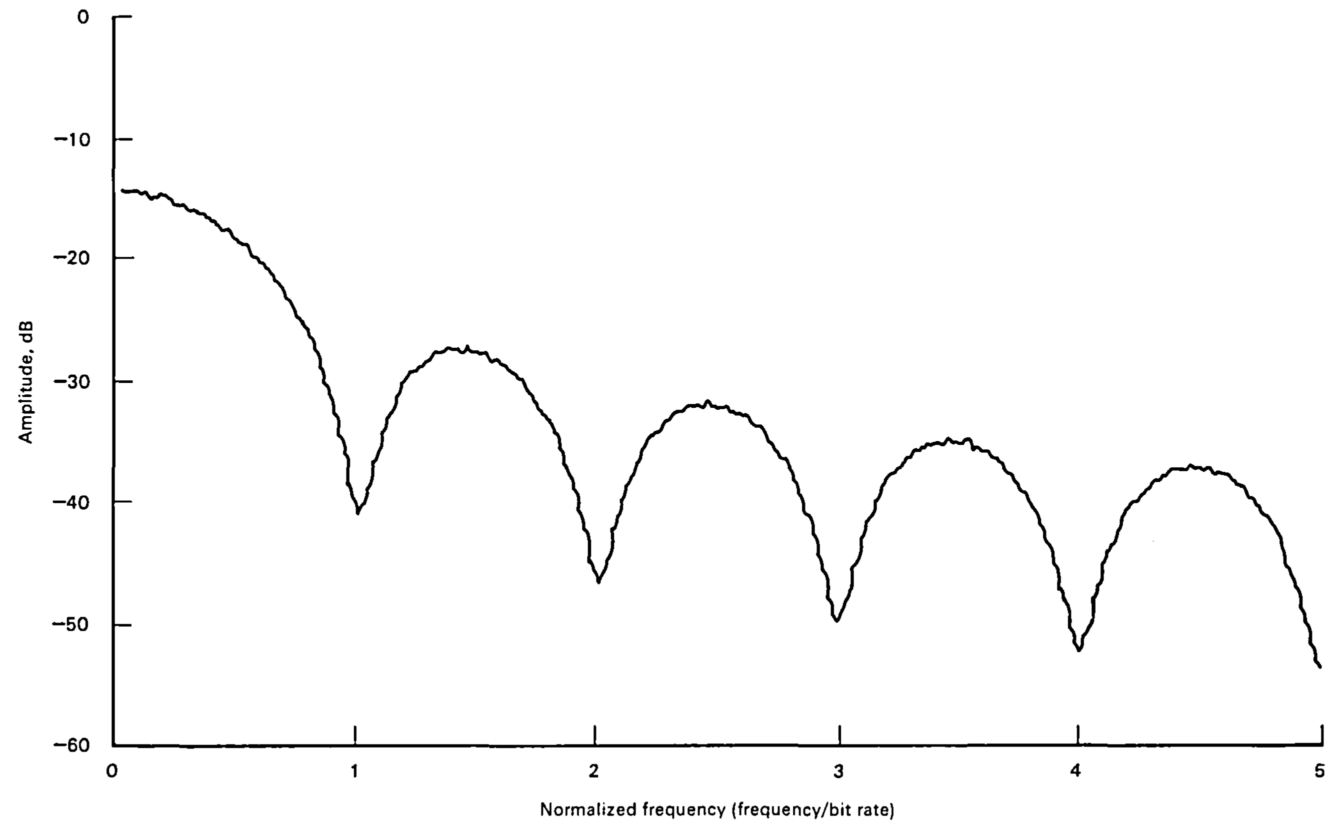

Figure 6-23.—NRZ—L, 2047-bit pseudorandom sequence.

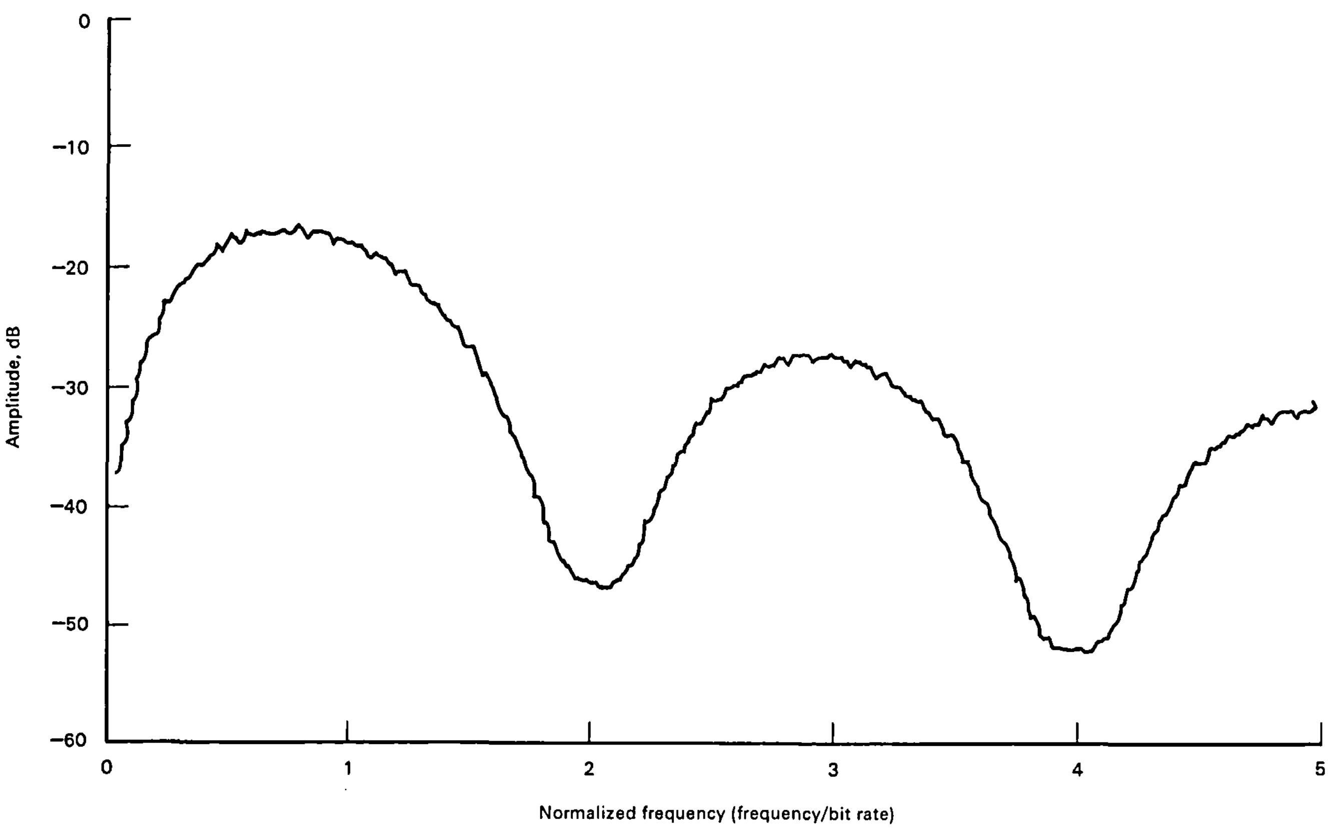

Figure 6-24.—Biϕ—L, 2047-bit pseudorandom sequence.

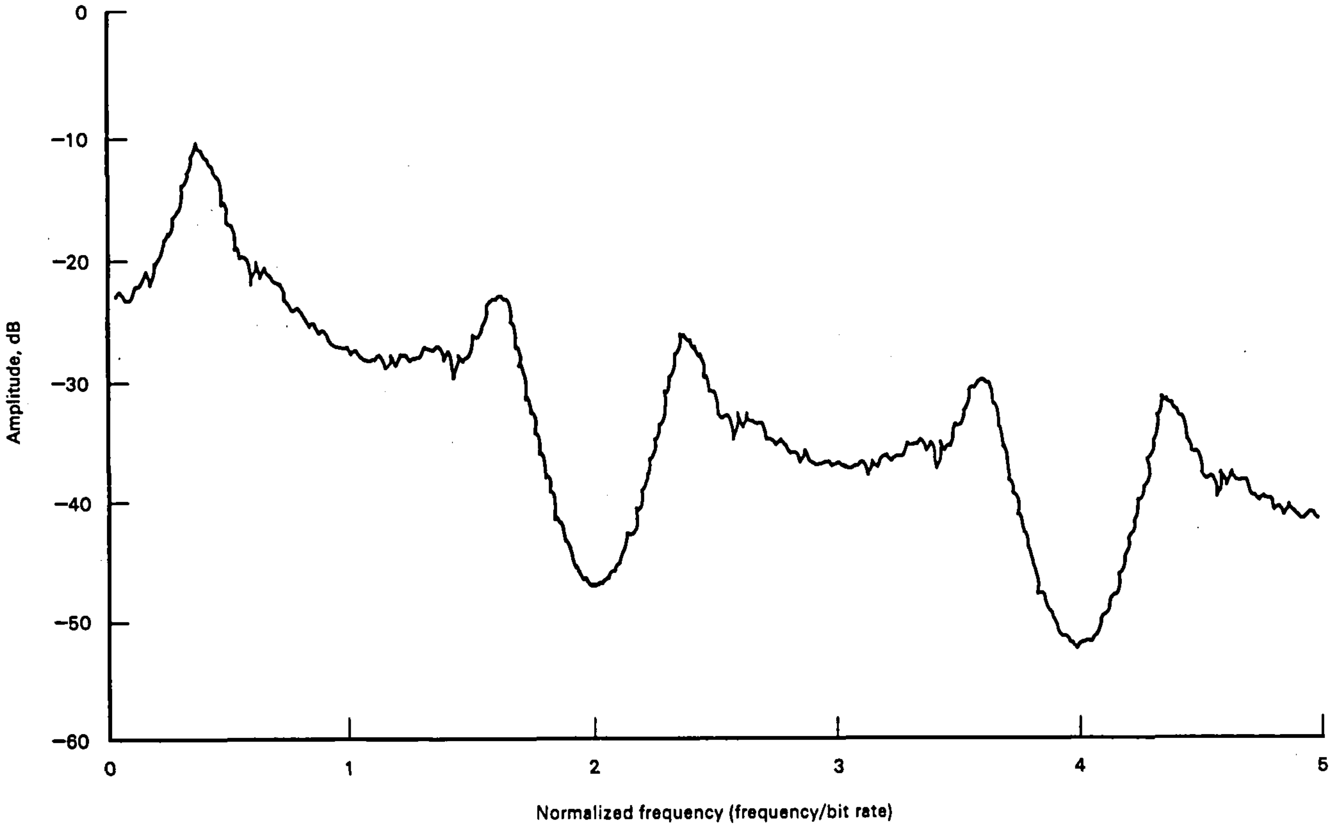

Figure 6–25.—Delay modulation, 2047-bit pseudorandom sequence.

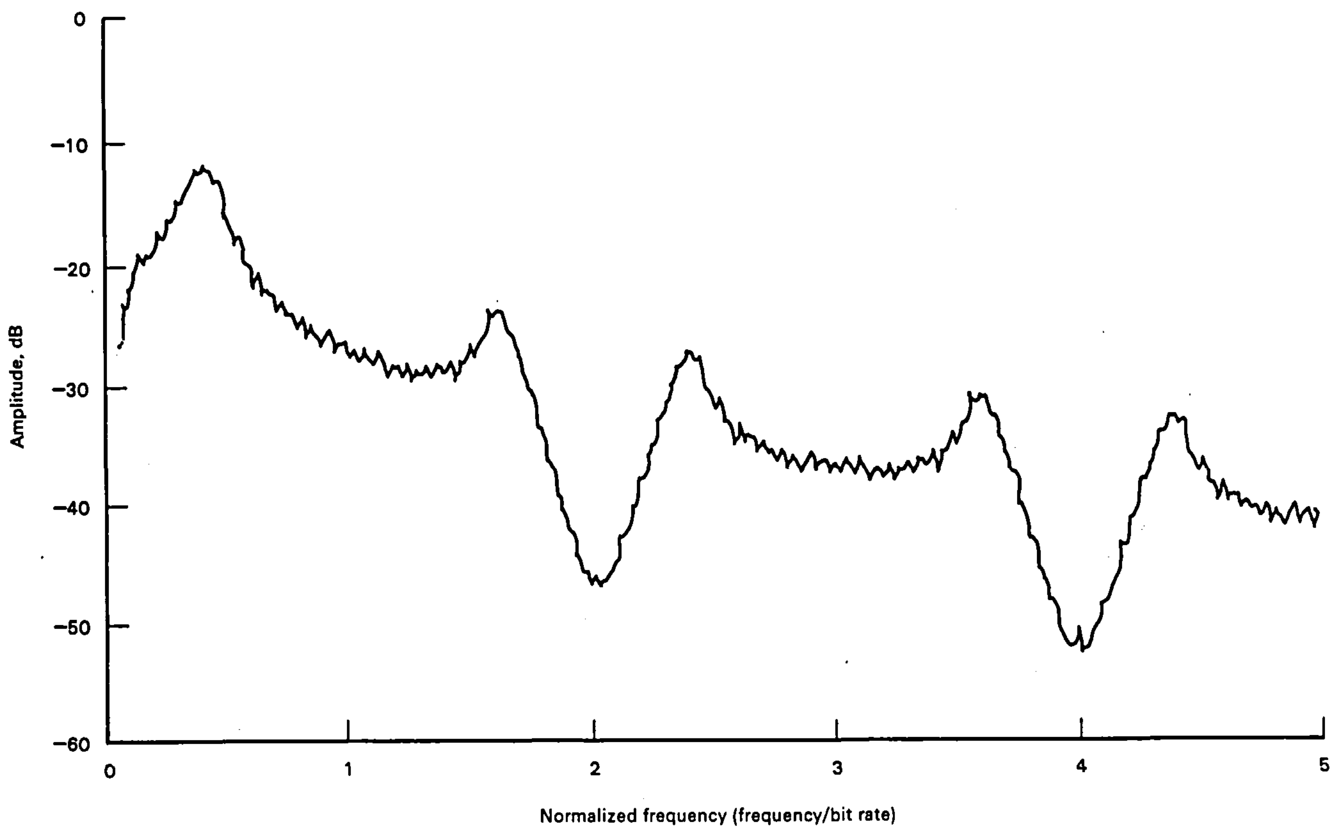

Figure 6–26.—Miller[2], 2047-bit pseudorandom sequence.

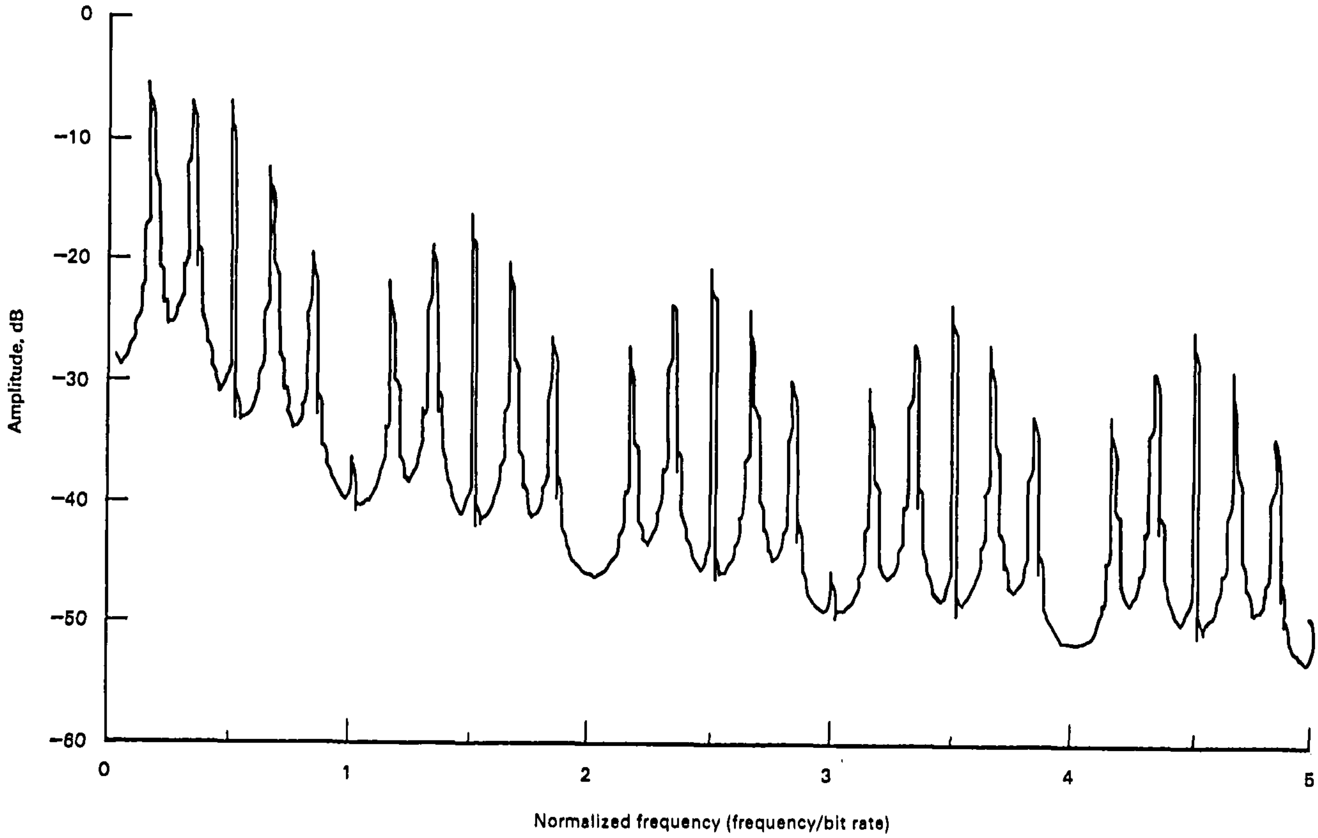

Figure 6-27.—NRZ—L, 6-bit ramp with 64 repetitions of each step.

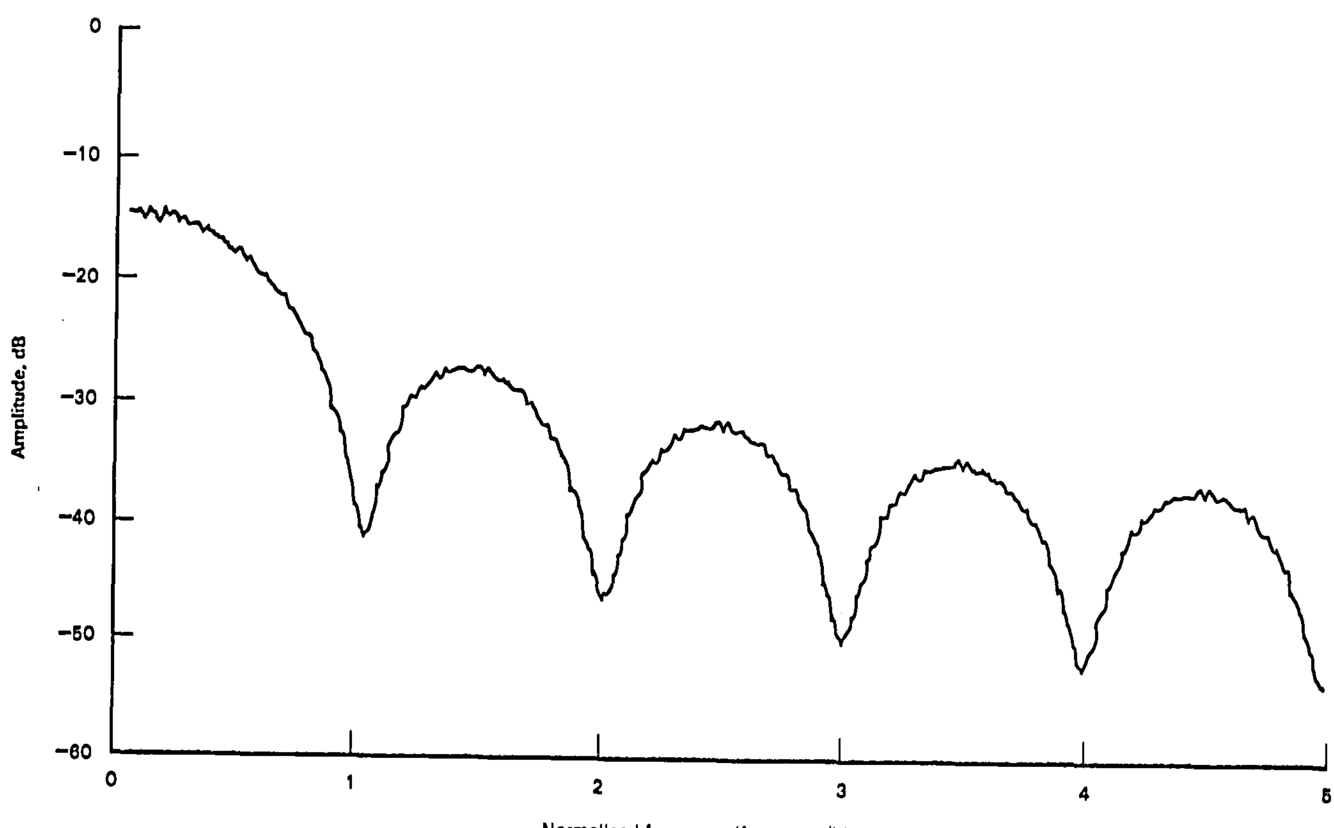

Figure 6-28.—R-NRZ—L, 6-bit ramp with 64 repetitions of each step.

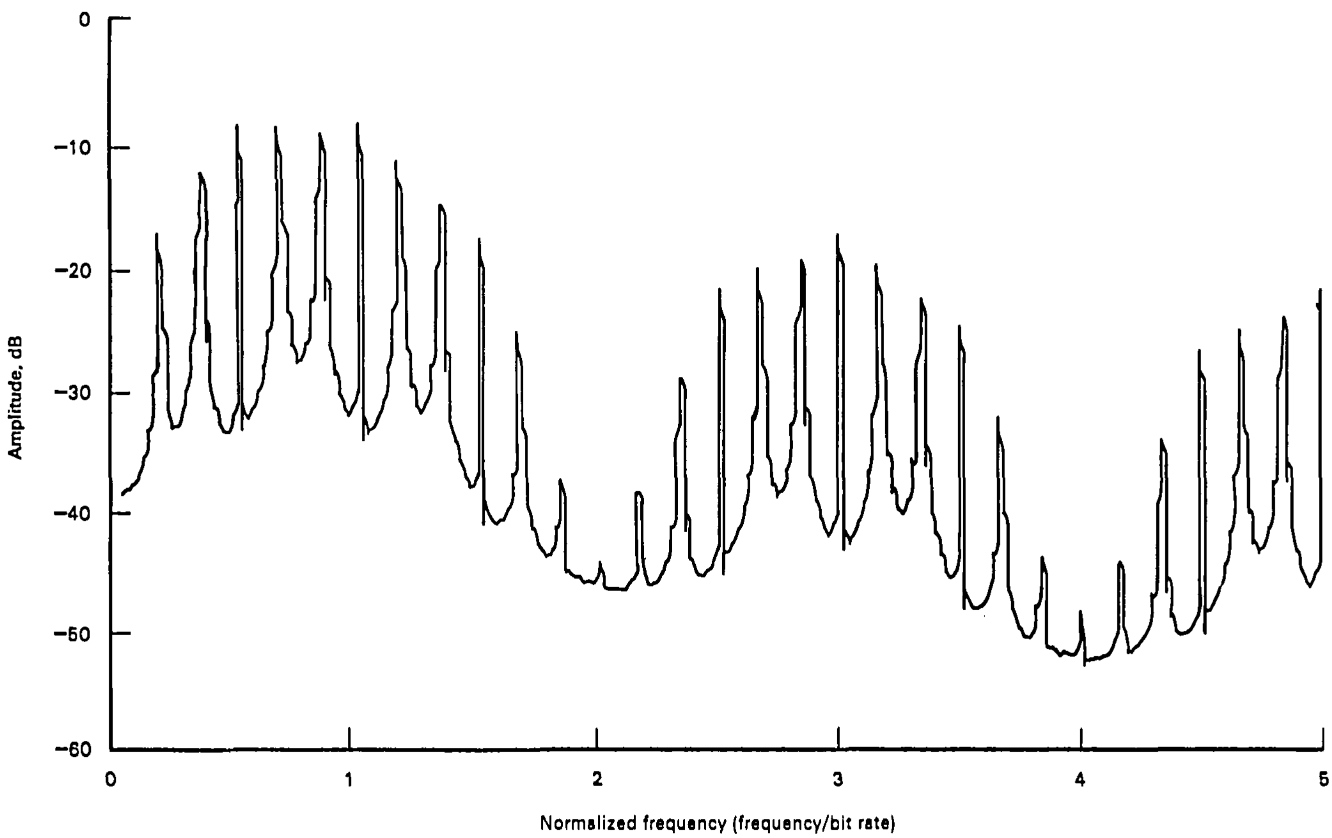

Figure 6–29.—Biφ—L, 6-bit ramp with 64 repetitions of each step.

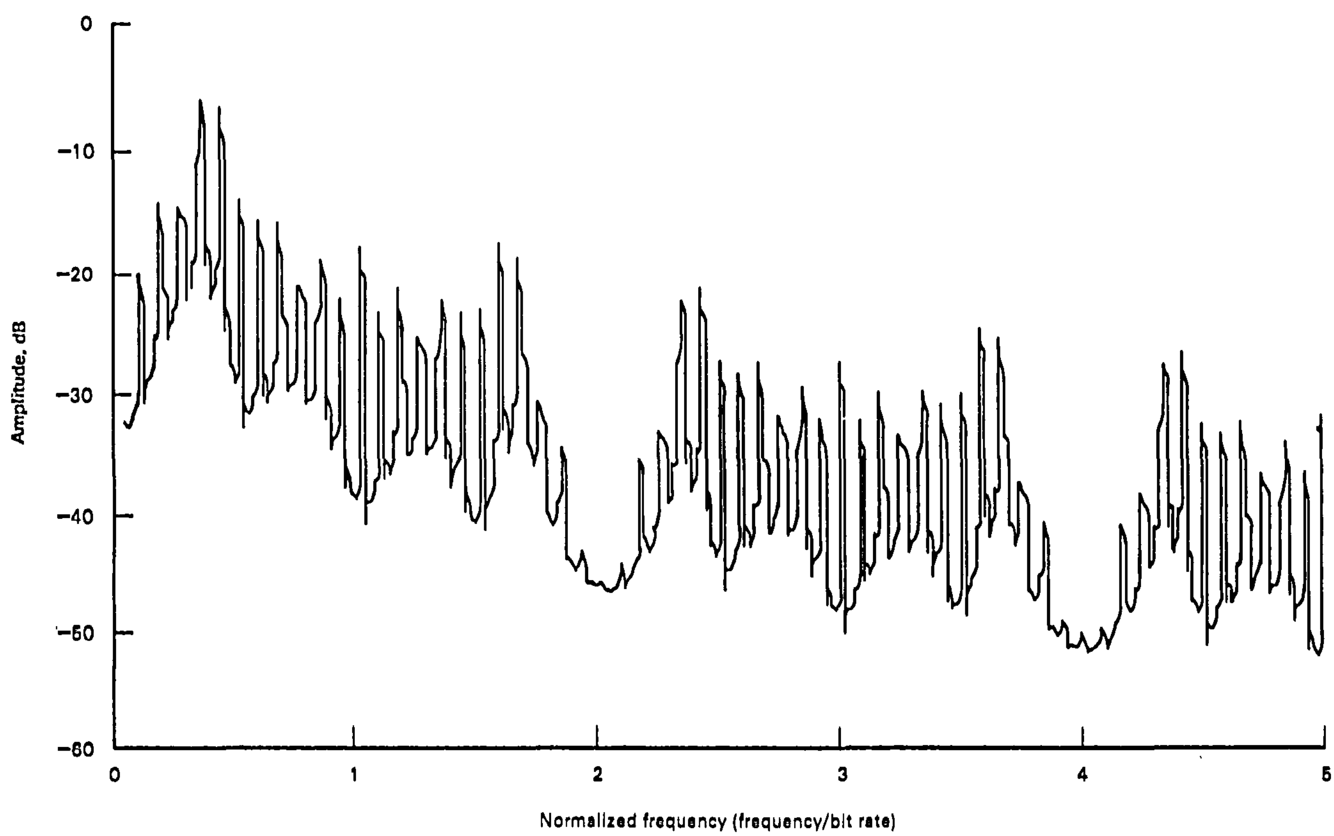

Figure 6–30.—Delay modulation, 6-bit ramp with 64 repetitions of each step.

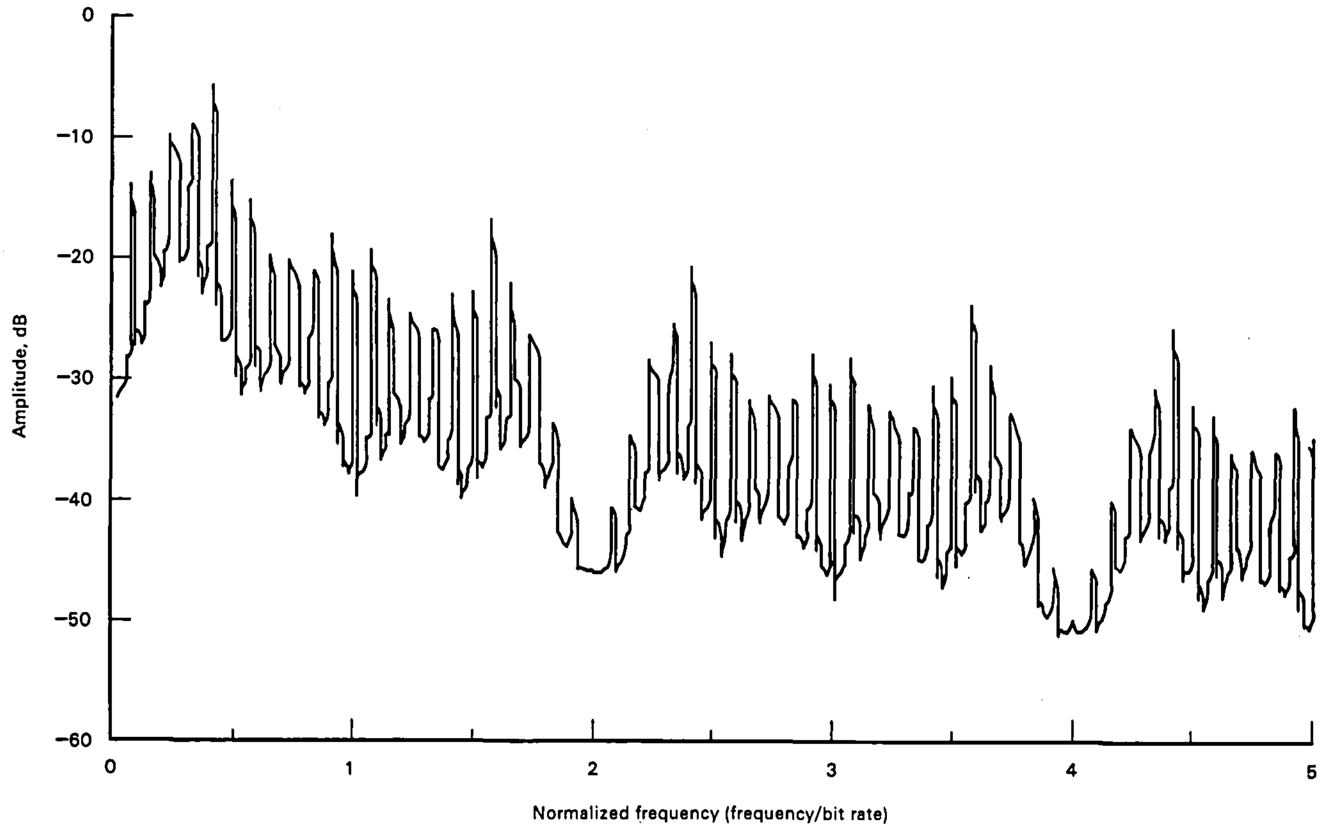

Figure 6–31.—Miller², 6-bit ramp with 64 repetitions of each step.

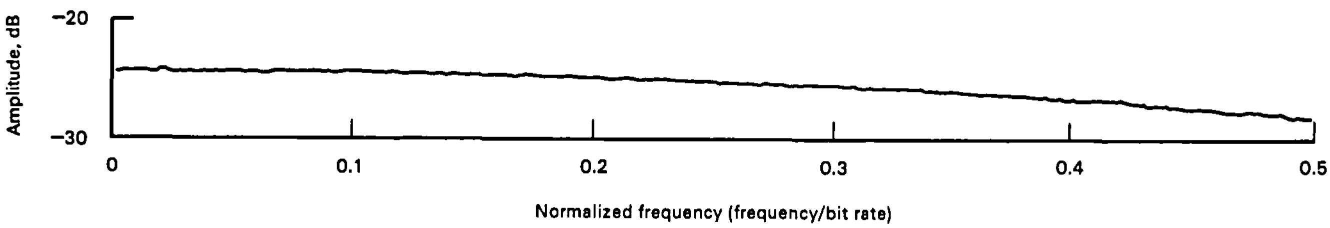

Figure 6–32.—NRZ—L, 2047-bit pseudorandom sequence.

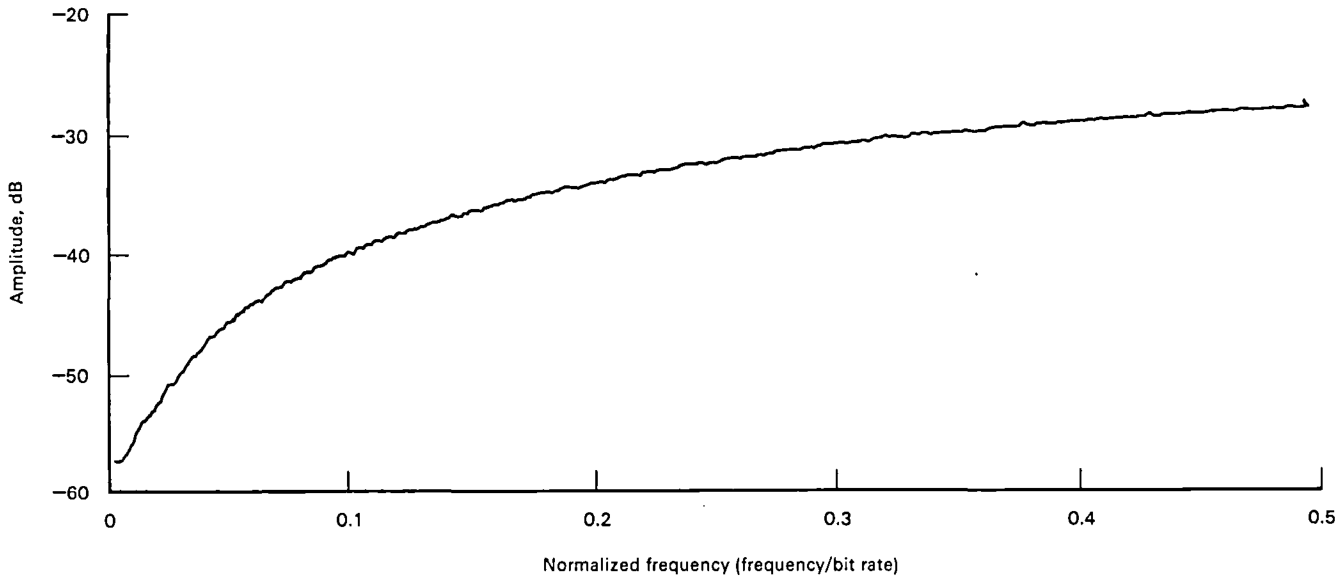

Figure 6–33.—Biϕ—L, 2047-bit pseudorandom sequence.

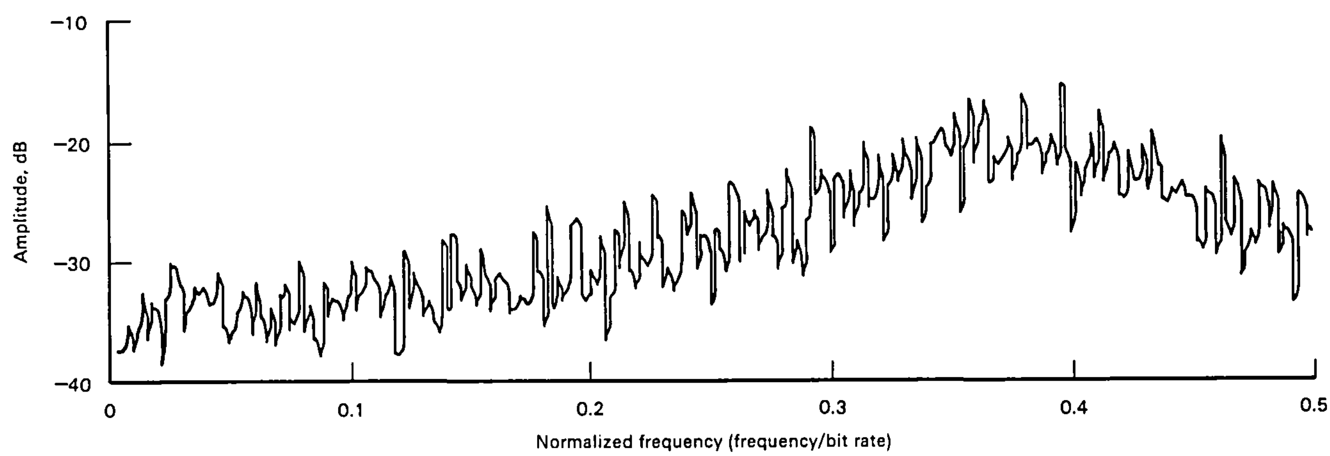

Figure 6–34.—Delay modulation, 2047-bit pseudorandom sequence.

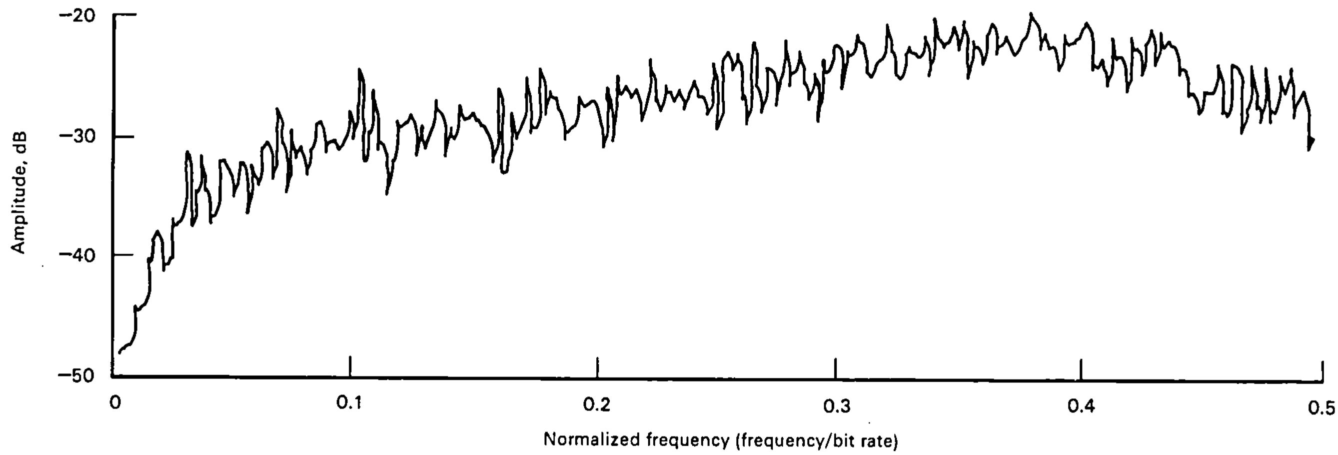

Figure 6–35.—Miller[2], 2047-bit pseudorandom sequence.

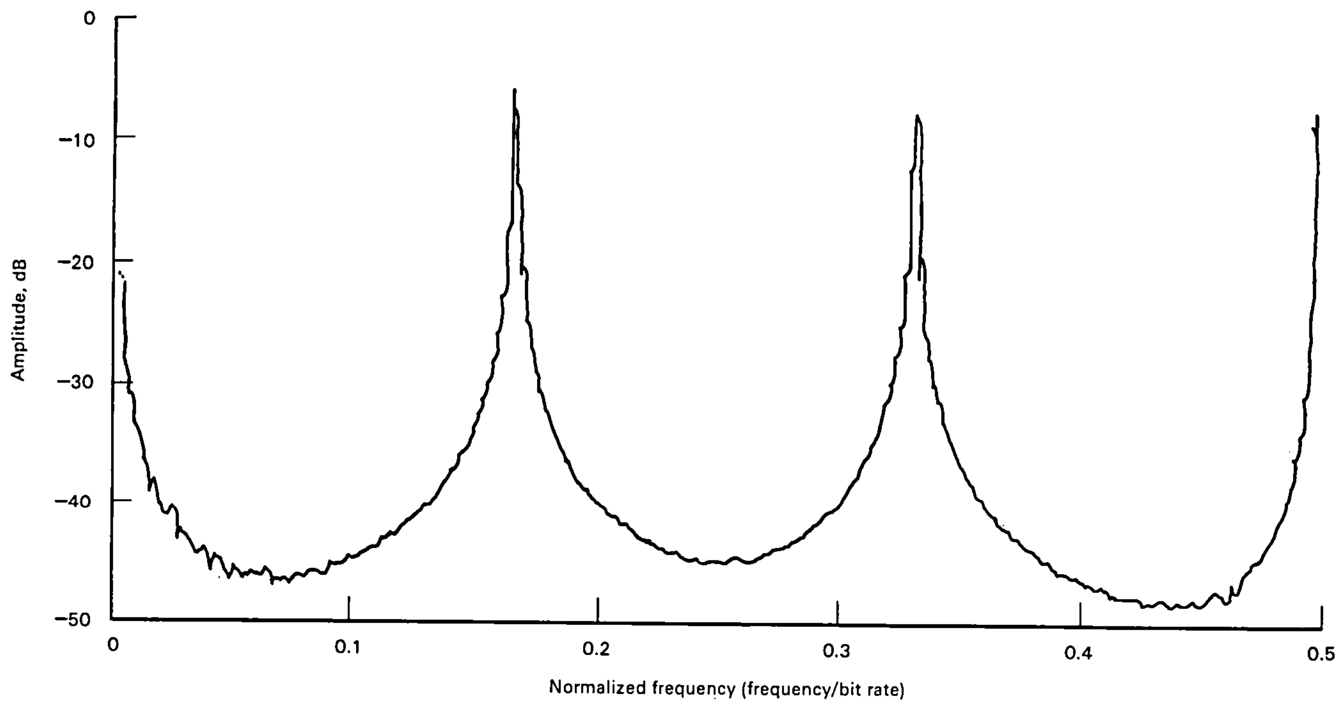

Figure 6–36.—NRZ—L, 6-bit ramp with 64 repetitions of each step.

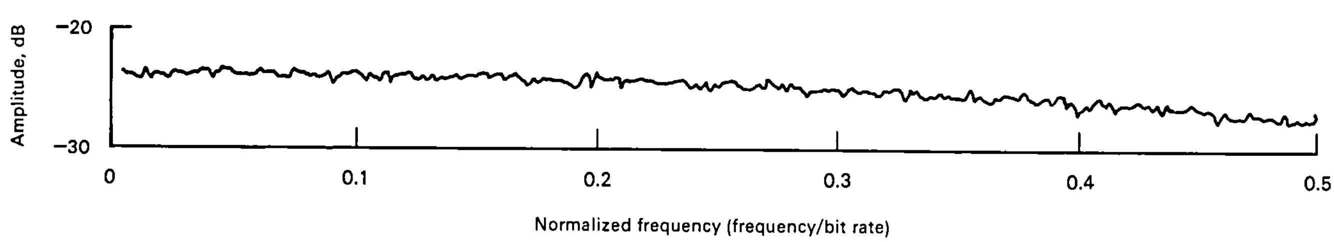

Figure 6–37.—R-NRZ—L, 6-bit ramp with 64 repetitions of each step.

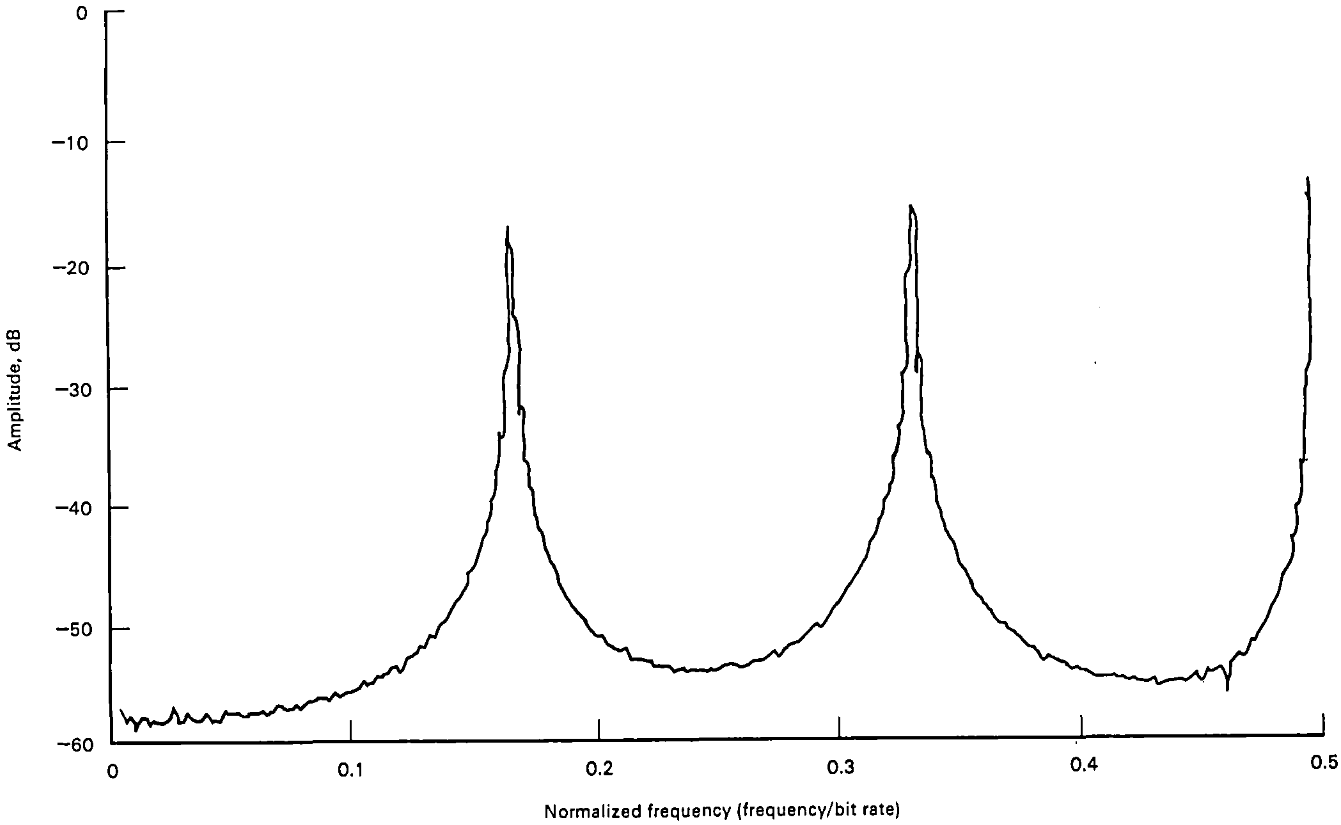

Figure 6–38.—Biϕ—L, 6-bit ramp with 64 repetitions of each step.

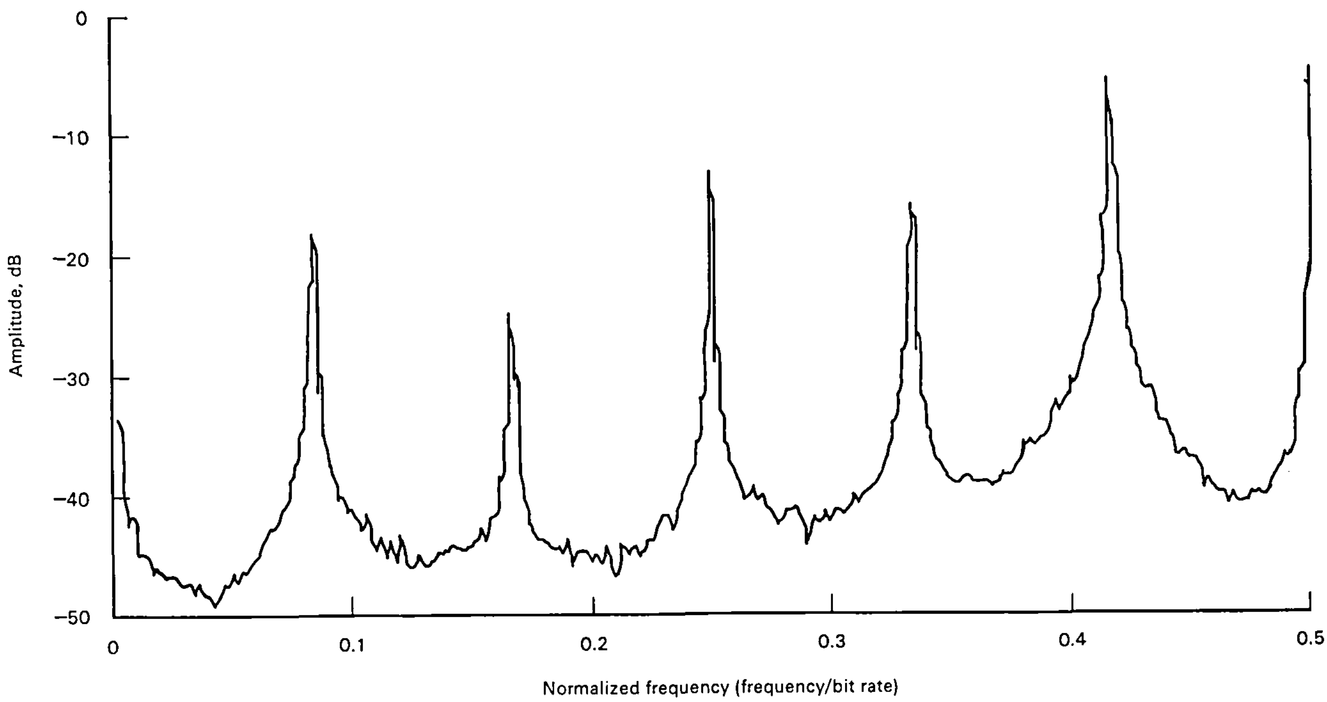

Figure 6–39.—Delay modulation, 6-bit ramp with 64 repetitions of each step.

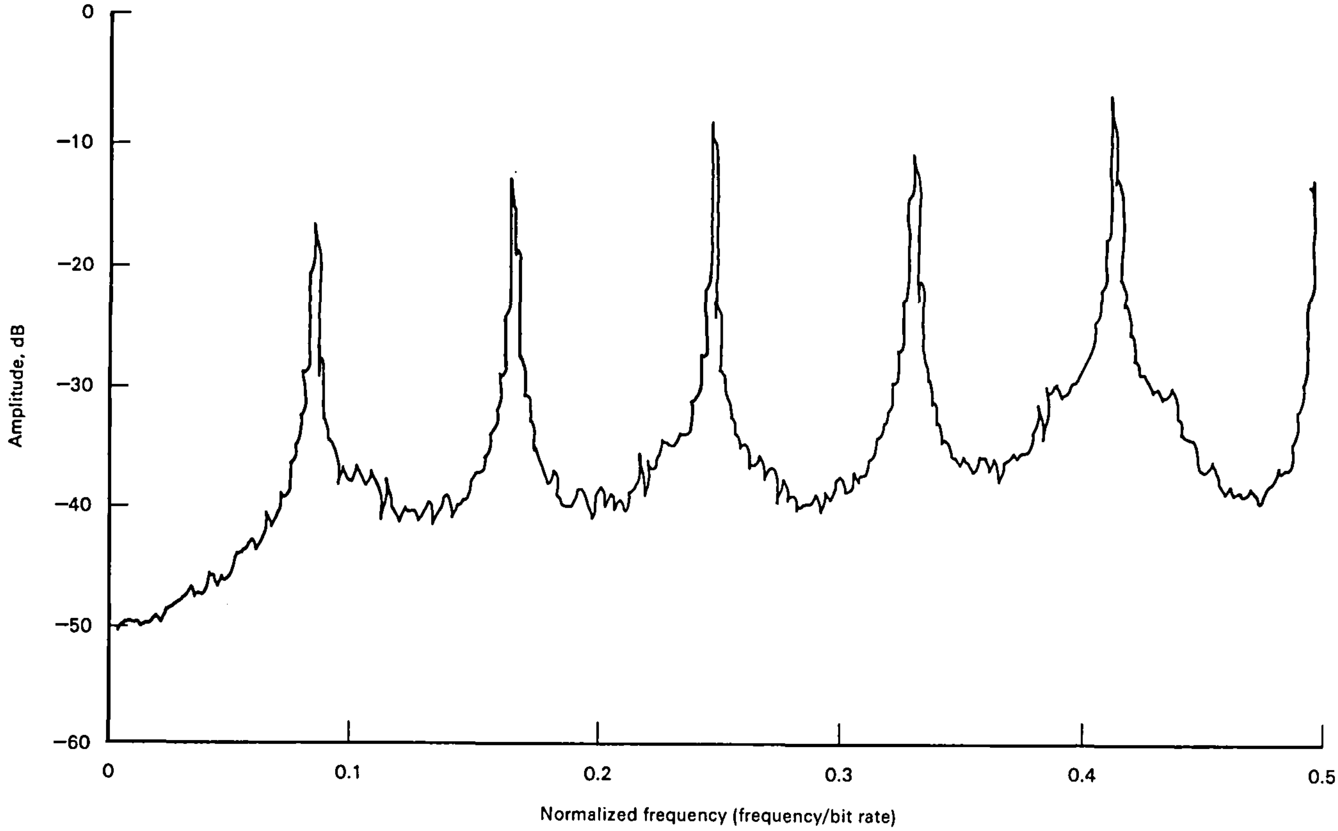

Figure 6–40.—Miller[2], 6-bit ramp with 64 repetitions of each step.

CHAPTER 7

Bit Error Rate Performance of Image Processing Facility High-Density Tape Recorders

Paul Heffner
NASA Goddard Space Flight Center

The Image Processing Facility (IPF) at the NASA Goddard Space Flight Center (GSFC) uses high-density tape recorders (HDTR's) to transfer high-volume image data and ancillary information from one system to another. For ancillary information it is mandatory that very low bit error rates (BER's) accompany the transfers. The facility processes approximately 10^{11} bits of image data per day from many sensors, involving 15 independent processing systems that require the use of HDTR's.

This chapter provides the background, technical approach, and final results of BER modifications. Also included are general discussions of the format of the data recorded by the HDTR, the magnetic tape format, magnetic tape dropout characteristics as experienced in the Image Processing Facility, head life history, and reliability of the HDTR's.

A simplified block diagram of the IPF is shown in figure 7-1. The principal elements within the facility have digital interface media. The front end elements are preprocessors that are designed and dedicated to process unique spacecraft sensor data as they appear on incoming video tapes. The preprocessed image data are transferred by high-density digital tape to an image processor where image framing, radiometric correction, geometric correction, etc., are applied to the data. Processed data are transferred to users via high-density tape, by conversion from high-density tape to computer tapes, and by conversion to film and photoprints.

A key requirement of the 16 HDTR's was that the HDTR record and reproduce a serial bit stream in the range of 500 kbps to 20 Mbps. Coupling image processing systems by a serial telemetrylike bit stream at any rate between these two limits essentially allowed any of the image processing systems to be optimized for throughput without the HDTR being a limiting factor. Only one preprocessor system in the IPF was required to be slowed down because of the 20 Mbps upper limit of the HDTR. The BER specification was 10^{-6}, the state of the art at that time. Martin Marietta developed (under contract awarded after competitive bidding) the serial-in/serial-out electronics that were packaged in the Honeywell Model 96 Wideband II longitudinal recorders.

SERIAL IMAGE PROCESSING FORMAT

The serial format was chosen to conform to the NASA pulse code modulation telemetry standard. The format consists of major frames that contain a given number of minor frames depending on system-driven design constraints, not on HDTR constraints. In all video data processed in the IPF, one image scan line, or one row of an image matrix, corresponds to one major frame. There is a hard requirement that each minor frame contain a 32-bit synchronization code followed by two bytes of minor frame identification. The flexibility of the general format allowed for optimized design of the image processing systems.

There are seven types of major frames:

(1) Preamble
(2) Tape direction
(3) Header
(4) Annotation
(5) Ancillary
(6) Image
(7) Trailer

Image major frames constitute the vast majority of all data on high-density tapes. Preamble major frames do not carry data but serve instead as a pilot tone and as a filler to maintain bit stream continuity. Only one tape directory major frame will appear on a tape, while there may be a header annotation, ancillary, and trailer major frames with each image array on the tape. Mapping information, for example, is carried in the annotation major frame, and geometric correction coefficients are carried in the ancillary major frame.

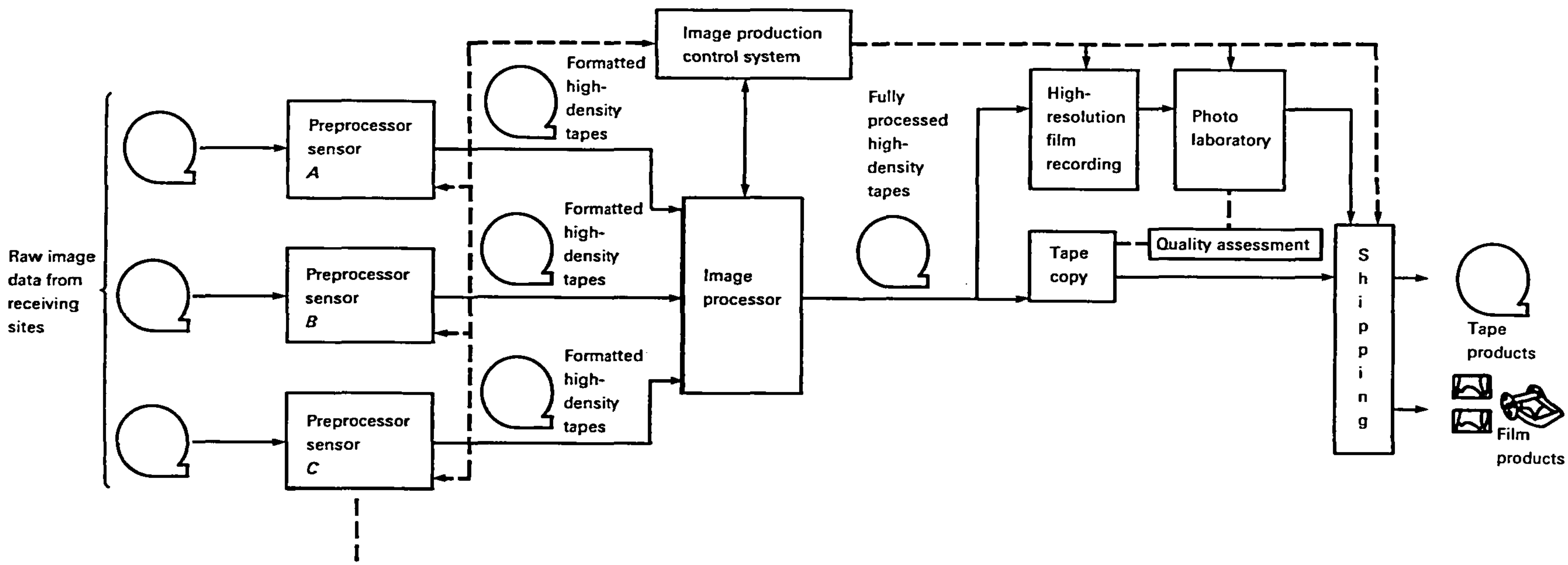

Figure 7–1.—Simplified diagram of key elements within the IPF.

PHYSICAL TAPE FORMAT

The HDTR physical tape format is independent of the format of the incoming serial bit stream. The HDTR does not establish synchronization between the two formats. Only bit synchronization is maintained during record. During playback, the synchronization objective is to maintain integrity of the order of the reconstructed output bits as well as the periodicity of the bit rate.

The physical tape format employs 10 of the 14 available tape channels for data. Each longitudinal channel includes overhead bits for both synchronization and data parity. In discussion of the physical tape format, data implies all bits that stream into the recorder. During playback, the channel synchronization words allow for deskewing the 10 channels of data and reconstruction of the data to serial form. During reconstruction, the parity bits are also removed so that the output data stream is an exact replica of the recorded input data stream, in the absence of bit errors.

Data and overhead bits are packed at 20 000 bits per track inch (25.4 mm) in the nonreturn to zero code. Two Inter-Range Instrumentation Group[1] (IRIG) standard heads are used for record so that each head stack records seven channels interleaved with the other head stack. Each head has a 3.56-mm lateral separation in tracks. A simplified representation of the tape format is given in figure 7-2. (The ECC track was an unused track in the delivered system.) The HDTR individual channel synchronization words are 24 bits in length. Odd parity is inserted after every seven data bits. Each channel has a fixed longitudinal frame length of 504 bits, including the synchronization word and parity bits. As illustrated in the figure, if incoming bit n is being recorded on channel 12, an even head, then bit $n + 1$ is recorded on the odd head stack of channel 11, bit $n + 3$ on channel 10 of the even head, etc. Because of the separation of the two heads, all even head recorded bits will be greatly displaced from the simultaneously recorded odd head bits due to the IRIG standard longitudinal head spacing of 3.81 cm. The two-head configuration is an advantage to error correction implementation and is discussed later in this chapter.

[1]Now the Range Commanders Council.

BIT ERROR RATE PERFORMANCE TESTING

In testing the HDTR's, the IPF uses two types of test instruments. One is a standard commercially available pseudorandom bit generator/receiver using a 2^{15} pseudorandom sequence. Pseudorandom code generators provide a uniform power spectrum and long frame lengths. In many cases, the pseudorandom codes provide a good measure of tape/head performance, but do not measure the end-to-end performance with the power spectrum of the actual data. The other test instrument was specially designed for the IPF by the Bendix Aerospace Corp. It outputs a serial format similar to the serial format used to transfer image data from one system to another and it generates the periodic major/minor frame sequence with the standard IPF frame synchronization pattern, frame type code, etc. It outputs preamble major frames, then a header major frame, followed by a series of image major frames comparable in volume to an image matrix of a typical scene.

Track			24-bit synchronization word					Data bits								Data bits						24-bit synchronization word		
2	ECC	P	1	2	3	23	24	P'	P'	P'	P'	P'	P'	P'	P	P'	P'	P'	P'	P'	P	1	2	3
3	Data	P	1	2	3	23	24	10	20	30	40	50	60	70	P	80	90	.	.	4200	P	1	2	3
4	Data	P	1	.	.	.	24	9	19	29	.	.	.	.	P	.	.	.	.	4199	P	.	.	.
5	Data	P	1	.	.	.	24	8	18	28	.	.	.	.	P	.	.	.	.	4198	P	.	.	.
6	Data	P	1	.	.	.	24	7	17	27	.	.	.	.	P	.	.	.	.	4197	P	.	.	.
7	Data	P	1	.	.	.	24	6	16	26	.	.	.	.	P	.	.	.	.	4196	P	.	.	.
8	Data	P	1	.	.	.	24	5	15	25	.	.	.	.	P	.	.	.	.	4195	P	.	.	.
9	Data	P	1	.	.	.	24	4	14	24	34	.	.	.	P	.	.	.	.	4194	P	.	.	.
10	Data	P	1	.	.	.	24	3	13	23	33	.	.	.	P	73	.	.	.	4193	P	.	.	.
11	Data	P	1	.	.	.	24	2	12	22	32	.	.	.	P	72	.	.	.	4192	P	.	.	.
12	Data	P	1	2	3	23	24	1	11	21	31	41	51	61	P	71	81	.	.	4191	P	1	2	3

Figure 7-2.—Simplified representation of recorded tape format. Head displacement skew not shown; ECC (error correction code) track was unused until later modification of the HDTR for error correction. (P = longitudinal parity; P' = lateral parity.)

The six-bit video words are programmable so that the user can select various six-bit combinations in order to exercise the HDTR with patterns. As a receiver, the unit synchronizes with the playback serial data stream and begins a correlation with each bit, making a cumulative count of all errors. Data rates can vary from 500 kbps to 20 Mbps.

A staircase ramp pattern is most frequently used during pattern testing, although other patterns can be programmed. This ramp pattern consists of 9360 major frames and provides a total of 3×10^8 bits per scene. Embedded in the video portions of the major frame is the ramp pattern, which consists of the six-bit data words. Each word is repeated 56 times per ramp step. The word value starts at 0; on the 57th word the value is stepped to 1, next to 2, and so on to the end of the major frame where the last 56 words have a value of 63. The next major frame repeats this sequence. After the scene of 9360 major frames, there are 200 major frames of preamble, followed by another scene, and so on. Unless otherwise noted, this test pattern was used in all tests discussed in this chapter.

The specially designed pattern generator has been an important asset to the IPF because it exercises the HDTR's with a controlled serial format that so closely resembles actual data transfers.

INITIAL ACCEPTANCE TEST RESULTS

Acceptance testing of the HDTR's occurred after delivery in early 1977. The BER performance met the 10^{-6} specification under all conditions of machine-to-machine compatibility with pattern data and with pseudorandom data over all tape speeds from 3¾ to 120 ips. A plot of the resultant tests appears in figure 7-3. Note that the average BER for all units was just under 1×10^{-7} and that only one test resulted in a BER near the specified limit of 10^{-6}.

PSEUDORANDOM MODULATION MODIFICATION

In 1977, GSFC contracted with Martin Marietta to modify each HDTR with logic that would perform a 2^7 pseudorandom modulation of the data prior to record and to derandomize the reconstructed data during playback. The modification was implemented to minimize the effects of pattern data in record and playback. The BER rate for a given pattern tended to depend on the particular HDTR calibration procedure used. By randomizing the data, there were no tradeoff calibration procedures required. Figure 7–4 shows how randomizing the serial bits was accomplished. Improvement in BER was mildly successful, as shown in figure 7-5. The BER of the test population of the HDTR before and after the modification changed by an approximate factor of 2. This, coupled with the better performance of Ampex 79A tapes over Ampex 787, allowed the IPF to specify HDTR BER performance at 2×10^{-7}.

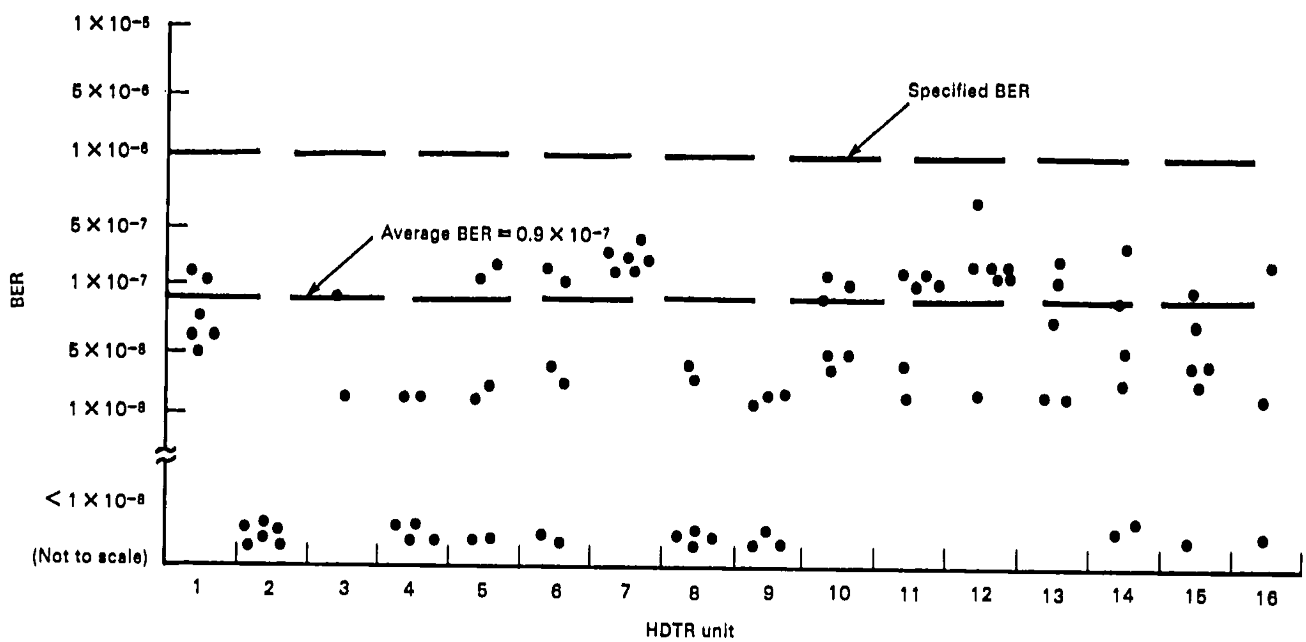

Figure 7–3.—Acceptance test results from original procurement of HDTR's. (Test pattern: ramp; tape: Ampex 787; end of test period: Oct. 1977.)

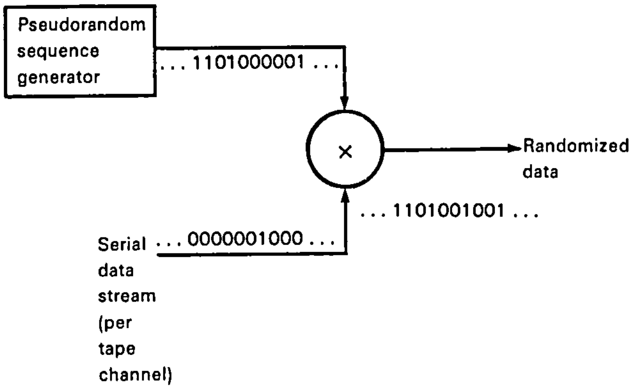

Figure 7–4.—Randomizing the serial data.

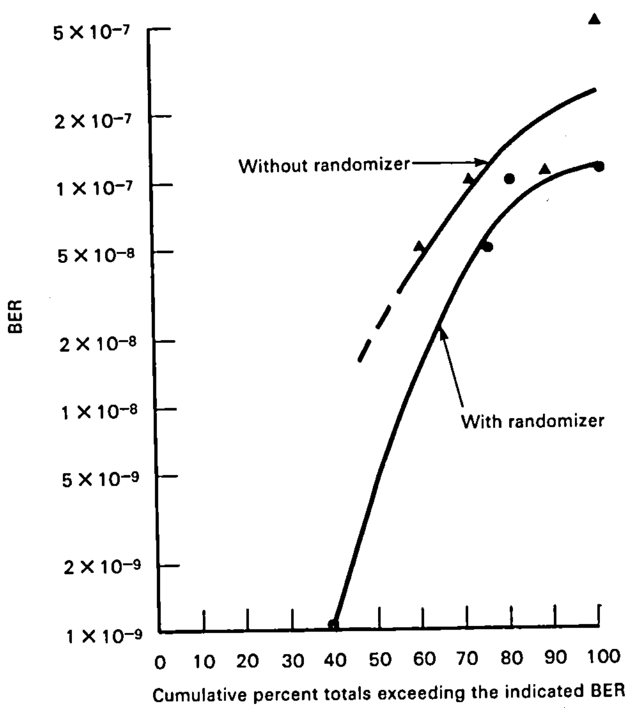

Figure 7–5.—Cumulative BER with and without HDTR randomizer modification. (Test pattern: pseudorandom and ramp; tape: Ampex 79A; end of test period: Feb. 1978.)

ANALYSES OF BIT ERRORS

Of particular concern were the magnetic tapes being used. The original specification for the HDTR's called for the use of conventional 1-in. instrumentation tape as supplied by the General Services Administration (GSA). All acceptance tests were run with the standard at that time, which was Ampex 787 tape. By 1978, GSA was supplying Ampex 79A tape. Both the 787 and 79A tapes were uncertified tapes, subjected only to sampled testing prior to delivery. The cost for certified tapes that were 100 percent tested was prohibitive for voluminous use of tapes in the operational environment; and the certified tape was not specified as a perfect tape.

A sequence of tests was run to ascertain the error profile of repeated playbacks of prerecorded data on GSA-supplied tape. One typical error profile is plotted in figure 7-6. The fact that most of the clustered errors repeated in the same place on tape gave support to the growing belief that bit errors were now primarily tape dependent. It was also learned that the vast majority of all errors were single track errors by observation of individual track parity indicators on the front panel during playback.

Further cluster error data were gathered during the testing of recorded test tapes that were used for compatibility testing with the Department of the Interior, a user of IPF image data. Table 7-1 shows the error data of that testing. The result was that 94 percent of all errors consisted of error clusters greater than 25 bits.

Further characteristics of HDTR and tape performance were sought. There was concern over how many times a recorded tape could be usefully reproduced. The first test was conducted using Ampex 787 tape with a recorded ramp pattern. The tape data was reproduced once every day for 38 days on the same HDTR. The HDTR was not adjusted during that time. Figure 7-7 shows the repeated performance of this test. In late 1978, five Ampex 79A tapes were similarly subjected to 20 repeated runs. Repeatability was similar to that shown in figure 7-7. One tape was repeated 50 times with no sign of degradation, proving that if the tape is handled correctly and the HDTR heads are cleaned properly, then tape wear out is not an operational problem. It was also noted during testing and operational use that rarely, if ever, did the HDTR's lose bit synchronization.

The HDTR and tape performance were well understood. The HDTR's were stable and predictable in performance. Although the tapes met specification, the physical magnetic tape was now known to be the principal limitation in BER performance.

ERROR CORRECTION MODIFICATION

Even though the BER over an entire tape may have been within the 2×10^{-7} BER specification, single track burst errors at times caused the receiving image processing system to lose identity with key ancillary information. At such occurrences the receiving system may have aborted or may have taken a wrong path with the data. Complex system-to-system interface problems were tougher to isolate and characterize when data transfer from the HDTR was questionable.

There was constant effort to improve performance at the interfaces. In 1978, Martin Marietta began experimenting with various techniques of applying error

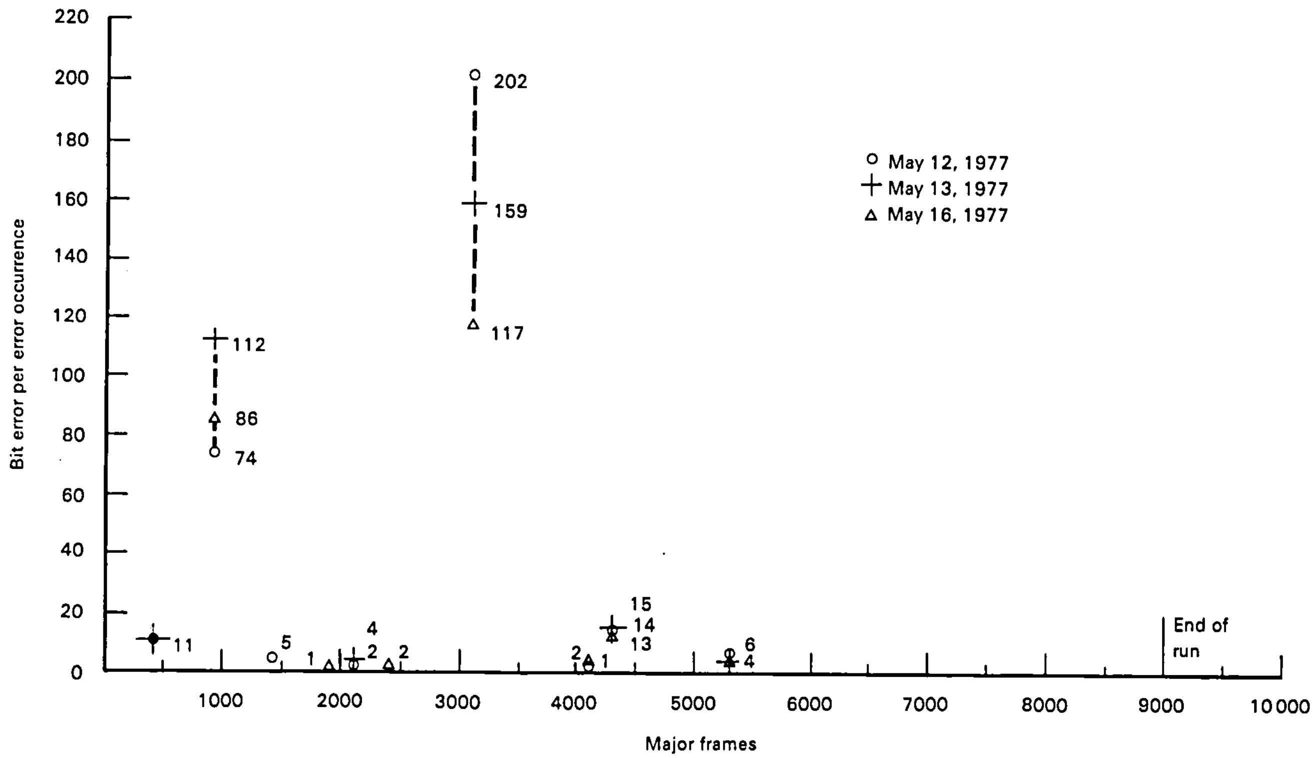

Figure 7–6.—HDTR error distribution on Ampex 787 tape at 15 ips (2.5 Mbps). (Test pattern: horizontal gray scale; 9360 major frames = 3 × 10⁸ bits.)

Table 7-1.—*Bit Errors in Clusters*[a]

Tape no.	Total bits in run, $\times 10^{10}$	Total bits in error	Total error bits in clusters greater than 25 bits	Total cluster bits / Total error bits, percent
1	1.10	934	866	33
2	1.56	2798	2640	94
3	1.04	2	0	0
4	1.04	4	0	0
5	1.04	851	829	97
6	1.03	514	480	93
Total	6.81	5103	4810	94

[a]Test pattern: pseudorandom; tape: Ampex 79A; end of test period: Nov. 1978.

correction to high-density tape recording. In 1979, GSFC established a contract with Martin Marietta to modify the IPF HDTR's with a single-loop error correction capability.

The single-loop system herein is defined as the error correction method that employs one extra track of the longitudinal tape. Logic hardware is added so that this extra track carries a lateral (across track) odd parity. The parity bit is determined prior to recording each 10 bits of lateral data on the 10 tracks of tape. Longitudinal parity had already been included in the record process as discussed earlier.

For the reproduce function, the data are deskewed, realigned in matrix form, and temporarily stored prior to removing the data in serial form. This matrix can be represented by figure 7-2, with the inclusion of the error correction code (ECC) track. Logic is readily designed to monitor the individual longitudinal track parity bits during this process. The logic also monitors the extra lateral parity channel. Any channel determined to have bit errors is examined along a given region surrounding its parity errors. For that region, the lateral parity bits in the outside channel are also examined. Data bit errors are then located by the intersection of the error produc-

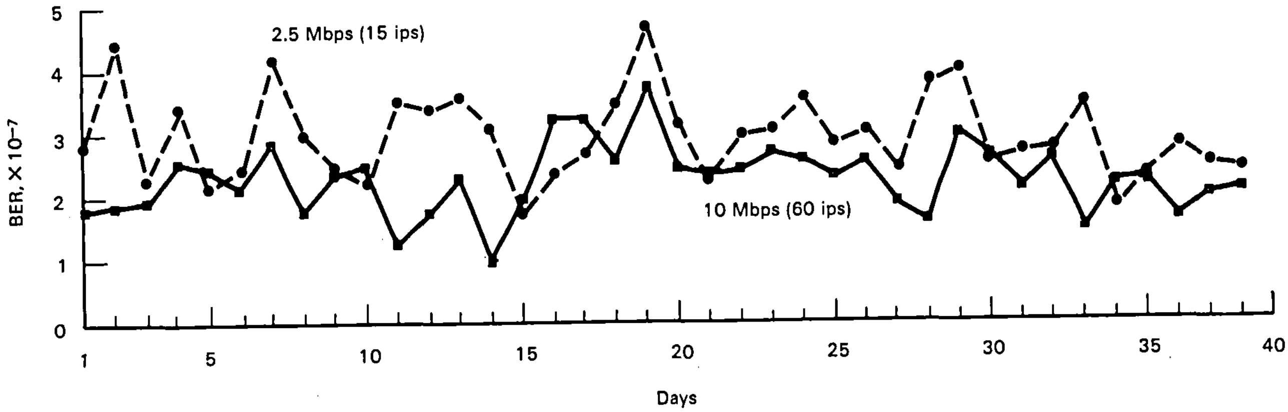

Figure 7–7.—Repeatability of HDTR unit and tape over 38 days without readjustment of HDTR. (Greater than 1.2 $\times$ 10^9 bits per test run; test pattern: ramp; tape: Ampex 787; end of test period: May 1977.)

ing longitudinal track and the error producing sets of 10 lateral bits as determined from lateral parity errors. Each bit in error is changed to complete the correction process. (See fig. 7-8.)

The reason the single-loop system was preferred over multiple-loop systems was to conserve on track usage, cost, complexity, and risk of modification. In addition, the causes of bit errors by past history in the IPF were well characterized. As shown previously, the majority of errors were in clusters and by observation were known to be almost entirely single track oriented at any one time. A review of existing documentation also supported the generally accepted view that tape dropouts of state-of-the-art commercially available instrumentation tape were usually less than 0.76 mm. The two head configuration provides an equivalent track spacing of 3.56 mm for simultaneous errors on a single head. A dropout on tape that covers two of its adjacent tracks does not reach the next record head until approximately 10^5 bits later. Therefore, simultaneous two track errors for a single head system become two time-separated single track errors; such a dropout is recoverable by a single-loop system. Dropouts larger than 3.56 mm (three tracks or over) were expected to be extremely rare.

Acceptance of each modified HDTR was made after exercising the HDTR at all tape speeds with 10 randomly picked Ampex 79A tapes. After making all runs, the error correction logic was disabled and the HDTR was retested in its old configuration. Figure 7-9 provides the results of this testing. With the error correction logic in place, 67 percent of all tape runs gave a perfect reproduction of the input data; i.e., no errors. Note that the average BER of all runs was a very low 3.6 $\times$ 10^{-10}. This average BER was 389 times better than the average of all runs with the error correction logic disabled. Over 300 km of tape were recorded and played back to verify the performance. The advantage of the error correction is clearly seen. The last HDTR unit was modified and put back on line in May 1980.

OPERATIONAL PERFORMANCE

The IPF performs routine operational level testing. In this testing each HDTR interface pair (the output

```
                                     ┌───Bad column
                                     ▼
LP channel ... P P P P P P P P P P P P P P P P P P P P P P P P P P P P P P P P P ...
Channel  1 ... o o o o o o o B o o o o o o o B o o o o o o o B o o o o o o o B o ...
Channel  2 ... o o o o o o o B o o o o o o o B o o o o o o o B o o o o o o o B o ...
Channel  3 ... o o o o o o o B o o o o o o o B o o o o o o o B o o o o o o o B o ...
Channel  4 ... o o o o o o o B o o o o o o o B o o o o o o o B o o o o o o o B o ...
Channel  5 ... o o o o o o o B o o o o o o o B o o o o o o o B o o o o o o o B o ...
Channel  6 ... o o o o o o o B o o o o o o o B o o o o o o o B o o o o o o o B o ...
Channel  7 ... o o o o o o o B o o o o[X]o o B o o o o o o o B o o o o o o o B o ...◄─┐
Channel  8 ... o o o o o o o B o o o o o o o B o o o o o o o B o o o o o o o B o ...  │
Channel  9 ... o o o o o o o B o o o o o o o B o o o o o o o B o o o o o o o B o ...  │
Channel 10 ... o o o o o o o B o o o o o o o B o o o o o o o B o o o o o o o B o ...  │
                                                                                      │
o──►Data bit                                                        Bad row ──────────┘
P──►Lateral parity                                                  (channel)
B──►Longitudinal parity
```

Figure 7–8.—Error detection during reproduce.

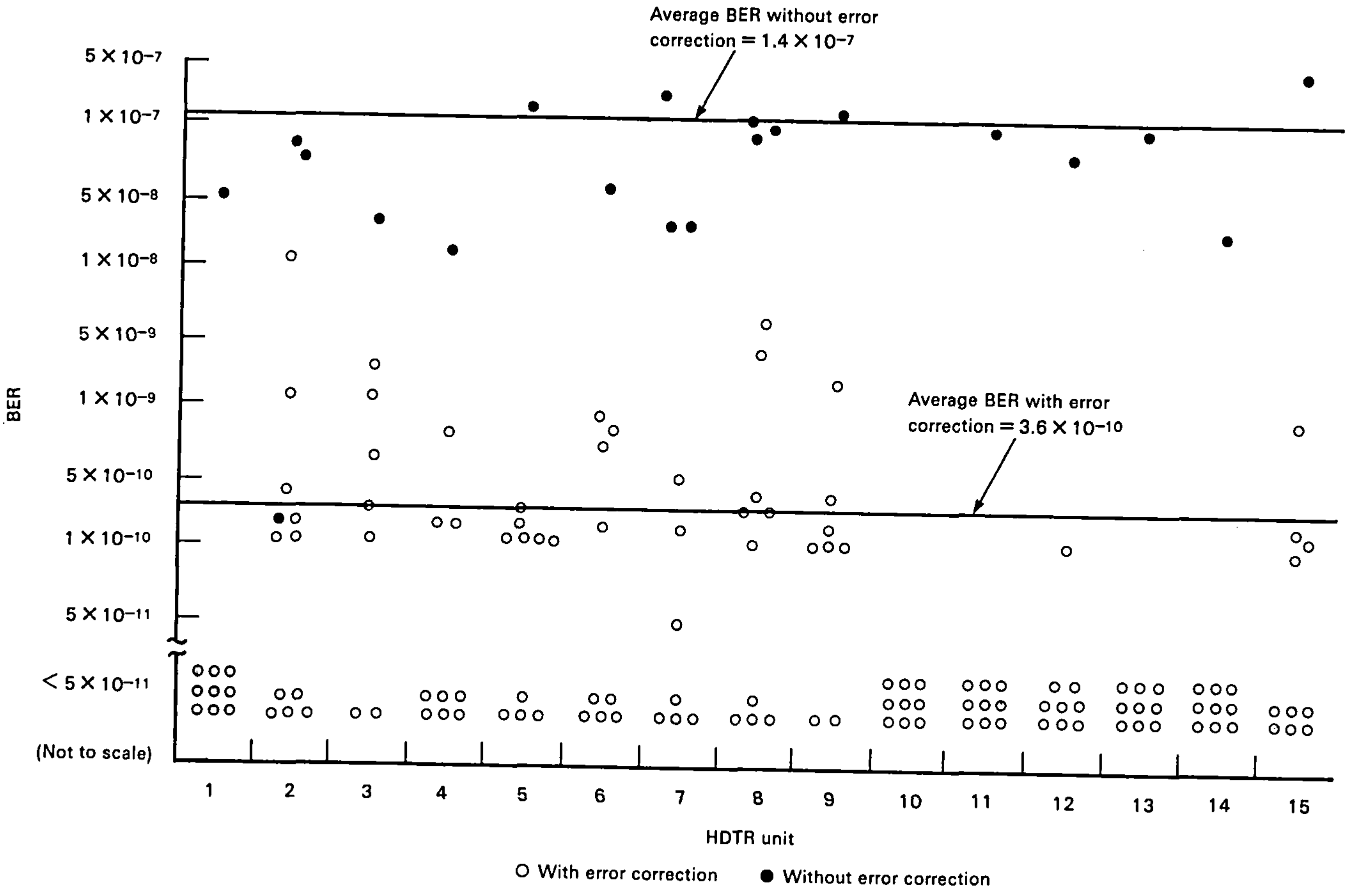

Figure 7–9.—Error correction modification test results. (Test pattern: ramp; tape: Ampex 79A; end of test period: May 1980.)

HDTR on one system to the input HDTR on the receiving system) is exercised. The bit pattern generator is used to record on the first HDTR at the exact same data rate used by that unit. The recorded test tape is then played back on the receiving system at the exact reproduce rate of that HDTR, and the BER is tabulated. This is performed for every operational pair combination in the IPF. Twenty-one pair combinations are tested every 2 weeks.

In addition to BER performance, the IPF monitors emergency and fractional failures of all equipment, a fractional failure being a failure that does not put the system down. From October 1976 to January 1981, the average of all HDTR mean time between failures for emergency failures was 2699.2 hr. The worst-case HDTR had an emergency mean time between failures of 555.2 hr. During the same time period the average mean time to fractional failure was 1780.2 hr, and the worst-case HDTR had a fractional failure at 416.4 hr.

Also of interest is the headlife of the HDTR's. The HDTR's employ solid ferrite heads. Tape tension is set at 8 oz. During operation the heads are lightly cleaned during each change of tapes. A plot of the head run time for the most heavily used HDTR's is given in figure 7–10. Each plot is a least-square fit to monthly HDTR data. Note that one set of heads lasted beyond 5000 hr, and none have failed below 2000 hr. Three other units are beyond the projected 3000-hr lifetime of the ferrite heads.

CONCLUSIONS

GSFC successfully improved the performance of its HDTR's in the IPF. The first improvement was the addition of pseudorandomization of the data just prior to actual recording to reduce the adverse effect of pattern data. This was mildly successful and afforded a BER improvement of about two to one. This coupled with the use of newer and better uncertified tape, Ampex 79A, allowed GSFC to improve the BER specification to 2×10^{-7}.

Investigative work at GSFC included characterization of the types and causes of bit errors, in addition to research being done in the field, and led to the final modification of HDTR's. The modification of the recorders for error correction was highly successful.

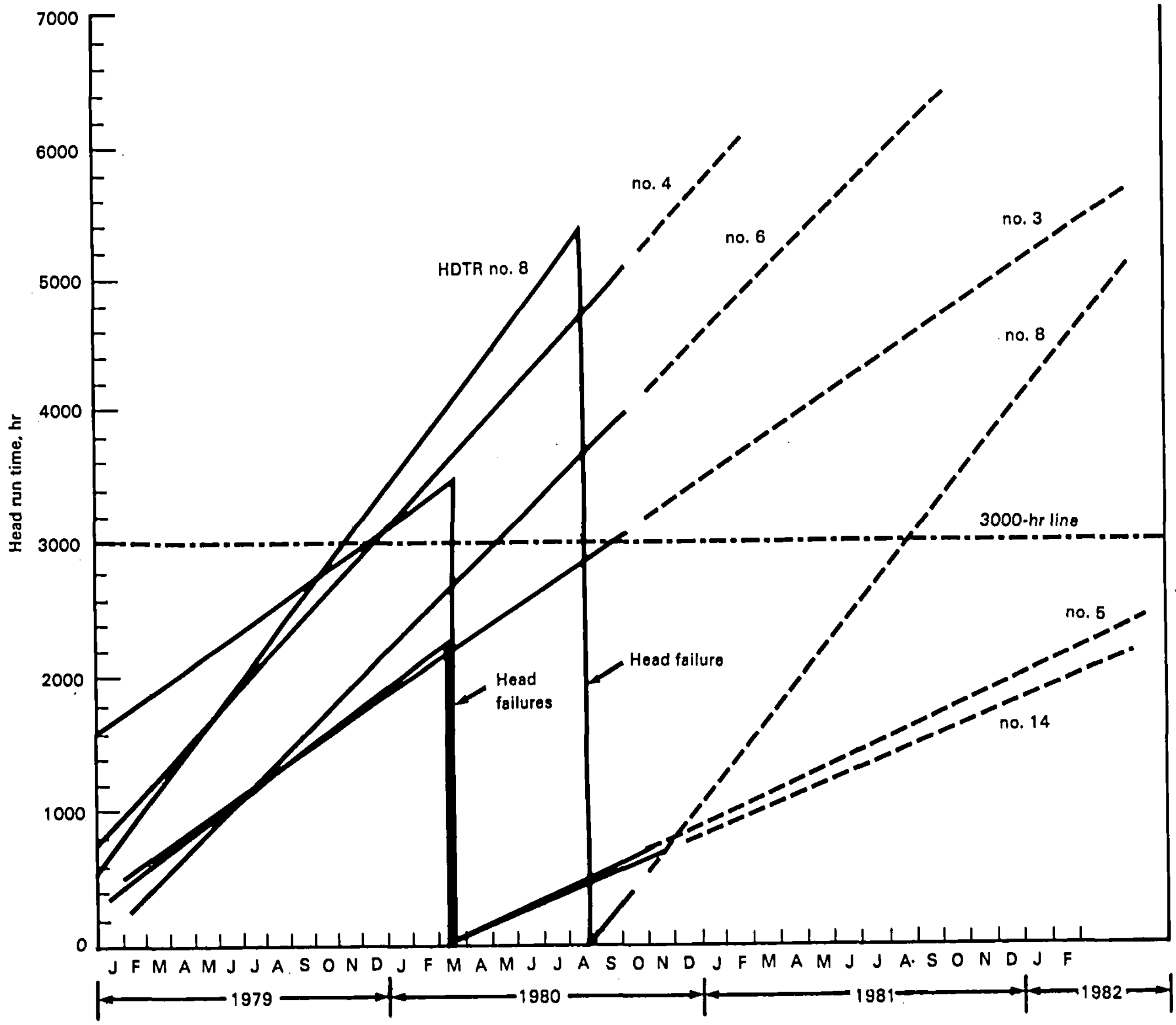

Figure 7–10.—Head run time for HDTR's. (Least-square fit to data from Feb. 1979 to Sept. 1980.)

After extensive testing of all recorders, the average BER was shown to improve by a factor of 389.

The new performance of the recorders allowed the BER specification to be changed to 2×10^{-9}, an improvement of 500 to 1 over the original state-of-the-art specification for HDTR's. This improvement coupled with the statistically proven operational reliability of the HDTR's has enabled IPF to accurately transfer data from one system to another during image processing.

ACKNOWLEDGMENTS

The author acknowledges the testing and bit error rate tabulations made by Joseph Heinig of GSFC and the conceptual design of the pattern generator by Robert Powless of GSFC. In addition, an acknowledgment is extended to Constantin Rauta of the Computer Science Technicolor Associates for independent determination of mean times between failure and head life statistics.

BIBLIOGRAPHY

Heffner, Paul; Connell, Edward; and McCaleb, Fred: "High Data Volume and Transfer Rate Techniques Used at NASA's Image Processing Facility." Marshall Space Flight Center/University of Alabama (Huntsville) *Data Management Symp.*, 1977.

Heffner, Paul: "The Application of High Density Recording to Image Processing." vol. VII, *Int. Telemetering Conf.* 1976.

Waltz, Edward: "A Serial Signal Simulator/Synchronizer for True Measurement of HDDR Bit Error Rates." THIC meeting, Mar. 7, 1978.

CHAPTER 8

The Density Upgrade: Mark III A (A Future Improvement of the Mark III Very Low Baseband Interferometry System)

H. F. Hinteregger
Haystack Observatory

At present, the Mark III acquisition system records up to 28 channels, each with up to 4-MHz (normally 2 MHz) bandwidth from two separate intermediate frequency bands, onto 28 tracks on 1-in.-wide tape, using a longitudinal recorder with 2 fixed heads per track. One head writes and a corresponding head reads each formatted channel. The bit (transition) density is 1.3/μm (33 333/in.), and tracks are 640 μm (0.025 in.) wide.

A long-sought order-of-magnitude density increase, called Mark III A, has been planned for the recording system. We expect to reduce trackwidth to 40 μm initially so that 336 tracks can be recorded in 12 passes of the tape. Thus, one 9200-ft tape will last for 3 hr while recording 56-MHz bandwidth, or a total of about one terabit (10^{12} bits).

Development efforts at Haystack Observatory during 1980-82 have been funded by NASA in support of geodetic applications under the crustal dynamics project. The density upgrade is probably even more useful to astronomy than geodesy, however.

In the near future both conventional geodetic and astronomical very low baseband interferometry systems (the former with more widespread use of small transportable antennas and the latter with dedicated networks of large fixed stations) will be pressed to conduct observations with high duty cycle as well as wide bandwidth. However, with the original density of Mark III recording, supporting observations at 56- or 112-MHz recorded bandwidth for more than a few percent of real time is not practical. (See table 8-1.) Clearly an order-of-magnitude increase in density is needed to make high duty cycle use of such a wideband system sufficiently economic and manageable.

The need for a major density upgrade was anticipated early in the design of the Mark III system. But technology was not sufficiently advanced in 1975 to permit a first implementation with much higher recording density. Nevertheless, we attempted from the outset to judge the degree to which critical components (tape transport, heads, and tapes) could support a major density increase and to select those which appeared to maximize "upgradeability."

Table 8-1.—*Cost Comparison of Mark III and Mark III A Acquisition Systems*[a]

Item	Mark III, 10^3 dollars	Mark III A,[b] 10^3 dollars
Tape shipping	100	8
Tape stock	100	10
Head replacement	15	7
Total	215	25

[a]30-percent duty cycle; 56-MHz bandwidth; per year. Mark III A would increase density by a factor of 12, reduce trackwidth by a factor of 16 from 640 to 40 μm, and move the headstack at a rate of 60 μm/pass for 12 passes.

[b]The cost to modify an M 96 tape recorder for a Mark III A application is $20,000.

Certainly most fortunate in this regard was the choice of the Honeywell 96 (longitudinal) tape transport. To the best of our knowledge, the ± 0.25-μm tracking consistency of the Model 96, measured independently by optical (edge detection) and magnetic (offset playback) tests and maintained under machine interchange, is unmatched by even the best of narrow track videocassette recorders (VCRs). This is an upper bound on tracking inconsistency that excludes characterizable (hence removable) machine and direction-dependent fixed offsets and the slight but systematic differences between the forward and reverse tracking "signature" of a given piece of tape. The Model 96 will contribute negligibly (less than 0.1 dB) to head/track misregistration losses when trackwidth is reduced to 40 μm. It could even support tracks as narrow as 2.5 micrometers.

Our present goal, an order-of-magnitude increase in density, can be met by taking advantage of the second, now fully mature, generation of tape. The second-generation tapes are variously termed "professional

video" (PV), "digital audio," "advanced instrumentation", or "video home system (VHS) equivalent." These high-coercivity (650-Oe) tapes represent at least a 12-dB improvement upon first-generation instrumentation tape in the present system. This 12-dB signal-to-noise ratio (SNR) improvement can be traded exactly, in theory, for a 16-fold reduction of trackwidth.

An additional 12-dB improvement provided by third-generation tape in the future will encourage another trackwidth reduction to 2.5 μm, with no net reduction of SNR or increase in error rate. One such third-generation tape has been developed; its generic name is "vacuum video" (VV) tape. A hand-held camera/VCR using VV tape is expected to be on the consumer market within a year.

Thus, 3-μm track spacing or 8000-tpi recording begins to seem feasible, given mature third-generation tape and the ± 0.25-μm tracking of the Model 96. A ± 0.25-μm accurate headstack, and environmental control of tapewidth and headstack length would also be needed. In addition to a 20-fold further reduction in track spacing, we can anticipate, with third-generation tape, a halving of tape thickness and a 2- to 3-fold increase in transition density. We project that a full and natural evolution of the upgrade will, by 1990, make possible recording 80 to 120 terabits on a single 14-in.-diameter reel of inch-wide tape. A total recorded bandwidth of about 1 GHz can be obtained by quadrupling the normal (2-MHz) channel bandwidth and quadrupling the number of channels (all within the framework of the present parallel Mark III system architecture). By 1990 it should, therefore, be practical to record 2 Gbps of data continuously because it will take about 12 hr to fill the 100-terrabit bucket.

THE CHOICE OF MEANS

Volume density of magnetic tape recording can be improved in three ways: Bits can be made (1) shorter by increasing transition density, (2) thinner by reducing tape thickness, and (3) narrower by reducing trackwidth (and guard band).

Significant but inherently sharply limited density improvements can be anticipated from the first two approaches: Specifically, the higher resolution channel resulting from the combination of VHS-equivalent (0.33-μm gap) heads and VHS-equivalent tape encourages a 50-percent increase in transition density from 1.3 to 2.0 per micrometer (33.3 to 50 kiloflux changes per inch (kfci)), with only a 6- to 7-dB response rolloff. Also, consider that currently available inch-wide tape is 26 μm thick, while VHS cassette tape is now supplied in 13- as well as 17-μm thicknesses. As much as a doubling of volume density therefore depends only on manufacturer's willingness to supply the thinner tape appropriately slit and packaged. Taken together, these two improvements should alone eventually yield a three-fold increase in volume density. The planned density upgrade would automatically accept such improvements but is not dependent on them.

Order-of-magnitude increases in volume density, however, can come only from the third approach, drastic reduction of trackwidth and spacing. This is because the SNR of a tape-noise-limited magnetic recording varies only as the square root of the trackwidth. Thus, every 3 dB of excess SNR above that required in practice to maintain an acceptably small error rate is expended most efficiently by halving trackwidth, hence doubling density.

Numerous tests have been performed to estabish that certain modern tapes such as Fuji H621, Sony V16, 3M5198, and Ampex 721 can guarantee an SNR more than 12 dB higher than that which can only now be maintained as an acceptable worst case with instrumentation tape. The new tapes are replacing conventional instrumentation tape like Ampex 795 and 3M892 in the Mark III system.

We plan, therefore, to exchange this 12 dB of excess SNR for a 16-fold reduction in trackwidth. Because our present (fixed) heads are 640 μm wide, the trackwidth of new heads will be 40 μm.

We plan to use headstacks organized like the present (fixed) ones. A stack is an array of heads uniformly spaced along a single (gap) line so as to span (slightly less than) the full 1 in. width of tape. The simplest system results if all 28 channels are carried in a single stack. We prefer in addition to have at each end of a stack an extra head used to monitor head-to-track registration near both edges of the tape; the case is thereby anticipated in which normal guard bands between adjacent tracks on tape are allowed to shrink to a small fraction of trackwidth. Thus a single stack of at least 30 or a pair of 16-head stacks is desirable. Specifically, because it fits these needs nicely, we now advocate adopting the IRIG PCM-format head pitch of 762 μm (0.030 in.) as a standard for Mark III A, which should be maintained by any future replacement stacks featuring further reduced trackwidth and greater accuracy of head placement within the stack.

We plan to provide an electrical headstack interface, similar to our present separate read and write head interfaces, which under electronic control will permit reading or writing with the same stack. One 30-head single-stack assembly interfaced in this way will then support the entire Mark III system. A pair of identical, independent assemblies would provide not only highly desirable redundancy for this critical subsystem, but also (probably) a bidirectional read-while-writing capability, and certainly the option to double the number of channels simultaneously available (doubling the maximum system bandwidth).

We expect to be able to replace any of the present four fixed headstacks by a new assembly or "headblock." This headblock will house not only the narrow-track headstack, but also position actuator, position sensor, temperature sensor, ballast resistor, and intimate head interface electronics.

The required positioner must be capable of translating the block at least one head spacing, specifically 762 μm (0.030 in.), in the cross-tape direction so that the wide space between narrow heads can be accessed in trackwidth-plus-guardband increments and the tape fully recorded in multiple passes. The positioner is admittedly a complication of the recorder. Its complications, however, are small in comparison to those introduced by other conceivable means of achieving the same required combination of bandwidth and density in a longitudinal machine. Assuming an initial 12-pass format, an equivalent fixed head-per-track system would, for example, require 336 heads to be supported. Sufficiently dense packaging of heads for such a system is, among other things, beyond current state of the art.

An equivalent to the upgraded 28-channel, longitudinal recorder would be a "black box" consisting of a bank of 28 VCRs, each supporting one channel. Only with 28 VCRs is the comparison fair, because, with equivalent tape and heads, channel bandwidth limitations are the same for both kinds of machine. The bank of VCRs would be no more expensive than a single properly outfitted longitudinal machine, and to make it operational for VLBI would probably require the least engineering effort (none in the critical and specialized area of the head/tape interface). The drawbacks of this approach are perhaps largely a matter of taste, especially if only short-term benefits are considered. A bank of 28 VCRs is awkwardly large. Any straightforward parallel growth of the system for increased bandwidth results necessarily in a proportional increase in hardware and hence in physical size. Not so for the longitudinal machine that would not grow even if it were outfitted with four blocks of 28 channels. The number of cassettes to be handled, too, would be at least an order of magnitude larger in a multi-VCR system than the number of reels in the multichannel recorder system (because the tape area of the standard 9200 ft $\times$ 1-in. reel is 22 times that of a VHS T-120 cassette).

The decision in 1980 to stay with the longitudinal multichannel approach was based on the following judgments: (1) providing a sufficiently accurate positioner (actuator and sensor) was considered a straightforward task, especially because no active tracking servo was required; (2) critical aspects of VCR head as well as tape technology could simply be transferred to the multichannel recorder; and (3) the longitudinal Honeywell 96 system would remain much more naturally open to at least another order-of-magnitude improvement in both bandwidth and density in the not-too-distant future.

As has already been discussed, our efforts to date leave no doubt that the third judgment (above) was correct.

The first judgment, too, has been confirmed. From among several devices that could in principle satisfy reasonable specifications for a positioner, we have selected the piezoelectric "inchworm" as actuator and a linear variable differential transformer as sensor.

The second judgment, that VCR head and tape technology could easily be transferred to the longitudinal machine, was optimistic, however. Every critical aspect of feasibility has now been demonstrated, but a full prototype is still incomplete. This is because though one prime requirement (VHS-equivalent performance) was met by our contractor's early prototype headstacks, and the other one ($\pm$3-μm head placement accuracy) was met by later prototypes, no headstack has yet been received that meets both.

PROGRESS AND PERFORMANCE BUDGET

Aspects of feasibility that have now been demonstrated include the following:

(1) $\pm$0.25-μm tracking consistency with the Honeywell 96

(2) "Inchworm" plus linear variable differential transformer positioner with submicrometer accuracy

(3) Several sources of suitably high-output, consistent, low-abrasivity tape capable of maintaining and/or restoring head performance

(4) Method of contouring heads to maintain high-speed performance

(5) Prototype headstacks with all head edges accurately located within $\pm$3-μm

(6) 60-dB bandedge SNR (2 MHz at 120 ips, 3-KHz slot) from 50-μm-wide heads and Fuji H621 tape, about 3-dB higher than can be maintained on 640-μm-wide ferrite heads and average instrumentation tape

The expectation of at least 59-dB average bandedge SNR (see table 8-2) is obtained by derating that obtained with 50-μm wide heads 1 dB. The bandedge SNR is intended to be a measure of intrinsic head performance and is, therefore, obtained by using the same head to write and read a reference tape. The 73- to 75-dB SNR often obtained for all 640-μm-wide heads in a Honeywell ferrite headstack suggests that 40-μm-wide heads could average 61 to 63 dB, perhaps 3 dB better than our minimum expectation.

We budget for $\pm$1-dB variations in the intrinsic

Table 8-2.—*Expected Head/Tape Performance*[a]

Parameter	Value
Minimum Average Bandedge SNR (2 MHz at 120 ips, 3-kHz slot), dB	59
Tape variations (Fuji H621 reference), dB	±1
Head variations, dB	±1
Temporary degradation, dB	<1
Permanent degradation, dB	0
Intrinsic worst-case SNR, dB	56
Interchange loss:	
Head edge location toleranced ±3 μm (implies 6 μm or 15 percent maximum loss), dB	−1.5
Environmental tape width change:	
ΔT = 6 C (implies 2 μm or 5 percent maximum loss), dB	−0.5
ΔH = 30 percent relative humidity (implies 4 μm or 10 percent maximum loss), dB	−1.0
Maximum total interchange losses, dB	−3
Total worst-case SNR, dB	53
Theoretical guaranteed bit error rate	$<10^{-4}$

[a]40-μm trackwidth.

1.5-μm wavelength response of suitable new tape. Fuji H621 became our standard of reference when we found it had tape-to-tape variations of only ±0.5 dB. The implicit reference to the Fuji "centerline" in our performance budget makes it a little optimistic because, for example, 3 M 5198 average response is about 1 dB lower. The consistency of tape response required is far higher than that obtained with conventional instrumentation tape, for which a +3- to −8-dB spread, about a 9-dB inferior centerline, is not uncommon. Such variations were not expected when Mark III first became operational; we have now decommissioned more than 35% of our instrumentation tapes for failure to meet our original −2 dB worst-case expectation.

In addition, new tapes like Fuji H621 and Sony V16 cause no measurable degradation, unlike instrumentation tapes, which have been found to rapidly and severely degrade (ferrite) head performance. In our experience, if 10 instrumentation tapes are run once each over fresh heads, a 6-dB degradation of initial (optimum) bandedge response typically results.

We have found that Sony V16 is too abrasive for full-time use in our system, but that it acts to restore degraded performance. If used on a 10-percent basis, it limits the slight and very gradual degradation caused by 3M 5198 to 1 dB.

On the other hand, we can project an extremely long 12 000-hr head life with Fuji H621 tape under extremely (greater than 70 percent) high humidity conditions. The abrasivity of 3M 5198 appears to be at least equally low.

To maintain initial optimum performance for the life of a head, it is necessary to optimize and stabilize the tape-to-head pressure, thus geometry as well as the surface condition of the head/tape interface is important. We have developed a "stepped" head contour that does this successfully. A pair of shallow steps cut 150 μm equidistant from and parallel to the gap line limits the areas of head/tape contact and discourages an air bearing from forming. The radius of the sharply defined contact area quickly stabilizes. As a result, we can now guarantee that initial performance at high (120 to 360 ips) speeds will be maintained, even with the smoothest tapes like 3M 5198.

The stepped-head contour has a major side benefit. It cleans even the best of the new tapes. This is evidenced by a typical 10-fold reduction in error and bit-slip rates after a single pass. The stepped head contour has been fielded in the present system as a modification of existing Honeywell heads. Only with this modification has it been possible to limit the degradation caused by instrumentation tape so as to maintain a −4- to −6 dB-degraded "operating point" and, in spite of that, error rates of about 10^{-6}.

The figure for intrinsic worst case SNR takes into account all factors except losses due to head/track misregistration. Assuming past experience with wider tracks and instrumentation tape yielding the same 56-dB bandedge SNR is relevant, error rates of 10^{-6} to 10^{-7} are expected. Error rates of about 10^{-6} have, in fact, been obtained with 50-μm wide heads and Fuji tape using the present head interface electronics with quickly made (probably not optimum) gain and equalizer modifications.

Head/track misregistration losses must also be taken into account. Narrow 40-μm-wide tracks and the requirement on machine interchange to read simultaneously all simultaneously written tracks lead to the new and stringent head edge location tolerance of ±3 μm for all heads in a stack. This tolerance permits a 1.5-dB loss of signal corresponding to minimum head/track overlap of 34 μm.

Not to be overlooked is the fact that tape width depends on temperature and humidity. The respective expansion coefficients are such that a change of 6 C moves the edge of an inch-wide tape 2 μm with respect to its center, and that a 30-percent change in relative humidity moves it 4 μm. A worst-case combination results in an additional 1.5-dB loss for edge tracks. No extraordinary environmental controls are needed to keep room temperature between 20 and 26 C and relative humidity between 25 and 55 percent.

Note, we must also take care to keep stable the temperature of each headstack so that its thermal expansion does not also contribute to misregistration loss. When, in the future, it becomes possible to obtain

headstacks with substantially improved head edge location tolerance, narrower heads and smaller guard bands (continued evolutionary density improvement) will be desirable. It should not be difficult to support further improvement and compensate for environmental instability by controlling head temperature and/or tape tension (vacuum). The effective gain of the latter can be increased by placing grooves between heads.

In July 1980 we let a contract to develop the narrow-track headstack to "production readiness" in, we were led to expect, 2 months. Partial prototype stacks that just met performance expectations were delivered in January 1981.

The improperly contoured "samples" sent in October 1980 were then modified and also found to perform comparably well. The partials of January 1981 and the samples of October 1980 failed, however, to meet the basic head placement accuracy specification by an order of magnitude.

A third generation of partial prototype stacks, delivered in June 1981, met that requirement, but only at the expense of adequate azimuth accuracy. Performance was 14 dB or more below expectation.

In January 1982 four full 32-head stacks were delivered that, except for systematic pitch errors later brought under control, met the head placement accuracy specification. These last prototypes under our original contract also represented a switch from superaccurate discrete head-tip assembly methods to an easy-to-manufacture "comb" headstack construction.

We had expressed a preference for the latter approach from the outset. From our point of view, the headstack required could most easily be obtained with the least technological risk by using (1) a mass-produced VHS "gapped bar" to obtain both the intrinsic consistent performance of the VHS head and the sufficiently accurate head pattern that specialized production grinding machines can put into such a bar and (2) a simple "comb" construction similar to that employed by Honeywell to adapt such a "patterned" bar by making it into a "tip-plate" that when bonded to a base containing an appropriately matched array of wound "back cores" (fluxors) becomes the completed stack.

Unfortunately, the January 1982 as well as the June 1981 prototypes exhibit very poor performance. One difference between the early prototypes with acceptable performance and the later prototypes stands out: Only the early prototypes used production VHS head tips. The later ones appear to be an unsuccessful attempt to "reinvent" the earlier technology.

Our contractor concluded in May 1982 that the performance problem was due to the use of improperly oriented single crystal ferrite in the later prototypes. A voluntary continuation of our contractor's effort (not under contract) has led to a fifth generation of prototypes, and a sixth is expected shortly. The fifth prototypes, obtained in July 1982, were once again made from hot pressed ferrite like the early ones, but worked no better than the third or fourth generations, thereby proving that single crystal orientation is not the (main) problem. The solution to the problem, it seems, lies in direct use of the VHS gapped bar or in an exactly copied process. Alternatively, by making use of the highly evolved grinding techniques used to pattern gap bars, we may now be able to accurately trim even used Honeywell headstacks to our new requirements.

CONCLUSION

The groundwork for Mark III A has been carefully laid. All known aspects of feasibility have been demonstrated. Solutions have been found to the subtle but extremely important problems of consistency and maintenance of head/tape channel performance. These solutions have been applied to the present system, and hence verified by operational use as well as by extensive laboratory tests. The delay caused by the inability, for more than 1 year, to reproduce the excellent performance of early prototypes is a real concern, but the remaining question about Mark III A is "When?" not "Whether?"

CHAPTER 9

Modular High-Density Recording System Using an Alternating Disparity Block Coding Scheme

Martin Davidson

The Johns Hopkins University Applied Physics Laboratory

The high-density digital array tape recording and reproducing system (DATARRS) was developed for use in The Johns Hopkins University Applied Physics Laboratory's (APL's) oceanographic measurement programs. The electronic interface equipment enables any standard 14-track wideband analog tape recorder/reproducer to be used as a digital recorder with a high throughput rate. Data with throughput rates of up to 45 Mbps are recorded on magnetic tape at bit packing densities of up to 33 kbpi per track. The recorded data can be reproduced at or below the recorded rate with an average bit error rate of 1 in 10^7.

The digital interface is packaged for field use with APL-owned portable tape recorders/reproducers; however, the interface can be used with the laboratory or portable standard instrumentation recorders of any manufacturer. DATARRS also can be used with error correction equipment at a throughput rate of 38 Mbps to provide a reduced bit error rate of 1 in 10^{10}. The interface provides a high-density digital recording capability for many data acquisition and processing applications where low error rates are required.

RECORDING OPERATION

Figure 9–1 is a simplified block diagram of the system in which DATARRS is designed to operate. Control lines and clocks are omitted for simplicity. Fourteen data channels can be accommodated. If error correction is desired, either 2 or 6 of the 14 channels will be preempted for parity bits and 12 or 8 of the channels for data bits.

The record digital interface accepts up to 14 parallel lines of clocked NRZ-L data or parity bits. It converts the NRZ-L bits to a recording code that is more suitable for the channel bandwidth of the tape recorder/reproducer and controls the recorder speed. The encoding data are recorded on magnetic tape using standard analog techniques.

The data are recorded at bit packing densities that depend on the data bit rates and the tape speed. Figure 9–2 indicates the operating points for the specified upper limit of 33 kbpi per track, and for a "typical" density of 21.5 kbpi per track. The points are indicated for operation with and without the error correction equipment.

REPRODUCING OPERATION

During tape playback, the DATARRS playback digital interface controls the tape recorder playback speed; synchronizes, channel decodes, deskews, and dejitters the data; and checks the data for channel coding errors. As a result of the last operation, the playback digital interface generates information on data quality on a line-for-line basis with channel decoded data. The playback digital interface data and data-quality information are fed to the error correction equipment for correction and transfer to a processor. DATARRS can function with the tape recorder/reproducer as a standalone unit or in conjunction with APL error correction equipment.

CHANNEL ENCODING

The tape recorders/reproducers for DATARRS are longitudinal 14-track instruments that use a nonsaturation direct-record method with bias to record the digital data on tape. Each track is essentially a baseband channel that usually requires the source binary information to be encoded in a format more suitable for transmission. The selected coding scheme is a low disparity block code $(N,c;D)$, where

N = number of NRZ–L binary "data" bits that constitute a source code block

c = number of binary bits in the recording channel code word or character

D = disparity of a recorded code word or character; i.e., the excess number of $+1$'s over -1's

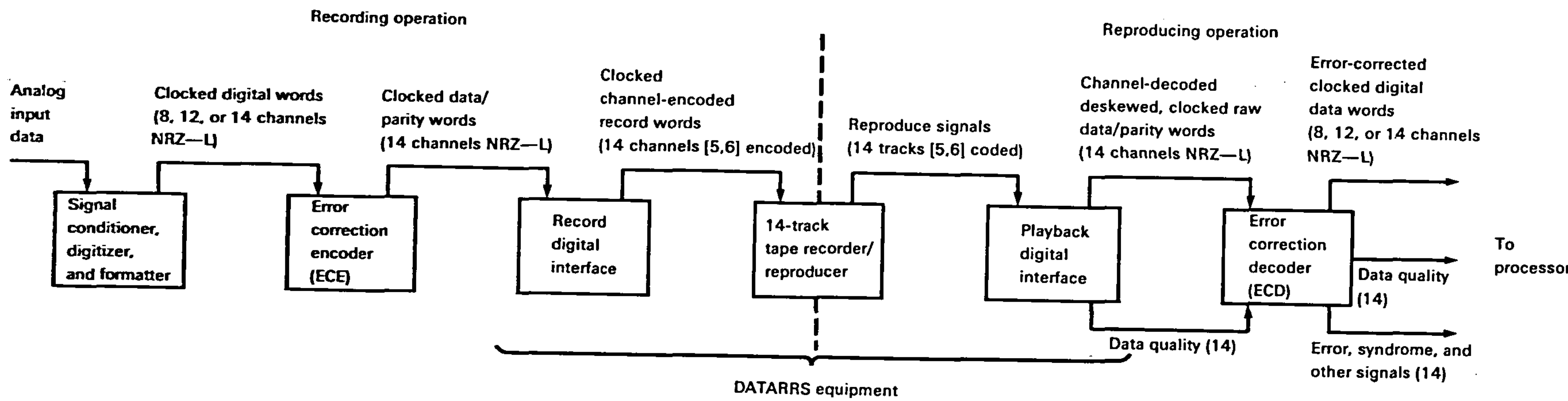

Figure 9–1.—Simplified block diagram of error correcting high-density digital tape recording/ reproducing system.

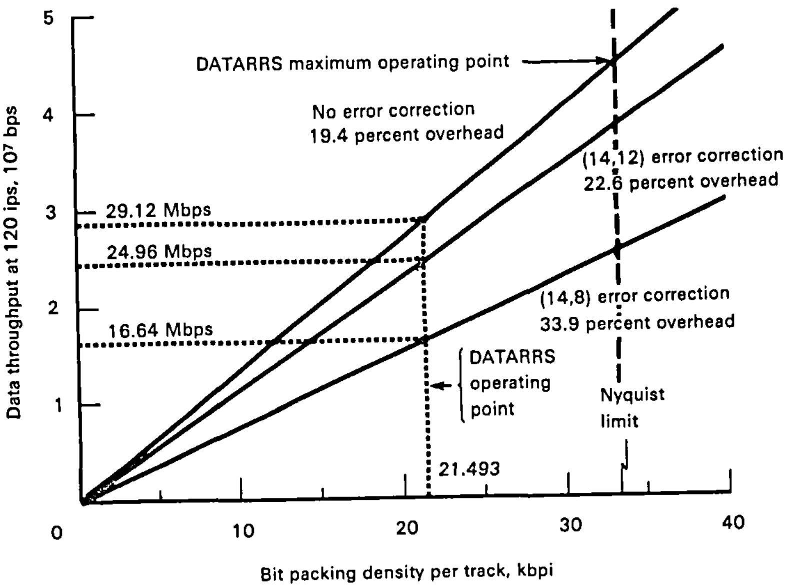

Figure 9–2.—Throughput rate versus bit packing density.

In particular, the code is a combination of the (5,6;0) and (5,6;±2) block codes; it contains a set of zero-disparity words and a set of word pairs with complementary disparities of ±2. See table 9–1. Word selection from the complementary subcodes is performed in alternation. Thus the encoded bit stream exhibits a tightly bounded digital sum variation that, word by word, can alternate only between ±2.

The code words, with zero-disparity or alternating ±2 bit disparity, are grouped with a unique tape synchronization word and are outputted as continuous bit streams that match the channel bandwidth better than the source data, while maintaining a reasonable overall efficiency. The data throughput when overhead bits are used is shown in figure 9–2 for the channel encoding, with and without error correction.

BLOCK CODING CONSIDERATIONS

Low disparity block codes could be more useful in high-density recording applications than some other coding schemes now being used. In particular, zero disparity and alternating disparity block codes, having no spectral content at dc, do not exhibit the baseline shift that NRZ–L data can dramatically exhibit when recorded on tape, and which delay-modulation coding and enhanced NRZ coding also exhibit.

Properties of some codes that are used in high-density and computer peripheral digital recording, and of some low disparity block codes that may be useful in those applications are listed in table 9–2. All the codes listed are either linear block codes or, for our purposes, can be considered to be variants of linear block codes. For a definition of linear block codes see textbooks on error correction or reference 9–21.

Cattermole (ref. 9–6, ch. 4) discusses low disparity block codes in a general pulse code modulation (PCM) context. Franklin and Pierce (ref. 9–22) discuss zero-disparity codes in particular. The familiar Manchester code is the simplest of zero-disparity block codes. (See table 9–3). Halpern (ref. 9–23) has proposed the (4,6;0) code for high-density wideband magnetic recording. His approach also involves the use of a linear receiver and maximum-likelihood symbol detection. Morizono et al. (ref. 9–8) report the use of the (8,10;0) code. Enhanced-NRZ (ref. 9–9), on the other hand, is a disparity reduction scheme rather than a low disparity scheme.

If we assume that NRZ–L data of a given bit rate is presented to the encoder, the "code rate" (table 9–2) of a block code is taken to be N/c, the ratio of source data bits to code word bits recorded on tape.

The relative bandwidth is the bandwidth required for the synchronous detection of a single code bit, relative to that required for an NRZ–L data bit. We assume equal energy difference signals and correlation (optimum) detection in Gaussian noise. Under these assumptions all codes will have the same bit error rate, providing the relative channel base bandwidth of each code is equal to c/N, reciprocal of the code rate. Thus both the Manchester and delay modulation code (DM) require twice the bandwidth of NRZ–L to achieve as low a BER as NRZ–L.

In a tape recorder, all binary code bits are constrained in amplitude between fixed levels, say ±1 V, hence difference signal energies per code bit will differ. Each is proportional to the code rate N/c. Thus the delay modulation and three position modulation (3PM) codes are poorer than NRZ–L by a factor of 2. That is, they

Table 9-1.—*Alphabet of the (5,6) Alternating Disparity Code*[a]

Code character No.[b]	(5,6;0) subcode[c]	Alternating subcodes (5,6;−2) subcode	Alternating subcodes (5,6;+2) subcode
1		000011	111100
2		000101	111010
3		000110	111001
4	000111		
5		001001	110110
6		001010	110101
7	001011		
8		001100	110011
9	001101		
10	001110		
11		010001	101110
12		010010	101101
13	010011		
14		010100	101011
15	010101		
16	010110		
17		011000	100111
18	011001		
19	011010		
20	011100		
21		100001	011110
22		100010	011101
23	100011		
24		100100	011011
25	100101		
26	100110		
27		101000	010111
28	101001		
29	101010		
30	101100		
31		110000	001111
32	110001		
33	110010		
34	110100		
35	111000		

[a]More formally, the (5,6; −2,0, +2) code; "0's" represent "−1's".
[b]Only 2^5 code characters are needed to represent data.
[c]This subcode is essentially the (4,6;0) code.

each suffer a signal-to-noise energy loss of 3 dB relative to NRZ−L, with consequent deleterious effect on their BER performance in Gaussian noise.

Consider the bits of a code to consist of +1 and −1 amplitudes. The running sum of a set of such bits is called the digital sum variation (DSV). (See ref. 9-24.) The DSV of a zero-disparity code word is zero. If a NRZ−L source emits all +1's, its DSV, being unbounded, tends to positive infinity. All the codes listed as "unbounded" can exhibit dc baseline shift problems in the reproduce mode. Those codes with "bounded" DSV's are such that no arrangement of source data can be found that will cause dc shift problems in the reproduced code bit stream.

Tests of Two Zero-Disparity Codes

Tests were run to compare the BER performance of the (4,6;0) and (6,8;0) codes with that of the delay modulation code. (See ref. 9-8.) The (6,8;0) zero-disparity code, as an example, has an unrestricted source alphabet consisting of 2^6 data blocks of 6 bits each in NRZ−L format. These blocks are encoded into a recording channel alphabet of 8-bit code words or characters, consisting only of various combinations of four +1's and four −1's. This recording channel alphabet has 70 characters available (ref. 9-6), six more than the number required to match the source alphabet.

It was of interest to determine what maximum bit-packing densities could be achieved at a BER of 1 in 10^7. Measurements of BER of serially recorded codes were performed with the setup of figure 9-3. The code word waveforms are essentially NRZ; hence commercially available NRZ bit synchronizers can be used to recover both waveforms and clock.

In measurements involving delay modulation (DM) code, a bit synchronizer incorporating a DM-to-NRZ−L decoder was used. The synchronization or framing word detector and the code word boundary counter were not needed.

The results of the tests with a 4095-length PR sequence are shown in fig. 9-4. It is seen that in the region of a BER of 1 in 10^7, the (4,6;0) code attains a higher equivalent bit-packing density than the DM code. In terms of its code rate, the (6,8;0) code is 8 percent more efficient than the (4,6;0) code and, predictably, achieves an increase in equivalent bit-packing density.

The remarkable thing about the equivalent bit-packing densities achieved by these two zero-disparity codes is that they actually represent recorded-on-tape bit-packing densities of close to 40 000 bpi. The recorded densities of these two codes where their interpolated performance curves cross the 1 in 10^7 bit error ordinate are indicated in figure 9-4.

Test of the (5,6) Alternating Disparity Code for Baseline Shift

To check the absence of baseline shift, a long (2^{20} −1) maximal length PR sequence was (5,6) encoded and recorded on tape. The reproduced output was examined, and no baseline shift was observed. Figure 9-5 shows a typical portion of the waveform comprising approximately 22 of the six-bit code words. (See also ref. 9-7).

In a second, more stringent test, runs of +1's and of −1's were inserted in the PR encoding sequence. Both this modified PR encoding sequence, in NRZ−L format, and the concomitant (5,6) encoded waveform were parallel recorded on two separate tracks. A portion of the reproduced encoding waveform that has undergone severe baseline shift is shown in figure 9-6(*a*). It consists

Table 9-2.—*Properties of Recording Channel Codes*

Block Code Type	Code designation (N,c;D)	Common terminology	Code rate	Relative bandwidth	Relative difference signal energy, dB	Bounded digital sum variation	Other designations or similar codes	Comments	References
Basic code	(1,1)	NRZ–L	1	1	0	No		Bit packing density at Nyquist rate of 2 bits/Hz of bandwidth	9-1, 9-2, 9-3
Scrambled basic code	(1,1)	Pseudorandom-noise-sequence modulated NRZ–L	1	1	0	No			9-4, 9-5
Linear block codes:									
0-disparity or low-disparity codes	(1,2;0)	Manchester code; biphase level	.5	2	−3	Yes	Phase encoding; bi-phase, mark; bi-phase, space; split phase; FM encoding		9-1, 9-2, 9-3
	(4,6;0)		.666	1.5	−1.8	Yes	H-code	20 0-disparity characters	9-6, 9-7
	(5,6;−2,0,+2)		.833	1.2	−.8	Yes		3 subcodes: 20 0-disparity characters plus 15 alternating disparity character pairs	9-6, 9-7
	(6,8;0)		.75	1.333	−1.2	Yes		70 0-disparity characters	9-6, 9-7
	(8,10;−2,0,+2)		.8	1.25	−1	Yes		3 subcodes: 252 0-disparity characters plus 210 alternating disparity character pairs	9-6, 9-8
Systematic code	(7,8)	Enhanced NRZ	.875	1.143	−.6	No	Bit stuffing code	Also implemented as a nonsystematic code by reversing selected data bits	9-9, 9-10
	(1,2)	Delay modulation	.5	2	−3	No	Miller code; Wood code; HDDR II; modified FM (MFM)	State sequential encoding	9-3, 9-11, 9-12
Adaptive block codes	(1,2)	Modified delay modulation	.5	2	−3	No	M^2FM	State sequential encoding	9-13
	(1,2)	Miller squared	.5	2	−3	Yes	M^2	State sequential encoding; digital sum variation constrained following even runs of data "1" bits	9-14

Table 9-2.—*Properties of Recording Channel Codes*—Concluded

Block Code Type	Code designation (N,c;D)	Common terminology	Code rate	Relative bandwidth	Relative difference signal energy, dB	Bounded digital sum variation	Other designations or similar codes	Comments	References
Run-length-limited codes:									
Adaptive block codes	(1,2)	Zero modulation	.5	2	−3	Yes	Patel code	Runs of "0" bits ≥1 and ≤3 between any 2 "1" bits; state sequential encoding	9-15
	(2,3)		.666	1.5	−1.8	No	A. Gabor code	Runs of "0" bits limited to not more than 1 between any 2 "1" bits; state sequential encoding	9-16
	(3,6)	3-position modulation	.5	2	−3	No		Runs of "0" bits ≥2 and ≤9 between any 2 "1" bits	9-17, 9-18
Linear block code	(4,5)	Group-coded recording	.8	1.25	−1	No		Runs of "0" bits limited to not more than 2 between any 2 "1" bits	9-19, 9-20

Table 9-3.—*Biphase and Delay Modulation (DM) Codes as Block Codes*

Code	Data word	Code word(s)
Biphase	0	01
	1	10
Delay modulation	0	00 or 11
	1	01 or 10
Modified DM	0	00 or 11
	1	01 or 10
Miller squared	0	00 or 11
	1	00, 01, 10, or 11

of a string of − 1's and a long string of + 1's, separated by some alternating bits. Unseen predecessor bits actually cause the shift at this point. The corresponding portion of the reproduced (5,6) encoded waveform, shown in figure 9-6(*b*), exhibits no base line shift.

The bit packing density of the (5,6) code bits on tape was 25.9 kbpi, by no means the upper limit.

The rate of the (5,6) code is only 4 percent less than the rate of the (7,8) enhanced NRZ code, which is highly pattern sensitive. Overall, then, (5,6) coding may prove to be a more useful scheme than enhanced NRZ. (See ref. 9-25.)

Excess Code Words

Each of the low disparity codes discussed has more characters available than are needed to match the number of code blocks of the NRZ−L source code. These excess characters can be used for frame synchronization, especially when deskewing is required, and for data or event "tagging" purposes. Unlike framing word Barker sequences, used in random NRZ−L bit streams, these excess characters will not occur in the code word bit stream, assuming that the recovered clock accurately denotes character boundaries.

Furthermore, the (4,6;0) and (6,8;0) codes contain pairs of characters that are truly unique in the sense that not even a bit-by-bit correlation of the entire bit stream could yield a false framing word. For the (6,8;0) code, the character pair is "truly unique" in the above sense.

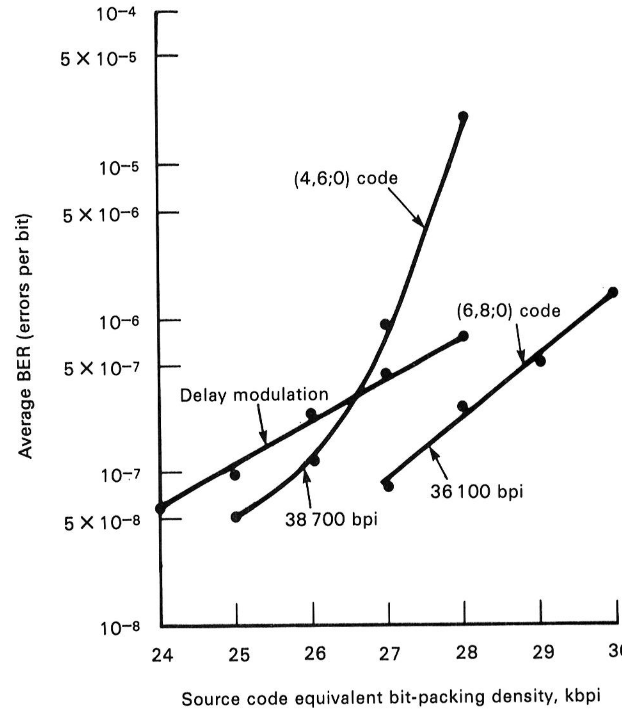

Figure 9–4.—BER versus equivalent bit packing density.

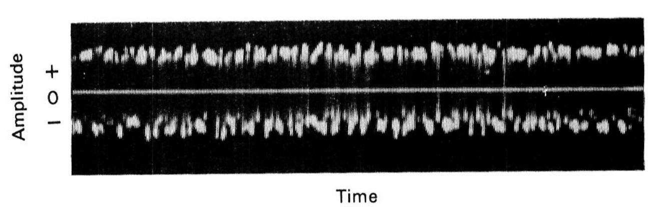

Figure 9–5.—Reproduce waveform of (5,6) code at 3.1 Mbps corresponding to PR data. (0 dc horizontal axis touched up for emphasis.)

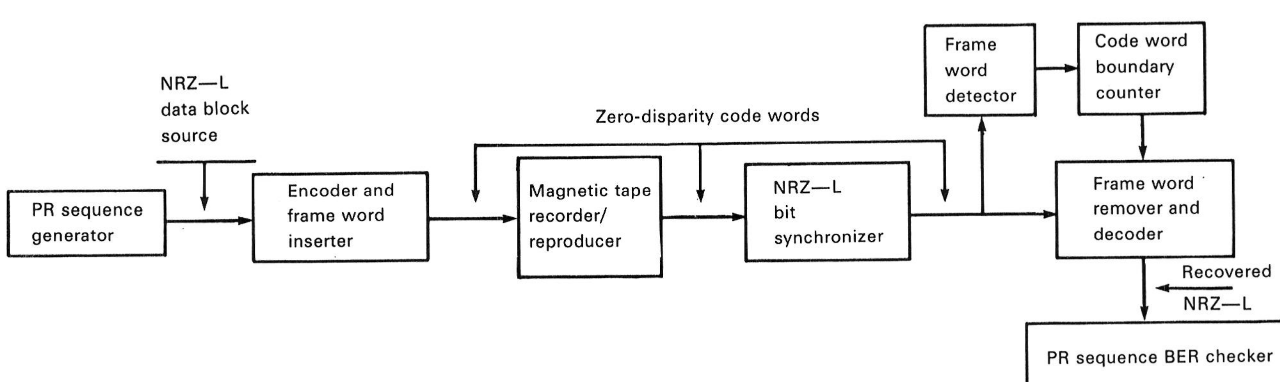

Figure 9–3.—BER measurement of recorded (4,6;0) and (6,8;0) codes. (PR = pseudorandom; PR code length = $2^{12} - 1$ bits.)

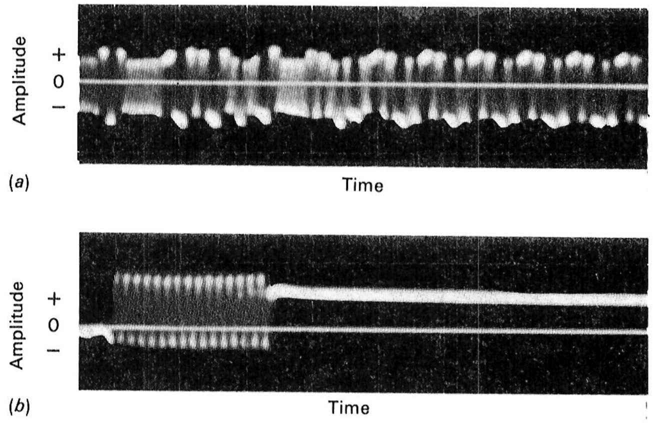

Figure 9–6.—Reproduce waveforms of NRZ data and corresponding (5,6) code. (0 dc horizontal axis touched up for emphasis.) (*a*) NRZ data at 2.5 Mbps. (*b*) (5,6) code at 3.1 Mbps.

Advantages of Low Disparity Block Codes

Zero-disparity codes are useful in high-density recording because of the following:

(1) Each code has a spectral null at dc, which eliminates problems associated with dc baseline fluctuations. The codes are pattern insensitive; i.e., neither recurrent nor random patterns of binary source data of any sort can induce baseline shifting.

(2) High code rates are attainable with relatively simple codes; e.g., the (6,8;0) code and (5,6) alternating disparity code.

(3) The zero-disparity property makes parity checking a simple procedure. In the case of the (5,6) alternating disparity code, an even-parity check can be made. Such parity error checks provide an indirect means of on-line monitoring of BER.

APL ERROR CORRECTION TECHNIQUE

The APL technique for detecting and correcting error bursts of indefinite length that occur in parallel data streams produced in the recording (as on magnetic tape) and reproduction of high-density digital data has a sequence of operations as follows:

(1) Generation of coded parity information from the input data
(2) Transmission of the information on lines parallel to but distinct from the data lines
(3) Recording the information on separate tracks
(4) Decoding the parity information on playback
(5) Determining the error syndrome
(6) From the syndrome, correcting the errors

This method continuously encodes and decodes the parity information and, therefore, continuously corrects error bursts. Thus the recording medium need not be rewound or backed up and reread to correct an error. The error correction power of this method may be augmented by the use of data quality information obtained from other, associated equipment. Such information, generated on playback, indicates tracks having a high probability of containing erroneous data.

APL has implemented this method in hardware as an ECE and an ECD, which were designed for use with a 14-track, 33-kbpi per track, tape recorder/reproducer having an inherent BER of 1 in 10^6. In that environment the ECE and ECD would reduce the overall BER to 3 in 10^{11} if all errors were independent. This error correction method is not inherently limited to any particular number of data channels, but can be used with equal advantage in systems employing far more than 14 channels.

Although this error correction method admits of many different coding schemes, the APL-built ECE and ECD implement only two, (14,12) and (14,8), for handling 12-bit and 8-bit data words, respectively. Figure 9-7 shows the formats of data on tape and the types of errors that can be corrected. In the (14,12) mode, the ECE adds eight parity bits (four on each edge track) to every block of four sequential 12-bit words, thus forming a 4-by-14 code word. On playback of the (14,12) data, the ECD can correct a burst of errors of any length occurring in any one channel.

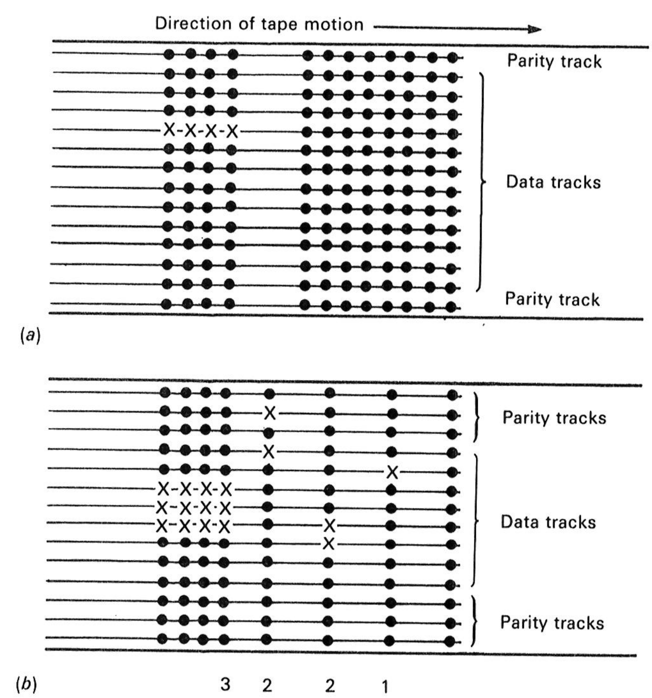

Figure 9–7.—Formats of data on tape and correctable error types. (*a*) (14,12) code; single channel errors of any length. (*b*) (14,8) code; simultaneous errors on parallel channels.

In the (14,8) mode, the ECE adds six parity bits (three on each set of edge tracks) to every eight-bit word, thus forming a 1-by-14 code word. On playback of the (14,8) data, the ECD can correct errors occurring simultaneously in as many as three adjacent channels.

In addition to this error correction mode of operation, an "error erasure" mode is available. In error erasure, data quality information from other equipment is used to resolve a limited number of uncertainties arising from ambiguous error indications, thereby further increasing the types of errors that can be corrected. The error correction and error erasure capabilities for the two coding modes are summarized as follows:

Mode and technique	*Type of data errors corrected*
(14,8) error correction	3 adjacent track errors
	2 adjacent track errors
	2 track errors separated by one good track
	Single track errors
	Double errors, parity tracks 0 and 13 (no error indication)
(14,8) erasure correction	Single track error, where the track number matches the data-quality line indicating "bad-data" or matches 1 of 2 data-quality lines indicating "bad data"
	Any 2 track errors where the track numbers match the data-quality lines indicating "bad data"
(14,12) error correction	Byte errors on any single data track (a byte error can be 1 of the 15 nonzero combinations of the 4 bits)
(14,12) error correction	Single byte errors on any single data track, where the track number matches the data-quality line indicating "bad data" or the track number matches either 1 of 2 data-quality lines indicating "bad data"
	2 byte errors on any 2 tracks where the track numbers match the data-quality lines indicating "bad data"

Tests of the system are described in reference 9-26. The DATARRS equipment had not been built at that time. With (14,12) error correction, 3.5×10^{10} effective data bits were recorded on 9200-ft lengths of tape and reproduced routinely with no bit errors.

The design basis of the system is covered in detail in reference 9-27. The simplified block diagram of figure 9-1 shows the ECE and ECD in a typical operating environment. The ECE and ECD operate as "pipeline" devices; each passes data through its internal stages at a constant rate and without buffering. Both can operate at any rate from 1 bps to 10^7 bps per channel.

Analog input data enter the signal conditioner and digitizer, which produces either 8- or 12-bit digital words, depending on the mode selected. If the (14,8) mode has been selected, modulo-2 adder circuits in the ECE generate the six parity bits for every eight-bit word. These parity bits are aligned and synchronized with the 8 data bits making each 14-bit code word an independent entity as far as error correction is concerned. If the (14,12) mode has been selected, modulo-2 adder circuits operate on blocks of four contiguous words, generating eight parity bits that are packed two in each word. In this case, each 4-by-14 code word is an independent entity. Outputs from the ECE are applied to a conventional record digital interface, which prepares the signals for recording by a magnetic tape recorder/reproducer.

On playback, the playback digital interface synchronizes and deskews the data and checks for signal dropouts. This interface incorporates circuitry for checking data quality; thus any signal below the threshold level causes a "bad data" indication on the corresponding data quality line. The ECD decodes the parity bits and calculates the corresponding syndrome. These syndrome bits address a read-only memory, whose output is used to correct certain kinds of errors. If an uncorrectable error is detected, an error signal is generated and transmitted synchronously with the data on another line.

Circuitry in the ECD uses the data quality information received from the playback digital interface in an error erasure mode. When that mode is operative, indications of bad data are used along with the parity information to compute syndromes that enhance the error correction capabilities of the system. (The ECD switches automatically from the error correction mode to the error erasure mode on the occurrence of a bad data indication.)

Data, data quality, error, and syndrome information are transmitted synchronously to an external processor along with clock pulses and bookkeeping information.

APPENDIX 9-A: THE DIFFERENCE SIGNAL CONCEPT AND ITS APPLICATION TO SOME CODES USED IN HIGH-DENSITY DIGITAL RECORDING

In evaluating binary codes for use in high-density digital recording, the importance of the spectral energy of the difference signal is usually overlooked. The spectrum of the difference signal can have a different shape and be wider than the spectrum of the code waveform. If the transmission channel bandwidth is shaped to match only the code waveform, a significant amount of the higher frequency energy that is necessary for cross-

correlating with the difference signal might be excluded, thereby resulting in a detection loss.

Much has been written about the difference signal concept:

To communicate information . . . different transmitted code words must be distinguishable at the receiver, and this requires that the channel be sufficiently wide to allow the difference waveform to propagate. [See ref. 9-28.]

The ability to distinguish between symbols is proportional to the energy difference between the signals. [See ref. 9-29.]

Both spectral matching and the enhancement of difference signals are needed to use the channel to its full capacity . . . The data should be handled in a manner to optimize the energy difference in the transmitted signals. [See ref. 9-30.]

When, as we are assuming here, the phases of the two coherent signals $s_0(t)$ and $s_1(t)$, as well as their complex envelopes, are known, a signal equal to $s_0(t)$ can be subtracted from the input, and the receiver needs only to decide whether the remainder contains the difference signal $s_\Delta(t) = s_1(t) - s_0(t)$ or no signal at all. We can, therefore, without loss of generality assume that one signal, say $s_0(t)$, is zero, and we do so henceforth. [See ref. 9-31.]

The receiver can just as well make its decisions after passing the input through a filter matched to the difference signal. [See ref. 9-32.]

The optimum detector for distinguishing between two signals in the presence of noise is a matched filter whose impulse response is matched to the difference between the signals to be distinguished. [See ref. 9-29.]

. . . the probability of error, which determines the optimum noise immunity, depends on two factors. . . . The first factor depends exclusively on the transmitted messages. The second factor depends on the ratio of the specific energy of the signal difference to . . . the square of the noise intensity. [See ref. 9-33.]

Equation 4.76b [in ref. 9-34] is the minimum error probability for any pair of equally likely signal vectors separated by a distance d, regardless of their actual location in signal space.

. . . if the channel is power limited, but bandwidth is available, one should use signals having good 'distance' properties [See ref. 9-35.]

The per-symbol transmission quality, measured by error rate, is (conceptually) entirely a function of the average received signal power, the noise level, the 'distance' between alternative signals, and the symbol integrating time. [See ref. 9-35.]

Optimum Receiver for Binary Signals

The material in this section is taken partly from Whalen [ref. 9-36] in a condensed form and is not intended to be a derivation.

In this brief outline we are concerned with the detection of signals of known form to which noise is added. If a signal is present, its amplitude, frequency, time of arrival, etc., are completely known. A hypothesis associated with such a signal will be simple. Some systems in practice do approach this ideal. In other cases, the performance of the ideal systems may be used as standards against which nonideal systems are compared. The material assumes that the noise is additive, white, and Gaussian.

Consider a binary communication model in which one of two signals $s_0(t)$ or $s_1(t)$ is received in the time interval $(0,T)$. At the receiver, white Gaussian noise $n(t)$ with zero mean and spectral density $N_0/2$ is unavoidably added to the signal. The observable signal is then

$$r(t) = \left\{ \begin{matrix} s_0(t) \\ \text{or} \\ s_1(t) \end{matrix} \right\} + n(t) \qquad (9\text{-}1)$$

The objective is to design a receiver that operates on $r(t)$ and chooses one of the following hypotheses:

$$H_0\text{: } r(t) = s_0(t) + n(t)$$

or

$$H_1\text{: } r(t) = s_1(t) + n(t)$$

The optimum decision rule is to compare the likelihood ratio $\lambda(r)$ to some threshold λ_0. The likelihood receiver is illustrated in figure 9-8.

The decision rule can be stated as follows: choose H_1 if

$$\int_0^T r(t)s_1(t)\,dt - \int_0^T r(t)s_0(t)\,dt \geq V_T \qquad (9\text{-}2)$$

where the threshold is

$$V_T = \frac{1}{2}N_0 \ln \lambda_0 - \frac{1}{2}\int_0^T [s_0^2(t) - s_1^2(t)]\,dt \qquad (9\text{-}3)$$

Otherwise, choose H_0. The decision rule may be implemented as shown in figure 9-9, a diagram of the correlation receiver, in which the input $r(t)$ is cross-correlated with the signal $s_0(t)$ and $s_1(t)$.

To determine the performance of the correlation receiver as applied to communications, assume that the probabilities of H_0 and H_1 are each ½ and that the cost of each kind of error is equal. This will result in a

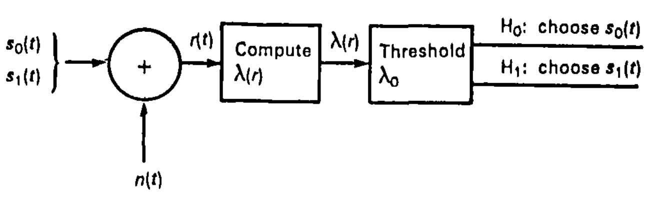

Figure 9-8.—Optimum receiver.

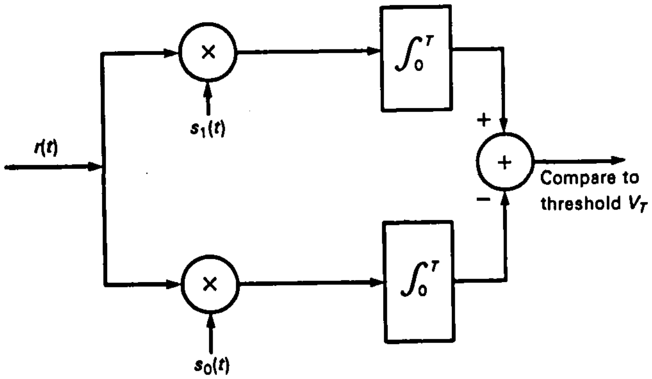

Figure 9–9.—Correlation receiver for binary signals.

minimum error probability. With these assumptions, $\lambda_0 = 1$, so the decision rule may be expressed as follows: choose H_1 if

$$\int_0^T r(t)s_1(t)\,dt - \int_0^T r(t)s_0(t)\,dt \geq \frac{1}{2}\int_0^T [s_1^2(t) - s_0^2(t)]\,dt \tag{9-4}$$

Otherwise choose H_0. Define

$$E = \frac{1}{2}\int_0^T [s_0^2(t) + s_1^2(t)]\,dt \tag{9-5}$$

and

$$\rho = \frac{1}{E}\int_0^T s_0(t)s_1(t)\,dt \tag{9-6}$$

The error probability can be written

$$P_e = \int_{[(1-\rho)E/N_0]^{1/2}}^{\infty} \frac{1}{(2\pi)^{1/2}}\,e^{-z^2/2}\,dz \tag{9-7}$$

This result gives a measure of the performance of the correlation receiver for detecting completely known signals in additive white Gaussian noise. The error performance depends on only three parameters:

(1) The average signal energy E
(2) The level of the noise spectral density N_0
(3) The time cross-correlation between signals ρ

The performance is otherwise independent of the particular signal waveforms used.

As $(1 - \rho)E/N_0$ increases, the error probability decreases. For fixed E/N_0, the optimum system is that for which the correlation coefficient $\rho = -1$. This is realizable only with "antipodal" signals, where

$$s_0(t) = -s_1(t)$$

The left-hand site of equation (9–4) can be written as

$$\int_0^T r(t)[s_1(t) - s_0(t)]\,dt$$

which makes explicit the fact that the test statistic is obtained by multiplying the noisy received signal $r(t)$ by the difference signal, which we define as

$$\Delta = s_1(t) - s_0(t) \tag{9-8}$$

The receiver block diagram of figure 9–9 can be redrawn to emphasize the role of Δ in the correlation detection process. (See figure 9–10.) Correlation detection thus requires that both signal waveforms $s_0(t)$ and $s_1(t)$ be available at the receiver or that Δ alone be available.

In the quotation from Helstrom (ref. 9–31), it is pointed out that a system in which the receiver is required to distinguish between two nonzero signals $s_1(t)$ and $s_0(t)$ is equivalent to a system in which

$$s_1(t) = \Delta$$

and

$$s_0(t) = 0$$

are the transmitted signals. That is, either Δ is transmitted or nothing is transmitted. The received signal is then

$$r(t) = \begin{Bmatrix} \Delta \\ \text{or} \\ 0 \end{Bmatrix} + n(t)$$

The correlation receiver for $r(t)$ is shown in figure 9–11. This provides another rationale for the statement that "the channel should be sufficiently wide to allow the difference signal to propagate" (ref. 9–28).

Alternatively, a matched filter receiver, which does not require the explicit presence of any of the signals, can be used to perform the computation represented by

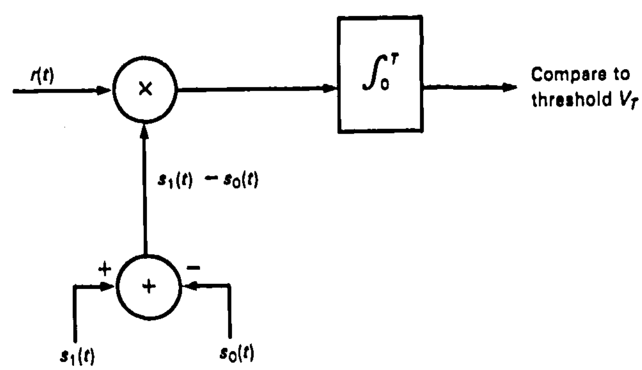

Figure 9–10.—Alternate version of correlation receiver for binary signals.

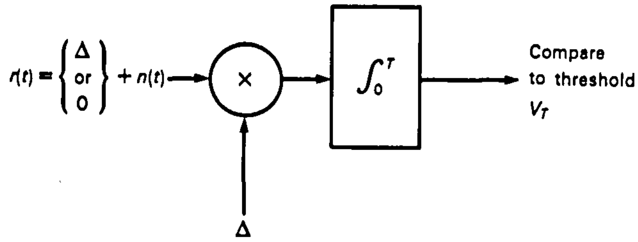

Figure 9-11.—Equivalent correlation receiver for binary signals.

the left-hand side of equation (9-4). In this case the signal properties are implicit in the impulse responses of the receiver filters. Matched filter detection can be shown to be mathematically equivalent to correlation detection and will not be further discussed.

P_e as a Function of the Difference Signal

The difference signal energy is given by

$$D = \int_0^T [s_1(t) - s_0(t)]^2 \, dt \tag{9-9}$$

By substituting equations (9-5) and (9-6) into the lower limit of the integral of equation (9-7), it is not difficult to show (ref. 9-35) that

$$(1 - \rho)E = \frac{D}{2} \tag{9-10}$$

The integral in equation (9-7) can thus be rewritten in terms of the difference signal energy as follows:

$$P_e = \int_{[D/2N_0]^{1/2}}^{\infty} \frac{1}{(2\pi)^{1/2}} e^{-z^2/2} \, dz \tag{9-11}$$

Consequently, an alternate statement concerning error performance is that P_e depends on only two parameters:

(1) The difference signal energy D
(2) The level of the noise spectral density N_0

In using a correlation receiver to distinguish between two binary signals, to obtain minimum P_e, the signal-to-noise ratio one should try to maximize is the difference signal-to-noise ratio and not necessarily the transmitted signal-to-noise ratio.

Difference Signal Waveforms of Some Binary Codes

The codes listed in table 9-4 and the spectra of their waveforms are given in Deffebach and Frost (ref. 9-1). The table shows the waveforms of $s_0(t)$, $s_1(t)$, and Δ. The time interval between the heavy dots is the bit interval $(0,T)$. These dots also represent the zero dc level of the waveform.

For each of these three codes,

$$\Delta = 2s_1(t) \tag{9-12}$$

Thus the difference signals do not impose any requirements on the bandwidths of their channels beyond that which the transmission of the signals themselves

Table 9-4.—*Some Binary Signals and Their Differences*

Code	Code signals $s_1(t)$	Code signals $s_0(t)$	Difference signal $\Delta = s_1(t) - s_0(t)$	Difference signal energy	Difference signal baseband width[a]
NRZ–L	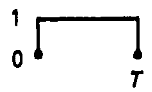		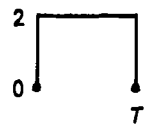	$4T$	$\frac{1}{T}$
RZ			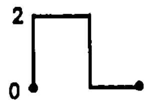	$2T$	$\frac{1}{2T}$
Biphase level (Manchester)	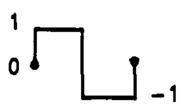	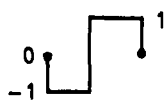	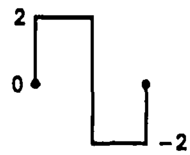	$4T$	$\frac{1}{2T}$

[a]Frequency at the first null.

imposes. In addition, the energies of the difference signals are proportional to the energies of the signals, because, very simply

$$(\Delta)^2 = 4[s_1(t)]^2 = 4[s_0(t)]^2 \qquad (9\text{-}13)$$

Code With a Wide Difference Signal Spectrum

We shall now contrive an example of a code in which the difference signal spectrum width differs greatly from that of the signals themselves. Assume that the RZ code is being used to represent one class of data and that it is decided to use a small amount of binary pulse duration modulation on the trailing edge of the RZ pulse to represent some other set of data. If the amount of PDM is represented by $\pm\epsilon T/2$, where ϵ is a constant, we now have four signals to distinguish, as shown in figure 9-12.

If ϵ is of the order of 0.01, we can use two correlation receivers, of which one processes only the RZ content of the received signals and the other processes only the PDM content of the same signals. To optimally detect the RZ code, the correlation receiver of figure 9-10 is used. We let

$$s_1(t) = \begin{cases} 1 \text{ for } 0 \le t \le T/2 \\ 0 \text{ otherwise} \end{cases} \qquad (9\text{-}14)$$

and

$$s_0(t) = \begin{cases} -1 \text{ for } 0 \le t \le T/2 \\ 0 \text{ otherwise} \end{cases} \qquad (9\text{-}15)$$

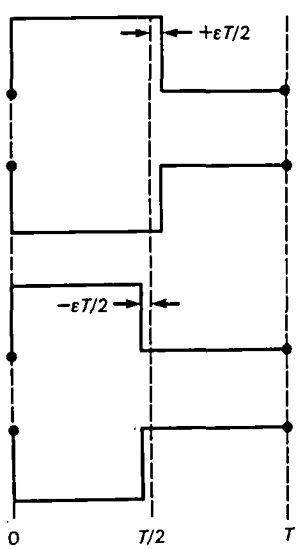

Figure 9-12.—Set of four distinguishable PDM signals.

We characterize the noisy received signals as follows:

$$r(t) = \begin{cases} s_1(t) + n(t) + n(\pm\epsilon T/2) \\ s_0(t) + n(t) + n(\pm\epsilon T/2) \end{cases} \qquad (9\text{-}16)$$

As before, $n(t)$ represents additive Gaussian noise. We treat the small duration modulation component on the RZ signal as an additional noise component, representing it by $n(\pm\epsilon T/2)$. Using this artifice, the RZ difference signal is again

$$\Delta = s_1(t) - s_0(t) = \begin{cases} 2 \text{ for } 0 \le t \le T/2 \\ 0 \text{ otherwise} \end{cases} \qquad (9\text{-}17)$$

as shown in table 9-4.

To detect the PDM component of the signal, we use the receiver shown in figure 9-13, where a second correlation receiver is preceded by an absolute value circuit. Only two signals (plus noise) that need to be distinguished can appear at the output of the absolute value circuit. They are

$$s_1'(t) = \begin{cases} 1 \text{ for } 0 \le t \le (1+\epsilon)T/2 \\ 0 \text{ otherwise} \end{cases} \qquad (9\text{-}18)$$

and

$$s_0'(t) = \begin{cases} 1 \text{ for } 0 \le t \le (1-\epsilon)T/2 \\ 0 \text{ otherwise} \end{cases} \qquad (9\text{-}19)$$

The signals are both positive and their difference signal is

$$\Delta' = \begin{cases} 1 \text{ for } \dfrac{(1-\epsilon)T}{2} \le t \le \dfrac{(1+\epsilon)T}{2} \\ 0 \text{ otherwise} \end{cases} \qquad (9\text{-}20)$$

This is a pulse of width ϵT, which occurs in the center of the bit interval $(0,T)$. (See fig. 9-14). The spectrum of this pulse is $1/2\epsilon$ times as wide as the spectrum of the RZ waveform. If the PDM is 1 percent, the difference signal

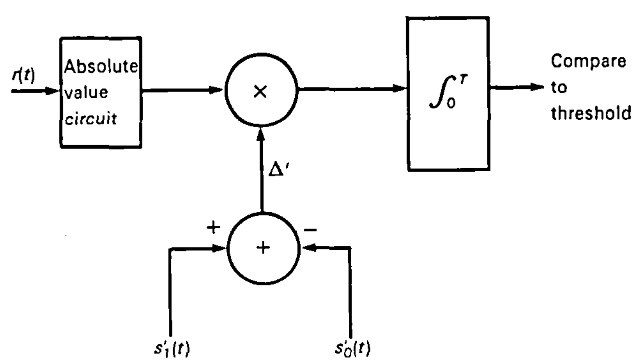

Figure 9-13.—Correlation receiver for binary PDM signals.

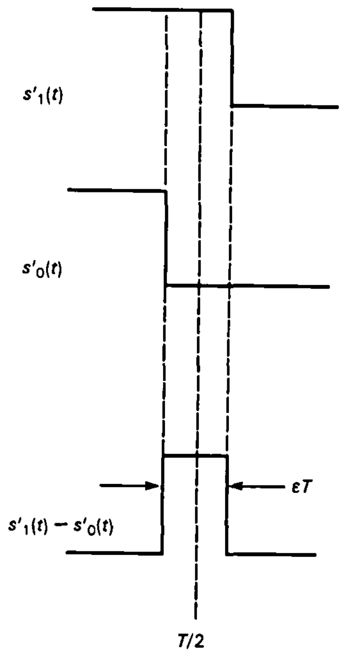

Figure 9–14.—Width of PDM difference signal.

spectral width will exceed the RZ waveform spectral width by a factor of 50.

Waveforms cannot be propagated over infinite bandwidths. Restriction of the baseband width of the system will put finite slope on the trailing edge of waveforms $s_0'(t)$ and $s_1'(t)$. The three difference signals corresponding to cases of infinite bandwidth, moderate bandwidth, and excessively narrow bandwidth are shown in figure 9–15, where linear slopes are used to approximate finite fall times.

From graphical considerations, it is apparent that the difference signal for moderate bandwidth has less energy than that for infinite bandwidth and that for narrow bandwidth has less energy than that for moderate bandwidth. With a trailing edge slope of $-1/n\epsilon T$, the energy of the difference signal for narrow bandwidth will be

$$D_N \approx \frac{D_\infty}{n} = \frac{\epsilon T}{n} \tag{9-21}$$

for large n.

The various values of D are computed by means of equation (9-9). Thus, if $s_0'(t)$ and $s_1'(t)$ are finite slope waveforms, then, for sufficiently large n, the energy in the difference signal will be reduced by a factor of $1/n$. This will cause an increase in the error probability P_e given by equation (9–11).

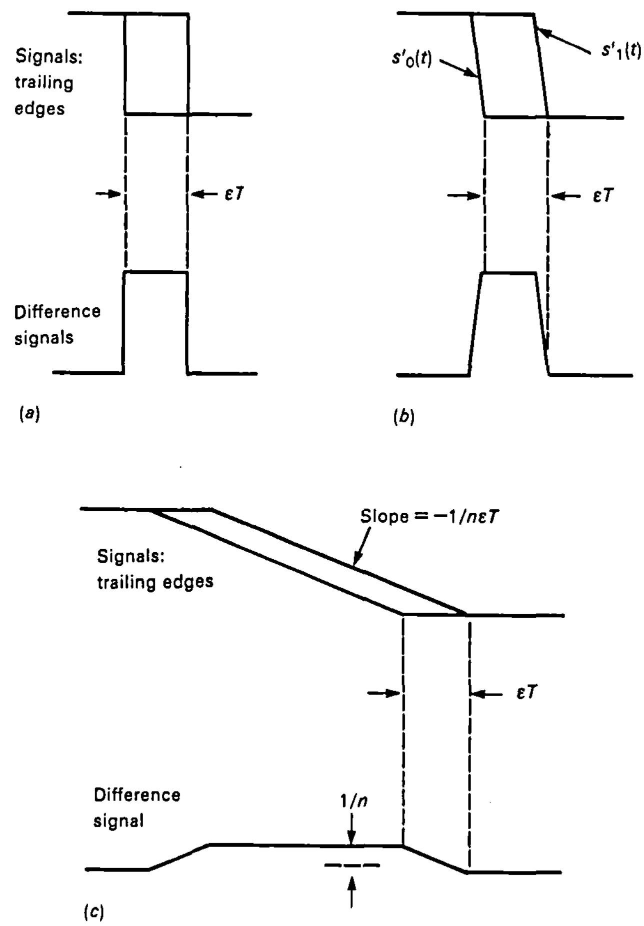

Figure 9–15.—Difference signal shape as a function of bandwidth. (*a*) Infinite bandwidth. (*b*) Moderate bandwidth. (*c*) Narrow bandwidth.

The consequence of adding a small amount of PDM modulation to the RZ waveform is seen to be the widening of the channel bandwidth well beyond that required by the RZ coding alone. Even though the difference signal is not actually transmitted, the bandwidth of the transmission channel nevertheless should be wide enough to accommodate the maximum-energy difference signal waveform, if it is desired to achieve minimum P_e.

An example of a binary code whose difference signal spectrum is only half as wide as the signal spectrum is as follows: Over the interval $(0,T)$, let

$$s_1(t) = \begin{cases} 1 \text{ for } 0 \le t \le T/2 \\ 0 \text{ otherwise} \end{cases}$$

and

$$s_0(t) = \begin{cases} -1 \text{ for } T/2 < t \le T \\ 0 \text{ otherwise} \end{cases}$$

Then, $\Delta = 1$ over the entire interval $(0,T)$. Thus Δ,

being twice as wide as either $s_1(t)$ or $s_0(t)$, has a spectrum half as wide.

Delay Modulation and the Difference Signal Concept

DM is often compared to NRZ and biphase in the following manner:

(1) It is a bandwidth compaction code (ref. 9-28, p. 833) whose average spectrum peaks at a frequency equal to about 0.4 of the bandwidth required by NRZ.

(2) It does not require much more bandwidth than NRZ, whereas biphase requires twice the NRZ bandwidth.

(3) It has relatively little power spectral density at dc, in contrast to NRZ, which is severely pattern sensitive.

(4) It is a desirable compromise choice over NRZ or biphase.

A graph of the DM spectrum that supports this reasoning is widely published (refs. 9-2 and 9-37). This graph is reproduced in figure 9-16. The Miller code is effectively a DM code. The statements presented below (in slightly paraphrased form) concerning Miller coding are typical.

> [Miller coding] . . . at once offers the virtue of very little power spectral density at dc, while maintaining the minimum interval between transitions at one bit cell; the maximum run length between transitions cannot be longer than two bit cells. Thus, the number of transitions per unit is neither so high as to require wide bandwidth, nor so low as to demand dc response [See ref. 9-38.]

> The great virtue of Miller code is that, since isolated zeroes are ignored, the . . . [ratio of data density to highest transition density] . . . remains unity as in NRZ; the bandwidth requirements of Miller code are, consequently, little greater than in NRZ [See ref. 9-39.]

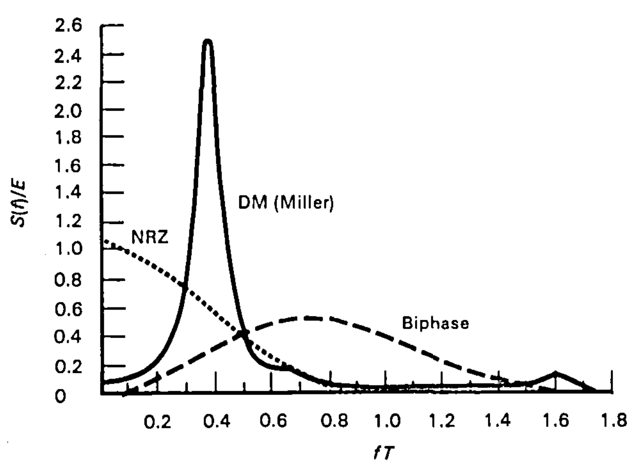

Figure 9-16.—Spectral density of NRZ, biphase, and DM coding. $S(f)/E$ = power spectral density normalized with respect to signal energy per bit; f = frequency; and T = bit period.

As we have seen, if we are interested in achieving minimum P_e, then we must make certain that the channel bandwidth can accommodate the spectrum of the difference signal waveform, not only that of the code signal waveform.

In dealing with the DM code, we no longer are concerned with distinguishing between only two signals. If the detections are made over a single data bit interval $(0,T)$, then it is necessary to distinguish between the four DM code signals listed in table 9-5. If one wants to take advantage of the redundancy in the DM code, then it is necessary to be able to distinguish between the eight code signals that can occur over an interval of $(0,2T)$ or two bit periods. (See Fig. 9-17.)

The receiver that can distinguish between more than two signals in an optimum manner is known as the maximum-likelihood receiver (ref. 9-32, p. 193, and ref. 9-40). In effect it is a means of separately correlating $r(t)$ with all possible signals, and choosing as the most plausible hypothesis H_k the signal $s_k(t)$, which corresponds to the correlator with the maximum peak output. It can also be shown that this is equivalent to processing $r(t)$ with a bank of matched filters.

We shall not concern ourselves with this more general approach, nor shall we consider the problem of detecting the four-bit DM waveform over two data bit intervals $(0,2T)$. (See fig. 9-17 and ref. 9-29.) The remainder of this section discusses DM detection over only a single data bit interval $(0,T)$.

Although four different signals are involved, the nature of the rules for DM coding allows us to construct a correlation receiver in which binary waveform difference signal concepts still apply in a straightforward manner. The DM signals used to represent single data bits are listed in table 9-5. The coding rules are such that the immediately preceding DM signal or code word influences the encoding of the latest data bit. Table 9-6 shows what the choices are as a function of the preceding DM code word. For example, if the immediately preceding DM code word is $-1,1$, then, depending on whether the new data bit is a 1 or a -1, the new DM code word will be either 1,1 or $1,-1$. The pairs of code word possibilities are listed in the center column. Each pair of possible DM code words is distinctive

Table 9-5.—*Codes for DM*

NRZ–L	DM code[a]
1	$-1,1$ or $1,-1$
-1	$-1,-1$ or 1,1

[a]Rules require that runs of "1's" or "-1's" be limited to 2, 3, or 4.

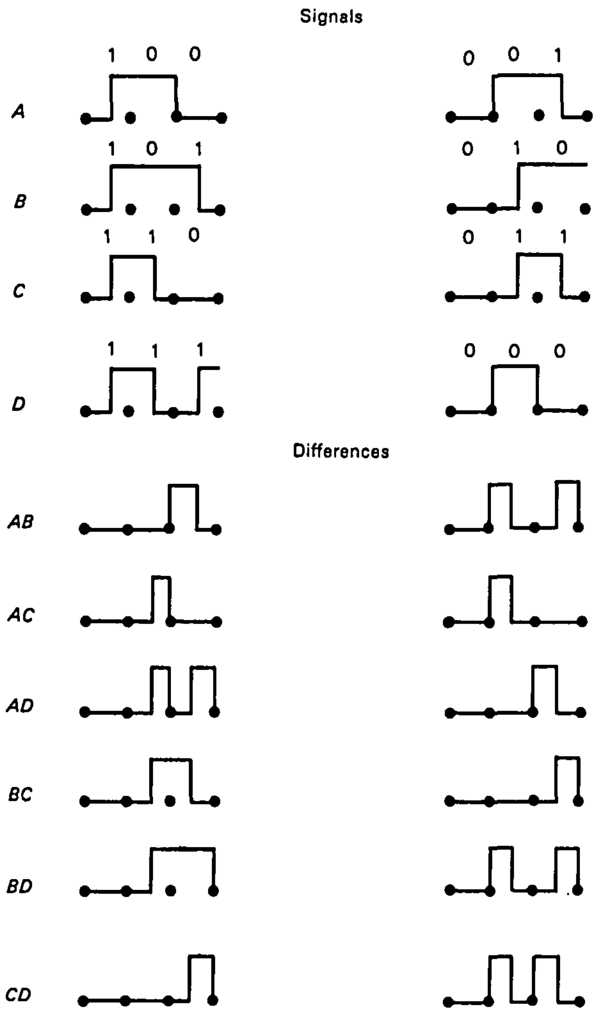

Figure 9–17.—DM signals and their differences over the interval (0,2*T*) (ref. 9–29).

Table 9-6.—*DM Code Expectancies*

If preceding DM bits* were	New DM bits will be	Applicable difference signal
−1, −1	1,1 or −1,1	2,0
−1,1	1,1 or 1, −1	0,2
1, −1	−1, −1 or −1,1	0, −2
1,1	−1, −1 or 1, −1	−2,0

*2 DM bits occupy the data bit interval (0,*T*).

and has a distinctive difference signal, as shown in the last column.

Having knowledge of the preceding DM code word allows us to apply the appropriate difference signal to the correlator multiplier in the manner shown in figure 9-18. When a hypothesis is chosen at the end of data bit interval (0,*T*), the appropriate one of the four difference signal generator outputs is immediately switched to the

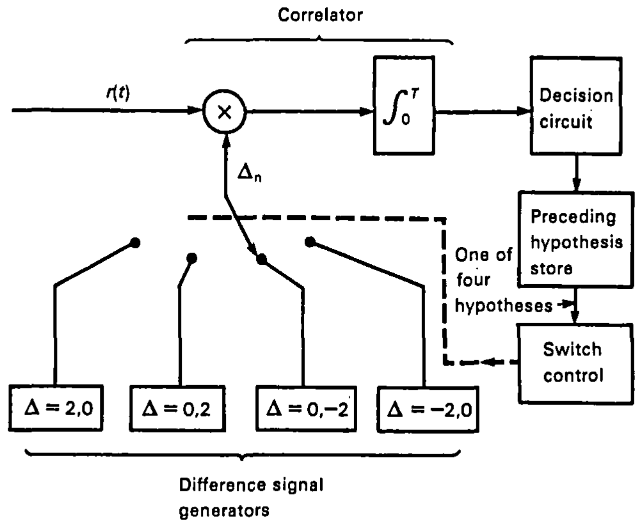

Figure 9–18.—Difference signal processing of DM code.

multiplier for use during the next bit interval (*T*, 2*T*), etc.

With this scheme of correlation detection, the DM difference signals are equivalent to either RZ or "delayed" RZ. Their bandwidth is twice that of NRZ and their energy is half that of NRZ.

If the fact that knowledge of the preceding DM code word was used in making the decision is ignored, then the P_e of the DM code will be no better than that of the RZ code. Furthermore, to achieve the P_e of the RZ code, the transmission channel bandwidth for DM should be as wide as that for RZ, which, of course, is twice as wide as that for NRZ.

It is notable that the RZ-shaped spectra of the DM difference signals exhibit no midfrequency peaking and no dropoff near dc. This is an indication that the DM code is essentially pattern sensitive and could suffer further detection losses in ac-coupled transmission systems such as direct-record magnetic tape recorder/reproducers.

It should now be clear that figure 9-16 must be used with caution. It is a signal waveform average spectrum corresponding to a bit-by-bit random data NRZ source code. Conclusions concerning "instantaneous" and worst-case pattern sensitivities of DM based on the interpretation of figure 9-16 can be misleading.

Conclusion

This paper is a discussion of the difference signal concept as it applies to some of the codes used to record digitally on magnetic tape at high bit-packing densities. Generally it has been assumed that unlimited bandwidth is available and that bit synchronization is flawless; that is, the time of arrival is completely known. The conse-

quence of operating in a bandwidth-limited manner was considered only briefly.

For economic reasons the user usually decides to maximize bit packing density rather than minimize probability of error P_e, thereby operating his system as close to an upper "band edge" bit rate as possible. Considerations of intersymbol interference now complicate the notion of the difference signal. Despite this the energy of the "distorted" difference signal remains a fundamental property of the binary signal detection process.

Although the more general notion of "distance" (ref. 9-34) should be applied when the number of alternative signals exceeds two, by considering the worst-case difference signal, the minumum "ideal" bandwidth for a system can be determined, as in the case of the PDM system outlined.

REFERENCES

9-1. Deffebach, H. L; and Frost, W. O.: "A Survey of Digital Baseband Signaling Techniques." NASA TM X-64615, June 1971. (Available from NTIS, N71-37703.)

9-2. Inter-Range Instrumentation Group: *Telemetry Standards.* IRIG 106-73, Revised, Nov. 1975.

9-3. Lindsey, W. C.; and Simon, M. K.: *Telecommunications Systems Engineering.* Prentice Hall, Inc., 1973, Ch. 1.

9-4. Castle, C. A.: "High Density PCM Tape Recording." *IEEE Trans. Instrum. Meas.* 24: 266-271, Sept. 1975.

9-5. Hopkins, P. M.; and Simpson, R. S.: "Probability of Error in Pseudonoise (PN)-Modulated Spread Spectrum Binary Communication Systems." *IEEE Trans. Comm. Technol.* 23: 467-472, Apr. 1975.

9-6. Cattermole, K. W.: *Principles of Pulse Code Modulation.* Amer. Elsevier Pub. Co., Inc., 1969.

9-7. Davidson, M.; Haase, S.; Machamer, J., and Wallman, L.: "High Density Magnetic Recording Using Digital Block Codes of Low Disparity." *IEEE Trans. Magn.* 12: 584-586, Sept. 1976.

9-8. Morizono, M.; Yoshida, H.; and Hashaimot, Y.: "Digital Video Recording—Some Experiments and Future Considerations", *Soc. Motion Pict. Telev. Eng. J.* 89: 658-662, Sept. 1980.

9-9. Wells, J. B.: "High Density PCM Magnetic Tape Recording." Vol.IX, *Int. Telemetering Conf.,Proc.*, 1973, pp. 66-73.

9-10. Hedeman, W. R.: "Baseband Frequency Response Requirements of an NRZ Pulse Train With Periodic Forced Transitions." *Telemetry J.*, pp. 30-31, Aug./Sept.1968.

9-11. Hecht, M.; and Guida, A.: "Delay Modulation." *Proc. IEEE* 57: 1314-1316, July 1969.

9-12. Spitzer, C. F.; "Digital Magnetic Recording of Wideband Analog Signals." *Comput. Design* 12: 83-90, Oct. 1973.

9-13. Kalstrom, D. J.: "Simple Encoding Schemes Double Capacity of Flexible Disc." *Comput. Design* 15: 98-102, Sept. 1976.

9-14. Mallinson, J. C.; and Miller, J. W.: "Optimal Codes for Digital Magnetic Recording." *Radio Electron. Eng.* 47: 172-176, Apr. 1977.

9-15. Patel, A. M.: "New Method for Magnetic Encoding Combines Advantages of Older Techniques." *Comput. Design* 15: 85-91, Aug. 1976.

9-16. Gabor, A.: "Adaptive Coding for Self-Clocking Recording." *IEEE Trans. Electron. Comput.*:16: 866-868, Dec. 1967.

9-17. Jacoby, G. V.: "A New Look-Ahead Code for Increased Data Density." *IEEE Trans. Magn.* 13: 1202-1204, Sept. 1977.

9-18. Mackintosh, N. D.: "The Choice of a Recording Code." *Radio Electron. Eng.* 50: 177-193, Apr. 1980.

9-19. Tamura, T.; Tsutsumi, M., Aoi, H.; Matsuishi, H.; Nakagoski, K.; Kawano, S.; and Makita, M.: "A Coding Method in Digital Magnetic Recording." *IEEE Trans. Magn.* 8: 612-614, Sept. 1972.

9-20. Ringkjøb, E. T.: "Achieving a Fast Data-Transfer Rate by Optimizing Existing Technology." *Electronics* 48: 86-91, May 1, 1975.

9-21. Trafton, P. J.; McAllister, N. F.; Turnstall, B. T.; Brenza, N.; Elliot, J. C.; Paul, H. I.; and Fox, P. W.: *Error Protection Manual for AFCS.* AD 759-836, Nov. 1972. (Available from the National Technical Information Service.)

9-22. Franklin, J. N., and Pierce, J. R.: "Spectra and Efficiency of Codes Without dc." *IEEE Trans. Commun. Technol.* 20: 1182-1184, Dec. 1972.

9-23. Halpern, P. H.: "High Density Data Processing System." U.S. Patent 4,020,282, Apr. 26, 1977.

9-24. Franaszek, J. A.: "Sequence State Coding for Digital Transmission." *Bell Syst.Tech. J.* 47: 144, 1968.

9-25. Davidson, M.; and Machamer, J. L.: "High Density Digital Magnetic Recording Using the (5,6) Alternating Disparity Block Code." *Electron. Lett.* 14: 459-460, July 1978.

9-26. Davidson, M.: "Results of Testing an Error Correction Encoding/Decoding System." Paper presented at meeting, THIC, Oct. 19, 1976.

9-27. Luke, P. J.; Machamer, J. L.; and Becraft, W. A.: "Error Correction Encoder and Decoder." U.S. Patent 4,107,650, Aug. 15, 1978.

9-28. Pelchat, M. G.; and Geist, J. M.: "Surprising Properties of Two-Level 'Bandwidth Compaction' Codes." *IEEE Trans. Commun. Technol.* 23: 878-883, Sept. 1975.

9-29. Waggener, W. N.: *Optimum Detection of Delay Modulation.* Tech. Note TN-72-001, EMR Telemetry, Feb. 1972.

9-30. Halpern, P.: "High Density Data Processing System." U.S. Patent 3,921,210, Jan. 14, 1974.

9-31. Helstrom, C. W.: *Quantum Detection and Estimation Theory.* Academic Press, Inc., 1976, p. 165.

9-32. Helstrom, C. W.: *Statistical Theory of Signal Detection.* Pergamon Press, 2d ed. 1968, p. 188.

9-33. Kotel'nikov, V. A. (R. A. Silverman, Trans.):*The Theory of Optimum Noise Immunity.* Doctoral dissertation (1947), McGraw-Hill Book Co., Inc., 1959, p. 26.

9-34. Wozencraft, J. M.; and Jacobs, I. M.: *Principles of Communication Engineering*. John Wiley & Sons, Inc., 1965, p. 250.

9-35. Ristenbatt, M. P.: "Alternatives in Digital Communications." *Proc IEEE*, 61(6): 703-721, June 1973.

9-36. Whalen, A. D.: *Detection of Signals in Noise*. Academic Press, Inc., 1971, ch. 6.

9-37. Spitzer, C. F.: "Digital Recording of Video Signals Up to 50 MHz." *Proc. Soc. Photoopt. Instrum. Eng.* 36, 1973.

9-38. Spitzer, C. F.; Jensen, T. A.; and Utschig, J. M.: *Study, Tests, and Evaluation for Wideband High-Density Data Acquisition (WHIDDA)*. Final Report (Wright-Patterson Air Force Base AFAL-TR-76-115), Ampex Corp., Redwood City, Ca., Apr. 1976 (Available from NTIS.)

9-39. Mallinson, J. C.; and Miller, J. W.: "On Optimal Codes for Digital Magnetic Recording." *Proc. IERE Conf. Video and Data Recording*, 1973. (Also available from Ampex Corp., Redwood City, CA.)

9-40. Lucky, R. W.; Salz, J.; and Weldon, E. J.: *Principles of Data Communication*. McGraw-Hill Book Co., Inc., 1968, p. 96.

CHAPTER 10

Miller Squared Coding

James Kelly
Ampex Corporation

DIGITAL RECORDING ON LONGITUDINAL RECORDERS

History of PCM

PCM was used as early as 1932 by Bell Telephone Laboratories for the transmission and storage of audio information. Because FM/FM had been developed earlier and was already quite reliable, these early PCM systems were used primarily for digitizing the output of the FM/FM systems to provide compatible inputs to computation devices. With the advent of the transistor, however, the complex circuitry of the PCM systems was reduced in size to that comparable with the FM/FM systems, and thus it gradually developed into more widespread use in the telemetry field.

Advantages of PCM

PCM is a form of data transmission and recording that depends on the coding of information in the form of discrete pulses. The codes used may be identical to those used for digital computer use, or, more likely, they may be different. Over the years, a number of coding schemes were developed depending on the requirements of the user's system.

PCM data transmission and recording were developed because of the need for higher accuracies. While pulse amplitude modulation and pulse duration modulation are capable of handling data with accuracies up to about 1 to 2 percent of full scale (though normally closer to 5 percent), there is a need for much higher accuracies in some cases. PCM affords a means for transmitting information with accuracies in excess of 1/2 percent of full scale.

When comparing PCM with FM/FM, one should compare the required bandwidths and power for accuracy obtainable. PCM can be 10 to 20 times more accurate than FM/FM, given the same bandwidth and power limitations.

There are also other advantages to PCM, particularly when data frequencies are very high. Once the data are in digital form, they can be stored for any length of time, transmitted over any distance, retransmitted, detected, or read out as many times as necessary without loss of accuracy. Analog signals become distorted and lose accuracy with each process. Digital signals are inherently less sensitive to noise, such as stray pickup, drift, environmental effects, attenuation, etc. This is because a digital system is concerned only with the presence or absence of a signal, and does not provide a precise measurement of the signal conditions.

Coding Schemes

NRZ Code

The most commonly used format for digital data recording is the NRZ data code. The NRZ code is characterized as a two-level signal with the data either at one voltage level or the other. The type of code used defines the meaning of these levels and the position of the transition between them. Because the data may occupy one of the two given voltage states for a significant period of time, the recorder low-frequency response must extend very close to dc to prevent distortion of the signal wave shape in the form of baseline galloping. Such a condition is not necessarily a result of low data rate, but may be caused by a succession of missing values in a given PCM frame with a resulting long string of "0's."

The reproduced NRZ signal must usually be reshaped before further processing can occur, which compounds the design problems. The circuit design is also compromised and becomes more susceptible to noise and loss of level due to tape dropouts.

Another incompatibility between NRZ codes and the direct recorder system is the pulse-to-pulse jitter or timing error. A clock can be extracted from the data as long as the timing error does not exceed plus or minus one half a bit cell. NRZ data can have long strings of "1's" and "0's," during which time no changes in the signal occur. If the timing errors exceed the half bit cell, then the bit cell must be increased, which reduces the packing

density. One other limitation is the system SNR. Noise, like jitter, reduces the ability to extract a clock from the data. The high-frequency response required for an NRZ code is approximately a sine wave response of one-half the digital bit rate. This means that a data channel with a sine wave frequency response of 2 MHz could handle 4-Mbps NRZ data.

There are two general types of NRZ codes in use. The first is NRZ−L. In this code the data remain at one voltage level during the total time a digital "1" is present in the data and return to the other voltage level for a digital "0." In NRZ−M, a digital "1" is indicated by a transition between the two voltage levels and a digital "0" is indicated by the absence of a transition. Due to the lack of transitions in the NRZ−L code during a continuous string of data "1's," there is no data correction signal before a following "1"/"0" transition in case of a missed bit. This means that a number of bits may be incorrectly sensed if a single transition is missed in NRZ−L. With NRZ−M data, this type of error is confined to a single bit transition, thus giving NRZ−M a distinct advantage in data reliability. Both have the same bandwidth requirements. The actual comparison of these signal waveforms for a given set of digital data is indicated in figure 10-1.

The NRZ codes have two major limitations, the requirement for dc response and the susceptibility to time base errors. The packing density for NRZ codes in most applications has been limited to approximately 6 kbpi/channel with bit error reliability of 1 in 10^6.

Self-Clocking Codes

It is sometimes desirable to simplify the data detection process by the use of a digital recording code that carries both the data and clock information in a single signal format. Such a recording code normally requires more bandwidth than data recorded in the NRZ manner but does offer some peripheral benefits. The Biϕ−L and Biϕ−M (Manchester codes) shown in figure 10-1 are typical examples of this type of recording. In the Biϕ−L code, the polarity of the transition in the middle of the bit period determines the polarity of the data recorded. In the case shown, a positive signal represents a data "1" and a negative signal represents a data "0." The necessary manipulations to provide transitions at the clock times are provided by the data encoding electronics. In the Biϕ−M code, the existence of a digital "1" is shown by the presence of a data transition in the center of the bit period. A digital "0" is shown by an absence of a transition.

When this method of data encoding is used, the frequency spectrum of the recorded signal is limited to a range of two octaves. The low-frequency response of the channel required is one-half the clock frequency rather than the dc frequency response required for accurate reproduction of NRZ codes. The high-frequency

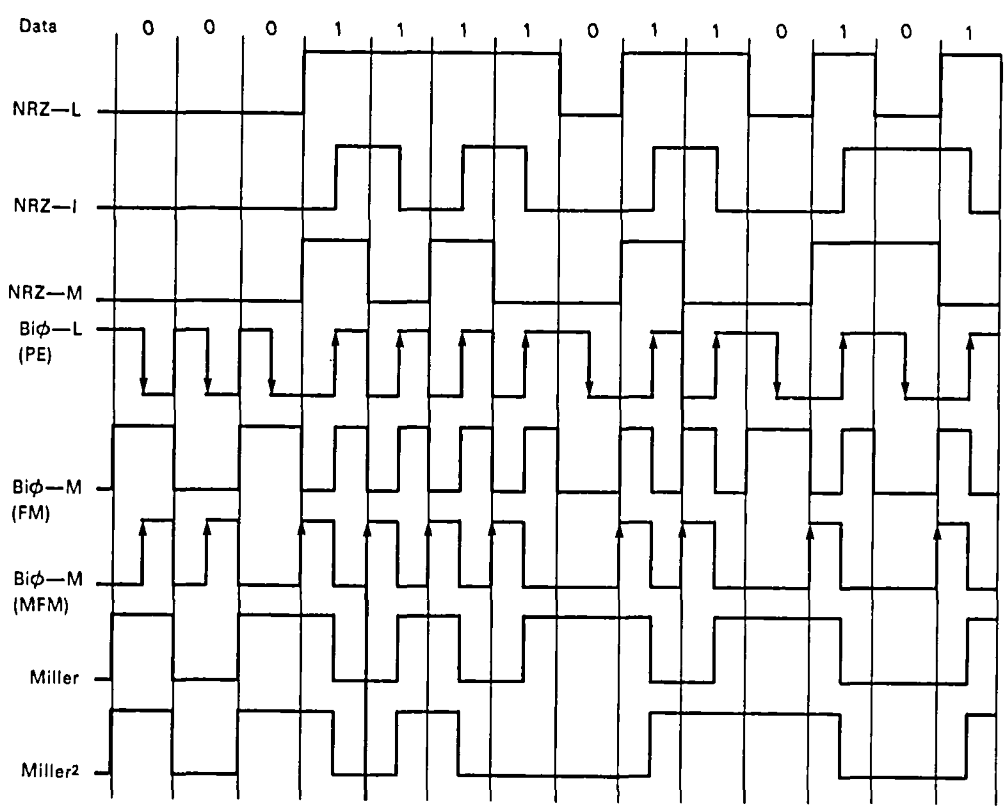

Figure 10-1.—Binary codes.

limit corresponds to that of the clock frequency that would be produced in the Biϕ – M code by a continuous string of data "1's"; bit rate and upper frequency response are the same. In practice, the signal is usually filtered on reproduction to eliminate noise occurring outside this range, and thus the SNR and bit reliability are improved.

In summary, recorder systems employing the Manchester codes have avoided some of the disadvantages of the NRZ codes. The major advantages are that dc response is not required and the pulse-to-pulse jitter becomes negligible because biphase data contain data transitions every clock period regardless of the data content. These advantages are outweighed for the most part, however, by the additional bandwidth required. The packing densities for Manchester codes have approached 12 kbpi/channel with bit error reliability of 1 in 10^6.

RZ/RB Codes

Two of the simplest pulse waveforms, conceptually, are the return-to-zero (RZ) and return-to-bias (RB) codes. In the RZ code, a "1" is represented by a positive pulse, and a "0" by a negative pulse. The RB code is a simpler form of this code in which a single pulse (either polarity) is generated for each data "1," and the absence of a pulse signifies a data "0." The codes are not self-clocking and require a bandwidth equal to or greater than NRZ data, due to the narrow pulsewidths normally used. The RB code is a two-level nonsymmetrical signal, so the low-frequency bandwidth approximating dc is again required to prevent baseline galloping and its corresponding loss of data. The high-frequency response required for these codes is greater than either the NRZ or self-clocking phase shift codes.

The RZ multilevel code inserts another set of pulses of a different amplitude for data "0's." In addition, a third level is sometimes used that provides word-by-word separation. Here we have the same low-frequency response requirements as the basic RZ code but with two or three times the high-frequency response needed. In addition, we also increase the required SNR for the same data reliability due to the multiple amplitude coding used. If the SNR is available on the data channel, this code might find special use; however, in most cases an RZ coding scheme is technically obsolete.

PRINCIPLE OF WIDEBAND ANALOG/DIGITAL/ANALOG SYSTEMS

The basic signal system of an analog/digital/analog (A/D/A) recorder/reproducer based on the multitrack longitudinal concept is shown in figure 10-2.

The sampling theorem can be stated as follows: Any two f_m independent samples per second will completely characterize a signal band limited at frequency f_m (ref. 10-1).

There are practical difficulties in designing a low-pass filter with sharp cutoff characteristics (to achieve true band limiting at f_m). In addition a gradual rolloff is needed to avoid undesirable phase shifts. A higher sampling rate, therefore, is used. For instance, we could elect to sample at a rate of three f_m samples per second. If we choose a multilevel code of base n, and each sample is represented by m such code groups, the signal is digitized into n^m quantization levels.

The digit rate becomes, therefore,

$$(m \text{ digits/sample}) \times (3 f_m \text{ samples/s}) = 3\, mf_m \text{ digits/s}$$

For a recorder with N parallel tracks, the required digit rate is

$$3mf_m/N \text{ digits/s/track}$$

If we decide on 128 quantization levels in the binary code (i.e., $2^m = 128$, $m = 7$), use a 42-track machine ($N = 42$), and wish to record $f_m = 10$ MHz, the rate of binary pulses becomes 5.0 Mb/s/track.

If, on the other hand, we choose a quaternary code ($n = 4$) for 128 quantization levels, the same machine could record 20 MHz, at a rate of 5×10^6 quaternary digits/s/track, although with a higher error rate.

We now must examine the system of figure 10-2 in more detail to show that the proposed A/D/A record/reproduce system is, in fact, feasible. (Refer to fig. 10-3.)

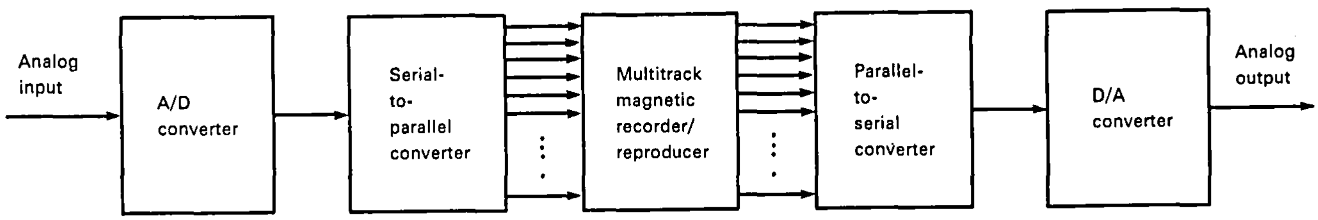

Figure 10-2.—Simplified block diagram of an A/D/A record/reproduce system.

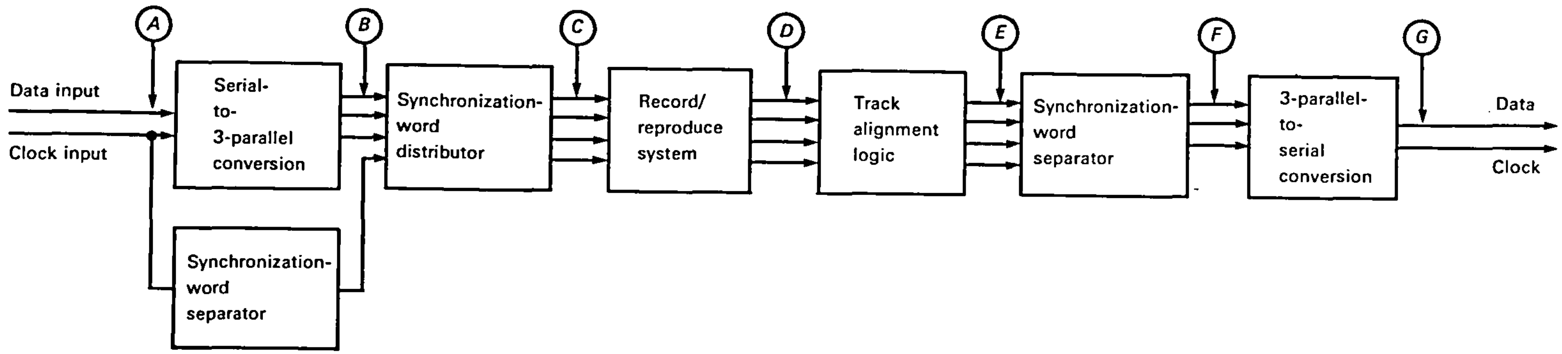

1	2	3	4	5	6	7	8	9	10	11	12	13	14	15	16	17	18	19	20	21	22	23	24	25	26	27	28	29	30	31	32	33	34	35	36	37	38	39	40	41	42	43	44	45	46	47	48	49	50	51	52	53	54	55	56	57	58	59	60	61	62	63	64	65	66	67	68	69	70

A

1	4	7	10	13	16	19	22	25	28	31	34	37	40	43	46	49	52	55	58	61	64	67	70
2	5	8	11	14	17	20	23	26	29	32	35	38	41	44	47	50	53	56	59	62	65	68	71
3	6	9	12	15	18	21	24	27	30	33	36	39	42	45	48	51	54	57	60	63	66	69	72
S1	S2	S3	S4	S1	S2	S3	S4	S1	S2	S3	S4	S1	S2	S3	S4	S1	S2	S3	S4	S1	S2	S3	S4

B

1	4	7	10	S1	S2	S3	S4	25	28	31	34	37	40	43	46	49	52	55	58	S1	S2	S3	S4
2	5	8	11	13	16	19	22	S1	S2	S3	S4	38	41	44	47	50	53	56	59	61	64	67	70
3	6	9	12	14	17	20	23	26	29	32	35	S1	S2	S3	S4	51	54	57	60	62	65	68	71
S1	S2	S3	S4	15	18	21	24	27	30	33	36	39	42	45	48	S1	S2	S3	S4	63	66	69	72

C

E Equals C plus delay

F Equals first three lines of B plus delay

G Equals A plus delay

1	4	7	10	S1	S2	S3	S4	25	28	31	34	37	40	43	46	49	52	55	58	S1	S2	S3	S4
2	5	8	11	13	16	19	22	S1	S2	S3	S4	38	41	44	47	50	53	56	59	61	64	67	70
3	6	9	12	14	17	20	23	26	29	32	35	S1	S2	S3	S4	51	54	57	60	62	65	68	71
S1	S2	S3	S4	15	18	21	24	27	30	33	36	39	42	45	48	S1	S2	S3	S4	63	66	69	72

D Master

Figure 10–3.—Complete data handling and timing diagram.

A/D Converter

At Ampex, substantial work is being done in digital television recording. Typically, the signal is digitized to 256 levels, i.e., 8 bits/sample. With Motorola MECL III logic (or equivalent), and to a resolution adequate for our purpose (e.g., 128 levels), signals of 16 MHz, for example, could be readily digitized.

Serial-to-Parallel Converter

This device is a logic system performing a "fan out" function on the high bit rate data stream. Work at Ampex has resulted in logic circuits, using MECL III components, operating at over 175 Mbps; even faster logic components are becoming commercially available. We already have substantial experience in the design of serial-to-parallel converters.

Several Multitrack Recorder/Reproducer systems exist as flight-qualified hardware and are capable of accommodating up to 42 tpi on 1-in.-wide tape. A significant task will consist of distributing the data stream over the available tracks in such a way that reassembly into a single bit stream becomes feasible upon playback. To this end, the simple block diagram of figure 10-2 must be replaced by that of figure 10-3. The timing diagrams indicate the data distribution for a 4-track system, although in a more realistic situation 40 data tracks or even more may be required. However, the principles illustrated in this example are equally applicable to a larger number of parallel tracks. The input data stream at point *A* consists of serial digital data as shown in line *A* of the timing diagram.

The serial-to-parallel converter fans out the data stream into three parallel tracks, each operating at a bit rate compatible with reliable recorder operation. However, in anticipation of timing problems introduced in recording and reproducing, a synchronization word is now added to the data to later aid in the process of bit synchronization. In the example, line *B* shows that the fourth track at point *B* carries the 4-bit synchronization word, S_1, S_2, S_3, S_4. The bit rate per track is clearly 1/3 of the system input bit rate. In general, therefore, we require $n+1$ tracks if the input bit rate is to be n times as high as the recorded track rate.

Synchronization Word Insertion

The synchronization word distributor serves to replace, in one track after the other, four data bits with a synchronization word. The displaced data bits are meanwhile transferred to the original synchronization word track. In this manner no data are lost, each track carries a 4-bit synchronization word after every 12 data bits, and the track bit rate is ⅓ of the serial input data rate. Line *C* of the timing diagram illustrates the conditions at point *C*.

Recording/Reproducing and Bit Synchronization

Uncontrollable dynamic skew motion of the tape in the recorder, track-to-track variations in record-gap-to-reproduce-gap distance, and other effects bring about dynamic changes in the relative bit positions during playback as suggested in line *D* of the timing diagram for point *D* of figure 10-3. The sources and magnitudes of such bit displacement errors are as follows:

Source of error	*Distance on tape peak to peak, μin.*
Within the same head stack:	
Static	
Gap azimuth (1 arcmin, 1 in. head); combined effect of recorder/reproducer (ref. 10-2, sec. 5.6.2.2.2(g))	600
Gap scatter (100-μin. band); combined effect of recorder/reproducer (ref. 10-2, sec. 5.6.2.2.2(f))	200
Total static error (worst case)	800
Dynamic	
Track-to-track: 0.15-μs zero to peak at 120 ips (ref. 10-3)	36
Dynamic skew over one head stack 6×36	216
Total skew within a head stack	1016
Between head stacks:	
Static (ref. 10-2, sec. 5.6.2.2.2(b))	4000
Dynamic	
From experience	500
Total worst-case skew error at 120 ips	5516
Time base error at 120 ips ±0.30 μs (ref. 10-3)	72
Total worst-case timing variation at 120 ips	5588

The timing of the synchronization is used as a means to resynchronize the data bits; the track alignment logic delays the data in suitable shift registers that are in turn timed by a clock signal extracted from the reproduced data. (One track is arbitrarily appointed "master" channel for this purpose). The result of the track alignment at point *E* is a reproduction of timing diagram line *C*. The conditions of point *C* are, therefore, established.

Synchronization Word Separation

It merely remains now to "strip" the synchronization words in the synchronization word separator and to discard them. At point *F* the three data tracks carry properly synchronized data words just as at point *B*.

Parallel-to-Serial Conversion

Finally, a parallel-to-serial converter reassembles the data from the three parallel tracks into a single output data stream except for such occasional bit errors as may result from dropouts during the record/reproduce sequence. Typically, such errors can be held as low as one error in 10^7 bits. Error correcting codes can reduce such errors even further.

BASIC LIMITATIONS OF RECORDER/REPRODUCER SYSTEMS

In recording high-density digital data on a longitudinal instrumentation recorder several recorder parameters play a significant part in determining the BER of the data storage system:

(1) High-frequency response
(2) Signal amplitude stability
(3) Low-frequency response
(4) Phase response
(5) System noise
(6) Tape speed errors (jitter, time base error, etc.)
(7) Magnetic tape performance

Because performance relating to these parameters varies widely according to machine type, the following sections are included to identify the type of information required before an estimate of the capabilities of any system can be made and to highlight the advantage of Miller code in circumventing these limitations.

The instrumentation recorders used at the majority of the data gathering installations are normally configured to handle analog signals and are optimized for this type of waveform. The use of these recorders in conjunction with the Miller code to handle serial digital information requires consideration of the following nonoptimized parameters of the recorder to assure accurate digital signal reproduction.

High-Frequency Response

The basic limitation to the upper digital packing density limit obtainable on any recorder is the maximum frequency that can be recorded and reproduced on the data track. For an NRZ or Miller type code the maximum digital recording density that can be assumed is 1.5 bits/sine wave cycle of channel bandwidth. This corresponds to a data rate of 3 Mbps with a 2-MHz signal channel. Another consideration is the signal-to-noise ratio (SNR) at the high-frequency end of the signal bandpass. It must be sufficient to allow accurate signal reproduction. Otherwise, the high data rate will be obtained only at great expense in data reliability.

Signal Amplitude Stability

An analogous problem and one dependent upon the upper frequency limit of the recorder is the signal amplitude stability. The amplitude stability of the reproduced signal on all records is degraded more and more as the upper bandwidth of the signal is approached because of the shorter wavelengths being recorded. If direct recording methods are used, the envelope of an upper band edge signal is not entirely constant. These variations in signal amplitude caused by head-to-tape perturbations or dropouts may range from 4 to 10 dB in amplitude. The only known method for minimizing this problem involves the use of a tape transport with closely controlled head-to-tape contact.

Low-Frequency Response

When direct recording is used with digital data codes, the low-frequency response of the recorder/reproducer can become critical. Under worst-case conditions some methods of digital signal encoding produce nonsymmetrical waveforms with long periods separating signal transitions. The limited low-frequency response of the direct channel (400 Hz) causes a phenomenon known as "baseline shifting," a change in the dc baseline caused by the random combinations inherent in digital data. The only way to minimize this effect in direct recording with NRZ-type data format is to control the total time allowed between data transitions under worst-case conditions. In this manner at least one digital bit is inserted per word, thus limiting the time allowed for one unchanging data level.

Baseline instability can also be eliminated through FM recording of the NRZ digital signals. Because of limitations in the FM detection process, the signal amplitude stability of the detected FM signal is much better than in a direct system, thus eliminating the effect of minor dropouts. Due to the dc response of the FM method, the baseline instability is also eliminated. Unfortunately, the limited signal bandwidth of an FM system also limits its suitability for use in storage of large volumes of digital data. For low bit packing densities, however, the NRZ code in conjunction with an FM record system will provide equal or better performance than the Miller code system.

Phase Response

Nonlinearities in the phase frequency response characteristic of the record/reproduce process have

been found to seriously affect bit reliability. The exact relationships between phase shift and error rate are not established.

System Noise

The SNR of the basic data channel, including the recorder/reproducer link, is vitally important for digital applications. A significant amount of literature has been published on this subject; therefore, no attempt will be made to cover it in detail in this chapter. Suffice it to say, the recorder/reproducer must offer an SNR exceeding the theoretical value required to achieve the desired bit error rate.

Tape Speed Errors

Another problem that has historically plagued the recording and reproduction of a digital waveform is the time instability introduced by the tape transport. In the past the allowable low-frequency jitter, or time base error, was drastically limited by the ability of the synchronizer to track a signal of varying bit rate and maintain lock. High-frequency jitter appears to the synchronizer as a reduced SNR, either degrading bit error performance or requiring a better channel SNR for the same BER.

Summary of Limitations

The primary function of the Miller code is to provide an improved method of encoding digital information for storage of large volumes of data on the magnetic tape recorder. These data can then be played back at normal or reduced speed (time base expansion). The code possesses several unique features that make it ideally suited to circumvent the problems normally associated with the recording of digital data on the longitudinal tape recorder, thus allowing higher bit packing densities to be achieved at stringent BER's.

SYSTEM PERFORMANCE

Digitization of a signal offers significant advantages in situtations of noise contamination, limited dynamic range, or perturbations of the time base. Such problems are typically encountered in some forms of data transmission and even more so in magnetic tape data recording and reproducing. In this section we estimate the effect of A/D/A operation on the performance specifications of a practical magnetic recorder/reproducer.

SNR and Basic Recorder Design

If a signal voltage is sampled and digitized, an error is necessarily incurred because the signal will probably not have been at the exact quantizing level at the instant of sampling, even if the sample was taken at precisely the correct instant. The rms value of the resulting digitizing error, or "quantization noise," is given by

$$\text{rms error} = -(6m + 10.8) \quad \text{decibels}$$

where m is the number of bits per sample. (From this equation we derived the values in table 10-1.) If the effect of gaussian noise can be made small compared to the quantization noise, we might select a 7-bit (128-level) system yielding a quantization noise of about −53 dB. The effective peak-to-peak signal/rms noise will actually be degraded if white noise is artificially introduced.

Signal Dynamic Range

Signal dynamic range (SDR) and SNR are often considered synonymous. In our system, however, we are free to trade SDR for system complexity. For example, a 4-MHz signal could be recorded with an SDR as high as 58 dB or even higher on a machine of suitable design. In other words, an unprecedented SDR becomes possible provided effective channel bandwidth is increased by the addition of recorder tracks.

Time Base Error

Time base errors can be introduced from several sources such as inaccuracies in sampling intervals, fluctuating duration of sampling pulses, tolerances on the quantizing levels, and corresponding errors in the reconversion process to reconstitute the analog output signal. It has been found, however, that a 256-level (8-bit) code will provide better than 4° phase resolution at a 5.0-MHz signal bandwidth. This performance would be degraded, however, by such factors as fewer levels, wider bandwidth, and D/A converter inaccuracies. Analogous to the case of rotary head transverse magnetic recorders, a pilot signal exists, in the form of clock pulses extracted from the reproduced signal, and is subsequently compared with a stable clock to control tape speed (to remove a major error source) as well as to act as a digital buffer of suitable length to further decrease the time base error in the output data.

Table 10-1.—*RMS Values of Quantization Noise for Selected Numbers of Bits Per Sample*

Bits per sample	Voltage levels per sample	RMS value of quantization noise, dB
3	8	−28.8
4	16	−34.8
5	32	−40.8
6	64	−46.8
7	128	−52.8

Spurious Signals

Spurious signals can be introduced in the quantization process as a result of coherent quantization errors. This nonlinear effect will cause harmonic and intermodulation products but can be essentially removed through the introduction of white noise of a magnitude of two to three quantization levels.

The largest contribution of spurious signals will probably be at the sampling frequency; i.e., at three times the highest signal frequency. Because this is well beyond the system passband, significant disturbances to the output signal from this source can only arise as a result of intermodulation in the final D/A conversion process. The signal in digital form typically is comparatively immune to nonlinear distortion. It is conceivable that for "pathological" data sequences this immunity may be somewhat compromised. On the whole, therefore, provided adequate care was taken with the design of the D/A converter, spurious signals from any source (including nonlinear products) should be less than −30 dB in the A/D/A record/reproduce system.

Bandwidth Reduction

Because the bandwidth of the recorder/reproducer is severely limited by head response and head-to-tape interface problems, it is clearly essential to reduce the required recording bandwidth and to match the spectral response requirements of the code to those of the recorder. This can be accomplished by several means.

Code Selection

Certain codes have lower spectral content than others. For example, the Ampex Miller code has about half the spectral content of other commonly used codes.

Data Compression

Data compression through redundance removal has been used for many years in an attempt to reduce the bandwidth required for television image transmission. For example, if the signal does not change over a significant number of sampling intervals, it may be more economical to record the value and the start and finish times of the unchanging data sequence than to record each sample. In addition, one might apply similar reasoning to the first derivative of the analog input signal.

Data compression ratios of 5:1 have been achieved in image transmission with tolerable degradation. Unquestionably, the requirements of instrumentation recording are more severe, but even a 2:1 compression ratio may be worthwhile, provided equipment complexity and cost are not prohibitive.

Calculation of the RMS Value of Quantization Noise[1]

An increase in effective recorder channel bandwidth may be achieved through an increase in the number of tracks (i.e., space multiplexing of the digitized input signal).

Improvement of Wideband SNR

If the available channel bandwidth can be made wider than needed to accommodate the maximum signal frequency f_m, then bandwidth can be traded off for an improvement in the recorder SNR. It can be shown that in the case of coded systems, such as PCM, in which the signals are digitized prior to data recording, the improvement is exponential with bandwidth:

$$(\mathrm{SNR})_{\mathrm{coded}} = (\mathrm{SNR})_{\mathrm{dir}}^{B/f_m}$$

where

B = total of effective bandwidth of the multitrack recorder/reproducer, Hz
f_m = maximum signal frequency, Hz
$(\mathrm{SNR})_{\mathrm{dir}}$ = recorder/reproducer SNR for direct recorded signals, dB

whereas, in uncoded systems, analog systems such as AM, FM, PAM, and PPM, the improvement is linear:

$$(\mathrm{SNR})_{\mathrm{uncoded}} = K\frac{B}{f_m}(\mathrm{SNR})_{\mathrm{dir}}$$

where K = constant of proportionality (e.g., $K=\sqrt{3}$ for FM and $K = 1/\sqrt{2}$ for PPM). Because $B=f_m$ in AM and PAM, there is no improvement. Because there is rapid improvement in system SNR results as B/f_m increases beyond unity, full and efficient use should be made of the potentially available system bandwidth together with a coded modulation system. For a given system bandwidth, this is accomplished by designing the code for the minimum number of levels compatible with the desired SNR.

Signal Quantization and Quantization Noise

When a continuous signal is to be coded, it must first be quantized. At each sampling instant the instantaneous signal value is replaced by the nearest "allowed" level. Intermediate signal values are "forbidden." This procedure results in a random sequence of instantaneous "errors" the magnitudes of which range from

[1] This section is based on a presentation by Mischa Schwartz (ref. 10-1).

zero to half a quantizing level. This random error sequence replaces the fluctuation noise modulating the signal in an uncoded system and is termed "quantization noise."

The gaussian fluctuation noise inherent in any recording process is not entirely absent, of course. However, aside from an occasional signal error (resulting in an incorrect analog sample), it will have no effect on the output signal in an ideal coded system. In an uncoded signal system fluctuation noise has a continuous effect.

In a typical tape recorder, fluctuation noise will have a more serious effect on a practical coded system than on the ideal coded system. The time available for a decision as to whether a digital "1" or a "0" was recorded is reduced by various causes including sampling pulses of finite duration and rise time, clock jitter, amplitude instabilities and dropouts due to changing head-to-tape interface conditions, phase shift, and rolloff at high and low ends of the system frequency response. This is illustrated in the so-called "eye pattern" of figure 10-4 which results from a superposition of the pulses of a random sequence. The square wave shape is lost by the limited high-frequency response; fluctuation noise adds to the signal and broadens the pulses in the y direction; timing jitter broadens the pulses in the x direction; and high-frequency rolloff causes a smaller reproduction of short pulses than longer ones. The interval uncontaminated by these deleterious effects and available for determination of the recorded bit is, therefore, substantially shorter than a bit period, and bit errors are introduced in the readout process. Errors of one in 10^7 have been achieved, however, even without error correcting codes. Thus, although a basic analysis of quantization noise can be made and is reviewed subsequently, an experimental evaluation will need to be performed to confirm the superiority of the A/D/A cases where bit packing density, signal system bit rate, or head-to-tape velocity are near their upper limits of the state of the art.

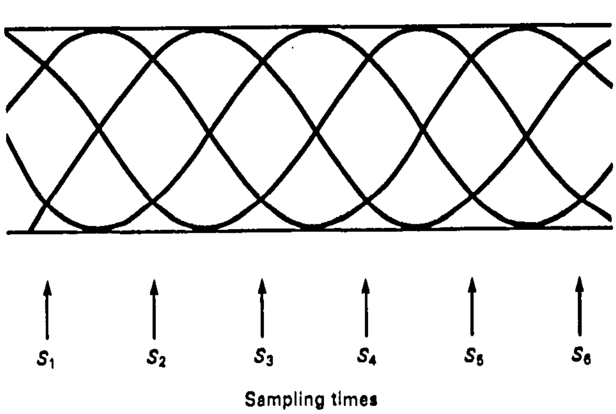

Figure 10-4.—Miller eye patterns.

RMS Value of Quantization Noise

To obtain an unambiguous measure of the quantization noise we assume that the dc component has been removed from the signal. The remaining signal can now be quantized as follows (see fig. 10-5):

$$a = \frac{P}{s}$$

where

P = peak-to-peak signal voltage
s = number of quantizing levels
a = quantum step

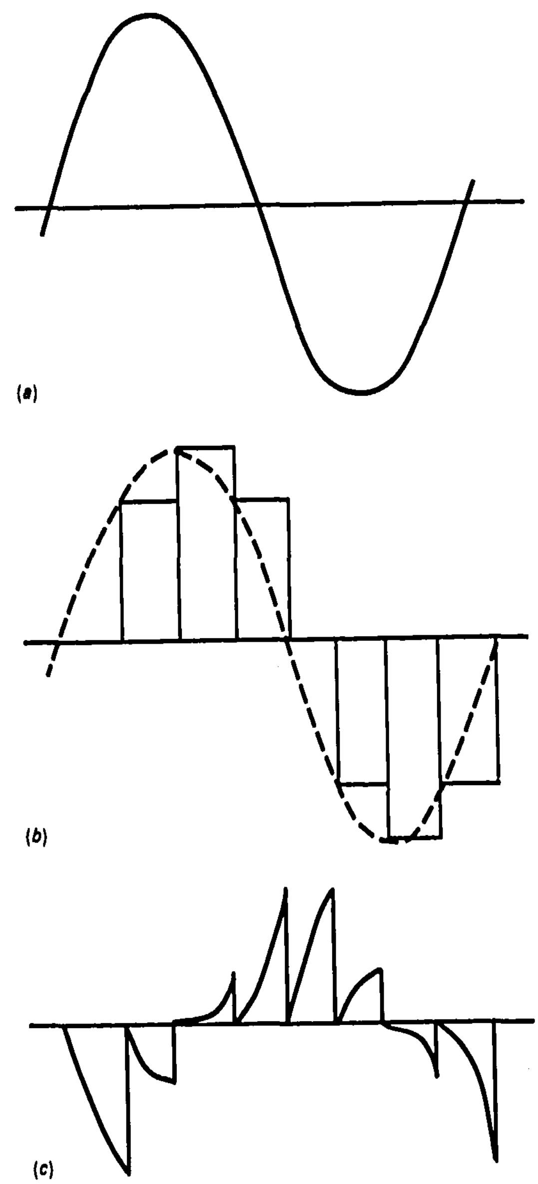

Figure 10-5.—Quantizing of a signal having zero average value. (*a*) Original signal. (*b*) Quantized signal. (*c*) Quantization error.

This process introduces an irreversible error because the instantaneous signal value after quantization will, in general, differ from the true value before quantization. The resultant error will, therefore, range from 0 to $\pm a/2$. Moreover, if the signal is unpredictable we must assume that all error values are equally probable. The "mean squared" value of this error is

$$\overline{E^2} = \frac{1}{a}\int_{-a/2}^{a/2} E^2 dE$$

$$= \frac{a^2}{12}$$

The rms value of quantizing noise is then

$$\sqrt{\overline{E^2}} = \frac{a}{2\sqrt{3}}$$

The voltage peak-to-peak signal-to-rms noise ratio SNR now becomes

$$\mathrm{SNR} = 2s\sqrt{3}$$

or

$$\mathrm{SNR} = 10.8 + 20 \log s \quad \text{decibels}$$

It can be seen from this relation that SNR based on rms noise is 10.8 dB higher than SNR based on the peak-to-peak error due to quantization. The number of quantization levels s is related to the number of bits m in the chosen binary code

$$s = 2^m$$

The voltage SNR in decibels is then

$$\mathrm{SNR} = 2^{m+1}\sqrt{3}$$

or

$$\mathrm{SNR}_{dB} = 10.8 + 6m$$

B is proportional to the bit rate, and the SNR can, therefore, be seen to increase exponentially with the number of bits per sample. If the system bandwidth allows, the SNR can be arbitrarily increased until the available system bandwidth has been fully used.

DEVELOPMENT OF MILLER SQUARED CODING

In channel coding the data streams are modified for best possible performance within the limitations of the transfer function of magnetic recording. The importance of each of many characteristics of a channel code varies from one application to another. Moreover, these different areas of performance are often in conflict. Miller² coding, developed by Ampex Corp. for use in its high-density digital recorders, provides an optimum overall compromise among these various areas of performance.

Miller code, the forerunner of Miller² code, first appeared in the 1960's. This code is also known as delay modulation (DM) and modified frequency modulation, MFM (a misnomer). This coding system saw extensive use in early high-density digital recording (HDDR) systems and in computer disk memory.

Miller² code, devised by J. W. Miller of Ampex Corp., debuted in the mid 1970's. This extension of the Miller code technique has no dc offset (digital sum variation). Consequently, it resolves the critical problem of pattern sensitivity, which plagues HDDR.

To visualize Miller² coding, first consider NRZ−M (fig. 10-1). In this coding technique "1's" are marked by a transition in the middle of the bit cell. "0's" are not marked. This technique has potential for very low frequency content down to dc and, consequently, is not at all compatible with magnetic recording.

Biϕ−M resolves this problem by simply having a transition at the beginning of every bit cell, and, as before, a transition in the middle of the bit cell to mark a "1." The weakness of this system is that the digital "1" now has two transitions within the same bit cell: one at the beginning, the second at the middle to mark the "1." Within a recording channel of fixed upper frequency limit, we now can have only 1/2 the throughput of NRZ-M.

Aaron Miller (Miller code) addressed this problem by adding two coding rules to Biϕ−M. The first is that in the case of a digital "1" there will be no transition at the beginning of the bit cell, only at the middle. The second is that in the case of a "1" followed by a "0" there would be no transition at the beginning of the bit cell containing the "0." This is Miller code.

The most objectionable facet of this coding is a sequence of "1," "0," "1," which encodes a pulse two bit cells long. A lengthy sequence of these two bit cell pulses results in a dc offset. This can be compensated with restoration as is done in most other high density codes; however, elimination of this dc offset condition would be far more desirable than trying to compensate for it. Miller² coding resolves this dc offset problem by employing the Miller code technique plus one additional

rule. This additional rule states that the coding will be the same as in Miller code except whenever there is an even number of "1's", the final "1" will not be marked.

ALGORITHM FOR MILLER AND MILLER² CODING

Digital Sum Variations

Digital sum variation (DSV) is the running integral of the area beneath the coded sequence. In computing DSV, the binary levels are assumed to be ± 1. If the DSV of the code can grow indefinitely, the code has a dc content. If the DSV is bounded, the code is dc free.

Density Ratio

Density ratio (DR) is given by

$$DR = \frac{\text{data density}}{\text{highest transition density}}$$

$$= \frac{x}{y}(d + 1)$$

where

x = nonreturn-to-zero bits
y = channel code bits
d = shortest run of "0's" between "1's"

The density ratio of M^2 code is unity. Generally high-frequency response of the channel must extend somewhat above the Nyquist frequency corresponding to the maximum transition density. This frequency is $(2\ DR \times T)^{-1}$, where T is the time interval between data bits in seconds. The larger the DR, the lower the bandwidth of the code.

Miller Coding Rules

Data "1's" are coded as in NRZ-M, with the addition of transitions in the middle of the bit cell. Isolated data "0's" are ignored (or delayed). Transitions are inserted at the beginning of the bit cell between pairs of data "0's." Because isolated "0's" are ignored, the DR remains unity as in NRZ, and, consequently, bandwidth requirements are little greater than NRZ.

Miller² Algorithm

In Miller² coding the basic Miller code is modified such that it becomes dc free. This is achieved by modifying the sequences that have non-zero digital sum variation. To limit the memory requirements, however, the changes are introduced only at the end of the sequences. In the sequences of non-zero DSV, Miller² encodes all the "1's" except the last. The final "1" is ignored. For example, in figure 10-1 the DSV returns to "0" after the final data "1" and, consequently, the final data "0" is to be counted again for the next sequence. All other sequences are coded as in Miller code. Miller² coding produces characteristic transition-free runs of 2½ and 3 intervals, which do not occur in Miller code—this insures unique decoding. The bandwidth requirements of this dc-free code are little greater than NRZ. Negligible baseline wander or eye pattern closure occur. The effective worst pattern signal to noise ratio (SNR) expected in Miller² coding is 3 to 5 dB better than in Miller coding.

MILLER² CODE PERFORMANCE

Typical Miller² code performance without the addition of error correcting code (ECC) is as follows:

Track density, kbpi	Up to 33.3
Areal density, bit/in²	Up to 10^6
Bit rate expansion/ reduction	32:1
Maximum throughput rate (28-track system), Mbps	Up to 130
Bit error rate	10^{-6}
Input/output formats	Bit serial or bit parallel
Bit parallel words, words/s	To 6×10^6
Bit serial streams, Mbps	To 96

Typical Miller² code performance with ECC is as follows:

Track density with standard tape, kbpi	Up to 43
Areal density, bit/in²	Up to 1.3×10^6
Bit rate expansion/reduction	64:1
Maximum throughput rate, Mbps	120
Bit error rate	10^{-8} to 10^{-9}
Input/output formats	Bit serial or bit parallel
Bit parallel words, words/s	To 6×10^6
Bit serial streams, Mbps	To 150

MILLER² CODE CHARACTERISTICS

There are numerous characteristics of a channel code that must be evaluated in judging its performance in a given application. The characteristics of Miller² coding in the following performance areas are evaluated:

(1) Packing density
(2) Code overhead

(3) Transition density
(4) Pattern sensitivity
(5) dc response/dc restoration
(6) Amplitude and phase requirements versus frequency
(7) Bit slip
(8) Effect of SNR
(9) Polarity sensitivity

Packing Density

Miller² coding requires no more than one transition per bit cell just as in NRZ coding. A typical tape recording unit using this channel code would have a capability of passing a 2-MHz sine wave at a tape speed of 120 ips. With these numbers the Nyquist frequency tells us the system will pass 4 Mbps. Consequently, the packing density per linear inch is 33.3 kilobits. Miller² coding will indeed perform admirably with these numbers; however, the Nyquist frequency is a theoretical number assuming a brick wall filter. Practical considerations must be examined to determine whether this channel code can perform at rates above 33.3 kbpi. The bit synchronizer/decoder must accurately detect axis crossings of the signal; therefore, the point must be determined at which these axis crossings become obscure by inadequate rise time, phase distortion, system noise, and noise caused by the beating of the various frequencies created in a given channel code. "Obscure" is commonly defined as the point at which the raw error rate reaches 1 in 10^6 bits. Bit error rate is measured by counting errors in a pseudorandom word. In many applications, however, this technique could be deceptive. The real world data in these applications could be quite different from a pseudorandom word. The most meaningful way to evaluate a channel code in a specific application is to try to determine the worst-case word pattern and evaluate the packing density under these conditions. Judged in this manner, Miller² coding is unusually strong because of its freedom from pattern sensitivity.

Code Overhead

Miller² coding requires no insertion of extraneous bits in the recording channel. This fact is pertinent because a number of channel codes do require that additional bits be added to the user data. This overhead data, typically 12 percent, must be deducted from the packing density and throughput specifications for those channel codes.

Transition Density

Transition density is a channel code parameter that describes the worst-case number of bit cells without a transition. It is essential to keep the number of bit cells without a transition as short as possible. Channel codes are self-clocking codes. The bit synchronizer must reestablish the clock using the transitions in the channel code as its reference. Codes having fewer transitions make this far more difficult. This, in turn, requires a narrow finely tuned tracking loop. More important, it tends to make the system considerably more unreliable in situations of time base expansion. The Miller² algorithm assures a transition at least once every three bit cells. The transition density is never less than 3.33. In situations involving time base expansion on playback this is an important consideration when compared with other channel codes that may guarantee a transition no more frequently than once every eight bit cells.

Pattern Sensitivity

Perhaps the most important single characteristic of Miller² coding is its freedom from pattern sensitivity. There is a tendency to fall into the trap of considering only packing density when addressing a channel code. To do this is perhaps a fallacy. Packing density is critical only in situations in which the recording system is being pressed to the limit for throughput. On the other hand, pattern sensitivity has caused great difficulty in many HDDR applications.

Pattern sensitivity goes by a number of names: the "pathological data sequence" and, more euphemistically, the "dirty word." When modified into a given channel code this "dirty word" can create a power spectral density far from optimum. The marginal system performance that results from this is pattern sensitivity.

Pattern sensitivity is the villain that is not identifiable in the specifications of a channel code. Only when the system goes on line is it sometimes found very difficult to maintain the prescribed error rate. In addition, machine to machine compatibility of tapes may be difficult, and the system may require frequent fine tuning by the operators. The cause is as follows. The real world data can contain certain patterns of "1's" and "0's" that when modified to the channel code result in a waveform on tape that is far from optimum. This is a very asymmetrical waveform. As this pattern of "1's" and "0's" repeats frequently, frequent cycles of this asymmetrical wave result in a dc offset, digital sum variation. It is this dc offset that will cause the bit synchronizer to miss access crossings. The approach in many channel codes is not to eliminate this problem, but instead to try and compensate for it by using dc restoration and attempting to predict the bit patterns in the missing data and modifying the channel code so that its particular "dirty word" is not likely to occur frequently. Perhaps the most significant advantage of Miller² coding is its freedom from pattern sensitivity. Unlike other channel codes that attempt to compensate for the pattern sensitivity problem after the data are put on tape, Miller² coding recognizes the potential worst-case pattern on the record side and modifies that data such that this pat-

tern is not put on tape. The algorithm for Miller² coding outlines how this comes about. Figure 10-6 illustrates how the DSV does not accumulate in Miller² coding as contrasted to the older Miller code.

dc Response/dc Restoration

Miller² coding intrinsically has no DSV and, consequently, has no need for dc restoration. Miller code, the predecessor to Miller² coding, is vulnerable to DSV (fig. 10-6) and, therefore, pattern sensitivity. It is less vulnerable than many other channel codes, but, nevertheless, the problem is present. The older Miller code systems do contain dc restoration circuitry.

Amplitude and Phase Requirements Versus Frequency

In all channel codes the goal is to present the bit synchronizer/decoder with a waveform eye pattern (fig. 10-4) that is optimum so that the bit synchronizer has the best possible opportunity to detect the axis crossing of the signal.

Amplitude versus frequency equalization is important because inadequacy here will cause the eye pattern to close down at some frequencies, making the axis crossing less identifiable (fig. 10-7). Equally important is phase versus frequency compensation. Lack of linearity

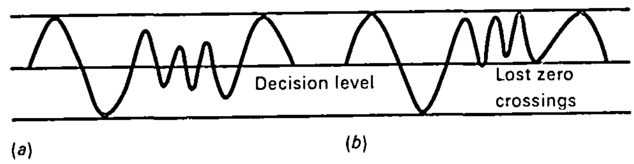

Figure 10–7.—(*a*) Acceptable eye pattern. (*b*) Eye pattern with lost axis crossings.

in phase compensation will shift the timing of the axis crossing at some of the frequencies. This is critical in Miller² coding, just as with Manchester code. In both systems it is necessary to differentiate between the beginning and middle of a bit cell. This makes the system more critical to phase equalization. In Miller² coding this problem is relieved somewhat because the power spectral density of Miller² coding has the benefit of being limited to a narrow band of frequencies. Consequently, phase linearity need be maintained only over a narrow band. In Miller² coding systems phase equalization for each tape speed is provided to a tolerance of ± 1/10 bit cell or better.

Bit Slip

Intrinsic in all channel codes is the problem of bit slip. To properly decode the data on playback the bit syn-

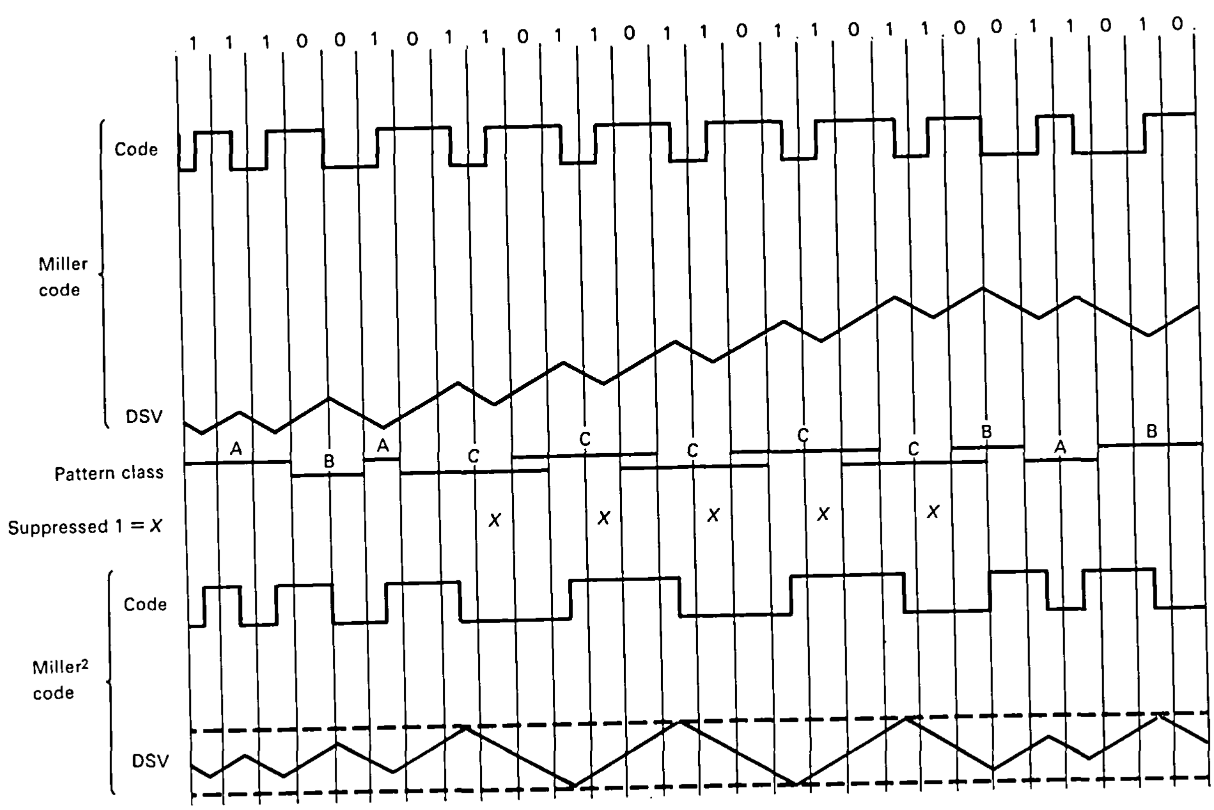

Figure 10–6.—Miller and Miller² coding.

chronizer must reestablish the data clock in each track. In Manchester and Miller^2 coding format this clock must be more precise to firmly identify the beginning and the center of the bit cells. Typically, the clock is held in proper relation with the signal by means of a phase-locked loop. A prolonged dropout on tape and the loss of signal transitions in the phase-locked loop could allow the clock to lose its phase relationship with the signal. The effect of this is bit errors continuing until the bit synchronizer can correct itself. This is bit slip. Virtually all channel codes incorporate periodic synchronization words in each track to bring the clock back into phase. In addition to this technique, Miller^2 and Miller coding resynchronize the clock whenever a suitable bit combination appears at random in the data. The technique is this: In Miller^2 format, "1," "1," "0," "1" encodes as a unique pulse, three bit cells in duration. Consequently, the bit synchronizer identifies the trailing edge of a pulse three bit cells long as a "1" and the trailing edge of the pulse is immediately identified as the middle of the bit cell. From this the phase of the clock can be established. In the case of Miller code, "1," "0", "1" uniquely encodes as a pulse two bit cells long; from this the phase of the clock can be established. Therefore, in the event of bit slip, the proper phase of the clock can be reestablished as soon as the "1," "1," "0", "1" combination occurs at random in the data. In the rare instance this were not to happen randomly in the data, the "1," "1," "0", "1" combination is an intrinsic part of the deskew synchronization word that is inserted every 512 bits.

Effect of SNR

In previous discussions it was seen that precise identification of axis crossings by the signal is essential to the performance of a high-density channel code. It follows then that excessive noise in the signal will obscure this axis crossing and degrade the system performance. The trend has been to address a raw bit error of 1 in 10^6 as the norm for a channel code (ref. 10-1). It has been shown that an SNR of 14 dB theoretically should yield a bit error rate (BER) of 1 in 10^6. In actual practice, SNR values of 24 to 28 dB are more typically related to a BER of 1 in 10^6. This requirement for additional dynamic range is brought about by tape surface imperfections. Miller^2 code, like Manchester code, is perhaps 3 dB more sensitive to noise than NRZ format. This 3 dB added to the typical 24- to 28-dB requirement still is well within the range of magnetic recording systems.

An error correcting code adjunct to Miller^2 code hardware is available from the manufacturer. Error correcting code would be employed in instances where bit error performance considerably better than 1 in 10^6 is required or where severely degraded recordings can be anticipated.

Polarity Sensitivity

In a number of channel codes including NRZ−L, the polarity of transition is essential in identifying a "1" or a "0." When cross-playing tapes between machines, the operator must be concerned about the possibility of a polarity reversal (i.e., one more stage of amplification with its ensuing 180° phase shift). Miller^2 code is insensitive to polarity because it is dependent only on the timing of the transition and not its polarity.

Summary

Numerous different programs and applications for collecting data in high-density digital format have been satisfied with high-density digital tape recorders (HDTR's). Each application has had its own unique needs and priorities; consequently, all performance areas must be equated against the needs in a given application.

OTHER FACTORS CLOSELY RELATED TO THE CHANNEL CODE

Deskewing schemes and error correcting codes are not an intrinsic part of the channel code. These operations are generally performed in the NRZ format before the NRZ is translated to a channel code. Nevertheless, the manufacturer of Miller^2 coding hardware (Ampex Corp.) incorporates deskewing and error correction in the tape recording systems using the Miller^2 channel code.

Deskewing

A tape transport used in HDDR will have a skew specification typically 0.6 μs at a tape speed of 120 ips. The angular skewing of the tape as it crosses the head can create a timing difference between the tracks on opposite sides of the tape varying from 0 to 0.6 μs. If, hypothetically, the system is being used to record at a bit rate of 4 megabits in each track, the duration of each bit cell is 0.25 μs. Obviously, the skewing of the tape will cause an intolerable error if the system is to correlate between bits in each track (parallel words). All HDDR systems in which there is to be cross correlation inject periodic deskew words in each of the tracks.

There are a number of ways of dealing with this overhead information. In the system employed in HDDR recorders produced by Ampex Corp., 32-bit deskew words are injected every 512 bits in each of the

tracks. The bit rate in each track remains unchanged. The overhead is handled by the use of an additional track (2 overhead tracks in a 28-track system). The 32-bit deskew words are not injected into all the tracks simultaneously but are staggered. The technique of the overhead track is to use it to alternately store the raw data from each of the other tracks during the intervals of time when the deskew word is being injected into each data track (fig. 10-8).

To evaluate this technique it must be compared to an alternate approach that would not use an overhead track. Instead, the alternate approach would increase the data rate per track greater than the raw data rate to accommodate the overhead. The disadvantage of the Ampex approach is the need for an additional overhead track on tape. The disadvantages of the alternate, bit stuffing, approach are twofold. First, the packing density and data rate in the tracks are made greater than the raw data rate. Increases in data rate and packing density make performance of the system more marginal. Second, and perhaps more important, the bit stuffing technique takes away the flexibility of the record system. With bit stuffing there is rate-sensitive circuitry in the record side of the system. In contrast, the Ampex technique can follow changes in record data rate without altering the system.

Error Correction

The error correcting system employed by Ampex Corp. in its HDDR systems involves the use of a simple transverse parity track (2 parity tracks in the case of the 28-track system) and a cyclic redundancy check (CRC) word inserted in each of the longitudinal tracks. The CRC word is a 16-bit word injected once in each 512-bit block. This format allows the detection and correction of any errors occurring in a single track. Errors are principally the result of dropouts caused by anomalies in the tape surface. These dropouts generally occur in groups and are isolated to one track. As with all ECC's of this type, if errors occur simultaneously in two tracks, simple transverse parity will fail to identify the tracks. In this instance an uncorrected error is flagged by the system. The probability of this event occurring has been statistically determined to be approximately 1 in 10^9. This then is the error performance that can be anticipated with this system. Improvements in tape quality will, therefore, enhance the performance of the system.

Overhead

The only overhead burden the ECC system will add is that of the transverse parity track. The CRC words do

Channel	Synchronization word bit numbers and source of data in master channel														
	1–32	33–64	65–96	97–128	129–160	161–192	193–224	225–256	257–288	289–320	321–352	353–384	385–416	417–448	449–512
Data 1	S	D	→	→	→	→	→	→	→	→	→	→	→	→	→ D
Data 2	D	S	D	→	→	→	→	→	→	→	→	→	→	→	→ D
Data 3	D	D	S	D	→	→	→	→	→	→	→	→	→	→	→ D
Data 4	D	→	→ D	S	D	→	→	→	→	→	→	→	→	→	→ D
Data 5	D	→	→	→ D	S	D	→	→	→	→	→	→	→	→	→ D
Data 6	D	→	→	→	→ D	S	D	→	→	→	→	→	→	→	→ D
Master	1	2	3	4	5	6	S	7	8	9	10	11	12	13	Special words
Data 7	D	→	→	→	→	→	→ D	S	D	→	→	→	→	→	→ D
Data 8	D	→	→	→	→	→	→	→ D	S	D	→	→	→	→	→ D
Data 9	D	→	→	→	→	→	→	→	→ D	S	D	→	→	→	→ D
Data 10	D	→	→	→	→	→	→	→	→	→ D	S	D	→	→	→ D
Data 11	D	→	→	→	→	→	→	→	→	→	→ D	S	D	→	→ D
Data 12	D	→	→	→	→	→	→	→	→	→	→	→ D	S	D	D
Data 13	D	→	→	→	→	→	→	→	→	→	→	→	→ D	S	D

Figure 10-8.—Typical synchronization word distribution. (512 bits between synchronizations; 13 data channels plus master channel; D = data; S = synchronization word. If any channels are unused, or contain unsynchronized data, no synchronization word is recorded on the tape. Nonsignificant signals are recorded on the master track during the periods that would normally be used for data transfer from these channels.)

not impact on the overhead of the system. These 16-bit words are inserted in the middle of the deskew words. Consequently, the bit rate in each track remains the same as the raw data rate.

Flexibility

This system enjoys the flexibility of not being hardwired for a specific number of tracks. By means of switches, the operator when recording dictates the number of tracks to be incorporated into the error correcting scheme. This not only sets up the appropriate logic for error correction but also tells the reproduce system the format being recorded by recording an identifying word in the overhead deskew track. On playback, even on another machine, the error correcting system will set itself up properly without operator intervention. When ECC is not employed, the reproduce system recognizes this also. The available space for recording the word that defines the error correcting format is available in this way: The master deskew track stores the user data while deskew words are being inserted in the data tracks. This is done in a 512-bit block. The user data is in the form of 32-bit segments that are displaced while the deskew words are inserted in the data tracks. There can be as many as 13 of these 32-bit segments during a 512-bit block. These thirteen 32-bit segments will occupy 416 bits. Consequently, 96 bits remain available in the master deskew track before the end of the 512-bit block. This is the space used to store the word that identifies the deskew format.

BACKWARD COMPATIBILITY OF AMPEX HDDR SYSTEMS

The Miller² hardware that has been in production since the early 1970's intrinsically contains Miller code circuitry. Consequently, Miller² code format systems will be compatible with the older Miller format. Similarly, the ECC format used with these systems will be completely compatible for playback of earlier tapes made without ECC. They will not even require operator intervention. The system with ECC capability will immediately recognize a tape recorder without ECC and implement the necessary circuit changes.

SUMMARY

The Miller² coding technique is the best possible compromise of the many characteristics of a high-density channel code affording maximum flexibility to fit various applications.

REFERENCES

10-1 Schwartz, Mischa: *Information Transmission, Modulation and Noise.* McGraw-Hill Book Co., Inc., 1959.

10-2 Telemetry Group: *Telemetry Standards.* IRIG 106-69, Inter-Range Instrumentation Group, Range Commanders Council, revised 1969.

10-3 "FR2000 Tape Recorder." Specification data sheet, Ampex Corp.

BIBLIOGRAPHY

Mackintosh, M. D.: "The Choice of a Recording Code." *Proc. IERE Conf. Video Data Record.*, July 24, 1979.

Malinson, J. C.; and Miller, J. W.: "Optimum Codes for Digital Magnetic Recording." *Radio Electron. Eng.* 47 (4), Apr. 1977.

Lindholm, J.: "Power Spectra of Channel Codes for Digital Magnetic Recording." *IEEE Trans. Magn.* 14 (5), Sept. 1978.

Baldwinn, J. L. E.: "Codes for Digital Video Tape Recording at 10 Mb/square inch." *Proc. IERE Conf. Video Data Record.*, July 24, 1979.

CHAPTER 11

Parallel Mode High-Density Digital Recording: Technical Fundamentals

Technical Staff
*Datatape, Incorporated**

This chapter is an introduction to parallel mode high-density digital recording (HDDR) techniques using the enhanced-NRZ (E-NRZ) encoding scheme.

Every attempt has been made to assemble all the basic information necessary to understand the fundamental principles of parallel mode high-density digital tape recorders (HDTR's).

It is assumed that the reader has a technical background and is familiar with the principles of magnetic tape recording, but has had no previous experience with HDDR techniques.

INTRODUCTION

HDDR is a relatively new method of recording information on magnetic tape that offers several significant advantages over conventional analog recording methods. First, the data are recorded in a format that is directly compatible with electronic data processing equipment, without the need for additional analog-to-digital (A/D) or digital-to-analog (D/A) conversion. Second, the data are reproduced with a much higher degree of accuracy because of the relative insensitivity of digital data to the effects of flutter and time base error, which tend to degrade analog signals.

Perhaps the most significant advantage of all, however, lies in the extremely high packing density made possible by this new recording method—up to 45 000 bpi/track. Such high packing density results in practical data transfer rates as high as 50, 100, or even 450 Mbps, with bit error rates of less than one error per 10^7 bits. Even more advanced recorders have been developed with data rate capabilities as high as 600 Mbps, and the development of a 10^9 bps recorder seems well within the practical limits of current technology.

HDDR is usually considered to be any digital recording at per-track densities of 20 000 bpi or greater, using longitudinal recording techniques. When individual bit streams are recorded one bit stream per track, the associated system is termed a "serial" HDDR system. If the bit stream is, instead, converted to parallel bytes of N bits and recorded across N tracks on tape, the associated system is termed a "parallel" HDDR system. This chapter concentrates on the discussion of parallel mode HDDR systems only.

When something such as HDDR is developed, there are bound to be many questions, such as will HDDR totally replace conventional analog recording methods? To answer this question so soon after the introduction of this new recording method would amount to little more than speculation; however, such a possibility is well within reason. HDDR has already gained rapid and widespread acceptance in such areas as satellite communications, radar signal analysis, digital imagery and X-ray, interferometry, and as mass storage systems for digital computers. Near future applications will probably include digitized television and advanced digital instrumentation. Beyond that the list is virtually endless—limited only by the imagination and creativity of the systems engineer.

ADVANTAGES OF ENHANCED NONRETURN TO ZERO ENCODING

Most of today's digital data are supplied as pulse code modulated (PCM) signals using a nonreturn-to-zero (NRZ) code format—a code format both rich in dc content, and one requiring a high degree of time base stability to maintain bit synchronization with a separate

*A Kodak company; formerly Datatape Division of Bell & Howell Company.

Editor's Note: DATATAPE, MARS, and M-14 are registered trademarks of Datatape, Incorporated. Enhanced-NRZ, E-NRZ, EDAC, and HI-D are trademarks of Datatape, Incorporated.

coincident clock signal. In apparent conflict with these code characteristics, magnetic tape recorders suffer from two major shortcomings that limit their suitability for recording and reproducing straight NRZ signals: time base instability and an absolute inability to reproduce dc signal components. What then is being done to eliminate, or at least minimize, these shortcomings to make recorders compatible with digital recording requirements? The answer lies in the development of an encoding scheme whereby the NRZ data are somehow modified (changed) to eliminate or minimize the dc component and provide the necessary time base stability to prevent loss of bit synchronization. Several such encoding schemes have been developed and have proven quite effective in overcoming these recorder shortcomings. Included among these encoding schemes are such contenders as delay modulation (DM; also known as Miller codes), randomized NRZ (R-NRZ), and enhanced NRZ (E-NRZ) encoding. Of the several encoding schemes currently available, Datatape, Incorporated's E-NRZ encoding scheme is rapidly proving to be the most acceptable for HDDR. The reason for this higher level of acceptance is the subject of the discussion that follows.

Encoding Scheme Classifications

Later in this chapter we shall explore the advantages and disadvantages of various encoding schemes on a point-by-point basis. Before engaging in such detailed analysis, though, let us review some of the many ways in which PCM data can be encoded and establish a fundamental baseline for their classification.

Virtually all encoding schemes, whether suitable for HDDR or not, can be classified as belonging to one of four basic family groups. The four groups are: return-to-zero (RZ) codes; nonreturn-to-zero (NRZ) codes; biphase codes (Biϕ); and delay modulation (DM or Miller) codes. The four classifications are identified in figure 11-1 along with the waveforms for several of the separate codes belonging to each group.

RZ Codes

RZ codes are far too inefficient for use in HDDR, but, because of their simple structure, they are included in this discussion to serve as a convenient starting point toward an understanding of more sophisticated encoding schemes.

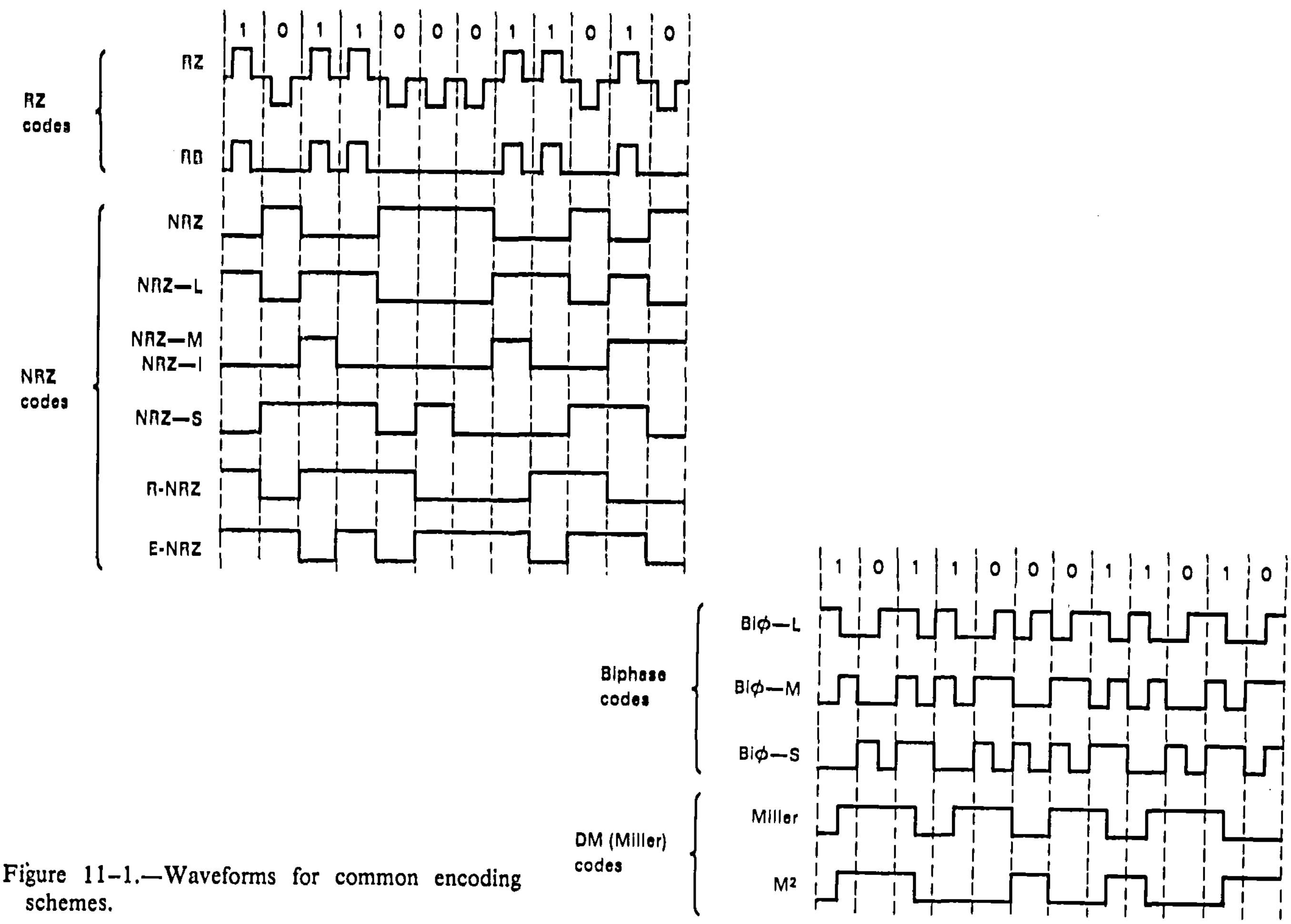

Figure 11-1.—Waveforms for common encoding schemes.

RZ (Return-to-Zero)

The simplest encoding scheme conceptually is the RZ code. A "1" is represented by a positive-going pulse, and a "0" by a negative-going pulse. This particular code may find applications in elementary equipment, but its inefficient use of bandwidth restricts its use from HDDR applications. It is a redundant coding scheme because two flux transitions are required for each bit.

RB (Return-to-Bias)

A slightly more efficient encoding scheme is one that remains at either the positive or the negative maximum excursion possible in the absence of a signal. A "1" in this encoding scheme is represented by an isolated pulse from one extreme signal to the other, or in the case of tape, from saturation in one direction to saturation in the other direction. At the end of the pulse the original value is resumed and a total of two flux transitions are required for each "1." A "0" is represented by the absence of a pulse.

NRZ Codes

Of the four code classifications, NRZ codes provide the most efficient use of available bandwidth and are the easiest to engineer and maintain. They are the most widely used codes for electronic data processing (EDP), and are generally suitable for high, medium, and low density EDP applications. The two outstanding characteristics that make the NRZ codes so widely accepted by the EDP industry, bandwidth efficiency and simplicity, make them equally attractive for HDDR. There are, however, two limitations that must be overcome to make NRZ codes compatible with magnetic recorders.

The first of these limitations is the presence of a substantial dc component in the straight (unencoded) variations of the NRZ code, which is unacceptable to the recorder. This dc component results because straight NRZ codes are not "run-length-limited"—meaning that there are no built-in safeguards to prevent the data stream from containing long uninterrupted strings of "1's" or "0's." To preserve such long strings of "1's" or "0's" without distortion, it becomes necessary for the response of the recorder to extend very close to dc, which is not possible.

The second limitation imposed by straight NRZ codes is the requirement for an extremely stable time base to prevent loss of bit synchronization as data is clocked through the recorder. At very low bit densities (up to approximately 800 bpi), the degree of time base stability provided by the recorder is normally sufficient to maintain bit synchronization through the use of an external synchronous clock signal supplied along with the NRZ data, on a separate line. As bit density increases above 1000 bpi, however, the degree of time base stability provided by the recorder becomes inadequate to maintain bit synchronization by this means, and a more effective means must be used. One of the most effective means of achieving the necessary time base stability is to extract the timing clock signal directly from the transitions in the data stream. This assumes, however, that a sufficient number of transitions exist in the data to insure "lock-on" by an internal timing oscillator. Unfortunately, with straight NRZ, there are no safeguards to prevent long uninterrupted strings of "1's" or "0's"; therefore, there is no assurance that a sufficient number of transitions will be present to insure lock-on by the timing oscillator.

In reviewing the two major limitations imposed by straight NRZ codes (i.e., the presence of a dc component and the requirement for an extremely stable time base) a definite commonality between them becomes apparent. That is, both limitations can be minimized by simply providing a safeguard that will guarantee the necessary minimum number of transitions in the data stream. This, in essence, is exactly what is done in the case of the "modified" NRZ codes (i.e., E-NRZ and R-NRZ) to make straight NRZ encoded data acceptable to the recorder. Increasing the transition density does not of itself provide the most acceptable encoding scheme, however, as there are still many other factors that must be taken into consideration, as will be explained later.

NRZ (Nonreturn-to-Zero)

In comparing NRZ encoding with RZ encoding, redundancy is sharply reduced by assigning, at most, a single transition to each separate bit. The information derived by the recorder from this encoding scheme is whether the flux changed or not. There are several ways in which these two pieces of information can be used to give a binary coding scheme. In straight NRZ, a flux change indicates that the bit following a given bit is different from the first bit. Thus, a change from "1" to "0" is indicated by a flux change. When a series of "1's" follow each other, no flux change is indicated, but when the last "1" is followed by a "0," there is another flux change.

NRZ—L (Nonreturn-to-Zero, Level)

NRZ—L is a straight NRZ code that is not acceptable for HDDR. A "1" is represented by one level, and "0" is represented by the other level.

NRZ—M/NRZ—I (Nonreturn-to-Zero, Mark)

NRZ—M/NRZ—I is a straight NRZ code that is not acceptable for HDDR. A "1" is represented by a change

in level, and "0" is represented by no change in level. The NRZ–M encoding scheme indicates a "1" by a flux change and a "0" by no flux change. The main advantage of NRZ–M over NRZ is that there is a one-to-one relationship between the signal and the bit. If there is an error, only the bit for which the error is made is lost. In straight NRZ, on the other hand, if a flux transition is missing all successive bits will be exactly opposite of what they should be, until bit synchronization is somehow regained. NRZ–M/NRZ–I encoding is used in 800 bpi IBM-compatible tape drives.

NRZ–S (Nonreturn-to-Zero, Space)

NRZ–S is a straight NRZ code that is not acceptable for HDDR. A "1" is represented by no change in level, and "0" is represented by a change in level.

R-NRZ (Randomized-NRZ)

R-NRZ is a modified NRZ code acceptable for HDDR at packing densities up to 30 000 bpi/track (typical for a 28-track recorder with a 2.0-MHz passband), with a bit error probability (BEP) of 1 BEP in 10^6 bits. As the name suggests, straight NRZ data are processed through a randomizer before being recorded on tape to increase the number of level transitions, which reduces the dc component and makes the data more acceptable to the recorder. The code is not run-length-limited, however, so there exists a definite, though remote, possibility that under certain conditions a given NRZ bit pattern could exactly nullify the randomizing process to produce unacceptable long strings of "1's" or "0's". A typical bit randomizer, such as used in R-NRZ encoding, is shown schematically in figure 11-2.

E-NRZ (Enhanced-NRZ)

Datatape, Incorporated's, E-NRZ is a modified NRZ code that is acceptable for HDDR at packing densities up to 33 000 bpi/track, with a BEP of 1 in 10^6 bits. As shown in figure 11-3, E-NRZ encoding entails separating the NRZ–L data stream into seven-bit words; inverting bits 2, 3, 6, and 7; and adding one parity (enhancement) bit to each of the words. This parity bit is added at the end of each word to make the total number of "1's" in the eight-bit word an odd count. Enhancement offers several advantages over straight NRZ and over R-NRZ. First, it assures a minimum transition rate sufficient to minimize dc components and to maintain phase lock in the playback timing oscillator. Second, E-NRZ is run-length-limited–providing, even under worst-case conditions, a minimum of 1 transition for every 14 bits. Third, by means of parity checks during playback, E-NRZ provides a good indication of the error rate with which the data were recorded and reproduced. Several other advantages are also realized with E-NRZ encoding, and will be discussed later in this chapter.

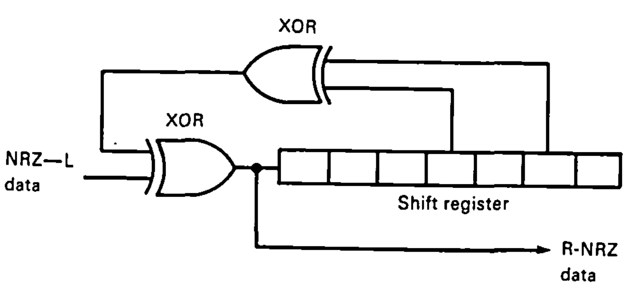

Figure 11-2.—Typical bit randomizer.

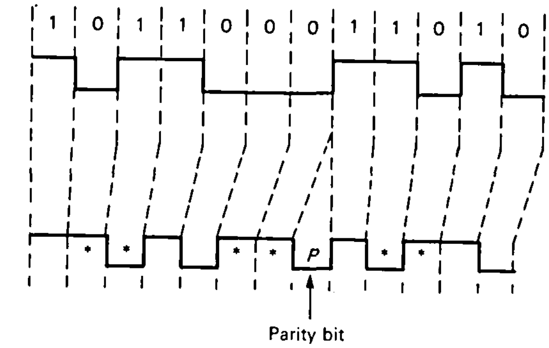

Figure 11-3.—Datatape, Incorporated's, E-NRZ encoding. (* = inverted bit.)

Biphase Codes

Biphase codes have appeared in several variations and are known by as many different names. Included in the variations are Manchester encoding, biphase encoding, double-frequency encoding, phase encoding, and frequency-shift encoding. All are characterized by having a minimum of one level transition per bit. The coding rules for biphase codes are the same as those for NRZ–M/NRZ–I, with the addition of one extra transition at the beginning of every bit cell. This results in a high transition density, which makes the code totally dc-free and run length limited–which is highly compatible with magnetic recorders. Unfortunately, this same high transition density requires twice as much bandwidth as NRZ codes to provide the same packing density. This inefficient use of bandwidth limits maximim packing density to approximately 12 000 bpi, which is well below the minimum requirements for HDDR. Biphase encoding is used in 1600-bpi IBM-compatible tape drives.

Biϕ–L (Biphase, Level)

Biphase, level, is also known as split-phase encoding. Level change occurs at the center of every bit period. A

"1" is represented by a "1" level with a transition to the "0" level, and "0" is represented by a "0" level with a transition to the "1" level.

Biϕ−M (Biphase, Mark)

Level change occurs at the beginning of every bit period. A "1" is represented by a midbit level change, and "0" is represented by no midbit level change.

Biϕ−S (Biphase, Space)

Level change occurs at the beginning of every bit period. A "1" is represented by no midbit level change, and "0" is represented by a midbit level change.

Delay Modulation (Miller) Codes

Miller and Miller squared (M^2) are perhaps the most familiar members of a code group known as delay modulation (DM) codes. These codes are characterized by having a minimum of one transition for every other bit cell. This transition density is sufficient to minimize any dc component and provides run length limiting. Miller codes are acceptable for HDDR at packing densities up to 22 000 bpi/track, with a BEP of 1 in 10^6 bits.

Miller Code

A "1" is represented by a midbit level change. A "0" has no level change—unless it is followed by another "0," in which case there is a level change at the end of the first "0" bit period.

Miller Squared (M^2)

The rules for M^2 encoding are the same as for Miller, except when an isolated "0" is followed by an even number of "1's", the midbit level change corresponding to the final "1" is inhibited.

Three Acceptable Encoding Schemes

In summarizing our review of the various encoding schemes, we discovered that most were unsuitable for HDDR. Both RZ and biphase codes suffer from inefficient bandwidth use. Straight NRZ codes, on the other hand, are handicapped by too few level transitions, which results in the presence of a dc component unacceptable to the recorder. This narrows the field to only three encoding schemes that have received official recognition as being suitable for HDDR: E-NRZ, R-NRZ, and M^2. Unfortunately, these codes are not compatible, nor directly interchangeable. The prospective buyer of HDDR equipment is, therefore, urged to give careful and thoughtful consideration to all the advantages and disadvantages of the encoding scheme to which his data will ultimately be dedicated. Many of these advantages and disadvantages are discussed in the paragraphs that follow.

Maximum Theoretical Per-Track Bit Rate

The maximum theoretical per-track bit rate is the maximum number of bits, per track per second, that successfully can be recorded and reproduced with any given recorder passband. This bit rate, known as the Nyquist rate (for NRZ codes), is equal to twice the upper band edge (UBE) frequency limit of the recorder passband.

$$\text{Nyquist rate} = \text{bps}_{max} = 2\ \text{UBE}$$

For example, calculate the Nyquist rate for a recorder with a 2.0 MHz passband:

$$\begin{aligned}\text{Nyquist rate} &= 2\ (\text{UBE}) \\ &= 2\ (2 \times 10^6) \\ &= 4\ \text{Mbps/track}\end{aligned}$$

Maximum Theoretical Per-Track Bit Packing Density

The maximum theoretical per-track bit packing density is the maximum number of bits, per unit length of tape per track, that successfully can be recorded and reproduced with any given recorded passband. This packing density—which, for lack of a better term, we shall call the Nyquist packing density—is equal to the Nyquist rate divided by the tape speed:

$$\text{Nyquist packing density} = \frac{2\ \text{UBE}}{\text{tape speed}}$$

For example, calculate the Nyquist packing density for a recorder with a 2.0 MHz passband operated at 120 ips.

$$\begin{aligned}\text{Nyquist packing density} &= \frac{2\ \text{UBE}}{\text{tape speed}} \\ &= \frac{2(2 \times 10^6)}{120} \\ &= \frac{4 \times 10^6}{120} \\ &= 33\ 333\ \text{bpi/track}\end{aligned}$$

Both the Nyquist rate and the Nyquist packing density are important for more than purely academic reasons because they govern the maximum performance attainable under ideal conditions with a perfect recorder

and a perfect encoding scheme. In other words, they set the goal toward which the design engineer must work to achieve maximum overall equipment performance. With parallel mode HDDR, however, there are two main limitations that prevent this goal from being fully attained: the ratio of actual user bits to the total number of bits recorded (i.e., overhead) and the maximum practical bit rate attainable for a given bit error probability.

Code Overhead

In parallel mode HDDR, not all bits recorded on tape are actual user bits. Others include the parity and synchronization word bits added to the data during the encoding process. These added bits are called "overhead" because they occupy space on tape that would otherwise be occupied by actual user bits. Depending on the particular encoding scheme used, the amount of space required for this overhead varies between approximately 3 and 22 percent of the total space available.

Low overhead does not always mean best performance. Low overhead is one characteristic of an encoding scheme that is, in many cases, the most oversold characteristic of all. The lower the overhead, the better the encoding scheme, or so the argument would have you believe. Why then, you might ask, does E-NRZ, with the highest overhead of all (21.43 percent), provide the second highest throughput rate? Code overhead calculations for the three major encoding schemes are discussed in the paragraphs that follow.

Straight NRZ

Straight NRZ has no overhead at all because all bits present are actual user bits. Unfortunately, this complete lack of overhead is what makes NRZ unsuitable for HDDR; that is, the code is not run limited and contains no synchronization to insure proper bit synchronization at the recorder output. Nevertheless, this lack of overhead makes straight NRZ the standard by which other code overheads are compared.

Randomized-NRZ

Randomized-NRZ has a code overhead of 3.2 percent, the lowest of the three major encoding schemes used for HDDR. With R-NRZ, a 16-bit deskew synchronizing word is inserted into the data stream once for every 496 data bits. These 16 synchronization bits added to every 496 data bits result in a code overhead calculated as follows:

$$\text{Percent overhead} = \frac{(496 + 16) - 496}{496} \times 100$$

$$= \frac{512 - 496}{496} \times 100$$

$$= \frac{16}{496} \times 100$$

$$= 0.0323 \times 100$$

$$= 3.23 \text{ percent}$$

Miller and M^2

Both Miller and M^2 codes require one additional master channel for every 12 data channels; i.e., one extra record/reproduce track. With Miller and M^2 codes, a 32-bit synchronizing word is inserted into each of the 12 data streams once for every 512 data bits. To accomplish this, 32 data bits are extracted from the normal data stream and placed on the 13th master channel. The 32-bit synchronization words are then inserted into the data stream to occupy the same space from which the data bits were extracted. To arrive at a meaningful overhead figure for these codes, we have to consider the number of tracks used rather than the number of added bits:

$$\text{Percent overhead} = \frac{(12 \text{ tracks} + 1 \text{ track}) - 12 \text{ tracks}}{12 \text{ tracks}} \times 100$$

$$= \frac{13 - 12}{12} \times 100$$

$$= \frac{1}{12} \times 100$$

$$= 0.0833 \times 100$$

$$= 8.33 \text{ percent}$$

E-NRZ

In the case of E-NRZ encoding, 80 parity bits and 40 synchronizing bits are added to every 560-bit data frame. The 120 overhead bits added to the 560 data bits result in an E-NRZ data frame containing 680 bits. E-NRZ overhead is calculated as follows:

$$\text{Percent overhead} = \frac{(560 + 80 + 40) - 560}{560} \times 100$$

$$= \frac{680 - 560}{560} \times 100$$

$$= \frac{120}{560} \times 100$$

$$= 0.2143 \times 100$$

$$= 21.43 \text{ percent}$$

Code Efficiency

Code efficiency provides a more meaningful insight into code performance than does code overhead. Efficiency is the ratio of usable per-track bit rate to the maximum theoretical per-track bit rate (i.e., Nyquist rate) for the recorder passband, assuming equal bit error probability:

$$\text{Code efficiency} = \frac{\text{usable per-track bit rate}}{\text{Nyquist per-track bit rate}} \times 100$$

Shown in table 11-1 are the comparative code efficiency ratings for the major encoding schemes used for HDDR. The efficiency figures specified assume a 28-track recorder with a 2.0 MHz passband, and a bit error probability of 1 in 10^6 bits.

Spectral Density Comparison for NRZ, Biϕ, and DM

Because the ultimate objective of an HDDR system is to maximize the amount of information that can be stored on a reel of tape, it follows that the slowest possible tape speed is desired. Consequently, digital encoding schemes are required that make efficient use of the recorder passband—thereby maximizing the bit packing density (i.e., bits recorded per linear inch of tape).

Determination of passband requirements for the various encoding schemes is often made by examination of the signal power spectrum. Some arbitrary portion of the total power is then assumed to be required for adequate recovery of the data, and the recording system is designed accordingly. The power spectrum does not, however, provide sufficient insight as to how the mechanism of restricting the passband affects the signal wave shape. Thus looking only at the spectral power density does not of itself provide the system designer ample indication of what happens when the digital signal is processed through a channel having finite attenuation rates in the stop band and imperfect phase linearity, as in the case of magnetic tape recorders.

Plotted in figure 11-4 are the power spectral densities of NRZ, Biϕ, and Miller coding. At first glance it may appear that the spectral density of the Miller scheme is the more suitable for HDDR because of the apparent narrow passband requirements and the apparent reduction in spectral energy in the vicinity of $f = 0$. Note that the emphasis here is on the word apparent. With Miller coding, the majority of the signaling energy appears to lie in frequencies less than one half the bit rate. The appearance is somewhat misleading, however, because in actual practice Miller requires a wider passband (up to 33 percent wider) than NRZ coding to achieve the same packing density.

Table 11-1.—*Comparison of Code Efficiencies*

Code	Nyquist bit rate, Mbps/track	Usable bit rate, Mbps/track	Efficiency, percent
R-NRZ	4	3.600	90.00
E-NRZ	4	3.294	82.35
M²	4	2.640	66.00

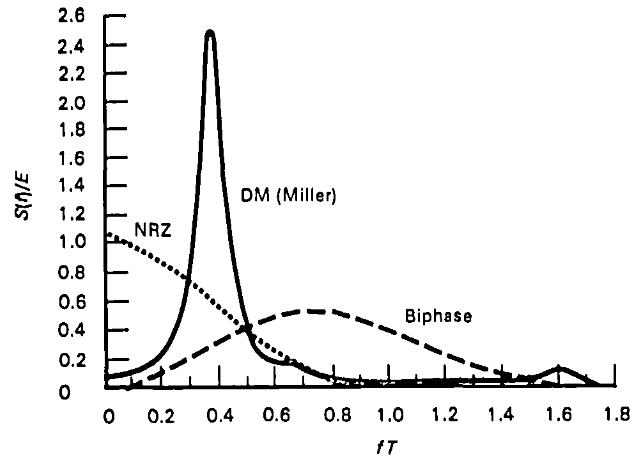

Figure 11-4.—Spectral density of NRZ, biphase, and DM coding. ($S(f)/E$ = power spectral density normalized with respect to signal energy per bit; f = frequency; T = bit period.)

The Miller spectrum appears to be small at $f = 0$. Once again, this appears to be an advantage because recorder response at low frequencies is quite poor when using the direct method of recording, as in the case of high density. In actual practice, however, the dc component of the Miller spectrum can reach as much as 33 percent of the peak-to-peak value when worst-case bit patterns are encountered.

As a direct result of the two factors just discussed, it begins to become apparent that higher packing density can only be achieved with NRZ-derived codes such as Datatape, Incorporated's E-NRZ.

BEP Versus SNR

Plotted in figure 11-5 are the theoretical bit error probability (BEP) versus signal-to-noise ratio (SNR) curves for NRZ, Biϕ, and Miller coding. As shown, a BEP of 1 in 10^6 would require a recorder SNR of 17 dB or better using the Miller encoding scheme but only 14 dB when using NRZ or Biϕ encoding. A recorder having a 12 dB SNR would (theoretically) provide a BEP of only 1 in $10^{2.5}$ using Miller encoding while the same 12 dB SNR would provide a BEP of 1 in $10^{4.5}$ using NRZ encoding—an improvement equal to two orders of magnitude.

The inherent BEP versus SNR performance of NRZ codes applies directly to E-NRZ. A number of authors

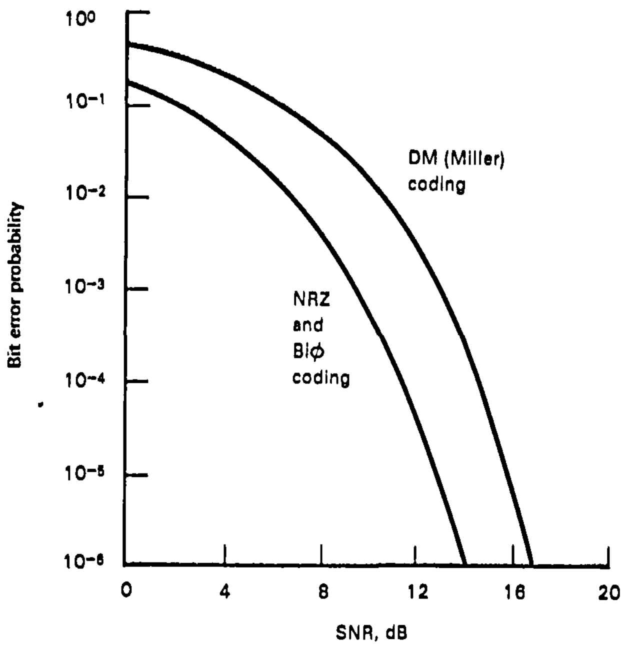

Figure 11-5.—Theoretical BEP versus SNR curves for NRZ, biphase, and DM (Miller) coding.

have published both theoretical curves as well as experimental curves on this important NRZ relationship. (See refs. 11-1 to 11-3.) This well-established relationship for NRZ and E-NRZ is not shared by other encoding schemes. W. N. Waggener from EMR-Schlumberger states (ref. 11-2):

> The performance of delay modulation (DM) has been widely misunderstood. The small low frequency content and a sharply peaked spectrum at about 0.4 bit rate has led potential users to conclude that DM is an efficient coding technique. Such a conclusion is unwarranted and, in fact, the performance of DM is 3.5 dB poorer than NRZ using an optimum detection bandwidth of twice that of NRZ. If the bandwidth of DM is limited to the spectral region less than the bit rate, a considerable penalty in bit error performance is paid.

Experiments at Datatape, Incorporated, with Miller and E-NRZ show the detection superiority of E-NRZ over Miller by the margin of opening in the eye pattern. (See fig. 11-6.)

Long-time proponents of Miller now recognize the 3.5-dB penalty cited by Waggener (ref. 11-3) but tend to discount its importance although this importance is quite obvious:

(1) An SNR margin of 3.5 dB provides a safeguard against operational problems of head varnish, head azimuth and electronic misalignment, and crossplay.

(2) Tape dropouts of a magnitude at or near detection and bit synchronization threshold will be successfully accommodated using NRZ or E-NRZ while errors will result with Miller.

(3) Increased packing density can be achieved with a superior BEP versus SNR code like E-NRZ if the criterion of packing density is established by increasing density until a given error rate results. (This is King's method of code evaluation and he, in fact, found that NRZ can be packed at higher densities than Miller, see ref. 11-4.)

Minimum Transition Density

Minimum transition density is the average number of transitions in the bit stream.

Transitions are necessary to maintain bit synchronization. EMR (ref. 11-5) describes the capability of its Model 720 Bit Synchronizer as follows: "Minimum transition density: Sync is maintained with transition densities as low as one transition in 64 bits (1.56 percent), with an SNR of 10 dB."

The minimum transition density for any given encoding scheme is important because it governs the low-frequency requirement of the recorder passband. That is, the fewer the number of transitions the lower the frequency requirement. In the extreme case where there are no (or very few) transitions, the low-frequency requirement would have to extend down to dc—below the capability of wideband direct record/reproduce systems.

Miller coding boasts a transition density of 50 percent regardless of bit pattern. This apparent advantage of Miller is obtained at the expense of compressing the spectrum, which has been previously shown to be detrimental (refs. 11-2 and 11-3). The Miller transition density of 50 percent seems beyond the point of diminishing returns and is an overreaction when viewed from the performance baseline of a well-designed bit synchronizer. The transition density of M^2 encoding (33 percent) is only a slight improvement over Miller and, here again, seems beyond the point of diminishing returns.

No claim is made by J. H. Stein (ref. 11-6) for the minimum transition density of randomized-NRZ. However, it is not difficult to envision a string of "0's" 20 to 40 bits long, resulting in a randomized output with no transitions. It would be difficult, if not impossible, to specify the minimum transition density of randomized-NRZ.

The worst-case transition density with E-NRZ encoding is 1 transition in 14 bits (7.15 percent). This minimum transition density is a major improvement over R-NRZ, which has no guarantee of transition density. The minimum transition density of E-NRZ (1 transition in 14 bits) brings the low-frequency requirement necessary to process the code well within the passband of standard wideband direct record/reproduce systems, with well-defined performance parameters for dc restoration.

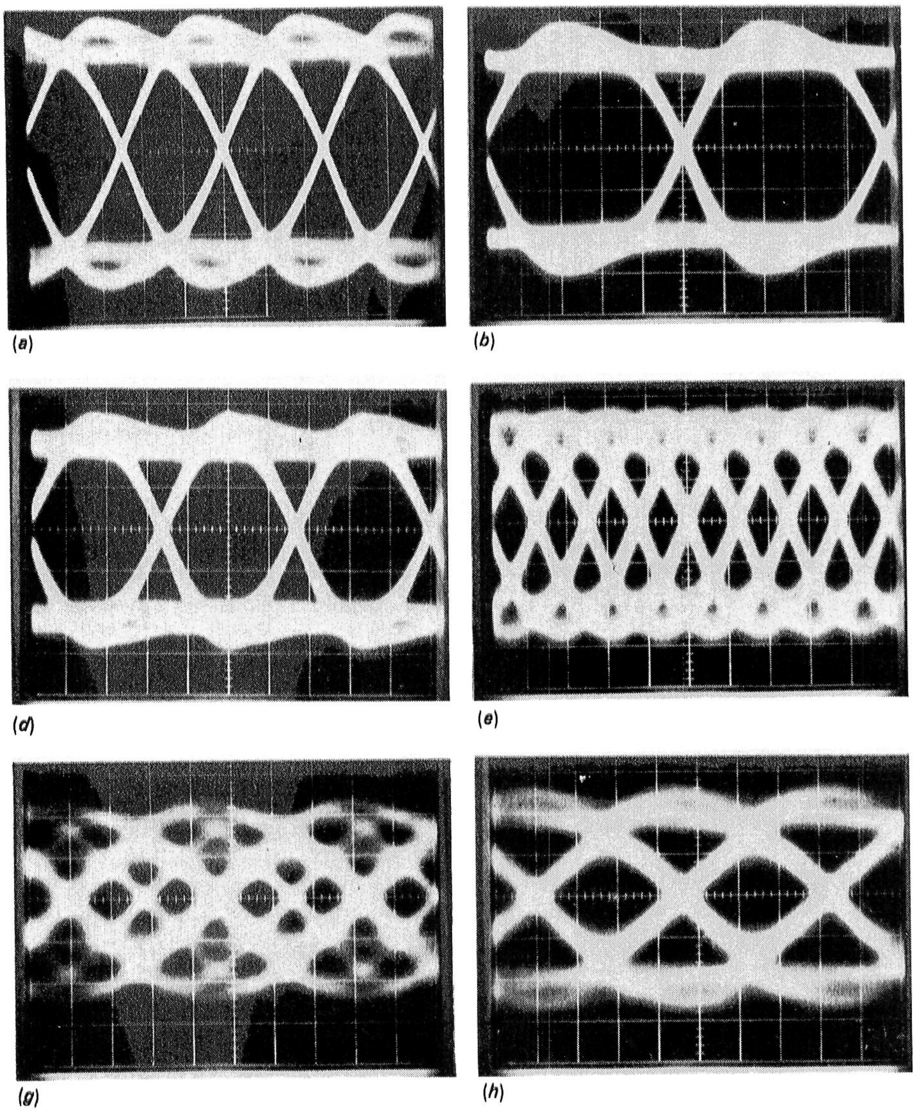

Figure 11–6.—Comparison of Miller and E-NRZ eye patterns for different bit packing densities. (*a*) Miller code; 16.70 kbpi. (*b*) E-NRZ code; 16.70 kbpi. (*c*) Miller code; 24.75 kbpi. (*d*) E-NRZ code; 24.75 kbpi. (*e*) Miller code; 33.0 kbpi. (*f*) E-NRZ code; 33.0 kbpi. (*g*) Miller code; 45.00 kbpi. (*h*) E-NRZ code; 45.00 kbpi.

Bit Pattern Sensitivity

Bit pattern sensitivity is the susceptibility of a code to certain bit patterns that will result in an increase in bit error rate over and above the bit error rate for more benign bit patterns.

Codes with low transition density suffer most. In practice, bit pattern sensitivity is usually the result of low transition density coupled with highly asymmetrical bit streams; that is, long strings of "1's" or "0's". This type of bit pattern is most responsible for baseline shift due to the recorder's inability to pass dc or very-low-frequency components.

E-NRZ is unaffected by bit patterns. E-NRZ encoding limits dc baseline shift so that it can never reach zero, or 100 percent, of the pulse train amplitude; specifically, the baseline is bounded between 12.5 percent and 87.5 percent of the peak-to-peak pulse amplitude.

Implementation of dc restoration reduces bit pattern sensitivity. The percent of baseline shift experienced with different encoding schemes can be reduced, even totally eliminated, through the use of effective dc restoration circuits in the recorder. In weighing the various merits of one HDTR versus another, consideration should be given to both the presence and effectiveness of dc restoration circuitry.

Datatape, Incorporated, recommends the use of dc restoration in all HDTR's, regardless of the encoding scheme used. Both the nominal cost and complexity of including this feature are low compared with its effectiveness in reducing baseline shift. Datatape, Incorporated, further recommends that all multispeed recorders incorporate scaled dc restoration circuitry to change the time constants of the dc restoration circuits automatically and proportionately with tape speed. The effectiveness of a properly designed dc restoration circuit in reducing baseline shift is shown in figure 11–7.

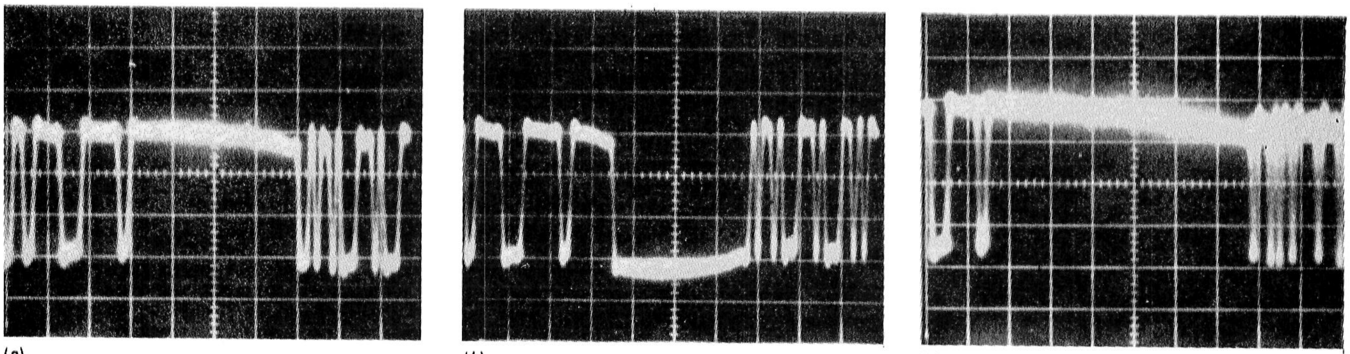

(a) (b) (c)

Figure 11–7.—Effectiveness of dc restoration. (*a*) Twenty-four consecutive "1" bits without transitions. (*b*) Twenty-four consecutive "0" bits without transitions. (*c*) Fifty-five consecutive "1" bits without transitions.

The photographs clearly show the effectiveness of Datatape, Incorporated's dc restoration circuitry in reducing baseline shift. Tests were performed using straight NRZ–L encoding at a packing density of 33 000 bpi. Tape speed was 60 ips, and a standard 28-track recorder with 1-in.-wide tape was used.

Claims of "superior dc-free codes" are often misleading. The reader is cautioned against reports of the comparative superiority of dc-free codes over E-NRZ when tested at various record levels and bit packing densities (ref. 11–7). Such tests have been performed with no (or marginal) dc restoration. In effect, these tests were merely measurements of dc restoration inferiority, rather than proof of code superiority.

Bandwidth Sensitivity

E-NRZ, like straight NRZ, enjoys an additional bandwidth related advantage over non-NRZ codes—low sensitivity to changes in bandwidth that may occur between reels of tape, or within a single reel of tape. D. A. King (ref. 11–4) reports: "NRZ bit packing was more sensitive to tape recorder bandwidth changes than biphase, but less sensitive than delay modulation." This is explained by King: "It is the compacting of delay modulation spectral energy that makes its bit packing density more sensitive to bandwidth changes."

Instead of being compressed into a narrow band of spectral energy, as in the case of delay modulation, E-NRZ makes better use of the full recorder passband. Hence, E-NRZ is less sensitive to UBE phenomena such as head varnish, azimuth misadjustment, and imperfect equalization. This relative insensitivity to UBE makes E-NRZ signal electronics easier to align and calibrate than DM electronics.

Bias Level Sensitivity

A second shortcoming of DM over NRZ was reported by King—bias level sensitivity (ref. 11–4): "NRZ was also more sensitive to bias changes than biphase, but less sensitive than delay modulation. NRZ showed only a 3 percent loss in bit packing [density] at 0 dB for [a tape of] 30 ips." Although not explained by King, it is likely that the band edge self-erasure from the bias level changes created phase response changes, which reduce the phase margin (intersymbol interference) for proper decoding of Miller and similar codes.

Datatape, Incorporated, recommends recording E-NRZ, or any other bilevel signal, without bias. Tests conducted at Datatape, Incorporated, laboratories have shown consistently better recorded levels, and lower bit error rates, with non-biased recording. The net improvement in the recorded level alone can be as great at 3 dB, which improves the off-tape SNR. The choice of E-NRZ encoding does not, however, require the elimination of high-frequency bias, if the user wishes to retain an Inter-Range Instrumentation Group[1] compatible direct record configuration. R. O. Leighou (ref. 11–8) reports successful operation at 32 kbpi/track with high-frequency bias, using "odd parity in every eight-bit byte". Although not stated by Leighou, he appears to be describing an NRZ code exactly equivalent to E-NRZ.

Sensitivity to Crossplay

D. A. King (ref. 11–4) reports on the sensitivity of various encoding schemes to crossplay between two recorders. Part of his experiment using two different 2 MHz wideband recorders possessing different SNR's is summarized in table 11–2.

The results of this experiment are not surprising, considering the compacting of the Miller spectrum, coupled with the 2 × clock requirement of that encoding scheme. Both of these shortcomings are apparent when crossplaying tapes between two different recorders. Here again, the wider frequency distribution of E-NRZ over Miller provides greater immunity to crossplay problems

[1]Now Range Commanders Council.

Table 11-2.—*Reduction in Packing Density Caused by Crossplay*

Tape speed, ips	Reduction in packing density, percent	
	NRZ	Miller
30	23	30
120	11	33

(ref. 11-4). The results of King's experiments are even more dramatic when it is realized that the NRZ data were recorded at a higher packing density, at the start of the experiment, than the Miller data.

Error Multiplication

Error multiplication is the property of an encoding scheme that results in an increase in decoder output errors over and above the output errors that would have been present using a code with zero error multiplication.

Error multiplication is one code property that has not yet received adequate exposure by past authors in the field of digital encoding schemes. R-NRZ, tested by King and described by Stein (ref. 11-6), is one example of an error multiplication code. Specifically, the derandomizing process inherently contains two types of error multiplication: from circulation through the feedback loops and from bit slip.

Circulation Error Multiplication

Some typical errors encountered when using analog tape for HDDR are as follows:

(1) A single bit in error, present at the input to the derandomizer, will result in three errors at the output, using any shift register size.
(2) A string of 23 bits in error at the input to the derandomizer will result in 46 bits in error at the output when using the 23-bit shift register.
(3) A string of 46 bits in error at the input to the derandomizer will result in 69 bits in error, 1.5 times the off-tape error rate, using the 23-bit shift register.

Bit Slip Error Multiplication

A single bit slip occurring before the derandomizer buffer will interrupt the synchronism of the buffer's derandomizing process. Twenty-three error-free, unslipped bits must purge the derandomizing buffer before an error-free output results.

Miller encoding is characterized by error multiplication. Miller encoding possesses a trait similar to R-NRZ—specifically, the Miller decoder must receive a 1-0-1 pattern to be synchronized for proper decoding. If either bit slip or burst errors occur, the Miller decoder must be purged by the 1-0-1 pattern to produce correct bit patterns at the output. The M^2 code is likewise disadvantaged.

The E-NRZ code is an example of a zero error multiplication code. It contains no inherent mechanism for the multiplication of errors, over and above the flaw rate of the tape being recorded and reproduced. Neither NRZ nor E-NRZ require purging of the decoder to reestablish error-free output. A single bit in error off tape will result in only a single bit error at the decoder output.

Bit Slip

Bit slip is the increase or decrease in clock frequency by one or more bit times with respect to the input signal.

One of the unique characteristics of E-NRZ encoding is its recovery potential from bit slip. The incorporation of parity bits in every eighth bit position of the E-NRZ encoding scheme provides, in effect, an electronic sprocket that can be used during playback decoding to combat bit slip. If bit slip occurs, the parity bit position will move ahead or backward in time by one or more bits. By inspecting for odd parity over a group of 8-bit words (five 8-bit words are usually adequate, with a 40-bit register), it becomes possible to detect the slip that has occurred and determine the direction and magnitude of the slip. Once the slip direction and magnitude have been determined, correction is greatly simplified. Encoding schemes that do not have the sprocket property of E-NRZ do not enable bit slip recovery until a unique bit pattern arrives (such as the 1-0-1 pattern required by Miller), or until a suitable time period has elapsed (such as the 23 bits required for R-NRZ).

In a parallel-mode digital recorder, if bit slip is not corrected with deskew buffers, the track experiencing bit slip will not be properly deskewed until the arrival of the next deskew frame synchronizing word, typically 500 to 600 bits later. E-NRZ tracks can be corrected for bit slip immediately without waiting for the next deskew frame synchronizing word.

Confidence Monitoring

The structure of E-NRZ encoding makes real-time confidence monitoring relatively easy. As soon as an error burst begins, odd parity will no longer be satisfied, a condition easily detected with conventional parity check circuitry. Error monitoring is accomplished by simply adding a parity error bus and indicator for each track to indicate error activity.

A single parity error can mean that an error burst of from one to seven bits in duration has occurred. Because of the fixed relationship between word bits and

parity bits (one parity bit for every seven word bits), the occurrence rate of parity (word) errors is a highly reliable indicator of recorded data quality.

Other codes may possess structuring suitable for confidence monitoring, but implementation is usually more costly. Examples are block codes, as described by Davidson (ref. 11-9) who states: "In the case of the (5, 6) alternating disparity code, an even parity check can be made. Such parity error checks can provide an indirect means of on-line monitoring BER [bit error rate]." Davidson concludes with the following comment on block code complexity: "Some drawbacks of these low disparity codes compared to biphase and delay modulation are as follows:

(1) Slightly more complex digital methods of generation are required.
(2) Moderately more complex (but nevertheless practical) digital methods of decoding are required. Not only must bit boundaries be determined, but character boundaries as well."

Eye Patterns

Indicator of System Performance

The overall performance characteristics of HDTR can be quickly determined by observing the analog output waveform from the reproduce amplifier. (See fig. 11-8). This waveform is often called the "eye pattern" because of its shape, which is similar to that of a human eye. The opening in the pattern (that is, the open area between the top and bottom) is called the "decision area" and it is within this decision area that the determination between a logic 1 and logic 0 is made. A wide decision area that is relatively free of unwanted transitions results in fewer bit errors in the reproduced data. Both the width of the decision area and the number of unwanted transitions are directly related to bit packing density and to the encoding scheme used.

Formation

Through mathematical analysis it can be shown that any step function waveform, such as the digital data, is actually composed of a fundamental sine wave frequency and an infinite number of harmonic components. To pass such a signal without distortion, a device must have sufficient bandwidth to pass not only the fundamental frequency but a certain number of the harmonic components as well. If, as in the case of the analog reproduce electronics, the passband is only sufficient to pass the fundamental, the harmonics will be filtered out and only the fundamental sine wave will appear at the output. This, in essence, is the basis for the formation of the eye pattern. The filtering effect of the reproduce

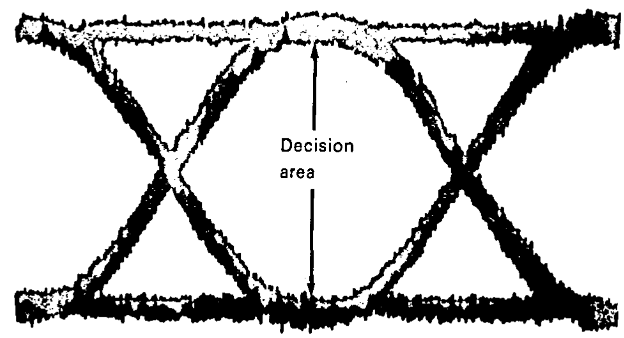

Figure 11-8.—Typical eye pattern.

electronics can be seen by comparing waveforms in figures 11-9(*a*) and (*b*).

If the filtered output of the reproduce amplifier (waveform (*b*)) is applied to the vertical input of an oscilloscope, and if the oscilloscope is triggered externally from the clock signal that accompanies the waveform (fig. 11-9 (*c*)), the various segments of the data stream will be superimposed on one another to form the characteristic eye pattern. This formation of the eye pattern by superimposing one segment on another is shown in progressive steps in figures 11-9 (*d*) to 11-9 (*g*).

To see the effects of bit packing density on the eye patterns for different encoding schemes, see figure 11-6.

Complexity and Cost

E-NRZ is an uncomplicated code that is readily understood, simple to engineer, and easy to maintain. E-NRZ requires no complicated algorithms, no truth tables or look up tables, and no complex circuitry. As a result of this relative simplicity, total cost to the user is less than more complicated encoding schemes. Reliability is better. Mean time between failures and mean time to repair are likewise better than more complicated codes. E-NRZ alignment procedures are less complicated because of wider adjustment margins, and the time interval between recorder recalibration and alignment is also greater.

Determination of Best Encoding Scheme

The list of superior properties of E-NRZ is important to any organization studying HDDR. Competing code schemes may match E-NRZ in one or more properties but no one code can match E-NRZ on a one-to-one basis, using the list of properties in table 11-3.

PRINCIPLES OF PARALLEL E-NRZ RECORDING

This section describes the operating principles of parallel E-NRZ HDTR's and the basic components that

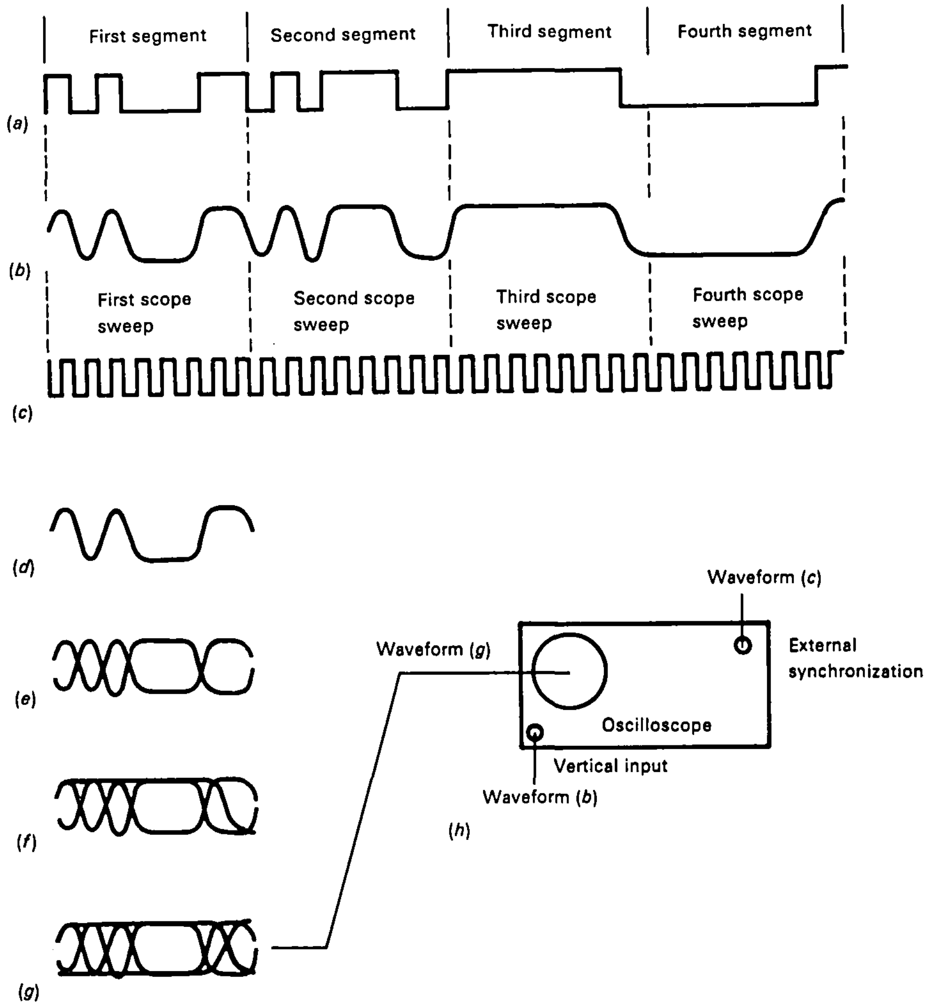

Figure 11-9.—Formation of the eye pattern. (*a*) Step function digital data. (*b*) Signal at output of reproduce electronics. (*c*) Clock signal. (*d*) First segment alone. (*e*) First and second segments superimposed. (*f*) First, second, and third segments superimposed. (*g*) First, second, third, and fourth segments superimposed to form eye pattern. (*h*) Connection of oscilloscope to observe eye pattern.

Table 11-3.—*Code Comparison for Parallel Mode HDDR*

Characteristics	Code			
	Miller	M²	R-NRZ	E-NRZ
Theoretical maximum per track packing density,[a] kbpi	33.33	33.33	33.33	33.33
Maximum user data per track packing density[b] for BEP of 1 in 10^6, kbpi	22.00	22.00	30.00	27.45
Code efficiency, percent	66.00	66.00	90.00	82.35
Code overhead, percent	8.33[c]	8.33[c]	3.22[d]	21.43[e]
SNR required for 1 in 10^6 BEP, dB	17.00	17.00	14.00	14.00
Stability of baseline even when transition density is low	Yes	Yes[f]	No	Yes
Immunity to error multiplication problems	No	No	No	Yes
Ability to recover from bit slip errors	Fair	Fair	Fair	Excellent
Immunity to bandwidth changes due to changes in record current and/or differences in tape	Fair	Fair	Good	Good
Error correction capability	No	No	No	Yes
Synchronous clock requirement	2× bit rate	2× bit rate	1× bit rate	1× bit rate

[a]Maximum packing densities specified assume passband of 2.0 MHz at 120 ips.
[b]Packing densities are for 28-track recorders with 2.0-MHz passbands.
[c]One extra synchronization track required for every 12 data tracks.
[d]16 synchronization bits added to every 496 data bits.
[e]80 parity and 40 synchronization bits added to every 560 data bits.
[f]Certain bit patterns will result in considerable dc (or near dc) spectral components that will produce baseline shift or "gallop."

make them work. To assist the reader in comprehending the function and interrelationship of these components, figure 11-10 contains a complete block diagram of a typical seven-track HDTR.

Comparison of NRZ–L and E-NRZ Data Streams

The principles of E-NRZ recording are easier to master if both the differences and the similarities between the NRZ–L and E-NRZ data streams are kept clearly in mind. As shown in figure 11-11, both data streams are divided into a series of sections called frames. These frames, in turn, are further divided into segments; and the segments, in turn, to a specific number of data bits. Note that the use of the term "divided" here is somewhat misleading because there is no actual physical separation between the various divisions; instead, the data are processed as continuous, uninterrupted, bit streams while the terms frame and segment merely serve as a convenient means of identifying the particular portion of the data stream being discussed.

It is important from the very onset of this discussion to recognize that the period of time occupied by a frame is the same for both the NRZ–L and the E-NRZ data streams. The only difference between the two data streams lies in the number and type of data bits contained in the frames.

The frames of the NRZ–L data stream each contain 560 bits. Note that all 560 bits are signal bits; there are no parity or synchronizing word bits present in the NRZ–L data stream. These 560 bits are grouped into 10 segments of 56 bits each. Each segment, in turn, contains eight seven-bit words.

The frames of the E-NRZ data stream contain 680 bits, 120 more than the frames of the NRZ–L data stream. The 120 additional bits consist of 80 parity bits and 40 synchronizing word bits, which are added to each 560-bit data frame of the NRZ–L data stream during the encoding process. The 680 bits of each E-NRZ frame are grouped into 17 segments of 40 bits each. Sixteen of the 17 segments are data segments, while the 17th segment consists of a 40-bit deskew synchronizing word used to realign (deskew) the NRZ–L data before final output from the recorder.

Each segment of the E-NRZ data stream, with the exception of the synchronizing word segment, contains five eight-bit words. The first seven bits of each eight-bit word are identical to the seven bits that make up the corresponding word of the NRZ–L data, except that bits 2, 3, 6, and 7 of the E-NRZ word have been inverted. This is a normal part of the E-NRZ encoding process and is done to increase the number of transitions in the data stream whenever long strings of "1's" or "0's" are present in the NRZ–L data.

The eighth bit in every eight-bit word of the E-NRZ data is a parity bit, denoted in the illustration by the letter *P*. This bit is inserted to make the total number of "1's" contained in each eight-bit word an odd count. In other words, with the insertion of the parity bit, every eight-bit word of the E-NRZ data stream will have odd parity.

The deskew synchronizing word is inserted at the center of each E-NRZ data frame and, like all E-NRZ data segments, contains 40 bits. This segment consists of 20 alternating "1's" and "0's" followed by 20 alternating "0's" and "1's". If the synchronizing word segment were divided into five eight-bit words, as in the case of the data segments, it would be discovered that each eight-bit word has even parity: Each eight-bit word of the synchronizing segment would contain an even number of "1's" as opposed to the data words, which contain an odd number of "1's". This provides the means for the decoder/deskew assembly of the recorder to differentiate between data segments and the synchronizing word segment during data reproduction.

Notice the structure of the deskew synchronizing word in figure 11-11, 10 "1-0" pairs followed by ten "0-1" pairs. The structure is unique in that the bit pattern reads the same in either the forward or the reverse direction. This permits the E-NRZ data to be read in forward or reverse direction during reproduction without loss of data synchronization. The unique structure of the synchronizing word also insures positive identification by the decoder/deskew assembly, and eliminates any possibility of the synchronizing word being misinterpreted as data bits.

Earlier in our discussion, we stated that the period of time occupied by each data frame remained the same for both the NRZ–L and the E-NRZ data streams despite the fact that there are 120 more bits in the E-NRZ frame. How is this possible without making the E-NRZ frames longer than the corresponding NRZ–L frames? The answer lies in the use of two separate clock signals—one at the normal bit rate of the NRZ–L data and the other at the bit rate of the E-NRZ data, which is 1.21 times faster than the NRZ–L bit rate. During the encoding process, the NRZ–L data, having fewer bits per frame, is clocked into the encoder at the normal NRZ–L bit rate then, later, clocked out at the slightly faster bit rate of the E-NRZ data, to provide the extra space required for the parity bits and the synchronizing word segment. During the decoding process, the E-NRZ data, having more bits per frame, is clocked into the decoder/deskew buffer at the faster rate. The parity bits and the deskew synchronizing word segment are stripped away during the decoding process, leaving only the original NRZ–L data bits, which are clocked out of the decoder at the normal (i.e., original) bit rate.

The block diagram in figure 11-10 illustrates the basic components of a typical seven-track high HDTR and in-

dicates the major paths of signal flow. The eight basic components considered in this discussion are as follows:

(1) Encoder assembly
(2) Input timing clock
(3) Magnetic head assembly
(4) Tape transport
(5) Preamplifier assembly
(6) Digital reproduce assembly
(7) Decoder/deskew assembly
(8) Output timing clock.

The principles of operation discussed in the paragraphs that follow apply to all Datatape, Incorporated, parallel mode HDTR's regardless of the number of tracks provided.

Encoder Assembly

The encoder assembly accepts up to seven lines of bit parallel NRZ–L input data, converts the NRZ–L data to E-NRZ data, and supplies the necessary signal current to drive the magnetic record heads. A separate encoder circuit card is provided for each NRZ–L data input line.

Typically a minimum of four input lines are required for normal recorder operation: tracks 1, 3, 5, and 7. This insures the availability of the four synchronizing word detect time signals (SWDT 1, SWDT 3, SWDT 5, and SWDT 7) at the output of the decoder/deskew assembly, used by the output timing clock to generate output timing signals. When less than four input lines are used, two or more of the SWDT inputs to the output timing clock must be connected in parallel for proper recorder operation.

During the NRZ–L to E-NRZ conversion process, the NRZ–L data stream is separated into seven-bit words, each of which is temporarily stored in one of eight storage registers contained by the encoder. Later, as data are clocked out of the storage registers, bits 2, 3, 6, and 7 of each seven-bit word are inverted to help increase the number of transitions in the data stream. This insures that the data stream will have sufficient transition density to support the regeneration of an output timing clock signal, even when the NRZ–L input consists of long uninterrupted strings of "1's" or "0's".

In addition to inverting bits 2, 3, 6, and 7 the encoder performs a parity check on each seven-bit word as it is clocked out of the storage registers to determine the number of "1's" present. From this check, an eighth parity bit is generated and inserted into the data stream directly after the seven-bit word to which it applies. If the number of "1's" is an odd count, the parity bit is a "0." If the number of "1's" is an even count, the parity bit is a "1" to make the count odd. Thus, with the addition of this parity bit each of the seven-bit words becomes an eight-bit word, and the E-NRZ encoding process is complete.

After every 16 data segments (640 bits), the encoder inserts a 40-bit deskew synchronizing word into the E-NRZ data stream. This synchronizing word consists of ten "1-0" pairs followed by ten "0-1" pairs and is used by the decoder/deskew assembly during data reproduction to align all parallel data tracks before final output from the recorder. Detection of the synchronizing word by the decoder/deskew assembly also initiates the four SWDT signals (SWDT 1, SWDT 3, SWDT 5, and SWDT 7) used by the output timing clock to create output timing signals. The addition of the deskew synchronizing word separates the E-NRZ data steam into frames, each consisting of 680 bits: The forty eight-bit words preceding the synchronizing word (320 bits), the synchronizing word (40 bits), and the forty eight-bit words following the synchronizing word (320 bits) constitute an E-NRZ data frame.

Exact timing of the encoding sequence is essential for proper encoder operation, because there are several more signal bits in the output data stream than were present in the input data stream. To preserve the same time base at the output of the encoder that is present at the input, yet provide the extra space needed to accommodate the added bits, the bits must be clocked out of the encoder at a faster rate than they were clocked in. This is accomplished by using two separate clock signals, supplied by the input timing clock. The slower of the two clock signals (ENCDR INPCLK) operates at the same rate as the synchronous clock signal that accompanies the NRZ–L data at the recorder input, and serves to clock data bits into the encoder storage registers. The faster clock (ENCDR OUTCLK) operates at a slightly faster rate than the ENCDR INPCLK ($680/560 = 17/14 = 1.21$ times), and serves to clock data bits out of the encoder storage registers. Thus, the actual time period occupied by the E-NRZ encoded data, including the deskew synchronizing words, remains exactly the same as the time period occupied by the original NRZ–L data present at the recorder input.

Encoder Input Timing Chart

The NRZ–L input data are clocked into eight encoder storage registers by the input clock signal (ENCDR INPCLK) from the input timing clock (fig. 11-12). The first seven input bits are clocked into the first storage register, the next seven bits into the second register, etc. This separates the NRZ–L data into seven-bit words to permit the insertion of appropriate parity bits. An input synchronizing pulse (ENCDR INPSYNC) is provided by the input timing clock at the beginning of the load sequence to insure the words are loaded into the proper storage registers. This synchronizing pulse occurs once for every four input data frames ($560 \times 4 = 2240$ bits) to maintain input synchronization. When four of the eight storage registers

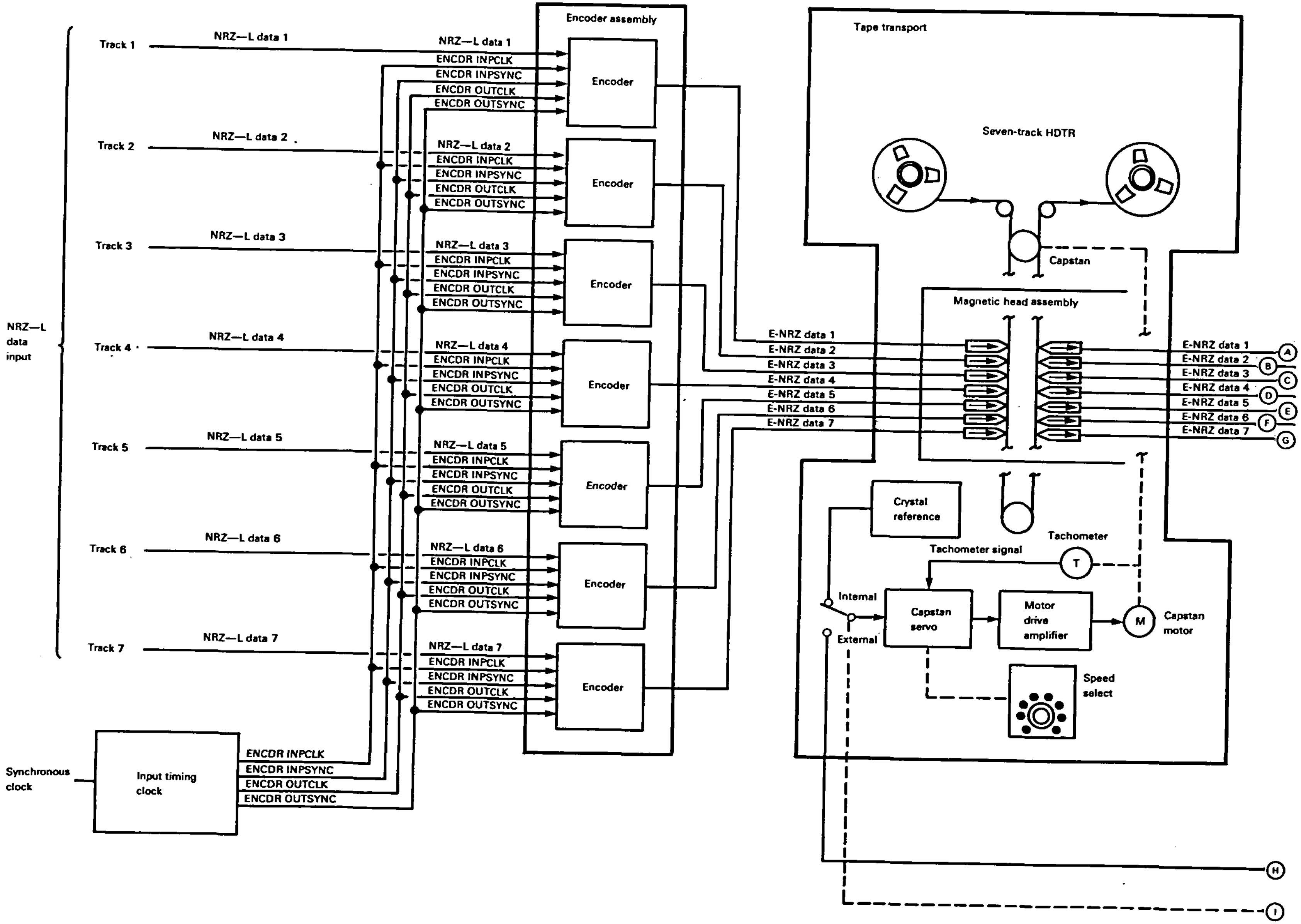
NRZ—L data input
Track 1
NRZ—L data 1
Track 2
NRZ—L data 2
Track 3
NRZ—L data 3
Track 4
NRZ—L data 4
Track 5
NRZ—L data 5
Track 6
NRZ—L data 6
Track 7
NRZ—L data 7
Encoder assembly
ENCDR INPCLK
ENCDR INPSYNC
ENCDR OUTCLK
ENCDR OUTSYNC
Encoder
Synchronous clock
Input timing clock
Tape transport
Seven-track HDTR
Capstan
Magnetic head assembly
E-NRZ data 1
E-NRZ data 2
E-NRZ data 3
E-NRZ data 4
E-NRZ data 5
E-NRZ data 6
E-NRZ data 7
A
B
C
D
E
F
G
Crystal reference
Tachometer
Tachometer signal
T
Internal
External
Capstan servo
Motor drive amplifier
M
Capstan motor
Speed select
H
I

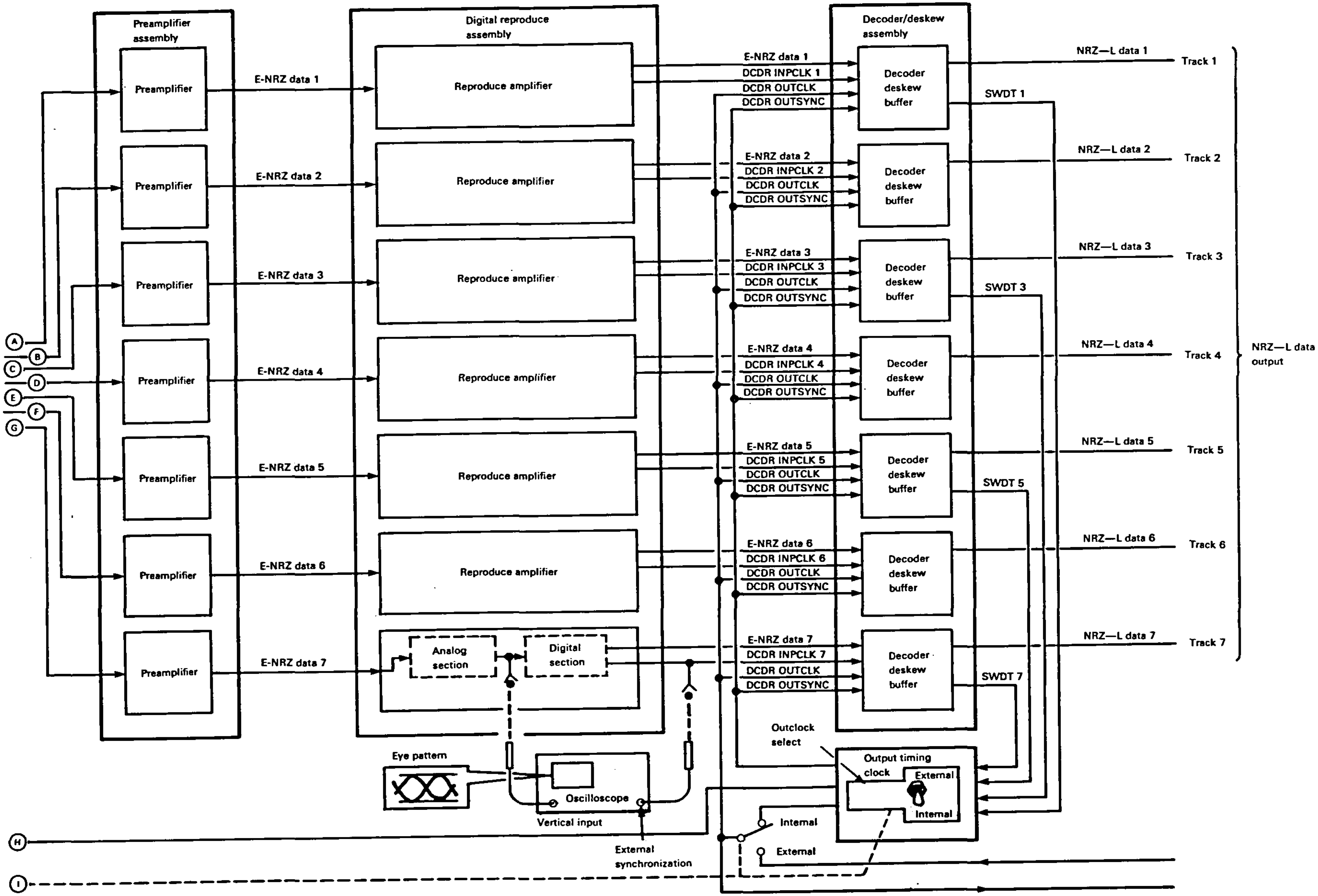

Figure 11–10.—Simplified block diagram of seven-track HDTR.

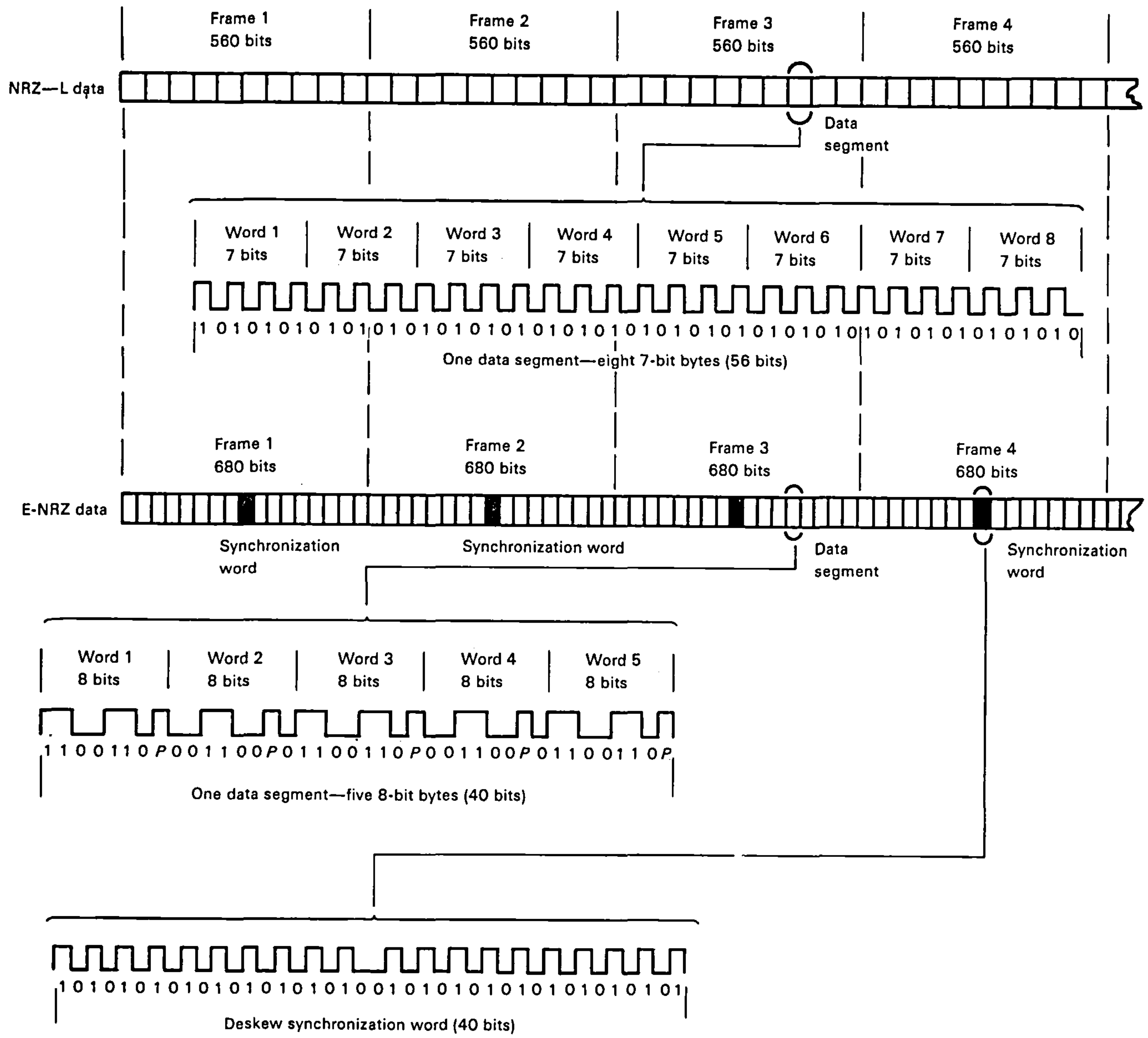

Figure 11–11.—Comparison of NRZ—L and E-NRZ data streams.

are loaded, each with a seven-bit word, an output sync pulse (ENCDR OUTSYNC) is provided to begin the unloading sequence. This synchronizing pulse occurs once for every four output data frames ($680 \times 4 = 2720$ bits) to maintain output synchronization.

Encoder Output Timing Chart

Unloading of the stored NRZ—L data from the encoder storage registers begins with the arrival of the output sync pulse (ENCDR OUTSYNC) from the input timing clock, which insures that the seven-bit words are unloaded in the same sequence in which they were loaded (fig. 11-13). Data are clocked out of the storage registers by the output clock signal (ENCDR OUTCLK), which operates at a slightly faster rate (1.21 times) than the encoder input clock to permit the insertion of parity bits and the deskew synchronizing words. During the output sequence, bits 2, 3, 6, and 7 of each seven-bit word are inverted to help increase data transition density. Then, following a parity check, an eighth bit is added to each seven-bit word to make the total number of "1's" contained in the eight-bit word an odd count.

Encoder Output Data Stream

The output from each E-NRZ encoder is a serial data stream consisting of 40-bit segments, each containing

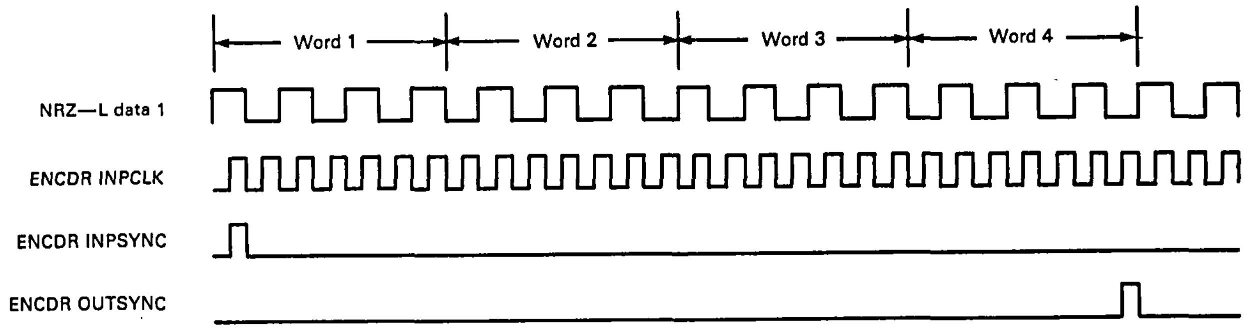

Figure 11-12.—Encoder input timing chart.

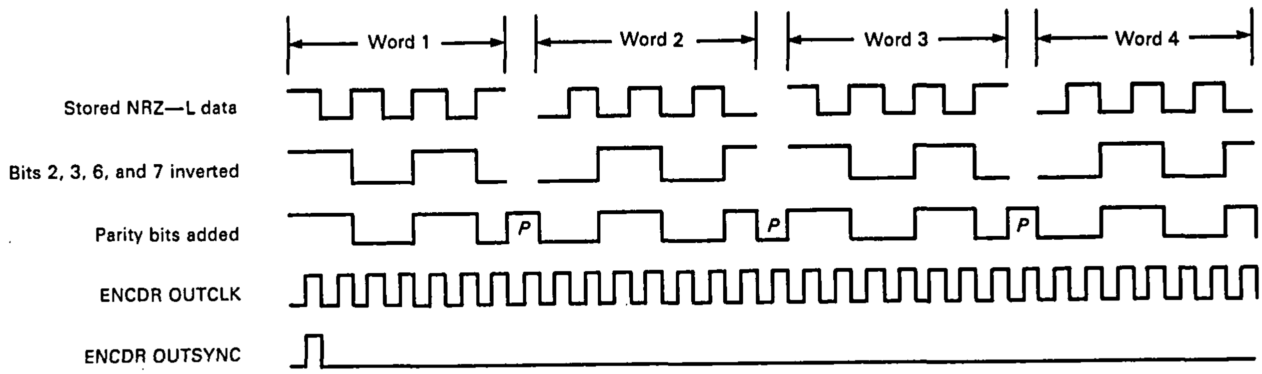

Figure 11-13.—Encoder output timing chart.

five eight-bit words, and the 40-bit deskew synchronizing word (fig. 11-14). The synchronizing word segment, plus the eight data segments preceding the synchronizing word, and the eight segments following the synchronizing word, constitute a data frame of 680 bits.

Input Timing Clock

The input timing clock accepts the synchronous clock signal supplied with the NRZ−L input data and supplies the four timing signals necessary to clock data into and out of the encoder assembly. The four outputs from the input timing clock are the encoder input clock (ENCDR INPCLK), encoder input synchronization (ENCDR INPSYNC), encoder output clock (ENCDR OUTCLK), and encoder output synchronization (ENCDR OUTSYNC).

As shown in the timing chart (fig. 11-15), the pulse rate of the ENCDR INPCLK signal is exactly the same

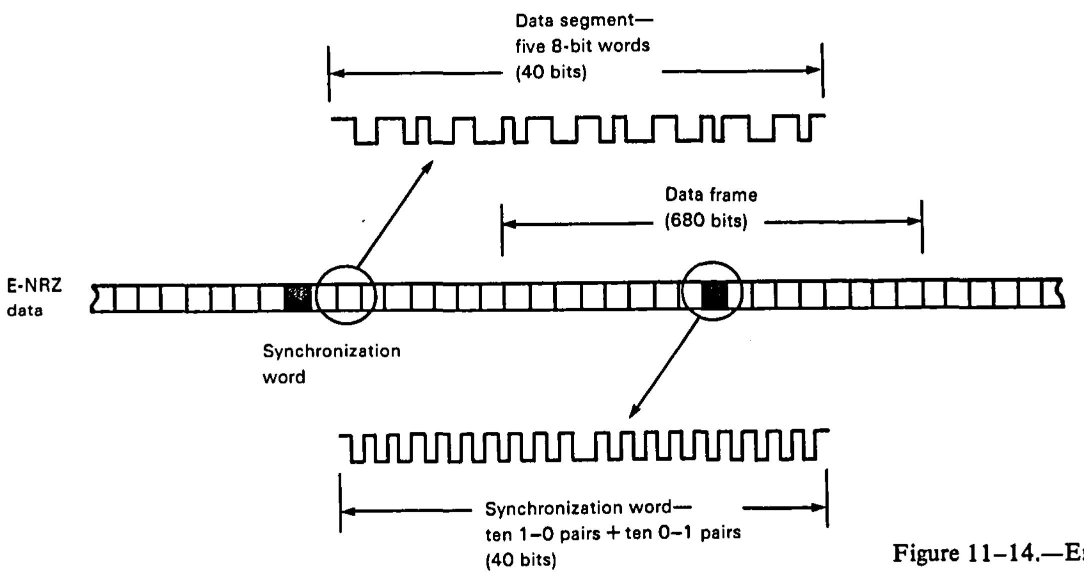

Figure 11-14.—Encoder output data stream.

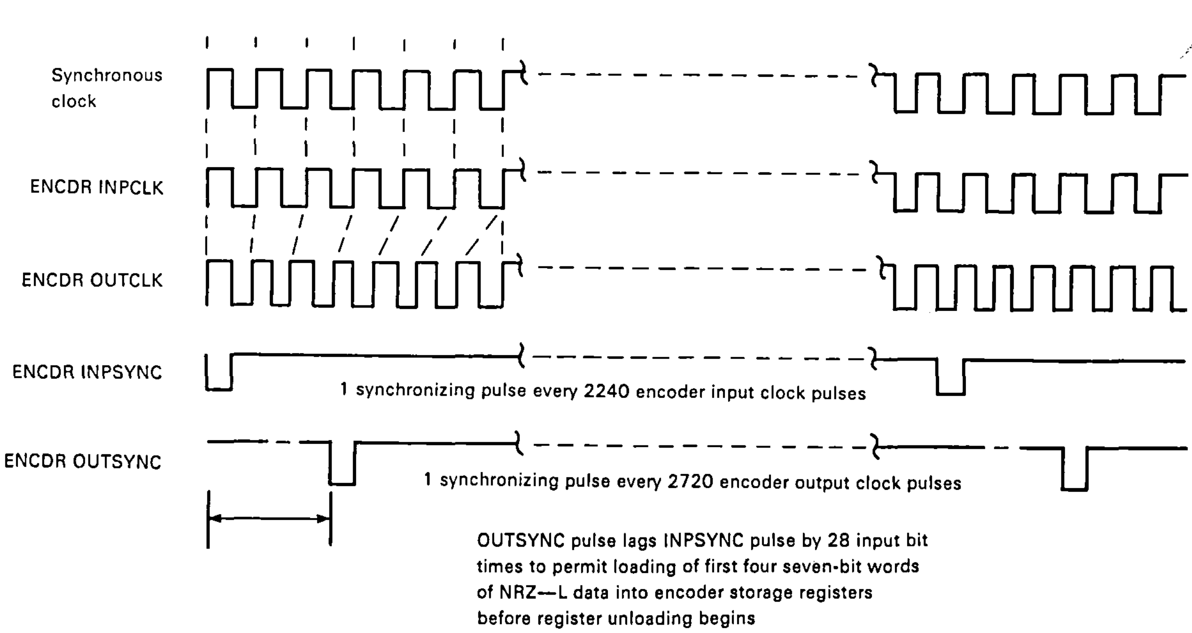

Figure 11–15.—Input clock timing chart.

as the synchronous clock input supplied with the NRZ–L input data. This signal is used to clock data into the encoders. The pulse rate of the ENCDR OUTCLK is slightly more than 1.21 (17/14) times the pulse rate of the ENCDR INPCLK signal and is used to clock data out of the encoders. This slight increase in clock rate is necessary to permit the insertion of parity (enchancement) bits and the deskew synchronizing words into the data stream without changing the time base of the original NRZ–L data.

The ENCDR INPSYNC pulse occurs once for every 2240 ENCDR INPCLK pulses and is used to insure that data are loaded into the proper encoder storage registers. The ENCDR OUTSYNC pulse occurs once for every 2720 ENCDR OUTCLK pulses to insure that data are unloaded from the encoder storage registers in the proper sequence. The two synchronizing pulses occur at exactly the same rate, but the ENCDR OUTSYNC pulse lags the ENCDR INPSYNC pulse by a period equal to 28 input bit times (i.e., a period equal to four seven-bit words), to delay the unloading of the eight encoder storage registers until loading of the first four has been completed.

Magnetic Head Assembly

The Magnetic Head Assembly performs two important functions. First, during the record process, the head assembly converts the signal current transitions from the encoder assembly to equivalent magnetic flux transitions to magnetize the tape. Then, during the reproduce process, the head assembly reconverts the recorded flux transitions on tape to equivalent electrical signal currents to drive the preamplifier assembly.

Tape Transport

The function of the tape transport is to move the magnetic tape past the magnetic head assembly at a fixed rate of speed, determined by the position of the "speed select" switch.

During the record mode of operation, capstan motor speed (and hence tape speed) is controlled by an internally generated crystal reference frequency supplied by the tape transport. This fixed frequency reference is routed to the capstan servo through the INT contacts of the "outclock select" switch (located on the output timing clock). Here, in the capstan servo, the reference frequency is compared with the output signal from an optical tachometer driven directly by the capstan motor. Any change in motor speed results in a corresponding change in tachometer frequency, which the servo immediately acts to correct.

During the reproduce mode of operation, tape speed may be controlled either internally or externally, depending on the method used to clock data out of the recorder. The choice of internal or external control is made possible by the outclock select switch (located on the output timing clock). When this switch is placed in the INT position, tape speed is controlled by the internally generated crystal reference frequency supplied by the tape transport, in exactly the same manner used during the record mode of operation.

When the switch is placed in the EXT position, capstan motor speed (and hence tape speed) is controlled by the 400-kHz servo reference signal from the output timing clock. In this case, an external clock signal (supplied by the user) is applied to the synchronous clock (input) connector of the recorder and

routed through the EXT contacts of the outclock select switch to the decoder/deskew assembly, where it serves as the DCDR OUTCLK signal. The clock rate of the user supplied clock signal determines the rate at which data bits are clocked out of the decoder/deskew buffers, and also the rate at which SWDT pulses are clocked into the output timing clock. The rate of the SWDT pulses, in turn, controls the 400-kHz servo reference frequency. This method of motor speed control serves as a "coarse data rate control" to prevent overflow of the storage registers in the decoder/deskew assembly. If, for any reason, the rate of data transfer into the storage registers becomes too great, and the possibility of an overflow condition exists, the frequency of the 400-kHz servo reference is decreased, causing the capstan motor to slow down and reduce the data transfer rate. As soon as the threat of register overflow has passed, the servo reference is again increased to 400 kHz to return the capstan motor to normal operating speed, and to restore the normal data transfer rate.

Preamplifier Assembly

The function of the preamplifier assembly is to amplify the low-level E-NRZ data signals from the reproduce heads to a level sufficient to drive the reproduce amplifiers in the digital reproduce assembly. It is significant, at this point, to mention that the output signal from the preamplifiers is an analog signal that does not contain the sharp rise and fall times of the digital signal that was recorded. This phenomenon is the result of the inherent nonlinear response characteristics of the reproduce head and must be compensated for by the reproduce amplifiers that follow. A separate preamplifier is provided for each reproduce data track.

Digital Reproduce Assembly

The digital reproduce assembly accepts unequalized analog signals from the preamplifier assembly and supplies digital E-NRZ data, and an input clock signal, to the decoder/deskew assembly. A separate reproduce amplifier is provided for each data track.

Each reproduce amplifier contains two sections: an analog section and a digital section. The function of the analog section is to amplify and equalize the analog signal from the preamplifier to restore normal amplitude and phase relationships. Then, the equalized data signal is routed to the digital section where it is reconverted to digital format for further processing by the decoder/deskew assembly. The digital section also reconstructs a clock signal proportional to the E-NRZ data rate for use by the decoder/deskew buffers in the decoder/deskew assembly. A separate decoder input clock signal (DCDR INPCLK) is generated for each data track and serves to clock E-NRZ data bits into the decoder/deskew buffers.

A test point provided at the output of the analog section of each reproduce amplifier permits monitoring the reproduce "eye pattern" to determine data quality. When monitoring these eye patterns, the oscilloscope sweep circuit should be synchronized to the data bit rate of the track being monitored. This may be accomplished by triggering the oscilloscope sweep from the DCDR INPCLK signal supplied by the reproduce amplifier, as shown in figure 11–10.

Decoder/Deskew Assembly

The decoder/deskew assembly converts the seven lines of bit parallel E-NRZ data from the digital reproduce assembly to NRZ–L data that exactly duplicates the original NRZ–L data supplied to the input of the recorder. A separate decoder/deskew buffer circuit card is provided for each data track.

The E-NRZ data stream is clocked into the decoder/deskew buffer in 40-bit segments; i.e., five eight-bit words at a time. Input timing is controlled by the DCDR INPCLK signal from the corresponding reproduce amplifier. Each of the five eight-bit words is loaded into a separate storage register and checked for parity. Odd parity in all five registers signifies the presence of a data segment, whereas even parity in all five registers signifies the presence of the deskew synchronizing word segments. The data segments are clocked out of the storage registers and into the deskew buffer for further processing. The synchronizing word segment, on the other hand, is clocked out of the storage registers and discarded.

The presence of the deskew synchronizing word segment in the input storage registers causes the SWDT output of the decoder/deskew buffer to switch from a logic 1 to a logic 0 level (fig. 11–16). The output remains at the logic 0 level for the next 40 bit times, while the synchronizing word is being clocked out of the storage registers, then returns to the logic 1 level. The SWDT pulse thus generated is routed to the output timing clock where it is used to create the DCDR OUTCLK signal.

Bits 2, 3, 6, and 7 of each eight-bit word are reinverted as the E-NRZ data are clocked from the input storage registers to the deskewing buffer (fig. 11–17). This compensates for the inversion of these bits that occurred in the encoder assembly and restores proper word content to the data stream.

In the deskew buffer, the E-NRZ data is aligned bit-for-bit with the corresponding data streams for all other data tracks (fig. 11–18). This corrects any "slip" in synchronization that may have occurred between the data tracks as a result of the record/reproduce process. Once all tracks are properly aligned, a DCDR OUTSYNC

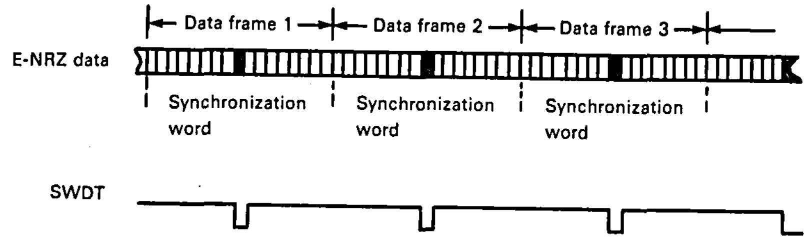

Figure 11-16.—Synchronization word detect time pulses.

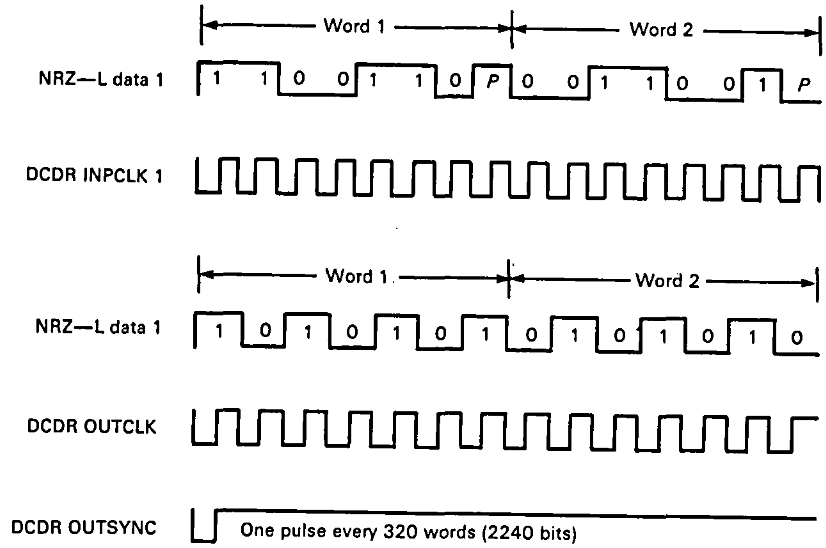

Figure 11-17.—Decoder input/output timing chart.

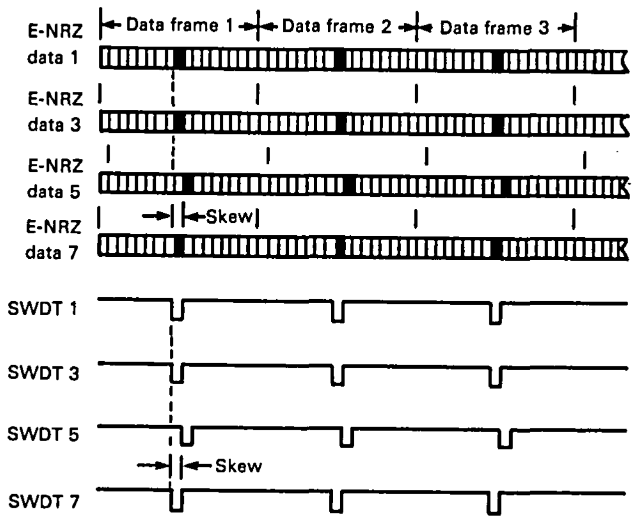

Figure 11-18.—Example of skew.

pulse from the output timing clock initiates the simultaneous unloading of the deskew buffers by the DCDR OUTCLK signal. The parity bits are stripped from the E-NRZ data streams during the output sequence, which restores the data stream to the original NRZ−L format.

Output Timing Clock

When the outclock select switch is placed in the INT position, the output timing clock accepts the SWDT outputs from the decoder/deskew buffers of tracks 1, 3, 5, and 7 and supplies the two timing signals necessary to clock data out of the decoder/deskew assembly: the decoder output clock (DCDR OUTCLK) and the decoder output synchronization (DCDR OUTSYNC) signals. The output timing clock also supplies the synchronous clock (output) signal that accompanies the NRZ−L data at the recorder output.

When the outclock select switch is placed in the EXT position, the DCDR OUTCLK signal normally supplied by the output timing clock is replaced by an external clock signal (supplied by the user) from the synchronous clock (input) connector. In the EXT mode, the output timing clock supples a 400-kHz servo reference signal used to control capstan motor speed when data are reproduced.

ERROR DETECTION AND CORRECTION

Errors in digital recording are always a problem because they degrade the integrity of the digital data. The seriousness of this problem depends, to a large ex-

tent, on the nature of the data to be processed and the ultimate accuracy required. For most scientific data, a certain number of errors can usually be tolerated without serious harm being done. On the other hand, business data almost always require extremely high accuracy where even a single error can result in a costly mistake. Errors can and do occur whenever magnetic tape is used as the medium for recording and reproducing digital data, especially when bit packing density is extremely high, as in the case of HDDR. It is important, therefore, that an efficient and effective method of detecting and correcting such errors be included as a standard, or optional, feature for any HDTR where data integrity is to be maintained. This section explores the subject of data errors and describes the basic principles of error detection and correction (EDAC) that apply to parallel mode HDTR's using E-NRZ encoding.

The Main Cause of Data Errors

Errors can occur one at a time, as in the case of isolated bit errors, or in strings ranging from two to as many as several thousand. Such strings are called burst errors. Most bit and burst errors are directly related to the medium on which the digital data are recorded; i.e., the magnetic tape itself. This is because any slight imperfections in the oxide coating of the tape will cause "dropouts," areas where no information is recorded, or is recorded at such low levels as to be undetectable during the reproduce process. Dust, lint, and other foreign material on the surface of the tape can also result in dropouts. Tape that has become excessively worn is yet another cause of bit and/or burst errors. There are other reasons for the occurrence of errors, of course, but none that contribute as significantly to the problem as the magnetic tape itself.

Types of Bit Errors

There are three types of bit errors that can occur as a result of imperfections in the magnetic tape: isolated bit errors, simultaneous bit errors, and even parity word errors. To simplify the discussion, we shall assume that the data are arranged in blocks. The width of each block shall be eight bits, corresponding to the eight bits that make up an E-NRZ data word. The height of each block shall correspond to the number of parallel tape tracks used to record and reproduce the E-NRZ data, in this case, four.

Isolated Bit Error

An isolated bit error is the occurrence of a single bit error in any given data block (fig. 11-19).

E-NRZ data 1	0	0	0	0	1	X	0	1
E-NRZ data 2	0	0	0	1	0	0	0	0
E-NRZ data 3	0	0	0	1	0	1	0	1
E-NRZ data 4	0	0	0	1	1	0	0	1

Figure 11-19.—Data block with isolated bit error. (X denotes position of bit error.)

Simultaneous Bit Errors

A simultaneous bit error is the occurrence of two (or more) isolated bit errors in the same bit column, within the same data block (fig. 11-20).

Even Parity Word Error

An even parity word error is the occurrence of any even number of bit errors in a single data word (fig. 11-21).

Burst Errors

Burst errors occur in strings ranging in length from two to as many as several thousand bits, and can extend across the width of more than one data track (fig. 11-22). Experiments at Datatape, Incorporated, laboratories have shown that the average burst error length is approximately 300 to 350 bits in duration, at packing densities of 30 000 to 33 333 bpi using a 28-track recorder and magnetic tape recommended for HDDR use. These experiments are in no way conclusive, however, because burst errors as short as 190 bits and as long as 8356 bits were also encountered during these experiments.

E-NRZ data 1	0	0	0	0	0	0	1	0
E-NRZ data 2	0	0	0	0	0	1	1	1
E-NRZ data 3	0	0	0	0	1	0	X	1
E-NRZ data 4	0	0	0	0	1	1	X	0

Figure 11-20.—Data block with simultaneous bit errors. (X denotes position of bit error.)

E-NRZ data 1	0	0	0	0	0	1	1	1
E-NRZ data 2	0	0	0	0	1	0	1	1
E-NRZ data 3	0	0	0	0	1	X	X	0
E-NRZ data 4	0	0	0	1	0	0	1	1

(*a*)

E-NRZ data 1	0	0	0	0	0	1	1	1
E-NRZ data 2	0	0	X	X	X	X	1	1
E-NRZ data 3	0	0	0	0	1	1	1	0
E-NRZ data 4	0	0	0	1	0	0	1	1

(*b*)

Figure 11-21.—Data blocks with even parity word errors. (X denotes position of bit error.) (*a*) Example 1. (*b*) Example 2.

E-NRZ data 1	X	X	X	X	X	X	X	X
E-NRZ data 2	0	0	0	0	1	0	1	1
E-NRZ data 3	0	0	0	1	0	1	0	1
E-NRZ data 4	0	0	0	1	1	0	0	1

(*a*)

E-NRZ data 1	X	X	X	X	X	X	X	X
E-NRZ data 2	X	X	X	X	X	X	X	X
E-NRZ data 3	0	0	0	1	0	1	0	1
E-NRZ data 4	0	0	0	1	1	0	0	1

(*b*)

Figure 11–22.—Data blocks with burst errors. (X denotes position of bit error.) (*a*) Single track burst error. (*b*) Multiple track burst error.

Methods of Error Reduction

Certified Tape

Bit errors occurring as a result of the record/reproduce process are almost always directly related to the type and condition of the magnetic tape used. Consequently, considerable care should be exercised in the selection of all tape used to record high-density digital data. Some manufacturers of instrumentation quality magnetic tape offer a complete line of tapes that are especially certified for digital use. As a rule, these tapes are no different than the manufacturer's line of noncertified tapes, except for the additional steps taken to prescreen and test the tapes for bit error rate (BER) before shipment from the factory. The steps taken to prescreen and test the tapes for certification are relatively uncomplicated, but they do require a certain amount of time and effort on the part of the manufacturer, which accounts for the much higher cost of the certified tapes. For those who wish to prescreen and test their own tapes, the use of Datatape, Incorporated's tape cleaner/certifier is recommended. It should be made clear, however, that the exclusive use of certified tape does not, of itself, guarantee error-free data because the protection offered is strictly of a preventive rather than a corrective nature.

Electronic EDAC

EDAC is Datatape, Incorporated's best solution to the problem of data errors (ref. 11-10), and is available as an optional feature on all Datatape, Incorporated parallel mode HDTR's. Better, more efficient, and less costly than the use of certified tapes, EDAC provides the capability to isolate and eliminate virtually all bit and burst errors from the digital data.

The EDAC feature provides a significant improvement in the BER specification of any parallel E-NRZ recorder. It is based on a track interleaving and parity check technique in which the data tracks are checked for parity both longitudinally and laterally to determine the exact coordinates of data errors.

EDAC is available in one, two, or three loop configurations, depending on the degree of error correction desired. Each loop consists of an EDAC encoder and decoder combination and requires one additional track on tape. A one-loop EDAC, for example, is the simplest configuration and is designed to detect and correct only isolated bit errors. This configuration requires one additional track on tape. A two-loop EDAC, on the other hand, will detect and correct both isolated bit errors and simultaneous bit errors and requires two additional tracks on tape. The most sophisticated EDAC is the three-loop EDAC, which will detect and correct all known types of bit errors (isolated bit errors, simultaneous bit errors, even parity word errors, and burst errors). The three-loop EDAC requires three additional tracks on tape and has been shown to be so effective in correcting data errors that one complete reproduce track may be totally disabled with no measurable increase in BER.

To illustrate the effectiveness of EDAC, if a two-loop EDAC is used in conjunction with a 14-track recorder, a correction of two to three orders of magnitude can be expected. Likewise, a three-loop EDAC used with a 28-track recorder would also exhibit two to three orders of magnitude of correction. For example, using a two-loop EDAC with a 14-track recorder having a BER of 1 in 10^6 could improve BER to better than 1 in 10^9. In a similar fashion, a three-loop EDAC used with a 28-track recorder having a BER of 1 in 10^6 would permit operation to 1 in 10^{10} or better.

Principles of Error Detection

Detecting Isolated Bit Errors

To pinpoint the exact location of isolated bit errors in the digital data, both the longitudinal and lateral coordinates of the bit error must be defined. In the case of E-NRZ encoding, the parity bits added to each word provide the means of defining the longitudinal coordinate. By simply adding column parity to the digital data it becomes possible to define the lateral coordinates as well. This column parity is added to the NRZ–L data at the input of the recorder, then encoded in the same manner as the other data streams and recorded on a separate track in bit-for-bit synchronization with the digital data. During reproduction, the presence of a bit error will result in the detection of even parity in both the word and the column in which the error occurs. Because there is only one location within the data block that will satisfy any given set of longitudinal and lateral coordinates, the exact position of the isolated bit error becomes known. The added parity track, known as a correction track, is shown in figure 11–23.

E-NRZ data 1	~~0~~	~~0~~	~~0~~	~~0~~	~~1~~	X	~~0~~	~~1~~	E
E-NRZ data 2	0	0	0	1	0	0	0	0	—
E-NRZ data 3	0	0	0	1	0	1	0	1	—
E-NRZ data 4	0	0	0	1	1	0	0	1	—
Correction track 1	1	1	1	0	1	1	1	1	—
	—	—	—	—	—	E	—	P	

Key
X Denotes position of bit error
— Denotes word or column having odd parity
E Denotes word or column having even parity
P Denotes column containing word parity bits

Figure 11–23.—Detection of isolated bit errors.

Detecting Simultaneous Bit Errors

When an even number of bit errors occurs in the same bit column, the parity for that column is the same as in the case in which no bit errors occurred. This complicates the matter of error detection considerably because the lateral coordinates required to pinpoint the exact location of the errors are not available (fig. 11–24).

To effectively detect simultaneous bit errors, the data words containing the errors must be separated from each other and the errors then detected individually as in the case for isolated bit errors. This requires the availability of a second correction track, because any displacement of the data words will change the original column parity. To achieve the necessary separation, a special circuit known as an interleaver is used to displace each of the data words into a different data block before the data are encoded. During reproduction, the data words must be deinterleaved to reestablish word coincidence before final output from the recorder. The detection of simultaneous bit errors through the use of interleavers and deinterleavers is shown in figure 11–25.

E-NRZ data 1	0	0	0	0	0	0	1	0	—
E-NRZ data 2	0	0	0	0	0	1	1	1	—
E-NRZ data 3	~~0~~	~~0~~	~~0~~	~~0~~	~~1~~	~~0~~	X	~~1~~	E
E-NRZ data 4	~~0~~	~~0~~	~~0~~	~~0~~	~~1~~	~~1~~	X	~~0~~	E
Correction track 1	1	1	1	1	1	1	1	0	—
	—	—	—	—	—	—	?	P	

Key
X Denotes position of bit error
— Denotes word or column having odd parity
E Denotes word or column having even parity
? Denotes word or column in error but not detectable due to the presence of an even number of bit errors
P Denotes column containing word parity bits

Figure 11–24.—Detection of simultaneous bit errors may not be successful with only one correction track.

Detecting Even Parity Word Errors

An even parity word error is the simultaneous occurrence of an even number of bit errors (e.g., 2, 4, or 6) in the same data word. When such an error occurs, the parity for that word is still odd, just as if no errors existed. This complicates the matter of error detection. In figure 11–26, however, it is the longitudinal rather than the lateral coordinate that is missing.

To effectively detect even parity word errors, at least two separate column parity checks are required, and the results of the checks must be compared to identify the data word in error. The steps involved in the process of detecting even parity word errors are as follows:

(1) The parity pattern resulting from the first column parity check is temporarily stored in a memory register that serves as one input to a pattern comparator circuit.

(2) Next, the data tracks are deinterleaved to restore the original time coincident structure to the data. The correction track from which the first parity pattern was obtained is discarded during this deinterleaving.

(3) Then, beginning with the first data block, the stored parity pattern is sequentially compared to each of the column parity patterns resulting from the second column parity check. If a pattern match occurs in the first data block, track 1 contains the word in error. If a match occurs in the second data block, track 2 contains the error, etc. In this manner, the exact location of the word containing the even parity error can be located. Figure 11–27 illustrates the comparison of column parity patterns to identify even parity word errors.

EDAC Encoder

Figure 11–28 is a simplified block diagram of a three-loop EDAC encoder that, when used in conjunction with a compatible EDAC decoder, constitutes a complete three-loop EDAC system. The function of the EDAC encoder is to encode the parallel NRZ–L digital data with column parity and to interleave the separate data tracks to disperse their original time coincident structure. Three encoder stages and two interleaver stages are used in the three-loop EDAC system shown.

The block diagram includes shaded bit maps that show the dispersion of data words before, during, and after processing by the EDAC decoder.

EDAC Encoder 1

The first EDAC encoder scans each lateral data column to determine whether there is an odd or an even number of "1's" in the column. If the number is even, the encoder generates a "1" to make the total number of "1's" an odd count. If the number is already odd, the encoder outputs a "0." The resulting encoder output is a column-by-column parity record of the incoming

	A	B	C	D	E
NRZ—L data 1	0001001	0001000	0000111	0000110	0000101
NRZ—L data 2	0001001	0001000	0000111	0000110	0000101
NRZ—L data 3	0001001	0001000	0000111	0000110	0000101
NRZ—L data 4	0001001	0001000	0000111	0000110	0000101

(*a*)

	A	B	C	D	E
NRZ—L data 1	0001001	0001000	0000111	0000110	0000101
NRZ—L data 2	0001001	0001000	0000111	0000110	0000101
NRZ—L data 3	0001001	0001000	0000111	0000110	0000101
NRZ—L data 4	0001001	0001000	0000111	0000110	0000101
Correction track 1	[illegible]	1111111	1111111	1111111	1111111

(*b*)

	A	B	C	D	E
NRZ—L data 1	0001001	0001000	0000111	0000110	0000101
NRZ—L data 2	0001010	0001001	0001000	0000111	0000110
NRZ—L data 3	0001011	0001010	0001001	0001000	0000111
NRZ—L data 4	0001100	0001011	0001010	0001001	0001000
Correction track 1	1111111	1111111	1111111	1111111	1111111

(*c*)

	A	B	C	D	E
NRZ—L data 1	0001001	0001000	0000111	0000110	0000101
NRZ—L data 2	0001010	0001001	0001000	0000111	0000110
NRZ—L data 3	0001011	0001010	0001001	0001000	0000111
NRZ—L data 4	0001100	0001011	0001010	0001001	0001000
Correction track 1	1111111	1111111	1111111	1111111	1111111
Correction track 2	0000100	0000000	0001100	0000000	0001100

(*d*)

Figure 11-25.—Detecting simultaneous bit errors. (*a*) Unencoded NRZ—L data. (*b*) Unencoded NRZ—L data plus first correction track. (*c*) Interleaved NRZ—L data and first correction track. (*d*) Interleaved NRZ—L data plus first and second correction tracks.

NRZ−L data and becomes the first correction track added to the digital data.

Interleaver 1

The function of the first interleaver is to disperse the parallel NRZ−L data, including the first correction track, such that it no longer contains its original time-coincident structure. This is accomplished by delaying each bit row (track) with respect to its adjacent bit rows. By comparing bit map 1 with bit map 3 in figure 11-28 it can be seen that NRZ−L data 1 is not delayed; NRZ−L data 2 is delayed by a period equal to one seven-bit word; NRZ−L data 3 by a period equal to two seven-bit words; and NRZ−L data 4 by a period equal to three seven-bit words. Correction track 1 is delayed by a period equal to four seven-bit words.

EDAC Encoder 2

The function of the second EDAC encoder is to generate a second correction track; see bit map 4 in figure 11-28. The operation of this circuit is identical to the operation of the first EDAC encoder.

	A	B	C	D	E
E-NRZ data 1	00010011	00010000	00001110	00001101	00001011
E-NRZ data 2	00010101	00010011	00010000	00001110	00001101
E-NRZ data 3	00010110	00010101	00010011	00010000	00001110
E-NRZ data 4	00011001	00010110	00010101	00010011	00001000
Correction track 1	11111110	11111110	11111110	11111110	11111110
Correction track 2	00001000	00000001	00011001	00000001	00011001

(*e*)

	A	B	C	D	E
E-NRZ data 1	00010011	00010000	00001110	00001101	00001011
E-NRZ data 2	00010101	00010011	00010000	00001110	**00001x01**
E-NRZ data 3	00010110	00010101	00010011	00010000	**00001x10**
E-NRZ data 4	00011001	00010110	00010101	00010011	00001000
Correction track 1	11111110	11111110	11111110	11111110	11111110
Correction track 2	00001000	00000001	00011001	00000001	00011001

(*f*)

	A	B	C	D	E
E-NRZ data 1	00010011	00010000	00001110	00001101	00001011
E-NRZ data 2	00010011	00010000	00001110	**00001x01**	00001011
E-NRZ data 3	00010011	00010000	**00001x01**	00001101	00001011
E-NRZ data 4	00010011	00010000	00001110	00001101	00001011
Correction track 1	11111110	11111110	11111110	11111110	11111110

(*g*)

	A	B	C	D	E
NRZ—L data 1	0001001	0001000	0000111	0000110	0000101
NRZ—L data 2	0001001	0001000	0000111	***0000110***	0000101
NRZ—L data 3	0001001	0001000	***0000111***	0000110	0000101
NRZ—L data 4	0001001	0001000	0000111	0000110	0000101

(*h*)

Key

- (black) Denotes data words belonging to block A
- **bold** Denotes data words containing bit errors
- ***italic*** Denotes position of corrected error

Figure 11–25 (continued).—Detecting simultaneous bit errors. (*e*) Encoded E-NRZ data as recorded on tape. (*f*) Reproduced E-NRZ data with simultaneous bit errors in block E. (*g*) Deinterleaved E-NRZ data showing displacement of simultaneous bit errors. (*h*) Decoded NRZ—L data showing corrected data in blocks C and D.

Key

X Denotes position of bit error
— Denotes word or column having odd parity
E Denotes word or column having even parity
? Denotes word or column in error but not detectable due to the presence of an even number of bit errors
P Denotes column containing word parity bits

E-NRZ data 1	0	0	0	0	0			1	—
E-NRZ data 2	0	0	0	0	1	0		1	—
E-NRZ data 3	0	0	0	0	1	X	X	0	?
E-NRZ data 4	0	0	0	1	0	0		1	—
Correction track 1	1	1	1	0	1			0	—
	—	—	—	—	—	E	E	P	

Figure 11–26.—Illustration of difficulty in detecting even parity word errors.

(a)

	A	B	C	D	E
E-NRZ data 1	00010011	00010000	00001110	00001101	00001011
E-NRZ data 2	00010011	00010000	00001110	00001101	00001011
E-NRZ data 3	00010011	00010000	**00001xx0**	00001101	00001011
E-NRZ data 4	00010011	00010000	00001110	00001101	00001011
Correction track 1	11111110	11111110	11111110	11111110	11111110

	A	B	C	D	E
Column parity pattern	-----	-----	--- EE	-----	-----
Stored parity pattern	--- EE				

Match? No

(b)

	A	B	C	D	E
E-NRZ data 1	00010011	00010000	00001110	00001101	00001011
E-NRZ data 2	00010011	00010000	00001110	00001101	00001011
E-NRZ data 3	00010011	00010000	**00001xx0**	00001101	00001011
E-NRZ data 4	00010011	00010000	00001110	00001101	00001011
Correction track 1	11111110	11111110	11111110	11111110	11111110

	A	B	C	D	E
Column parity pattern	-----	-----	--- EE	-----	-----
Stored parity pattern		--- EE			

Match? No

(c)

	A	B	C	D	E
E-NRZ data 1	00010011	00010000	00001110	00001101	00001011
E-NRZ data 2	00010011	00010000	00001110	00001101	00001011
E-NRZ data 3	00010011	00010000	**00001xx0**	00001101	00001011
E-NRZ data 4	00010011	00010000	00001110	00001101	00001011
Correction track 1	11111110	11111110	11111110	11111110	11111110

	A	B	C	D	E
Column parity pattern	-----	-----	--- EE	-----	-----
Stored parity pattern			--- EE		

Match? Yes

Key

Signifies relationship between parity comparisons and track containing even parity error

bold Indicates location of error (in block C)

Figure 11–27.—Comparison of column parity patterns to isolate even parity word errors. In (*a*), the stored parity pattern is first compared with the column parity pattern for block A. The patterns do not match, indicating the first data track (E-NRZ data 1) does not contain the error. In (*b*), the stored parity pattern is compared with the column parity pattern for block B, but the patterns do not match, indicating the second data track (E-NRZ data 2) does not contain the error. In (*c*), the stored parity pattern is compared with the column parity pattern for block C. This time the patterns match, indicating the third data track (E-NRZ data 3) contains the even parity word error.

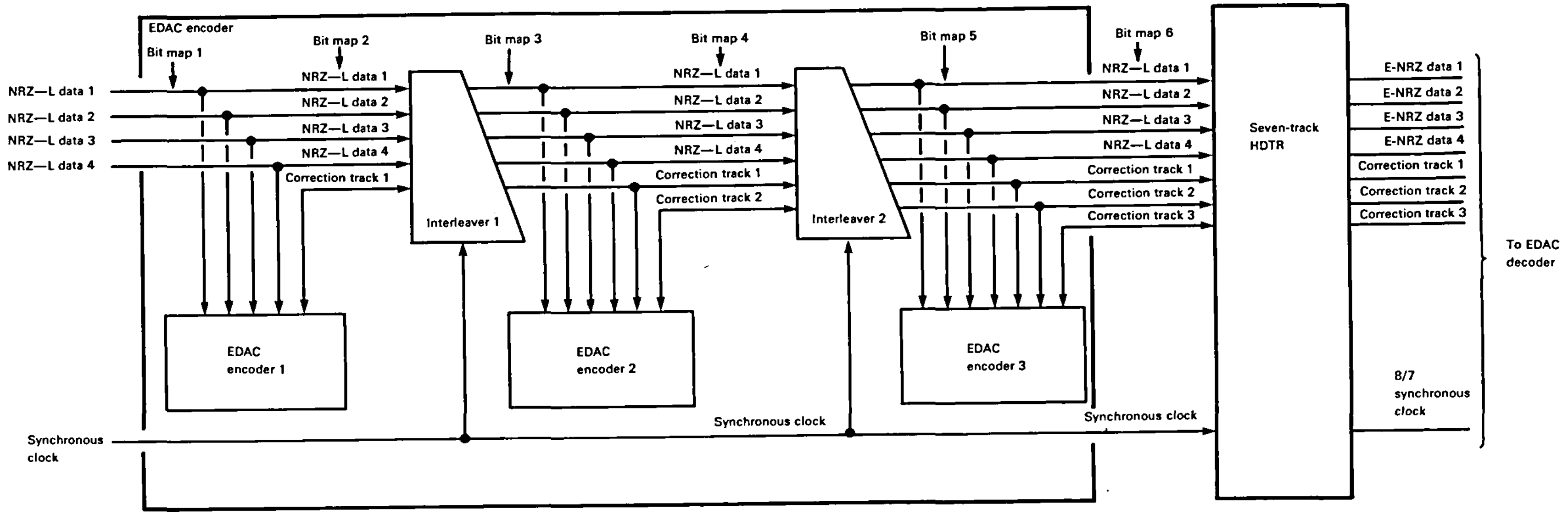

(a)

	A	B
NRZ—L data 1	0001001	0001000
NRZ—L data 2	0001001	0001000
NRZ—L data 3	0001001	0001000
NRZ—L data 4	0001001	0001000

(b)

	A	B
NRZ—L data 1	0001001	0001000
NRZ—L data 2	0001001	0001000
NRZ—L data 3	0001001	0001000
NRZ—L data 4	0001001	0001000
Correction track 1	1111111	1111111

(c)

	A	B	C	D	E	F
NRZ—L data 1	0001001	0001000	0000111	0000110	0000101	0000100
NRZ—L data 2	0001010	0001001	0001000	0000111	0000110	0000101
NRZ—L data 3	0001011	0001010	0001001	0001000	0000111	0000110
NRZ—L data 4	0001100	0001011	0001010	0001001	0001000	0000111
Correction track 1	1111111	1111111	1111111	1111111	1111111	1111111

(d)

	A	B
NRZ—L data 1	0001001	0001000
NRZ—L data 2	0001010	0001001
NRZ—L data 3	0001011	0001010
NRZ—L data 4	0001100	0001011
Correction track 1	1111111	1111111
Correction track 2	0000100	0000000

(e)

Key

Denotes data words belonging to block A

Denotes data words moved into block A after first interleaver

Figure 11–28.—EDAC encoder. (*a*) Simplified block diagram. (*b*) Bit map 1. (*c*) Bit map 2. (*d*) Bit map 3. (*e*) Bit map 4.

	A	B	C	D	E	F	G	H	I
NRZ—L data 1	0001001	0001000	0000111	0000110	0000101	0000100	0000011	0000010	0000001
NRZ—L data 2	0001011	0001010	0001001	0001000	0000111	0000110	0000101	0000100	0000011
NRZ—L data 3	0001101	0001100	0001011	0001010	0001001	0001000	0000111	0000110	0000101
NRZ—L data 4	0001111	0001110	0001101	0001100	0001011	0001010	0001001	0001000	0000111
Correction track 1	1111111	1111111	1111111	1111111	1111111	1111111	1111111	1111111	1111111
Correction track 2	0011000	0000000	0000000	0000000	0000000	0000100	0000000	0001100	0000000

(*f*)

	A	B	C	D	E	F	G	H	I
NRZ—L data 1	0001001	0001000	0000111	0000110	0000101	0000100	0000011	0000010	0000001
NRZ—L data 2	0001011	0001010	0001001	0001000	0000111	0000110	0000101	0000100	0000011
NRZ—L data 3	0001101	0001100	0001011	0001010	0001001	0001000	0000111	0000110	0000101
NRZ—L data 4	0001111	0001110	0001101	0001100	0001011	0001010	0001001	0001000	0000111
Correction track 1	1111111	1111111	1111111	1111111	1111111	1111111	1111111	1111111	1111111
Correction track 2	0011000	0000000	0000000	0000100	0000000	0000100	0000000	0001100	0000000
Correction track 3	0011000	0000000	0001000	0001100	0000000	0000100	0001000	0000100	0000000

(*g*)

Key

Denotes data words belonging to block A

Denotes data words moved into block A after first interleaver

Denotes data words moved into block A after second interleaver

Figure 11–28 (continued).—EDAC encoder. (*f*) Bit map 5. (*g*) Bit map 6.

Interleaver 2

The function of the second interleaver is similar to that of the first interleaver; that is, to disperse the parallel NRZ–L data, including the first and second correction tracks, so that it no longer contains its previous time-coincident structure. In actual practice, the bit-row delays provided by the second interleaver are much greater than those of the first interleaver (up to 65 times as great), but for purposes of this discussion, the delays are assumed to be equal, see bit map 5 in figure 11-28.

EDAC Encoder 3

The third EDAC encoder operates exactly like the first and second encoders, and serves to generate the third correction track. After processing through the third encoder, the NRZ–L data, along with the three correction tracks, are routed to the recorder to be converted to E-NRZ data and subsequently recorded on tape, see bit map 6 in figure 11-28.

EDAC Decoder

Figure 11-29 is a simplified block diagram of a three-loop EDAC decoder that is compatible with the EDAC encoder shown in figure 11-28. Its function is fourfold: (1) to detect and correct bit errors in E-NRZ digital data, (2) to restore the twice-interleaved digital data to its original time-coincident structure, (3) to reconvert the encoded E-NRZ data back to its original NRZ–L format, and (4) to reconstruct the synchronous clock signal required to maintain time-coincident structure once the parallel digital data leaves the recorder. The three-loop decoder system shown consists of three error detector/corrector stages, two deinterleaver stages, a parity stripper, and a clock converter stage.

Inputs to the EDAC decoder of figure 11-29 consist of four E-NRZ data tracks, three correction tracks, and the 8/7 synchronous clock signal from the recorder. It should be noted that the 40-bit synchronizing words that were added to the E-NRZ data during the encoding process have already been stripped from the data before the data reaches the EDAC decoder. The absence of these synchronizing words accounts for the use of the 8/7 synchronous clock signal rather than the 17/14 clock signal (ENCDR OUTCLK and DCDR INPCLK) discussed previously.

Shaded Bit Maps

The block diagram of figure 11-29 includes shaded bit maps that show the dispersion of data words before, during, and after processing by the EDAC decoder. In bit map 1, block D contains an isolated bit error; block G an even parity word error; and block I simultaneous bit errors. The detection and correction of these bit errors is discussed in detail in the following paragraphs.

Error Detector 1

The first error detector works in conjunction with the first error corrector to detect and correct isolated bit errors. The function of this detector is to perform a column-by-column parity check of the twice-interleaved E-NRZ data and supply an output that identifies any column with even parity—that is, any column containing an isolated bit error. This output defines the longitudinal coordinate of the bit error and, when combined with the lateral coordinate, will define the precise location of the error. Following the completion of this parity check, correction track 3 is discarded from the digital data.

Error Corrector 1

The first error corrector performs a serial parity check on each word of the digital data to identify any word with even parity—that is, any word containing a single bit error. This information defines the lateral coordinate of the bit error and, when correlated with the longitudinal coordinate information from the first error detector, defines the precise location of the isolated bit error. This bit error is then corrected (inverted), and the digital data routed to deinterleaver 1 for further processing. (See bit map 2 in figure 11-29.)

Deinterleaver 1

The function of deinterleaver 1 is to partially restore the time-coincident structure of the E-NRZ data by an exact amount, equal and opposite to the dispersion created by the second interleaver in the EDAC encoder. As a result of this deinterleaving, any simultaneous bit errors in the data are separated for subsequent detection and correction as isolated bit errors. This separation of simultaneous bit errors can be seen by comparing bit maps 1 and 3 in figure 11-29. Note that the simultaneous errors in block I of bit map 1 have been shifted to blocks F and G of bit map 3 as a result of deinterleaver 1.

Error Detector 2

The function of the second error detector is twofold: (1) to work in conjunction with the second error corrector to detect and correct simultaneous bit errors (which now appear as isolated bit errors due to the action of deinterleaver 1 and (2) to detect the presence of even parity word errors, which activates the pattern comparator in loop 3.

The first function performed by the second error detector is identical to that of the first error detector;

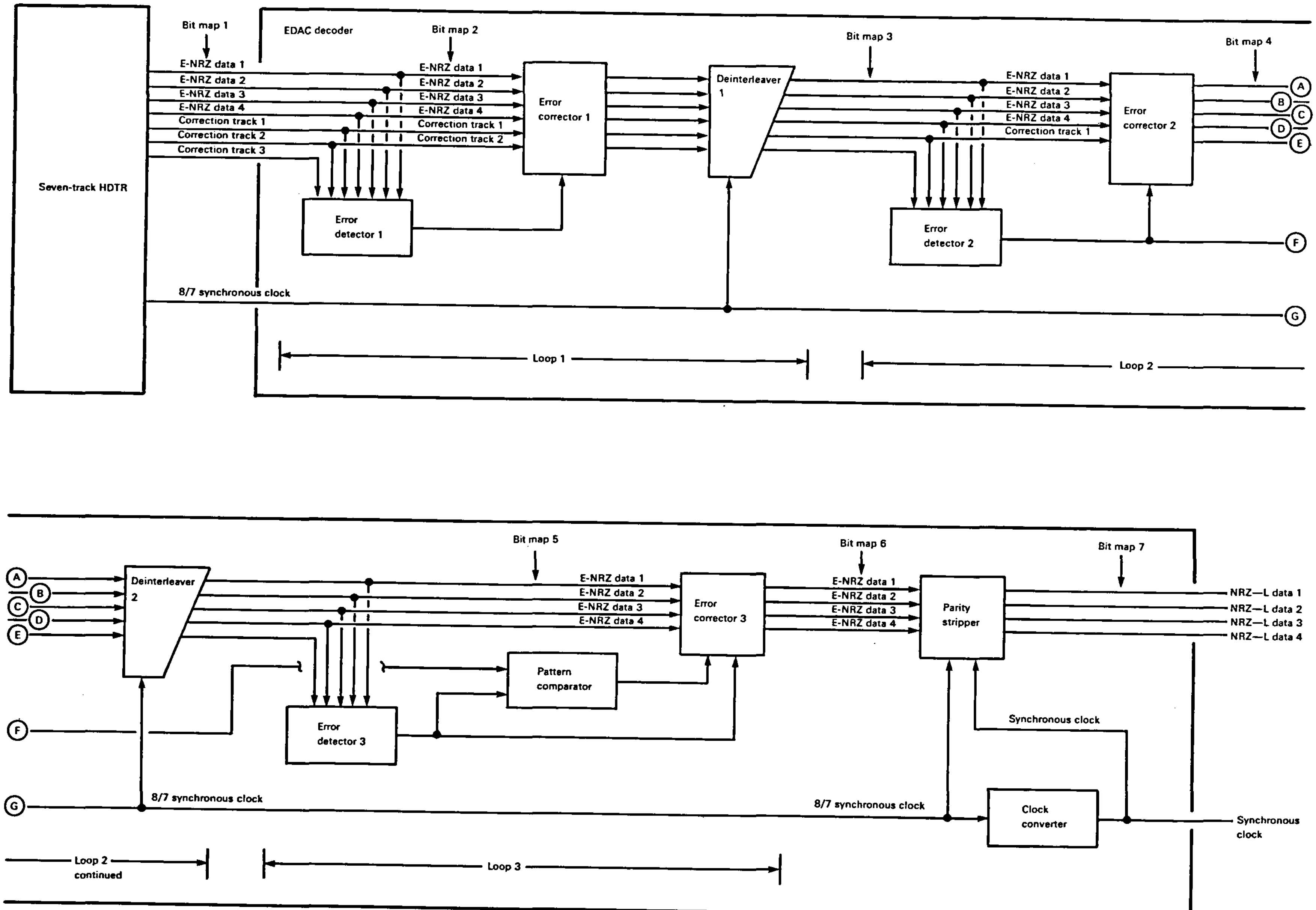

Seven-track HDTR
EDAC decoder
Bit map 1
Bit map 2
Bit map 3
Bit map 4
E-NRZ data 1
E-NRZ data 2
E-NRZ data 3
E-NRZ data 4
Correction track 1
Correction track 2
Correction track 3
Error corrector 1
Error detector 1
Deinterleaver 1
Error corrector 2
Error detector 2
8/7 synchronous clock
Loop 1
Loop 2
A
B
C
D
E
F
G
Deinterleaver 2
Bit map 5
Bit map 6
Bit map 7
Error corrector 3
Error detector 3
Pattern comparator
Parity stripper
NRZ—L data 1
NRZ—L data 2
NRZ—L data 3
NRZ—L data 4
Synchronous clock
Clock converter
Loop 2 continued
Loop 3

(a)

Isolated bit error | Even parity word error | Simultaneous bit errors

	A	B	C	D	E	F	G	H	I
E-NRZ data 1	00010011	00010000	00001110	**00001x01**	00001011	00001000	00000111	00000100	00000010
E-NRZ data 2	00010110	00010101	00010011	00010000	00001110	00001101	00001011	00001000	00000111
E-NRZ data 3	00011010	00011001	00010110	00010101	00010011	00010000	**00001xx0**	00001101	**000010x1**
E-NRZ data 4	00011111	00011100	00011010	00011001	00010110	00010101	00010011	00010000	**000011x0**
Correction track 1	11111110	11111110	11111110	11111110	11111110	11111110	11111110	11111110	11111110
Correction track 2	0011001	00000001	00000001	00001000	00000001	00001000	00000001	00011001	00000001
Correction track 3	00110001	00000001	00010000	00011001	00000001	00001000	00010000	00001000	00000001

(*b*)

	A	B	C	D	E
E-NRZ data 1	00010011	00010000	00001110	***00001101***	00001011
E-NRZ data 2	00010110	00010101	00010011	00010000	00001110
E-NRZ data 3	00011010	00011001	00010110	00010101	00010011
E-NRZ data 4	00011111	00011100	00011010	00011001	00010110
Correction track 1	11111110	11111110	11111110	11111110	11111110
Correction track 2	00110001	00000001	00000001	00001000	00000001

(*c*)

Key:

- Denotes data words belonging to block A
- Denotes data words moved into block A after first interleaver
- Denotes data words moved into block A after second interleaver
- **bold** Denotes data words containing bit errors
- ***italic*** Denotes position of corrected errors

Even parity word error | Isolated bit errors

	A	B	C	D	E	F	G	H	I
E-NRZ data 1	00010011	00010000	00001110	00001101	00001011	00001000	00000111	00000100	00000010
E-NRZ data 2	00010101	00010011	00010000	00001110	00001101	00001011	00001000	00000111	00000100
E-NRZ data 3	00010110	00010101	00010011	00010000	**00001xx0**	00001101	**000010x1**	00001000	00000111
E-NRZ data 4	00011001	00010110	00010101	00010011	00010000	**000011x0**	00001101	00001011	00001000
Correction track 1	11111110	11111110	11111110	,11111110	11111110	11111110	11111110	11111110	11111110
Correction track 2	00001000	00000001	00011001	00000001	00011001	00000001	00001000	00000001	00001000

(*d*)

Figure 11–29.—EDAC decoder. (*a*) Simplified block diagram. (*b*) Bit map 1. (*c*) Bit map 2. (*d*) Bit map 3.

Even parity word error

	A	B	C	D	E	F	G	H	I
E-NRZ data 1	00010011	00010000	00001110	00001101	00001011	00001000	00000111	00000100	00000010
E-NRZ data 2	00010101	00010011	00010000	00001110	00001101	00001011	00001000	00000111	00000100
E-NRZ data 3	00010110	00010101	00010011	00010000	**00001xx0**	00001101	***00001011***	00001000	00000111
E-NRZ data 4	00011001	00010110	00010101	00010011	00010000	***00001110***	00001101	00001011	00001000
Correction track 1	11111110	11111110	11111110	11111110	11111110	11111110	11111110	11111110	11111110

(*e*)

Even parity word error

	A	B	C	D	E	F	G	H	I
E-NRZ data 1	00010011	00010000	00001110	11110010	00001011	00001000	00000111	00000100	00000010
E-NRZ data 2	00010011	00010000	00001110	00001101	00001011	00001000	00000111	00000100	00000010
E-NRZ data 3	00010011	00010000	**00001xx0**	00001101	00001011	00001000	00000111	00000100	00000010
E-NRZ data 4	00010011	00010000	00001110	00001101	00001011	00001000	00000111	00000100	00000010

(*f*)

	A	B	C	D
E-NRZ data 1	00010011	00010000	00001110	00001101
E-NRZ data 2	00010011	00010000	00001110	00001101
E-NRZ data 3	00010011	00010000	***00001110***	00001101
E-NRZ data 4	00010011	00010000	00001110	00001101

(*g*)

	A	B	C	D	E	F	G	H	I
NRZ—L data 1	0001001	0001000	0000111	0000110	0000101	0000100	0000011	0000010	0000001
NRZ—L data 2	0001001	0001000	0000111	0000110	0000101	0000100	0000011	0000010	0000001
NRZ—L data 3	0001001	0001000	0000111	0000110	0000101	0000100	0000011	0000010	0000001
NRZ—L data 4	0001001	0001000	0000111	0000110	0000101	0000100	0000011	0000010	0000001

(*h*)

Key:

Denotes data words belonging to block A

Denotes data words moved into block A after first interleaver

Denotes data words moved into block A after second interleaver

bold Denotes data words containing bit errors

italic Denotes position of corrected errors

Figure 11–29 (continued).—EDAC decoder. (*e*) Bit map 4. (*f*) Bit map 5. (*g*) Bit map 6. (*h*) Bit map 7.

i.e., to define the longitudinal coordinate of the bit error(s) so that when combined with the lateral coordinate supplied by the second error corrector the precise location of the bit error(s) will be known.

The parity pattern generated by the second error detector is also routed to the pattern comparator in loop 3 where it is stored for comparison with subsequent column parity patterns to detect even parity word errors.

Error Corrector 2

The operation of the second error corrector is identical to that of the first error corrector, i.e., to define the lateral coordinate of the bit error(s) and combine this information with the longitudinal coordinate information supplied by the second error detector to define the precise location of the bit error(s). The bit error(s) is/are then corrected (inverted), and the digital data routed to deinterleaver 2 for further processing.

Deinterleaver 2

The function of deinterleaver 2 is to completely restore the original time-coincident structure of the E-NRZ data. The delays provided by this circuit are exactly equal and opposite to the dispersion created by the first interleaver in the EDAC encoder.

Error Detector 3

The function of the third error detector is identical to that of the second error detector: (1) to work in conjunction with the third error corrector to detect and correct any remaining isolated bit errors and (2) to detect and confirm the presence of even parity word errors, which activates the pattern comparator in loop 3.

Pattern Comparator

The pattern comparator accepts two inputs: (1) the column parity pattern generated by the second error detector and (2) the column parity pattern generated by the third error detector. The function of this circuit is to identify the exact location of even parity word errors in the digital data. (See block C in bit map 5 in figure 11-29.)

The parity pattern from the second error detector is stored by the pattern comparator until the digital data is processed through deinterleaver 2. Then the pattern comparator begins a count sequence during which the stored pattern is sequentially compared block-by-block with the parity pattern from the third error detector. When the parity patterns match, the track containing the even parity word error is identified, and the comparator enables the third error corrector to correct the error.

Error Corrector 3

The function of the third error corrector is twofold: (1) to correct any remaining isolated bit errors present in the digital data and (2) to correct even parity word errors based on the error location information provided by the pattern comparator. The action of the third error corrector in correcting even parity word errors can be seen by comparing bit maps 5 and 6 in figure 11-29.

Parity Stripper

The parity stripper removes (strips) the parity bits from the E-NRZ data to restore the original NRZ–L format. During this process, the E-NRZ data, consisting of eight-bit words, is clocked into the parity stripper by the 8/7 synchronous clock signal. After removal of the parity bits, the NRZ–L data, consisting of seven-bit words, are clocked out of the parity stripper by the synchronous clock signal from the clock converter, which restores the original time base to the NRZ–L data. The removal of the eighth parity bit from each of the data words can be seen by comparing bit maps 6 and 7 in figure 11-29.

Clock Converter

The function of the clock converter is to convert the 8/7 synchronous clock signal, compatible with the bit rate of the E-NRZ data, to a synchronous clock signal compatible with the bit rate of the NRZ–L data.

Other EDAC Variations

The three-loop EDAC system described offers the highest attainable degree of data integrity and lowest possible BER. Thus, for the most demanding data requirements, there is no substitute for the three-loop EDAC configuration. There is, however, one limitation associated with two-loop or three-loop EDAC about which the user should be aware before deciding on this approach to insure maximum data integrity. Because of the track interleaving required with the two- and three-loop EDAC system, tapes cannot be crossplayed between EDAC configured recorders and non-EDAC configured recorders. Both the recorder and the reproducer must be compatible.

There are, however, other instances when the extremely high order of data integrity provided by two- or three-loop EDAC is secondary to maintaining a high degree of recorder flexibility. One example of such flexibility would be the ability to reproduce prerecorded tapes made on recorders not configured with the EDAC feature, yet retain the ability to reproduce tapes that were recorded with supplemental EDAC tracks. This can be accomplished by using only one EDAC loop.

Only one correction track is required with single-loop EDAC, so track interleaving is not used. This insures complete crossplay compatibility between E-NRZ recorders with and without the EDAC feature. When tapes recorded on a single-loop EDAC recorder are played on a non-EDAC reproducer, the added correction track is simply ignored.

Figure 11-30 is a simplified block diagram showing one application of a single-loop EDAC. The 24 parallel lines to be recorded are divided into 4 groups, each containing 6 parallel lines. One additional EDAC correction track is provided for each of the four groups. An even simpler configuration would be to provide one EDAC track for every 12 data tracks. As a general rule, however, the fewer the number of data tracks assigned to each EDAC track, the lower the bit error rate.

DATA FORMATTERS

In the interest of overall system efficiency, some degree of data restructuring (formatting) is often needed to interface an HDTR with a specific recording situation. Data formatters (available on special order for all Datatape, Incorporated, HDTR's) serve this need by providing the user with a convenient means of customizing the recorder for optimum performance efficiency and best tape utilization.

Using a Data Formatter

Data formatters can be used in one of two ways. First, to demultiplex a single data line with a relatively high data rate and distribute the demultiplexed output to two or more data lines at a lower per-line data rate, or second, to multiplex two or more data lines with a relatively low per-line data rate onto a single data line at a relatively high data rate. The first application of a data formatter is especially useful when the per-line data rate to be recorded exceeds the maximum throughput capability for a given record/reproduce track. In this case, each of the data input lines is demultiplexed and distributed to several record/reproduce tracks at a much lower per-line data rate. The second application is useful when the number of parallel data lines is large, and the per-line data rate is relatively low because several data lines can be multiplexed together and recorded on a single track at a much higher data rate, thereby reducing the total number of record/reproduce tracks required.

Selecting a Data Formatter

Data formatters are not normally supplied as "off the shelf" items. They are custom designed and manufactured to meet specific user requirements. It is important, therefore, to know and understand the basic factors that determine the manner in which the formatter will be configured. The factors to be considered are as follows:

(1) Number of parallel data lines to be recorded
(2) Maximum throughput rate required
(3) Record time required

Parallel Data Lines

The number of parallel data lines to be recorded will be determined by the electronic data processing equipment supplying inputs to the recorder. The minimum number of lines that can be accommodated is typically four, but as few as two can be accommodated if jumpers are installed to parallel the SWDT outputs of the decoder/deskew buffers in the recorder. (See fig. 11-10.) The maximum number of lines is essentially

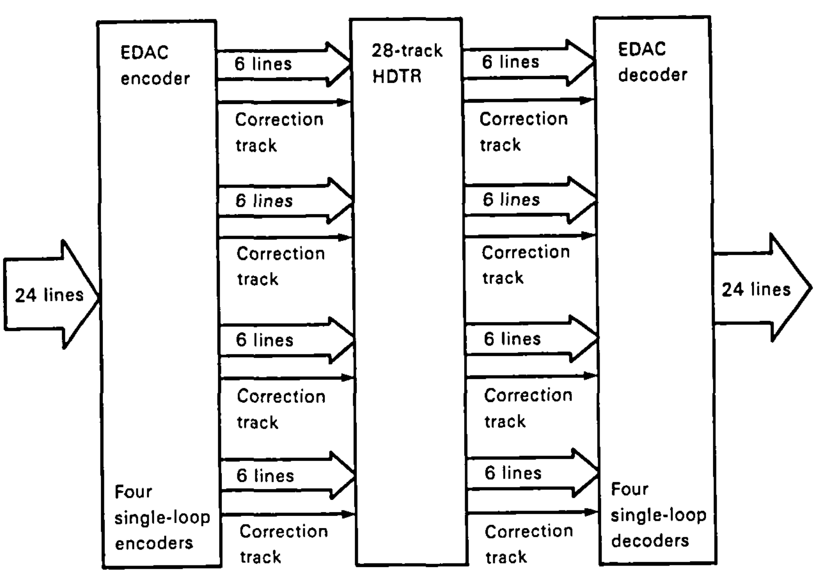

Figure 11-30.—Quad single-loop EDAC.

unlimited, but practical considerations will usually dictate that the total number will not exceed 32. Line counts of 4, 6, 8, 16, 24, and 32 are most frequently used.

Maximum Throughput Rate

Throughput rate is the total number of actual signal bits per second to be recorded on tape. It does not take into account any parity bits or synchronizing words (overhead) that are added to the data during the encoding process. Throughput rate may be calculated by multiplying the per-line bit rate (also known as the byte rate) by the number of data lines used. For example, calculate the throughput rate for a 16-line system with a per-line bit rate of 1.6 Mbps:

$$\begin{aligned}\text{Throughput rate} &= \text{per-line bit rate} \times \text{no. of lines}\\ &= 1.6 \times 10^6 \times 16\\ &= 25.6 \times 10^6\\ &= 25.6\ \text{Mbps}\end{aligned}$$

Record Time

The amount of record time required is a significant factor because it governs the selection of tape speed. Normally, HDTR's are designed to operate at the standard tape speed most frequently used for instrumentation recorders; that is, 120, 60, 30, 15, 7.5, 3.75, and 1.87 ips. The length of magnetic tape used to record the data is also a significant factor governing available record time. Here, as in the case of tape speed, a considerable degree of standardization exists and should be taken into account. Tapes used for recording high-density digital data are usually supplied in 9200-ft lengths, on 14-in.-diameter tape reels. Using these tapes in conjunction with the standard tape speeds mentioned provides recording times from 15 min. to 16 h:

Tape speed, ips	*Record time, hr*
120	¼
60	½
30	1
15	2
7.5	4
3.75	8
1.87	16

Tape lengths of 4600, 7200 and 10 800 ft are also commonly used for recording high-density data.

Reducing Per-Line Data Rate

In many instances the per-line data rate required for a particular recorder application exceeds the maximum throughput capability of the basic recorder selected to do the recording. In this case, the function of the data formatter is one of reducing the per-line data rate to a rate that is acceptable to the recorder.

Selecting a Formatter

The steps involved in reducing per-line data rate are listed as follows and are illustrated in figure 11-31.

	Known factors	*Sample values*
(*a*)	Number of parallel NRZ–L lines to be recorded	8
(*b*)	Maximum throughput rate required, Mbps	76.8
(*c*)	Per-line NRZ–L data rate (*b*)/(*a*), Mbps	9.6
(*d*)	Record time required, min	15

Step	*Procedure*
(1)	Under no. of tracks, circle number corresponding to (*a*), then circle numbers corresponding to multiples of (*a*), throughout remainder of column.
(2)	At the bottom of figure 11-31, locate approximate record time column equal to, or greater than, (*d*) above.
(3)	Beginning at the top of figure 11-31, place a straightedge under each of the numbers circled in step (1), and read across the straightedge to the number in the column identified in step (2). This number should be equal to, or greater than, (*b*). If not, move down to the next circled number. Stop when the field number is equal to or greater than (*b*). Number of fanout tracks required is the same as the circled number in the no. of tracks column directly above straightedge. *Answer = 24 tracks.*

Discussion

The use of a data formatter to reduce per-line data rate is shown in figure 11-32. Any attempt to record eight lines of parallel data having a combined total throughput rate of 76.8 Mbps is clearly impossible because the maximum throughput rate that can be accommodated by eight tracks is only 52.704 Mbps. The use of a suitable data formatter in this case is not only desirable but actually necessary to reduce per-line data rate to a rate that can be accommodated by the recorder.

The block diagram in figure 11-32 shows how the per-line data rate is reduced through the use of a data formatter. In this case, each of the eight data input lines is demultiplexed to three separate parallel lines to reduce the per-line data rate from 9.6 to 3.2 Mbps, a rate acceptable to the recorder at a tape speed of 120 ips. To

No. of tracks		Typical NRZ—L throughput rates for 2-MHz IRIG heads, Mbps							
		150 ips	120 ips	60 ips	30 ips	15 ips	7.5 ips	3.75 ips	1.87 ips
7	1	4.117	3.294	1.647	0.823	0.412	0.206	0.103	0.051
	2	8.235	6.588	3.294	1.647	0.823	0.412	0.206	0.103
	3	12.352	9.882	4.941	2.470	1.235	0.618	0.309	0.154
	4	16.470	13.176	6.588	3.294	1.647	0.823	0.412	0.206
	5	20.059	16.470	8.235	4.117	2.059	1.030	0.515	0.257
	6	24.705	19.764	9.882	4.941	2.470	1.235	0.618	0.309
	7	28.823	23.058	11.529	5.764	2.882	1.441	0.720	0.360
14	8	32.940	26.352	13.176	6.588	3.294	1.647	0.823	0.412
	9	37.058	29.646	14.823	7.411	3.706	1.853	0.926	0.463
	10	41.175	32.940	16.470	8.235	4.117	2.059	1.030	0.515
	11	45.293	36.234	18.117	9.058	4.529	2.265	1.132	0.566
	12	49.410	39.528	19.764	9.882	4.941	2.470	1.235	0.618
	13	53.528	42.882	21.411	10.705	5.353	2.676	1.338	0.669
	14	57.645	46.116	23.058	11.529	5.764	2.882	1.441	0.720
28	15	61.763	49.410	24.705	12.352	6.176	3.088	1.544	0.772
	16	65.880	52.704	26.352	13.176	6.588	3.294	1.647	0.823
	17	69.998	55.998	27.999	13.999	7.000	3.500	1.750	0.875
	18	74.115	59.292	29.646	14.823	7.411	3.706	1.853	0.926
	19	78.233	62.586	31.293	15.646	7.823	3.911	1.956	0.978
	20	82.350	65.880	32.940	16.470	8.235	4.117	2.059	1.030
	21	86.468	69.174	34.587	17.293	8.647	4.323	2.162	1.081
	22	90.585	72.468	36.234	18.117	9.058	4.529	2.264	1.132
	23	94.703	75.762	37.881	18.940	9.470	4.735	2.367	1.184
	24	98.820	79.056	39.528	19.764	9.882	4.941	2.470	1.235
	25	102.940	82.350	41.175	20.587	10.293	5.147	2.573	1.287
	26	107.060	85.644	42.822	21.411	10.705	5.353	2.676	1.338
	27	111.170	88.938	44.469	22.234	11.117	5.559	2.779	1.390
	28	115.290	92.232	46.116	23.058	11.529	5.764	2.882	1.441
42	29	119.410	95.526	47.763	23.881	11.941	5.970	2.985	1.492
	30	123.530	98.820	49.410	24.750	12.352	6.176	3.088	1.544
	31	127.640	102.114	51.057	25.528	12.764	6.382	3.191	1.595
	32	131.760	105.408	52.704	26.352	13.176	6.588	3.294	1.647
	33	135.880	108.702	54.351	27.175	13.588	6.794	3.397	1.698
	34	140.000	111.996	55.998	27.999	13.999	7.000	3.500	1.750
	35	144.110	115.290	57.645	28.822	14.411	7.206	3.603	1.801
	36	148.230	118.584	59.292	29.646	14.823	7.411	3.706	1.853
	37	152.350	121.878	60.939	30.469	15.235	7.617	3.809	1.904
	38	156.470	125.172	62.586	31.293	15.646	7.823	3.912	1.956
	39	160.580	128.466	64.233	32.116	16.058	8.029	4.014	2.007
	40	164.700	131.760	65.880	32.940	16.470	8.235	4.117	2.059
	41	168.820	135.054	67.527	33.763	16.882	8.441	4.220	2.110
	42	172.940	138.348	69.174	34.587	17.293	8.647	4.323	2.162
		12.3 min	15 min	30 min	1 hr	2 hr	4 hr	8 hr	16 hr
		Approximate record time for 9200 ft of tape							

1 2 3

Figure 11–31.—Selecting a formatter to reduce per-line data rate.

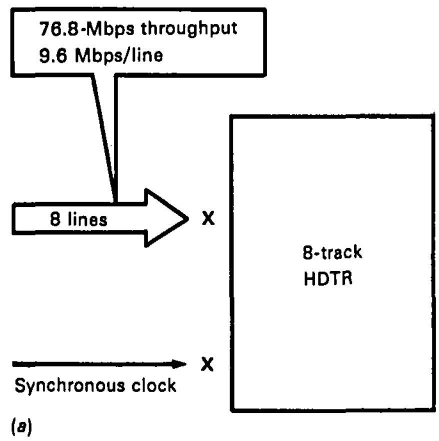

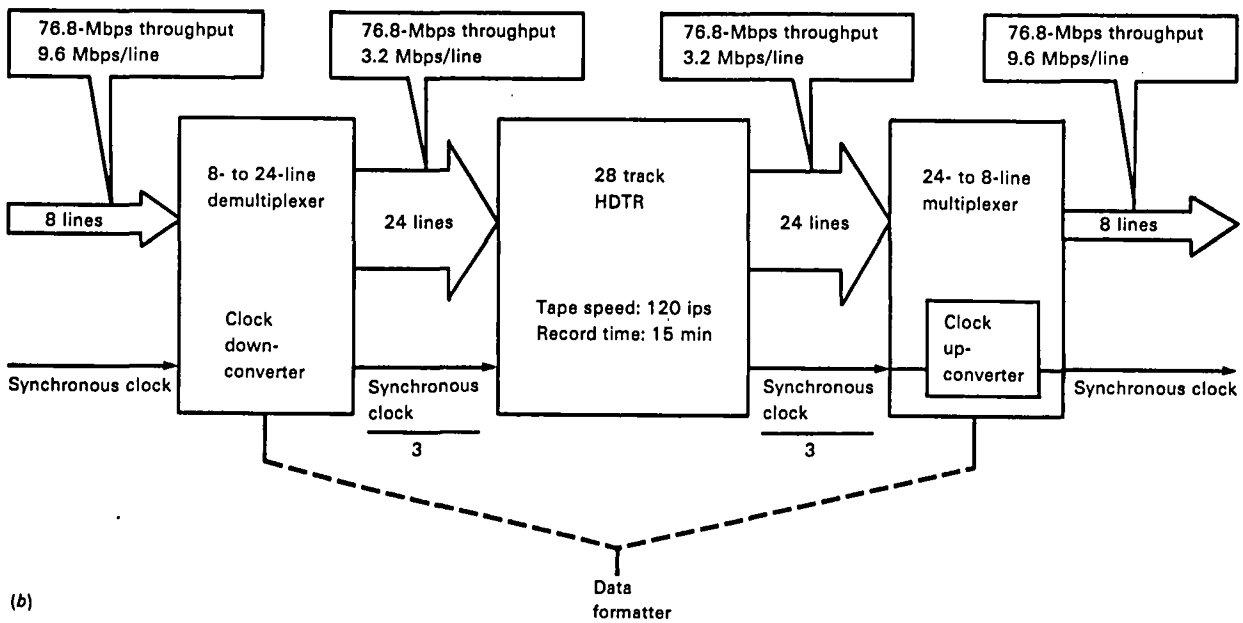

Figure 11–32.—Example of data formatter used to reduce per-line data rate. Recorder cannot throughput data rates as high as 76.8 Mbps on only eight lines without use of a data formatter. (*a*) Without data formatter. (*b*) With data formatter.

accommodate all 8 input lines, it is necessary to use a total of 24 separate lines, each of which requires a separate record track. Note that the conversion of each input line to 3 separate lines requires a corresponding conversion of the synchronous clock signal by the same 3:1 ratio to maintain proper timing through the recorder.

Increasing Record Time

When used to increase record time, the function of a data formatter is the same as when used to reduce per-line data rate; that is, to distribute the data over a greater number of record tracks. In this case, however, the purpose of the data formatter becomes one of extending record time rather than reducing data rate to a rate acceptable to the recorder.

Selecting a Formatter

The steps involved in increasing record time are listed as follows and are illustrated in figure 11-33.

	Known factors	*Sample values*
(*a*)	Number of parallel NRZ–L lines to be recorded	4
(*b*)	Maximum throughput rate required, Mbps	9.36
(*c*)	Per-line NRZ–L data rate (*b*)/(*a*), Mbps	2.34
(*d*)	Existing record time, min	15
(*e*)	Record time required, hr	1.25

Step	*Procedure*
(1)	Under no. of tracks in figure 11-33, circle number corresponding to (*a*), then circle

No. of tracks		Typical NRZ—L throughput rates for 2-MHz IRIG heads, Mbps							
		150 ips	120 ips	60 ips	30 ips	15 ips	7.5 ips	3.75 ips	1.87 ips
7	1	4.117	3.294	1.647	0.823	0.412	0.206	0.103	0.051
	2	8.235	6.588	3.294	1.647	0.823	0.412	0.206	0.103
	3	12.352	9.882	4.941	2.470	1.235	0.618	0.309	0.154
	4	16.470	13.176	6.588	3.294	1.647	0.823	0.412	0.206
	5	20.059	16.470	8.235	4.117	2.059	1.030	0.515	0.257
	6	24.705	19.764	9.882	4.941	2.470	1.235	0.618	0.309
	7	28.823	23.058	11.529	5.764	2.882	1.441	0.720	0.360
14	8	32.940	26.352	13.176	6.588	3.294	1.647	0.823	0.412
	9	37.058	29.646	14.823	7.411	3.706	1.853	0.926	0.463
	10	41.175	32.940	16.470	8.235	4.117	2.059	1.030	0.515
	11	45.293	36.234	18.117	9.058	4.529	2.265	1.132	0.566
	12	49.410	39.528	19.764	9.882	4.941	2.470	1.235	0.618
	13	53.528	42.882	21.411	10.705	5.353	2.676	1.338	0.669
	14	57.645	46.116	23.058	11.529	5.764	2.882	1.441	0.720
28	15	61.763	49.410	24.705	12.352	6.176	3.088	1.544	0.772
	16	65.880	52.704	26.352	13.176	6.588	3.294	1.647	0.823
	17	69.998	55.998	27.999	13.999	7.000	3.500	1.750	0.875
	18	74.115	59.292	29.646	14.823	7.411	3.706	1.853	0.926
	19	78.233	62.586	31.293	15.646	7.823	3.911	1.956	0.978
	20	82.350	65.880	32.940	16.470	8.235	4.117	2.059	1.030
	21	86.468	69.174	34.587	17.293	8.647	4.323	2.162	1.081
	22	90.585	72.468	36.234	18.117	9.058	4.529	2.264	1.132
	23	94.703	75.762	37.881	18.940	9.470	4.735	2.367	1.184
	24	98.820	79.056	39.528	19.764	9.882	4.941	2.470	1.235
	25	102.940	82.350	41.175	20.587	10.293	5.147	2.573	1.287
	26	107.060	85.644	42.822	21.411	10.705	5.353	2.676	1.338
	27	111.170	88.938	44.469	22.234	11.117	5.559	2.779	1.390
	28	115.290	92.232	46.116	23.058	11.529	5.764	2.882	1.441
42	29	119.410	95.526	47.763	23.881	11.941	5.970	2.985	1.492
	30	123.530	98.820	49.410	24.750	12.352	6.176	3.088	1.544
	31	127.640	102.114	51.057	25.528	12.764	6.382	3.191	1.595
	32	131.760	105.408	52.704	26.352	13.176	6.588	3.294	1.647
	33	135.880	108.702	54.351	27.175	13.588	6.794	3.397	1.698
	34	140.000	111.996	55.998	27.999	13.999	7.000	3.500	1.750
	35	144.110	115.290	57.645	28.822	14.411	7.206	3.603	1.801
	36	148.230	118.584	59.292	29.646	14.823	7.411	3.706	1.853
	37	152.350	121.878	60.939	30.469	15.235	7.617	3.809	1.904
	38	156.470	125.172	62.586	31.293	15.646	7.823	3.912	1.956
	39	160.580	128.466	64.233	32.116	16.058	8.029	4.014	2.007
	40	164.700	131.760	65.880	32.940	16.470	8.235	4.117	2.059
	41	168.820	135.054	67.527	33.763	16.882	8.441	4.220	2.110
	42	172.940	138.348	69.174	34.587	17.293	8.647	4.323	2.162
		12.3 min	15 min	30 min	1 hr	2 hr	4 hr	8 hr	16 hr
		Approximate record time for 9200 ft of tape							

1 2 3

Figure 11–33.—Selecting a formatter to increase record time.

numbers corresponding to multiples of (*a*) throughout remainder of column.

(2) At bottom of figure 11-33, locate approximate record time column equal to, or greater than, (*e*) above.

(3) Beginning at the top of figure 11-33, place a straightedge under each of the numbers circled in step (1), and read across the straightedge to the number in the column identified in step (2). This number should be equal to or greater than (*b*). If not, move down to the next circled number. Stop when the field number is equal to or greater than (*b*). Number of fanout tracks required is the same as the circled number in no. of tracks column directly above straightedge. *Answer = 24 tracks.*

Discussion

The use of a data formatter to increase record time is shown in figure 11-34. Part (*a*) depicts a basic digital recorder without a data formatter configured to accept four parallel lines of NRZ−L input data at a per-line data rate of 2.34 Mbps and a synchronous clock signal. The combined throughput rate for this configuration is relatively high considering there are only four lines of data (i.e., 2.34 Mbps/line × 4 = 9.36 Mbps). To accommodate this relatively high throughput rate, the seven-track recorder must be operated at a relatively high tape speed of 120 ips, providing only 15 min of usable record time.

Figure 11-34(*b*) shows how the record time for the basic recorder was extended from 15 min to 2 hr by us-

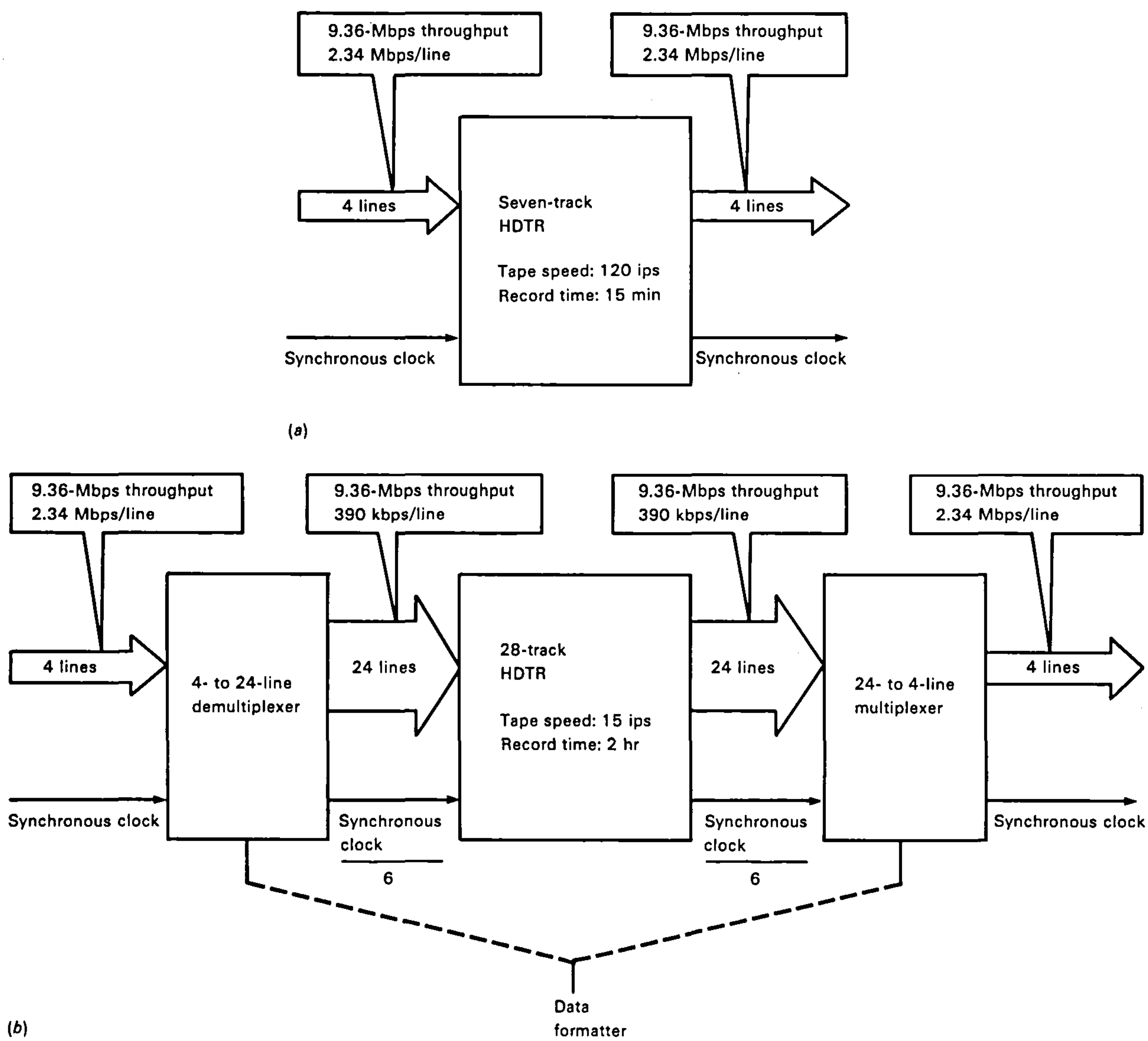

Figure 11-34.—Example of data formatter used to increase record time for a four-line, 9.36-Mbps recorder. (*a*) Without data formatter. (*b*) With data formatter.

ing a suitable data formatter. In this case, each of the four data input lines is demultiplexed and distributed to six separate parallel lines at a reduced data rate of 390 kbps/line. To accommodate all four input lines, it is necessary to use a total of 24 separate lines, each requiring a separate record track. It should be noted that the conversion of each input line to six separate lines requires a corresponding conversion of the synchronous clock signal by the same 1:6 ratio to maintain proper timing through the recorder.

Reducing Number of Record Tracks

In the previous two sections, the use of a data formatter resulted in an increase in the number of record tracks required. There are instances, however, when the use of a data formatter can actually reduce rather than increase the number of record tracks required and thereby provide the user with a significant reduction in overall recorder cost.

Selecting a Formatter

The steps involved in reducing the number of record tracks are listed as follows and are illustrated in figure 11-35.

	Known factors	*Sample values*
(*a*)	Number of parallel NRZ–L lines to be recorded	32
(*b*)	Maximum throughput rate required, Mbps	3.2
(*c*)	Per-line NRZ–L data rate (*b*)/(*a*), kbps	100
(*d*)	Available record time, hr	8

Step	*Procedure*
(1)	Under no. of tracks in figure 11-35, circle number corresponding to (*a*), then circle numbers corresponding to (*a*) divided by its factors throughout remainder of column.
(2)	Beginning at the top of figure 11-35, place a straightedge under each of the numbers circled in step (1), and read across the straightedge to locate the smallest number that is equal to or greater than (*b*). If none of the numbers is equal to or greater than (*b*) move down to the next circled number. Stop when a field number is equal to or greater than (*b*). The minimum number of tracks needed to record the specified throughput rate is the same as the circled number in no. of tracks column directly above straightedge. *Answer = 4 tracks.*

Discussion

The use of a data formatter to reduce the number of record tracks is shown in figure 11-36. Part (*a*) depicts a basic digital recorder without a data formatter configured to accept 32 parallel lines of NRZ–L input data at a per-line data rate of 100 kbps and a synchronous clock signal. The combined throughput rate for this configuration is relatively low considering there are 32 lines of data (i.e., 100 kbps/line × 32 lines = 3.2 Mbps). To accommodate this many lines, a 42-track recorder is used, operating at 3.75 ips and providing up to 8 hr of record time.

Figure 11-36(*b*) shows how the number of lines (and hence the number of record/reproduce tracks) is reduced from 32 lines to only 4 lines by using a suitable data formatter. In this case, each group of eight input lines is multiplexed to a single line at an increased data rate of 800 kbps. To accommodate all 32 input lines, it is necessary to use only 4 separate parallel lines. The total number of lines (and tracks) to be recorded has thus been reduced by a factor of 8, through the use of the data formatter. It should be noted that the conversion of each group of eight input lines to a single line requires a corresponding conversion of the synchronization clock signal by the same 8:1 ratio to maintain proper timing through the recorder.

ACKNOWLEDGMENTS

Grateful acknowledgment is extended to the members of the Datatape, Incorporated, technical staff who, in one way or another, have contributed to the preparation of this chapter. These include the members of the Marketing Department, Engineering Department, Technical Publications Department, and Customer Services Department, whose untiring efforts have made the preparation of this chapter much easier.

REFERENCES

11-1. DeWitt, K. I.; and Perez, P. E.: "Theoretical and Experimental Error Rates of PCM Codes." Vol. III, *Int. Telemetering Conf. Proc.*, Washington, D.C., 1967.

11-2. Waggener, W. N.: *Considerations in Choosing PCM Codes for Band-Limited Channels.* TR-75-003, EMR-Schlumberger publication, May 1, 1975.

11-3. Waggener, W. N.: *Optimum Detection of Delay Modulation.* EMR-Schlumberger publication, undated.

11-4. King, D. A.: "Comparison of PCM Codes for Direct Recording". *Int. Telemetering Conf. Proc.*, Los Angeles, 1976.

11-5. *EMR 720 PCM Bit Synchronizer.* EMR-Schlumberger Specification No. 720-071, July 1971.

11-6. Stein, J. H.: "The Sangamo HDR System," Sangamo publication, paper presented at THIC/ANSI meeting, San Mateo, CA., Jan. 1977.

11-7. Spitzer, C. F.; Jensen, T. A.; Utschig, J. M.: "High Bit Rate, High Density Magnetic Tape Recording." *Proc. Video and Data Recording Conf.*, Inst. Elec-

No. of tracks		Typical NRZ—L throughput rates for 2-MHz IRIG heads, Mbps							
		150 ips	120 ips	60 ips	30 ips	15 ips	7.5 ips	3.75 ips	1.87 ips
7	1	4.117	3.294	1.647	0.823	0.412	0.206	0.103	0.051
	2	8.235	6.588	3.294	1.647	0.823	0.412	0.206	0.103
	3	12.352	9.882	4.941	2.470	1.235	0.618	0.309	0.154
	4	16.470	13.176	6.588	3.294	1.647	0.823	0.412	0.206
	5	20.059	16.470	8.235	4.117	2.059	1.030	0.515	0.257
	6	24.705	19.764	9.882	4.941	2.470	1.235	0.618	0.309
	7	28.823	23.058	11.529	5.764	2.882	1.441	0.720	0.360
14	8	32.940	26.352	13.176	6.588	3.294	1.647	0.823	0.412
	9	37.058	29.646	14.823	7.411	3.706	1.853	0.926	0.463
	10	41.175	32.940	16.470	8.235	4.117	2.059	1.030	0.515
	11	45.293	36.234	18.117	9.058	4.529	2.265	1.132	0.566
	12	49.410	39.528	19.764	9.882	4.941	2.470	1.235	0.618
	13	53.528	42.882	21.411	10.705	5.353	2.676	1.338	0.669
	14	57.645	46.116	23.058	11.529	5.764	2.882	1.441	0.720
28	15	61.763	49.410	24.705	12.352	6.176	3.088	1.544	0.772
	16	65.880	52.704	26.352	13.176	6.588	3.294	1.647	0.823
	17	69.998	55.998	27.999	13.999	7.000	3.500	1.750	0.875
	18	74.115	59.292	29.646	14.823	7.411	3.706	1.853	0.926
	19	78.233	62.586	31.293	15.646	7.823	3.911	1.956	0.978
	20	82.350	65.880	32.940	16.470	8.235	4.117	2.059	1.030
	21	86.468	69.174	34.587	17.293	8.647	4.323	2.162	1.081
	22	90.585	72.468	36.234	18.117	9.058	4.529	2.264	1.132
	23	94.703	75.762	37.881	18.940	9.470	4.735	2.367	1.184
	24	98.820	79.056	39.528	19.764	9.882	4.941	2.470	1.235
	25	102.940	82.350	41.175	20.587	10.293	5.147	2.573	1.287
	26	107.060	85.644	42.822	21.411	10.705	5.353	2.676	1.338
	27	111.170	88.938	44.469	22.234	11.117	5.559	2.779	1.390
	28	115.290	92.232	46.116	23.058	11.529	5.764	2.882	1.441
42	29	119.410	95.526	47.763	23.881	11.941	5.970	2.985	1.492
	30	123.530	98.820	49.410	24.750	12.352	6.176	3.088	1.544
	31	127.640	102.114	51.057	25.528	12.764	6.382	3.191	1.595
	32	131.760	105.408	52.704	26.352	13.176	6.588	3.294	1.647
	33	135.880	108.702	54.351	27.175	13.588	6.794	3.397	1.698
	34	140.000	111.996	55.998	27.999	13.999	7.000	3.500	1.750
	35	144.110	115.290	57.645	28.822	14.411	7.206	3.603	1.801
	36	148.230	118.584	59.292	29.646	14.823	7.411	3.706	1.853
	37	152.350	121.878	60.939	30.469	15.235	7.617	3.809	1.904
	38	156.470	125.172	62.586	31.293	15.646	7.823	3.912	1.956
	39	160.580	128.466	64.233	32.116	16.058	8.029	4.014	2.007
	40	164.700	131.760	65.880	32.940	16.470	8.235	4.117	2.059
	41	168.820	135.054	67.527	33.763	16.882	8.441	4.220	2.110
	42	172.940	138.348	69.174	34.587	17.293	8.647	4.323	2.162
		12.3 min	15 min	30 min	1 hr	2 hr	4 hr	8 hr	16 hr
		Approximate record time for 9200 ft of tape							

Figure 11–35.—Selecting a formatter to reduce number of record tracks.

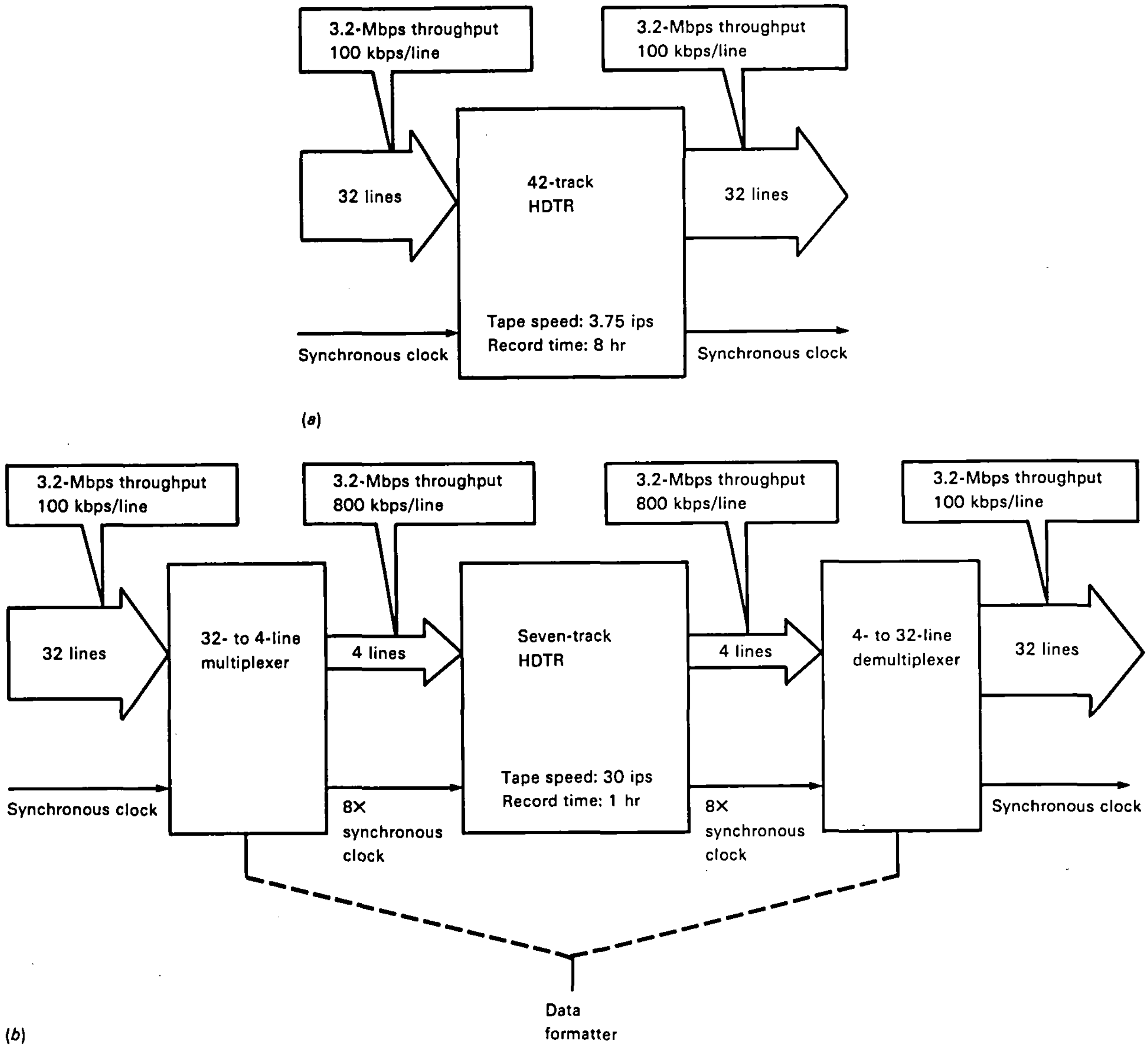

Figure 11-36.—Example of data formatter used to reduce number of record tracks for a 32-line, 3.2-Mbps recorder. (*a*) Without data formatter. (*b*) With data formatter.

tron. Radio Eng. Birmingham, United Kingdom, July 1976.

11-8. Leighou, R. O., "High Density Data Recording/ Reproducing System." *Int. Telemetering Conf. Proc.*, Los Angeles, 1976.

11-9. Davidson, M.; Hasse, S. F.; Machamer, J. L.; Wallman, L. H.: "High Density Magnetic Recording Using Digital Block Codes of Low Disparity." *IEEE Trans. Magn.*, Sept. 1976.

11-10. Herff, A. P.: *Error Detection and Correction Techniques for Longitudinal HI-D Digital Magnetic Tape Recording*. Bell & Howell publication, June 1976.

APPENDIX—AN ULTRAHIGH DATA RATE MASS STORAGE SYSTEM

M. A. Zoeller
Datatape, Incorporated

This appendix describes the mechanical, electronic, and signal processing capabilities of a special purpose instrumentation mass storage system developed by Datatape, Incorporated. The system is presently operational and encompasses many of the features of computer storage systems, including vacuum column tape handling and fast start/stop capability. Throughput rates of up to 450 Mbps and total user storage capacity

of 2.9×10^{11} bits are operational specifications of the system. Bit error rates of 1×10^{-9} are achievable using error detection and correction techniques that complement the E-NRZ source encoding scheme. Search speeds of up to 1140 cm/s (450 ips) provide worst-case access times of approximately 4 min to any portion of the data. Very high data rates and storage densities characteristic of instrumentation recorders are now coupled with the high-speed transport capabilities of computer data storage; the result is a hybrid system of exceptional capability.

System Capabilities

As a special purpose instrumentation recorder, the system described in this appendix, designated the System 600 Magnetic Tape Unit (MTU), exhibits a number of operational features that are similar to existing computer tape drives. However, because of the nature of specific instrumentation requirements, the data transfer rate, storage capacity, and storage density are significantly higher than its computer counterparts. The important system capabilities of the System 600 MTU are as follows:

Data transfer rate	16 selectable rates; 50 to 450 Mpbs
Storage capacity	4.1×10^{11} total, 2.9×10^{11} user bits on a 35.6-cm (14-in.) diameter reel
Bit error rate with EDAC	1×10^{-9}
Number of tracks	84; 72 data, 11 EDAC, 1 search
Storage density (per reel)	2.9×10^5 bits/cm^2 (1.9×10^6 bits/in^2)
Storage density (per track)	17.7 bits/cm (45 kbpi)
Tape width	5.08 cm (2.0 in.)
Tape diameter	35.6 cm (14.0 in.)
Tape length	2804 m (9200 ft)
Tape speed	16 selectable speeds: 49.5 cm/s (19.5 ips) to 428.6 cm/s (168.75 ips): Search: 1143 cm/s (450 ips) Wind/Rewind: >1397 cm/s (550 ips)
Start/stop time (tape)	Start: 5.0 ms valid data at 450 Mbps Stop: 2.0 ms at 381 cm/s (150 ips)
Access time	Worst case: 245 s Typical (center of reel): 122 s
Features	Auto Thread Remote Digital Calibration

Those knowledgeable in the design of instrumentation recorders will note that the vacuum/pressure tape handling treatment of the System 600 is an unusual feature for this class of equipment. The tape handling design arises from a key operational requirement to record data which is received by the system in "bursts" of very high rate. The fast start/stop transport allows this data to be recorded with minimum interrecord gap and to be accessed for reproduction at very high search speeds. The following sections of this paper briefly outline the mechanical, electrical and signal handling design features of the System 600 MTU and point out the formidable mass data storage aspects of the system.

MTU Mechanical Configuration

The System 600 transport (fig. 11-37) is a fast start/stop transport designed to operate with 5.1-cm (2-in.) wide tape and reels up to 40.6 cm (16 in.) in diameter. Because of the large reel diameter and tape width, the resultant reel inertia must be isolated from high tape acceleration at the capstan by vacuum columns of sufficient length to accommodate the effective inertia and motor torque. In this regard, the MTU is similar to a high-performance computer peripheral tape drive with the additional design extensions required to handle the quadrupling of tape width and the increase (by a factor of at least 5) of both the tape length and the packing density. Figure 11-37 illustrates the MTU configuration and exhibits the three principal visible parts of the transport: the upper reel drives, the center tape guiding group, and the lower vacuum columns.

Reel Drive Assembly

The reel drive requirements are defined by the length of the vacuum column and the size of the tape reel. The active storage capability in the vacuum columns is 152 cm (60 in.) of tape, and the reels requiring the fast start/stop capability vary up to 35.6 cm (14 in.) in diameter. Under conditions of instant capstan reversal at 380 cm/s (150 ips), the reel must stop and reverse to speed in 400 ms. Start or stop can be accomplished in either direction from the center of the vacuum column with half of the tape storage available.

To optimize the fast rewind speeds for the various reel sizes, two drive ratios from the motor to the reel hub have been implemented. For the 35.6 cm (14-in.) reel or larger, the speed reduction is 2.5:1. For a 26.7-cm (10½-in.) reel or smaller, the reduction is 1.25:1.

The motors and reel jackshifts are coupled with cogged timing belts and pulleys to prevent slippage and are mounted on adjustable frames so that the belt can be loosened to shift it from one set of pulleys to the other for the drive ratio change. The jackshaft assembly is constructed to allow quick belt changes in the field and to assure interchangeability without affecting tape stacking on the reels.

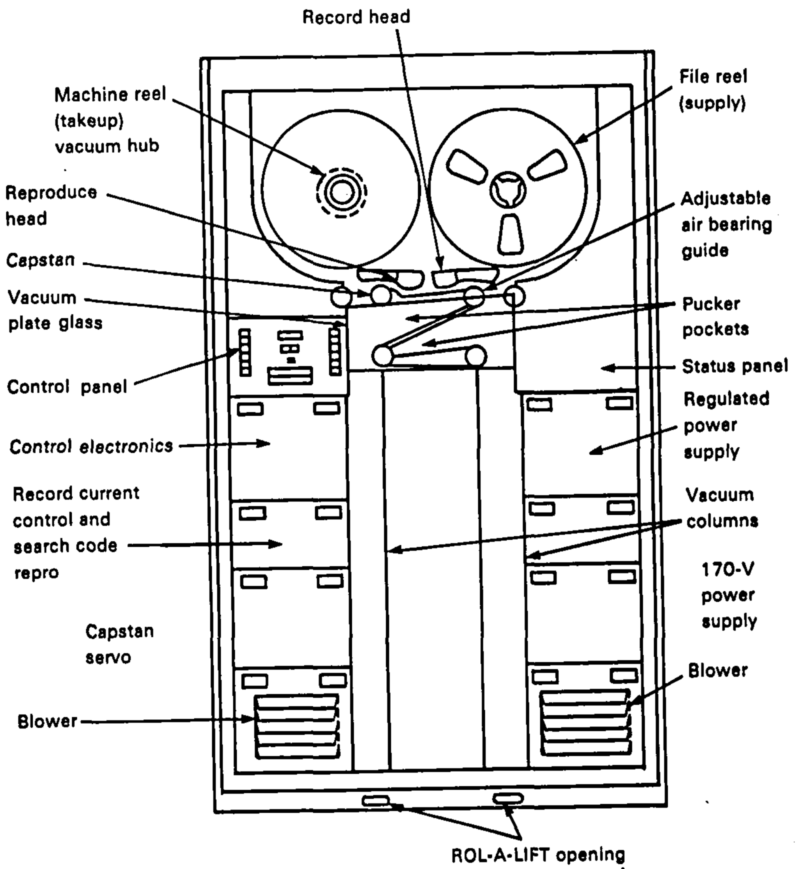

Figure 11-37.—MTU configuration.

Because of the high torque transmitted to the reel hub from the motor (as much as 5.93 N-m (840 oz-in.) during reversal), a special reel hub was developed to prevent loosening or slippage. A mechanical brake is mounted to the rear shaft of the motor to lock the reels in no-power modes and to assist in braking during power loss. During power loss, the maximum braking effect is accomplished by shorting the motor windings through resistors, thus slowing the reels adequately to prevent tape breaking or stretching and to avoid an excessive accumulation in the columns.

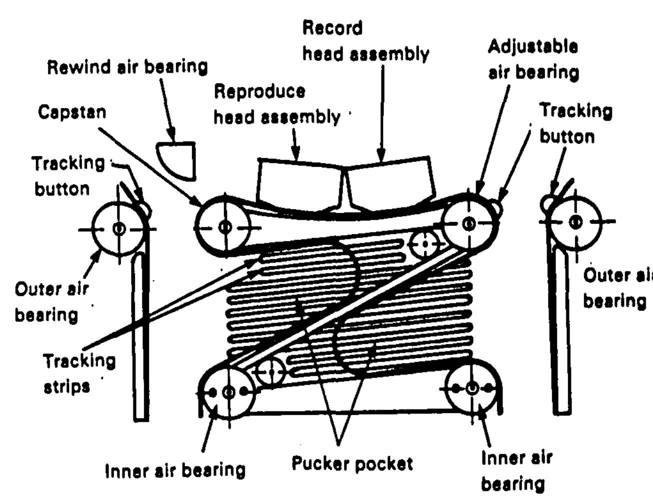

Figure 11-38.—Tape guidance configuration.

Air Bearing

As shown in figure 11-38, there are six air bearings on the transport to provide virtually frictionless support and negligible change in tape tension across the bearing. This is achieved by forcing air supplied by the vacuum-pressure system through the bearing and into an air layer between the bearing structure and the tape.

To provide an air bearing that acts independently of the air gap between the tape and bearing shell, the bearing is made as shown in figure 11-39. The outer diameter D, 0.079 cm (0.031 in.), is larger and acts as a plenum or reservoir while the restrictive orifice is provided by the smaller diameter d, 0.020 cm (0.008 in.). This results in an effective orifice area that is significantly less dependent on the tape air gap and also provides a lower velocity air cushion to minimize tape distortion during periods when the tape is at rest on a bearing.

The small diameter holes are provided by a chemically etched screen, which fits inside the air bearing shell as

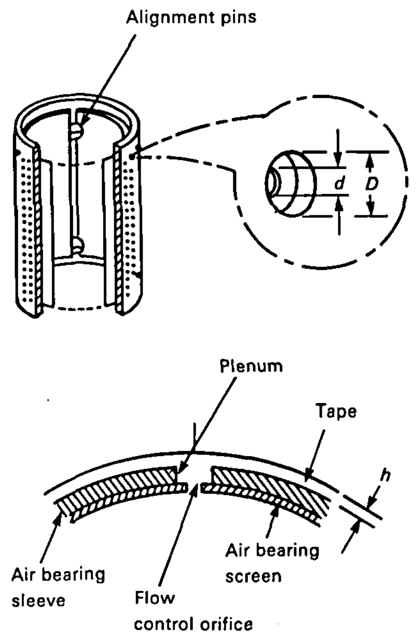

Figure 11–39.—Air bearing configuration.

shown in the figure. The hole pattern of the screen is common to all six bearings, and alignment is maintained by swaged precision alignment pins in the shell.

Pucker Pockets

As indicated in figure 11-38, the pucker pockets are located immediately adjacent to the capstan and the adjustable air bearing guide. These pockets are necessary to isolate the inertia of the tape and air mass within the vacuum columns from the high acceleration of tape at the capstan.

Pucker pocket dynamics were simulated in a computer study in which tape tension and velocity characteristics were determined for particular capstan motions and time periods. The analysis considered the geometry of the pocket including the angle and the orifice size, the flow into and out of the pocket from the orifice and the edge gap (assuming air is an ideal gas), the position of the tape in the pocket, and the amount of tape in the vacuum column.

The back surfaces of the pucker pockets are grooved to aid in guiding the tape against the back reference surface. As in the vacuum columns, the walls of the pockets are coated with "Scotchlite," a low-friction glass bead material, and the air bearings are overhung into the pockets to minimize friction.

Tape Guidance

For optimum recording performance and maximum tape life, careful guidance of the tape is essential. On the System 600 transport, the tape is single-edge guided to avoid problems due to variations in tape width.

The reference surface against which the tape registers is defined by the adjustable air bearing tracking button, the tracking strips, and the capstan perpendicularity.

The adjustable air bearing (fig. 11-38) has a slight adjustable taper on the outer edge, which provides a small tape guiding force moving it toward the tracking button. To protect the tape, the adjustable air bearing is visually adjusted so that the tape just contacts the button. This air bearing is particularly useful in the forward direction because it directly precedes the recording head.

The grooves of the pucker pocket also aid in guiding in the tape. Air flows past both edges of the tape into the vacuum pockets where the grooves are so designed that an equal amount of air flows past both edges with the tape biased against the reference surface. Because there are grooves in both pockets, they are useful guiding elements in either forward or reverse directions.

Auto Thread

The autothread features of the transport use no special leader or grooming of the tape end. Three air jets blow the tape through the head area and up to the dedicated vacuum reel that captures the tape.

Capstan/Motor/Stripper Assembly

The capstan/motor/stripper assembly is a completely interchangeable subsystem consisting of drive motor, tachometer, capstan, and stripper assembly.

The capstan itself (fig. 11-40) is of four-piece construction consisting of a grooved magnesium outer cylinder capped by slightly conical end disks, which attach to a cylindrical hub mounted on the motor shaft. The disks are dished to afford more axial stiffness, and the outer shell is grooved to provide a more effective vacuum area on the tape surface and a minimum of vacuum at the engagement and disengagement tangent points of the tape and capstan. The fingers of the tape stripper extend under the tape and beyond the tangent point within the grooves of the capstan. Before 3-axis adjustment on the transport, the capstan is assembled on the motor shaft and then ground in place achieving runouts of less than 5 μm (0.0002 in.).

Tape Servo Systems

The capstan servo implemented in the System 600 is designed to accelerate to 380 cm/s (150 ips) in 2.0 ms, allowing a complete reversal from 380 cm/s (150 ips) forward to 380 cm/s (150 ips) reverse in 4 ms.

To accomplish the required acceleration, a low inertia motor capable of the system torque requirements was selected. The motor, when coupled with a low inertia capstan and high resolution optical encoder, exhibits a calculated torsional shaft resonance of 2.6 kHz. This

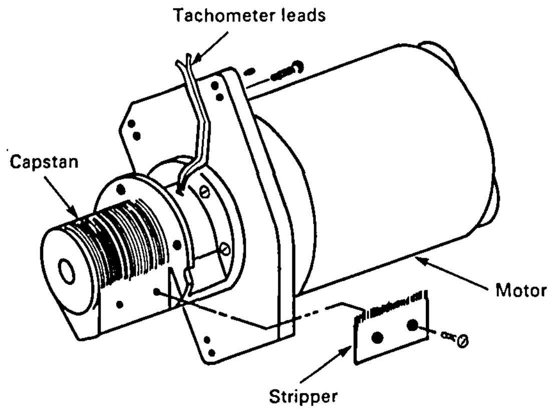

Figure 11-40.—Capstan/motor/stripper assembly.

resonance limits the design of the capstan servo bandwidth to 350 Hz. A controlled speed of 380 cm/s (150 ips) in 2 ms with a servo bandwidth of only 350 Hz is achieved through the use of an open-loop start/stop pulse generator to quickly accelerate the capstan with a linear velocity profile.

The reeling servos for the system are position servos operating to keep tape within the vacuum column at all times. The vacuum columns are of adequate size to absorb any instantaneous velocity difference between the capstan and the reels normally encountered in the legitimate start/stop/reversal maneuvers of this transport.

Tape is stored during these maneuvers in vacuum columns that have a storage capacity to accommodate a maximum reel accleration time of 200 ms and a reversal time of 400 ms.

To achieve the required torque, the motors are supplied with a maximum of 40 A at a voltage of 170 V. This high voltage is necessary to overcome the back emf produced by the motors at high speeds.

Vacuum Columns

The vacuum columns, as shown in figure 11-37, are functionally located between the reels and the pucker pocket/capstan/head area, isolating the inertia of the reels from the capstan and allowing the capstan to accelerate at much higher rates than the reels. Each column has an active length of 76 cm (30 in.), or a total of 152 cm (60 in.) of tape compliance per column. This compliance is necessary to interface the capstan 4 ms reversal time with the 400-ms reversal time of the reels.

Each column consists of three walls and a front glass door that can be hinged open for maintenance and cleaning. A good seal between the door and the column walls is achieved by grinding the column walls. The two side walls against which the Mylar side of the tape runs are coated with "Scotchlite."

Magnetic Heads

In virtually all high-density instrumentation systems, the magnetic record/reproduce head assembly represents the single most critical element determining the performance of the system. The unusual 84-track, 5.1 cm (2-in.) configuration coupled with extremely high storage density requirements represents a formidable design task in itself. The record and reproduce heads for the System 600 are an 84-track longitudinal design interleaved on two stacks. The tracks are 0.045 cm (0.018 in.) wide with 0.013-cm (0.005-in.) guard bands and are designed for 17.7 kilobit/cm (45-kbpi) track storage density at a maximum speed of 406 cm/s (160 ips).

The heads are positioned with a 3° angle of wrap on each side of the head, which is necessary for good head-to-tape contact at the higher speeds. The tape contacts the heads at all times except during the fast wind/rewind mode when the tape is pulled down into the vacuum rewind pocket to reduce wear.

Electronic and Signal Processing Design

A block diagram of the System 600 signal processing design is shown in figure 11-41. The major processing functions of the design include source encoding, reproduce amplification, and bit synchronization and deskew. A brief description of these functions is presented in this section.

EDAC Encoder

Each of the two input formatters of the system converts 18 channels of 12.5-Mbit input data to 36 tracks of 6.25 Mbit each and directs these data to the EDAC encoder.

The System 600 EDAC scheme can generally be described as a three-loop process composed of multiple first, second, and third loops. The first and second loops correct parity detectable errors using serial parity information inherent to the E-NRZ data format along with pre-encoded data recorded on correction tracks. The third loops detect and correct nonparity-detectable errors (even numbers of bits in error) using information recorded on correction tracks.

In the EDAC encode section, parallel tracks of data are blocked and checked for lateral parity. The adjacent parallel data tracks are then separated or staggered longitudinally in position by the use of delay networks (interleavers), the lateral parity information being recorded on a separate dedicated track (correction track). This lateral parity checking of the data is performed a total of 11 times during the EDAC encoding process to generate 11 correction tracks—one for each of seven first loops, one for each of two second loops, and one for each of two third loops.

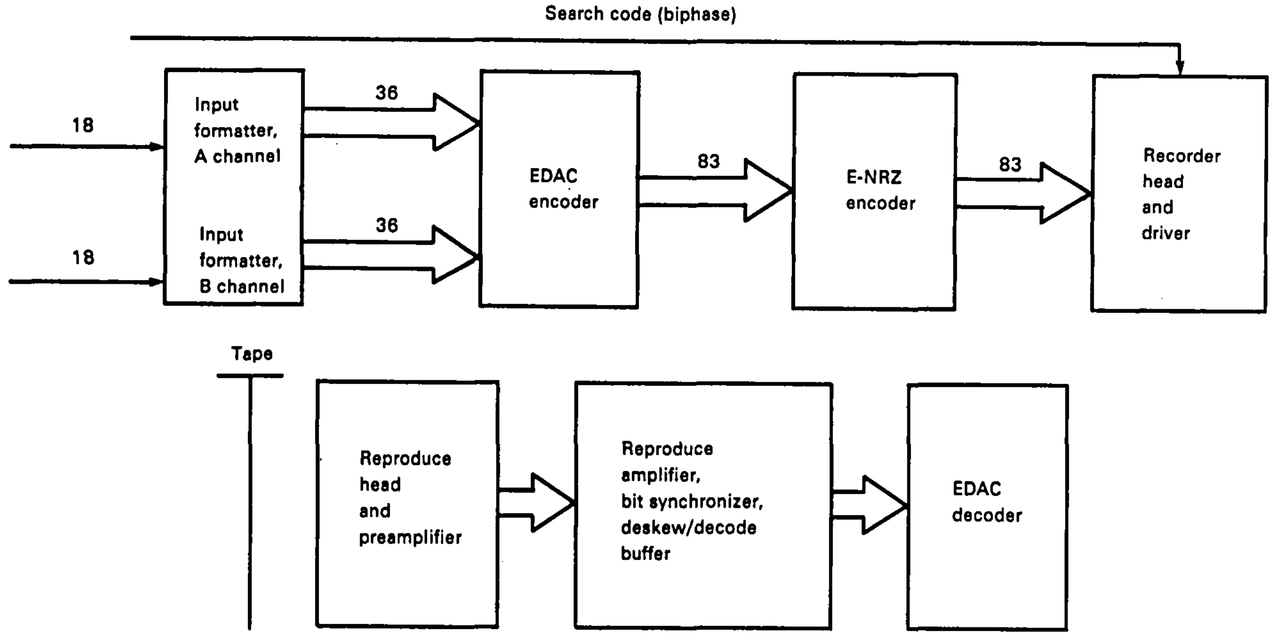

Figure 11–41.—System 600 signal processing design.

In the EDAC decode section, reproduced data and data parity information are correlated with correction track information for identification and correction of bit errors. Following each loop correction process, the data are restored to the original lateral relationship using delay elements (deinterleavers) so that the data may be processed in next loop with the corresponding correction track. Data leaving the final loop of correction have the same lateral relationship as the input data.

E-NRZ Encoder

The encoder provides the buffering of input write data, the insertion of a serial odd parity bit every seven data bits, the inversion of selected data bits, and the insertion of a 40-bit synchronization word every 560 data bits (fig. 11–42).

Input data are loaded into a 128-bit deep first in, first out (FIFO) memory that compensates for small variations between the user and transport clock rates and accumulates data when the synchronization word is being written. A serial parity flip-flop generates an odd parity for every byte of data. The data bits and the parity bit are combined to form an 8-bit enhanced word. The modified data and the associated parity bit, along with the 40-bit synchronization word, are sent to the record head driver to complete the record process of the system.

Digital Calibration

An important feature of the System 600 MTU is the capability to accept microcomputer-controlled read/write calibration signals and to perform digitally controlled equalization. A read/write calibration (RWC) controller provides equalization data to the record and reproduce electronics for each track and for each speed. In the online control mode, these data are provided to the MTU based on a stored set of equalization parameters characteristic of the unit. The data are sufficient to provide information for midband, phase, band edge, range (speed), frequency, and record current correction in response to commands from the system controller.

The RWC controller is capable of controlling the calibration of several tape transports by generating and storing the parameter datasets of each MTU and performing the calibration control on the units individually.

While programming of the calibration datasets is accomplished manually, the process is aided by the use of spring return-to-center switches and light-emitting diode displays for each calibration variable and an integral scope display for eye pattern examination. This calibration approach provides a significant reduction in labor compared with conventional designs requiring individual potentiometer adjustments on record and reproduce electronic boards. Fully automatic calibration of the MTU is anticipated in future designs.

Reproduce Amplifier

The reproduce amplifier is located on a single board with the bit synchronizer and deskew buffer. The board is digitally programmed to perform a number of calibration functions and interfaces to the control busses via an

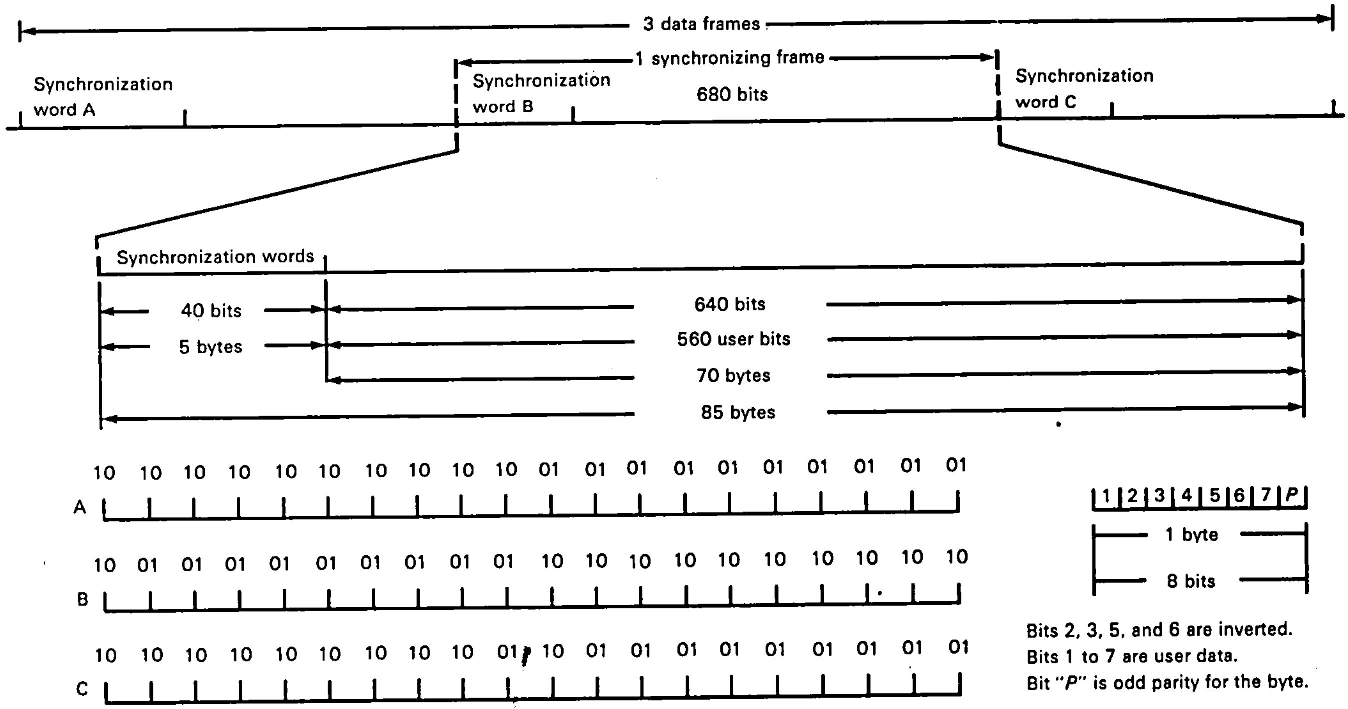

Figure 11-42.—Data format.

interface card mounted in each drawer of 16 reproduce amplifiers.

Preamplifier signals are fed differentially into the reproduce amplifier and proceed through a band-edge peaking circuit. Both the peaking frequency and the magnitude of the peaking are digitally controlled with analog multiplexers that select 1 of 16 peaking frequencies and 1 of 8 magnitudes.

This conditioned signal is then integrated to give the proper low-frequency response and fed to the midband amplifier. The gain of the amplifier, which is controlled by two four-bit digital words in a manner analogous to the band-edge amplifier, adjusts the amplitude of the midband signals. In addition to performing midband amplification, this circuit simultaneously performs phase equalization adjusted by a digital control word. Following equalization, the signal is dc restored and buffered before being fed to the bit synchronizer.

Bit Synchronizer

The bit synchronizer is located on the same boards as the reproduce amplifier and deskew buffer. The function of the bit synchronizer is to synchronize a clock to E-NRZ data taken from the reproduce amplifier. The circuit consists of a zero crossing detector that acts on the equalized data to determine data transitions, which are fed to a high-speed phase comparator and compared with the synchronized clock. The error is then fed through a charge pump and compensation amplifier, and finally as an error signal to a voltage-controlled oscillator (VCO). The VCO also has digital inputs to program its center frequency for the data rate of operation. The output of the VCO is appropriately scaled and returned to the phase comparator to close the loop. Acquisition range of the bit synchronizer is ±3 percent. Tracking range is +10 percent for frequencies normally encountered in flutter.

Decode/Deskew Buffer

The data clock received from the bit synchronization is first sent to the synchronizing word detection logic. The data are stripped of synchronization and converted to 8-bit words aligned so that the word consists of 7 data bits and the associated parity bit.

When a complete new word is present, it is clocked into a FIFO memory, which internally stacks consecutive words behind one another, ready for the output timing control signals to unload them. The data are sent through an exclusive OR gate where the encoded bit inversions are removed. The 8-bit words are checked for parity errors, and the 7 data bits are reconverted to a serial stream and sent, along with the parity status information, to the EDAC circuit.

EDAC Decoder

The EDAC decoder performs two primary functions. First, it senses and corrects errors on both data and correction tracks; and, second, it restores data to the same time-coinciding relationship as existed at the input to the EDAC encoder.

During decoding data are parity checked laterally ("columnwise") by each loop to detect the presence of errors. This information, used in conjunction with the serial parity check information from each track, is used to locate both the track and the bits that are in error, and thus enable correction of the data.

Summary

This appendix describes a special purpose instrumentation tape recording system with exceptional storage capacity, data transfer rate, and tape handling capability. Because of the demanding requirements under which the system was developed, the system design exhibits many of the features of existing computer mass memory systems. This "hybrid" character of the system makes it unique in the instrumentation world and provides a baseline for possible future development of extremely high-density, rapid access mass memory systems.

CHAPTER 12

The Application of 3-Position Modulation Coding to Longitudinal Instrumentation Tape Recording

John M. Howard
Thorn EMI Technology Incorporated

The state of the art for high-density digital recording (HDDR) bit packing density for conventional systems using standard wideband headstacks and general purpose tape has been static for several years in the region of 28 to 33 kbpi. The only generally accepted method of exceeding this packing density has up to now been to use so called "half-wavelength" recording techniques involving very narrow gap heads, high-energy tape, etc.

This paper discusses how a coding scheme, designated 3-position modulation (3PM), has been adapted from its original fixed-speed computer disk application to the special needs of multispeed, bidirectional instrumentation tape recording. Using a development of this code, it has been possible to extend packing density, using standard wideband heads and tapes, up to about 45 kbpi and to lower the minimum data rate to 5 kbps.

The increase of about 50 percent in packing density over that possible with the use of conventional systems is of immediate benefit to the user in significant tape economy and increased data throughput at a given tape speed or a combination of both. The extended low data rate capability permits two or more asynchronous bit streams of widely different rates to be recorded simultaneously using the same coding scheme.

3PM coding is simple to implement and will prove an attractive alternative wherever tape economy, recorder/recorder interchange (crossplay), adjustment free operation over extended periods, high data throughput, and bidirectional operation at regular and nonstandard tape speeds are primary requirements.

Before discussing the 3PM coding process in detail, it is important to draw a clear distinction between "bits" and "transitions." Consider the waveform shown in figure 12-1, which we can take to represent the current flowing in a magnetic tape record head. We know that if certain conditions are satisfied, then flux transitions corresponding to the current transitions will be recorded on the tape as it moves past the recording gap.

What we cannot say, simply by inspection of the

Figure 12–1.—Voltage at magnetic tape record head.

waveform, is what the series of transitions is meant to represent, even if we assume that it is serial binary data. Additional information is required regarding the coding scheme being used and the relationship of the transitions to the associated data clock. Figure 12-2 shows three possible "interpretations" of the transition pattern; there could, of course, be many more. Note that this sample transition pattern carries about 10 bits of information if delay modulation, mark (DM–M), or nonreturn-to-zero (NRZ) codes are used but only about 6 bits for biphase.

Because so many codes in general use today involve one transition (or the absence of one transition) to describe one data bit, it is sometimes mistakenly felt that it has to be that way. Users are prepared to accept the fact that biphase data contains additional "reset" transitions, which tend to limit the possible data packing density, but they cannot always readily accept the possibility of describing bits with less than one transition per clock period. We are not talking about transitionless periods in the basic NRZ–L data, because such a system is quite prepared to accommodate transitions at the clock rate and the rules of NRZ coding state that the absence of a transition carries just as much data as the presence of one. It will be shown later that codes such as 3PM never have transitions occurring at the data clock rate regardless of the data sequence.

The recording/reproducing process is, of course, more concerned with the problems of faithfully recording and reproducing the series of transitions than with any information that might be contained by those transitions, their relationship in time to one another, etc. The limitations of such a system will be well known to anyone working in the field.

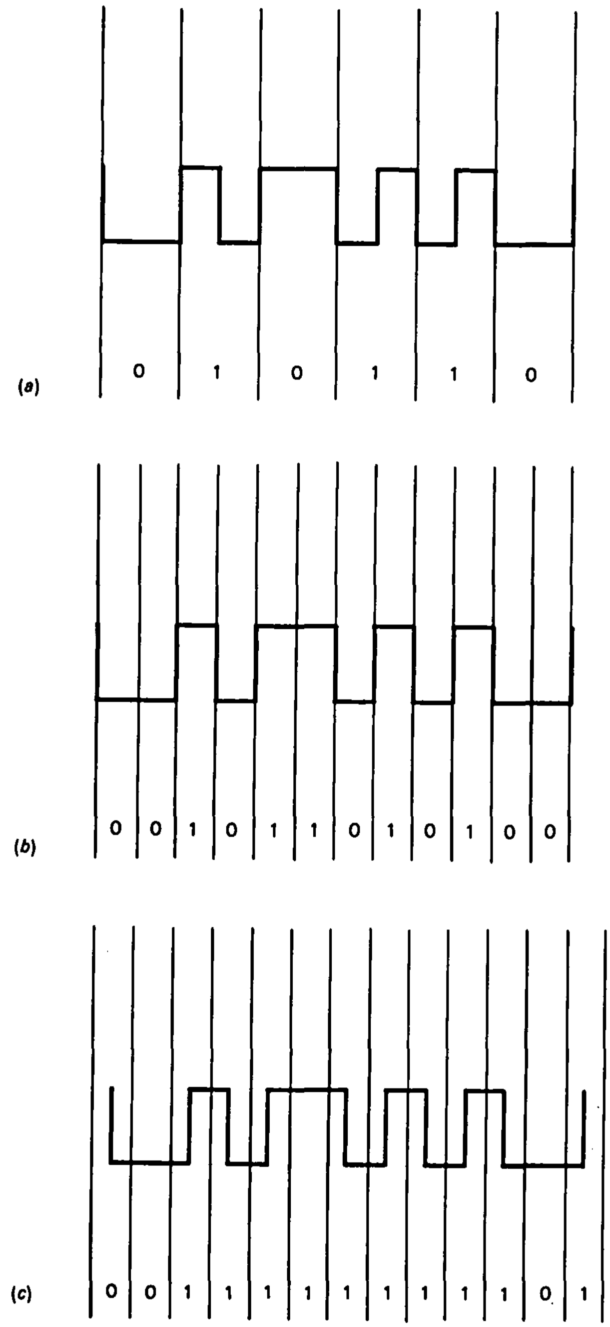

Figure 12–2.—Three possible interpretations of transition pattern of figure 12–1. (*a*) Biphase. (*b*) Nonreturn to zero, level. (*c*) Delay modulation, mark.

At one end of the scale we are limited in how closely we can pack our transitions (fig. 12–3). The output from the reproduce head falls sharply as the recorded wavelength approaches the length of the reproduce gap. Under certain circumstances, bit crowding can take place. This is the situation in which a transition placed close to another may appear to "migrate" into the larger space available between it and the transition on its other side.

At the low end we are faced with the problem that the direct reproduction process has a low-frequency rolloff in the region of 400 Hz for a typical wideband recorder. This means that if the tape speed is kept constant while the transition rate is gradually reduced, there will come a time when a significant amount of the spectrum is below the passband of the recorder with consequent results. A similar effect can be created by reproducing a recorded data stream at a sufficiently low replay speed so that the spectrum is once more outside the passband. It is for this reason, incidentally, that it is not normally possible to state a lower limit for transition packing density, because the constraints are related to frequency rather than recorded wavelength. Note that the actual lower data rate at which the system becomes unreliable is related to the longest transition-free interval that can occur in the data. For example, a code in which the maximum transition-free interval is 3 clock periods is likely to be capable of lower reproduced data rates than one where 16 period intervals are possible.

An associated problem is concerned with clock-recovery because virtually all HDDR schemes require "self-clocking" properties of their codes. Even if the transitions are being reproduced they must occur frequently enough for a bit synchronizer to remain locked to them.

All the problems have been discussed in terms of transitions—not what those transitions might mean. A given digital code simply sets out to insure that these constraints are accommodated, while at the same time packing as much data onto a given length of tape as possible.

It is assumed that the reader is familiar with the more common coding schemes in use in HDDR recorders today. Further information is given in reference 12–1 and appendix D to this publication.

All that needs to be said here is that NRZ in all its forms and delay modulation (DM–M, Miller, Miller squared, etc.) are all examples of codes in which transitions can occur at the data clock rate, meaning that the maximum transition density is equal to the maximum data density. Biphase is an example of a code in which the maximum bit density can be one-half of the maximum transition density.

3PM is a code in which data density actually exceeds transition density by 50 percent, giving the code its interesting and important properties.

3PM CODING

Consider the serial bit stream shown in figure 12–4. This is first divided into three-bit bytes, and each byte is divided into six half-periods. The boundaries between half periods are called "positions" and designated P_1 to P_6 as shown. Each three-bit byte is recoded according to

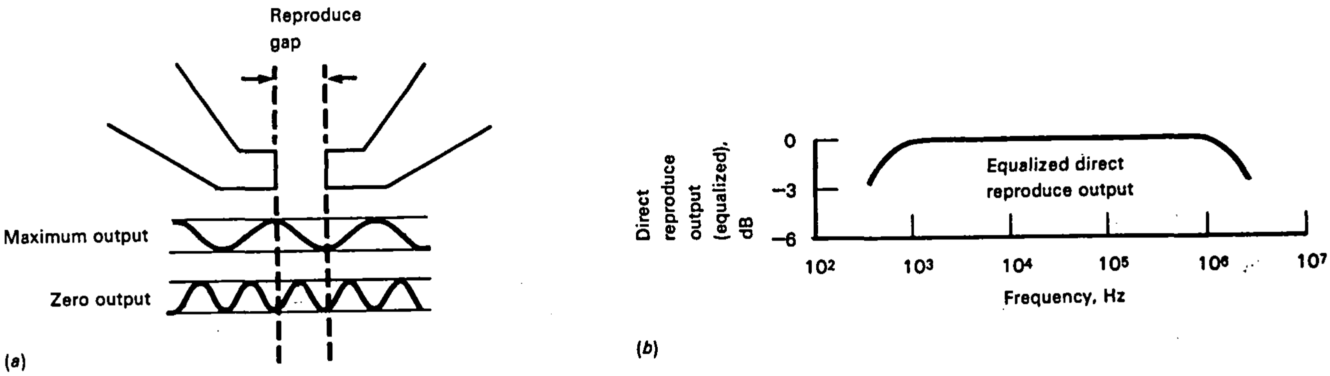

Figure 12–3.—(*a*) Relationship between wavelength and reproduce gap. (*b*) Frequency response at 120 ips.

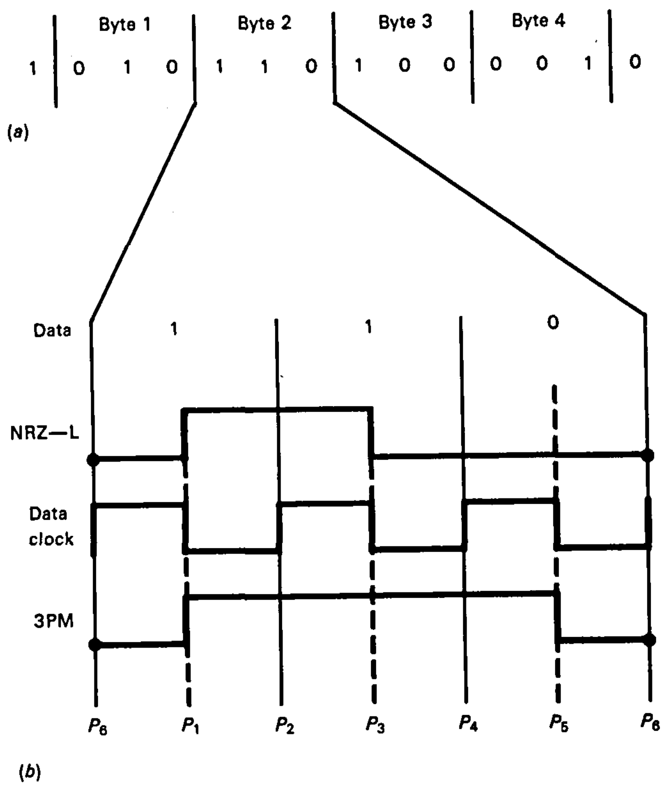

Figure 12–4.—(*a*) Data stream. (*b*) Typical 3PM waveform.

Table 12–1.—*Basic 3PM Coding Scheme*

Data byte	Transition positions P_1	P_2	P_3	P_4	P_5	P_6
000	0	0	0	0	1	0
001	0	0	0	1	0	0
010	0	1	0	0	0	0
011	0	1	0	0	1	0
100	0	0	1	0	0	0
101	1	0	0	0	0	0
110	1	0	0	0	1	0
111	1	0	0	1	0	0

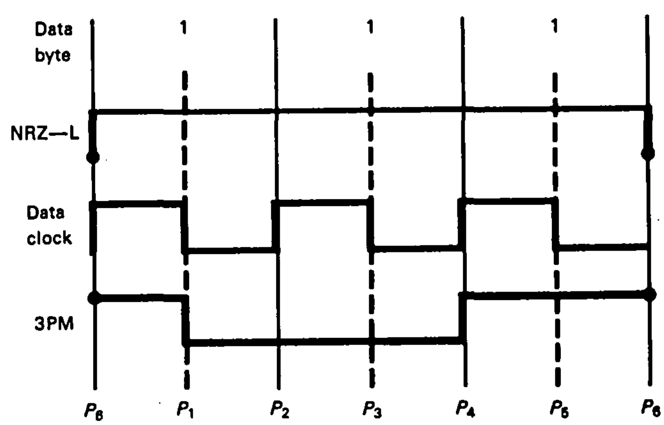

Figure 12–5.—Typical 1½-period interval 3PM waveform.

table 12–1 with transitions being assigned to one or more "positions" within the byte. Notice that there can be either one or two transitions in a recoded group but there must always be at least two transition-free positions between transitions, corresponding to an interval of 1½ data clock periods. Figure 12–5 illustrates this.

There is one further rule: No transition is ever assigned automatically to position P_6 in the basic code groups. Looking at table 12–1, it can be seen that there are certain data bytes that if arranged serially, can cause transitions to occur without the desired two-position (1½-clock period) interval between them. One such example might be

011 101

where transitions would occur at byte 1, P_5, and byte 2, P_1, leaving only byte 1, P_6, as a transition-free position. Such a condition would produce transitions at the data

clock rate and defeat the object of the exercise. In this case, the offending transitions are merged to form a single transition at byte 1, P_6, by which means the minimum transition interval of 1½ data clock periods is guaranteed. (See fig. 12-6.)

If the reader cares to experiment with various byte combinations (observing the merging rules where appropriate), it will be found that a finite number of intervals between transitions are possible: 1½, 2, 2½, 3, 3½, 4, 4½, 5, 5½, and 6. For example, the longest interval (six periods) is given by the data combination 101000 preceded by 000, 011, or 110 and followed by 101, 110, or 111. (See fig. 12-7).

Anyone familiar with the 1-, 1½-, 2-, 2½-, and 3-period intervals that characterize the Miller squared system may see 3PM as a logical extension of the technique except that the critical 1-period interval has now been eliminated.

Some figures may help to emphasize what we have achieved at this point. For example, take a recorder/reproducer that is capable of resolving 30 000 flux transitions per inch: If the code being used is randomized NRZ, then the bit packing density will also be

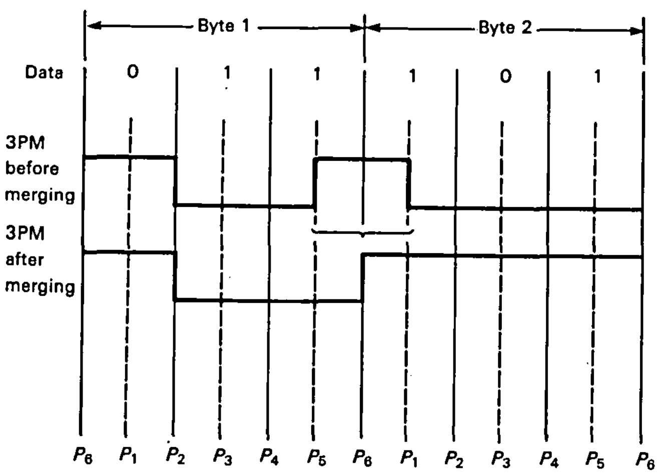

Figure 12-6.—Merging.

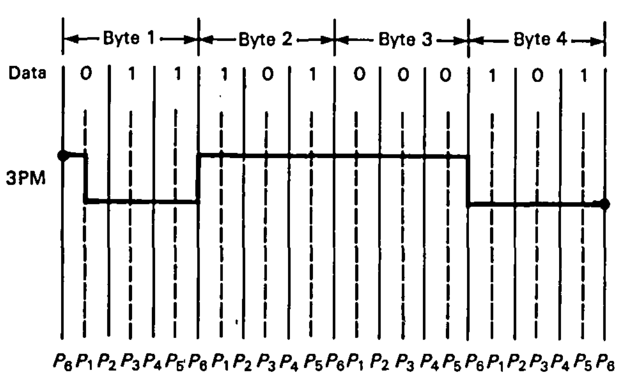

Figure 12-7.—Example of six-period interval.

30 kbpi, because maximum transition density and maximum bit packing density are the same in the case of R-NRZ.

With 3PM coding, the maximum transition density has been shown to be only two-thirds the data density, so a transition density of 30 ktpi will be equivalent to a bit packing density 50 percent higher, namely 45 kbpi. (See table 12-2.)

So, by changing nothing but the rules by which the transition pattern is decoded (and the associated electronics, of course), we have significantly increased the amount of data that a given length of tape can accommodate.

SYNCHRONIZING WORD

The selection of a synchronizing word in any HDDR format is generally a compromise between several conflicting requirements. It is important that it should not be possible to confuse the synchronizing word with normal data. So with many NRZ-based codes it is customary to write a fairly long sequence (maybe 16 bits or more) that cannot occur naturally. On the other hand, code efficiency requirements suggest that we should not waste more tape than necessary on overhead bits.

Similarly, it should be remembered that if synchronization is lost, following an error burst, for example, then correct lock often cannot be reestablished until the next synchronizing word is detected. With this in mind, we would like to repeat synchronizing words frequently, but not so frequently that efficiency suffers unduly.

Like DM, 3PM has a finite number of possible intervals between transitions (1½ to 6), and we can take advantage of this fact by writing a unique interval by means of a code violation. A 7-period interval is chosen and placed symmetrically in a 10-period window as shown in figure 12-8. If we had chosen a window smaller than 10 periods, it would be possible for a first data transition occurring after the synchronizing word to be closer to the trailing edge of the synchronizing word than the required 1½ clock periods. The properties of a synchronizing word are as follows:

(1) It cannot be confused with data because it is a violation of the code

(2) It can be read in both directions

Table 12-2.—*Comparison of Required Bit Packing Densities*

Flux transition density, ktpi	Data density, kbpi		
	Biphase	NRZ and DM	3PM
30	15	30	45
20	10	20	30

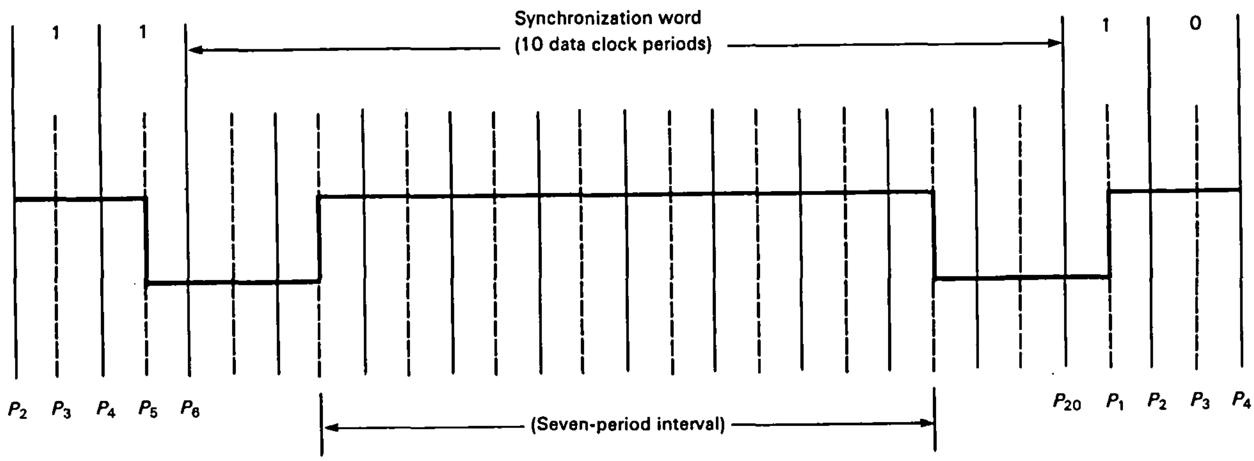

Figure 12–8.—Unique synchronization word.

(3) It occupies only 10 clock periods

(4) It provides both clock frequency and phasing information

(5) It also has all the properties necessary for a parallel deskewing marker

While it is tempting to only place these synchronizing words infrequently in the data, practical experience has shown that the optimum block length between synchronizing words is 260 data bits. Space for the synchronizing word in a continuous data stream is achieved by conventional "stuffing" techniques.

SLOW DATA RATES

So far we have considered only how it has been possible to extend the upper limit of packing density using the 3PM code; for many applications, this is the primary requirement. However, there are also many requirements to record low data rates. Even worse, it can be necessary to record high rates and low rates simultaneously; traditionally this has posed special problems.

For example, one recent specification involved the need to be able to record a 50-Mbps serial bit stream at the same time as a parallel 100-kbps serial stream. For operational reasons, the 50-Mbps stream was to be fanned out over 22 tracks while the 100-kbps stream would be fanned out over 2 tracks. Needless to say, the high rate data (see fig. 12-9) took precedence when choosing a tape speed:

$$50\ \text{Mbps} \div 22\ \text{tracks} = 2.272\ \text{Mbps per track}$$

At a packing density of 30 kbpi, tape speed is given by

$$\text{Tape speed (ips)} = \frac{\text{Bit rate (bps)}}{\text{Packing density (bpi)}} = \frac{2.272\ \text{Mbps}}{30\ 000\ \text{bpi}} = 75\ \text{ips}$$

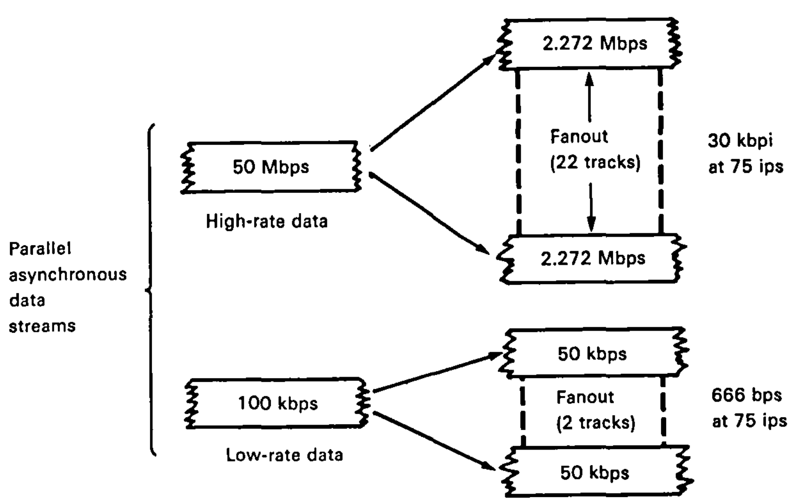

Figure 12–9.—Recording at high and low data rates simultaneously.

Keeping these numbers constant, the packing density, per track, for the low data rate channel became

$$100 \text{ kbps} + 2 \ + 75 \text{ ips} = 666 \text{ bpi}$$

It must be remembered that, with six-period intervals occurring naturally in the encoded waveform, together with seven-period synchronizing words, a significant frequency component of around 3.5 kHz would be present in the recorded waveform. This cannot be reliably reproduced. This problem is compounded when it is noted that an additional requirement was to reproduce the high-rate data at 1/32 of recording speed. This would necessitate playing back the slow data at

$$50 \text{ kbps} + 32 = 1.5625 \text{ kbps}$$

with components in the region of 120 Hz. For this particular application, it was desirable for various reasons not to use more than one basic coding method, so this posed a serious problem for the HDDR formatting electronics.

The IRIG document 106-80 (ref. 12-2) acknowledges this difficulty by recommending different codes for high and low rate applications. Biphase, level (Biφ–L), is used up to a packing density of 15 kbpi, and R-NRZ–L is used in the region of 15 to 25 kbpi. The minimum recommended reproduce bit rates are 5 kbps for Biφ–L and 200 kbps for R-NRZ–L.

The 3PM code has been extended to provide a very convenient solution. Without going too deeply into the mathematics at this stage, it happens that the minimum data rate at which 3PM (as discussed so far) can be safely reproduced is 40 kbps. Therefore, when slow-rate data are to be recorded, and it is known that it will be impossible to reproduce the data in real time or at any other speed where the rate will be lower than 50 kbps, we use a simple variation of the original 3PM code. The 3PM waveform and the write clock are combined in an exclusive OR gate as shown in figure 12-10. It can be seen that data integrity is maintained: the original transitions have now become nontransitions while places where no transition would have occurred are now provided with transitions. The decoding system now has to look for spaces rather than marks, but the recording now has between four and five transitions per three-bit byte to work with rather than one or two, thus reducing the minimum data rate from 50 to 5 kbps.

The synchronizing word is treated similarly and becomes a unique 13-transition group at double the clock rate instead of a 7-bit interval. Therefore, the reproduce electronics has a convenient method of detecting which form of the code was used in the recording process. The low rate version is called Yφ.

Thus 3PM coding combines both the low-frequency properties of biphase (5 kbps minimum data rate) with the important ability to pack data at densities considerably in excess of those recommended by the Inter-Range Instrumentation Group[1] for R-NRZ (45 kbpi rather than 25 kbpi).

[1]Now the Range Commanders Council.

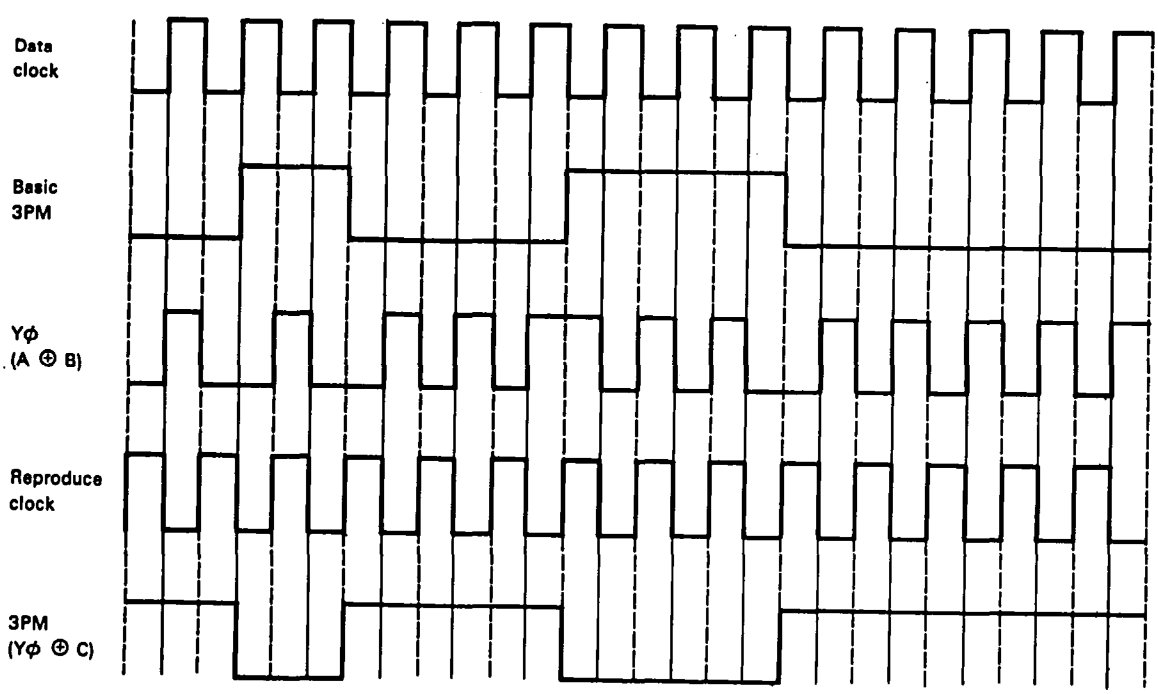

Figure 12–10.—Yφ waveform for low data rates.

SAFETY MARGINS

Before leaving the theoretical aspects of 3PM coding, it is appropriate to discuss briefly some of the less obvious reasons for wishing to extend the maximum packing density beyond the traditional limits. Major users of tape will already have calculated for themselves what a 30 percent saving in tape usage would mean to them, but there are other benefits also. Some of these, if not all, will be relevant to most users.

(1) *Recording and reproducing at different tape speeds.*—It is generally found that with any code if the packing density is maximized at one particular speed by adjustment of record current and bias (if used), data cannot necessarily be reproduced over the entire speed range of the recorder. Even if only standard tape speeds (suitably equalized) are used in the forward direction, it is often necessary to make an allowance of 1 to 2 kbpi to accommodate this problem.

(2) *Recording and reproducing at nonstandard speeds.*—The problem mentioned in (1) is compounded at nonstandard (intermediate) speeds where equalization may be less than ideal. If only the "nearest" equalizer may be used and no adjustments are permitted, then typically the maximum packing density drops by about 15 percent for a 35 percent change in tape speed from that at which the equalization was optimized.

(3) *Reverse reproduce.*—Assuming reverse phase equalization is provided and that the coding format is designed to be read in both directions (including error detection), it is still desirable to make a reduction in packing density of about 10 percent.

(4) *Recorder-recorder compatibility (crossplay).*—It is known that all codes suffer to some extent from a loss of usable packing density when universal crossplay is required. Therefore, a safety margin of approximately 5 percent should be allowed, even if all recorders are of the same type and vintage.

(5) *Tolerance to setting inaccuracies and changes in operating conditions.*—If several recorders are to be used in a network under operational conditions by a number of different technicians, it is considered unacceptable that the performance should be specified in such a way that it can be maintained only by frequent "knife-edge" adjustments so safety margins and fundamental immunity to these problems must be provided. It is well known that the majority of problems occur at the high-frequency, short-wavelength end of the scale (changes in bandedge output with time, dropout susceptibility, phase equalization, etc.). It follows that the more the absolute performance can be derated, the more stable and troublefree should be system operation.

For example, if a 3PM recording system could pack data at, say, 45 kbpi under ideal conditions, then we could derate that figure by 30 percent to accommodate some or all of the five points mentioned and still be recording at around 30 kbpi.

On the other hand, a recording code rated at 30 kbpi might have to be downgraded to, say, 20 to 25 kbpi to solve the same problems. In practice, the user of such a system is probably accepting the need for frequent adjustment to force up the packing density. He would certainly find operational (and cost) benefits from using a code such as 3PM.

Typical eye patterns are shown in figure 12–11, and power density spectral curves are given in figure 12–12.

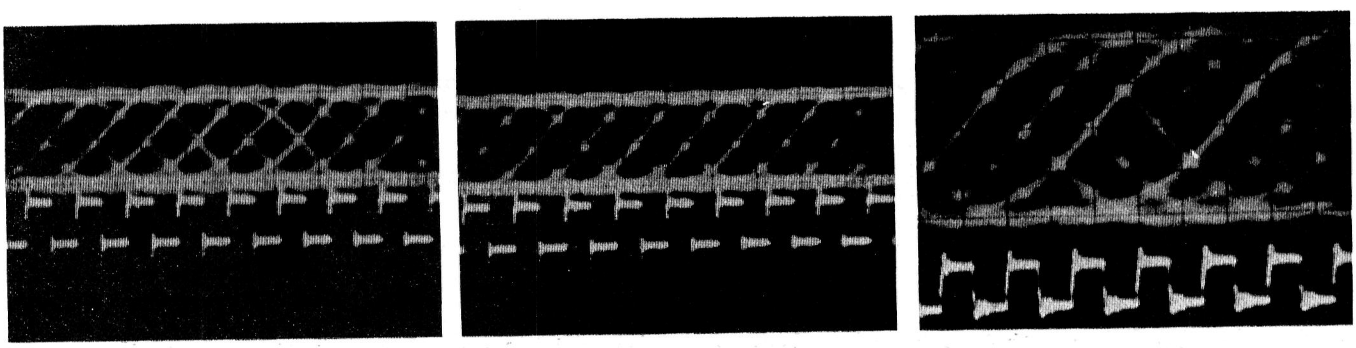

Tape speed	15 ips
Data density	29 kbpi
Data rate	435 kbps
Data	Pseudorandom noise
Bit synchronization shown	2 × bit frequency clock
Sweep speed	1 μs/cm
Record mode	Saturation

(*a*)

(*b*)

Tape speed	15 ips
Data density	45 kbpi
Data rate	675 kbps
Data	Pseudorandom noise
Bit synchronization shown	2 × bit frequency clock
Sweep speed	0.5 μs/cm
Record mode	Saturation

(*c*)

Figure 12–11.—Typical eye patterns for 3PM. (*a*) Forward reproduce. (*b*) Reverse reproduce of (*a*). (*c*) Forward reproduce with different parameters.

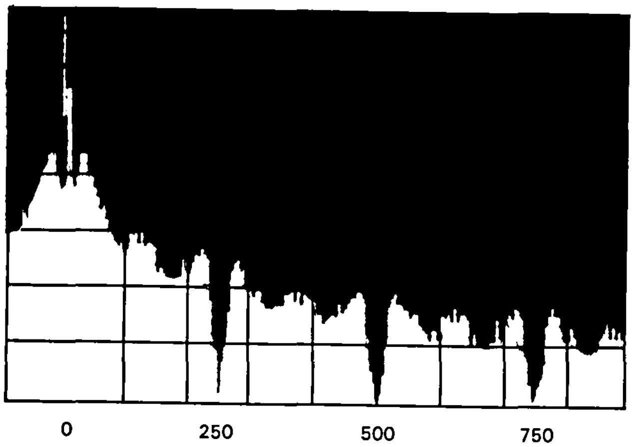

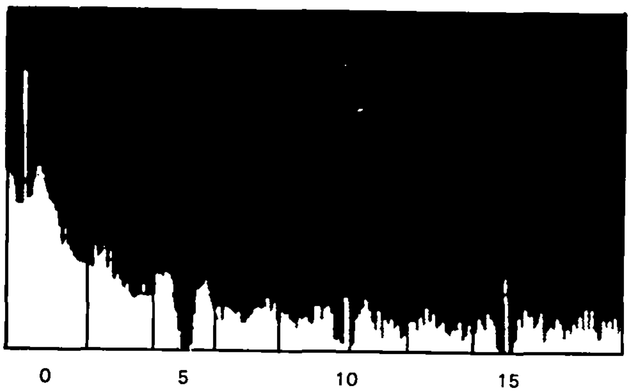

Figure 12–12.—Typical spectral distribution curves. (260 pseudorandom data bits, 16-bit cyclic redundancy check (CRC) plus 10-bit synchronization word, repeated in 286-bit block length.) (*a*) Data clock = 125 kbps. (*b*) Data clock = 2.5 Mbps.

BIT ERROR RATE

If we assume that the bit error rate (BER) performance of a well-engineered system is related predominantly to momentary discontinuities at the tape/head interface (dropouts, etc.), we can draw some rough comparisons for BER with 3PM compared with other codes.

If a 3PM system is writing data at 30 kbpi, then the transition density is 20 000 transitions/in., which means that its dropout performance will be roughly equal to an NRZ system working at 20 kbpi.

Similarly, working at over 40 kbpi, the 3PM recorder will have a BER equivalent to an NRZ system working at around 27 kbpi.

Typical "uncorrected" BER's are given in table 12-3. We can use a few percent of our increased packing density capability with 3PM to provide error detection and correction. Using a 6 percent longitudinal overhead (16 CRC bits per 260 data bits), it is possible to achieve BER improvement factors on the order of 10^3 or greater.

Table 12-3.—*Typical Uncorrected BER's With Ampex 797 Tapes*[a]

No. of tracks	Packing density	
	30 kbpi	40 kbpi
14	1×10^{-7}	3×10^{-7}
28	3×10^{-7}	5×10^{-7}

[a]Improvement of 3 orders of magnitude or greater is possible with error correction.

TYPICAL 3PM FORMAT

The complete parallel recording format used in a typical 3PM system is shown in figure 12–13. Data are blocked into 260 bit blocks and compressed to accommodate the unique 10-bit block marker (synchronizing word) and a 16-bit CRC character. The 260 data bits plus 16 CRC bits are encoded in 3PM ($276 \div 3 = 92$ bytes). Lateral parity tracks are treated exactly like data for the purpose of recording.

A TYPICAL 3PM SYSTEM

Figure 12–14 shows a typical high data rate serial HDDR formatting/recording system. Figure 12–15 shows its basic operation in more detail. The input and output interfaces will often be custom-designed to accommodate specific user requirements in terms of serial data rate and number of tracks over which the data are to be fanned out to accommodate minimum recording duration, maximize tape economy, etc. A lateral parity bit stream is developed at the same time as serial-to-parallel conversion takes place, and this parity channel is subsequently treated exactly as any other data channel throughout the system.

The parallel data and parity channels are blocked into 260-bit blocks plus 16-bit CRC character and 10-bit block marker (synchronizing word) in the stuffing and

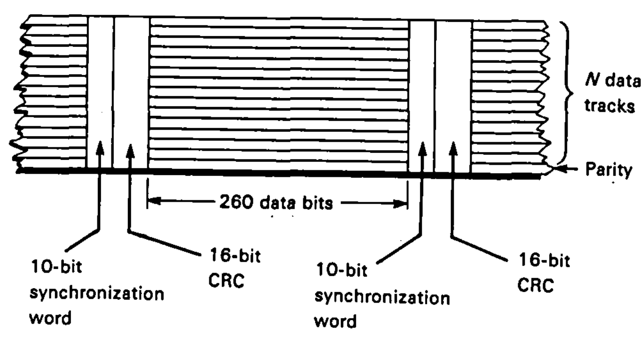

Figure 12–13.—3PM recording format.

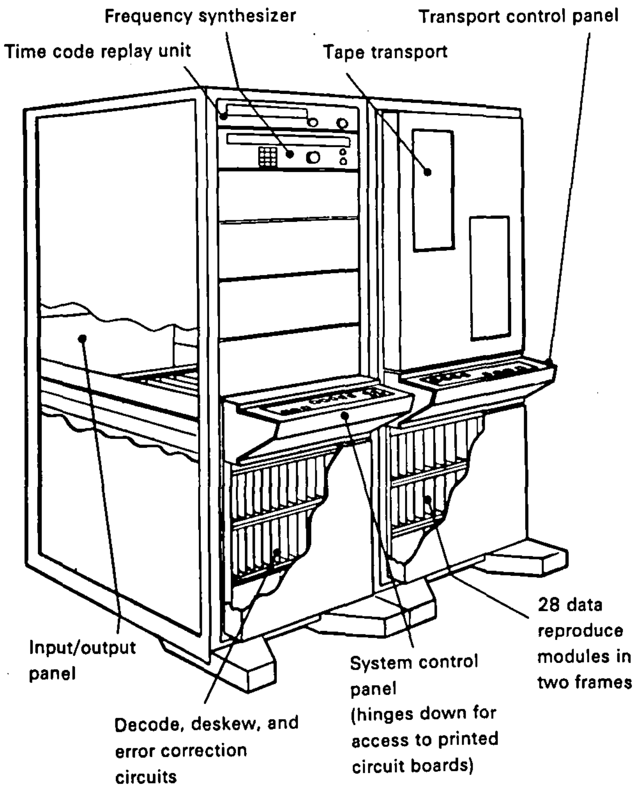

Figure 12–14.—Typical high data rate system configuration.

encoding modules. (The CRC is encoded into 3PM along with the data bits.)

The encoded waveform is recorded by conventional direct recording modules, using standard IRIG wideband II record headstacks. The number of tracks chosen (up to 42) will generally depend upon such factors as user preference and the number of tracks over which data must be fanned out.

Direct reproduce modules amplify and equalize the reproduced data before decoding can take place. Reproduce modules can either be of the conventional type with unidirectional equalization in octave steps or of a new type capable of bidirectional operation together with equalizers controlled by the frequency translator at nonstandard tape speeds. This latter feature insures that high packing densities can be maintained even at intermediate speeds.

Following equalization, data are synchronized in the 3PM/CRC decoder and bit synchronization module. Two versions are available. One has conventional manual adjustment of the phase lock loop synchronization circuits, the other incorporates a microprocessor-based automatic adjustment system involving no manual adjustments if the bit rate should suddenly change. This feature is particularly useful for applications in which bit rate changes are a frequent occurrence.

The parallel data channels are deskewed and checked for longitudinal parity errors before being routed to the destuffing and error correction circuits. Once error correction has taken place, the parallel bit streams are once more combined to form a high-rate serial bit stream.

The tape speed control system is of particular interest because the system is capable of calculating automatically the tape speed given the proposed input rate and desired linear packing density. If the input data rate should be slowly varying, constant packing density can be maintained by deriving a capstan tape speed control signal from the input data clock.

There are a total of three possible sources for the controlling (reference) input:

(1) The tape transport's built-in crystal reference oscillator.

(2) A similar, but externally supplied, reference frequency. This can be varied to produce any tape speed within the range of the tape transport.

(3) A reference frequency derived from the input data bit stream as processed by the variable frequency translator.

The system block diagram also shows the self-check and calibration facility provided. This comprises a built-in pseudorandom word generator the input of which is clocked out at any frequency selected by means of the frequency synthesizer. This bit sequence is applied to the stuffing module input and passed through the entire signal chain, either via tape record/reproduce or bypassing the actual record/reproduce process by means of the electronics-electronics (E-E) facility. The resulting output is compared with the general sequence on a bit-to-bit basis and any bit errors are counted, the count being displayed on the built-in digital indicator. Three sampling periods are switch selectable: 5×10^6 clock periods, 5×10^8 clock periods, or infinity. System control is by means of two sloping control panels shown in figure 12–14.

The right-hand unit (fig. 12–16) is basically a conventional tape transport control unit except that tape speed and servo parameters may be governed at the system control panel. The control enable switch is provided to select either local control or remote control via the TTL or IEEE-488 interfaces.

A convenient visual indication of the operation of the HDDR electronics is given by the array of light emitting diodes (one per channel) that indicate CRC errors during reproduce. Because these displays are operational regardless of whether the error correction system is enabled, it is possible to tell very easily whether a certain channel is behaving erratically.

The left-hand panel contains the controls necessary to operate the HDDR electronics (fig. 12–17). The extreme left block will generally be specifically designed with the

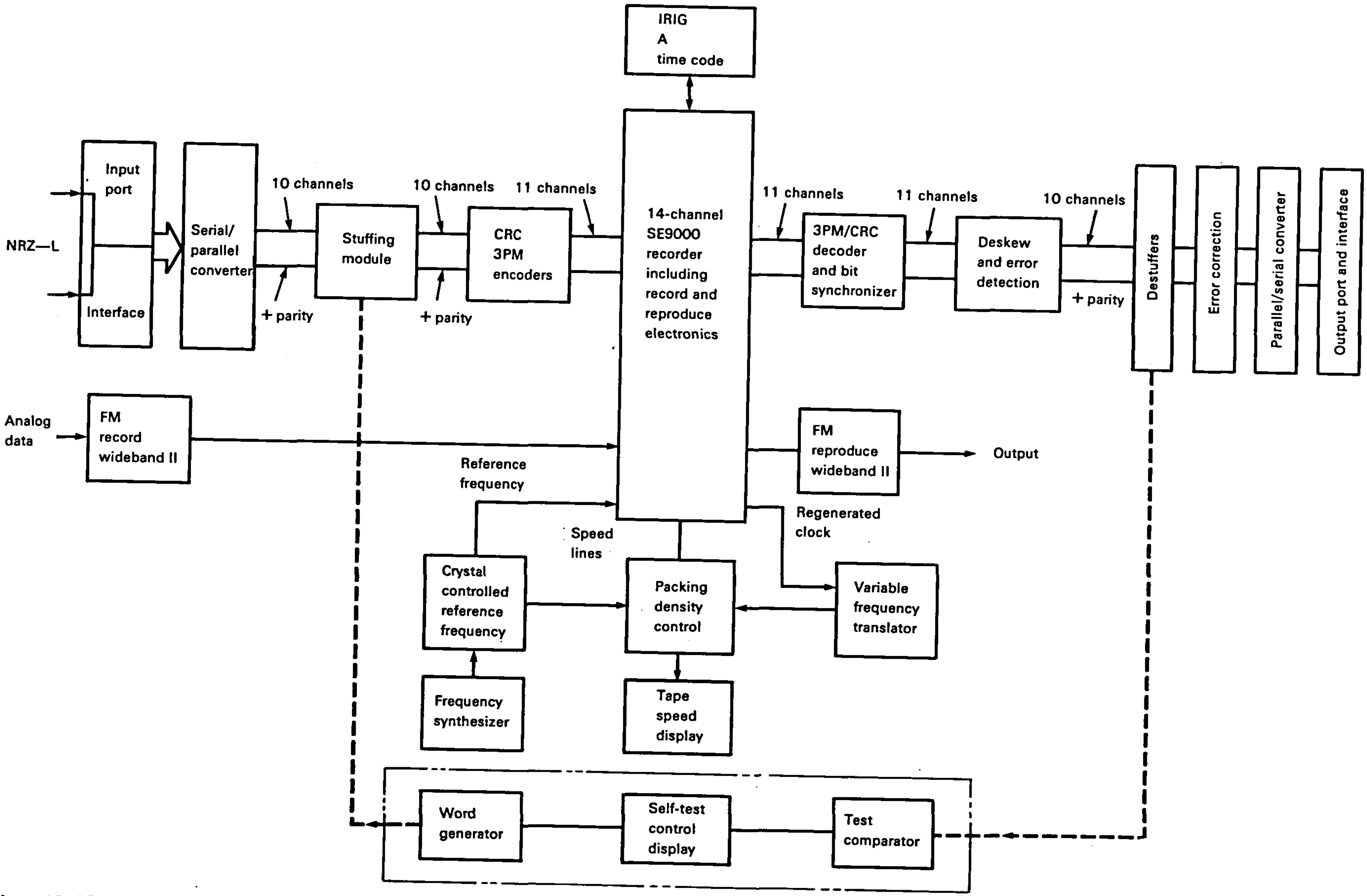

Figure 12–15.—System block diagram.

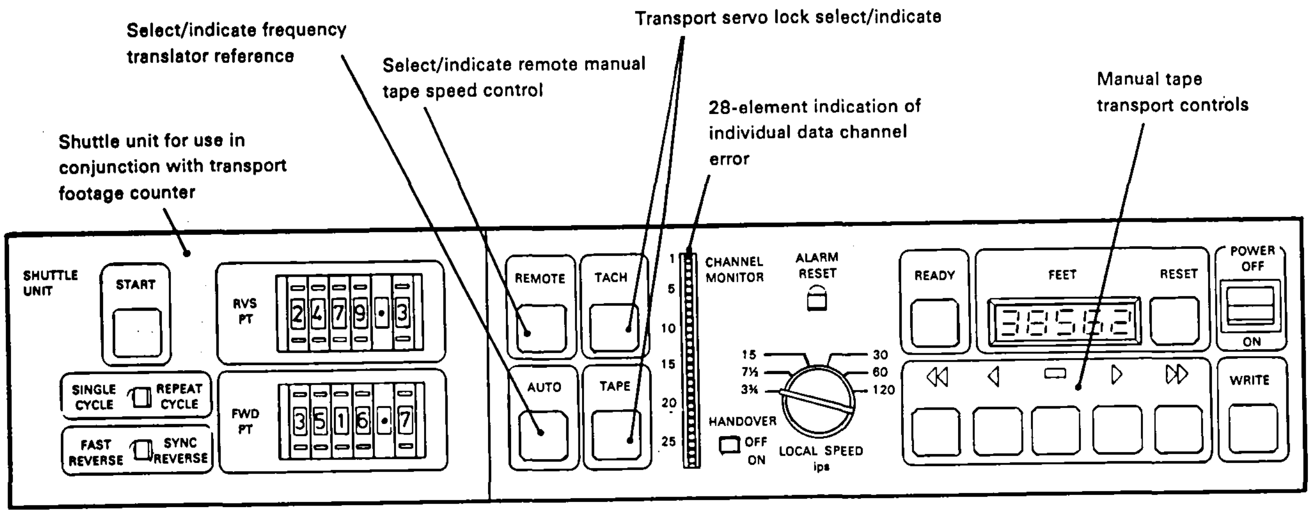

Figure 12-16.—Transport control panel.

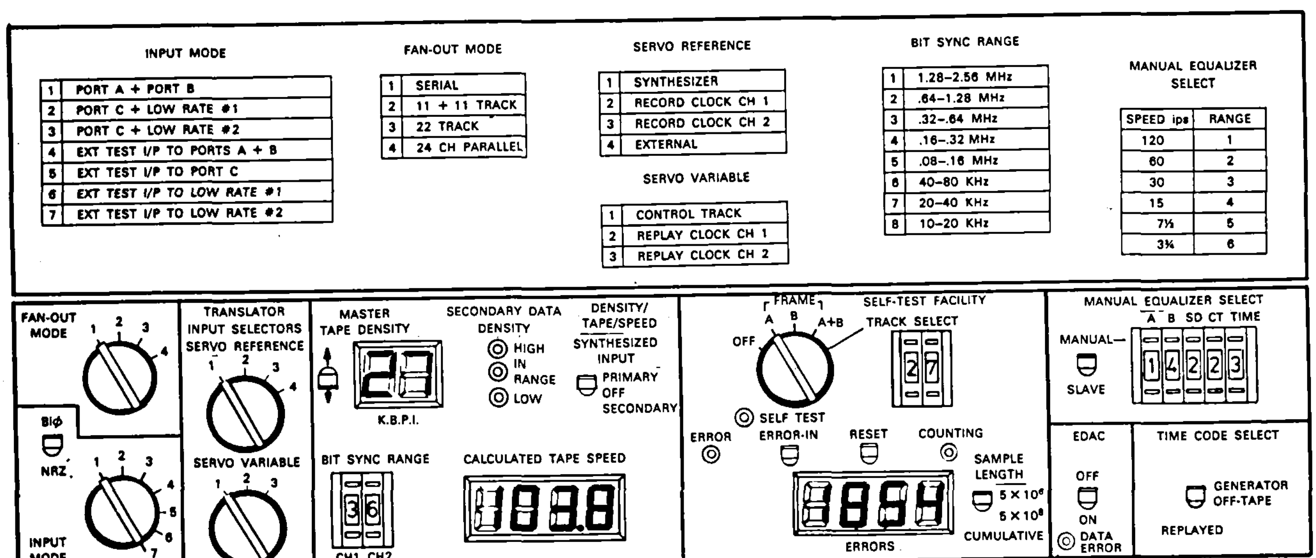

Figure 12-17.—System control panel.

user's inputs in mind. It could be as simple as a HI/LO data rate switch (as illustrated in fig. 12-18) or a method of selecting groups of asynchronous data streams presented to the recorder in more than one input code.

The large block in the upper center contains selectors for automatically calculating tape speed, based on a desired packing density and known input rate. If only one data stream is to be recorded, this simply involves applying either the actual data to the system input, or a simulated data clock derived from the synthesizer (switch selectable). The desired bit packing density is selected by the up/down pushbutton switches, and a microprocessor determines and displays the resultant tape speed.

If two asynchronous bit streams are to be recorded in parallel on separate groups of tracks, then the procedure for selecting tape speed is slightly different. If the two bit rates are considerably different, it could be possible to select a packing density/tape speed combination for one channel that produces a tape speed unacceptable to the other (outside its packing density/tape speed range). To avoid this, the two clocks (or simulated clocks) are applied to the inputs and one is taken to be the "primary" channel. A packing density is selected and indicated as before. Additional indicators show whether the resultant packing density for the other channel is within its operating range. If it is too high or too low, the conflict is overcome by changing another packing density/tape speed for the primary channel until the second situation is accommodated.

The middle/lower block is generally system oriented depending upon operational requirements. In the il-

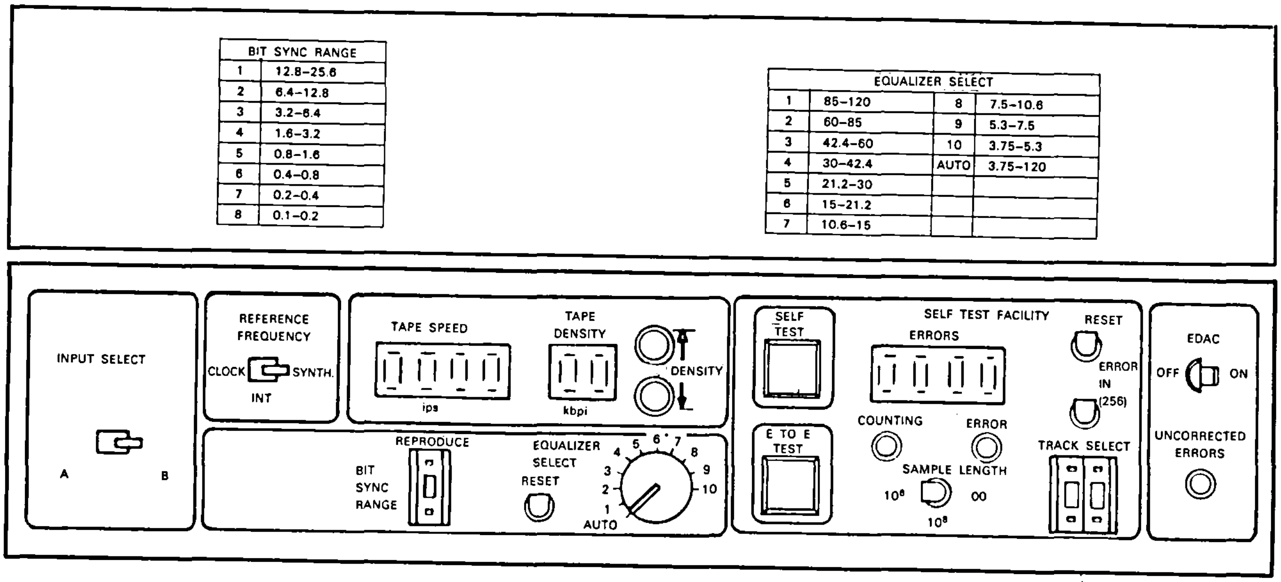

Figure 12–18.—Alternate system control panel.

lustration, the automatic equalization facility is shown along with a method of overriding the automatic bit synchronizing feature.

The self-test facility has already been discussed.

The extreme right block is associated with error detection and correction (EDAC). A correction disable switch is provided together with an indication of when uncorrected errors are occurring. The visual relationship between the individual channel CRC error indicators and the uncorrected error indicator shows very clearly the health of the system as it processes data and how well the error correction system is coping with any raw errors. For example, it would be possible to tell immediately that one channel was not functioning at all and the error correction system was working full time to correct the data on that track.

A brief technical specification of the SE9000 system HDDR is as follows:

Tape speeds	120 to 3¾ ips (1⅞ and 15/16 ips optional)
Recording formats	7 track (1/2 in.) 14 track (1 in.) 28 track (1 in.) 42 track (1 in.)
Coding format	3 PM/Yϕ
Block length	260 bits
Synchronizing word	Unique 10-bit word
Longitudinal parity	16-bit polynominal CRC
Lateral parity	One or two parallel tracks depending upon system configuration
Serial overhead	10 percent
Parallel overhead	Dependent upon number of parallel data tracks used and number of error correction tracks; typically 9 percent for 28-track system
Maximum bit packing density (gross)	Up to 45 kbpi with standard wideband heads and tape, depending upon mode of operation
Data rate	50 Mbps at 78 ips using 22 track fanout; other tape speed/fanout combinations proportional
Minimum data rate (reproduce)	40 kbps per track with 3 PM 5 kbps per track with Yϕ
Bit error rates	Better than 1 in 10^6 (uncorrected) Better than 1 in 10^8 (corrected)
Input/outputs	Transistor-to-transister logic (TTL) or emitter-to-collector logic (ECL)
Error correction	Standard: 16-bit CRC plus one or two lateral correction channels
Analog channel	FM or direct recording channels can be used in parallel with HDDR data channels

A LOOK AHEAD

3PM coding as available for longitudinal instrumentation recording represents an important breakthrough in terms of increased linear packing density using standard heads and tape. Using 40 tracks for data plus 2 parity tracks, it is possible to pack safely in excess of 40 kbpi per track, giving a total throughput at 120 ips of almost

200 Mbps. (Note that 40 kbpi in 3PM is equivalent to a transition density of only 26.6 kbpi—safely inside current wideband recording limits.)

There are manufacturers who have elected to achieve additional packing density by means of half-wave length recording. Assuming that 50 kbpi can be recorded using such a system, then further development of the 3PM system could, in fact, result in achieving the "best of both worlds": 50 ktpi represents 50 + 50 percent, or 75 kbpi using 3PM. When that is multiplied by 40 tracks and 240 ips, we have 720 Mbps. The uncorrected error rate for such a system might be no better than 1 in 10^4 or 10^5, but because error correction is becoming a standard component of an HDDR system, we would probably be talking in terms of a "corrected" BER in the region of 1 in 10^8.

APPENDIX—3-POSITION MODULATION FORMAT—AN ENGINEERING VIEWPOINT

Geoffrey C. Nottley
Thorn EMI Technology Incorporated

This appendix discusses the 3PM format from the engineering point of view, giving the rationale behind the selection of the basic coding scheme and its implementation in HDDR applications. Key parameters such as bandwidth sensitivity, adjustment margins, SNR dependence, tolerance to phase nonlinearity, and error correction strategies are discussed in detail.

The selection of our new HDDR format began with a detailed analysis of system requirements based partly on Thorn EMI's 10 years of experience in the field, but also on a critical study of trends in the industry. Our studies included future user requirements, developments in hardware and tape technology, and a rigorous return to basics, placing ourselves in the user's position and attempting to establish the most desirable features of a general purpose, easy to use system.

Because HDDR is being adopted for an increasingly varied range of applications, the basic rules of economics dictate that our proposed system should be suitable for the widest number of users. This meant that we had to incorporate considerable flexibility within the system without imposing price penalties that would render the system noncompetitive.

SYSTEM REQUIREMENTS

The outcome of our studies was the following list of features considered essential or desirable:

(1) Suitability for both parallel and serial operation
(2) Bidirectional (time-inverse) capacity
(3) Low overhead synchronizing word
(4) Low overhead EDAC suitable for both individual bit errors and error bursts
(5) Wide range, continuously variable time translation
(6) Low-rate operation without the need to reconfigure
(7) High data packing with large adjustment margins
(8) Tolerance to variation in off-tape conditions
(9) Adjustment-free operation regardless of changes in operating conditions
(10) Crossplay
(11) Suitability for use with standard analog (IRIG) data channels and headstacks.

No doubt the list is incomplete, but it provided a good starting point. The order in which the various parameters are listed is arbitrary because the weighting applied to each varies with the application.

CHOICE OF 3PM

It was evident that despite considerable debate during the last 5 years or so, no traditional coding scheme had emerged as being clearly superior to all others for a wide range of applications. Undoubtedly each has its intrinsic good and bad points, but these have sometimes been masked by practical implementation in terms of system hardware. (When reading the literature it is often difficult to determine whether we are learning about the fundamental properties of a particular code or the excellence or shortcomings of its associated electronics.) For example, what is the point of belaboring the fact that a certain code is dc free if a certain amount of dc content can be tolerated and allowed by standard design techniques. Similarly, why draw attention to the point that a certain code needs a more sophisticated clock recovery circuit if such a circuit is available and simple and cheap to implement.

Clearly we had to get back to basics, sift and disregard the traditional dogma, and develop a new rationale based on our objective to record as many of the users' data bits as possible in the smallest possible space and with the minimum of user involvement. It was important also that the system should have the highest possible data integrity.

It was traditional but incorrect to assume that the best data packing density that could be achieved was 1 flux transition per recorded bit. (NRZ—L, NRZ—M, E-NRZ, R-NRZ, DM—M and Miller squared (M^2) are

all examples of this.) We often read that the Nyquist data packing density is twice the upper bandedge frequency. By this thought process, the only way that data density could be increased would be to increase the upper bandedge frequency for a given tape speed by reducing the gap length in the headstack and implementing the associated changes to electronic components. Because the vast majority of problems in a magnetic tape recorder involve the difficulty of recording, resolving, reproducing, and equalizing the shortest wavelengths, this is without question an undesirable approach.

A better approach is to adopt one of the codes that, in effect, uses less than 1 flux transition per recorded bit (figure 12–19). The code we selected is known as 3PM and was first discussed in a paper by George Jacoby of Sperry Univac in 1976 (ref. 12–3).

The important feature of 3PM code is that, as with DM codes, a finite number of intervals are possible (1½, 2, 2½, 3, 3½, 4, 4½, 5, 5½, and 6 write clock periods), but because the shortest interval is 1½ periods, it can be seen that the maximum transition density is only 66⅔ percent of the data density, unlike most conventional codes in which transition density and data density are numerically the same. Theoretically this means that the 3PM code should be capable of recording and reproducing at data densities far beyond the "Nyquist maximum," but as we shall see later, the code has more subtle advantages than low transition density alone.

SYNCHRONIZATION

Unlike some serial recording systems that rely on random synchronization on certain bit patterns, which may or may not occur naturally at sufficient frequency, it is found desirable to use the unique block marker technique. By this means, regular rechecking of phase and polarity is assured. This is an important change in philosophy compared with earlier designs where "code efficiency" was considered to be sacrosanct.

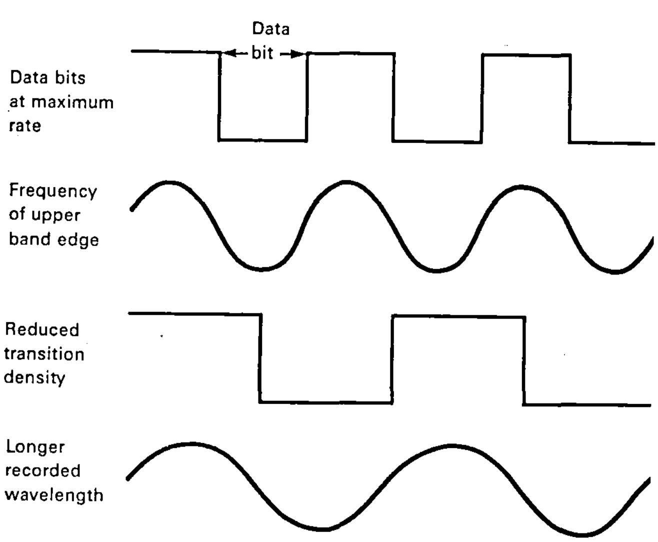

Figure 12–19.—Reducing transition density.

ERROR DETECTION

The longitudinal format is completed by the addition of a 16-bit CRC character immediately following each 260 data bits before encoding. The mathematics behind the choice of this type of check character is outside the scope of this paper, but its ability to detect both individual and burst errors within its associated data block without giving false alarms is extraordinarily good.

During the recording process, data are broken into blocks of 260 data bits. The 260-bit block is treated as a binary number that is then divided by a "generator" having the expression $x^{16} + x^{15} + 5x + x + 1$ (see chapter 3). At the end of the division process, the 16-digit remainder is recorded immediately following the data block. During reproduction, each 260-bit block is divided by the same generator and the resultant remainder is compared with that which was recorded. If the two remainders agree, the probability that the data block was recorded and reproduced without error is extremely high. Conversely, if the remainders differ, the probability that one or more errors occurred is extremely high. This system is good for detecting error bursts as well as individual errors. When used in conjunction with a lateral parity track (fig. 12-20), this system gives error rate improvements of several orders of magnitude. Longitudinal polynomial error checking is used for detecting errors only. Lateral parity tracks are used to correct errors that have been detected by the longitudinal CRC. If an error is detected in a track, the whole track is recalculated from other data tracks and the parity track, because all columns must contain an odd number of "1's."

	Track 1	1 1 0 0 1 0 1 0
	Track 2	0 1 0 1 0 1 1 0
	Track 3	0 0 0 1 0 1 0 1
(*a*)	Odd parity	0 1 1 1 0 1 1 0

	Track 1	1 0 1 0 1 1 0 1 1
	Track 2 (with error)	X X X X X X X X X
	Track 3	0 0 1 0 0 1 0 0 1
	Odd parity	1 0 0 1 0 0 1 0 1
(*b*)	Track 2 (recalculated)	1 1 1 0 0 1 0 0 1

Figure 12–20.—Lateral parity correction. (*a*) Three data tracks plus parity track. (*b*) Recalculation of data in a track with error.

It is now no longer cost effective to use premium-priced certified tapes for the majority of applications where corrected error rates in the region of 1 in 10^8 or 10^9 are required, although we would obviously not question their effect on the "raw" error rate if properly maintained.

COMPLETE FORMAT

Figure 12–13 shows the complete 3PM format. The number of parallel data channels can vary depending upon the application. The lateral parity channel, although desirable, is optional.

Because the longitudinal format is fixed for all applications, the only parameter that must be agreed upon by interchange parties is the value of *N*. The recording facility can fan out the data over any suitable number of tracks, depending upon the application; the reproducing facility only needs to have that many channels available and a compatible fan-in capability to reproduce the tapes.

BANDWIDTH

Figures 12–21 to 12–23 show the eye patterns for DM, R-NRZ, and 3PM at various packing densities. For the

(*a*)

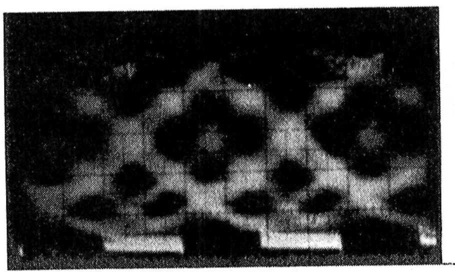

(*b*)

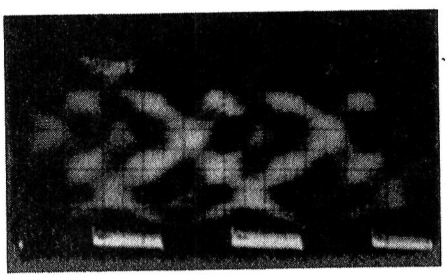

(*c*)

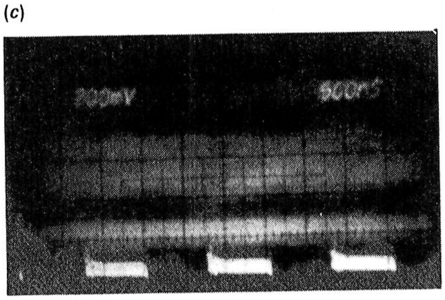

(*d*)

Figure 12–21.—DM, 15 ips. (CF = capability factor.) (*a*) 30 kbpi; CF, 1:3. (*b*) 35 kbpi; CF, 1:2 (*c*) 40 kbpi; CF, unresolvable. (*d*) 45 kbpi; CF, unresolvable.

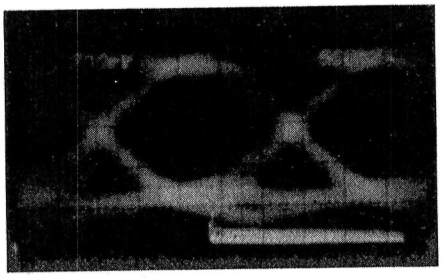

(*a*)

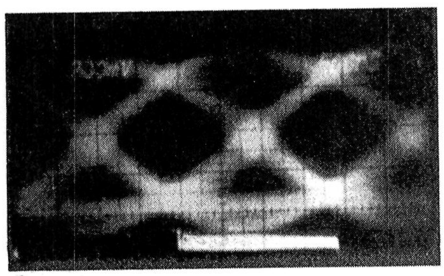

(*b*)

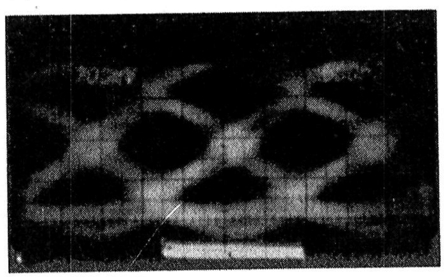

(*c*)

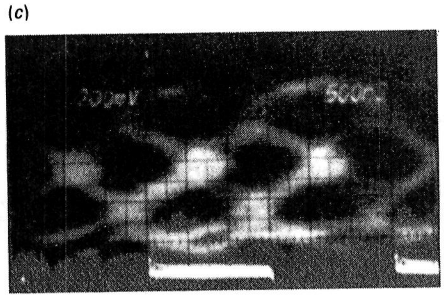

(*d*)

Figure 12–22.—R-NRZ, 15 ips. (*a*) 30 kbpi; CF, 1:6. (*b*) 35 kbpi; CF, 1:4. (*c*) 40 kbpi; CF, 1:3. (*d*) 45 kbpi; CF, 1:2.4.

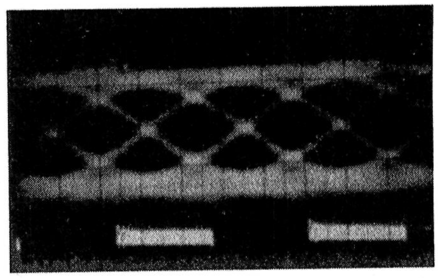

(*a*)

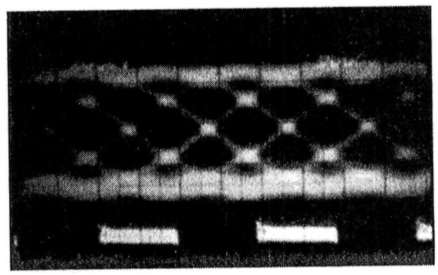

(*b*)

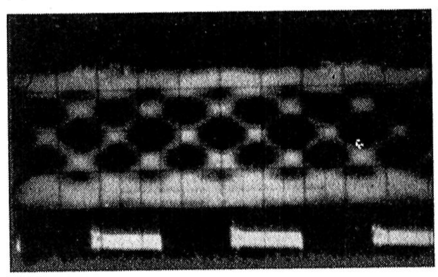

(*c*)

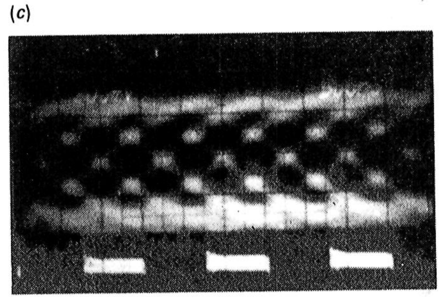

(*d*)

Figure 12–23.—3PM, 15 ips. (*a*) 30 kbpi; CF, 1:6.1. (*b*) 35 kbpi; CF, 1:6. (*c*) 40 kbpi; CF, 1:4.3. (*d*) 45 kbpi; CF, 1:3.8.

purpose of this experiment, we used a standard IRIG wideband II direct record/reproduce channel set up to IRIG 106-80 standards (ref. 12-2) using Ampex 797 tape. It is acknowledged that some optimization might be possible in each case by readjusting the channel, but this was not done in the interests of direct comparison. As a means of comparison a capability factor CF (the ratio of trace thickness *a* to the total width of the eye *b* at the center of the waveform) was measured from the photographs, which were taken using a storage oscilloscope having the same sample time in each case (fig. 12-24). These ratios are summarized in figure 12-25. The comparison is crude, but the message is clear: 3PM lives up to its promise of more bits per linear inch of tape than the previously used codes when compared under the same conditions.

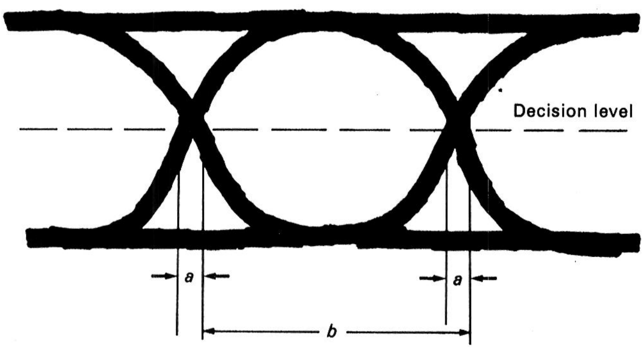

Figure 12-24.—Capability factor *b/a*. (*a* = uncertainty; *b* = bit or half bit period.)

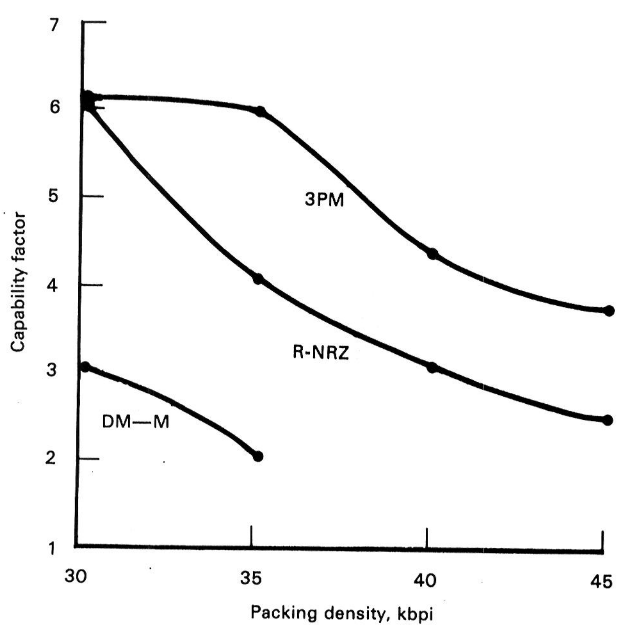

Figure 12-25.—Capability factor versus packing density for selected codes.

The fact that the new code can have transitions at both the bit cell ends and in the center of the bit cell immediately equates 3PM to DM and M² in some minds. As a result, a clock two times bit frequency has to be provided from the bit synchronizer rather than the bit frequency for NRZ-based codes. However, this is where the similarity ends. As can be seen very clearly from figure 12-26, although the clock period is halved compared to NRZ (that is, a decision window of ± 25 percent is necessary) the pulse crowding and other noise- and linearity-related effects are considerably reduced. This effect is noticeable even at densities as low as 30 kbpi and becomes of even greater significance as packing density is increased.

Figure 12-27 shows a typical wideband II reproduce head output frequency response. Shown on this curve is an approximation of the spread of fundamental frequencies present in various codes operating near their typical maximum data rates. Starting with E-NRZ, the spread of fundamental frequencies is from upper bandedge (UBE) to about 0.15 UBE: around 140 kHz. In a typical headstack, the output at UBE will be 15 ± 2

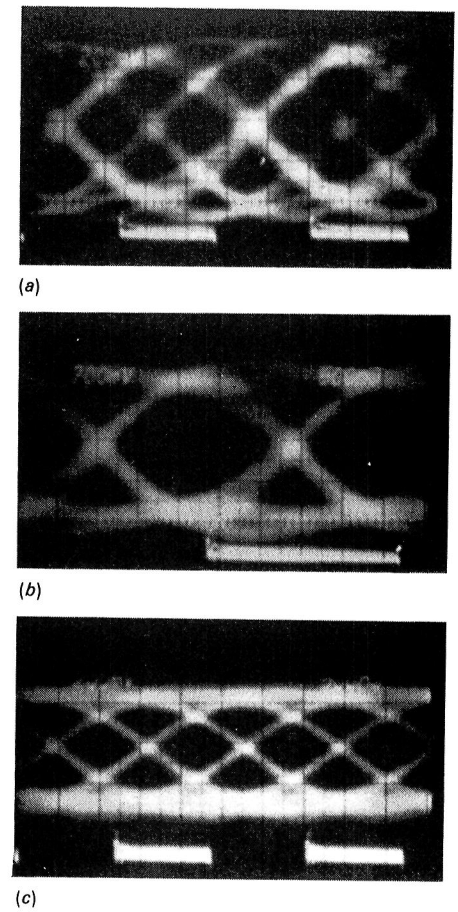

Figure 12-26.—Selected codes. (*a*) DM—M; CF, 1:3. (*b*) R-NRZ; CF, 1:6. (*c*) 3PM; CF, 1:6.1.

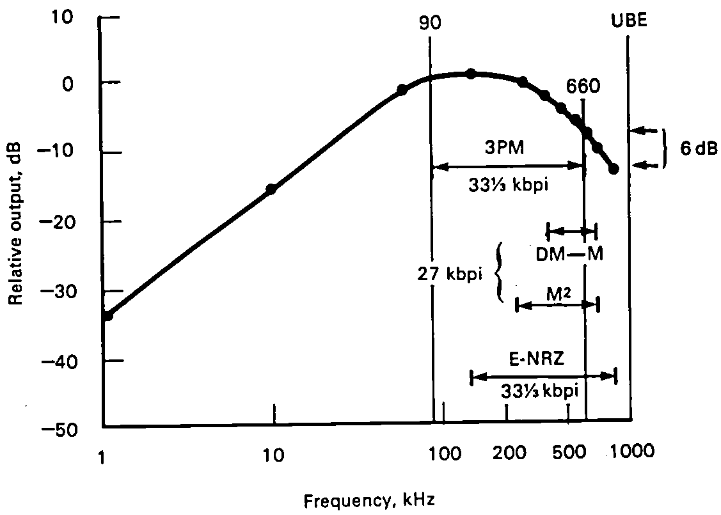

Figure 12–27.—Wideband II head output at 60 ips.

dB "down" on the peak output level, which occurs at about 0.15 UBE. Obviously, the amount of gain required at UBE to give a "flat" amplitude response amplifies the high-frequency content of the noise, but the ± 50 percent decision window that is possible with the code permits a total bit packing density in excess of 30 kbpi to be used reliably. (Note the word total—not all the recorded bits are actual data.)

It will be noticed that the spread of fundamentals for DM−M and M² is compressed considerably compared with E-NRZ. The ratio of minimum/maximum is 1:2 for DM−M and 1:3 for M². The upper bit packing density is considerably limited because the effect of a given noise level will be greater on a system with a ±25 percent window than one with a ±50 percent window, given that transitions can occur at the clock rate. This effect was clearly illustrated in figure 12–21.

The case of 3PM is somewhat different because transition density and bit packing density are not the same. The top frequency present in the 3PM waveform is only 66 percent of that which would be found in the other codes for a given data rate. This improves the situation in several ways:

(1) The head output at this frequency is 6 dB higher than at UBE, giving an improvement in signal-to-noise ratio of 6 dB.

(2) The frequencies involved are further away from the peak of the equalizer curve. For good pulse reproduction a linear phase characteristic (fig. 12–28) is required, and care is usually taken to provide a phase equalization adjustment in the reproduce chain. This is usually only effective at the middle bandwidths. At the peak in the equalization curve (which is generally a tuned circuit), the phase characteristic departs violently from any sort of linearity.

(3) The effect on spacing loss is reduced. The well-

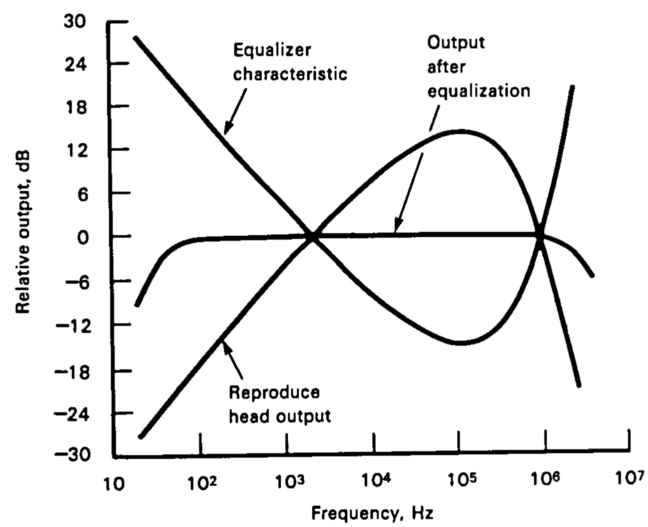

Figure 12–28.—Output versus frequency characteristic of a wideband reproduce head, electronic equalization, and resultant equalizer output.

known spacing loss of $55d/\lambda$ dB is improved in the direct ratio of 2:3.

All these factors contribute to the clean appearance of the 3PM waveform. As packing density is increased, the spectra move down the ever-steepening and unequalized characteristic. The waveforms become more indeterminate. It can be seen that the NRZ waveform deteriorates faster than 3PM, with DM−M having degenerated at a much earlier point.

At the time the photographs shown in figures 12–21 to 12–23 were taken, BER measurements using standard 2 MHz analog record and reproduce headstacks were made and are summarized in tables 12–4 and 12–5 and in figures 12–29 and 12–30.

First, BER's were taken using a standard direct re-

Table 12-4.—*Test 1: Direct Channel Setup According to IRIG 106-80 Standards*

Packing density, kbpi	Uncorrected BER × 10^{-6}		
	3PM	NRZ	DM–M
30	0	0	0
35	0.2	0.02	2.1
37	1.5	8.0	2 500
40	25.3	4 400	30 000
42	101	13 000	(a)
45	2300	33 000	(a)

[a]Synchronization lost.

Table 12-5.—*Test 2: Direct Channel Optimized for Minimum BER*

Packing density, kbpi	Uncorrected BER × 10^{-6}		
	3PM	NRZ	DM–M
30	0	0	0
35	0	0	0.2
37	0.1	0.01	4.0
40	2.3	15.8	2 100
42	2.5	45.3	11 000
45	27.6	7000	(a)
47	44.3	(a)	(a)

[a]Synchronization lost.

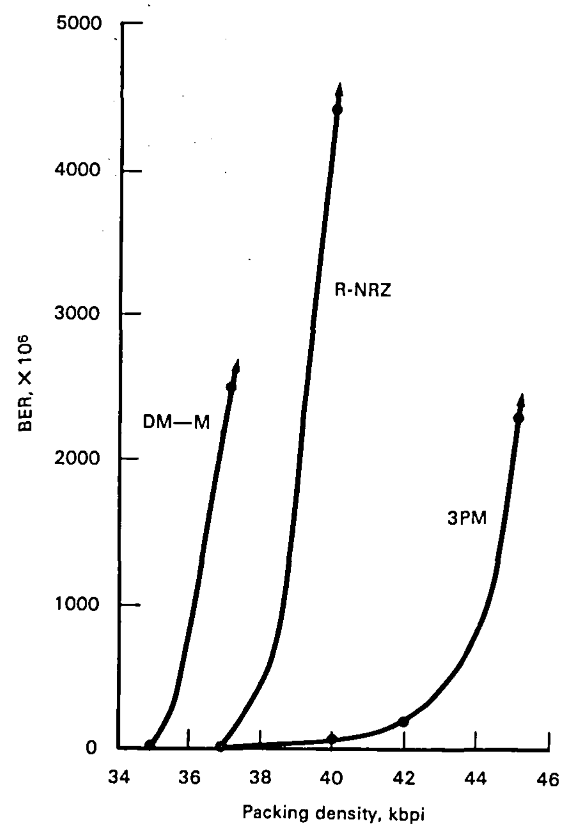

Figure 12-29.—Test 1: Direct channel setup according to IRIG 106–80 standards.

cording channel set up to IRIG 106-80 (ref. 12-2). Total errors were counted over 100 meters of tape, and these errors were divided by the total number of recorded bits. The tape used was Ampex 797, and the tape speed was 15 ips. (See fig. 12-29 and table 12-4.)

A second experiment was then conducted in which the settings of the direct channel were optimized for minimum BER, confirming that all three coding methods respond significantly to this procedure, but particularly 3PM, whose error rate dropped to 44.3 in 10^6 at 47 kbpi. (See fig. 12-30 and table 12-5.)

Last, BER's were taken using our specially designed record and reproduce modules, showing that it is important to design equalization circuits specifically for HDDR:

Packing density, kbpi	*Uncorrected BER, × 10^{-6}*
30	0
35	0.15
37	0.4
40	0.95
42	1.2
45	2.9
47	24.8

If 3PM is to be used at conventional data densities (e.g., 30 kbpi), we can take advantage of the fact that its spectrum is lower and optimize the channel by reducing the amount of high-frequency equalization, which reduces the signal-to-noise ratio still further and also has the important effect of improving phase response. Figure 12-31 compares the phase response of a conventional IRIG channel with one optimized for 30-kbpi 3PM.

The advantages shown for 3PM can be utilized in three ways:

(1) 3PM may be used at equivalent densities to NRZ with less critical operator settings.

(2) 3PM may be used at much higher densities than NRZ with somewhat reduced tolerance to setting errors.

(3) Some compromise between options (1) and (2) may be used—the exact compromise will depend upon the application.

LOW FREQUENCIES

It is possible that more has been written about dc content than any other single aspect of HDDR. There are those who feel that a code must be totally dc-free, while

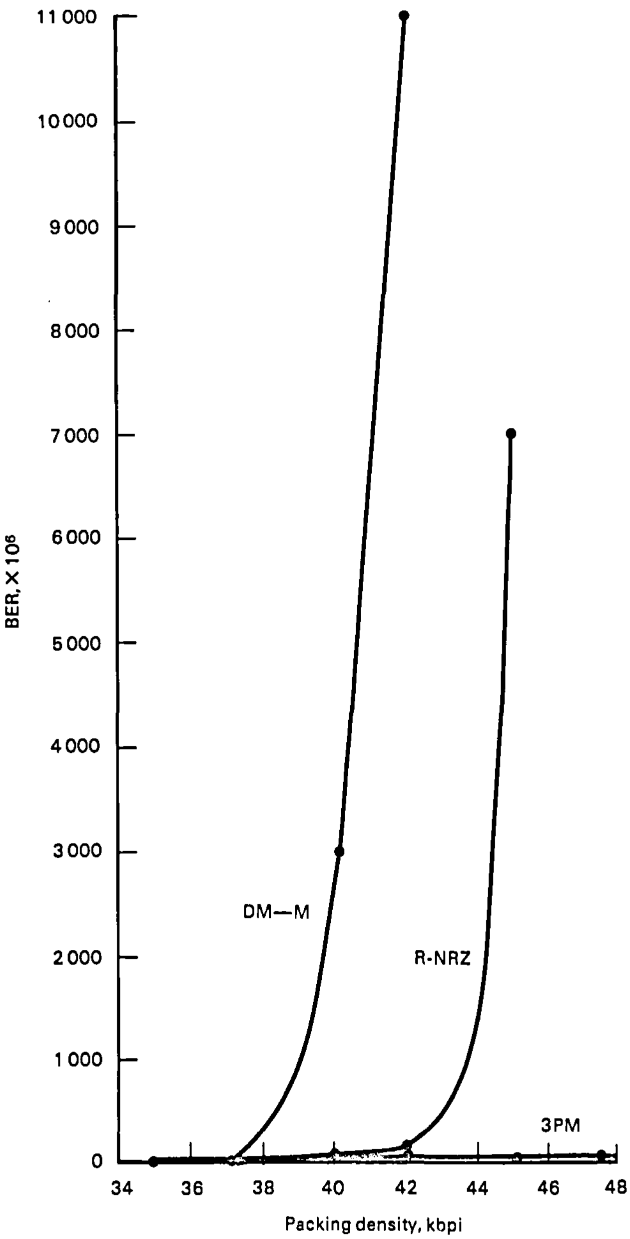

Figure 12–30.—Test 2: Direct channel optimized for minimum BER.

others point to the fact that there are systems operating successfully with considerable dc content in their recorded waveform.

Our feeling is that a typical HDDR waveform lends itself to standard dc restoration techniques provided that a minimum transition density can be guaranteed.

Looking again at figure 12–26 and remembering that we chose a 7-bit interval for our block marker, the lowest fundamental frequency is around 0.15 UBE.

We use a standard half double-peak dc restoration technique, which has proved entirely satisfactory under operational conditions down to bit rates as low as 40 kbps. We see no reason to employ bandwidth compres-

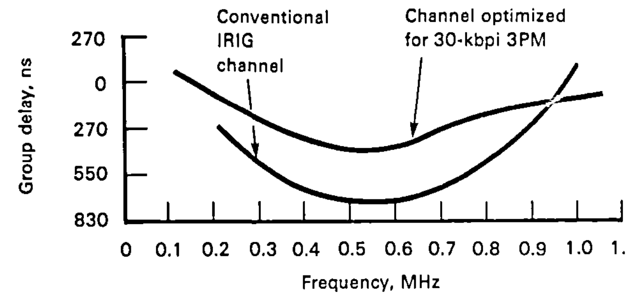

Figure 12–31.—Group delay versus frequency. (Reference frequency: 100 kHz at 60 ips.)

sion to the point where dc content is eliminated completely.

IRIG's recommendations for recording serial data streams were duly noted, but for our parallel recorder we were anxious not to have two entirely different signal processing chains for high and low data rates. We have been associated with a number of projects where high and low rates must be handled simultaneously and we felt that it was undesirable to have to reconfigure the system as bit rates changed. Our solution was to produce a variation of the basic 3PM code, called Yϕ. Because Yϕ behaves very much like biphase, we cannot claim any originality for the waveform itself. But what makes this approach of interest is that both high and low data rates can be handled by a common signal formatting chain without the need to reconfigure.

SERIAL DATA

The 3PM/Yϕ coding technique is also ideal for serial recording for those applications where the "random" synchronization problems associated with some zero overhead codes are unacceptable. We would not recommend a system that relies on a certain bit sequence to occur in the data stream for synchronization to be possible. It is therefore better to use a few of the extra bits available with 3PM on a positive synchronization word.

The 16-bit CRC is also recommended for serial application as a positive indication of data integrity (not to be confused with the rather arbitary "confidence monitoring" associated with simple parity systems).

For serial applications where two recording tracks are available per data channel, we record on two tracks and use the CRC's to choose which data block to clock out. Because probability of simultaneous errors is low, the remaining error count is extremely low.

CONCLUSION

Returning to our list of system requirements, we see its close match to the 3PM format:

(1) All features necessary for both parallel and serial operation.

(2) Bidirectional block marker and CRC calculation in both directions.

(3) Low overhead synchronizing word: 3.85 percent.

(4) Low overhead error detection: 6.15 percent; low overhead error correction: typically 9 percent.

(5) Wide-range, continuously variable time translation.

(6) Low rate operation without need to reconfigure with $Y\phi$.

(7) High data packing with large adjustment margins with considerably less susceptibility to short-wavelength effects and maladjustments of record and reproduce settings.

(8) Tolerance to variations in off-tape conditions (the longer minimum recorded wavelengths significantly reduce this problem).

(9) Adjustment-free operation with no recalibration or other manual intervention when recording or reproducing parameters change.

(10) Universal crossplay insured by longer minimum recorded wavelengths.

(11) Suitable for use with standard (IRIG) data channels and headstacks. Data packing densities and rate considerably in excess of those achieved with other HDDR recorders are possible. Naturally, if 3PM is used with optimized record and reproduce electronics, then even greater performance is possible.

In summary, our original objective of producing a user-oriented HDDR system has been achieved, and the system is in use. This was accomplished by applying original thinking to the increasing volume of experience with complementary systems to point the way for the future.

REFERENCES

12–1. International Standards Organization: ISO TC/97/SC 12 N222. Geneva, Nov. 1980.

12–2. Inter-Range Instrumentation Group: *Telemetry Standards.* IRIG 106–80, Range Commanders Council, White Sands Missile Range, N. Mex., revised May 1980.

12–3. Jacoby, George: "A New Lookahead Code for Increased Density." *IEEE Trans. Magn.* 13(5), Sept. 1977.

CHAPTER 13

The Honeywell HD-96 High-Density Digital Tape Record/Reproduce System

Leighton Meeks
Honeywell, Inc.

In its Model HD-96 high density digital tape record/reproduce systems, Honeywell uses its multitrack (fixed head) instrument transports and installs specially designed digital electronics to provide serial-in/serial-out or parallel-in/parallel-out operation. A modular design permits the number of active tracks to be adjusted to match the aggregate total bit rate capability needed for the particular application.

One advantage of this basic concept is that when the number of digital tracks required is less than the number of tracks available, the extra tracks can be used independently for recording time codes, voice, low-data-rate pulse code modulation (PCM) or similar editing/processing aids. The standard design provides for up to four such tracks, which are interchangeably connected either for high-density digital or for analog auxiliary track service.

BIT ERROR RATE PERFORMANCE

Standard bit error rate performance is 10^{-6} without error correction using 28-track heads and high-quality gamma ferric oxide magnetic tapes at packing densities of 33 to 34 kbpi. This BER is maintained under the following conditions:

(1) Tapes are recorded and reproduced on the same machine.
(2) Tapes are recorded on one machine and reproduced on another machine of like design.
(3) Tapes are recorded at a given speed and reproduced at the same or a different speed.
(4) Tapes are recorded with the conditions (1), (2), and (3) occurring singly or in combination.

Honeywell's Model 96 has superior tape path design, which provides high signal-to-noise ratio (SNR) due to head/tape contact and solid ferrite head construction, and low pulse-to-pulse jitter because of stable speed performance.

To further improve high-density digital recording (HDDR) performance, Honeywell has developed the following:

(1) Improved SNR and phase linearity
  (a) Record/reproduce electronics have been optimized for ditigal service.
  (b) A microgap record head is used, which reduces pulse-to-pulse crowding and increases signal flux margin on tape.

(2) Fully automatic operation (no recalibration over a 128:1 speed range and elimination of the traditional binary speed steps)
  (a) A digital reproduce amplifier and digital bit synchronizer have replaced the traditional binary equalizer and the traditional phase-locked loop bit synchronizer.
  (b) A control panel and an associated clock frequency synthesizer that permits thumbwheel selection of bit rate and packing density. Built-in electronics automatically computes and sets tape speed and reproduce equalization. The synthesizer will phase lock to either an external bit rate source or a built-in crystal reference.
  (c) Development of bit slip protection during tape dropouts by circuits that use the digital bit synchronizer to maintain each channel bit rate clock and to control reproduce tape speed without requiring a separate recorded tape servo track.

(3) An error correction technique
  (a) Tape signal dropouts are used for error detection.
  (b) The number of components required to incorporate error correction is minimized.

(c) When error correction is not required, parity tracks can be converted to regular data tracks.

(4) A deskewing format with on-tape coding

(a) Minimum demands are placed on a limited bandwidth record/reproduce channel.
(b) Decoding accuracy is not dependent on input data patterns (i.e., provides freedom from pattern sensitivity).
(c) Synchronization frequency is high enough to track dynamic skew and permit rapid initial acquisition and reliable maintenance of frame lock.
(d) Synchronization frequency is low enough to avoid aliasing and mis-framing of data from worst-case skew, tape stretch, etc.
(e) A synchronization pattern in which both the length and the bit pattern are "unique" is used (i.e., cannot appear in the input data stream) and are chosen to provide reliable and rapid synchronization detection.

(5) Special hardware techniques compensating for any remaining weakness in coding and format (because the perfect code has not been found and may not exist, the perfect format has not been found and may not exist, and the magnetic tape commercially available is not perfect)

MODULAR CONSTRUCTION

Figure 13-1 illustrates the building block concept used. A single diagram serves for all system levels. The basic differences between systems relate primarily to the maximum number of digital channels (provided by selection of 14- and 28-track Inter-range Instrumentation Group[1] heads) that use 1-in.-wide tape. To meet a given requirement, one of these heads with a sufficient number of tracks is selected. Because of common function, many of the functional elements are of modular "building block" construction. This method permits covering a wide range of system configurations with a minimum need for costly and time-consuming special designs.

MULTIPLEXER/DEMULTIPLEXER

The basic purpose of this digital logic module is to accept a high rate PCM data stream and divide (demultiplex) this stream into individual parallel streams running at a sufficiently slow rate such that they can be recorded on multiple, but limited bandwidth record/reproduce tracks. During reproduction, these individual streams are reassembled (multiplexed) into the original serial data stream.

Plug-in demultiplex and plug-in multiplex modules are available in the following basic variations, which handle the number of channels divided by 4 to the number of channels divided by 56:

(1) Serial to 4 minimum to serial to 14 maximum parallel channels; maximum serial in/out rate of 80 Mbps.

(2) Serial in/out to 4 minimum to 28 maximum parallel channels; maximum in/out rate of 160 Mbps.

The demultiplex also contains a built-in pseudorandom noise (PRN) test signal generator and the multiplex contains a companion decoder. This capability is useful and convenient for a quick, complete, throughput digital diagnostic test.

PARALLEL DATA TRACK ENCODER

Deskewing With Multitrack Recording

With fixed-head multitrack recording at high packing density (20 000 or greater bpi), it is essential to reestablish precise intertrack timing during the reproduction process before final output in parallel form or conversion from parallel back into serial form.

To facilitate deskewing, each input parallel NRZ−L data recording channel (track) is organized into synchronous frames of 504 bits. A 24-bit synchronization pattern (001111000011110000111100) is injected to mark the beginning of each frame. The remaining 480 bits consist of 420 bits of input data plus 60 parity bits. The 480 bits are divided into 60 data words in which each word consists of 7 data bits plus 1 injected (odd-parity) bit. The 420 data bits are randomized. Parity bits and synchronization bits are not randomized, and parity is formed on each randomized data word. The randomization consists of adding (modulo 2) the sum of data bits and a pseudorandom sequence. The sequence is itself modified by inhibiting certain data clock pulses to the sequence generator. The sequence generator is reset each new frame at the end of the 24-bit synchronization pattern. For convenience in interfacing, a data sense inversion is provided. When activated, every input data bit is inverted (complemented) on a per-channel basis. Capability for reverse (time-inverse) reproduce is also included.

During reproduction the data are restored to bilevel form and deskewed. Synchronization bits, parity bits, and randomized bits added during the recording process are removed and the data streams are restored to their original NRZ−L form without leaving time gaps.

The function of the parallel data encoders is to generate the data frame set described and illustrated in figure 13-2. The parallel data inputs are the common

[1]Now Range Commanders Council.

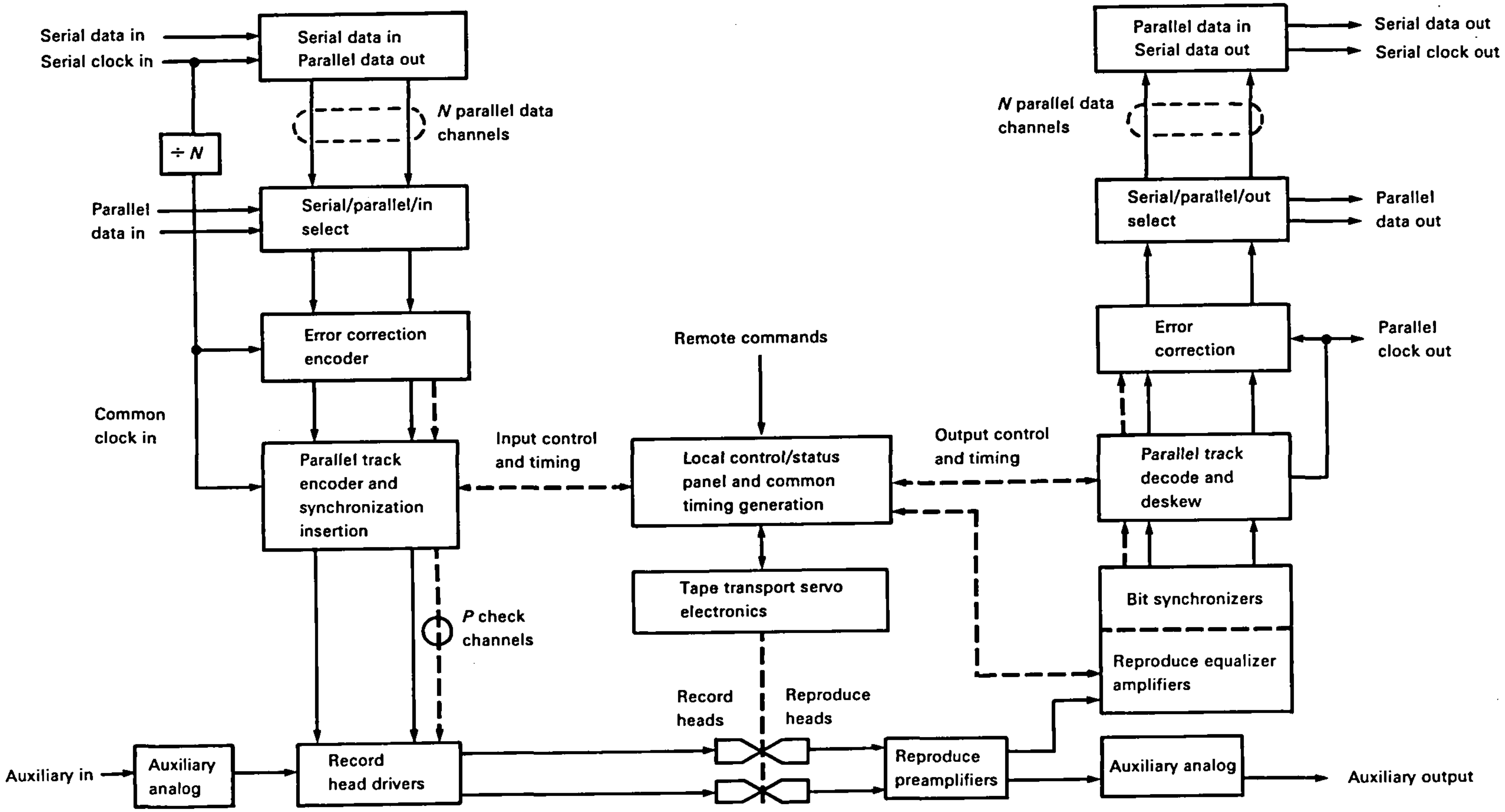

Figure 13–1.—Overall modular concept.

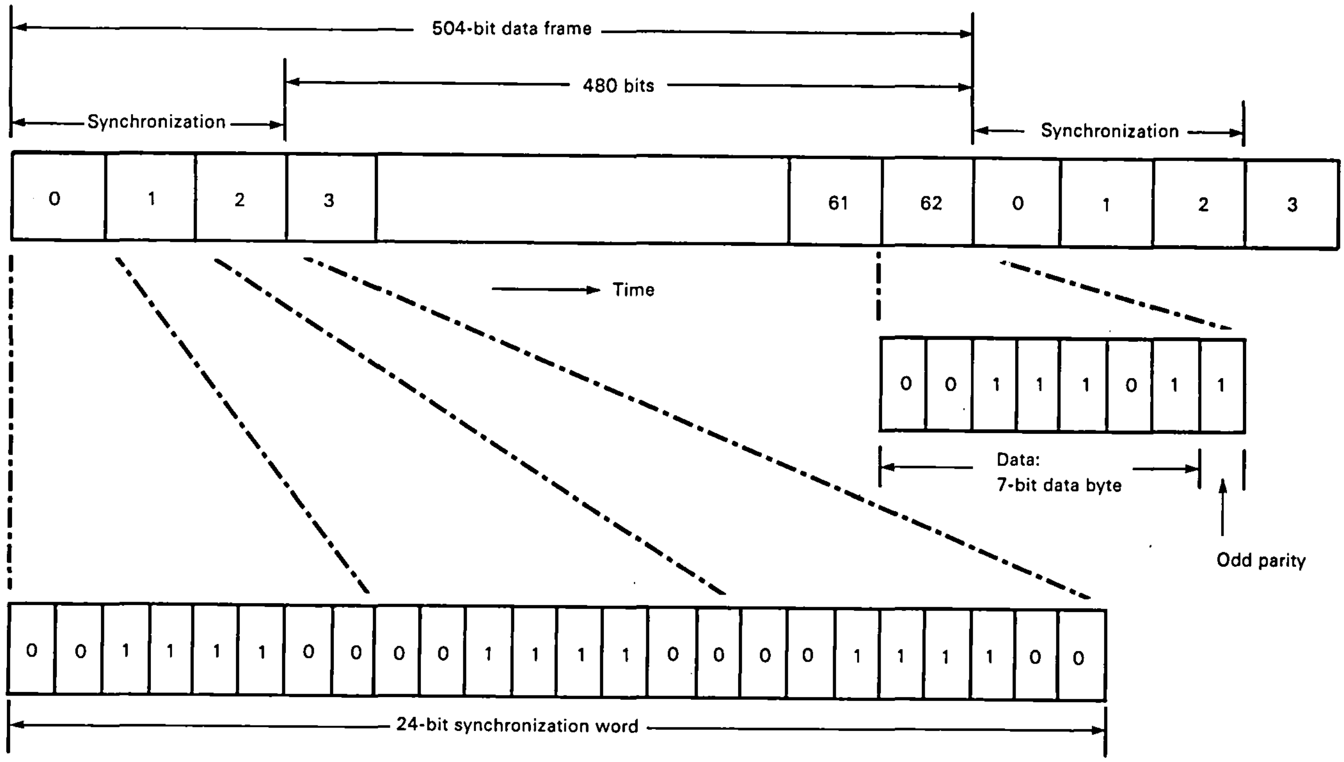

Figure 13–2.—Frame set. Overhead = 20 percent. (Overhead = (no. of bits per frame/no. of data bits per frame − 1) × 100.)

clocked outputs from the demultiplexer or from the external parallal data inputs. The data frame set (figure 13–2) is the same for all digital tracks (including check tracks if error correction is used). The outputs of the parallel data encoders are inputs to the record head drivers. The data frame set results in insuring the additional overhead bits needed to facilitate data recovery during the reproduce process.

As shown in figure 13–3, the parallel data encoders are implemented based on the use of FIFO memories. The logic is partitioned into two main sections: a typical channel section that is repeated for each digital recording channel (track) and an input timing and format control section that is used once per system. Each data input (serial format) is common-clocked, modulated by a PRN sequence, and collected into eight-bit groups (words) of seven bits data plus one odd parity bit by means of a temporary holding register for writing (storing) into a FIFO memory. The FIFO memory is fast enough to permit operation at a variable input storage rate and output at a constant, but higher rate.

Synchronization of all channels is accomplished by entering a channel marker pulse (from the common input frame counter) into the FIFO memory of each channel and then programming FIFO memory dump (i.e., clear) pulses until all channels read out channel marker pulses simultaneously. The PRN modulating sequence generator is reset at the beginning of the first data word in each frame. Note that only the data portion of the frame is PRN modulated. The synchronization is recorded in the "clear," and the odd parity is formed after PRN modulation of the data.

Packaging

The common input timing format control is constructed as a dual channel plug-in module. The parallel data encoders on a single plug-in module are grouped two channels to a board along with a corresponding two channels of deskew logic on the same board. An input timing format module is used once per system. Fourteen of the dual channel encoder/decoder modules are used for a 28-channel system.

RECORD HEAD DRIVERS

The record head driver inputs are the outputs from the parallel data encoders and produce drive signal current to the record magnetic heads. The record head drivers are installed behind the record heads on the transport deck plate. These are modular plug-in units.

Digital Recording

Non-bias recording techniques are used to record the digital outputs from the parallel data encoders via a head driver interface board that permits quick and easy

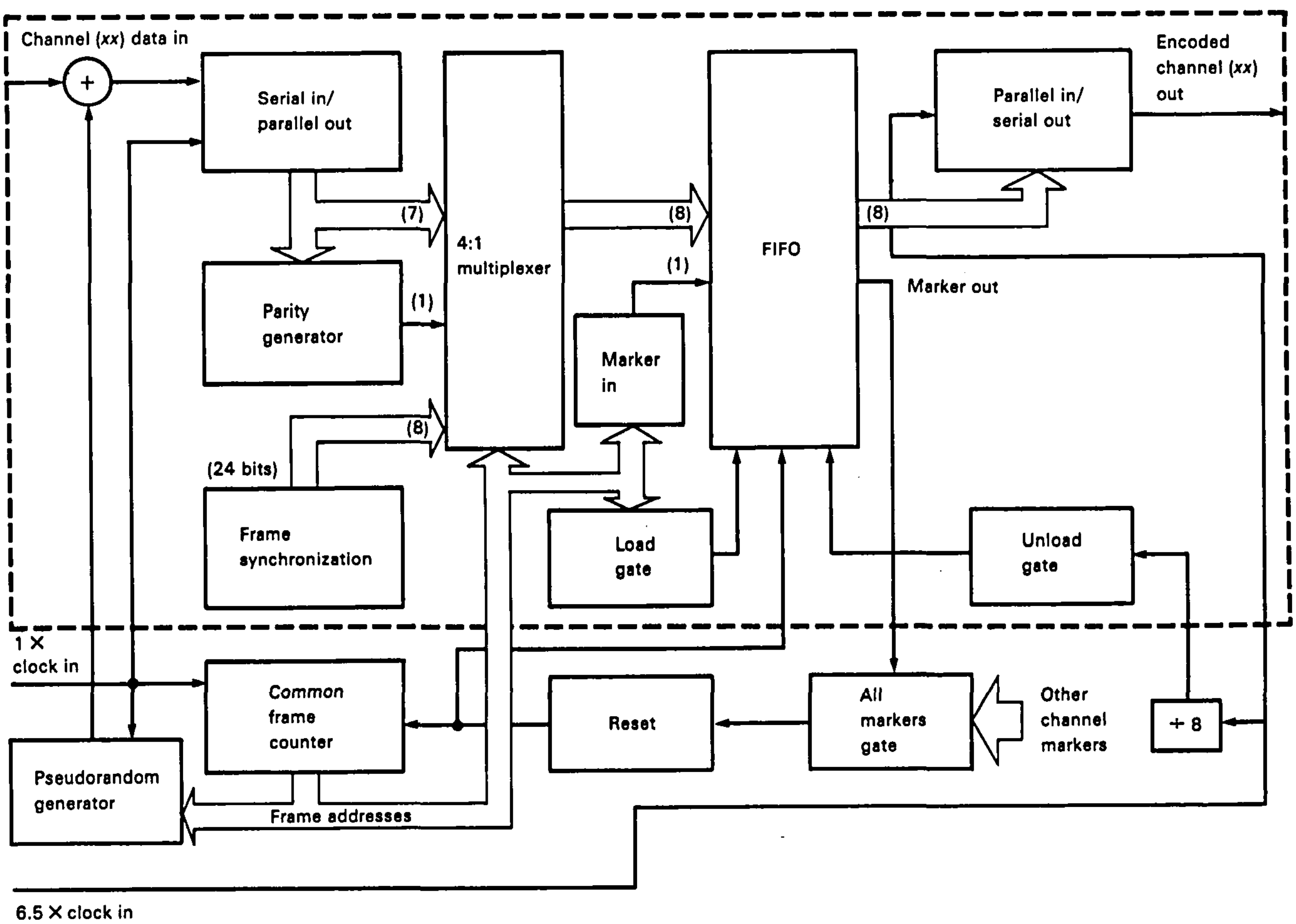

Figure 13–3.—Parallel data encoder logic.

accommodation of different magnetic head track formats (e.g., 14 and 28 tracks). The digital driver circuit contains a clamping means to immunize the head currents from transistor-to-transistor logic (TTL) level and power supply variation. This circuit contains only one single head current level adjustment per channel to optimize record current for the tape type being used. The head driver electronics are automatically equalized for recording losses at all speeds so that the single adjustment for tape type is all that is required. Construction is seven channels (heptad) per plug-in module. Four such modules are required for a 28-track system.

Analog Recording and Analog Patch

Bias recording techniques are used to satisfy the auxiliary analog signal recording requirements. A four-channel (quad) plug-in module is installed if required for this purpose. The capability to convert between analog bias recording and digital recording is provided by means of a patch capability on the head driver housing. Conversion is accomplished by simple jumper change for each of the channels individually.

TAPE/HEAD CONFIGURATION AND ALIGNMENT PRECISION

The tape transport is supplied configured for 1-in. tape and appropriate number of tracks using interleaved (two-stack) heads as required for the application. Heads are of long-wearing solid ferrite construction. Honeywell does not believe it is necessary to lift heads from the tape during wind or rewind as do some suppliers. New head pole face depth is 1.5 mils on the reproduce stacks and 3 mils on the record stacks. Azimuth adjustment range is plus or minus 12 min of arc for not only the reproduce head stacks but for the record stacks as well. The ability to azimuth align both the record side and the reproduce side is of special significance to high-density recording because it provides a means to maximize machine-to-machine crossplay margin. This is because this feature provides a means to align all transports for peaked signal response using a common recorded reference tape. Once aligned in this manner, interchangeability of tapes recorded on a multiplicity of different recording transports is assured without the time-consuming effort of adjusting

the reproduce azimuth each time a tape is reproduced from a different transport.

Because of unique construction and optical methods used in the factory, Honeywell solid ferrite heads are an advance on IRIG tolerances. To insure maintenance of tolerances in the field, Honeywell prerecorded alignment tapes are available.

REPRODUCE HEAD PREAMPLIFIERS

Reproduce heads are equipped (integral to the head assemblies) with an active gain first stage to minimize phase shift (i.e., group delay distortion) and maximize SNR. Additional gain is provided by main stage preamplifiers mounted in a housing on the transport deck plate immediately behind the reproduce heads. The main stage preamplifiers are arranged as seven channels per module (heptad) plug-in units. Four such modules are required for a 28-track system. The combination of head-mounted first stage and main preamplifier provides approximately 40 dB of fixed gain.

REPRODUCE DATA SYNCHRONIZERS

After reproduce preamplification and prior to digital processing, the reproduce head outputs must be "equalized." In addition, the binary message and associated bit rate clock must be extracted from an analog signal that is highly variable in amplitude, sometimes noisy (during flaws), and jittery. These functions are performed by the data synchronizer.

For HDDR application, a very significant operational advantage results from a data synchronization method that provides:

(1) Automatic and optimum speed equalization over a continous tape speed range from 1 ⅞ to 240 ips as well as the traditional (binary related) discrete step operating speeds.

(2) Automatic bit synchronization over the 1 ⅞ to 240-ips speed range without the necessity to take time to recalibrate each time a new operating requirement calls for reproducing at a bit rate different from the old preset value.

(3) Complete freedom from the operating constraints imposed by the binary speed selection of traditionally designed instrument transports.

(4) Elimination of special bit synchronizer calibration equipment.

All these desirable operating features are achieved by the reproduce data synchronizer module. This module contains both a 64-speed step equalizer section and a digital bit synchronizer on one printed circuit package.

Reproduce Amplifiers

When data are recorded and subsequently reproduced at a given tape speed, the amplitude-versus-frequency transfer function at the output of the reproduce head appears as in figure 13-4 (plotted from an actual circuit). Because such a large amplitude variation is not suitable for most applications, including HDDR, equalization circuits are required to linearize the head output by performing the inverse amplitude versus frequency characteristic shown in figure 13-5. There is a unique reproduce head output curve for each speed (binarily related or not) within the transport operating range as illustrated in figure 13-6. These transfer functions at a given speed are the same for all recorder tracks and, furthermore, are not all related to the individual

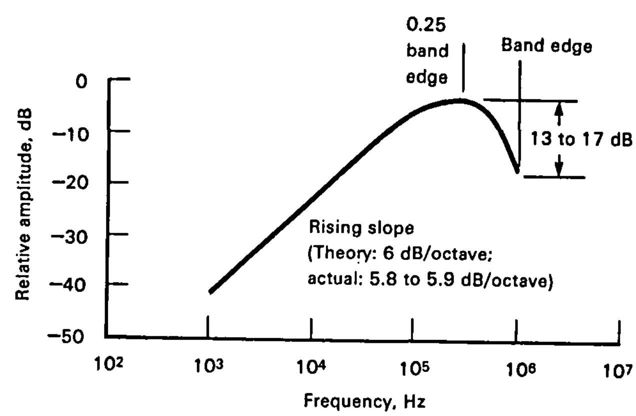

Figure 13–4.—28-track ferrite wideband reproduce head output versus logarithm of frequency. (tape speed: 60 ips.)

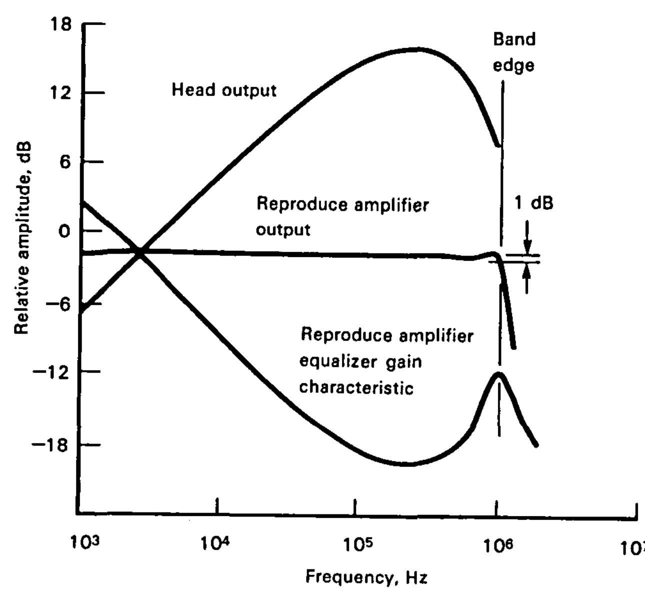

Figure 13–5.—Equalization for 60-ips tape speed using 60-ips equalizer.

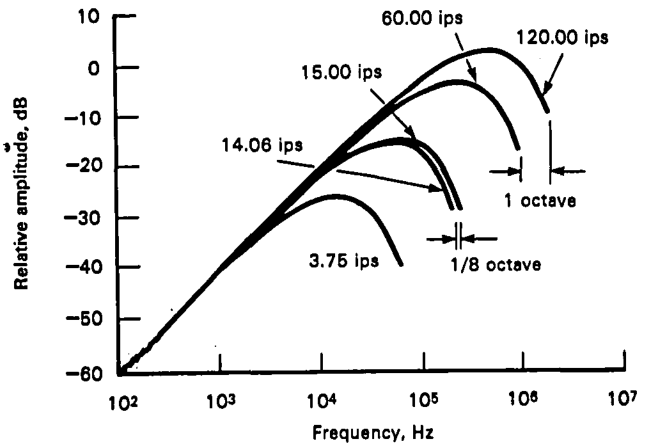

Figure 13–6.—28-track ferrite wideband reproduce head output versus logarithm of frequency at multiple tape speeds.

channel bit rates. Consequently, an equalizer selection based on any reason other than matching playback speed serves no useful purpose and unnecessarily complicates use of the recording system in an operational environment.

The reproduce amplifiers described fully address the requirement to reproduce data at the standard IRIG tape speeds as well as at "variable" speeds in between. Furthermore, there is no need to retune the equalization networks. The method also permits reading the data while recording so that data quality may be assessed in real time. An indication of malfunction in an active recorder could be used to bring a standby recorder system on line quickly to reduce loss of valuable information. Fully equalized reverse tape motion reproduce is also provided.

The equalization amplifier shown in figure 13-7 provides 64-equalization speed steps to cover the tape speed range from 1⅞ to 240 ips. The amplifier will provide 8 intermediate steps within each octave range for a total of 64 speed steps being used. Figure 13-8 shows the worst-case mismatch that would result in amplitude versus frequency response from using a single equalizer network to equalize two speeds separated by 6¼ percent (1/8 speed octave). This design provides a very good margin dictated by experience which has shown that varying the tape speed more than about 10 percent from a given equalizer set point causes bit errors to increase noticeably.

Only 6 adjustments are required to fully equalize each amplifier (as compared to 27 for some other designs for the nine speed ranges) during initial calibration, and this calibration need be done only at a single tape speed. Equalization at all other "fixed" and "variable" speeds is done automatically. The tape speed equalizer set information is communicated from the frequency synthesizer to the amplifier via 12 binary coded lines (11 lines for speed and 1 line for forward/reverse). This binary code is presented to all amplifiers simultaneously via the amplifier/bit synchronizer housing.

Digital Bit Synchronizers

Figure 13-9 shows the digital bit synchronizer section of the reproduce/bit synchronizer plug-in module. Several features significant to minimum bit errors are incorporated. Digital techniques are used for precision bit rate clock synchronization and freedom from tuning adjustments. The digital methods employed completely eliminate the restrictions imposed by conventional phase-locked loops on system operation such as narrow margins of bit rate range for acquisition and tracking. The synchronizer will easily operate over the entire specified bit rate ranges and tape speed ranges with no expensive auxiliary tuning and calibration equipment required during operation. Because there is no calibration setup time required, there is no system operating time lost for recalibration.

To facilitate initial system debugging and labor troubleshooting, an input field effect transistor switch (remotely controllable) is provided. The bit synchronizer section can be operated either from the reproduce output (on the same module) or from an external source. For example, when the encoder output is connected, the HDDR system can be operated in a "transport bypass" mode, which permits rapid digital system checkout initially and enhances system troubleshooting later.

Baseline correction is incorporated to restore the signal dc level for maximum SNR and accurate data bit decisions. The amount of correction is based on integration of the average dc level of the signal waveform. The baseline correction is automatically scaled to eliminate sensitivity to tape-to-tape and channel-to-channel variations, but the signal level is not gain controlled automatically. This is to maximize SNR, especially during tape flaws. To prevent overcorrection during tape flaws, a dual (two-level) hysteresis scheme is employed to accurately determine the presence of signal dropouts and prevent inappropriate baseline correction action. This flaw detector signal is made available as a data "dropout" signal to the status monitor panel and to the error correction logic in the decoder.

The data comparator converts the baseline corrected but variable amplitude reproduce signal to bilevel form. The data comparator operates as a 0-level axis-crossing detector with minimum hysteresis. The digital synchronizing logic uses the transition edges of the bilevel signal to recover the bit rate clock. The bit rate clock phase is continuously adjusted to select the nearest transition match with the 22× reference clock (plus or minus one cycle of the reference). If no data transitions occur, then the digital synchronizer logic automatically

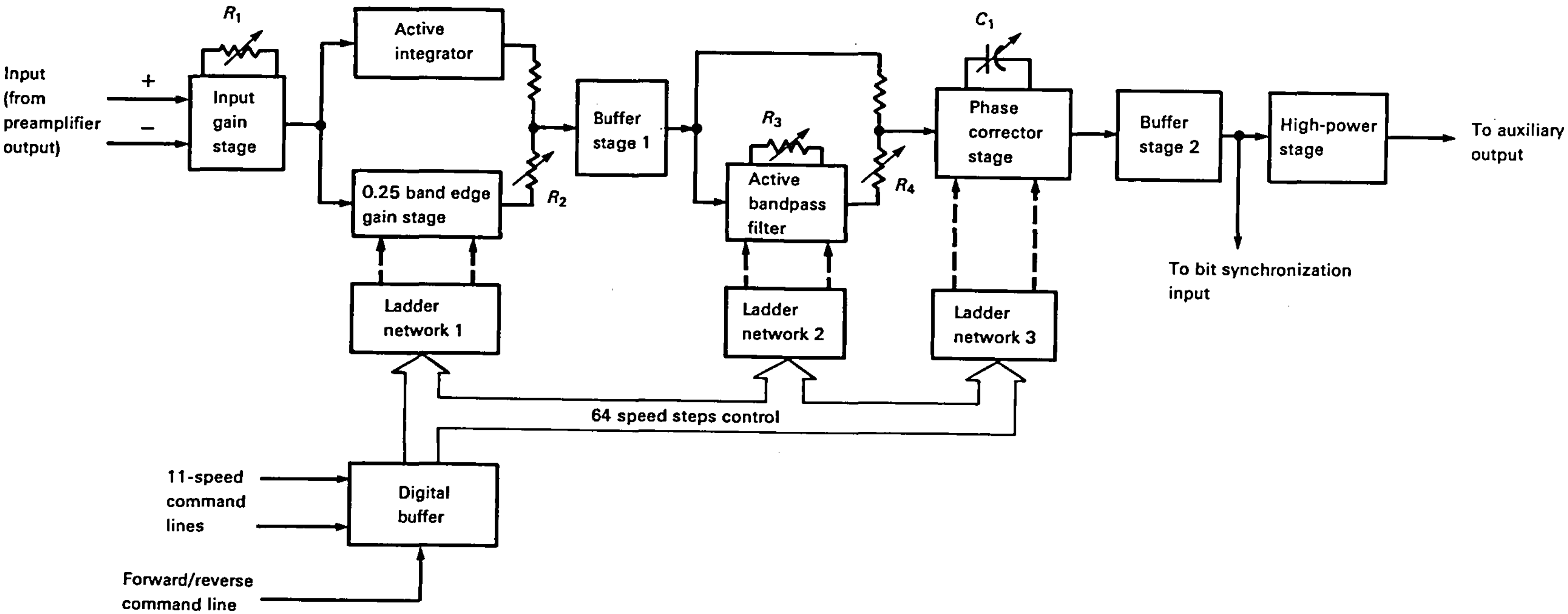

Figure 13–7.—64-speed reproduce equalizer amplifier simplified block diagram. (Fine tune adjustments—one each per amplifier; R_1 = gain set; R_2 = Y_4 band edge set; R_3 = band edge set; R_4 = 8/10 band edge set; and C_1 = phase set.)

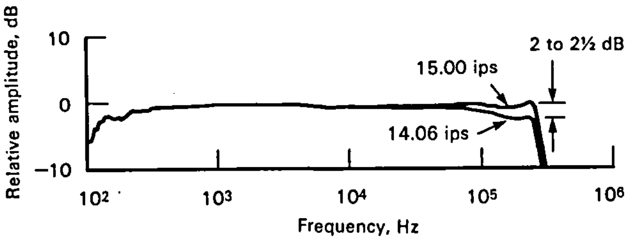

Figure 13–8.—Worst-case equalization output degradation using 15.00-ips equalizer at 14.06 ips tape speed. (Δ speed ≃ 1/8 octave.)

retains the last transition setting and outputs a 1× data rate clock accordingly. Thus the bit rate clock can "flywheel" indefinitely, limited only by the stability of the 22× reference clock.

To restore maximum timing margin (data versus clock) for the following deskew logic, the bilevel data signal is reclocked via a *D*-type flip flop prior to output. Although not shown in figure 13-9, all output signals (dropout, data, and bit rate clock) are transmitted via differential voltage mode line drivers to provide a maximum noise immunity interface.

PARALLEL DATA DECODERS

The function of the decoders is to accept outputs from the data synchronizer and to perform data recovery and realignment (deskew) of the original parallel recorded data. The design is based on FIFO memories and contains provision for error correction based on association of reproduced bit errors with data dropouts.

As shown in figure 13–10, the decoder is partitioned into two sections: a typical channel section, which is repeated one per recorded channel (including check tracks if error correction is used), and an output timing and format control section shared by all channel sections. The basic operation is as described in the remainder of this section.

Time-skewed data after conversion to bilevel form from the data bit synchronizer is first shifted into an 8-stage serial input/parallel output data register and simultaneously into a 24-stage serial input/parallel output synchronization pattern detection register. The shift rate is controlled by the data rate clock, which also advances the channel frame counter, which is reset controlled by synchronization pattern detection pulses.

The individual channel frame synchronization logic contains a scoring register scheme that initially requires two successive frame synchronizations to establish channel lock. Thereafter, the scoring register maintains lock during missed (due to data dropouts) synchronizations or reestablishes channel lock without requiring master (all channels) lock to be reacquired.

With channel lock established, the time-skewed data words (seven bits) are stored into the channel FIFO memory, which also stores a parity check bit and the bit-synchronizer-furnished two drop-out signals (if they are present) as one bit per data word.

Frame synchronization bits added during the encode/recording process are removed by blocking storage into the FIFO. Instead, a synchronizer marker bit is added in parallel with the first data byte of each data frame.

Data readout occurs simultaneously for all channel FIFO's using a common clock running at a rate corresponding to the channel data rate less the added overhead.

The readout is set to lag the first-in time arriving channel by a constant number of bits (set large compared to the worst-case skew plus a margin to insure adequate FIFO storage) by controlling the common readout frame reset.

Channel deskew is continuously monitored by comparing the channel synchronization marker readout for simultaneous comparison to the common frame synchronization marker. Should this not occur, the FIFO is cleared automatically. Because clearing action causes a burst of errors, the design has included measures to prevent bit slip. These include the use of a digital bit synchronizer, tape speed servo loop, and a special clock synthesizer.

Pseudorandom noise modulation added during the encode/record process is removed during simultaneous readout of the deskew data by modulo 2 addition of the same pseudorandom noise sequence. Synchronization noise for this modulation removal is assured by using the common synchronization marker to synchronize the pseudorandom noise generator that is shared by all channels.

CONTROLS AND INDICATORS

Transport Controls and Indicators

The transport is equipped with the following standard pushbutton controls and lighted indicators on the front panel of the transport tape deck:

(1) Reverse
(2) Fast
(3) Forward
(4) Stop
(5) Record
(6) Tape speed synchronization (indicator)
(7) Low tape
(8) Footage reset
(9) Tape footage (indicator) counter
(10) Shuttle set reverse (optional)
(11) Shuttle set forward (optional)
(12) Select track record (optional)

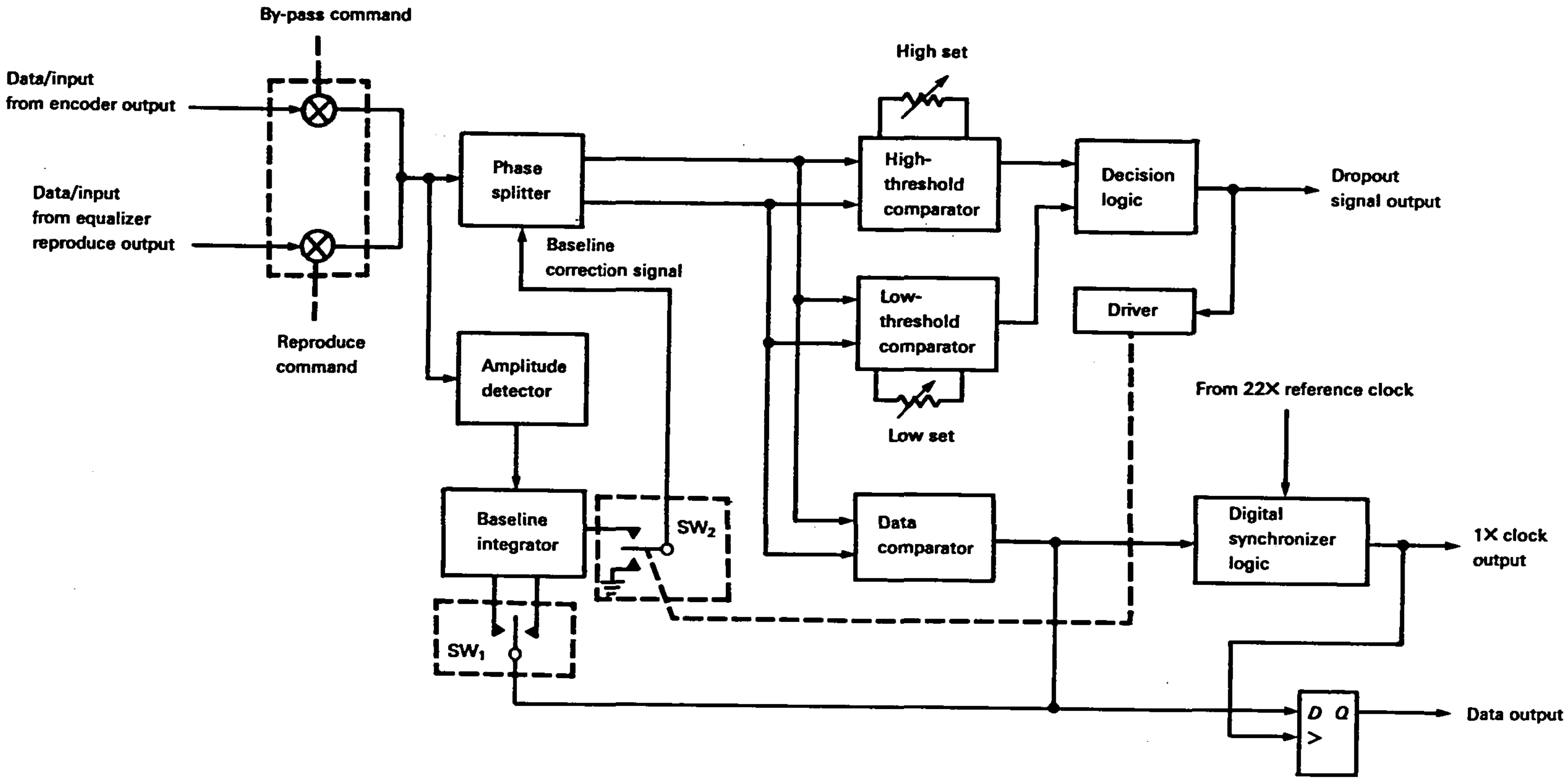

Figure 13–9.—Digital bit synchronizer simplified block diagram.

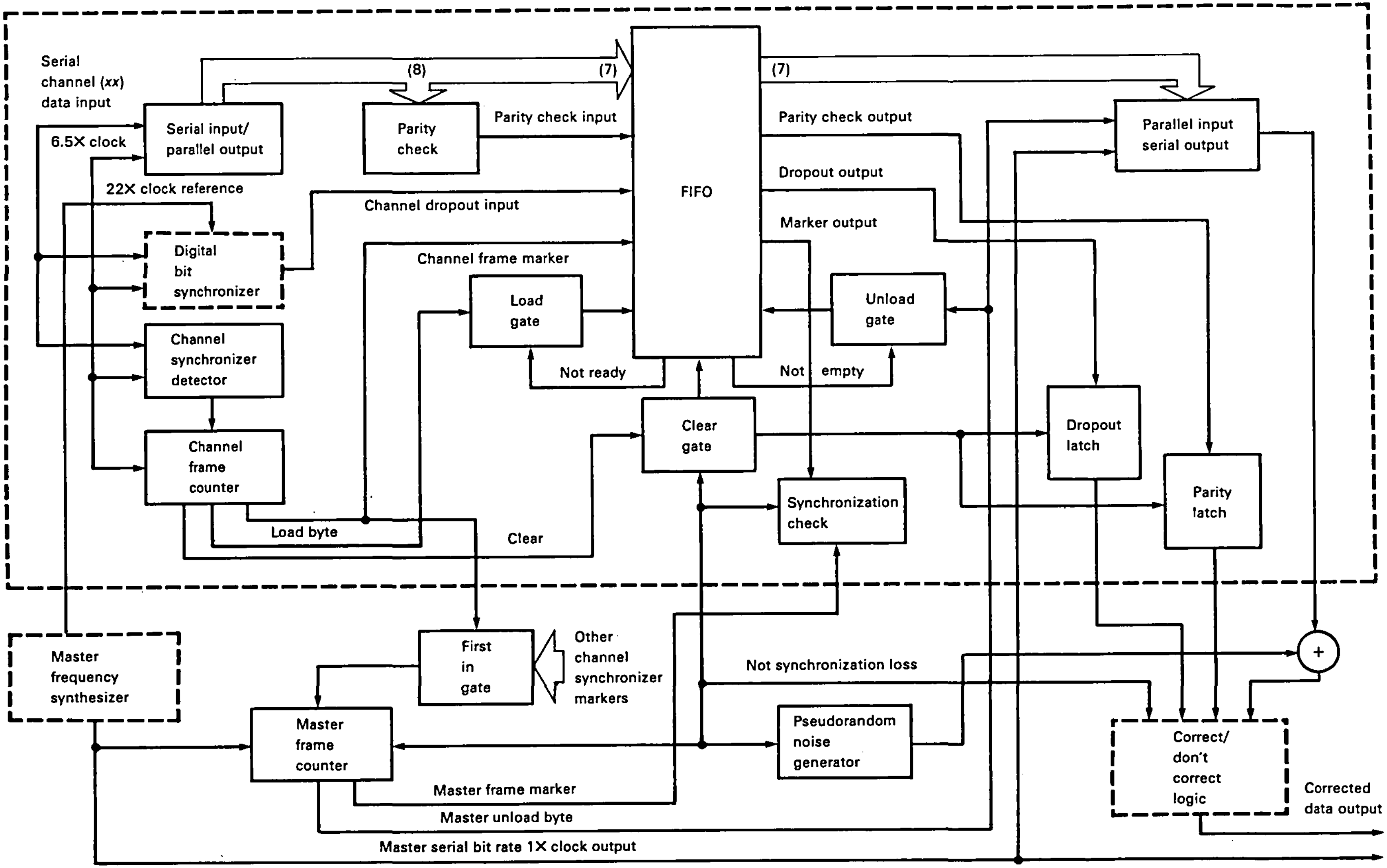

Figure 13–10.—Parallel channel decode/logic deskew.

Traditional tape speed select pushbuttons are not used on Honeywell HDDR systems. This function is accomplished via the digital control and display panel discussed in the next section.

Digital System Controls and Indicators

Figure 13-11 shows the digital local control and status panel for a 28-channel (track) system. This panel provides three light-emitting diode (LED) indicators for each active tape channel for reproduce signal loss, frame synchronization search (loss), and parity error. In addition, a master (system) synchronization lock (LED indicator) is provided.

Lighted message displays are provided for the on-tape code used; the functional conditions of forward reproduce, reverse reproduce operation (i.e., time-inverse reproduce), tape transport bypass operation (a test mode); total (i.e., serial) aggregate bit rate; and a three-decimal digit tape speed (ips) display.

One set of thumbwheels selects the desired operating channel (track) bit rate (to the nearest 0.1 percent) from 31.25 kbps to 6.667 Mbps. A second set of thumb wheels selects the desired operating packing density (kbpi) expressed as a percent where 100 percent corresponds to 33.33 kbpi. The packing density thumbwheels are calibrated to take into account the 20-percent overhead used. The channel bit rate thumbwheels are calibrated for the customer's channel bit rate.

Clock status and controls are provided with lighted switch selection of internal bit rate clock source or external (customer-supplied) bit rate clock source. If thumbwheel selection and/or clock rates are inadvertently set outside system design capabilities, an "out-of-range" light flashes red. When normal (in-range) conditions are met, then a "lock" light shows steady green color. A convenient "push-to-test" lamp test switch is provided for quick operator verification of active lamps and LED's during operation.

To accommodate a lesser or greater number of channels (tracks), the number of active LED status indicators for reproduce data loss, synchronization loss, and parity error are adjusted as required.

A lighted remote/local control selector switch is provided. All digital controls and transport controls are capable of remote control. Critical status signals are also available. Remote control (TTL) via IEEE-488 is interfaced via a connector on the back input/output panel.

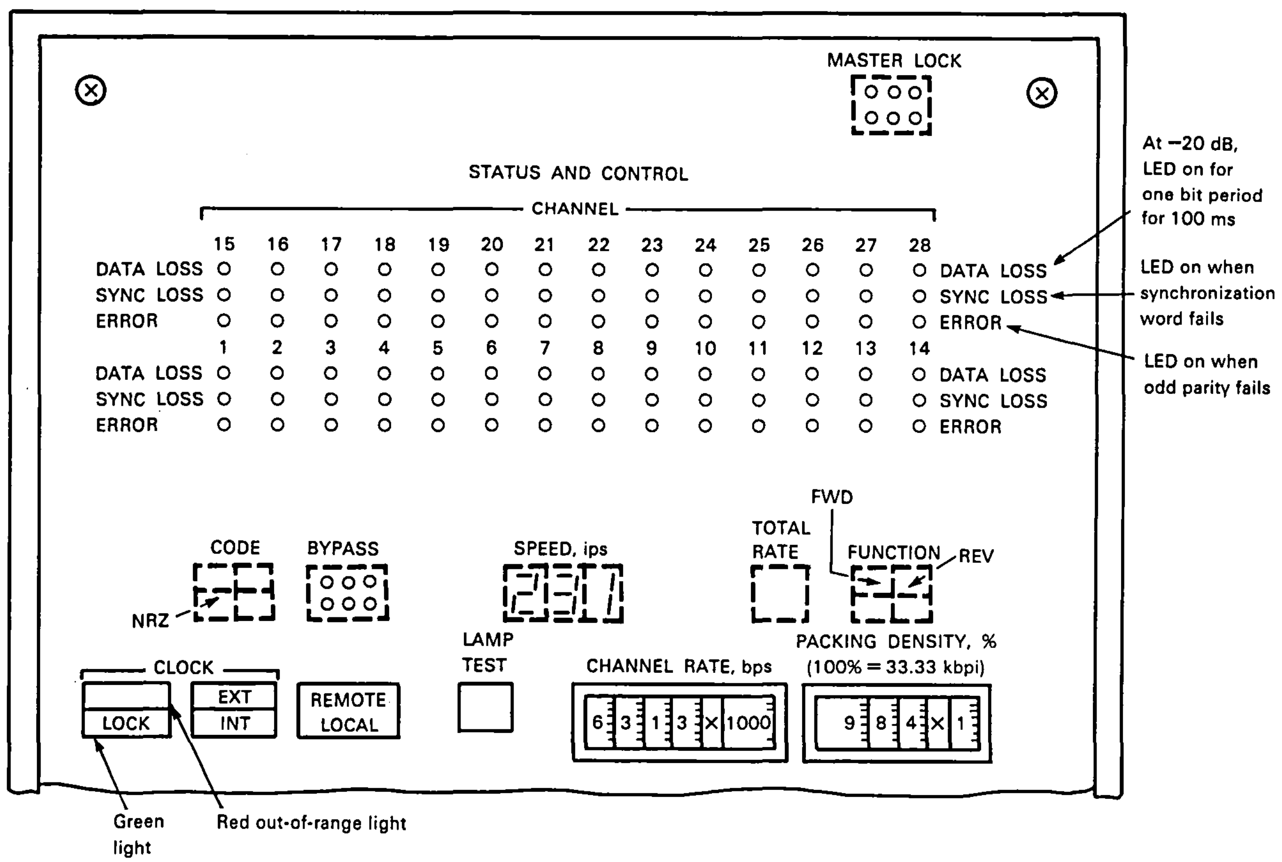

Figure 13-11.—28-channel control/display panel.

FREQUENCY SYNTHESIZERS

A common clock frequency synthesizer functional module is shown in figure 13-12. This module uses the thumbwheel settings and control switch settings of the digital control panel to derive all clocking signals needed to operate the HDDR system data logic and automatically selects speed control lines for the transport and reproduce amplifier equalizer networks. The clock synthesizer output clocks are phase locked to either an internal crystal reference or to an external source. Packing density range is from 48 to 200 percent (where 100 percent corresponds to 33.33 kbpi).

TRANSPORT SPEED CONTROL LOOP

The method of servo-controlling tape speed is illustrated in figure 13-13. The basic purpose of the loop is to provide a means for regulating instantaneous tape speed (especially during reproduce) to force the reproduced data rate to match, on the average, the bit rate demanded either from an external source or the internal source and to accomplish this without need for a special tape-recorded servo track. Without such a scheme, slight variations from machine to machine in capstan diameter and tape-to-tape stretch/contraction could cause a slowly varying average rate offset. The speed control loop uses the reconstructed bit rate clock (from a bit synchronizer) off-tape as a measure of instantaneous tape speed and, via a phase-locked loop comparison with the common clock generated tape rate reference, causes the tape speed reference to vary so as to reduce the difference between demanded bit rate and the instantaneous rate. In this manner, the reproduced data rate is forced to match (on the average) the demanded rate.

During record, the phase-locked loop bit synchronization clock input is switched to a feedback divider output; this procedure is used because it is not possible to servo off tape feedback while recording, because the data rate at the reproduce heads is the same as the record input independent of tape speed; therefore, during record, tape speed servo is via the capstan tachometer phase locked to a fixed (via the common clock synthesizer) tape speed reference. Fortunately, the need to servo with off-tape feedback is not required during simultaneous reproduce while recording. This is because, as previously stated, the reproduced rate is the same as the input record rate independent of tape speed. The loop closing control logic permits the loop to be closed only during reproduce and after the transport has reached stable speed (i.e., capstan tachometer synchronization).

To protect the loop security during reproduce operation from tape dropouts, two bit synchronizers are used: bit synchronizer "A" is the primary off-tape clock source and bit synchronizer "B" is its "helper." During a tape dropout on bit synchronizer "A", a 4× clock from the bit synchronizer "B" is used by "A" to avoid bit slipping during the noisy flaw period. This method provides very secure operation because experience has shown that simultaneous dropouts on two tracks on the same head

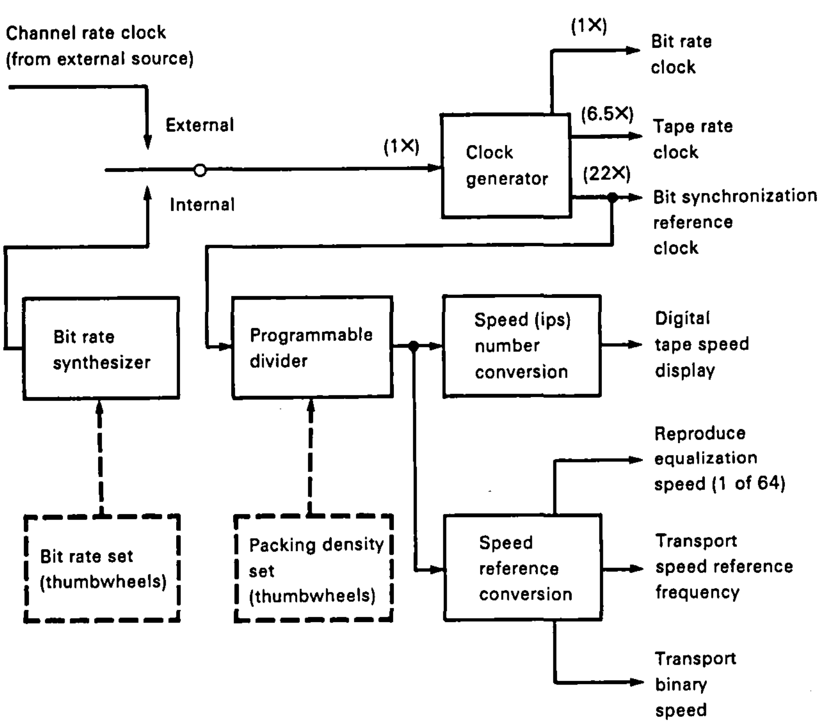

Figure 13-12.—Common clock synthesizer.

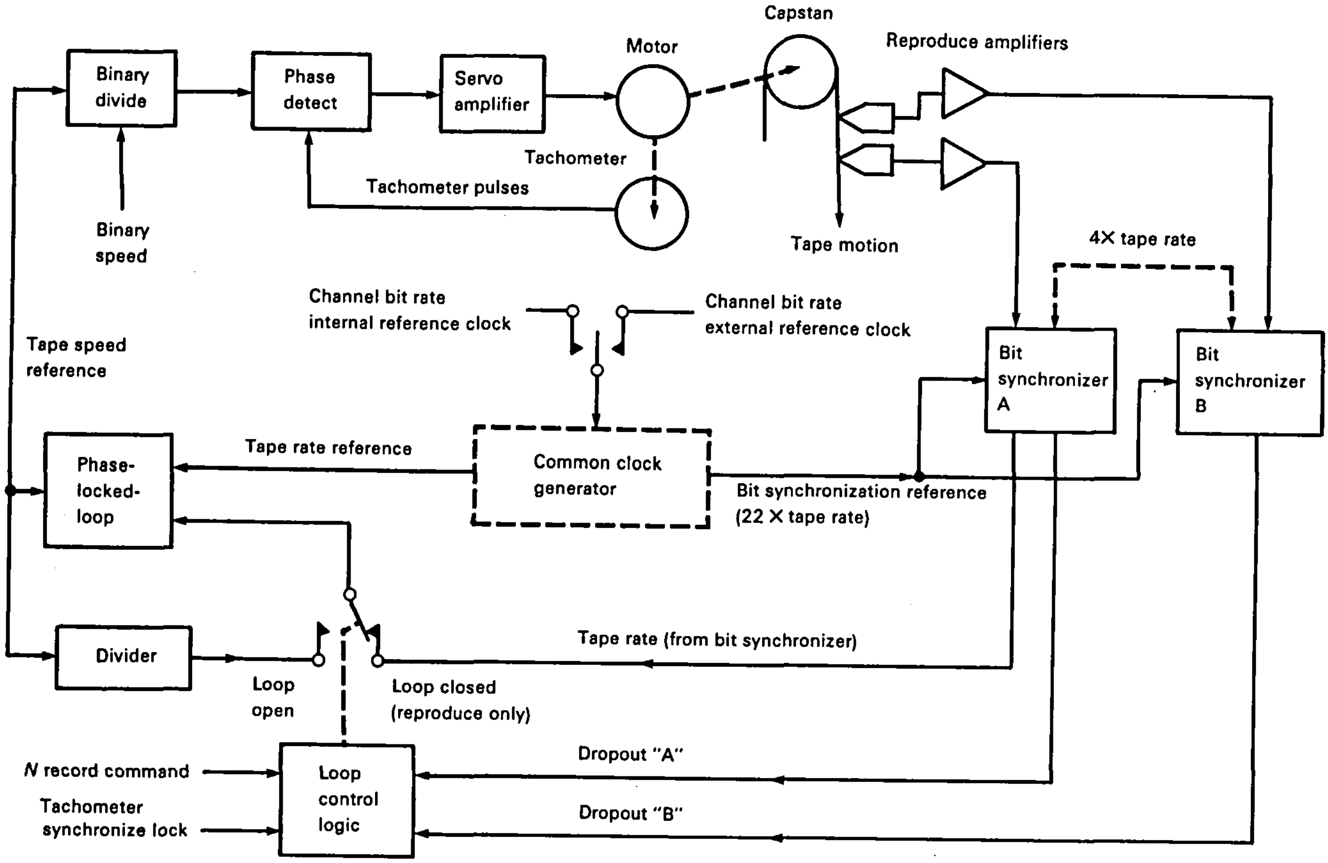

Figure 13–13.—Tape speed control loop.

stack where tracks are spaced apart by at least 70 mils are very rare.

INPUT/OUTPUT DATA PANEL

All input and output signals entering or leaving the high-density digital tape recorder are connected via swingout input/output panels located on the rear of the cabinet as shown in figure 13–14. For a 14-channel system, only the upper section is required. For 28 channels and up, the lower section is also supplied. Standard system capability is as follows:

(1) Input parallel—TTL level parallel input NRZ–L data consisting of a minimum of four data channels plus a 0° clock are terminated to 100 Ω with a differential receiver. The inputs can be single ended or differential. The differential connection is preferred for maximum noise immunity. Connection is via groups of 40-pin connectors that accommodate flat "Twist-N-Flat" cables. This arrangement allows each channel to be a twisted pair.

(2) Output parallel—TTL level parallel output NRZ–L data consisting of a minimum of four data channels plus a 0° clock are outputted via differential drivers. In all other ways parallel output interfaces are like the inputs.

The following types of input data and clock can be selected for optional serial inputs and outputs:

(1) TTL single ended (up to 20 Mb): Bayonet nut coupling (BNC)

(2) TTL differential (up to 15 Mb): keyed twinax

(3) Emitter-coupled logic (ECL) single ended (up to 160 Mb): type CUG568/U

(4) ECL differential (up to 110 Mb): dual coax, type C

The HDDR system can be patched for operation either in the serial or parallel mode, but not both at the same time.

SIGNAL MONITORING

Where frequencies permit, critical signal test points are provided for monitoring on a suitable oscilloscope while the system is operating and such monitoring does not interfere with normal operation. As a minimum, waveform and level monitoring is possible for the following:

(1) If supplied, high-speed serial-to-parallel demultiplexer inputs (data and clock) and high-speed parallel-to-serial multiplexer outputs (data and clock)

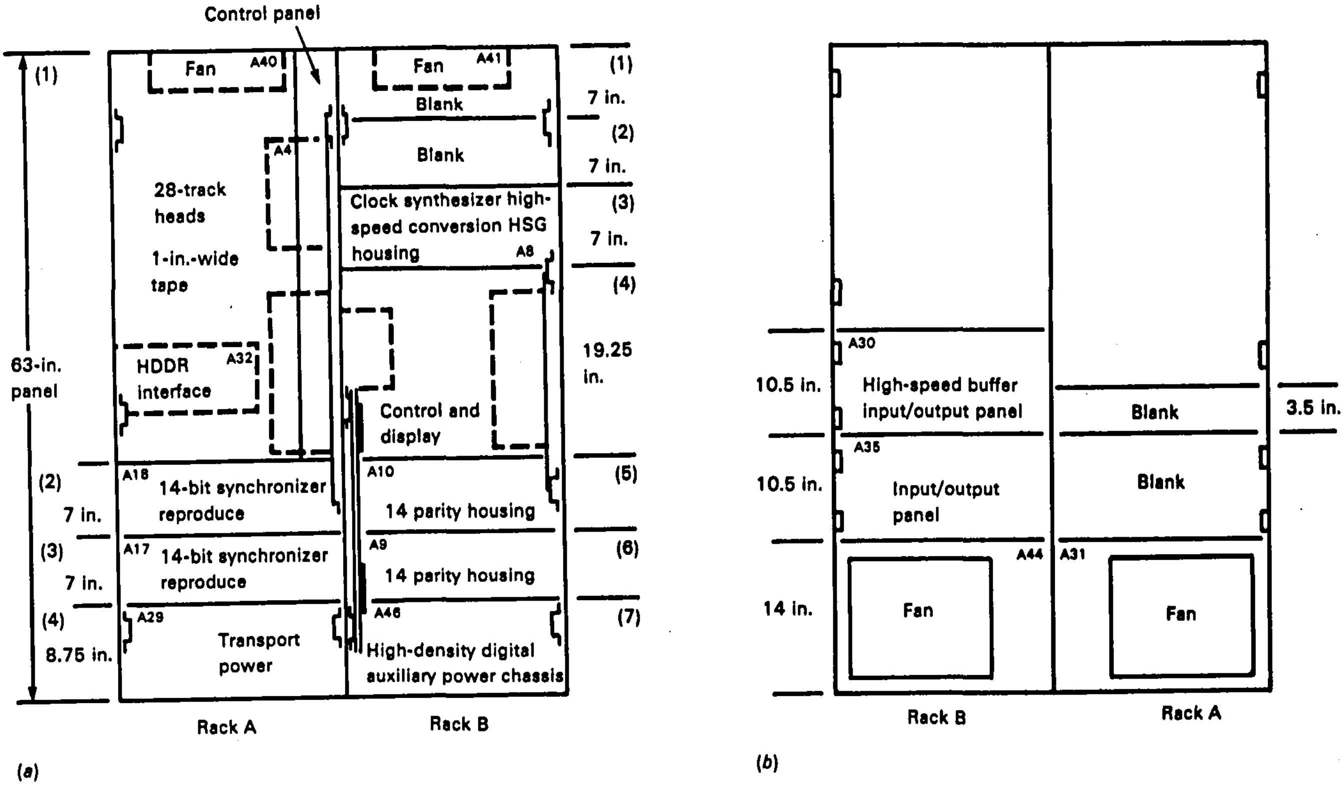

Figure 13–14.—Basic 28-channel HDDR panel configuration. (*a*) Front view. (*b*) Rear view.

(2) Each input channel to the parallel encoders

(3) Each output channel to the record head driver amplifiers

(4) Each reproduce output channel from the reproduce head amplifiers

(5) Each output (data, clock, and dropout) signal from the data bit synchronizers and each reproduce output after base line compensation

(6) Tape speed servo reference

(7) Critical timing and control waveforms required for monitoring during signal electronic alignment and system test debugging.

To facilitate signal monitoring, a deluxe maintenance kit is supplied with each system. The kit contains "extender boards" for all plug-in modules. When mounted on these extender boards, full front access to both sides of the plug-in module is provided.

ERROR CORRECTION

The HD-96 employs a dropout-based error correction method as depicted by figure 13-15. The large block labeled "HD-96 28-track head" represents a 28-channel system complete with parallel encode and deskew electronics. The concept is based upon product code error location where cross-track parity corresponds to "checks on rows" and data channel dropout signals correspond to "checks on columns." Cross-track parity is formed for groups of 14 parallel tracks where up to 13 of these can be assigned to data and 1 of these tracks is the odd parity for the group of 14. Thus, for a 28-track system, 26 can be data and 2 are check tracks. In a 14-track system, the parity track is track 8; in a 28-track system, the parity tracks are numbers 15 and 22.

The parity tracks are formed prior to encoding and synchronization insertion on the record side. Correction is performed after data is deskewed and realigned on the reproduce side. Cross-track parity is reformed and checked against the reproduce parity for each corresponding cross-track group. If these parity checks do not agree, then at least one track has an error at this precise bit time. The channel dropout signals are used to locate which track. As long as only one channel dropout exists, the error can be corrected by simple inversion (adding a "1" to the corresponding channel modulo 2 and gate). As shown, this system is capable of correcting all single-track burst errors and isolated single-track errors plus half of the double-track errors. Because of the tape flaw distributions encountered in practice, this

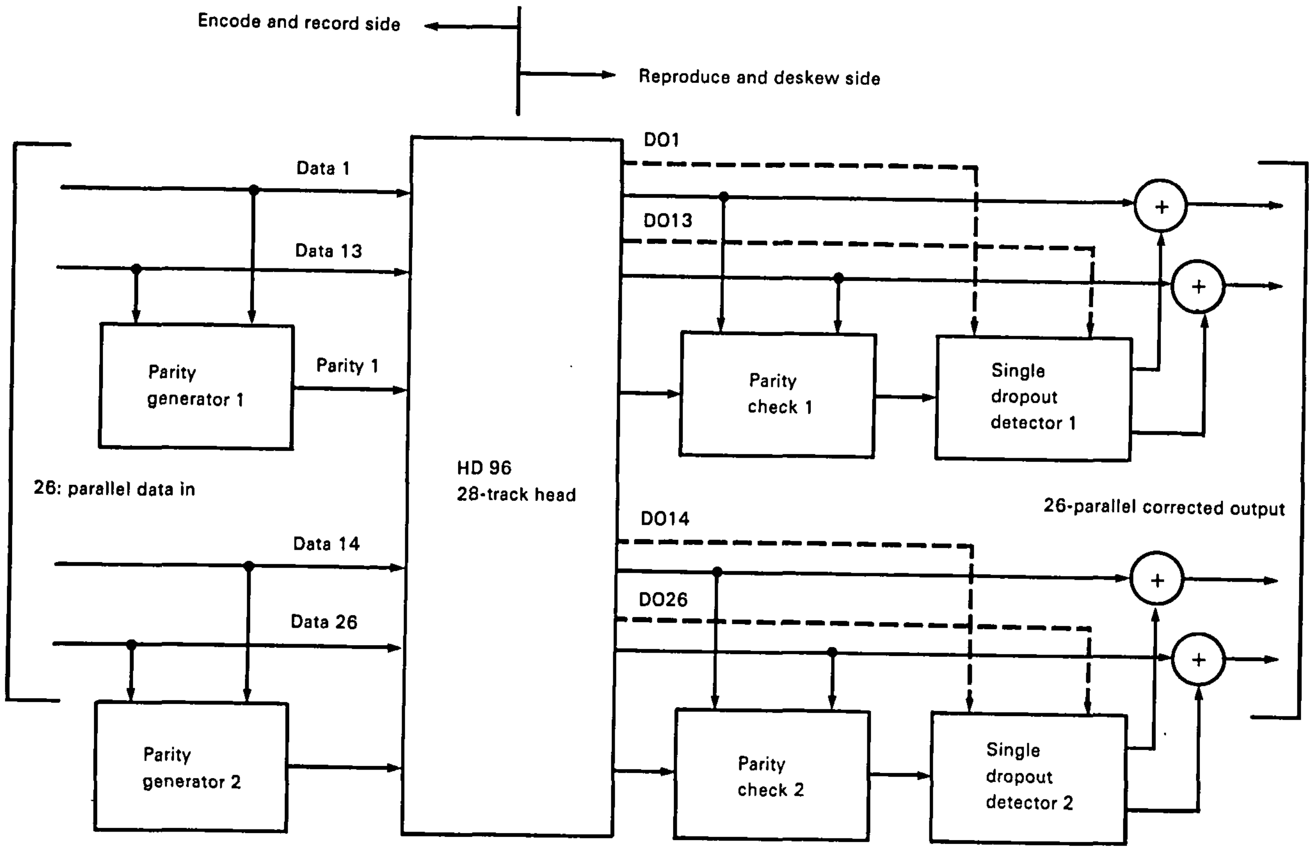

Figure 13-15.—Dropout-based error correction concept. (DO = data out.)

system is very effective and improves "raw" error performance by factors of 50 to 500.

AUXILIARY ELECTRONICS

When not all tracks are required for digital service, the extra tracks are available for auxiliary data recording of such items as time code, voice, and PCM. The standard HDDR design provides for up to four such channels. This capability is provided by using standard FM, direct, servo-reference analog accessories of the basic model 96 transport.

CABINET LAYOUT AND PHYSICAL CHARACTERISTICS

The HDDR system is designed for housing within standard Honeywell transport racks for ground-based systems, or alternatively in standard Electronic Industries Association racks having a panel width opening for 19-in. wide panels and an equipment depth of a minimum of 25½ in. Controls and other extensions do not protrude more than 3¾ in. in front of the panel frame. A typical panel arrangement is illustrated in figure 13-14.

CHAPTER 14

The Development of a High-Performance High-Density Digital Recording Error Correction System

James H. Stein and W. D. Kessler
Fairchild Weston Systems, Incorporated

This chapter describes HDDR (high-density digital recording) systems developed by Fairchild Weston Systems, Inc. (commonly referred to as Fairchild Weston) and includes systems both without and with error detection/correction. It is organized sequentially (much as the systems were developed, historically), proceeding from the simplest hardware to more sophisticated error correcting systems that provide essentially error-free recording and reproducing.

HISTORY

Within Fairchild Weston, there is a group, previously Sangamo, that has been developing and producing magnetic tape recorders since the early 1960's and HDDR systems for these recorders since the inception of these techniques in the early 1970's (refs. 14-1 and 14-2). Another group within Fairchild Weston, EMR Telemetry, has been working an equally long time with recorder encoding and decoding techniques and devices as well as with bit error test sets (ref. 14-3). These two groups pooled their talents in 1978 and now reside in Sarasota, Fla. As a result of this combination, mature systems worthy of description have been developed.

HDDR was first implemented on a "per track" basis as serial systems. The only processing involved encoding of data to make its frequency spectrum more compatible with the frequency response characteristic of the magnetic tape. Parallel HDDR systems were not practical because economic dynamic skew correction had not been developed.

As large-scale integration became available, dynamic skew correction was instituted so parallel data streams could be recorded and reproduced with proper time coherence. This deskewing required portioning the data into frames and the addition of frame synchronizing words. Naturally, these additional overhead bits reduced the recorder efficiency as less user data could be recorded. However, the overall effect was very positive because parallel data bytes could be recorded. This made possible the recording of higher input data rates because the data could be demultiplexed, or spread over several parallel recorder channels. Bit rates to 100 Mbps could be accommodated on a 32-track, 120-ips recorder. These serial and parallel recording systems have become standard and are in wide use today—using the same formats originally adopted and making interplay between recorders possible. The standard systems will continue to be used for years to come. In fact, this serial format is now a Range Commanders Council (RCC; formerly Inter-Range Instrumentation Group) Recording Standard.

Still later, as error detection and correction began to be implemented (often by the "user" completely external to the recorder), more redundant parity bits were added. Again, although the overall effect was positive, user efficiency was further decreased.

This set the stage for a fresh look at the overall problem within Fairchild Weston and, with the aid of its consultant CNR, Inc., the present error detecting/correcting system, which provides essentially error-free recording and reproducing, was developed.

HDDR ENCODING

HDDR is digital recording that makes use of the full analog bandwidth of the tape recorder. The name implies that there must also be a "low density" technique. Such a name is not in common use in the instrumentation field; however, recording at lower densities is applied where extreme reliability and accuracy are paramount, such as with computers.

Digital recording is used in instrumentation because it allows precise reproduction of data, although at the expense of bandwidth. Recorder-induced flaws, such as noise and distortion, can be reduced to almost any desired level by sacrificing sufficient bandwidth. When

this is important, HDDR may be used instead of direct or FM recording.

The HDDR encoding process must solve two basic problems. One is to allow the recording of any legal stream of data. The other is to record data and clock on a single track. Suitable conditioning or encoding of the data so as to introduce a plentiful supply of transitions between "0" and "1" values will solve both these problems.

When the data rate is sufficiently low, the use of a biphase code will serve the purpose. Any of the biphase codes will guarantee at least one transition for every bit. Reproduction of the data then becomes a simple matter because there are no long regions without a signal. Reconstruction of a clock from the reproduced data is easy for the same reason; there are many transitions of data upon which to synchronize a clock oscillator. Thus, biphase is one method of encoding HDDR for recording.

Biphase, however, entails a penalty in that it requires twice the bandwidth that nonreturn to zero (NRZ) requires for the same data rate. Therefore, the coding problem in HDDR becomes one of supplying enough transitions in the recorded signal without appreciably decreasing the bit rate from the NRZ bit rate.

All HDDR systems manufacturers use some method to achieve this modulation or "signal conditioning" prior to recording.

The most popular methods of signal conditioning for HDDR recording are described in detail in the ANSI document on standardization of HDDR recorded tapes (ref. 14-4), in draft form at this writing, and in other chapters of this book. All have certain advantages and disadvantages. Long ago, Fairchild Weston selected randomizing as its method of signal conditioning, for reasons to be set forth.

Randomizing

Randomizing is a form of polynomial division, modulo 2, of the data stream by a special number defined by the shift register circuit. It produces an output resembling, to a degree, a random sequence. This sequence, however, is an encoded form of the original sequence and can be decoded by the corresponding polynomial multiplication. Figure 14-1 shows the standard 15-cell randomizer and derandomizer. The reader may readily test, on paper, how these work by applying a data stream containing all "0" values except for a single "1."

History of Randomizing

J. E. Savage (ref. 14-5), in 1967, gave a thorough and understandable presentation of this subject. Savage listed 13 references going back to 1941. His use of the

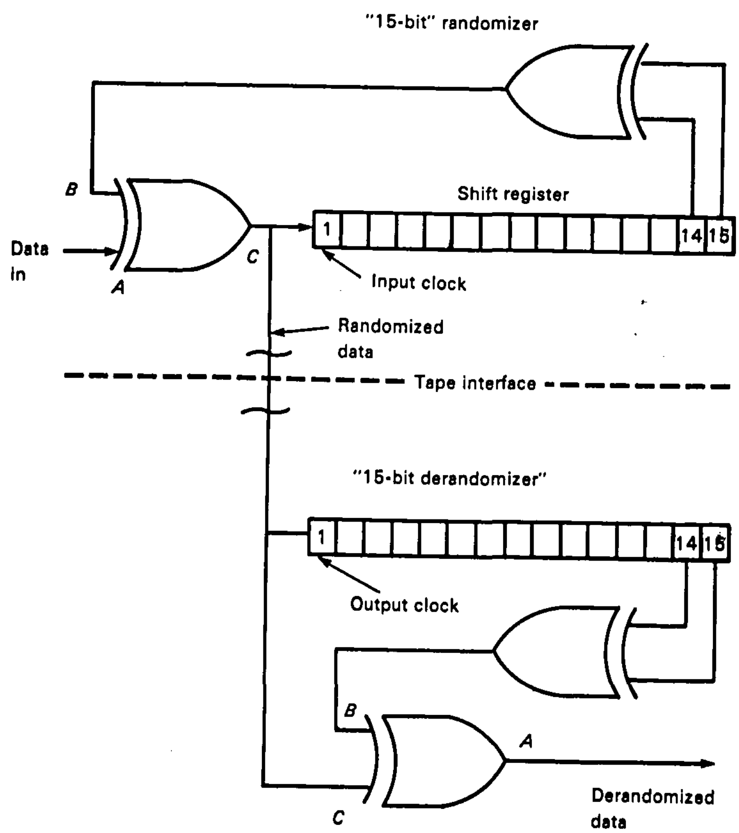

Figure 14-1.—15-bit randomizer and derandomizer.

term scrambler indicates that it need not be considered slang; therefore, it is used here interchangeably with randomizing.

At the time the Fairchild Weston HDDR system was developed, the company (then Sangamo Electric) was building modems with scramblers. It is from that technology that scramblers became a part of Fairchild HDDR. Also, prior to the acquisition of Sangamo Electric by Schlumberger, the latter was using scrambling in its HDDR, having made the decision to do so quite independently of Sangamo Electric.

Sangamo (now Fairchild) was the first manufacturer to use randomizing as a routine method for conditioning data in HDDR.

In the intervening years, scrambling has been vigorously attacked by competitors who did not offer it, and has been feared or avoided by users who misunderstood it. But, in 1980, RCC adopted scrambling as the standard method for signal conditioning serial HDDR (ref. 14–6). With this recognition, scrambling in HDDR was no longer the "ugly duckling" it once was, but has been marketed (although in a noncompatible form) by other manufacturers.

Advantages of Randomizing

Compared with other methods of signal conditioning for HDDR, randomizing has the following advantages:

(1) It does not add any overhead bits.

(2) It is practically dc free.

(3) It has an extremely low probability of being defeated by a chance data pattern (low pattern sensitivity).

(4) It does not require a change in clock rate.

(5) It does not require a special sequence for decoding.

(6) Decoding does not involve a double-frequency clock.

(7) The encoded data remains in NRZ form; i.e., transitions occur only on bit boundaries.

(8) It does not involve phase modulation with resultant reduced phase margin.

(9) It does not "multiply" errors (it adds two errors to the end of an error burst).

The overall result is better performance with fewer errors.

HDDR SYSTEMS

Serial HDDR

Serial HDDR is the recording of serial digital information on a single tape track without the need to retain any exact time relationship to other tracks. In other words, tape skew is ignored. Serial channels ordinarily have their own clock accompanying the data, and each serial channel can have a different bit rate.

Parallel HDDR

Parallel HDDR requires that the reproduced data be deskewed so that bits recorded together as a parallel byte may be reproduced together to regenerate the same byte.

To accomplish deskewing, parallal HDDR requires the use of occasional markers inserted in series with the data, at intervals exceeding the maximum skew. These markers are called "synchronizing words." They must be recognized in the reproduce circuits and used to realign the data in deskew buffers.

To "make room" for the synchronizing words, the data rate must be increased prior to recording. The ratio of added bits to original bits is known as "overhead." High overhead is undesirable because it restricts the data rate that can be handled.

THE FAIRCHILD WESTON HDDR SYSTEM

Format is defined, here, as the pattern of data on the tape, other than the data message. The very basic format items of track number and dimensions are covered by RCC and ANSI standards and will not be discussed here. Serial HDDR has no actual format; it has only a "code." The code used by Fairchild Weston is randomized NRZ–L, as mentioned earlier. Parallel HDDR has a format that consists of the details of frame and synchronizing words recorded on tape. The format used by Fairchild Weston is shown in figure 14–2. In this figure, line 1 shows the original data as applied to the system. The data are blocked into 496-bit blocks, and the data rate is increased in the ratio of 31 to 32, leaving 16 bits, as shown on line 2. Line 3 shows the synchronizing word, 16 bits long, generated once for each frame. Line 4 shows the data and synchronizing word, with the synchronizing word inserted into the gaps in the data, making the full 512-bit block.

Line 5 shows a detail of the synchronizing word. It is seen that the 16th bit is not actually part of the synchronizing word, but is a single odd parity bit taken over the intervening region of 511 bits. It is used solely for visual monitoring, flashing an indicator on the deskew card panel should a synchronizing word not be detected when expected.

In some models, the first bit of the synchronizing word is a "don't care" bit. This allows reverse play without synchronizing errors because of the parity bit that becomes bit one, in reverse. For reverse operation, the user may select either a symmetrical synchronizing word, or may reverse the reproduce synchronizing word

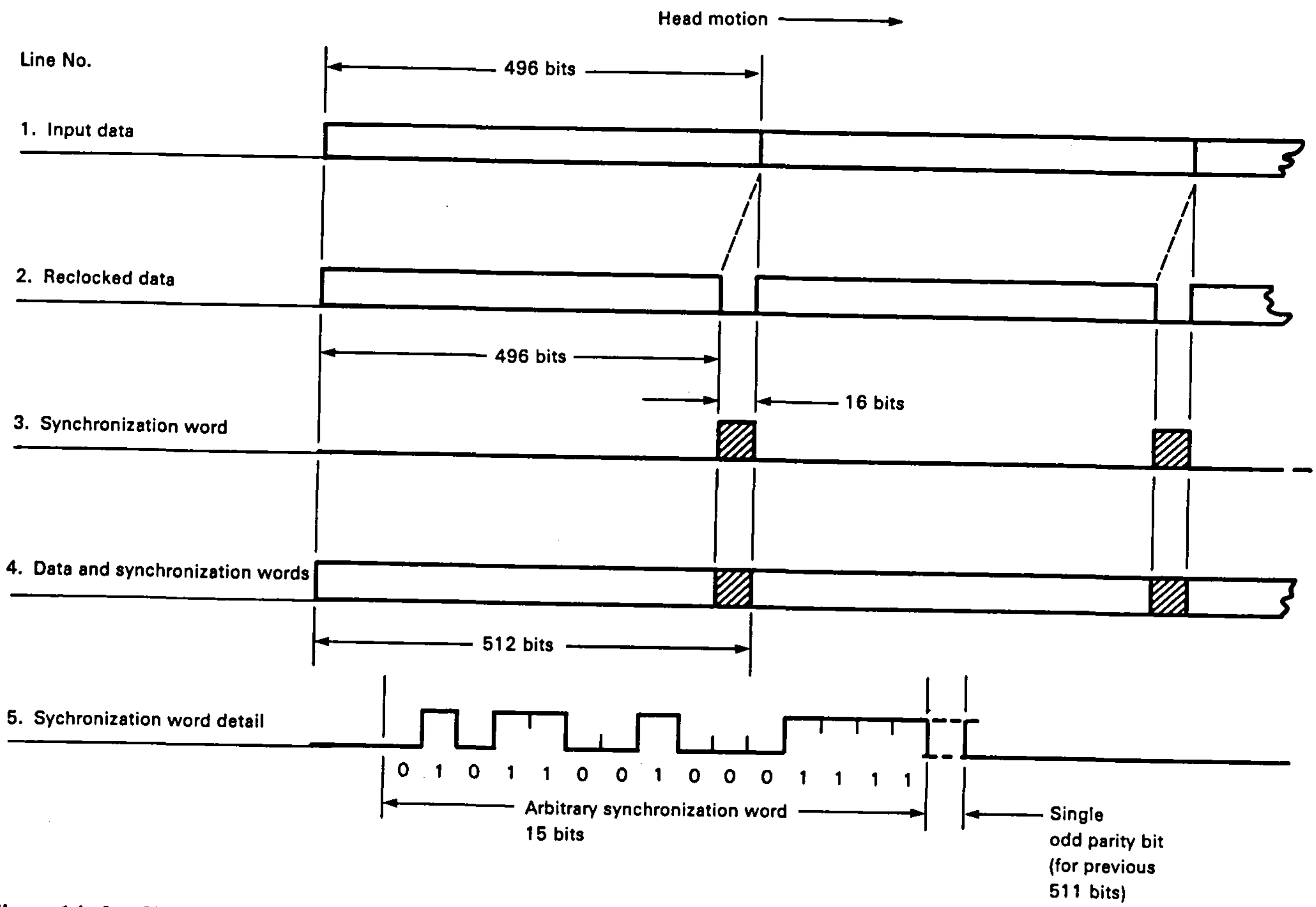

Figure 14–2.—Format for HDDR.

as compared with the record synchronizing word. Each bit of the synchronizing word is programmable for both record and reproduce.

This block of 496 bits of data plus 16 overhead bits remains unchanged through scrambling, code conversions, and recording. It is the recorded format.

It is important to note that this format has remained unchanged in Fairchild Weston HDDR tape transports since the first system, and continues through the present. This assures users of compatibility with past or future systems. Similarly, the synchronizing words and the scrambling options are compatible.

Advantages of the Fairchild Weston HDDR Format

Low Overhead

The use of randomizing as an encoding method in serial HDDR has the advantage of introducing no overhead. The resulting signal spectrum, consisting of ac signals only, can be handled efficiently by the tape transport without the need for further encoding or modulation. The low overhead of the parallel system is a direct result of building on the zero overhead of the serial system and using a low ratio of synchronizing word length to synchronizing word spacing. This ratio is 1/31, giving an overhead of 3.23 percent. This overhead figure is so low as to be practically negligible.

Cross-Play Capability

All Fairchild systems without error correction are compatible in serial codes and parallel format. The basic serial code is randomizing, from the earliest to the latest. Most serial cards offer three scrambler codes. The parallel frame has remained at 496 data plus 16 overhead bits since the first system, and there appears to be no reason to change it. The synchronizing word is programmable bit by bit; however, an identical standard synchronizing word has been recommended to all users.

Skew Correction Ability

The Fairchild Weston parallel HDDR has a deskew capability of about 490 bits, peak to peak, at the tape rate. This is more than enough for the extreme skew that might be encountered when allowing for interleaved

heads, mechanical head tolerances, and cross-play between machines, with maximum tension, temperature, and humidity effects on the tape. With double-density data, this deskew capability is reduced to one-half the distance on tape, or 245 normal density bits. This is still adequate for any expected demands; however, the point should be made that any system that does not have comparable deskew capability may be expected to show problems at double-density rates, when used in conditions of extreme skew.

Implementation

Figure 14-3 is a block diagram of a typical Fairchild Weston HDDR system. Four parallel tracks are shown, although this number could be any from 2 to 32 (or more).

Serial HDDR

In figure 14-3, the shortest brace, labeled "Serial," shows the elements of a serial system. These are, typically, the encoders (E) and the decoders (D). The encoder accepts data and a clock; performs standard scrambling, biphase encoding, other code conversion, or complete bypass; then sends the encoded data stream on to be recorded. The encoding functions are normally on a single card that is interchangeable with the direct or FM record cards.

On the reproduce side of the tape, the signal from the tape goes to a decoder where it is amplified, equalized, converted to NRZ–L code, if desired, and descrambled. Also, a clock is generated by the bit sychronizer portion of the decoder. The data and clock then leave the card. The decoders are interchangeable with direct and FM reproduce cards. These two types of cards, encoder and decoder, form a serial channel meeting the RCC standards as stated in reference 14-6.

Parallel HDDR

Again, in figure 14-3, the next longer brace shows the elements of a parallel system without demultiplexing and multiplexing. Note that the parallel system is composed of four serial systems plus the extra functions in blocks S, C1, B, and C2. The parallel system can be composed of any number of tracks from two up to the limit of the tape transport.

Block S represents the synchronizing word insertion operation in which the data rate is increased and the synchronizing sequence is inserted every 496 bits. Block S is, typically, a four-channel card. It uses timing signals generated by block C1, the synchronizing clock card.

On the reproduce side of the tape transport, the parallel system is formed by adding deskew buffers (B) and a deskew clock card (C2) to the serial decoders. These cards restore the parallel data to its original form by removing skew, changing the data rate, and deleting the synchronizing words.

Deskewing is accomplished using random access memories (RAM's). Track clocks generate "load" addresses for the RAM's and load 512-bit blocks into the RAM's under control of the individual synchronizing words. Data are read out of the RAM's in 496-bit blocks by the master clock, thereby accomplishing both deskewing and removal of the synchronizing word.

False synchronizing word detection is never a problem because synchronizing words lying outside the expected zone are gated out. Only after two successive missed words is the gate removed. Similarly, after two successive synchronizing words are detected, the gate is reinstalled around the synchronizing region. Once synchronization is achieved on any track, further synchronizing indications are only precautionary and are not needed unless bit slip occurs.

Experience shows that bit slip rarely occurs even from large, deep dropouts, unless there is tape damage. For this same reason, the single master track has proven to be adequate.

Serial Data Demultiplexing and Multiplexing Option

When the incoming data rate is too high to be recorded directly onto tape (as may happen when it is a high-rate serial channel), it can be demultiplexed onto two or more tracks, as necessary, to reduce the data rate to one which is within the limits of the tape transport. After reproduce, the several tracks of parallel data can then be multiplexed back to the original rate, or a scaled version of it at a different tape speed.

Referring once more to figure 14-3, we see a demultiplex function preceding the parallel system and a multiplex function following it. This shows how the parallel system can be used with demultiplexing and multiplexing operations.

Fairchild Weston offers two sets of demultiplexing/multiplexing cards. One is implemented in Schottky logic for use up to about 30 Mbps, and the other is emitter-coupled logic (ECL) for higher data rates.

The demultiplexing cards have 4 inputs and 16 outputs to allow numerous options to be programmed. Similarly, the multiplexing cards have 16 inputs and 4 outputs. Both are cascadable for ratios higher than 16:1.

Configurations

Parallel HDDR is available with any of the Fairchild Weston tape transport models. The first generation cards are used in Models 3, 4, 5, and 80. Models 9 and 10 have improvements bearing on user convenience, but

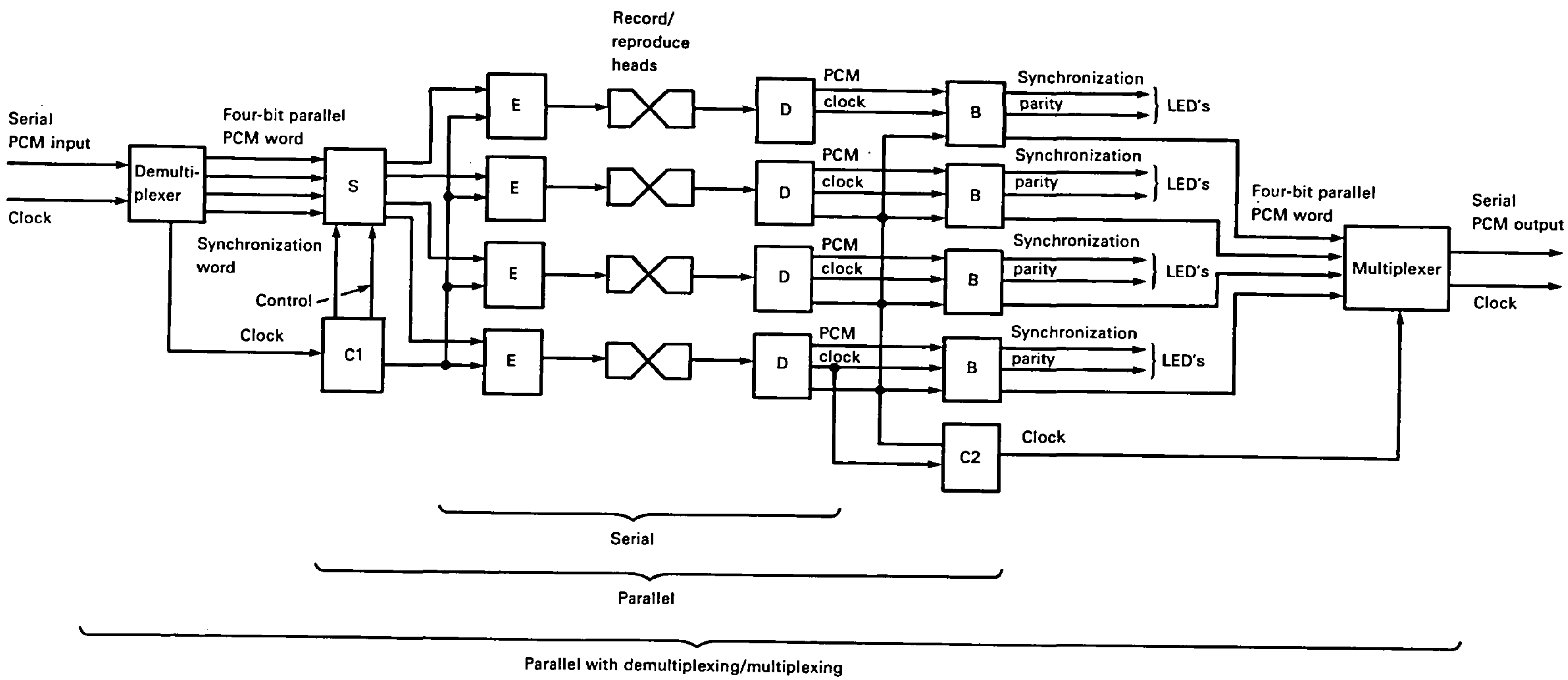

Figure 14–3.—Typical Fairchild Weston HDDR system. (LED = light emitting diode.)

the tape format remains compatible with formats of earlier models. The laboratory Model 10, for example, has bit synchronization with two clock rates, to allow rapid change of data rate, and allows for reverse operation of the descrambler. Model 9 programming is controlled through a touch membrane and microprocessor. It also has reversible logic, but the primary advantage is that the track bit synchronizations may be programmed together, singly or simultaneously, in groups of the user's choice, to accept any bit rate from band edge down to 15 kbps, and at any speed.

The range of operation is secured by first changing the frequency of the oscillator in 2 percent increments for a total 2-to-1 variation. Greater requirements then act to combine this with one or more divider stages to give the requested bit rate. This is done, automatically, with the touch of a finger.

In all Fairchild Weston models, tracks not required for parallel HDDR may be used for direct recording, frequency modulation, or serial HDDR. The serial HDDR option retains the scrambling and bit synchronizing features that are present in the parallel system for that tape recorder model.

Performance Monitoring

Fairchild Weston parallel systems are equipped with light-emitting diodes (LED's) that provide a visual indication of data quality. Each track has, on the deskew card panel, two LED's. One will flash when the serial parity does not check; the other will flash when a synchronizing word is not detected in any frame. Repeated flashing of either of these lights indicates a problem in that track, such as wrong head current, poor equalization, or a dirty head. A constant "ON" condition may indicate a setup problem such as wrong polarity, etc. The signals to these LED's are "stretched" to give good visibility; however, "unstretched" signals are also available should the user wish to use them.

Features

The more important features and options of the Fairchild HDDR recorders (HDTR) are the following:

(1) IRIG heads
(2) Readout by external clock
(3) Ability to use the same electronics (Lab Model 4 and portable Models 3 and 5)
(4) 32 tracks and front access boards in 28-in. panel height (Models 3, 4, and 5)
(5) 28 tracks and front access plus versatile multiplexing/demultiplexing system in 28-in. panel height
(6) Minimized circuits for reliability and lower cost
(7) 64-to-1 speed change, up or down
(8) Line drivers and receivers
(9) Optional synchronizing word composition
(10) Optional scrambler length (11, 15, or 17 bits), or complete bypass
(11) Optional code formats: NRZ mark, NRZ space, NRZ level, biphase mark, biphase space, and biphase level
(12) No pattern sensitivity
(13) Performance monitoring LED's
(14) Decoding without key words
(15) 1024-bit RAM buffer for 490-bit peak-to-peak deskewing
(16) Reversible code operation in Models 9 and 10
(17) Programmable bit synchronizing clock rates

Nearly all of these features that apply to parallel systems are also available in the error correction/detection system (ECDS).

Performance

The error rates experienced with non-correcting HDDR depend more upon the tape and its cleanliness than upon the electronics. The experience of Fairchild Weston and of users of our machines leads to the following guidelines:

(1) New tape causes more errors than tape that has experienced 10 to 20 passes over the heads.
(2) New or dirty tape can be greatly improved by processing through a cleaner/burnisher.
(3) Solid ("glass") reels should be used in the most critical applications, as they help keep the tape clean.
(4) The wider tracks of the 14-track format give 10 to 100 times reduction in error count over 28- and 32-track formats.
(5) Adverse tape/head contact can cause errors, especially at the 120-ips speed. The presence of "brown stain" on the heads in dry environments can be troublesome.
(6) Users with critical applications are advised to obtain a copy of *Magnetic Tape Recording for the Eighties* and to heed the precautions in appendix B (ref. 14-7).

Measured performance of HDDR depends, primarily, on the condition of the tape used and is so variable as to have little meaning relevant to the system. Typical figures are shown in table 14-1.

When serial channels are demultiplexed and multiplexed, the error rate of the entire tape system can be measured easily using a bit error test set of suitable speed, such as one of the Tau-Tron models.

When demultiplexing and multiplexing cards are not used, there are two alternatives:

(1) Measure single tracks.
(2) Use fanout logic to drive all tracks and use an "error funnel" to provide the "OR" of all channel errors.

Table 14-1.—*Typical Tape Performance Under Various Conditions*[a]

Tape condition	Trackwidth, mils	Speed, ips	Error rate
New	25	60	$2/10^6$
	50	120	$1/10^6$
Wiped	25	60	$2/10^7$
Used	50	120	$1/10^8$

[a]Ampex 799 tape; density: 33 000 bpi.

Measurement of single tracks, method (1), is convenient for "go/no-go" testing, but does not prove performance because there is no check of deskewing.

Method (2) is strongly recommended. The fanout logic requires no explanation. Note, however, that a simple "OR" circuit will detect errors of only one polarity—that which passes through the OR gate. For rigorous testing, the outputs of an OR gate and of an AND gate should be added to give total errors. Simultaneous errors on two or more tracks will be counted only once, as though from only a single track. This occurrence is infrequent enough that it may be ignored.

THE NEED FOR ERROR CORRECTION

In chapter 4 of the NASA Reference Publication 1075 (ref. 14-8), Al Buschman lists 12 sources of tape anomalies causing dropout errors. When one realizes that all tape, dirty or clean, old or new, causes errors, the question arises, what can be done about it? The obvious answer is to use an HDDR system with the ability to correct most tape errors.

Over the years, manufacturers of HDDR systems have produced add-on error correcting systems, but such systems were less effective than if they had been an integral part of the system.

The time was ripe, in 1980, for the introduction of the best practical error correction system for HDDR. Fairchild Weston first announced its double-track error correcting system at the International Telemetering Conference Meeting in October 1981 (ref. 14-9) and also at the September 1981 meeting of the Tape Head Interface Committee (ref. 14-10).

THE FAIRCHILD WESTON ERROR CORRECTING HDDR SYSTEM

As stated earlier, the Fairchild Weston error detection and correction system (EDCS) is the result of a cooperative effort by Fairchild and CNR, Inc. Its parameters have been chosen with the goal of designing the best possible error correction system for HDDR without any great increase in hardware complexity beyond that commonly used in less powerful systems.

Figure 14-4 is a simplified block diagram of the system. It shows that two main functions are performed on the record side; outer encoding and inner encoding. Similarly, on the reproduce side are the inverse operations: inner decoding and outer decoding. These functions generate and check orthogonal parities on the tape, thereby allowing the exact bits in error to be located and corrected.

The parameters of the codes (i.e., the numbers involved) are not arbitrary, but are chosen as a set that fits together well. It would be difficult to change them without reducing the effectiveness of the system.

Outer Encoder

The reader's attention is directed to the upper left corner of figure 14-4. The outer encoder generates cross-tape parity from the data tracks. In one mode, it generates a simple parity from a maximum of 15 tracks; in the full double correction mode it uses a (16, 14) modified Reed-Solomon (R-S) code (refs. 14-11 and 14-12) and generates two tracks of parity. The two transverse parities must, of course, be derived according to different rules; the use of the base 16 number system and 4-bit characters makes this possible. The two parity tracks are then processed in the inner decoder in the same manner as the data tracks.

Inner Encoder

The purpose of the inner encoder is to generate a longitudinal (serial) parity for each individual track, data and parity, alike. This longitudinal parity is used during reproduce for synchronization, skew correction, and error correction. To provide room for this longitudinal parity, the data rate is "speeded up" by a factor of 10/9, leaving a hole at the end of the frame of data into which the longitudinal parity is inserted. A coset is also added modulo 2 at this point. In fact, three frames use one coset and the fourth frame uses a second different coset. This provides a unique synchronization pattern each fourth frame (or 960 bits) that is used for deskewing during the reproduce process.

The pseudorandom characteristics of this coset help to spectrally condition the data for recording. The data are then further spectrally conditioned by randomizing if the packing density is above 15 kbpi or by converting to biphase if lower packing densities are to be used. It is important to note that although biphase and randomization are the two standard forms of conditioning used by Fairchild Weston, this system is not restricted to them—any other appropriate form could be used. The spectrally conditioned data and parity are output from the inner encoders and are saturate recorded on the magnetic tape. Again, saturate recording is not a necessity; bias recording could be used, but the addi-

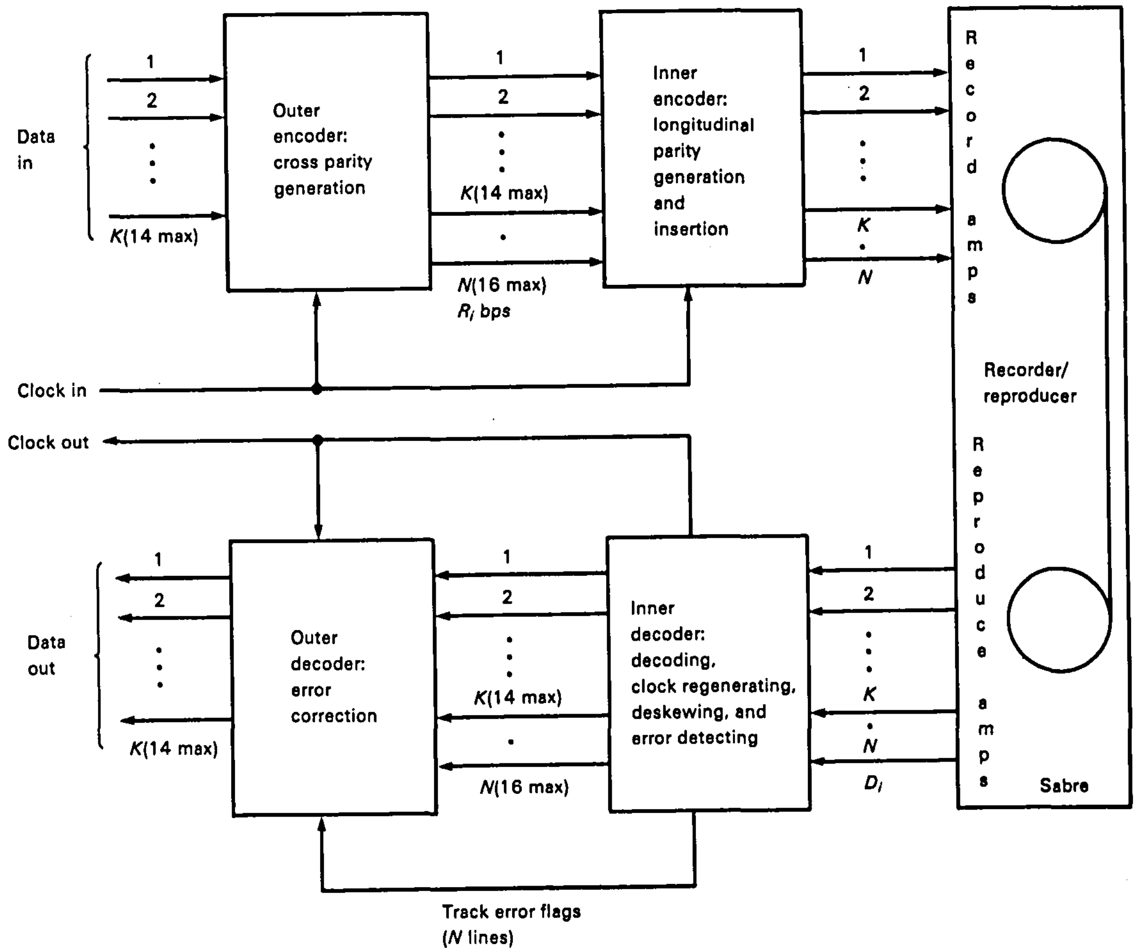

Figure 14–4.—Fairchild Weston EDCS with Sabre recorder. (K = tracks of data; $N-K$ = tracks of parity; R_i = input data rate; and D_i = recorded (data plus parity) rate = 10/9 R_i.)

tional signal-to-noise advantage obtained by saturate recording is desirable.

Tape Format

Figure 14–5 illustrates how a frame of data is recorded on tape, excluding for a moment the effect of the normally specified 1.5-in. spacing of the interleaved heads. A "block" has a length of 216 bits of data plus 24 bits of longitudinal block control header (BCH) (refs. 14–11 and 14–12) parity for a total length of 240 bits. The block width is K (maximum of 14) data tracks and $N-K$ (normally 2) cross-parity tracks for a total of N (maximum 16) tracks. As indicated previously, the outer code is a simple parity for one track and a modified R-S code for the second track. Note in figure 14–5 that the inner BCH parity is generated for the two tracks of cross-parity as well as for the data tracks. The simple parity is calculated on a bit-by-bit basis across the frame and includes the track of R-S parity whenever two tracks of parity are used. The R-S parity is computed using 4-bit symbols (shown as Q) across the frame. These symbols are formed by grouping four sequential bits from the same track; Galois field arithmetic over GF(16) (refs. 14–10 and 14–11) is used in the computation. Thus, the R-S parity is, in itself, a 4-bit symbol. However, all outputs remain serial with the R-S parity being shifted out serially along with the data and simple parity tracks. The overhead per track, using N = 240 bits and K = 216 bits, is

$$\left(\frac{N}{K}-1\right) \times 100 = \left(\frac{240}{216}-1\right) \times 100 = 11 \text{ percent}$$

For the Fairchild Weston system, this track overhead remains the same in every case.

The system overhead, assuming 2 tracks of parity and 14 tracks of data, and including the track overhead, is

$$\left(\frac{10N}{9K}-1\right) \times 100 = \left(\frac{160}{126}-1\right) \times 100$$

$$= 27 \text{ percent}$$

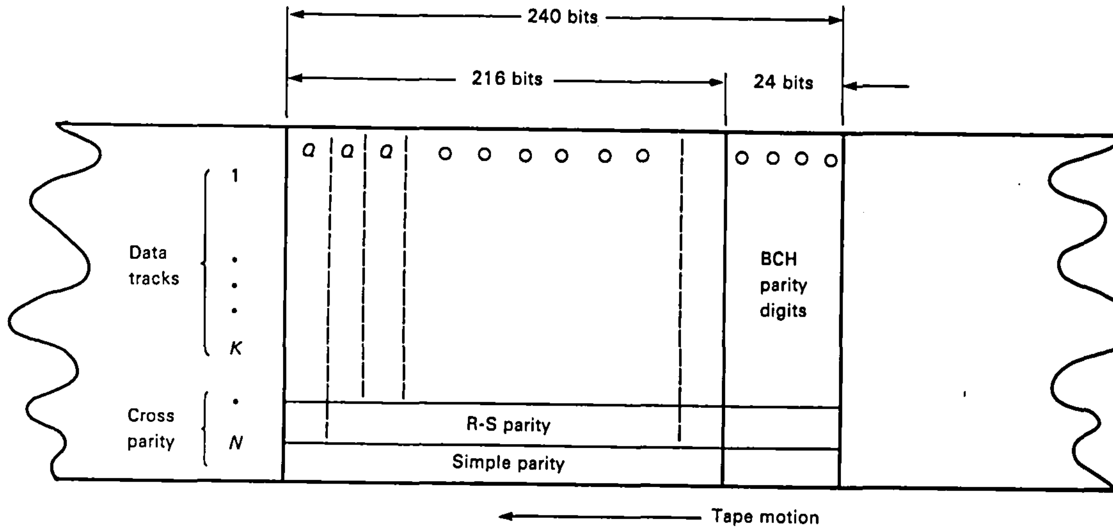

Figure 14–5.—Recording onto tape. (Q = 4 bits in length.)

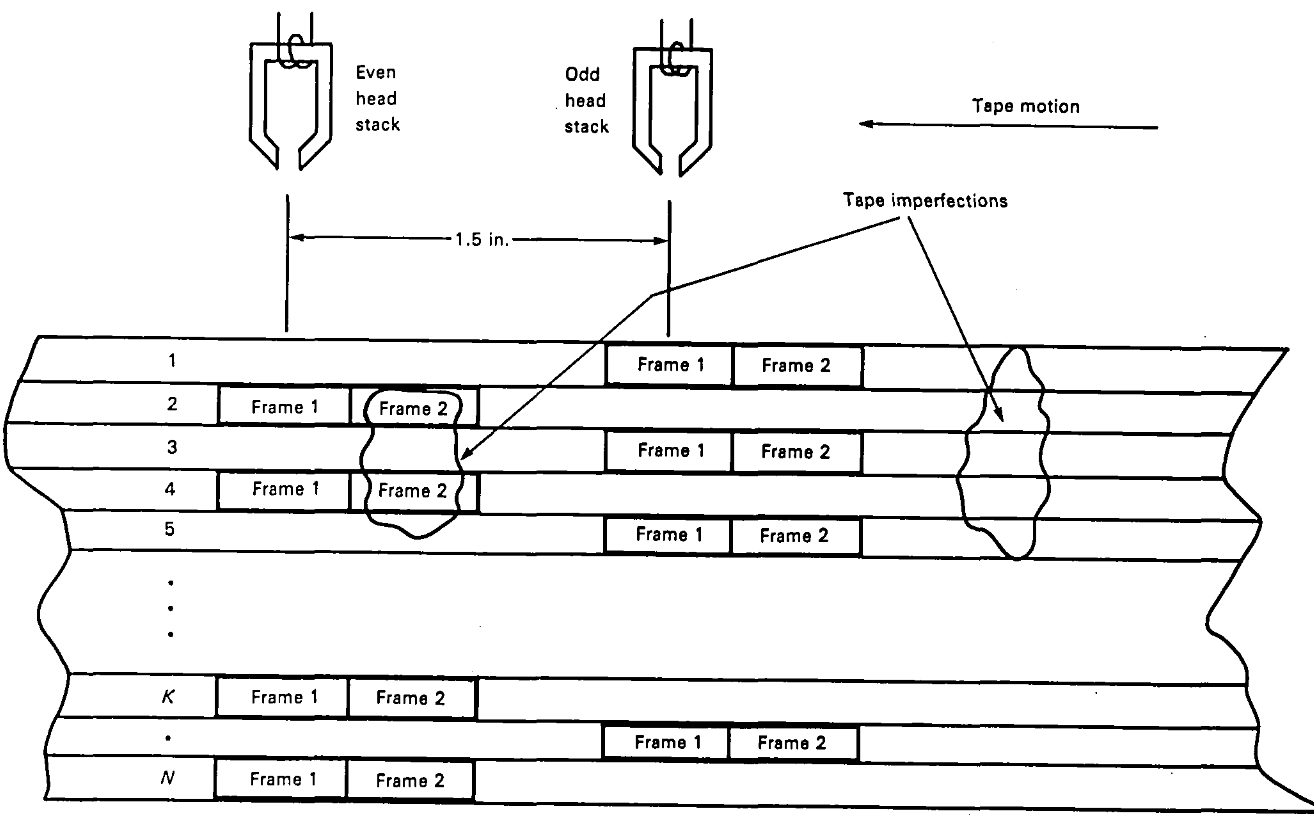

Figure 14–6.—Frame offset due to interleaved headstacks.

This is an unusually low system overhead for the powerful results obtained. Note that no frame synchronizing words, in the conventional sense, are included within the frame of data. As will later be seen, the longitudinal parity is, in effect, used as a synchronizing word, which allows all the bits within the frame to be used as either data or parity.

The reader is reminded that, as shown in figure 14-6, the data on every other track is displaced 1.5 in. due to the normal interleaved head construction as specified by RCC (ref. 14-6). This provides a protection against tape imperfections large enough to encompass up to four adjacent tracks because it places the resulting error burst of each pair of tracks in a different frame and the

system is capable of correcting for errors occurring within the same frame on two tracks, simultaneously. This is illustrated by the tape imperfections encompassing frame 2 on tracks 2 and 4 of figure 14-6. This error burst would be corrected by the system. The tape imperfection shown on the right-hand side of figure 14-6 encompasses more than four tracks, so error bursts would occur in three tracks of the frame, simultaneously, and the system would not correct for these. However, it would flag the fact that error bursts occurred and would output data as decoded.

Reproduce Data Conditioning

Referring back to the lower half of figure 14-4, as data is reproduced from each track, it is amplified, equalized, and bit-synchronized to produce serial data streams plus clock. Also, at this point, the spectral conditioning (either randomizing or biphase encoding) that was applied to the bit stream just before recording is removed. Following this, the data and parity (now in reconstructed digital form) proceed to the inner decoders.

Inner Decoders

The primary function of the inner decoders is to detect errors as they occur and to send error flags to the outer decoder, indicating the tracks in which these errors occurred so that the outer decoder can use the cross-parity tracks to correct them. But, before this can be done, skew created by the magnetic tape recorder must be corrected.

A unique feature of this system is that deskewing is accomplished without a conventional frame synchronizing word. For each track, each time the data stream advances one bit into the decoder, it is stored in a deskew buffer. Also, each time the data advances one bit, longitudinal parity is calculated and compared with the recorded parity and coset (which was added modulo 2 in the inner encoder). Eventually, the calculated and recorded parities will compare, allowing the coset to be recognized; this coset then acts as a frame synchronizing word to be used to align the frame boundary for deskewing. During this process of parity verification and coset recognition, the effects of the bits preceding the block under consideration are removed by logic circuits that simulate clearing the parity generators prior to parity calculation. As the frame boundary is determined for that particular track, the data of that frame are clocked to the output side of the first-in, first-out (FIFO) deskew buffer. This process is repeated for each track, and when frame boundaries for all tracks have been determined and all data corresponding to these frame boundaries are poised on the output side of the deskew FIFO's, a completely deskewed parallel word is clocked out of the deskew buffers. A frame synchronizing pulse is also generated at the boundary side of the frame.

Once synchronization is achieved and the frame boundary is defined, the system calculates the location of the next frame synchronizing pulse and compares this with the actual occurrence. Normally the expected pulse occurs at the proper location because the error rate is so low. If it does not, the system "knows" that an error has occurred or that the system has lost synchronization. It is first assumed that errors in that block have occurred and corrects them. If the parity fails to check for several contiguous frames, the system assumes that synchronization has been lost, and the process starts over for the track involved.

As stated previously, the inner decoders calculate the parity for each frame on a track-by-track basis and compare this calculated parity with the recorded parity. If they do not agree, an error flag is sent to the outer decoder indicating that an error has occurred in that track for that particular frame. If two tracks have errors, two flags are sent to the outer decoder. Indeed, each track, including the cross-parity tracks, has a flag that is set for that frame when an error occurs on that track. At the end of each frame, all error flags are reset. These flags, together with the transverse parities, allow the outer decoder to correct for errors. As seen in figure 14-4, the data stream and the error flags are output to the outer decoder.

Outer Decoder

The outer decoder performs a number of functions, in addition to correcting errors detected by the inner decoder. These additional functions are described first, assuming that no errors have occurred on any tracks for the frame under consideration. On a track-by-track basis, the coset added modulo 2 to the data in the inner decoder is removed. Further, the longitudinal BCH parity, also added to the data in the inner encoder, is removed from the frame and the data slowed down by 9/10 to fill in the hole left by removing the 24-bit parity word. Following this, the fully restored data, identical to the input data, are clocked out and returned to the user, along with a clock.

Assume now that errors have occurred in the reproduced data for this particular frame. If two tracks of cross-parity have been recorded, and this is normally the case, then errors can occur in two tracks (either data or cross parity) simultaneously and be corrected because the serial parity flags the tracks with errors. This requires the solution of two equations to determine two unknowns. Modulo 16 arithmetic is used.

It is important to note that in this system any two of

the K tracks can have errors and be corrected. Some systems with two tracks of redundancy split the data tracks into groups, such as odd and even, and use one parity track for each group. That method has the disadvantage that, if errors occur in two tracks within the one group, simultaneously, correction cannot occur, even if no errors occur in the other group. The Fairchild system allows any two tracks to have errors and to be corrected.

If errors occur on three tracks, simultaneously, correction is mathematically impossible and cannot occur. In this case, the data are output as they are decoded, but a "correction for this frame not possible" flag occurs. The channel error flags also are made available so data deletion or weighting can be accomplished by the user, if desirable; however, the occurrence of errors on three tracks, simultaneously, occurs only very rarely, less than once per 14 in. reel of tape. Normally, the errors are confined to one or two tracks and are completely detected and corrected, as we shall see in the later sections on performance.

System Condition Monitor

By its very nature, a system such as this accommodates degradation and even some types of failures within itself. One track of recorder electronics can fail, and the normal user may not even recognize the failure. The error rate is somewhat increased, but that may not be noticeable. In a sense, this is very good. However, to obtain the maximum use of the equipment, it must be self-diagnosing when internal problems occur. To accomplish this, an error monitor panel continuously displays either raw track error rate, composite error rate, or error count, as selected by the user.

For "raw error rate," the error monitor panel actually counts error corrections made on the track being monitored. The track selection may be made manually or through a computer interface (IEEE 488 or RS 232).

"Composite error rate" is actually a sampling of the track-by-track "raw error rate" measurement and then a manipulation of the data to account for the sampling process. It provides a measure of the overall effectiveness of the system. Normally, it is used until problems are suspected, then track-by-track monitoring serves to localize problems.

It is clear that if a track fails, this failure is indicated even though the system normally continues to correct for most of the errors generated. Thus, system repairs can be implemented at user convenience without full failure occurring.

Hardware

Figure 14–7 is a photograph of a 32-track EDCS, which includes record, reproduce, monitoring, and power for 2 modules, each of 14 tracks of data, plus 2 parity tracks. From the top down, figure 14–7 shows the first card rack, the monitor chassis, the second card rack, and the power supply.

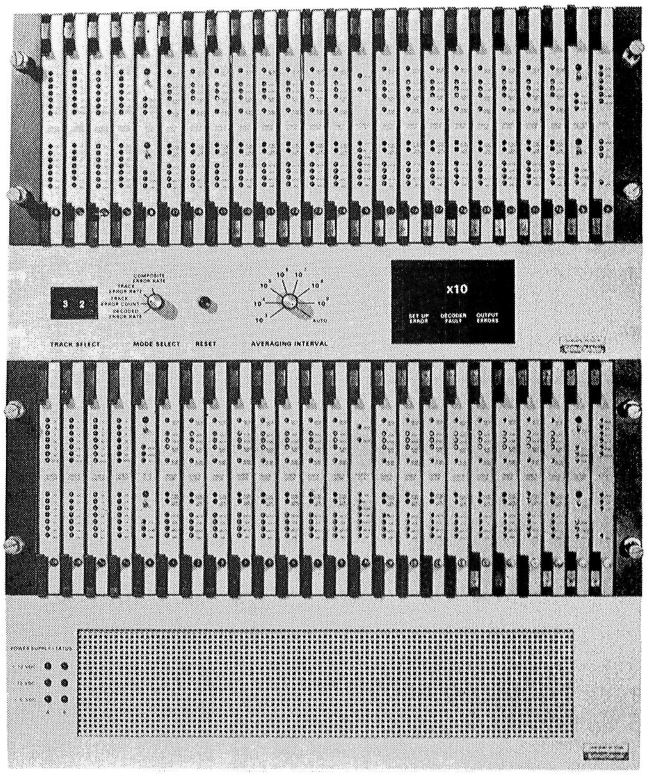

Figure 14–7.—32-track EDCS.

A 16-track system requires only a single card rack and replacement of the 32-track power supply with one for 16 tracks. Both power supplies use the same rack space.

The hardware shown includes all signal electronics functions, except head drivers and preamplifiers. Two equalizers per track are included. For installation of all eight equalizers, direct reproduce cards may be used ahead of the reproduce part of the EDCS.

Figure 14–8 shows a Model 5 transport with 28 tracks and EDCS, 14 in each card module. Figure 14–9 depicts a Model 10 transport with 27 tracks; 16 tracks of cards are in the upper module and 11 are in the lower.

THEORETICAL PERFORMANCE PREDICTION

There are a number of phenomena associated with magnetic tape recording and the magnetic tape itself that make theoretical performance prediction less than exact. The most predominant of these is probably the variable nature of the error bursts themselves: They can be random, single-bit errors, or bursts. Most authorities would agree that the majority of these errors occur not as random single-bit errors, but as multibit bursts of variable length created by foreign particles on or in the

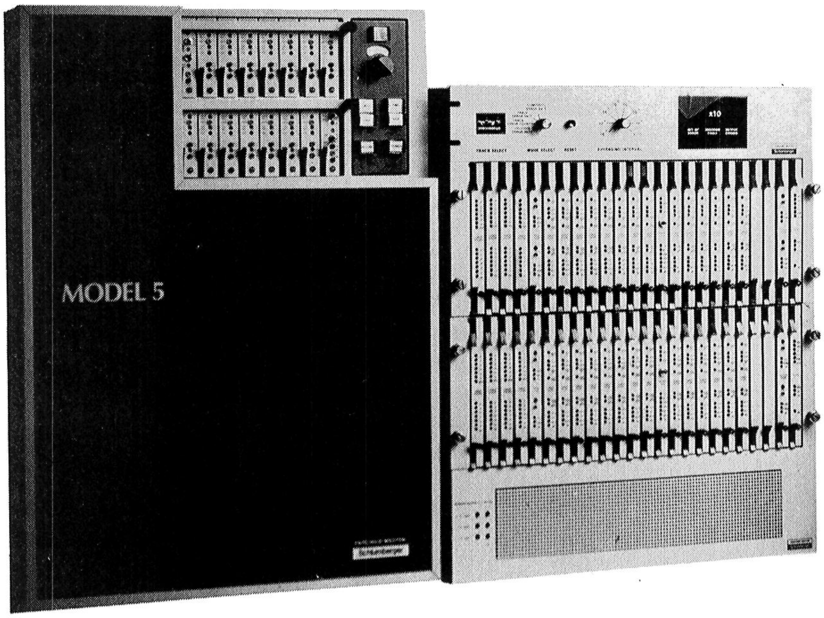

Figure 14–8.—Model 5 transport with 28 tracks and EDCS.

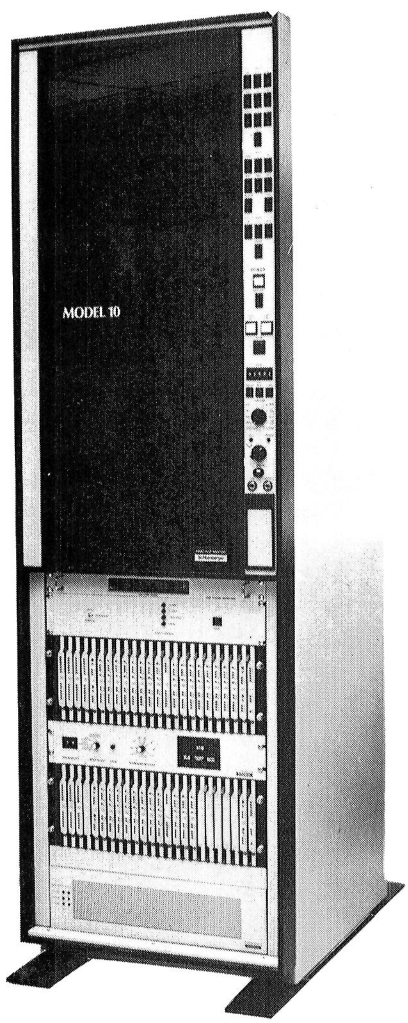

Figure 14–9.—Model 10 transport with 27 tracks and EDCS.

surface of the tape, and much work has been done to classify the length and width of these bursts (ref. 14–8).

Recognizing the variability of these conditions, Dr. Chase, in a paper presented to the Tape Head Interface Committee in September 1981 (ref. 14–10), provided equations and curves describing the theoretical performance of this error correction system as a function of the error burst characteristics.

His plots of the decoded error rate as a function of the raw error rate for different burst lengths are presented in figures 14–10 to 14–12. These provide an insight into the performance capabilities of the system. They also show the wide range of answers one can get by using different burst characteristics.

For all plots, the abscissa is the raw error rate (the bit error rate (BER) without or before correction); the ordinate is the decoded error rate, or the BER after correction; and the inner code is the (240, 216) BCH code.

Figure 14–10 compares performance of double-track correction for burst errors of different lengths. Curves are shown for values of B, the length of the error burst, from 1 bit to the other limiting case of infinitely long bursts.

Figure 14–11 provides similar curves for single-track correction. From these two plots, one can grasp an idea of the error performance, based on one's concept of the nature of the errors. In today's world, and the writer continues to stress the changing nature of dropouts with new tape and tape-handling procedures, one tends to consider that most errors are of the burst variety in lengths of 100 to 300 bits. Using these burst lengths as the primary effect, one concludes that the performances indicated in figure 14–12 can be expected. This curve

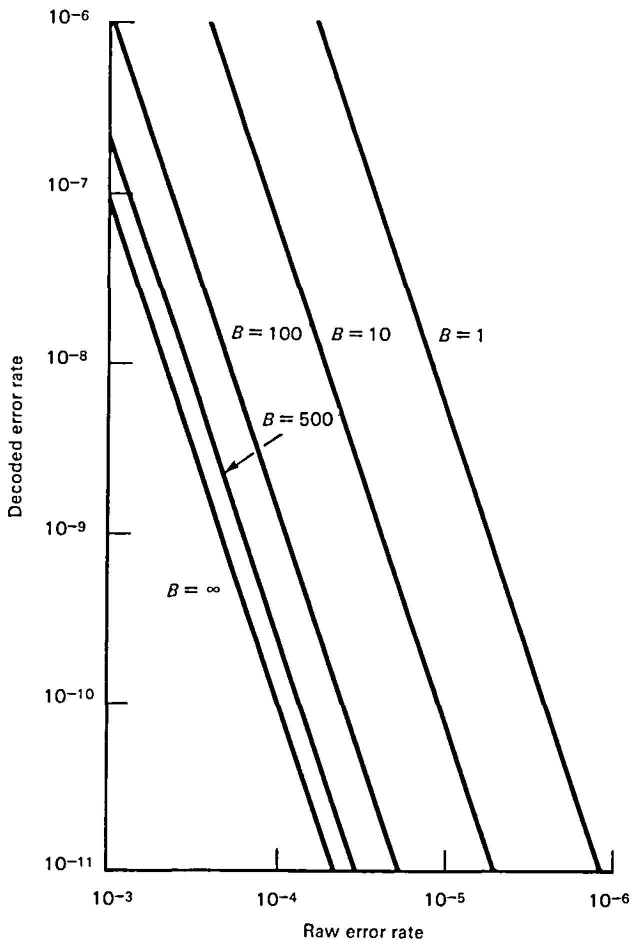

Figure 14–10.—Performance comparison for bursts of different lengths with two-track correction; (16, 14) system. (B = length of error burst in bits.)

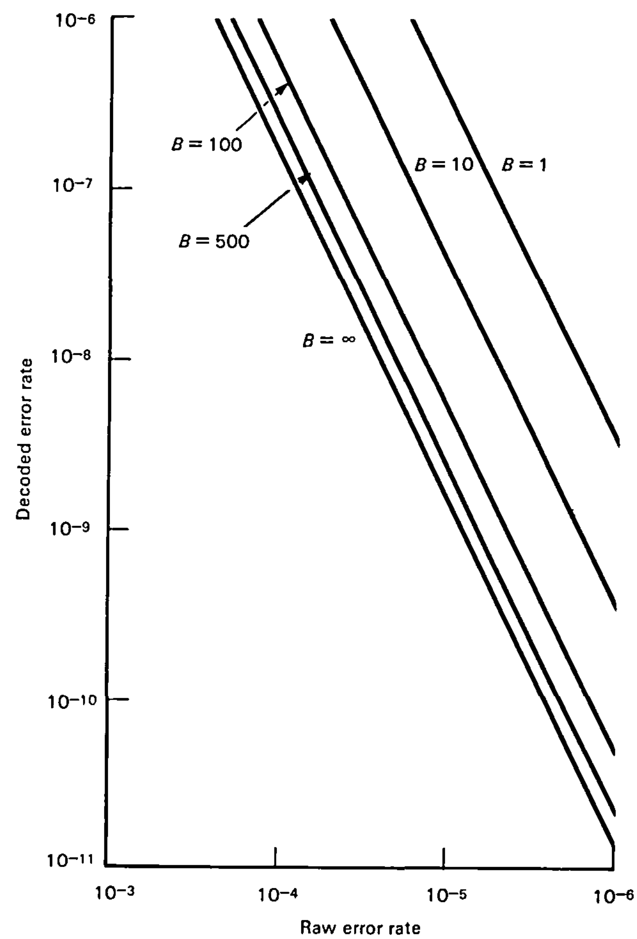

Figure 14–11.—Performance comparison for bursts of different lengths with single-track correction; (16, 15) system.

shows that an improvement in bit error rate of about six orders of magnitude can be expected from the two-channel (16, 14) correction system and about three orders of magnitude for the single-channel (16, 15) correction system.

MEASURED PERFORMANCE

Measuring the performance of a double-channel (16, 14) correcting system such as this is, at best, very time consuming because so few errors occur in the output. As seen from the theoretical curves of the previous section, the expected BER is about 1 error in 10^{11} bits, if reasonably good tape is used. Because there are about 10^{11} bits on a 14-in. reel of tape (28 tracks at 33 kbpi) and because errors usually occur in bursts, several reels of tape must be measured before an uncorrected error burst in the output is to be expected. Such is normally the case, and the following experiment demonstrates the double-channel (16, 14) correcting system when used with new but relatively dirty tape.

Five reels of new Ampex 797 tape were obtained from stock. They were removed from their original cartons and, without any cleaning or preconditioning, were recorded at 25 kbpi of user data (27.7 kbpi including overhead) on a double-channel correcting system. Record trackwidth was 25 mils, which provided the signal-to-noise ratio of a 28-track recorder. Both record and reproduce occurred at 60 ips, and a Tau-Tron provided a 2^{20}-bit pseudorandom test word.

The results are given in figure 14–13. Figure 14–13(*a*) provides the error rate before correction while figure 14–13(*b*) shows the actual errors in the output after correction. Note that four of the five reels of data reproduced without any errors while the fifth had a burst of 12 uncorrected errors. The composite corrected error rate for the five reels is 5.4 errors in 10^{11} bits.

SUMMARY

This chapter has described the two parallel HDDR systems offered by Fairchild Weston; one being a non-

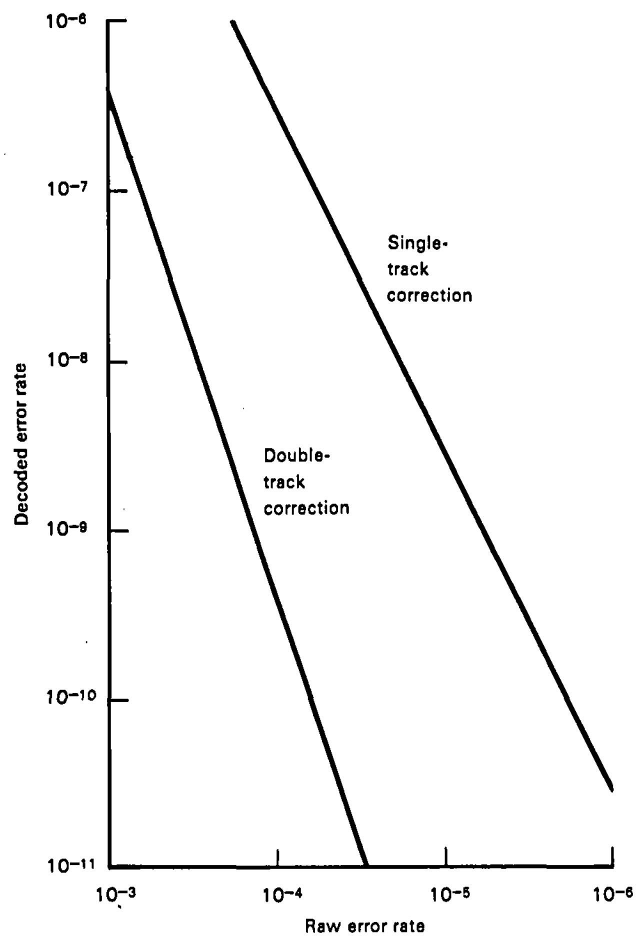

Figure 14–12.—Burst error performance (burst error length = 300 bits) for both double-track (16, 14) and single-track (16, 15) correction systems.

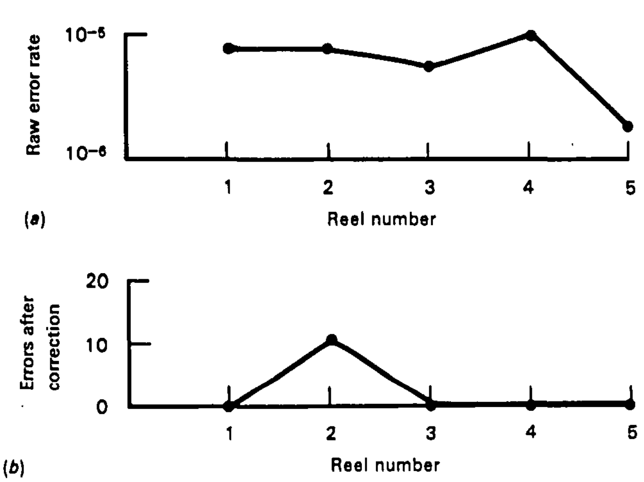

Figure 14–13.—Performance curves for a Model 10 EDCS with 797 tape from the National Security Agency, 14-in. reel, 25 kbpi input data, 25-mil tracks, and a (16, 14) configuration. (*a*) Error rate. (*b*) Number of errors remaining after correction. (Composite corrected error rate for 5 reels: 5.4×10^{-11}.)

error-correcting HDDR system and the other, the EDCS. Randomizing is used in both systems as a means of signal conditioning because it has no detectable pattern sensitivity and it adds no overhead. In the non-error-correcting system, the 16-bit synchronizing word every 496 bits offers reliable deskewing with only 3.23 percent overhead. The EDCS uses 24 serial parity bits for strong error detection and two parity tracks for two-track correcting ability. The values of the parameters are selected as the best compromise found between performance and overhead.

The error rate of the non-correcting system largely depends on tape condition. The error rate of the EDCS is essentially zero through a reel of tape.

The non-error-correcting system uses an unchanging format that is compatible with all Fairchild Weston HDDR systems delivered in the past, and this format is expected to continue. The EDCS, by necessity, uses a separate format as dictated by the features of the powerful correcting capabilities.

With these two systems, the user has a choice as to which best suits his requirements: (1) a minimum overhead system without error correction with performance limited by the tape; or (2) the powerful error correction ability of EDCS, giving performance essentially independent of tape dirt and defects.

The reader should bear in mind that the BER's (especially without error correction) and the packing densities of today are primarily limited by the magnetic tape and heads in use.

The recorder/reproducers and encoding/decoding techniques and electronics are designed to handle magnetic tape capable of much higher packing densities. Already, 66 kbpi with high-energy tape and double density heads is becoming commonplace. The reader should, in future years, update his thinking in light of the magnetic tapes that become available with time.

REFERENCES

14-1. Castle, C. A.: "High Density PCM Tape Recording." *IEEE Trans. Instrum. Meas.* **24**: 266–271, Sept. 1975.

14-2. Stein, J. H.: "The Sangamo HDR System." Sangamo publication, paper presented at meeting, THIC/ANSI (San Mateo, CA.) Jan. 1977.

14-3. Waggener, W. N.: *PCM Code Selection for Band-Limited Transmission and Tape Recording.* TP-75-005, EMR-Schlumberger, Dec. 1975.

14-4. American National Standards Institute (ANSI): "Interchange Practices and Recommended Test Methods for High Density Digital Recorder (HDDR) Systems (Including the Recording Characteristics of Instrumentation Magnetic Tape)." *HDDR Recorded Tape Standard X3B6/628R*, Working Paper, Sept. 7, 1982.

14-5. Savage, J. E.: "Some Simple Self-Synchronizing Digital Data Scramblers." *Bell Systems Tech. J.* **46**: 449–487, Feb. 1967.

14-6. Inter-Range Instrumentation Group: Ch. 6, *Telemetry Standards*. IRIG 106-80, Range Commanders Council, White Sands Missile Range, N. Mex., revised May 1980.

14-7. Kalil, F., editor: "A Care and Handling Manual for Magnetic Tape Recording." App. B of *Magnetic Tape Recording for the Eighties*, NASA RP-1075, Apr. 1982, pp. 127-147.

14-8. Buschman, A.: "Magnetic Tape Certification," Ch. 4 of *Magnetic Tape Recording for the Eighties*, NASA RP-1075, Apr. 1982, pp. 35-44.

14-9. Kessler, W. D.; and Stein, J. H.: "A High-Performance Error Correction System for Digital Tape Recorders." *Int. Telem. Conf. Proc.*, Session XI, Oct. 1981.

14-10. Chase, D.; and Kessler, W.: "The Sangamo/CNR Error Correction System." Paper presented to the Tape Head Interface Committee, Sept. 6, 1981.

14-11. Peterson, W.; and Weldon, J.: *Error Correcting Codes*. MIT Press, 1961, 1972.

14-12. Lin, Shu.: *An Introduction to Error Correcting Codes*. Prentice-Hall, Inc., 1970.

CHAPTER 15

Error Correction for High-Density Digital Tape Recorders

John Montgomery
Martin Marietta Corporation

High-density digital recording (HDDR) is rapidly becoming a valuable and reliable data storage technique. For the last several years HDDR systems, built on a production basis, have been satisfying many of the needs of modern technology with a large storage capacity and high data rate capability.

System designers using high-density digital recorders (HDDR's) are now focusing their attention on accuracy, with the result that bit error rate (BER) is becoming an increasingly important specification. An HDDR is usually one component of a larger data system. Minimizing the data errors created by the HDDR is often the key to improving or to simplifying the data system.

Example.—In a data retrieval and processing system, the information rate is often too high to fully process in real time. Therefore, the computer must receive slower playback data from an HDDR. However, the software must be designed to accommodate perhaps 1 error in 10^6 bits from the HDDR. If errors occur in critical synchronization data, for instance, the information may be lost or the software must enter a time-consuming analysis routine. A 1 in 10^9 BER on the other hand might save processing time or allow the software to be simplified or both.

Example.—A data system may use hundreds or thousands of expensive high quality HDDR tapes each year. If the BER of the hardware is improved, money may be saved by allowing lower quality tapes to be used without sacrificing overall performance.

The bit error performance of an HDDR is a function of the tape and of the HDDR design. Typical performance is in the range of 10^{-6} plus or minus an order of magnitude. Exceptions to typical performance exist at both ends of the range, of course. One manufacturer's HDDR may perform better than another's; also, the quality of the tape, the number of tracks, the coding approach, and the bit packing density are among the variables that affect results. The performance ranges in figure 15-1 were obtained using Martin Marietta HDDR's based on the Honeywell Model 96. The results were compiled using data from many HDDR's with scores of tapes over a period of approximately 2 years.

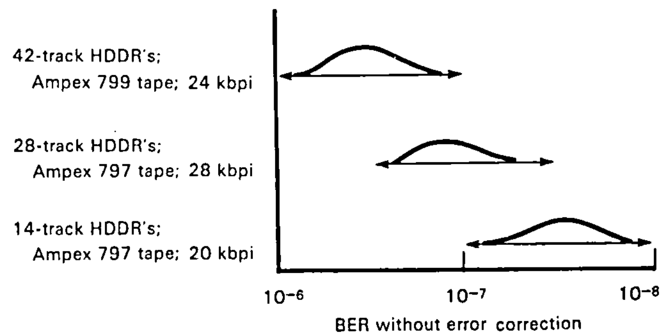

Figure 15-1.—Performance ranges for Martin Marietta HDDR's based on Honeywell Model 96.

The subject of this paper is a simple technique for error correction that can improve typical results to 10^{-9}, plus or minus an order of magnitude. The technique is a digital correction method that does not affect the transparency of the HDDR system and, with the exception of requiring one or more overhead tracks, does not affect the head/tape interface or associated record/reproduce circuitry. This error correction approach for HDDR's is easily implemented. Its trade name is EC^2 (error correction code). EC^2 has been incorporated and tested in numerous Martin Marietta HDDR's; therefore, the discussion begins with an overview of these systems.

THE BASIC HDDR SYSTEM (without error correction)

An HDDR required to record and reproduce a high-speed serial data stream is, in general, described by figure 15-2.

The term "high speed" in this case refers to a rate greater than an individual tape channel can carry (i.e., greater than 4 to 8 Mbps for a typical longitudinal machine). This type of system is called "parallel

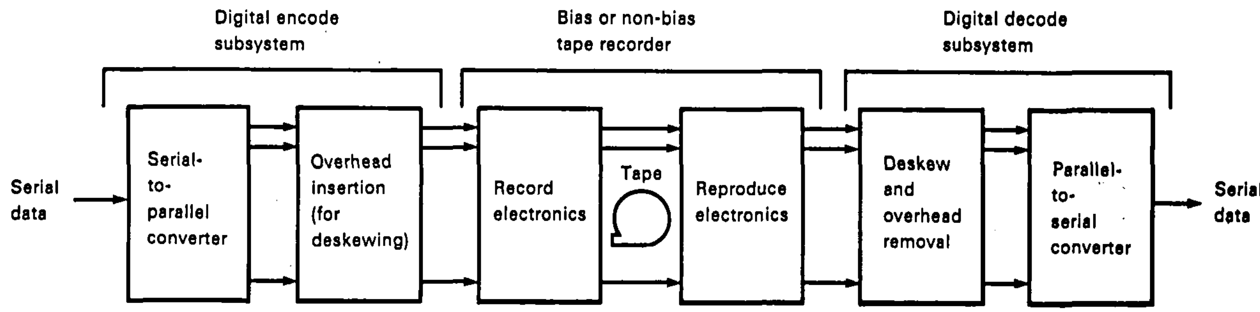

Figure 15-2.—Basic high-speed HDDR system.

HDDR," which refers to the necessary parallel format and the corresponding need for deskewing.

The EC² method is applicable to parallel HDDR systems and affects the block diagram by modifying the overhead insertion/removal logic and by adding one or more channels to be recorded.

CHANNEL DATA FORMAT

The HDDR systems in which EC² has been incorporated have all used the same channel format. Briefly, each parallel channel is modified by the following four steps:

(1) A counter is used to subdivide the incoming data into 420 bit groups called "frames" (fig. 15-3).

(2) Each frame of data is mixed with a 420-bit pseudorandom noise (PRN) sequence (fig. 15-4).

This "randomization" is performed to increase the probability of bit transitions on the tape, which in turn assists the reproduce and bit synchronization processes. Randomization improves the behavior of data with long strings of "1's" or "0's".

(3) Next, each frame of data is subdivided into 60 seven-bit bytes. Odd parity is computed for each byte, and the result is 60 eight-bit bytes per frame (fig. 15-5).

(4) Finally, a 24-bit deskew synchronization word is inserted at the beginning of each 60-byte frame. The result is the recorded format shown in figure 15-6.

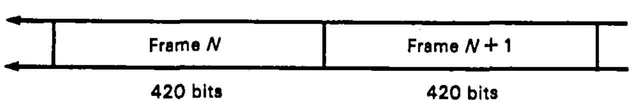

Figure 15-3.—Data divided by counter into frames.

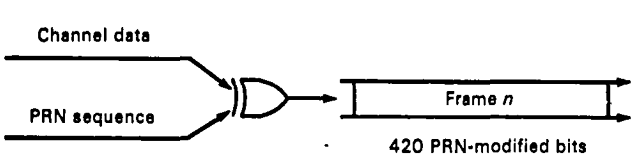

Figure 15-4.—Data mixed with a PRN sequence.

A data frame, therefore, consists of the following:

(1) 420 PRN-modified data bits
(2) 60 byte parity bits
(3) 24 deskew synchronization bits

Therefore, there are 504 total bits per frame for an overhead of 20 percent.

HDDR WITH ERROR CORRECTION

Conceptually, the process of error correction involves two steps:

(1) *Error detection*—In general, redundancy must exist in the data so that invalid data may be distinguished from valid data. If redundancy does not exist, it must be added in the form of overhead, which may be called "detection overhead." The efficiency of detection (or probability of detection) is measured as the percent of possible error combinations which will be detected.

(2) *Error correction*—Additional redundancy must exist or be added to the data so that in the presence of error combinations, it becomes possible to choose among alternate combinations with the correct alternate being the most probable. This redundancy may be called "correction overhead."

It is not within the scope of this chapter to present the full range of tradeoff arguments applicable to the selection of an error correction approach. The practicality of the approach must be given very serious consideration. The EC² approach is quite compatible with the basic HDDR format. A block code was chosen over a convolutional code because the necessary data framing is already performed in the system. The fact that simultaneous errors across the tape tracks within the space of a frame are quite rare suggested a matrix code in which simple parity bits were formed from each column of data bits across the tape. The effectiveness of the error correction was determined to be a strong function of detection efficiency. The best detection code consistent with reasonable overhead was the ideal. A product code was chosen.

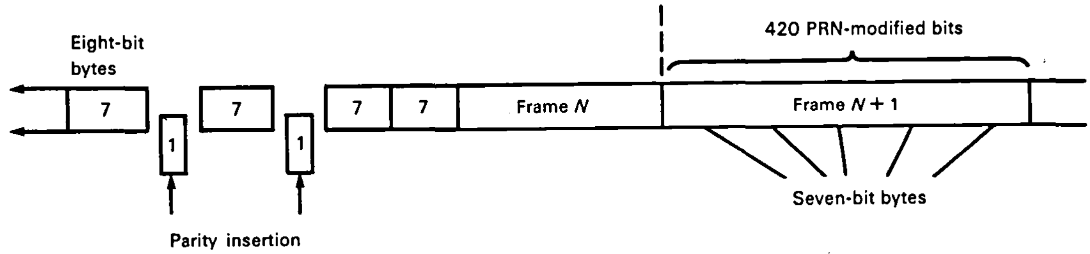

Figure 15-5.—Data divided into bytes.

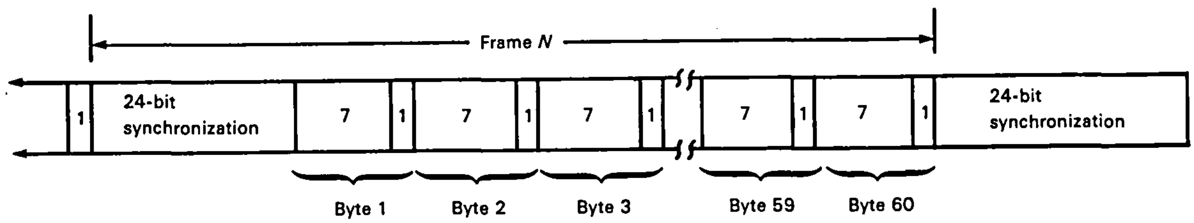

Figure 15-6.—Addition of 24-bit deskew synchronization word at beginning of 60-byte frame.

EC² Format

Figure 15-7 presents the EC² format. Two changes have been made in the basic HDDR format; however, the 60 data/parity bytes per frame remains unaltered. The two changes are as follows:

(1) 12 bits of the synchronization word are replaced by a 12-bit cyclic redundancy check (CRC) word. This is the detection overhead referred to previously. The role of the existing byte parity bits is discussed later.

(2) An $N + 1$ channel is added. Its bits are the result of vertical parity checks of the bits in each data channel. The $N + 1$ channel (or "EC² track") is the correction overhead.

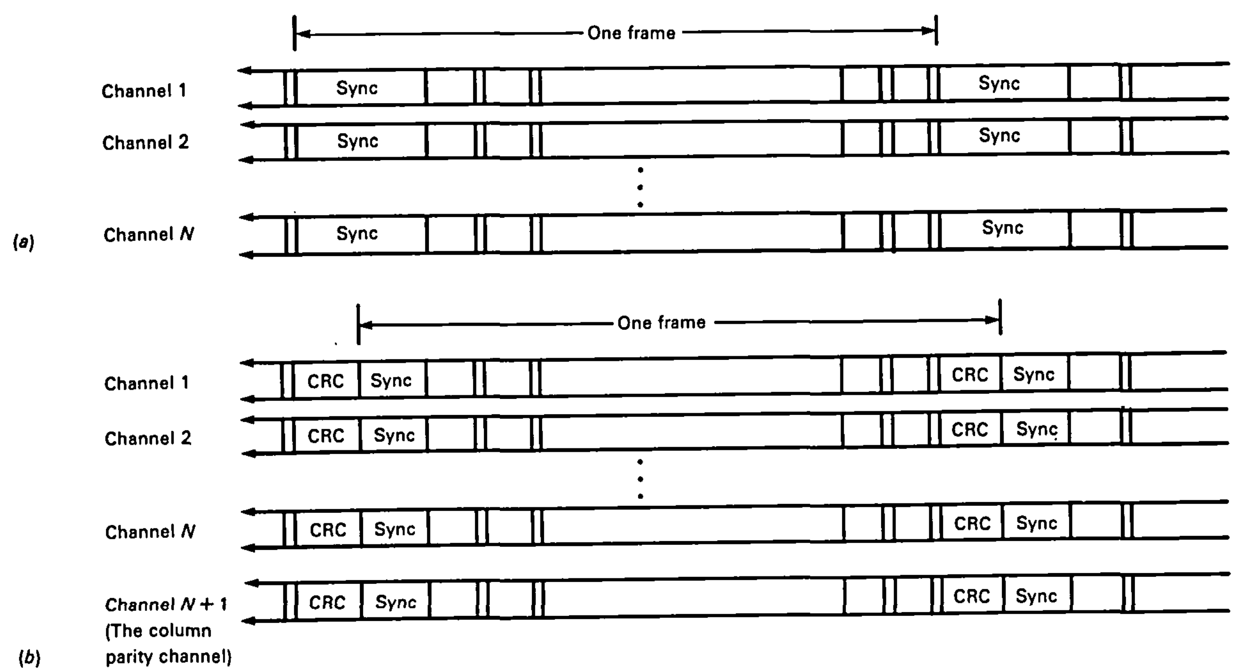

Figure 15-7.—Addition of EC². (Sync = synchronization word.) (*a*) A group of *N* data channels without EC². (*b*) A group of *N* data channels with EC². (Each frame contains 504 bits and still contains 60 bytes; the 24-bit synchronization word becomes 12 bits CRC + 12 bits synchronization; an N + 1st channel (the data bits of which are the result of vertical parity checks of the bits in each data channel) is added.)

CRC Error Detection

The cyclic redundancy check (CRC) has been shown by both theory (ref. 15-1) and experiment to be a powerful error detecting code. The CRC is perhaps best known in its various forms as the generator polynomial in cyclic error correction codes such as the block check header. Constructing and decoding a CRC for error correction is usually quite complicated; however, the process for error detection is quite simple.

The CRC bits are generated during the HDDR record process by serially shifting each frame of 60 data/parity bytes into a CRC generator. The generator is an integrated circuit consisting of a feedback shift register with modulo 2 adders between certain stages.

Figure 15-8 is a block diagram of the 12-bit CRC configuration used in the HDDR systems.

Serially shifting a frame's worth of data into the CRC is equivalent to dividing the frame by the polynomial $X^{12} + X^{11} + X^3 + X^2 + X + 1$. At the end of the division, the generator contains a 12-bit remainder that is appended to the data frame as the CRC word.

On the decode side, during reproduce, each received frame is shifted into a CRC detector. The detector, which is identical to the generator, divides the received frame and the remainder by the same polynomial, $X^{12} + X^{11} + X^3 + X^2 + X + 1$. If the result of this division is a zero remainder, then either there were no errors in the frame or else the error pattern was an undetectable permutation of the frame. If a non-zero remainder is detected, then at least one error must have occurred in the frame (ref. 15-2).

The error detection efficiency of this CRC cyclic code is 100 percent of all error bursts of 12 bits or less and $(1 - 2^{-12}) = 99.98$ percent of all bursts greater than 12 bits (ref. 15-1).

Although CRC is a highly effective approach, even greater detection efficiency is obtained through the use of the byte parity bits that already exist in the frame.

Error Correction

The matrix code error correction approach, ideal for parallel HDDR, is the process of horizontal (or longitudinal) detection of channels followed by vertical correction.

When a frame is found to be in error by the CRC, the overhead EC^2 track may be used to correct it. The process consists simply of recomputing vertical column parity bits across all channels through the entire frame, inverting those bits in the erroneous frame for which the parity check fails. A block diagram is shown in figure 15-9.

Two conditions must be satisfied, however, for this CRC form of matrix correction to work with a single EC^2 track:

(1) The erroneous track must be known (i.e., detected)

(2) Only one track can be in error within any given frame time

The overall effectiveness of matrix correction depends on how well these two conditions are met in actual practice. In statistical language, the probability of uncorrected errors, $P(\text{uce})$, is a function of the probability of not detecting the errors $P(\text{miss})$ and the probability of two or more tracks simultaneously in error $P(\text{se})$.

Because the two conditions are independent

$$P(\text{uce}) = P(\text{miss}) + P(\text{se}) - P(\text{miss})P(\text{se})$$

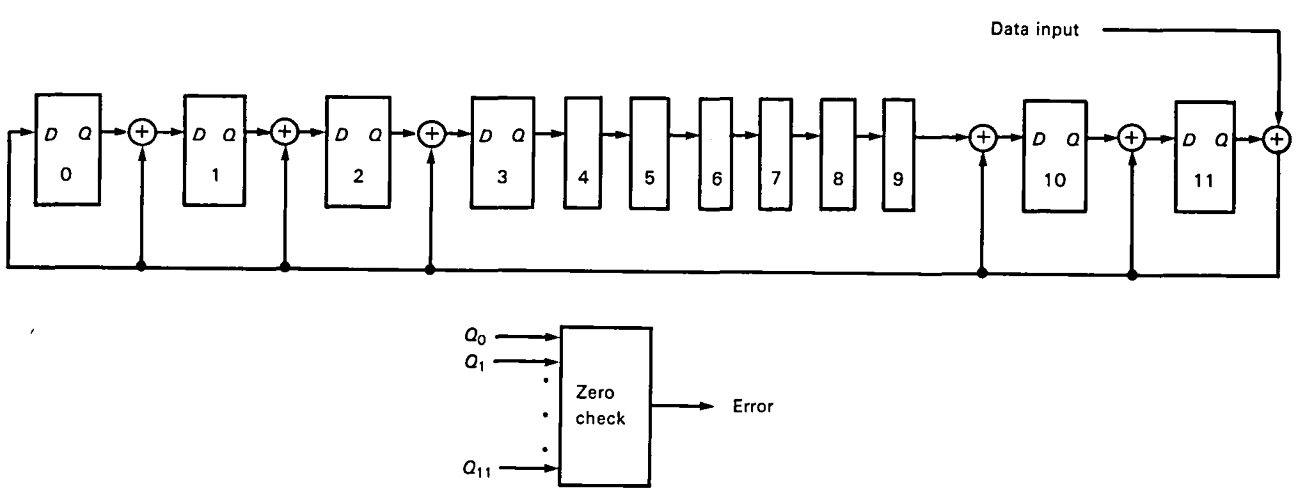

Figure 15-8.—CRC generator/checker (Fairchild 9401). Division polynomial $= X^{12} + X^{11} + X^3 + X^2 + X + 1$.

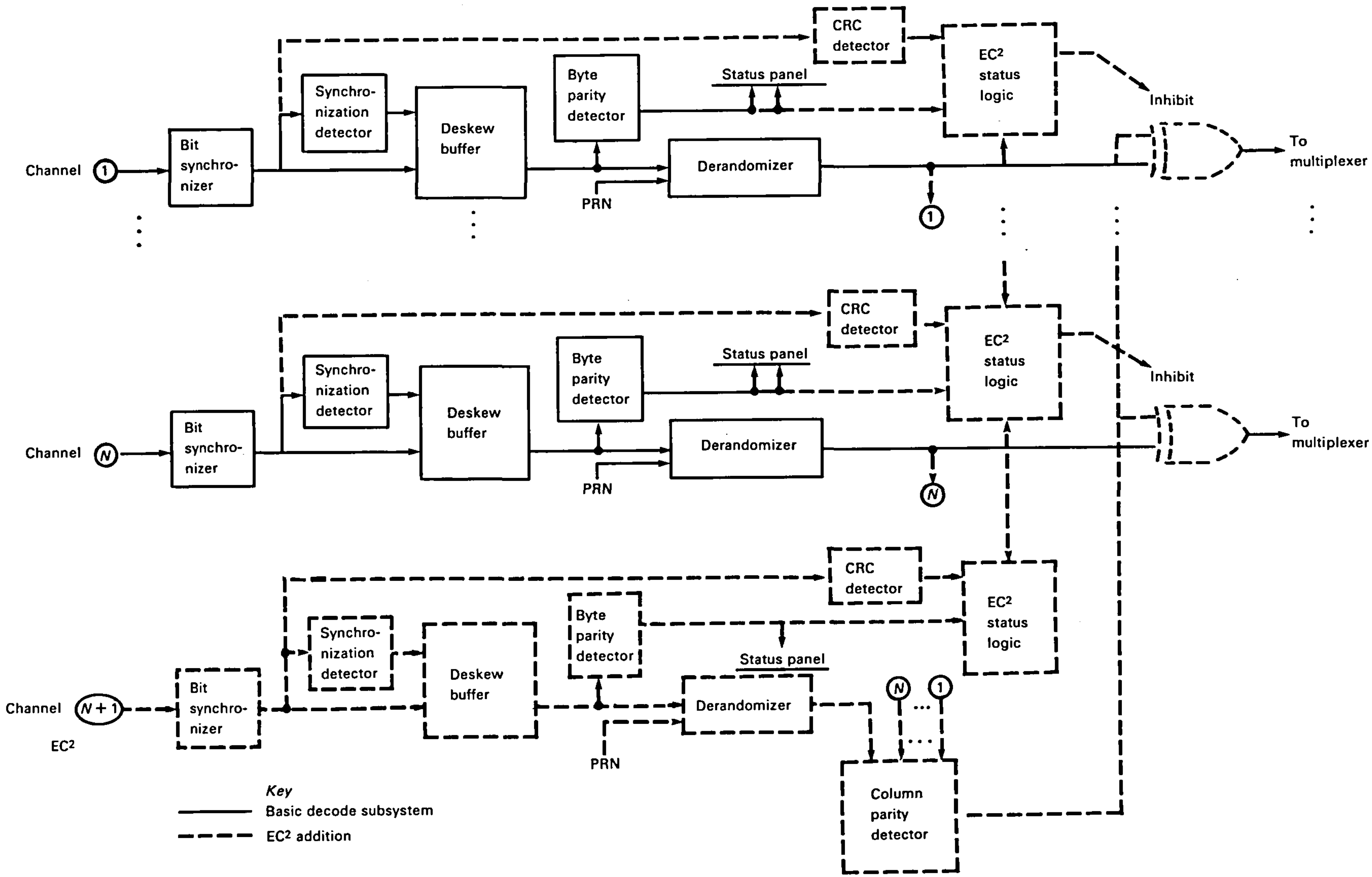

Figure 15-9.—The decode subsystem with EC2.

If P(miss) and P(se) are reasonably small numbers, then the last term may be neglected. The result is a simple expression that can be used to quantify the performance of the EC² system:

$$P(\text{uce}) \leq P(\text{miss}) + P(\text{se}) \qquad (15\text{–}1)$$

Condition 1, Detection

Detection may be considered the key to effective error correction. Poor detection could cause P(miss) to be far higher than P(se).

Let P(fe) be the probability of one or more errors within an HDDR data frame. Because errors in the 12-bit deskew synchronization word do not affect BER performance (within limits), the size of the frames here is 504 − 12 = 492 bits.

P(fe) can be related to the raw BER by the expression

$$P(\text{fe}) = 1 - (1 - \text{BER})^{492} \qquad (15\text{–}2)$$

The detection ability of a 12-bit CRC is $1 - 2^{-12}$. Therefore, the probability of missing a frame error is

$$P(\text{miss}) = P(\text{fe})\,(2^{-12}) \qquad (15\text{–}3)$$

Condition 2, Simultaneous Errors

In the derivation of P(se), a basic assumption is made that the distribution of single-frame errors is random. This assumption breaks down in the presence of a tape flaw large enough to encompass two tracks. The likelihood of this occurrence is difficult to assess, but experience has shown that the vast majority of instrumentation tape flaws are 20 mils or less.

The following system configurations of EC² have been used:

(1) *14-track HDDR's.*—Trackwidths are 50 mils. The likelihood of flaws large enough to seriously affect two adjacent tracks is considered "acceptably" small. Test results have shown one EC² track to be more than adequate.

(2) *28-track HDDR's.*—Trackwidths are 25 mils. The standard EC² configuration here is to separate the tracks into two interleaved groups and provide an EC² track for each. A flaw must now span three tracks to create a problem.

(3) *42-track HDDR's.*—With trackwidths of 17 mils, three or four EC² groups are advantageous. Standard systems using four groups have produced excellent results.

The occurrence of large flaws appears to be perhaps one or two per tape for tapes of Ampex 797 quality and considerably less for tapes of Ampex 799 quality. The rate of occurrence does not seriously affect the derivation of P(se).

P(se) can be expressed from the point of view of a particular track within an EC² group of $N + 1$ tracks. (N data tracks plus one overhead track.) The particular track must be in error and at least one of the other N tracks must also be in error.

$$P(\text{se}) = P(\text{fe})\,\{1 - [1 - P(\text{fe})]^N\} \qquad (15\text{–}4)$$

The total expression for uncorrected frame errors for a particular track in an EC² group is

$$P(\text{uce}) \leq P(\text{fe})(2^{-12}) + P(\text{fe})\{1 - [1 - P(\text{fe})]^N\} \qquad (15\text{–}5)$$

Also P(fe) can be related to the raw bit error rate B_r as

$$P(\text{fe}) = 1 - (1 - B_r)^{492} \qquad (15\text{–}6)$$

P(uce) can be related to the corrected bit error rate $\overline{B_c}$ as

$$P(\text{uce}) = 1 + (1 - B_c)^{492} \qquad (15\text{–}7)$$

Solving for B_c gives

$$B_c = 1 - \exp_{10} \frac{\log[1 - P(\text{uce})]}{492} \qquad (15\text{–}8)$$

where P(uce) is in terms of N and raw BER. Figure 15–10 presents the results of this equation for several values of N.

The Use of Byte Parity

Equation (15–1) states

$$P(\text{uce}) \leq P(\text{miss}) + P(\text{se})$$

The efficiency of the CRC detector is so close to 100 percent that the probability of an undetected error is much smaller than the probability of simultaneous errors. (Only if N and raw BER are very low will P(miss) and P(se) be approximately the same.) The conclusion is that simultaneous errors are the source of most of the errors in an EC² system with CRC detection.

P(se) could be reduced if the frame length (504 bits) were smaller; however, there is a more convenient alternative: The existing byte parity bits may be used as backup to the CRC. Whenever CRC detects simultaneous frame errors, the individual byte parity checks on the erroneous frames may be used as a higher resolution detection mechanism. For example: CRC detects tracks 2 and 8 to be in error. Byte parity detection discovers errors only in the first 100 bits of the track 2 frame and only in the second 100 bits of the track 8 frame. Error correction is enabled and both tracks are corrected.

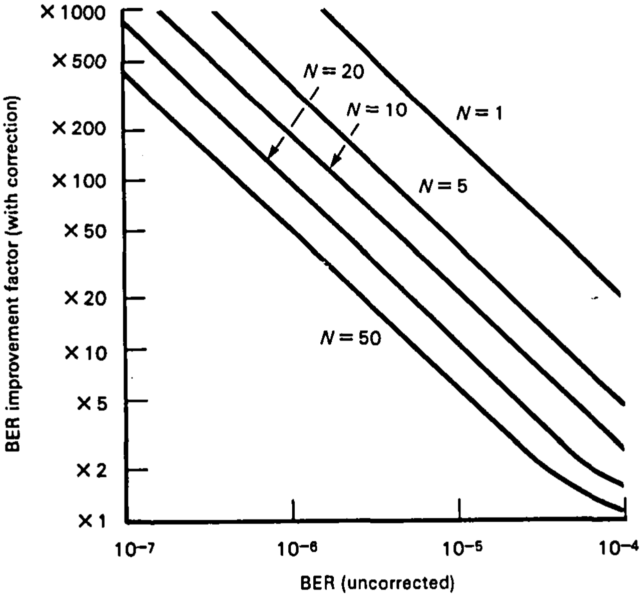

Figure 15–10.—BER improvement with EC² (CRC only). (One EC² group = N data tracks plus one parity track; empirical results indicate that byte parity adds approximately one order of magnitude to the improvement factor.

A tradeoff is involved here. The "window" of byte parity correction must be small to achieve resolution; yet on the other hand byte parity detection efficiency is not very high (50 percent per byte). We know that tape errors tend to be produced in bursts (from dropouts or bit slips). The CRC will detect all bursts 12 bits or less in length. Therefore, the byte window should be somewhere between 2 bytes and half a frame. In 28- and 42-track systems, the choice has been a 7-byte window.

The implementation is as follows: When a byte parity error is sensed, it is assumed that a burst error is occurring. Correction begins with the fourth byte prior to the detection and continues for three additional bytes. In this way, detection efficiency is improved from 50 percent to at least

$$1 - (0.5)(0.5)(0.5)(0.5) = 93.75 \text{ percent}$$

Table 15-1 provides test results on a 42-track HDDR. The tapes used were Ampex 799 and a series of Ampex 79A tapes (similar to 797). Bit packing densities of 24 and 33 kbpi were used in conjuction with an EC² group with N = 10. General results of tests with a 42-track HDDR system are as follows:

(1) The CRC improvement factor for Ampex 79A is about 150. Theory predicts about 50.

(2) The CRC improvement factor for Ampex 799 is 200 to 500. Theory predicts 400.

(3) Byte parity produces roughly an order of magnitude improvement in the CRC.

Table 15-1.—*Results of 42-Track HDDR Tests*

Bit packing density, kbpi	Tape	Raw BER	CRC	CRC + BP
24	79A	3.2×10^{-6}	2.2×10^{-8}	2.8×10^{-9}
	799	4.5×10^{-7}	9.0×10^{-10}	Zero errors
33	79A	5.1×10^{-6}	3.0×10^{-8}	3.6×10^{-9}
	799	4.3×10^{-7}	2.4×10^{-9}	Zero errors

BP = byte parity.

Tests conducted on a 28-track Landsat D system with two EC² groups of 12 data tracks each show BER's that are too low to measure accurately. Ampex 79A tapes were used, with bit packing density of 33⅓ kbpi. General results are as follows:

(1) Many runs produced zero errors through the entire tape.

(2) Other runs produced one or more burst errors. (Printer results for a tape were displayed in 65 samples of 10^9 bits each. The vast majority of samples produced zero errors. Occasionally a tape produced one or two samples with burst readings to several bits.)

(3) The average of results was a BER $<10^{-9}$.

14-track systems have thus far used an EC² system based solely on byte parity detection (with a 15-byte window). With Ampex 79A tapes and 20 kbpi, approximately 90 percent of tapes produce zero errors. The BER over 10 tapes typically is less than 10^{-10}.

REFERENCES

15-1. Stites, Randy; and Leighou, Robert O.: *Error Correction for High Density Tape Recording.* R77-48610-003, Martin Marietta Corp., Dec. 1977.

15-2. Spurr, Robert: *High Density Tape Recorded Error Correction Hardware.* Martin Marietta Corp., 1979.

APPENDIX A

Pulse-Code-Modulated Tapes for High-Density Digital Recording Requirements

Walter Shaffer
Ampex Corporation

This chapter describes how pulse-code-modulated (PCM) tapes differ from other tapes, why they are so important, and the use and importance of each type of PCM tape.

REQUIREMENTS

Higher Data Rates

Today we are asked to record higher data rates or store more data on a given piece of tape. Many of these requirements can still be met with Inter-Range Instrumentation Group[1] (IRIG) compliant high-density digital tape recorders (14-, 28-, or 42-track format with 2-MHz heads and electronics) using standard-energy high-bit-rate PCM tape. Some of the newer requirements go beyond this and necessitate increasing the bit packing density (higher bandwidth), increasing the trade density (narrower tracks), or both to meet their mission: the need for higher areal packing density.

In either case, the impact on the tape is the same: The relative output from the tape is reduced. We know that as track densities are increased, the trackwidth is decreased with a calculated loss in output. We also know that as we increase the bit packing density, the output drops because the shorter recorded wavelength on tape is approaching the reproduce gap width (gap null effect). (See ref. A-1.) If we make the head gap shorter to move out of the gap null, the overall output from the tape will decrease. If we increase track and packing densities, we have a combined loss in output.

In addition, as the wavelength on tape becomes shorter, the magnetic domains on the tape form very short, wide magnets. Some of the domains will switch to conserve energy (self-demagnetization), with a resulting loss of output. The higher the coercivity of the tape, the less will be the tendency to switch. To combat these losses, particularly when packing densities are greater than 33.3 kbpi (60-μin. wavelength), a high-energy PCM tape is required.

High-Energy PCM Tape

There is no industry specification or agreement as to what constitutes a high-energy PCM tape. Tape specifications normally have a magnetic coating characteristic indicator that defines a coating in terms of its short-wavelength recording capabilities. Standard energy (gamma ferric particle) has an "E" indicator (high resolution), denoting tape intended for use on wideband recorder/reproducers having a recorded wavelength down to 60 μin. (1.5 μm). These tape[illegible] a coercivity of 325 to 350 Oe.

For a high-energy tape, oxide or particles can be obtained in many coercivities. For example, chromium dioxide can be obtained from 450 to 650 Oe. Cobalt-doped gamma ferric is available from 400 to 2000 Oe. Other metal oxides and isotropic particles are available. The problem now is for the tape manufacturer to define and supply a product he feels will meet these new high-density digital recording (HDDR) PCM requirements. Our high-energy PCM tape is defined as having a coercivity of 650 Oe and is for use on recorder/reproducers having a record wavelength as small 30 μin. (0.75 μm).

Uniformity

Whether high-energy or standard-energy tape is to be used, one factor is equally important: uniformity of output within a tape and between tapes. When maximizing the performance of an HDDR, the signal-to-noise margin may become much less. A 6- to 8-dB difference in band-edge output, permitted on some analog tapes, is not acceptable. Variations of 4 dB or less, offered by the HDDR/PCM family of tapes, are required.

[1]Now Range Commanders Council.

Low Raw Error Rates

Bit error requirements are becoming more stringent. Where one error in 10^6 bits was once acceptable, today's users are asking for one error in 10^7 bits or better. The surface integrity of the tape is a key factor.

We are all aware that for some requirements we can certify a tape. This is very specific in nature and very expensive. There is no standard code or format. Data rates, packing densities, and tape speeds differ. Each requirement would have to be tested on the particular equipment used. From a tape supplier's point of view, the expense incurred would be prohibitive; the certification will have to be done or contracted for by the user.

A more economical alternative is the 100-percent-tested PCM tape in which the dropout is defined in terms that insure the required surface integrity. Instead of a 6 dB (50 percent) loss of signal for 10 μs, which is used for analog tape, the PCM dropout is redefined as 12 dB (75 percent) loss of signal for 1 μs and then allows an average of only 2 per 100 ft, in comparison with the 10 dropouts per 100 ft allowed for analog tapes. The full length of the tape, excluding the first and last 200 ft, is tested on tracks randomly spaced across the tape. This form of testing (testing for surface integrity) accomplishes the following: (1) insures that the raw bit error rate is low and (2) insures that the probability for two simultaneous burst errors (of the type that can override error detection and correction schemes) is minuscule.

Durability

As with any magnetic tape, an HDDR/PCM tape must be able to be used again and again and again and still meet its state-of-the-art performance criteria. Durability and the ability to recover from adverse conditions and environment and improper handling are important. A good example of this was the qualification of a standard-energy PCM tape for a special program: 25 000 passes were asked; 35 000 were achieved, with no measurable change in performance.

Then there are cases where the tape gets handled a lot, or people smoke or eat around the recorder and the tape gets dirty. A PCM tape must be able to stand many passes on a cleaner/winder with many different types of cleaning configurations and return to its original condition with no sacrifice in tape life. (See ref. A-1.) Of course, if the tape has been damaged (e.g., edge curl or stretching), full recovery is normally not possible.

PCM TESTED TAPES

As can be seen, the needs of modern HDDR place great demands on the tape. PCM tapes must provide the maximum output for a given coercivity and must have outstanding uniformity, durability, and surface integrity. To meet these requirements, better base films had to be developed. Oxides had to be improved. Variations in raw materials were reduced. It was only through attention to detail that the PCM tape became a reality—a tape that was designed for, and tested to, PCM requirements.

There is no general purpose tape, no tape that can record everything. Each tape is designed, formulated, and manufactured for a specific usage. Tradeoffs must be made and will be weighted toward the end purpose of the product. The key parameters for a PCM tape are output and surface integrity. These are weighted the heaviest, with other parameters such as abrasivity and durability rated slightly behind.

A helical videotape, for example, is designed for a different application and will have different key parameters. Given the choice of output versus still framing durability, the durability is the more important. Abrasivity is normally higher on a video tape to keep the ferrite head clean.

In summary, those that have an IRIG-compliant recorder in their HDDR system can use a standard-energy high-bit-rate PCM tape. For a better record margin, a high-energy PCM tape would be used. For packing densities greater than 33.3 kbpi, or when trackwidths are less than 25 mils, a high-energy PCM tape should be used. In any case, PCM-tested tape has been proven to meet the requirements of the HDDR community.

REFERENCE

A-1. Kalil, Ford, ed.: *Magnetic Tape Recording for the Eighties.* NASA RP-1075, Apr. 1982.

APPENDIX B

Testing Magnetic Tape for High-Density Digital Recording Systems

R. A. Schultz
Illinois Institute of Technology Research Institute

Illinois Institute of Technology Research Institute, under contract to NASA Goddard Space Flight Center, evaluated five types of magnetic tape for satellite recording systems:

(1) Ampex 466
(2) Ampex 721
(3) Ampex 797
(4) Fuji H621
(5) 3M 5198

These tapes are considered adequate for 150 Mbps data transfer rates for satellite applications. Reference B–1 is a summary report describing test methods and results.

Only the test procedures from reference B–1 are presented here to allow others to test tapes for a variety of applications. Tape testing for analog systems is covered in reference B–2. As specified in reference B–2, the tape should be tested according to its end use. Not all testing presented here is required of all tape, and overtesting is wasteful. It is the responsibility of the system designer to know the requirements of the user and be able to specify critical parameters for tape testing. For use in space, the given tape to be used might be tested 100 percent; however, normally only some of the tests presented here are performed and even then they are usually performed on a sample basis, perhaps three reels per lot of 100.

PHYSICAL PROPERTIES

This section describes the physical characteristics that may affect the long-term durability and reliability of the tape as well as the integrity of the head/tape interface. Physical dimensions and dimensional variability should be determined for each tape type. Relative flexibility and dynamic tracking and guidance measurements, which are dependent mainly on the base film properties of the tapes, should be investigated. Bulk properties of the oxide binder systems including abrasion resistance, binder strength, and lubricant content need to be investigated. Oxide surfaces can be characterized by scanning electron microscopy, coefficient of friction measurements, relative head material abrasivity tests, and elemental analysis.

Tape Thickness

Although slight thickness differences between tape types are not expected to have a large effect on their relative performance, thickness variation within a given tape type may be an indication of poor manufacturing process controls.

Ten or more layers of tape are measured with a micrometer and the results divided by the number of layers measured. The measurements are made on the total thickness of the tape, on the tape with the back coating removed, and on the Mylar base alone with both the back coating and the magnetic oxide coating removed. The back coating and oxide thickness are determined by subtracting the sequential measurements.

The possible effects of solvents on the tape Mylar were examined during this tape thickness measurement procedure. Mylar samples were exposed to solvents for 1-hr periods after the initial thickness measurement. The long exposure did not change the measured Mylar thickness, indicating that short exposures do not cause errors as a result of Mylar dissolving, swelling, or softening.

The micrometer must be accurately zeroed and must have a slip mechanism that provides a low and repeatable measurement pressure. The micrometer may have a 0.1-mil vernier scale, or 0.2-mil resolution can be observed between 1.0-mil divisions if a vernier scale is not available. Several measurements of a single 16-layer sample should not vary by more than ± 0.2 mil, and the median value of those measurements is recorded. The test method produces average measurements for tape sections less than 3 ft long. The precision of the average measurement technique approaches 20 μin. (0.02 mil).

Flexibility

Measurement of tape flexibility is a simple test that may indicate the tendency of a tape to produce oxide binder debris. The relative flexibilities of the magnetic tapes are measured. The test fixture includes a horizontal clamping surface, a coordinate grid to indicate the position of the free end of the tape, and a swingaway support that maintains the tape sample horizontally during mounting and allows the sample to bend freely for the measurement. The angle of curvature (deflection from the horizontal) is measured for the line extending between the clamping point and the free end of the tape sample. All tapes should be maintained in the same environment prior to and during the testing, an environment that approximates the environmental conditions specified for the test, 70° ± 3° F and 30 ± 3 percent relative humidity.

Abrasion Resistance

This test provides a relative measure of the resistance to abrasion of magnetic tape oxide binder systems. The raw data that is presented allows ranking of tapes according to their abrasion resistance, but the correlation between the test results and the useful life of tape oxide during normal or abusive conditions has not been determined. Nonlinear effects of the test method are under study.

Grade 25 chrome steel balls 0.125 in. in diameter are employed. The balls have a Rockwell C scale hardness specification of 62–66 and a roundness tolerance of 25 μin.

Prior to use, shipping lubricant and contaminants are removed from the balls with benzene. Skin contact is prevented during mounting of the balls in the test fixture and during tape preparation and mounting. A new ball is employed for each test.

Prior to mounting the virgin tape samples, a small part of the back coating is removed with methyl ethyl ketone (MEK) and cotton swabs. Contact between MEK and the oxide coating is to be avoided. Abrasion during coating removal is minimized by preparation without motion on a clean polyester sheet.

A 0.227-N (23.1-g) normal force is applied to the tape through the steel ball as it is dragged back and forth across the tape along a 2.67-in. path. The ball passes are counted until a tungsten lamp behind the sample is visible through the clear polyester base material of the sample. Multiple samples of each tape type are tested and the mean value and standard deviation of the number of passes until failure are calculated. For highly abrasion resistant tape types (more than 500 passes), the wear is monitored periodically, and the number of passes between the last unworn observation and the first worn observation is averaged.

Lubricant Content

This test measures the weight of lubricants and other low molecular weight compounds that are extractable by a solvent as a percent of oxide binder system weight. Lubricant is added to the oxide binder system to reduce friction, but excessive lubricant may weaken the integrity of the binder polymer. Benzene is the usual extraction solvent for this test, but the possible use of fluorocarbon lubricants suggested the use of Freon TF as the extraction solvent.

Virgin samples of each tape are determined. The samples must not be contaminated with body oils, lint, or dirt. Tweezers, petri dishes, and work surfaces covered with clean polyester sheets are required to facilitate sample handling and preparation.

All samples should be 18 in² ± 1%. Two tape strips 0.248 ± 0.002 in. wide and 36 ± 0.03 in. long provide this area tolerance.

Each tape sample is labeled and weighed prior to treatments. An analytical balance with 10-μg resolution is suitable. The preweighed samples are divided into groups for oxide binder system removal and lubricant extractions.

The oxide binder system is removed with MEK and cotton swabs or lint-free wipes. Contact of MEK and the back coating is unavoidable; however, if the tape is placed with the oxide side up on a polyester sheet and stroked lightly with an MEK-saturated wipe, the back coating will adhere firmly to the polyester sheet before it is loosened significantly. The adhesion will prevent mechanized disruption of the MEK-wetted back coating and will minimize addition of dissolved oxide binder to the back coating. A subjective indication of the oxide binder system strength is given by the ease of oxide removal with MEK.

The lubricant is extracted from the other groups of samples by soaking for at least 12 hr in selected solvents. The tape is placed in petri dishes on edge during benzene treatment to facilitate complete wetting. Freon-treated samples may be soaked in loosely capped polypropylene bottles. The oxide binder system and back coating should remain intact during extraction and subsequent sample drying.

The samples are dried thoroughly and reweighed. The mean weight losses following treatment are calculated for each group. The lubricant weight as a percent of the oxide binder system weight is calculated as follows:

$$\frac{\text{Lubricant weight}}{\text{Binder weight}} \times 100 = \text{Percent lubricant content}$$

Elemental Surface Analysis

Detection and measurement of elements present near the oxide coating surface of magnetic tapes provide in-

dications of the types and relative amounts of metal oxides, binders, and lubricants on the tape surfaces. Two methods, electron microprobe analysis (EMA) and ion microprobe analysis (IMA), have been employed for elemental analysis. Both methods direct beams of high-energy charged particles onto the surface of the tapes, which induce the emission of small ions or X-rays from materials on the oxide surface. During these probes, the sample size and depth can be controlled by the focus, energy, and intensity of the particle beams.

The ions released from the tape surface by IMA beams are directed to a mass spectrometer, which separates, detects, and counts the individual atoms or, in some cases, small polyatomic ions released from the tape surface. The X-rays emitted by the electron probe are characteristic of the elements in the sample.

Of the two methods, EMA is considered more repeatable and quantitative than IMA, but IMA is considered more sensitive and can detect all elements while EMA is restricted to measurement of elements with atomic weights between 5 and 20 at trace levels by wavelength analysis. EMA can identify heavier elements only as major constituents (>10 percent).

Electron microprobe wavelength dispersion analysis intensity measurements are based on several standards such as SiO_2 for silicon, Teflon for fluorine, sodium chloride for chlorine, metallic iron for iron, and metallic cobalt for cobalt. Because the matrices of the tape samples and the standards are very different, the precision of the EMA measurements is not better than 30 percent relative.

Although IMA counts individual atoms or ions, matrix effects are even more pronounced on the generation of ions during IMA. Quantitative results from IMA obtained by computer analysis of the data employed relative sensitivity factors that give even poorer precision than EMA, not better than ± 50 percent under the best of conditions. It is felt that higher precision for a surface analysis is virtually impossible.

Virgin tape samples are placed in polyethylene bags to prevent chemical contamination and are submitted for analysis of the outer 2-μin. (500-Å) surface layer of the oxide binder coating. Each tape type is mounted on an aluminum substrate with conductive aluminum paint for analysis.

Electron-excited X-ray analysis is conducted with an electron microprobe employing a 6-kV accelerating voltage, a 15-nA sample current, and a 3.2-mil (80-μm) beam diameter. These conditions are intended to produce a 2-μin. penetration depth and essentially no damage to the sample surface. Intensities of silicon, fluorine, oxygen, and carbon are measured during this analysis.

IMA is conducted with an oxygen ion beam accelerated to 20 kV with a 1-nA beam current and a 100-μm beam diameter. These conditions are intended to sputter away the oxide binder system surface to a 2-μin. depth. Secondary ions generated by the sputtering are analyzed in a mass spectrometer. Mass spectra of positive and negative ions are obtained for each sample. Chlorine and cyanide intensities are measured from the negative ion spectra. Iron and cobalt intensities are measured from the positive ion spectra.

Coefficient of Friction

This test measures the coefficient of friction between the tape oxide binder system and the tape head. The symbol μ_s represents the coefficient for the static case when there is no relative motion between the tape and the head, while μ_d represents the dynamic case when the tape moves across the head. The coefficients are dimensionless ratios that increase as the friction between the tape and the head increases. Low values of μ are desirable for overall performance, and critical stick-slip speed generally increases as the difference between μ_s and μ_d decreases.

The standard equation for "belt friction" is

$$\mu = \frac{1}{\beta} \ln \frac{T_1}{T_2}$$

where μ is the coefficient of friction, β is the total wrap angle in radians, T_1 is the takeup tension, and T_2 is the supply tension. For small total wrap angles and equilibrium conditions, the dynamic friction force F_d of the tape across the head is approximately the difference between the takeup and supply tensions:

$$F_d = T_1 - T_2$$

or

$$T_2 = T_1 - F_d \tag{B-1}$$

therefore,

$$\mu = \frac{1}{\beta} \ln \frac{T_1}{T_1 - F_d} \tag{B-2}$$

When the tape changes direction, there is no relative motion or acceleration between the tape and the head for a brief instant, and a peak static friction force F_s occurs just before the tape begins to slip across the head. Once forward tape motion across the head begins, the dynamic friction force F_d occurs between the tape and the head. Although the tape accelerates with respect to the head after slippage begins, very little force is required to accelerate the low mass of the tape, and the test conditions may be assumed to have a nominal effect

on the force tension relation of equation (B-1), which assumes equilibrium conditions.

A Video Research Corp. Model 9209 Tape Tester with a recorder head mounted on a strain gage and a Minnetech Laboratories Model MTM 106 Tension Meter are employed. The head position is adjusted for a 15° total wrap angle, and the tape tester tension control is adjusted for a tape tension close to 8 oz. The tape tester speed control is set as low as possible to allow acceptable and repeatable operation of the tester while minimizing tape acceleration with respect to the head. The speed and tension controls are not readjusted during the test series.

The strain gage measures the frictional drag force F_d associated with the tape movement across the head, while the tension meter measures the takeup tension T_t in the tape following reverse-to-forward changes of tape motion. The transducers are calibrated under static conditions by orienting the tester so that weights can be hung from the free end of a tape secured across the face of the head and threaded through the tension sensor. The drag force strain gage amplifier gain is adjusted for a 10-g/division deflection on a Tektronix Model 7623A Storage Oscilloscope with a Model 7A18 Dual Trace Amplifier set at 50 mV/division; a 4-g/division scale is obtained by changing the calibrated sensitivity control 20mV/division. The second oscilloscope channel is connected to the tension meter output, and the oscilloscope sensitivity is adjusted for a 50g/division deflection. The channels are rezeroed after reorienting the tape tester in its normal operating position, and the zero levels are checked frequently to reduce errors in the absolute value of force and tension that would result from zero level drift.

Samples of virgin ½-in. tape maintained at 70 °F and 30 percent relative humidity prior to and during testing are placed on the tester, the frictional forces are monitored while reversing the tester direction, and five oscilloscope traces of each tape type with reverse-to-forward direction changes are stored and photographed. A new section of tape is positioned near the head for each photograph to maintain the virgin condition of the tape. The tape head is cleaned with ethanol and cotton swabs between each change of tape type.

Static and dynamic friction forces along with simultaneous takeup tensions are calculated from measurements of the photographs, and the coefficients of friction are calculated from equation (B-2). Mean values and standard deviations are obtained for each coefficient and each tape type from the photographic data of each tape type.

Abrasivity

Oxide surface abrasivity or the rates of head wear produced by different tape types can be affected by many variables of the heads, the transport, the tape surface, and the environment. Some abrasion is desirable to prevent buildup of varnish on the surface of the head, but excessive head wear would be disastrous to a satellite recorder. Considerable controversy exists in the field of abrasivity testing. Although several test methods have been developed, little has been done to correlate results of various methods with actual rates of head wear or varnish buildup.

The alfesil bar test was selected for tape abrasivity measurements because the method is simple, is in widespread use, and offers a relatively high degree of precision. The test is also under consideration by the American National Standards Institute as a standard and is the subject of active research. Current studies by several laboratories to assess repeatability and correlation between results and actual head wear will be monitored and reviewed prior to further testing.

The most obvious factor that would affect the test results is the force of the tape against the alfesil bar, which in turn is related to the tape tension at the bar. Tape tension is usually measured at the takeup reel, but the friction of the tape (usually the back coating) or transport bearings as the tape passes over guides, rollers, and capstans along with the force of a vacuum column against the tape can change the tape tension between the takeup reel and the location of the abrasivity test bar. Bearing friction and vacuum column force may produce relatively constant tension changes for different tape types, but preliminary measurements of tension at the abrasivity test fixture with three different ½-in. tape types and 7.5-oz takeup tension resulted in tension at the test bar from 5.5 to 6.5 oz, which suggests that tape friction and transport configuration are important variables in this test.

On the alfesil test bar, the width of the worn surface is approximately twice the depth of the worn surface, so the contact area between the tape and the test bar increases with the wear depth, in contrast to an actual head where the contact surface would not change as much as the wear depth increases. Assuming the pressure of the tape against the worn surface of the test bar decreases in inverse proportion to the area of the worn surface, the rate of wear probably decreases as the wear depth and the area of the worn surface increase. If the wear rate is directly proportional to the area of the worn surface, the amount of wear will be proportional to the square of the wear width that is measured in this test. This relationship could be tested with different lengths of a single tape type.

If tape tension and width are varied in direct proportion, the pressure (force per unit area) of the tape against the alfesil test bar should be constant at any given wear width. If the wear rate is assumed proportional to the wear width and the pressure for a given

tape, this relationship and the constant tension per unit tape width specified in the procedure permits comparison of test results with different tape widths. However, a test series with a constant width for all tape types is recommended if results of current research indicate that the test results are a valid indicator of head wear.

For this test, virgin tape, 1700 ft in length, is wound onto a supply reel. A clean alfesil test bar is mounted with an unworn edge on the test fixture, and the test fixture is installed on the tape transport. The test fixture provides a 16° total wrap angle with 8° of wrap on each side of the bar. The transport tape is set at 3¾ ips, and the tape tension is set at 16 oz/in. of tape width. The test tape is run end to end for one pass only. The reference end of the wear pattern is the end toward lower track numbers of a tape recorder head. For recorders with supply reels that turn counterclockwise for the forward tape direction, the reference end of the wear pattern is the end closest to the tape recorder. The test bar is removed and mounted on a microscope with a calibrated scale and 400× optics.

The width of the wear is measured at three points by sharply focusing the edges of the wear pattern, observing the width against the microscope scale, and multiplying the divisions by the microscope scale calibration factor. The measurement points are one-fourth, one-half, and three-fourths of the distance from the reference end to the opposite end of the wear pattern. During microscopic observation, unusual wear patterns such as scalloping of the work surface or flaking of the worn bar edge should be noted and recorded. Figure B-1 illustrates a typical wear pattern and the points of wear width measurements.

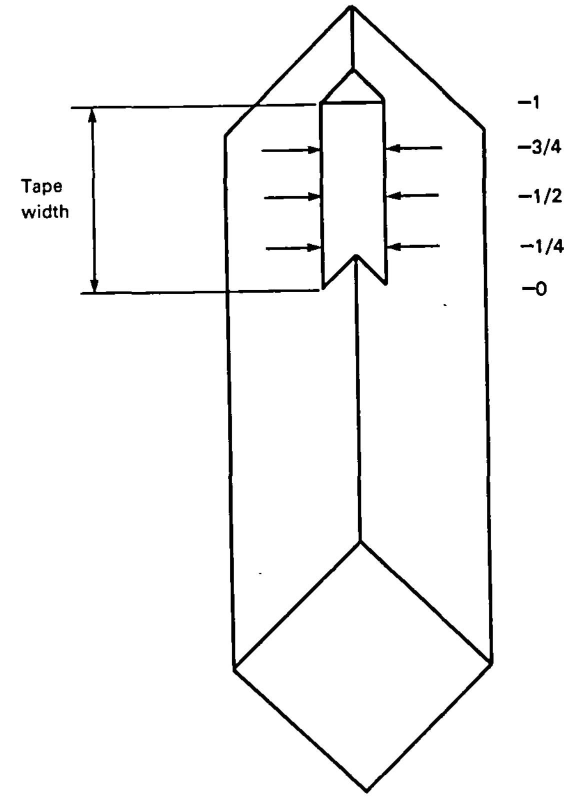

Figure B–1.—Alfesil bar following abrasivity test illustrating three locations for measuring wear width. (See horizontal arrows.) Amount of wear has been greatly exaggerated for clarity.

Scanning Electron Microscopy

The appearance of a magnetic tape oxide surface on a scanning electron micrograph (SEM) may provide evidence regarding oxide particle size, distribution and orientation, surface roughness, and the presence of dirt or debris. The appearance can then be correlated with other surface properties such as abrasivity and coefficient of friction. The surface appearance may also indicate features responsible for bulk performance properties including abrasion resistance, orientation ratio of the particles, and surface dc noise. Production variations that affect tape performance may be analyzed by comparing SEM's from different tape lots.

SEM's of oxide surfaces are made from virgin samples of each tape to be tested. Each sample is micrographed at approximately 2400× and 12 000 × at viewing angles perpendicular to the tape surface and 45° from the long axis of the tape. The long dimension of each SEM corresponds to the transverse direction across the tape, and the short dimension of the micrographs corresponds to the long axis of the tape. Each view is selected to represent a typical portion of tape surface. This procedure does not include a search for defects or surface variations over large areas or between tape lots.

Oxide Surface Cleanliness

Debris on a tape oxide surface can lift the tape away from the head and may constitute a major source of dropouts. The following test can be used to compare two tape types. Virgin tape samples are mounted on the transport of a Kybe Corp. Model CT-100 Tape Tester. The tester can be modified by replacing conventional tape guides with crowned guide rollers, eliminating the oxide surface scraper blade, and stopping the cleaning tissue drive mechanism so that the entire length of the test tape will contact the same spot on the cleaning tissue during a given test run. After each forward end-to-end pass of the tape samples, the tissue cartridges are removed, the tissues are advanced a few inches and marked to indicate the run number, the tapes are rewound, and the tissue cartridges are reinstalled for the next run. The amount of debris on the tissues is ob-

served subjectively, and tissues from different tape types are compared.

MAGNETIC PROPERTIES

Reference B–1 presents the results from three series of *M-H* measurements on the subject tape types and parameters derived from the measurements. The first test series includes measurements of longitudinal properties at 20° C and 20 percent relative humidity, including measurements of four or more samples of three of the tape types. The second test series shows the relationship between temperature and the coercivity and residual induction of single longitudinal tape samples. Finally, the magnetic properties of single transverse samples and orientation ratios of the tapes are reported.

An accurate calibration method or standard has not yet been obtained for the remanence *M*-axis of the *M-H* curve plotter. Comparison of results presented in reference B–1 with various manufacturer's specifications suggests that the reported results are only 0.7 times other manufacturer's specifications. Saturation induction and residual induction are directly dependent on the maximum applied field, and this effect is under investigation as the source of the *M*-axis calibration inaccuracy. Discrepancies in the *M*-axis calibration will only affect the values of saturation induction M_s and residual induction M_r, which can easily be corrected in future reports when a more accurate calibration is obtained. The squareness and orientation ratios, and the switching field distributions (SFD) can be calculated with arbitrary *M*-axis scales and do not depend on the absolute accuracy of the calibration.

Theory of *B-H* Measurements

According to classical electromagnetic theory, a changing magnetic flux ϕ_B induces an electromotive force:

$$\epsilon = -\frac{d\phi_B}{dt} \tag{B-3}$$

If the flux density B is constant over a given area A, then the flux equals the flux density multiplied by the area:

$$\phi_B = BA \tag{B-4}$$

Substitution of equation (B–4) into (B–3) and integrating shows that the flux density is equal to the integral of the induced electromotive force divided by the area:

$$B = -\frac{1}{A}\int \epsilon \, dt \tag{B-5}$$

Equation (B–5) is valid for a magnetic field in a vacuum and is a close approximation when weak magnetic materials such as air, glass, Mylar, or wood are present. When a ferromagnetic material is present, an external field aligns magnetic domains in the material, and the resultant flux density can be described by

$$B = \mu_0 H + J \tag{B-6}$$

where μ_0 is the permeability of free space and is equal to 1 G/Oe in the centimeter-gram-second (cgs) system of units, H is the applied magnetizing field, and J is the magetization induced in the ferromagnetic material by the applied field H. Equation (B–6) is often written

$$B = \mu_0 (H + M)$$

where $M = J/\mu_0$. Because the magnitude of μ_0 is unity in the cgs system, we can ignore dimensions and write

$$B = H + M$$

The flux density in the sample produced directly by H cannot be measured directly; only the induced magnetization M (or J) is measured.

Figure B–2 is a simplified schematic of the IITRI *M-H* curve plotter. The 120-V, 60-Hz input power is coupled through isolation transformer T1 and circuit breaker CB1 to the H field control variable autotransformer T2 and the H field range autotransformer T3 to produce a drive voltage across the excitation solenoid L, which produces a uniform magnetic field at the H and M pickup coils. The H range switch S1 selects one of two taps on T3 and one of two resistors R1 or R2 in series with the H meter that are connected across the excitation solenoid to indicate the fraction of the selected H range produced by the solenoid. The value of a bank of capacitors C1 places the excitation circuit near resonance to reduce the input current required by the curve plotter.

The voltage across the excitation solenoid is also applied to calibration network including R15, R16, and the sample size precision voltage divider. When S3 is in the calibrate position, known in-phase sinusoidal voltages developed by the networks are applied to the inputs of the H and M amplifiers to allow adjustment of the oscilloscope input sensitivities. The sample size voltage divider provides an M calibration voltage that is proportional to the sample cross-sectional area so that the vertical sensitivity of the oscilloscope can be adjusted in inverse proportion to the sample area as required by the $1/A$ term of equation (B–5).

The H cal and B cal variable resistors R15 and R16, respectively, are internal controls that set the output voltages of the calibration networks equal to the output

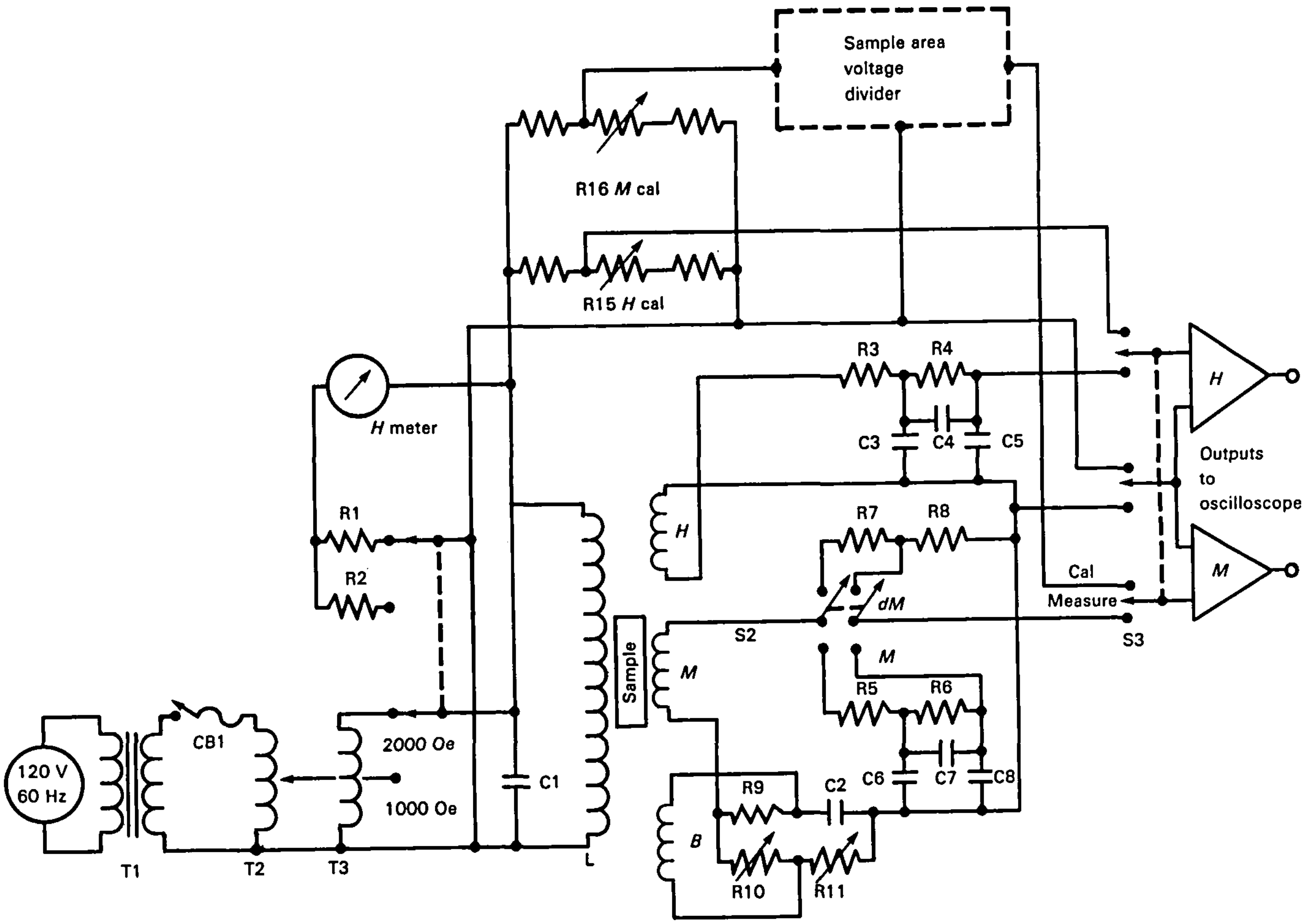

Figure B-2.—Simplified schematic of IITRI *M-H* curve plotter. (CB = circuit breaker.)

voltages of the *H* and *M* integrators. A standard sample is required for the adjustment of R16. The peak magnetizing field H_m can be calculated from the solenoid geometry and current or measured by a calibrated magnetometer with an axial probe inserted into the sample holder of the curve plotter. R15 is adjusted for equal horizontal trace size in the measure and calibrate modes.

Two pickup coils *H* and *M* are located in the uniform magnetic field region within the solenoid. The *M* pickup coil encircles the sample tube so that the voltage induced in *M* is caused by both the applied field over the cross-sectional area of *M* and the induced magnetization of the sample over the cross-sectional area of the sample. Because the *M* coil area is much greater than the sample area, it is necessary to apply a voltage in series with the *M* coil to cancel the voltage induced by the applied field. To accomplish this, a sinusoidal voltage is induced in the balance pickup coil *B* located at one end of the solenoid. This voltage is applied across bridge R9, R10, R11, and C2, and the bridge output is connected in series with the *M* pickup coil. R10 controls the in-phase amplitude of the balance voltage while R11 sets the phase of the balance voltage equal to the voltage induced in *M* by the field. Together, these controls are adjusted with the sample holder empty to cancel the voltage induced in *M* by the field, and the voltage induced by the sample magnetization is applied through switch S2 to the *M* amplifier. With switch S2 in the *M* position, this voltage is integrated by R5, R6, C6, C7, and C8 before application to the amplifier. With S2 in the *dM* position, the voltage is attenuated by R7 and R8 and is applied to the amplifier without integration.

The *H* pickup coil is wound around the *M* pickup coil so that its area is so large with respect to a sample area that the voltage induced in *H* by the sample magnetization is insignificant with respect to the voltage induced by the field. The voltage can be integrated by R3, R4, C3, C4, and C5 before application to the *H* amplifier.

The *M* and *H* outputs of the *M-H* curve plotter are connected to the vertical and horizontal inputs respectively of an oscilloscope. The horizontal *H*-axis sensitivity of the oscilloscope can be adjusted for a convenient *H*-axis scale factor. In the calibrate mode, the

signal applied to the vertical axis of the oscilloscope is equal to 0.5 G/Oe of the applied field setting, which permits the adjustment of the vertical M-axis sensitivity for a convenient scale factor. Oscilloscope calibration is discussed in the section entitled "M-H curve plotter operation and curve measurements."

Three parameters can be measured directly from oscilloscope photographs of magnetic hysteresis loops. The values are calculated by multiplying photograph measurements by scale factors. The saturation induction M_s is represented by the distance between the value of M at $H = H_m$ and the H-axis. The residual induction M_r or remanence is the value of M at $H = 0$, which is the induction in the sample with no applied field following saturation of the sample. M_r is represented by the distance between the M-axis intercept and the origin. The coercivity H_c or coercive force is the value of H at $M = 0$, which is the applied field required to reduce the remanence to zero following saturation of the sample. H_c is represented by the distance between the H-axis intercept and the origin. These parameters are illustrated in figure B-3.

Definition and Calculation of Derived Parameters

The saturation induction M_s, residual induction or remanence M_r, and coercivity H_c are measured directly from M-H curves produced by the M-H curve plotter. The squareness ratio is defined as the residual induction

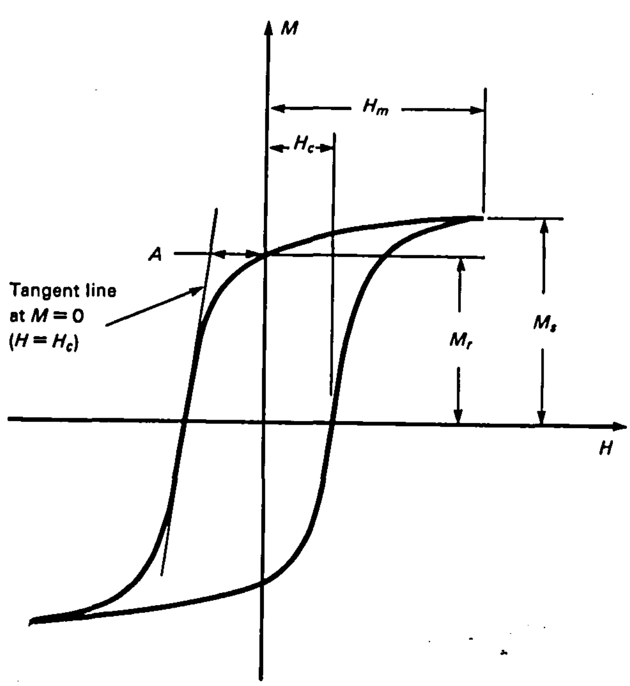

Figure B-3.—Typical M-H hysteresis loop illustrating H_m, H_c, M_s, M_r, and $S^* = A/H_c$.

divided by the saturation induction, or squareness = M_r/M_s. When the magnetic particles are oriented during the tape manufacturing processes, the values of M_s, M_r, and H_c depend on the orientation of the tape with respect to the H field applied by the M-H curve plotter. The orientation ratio (O.R.) is defined as the longitudinal remanence divided by the transverse remanence of a given tape: O.R. = M_{rL}/M_{rT}. Squareness and orientation are dimensionless ratios that generally have higher values for tape with greater particle orientation (transverse samples of tape with greater orientation have lower squareness values). Squareness is always less than 1, while orientation ratio is equal to 1 for unoriented particles and greater than 1 for longitudinal oriented particles.

The parameter symbolized by S^* in figure B-3 can be measured from a magnetic hysteresis loop by constructing a line tangent to the curve at $H = H_c$ ($M = 0$), measuring the horizontal distance A between the vertical axis and that line at the level of M_r, and dividing the resultant value by H_c.

SFD is defined as the width of the dM/dH-H curve in Oersteds at the half amplitude level of the curve (fig. B-4). The dM/dH curve can be produced electronically by defeating the integration of the voltage induced in the M pickup coil by the sample, or it can be plotted from slope measurements of the M-H curve. The half amplitude level of the dM/dH-H curve is measured from the horizonal axis and is half the distance between the horizontal axis and the maximum positive or negative value on the curve.

The parameters SFD/H_c and S^* are associated with the slope of the M-H loop at or around $M = 0$ and are less than 1 for longitudinal samples. They are related to the number of magnetic particles that will switch their orientation for a change in the applied field around the value of H_c. In general, lower values of SFD/H_c and higher values of S^* are associated with shorter transition zones and higher digital output for magnetic media. However, coercivity and residual induction can have a much greater effect on high-density digital recording output than switching parameters.

Sample Preparation

The thickness of the oxide coating of the tape to be tested is determined by measuring with a micrometer the thickness of 16 layers of tape adjacent to the tape sample for M-H measurements. This measurement is divided by 16 to obtain the total thickness of one tape layer. The oxide coating is then removed from the Mylar base. The thickness tape sample is placed with oxide side up on a clean smooth surface. The oxide is rubbed off with cotton swabs or Kim Wipes saturated with a solvent such as MEK. The thickness of the 16 base layers with

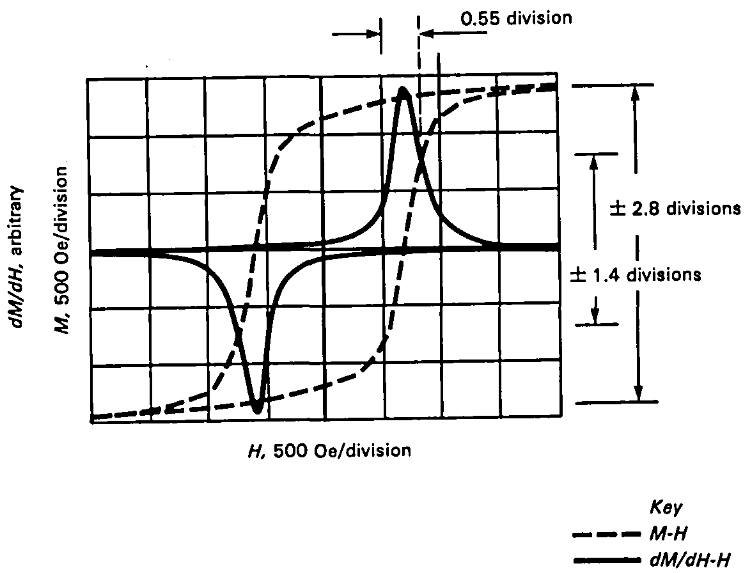

Figure B-4.—Typical *M-H* curve with ***dM/dH-H*** curve. The half amplitude level of ***dM/dH-H*** curve is 1.4 divisions above or below the horizontal axis, and the width of the ***dM/dH-H*** curve at that level is 0.55 division × 500 Oe/division = 275 Oe.

the oxide coating removed is measured and divided by 16. The Mylar thickness is subtracted from the total thickness to determine the oxide coating thickness. The micrometer must be accurately zeroed and must not apply so much pressure that the tape sample deforms and causes measurement errors. Micrometers with slip mechanisms produce low and repeatable measurement pressure. The micrometer measurements should be read to the nearest 0.1 mil, and a median value of several measurements that do not vary by more than ±0.2 mil can be employed for the thickness calculations.

The sample width is determined next. For longitudinal *M-H* measurements, tape widths of 250, 500, and 1000 mils may be assumed for 1/4-in., 1/2-in. and 1-in.-wide samples, respectively. For transverse measurements, tape samples should be cut to suitable lengths with an accuracy of ±1 percent.

The cross-sectional area of the tape samples is then calculated in square mils. For longitudinal measurements,

$$\text{Total area} = \text{width} \times \text{thickness} \times \text{number of layers}$$

For transverse measurements,

$$\text{Total area} = \text{length} \times \text{thickness}$$

For either type of measurement, the sample size must be large enough to provide an adequate signal-to-noise ratio, but it must be small enough to fit within and allow ventilation of a sample tube, and to prevent saturation of the *M-H* curve plotter amplifiers by large induced voltages. Total areas between 400 and 2000 mil^2 are suitable for electronic considerations, but areas toward the low end of that range are suggested for sample holder considerations. For oxide dimensions of 250 by 0.2 mils, 10 layers will fit within the recommended glass tube sample holders.

The sample holder of the IITRI *M-H* curve plotter accepts sample tubes up to 5/16 in. in diameter. Standard 7-mm glass tubing may be cut to 16-in. lengths. Fire polishing of the cut ends should be minimized to prevent narrowing of the ends, which may interfere with sample insertion into the tubing.

A sample at least 6 in. in length is inserted into the sample holder. This minimum size allows for excess tape and positioning variability within the sample holder of the *M-H* curve plotter.

For longitudinal measurements, the tapes employed in the total area calculation should be cut to lengths greater than 6 in. and aligned. End alignment can be achieved by trimming. Then the aligned tapes can be folded longitudinally and inserted into a sample tube. The final fold should be made while inserting the sample. A sharp crease is not required for the final fold. The sample must not be twisted or kinked within the sample tube. If a twist or kink develops, it can often be removed by slightly withdrawing the sample. After at least 6 in. of sample have been inserted, any tape extending from the end of the sample tube can be trimmed. The ends of the sample tube should remain unrestricted.

For transverse measurements, the tape should be cut to the length employed in the total area calculation. A minimum of 6, 12, or 24 accurately cut lengths are required for 1-in., ½-in., and ¼-in. tapes, respectively, to insure adequate sample length. Each cut length must be rolled and/or folded transversely and inserted sequentially into the sample tube. The first cut and rolled tape section should be pushed 6 in. into the sample tube with a rigid instrument, and each subsequent section should be pushed into the sample tube so that it just touches the preceding section. If the recommended lengths have

been used, the total sample length should be within 1 percent of 6 in. A longer sample length indicates gaps between tape sections while a shorter sample length indicates deformation of the tape edges produced by pushing the sections too hard against each other.

Sample code and cross-sectional area should be marked on pressure sensitive paper applied to the empty end of the sample tube.

M-H Curve Plotter Operation and Curve Measurements

An oscilloscope with *X-Y* display capabilities, continuously variable sensitivity controls, dc coupled inputs, and a camera are required. A horizontal sensitivity between 0.2 and 0.5 V/cm is required. A 500 mil² sample size requires a vertical sensitivity of about 20 mV/cm. A wide bandwidth is not required due to the low excitation frequency. The 500-kHz bandwidth and control features of a Tektronix Type 503 oscilloscope are suitable.

The *M* output of the curve plotter is connected to the vertical or *Y* input of the oscilloscope. Connect the *H* output of the curve plotter to the horizontal input of the oscilloscope.

The field H_m control should be checked to see that it is fully counterclockwise, and the field range must be selected before applying power to the curve plotter. The 2000-Oe range is suitable for high-coercivity samples such as cobalt-doped γ-Fe_2O_3 tape. (*Warning:* the field solenoid is not designed for continuous operation at high field strengths. Do not operate the solenoid at 2000 Oe for more than 1 min. at a time or at a duty cycle greater than 10 percent.) The phase and quadrature adjustments must be repeated as the solenoid heats the pickup coils.

The blower, the amplifiers, the field circuit breaker, and the oscilloscope are turned on and allowed at least 10 min to warm up. The field control should be left fully counterclockwise except during short periods when the field is required for calibration or measurements. The field range selector and the field circuit breaker should be switched only when the field control is turned fully counterclockwise to prevent the induction of high-voltage transients due to sudden interruption of the field current.

The *M-dM* switch is set on the *M* position, and the *H* gain switch is set on the $H \times 1$ position. Any sample present in the sample holder is removed, the mode switch is set to the "measure" position, and the field control is adjusted for full-scale deflection of the *H* meter. The in-phase balance and quadrature balance controls are adjusted for a horizontal trace on the oscilloscope. The in-phase control affects the tilt of the trace, and the quadrature control prevents the elliptical loop appearance of the trace. These controls can be adjusted more accurately by increasing the vertical sensitivity of the oscilloscope. The controls do not affect the trace when the plotter is in the calibrate mode, but their setting should be checked whenever operation of the field solenoid is likely to change the temperature of the pickup coils. The blower directs air over the pickup coils to minimize these temperature changes.

The calibration voltage divider is set to 0.0001/mil² of the sample cross-sectional area. With the field control counterclockwise ($H = 0$) and the *M-H* curve plotter in the calibrate mode, the trace should be centered on the oscilloscope with the vertical and horizontal position controls. The field control is adjusted for full-scale deflection on the *H* meter. At this point, a diagonal trace will appear on the oscilloscope. The signal amplitude applied to the horizontal *H* input of the oscilloscope represents twice the applied peak field, and the signal amplitude applied to the vertical *B* input of the oscilloscope represents 0.5 G/Oe of applied field. For example, if H_m is 2000 Oe (4000 Oe peak to peak), the *M* signal represents 1000 G (2000 G peak to peak). The vertical and horizontal sensitivity controls of the oscilloscope are adjusted for convenient trace width and height. To calculate the scale factors, the peak-to-peak *H* and *M* values are divided by the width and height, respectively, of the diagonal trace. For example, if the oscilloscope sensitivities are adjusted for a diagonal six divisions high by eight divisions wide and $H_m = 2000$ Oe, the scale factors will be 4000 Oe $\div$ 8 divisions = 500 Oe/division and 2000 G $\div$ 6 divisions = 333 G/division. The oscilloscope calibration must be repeated each time the sample cross-sectional area is changed.

With the field control fully counterclockwise and the sample holder empty, the *M-H* curve plotter is set to the measure position. The oscilloscope trace is centered, and the field control is adjusted for full-scale deflection of the *H* meter. The phase and quadrature adjustment must then be checked. The sample tube is then inserted in the sample holder. Adequate sample length and uniformity are insured by observing the hysteresis loop on the oscilloscope while positioning the sample. The trace should remain stable for a variation of at least 1 in. in sample position, and the sample should be placed near the center of the position range that produces a stable trace. The *M-H* hysteresis loop is photographed. If SFD measurements are required, the *M-dM* switch is set to the *dM* position, the vertical gain and position controls of the oscilloscope are adjusted for a convenient *dM/dH-H* curve amplitude, and the curve is photographed.

When measuring H_c and M_r on the photographs, the intercept-to-intercept distances are measured, multiplied by the scale factor, and divided by 2 to reduce parallax error. M_s can also be measured peak to peak

and divided by 2. When measuring SFD from the *dM/dH-H* curve, the width of the curve at the half amplitude level is measured and multiplied by the horizontal scale factor. This result is not to be divided by 2.

Figure B-5 is a calibration record of the *M-H* curve plotter. The "standard" Ampex 721 sample with a published M_r value of 1000 G ± 10 percent was inserted into the plotter, and the oscilloscope sensitivity controls were adjusted for $M_r = \pm 3$ divisions and $H_m = \pm 4$ divisions, which produce scale factors of 333 G/division along the vertical axis and 500 Oe/division along the horizontal axis. Then the calibration voltage divider was set for the sample size, the plotter was switched to the calibrate mode, and the internal calibration controls *H* cal and *B* cal were adjusted without changing the oscilloscope sensitivity controls to produce the eight-division-wide by six-division-high diagonal calibration trace. The apparatus is now ready to be recalibrated for different sample sizes and scale factors. This is done by resetting the calibration voltage divider to the sample size and readjusting the oscilloscope sensitivity controls for the desired diagonal calibration trace size without changing the internal calibration controls.

A horizontal trace on figure B-5 just below the horizontal axis is the no-sample signal with proper adjustment of the balance phase and quadrature controls. The positive and negative pulse waveforms in the first and third quadrants are the *dM/dH-H* curve with an arbitrary vertical scale that can be calibrated by graphically measuring the maximum slopes of the *M-H* curve. Figure B-5 also indicates that the camera has slight parallax errors that are apparent from the asymmetric horizontal centering and an apparent *M*-intercept to *M*-intercept distance of 5.95 divisions rather than the 6.00-division distance intended for the calibration procedure.

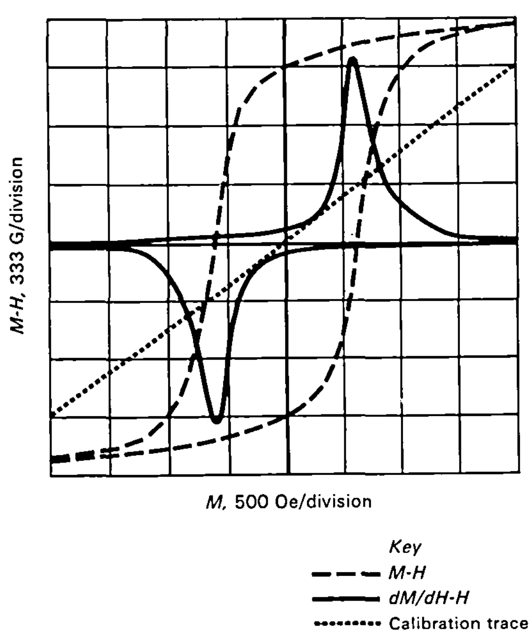

Figure B-5.—*M*-axis calibration record with Ampex 721 tape and manufacturer's specification of $M_r = 1000$ G as the "standard." Vertical scale for *dM/dH-H* curve (pulse waveforms in first and third quadrants) is arbitrary because only the width at the half-amplitude level is required to determine the SFD. Horizontal trace just below horizontal axis indicates correct adjustment of balance controls with no sample in the curve plotter.

Sample Selection and Test Methods

All prepared samples should be conditioned at 70° ± 5° F and 20 ± 10 percent relative humidity for at least 16 hr prior to any testing. The small samples and their glass sample tubes are maintained for at least 16 hr at test temperatures below 20° C and for at least 3 hr at temperatures above 20° C. Sample temperature was maintained in the sample holder by blowing air through the sample tubes and by limiting the time between insertion of the sample and photographing the *M-H* curves to less than 1 min. One end of the sample tubes was always occluded during transfer of the sample tubes to the sample holder, requiring exposure of the sample tubes to ambient room conditions for approximately 10 s. No condensation was observed in the sample tubes following their transfers.

ELECTRICAL PROPERTIES

This section describes the electrical properties of tapes. The tests compare tape performance with respect to record currents required to achieve maximum outputs at different wavelengths, the magnitude of these maximum outputs, and the output magnitude in response to a constant record current, the resistivities of the tape coatings, and the distribution and size of oxide defects that cause momentary reductions in signal output or "dropouts." The results of these tests permit predictions of high-density digital recording system performance with specified coding, signal-to-noise ratio tolerance, and minimum distance between flux reversals.

Record Current Without Bias

This test measures and compares the record current at selected wavelengths required to achieve the maximum attainable reproduce signal level. A square wave current source is applied to the record head, and the current is increased and measured while the reproduce level is monitored to detect its maximum level. A frequency range is selected that allows application of adequately square current waveforms to the record head by the available test equipment, and then the tape transport

speed is selected so that the record frequency range corresponds to the range of wavelengths under consideration for a specific application.

As shown in figure B–6, a square wave output voltage from a Krohn-Hite Model 5300 Function Generator is applied to inputs of an Instruments for Industry Model 5100 Wideband Amplifier and a Heathkit Model 1B-1100 Frequency Counter. The output level of the function generator is set just below the specified maximum input level of the wideband amplifier.

The output of the wideband amplifier is connected to the Honeywell 1-in. record head in series with a 3-Ω resistor and a 2-A fuse. That resistor and the 50-Ω output impedance of the amplifier make the amplifier output appear as a current source to the very low impedance record head. The phase response of the amplifier produces nominal distortion of the applied square wave over the range of 100 kHz to 1.0 MHz, and to achieve record wavelengths in the range of 30 to 300 μin. a tape transport speed of 30 ips is selected. Intermediate wavelengths of 150 and 60 μin. may be selected for record current measurements.

The current through the record head is monitored and measured with a Tektronix Type P6019 Current Probe connected to channel 2 of a Tektronix Type 454 Oscilloscope and to a Hewlett-Packard Model 3403C True Root-Mean-Square Voltmeter operating in the auto ranging ac mode.

The record head and a Honeywell 42-track, 1-in. (17-mil) Reproduce Head are mounted on a Honeywell Model 96HD Tape Recorder. Signals recorded on the test tapes can be reproduced through track 39 of the reproduce head and preamplifier and the 4-MHz direct reproduce amplifier supplied with the tape recorder. The reproduced signal is measured and monitored at test points 1 and 2 of the direct reproduce amplifier, which are located before the equalizer circuits of the direct reproduce amplifier. The reproduced output is monitored on channel 1 of the oscilloscope, and the output level is measured with a Hewlett-Packard Model 3400A True Root-Mean-Square Voltmeter.

For each test tape and record wavelength, the output level control of the record amplifier is increased until the maximum output level is observed, and the record

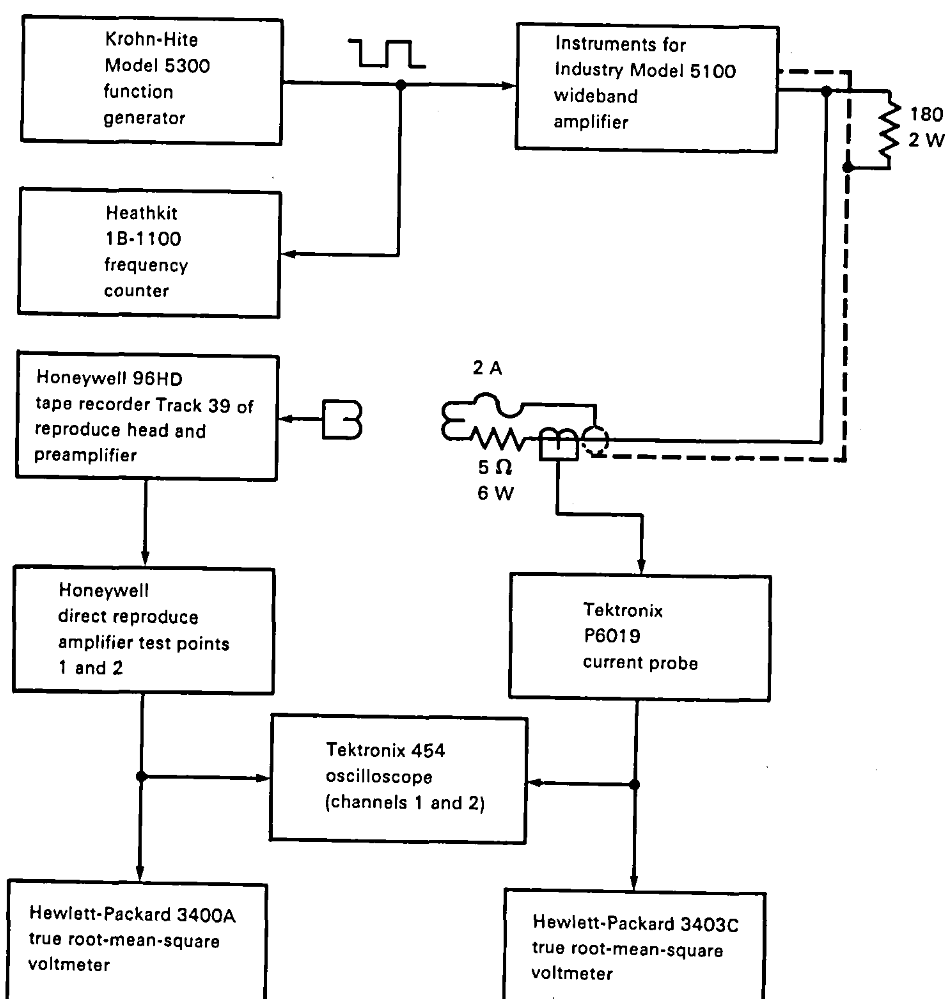

Figure B–6.—Test equipment for record current and wavelength response tests.

current that produced the observed maximum output is measured. Recording continues at the maximum output level for at least 20 s after noting the footage counter reading at which maximum output is achieved. Then the record current is turned off, the tape is rewound to the noted footage counter reading, and the maximum output level is measured while reproducing the recorded signal with no record current. This procedure eliminates "feed through" from the record head to the reproduce head during the output level measurement. Although feed through increases as the record current increases and some feed through is present during the maximum output level observation, the output level always decreases for shorter wavelengths ($\lambda \leq 150$ μin.) and record currents slightly above the level that produces the maximum output before the feed through interferes with the maximum output level observation. For 300-μin. wavelengths, the output level approaches a plateau as the record current is increased, and the record current that produces the maximum output level is difficult to measure accurately.

A broadband noise measurement may also be conducted on each tape with no record current and no recorded signal. Most of this noise is generated or picked up within the reproduce electronics and is not a function of the test tapes.

Wavelength Response

This test measures the reproduce level from the direct reproduce amplifier for each tape at selected wavelengths with a constant record current. The record current that produces the maximum output level with a 30-μin. wavelength for a given tape type is employed for that tape type.

The test equipment, tape speed, and wavelengths are identical to those employed for the record current test described in the preceding section. For each wavelength, the record current is adjusted by varying the output level control of the wideband amplifier until the indicated record current is obtained. Then the reproduce voltage in decibels is measured. For each tape, the reproduce voltages are normalized to a reference level of 0.0 dB corresponding to the output level at the 300-μin. wavelength.

Coating Resistivity

The surface resistance on the coatings of the tape is related to the amount of carbon or graphite added to the overall binder composition. Carbon is generally added to the binder to increase conductivity, thereby reducing possible buildup of static charges when operated in a dry atmosphere. However, the addition of excessive carbon may have a weakening effect on the integrity of the binder system. In other studies, carbon has been observed as a constituent of excessive debris accumulation.

The coating resistivity of the magnetic oxides and the back coatings of the tape samples are measured with a Hewlett-Packard Model 4329A High Resistance Meter. The test fixture permits five measurements on each sample. The reported oxide results are for 500 V_{dc} test potentials. The coating resistivity test procedure generally follows methods specified in volume III, appendix B, paragraph 3-61(b) of IRIG 106-80 and the Electronic Industries Association (EIA) *Recommended Test Method—Magnetic Tape Electrical Resistance Coating,* RS-342 (ANSI C83.36-1968), which differ mainly in the applied test potential: 500 V_{dc} required in the IRIG standard and 100 V_{dc} preferred in the EIA standard. The relationship between resistance and test voltage is probably nonlinear, with lower resistance occurring as the test potential is increased. Because low coating resistivity is desirable to prevent the buildup of static electricity, a phenomenon associated with high voltage, the higher test potential appears to be the most rational choice for future tests. However, the higher power dissipation in the tape samples, which results from a high test potential, may increase two technical problems in an objective, unbiased evaluation of coating resistivity. First, the test electrodes are secured at each end, and the contact resistance between the tape samples and the electrodes may be less at the tape edges than at the center. Melting of the Mylar base at the sample tape edge is evident following some tests. On the other hand, the contact force between the electrodes and the samples does not have a large effect on the measured resistivities. Therefore, this first problem can be reduced by applying nominal torque to the screws that secure the electrodes. We found that "finger tight" screws were adequate. The standards do not specify electrode forces.

The second problem that may be associated with power dissipation in tape samples is the tendency for the resistance to increase during the application of the test potential, especially with high-resistance tape samples. The measurements can be completed within a 2-min limit, and the resistance values appear to stabilize within that time period. The resistance change is very rapid upon initial application of the test potential, and the initial resistance cannot be resolved with slowly responding test equipment. Increasing resistance may result from moisture loss while power is dissipated by the test samples.

One final procedure problem that is not answered in the standards is the possibility of contact between the tape backing and the electrodes if the back-to-back strips are not perfectly aligned on the electrodes. A wide uncoated Mylar strip can be inserted between the two sample strips to perform the tests.

Dropouts With 18-Mil Trackwidth

Square wave currents from a 500-kHz source are applied to a single track record head. The record current and reproduce head azimuth are adjusted to produce maximum reproduce output levels. A 500-kHz record frequency is selected to achieve the best record current waveform, and the tapes are recorded at 30 ips to achieve 60-μin. wavelengths (one wavelength is equivalent to two flux reversals).

Data are obtained with a dropout detector, a 500-kHz oscillator, and two electronic counters. One counter is used to register total dropouts and one to register total duration of dropouts in units of wavelength. Counts are recorded after every 100 ft of tape, and the sequential readings are subtracted to determine dropouts per 100 ft and errors per 10^6 wavelengths (100 ft $\times$ 12 in./ft $\times$ 1 wavelength/60 $\times$ 10^{-6} in. = 2$\times$ 10^7 wavelengths). The average number of errors per dropout is calculated for each 100-ft tape segment. Average values of each parameter are also calculated over the entire 1600-ft sample lengths.

The dropout detector receives the signal from one preamplifier of the Honeywell Model 96HD Recorder, amplifies the signal and provides automatic gain control with a very long time constant in comparison to the longest detected dropouts, rectifies and filters the gain controlled output, and compares the filtered output to a selectable reference voltage corresponding to the specified threshold level below the normal gain-controlled output level. In the preliminary trials, the comparator output is filtered to remove "glitches" at the leading edge of dropouts just below the threshold level, and the filtered comparator output is applied to the electronic counter that registers dropouts. The filtered comparator output is also employed to enable the 500-kHz oscillator signal to the second electronic counter that registered errors. Thus an error is defined as one wavelength (two flux reversals) that produces an output signal below the threshold level, and a dropout is defined as a series of consecutive errors.

The threshold levels are calibrated by applying a square wave modulated sinusoidal waveform to the dropout detector input and varying the degree of modulation while observing the input signal and the comparator output on an oscilloscope. The accuracy of the calibration method approaches ± 1 dB for the 6- and 12-dB thresholds, but some distortion of the modulated input signal may reduce the accuracy to around ± 2 dB during the 20-dB threshold calibration. During the calibration, the dropout detection signal did not enable the error signal until after the first wavelength of a dropout had passed. This source of error does not appear to be significant with respect to the typical length of dropouts detected on the sample tapes. The filtered dropout detector signal occasionally fails to trigger the dropout counter or triggers it twice for what appears to be a single dropout. These two sources of error tend to cancel each other, but their overall effect on the data are not quantified. Digital filtering of the detected reproduce signal of the tape and the addition of a one-shot pulse generator to the comparator output should eliminate all sources of count errors.

The errors per 10^6 wavelengths parameter should be equivalent to bit error rate for randomized nonreturn-to-zero recordings with an equal number of "1's" and "0's."

Dropouts With 7.3-Mil Trackwidth

This narrow track video head was designed for high frequencies, and it is necessary to increase the tape speed to 60 ips to maintain a signal-to-noise ratio greater than 20 dB. Tapes must also be recorded at 60 ips with a 1.0-MHz record signal to maintain the 60-μin. wavelength. The record current at this higher frequency is slightly less square than the 500-kHz square wave record current of the 18-mil trackwidth measurements.

Dropouts are measured on 13 tracks near the center of each 1-in.-wide tape sample during sequential passes. The distance between track centers is 20.8 mils. The first is 315 $\pm$ 5 mils from the edges of the tape samples, and the last track is 565 $\pm$ 5 mils from the edges of the samples. Dropout locations along the length of the samples are calculated to within ± 10 ft.

The total errors registered on the error counter are printed once every 2 s, or every 10 ft of tape, and each change of error registrations between adjacent 10-ft tape segments is considered a single dropout. Oscilloscope monitoring of the comparator input demonstrates that this dropout counting method is accurate for low dropout rates (less than 1 dropout per 100 ft), and that very few of the error registration changes on higher dropout rate samples are caused by more than one dropout per 10-ft tape segment. This dropout counting method is more accurate than the counter method employed with the 18-mil trackwidth measurements. Other details of the dropout measurement procedure are the same as for the 18-mil trackwidth.

REFERENCES

B-1. Schultz, R. A.: *Technical and Investigative Support for High Density Digital Satellite Recording Systems.* IITRI Progress Report 8-11, IITRI Project No. K06003, July 1982.

B-2. Buschman, Al: "Magnetic Tape Certification." Ch. 4 of *Magnetic Tape Recording for the Eighties,* NASA RP-1075, Apr. 1982.

APPENDIX C

*Increasing Head Life**

SECTION 1 – EXTENDED-LIFE INSTRUMENTATION HEADS

David Cristofar
Spin Physics

In September 1982, at the International Telemetry Conference in San Diego, Spin Physics formally announced the development of two new products. One of these was the instrumentation head with integral wideband preamplifier. The other was a 3000-hr, extended-life instrumentation head. This new, extended-life head represents an improvement in life of 3:1 over previous offerings. Like many technical solutions we run across today, Spin Physics' approach appears simple and straightforward in retrospect, but it took a great deal of time and effort to develop.

The Need for Long-life Heads

The extended-life instrumentation head represents further development of technology at Spin Physics in the production of long-life and high-performance heads. It was developed in response to a market need for high-speed tape operation, high data reliability over extended periods, and life and maintenance cycles consistent with the electronics and other transport elements.

Several years ago, Spin Physics introduced the Spinalloy™-tipped head. This head provided improved wear performance of two to four times that of conventional metal heads. The warranty offered on this head was 1000 hr. The Spinalloy™ head has had an excellent record since introduction, often lasting several times the warranted life. The new generation of extended-life heads uses new fabrication techniques developed at Spin Physics and is capable of over 3000 hr of life; the new design combines optimum performance with long life.

Editor's note: This appendix consists of three sections. Each section was written by a different head manufacturer expressing its technical point of view. It is not the intent of this presentation to imply that only three sources for heads exist or that only these manufacturers have 3000-hr heads.

Head Wear

In analyzing the problem over the years, Spin Physics has tested and documented head wear with most instrumentation tapes. We have learned that this is quite a complex phenomenon: head wear is affected by tape characteristics and tape chemistry reacting with materials in contact with the tape. These effects are accelerated by temperature and humidity combinations, and are directly affected by tape pressure and speed.

There are a number of effective materials, including glass, ceramics, and anodized metals, that offer a significant improvement in wear over aluminum when used in the faceplate area. At the same time, though, not all of these materials produce the best results under all conditions. Debris buildup, as well as the hardness of the faceplate material, must be considered in an effort to reduce maintenance and achieve reliability.

Typical Head

Figure C–1 depicts a typical head: a 14-track, interleaved head with a 0.050-in. trackwidth and a 0.140-in. pitch. This head is characterized by a very thin

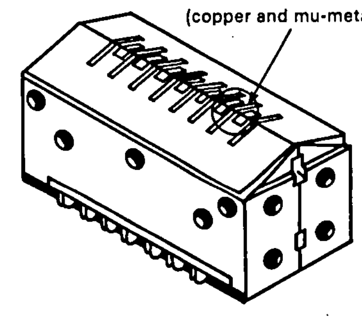

Figure C–1.—Typical head: 14 tracks, interleaved, 0.050-in. trackwidth, and 0.140-in. pitch.

shield and a large island between the shield and track representing the soft aluminum of the faceplate. The Spinalloy™ on the pole tips wears very well. It is the area between the tracks, the intertrack shield and aluminum faceplate, in which wear occurs. Both the aluminum faceplate and the mu-metal/copper shield are relatively soft, mechanically.

Figure C-2 shows the effect of "scalloping," or wear occurring in the intertrack area. Although a certain degree of scalloping is desirable, to improve tape-to-head contact in the gap area, on the typical head it reaches excessive amounts. The eventual result is wear-through at the track edge.

Figure C-3 shows that the faceplate occupies a large area between tracks. Head life can be increased if the typical aluminum material used here is replaced with a harder material, increasing the area of hard material in tape contact. To effectively maximize this area, it is also necessary to minimize the thickness of the mechanically soft shield, thereby maximizing the width of the hard material now in contact with the tape.

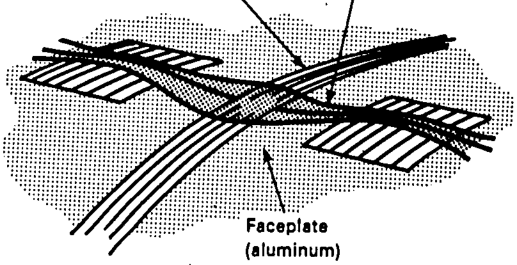

Figure C-2.—Scalloping. (Dark area shows tape contact and wear.)

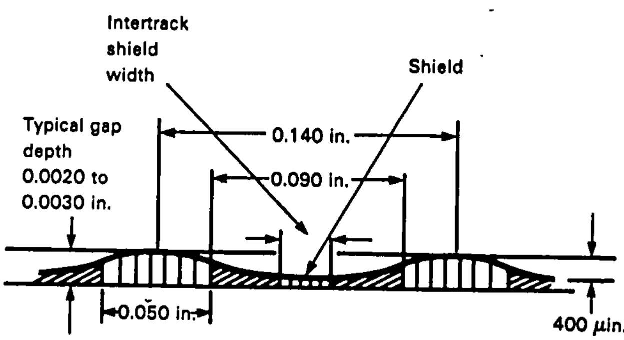

Figure C-3.—Cross section of figure C-2. To increase head life the faceplate should be made as wide as possible and of a hard material. The shield should be as wide as possible to reduce electrostatic and electromagnetic coupling and prevent crosstalk. The selection of tip plate material is also critical—it should wear slightly faster than the pole tips.

The selection of the material used in the faceplate is critical. Material with a lower wear than the pole tips can actually result in the loss of tape/head contact, and will encourage debris buildup. This phenomenon is referred to as "negative wear." Ideally, the tip plate should wear at the same, or a slightly higher rate than the pole tips. Also, material must be selected that does not promote debris buildup with any tapes or environments encountered.

Goals and Compromises

In trying to achieve the desired head life, several compromises are involved. First is the effort to maximize tape contact area with hard material to achieve low wear. This could be done by putting hard material between the tracks. At the same time, it is desirable to maximize the thickness of the shields to reduce electrostatic coupling so cross-talk is minimized, particularly between tracks of an interleaved head. Also, to improve the wear factors, a hard pole tip and other intertrack materials could be used in contact with the tape; however, at the same time negative wear should be avoided: The intertrack material should wear at the same rate, or slightly faster than the pole tip material. In addition, the number of material types in contact with the tape should be minimized. This is to avoid the buildup of oxide, brown stain, and other debris, and to minimize the unknown factors of materials and environment acting in combination.

Solution

The Spin Physics solution for achieving an extended head life lies in the unique characteristics of its "hybrid shield." This patented, laminated shield is typically the same width as the track. It produces an improvement in cross-talk of 3 to 6 dB. In addition, a Spinalloy™ tip has been placed in the shield so that Spinalloy™ is on both the pole tip and the shield. This creates a hard, nonabrasive surface for low wear over a maximum area without sacrificing shielding capabilities. Even wear is achieved because a very limited number of materials are used in tape contact. Furthermore, the materials that are used do not encourage debris buildup. These materials are as follows:

(1) Spinalloy™, which has demonstrated wear improvement
(2) Aluminum
(3) Thin epoxy lines between laminations

Each of these materials is well known and well characterized. The result is an expected life in excess of 3000 hr at 120 ips.

Spin Physics' extended-life head is depicted in figure C-4. Its much wider cross-talk shield has a Spinalloy™ insert at the crown area only.

Figure C-5 shows an enlarged view with the Spinalloy™ insert visible at the crown. The Spinalloy™ material is identical to the material used on the pole tip. This is what produces an even, long wear because both areas are made of hard material. The darker area in the center of the illustration represents the area of actual tape contact where wear occurs. The basic shield is still mu-metal and copper.

The cross section in figure C-6 puts the relative amount of contact area with hard material in perspective. The shield with Spinalloy™ insert is essentially the same width as the track. There is only a small area of soft aluminum, the faceplate, between the hard shield and the track.

An actual head test is shown in the profilometer graph in figure C-7. This was a test conducted at Spin Physics under laboratory conditions, though presently there are a number of ongoing field tests. Tests were conducted on a Honeywell 7600 transport with a 14-track, 1-in. head with a 0.050-in. trackwidth and

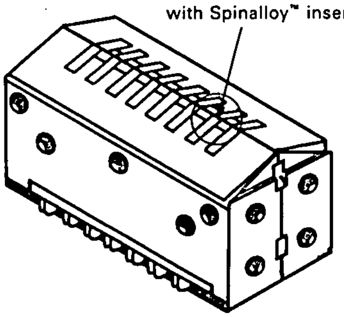

Figure C-4.—Extended-life head.

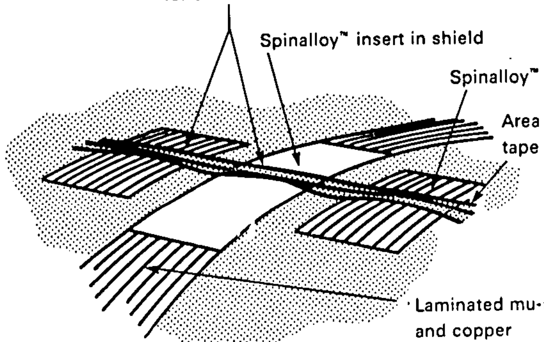

Figure C-5.—Enlarged view of segment of figure C-4.

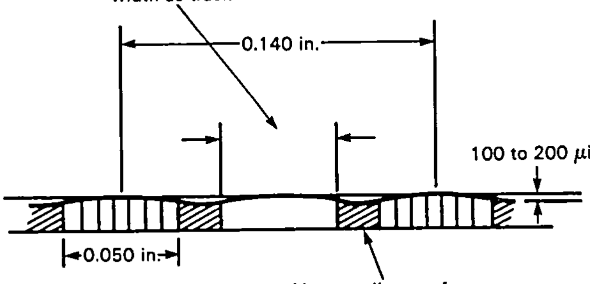

Figure C-6.—Cross section of figure C-5.

0.050-in. shields. Ampex 797 tape was used, with a tape speed of 60 ips and a tape tension of 12 oz. The total number of hours shown on this test is 860. The test results are as follows:

(1) Even wear on pole tips and shields
(2) Wear rate: 0.2 μin./hr at track edges (200 μin. total)
(3) No debris buildup (laboratory or field tests)
(4) Initial wear step established in a few hours
(5) With a 2- to 3-mil gap depth there is ample margin at 3000 hr

The scale on the graph is extremely compressed to depict the number of tracks. The vertical scale is 50 μin. per division; the horizontal scale is 11 mils per division. This represents a compression ratio of 220:1. Because of this, there appears to be a sharp gradient between tracks. Actually, the gradient is quite flat.

Looking very carefully at the graph, the pole tips can be distinguished by the very slight lines where the laminations occur. Three tracks are shown. The raised area between the pole tips is the shield. The upper trace was run at 10 hr to develop a reference point; the lower trace was run at 860 hr.

As theorized, the first thing noticed is that the pole tips and shields wear evenly because the material is the same. Second, the wear rate is very low. Looking at the actual track edge, total wear is approximately 200 μin. This corresponds to a little less than 0.2 μin./hr at the edge of the track. In addition, there is no debris buildup, an occurrence consistent with results received from field tests to date. The initial wear in the faceplate area is established in just a few hours, as shown in the first trace. This is desirable because it helps the tape maintain contact with the pole tips.

The graph illustrates that with a 0.002- to 0.003-in. gap depth there is ample design margin at 3000 hr. Because this test was run at 60 ips, we can project wear

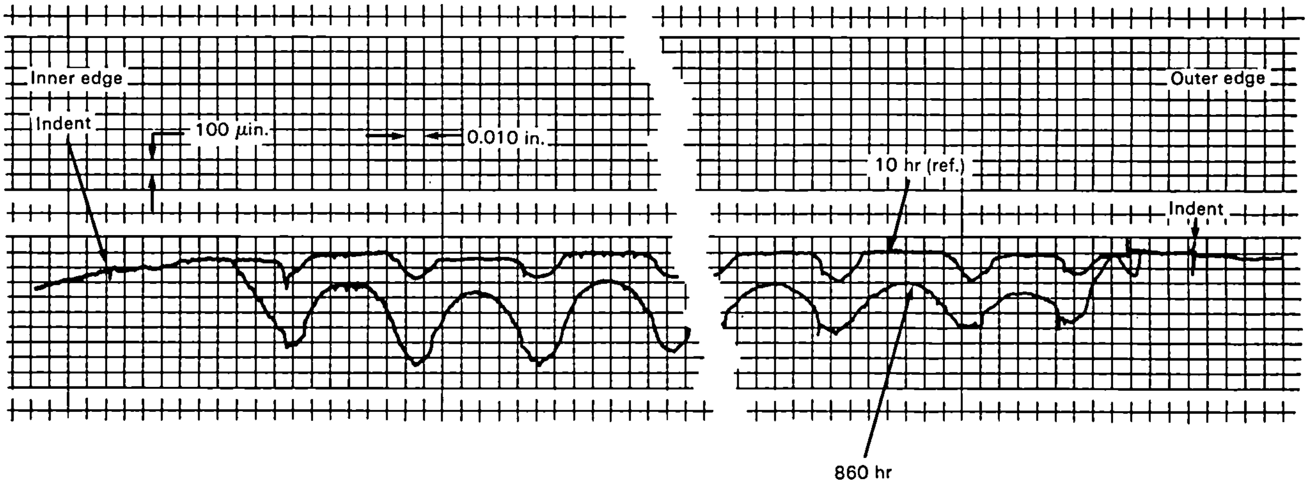

Figure C–7.—Head test. (Vertical scale: 100 μin./division; horizontal: 10 mils/division (220:1).)

at 120 ips by assuming an increased wear rate of 50 percent, or 0.3 μin. per hour. At 3000 hr, wear would still be only 0.9 mil.

Conclusion

The use of Spinalloy™ on the pole tips and on the shields, and use of a full-width shield, has enabled Spin Physics to achieve a hard, nonabrasive surface that wears slowly and uniformly. It also increases shielding, which provides superior cross-talk performance with an improvement of 3 to 6 dB. Spin Physics is manufacturing the long-life head, which is offered with a 3000-hr warranty, for most recorders. Spin Physics has a patent pending for this design concept.

SECTION 2—WEAR CHARACTERISTICS OF ULTRASIL™ VERSUS ALFESIL INSTRUMENTATION HEADS

Roger Mersing
Ampex Corporation

Instrumentation recorder heads capable of wideband performance are very expensive (several thousand dollars) and wear out because of the abrasive effect of magnetic tape passing across the head gaps. The heads, therefore, can be considered a consumable product and, depending on operating conditions, can have a significant impact on operating expense.

Various techniques have been developed (refs. C–1 to C–4) to study tape abrasivity and associated parameters contributing to head wear resulting in a better understanding of the effects of various wear factors. Figure C–8 illustrates in a broad sense the more important factors that have been found to influence recorder head life. These factors also have an effect on electrical performance, as illustrated in figure C–9. For example, as gap depth increases head life increases but performance decreases (because head efficiency is inversely related to gap depth).

Comparing figures C–8 and C–9, it is readily seen that in all but two cases if the factors are adjusted toward an improvement in head life, performance is adversely affected. However, there is a range over which tape abrasivity may be reduced that tends to increase head life while having positive effects on head performance. As a matter of fact, tape manufacturers have made considerable progress in recent years in maintaining the correct level of abrasivity, which has been defined loosely as the minimum required to keep the head gaps and contact surfaces well polished and stain free.

The other important factor allowing improved performance with improvements in head life is the hardness of the materials used in the head contact areas. Although a direct mathematical relationship between material hardness and abrasive wear has not been shown to exist, harder materials generally wear longer than soft materials. As a result, soft mu-metal pole pieces are seldom used in wideband heads in preference for the much harder alfesil or sendust pole pieces, which exhibit significantly longer head life as well as improved performance due to better gap definition and reduced gap smearing. Therefore, lacking some definitive physical laws regarding abrasive wear, one must resort to experiment to arrive at useful conclusions. Such was the case in developing Ultrasil™ heads.

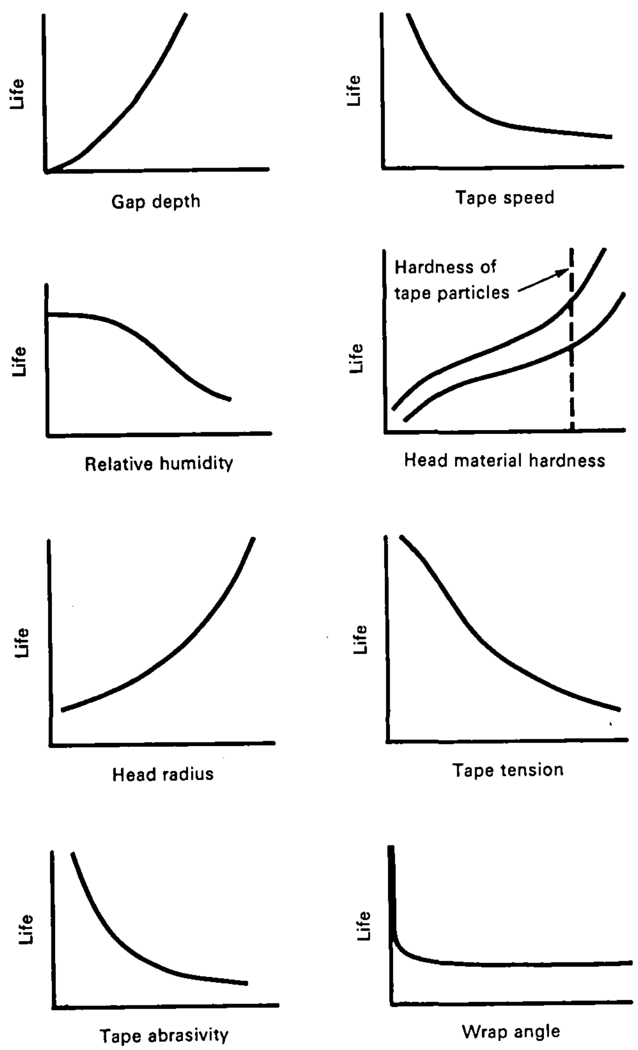

Figure C-8.—Factors influencing head life.

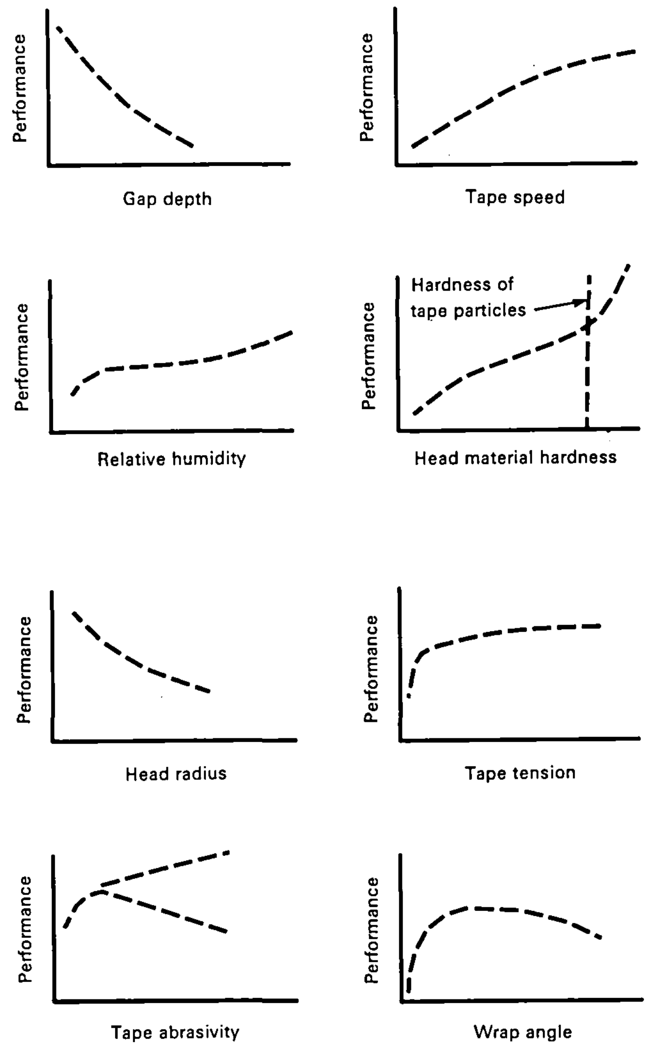

Figure C-9.—Life factors versus performance.

Materials Selection

The tape contact surface of a conventional hard-tipped head consists of alfesil or sendust pole tips, aluminum separators, mu-metal/copper shields, and thin adhesive bond lines (figure C-10). The alfesil head, a hard-tipped ferrite head design, is composed essentially of aluminum, iron and silicon. The pole tips have extreme hardness, excellent gap definition, low distortion, and high saturation magnetization. The alfesil head provides more than 10 times the life of mu-metal heads and has superb wideband performance characteristics without the need for frequent circuit readjustments.

Alfesil has a Vickers hardness of about 525 and is a great deal harder (and wears much slower) than aluminum or mu-metal, but alfesil represents only 35 percent of the total contact surface. Therefore, if the softer aluminum and mu-metal materials, representing 61 percent of the surface, are replaced by harder materials, a reduction in head wear should result. After much experimentation, a polycrystalline glass ceramic was chosen for the separator (tip plate) material because of three reasons: (1) it is hard, stable, and 100 percent dense; (2) it is easily machineable so that core and shield slots can be easily and accurately made; and (3) it wears faster than alfesil so that the alfesil pole tips will protrude slightly from the surrounding glass ceramic for intimate head/tape contact.

A wear evaluation stack was prepared (figure C-11) by machining a block of glass ceramic and adding inserts of hard materials commonly used in recording heads. The evaluation stack was contoured on a hard lapping plate to provide a uniform tape contact surface and then mounted onto an Ampex FR-3030 for wear testing. The test conditions and results are shown in figure C-12. The results clearly indicate the relative wear rates of alfesil and low-wear alfesil are less than that of glass ceramic. This is of profound importance in insuring intimate head-to-tape contact for the varied operational conditions that might be encountered.

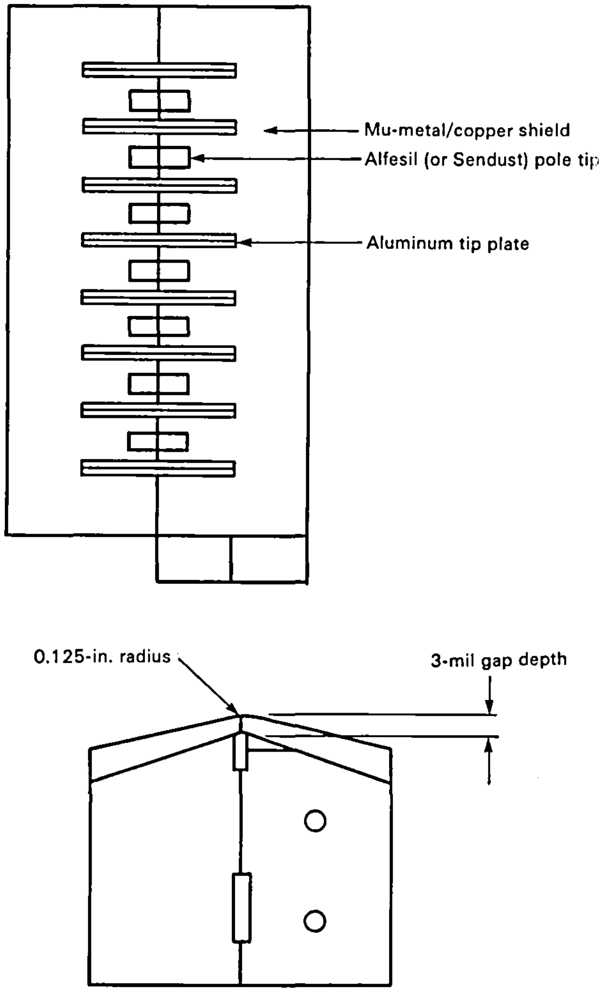

Figure C-10.—Conventional hard-tipped head stack.

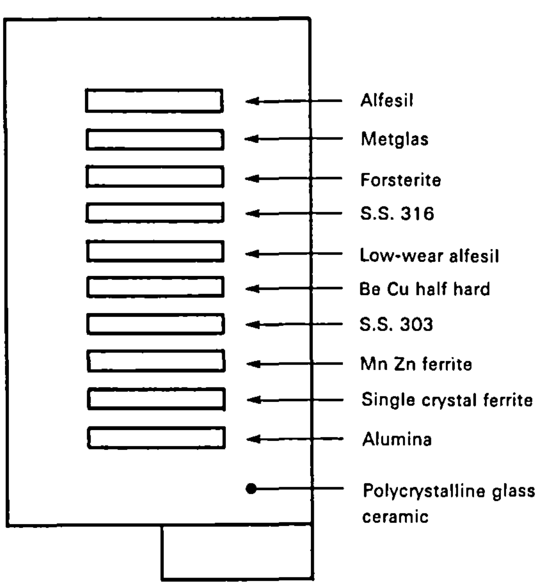

Figure C-11.—Wear evaluation stack.

The materials for the intertrack head shields must have good electromagnetic shielding properties and wear as fast or faster than the pole tip material. A sandwich structure consisting of laminations of alfesil and half-hard beryllium copper was chosen because it met both the shielding and wear rate requirements. The thickness of the beryllium copper laminations was minimized to reduce the "copper carryover" effect.

The pole tip material selected is the recently developed low-wear alfesil, which differs from alfesil in that it has a greater hardness (550-575 Vickers); smaller grain size; and reduced low-frequency permeability resulting in longer life, better gap definition, and a flatter permeability spectrum than regular alfesil. Figure C-13 illustrates the details of the Ultrasil™ head glass construction.

Wear Tests

Wear tests were conducted at tape speeds of 15 and 120 ips on an Ampex FR-3030 tape transport using Ampex 797 tape. Two 1-in. 7-track Ultrasil™ and two alfesil stacks having the same contour were prepared for the wear tests. In both tests, one Ultrasil™ stack was mounted in the odd record position and one alfesil stack in the even reproduce position with stainless steel dummy stacks in the even record and odd reproduce positions. Relative humidity was maintained at 50 to 55 percent, and the tape was changed every 16 hr.

15-ips Tests

The run time to achieve 250 μin. of wear on the alfesil head pole tip of track number 5 was 176 hr. The run time to achieve 250 μin. of wear on the Ultrasil™ track 5 was 369 hr, or more than twice as long as for the alfesil head.

120-ips Tests

The run time to achieve 500 μin. of wear on the alfesil head track 5 was 154 hr. The run time to achieve 500 μin. of wear on the Ultrasil™ track 5 was 438 hr, or about three times as long as for the alfesil head. The wear test was continued to 500 hr, and profilometer recordings were made of the tape contact area along the gap lines of both stacks.

The Ultrasil™ stack exhibited much less scalloping than the alfesil stack (fig. C-14).

Readings were made after 500 hr of use. The alfesil head exhibits 1000 μin. of wear and the normal 300 to 400 μin. of scalloping. The Ultrasil™ head exhibits only 570 μin. of wear and about 50 μin. of scalloping.

Wideband Performance

Frequency response of the Ultrasil™ head is outstanding across the entire bandwidth from 800 Hz to 4 MHz. Measured in voltage output, peak performance of

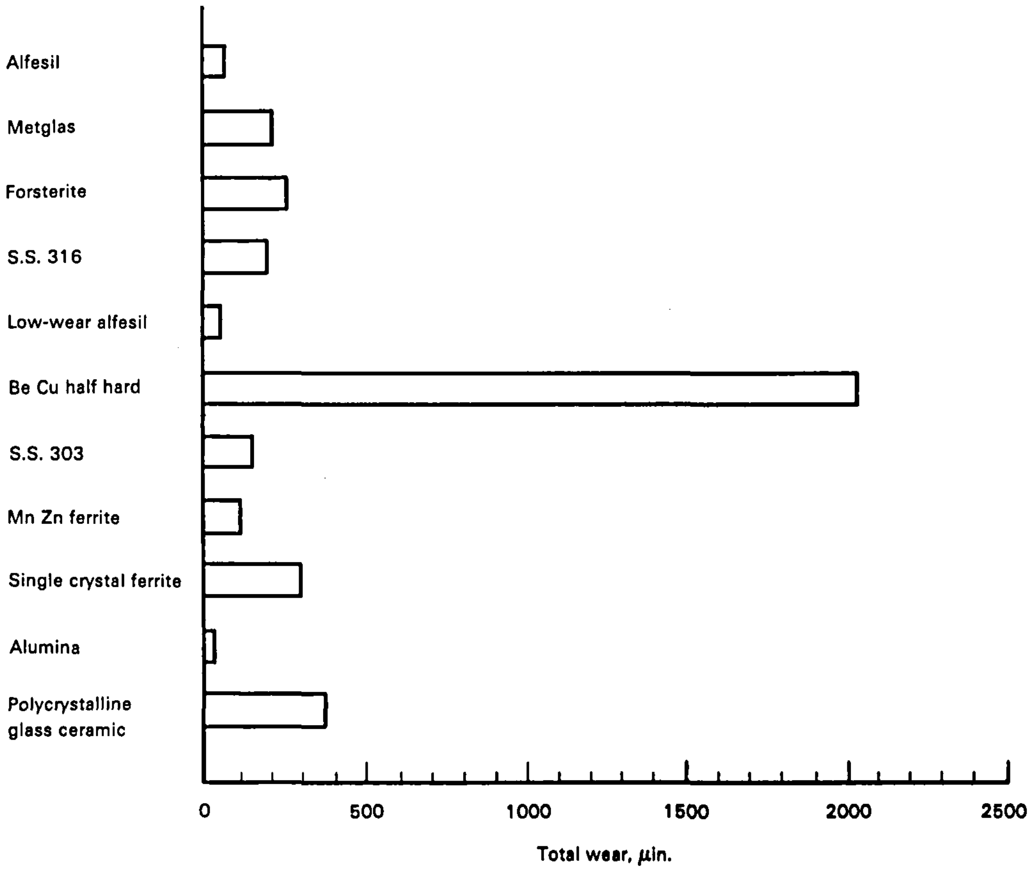

Figure C–12.—Wear results. (Transport: Ampex FR-3030; tape: 1-in. Ampex 797; speed: 120 ips; tension: 11 oz; humidity: 55 percent; radius: 0.118 in.; wrap: 7°; and run time: 113 hr.

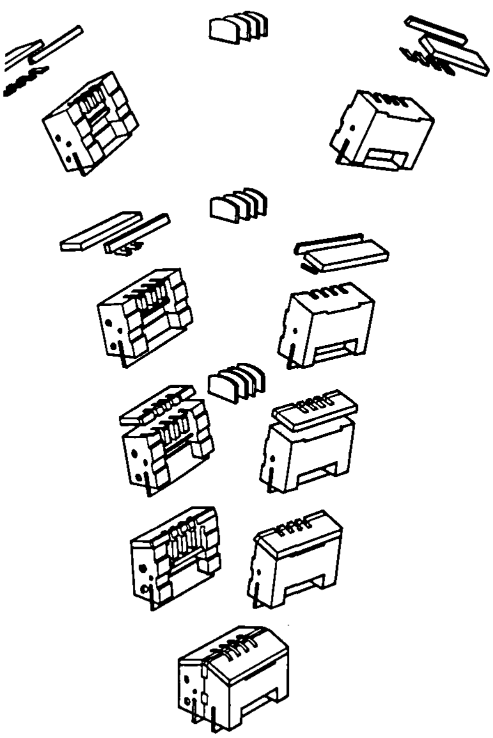

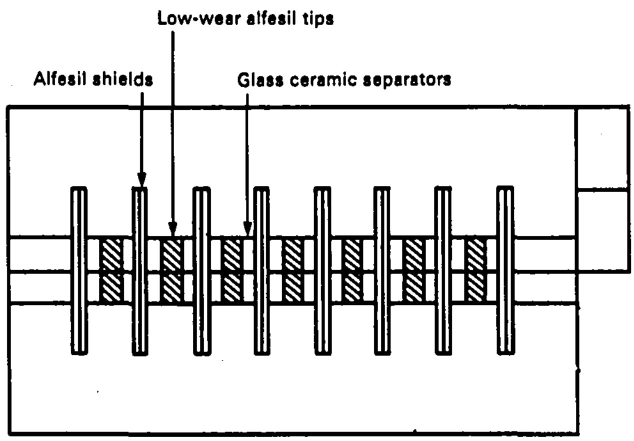

Figure C–13.—Ultrasil™/glass construction.

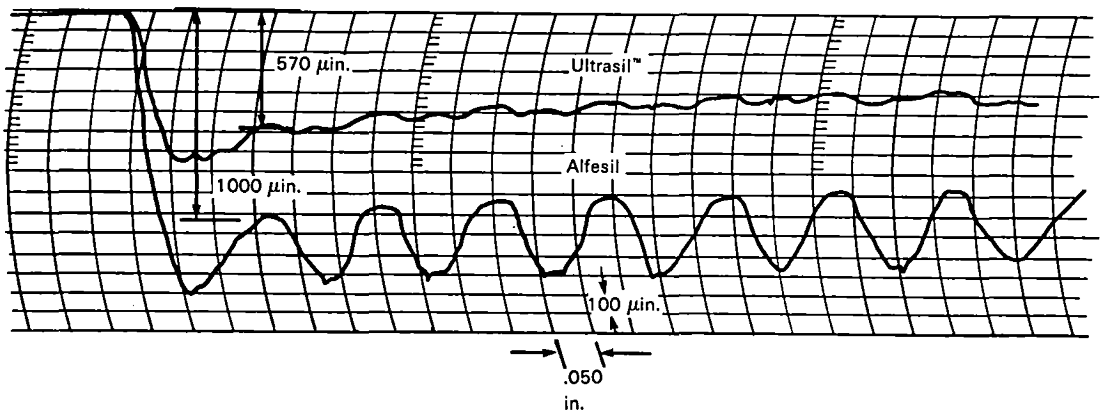

Figure C-14.—Ultrasil™ versus alfesil wear comparison. (Transport: Ampex FR-3030; tape: Ampex 797; speed: 120 ips; humidity: 50 to 55 percent; and run time: 500 hr.)

the Ultrasil™ head occurs at just under 1 MHz and exhibits very shallow rolloff to 4 MHz. (See fig. C-15.)

Operating Costs

The Ultrasil head is a very cost-effective technology improvement. It is comparable in price to an alfesil head yet has far greater intervals between replacement, the result of longer life cycle. (See fig. C-16.)

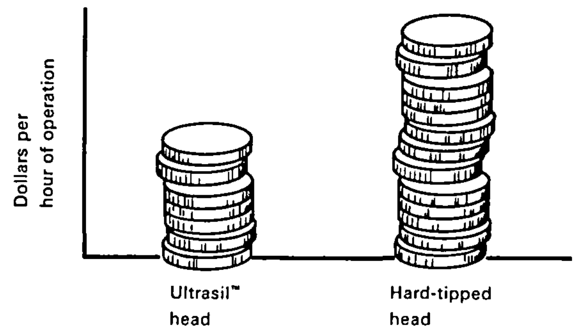

Figure C-16.—Comparison of operating costs for hard-tipped and Ultrasil™ heads.

Conclusions

The harder materials used in Ultrasil™ glass heads have been shown to provide a wear reduction of 2 to 1 at 15 ips and 3 to 1 at 120 ips compared with conventional hard-tipped alfesil heads. The reason for the ratio differential between 15 and 120 ips was not determined and is a possible subject for further investigation.

In both analog and high-bit-rate digital applications, electrical and mechanical performance of the heads is equivalent and usually superior to that of conventional alfesil heads. Head surface undulations (scalloping) are markedly reduced, assuring intimate head-to-tape contact. Galvanic effects in the head-to-tape contact area are eliminated. Stiction is reduced. "Copper carryover" effect is greatly reduced, minimizing staining problems.

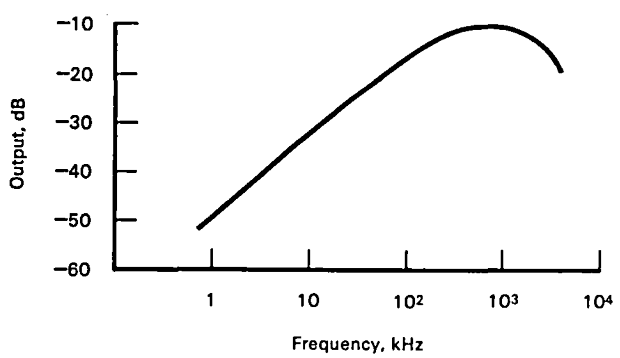

Figure C-15.—Frequency response at 240 ips.

SECTION 3—LONG-LIFE INSTRUMENTATION HEAD

Anthony Bucher
Odetics, Incorporated

For many years magnetic head technology concentrated largely on the improvement of the three dynamic factors that are desired in head performance: frequency, amplitude, and phase response. Head life was not of prime consideration so mechanical and metallurgical factors that were vital to the tape-to-head interface were largely ignored. Typical head life in those years was anywhere from 50 to 250 hr.

The next generation was what we now refer to as the hard-tipped heads. These had an order of magnitude improvement over previous technologies in signal qualities and head wear. Thus, the 1000-hr head warranty era was ushered in by the head manufacturers.

During this same time a marked improvement in ferrite head technology was attained that could have directed the industry into opportunities heretofore unexplored. However, it largely remained the domain of only a few companies due to reasons that are beyond the scope of this discussion.

Increased life requirements necessitated further improvements on head wear from head suppliers, and the next increment on warranties became 3000 hr.

Head Wear

Traditionally, failures due to headwear start to take place in between active tracks of a head assembly. The softer material simply wears at a faster rate and causes a "washboard" effect on the radius of the head. As this wear progresses, it will start affecting the track edges and from these ultimate failure will occur due to signal losses. The visual effect is a flaring of the gap at the outer edges of the track, commonly called an "open" gap.

Remedy

On October 1, 1979, Omutec introduced a new technology that allowed a conventional hard-tipped head to wear 3000 hr. Conventional here means that nothing was done that interfered with any standards that were set up by the industry, nor were any other parameters altered that are normally connected with head design, such as trackwidth, radius, and shielding.

Omutec's heads provide a hard wearing surface between the track material and the intertrack shielding material, thus preventing accelerated wear of that area. The wear rate is still such that a minimum amount of scalloping takes place so that the tape "seats" properly on the track material and allows the air boundary layer of the tape to bleed off at higher tape speeds (120 and 240 ips), thus minimizing the flying effect of the recording tape.

Method

Magnetic heads are manufactured in two opposing halves. Each carries a holding plate for the alfesil tips commonly referred to as the tip plate. (See fig. C-17.) This tip plate is made of the same material as the half-brackets, a high-grade aluminum. Through a series of lapping procedures the top surface of the half brackets and the bottom surface of the tip plate are carefully brought to a finite degree of flatness. They are then matched with the half bracket and bonded together. The two head halves with the tip plates in place are further submitted for flat lapping of the gap surface, and, in turn, carefully mated.

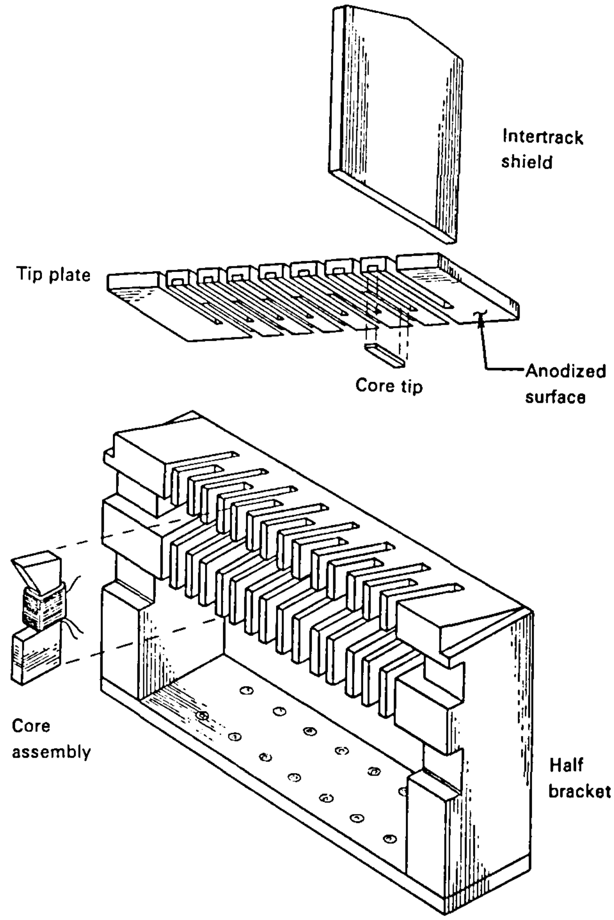

Figure C-17.—Components of half of a magnetic head.

The intertrack shields are lowered into the slots provided in the tip plates and the brackets, and the assembly is back-filled with epoxy, cured, and submitted for further processing, which includes removal of the top layer of aluminum to expose the alfesil core tips. All this is done on lapping machines so no work hardening of the magnetic materials used on the face of the head will occur.

As previously described, the problem of head life is one in which the softer material of the tip plate and interchannel shields is worn at a faster rate than the hard alfesil material in the core tips.

It is evident that a continuous surface of a greater and more consistent hardness at the tape contact area would lessen the "washboard" effect and slow head wear. Our solution to this problem was to develop a process whereby any application of a special hard anodize to the bottom of each tip plate half would present a continuous hard wear surface. Anodization is applied by an

electrolytic oxidation process in which the slotted aluminum tip plate becomes the anode in an electrolyte solution.

Head manufacture then proceeds in a more or less normal operational sequence. During the contour polishing operations the excess aluminum of the tip plate is removed, exposing both the hard alfesil core tips and the hard anodized surface surrounding the gap surfaces. Thus, when the head stack is placed in operation, the areas adjacent to the core tips are essentially the same hardness as the core tips, substantially reducing the "washboard" effect due to the abrasive nature of recording media. This reduction, or slowing down of head wear, has been accomplished without any head performance losses. The result has been to increase the functional life of hard-tipped heads from approximately 1000 hr up to 3000 hr.

REFERENCES

C-1. Carroll, J. F.; and Gotham, R. C.: "The Measurement of Abrasiveness of Magnetic Tape," *IEEE Trans Magn.*, pp. 6-13, Mar. 1966.

C-2. Ragle, H. U.; and Daniel, E. D.: *Considerations of Head Wear in Magnetic Recording,* Memorex Monograph 2, Memorex Corp., 1963.

C-3. Cash, J.; and Pagel, R.: "Wear in Recorder Heads by Magnetic Tapes." *Proc. Video Data Recording Conf.*, Inst. Electron. Radio Eng. (Birmingham, United Kingdom), July 1976.

C-4. Buchanan, J. D.; and Tuttle, J. D.: "A Sensitive Radiotracer Technique for Measuring Abrasivity of Magnetic Recording Tapes." *Int. J. of Appl. Radiat. Isotop.* 19: 101-121, 1968.

APPENDIX D

High-Density Digital Recording (HDDR) Users Subcommittee Evaluation of Parallel HDDR Systems

R. S. Reynolds
Subcommittee Chairman

The HDDR Users Subcommittee was established by the Tape Head Interface Committee (THIC) in November 1980 to investigate the feasibility of selecting a single parallel HDDR coding scheme acceptable to the user community and to recommend to standards committees the adoption of the system as a standard. At its charter meeting (November 1980) the subcommittee adopted two main objectives:

(1) To draft a letter to executives of HDDR system suppliers voicing the concern of users regarding the proliferation of HDDR coding schemes

(2) To implement action to define, if possible, a single parallel HDDR standard and to recommend such a standard to ANSI X3B6 and to the Range Commanders Council (RCC) Telemetry Group (formerly Inter-Range Instrumentation Group Telemetry Group).

Over a 2-year period the subcommittee reviewed previous American National Standards Institute (ANSI) X3B6 efforts, revised and redefined parameters, reviewed procedures with manufacturers, and queried users on relative importance of system parameters. Based on input from manufacturers in early 1983, the subcommittee evaluated the six HDDR systems under consideration and is preparing the final recommendation for THIC consideration.

BACKGROUND

HDDR systems were developed in response to the need of various users to record high bit-rate pulse-code-modulated telemetry data or digitized instrumentation data that could not readily be buffered and recorded on computer-type digital recorders. The advent of 2-MHz bandwidth analog recorders in the 1970's gave impetus to HDDR schemes with bit rates well above 4 Mbps/track.

Early in the development of HDDR systems the basic limitations of magnetic recorders were encountered at both high and low frequencies. On the low-frequency end, NRZ systems that made good use of the upper frequency response ran into low-frequency components approaching dc when long strings of "1's" or "0's" were encountered in the data. Biphase systems, on the other hand, nicely sidestepped the low-frequency limitations by having at least one transition per bit, but the same characteristic requires a bandwidth equal to the bit rate to accommodate repeated "1's" in the data. To avoid these problems, the input data were modified or encoded in various ways. Among those who chose to use NRZ recording, Bell and Howell inserted a parity bit after each seven data bits and employed a fixed pattern of bit inversion to minimize the possibility of long intervals without a transition. Sangamo (now Fairchild Weston) employed a feedback shift register to "randomize" the input data to minimize long intervals without a transition. The data could be recovered upon playback through an identical feedback shift register. Other manufacturers chose to work on the characteristics of phase modulation to reduce the upper bandwidth requirements. An early development was the delay modulation (or Miller) code chosen by Ampex. This scheme suppressed transitions after various combinations of input data bits, thus reducing the upper bandwidth to about 75 percent of the input bit rate. The delay modulation code still resulted in some long periods without transitions and was modified to "Miller Squared" by Ampex, resulting in a "dc-free" code.

By 1975 enough HDDR systems were being procured that the question of standards in this area was raised. The Recorders and Reproducers Committee of the RCC Telemetry Group was approached by some of the manufacturers with the suggestion that standards be developed. At that time there was little or no usage of HDDR systems among RCC members, and the committee declined to undertake the task. About a year later the ANSI X3B6 Committee recognized that enough

HDDR systems were in use or contemplated that standards were desirable. Accordingly, X3B6 proposed to the Standards Planning and Requirements Committee of ANSI that X3B6 undertake the preparation of HDDR standards. The project was approved and was started in 1977.

The X3B6 Committee quickly found that the modulation format or encoding of HDDR systems would be the most difficult area for standardization and, therefore, undertook to develop a three-part standard:

(1) Unrecorded tape standards
(2) Recorded tape standards
(3) HDDR codes

The first two parts were based on existing wideband instrumentation recording standards and were not controversial. However, each manufacturer advocated standardization of his own code, and each discussed the merits of the particular scheme in technical presentations to the committee. As a result, X3B6 undertook to evaluate the merits of each coding scheme to try to arrive at a best code for standardization. A users group was established within X3B6 to establish the criteria for evaluating the codes.

Several users who had been involved with large system procurement proposal evaluation suggested a formalized approach for the X3B6 exercise. This approach required establishing a list of system parameters important to the use of the system, then defining a means of comparatively evaluating how well a proposed system approached the performance of an ideal system. The parameter values for all systems would then be processed to give an overall system evaluation. The method adopted by the X3B6 users was a multiplicative scheme wherein each parameter was given a rating between 0 and 1. The numbers were multiplied to give an overall system evaluation number. Addendum A is an excerpt of an X3B6 document explaining this method.

After several surveys and many meetings of the Users Group, a list of 14 parameters was adopted. The performance "valuation function" of each parameter was defined, and the importance of the parameter to the users was included as an exponential weighting factor for the parameter. The product of the 14 weighted valuation factors then became the utility score for a system. Because the product of 14 numbers less than 1 becomes a small fraction, the utility scores were normalized by taking the 14th root of the overall product, resulting in a number nearer to 1 and esthetically more pleasing.

By mid 1978 the X3B6 Users Group had evaluated the three systems then in contention for standardization and had made a preliminary suggestion to X3B6. However, the choice was not acceptable to all of the committee, and some members stated that they would veto the standard if carried through. Under ANSI rules, a veto by a committee member stops the progress of a standard until the problem that created the veto is resolved. In this case, there was no prospect of resolving the issues, so the standardization effort was shelved.

The RCC Telemetry Group began to show some interest in HDDR systems during 1977. Several of its members and associates participated in the X3B6 Users Group efforts. In 1978, *Telemetry Standards* (IRIG-106-77) was being reviewed for possible updating, and it was felt that the next issue, due to be published in 1980, should contain a section on HDDR. The RCC representatives were mostly interested in converting one or several channels on a wideband analog recorder to serial HDDR service. Little need was seen for full-blown parallel HDDR systems in the test range applications. A joint meeting between the RCC Telemetry Group Recorders and Reproducers Committee and ANSI X3B6 was held in January 1979. At that meeting it was decided that the RCC committee would proceed to develop serial HDDR standards. The X3B6 Committee agreed to proceed to try to establish standards for parallel HDDR systems and to avoid the issue of code selection by making the coding scheme optional from among the contending systems. (By that time, a fourth code, PC^2, had been submitted for the consideration of X3B6 by Martin Marietta Aerospace.) Based on results of the X3B6 studies, the systems favored by the RCC Telemetry Group were biphase recording for up to 15 kbpi and randomized NRZ for up to 25 kbpi. The IRIG Standard 106-80 was published in September 1980 with the two codes included.

At the time of the November 1980 THIC meeting, the following situation prevailed: RCC had published the conservative serial HDDR standards in IRIG 106-80, and ANSI X3B6 was proceeding to generate a standard containing four optional codes that were not directly interchangeable, although some manufacturers could accommodate some other formats by switch selection.

At its November 1980 meeting the THIC Steering Committee voted to try to give some impetus to HDDR standardization by establishing a subcommittee of users only. The subcommittee was to be tasked to select a coding system and to propose its adoption to ANSI X3B6 and to the RCC Telemetry Group. The THIC membership approved the recommendation, and the subcommittee was formed.

HDDR USERS SUBCOMMITTEE ACTIONS

During the subcommittee's charter meeting it was decided that the ANSI evaluation scheme would be revived and that manufacturers or suppliers of HDDR

systems would be invited to participate in the evaluation. A letter explaining the subcommittee's objectives and approach was prepared for the THIC Chairman's signature and sent to manufacturers who were known to be active in HDDR systems in December 1980. (See specimen letter, addendum B.)

In January 1981 HDDR subcommittee members met with representatives of manufacturers who had expressed interest in participating in the evaluation. Individual meetings were held with people from five different manufacturers to explore opinions on how the evaluation should be conducted. A sixth manufacturer asked to be considered at the March THIC meeting. As a result of these sessions, the parameter definitions used by X3B6 were revised to reflect the limitation to parallel HDDR systems and to reflect significant differences between 1977 and 1981 systems. After several iterations, 11 parameters were retained. The list of parameters was submitted to subcommittee members and other users with a request that the parameters be ranked in order of their importance to each user. Rankings were from 1 (most important) to 11 (least important). Two classes of use were identified (rankings were requested for either or both classes):

(1) A large number of data channels with medium to high data rates, modest bit error rate requirements, and full reel recording time,

(2) One or many high data rate channels requiring some mix of high sampling rate, high amplitude resolution, and few (or no) bit errors.

Recording time could be from a few seconds to a full reel.

Results of the user survey were used by the subcommittee to establish weighting factors for the 11 parameters. For each system the rankings were averaged over the numbers of responses, and the average ranking was used to establish a weighting factor with a possible range from 0.45 to 5.00 by the following formula:

$$W = 5\left(1 - \frac{R - 1}{11}\right)$$

where W is the weighting factor obtained from the averaged ranking R. Parameter definitions and suggested test procedures are shown in addendum C.

In December 1982 the refined parameter definitions were sent to the six participating manufacturers with a request that valuation factors based on the corresponding test procedures be returned to the subcommittee. Responses received were satisfactory for all but two parameters. The subcommittee felt that further tests were required for the interchange signal-to-noise-ratio margin parameter. Manufacturers were requested to conduct further tests with a subcommittee member present. Conclusion of these tests will permit a final evaluation to be made.

CONCLUSIONS

The importance of careful definition of system parameters and corresponding test procedures when evaluating complex systems has been highlighted many times during this evaluation. The utility function method of ranking contending systems is very sensitive to small differences in parameters considered most important to the evaluators. It also serves to immediately reject systems that do not comply with any of the parameters. It falls upon the evaluators to carefully define the weights applied to the valuation factors so that a single parameter does not completely dominate the evaluation. Evolution of system technology over the span of time taken by this exercise has made it difficult to hold to original objectives. Error correction systems, for example, have become universally available and of greater importance than when the task was started.

HDDR USERS SUBCOMMITTEE

The Subcommittee members were users or potential users of HDDR systems, and all were from government facilities including the National Aeronautics and Space Administration, the Department of Defense, the Federal Aviation Administration, and the Department of Energy.

Bill Poland, Chairman of the ANSI X3B6 Committee, was most helpful in providing background and guidance for application of the value function method. Other subcommittee members who endured many hours of discussions and read through many iterations of documents were Alan Montgomery, Ed Mack, Al Buschman, George Rosset, Paul Ash, Mark Smith, Jim Keeler, Don Tinari, Eugene Law, Don Hust, and Al Zupan. Their participation and contributions are gratefully acknowledged.

MANUFACTURER PARTICIPANTS

The following manufacturers participated in the HDDR evaluation:

Ampex Data Systems
Bell and Howell Datatape Division
Fairchild Weston Division, Schlumberge
Honeywell Test Instruments Division
Martin Marietta Aerospace
Thorn EMI Technology, Incorporated

ADDENDUM A – DISCUSSION OF UTILITY FUNCTION AS AN EVALUATION TECHNIQUE[1]

In cases where a selection between contenders is to be based on evaluation of performance factors or parameters *all* of which must be maintained at a satisfactory level, it is useful to measure each contender's performance by means of a "Utility Function" derived from weighted parameter ratings. This technique can have the property that, irrespective of the number of parameters entering into the evaluation, one substandard rating for any one parameter will eliminate a contender, no matter how high his ratings in the other parameters. The technique also provides a means for applying weights to the various parameters to reflect their relative importance in the evaluation.

The basic approach is: select parameters, define a normalized value function for each parameter, and determine a weight for each value function. Then for a given contender a weighted value rating is obtained for each parameter. In the approach discussed herein, these value ratings are multiplied together to produce the contender's final "utility" score. The contender having the highest score is selected. Both value functions and utility scores are so defined that they fall between 0 and 1, and the weights are in the form of exponents rather than multipliers.

The approach outlined is not totally "objective"; in fact, it is doubtful that such an approach could be defined. Judgmental factors enter into the procedure at three points: in choosing parameters, in defining value functions for the parameters, and in establishing weights for the value functions. All other parts of the procedure are arithmetic. The judgmental factors, once chosen, are applied equally to all contenders (however, care must be taken that they are not chosen so as to arbitrarily favor some contenders).

A principal characteristic of the approach is that it permits exposure of the major steps of the selection process to quantitative examinations by all interested parties.

The procedure for obtaining utility scores consists of the steps listed below; guidelines for precision in carrying out the computations are to be found in appendix B [not included in this publication].

1. Define parameter categories P_i for all relevant aspects of the evaluation (for easy interpretation of the results, a mutually exclusive set is desirable). The parameters may have any range of values, including negative values. The parameter value in the ith category for the jth contender is P_{ij}.

2. Define a value function $V_i(P_i)$ for each parameter. The value functions all range in value between zero and one: $0 \leq V_i \leq 1$ (see section on Value Functions below). If there is a threshold value for a parameter beyond which the system performance is rendered unacceptable, the value function for that parameter should be set to zero beyond threshold. It is desirable to normalize the value function so that average or reasonably acceptable behavior falls at a chosen level $\overline{V}$ for each parameter (see Value Functions section below). This level might be made dependent somewhat; $\overline{V}=0.9$ is suggested. For Yes/No parameter:

$$V(\text{Yes}) = 1, \; V(\text{No}) = \text{(arbitrary)}$$

3. Define a weight W_i for each value function. This weight reflects the relative importance of the corresponding parameter. The weight may be any positive number; for convenience, unity weight may be chosen as the point of departure. A weight greater than 1 has the effect of diminishing values of the value function which are substantially less than 1, while having little effect on values close to 1. A weight less than 1 brings all values of the value function closer to 1 but has a small effect on those values near 0. In this way, weights greater than 1 tend to eliminate contenders with low value functions more rapidly than lower weights, and conversely. Guidelines for assigning weights are to be found in appendix A [not included in this publication].

4. For each parameter, compute each contender's value rating r_{ij}; i.e., compute the weighted value for the jth contender's performance with respect to each ith parameter:

$$R_{ij} = \left[V_i(P_{ij})\right]^{w_i}$$

5. To determine the utility score U_j for the jth contender, multiply together all the entries $i = 1$ through $i = n$ in jth column of R's (see also comment (*c*) in the Properties section below and the section on normalization):

$$U_j = \prod_{i=1}^{n} R_{ij} = \prod_{i=1}^{n} \left[V_i(P_{ij})\right]^{w_i}$$

6. These utility scores for the contenders lie between 0 and 1. The contender having the score closest to 1 is selected.

Properties

In contrast to a multiplicative system such as that described above, an evaluation technique which adds weighted factors suffers from the difficulty that only one or at most a few factors can have a decisive individual influence on the final score no matter what weighting factors are used. An example was provided by an actual magnetic recorder/reproducer procurement based on a specification containing about 90 quantitative requirements. It was found during the evaluation of proposals that a contender whose system failed to reproduce any signal whatsoever could quite possibly win the competition if he scored well in other areas, in spite of heavy weighting for signal reproduction, and it was found necessary to depart from the pre-established scoring technique. The greater the number of factors, the smaller the effect of most individual factors in an additive approach, no matter how important they may be.

The utility function technique has the following properties worth noting:

a) The final utility score for a contender cannot exceed his lowest weighted-value rating.

b) When a parameter value is in the highly satisfactory range, the corresponding value function approaches 1, and the parameter does not materially affect the utility score; i.e., the utility function technique effectively sets aside parameters

[1]Excerpt from "Discussion of Utility Functions As an Evaluation Technique," ANSI X3B6/299R 1978-10-11.

which are highly satisfactory and directs attention to those that are marginal or unsatisfactory. A factor which far exceeds the acceptable level does not compensate for one which is substandard.

c) If the weighting factors W_i are all multiplied by a positive constant greater than 1, the effect is to alter the separation between utility scores without changing the ranking. This effect is reversed for a multiplier between 0 and 1; i.e., scores are compressed but rank is preserved. However, if it is desired to bring the final scores back into the same numerical range as the value functions, irrespective of the number of parameters used, it may be desirable to divide W_i by n (refer to the section on normalization below).

d) If desired, the log of the value functions can be used instead of the function itself in arriving at the utility score. If this is done, all values on the vertical axis [fig. D-1] become negative, zero becomes $-\infty$, and weights become multipliers of basic factor rating logarithms. These weighted logs are then added to obtain the log of the utility function. Use of the log scale in place of direct representation is merely stenographic and does not affect ranking.

e) Threshold criteria should be applied to given parameters at the value function level rather than to the score as a whole at the utility function level of the evaluation if the threshold criterion is to be kept insensitive to varying choice of weighting functions and normalizations.

Parameter Values

The choice of parameters generally should avoid overlap with respect to performance criteria; i.e., the parameters should be a mutually exclusive, but not necessarily an exhaustive set. If this is not done, the redundant factors may inadvertently be given an undue emphasis in the final scoring, and this emphasis may be hard to detect. For this reason, it is usually preferable in evaluating systems to choose parameters representing external performance characteristics rather than internal or fabrication characteristics.

An inactive parameter may be omitted or its value function may be set to unity without affecting the final results.

The number of parameters involved in an evaluation may affect the utility score but does not of itself have any effect on ranking; i.e., introduction of a new parameter for which all contenders have the same value rating may change the utility score except as indicated in (c) above but does not change ranking among contenders.

Value Functions

The figures provide a few examples of value functions which may be useful. Since a high degree of precision in shaping value functions ordinarily is not needed, the two constants P_0 and P_x and the shape factor N usually provide sufficient flexibility to fit these functions to a given application. Whatever function is used as the value function must be confined to the range $0 \leq V_i \leq 1$ within the entire range of the corresponding parameter P_i. (See figs. D-2 to D-6, for example.)

Weighting Factor

The weighting factor W_i provides emphasis for relative importance among normalized value functions so as to represent the effect of the various parameters in accordance with their relative importance. Appendix A [not included in this publication] gives some guidelines for choosing weights.

Thresholds and Decisions

Threshold criteria for individual parameters may be applied by, in effect, multiplying the value function by a unit step function. Approximately the same result may sometimes be

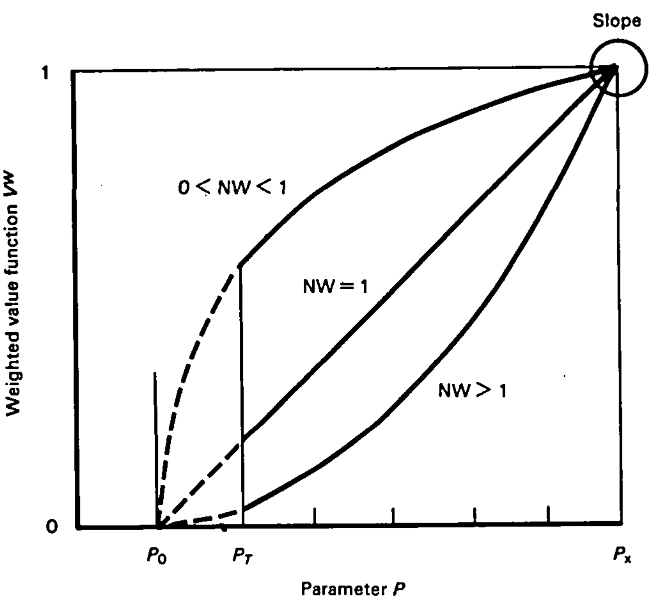

Figure D–1.—Weighted exponential value functions monotonically increasing with P. $N > 0$. $VW = \{[(P - P_0)/(P_x - P_0)]^N\}^W$. Slope $\cong NW/(P_x - P_0)$.

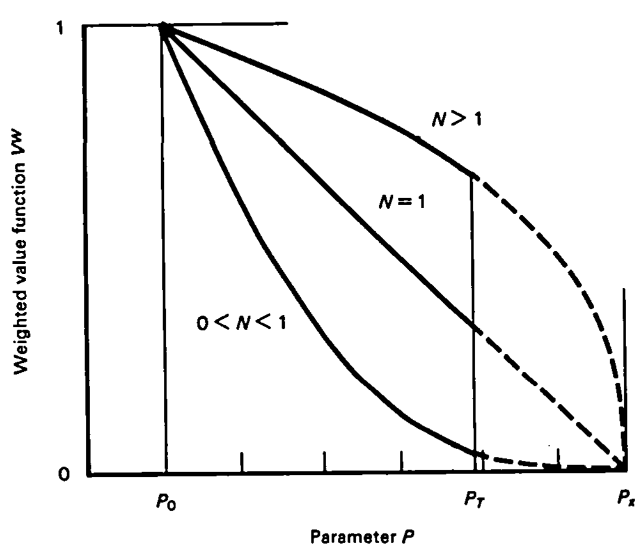

Figure D–2.—Weighted exponential value functions monotonically decreasing with P. $N > 0$. $VW = \{1 - [(P - P_0)/(P_x - P_0)]^N\}^W$.

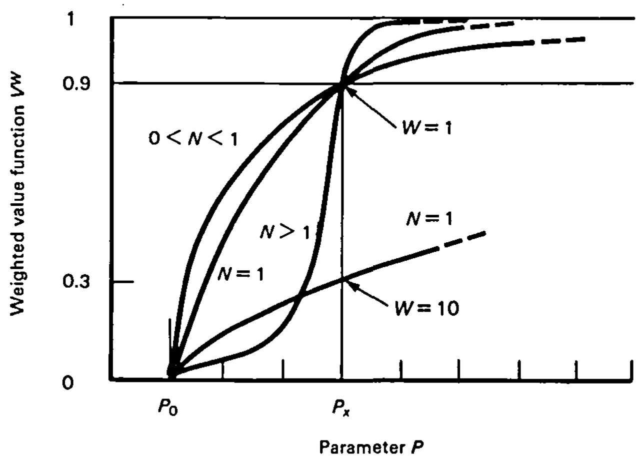

Figure D-3.—Weighted sigmoid value functions monotonically increasing with P. $N > 0$; P_T undefined. $VW = \{1 + (1/9)[(P - P_0)/(P_x - P_0)]^{-N}\}^{-W}$.

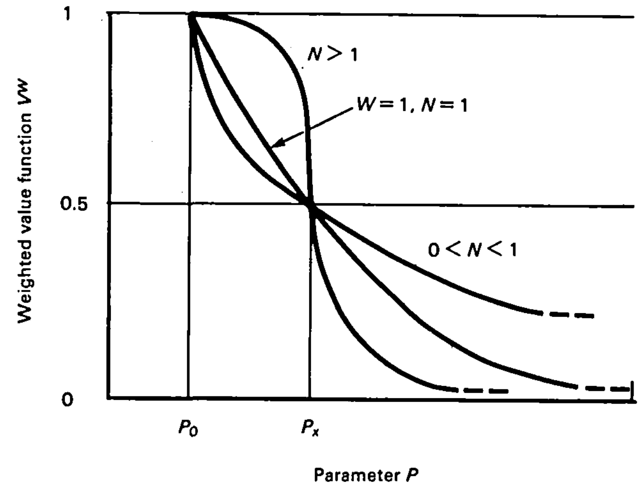

Figure D-6.—Weighted decreasing asymptotic value functions. $VW = \{1 + [(P - P_0)/(P_x - P_0)]^{N}\}^{-W}$.

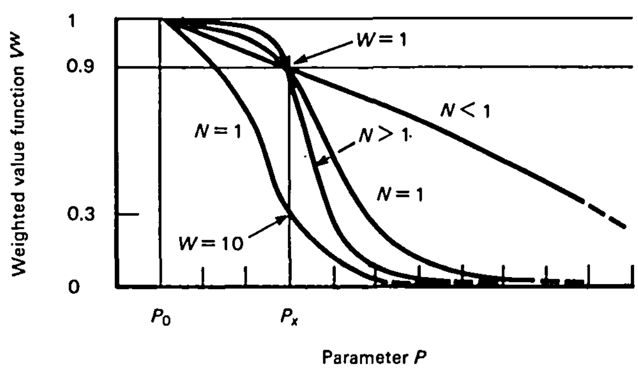

Figure D-4.—Weighted sigmoid value functions monotonically decreasing with P. $N > 0$; P_T undefined. $VW = \{1 + (1/9)[(P - P_0)/(P_x - P_0)]^{N}\}^{-W}$.

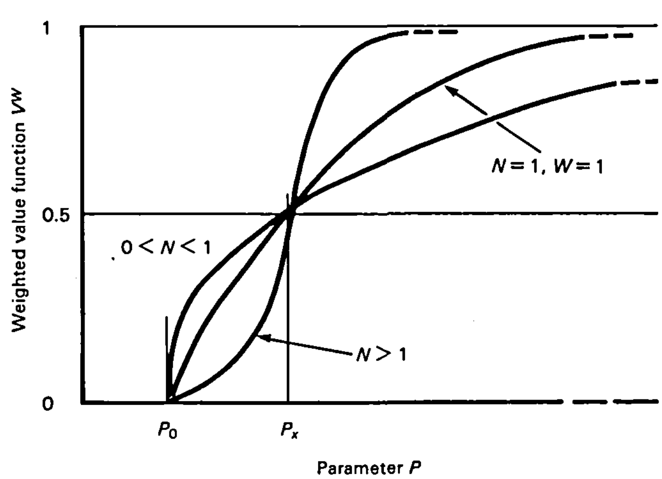

Figure D-5.—Weighted increasing asymptotic value functions. $VW = (1 - 1/\{1 + [(P - P_0)/(P_x - P_0)]^{N}\})^{W}$.

obtained by suitable choice of normalization; e.g. [in figures D-3 and D-4], choosing a large N effectively sets a soft threshold at $P - P_x$.

The level of the value function at $P - P_x$ is unaffected by the magnitude of N but the shape of the function is strongly affected. On the other hand, the basic shape of the function is not changed by the weighting constant W, but the level of the weighted value function at all points on the value axis, including the weighted value for $P - P_x$, is controlled by W.

Normalization

The application of large weighting factors can produce individual ratings R_{ij} which are very small numbers. Also, U_j depends on the number of factors n that it contains. If these conditions are considered undesirable, they can be improved by a minor redefinition of the utility and rating functions:

$$R_{ij} = \left[V_i(P_{ij})\right]^{W_i/n}$$

$$U_j = \prod_{i=1}^{n} R_{ij} = \prod_{i=1}^{n} \left[V_i(P_{ij})\right]^{W_i/n}$$

This change has the effect of bringing U_j to a value closer to 1. There is no change in relative ranking resulting from this redefinition.

ADDENDUM B

12 December 1980

Mr. J. Jones, President
HDDR Manufacturing Co.
United States

Dear Mr. Jones:

The Tape Head Interface Committee (THIC) is an informal association which provides a continuing forum for interchange of information between users and manufacturers of instrumentation magnetic tape recording systems and magnetic

tape concerning problems arising at the tape/head interface, and techniques, including advances in the state-of-the-art, available to solve such problems. Your support of THIC and participation by your people in THIC activities is very much appreciated.

At its November 18 meeting in Maryland, THIC formed a Subcommittee of HDDR system users. Each member of the Subcommittee represents a single government agency which is now using high-density digital recording systems or expects to be procuring systems to meet defined requirements.

The Subcommittee has two major objectives: (1) to convey to the HDDR system development and manufacturing industry the deep and urgent concern of the users over the proliferation of HDDR coding techniques; and (2) to attempt to find an approach which will eventually result in a single American National Standards Institute (ANSI) standard—acceptable to users and manufacturers—for the interchange of HDDR tapes without intermediate code conversion.

As you are aware, the ANSI X3B6 Committee has been and is currently in the process of developing a standard which includes: (a) IRIG-compatible serial bi-phase and randomized NRZ codes at conservative bit-packing densities; (b) 33 kilobit-per-inch serial Randomized NRZ (Sangamo Weston), Enhanced NRZ (Bell & Howell), and Miller Squared (Ampex) codes; and (c) 33 kilobit-per-inch-per-track parallel Randomized NRZ, Enhanced NRZ, Miller Squared, and Pattern Compatible Code (Martin-Marietta). This standard will be presented to the international community as a working paper for consideration as an International Standard at the January 1981 meeting of the International Standards Organization's ISO SC-12 Committee. At least three other manufacturers have asked that their codes be considered for standardization and others have been proposed. For agencies faced with the need to reproduce data from many formats, the situation is becoming impossible to manage (and finance).

To get a start on its second objective, the THIC/HDDR Users Subcommittee proposes to make use of the approach used by the ANSI X3B6 Users Committee in 1977-78 to establish a relative ranking of the three codes which were then candidates for the ANSI Standard. The X3B6 effort was suspended when some of the manufacturers represented on X3B6 could not accept the preliminary conclusions of the Committee. This "Utility Function" evaluation method, adapted from strategies used by some agencies in evaluating and ranking complex technical proposals, was felt to have merit as a starting point for the THIC Subcommittee. The list of system characteristics to be considered are parameters which were generated by the ANSI Committee and which survived many iterations of the evaluation. An explanation of the Value Function approach, lists of evaluation parameters, and definitions are attached. One of the important tasks of the Subcommittee will be to review and define weighting functions to be applied to the Value Functions in the evaluation. In the years that have elapsed since the ANSI evaluation stopped, new codes have evolved and systems previously considered may have been improved. The Subcommittee therefore plans to evaluate all candidate existing and proposed HDDR codes with the most recent data obtainable. Only the 33 kilobit-per-inch categories will be considered, with emphasis on parallel-track formats.

Results of the evaluation will be used as a point of departure in the preparation of a users recommendation to standards committees (ANSI and IRIG) for generation of an HDDR recorded tape interchange standard with as few format options as are found to be feasible.

You are invited to submit the 14 required parameter values in the requested format, based on your most current HDDR system data, to the THIC/HDDR Users Subcommittee Chairman at the address below prior to January 5, 1981. As an alternative, you may choose to meet with the Subcommittee (without other suppliers present) in Pasadena during the week of January 12 at a time not conflicting with scheduled ISO or THIC functions. If you choose the latter course, a time must be prearranged with the Subcommittee. If you choose not to reply, the Subcommittee will assume your system should not be considered in the evaluation.

If you need further information or have questions on this matter, please contact:

R. S. Reynolds
Chairman, THIC/HDDR Users Subcommittee
Sandia National Laboratories
Organization 1535
Albuquerque, NM 87185
Phone: (505) 844-4435

Sincerely yours,

C. Don Wright,
Chairman, THIC

RSReynolds:amc
Attachments

ADDENDUM C—THIC HDDR USERS SUBCOMMITTEE PARALLEL HDDR SYSTEM EVALUATION PARAMETERS AND SUGGESTED TEST PROCEDURES, OCTOBER, 1982

The following guidelines and evaluation parameters with associated suggested test procedures will be used by the HDDR Users Subcommittee of THIC in preparing a recommendation to ANSI X3B6 and the RCC Telemetry Group for parallel HDDR Standards.

1. Evaluation Ground Rules

1.1 A 1-in. 14-track HDDR system is presumed. Only parallel HDDR systems of ANSI X3B6 categories B and C are considered.

1.2 Unless otherwise noted, an 11-bit pseudorandom noise (e.g., see attachment 3) is to be used in establishing performance levels. Data output errors must not exceed 1 in 10^6 information bits. The maximum tape speed considered for the evalution is 120 ips. Minimum speed considered is 1⅞ ips.

1.3 Two general classes of use with differing requirements are identified: (1) a large number of

data channels with medium to high data rates, modest bit error rate requirements, and full reel recording, and (2) one or many high data rate channels requiring some mix of high sampling rate, high amplitude resolution, and few (or no) bit errors. Recording time may be from a few microseconds to a full reel.

1.4 Conformance to ANSI patent policy is assumed and is, therefore, not listed in the parameters for this evaluation. (See attachment 4.)

2. Parameters

2.1 Longitudinal Packing Density

Definition: Longitudinal packing density is the average effective density of source data bits per lineal inch of tape, per track.

Note: This parameter represents the number of bits per inch per track of the NRZ source data irrespective of the number of flux transitions actually recorded, with the additional limitation that the number of flux transitions must not exceed 33⅓ ktpi. Bits required strictly for parallel system operation, such as deskew or parallel synchronization words are considered data bits for this parameter.

Test Procedure: Using Ampex 799 type tape, operate one serial track at 120 ips with the maximum recorded packing density (see preceding paragraph). Record and reproduce an 11-bit pseudorandom test pattern for a continuous run of at least 10^9 bits and measure error rate. Rewind, replay at lowest tape speed consistent with the parameter in section 2.7. If either speed shows errors in excess of 10^{-6}, reduce the packing density about 10 percent and repeat. When the error rate is met, compute the effective packing density. (Selection of a particular roll of tape is allowed for this test.)

Value Function: Increasing weighted exponential

$$V = \left[\left(\frac{P - P_0}{P_x - P_0}\right)^N\right]^w$$

where

$$P_0 = 0 \text{ data bpi}$$
$$P_x = 33\tfrac{1}{3} \times 10^3 \text{ ftpi}$$
$$N = 1$$
$$P_T(\text{threshold}) = 15 \times 10^3 \text{ data bpi}$$
$$(P < P_T) \rightarrow V = 0$$

2.2 Minimum Transition Density Measured in a Parallel System

Definition: Minimum transition density is the reciprocal of the maximum number of bit intervals without a flux transition that can occur on any track of a parallel system.

Test Procedure: Determine by analysis the maximum number of encoded bits that can occur without a transition in the recorded signal. The reciprocal of the quantity so obtained is used as the value of this parameter. The worst-case input for each code must be assumed, however improbable. Raw NRZ, for example, can extend from one synchronization word to the next with no transitions.

Value Function: Increasing weighted exponential (see sec. 2.1) where

$$P_0 = 0$$
$$P_x = 1$$
$$N = 0.025$$

2.3 Recovery From Burst Errors (Longitudinal Without Bit Slip)

Definition: Recovery from burst errors without bit slip is the number of information bit periods required by a system to restore normal operation after an error burst, assuming bit synchronization is not lost. "Normal" implies that the expected interval before the next bit error is 10^6 bits.

Test Procedures: Determine by analysis.

Value Function: Weighted decreasing asymptotic

$$V = \left[\frac{1}{1 + \left(\frac{P - P_0}{P_x + P_0}\right)^N}\right]^w$$

where

$$P_0 = 0 \text{ data bit periods}$$
$$P_x = 250 \text{ data bit periods}$$
$$N = 1$$

2.4 Recovery From Burst Errors (Longitudinal With Worst-Case Bit Slip)

Definition: Recovery from burst errors with worst-case bit slip is the maximum number of information bit periods required by a system to reestablish normal operation beginning with the establishment of transition timing after an error burst during which bit synchronization was lost. If recovery depends upon the eventual occurrence of a synchronization word, the synchronization word spacing must be consistent with that used in section 2.1.

Test Procedure: Determine by analysis. This parameter represents the maximum number of

bits required before data sequences essential for decoding can be guaranteed to appear, or before erroneous data sequences can be guaranteed to be interrupted, so as to permit, in either case, successful decoding. This parameter can never be smaller than that in section 2.3.

Value Function: Weighted decreasing asymptotic (see sec. 2.3) where

P_0 = 0 data bit periods
P_x = 512 data bit periods
$N = 1$

2.5 Pattern Sensitivity (Parallel)

Definition: The system is pattern sensitive if a pattern of data bits (repetitive or not) can be found that when recorded by a parallel HDDR system will cause excessive bit errors or will significantly reduce interchange margin.

Test Procedure: Using the output of an 11-bit counter operating at 1 Mbps as data input to the HDDR system, read out each counter level (including all "0's" and "1's") 1000 times and record at 3¾ ips. Report any pattern that results in a bit error rate (BER) of 10^{-6} or worse.

Value Function: Yes/No

V(yes) = 0.7
V(no) = 1

2.6 Reverse Play

Definition: Reverse play capability requires ability to play back a given tape in either direction without manual adjustments.

Test Procedure: Determine by analysis. A "yes" rating requires the presence of the following:

(1) Reverse synchronization word detection
(2) Reverse equalization
(3) Reverse signal polarity accommodation
(4) Processing of overhead bits in reverse
(5) Attainment of synchronization to correct clock

All the above must be automatically selected or be direction independent.

Note: The forward and reverse speeds available must be operable in any combination. Reverse play must be compatible with the tape speeds discussed in section 2.7.

Value Function: Yes/No

V(yes) = 1
V(no) = 0.9

2.7 Record/Reproduce Speed Ratio

Definition: The record/reproduce speed ratio is the ratio of the maximum record to the minimum playback operating speeds at which all performance criteria are met (e.g., 120 ÷ 1⅞ = 64).

Test Procedure: Determine by analysis.

Value Function: Increasing weighted exponential

$$V = \left[\left(\frac{P - P_0}{P_x - P_0} \right)^N \right]^W$$

where

$P_0 = 1$

$P_x = 64$

$N = 1/6$

2.8 Polarity Insensitivity

Definition: Polarity insensitivity is that property of a pulse code modulation code that renders it insensitive to signal polarity reversal, such as might occur with miswired magnetic head windings (e.g., NRZ-M is polarity insensitive).

Test Procedure: Determine by analysis.

Value Function: Yes/No

V(yes) = 1
V(no) = 0.9

2.9 Interchange Signal-to-Noise Ratio Margin Between Record and Reproduce

Definition: The interchange signal-to-noise ratio (SNR) margin between record and reproduce is the excess SNR available at the reproduce output that results in a BER of 10^{-6}.

Test Procedure (see fig. D-7):

2.9.1 Record on two tracks of the HDDR recorder with no digital signal applied to the record head. All other record conditions are to be maintained. Reproduce at the minimum tape speed obtained in section 2.7. Measure the noise power output of both tracks. The power output of the first track is N; that of the second track is KN. (The noise power and noise spectra of the two tracks must be similar.)

2.9.2 Record a serial bit stream on the first track at the maximum bit packing density determined in section 2.1 while recording a zero-level input on the second track. While reproducing at the minimum tape speed from section 2.7, sum the analog output of the second track with the output of an attenuator inserted between the output of the

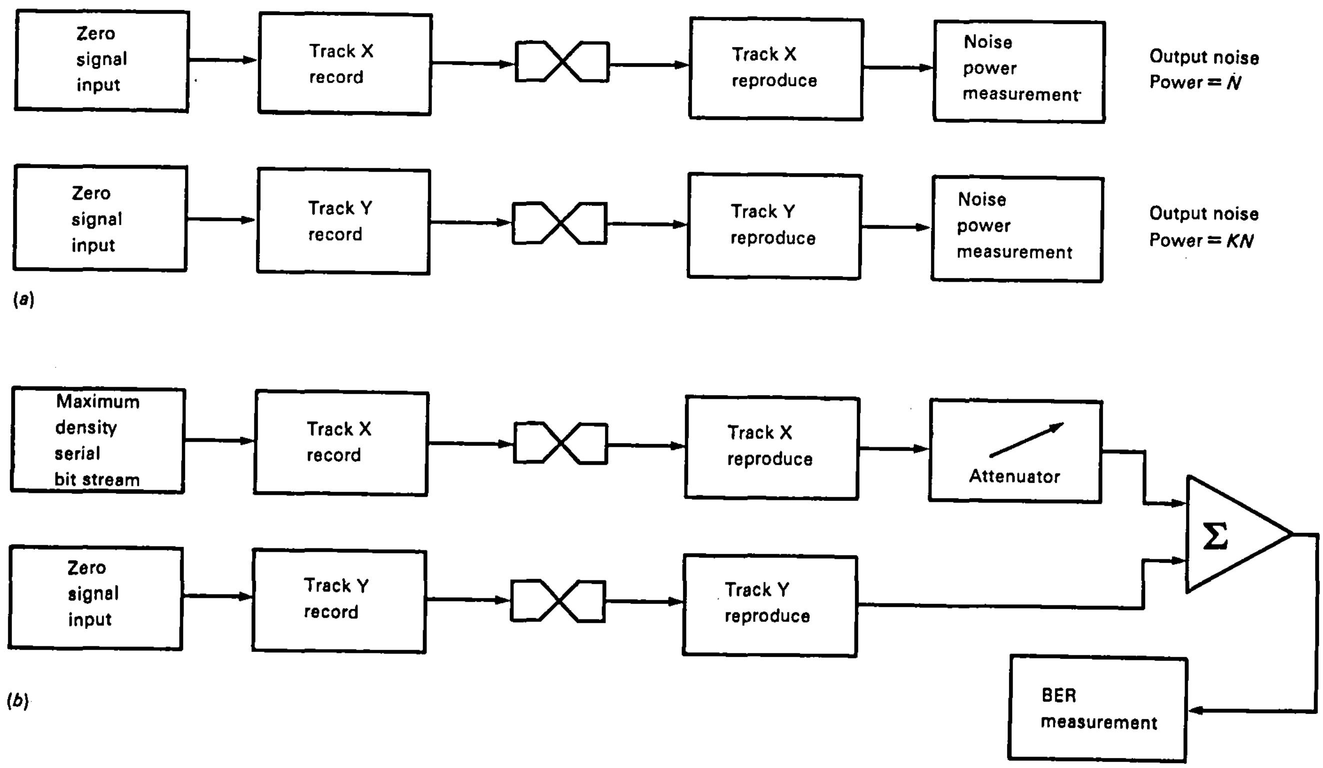

Figure D-7.—Interchange SNR margin test setup. (*a*) Determination of noise ratio of two tracks (factor K). (*b*) Determination of interchange SNR margin.

first track and the summing circuit. Attenuate the signal from the first track until the BER is approximately 10^{-6}. (If the BER is no greater than 10^{-6} with no attenuation, the margin is less than 3 dB, and the system under test has insufficient margin for interchange.) For an attenuation of A dB, as measured above,

$$\mathrm{SNR}_{\mathrm{output}} \approx \frac{10^{-A/10}}{K + 10^{-A/10}}$$

and the excess SNR is approximately

$$10 \log 1 + \frac{k}{10^{-A/10}} \quad \mathrm{dB}$$

Value Function: Increasing sigmoid

$$V = \left[\frac{1}{1 + \frac{1}{9} \left(\frac{P - P_0}{P_x - P_0} \right)^{-N}} \right]^{W}$$

where

$P_0 = 3$ dB
$P_x = 10$ dB
$N = 2$
$P_t = 3$ dB

2.10 Error Detection

(See also sec. 2.11.)

Definition: Error detection is that property of a code (E-NRZ [Datatape, Incorporated], M[2] [Ampex Corporation], R-NRZ [Fairchild Weston Systems Incorporated], PC[2] [Martin Marietta], 3PM [Thorn EMI Technology Incorporated], or PROP [Honeywell]) that permits detecting all single-bit errors.

Test Procedure: Determine by analysis whether the code contains the necessary properties to support detection of all single-bit errors.

Value Function: Yes/No

$V(\text{yes}) = 1$
$V(\text{no}) = 0.9$

2.11 Error Correction

(See also sec. 2.10.)

Definition: Error correction compatibility, if present, permits correcting all single-bit errors in a serial word and some multiple errors by making use of redundancy in the recorded signals. To be "compatible" the system must permit the incorporation of error correction at no increase in

overhead beyond the addition of one or more parity tracks to the parallel system.

Test Procedure: Analysis may be used to show that the code as formatted on tape by the system is compatible with error correction.

Value Function: Yes/No

$$V(\text{yes}) = 1$$
$$V(\text{no}) = 0.9$$

Attachment 1—Categories of High Density PCM Recording and Cross-Play Criteria[2]

Three categories—A, B, and C—of high density PCM recording performance are covered in this standard as defined below.

Category A. This category covers Serial High Density PCM recording performance using 14-track analog 1-inch heads of Table 3-4 on wideband (2 megahertz at 120 inches per second) analog recorder/reproducers adjusted for analog service and using standard record head gap lengths.

Category B. This category covers Serial or Parallel PCM Recording performance using 1-inch 14-track, 28-track, or 42-track heads on wideband (2 megahertz at 120 inches per second) recorder/reproducers adjusted for optimal digital service using bias or non-bias recording techniques and using standard record gap lengths. Since this category allows both bias and non-bias recording, a significant tolerance spread in record gap lengths, and a significant tolerance spread in magnetic tape uniformity, interchange parties should be aware that fine tuning may be necessary on the reproducing machine to realize the full performance of any individual tape.

Category C. This category covers Parallel High Density PCM recording performance using wideband recorder/reproducers equipped with optimized record gap lengths and special digital electronics using non-bias recording. For this category, packing densities above 25 000 flux transitions per inch may be used.

See the following table for a summary of performance category versus important recording parameters.

Attachment 2—Summary of Performance Category Versus Record Parameters[3]

Recording parameter	*Performance category*
Track densities, one inch tape	
1. 14 tracks	A, B, C
2. 28 and 42 tracks	B, C
Data configuration	
1. Serial PCM	A, B, C
2. Parallel PCM	B, C
Packing densities	
1. 15 to 25 KTI	A, B
2. 15 to 33.33 KTI	C
Recorder/reproducer	
1. Wideband Analog Service	A
2. Wideband Digital Service	B, C
Adjustments between routine maintenance	
1. No adjustments after standard setup	A, C
2. Fine adjustments allowed for individual tape reproduce	B
3. Fine adjustments allowed for tape type and record mode	B, C
Record gap length	
1. 85 ± 20 micro-inches	A, B
2. 20 ± 5 micro-inches	C
Record mode	
1. With bias	A, B
2. Without bias	B, C

[2] From "HDDR Recorded Tape Standard," ANSI X3B6 403R.
[3] From ANSI X3B6 403R.

Attachment 3—Pseudorandom Test Pattern[4]

2.1.1.3.3.3 Procedure:

2.1.1.3.3.3.1 It is recommended that a PN [pseudorandom noise] test pattern be utilized whenever possible. One reason for this is that a PN sequence can be generated and synchronized economically by a shift register with feedback configured for a maximum length sequence. The number of positions in the shift register and the feedback connections uniquely determine the test pattern which has been adopted by ranges and users and allows the exchange of test data without ambiguity. In this connection an 11-position shift register is recommended with feedback summed modulo two from positions 9 and 11. The sequence will be 2047 bits long which corresponds roughly to the frame lengths used for nonreturn to zero (NRZ) and exercises the low-frequency response of elements of the system. This is important because with NRZ the lack of d.c. response causes zero wander of the bit stream in accordance with the fractional amount of near-d.c. power lost. In addition, the sequence will contain 11 binary "1's" followed by 9 binary "0's", thus exercising the bit synchronizer with only 1 NRZ transition in 19 bits, 3 in 29 bits, 5 in 39 bits, 7 in 49 bits, etc.

[4] From Telemetry Group: *Test Methods for Telemetry Systems and Subsystems.* IRIG 118-79, Vol. IV, Inter-Range Instrumentation Group, May 1979.

Attachment 4—ANSI Patent Policy[5]

7.4 Patents. There is no objection in principle to drafting a proposed American National Standard in terms that include the use of a patented item, if it is considered that technical reasons justify this approach.

If the Institute receives a notice that a proposed American National Standard may require the use of a patented invention, the procedures in 7.4.1 through 7.4.4 shall be followed.

7.4.1 Prior to approval of such a proposed American National Standard, the Institute shall receive from the patent holder (in a form approved by the Institute) either: assurance in the form of a general disclaimer to the effect that the patentee does not hold and does not anticipate holding any United States patent covering any invention whose use would be required for compliance with the proposed American National Standard: or assurance that:

(1) A license shall be made available without compensation to applicants desiring to utilize the license for the purpose of implementing the standard, or

(2) A license shall be made available to applicants under reasonable terms and conditions that are demonstrably free of any unfair discrimination.

The terms and conditions of any license shall be submitted to ANSI for review by its counsel, together with a statement of the number of independent licensees, if any, which have accepted or indicated their acceptance of the terms and conditions of the license. On the advice of Institute counsel the Executive Standards Council shall determine, prior to approval, whether or not the patent situation would disqualify the standard for consideration.

7.4.2 A record of the patent holder's statement (and a statement of the basis for considering such terms and conditions free of any unfair discrimination) shall be placed and retained in the files of the Institute.

7.4.3 When the Institute receives from a patent holder assurance set forth in 7.4.1(1) or (2) the standard shall include a note as follows:

> The user's attention is called to the possibility that compliance with this standard may require use of an invention covered by patent rights.
>
> By publication of this standard, no position is taken with respect to the validity of this claim or of any patent rights in connection therewith. The patent holder has, however, filed a statement of willingness to grant a license under these rights on reasonable and nondiscriminatory terms and conditions to applicants desiring to obtain such a license. Details may be obtained from the publisher.
>
> No representation or warranty is made or implied that this is the only license that may be required to avoid infringement in the use of this standard.

7.4.4 The Institute shall not be responsible for indentifying all patents for which a license may be required by an American National Standard or for conducting inquiries into the legal validity or scope of those patents which are brought to its attention.

7.4.5 Compliance with the procedures in 7.4.1 through 7.4.4 is mandatory for Institute approval of a proposed standard that may require use of a patented item.

[5] From "ANSI's Patent Policy." App. D of *ANSI Procedures for the Development and Coordination of American National Standards*, Mar. 30, 1983.

APPENDIX E

Care and Handling of Magnetic Tape Heads

The Headwear Advisory Committee
of the Tape Head Interface Committee

The information in this appendix is intended for general use by users of magnetic tape recording heads. It does not replace information or instructions provided by a manufacturer.

Tape heads have changed significantly over the past 10 years. Increased packing density has required performance improvements and the resolution of wear problems. Tape heads are the most costly component in a tape recording system. It is important to understand what causes them to fail and how they should be handled to extend their usefulness.

Generally the tape contact surface of the head is most susceptible to damage, but the mounting surface and pins or cable are also easily damaged. For the purpose of this document, handling damage will be defined as damage caused by either of two categories:

(1) Wear at the interface occurring while installed in a computer tape drive or instrumentation recorder

(2) Mishandling during installation, cleaning, or removal of a head from a recording device.

HEAD WEAR

The tape/head interface is critical to the performance of a tape recording system; therefore, a significant factor for improving or extending performance is to control variables affecting the interface. The variables include tape tension, tape speed, tape guiding, head contour, surface material, and environmental conditions. Understanding the interrelationship among these factors can help explain many of the reasons for head failures. One factor affected by all of the variables at the interface is the degree of contact required between the head and tape. The tape must remain in intimate contact with the head to sustain adequate performance. As a result of this contact, head wear begins as soon as a head is exposed to tape. As the surface of the head wears, the interface changes. The changes that take place can cause the tape to separate from the head. In high-density recording, an increase of a few millionths of an inch in tape/head separation can cause a significant decrease in output. Some of the factors influencing the rate of head wear are described in the following paragraphs.

Head Alignment

Head alignment is a critical factor in controlling head wear. When heads are manufactured, the mounting surface and tape contact surface are held perpendicular to each other within 1 arcmin. If the head is tilted relative to the tape path, one side of the head will wear faster than the other. If the head is not aligned for accurate tape wrap, the result will be nonsymmetrical wear. This will eventually cause loss of output and failure.

Tape Tension

Tape tension must be accurately adjusted for proper performance. Too little tension will cause the tape to fly over the heads and decrease signal amplitude. If there is too much tension, the wear rate will increase and shorten the life of the head.

Tape

Tape is a variable that is not easily controlled. Abrasivity can vary drastically from one type of tape to another. If a tape is too abrasive, it will accelerate head wear. Insufficient abrasivity will permit oxide and other materials to build up on the surface of the head. Improper storage and handling of tape can also cause a variety of problems. Rapid temperature or humidity changes in a storage area can alter the oxide and cause performance problems. If the oxide surface becomes contaminated by exposure to cleaning solvents, contaminants can be transferred to the surface of the head, causing tape/head separation problems. Tape must be handled carefully so that fingerprints, dust, and other contamination are not transferred to the oxide surface during installation of a reel. Tape reels should be

carefully inspected. Cracked or warped reel flanges cause tape to stack improperly and can cause tape edge damage. New tape is contaminated and consequently highly abrasive. All new tape should be degaussed and cleaned before being used.

Tape Head and Tape Path Cleaning

Frequent cleaning of the tape head and tape path can help significantly in maintaining performance. Removal of contamination from head surfaces will decrease friction between tape and the head. Solvents recommended by the drive manufacturer should be used to clean the head and tape path. Devices used to apply the solvent should also be approved and used carefully. Only soft, lint-free materials should be used to clean the surface of the head. Any hard material can cause microscopic scratches and increase the rate of head wear.

The tape contact surface of a head is a smooth, highly polished surface. This smooth surface is necessary to reduce friction between the tape and head and to allow intimate head/tape contact. Scratches or other damage to this precision surface may allow microscopic oxide particles and airborne contaminants to accumulate on the surface. Eventually, accumulation may cause head/tape separation and loss of output.

MISHANDLING

One of the major causes of surface damage to tape heads is mishandling. If the surface of a tape head is even lightly bumped against a hard surface, it can be damaged and eventually cause a head failure. Generally the damage is not visible without the aid of a microscope, so no one is aware that the surface has been damaged. There are a number of techniques available for visually inspecting a precision tape head surface for defects. The most common method is inspection with a high-magnification microscope. Many defects on the surface of a head will become visible when magnified 10 to 15 times. Other defects require magnifications of 50 to 100 times before they can be seen. To accurately measure or inspect a head, it must be magnified several hundred times. The gaps for many heads are less than 60 millionths of an inch in length.

Other techniques for surface inspection include interference contrast, noncontact interferometry, and profilometer measurement. Interference contrast and interferometry use the wavelengths of different colors of light to accurately measure deviations on a surface. A profilometer is a precision device that moves a sensitive stylus across the surface to measure the surface profile. Any deviation in the surface is recorded on a chart connected to the stylus. Another type of defect measured by this equipment is stepped gaps and core undercut. Stepped gaps are caused, generally, when a head is bumped or dropped. One side of the head shifts, causing a step at the gap. Tape is then separated from the core surface by the amount of the step, causing a decrease in output. Core undercut is a condition in which the core material wears faster than the harder material on either side of the core. The tape is in contact with the harder material so it becomes separated from the core surface and the gap.

Handling damage to the tape heads can occur whenever a head is not in its protective container. When heads are removed, they should be handled carefully without touching the head stacks. Only the base plate should be handled. Heads are most vulnerable to damage during installation or removal from a tape drive. Heads damaged during installation or alignment may perform sufficiently for many hours before the damage causes the drive to fail. Unfortunately, many heads are not checked for handling damage when they fail. Consequently, many types of handling damage are not found and the problem continues.

Use of the following guidelines may help in preventing handling damage to tape heads:

(1) Use only authorized solvents and cleaning devices to clean the tape head.

(2) Never tap or pry (however lightly) on any part of the head.

(3) Never apply any hand tools to the head or screws contained within the head.

(4) Never lift or carry a head by its cables.

(5) Avoid contamination of the head by dust, oil, solvents, or tobacco smoke.

(6) Keep the tape contact surface covered with a soft material when the head is not installed.

A drive problem may be corrected temporarily by head replacement, but the drive itself may have damaged the head. In that case head replacement will only mask the problem.

Heads are expensive, precision devices and should always be handled carefully. Only technically qualified and fully trained personnel should be removing or installing tape heads.

In summary, the major causes of tape head failures are head wear and mishandling. Head wear cannot be prevented, but the wear rate can be slowed by careful alignment of the head, using correct tape tension, proper cleaning of the bearing surface of the head, and controlling the environment at the head. Mishandling can be prevented by understanding how to handle heads in a manner that will keep them from being damaged. Handling tape heads carefully can decrease the number of heads that would have to be replaced, thus reducing cost of operation. The number of head failures will decrease and reliability will improve only when everyone handles tape heads properly.

HEAD HANDLING PROCEDURE

Unpacking from Shipping Box

Remove the head assembly from its protective shipping container, taking care when opening bag with knife or scissors not to damage wires or heads. If possible, always grasp head by the base. Never hold head by the leads. Do not hold head assembly with fingers on the face of the head.

Preliminary Visual Inspection

Visually inspect head for any obvious damage with or without the aid of the microscope. Check head for scratches and dents in the tape contact area. Inspect wires for broken connections and for broken connectors. If cleaning of the head is required, follow the recommended cleaning procedure.

Cleaning and Degaussing

Clean tape head surface according to the manufacturer's recommended procedure. Clean tape guides and the entire tape path using recommended cleaning materials. During cleaning, the tape should not be returned to drive until all solvents and residues have been removed and cleaning is complete. Degauss tape heads periodically with an approved head degausser.

Mounting Head on Transport

Use prescribed torque and assembly hardware for head mounting and mount according to the system instruction manual. Use only degaussed tools and hardware.

Storage

Protect heads from heat or cold extremes. Storage temperatures, in general, should be from 5° to 52°C.

Place head in moisture barrier bag with desiccant, and always try to store in original shipping box.

RECOMMENDED HEAD AND DRIVE CLEANING PROCEDURE

Follow the manufacturer's procedure using the recommended solvents. In the absence of manufacturer instruction, use acceptable in-house procedures.

Frequency

Heads should be cleaned—

(1) Before critical recordings
(2) Whenever loss of signal or poor frequency response occurs
(3) When there is visual evidence of tape oxide shedding of surface of head
(4) When error rates increase
(5) When called for according to the periodic schedule specified by the manufacturer

Tools

(1) Foam applicators or cotton swabs (Use applicators or cotton swabs that do not contain adhesives.)
(2) Lintless wipers
(3) Manufacturer's recommended solvents
(4) Tools to remove or access heads and guides, if necessary
(5) Magnifier (to check for deposits or debris on heads)

Method

The recommended head cleaning procedure is as follows:

(1) Remove tape from the tape recorder so that all guides and heads are exposed for inspection.
(2) Moisten applicator with approved solvent. (Applicant should not be dripping wet, only moist.)
(3) Wipe using minimal pressure (do not scrub) in the direction of tape travel. Be sure that fibers of applicator do not adhere to surface or any part of the head.
(4) Wipe dry with lintless wiper.
(5) Clean guides and entire tape path.
(6) Degauss heads with manufacturer's recommended head degausser according to specified degaussing procedures.
(7) Replace heads on transport or engage heads to operating positions (as required).

CAUSES OF DIRTY HEADS

The major causes of dirty heads are as follows:

(1) Contamination with oil, fingerprints, airborne lint, smoke, etc.
(2) Tape oxide shed or binder/lubricant exudation
(3) Tape splices with oozing adhesive
(4) Dirty tape
(5) Bad tape

Even with optimum conditions, heads need periodic cleaning. A minimum rate should be once every 8 hr. Cleaning before mounting each tape is a good practice.

DEGAUSSING TAPE HEADS

The importance of head degaussing on a routine preventive maintenance basis cannot be overemphasized. Magnetized record/reproduce heads can cause reduced signal-to-noise ratios, loss of high-frequency

response, second harmonic distortion, or even loss of data due to tape erasure.

Magnetic heads become magnetized during the course of normal operation by power interruptions or even by Earth's magnetic field over a period of time. Periodic degaussing is necessary for continued optimum equipment performance. Symptoms of magnetized heads are increased noise, increased distortion, and decreased high-frequency response.

Degaussing should be done carefully so head surfaces are not damaged. Transport power should be off and tape, reels, head covers, and shields removed before the degaussing procedure is started. The head degausser should be energized at least 3 ft from the tape head and brought slowly into the head area. The degausser pole tips should be moved slowly back and forth across all gaps of all head stacks. The degausser pole tips should have a protective coating to prevent scratches. After the heads are degaussed, the degausser should be moved a minimum of 3 ft from the head area before being deenergized.

BIBLIOGRAPHY

Bucher, Anton: *Magnetic Head Technology.* Omutec, Pomona, Calif.

Jorgensen, F.: *The Complete Handbook of Magnetic Recording.* Tab Books, Inc., Blue Ridge Summit, Pa., 1980.

Kasai, D.: *The Commandments for Handling Tape Heads.* Applied Magnetic Corp., Goleta, Calif.

Pear, Charles B., Jr.: *A Solution to Tape Recording Head Wear.*

Sillers, Robert A.: *Tape Head Failures, Causes and Cures.* Magnetic Recovery Technologists, Inc., Valencia, Calif.

APPENDIX F

Acronyms

A/D	Analog to digital
A/D/A	Analog to digital to analog
BCC	Block check character
BEP	Bit error probability
BER	Bit error rate
Biφ–L	Biphase, level
Biφ–M	Biphase, mark
Biφ–S	Biphase, space
BNC	Bayonet nut coupling
bpi	Bits per inch
bps	Bits per second
CPU	Central processing unit
CRC	Cyclic redundancy check
CRO	Cathode ray oscilloscope
DED	Double error detecting
DM	Delay modulation
DM–M	Delay modulation, mark (Miller code)
DM–S	Delay modulation, space
DMX	Demultiplexing
DR	Density ratio
DSV	Digital sum variation
ECC	Error correction code
ECD	Error correction decoder
ECE	Error correction encoder
ECL	Emitter-coupled logic
EDAC	Error detection and correction
EDP	Electronic data processing
EMA	Electron microprobe analysis
E-NRZ	Enhanced nonreturn to zero
fci	Flux changes per inch
FET	Field effect transistor
FFT	Fast Fourier transform
FIFO	First in, first out
Gbps	Gigabits per inch
GCR	Group-coded recording
HDDR	High-density digital recording
HDTR	High-density tape recorder
IMA	Ion microprobe analysis
I/O	Input/output
IPF	Image processing format; Image Processing Facility
IRIG	Inter-Range Instrumentation Group; now Range Commanders Council (RCC)
kbpi	Kilobits per inch
kbps	Kilobits per second
ktpi	Kilotransitions per inch
LED	Light-emitting diode
LSC	Linear sequential circuit
LSR	Linear shift register
LVDT	Linear variable differential transformer
Mb	Magabits
MB	Megabytes
Mbps	Megabits per second
MFM	Modified frequency modulation
MIG	Metal in gap
MR	Residual induction
MS	Saturation induction
MTBF	Mean time between failures
MTRR	Magnetic tape recorder/reproducer
MTTR	Mean time to repair
MTU	Magnetic tape unit
MUX	Multiplexer
MX	Multiplexing
NRZ	Nonreturn to zero
NRZ–I	Nonreturn to zero, inverted
NRZ–L	Nonreturn to zero, level
NRZ–M	Nonreturn to zero, mark
NRZ–S	Nonreturn to zero, space
OEM	Original equipment manufacturer
OR	Orientation ratio
PAM	Pulse amplitude modulation
PCM	Pulse code modulation
PDM	Pulse duration modulation
PET	Polyethylene terephthalate
PLL	Phase-locked loop
P-P	Peak to peak
PPM	Pulse position modulation
PR	Pseudorandom
PRBS	Pseudorandom bit sequence
PRN	Pseudorandom noise
PV	Professional video
RAM	Random access memory
RB	Return to bias
RH	Relative humidity
RLL	Run length limited
RMS	Root mean square
R-NRZ	Randomized nonreturn to zero

R-NRZ–L	Randomized nonreturn to zero, level
ROM	Read-only memory
RWC	Read/write calibration
RZ	Return to zero
SDR	Signal dynamic range
SEC	Single error correcting
SED	Single error detecting
SEM	Scanning electron microscopy
SFD	Switching field distribution
SNR	Signal-to-noise ratio
SWDT	Synchronization word detect time
TBC	Time base correction
TBE	Time base error
THIC	Tape Head Interface Committee
3PM	Three-position modulation
tpi	Tracks per inch
TTL	Transistor-to-transistor logic
UBE	Upper band edge
VCO	Voltage-controlled oscillator
VCR	Video cartridge (cassette) recorder
VV	Vacuum video
$Y\phi$	Y-phase

APPENDIX G

Glossary

Aliasing: The misinterpretation of a high-frequency tonal as a lower frequency tonal due to sampling at less than twice the highest frequency of interest.

Align: To adjust circuits, equipment, or systems so that their functions are properly synchronized or their relative positions properly oriented.

Analog: Pertaining to representation by means of continuously variable physical quantities, as contrasted to digital, or discrete, representation.

Analog to digital (A/D): The process of converting from analog format to digital format.

Analog to digital to analog (A/D/A): The process of converting from analog format to digital format and back to analog format; usually required when digital tapes are used to provide data for analog systems.

Ancillary frame: In image processing format, a tape format element carrying all geometric correction coefficients.

AND gate: A multiple-input, single-output gate that has a "1" output only when all inputs are "1's".

Annotation frame: In image processing format, a tape format element carrying mapping and other information.

Antiferromagnet: A material in which spontaneous magnetization occurs in two equivalent sublattices.

Bandwidth: The range of frequency within which the performance of a recorder is measured.

Bandwidth sensitivity: The tendency of a code to increase bit error rate with increasing bandwidth.

Baseband: The frequency band occupied by data before modulating a carrier.

Baseline shift: A shift of the average direct current of a bit sequence relative to the peak value, caused by lack of low-frequency response of the recorder.

Baud: The baud, named for Emile Baudot, is the signaling rate in code elements per second; usually 1 baud equals 1 bit per second.

Bias (sometimes called ac bias): A high-frequency signal, usually three to five times the highest data frequency, that is linearly mixed with the data signal and fed to the record heads to compensate for the hysteresis effect of the tape. The use of bias improves the linearity and sensitivity of the system and provides maximum undistorted output levels. The amount of bias current used represents the best compromise of low distortion, extended high-frequency response, and high output.

Bias level: Normally, the level of an ac signal required to maximize the upper band edge when mixed with signals of interest and recorded on tape. A plus 2-dB bias level is defined by further increasing the bias level until the output decreases by 2 dB from maximum.

Biphase encoding: Double frequency encoding in which an extra transition occurs either at the beginning or in the middle of every bit cell.

Biphase, level (Biϕ−L): Biphase, level, is also known as split-phase encoding. Level change occurs at the center of every bit period. A "1" is represented by a "1" level with a transition to the "0" level; "0" is represented by a "0" level with a transition to the "1" level.

Biphase, mark (Biϕ−M): Level change occurs at the beginning of every bit period. A "1" is represented by a midbit level change; "0" is represented by no midbit level change. (See fig. G-1.)

Biphase, space (Biϕ−S): Level change occurs at the beginning of every bit period. A "1" is represented by no midbit level change; "0" is represented by a midbit level change. (See fig. G-1.)

Bit: Binary digit.

Bit cell time: The average bit duration during the process of recording at continuous maximum flux reversal rates.

Bit crowding: A condition in magnetic recording wherein a transition placed close to another appears to migrate into the larger space available between it and the transition on its other side.

Bit density: Bits per unit length, area, or volume of the recording medium; for example, the number of bits per square centimeter of magnetic tape.

Bit error rate (BER): The fraction of bits that are in error. BER = e/N where e is the number of errors and N is the total number of bits (correct bits plus erroneous bits).

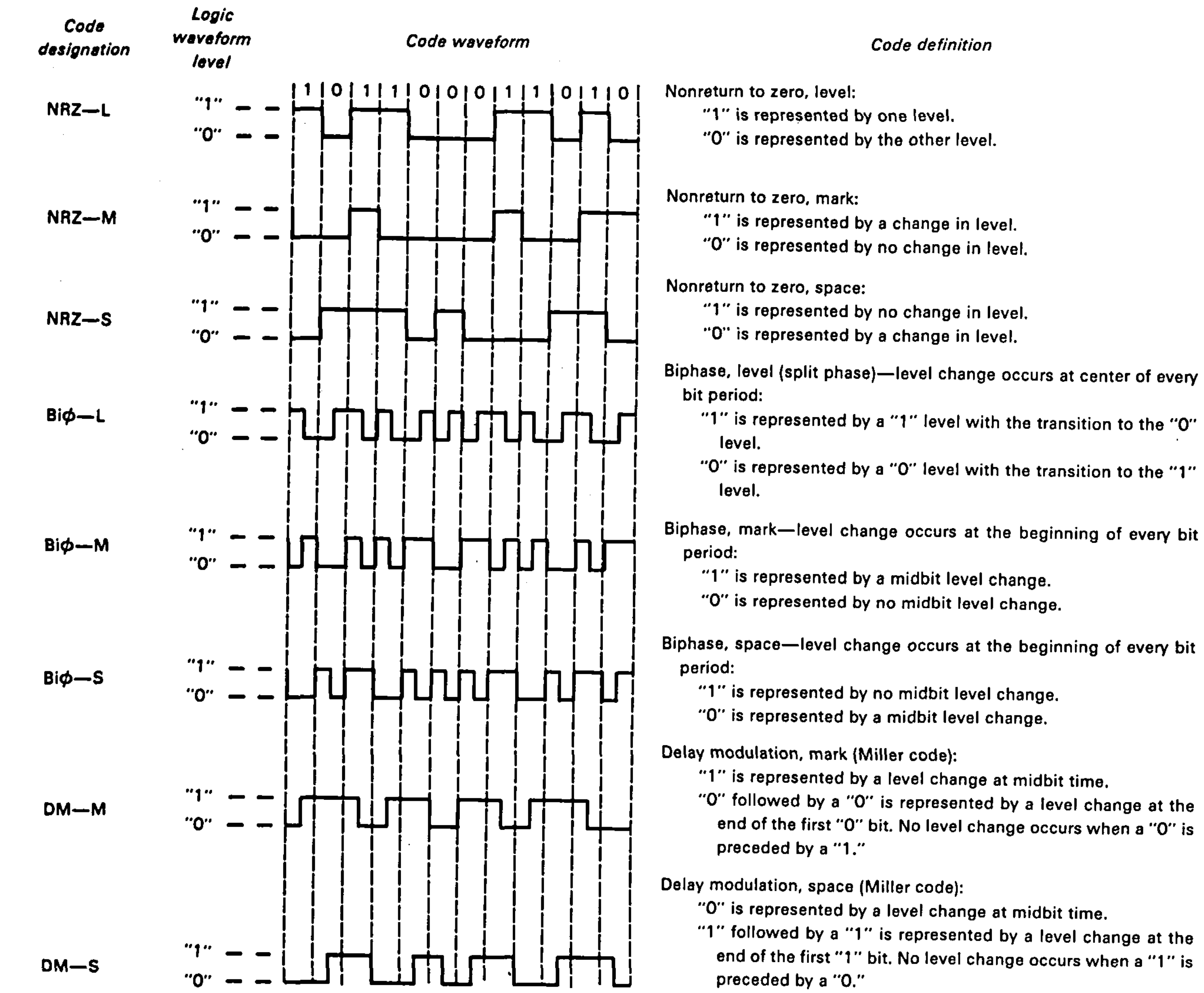

Figure G-1.—PCM code definitions. The definitions for Biφ—M and Biφ—S represent the accepted standard as previously defined in Range Commanders Council (RCC) documents 106-66 and 106-73 (revised Nov. 1975).

Bit parallel: Information transfer in which all bits constituting one word are transmitted simultaneously in different parallel channels.

Bit rate (bit frequency): Speed at which bits are transmitted or handled.

Bit serial: Information transfer in which all bits are transmitted one after the other in a single channel.

Bit slip: Reconstructed bit stream out of synchronization with the actual bit stream because the reconstructed clock has gained or lost one or more cycles with respect to the correct clock. Continuous errors result until recovery is made, because the "interpreter," such as a D/A converter, needs to know exactly which bit is the first bit of a word.

Bit stuffing: Insertion of overhead bits on the data tracks.

Block check character (BCC): Contained in the trailer field of a transmission block, such a character is generated by a checking algorithm applied to the block data.

Block data: Groups of words, frames, or characters handled as single units separated by interblock characters.

Bookkeeping (housekeeping): Computer coding that reserves, restores, and clears memory areas or sets up constants and variables to be used by the program.

Boolean logic: The logic resulting from the use of the AND, OR, and NOT functions (gates).

Buffer register: A storage register capable of receiving and transmitting data at different I/O rates.

Capability factor: As obtained from an eye pattern, the ratio of trace thickness (measured normal to the trace) to the total width (opening) of the eye at the center of the waveform.

Certified tape: Tape that is electrically tested on a specified number of tracks with a specific drive and electronics using a defined code at a specified tape speed and data rate, and certified by the supplier to have less than a certain total number of permanent errors of a specified duration.

Channels: Subcircuits of a large system allowing processing of data streams.

Check bit: A bit generated periodically to assist in error detection and correction.

Clock: A timing reference required to decode digital signals; i.e., a timing reference for digital data to keep track of bits during periods of no transitions and to indicate instants when to sample data.

Clock efficiency: The ratio of data bits to total bits (data bits plus overhead bits) for a given bit error rate.

Coercivity or coercive force: The field strength required to bring the remanence to zero in a magnetic material, thus removing the residual magnetism.

Compatibility: The ability of two types of recording equipment to perform similar functions and operate interchangeably.

Crossplay: Playback on a device different in design and manufacturer from that on which the data was originally recorded.

Cyclic redundancy check (CRC): An error detection method in which check bits are generated by taking the remainder after dividing the data bits by a cyclic code polynomial.

Data compression: A communications technique in which short code words are substituted for data strings whenever possible.

Data formatter: Custom-designed equipment used to multiplex or demultiplex a single data line with a relatively high data rate, distributing the output to two or more data lines at a lower per-line data rate, or the reverse.

dc restorer: Circuitry designed to reduce baseline shift.

Decoder/deskew assembly: A component of a typical N-track high-density digital recorder that accepts up to N lines of bit parallel data in whatever code was recorded, converts it to NRZ–L data, time aligns all tracks, and outputs serial or parallel NRZ–L data and clock.

Decoding: To recover the original data stream from an encoded form of the data stream.

Delay modulation code (DM): Code characterized by having a minimum of one transition for every other bit cell. Transitions occur at the middle of all "1" bits and between all "0" bits. (Also known as delay modulation, mark (DM–M); see fig. G-1.)

Delay modulation, space (DM–S): Transitions occur at the middle of all "0" bits and between all "1" bits. (See fig. G-1).

Demultiplexing (DMX): Separation of independent channels from a single high-speed data stream.

Density ratio (DR): Data density divided by high translation density.

Difference signal: In communication theory models, a convenient function of two known signals on which the correlation detection process is based.

Digital data: Information in a series of digits having only two possible values, "0" or "1."

Digital recording: A method of recording in which the analog information is first digitized and then recorded on tape. Usually a binary code is used and two discrete values are recorded.

Digital sum variations (DSV's): Values of the running integral of a bit sequence whose levels are assumed to be ± 1.

Disparity: In a code word or character, the excess number of "$+1$" bits over "-1" bits.

Distortion (harmonic): A nonlinear change in signal waveform upon reproduction in which undesired harmonics of a sinusoidal input are generated.

Double-density code: A code in which the bit density is doubled, the bandwidth remaining the same; i.e., codes that allow doubling the bit density for the same bandwidth as compared to a biphase code.

Double-frequency clock: A clock at twice the bit rate.

Dropout: Variation (reduction) in signal level of reproduced, tape-recorded data, resulting in an error in data reproduction. More specifically, a loss in output from a magnetic tape of more than a certain predetermined amount (depth), expressed in terms of the percent of reduction or decibel loss for a specified time period (length); e.g., 12 dB (75 percent) for 1 μs.

EDAC: Error detection and correction of recorded data using simultaneously recorded correction data either added to the data stream or recorded separately on an auxiliary track.

Encoding: To express a single character or a data stream in terms of digital bit code.

Enhanced nonreturn to zero (E-NRZ): A modification of NRZ encoding in which the bit stream is separated into 7-bit words, bits 2, 3, 6, and 7 inverted, and a parity bit is added to minimize dc components and maintain phase lock in the playback timing oscillator.

Environmental conditions: External factors such as room temperature and relative humidity that affect tape performance.

Equalization: The process of reducing amplitude or phase distortion of a circuit by compensating for dif-

ferences in attenuation or time delay throughout the transmission band.

Error burst: Multiple errors caused by a common event such as large voids in the magnetic media of a tape.

Error log: A capability for storing the location and number of errors found on a magnetic medium.

Error multiplication: A property of code process converters whereby a single incorrect digit in the input signal can cause more than one digital error in the output signal.

Error recovery strategy: Selection of error detection and correction processes to minimize the probability of undetected erroneous data, entailing reduction of burst error rate, miscorrection probability, and catastrophic probability.

Euclidean division algorithm: A formal method allowing the selection of check bits, based on the remainder formed when a data polynomial is divided by a generator polynomial.

Even parity: A block of data with an even number of "1" bits, either vertically or longitudinally along the tape.

Eye patterns: The reproduce system output is applied to the vertical input of an oscilloscope with the horizontal input synchronized to the bit rate clock. The oscilloscope display gives an insight into the quality of the reproduced data.

Ferrite: A magnetic ceramic compound such as those used in the construction of magnetic recorder heads.

Fire code: An error correction code for which the generator polynomial has a particular form.

FM code: A pulse code for which a flux reversal at the beginning of a cell time represents a clock bit, a flux reversal at the center of the cell time represents a "1" bit, and an absence of a flux reversal represents a "0" bit.

4/5 code: A group-coded recording code developed by IBM in which the 16 possible combinations of 4 bits are encoded in sixteen 5-bit groups selected such that each has at least two "1" bits and no more than two "0" bits in sequence.

Frame: In high-density digital recording, an entity containing data bits and overhead bits. It is preceded and followed by synchronization words.

Frame synchronization: The process whereby a given receiving channel is aligned in time with the corresponding transmitting channel.

Frequency-division multiplexing: The process of dividing the available frequency passband into a number of narrower frequency bands, each available for a separate signal.

Gap: The space in a ring-type magnetic head at which tape read and write operations take place.

Gate: A device having one output channel and two or more input channels such that the output channel state is completely determined by contemporaneous input channel states.

Group-coded recording (GCR) code: A code that groups characters and encodes them, using a lookup table, allowing a maximum of two "0" values in sequence.

Hamming code: A data transmission code that is correctable.

Hardware: Equipment, as contrasted to computer programs (software), used for data processing.

Head: A transducer to convert electrical signals into magnetic signals for recording on magnetic tape and vice versa.

Headblock: A specialized head assembly containing recording headstacks, position sensors, temperature sensors, a ballast resistor, and interface electronics.

Image major frame: In image processing format, a tape format element that carries most of the data.

Interface: A shared boundary between two systems, or parts of a system, through which data are transmitted, consisting in practice of mechanical or electronic elements, or both.

Interleaver: A special circuit used to separate (displace into different data blocks) data words to minimize the effects of burst errors.

Jitters: Sudden, small, irregular departures from phase, amplitude, or pulse duration of a signal caused by the recording/reproducing mechanisms.

Latch: A single-input, single-output circuit whose output at a point of time is the bit that appeared on its input when the latching command was issued.

Linear function: A function satisfying the relation

$$f(x + y + \dots + n) = f(y) + \dots + f(n)$$

Linear sequential circuits (LSC's): Circuits constructed with modulo 2 addition (XOR gates), memory circuits (latches), and constant multipliers.

Logic levels: Nominal voltages that represent binary conditions in a logic circuit.

Longitudinal recording: (1) Recording in which the tape tracks are parallel to the direction of tape motion, contrary to rotary recording. (2) Recording in which the magnetic vector of tape magnetization parallels the track surface on the tape. Horizontal recording is more acceptable for the second definition.

Magnetic field strength: The magnitude of a magnetic field vector, usually expressed in oersteds or ampere-turns per meter.

Magnetic flux: The magnetic lines of force produced by a magnet or electric current.

Magnetomotive force: The magnetic analog of electromotive force, which, when due to a current in a coil, is proportional to the product of current in amperes and the number of turns.

Magnetoresistance: The change in electrical resistance of a conductor or semiconductor due to a change in the applied magnetic field.

Magnetostriction: The change in dimensions of a ferromagnetic body when placed in a magnetic field.

Manchester codes: Biphase, level (Biϕ—L), and biphase, mark (Biϕ—M), codes, which are self-clocking and avoid the necessity of dc response, although at the expense of required additional bandwidth.

Maximum-likelihood receiver: A receiver that can determine the coded signal or word that was most probably transmitted.

Merging: In three-position modulation (3PM) code, combination of two transitions to form a single transition when there is only one transition-free position between them.

MFM code: See **Delay modulation (DM) code.**

Microcode: Computer programming using elementary machine instructions.

Microdiagnostics: Data testing required to implement error correction circuits of data storage devices.

Miller code: A biphase encoding scheme in which a minimum of one transition occurs in every two bit cells, minimizing signal dc components and providing run length limitation. See also **Delay modulation (DM) code.** See figure G-1.

Miller^2 code: A modification of Miller code having a bounded digital sum variation and, therefore, zero dc content.

Minimum transition density: The least transition density that allows maintaining synchronization without extending the low-frequency response requirement below the capability of wideband direct record/reproduce systems.

Miscorrection: An error condition that occurs when three bits are in error on three corners of a rectangle within a data block.

Misdetection: An error condition that occurs when four bits are in error on four corners of a rectangle within a data block.

Misregistration: The improper interpretation of a word, while passing, for example, between a head and a track during read or write operations.

Modem: A data station device capable of modulating the transmitted signal and demodulating the received signal, and also capable of related functions such as multiplexing.

Modular packaging: Assembling electronic equipment from already completed states (in boxes or blocks).

Modulo 2 adder: A logic element whose output at a point of time is the modulo 2 sum of its inputs at that time.

Multiplexing: Interleaving of two or more independent channels (of various data rates) into a single high-speed data stream; or, in tape recording, time or frequency sharing (i.e., time division or frequency division) of a single track on tape by two or more signals, each occupying a different time or frequency domain.

Nonreturn to zero code (NRZ): A binary digital code in which transitions between signal levels, rather than the levels themselves, represent bits. See figure G-1.

Nonreturn to zero, inverted (NRZ—I): Same as **Nonreturn to zero, mark.**

Nonreturn to zero, level (NRZ—L): A binary digital code in which a "1" is represented by one level and a "0" by the other level. (See fig. G-1.)

Nonreturn to zero, mark (NRZ—M): A binary digital code in which a "1" is represented by a transition at the beginning of the bit cell, and a "0" is represented by no transition. (See fig. G-1.)

Nonreturn to zero, space (NRZ—S): A binary digital code in which a "1" is represented by no transition, and a "0" is represented by a transition at the beginning of the bit cell. (Seee fig. G-1.)

NOT function (gate): An inverting function (inverter).

Nyquist rate: Minimum sampling rate required to avoid aliasing. Should be twice the highest frequency of interest.

Odd parity: A property of a vector, word, or data stream with an odd number of "1" bits.

Oligimers: Low molecular weight components of polymer films.

OR gate: A multiple-input, single-output gate that has a "0" output only when all inputs are "0's".

Orientation ratio: As used in this document, the ratio of squareness in the longitudinal direction (direction of orientation of magnetic particles on magnetic tape) to the squareness in the transverse direction where squareness is the ratio of the remanence B_r to saturation B_s.

Overhead: Information added to the data stream, such as parity bits, and cyclic redundancy check characters and synchronization words.

Parallel-mode high-density digital recording: Process of converting a bit stream to parallel bytes of N bits, to be recorded across N tracks on tape.

Parity: The property of oddness or evenness of the number of "1" bits in a word.

Parity channel: A channel added or used to contain bits generated to maintain odd/even parity across all channels for detection of bit errors.

Pattern sensitivity: Vulnerability of a given code to certain patterns of "1" and "0" bits resulting in a higher bit error rate.

Pulse code modulation (PCM) multiplexing: A combination of pulse code modulation with time division multiplexing to produce a single digital signal consisting of a given number of channels.

Permalloy: A magnetic alloy, consisting of iron, nickel,

and small quantities of other metals, used to make magnetic heads.

Permeability: The ratio of magnetic induction (B in gauss) to magnetizing force (H in oersteds) for a given material ($\mu = B/H$).

Perpendicular recording: Recording in which the detected magnetic vector of tape magnetization is perpendicular to the track surface on the tape. Also known as vertical recording.

Phase-locked loop: A circuit containing an oscillator whose output phase and frequency is in synchronization with a reference.

Polarity reversal: A 180° phase shift in signal caused by each stage of amplification. Some codes are polarity sensitive, others are not.

Polynomial error detection: Use of a polynomial expression applied to blocks of data to generate remainders for both input and output data, the comparison of which indicates whether reproduction errors have occurred.

Power spectrum: Signal power graphed as a function of frequency.

Preamble major frame: In image processing format, a tape format element that does not carry data but serves as a pilot tone and filler to maintain bit stream continuity.

Probe head: A head suited for writing on perpendicular media. See also **Perpendicular recording.**

Pseudorandom bit sequence (PRBS): A digital code having the appearance of random bit sequence, but of finite length. It is usually achieved by the use of a feedback shift register to modify sequences or patterns or bits in a predetermined manner or to restore each modified bit patterns to their original sequence. The repeating sequences exhibit many of the statistical properties of uniformly distributed random number sequences: hence, they are called pseudorandom.

Pulse: A transient signal that is usually of short duration. In digital applications, it is of constant amplitude and polarity.

Pulse code: Codes in which groups of pulses/bits represent digits/amplitude.

Pulse code modulation (PCM): Use of a pulse code to record digital data on magnetic tape. (See also fig. G-1.)

Quantization: Process of replacing instantaneous (analog) signal values by the nearest allowed step in level, resulting in a random sequence of instantaneous errors whose magnitudes range from zero to half a quantization level.

Quantization noise: The sequence of quantization errors.

Ramp signal: A test signal that changes linearly with time.

Randomization: A modification of nonreturn to zero (NRZ) encoding in which the bit stream is randomized to reduce dc components before being recorded on tape.

Random noise: Noise caused by a large number of superimposed elementary disturbances, characterized by random occurrences in time and amplitude.

Real time: Operation of a computer on demand as and when required by a user, process, or system interacting with the computer. Also means playback of recorded data at record speed.

Reconstruction: The process of forming the output data stream to be an exact replica of the input data stream in the absence of bit errors.

Redundancy: The fraction of the gross information content of a message that can be eliminated without loss of essential information.

Reluctance: For an element of a magnetic circuit, the magnetomotive force per unit magnetic flux.

Remanence: The magnetic flux density remaining in an element of a magnetic circuit after the removal of the applied magnetomotive force.

Reread: Repetition of signal receiving process to improve syndrome errors. Correction is best performed only after a consistent syndrome has been received.

Return to zero (RZ): A binary digital code using a signal with a positive pulse to indicate a "1" and a negative or zero pulse to indicate "0". The signal level returns to zero during each bit period.

Ring head: A recording head with geometry that is particularly suited for high flux-gathering efficiency.

Rolloff: A gradually increasing loss or attenuation with change of frequency beyond the substantially flat portion of the amplitude-frequency response characteristic of a system.

Run-length limitation: A safeguard to prevent the data stream from containing long uninterrupted strings of "1's" or "0's".

Sampling theorem: The statement that $2f$ equally spaced samples per second completely characterize a signal that is band limited at frequency f.

Saturation: A condition in which increasing field strength H provides no increases in remanence B.

Self-clocking code: A binary digital code that permits intrinsic timing of pulses for both "0" and "1" bits, such as a biphase code.

Sendust: A magnetic alloy with a high coercivity used in the construction of pole tips for recorder heads.

Sensitivity: The ability or tendency of a circuit or device to respond to a low-level applied stimulus.

Sensor: A device directly responsive to the value of a measured quantity.

Servo: In general, a self-correcting, closed-loop control system. In magnetic tape recording, a speed correcting, closed-loop control system that generates an

error signal when tape is not moving at the speed selected. Recorder can servo from either a built-in tachometer or a signal recorded on tape.

Signal bits: Data stream bits other than check bits and synchronization word bits.

Signal-to-noise ratio (SNR): The ratio of the power output of a given signal to the noise power in a given bandwidth without the signal.

Simultaneous bit errors: The occurrence of two isolated bit errors in the same bit column within the same data block.

Skew: In parallel data recording, the tendency for pulses from the same word to fail to appear simultaneously at the reproduce gap.

Slip agent: A compound such as ultrafine silica that is dusted on films to facilitate winding and unwinding.

Software: Computer programs and associated documentation defining the operation of a data processing system.

Source codes: Codes that are inputs to a given encoding system.

Split-phase encoding: Double-frequency encoding similar to biphase, level, in which a transition always occurs at the center of every bit period.

Sputtering: A process allowing fabrication of flexible magnetic disks by deposition of magnetic media on a polymer substrate.

Staircase ramp: A test pattern in which a data word is repeated a fixed number of times per ramp step, then incremented by one for the next step, and so on, to the end of a major frame.

Switching field: A magnetizing field of such strength that when applied to a specimen magnetized to saturation in the opposite direction will cause the specimen to become saturated in the direction of the applied field.

Switching field distribution (SFD): The coercivity range of individual particles that determines the length of a transition zone when switching fields are applied by the head.

Symptom: An element of the syndrome vector, the value of which is "0" unless a parity error has been detected.

Synchronization words: Channel words allowing deskew of channel data and reconstruction of the data to serial form. Also, words inserted at the beginning of a sequence/frame/block of bits to inform the "interpreter," such as a D/A converter, which bit is the first bit in the sequence.

Synchronizer: A device used at a receiving site to achieve coherence with a transmitted signal.

Synchronizing signal: A signal used to synchronize another signal, usually in frequency.

Synchronous clock: The timing source in a synchronous computer.

Synchronous computer: A computer whose operations are timed by single-frequency clock signals.

Synchronous inputs: In a computer flip-flop circuit, inputs that accept pulses only at the command of the clock.

Synchronous transmission: Data transmission in which synchronization of characters is controlled by timing signals generated at the sending and receiving stations.

Synchronizing pulse: A pulse used to control the frequency of an oscillator or a system to maintain lock with a reference.

Syndrome: A vector generated by taking the XOR sum of a set of parity checks generated on receive with a set of parity checks generated on transmit; a symptom of an error.

Thermal noise: Electronic noise due to thermal excitation of electrons in conductors and semiconductors.

Thin-film heads: Heads that are constructed using standard thin-film deposition and lithography techniques; for example, sputtering and ion etching.

Three position modulation (3PM): A coding scheme employed by Thorn EMI Technology Incorporated in which data are grouped into three-bit bytes. Each byte is divided into six periods. A lookup table is used to determine the location of transitions, not bits, within the six periods to represent each byte.

Time base correction (TBC): Methods employed to reduce time base errors in analog recordings.

Time base errors (TBE's): Errors introduced because of short-term speed inaccuracy.

Time base expansion: Playback at reduced tape speed.

Time division multiplexing: The process of interleaving in time two or more digital signals for transmission over a common channel.

Track density: Number of bits stored in a track per unit length.

Tracks: Portions of a tape accessible to given head positions.

Transducer: Any device that converts energy from one form to another. In high-density digital recording, a magnetic recording head assembly that converts magnetic pulses into corresponding voltage or current pulses, or vice versa.

Transfer function: A mathematical function that relates the input to the output of a system.

Transition density: On a magnetic tape, the number of available magnetic transitions per unit length of tape.

Transitions: Changes from one circuit condition to the other; e.g., change from mark to space ("1's" to "0's") or from north to south, and vice versa.

Tunnel erase: A coil contained in a head structure designed for perpendicular recording, providing erasure capability for disks.

Wideband channel: In magnetic recording, a channel that will satisfactorily record and reproduce a signal with an on-tape wavelength of 80 μin.

Wood code: See **Delay modulation (DM) code; Miller code.**

Word: A group of bits, usually of a fixed length, in a given system.

XOR gate: Exclusive OR gate requires both a "0" and a "1" input for a "1" output. Two "0" bits or two "1" bits give a "0" output. A combinatorial logic circuit often used to show whether two inputs are alike or different on a bit-by-bit basis.

Y-phase (Yϕ): Thorn EMI Technology Incorporated's low-rate code. The three-position modulation waveform and the write clock are combined in an exclusive OR gate prior to recording. Upon reproducing, the data are combined with a reproduce clock in an exclusive OR gate to obtain the low-rate transition positions.

Index

ANSI X3B6 Committee, 281, 282, 283, 287
APL. *See* Applied Physics Laboratory
A/D conversion. *See* Analog-to-digital conversion
A/D/A system. *See* Analog-to-digital-to-analog system
Airborne recorder, 7, 9
Aircraft, 3
Aircraft carrier, 3, 10
Alfesil, 261, 274–279
Aliasing, 216
Alternating-disparity code, 109, 112, 116
Aluminum, 63, 271, 272, 273, 275, 279
Ampex Corp., 136, 281, 283, 290
Ampex 79A tape, 96, 97, 98, 99, 100, 253
Ampex 466 tape, 257
Ampex 721 tape, 104, 257, 267
Ampex 786 tape, 72
Ampex 787 tape, 96, 97, 98, 99
Ampex 795 tape, 9, 10, 104
Ampex 797 tape, 202, 210, 212, 244, 247, 253, 257, 273, 276, 278
Ampex 799 tape, 10, 238, 247, 253, 288
Amplifier, 159, 192–193, 215, 217, 220–223, 229
Amplifier noise, 43
Amplitude error, 5, 11
Amplitude stability, 132
Analog channel, 206
Analog headstack, 211
Analog signal, 163
Analog system, 3, 5, 8, 9, 67, 109, 110, 127
Analog tape, 256
Analog-to-digital conversion, 5, 129, 131, 143
Analog-to-digital-to-analog system, 129, 133–135
Analog track, 215, 217
AN/AQH-4(V)2 recording system, 9
AN/AQH-5(V)XD recording system, 9, 10
AND gate, 28, 34
AN/SQR-18 recording system, 8
Antisubmarine warfare, 1, 2, 9, 11, 12
AN/USH-24(V) recorder, 11
AN/USH-31(V) reproducer, 10
AN/USH-32 recording system, 11
Applied Physics Laboratory, 109, 116–117
Asynchronous bit stream, 195, 199, 215
Asynchronous clock, 9
Auxiliary pole, 60, 61

Bandwidth, 2, 3, 5, 15, 17, 69, 78, 81, 83, 103–105, 111, 125, 128, 134, 137, 146–152, 155, 196, 209–213, 232, 266, 276, 281
Baseline gallop, 127, 129, 155
Baseline shift, 112, 117, 132, 151, 152, 155
Bell and Howell, Inc., 11, 281, 283
Bendix Aerospace Corp., 95
Bias recording, 5, 45, 54, 67–68, 81, 152, 291
Biϕ code. *See* Biphase code
Bidirectional operation, 195, 207, 214
Biϕ—L code, 16, 17, 67, 68, 69, 70, 71, 73, 78, 79, 82, 84, 87, 89, 91, 113, 128, 144, 146–147, 200, 237
Biϕ—M code, 16, 17, 113, 128, 129, 136, 144, 147, 237
Biphase code, 16, 17, 113, 115, 144–152, 192, 195, 196, 213, 232, 241, 281, 282, 287
Biϕ—S code, 113, 144, 147, 237
Bit, 5, 13, 14, 25, 26, 27, 33
Bit cell, 18, 19, 20, 21, 127, 136, 138, 140
Bit crowding, 196, 210
Bit error, 165–167, 169, 173, 175, 177, 178, 203
Bit error probability. *See* Bit error rate
Bit error rate, 6, 8–14, 19, 67, 70–73, 76–83, 93–101, 106, 109, 111, 112, 115, 116, 132, 137, 138, 140, 143, 146–155, 166, 188, 202, 206, 207, 212–216, 243–247, 252, 253, 256, 283, 288–290
Bit length, 58
Bit map, 170–177
Bit packing density, 15, 67–71, 73, 74, 77, 81, 82, 83, 95, 103, 109–115, 125, 127, 137, 138, 141–149, 152, 155, 165, 195, 198, 199, 201, 204–214, 247, 253, 255
Bit period, 15, 78
Bit rate, 15, 71, 72, 73, 78, 109, 111, 125, 137, 148, 149, 180, 184, 185, 186, 187, 200, 203, 210, 213, 214, 215, 223, 227, 232, 255, 281
Bit slip, 77, 139–140, 153, 155, 215, 223, 227, 235, 288
Bit stream. *See* Digital stream
Bit stuffing, 113, 141, 199, 202, 203, 204
Bit synchronization, 8, 9, 10, 11, 67, 68, 71, 73, 77, 82, 83, 95, 97, 112, 124, 131, 138, 139, 140, 143, 145, 150, 193, 196, 201, 203, 206, 210, 215, 216, 217, 220, 221, 223, 224, 227, 228, 229, 251, 291
Block code, 74, 111–116, 154, 248
Brown stain, 237, 272
Buffer register, 21, 32, 33, 34, 163, 164, 178, 192, 230
Byte, 25, 143, 196–197

Calibration, 96, 192, 203, 214, 221, 226, 267, 270
Capability factor, 210
Certified tape, 11, 166, 209
Channel synchronization, 218, 219, 223, 225
Check bit, 29, 30, 31, 32, 37, 38, 39, 41
Check byte, 36, 39, 41
Check polynomial, 30
Chief of Naval Operations, 1

Chinese remainder, 28, 29
Clean room, 64, 65, 66
Cleaning, 5, 7, 100, 165, 166, 256, 258, 261–262, 271, 272, 294, 295
Clock, common, 223, 228
Clock recovery, 196
Clock signal, 4, 16, 17, 20
Clock slip, 72, 73, 74–75, 77
Clocked data, 110, 127, 130, 131, 140, 195
Cobalt, 255, 266
Cobalt-chromium film, 49, 57, 58, 61, 62, 63, 64, 65
Code efficiency, 19–21, 30, 149, 155, 198, 208
Coercivity, 43, 45, 46, 49, 51, 56, 58, 255, 256, 262, 264
Column parity. *See* Lateral parity
Compatibility, 1, 2, 96, 142, 146, 178, 179, 201
Composite head, 60, 61
Computer-generated code, 37, 39
Confidence monitoring, 153–154
Constant multiplier circuit, 25, 26
Controls and indicator, 205, 206, 225–226
Correction track. *See* Parity track
Cost, 1, 2, 3, 4, 5, 97, 99, 103, 207, 209
Cross parity. *See* Lateral parity
Crossplay, 2, 3, 5, 70, 150, 152–153, 179, 195, 201, 207, 214, 234, 235, 291
Crystalline anisotropy, 58, 62
Cyclic redundancy check, 13, 20, 36, 38, 141, 202, 204, 206, 208, 213, 214, 249, 249–253

Data accuracy, 36, 37, 38, 39
Data bit, 32, 33, 41
Data capacity, 15
Data channel, 7, 8, 9, 11, 14, 109, 110, 202, 248, 249
Data clock, 32, 33, 34, 196, 200, 202, 205, 216, 223
Data comparator, 174, 178, 221, 224
Data compression, 134, 202
Data density, 196, 198, 201, 208, 212
Data formatting, 179–187, 191, 202
Data integrity, 200
Data polynomial, 30
Data rate, 15, 19, 142, 180–183, 188, 195, 199–203, 206, 210, 211, 232, 238, 239, 255
Data recoverability, 36
Data reliability, 15, 23
Data segment, 156, 157, 160, 161, 163
Data storage system, 5, 15, 19, 39, 143, 187–194
Data string, 27, 28
Data timing. *See* Clocked data
Data track, 116, 142, 163, 179, 216–218, 239
Datatape, Inc., 143, 144, 146, 149, 150, 151, 152, 157, 165, 166, 179, 185, 187
dc response, 73, 74, 75, 77, 116, 127, 128, 139, 291
dc restoration, 81, 82, 139, 150, 151, 152, 213
dc signal, 18, 74, 78, 143, 144, 145, 146, 147, 149, 221
dc-free code, 152, 207, 212, 233, 281
Decision window, 210, 211
Decoder/deskew assembly, 156, 157, 159, 163, 164, 193
Decoding, 14, 16, 20, 21, 32, 34, 74, 76, 164, 167, 174, 179, 223, 225, 239, 241–242
Degaussing, 5, 295–296
Deinterleaver, 167, 169, 173, 178, 192
Delay modulation code, 17, 67–73, 78–81, 85, 87, 89, 91, 111–115, 123–124, 144, 147, 149, 150, 152, 208, 209, 281
Delay modulation—mark code, 8, 9, 10, 195, 196, 210–213
Demagnetization, 43, 54, 58, 62
Density ratio, 137
Department of the Interior, 97
Derandomizer, 76, 153
Design optimization, 43–56
Deskewing, 77, 95, 98, 109, 115, 117, 140–142, 153, 156, 160, 162, 163, 199, 216, 218, 223, 225, 229, 231, 234, 235, 238, 239, 241, 245–249, 251, 288
Diagnostic Retrieval Systems, Inc., 10
Diagnostics, 12, 39, 41
Difference signal, 111, 113, 114, 117–125
Digital array tape recording and reproducing system, 109–111, 117
Digital audio tape, 104
Digital image processing, 143
Digital recording, 4, 8, 10, 109
Digital stream, 9, 11, 14, 19, 20, 25, 26, 27, 72, 75, 76, 78, 96, 115, 143, 148, 151, 156, 195
Digital sum variation, 112, 113, 114, 137, 139
Digital-to-analog conversion, 143
Digitized television, 143
Dipulse response, 60
Direct recording, 4, 5, 9, 10
Disk controller, 38, 39
Disk drive error, 38
Disk storage, 45
Disk system, 36
Distortion, 3
Double-bit error, 28, 31, 34
Double-burst error, 31
Double-density code, 17, 18
Double-frequency clock, 20
Dropout, 3, 5, 6, 10, 11, 14, 21, 71, 72–73, 77, 81, 82, 83, 99, 141, 150, 165, 202, 221–230, 238, 243, 256, 261, 267, 270
Dynamic range, 133

Eddy current, 46
Edge track, 82, 106
Eight-bit processor, 28
Electron microprobe analysis, 259
Electron microscopy, 64
Electronic noise, 8, 11, 15, 19, 55
Emerson Electric, Inc., 9
EMR 1510 spectrum analyzer, 83–92
EMR-Schlumberger, Inc., 150
Encoding, 14, 15, 20, 32, 34, 74, 78, 109, 113, 128, 144–147, 157–162, 166–173, 179, 191, 192, 203, 216–219, 229, 231–235, 238
E-NRZ code, 18, 19, 21, 111, 113, 115, 143–161, 164–179, 188, 191, 192, 210, 211, 287, 290
Environmental condition, 2, 5, 6, 106, 127, 258
Equalization, 139, 192, 193, 201, 203, 206, 211, 212, 220, 221, 223
Error burst, 29, 31, 34–38, 72, 75, 76, 116, 153, 165, 198, 199, 208, 223, 233, 240, 243, 244, 245, 288
Error cluster, 97, 98, 99

Error control system, 39
Error correction, 100, 110, 116, 117, 247–253, 290–291
Error correction circuit, 28, 36, 38, 39, 41
Error correction code, 38, 39, 41, 95, 98, 137, 142, 247–253
Error detection, 35–36, 248, 250, 252, 290
Error detection/correction, 8, 14, 19–25, 29, 81, 97–100, 109, 110, 116–117, 128, 140–142, 164–179, 191–194, 202, 206, 208, 214, 215, 217, 229–230, 231–245
Error erasure mode, 117
Error forcing, 40
Error logging, 40
Error multiplication, 76, 153, 155
Error polynomial, 30, 36
Error recovery, 37
Euclidean division algorithm, 29, 30
Eye pattern, 78, 79, 135, 137, 139, 150, 151, 154, 155, 159, 163, 201, 209

Fabrication, 44, 57, 63, 66
Fairchild Weston Systems, Inc., 231–245, 281, 283, 290
Fanout, 180, 184, 199, 202, 203, 205, 206, 209, 237
Fault isolation, 12
Feedback loop, 40, 53
γ-Fe_2O_3 tape, 45, 57, 215, 255, 266
Ferrite core, 45, 46, 61
Ferrite head, 43, 49, 51, 55, 100, 105, 106, 215, 219, 220, 221, 275, 276, 277
Film thickness, 62, 65
Fire code, 36, 37, 39
First in, first out memory, 32, 192, 193, 218, 219, 223, 225
Floppy disk, 60, 61, 62–66
Fluctuation noise, 135
Flutter, 3, 4, 5, 19, 193
Flux transition. *See* Magnetization transition
Four-bit error, 28
Fourier transform, 2, 83
Frame, 20, 21, 23, 93, 96, 156, 157, 160, 161
Frame synchronization, 38, 39, 75, 77, 93, 95, 115, 216, 219, 226, 231, 240, 241
FM recording, 2, 4, 5, 8, 9, 10, 11, 127, 132, 134, 204, 206, 232, 237
Frequency response, 51, 54, 59, 78, 197, 210, 211, 223, 269, 276, 278
Frequency synthesizer, 203, 204, 227
Friction, 259–260, 294
Fuji H621 tape, 104, 105, 106, 257

GSA. *See* General Services Administration
GSFC. *See* Goddard Space Flight Center
Gain control, 221, 222, 270
Gap corner saturation, 45
Gap depth, 44, 47, 276
Gap edge saturation, 43
Gap edge straightness, 51
Gap field, 43, 45, 47, 49, 58
Gap length, 5, 6, 70, 196, 197, 208, 291
Gap loss, 43, 50, 51, 211
Gap null frequency, 51
Gap reluctance, 44
Gap width, 44, 45, 46, 47, 48, 49, 50, 255
Gate enablement, 33, 34
Gaussian noise, 111, 112, 119, 121, 133, 135
General Services Administration, 3, 6, 7, 97
Generator polynomial, 29–40, 208, 250
Glass, 262, 271, 275, 276, 277, 278
Goddard Space Flight Center, 93, 96, 98, 100
Gold, 54
Grain size, 58
Group code, 18, 19, 21, 114
Guard band, 104, 105

Hamming code, 33, 34
Hardness, 271, 274, 275, 279, 294
Hardware, 3, 5, 10, 12, 23, 39, 40, 41
Harmonic distortion, 69, 70, 296
Haystack Observatory, 103
HDDR™ code, 16
HDDR™ II code, 17, 20, 21, 23
Head assembly, 43–56, 157, 158, 162, 181, 183, 186, 191
Head contour, 106
Head current, 50, 51, 195, 267
Head driver, 217, 218–219, 229
Head flux, 49
Head life, 100, 101, 106, 271–279
Head noise, 43, 54–56, 211
Head output. *See* Output signal
Head pitch, 104
Head placement, 104, 105
Head saturation, 60
Head stack, 95, 104, 105, 107, 131
Head-tape contact, 14, 43, 45, 106, 215, 237, 275, 278, 293, 294
Head-tape interface, 104, 105, 106, 135, 202, 247, 257, 278, 287
Head-tape performance, 106, 107
Head/tape separation, 44, 50, 293, 294
Head-track registration, 103, 104, 106, 130, 131
Head wear, 43, 48, 271–279, 293, 294
Hedeman code, 81
Helicopter, 3, 9
Hexagonal close-packed crystal, 62
High-coercivity tape, 104
High-density tape recorder, 93–101, 151, 154, 156, 157, 158, 165, 166, 171, 174, 179, 180, 184, 187, 215–230, 236, 237, 247
High-frequency noise, 211
High-frequency response, 73, 127, 129, 132, 135
High-resolution film recording, 94
Honeywell Model 96 Recorder, 9, 93, 103, 105, 215–230, 247, 268, 270
HP–85 computer, 50
Humidity, 106, 258, 267, 295
Hunt head, 54
Hysteresis, 264, 266

IBM, Inc., 18, 19, 57, 146
IPF. *See* Image Processing Facility
IRIG. *See* Inter-Range Instrumentation Group
IRIG A time code, 204
IRIG head, 207, 214, 216, 237

IRIG recorder, 255, 256
IRIG standard, 81, 93, 203
IRIG Standard 106–77, 282
IRIG Standard 106–80, 3, 81, 200, 210, 212, 269, 282
Illinois Institute of Technology Research Institute, 257, 265
Image Processing Facility, 93–101
Impedance, 55, 71
Inductance, 55
Input timing, 157, 158, 161–162, 163, 218
Instrumentation recording, 231, 281, 286, 293
Instrumentation tape, 81, 97, 104, 105, 106, 194, 195, 252
Integrated circuit, 21
Interface, 1, 2, 97, 99, 109, 117, 202, 203
Interference intersymbol, 70, 73, 125, 152
Interferometry, 103–107, 294
Interleaving, 36, 95, 167, 168, 171, 172, 173, 177, 178, 191, 240
Inter-Range Instrumentation Group, 2, 3, 67, 95, 200, 231, 281
Inverted bit, 28
Ion microprobe analysis, 259
Isomax tape, 55, 56

Jitter, 21, 127, 132, 133, 135, 215

Karlqvist approximation, 48, 49

Ladder network, 222
LAMPS MK–I (AN/SQR–17) system, 7, 8
Landsat D system, 253
Latch, 25, 26, 41, 225
Lateral parity, 2, 14, 16, 27, 28, 170, 208, 241, 249, 250
Light-emitting diode, 226, 236–237
Linear sequential circuit, 25, 26, 27
Linear shift register, 26
Lockheed Electronics Co., Inc., 16
Logic hardware, 98
Longitudinal parity, 14, 238, 240
Longitudinal recording, 15, 57, 58, 59, 103, 105, 109, 127, 195–214
Lorentz micrograph, 62, 63
Low-disparity code, 109, 111, 113, 116
Low-frequency response, 127, 128, 132
Lubricant, 258

Magnetic disk, 36
Magnetic film, 63, 65
MTU. *See* System 600 Magnetic Tape Unit
Magnetization, 15, 262–267
Magnetization transition, 4, 58, 59, 74, 77, 78, 136, 138, 162, 195, 207, 208
Magnetomotive force, 44, 49
Magnetoresistive head, 54, 55, 61
Magnetostriction, 46, 47, 55
Manchester code, 111, 113
MnZn ferrite, 45, 46
Mark III A VLBI system, 103–107
Martin Marietta Corp., 93, 96, 97, 98, 247, 283, 387
Master bit rate, 225
Master channel, 148
Mean time between failure, 154
Mean time to repair, 14, 154
Meissner trap, 66
Memory circuit. *See* Latch
Metal head, 43, 46
Metal-in-gap head, 43, 46, 48
Methyl ethyl ketone, 258, 264
M–14 recorder, 11
Microdiagnostics. *See* Diagnostics
Microgap head, 215
MIL–STD–1610, 1, 3, 4, 5, 8, 9, 11, 12
Miller code, 8, 9, 10, 17, 19, 20, 21, 67, 71, 113, 128, 134, 135, 136, 137, 139, 142, 144, 145, 147, 148, 149, 151, 153
Miller^2 code, 18, 19, 20, 23, 73, 78–81, 85, 88, 90, 92, 113, 115, 128, 132, 133, 136–140, 142, 147, 148, 149, 153, 210, 211
Miscorrection, 28, 34
Miscorrection probability, 36, 37, 38
Misdetection, 28, 31, 35
Modular system, 3, 109–110, 203, 215–230
Modulo 2 addition, 26, 117, 238, 241, 291
Multiplexing, 7, 8, 30, 32, 179, 184, 185, 193, 216, 219, 235, 236, 237
Multitrack recording, 21, 131, 216
Mylar, 191, 257, 262, 264, 265, 269

National Security Agency, 245
Naval Air Development Center, 2, 9
Nibble, 25
NiFe film, 46, 61
Noise spectrum, 69, 78, 80, 289
Nonreturn-to-zero code, 16, 17, 18, 95, 127–129, 132, 144–152, 195, 198, 210, 212, 232, 281, 288, 291
NRZ—I code, 144, 146
NRZ—L code, 16, 17, 67–84, 86, 88, 90, 109–115, 128, 144, 145, 152, 156–164, 167, 168, 171, 172, 173, 177–186, 195, 196, 197, 216, 228, 235, 237
NRZ—M code, 16, 17, 73, 74, 128, 136, 137, 144, 145–146, 237
NRZ—S code, 73, 74, 144, 146, 237
Normalized frequency, 79, 84–92
Null, output, 59, 117
Nyquist frequency, 137, 138
Nyquist packing density, 147, 208
Nyquist rate, 111, 113, 147, 149

Oligimer, 63, 64
OR gate, 16, 22, 200
Oscilloscope, 68, 154, 155, 260, 262–268, 270
Output data, 6, 21, 77
Output signal, 49, 59, 197, 210–211, 220–221, 269
Output spectrum, 76, 78
Output timing clock, 157, 159, 160–161, 164
Overall check, 28, 31
Overhead, 13, 14, 16, 17, 19, 77, 95, 111, 137, 138, 141–142, 148, 155, 198, 206, 207, 214, 218, 226, 233, 234, 245, 247, 249, 250, 252, 289, 291
Oxide coating, 6, 9, 10, 12, 165

Parallel stream, 199, 203, 216
Parallel recording, 11, 14, 16, 77, 81, 143, 154–194, 213, 216–218, 228, 231, 233, 235, 236, 237, 250, 287, 288, 291
Parallel-to-serial conversion, 132, 204, 216, 248
Parametric model, 6
Parity bit, 13, 16, 20, 21, 25, 26, 27, 40, 41, 77, 95, 98, 146, 148, 156, 157, 164, 166, 216
Parity channel, 21, 202, 209
Parity check, 26, 27, 31, 41, 116, 146, 153, 154, 157, 163, 173, 191, 194, 225, 229
Parity error, 165, 167, 169, 170, 173, 175, 176, 178, 191, 193, 203, 226
Parity function, 27
Parity prediction circuit, 41
Parity stripper, 173, 174, 178
Parity track, 21, 23, 116, 141, 166–176, 179, 191, 202, 208, 229, 239, 245, 253, 291
Parity tree, 25, 41
Patent, 292
Pattern compatible code, 287, 290
Pattern sensitivity, 35, 36, 37, 39, 117, 123, 136, 138–139, 151–152, 216, 289
Performance, 3, 45, 59–60, 93–101, 150, 154, 237–238, 242–245, 256, 291
Permalloy, 48, 54, 57, 58, 60, 62, 65
Permeability, 44, 47
Perpendicular recording, 57–66
Phase equalization, 69
Phase-locked loop, 5, 9, 140, 203, 215, 221, 227
Phase response, 132
PI–214 recorder, 7
Playback, 95, 109, 116, 117, 139, 142, 281
Polarity sensitivity, 138, 140, 289
Pole thickness, 47, 49
Pole tip erosion, 48
Pole tip saturation, 58
Pole winding, 49, 50
Polished tape, 82
Polyamide, 63
Polyethylene terephthalate, 62–66
Polyimide, 63
Polynomial, 29, 30, 31, 232
Portable system, 109
Power failure, 36, 41
Power spectrum, 78, 79, 80, 83–92, 95, 149
Preamplifier, 159, 162, 163, 192, 193, 220
Precision Echo, Inc., 7, 9
Precision Instruments, Inc., 7
Primitive polynomial, 35
Probe head, 57, 58, 60
Probe write/ring read head, 61
Procurement, 3, 6, 7
Professional video tape, 104
Profilometry, 294
Prototype, 105, 107
Provisioning, 3
Pseudorandom noise, 2, 18, 75–80, 83–85, 88–90, 95, 97, 112, 115, 216, 218, 223, 225, 248, 251, 287, 291
P–3C aircraft, 9
Pulse code modulation, 67, 70, 71, 74, 83–92, 93, 111, 127, 215, 236
PCM tape, 255, 256

Quadra-Phase code, 81
Quality control, 11
Quantization error, 134, 135
Quantization level, 129, 134, 135
Quantization noise, 133, 134–136
Quantization signal, 5, 134, 135

Rack, 230, 242
Radar signal analysis, 143
Ramp, 76, 78, 83, 86–88, 90–92, 96, 97, 99, 100
Random access memory, 235
Randomization, 18, 75–77, 96, 97, 100, 146, 232–233, 241, 248, 251, 281
R-NRZ code, 18–21, 144–150, 153, 155, 198, 200, 209, 212, 213, 282, 287, 290
R-NRZ—L code, 67, 71–83, 86, 90, 200
Range Commanders Council. *See* Inter-Range Instrumentation Group
RCC Telemetry Group, 281, 282
RD–420 recorder, 7, 8, 9
Read-back mode, 60
Read head, 49, 54
Read-only memory, 77
Readout, 135
Real time monitoring, 66
Receive polynomial, 30
Reciprocal polynomial, 35
Record head, 48, 51, 203, 217, 219, 229
Record level, 69–70, 267
Record mode, 43–45, 162, 201
Record/reproduce channel, 210
Record/reproduce head, 46, 191, 192, 236
Record/reproduce track, 148, 179, 185, 186
Record time, 180–186, 283
Record wavelength, 45, 50, 54, 196, 197, 208, 255, 268
Record zone, 45
Redundancy, 30, 37, 104, 248, 290
Reed-Solomon code, 36, 38, 39, 238
Reformatting, 8
Relative bandwidth, 111, 113, 114
Reluctance, 44
Remainder, 28, 29, 30, 208, 250
Remanence, 43, 50, 56
Replay, 2, 3, 7, 8, 9
Reproduce clock, 200
Reproduce head, 15, 16, 45, 49, 50, 51, 211, 217, 219, 220, 221, 227
Reproduce level, 69, 71
Reproduce mode, 47, 162
Reproduce signal, 18
Resistance, dc, 55
Response, 8
Return-to-bias code, 129, 145
Return-to-zero code, 16, 17, 121–122, 124, 129, 144–145
Ring head, 43, 49, 57, 58, 60, 61
Ring write/ring read head, 61

Roller, 65
Rolloff, 78, 104, 129, 135, 196, 278
Row check, 27, 28
Royal Australian Air Force, 9
Run-length-limited code, 145, 146, 147

Sabre recorder, 239
Sampling theorem, 129
Sapphire, 48, 55
Satellite communications, 143
Saturation, 46, 47, 55, 58
Scanning electron microscopy, 62, 63, 257, 261
Sealing, 5
Sector, 38, 39
Security, 18
Self-checking code, 38, 39, 40, 41
Self-clocking code, 4, 8, 17, 128, 129, 138, 196
Self-demagnetization, 58, 59, 255
Self-synchronization, 77
Sendust, 45, 46, 47, 51, 55, 56, 275
SE9000 recorder, 203–206
Sensor data, 1, 2, 3, 94
Separation loss, 44, 50, 61
Separation/wavelength ratio, 58, 61
Serial bit stream, 93–97, 160–164, 196, 197, 199, 203, 213, 241, 247, 289
Serial image processing, 93
Serial recording, 67, 77–82, 213, 231, 233, 235, 291
Serial-to-parallel conversion, 130, 131, 202, 204, 248
Servomechanism, 2, 4, 5, 8, 10, 60, 162, 163, 189, 191, 227, 228
Shift register, 20, 25, 26, 29–35, 37, 40, 41, 75, 76, 77, 153, 232, 281, 291
Shim, 59, 60, 61
Shipping, 5
Shore station, 3
SH–3H helicopter, 9
Sideband, 2
Signal level, 43, 48, 49, 50, 51, 54, 55, 56, 58
Signal monitoring, 12, 228–229
Signal-to-noise ratio, 2, 4, 11, 15, 19, 56, 59, 70–72, 76, 78, 81, 105, 106, 127, 129, 133, 134, 136, 138, 140, 149, 150, 152, 155, 211, 212, 215, 289, 290
Silica, 63
Simulation, 83
Simultaneous error, 2, 166, 167, 173, 252
Sine wave signal, 51, 83
Single-bit error, 27, 28, 31, 32, 33, 34, 290
Single-burst error, 31
Single-symbol error, 36
Skew, 3, 4, 16, 95, 131, 140, 164, 216, 223
Slip agent, 63
SNR degradation, 106
Sonar, tactical towed array, 8
Software, 10, 39, 41
Sony V16 tape, 104, 106
Source data, 6
Speedup, 2
Spin Physics, Inc., 272, 273, 274
Spinalloy™, 271–274
Split-phase encoding. *See* Biϕ—L code
Sputtering, 57, 62–66
Square wave signal, 51
Standardization, 3
Storage register, 157
Storage system. *See* Data storage system
Submarine, 3
Subsequent cycle erasure, 44
Substrate, 50, 54
Surface vessel, 3
Symbol, 36, 73
Symptom, 27
Synchronization, 8, 11, 20, 93
Synchronization bit, 155
Synchronization pulse, 160, 161, 162
Synchronization track, 155
Synchronization word, 20, 21, 74, 77, 95, 130–132, 140, 141, 148, 156, 157, 160–164, 173, 192, 193, 198–202, 206, 214, 233, 234, 235, 236, 245, 248, 249, 288
Synchronous clock, 26, 145, 155, 158, 162, 171, 173, 174, 178, 182, 184, 185, 187
Syndrome, 27, 28, 32, 33, 34, 38, 39, 116
System 600 Magnetic Tape Unit, 188–194

THIC. *See* Tape Head Interface Committee
Tape abrasivity, 105, 106, 256–261, 274, 275, 293
Tape coating resistivity, 269
Tape damage, 6, 7
Tape drive, 14
Tape economy, 195
Tape format, 1
Tape handling, 3, 187, 243
Tape-head alignment, 219, 293
Tape Head Interface Committee, 238, 243, 281, 282, 283, 286, 287
Tape-head performance, 95
Tape imperfection, 21
Tape life, 7
Tape Recorder Steering Group, 1, 3
Tape speed, 14, 67, 70, 71, 78, 79, 81, 96, 99, 109, 133, 153, 180, 184, 188, 195, 196, 199, 201, 203, 205, 206, 208, 215, 220, 221, 223, 226, 227, 228, 270, 271, 272, 273, 274, 275, 278, 279, 287, 288, 289
Tape surface, 43
Tape tension, 100, 107, 189, 259, 260, 275, 293, 294
Tape thickness, 48, 104, 257
Tape track, 4, 8, 9, 95, 99
Tape transport, 7, 103, 133, 157, 158, 162–163, 188–191, 203, 205, 215, 217, 219, 223, 227, 235, 242, 243, 260, 268, 276, 295
Tape wear, 97
Tape width, 6, 188
Technical manual, 3
Telemetry data, 67, 81, 93, 281
Temperature, 55, 107, 258, 267, 295
Temperature coefficient of resistance, 55
Test configuration, 83
Testing, acceptance, 96
Thermal noise, 55
Thin film, 48–49, 58–59

Thin film head, 43, 46, 47
Thorn EMI Technology, Inc., 207, 283, 290
Three-bit error, 28, 31, 34
3M892 tape, 104
3M5198 tape, 104, 106, 257
Three-position modulation code, 21, 81, 111, 114, 195–214
Throughput rate, 148, 179–187, 195
Time base correction, 4, 5
Time base error, 131, 132, 133
Time base stability, 143, 144, 145
Track clock, 235
Track density, 15, 291
Track spacing, 99, 104
Track width, 67, 77, 81, 103, 104, 105, 106, 270
Transducer, 15
Transistor-to-transistor logic, 206, 219, 226, 228
Transition. *See* Magnetization transition
Transition density, 49, 58, 59, 61, 103, 104, 137, 138, 146, 150, 151, 155, 196, 197, 198, 202, 207, 208, 211, 213, 288
Transmit polynomial, 30
Troubleshooting, 221
Tunnel erase, 60, 61

Ultrasil™, 274–278
U.S. Navy, 1, 5, 7, 9, 12
Upper bandedge, 83, 208, 210, 211, 213
Utility function, 282, 284–286

Vacuum video tape, 104
Value function, 284–291
Vertical media, 43, 49
Vertical parity. *See* Lateral parity
Vertical pole head, 43, 49, 50
Vibration, 3
Video display, 10
Video home system, 104, 105, 107
Video word, 96
Videocassette recorder, 103, 105
Voice recording, 4, 8, 9
Voltage level, 16

White noise, 83, 134
Wideband recorder, 5, 8, 67–92, 129–132, 134, 152, 207, 255, 291
Wideband II recorder, 8, 93, 203, 204, 210, 211
Winchester media, 38
Winding, 7, 63, 65, 66, 188
Wood code, 13, 17
Wrapping, 5
Write clock, 200, 208

XOR gate, 25, 26, 28, 30, 39, 77
X-ray diffraction, 62
X-ray interferometry, 143

Yoke head, 43, 50, 54, 55
Yϕ code, 200, 206, 213, 214

Zero-disparity code, 111, 112, 113, 116

1. Report No. NASA RP-1111	2. Government Accession No.	3. Recipient's Catalog No.
4. Title and Subtitle HIGH-DENSITY DIGITAL RECORDING		5. Report Date September 1985
		6. Performing Organization Code TX
7. Author(s) Ford Kalil and Al Buschman,* editors		8. Performing Organization Report No.
9. Performing Organization Name and Address Tracking and Data Relay Satellite Systems Office of Space Tracking and Data Systems		10. Work Unit No.
		11. Contract or Grant No.
12. Sponsoring Agency Name and Address National Aeronautics and Space Administration Washington, D.C. 20546		13. Type of Report and Period Covered Reference Publication
		14. Sponsoring Agency Code

15. Supplementary Notes *Naval Intelligence Support Center

This book contains technical papers presented at meetings of the Tape Head Interface Committee (THIC, Inc.), a professional society consisting of both users and manufacturers. Its primary purpose is to advance the technology of data storage design.

16. Abstract

This book deals with the problems associated with high-density digital recording (HDDR). Chapters 1, 6, 7, 8, and 9 were written by five independent users of HDDR systems. Their problems, solutions, and insights are provided as guidance for other users of HDDR systems. Chapter 2 is a review of various pulse code modulation coding techniques. Chapter 3 provides an introduction to error detection and correction. Head optimization theory and perpendicular recording are covered in chapters 4 and 5, respectively.

Competitive tape recorder manufacturers apply all of the above theories and techniques and present their offerings in chapters 10 to 15. Appendixes A and B address tape. The former presents a manufacturer's thoughts, and the latter shows results of an independent evaluation of magnetic tape for a NASA space application. Appendix C presents three head manufacturers' efforts toward long life heads, with Appendix E giving guidance for the care and handling of magnetic heads. Appendix D presents the methodology used by the HDDR Users Subcommittee of THIC to evaluate parallel HDDR systems.

This book should be read by anyone interested in high-density recording. The recorder can be tailored to the user's needs.

17. Key Words (Suggested by Author(s))	18. Distribution Statement
Bit error rates, Bit packing density, Error detection and correction, Head theory, High-density digital recording, Perpendicular or vertical recording, Pulse code modulation coding, Systems evaluation criteria, Tape evaluation	Unclassified—Unlimited Subject category 33

19. Security Classif. (of this report)	20. Security Classif. (of this page)	21. No. of Pages	22. Price
Unclassified	Unclassified	320	

N-305

☆U.S. GOVERNMENT PRINTING OFFICE: 1985 489 506 42147

B. INDEX OF INFRARED SOURCE POSITIONS

The *Index of Infrared Source Positions* gives the position of infrared sources listed alphabetically by source name. Thus, the celestial position of an infrared source can be found, and the source quickly located in the main Catalog.

The "POS REF" column is left blank when the position of the observation was given in the original reference. If the source position was not given by the original authors, which is true in a large number of cases (primarily well known visible sources), a supplementary position was obtained by the editors from visible star catalogs, or from references listed in the Bibliography, and the reference is listed in the "POS REF" column (see abbreviations below). If the source position had to be determined by the editors from source maps or other non-tabular material in the article, the term "ED" (meaning "editors") is listed as the position reference. The six-digit bibliographic reference number is given when the position was obtained from another publication contained in the Infrared Astronomical Data Base.

Supplementary positional references frequently used in the Index include:

AFGL	Air Force Geophysics Laboratory Four-Color Sky Survey (760913, 770706)
AS	Mount Wilson Additional Stars (509901)
CSI	Catalogue of Stellar Identifications - 1979 (719902)
3CR	Third Cambridge Revised Catalog
ED	Editors
GCVS	General Catalogue of Variable Stars (699901)
IC	Index Catalogue (958901)
IRC	Caltech Two-micron Sky Survey (690001)
MCG	Morphological Catalog of Galaxies
MWC	Mount Wilson Catalog (339901, 439901, 499901)
P-K	Catalogue of Galactic Planetary Nebulae (679901)
RA42	Master List of Radio Sources (769905)
RNGC	Revised New General Catalogue (739906)
YALE	Yale Trigonometric Parallax Catalog (639902)
UGC	Uppsala Galaxy Catalog (739908)

NAME	RA (1950) h m s	DEC ° ′ ″	POS REF
+40 IR1	20 18 57.6	+41 11 31	ED
+40 IR2	20 18 34.4	+41 10 29	"
AB 9	12 46 28.7	+37 46 50	809908
AB 78	12 57 26.7	+34 39 31	
AB 133	13 04 48.0	+34 40 24	
ABELL 78	21 33 24	+31 28	P–K
ABELL 78 9"E	21 33 25	+31 28	ED
ABELL 78 9"W	21 33 23	+31 28	"
ADS 4209 IRS2	5 33 55.4	− 6 47 27	
ADS 5165 IRS2	6 29 22.1	+ 5 03 49	
ADS 5165 IRS3	6 29 13.1	+ 4 59 20	
ADS 6033 IRS1	7 21 09.2	−25 38 51	
ADS 6033 IRS2	7 21 03.8	−25 39 36	
AFCRL IRS	20 27 34	+40 01 54	
AFCRL809−2992	"	"	730703
AFGL 2S	0 00 14	+73 43 30	
AFGL 3S	0 00 15	+24 37 12	
AFGL 4S	0 00 20	+58 17 30	
AFGL 5	0 00 42	+55 25 06	
AFGL 7	0 01 13	+66 25 18	
AFGL 8	0 01 54	+39 49 42	
AFGL 9	0 01 59	+41 50 36	
AFGL 12	0 03 40	+69 46 24	
AFGL 13	0 03 54	+26 46 48	
AFGL 14	0 04 15	+42 49 12	
AFGL 17	0 05 11	−25 45 36	
AFGL 18	0 05 53	−17 51 54	
AFGL 20	0 06 14	+33 35 12	
AFGL 21	0 06 28	+58 52 42	
AFGL 22	0 06 59	+63 40 24	
AFGL 24	0 07 38	+54 36 36	
AFGL 25S	0 07 42	+38 09 06	
AFGL 26S	0 07 45	+33 23 00	
AFGL 27	0 07 49	+28 21 54	
AFGL 28	0 08 07	+31 58 06	
AFGL 29	0 08 23	−18 51 24	
AFGL 30S	0 09 07	+27 57 18	
AFGL 31S	0 09 11	− 6 17 48	
AFGL 32	0 09 28	−24 53 24	
AFGL 33S	0 09 33	+28 08 00	
AFGL 34S	0 10 04	+24 52 30	
AFGL 35S	0 11 03	+73 06 00	
AFGL 37	0 11 56	− 8 03 48	
AFGL 38	0 12 01	−19 12 12	
AFGL 39S	0 12 44	+60 57 18	
AFGL 40	0 12 54	−32 19 12	
AFGL 41	0 14 03	+49 11 30	
AFGL 42	0 14 07	+ 1 36 12	
AFGL 43	0 14 18	+ 9 59 00	
AFGL 44S	0 14 32	+33 20 54	
AFGL 45	0 14 26	+74 20 12	
AFGL 46S	0 15 01	+33 30 48	
AFGL 47	0 15 44	+16 04 54	
AFGL 48	0 16 50	− 9 05 42	
AFGL 50	0 17 14	+44 25 24	
AFGL 53	0 19 15	−20 19 42	
AFGL 54S	0 19 47	+53 18 54	
AFGL 55	0 19 35	+58 55 36	
AFGL 56	0 20 30	+38 27 54	
AFGL 57	0 20 21	+55 31 12	
AFGL 58S	0 20 30	−16 16 54	
AFGL 59	0 21 07	+38 18 12	
AFGL 60	0 22 11	+69 52 06	
AFGL 62	0 22 26	+47 23 00	
AFGL 63S	0 22 32	+48 33 42	
AFGL 64	0 23 46	−42 37 48	
AFGL 66	0 24 26	− 6 54 54	
AFGL 67	0 24 29	+69 21 24	
AFGL 68	0 24 49	+35 19 06	
AFGL 69S	0 25 12	−36 03 18	
AFGL 70	0 25 15	−33 17 00	
AFGL 71	0 25 27	+17 37 18	
AFGL 72	0 25 29	− 4 14 18	
AFGL 73	0 26 07	+48 08 54	
AFGL 74S	0 27 05	+57 00 00	
AFGL 75	0 27 24	− 4 15 24	
AFGL 76	0 27 21	+82 20 18	
AFGL 79S	0 28 23	+76 18 12	
AFGL 82	0 29 39	+25 45 36	
AFGL 85	0 32 57	−11 46 00	
AFGL 86S	0 33 00	+70 15 00	
AFGL 87S	0 33 30	−14 44 54	
AFGL 88	0 33 57	+48 40 24	
AFGL 89	0 34 03	+44 12 12	
AFGL 90	0 34 27	+53 26 06	
AFGL 91S	0 35 24	+68 19 00	
AFGL 92	0 36 11	+59 24 42	
AFGL 94	0 36 26	+30 35 12	
AFGL 95S	0 36 28	+49 04 30	
AFGL 96	0 36 55	+37 56 30	
AFGL 97S	0 36 59	+71 47 48	
AFGL 99	0 37 31	+59 12 42	
AFGL 100	0 37 42	+56 16 12	
AFGL 101S	0 37 49	+36 55 42	
AFGL 103S	0 38 07	− 3 57 12	
AFGL 104	0 39 59	+41 00 30	
AFGL 106	0 41 05	−18 17 18	
AFGL 107	0 42 29	+68 55 36	
AFGL 108	0 43 55	+15 12 24	
AFGL 108	0 43 55.7	+15 12 12	
AFGL 109	0 44 53	+32 25 24	
AFGL 110S	0 45 31	+ 8 24 24	
AFGL 111	0 46 05.1	+ 7 18 48	
AFGL 111	0 46 11	+ 7 19 06	
AFGL 112S	0 46 13	+57 31 30	
AFGL 113	0 46 18.9	+56 48 10	
AFGL 113	0 46 30	+56 46 00	
AFGL 114S	0 46 56	+64 27 12	
AFGL 115	0 47 25	−16 45 00	
AFGL 116	0 48 22	+62 38 54	
AFGL 117	0 48 25	+61 32 54	
AFGL 119S	0 49 06	+56 17 00	
AFGL 120	0 49 01.8	+59 18 06	
AFGL 120	0 49 21	+59 25 54	
AFGL 121	0 49 53	+69 41 18	
AFGL 122	0 49 53	+47 08 36	
AFGL 122	0 49 55	+47 08 18	
AFGL 123	0 50 25	− 1 25 30	
AFGL 123	0 50 27.0	− 1 24 56	
AFGL 124	0 50 26	+17 15 42	
AFGL 125S	0 50 48	+52 23 18	
AFGL 126	0 50 56	+ 6 33 54	
AFGL 127	0 52 00	+48 25 18	
AFGL 127	0 52 14.0	+48 24 29	
AFGL 128	0 52 06	+58 42 00	
AFGL 129	0 52 31	+24 16 48	
AFGL 129	0 52 33.8	+24 17 12	
AFGL 130S	0 52 45	−23 50 00	
AFGL 131S	0 53 00	− 7 34 36	
AFGL 132	0 53 13.8	+57 43 35	
AFGL 132	0 53 28	+57 43 30	
AFGL 133	0 53 41	+60 27 42	
AFGL 134	0 53 53	+48 26 12	
AFGL 135	0 53 57	+58 53 36	
AFGL 136	0 54 24	+23 09 18	
AFGL 137	0 54 32	+58 09 12	
AFGL 139S	0 56 58	+32 38 54	
AFGL 140S	0 56 59	− 8 48 42	
AFGL 141	0 57 41	+56 21 12	
AFGL 143	0 57 59	− 1 57 00	
AFGL 143	0 58 07.2	− 1 55 40	
AFGL 144	0 58 39	+29 39 54	
AFGL 146S	0 59 33	+61 34 06	
AFGL 147	1 00 06	+52 52 30	
AFGL 149	1 01 09	+74 33 18	
AFGL 150S	1 01 51	+28 33 12	
AFGL 151S	1 02 06	− 7 03 06	
AFGL 152	1 02 19	+18 53 42	
AFGL 153	1 02 38	+85 57 24	
AFGL 154	1 02 47	+65 33 18	
AFGL 155S	1 02 47	+19 58 54	
AFGL 156	1 03 04	−32 00 24	
AFGL 157	1 03 40	+12 19 06	
AFGL 158	1 03 50	−20 49 00	
AFGL 159S	1 05 02	− 2 06 54	
AFGL 160	1 05 20	+63 18 12	
AFGL 161	1 06 05	−10 28 00	
AFGL 162	1 06 25	− 5 50 48	
AFGL 163	1 06 48	+65 52 36	
AFGL 164	1 06 52	+35 21 30	
AFGL 165	1 07 30	+15 26 00	
AFGL 166S	1 07 47	+10 33 24	
AFGL 167	1 08 02	+53 28 36	
AFGL 168	1 08 20	+30 22 24	
AFGL 169	1 08 44	−13 47 12	
AFGL 170S	1 09 23	+21 57 12	
AFGL 172	1 09 39	− 3 40 54	
AFGL 174S	1 09 52	− 1 09 06	
AFGL 175	1 09 53	+67 31 30	
AFGL 176S	1 09 54	−32 16 24	
AFGL 177	1 10 23	+62 42 00	
AFGL 178S	1 10 51	+13 03 12	
AFGL 179	1 10 52	+26 53 00	
AFGL 180S	1 11 04	−43 09 24	
AFGL 182	1 11 42	− 2 26 30	
AFGL 184	1 11 49	+66 23 36	
AFGL 185S	1 12 20	+78 58 06	
AFGL 186	1 12 27	+71 27 36	
AFGL 187S	1 12 48	+48 59 12	
AFGL 188	1 13 18	+25 30 42	
AFGL 189	1 14 32	+59 02 12	
AFGL 190	1 14 25	+66 57 12	
AFGL 192	1 14 50	+13 38 48	
AFGL 193	1 15 00	+57 32 42	
AFGL 194	1 15 50	+72 21 06	
AFGL 195	1 16 05	+35 29 54	
AFGL 196S	1 16 10	−27 33 48	
AFGL 197	1 16 17	+56 04 00	
AFGL 198S	1 16 36	+ 1 16 18	
AFGL 200	1 17 13	+63 43 42	
AFGL 201S	1 18 21	+18 54 54	
AFGL 202S	1 18 41	+76 37 12	
AFGL 203	1 18 47	+66 32 36	
AFGL 204S	1 19 03	− 1 10 42	
AFGL 205	1 19 40	+61 35 36	
AFGL 206	1 19 42	+ 1 52 00	
AFGL 208S	1 20 47	− 9 00 42	
AFGL 209S	1 21 13	−31 14 24	
AFGL 210	1 21 35	− 8 26 48	
AFGL 211	1 21 37	+60 48 54	
AFGL 212S	1 21 39	+19 01 06	
AFGL 213S	1 22 15	+67 51 30	
AFGL 214	1 24 26	+16 40 30	
AFGL 215	1 24 38	−32 49 42	
AFGL 216	1 25 05	+16 25 54	
AFGL 218	1 26 07	−43 36 18	
AFGL 220	1 26 10	+51 24 36	
AFGL 221S	1 26 02	+79 25 18	
AFGL 222S	1 26 36	+35 40 06	
AFGL 224	1 27 38	+ 5 53 18	
AFGL 225	1 27 44	+15 25 00	
AFGL 226	1 28 11	+ 2 37 54	
AFGL 227	1 28 30	+62 04 24	
AFGL 228	1 28 53	+15 04 00	
AFGL 230	1 30 27.2	+62 11 31	
AFGL 230	1 30 40	+62 10 54	
AFGL 231	1 31 16	+65 32 12	
AFGL 232S	1 31 48	+15 06 00	
AFGL 233S	1 32 22	+23 21 06	
AFGL 236	1 34 06	+ 7 35 06	
AFGL 237	1 34 42	+48 22 00	
AFGL 239S	1 35 20	+ 8 25 18	
AFGL 240	1 35 29	+65 15 42	
AFGL 241S	1 37 00	+ 8 40 42	
AFGL 242S	1 37 28	+55 47 24	
AFGL 243	1 38 50	+ 5 15 36	
AFGL 245	1 39 57	+28 18 00	
AFGL 247	1 43 59	+10 08 06	
AFGL 248S	1 44 14	+64 17 30	
AFGL 250	1 46 04	+29 34 42	
AFGL 251	1 47 18	+64 37 06	
AFGL 252	1 47 24	− 5 06 24	
AFGL 253	1 47 14.1	+53 29 43	
AFGL 253	1 47 30	+53 28 00	
AFGL 254	1 47 48	−13 06 54	
AFGL 255	1 48 58	−10 36 06	
AFGL 256	1 49 03	− 6 41 54	
AFGL 257	1 49 03	+38 53 54	
AFGL 258S	1 50 29	+54 01 12	
AFGL 258S	1 50 33	+53 59 54	
AFGL 259	1 50 33	+59 55 18	
AFGL 260S	1 51 25	+ 6 46 36	
AFGL 261	1 51 39	−46 32 06	
AFGL 262	1 51 41	+ 8 32 00	
AFGL 262	1 51 47	+ 8 30 42	
AFGL 263S	1 52 10	−31 52 24	
AFGL 264S	1 52 17	+ 6 58 36	
AFGL 265	1 52 20	+69 58 12	
AFGL 266S	1 52 22	+24 50 54	
AFGL 267S	1 52 28	+ 7 42 36	
AFGL 269S	1 52 59	+43 32 24	
AFGL 270S	1 53 03	+59 02 12	
AFGL 272	1 54 20	−22 46 42	
AFGL 273	1 53 30	+89 00 00	
AFGL 274	1 54 49	+27 33 48	
AFGL 274	1 54 52.9	+27 33 43	
AFGL 275S	1 55 13	+ 5 47 06	
AFGL 276	1 55 10.7	+30 53 31	
AFGL 276	1 55 13	+30 53 42	
AFGL 277	1 55 16	−48 45 18	
AFGL 278	1 55 31	+45 11 42	
AFGL 278	1 55 37.3	+45 11 32	
AFGL 279	1 50 11.7	− 7 54 32	
AFGL 279	1 55 56	− 7 19 06	
AFGL 280	1 56 07	+54 34 48	
AFGL 280	1 56 14.8	+54 34 49	
AFGL 282S	1 56 29	+75 41 48	
AFGL 283	1 57 04	−14 07 54	
AFGL 284	1 57 23	−21 03 06	
AFGL 285	1 57 28	+63 53 24	
AFGL 286	1 57 37	−21 19 06	
AFGL 287	1 57 57	− 8 47 24	
AFGL 288S	1 58 19	+71 01 12	
AFGL 289	1 58 26	+61 41 06	
AFGL 290	1 59 48	+13 14 54	
AFGL 292	2 00 16	+ 7 27 54	
AFGL 293S	2 00 20	−45 36 12	
AFGL 294	2 00 45	+42 05 48	
AFGL 295	2 01 06	− 4 21 00	
AFGL 297	2 03 40	−10 27 18	
AFGL 298S	2 04 58	+59 01 00	
AFGL 299	2 05 22	+51 33 24	
AFGL 301	2 06 21	−18 01 54	
AFGL 302S	2 06 46	+16 32 42	
AFGL 303	2 07 55	+19 16 54	
AFGL 304S	2 08 11	+22 14 42	
AFGL 305	2 08 41	+63 56 06	
AFGL 310	2 14 18	+44 04 18	
AFGL 311	2 14 25	+78 31 48	
AFGL 312S	2 14 36	−14 54 36	
AFGL 313	2 15 28	+57 12 00	
AFGL 314	2 15 46	−14 22 42	
AFGL 315S	2 16 17	+63 55 48	
AFGL 316S	2 16 28	+33 36 54	
AFGL 317	2 16 36	+24 12 18	
AFGL 318	2 16 51	− 3 11 42	
AFGL 319	2 18 02	+60 41 36	
AFGL 320	2 18 43	+56 52 00	
AFGL 321	2 19 17	+ 0 10 54	
AFGL 323	2 19 21	+58 22 24	
AFGL 324S	2 19 26	+70 45 24	
AFGL 326	2 21 53	+61 51 42	
AFGL 327	2 22 00	+57 11 36	
AFGL 328	2 23 10	+62 03 06	
AFGL 331	2 23 22	+61 38 48	
AFGL 332	2 23 34	+60 28 30	
AFGL 333	2 24 13	+61 18 06	
AFGL 333	2 24 30	+61 15	ED
AFGL 333	2 24 38	+61 15 20	"
AFGL 334S	2 24 33	+26 43 18	
AFGL 335	2 24 44	+51 05 24	
AFGL 337	2 26 57	−26 20 00	
AFGL 338S	2 28 12	−21 17 18	
AFGL 339	2 28 14	−22 44 36	
AFGL 340	2 29 10	+76 29 48	
AFGL 341	2 29 15	+57 50 12	
AFGL 342	2 29 22	+14 14 36	
AFGL 343S	2 30 01	−26 50 00	
AFGL 344S	2 30 18	+ 0 18 36	
AFGL 346S	2 30 20	−16 54 54	
AFGL 347	2 30 29	+45 25 12	
AFGL 348	2 31 19	−13 20 54	
AFGL 349	2 31 41	+64 56 12	
AFGL 350	2 32 35	+53 16 00	
AFGL 351	2 32 36	+34 28 06	
AFGL 352	2 33 04	−42 24 42	
AFGL 354	2 33 37	− 8 02 18	
AFGL 355	2 34 04	+34 02 24	
AFGL 356S	2 34 11	+27 29 12	
AFGL 357	2 35 14	−27 10 30	
AFGL 358S	2 35 43	− 9 47 48	
AFGL 359	2 36 03	+59 21 24	
AFGL 360	2 36 06	+80 55 36	
AFGL 361	2 36 16	+60 12 18	
AFGL 362S	2 36 30	+55 45 18	
AFGL 363	2 36 40	+ 6 08 18	
AFGL 365	2 36 55	+39 37 18	
AFGL 367	2 38 06	+30 59 00	
AFGL 368S	2 38 16	+62 03 18	
AFGL 369	2 39 55	− 5 46 36	
AFGL 370S	2 40 01	−23 50 42	
AFGL 371	2 40 44	+36 02 18	
AFGL 371	2 40 47	+36 02 24	
AFGL 372	2 42 17	−29 27 30	
AFGL 373	2 42 40	+62 48 30	
AFGL 374S	2 43 50	−28 16 12	
AFGL 377	2 44 55.5	+29 02 27	
AFGL 377	2 45 06	+29 03 24	
AFGL 378	2 45 29	−12 39 18	
AFGL 378	2 45 32.1	−12 40 04	
AFGL 379	2 45 32.0	+17 18 07	
AFGL 379	2 45 34	+17 17 54	
AFGL 380	2 45 49	+60 50 18	
AFGL 381	2 46 36	+56 46 00	

NAME	RA (1950)	DEC	POS REF
AFGL 381	2 46 55.3	+56 46 38	
AFGL 382	2 46 58	+55 40 54	
AFGL 383	2 47 12	−45 03 36	
AFGL 384	2 47 07	+57 39 24	
AFGL 385	2 48 29	+34 51 00	
AFGL 386	2 48 44	+53 48 06	
AFGL 387	2 48 56	+54 40 42	
AFGL 388S	2 49 04	+47 16 48	
AFGL 389	2 49 13	+14 12 48	
AFGL 391S	2 49 48	+27 43 12	
AFGL 392	2 49 48	− 8 28 18	
AFGL 393	2 50 15	+74 07 24	
AFGL 396	2 51 09	+ 9 07 12	
AFGL 400	2 53 05	+54 27 00	
AFGL 401	2 53 08	+18 07 30	
AFGL 402S	2 53 32	+55 44 42	
AFGL 403	2 54 00	− 9 05 06	
AFGL 404	2 54 07	+14 25 06	
AFGL 405	2 54 21	+ 4 19 30	
AFGL 406	2 55 15	+62 54 48	
AFGL 409	2 56 52	+41 19 18	
AFGL 410	2 57 11	+43 58 18	
AFGL 412	2 58 12	+13 46 42	
AFGL 413	2 58 17	− 3 03 36	
AFGL 414	2 58 34	+21 36 18	
AFGL 415S	2 59 19	−16 33 00	
AFGL 416	2 59 13	+60 18 30	
AFGL 416	2 59 22.0	+60 16 15	
AFGL 416.1	2 59 13	+60 18 30	ED
AFGL 416.2	"	"	"
AFGL 417S	2 59 33	+16 25 12	
AFGL 418	2 59 36	+79 12 48	
AFGL 419	2 59 42	+ 3 53 06	
AFGL 421S	3 00 06	−22 58 24	
AFGL 422S	3 00 09	+43 41 24	
AFGL 423S	3 00 12	− 9 16 30	
AFGL 424S	3 00 36	+38 44 30	
AFGL 425	3 01 13	+53 18 18	
AFGL 426S	3 01 33	+31 18 18	
AFGL 428	3 01 54	+38 38 48	
AFGL 432	3 02 26	+75 33 30	
AFGL 434	3 03 00	+55 33 36	
AFGL 436S	3 03 56	+31 12 48	
AFGL 437	3 03 31.7	+58 19 07	ED
AFGL 437	3 03 58	+58 16 42	
AFGL 437N	3 03 32.0	+58 19 23	
AFGL 437S	3 03 32.2	+58 19 13	
AFGL 437W	3 03 31.3	+58 19 19	
AFGL 438S	3 03 59	+38 45 36	
AFGL 439	3 04 03	− 6 17 00	
AFGL 440	3 04 03	+58 50 12	
AFGL 441	3 04 09	−47 03 30	
AFGL 443	3 04 59	+40 46 24	
AFGL 445S	3 05 34	−24 13 30	
AFGL 449	3 06 21	+44 40 06	
AFGL 453	3 07 38	+57 42 36	
AFGL 454	3 08 04	−47 56 48	
AFGL 455	3 08 24	+14 35 48	
AFGL 456S	3 08 37	−43 51 42	
AFGL 457	3 08 49	+74 03 12	
AFGL 458	3 08 56	−33 43 48	
AFGL 459S	3 09 12	+23 31 54	
AFGL 460S	3 09 44	+65 23 48	
AFGL 461	3 09 54	+ 6 29 12	
AFGL 462S	3 10 35	+47 06 36	
AFGL 463	3 11 22	−44 35 36	
AFGL 464	3 11 58	+46 23 54	
AFGL 465	3 12 16	− 2 31 48	
AFGL 466	3 12 14	+64 34 06	
AFGL 467	3 12 32	+45 10 12	
AFGL 468S	3 12 50	−25 44 18	
AFGL 469S	3 13 05	−23 47 24	
AFGL 470S	3 13 54	− 8 45 48	
AFGL 471	3 14 48	+32 45 30	
AFGL 472	3 14 53	+81 58 30	
AFGL 473S	3 17 01	+70 32 42	
AFGL 474	3 17 14	+31 49 24	
AFGL 475	3 17 22	−21 57 06	
AFGL 476	3 17 25	−24 18 00	
AFGL 477	3 17 29	+28 51 30	
AFGL 478S	3 17 54	+31 46 06	
AFGL 480S	3 18 17	− 7 36 54	
AFGL 481	3 18 20	+22 48 18	
AFGL 482	3 18 38	+70 16 54	
AFGL 483	3 19 31	+32 03 54	
AFGL 484S	3 19 50	+29 26 00	
AFGL 485	3 20 18	+64 25 18	
AFGL 487	3 20 49	+49 40 36	
AFGL 488	3 22 57	−12 30 12	
AFGL 489	3 22 56	+47 21 12	
AFGL 490	3 23 38.9	+58 36 49	
AFGL 490	3 23 43.0	+58 36 52	
AFGL 490	3 23 59	+58 35 24	
AFGL 491	3 25 11	+71 42 06	
AFGL 492	3 26 55	+47 48 24	
AFGL 494	3 28 04	− 2 05 48	
AFGL 496	3 29 02	+19 54 48	
AFGL 497	3 30 35	− 9 38 54	
AFGL 500	3 31 54	−16 20 12	
AFGL 502S	3 34 37	− 6 51 12	
AFGL 503	3 36 06	−33 00 48	
AFGL 504S	3 37 11	+61 36 24	
AFGL 505	3 37 23	+62 29 24	
AFGL 506	3 37 44	+63 03 00	
AFGL 507	3 37 57	+51 18 18	
AFGL 511	3 38 54	−10 54 24	
AFGL 512	3 40 31.9	+12 38 11	
AFGL 512	3 40 44	+12 37 24	
AFGL 513	3 40 47	− 9 57 24	
AFGL 514	3 41 08	+80 10 36	
AFGL 515	3 41 18	−31 10 24	
AFGL 516	3 41 47	−43 03 06	
AFGL 517	3 42 26	+53 45 30	
AFGL 519	3 43 45	−12 16 06	
AFGL 519	3 43 46.5	−12 15 26	
AFGL 520	3 44 55	+65 22 24	
AFGL 521	3 44 56.8	+50 41 32	
AFGL 521	3 44 59	+50 41 30	
AFGL 522	3 45 52	+50 54 12	
AFGL 522	3 45 56	+50 55 30	
AFGL 523	3 46 03	+63 30 24	
AFGL 524	3 46 10	+67 29 12	
AFGL 525	3 46 16	− 7 09 54	
AFGL 525	3 46 20.8	− 7 10 00	
AFGL 526	3 48 21	−32 25 54	
AFGL 527	3 49 05	+39 43 30	
AFGL 528	3 49 16	+44 55 30	
AFGL 529	3 50 55	+11 14 18	
AFGL 530	3 51 22	−11 45 36	
AFGL 531	3 51 43	+57 31 36	
AFGL 532S	3 51 44	−17 29 30	
AFGL 533S	3 53 56	−34 24 54	
AFGL 534	3 54 05	−13 45 36	
AFGL 535S	3 54 27	+12 56 12	
AFGL 537	3 55 43	−13 39 00	
AFGL 538	3 58 00.5	+56 56 20	
AFGL 538	3 58 13	+57 02 36	
AFGL 539S	4 01 15	−33 52 00	
AFGL 540	4 01 20	−24 34 12	
AFGL 542	4 02 03	−15 53 12	
AFGL 543	4 03 32	−10 26 06	
AFGL 544S	4 04 00	+23 39 42	
AFGL 545	4 04 20	+42 53 12	
AFGL 547S	4 06 19	−38 07 30	
AFGL 548	4 06 31	− 8 14 54	
AFGL 549	4 07 04	+42 03 48	
AFGL 550	4 07 15	+51 02 30	
AFGL 551	4 08 35	+ 2 14 42	
AFGL 552	4 09 25	−25 15 18	
AFGL 553	4 11 07	−10 32 00	
AFGL 555	4 12 27	+23 57 24	
AFGL 556	4 12 33	+33 42 42	
AFGL 557S	4 13 01	−13 21 42	
AFGL 558	4 13 01	+50 32 12	
AFGL 559	4 13 15	+62 13 30	
AFGL 560	4 13 38	+31 14 54	
AFGL 562	4 15 07	−38 13 42	
AFGL 563	4 15 37	−18 38 00	
AFGL 564	4 16 01	−20 49 54	
AFGL 565	4 16 28	+40 56 42	
AFGL 566	4 16 54	+15 31 42	
AFGL 567	4 17 25	+60 37 42	
AFGL 570	4 18 52	+68 07 12	
AFGL 571	4 19 11	−22 18 42	
AFGL 572	4 19 23	+20 42 48	
AFGL 574	4 20 42	−13 00 18	
AFGL 575S	4 20 46	+73 12 30	
AFGL 578S	4 21 40	−27 55 18	
AFGL 579	4 22 18	−34 09 06	
AFGL 580S	4 25 42	− 5 13 48	
AFGL 581	4 25 51	+10 00 24	
AFGL 582	4 26 12	+39 46 30	
AFGL 583	4 26 14	+57 18 18	
AFGL 584S	4 26 51	+ 5 05 00	
AFGL 585	4 27 07	+35 09 54	
AFGL 586	4 27 55	+27 24 06	
AFGL 589	4 29 04	+22 45 12	
AFGL 590	4 29 28	+31 00 36	
AFGL 591	4 29 28	−37 09 36	
AFGL 592	4 29 29	+ 8 51 00	
AFGL 593	4 29 42	+48 36 24	
AFGL 595	4 30 40	+62 08 36	
AFGL 596S	4 31 26	−29 50 18	
AFGL 598	4 31 48	− 8 20 06	
AFGL 599	4 31 49	− 9 03 36	
AFGL 600	4 32 36	+28 25 48	
AFGL 601	4 33 10	+16 23 18	
AFGL 602	4 33 29	+41 09 36	
AFGL 603	4 33 39	−30 42 36	
AFGL 604	4 33 47	− 5 25 30	
AFGL 605	4 34 28	−27 42 18	
AFGL 606	4 34 58	+66 03 18	
AFGL 608	4 35 29	+ 8 14 24	
AFGL 610	4 35 56	−14 26 42	
AFGL 611S	4 36 00	+59 58 42	
AFGL 612	4 37 27	+17 25 30	
AFGL 614	4 38 11	−19 45 12	
AFGL 615	4 38 15	−14 19 00	
AFGL 617	4 38 41	−38 18 18	
AFGL 618	4 39 30	+36 01 48	
AFGL 619	4 39 37	+ 6 47 12	
AFGL 621	4 40 42	+17 13 54	
AFGL 622	4 40 56	+20 40 42	
AFGL 622	4 40 59	+20 40 48	
AFGL 624	4 40 34.0	+32 46 24	
AFGL 624	4 41 43	+32 51 36	
AFGL 625S	4 41 49	− 8 23 24	
AFGL 627	4 41 58	−12 46 30	
AFGL 630S	4 43 22	+14 58 00	
AFGL 631S	4 43 56	+14 47 48	
AFGL 632	4 44 38	+61 25 48	
AFGL 633	4 46 08	+68 05 48	
AFGL 634	4 46 12	− 3 57 30	
AFGL 635	4 46 32.4	+37 24 07	
AFGL 635	4 46 43	+37 23 24	
AFGL 636	4 47 34	+63 25 30	
AFGL 637S	4 48 01	+ 8 49 24	
AFGL 639	4 48 23	+28 26 36	
AFGL 639	4 48 33	+28 25 36	
AFGL 641S	4 49 01	− 4 58 42	
AFGL 643	4 49 21	+38 25 24	
AFGL 644	4 49 45	+14 09 06	
AFGL 645	4 50 09	+22 51 18	
AFGL 646S	4 50 39	+38 09 00	
AFGL 647	4 50 39	+ 2 25 24	
AFGL 648	4 52 55	+59 03 48	
AFGL 649	4 52 56	− 2 58 42	
AFGL 650	4 53 18	− 4 45 36	
AFGL 652	4 53 26	+13 28 12	
AFGL 654	4 53 50	+33 04 36	
AFGL 655S	4 54 17	+48 28 12	
AFGL 657S	4 55 21	−34 23 12	
AFGL 659	4 55 52	+ 1 38 06	
AFGL 661	4 56 06	−16 43 54	
AFGL 663	4 56 32	+74 10 36	
AFGL 664	4 56 44	+56 06 48	
AFGL 667	4 57 19	−14 53 54	
AFGL 668S	4 57 26	+32 43 48	
AFGL 669	4 57 56	−28 07 18	
AFGL 670S	4 58 19	+43 45 18	
AFGL 671	4 58 57	+60 23	
AFGL 671	4 58 59	+60 22 36	
AFGL 672	4 59 05	+50 35 06	
AFGL 673S	4 59 10	− 1 55 54	
AFGL 674	4 58 59	+41 01	
AFGL 674	4 59 11	+41 00 00	
AFGL 677S	5 00 24	+ 9 17 06	
AFGL 679S	5 02 27	+21 35 00	
AFGL 681	5 02 41	+44 47 30	
AFGL 682	5 02 42	−21 58 48	
AFGL 683	5 02 45	+ 1 05 48	
AFGL 684S	5 02 51	+38 39 12	
AFGL 686	5 03 12	+34 46 42	
AFGL 687	5 03 13	+50 19 18	
AFGL 688	5 03 26	−22 27 00	
AFGL 692	5 05 17	+42 30 54	
AFGL 693	5 05 24	+68 36 30	
AFGL 694	5 05 31	−12 40 42	
AFGL 696S	5 06 19	+79 41 18	
AFGL 697	5 06 26	+22 59 12	
AFGL 698	5 06 28	+14 17 42	
AFGL 699	5 07 02	−34 37 00	
AFGL 700	5 07 23	+52 48 30	
AFGL 701S	5 07 50	−12 18 42	
AFGL 702	5 08 57	−11 53 06	
AFGL 703S	5 09 04	+38 35 36	
AFGL 705S	5 10 07	− 8 08 00	
AFGL 706	5 10 30	+ 2 48 12	
AFGL 707	5 11 11	+ 0 31 48	
AFGL 708	5 11 58	+ 0 36 42	
AFGL 709	5 12 04	+49 30 00	
AFGL 710	5 12 19	− 8 17 06	
AFGL 712S	5 12 57	+45 31 06	
AFGL 713	5 13 02	+45 56 18	
AFGL 714	5 13 12	+11 56 48	
AFGL 715	5 13 16	+53 32 30	
AFGL 718S	5 14 01	+51 22 12	
AFGL 719S	5 14 26	+27 13 30	
AFGL 720	5 14 34	+42 44 18	
AFGL 721	5 14 34	+29 33 42	
AFGL 722	5 15 01	+33 18 00	
AFGL 724	5 15 08	+63 13 00	
AFGL 725	5 15 14	+13 20 12	
AFGL 726S	5 15 26	−25 45 48	
AFGL 727S	5 15 45	+43 15 42	
AFGL 728	5 15 49	+62 36 36	
AFGL 729	5 16 10	−10 12 06	
AFGL 732	5 17 22	−25 09 48	
AFGL 733	5 17 43	−17 56 36	
AFGL 735	5 18 26	+32 29 12	
AFGL 736S	5 19 48	− 8 42 36	
AFGL 737S	5 21 08	+20 14 18	
AFGL 739	5 21 42	+36 08 12	
AFGL 740	5 22 06	− 6 12 48	
AFGL 741S	5 22 07	+33 53 12	
AFGL 742S	5 22 42	+ 0 18 18	
AFGL 744	5 23 36	+ 0 40 48	
AFGL 745S	5 23 39	−33 34 24	
AFGL 746	5 23 50	+48 40 36	
AFGL 747S	5 23 46	+36 50 54	
AFGL 748	5 23 51	+34 06 24	
AFGL 749	5 23 58	+29 52 30	
AFGL 751	5 24 16	+23 03 24	
AFGL 752	5 25 19	+17 11 48	
AFGL 753	5 25 21	+63 00 00	
AFGL 754	5 25 28	+32 25 12	
AFGL 755	5 25 30	+38 59 18	
AFGL 756	5 26 05	−20 49 06	
AFGL 757	5 26 40	− 4 46 48	
AFGL 759	5 27 15	− 1 09 30	
AFGL 760S	5 27 34	+15 06 18	
AFGL 761	5 28 08	+18 30 48	
AFGL 765S	5 29 13	−12 24 48	
AFGL 766	5 29 23	−35 29 54	
AFGL 767	5 29 06	+18 31 18	
AFGL 768	5 29 36	+65 01 54	
AFGL 769	5 30 07	+12 59 12	
AFGL 771	5 30 30	−17 49 12	
AFGL 772S	5 31 13	− 5 19 18	
AFGL 774S	5 31 53	+54 54 06	
AFGL 776	5 31 57	− 5 14 48	
AFGL 777	5 32 06	+54 24 30	
AFGL 778	5 32 26	+67 25 24	
AFGL 779	5 32 50	− 5 26 36	
AFGL 779.1	"	"	ED
AFGL 780	5 32 35	+ 8 40 06	
AFGL 781	5 32 36	− 4 56 24	
AFGL 782	5 32 45	+38 00 36	
AFGL 783S	5 32 52	− 5 08 30	
AFGL 784S	5 33 01	+20 58 18	
AFGL 786	5 35 03	− 1 48 12	
AFGL 787	5 35 26	+42 35 42	
AFGL 788	5 35 31	+24 57 42	
AFGL 789	5 35 54	+18 25 48	
AFGL 791	5 36 09	+46 44 06	
AFGL 792	5 36 23	−35 30 36	
AFGL 793	5 36 37	−14 04 36	
AFGL 794	5 36 44	+37 36 00	
AFGL 795	5 37 11	−12 28 36	
AFGL 796	5 37 19	− 8 11 24	
AFGL 797	5 37 29	+31 53 54	
AFGL 799	5 37 56	+13 45 42	
AFGL 799.1	"	"	ED
AFGL 800	5 37 56	+28 03 36	
AFGL 801	5 38 19	+12 16 06	
AFGL 802	5 38 26	+38 55 30	
AFGL 803	5 38 38	+17 28 00	
AFGL 804	5 39 03	− 4 08 54	
AFGL 805	5 39 04	+32 00 24	
AFGL 806	5 39 06	− 2 17 00	
AFGL 807	5 39 12	− 1 56 54	
AFGL 807.1	"	"	ED
AFGL 807.2	"	"	"
AFGL 808S	5 39 19	−20 47 36	

NAME	RA (1950)	DEC	POS REF
	h m s	° ′ ″	
AFGL 809	5 40 33.3	+32 40 58	
AFGL 809	5 40 36	+32 41 06	
AFGL 810S	5 40 45	−23 47 36	
AFGL 811	5 41 11	+69 58 06	
AFGL 812	5 42 09.7	+24 24 01	
AFGL 812	5 42 13	+24 22 42	
AFGL 813S	5 44 00	+ 2 09 36	
AFGL 814S	5 44 06	+ 0 04 24	
AFGL 815	5 44 03	+43 11 36	
AFGL 815	5 44 07	+43 11 54	
AFGL 818	5 44 29	+ 0 18 06	
AFGL 819	5 44 55.5	−12 49 18	
AFGL 819	5 45 06	−12 52 12	
AFGL 820	5 45 05	−21 34 06	
AFGL 821	5 47 10	+18 27 18	
AFGL 822	5 47 41	+37 17 54	
AFGL 823	5 48 20	+32 05 06	
AFGL 825S	5 48 37	+ 0 12 54	
AFGL 826	5 49 05	+63 01 54	
AFGL 827S	5 49 21	+61 31 00	
AFGL 828	5 49 07	−20 53 18	
AFGL 829	5 49 11	−35 48 54	
AFGL 830	5 49 49	+ 1 51 06	
AFGL 831	5 50 15	+64 57 06	ED
AFGL 831S	5 50 15	+64 57 00	
AFGL 832	5 50 39	+39 30 54	
AFGL 833S	5 51 40	− 1 03 36	
AFGL 834	5 52 10	+ 0 57 36	
AFGL 835S	5 52 24	+41 29 18	
AFGL 836	5 52 25	+ 7 24 42	
AFGL 837	5 52 57	+20 09 12	
AFGL 838S	5 53 06	+ 2 18 42	
AFGL 839	5 53 21	+45 30 12	
AFGL 841	5 53 34	+35 34 54	
AFGL 842	5 53 43	+48 21 36	
AFGL 843	5 53 45	+22 50 24	
AFGL 844S	5 53 49	+ 6 45 24	
AFGL 845	5 54 38	+15 45 18	
AFGL 846	5 55 06	+ 2 42 06	
AFGL 847	5 55 32	−33 06 48	
AFGL 848	5 55 34	+54 16 48	
AFGL 849	5 55 59	+74 32 00	
AFGL 850	5 55 58	+38 24 54	
AFGL 851	5 56 13	+45 56 36	
AFGL 853	5 57 39	+39 38 48	
AFGL 855S	5 58 34	+ 6 01 42	
AFGL 856	5 58 53	+10 54 48	
AFGL 856	5 58 54	+10 54 36	
AFGL 857	5 59 08	− 7 36 06	
AFGL 858	5 59 11	− 2 19 48	
AFGL 858	5 59 16	− 2 21 12	
AFGL 859S	5 59 21	+ 1 51 00	
AFGL 860	5 59 27	+37 43 54	
AFGL 861S	5 59 31	− 2 56 12	
AFGL 862	5 59 47.3	+50 36 53	
AFGL 862	5 59 56	+50 37 36	
AFGL 864	6 01 06	+28 28 06	
AFGL 865	6 01 18	+ 7 25 24	
AFGL 866	6 01 27	+67 44 24	
AFGL 869S	6 02 30	+68 48 36	
AFGL 870	6 02 41	−16 28 36	
AFGL 871	6 03 14	+10 07 00	
AFGL 872	6 03 43	−24 11 30	
AFGL 873	6 03 53	− 5 42 48	
AFGL 873	6 03 55	− 5 43 18	
AFGL 874	6 04 50	−21 48 00	
AFGL 876	6 05 18	+34 53 42	
AFGL 877	6 05 19	− 6 23 18	
AFGL 878	6 05 25	−19 08 00	
AFGL 881	6 06 38	+47 44 30	
AFGL 882	6 06 50	+60 28 30	
AFGL 883	6 07 01	+31 23 30	
AFGL 884	6 07 40	+65 44 18	
AFGL 885S	6 07 34	−19 07 48	
AFGL 887S	6 08 02	+34 52 00	
AFGL 888	6 08 05	+ 3 46 30	
AFGL 889S	6 08 10	−31 42 42	
AFGL 890S	6 08 25	− 6 11 54	
AFGL 891	6 08 27	+11 15 18	
AFGL 892	6 08 56	− 7 13 54	
AFGL 893	6 09 07	+21 50 30	
AFGL 894	6 09 10	+32 42 12	
AFGL 895	6 09 22	+22 53 48	
AFGL 896	6 10 04	+17 59 18	
AFGL 897	6 10 08	+18 33 36	
AFGL 899S	6 10 45	− 2 13 06	
AFGL 900	6 11 02	+76 42 00	
AFGL 901	6 11 12	+60 01 42	
AFGL 902	6 11 31	+13 52 12	
AFGL 903	6 12 08	+56 45 48	
AFGL 905	6 12 22	− 6 15 48	
AFGL 906	6 13 06	−10 57 48	
AFGL 907	6 13 14	+61 31 00	
AFGL 908	6 14 00	−27 27 06	
AFGL 909	6 14 03	+33 13 06	
AFGL 910	6 15 02	+ 8 31 24	
AFGL 911S	6 16 38	+83 52 18	
AFGL 912	6 17 05	−12 36 36	
AFGL 913	6 17 19	− 2 54 12	
AFGL 915	6 17 35	−10 36 00	
AFGL 916	6 18 04	+11 59 30	
AFGL 918	6 18 13	+11 35 00	
AFGL 918	6 18 20.0	+11 35 42	
AFGL 919	6 18 16	+ 2 37 24	
AFGL 920	6 19 13	+ 7 22 30	
AFGL 921	6 19 21	− 3 51 00	
AFGL 922	6 19 44	+22 32 12	
AFGL 923	6 19 47	+ 3 27 12	
AFGL 924	6 20 07	−33 21 54	
AFGL 925	6 20 08	− 2 10 54	
AFGL 926S	6 20 36	+59 11 30	
AFGL 927	6 20 45	+49 18 30	
AFGL 928	6 21 39	+ 0 04 42	
AFGL 930S	6 22 25	− 2 57 42	
AFGL 931	6 22 32	+58 27 24	
AFGL 932S	6 22 38	−32 07 00	
AFGL 933	6 22 39	− 9 06 30	
AFGL 934	6 22 43	+14 44 06	
AFGL 935	6 23 02	− 9 29 06	
AFGL 936	6 23 15	+ 5 35 06	
AFGL 937	6 23 15	+19 06 00	
AFGL 938	6 23 32	+68 57 24	
AFGL 939S	6 23 44	−18 20 06	
AFGL 940	6 23 59	+ 9 02 54	
AFGL 941	6 24 04	+ 3 45 12	
AFGL 942S	6 24 08	− 7 49 12	
AFGL 943	6 24 20	+ 5 25 18	
AFGL 944	6 24 34	−19 35 18	
AFGL 945	6 25 12	+61 35 12	
AFGL 947	6 26 09	+16 36 24	
AFGL 948S	6 26 51	− 8 03 42	
AFGL 949	6 27 36	+ 8 08 00	
AFGL 950	6 27 56	+27 28 42	
AFGL 951S	6 28 18	+10 27 30	
AFGL 953S	6 28 49	+46 56 48	
AFGL 954	6 29 22	+43 19 24	
AFGL 955	6 29 39	+40 44 36	
AFGL 956	6 29 57	+60 59 18	
AFGL 957	6 30 16	+55 24 06	
AFGL 958	6 30 26	+64 07 06	
AFGL 959	6 31 41	+16 04 54	
AFGL 960S	6 31 51	+60 42 12	
AFGL 961	6 31 54	+ 4 16 36	
AFGL 961	6 31 58.9	+ 4 15 07	
AFGL 961	6 31 59	+ 4 15 09	
AFGL 962	6 31 55	+45 41 00	
AFGL 963S	6 32 00	−29 13 42	
AFGL 964	6 32 01	+ 4 59 06	
AFGL 965	6 32 19	−12 26 24	
AFGL 966	6 33 06	+38 28 42	
AFGL 967	6 33 06	+14 15 06	
AFGL 968	6 33 19	− 5 20 30	
AFGL 969	6 33 57	+17 46 18	
AFGL 970	6 34 08	+21 09 12	
AFGL 971	6 34 19	+ 3 26 24	
AFGL 972S	6 34 32	−19 13 36	
AFGL 973S	6 34 38	+81 46 48	
AFGL 974S	6 34 41	+10 57 12	
AFGL 975	6 34 44	+16 26 42	
AFGL 976	6 34 47	+14 42 42	
AFGL 977	6 34 56	− 1 21 18	
AFGL 978S	6 35 07	− 2 46 36	
AFGL 980	6 35 44	−18 12 18	
AFGL 981	6 35 49	+ 5 16 24	
AFGL 982	6 36 09	+59 54 30	
AFGL 985	6 36 51	−14 04 36	
AFGL 986	6 36 56	− 2 25 12	
AFGL 987S	6 37 01	+20 31 30	
AFGL 988	6 38 34	+27 06 42	
AFGL 989	6 38 26	+ 9 32 18	
AFGL 990	6 38 48	+ 2 48 30	
AFGL 991	6 38 52	+55 32 06	
AFGL 992S	6 39 10	− 4 33 06	
AFGL 993S	6 39 15	−16 57 54	
AFGL 994	6 39 15	+44 33 54	
AFGL 995	6 39 23	+ 8 50 06	
AFGL 996	6 39 38	+ 1 24 06	
AFGL 997	6 40 09	−18 56 12	
AFGL 998	6 40 40	+57 58 30	
AFGL 999	6 40 18	−14 23 42	
AFGL 1001	6 40 51.4	+25 10 57	
AFGL 1001	6 40 52	+25 10 06	
AFGL 1002	6 41 05	−27 23 30	
AFGL 1003	6 41 26	+77 02 18	
AFGL 1004	6 41 35.4	+29 01 24	
AFGL 1004	6 41 36	+29 00 24	
AFGL 1007	6 42 48	−16 37 30	
AFGL 1008	6 43 27	−36 30 06	
AFGL 1009	6 44 04	+30 18 54	
AFGL 1010	6 44 27	+ 8 06 36	
AFGL 1012	6 44 52	−20 14 48	
AFGL 1014	6 45 06	− 8 54 24	
AFGL 1016S	6 45 59	−16 13 54	
AFGL 1017	6 47 04	+ 3 01 24	
AFGL 1018	6 47 22	+11 22 36	
AFGL 1020	6 49 01	+ 5 49 30	
AFGL 1021	6 49 17	+61 04 30	
AFGL 1022	6 49 21	+ 4 49 06	
AFGL 1023	6 49 23	−33 27 00	
AFGL 1024	6 49 27	+20 54 00	
AFGL 1026	6 49 49	+ 4 10 36	
AFGL 1027	6 50 03	+ 1 02 36	
AFGL 1028	6 50 07	+ 8 27 54	
AFGL 1029S	6 50 30	+ 4 51 42	
AFGL 1030S	6 50 32	−37 09 00	
AFGL 1031S	6 51 03	−10 01 24	
AFGL 1032S	6 51 08	−27 42 24	
AFGL 1033	6 51 38	−14 18 24	
AFGL 1034	6 51 44	−11 55 48	
AFGL 1035	6 52 08	−24 10 06	
AFGL 1036	6 52 27	+77 02 36	
AFGL 1037S	6 52 40	−14 47 00	
AFGL 1038	6 53 04	+ 6 24 54	
AFGL 1039	6 53 09.7	− 2 16 18	
AFGL 1039	6 53 12	− 2 16 06	
AFGL 1041	6 53 53	−14 00 24	
AFGL 1042	6 53 53	+37 27 06	
AFGL 1043	6 55 10	+ 3 21 48	
AFGL 1044	6 55 36	− 8 55 12	
AFGL 1045	6 55 35	+ 6 15 18	
AFGL 1046S	6 55 38	+15 45 42	
AFGL 1047S	6 55 54	−19 12 06	
AFGL 1048S	6 56 03	+ 8 31 30	
AFGL 1050	6 57 00	+55 23 36	
AFGL 1051	6 57 23	+16 09 12	
AFGL 1052	6 58 17	+30 35 18	
AFGL 1053	6 58 36	− 3 11 18	
AFGL 1054S	6 59 04	+15 43 54	
AFGL 1055	6 59 20	+17 50 36	
AFGL 1056	6 59 36	+16 44 18	
AFGL 1057	6 59 38	−27 52 24	
AFGL 1058	7 00 03	− 4 33 36	
AFGL 1059	7 01 22	−11 28 42	
AFGL 1060	7 02 08	− 8 53 06	
AFGL 1061	7 02 35	+10 38 36	
AFGL 1062	7 02 40	−14 57 06	
AFGL 1063S	7 03 16	−40 58 42	
AFGL 1064	7 03 21	−35 51 24	
AFGL 1065	7 03 29	−25 02 30	
AFGL 1066S	7 03 32	+12 44 06	
AFGL 1067	7 04 05	+ 8 58 18	
AFGL 1068S	7 04 09	+28 22 42	
AFGL 1070	7 04 31	− 7 29 30	
AFGL 1071	7 04 57	−32 23 12	
AFGL 1072	7 04 57	+66 01 30	
AFGL 1073	7 05 16	+24 10 06	
AFGL 1074	7 05 26	−10 39 30	
AFGL 1074	7 05 27	−10 39 18	
AFGL 1075	7 05 43	−11 50 36	
AFGL 1077	7 06 13	+ 4 12 18	
AFGL 1078	7 06 14	−26 16 00	
AFGL 1080	7 07 57	+30 19 12	
AFGL 1081	7 08 21	+39 24 42	
AFGL 1082	7 08 59	−29 00 42	
AFGL 1083	7 09 23	+51 31 18	
AFGL 1084	7 09 37	+68 53 18	
AFGL 1085	7 09 55	−20 13 18	
AFGL 1086	7 10 28	+16 14 54	
AFGL 1087	7 10 34	− 7 52 30	
AFGL 1088S	7 11 02	− 6 02 12	
AFGL 1089S	7 11 40	+24 58 24	
AFGL 1090S	7 12 36	− 9 31 00	
AFGL 1091	7 12 48	+28 00 00	
AFGL 1092	7 13 04	+ 5 08 36	
AFGL 1094	7 14 25	+48 36 12	
AFGL 1095	7 14 34	−23 15 18	
AFGL 1096	7 14 37	−27 49 24	
AFGL 1097S	7 14 46	+39 12 48	
AFGL 1098	7 15 02	+38 09 12	
AFGL 1099	7 15 14	−34 44 42	
AFGL 1100S	7 15 24	+76 15 48	
AFGL 1101	7 16 21	−15 44 54	
AFGL 1102	7 16 34	+79 52 42	
AFGL 1103	7 16 56	+22 03 06	
AFGL 1104	7 17 56	+55 55 00	
AFGL 1105	7 18 48	+ 4 44 42	
AFGL 1106	7 18 53	+87 07 18	
AFGL 1107S	7 19 08	−11 21 18	
AFGL 1108	7 20 13	−20 25 42	
AFGL 1109	7 20 37	+47 15 54	
AFGL 1110	7 20 37	+82 31 00	
AFGL 1110	7 20 41.0	+82 30 50	
AFGL 1111	7 20 56	−25 41 00	
AFGL 1112	7 21 25	−27 44 36	
AFGL 1113	7 22 26	−21 25 12	
AFGL 1114	7 22 44	+27 54 06	
AFGL 1115	7 22 52	+ 6 10 42	
AFGL 1117	7 23 01	+33 27 42	
AFGL 1118	7 23 12	− 5 45 18	
AFGL 1119S	7 23 48	+12 47 48	
AFGL 1120	7 24 39	+46 05 48	
AFGL 1121S	7 24 41	+75 11 00	
AFGL 1122	7 24 53	+41 03 54	
AFGL 1123	7 25 02	+48 02 12	
AFGL 1124	7 25 04	−26 18 48	
AFGL 1125S	7 25 15	−26 45 24	
AFGL 1126S	7 25 23	+68 33 12	
AFGL 1127	7 25 29	+ 9 01 30	
AFGL 1129	7 26 37	−10 15 06	
AFGL 1130	7 26 50	+28 01 30	
AFGL 1131	7 26 54	−19 20 48	
AFGL 1131	7 27 01	−19 21 24	
AFGL 1132S	7 27 06	− 7 01 48	
AFGL 1133	7 27 11	+50 07 54	
AFGL 1134	7 27 58	+51 53 06	
AFGL 1135	7 28 08	− 9 38 42	
AFGL 1136	7 28 17	+20 37 24	
AFGL 1138	7 30 01	+ 8 26 18	
AFGL 1139	7 30 34	+11 08 54	
AFGL 1140	7 30 34	−20 34 42	
AFGL 1141	7 30 45	+30 37 48	
AFGL 1142S	7 31 05	+67 33 30	
AFGL 1143	7 31 12	+66 35 48	
AFGL 1144	7 31 22	+31 59 00	
AFGL 1145	7 31 25	−14 24 00	
AFGL 1146S	7 31 34	− 9 58 24	
AFGL 1147S	7 31 54	+ 5 47 36	
AFGL 1148	7 31 59	+37 09 48	
AFGL 1150	7 32 58	+27 02 18	
AFGL 1151	7 33 02	−23 53 30	
AFGL 1153S	7 34 51	+29 17 42	
AFGL 1154S	7 34 59	+ 8 44 30	
AFGL 1156S	7 35 27	+13 46 12	
AFGL 1157S	7 35 30	+13 12 00	
AFGL 1158S	7 35 58	− 7 32 48	
AFGL 1159	7 36 42	− 8 21 06	
AFGL 1160	7 36 46	+38 27 54	
AFGL 1161	7 36 48	+ 5 19 48	
AFGL 1162	7 37 38	−21 35 54	
AFGL 1163	7 38 09	+20 34 00	
AFGL 1164	7 38 30	−23 21 00	
AFGL 1165S	7 38 36	−28 23 18	
AFGL 1167	7 38 53	+13 35 48	
AFGL 1168	7 39 13	+14 18 36	
AFGL 1169	7 39 15	− 4 03 42	
AFGL 1170S	7 39 16	+ 8 34 54	
AFGL 1171	7 39 20	−37 20 42	
AFGL 1172S	7 39 35	+25 57 48	
AFGL 1173	7 40 01	−10 46 54	
AFGL 1174	7 40 07	+29 01 06	
AFGL 1175	7 40 46	+38 58 36	
AFGL 1176	7 40 59	+25 54 12	
AFGL 1178	7 41 26	+24 29 36	
AFGL 1179	7 41 32	−28 17 36	
AFGL 1180S	7 41 43	−19 26 24	
AFGL 1181	7 41 45	−28 50 18	
AFGL 1182S	7 41 59	+26 45 06	
AFGL 1183	7 42 18	+28 08 06	
AFGL 1184	7 42 20	+30 54 24	
AFGL 1185S	7 43 02	+ 3 42 54	
AFGL 1186	7 43 02	+18 39 48	
AFGL 1187	7 43 15	+37 39 36	
AFGL 1188	7 43 59	− 5 28 24	
AFGL 1189	7 44 05	+25 31 48	

NAME	RA (1950)	DEC	POS REF
	h m s	° ′ ″	
AFGL 1191	7 44 11	+33 31 18	
AFGL 1191	7 44 17.1	+33 32 25	
AFGL 1192	7 44 28	−26 10 30	
AFGL 1193S	7 46 14	−15 49 00	
AFGL 1194S	7 46 26	+10 53 54	
AFGL 1195	7 47 07	−24 41 48	
AFGL 1198S	7 48 43	−34 48 42	
AFGL 1199	7 48 43	− 2 32 06	
AFGL 1200	7 49 28	+ 3 24 30	
AFGL 1201S	7 50 21	+60 04 36	
AFGL 1202S	7 50 58	+47 40 48	
AFGL 1203S	7 51 34	−28 49 24	
AFGL 1204	7 51 51	−26 12 42	
AFGL 1206S	7 52 18	+30 37 42	
AFGL 1207S	7 52 44	− 6 16 36	
AFGL 1208S	7 52 56	+20 06 18	
AFGL 1209	7 52 57	−36 03 00	
AFGL 1210S	7 53 17	+ 8 59 18	
AFGL 1211S	7 53 29	+16 54 36	
AFGL 1212S	7 53 46	+11 02 06	
AFGL 1214S	7 56 08	+ 0 50 12	
AFGL 1215	7 58 27	−12 43 06	
AFGL 1216	7 58 36	− 1 14 24	
AFGL 1216	7 58 40.7	− 1 15 09	
AFGL 1218	7 59 31	+ 2 28 18	
AFGL 1218	7 59 39.9	+ 2 28 24	
AFGL 1219S	8 00 13	+47 06 06	
AFGL 1220	8 00 21	+36 29 12	
AFGL 1221	8 00 46	− 5 32 30	
AFGL 1222S	8 01 22	+62 16 42	
AFGL 1223	8 01 53	−31 21 42	
AFGL 1224	8 02 10	−32 29 42	
AFGL 1225S	8 02 37	+34 16 24	
AFGL 1227	8 03 21	+22 46 36	
AFGL 1228	8 03 23	+ 5 43 48	
AFGL 1229S	8 03 31	+60 52 00	
AFGL 1230S	8 03 33	+ 0 32 06	
AFGL 1231	8 05 30	−20 31 30	
AFGL 1232	8 06 03	+65 22 06	
AFGL 1233	8 08 24	+19 17 12	
AFGL 1234S	8 08 51	+ 3 39 18	
AFGL 1235	8 09 02	−32 44 42	
AFGL 1236S	8 09 51	+ 2 02 30	
AFGL 1237S	8 10 34	−32 40 00	
AFGL 1238	8 11 20	+20 29 24	
AFGL 1239S	8 11 32	−28 00 54	
AFGL 1240	8 11 58	+24 53 30	
AFGL 1241	8 13 44	+11 52 42	
AFGL 1242S	8 15 22	+85 16 48	
AFGL 1243	8 17 22	+ 2 54 18	
AFGL 1244	8 18 55	+ 5 05 42	
AFGL 1245	8 19 30	+43 20 30	
AFGL 1246S	8 19 35	+33 40 00	
AFGL 1247	8 19 39	+15 08 00	
AFGL 1248S	8 20 58	+ 1 33 06	
AFGL 1249	8 21 59	+52 27 18	
AFGL 1250	8 22 09	− 8 22 54	
AFGL 1252S	8 23 13	+44 57 06	
AFGL 1253	8 23 40	− 4 45 24	
AFGL 1254	8 23 43	+ 3 53 00	
AFGL 1255	8 24 01	+12 48 24	
AFGL 1256S	8 24 34	+13 08 54	
AFGL 1257S	8 24 50	−27 35 54	
AFGL 1258	8 27 05	− 6 08 06	
AFGL 1259S	8 27 03	+ 2 51 48	
AFGL 1260	8 27 44	−21 17 36	
AFGL 1261	8 28 08	+ 9 18 24	
AFGL 1262	8 28 40	+18 15 54	
AFGL 1263	8 28 52	−22 36 30	
AFGL 1264S	8 28 49	+24 10 06	
AFGL 1265	8 29 40	+67 21 18	
AFGL 1269S	8 31 30	+ 4 07 24	
AFGL 1270S	8 33 01	+ 9 44 42	
AFGL 1271	8 34 29	−17 45 30	
AFGL 1272S	8 34 39	+19 49 30	
AFGL 1273	8 34 40	− 8 39 24	
AFGL 1274	8 35 52	−10 16 42	
AFGL 1275	8 36 01	+11 11 36	
AFGL 1276	8 36 06	+ 3 29 48	
AFGL 1277S	8 36 19	+64 31 54	
AFGL 1278	8 36 23	− 3 59 12	
AFGL 1279S	8 37 07	−23 55 36	
AFGL 1280	8 37 17	− 9 24 36	
AFGL 1281	8 37 30	−17 06 36	
AFGL 1282	8 38 22	+ 0 33 30	
AFGL 1283	8 39 06	+ 2 21 42	
AFGL 1285	8 41 45	+18 19 54	
AFGL 1285	8 41 50.7	+18 20 22	
AFGL 1286S	8 43 29	+79 09 54	
AFGL 1287	8 43 35	+28 56 54	
AFGL 1288	8 43 44	+ 1 49 24	
AFGL 1288	8 43 46.0	+ 1 48 57	
AFGL 1289	8 44 06	+ 6 35 42	
AFGL 1289	8 44 07.8	+ 6 36 12	
AFGL 1290S	8 44 27	+ 1 18 06	
AFGL 1291	8 44 40	+78 21 30	
AFGL 1292	8 45 53	+18 13 12	
AFGL 1293	8 45 54.7	+12 43 58	
AFGL 1293	8 46 01	+12 42 00	
AFGL 1294S	8 46 40	+73 16 30	
AFGL 1295	8 47 40	+40 14 00	
AFGL 1296	8 49 24	+28 26 06	
AFGL 1297S	8 51 21	−12 51 30	
AFGL 1298	8 52 33	+17 25 24	
AFGL 1298	8 52 34.0	+17 25 22	
AFGL 1299	8 52 40	+ 6 07 48	
AFGL 1300	8 53 31	−19 02 48	
AFGL 1301	8 53 40	+20 02 18	
AFGL 1301	8 53 48.9	+20 02 30	
AFGL 1302	8 55 28	+11 01 48	
AFGL 1302	8 55 33.1	+11 02 23	
AFGL 1304	8 57 57	+67 50 30	
AFGL 1305S	8 59 01	+ 4 35 18	
AFGL 1306S	9 00 08	−20 50 36	
AFGL 1307	9 00 31	+38 57 00	
AFGL 1308	9 01 11	+60 29 00	
AFGL 1309	9 01 22	+ 9 04 12	
AFGL 1310	9 02 18	+64 58 30	

NAME	RA (1950)	DEC	POS REF
	h m s	° ′ ″	
AFGL 1311	9 02 20	+12 53 30	
AFGL 1312S	9 02 30	− 5 56 12	
AFGL 1313S	9 02 31	− 7 06 12	
AFGL 1314	9 03 04	+38 38 42	
AFGL 1315	9 03 39	− 9 43 36	
AFGL 1316	9 03 48	+67 03 48	
AFGL 1317	9 04 24	+ 1 41 06	
AFGL 1318S	9 04 35	− 8 36 36	
AFGL 1319	9 04 49	−15 30 48	
AFGL 1320	9 04 47	+69 24 18	
AFGL 1321	9 05 45	+13 24 48	
AFGL 1322S	9 06 37	+ 3 34 12	
AFGL 1323	9 06 51	+25 27 00	
AFGL 1324	9 07 16	+ 6 39 12	
AFGL 1326	9 07 36	+31 10 12	
AFGL 1327	9 07 44	− 6 05 00	
AFGL 1329S	9 08 36	+19 11 12	
AFGL 1331S	9 11 46	+ 0 48 54	
AFGL 1332	9 12 15	+56 56 30	
AFGL 1333S	9 12 27	+ 9 49 12	
AFGL 1334	9 12 34	− 1 40 30	
AFGL 1335	9 12 38	− 3 46 54	
AFGL 1337S	9 14 10	+37 38 00	
AFGL 1338S	9 15 47	+ 5 57 06	
AFGL 1339S	9 17 40	+ 3 12 24	
AFGL 1340S	9 17 56	+ 6 55 00	
AFGL 1341	9 17 59	+34 36 30	
AFGL 1342	9 18 02	+ 0 22 30	
AFGL 1343S	9 18 10	− 9 29 54	
AFGL 1344	9 18 18	+56 55 30	
AFGL 1345S	9 19 28	+41 40 30	
AFGL 1346S	9 19 45	− 6 33 54	
AFGL 1347S	9 20 29	+31 58 12	
AFGL 1348	9 20 45	+ 7 55 12	
AFGL 1349S	9 20 48	+21 35 18	
AFGL 1350	9 21 18	+64 08 48	
AFGL 1351	9 21 52	+26 22 42	
AFGL 1352	9 23 40	+21 00 24	
AFGL 1353	9 25 05	− 8 28 18	
AFGL 1354	9 25 37	+36 23 18	
AFGL 1355	9 27 51	+44 53 12	
AFGL 1357	9 28 24	+35 19 24	
AFGL 1358	9 28 50	+23 11 42	
AFGL 1359S	9 29 31	− 7 27 36	
AFGL 1360	9 29 46	+70 02 42	
AFGL 1363	9 30 07.4	+81 33 00	
AFGL 1363	9 31 02	+81 34 36	
AFGL 1364S	9 31 08	− 9 03 54	
AFGL 1366	9 33 45	+31 23 42	
AFGL 1367S	9 34 53	+11 55 00	
AFGL 1369	9 37 29	+ 0 54 54	
AFGL 1370S	9 38 11	+19 27 00	
AFGL 1371	9 38 54	+31 30 42	
AFGL 1372	9 41 00.6	+14 15 05	
AFGL 1372	9 41 06	+14 15 54	
AFGL 1373S	9 41 33	+46 17 36	
AFGL 1374S	9 42 01	+69 43 06	
AFGL 1375S	9 42 13	+18 01 42	
AFGL 1376	9 42 27	+34 43 54	
AFGL 1376	9 42 34.7	+34 44 34	
AFGL 1377S	9 42 55	+16 16 42	
AFGL 1378	9 43 00.1	+57 21 32	
AFGL 1378	9 43 03	+57 19 42	
AFGL 1379	9 43 31.8	+ 6 56 25	
AFGL 1379	9 43 34	+ 6 56 06	
AFGL 1380	9 44 48	+11 39 24	
AFGL 1380	9 44 52.2	+11 39 42	
AFGL 1381	9 45 10	+13 30 42	
AFGL 1382S	9 47 56	+ 2 23 42	
AFGL 1383S	9 48 09	+16 13 42	
AFGL 1384S	9 48 46	+ 0 02 06	
AFGL 1386	9 50 00	+26 15 06	
AFGL 1387	9 51 05.4	+ 6 11 41	
AFGL 1387	9 51 07	+ 6 10 36	
AFGL 1388	9 52 10	+69 54 42	
AFGL 1389	9 52 40	−18 44 36	
AFGL 1390S	9 52 55	+58 27 36	
AFGL 1391S	9 53 08	+55 31 24	
AFGL 1392	9 53 39	+16 56 42	
AFGL 1393S	10 00 31	+20 57 18	
AFGL 1394S	10 01 05	+45 08 18	
AFGL 1395	10 01 55	− 2 39 42	
AFGL 1396	10 02 13	+ 4 50 00	
AFGL 1398S	10 05 09	+10 58 18	
AFGL 1399	10 05 15	+10 15 30	
AFGL 1401S	10 10 57	+59 39 48	
AFGL 1402S	10 11 24	+56 36 30	
AFGL 1403	10 13 01	+30 49 30	
AFGL 1404	10 13 41	+23 37 54	
AFGL 1405	10 14 13	+14 00 54	
AFGL 1406	10 14 36	−14 24 00	
AFGL 1408S	10 16 10	+18 50 18	
AFGL 1409S	10 16 33	+21 30 00	
AFGL 1410	10 17 15	+20 05 18	
AFGL 1411	10 19 13	+41 45 00	
AFGL 1416	10 23 43	−16 33 06	
AFGL 1417	10 24 21	+ 5 52 54	
AFGL 1418S	10 27 41	+75 09 00	
AFGL 1419	10 29 36	+14 24 42	
AFGL 1421S	10 29 45	+44 07 30	
AFGL 1423	10 30 36	+70 01 24	
AFGL 1424	10 30 47	− 7 12 54	
AFGL 1425S	10 32 32	+14 37 30	
AFGL 1426	10 34 31	− 3 47 36	
AFGL 1427	10 35 08	−13 06 06	
AFGL 1428	10 35 16	−11 46 48	
AFGL 1429S	10 37 07	+72 54 12	
AFGL 1430S	10 37 12	−22 03 42	
AFGL 1431	10 39 41	+69 21 00	
AFGL 1432	10 41 12	+69 03 54	
AFGL 1433	10 41 45	+67 41 48	
AFGL 1434	10 42 28	− 6 35 12	
AFGL 1435S	10 42 45	+52 30 54	
AFGL 1437	10 46 10	+ 8 55 48	
AFGL 1437	10 46 11	+ 8 56 48	
AFGL 1438	10 47 07	−15 54 54	
AFGL 1439	10 49 11	−21 00 00	
AFGL 1440	10 50 27	+34 29 48	

NAME	RA (1950)	DEC	POS REF
	h m s	° ′ ″	
AFGL 1441	10 50 59	+13 58 54	
AFGL 1441	10 50 59	+14 00 06	
AFGL 1442	10 51 12	+77 19 48	
AFGL 1443	10 52 01	+72 08 42	
AFGL 1445S	10 52 39	+22 25 00	
AFGL 1446	10 53 18	+ 6 25 30	
AFGL 1446	10 53 25.7	+ 6 27 09	
AFGL 1447S	10 53 33	+74 24 36	
AFGL 1448	10 53 48	+74 35 36	
AFGL 1449	10 55 53	+70 16 54	
AFGL 1450	10 58 06	−18 03 24	
AFGL 1451S	10 59 01	+73 08 12	
AFGL 1452	10 59 20	− 2 11 24	
AFGL 1453	10 59 26	+46 36 06	
AFGL 1454	11 00 29	+62 00 00	
AFGL 1455	11 01 03	− 2 56 48	
AFGL 1456S	11 02 45	+72 57 24	
AFGL 1457	11 04 50	+49 27 24	
AFGL 1458	11 04 53	−11 11 42	
AFGL 1459S	11 05 07	+77 38 42	
AFGL 1460	11 06 30	+44 46 48	
AFGL 1461	11 06 38	+31 26 12	
AFGL 1462	11 06 40	+36 34 06	
AFGL 1463	11 06 46	+43 29 24	
AFGL 1465S	11 07 00	+31 07 36	
AFGL 1466S	11 07 53	+ 1 18 36	
AFGL 1468S	11 09 45	+28 49 12	
AFGL 1469S	11 11 20	− 8 43 36	
AFGL 1470S	11 11 50	+27 10 00	
AFGL 1473	11 12 28	+23 22 12	
AFGL 1474	11 12 39	+75 23 42	
AFGL 1475	11 15 46	+33 22 00	
AFGL 1476	11 16 26	−30 10 00	
AFGL 1477	11 16 46	−14 32 48	
AFGL 1478S	11 18 32	+ 4 33 42	
AFGL 1479	11 19 57	+43 44 36	
AFGL 1481	11 20 29	+24 24 18	
AFGL 1482	11 21 27	−19 36 30	
AFGL 1483	11 22 06	−10 36 00	
AFGL 1484	11 22 27	+16 29 48	
AFGL 1486	11 23 02	−12 14 06	
AFGL 1487	11 23 20	+ 9 30 30	
AFGL 1488	11 25 10	+15 25 06	
AFGL 1489	11 25 16	+45 28 30	
AFGL 1490S	11 25 47	+24 07 18	
AFGL 1491S	11 26 08	+ 1 42 06	
AFGL 1492	11 27 46	− 2 43 42	
AFGL 1493	11 27 57	−22 21 06	
AFGL 1494	11 28 25	+69 35 00	
AFGL 1495	11 29 13	−12 05 18	
AFGL 1496S	11 29 55	+ 5 22 24	
AFGL 1497	11 30 19	−30 50 54	
AFGL 1498	11 32 28	+19 27 12	
AFGL 1499	11 32 57	+35 09 36	
AFGL 1500	11 34 11	+77 51 06	
AFGL 1501S	11 35 19	+ 2 57 06	
AFGL 1502	11 35 55	+ 8 25 18	
AFGL 1503	11 37 17	−16 20 24	
AFGL 1504S	11 37 37	+16 13 30	
AFGL 1505S	11 38 27	+26 19 12	
AFGL 1506S	11 39 19	+55 27 06	
AFGL 1507S	11 42 16	+53 46 54	
AFGL 1508	11 43 05	+36 11 42	
AFGL 1509	11 43 12	+ 6 48 54	
AFGL 1509	11 43 17.3	+ 6 48 35	
AFGL 1510	11 43 22	+48 04 06	
AFGL 1510	11 43 25.0	+48 03 24	
AFGL 1511	11 44 31	+43 45 30	
AFGL 1511	11 44 36.1	+43 44 57	
AFGL 1512	11 46 19	−26 25 36	
AFGL 1513S	11 46 41	− 3 02 24	
AFGL 1514	11 46 50	+ 3 46 48	
AFGL 1515	11 47 23	−27 17 36	
AFGL 1516	11 48 35	−10 56 12	
AFGL 1517	11 51 45	+86 30 06	
AFGL 1518S	11 52 18	−17 39 54	
AFGL 1519	11 53 31	+58 07 00	
AFGL 1520S	11 53 36	−29 17 18	
AFGL 1521	11 54 17	+64 05 36	
AFGL 1523	11 56 20	+53 00 36	
AFGL 1524S	11 56 57	+49 10 24	
AFGL 1525S	11 57 14	−13 14 06	
AFGL 1526	11 57 38	+81 07 30	
AFGL 1527	11 57 39	+19 43 36	
AFGL 1528S	11 58 21	+ 3 05 36	
AFGL 1529S	11 59 49	+35 37 42	
AFGL 1530S	11 59 52	+21 16 24	
AFGL 1532	12 01 56	+42 58 24	
AFGL 1533S	12 03 03	−24 36 12	
AFGL 1534S	12 04 20	+19 58 30	
AFGL 1535	12 04 43	− 6 29 00	
AFGL 1536	12 07 28	−22 20 00	
AFGL 1537S	12 08 08	+35 24 30	
AFGL 1538S	12 08 57	+51 28 54	
AFGL 1539	12 09 55	+45 44 06	
AFGL 1540S	12 10 00	+21 05 24	
AFGL 1541S	12 12 10	+48 11 18	
AFGL 1542	12 12 30	+19 18 54	
AFGL 1543	12 13 35	+40 58 36	
AFGL 1545	12 17 18	+49 17 06	
AFGL 1546S	12 19 24	−10 02 30	
AFGL 1547	12 20 41	−11 34 06	
AFGL 1549	12 22 38	+ 1 01 24	
AFGL 1550	12 22 50	+57 03 18	
AFGL 1551	12 24 33	+28 33 12	
AFGL 1552	12 25 26	+55 58 24	
AFGL 1553S	12 25 52	− 8 23 12	
AFGL 1554	12 27 48	+ 4 42 48	
AFGL 1555	12 28 13	+69 28 30	
AFGL 1556S	12 28 17	+69 54 06	
AFGL 1557S	12 30 39	+40 32 24	
AFGL 1558	12 31 47	−23 04 00	
AFGL 1561S	12 32 33	+70 17 48	
AFGL 1562S	12 33 30	+21 00 48	
AFGL 1564	12 34 26	+27 21 06	
AFGL 1565	12 34 28	−17 15 48	
AFGL 1566	12 35 46	+ 2 06 12	
AFGL 1568S	12 37 20	+36 42 36	

NAME	RA (1950)	DEC	POS REF
	h m s	° ′ ″	
AFGL 1570	12 37 57	+56 06 12	
AFGL 1571	12 39 06	− 1 11 00	
AFGL 1572S	12 39 42	−13 50 24	
AFGL 1574S	12 40 40	+ 9 31 30	
AFGL 1575	12 42 41	− 6 14 54	
AFGL 1576	12 42 48	+45 43 12	
AFGL 1577S	12 43 30	+47 58 18	
AFGL 1578S	12 43 46	+53 28 00	
AFGL 1579	12 44 41	+ 4 24 48	
AFGL 1579	12 44 46	+ 4 25 06	
AFGL 1581	12 47 07	−14 50 12	
AFGL 1583	12 51 39	− 9 15 48	
AFGL 1583	12 51 45	− 9 16	
AFGL 1584	12 51 53	+56 12 48	
AFGL 1585	12 52 39	+47 27 30	
AFGL 1586	12 52 54	+ 3 38 36	
AFGL 1587S	12 54 15	−22 59 12	
AFGL 1588	12 54 17	+66 16 42	
AFGL 1589	12 56 12	+17 40 24	
AFGL 1590S	12 56 46	+ 0 29 00	
AFGL 1591S	12 57 22	+19 38 00	
AFGL 1593	12 59 47	+11 14 30	
AFGL 1594	12 59 56	+ 5 25 54	
AFGL 1594	13 00 06	+ 5 27 12	
AFGL 1595S	13 00 01	+17 07 48	
AFGL 1596	13 01 01	+ 6 34 48	
AFGL 1597	13 01 21	+ 7 19 30	
AFGL 1598S	13 02 07	+69 25 36	
AFGL 1600S	13 05 58	+39 26 48	
AFGL 1601S	13 08 36	−30 38 06	
AFGL 1602	13 08 48	−10 14 18	
AFGL 1603S	13 08 54	−29 35 18	
AFGL 1604	13 10 18	− 1 32 12	
AFGL 1605S	13 10 22	+42 29 42	
AFGL 1606	13 11 31	− 2 32 12	
AFGL 1607S	13 11 34	+ 5 37 06	
AFGL 1608	13 11 55	+11 34 48	
AFGL 1609S	13 13 33	+ 0 54 54	
AFGL 1610	13 13 40	+ 6 43 24	
AFGL 1611	13 15 04	+ 5 44 42	
AFGL 1612	13 15 21	+55 54 00	
AFGL 1613S	13 15 41	+32 28 54	
AFGL 1614	13 16 11	−22 54 30	
AFGL 1615	13 17 03	+45 46 30	
AFGL 1616S	13 18 05	+71 04 54	
AFGL 1617	13 19 57	− 3 31 54	
AFGL 1618	13 20 40	+47 13 42	
AFGL 1619S	13 20 43	+42 21 18	
AFGL 1620	13 21 42	+37 17 36	
AFGL 1621S	13 21 50	+55 10 12	
AFGL 1622	13 22 32	−10 53 36	
AFGL 1623S	13 24 58	−22 47 54	
AFGL 1624	13 25 31	+40 07 36	
AFGL 1625	13 26 12	+55 24 12	
AFGL 1626S	13 26 46	−10 50 48	
AFGL 1627	13 27 02	−23 02 06	
AFGL 1630S	13 29 12	+23 06 30	
AFGL 1631	13 29 24	− 5 59 24	
AFGL 1633	13 30 18	− 6 56 42	
AFGL 1634	13 30 47	−26 19 30	
AFGL 1635S	13 31 41	+25 18 36	
AFGL 1637	13 33 20	+76 46 00	
AFGL 1638S	13 33 43	− 2 59 18	
AFGL 1639S	13 36 07	−11 11 48	
AFGL 1640S	13 36 18	+ 1 26 36	
AFGL 1641S	13 38 08	−30 14 24	
AFGL 1642	13 38 21	+54 54 12	
AFGL 1643	13 38 58	− 8 27 54	
AFGL 1644S	13 41 08	− 9 20 18	
AFGL 1647S	13 44 21	+25 27 06	
AFGL 1648	13 44 42	−17 35 24	
AFGL 1649S	13 45 07	+12 56 24	
AFGL 1650	13 46 09	−28 07 18	
AFGL 1651	13 46 47	+16 00 18	
AFGL 1652	13 46 53	+39 47 36	
AFGL 1653	13 49 13	− 3 25 18	
AFGL 1654	13 49 32	+34 40 42	
AFGL 1656	13 49 56	+64 58 54	
AFGL 1657S	13 50 03	−17 21 48	
AFGL 1658	13 51 20	+52 33 42	
AFGL 1659	13 51 48	+16 25 36	
AFGL 1660	13 52 29.9	−26 11 13	
AFGL 1660	13 52 32	−26 12 00	
AFGL 1661	13 54 02	+27 42 18	
AFGL 1662S	13 54 06	−11 10 36	
AFGL 1663	13 54 46	−30 50 30	
AFGL 1664S	13 56 08	+11 11 12	
AFGL 1665S	13 56 18	+59 50 06	
AFGL 1666S	13 56 31	− 5 20 06	
AFGL 1667S	13 56 55	−18 41 30	
AFGL 1668S	13 57 04	+40 32 06	
AFGL 1669	13 57 31	+37 27 00	
AFGL 1670S	13 58 06	+62 13 00	
AFGL 1671	13 58 16.7	+39 16 17	
AFGL 1671S	13 58 10	+39 15 42	
AFGL 1672S	13 58 51	+39 42 36	
AFGL 1673	13 59 33	−27 09 00	
AFGL 1676	14 03 30	−26 28 18	
AFGL 1677	14 03 58	−13 58 24	
AFGL 1678S	14 04 44	− 7 44 24	
AFGL 1679S	14 04 48	+20 38 00	
AFGL 1680	14 05 57	+44 05 36	
AFGL 1681S	14 05 58	+24 12 06	
AFGL 1682S	14 06 40	−14 37 06	
AFGL 1683S	14 07 33	−15 08 18	
AFGL 1684	14 08 11	−16 04 48	
AFGL 1685	14 08 36	−28 37 36	
AFGL 1686	14 08 38	− 7 33 54	
AFGL 1687	14 08 40	+77 48 00	
AFGL 1688	14 10 13	−10 02 42	
AFGL 1689	14 10 30	−13 36 06	
AFGL 1690	14 11 16	+69 39 06	
AFGL 1692	14 13 09	+19 44 42	
AFGL 1693	14 13 20	+19 25 30	
AFGL 1694	14 14 08	−16 10 36	
AFGL 1696	14 15 58	+67 01 24	
AFGL 1697	14 16 29	−14 09 12	
AFGL 1698	14 16 31	−13 09 30	
AFGL 1699S	14 16 42	−20 25 54	
AFGL 1700	14 16 49	+ 3 01 00	
AFGL 1702S	14 20 40	− 1 44 36	
AFGL 1705S	14 21 52	+84 03 48	
AFGL 1706	14 21 46	+25 54 36	
AFGL 1707S	14 22 38	+33 07 24	
AFGL 1709S	14 24 38	−24 59 00	
AFGL 1710	14 24 42	+ 4 53 42	
AFGL 1711	14 26 02	− 6 37 30	
AFGL 1713	14 26 33	+38 09 36	
AFGL 1714	14 27 27	+75 54 18	
AFGL 1715	14 28 04	−29 52 12	
AFGL 1716	14 29 40	+30 34 36	
AFGL 1717S	14 30 23	+ 7 19 36	
AFGL 1719	14 37 10	+32 44 24	
AFGL 1720	14 39 13	+31 47 18	
AFGL 1721S	14 39 19	−26 03 42	
AFGL 1723S	14 40 32	−26 35 00	
AFGL 1724	14 41 02	+26 43 18	
AFGL 1726	14 42 48	+56 19 54	
AFGL 1727S	14 43 02	−25 58 54	
AFGL 1728	14 43 54	+15 19 30	
AFGL 1729S	14 43 53	−20 20 42	
AFGL 1730S	14 44 33	+ 0 22 12	
AFGL 1731S	14 44 43	−12 29 18	
AFGL 1732	14 45 31	−36 27 12	
AFGL 1734	14 46 52	− 7 55 30	
AFGL 1735	14 47 07	+12 54 42	
AFGL 1736	14 47 20	−27 43 48	
AFGL 1737S	14 49 53	−28 31 42	
AFGL 1739S	14 50 37	+21 33 06	
AFGL 1740	14 51 07	+74 22 30	
AFGL 1741S	14 52 12	− 2 29 36	
AFGL 1742S	14 53 41	−25 12 54	
AFGL 1743	14 54 59	−12 15 54	
AFGL 1743	14 55 02.6	−12 14 15	
AFGL 1744	14 56 41	+66 08 48	
AFGL 1745	14 57 02	+ 4 45 12	
AFGL 1746	14 58 00	−34 16 48	
AFGL 1747S	14 58 41	−18 36 18	
AFGL 1748	14 59 36	+40 33 54	
AFGL 1749S	15 00 16	+ 2 18 54	
AFGL 1750	15 01 09	−25 03 18	
AFGL 1754	15 09 46	+19 09 06	
AFGL 1755S	15 12 12	+15 20 18	
AFGL 1756	15 12 20	− 2 16 18	
AFGL 1759S	15 14 13	−12 33 00	
AFGL 1760	15 15 47	+15 56 18	
AFGL 1761	15 16 39	− 9 00 18	
AFGL 1762S	15 18 09	+16 46 24	
AFGL 1763	15 18 37	−36 03 24	
AFGL 1764	15 18 55	−32 04 30	
AFGL 1765	15 19 11	+14 28 12	
AFGL 1766	15 21 21	−33 46 18	
AFGL 1767	15 21 22	−22 42 12	
AFGL 1768S	15 22 10	+ 9 05 06	
AFGL 1769	15 22 17	− 2 04 24	
AFGL 1771	15 22 36	−36 04 18	
AFGL 1772	15 23 21	+15 36 00	
AFGL 1773	15 25 27	+19 43 36	
AFGL 1774S	15 27 48	−13 13 24	
AFGL 1775S	15 28 26	−22 45 54	
AFGL 1776	15 29 18	−23 43 00	
AFGL 1777	15 29 55	+ 3 50 42	
AFGL 1778S	15 30 00	−16 53 48	
AFGL 1779S	15 30 19	+13 42 36	
AFGL 1780	15 30 55	+78 48 12	
AFGL 1781S	15 31 23	−18 21 48	
AFGL 1783	15 32 52	+77 31 30	
AFGL 1787	15 33 55	−28 01 12	
AFGL 1788	15 34 06	+15 16 06	
AFGL 1789	15 34 04	+21 48 12	
AFGL 1790	15 35 55	+24 42 06	
AFGL 1791S	15 36 09	− 8 24 00	
AFGL 1792	15 39 01	−19 30 54	
AFGL 1793	15 41 04	− 1 33 00	
AFGL 1794	15 41 54	+ 6 33 12	
AFGL 1795S	15 44 43	+11 24 24	
AFGL 1796	15 45 54	−20 14 12	
AFGL 1797S	15 46 20	+ 5 00 06	
AFGL 1799	15 46 35	+18 17 18	
AFGL 1801	15 48 16	+15 17 30	
AFGL 1801	15 48 23.2	+15 17 02	
AFGL 1803	15 48 57	+21 08 48	
AFGL 1804	15 49 44	−25 57 36	
AFGL 1805	15 51 00	−16 32 36	
AFGL 1806	15 51 47	−10 43 00	
AFGL 1807	15 51 55	−37 11 30	
AFGL 1808S	15 52 36	+ 5 05 12	
AFGL 1809	15 52 37	− 3 48 42	
AFGL 1810S	15 52 45	−12 40 48	
AFGL 1811	15 52 50	−18 38 54	
AFGL 1812S	15 52 56	− 8 05 06	
AFGL 1813S	15 54 08	−18 32 06	
AFGL 1814	15 54 11	−15 53 54	
AFGL 1815S	15 54 46	−29 08 06	
AFGL 1816	15 55 36	+27 01 30	
AFGL 1818	15 57 35	−12 12 18	
AFGL 1820S	16 01 35	+15 01 36	
AFGL 1821	16 02 55	−21 38 06	
AFGL 1822	16 02 59	−30 40 30	
AFGL 1823	16 05 03	−26 10 30	
AFGL 1824S	16 05 55	+ 0 54 12	
AFGL 1825	16 06 05	+ 8 39 24	
AFGL 1826	16 06 04	− 1 25 30	
AFGL 1827S	16 06 40	− 3 01 42	
AFGL 1828	16 07 13	− 3 18 36	
AFGL 1830	16 07 27	−27 40 30	
AFGL 1832	16 08 09	+25 12 12	
AFGL 1833S	16 09 28	+ 3 51 36	
AFGL 1834	16 09 29	+23 37 42	
AFGL 1835	16 10 59	−11 45 18	
AFGL 1836S	16 11 31	−36 40 18	
AFGL 1837	16 11 46	− 3 33 30	
AFGL 1838	16 15 46	− 4 35 12	
AFGL 1839S	16 16 04	− 1 37 36	
AFGL 1840S	16 16 07	−14 46 24	
AFGL 1841	16 16 08	+59 52 36	
AFGL 1842S	16 16 47	−17 44 30	
AFGL 1843	16 17 07	−14 31 12	
AFGL 1844	16 17 40	−24 02 54	
AFGL 1845	16 18 09	−25 28 12	
AFGL 1847	16 18 41	− 7 34 24	
AFGL 1849S	16 19 46	+64 11 42	
AFGL 1850	16 19 53	−25 31 18	
AFGL 1851	16 20 16	− 7 08 30	
AFGL 1852	16 20 24	+30 59 24	
AFGL 1853	16 20 45	+33 53 36	
AFGL 1854	16 20 52	−22 14 18	
AFGL 1855	16 22 23	−24 17 54	
AFGL 1856	16 23 16	−33 42 54	
AFGL 1857	16 23 28	− 1 19 24	
AFGL 1858	16 23 30	+19 00 00	
AFGL 1859	16 23 58	−12 18 24	
AFGL 1861	16 24 59	− 7 30 42	
AFGL 1862	16 26 02	+34 54 12	
AFGL 1863	16 26 20	−26 19 24	
AFGL 1864	16 26 59	+41 59 12	
AFGL 1865S	16 29 54	+56 39 36	
AFGL 1866S	16 29 59	−16 00 36	
AFGL 1867S	16 30 02	+50 59 00	
AFGL 1868	16 30 15	+72 23 00	
AFGL 1869	16 30 48	−16 02 48	
AFGL 1870	16 33 22	−31 06 36	
AFGL 1872	16 34 22	+60 33 48	
AFGL 1873	16 35 42	+22 30 48	
AFGL 1874	16 36 02	− 8 31 18	
AFGL 1875	16 36 15	−21 48 42	
AFGL 1876	16 36 47	−20 47 30	
AFGL 1877S	16 37 18	−33 56 30	
AFGL 1878	16 37 27	−32 19 42	
AFGL 1879	16 37 38	+49 01 06	
AFGL 1880	16 38 18	−19 50 54	
AFGL 1881S	16 38 20	−11 42 42	
AFGL 1882S	16 38 43	−17 41 24	
AFGL 1883	16 38 45	−27 01 18	
AFGL 1885	16 41 03	+39 01 12	
AFGL 1886	16 42 06	+54 59 18	
AFGL 1887	16 42 30	− 3 00 54	
AFGL 1888	16 43 00	+15 50 36	
AFGL 1889	16 43 02	+12 16 30	
AFGL 1890	16 43 53	−11 34 54	
AFGL 1891	16 45 48	+42 19 12	
AFGL 1892S	16 45 51	−28 00 48	
AFGL 1893	16 46 01	−36 11 18	
AFGL 1894	16 46 16	−19 27 00	
AFGL 1895	16 46 36	−21 45 00	
AFGL 1897S	16 47 18	−13 36 30	
AFGL 1898	16 47 20	+57 54 12	
AFGL 1899	16 47 30	+63 02 06	
AFGL 1900	16 47 49	+11 04 42	
AFGL 1901S	16 48 33	−23 30 36	
AFGL 1902	16 49 04	−12 20 30	
AFGL 1904	16 49 26	−12 49 18	
AFGL 1905	16 49 24	+15 02 18	
AFGL 1906	16 51 29	+ 6 36 24	
AFGL 1907S	16 51 31	− 6 38 54	
AFGL 1908	16 52 08	−21 52 30	
AFGL 1909	16 53 12	−32 45 36	
AFGL 1910	16 53 30	−30 30 42	
AFGL 1911	16 54 07	−10 23 00	
AFGL 1912S	16 55 01	+ 9 19 12	
AFGL 1913S	16 55 10	− 1 15 36	
AFGL 1914	16 55 25	+ 9 27 00	
AFGL 1915S	16 55 48	+16 22 30	
AFGL 1916	16 56 55	−24 58 24	
AFGL 1917	16 57 16	−10 51 42	
AFGL 1920	17 00 08	−20 27 54	
AFGL 1921S	17 04 47	− 9 18 06	
AFGL 1922	17 04 53	−24 39 00	
AFGL 1923	17 04 54	−16 01 12	
AFGL 1925S	17 06 51	+49 05 42	
AFGL 1927	17 07 57	−32 13 24	
AFGL 1929	17 08 26	+40 46 00	
AFGL 1930	17 08 28	+64 24 24	
AFGL 1931S	17 09 59	+29 46 00	
AFGL 1932	17 10 05	+10 39 42	
AFGL 1933	17 10 10	−14 47 42	
AFGL 1934	17 10 13	−10 29 00	
AFGL 1935	17 10 58	+ 0 03 36	
AFGL 1936S	17 11 22	+ 4 56 48	
AFGL 1937	17 11 38	−33 21 24	
AFGL 1938	17 11 49	+14 08 24	
AFGL 1939S	17 11 50	− 4 44 24	
AFGL 1940	17 11 54	+ 8 58 06	
AFGL 1941	17 11 58	+ 0 42 06	
AFGL 1942	17 12 00	+57 56 06	
AFGL 1943	17 12 01	−30 27 42	
AFGL 1944	17 12 18	+11 08 24	
AFGL 1945	17 12 21	−21 22 12	
AFGL 1946S	17 12 25	− 9 53 54	
AFGL 1947	17 12 22	+14 26 48	
AFGL 1948	17 12 46	+36 25 18	
AFGL 1949S	17 12 56	− 3 10 48	
AFGL 1950	17 13 17	+36 51 42	
AFGL 1951	17 13 20	−15 07 48	
AFGL 1954	17 16 14	−19 32 48	
AFGL 1955	17 17 16	+ 2 11 48	
AFGL 1956	17 17 51	+18 08 42	
AFGL 1958	17 19 20	+16 47 00	
AFGL 1959	17 19 22	−13 05 48	
AFGL 1960	17 20 29	+ 0 56 18	
AFGL 1961	17 20 43	−29 15 54	
AFGL 1962S	17 21 31	+10 07 36	
AFGL 1963	17 22 00	−24 38 12	
AFGL 1964	17 22 31	−26 49 36	
AFGL 1965	17 22 55	− 3 00 30	
AFGL 1966S	17 23 27	+22 06 18	
AFGL 1967	17 23 31	+16 58 30	
AFGL 1968	17 23 24	+71 54 48	
AFGL 1969	17 24 00	+ 4 11 30	
AFGL 1970	17 26 35	− 7 26 30	
AFGL 1971	17 26 41	−19 26 30	
AFGL 1972	17 26 52	−26 25 06	
AFGL 1973S	17 27 16	−18 54 18	
AFGL 1974	17 27 23	−26 41 06	

NAME	RA (1950)	DEC	POS REF
	h m s	° ′ ″	
AFGL 1976	17 28 45	+26 09 00	
AFGL 1977	17 29 38	+17 49 12	
AFGL 1979S	17 30 05	−22 24 24	
AFGL 1981	17 30 41	+ 0 09 36	
AFGL 1982S	17 31 05	−24 49 06	
AFGL 1983	17 31 16	− 1 55 24	
AFGL 1985	17 31 46	−23 42 54	
AFGL 1986S	17 32 22	+15 20 12	
AFGL 1987	17 33 13	+53 59 00	
AFGL 1988	17 33 19	+15 35 48	
AFGL 1989	17 33 22	+17 39 54	
AFGL 1990S	17 34 27	−16 17 42	
AFGL 1991	17 35 16	−20 48 00	
AFGL 1992	17 36 05	−30 13 18	
AFGL 1993	17 36 12	+57 46 00	
AFGL 1995	17 37 34	− 2 09 30	
AFGL 1996	17 38 50	−20 48 36	
AFGL 1997	17 39 25	−30 03 54	
AFGL 1998	17 39 56	− 4 51 12	
AFGL 1999	17 40 05	+62 36 18	
AFGL 2000	17 41 03	+ 4 34 30	
AFGL 2001S	17 41 22	−29 26 30	
AFGL 2002	17 42 11	−29 16 12	
AFGL 2003	17 42 32	−28 56 00	
AFGL 2004	17 43 00	−28 50 48	
AFGL 2004.1	"	"	ED
AFGL 2004.2	"	"	"
AFGL 2005S	17 43 37	−20 53 36	
AFGL 2006	17 43 50	−28 32 36	
AFGL 2007S	17 44 56	+ 7 00 54	
AFGL 2008	17 45 06	− 3 37 36	
AFGL 2009	17 45 45.5	−28 53 00	
AFGL 2009	17 45 50	−28 48 18	
AFGL 2010	17 46 09	−29 00 12	
AFGL 2011	17 46 13	−28 42 12	
AFGL 2012	17 46 16	− 9 08 42	
AFGL 2013	17 46 48	−29 01 30	
AFGL 2014	17 47 09	+45 43 18	
AFGL 2015	17 47 29	−27 51 12	
AFGL 2016	17 48 24	− 8 00 12	
AFGL 2017	17 48 54	−28 00 18	
AFGL 2018	17 49 04	− 2 27 06	
AFGL 2019	17 50 10	−26 56 54	
AFGL 2020	17 50 23	− 2 32 30	
AFGL 2021S	17 50 41	+10 46 48	
AFGL 2023	17 51 15	−25 47 18	
AFGL 2023.1	"	"	ED
AFGL 2023.2	"	"	"
AFGL 2024	17 51 21	−23 14 00	
AFGL 2025	17 51 53	+28 12 12	
AFGL 2026	17 53 00	+56 52 42	
AFGL 2027	17 53 11	+57 05 48	
AFGL 2028	17 53 29	+26 02 30	
AFGL 2029S	17 53 38	− 1 26 42	
AFGL 2032	17 53 50	+11 34 42	
AFGL 2033	17 53 53	+10 38 48	
AFGL 2034	17 54 01	−23 54 06	
AFGL 2036	17 54 06	−19 19 42	
AFGL 2037	17 54 17	+11 11 42	
AFGL 2038	17 54 47	+37 13 18	
AFGL 2039	17 55 16	+51 29 36	
AFGL 2040	17 55 31	+58 13 06	
AFGL 2041	17 55 30	+45 23 54	
AFGL 2042	17 56 19	− 9 46 48	
AFGL 2043S	17 56 35	−20 35 18	
AFGL 2045S	17 57 16	− 8 04 30	
AFGL 2046	17 57 23	−24 05 06	
AFGL 2046.1	"	"	ED
AFGL 2047	17 57 59.3	−17 44 34	
AFGL 2047	17 58 11	−17 44 00	
AFGL 2048	17 58 58	−23 35 30	
AFGL 2049S	17 59 14	−23 27 24	
AFGL 2050	17 59 14	−23 02 42	
AFGL 2051	17 59 55	−21 46 30	
AFGL 2052	18 00 38	−24 20 42	
AFGL 2052.1	"	"	ED
AFGL 2053	18 00 53	−24 05 00	
AFGL 2054	18 00 58	−20 19 00	
AFGL 2055S	18 01 07	−16 57 24	
AFGL 2056	18 01 08	+19 33 48	
AFGL 2057	18 01 21	+ 8 26 36	
AFGL 2059	18 01 48	−24 29 48	
AFGL 2061	18 01 53	−28 06 42	
AFGL 2062	18 02 36	−21 13 24	
AFGL 2063	18 02 54	−20 49 06	
AFGL 2063.1	"	"	ED
AFGL 2064	18 03 54	+22 12 12	
AFGL 2065	18 03 58	− 8 14 18	
AFGL 2066	18 04 01	− 4 54 12	
AFGL 2067	18 04 04	− 9 41 48	
AFGL 2068	18 04 26	+62 37 12	
AFGL 2069	18 04 28	−29 25 12	
AFGL 2070	18 04 45	+ 6 33 24	
AFGL 2071	18 05 00	−22 15 36	
AFGL 2072	18 05 23	+43 27 18	
AFGL 2073S	18 05 26	−20 01 48	
AFGL 2074	18 06 01	−18 13 12	
AFGL 2075	18 06 07	+ 5 17 36	
AFGL 2076	18 06 11	−27 40 48	
AFGL 2077	18 06 19	+42 13 48	
AFGL 2078	18 06 24	−20 20 06	
AFGL 2079	18 06 24	−23 06 18	
AFGL 2080.2	18 06 59	−24 07 24	ED
AFGL 2080.3	"	"	"
AFGL 2081S	18 07 04	−23 34 42	
AFGL 2082	18 07 22	−26 52 00	
AFGL 2083	18 07 38	−10 33 30	
AFGL 2084	18 07 37	− 7 18 30	
AFGL 2085	18 07 52	−20 24 30	
AFGL 2086	18 08 23	−26 29 00	
AFGL 2087	18 09 06	−18 53 36	
AFGL 2088	18 09 10	− 4 35 48	
AFGL 2089	18 09 52	+31 24 18	
AFGL 2090	18 11 16	−17 56 42	
AFGL 2091S	18 11 15	−12 39 42	
AFGL 2092	18 11 17	−21 43 06	
AFGL 2094	18 11 47	−16 49 12	
AFGL 2096	18 12 00	−22 47 48	

NAME	RA (1950)	DEC	POS REF
	h m s	° ′ ″	
AFGL 2097	18 12 33	+15 34 54	
AFGL 2098	18 12 43	+30 10 36	
AFGL 2099S	18 12 56	+25 55 54	
AFGL 2100S	18 13 22	+27 33 30	
AFGL 2101	18 13 25	−16 51 42	
AFGL 2102	18 13 28	−17 40 36	
AFGL 2103	18 13 30	−16 42 12	
AFGL 2104	18 13 41	−19 00 00	
AFGL 2105	18 13 43	−16 12 00	
AFGL 2105.1	"	"	ED
AFGL 2105.2	"	"	"
AFGL 2106	18 13 48	+ 2 18 24	
AFGL 2107	18 13 57	−18 40 48	
AFGL 2107.1	"	"	ED
AFGL 2107.2	"	"	"
AFGL 2108	18 14 05	−12 11 36	
AFGL 2109	18 14 07	−16 27 24	
AFGL 2110	18 14 42	−22 15 06	
AFGL 2111S	18 14 56	+36 42 48	
AFGL 2112	18 15 00	−27 00 00	
AFGL 2113	18 15 05	−11 46 48	
AFGL 2113.1	"	"	ED
AFGL 2113.2	"	"	"
AFGL 2114	18 15 32	−13 28 24	
AFGL 2115	18 15 35	−15 21 30	
AFGL 2116	18 15 41	+17 58 36	
AFGL 2117	18 15 43	−13 46 24	
AFGL 2118	18 15 42	− 6 55 00	
AFGL 2119	18 16 06	−13 57 48	
AFGL 2120S	18 16 12	−11 41 54	
AFGL 2121S	18 16 17	−20 45 06	
AFGL 2122	18 16 25	−15 48 12	
AFGL 2123	18 17 05	−12 20 36	
AFGL 2124	18 17 36	−16 12 48	
AFGL 2125S	18 17 38	−14 09 54	
AFGL 2126	18 17 47	−29 49 24	
AFGL 2127	18 17 55	−13 48 12	
AFGL 2128	18 18 14	+21 56 48	
AFGL 2129	18 18 17	+36 01 30	
AFGL 2130	18 18 19	+25 49 06	
AFGL 2131	18 18 22	−24 53 18	
AFGL 2132	18 18 29	−13 04 18	
AFGL 2133	18 18 31	+31 43 06	
AFGL 2134	18 18 46	− 2 53 48	
AFGL 2135	18 19 32	−27 03 48	
AFGL 2136	18 19 34	−13 31 54	
AFGL 2137	18 20 02	+23 15 42	
AFGL 2138	18 20 21	+49 06 18	
AFGL 2139	18 20 25	−13 42 54	
AFGL 2140S	18 20 29	+50 42 24	
AFGL 2141S	18 20 49	− 4 30 30	
AFGL 2142	18 21 28	+ 3 35 42	
AFGL 2143	18 21 33	−16 15 24	
AFGL 2143.1	"	"	ED
AFGL 2143.2	"	"	"
AFGL 2144S	18 21 33	+72 41 36	
AFGL 2145	18 21 33	+21 43 48	
AFGL 2147	18 22 08	−13 16 06	
AFGL 2148	18 22 12	+39 33 06	
AFGL 2149	18 22 15	−20 31 00	
AFGL 2150	18 23 02.2	+ 5 44 16	
AFGL 2150	18 23 07	+ 5 43 48	
AFGL 2151	18 23 26	−22 05 30	
AFGL 2152	18 23 39	−11 51 18	
AFGL 2153	18 23 52	−12 26 48	
AFGL 2154	18 23 52	− 6 55 30	
AFGL 2155	18 24 04	+23 27 42	
AFGL 2155.1	"	"	ED
AFGL 2156	18 24 16	+ 3 55 00	
AFGL 2157	18 24 22	−12 42 00	
AFGL 2158	18 24 31	+ 1 06 48	
AFGL 2159	18 24 34	+ 7 31 12	
AFGL 2160	18 24 39	+10 50 36	
AFGL 2161	18 24 47	−12 00 00	
AFGL 2162	18 24 47	−12 28 30	
AFGL 2163	18 24 53	−25 26 36	
AFGL 2164	18 24 59	− 8 42 36	
AFGL 2165	18 24 59	− 3 51 30	
AFGL 2166	18 25 11	−13 04 06	
AFGL 2167	18 26 02	−17 45 54	
AFGL 2168	18 26 15	−11 34 42	
AFGL 2169	18 26 30	−10 55 12	
AFGL 2170S	18 26 38	− 6 06 18	
AFGL 2171	18 27 07	+82 35 54	
AFGL 2172	18 27 32	+24 19 42	
AFGL 2173	18 27 44	− 1 24 12	
AFGL 2174	18 28 18	− 9 45 12	
AFGL 2174.1	"	"	ED
AFGL 2174.2	"	"	"
AFGL 2176S	18 28 44	+12 49 36	
AFGL 2177	18 28 47	− 2 07 36	
AFGL 2177	18 28 47.7	− 2 07 42	
AFGL 2178	18 28 50	− 8 38 12	
AFGL 2179	18 28 55	−10 00 18	
AFGL 2180	18 28 55	+ 4 20 42	
AFGL 2181	18 28 57	+38 35 36	
AFGL 2182	18 29 48	−14 53 18	
AFGL 2183S	18 30 09	+23 11 12	
AFGL 2184	18 30 10	+86 39 30	
AFGL 2185	18 30 26	− 7 30 06	
AFGL 2186	18 30 37	−14 10 48	
AFGL 2187	18 30 39	+36 58 36	
AFGL 2188	18 30 53	− 9 10 42	
AFGL 2188.2	"	"	ED
AFGL 2188.3	"	"	"
AFGL 2189	18 31 23	+14 12 06	
AFGL 2190	18 31 26	− 7 20 54	
AFGL 2191	18 31 32	−21 03 30	
AFGL 2192	18 31 37	−11 33 18	
AFGL 2193	18 31 46	− 8 45 42	
AFGL 2194	18 31 49	− 7 59 18	
AFGL 2195	18 32 02	− 8 36 06	
AFGL 2196	18 32 27	−19 18 42	
AFGL 2197	18 32 27	− 8 16 06	
AFGL 2198	18 33 10	+51 44 54	
AFGL 2199	18 33 17	+ 5 32 42	
AFGL 2200	18 33 30	− 7 11 48	
AFGL 2201	18 33 49	−19 58 06	

NAME	RA (1950)	DEC	POS REF
	h m s	° ′ ″	
AFGL 2202	18 33 51	− 7 23 24	
AFGL 2203	18 34 13	− 7 38 18	
AFGL 2204	18 34 44	− 2 43 06	
AFGL 2205	18 34 47	− 5 27 42	
AFGL 2206	18 34 52	+10 24 06	
AFGL 2207	18 35 04	− 6 22 18	
AFGL 2208	18 35 13	+38 44 30	
AFGL 2209S	18 35 14	−12 22 24	
AFGL 2210	18 35 33	− 6 50 42	
AFGL 2210	18 35 34.4	− 6 50 57	
AFGL 2211	18 35 39	− 5 32 30	
AFGL 2212S	18 35 57	+22 38 54	
AFGL 2213	18 35 59	+ 8 45 36	
AFGL 2214	18 36 07	−13 50 12	
AFGL 2215	18 36 08	−15 04 18	
AFGL 2216S	18 36 18	− 5 20 48	
AFGL 2217	18 36 28	+39 37 36	
AFGL 2218	18 36 33	+18 23 12	
AFGL 2219	18 37 00	+11 48 30	
AFGL 2220	18 37 10	− 7 49 00	
AFGL 2222	18 37 31	− 0 23 36	
AFGL 2223	18 37 32	− 5 45 30	
AFGL 2224	18 37 53	−25 46 48	
AFGL 2225	18 38 03	+40 17 48	
AFGL 2226S	18 38 18	− 5 42 36	
AFGL 2227	18 38 46	− 4 24 12	
AFGL 2228	18 39 22	+28 46 12	
AFGL 2229	18 39 28	− 5 05 12	
AFGL 2230	18 39 31	− 2 49 36	
AFGL 2231S	18 39 36	+74 17 42	
AFGL 2232	18 39 42	+17 38 42	
AFGL 2233	18 39 53	− 2 21 06	
AFGL 2234S	18 39 53	− 2 07 42	
AFGL 2235	18 40 04	−19 20 18	
AFGL 2236	18 40 04	+28 55 24	
AFGL 2237S	18 40 10	− 4 36 00	
AFGL 2238	18 40 24	− 3 36 18	
AFGL 2239	18 40 49	+12 21 42	
AFGL 2240	18 41 07	+36 55 06	
AFGL 2241	18 41 15	+13 53 06	
AFGL 2242	18 41 44	+32 38 24	
AFGL 2243	18 41 42	− 4 23 18	
AFGL 2244	18 43 01	−19 38 36	
AFGL 2245	18 43 23	− 2 42 36	
AFGL 2246	18 43 39	+43 34 48	
AFGL 2247	18 44 07	+26 38 00	
AFGL 2248	18 44 26	− 4 47 48	
AFGL 2249S	18 44 39	− 2 24 24	
AFGL 2250S	18 44 56	−12 21 30	
AFGL 2251	18 45 02	− 2 03 00	
AFGL 2252	18 45 03	− 9 21 36	
AFGL 2252 #1	"	"	
AFGL 2252 #2	18 45 03.7	− 9 22 45	
AFGL 2252.1	18 45 03	− 9 21 36	ED
AFGL 2252.2	"	"	"
AFGL 2253S	18 45 30	−19 55 36	
AFGL 2254	18 45 39	− 2 03 36	
AFGL 2255S	18 46 09	− 9 40 00	
AFGL 2256	18 46 28.8	− 6 56 32	
AFGL 2256	18 46 37	− 6 58 24	
AFGL 2257S	18 46 38	− 2 30 54	
AFGL 2258	18 47 08	− 1 32 00	
AFGL 2259	18 47 25	+ 9 29 30	
AFGL 2260	18 47 38	− 7 57 48	
AFGL 2261	18 48 00	+47 27 54	
AFGL 2262S	18 48 05	− 6 45 24	
AFGL 2263S	18 48 17	+23 43 48	
AFGL 2264	18 48 57	−29 04 36	
AFGL 2265S	18 49 05	− 1 36 18	
AFGL 2266	18 49 35	+12 07 30	
AFGL 2267	18 49 45	− 3 47 48	
AFGL 2268	18 49 50	− 5 23 12	
AFGL 2269S	18 49 55	+46 41 18	
AFGL 2270	18 50 08	−21 33 06	
AFGL 2271	18 50 50	+ 1 10 24	
AFGL 2272	18 51 13	+ 0 36 12	
AFGL 2273S	18 51 15	+30 37 54	
AFGL 2274	18 51 39	+40 57 12	
AFGL 2275	18 52 02	−16 35 06	
AFGL 2276	18 52 16	+10 35 18	
AFGL 2277S	18 52 38	+41 25 54	
AFGL 2278	18 52 40	+36 50 54	
AFGL 2279	18 52 48	+42 25 18	
AFGL 2280	18 53 09	−11 04 48	
AFGL 2281S	18 53 13	− 4 50 00	
AFGL 2282	18 53 41	−10 36 18	
AFGL 2284	18 53 47	+ 7 51 06	
AFGL 2285	18 53 55	+43 52 30	
AFGL 2286	18 54 47	−21 11 00	
AFGL 2287	18 55 15	+ 3 22 54	
AFGL 2288	18 55 53	+ 4 35 24	
AFGL 2289	18 56 03	−29 55 12	
AFGL 2290	18 56 04	+ 6 38 18	
AFGL 2290	18 56 04.0	+ 6 38 50	
AFGL 2291	18 56 12	+12 56 06	
AFGL 2292	18 56 25	+14 19 00	
AFGL 2293	18 56 27	−19 16 42	
AFGL 2294S	18 56 33	+25 11 30	
AFGL 2295S	18 57 04	− 6 56 12	
AFGL 2296	18 57 10	+ 5 16 00	
AFGL 2297	18 57 57	+22 44 30	
AFGL 2298S	18 57 59	+ 3 39 36	
AFGL 2300	18 58 45	−12 50 42	
AFGL 2301	18 58 47	+40 36 36	
AFGL 2302	18 58 59	− 5 50 54	
AFGL 2303	18 59 14	+ 4 07 42	
AFGL 2304	18 59 21	+ 1 07 42	
AFGL 2305	19 00 05	+ 8 25 18	
AFGL 2306S	19 00 09	+22 45 30	
AFGL 2307S	19 00 17	+25 15 54	
AFGL 2308	19 00 35	+20 39 36	
AFGL 2309	19 00 41	−22 45 30	
AFGL 2310	19 00 45	+ 7 24 36	
AFGL 2312	19 00 56	+12 09 30	
AFGL 2313S	19 01 10	+ 5 26 48	
AFGL 2314	19 01 39	− 5 46 24	
AFGL 2315	19 01 58	−13 50 12	
AFGL 2316	19 02 53	+ 8 09 48	

NAME	RA (1950)	DEC	POS REF
	h m s	° ′ ″	
AFGL 2317	19 03 08	+30 40 36	
AFGL 2318	19 03 04	+20 17 18	
AFGL 2319	19 03 17	+27 02 18	
AFGL 2320	19 03 24	+39 36 12	
AFGL 2321	19 03 47	+ 6 28 36	
AFGL 2322S	19 03 44	+29 49 18	
AFGL 2323	19 03 51	−27 45 42	
AFGL 2324	19 04 05	+ 8 07 48	
AFGL 2326	19 04 33	+ 7 05 00	
AFGL 2327	19 04 42	−17 04 48	
AFGL 2328S	19 05 30	−12 45 18	
AFGL 2329	19 05 40	+ 6 12 36	
AFGL 2330	19 05 56	−22 16 48	
AFGL 2331	19 06 30	+39 04 18	
AFGL 2333	19 07 33	+ 9 20 06	
AFGL 2334	19 07 54	+ 9 00 48	
AFGL 2335	19 08 07	−15 09 12	
AFGL 2337S	19 09 29	+10 03 06	
AFGL 2338	19 09 59	+66 00 42	
AFGL 2339S	19 10 14	+67 12 12	
AFGL 2341	19 11 02	+10 47 30	
AFGL 2342S	19 11 04	+25 55 36	
AFGL 2343	19 11 22	+ 0 03 30	
AFGL 2344S	19 11 27	+27 39 54	
AFGL 2345	19 11 58	+11 04 54	
AFGL 2345.1	"	"	ED
AFGL 2345.2	"	"	"
AFGL 2346	19 12 00	+46 53 18	
AFGL 2348	19 12 39	+67 33 48	
AFGL 2349	19 12 40	− 7 08 18	
AFGL 2350	19 13 28	+ 9 34 06	
AFGL 2351	19 13 25	+30 26 12	
AFGL 2352S	19 13 36	−10 07 24	
AFGL 2353	19 13 49	−19 25 24	
AFGL 2354S	19 14 08	− 8 24 12	
AFGL 2355S	19 14 08	+34 35 18	
AFGL 2356	19 14 16	+67 26 48	
AFGL 2357	19 14 33	+38 02 24	
AFGL 2358	19 14 37	+21 48 42	
AFGL 2359	19 15 09	+11 50 54	
AFGL 2359.2	"	"	ED
AFGL 2360	19 15 15	+12 04 12	
AFGL 2361	19 15 52	−17 08 30	
AFGL 2362	19 16 01	+23 45 48	
AFGL 2363	19 16 17	−15 58 12	
AFGL 2364S	19 16 29	+73 16 06	
AFGL 2365	19 16 46	+ 3 18 48	
AFGL 2366	19 17 32	+22 27 06	
AFGL 2367	19 17 35	+22 57 06	
AFGL 2368	19 17 36	− 8 06 06	
AFGL 2369	19 17 43	−10 42 48	
AFGL 2370	19 17 49	−26 15 36	
AFGL 2371	19 18 13	+13 49 48	
AFGL 2372S	19 18 17	+40 41 06	
AFGL 2373	19 18 50	−16 00 42	
AFGL 2374	19 19 13.2	+ 9 22 14	
AFGL 2374	19 19 15	+ 9 23 12	
AFGL 2375	19 19 25	+17 33 54	
AFGL 2376	19 20 09	+13 58 30	
AFGL 2376.1	"	"	ED
AFGL 2376.2	"	"	"
AFGL 2377S	19 20 25	+ 7 20 12	
AFGL 2378	19 20 38	+14 23 00	
AFGL 2379	19 20 44	+14 10 00	
AFGL 2380	19 20 55	+14 47 42	
AFGL 2381	19 21 24	+14 24 30	
AFGL 2382	19 22 17	−13 28 54	
AFGL 2383	19 23 10	+50 09 24	
AFGL 2384	19 23 11	+76 27 36	
AFGL 2385S	19 23 21	+53 32 00	
AFGL 2386S	19 23 41	+60 55 30	
AFGL 2387S	19 23 45	+65 33 12	
AFGL 2388	19 24 13	+71 34 12	
AFGL 2389	19 24 14	+36 07 06	
AFGL 2390	19 24 30	+11 15 36	
AFGL 2391	19 24 51	−17 25 12	
AFGL 2392	19 24 55	+ 6 56 54	
AFGL 2393S	19 25 40	+33 25 06	
AFGL 2394S	19 26 17	+12 45 24	
AFGL 2395	19 26 41	+24 32 30	
AFGL 2396	19 27 13	+45 56 42	
AFGL 2397S	19 27 20	+13 55 54	
AFGL 2398	19 27 38	+ 2 49 36	
AFGL 2400	19 27 37	+ 0 56 36	
AFGL 2402	19 28 06	− 2 54 06	
AFGL 2403	19 28 17	+19 42 30	
AFGL 2403	19 28 18.0	+19 44 21	
AFGL 2404	19 28 26	+48 53 54	
AFGL 2405S	19 28 33	+15 32 54	
AFGL 2406	19 28 38	+27 52 06	
AFGL 2407	19 28 53	+46 02 42	
AFGL 2408	19 29 24	+18 36 48	
AFGL 2409	19 29 36	+43 31 24	
AFGL 2410	19 30 03	+13 15 12	
AFGL 2412	19 30 41	+ 4 56 24	
AFGL 2414	19 31 11	+23 31 54	
AFGL 2415	19 31 22	+ 5 21 42	
AFGL 2416	19 31 28	−16 28 48	
AFGL 2417	19 32 12	+27 57 54	
AFGL 2418	19 32 19	+49 09 06	
AFGL 2419S	19 33 09	+72 49 24	
AFGL 2420	19 33 12	+33 41 36	
AFGL 2421S	19 34 52	+12 02 36	
AFGL 2422	19 35 37	+50 05 36	
AFGL 2423	19 35 40	+11 38 12	
AFGL 2424	19 35 40	+69 41 12	
AFGL 2425	19 36 11	−16 57 30	
AFGL 2426	19 36 52	+28 22 24	
AFGL 2428	19 38 08	+33 15 42	
AFGL 2428.1	"	"	ED
AFGL 2428.2	"	"	"
AFGL 2429	19 38 23	+43 48 24	
AFGL 2430	19 38 27	− 4 00 48	
AFGL 2431S	19 38 27	+32 42 42	
AFGL 2432	19 38 52	+32 29 54	
AFGL 2433	19 38 58	+39 56 12	
AFGL 2434	19 39 02	+17 20 36	
AFGL 2435	19 39 04	+42 58 30	
AFGL 2436	19 39 37	+48 41 06	
AFGL 2439	19 41 07	+55 21 18	
AFGL 2440	19 41 14	+ 3 38 12	
AFGL 2443	19 41 47	+34 22 24	
AFGL 2444S	19 42 13	+32 23 18	
AFGL 2445	19 42 21	+35 07 54	
AFGL 2446	19 42 40	+34 17 30	
AFGL 2447S	19 42 51	+33 15 30	
AFGL 2448	19 43 07	+19 46 30	
AFGL 2450	19 43 19	+40 35 42	
AFGL 2451S	19 43 27	+31 21 18	
AFGL 2452	19 43 42	+ 1 33 36	
AFGL 2453	19 43 57	+10 30 42	
AFGL 2454	19 44 10	+24 27 18	
AFGL 2455	19 44 41	+25 05 12	
AFGL 2456	19 45 08	+18 24 54	
AFGL 2457S	19 46 04	+23 46 36	
AFGL 2458	19 46 04	+ 3 36 06	
AFCL 2459	19 46 13	+47 46 48	
AFGL 2460	19 47 10	+26 43 00	
AFGL 2461	19 47 24	− 7 43 24	
AFGL 2462	19 48 09	+24 46 12	
AFGL 2463	19 48 18	+ 8 44 24	
AFGL 2464	19 48 35	+70 09 54	
AFGL 2465	19 48 35	+32 47 18	
AFGL 2466	19 48 48	+38 35 42	
AFGL 2467	19 48 55	+37 41 54	
AFGL 2468S	19 49 15	+22 24 06	
AFGL 2471	19 50 18	+22 18 18	
AFGL 2472	19 52 23	+49 27 48	
AFGL 2473S	19 53 00	+23 15 12	
AFGL 2475	19 54 19	+34 57 12	
AFGL 2476	19 54 43	+58 43 12	
AFGL 2477	19 54 43	+30 35 18	
AFGL 2477	19 54 50.0	+30 35 57	
AFGL 2478S	19 54 55	+33 53 36	
AFGL 2479	19 54 56	− 2 00 24	
AFGL 2480	19 55 36	+44 08 48	
AFGL 2481	19 55 42	− 3 40 12	
AFGL 2481	19 55 55.0	− 3 41 24	
AFGL 2482	19 55 56	+33 00 18	
AFGL 2483	19 56 01	−13 44 12	
AFGL 2484	19 56 15	+15 51 30	
AFGL 2485	19 56 39	+19 21 00	
AFGL 2486	19 57 42	+17 22 48	
AFGL 2487S	19 57 43	−13 40 06	
AFGL 2488	19 58 34	+36 38 36	
AFGL 2489S	19 58 41	−10 05 42	
AFGL 2490	19 58 42	+52 00 24	
AFGL 2491	19 58 54	+36 58 54	
AFGL 2492	19 59 08	+33 02 00	
AFGL 2493	19 59 20	+33 47 12	
AFGL 2494	19 59 21	+40 45 42	
AFGL 2495	19 59 55	+33 25 06	
AFGL 2496	20 00 51	+76 23 18	
AFGL 2497	20 00 55	+64 40 42	
AFGL 2498	20 00 55	+30 11 42	
AFGL 2499S	20 01 30	+21 22 06	
AFGL 2500	20 01 38	+30 19 12	
AFGL 2501	20 02 19	+67 44 06	
AFGL 2502	20 02 24	+40 17 48	
AFGL 2503	20 02 33	+36 40 42	
AFGL 2504	20 02 56	+20 31 30	
AFGL 2505	20 03 12	+15 21 36	
AFGL 2506	20 03 38	+51 41 30	
AFGL 2507	20 03 45	+25 26 30	
AFGL 2508	20 03 45	−27 22 24	
AFGL 2509	20 04 12	+66 19 12	
AFGL 2511	20 05 23	+ 5 56 42	
AFGL 2512	20 06 09	+56 51 00	
AFGL 2513	20 07 13	+31 17 42	
AFGL 2514	20 07 46	− 6 25 24	
AFGL 2515	20 07 49	− 1 45 36	
AFGL 2516	20 07 55	+47 44 54	
AFGL 2517	20 08 02	+26 08 24	
AFGL 2518S	20 08 49	− 7 48 00	
AFGL 2519	20 09 16	+35 59 18	
AFGL 2520	20 09 30	−11 22 42	
AFGL 2521S	20 09 41	+ 9 46 48	
AFGL 2522	20 10 18	+ 0 24 54	
AFGL 2523	20 10 35	− 1 12 00	
AFGL 2525S	20 10 56	+32 05 48	
AFGL 2526	20 11 16	+49 18 12	
AFGL 2527S	20 11 20	+18 48 18	
AFGL 2528	20 11 44	+38 34 48	
AFGL 2529S	20 11 44	+17 34 06	
AFGL 2531	20 12 08	+46 35 54	
AFGL 2532	20 12 19	− 4 44 12	
AFGL 2533	20 12 21	+39 14 00	
AFGL 2534	20 12 26	+26 16 48	
AFGL 2535	20 12 37	+66 05 42	
AFGL 2537	20 13 18	+ 7 31 00	
AFGL 2538	20 13 26	+30 54 48	
AFGL 2539S	20 13 40	+36 53 00	
AFGL 2540	20 13 51	+47 32 48	
AFGL 2541	20 13 54	+23 18 36	
AFGL 2542	20 14 10	−21 28 36	
AFGL 2543S	20 14 10	+80 00 54	
AFGL 2544	20 14 52	+40 14 18	
AFGL 2545S	20 15 36	+36 38 00	
AFGL 2546S	20 15 46	−15 03 42	
AFGL 2547	20 16 05	+33 56 30	
AFGL 2548S	20 16 08	+43 09 12	
AFGL 2549	20 16 10	+39 12 30	
AFGL 2550	20 16 36	+34 14 54	
AFGL 2551	20 16 58	+66 52 12	
AFGL 2552	20 17 07	− 7 42 48	
AFGL 2554	20 17 33	+40 48 18	
AFGL 2554.2	"	"	ED
AFGL 2555	20 18 07	−14 59 06	
AFGL 2556	20 18 12	+47 44 54	
AFGL 2557	20 18 45.0	+41 11 52	
AFGL 2557	20 18 54	+41 12 54	
AFGL 2558	20 19 25	+35 27 48	
AFGL 2559	20 19 28	+36 46 54	
AFGL 2560	20 19 46	+37 21 48	
AFGL 2561	20 19 43	+40 17 06	
AFGL 2562	20 19 48	+68 42 24	
AFGL 2563	20 19 52	+16 44 06	
AFGL 2565	20 20 35	+40 05 30	
AFGL 2566	20 20 45	+63 48 36	
AFGL 2567	20 20 49	+ 0 37 48	
AFGL 2568	20 21 15	+ 0 45 36	
AFGL 2569	20 21 27	+51 51 42	
AFGL 2570	20 21 29	+62 42 54	
AFGL 2571	20 21 49	+32 02 00	
AFGL 2572S	20 22 23	+24 07 18	
AFGL 2573S	20 23 25	+33 45 48	
AFGL 2574	20 24 01	− 2 12 42	
AFGL 2575	20 24 11	+38 11 18	
AFGL 2577	20 25 03	− 5 49 00	
AFGL 2578	20 25 17	+39 15 30	
AFGL 2579	20 25 19	+39 53 06	
AFGL 2580	20 25 18	+36 22 42	
AFGL 2581	20 25 18	+75 05 42	
AFGL 2582	20 25 21	+55 35 42	
AFGL 2583	20 25 29	+40 54 24	
AFGL 2584	20 25 31	+37 12 06	
AFGL 2585	20 26 29	+37 37 54	
AFGL 2586	20 26 29	+40 42 30	
AFGL 2588	20 26 50	+16 06 48	
AFGL 2589	20 27 02	+ 9 44 30	
AFGL 2590	20 27 11	+39 48 18	
AFGL 2591	20 27 25	+40 01 54	
AFGL 2591	20 27 35	+40 01	
AFGL 2592	20 27 41	− 4 54 54	
AFGL 2593	20 27 42	+38 50 18	
AFGL 2596	20 29 36	+39 43 00	
AFGL 2597	20 29 40	+32 22 06	
AFGL 2598	20 29 47	+49 03 06	
AFGL 2599	20 30 04	+62 46 30	
AFGL 2600	20 29 52	+40 28 36	
AFGL 2601	20 30 15	+35 16 36	
AFGL 2602	20 30 44	+40 06 48	
AFGL 2602	20 30 46.4	+40 05 48	
AFGL 2603	20 30 59	+40 29 30	
AFGL 2604	20 31 09	+42 22 48	
AFGL 2605	20 31 17	+40 35 24	
AFGL 2606	20 31 37	+54 17 00	
AFGL 2607	20 31 44	+38 30 36	
AFGL 2608	20 31 50	+35 04 36	
AFGL 2609	20 32 15	+42 15 36	
AFGL 2610	20 32 18	− 7 35 48	
AFGL 2612	20 33 32	+41 04 18	
AFGL 2613	20 34 08	+53 39 00	
AFGL 2614	20 34 13	− 2 42 12	
AFGL 2616	20 35 00	+41 24 54	
AFGL 2617	20 35 03	+37 42 06	
AFGL 2618	20 35 41	+18 05 54	
AFGL 2620	20 36 31	+41 55 42	
AFGL 2621	20 36 34	+42 27 54	
AFGL 2623	20 37 08	−18 17 30	
AFGL 2624	20 37 17	+42 09 48	
AFGL 2625	20 37 28	+41 08 06	
AFGL 2626	20 37 46	+39 01 18	
AFGL 2627	20 37 48	+53 20 48	
AFGL 2628S	20 37 55	+50 00 12	
AFGL 2629	20 38 20	+ 1 00 42	
AFGL 2631	20 39 26	+41 40 24	
AFGL 2632	20 39 31	+47 57 42	
AFGL 2633	20 39 35	+45 06 18	
AFGL 2634S	20 39 43	+62 17 24	
AFGL 2635	20 40 39	+38 31 48	
AFGL 2636	20 40 42	+42 46 42	
AFGL 2636	20 40 47.0	+42 45 52	
AFGL 2636	20 41	+42 50	ED
AFGL 2636.1	20 40 42	+42 46 42	"
AFGL 2636.2	"	"	"
AFGL 2636IRS1	20 40 47.3	+42 46 01	
AFGL 2636IRS2	20 40 46.6	+42 45 59	
AFGL 2637	20 41 36	+43 00 30	
AFGL 2639	20 41 57	+19 04 24	
AFGL 2640	20 42 46	+80 19 42	
AFGL 2641	20 43 07	+17 55 36	
AFGL 2642S	20 43 20	+42 09 06	
AFGL 2643	20 43 21	+30 29 42	
AFGL 2644	20 43 06	+56 19 30	
AFGL 2645	20 43 48	− 4 17 06	
AFGL 2646	20 43 55	− 1 04 36	
AFGL 2648	20 44 14	+33 47 18	
AFGL 2649	20 44 18	+61 38 54	
AFGL 2650	20 44 34	+39 56 36	
AFGL 2651S	20 44 47	− 3 57 54	
AFGL 2652	20 45 07	− 5 11 18	
AFGL 2653	20 45 14	+45 22 30	
AFGL 2654	20 45 32	+19 09 00	
AFGL 2655	20 45 44	+58 14 30	
AFGL 2656S	20 45 53	+44 14 12	
AFGL 2657	20 46 16	+28 03 54	
AFGL 2658	20 46 49	+ 0 44 30	
AFGL 2659	20 46 49	+22 49 06	
AFGL 2660	20 47 06	+31 40 06	
AFGL 2661S	20 47 23	− 3 12 18	
AFGL 2662	20 47 48	+ 5 53 42	
AFGL 2663	20 48 02	+49 56 24	
AFGL 2665	20 48 34	−27 05 30	
AFGL 2666	20 48 44	−11 16 00	
AFGL 2667	20 50 02	+47 09 36	
AFGL 2668	20 50 16	+80 22 30	
AFGL 2670	20 50 21	−12 33 30	
AFGL 2672	20 50 43	+23 10 00	
AFGL 2673S	20 51 00	+29 29 36	
AFGL 2674S	20 51 09	+32 55 18	
AFGL 2675	20 51 11	+25 22 54	
AFGL 2676	20 52 21	+27 52 12	
AFGL 2677	20 53 04	+30 12 00	
AFGL 2678	20 54 49	+16 03 24	
AFGL 2679	20 54 55	+37 13 00	
AFGL 2679	20 54 55.8	+37 13 35	
AFGL 2681	20 56 11	+56 13 30	
AFGL 2682	20 56 18	+44 35 24	
AFGL 2683	20 56 25	+46 16 30	
AFGL 2685S	20 56 59	+41 07 24	
AFGL 2686	20 57 00.7	+27 14 42	
AFGL 2686	20 57 09	+27 15 48	
AFGL 2687	20 59 59	+61 45 06	

NAME	RA (1950)	DEC	POS REF
AFGL 2688	21 00 16	+36 30 00	
AFGL 2689	21 00 33	+44 35 36	
AFGL 2690	21 00 01.8	+82 51 41	
AFGL 2690	21 00 48	+82 52 42	
AFGL 2691	21 00 51	+35 39 24	
AFGL 2692S	21 00 53	− 2 32 54	
AFGL 2693S	21 00 56	+59 30 12	
AFGL 2694	21 01 18	+23 48 18	
AFGL 2695	21 00 59.7	+67 57 56	
AFGL 2695	21 01 19	+67 58 42	
AFGL 2696S	21 02 11	+25 34 54	
AFGL 2697	21 02 16	+37 39 24	
AFGL 2698	21 02 35	+37 04 42	
AFGL 2699	21 02 49	+53 08 54	
AFGL 2700	21 02 52	+27 11 30	
AFGL 2701S	21 03 11	−18 19 42	
AFGL 2702	21 03 18	+ 0 24 54	
AFGL 2703	21 03 24	+43 43 36	
AFGL 2704	21 03 28	+51 36 30	
AFGL 2705S	21 03 40	+ 7 38 42	
AFGL 2707	21 04 18	−25 11 06	
AFGL 2708	21 04 23	−16 37 12	
AFGL 2709	21 04 36	+47 27 24	
AFGL 2712	21 04 56	+ 0 21 06	
AFGL 2713	21 05 08	+42 01 48	
AFGL 2716	21 05 52	+ 6 48 36	
AFGL 2717	21 06 02	+ 2 58 06	
AFGL 2718S	21 07 32	+37 42 48	
AFGL 2719	21 08 39	+47 27 36	
AFGL 2720	21 08 52	+52 38 24	
AFGL 2721	21 09 05	+68 17 30	
AFGL 2722	21 09 53	−14 35 24	
AFGL 2723	21 10 34	+30 00 30	
AFGL 2724S	21 11 11	+70 51 24	
AFGL 2725	21 11 27	+59 53 18	
AFGL 2726S	21 13 00	− 1 19 12	
AFGL 2727	21 13 01	−15 22 00	
AFGL 2728	21 13 36	− 9 26 12	
AFGL 2731	21 14 07	+53 49 18	
AFGL 2732S	21 14 40	+ 8 27 18	
AFGL 2733S	21 14 47	+41 45 36	
AFGL 2734S	21 15 09	+11 13 42	
AFGL 2735	21 15 13	+40 49 24	
AFGL 2737	21 15 55	+ 7 32 42	
AFGL 2738S	21 16 05	− 1 27 48	
AFGL 2739	21 16 26	+10 58 36	
AFGL 2740	21 16 34	+76 46 06	
AFGL 2741S	21 16 37	+19 52 42	
AFGL 2743	21 17 01	+55 03 48	
AFGL 2744S	21 17 03	+ 8 21 24	
AFGL 2745	21 17 26	+63 22 00	
AFGL 2746	21 17 28	+60 58 18	
AFGL 2747	21 17 36	+50 35 06	
AFGL 2748	21 17 43	+58 24 42	
AFGL 2750	21 18 18	+55 14 36	
AFGL 2751	21 18 41	+ 7 08 12	
AFGL 2752	21 18 42	+49 07 48	
AFGL 2753	21 20 01	−22 56 42	
AFGL 2754	21 20 07	+21 47 24	
AFGL 2755	21 20 32	+42 09 36	
AFGL 2756	21 20 45	+23 14 54	
AFGL 2757	21 20 54	+77 38 30	
AFGL 2759	21 20 57	+40 42 48	
AFGL 2761	21 22 46	+79 34 00	
AFGL 2762S	21 23 38	+16 05 24	
AFGL 2763S	21 23 40	−31 18 06	
AFGL 2764	21 23 52	−22 37 06	
AFGL 2765	21 24 13	+62 22 06	
AFGL 2767	21 26 01	+59 31 54	
AFGL 2768	21 26 40	+70 00 00	
AFGL 2769	21 26 39	+21 57 42	
AFGL 2770S	21 26 54	+51 02 30	
AFGL 2771	21 27 03	+71 35 36	
AFGL 2772	21 27 42	+23 24 18	
AFGL 2774S	21 28 20	+12 44 12	
AFGL 2775	21 28 38	+10 55 48	
AFGL 2776	21 28 49	− 5 48 42	
AFGL 2777	21 29 39	+60 39 36	
AFGL 2778S	21 30 14	+74 30 24	
AFGL 2779	21 31 15	+54 04 54	
AFGL 2781	21 32 03	+38 49 48	
AFGL 2782	21 32 14	+ 1 37 12	
AFGL 2783S	21 32 20	+13 39 54	
AFGL 2784	21 34 15	+31 52 18	
AFGL 2785	21 36 21	+78 23 36	
AFGL 2787	21 37 40	− 1 59 12	
AFGL 2788	21 38 10	+43 03 06	
AFGL 2789	21 38 12	+50 00 48	
AFGL 2789	21 38 23	+50 01 12	
AFGL 2790	21 38 57	+54 06 06	
AFGL 2791S	21 38 47	+51 30 42	
AFGL 2792	21 39 43	+ 5 25 42	
AFGL 2793	21 39 47	+35 16 00	
AFGL 2794	21 39 52	+45 32 12	
AFGL 2795	21 40 12	+54 37 00	
AFGL 2796	21 40 49	+40 55 24	
AFGL 2797S	21 40 50	+61 31 24	
AFGL 2798	21 41 20	+37 47 12	
AFGL 2799	21 41 42	+76 09 12	
AFGL 2800	21 41 45	+ 9 39 18	
AFGL 2801S	21 42 08	+17 04 36	
AFGL 2802	21 41 11	+58 32 42	
AFGL 2803	21 42 16	− 9 19 06	
AFGL 2804	21 42 49	+12 27 48	
AFGL 2805	21 43 47	+73 24 18	
AFGL 2806	21 44 01	− 2 26 06	
AFGL 2807	21 44 55	+57 50 42	
AFGL 2808	21 45 40	+64 21 54	
AFGL 2809S	21 46 15	+60 27 30	
AFGL 2810	21 47 18	+61 01 54	
AFGL 2811	21 47 27	+52 11 36	
AFGL 2812	21 50 01	+21 01 42	
AFGL 2813	21 50 35	+55 44 18	
AFGL 2814S	21 52 30	+79 19 00	
AFGL 2815	21 52 57	+51 14 24	
AFGL 2816	21 53 03	+54 14 48	
AFGL 2817	21 53 11	+50 14 06	
AFGL 2818	21 53 58	+22 37 42	

NAME	RA (1950)	DEC	POS REF
AFGL 2819	21 54 26	−14 20 36	
AFGL 2820	21 54 57	+17 32 00	
AFGL 2821	21 55 15	+63 23 24	
AFGL 2822	21 55 26	+80 04 06	
AFGL 2823	21 55 44	−21 30 00	
AFGL 2824	21 55 50	+23 26 06	
AFGL 2825	21 56 10	+56 29 42	
AFGL 2826	21 56 48	+54 19 24	
AFGL 2827	21 57 27	+62 27 00	
AFGL 2828	21 57 30	+23 42 00	
AFGL 2829S	21 58 36	+76 25 30	
AFGL 2831	21 59 08	+33 28 42	
AFGL 2832	21 59 56	+48 29 18	
AFGL 2833	21 59 56	+56 42 30	
AFGL 2834S	22 00 20	+54 29 30	
AFGL 2835	22 00 23	+ 0 08 18	
AFGL 2836	22 00 28	−31 39 54	
AFGL 2837	22 01 43	+28 07 06	
AFGL 2839	22 02 23	+62 53 42	
AFGL 2841S	22 03 09	+59 53 30	
AFGL 2842	22 03 10	+46 29 24	
AFGL 2843	22 03 11	+ 4 49 00	
AFGL 2844	22 03 17	+ 0 34 12	
AFGL 2845	22 03 24	+35 06 00	
AFGL 2846S	22 03 34	+10 18 48	
AFGL 2847	22 03 59	+62 49 30	
AFGL 2848	22 04 08	+62 14 48	
AFGL 2849S	22 04 33	+41 37 06	
AFGL 2851	22 04 48	+11 38 12	
AFGL 2852	22 05 26	−34 19 36	
AFGL 2853S	22 05 28	+17 31 18	
AFGL 2854	22 06 21	+12 18 00	
AFGL 2855	22 06 23	+74 30 18	
AFGL 2856	22 06 23	+49 30 54	
AFGL 2857	22 06 38	+59 18 06	
AFGL 2859	22 07 05	+72 31 24	
AFGL 2862	22 08 13	+11 23 42	
AFGL 2864	22 09 02	+57 57 36	
AFGL 2865	22 09 34	+56 46 54	
AFGL 2866	22 09 44	+14 17 06	
AFGL 2867	22 10 40	+63 02 48	
AFGL 2868	22 11 31	+25 10 42	
AFGL 2869	22 11 40	+39 28 12	
AFGL 2872	22 12 20	+57 45 00	
AFGL 2874S	22 13 45	+ 3 06 00	
AFGL 2875	22 13 45	+37 29 36	
AFGL 2878S	22 14 57	+66 45 42	
AFGL 2879	22 15 39	+ 2 27 36	
AFGL 2880	22 16 01	+13 21 12	
AFGL 2881	22 16 36	+43 31 00	
AFGL 2881.1	"	"	ED
AFGL 2881.2	"	"	"
AFGL 2882S	22 16 54	+51 11 24	
AFGL 2884	22 17 29	+63 03 18	
AFGL 2885	22 17 41	+59 35 24	
AFGL 2887	22 18 27	+61 54 42	
AFGL 2888	22 18 42	+26 41 00	
AFGL 2889	22 19 00	− 7 52 06	
AFGL 2891	22 19 23	+45 23 36	
AFGL 2893	22 20 37	−22 17 30	
AFGL 2895	22 21 30	+31 00 36	
AFGL 2896	22 21 38	+55 42 18	
AFGL 2897S	22 21 43	+35 46 00	
AFGL 2900	22 23 13	+30 13 00	
AFGL 2901	22 24 04	+60 04 30	
AFGL 2902S	22 24 10	+63 03 06	
AFGL 2904	22 24 36	+45 08 36	
AFGL 2908	22 26 05	+35 16 12	
AFGL 2910	22 26 36	+58 58 06	
AFGL 2911	22 26 49	+ 8 53 30	
AFGL 2912	22 26 52	+49 52 12	
AFGL 2913	22 27 20	+47 26 18	
AFGL 2916	22 28 20	+56 44 42	
AFGL 2917S	22 28 41	−31 56 06	
AFGL 2918	22 30 19	+52 57 42	
AFGL 2919	22 30 37	+55 10 30	
AFGL 2920S	22 31 36	+66 40 42	
AFGL 2921	22 31 39	+24 16 42	
AFGL 2922	22 31 45	+58 38 30	
AFGL 2924	22 34 09	− 9 00 42	
AFGL 2925	22 34 25	+58 10 12	
AFGL 2926S	22 34 36	+65 34 42	
AFGL 2927S	22 36 26	+72 48 36	
AFGL 2928	22 36 28	+56 32 00	
AFGL 2929	22 36 50	+75 06 00	
AFGL 2931	22 37 56	+40 24 30	
AFGL 2932	22 38 29	+49 45 18	
AFGL 2932	22 38 34	+49 45 36	
AFGL 2933S	22 38 54	+10 45 24	
AFGL 2934	22 39 20	+20 55 18	
AFGL 2935	22 39 22	− 5 23 24	
AFGL 2936	22 39 38	+42 16 12	
AFGL 2937S	22 40 12	+53 38 12	
AFGL 2938	22 40 31	+29 57 12	
AFGL 2939	22 40 31	+13 18 30	
AFGL 2940	22 40 32	+27 54 48	
AFGL 2940	22 40 37.0	+27 53 42	
AFGL 2941	22 40 55	+59 30 18	
AFGL 2941	22 41 16	+59 29 30	
AFGL 2942	22 40 55	−19 05 24	
AFGL 2943	22 40 58	+22 55 48	
AFGL 2946	22 41 54	+29 19 48	
AFGL 2948	22 42 19	+61 26 54	
AFGL 2949	22 42 25.3	+74 31 51	
AFGL 2949	22 42 38	+74 32 36	
AFGL 2950S	22 42 49	+46 55 00	
AFGL 2951S	22 42 50	+ 6 37 00	
AFGL 2956S	22 45 20	+12 02 48	
AFGL 2957	22 45 38	+54 53 06	
AFGL 2959S	22 46 10	+18 19 12	
AFGL 2960	22 46 42	+27 05 36	
AFGL 2961	22 46 48	−14 25 06	
AFGL 2962	22 46 59	−13 50 00	
AFGL 2963	22 47 23	+59 40 30	
AFGL 2964	22 47 24	+55 39 24	
AFGL 2965	22 47 34	+40 47 00	
AFGL 2966	22 47 44	+24 20 42	
AFGL 2967	22 47 53	+65 56 00	

NAME	RA (1950)	DEC	POS REF
AFGL 2968	22 48 04	+60 01 30	
AFGL 2969	22 48 51	+61 31 24	
AFGL 2970	22 48 55	+17 50 54	
AFGL 2971	22 49 04	+64 00 00	
AFGL 2972S	22 49 07	+ 7 01 00	
AFGL 2973S	22 49 15	+47 48 42	
AFGL 2974	22 49 29	−25 33 06	
AFGL 2976	22 49 42	+43 02 06	
AFGL 2977	22 49 57	− 7 51 12	
AFGL 2978S	22 49 56	+17 29 00	
AFGL 2979S	22 49 57	+50 42 12	
AFGL 2980S	22 50 25	+50 27 18	
AFGL 2982	22 51 19	+61 01 24	
AFGL 2984	22 51 44	+ 8 37 42	
AFGL 2985	22 51 54	+66 00 00	
AFGL 2986	22 52 11	+16 40 12	
AFGL 2987	22 52 33	+60 33 36	
AFGL 2988	22 52 37	+84 49 00	
AFGL 2988	22 52 38.3	+84 46 49	
AFGL 2989	22 52 33	−29 51 48	
AFGL 2991	22 54 13	+58 15 48	
AFGL 2992	22 54 21	+49 27 12	
AFGL 2993	22 54 21	−20 36 24	
AFGL 2994S	22 54 42	+54 25 54	
AFGL 2995	22 54 53	−29 50 12	
AFGL 2996S	22 54 53	+61 15 30	
AFGL 2997S	22 54 54	+61 46 54	
AFGL 2999	22 55 29	+58 34 18	
AFGL 3000	22 55 31	+62 21 30	
AFGL 3001	22 55 39	+21 13 18	
AFGL 3002S	22 55 51	+28 20 06	
AFGL 3003S	22 56 32	+24 38 48	
AFGL 3004	22 56 19	+58 31 06	
AFGL 3005	22 56 59	−13 23 00	
AFGL 3006	22 57 51	+56 40 42	
AFGL 3007	22 57 54	+35 38 24	
AFGL 3008	22 58 22	+ 0 11 54	
AFGL 3010	22 58 41	+46 14 00	
AFGL 3011	22 58 47	+64 02 48	
AFGL 3012	22 59 08	+32 20 36	
AFGL 3013	22 59 10	+61 17 36	
AFGL 3014S	22 59 12	+56 48 36	
AFGL 3015	22 59 35	+45 37 18	
AFGL 3016	23 00 00	+59 32 06	
AFGL 3017	23 01 18	+27 48 30	
AFGL 3018	23 01 29	+37 34 54	
AFGL 3019	23 02 39	−22 44 36	
AFGL 3020	23 02 41	+56 52 18	
AFGL 3021S	23 03 16	+65 07 54	
AFGL 3022	23 03 26	+60 00 00	
AFGL 3023	23 04 06	+10 15 30	
AFGL 3024	23 04 28	+ 9 07 24	
AFGL 3025S	23 04 35	−25 53 48	
AFGL 3026	23 04 39	+25 11 24	
AFGL 3027S	23 05 02	+46 06 24	
AFGL 3029	23 06 26	−30 24 00	
AFGL 3030	23 06 50	−21 23 42	
AFGL 3031	23 06 58	+ 8 23 54	
AFGL 3032S	23 06 50	+75 08 00	
AFGL 3033	23 07 21	−40 51 48	
AFGL 3034	23 07 40	+33 29 54	
AFGL 3035S	23 07 46	+17 48 00	
AFGL 3036S	23 07 50	+ 0 01 54	
AFGL 3037S	23 07 54	+39 55 12	
AFGL 3038S	23 08 11	−11 58 00	
AFGL 3039	23 08 37	+ 4 42 54	
AFGL 3040S	23 08 51	+ 0 11 06	
AFGL 3041	23 09 09	+52 37 12	
AFGL 3042	23 09 14	+48 43 36	
AFGL 3044	23 09 33	+59 24 36	
AFGL 3045	23 10 21	+63 41 42	
AFGL 3046	23 11 00	+66 46 54	
AFGL 3048	23 11 33	+61 12 30	
AFGL 3048.1	"	"	ED
AFGL 3048.2	"	"	"
AFGL 3049	23 11 40	− 6 20 48	
AFGL 3050S	23 11 54	−34 09 36	
AFGL 3051	23 12 16	+40 30 48	
AFGL 3052	23 13 00	+63 55 12	
AFGL 3053	23 13 20	+60 50 06	
AFGL 3053.1	"	"	ED
AFGL 3053.2	"	"	"
AFGL 3054	23 13 22	− 9 19 24	
AFGL 3056	23 13 51	+62 04 00	
AFGL 3057	23 13 53	+59 45 42	
AFGL 3058	23 14 17	− 8 01 18	
AFGL 3059	23 14 15	+10 18 18	
AFGL 3060S	23 14 27	−28 43 54	
AFGL 3061	23 14 34	+60 09 36	
AFGL 3062	23 14 36	+ 3 01 06	
AFGL 3063S	23 14 38	+32 00 06	
AFGL 3064	23 15 13	+40 35 06	
AFGL 3065	23 15 21	+48 44 12	
AFGL 3066	23 16 01	−32 52 06	
AFGL 3067	23 16 27	+82 45 42	
AFGL 3068	23 16 41	+16 54 36	
AFGL 3068	23 16 43.1	+16 55 05	760605
AFGL 3069S	23 16 46	−38 04 12	
AFGL 3070S	23 16 53	+56 55 36	
AFGL 3073	23 17 15	+62 28 54	
AFGL 3074	23 17 23	+48 23 00	
AFGL 3075	23 17 25	+26 00 00	
AFGL 3076	23 17 52	+ 8 36 36	
AFGL 3077S	23 17 53	+46 57 30	
AFGL 3078	23 18 12	+30 08 54	
AFGL 3079	23 18 25	+60 53 42	
AFGL 3080S	23 18 32	+39 20 48	
AFGL 3082	23 19 32	−10 43 54	
AFGL 3083	23 20 06	−11 07 24	
AFGL 3085	23 20 12	+59 01 54	
AFGL 3086	23 20 16	−20 24 06	
AFGL 3087	23 20 16	+59 50 30	
AFGL 3088	23 21 16	+39 26 18	
AFGL 3089	23 21 47	+ 3 23 48	
AFGL 3090	23 21 51	− 2 06 30	
AFGL 3091	23 22 18	+62 00 54	
AFGL 3092S	23 23 14	−11 27 06	
AFGL 3093	23 23 18	−20 56 54	

NAME	RA (1950)	DEC	POS REF
	h m s	° ′ ″	
AFGL 3094	23 23 28	+52 42 42	
AFGL 3097S	23 24 26	+ 5 23 18	
AFGL 3099	23 25 45	+10 38 24	
AFGL 3101	23 26 52	+38 21 36	
AFGL 3102	23 26 59	+50 57 12	
AFGL 3103S	23 27 00	+56 24 06	
AFGL 3104	23 26 54	+51 26 30	
AFGL 3107	23 27 36	+59 09 12	
AFGL 3108S	23 27 39	−17 19 30	
AFGL 3109	23 27 51	+60 00 00	
AFGL 3110	23 28 16	+57 42 18	
AFGL 3111	23 30 20	+31 57 00	
AFGL 3112	23 30 21	+45 51 06	
AFGL 3113	23 30 49	+22 13 30	
AFGL 3114	23 31 16	+31 04 00	
AFGL 3115	23 31 29	+20 34 06	
AFGL 3116	23 31 59	+43 15 54	
AFGL 3117S	23 32 18	+71 22 12	
AFGL 3118	23 32 23	− 5 34 30	
AFGL 3119	23 32 33	+ 2 49 54	
AFGL 3120	23 33 24	+24 15 48	
AFGL 3122	23 34 58	+46 13 00	
AFGL 3123	23 35 06	− 5 00 24	
AFGL 3124	23 36 00	+61 38 00	
AFGL 3125	23 36 36	+51 58 24	
AFGL 3126	23 37 01	+32 03 24	
AFGL 3127	23 37 10	+77 20 24	
AFGL 3128	23 38 18	+70 07 12	
AFGL 3131	23 39 47	+18 10 00	
AFGL 3132S	23 39 55	+44 39 42	
AFGL 3133	23 39 56	+64 14 00	
AFGL 3134S	23 40 03	+32 55 30	
AFGL 3135	23 40 45	+10 02 24	
AFGL 3136	23 41 10	−15 34 24	
AFGL 3137S	23 41 23	+24 25 42	
AFGL 3138	23 41 40	+61 30 06	
AFGL 3139	23 41 46	+55 30 30	
AFGL 3140	23 42 03	+41 47 06	
AFGL 3140	23 42 10.6	+41 46 52	
AFGL 3141	23 42 10	+56 17 24	
AFGL 3142S	23 42 15	+56 57 24	
AFGL 3143	23 42 32	+43 38 48	
AFGL 3143	23 42 33	+43 38 12	
AFGL 3144	23 43 06	+41 06 00	
AFGL 3145	23 43 23	+60 12 06	
AFGL 3146S	23 43 39	− 7 09 30	
AFGL 3147	23 43 48	+ 3 11 18	
AFGL 3148	23 43 54	+54 13 00	
AFGL 3150	23 44 28	+28 09 48	
AFGL 3151	23 44 43	+39 14 54	
AFGL 3152	23 44 45	+57 09 36	
AFGL 3153	23 45 00	+25 51 12	
AFGL 3154	23 45 02	+68 17 36	
AFGL 3155S	23 46 22	+21 47 54	
AFGL 3156S	23 46 40	+76 39 18	
AFGL 3158	23 48 17	+47 13 30	
AFGL 3159	23 48 33	+20 07 36	
AFGL 3160	23 48 35	+ 9 00 54	
AFGL 3161S	23 48 45	+26 53 24	
AFGL 3162S	23 48 51	+ 5 25 48	
AFGL 3163	23 49 11	+ 8 46 42	
AFGL 3164	23 49 28	+ 2 37 42	
AFGL 3165	23 49 35	+61 31 36	
AFGL 3166	23 49 47	+18 50 24	
AFGL 3167	23 50 13	−12 16 24	
AFGL 3168	23 50 19	+60 42 30	
AFGL 3169S	23 50 34	− 1 38 06	
AFGL 3170	23 50 44	+66 16 24	
AFGL 3173	23 52 01	+57 12 24	
AFGL 3174	23 52 05	+ 0 12 18	
AFGL 3176	23 52 48	+48 21 54	
AFGL 3177	23 53 27	+14 57 06	
AFGL 3178	23 53 51	−19 09 12	
AFGL 3180	23 54 05	+22 22 00	
AFGL 3181	23 54 16	+70 30 48	
AFGL 3183	23 54 27	+32 03 24	
AFGL 3184S	23 55 01	+60 44 18	
AFGL 3185	23 55 07	+23 45 18	
AFGL 3186	23 55 11	+24 51 00	
AFGL 3187	23 55 37	+56 12 24	
AFGL 3188	23 55 59	+51 05 54	
AFGL 3189	23 56 11	−39 42 54	
AFGL 3190	23 56 56	−29 50 36	
AFGL 3193	23 57 17	+67 04 24	
AFGL 3194	23 57 35	+25 35 54	
AFGL 3195S	23 57 41	+14 44 30	
AFGL 3196	23 58 30	+60 04 12	
AFGL 3196	23 58 41.9	+60 04 37	
AFGL 3197	23 59 28	− 6 16 24	
AFGL 3198S	23 59 43	−21 17 06	
AFGL 4001	0 12 05	+19 56 12	
AFGL 4001S	0 00 10	+60 24 30	
AFGL 4002	0 20 07	−66 29 12	
AFGL 4002S	0 00 31	+59 27 36	
AFGL 4003	0 25 35	+31 19 48	
AFGL 4003S	0 01 06	+64 52 42	
AFGL 4004	0 31 03	− 7 56 00	
AFGL 4004S	0 02 25	−11 50 42	
AFGL 4005	0 35 11	+45 19 42	
AFGL 4005S	0 03 30	+56 03 24	
AFGL 4006	0 37 20	−57 07 06	
AFGL 4006S	0 04 04	−32 50 30	
AFGL 4007	0 41 37	−10 55 00	
AFGL 4007S	0 04 43	−11 09 48	
AFGL 4008	0 49 42	+49 26 00	
AFGL 4008S	0 05 12	+ 1 05 24	
AFGL 4009	1 43 59	−24 47 30	
AFGL 4009S	0 06 23	−22 27 00	
AFGL 4010	1 48 03	−23 05 06	
AFGL 4010S	0 07 09	− 2 54 30	
AFGL 4011	1 48 13	−17 52 18	
AFGL 4011S	0 07 44	+71 01 30	
AFGL 4012	1 49 41	− 2 31 24	
AFGL 4012S	0 08 09	+71 09 12	
AFGL 4013	1 52 46	+16 56 18	
AFGL 4013	1 52 47.6	+16 56 41	
AFGL 4013S	0 09 35	−18 15 30	
AFGL 4014	1 58 44	+ 0 14 36	
AFGL 4014S	0 09 38	+22 15 54	
AFGL 4015	2 03 27	−28 01 12	
AFGL 4015S	0 10 01	+70 42 48	
AFGL 4016	2 04 14	−67 45 00	
AFGL 4016S	0 10 21	− 3 39 42	
AFGL 4017	2 08 28	+47 33 24	
AFGL 4017S	0 11 17	−26 17 54	
AFGL 4018	2 08 41	− 4 23 00	
AFGL 4018S	0 11 45	+75 48 30	
AFGL 4019	2 13 29	+ 0 17 24	
AFGL 4019S	0 12 56	+66 19 24	
AFGL 4020	2 19 23	−53 53 18	
AFGL 4020S	0 14 26	− 1 34 30	
AFGL 4021	2 22 06	+38 34 48	
AFGL 4021S	0 15 29	+19 57 30	
AFGL 4022	2 22 20	+50 03 30	
AFGL 4022S	0 17 53	+61 35 18	
AFGL 4023	2 32 11	+21 38 54	
AFGL 4023S	0 17 59	+ 7 53 36	
AFGL 4024	2 32 53	−70 53 24	
AFGL 4024S	0 18 33	+59 41 24	
AFGL 4025	2 37 05	− 6 28 06	
AFGL 4025S	0 18 36	− 2 38 48	
AFGL 4026	2 46 52	+60 32 12	
AFGL 4026S	0 18 43	+50 39 24	
AFGL 4027	2 47 26	+59 03 06	
AFGL 4027S	0 18 56	+86 36 18	
AFGL 4028	2 52 21	+64 09 18	
AFGL 4028S	0 19 20	+43 53 12	
AFGL 4029	2 57 17	+60 16 54	
AFGL 4029	2 57 32.5	+60 17 22	
AFGL 4029.1	2 57 17	+60 16 54	ED
AFGL 4029.2	"	"	"
AFGL 4029S	0 20 14	+69 07 30	
AFGL 4030	3 08 33	−56 32 24	
AFGL 4030S	0 20 51	−30 03 54	
AFGL 4031	3 09 57	−29 12 18	
AFGL 4031S	0 21 52	− 4 56 54	
AFGL 4032	3 15 05	− 9 36 12	
AFGL 4032S	0 25 25	−11 55 36	
AFGL 4033	3 27 50	−19 24 18	
AFGL 4033S	0 25 27	−49 52 42	
AFGL 4034	3 31 30	−12 57 48	
AFGL 4034S	0 25 47	+16 12 12	
AFGL 4035	3 33 16	−18 52 18	
AFGL 4035S	0 26 00	−40 13 06	
AFGL 4036	3 44 35	− 3 55 54	
AFGL 4036S	0 29 16	+19 22 00	
AFGL 4037	3 46 26	−20 58 18	
AFGL 4037S	0 29 26	+14 19 24	
AFGL 4038	3 47 25	−18 53 30	
AFGL 4038S	0 30 08	+50 53 54	
AFGL 4039	3 52 56	+60 58 12	
AFGL 4039S	0 31 14	−29 51 42	
AFGL 4040	3 55 45	− 5 48 24	
AFGL 4040S	0 34 56	− 7 31 36	
AFGL 4041	3 56 47	−13 48 00	
AFGL 4041S	0 36 52	−15 44 54	
AFGL 4042	3 57 12	−12 42 06	
AFGL 4042S	0 37 37	+54 30 00	
AFGL 4043	4 01 02	+68 33 36	
AFGL 4043S	0 38 53	−46 26 24	
AFGL 4044	4 05 14	+68 33 30	
AFGL 4044S	0 39 30	− 9 55 18	
AFGL 4045	4 13 36	−21 08 54	
AFGL 4045S	0 41 58	−79 38 42	
AFGL 4046	4 13 53	−81 59 18	
AFGL 4046S	0 42 01	+38 51 30	
AFGL 4047	4 24 22	+69 16 12	
AFGL 4047S	0 42 50	+58 09 12	
AFGL 4048	4 25 41	−23 10 54	
AFGL 4048S	0 43 04	− 4 52 42	
AFGL 4049	5 08 23	+29 49 30	
AFGL 4049S	0 43 16	+57 43 54	
AFGL 4050	5 16 41	−65 02 00	
AFGL 4050S	0 43 45	+47 57 18	
AFGL 4051	5 20 56	− 4 39 06	
AFGL 4051S	0 43 50	−17 19 12	
AFGL 4052	5 21 26	−20 35 18	
AFGL 4052S	0 44 29	−22 58 12	
AFGL 4053	5 22 32	+38 20 06	
AFGL 4053S	0 44 56	+53 15 24	
AFGL 4054	5 35 39	−47 57 30	
AFGL 4054S	0 46 53	−10 54 42	
AFGL 4055	5 38 27	−69 12 36	
AFGL 4055S	0 47 10	−13 47 48	
AFGL 4056	5 39 57	−69 45 42	
AFGL 4056S	0 47 31	+44 27 48	
AFGL 4057	5 43 45	−66 26 54	
AFGL 4057S	0 49 31	+47 45 12	
AFGL 4058	6 08 34	−40 16 36	
AFGL 4058S	0 50 03	+53 34 48	
AFGL 4059	6 18 12	+49 04 42	
AFGL 4059S	0 50 09	−24 17 00	
AFGL 4060	6 21 40	+ 0 16 48	
AFGL 4060S	0 50 10	+44 50 30	
AFGL 4061	6 26 02	+44 47 00	
AFGL 4061S	0 50 57	+73 52 36	
AFGL 4062	6 27 04	−72 47 24	
AFGL 4062S	0 52 04	+58 17 18	
AFGL 4063	6 29 05	+45 56 30	
AFGL 4063S	0 53 23	−65 12 36	
AFGL 4064	6 47 17	−66 50 30	
AFGL 4064S	0 53 29	−28 01 12	
AFGL 4065	6 54 39	−23 54 18	
AFGL 4065S	0 53 35	−11 31 00	
AFGL 4066	6 58 59	−76 55 12	
AFGL 4066S	0 54 10	+26 12 06	
AFGL 4067	6 59 50	+70 48 24	
AFGL 4067S	0 54 30	−60 56 30	
AFGL 4068	7 04 00	+59 31 12	
AFGL 4068S	0 55 08	−30 09 42	
AFGL 4069	7 06 30	+58 32 42	
AFGL 4069S	0 56 18	+39 22 00	
AFGL 4070	7 06 33	−72 54 54	
AFGL 4070S	0 56 42	+42 33 48	
AFGL 4071	7 16 52	+31 24 06	
AFGL 4071S	0 57 08	+ 6 12 24	
AFGL 4072	7 25 22	−66 44 00	
AFGL 4072S	0 57 59	+46 38 54	
AFGL 4073	7 32 57	+46 18 54	
AFGL 4073S	0 58 46	−12 19 48	
AFGL 4074	7 34 42	+38 22 36	
AFGL 4074S	0 59 29	+69 04 06	
AFGL 4075	7 37 19	−84 57 06	
AFGL 4075S	1 00 01	+62 49 42	
AFGL 4076	7 37 34	− 8 45 36	
AFGL 4076S	1 00 01	+ 7 34 36	
AFGL 4077	7 43 33	−58 19 36	
AFGL 4077S	1 00 27	− 5 06 54	
AFGL 4078	7 45 37	−71 10 06	
AFGL 4078S	1 01 12	+52 15 18	
AFGL 4079	7 47 09	+57 35 54	
AFGL 4079S	1 03 05	+49 36 00	
AFGL 4080	7 54 17	−22 19 12	
AFGL 4080S	1 04 21	+53 15 24	
AFGL 4081	8 10 42	−62 36 42	
AFGL 4081S	1 04 23	+45 21 12	
AFGL 4082	8 15 24	+72 34 48	
AFGL 4082S	1 04 27	+49 07 30	
AFGL 4083	8 21 17	+10 45 36	
AFGL 4083S	1 05 36	+ 9 38 12	
AFGL 4084	8 25 41	+72 33 12	
AFGL 4084S	1 07 21	+25 12 24	
AFGL 4085	8 26 39	+60 54 24	
AFGL 4085S	1 07 22	−65 24 54	
AFGL 4086	8 27 39	−61 14 06	
AFGL 4086S	1 07 45	+ 2 10 36	
AFGL 4087	8 36 26	+46 09 42	
AFGL 4087S	1 08 25	+20 41 00	
AFGL 4088	8 45 35	+70 28 12	
AFGL 4088S	1 08 30	−33 46 36	
AFGL 4089	8 50 54	−18 07 42	
AFGL 4089S	1 08 57	+20 46 30	
AFGL 4090	8 55 08	+55 36 12	
AFGL 4090S	1 11 23	+28 15 48	
AFGL 4091	9 11 03	+51 17 36	
AFGL 4091S	1 11 51	+74 56 54	
AFGL 4092	9 16 27	+49 58 12	
AFGL 4092S	1 12 10	− 7 21 48	
AFGL 4093	9 22 46	−57 26 30	
AFGL 4093S	1 12 36	+57 45 54	
AFGL 4094	9 28 21	+44 56 06	
AFGL 4094S	1 14 04	−13 35 36	
AFGL 4095	9 30 53	−62 34 42	
AFGL 4095S	1 17 08	+57 15 18	
AFGL 4096	9 35 37	+67 31 12	
AFGL 4096S	1 17 43	+67 07 54	
AFGL 4097	9 51 58	−67 20 00	
AFGL 4097S	1 18 24	−17 16 00	
AFGL 4098	9 52 14	−75 07 36	
AFGL 4098S	1 19 53	+ 1 23 30	
AFGL 4099	9 56 31	−58 38 48	
AFGL 4099S	1 20 04	−69 15 42	
AFGL 4100	9 57 35	+ 8 16 30	
AFGL 4100S	1 21 03	−18 08 36	
AFGL 4101	10 04 50	−56 56 24	
AFGL 4101S	1 22 26	+14 35 24	
AFGL 4102	10 05 39	−53 00 00	
AFGL 4102S	1 22 51	+57 20 18	
AFGL 4103	10 17 54	−57 41 54	
AFGL 4103S	1 22 55	−46 15 24	
AFGL 4104	10 18 12	−57 50 30	
AFGL 4104S	1 23 15	+17 54 06	
AFGL 4105	10 18 32	−60 10 30	
AFGL 4105S	1 23 49	−17 13 18	
AFGL 4106	10 21 32	−59 17 48	
AFGL 4106S	1 24 34	+14 29 54	
AFGL 4107	10 22 12	−57 31 06	
AFGL 4107S	1 25 01	−22 48 24	
AFGL 4108	10 29 05	−57 36 48	
AFGL 4108S	1 25 39	+ 7 39 18	
AFGL 4109	10 29 35	−57 45 36	
AFGL 4109S	1 25 55	+61 29 00	
AFGL 4110	10 35 22	−58 20 30	
AFGL 4110S	1 26 15	−22 01 06	
AFGL 4111	10 35 55	−58 30 18	
AFGL 4111S	1 27 19	−47 03 24	
AFGL 4112	10 38 31	−59 09 42	
AFGL 4112S	1 28 08	+14 44 18	
AFGL 4113	10 42 29	−59 50 12	
AFGL 4113S	1 29 06	+15 23 00	
AFGL 4114	10 43 07	−59 23 36	
AFGL 4114S	1 29 58	+58 03 36	
AFGL 4115	10 43 16	+57 38 42	
AFGL 4115S	1 30 06	+77 18 54	
AFGL 4116	10 45 14	−59 45 42	
AFGL 4116S	1 30 23	+ 0 09 30	
AFGL 4117	10 48 03	+59 36 12	
AFGL 4117S	1 30 32	+58 59 30	
AFGL 4118	10 53 50	−60 09 36	
AFGL 4118S	1 31 47	+37 57 00	
AFGL 4119	10 54 14	−59 50 18	
AFGL 4119S	1 31 54	−19 16 12	
AFGL 4120	10 56 46	−60 55 30	
AFGL 4120S	1 32 15	+12 20 48	
AFGL 4121	10 58 39	−59 33 30	
AFGL 4121S	1 32 22	+18 12 12	
AFGL 4122	10 58 50	−60 33 36	
AFGL 4122S	1 33 37	−15 37 42	
AFGL 4123	11 03 59	−41 53 00	
AFGL 4123S	1 33 41	−36 38 48	
AFGL 4124	11 09 39	−61 02 30	
AFGL 4124S	1 35 17	− 3 40 30	
AFGL 4125	11 10 32	−60 34 54	
AFGL 4125S	1 36 03	+ 1 07 54	
AFGL 4126	11 12 48	−60 58 12	
AFGL 4126S	1 36 30	−18 13 24	
AFGL 4127	11 14 27	−61 12 36	
AFGL 4127S	1 36 53	+60 37 00	
AFGL 4128	11 15 16	−65 34 42	
AFGL 4128S	1 37 32	− 2 07 06	
AFGL 4129	11 15 17	−21 54 00	
AFGL 4129S	1 38 43	− 1 51 12	
AFGL 4130	11 19 04	−55 30 30	
AFGL 4130S	1 39 10	− 3 19 42	

NAME	RA (1950)	DEC	POS REF
	h m s	° ′ ″	
AFGL 4131	11 22 06	+48 53 00	
AFGL 4131S	1 39 56	+48 15 12	
AFGL 4132	11 26 07	−62 41 48	
AFGL 4132S	1 40 14	+58 32 48	
AFGL 4133	11 32 26	−72 57 24	
AFGL 4133S	1 40 15	− 3 58 12	
AFGL 4134	11 36 20	−63 10 00	
AFGL 4134S	1 40 47	−22 54 18	
AFGL 4135	11 41 00	−62 11 00	
AFGL 4135S	1 41 35	−16 10 48	
AFGL 4136	11 46 08	−35 43 12	
AFGL 4136S	1 42 02	+60 46 30	
AFGL 4137	11 46 49	−41 29 30	
AFGL 4137S	1 42 31	+ 8 51 06	
AFGL 4138	11 51 48	+37 24 30	
AFGL 4138	11 52 03	+37 25 12	
AFGL 4138S	1 43 17	− 5 55 36	
AFGL 4139	11 52 35	+37 03 18	
AFGL 4139	11 52 39.3	+37 02 37	
AFGL 4139S	1 43 44	+62 21 00	
AFGL 4140	11 53 52	−39 08 12	
AFGL 4140S	1 44 20	−42 29 30	
AFGL 4141	11 56 47	+33 28 18	
AFGL 4141S	1 44 48	−25 35 54	
AFGL 4142	12 01 05	−34 11 24	
AFGL 4142S	1 45 41	−46 27 06	
AFGL 4143	12 03 18	−51 41 00	
AFGL 4143S	1 45 43	+33 54 36	
AFGL 4144	12 06 22	−63 00 30	
AFGL 4144S	1 48 02	+37 46 06	
AFGL 4145	12 06 32	+29 26 48	
AFGL 4145S	1 49 44	− 7 16 24	
AFGL 4146	12 07 14	−62 32 00	
AFGL 4146S	1 50 07	+68 57 12	
AFGL 4147	12 09 04	+26 09 18	
AFGL 4147S	1 50 23	+60 49 54	
AFGL 4148	12 12 40	−62 43 42	
AFGL 4148S	1 51 56	+ 4 28 24	
AFGL 4149	12 14 59	−67 41 54	
AFGL 4149S	1 53 20	+37 00 24	
AFGL 4150	12 28 16	−56 51 30	
AFGL 4150S	1 55 14	−70 23 00	
AFGL 4151	12 30 02	−57 55 06	
AFGL 4151S	1 55 22	+59 01 12	
AFGL 4152	12 31 33	−61 21 00	
AFGL 4152S	1 56 08	+ 2 42 36	
AFGL 4153	12 32 03	+ 8 27 36	
AFGL 4153S	1 59 19	+55 00 24	
AFGL 4154	12 32 42	−61 34 12	
AFGL 4154S	1 59 26	− 6 12 36	
AFGL 4155	12 32 49	+ 8 22 42	
AFGL 4155S	1 59 34	− 7 33 30	
AFGL 4156	12 32 51	+ 6 18 36	
AFGL 4156S	1 59 45	+16 01 48	
AFGL 4157	12 36 00	+ 7 16 18	
AFGL 4157S	2 01 40	−12 07 24	
AFGL 4158	12 52 51	−52 43 18	
AFGL 4158S	2 01 40	−10 40 36	
AFGL 4159	12 53 15	−68 46 36	
AFGL 4159S	2 02 16	− 3 04 24	
AFGL 4160	13 01 27	+11 29 48	
AFGL 4160S	2 02 28	−17 30 12	
AFGL 4161	13 05 32	−61 58 54	
AFGL 4161S	2 04 02	−39 47 18	
AFGL 4162	13 08 25	−48 31 24	
AFGL 4162S	2 04 54	+ 0 28 36	
AFGL 4163	13 08 31	−62 18 24	
AFGL 4163S	2 06 08	−11 57 42	
AFGL 4164	13 11 02	−60 51 36	
AFGL 4164S	2 06 21	− 4 53 24	
AFGL 4165	13 11 06	−62 28 48	
AFGL 4165S	2 07 16	−13 58 12	
AFGL 4166	13 19 53	−11 24 12	
AFGL 4166S	2 08 38	+ 4 28 48	
AFGL 4167	13 23 20	−40 18 48	
AFGL 4167S	2 09 14	−27 00 36	
AFGL 4168	13 24 15	−37 14 42	
AFGL 4168S	2 09 22	−23 52 00	
AFGL 4169	13 25 15	−36 44 42	
AFGL 4169S	2 09 50	+44 00 54	
AFGL 4170	13 26 12	−36 15 48	
AFGL 4170S	2 10 16	+15 02 12	
AFGL 4171	13 27 44	−38 00 00	
AFGL 4171S	2 11 23	− 5 47 12	
AFGL 4172	13 29 18	−62 32 12	
AFGL 4172S	2 11 43	−19 47 54	
AFGL 4173	13 32 51	− 4 08 24	
AFGL 4173S	2 12 51	+67 02 36	
AFGL 4174	13 36 31	−61 28 36	
AFGL 4174S	2 13 14	+75 06 54	
AFGL 4175	13 36 52	−49 41 36	
AFGL 4175S	2 13 20	−23 32 24	
AFGL 4176	13 39 41	−61 52 42	
AFGL 4176S	2 13 28	−20 47 12	
AFGL 4177	13 43 59	−62 22 06	
AFGL 4177S	2 13 35	−25 48 48	
AFGL 4178	13 44 08	−61 08 06	
AFGL 4178S	2 13 52	+72 29 12	
AFGL 4179	13 45 10	−31 15 18	
AFGL 4179S	2 15 37	+31 53 06	
AFGL 4180	13 45 49	−62 33 24	
AFGL 4180S	2 15 43	− 1 33 36	
AFGL 4181	13 46 31	−34 11 18	
AFGL 4181S	2 15 59	− 5 36 24	
AFGL 4182	13 47 03	−61 21 30	
AFGL 4182S	2 16 55	+56 46 06	
AFGL 4183	13 47 36	−65 31 48	
AFGL 4183S	2 17 03	−19 02 18	
AFGL 4184	13 52 31	+ 5 46 36	
AFGL 4184S	2 17 38	−12 29 30	
AFGL 4185	13 55 29	−61 07 30	
AFGL 4185S	2 17 47	+60 32 06	
AFGL 4186	13 57 46	−59 30 48	
AFGL 4186S	2 17 48	−22 45 54	
AFGL 4187	13 59 53	−76 32 48	
AFGL 4187S	2 18 25	+23 12 42	
AFGL 4188	14 00 35	−61 05 18	
AFGL 4188S	2 18 36	+57 36 12	
AFGL 4189	14 02 25	−62 07 00	
AFGL 4189S	2 19 44	+56 59 00	
AFGL 4190	14 03 57	−61 12 30	
AFGL 4190S	2 20 09	−10 26 30	
AFGL 4191	14 13 02	−59 41 12	
AFGL 4191S	2 20 31	− 9 24 24	
AFGL 4192	14 13 54	−13 52 48	
AFGL 4192S	2 20 35	− 3 03 30	
AFGL 4193	14 17 00	−36 38 30	
AFGL 4193S	2 22 43	−13 23 06	
AFGL 4194	14 19 50	+29 34 06	
AFGL 4194S	2 23 06	+37 53 36	
AFGL 4195	14 20 57	−60 10 54	
AFGL 4195S	2 23 29	+ 0 22 54	
AFGL 4196	14 25 44	−68 43 12	
AFGL 4196S	2 24 09	+36 44 48	
AFGL 4197	14 36 35	−60 36 48	
AFGL 4197S	2 25 49	+68 57 36	
AFGL 4198	14 40 55	+55 01 18	
AFGL 4198S	2 28 12	−34 34 06	
AFGL 4199	14 41 31	−59 36 42	
AFGL 4199S	2 28 17	+49 58 48	
AFGL 4200	14 42 32	−59 10 30	
AFGL 4200S	2 29 06	+35 55 48	
AFGL 4201	14 42 55	+27 16 54	
AFGL 4201S	2 30 29	−70 39 54	
AFGL 4202	14 48 02	−61 52 00	
AFGL 4202S	2 30 31	− 5 42 48	
AFGL 4203	14 51 44	−72 37 42	
AFGL 4203S	2 31 21	+67 44 42	
AFGL 4204	14 51 54	−58 48 36	
AFGL 4204S	2 31 49	− 3 49 00	
AFGL 4205	14 56 15	−54 06 18	
AFGL 4205S	2 31 51	+22 14 00	
AFGL 4206	14 58 39	−59 27 00	
AFGL 4206S	2 31 59	−34 48 48	
AFGL 4207	14 59 02	−58 25 42	
AFGL 4207S	2 32 54	+37 05 24	
AFGL 4208	14 59 48	−58 50 12	
AFGL 4208S	2 33 10	+ 5 22 36	
AFGL 4209	15 01 33	−57 19 06	
AFGL 4209S	2 33 27	+65 30 12	
AFGL 4210	15 07 22	−57 31 54	
AFGL 4210S	2 34 31	+56 48 24	
AFGL 4211	15 08 18	−48 08 48	
AFGL 4211S	2 34 33	−36 01 42	
AFGL 4212	15 09 48	−55 11 24	
AFGL 4212S	2 35 03	− 3 00 00	
AFGL 4213	15 12 22	−58 01 48	
AFGL 4213S	2 35 04	+64 47 48	
AFGL 4214	15 20 56	+16 32 12	
AFGL 4214S	2 35 32	+27 18 18	
AFGL 4215	15 26 16	+17 34 00	
AFGL 4215S	2 35 45	−14 37 12	
AFGL 4216	15 27 59	−62 08 30	
AFGL 4216S	2 38 36	−40 03 54	
AFGL 4217	15 35 05	−15 12 36	
AFGL 4217S	2 38 49	+34 17 48	
AFGL 4218	15 40 21	−37 00 36	
AFGL 4218S	2 39 34	−26 15 18	
AFGL 4219	15 46 30.7	+28 18 32	
AFGL 4219	15 46 38	+28 17 54	
AFGL 4219S	2 39 45	−22 50 18	
AFGL 4220	15 53 32	−18 08 48	
AFGL 4220S	2 40 18	+ 0 12 24	
AFGL 4221	16 08 06	− 1 56 06	
AFGL 4221S	2 41 00	+17 19 48	
AFGL 4222	16 23 14	−24 29 54	
AFGL 4222S	2 43 00	− 1 29 42	
AFGL 4223	16 23 42	+61 38 24	
AFGL 4223S	2 43 08	+71 41 54	
AFGL 4224	16 23 44	−24 17 48	
AFGL 4224S	2 43 11	−14 15 42	
AFGL 4225	16 26 08	−82 09 30	
AFGL 4225S	2 44 23	−17 10 06	
AFGL 4226	16 30 11	− 2 20 12	
AFGL 4226S	2 46 18	−19 17 18	
AFGL 4227	16 32 48	− 8 19 42	
AFGL 4227S	2 46 22	− 4 29 00	
AFGL 4228	16 33 08	−35 08 30	
AFGL 4228S	2 46 59	+51 51 18	
AFGL 4229	16 59 37	+ 2 44 42	
AFGL 4229S	2 47 29	−15 52 00	
AFGL 4230	17 10 49	−75 32 06	
AFGL 4230S	2 49 12	−41 09 36	
AFGL 4231	17 28 14	+ 4 49 54	
AFGL 4231S	2 51 05	+52 31 42	
AFGL 4232	17 33 46	+36 00 12	
AFGL 4232S	2 52 55	+57 22 18	
AFGL 4233	17 45 34	−77 51 36	
AFGL 4233S	2 53 00	+51 05 42	
AFGL 4234	18 03 32	+ 5 30 54	
AFGL 4234S	2 53 47	− 6 17 00	
AFGL 4235	18 06 02	−20 06 12	
AFGL 4235S	2 55 16	−12 13 48	
AFGL 4236	18 14 03	+31 36 18	
AFGL 4236S	2 55 51	−23 51 30	
AFGL 4237	18 22 42	−13 18 00	
AFGL 4237S	2 55 57	+35 00 06	
AFGL 4238	18 28 33	+89 06 00	
AFGL 4238S	2 56 45	+29 38 18	
AFGL 4239	18 45 27	−22 35 30	
AFGL 4239S	2 57 54	+10 39 48	
AFGL 4240	18 49 50	+25 36 18	
AFGL 4240S	2 58 08	−13 08 30	
AFGL 4241	18 54 01	+30 03 30	
AFGL 4241S	2 59 45	− 5 08 18	
AFGL 4242	18 59 57	+ 4 57 06	
AFGL 4242S	3 00 13	− 7 54 12	
AFGL 4243	19 01 13	+57 46 18	
AFGL 4243S	3 01 23	+35 40 42	
AFGL 4244	19 11 51	+32 30 06	
AFGL 4244S	3 01 39	−15 24 00	
AFGL 4245	19 13 22	−17 05 24	
AFGL 4245S	3 01 51	−12 59 24	
AFGL 4246	19 14 39	−20 47 36	
AFGL 4246S	3 02 22	−26 00 48	
AFGL 4247	19 16 44	+49 05 06	
AFGL 4247S	3 03 16	+74 31 48	
AFGL 4248	19 19 49	+57 30 12	
AFGL 4248S	3 03 44	+11 29 06	
AFGL 4249	19 28 05	+18 11 36	
AFGL 4249S	3 03 45	+60 19 06	
AFGL 4250	19 30 39	+13 37 30	
AFGL 4250S	3 04 08	+66 11 36	
AFGL 4251	19 32 45	+30 23 00	
AFGL 4251S	3 05 05	−11 10 12	
AFGL 4252	19 41 07	+ 0 04 30	
AFGL 4252S	3 06 24	−26 36 06	
AFGL 4253	19 45 26	+ 9 21 54	
AFGL 4253	19 45 31.7	+ 9 20 39	
AFGL 4253S	3 08 06	+39 25 06	
AFGL 4254	19 47 40	+ 8 23 30	
AFGL 4254S	3 08 11	+37 52 48	
AFGL 4255	19 51 15	+ 0 41 12	
AFGL 4255S	3 08 19	−21 53 18	
AFGL 4256	19 53 05	+27 04 12	
AFGL 4256S	3 08 44	− 4 01 00	
AFGL 4257	19 57 47	+ 1 11 48	
AFGL 4257S	3 09 03	−23 56 00	
AFGL 4258	19 58 36	+ 1 14 54	
AFGL 4258S	3 09 33	+55 31 12	
AFGL 4259	20 04 21	+26 51 18	
AFGL 4259S	3 10 01	−29 51 18	
AFGL 4260	20 10 01	+ 0 33 18	
AFGL 4260S	3 11 29	+54 42 00	
AFGL 4261	20 11 56	+ 0 09 06	
AFGL 4261S	3 12 26	+ 1 25 36	
AFGL 4262	20 16 13	−16 02 18	
AFGL 4262S	3 12 44	+ 1 31 36	
AFGL 4263	20 18 42	+39 31 12	
AFGL 4263S	3 12 58	−30 48 18	
AFGL 4264	20 20 09	+39 46 06	
AFGL 4264S	3 13 18	−24 34 36	
AFGL 4265	20 22 41	− 7 19 18	
AFGL 4265S	3 13 49	− 5 54 36	
AFGL 4266	20 24 02	− 6 28 06	
AFGL 4266S	3 14 12	−76 50 48	
AFGL 4267	20 29 58	+38 48 00	
AFGL 4267S	3 15 32	+34 03 42	
AFGL 4268	20 33 49	− 8 44 18	
AFGL 4268S	3 16 35	+32 57 12	
AFGL 4269	20 41 45	− 5 01 30	
AFGL 4269S	3 17 21	−17 21 24	
AFGL 4270	20 58 42	−74 15 36	
AFGL 4270S	3 18 26	−15 29 48	
AFGL 4271	21 08 26	−18 42 12	
AFGL 4271S	3 19 02	+74 51 54	
AFGL 4272	21 08 53	+54 18 54	
AFGL 4272S	3 19 24	−27 45 06	
AFGL 4273	21 16 01	−19 25 00	
AFGL 4273S	3 21 12	+ 3 44 00	
AFGL 4274	21 25 34	+10 15 48	
AFGL 4274S	3 21 15	+11 42 06	
AFGL 4275	21 26 17	− 2 58 06	
AFGL 4275S	3 22 51	+ 0 52 24	
AFGL 4276	21 29 34	−27 47 36	
AFGL 4276S	3 23 45	+74 16 54	
AFGL 4277	21 29 43	−57 03 30	
AFGL 4277S	3 24 13	+60 32 06	
AFGL 4278	21 30 16	−56 46 30	
AFGL 4278S	3 25 12	−10 01 54	
AFGL 4279	21 36 15	−36 29 36	
AFGL 4279S	3 25 32	+48 34 36	
AFGL 4280	21 37 24	−36 16 36	
AFGL 4280S	3 25 55	+58 44 30	
AFGL 4281	21 37 41	−54 46 18	
AFGL 4281S	3 28 24	−14 25 54	
AFGL 4282	21 37 57	−34 47 00	
AFGL 4282S	3 29 05	+60 40 30	
AFGL 4283	21 39 32	−45 50 42	
AFGL 4283S	3 30 21	−25 49 00	
AFGL 4284	21 41 21	−50 28 30	
AFGL 4284S	3 31 12	−15 28 30	
AFGL 4285	21 43 42	− 9 31 42	
AFGL 4285S	3 31 56	+63 01 42	
AFGL 4286	22 05 08	+59 14 30	
AFGL 4286S	3 34 30	−19 11 30	
AFGL 4287	22 05 41	−50 10 12	
AFGL 4287S	3 35 36	−16 39 42	
AFGL 4288	22 13 44	−80 41 06	
AFGL 4288S	3 36 26	+24 49 36	
AFGL 4289	22 19 48	−46 10 18	
AFGL 4289S	3 38 00	+89 29 54	
AFGL 4290	22 20 37	− 2 46 00	
AFGL 4290S	3 38 15	+59 49 42	
AFGL 4291	22 36 26	+77 21 12	
AFGL 4291S	3 39 10	+36 20 36	
AFGL 4292	22 39 34	−47 09 12	
AFGL 4292S	3 41 14	−32 54 42	
AFGL 4293	22 54 03	−57 39 36	
AFGL 4293S	3 43 11	−16 21 12	
AFGL 4294	22 55 21	+84 06 24	
AFGL 4294S	3 44 34	+59 26 12	
AFGL 4295	22 59 35	+10 19 12	
AFGL 4295	22 59 37	+10 20 00	
AFGL 4295S	3 45 11	+24 50 24	
AFGL 4296	23 21 23	−45 21 42	
AFGL 4296S	3 46 33	+65 07 48	
AFGL 4297	23 24 12	+27 18 36	
AFGL 4297S	3 47 09	+42 26 12	
AFGL 4298	23 26 40	+11 16 12	
AFGL 4298S	3 48 23	+63 52 30	
AFGL 4299	23 28 53	+59 57 00	
AFGL 4299S	3 48 56	− 1 31 30	
AFGL 4300	23 38 30	+44 32 48	
AFGL 4300S	3 49 56	−40 17 06	
AFGL 4301	23 44 13	+58 22 00	
AFGL 4301S	3 50 12	+60 47 12	
AFGL 4302	23 46 04	+63 24 36	
AFGL 4302S	3 51 28	+24 33 12	
AFGL 4303	23 48 59	+62 44 48	
AFGL 4303S	3 52 39	+53 07 30	
AFGL 4304	23 57 18	−51 47 12	
AFGL 4304S	3 52 43	−15 02 24	
AFGL 4305	23 59 15	+67 07 18	

NAME	RA (1950)	DEC	POS REF
	h m s	° ′ ″	
AFGL 4305S	3 53 10	−24 09 48	
AFGL 4306	23 59 53	+56 46 12	
AFGL 4306S	3 56 00	+10 52 36	
AFGL 4307S	3 57 13	+55 08 36	
AFGL 4308S	3 57 36	− 6 28 36	
AFGL 4309S	3 58 13	−16 07 18	
AFGL 4310S	3 59 50	− 6 03 30	
AFGL 4311S	3 59 51	−13 53 06	
AFGL 4312S	4 00 18	−10 54 36	
AFGL 4313S	4 00 39	−10 47 30	
AFGL 4314S	4 01 08	−20 48 12	
AFGL 4315S	4 01 08	− 7 07 06	
AFGL 4316S	4 01 10	+61 38 42	
AFGL 4317S	4 01 33	−25 58 12	
AFGL 4318S	4 01 47	+12 21 42	
AFGL 4319S	4 01 47	+26 04 24	
AFGL 4320S	4 04 38	− 7 51 06	
AFGL 4321S	4 04 46	+55 05 00	
AFGL 4322S	4 05 47	+10 00 12	
AFGL 4323S	4 08 02	−34 42 00	
AFGL 4324S	4 09 52	− 9 56 48	
AFGL 4325S	4 09 57	− 4 34 00	
AFGL 4326S	4 10 26	−23 58 18	
AFGL 4327S	4 10 48	− 4 04 36	
AFGL 4328S	4 11 56	−10 22 42	
AFGL 4329S	4 12 25	−42 24 24	
AFGL 4330S	4 12 48	− 7 42 18	
AFGL 4331S	4 13 10	+50 43 42	
AFGL 4332S	4 14 06	−28 30 00	
AFGL 4333S	4 14 19	+42 37 06	
AFGL 4334S	4 14 22	+49 43 18	
AFGL 4335S	4 15 20	+54 42 54	
AFGL 4336S	4 16 39	+37 06 24	
AFGL 4337S	4 18 17	−17 00 24	
AFGL 4338S	4 18 43	+80 42 00	
AFGL 4339S	4 19 43	+36 06 48	
AFGL 4340S	4 19 49	+17 26 48	
AFGL 4341S	4 20 01	− 5 34 36	
AFGL 4342S	4 20 23	+62 47 54	
AFGL 4343S	4 20 30	−12 43 36	
AFGL 4344S	4 22 15	+57 48 24	
AFGL 4345S	4 25 29	+19 05 42	
AFGL 4346S	4 26 04	−29 23 48	
AFGL 4347S	4 26 11	+64 17 24	
AFGL 4348S	4 26 27	+45 50 24	
AFGL 4349S	4 27 18	+16 03 36	
AFGL 4350S	4 28 00	+15 01 36	
AFGL 4351S	4 29 26	+52 41 54	
AFGL 4352S	4 29 49	−20 46 48	
AFGL 4353S	4 31 08	+ 0 04 30	
AFGL 4354S	4 31 50	+29 38 12	
AFGL 4355S	4 35 18	−24 23 24	
AFGL 4356S	4 36 05	+41 32 48	
AFGL 4357S	4 36 16	−20 29 00	
AFGL 4358S	4 37 10	−33 00 00	
AFGL 4359S	4 37 56	+40 05 48	
AFGL 4360S	4 38 47	+79 03 42	
AFGL 4361S	4 38 47	−20 05 48	
AFGL 4362S	4 39 34	−32 35 48	
AFGL 4363S	4 39 36	−24 07 36	
AFGL 4364S	4 39 46	−27 28 30	
AFGL 4365S	4 40 04	+48 37 30	
AFGL 4366S	4 40 58	+25 16 06	
AFGL 4367S	4 41 16	−30 50 54	
AFGL 4368S	4 41 34	+11 36 00	
AFGL 4369S	4 42 20	−17 50 12	
AFGL 4370S	4 42 26	− 2 41 24	
AFGL 4371S	4 42 52	−21 24 42	
AFGL 4372S	4 43 29	−30 44 48	
AFGL 4373S	4 43 32	+35 45 06	
AFGL 4374S	4 43 51	−26 30 18	
AFGL 4375S	4 43 54	+25 30 54	
AFGL 4376S	4 45 45	−36 17 48	
AFGL 4377S	4 45 52	− 5 26 18	
AFGL 4378S	4 46 22	+31 22 24	
AFGL 4379S	4 47 14	+28 01 48	
AFGL 4380S	4 47 23	+ 6 50 06	
AFGL 4381S	4 47 38	+52 08 36	
AFGL 4382S	4 47 44	+68 51 30	
AFGL 4383S	4 49 13	+28 53 48	
AFGL 4384S	4 49 28	+36 36 36	
AFGL 4385S	4 50 32	+49 49 12	
AFGL 4386S	4 50 51	−22 05 42	
AFGL 4387S	4 51 17	+69 17 06	
AFGL 4388S	4 59 43	−26 16 48	
AFGL 4389S	5 00 48	−22 54 18	
AFGL 4390S	5 02 32	−35 35 30	
AFGL 4391S	5 03 59	+ 0 28 00	
AFGL 4392S	5 05 39	+38 55 54	
AFGL 4393S	5 06 34	−24 53 12	
AFGL 4394S	5 06 56	− 8 52 36	
AFGL 4395S	5 07 02	+37 14 18	
AFGL 4396S	5 08 43	+15 58 30	
AFGL 4397S	5 09 24	+80 48 54	
AFGL 4398S	5 11 07	−27 09 36	
AFGL 4399S	5 11 27	+77 09 12	
AFGL 4400S	5 13 26	+47 24 12	
AFGL 4401S	5 15 54	+35 44 06	
AFGL 4402S	5 16 18	−49 11 36	
AFGL 4403S	5 17 26	−33 46 36	
AFGL 4404S	5 18 25	+ 7 19 24	
AFGL 4405S	5 18 29	+73 40 18	
AFGL 4406S	5 19 14	+60 38 06	
AFGL 4407S	5 19 22	+46 57 12	
AFGL 4408S	5 19 50	+50 10 24	
AFGL 4409S	5 22 21	+ 1 09 48	
AFGL 4410S	5 22 50	−10 23 24	
AFGL 4411S	5 22 52	+50 04 12	
AFGL 4412S	5 23 16	+20 33 48	
AFGL 4413S	5 23 23	−29 49 18	
AFGL 4414S	5 23 26	+32 00 12	
AFGL 4415S	5 24 13	+34 24 36	
AFGL 4416S	5 26 04	+ 0 03 42	
AFGL 4417S	5 27 13	+31 29 06	
AFGL 4418S	5 27 54	−42 39 30	
AFGL 4419S	5 28 28	− 6 55 48	
AFGL 4420S	5 30 08	− 6 17 42	
AFGL 4421S	5 30 29	+41 04 30	
AFGL 4422S	5 31 00	−25 23 12	
AFGL 4423S	5 31 22	+60 33 42	
AFGL 4424S	5 31 40	− 1 30 54	
AFGL 4425S	5 32 29	− 6 09 12	
AFGL 4426S	5 33 36	+75 02 36	
AFGL 4427S	5 33 39	− 3 50 18	
AFGL 4428S	5 33 41	− 1 14 48	
AFGL 4429S	5 33 46	−25 45 42	
AFGL 4430S	5 34 14	+ 9 16 00	
AFGL 4431S	5 34 26	−44 09 12	
AFGL 4432S	5 35 11	+21 54 36	
AFGL 4433S	5 36 29	− 7 20 06	
AFGL 4434S	5 37 14	+65 40 30	
AFGL 4435S	5 37 15	+51 36 30	
AFGL 4436S	5 37 59	−34 08 06	
AFGL 4437S	5 38 58	−27 55 24	
AFGL 4438S	5 39 21	+14 47 42	
AFGL 4439S	5 39 37	+21 58 24	
AFGL 4440S	5 39 40	+ 1 29 24	
AFGL 4441S	5 41 08	+64 45 24	
AFGL 4442S	5 41 29	−33 27 54	
AFGL 4443S	5 42 02	+37 39 54	
AFGL 4444S	5 42 23	−22 24 24	
AFGL 4445S	5 43 21	+47 17 54	
AFGL 4446S	5 44 05	−23 37 54	
AFGL 4447S	5 45 04	+28 30 18	
AFGL 4448S	5 45 41	+39 09 18	
AFGL 4449S	5 46 14	−15 33 12	
AFGL 4450S	5 46 41	+13 10 24	
AFGL 4451S	5 47 51	+39 08 06	
AFGL 4452S	5 48 09	+65 43 00	
AFGL 4453S	5 51 45	+20 14 06	
AFGL 4454S	5 52 17	−47 00 48	
AFGL 4455S	5 53 44	+20 17 00	
AFGL 4456S	5 54 09	−14 10 54	
AFGL 4457S	5 56 28	− 1 06 42	
AFGL 4458S	5 56 41	−10 53 30	
AFGL 4459S	5 57 43	− 3 06 24	
AFGL 4460S	5 58 50	+10 38 24	
AFGL 4461S	5 59 09	+75 37 18	
AFGL 4462S	5 59 20	−19 40 54	
AFGL 4463S	5 59 28	−33 54 00	
AFGL 4464S	5 59 29	+ 8 25 42	
AFGL 4465S	5 59 40	−21 07 18	
AFGL 4466S	6 00 00	+46 17 42	
AFGL 4467S	6 00 08	−50 41 54	
AFGL 4468S	6 01 16	−26 20 00	
AFGL 4469S	6 01 21	− 3 56 30	
AFGL 4470S	6 01 21	+75 44 06	
AFGL 4471S	6 01 49	+47 54 30	
AFGL 4472S	6 06 07	−18 17 12	
AFGL 4473S	6 06 42	−14 48 48	
AFGL 4474S	6 07 15	−14 28 54	
AFGL 4475S	6 07 24	+64 14 18	
AFGL 4476S	6 09 48	−14 38 12	
AFGL 4477S	6 10 30	− 7 16 36	
AFGL 4478S	6 11 54	+22 29 54	
AFGL 4479S	6 12 50	−20 11 30	
AFGL 4480S	6 13 59	−15 33 54	
AFGL 4481S	6 14 13	+39 30 12	
AFGL 4482S	6 14 48	+35 35 54	
AFGL 4483S	6 15 17	−30 58 24	
AFGL 4484S	6 15 36	−16 50 18	
AFGL 4485S	6 16 34	−14 57 48	
AFGL 4486S	6 17 08	+14 40 36	
AFGL 4487S	6 17 56	+52 32 00	
AFGL 4488S	6 18 04	+ 5 47 00	
AFGL 4489S	6 18 49	+13 15 36	
AFGL 4490S	6 21 15	− 9 50 42	
AFGL 4491S	6 21 25	−26 18 18	
AFGL 4492S	6 21 27	+ 3 45 06	
AFGL 4493S	6 21 48	−25 32 06	
AFGL 4494S	6 22 25	+ 3 44 30	
AFGL 4495S	6 23 30	+46 16 06	
AFGL 4496S	6 24 05	+10 25 48	
AFGL 4497S	6 24 57	+ 0 16 30	
AFGL 4498S	6 25 13	+49 32 54	
AFGL 4499S	6 26 39	+ 2 40 24	
AFGL 4500S	6 27 52	−19 09 12	
AFGL 4501S	6 27 57	−10 05 06	
AFGL 4502S	6 29 20	−40 49 54	
AFGL 4503S	6 29 32	−32 51 54	
AFGL 4504S	6 29 52	−36 55 42	
AFGL 4505S	6 30 01	−27 04 24	
AFGL 4506S	6 30 37	+30 18 12	
AFGL 4507S	6 30 38	− 9 54 30	
AFGL 4508S	6 30 40	+10 20 00	
AFGL 4509S	6 32 07	−36 11 42	
AFGL 4510S	6 32 34	− 1 26 48	
AFGL 4511S	6 33 01	+78 03 30	
AFGL 4512S	6 34 48	−22 14 12	
AFGL 4513S	6 34 51	+ 0 57 36	
AFGL 4514S	6 36 02	+42 31 12	
AFGL 4515S	6 36 04	− 2 32 24	
AFGL 4516S	6 36 30	+26 10 30	
AFGL 4517S	6 36 33	+13 17 24	
AFGL 4518S	6 37 40	− 6 14 54	
AFGL 4519S	6 38 08	+ 9 47 48	
AFGL 4520S	6 38 33	+11 03 18	
AFGL 4521S	6 39 09	−22 16 12	
AFGL 4522S	6 39 22	− 9 06 00	
AFGL 4523S	6 40 36	+71 25 18	
AFGL 4524S	6 40 40	−20 06 18	
AFGL 4525S	6 41 10	+13 18 18	
AFGL 4526S	6 41 12	+40 39 18	
AFGL 4527S	6 42 49	+ 8 06 48	
AFGL 4528S	6 44 07	+49 19 42	
AFGL 4529S	6 44 18	+48 50 30	
AFGL 4530S	6 44 35	+ 1 35 00	
AFGL 4531S	6 45 04	+ 0 43 42	
AFGL 4532S	6 45 43	+ 5 35 00	
AFGL 4533S	6 46 23	+32 37 18	
AFGL 4534S	6 46 43	− 1 38 24	
AFGL 4535S	6 47 05	+12 09 36	
AFGL 4536S	6 48 01	+15 10 18	
AFGL 4537S	6 49 27	+18 44 24	
AFGL 4538S	6 50 24	−12 06 18	
AFGL 4539S	6 51 00	−21 49 54	
AFGL 4540S	6 51 26	+33 15 24	
AFGL 4541S	6 51 34	+ 0 49 42	
AFGL 4542S	6 52 23	+58 30 42	
AFGL 4543S	6 52 33	+57 34 30	
AFGL 4544S	6 52 59	−42 21 42	
AFGL 4545S	6 53 23	+47 39 48	
AFGL 4546S	6 56 30	+26 05 06	
AFGL 4547S	6 58 27	−14 17 06	
AFGL 4548S	6 59 25	− 3 38 36	
AFGL 4549S	6 59 39	− 5 40 30	
AFGL 4550S	6 59 58	−15 35 06	
AFGL 4551S	7 00 54	+11 02 12	
AFGL 4552S	7 01 04	+20 39 00	
AFGL 4553S	7 01 17	− 5 14 06	
AFGL 4554S	7 01 48	+41 54 54	
AFGL 4555S	7 01 56	−16 29 18	
AFGL 4556S	7 01 59	− 9 54 54	
AFGL 4557S	7 02 17	+31 27 24	
AFGL 4558S	7 02 31	−68 06 54	
AFGL 4559S	7 02 45	+ 9 16 06	
AFGL 4560S	7 02 45	+55 58 24	
AFGL 4561S	7 03 28	+51 28 36	
AFGL 4562S	7 04 07	+33 21 00	
AFGL 4563S	7 04 10	+32 32 36	
AFGL 4564S	7 04 15	−24 33 42	
AFGL 4565S	7 05 04	−11 58 48	
AFGL 4566S	7 05 39	+36 58 36	
AFGL 4567S	7 05 45	+10 06 48	
AFGL 4568S	7 07 45	−27 50 12	
AFGL 4569S	7 09 05	+ 7 40 12	
AFGL 4570S	7 09 37	+34 39 54	
AFGL 4571S	7 09 45	+17 46 48	
AFGL 4572S	7 09 46	− 1 19 42	
AFGL 4573S	7 09 53	− 9 17 54	
AFGL 4574S	7 09 55	+14 42 06	
AFGL 4575S	7 11 24	−22 39 36	
AFGL 4576S	7 11 31	+27 43 36	
AFGL 4577S	7 11 41	+60 09 48	
AFGL 4578S	7 11 57	+ 3 09 54	
AFGL 4579S	7 11 59	+55 51 36	
AFGL 4580S	7 15 07	− 6 36 06	
AFGL 4581S	7 16 18	+ 3 38 06	
AFGL 4582S	7 16 18	−17 12 18	
AFGL 4583S	7 16 56	−10 47 12	
AFGL 4584S	7 16 59	−11 25 18	
AFGL 4585S	7 16 59	−26 33 06	
AFGL 4586S	7 17 24	+53 36 00	
AFGL 4587S	7 18 18	+36 50 54	
AFGL 4588S	7 18 25	+35 00 18	
AFGL 4589S	7 19 07	+20 31 06	
AFGL 4590S	7 19 20	+26 06 00	
AFGL 4591S	7 19 24	−24 06 54	
AFGL 4592S	7 19 32	+43 07 36	
AFGL 4593S	7 19 37	−14 49 24	
AFGL 4594S	7 20 06	+69 14 48	
AFGL 4595S	7 20 23	+36 40 00	
AFGL 4596S	7 20 44	+40 45 00	
AFGL 4597S	7 20 54	−29 13 42	
AFGL 4598S	7 21 12	+37 42 36	
AFGL 4599S	7 21 45	+35 41 06	
AFGL 4600S	7 25 28	+40 47 24	
AFGL 4601S	7 26 39	− 1 51 00	
AFGL 4602S	7 26 47	−10 10 18	
AFGL 4603S	7 26 53	− 4 12 18	
AFGL 4604S	7 26 58	+12 07 06	
AFGL 4605S	7 27 18	−17 28 24	
AFGL 4606S	7 27 55	− 9 19 54	
AFGL 4607S	7 28 56	−10 02 42	
AFGL 4608S	7 28 58	+40 47 18	
AFGL 4609S	7 30 59	+18 31 18	
AFGL 4610S	7 31 26	+31 19 30	
AFGL 4611S	7 31 49	+28 50 12	
AFGL 4612S	7 31 50	+ 2 56 12	
AFGL 4613S	7 33 06	−18 37 36	
AFGL 4614S	7 33 43	−19 43 48	
AFGL 4615S	7 33 45	− 8 10 30	
AFGL 4616S	7 33 50	+40 08 42	
AFGL 4617S	7 36 32	+36 52 42	
AFGL 4618S	7 36 41	+43 33 30	
AFGL 4619S	7 36 54	+57 13 54	
AFGL 4620S	7 37 26	+34 21 18	
AFGL 4621S	7 37 35	−27 36 06	
AFGL 4622S	7 38 04	−15 09 36	
AFGL 4623S	7 38 42	− 9 24 18	
AFGL 4624S	7 38 59	+53 00 00	
AFGL 4625S	7 39 25	−22 16 24	
AFGL 4626S	7 39 56	+23 34 54	
AFGL 4627S	7 40 21	+44 21 18	
AFGL 4628S	7 41 25	−33 13 54	
AFGL 4629S	7 41 37	+42 13 48	
AFGL 4630S	7 42 18	+51 09 12	
AFGL 4631S	7 43 23	− 6 36 24	
AFGL 4632S	7 44 12	−21 24 24	
AFGL 4633S	7 44 47	−32 13 06	
AFGL 4634S	7 45 11	+24 09 12	
AFGL 4635S	7 45 13	−19 19 54	
AFGL 4636S	7 45 18	−15 49 24	
AFGL 4637S	7 46 29	+13 27 36	
AFGL 4638S	7 46 49	−35 33 54	
AFGL 4639S	7 47 24	−13 58 12	
AFGL 4640S	7 47 52	−33 13 18	
AFGL 4641S	7 48 09	−27 48 42	
AFGL 4642S	7 49 49	−35 08 36	
AFGL 4643S	7 50 40	− 7 52 30	
AFGL 4644S	7 51 30	+ 1 53 12	
AFGL 4645S	7 52 40	−34 43 42	
AFGL 4646S	7 53 30	−28 29 48	
AFGL 4647S	7 53 48	+68 00 12	
AFGL 4648S	7 53 56	+74 02 18	
AFGL 4649S	7 53 57	+11 13 18	
AFGL 4650S	7 54 03	+21 26 36	
AFGL 4651S	7 54 26	+15 51 54	
AFGL 4652S	7 54 39	−22 43 12	
AFGL 4653S	7 55 19	−15 05 00	
AFGL 4654S	7 55 34	+16 41 48	
AFGL 4655S	7 56 42	−32 24 24	
AFGL 4656S	7 58 19	−32 35 48	
AFGL 4657S	7 58 36	−29 56 00	

NAME	RA (1950)	DEC	POS REF
	h m s	° ′ ″	
AFGL 4658S	7 59 07	−31 33 36	
AFGL 4659S	8 00 06	−26 03 42	
AFGL 4660S	8 00 40	+27 57 30	
AFGL 4661S	8 00 45	−12 06 48	
AFGL 4662S	8 02 43	−29 52 06	
AFGL 4663S	8 03 04	−16 56 24	
AFGL 4664S	8 05 13	+ 6 41 36	
AFGL 4665S	8 05 14	− 3 17 48	
AFGL 4666S	8 05 17	−22 46 24	
AFGL 4667S	8 05 27	+47 28 12	
AFGL 4668S	8 06 46	+55 40 48	
AFGL 4669S	8 07 10	+17 12 12	
AFGL 4670S	8 09 11	+43 42 42	
AFGL 4671S	8 09 32	+44 21 54	
AFGL 4672S	8 09 35	+19 11 30	
AFGL 4673S	8 10 50	+45 55 54	
AFGL 4674S	8 11 40	+40 32 06	
AFGL 4675S	8 11 48	+37 49 36	
AFGL 4676S	8 11 58	+ 8 40 42	
AFGL 4677S	8 12 24	+ 4 45 18	
AFGL 4678S	8 12 26	+17 17 24	
AFGL 4679S	8 13 20	+23 35 24	
AFGL 4680S	8 13 37	+ 9 21 36	
AFGL 4681S	8 15 14	+39 37 12	
AFGL 4682S	8 16 47	+23 06 48	
AFGL 4683S	8 16 54	+39 36 18	
AFGL 4684S	8 20 08	−25 30 48	
AFGL 4685S	8 20 35	+18 55 48	
AFGL 4686S	8 20 35	− 7 25 00	
AFGL 4687S	8 20 44	+19 08 12	
AFGL 4688S	8 21 33	+42 11 48	
AFGL 4689S	8 22 03	+28 04 42	
AFGL 4690S	8 22 47	−23 52 06	
AFGL 4691S	8 22 51	+19 41 18	
AFGL 4692S	8 22 52	+ 2 14 00	
AFGL 4693S	8 23 57	+59 14 48	
AFGL 4694S	8 26 31	+21 52 24	
AFGL 4695S	8 26 51	+44 18 54	
AFGL 4696S	8 28 01	+43 49 30	
AFGL 4697S	8 28 08	+67 11 36	
AFGL 4698S	8 30 25	−67 37 12	
AFGL 4699S	8 31 22	− 9 48 48	
AFGL 4700S	8 31 54	+38 54 30	
AFGL 4701S	8 31 58	+ 5 41 24	
AFGL 4702S	8 32 01	+29 57 06	
AFGL 4703S	8 32 33	+57 42 30	
AFGL 4704S	8 36 36	−19 35 12	
AFGL 4705S	8 37 35	−12 18 42	
AFGL 4706S	8 37 36	+46 02 48	
AFGL 4707S	8 37 36	+16 26 12	
AFGL 4708S	8 39 28	− 2 55 36	
AFGL 4709S	8 39 45	− 2 51 42	
AFGL 4710S	8 41 51	+59 35 30	
AFGL 4711S	8 42 26	+72 34 06	
AFGL 4712S	8 43 53	−13 20 42	
AFGL 4713S	8 43 58	−10 42 12	
AFGL 4714S	8 44 48	+49 15 06	
AFGL 4715S	8 47 45	+44 22 42	
AFGL 4716S	8 48 23	+63 54 12	
AFGL 4717S	8 49 35	− 3 14 06	
AFGL 4718S	8 52 41	+23 00 30	
AFGL 4719S	8 54 14	+41 33 12	
AFGL 4720S	8 54 34	+11 04 24	
AFGL 4721S	8 55 37	+29 08 12	
AFGL 4722S	8 57 10	−13 38 30	
AFGL 4723S	8 57 18	+37 49 06	
AFGL 4724S	8 57 26	+41 58 54	
AFGL 4725S	9 01 52	+52 50 48	
AFGL 4726S	9 03 21	+ 5 13 48	
AFGL 4727S	9 03 52	+27 44 54	
AFGL 4728S	9 04 26	+37 22 54	
AFGL 4729S	9 04 37	+32 54 30	
AFGL 4730S	9 05 18	− 9 19 00	
AFGL 4731S	9 06 24	+59 06 00	
AFGL 4732S	9 07 42	+58 14 00	
AFGL 4733S	9 08 08	−62 51 00	
AFGL 4734S	9 08 57	+73 35 12	
AFGL 4735S	9 12 42	+23 40 12	
AFGL 4736S	9 12 43	+48 42 06	
AFGL 4737S	9 13 12	−15 28 06	
AFGL 4738S	9 15 23	+47 28 18	
AFGL 4739S	9 16 05	+36 35 36	
AFGL 4740S	9 16 46	+42 58 18	
AFGL 4741S	9 17 15	+45 25 30	
AFGL 4742S	9 21 57	+41 55 36	
AFGL 4743S	9 25 55	− 7 26 24	
AFGL 4744S	9 26 53	+63 18 42	
AFGL 4745S	9 28 15	+25 16 30	
AFGL 4746S	9 29 03	+51 52 42	
AFGL 4747S	9 32 03	+39 50 48	
AFGL 4748S	9 32 51	−14 30 54	
AFGL 4749S	9 35 18	+58 46 36	
AFGL 4750S	9 36 01	+ 4 51 54	
AFGL 4751S	9 38 39	+10 10 36	
AFGL 4752S	9 39 16	+72 25 12	
AFGL 4753S	9 40 15	+53 58 30	
AFGL 4754S	9 43 48	− 5 51 48	
AFGL 4755S	9 44 24	+ 5 55 54	
AFGL 4756S	9 45 41	+53 47 12	
AFGL 4757S	9 48 09	+13 14 48	
AFGL 4758S	9 51 01	+10 31 54	
AFGL 4759S	9 51 02	−17 42 00	
AFGL 4760S	9 56 18	+ 5 03 12	
AFGL 4761S	9 56 22	+57 02 42	
AFGL 4762S	9 57 34	+70 12 06	
AFGL 4763S	10 00 07	+41 32 36	
AFGL 4764S	10 01 14	− 9 20 12	
AFGL 4765S	10 02 06	+84 04 54	
AFGL 4766S	10 02 17	+86 48 54	
AFGL 4767S	10 02 59	−58 26 54	
AFGL 4768S	10 03 06	+18 18 42	
AFGL 4769S	10 05 13	+ 1 13 36	
AFGL 4770S	10 05 29	+17 35 48	
AFGL 4771S	10 05 39	+12 12 48	
AFGL 4772S	10 07 27	+24 36 36	
AFGL 4773S	10 08 56	−18 43 18	
AFGL 4774S	10 12 46	−57 34 12	
AFGL 4775S	10 12 49	+79 34 24	
AFGL 4776S	10 13 21	−54 12 24	
AFGL 4777S	10 15 02	−57 40 36	
AFGL 4778S	10 16 21	−53 45 00	
AFGL 4779S	10 19 38	+25 44 24	
AFGL 4780S	10 21 03	− 3 22 00	
AFGL 4781S	10 24 52	−25 17 54	
AFGL 4782S	10 25 00	+36 57 24	
AFGL 4783S	10 25 24	−21 33 24	
AFGL 4784S	10 26 34	+84 00 18	
AFGL 4785S	10 28 29	− 7 22 00	
AFGL 4786S	10 31 17	+68 44 18	
AFGL 4787S	10 32 08	+ 7 11 24	
AFGL 4788S	10 32 47	−48 36 54	
AFGL 4789S	10 33 32	−63 20 54	
AFGL 4790S	10 34 26	+79 00 18	
AFGL 4791S	10 38 05	+68 42 30	
AFGL 4792S	10 39 06	+31 57 30	
AFGL 4793S	10 43 42	−59 52 48	
AFGL 4794S	10 44 04	+65 51 30	
AFGL 4795S	10 45 57	− 1 43 30	
AFGL 4796S	10 56 27	+36 20 36	
AFGL 4797S	10 57 00	+45 48 36	
AFGL 4798S	10 57 02	−16 06 18	
AFGL 4799S	11 03 50	−62 13 30	
AFGL 4800S	11 06 29	+20 33 00	
AFGL 4801S	11 07 26	−43 47 42	
AFGL 4802S	11 08 02	+11 34 24	
AFGL 4803S	11 12 10	+73 29 54	
AFGL 4804S	11 12 52	−11 21 06	
AFGL 4805S	11 13 20	+13 34 18	
AFGL 4806S	11 14 13	+10 03 54	
AFGL 4807S	11 15 43	−39 37 36	
AFGL 4808S	11 16 10	−61 09 06	
AFGL 4809S	11 16 15	−46 05 18	
AFGL 4810S	11 17 27	+12 23 12	
AFGL 4811S	11 20 48	+17 05 24	
AFGL 4812S	11 22 17	−48 07 00	
AFGL 4813S	11 22 22	+77 36 42	
AFGL 4814S	11 23 28	−13 28 36	
AFGL 4815S	11 23 57	+72 45 36	
AFGL 4816S	11 24 22	+13 09 06	
AFGL 4817S	11 24 59	+ 3 08 00	
AFGL 4818S	11 27 27	−62 23 54	
AFGL 4819S	11 29 57	−26 30 12	
AFGL 4820S	11 31 10	+ 2 47 24	
AFGL 4821S	11 34 02	+80 06 36	
AFGL 4822S	11 37 15	−58 35 06	
AFGL 4823S	11 37 43	−30 01 00	
AFGL 4824S	11 39 14	−32 09 42	
AFGL 4825S	11 39 47	−48 12 42	
AFGL 4826S	11 43 31	−24 40 36	
AFGL 4827S	11 44 03	−63 30 42	
AFGL 4828S	11 45 47	−43 46 12	
AFGL 4829S	11 47 42	+51 41 42	
AFGL 4830S	11 50 09	− 7 20 30	
AFGL 4831S	11 50 53	+53 56 48	
AFGL 4832S	11 56 46	−29 44 18	
AFGL 4833S	11 58 09	−27 26 06	
AFGL 4834S	11 58 42	−62 53 00	
AFGL 4835S	12 01 43	+19 03 30	
AFGL 4836S	12 07 34	−58 44 48	
AFGL 4837S	12 17 20	+11 53 24	
AFGL 4838S	12 17 46	− 8 42 42	
AFGL 4839S	12 17 47	+ 3 35 06	
AFGL 4840S	12 19 45	+ 5 08 24	
AFGL 4841S	12 20 12	+77 10 18	
AFGL 4842S	12 21 33	+ 6 15 36	
AFGL 4843S	12 21 35	+25 49 54	
AFGL 4844S	12 23 03	−59 42 06	
AFGL 4845S	12 23 43	−59 19 48	
AFGL 4846S	12 26 37	− 3 48 00	
AFGL 4847S	12 26 37	− 2 06 42	
AFGL 4848S	12 26 56	−76 46 00	
AFGL 4849S	12 27 55	+31 49 00	
AFGL 4850S	12 29 55	+15 35 54	
AFGL 4851S	12 31 11	− 7 03 48	
AFGL 4852S	12 31 19	+41 39 00	
AFGL 4853S	12 32 43	+18 39 24	
AFGL 4854S	12 36 12	− 4 04 42	
AFGL 4855S	12 36 31	−30 13 54	
AFGL 4856S	12 38 12	−61 28 06	
AFGL 4857S	12 38 35	−27 33 54	
AFGL 4858S	12 38 41	+11 41 42	
AFGL 4859S	12 39 02	−37 21 54	
AFGL 4860S	12 39 19	− 7 14 30	
AFGL 4861S	12 40 36	−24 42 48	
AFGL 4862S	12 40 47	+10 23 30	
AFGL 4863S	12 40 59	+77 52 06	
AFGL 4864S	12 44 08	−33 06 54	
AFGL 4865S	12 44 48	+38 40 18	
AFGL 4866S	12 45 07	+67 06 18	
AFGL 4867S	12 45 24	+30 02 42	
AFGL 4868S	12 50 00	+17 22 36	
AFGL 4869S	12 50 08	−25 43 42	
AFGL 4870S	12 51 26	+46 55 00	
AFGL 4871S	12 52 49	+11 44 48	
AFGL 4872S	12 57 05	+76 41 54	
AFGL 4873S	12 57 49	−51 51 36	
AFGL 4874S	12 57 54	+66 53 06	
AFGL 4875S	13 00 30	−63 23 06	
AFGL 4876S	13 00 42	+ 5 08 24	
AFGL 4877S	13 04 14	− 5 38 36	
AFGL 4878S	13 04 41	+27 54 06	
AFGL 4879S	13 06 07	−32 47 48	
AFGL 4880S	13 07 28	−55 34 54	
AFGL 4881S	13 08 52	−62 50 24	
AFGL 4882S	13 09 05	−47 55 42	
AFGL 4883S	13 09 46	+56 40 48	
AFGL 4884S	13 09 59	+11 49 12	
AFGL 4885S	13 12 35	+ 4 47 36	
AFGL 4886S	13 12 42	−12 11 00	
AFGL 4887S	13 13 17	−19 44 12	
AFGL 4888S	13 18 02	−11 12 54	
AFGL 4889S	13 18 55	+75 52 24	
AFGL 4890S	13 19 35	−62 24 06	
AFGL 4891S	13 20 27	−18 03 42	
AFGL 4892S	13 20 28	+59 29 36	
AFGL 4893S	13 20 44	−24 22 48	
AFGL 4894S	13 20 50	− 4 38 48	
AFGL 4895S	13 23 54	−40 26 42	
AFGL 4896S	13 24 26	+72 37 24	
AFGL 4897S	13 25 05	−27 05 54	
AFGL 4898S	13 26 47	−38 05 12	
AFGL 4899S	13 28 43	−25 37 30	
AFGL 4900S	13 30 22	− 9 52 42	
AFGL 4901S	13 31 12	−59 58 30	
AFGL 4902S	13 33 27	−62 35 18	
AFGL 4903S	13 34 20	−33 49 48	
AFGL 4904S	13 34 40	+24 52 30	
AFGL 4905S	13 35 34	+50 58 00	
AFGL 4906S	13 35 38	−33 37 48	
AFGL 4907S	13 36 38	−62 50 18	
AFGL 4908S	13 38 08	−52 15 12	
AFGL 4909S	13 38 42	−33 20 42	
AFGL 4910S	13 39 39	−19 07 48	
AFGL 4911S	13 39 59	+23 32 12	
AFGL 4912S	13 41 13	−61 49 06	
AFGL 4913S	13 43 05	+ 0 11 00	
AFGL 4914S	13 45 17	+47 58 06	
AFGL 4915S	13 45 42	−27 55 48	
AFGL 4916S	13 45 57	+49 34 36	
AFGL 4917S	13 47 03	+ 0 17 42	
AFGL 4918S	13 47 19	−67 16 30	
AFGL 4919S	13 48 39	+34 53 42	
AFGL 4920S	13 49 28	+11 29 36	
AFGL 4921S	13 49 45	+39 54 54	
AFGL 4922S	13 51 56	− 5 31 24	
AFGL 4923S	13 52 30	+18 39 42	
AFGL 4924S	13 57 59	+38 05 24	
AFGL 4925S	13 58 00	−10 21 00	
AFGL 4926S	14 00 17	− 7 20 00	
AFGL 4927S	14 02 53	−35 14 36	
AFGL 4928S	14 03 58	+17 09 54	
AFGL 4929S	14 05 30	−60 55 42	
AFGL 4930S	14 05 44	− 8 37 42	
AFGL 4931S	14 06 08	−18 56 12	
AFGL 4932S	14 06 33	+49 41 24	
AFGL 4933S	14 07 28	−30 35 24	
AFGL 4934S	14 07 44	−19 01 54	
AFGL 4935S	14 08 04	− 4 11 30	
AFGL 4936S	14 12 22	−12 43 42	
AFGL 4937S	14 15 19	−14 27 18	
AFGL 4938S	14 16 04	−61 11 00	
AFGL 4939S	14 18 13	+ 5 42 00	
AFGL 4940S	14 18 56	− 2 05 48	
AFGL 4941S	14 21 25	+54 00 54	
AFGL 4942S	14 21 56	−69 39 06	
AFGL 4943S	14 22 02	+27 39 12	
AFGL 4944S	14 26 02	−56 35 18	
AFGL 4945S	14 26 16	−53 57 30	
AFGL 4946S	14 26 45	+26 06 36	
AFGL 4947S	14 27 50	+39 04 30	
AFGL 4948S	14 29 45	+38 29 42	
AFGL 4949S	14 34 23	−14 17 30	
AFGL 4950S	14 34 48	+26 55 42	
AFGL 4951S	14 35 32	+ 3 40 18	
AFGL 4952S	14 35 48	− 3 20 24	
AFGL 4953S	14 36 38	−10 23 54	
AFGL 4954S	14 38 16	−25 08 18	
AFGL 4955S	14 38 16	+15 42 06	
AFGL 4956S	14 39 06	−28 47 42	
AFGL 4957S	14 39 31	− 3 21 30	
AFGL 4958S	14 40 49	−48 55 12	
AFGL 4959S	14 42 21	−37 25 30	
AFGL 4960S	14 44 20	+ 7 28 24	
AFGL 4961S	14 44 30	+ 5 03 42	
AFGL 4962S	14 46 29	−24 02 30	
AFGL 4963S	14 47 35	−43 21 18	
AFGL 4964S	14 48 25	+37 28 24	
AFGL 4965S	14 52 25	−21 49 00	
AFGL 4966S	14 53 45	+ 6 02 42	
AFGL 4967S	14 54 05	−11 10 06	
AFGL 4968S	14 54 34	−59 48 24	
AFGL 4969S	14 54 43	+75 01 12	
AFGL 4970S	14 54 52	−27 52 12	
AFGL 4971S	14 54 59	−28 58 12	
AFGL 4972S	14 57 18	−58 45 06	
AFGL 4973S	14 58 35	− 2 31 12	
AFGL 4974S	14 59 18	+ 0 03 30	
AFGL 4975S	15 00 20	+31 52 06	
AFGL 4976S	15 02 11	− 7 50 42	
AFGL 4977S	15 02 32	+27 10 06	
AFGL 4978S	15 03 34	−57 33 42	
AFGL 4979S	15 03 55	−16 02 48	
AFGL 4980S	15 05 43	−68 58 06	
AFGL 4981S	15 05 48	−58 26 12	
AFGL 4982S	15 06 08	+ 0 48 54	
AFGL 4983S	15 07 38	+65 57 54	
AFGL 4984S	15 08 05	+11 51 48	
AFGL 4985S	15 09 10	−69 53 06	
AFGL 4986S	15 09 48	+22 30 12	
AFGL 4987S	15 15 24	−27 43 12	
AFGL 4988S	15 15 44	+ 0 16 36	
AFGL 4989S	15 16 33	+72 02 12	
AFGL 4990S	15 19 17	+31 36 00	
AFGL 4991S	15 20 14	−14 54 42	
AFGL 4992S	15 20 49	− 9 32 00	
AFGL 4993S	15 21 59	+15 39 18	
AFGL 4994S	15 22 06	−26 32 30	
AFGL 4995S	15 24 02	+17 08 30	
AFGL 4996S	15 24 53	−37 08 48	
AFGL 4997S	15 25 15	+25 15 24	
AFGL 4998S	15 25 35	−16 36 30	
AFGL 4999S	15 26 09	−11 44 18	
AFGL 5000S	15 27 11	+17 44 12	
AFGL 5001S	15 27 27	−12 44 24	
AFGL 5002S	15 28 31	−70 18 12	
AFGL 5003S	15 30 21	−27 02 18	
AFGL 5004S	15 30 39	−37 28 30	
AFGL 5005S	15 31 38	−27 52 24	
AFGL 5006S	15 32 21	−23 43 48	
AFGL 5007S	15 32 45	−14 34 36	
AFGL 5008S	15 33 42	−37 38 18	
AFGL 5009S	15 36 46	+33 02 42	
AFGL 5010S	15 36 57	+10 47 42	
AFGL 5011S	15 41 40	+ 2 36 24	

NAME	RA (1950)	DEC	POS REF
	h m s	° ′ ″	
AFGL 5012S	15 42 21	+20 02 24	
AFGL 5013S	15 47 49	−12 39 54	
AFGL 5014S	15 47 54	−34 55 48	
AFGL 5015S	15 48 19	−31 33 48	
AFGL 5016S	15 48 28	−37 58 24	
AFGL 5017S	15 50 02	−36 27 42	
AFGL 5018S	15 50 53	−18 50 54	
AFGL 5019S	15 51 42	−20 35 36	
AFGL 5020S	15 51 52	−20 44 42	
AFGL 5021S	15 52 29	+20 25 54	
AFGL 5022S	15 54 11	−36 03 36	
AFGL 5023S	15 54 12	−34 14 30	
AFGL 5024S	15 57 15	−22 33 48	
AFGL 5025S	15 59 15	+25 16 30	
AFGL 5026S	16 00 24	−25 46 24	
AFGL 5027S	16 01 56	+85 41 00	
AFGL 5028S	16 03 09	−37 49 54	
AFGL 5029S	16 04 24	− 3 43 36	
AFGL 5030S	16 04 50	− 4 57 48	
AFGL 5031S	16 05 07	− 6 13 12	
AFGL 5032S	16 07 48	−29 15 00	
AFGL 5033S	16 07 55	+10 44 06	
AFGL 5034S	16 10 16	+25 03 18	
AFGL 5035S	16 10 32	−10 12 12	
AFGL 5036S	16 10 55	+ 5 05 48	
AFGL 5037S	16 12 46	− 6 28 54	
AFGL 5038S	16 12 54	+11 31 24	
AFGL 5039S	16 15 42	−28 34 42	
AFGL 5040S	16 15 55	+25 59 18	
AFGL 5041S	16 16 57	−22 09 48	
AFGL 5042S	16 18 48	+81 35 54	
AFGL 5043S	16 19 31	+24 29 54	
AFGL 5044S	16 21 01	+30 54 42	
AFGL 5045S	16 24 04	−31 10 12	
AFGL 5046S	16 24 06	− 9 41 36	
AFGL 5047S	16 24 11	− 2 30 18	
AFGL 5048S	16 24 37	−35 01 18	
AFGL 5049S	16 25 07	+ 3 00 00	
AFGL 5050S	16 25 31	−35 34 12	
AFGL 5051S	16 26 35	−19 12 42	
AFGL 5052S	16 26 50	− 3 26 48	
AFGL 5053S	16 27 15	+ 0 01 48	
AFGL 5054S	16 28 31	−10 26 42	
AFGL 5055S	16 30 30	+11 32 36	
AFGL 5056S	16 32 25	−24 46 06	
AFGL 5057S	16 33 48	−27 56 42	
AFGL 5058S	16 34 01	+ 5 02 36	
AFGL 5059S	16 34 18	+ 5 06 06	
AFGL 5060S	16 34 27	−10 26 18	
AFGL 5061S	16 34 45	−35 19 30	
AFGL 5062S	16 37 39	−20 21 42	
AFGL 5063S	16 39 48	+16 49 00	
AFGL 5064S	16 41 57	−14 00 24	
AFGL 5065S	16 43 24	−16 50 54	
AFGL 5066S	16 48 58	− 7 03 06	
AFGL 5067S	16 50 14	−21 36 30	
AFGL 5068S	16 50 20	+ 5 27 06	
AFGL 5069S	16 52 03	− 6 07 54	
AFGL 5070S	16 52 38	−33 21 36	
AFGL 5071S	16 52 41	+49 00 48	
AFGL 5072S	16 52 41	+82 09 48	
AFGL 5073S	16 52 59	+18 31 18	
AFGL 5074S	16 54 07	−33 14 48	
AFGL 5075S	16 54 41	+50 07 12	
AFGL 5076S	16 55 03	− 9 25 48	
AFGL 5077S	16 55 06	−19 46 12	
AFGL 5078S	16 55 12	− 2 41 24	
AFGL 5079S	16 57 05	− 7 34 54	
AFGL 5080S	16 57 30	−10 32 30	
AFGL 5081S	16 58 03	−25 29 36	
AFGL 5082S	16 58 22	− 4 08 30	
AFGL 5083S	16 59 38	+20 32 24	
AFGL 5084S	17 01 30	+42 41 18	
AFGL 5085S	17 03 41	+72 18 48	
AFGL 5086S	17 04 24	+22 07 42	
AFGL 5087S	17 04 24	−31 48 36	
AFGL 5088S	17 05 44	+76 21 30	
AFGL 5089S	17 06 02	+72 13 00	
AFGL 5090S	17 06 35	−31 17 42	
AFGL 5091S	17 08 51	+27 38 06	
AFGL 5092S	17 10 11	+ 4 17 30	
AFGL 5093S	17 10 38	−31 23 42	
AFGL 5094S	17 11 07	−22 04 54	
AFGL 5095S	17 12 12	−15 12 48	
AFGL 5096S	17 12 33	−26 29 36	
AFGL 5097S	17 13 11	+45 13 42	
AFGL 5098S	17 14 07	+ 4 46 36	
AFGL 5099S	17 15 12	−11 57 12	
AFGL 5100S	17 15 21	−16 13 24	
AFGL 5101S	17 16 24	+10 52 12	
AFGL 5102S	17 16 44	−23 47 00	
AFGL 5103S	17 16 57	+41 36 48	
AFGL 5104S	17 18 54	−14 33 36	
AFGL 5105S	17 18 56	+46 16 24	
AFGL 5106S	17 20 05	−28 04 24	
AFGL 5107S	17 21 22	−22 19 54	
AFGL 5108S	17 21 57	− 6 57 48	
AFGL 5109S	17 22 43	+16 49 48	
AFGL 5110S	17 23 42	+12 38 42	
AFGL 5111S	17 23 46	−31 04 24	
AFGL 5112S	17 24 48	− 6 14 00	
AFGL 5113S	17 24 52	+ 4 14 48	
AFGL 5114S	17 25 27	+ 8 27 42	
AFGL 5115S	17 25 59	+15 55 42	
AFGL 5116S	17 27 59	−23 34 30	
AFGL 5117S	17 29 38	+39 42 48	
AFGL 5118S	17 29 38	+52 24 00	
AFGL 5119S	17 32 08	− 7 12 30	
AFGL 5120S	17 32 43	− 1 18 24	
AFGL 5121S	17 32 47	−14 17 18	
AFGL 5122S	17 33 16	−22 24 12	
AFGL 5123S	17 34 30	−15 19 18	
AFGL 5124S	17 35 23	−10 51 42	
AFGL 5125S	17 35 48	−14 07 24	
AFGL 5126S	17 36 01	−21 37 06	
AFGL 5127S	17 37 08	−24 37 36	
AFGL 5128S	17 38 00	+46 10 12	
AFGL 5129S	17 39 05	− 6 25 30	
AFGL 5130S	17 39 16	+11 42 30	
AFGL 5131S	17 39 55	−17 29 36	
AFGL 5132S	17 40 27	+24 35 12	
AFGL 5133S	17 40 41	− 3 53 30	
AFGL 5134S	17 41 58	−18 38 00	
AFGL 5135S	17 42 09	− 1 33 30	
AFGL 5136S	17 42 38	−28 34 24	
AFGL 5137S	17 42 56	+21 30 12	
AFGL 5138S	17 43 59	−26 58 12	
AFGL 5139S	17 44 31	+27 43 42	
AFGL 5140S	17 44 57	−24 45 30	
AFGL 5141S	17 45 43	−19 46 42	
AFGL 5142S	17 45 48	+28 47 12	
AFGL 5143S	17 46 12	−28 04 00	
AFGL 5144S	17 47 10	−22 27 30	
AFGL 5145S	17 47 14	+22 28 54	
AFGL 5146S	17 48 25	−28 26 00	
AFGL 5147S	17 48 55	−22 35 00	
AFGL 5148S	17 48 55	−29 41 06	
AFGL 5149S	17 49 20	+19 02 18	
AFGL 5150S	17 49 34	−28 15 18	
AFGL 5151S	17 50 39	−28 09 48	
AFGL 5152S	17 50 39	+45 28 42	
AFGL 5153S	17 51 37	+13 06 42	
AFGL 5154S	17 52 15	+56 31 06	
AFGL 5155S	17 52 51	−13 38 30	
AFGL 5156S	17 52 54	−27 58 54	
AFGL 5157S	17 53 18	−12 54 42	
AFGL 5158S	17 54 20	+ 5 53 06	
AFGL 5159S	17 54 25	−29 52 30	
AFGL 5160S	17 55 50	−16 36 48	
AFGL 5161S	17 55 57	−26 35 00	
AFGL 5162S	17 56 12	+29 13 06	
AFGL 5163S	17 56 18	+80 36 12	
AFGL 5164S	17 56 31	− 6 41 18	
AFGL 5165S	17 56 35	−23 27 42	
AFGL 5166S	17 56 40	− 6 06 54	
AFGL 5167S	17 57 03	−20 23 30	
AFGL 5168S	17 57 47	+16 45 00	
AFGL 5169S	17 57 54	+23 38 24	
AFGL 5170S	17 58 02	−22 58 48	
AFGL 5171S	17 58 14	+ 5 34 42	
AFGL 5172S	17 58 14	+45 29 24	
AFGL 5173S	17 58 23	−15 18 30	
AFGL 5174S	17 58 36	−15 26 00	
AFGL 5175S	17 58 36	−17 12 36	
AFGL 5176S	17 58 53	−23 59 06	
AFGL 5177S	17 58 59	+33 13 00	
AFGL 5178S	17 59 18	−12 16 54	
AFGL 5179S	17 59 20	+ 8 28 48	
AFGL 5180S	17 59 22	+21 37 18	
AFGL 5181S	17 59 24	−19 13 24	
AFGL 5182S	17 59 56	−22 00 00	
AFGL 5183S	18 00 10	−25 15 30	
AFGL 5184S	18 00 13	+ 1 42 36	
AFGL 5185S	18 00 20	+49 51 42	
AFGL 5186S	18 00 34	+26 58 18	
AFGL 5187S	18 00 38	+15 02 12	
AFGL 5188S	18 00 49	−13 14 06	
AFGL 5189S	18 01 31	−12 43 54	
AFGL 5190S	18 01 36	−26 01 00	
AFGL 5191S	18 02 14	−16 57 06	
AFGL 5192S	18 02 28	−27 03 48	
AFGL 5193S	18 02 38	−25 17 12	
AFGL 5194S	18 02 51	−25 25 54	
AFGL 5195S	18 03 28	+50 40 00	
AFGL 5196S	18 03 50	−27 50 18	
AFGL 5197S	18 04 13	−14 34 30	
AFGL 5198S	18 05 18	−23 52 00	
AFGL 5199S	18 06 50	−24 04 12	
AFGL 5200S	18 07 07	−24 10 36	
AFGL 5201S	18 07 35	− 6 52 24	
AFGL 5202S	18 07 37	−23 38 00	
AFGL 5203S	18 08 05	−18 50 48	
AFGL 5204S	18 08 08	− 6 07 24	
AFGL 5205S	18 09 10	−14 56 06	
AFGL 5206S	18 09 45	+ 6 48 42	
AFGL 5207S	18 09 54	−24 55 12	
AFGL 5208S	18 09 56	−16 18 06	
AFGL 5209S	18 10 37	+25 07 48	
AFGL 5210S	18 10 41	+ 4 05 12	
AFGL 5211S	18 11 22	+12 26 24	
AFGL 5212S	18 12 14	− 2 40 48	
AFGL 5213S	18 12 55	+16 15 00	
AFGL 5214S	18 14 19	−25 35 48	
AFGL 5215S	18 14 33	−25 18 24	
AFGL 5216S	18 14 37	−15 15 42	
AFGL 5217S	18 15 02	−17 52 48	
AFGL 5218S	18 15 23	+47 47 30	
AFGL 5219S	18 16 00	−25 37 30	
AFGL 5220S	18 16 13	+60 44 18	
AFGL 5221S	18 16 32	+36 41 12	
AFGL 5222S	18 17 17	−15 49 54	
AFGL 5223S	18 18 11	−15 15 30	
AFGL 5224S	18 18 26	+ 5 54 06	
AFGL 5225S	18 19 02	−23 35 06	
AFGL 5226S	18 19 20	−14 40 48	
AFGL 5227S	18 19 40	−19 22 36	
AFGL 5228S	18 20 19	−12 40 30	
AFGL 5229S	18 20 25	−20 40 12	
AFGL 5230S	18 20 27	−23 05 12	
AFGL 5231S	18 20 58	− 9 00 00	
AFGL 5232S	18 22 14	+43 52 00	
AFGL 5233S	18 22 28	− 6 54 54	
AFGL 5234S	18 22 43	−13 47 36	
AFGL 5235S	18 22 44	−12 43 06	
AFGL 5236S	18 23 56	−21 10 24	
AFGL 5237S	18 25 05	−16 45 24	
AFGL 5238S	18 25 12	−21 18 48	
AFGL 5239S	18 25 39	−19 47 06	
AFGL 5240S	18 26 05	+65 33 06	
AFGL 5241S	18 26 26	+49 17 54	
AFGL 5242S	18 26 26	+ 6 16 54	
AFGL 5243S	18 26 58	−11 11 06	
AFGL 5244S	18 27 05	+16 11 06	
AFGL 5245S	18 28 08	−21 15 48	
AFGL 5246S	18 28 25	− 8 26 42	
AFGL 5247S	18 28 31	− 9 23 00	
AFGL 5248S	18 29 07	+25 08 06	
AFGL 5249S	18 29 59	+ 4 18 12	
AFGL 5250S	18 30 05	−19 48 30	
AFGL 5251S	18 30 15	−21 00 00	
AFGL 5252S	18 30 17	−20 06 42	
AFGL 5253S	18 30 18	+20 19 54	
AFGL 5254S	18 30 50	+23 34 06	
AFGL 5255S	18 30 51	−24 07 06	
AFGL 5256S	18 31 13	+ 3 41 48	
AFGL 5257S	18 31 29	−13 08 06	
AFGL 5258S	18 31 46	−19 37 06	
AFGL 5259S	18 31 51	+10 25 54	
AFGL 5260S	18 32 48	+ 6 26 36	
AFGL 5261S	18 33 18	−23 55 36	
AFGL 5262S	18 33 31	+28 44 12	
AFGL 5263S	18 33 37	− 6 42 00	
AFGL 5264S	18 33 38	− 8 58 00	
AFGL 5265S	18 34 14	−19 11 48	
AFGL 5266S	18 34 23	+30 26 18	
AFGL 5267S	18 35 13	+31 17 36	
AFGL 5268S	18 35 18	− 6 53 48	
AFGL 5269S	18 35 25	+35 11 54	
AFGL 5270S	18 35 28	+ 5 00 24	
AFGL 5271S	18 35 43	+14 42 42	
AFGL 5272S	18 36 28	+ 1 38 48	
AFGL 5273S	18 36 41	+30 26 12	
AFGL 5274S	18 36 45	−28 42 36	
AFGL 5275S	18 38 36	− 6 24 18	
AFGL 5276S	18 39 16	+ 6 22 24	
AFGL 5277S	18 39 23	+46 02 12	
AFGL 5278S	18 39 32	− 7 22 48	
AFGL 5279S	18 40 07	+10 18 12	
AFGL 5280S	18 40 45	− 8 23 36	
AFGL 5281S	18 40 54	− 1 35 24	
AFGL 5282S	18 40 58	−11 25 48	
AFGL 5283S	18 41 07	+29 45 18	
AFGL 5284S	18 41 30	− 2 34 24	
AFGL 5285S	18 41 38	− 3 51 18	
AFGL 5286S	18 42 02	+11 14 00	
AFGL 5287S	18 42 26	+17 27 12	
AFGL 5288S	18 42 57	−17 20 42	
AFGL 5289S	18 43 01	+ 4 10 12	
AFGL 5290S	18 43 13	+ 8 42 24	
AFGL 5291S	18 43 22	−22 22 42	
AFGL 5292S	18 43 36	−29 37 24	
AFGL 5293S	18 43 40	− 3 00 00	
AFGL 5294S	18 44 07	+22 25 12	
AFGL 5295S	18 44 40	+ 5 25 18	
AFGL 5296S	18 44 50	− 5 44 00	
AFGL 5297S	18 45 00	+42 43 48	
AFGL 5298S	18 46 07	+19 04 06	
AFGL 5299S	18 46 22	+15 44 24	
AFGL 5300S	18 46 25	+ 2 21 30	
AFGL 5301S	18 46 38	+69 37 42	
AFGL 5302S	18 46 59	− 5 58 36	
AFGL 5303S	18 47 28	−10 45 24	
AFGL 5304S	18 47 36	+28 04 18	
AFGL 5305S	18 48 04	+33 19 06	
AFGL 5306S	18 48 26	+24 02 42	
AFGL 5307S	18 48 34	−12 42 36	
AFGL 5308S	18 48 37	− 9 38 00	
AFGL 5309S	18 48 59	+25 00 00	
AFGL 5310S	18 49 01	+ 0 09 12	
AFGL 5311S	18 50 01	− 3 16 18	
AFGL 5312S	18 50 13	− 7 57 18	
AFGL 5313S	18 50 16	+33 30 42	
AFGL 5314S	18 50 31	+59 20 30	
AFGL 5315S	18 50 56	+17 03 12	
AFGL 5316S	18 50 56	−12 40 54	
AFGL 5317S	18 50 59	+ 9 39 48	
AFGL 5318S	18 51 10	+42 07 00	
AFGL 5319S	18 51 52	+36 49 18	
AFGL 5320S	18 52 06	+50 38 48	
AFGL 5321S	18 52 17	+ 0 22 00	
AFGL 5322S	18 52 20	+27 50 24	
AFGL 5323S	18 52 22	+ 8 12 24	
AFGL 5324S	18 52 41	− 8 14 06	
AFGL 5325S	18 53 17	−29 40 06	
AFGL 5326S	18 54 52	+71 13 54	
AFGL 5327S	18 55 07	+ 0 22 36	
AFGL 5328S	18 56 49	+10 20 36	
AFGL 5329S	18 58 17	+32 04 36	
AFGL 5330S	18 59 29	+ 5 07 36	
AFGL 5331S	19 00 03	+ 1 24 36	
AFGL 5332S	19 01 22	+29 08 18	
AFGL 5333S	19 01 40	−21 47 54	
AFGL 5334S	19 02 25	+ 1 31 30	
AFGL 5335S	19 02 26	− 7 15 30	
AFGL 5336S	19 02 42	−12 42 00	
AFGL 5337S	19 02 52	+39 10 30	
AFGL 5338S	19 02 52	+31 39 06	
AFGL 5339S	19 03 05	+17 18 24	
AFGL 5340S	19 03 32	+ 3 06 06	
AFGL 5341S	19 03 37	− 8 57 36	
AFGL 5342S	19 05 36	+31 06 48	
AFGL 5343S	19 06 11	− 4 07 54	
AFGL 5344S	19 06 52	+24 04 36	
AFGL 5345S	19 07 58	+ 7 43 30	
AFGL 5346S	19 07 59	+35 08 00	
AFGL 5347S	19 08 37	+21 57 12	
AFGL 5348S	19 08 38	+36 30 30	
AFGL 5349S	19 09 34	+32 32 30	
AFGL 5350S	19 11 18	+ 2 33 48	
AFGL 5351S	19 12 00	+11 37 06	
AFGL 5352S	19 12 47	+22 00 00	
AFGL 5353S	19 12 53	+14 36 54	
AFGL 5354S	19 12 55	+57 38 30	
AFGL 5355S	19 13 22	+18 25 48	
AFGL 5356S	19 13 44	+22 54 00	
AFGL 5357S	19 14 23	+29 14 54	
AFGL 5358S	19 14 26	+22 24 06	
AFGL 5359S	19 15 29	−19 30 42	
AFGL 5360S	19 15 53	+53 15 48	
AFGL 5361S	19 16 13	−15 40 30	
AFGL 5362S	19 17 05	+27 12 36	
AFGL 5363S	19 17 22	− 6 39 42	
AFGL 5364S	19 17 33	+68 48 30	
AFGL 5365S	19 17 47	+46 04 48	

NAME	RA (1950)	DEC	POS REF
	h m s	° ′ ″	
AFGL 5366S	19 18 12	− 4 39 48	
AFGL 5367S	19 18 19	+37 47 06	
AFGL 5368S	19 18 39	+41 37 12	
AFGL 5369S	19 20 02	− 3 19 42	
AFGL 5370S	19 20 54	− 2 42 54	
AFGL 5371S	19 22 13	− 8 56 12	
AFGL 5372S	19 22 38	+21 22 54	
AFGL 5373S	19 22 47	+17 37 48	
AFGL 5374S	19 23 13	+35 56 00	
AFGL 5375S	19 23 54	+68 55 36	
AFGL 5376S	19 23 58	−18 33 18	
AFGL 5377S	19 24 10	+16 36 12	
AFGL 5378S	19 24 18	+19 47 24	
AFGL 5379S	19 24 41	+ 0 56 30	
AFGL 5380S	19 26 43	−16 11 54	
AFGL 5381S	19 26 47	+17 54 18	
AFGL 5382S	19 26 48	+ 3 46 06	
AFGL 5383S	19 27 09	+ 4 27 12	
AFGL 5384S	19 28 05	+11 16 54	
AFGL 5385S	19 28 51	−10 57 42	
AFGL 5386S	19 29 07	+23 24 24	
AFGL 5387S	19 29 12	+49 46 24	
AFGL 5388S	19 29 54	− 6 31 12	
AFGL 5389S	19 30 46	+ 6 11 06	
AFGL 5390S	19 30 48	+36 44 42	
AFGL 5391S	19 31 04	+ 2 50 42	
AFGL 5392S	19 31 05	−22 45 06	
AFGL 5393S	19 31 11	+ 1 32 18	
AFGL 5394S	19 31 14	+32 35 36	
AFGL 5395S	19 31 37	+45 21 48	
AFGL 5396S	19 31 41	+ 7 16 54	
AFGL 5397S	19 32 29	+69 33 48	
AFGL 5398S	19 32 34	+23 44 48	
AFGL 5399S	19 32 43	+30 40 18	
AFGL 5400S	19 32 54	+ 0 36 18	
AFGL 5401S	19 32 57	+60 04 06	
AFGL 5402S	19 33 06	+63 31 12	
AFGL 5403S	19 33 08	+ 0 14 30	
AFGL 5404S	19 33 21	+48 07 36	
AFGL 5405S	19 33 26	+47 41 12	
AFGL 5406S	19 33 43	+ 0 35 30	
AFGL 5407S	19 34 38	+21 36 36	
AFGL 5408S	19 35 09	+20 28 18	
AFGL 5409S	19 35 53	+ 6 19 12	
AFGL 5410S	19 36 46	+30 55 48	
AFGL 5411S	19 36 55	+16 26 00	
AFGL 5412S	19 37 02	+12 03 30	
AFGL 5413S	19 37 08	+20 02 54	
AFGL 5414S	19 37 32	+30 03 54	
AFGL 5415S	19 40 11	+59 30 12	
AFGL 5416S	19 40 33	+42 06 12	
AFGL 5417S	19 41 06	+58 46 36	
AFGL 5418S	19 41 40	+23 04 48	
AFGL 5419S	19 42 01	+14 36 12	
AFGL 5420S	19 42 02	+48 41 42	
AFGL 5421S	19 42 07	+37 15 06	
AFGL 5422S	19 42 19	+41 39 54	
AFGL 5423S	19 42 36	+ 0 51 48	
AFGL 5424S	19 42 38	+50 55 30	
AFGL 5425S	19 43 15	+58 12 36	
AFGL 5426S	19 43 38	+30 07 00	
AFGL 5427S	19 44 15	−17 12 12	
AFGL 5428S	19 44 50	+53 05 00	
AFGL 5429S	19 45 10	+15 55 00	
AFGL 5430S	19 45 22	+59 28 24	
AFGL 5431S	19 46 46	+26 00 18	
AFGL 5432S	19 46 54	+30 18 30	
AFGL 5433S	19 47 13	+21 27 12	
AFGL 5434S	19 48 24	+26 12 30	
AFGL 5435S	19 49 20	+52 51 48	
AFGL 5436S	19 49 40	+ 0 32 54	
AFGL 5437S	19 50 04	+ 0 48 18	
AFGL 5438S	19 50 13	+42 22 24	
AFGL 5439S	19 51 05	+29 30 30	
AFGL 5440S	19 51 16	+33 50 00	
AFGL 5441S	19 51 21	− 8 43 42	
AFGL 5442S	19 52 48	+ 6 16 06	
AFGL 5443S	19 53 38	+15 28 18	
AFGL 5444S	19 53 50	+32 36 42	
AFGL 5445S	19 54 41	+17 12 06	
AFGL 5446S	19 55 17	+24 06 54	
AFGL 5447S	19 55 32	+39 41 24	
AFGL 5448S	19 56 12	− 8 04 24	
AFGL 5449S	19 56 30	+10 12 00	
AFGL 5450S	19 57 10	− 4 07 18	
AFGL 5451S	19 57 10	−16 35 54	
AFGL 5452S	19 57 55	+ 9 28 12	
AFGL 5453S	19 57 57	+35 09 12	
AFGL 5454S	19 59 09	+40 01 36	
AFGL 5455S	20 00 10	+30 39 30	
AFGL 5456S	20 00 14	+49 54 48	
AFGL 5457S	20 00 26	+ 4 33 24	
AFGL 5458S	20 02 05	+44 34 24	
AFGL 5459S	20 02 59	+44 40 24	
AFGL 5460S	20 03 04	+19 50 42	
AFGL 5461S	20 04 19	+24 18 18	
AFGL 5462S	20 04 36	+61 51 42	
AFGL 5463S	20 04 42	+13 10 06	
AFGL 5464S	20 04 49	+67 52 42	
AFGL 5465S	20 05 08	+52 52 48	
AFGL 5466S	20 05 54	+16 30 48	
AFGL 5467S	20 06 22	− 1 48 06	
AFGL 5468S	20 06 36	+56 25 24	
AFGL 5469S	20 06 41	+33 06 12	
AFGL 5470S	20 06 43	−25 41 24	
AFGL 5471S	20 06 55	+36 48 06	
AFGL 5472S	20 07 49	+28 11 36	
AFGL 5473S	20 08 07	+29 13 00	
AFGL 5474S	20 08 34	−14 27 12	
AFGL 5475S	20 08 35	+48 41 30	
AFGL 5476S	20 08 39	+33 18 06	
AFGL 5477S	20 08 54	+73 50 54	
AFGL 5478S	20 09 03	− 8 17 18	
AFGL 5479S	20 09 12	−11 51 48	
AFGL 5480S	20 09 21	+ 0 47 54	
AFGL 5481S	20 09 26	+ 0 34 42	
AFGL 5482S	20 09 32	+36 26 36	
AFGL 5483S	20 11 05	+25 05 06	
AFGL 5484S	20 11 25	+41 11 24	
AFGL 5485S	20 12 32	+60 29 18	
AFGL 5486S	20 13 07	+29 38 06	
AFGL 5487S	20 13 43	−18 32 42	
AFGL 5488S	20 13 51	+27 40 00	
AFGL 5489S	20 13 57	− 7 19 06	
AFGL 5490S	20 14 39	+49 51 24	
AFGL 5491S	20 14 41	+ 6 54 42	
AFGL 5492S	20 15 31	+72 26 18	
AFGL 5493S	20 15 59	+37 51 36	
AFGL 5494S	20 16 10	+42 35 12	
AFGL 5495S	20 16 24	+37 19 06	
AFGL 5496S	20 17 12	+38 50 24	
AFGL 5497S	20 20 52	+18 11 30	
AFGL 5498S	20 20 59	+ 7 48 18	
AFGL 5499S	20 21 14	+36 41 42	
AFGL 5500S	20 21 45	− 2 52 48	
AFGL 5501S	20 22 09	+37 27 00	
AFGL 5502S	20 22 53	+58 40 36	
AFGL 5503S	20 22 57	+16 49 54	
AFGL 5504S	20 23 12	+55 02 06	
AFGL 5505S	20 23 19	+23 50 42	
AFGL 5506S	20 24 02	+26 05 18	
AFGL 5507S	20 24 59	+40 09 48	
AFGL 5508S	20 25 16	−15 52 30	
AFGL 5509S	20 26 50	+41 43 00	
AFGL 5510S	20 29 07	+44 45 12	
AFGL 5511S	20 29 49	+18 26 42	
AFGL 5512S	20 30 29	+56 35 24	
AFGL 5513S	20 31 09	+54 44 54	
AFGL 5514S	20 31 36	+ 2 09 24	
AFGL 5515S	20 32 08	+19 22 06	
AFGL 5516S	20 32 17	+28 06 00	
AFGL 5517S	20 32 44	+52 51 12	
AFGL 5518S	20 32 45	+28 24 00	
AFGL 5519S	20 33 34	+42 23 30	
AFGL 5520S	20 33 41	+61 36 24	
AFGL 5521S	20 33 59	+34 57 18	
AFGL 5522S	20 34 02	+61 09 42	
AFGL 5523S	20 34 22	+32 14 00	
AFGL 5524S	20 35 28	+59 53 42	
AFGL 5525S	20 35 53	+33 34 30	
AFGL 5526S	20 35 56	+36 39 54	
AFGL 5527S	20 36 16	+68 23 48	
AFGL 5528S	20 36 49	+37 43 06	
AFGL 5529S	20 37 00	+44 53 36	
AFGL 5530S	20 38 25	+59 19 36	
AFGL 5531S	20 38 51	+52 52 06	
AFGL 5532S	20 41 18	+11 40 24	
AFGL 5533S	20 41 28	+27 04 24	
AFGL 5534S	20 42 29	+72 12 12	
AFGL 5535S	20 42 40	+32 20 12	
AFGL 5536S	20 43 02	+54 04 18	
AFGL 5537S	20 43 13	+40 13 54	
AFGL 5538S	20 43 18	+67 12 12	
AFGL 5539S	20 43 23	+32 17 06	
AFGL 5540S	20 44 03	+29 58 06	
AFGL 5541S	20 44 15	+ 2 15 42	
AFGL 5542S	20 44 55	+45 50 06	
AFGL 5543S	20 44 59	+39 40 42	
AFGL 5544S	20 45 12	+15 37 48	
AFGL 5545S	20 45 36	+35 40 42	
AFGL 5546S	20 47 04	+40 49 42	
AFGL 5547S	20 47 25	+33 03 42	
AFGL 5548S	20 47 59	+50 34 54	
AFGL 5549S	20 49 05	+39 38 12	
AFGL 5550S	20 49 42	− 3 21 24	
AFGL 5551S	20 50 06	− 7 58 54	
AFGL 5552S	20 50 11	+35 01 36	
AFGL 5553S	20 51 08	+20 44 00	
AFGL 5554S	20 52 08	+33 15 24	
AFGL 5555S	20 54 11	+ 8 37 24	
AFGL 5556S	20 55 29	+25 20 54	
AFGL 5557S	20 56 16	+22 07 30	
AFGL 5558S	20 56 26	+47 28 06	
AFGL 5559S	20 56 56	+36 31 48	
AFGL 5560S	20 58 06	+13 26 00	
AFGL 5561S	20 58 18	+19 08 24	
AFGL 5562S	20 58 36	+59 14 42	
AFGL 5563S	20 59 07	+49 56 12	
AFGL 5564S	20 59 12	− 4 22 18	
AFGL 5565S	20 59 13	+45 10 48	
AFGL 5566S	20 59 34	+18 46 54	
AFGL 5567S	20 59 55	−10 11 54	
AFGL 5568S	21 00 30	+34 34 36	
AFGL 5569S	21 00 47	+48 00 54	
AFGL 5570S	21 00 52	+14 33 48	
AFGL 5571S	21 00 55	+27 06 48	
AFGL 5572S	21 02 22	+ 5 21 00	
AFGL 5573S	21 02 47	+42 14 18	
AFGL 5574S	21 05 08	+ 7 10 06	
AFGL 5575S	21 06 02	+ 4 44 42	
AFGL 5576S	21 06 03	+32 01 12	
AFGL 5577S	21 06 09	+66 44 42	
AFGL 5578S	21 07 12	−29 53 06	
AFGL 5579S	21 08 22	+ 4 51 00	
AFGL 5580S	21 09 03	+67 05 00	
AFGL 5581S	21 09 22	+44 00 00	
AFGL 5582S	21 10 04	+41 39 18	
AFGL 5583S	21 10 10	+79 07 12	
AFGL 5584S	21 10 24	+75 41 24	
AFGL 5585S	21 11 08	+55 50 12	
AFGL 5586S	21 11 21	+31 53 48	
AFGL 5587S	21 11 47	+42 44 24	
AFGL 5588S	21 12 03	+ 0 08 36	
AFGL 5589S	21 12 20	+82 33 36	
AFGL 5590S	21 12 50	+61 40 18	
AFGL 5591S	21 12 59	+37 49 30	
AFGL 5592S	21 13 11	+46 13 42	
AFGL 5593S	21 13 26	+ 9 06 12	
AFGL 5594S	21 13 45	+38 00 18	
AFGL 5595S	21 14 00	+57 23 36	
AFGL 5596S	21 14 25	+36 38 18	
AFGL 5597S	21 14 27	−20 35 06	
AFGL 5598S	21 15 03	+49 46 18	
AFGL 5599S	21 15 35	+47 53 12	
AFGL 5600S	21 16 01	−68 49 42	
AFGL 5601S	21 16 09	−13 20 24	
AFGL 5602S	21 16 41	+40 46 18	
AFGL 5603S	21 17 00	+17 02 00	
AFGL 5604S	21 17 04	+23 16 54	
AFGL 5605S	21 17 50	+62 16 00	
AFGL 5606S	21 19 33	+56 09 18	
AFGL 5607S	21 19 50	+57 11 36	
AFGL 5608S	21 19 50	+19 35 24	
AFGL 5609S	21 20 12	− 5 49 12	
AFGL 5610S	21 20 20	− 9 31 06	
AFGL 5611S	21 20 20	−19 53 12	
AFGL 5612S	21 20 29	− 7 22 18	
AFGL 5613S	21 23 53	−24 10 12	
AFGL 5614S	21 25 05	+13 54 54	
AFGL 5615S	21 25 26	+36 27 54	
AFGL 5616S	21 25 44	+ 7 55 30	
AFGL 5617S	21 26 04	+24 27 06	
AFGL 5618S	21 27 38	+55 11 36	
AFGL 5619S	21 28 04	+47 07 24	
AFGL 5620S	21 28 05	−14 20 18	
AFGL 5621S	21 28 46	+12 56 42	
AFGL 5622S	21 28 59	+50 27 54	
AFGL 5623S	21 29 25	+61 27 48	
AFGL 5624S	21 29 48	+ 0 33 00	
AFGL 5625S	21 31 32	+56 32 18	
AFGL 5626S	21 32 19	−65 08 12	
AFGL 5627S	21 33 29	+60 39 00	
AFGL 5628S	21 33 55	+32 17 06	
AFGL 5629S	21 35 02	−35 20 18	
AFGL 5630S	21 35 58	− 4 24 42	
AFGL 5631S	21 36 43	+ 9 01 36	
AFGL 5632S	21 36 43	+ 8 04 06	
AFGL 5633S	21 37 26	+44 56 18	
AFGL 5634S	21 38 05	− 7 38 30	
AFGL 5635S	21 38 43	+65 35 24	
AFGL 5636S	21 40 43	+22 13 42	
AFGL 5637S	21 41 42	+71 01 54	
AFGL 5638S	21 43 28	+67 21 48	
AFGL 5639S	21 43 48	+22 44 42	
AFGL 5640S	21 44 00	+65 38 42	
AFGL 5641S	21 44 48	+25 17 24	
AFGL 5642S	21 46 10	+42 06 12	
AFGL 5643S	21 47 13	+78 45 24	
AFGL 5644S	21 49 42	+74 35 54	
AFGL 5645S	21 49 44	−46 34 00	
AFGL 5646S	21 50 42	+62 34 48	
AFGL 5647S	21 53 43	− 9 51 54	
AFGL 5648S	21 54 07	+21 00 00	
AFGL 5649S	21 54 39	−66 45 30	
AFGL 5650S	21 54 42	+39 41 30	
AFGL 5651S	21 56 11	−15 18 54	
AFGL 5652S	21 56 13	+65 54 00	
AFGL 5653S	21 56 32	−25 30 00	
AFGL 5654S	21 57 23	−42 06 06	
AFGL 5655S	21 57 42	+76 11 36	
AFGL 5656S	21 57 52	+57 07 18	
AFGL 5657S	21 58 38	+ 8 00 36	
AFGL 5658S	21 58 38	+ 5 52 54	
AFGL 5659S	21 59 00	+48 16 48	
AFGL 5660S	22 01 39	−30 06 54	
AFGL 5661S	22 01 46	−35 53 24	
AFGL 5662S	22 02 36	+14 34 48	
AFGL 5663S	22 02 41	+67 31 12	
AFGL 5664S	22 03 13	−39 44 18	
AFGL 5665S	22 03 25	+62 33 54	
AFGL 5666S	22 04 13	+ 0 40 36	
AFGL 5667S	22 04 23	+25 05 42	
AFGL 5668S	22 04 28	+81 38 06	
AFGL 5669S	22 04 39	−40 39 12	
AFGL 5670S	22 04 46	+48 13 42	
AFGL 5671S	22 05 30	+47 28 42	
AFGL 5672S	22 05 31	−34 49 18	
AFGL 5673S	22 06 49	+44 45 42	
AFGL 5674S	22 09 31	+38 10 42	
AFGL 5675S	22 09 43	+24 43 30	
AFGL 5676S	22 09 59	− 5 38 54	
AFGL 5677S	22 11 47	+53 20 42	
AFGL 5678S	22 14 13	− 8 01 42	
AFGL 5679S	22 14 14	+47 28 30	
AFGL 5680S	22 15 09	−10 17 12	
AFGL 5681S	22 15 37	+61 17 18	
AFGL 5682S	22 18 38	−61 05 36	
AFGL 5683S	22 19 40	−51 01 06	
AFGL 5684S	22 21 46	+51 58 12	
AFGL 5685S	22 22 56	+51 01 00	
AFGL 5686S	22 23 09	+68 46 36	
AFGL 5687S	22 23 12	−48 40 12	
AFGL 5688S	22 25 39	+43 52 18	
AFGL 5689S	22 25 51	+31 34 54	
AFGL 5690S	22 26 06	−65 41 30	
AFGL 5691S	22 26 57	+40 02 12	
AFGL 5692S	22 27 37	+34 28 54	
AFGL 5693S	22 27 52	− 5 40 00	
AFGL 5694S	22 28 06	+12 49 36	
AFGL 5695S	22 28 20	+37 16 24	
AFGL 5696S	22 30 59	+ 0 57 42	
AFGL 5697S	22 31 19	+58 11 12	
AFGL 5698S	22 32 08	+56 21 48	
AFGL 5699S	22 33 29	− 7 50 48	
AFGL 5700S	22 34 22	+48 03 00	
AFGL 5701S	22 34 31	+52 20 42	
AFGL 5702S	22 35 53	−14 18 48	
AFGL 5703S	22 36 47	+20 53 00	
AFGL 5704S	22 36 56	−61 50 30	
AFGL 5705S	22 38 06	+44 00 36	
AFGL 5706S	22 39 21	+30 41 36	
AFGL 5707S	22 39 38	−29 35 06	
AFGL 5708S	22 40 44	+77 13 30	
AFGL 5709S	22 41 36	+41 33 24	
AFGL 5710S	22 43 06	+56 19 36	
AFGL 5711S	22 43 06	+52 16 54	
AFGL 5712S	22 43 38	−10 36 24	
AFGL 5713S	22 43 48	−11 24 54	
AFGL 5714S	22 44 10	+11 55 18	
AFGL 5715S	22 45 46	+61 00 00	
AFGL 5716S	22 46 09	+49 19 06	
AFGL 5717S	22 46 10	+32 03 12	
AFGL 5718S	22 47 26	+59 24 06	
AFGL 5719S	22 47 26	−40 08 42	

NAME	RA (1950) DEC	POS REF
AFGL 5720S	22 48 14 +17 38 36	
AFGL 5721S	22 49 45 +52 00 48	
AFGL 5722S	22 51 11 +59 50 30	
AFGL 5723S	22 51 57 +24 05 36	
AFGL 5724S	22 52 14 − 9 39 00	
AFGL 5725S	22 52 30 +20 03 24	
AFGL 5726S	22 53 36 +20 11 48	
AFGL 5727S	22 54 46 −53 46 36	
AFGL 5728S	22 55 03 −26 30 06	
AFGL 5729S	22 55 11 +17 47 06	
AFGL 5730S	22 55 25 +19 21 18	
AFGL 5731S	22 56 00 +64 53 24	
AFGL 5732S	22 56 10 +56 42 18	
AFGL 5733S	22 59 42 +50 32 18	
AFGL 5734S	22 59 56 − 6 52 00	
AFGL 5735S	23 02 05 +66 57 24	
AFGL 5736S	23 02 52 +28 43 12	
AFGL 5737S	23 03 00 +58 18 12	
AFGL 5738S	23 04 08 −23 59 18	
AFGL 5739S	23 04 11 −30 33 18	
AFGL 5740S	23 07 26 +60 58 24	
AFGL 5741S	23 07 36 +80 12 48	
AFGL 5742S	23 10 09 +13 06 54	
AFGL 5743S	23 10 41 + 8 41 30	
AFGL 5744S	23 10 54 +12 25 24	
AFGL 5745S	23 11 54 +29 08 54	
AFGL 5746S	23 11 58 +66 16 06	
AFGL 5747S	23 13 11 +34 27 54	
AFGL 5748S	23 14 29 +29 35 36	
AFGL 5749S	23 15 05 +73 29 18	
AFGL 5750S	23 16 13 −28 39 36	
AFGL 5751S	23 16 52 +67 51 24	
AFGL 5752S	23 17 25 +41 49 06	
AFGL 5753S	23 17 43 +32 39 48	
AFGL 5754S	23 17 53 + 5 06 36	
AFGL 5755S	23 18 28 +61 56 12	
AFGL 5756S	23 19 00 +20 18 18	
AFGL 5757S	23 19 27 +63 23 12	
AFGL 5758S	23 19 44 +25 33 54	
AFGL 5759S	23 19 49 −59 16 00	
AFGL 5760S	23 20 11 +28 28 00	
AFGL 5761S	23 20 13 +26 41 30	
AFGL 5762S	23 20 16 +25 39 48	
AFGL 5763S	23 20 34 +12 00 30	
AFGL 5764S	23 21 04 +55 53 30	
AFGL 5765S	23 21 46 +41 19 06	
AFGL 5766S	23 21 50 −17 34 48	
AFGL 5767S	23 21 59 +12 40 00	
AFGL 5768S	23 23 37 +27 33 30	
AFGL 5769S	23 25 19 +59 04 12	
AFGL 5770S	23 25 37 +44 58 48	
AFGL 5771S	23 26 24 − 9 30 48	
AFGL 5772S	23 26 38 +59 27 42	
AFGL 5773S	23 28 16 +53 35 18	
AFGL 5774S	23 30 16 +23 35 42	
AFGL 5775S	23 31 06 + 5 56 54	
AFGL 5776S	23 31 43 +12 40 30	
AFGL 5777S	23 32 09 +51 52 18	
AFGL 5778S	23 33 51 −69 54 42	
AFGL 5779S	23 34 44 +46 49 54	
AFGL 5780S	23 35 06 +71 05 48	
AFGL 5781S	23 35 10 +55 33 00	
AFGL 5782S	23 37 24 +51 47 36	
AFGL 5783S	23 38 58 −18 16 30	
AFGL 5784S	23 41 22 + 0 04 18	
AFGL 5785S	23 41 47 +29 05 12	
AFGL 5786S	23 46 32 +68 25 36	
AFGL 5787S	23 47 37 +60 48 36	
AFGL 5788S	23 48 18 +48 43 54	
AFGL 5789S	23 48 59 +29 26 54	
AFGL 5790S	23 50 11 −16 43 30	
AFGL 5791S	23 51 10 +53 19 06	
AFGL 5792S	23 51 20 + 0 17 24	
AFGL 5793S	23 52 06 −31 00 54	
AFGL 5794S	23 53 31 −22 21 54	
AFGL 5795S	23 53 36 −22 13 12	
AFGL 5796S	23 54 09 +26 04 36	
AFGL 5797S	23 55 08 +49 39 54	
AFGL 5798S	23 57 38 +19 57 06	
AFGL 5799S	23 58 26 +38 12 42	
AFGL 5800S	23 59 03 −51 40 18	
ALDEBARAN	4 33 02.9 +16 24 36	CSI 79
ALGOL	3 04 54.4 +40 45 52	779907
ALLEN IRS	6 38 24.9 + 9 32 29	720302
AB AND	23 09 08.7 +36 37 19	CSI 79
AE AND	0 40 20 +41 32 46	GCVS
AF AND	0 40 49 +40 55 52	"
ALF AND	0 05 47.7 +28 48 50	CSI 79
AQ AND	0 24 52.5 +35 18 40	779907
BET AND	1 06 55.3 +35 21 20	CSI 79
BM AND	23 35 13 +48 07 36	GCVS
DEL AND	0 36 38.7 +30 35 14	CSI 79
EPS AND	0 35 54.3 +29 02 25	"
EW AND	23 24 35.2 +49 14 28	779907
EY AND	23 42 32 +43 38 51	GCVS
GAM AND	2 00 49.1 +42 05 25	CSI 79
GAM 1 AND	" "	"
LAM AND	23 35 06.6 +46 11 11	779907
MUU AND	0 53 58.1 +38 13 42	CSI 79
NUU AND	0 47 02.7 +40 48 24	"
OMI AND	22 59 36.9 +42 03 25	779907
PHI AND	1 06 35.3 +46 58 32	CSI 79
R AND	0 21 23.0 +38 18 03	779907
RR AND	0 48 39.9 +34 05 30	CSI 79
RU AND	1 35 40.7 +38 25 00	779907
RW AND	0 44 36.6 +32 24 46	"
RX AND	1 01 45.9 +41 01 56	"
ST AND	23 36 16.1 +35 29 44	"
SU AND	0 02 01.7 +43 16 23	"
SV AND	0 01 45.5 +39 49 55	"
T AND	0 19 46.3 +26 43 09	CSI 79
U AND	1 12 37.7 +40 27 19	779907
UPS AND	1 33 51.1 +41 09 21	CSI 79
UX AND	2 30 13.1 +45 26 06	779907
UZ AND	1 13 20.7 +41 28 33	"
V AND	0 47 22.5 +35 22 51	"
VX AND	0 17 15.0 +44 25 56	"
VY AND	22 59 33.2 +45 37 00	CSI 79

NAME	RA (1950) DEC	POS REF
W AND	2 14 23.1 +44 04 30	779907
Y AND	1 36 40.4 +39 05 26	"
Z AND	23 31 15.4 +48 32 32	"
ZET AND	0 44 40.9 +23 59 42	CSI 79
2 AND	23 00 17.7 +42 29 18	"
41 AND	1 05 07.9 +43 40 34	"
50 AND	1 33 51.1 +41 09 21	"
ANOMALOUS	17 34 −33 40	ED
ANON	4 20 32.0 −38 52 17	
ANON	15 16 39 −56 59	
ANON	18 02 48 −25 40	
ANON	18 08 34 −17 35 00	
ANON	18 36 47 −11 13	
ANON #1	7 48 54.0 −33 36 26	
ANON #10	12 54 19.2 −61 15 22	
ANON 1	18 58 12.4 −37 05 13	760503
ANON 2	18 57 44.5 −37 02 16	"
U ANT	10 32 59.3 −39 18 12	CSI 79
V ANT	10 18 54.9 −34 32 44	"
Z ANT	10 43 40.3 −34 59 16	"
AO 0235+16	2 35 52.6 +16 24 05	809908
AO 0235+164	" "	"
KAP 1 APS	15 26 01.0 −73 13 06	CSI 79
S APS	15 04 13.7 −71 51 49	"
THE APS	14 00 23.2 −76 33 24	"
U APS	15 21 55.5 −75 44 55	"
VY APS	15 54 47.0 −74 53 07	"
AP1−1	17 25 37.4 −29 02 59	769910
AP1−2	17 25 56.4 −29 10 48	"
AP1−3	17 28 04 −28 21 18	819916
AP1−8	18 01 19 −28 21 42	789908
AP1−9	18 07 19.5 −28 08 21	769910
AP1−10	18 07 34.6 −27 58 30	"
AP1−11	18 07 51.6 −28 33 21	"
AP3−1	19 08 05.4 + 2 44 33	"
AD AQL	18 56 25.0 − 8 14 30	CSI 79
ALF AQL	19 48 19.7 + 8 43 58	"
ALF AQL	19 48 24 + 8 44	
BET AQL	19 52 51.3 + 6 16 48	CSI 79
DEL AQL	19 22 58.5 + 3 00 48	"
DY AQL	19 43 44.3 −11 04 22	"
EPS AQL	18 57 21.0 +14 59 55	"
ETA AQL	19 49 55.4 + 0 52 31	"
FF AQL	18 56 01.1 +17 17 31	"
GAM AQL	19 43 52.9 +10 29 23	"
GAM AQL	19 43 55 +10 29 02	
GY AQL	19 47 25 − 7 44 33	GCVS
KAP AQL	19 34 12.0 − 7 08 23	CSI 79
NOVA AQL 1970	19 22 16 + 4 08 51	
NOVA AQL 1975	19 15 26 + 4 41 43	GCVS
NOVA AQL 1982	19 20 50.1 + 2 23 35	829901
R AQL	19 03 57.6 + 8 09 09	CSI 79
R AQL	19 03 58.0 + 8 09 06	
RR AQL	19 54 58.0 − 2 01 12	
RR AQL	19 54 59.7 − 2 01 06	CSI 79
RS AQL	19 56 23.9 − 8 01 01	"
RT AQL	19 35 36.0 +11 36 16	
RT AQL	19 35 38.3 +11 35 02	CSI 79
RU AQL	20 10 00.1 +12 50 59	"
RV AQL	19 38 17.1 + 9 48 46	"
S AQL	20 09 19.3 +15 28 12	"
SY AQL	20 04 43.0 +12 48 10	
SY AQL	20 04 44.6 +12 48 30	CSI 79
THE AQL	20 08 43.4 − 0 58 15	"
U AQL	19 26 39.9 − 7 08 52	"
UV AQL	18 56 17.0 +14 17 53	"
UW AQL	18 55 00.2 + 0 23 16	"
V AQL	19 01 43.9 − 5 45 37	"
VX AQL	18 57 29 − 1 37 57	GCVS
V347 AQL	19 05 33 + 6 13 13	"
V450 AQL	19 31 17.9 + 5 21 22	CSI 79
V492 AQL	18 56 58 + 5 18 31	GCVS
V536 AQL	19 36 34 +10 23 21	"
V603 AQL	18 46 21.0 + 0 31 10	CSI 79
V733 AQL	19 55 10.4 +10 54 30	"
V844 AQL	19 04 30.9 + 7 04 22	"
V915 AQL	19 00 49.9 +12 10 39	"
V923 AQL	19 28 03 + 3 20 16	GCVS
V925 AQL	19 39 41 +11 43 10	"
W AQL	19 12 41.6 − 7 08 08	CSI 79
X AQL	19 48 59.0 + 4 20 28	"
Z AQL	20 12 31.0 − 6 18 16	"
58 AQL	19 52 11.0 + 0 08 29	"
AE AQR	20 37 33.9 − 1 02 53	"
ALF AQR	22 03 12.9 − 0 33 47	"
BET AQR	21 28 55.6 − 5 47 30	"
CHI AQR	23 14 15.3 − 7 59 56	"
EPS AQR	20 44 58.2 − 9 40 46	"
GAM AQR	22 19 04.3 − 1 38 23	"
LAM AQR	22 50 00 − 7 50 37	
LAM AQR	22 50 00.3 − 7 50 45	CSI 79
OMI AQR	22 00 43.6 − 2 23 49	"
PHI AQR	23 11 43.9 − 6 19 06	"
PI AQR	22 22 43.3 + 1 07 21	"
R AQR	23 41 14.1 −15 33 40	"
RR AQR	21 12 24.0 − 3 06 40	"
RS AQR	21 08 21.1 − 4 13 58	"
RT AQR	22 20 27.6 −22 18 34	"
S AQR	22 54 25.7 −20 36 37	"
SS AQR	22 17 13.4 −14 39 12	"
SZ AQR	22 40 07.6 −21 26 27	"
T AQR	20 47 18.0 − 5 19 59	"
THE AQR	22 14 11.7 − 8 01 57	"
W AQR	20 43 47.5 − 4 16 04	"
X AQR	22 15 57.3 −21 09 02	"
Y AQR	20 41 47.2 − 5 01 00	"
Z AQR	23 49 40.0 −16 07 56	"
ZET AQR	22 26 15.4 − 0 16 35	"
ZET AQR A		"
ZET AQR B	22 26 15.2 − 0 16 33	"
ZET AQR B(A)	" "	"
ZET AQR B(B)	" "	"
3 AQR	20 45 05.9 − 5 12 42	"
AQUILA REGION	19 17 +15 00	ED
AQUILA REGION	19 30 +11 36	
ARA #A	16 43 25.7 −45 45 17	
ARA #A	16 43 27.1 −45 45 18	
ARA #ALF	16 43 17 −45 48 40	ED

NAME	RA (1950) DEC	POS REF
ARA #B	16 43 24.3 −45 47 00	
ARA #B	16 43 24.7 −45 47 00	700103
ARA #C	16 43 25.4 −45 45 11	
ARA #C	16 43 26.0 −45 45 12	700103
ARA #D	16 43 26.0 −45 46 04	
ARA #D	16 43 26.4 −45 46 06	700103
ARA #E	16 43 30.2 −45 44 39	
ARA #E	16 43 31 −45 44 42	700103
ARA #F	16 43 25.0 −45 45 24	
ARA #F	16 43 25.5 −45 45 24	700103
ARA #G	16 43 28.7 −45 47 10	
ARA #G	16 43 29.1 −45 47 12	700103
ARA #H	16 43 22.7 −45 45 17	
ARA #H	16 43 23.2 −45 45 18	700103
ARA #I	16 43 28.5 −45 44 00	"
ARA #K	16 43 24 −45 45 30	"
ARA #L	16 43 21.9 −45 45 23	
ARA #L	16 43 28.6 −45 45 24	700103
ARA #M	16 43 25 −45 45 00	"
ARA #S	16 43 02.7 −45 44 12	
ARA #Z	16 43 25 −45 45 08	
ARA NOM.	" "	ED
ALF ARA	17 27 58.3 −49 50 18	CSI 79
IOT ARA	17 19 30.5 −47 25 15	"
LQ ARA	16 47 11.6 −60 56 48	"
LS ARA	16 54 42 −60 00 45	GCVS
RT ARA	17 22 10 −55 11 29	"
RY ARA	17 17 09.1 −51 04 14	CSI 79
SZ ARA	17 06 32 −61 53 07	GCVS
T ARA	16 58 28.7 −54 59 41	CSI 79
U ARA	17 49 39.7 −51 40 00	"
ARAK 120	5 13 38.0 − 0 12 17	819908
ARAK 253	10 41 19.2 − 1 01 55	789906
ARCTURUS	14 13 22.7 +19 26 30	CSI 79
ALF ARI	2 04 20.9 +23 13 35	"
BET ARI	1 51 52.3 +20 33 50	"
R ARI	2 13 16.0 +24 49 28	"
RZ ARI	2 52 59.5 +18 07 47	"
S ARI	2 01 58.6 +12 17 28	"
T ARI	2 45 31.9 +17 18 06	"
TT ARI	2 04 10 +15 02 34	GCVS
U ARI	3 08 15.9 +14 36 31	CSI 79
V ARI	2 12 18.1 +12 00 23	"
AS 201	8 29 36 −27 35	AS
AS 205	16 08 41 −18 31 00	GCVS
AS 209	16 46 26 −14 18 22	"
AS 210	16 48 12 −25 54	AS
AS 222	17 10 50 −38 56	"
AS 225	17 17 31 −37 57	"
AS 239	17 40 24 −22 45	"
AS 239	17 40 30.8 −22 44 16	
AS 296	18 12 34 − 0 20	AS
AS 299	18 14 09 −28 11	"
AS 310	18 30 45 − 5 01	
AS 319	18 40 40 − 5 08	
AS 320	18 41 34.9 − 3 51 02	CSI 79
AS 327	18 50 15 −24 26	AS
AS 341	19 07 19 − 2 52	"
AS 353	19 18 10 +10 56	"
AS 353A	" "	"
AS 360	19 43 38 +18 29	"
AS 374	19 57 16 +31 19	"
AS 422	20 30 18 +40 38	"
AS 441	20 44 58 +43 34	"
AS 442	20 45 52 +43 35	"
AS 501	22 55 39 +58 31	"
AS 513	23 41 06.5 +61 39 02	CSI 79
AB AUR	4 52 34.4 +30 28 22	760504
AE AUR	5 12 59.8 +34 15 26	779907
AF AUR	5 45 03.7 +44 51 21	CSI 79
ALF AUR	5 12 59.4 +45 56 56	"
AZ AUR	5 57 38.9 +39 40 13	"
BS AUR	6 01 07 +28 28 02	GCVS
CHI AUR	5 29 28.2 +32 09 24	CSI 79
EPS AUR	4 58 22.4 +43 45 03	"
ETA AUR	5 03 00.2 +41 10 07	"
FU AUR	5 44 54.9 +30 36 52	"
GM AUR	4 52 00 +30 17 11	GCVS
HH AUR	5 36 17.9 +29 48 24	CSI 79
IOT AUR	4 53 43.9 +33 05 18	"
KR AUR	6 12 35 +28 35 18	GCVS
LAM AUR	5 15 37.2 +40 03 23	CSI 79
LO AUR	5 53 34 +48 22 36	GCVS
NO AUR	5 37 26.9 +31 53 42	CSI 79
NUU AUR	5 48 01.3 +39 08 08	"
PSI 1 AUR	6 21 02.9 +49 18 57	779907
PSI 9 AUR	6 52 50.4 +46 20 21	CSI 79
R AUR	5 13 15.1 +53 31 57	779907
RT AUR	6 25 21.2 +30 31 32	CSI 79
RU AUR	5 36 42.6 +37 36 44	"
RW AUR	5 04 37.6 +30 20 13	"
S AUR	5 23 48.0 +34 06 51	"
SU AUR	4 52 47.8 +30 29 19	760504
THE AUR	5 56 18.6 +37 12 38	CSI 79
TX AUR	5 05 39.2 +38 56 21	779907
U AUR	5 38 51.0 +32 00 46	CSI 79
UU AUR	6 33 06.6 +38 29 16	779907
UV AUR	5 18 33.3 +32 27 51	"
UY AUR	4 48 36.0 +30 42 21	CSI 79
V AUR	6 20 16.9 +47 43 47	"
W AUR	5 23 31.3 +36 51 40	779907
X AUR	6 08 19.4 +50 14 26	"
ZET AUR	4 58 58.6 +41 00 17	CSI 79
16 AUR	5 14 53.5 +33 19 16	"
A0035	0 35 00 −33 52 30	
A0202−06	2 02 01.4 − 6 26 18	
A0311−25	3 11 30.2 −25 22 23	
A0316−26	3 16 23.8 −26 01 05	
A0419−21	4 19 04.0 −21 57 42	
A0620−00	6 20 11.2 − 0 19 10	769904
A0945−30	9 45 28 −30 43 36	809909
A1718+49A	17 17 35.6 +49 56 00	769909
A2020−44	20 20 −44	ED
A28		
A30	8 44 00 +18 04	P−K
A36	13 37 57.8 −19 37 33	769910
A43	17 51 11.1 +10 37 57	"
A46	18 29 18.0 +26 54 05	739909

NAME	RA (1950) DEC h m s ° ′ ″	POS REF
A63	19 39 55.2 +16 58 00	769910
A370		
A1246		
A1759		
B #38		
B #64		
B #67		
B #70		
B #73		
B SUPERGIANT	20 40 48.7 +42 45 46	
B 4 #80		
B 35	5 41 56.7 + 9 10 00	
B 35 ANON	5 40 46.1 + 9 11 56	ED
B 35 IRS1	5 41 24.6 + 9 08 00	
B 35 IRS2A	5 41 31.9 + 9 09 29	
B 35 IRS2B	5 41 33.0 + 9 09 45	
B 35 IRS3	5 41 38.8 + 9 10 50	
B 35 IRS4	5 41 44.3 + 9 09 57	
B 35 IRS5	5 41 53.3 + 9 15 09	
B 35 IRS6	5 42 04.5 + 9 11 56	
B 35 IRS7	5 42 08.3 + 9 19 05	
B 35 IRS8	5 42 09.3 + 9 15 47	
B 35 IRS9A	5 42 12.1 + 9 13 50	
B 35 IRS9B	5 42 12.6 + 9 13 30	
B 35 IRS10	5 42 13.7 + 9 14 16	
B 133	19 03 30 − 6 58 00	
B 133 2'E,2'S	19 03 38 − 7 00 00	ED
B 133 2'W,2'N	19 03 22 − 6 56 00	"
B 134	19 04 15 − 5 19 36	
B 163	21 40 39 +56 30 00	
B 179		
B 180		
B 227	6 04 31 +19 28 30	
B 234	13 00 42.5 +36 07 34	789905
B 264	12 59 30.9 +32 21 58	689904
B 267		
B 272	13 01 34.6 +37 30 07	789905
B 335	19 34 35 + 7 27 30	
B 335 0.2M W	19 34 23 + 7 27 30	ED
B 335 0.5M E	19 35 05 + 7 27 30	"
B 335 1.1M E	19 35 41 + 7 27 30	"
B 340	13 04 48.0 +34 40 24	789905
B 361	21 10 40 +47 10 30	
B 361 2'E	21 10 52 +47 10 30	ED
B 361 2'W	21 10 28 +47 10 30	"
B 361 4'W	21 10 16 +47 10 30	"
B 361 6'W	21 10 00 +47 10 30	"
B 382		
B 1985	7 31 30.0 −14 24 50	CSI 79
B 5481	21 17 52.6 +58 24 40	"
BARNARDS STAR	17 55 22.9 + 4 33 18	"
BD+ 0 1694	6 52 07.3 + 0 00 52	
BD+ 0 4030	18 47 51.3 + 0 43 45	BD
BD+ 1 2341P	9 38 10.4 + 1 15 31	CSI 79
BD+ 1 2916	14 19 12.1 + 1 00 38	"
BD+ 1 3694	18 27 52.3 + 1 11 15	"
BD+ 2 1451	6 50 51.3 + 1 56 08	"
BD+ 2 2957	15 22 29.0 + 1 41 06	
BD+ 2 3336	17 28 51.7 + 2 00 42	CSI 79
BD+ 3 2954	14 52 23.2 + 3 11 33	
BD+ 4 3561	17 55 28.0 + 4 15 05	CSI 79
BD+ 4 4048B	19 14 31.9 + 5 04 42	"
BD+ 5 168	1 17 08.4 + 5 53 57	"
BD+ 5 593	4 05 36.6 + 6 04 44	"
BD+ 5 1198	6 18 07.9 + 5 45 48	"
BD+ 6 319	2 00 00.2 + 7 26 11	"
BD+ 8 2654	12 49 57.5 + 7 28 43	"
BD+ 9 880	5 32 24 +10 00 28	BD
BD+ 9 1330	6 37 39.6 + 9 49 04	
BD+ 9 2870	14 14 01.9 + 8 41 44	CSI 79
BD+ 9 3920	18 52 19.7 +10 03 23	BD
BD+10 1085	6 16 13.0 +10 20 49	CSI 79
BD+10 2179	10 36 17.2 +10 19 25	"
BD+10 3721	18 52 07.3 +10 34 06	"
BD+12 3703	18 51 20.4 +12 46 39	BD
BD+13 1110	6 04 01.9 +13 36 11	CSI 79
BD+13 1212	6 18 12.0 +13 56 38	"
BD+13 1994	8 45 54.6 +12 43 57	"
BD+14 3887	19 19 17.3 +14 47 08	"
BD+15 635	4 27 13.6 +16 03 47	"
BD+16 625	4 32 09.3 +17 05 54	"
BD+17 734	4 26 37.6 +17 47 04	"
BD+17 3325	17 43 29.6 +17 13 58	"
BD+17 4282	20 15 58.7 +18 10 15	"
BD+17 4708	22 09 05.5 +17 50 40	"
BD+19 1183	5 59 56.1 +19 28 54	BD
BD+19 3109	16 27 13.9 +19 36 48	CSI 79
BD+22 1808	7 52 11.4 +21 48 12	"
BD+22 3840	19 50 20.5 +22 19 24	"
BD+23 1138	5 56 22.7 +23 43 36	"
BD+23 1240	6 20 21.5 +24 19 00	BD
BD+23 2998	16 45 18.1 +23 18 13	CSI 79
BD+23 3745	19 40 41.9 +23 20 37	"
BD+24 1072	5 59 43.9 +24 54 47	"
BD+24 3866	19 43 34.7 +25 00 12	"
BD+24 3881	19 44 56.5 +24 43 28	"
BD+24 3902	19 48 04.7 +24 49 30	"
BD+25 1131	6 05 41.9 +25 39 17	"
BD+25 1981	8 41 27.9 +24 58 58	"
BD+25 4097	20 03 43.7 +25 27 23	"
BD+27 2174	12 46 44.7 +27 09 24	"
BD+27 2178	12 48 05.4 +27 28 05	"
BD+27 2183	12 49 54.2 +27 15 15	"
BD+27 2187	12 50 36.3 +27 03 59	"
BD+27 2188	12 51 15.6 +27 15 40	"
BD+27 2189	12 51 29.6 +27 03 02	"
BD+27 2190	12 51 52.9 +27 21 03	"
BD+27 3687A	19 22 38 +22 40 48	
BD+28 834	5 08 48.6 +29 27 09	BD
BD+28 2153	12 46 51.3 +27 49 26	CSI 79
BD+28 2154	12 48 49.7 +27 36 45	"
BD+28 2155	12 49 01.5 +27 30 19	"
BD+28 2156	12 49 15.7 +27 48 45	"
BD+28 2162	12 51 44.5 +27 34 14	"
BD+28 2167	12 52 42.7 +28 02 16	"
BD+28 2169	12 54 26.4 +28 04 24	"
BD+29 3730	19 43 43.9 +30 08 01	"
BD+30 2512	14 19 47.7 +29 51 39	"
BD+30 2611	15 04 48.0 +30 12 06	"
BD+30 3526	19 19 44.1 +31 03 58	"
BD+30 3639	19 32 47.4 +30 24 20	"
BD+31 643	3 41 25.7 +32 00 21	"
BD+31 643AB	" "	"
BD+31 653	3 45 18.3 +32 09 20	"
BD+31 689	3 58 47.6 +31 50 48	"
BD+31 1049	5 37 26.9 +31 53 42	"
BD+32 666	3 44 17.4 +33 10 15	"
BD+32 1113	5 49 02.4 +32 32 28	"
BD+33 706	3 40 46.0 +34 01 30	"
BD+33 743	3 52 53.6 +34 14 30	"
BD+33 753	3 57 09.7 +34 12 08	"
BD+35 3955	20 04 05.9 +35 39 10	"
BD+35 4077	20 19 17.4 +35 27 34	"
BD+35 4138	20 27 00.5 +35 22 23	"
BD+36 724	3 30 42.9 +36 50 15	"
BD+36 746	3 41 56.3 +37 14 00	"
BD+36 2147	11 00 36.5 +36 18 19	"
BD+37 782	3 28 48.6 +37 39 42	"
BD+38 1162	5 23 34.8 +30 57 14	BD
BD+38 4003	20 17 08.2 +38 50 47	CSI 79
BD+39 1070	4 44 51.0 +39 51 40	"
BD+39 1328	5 28 44.3 +40 01 48	"
BD+39 4926	22 43 55.3 +39 50 37	"
BD+40 4124	20 18 42.5 +41 12 20	"
BD+40 4219	20 30 26.3 +41 16 57	"
BD+40 4220	20 30 34.8 +41 08 04	779907
BD+40 4227	20 31 27.3 +41 08 31	CSI 79
BD+40 4243	20 33 59.1 +41 11 48	"
BD+41 3306	19 17 22.0 +41 33 03	"
BD+41 3731	20 22 31.7 +42 08 14	"
BD+41 3804	20 31 58.6 +41 22 39	"
BD+41 4021	21 07 46.4 +42 13 44	"
BD+41 4064	21 14 16.0 +42 19 52	"
BD+42 1065	4 44 59.8 +43 43 36	BD
BD+43 44A	0 15 30.9 +43 44 21	CSI 79
BD+43 1131	4 52 28.9 +43 24 53	"
BD+43 1183	5 02 29.7 +43 52 14	BD
BD+43 3477	20 03 15.6 +43 28 10	"
BD+43 4108	21 58 35.1 +43 51 51	CSI 79
BD+43 4109	21 58 38.7 +43 47 43	"
BD+44 1005	4 53 10.7 +46 02 02	BD
BD+44 4014	21 58 12.3 +45 21 33	CSI 79
BD+46 3471	21 50 39.6 +46 59 20	"
BD+47 3487	21 34 01.3 +47 41 15	"
BD+48 1958	11 34 42.6 +47 44 22	"
BD+52 1601	11 57 24.9 +52 02 58	"
BD+52 3147	22 11 43.7 +53 22 20	"
BD+54 651	3 10 13.4 +54 44 58	"
BD+54 739	4 04 58 +55 01 12	IRC
BD+54 1323	9 38 53.9 +53 42 09	CSI 79
BD+54 2698	22 09 45.9 +55 01 13	"
BD+55 388	1 39 45.9 +56 15 40	"
BD+55 529	2 06 48.4 +56 19 24	779907
BD+55 778	3 23 +56 16	ED
BD+56 563	2 18 11.2 +56 53 46	CSI 79
BD+56 595	2 19 37.5 +56 58 19	"
BD+56 597	2 19 50.4 +56 59 05	"
BD+56 609	2 21 46.9 +57 12 42	"
BD+56 624	2 23 05.7 +56 52 05	"
BD+57 258	1 16 43.9 +58 02 47	779907
BD+57 524	2 11 40.5 +57 54 35	CSI 79
BD+57 550	2 18 08.1 +57 38 06	779907
BD+57 641	2 45 24.0 +57 48 20	CSI 79
BD+57 647	2 47 18.7 +57 38 59	"
BD+58 342	1 55 00.5 +59 01 33	"
BD+58 373	2 03 41.1 +58 33 00	"
BD+58 445	2 16 44.0 +59 26 32	"
BD+58 1218	9 49 07.7 +58 09 05	"
BD+58 2249	21 17 52.6 +58 24 40	"
BD+59 274	1 30 09.3 +60 23 24	"
BD+59 319	1 43 34.3 +60 07 22	"
BD+59 372	1 56 07.3 +60 00 42	"
BD+59 580	2 56 46.7 +59 46 15	"
BD+59 594	3 03 42.3 +60 17 52	"
BD+59 618IRS2	3 12 48.0 +59 44 53	
BD+59 2541	22 32 +60 22	ED
BD+60 261	1 29 12.3 +60 52 21	CSI 79
BD+60 335	1 42 38.9 +60 44 36	"
BD+60 478	2 23 44.1 +60 29 48	"
BD+60 497	2 28 08.3 +61 23 27	"
BD+60 2522	23 18 31.7 +60 55 13	"
BD+61 40	0 17 41.2 +62 07 08	"
BD+61 154	0 40 21.7 +61 38 12	"
BD+61 219	1 07 08 +62 15 00	IRC
BD+61 2068	20 52 17.7 +61 58 33	CSI 79
BD+61 2352	22 47 53.9 +62 04 00	"
BD+63 3	0 06 47.7 +63 40 31	"
BD+63 261	1 53 49.5 +63 47 50	"
BD+63 2073	23 51 26.2 +63 59 46	"
BD+64 1842	23 39 50.4 +65 22 30	"
BD+65 1055	15 27 18.9 +65 35 33	"
BD+65 1637	21 41 42.9 +65 52 36	"
BD+65 1638	21 41 50.9 +65 52 07	"
BD+68 946	17 36 42.3 +68 23 05	"
BD− 0 1050	5 38 04.2 − 0 19 30	"
BD− 0 4234	21 29 36 + 0 00	
BD− 4 4225	17 02 27.9 − 4 58 39	CSI 79
BD− 5 1318	5 32 53.2 − 5 23 29	"
BD− 5 4743	18 41 57.6 − 5 07 22	BD
BD− 6 4827	18 37 28.3 − 6 39 59	"
BD− 8 4645	18 33 37.5 − 8 55 01	"
BD− 9 1649	6 45 00.4 − 9 54 22	CSI 79
BD−10 1839	7 01 02.9 −10 38 11	"
BD−10 4662	18 12 22.9 −10 14 54	BD
BD−10 4738	18 42 40.4 −10 57 05	"
BD−11 3841	14 55 02.5 −12 14 13	CSI 79
BD−11 4747	18 44 18 −11 44	
BD−12 2669	8 44 21.3 −13 09 59	CSI 79
BD−13 3407	11 33 10.9 −14 18 58	"
BD−13 4930	18 16 02.3 −13 50 56	"
BD−14 1971	7 31 30.0 −14 24 50	"
BD−14 5037	18 22 14.9 −14 40 40	"
BD−14 5105	18 30 32.5 −14 08 45	"
BD−15 4221	15 54 15.0 −15 53 24	"
BD−16 4816	18 17 34.4 −16 13 23	"
BD−16 5440	19 45 42.7 −16 17 20	"
BD−18 4320	16 42 34.5 −19 02 46	"
BD−18 4489	17 16 33.5 −18 54 13	"
BD−19 967	4 34 07.3 −19 22 49	BD
BD−19 4708	17 45 43.7 −19 45 50	CSI 79
BD−19 4907	18 10 46.1 −19 16 00	BD
BD−19 5039	18 28 31.7 −19 20 29	CSI 79
BD−19 5077	18 32 26.5 −19 18 33	"
BD−19 5250	18 55 33.0 −19 14 42	"
BD−19 5255	18 56 27.3 −19 20 51	"
BD−20 5056	18 12 25.3 −20 47 50	BD
BD−20 5118	18 20 20.9 −20 40 47	CSI 79
BD−21 4897	18 09 21.5 −21 07 35	"
BECKLINS STAR	5 32 46.8 − 5 24 17	670701
BETELGEUSE	5 52 27.7 + 7 23 56	CSI 79
BICON. NEB A	20 22 03.2 +42 02 40	
BIPOLAR NEB	12 41 55 −54 14 54	
BL L	17 50 01 −30 17 36	789908
BL Q	17 51 25 −28 12 18	
BL2−1	22 18 28.0 +57 59 01	819914
BL3−5	17 39 06 −30 25 30	819916
BL3−10	17 52 09 −29 57 30	789908
BL3−11	17 45 07.5 −27 59 49	769910
BL3−13	17 52 50.7 −29 10 53	"
BN	5 32 46.7 − 5 24 17	
BN	5 32 46.8 − 5 24 17	670701
BN OBJECT		ED
BN SOURCE	" "	670701
BN 12"S	5 32 46.8 − 5 24 29	ED
BN 16"S,4"E	5 32 47.0 − 5 24 33	"
BN 6"S,1"E	5 32 46.9 − 5 24 23	"
BN 6"S,3"E	5 32 47.0 − 5 24 23	"
BN−KL	5 32 46.7 − 5 24 16	"
BN−KL	5 32 46.7 − 5 24 34	670701
BO 11 IRS1	10 45 32.2 −59 48 24	
ALF BOO	14 13 22.7 +19 26 30	
BET BOO	15 00 03.6 +40 35 12	CSI 79
DEL BOO	15 13 29.0 +33 30 00	"
EPS BOO	14 42 47.9 +27 17 04	"
ETA BOO	13 52 18.1 +18 38 50	"
LAM BOO	14 14 28.9 +46 19 01	"
R BOO	14 34 59.2 +26 57 08	"
RHO BOO	14 29 40.3 +30 35 23	"
RR BOO	14 45 08.3 +39 31 30	"
RV BOO	14 37 09.3 +32 45 15	779907
RW BOO	14 39 06.1 +31 47 05	CSI 79
RX BOO	14 21 56.6 +25 55 47	"
RX BOO	14 21 58.0 +25 55 54	
S BOO	14 21 12.4 +54 02 13	779907
SIG BOO	14 32 30.1 +29 57 40	CSI 79
THE BOO	14 23 29.5 +52 04 50	"
U BOO	14 52 00.7 +17 53 52	"
UPS BOO	13 47 03.7 +16 02 41	"
V BOO	14 27 44.1 +39 04 59	779907
W BOO	14 41 13.3 +26 44 20	CSI 79
XI BOO A	14 49 04.7 +19 18 25	"
Z BOO	14 04 04.2 +13 43 20	"
44 I BOO	15 02 10.4 +47 50 52	779907
BPM 4729	7 52 47 −67 38	BPM
BRETZ 3	6 05 44 +18 08 41	729902
BRETZ 4	6 10 20 − 6 13	"
BRUN 2	5 30 18.4 − 4 59 42	CSI 79
BRUN 17	5 30 25.2 − 5 11 19	"
BRUN 19	5 30 27 − 4 36 42	829909
BRUN 21		
BRUN 25	5 30 28.6 − 4 36 00	CSI 79
BRUN 29		
BRUN 43		
BRUN 50	5 30 39.9 − 5 22 27	CSI 79
BRUN 59	5 30 45.7 − 4 40 06	"
BRUN 60		
BRUN 62	5 30 48.7 − 4 23 13	CSI 79
BRUN 70		
BRUN 100	5 31 02.4 − 6 05 40	CSI 79
BRUN 111	5 31 06.3 − 5 07 02	749905
BRUN 131		
BRUN 145	5 31 22.3 − 5 34 06	CSI 79
BRUN 161	5 31 27.9 − 5 38 20	"
BRUN 162	5 31 28.0 − 5 40 41	"
BRUN 218		
BRUN 224		
BRUN 238		
BRUN 243	5 31 55.9 − 4 50 12	CSI 79
BRUN 246	5 31 57.5 − 4 24 11	"
BRUN 281	5 32 03.9 − 4 31 11	"
BRUN 295	5 32 06.6 − 5 04 56	"
BRUN 300	5 32 03 − 5 48	779904
BRUN 304	5 32 02.9 − 5 44 45	CSI 79
BRUN 312		
BRUN 328	5 32 10 − 5 12	779904
BRUN 330	5 32 14.6 − 4 25 26	CSI 79
BRUN 342	5 32 15.5 − 5 09 46	"
BRUN 352		
BRUN 359	5 32 15 − 5 20	779904
BRUN 388	5 32 19.6 − 5 36 09	CSI 79
BRUN 405	5 32 22.4 − 5 20 32	"
BRUN 414	5 32 20.5 − 6 01 47	"
BRUN 417	5 32 22.3 − 6 02 17	"
BRUN 430	5 32 24.9 − 5 34 56	"
BRUN 437	5 32 27.9 − 4 47 51	"
BRUN 440	5 32 30.3 − 4 23 08	"
BRUN 442	5 32 27.1 − 5 31 47	"
BRUN 454	5 32 28.2 − 4 33 47	"
BRUN 464	5 32 30.9 − 5 06 58	"
BRUN 466	5 32 32 − 5 27 13	GCVS
BRUN 472	5 32 35.0 − 4 24 58	CSI 79
BRUN 479	5 32 32.9 − 5 07 39	"
BRUN 480	5 32 36.5 − 4 45 47	"
BRUN 482	5 32 34.2 − 6 02 26	"
BRUN 486	5 32 40 − 4 45	779904
BRUN 490		
BRUN 493	5 32 35.9 − 6 02 00	CSI 79
BRUN 497		
BRUN 502	5 32 38.4 − 5 14 08	CSI 79
BRUN 508	5 32 36.9 − 6 00 55	749905
BRUN 510		
BRUN 520	5 32 40.6 − 5 54 01	CSI 79
BRUN 529	5 32 44.7 − 4 37 33	"
BRUN 530	5 32 42.4 − 5 29 45	"

NAME	RA (1950) DEC	POS REF
	h m s ° ′ ″	
BRUN 541		
BRUN 545	5 32 45.3 - 4 53 31	CSI 79
BRUN 552	5 32 44.1 - 5 57 29	"
BRUN 581	5 32 46.9 - 5 51 28	"
BRUN 582	5 32 48.9 - 4 43 34	"
BRUN 598	5 32 48.9 - 5 25 13	"
BRUN 599	5 32 52 - 4 43	779904
BRUN 604		
BRUN 608	5 32 50.2 - 5 05 46	CSI 79
BRUN 621	5 32 48.9 - 6 03 50	"
BRUN 631	5 32 53.7 - 4 27 20	"
BRUN 632	5 32 53.3 - 4 31 30	"
BRUN 643		
BRUN 653	5 32 53.5 - 5 11 01	CSI 79
BRUN 655	5 32 53.2 - 5 23 29	"
BRUN 659	5 32 55.0 - 4 52 09	"
BRUN 682	5 32 55.3 - 5 26 49	"
BRUN 708		
BRUN 714	5 32 58.9 - 5 26 51	CSI 79
BRUN 720	5 32 59.2 - 5 50 01	"
BRUN 721	5 32 59.1 - 5 56 27	"
BRUN 722A(SW)	5 33 02.3 - 4 23 42	"
BRUN 734	5 33 01.0 - 5 28 11	"
BRUN 736	5 33 03.0 - 4 56 05	"
BRUN 747	5 33 03.7 - 5 17 53	"
BRUN 749		
BRUN 760	5 33 03.9 - 5 27 07	CSI 79
BRUN 761	5 33 05.2 - 4 52 06	"
BRUN 767	5 33 04.1 - 5 34 53	"
BRUN 776	5 33 06.3 - 5 08 12	"
BRUN 786	5 33 08.1 - 5 14 04	"
BRUN 796	5 33 08.0 - 6 06 50	"
BRUN 862		
BRUN 884	5 33 23.1 - 5 30 17	CSI 79
BRUN 885	5 33 21 - 5 42	779904
BRUN 907	5 33 26.9 - 5 38 49	CSI 79
BRUN 920	5 33 30.9 - 5 24 20	"
BRUN 929	5 33 33.9 - 4 46 52	"
BRUN 940	5 33 37.6 - 4 27 21	"
BRUN 980	5 33 47.7 - 5 40 40	"
BRUN 982		
BRUN 992	5 33 59.7 - 5 26 17	CSI 79
BRUN 1001	5 34 02.2 - 5 47 58	"
BRUN 1016	5 34 10.9 - 5 09 39	"
BRUN 1018	5 34 10.8 - 5 30 23	749905
BRUN 1019	5 34 11.9 - 5 21 32	CSI 79
BRUN 1037		
BRUN 1045		
BRUN 1048		
BRUN 1050		
BRUN 1051	5 34 32.6 - 6 11 01	CSI 79
BRUN 1073	5 34 45 - 5 42	779904
BRUN 1082	5 34 52 - 4 42	"
BRUN 1083	5 34 51 - 5 34	"
BRUN 1098	5 35 00.5 - 5 58 01	CSI 79
BRUN 1109	5 35 08.7 - 4 57 44	"
BRUN 1112		
BRUN 1117		
BRUN 1129	5 35 25.2 - 4 50 30	CSI 79
BRUN 1131	5 35 28 - 4 49	779904
BS 3	0 02 46.5 - 5 59 14	
BS 3	0 02 46.5 - 5 59 15	CSI 79
BS 15	0 05 47.7 +28 48 50	"
BS 15	0 05 47.8 +28 48 52	
BS 21	0 06 30.2 +58 52 26	779907
BS 25	0 06 52.7 -46 01 22	CSI 79
BS 27	0 07 42.7 +45 47 37	"
BS 33	0 08 43.1 -15 44 31	"
BS 39	0 10 39.3 +14 54 19	"
BS 39	0 10 39.4 +14 54 21	
BS 45	0 12 00.6 +19 55 42	CSI 79
BS 46	0 11 54.1 - 8 03 29	"
BS 48	0 12 06.0 -19 12 33	"
BS 72	0 16 07.3 - 8 19 42	"
BS 74	0 16 52.7 - 9 06 01	"
BS 74	0 16 52.8 - 9 06 03	
BS 77	0 17 28.7 -65 10 05	CSI 79
BS 77	0 17 28.8 -65 10 07	
BS 85	0 19 14.4 -20 20 05	CSI 79
BS 88	0 20 18.0 -12 29 15	
BS 90	0 21 23.0 +38 18 03	779907
BS 98	0 23 09.3 -77 32 07	CSI 79
BS 98	0 23 09.4 -77 32 09	
BS 109	0 25 58.7 -40 11 25	CSI 79
BS 113	0 27 31.5 +59 42 04	"
BS 117	0 27 29.1 - 4 13 59	"
BS 130	0 30 08.3 +62 39 21	"
BS 134	0 30 10.3 +28 00 15	"
BS 153	0 34 10.3 +53 37 19	"
BS 163	0 35 54.3 +29 02 25	"
BS 165	0 36 38.7 +30 35 14	"
BS 166	0 36 45.3 +20 58 51	"
BS 168	0 37 39.3 +56 15 47	"
BS 179	0 39 15.7 +50 14 18	"
BS 180	0 38 57.9 -46 21 32	"
BS 188	0 41 04.7 -18 15 37	"
BS 193	0 41 55.6 +48 00 38	"
BS 215	0 44 40.9 +23 59 42	"
BS 219	0 46 03.6 +57 33 02	"
BS 222	0 45 45.3 + 5 01 24	"
BS 224	0 46 05.0 + 7 18 47	"
BS 244	0 50 03.9 +60 51 01	"
BS 248	0 50 27.0 - 1 24 54	"
BS 258	0 52 17.0 +23 21 27	"
BS 263	0 53 10.7 - 7 37 01	"
BS 264	0 53 40.3 +60 26 47	779907
BS 284	0 57 13.9 + 6 12 48	CSI 79
BS 294	1 00 20.6 + 7 37 16	"
BS 321	1 04 55.6 +54 40 32	"
BS 322	1 03 51.3 -46 59 08	"
BS 334	1 06 04.3 -10 26 48	"
BS 337	1 06 55.3 +35 21 20	"
BS 360	1 11 01.6 +24 19 08	"
BS 363	1 11 19.6 +28 15 57	"
BS 382	1 16 55.0 +57 58 08	"
BS 402	1 21 31.3 - 8 26 26	"
BS 403	1 22 31.4 +59 58 33	"
BS 423	1 24 39.9 -32 48 05	"

NAME	RA (1950) DEC	POS REF
BS 434	1 27 33.7 + 5 53 10	"
BS 437	1 28 48.1 +15 05 18	"
BS 458	1 33 51.1 +41 09 21	"
BS 464	1 34 54.6 +48 22 32	"
BS 472	1 35 51.3 -57 29 24	"
BS 483	1 38 43.7 +42 21 48	"
BS 489	1 38 49.5 + 5 14 06	"
BS 493	1 39 46.5 +20 01 33	"
BS 495	1 40 13.1 +45 04 15	"
BS 496	1 40 30.7 +50 26 15	"
BS 509	1 41 44.6 -16 11 59	"
BS 510	1 42 45.0 + 8 54 23	
BS 512	1 39 08.9 -83 13 47	
BS 519	1 44 08.3 -51 03 56	CSI 79
BS 519	1 44 08.4 -51 03 57	
BS 539	1 48 59.3 -10 34 51	CSI 79
BS 542	1 50 46.3 +63 25 29	"
BS 544	1 50 13.3 +29 20 09	"
BS 553	1 51 52.3 +20 33 50	"
BS 585	1 57 38.9 -21 19 08	"
BS 587	1 57 57.7 - 8 45 53	"
BS 591	1 57 11.6 -61 48 45	"
BS 601	1 59 53.3 +13 14 10	"
BS 602	1 59 42.1 -44 57 12	"
BS 603/4	2 00 49.1 +42 05 25	"
BS 612	2 02 15.0 -29 32 08	"
BS 617	2 04 20.9 +23 13 35	"
BS 618	2 05 09.7 +58 11 12	"
BS 622	2 06 33.5 +34 45 05	"
BS 648	2 10 19.3 +15 02 46	"
BS 649	2 10 20.7 + 8 36 46	"
BS 681	2 16 49.0 - 3 12 12	"
BS 686	2 17 25.0 -42 04 39	"
BS 696	2 21 43.0 +56 23 03	"
BS 718	2 25 29.7 + 8 14 12	"
BS 718	2 25 29.8 + 8 14 13	
BS 721	2 25 09.1 -47 55 38	CSI 79
BS 721	2 25 09.2 -47 55 39	
BS 740	2 29 42.9 -15 27 46	CSI 79
BS 788	2 39 04.9 +39 59 00	"
BS 799	2 40 46.2 +49 01 06	"
BS 804	2 40 42.3 + 3 01 32	"
BS 818	2 42 46.0 -18 46 58	"
BS 824	2 44 55.4 +29 02 25	"
BS 834	2 47 01.9 +55 41 22	"
BS 841	2 46 59.7 -32 36 53	"
BS 843	2 48 25.4 +34 51 18	"
BS 850	2 48 46.1 -21 12 31	"
BS 854	2 50 41.7 +52 33 32	"
BS 857	2 50 07.3 -12 58 14	"
BS 867	2 52 59.5 +18 07 47	"
BS 874	2 53 58.9 - 9 05 44	"
BS 897/8	2 56 21.9 -40 30 14	"
BS 911	2 59 39.7 + 3 53 39	"
BS 915	3 01 09.5 +53 18 43	
BS 921	3 01 57.9 +38 38 52	779907
BS 923	3 02 06.3 +40 23 18	CSI 79
BS 936	3 04 54.4 +40 45 52	779907
BS 937	3 05 26.7 +49 25 25	CSI 79
BS 941	3 06 06.7 +44 40 08	"
BS 951	3 08 45.9 +19 32 18	"
BS 963	3 09 56.3 -29 11 08	"
BS 977	3 11 16.9 -57 30 29	"
BS 991	3 15 35.7 +34 02 27	"
BS 1003	3 17 17.4 -21 56 18	"
BS 1003	3 17 17.5 -21 56 20	
BS 1006	3 16 40.8 -62 45 58	
BS 1007	3 18 29.6 + 3 29 47	CSI 79
BS 1008	3 17 55.7 -43 15 35	"
BS 1008	3 17 55.9 -43 15 36	
BS 1009	3 20 18.5 +64 24 33	CSI 79
BS 1017	3 20 44.3 +49 41 05	"
BS 1030	3 22 07.0 + 8 51 14	"
BS 1035	3 25 00.0 +59 46 04	"
BS 1040	3 25 54.1 +58 42 26	"
BS 1052	3 27 02.2 +47 49 27	"
BS 1066	3 28 06.4 +12 45 59	"
BS 1069	3 28 57.7 +45 53 20	"
BS 1084	3 30 34.3 - 9 37 34	"
BS 1084	3 30 34.4 - 9 37 35	
BS 1101	3 34 19.0 + 0 14 38	CSI 79
BS 1105	3 37 47.6 +63 03 24	"
BS 1105	3 37 47.7 +63 03 25	
BS 1106	3 35 17.9 -40 26 15	CSI 79
BS 1112	3 38 34.3 +59 48 36	"
BS 1122	3 39 21.2 +47 37 45	"
BS 1135	3 41 47.2 +42 25 19	"
BS 1136	3 40 50.9 - 9 55 51	"
BS 1140	3 41 49.4 +24 08 00	"
BS 1142	3 41 54.0 +23 57 26	"
BS 1144	3 42 10.3 +24 41 01	"
BS 1145	3 42 13.5 +24 18 42	"
BS 1149	3 42 50.7 +24 12 46	"
BS 1151	3 42 55.3 +24 23 58	"
BS 1155	3 44 55.1 +65 22 25	"
BS 1156	3 43 21.1 +23 47 38	"
BS 1162	3 43 46.4 -12 15 25	"
BS 1165	3 44 30.3 +23 57 07	"
BS 1172	3 45 22.9 +23 16 07	"
BS 1178	3 46 10.9 +23 54 06	"
BS 1180	3 46 12.3 +23 59 07	"
BS 1195	3 47 34.9 -36 21 01	
BS 1195	3 47 34.9 -36 21 02	
BS 1203	3 50 58.9 +31 44 11	CSI 79
BS 1208	3 47 59.4 -74 23 32	"
BS 1220	3 54 29.3 +39 52 01	"
BS 1228	3 56 42.7 +35 38 55	"
BS 1231	3 55 41.6 -13 38 57	"
BS 1239	3 57 54.3 +12 21 01	"
BS 1239	3 57 54.4 +12 21 02	
BS 1242	4 00 16.2 +59 01 07	CSI 79
BS 1247	3 57 56.9 -61 32 26	"
BS 1256	4 01 44.0 +21 56 47	"
BS 1264	4 00 10.0 -62 17 54	
BS 1264	4 00 10.1 -62 17 55	
BS 1286	4 07 46.0 +33 27 27	CSI 79
BS 1302	4 09 09.3 -42 07 21	"
BS 1303	4 11 12.9 +48 17 02	"

NAME	RA (1950) DEC	POS REF
BS 1309	4 10 51.3 + 7 35 22	"
BS 1318	4 12 00.7 -10 22 43	"
BS 1325	4 12 58.1 - 7 43 45	"
BS 1326	4 12 20.5 -42 24 59	"
BS 1327	4 15 56.9 +65 01 15	"
BS 1336	4 13 46.5 -62 35 54	"
BS 1346	4 16 56.6 +15 30 29	"
BS 1347	4 15 59.9 -33 55 08	"
BS 1355	4 15 36.9 -59 25 17	"
BS 1373	4 20 02.7 +17 25 35	"
BS 1393	4 22 09.3 -34 07 53	"
BS 1407	4 25 34.6 +16 14 57	"
BS 1409	4 25 41.5 +19 04 15	"
BS 1411	4 25 42.9 +15 51 09	"
BS 1412	4 25 48.2 +15 45 40	"
BS 1423	4 26 47.4 -13 09 24	"
BS 1453	4 31 32.7 -29 51 59	"
BS 1454	4 33 13.0 +41 09 49	"
BS 1457	4 33 02.9 +16 24 36	"
BS 1457	4 33 02.9 +16 24 38	
BS 1464	4 33 36.3 -30 39 47	CSI 79
BS 1481	4 35 53.3 -14 24 00	"
BS 1496	4 38 15.1 -19 45 57	"
BS 1502	4 38 56.9 -41 57 28	"
BS 1543	4 47 07.3 + 6 52 31	"
BS 1552	4 48 32.3 + 5 31 15	"
BS 1556	4 49 42.0 +14 10 07	"
BS 1577	4 53 43.9 +33 05 18	"
BS 1580	4 53 33.3 +13 26 12	"
BS 1603	4 58 57.5 +60 22 18	"
BS 1605	4 58 22.4 +43 45 03	"
BS 1612	4 58 58.6 +41 00 17	"
BS 1614	4 58 19.9 - 5 48 37	"
BS 1641	5 03 00.2 +41 10 07	"
BS 1648	5 02 48.5 + 1 06 37	"
BS 1652	5 02 36.3 -35 33 00	"
BS 1654	5 03 20.5 -22 26 11	"
BS 1663	5 03 39.7 -49 38 36	"
BS 1666	5 05 23.3 - 5 08 57	"
BS 1698	5 10 40.4 + 2 48 10	"
BS 1702	5 10 40.9 -16 15 46	"
BS 1708	5 12 59.4 +45 56 56	"
BS 1713	5 12 07.9 - 8 15 27	
BS 1713	5 12 08.0 - 8 15 29	
BS 1729	5 15 37.2 +40 03 23	CSI 79
BS 1743	5 15 40.7 -34 56 34	"
BS 1744	5 13 47.3 -67 14 29	"
BS 1748	5 17 03.1 - 1 27 42	"
BS 1763	5 19 00.0 + 8 22 50	"
BS 1765	5 19 12.4 - 0 25 47	"
BS 1770	5 20 12.1 + 3 29 50	"
BS 1784	5 21 32.1 - 7 51 07	"
BS 1788	5 21 57.6 - 2 26 27	"
BS 1790	5 22 26.7 + 6 18 21	
BS 1790	5 22 26.8 + 6 18 22	
BS 1791	5 23 07.7 +28 34 00	CSI 79
BS 1791	5 23 07.7 +28 34 02	
BS 1829	5 26 06.0 -20 47 52	CSI 79
BS 1830	5 26 53.9 - 3 29 03	"
BS 1839	5 28 06.3 + 5 54 40	"
BS 1842	5 28 36.9 + 3 15 19	"
BS 1845	5 29 16.7 +18 33 31	"
BS 1852	5 29 26.9 - 0 20 01	"
BS 1855	5 29 30.5 - 7 20 11	"
BS 1862	5 29 26.1 -35 30 21	"
BS 1863	5 30 35.4 - 1 45 06	"
BS 1865	5 30 31.3 -17 51 22	"
BS 1868	5 30 59.0 - 1 11 21	"
BS 1876	5 32 04.3 + 9 27 25	"
BS 1879/80	5 32 22.9 + 9 54 10	"
BS 1893/4	5 32 48.9 - 5 25 13	"
BS 1897	5 32 55.3 - 5 26 49	"
BS 1899	5 32 59.1 - 5 56 27	"
BS 1903	5 33 40.4 - 1 13 54	"
BS 1907	5 34 09.3 + 9 15 53	"
BS 1908	5 34 17.4 +11 00 20	"
BS 1910	5 34 39.2 +21 06 49	"
BS 1925	5 37 16.7 +53 27 46	"
BS 1931	5 36 13.9 - 2 37 36	"
BS 1934	5 36 32.5 + 4 05 38	"
BS 1938	5 37 21.7 +31 19 57	"
BS 1948	5 38 13.9 - 1 58 00	"
BS 1948/9	" "	"
BS 1953	5 33 51.2 -76 22 40	"
BS 1956	5 37 50.2 -34 05 57	"
BS 1963	5 39 53.3 + 1 27 05	"
BS 1977	5 42 40.4 +20 40 32	"
BS 1983	5 42 22.6 -22 27 46	"
BS 1995	5 45 42.4 +39 09 57	"
BS 2004	5 45 22.9 - 9 41 07	"
BS 2011	5 47 37.7 +37 17 35	"
BS 2012	5 48 01.3 +39 08 08	"
BS 2015	5 44 40.9 -65 45 14	"
BS 2018	5 48 10.0 +32 06 43	"
BS 2020	5 46 05.9 -51 05 00	"
BS 2035	5 49 10.1 -20 52 53	"
BS 2040	5 49 11.7 -35 47 08	"
BS 2047	5 51 25.1 +20 16 06	"
BS 2056	5 51 17.7 -33 48 40	"
BS 2061	5 52 27.7 + 7 23 56	"
BS 2065	5 52 23.4 -11 46 55	"
BS 2077	5 55 24.4 +54 16 59	"
BS 2085	5 54 07.5 -14 10 30	"
BS 2088	5 55 51.5 +44 56 40	"
BS 2091	5 56 13.3 +45 56 03	"
BS 2095	5 56 18.6 +37 12 38	"
BS 2102	5 53 42.9 -63 06 16	"
BS 2106	5 55 45.7 -35 17 13	"
BS 2113	5 57 33.1 - 3 04 28	"
BS 2120	5 57 36.9 -42 49 00	"
BS 2134	6 01 04.7 +23 16 03	"
BS 2135	6 00 56.9 +20 08 27	"
BS 2140	6 01 14.5 -26 16 58	"
BS 2142	6 01 47.5 - 6 42 18	"
BS 2199	6 09 05.7 +14 13 17	"
BS 2216	6 11 51.4 +22 31 21	"
BS 2219	6 12 11.4 +29 31 05	"
BS 2227	6 12 24.9 - 6 15 28	"

NAME	RA (1950) DEC	POS REF
BS 2249	6 13 53.7 −16 35 57	"
BS 2256	6 14 46.2 −35 07 21	"
BS 2263	6 15 18.9 −37 43 08	"
BS 2284	6 19 04.7 −11 44 54	"
BS 2286	6 19 56.0 +22 32 27	"
BS 2290	6 18 47.1 −48 42 50	
BS 2294	6 20 29.7 −17 55 45	CSI 79
BS 2296	6 20 17.0 −33 24 35	"
BS 2308	6 22 36.9 +14 45 03	"
BS 2318	6 22 47.3 −28 44 59	
BS 2326	6 22 50.4 −52 40 03	CSI 79
BS 2326	6 22 50.5 −52 40 03	
BS 2354	6 24 05.4 −63 23 52	CSI 79
BS 2354	6 24 05.5 −63 23 53	
BS 2361	6 26 18.7 −32 32 49	CSI 79
BS 2392	6 30 26.2 −11 07 40	"
BS 2405	6 33 06.6 +38 29 16	779907
BS 2421	6 34 49.3 +16 26 36	CSI 79
BS 2422	6 34 43.2 + 6 10 42	"
BS 2427	6 35 45.6 +42 32 04	"
BS 2429	6 34 30.0 −19 12 42	"
BS 2443	6 35 41.3 −18 11 32	"
BS 2451	6 36 13.7 −43 09 03	"
BS 2456	6 38 13.3 + 9 56 36	"
BS 2467	6 39 18.1 + 6 23 38	"
BS 2469	6 39 33.1 − 9 07 02	"
BS 2473	6 40 51.3 +25 10 55	"
BS 2478	6 41 10.0 +13 16 47	"
BS 2484	6 42 28.9 +12 57 03	"
BS 2491	6 42 56.7 −16 38 45	"
BS 2491	6 42 56.7 −16 38 46	
BS 2527	6 52 48.3 +77 02 42	CSI 79
BS 2549	6 49 03.1 −34 18 25	"
BS 2560	6 52 57.1 +58 29 26	"
BS 2574	6 51 51.9 −11 58 28	"
BS 2580	6 52 03.3 −24 07 11	"
BS 2580	6 52 03.4 −24 07 13	
BS 2591	6 52 52.1 −42 18 03	CSI 79
BS 2608	6 54 56.0 −48 39 14	"
BS 2609	7 17 50.5 +87 07 34	"
BS 2615	6 57 23.3 +16 08 57	"
BS 2618	6 56 39.5 −28 54 09	"
BS 2646	6 59 43.5 −27 51 42	"
BS 2653	7 00 56.1 −23 45 31	"
BS 2667	7 02 25.2 −43 32 16	
BS 2668	7 02 26.8 −43 32 28	
BS 2693	7 06 21.3 −26 18 45	CSI 79
BS 2693	7 06 21.4 −26 18 45	
BS 2697	7 07 57.4 +30 19 43	CSI 79
BS 2701	7 07 44.5 − 4 09 26	"
BS 2702	7 07 10.2 −39 34 27	"
BS 2717	7 10 30.0 +16 14 42	"
BS 2719	7 09 26.7 −48 51 01	"
BS 2740	7 11 07.9 −46 40 29	"
BS 2742	7 20 40.9 +82 30 49	"
BS 2745	7 12 12.7 −26 15 52	"
BS 2748	7 12 00.6 −44 33 26	"
BS 2749	7 12 46.9 −26 41 04	"
BS 2762	7 13 15.3 −48 11 00	"
BS 2766	7 14 34.6 −27 47 28	"
BS 2773	7 15 22.5 −37 00 23	"
BS 2777	7 17 08.2 +22 04 32	"
BS 2787	7 16 31.6 −36 38 29	"
BS 2790	7 16 51.3 −36 38 59	"
BS 2803	7 16 51.6 −67 51 55	"
BS 2821	7 22 37.3 +27 53 55	"
BS 2825	7 22 24.4 −16 06 05	"
BS 2827	7 22 06.9 −29 12 14	"
BS 2845	7 24 26.3 + 8 23 28	"
BS 2852	7 25 53.7 +31 53 07	"
BS 2854	7 25 26.3 + 9 01 41	"
BS 2878	7 27 38.5 −43 11 56	"
BS 2881	7 28 45.7 −30 51 21	"
BS 2882	7 28 56.1 −37 14 02	
BS 2890/1	7 31 24.6 +32 00 00	CSI 79
BS 2902	7 31 30.1 −14 24 52	
BS 2905	7 32 50.5 +27 00 29	CSI 79
BS 2911	7 32 02.3 −36 13 42	"
BS 2919	7 28 25.5 −78 59 27	"
BS 2921	7 33 45.9 −14 22 49	"
BS 2937	7 35 30.9 −34 51 17	"
BS 2938	7 36 35.3 +17 47 22	"
BS 2943	7 36 41.0 + 5 21 16	"
BS 2943	7 36 41.1 + 5 21 17	
BS 2961	7 37 41.5 −38 11 31	CSI 79
BS 2970	7 38 51.4 − 9 25 58	"
BS 2973	7 40 11.3 +29 00 21	"
BS 2985	7 41 25.7 +24 31 08	"
BS 2990	7 42 15.4 +28 08 54	"
BS 2993	7 41 31.1 −28 17 26	"
BS 3002	7 41 59.7 −40 48 37	"
BS 3003	7 43 13.7 +18 37 59	"
BS 3017	7 43 28.3 −37 50 45	"
BS 3027	7 45 28.5 −15 53 21	"
BS 3045	7 47 11.3 −24 43 57	"
BS 3046	7 46 50.9 −46 57 01	"
BS 3061	7 49 29.7 + 3 24 27	"
BS 3095	7 54 09.1 +15 55 30	"
BS 3105	7 53 51.1 −57 10 11	"
BS 3113	7 55 40.3 −30 11 55	"
BS 3126	7 55 54.5 −58 59 25	"
BS 3135	7 58 13.2 − 2 44 34	"
BS 3138	7 56 51.6 −60 10 06	
BS 3145	7 59 39.7 + 2 28 22	CSI 79
BS 3147	7 58 00.5 −60 41 12	"
BS 3165	8 01 49.5 −39 51 40	"
BS 3176	8 04 49.4 +21 43 42	
BS 3185	8 05 24.7 −24 09 31	CSI 79
BS 3188	8 06 04.7 − 2 50 11	"
BS 3207	8 07 59.3 −47 11 17	"
BS 3211	8 08 55.4 −12 46 37	"
BS 3225	8 09 34.2 −39 28 06	"
BS 3226	8 09 44.4 −42 50 12	"
BS 3237	8 11 36.1 −35 44 49	"
BS 3243	8 12 16.2 −40 11 38	"
BS 3249	8 13 48.2 + 9 20 26	"
BS 3270	8 16 40.9 −36 30 11	"
BS 3275	8 19 25.1 +43 21 00	"
BS 3282	8 19 24.7 −32 53 39	"
BS 3294	8 20 59.2 −48 19 43	"
BS 3304	8 23 25.3 +28 03 37	"
BS 3314	8 23 09.7 − 3 44 30	"
BS 3315	8 22 54.1 −23 52 57	"
BS 3319	8 23 58.0 +12 49 14	"
BS 3323	8 26 07.6 +60 53 13	"
BS 3357	8 28 44.7 +18 15 52	"
BS 3403	8 35 51.9 +64 30 15	"
BS 3407	8 33 11.9 −49 46 15	"
BS 3418	8 36 08.6 + 3 31 03	"
BS 3426	8 35 53.0 −42 48 47	"
BS 3427	8 37 13.9 +20 11 07	"
BS 3428	8 37 30.0 +19 50 52	"
BS 3461	8 41 50.7 +18 20 20	"
BS 3474/5	8 43 40.4 +28 56 38	"
BS 3482	8 44 07.6 + 6 36 08	"
BS 3484	8 44 00.7 −13 21 48	"
BS 3498	8 45 24.9 −56 35 06	"
BS 3518	8 48 24.4 −27 31 23	"
BS 3541	8 52 33.9 +17 25 21	"
BS 3547	8 52 45.0 + 6 08 11	"
BS 3569	8 55 47.6 +48 14 21	"
BS 3576	8 58 03.9 +67 49 34	"
BS 3579	8 57 24.0 +41 58 55	"
BS 3593	8 58 32.7 −42 58 36	"
BS 3614	9 02 25.6 −46 53 51	"
BS 3628	9 05 51.0 −25 39 20	"
BS 3634	9 06 09.3 −43 13 46	"
BS 3634	9 06 09.3 −43 13 48	
BS 3654	9 09 15.3 −44 39 40	CSI 79
BS 3682	9 13 38.3 −38 21 38	"
BS 3684	9 13 44.9 −37 12 12	"
BS 3685	9 12 39.6 −69 30 38	"
BS 3699	9 15 45.0 −59 03 52	"
BS 3705	9 18 00.7 +34 36 17	"
BS 3718	9 19 16.6 −25 45 04	"
BS 3731	9 21 44.7 +26 23 54	"
BS 3733	9 21 02.2 −28 37 07	"
BS 3748	9 25 07.7 − 8 26 26	"
BS 3748	9 25 07.8 − 8 26 28	
BS 3757	9 27 36.5 +63 16 54	CSI 79
BS 3765	9 27 10.7 −35 43 54	"
BS 3771	9 30 05.7 +70 03 06	"
BS 3773	9 28 52.2 +23 11 20	"
BS 3775	9 29 31.4 +51 54 21	"
BS 3777	9 26 37.3 −71 23 04	"
BS 3779	9 29 16.7 + 9 56 12	"
BS 3786	9 28 43.6 −40 14 48	"
BS 3834	9 35 50.7 + 4 52 32	"
BS 3836	9 35 02.1 −49 07 47	"
BS 3842	9 36 04.0 −42 57 51	"
BS 3845	9 37 18.1 − 0 54 52	"
BS 3852	9 38 28.9 +10 07 13	"
BS 3858	9 39 00.0 −23 21 47	"
BS 3871	9 41 58.2 −27 32 22	"
BS 3873	9 43 00.9 +24 00 18	"
BS 3881	9 45 22.3 +46 15 17	"
BS 3888	9 47 27.0 +59 16 29	"
BS 3903	9 49 04.3 −14 36 39	"
BS 3905	9 49 55.3 +26 14 34	"
BS 3912	9 49 44.6 −46 18 45	"
BS 3919	9 51 56.2 −25 41 45	"
BS 3946	9 56 47.4 −23 42 38	"
BS 3950	9 57 34.3 + 8 17 05	"
BS 3975	10 04 36.4 +17 00 24	"
BS 3980	10 05 15.1 +10 14 35	"
BS 3982	10 05 42.6 +12 12 43	"
BS 3982	10 05 42.6 +12 12 45	
BS 3994	10 08 08.9 −12 06 21	CSI 79
BS 4008	10 11 41.6 +60 14 01	"
BS 4009	10 10 01.6 −57 48 46	"
BS 4023	10 12 37.9 −41 52 24	"
BS 4023	10 12 38.0 −41 52 25	
BS 4030	10 13 46.3 +23 45 08	
BS 4031	10 13 54.7 +23 40 01	CSI 79
BS 4033	10 14 05.3 +43 09 52	"
BS 4039	10 14 29.7 +23 21 26	"
BS 4057/8	10 17 13.0 +20 05 42	"
BS 4069	10 19 21.4 +41 45 05	"
BS 4080	10 20 10.6 −41 23 51	"
BS 4092	10 23 14.2 − 6 48 24	"
BS 4094	10 23 40.2 −16 34 48	"
BS 4100	10 24 59.9 +36 57 50	"
BS 4102	10 23 24.4 −73 46 36	"
BS 4104	10 24 51.6 −30 48 45	"
BS 4127	10 29 31.7 +14 23 39	"
BS 4133	10 30 10.7 + 9 33 51	"
BS 4156	10 33 50.0 −16 05 05	"
BS 4163	10 35 04.9 −13 07 24	"
BS 4167	10 35 11.6 −47 57 54	"
BS 4167	10 35 11.7 −47 57 56	
BS 4174	10 34 53.6 −78 20 54	
BS 4195	10 41 37.2 +67 40 27	779907
BS 4216	10 44 36.7 −49 09 18	CSI 79
BS 4216	10 44 36.8 −49 09 20	
BS 4232	10 47 09.3 −15 55 52	CSI 79
BS 4247	10 50 31.2 +34 29 05	"
BS 4257	10 51 27.3 −58 35 13	"
BS 4273	10 54 22.9 −36 52 06	"
BS 4287	10 57 20.1 −18 01 54	"
BS 4293	10 57 51.2 −41 57 26	"
BS 4295	10 58 50.2 +56 39 02	"
BS 4299	10 59 16.5 − 2 12 53	"
BS 4301	11 00 39.5 +62 01 15	"
BS 4335	11 06 51.5 +44 46 12	"
BS 4336	11 06 50.9 +43 28 43	"
BS 4337	11 06 26.7 −58 42 12	"
BS 4357	11 11 27.0 +20 47 51	"
BS 4359	11 11 37.0 +15 42 10	"
BS 4362	11 12 32.7 +23 22 04	"
BS 4371	11 14 42.9 + 2 17 07	"
BS 4374/5	11 15 31.1 +31 48 39	"
BS 4377	11 15 46.9 +33 22 02	"
BS 4382	11 16 50.3 −14 30 27	"
BS 4392	11 20 05.3 +43 45 25	"
BS 4432	11 27 45.4 − 2 43 37	"
BS 4434	11 28 27.5 +69 36 25	"
BS 4450	11 30 32.2 −31 34 50	"
BS 4450	11 30 32.3 −31 34 51	
BS 4471	11 34 23.2 − 0 32 49	CSI 79
BS 4483	11 35 52.9 + 8 24 38	"
BS 4494	11 37 43.4 −34 28 01	"
BS 4496	11 38 25.2 +34 29 01	"
BS 4511	11 41 07.3 −62 12 41	"
BS 4517	11 43 17.3 + 6 48 34	"
BS 4518	11 43 24.9 +48 03 22	"
BS 4520	11 43 13.9 −66 27 04	"
BS 4523	11 44 07.6 −40 13 41	
BS 4532	11 46 13.2 −26 28 16	CSI 79
BS 4534	11 46 30.5 +14 51 04	"
BS 4540	11 48 05.3 + 2 02 46	"
BS 4546	11 48 38.1 −44 53 40	"
BS 4550	11 50 06.1 +38 04 38	"
BS 4552	11 50 22.6 −33 37 46	"
BS 4554	11 51 12.5 +53 58 21	"
BS 4562	11 52 39.2 +37 02 06	"
BS 4586	11 57 44.3 +81 07 54	"
BS 4608	12 02 39.6 + 9 00 36	"
BS 4618	12 05 29.2 −50 22 57	"
BS 4630	12 07 32.9 −22 20 29	"
BS 4638	12 09 01.6 −52 05 24	"
BS 4660	12 12 57.5 +57 18 35	"
BS 4662	12 13 13.7 −17 15 50	"
BS 4671	12 14 50.9 −67 40 56	"
BS 4682	12 16 19.0 −54 51 54	"
BS 4689	12 17 20.7 − 0 23 19	"
BS 4690	12 17 21.2 +49 15 39	"
BS 4694	12 17 47.2 +26 16 43	"
BS 4695	12 17 48.4 + 3 35 25	"
BS 4700	12 18 38.7 −60 07 30	"
BS 4707	12 19 59.5 +26 07 23	"
BS 4737	12 24 26.7 +28 32 45	"
BS 4743	12 25 19.4 −49 57 12	"
BS 4757	12 27 16.3 −16 14 12	"
BS 4763	12 28 22.7 −56 50 00	
BS 4773	12 29 27.1 −71 51 24	CSI 79
BS 4785	12 31 22.2 +41 37 43	"
BS 4786	12 31 45.3 −23 07 12	"
BS 4787	12 31 21.5 +70 03 48	"
BS 4801	12 34 27.9 +17 21 52	"
BS 4802	12 34 57.3 −48 15 56	"
BS 4807	12 35 49.3 + 2 07 45	"
BS 4813	12 36 39.7 − 7 43 13	"
BS 4817	12 37 09.5 −39 42 44	"
BS 4819	12 38 44.7 −48 41 06	"
BS 4825	12 39 07.3 − 1 10 30	"
BS 4825/6	" "	"
BS 4828	12 39 21.1 +10 30 37	"
BS 4830	12 39 53.1 −62 47 04	"
BS 4831	12 39 48.6 −48 32 18	"
BS 4845	12 42 37.6 +39 32 59	"
BS 4846	12 42 47.0 +45 42 48	779907
BS 4853	12 44 46.9 −59 24 56	CSI 79
BS 4883	12 49 15.7 +27 48 45	"
BS 4883	12 49 15.9 +27 48 45	
BS 4888	12 50 16.3 −48 40 16	CSI 79
BS 4889	12 50 39.4 −39 54 24	"
BS 4902	12 51 44.9 − 9 16 02	"
BS 4905	12 51 50.2 +56 13 51	779907
BS 4908	12 52 59.3 −56 33 53	CSI 79
BS 4910	12 53 04.9 + 3 40 06	"
BS 4914	12 53 40.1 +38 35 02	
BS 4915	12 53 41.5 +38 35 17	779907
BS 4920	12 56 27.0 +17 40 41	CSI 79
BS 4930	12 59 39.3 −71 12 25	"
BS 4932	12 59 41.2 +11 13 37	"
BS 4949	13 03 56.5 +22 53 00	"
BS 4952	13 04 51.7 −65 02 17	"
BS 4979	13 09 15.3 −37 32 17	"
BS 4983	13 09 32.3 +28 07 51	"
BS 4989	13 11 08.3 −58 50 11	"
BS 5020	13 16 11.7 −22 54 28	"
BS 5028	13 17 46.6 −36 26 56	"
BS 5054/5	13 21 54.9 +55 11 09	"
BS 5056	13 22 33.3 −10 54 01	"
BS 5056	13 22 33.3 −10 54 03	
BS 5080	13 26 58.4 −23 01 23	CSI 79
BS 5089	13 28 08.1 −39 08 58	"
BS 5095	13 29 21.7 − 5 59 52	"
BS 5097	13 29 48.3 −28 26 08	"
BS 5107	13 32 08.5 − 0 20 26	"
BS 5132	13 36 42.3 −53 12 45	"
BS 5134	13 36 53.5 −49 41 48	"
BS 5150	13 38 59.0 − 8 27 04	"
BS 5154	13 38 50.5 +54 56 01	"
BS 5168	13 42 50.9 −32 47 25	"
BS 5171	13 43 40.1 −62 20 24	"
BS 5171A	" "	"
BS 5181	13 44 41.7 −17 36 36	"
BS 5191	13 45 34.3 +49 33 43	"
BS 5192	13 46 32.3 −34 12 05	
BS 5192	13 46 32.4 −34 12 07	
BS 5200	13 47 03.7 +16 02 41	CSI 79
BS 5219	13 49 35.1 +34 41 28	"
BS 5223	13 50 49.5 −46 52 55	"
BS 5226	13 49 58.2 +64 58 10	"
BS 5231	13 52 24.4 −47 02 34	"
BS 5235	13 52 18.1 +18 38 50	"
BS 5249	13 55 34.7 −44 33 37	"
BS 5270	14 00 04.5 + 9 55 38	"
BS 5287	14 03 31.0 −26 26 31	"
BS 5288	14 03 43.9 −36 07 28	"
BS 5288	14 03 43.9 −36 07 30	
BS 5299	14 05 55.7 +44 05 28	CSI 79
BS 5301	14 08 06.3 −16 03 59	"
BS 5315	14 10 13.3 −10 02 29	"
BS 5316	14 11 27.0 −56 51 09	"
BS 5339	14 18 39.0 −83 26 28	"
BS 5340	14 13 22.7 +19 26 30	"
BS 5384	14 20 41.6 + 1 28 28	"
BS 5384	14 20 41.7 + 1 28 30	
BS 5394	14 21 50.5 + 8 18 42	CSI 79
BS 5429	14 29 40.3 +30 35 23	"
BS 5435	14 30 03.7 +38 31 33	"
BS 5447	14 32 30.1 +29 57 40	"

NAME	RA (1950) DEC	POS REF
BS 5459	14 36 11.2 −60 37 49	
BS 5460	" "	
BS 5470	14 41 32.9 −78 50 04	CSI 79
BS 5487	14 40 25.2 − 5 26 30	"
BS 5490	14 41 13.3 +26 44 20	"
BS 5502	14 42 54.3 +17 10 29	"
BS 5505/6	14 42 47.9 +27 17 04	"
BS 5510	14 43 08.1 +32 59 56	"
BS 5512	14 43 44.4 +15 20 25	"
BS 5526	14 47 20.7 −27 45 10	"
BS 5530	14 47 54.9 −15 47 24	"
BS 5531	14 48 06.3 −15 50 05	"
BS 5544	14 49 04.7 +19 18 25	"
BS 5568	14 54 32.3 −21 11 27	"
BS 5589	14 56 46.7 +66 07 52	779907
BS 5601	15 00 22.2 + 2 17 10	CSI 79
BS 5602	15 00 03.6 +40 35 12	"
BS 5603	15 01 08.2 −25 05 10	
BS 5603	15 01 08.2 −25 05 12	
BS 5616	15 02 18.0 +27 08 29	CSI 79
BS 5622	15 03 49.9 −16 03 49	"
BS 5634	15 05 06.1 +25 03 45	"
BS 5635	15 04 50.7 +54 44 51	"
BS 5649	15 08 40.7 −51 54 36	"
BS 5681	15 13 29.0 +33 30 00	"
BS 5685	15 14 18.7 − 9 11 57	"
BS 5686	15 14 46.7 −29 57 57	"
BS 5705	15 18 37.4 −36 04 52	"
BS 5739	15 23 28.0 +15 36 08	"
BS 5743	15 25 25.9 −16 32 36	"
BS 5744	15 23 48.6 +59 08 26	"
BS 5747	15 25 45.9 +29 16 35	"
BS 5777	15 31 26.4 − 9 53 39	"
BS 5787	15 32 43.4 −14 37 26	"
BS 5793	15 32 34.1 +26 52 53	"
BS 5824	15 37 19.1 −23 39 24	"
BS 5824	15 37 19.2 −23 39 26	
BS 5854	15 41 48.1 + 6 34 52	CSI 79
BS 5868	15 44 00.7 + 7 30 29	"
BS 5879	15 46 29.2 +18 17 39	"
BS 5897	15 50 42.9 −63 16 41	"
BS 5908	15 50 58.3 −16 35 02	"
BS 5914	15 50 56.6 +42 35 25	"
BS 5924	15 52 22.2 +20 27 21	"
BS 5932	15 52 57.7 +43 16 59	"
BS 5933	15 54 08.3 +15 49 23	"
BS 5947	15 55 30.9 +27 01 16	"
BS 5953	15 57 22.3 −22 28 49	"
BS 5964	15 57 38.9 +50 01 20	"
BS 5984/5	16 02 31.4 −19 40 10	"
BS 5993	16 03 52.6 −20 32 05	"
BS 5997	16 04 28.0 −20 44 04	"
BS 5999	16 05 12.7 −38 58 21	"
BS 6001	16 05 04.3 −26 11 39	"
BS 6018	16 07 08.4 +36 36 59	"
BS 6020	16 12 48.0 −78 34 25	"
BS 6021	16 12 54.6 −78 32 44	"
BS 6027	16 09 05.0 −19 19 54	"
BS 6056	16 11 43.3 − 3 34 00	"
BS 6072	16 16 05.3 −50 02 06	
BS 6075	16 15 40.3 − 4 34 18	CSI 79
BS 6084	16 18 08.6 −25 28 27	"
BS 6084	16 18 08.7 −25 28 28	
BS 6086	16 16 24.9 +59 52 32	CSI 79
BS 6092	16 18 14.0 +46 25 53	"
BS 6095	16 19 42.7 +19 16 08	"
BS 6104	16 21 10.3 −19 55 18	"
BS 6132	16 23 18.4 +61 37 36	"
BS 6134	16 26 20.1 −26 19 21	"
BS 6136	16 26 00.9 + 0 46 30	"
BS 6146	16 26 59.9 +41 59 26	779907
BS 6147	16 28 16.3 −16 30 17	CSI 79
BS 6148	16 28 04.0 +21 35 49	"
BS 6159	16 30 15.7 +11 35 37	"
BS 6163	16 35 53.0 −77 25 00	"
BS 6175	16 34 24.1 −10 28 02	"
BS 6212	16 39 23.9 +31 41 30	"
BS 6220	16 41 10.7 +39 00 57	"
BS 6228	16 43 25.7 + 8 40 19	"
BS 6241	16 46 55.1 −34 12 14	"
BS 6258	16 48 41.7 +29 53 25	"
BS 6272	16 51 28.7 −41 04 14	"
BS 6285	16 54 28.3 −55 54 48	"
BS 6293	16 53 10.2 +18 30 42	"
BS 6299	16 55 17.9 + 9 27 03	"
BS 6304	16 57 26.5 −58 53 07	"
BS 6337	17 00 50.2 +14 09 43	"
BS 6353	17 02 57.5 − 0 49 29	
BS 6378	17 07 30.3 −15 39 50	CSI 79
BS 6392	17 10 59.4 −39 42 34	"
BS 6396	17 08 38.1 +65 46 33	"
BS 6397	17 12 02.0 −33 29 32	"
BS 6406	17 12 21.9 +14 26 44	"
BS 6410	17 12 58.5 +24 53 47	"
BS 6418	17 13 18.2 +36 51 50	"
BS 6453	17 18 56.1 −24 57 03	"
BS 6461	17 21 08.2 −55 29 05	"
BS 6461	17 21 08.3 −55 29 06	
BS 6464	17 18 56.2 +46 17 20	CSI 79
BS 6497	17 23 54.0 + 7 38 15	"
BS 6498	17 24 01.9 + 4 10 55	"
BS 6526	17 28 42.9 +26 08 48	"
BS 6536	17 29 17.9 +52 20 15	"
BS 6543	17 31 26.4 +14 52 31	"
BS 6556	17 32 36.6 +12 35 41	"
BS 6601	17 41 05.0 − 7 03 28	
BS 6603	17 41 00.0 + 4 35 11	CSI 79
BS 6603	17 41 00.0 + 4 35 12	
BS 6623	17 44 30.0 +27 44 54	CSI 79
BS 6630	17 46 27.1 −37 01 45	"
BS 6688	17 52 39.6 +56 52 47	"
BS 6693	17 55 52.3 −30 14 58	"
BS 6695	17 54 32.1 +37 15 20	"
BS 6698	17 56 16.3 − 9 46 08	
BS 6698	17 56 16.3 − 9 46 09	
BS 6702	17 55 22.3 +45 21 21	779907
BS 6703	17 55 49.2 +29 15 06	CSI 79
BS 6705	17 55 26.5 +51 29 37	"

NAME	RA (1950) DEC	POS REF
BS 6707	17 56 35.2 +30 11 30	"
BS 6736	18 00 48.3 −24 21 47	"
BS 6736	18 00 48.4 −24 21 49	
BS 6746	18 02 35.6 −30 25 34	CSI 79
BS 6746	18 02 35.7 −30 25 36	
BS 6752	18 02 55.5 + 2 30 33	CSI 79
BS 6766	18 04 54.9 −28 27 51	"
BS 6806	18 07 57.9 +38 27 11	"
BS 6815	18 10 01.1 +31 23 29	"
BS 6819	18 12 54.7 −56 02 27	"
BS 6832	18 14 14.6 −36 46 44	
BS 6859	18 17 47.5 −29 51 03	CSI 79
BS 6861	18 18 26.6 −24 56 20	"
BS 6868	18 18 10.9 +21 56 18	"
BS 6869	18 18 43.2 − 2 54 47	"
BS 6872	18 18 06.3 +36 02 26	"
BS 6879	18 20 51.1 −34 24 35	"
BS 6891	18 20 15.7 +49 05 43	"
BS 6895	18 21 33.9 +21 44 43	"
BS 6913	18 24 53.0 −25 27 03	"
BS 6929	18 26 16.9 −25 17 23	"
BS 6973	18 32 29.0 − 8 16 49	"
BS 6982	18 37 12.3 −71 28 28	"
BS 7001	18 35 14.6 +38 44 09	"
BS 7023	18 39 58.3 −19 20 00	"
BS 7063	18 44 31.2 − 4 48 10	"
BS 7064	18 44 03.4 +26 36 26	"
BS 7066	18 44 48.7 − 5 45 35	"
BS 7106	18 48 14.0 +33 18 12	779907
BS 7120	18 52 05.7 −22 44 06	CSI 79
BS 7120	18 52 05.8 −22 44 08	
BS 7133	18 52 38.1 +22 34 49	CSI 79
BS 7139	18 52 45.2 +36 50 02	779907
BS 7150	18 54 44.7 −21 10 25	CSI 79
BS 7157	18 53 48.7 +43 52 46	779907
BS 7169	18 57 40.5 −37 07 53	CSI 79
BS 7170	18 57 41.6 −37 07 57	"
BS 7176	18 57 21.0 +14 59 55	"
BS 7178	18 57 04.3 +32 37 10	"
BS 7193	18 59 00.5 − 5 48 38	"
BS 7217	19 01 41.2 −21 48 58	"
BS 7217	19 01 41.2 −21 49 00	
BS 7234	19 03 49.1 −27 44 42	CSI 79
BS 7235	19 03 06.6 +13 47 15	"
BS 7236	19 03 35.6 − 4 57 31	"
BS 7236	19 03 35.7 − 4 57 33	
BS 7264	19 06 47.3 −21 06 16	CSI 79
BS 7275	19 07 15.4 +52 20 41	"
BS 7310	19 12 32.7 +67 34 23	"
BS 7314	19 14 37.7 +38 02 36	"
BS 7317	19 16 08.9 −15 37 28	"
BS 7328	19 15 56.7 +53 16 30	"
BS 7340	19 18 46.3 −17 56 34	"
BS 7352	19 16 31.4 +73 15 47	"
BS 7377	19 22 58.5 + 3 00 48	"
BS 7405	19 26 37.3 +24 33 43	"
BS 7417	19 28 42.2 +27 51 11	"
BS 7429	19 31 38.7 + 7 16 15	"
BS 7429	19 31 38.8 + 7 16 17	
BS 7446	19 34 12.0 − 7 08 23	CSI 79
BS 7446	19 34 12.1 − 7 08 25	
BS 7462	19 32 27.5 +69 34 33	CSI 79
BS 7475	19 37 09.5 +16 27 18	"
BS 7479	19 37 51.5 +17 53 49	
BS 7482	19 37 48.8 +42 42 06	
BS 7488	19 38 48.1 +17 21 30	CSI 79
BS 7503	19 40 29.0 +50 24 29	"
BS 7504	19 40 32.0 +50 24 02	"
BS 7525	19 43 52.9 +10 29 23	
BS 7525	19 43 52.9 +10 29 24	
BS 7528	19 43 24.6 +45 00 27	CSI 79
BS 7536	19 45 09.3 +18 24 33	"
BS 7541	19 46 16.7 −10 59 46	"
BS 7557	19 48 19.7 + 8 43 58	
BS 7557	19 48 20.6 + 8 44 06	
BS 7564	19 48 38.5 +32 47 11	779907
BS 7569	19 49 55.2 +24 51 44	CSI 79
BS 7582	19 48 21.0 +70 08 26	"
BS 7602	19 52 51.3 + 6 16 48	"
BS 7615	19 54 25.7 +34 56 57	"
BS 7635	19 56 31.9 +19 21 17	"
BS 7652	20 00 14.3 −38 04 49	"
BS 7665	20 03 50.3 −66 18 42	"
BS 7676	20 00 56.9 +64 40 49	"
BS 7678	20 02 38.3 +32 04 31	"
BS 7685	20 02 35.9 +67 43 51	"
BS 7686	20 01 02.3 +76 20 32	"
BS 7704	20 04 40.7 +67 52 58	"
BS 7710	20 08 43.4 − 0 58 15	"
BS 7710	20 08 43.5 − 0 58 16	
BS 7735	20 12 03.3 +46 35 19	CSI 79
BS 7747	20 14 52.6 −12 39 49	"
BS 7751	20 13 55.4 +47 33 34	"
BS 7754	20 15 16.9 −12 42 03	
BS 7754	20 15 16.9 −12 42 05	
BS 7763	20 15 56.5 +37 52 35	779907
BS 7769	20 16 36.0 +36 50 31	CSI 79
BS 7773	20 17 53.4 −12 55 03	"
BS 7776	20 18 12.1 −14 56 25	"
BS 7796	20 20 25.9 +40 05 43	"
BS 7806	20 21 51.6 +32 01 39	"
BS 7847	20 29 05.1 +36 45 58	"
BS 7869	20 34 03.4 −47 28 02	"
BS 7882	20 35 11.7 +14 25 08	"
BS 7884	20 35 45.3 − 1 16 50	"
BS 7892	20 36 22.3 +13 08 16	"
BS 7900	20 37 12.3 −18 18 56	"
BS 7924	20 39 43.4 +45 06 02	"
BS 7939	20 42 42.5 +25 05 25	"
BS 7940	20 41 57.9 +56 55 58	
BS 7942	20 43 35.7 +30 32 09	CSI 79
BS 7949	20 44 11.1 +33 46 54	"
BS 7950	20 44 58.2 − 9 40 46	"
BS 7951	20 45 05.9 − 5 12 42	"
BS 7951	20 45 06.0 − 5 12 43	
BS 7957	20 44 16.4 +61 38 38	CSI 79
BS 7980	20 48 50.4 −27 06 25	"
BS 7986	20 50 55.0 −58 38 38	"

NAME	RA (1950) DEC	POS REF
BS 8006	20 52 33.0 − 1 33 52	"
BS 8023	20 54 48.7 +44 43 53	"
BS 8042	20 58 54.4 −43 11 52	
BS 8062	21 00 36.7 +44 35 35	CSI 79
BS 8079	21 03 06.5 +43 43 38	"
BS 8085	21 04 39.9 +38 29 58	"
BS 8086	21 04 38.3 +38 29 29	"
BS 8093	21 06 52.3 −11 34 30	"
BS 8110	21 10 19.6 −27 49 27	"
BS 8115	21 10 48.3 +30 01 14	"
BS 8128	21 12 58.9 −15 22 48	"
BS 8130	21 12 47.5 +37 49 51	"
BS 8143	21 15 26.9 +39 11 03	"
BS 8162	21 17 23.1 +62 22 22	"
BS 8164	21 17 52.6 +58 24 40	"
BS 8167	21 19 27.9 −17 02 54	"
BS 8173	21 19 46.3 +19 35 21	"
BS 8181	21 22 20.1 −65 35 38	"
BS 8183	21 21 19.6 −21 03 55	"
BS 8204	21 23 48.9 −22 37 42	
BS 8204	21 23 48.9 −22 37 44	
BS 8213	21 25 52.4 −22 01 32	CSI 79
BS 8225	21 27 40.7 +23 25 06	"
BS 8232	21 28 55.6 − 5 47 30	"
BS 8232	21 28 55.6 − 5 47 32	
BS 8238	21 28 01.3 +70 20 26	CSI 79
BS 8252	21 32 05.7 +45 22 11	"
BS 8255	21 32 43.7 +38 18 31	"
BS 8262	21 34 08.3 +45 09 00	779907
BS 8278	21 37 19.3 −16 53 19	CSI 79
BS 8279	21 36 34.6 +61 51 20	"
BS 8283	21 38 49.8 −14 16 17	
BS 8297	21 39 54.4 +35 16 53	779907
BS 8308	21 41 43.7 + 9 38 40	CSI 79
BS 8313	21 42 08.4 +17 07 10	"
BS 8316	21 41 58.5 +58 33 01	779907
BS 8318	21 43 36.2 − 9 30 26	CSI 79
BS 8321	21 43 46.1 +22 43 02	"
BS 8322	21 44 16.9 −16 21 17	"
BS 8327	21 43 30.7 +62 13 46	"
BS 8334	21 44 00.2 +60 53 22	"
BS 8383	21 55 14.5 +63 23 14	779907
BS 8413	22 03 09.3 + 4 48 47	CSI 79
BS 8414	22 03 12.9 − 0 33 47	"
BS 8421	22 03 16.9 +46 30 04	"
BS 8424	22 04 00.2 +44 46 13	"
BS 8425	22 05 05.4 −47 12 14	"
BS 8428	22 03 36.2 +62 02 10	"
BS 8430	22 04 40.7 +25 06 00	"
BS 8430	22 04 40.8 +25 06 01	
BS 8465	22 09 06.9 +57 57 14	CSI 79
BS 8469	22 09 48.5 +59 10 02	"
BS 8477	22 11 35.7 −41 37 10	
BS 8481	22 14 32.5 −80 41 23	CSI 79
BS 8485	22 11 43.6 +39 27 57	"
BS 8498	22 13 47.1 +37 29 55	"
BS 8499	22 14 11.7 − 8 01 57	"
BS 8502	22 15 05.6 −60 30 33	"
BS 8521	22 19 41.1 −46 12 01	"
BS 8531	22 21 38.0 −58 02 48	
BS 8538	22 21 35.3 +51 58 40	CSI 79
BS 8541	22 22 28.9 +49 13 20	"
BS 8551	22 25 19.4 + 4 26 38	"
BS 8560	22 26 46.6 −44 00 19	"
BS 8560	22 26 46.7 −44 00 21	
BS 8572	22 27 26.4 +47 27 00	CSI 79
BS 8575	22 28 02.7 +49 05 59	"
BS 8621	22 36 39.4 +56 32 07	"
BS 8622	22 37 00.7 +38 47 21	"
BS 8632	22 38 18.9 +44 00 53	"
BS 8650	22 40 39.2 +29 57 32	"
BS 8667	22 44 07.1 +23 18 06	"
BS 8677	22 45 23.5 +58 13 06	"
BS 8679	22 46 56.7 −13 51 23	"
BS 8681	22 47 01.9 +10 12 50	"
BS 8684	22 47 35.1 +24 20 12	"
BS 8685	22 48 11.7 −39 25 18	"
BS 8694	22 47 53.5 +65 56 13	"
BS 8698	22 50 00.3 − 7 50 45	
BS 8700	22 50 40.8 −48 51 48	
BS 8701	22 51 12.6 −70 20 29	
BS 8709	22 51 59.9 −16 05 12	CSI 79
BS 8714	22 52 07.5 +16 40 29	"
BS 8726	22 54 14.0 +49 27 57	"
BS 8728	22 54 53.4 −29 53 14	
BS 8728	22 54 53.5 −29 53 16	
BS 8729	22 55 00.3 +20 30 00	CSI 79
BS 8752	22 57 58.1 +56 40 36	"
BS 8775	23 01 20.7 +27 48 39	"
BS 8781	23 02 16.0 +14 56 08	"
BS 8781	23 02 16.1 +14 56 09	
BS 8795	23 04 28.9 + 9 08 19	CSI 79
BS 8799	23 05 00.5 +20 51 49	"
BS 8808	23 05 44.7 +63 21 44	"
BS 8812	23 06 46.9 −21 26 38	"
BS 8832	23 10 51.7 +56 53 30	"
BS 8834	23 11 43.9 − 6 19 06	"
BS 8841	23 13 16.3 − 9 21 36	"
BS 8848	23 14 31.4 −58 30 35	"
BS 8850	23 14 15.3 − 7 59 56	"
BS 8852	23 14 34.3 + 3 00 30	"
BS 8860	23 15 25.1 +48 44 29	"
BS 8892	23 20 20.7 −20 22 24	"
BS 8905	23 22 52.7 +23 07 42	"
BS 8906	23 23 25.3 −20 54 57	"
BS 8916	23 25 25.7 + 6 06 13	"
BS 8923	23 26 37.3 +12 29 03	"
BS 8924	23 26 56.9 − 4 48 17	"
BS 8961	23 35 06.6 +46 11 11	779907
BS 8989	23 39 58.3 +64 14 16	CSI 79
BS 9004	23 43 50.0 + 3 12 32	"
BS 9045	23 51 52.4 +57 13 16	779907
BS 9047	23 52 12.9 − 0 10 05	CSI 79
BS 9064	23 55 12.3 +24 51 47	"
BS 9088	23 59 33.1 +26 49 02	"
BS 9089	23 59 23.7 − 6 17 30	"
BS #2	18 00 02.0 −24 29 25	
BS #3	18 00 16.8 −24 22 55	

NAME	RA (1950)	DEC	POS REF
	h m s	° ' ''	
BS4	2 23 46.5	+61 42 30	
BW 25	5 08 05.1	−69 13 43	809910
BW 45	5 08 41.6	−69 15 05	"
BW 89	5 09 54.7	−69 08 09	"
B2 0912+29	9 12 53.5	+29 45 55	809908
B2 1128+315	11 28 30.3	+31 30 40	"
B2 1215+30	12 15 21.1	+30 23 40	"
B2 1225+31	12 25 55.9	+31 45 13	"
B2 1225+317	"	"	"
B2 1308+326	13 08 07.6	+32 36 41	"
C−891			
ALF CAE	4 38 56.9	−41 57 28	CSI 79
R CAE	4 38 43.9	−38 20 02	"
T CAE	4 45 31.7	−36 17 49	"
ALF CAM	4 49 03.7	+66 15 37	"
BET CAM	4 58 57.5	+60 22 18	"
R CAM	14 21 17.4	+84 03 36	779907
RU CAM	7 16 20.2	+69 45 54	"
S CAM	5 35 37.4	+68 46 21	"
ST CAM	4 46 01.2	+68 05 01	"
T CAM	4 35 14.1	+66 02 57	"
TW CAM	4 16 39.6	+57 19 21	"
TX CAM	4 56 42	+56 06 42	GCVS
U CAM	3 37 28.8	+62 29 18	779907
UV CAM	4 01 31.6	+61 39 33	"
V CAM	5 55 57.5	+74 30 24	"
X CAM	4 39 12.3	+75 00 31	"
XX CAM	4 04 46.1	+53 13 44	"
Z CAM	8 19 39.9	+73 16 24	"
2 H CAM	4 35 59.7	+53 22 36	CSI 79
2 H CAM	4 35 59.8	+53 22 37	"
11 CAM	5 01 47.1	+58 54 18	CSI 79
12 CAM	5 01 50.5	+58 57 14	"
AE CAP	20 16 07.4	−16 00 51	
ALF 1 CAP	20 14 52.6	−12 39 49	CSI 79
BET CAP	20 18 12.1	−14 56 25	"
EPS CAP	21 34 16.9	−19 41 26	"
ETA CAP	21 01 33.5	−20 03 11	"
IOT CAP	21 19 27.9	−17 02 54	"
RR CAP	20 59 22.5	−27 17 20	"
RS CAP	21 04 27.9	−16 37 25	"
RT CAP	20 14 13.7	−21 28 55	"
RX CAP	20 12 08.9	−13 05 50	"
T CAP	21 19 15.3	−15 22 20	"
U CAP	20 45 21.3	−14 58 11	"
UPS CAP	20 37 12.3	−18 18 56	"
V CAP	21 04 42.6	−24 07 04	"
W CAP	20 11 33.0	−22 07 40	"
X CAP	21 05 41.1	−21 33 07	"
Z CAP	21 07 50.4	−16 22 40	"
47 CAP	21 43 36.2	− 9 30 26	"
AC CAR	7 05 58.0	−58 18 05	"
AG CAR	10 54 10.5	−60 11 09	"
ALF CAR	6 22 50.4	−52 40 03	"
BO CAR	10 43 53.1	−59 13 30	"
BZ CAR	10 52 08.5	−61 46 33	"
CK CAR	10 22 38.9	−59 56 15	"
CL CAR	10 52 03.9	−60 49 54	"
DI CAR	11 13 54.6	−69 38 30	"
ETA CAR	10 43 06.4	−59 26 22	
ETA CAR	10 43 06.9	−59 25 14	CSI 79
EV CAR	10 18 37.3	−60 12 01	"
GG CAR	10 53 57.9	−60 07 30	"
HR CAR	10 21 07.2	−59 22 16	"
IW CAR	9 25 42.9	−63 24 42	"
IX CAR	10 48 27.4	−59 43 01	"
KL CAR	9 41 37	−63 27 31	GCVS
KN CAR	10 01 51	−70 12 37	"
OME CAR	10 12 33.0	−69 47 20	CSI 79
OY CAR	10 05 21	−69 59 32	GCVS
P CAR	10 30 14.4	−61 25 38	CSI 79
PP CAR	10 30 15	−61 25 43	GCVS
R CAR	9 30 59.2	−62 34 01	CSI 79
RT CAR	10 42 50.2	−59 08 59	"
RU CAR	9 14 24.7	−66 00 27	"
RW CAR	9 18 56.4	−68 32 41	"
RY CAR	11 17 56	−61 35 54	GCVS
RZ CAR	10 34 12.6	−70 27 29	CSI 79
S CAR	10 07 46.1	−61 18 13	"
SY CAR	11 13 23.4	−57 39 18	"
SZ CAR	9 58 16.9	−59 58 19	"
THE CAR	10 41 10.0	−64 07 54	"
TZ CAR	10 44 16.3	−65 21 02	"
CARINA	10 41 39	−59 18 02	
CARINA	10 42 34	−59 24 02	
CARINA A1	6 39 48.6	−51 02 53	
CARINA C1	6 40 34.5	−50 55 20	
CARINA C2	6 40 33.6	−50 55 54	
CARINA C3	6 40 28.8	−50 55 06	
CARINA C4	6 40 31.9	−50 57 20	
CARINA C5	6 40 57.6	−50 53 23	
CARINA C6	6 40 11.9	−51 00 25	
CARINA I	10 41 27	−59 19 00	
CARINA II	10 42 57	−59 23 00	
CAS A	23 20 56	+58 32 12	
CAS A	23 21	+58 32	ED
CAS A	23 21 10	+58 31 18	
CAS A	23 21 10	+58 33 54	
CAS A #A	23 21 05	+58 34 06	
CAS A #B	23 21 07	+58 32 48	
CAS A #C	23 21 15	+58 31 06	
CAS A #D	23 21 40	+58 31 06	
CAS A CK1	23 21 20.2	+58 33 30	ED
CAS A KB33	23 21 01.2	+58 33 37	"
CAS A KB42	23 21	+58 33	"
CAS A KB61	23 21 09.3	+58 33 53	"
CAS A KB93	23 21 19.2	+58 33 34	"
CAS A KB98	23 21 22.1	+58 33 30	"
ALF CAS	0 37 39.3	+56 15 47	CSI 79
AO CAS	0 15 03.5	+51 09 19	779907
AZ CAS	1 38 51.0	+61 10 09	"
BET CAS	0 06 30.2	+58 52 26	"
DEL CAS	1 22 31.4	+59 58 33	CSI 79
EPS CAS	1 50 46.3	+63 25 29	"
EQ CAS	23 50 23	+54 44 05	GCVS
ETA CAS	0 46 03.6	+57 33 02	CSI 79
ETA CAS A	"	"	
FZ CAS	0 36 09	+59 24 30	GCVS
GAM CAS	0 53 40.3	+60 26 47	779907
GP CAS	2 36 04.7	+59 22 57	"
HO CAS	0 59 36.9	+61 35 04	CSI 79
HS CAS	1 05 07.8	+63 19 12	779907
HT CAS	1 07 00	+59 48 01	GCVS
HV CAS	1 08 04.5	+53 26 01	CSI 79
KAP CAS	0 30 08.3	+62 39 21	"
KN CAS	0 06 58.0	+62 23 23	779907
LW CAS	2 53 26	+60 29 09	GCVS
MUU CAS	1 04 55.6	+54 40 32	CSI 79
MZ CAS	0 18 40.4	+59 40 33	779907
OMI CAS	0 41 55.6	+48 00 38	CSI 79
OMI CAS	0 41 56	+48 00 27	
PHI CAS	1 16 55.0	+57 58 08	CSI 79
PZ CAS	23 41 38.9	+61 30 44	779907
PZ CAS	23 41 41.0	+61 31 00	
R CAS	23 55 50.0	+51 07 01	779907
R CAS	23 55 53.0	+51 06 36	
RHO CAS	23 51 52.4	+57 13 16	779907
RR CAS	23 52 17.6	+53 13 09	CSI 79
RV CAS	0 49 54.1	+47 09 21	"
S CAS	1 15 57.8	+72 20 56	779907
SS CAS	0 06 59.7	+51 17 20	"
ST CAS	0 14 52.7	+50 00 36	"
SU CAS	2 47 28.8	+68 41 00	"
SZ CAS	2 23 33.3	+59 14 11	"
T CAS	0 20 31.1	+55 30 56	"
TU CAS	0 23 36.7	+51 00 13	"
TV CAS	0 16 36.1	+58 51 42	"
TZ CAS	23 50 26.9	+60 43 27	"
U CAS	0 43 33.2	+47 58 17	"
UV CAS	23 00 09.6	+59 20 28	"
V CAS	23 09 31.1	+59 25 40	"
VX CAS	0 28 30	+61 43 23	GCVS
V338 CAS	0 10 29	+48 49 41	"
V358 CAS	23 28 00.9	+57 42 42	CSI 79
V376 CAS	0 08 43	+58 34 17	GCVS
V466 CAS	1 16 43.9	+58 02 47	779907
W CAS	0 51 55.0	+58 17 35	"
WW CAS	1 30 16.0	+57 29 48	CSI 79
WX CAS	1 50 33.3	+60 51 49	779907
WZ CAS	23 58 42.1	+60 04 38	"
X CAS	1 53 10.3	+59 00 59	CSI 79
Y CAS	0 00 44.7	+55 23 41	"
Y CAS	0 00 45.0	+55 24 21	
Z CAS	23 42 05.1	+56 18 13	779907
ZET CAS	0 34 10.3	+53 37 19	CSI 79
6 CAS	23 46 23.2	+61 56 10	"
CASE 23	0 46 24	+64 29 23	ED
CASE 31	2 53 08	+57 20 15	"
CASE 33	3 03 41.2	+55 33 34	CSI 79
CASE 34	3 11 24	+54 42 18	ED
CASE 39	4 48 03.2	+39 54 14	549901
CASE 49	18 22 44	−13 47 26	ED
CASE 62	19 59 15.8	+30 43 04	549901
CASE 75	22 31 40	+58 38 27	ED
CASE 78	22 47 22	+59 01 51	"
CASE 79	22 52	+61 03	
CASE 81	23 11 20	+60 14 18	ED
CCS 1	0 03 35	+69 48	739907
CCS 39	0 51 32.4	+23 47 46	CSI 79
CCS 59	1 10 24	+62 41	739907
CCS 62	1 12 22.5	−48 31 02	CSI 79
CCS 77	1 37 58.7	−59 30 43	"
CCS 110	2 32 39.6	− 9 39 37	"
CCS 131	3 07 33.4	+57 42 51	"
CCS 134	3 10 08.5	+47 38 27	"
CCS 136	3 11 16.9	−57 30 29	"
CCS 142	3 23 23	+47 22	739907
CCS 144	3 22 10	−65 27	
CCS 155	3 37 47.2	+51 20 36	CSI 79
CCS 164	3 48 25.5	−43 41 02	"
CCS 187	4 09 07	+29 15	739907
CCS 191	4 07 51.0	−69 55 07	CSI 79
CCS 225	4 30 30.6	−66 05 36	"
CCS 313	5 15 49.1	+35 44 27	"
CCS 373	5 33 45.9	−25 46 07	"
CCS 503	6 21 08	+ 8 32	739907
CCS 524	6 28 27	− 5 29	
CCS 574	6 38 40.9	−70 02 55	CSI 79
CCS 589	6 47 01	+ 3 02	739907
CCS 623	6 52 52.1	−42 18 03	CSI 79
CCS 633	6 55 24	−27 44	
CCS 645	6 58 31.7	− 3 10 48	CSI 79
CCS 695	7 12 59.0	+ 5 07 59	"
CCS 704	7 13 05	−39 27	
CCS 715	7 16 11	−36 15	
CCS 721	7 17 29	−42 52	
CCS 734	7 19 35	−28 52	
CCS 776	7 27 00.5	−19 21 29	739907
CCS 779	7 28 52.6	+24 36 36	CSI 79
CCS 844	7 36 57	−35 17	
CCS 869	7 40 21	−26 54	
CCS 893	7 44 11	−41 25	
CCS 915	7 47 20	−48 36	
CCS 918	7 48 42.6	− 2 29 32	739907
CCS 921	7 48 46	−38 41	
CCS 936	7 50 20	−46 22	
CCS 947	7 52 33	−32 13	
CCS 954	7 53 12	−29 31	
CCS 955	7 52 49	−43 47	
CCS 967	7 54 56.4	−49 50 48	CSI 79
CCS 988	7 58 07	−33 45	
CCS 1002	8 00 24	−30 24	
CCS 1013	8 01 32	−23 40 23	GCVS
CCS 1014	8 01 23	−31 21	
CCS 1027	8 02 27	−43 27	
CCS 1184	8 26 06	−27 06	
CCS 1193	8 28 06	−27 32	
CCS 1209	8 31 21	−29 46	
CCS 1217	8 32 56	−30 44	
CCS 1232	8 35 08	−52 24	
CCS 1275	8 40 57	−47 02	
CCS 1281	8 42 45	−35 32	
CCS 1290	8 44 31.0	−29 32 37	CSI 79
CCS 1311	8 48 46	−35 53	
CCS 1323	8 49 36	−49 40	
CCS 1386	9 04 55	−58 24	
CCS 1401	9 09 48	−41 11	
CCS 1539	9 42 48	−46 30	
CCS 1568	9 48 59	−43 54	
CCS 1570	9 48 52	−56 12	
CCS 1606	9 58 14	−71 57	
CCS 1621	10 04 25	−53 55	
CCS 1630	10 09 41.7	−35 04 37	CSI 79
CCS 1636	10 11 23	−43 34	
CCS 1705	10 32 34	−62 27	
CCS 1776	10 51 40	−61 11	
CCS 1824	11 06 33	−81 31	
CCS 1841	11 19 03.5	−55 29 22	CSI 79
CCS 1842	11 19 07	−60 01	
CCS 1935	11 54 18	−63 06	
CCS 1942	11 57 31.2	−58 18 39	CSI 79
CCS 1944	11 57 49.6	−54 49 41	"
CCS 1971	12 08 56	−63 30	
CCS 1986	12 17 17	−58 40	
CCS 2008	12 26 40.7	−37 59 14	CSI 79
CCS 2023	12 37 26	−57 06	
CCS 2031	12 44 49	−59 16	
CCS 2055	13 00 45	−60 16	
CCS 2099	13 29 30.5	−53 34 29	CSI 79
CCS 2134	13 54 54.7	−56 06 34	"
CCS 2148	14 10 43.6	−53 41 54	"
CCS 2250	15 24 49.9	−24 59 45	"
CCS 2301	15 59 18	−41 14	
CCS 2333	16 24 37.0	−43 33 57	CSI 79
CCS 2342	16 30 45.2	−67 01 26	"
CCS 2388	16 58 51	−32 41	
CCS 2416	17 12 43	−34 37	
CCS 2417	17 11 56.5	+42 09 48	CSI 79
CCS 2421	17 15 16.9	−45 55 28	"
CCS 2426	17 16 10	−28 45	
CCS 2429	17 17 16.3	−40 19 53	CSI 79
CCS 2455	17 30 10	−36 14	
CCS 2586	18 24 26	+ 1 07	739907
CCS 2593	18 26 50.3	−38 27 16	CSI 79
CCS 2689	18 58 26	−31 38	
CCS 2692	18 59 53.9	+10 10 03	CSI 79
CCS 2694	19 00 49	+ 7 26	739907
CCS 2721	19 16 17.7	−16 00 02	CSI 79
CCS 2733	19 25 01	+23 30	739907
CCS 2783	19 41 46	+34 22	"
CCS 2801	19 46 35	+26 01 13	"
CCS 2817	19 51 45.1	−65 29 27	CSI 79
CCS 2849	20 00 54	+30 37 51	739907
CCS 2871	20 08 20	+29 11	"
CCS 2874	20 09 13.9	+35 57 59	CSI 79
CCS 2885	20 16 34.4	−49 58 49	"
CCS 2904	20 24 51	+38 08	739907
CCS 2918	20 35 43	+36 40	
CCS 2924	20 41 30.5	+31 56 36	CSI 79
CCS 2935	20 47 13.9	+33 02 30	"
CCS 2976	21 03 29	+51 37	739907
CCS 2980	21 06 49.9	−53 54 59	CSI 79
CCS 3040	21 31 13.9	+43 42 22	"
CCS 3041	21 32 01	+38 51	739907
CCS 3056	21 40 35.3	−65 16 26	CSI 79
CCS 3060	21 39 54.4	+35 16 53	779907
CCS 3140	22 30 28	+58 22	739907
CCS 3170	22 52 47	+60 31	"
CCS 3186	23 21 17	+55 52	"
CCS 3204	23 46 31.9	+ 6 06 14	CSI 79
CD−24 5721	7 37 00.4	−24 38 08	CD
CD−24 12698	16 28 38.9	−24 18 51	CSI 79
CD−24 13785	17 59 35.7	−24 14 51	"
CD−27 3544	6 59 43.5	−27 51 42	"
CD−31 4916	7 39 05.9	−31 33 47	"
CD−33 10685	15 42 01.9	−34 08 00	CD
CD−35 10525	15 45 56.1	−35 29 57	"
CD−36 8436	13 13 11	−36 44 16	"
CD−37 7613	11 59 40.3	−37 53 09	"
CD−41 11303	17 05 42	−41 07 46	"
CD−42 11721	16 55 32	−42 37 26	"
CD−42 11721#1	"	"	ED
CD−42 11721#2	"	"	"
CD−42 11721#3	"	"	"
CD−44 9880	15 04 57	−44 33	
CD−44 11324	16 55 21	−44 19 22	CD
CD−56 3464	10 36 05	−56 33 34	"
CD−57 3459	10 42 22	−57 47 43	"
CD−57 3493	10 45 40	−57 39 49	"
CD−58 3538	10 42 50.2	−59 08 59	CSI 79
CD−59 3174	10 34 00	−59 46 31	CD
CD−59 4459	12 50 41	−60 04 19	"
CD−59 4549	12 50 44.5	−60 06 12	ED
CD−60 3227	10 48 27	−60 31 52	CD
CD−60 3621	11 33 26	−61 18 34	"
CD−60 3636	11 33 54	−61 19 35	"
CD−68 840	10 53 13	−69 00	
CD−82 174	8 59 00	−82 57	
CED 110	11 04 54	−77 06	ED
CEN A	13 22 30	−42 46	
CEN A	13 22 32.0	−42 46 00	
CEN X−3	11 19	−60	
AL CEN	12 35 21.3	−53 19 31	CSI 79
ALF CEN	14 36 11.1	−60 37 45	"
ALF CEN A	"	"	"
ALF CEN B			"
AM CEN	13 44 03.1	−53 06 30	"
AW CEN	13 10 38.7	−56 41 57	"
DEL CEN	12 05 45.3	−50 26 37	"
DY CEN	13 22 25	−53 59 11	GCVS
ETA CEN	14 32 19.3	−41 56 20	CSI 79
KQ CEN	14 21 30	−63 46 06	GCVS
MUU CEN	13 46 35.6	−42 13 31	CSI 79
NZ CEN	13 22 42	−63 02 46	GCVS
OME CEN #1	13 23 48	−47 13 36	779909
OME CEN G55	"	"	"
OME CEN G78	"	"	"
OME CEN G318	"	"	"
OME CEN NOM.	"	"	"
OME CEN RGO40	"	"	"
OME CEN RGO43	"	"	"
OME CEN RGO56	"	"	"
OME CEN RGO66	"	"	"
OME CEN V6	"	"	"

NAME	RA (1950)	DEC	POS REF
	h m s	° ' "	
OME CEN V17	"	"	"
OME CEN V53	"	"	"
OME CEN V138	"	"	"
OME CEN V148	"	"	"
OME CEN V162	"	"	"
OME CEN V164	"	"	"
OMI CEN	11 29 26.7	−59 09 56	CSI 79
OMI 1 CEN	"	"	"
PROX CEN	14 26 18.9	−62 28 05	"
R CEN	14 12 56.9	−59 40 53	"
RS CEN	11 18 16.3	−61 36 22	"
RT CEN	13 45 24.7	−36 36 49	"
RU CEN	12 06 47.5	−45 08 51	"
RV CEN	13 34 17.9	−56 13 22	"
RW CEN	11 05 04.3	−54 51 10	"
RX CEN	13 48 29.9	−36 41 57	"
S CEN	12 21 52.3	−49 09 45	"
SX CEN	12 18 32.2	−48 56 00	"
T CEN	13 38 53.2	−33 20 40	"
TT CEN	13 16 26.3	−60 31 25	"
TV CEN	12 11 53.1	−51 15 14	"
UW CEN	12 40 25.5	−54 15 15	"
UX CEN	13 18 47.3	−63 57 46	"
UY CEN	13 13 36.9	−44 26 25	"
VX CEN	13 47 48.3	−60 09 59	"
V368 CEN	12 10 28.0	−49 55 41	"
V369 CEN	12 12 20.3	−54 32 31	"
V381 CEN	13 47 22.4	−57 19 57	"
V396 CEN	13 14 11.3	−61 19 13	"
V682 CEN	14 27 20	−34 33 14	GCVS
V744 CEN	13 36 53.5	−49 41 48	CSI 79
V748 CEN	14 56 32	−33 13 28	GCVS
V771 CEN	11 24 43.9	−61 05 37	CSI 79
V772 CEN	11 39 26.9	−63 08 12	"
W CEN	11 52 28.7	−58 58 40	"
WW CEN	13 06 16.7	−59 59 02	"
X CEN	11 46 41.5	−41 28 38	"
Y CEN	14 28 01.6	−29 52 33	"
2 CEN	13 46 32.3	−34 12 05	
CEP A	22 54 19.9	+61 45 56	
CEP A #1	22 54 09.0	+61 45 07	ED
CEP A #2	22 54 10.7	+61 45 43	"
CEP A #3	22 54 12.1	+61 46 16	"
CEP A #4	22 54 13.2	+61 44 50	"
CEP A #5	22 54 14.9	+61 46 52	"
CEP A #6	22 54 15.8	+61 45 25	"
CEP A #7	22 54 15.9	+61 47 28	"
CEP A #8	22 54 17.1	+61 46 01	"
CEP A #9	22 54 18.3	+61 48 04	"
CEP A #10	22 54 18.3	+61 44 22	"
CEP A #11	22 54 19.2	+61 46 34	"
CEP A #12	22 54 20.9	+61 47 12	"
CEP A #13	22 54 20.9	+61 45 07	"
CEP A #14	22 54 21.7	+61 45 43	"
CEP A #15	22 54 22.1	+61 44 16	"
CEP A #16	22 54 23.0	+61 47 43	"
CEP A #17	22 54 23.8	+61 46 16	"
CEP A #18	22 54 25.0	+61 46 52	"
CEP A #19	22 54 25.8	+61 44 49	"
CEP A #20	22 54 26.1	+61 45 25	"
CEP A #21	22 54 27.2	+61 43 56	"
CEP A #22	22 54 27.2	+61 47 22	"
CEP A #23	22 54 28.9	+61 46 01	"
CEP A #24	22 54 30.2	+61 44 28	"
CEP A #25	22 54 30.2	+61 46 34	"
CEP A #26	22 54 30.6	+61 45 07	"
CEP A #27	22 54 32.2	+61 47 02	"
CEP A #28	22 54 33.3	+61 45 39	"
CEP A #29	22 54 34.0	+61 46 16	"
CEP A #30	22 54 36.0	+61 46 46	"
CEP B	22 55 08.7	+62 21 30	CSI 79
CEP OB3 FIRS1	22 54 42	+61 47 12	
AZ CEP	22 06 57.9	+59 18 17	779907
CQ CEP	22 34 56.8	+56 38 46	"
DEL CEP	22 27 18.5	+58 09 32	"
DG CEP	22 42 18.0	+61 27 56	"
DI CEP	22 54 08.4	+58 24 00	"
EH CEP	21 02 53	+67 47 32	GCVS
GL CEP	21 36 12	+57 30 59	
GP CEP	22 16 54.5	+55 52 30	779907
GU CEP	23 08 03.9	+60 58 13	"
LAM CEP	22 09 48.5	+59 10 02	CSI 79
MUU CEP	21 41 58.5	+58 33 01	779907
NOVA CEP 1971	22 02 47	+53 15 50	GCVS
NUU CEP	21 44 00.2	+60 53 22	CSI 79
PV CEP	20 45 23.5	+67 46 37	
PV CEP 10"S	20 45 23.5	+67 46 27	
PV CEP 8"E	20 45 24.9	+67 46 37	
PV CEP 8"N8"E	20 45 24.9	+67 46 45	
PV CEP 8"W	20 45 22.1	+67 46 37	
RR CEP	2 36 12	+80 55 26	GCVS
RW CEP	22 21 14.0	+55 42 36	779907
S CEP	21 35 52.6	+78 23 58	CSI 79
ST CEP	22 28 16.5	+56 44 39	779907
SV CEP	22 20 34.3	+73 25 16	"
SW CEP	21 24 32.3	+62 21 25	"
T CEP	21 08 52.7	+68 17 13	"
U CEP	0 57 44.3	+81 36 25	"
VV CEP	21 55 14.5	+63 23 14	"
W CEP	22 34 32.8	+58 10 00	"
X CEP	21 00 01.8	+82 51 41	"
Y CEP	0 34 47.2	+80 04 55	
Z CEP	2 19 21	+81 27 09	GCVS
9 CEP	21 36 34.6	+61 51 20	CSI 79
11 CEP	21 41 11.7	+71 04 51	"
13 CEP	21 53 12.0	+56 22 25	"
21 CEP	22 09 06.9	+57 57 14	"
ALF CET	2 59 39.7	+ 3 53 39	"
ALF CET	2 59 41	+ 3 53 38	
GAM CET	2 40 42.3	+ 3 01 32	CSI 79
IOT CET	0 16 52.7	− 9 06 01	"
KAP CET	3 16 44.1	+ 3 11 16	"
OMI CET	2 16 49.0	− 3 12 12	"
R CET	2 23 28.7	− 0 24 09	"
S CET	0 21 30.9	− 9 36 14	"
TAU CET	1 41 44.6	−16 11 59	"
U CET	2 31 19.5	−13 22 01	"
UV CET A+B	1 36 24.9	−18 12 40	"

NAME	RA (1950)	DEC	POS REF
	h m s	° ' "	
UZ CET	2 03 38.2	−10 27 01	"
V CET	23 55 20.2	− 9 14 13	"
W CET	23 59 33.6	−14 57 13	"
X CET	3 16 53.2	− 1 14 44	"
XI 2 CET	2 25 29.7	+ 8 14 12	"
Z CET	1 04 08.9	− 1 44 52	"
84 CET	2 38 40.0	− 0 54 25	"
CHA T #A	11 07	−76 33	ED
CHA T #B	11 05	−76 58	"
CHA T #C	11 02	−76 06	"
CHA T #D	11 03	−77 00	"
CHA T #E	11 04	−77 00	"
CHA T #F	11 05	−77 06	"
CHA T #G	11 06	−77 11	"
CHA T #H	11 06	−77 12	"
CHA T #I	11 07	−77 17	"
CHA T #J	11 01	−77 20	"
CHA T #K	11 01	−77 23	"
CHA T #L	11 02	−77 25	"
CHA T #M	11 02	−77 24	"
CHA T #N	11 07	−77 34	"
CHA T #O	11 08	−77 31	"
CHA T #P	11 09	−77 14	"
CHA T #Q	11 09	−77 15	"
CHA T #R	11 08	−76 13	"
CHA T #S	11 06	−76 34	"
CHA T #T	11 03	−76 36	"
CHA T #U	11 02	−76 14	"
CHA T #V	10 56	−77 00	
CHA T C1−1	11 09 14.9	−76 15 26	
CHA T C1−2	11 08 20.7	−76 16 24	
CHA T C1−3	11 07 52.0	−76 17 20	
CHA T C1−4	11 08 29.7	−76 17 15	
CHA T C1−5	11 08 19.4	−76 18 13	
CHA T C1−6	11 07 49.5	−76 18 19	
CHA T C1−7	11 08 26.1	−76 18 44	
CHA T C1−8	11 08 37.5	−76 19 13	
CHA T C1−9	11 08 30.8	−76 19 29	
CHA T C1−10	11 07 08.5	−76 19 54	
CHA T C1−11	11 08 16.6	−76 20 33	
CHA T C1−12	11 08 56.0	−76 21 03	
CHA T C1−13	11 07 40.7	−76 21 39	
CHA T C2−1	11 09 01.8	−76 24 25	
CHA T C2−2	11 07 52.1	−76 25 52	
CHA T C2−3	11 08 12.7	−76 27 38	
CHA T C2−4	11 08 18.2	−76 29 30	
CHA T C2−5	11 09 21.5	−76 29 16	
CHA T C3−1	11 07 23.0	−76 35 13	
CHA T C3−2	11 09 37.0	−76 41 05	
CHA T C4−1	11 08 20.1	−76 41 44	
CHA T C4−2/3	11 08 20.1	−76 42 42	
CHA T C4−4	11 07 32.8	−76 44 36	
CHA T C4−5	11 07 24.8	−76 45 58	
CHA T C4−6	11 07 25.5	−76 48 36	
CHA T C4−7	11 09 31.5	−76 50 10	
CHA T C5−1	11 07 35.0	−76 51 30	
CHA T C5−2	11 09 21.5	−76 53 11	
CHA T C5−3	11 08 09.0	−76 54 24	
CHA T C5−4	11 07 52.6	−76 57 42	
CHA T C6−1	11 07 12.0	−76 59 47	
CHA T C6−2	11 08 59.7	−77 00 43	
CHA T C6−4	11 09 36.7	−77 01 42	
CHA T C6−5	11 08 28.3	−77 02 08	
CHA T C6−6	11 07 21.5	−77 02 08	
CHA T C7−1	11 08 15.5	−77 09 43	
CHA T C7−2	11 07 59.4	−77 10 08	
CHA T C7−3	11 08 31.7	−77 10 17	
CHA T C7−5	11 08 10.3	−77 10 19	
CHA T C7−7	11 07 43.4	−77 13 08	
CHA T C7−8	11 09 38.9	−77 15 10	
CHA T C7−10	11 07 28.3	−77 15 50	
CHA T C7−11	11 09 08.2	−77 16 34	
CHA T C8−3	11 08 29.9	−77 20 59	
CHA T C9−1	11 07 25.6	−77 27 23	
CHA T C9−2	11 07 12.2	−77 27 37	
CHA T C9−3	11 07 19.9	−77 27 43	
CHA T C9−4	11 08 23.1	−77 29 30	
CHA T C9−5	11 07 50.4	−77 31 28	
CHA T C10−6	11 08 47.5	−77 41 48	
CHA T C10−8	11 07 38.9	−77 44 13	
CHA T C10−9	11 09 26.2	−77 44 37	
CHA T E1−1	11 09 44.7	−76 16 13	
CHA T E1−2	11 10 41.4	−76 16 22	
CHA T E1−4	11 11 49.7	−76 18 03	
CHA T E1−5	11 10 33.7	−76 18 24	
CHA T E1−6	11 11 55.9	−76 19 23	
CHA T E1−7	11 09 58.5	−76 20 09	
CHA T E1−8	11 11 06.3	−76 20 51	
CHA T E1−9A	11 10 48.2	−76 20 53	
CHA T E1−9B	11 10 51.0	−76 20 47	
CHA T E1−10	11 10 27.4	−76 20 46	
CHA T E2−1	11 11 46.0	−76 24 07	
CHA T E2−3	11 11 22.2	−76 27 23	
CHA T E2−4	11 10 52.5	−76 28 09	
CHA T E2−5	11 11 14.2	−76 28 07	
CHA T E2−6	11 10 36.6	−76 28 46	
CHA T E2−7	11 11 36.7	−76 29 24	
CHA T E2−8	11 10 09.4	−76 29 39	
CHA T E2−9	11 11 13.1	−76 30 53	
CHA T E2−10	11 11 35.9	−76 31 26	
CHA T E2−11	11 10 12.9	−76 31 33	
CHA T E3−1	11 11 05.1	−76 34 26	
CHA T E3−2	11 10 29.8	−76 34 42	
CHA T E3−3	11 09 36.9	−76 35 38	
CHA T E3−4	11 10 18.5	−76 35 47	
CHA T E3−5	11 09 38.3	−76 41 08	
CHA T E3−6	11 11 15.7	−76 41 30	
CHA T E4−2	11 10 37.9	−76 41 54	
CHA T E4−3	11 11 08.5	−76 42 26	
CHA T E4−4	11 11 45.8	−76 44 50	
CHA T E4−6	11 10 40.4	−76 49 11	
CHA T E4−7	11 09 51.4	−76 49 42	
CHA T E4−8	11 12 15.7	−76 50 26	
CHA 16	11 06 36	−77 23	739913
ST CHA	10 46 37	−79 11 57	GCVS
SZ CHA	10 57 06	−77 01 16	"
T CHA	11 54 48	−79 05 06	"
TW CHA	10 57 47	−77 06 53	"

NAME	RA (1950)	DEC	POS REF
	h m s	° ' "	
VW CHA	11 06 33	−77 26 38	"
Z CHA	8 08 38	−76 23 32	"
CIR X−1	15 16 48	−56 59 14	769903
AS CIR	15 09 40	−60 08 36	GCVS
R CIR	15 23 53.4	−57 32 42	CSI 79
U CIR	14 01 49	−66 46 16	GCVS
CIT 1	0 04 18	+42 48	661001
CIT 2	0 44 36	+32 25	"
CIT 3	1 03 48	+12 20	
CIT 3	1 03 49.0	+12 18 42	
CIT 4	2 31 42	+64 55	661001
CIT 5	3 23 12	+47 22	"
CIT 6	10 13 18	+30 49	"
CIT 7	15 25 30	+19 44	"
CIT 8	16 08 12	+25 12	"
CIT 9	17 33 24	+15 37	"
CIT 10	20 31 48	+38 29	"
CIT 11	20 37 42	+39 01	"
CIT 12	20 41 36	+43 01	"
CIT 13	21 32 06	+38 51	"
CIT 14	23 42 36	+43 39	"
CLNEAR3C323.1	15 45 31.1	+21 01 33	
CMA R1 #2	6 59 28.5	−11 13 39	CSI 79
CMA R1 #3	6 59 28.8	−11 16 18	
CMA R1 #4	7 00 19.3	−12 09 36	820108
CMA R1 #5	7 00 21.9	−11 22 46	"
CMA R1 #6	7 00 38.4	−11 22 58	"
CMA R1 #7	7 00 50.5	−11 33 59	"
CMA R1 #8	7 01 02.8	−10 37 47	"
CMA R1 #9	7 01 22.5	−11 28 34	CSI 79
CMA R1 #11	7 01 31.7	−11 30 20	820108
CMA R1 #12	7 01 34.3	−11 29 08	"
CMA R1 #13	7 01 34.5	−11 29 59	"
CMA R1 #14	7 01 36.4	−11 30 10	"
CMA R1 #15	7 01 38.2	−11 07 24	"
CMA R1 #16	7 01 46.7	−11 14 23	"
CMA R1 #17	7 01 52.6	−11 14 25	"
CMA R1 #18	7 01 56.8	−11 13 34	"
CMA R1 #19	7 01 58.3	−11 12 38	"
CMA R1 #20	7 02 03.5	−10 22 42	CSI 79
CMA R1 #21	7 02 14.9	−11 00 12	
CMA R1 #23	7 02 23.4	−10 29 32	820108
CMA R1 #24	7 02 26.2	−10 51 41	"
CMA R1 #25	7 02 26.7	−11 01 57	"
CMA R1 #26	7 02 32.4	−10 34 12	"
CMA R1 #27	7 02 57.0	−12 14 57	"
CMA R1 #28	7 03 16.5	−11 04 49	
CMA R1 #29	7 04 19.7	−11 12 55	CSI 79
CMA R1 #30	7 04 29.0	−11 14 30	820108
ALF CMA	6 42 56.7	−16 38 45	CSI 79
ALF CMA	6 42 59	−16 39 18	
ALF CMA A	6 42 56.7	−16 38 45	CSI 79
CO CMA	7 11 58.2	−26 01 20	"
DEL CMA	7 06 21.3	−26 18 45	"
EPS CMA	6 56 39.5	−28 54 09	"
ETA CMA	7 22 06.9	−29 12 14	"
EZ CMA	6 52 08.0	−23 51 50	"
KAP CMA	6 47 58.3	−32 26 57	"
OME CMA	7 12 46.9	−26 41 04	"
OMI 1 CMA	6 52 03.3	−24 07 11	"
OMI 2 CMA	7 00 56.1	−23 45 31	"
R CMA	7 17 12.3	−16 17 58	"
SIG CMA	6 59 43.5	−27 51 42	"
TAU CMA	7 16 37.9	−24 51 41	"
THE CMA	6 51 51.9	−11 58 28	"
U CMA	6 16 49.9	−26 08 58	"
UW CMA	7 16 35.3	−24 27 57	
VY CMA	7 20 53.0	−25 40 24	
VY CMA	7 20 54.5	−25 40 10	CSI 79
VY CMA	7 20 55	−25 40 11	
W CMA	7 05 43.1	−11 50 34	CSI 79
Z CMA	7 01 22.5	−11 28 34	"
Z CMA	7 01 22.6	−11 28 36	
27 CMA	7 12 12.7	−26 15 52	CSI 79
ALF CMI	6 42 56.7	−16 38 45	"
ALF CMI	7 36 41.0	+ 5 21 16	"
BET CMI	7 24 26.3	+ 8 23 28	"
R CMI	7 05 57.5	+10 06 14	"
S CMI	7 30 00.2	+ 8 25 34	"
T CMI	7 31 12.9	+11 51 15	"
U CMI	7 38 36.7	+ 8 30 12	"
V CMI	7 04 13.7	+ 8 56 33	"
VY CMI	7 53 28	+ 4 23 03	GCVS
W CMI	7 46 06.0	+ 5 31 08	CSI 79
ZZ CMI	7 21 29.9	+ 8 59 54	"
BET CNC	8 13 48.2	+ 9 20 26	"
R CNC	8 13 48.4	+11 52 51	"
RHO 1 CNC	8 49 37.3	+28 31 22	
RS CNC	9 07 37.8	+31 10 05	779907
RT CNC	8 55 33.0	+11 02 22	CSI 79
RX CNC	8 11 43.9	+24 53 15	"
RZ CNC	8 36 02.7	+31 58 21	779907
SY CNC	8 58 13.4	+18 06 07	CSI 79
T CNC	8 53 48.9	+20 02 28	"
U CNC	8 32 54.6	+19 04 09	"
V CNC	8 18 52.0	+17 26 41	"
VV CNC	8 08 22.9	+19 17 51	"
VZ CNC	8 38 09.4	+10 00 09	"
W CNC	9 06 55.9	+25 26 58	"
X CNC	8 52 33.9	+17 25 21	"
YZ CNC	8 07 52	+28 17 33	GCVS
Z CNC	8 19 36.9	+15 09 10	CSI 79
CNMY 17	18 12 11.7	−30 32 54	769910
CN1−1	15 47 38.5	−48 36 00	"
CN1−2	16 40 00.5	−62 31 27	"
CN1−3	17 22 34	−44 08 54	779909
CN1−4	17 24 04	−46 53 06	"
CN1−5	18 25 57	−31 32 00	809909
CN2−1	17 51 13.6	−34 21 50	769910
CN3−1	18 15 10.7	+10 08 02	739909
COALSACK D−0	12 28 00.6	−63 28 58	
COALSACK D−1	12 28 11.0	−63 30 57	
COALSACK D−2	12 28 07.1	−63 31 05	
COALSACK D−3	12 28 06.9	−63 29 31	
COALSACK D−4	12 28 13.0	−63 23 52	
COALSACK D−5	12 28 14.9	−63 31 58	
COALSACK D−6	12 28 16.7	−63 24 37	
COALSACK D−6A	12 28 21.7	−63 30 30	

NAME	RA (1950)	DEC	POS REF
	h m s	° ' "	
COALSACK D−7	12 28 23.0	−63 29 05	
COALSACK D−8	12 28 22.2	−63 23 47	
COALSACK D−9	12 28 25.5	−63 23 37	
COALSACK D−10	12 28 31.4	−63 23 52	
COALSACK D−11	12 28 33.1	−63 24 33	
COALSACK D−11A	12 28 38.7	−63 24 21	
COALSACK D−12	12 28 38.7	−63 26 07	
COALSACK D−13	12 28 45.7	−63 24 16	
COALSACK D−14	12 28 48.2	−63 30 55	
COALSACK D−15	12 28 58.6	−63 31 10	
COALSACK D−15A	12 28 53.0	−63 32 34	
COALSACK D−15B	12 29 00.5	−63 27 43	
COALSACK D−16	12 29 06.2	−63 25 48	
COALSACK D−17	12 29 07.9	−63 27 07	
COALSACK D−18	12 29 07.6	−63 25 09	
COALSACK D−19	12 29 07.9	−63 30 58	
COALSACK D−20	12 29 12.3	−63 27 13	
COALSACK D−21	12 29 19.2	−63 26 43	
COALSACK D−22	12 29 19.1	−63 23 32	
COALSACK D−23	12 28 39.9	−63 27 11	
COALSACK D−24	12 28 30.9	−63 27 21	
COALSACK D−26	12 29 02.4	−63 27 36	
COALSACK D−27	12 28 41.5	−63 27 49	
COALSACK D−28	12 28 50.6	−63 28 41	
COALSACK D−29	12 28 56.0	−63 29 39	
COALSACK D−30	12 28 59.2	−63 29 50	
COALSACK D−31	12 28 51.7	−63 29 52	
COALSACK D−32	12 28 29.5	−63 29 53	
COALSACK D−33	12 28 24.7	−63 29 50	
COALSACK D−34	12 28 32.3	−63 30 11	
COALSACK D−35	12 28 42.2	−63 30 22	
COALSACK D−37	12 28 38.7	−63 30 38	
COALSACK D−38	12 28 48.8	−63 30 54	
COALSACK E−1	12 28 01.8	−63 14 43	
COALSACK E−2	12 28 02.4	−63 20 58	
COALSACK E−3	12 28 04.2	−63 18 27	
COALSACK E−4	12 28 11.8	−63 21 30	
COALSACK E−5	12 28 18.5	−63 18 17	
COALSACK E−6	12 28 25.3	−63 19 51	
COALSACK E−7	12 28 21.1	−63 14 54	
COALSACK E−9	12 28 39.2	−63 18 16	
COALSACK E−10	12 28 41.1	−63 15 05	
COALSACK E−11	12 28 49.8	−63 14 31	
COALSACK E−12	12 28 51.8	−63 21 27	
COALSACK E−13	12 28 49.1	−63 23 12	
COALSACK E−14	12 28 52.9	−63 19 23	
COALSACK E−15	12 28 51.4	−63 19 53	
COALSACK E−16	12 28 53.4	−63 21 30	
COALSACK E−17	12 28 55.3	−63 15 16	
COALSACK E−18	12 28 59.7	−63 16 40	
COALSACK E−19	12 28 59.2	−63 14 51	
COALSACK E−20	12 29 02.9	−63 16 36	
COALSACK E−22	12 29 03.9	−63 18 12	
COALSACK E−23	12 29 04.5	−63 21 10	
COALSACK E−24	12 29 05.3	−63 23 26	
COALSACK E−25	12 29 10.0	−63 16 49	
COALSACK E−26	12 29 11.2	−63 15 15	
COALSACK E−27	12 29 20.7	−63 19 41	
COALSACK F−4	12 28 00.7	−63 34 46	
COALSACK F−9B	12 28 40.4	−63 33 06	
COALSACK F−12	12 28 38.7	−63 34 29	
COALSACK F−13A	12 28 48.0	−63 34 29	
COALSACK F−14	12 28 44.6	−63 34 09	
COALSACK F−14A	12 28 54.3	−63 33 03	
COALSACK F−18	12 29 10.3	−63 33 05	
COALSACK F−20	12 29 17.6	−63 35 46	
COALSACK F−22	12 29 19.8	−63 34 44	
COALSACK F−23	12 29 21.9	−63 36 56	
COALSACK 1−1	12 31 02	−63 26 08	
COALSACK 1−2	12 30 26	−63 27 02	
COALSACK 1−3	12 30 16	−63 25 32	
COALSACK 2−1	12 29 07	−63 27 25	
COALSACK 2−2	12 28 22	−63 29 07	
COALSACK 3−1	12 27 14	−63 30 49	
COALSACK 9−1	12 33 12	−62 55 56	
COHEN IRS	6 31 59.0	+ 4 15 09	731003
ALF COL	5 37 50.2	−34 05 57	CSI 79
RV COL	5 33 49.9	−30 51 24	"
S COL	5 45 03.7	−31 42 25	"
T COL	5 17 27.4	−33 45 28	"
BET COM	13 09 32.3	+28 07 51	"
GQ COM	12 02 08.9	+28 10 53	809908
R COM	12 01 41.6	+19 03 38	CSI 79
W COM	12 19 01.1	+28 30 36	809908
14 COM	12 23 54.1	+27 32 41	CSI 79
31 COM	12 49 15.7	+27 48 45	"
36 COM	12 56 27.0	+17 40 41	"
40 COM	13 03 56.5	+22 53 00	"
CORDOBA 12403	18 00 42.2	−24 21 21	740903
CP−44 3129	8 48 17.2	−44 23 24	CSI 79
CP−45 3218	8 51 38.5	−45 50 45	"
CP−46 3272	8 55 13.7	−46 51 07	"
CP−52 9243	16 03 06	−52 55	
CP−52 9243	16 03 12	−52 56	
CP−56 8032	17 04 47.5	−56 51 00	
CP−56 8032	17 04 48	−56 51	
CP−57 2874	10 13 36	−57 37	730001
CP−57 3502	10 33 48.9	−57 59 09	CSI 79
CP−57 3635ABC	10 37 13.9	−58 21 23	
CP−57 3635IRS	10 37 32.9	−58 23 13	
CP−59 2505	10 40 50.6	−59 56 19	
CP−59 2505IR2	10 40 51.5	−59 54 41	
CP−59 2505IR3	10 40 58.9	−59 57 09	
CP−59 2505IR4	10 40 31.3	−59 53 36	
CP−61 2935	12 02 12.8	−61 43 23	CSI 79
CP−62 1837ABC	10 56 17.5	−62 35 57	
CRA H−H	18 58 28.3	−37 02 27	
AM CRA	18 37 51.1	−37 31 55	CSI 79
DG CRA	18 58 32	−37 27 54	GCVS
NOVA CRA 1981	18 38 33.6	−37 34 09	819915
QT CRA	18 05 42.0	−40 12 48	CSI 79
R CRA	18 54 23.9	−37 01 57	"
R CRA	18 58 31.4	−37 01 30	
R CRA	18 58 31.5	−37 01 22	
R CRA #A	18 58 28.3	−37 02 27	740103
R CRA #A2	18 58 39.2	−37 12 08	CD
R CRA #B	18 57	−37 02	ED
R CRA #B2	18 58	−37 13	"

NAME	RA (1950)	DEC	POS REF
	h m s	° ' "	
R CRA #C	18 56 54.7	−37 02 49	CD
R CRA #C2	18 58	−37 09	ED
R CRA #D	18 57	−37 01	"
R CRA #D2	19 00	−37 22	"
R CRA #E	18 58	−37 05	"
R CRA #E2	18 58	−37 03	"
R CRA #F	18 58	−37 09	"
R CRA #F2	18 58	−36 52	"
R CRA #G	18 58	−37 11	"
R CRA #G2	18 57	−36 59	"
R CRA #H	18 57	−37 11	"
R CRA #H2	18 55	−37 09	"
R CRA #I	18 58	−37 04	"
R CRA #I2	18 58	−37 05	"
R CRA #J	18 58	−37 10	"
R CRA #J2	18 58	−37 02	"
R CRA #K	18 57 41.6	−37 07 57	CSI 79
R CRA #K2	19 00	−36 58	ED
R CRA #L	18 57 40.5	−37 07 53	CSI 79
R CRA #L2	18 59	−37 03	ED
R CRA #M	18 58	−37 06	"
R CRA #N	18 58	−37 07	"
R CRA #O	18 58	−37 06	"
R CRA #P	18 58 16.5	−36 57 44	CSI 79
R CRA #Q	18 58	−36 54	ED
R CRA #R	18 58	−36 51	"
R CRA #S	18 58	−36 52	"
R CRA #T	18 58	−36 51	"
R CRA #U	18 59	−36 52	"
R CRA #V	18 59	−36 55	"
R CRA #W	18 59	−37 00	"
R CRA #X	18 58 39.8	−37 27 38	CD
R CRA #Y	18 59	−37 25	ED
R CRA #Z	18 58	−37 03	"
R CRA #6	18 57 48.2	−36 57 36	
R CRA #7	18 58 45.2	−36 57 34	
R CRA #10	18 59 54.1	−37 18 29	
R CRA #11	18 59 30.1	−37 14 14	
R CRA #12	19 00 16.1	−37 13 54	
R CRA #13	19 01 58.8	−37 30 03	761101
R CRA #17	18 57 56.2	−37 01 06	
R CRA #18	18 58 04.2	−37 03 36	
R CRA #36	19 06 21.0	−37 08 57	761101
R CRA #41	18 56 12.9	−37 04 25	"
R CRA #42	18 56 13.2	−37 11 42	"
S CRA	18 57 47.6	−37 01 21	CSI 79
T CRA	18 58 37	−37 02 18	GCVS
TY CRA	18 58 18.5	−36 56 50	CSI 79
TY CRA	18 58 19.5	−36 55 35	
V CRA	18 44 06.9	−38 12 50	CSI 79
VV CRA	18 59 44.1	−37 17 14	
VV CRA	18 59 45	−37 17 01	GCVS
WX CRA	18 05 25.9	−37 20 28	CSI 79
CRAB #A	5 31 30	+21 59 43	
CRAB #B	5 31 25	+22 00 00	
CRAB #C	5 31 35	+21 59 50	
CRAB #D	5 31 34	+21 57 55	
CRAB #E	5 31 28	+21 58 40	
CRAB NEBULA	5 31 30	+21 59	RNGC
CRAB NEBULA	5 31 31.7	+21 59 29	
CRAB PULSAR	5 31 31.5	+21 58 55	760601
CRAB 2' SW	5 31 22	+21 58	ED
ALF CRB	15 32 34.1	+26 52 53	CSI 79
DEL CRB	15 47 29.7	+26 13 11	"
EPS CRB	15 55 30.9	+27 01 16	"
KAP CRB	15 49 20.7	+35 48 39	"
R CRB	15 46 30.6	+28 18 31	"
RR CRB	15 39 36.2	+38 43 01	779907
RY CRB	16 21 07.8	+30 57 56	"
S CRB	15 19 19.0	+31 32 36	
S CRB	15 19 21.5	+31 32 46	779907
SIG CRB	16 12 48.1	+33 59 03	CSI 79
T CRB	15 57 24.4	+26 03 38	"
THE CRB	15 30 54.6	+31 31 35	"
THE 1 CRB	"	"	"
V CRB	15 47 44.0	+39 43 22	"
W CRB	16 13 37.3	+37 55 10	779907
X CRB	15 47 00.9	+36 23 59	"
Z CRB	15 54 13.4	+29 23 08	CSI 79
CRL 67	0 24 47.0	+69 22 16	
CRL 107	0 42 29	+68 55 36	
CRL 190	1 14 22.4	+66 58 00	
CRL 190	1 14 26.3	+66 58 08	
CRL 230	1 31 07.2	+62 11 31	
CRL 341	2 29 19.2	+57 49 27	
CRL 341	2 29 21.1	+57 48 53	
CRL 437	3 03 31.3	+58 19 19	
CRL 482	3 18 38	+70 16 54	
CRL 482	3 18 38.8	+70 16 27	
CRL 482	3 18 38.8	+70 16 47	
CRL 490	3 23 38.8	+58 36 39	
CRL 490	3 23 41.4	+58 36 52	
CRL 490	3 23 44.8	+58 36 48	
CRL 490	3 23 59	+58 35 24	
CRL 568	4 17 52.3	−13 34 26	
CRL 601	4 33 10	+16 23 18	
CRL 618	4 39 30	+36 01 48	
CRL 618	4 39 33.8	+36 01 15	
CRL 712	5 13 07.3	+45 30 50	
CRL 799	5 37 46.6	+13 46 45	
CRL 799	5 37 46.8	+13 46 55	
CRL 799	5 37 56	+13 45 42	
CRL 809	5 40 33.3	+32 40 49	
CRL 809	5 40 36	+32 41 06	
CRL 865	6 01 17.4	+ 7 26 06	
CRL 865	6 01 17.5	+ 7 26 03	
CRL 865	6 01 18	+ 7 25 24	
CRL 877	6 05 19	− 6 23 18	
CRL 877	6 05 22	− 6 22 30	
CRL 915	6 17 35	−10 36 00	
CRL 915	6 17 37.0	−10 36 52	
CRL 935	6 23 02	− 9 29 06	
CRL 935	6 23 04.7	− 9 30 21	
CRL 935	6 23 04.8	− 9 30 57	
CRL 954	6 29 05.8	+43 19 30	
CRL 956	6 30 00.3	+60 58 48	
CRL 961	6 31 57.1	+ 4 15 03	
CRL 961	6 31 57.3	+ 4 15 12	

NAME	RA (1950)	DEC	POS REF
	h m s	° ' "	
CRL 971	6 34 16.5	+ 3 28 04	
CRL 971	6 34 16.6	+ 3 28 07	
CRL 971	6 34 19	+ 3 26 24	
CRL 989	6 38 24.9	+ 9 32 29	
CRL 989	6 38 25.7	+ 9 32 16	
CRL 989	6 38 26	+ 9 32 18	
CRL 1011	6 44 03.1	− 4 20 18	
CRL 1047	6 56 21.2	−19 05 48	
CRL 1059	7 01 22.6	−11 28 36	
CRL 1062	7 02 48.8	−14 56 21	
CRL 1062	7 02 49.4	−14 56 23	
CRL 1085	7 09 53.7	−20 12 18	
CRL 1085	7 09 53.8	−20 12 20	
CRL 1085	7 09 54.9	−20 13 06	
CRL 1085	7 09 55	−20 13 18	
CRL 1099	7 15 15.8	−34 44 14	
CRL 1101	7 16 31.4	−15 47 46	
CRL 1113	7 22 40.3	−21 22 11	
CRL 1162	7 37 43.2	−21 35 38	
CRL 1164	7 38 10.8	−23 18 25	
CRL 1192	7 44 34.0	−26 13 11	
CRL 1198	7 48 42.7	−34 44 32	
CRL 1235	8 08 51.3	−32 43 07	
CRL 1235	8 08 51.6	−32 43 08	
CRL 1258	8 27 13.3	− 6 09 00	
CRL 1274	8 35 44.3	−10 13 40	
CRL 1274	8 35 44.5	−10 13 40	
CRL 1274	8 35 44.6	−10 13 41	
CRL 1274	8 35 52	−10 16 42	
CRL 1283	8 39 06	+ 2 21 42	
CRL 1283	8 39 10.1	+ 2 22 05	
CRL 1283	8 39 10.6	+ 2 22 08	
CRL 1283	8 39 12.2	+ 2 22 48	
CRL 1368	9 36 50.0	+78 04 41	
CRL 1686	14 08 38	− 7 33 54	
CRL 1686	14 08 39.0	− 7 30 44	
CRL 1686	14 08 39.5	− 7 30 42	
CRL 1686	14 08 40.0	− 7 30 32	
CRL 1771	15 22 35.9	−36 03 26	
CRL 1822	16 02 59	−30 40 30	
CRL 1822	16 02 59.6	−30 41 25	
CRL 1822	16 02 59.6	−30 41 33	
CRL 1822	16 02 59.7	−30 40 48	
CRL 1830	16 07 20.0	−27 46 30	
CRL 1922	17 04 53	−24 39 00	
CRL 1922	17 04 54.4	−24 40 39	
CRL 1922	17 04 54.6	−24 40 39	
CRL 1922	17 04 54.8	−24 40 36	
CRL 1937	17 11 35.5	−33 22 45	
CRL 1954	17 16 14.3	−19 34 40	
CRL 1954	17 16 14.4	−19 34 41	
CRL 1992	17 36 01.9	−30 12 54	
CRL 1992	17 36 02.7	−30 12 55	
CRL 1992	17 36 03.0	−30 12 46	
CRL 1992	17 36 05	−30 13 18	
CRL 2004	17 43 03.6	−28 48 41	
CRL 2015	17 47 21.0	−27 51 12	
CRL 2015	17 47 22.1	−27 51 08	
CRL 2019	17 50 11.1	−26 55 57	
CRL 2019	17 50 11.2	−26 56 00	
CRL 2019	17 50 13.4	−26 56 20	
CRL 2023	17 51 13.6	−25 49 04	
CRL 2023	17 51 13.7	−25 49 03	
CRL 2023	17 51 13.9	−25 49 00	
CRL 2046	17 57 24.5	−24 03 56	
CRL 2047	17 58 11.0	−17 44 22	
CRL 2059	18 01 48.8	−24 26 56	
CRL 2059	18 01 49.0	−24 27 00	
CRL 2080 NOM.	18 06 59	−24 07 24	ED
CRL 2085	18 07 53.4	−20 22 48	
CRL 2086	18 08 26.0	−26 30 49	
CRL 2086	18 08 26.2	−26 30 03	
CRL 2086	18 08 26.2	−26 30 15	
CRL 2088	18 09 17.1	− 4 37 11	
CRL 2088	18 09 17.3	− 4 37 11	
CRL 2096	18 11 59.2	−22 44 53	
CRL 2096	18 11 59.2	−22 45 14	
CRL 2096	18 11 59.6	−22 44 59	
CRL 2104	18 13 36.7	−18 59 48	
CRL 2104	18 13 36.8	−18 59 48	
CRL 2104	18 13 37.0	−18 59 49	760604
CRL 2104	18 13 41	−19 00 00	
CRL 2110	18 14 41.8	−22 15 46	
CRL 2110	18 14 42.0	−22 15 53	
CRL 2110	18 14 44.6	−22 15 40	
CRL 2113	18 15 25.6	−11 46 24	
CRL 2118	18 15 37.2	− 6 53 03	
CRL 2118	18 15 37.2	− 6 53 06	
CRL 2118	18 15 38.2	− 6 53 01	
CRL 2121	18 16 09.7	−20 46 30	
CRL 2132	18 18 26.7	−13 02 52	
CRL 2132	18 18 26.9	−13 02 52	
CRL 2132	18 18 29	−13 04 18	
CRL 2135	18 19 26.7	−27 08 02	
CRL 2135	18 19 26.9	−27 08 05	
CRL 2135	18 19 27.5	−27 08 03	
CRL 2136	18 19 36.6	−13 31 40	
CRL 2136	18 19 36.9	−13 31 47	
CRL 2136	18 19 39.3	−13 31 18	
CRL 2143	18 21 38.7	−16 17 45	
CRL 2154	18 23 57.0	− 6 55 35	
CRL 2154	18 23 57.5	− 6 55 55	
CRL 2154	18 23 57.9	− 6 55 55	
CRL 2155	18 24 00.4	+23 26 50	
CRL 2155	18 24 00.8	+23 27 01	
CRL 2161	18 24 29.3	−12 01 36	
CRL 2165	18 24 59	− 3 51 30	
CRL 2165	18 25 00.9	− 3 51 29	
CRL 2165	18 25 00.9	− 3 51 39	
CRL 2165	18 25 01.6	− 3 51 44	
CRL 2170	18 26 44.7	− 6 06 45	
CRL 2171	18 27 37.2	+82 36 52	
CRL 2174	18 28 26.4	− 9 46 54	
CRL 2174	18 28 27.0	− 9 47 14	
CRL 2174	18 28 28.5	− 9 47 02	
CRL 2178	18 28 50	− 8 38 12	
CRL 2178	18 28 52.4	− 8 37 27	
CRL 2178	18 28 52.7	− 8 37 41	

NAME	RA (1950) DEC	POS REF
CRL 2178	18 28 54 − 8 38	
CRL 2179	18 28 55 −10 00 18	
CRL 2179	18 28 56.5 −10 01 24	
CRL 2179	18 28 56.8 −10 01 31	
CRL 2179	18 28 59 −10 00 36	
CRL 2188A	18 30 41.6 − 9 06 10	
CRL 2188B	18 30 56.1 − 9 11 31	
CRL 2192	18 31 29.0 −11 31 47	
CRL 2192	18 31 29.1 −11 31 54	
CRL 2192	18 31 29.6 −11 31 45	
CRL 2192	18 31 37 −11 33 18	
CRL 2199	18 33 18.9 + 5 33	
CRL 2199	18 33 19.2 + 5 33 16	
CRL 2199	18 33 19.6 + 5 33 17	
CRL 2205	18 34 47 − 5 27 42	
CRL 2205	18 34 51.9 − 5 26 35	
CRL 2205	18 34 52.3 − 5 26 34	
CRL 2205	18 34 52.5 − 5 26 42	
CRL 2208	18 35 13 +38 44 30	
CRL 2222	18 37 20.7 − 0 21 26	
CRL 2222	18 37 20.9 − 0 21 27	
CRL 2222	18 37 21.3 − 0 21 30	
CRL 2259	18 47 25 + 9 29 30	
CRL 2259	18 47 31.1 + 9 26 34	
CRL 2259	18 47 31.6 + 9 26 39	
CRL 2266	18 49 23.6 +12 08 50	
CRL 2266	18 49 25.5 +12 09 30	
CRL 2290	18 56 03.8 + 6 38 52	
CRL 2290	18 56 04 + 6 38 18	
CRL 2290	18 56 04.1 + 6 38 50	
CRL 2316	19 02 57.0 + 8 07 51	
CRL 2316	19 02 58.2 + 8 08 28	
CRL 2316	19 03 00.0 + 8 08 20	
CRL 2318	19 02 56.9 +20 17 25	
CRL 2318	19 02 57.1 +20 17 26	
CRL 2341	19 10 52.3 +10 49 30	
CRL 2341	19 10 53 +10 48 06	
CRL 2350	19 13 25.6 + 9 32	
CRL 2350	19 13 28 + 9 34 06	
CRL 2350	19 13 28.9 + 9 31 39	
CRL 2350	19 13 30.9 + 9 31 38	
CRL 2361	19 15 46.5 −17 06 36	
CRL 2362	19 16 06.9 +23 43 58	
CRL 2362	19 16 08.0 +23 43 53	
CRL 2370	19 17 48.1 −26 20 02	
CRL 2370	19 17 50.8 −26 20 18	
CRL 2370	19 17 51.5 −26 20 22	
CRL 2392	19 24 48.8 + 6 58 06	
CRL 2392	19 24 49.0 + 6 57 36	
CRL 2413	19 30 42.9 +13 38 14	
CRL 2425	19 36 08.7 −16 58 50	
CRL 2428	19 38 06.9 +33 15 04	
CRL 2428	19 38 07.6 +33 15 27	
CRL 2445	19 42 15.7 +35 06 52	
CRL 2445	19 42 16.1 +35 06 50	
CRL 2474	19 53 46 +22 14 06	
CRL 2477	19 54 49.2 +30 35 54	
CRL 2477	19 54 55.9 +30 35 55	
CRL 2494	19 59 21 +40 45 42	
CRL 2494	19 59 24.5 +40 47 30	
CRL 2494	19 59 24.8 +40 47 18	
CRL 2513	20 07 13 +31 17 42	
CRL 2513	20 07 15.0 +31 16 52	
CRL 2513	20 07 22.1 +31 17 30	
CRL 2591	20 27 25 +40 01 54	
CRL 2591	20 27 35.9 +40 01 05	
CRL 2591	20 27 35.9 +40 01 16	
CRL 2603	20 30 57.3 +40 29 32	
CRL 2604	20 31 09.0 +42 22 24	
CRL 2604	20 31 09.1 +42 22 43	
CRL 2613	20 34 04.4 +53 38 57	
CRL 2613	20 34 08 +53 39 00	
CRL 2679	20 54 56.3 +37 13 36	
CRL 2686	20 56 59.8 +27 14 59	
CRL 2686	20 57 00.5 +27 15 08	
CRL 2686	20 57 09 +27 15 48	
CRL 2688	21 00 16 +36 30 00	
CRL 2688	21 00 19.9 +36 29 45	
CRL 2699	21 02 42.9 +53 09 07	
CRL 2699	21 02 43.3 +53 09 00	
CRL 2699	21 02 49 +53 08 54	
CRL 2789	21 38 10.4 +50 00 35	
CRL 2789	21 38 10.4 +50 00 44	
CRL 2881	22 16 32.0 +43 31 45	
CRL 2881	22 16 36 +43 31 00	
CRL 2885	22 17 41 +59 35 24	
CRL 2885	22 17 42.1 +59 36 06	
CRL 2885	22 17 42.7 +59 36 17	
CRL 2901	22 24 04 +60 04 30	
CRL 2901	22 24 08.1 +60 05 25	
CRL 2985	22 51 51.9 +66 00 49	
CRL 2999	22 55 00.3 +58 32 39	
CRL 2999	22 55 29 +58 34 18	
CRL 2999	22 55 39.5 +58 33 28	
CRL 3011	22 58 29.7 +64 02 38	
CRL 3011	22 58 32.0 +64 02 44	
CRL 3011	22 58 47 +64 02 48	
CRL 3022	23 03 52.3 +59 58 45	
CRL 3068	23 16 42.4 +16 55 10	
CRL 3068	23 16 42.6 +16 55 07	
CRL 3068	23 16 43 +16 55 06	
CRL 3068	23 16 43.1 +16 55 05	
CRL 3099	23 25 43.5 +10 37 55	
CRL 3099	23 25 45 +10 38 24	
CRL 3099	23 25 45.0 +10 38 08	
CRL 3099	23 25 45.0 +10 38 14	
CRL 3099	23 25 45.6 +10 38 03	
CRL 3181	23 54 05.5 +70 31 35	
CRL 825−2650	19 49 33.0 + 8 36 13	
CRL 825−2650	19 49 33.1 + 8 35 08	
R CRT	10 58 05.9 −18 03 20	CSI 79
R CRT	10 58 09.0 −18 03 36	
S CRT	11 50 11.6 − 7 19 04	CSI 79
THE CRT	11 34 08.5 − 9 31 30	"
AZ CRU	12 08 53 −61 29 36	GCVS
GAM CRU	12 28 22.7 −56 49 59	CSI 79
MUU 2 CRU	12 51 39.5 −56 53 49	"
V CRU	12 53 38.4 −57 38 16	"

NAME	RA (1950) DEC	POS REF
Z CRU	12 08 32.9 −64 10 58	"
BET CRV	12 31 45.3 −23 07 12	"
DEL CRV	12 27 16.3 −16 14 12	"
GAM CRV	12 13 13.7 −17 15 50	"
R CRV	12 17 02.3 −18 58 40	"
ZET CRV	12 17 57.9 −21 56 15	"
CR228 IRS6	10 41 49.4 −59 47 25	
CR228 IRS7	10 41 41.4 −59 49 16	
CR228−67,68	10 42 04.9 −59 50 19	
CSS 3	0 05 07 −62 36	
CSS 30	1 30 53.6 −79 13 02	CSI 79
CSS 64	4 03 04.0 +24 35 52	"
CSS 76	4 37 25.7 −30 33 13	"
CSS 79	4 31 08 −84 16	
CSS 98	5 19 54.7 − 8 42 46	CSI 79
CSS 102	5 22 25 −33 54	
CSS 105	5 26 29 −51 14	
CSS 125	5 57 09.6 −38 04 33	CSI 79
CSS 140	6 11 09 −39 32	
CSS 142	6 11 40 −60 57	
CSS 149	6 24 10.5 +15 55 40	CSI 79
CSS 154	6 30 49 −26 08	
CSS 155	6 31 18 −43 52	
CSS 164	6 38 00 −34 50	
CSS 167	6 38 29 −27 39	
CSS 169	6 38 52 −38 58	
CSS 179	6 45 40 + 5 36	
CSS 200	6 59 10 −29 02	
CSS 218	7 14 51 −30 14	
CSS 226	7 20 49 −45 11	
CSS 233	7 24 42.9 −11 37 06	CSI 79
CSS 239	7 27 16 −53 31	
CSS 241	7 28 57 −30 56	
CSS 253	7 29 13 −82 37	
CSS 257	7 38 03.5 −70 13 55	CSI 79
CSS 259	7 40 41 −25 43	
CSS 266	7 47 32.3 −18 52 45	CSI 79
CSS 270	7 50 43.5 −11 29 38	"
CSS 277	7 53 04.9 −60 27 02	"
CSS 285	7 56 47 −71 24	
CSS 286	7 59 30.0 −31 39 17	CSI 79
CSS 287	8 02 24 −41 53	
CSS 290	8 02 21 −65 41	
CSS 294	8 07 24 −30 41	
CSS 296	8 09 51 −28 09	
CSS 300	8 14 54 −26 32	
CSS 301	8 16 26 −29 47	
CSS 302	8 16 40 −32 39	
CSS 307	8 19 58 −37 08	
CSS 311	8 23 31 −35 38	
CSS 316	8 30 27 −29 50	
CSS 320	8 34 55 −36 17	
CSS 324	8 41 08 −86 39	
CSS 325	8 39 00 −51 12	
CSS 326	8 39 04 −49 14	
CSS 327	8 40 16 −38 54	
CSS 328	8 41 37 −32 20	
CSS 331	8 45 48 −45 47	
CSS 333	8 46 10 −70 52	
CSS 335	8 49 04 −50 26	
CSS 339	8 54 49 −70 58	
CSS 346	9 01 42 −40 21	
CSS 350	9 06 15 −33 20	
CSS 352	9 07 02 −28 48	
CSS 353	9 06 59 −41 45	
CSS 354	9 08 09 −34 13	
CSS 363	9 35 55 −65 36	
CSS 366	9 39 59 −46 42	
CSS 368	9 41 21 −64 17	
CSS 374	9 47 09 −61 11	
CSS 377	9 54 53 −32 44	
CSS 378	9 57 17 −49 43	
CSS 379	10 01 35 −46 33	
CSS 382	10 03 53 −60 55	
CSS 384	10 04 41 −51 37	
CSS 385	10 04 38 −59 54	
CSS 386	10 05 18 −46 02	
CSS 387	10 05 36 −40 16	
CSS 388	10 05 18 −60 43	
CSS 390	10 13 53.7 −30 45 21	CSI 79
CSS 391	10 13 40 −60 46	
CSS 392	10 15 10 −54 38	
CSS 393	10 16 23 −60 44	
CSS 399	10 25 35 −51 58	
CSS 401	10 30 51 −67 08	
CSS 406	10 36 03 −60 20	
CSS 409	10 38 58.3 −51 49 25	CSI 79
CSS 410	10 42 00 −56 23	
CSS 412	10 42 14 −54 49	
CSS 418	10 55 08.3 −52 49 57	CSI 79
CSS 419	10 55 19 −60 26	
CSS 421	10 59 55 −56 15	
CSS 422	11 00 43.6 −56 00 05	CSI 79
CSS 427	11 07 49 −59 59	
CSS 429	11 16 17 −65 52	
CSS 439	11 58 25.7 −55 48 40	CSI 79
CSS 443	12 21 55 −28 03	
CSS 444	12 23 48 −52 09	
CSS 445	12 16 12 −47 36	
CSS 447	12 31 12 −42 19	
CSS 451	12 40 49 −53 27	
CSS 453	13 07 57.3 −89 31 16	CSI 79
CSS 454	12 46 28 −42 48	
CSS 455	12 50 31 −46 54	
CSS 457	12 58 11 −66 38	
CSS 458	12 59 58 −60 42	
CSS 460	13 07 29 −72 56	
CSS 461	13 09 20.3 −56 43 59	CSI 79
CSS 462	13 11 52 −31 10	
CSS 467	13 32 47 −50 57	
CSS 468	13 37 15.3 −71 36 57	CSI 79
CSS 472	13 45 56.7 −55 08 02	"
CSS 476	13 59 43.7 −41 44 49	"
CSS 484	14 29 47 −25 57	
CSS 486	14 48 31.4 −37 46 18	CSI 79
CSS 488	14 51 00.7 −60 52 21	"
CSS 494	15 21 01 −32 52	
CSS 508	16 38 05 −57 27	

NAME	RA (1950) DEC	POS REF
CSS 509	16 39 35 −55 43	
CSS 513	16 55 12 −53 34	
CSS 516	17 10 27 −32 20	
CSS 520	17 16 56 −23 12	
CSS 531	17 38 28.7 −53 56 50	CSI 79
CSS 541	18 00 38.6 −65 10 05	"
CSS 544	18 05 53.0 −36 58 29	"
CSS 623	19 47 42 −32 21	
CSS 636	20 10 05.1 −62 25 51	CSI 79
CSS 646	20 21 21.3 + 0 44 37	"
CSS 647	20 23 09 −40 46	
CSS 681	21 17 17 −48 19	
CSS 686	21 30 48 −25 59	
CSS 703	22 20 02 −54 12	
CSS 709	22 42 09 −45 08	
CSS 718	22 52 07.5 +16 40 29	CSI 79
CSS 725	23 15 19 −86 04	
CSV 2694	16 26 14 −53 23	
CTA 102	22 30 07.7 +11 28 23	809908
ALF 2 CVN	12 53 41.5 +38 35 17	779907
BET CVN	12 31 22.2 +41 37 43	CSI 79
R CVN	13 46 48.4 +39 47 27	779907
T CVN	12 27 43.8 +31 46 46	"
TU CVN	12 52 39.7 +47 28 03	"
TX CVN	12 42 17.8 +37 02 15	"
U CVN	12 44 57.0 +38 38 24	
U CVN	12 44 59.6 +38 38 35	CSI 79
V CVN	13 17 17.1 +45 47 22	779907
Y CVN	12 42 47.0 +45 42 48	"
10 CVN	12 42 37.6 +39 32 59	CSI 79
20 CVN	13 15 18.1 +40 50 06	"
CW 1103+254	11 03 +25 24	ED
CYG A	19 58 31.0 +40 39 36	720901
CYG OB II−12	20 30 53.4 +41 04 12	"
CYG OB2 #26	20 32 30 +41 10	ED
CYG OB2 #27	20 33 00 +41 07	"
CYG OB2 #28	20 32 21.1 +41 26 38	CSI 79
CYG OB2 #29	20 32 25 +41 24 30	ED
CYG OB2 #30	20 33 00 +41 18	"
CYG OB2 #31	20 30 55 +41 05 30	"
CYG OB2 #32	20 30 55 +41 04 10	"
CYG OB2 #33	20 30 55 +41 07	"
CYG OB2 #34	" "	"
CYG OB2 #35	20 31 00 +41 05 30	"
CYG OB2 #36	20 31 00 +41 05 00	"
CYG OB2 #37	20 31 00 +41 04 30	"
CYG OB2 #38	20 31 00 +41 02	"
CYG OB2 #39	20 31 10 +41 02	"
CYG OB2 #40	20 31 10 +41 04 00	"
CYG OB2 #41	20 31 10 +41 04 30	"
CYG OB2 #111	20 31 30 +41 16	
CYG OB2 #210	" "	
CYG OB2 #266	" "	
CYG OB2 #274	" "	
CYG OB2 #280	" "	
CYG OB2 #284	" "	
CYG OB2 #295	" "	
CYG OB2 #303	" "	
CYG OB2 #311	" "	
CYG OB2 #312	" "	
CYG OB2 #324	" "	
CYG OB2 #349	" "	
CYG OB2 #360	" "	
CYG OB2 #392	" "	
CYG OB2 #413	" "	
CYG OB2 #426	" "	
CYG OB2 #451	" "	
CYG OB2 #492	" "	
CYG OB2 #500	" "	
CYG OB2 #502	" "	
CYG OB2 #545	" "	
CYG OB2 #560	" "	
CYG OB2 #570	" "	
CYG OB2 #603	" "	
CYG OB2 #629	" "	
CYG OB2 #661	" "	
CYG OB2 #662	" "	
CYG OB2 #664	" "	
CYG OB2 #666	" "	
CYG OB2 #668	" "	
CYG OB2 #680	" "	
CYG OB2 #683	" "	
CYG OB2 #689	" "	
CYG OB2 #692	" "	
CYG OB2 #702	" "	
CYG OB2 #706	" "	
CYG OB2 #738	" "	
CYG OB2 #741	" "	
CYG OB2 #748	" "	
CYG OB2 #749	" "	
CYG OB2 #766	" "	
CYG OB2 #814	" "	
CYG OB2 #815	" "	
CYG OB2 #840	" "	
CYG OB2 #841	" "	
CYG OB2 #852	" "	
CYG OB2 #853	" "	
CYG OB2 #856	" "	
CYG OB2 #887	" "	
CYG OB2 #920	" "	
CYG OB2 #922	" "	
CYG OB2 #953	" "	
CYG OB2 #984	" "	
CYG OB2 #986	" "	
CYG OB2 #1029	" "	
CYG OB2 #1030	" "	
CYG OB2 #1031	" "	
CYG OB2 #1032	" "	
CYG OB2 #1069	" "	
CYG OB2 #1074	" "	
CYG OB2 #1076	" "	
CYG OB2 #1093	" "	
CYG OB2 #1121	" "	
CYG OB2 #1144	" "	
CYG OB2 #1171	" "	
CYG OB2 #1245	" "	
CYG OB2 #1252	" "	
CYG OB2 #1359	" "	

NAME	RA (1950) DEC	POS REF
CYG OB2 #1384	h m s " ° ' " "	
CYG OB2 #1419	" "	
CYG OB2 #1420	" "	
CYG OB2 #1430	" "	
CYG OB2 #1489	" "	
CYG OB2 #1492	" "	
CYG OB2 #1494	" "	
CYG OB2 #1512	" "	
CYG OB2 #1542	" "	
CYG OB2 #1590	" "	
CYG OB2 #1592	" "	
CYG OB2 B	20 31 26.9 +41 08 32	CSI 79
CYG OB2 D	20 31 28.4 +41 08 43	"
CYG OB2 E	20 31 30 +41 16	
CYG OB2 IRS1	20 31 22.9 +41 04 48	
CYG OB2 IRS2	20 31 26.4 +41 10 04	
CYG OB2 IRS3	20 31 37.8 +41 10 29	
CYG OB2 IRS4	20 31 44.0 +41 08 35	
CYG OB2 IRS5	20 31 43.0 +41 05 02	
CYG OB2 IRS6	20 31 51.3 +41 09 08	
CYG OB2 IRS7	20 31 51.9 +41 12 15	
CYG OB2 NOM.	20 31 30 +41 16	ED
CYG OB2 1	20 29 20 +41 21	"
CYG OB2 2	20 29 30 +41 21	"
CYG OB2 3	20 29 49.9 +41 03 08	CSI 79
CYG OB2 4	20 30 26.3 +41 16 57	"
CYG OB2 5	20 30 34.7 +41 08 04	779907
CYG OB2 6	20 31 00 +41 17	ED
CYG OB2 7	20 31 26.5 +41 10 04	819910
CYG OB2 8A	20 31 27.3 +41 08 31	CSI 79
CYG OB2 8B	20 31 26.9 +41 08 32	"
CYG OB2 8C	20 31 28.4 +41 08 43	"
CYG OB2 8D	20 31 30.3 +41 08 13	829906
CYG OB2 9	20 31 23.0 +41 04 51	819910
CYG OB2 10	20 31 58.6 +41 22 39	CSI 79
CYG OB2 11	20 32 21.1 +41 26 38	"
CYG OB2 12	20 30 53.4 +41 04 12	780403
CYG OB2 15	20 30 40 +41 16 40	ED
CYG OB2 16	20 30 50 +41 16 20	"
CYG OB2 19	20 32 20 +41 08 50	"
CYG OB2 21	20 30 40 +41 17 20	"
CYG OB2 22	20 31 20 +41 03	"
CYG OB2 23	20 31 25 +41 09	"
CYG OB2 24	20 31 30 +41 06	"
CYG X	20 19 36 +40 06	
CYG X FIR 1	20 20 56 +39 59 25	
CYG X FIR 2	20 21 41 +41 17 51	
CYG X FIR 3	20 22 18 +39 48 52	
CYG X FIR 4	20 22 26 +37 37 41	
CYG X FIR 5	20 25 48 +37 03 04	
CYG X FIR 6	20 25 51 +39 58 45	
CYG X FIR 7	20 25 54 +39 21 50	
CYG X FIR 8	20 26 31 +37 37 02	
CYG X FIR 9	20 26 55 +40 49 31	
CYG X FIR 10	20 28 03 +40 04 54	
CYG X FIR 11	20 28 08 +41 23 18	
CYG X FIR 12	20 28 40 +38 58 07	
CYG X FIR 13	20 30 04 +37 19 14	
CYG X FIR 14	20 30 28 +36 28 29	
CYG X FIR 15	20 30 49 +41 03 51	
CYG X FIR 16	20 30 54 +43 00 02	
CYG X FIR 17	20 30 57 +41 57 24	
CYG X FIR 18	20 30 59 +38 53 40	
CYG X FIR 19	20 31 13 +39 23 49	
CYG X FIR 20	20 31 33 +40 16 07	
CYG X FIR 21	20 31 55 +46 17 07	
CYG X FIR 22	20 31 58 +43 43 32	
CYG X FIR 23	20 32 03 +45 16 29	
CYG X FIR 24	20 32 19 +41 16 32	
CYG X FIR 25	20 33 19 +42 04 00	
CYG X FIR 26	20 33 21 +39 46 54	
CYG X FIR 27	20 33 40 +41 06 17	
CYG X FIR 28	20 34 31 +40 29 05	
CYG X FIR 29	20 35 02 +41 15 33	
CYG X FIR 30	20 35 06 +42 37 16	
CYG X FIR 31	20 35 52 +41 50 41	
CYG X FIR 32	20 36 35 +38 33 43	
CYG X FIR 33	20 36 47 +42 24 21	
CYG X FIR 34	20 36 59 +40 27 56	
CYG X FIR 35	20 37 23 +43 10 22	
CYG X FIR 36	20 37 24 +42 06 20	
CYG X FIR 37	20 37 37 +39 13 07	
CYG X FIR 38	20 37 57 +41 04 26	
CYG X FIR 39	20 38 52 +41 42 46	
CYG X FIR 40	20 40 22 +38 40 29	
CYG X FIR 41	20 40 35 +42 41 00	
CYG X FIR 42	20 43 53 +43 56 03	
CYG X FIR 43	20 44 43 +40 48 36	
CYG X FIR 44	20 44 54 +39 13 27	
CYG X FIR 45	20 45 41 +43 16 55	
CYG X FIR 46	20 47 29 +44 21 46	
CYG X FIR 47	20 51 45 +44 18 55	
CYG X FIR 48	20 52 16 +47 11 50	
CYG X FIR 49	20 54 43 +43 21 07	
CYG X−1	19 56 28.7 +35 03 54	CSI 79
CYG X−3	20 30 34 +40 47 17	ED
CYG X−3	20 30 37.6 +40 47 13	
CYG XR−1	19 52 19 +32 47	
AB CYG	21 34 24.4 +31 52 38	CSI 79
AC CYG	20 11 21.3 +49 17 56	779907
AF CYG	19 28 43.1 +46 02 31	"
ALF CYG	20 39 43.4 +45 06 02	CSI 79
AW CYG	19 27 17.9 +45 56 22	"
AX CYG	19 55 35.7 +44 07 33	779907
AZ CYG	20 56 15.8 +46 16 22	"
BC CYG	20 19 46.6 +37 22 21	"
BET CYG	19 28 42.2 +27 51 11	CSI 79
BET 1 CYG	" "	"
BET 2 CYG	19 28 44.3 +27 51 31	"
BF CYG	19 21 55.0 +29 34 31	"
BG CYG	19 36 55 +28 23 47	GCVS
BI CYG	20 19 29.1 +36 46 20	779907
CH CYG	19 23 14.1 +50 08 31	"
CHI CYG	19 48 38.5 +32 47 11	"
CI CYG	19 48 20.6 +35 33 23	"
DEL CYG	19 43 24.6 +45 00 27	CSI 79
DF CYG	19 47 15.7 +42 54 40	779907
DG CYG	20 41 37 +43 00 53	GCVS

NAME	RA (1950) DEC	POS REF
DT CYG	h m s ° ' " 21 04 24.2 +30 58 58	CSI 79
EM CYG	19 36 42 +30 23 41	GCVS
EPS CYG	20 44 11.1 +33 46 54	CSI 79
ETA CYG	19 54 25.7 +34 56 57	"
GAM CYG	20 20 25.9 +40 05 43	"
KY CYG	20 24 06 +38 11 16	GCVS
LAM CYG	20 45 27.4 +36 18 20	CSI 79
LW CYG	21 53 27.1 +50 16 08	"
MUU 1 CYG	21 41 54.2 +28 30 56	"
NML CYG	20 44 33.9 +39 55 58	
NML CYG	20 44 39 +39 56	650701
NOVA CYG 1975	21 09 53 +47 56 42	GCVS
NOVA CYG 1978	21 40 38.1 +43 48 11	780911
NOVA CYG 1980	21 40 46.2 +31 13 45	801210
P CYG	20 15 56.5 +37 52 35	779907
R CYG	19 35 28.7 +50 05 12	"
RHO CYG	21 32 05.7 +45 22 11	CSI 79
RS CYG	20 11 34.6 +38 34 36	779907
RT CYG	19 42 12.5 +48 39 26	"
RU CYG	21 38 58.6 +54 05 49	"
RV CYG	21 41 11.9 +37 47 17	"
RW CYG	20 27 01.5 +39 48 52	"
RY CYG	20 08 30.4 +35 47 53	"
RZ CYG	20 50 12.5 +47 10 00	"
S CYG	20 04 27.6 +57 51 14	"
SIG CYG	21 15 26.9 +39 11 03	CSI 79
SS CYG	21 40 43.9 +43 21 21	779907
ST CYG	20 31 14.6 +54 46 44	"
SU CYG	19 42 48.4 +29 08 33	CSI 79
SV CYG	20 07 58.7 +47 43 24	779907
SX CYG	20 13 36.1 +30 55 03	CSI 79
TT CYG	19 39 01.9 +32 30 02	779907
TU CYG	19 44 48.7 +48 57 16	CSI 79
TW CYG	21 03 41.7 +29 19 27	"
U CYG	20 18 03.4 +47 44 09	779907
UPS CYG	21 15 51.5 +34 41 09	CSI 79
UX CYG	20 52 59.1 +30 13 19	"
UX CYG	20 53 00.0 +30 13 24	
V CYG	20 39 41.3 +47 57 44	CSI 79
VI CYG 3		
VI CYG 5	20 30 34.8 +41 08 04	779907
VI CYG 7	20 31 26.5 +41 10 04	819910
VI CYG 8C	20 31 28.4 +41 08 43	CSI 79
VI CYG 9	20 31 23.0 +41 04 51	819910
VI CYG 10	20 31 58.6 +41 22 39	CSI 79
VI CYG 11	20 32 21.1 +41 26 38	"
VI CYG 12	20 30 53.4 +41 04 12	780403
VI CYG 103		
VI CYG 629		
VI CYG #1245		
VI CYG #1359		
VI CYG A		
V360 CYG	21 08 28.7 +30 28 02	CSI 79
V425 CYG	20 06 12.1 +35 58 39	779907
V441 CYG	20 25 14.0 +36 23 09	"
V444 CYG	20 17 42.6 +38 34 24	"
V457 CYG	20 35 57 +30 14 39	GCVS
V460 CYG	21 39 54.4 +35 16 53	779907
V517 CYG	20 45 37 +43 33 54	GCVS
V644 CYG	21 38 19 +45 10 34	"
V645 CYG	21 38 12 +50 00 46	"
V717 CYG	19 59 05 +30 42 12	"
V729 CYG	20 30 34.8 +41 08 04	779907
V786 CYG	20 13 29 +59 35 09	GCVS
V1016 CYG	19 55 19.9 +39 41 38	CSI 79
V1042 CYG	20 10 00.8 +36 02 49	779907
V1057 CYG	20 57 06 +44 03 49	GCVS
V1195 CYG	20 22 43 +55 01 43	"
V1329 CYG	20 49 02.6 +35 23 37	749903
V1331 CYG	20 59 31 +50 09 45	GCVS
V1515 CYG	20 22 03 +42 03	769913
W CYG	21 34 08.3 +45 09 00	779907
WX CYG	20 16 41.6 +37 17 34	"
X CYG	20 41 26.6 +35 24 24	"
XI CYG	21 03 06.5 +43 43 38	CSI 79
Z CYG	20 00 00.0 +49 54 06	
Z CYG	20 00 02.4 +49 54 09	779907
ZET CYG	21 10 48.3 +30 01 14	CSI 79
16 CYG A	19 40 29.0 +50 24 29	"
16 CYG B	19 40 32.0 +50 24 02	"
29 CYG	20 12 39.5 +36 39 06	"
44 CYG	20 29 05.1 +36 45 58	"
55 CYG	20 47 13.9 +45 55 40	"
61 CYG	21 04 39.9 +38 29 58	"
61 CYG A	" "	"
61 CYG B	21 04 38.3 +38 29 29	"
62 CYG	21 03 06.5 +43 43 38	"
68 CYG	21 16 35.1 +43 44 04	"
75 CYG	21 38 13.1 +43 02 45	"
CYGNUS EGG	21 00 16 +36 30 00	
CYGNUS LOOP	20 40 +41 50	ED
CYGNUS REGION	20 42 +41 48	
C1715−387 NOM	17 15 36 −38 46	ED
C1715−387 1	" "	
C1715−387 2	" "	
C1715−387 3	" "	
C1715−387 6	17 15 36 −33 46	
EU DEL	20 35 37.7 +18 05 29	CSI 79
GAM DEL	20 44 20.1 +15 56 37	"
NOVA DEL 1967	20 40 04 +18 58 47	GCVS
R DEL	20 12 30.2 + 8 56 07	CSI 79
RS DEL	20 26 51.2 +16 06 20	"
S DEL	20 40 46.5 +16 54 26	"
T DEL	20 43 01.9 +16 12 57	"
TX DEL	20 47 41.9 + 3 27 53	"
U DEL	20 43 10.7 +17 54 25	"
V DEL	20 45 28.1 +19 08 54	"
X DEL	20 52 35.6 +17 27 00	"
Y DEL	20 39 16 +11 41 50	GCVS
Z DEL	20 30 21.7 +17 16 48	CSI 79
1 DEL	20 27 54.2 +10 43 37	"
DK 2	2 37 −34	
DK 3	" "	
DK 4	" "	
DK 6	" "	
DK 7	" "	
DK 10	" "	
DK 22	" "	

NAME	RA (1950) DEC	POS REF
DK 33	h m s " ° ' " "	
DK 46	" "	
DK 49	" "	
DK 58	" "	
DK 60	" "	
DK 64	" "	
DKH 6737	" "	
DKH 11179	" "	
DKH 11325	" "	
DO−AR 9	16 16 11 −23 09	599902
DO−AR 21	16 23 01.7 −24 16 50	780902
DO−AR 24	16 23 15.8 −24 13 37	"
DO−AR 24E	16 23 21.4 −24 14 13	
DO−AR 24E	16 23 22.0 −24 14 15	780902
DO−AR 51	16 29 08 −24 34	599902
DO−AR 52	16 29 20 −24 34	"
DO−AR 58	16 31 25.0 −24 07 32	729902
DOR #1	5 37 51.4 −69 04 14	
DOR #2	5 38 11.1 −69 06 00	
DOR #3	5 38 15.7 −69 10 44	
DOR #4	5 38 27.2 −69 05 29	
DOR #5	5 38 30.9 −69 08 04	
DOR #6	5 38 37.7 −69 11 50	
DOR #7	5 38 37.9 −69 05 40	
DOR #8	5 38 38.5 −69 05 51	
DOR #9	5 38 44.7 −69 12 04	
DOR #10	5 38 48.6 −69 10 33	
DOR #11	5 38 51.4 −69 02 53	
DOR #12	5 39 02.2 −69 05 35	
DOR #13	5 39 02.6 −69 09 53	
DOR #14	5 39 02.8 −69 06 56	
DOR #15	5 39 03.7 −69 07 42	
DOR #16	5 39 04.8 −69 06 36	
DOR #17	5 39 05.8 −69 07 20	
DOR #18	5 39 09.5 −69 07 13	
DOR #19	5 39 12.7 −69 09 49	
DOR #20	5 39 17.5 −69 09 18	
DOR #21	5 39 26.9 −69 03 33	
DOR #22	5 39 48.2 −69 13 12	
DOR #23	5 40 01.9 −69 13 24	
DOR #24	5 40 04.0 −69 13 03	
BET DOR	5 33 11.3 −62 31 19	CSI 79
R DOR	4 36 10.3 −62 10 30	"
S DOR	5 18 34.3 −69 18 00	"
T DOR	4 45 02.2 −59 52 33	"
U DOR	5 09 52.9 −64 22 53	"
30 DOR #1	5 38 32 −69 07 35	
30 DOR #2	5 38 42 −69 06 35	
30 DOR #3	5 38 42 −69 07 35	
30 DOR #4	5 38 42 −69 08 35	
30 DOR #5	5 38 42 −69 09 35	
30 DOR #6	5 38 48 −69 06 05	
30 DOR #7	5 38 48 −69 07 05	
30 DOR #8	5 38 48 −69 07 35	
30 DOR #9	5 38 48 −69 08 05	
30 DOR #10	5 38 48 −69 08 35	
30 DOR #11	5 38 54 −69 06 35	
30 DOR #12	5 38 54 −69 07 05	
30 DOR #13	5 38 54 −69 07 35	
30 DOR #14	5 38 54 −69 08 05	
30 DOR #15	5 38 54 −69 08 35	
30 DOR #16	5 38 54 −69 09 35	
30 DOR #17	5 38 54 −69 10 05	
30 DOR #18	5 38 59 −69 05 05	
30 DOR #19	5 38 59 −69 05 35	
30 DOR #20	5 38 59 −69 06 05	
30 DOR #21	5 38 59 −69 06 35	
30 DOR #22	5 38 59 −69 07 05	
30 DOR #23	5 38 59 −69 07 35	
30 DOR #24	5 38 59 −69 08 05	
30 DOR #25	5 38 59 −69 08 35	
30 DOR #26	5 39 04 −69 03 35	
30 DOR #27	5 39 04 −69 04 35	
30 DOR #28	5 39 04 −69 05 05	
30 DOR #29	5 39 04 −69 05 35	
30 DOR #30	5 39 04 −69 06 05	
30 DOR #31	5 39 04 −69 06 35	
30 DOR #32	5 39 04 −69 07 05	
30 DOR #33	5 39 04 −69 07 35	
30 DOR #34	5 39 04 −69 08 35	
30 DOR #35	5 39 04 −69 19 35	
30 DOR #36	5 39 04 −69 10 35	
30 DOR #37	5 39 09 −69 05 35	
30 DOR #38	5 39 09 −69 06 05	
30 DOR #39	5 39 09 −69 06 35	
30 DOR #40	5 39 09 −69 07 05	
30 DOR #41	5 39 09 −69 08 05	
30 DOR #42	5 39 14 −69 05 05	
30 DOR #43	5 39 14 −69 05 35	
30 DOR #44	5 39 14 −69 06 05	
30 DOR #45	5 39 14 −69 06 35	
30 DOR #46	5 39 14 −69 07 05	
30 DOR #47	5 39 14 −69 07 35	
30 DOR #48	5 39 14 −69 08 35	
30 DOR #49	5 39 19 −69 05 35	
30 DOR #50	5 39 19 −69 06 05	
30 DOR #51	5 39 19 −69 06 35	
30 DOR #52	5 39 19 −69 07 05	
30 DOR #53	5 39 24 −69 05 05	
30 DOR #54	5 39 24 −69 06 05	
30 DOR #55	5 39 24 −69 07 05	
30 DOR #56	5 39 24 −69 07 35	
30 DOR #57	5 39 29 −69 06 05	
30 DOR #58	5 39 34 −69 07 35	
30 DOR IR 1	5 37 51.4 −69 04 14	
30 DOR IR 2	5 38 11.1 −69 06 00	
30 DOR IR 3	5 38 15.7 −69 10 44	
30 DOR IR 4	5 38 27.2 −69 05 29	
30 DOR IR 5	5 38 30.9 −69 08 04	
30 DOR IR 6	5 38 37.7 −69 11 50	
30 DOR IR 7	5 38 37.9 −69 05 40	
30 DOR IR 8	5 38 38.5 −69 05 51	
30 DOR IR 10	5 38 48.6 −69 10 33	
30 DOR IR 11	5 38 51.4 −69 02 53	
30 DOR IR 13	5 39 02.6 −69 09 53	
30 DOR IR 14	5 39 02.8 −69 06 56	
30 DOR IR 15	5 39 03.7 −69 07 42	
30 DOR IR 16	5 39 04.8 −69 06 36	

NAME	RA (1950)	DEC	POS REF
30 DOR IR 17	5 39 05.8	−69 07 20	
30 DOR IR 18	5 39 09.5	−69 07 13	
30 DOR IR 19	5 39 12.7	−69 09 49	
30 DOR IR 20	5 39 17.5	−69 09 18	
30 DOR IR 21	5 39 32.5	−69 03 36	
30 DOR IR 22	5 39 48.2	−69 13 12	
30 DOR IR 23	5 40 01.9	−69 13 24	
30 DOR IR 24	5 40 04.0	−69 13 03	
30 DOR IR 25	5 39 27.3	−69 03 28	
30 DOR IR 26	5 39 33.6	−69 03 44	
30 DOR IR 27	5 39 18.9	−69 07 38	
30 DOR IR 28	5 39 03.9	−69 07 20	
30 DOR IR 29	5 39 05.4	−69 06 47	
30 DOR IR 30	5 38 55.1	−69 06 26	
30 DOR IR 31	5 39 05.4	−69 06 29	
30 DOR IR 32	5 38 57.0	−69 07 46	
30 DOR IR 33	5 38 57.1	−69 07 35	
30 DOR IR 34	5 38 58.6	−69 06 42	
30 DOR IR 35	5 38 37.4	−69 05 50	
DR 4	20 20 20	+40 00	
DR 5	20 24 25	+40 00	
DR 6	20 25 25	+39 21	
DR 7	20 26 25	+40 47	
DR 12	20 30 45	+39 18	
DR 13	20 30 05	+39 49	
DR 15	20 30 34	+40 04 24	
DR 15	20 30 50	+40 13	
DR 15 #A	20 30 34	+40 04 24	
DR 15 #B	20 30 22	+40 03 00	
DR 17	20 34	+42 20	ED
DR 20	20 35	+41 30	”
DR 21	20 37 12	+42 09	
DR 21	20 37 13	+42 09	
DR 21	20 37 13.5	+42 03 51	
DR 21	20 37 14	+42 08 55	ED
DR 21	20 37 14	+42 09 00	
DR 21	20 37 14.0	+42 09 00	ED
DR 21	20 37 14.1	+42 09 18	”
DR 21	20 37 14.2	+42 09 07	
DR 21	20 37 14.3	+42 09 25	ED
DR 21	20 37 14.8	+42 08 57	770208
DR 21	20 37 14.9	+42 09 12	
DR 21	20 37 21.9	+42 09 18	
DR 21	20 38	+42 10	ED
DR 21 A	20 37 13.7	+42 08 57	
DR 21 B	20 37 14.0	+42 09 03	
DR 21 B(0.2E)	20 37 14.2	+42 09 03	
DR 21 C(0.1E)	20 37 14.2	+42 08 54	
DR 21 D	20 37 14.2	+42 09 16	
DR 21 H2	20 37 21.9	+42 09 18	
DR 21 IRS	20 37 14.8	+42 08 57	
DR 21 N	20 37 12.7	+42 09 09	770104
DR 21 N	20 37 14.0	+42 09 17	
DR 21 N	20 37 14.5	+42 09 20	ED
DR 21 N+S	20 37 12.7	+42 09 09	
DR 21 OH	20 37 14	+42 11 45	ED
DR 21 OH	20 37 14	+42 12 00	
DR 21 OH	20 37 14.1	+42 09 18	770208
DR 21 OH	20 37 14.5	+42 12 00	
DR 21 POS1	20 37 17	+42 10 25	ED
DR 21 POS2	20 37 17	+42 09 18	”
DR 21 POS3	20 37 19	+42 09 45	”
DR 21 POS4	20 37 19	+42 09 18	”
DR 21 POS5	20 37 19	+42 08 45	”
DR 21 POS6	20 37 22	+42 10 25	”
DR 21 POS7	20 37 22	+42 09 45	”
DR 21 POS8	20 37 22	+42 10 25	”
DR 21 POS9	20 37 25	+42 09 45	”
DR 21 POS10	20 37 25	+42 08 45	”
DR 21 POS11	20 37 27	+42 10 25	”
DR 21 S	20 37 13.3	+42 09 04	
DR 22	20 38	+41 10	ED
DR 23	20 39	+41 50	”
AB DRA	19 51 04	+77 37 03	GCVS
AC DRA	20 19 53.1	+68 43 14	779907
AG DRA	16 01 23.3	+66 56 25	”
AH DRA	16 47 23.9	+57 54 00	”
BET DRA	17 29 17.9	+52 20 15	CSI 79
BY DRA	18 32 44.5	+51 40 58	779907
CM DRA	16 33 24	+57 14 48	GCVS
GAM DRA	17 55 26.5	+51 29 37	CSI 79
KAP DRA	12 31 21.5	+70 03 48	”
LAM DRA	11 28 27.5	+69 36 25	”
R DRA	16 32 31.3	+66 51 31	779907
RY DRA	12 54 28.3	+66 15 53	”
SIG DRA	19 32 27.5	+69 34 33	CSI 79
SV DRA	18 32 21.6	+49 19 52	”
T DRA	17 55 36.1	+58 13 11	779907
TX DRA	16 34 17.3	+60 34 09	”
TY DRA	17 36 11.7	+57 46 08	”
U DRA	19 09 56.5	+67 12 00	CSI 79
UX DRA	19 23 22.4	+76 27 42	779907
V DRA	17 57 15.9	+54 52 47	CSI 79
W DRA	18 05 30.5	+65 56 56	779907
WZ DRA	16 58 39.6	+52 23 28	”
X DRA	18 06 50.2	+66 08 48	”
Y DRA	9 37 23.4	+78 04 55	CSI 79
ZET DRA	17 08 38.1	+65 46 33	”
64 DRA	20 00 56.9	+64 40 49	”
D0637.2+09ABC	6 39 53.0	+ 9 04 08	
D0637.2+09IRS	6 39 56	+ 9 07 06	
D1827.6−08ABC	18 30 19.8	− 8 47 13	
D1827.6−08IR1	18 30 34.3	− 8 46 06	
D1827.6−08IR3	18 30 28.7	− 8 48 33	
D1827.6−08IR5	18 30 22.7	− 8 44 16	
D1827.6−08IR6	18 30 24.3	− 8 49 21	
D1827.6−08IR7	18 30 14.5	− 8 48 37	
D1827.6−08IR8	18 30 11.6	− 8 50 36	
EIC 1	0 04 28.3	+ 5 00 34	
EIC 2	0 05 44.0	− 9 06 07	
EIC 3	0 11 54.1	− 8 03 29	
EIC 4	0 16 52.6	− 9 00 53	
EIC 5	0 17 30.6	+ 6 00 55	
EIC 6	0 17 35.5	+ 2 45 19	
EIC 7	0 18 01.1	+ 7 54 47	
EIC 8	0 23 07.1	+ 7 24 51	
EIC 9	0 24 33.3	− 6 52 51	
EIC 10	0 34 55.8	+ 2 51 37	
EIC 11	0 42 20.7	+ 2 55 39	
EIC 12	0 45 41.7	+ 7 01 39	
EIC 13	0 46 05.1	+ 7 18 45	
EIC 14	0 50 26.9	− 1 24 55	
EIC 15	0 57 13.8	+ 6 12 49	
EIC 16	1 00 20.4	+ 7 37 17	
EIC 17	1 02 16.9	+ 5 23 17	
EIC 18	1 11 34.7	+ 7 02 52	
EIC 19	1 17 08.3	+ 5 53 57	
EIC 20	1 21 31.0	− 8 26 32	
EIC 21	1 25 45.6	+ 7 42 09	
EIC 22	1 27 34.1	+ 5 53 09	
EIC 23	1 28 03.0	+ 2 37 25	
EIC 24	1 30 40.7	+ 7 57 08	
EIC 25	1 34 05.9	+ 7 34 36	
EIC 26	1 38 49.4	+ 5 14 04	
EIC 27	1 42 00.5	+ 2 58 21	
EIC 28	1 45 50.4	+ 3 26 11	
EIC 29	1 51 58.9	+ 4 28 00	
EIC 30	1 57 34.8	+ 6 40 34	
EIC 31	1 57 57.8	− 8 45 55	
EIC 32	2 00 00.2	+ 7 26 11	
EIC 33	2 03 33.3	+ 8 00 35	
EIC 34	2 05 09.5	+ 5 44 51	
EIC 35	2 11 25.3	− 9 17 51	
EIC 36	2 15 38.3	+ 6 28 22	
EIC 37	2 16 49.0	− 3 12 19	
EIC 38	2 19 22.7	+ 0 10 03	
EIC 39	2 26 19.8	+ 8 09 24	
EIC 40	2 32 24.9	+ 7 15 10	
EIC 41	2 33 23.1	+ 6 39 32	
EIC 42	2 33 32.1	− 8 02 54	
EIC 43	2 33 55.7	+ 7 30 46	
EIC 44	2 49 47.0	− 8 28 17	
EIC 45	2 53 58.9	− 9 05 51	
EIC 46	2 54 27.1	+ 4 18 01	
EIC 47	2 59 39.6	+ 3 53 37	
EIC 48	3 04 04.9	− 6 16 50	
EIC 49	3 05 57.7	+ 8 16 50	
EIC 50	3 09 46.7	+ 6 28 26	
EIC 51	3 12 50.5	+ 1 30 03	
EIC 52	3 28 09.5	− 2 06 27	
EIC 53	3 37 49.3	+ 4 57 54	
EIC 54	3 43 29.0	+ 6 38 55	
EIC 55	3 46 20.6	− 7 10 00	
EIC 56	3 48 54.6	− 1 31 12	
EIC 57	4 01 24.3	+ 2 24 04	
EIC 58	4 06 30.3	− 8 13 56	
EIC 59	4 08 36.3	+ 8 09 33	
EIC 60	4 13 00.0	+ 6 06 21	
EIC 61	4 13 24.2	+ 7 48 21	
EIC 62	4 18 01.1	+ 6 00 43	
EIC 63	4 26 59.6	+ 5 03 21	
EIC 64	4 29 19.0	− 0 08 54	
EIC 65	4 31 46.8	− 8 20 04	
EIC 66	4 31 48.0	− 6 56 28	
EIC 67	4 33 44.6	− 5 22 22	
EIC 68	4 35 31.6	+ 8 14 12	
EIC 69	4 36 04.9	+ 6 43 19	
EIC 70	4 39 40.0	+ 6 47 00	
EIC 71	4 47 08.3	+ 6 52 31	
EIC 72	4 48 19.9	+ 7 36 50	
EIC 73	4 49 37.4	+ 8 26 04	
EIC 74	4 50 46.1	+ 2 25 36	
EIC 75	4 52 05.3	+ 7 41 56	
EIC 76	4 55 57.2	+ 1 38 24	
EIC 77	4 58 29.5	+ 5 15 59	
EIC 78	4 59 03.4	+ 6 35 36	
EIC 79	5 02 48.6	+ 1 06 37	
EIC 80	5 04 01.7	+ 0 28 57	
EIC 81	5 05 22.1	+ 7 50 03	
EIC 82	5 09 00.8	+ 8 32 55	
EIC 83	5 09 26.1	+ 6 48 00	
EIC 84	5 10 40.2	+ 2 48 10	
EIC 85	5 12 03.6	− 0 37 09	
EIC 86	5 12 04.4	+ 5 06 00	
EIC 87	5 12 07.8	− 8 15 29	
EIC 88	5 12 29.6	+ 6 30 38	
EIC 89	5 18 05.3	+ 8 38 31	
EIC 90	5 18 31.1	+ 7 18 24	
EIC 91	5 21 31.8	− 7 51 09	
EIC 92	5 22 02.2	− 6 11 28	
EIC 93	5 22 26.8	+ 6 18 19	
EIC 94	5 25 39.2	+ 8 39 02	
EIC 95	5 26 32.6	− 4 43 51	
EIC 96	5 27 11.5	− 1 07 47	
EIC 97	5 29 13.1	+ 7 34 39	
EIC 98	5 30 31.6	+ 7 07 08	
EIC 99	5 30 35.8	+ 8 30 16	
EIC 100	5 32 32.6	+ 8 40 06	
EIC 101	5 35 06.9	− 1 47 59	
EIC 102	5 35 38.2	+ 8 27 34	
EIC 103	5 39 53.1	+ 1 27 10	
EIC 104	5 46 02.3	+ 7 51 42	
EIC 105	5 49 50.3	+ 1 50 35	
EIC 106	5 51 11.6	+ 8 26 15	
EIC 107	5 51 38.3	+ 3 13 02	
EIC 108	5 52 27.7	+ 7 23 56	
EIC 109	5 56 21.5	+ 8 55 37	
EIC 110	5 59 15.8	− 2 21 11	
EIC 111	5 59 27.2	+ 8 27 07	
EIC 112	6 00 26.8	+ 7 37 42	
EIC 113	6 02 52.9	+ 7 32 32	
EIC 114	6 07 04.5	+ 8 45 16	
EIC 115	6 08 06.9	+ 3 46 03	
EIC 116	6 08 58.0	− 7 14 16	
EIC 117	6 10 18.7	+ 6 01 49	
EIC 118	6 10 25.6	− 7 17 07	
EIC 119	6 12 24.9	− 6 15 28	
EIC 120	6 14 58.2	+ 8 32 20	
EIC 121	6 17 29.1	− 2 55 14	
EIC 122	6 18 07.9	+ 5 45 50	
EIC 123	6 18 26.1	+ 2 35 36	
EIC 124	6 19 15.5	+ 7 22 26	
EIC 125	6 19 46.0	+ 3 26 59	
EIC 126	6 20 12.3	− 2 10 06	
EIC 127	6 21 04.0	+ 8 31 30	
EIC 128	6 21 08.0	+ 8 30 49	
EIC 129	6 21 24.5	+ 8 28 09	
EIC 130	6 22 08.7	+ 3 47 31	
EIC 131	6 23 57.0	+ 8 39 55	
EIC 132	6 26 10.6	+ 6 47 44	
EIC 133	6 26 37.9	+ 2 40 48	
EIC 134	6 26 50.8	− 8 03 58	
EIC 135	6 26 51.2	+ 8 49 18	
EIC 136	6 27 19.1	+ 7 57 19	
EIC 137	6 27 41.2	+ 8 05 44	
EIC 138	6 27 41.6	+ 9 03 35	
EIC 139	6 31 39.7	+ 9 07 31	
EIC 140	6 31 56.0	+ 5 00 28	
EIC 141	6 32 40.3	− 1 28 06	
EIC 142	6 33 18.8	− 5 20 07	
EIC 143	6 34 59.1	− 1 21 02	
EIC 144	6 35 13.2	+ 7 46 23	
EIC 145	6 36 11.0	+ 5 14 11	
EIC 146	6 36 26.0	+ 8 46 53	
EIC 147	6 37 52.2	− 6 17 57	
EIC 148	6 39 34.8	+ 7 26 48	
EIC 149	6 42 03.1	+ 3 22 06	
EIC 150	6 42 21.2	+ 9 05 28	
EIC 151	6 42 50.5	+ 8 05 30	
EIC 152	6 43 48.5	+ 9 15 30	
EIC 153	6 44 22.7	+ 8 04 11	
EIC 154	6 44 36.0	+ 1 35 05	
EIC 155	6 44 36.7	+ 8 05 32	
EIC 156	6 45 15.0	+ 2 28 07	
EIC 157	6 45 21.5	+ 8 20 12	
EIC 158	6 48 18.7	− 0 00 47	
EIC 159	6 49 18.0	+ 4 49 31	
EIC 160	6 50 03.5	+ 8 29 00	
EIC 161	6 50 13.4	+ 8 43 35	
EIC 162	6 52 55.6	+ 6 26 36	
EIC 163	6 53 29.7	+ 8 48 41	
EIC 164	6 54 35.5	+ 8 38 39	
EIC 165	6 55 07.6	+ 3 22 14	
EIC 166	6 55 40.7	+ 6 14 07	
EIC 167	6 58 31.7	− 3 10 49	
EIC 168	6 59 29.0	− 5 38 55	
EIC 169	6 59 37.1	− 3 40 54	
EIC 170	7 02 54.6	+ 9 15 46	
EIC 171	7 04 14.6	+ 8 57 19	
EIC 172	7 04 31.0	− 7 28 42	
EIC 173	7 05 58.4	+ 4 15 24	
EIC 174	7 07 44.7	− 4 09 20	
EIC 175	7 10 21.3	− 2 42 41	
EIC 176	7 11 15.7	− 3 51 46	
EIC 177	7 11 41.3	− 3 48 53	
EIC 178	7 11 42.8	+ 3 11 52	
EIC 179	7 12 09.5	+ 4 14 21	
EIC 180	7 12 31.4	+ 8 28 19	
EIC 181	7 12 56.6	+ 8 03 56	
EIC 182	7 12 58.2	+ 6 00 34	
EIC 183	7 12 59.4	+ 5 08 56	
EIC 184	7 14 56.6	+ 8 53 12	
EIC 185	7 16 25.0	+ 3 37 27	
EIC 186	7 19 21.2	+ 3 12 10	
EIC 187	7 21 30.3	+ 8 59 45	
EIC 188	7 22 54.8	+ 9 22 33	
EIC 189	7 24 21.2	+ 9 08 43	
EIC 190	7 24 34.2	+ 3 39 50	
EIC 191	7 25 26.1	+ 9 01 40	
EIC 192	7 30 00.1	+ 8 25 33	
EIC 193	7 32 22.3	+ 6 18 15	
EIC 194	7 33 51.5	− 8 11 56	
EIC 195	7 36 39.7	+ 5 20 47	
EIC 196	7 38 37.1	+ 8 29 51	
EIC 197	7 39 18.5	− 4 03 32	
EIC 198	7 42 54.4	+ 5 19 48	
EIC 199	7 43 35.0	− 6 38 56	
EIC 200	7 49 29.9	+ 3 24 26	
EIC 201	7 51 01.4	+ 9 07 56	
EIC 202	7 53 51.2	+ 6 32 24	
EIC 203	7 58 40.8	− 1 15 10	
EIC 204	7 59 39.6	+ 2 28 27	
EIC 205	8 03 02.7	+ 6 46 26	
EIC 206	8 03 29.2	+ 5 43 34	
EIC 207	8 09 11.4	+ 5 56 51	
EIC 208	8 09 53.4	+ 7 07 36	
EIC 209	8 13 48.1	+ 9 20 26	
EIC 210	8 14 58.0	+ 9 19 14	
EIC 211	8 16 47.5	− 7 24 00	
EIC 212	8 18 54.6	+ 5 07 04	
EIC 213	8 20 27.3	− 7 22 54	
EIC 214	8 20 49.6	+ 6 58 26	
EIC 215	8 22 01.9	− 8 21 27	
EIC 216	8 23 36.7	− 4 44 11	
EIC 217	8 27 13.1	− 6 09 01	
EIC 218	8 36 08.5	+ 3 31 06	
EIC 219	8 41 12.7	− 7 03 08	
EIC 220	8 43 45.8	+ 1 48 56	
EIC 221	8 44 07.2	+ 6 36 09	
EIC 222	8 45 36.6	− 6 22 22	
EIC 223	8 47 37.9	+ 9 27 29	
EIC 224	8 52 44.8	+ 6 08 12	
EIC 225	9 00 35.0	+ 8 24 40	
EIC 226	9 00 35.0	+ 7 00 47	
EIC 227	9 03 20.3	+ 5 17 34	
EIC 228	9 04 24.9	+ 1 39 53	
EIC 229	9 04 50.4	+ 6 31 28	
EIC 230	9 14 12.5	− 6 08 36	
EIC 231	9 18 02.6	+ 0 23 37	
EIC 232	9 20 49.7	+ 7 55 44	
EIC 233	9 22 53.7	− 4 54 08	
EIC 234	9 25 44.9	− 7 30 07	
EIC 235	9 25 46.9	+ 9 16 30	
EIC 236	9 25 49.4	+ 8 24 24	
EIC 237	9 32 01.7	+ 8 24 37	
EIC 238	9 32 02.9	− 5 41 29	
EIC 239	9 34 34.1	+ 7 03 38	
EIC 240	9 35 50.3	+ 4 52 32	
EIC 241	9 37 18.0	− 0 54 55	
EIC 242	9 43 31.6	+ 6 56 24	
EIC 243	9 43 48.2	+ 8 41 17	
EIC 244	9 51 05.3	+ 6 11 41	
EIC 245	9 51 29.8	+ 5 10 54	
EIC 246	9 52 16.5	+ 5 26 06	

NAME	RA (1950)	DEC	POS REF
	h m s	° ′ ″	
EIC 247	9 53 46.7	+ 9 10 14	
EIC 248	9 55 28.7	+ 8 33 10	
EIC 249	9 56 11.9	+ 5 02 53	
EIC 250	9 57 34.2	+ 8 17 03	
EIC 251	10 05 15.9	− 7 23 09	
EIC 252	10 06 37.7	+ 6 25 00	
EIC 253	10 06 52.2	+ 9 50 18	
EIC 254	10 19 35.8	+ 9 13 00	
EIC 255	10 20 23.6	+ 6 47 47	
EIC 256	10 22 37.0	+ 9 02 20	
EIC 257	10 23 13.8	− 6 48 19	
EIC 258	10 23 27.2	− 7 15 34	
EIC 259	10 28 28.2	− 7 22 48	
EIC 260	10 28 49.9	+ 9 36 31	
EIC 261	10 32 11.2	+ 7 12 42	
EIC 262	10 38 46.1	+ 8 49 25	
EIC 263	10 40 45.0	+ 5 00 39	
EIC 264	10 42 32.4	− 6 33 40	
EIC 265	10 46 07.1	− 1 41 41	
EIC 266	10 46 09.5	+ 8 55 48	
EIC 267	10 53 25.5	+ 6 27 06	
EIC 268	10 57 58.6	+ 3 53 11	
EIC 269	10 59 16.4	− 2 12 54	
EIC 270	10 59 40.6	+ 4 28 05	
EIC 271	11 01 05.3	− 2 56 04	
EIC 272	11 01 43.7	+ 5 29 40	
EIC 273	11 02 25.7	+ 7 36 20	
EIC 274	11 03 27.9	+ 1 28 49	
EIC 275	11 04 20.4	+ 2 13 36	
EIC 276	11 07 54.8	+ 8 09 47	
EIC 277	11 11 25.9	+ 8 20 01	
EIC 278	11 14 43.0	+ 2 17 07	
EIC 279	11 17 30.9	+ 5 55 27	
EIC 280	11 18 54.6	+ 4 12 41	
EIC 281	11 23 42.5	+ 8 56 03	
EIC 282	11 25 21.8	+ 3 07 53	
EIC 283	11 27 45.5	− 2 43 40	
EIC 284	11 28 52.4	+ 9 01 32	
EIC 285	11 30 14.6	− 7 33 04	
EIC 286	11 31 02.0	+ 2 46 30	
EIC 287	11 34 19.6	+ 9 48 20	
EIC 288	11 35 13.8	+ 4 35 59	
EIC 289	11 35 34.9	+ 9 09 37	
EIC 290	11 35 52.8	+ 8 24 38	
EIC 291	11 43 17.2	+ 6 48 28	
EIC 292	11 43 31.8	+ 7 27 05	
EIC 293	11 44 20.2	+ 1 52 53	
EIC 294	11 48 06.5	+ 2 02 39	
EIC 295	11 48 59.8	+ 7 09 15	
EIC 296	11 50 11.5	− 7 19 05	
EIC 297	11 51 30.5	+ 5 09 23	
EIC 298	11 52 28.9	+ 8 43 19	
EIC 299	11 55 10.9	+ 7 15 06	
EIC 300	11 55 40.1	+ 3 45 38	
EIC 301	11 56 49.9	+ 2 06 15	
EIC 302	12 00 01.2	+ 8 20 52	
EIC 303	12 00 17.6	− 7 24 18	
EIC 304	12 01 44.9	+ 5 12 36	
EIC 305	12 02 02.0	+ 2 53 53	
EIC 306	12 02 39.0	+ 9 00 38	
EIC 307	12 04 40.8	− 6 29 15	
EIC 308	12 07 12.7	+ 8 27 23	
EIC 309	12 17 47.7	+ 3 35 27	
EIC 310	12 19 41.6	+ 5 07 55	
EIC 311	12 21 38.2	+ 6 14 56	
EIC 312	12 22 40.5	+ 1 02 45	
EIC 313	12 25 09.2	+ 8 53 11	
EIC 314	12 27 47.8	+ 4 41 32	
EIC 315	12 28 48.7	+ 7 52 48	
EIC 316	12 30 35.5	+ 7 31 32	
EIC 317	12 35 49.0	+ 2 07 44	
EIC 318	12 35 57.4	+ 7 15 47	
EIC 319	12 36 39.2	− 7 43 15	
EIC 320	12 39 17.1	+ 6 08 30	
EIC 321	12 39 43.1	+ 4 33 59	
EIC 322	12 43 31.0	+ 7 43 03	
EIC 323	12 43 50.4	+ 9 48 54	
EIC 324	12 44 30.3	+ 9 20 12	
EIC 325	12 44 45.5	+ 4 25 02	
EIC 326	12 45 18.4	+ 3 50 44	
EIC 327	12 46 14.0	+ 7 38 13	
EIC 328	12 49 03.8	+ 3 19 44	
EIC 329	12 53 04.0	+ 3 40 05	
EIC 330	12 56 16.9	+ 8 28 46	
EIC 331	13 00 05.6	+ 5 27 13	
EIC 332	13 00 55.2	+ 5 10 35	
EIC 333	13 01 24.1	+ 7 20 08	
EIC 334	13 10 11.4	− 1 29 35	
EIC 335	13 10 52.6	+ 9 03 38	
EIC 336	13 11 24.3	+ 1 43 13	
EIC 337	13 11 29.6	− 2 32 34	
EIC 338	13 12 30.7	+ 4 46 51	
EIC 339	13 13 16.0	+ 8 13 01	
EIC 340	13 13 52.5	+ 6 46 05	
EIC 341	13 14 16.7	+ 9 41 08	
EIC 342	13 15 04.5	+ 5 43 56	
EIC 343	13 17 01.6	+ 8 54 25	
EIC 344	13 17 26.6	+ 8 44 57	
EIC 345	13 19 28.9	+ 3 01 05	
EIC 346	13 26 41.3	+ 4 07 44	
EIC 347	13 27 26.6	+ 6 16 14	
EIC 348	13 27 29.3	+ 7 26 11	
EIC 349	13 29 21.4	− 5 59 55	
EIC 350	13 30 23.1	− 6 56 19	
EIC 351	13 32 07.8	− 0 20 23	
EIC 352	13 32 56.1	− 4 08 03	
EIC 353	13 33 22.2	+ 8 32 49	
EIC 354	13 35 11.2	+ 2 38 09	
EIC 355	13 40 32.1	+ 3 47 22	
EIC 356	13 45 38.7	+ 8 04 08	
EIC 357	13 47 53.8	+ 5 44 40	
EIC 358	13 49 15.7	− 3 25 45	
EIC 359	13 52 07.5	− 1 15 23	
EIC 360	13 54 29.4	+ 6 49 05	
EIC 361	13 55 32.1	+ 7 42 21	
EIC 362	13 58 57.8	+ 9 32 24	
EIC 363	14 00 05.0	+ 8 08 14	
EIC 364	14 01 07.5	+ 7 47 08	
EIC 365	14 05 24.9	+ 8 19 27	
EIC 366	14 06 54.7	+ 5 11 59	
EIC 367	14 07 30.8	+ 7 34 42	
EIC 368	14 11 39.8	+ 8 06 49	
EIC 369	14 12 21.5	+ 3 34 05	
EIC 370	14 13 22.9	− 5 45 58	
EIC 371	14 14 41.8	+ 7 32 48	
EIC 372	14 17 05.1	+ 9 01 23	
EIC 373	14 18 55.8	+ 6 40 15	
EIC 374	14 21 50.2	+ 8 18 38	
EIC 375	14 23 25.6	+ 6 41 56	
EIC 376	14 24 45.7	+ 4 54 06	
EIC 377	14 25 58.8	+ 5 54 14	
EIC 378	14 26 02.9	− 6 40 38	
EIC 379	14 26 25.2	+ 3 56 33	
EIC 380	14 28 14.9	+ 4 59 35	
EIC 381	14 29 42.1	+ 4 21 45	
EIC 382	14 34 42.7	+ 4 41 02	
EIC 383	14 35 23.5	+ 3 44 15	
EIC 384	14 35 52.5	− 3 23 43	
EIC 385	14 37 35.4	+ 7 33 19	
EIC 386	14 39 11.1	+ 8 22 27	
EIC 387	14 39 22.0	− 3 18 38	
EIC 388	14 40 25.1	− 5 26 36	
EIC 389	14 43 08.4	+ 8 22 09	
EIC 390	14 44 15.9	+ 7 29 24	
EIC 391	14 44 33.5	+ 5 05 38	
EIC 392	14 46 01.1	+ 1 18 53	
EIC 393	14 51 11.0	+ 6 26 41	
EIC 394	14 52 54.5	+ 6 59 10	
EIC 395	14 52 59.0	+ 7 57 47	
EIC 396	14 54 59.1	+ 0 01 58	
EIC 397	14 56 08.3	− 0 21 19	
EIC 398	14 56 53.0	+ 4 45 57	
EIC 399	14 57 41.8	+ 3 27 33	
EIC 400	14 57 51.1	+ 7 50 44	
EIC 401	14 58 43.6	− 2 33 27	
EIC 402	14 59 14.9	+ 0 03 24	
EIC 403	14 59 23.2	− 8 08 54	
EIC 404	15 00 21.9	+ 2 17 12	
EIC 405	15 02 08.7	− 7 49 46	
EIC 406	15 04 35.0	+ 2 33 14	
EIC 407	15 04 52.9	+ 9 08 58	
EIC 408	15 05 05.6	+ 6 27 36	
EIC 409	15 05 11.0	+ 5 41 22	
EIC 410	15 05 58.0	− 0 49 18	
EIC 411	15 08 30.7	+ 3 22 19	
EIC 412	15 09 01.9	− 5 49 20	
EIC 413	15 10 03.4	− 0 11 39	
EIC 414	15 10 52.8	+ 8 25 49	
EIC 415	15 11 26.0	− 1 42 00	
EIC 416	15 12 11.8	− 5 19 00	
EIC 417	15 12 21.7	− 2 13 46	
EIC 418	15 12 41.9	+ 5 07 27	
EIC 419	15 13 25.4	+ 6 38 55	
EIC 420	15 13 30.7	+ 2 21 05	
EIC 421	15 15 49.5	+ 1 07 14	
EIC 422	15 15 51.8	− 0 16 45	
EIC 423	15 16 46.1	+ 1 56 56	
EIC 424	15 18 28.5	− 5 38 42	
EIC 425	15 18 28.9	+ 0 53 42	
EIC 426	15 21 11.3	+ 2 11 44	
EIC 427	15 21 34.3	+ 9 04 53	
EIC 428	15 22 19.4	− 2 03 34	
EIC 429	15 22 27.4	− 5 44 34	
EIC 430	15 26 13.3	+ 4 00 00	
EIC 431	15 27 58.2	+ 5 25 58	
EIC 432	15 28 19.3	− 4 00 57	
EIC 433	15 29 48.7	− 1 36 51	
EIC 434	15 29 53.8	+ 7 04 41	
EIC 435	15 29 54.4	+ 3 48 32	
EIC 436	15 30 23.1	− 1 01 04	
EIC 437	15 34 07.0	− 2 39 43	
EIC 438	15 34 13.1	− 5 51 46	
EIC 439	15 38 37.6	− 3 50 03	
EIC 440	15 41 01.3	− 1 33 09	
EIC 441	15 41 34.4	+ 2 32 50	
EIC 442	15 41 45.3	+ 8 17 52	
EIC 443	15 41 48.2	+ 6 34 53	
EIC 444	15 42 05.7	+ 8 16 09	
EIC 445	15 43 45.7	+ 6 15 54	
EIC 446	15 44 00.2	+ 7 30 27	
EIC 447	15 44 54.5	+ 1 42 01	
EIC 448	15 45 13.8	− 2 09 57	
EIC 449	15 45 18.8	+ 4 27 07	
EIC 450	15 45 20.4	+ 0 50 28	
EIC 451	15 46 18.2	− 0 50 56	
EIC 452	15 46 19.0	+ 5 33 16	
EIC 453	15 47 45.8	+ 2 20 49	
EIC 454	15 48 19.3	+ 4 37 36	
EIC 455	15 48 45.8	+ 8 01 12	
EIC 456	15 51 56.7	+ 5 26 22	
EIC 457	15 52 12.9	+ 4 52 26	
EIC 458	15 52 17.8	− 3 47 36	
EIC 459	15 52 18.0	+ 5 43 57	
EIC 460	15 52 21.9	− 2 01 53	
EIC 461	15 52 24.2	+ 8 43 48	
EIC 462	15 52 30.2	− 3 50 16	
EIC 463	15 53 13.2	+ 5 51 13	
EIC 464	15 53 39.9	+ 8 04 49	
EIC 465	15 54 19.2	− 0 48 43	
EIC 466	15 57 15.3	− 2 09 50	
EIC 467	15 57 28.9	+ 0 45 52	
EIC 468	15 58 04.2	+ 4 51 58	
EIC 469	15 58 21.9	+ 4 33 58	
EIC 470	15 59 11.2	+ 9 03 05	
EIC 471	15 59 59.8	− 8 21 23	
EIC 472	16 00 12.6	+ 8 59 02	
EIC 473	16 01 22.9	+ 3 51 50	
EIC 474	16 01 51.7	+ 6 08 49	
EIC 475	16 03 19.5	− 6 00 19	
EIC 476	16 04 23.1	− 3 44 37	
EIC 477	16 05 59.3	− 1 24 18	
EIC 478	16 06 03.1	+ 8 39 55	
EIC 479	16 06 11.6	+ 8 44 39	
EIC 480	16 06 28.7	+ 3 35 06	
EIC 481	16 06 43.5	+ 6 30 50	
EIC 482	16 06 45.7	+ 3 52 59	
EIC 483	16 07 13.0	− 3 20 09	
EIC 484	16 08 22.4	+ 7 54 28	
EIC 485	16 10 46.6	+ 5 08 50	
EIC 486	16 11 43.0	− 3 34 04	
EIC 487	16 11 45.9	+ 6 01 37	
EIC 488	16 12 16.7	+ 7 58 57	
EIC 489	16 13 11.2	− 2 16 05	
EIC 490	16 15 40.3	− 4 34 17	
EIC 491	16 16 08.2	+ 7 22 49	
EIC 492	16 17 46.2	+ 5 59 02	
EIC 493	16 18 42.0	− 7 34 56	
EIC 494	16 19 44.3	+ 2 59 27	
EIC 495	16 20 17.7	− 7 05 34	
EIC 496	16 21 12.0	− 7 47 34	
EIC 497	16 22 15.6	− 2 21 29	
EIC 498	16 23 47.7	+ 8 37 32	
EIC 499	16 25 01.4	− 7 29 11	
EIC 500	16 25 01.5	+ 2 58 51	
EIC 501	16 26 00.8	+ 0 46 27	
EIC 502	16 26 08.5	+ 0 09 51	
EIC 503	16 27 21.1	+ 7 51 25	
EIC 504	16 27 25.9	− 0 01 08	
EIC 505	16 29 35.6	− 1 31 53	
EIC 506	16 31 50.7	− 8 02 49	
EIC 507	16 32 03.1	+ 8 46 35	
EIC 508	16 32 44.5	+ 2 53 06	
EIC 509	16 34 13.5	+ 5 07 02	
EIC 510	16 35 05.7	+ 5 22 32	
EIC 511	16 37 43.4	+ 8 36 47	
EIC 512	16 37 48.0	+ 7 43 19	
EIC 513	16 40 17.9	− 3 33 17	
EIC 514	16 40 34.3	− 4 03 21	
EIC 515	16 41 52.2	+ 7 24 28	
EIC 516	16 42 25.3	− 0 31 23	
EIC 517	16 42 34.1	− 2 59 38	
EIC 518	16 43 18.4	− 3 55 21	
EIC 519	16 43 25.5	+ 8 40 19	
EIC 520	16 47 13.6	+ 6 33 31	
EIC 521	16 49 00.3	+ 8 23 47	
EIC 522	16 50 20.4	+ 5 29 21	
EIC 523	16 51 36.2	− 6 37 50	
EIC 524	16 51 48.5	− 7 28 48	
EIC 525	16 51 54.6	− 6 04 26	
EIC 526	16 54 24.5	+ 6 34 42	
EIC 527	16 54 53.4	+ 6 17 16	
EIC 528	16 55 50.3	+ 8 20 44	
EIC 529	16 56 54.1	− 7 32 21	
EIC 530	16 57 10.3	+ 8 06 03	
EIC 531	16 57 55.4	+ 5 05 52	
EIC 532	16 58 07.7	+ 8 51 55	
EIC 533	16 58 25.0	− 4 08 59	
EIC 534	16 58 31.2	− 6 57 19	
EIC 535	16 58 52.5	+ 7 30 03	
EIC 536	16 59 20.4	+ 6 40 50	
EIC 537	17 00 23.9	+ 6 12 12	
EIC 538	17 00 32.2	+ 4 49 01	
EIC 539	17 03 05.2	+ 3 50 02	
EIC 540	17 03 29.4	+ 5 06 14	
EIC 541	17 03 43.2	+ 8 41 21	
EIC 542	17 06 15.9	+ 8 29 35	
EIC 543	17 09 20.2	+ 7 57 14	
EIC 544	17 09 24.3	+ 2 14 44	
EIC 545	17 11 16.1	+ 5 51 56	
EIC 546	17 11 55.9	+ 8 59 26	
EIC 547	17 13 24.1	+ 6 53 52	
EIC 548	17 13 56.4	+ 4 46 29	
EIC 549	17 15 07.6	+ 6 48 52	
EIC 550	17 16 18.5	− 4 15 23	
EIC 551	17 17 15.0	+ 2 11 22	
EIC 552	17 20 22.2	+ 0 55 10	
EIC 553	17 21 32.4	+ 5 29 59	
EIC 554	17 21 33.9	+ 8 53 51	
EIC 555	17 21 34.2	+ 8 38 59	
EIC 556	17 21 54.7	+ 7 08 59	
EIC 557	17 22 55.4	+ 8 58 05	
EIC 558	17 23 54.0	+ 7 38 16	
EIC 559	17 24 01.8	+ 4 10 56	
EIC 560	17 25 19.9	+ 8 28 57	
EIC 561	17 25 40.2	+ 5 04 41	
EIC 562	17 26 32.0	− 7 25 30	
EIC 563	17 29 48.6	+ 8 21 19	
EIC 564	17 30 42.8	+ 2 28 24	
EIC 565	17 30 43.2	+ 0 08 09	
EIC 566	17 31 24.8	− 1 56 46	
EIC 567	17 32 22.3	+ 3 23 30	
EIC 568	17 33 04.4	+ 5 02 52	
EIC 569	17 35 17.5	+ 8 38 56	
EIC 570	17 35 32.5	+ 4 05 11	
EIC 571	17 35 43.8	+ 7 05 03	
EIC 572	17 36 30.3	+ 6 05 15	
EIC 573	17 36 41.8	+ 4 27 08	
EIC 574	17 36 55.0	+ 1 37 50	
EIC 575	17 37 01.2	+ 3 25 05	
EIC 576	17 37 31.1	+ 7 49 37	
EIC 577	17 37 35.6	− 2 07 35	
EIC 578	17 37 53.7	+ 6 35 22	
EIC 579	17 38 33.1	+ 4 33 46	
EIC 580	17 39 05.7	+ 6 20 12	
EIC 581	17 39 05.8	+ 6 45 07	
EIC 582	17 39 55.7	− 4 49 37	
EIC 583	17 40 29.5	+ 3 47 30	
EIC 584	17 40 37.3	− 3 52 10	
EIC 585	17 40 59.9	+ 4 35 15	
EIC 586	17 45 01.7	+ 5 37 14	
EIC 587	17 45 04.2	− 3 37 38	
EIC 588	17 45 26.3	+ 6 25 08	
EIC 589	17 46 17.0	+ 3 36 12	
EIC 590	17 48 15.0	+ 4 25 45	
EIC 591	17 48 34.0	+ 6 43 03	
EIC 592	17 48 37.0	− 5 14 27	
EIC 593	17 49 12.0	− 5 00 36	
EIC 594	17 49 31.4	+ 4 29 53	
EIC 595	17 49 34.0	+ 7 09 47	
EIC 596	17 49 55.0	+ 6 46 42	
EIC 597	17 49 57.6	− 6 07 59	
EIC 598	17 50 03.4	+ 1 18 52	
EIC 599	17 50 26.7	− 2 34 09	
EIC 600	17 50 34.4	− 5 55 07	

NAME	RA (1950) DEC	POS REF
	h m s ° ′ ″	
EIC 601	17 51 01.1 + 5 30 34	
EIC 602	17 52 49.6 + 5 42 41	
EIC 603	17 53 31.8 − 1 24 12	
EIC 604	17 54 08.9 − 6 25 37	
EIC 605	17 54 14.4 + 6 50 43	
EIC 606	17 56 19.9 − 6 38 32	
EIC 607	17 56 41.6 − 6 06 30	
EIC 608	17 56 57.3 − 4 49 06	
EIC 609	17 57 37.3 + 6 07 21	
EIC 610	17 58 03.9 + 5 37 01	
EIC 611	17 59 25.7 + 8 26 58	
EIC 612	18 00 04.7 + 7 45 33	
EIC 613	18 02 56.0 + 2 30 02	
EIC 614	18 03 45.6 + 3 23 45	
EIC 615	18 03 59.1 − 8 13 37	
EIC 616	18 04 33.3 − 5 45 11	
EIC 617	18 04 43.6 + 8 22 19	
EIC 618	18 04 54.6 + 8 43 33	
EIC 619	18 04 56.2 + 6 32 07	
EIC 620	18 05 11.2 + 8 00 24	
EIC 621	18 06 01.2 + 8 48 48	
EIC 622	18 06 09.0 + 5 16 43	
EIC 623	18 06 36.7 − 8 30 21	
EIC 624	18 07 14.0 − 8 31 03	
EIC 625	18 08 10.1 + 3 18 47	
EIC 626	18 08 34.4 + 7 52 23	
EIC 627	18 08 47.0 − 8 37 52	
EIC 628	18 09 01.8 − 7 26 51	
EIC 629	18 09 16.1 + 5 27 33	
EIC 630	18 09 45.9 + 8 12 47	
EIC 631	18 10 19.9 + 4 08 01	
EIC 632	18 11 21.0 + 2 22 40	
EIC 633	18 11 33.0 + 5 17 16	
EIC 634	18 11 39.3 + 4 12 47	
EIC 635	18 11 39.9 + 5 20 49	
EIC 636	18 13 34.4 + 2 21 34	
EIC 637	18 14 07.1 + 3 40 27	
EIC 638	18 15 41.4 + 6 55 03	
EIC 639	18 16 03.5 + 8 36 23	
EIC 640	18 16 44.0 + 7 14 17	
EIC 641	18 17 00.0 − 8 04 44	
EIC 642	18 18 20.7 + 5 54 48	
EIC 643	18 18 22.1 + 3 21 12	
EIC 644	18 18 28.8 − 8 19 34	
EIC 645	18 18 42.2 − 2 55 08	
EIC 646	18 20 23.5 + 7 10 50	
EIC 647	18 20 46.3 − 4 31 32	
EIC 648	18 21 02.4 − 8 54 09	
EIC 649	18 21 22.5 + 3 35 43	
EIC 650	18 21 57.1 + 8 44 03	
EIC 651	18 22 29.3 + 8 17 07	
EIC 652	18 23 01.8 + 5 44 16	
EIC 653	18 23 14.1 + 8 00 09	
EIC 654	18 24 23.4 + 3 52 55	
EIC 655	18 24 27.2 + 8 09 43	
EIC 656	18 24 43.9 + 7 29 33	
EIC 657	18 24 48.4 + 6 58 39	
EIC 658	18 24 49.9 − 7 45 14	
EIC 659	18 24 57.9 − 8 42 31	
EIC 660	18 25 10.8 − 8 43 51	
EIC 661	18 25 20.8 + 3 42 58	
EIC 662	18 25 46.1 + 7 55 17	
EIC 663	18 26 05.1 − 7 46 25	
EIC 664	18 26 22.1 + 6 15 51	
EIC 665	18 26 26.5 + 8 30 06	
EIC 666	18 27 27.8 − 8 13 23	
EIC 667	18 28 29.9 + 8 02 32	
EIC 668	18 28 48.6 + 7 52 18	
EIC 669	18 28 54.4 + 4 20 42	
EIC 670	18 29 01.3 + 7 59 24	
EIC 671	18 30 04.9 − 8 22 53	
EIC 672	18 30 09.7 + 4 15 29	
EIC 673	18 30 27.5 − 7 28 35	
EIC 674	18 31 22.2 + 3 40 23	
EIC 675	18 31 39.6 − 1 01 07	
EIC 676	18 31 51.0 + 8 42 26	
EIC 677	18 31 52.7 + 7 45 56	
EIC 678	18 31 55.0 − 8 37 12	
EIC 679	18 32 07.8 − 8 39 07	
EIC 680	18 32 26.1 + 7 01 35	
EIC 681	18 32 28.9 − 8 16 59	
EIC 682	18 32 46.8 − 8 43 52	
EIC 683	18 32 57.1 + 6 25 04	
EIC 684	18 33 35.5 + 7 38 36	
EIC 685	18 33 37.2 − 8 55 12	
EIC 686	18 34 21.3 − 7 38 46	
EIC 687	18 34 44.0 − 2 41 52	
EIC 688	18 34 56.9 + 3 10 34	
EIC 689	18 35 55.2 − 8 37 08	
EIC 690	18 35 57.4 + 8 47 20	
EIC 691	18 36 32.3 + 1 38 31	
EIC 692	18 37 15.7 + 8 41 08	
EIC 693	18 37 17.5 − 7 50 17	
EIC 694	18 39 15.1 + 6 23 12	
EIC 695	18 39 30.8 + 6 46 10	
EIC 696	18 39 31.2 − 2 48 13	
EIC 697	18 39 48.3 − 2 20 26	
EIC 698	18 39 51.8 − 8 35 00	
EIC 699	18 39 54.3 + 4 34 19	
EIC 700	18 40 06.6 + 8 35 02	
EIC 701	18 40 25.4 + 8 15 30	
EIC 702	18 40 38.8 + 6 43 19	
EIC 703	18 43 00.9 − 5 38 58	
EIC 704	18 43 17.2 − 8 38 31	
EIC 705	18 43 19.8 + 8 41 21	
EIC 706	18 43 38.8 + 8 09 49	
EIC 707	18 44 00.1 + 8 02 35	
EIC 708	18 44 48.5 − 5 45 40	
EIC 709	18 44 53.3 + 5 23 58	
EIC 710	18 47 00.0 + 8 32 09	
EIC 711	18 47 00.1 − 5 58 14	
EIC 712	18 47 36.9 − 7 58 00	
EIC 713	18 47 39.9 + 7 02 45	
EIC 714	18 48 00.4 + 7 23 56	
EIC 715	18 48 52.8 + 8 01 17	
EIC 716	18 51 19.4 + 0 35 40	
EIC 717	18 52 33.3 + 8 11 48	
EIC 718	18 52 44.2 − 8 15 06	
EIC 719	18 53 00.9 + 8 17 16	
EIC 720	18 54 24.2 + 4 37 00	
EIC 721	18 54 51.9 + 6 37 50	
EIC 722	18 55 39.6 + 8 11 22	
EIC 723	18 55 47.3 + 7 55 08	
EIC 724	18 55 55.6 + 4 35 46	
EIC 725	18 56 03.7 + 6 38 47	
EIC 726	18 56 59.4 + 5 18 27	
EIC 727	18 57 15.8 + 6 01 02	
EIC 728	18 57 26.9 + 8 12 30	
EIC 729	18 57 52.5 + 4 50 08	
EIC 730	18 58 58.8 + 8 15 06	
EIC 731	18 59 00.3 − 5 48 41	
EIC 732	18 59 15.4 + 5 21 54	
EIC 733	18 59 22.2 + 7 44 27	
EIC 734	18 59 56.5 + 4 45 31	
EIC 735	18 59 57.0 + 8 17 59	
EIC 736	19 00 14.4 + 8 22 54	
EIC 737	19 00 39.6 + 3 59 58	
EIC 738	19 00 52.9 + 7 26 15	
EIC 739	19 01 10.2 + 8 18 00	
EIC 740	19 01 43.7 − 5 45 37	
EIC 741	19 02 16.3 + 2 54 27	
EIC 742	19 02 22.5 + 3 55 54	
EIC 743	19 02 33.1 + 8 08 26	
EIC 744	19 02 33.3 + 1 31 55	
EIC 745	19 03 48.6 + 5 35 37	
EIC 746	19 03 57.4 + 8 09 07	
EIC 747	19 04 30.8 + 7 04 20	
EIC 748	19 05 13.7 + 5 20 59	
EIC 749	19 05 34.1 + 6 13 38	
EIC 750	19 06 15.6 + 3 11 15	
EIC 751	19 07 01.3 + 4 54 48	
EIC 752	19 07 22.4 + 7 08 57	
EIC 753	19 10 12.6 + 6 47 50	
EIC 754	19 11 23.4 + 2 32 17	
EIC 755	19 12 21.9 + 4 09 14	
EIC 756	19 12 41.5 − 7 08 09	
EIC 757	19 16 24.9 + 4 12 00	
EIC 758	19 16 46.2 + 5 00 31	
EIC 759	19 17 35.3 − 8 07 50	
EIC 760	19 17 51.9 + 7 47 35	
EIC 761	19 18 09.5 − 4 35 50	
EIC 762	19 18 35.2 + 5 01 01	
EIC 763	19 20 01.7 + 4 30 04	
EIC 764	19 20 05.7 − 3 19 48	
EIC 765	19 22 15.2 − 8 56 52	
EIC 766	19 22 24.9 + 7 32 52	
EIC 767	19 23 30.5 + 8 06 07	
EIC 768	19 24 48.6 + 6 58 03	
EIC 769	19 25 46.8 + 5 25 44	
EIC 770	19 26 18.9 + 4 44 22	
EIC 771	19 26 31.8 + 7 56 09	
EIC 772	19 26 42.5 + 3 45 26	
EIC 773	19 27 39.7 + 2 47 54	
EIC 774	19 27 40.0 − 0 56 26	
EIC 775	19 28 02.8 − 2 53 40	
EIC 776	19 28 14.8 + 3 32 42	
EIC 777	19 30 31.8 + 5 57 51	
EIC 778	19 30 39.1 + 4 55 13	
EIC 779	19 30 53.4 + 6 09 11	
EIC 780	19 31 17.8 + 5 21 22	
EIC 781	19 31 38.9 + 7 16 12	
EIC 782	19 32 17.1 + 7 02 06	
EIC 783	19 32 41.0 + 1 58 43	
EIC 784	19 35 12.4 + 5 11 07	
EIC 785	19 35 25.6 + 6 36 53	
EIC 786	19 37 25.4 + 5 50 56	
EIC 787	19 38 29.3 − 4 02 13	
EIC 788	19 41 15.2 + 3 37 17	
EIC 789	19 43 01.8 + 7 39 43	
EIC 790	19 43 44.9 + 1 34 05	
EIC 791	19 46 07.0 + 3 34 17	
EIC 792	19 47 24.3 − 7 44 32	
EIC 793	19 48 34.5 − 2 35 20	
EIC 794	19 48 57.1 + 3 57 35	
EIC 795	19 49 10.6 + 7 22 15	
EIC 796	19 51 25.4 − 8 42 20	
EIC 797	19 51 49.4 + 8 19 47	
EIC 798	19 52 02.2 + 6 51 28	
EIC 799	19 52 51.2 + 6 16 35	
EIC 800	19 53 22.4 + 6 03 25	
EIC 801	19 54 29.1 + 8 18 45	
EIC 802	19 55 00.1 − 2 01 15	
EIC 803	19 55 10.3 − 9 11 39	
EIC 804	19 55 11.7 + 6 25 37	
EIC 805	19 58 08.4 + 8 18 45	
EIC 806	19 58 18.2 + 4 18 19	
EIC 807	19 58 33.8 + 8 25 06	
EIC 808	20 00 43.4 + 4 35 19	
EIC 809	20 01 03.6 + 8 05 16	
EIC 810	20 01 41.6 + 7 08 07	
EIC 811	20 02 15.7 + 4 04 39	
EIC 812	20 02 34.0 + 4 26 03	
EIC 813	20 05 15.0 + 5 54 28	
EIC 814	20 07 47.6 − 6 25 08	
EIC 815	20 07 54.1 − 1 46 35	
EIC 816	20 08 41.9 + 6 11 56	
EIC 817	20 09 35.5 + 7 32 01	
EIC 818	20 10 21.9 + 6 08 55	
EIC 819	20 11 50.9 − 0 09 27	
EIC 820	20 13 27.0 + 7 30 57	
EIC 821	20 14 33.0 + 6 54 57	
EIC 822	20 16 02.1 + 7 25 38	
EIC 823	20 17 49.9 + 6 39 50	
EIC 824	20 20 41.7 + 5 10 53	
EIC 825	20 20 48.3 + 7 47 40	
EIC 826	20 21 21.6 + 0 46 59	
EIC 827	20 22 09.2 + 1 12 20	
EIC 828	20 28 47.2 + 6 11 11	
EIC 829	20 29 16.9 + 6 27 43	
EIC 830	20 29 48.3 + 1 57 45	
EIC 831	20 32 17.9 + 5 03 34	
EIC 832	20 33 08.3 + 3 49 29	
EIC 833	20 37 49.0 + 7 27 26	
EIC 834	20 39 34.0 + 8 07 33	
EIC 835	20 44 16.2 + 6 16 39	
EIC 836	20 44 17.5 + 2 15 12	
EIC 837	20 44 24.8 + 5 40 28	
EIC 838	20 45 05.8 − 5 12 43	
EIC 839	20 46 42.8 − 0 44 57	
EIC 840	20 47 56.3 + 5 54 25	
EIC 841	21 02 05.1 + 5 18 11	
EIC 842	21 03 17.5 − 0 24 42	
EIC 843	21 03 39.2 + 7 37 45	
EIC 844	21 04 58.6 − 0 21 56	
EIC 845	21 05 16.1 + 0 57 05	
EIC 846	21 05 38.1 + 1 17 57	
EIC 847	21 05 55.3 + 3 00 57	
EIC 848	21 05 59.6 + 6 47 10	
EIC 849	21 08 46.1 + 5 03 22	
EIC 850	21 12 00.5 + 4 28 55	
EIC 851	21 12 02.9 − 0 06 57	
EIC 852	21 13 19.4 + 5 02 21	
EIC 853	21 15 49.3 + 7 32 58	
EIC 854	21 18 36.3 + 7 08 29	
EIC 855	21 22 40.2 − 3 46 18	
EIC 856	21 25 56.8 + 7 58 36	
EIC 857	21 26 31.9 + 7 58 23	
EIC 858	21 28 39.2 + 5 21 31	
EIC 859	21 28 55.4 − 5 47 31	
EIC 860	21 30 38.4 + 6 55 37	
EIC 861	21 32 10.0 + 1 36 21	
EIC 862	21 36 44.1 + 8 04 26	
EIC 863	21 37 01.0 + 2 01 00	
EIC 864	21 37 44.5 − 2 00 47	
EIC 865	21 38 16.8 + 3 40 09	
EIC 866	21 39 45.3 + 5 27 06	
EIC 867	21 43 56.3 − 2 26 39	
EIC 868	21 44 29.3 + 6 56 37	
EIC 869	21 58 40.1 + 8 00 57	
EIC 870	21 59 24.0 + 6 02 57	
EIC 871	22 00 53.8 + 5 11 51	
EIC 872	22 03 09.4 + 4 48 48	
EIC 873	22 03 12.7 − 0 33 48	
EIC 874	22 07 41.0 + 5 57 04	
EIC 875	22 14 58.5 + 4 53 37	
EIC 876	22 19 03.8 − 7 51 37	
EIC 877	22 25 19.4 + 4 26 32	
EIC 878	22 39 29.8 − 5 21 45	
EIC 879	22 50 00.1 − 7 50 42	
EIC 880	22 57 15.9 + 7 05 13	
EIC 881	23 04 14.0 + 4 45 52	
EIC 882	23 06 59.8 + 8 24 23	
EIC 883	23 08 41.3 + 4 43 55	
EIC 884	23 11 43.8 − 6 19 13	
EIC 885	23 13 16.8 − 9 21 38	
EIC 886	23 14 15.1 − 7 59 57	
EIC 887	23 14 35.4 + 3 00 33	
EIC 888	23 17 47.5 + 5 06 26	
EIC 889	23 22 01.5 + 3 26 22	
EIC 890	23 25 25.4 + 6 06 13	
EIC 891	23 31 13.9 + 6 01 19	
EIC 892	23 32 53.9 + 8 14 34	
EIC 893	23 43 49.8 + 3 12 32	
EIC 894	23 52 12.7 − 0 10 06	
EIC 895	23 56 44.4 + 6 35 06	
EIC 896	23 59 23.6 − 6 17 29	
EL−24	16 23 22.9 −24 09 29	780902
DEL EQU	21 12 02.5 + 9 48 18	CSI 79
GAM EQU	21 07 54.5 + 9 55 44	"
R EQU	21 10 47.7 +12 35 42	"
RV EQU	21 12 27 + 8 47 10	GCVS
ALF ERI	1 35 51.3 −57 29 24	CSI 79
AU ERI	4 15 01.3 −25 08 03	"
BR ERI	3 46 20.7 − 7 09 59	"
EPS ERI	3 30 34.3 − 9 37 34	"
GAM ERI	3 55 41.6 −13 38 57	"
GAM ERI	3 55 44 −13 38 38	
NUU ERI	4 33 49.0 − 3 27 10	CSI 79
OMI 2 ERI	4 12 58.1 − 7 43 45	"
RT ERI	3 31 53.9 −16 19 46	"
SY ERI	5 07 20.9 − 5 34 35	"
T ERI	3 53 05.5 −24 10 39	"
TAU 4 ERI	3 17 17.4 −21 56 18	"
U ERI	3 48 19.2 −25 06 45	"
V ERI	4 02 01.5 −15 51 37	"
W ERI	4 09 23.6 −25 16 04	"
W ERI	4 09 26.0 −25 15 26	
Z ERI	2 45 32.0 −12 40 03	CSI 79
56 ERI	4 41 40.9 − 8 35 42	"
ESO 054−21	3 50 07.0 −71 47 06	
ESO 060−19	8 56 57.3 −68 51 59	
ESO 103−G35	18 33 22 −65 28 18	779909
ESO 116−12	3 11 48.0 −57 32 36	
ESO 122−01	6 39 57.0 −58 28 36	
ESO 138−14	17 02 23.9 −62 01 00	
ESO 141−G55	19 16 17 −58 45 54	759905
ESO 141−G55	19 16 57.0 −58 45 52	789906
ESO 154−23	2 55 24.5 −54 46 12	
ESO 209−09	7 56 50.0 −49 42 54	
ESO 219−21	12 59 26.5 −50 03 52	
ESO 240−11	23 35 08.0 −48 00 12	
ESO 300−G14	3 07 47 −41 13 12	789907
ESO 300−14	3 07 47.0 −41 13 12	
ESO 302−G09	3 45 44 −38 43 48	789909
ESO 346−G14	22 52 17 −38 51 06	789908
ESO 357−G12	3 14 56 −35 43 24	"
ESO 357−12	3 14 56.0 −35 43 24	
ESO 358−G63	3 44 24 −35 05 48	789908
ESO 423−02	5 13 21.0 −30 35 00	
ESO 469−15	23 06 13.0 −31 07 48	
ESO 482−46	3 47 36.5 −27 08 44	
ESPIN 1181	1 41 12 +61 22 09	ED
E1615+061	16 15 18.2 + 6 11 12	
F−9	1 21 54 −59 04	790117
F−51	18 40 12 −62 25	ED
FG 1	11 26 14.6 −52 39 34	769910
FG 2	17 35 41 −44 08 00	759905
FG 3	17 56 44.4 −38 49 45	739909
FIELD #1	16 37 27.9 −46 13 34	
FIELD #2	16 44 55.2 −44 51 10	
FIELD #3	16 45 33.2 −45 29 46	
FIELD #4	17 06 40.7 −39 08 20	
FIELD #5	17 08 24.7 −39 10 12	
FIELD #6	17 19 19.7 −35 46 17	

NAME	RA (1950) h m s	DEC ° ′ ″	POS REF
FIELD #7	17 27 04.8	−34 25 46	
FIELD #8	17 37 35.1	−31 34 53	
FIELD #9	17 46 13.0	−27 41 00	
FIELD I	5 32 47.9	− 5 25 12	ED
FIR #1	17 23 03	−35 26	"
FIR #2	17 23 54	−34 28	"
FIR #3	17 32 31	−32 18	"
FIR #4	17 35 56	−30 59	"
FIR #5	17 42 28	−28 55	"
FIR #6	17 44 31	−28 22	"
FIR #7	17 50 44	−26 17	"
FIR #8	17 54 28	−24 28	"
FIR #9	17 58 11	−23 48	"
FIR #10	17 59 36	−22 50	"
FIR #11	18 02 49	−21 32	"
FIR #12	18 06 58	−20 01	"
FIR #13	18 11 41	−18 00	"
FIR #14	18 17 12	−16 13	"
FIR #15	18 16 25	−13 50	"
FIR #16	18 19 29	−14 21	"
FIR #17	18 22 27	−12 35	"
FIR #18	18 25 22	−11 02	"
FIR #19	18 30 36	− 9 27	"
FIR #20	18 31 33	− 8 47	"
FIR #21	18 32 43	− 7 48	"
FIR #22	18 35 52	− 6 45	"
FIR #23	18 41 15	− 4 11	"
FIR #24	18 43 19	− 2 45	"
FIR #25	18 44 58	− 1 57	"
FIR #26	18 50 30	+ 0 43	"
FIR #27	18 53 03	+ 1 30	"
FIR #28	18 58 56	+ 4 07	"
FIR #29	19 04 12	+ 7 16	"
FIR #30	19 06 38	+ 8 26	"
FIRSSE 1	0 36 26	+66 35 00	
FIRSSE 2	0 37 33	+66 39 36	
FIRSSE 3	0 40 39	+66 34 42	
FIRSSE 4	0 46 44	+65 26 06	
FIRSSE 5	0 48 28	+65 31 48	
FIRSSE 6	0 51 46	+65 34 30	
FIRSSE 7	0 55 20	+65 22 24	
FIRSSE 8	1 02 36	+75 58 42	
FIRSSE 9	1 04 29	+65 04 24	
FIRSSE 10	1 13 33	+64 36 24	
FIRSSE 11	1 20 00	+61 37 12	
FIRSSE 12	1 30 14	+62 10 48	
FIRSSE 13	2 03 29	+73 23 36	
FIRSSE 14	2 04 24	+60 31 12	
FIRSSE 15	2 13 05	+55 08 30	
FIRSSE 16	2 18 57	+57 35 18	
FIRSSE 17	2 19 24	+61 38 42	
FIRSSE 18	2 21 55	+61 51 36	
FIRSSE 19	2 22 56	+61 21 48	
FIRSSE 20	2 23 22	+62 03 06	
FIRSSE 21	2 23 37	+61 40 06	
FIRSSE 22	2 24 40	+60 40 24	
FIRSSE 23	2 24 55	+61 17 36	
FIRSSE 24	2 38 01	+59 23 12	
FIRSSE 25	2 38 43	+53 18 24	
FIRSSE 26	2 39 01	+62 42 54	
FIRSSE 27	2 43 29	+61 45 18	
FIRSSE 28	2 45 44	+60 28 36	
FIRSSE 29	2 46 01	+59 30 00	
FIRSSE 30	2 46 02	+61 46 30	
FIRSSE 31	2 46 40	+55 40 24	
FIRSSE 32	2 47 27	+60 30 36	
FIRSSE 33	2 53 13	+60 08 48	
FIRSSE 34	2 53 52	+60 35 48	
FIRSSE 35	2 57 39	+60 17 18	
FIRSSE 36	2 59 00	+60 14 30	
FIRSSE 37	3 03 37	+58 19 06	
FIRSSE 38	3 03 51	+55 36 30	
FIRSSE 39	3 06 36	+56 38 54	
FIRSSE 40	3 21 06	+54 47 06	
FIRSSE 41	3 23 24	+58 35 42	
FIRSSE 42	3 25 34	+31 01 18	
FIRSSE 43	3 26 10	+31 12 18	
FIRSSE 44	3 41 21	+31 57 54	
FIRSSE 45	3 41 52	+23 58 24	
FIRSSE 46	3 42 11	+23 36 12	
FIRSSE 47	3 42 41	+24 11 30	
FIRSSE 48	3 42 48	+31 22 06	
FIRSSE 49	3 43 08	+23 39 36	
FIRSSE 50	3 43 40	+24 17 42	
FIRSSE 51	3 45 02	+65 22 36	
FIRSSE 52	3 51 53	+37 12 06	
FIRSSE 53	3 52 19	+53 43 30	
FIRSSE 54	3 59 34	+51 11 36	
FIRSSE 55	4 07 22	+51 02 18	
FIRSSE 56	4 15 32	+28 12 00	
FIRSSE 57	4 19 09	+19 25 24	
FIRSSE 58	4 27 04	+35 10 12	
FIRSSE 59	4 28 43	+18 02 06	
FIRSSE 60	4 32 31	+51 06 42	
FIRSSE 61	4 33 07	+50 46 36	
FIRSSE 62	4 36 56	+50 22 18	
FIRSSE 63	4 39 31	+36 01 06	
FIRSSE 64	4 52 26	+47 16 48	
FIRSSE 65	4 54 52	+47 53 54	
FIRSSE 66	4 56 38	+56 06 30	
FIRSSE 67	5 04 18	− 3 26 48	
FIRSSE 68	5 09 55	+37 23 06	
FIRSSE 69	5 13 11	+34 16 48	
FIRSSE 70	5 13 26	+45 31 00	
FIRSSE 71	5 13 26	+53 31 48	
FIRSSE 72	5 19 42	+33 55 30	
FIRSSE 73	5 19 56	+33 29 12	
FIRSSE 74	5 22 11	+41 39 54	
FIRSSE 75	5 23 49	+34 07 24	
FIRSSE 76	5 24 43	+34 22 06	
FIRSSE 77	5 27 26	+33 45 54	
FIRSSE 78	5 28 07	+34 13 54	
FIRSSE 79	5 30 20	+59 11 18	
FIRSSE 80	5 30 20	− 5 31 12	
FIRSSE 81	5 30 23	+30 28 18	
FIRSSE 82	5 31 32	+21 59 12	
FIRSSE 83	5 32 25	+57 23 06	
FIRSSE 84	5 32 32	− 6 08 06	
FIRSSE 85	5 32 40	− 4 44 12	
FIRSSE 86	5 32 46	− 4 52 30	
FIRSSE 87	5 32 50	− 5 24 36	
FIRSSE 88	5 32 52	+36 28 48	
FIRSSE 89	5 33 22	− 4 16 24	
FIRSSE 90	5 33 46	− 5 19 06	
FIRSSE 91	5 33 53	− 6 46 42	
FIRSSE 92	5 34 36	+31 58 06	
FIRSSE 93	5 35 00	− 4 56 36	
FIRSSE 94	5 35 11	+35 50 06	
FIRSSE 95	5 35 33	+30 40 24	
FIRSSE 96	5 36 11	+46 44 30	
FIRSSE 97	5 36 23	+36 01 36	
FIRSSE 98	5 37 07	+36 21 18	
FIRSSE 99	5 37 10	+35 48 48	
FIRSSE 100	5 37 41	+35 40 48	
FIRSSE 101	5 37 55	− 7 30 24	
FIRSSE 102	5 37 55	− 3 23 48	
FIRSSE 103	5 37 58	− 1 59 18	
FIRSSE 104	5 38 16	+35 48 48	
FIRSSE 105	5 39 01	− 2 18 24	
FIRSSE 106	5 39 14	− 1 56 36	
FIRSSE 107	5 40 38	+32 41 18	
FIRSSE 108	5 40 59	+30 55 00	
FIRSSE 109	5 41 24	− 1 18 48	
FIRSSE 110	5 44 02	+ 0 02 18	
FIRSSE 111	5 44 06	+30 34 30	
FIRSSE 112	5 44 31	+ 0 17 36	
FIRSSE 113	5 48 03	+25 45 12	
FIRSSE 114	5 48 00	+27 01 48	
FIRSSE 115	5 49 08	+27 00 12	
FIRSSE 116	5 50 37	+24 14 18	
FIRSSE 117	5 52 25	+ 7 23 18	
FIRSSE 118	5 55 17	+16 31 12	
FIRSSE 119	5 55 25	+20 13 24	
FIRSSE 120	5 57 16	+31 56 24	
FIRSSE 121	6 00 26	+75 43 36	
FIRSSE 122	6 00 46	+30 15 18	
FIRSSE 123	6 01 15	+30 29 48	
FIRSSE 124	6 01 18	− 9 40 54	
FIRSSE 125	6 04 15	+21 14 54	
FIRSSE 126	6 05 18	− 6 22 36	
FIRSSE 127	6 05 21	+20 38 12	
FIRSSE 128	6 05 42	+21 31 00	
FIRSSE 129	6 05 55	+21 37 48	
FIRSSE 130	6 05 59	+15 41 30	
FIRSSE 131	6 06 24	+20 41 30	
FIRSSE 132	6 06 58	+20 30 54	
FIRSSE 133	6 07 14	+21 41 48	
FIRSSE 134	6 07 22	+12 49 24	
FIRSSE 135	6 07 27	+16 43 42	
FIRSSE 136	6 08 03	+20 28 36	
FIRSSE 137	6 08 18	− 6 13 00	
FIRSSE 138	6 08 18	+20 39 36	
FIRSSE 139	6 08 37	+17 28 30	
FIRSSE 140	6 08 42	+21 03 48	
FIRSSE 141	6 08 58	+20 39 12	
FIRSSE 142	6 09 01	+17 55 36	
FIRSSE 143	6 09 13	− 6 12 30	
FIRSSE 144	6 09 33	+78 24 42	
FIRSSE 145	6 09 42	+62 38 42	
FIRSSE 146	6 09 56	+18 00 30	
FIRSSE 147	6 10 11	+18 47 00	
FIRSSE 148	6 10 19	+15 23 00	
FIRSSE 149	6 10 43	+17 58 36	
FIRSSE 150	6 10 56	+18 44 36	
FIRSSE 151	6 11 31	+17 46 00	
FIRSSE 152	6 11 52	+13 52 06	
FIRSSE 153	6 11 53	+19 01 24	
FIRSSE 154	6 12 03	+19 05 00	
FIRSSE 155	6 12 07	+12 21 18	
FIRSSE 156	6 12 47	+14 16 18	
FIRSSE 157	6 13 39	−15 58 18	
FIRSSE 158	6 15 40	+23 20 42	
FIRSSE 159	6 15 50	+15 17 18	
FIRSSE 160	6 17 32	−10 37 18	
FIRSSE 161	6 18 35	+66 18 12	
FIRSSE 162	6 20 53	+ 9 58 36	
FIRSSE 163	6 24 49	−10 09 42	
FIRSSE 164	6 26 50	+ 8 49 42	
FIRSSE 165	6 28 13	+13 18 18	
FIRSSE 166	6 28 20	− 9 35 18	
FIRSSE 167	6 28 23	+ 9 52 48	
FIRSSE 168	6 28 23	+10 29 30	
FIRSSE 169	6 28 53	+10 02 24	
FIRSSE 170	6 29 14	+ 4 22 24	
FIRSSE 171	6 30 00	+10 12 18	
FIRSSE 172	6 30 24	+10 23 30	
FIRSSE 173	6 30 43	+10 59 18	
FIRSSE 174	6 30 59	+ 4 03 24	
FIRSSE 175	6 31 59	+ 4 15 18	
FIRSSE 176	6 33 01	+11 01 48	
FIRSSE 177	6 33 52	+10 50 18	
FIRSSE 178	6 33 58	+10 27 42	
FIRSSE 179	6 35 56	− 1 36 06	
FIRSSE 180	6 36 27	+ 8 47 00	
FIRSSE 181	6 37 12	+10 40 54	
FIRSSE 182	6 38 00	+ 9 51 18	
FIRSSE 183	6 38 10	+10 39 18	
FIRSSE 184	6 38 28	+10 03 06	
FIRSSE 185	6 38 30	+ 9 33 24	
FIRSSE 186	6 41 19	− 1 04 48	
FIRSSE 187	6 42 59	−16 39 18	
FIRSSE 188	6 44 15	+ 1 20 30	
FIRSSE 189	6 50 00	+ 8 28 42	
FIRSSE 190	6 55 52	−13 58 18	
FIRSSE 191	6 56 16	+ 3 39 06	
FIRSSE 192	6 57 21	− 7 40 48	
FIRSSE 193	6 59 26	−11 13 24	
FIRSSE 194	7 01 21	−11 29 12	
FIRSSE 195	7 01 47	−11 13 48	
FIRSSE 196	7 02 01	−10 22 36	
FIRSSE 197	7 02 57	−12 14 30	
FIRSSE 198	7 06 53	−10 47 12	
FIRSSE 199	7 07 43	−18 26 54	
FIRSSE 200	7 09 08	−19 44 54	
FIRSSE 201	7 09 57	−20 11 00	
FIRSSE 202	7 14 11	− 9 20 36	
FIRSSE 203	7 15 54	−21 59 42	
FIRSSE 204	7 20 55	−25 39 48	
FIRSSE 205	7 27 28	−17 45 06	
FIRSSE 206	7 27 39	−18 04 48	
FIRSSE 207	7 27 58	−18 28 36	
FIRSSE 208	7 28 07	−17 49 42	
FIRSSE 209	7 28 25	−15 10 24	
FIRSSE 210	7 28 27	− 9 38 48	
FIRSSE 211	7 28 35	−17 34 36	
FIRSSE 212	7 29 40	−19 14 48	
FIRSSE 213	7 29 51	−16 51 24	
FIRSSE 214	7 31 14	−22 03 30	
FIRSSE 215	7 31 14	−21 56 36	
FIRSSE 216	7 32 30	−22 16 18	
FIRSSE 217	7 33 21	−22 15 18	
FIRSSE 218	7 33 22	−18 40 42	
FIRSSE 219	7 35 52	−32 44 48	
FIRSSE 220	7 38 23	−33 25 36	
FIRSSE 221	7 39 57	−14 36 54	
FIRSSE 222	7 42 15	−20 00 24	
FIRSSE 223	7 42 47	−23 59 42	
FIRSSE 224	7 43 00	−19 44 42	
FIRSSE 225	7 43 42	−19 48 48	
FIRSSE 226	7 43 49	−19 13 48	
FIRSSE 227	7 48 30	−33 29 30	
FIRSSE 228	7 50 10	−25 48 42	
FIRSSE 229	7 50 29	−26 16 06	
FIRSSE 230	7 53 00	−34 44 18	
FIRSSE 231	7 53 25	−20 34 12	
FIRSSE 232	8 00 42	−34 23 18	
FIRSSE 233	8 11 05	−33 09 30	
FIRSSE 234	8 11 15	− 2 49 24	
FIRSSE 235	8 13 07	−35 12 36	
FIRSSE 236	8 14 07	−35 58 24	
FIRSSE 237	8 14 51	−35 17 48	
FIRSSE 238	8 15 00	−35 27 06	
FIRSSE 239	8 16 01	−35 44 18	
FIRSSE 240	8 17 04	−21 35 06	
FIRSSE 241	8 19 03	−36 04 06	
FIRSSE 242	8 27 13	−28 09 30	
FIRSSE 243	8 31 56	−35 53 30	
FIRSSE 244	8 36 38	−27 53 06	
FIRSSE 245	8 41 22	−28 03 00	
FIRSSE 246	9 03 07	− 5 36 12	
FIRSSE 247	9 53 09	+75 51 42	
FIRSSE 248	9 55 03	+75 59 06	
FIRSSE 249	10 26 00	−28 48 48	
FIRSSE 250	10 31 54	−29 18 42	
FIRSSE 251	10 34 56	−28 51 06	
FIRSSE 252	10 49 12	−20 59 12	
FIRSSE 253	10 58 06	−18 04 06	
FIRSSE 254	11 25 56	−28 12 48	
FIRSSE 255	11 30 09	−27 33 06	
FIRSSE 256	11 30 25	−23 46 00	
FIRSSE 257	11 39 56	+ 4 15 24	
FIRSSE 258	11 40 35	+ 4 12 54	
FIRSSE 259	11 41 36	+ 3 39 36	
FIRSSE 260	11 45 27	−27 27 24	
FIRSSE 261	11 48 27	−21 56 54	
FIRSSE 262	11 50 26	−22 37 54	
FIRSSE 263	11 53 27	−24 52 12	
FIRSSE 264	11 59 18	−18 34 48	
FIRSSE 265	12 01 11	−26 08 18	
FIRSSE 266	12 02 51	−21 45 06	
FIRSSE 267	12 03 33	+16 51 36	
FIRSSE 268	12 04 21	+17 08 48	
FIRSSE 269	12 04 34	+16 58 00	
FIRSSE 270	12 09 36	−13 54 54	
FIRSSE 271	12 16 08	+14 42 48	
FIRSSE 272	12 27 51	+ 4 41 18	
FIRSSE 273	12 36 13	− 4 01 06	
FIRSSE 274	12 39 34	+32 47 36	
FIRSSE 275	12 40 06	+60 18 30	
FIRSSE 276	12 42 54	−11 00 18	
FIRSSE 277	12 48 35	+41 22 48	
FIRSSE 278	13 00 52	− 8 47 30	
FIRSSE 279	13 01 27	− 8 38 12	
FIRSSE 280	13 10 13	+44 19 30	
FIRSSE 281	13 13 45	+42 17 54	
FIRSSE 282	13 21 51	+54 36 00	
FIRSSE 283	13 52 24	+56 08 42	
FIRSSE 284	14 13 23	+19 25 54	
FIRSSE 285	14 21 49	+25 56 00	
FIRSSE 286	14 36 35	+44 46 30	
FIRSSE 287	15 50 27	+58 56 00	
FIRSSE 288	16 10 15	+66 29 24	
FIRSSE 289	16 56 38	+65 11 30	
FIRSSE 290	17 58 31	+66 38 48	
FIRSSE 291	18 32 01	+69 09 06	
FIRSSE 292	21 10 08	+81 29 18	
FIRSSE 293	21 11 46	+73 15 18	
FIRSSE 294	21 20 49	+77 40 42	
FIRSSE 295	21 26 35	+73 23 36	
FIRSSE 296	23 51 01	+75 50 18	
FIR10.70−0.17	18 06 52.1	−19 46 00	
FIR11.07−0.38	18 08 25.4	−19 32 48	
FIR11.11−0.40	18 08 34.8	−19 31 20	
FIR12.21−0.10	18 09 44.4	−18 25 04	
FIR12.40−0.46	18 11 25.2	−18 25 36	
FIR12.41+0.50	18 07 56.2	−17 57 41	
FIR12.43−1.12	18 13 56.9	−18 42 59	
FIR12.63−0.02	18 10 17.1	−18 00 44	
FIR12.70−0.17	18 10 58.6	−18 01 20	
FIR12.73−0.22	18 11 12.9	−18 01 00	
FIR12.78+0.33	18 09 17.4	−17 42 36	
FIR12.81−0.19	18 11 17.4	−17 56 16	
FIR12.84+0.54	18 08 40.0	−17 33 36	
FIR12.89+0.48	18 08 58.4	−17 32 24	
FIR12.91−0.26	18 11 44.8	−17 52 40	
FIR13.01−0.36	18 12 17.8	−17 50 24	
FIR13.19+0.05	18 11 09.3	−17 29 20	
FIR13.21−0.14	18 11 53.3	−17 33 36	
FIR13.39+0.08	18 11 26.9	−17 17 52	
FIR13.54−0.18	18 12 44.2	−17 17 28	
FIR13.66−0.60	18 14 29.6	−17 23 12	
FIR13.71−0.09	18 12 42.4	−17 05 56	
FIR13.88+0.29	18 11 40.8	−16 46 12	
FIR13.98−0.13	18 13 25.9	−16 52 40	

NAME	RA (1950) DEC	POS REF
	h m s ° ′ ″	
FIR14.01−0.12	18 13 27.9 −16 50 56	
FIR14.10+0.10	18 12 49.8 −16 39 44	
FIR14.11−0.56	18 15 14.4 −16 58 28	
FIR14.21−0.53	18 15 21.4 −16 52 00	
FIR14.33−0.64	18 15 59.2 −16 48 48	
FIR14.43−0.69	18 16 22.3 −16 45 12	
FIR14.44−0.07	18 14 06.6 −16 26 40	
FIR14.47−0.11	18 14 18.6 −16 26 16	
FIR14.48+0.02	18 13 52.6 −16 22 08	
FIR14.60+0.02	18 14 06.7 −16 15 36	
FIR14.63−0.59	18 16 24.1 −16 31 32	
FIR14.65+0.15	18 13 44.6 −16 09 28	
FIR14.89−0.39	18 16 12.2 −16 12 16	
FIR14.92+0.07	18 14 33.3 −15 57 24	
FIR15.02−0.67	18 17 28.0 −16 13 40	
FIR15.10−0.67	18 17 37.9 −16 09 04	
FIR15.19−0.15	18 15 53.6 −15 49 52	
FIR15.20−0.62	18 17 39.8 −16 02 32	
FJM 1	5 32 48 − 5 25	
FJM 2	5 39 − 1 55	
FJM 3	20 56 13 +57 37	
FJM 3 #1	20 56 30.1 +57 46 38	
FJM 3 #2	20 56 25.2 +57 45 47	
FJM 3 #3	20 56 28.6 +57 43 08	
FJM 3 #4	20 56 07.8 +57 40 02	
FJM 3 #5	20 56 09.4 +57 39 16	
FJM 3 #6	20 56 34.5 +57 35 28	
FJM 3 #7	20 56 00.2 +57 35 30	
FJM 3 #8	20 55 27.5 +57 39 26	
FJM 3 #9	20 55 41.9 +57 40 59	
FJM 3 #10	20 55 33.3 +57 46 26	
FJM 3 #11	20 56 25.6 +57 49 01	
FJM 3 #12	20 56 41.3 +57 48 24	
FJM 3 #13	20 56 57.2 +57 47 47	
FJM 3 #14	20 56 49.6 +57 53 22	
FJM 3 #15	20 56 29.7 +57 54 27	
FJM 3 #16	20 56 08.2 +57 55 12	
FJM 3 #17	20 56 58.6 +58 03 00	
FJM 3 #18	20 56 16.7 +58 04 58	
FJM 3 #19	20 55 40.6 +58 05 11	
FJM 3 #20	20 55 40.7 +57 45 21	
FJM 4	2 20 45 +61 52	
FJM 5	2 36 34 +64 51	
FJM 6	21 08 57 +47 17 00	751202
FJM 6 #1	21 11 05.5 +47 06 55	
FJM 6 #2	21 10 59.7 +47 10 28	
FJM 6 #3	21 10 47.5 +47 10 16	
FJM 6 #4	21 10 38.3 +47 10 53	
FJM 6 #5	21 10 31.0 +47 12 02	
FJM 6 #6	21 10 32.1 +47 07 54	
FJM 6 #7	21 10 30.5 +47 15 40	
FJM 6 #8	21 10 24.9 +47 10 16	
FJM 6 #9	21 10 20.2 +47 08 00	
FJ1	9 30 +54 30	
FJ2	7 27 − 9 48	
FJ3	1 18 +22 18	
FJ4	5 34 −21 48	
R FOR	2 26 59.9 −26 18 32	CSI 79
RZ FOR	3 30 18.5 −25 49 34	"
ST FOR	2 42 15.1 −29 26 10	"
X FOR	2 40 45.3 −26 19 49	"
FORNAX #2	2 36 06 −35 01	619901
FORNAX #3	2 37 48 −34 29	"
FORNAX #4	2 38 06 −34 45	"
FORNAX #5	2 40 24 −34 21	"
FORNAX BM 1	2 37 36 −34 32 51	
FORNAX BM 2	2 37 51 −34 35	ED
FORNAX BM 3	2 37 57 −34 35	"
FORNAX BM 5	2 37 52 −34 38	"
FORNAX BM 7	2 38 10 −34 45	"
FORNAX BM 9	2 38 07 −34 47	"
FORNAX BM 10	2 38 02 −34 47	"
FORNAX BM 11	2 38 04 −34 48	"
FORNAX BM 12	2 38 00 −34 49	"
FORNAX BM 13	2 37 52 −34 47	"
FORNAX BM 16	2 37 36 −34 45	"
FORNAX BM 22	2 37 27 −34 51	"
FORNAX BM 24	2 37 12 −34 52	"
FORNAX BM 28	2 37 20 −34 42	"
FORNAX BM 29	2 37 19 −34 41	"
FORNAX BM 32	2 36 47 −34 46	"
FORNAX GLOB2	2 37 −34	
FORNAX GLOB3	" "	
FORNAX GLOB4	" "	
FORNAX GLOB5	" "	
FORNAX NOM.	" "	ED
G 1	3 40 16 +32 08 04	"
G 2	3 40 43 +32 03 40	"
G 3	3 40 50 +32 00 22	"
G 4	3 41 00 +31 57 52	"
G 5	3 41 01 +31 57 40	"
G 6	3 41 11 +32 00 04	"
G 7	3 41 13 +31 58 10	"
G 8	3 41 16 +32 01 34	"
G 9	3 41 16 +32 00 46	"
G 10	3 41 22 +32 00 28	"
G 11	3 41 23 +31 56 58	"
G 12	3 41 27 +32 00 40	"
G 13	3 41 29 +31 57 22	"
G 14	3 41 40 +32 06 10	"
G 15	3 41 41 +32 07 28	"
G 16	3 41 42 +32 09 52	"
G 17	3 41 59 +32 01 04	"
G 18	3 41 59 +31 51 10	"
GAL A	18 45 50 +79 44	"
GAL ANTICEN	5 13 55 +22 18 41	"
GAL B	18 45 18 +79 42	"
GAL CEN	17 37 −33 06	"
GAL CEN	17 42 −29 00	"
GAL CEN	17 42 28 −28 55 00	"
GAL CEN	17 42 29.2 −28 59 12	"
GAL CEN	17 42 29.4 −28 59 23	"
GAL CEN	17 42 29.5 −28 59 18	
GAL CEN	17 42 29.9 −28 59 25	ED
GAL CEN	17 42 30 −28 59 24	
GAL CEN	17 42 32 −28 59 42	
GAL CEN	17 42 32.5 −28 59 22	ED
GAL CEN	17 42 32.6 −28 59 27	"

NAME	RA (1950) DEC	POS REF
	h m s ° ′ ″	
GAL CEN	17 43 −28 52	"
GAL CEN	17 44 −28 54	"
GAL CEN	18 00 −28	"
GAL CEN #A	17 42 29.6 −28 59 04	"
GAL CEN #B	17 42 29.6 −28 59 16	"
GAL CEN #C	17 42 29.6 −28 59 26	"
GAL CEN #D	17 42 28.8 −28 59 22	"
GAL CEN #E	17 42 28.9 −28 59 32	"
GAL CEN #F	17 42 28.9 −28 59 11	"
GAL CEN #G	17 42 29.2 −28 59 20	"
GAL CEN #H	17 42 28.8 −28 59 22	"
GAL CEN #I	17 42 28.5 −28 59 22	"
GAL CEN #III	17 42 28.9 −28 59 14	
GAL CEN #1	17 42 29.5 −28 59 17	
GAL CEN #1	17 42 29.6 −28 59 17	
GAL CEN #1	17 42 29.7 −28 59 17	
GAL CEN #1	17 42 29.7 −28 59 18	
GAL CEN #1	17 42 29.7 −28 59 19	
GAL CEN #1	17 42 30.6 −28 59 20	ED
GAL CEN #2	17 42 29.0 −28 59 21	750903
GAL CEN #2	17 42 29.1 −28 59 22	
GAL CEN #2	17 42 29.1 −28 59 26	
GAL CEN #2	17 42 30.0 −28 59 26	ED
GAL CEN #3	17 42 28.9 −28 59 14	
GAL CEN #3	17 42 29.0 −28 59 14	
GAL CEN #3	17 42 29.7 −28 59 18	ED
GAL CEN #4	17 42 30.3 −28 59 23	
GAL CEN #4	17 42 31.1 −28 59 28	ED
GAL CEN #5	17 42 29.7 −28 59 06	
GAL CEN #5	17 42 29.8 −28 59 08	
GAL CEN #5	17 42 29.9 −28 59 07	
GAL CEN #6	17 42 28.6 −28 59 15	750903
GAL CEN #7	17 42 29.2 −28 59 12	
GAL CEN #7	17 42 29.3 −28 59 12	
GAL CEN #8	17 42 29.3 −28 58 49	
GAL CEN #8	17 42 29.4 −28 58 48	
GAL CEN #9	17 42 29.6 −28 59 23	
GAL CEN #10	17 42 29.7 −28 59 13	
GAL CEN #10	17 42 29.8 −28 59 12	
GAL CEN #11	17 42 28.4 −28 59 06	
GAL CEN #12	17 42 28.9 −28 59 25	
GAL CEN #13	17 42 28.9 −28 59 19	
GAL CEN #14	17 42 29.2 −28 59 26	
GAL CEN #15	17 42 29.2 −28 59 08	
GAL CEN #16	17 42 29.3 −28 59 18	
GAL CEN #17	17 42 30.2 −28 59 12	
GAL CEN #18	17 42 30.3 −28 59 27	
GAL CEN #19	17 42 30.3 −28 59 35	
GAL CEN #22	17 42 29.1 −28 59 42	
GAL CEN IRS1	17 42 29.6 −28 59 17	
GAL CEN IRS1	17 42 29.7 −28 59 17	750903
GAL CEN IRS1	17 42 29.8 −28 59 18	
GAL CEN IRS1	17 42 29.8 −28 59 19	780109
GAL CEN IRS2	17 42 29.0 −28 59 21	750903
GAL CEN IRS2	17 42 29.0 −28 59 23	
GAL CEN IRS3	17 42 29.1 −28 59 15	
GAL CEN IRS4	17 42 30.4 −28 59 23	
GAL CEN IRS4	17 42 30.4 −28 59 24	780109
GAL CEN IRS5	17 42 29.9 −28 59 07	750903
GAL CEN IRS5	17 42 30.0 −28 59 09	
GAL CEN IRS5	17 42 30.0 −28 59 12	780109
GAL CEN IRS6	17 42 28.7 −28 59 17	
GAL CEN IRS6	17 42 28.7 −28 59 18	780109
GAL CEN IRS7	17 42 27.2 −28 59 13	ED
GAL CEN IRS7	17 42 29.2 −28 59 12	
GAL CEN IRS7	17 42 29.3 −28 58 41	ED
GAL CEN IRS7	17 42 29.3 −28 59 13	780109
GAL CEN IRS7	17 42 29.3 −28 59 45	ED
GAL CEN IRS7	17 42 31.4 −28 59 13	"
GAL CEN IRS8	17 42 29.5 −28 58 49	780109
GAL CEN IRS9	17 42 29.6 −28 59 23	750903
GAL CEN IRS9	17 42 29.6 −28 59 25	
GAL CEN IRS9	17 42 29.7 −28 59 26	780109
GAL CEN IRS10	17 42 29.6 −28 59 14	ED
GAL CEN IRS10	17 42 29.7 −28 59 13	750903
GAL CEN IRS10	17 42 29.8 −28 59 14	780109
GAL CEN IRS11	17 42 28.4 −28 59 06	
GAL CEN IRS11	17 42 28.6 −28 59 09	
GAL CEN IRS12	17 42 28.9 −28 59 25	
GAL CEN IRS13	17 42 28.9 −28 59 19	750903
GAL CEN IRS16	17 42 29.3 −28 59 18	
GAL CEN IRS17	17 42 30.2 −28 59 12	
GAL CEN IRS19	17 42 30.3 −28 59 35	750903
GAL CEN IRS20	17 42 29.1 −28 59 23	ED
GAL CEN IRS20	17 42 29.3 −28 59 24	780109
GAL CEN IRS22	17 42 29.1 −28 59 46	
GAL CEN IRS23	17 42 32.1 −28 58 58	
GAL CEN IRS24	17 42 31.8 −28 58 40	
GAL CEN IRS25	17 42 24.0 −28 58 24	
GAL CEN IRS26	17 42 23.9 −28 59 03	
GAL CEN IRS27	17 42 22.2 −28 59 48	
GAL. CENTER	17 51 −25 06	ED
GCS 1	17 41 50 −28 42 04	
GCS 2	17 42 55 −28 44 42	
GCS 3	17 43 05 −28 48 31	
GCS 4	17 43 05 −28 48 40	
GCS 5	17 42 36 −28 55 09	
GCS 6	17 42 38 −28 55 41	
GCS 7	17 42 52 −29 00 32	
GCS 8	17 42 39 −29 02 17	
GCS 9	" "	
GCS 10	17 41 35 −29 04 32	
GCS 11	17 40 53 −29 05 38	
GCS 12	17 43 34 −29 05 42	
GCS 13	17 41 53 −29 09 53	
GCS 14	17 42 22 −29 11 09	
GCS 15	17 40 59 −29 18 48	
GD 140	11 34 30 +30 05	679903
GD 190	15 42 06 +18 16	"
ALF GEM	7 31 24.6 +32 00 00	CSI 79
BET GEM	7 42 15.4 +28 08 54	"
BM GEM	7 17 55.9 +25 05 37	"
BN GEM	7 34 13.3 +17 01 00	"
BU GEM	6 09 17.1 +22 55 16	"
DY GEM	6 33 05.3 +14 14 11	"
EPS GEM	6 40 51.3 +25 10 55	"
ETA GEM	6 11 51.4 +22 31 21	"
GAM GEM	6 34 49.3 +16 26 36	"

NAME	RA (1950) DEC	POS REF
	h m s ° ′ ″	
GH GEM	7 01 18 +12 06 41	GCVS
MUU GEM	6 19 56.0 +22 32 27	CSI 79
NUU GEM	6 25 59.6 +20 14 43	"
OME GEM	6 59 21.9 +24 17 17	"
R GEM	7 04 20.7 +22 46 56	"
RHO GEM	7 25 53.7 +31 53 07	"
S GEM	7 40 02.5 +23 34 07	"
SS GEM	6 05 33.4 +22 37 31	"
ST GEM	7 35 45.9 +34 35 56	"
SU GEM	6 10 50.6 +27 42 26	"
T GEM	7 46 18.1 +23 51 38	"
TU GEM	6 07 46.7 +26 01 33	"
TV GEM	6 08 50.9 +21 52 50	"
U GEM	7 52 09.3 +22 13 11	"
UPS GEM	7 32 50.5 +27 00 29	"
V GEM	7 20 19.9 +13 11 19	"
VW GEM	6 38 54.6 +31 30 14	779907
VX GEM	7 10 02.3 +14 41 09	CSI 79
W GEM	6 32 05.5 +15 22 15	"
WY GEM	6 08 53.9 +23 13 09	"
X GEM	6 43 54.9 +30 19 52	"
XI GEM	6 42 28.9 +12 57 03	"
YY GEM	7 31 26.1 +31 58 49	779907
ZET GEM	7 01 08.6 +20 38 42	CSI 79
ZZ GEM	6 20 50.6 +25 02 26	"
3 GEM	6 06 41.7 +23 07 23	"
9 GEM	6 13 55.6 +23 45 33	"
12 GEM	6 16 18 +23 18	
12 GEM A	6 16 20.1 +23 17 45	CSI 79
12 GEM B	6 16 24.3 +23 17 48	"
12 GEM IRS1	6 16 27.0 +23 21 24	
12 GEM IRS2	6 16 23.6 +23 18 17	
48 GEM	7 09 24.1 +24 12 48	CSI 79
GICLAS 51−15	8 26 52 +26 57 06	
GLIESE 11AB	0 10 29.9 +69 02 11	CSI 79
GLIESE 15A	0 15 30.9 +43 44 21	"
GLIESE 15B	0 15 33.9 +43 44 45	"
GLIESE 29.1	0 40 04.9 +35 16 24	"
GLIESE 48	0 58 47.9 +71 25 00	"
GLIESE 49	0 59 23.9 +62 04 28	"
GLIESE 51	1 00 07.4 +62 05 50	"
GLIESE 65AB	1 36 24.9 −18 12 40	"
GLIESE 65B	" "	"
GLIESE 83.1	1 57 27.9 +12 50 06	"
GLIESE 84.2	2 03 47.9 +44 57 12	"
GLIESE 96	2 18 57.2 +47 39 05	"
GLIESE 102	2 30 42.9 +24 42 54	"
GLIESE 105.5	2 38 07.6 + 0 58 57	
GLIESE 105A	2 33 20.0 + 6 38 57	CSI 79
GLIESE 105B	2 33 30.4 + 6 38 03	"
GLIESE 109	2 41 17.6 +25 19 05	"
GLIESE 129	3 10 28.9 +18 39 23	"
GLIESE 144	3 30 34.3 − 9 37 34	"
GLIESE 157.1	3 56 47.7 +25 57 11	"
GLIESE 166C	4 13 03.6 − 7 44 05	"
GLIESE 169.1	4 26 49.9 +58 53 21	"
GLIESE 170	4 26 58.9 +39 44 53	"
GLIESE 176	4 39 57.9 +18 52 48	"
GLIESE 182	4 56 58.9 + 1 42 36	"
GLIESE 184	4 59 16.9 +53 04 47	"
GLIESE 185AB	5 00 19.9 −21 19 23	"
GLIESE 192	5 09 43.9 +19 36 12	"
GLIESE 199	5 16 43.7 −21 26 40	"
GLIESE 205	5 28 55.3 − 3 41 03	"
GLIESE 207.1	5 31 09.9 + 1 54 54	"
GLIESE 213	5 39 13.9 +12 29 18	"
GLIESE 228	6 08 08.7 +10 20 58	"
GLIESE 229	6 08 28.1 −21 50 34	"
GLIESE 232	6 21 35.2 +23 28 15	"
GLIESE 234AB	6 26 50.9 − 2 46 10	"
GLIESE 239	6 34 19.9 +17 36 08	"
GLIESE 247	6 45 26.6 +60 23 13	"
GLIESE 251	6 51 34.9 +33 20 18	"
GLIESE 268	7 06 38.9 +38 37 23	"
GLIESE 270	7 16 14.4 +32 55 48	"
GLIESE 273	7 24 42.9 + 5 22 42	"
GLIESE 277A	7 28 39.4 +36 19 44	"
GLIESE 277B	7 28 38.9 +36 20 24	"
GLIESE 278C	7 31 26.1 +31 58 49	779907
GLIESE 285	7 42 03.9 + 3 40 42	CSI 79
GLIESE 299	8 09 11 + 8 59 42	
GLIESE 299	8 09 11.3 + 9 01 34	CSI 79
GLIESE 300	8 10 29.9 −21 22 58	"
GLIESE 324A	8 49 37.3 +28 31 22	"
GLIESE 324B	8 49 41.9 +28 30 29	"
GLIESE 326AB	8 51 41.9 −12 55 35	"
GLIESE 338A	9 11 00.9 +52 54 09	"
GLIESE 338B	9 10 58.7 +52 54 06	"
GLIESE 347	9 26 24.9 − 7 08 40	"
GLIESE 347A	9 26 25 − 7 08 30	
GLIESE 352	9 28 51.5 −13 16 01	CSI 79
GLIESE 365	9 40 16.6 +42 55 56	"
GLIESE 369	9 48 39.5 −12 04 28	"
GLIESE 380	10 08 19.0 +49 42 27	"
GLIESE 382	10 09 46.3 − 3 29 39	"
GLIESE 388	10 16 53.9 +20 07 18	"
GLIESE 390	10 22 43.9 − 9 58 33	"
GLIESE 390	10 22 44 − 9 58 36	
GLIESE 393	10 26 23.4 + 1 06 28	CSI 79
GLIESE 402	10 48 18.9 + 7 05 06	"
GLIESE 406	10 54 05.9 + 7 19 14	
GLIESE 406	10 54 06 + 7 19 12	
GLIESE 411	11 00 36.5 +36 18 19	CSI 79
GLIESE 412A	11 02 59.7 +43 47 01	"
GLIESE 412B	11 03 01.9 +43 46 41	"
GLIESE 413	11 05 53.4 +16 02 39	"
GLIESE 424	11 17 28.5 +66 07 02	"
GLIESE 445	11 44 34.9 +78 57 42	"
GLIESE 447	11 45 08.9 + 1 06 00	"
GLIESE 463	12 20 44.9 +64 18 12	"
GLIESE 465	12 22 12.9 −17 55 59	"
GLIESE 473	12 30 50.9 + 9 17 32	"
GLIESE 473AB	" "	"
GLIESE 487	12 47 06.0 +66 23 03	"
GLIESE 488	12 48 10 − 0 29 24	709903
GLIESE 494	12 58 19.7 +12 38 43	CSI 79
GLIESE 512	13 25 45.9 − 2 05 28	"
GLIESE 513	13 26 53.9 +11 42 59	"

NAME	RA (1950)	DEC	POS REF
	h m s	° ′ ″	
GLIESE 514	13 27 26.6	+10 39 02	"
GLIESE 514.1	13 27 30.5	− 8 25 44	"
GLIESE 516AB	13 30 17.9	+17 04 12	"
GLIESE 526	13 43 11.7	+15 09 41	"
GLIESE 537AB	14 00 26.9	+46 34 53	"
GLIESE 544B	14 17 00.6	− 4 55 16	"
GLIESE 546	14 19 47.7	+29 51 39	"
GLIESE 550.1	14 25 30.9	+14 03 47	"
GLIESE 551	14 26 18.9	−62 28 05	"
GLIESE 553.1	14 28 19.9	−12 04 10	"
GLIESE 555	14 31 34.9	−12 18 33	"
GLIESE 568AB	14 51 41.5	+23 45 21	"
GLIESE 570B	14 54 31.0	−21 11 16	"
GLIESE 581	15 16 52.2	− 7 32 20	"
GLIESE 585	15 21 35.5	+17 39 38	"
GLIESE 595	15 39 19.9	−19 18 34	"
GLIESE 616.2	16 15 58.9	+55 23 47	"
GLIESE 617	16 16 36.9	+67 21 31	"
GLIESE 617A	"	"	"
GLIESE 617B	16 16 39.3	+67 22 34	"
GLIESE 628	16 27 31.0	−12 31 50	"
GLIESE 631	16 33 42.9	− 2 13 01	"
GLIESE 642	16 51 52.9	+11 59 29	"
GLIESE 643	16 52 45.0	− 8 13 47	"
GLIESE 644	16 52 48.3	− 8 14 39	"
GLIESE 653	17 02 27.9	− 4 58 39	"
GLIESE 654	17 02 38.2	− 5 00 19	"
GLIESE 661AB	17 10 39.6	+45 44 58	"
GLIESE 669A	17 17 53.9	+26 32 48	"
GLIESE 669B	17 17 52.9	+26 32 48	"
GLIESE 673	17 23 15.7	+ 2 10 12	"
GLIESE 679	17 30 13.3	+34 18 17	"
GLIESE 687	17 36 42.3	+68 23 05	"
GLIESE 695BC	17 44 27.7	+27 44 45	"
GLIESE 699	17 55 22.9	+ 4 33 18	"
GLIESE 702AB	18 02 55.4	+ 2 30 35	"
GLIESE 706	18 07 57.9	+38 27 11	"
GLIESE 717	18 30 42.3	−11 40 16	"
GLIESE 719	18 32 44.5	+51 40 58	779907
GLIESE 720	18 33 49.3	+45 41 40	CSI 79
GLIESE 725A	18 42 16.7	+59 32 38	"
GLIESE 725AB	"	"	"
GLIESE 725B	18 42 17.7	+59 32 23	"
GLIESE 729	18 46 44.9	−23 53 28	"
GLIESE 735	18 53 02.9	+ 8 20 17	"
GLIESE 740	18 55 33.6	+ 5 51 23	"
GLIESE 745A	19 04 58.6	+20 48 56	"
GLIESE 745B	19 05 04.9	+20 48 05	"
GLIESE 747AB	19 05 43.7	+32 26 42	"
GLIESE 748	19 09 35.2	+ 2 48 42	
GLIESE 748	19 09 38	+ 2 48 36	
GLIESE 752	19 14 29.3	+ 5 05 57	CSI 79
GLIESE 752A	"	"	"
GLIESE 766AB	19 43 42.7	+27 01 11	"
GLIESE 777	20 01 22.9	+29 43 54	"
GLIESE 778	20 01 46.6	+23 12 38	"
GLIESE 781	20 03 54.9	+54 18 12	"
GLIESE 786	20 12 24.0	+77 04 48	"
GLIESE 791.2	20 27 21.9	+ 9 31 18	"
GLIESE 806	20 43 16.0	+44 18 26	"
GLIESE 809	20 52 17.7	+61 58 33	"
GLIESE 811.1	20 54 04	−10 37 36	
GLIESE 811.1	20 54 04.3	−10 37 14	CSI 79
GLIESE 815AB	20 58 08.9	+39 52 42	"
GLIESE 829	21 27 11.9	+17 25 06	"
GLIESE 830	21 27 16.3	−12 43 33	"
GLIESE 860AB	22 26 14.3	+57 26 51	"
GLIESE 866	22 35 44.9	−15 35 35	"
GLIESE 867	22 36 01.2	−20 52 47	"
GLIESE 867A	"	"	"
GLIESE 867B	22 36 00.9	−20 52 24	"
GLIESE 873	22 44 41.2	+44 04 45	"
GLIESE 876	22 50 31.3	−14 31 00	"
GLIESE 880	22 54 10.0	+16 17 22	"
GLIESE 884	22 57 38.1	−22 47 37	"
GLIESE 892	23 10 51.7	+56 53 30	"
GLIESE 896AB	23 29 18.9	+19 39 43	"
GLIESE 897AB	23 30 08.9	−17 01 32	"
GLIESE 905	23 39 25.9	+43 55 12	"
GLIESE 908	23 46 35.5	+ 2 08 10	"
GMB 1830	11 50 06.1	+38 04 38	"
GP OBJECT	13 23 09.3	−42 41 02	809906
GPA	18 58 28.5	−37 02 33	
GRB 03/05/79	5 26 00	−66 08	829908
GRB 03/05/79M	"	"	
GRB 11/19/78B	1 16 27	−28 50 50	829908
BET GRU	22 39 41.3	−47 08 47	CSI 79
DEL 2 GRU	22 26 46.6	−44 00 19	"
PI 1 GRU	22 19 41.1	−46 12 01	"
R GRU	21 45 20.6	−47 08 11	"
S GRU	22 23 00.0	−48 41 50	"
T GRU	22 22 46.1	−37 49 22	"
ZET GRU	22 57 56.3	−53 01 21	"
GRW+70 5824	13 38	+70 33	ED
GRW+70 8247	19 00 39.1	+70 35 07	
GS 5	16 22 17.7	−24 20 06	730903
GS 8	16 22 20.5	−24 23 39	"
GS 8	16 22 20.8	−24 23 26	
GS 15	16 22 33.9	−24 27 13	780902
GS 23	16 23 01.6	−24 16 48	
GS 23	16 23 02.1	−24 16 44	730903
GS 26	16 23 08.9	−24 14 13	"
GS 28	16 23 15.7	−24 13 42	"
GS 29	16 23 15.7	−24 15 43	"
GS 30	16 23 19.7	−24 16 14	"
GS 31	16 23 21.4	−24 14 13	"
GS 32	16 23 22.5	−24 18 13	"
GS 35	16 23 32.7	−24 16 44	"
GS 39	16 23 43.3	−24 16 24	780902
GSS 1	16 23 32.7	−24 16 43	
GX 2+5 IR	17 29 00	−24 42	739912
GX 339−4	16 58	−48	ED
GX 354+0 C3	17 28 39	−33 48 01	"
GX 354+0 C4	17 28 40	−33 47 58	"
GX 354+0 C6	17 28 39	−33 45 40	"
G0.0−0.0	17 42 28	−28 55 00	"
G0.01+0.02	17 42 25	−28 53 52	"
G0.01−0.12	17 42 57	−28 58 16	"
G0.07+0.04	17 42 28	−28 50 10	"
G0.4−0.1	17 44	−28 38	"
G0.5+0.0(N)	17 43 55	−28 29 30	"
G0.5+0.0(S)	17 43 50	−28 32 00	"
G0.55−0.85	17 47 03.7	−28 53 41	
G0.6+0.0	17 44 02	−28 25 30	ED
G0.6−0.1	17 41 21	−29 22 06	
G0.7−0.0	17 44 10	−28 21 48	ED
G3.2−0.5	17 51 53	−26 26	"
G8.1+0.2	18 00 01.6	−21 48 39	
G9.62+0.19	18 03 15.7	−20 31 47	
G10.6−0.4	18 07 31	−19 58	
G12.2−0.1	18 09 45	−18 25 05	
G12.2−0.1IRS1	18 09 43.6	−18 25 10	
G12.2−0.1IRS2	18 09 50	−18 26 54	
G12.2−0.1IRS3	18 09 53	−18 23 36	
G12.8−0.2	18 11 19	−17 57	ED
G14.6+0.0	18 14 09.8	−16 15 40	
G19.6−0.2	18 24 50.5	−11 58 35	
G21.1−1.4	18 31 54	−11 12	ED
G23.95+0.15	18 31 42.1	− 7 57 24	
G24.29−0.15	18 33 24.3	− 7 47 43	
G24.49−0.04	18 33 22.9	− 7 34 07	
G28.86+0.07	18 41 08.3	− 3 38 27	
G29.9+0.0	18 43 30	− 2 43	
G29.9−0.0	18 43	− 2 45	ED
G29.9−0.0	18 43 27.7	− 2 42 48	750807
G31.4−0.3	18 46 57.4	− 1 32 21	
G33.9+0.1	18 50 14.9	+ 0 51 14	
G34.3+0.1	18 50 46.2	+ 1 11 21	
G35.2−1.7	18 59 14.1	+ 1 09 00	
G45.07+0.13	19 11 02	+10 46	ED
G45.1+0.1	19 11 06	+10 47 48	"
G45.1+0.1	19 11 06.4	+10 48 24	750706
G45.1+0.1 IRS	19 11 06	+10 47 48	ED
G45.1−0.1 IRS	"	"	"
G45.13+0.14A	19 12 00.0	+11 04 00	750706
G45.13+0.34	19 11 06.3	+10 48 29	
G45.18+0.13	19 11 46.9	+11 07 15	
G45.5+0.1	19 11 58.3	+11 05 20	771109
G45.5+0.1	19 12 00.0	+11 04 00	
G45.5+0.1 #2	19 11 58.3	+11 05 20	771109
G45.5+0.1IRS1	19 12 00.2	+11 04 06	
G45.5+0.1IRS2	19 11 57.8	+11 05 24	
G45.5+0.1IRS3	19 11 43.6	+11 07 45	
G45.5+0.1IRS4	19 11 39.5	+11 05 03	
G75.77+0.34	20 19 50.0	+37 16 16	
G75.84+0.4	20 19 47	+37 21 30	
G75.84+0.4	20 19 47.4	+37 21 32	770401
G75.84+0.40	"	"	
G110.25+0.01I	23 04 15.9	+59 59 55	
G133.7+1.2	2 21 52	+61 51 36	
G133.9+1.1	2 23 29	+61 38 54	
G268.0−1.1	8 57 27	−47 23 17	ED
G282.0−1.2	10 04 55.9	−56 57 49	
G282.0−1.2	10 04 55.9	−56 57 56	
G285.3−0.0	10 29 35.7	−57 46 37	
G287.6−0.6	10 43 16	−59 23 47	ED
G291.3−0.7	11 10	−61 02	"
G291.3−0.7	11 10 00	−61 02 10	"
G291.6−0.5	11 12 50.8	−60 59 37	"
G298.2−0.3	12 07	−62 30	"
G298.2−0.3	12 07 14	−62 30 39	"
G298.2−0.3	12 07 21	−62 33	
G298.2−0.3	12 07 22.5	−62 33 20	
G298.2−0.3	12 07 22.7	−62 33 14	
G298.2−0.3 E	12 07 21.7	−62 33 12	ED
G298.2−0.3 W	12 07 19.5	−62 33 12	"
G316.8−0.1 #1	14 41 02.7	−59 37 57	
G316.8−0.1 #2	14 41 02.8	−59 37 06	
G316.8−0.1 #3	14 41 02.8	−59 36 41	
G316.8−0.1 #4	14 41 04.4	−59 38 09	
G316.8−0.1 #5	14 41 05.1	−59 38 43	
G316.8−0.1 #6	14 41 25.0	−59 37 00	
G316.8−0.1 #7	14 41 28.5	−59 36 51	
G316.8−0.1 #8	14 41 30.2	−59 37 19	
G316.8−0.1 #9	14 41 31.8	−59 37 36	
G316.8−0.1#10	14 41 33.6	−59 36 53	
G316.8−0.1#11	14 41 37.9	−59 36 41	
G322.2+0.6	15 15	−56 28	ED
G324.2+0.1	15 29 01.0	−55 46 08	811014
G327.3−0.5	15 49	−54 24	ED
G330.9−0.4	16 07	−51 58	"
G331.5−0.1	16 08	−51 21	"
G332.8−0.6	16 16	−50 49	"
G333.1−0.4	16 17 14.6	−50 28 50	
G333.1−0.4#1	16 17 12.8	−50 28 05	ED
G333.1−0.4#3	16 17 11.3	−50 27 52	"
G333.3−0.4	16 17 44.1	−50 18 02	
G333.6−0.2	16 18 20	−49 58 36	ED
G333.6−0.2	16 18 22.5	−49 58 58	
G333.6−0.2	16 18 22.5	−49 59 00	
G333.6−0.2	16 18 22.6	−49 58 58	ED
G333.6−0.2	16 18 23.0	−49 58 54	
G333.6−0.2	16 18 23.4	−49 58 59	
G333.6−0.2	16 18 23.5	−49 58 45	ED
G333.6−0.2	16 18 23.5	−49 58 58	770403
G333.6−0.2	16 18 23.5	−49 59 11	ED
G333.6−0.2	16 18 23.6	−49 58 57	
G333.6−0.2	16 18 23.6	−49 59 03	
G333.6−0.2	16 18 24.4	−49 58 58	ED
G333.6−0.2	16 18 24.5	−49 59 50	
G333.6−0.2	16 18 26.1	−49 58 23	
G333.6−0.2	16 18 27.1	−49 58 54	
G333.6−0.2#1	16 18 23.1	−49 58 52	
G333.6−0.2#2	16 18 23.1	−49 58 55	
G333.6−0.2#3	16 18 23.1	−49 58 58	
G333.6−0.2#4	16 18 23.1	−49 59 01	
G333.6−0.2#5	16 18 23.6	−49 58 52	
G333.6−0.2#6	16 18 23.6	−49 58 55	
G333.6−0.2#7	16 18 23.6	−49 58 58	
G333.6−0.2#8	16 18 23.6	−49 59 01	
G333.6−0.2#9	16 18 24.1	−49 58 52	
G333.6−0.2#10	16 18 24.1	−49 58 55	
G333.6−0.2#11	16 18 24.1	−49 58 58	
G333.6−0.2#12	16 18 24.1	−49 59 01	
G335.6+2.3	17 22 28	−31 21	ED
G336.5−1.5	16 36	−48 40	"
G337.1−0.2	16 33	−47 27	"
G337.9−.5#1+2	16 37 27.1	−47 01 00	
G337.9−0.5	16 37	−47 04	ED
G337.9−0.5	16 37 33	−47 03 56	"
G337.9−0.5#1	16 37 27.1	−47 01 00	
G337.9−0.5#2	"	"	
G337.9−0.5N	"	"	
G337.9−0.5S	16 37 27.1	−47 01 58	
G345.4−0.9	17 06	−41 30	ED
G348.7−1.0	17 16	−38 54	"
G351.1+0.7	17 16	−35 58	"
G351.31+0.6	17 17	−35 51	"
G351.34+0.6	17 18	−35 49	"
G351.4+0.7	17 17	−35 43	"
G351.6−1.3	17 25 53.0	−36 37 49	
G351.6−1.3	17 26	−36 41	ED
G351.6−1.3	17 26 01	−36 41 06	"
G45−20	10 54 05.9	+ 7 19 14	CSI 79
G51−15	8 26 52	+26 57 06	
G64−12	13 37 29	+ 0 12 54	ED
G69−47	1 02 48	+28 13 36	
G77−31	3 10 40	+ 4 35 12	
G77−31	3 10 40.5	+ 4 35 12	
G95−59	3 46 45	+43 17 36	
G99−37	5 48	− 0 12	
G99−37	5 48 48	− 0 11	LTT
G99−44	5 52 39.9	− 4 08 46	CSI 79
G99−47	5 53 47	+ 5 22 00	GICLAS
G107−70	7 27 05.9	+48 17 24	CSI 79
G112−50	7 49 21	+ 0 08 00	GICLAS
G139−7	22 48	+29 24	
G139−12	17 05 17	+ 7 26 12	
G149−172			
G158−27	0 04 12	− 7 47 54	
G195−19	9 12 28.9	+53 38 54	CSI 79
G224−1	7 05 27.8	−10 39 15	
G231−27	21 06 44	+59 32 06	
G266−157	0 38 57	−22 37 18	799901
G191B2B			
H 0139−68	1 39 37.5	−68 08 32	819919
H 11 LE1			
H 11 LE2			
H−C #10			
H−C #13			
H−C #22			
H−C #23			
H−C #26			
H−C #38			
H−C #50			
H−C #52			
H−C #54			
H−C #57			
H−C #58			
H−C #61			
H−C 1	20 32 04	+42 09	
H−C 2	20 31 03	+40 27	
H−C 3	20 23 46	+40 34	
H−C 4	20 24 51	+39 39	
H−C 6	20 39 03	+40 54	650004
H−C 7	20 40 15	+40 11	
H−C 8	20 41 51	+40 43	
H−H 1	5 33 54.8	− 6 47 02	
H−H 1	5 33 54.9	− 6 47 02	749904
H−H 1	5 33 55.4	− 6 47 24	
H−H 1 (NW)	5 33 54.9	− 6 47 02	749904
H−H 1 STAR	5 33 56	− 6 47 30	ED
H−H 2	5 33 59.5	− 6 48 57	
H−H 2	5 34 01.1	− 6 48 56	
H−H 2 EAST	5 34 57.6	− 6 48 53	
H−H 2 EAST	5 35 01.8	− 6 48 22	
H−H 2A	5 33 59.4	− 6 49 00	749904
H−H 2E	5 34 00.7	− 6 49 00	"
H−H 2G	5 34 00.1	− 6 48 56	"
H−H 2H	5 33 59.7	− 6 49 02	"
H−H 3	5 33 41.9	− 6 44 54	
H−H 7	3 26 02.5	+31 05 13	749904
H−H 7−11	3 25 58.2	+31 05 46	
H−H 7−11	3 26 00.0	+31 06 27	
H−H 11	3 25 59.0	+31 05 35	749904
H−H 12	3 25 51.8	+31 09 38	
H−H 12	3 25 55.6	+31 10 10	
H−H 12	3 25 56.0	+31 10 05	
H−H 12 SOUTH#1	3 25 51.1	+31 08 27	
H−H 12 SOUTH#2	3 25 51.3	+31 06 05	
H−H 24	5 43 33.8	− 0 12 48	
H−H 24	5 43 34.4	− 0 11 17	
H−H 24	5 43 34.5	− 0 11 07	
H−H 24D	5 43 36.1	− 0 11 02	749904
H−H 24IR	5 43 34.4	− 0 11 17	800411
H−H 28	4 28 12.0	+17 57 01	
H−H 29	4 28 32.3	+17 59 30	
H−H 32	19 18 07.9	+10 56 21	749904
H−H 39	6 36 23.0	+ 8 53 12	
H−H 40	5 32 54.5	− 6 20 16	749904
H−H 41/42	5 33 35.8	− 5 05 45	
H−H 43	5 33 44.9	− 7 11 07	
H−H 46			
H−H 47			
H−H 48			
H−H 49			
H−H 50			
H−H 52			
H−H 53			
H−H 54B			
H−H 56			
H−H 57			
H−H 100	18 58 26.7	−37 02 36	
H−H 100	18 58 28.3	−37 02 27	
H−H 100IR	"	"	740103
H−H 101	18 58 12.3	−37 07 17	
H−H 103	21 41 15.8	+65 49 55	
NEAR H−H 1	5 33 59.4	− 6 47 24	ED
NEAR H−H 2	5 34 01.1	− 6 48 56	"
HARO S6−2			
HARO 1−1	16 18 31.1	−26 05 22	729902
HARO 1−4	16 22 10.5	−23 12 24	"
HARO 1−8	16 23 47.4	−23 08 09	"
HARO 1−14	16 28 03.1	−23 58 07	"

NAME	RA (1950) DEC	POS REF
	h m s ° ′ ″	
HARO 1−16	16 28 31.7 −24 21 13	"
HARO 13A	5 36 07 − 7 07	IC
HARO 14A	5 35 45.4 − 7 11 06	
HARO 2−249	5 36 23 − 7 12 47	
HARO 2−249C	5 36 22 − 7 12 50	
HARO 4−255	5 36 55 − 7 27	729902
HARO 6−5		
HARO 6−8		
HARO 6−8/C		
HARO 6−13	4 29 13.5 +24 22 40	780909
HARO 6−16	4 29 25 +24 11	ED
HARO 6−17	4 29 32 +24 13	"
HARO 6−18	4 29 34 +24 13	"
HARO 6−19	4 29 37.6 +24 15 08	
HARO 6−28	4 32 55.9 +22 48 30	ED
HARO 6−35		
HARO 6−37	4 44 05.9 +16 57 19	729902
HARO 7−2	5 39 26 − 8 02 19	"
HB 4	17 38 48.4 −24 40 34	739909
HB 5	17 44 44.5 −29 58 53	"
HB 6	17 52 06.8 −21 44 10	"
HB 7	18 52 23.8 −32 19 49	769910
HB 12	23 23 57 +57 54 24	709904
HBV 475	20 49 02.6 +35 23 37	749903
HD 26	0 02 47.3 + 8 30 35	CSI 79
HD 108	0 03 26.7 +63 24 05	"
HD 1032	0 11 28.0 −85 16 19	"
HD 1038	0 12 06.0 −19 12 33	"
HD 1160	0 13 23.1 + 3 58 24	
HD 1544	0 17 21.5 +61 47 19	CSI 79
HD 1613	0 17 59.3 +61 36 06	"
HD 2811	0 28 53.0 −43 52 58	
HD 2905	0 30 08.3 +62 39 21	CSI 79
HD 3029	0 31 02.3 +20 09 30	
HD 3369	0 34 12.1 +33 26 39	CSI 79
HD 3421	0 34 40.0 +35 07 27	"
HD 3651	0 36 45.3 +20 58 51	"
HD 4004	0 40 28.7 +64 29 17	"
HD 4174	0 41 52.6 +40 24 21	"
HD 4628	0 45 45.3 + 5 01 24	"
HD 4727	0 47 02.7 +40 48 24	"
HD 4817	0 48 15.9 +61 32 01	"
HD 5384	0 53 10.7 − 7 37 01	"
HD 5550	0 55 19.6 +66 04 56	"
HD 5996	0 59 35.3 +68 57 37	"
HD 6327	1 02 15.0 +60 09 08	"
HD 6582	1 04 55.6 +54 40 32	"
HD 6961	1 08 02.5 +54 53 03	"
HD 7636	1 14 18.3 +57 22 07	"
HD 7674	1 13 58.0 −13 48 40	"
HD 7902	1 16 41.9 +57 56 43	"
HD 7983	1 16 30.6 − 9 11 44	"
HD 8498	1 21 11.3 −31 12 19	"
HD 8538	1 22 31.4 +59 58 33	"
HD 8879	1 24 39.9 −32 48 05	"
HD 9105	1 27 53.9 +63 05 24	"
HD 9311	1 29 54.1 +60 25 45	"
HD 9974	1 35 38.9 +57 54 21	"
HD 10476	1 39 46.5 +20 01 33	"
HD 10494	1 40 44.0 +61 35 55	"
HD 10516	1 40 30.7 +50 26 15	"
HD 10700	1 41 44.6 −16 11 59	"
HD 10780	1 44 06.3 +63 36 23	"
HD 11092	1 47 38.2 +64 36 26	"
HD 11241	1 48 41.3 +54 54 01	"
HD 11636	1 51 52.3 +20 33 50	"
HD 11961	1 55 10.6 +30 53 30	"
HD 11979	1 55 37.3 +45 11 31	"
HD 12111	1 57 48.4 +70 39 56	"
HD 12302	1 59 05.3 +59 26 51	"
HD 12399	2 00 05.5 +63 59 50	"
HD 12953	2 05 09.7 +58 11 12	"
HD 13043	2 05 01.7 − 0 50 59	"
HD 13268	2 08 02.6 +55 55 25	"
HD 13476	2 10 08.5 +58 19 38	"
HD 13658	2 11 40.5 +57 54 35	"
HD 13661	2 11 28.1 +54 17 56	"
HD 13669	2 11 35.0 +55 33 37	"
HD 13854	2 13 20.9 +56 49 25	"
HD 14134	2 15 32.6 +56 54 19	"
HD 14142	2 15 45.7 +58 43 54	779907
HD 14143	2 15 41.9 +56 56 22	CSI 79
HD 14242	2 16 44.0 +59 26 32	"
HD 14270	2 16 57.0 +56 45 51	779907
HD 14322	2 17 13.0 +55 40 48	CSI 79
HD 14330	2 17 27.1 +56 55 47	779907
HD 14404	2 18 08.1 +57 38 06	"
HD 14422	2 18 17.3 +57 09 30	CSI 79
HD 14433	2 18 22.3 +57 00 52	"
HD 14434	2 18 20.0 +56 40 36	"
HD 14442	2 18 31.9 +59 19 18	"
HD 14489	2 18 51.1 +55 37 05	"
HD 14535	2 19 19.9 +57 01 04	"
HD 14542	2 19 26.5 +57 09 34	"
HD 14580	2 19 50.4 +56 59 05	"
HD 14605	2 20 03.1 +56 20 51	"
HD 14818	2 21 43.0 +56 23 03	"
HD 14826	2 21 46.9 +57 12 42	"
HD 14947	2 23 07.9 +58 39 04	"
HD 14956	2 23 09.5 +57 27 16	"
HD 15238	2 25 58.5 +60 27 17	"
HD 15253	2 25 52.7 +55 18 48	"
HD 15316	2 26 21.2 +57 35 54	"
HD 15497	2 28 15.3 +57 28 35	"
HD 15570	2 29 01.0 +61 09 29	"
HD 15629	2 29 31.3 +61 18 06	"
HD 15652	2 28 15.9 −22 45 58	"
HD 15963	2 32 31.9 +57 51 28	"
HD 16397	2 35 30.9 +30 36 22	"
HD 16429	2 36 53.5 +61 04 04	"
HD 16523	2 37 32.9 +56 30 59	"
HD 16691	2 39 12.2 +56 41 31	"
HD 16779	2 39 56.0 +57 36 57	"
HD 17145	2 43 40.9 +57 28 05	"
HD 17378	2 45 48.3 +56 52 37	"
HD 17378A	"	
HD 17505	2 47 15.3 +60 12 41	"
HD 17520	2 47 21.7 +60 10 48	"
HD 17603	2 48 04.6 +56 50 35	"
HD 17638	2 48 28.1 +56 43 33	"
HD 17738	2 48 08.3 −14 42 18	"
HD 17829	2 48 39.0 −35 52 49	"
HD 17925	2 50 07.3 −12 58 14	"
HD 17971	2 52 00.0 +60 11 28	"
HD 18391	2 56 01.2 +57 27 52	"
HD 18636	2 56 36.1 −38 11 27	"
HD 18881	3 00 20.5 +38 12 53	
HD 19445	3 05 28.6 +26 09 07	CSI 79
HD 19557	3 07 33.4 +57 42 51	"
HD 19820	3 10 07.3 +59 22 37	"
HD 19904	3 08 49.1 −39 14 24	
HD 20040	3 12 10.3 +59 55 54	
HD 20041	3 11 57.0 +56 57 21	CSI 79
HD 20336	3 15 33.7 +65 28 17	"
HD 20430	3 14 45.3 + 7 28 23	"
HD 20439	3 14 51.7 + 7 30 26	"
HD 20619	3 16 29.7 − 3 01 21	"
HD 20630	3 16 44.1 + 3 11 16	"
HD 20727	3 17 54.2 + 8 51 15	"
HD 21018	3 21 00.9 + 4 42 17	"
HD 21071	3 22 23.7 +48 56 45	"
HD 21110	3 22 18.1 +31 33 20	"
HD 21197	3 22 31.6 − 5 31 41	"
HD 21212	3 24 25.2 +62 19 12	"
HD 21291	3 25 00.0 +59 46 04	"
HD 21389	3 25 54.1 +58 42 26	"
HD 21447	3 26 10.4 +55 16 50	"
HD 21483	3 25 42.1 +30 12 11	"
HD 21943	3 30 23.7 +37 50 44	"
HD 22049	3 30 34.3 − 9 37 34	"
HD 22686	3 36 18.7 + 2 36 07	
HD 22879	3 37 49.1 − 3 22 28	CSI 79
HD 23060	3 40 13.0 +33 57 30	"
HD 23180	3 41 10.5 +32 07 53	779907
HD 23489	3 43 28.4 +24 06 02	CSI 79
HD 23512	3 43 36.2 +23 28 11	"
HD 23793	3 45 31.4 +10 59 27	"
HD 23802	3 45 58.3 +32 06 43	"
HD 23848	3 46 22.5 +32 56 22	"
HD 24039	3 47 49.7 +32 01 11	"
HD 24341	3 51 03.2 +52 16 30	"
HD 24398	3 50 58.9 +31 44 11	"
HD 24600	3 52 49.1 +32 01 04	"
HD 24706	3 52 00.2 −47 02 23	"
HD 24736	3 54 08.6 +32 44 40	"
HD 24916	3 54 56.7 − 1 18 01	"
HD 25329	3 59 53.1 +35 09 16	"
HD 25558	4 01 05.3 + 5 17 55	"
HD 25596	4 01 44.0 +26 03 53	"
HD 26571	4 09 53.0 +22 17 10	"
HD 26575	4 08 54.1 −35 24 06	"
HD 26736	4 11 32.1 +23 27 01	"
HD 26784	4 11 48.9 +10 34 33	"
HD 26846	4 12 00.7 −10 22 43	"
HD 26967	4 12 20.5 −42 24 59	"
HD 27282	4 16 14.9 +17 24 16	"
HD 27524	4 18 34.3 +20 55 21	"
HD 27829	4 16 54.5 −76 06 47	"
HD 27836	4 21 22.3 +14 38 36	"
HD 27901	4 22 01.9 +18 55 41	"
HD 28034	4 23 14.7 +15 24 42	"
HD 28068	4 23 31.9 +16 44 28	"
HD 28099	4 23 47.6 +16 38 06	"
HD 28099	4 23 47.7 +16 38 07	"
HD 28291	4 25 41.1 +19 37 51	CSI 79
HD 28343	4 26 01.9 +21 48 38	"
HD 28344	4 25 55.0 +17 10 32	"
HD 28406	4 26 36.5 +17 45 16	"
HD 28843	4 30 07.1 − 3 18 49	"
HD 28910	4 31 00.3 +14 44 26	"
HD 28932	4 30 56.7 + 0 55 06	"
HD 28992	4 31 43.9 +15 24 06	"
HD 29051	4 32 09.3 +17 05 54	"
HD 29587	4 38 03.4 +42 01 43	"
HD 29697	4 38 22.0 +20 48 33	"
HD 30353	4 45 19.9 +43 11 19	779907
HD 30614	4 49 03.7 +66 15 37	CSI 79
HD 30959	4 49 42.0 +14 10 07	"
HD 31237	4 51 38.6 + 2 21 36	"
HD 31274	4 50 36.3 −46 56 02	"
HD 31648	4 55 35.4 +29 46 05	"
HD 31869	4 56 11.7 −28 06 39	"
HD 32831	5 02 36.3 −35 33 00	"
HD 32990	5 05 03.5 +24 12 02	"
HD 33232	5 07 17.7 +40 56 28	"
HD 33461	5 08 43.6 +41 09 18	"
HD 34033	5 12 10.5 +12 57 27	"
HD 34078	5 12 59.8 +34 15 26	779907
HD 34085	5 12 07.9 − 8 15 27	CSI 79
HD 34454	5 15 14.3 +13 21 42	"
HD 34578	5 16 42.9 +33 54 26	"
HD 34664	5 13 54.9 −67 30 38	"
HD 34748	5 17 03.1 − 1 27 42	"
HD 34989	5 19 00.0 + 8 22 50	"
HD 35039	5 19 12.4 − 0 25 47	"
HD 35079	5 19 27.9 − 3 00 39	"
HD 35149	5 20 12.1 + 3 29 50	"
HD 35155	5 19 54.7 − 8 42 46	"
HD 35165	5 19 28.1 −34 23 34	"
HD 35299	5 21 08.7 − 0 12 17	"
HD 35468	5 22 26.7 + 6 18 21	"
HD 35502	5 22 30.7 − 2 51 33	"
HD 35601	5 23 58.4 +29 52 44	"
HD 35673	5 23 54.1 + 2 53 36	"
HD 35910	5 25 29.0 + 3 29 42	"
HD 35956	5 26 02.9 +12 30 51	"
HD 35972	5 25 51.7 − 0 44 29	"
HD 36003	5 25 57.3 − 3 31 40	"
HD 36267	5 28 06.3 + 5 54 40	"
HD 36351	5 28 36.9 + 3 15 19	"
HD 36486	5 29 26.9 − 0 20 01	"
HD 36512	5 29 30.5 − 7 20 11	"
HD 36552	5 28 49.1 −43 43 51	"
HD 36605	5 30 16.7 − 0 44 49	"
HD 36619	5 30 00.1 −23 27 52	"
HD 36629	5 30 28.6 − 4 36 00	"
HD 36646	5 30 35.4 − 1 45 06	"
HD 36781	5 31 28.7 − 1 47 13	"
HD 36811	5 31 38.1 − 1 56 04	"
HD 36819	5 32 23.7 +24 00 28	"
HD 36824	5 32 02.9 + 5 37 41	"
HD 36826	5 31 46.5 − 2 25 03	"
HD 36861	5 32 22.9 + 9 54 10	"
HD 36981	5 32 38.4 − 5 14 08	"
HD 37017	5 32 53.3 − 4 31 30	"
HD 37022	5 32 48.9 − 5 25 13	"
HD 37025	5 32 48.9 − 6 03 50	"
HD 37040	5 33 02.3 − 4 23 42	"
HD 37041	5 32 55.3 − 5 26 49	"
HD 37042	5 32 58.9 − 5 26 51	"
HD 37043	5 32 59.1 − 5 56 27	"
HD 37058	5 33 05.2 − 4 52 06	"
HD 37061	5 33 03.7 − 5 17 53	"
HD 37128	5 33 40.4 − 1 13 54	"
HD 37140	5 33 45.3 − 0 20 00	"
HD 37356	5 35 25.2 − 4 50 30	"
HD 37428	5 35 50.3 − 6 10 01	"
HD 37468	5 36 13.9 − 2 37 36	"
HD 37479	5 36 16.3 − 2 37 16	"
HD 37536	5 37 26.9 +31 53 42	"
HD 37742	5 38 13.9 − 1 58 00	"
HD 37744	5 38 06.7 − 2 50 59	"
HD 37776	5 38 24.3 − 1 31 53	"
HD 37806	5 38 31.6 − 2 44 28	"
HD 37836	5 35 45.5 −69 42 14	"
HD 37903	5 39 07.2 − 2 16 56	"
HD 37903	5 39 07.3 − 2 16 58	
HD 37903 40"E	5 39 10.0 − 2 16 58	
HD 37903 40"N	5 39 07.3 − 2 16 18	ED
HD 37903 40"S	5 39 07.3 − 2 17 38	"
HD 37903 40"W	5 39 04.6 − 2 16 58	"
HD 37903 60"E	5 39 11.3 − 2 16 58	
HD 37903 60"N	5 39 07.3 − 2 15 58	ED
HD 37903 60"S	5 39 07.3 − 2 17 58	"
HD 37903 60"W	5 39 03.3 − 2 16 58	"
HD 37903 80"E	5 39 12.6 − 2 16 58	
HD 37903 80"N	5 39 07.3 − 2 15 38	ED
HD 37903 80"S	5 39 07.3 − 2 18 18	"
HD 37903 80"W	5 39 02.0 − 2 16 58	"
HD 37903120"N	5 39 07.3 − 2 14 58	"
HD 37903120"S	5 39 07.3 − 2 18 58	"
HD 37903120"W	5 38 59.3 − 2 16 58	
HD 37903160"N	5 39 07.3 − 2 14 18	ED
HD 37903160"S	5 39 07.3 − 2 19 38	"
HD 37903160"W	5 38 56.6 − 2 16 58	"
HD 37903200"N	5 39 07.3 − 2 13 38	"
HD 37974	5 36 48.3 −69 24 18	CSI 79
HD 38051	5 40 17.7 − 4 39 29	"
HD 38087	5 40 29.4 − 2 20 03	"
HD 38165	5 41 11.1 − 0 57 34	"
HD 38230	5 42 35.3 +37 16 21	"
HD 38238	5 41 44.7 + 0 07 27	"
HD 38247	5 42 15.2 +18 41 03	"
HD 38268	5 41 38.3 −19 40 20	"
HD 38427	5 42 41.4 −22 51 59	"
HD 38563A	5 44 09.5 + 0 03 33	750301
HD 38563B	5 44 09.4 + 0 03 33	CSI 79
HD 38563B	5 44 10.9 + 0 04 17	750301
HD 38563C	5 44 11.5 + 0 01 38	
HD 38563N	5 44 10.9 + 0 04 17	
HD 38563S	5 44 09.5 + 0 03 33	
HD 38666	5 44 08.3 −32 19 26	CSI 79
HD 38708	5 45 42.7 +29 07 13	"
HD 38856	5 46 11.3 + 0 42 37	"
HD 38921	5 45 41.0 −38 14 51	
HD 39033	5 47 24.3 + 0 08 23	CSI 79
HD 39680	5 51 54.4 +13 50 46	"
HD 39746	5 52 31.3 +27 42 29	"
HD 40101	5 53 37.7 −28 57 36	"
HD 40111	5 54 53.3 +25 56 58	"
HD 40335	5 55 37.6 + 1 51 09	
HD 40402	5 55 19.6 −27 20 07	CSI 79
HD 41117	6 00 56.9 +20 08 27	"
HD 41312	6 01 14.5 −26 16 58	"
HD 41335	6 01 47.5 − 6 42 18	"
HD 41398	6 02 55.7 +28 56 23	"
HD 41511	6 02 45.1 −16 28 45	"
HD 41690	6 04 38.2 +21 52 49	"
HD 42087	6 06 41.7 +23 07 23	"
HD 42088	6 06 40.7 +20 29 50	"
HD 42111	6 06 21.2 + 2 30 31	"
HD 42259	6 07 05.7 − 5 03 23	"
HD 43039	6 12 11.4 +29 31 05	"
HD 43384	6 13 55.6 +23 45 33	"
HD 43818	6 16 16.6 +23 29 26	"
HD 44179	6 17 36.9 −10 36 51	"
HD 44213	6 18 07.9 + 5 45 48	"
HD 44351	6 19 08.0 +14 20 00	"
HD 44458	6 19 04.7 −11 44 54	"
HD 44594	6 18 47.0 −48 42 48	"
HD 44612	6 21 09.7 +43 34 35	
HD 44743	6 20 29.7 −17 55 45	CSI 79
HD 44965	6 22 25.6 +11 42 45	"
HD 45166	6 23 36.0 + 8 00 16	"
HD 45314	6 24 24.3 +14 55 13	"
HD 45391	6 25 24.3 +36 30 56	"
HD 45542	6 25 59.6 +20 14 43	"
HD 45626	6 25 53.9 − 4 25 44	"
HD 45677	6 25 59.0 −13 01 10	"
HD 45829	6 27 19.3 + 7 57 21	"
HD 45871	6 26 47.4 −32 20 14	"
HD 45910	6 27 52.3 + 5 54 06	"
HD 46106	6 28 58.7 + 5 03 46	"
HD 46149	6 29 12.9 + 5 04 10	"
HD 46150	6 29 16.0 + 4 58 46	"
HD 46223	6 29 29.9 + 4 51 37	"
HD 46380	6 30 18.2 − 7 28 14	"
HD 46407	6 30 26.2 −11 07 40	"
HD 46484	6 31 15.2 + 4 42 05	"
HD 46485	6 31 11.9 + 4 33 52	"
HD 46559	6 31 38.6 + 2 25 43	"
HD 46573	6 31 46.9 + 2 34 26	"
HD 46711	6 32 20.0 + 2 48 08	"
HD 46867	6 33 15.2 + 5 21 02	"

NAME	RA (1950) DEC	POS REF
	h m s ° ′ ″	
HD 46883	6 33 23.9 +10 19 35	"
HD 46966	6 33 45.0 + 6 07 30	"
HD 47032	6 34 07.3 + 4 44 12	"
HD 47105	6 34 49.3 +16 26 36	"
HD 47129	6 34 43.2 + 6 10 42	"
HD 47240	6 35 13.2 + 5 00 03	"
HD 47382	6 35 49.4 + 4 39 06	"
HD 47396	6 36 19.2 +22 39 34	"
HD 47432	6 36 02.5 + 1 39 29	"
HD 47755	6 37 53.1 + 9 50 06	"
HD 47839	6 38 13.3 + 9 56 36	"
HD 47887	6 38 24.7 + 9 30 48	"
HD 48217	6 39 33.1 − 9 07 02	"
HD 48279	6 40 04.7 + 1 45 56	"
HD 48434	6 41 00.3 + 3 58 59	"
HD 48915	6 42 56.7 −16 38 45	"
HD 49333	6 44 52.9 −20 57 35	"
HD 49960	6 47 46.3 −31 12 00	"
HD 49977	6 48 09.0 −14 03 13	"
HD 50064	6 49 00.0 + 0 21 26	"
HD 50091	6 48 43.9 −13 10 16	"
HD 50138	6 49 07.5 − 6 54 20	"
HD 50707	6 51 23.0 −20 09 39	"
HD 50896	6 52 08.0 −23 51 50	"
HD 51219	6 53 59.0 + 1 14 10	"
HD 51480	6 54 48.0 −10 45 22	"
HD 51585	6 55 40.7 +16 24 10	"
HD 52266	6 57 53.9 − 5 45 19	"
HD 52382	6 58 15.9 − 9 07 53	"
HD 52721	6 59 28.5 −11 13 39	"
HD 52721	6 59 28.6 −11 13 42	
HD 52942	7 00 21.9 −11 22 44	CSI 79
HD 53138	7 00 56.1 −23 45 31	"
HD 53244	7 01 29.7 −15 33 27	"
HD 53367	7 02 03.5 −10 22 42	"
HD 53367	7 02 04.0 −10 22 44	
HD 53667	7 03 11.3 − 8 39 06	CSI 79
HD 53755	7 03 27.9 −10 34 58	"
HD 53974	7 04 19.7 −11 12 55	
HD 53974	7 04 19.8 −11 12 57	
HD 53975	7 04 16.2 −12 18 55	CSI 79
HD 54439	7 06 02.7 −11 46 18	"
HD 54627	7 05 49.6 −46 32 12	"
HD 54662	7 06 58.1 −10 15 54	"
HD 54858	7 07 48.0 − 9 15 13	"
HD 55383	7 10 30.0 +16 14 42	"
HD 55879	7 12 05.9 −10 13 43	"
HD 56438	7 13 10.7 −47 02 48	"
HD 56847	7 15 53.4 −15 32 09	"
HD 56925	7 16 12.9 −13 08 15	"
HD 57061	7 16 37.9 −24 51 41	"
HD 57219	7 16 51.3 −36 38 59	"
HD 57682	7 19 38.0 − 8 52 59	"
HD 58131	7 21 13.7 −20 07 55	"
HD 58260	7 21 31.7 −36 14 32	"
HD 58343	7 22 24.4 −16 06 05	"
HD 58350	7 22 06.9 −29 12 14	"
HD 58715	7 24 26.3 + 8 23 28	"
HD 58978	7 24 52.1 −22 59 01	"
HD 59059	7 25 56.7 +15 12 46	"
HD 59075	7 25 23.9 −18 23 36	"
HD 59094	7 25 35.0 −15 59 27	"
HD 60325	7 31 04.0 −14 13 44	"
HD 60341	7 31 07.3 −19 18 08	"
HD 60479	7 31 33.1 −27 52 04	"
HD 60522	7 32 50.5 +27 00 29	"
HD 60848	7 34 13.3 +17 01 00	"
HD 61555A	7 36 46.3 −26 41 11	
HD 61555IRS	7 37 01 −26 42 40	
HD 61827	7 37 54.3 −32 27 43	CSI 79
HD 62150	7 39 18.2 −32 31 32	"
HD 62910	7 43 01.6 −31 47 09	
HD 63099	7 43 57.3 −34 12 29	
HD 63922	7 47 42.7 −46 14 46	CSI 79
HD 64090	7 50 21.6 +30 45 38	"
HD 64740	7 51 39.1 −49 28 54	"
HD 64760	7 51 49.9 −47 58 17	"
HD 65412	7 55 41.9 −20 17 33	"
HD 65750	7 55 54.5 −58 59 25	"
HD 65818	7 56 47.9 −49 06 27	"
HD 65865	7 57 44.2 −28 35 46	"
HD 65873	7 58 39.3 +16 35 39	"
HD 65875	7 58 13.2 − 2 44 34	"
HD 66552	8 01 51.9 +18 59 05	"
HD 66811	8 01 49.5 −39 51 40	"
HD 67728	8 06 24.3 −19 41 33	"
HD 68468	8 09 40.7 −14 01 05	"
HD 68980	8 11 36.1 −35 44 49	"
HD 69464	8 13 54.4 −35 28 36	"
HD 69882	8 15 34.4 −42 21 54	"
HD 70011	8 17 33.9 +24 10 51	"
HD 70946	8 21 26.0 −38 07 25	"
HD 71072	8 22 38.7 −12 36 02	"
HD 71304ABC	8 23 14.6 −44 08 15	
HD 73394	8 36 43.1 +51 55 49	CSI 79
HD 73665	8 37 13.9 +20 11 07	"
HD 73710	8 37 30.0 +19 50 52	"
HD 73882	8 37 19.4 −40 14 31	"
HD 74272	8 39 34.6 −47 08 15	"
HD 74377	8 41 52.7 +41 51 46	"
HD 74575	8 41 34.9 −33 00 18	"
HD 75021	8 44 31.0 −29 32 37	"
HD 75156	8 45 54.6 +12 43 57	"
HD 75211	8 45 16.0 −43 53 23	"
HD 75222	8 45 28.5 −36 33 56	"
HD 75223	8 45 29.8 −39 36 54	
HD 75821	8 48 51.5 −46 20 28	CSI 79
HD 75860	8 49 06.4 −43 33 47	"
HD 76534	8 53 20.6 −43 16 28	"
HD 76536	8 53 18.2 −47 24 02	
HD 76556	8 53 26.1 −47 24 56	CSI 79
HD 76644	8 55 47.6 +48 14 21	"
HD 76764	8 54 49.6 −43 00 31	"
HD 76830	8 56 21.4 +19 14 49	"
HD 76838	8 55 18.9 −43 03 45	"
HD 76868	8 56 22.3 + 3 51 01	"
HD 77281	8 59 05.4 − 1 16 45	
HD 77443	9 00 35.7 +38 56 26	CSI 79
HD 77581	9 00 13.1 −40 21 24	"
HD 78146	9 03 35.0 −27 52 55	"
HD 78344	9 04 08.3 −47 34 01	"
HD 78785	9 06 37.7 −46 03 01	"
HD 79210	9 10 58.7 +52 54 06	"
HD 79211	9 11 00.9 +52 54 09	"
HD 79452	9 12 10.3 +34 50 27	"
HD 79573	9 11 30.9 −49 54 00	
HD 80077	9 14 13.2 −49 45 49	CSI 79
HD 80558	9 17 03.0 −51 20 55	"
HD 81357	9 23 42.7 +58 21 36	"
HD 82595	9 29 54.3 −36 38 14	"
HD 82885	9 32 39.9 +36 02 14	"
HD 83618	9 37 18.1 − 0 54 52	"
HD 83943	9 38 07.3 −58 05 31	"
HD 83953	9 39 00.0 −23 21 47	"
HD 84542	9 43 31.7 + 6 56 23	"
HD 84748	9 44 52.2 +11 39 40	"
HD 84800	9 45 35.9 +43 53 56	
HD 84937	9 46 12.0 +13 59 15	CSI 79
HD 86440	9 55 06.2 −54 19 44	"
HD 86612	9 56 47.4 −23 42 38	"
HD 87643	10 02 49.7 −58 25 15	"
HD 87696	10 04 29.1 +35 29 20	"
HD 87737	10 04 36.4 +17 00 24	"
HD 87884	10 05 33.0 +12 14 29	"
HD 87901	10 05 42.6 +12 12 43	"
HD 88230	10 08 19.0 +49 42 27	"
HD 88609	10 11 14.2 +53 48 34	"
HD 88725	10 11 32.1 + 3 24 18	"
HD 89201	10 14 04.9 −57 07 30	"
HD 89249	10 14 29.7 −55 20 51	"
HD 89272	10 14 46.1 −49 06 50	"
HD 89884	10 19 34.7 −17 46 54	"
HD 90362	10 23 14.2 − 6 48 24	"
HD 90508	10 24 59.3 +49 03 08	"
HD 90586	10 24 18.5 −53 38 11	"
HD 90706	10 25 03.6 −57 21 05	"
HD 90707	10 25 03.1 −57 25 12	"
HD 90772	10 25 32.3 −57 22 59	"
HD 91093	10 27 39.7 −57 43 17	"
HD 91120	10 28 32.3 −13 19 51	"
HD 91316	10 30 10.7 + 9 33 51	"
HD 91323	10 29 34.9 −44 13 38	"
HD 91619	10 31 31.6 −57 55 54	"
HD 91805	10 33 00.1 −43 24 20	"
HD 92207	10 35 32.3 −58 28 23	"
HD 92693	10 38 55.5 −57 40 24	"
HD 92740	10 39 22.5 −59 24 53	"
HD 92809	10 39 41.7 −58 30 35	"
HD 92839	10 41 37.2 +67 40 27	779907
HD 92964	10 40 44.2 −58 57 11	CSI 79
HD 93027	10 41 22.3 −59 52 18	"
HD 93028	10 41 20.2 −59 56 17	"
HD 93030	10 41 10.0 −64 07 54	
HD 93129	10 41 53 −59 17 08	
HD 93129	10 42 01.0 −59 17 05	CSI 79
HD 93129AB	" "	"
HD 93130	10 42 04.3 −59 36 40	"
HD 93131	10 41 56.7 −59 51 16	"
HD 93146	10 42 04.3 −59 49 25	"
HD 93146	10 42 04.4 −59 49 25	
HD 93160	10 42 10.7 −59 18 45	CSI 79
HD 93160	10 42 10.8 −59 18 46	
HD 93161	10 42 12.4 −59 18 50	
HD 93162	10 42 14.2 −59 27 23	CSI 79
HD 93204	10 42 36.0 −59 28 43	"
HD 93205	10 42 37.0 −59 28 26	"
HD 93206	10 42 26.9 −59 43 48	"
HD 93222	10 42 40.3 −59 49 40	"
HD 93249ABC	10 42 46.9 −59 05 39	
HD 93250	10 42 48.3 −59 18 06	CSI 79
HD 93281	10 43 01.0 −59 40 18	"
HD 93540	10 44 27.4 −64 15 03	"
HD 93632ABC	10 45 15.6 −59 50 00	
HD 93632F	10 45 15 −59 50 00	ED
HD 93795	10 46 24.5 −59 16 33	CSI 79
HD 93890	10 47 03.6 −58 37 49	"
HD 94028	10 48 47.7 +20 32 56	"
HD 94237	10 50 02.3 + 0 03 52	"
HD 94367	10 50 27.5 −56 58 27	"
HD 94599	10 52 03.9 −60 49 54	"
HD 94909	10 54 19.9 −57 17 01	"
HD 94956	10 55 00.4 −29 00 46	"
HD 95687	10 59 32.7 −60 46 46	"
HD 95689	11 00 39.5 +62 01 15	"
HD 95731	10 59 52.9 −59 06 29	"
HD 95735	11 00 36.5 +36 18 19	"
HD 95880	11 00 40.7 −59 28 17	"
HD 95950	11 01 02.3 −60 38 27	"
HD 96088	11 01 52.6 −57 41 06	"
HD 96088	11 01 53.9 −57 41 06	"
HD 96446	11 03 59.3 −59 40 45	"
HD 96548	11 04 17.9 −65 14 20	"
HD 96880	11 06 16.4 −59 08 28	"
HD 96919	11 06 28.5 −61 40 32	"
HD 97048	11 06 38.5 −77 23 07	
HD 97048	11 06 39.5 −77 23 00	CSI 79
HD 97152	11 07 56.7 −60 42 25	"
HD 97300	11 08 17.9 −76 20 29	"
HD 97393	11 09 49.9 −32 09 41	"
HD 97534	11 10 26.7 −60 02 40	"
HD 97603	11 11 27.0 +20 47 51	"
HD 97670	11 11 20.4 −59 20 47	"
HD 97671	11 11 20.5 −59 49 15	"
HD 97707	11 11 29.0 −60 28 06	"
HD 97907	11 13 15.0 +13 34 48	"
HD 97950	11 12 59 −60 59 20	
HD 98624	11 17 53.1 −60 57 31	CSI 79
HD 98817	11 19 23.7 −60 42 23	"
HD 99171	11 21 58.1 −42 23 38	"
HD 99196	11 22 23.3 +11 42 17	"
HD 99953	11 27 00.0 −63 16 40	"
HD 100262	11 29 29.4 −59 14 22	"
HD 100307	11 29 53.9 −26 28 14	"
HD 100363	11 30 19.3 −11 45 24	"
HD 100841	11 33 27.7 −62 44 33	"
HD 100930	11 34 06.9 −61 02 33	"
HD 101007	11 34 37.2 −60 53 33	"
HD 101065	11 35 10.7 −46 25 59	"
HD 101190A	11 35 49.4 −62 55 11	"
HD 101190ABC	11 35 49.5 −62 55 12	
HD 101190B	11 35 47.8 −62 55 10	CSI 79
HD 101205	11 35 59.7 −63 05 44	"
HD 101452	11 37 45.1 −38 52 09	
HD 101501	11 38 25.2 +34 29 01	CSI 79
HD 101584	11 38 33.6 −55 17 46	"
HD 101606	11 38 58.3 +32 01 20	"
HD 101712	11 39 26.9 −63 08 12	"
HD 102647	11 46 30.5 +14 51 04	"
HD 102851	11 47 46.7 −51 11 32	"
HD 103052	11 49 14.2 −60 52 48	"
HD 103095	11 50 06.1 +38 04 38	"
HD 103287	11 51 12.5 +53 58 21	"
HD 103516	11 52 29.9 −63 00 02	"
HD 104216	11 57 44.3 +81 07 54	"
HD 104556	11 59 56.9 +43 22 09	"
HD 104901	12 02 11.2 −61 43 05	"
HD 104901A	" "	"
HD 104901C	" "	ED
HD 104901IRS1	12 02 22.3 −61 39 58	
HD 104901IRS3	12 01 56.7 −61 40 15	
HD 105546	12 06 32.9 +59 17 48	CSI 79
HD 105601	12 06 56.1 +38 54 39	
HD 105783	12 08 06.3 −41 45 10	CSI 79
HD 106068	12 09 42.0 −62 40 20	"
HD 106965	12 15 24.0 + 1 51 10	
HD 107328	12 17 48.4 + 3 35 25	CSI 79
HD 107906	12 21 25.2 +16 41 50	"
HD 108759	12 27 16.7 −41 27 32	"
HD 109011	12 28 57.1 +55 23 40	"
HD 109399	12 32 11.6 −72 26 28	"
HD 109995	12 36 23.2 +39 35 06	"
HD 110073	12 37 09.5 −39 42 44	"
HD 110184	12 37 42.0 + 8 48 05	"
HD 110432	12 39 53.1 −62 47 04	"
HD 110639	12 41 20.7 −61 07 15	"
HD 110833	12 42 36.2 +27 40 00	"
HD 110897	12 42 37.6 +39 32 59	"
HD 111124	12 44 50.7 −62 43 22	"
HD 111558	12 47 59.9 −69 22 22	"
HD 111631	12 48 09.6 − 0 29 25	"
HD 111908	12 49 57.5 + 7 28 43	"
HD 112127	12 51 29.6 +27 03 02	"
HD 112244	12 52 59.3 −56 33 53	"
HD 112758	12 56 27.7 − 9 34 01	"
HD 112769	12 56 27.0 +17 40 41	"
HD 112869	12 57 02.0 +38 05 13	"
HD 113034	12 58 46.7 −61 33 48	"
HD 113422	13 01 29.5 −61 26 30	"
HD 113801	13 03 44.3 −19 47 28	"
HD 114213	13 07 11.4 −61 12 22	"
HD 114340	13 07 56.0 −59 28 47	"
HD 114606	13 08 52.9 + 9 53 14	"
HD 115473	13 15 18.2 −57 52 51	"
HD 115842	13 17 41.3 −55 32 18	"
HD 116119	13 19 38.5 −61 45 03	"
HD 116658	13 22 33.3 −10 54 01	"
HD 116842	13 23 13.4 +55 14 52	"
HD 117797	13 30 48.7 −62 09 38	"
HD 119227	13 37 46.6 +74 33 48	"
HD 119256	13 40 17.4 −57 20 17	"
HD 119608	13 41 48.2 −17 41 09	"
HD 120033	13 44 34.5 − 9 27 33	"
HD 120170	13 45 20.3 − 8 32 24	"
HD 120213	13 49 05.6 −82 25 11	"
HD 120315	13 45 34.3 +49 33 43	"
HD 120678	13 49 22.5 −62 28 26	"
HD 120991	13 50 49.5 −46 52 55	"
HD 121190	13 51 57.7 −51 54 55	"
HD 122547	13 59 43.5 +33 03 58	"
HD 122563	14 00 04.5 + 9 55 38	"
HD 122669	14 01 42.7 −62 16 05	"
HD 122691	14 01 45.6 −62 20 54	"
HD 122879	14 02 52.3 −59 28 38	"
HD 124314	14 11 20.0 −61 28 25	"
HD 124448	14 11 46.5 −46 03 21	"
HD 124471	14 12 39.9 −66 21 21	"
HD 124721	14 13 13.7 −44 57 29	"
HD 124979	14 14 51.2 −51 16 22	"
HD 125206	14 16 27.0 −60 51 08	"
HD 125241	14 16 41.2 −60 39 36	"
HD 125823	14 19 56.7 −39 17 04	"
HD 125835	14 20 55.5 −67 58 08	"
HD 126053	14 20 41.6 + 1 28 28	"
HD 126587	14 24 10.4 −22 01 08	"
HD 127755	14 31 43.7 −60 25 18	"
HD 128167	14 32 30.1 +29 57 40	"
HD 129116	14 38 50.6 −37 34 47	"
HD 129653	14 40 38.2 +36 58 07	
HD 129655	14 41 11.0 − 2 17 38	
HD 130163	14 44 36.2 −39 43 04	
HD 130227	14 45 26.4 −56 27 30	CSI 79
HD 130694	14 47 20.7 −27 45 10	"
HD 132142	14 53 45.5 +53 52 28	"
HD 132776	14 58 26.3 − 2 40 20	"
HD 132950	14 59 09.3 +16 04 05	"
HD 132960	15 00 05.3 −41 04 33	"
HD 133332	15 01 23.5 − 2 39 51	"
HD 133518	15 03 20.5 −51 50 13	"
HD 134439	15 07 28.4 −16 08 26	"
HD 134440	15 07 28.3 −16 13 28	"
HD 134959	15 11 27.2 −58 53 21	"
HD 135159	15 12 25.9 −59 28 20	"
HD 135591	15 14 46.2 −60 18 50	"
HD 135742	15 14 18.7 − 9 11 57	"
HD 136488	15 19 58.1 −62 29 58	"
HD 136512	15 18 04.4 +29 47 48	"
HD 136664	15 19 57.1 −36 40 49	"
HD 136754	15 19 24.3 +24 31 19	
HD 137432	15 24 05.4 −36 35 36	CSI 79
HD 137595	15 24 54.0 −33 22 17	"
HD 137603	15 25 44.7 −58 24 32	"
HD 137613	15 24 49.9 −24 59 45	"
HD 138693	15 32 12.4 −51 43 28	"
HD 139006	15 32 34.1 +26 52 53	"

NAME	RA (1950)	DEC	POS REF
	h m s	° ′ ″	
HD 139254	15 34 51.3	−22 58 37	"
HD 139323	15 34 09.7	+39 59 41	"
HD 139341	15 34 15.4	+39 57 57	"
HD 140283	15 40 22.4	−10 46 17	"
HD 140301	15 40 36.3	−14 53 02	"
HD 142139	15 51 52.0	−60 20 08	"
HD 142267	15 50 52.2	+13 21 05	"
HD 142301	15 51 39.0	−25 05 47	"
HD 142373	15 50 56.6	+42 35 25	"
HD 142468	15 53 31.3	−54 11 16	"
HD 142669	15 53 47.4	−29 04 09	"
HD 142696	15 54 40.5	−54 34 53	"
HD 142754	15 54 25.9	−40 51 13	"
HD 142804	15 54 15.0	−15 53 24	"
HD 142983	15 55 23.0	−14 08 10	"
HD 142990	15 55 34.6	−24 41 18	"
HD 143183	15 57 39.4	−53 59 42	"
HD 143796	16 01 14.4	−56 12 13	"
HD 144334	16 03 07.0	−23 28 16	"
HD 144386	16 04 19.0	−52 56 45	"
HD 144542	16 02 14.4	+59 32 50	"
HD 144579	16 03 13.1	+39 17 25	"
HD 144844	16 05 44.2	−23 33 12	"
HD 144872	16 04 41.7	+38 46 21	"
HD 144900	16 06 40.5	−48 50 11	"
HD 144969	16 07 08.0	−48 39 54	"
HD 145675	16 08 46.7	+43 57 02	"
HD 145958	16 10 58.3	+13 39 34	"
HD 146116	16 12 04.2	− 0 16 25	"
HD 146145	16 13 27.7	−52 57 46	"
HD 146331	16 13 47.9	−25 44 22	"
HD 146479AB	16 15 08.9	−50 16 16	
HD 146706	16 15 28.6	−23 09 09	CSI 79
HD 146888	16 22 24.0	−23 20 47	"
HD 147012	16 17 16.2	−25 29 25	"
HD 147013	16 17 12.3	−25 31 34	"
HD 147084	16 17 37.3	−24 03 00	"
HD 147165	16 18 08.6	−25 28 27	"
HD 147165A	"	"	"
HD 147165B	16 18 07.1	−25 28 26	"
HD 147196	16 18 18.9	−23 35 21	"
HD 147283	16 18 56.3	−24 22 39	"
HD 147343	16 19 18.7	−24 14 45	"
HD 147384	16 19 35.5	−24 15 56	"
HD 147648	16 21 00.2	−25 17 58	"
HD 147701	16 21 19.2	−24 54 36	"
HD 147888	16 22 24.0	−23 20 46	"
HD 147889	16 22 22.7	−24 21 05	"
HD 147889	16 22 22.9	−24 21 07	
HD 147932	16 22 34.9	−23 17 29	CSI 79
HD 147933/4	16 22 34.9	−23 19 56	"
HD 147955	16 22 46.4	−26 27 17	"
HD 148184	16 24 07.2	−18 20 38	"
HD 148379	16 26 04.3	−46 08 02	"
HD 148546	16 27 01.5	−37 51 50	"
HD 148579	16 26 56.6	−25 02 20	"
HD 148605	16 27 09.9	−25 00 24	"
HD 148688	16 28 12.7	−41 42 36	"
HD 148703	16 28 06.5	−34 35 49	"
HD 148816	16 28 00.7	+ 4 18 16	"
HD 148839	16 30 45.2	−67 01 26	"
HD 148937	16 30 09.6	−48 00 23	"
HD 149019	16 30 36.0	−49 39 57	"
HD 149168	16 30 58.7	−26 24 04	"
HD 149228	16 31 20.7	−25 26 46	"
HD 149367	16 32 10.4	−26 22 31	"
HD 149438	16 32 45.9	−28 06 49	"
HD 149661	16 33 42.9	− 2 13 01	"
HD 149757	16 34 24.1	−10 28 02	"
HD 149827	16 35 11.9	−24 47 17	"
HD 150080	16 36 38.0	−24 54 37	"
HD 150136AB	16 37 35.0	−48 39 50	"
HD 150136C	16 37 35.3	−48 40 16	"
HD 150193	16 37 16.3	−23 47 55	"
HD 150207	16 37 22.9	−23 33 10	"
HD 150898	16 43 03.3	−58 15 06	"
HD 151213	16 44 36.3	−47 11 33	"
HD 151288	16 43 14.6	+33 35 37	"
HD 151346	16 44 44.6	−23 53 08	"
HD 151658	16 46 35.7	−21 45 57	"
HD 151804	16 48 04.1	−41 08 46	"
HD 151932	16 48 48.3	−41 46 16	"
HD 151937	16 47 18.3	+30 02 56	"
HD 152003	16 49 16.5	−41 42 10	"
HD 152147	16 49 57.1	−42 02 21	"
HD 152234	16 50 30.9	−41 43 30	"
HD 152235	16 50 27.5	−41 54 46	"
HD 152236	16 50 27.7	−42 16 50	"
HD 152408	16 51 28.7	−41 04 14	"
HD 152424	16 51 31.7	−42 00 37	"
HD 152478	16 52 16.9	−50 35 44	"
HD 152667	16 53 06.7	−40 44 43	"
HD 152723	16 53 26.1	−40 26 03	
HD 153261	16 57 26.5	−58 53 07	CSI 79
HD 153919	17 00 32.6	−37 46 28	"
HD 154043	17 01 35.5	−47 00 01	"
HD 154090	17 01 31.7	−34 03 15	"
HD 154276	17 01 36.2	+17 15 35	"
HD 154368	17 03 08.4	−35 23 04	"
HD 154445	17 02 57.4	− 0 49 28	"
HD 155737	17 11 45.3	−39 35 42	"
HD 155851	17 12 17.9	−32 38 00	"
HD 156074	17 11 56.5	+42 09 48	"
HD 156201	17 14 25.3	−35 10 13	"
HD 156385	17 15 48.9	−45 35 18	"
HD 156738	17 17 30.9	−36 01 21	"
HD 156860	17 17 15.0	+ 2 11 20	"
HD 157038	17 19 14.4	−37 45 26	"
HD 157089	17 18 35.4	+ 1 29 15	"
HD 157214	17 18 47.1	+32 31 50	"
HD 157246	17 21 10.7	−56 19 58	"
HD 157451	17 21 46.7	−43 26 51	"
HD 157504	17 21 49.9	−34 08 33	"
HD 157857	17 23 30.7	−10 56 59	"
HD 157881	17 23 15.7	+ 2 10 12	"
HD 158614	17 27 49.2	− 1 01 20	"
HD 159176ABC	17 31 26.2	−32 32 58	
HD 159864	17 34 43.9	−17 47 52	CSI 79
HD 160346	17 36 47.7	+ 3 34 58	"
HD 160529	17 38 41.1	−33 28 46	"
HD 160641	17 38 54.9	−17 52 42	"
HD 160810	17 40 05.0	−35 16 31	"
HD 161056	17 41 04.9	− 7 03 27	"
HD 161061	17 41 27.5	−28 09 26	"
HD 161261	17 41 48.6	+ 5 44 05	"
HD 161743	17 45 31.8	−38 06 11	
HD 161796	17 43 41.3	+50 03 47	CSI 79
HD 161903	17 45 43.3	− 1 47 34	
HD 161961	17 46 00.5	− 2 10 49	CSI 79
HD 162120A	17 47 30.0	−29 15 54	"
HD 162120BCD	17 47 28.8	−29 15 11	"
HD 162208	17 46 20.7	+39 59 40	
HD 162374	17 48 53.3	−34 47 14	CSI 79
HD 162978	17 51 49.2	−24 52 43	"
HD 163296	17 53 20.6	−21 56 56	"
HD 163428	17 54 03.9	−23 56 00	"
HD 163800	17 55 55.6	−22 30 49	"
HD 164270	17 58 26.3	−32 42 53	"
HD 164353	17 58 08.3	+ 2 55 55	"
HD 164492AB	17 59 21.3	−23 01 53	"
HD 164492CD	17 59 21.0	−23 02 08	"
HD 164514	17 59 29.7	−22 54 23	"
HD 164536AB	17 59 34.7	−24 15 23	"
HD 164740	18 00 36.3	−24 22 53	"
HD 164794	18 00 47.3	−24 21 48	"
HD 164865	18 01 11.1	−24 11 08	"
HD 164906	18 01 21.7	−24 23 21	"
HD 165024	18 02 44.1	−50 05 47	"
HD 165052	18 02 06.4	−24 24 09	"
HD 165195	18 02 10.7	+ 3 46 33	"
HD 165246	18 03 00	−24 12 06	
HD 165319	18 03 08.1	−14 12 11	CSI 79
HD 165401	18 03 09.2	+ 4 39 22	"
HD 165462	18 03 33.1	− 0 27 06	"
HD 165516	18 04 11.3	−21 27 01	"
HD 165634	18 04 54.9	−28 27 51	"
HD 165688	18 04 59.3	−19 24 24	"
HD 165705	18 05 18	−23 26 36	
HD 165763	18 05 28.7	−21 15 39	CSI 79
HD 165872N	18 06 06	−23 26 48	
HD 165872S	18 06 06	−23 26 54	
HD 165908	18 05 07.4	+30 33 12	CSI 79
HD 165921	18 06 16	−24 00 06	
HD 165999	18 06 34	−23 34 48	
HD 166033	18 06 44	−23 41 36	
HD 166056	18 06 54	−24 07 12	
HD 166079	18 06 45	−23 39 30	
HD 166097	18 06 22.6	+ 9 26 35	CSI 79
HD 166107	18 07 05	−23 47 12	
HD 166197	18 07 36.7	−33 48 39	CSI 79
HD 166620	18 07 57.9	+38 27 11	"
HD 166628	18 09 17.3	−19 26 43	"
HD 166734	18 09 38.2	−10 44 39	"
HD 166934 ABC	18 10 49.8	−18 49 29	
HD 166934IRS1	18 10 52.6	−18 47 25	
HD 166934IRS2	18 10 51.7	−18 47 25	
HD 166934IRS3	18 10 54.2	−18 47 11	
HD 166934IRS8	18 10 59.8	−18 43 50	
HD 166934IRS9	18 10 37.6	−18 45 51	
HD 166934IR10	18 10 52	−18 44 48	
HD 166934IR11	18 10 43	−18 45 41	
HD 166934IR12	18 10 56.0	−18 44 55	
HD 167287 AP	18 12 19.9	−19 00 32	CSI 79
HD 167287 BR	18 12 19.9	−19 00 14	"
HD 167356	18 12 34.4	−18 40 41	"
HD 167362	18 12 55.4	−30 53 16	"
HD 167451	18 13 04.9	−13 35 29	"
HD 167838	18 14 45.4	−15 26 59	"
HD 167971	18 15 17.5	−12 15 45	"
HD 168075	18 15 45.7	−13 48 51	"
HD 168076	18 15 46.2	−13 49 16	"
HD 168137	18 16 05.9	−13 49 45	"
HD 168206	18 16 19.7	−11 39 14	"
HD 168227	18 16 29.3	−15 38 03	"
HD 168476	18 18 59.7	−56 39 13	"
HD 168571	18 18 14.3	−17 24 18	"
HD 168607	18 18 21.4	−16 23 57	"
HD 168625	18 18 26.1	−16 23 52	"
HD 169010	18 20 19.9	−13 44 41	"
HD 169034	18 20 27.6	−13 37 13	"
HD 169226	18 21 23.5	−12 14 28	"
HD 169454	18 22 24.9	−14 00 24	"
HD 169754	18 23 55.4	−11 23 13	"
HD 169978	18 26 42.3	−62 18 45	"
HD 170153	18 21 57.4	+72 42 41	"
HD 170235	18 26 16.9	−25 17 23	"
HD 170740	18 28 39.2	−10 49 54	"
HD 170836	18 29 15.2	−19 18 45	"
HD 170938	18 29 45.3	−15 44 20	"
HD 171012	18 30 14.3	−18 24 23	"
HD 171094	18 30 32.5	−14 08 45	"
HD 172167	18 35 14.6	+38 44 09	"
HD 172252	18 36 52.1	−11 55 28	"
HD 172275	18 36 57.3	− 7 24 00	"
HD 172488	18 38 04.1	− 8 45 56	"
HD 172694	18 39 22.3	−15 54 19	"
HD 172910	18 40 58.3	−35 41 34	"
HD 173409	18 43 12.7	−31 23 46	"
HD 173438	18 42 49.4	− 4 39 09	"
HD 173654A	18 43 53.5	− 1 00 56	"
HD 173654B	18 43 54.3	− 1 01 02	"
HD 173654C	18 43 54.4	− 1 01 17	"
HD 174585	18 47 54.1	+32 45 13	"
HD 175305	18 48 27.3	+74 40 00	"
HD 175541	18 53 11.9	+ 4 12 03	"
HD 175754	18 54 39.3	−19 13 13	"
HD 175876	18 55 12.7	−20 29 29	"
HD 176124	18 56 27.3	−19 20 51	"
HD 176279	18 58 21.6	−54 09 03	"
HD 177230	19 01 20.6	− 4 23 44	"
HD 177291	19 01 52.3	−18 46 59	"
HD 178175	19 05 20.3	−19 22 11	"
HD 179343	19 09 32.3	+ 2 32 16	"
HD 179406	19 09 57.9	− 8 01 28	"
HD 180953	19 16 17.7	−16 00 02	"
HD 182040	19 20 24.3	−10 47 59	"
HD 182488	19 21 40.7	+33 07 17	"
HD 183143	19 25 13.2	+18 11 36	"
HD 183255	19 25 02.0	+49 21 08	"
HD 183914	19 28 44.3	+27 51 31	"
HD 184499	19 31 35.2	+33 05 19	"
HD 184915	19 34 12.0	− 7 08 23	"
HD 185144	19 32 27.5	+69 34 33	"
HD 185268A	19 35 09.8	+29 13 14	
HD 185737	19 37 43.1	+19 17 00	CSI 79
HD 185859	19 38 17.0	+20 21 35	"
HD 186427	19 40 32.0	+50 24 02	"
HD 186660	19 43 15.3	− 3 00 20	"
HD 186689	19 43 13.9	+ 7 29 25	"
HD 186745/6	19 43 17.0	+23 49 11	"
HD 186842	19 44 10.5	+ 7 32 42	"
HD 186943	19 44 14.2	+28 08 56	"
HD 186980	19 44 19.6	+31 59 33	"
HD 186994	19 44 03.9	+44 50 26	"
HD 187238	19 46 02.9	+22 38 13	"
HD 187282	19 46 17.9	+18 04 33	"
HD 187299	19 46 15.4	+24 53 01	"
HD 187399	19 46 41.5	+29 16 33	"
HD 187982/3	19 49 55.2	+24 51 44	"
HD 188001	19 50 07.9	+18 32 30	"
HD 188056	19 49 22.3	+52 51 36	"
HD 188209	19 50 28.5	+46 53 50	"
HD 188339	19 52 50.3	−38 27 34	"
HD 188485	19 52 23.7	+24 11 12	"
HD 188934	19 55 03.9	+ 0 06 23	"
HD 189103	19 56 29.1	−35 24 46	"
HD 189711	19 58 39.6	+ 9 22 30	"
HD 189864A	19 58 53.7	+36 27 02	"
HD 189864B	19 58 51.6	+36 25 55	"
HD 189864C	19 58 49.3	+36 26 00	"
HD 189864D	19 58 48.7	+36 26 15	"
HD 190002	19 59 44.7	+32 26 12	"
HD 190007	20 00 16.7	+ 3 10 59	"
HD 190073	20 00 34.3	+ 5 35 48	"
HD 190323	20 01 31.1	+14 50 27	"
HD 190404	20 01 46.6	+23 12 38	"
HD 190429	20 01 37.3	+35 52 58	"
HD 190429AB	20 01 37.2	+35 52 58	"
HD 190429C	20 01 35.4	+35 53 35	"
HD 190603	20 02 38.3	+32 04 31	"
HD 190864	20 03 46.9	+35 27 49	"
HD 190918	20 04 04.5	+35 38 37	"
HD 190944	20 03 52.3	+46 31 39	"
HD 191612	20 07 35.3	+35 35 07	"
HD 191639	20 08 27.3	− 8 59 28	"
HD 191765	20 08 21.5	+36 01 39	"
HD 191978	20 09 13.9	+41 12 10	"
HD 192103	20 10 00.8	+36 02 49	779907
HD 192163	20 10 17.0	+38 12 13	CSI 79
HD 192281	20 10 46.7	+40 07 00	"
HD 192422	20 11 33.3	+38 36 47	"
HD 192639	20 12 39.0	+37 12 01	"
HD 192641	20 12 39.3	+36 30 27	"
HD 192954	20 14 51.6	+15 43 00	"
HD 193077	20 15 08.5	+37 16 02	"
HD 193182	20 15 36.9	+39 26 15	"
HD 193322	20 16 20.5	+40 34 30	"
HD 193443	20 17 01.3	+38 07 19	"
HD 193514	20 17 19.6	+39 06 54	"
HD 193576	20 17 42.6	+38 34 24	779907
HD 193621	20 17 55.9	+36 58 26	CSI 79
HD 193793	20 18 46.7	+43 41 42	"
HD 193901	20 20 38.7	−21 31 04	"
HD 193928	20 19 40.5	+36 45 26	"
HD 194279	20 21 31.0	+40 35 49	"
HD 194334	20 21 45.3	+38 43 12	"
HD 194839	20 24 35.0	+41 12 51	"
HD 195050	20 25 42.9	+38 16 30	"
HD 195177	20 26 32.9	+38 26 50	"
HD 195358	20 27 59.2	+19 15 08	"
HD 195407	20 27 53.9	+36 48 43	"
HD 195592	20 28 52.7	+44 08 44	"
HD 196610	20 35 37.7	+18 05 29	"
HD 197076	20 38 29.3	+19 45 07	"
HD 197345	20 39 43.4	+45 06 02	"
HD 197406	20 39 51.1	+52 24 38	"
HD 197434	20 40 01.9	+54 01 47	"
HD 198478	20 47 13.9	+45 55 40	"
HD 198820	20 49 58.1	+32 39 36	"
HD 198931	20 50 23.7	+44 14 42	"
HD 199081	20 51 28.4	+44 11 49	"
HD 199216	20 52 15.4	+49 20 32	"
HD 199356	20 53 30.1	+40 06 27	"
HD 199476	20 52 04.3	+74 34 56	"
HD 199478	20 54 08.3	+47 13 30	"
HD 199579	20 54 48.7	+44 43 53	"
HD 199801	20 56 50.5	+ 8 26 32	"
HD 200775	21 00 59.6	+67 57 55	"
HD 200775 #1	21 00 59.6	+67 58 25	ED
HD 200775 #2	21 00 59.6	+67 58 55	"
HD 200775 #3	21 00 54.3	+67 58 25	"
HD 200775 #4	21 01 04.9	+67 58 40	"
HD 200775 #5	21 00 55.2	+67 58 40	"
HD 200775 #6	21 00 55.2	+67 59 25	"
HD 200857	21 02 25.9	+55 01 50	CSI 79
HD 201091	21 04 39.9	+38 29 58	"
HD 201092	21 04 38.3	+38 29 29	"
HD 201345	21 05 51.6	+33 11 39	"
HD 201626	21 07 48.3	+26 24 36	"
HD 201733	21 08 10.7	+45 17 52	"
HD 201891	21 09 39.9	+17 32 03	"
HD 201941	21 10 13.6	+ 2 26 12	
HD 202380	21 11 30.7	+59 53 26	CSI 79
HD 203532	21 25 57.9	−82 54 13	"
HD 203638	21 21 19.6	−21 03 55	"
HD 203856	21 21 37.1	+39 48 12	
HD 203938	21 22 01.7	+46 56 55	CSI 79
HD 204827	21 27 31.3	+58 31 12	"
HD 205772	21 35 33.6	−41 16 26	
HD 206183ABC	21 36 52.0	+56 44 50	CSI 79
HD 206773	21 40 50.3	+57 30 24	"
HD 207076	21 43 56.4	− 2 26 40	"
HD 207198	21 43 30.7	+62 13 46	"
HD 207260	21 44 00.2	+60 53 22	"

NAME	RA (1950) DEC	POS REF
	h m s ° ′ ″	
HD 207673	21 47 37.7 +40 54 53	"
HD 208501	21 53 12.0 +56 22 25	"
HD 208906	21 56 27.7 +29 34 42	"
HD 209008	21 57 37.9 + 6 28 35	"
HD 209975	22 03 36.2 +62 02 10	"
HD 210066	22 05 30.6 −34 17 17	"
HD 210418	22 07 40.5 + 5 57 03	"
HD 210594	22 08 35.9 +30 18 22	"
HD 210839	22 09 48.5 +59 10 02	"
HD 211564	22 14 44.3 +55 21 54	"
HD 211853	22 16 54.5 +55 52 30	779907
HD 212044	22 18 24.9 +51 36 31	CSI 79
HD 212571	22 22 43.3 + 1 07 21	"
HD 213049	22 25 35.4 +56 01 14	"
HD 213320	22 28 00.0 −10 56 03	"
HD 213470	22 28 24.7 +56 58 06	"
HD 214080	22 33 25.3 −16 38 48	"
HD 214419	22 34 56.8 +56 38 46	779907
HD 214454	22 35 18.7 +51 17 10	CSI 79
HD 214680	22 37 00.7 +38 47 21	"
HD 215773	22 44 40.3 +46 26 45	"
HD 216411	22 49 32.9 +58 44 34	"
HD 216777	22 53 11.7 − 8 05 19	"
HD 216898	22 53 44.1 +62 02 20	"
HD 217050	22 54 51.5 +48 25 00	779907
HD 217086	22 54 48.9 +62 27 34	CSI 79
HD 217101	22 55 21.7 +39 02 27	"
HD 217476	22 57 58.1 +56 40 36	"
HD 217490	22 58 04.9 +59 21 03	"
HD 217543	22 58 34.7 +38 26 21	"
HD 217701	22 59 56.7 − 6 50 32	"
HD 218209	23 03 07.4 +68 08 40	"
HD 218342	23 04 06.5 +62 56 33	"
HD 218393	23 04 51.1 +49 55 16	"
HD 218915	23 08 52.3 +52 47 10	"
HD 219134	23 10 51.7 +56 53 30	"
HD 219287	23 11 52.6 +59 06 07	"
HD 219460	23 13 01.9 +60 10 38	"
HD 219617	23 14 29.7 −14 06 27	"
HD 219688	23 15 18.3 − 9 27 19	"
HD 220300	23 19 53.5 +56 04 25	"
HD 220652	23 22 36.3 +62 00 28	"
HD 221170	23 27 00.4 +30 09 27	"
HD 221354	23 28 55.7 +58 53 15	"
HD 221861	23 32 47.9 +71 21 55	"
HD 222173	23 35 40.5 +42 59 27	"
HD 223385	23 46 23.2 +61 56 10	"
HD 223960	23 51 20.1 +60 34 31	"
HD 224151	23 53 02.5 +57 08 01	"
HD 224930	23 59 33.1 +26 49 02	"
HD 225023	0 00 11.8 +35 32 14	
HD 225094	0 00 50.7 +63 21 45	CSI 79
HD 225095	0 00 52.5 +55 16 20	"
HD 225146	0 01 22.2 +60 49 29	"
HD 225160	0 01 28.3 +61 56 36	"
HD 225239	0 02 16.0 +34 22 48	"
HD 225985	19 47 37.5 +32 49 45	"
HD 226868	19 56 28.7 +35 03 54	"
HD 227460	20 02 24.3 +36 07 23	"
HD 228368	20 11 24.2 +34 52 23	"
HD 228712	20 14 49.6 +40 43 48	"
HD 228854	20 16 53.9 +36 10 59	"
HD 229033	20 19 03.9 +37 34 20	"
HD 229059	20 19 23.3 +37 14 54	"
HD 231195	19 18 23.1 +14 19 27	"
HD 232078	19 35 56.5 +16 41 33	"
HD 236031	23 01 46.5 +53 55 42	"
HD 236689	1 15 23.7 +58 06 43	"
HD 236970	2 29 43.2 +56 05 52	"
HD 237211	3 59 14.2 +56 24 08	"
HD 248411	5 48 44.7 +28 15 00	"
HD 249845	5 56 15.0 +32 53 03	"
HD 250028	5 56 48.5 +25 05 10	"
HD 250550	5 59 06.3 +16 30 58	"
HD 254577	6 14 53.1 +22 25 44	"
HD 259597	6 30 48.7 + 8 22 27	"
HD 268743	4 57 39.9 −66 32 07	"
HD 268757	4 54 26.5 −69 17 13	"
HD 269006	5 02 50.1 −71 24 20	"
HD 269217	5 13 57.9 −69 24 38	"
HD 269227	5 14 16.9 −69 34 39	"
HD 269599	5 28 37.9 −69 10 34	"
HD 283447	4 11 31 +27 55	ED
HD 285773	4 26 37.6 +17 47 04	CSI 79
HD 290556	5 31 37.9 + 0 22 54	"
HD 290662	5 33 24.9 − 0 49 38	"
HD 290768	5 36 34.9 − 1 32 28	"
HD 290787	5 38 04.2 − 0 19 30	"
HD 290798	5 37 44.1 − 0 46 07	"
HD 290813	5 37 52.3 − 1 47 59	"
HD 294304	5 38 25.6 − 2 51 59	BD
HD 303492	10 49 51.7 −58 42 36	CSI 79
HD 306070	11 07 28.3 −60 15 24	"
HD 306097	11 09 10.9 −60 38 50	"
HD 316248	17 42 48 −30 11	
HD 316285	17 45 04.7 −27 59 54	CSI 79
HD 316285	17 45 06 −28 00	
HD 326823	17 03 18 −42 32	
HD 330036	15 47 38.5 −48 36 00	820620
HD 331777	20 01 13.5 +31 46 39	CSI 79
HD 333424	20 02 48 +29 01	
HD 334060	20 16 06 +30 17	
HD 351123	19 55 24 +17 14	
HDE 226868	19 56 28.7 +35 03 54	CSI 79
HDE 228368	20 11 24.2 +34 52 23	"
HDE 228766	20 15 37.9 +37 09 08	"
HDE 228854	20 16 53.9 +36 10 59	"
HDE 245770	5 35 47.9 +26 17 17	"
HDE 258686	6 28 02 +10 05 54	
HDE 258749	6 28 13 + 9 50 48	
HDE 258853	6 28 30 + 9 49 36	
HDE 258973	6 28 57 +10 22 36	
HDE 259431	6 30 19 +10 21 36	
HDE 259431	6 30 19.3 +10 21 36	CSI 79
HDE 290857	5 44 34 + 0 38	HDE
HDE 290859	5 42 52 + 0 27	"
HDE 290860	5 44 23.1 + 0 19 08	CSI 79
HDE 290861	5 44 33.6 + 0 16 54	"

NAME	RA (1950) DEC	POS REF
	h m s ° ′ ″	
HDE 290861 A	" "	"
HDE 290861 B	" "	"
HDE 303308	10 43 09.2 −59 24 16	"
HDE 303311	10 43 −59 16	ED
HDE 305523	10 42 33.4 −59 41 29	CSI 79
HDE 313706IRS1	18 00 15.3 −22 32 52	
HDE 313706IRS2	18 00 14.3 −22 35 34	
HDE 313706IRS3	18 00 15.8 −22 36 49	
HDE 313706IRS4	18 00 11.1 −22 32 05	
HDE 313706IRS5	18 00 12.7 −22 28 10	
HDE 313706IRS9	18 00 06.5 −22 32 01	
HDE 313706IR10	18 00 06.2 −22 34 17	
HDE 313706IR11	18 00 06 −22 32 01	
HDE 313706IR12	17 59 57.7 −22 25 21	
HDE 313706IR13	18 00 03 −22 32 07	
HDE 313706IR15	17 59 59.4 −22 36 32	
HDE 313706IR16	17 59 55.5 −22 30 30	
HDE 313706IR18	17 59 52 −22 35 30	
HDE 313706IR19	17 59 49 −22 35 18	
HDE 313706IR20	17 59 52.3 −22 32 45	
HDE 313643	18 01 43.7 −21 10 03	CSI 79
HDE 313875	18 05 48 −23 26 30	
HDE 314030	18 07 03 −23 39 30	
HDE 314031	18 06 50 −23 37 36	
HDE 314032	18 06 46 −23 40 06	
HDE 322426	16 53 33.2 −40 18 56	
HEN 1191	16 23 31.9 −48 32 45	ED
HEN S26	5 19 06 −68 00	
HEN S43	5 30 36 −67 19	
HEN S63	5 48 48 −67 36	
HEN S63	5 48 52.4 −67 37 02	
HEN S136	5 41 54 −69 26	
HEN 40	7 30 00 −41 29	
HEN 209	8 47 04 −45 53 54	709901
HEN 230	8 54 54 −46 12	
HEN 373	10 08 14 −56 47 36	709901
HEN 401	10 17 49 −59 58 18	"
HEN 485	10 44 00 −59 40 48	"
HEN 519	10 52 01 −60 10 30	"
HEN 591	11 06 33 −60 26 30	"
HEN 653	11 23 17 −59 40 06	"
HEN 664	11 28 58 −63 33 36	"
HEN 729	11 52 14 −62 56 48	"
HEN 748	12 02 27 −65 04 06	"
HEN 782	12 20 41 −62 21 36	"
HEN 794	12 26 46 −64 33 00	"
HEN 814		
HEN 938	13 49 01 −63 18 00	709901
HEN 1044	14 56 14.7 −54 06 09	820620
HEN 1044	14 56 18 −54 06	
HEN 1092	15 42 28.7 −66 19 53	769910
HEN 1125	15 55 51 −41 48 48	709901
HEN 1227	16 34 54 −45 18	
HEN 1242	16 40 00 −62 32	
HEN 1242	16 40 00.5 −62 31 27	769910
HEN 1481	17 44 04 −36 08 00	709901
HEN 1495	17 46 47 −47 21 42	"
HEN 1591	18 04 24 −25 55 00	"
HEN 1751	19 24 36 +23 48	
HEN 1835	20 07 42 +25 03	
AC HER	18 28 08.9 +21 49 52	CSI 79
AH HER	16 42 06 +25 20 34	GCVS
ALF HER	17 12 21.9 +14 26 44	CSI 79
ALF HER	17 12 22 +14 26 50	
ALF HER A	17 12 21.9 +14 26 44	CSI 79
ALF 1 HER	" "	"
AM HER	18 14 59 +49 50 51	GCVS
AM HER W	18 14 53 +49 52 14	ED
BET HER	16 28 04.0 +21 35 49	CSI 79
BL HER	17 58 59.9 +19 15 00	"
CHI HER	15 50 56.6 +42 35 25	"
DQ HER C	18 06 05.9 +45 52 00	"
DQ HER C NEB.	18 06 06 +45 50 55	ED
DQ HER NOVA	18 06 06 +45 51 00	
EPS HER	16 58 22.4 +30 59 55	CSI 79
G HER	16 26 59.9 +41 59 26	779907
LQ HER	16 09 30.1 +23 37 21	CSI 79
MUU HER	17 44 30.0 +27 44 54	"
MUU HER BC	17 44 27.7 +27 44 45	"
MW HER	17 33 25 +15 36 53	GCVS
NUU HER	17 56 35.2 +30 11 30	CSI 79
OP HER	17 55 22.3 +45 21 21	779907
PI HER	17 13 18.2 +36 51 50	CSI 79
PP HER	18 05 56 +36 21 22	GCVS
R HER	16 03 57.5 +18 30 13	CSI 79
RR HER	16 02 50.6 +50 38 04	779907
RS HER	17 19 36.4 +22 58 06	CSI 79
RT HER	17 08 48.1 +27 07 08	"
RU HER	16 08 05.7 +25 12 01	"
RV HER	16 58 25.9 +31 10 41	"
RY HER	17 57 35.3 +19 26 57	"
RZ HER	18 34 43.3 +26 00 21	"
S HER	16 49 37.1 +15 01 27	"
SS HER	16 30 29.3 + 6 57 41	"
ST HER	15 49 16.7 +48 37 58	779907
SV HER	18 24 20.5 +24 59 37	CSI 79
SX HER	16 05 20.9 +25 02 27	"
SY HER	16 59 22.1 +22 32 57	"
T HER	18 07 12.6 +31 00 40	779907
TAU HER	16 18 14.0 +46 25 53	CSI 79
THE HER	17 54 32.1 +37 15 20	"
TV HER	18 12 48.1 +31 48 09	779907
U HER	16 23 34.7 +19 00 16	CSI 79
U HER	16 23 35.0 +19 00 24	
UU HER	16 34 12.2 +38 04 05	779907
UW HER	17 12 39.0 +36 25 26	"
V396 HER	17 20 45 +24 36 05	GCVS
V441 HER	17 53 24.0 +26 02 23	CSI 79
V443 HER	18 20 05 +23 25 23	GCVS
W HER	16 33 26.1 +37 26 49	779907
X HER	16 01 08.7 +47 22 36	"
YY HER	18 12 25.9 +20 58 17	CSI 79
2 HER	15 52 57.7 +43 16 59	"
4 HER	15 53 49.3 +42 42 37	"
14 HER	16 08 46.7 +43 57 02	"
28 HER	16 30 07.9 + 5 37 33	"
30 HER	16 26 59.9 +41 59 26	779907
39 HER	16 39 34.9 +27 00 42	CSI 79

NAME	RA (1950) DEC	POS REF
	h m s ° ′ ″	
50 HER	16 48 41.7 +29 53 25	"
88 HER	17 48 44.7 +48 24 23	"
89 HER	17 53 24.0 +26 03 23	"
104 HER	18 10 01.1 +31 23 29	"
106 HER	18 18 10.9 +21 56 18	"
108 HER	18 19 01.3 +29 50 01	"
HERSCHEL 36	18 00 35.6 −24 23 07	ED
HETZLER 1−1	21 56 19 +56 29 37	379901
HETZLER 1−2	21 49 38 +56 29 50	"
HETZLER 4−1	19 33 34 +22 13 51	"
HETZLER 4−2	19 13 49 +22 51 53	"
HE1−3	19 46 15.5 +22 02 28	769910
HE1−5	20 09 42.9 +20 11 00	"
HE2−10	8 34 07.1 −26 14 04	761008
HE2−17	8 54 54 −46 12	730001
HE2−17	8 55 −46 12	
HE2−25	9 16 29 −54 26 42	779909
HE2−26	9 18 06.4 −58 59 23	769910
HE2−32	9 29 26 −57 23 42	779909
HE2−34	9 39 24 −49 09	P−K
HE2−35	9 39 47.9 −49 44 02	739909
HE2−38	9 53 03 −57 04 24	749906
HE2−41	10 05 54.0 −63 39 50	769910
HE2−47	10 21 24.0 −60 17 22	"
HE2−57	10 54 03 −61 12 00	759905
HE2−61	11 04 22 −54 33 06	779909
HE2−62	11 15 45 −70 33 06	789907
HE2−63	11 21 40.8 −52 34 52	769910
HE2−64	11 25 05 −57 01 24	779909
HE2−67	11 26 30.5 −59 50 00	769910
HE2−68	11 29 31.8 −65 41 40	"
HE2−71	11 36 54.1 −68 35 30	"
HE2−76	12 05 48 −63 55 30	779909
HE2−77	12 06 23.8 −62 59 20	769910
HE2−79	12 12 39 −63 22 42	779909
HE2−80	12 19 37 −63 00 54	"
HE2−80	12 20 −63 01	
HE2−81	12 20 16 −63 45 30	779909
HE2−84	12 25 57 −63 28 00	"
HE2−87	12 42 49 −62 44 12	"
HE2−88	13 02 45 −57 23 18	759905
HE2−90	13 06 −61 04	
HE2−90	13 06 27 −61 03 36	749906
HE2−91	13 06 53 −62 55 30	759905
HE2−97	13 41 24.0 −71 13 47	769910
HE2−99	13 48 46.3 −66 08 37	"
HE2−101	13 51 30 −58 12 30	759905
HE2−102	13 54 45.9 −58 39 54	769910
HE2−103	14 01 50.9 −64 26 37	"
HE2−104	14 08 33.5 −51 12 19	"
HE2−104	14 09 −51 12	
HE2−106	14 10 −63 12	
HE2−106	14 10 24.0 −63 11 47	769910
HE2−108	14 14 47.5 −51 56 50	"
HE2−113	14 56 14.7 −54 06 09	820620
HE2−113	14 56 18 −54 06	
HE2−118	15 02 55.2 −42 48 24	739909
HE2−119	15 06 23.1 −64 28 57	769910
HE2−127	15 21 18.3 −51 39 10	"
HE2−128	15 21 29.7 −51 09 08	"
HE2−131	15 31 54.0 −71 45 00	"
HE2−134	15 42 28.7 −66 19 53	"
HE2−138	15 51 19.2 −66 00 26	"
HE2−139	15 50 48 −55 20 42	779909
HE2−147	16 09 56 −56 51 54	"
HE2−151	16 11 25.4 −59 46 34	769910
HE2−156	16 17 38 −42 16 48	779909
HE2−157	16 18 17.1 −53 33 53	769910
HE2−162	16 23 53.6 −53 54 47	"
HE2−170	16 31 22.9 −53 43 59	"
HE2−171	16 30 47 −34 59 12	789908
HE2−173	16 32 59 −39 45 36	779907
HE2−174	16 34 52 −45 17 48	779909
HE2−174	16 35 −45 18	
HE2−176	16 37 54 −45 07 21	779909
HE2−179	16 39 37 −45 55 06	"
HE2−182	16 49 49.3 −64 09 39	769910
HE2−183	16 49 47 −44 47 54	779909
HE2−185	16 55 45.4 −70 01 40	769910
HE2−248	17 32 16.3 −49 23 43	"
HE2−260	17 36 01.5 −18 15 57	819914
HE2−275	17 42 05 −38 38 24	779909
HE2−294	17 48 29 −32 54 12	819916
HE2−325	17 57 59 −26 21 24	"
HE2−349	18 04 17 −36 06 48	"
HE2−354	18 06 35 −33 20 30	"
HE2−370	18 11 23 −29 50 18	789908
HE2−390	18 17 51.3 −26 49 53	769910
HE2−396	18 20 27 −21 26 18	819917
HE2−429	19 11 21.2 +14 54 18	769910
HE2−430	19 11 50.9 +17 26 20	"
HE2−432	19 21 14.8 +21 02 21	"
HE2−436	19 28 51.5 −34 18 59	739909
HE2−440	19 36 03.5 +25 09 00	819914
HE2−442	19 37 36 +26 24	
HE2−442	19 37 40.1 +26 22 48	769910
HE2−446	19 41 57.5 +23 19 42	"
HE2−446	19 42 +23 20	
HE2−446	19 42 00 +23 20	
HE2−447	19 43 11.7 +21 12 46	819914
HE2−459	20 11 54 +29 25	P−K
HE2−467	20 33 42.6 +20 01 07	769910
HE2−468	20 39 20.4 +34 34 09	819914
HFE 1	5 25 41 − 5 08	
HFE 2	5 26 56 − 4 46	
HFE 2#1	5 26 47.2 − 4 45 06	
HFE 2#2	5 27 00.5 − 4 43 43	
HFE 2#3	5 26 44.6 − 4 50 46	
HFE 2#4	5 26 59.8 − 4 51 39	
HFE 2#5	5 26 56.4 − 4 54 11	
HFE 2#6	5 26 32.9 − 4 56 37	
HFE 2#7	5 26 20.0 − 4 52 55	
HFE 2#8	5 26 09.1 − 5 01 57	
HFE 2#9	5 26 56.6 − 5 01 40	
HFE 3	5 28 48 − 4 55	
HFE 4	5 31 09 − 5 42	
HFE 5	5 32 56 − 4 46	
HFE 6	5 33 01 − 5 24	

NAME	RA (1950)	DEC	POS REF
	h m s	° ′ ″	
HFE 7	5 33 48	− 3 53	
HFE 8	5 37 33	− 6 30	
HFE 9	6 13 49	+ 4 11	
HFE 10	9 50 42	+70 42	
HFE 11	9 56 07	+71 24	
HFE 12	10 07 29	−59 10	
HFE 13	10 18 32	−57 22	
HFE 14	10 25 04	−57 38	
HFE 15	10 37 21	−56 51	
HFE 16	10 56 12	−57 01	
HFE 17	13 27 50	−43 25	
HFE 18	13 33 41	−42 26	
HFE 19	13 35 49	−40 40	
HFE 20	16 28 42	−19 00	
HFE 21	16 35 33	−22 13	
HFE 22	17 13 06	−36 20	
HFE 23	17 15 56	−38 51	
HFE 24	17 16 29	−35 52	
HFE 25	17 17 22	−34 33	
HFE 26	17 20 56	−34 12	
HFE 27	17 21 47	−34 22	
HFE 28	17 25 34	−34 31	
HFE 29	17 25 12	−36 38	
HFE 30	17 35 49	−31 32	
HFE 31	17 38 40	−29 58	
HFE 32	17 39 51	−29 47	
HFE 33	17 41 46	−29 22	
HFE 34	17 42 54	−28 59	
HFE 35	17 43 12	−28 47	
HFE 36	17 44 46	−28 22	
HFE 37	17 45 56	−28 01	
HFE 38	17 48 20	−27 24	
HFE 39	17 50 02	−26 45	
HFE 40	17 51 22	−26 13	
HFE 41	17 53 33	−25 00	
HFE 42	17 56 31	−23 55	
HFE 43	17 58 03	−23 58	
HFE 44	17 59 09	−23 42	
HFE 45	17 59 55	−26 57	
HFE 46	18 00 34	−24 20	
HFE 47	18 01 26	−19 43	
HFE 48	18 02 43	−21 44	
HFE 49	18 05 21	−20 20	
HFE 50	18 09 46	−17 58	
HFE 51	18 14 17	−16 22	
HFE 52	18 14 44	−15 53	
HFE 53	18 15 55	−16 08	
HFE 54	18 16 36	−16 46	
HFE 55	18 16 53	−16 12	
HFE 56	18 43 18	− 2 49	
HFE 57	18 44 49	− 2 07	
HFE 58	19 07 59	+ 9 03	
HFE 59	19 19 58	+14 08	
HFE 60	19 21 18	+14 21	
HFE 61	19 32 41	+21 56	
HFE 62	19 59 41	+40 18	
HFE 63	20 00 31	+33 24	
HFE 64	20 24 43	+40 12	
HFE 65	20 26 17	+39 34	
HFE 66	20 27 20	+40 55	
HFE 67	20 33 50	+42 22	
HFE 68	20 38 24	+42 27	
HFE 69	20 38 38	+41 29	
HFE 70	20 39 23	+42 03	
HFE 71	20 48 24	+43 26	
HFE 72	20 57 44	+43 20	
HI 263	2 19	+57	ED
HM 1	10 54 48	−77 09	739903
HM 2	10 55 25	−76 56 08	GCVS
HM 3	10 57 47	−77 06 53	"
HM 4	10 57 51	−76 46	739903
HM 5	10 58 56	−76 28	"
HM 6	10 59 18	−76 01	"
HM 7	11 01 06	−77 17	"
HM 8	11 01 38	−77 06	"
HM 9	11 02 41	−76 11	"
HM 10	11 03 13	−77 10	"
HM 11	11 05 35	−77 03	"
HM 12	11 05 50	−75 47	"
HM 13	11 06 00	−77 122	"
HM 14	11 05 58	−76 36	"
HM 15	11 06 18	−77 24	"
HM 16	11 06 36	−77 23	"
HM 17	11 06 36	−77 26	"
HM 18	11 06 39.5	−77 23 00	CSI 79
HM 19	11 06 54	−77 29	739903
HM 21	11 07 27	−76 46	
HM 22	11 07 51	−76 07 04	GCVS
HM 24	11 08 27	−76 18 46	"
HM 26	11 08 37	−76 14	739903
HM 28	11 09 19	−76 18	"
HM 29	11 10 06	−76 04	"
HM 30	11 10 55	−76 28	"
HM 31	11 11 01	−76 28	"
HM 32	11 15 58	−76 47	"
HO I/A936	9 36	+71	ED
HO II/A814	8 14	+70	"
HO IV			
R HOR	2 52 11.9	−50 05 32	CSI 79
S HOR	2 23 50.1	−59 47 23	"
T HOR	2 59 17.7	−50 50 03	"
U HOR	3 51 10.9	−45 58 58	"
V HOR	3 02 14.4	−59 07 37	"
X HOR	2 46 25.4	−59 15 32	"
HOURGLASS (N)	18 00 36.9	−24 23 04	ED
HTR 18	5 39 09.5	−69 07 13	780108
HU1−1	0 25 30	+55 41 20	709904
HU1−2	21 31 06	+39 25	P−K
HU2−1	18 47 39.2	+20 47 12	739909
HV 832	0 49 33	−72 55 23	ED
HV 838	0 53 55	−73 28 14	"
HV 859	1 08 50	−73 40 09	"
HV 873	4 55 04	−70 59	609903
HV 878			
HV 883	5 00 23	−68 31	609903
HV 884	5 01 44	−68 10 00	GCVS
HV 886			
HV 888			

NAME	RA (1950)	DEC	POS REF
	h m s	° ′ ″	
HV 894			
HV 900			
HV 902			
HV 909			
HV 914			
HV 916			
HV 928			
HV 953			
HV 995			
HV 1001			
HV 1002			
HV 1003			
HV 1004			
HV 1349	0 38 56	−73 40 08	ED
HV 1366	0 41 33	−73 11 59	"
HV 1375	0 40 59	−7[illegible] 07 37	"
HV 1455	0 46 30	−7[illegible] [illegible] 03	"
HV 1475	0 47 36	−73 34 53	"
HV 1645	0 53 32	−73 31 27	"
HV 1719	0 55 32	−73 17 58	"
HV 1865	0 59 58	−73 01 06	"
HV 1956	1 02 31	−72 46 02	"
HV 1963	1 02 50	−72 51 04	"
HV 2112	1 08 32	−72 53 07	"
HV 2251			
HV 2255			
HV 2257			
HV 2279			
HV 2294	5 06 17	−66 45	609903
HV 2337			
HV 2338			
HV 2360			
HV 2362			
HV 2369	5 13 55	−67 07	609903
HV 2405			
HV 2432			
HV 2447	5 19 56	−68 43	609903
HV 2450			
HV 2493			
HV 2523			
HV 2526			
HV 2527			
HV 2555			
HV 2575			
HV 2576			
HV 2578			
HV 2586			
HV 2595			
HV 2604			
HV 2677			
HV 2694			
HV 2749			
HV 2763			
HV 2793			
HV 2827			
HV 2883			
HV 5497	4 55 33	−66 30	609903
HV 5541			
HV 5593			
HV 5654			
HV 5715			
HV 5854			
HV 5870			
HV 5914			
HV 6065			
HV 6093			
HV 11223	0 30 03	−73 39 07	ED
HV 11262			
HV 11295	0 49 06	−73 08 55	ED
HV 11303	0 50 16	−71 53 24	"
HV 11329	0 52 00	−73 09 01	"
HV 11366	0 55 18	−72 30 26	"
HV 11417	0 59 05	−73 07 30	"
HV 11423	0 59 20	−71 54 11	"
HV 11427	0 59 55	−73 04 45	"
HV 11452	1 02 06	−73 49 11	"
HV 11984			
HV 12048			
HV 12070			
HV 12122	0 53 26	−72 22 13	ED
HV 12149	0 57 08	−72 35 07	"
HV 12179	1 03 25	−72 23 11	"
HV 12225			
HV 12247	6 01 20	−65 06 11	GCVS
HV 12249	6 07 04	−66 49 00	"
HV 12252			
HV 12667			
HV 12700			
HV 12747			
HV 12765			
HV 12797			
HV 12956	1 07 44	−71 36 55	ED
HV 13048			
AK HYA	8 37 35.7	−17 07 22	CSI 79
ALF HYA	9 25 07.7	− 8 26 26	"
CZ HYA	10 24 57.9	−25 17 47	"
ETA HYA	8 40 36.6	+ 3 34 45	"
EX HYA	12 49 42	−28 59 14	GCVS
FI HYA	12 37 11.9	−26 24 57	CSI 79
FK HYA	8 22 02.2	− 8 21 25	"
I HYA	9 39 00.0	−23 21 47	"
R HYA	13 26 58.4	−23 01 23	"
RR HYA	9 42 40.9	−23 47 39	"
RT HYA	8 27 13.1	− 6 08 59	"
RU HYA	14 08 40.7	−28 39 00	"
RU HYA	14 08 42.0	−28 38 24	
RV HYA	8 37 18.5	− 9 24 31	CSI 79
RW HYA	13 31 31.9	−25 07 27	"
RY HYA	8 17 30.5	+ 2 55 42	"
S HYA	8 50 57.4	+ 3 15 29	"
T HYA	8 53 13.7	− 8 56 56	"
THE HYA	9 11 45.7	+ 2 31 33	"
U HYA	10 35 04.9	−13 07 24	"
V HYA	10 49 11.3	−20 59 03	"
W HYA	13 46 12.2	−28 07 05	"
X HYA	9 33 06.9	−14 28 02	"
Y HYA	9 48 45.0	−22 46 56	"
ZET HYA	8 52 45.0	+ 6 08 11	"

NAME	RA (1950)	DEC	POS REF
	h m s	° ′ ″	
HYADES #15	4 11 32.1	+23 27 01	"
HYADES #25	4 15 27.7	+15 58 02	"
HYADES #30	4 17 08.4	+13 54 57	"
HYADES #32	4 17 30.4	+18 37 26	"
HYADES #33	4 17 45.9	+14 58 36	"
HYADES #34	4 18 03.7	+13 44 45	"
HYADES #43	4 20 27.0	+19 32 36	"
HYADES #50	4 21 22.3	+14 38 36	"
HYADES #52	4 21 35.7	+16 46 18	"
HYADES #54	4 22 23.0	+22 10 50	"
HYADES #65	4 24 44.7	+15 28 42	"
HYADES #69	4 25 41.1	+19 37 51	"
HYADES #72	4 25 48.2	+15 45 40	"
HYADES #78	4 26 36.5	+17 45 16	"
HYADES #79	4 26 37.6	+17 47 04	"
HYADES #174			
HYDRA G8+G9			
BET HYI	0 23 09.3	−77 32 07	CSI 79
GAM HYI	3 47 59.4	−74 23 32	"
UX HYI	3 49 00.6	−70 01 43	"
VW HYI	4 09 30	−71 25 22	GCVS
HZ 43			
HZ 44			
HZ 46			
HZ 133			
HZ 134			
HZ 357			
HZ 451			
HZ 489			
HZ 491			
HZ 625			
HZ 747	12 02 12.8	−61 43 23	CSI 79
HZ 793			
HZ 799			
HZ 1061			
HZ 1110			
HZ 1124			
HZ 1286			
HZ 1305			
HZ 1306			
HZ 1321			
HZ 1332			
HZ 1348			
HZ 1355			
HZ 1531			
HZ 1653			
HZ 2016			
HZ 2244			
HZ 2407			
HZ 2588			
HZ 2601			
HZ 2741			
HZ 3030			
HZ 3063			
H1−1	16 10 13	−34 28 06	789908
H1−2	16 45 34	−35 42 00	"
H1−4	16 50 24	−31 35 42	809909
H1−8	17 11 26.0	−33 21 23	739909
H1−9	17 18 20	−30 17 54	789908
H1−17	17 26 31	−28 38 12	819916
H1−18	17 26 32.0	−29 30 30	769910
H1−19	17 26 54	−27 57 06	819916
H1−21	17 29 17	−40 56 18	779909
H1−22	17 28 55	−37 55 30	"
H1−23	17 29 35	−29 58 18	819916
H1−25	17 32 10	−29 43 30	"
H1−29	17 40 55	−34 16 12	789908
H1−31	17 42 13	−34 32 42	"
H1−33	17 44 30	−34 07 06	"
H1−35	17 45 54.6	−34 21 59	769910
H1−36	17 46 24	−37 00 36	789908
H1−39	17 50 02	−33 55 24	819916
H1−40	17 52 23.0	−30 33 05	739909
H1−43	17 54 57	−33 47 24	819916
H1−44	17 54 56	−31 42 42	789908
H1−45	17 55 12	−28 14 42	"
H1−46	17 55 46.3	−32 21 33	769910
H1−47	17 57 26	−29 21 42	789908
H1−49	18 00 07.2	−32 42 30	769910
H1−50	18 00 37	−32 41 48	819916
H1−53	18 02 50.0	−26 30 01	769910
H1−54	18 03 56.1	−29 13 20	"
H1−55	18 04 02.7	−29 41 49	"
H1−56	18 04 42	−29 44 54	789908
H1−58	18 06 07	−26 03 06	819916
H1−60	18 09 16.2	−27 29 42	769910
H1−61	18 09 29	−24 50 42	819916
H1−62	18 10 02	−32 20 30	789908
H1−63	18 13 06.1	−30 08 40	769910
H1−65	18 17 05.0	−24 16 27	"
H134	15 42 32	−66 20	679907
H172	16 33 37.1	−55 36 25	769910
H177	16 40 04	−62 32	679907
H2−1	17 01 19.4	−33 55 05	739909
H2−2	17 04 04	−34 01 24	789908
H2−3	17 06 01.5	−41 32 20	
H2−3	17 06 02.3	−41 32 04	
H2−4	17 08 57	−32 34 12	789908
H2−5	17 12 05	−31 30 36	"
H2−10	17 24 23	−29 28 42	"
H2−11	17 26 18	−25 46 54	"
H2−14	17 28 51	−39 49 12	779909
H2−17	17 37 03.0	−24 24 11	769910
H2−18	17 40 29	−21 08 48	819917
H2−19	17 41 48	−38 16 12	779909
H2−23	17 45 39	−34 21 00	789908
H2−28	17 47 59.0	−22 18 48	769910
H2−32	17 53 12	−29 37 48	789908
H2−34	17 55 19	−28 33 30	"
H2−36	18 00 53	−31 39 24	"
H2−38	18 02 51	−28 17 18	"
H2−43	18 09 37	−28 20 48	"
H2−46	18 15 22	−31 56 06	809909
H2−47	18 25 46	−24 34 00	819916
H2−48	18 43 32	−23 30 06	"
H2O 0610+18	6 09 58	+18 00 07	
H2155−304	21 55 58.2	−30 27 52	809908
H222	2 37	−34	

NAME	RA (1950)	DEC	POS REF
	h m s	° ' "	
H2252−035	22 52	− 3 30	
H4−1	12 57 02.7	+27 54 24	819914
H453	2 37	−34	
I ZW 1	0 51 00.0	+12 25 00	809908
I ZW 92	14 39 12	+53 44	ED
I ZW 186	17 27	+50 18	
I ZW 187	17 27 04.3	+50 15 31	809908
I ZW 1727+50	17 27 06	+50 15	ED
IC 10	0 17 41.5	+59 00 52	739910
IC 65	0 58 02.8	+47 24 50	
IC 131	1 30 22	+30 30	IC
IC 132	1 30 27	+30 41	”
IC 133	1 30 27	+30 38	”
IC 142	1 31 06	+30 30	”
IC 163	1 46 30.4	+20 27 48	
IC 342	3 41 57.2	+67 56 27	
IC 342	3 41 58.6	+67 56 26	769909
IC 342 WEST	3 41 56.5	+67 56 27	
IC 348 IR	3 40 51.4	+31 52 29	
IC 351	3 44 20	+34 53 35	709904
IC 381	4 37 49.9	+75 32 44	
IC 418	5 25 09.5	−12 44 15	739909
IC 443	6 13 26	+22 29	IC
IC 446	6 28 21	+10 29 42	
IC 467	7 21 55.2	+79 58 29	
IC 529	9 13 28.0	+73 58 06	
IC 764	12 07 38.8	−29 27 30	
IC 769	12 09 58.5	+12 24 06	769909
IC 972	14 01 41.8	−16 59 13	769910
IC 1029	14 30 42.4	+50 07 27	
IC 1048	14 40 28.0	+ 5 06 03	
IC 1058	4 16 50.0	−56 03 18	
IC 1396 IRS1	21 37 31	+56 41 30	
IC 1470	23 03 05.5	+59 58 13	759901
IC 1575	0 41 03	− 4 25	IC
IC 1613	1 02 14.0	+ 1 51 09	719904
IC 1703	1 23 52	− 1 54	IC
IC 1747	1 53 58	+63 04 42	709904
IC 1805 2	2 29 01.0	+61 09 29	CSI 79
IC 1848 A	2 57 29	+60 17 30	
IC 1848A	2 57 37.8	+60 17 28	790906
IC 1848A IRS1	”	”	
IC 1898	3 08 07.0	−22 35 36	
IC 1954	3 30 06.0	−52 04 24	
IC 2003	3 53 12	+33 43 00	709904
IC 2087	4 36 51.9	+25 39 29	
IC 2087 IR	4 36 49.1	+25 39 10	
IC 2149	5 52 40.9	+46 05 53	749905
IC 2165	6 19 24.2	−12 57 40	739909
IC 2392	8 41 40	+18 28	IC
IC 2501	9 37 20.9	−59 51 52	769910
IC 2553	10 07 47	−62 22 00	759905
IC 2574	10 24 41.3	+68 40 18	769909
IC 2621	10 58 23.5	−64 58 47	769910
IC 2944 IRS1	11 35 46.9	−62 53 53	
IC 2944 IRS2	11 35 48.2	−62 56 35	
IC 3568	12 31 47.0	+82 50 22	749905
IC 3881	12 52 20.2	+19 26 53	
IC 3998	12 57 22.2	+28 14 36	769914
IC 4011	12 57 41.2	+28 16 21	739910
IC 4012	12 57 42.8	+28 20 49	”
IC 4021	12 57 49.6	+28 18 35	”
IC 4026	12 57 57.6	+28 18 54	769914
IC 4042	12 58 18	+28 14 18	”
IC 4191	13 05 28.0	−67 22 33	769910
IC 4320	13 41 15	−26 58 48	819916
IC 4329A	13 46 27.9	−30 03 41	789906
IC 4351	13 55 02.2	−29 04 18	
IC 4406	14 19 15.5	−43 55 27	739909
IC 4593	16 09 23.3	+12 12 08	”
IC 4634	16 58 34.6	−21 45 28	”
IC 4637	17 01 39.2	−40 48 52	”
IC 4701 IRS2	18 14 34.1	−16 38 59	
IC 4701 IRS3	18 14 31.7	−16 40 17	
IC 4701 IRS4	18 14 45.6	−16 40 38	
IC 4701 IRS6	18 14 39.6	−16 34 39	
IC 4701 IRS7	18 14 38	−16 36 04	
IC 4731	18 34 00	−62 59 12	779909
IC 4732	18 30 53.3	−22 40 57	739909
IC 4776	18 42 34.1	−33 23 52	”
IC 4830	19 09 28	−59 22 48	759905
IC 4846	19 13 44.9	− 9 08 06	739909
IC 4954	20 02 45	+29 07	IC
IC 4997	20 17 51.0	+16 34 27	739909
IC 5052	20 47 22.0	−69 23 30	
IC 5063	20 48 12	−57 15 30	779909
IC 5117	21 30 37	+44 22	IC
IC 5146 #1	21 45 03.0	+47 01 11	
IC 5146 #2	21 45 47.8	+47 05 59	
IC 5146 #3	21 47 42.4	+47 32 43	
IC 5146 #4	21 48 21.0	+47 33 58	
IC 5146 #5	21 50 33.5	+47 09 05	
IC 5146 #6	21 52 41.5	+47 15 06	
IC 5146 #7	21 56 59.2	+47 33 08	
IC 5146 #8	21 57 01.0	+47 18 47	
IC 5146 #9	21 58 02.8	+47 29 33	
IC 5146 #10	21 39 34.4	+47 12 59	
IC 5146 #11	21 42 03.5	+47 07 56	
IC 5146 #12	21 45 26.9	+47 18 08	
IC 5146 #13	21 49 52.5	+47 25 08	
IC 5146 #14	21 50 15.1	+47 35 05	
IC 5146 #15	21 50 38.5	+46 59 34	
IC 5146 #16	21 54 57.0	+47 25 24	
IC 5146 N	21 51 40	+47 03	ED
IC 5146 NOM.	21 51 30	+47 02	
IC 5146 SE	21 51 50	+46 58	ED
IC 5146 SW	21 51 15	+47 00	”
IC 5146 W2	21 51 30	+47 02	IC
IC 5146 W6	21 50 39.6	+46 59 20	CSI 79
IC 5146 W8	21 51 30	+47 02	IC
IC 5146 W9	”	”	”
IC 5146 W11	”	”	”
IC 5146 W14	”	”	”
IC 5146 W18	”	”	”
IC 5146 W32	”	”	”
IC 5146 W35	”	”	”
IC 5146 W42	21 51 32.9	+47 01 49	CSI 79
IC 5146 W44	21 51 30	+47 02	IC
IC 5146 W48	”	”	”
IC 5146 W53	”	”	”
IC 5146 W62	”	”	”
IC 5146 W64	”	”	”
IC 5146 W66	”	”	”
IC 5146 W70	”	”	”
IC 5146 W74	”	”	”
IC 5146 W76	”	”	”
IC 5176	22 11 10.0	−67 05 58	
IC 5217	22 21 56	+50 43	IC
IC 5240	22 38 56	−45 01 48	759905
IC 5267	22 54 22	−43 39 48	”
IC 5269B	22 53 49	−37 31 00	789908
IC 5269C	22 58 02	−35 38 24	”
IC 5270	22 55 08	−36 07 30	”
IC 5271	22 55 16	−34 00 36	”
IC 5273	22 56 38.3	−37 58 29	
II ZW 0553+03	5 53 06	+ 3 24	740903
II ZW 23	4 47 00	+ 3 15	”
II ZW 40	5 53 06	+ 3 24	”
II ZW 136	21 30 01.2	+ 9 55 01	789906
II+ 22 8	19 38 06	+22 25	
II+ 29 6			
III ZW 2	0 07 56.7	+10 41 48	809908
III ZW 55	3 38 38.3	−10 17 30	789906
III ZW 55 N	”	”	”
III ZW 77	16 22 06	+41 12	ED
R IND	22 32 30.9	−67 32 35	CSI 79
RR IND	21 42 23.5	−65 32 21	”
S IND	20 52 43.3	−54 30 45	”
T IND	21 16 52.1	−45 14 03	”
U IND	20 38 44.9	−51 16 31	”
INFRARED A	5 44 30.6	+ 0 20 43	
INFRARED B	5 44 31.2	+ 0 21 13	
INFRARED STAR	5 32 46.8	− 5 24 17	670701
IR 12.4+0.5	18 07 53.8	−17 57 10	
IR 12.4+0.5	18 07 57.9	−17 57 40	
IRC 00001	0 05 05	+ 1 04 24	
IRC 00002	0 05 37	− 2 43 42	
IRC 00003	0 07 19	− 2 49 42	
IRC 00004	0 10 24	− 3 39 36	
IRC 00005	0 12 22	− 3 18 00	
IRC 00006	0 14 05	+ 1 34 30	
IRC 00007	0 17 34	+ 2 45 24	
IRC 00008	0 18 35	− 2 37 54	
IRC 00009	0 21 55	− 4 55 42	
IRC 00010	0 27 28	− 4 14 00	
IRC 00011	0 42 22	+ 2 55 36	
IRC 00012	0 42 52	− 4 54 12	
IRC 00013	0 50 27	− 1 24 42	
IRC 00014	0 58 08	− 1 55 36	
IRC 00015	1 07 58	+ 2 10 30	
IRC 00016	1 09 11	− 2 31 00	
IRC 00017	1 11 43	− 2 26 42	
IRC 00018	1 20 01	+ 1 28 06	
IRC 00019	1 28 03	+ 2 37 24	
IRC 00020	1 30 26	− 0 08 12	
IRC 00021	1 35 21	− 3 41 24	
IRC 00022	1 36 01	+ 1 06 54	
IRC 00023	1 39 04	− 3 22 42	
IRC 00024	1 40 13	− 3 56 24	
IRC 00025	1 42 00	+ 2 58 06	
IRC 00026	1 42 46	− 3 24 30	
IRC 00027	1 50 57	+ 2 56 24	
IRC 00028	1 51 59	+ 4 27 54	
IRC 00029	2 01 10	− 4 20 24	
IRC 00030	2 16 49	− 3 12 12	
IRC 00031	2 19 22	+ 0 10 24	
IRC 00032	2 23 29	− 0 24 36	
IRC 00033	2 28 54	+ 2 03 06	
IRC 00034	2 46 28	− 4 25 12	
IRC 00035	2 48 47	+ 1 58 30	
IRC 00036	2 54 27	+ 4 18 00	
IRC 00037	2 58 17	− 3 04 36	
IRC 00038	2 59 40	+ 3 53 36	
IRC 00039	3 07 02	+ 4 11 30	
IRC 00040	3 08 51	− 3 59 54	
IRC 00041	3 12 04	− 2 31 06	
IRC 00042	3 12 20	+ 1 24 42	
IRC 00043	3 12 50	+ 1 30 24	
IRC 00044	3 15 49	− 1 06 54	
IRC 00045	3 21 04	+ 3 42 24	
IRC 00046	3 28 08	− 2 06 30	
IRC 00047	3 34 17	+ 0 14 54	
IRC 00048	3 42 28	− 0 27 24	
IRC 00049	3 48 44	− 0 24 30	
IRC 00050	3 48 55	− 1 31 30	
IRC 00051	3 51 43	− 3 05 54	
IRC 00052	4 01 23	+ 2 24 24	
IRC 00053	4 08 32	+ 2 11 24	
IRC 00054	4 09 54	− 4 32 36	
IRC 00055	4 10 44	+ 3 46 24	
IRC 00056	4 10 46	− 4 00 54	
IRC 00057	4 17 44	− 2 44 54	
IRC 00058	4 18 40	− 1 55 30	
IRC 00059	4 18 54	− 0 13 00	
IRC 00060	4 23 24	+ 4 15 42	
IRC 00061	4 29 22	− 0 09 12	
IRC 00062	4 31 13	− 0 05 06	
IRC 00063	4 42 25	− 2 42 42	
IRC 00064	4 50 49	+ 2 25 42	
IRC 00065	4 55 57	+ 1 38 12	
IRC 00066	5 02 47	+ 1 06 42	
IRC 00067	5 04 04	+ 0 28 42	
IRC 00068	5 10 41	+ 2 48 24	
IRC 00069	5 11 13	+ 0 30 12	
IRC 00070	5 12 05	− 0 37 06	
IRC 00071	5 20 52	− 4 36 30	
IRC 00072	5 21 55	− 0 56 24	
IRC 00073	5 22 30	+ 1 09 00	
IRC 00074	5 26 29	− 4 43 30	
IRC 00075	5 27 11	− 1 07 42	
IRC 00076	5 29 26	− 0 19 12	
IRC 00077	5 30 05	− 0 01 30	
IRC 00078	5 31 30	− 1 30 12	
IRC 00079	5 33 38	− 1 13 54	
IRC 00080	5 35 04	− 1 47 42	
IRC 00081	5 38 14	− 1 57 42	
IRC 00082	5 39 01	− 4 09 24	
IRC 00083	5 39 55	+ 1 26 54	
IRC 00084	5 40 37	− 1 37 12	
IRC 00085	5 42 57	− 4 15 36	
IRC 00086	5 43 53	+ 2 17 36	
IRC 00087	5 44 41	− 1 02 36	
IRC 00088	5 47 34	+ 4 24 42	
IRC 00089	5 49 52	+ 1 51 00	
IRC 00090	5 51 50	− 1 05 12	
IRC 00091	5 52 11	+ 0 57 00	
IRC 00092	5 55 07	+ 2 42 12	
IRC 00093	5 55 18	+ 1 13 06	
IRC 00094	5 56 24	− 1 07 00	
IRC 00095	5 57 32	− 3 04 36	
IRC 00096	5 59 13	− 2 21 06	
IRC 00097	6 01 30	− 3 57 00	
IRC 00098	6 02 46	+ 0 36 54	
IRC 00099	6 08 08	+ 3 46 12	
IRC 00100	6 17 29	− 2 55 12	
IRC 00101	6 18 26	+ 2 35 30	
IRC 00102	6 19 22	− 3 50 12	
IRC 00103	6 19 46	+ 3 26 42	
IRC 00104	6 20 11	− 2 10 00	
IRC 00105	6 21 30	− 0 15 36	
IRC 00106	6 21 41	− 0 04 00	
IRC 00107	6 21 41	+ 3 43 12	
IRC 00108	6 22 10	+ 3 47 30	
IRC 00109	6 22 23	− 2 56 36	
IRC 00110	6 24 36	+ 4 49 00	
IRC 00111	6 24 41	+ 0 19 36	
IRC 00112	6 24 42	− 0 14 36	
IRC 00113	6 26 37	+ 2 41 00	
IRC 00114	6 29 11	+ 1 22 30	
IRC 00115	6 30 28	+ 1 18 42	
IRC 00116	6 31 56	+ 0 14 06	
IRC 00117	6 32 39	− 1 28 06	
IRC 00118	6 34 44	+ 0 57 54	
IRC 00119	6 34 58	− 1 20 54	
IRC 00120	6 35 49	− 2 30 00	
IRC 00121	6 35 53	− 1 36 24	
IRC 00122	6 36 57	− 2 24 24	
IRC 00123	6 39 01	− 4 32 36	
IRC 00124	6 40 26	+ 3 05 42	
IRC 00125	6 41 59	+ 3 22 12	
IRC 00126	6 44 37	+ 1 35 12	
IRC 00127	6 45 02	+ 0 45 06	
IRC 00128	6 45 14	+ 2 28 12	
IRC 00129	6 46 29	− 1 36 30	
IRC 00130	6 46 58	+ 3 13 36	
IRC 00131	6 47 05	+ 3 02 06	
IRC 00132	6 48 15	− 0 00 30	
IRC 00133	6 48 56	+ 0 01 54	
IRC 00134	6 49 18	+ 4 49 30	
IRC 00135	6 49 37	− 3 58 12	
IRC 00136	6 50 45	− 4 30 42	
IRC 00137	6 51 30	+ 0 51 12	
IRC 00138	6 51 40	+ 2 57 06	
IRC 00139	6 54 11	+ 0 52 12	
IRC 00140	6 55 07	+ 3 22 24	
IRC 00141	6 58 30	− 3 10 42	
IRC 00142	6 58 44	− 2 04 12	
IRC 00143	6 59 36	− 3 40 30	
IRC 00144	7 01 07	− 3 06 24	
IRC 00145	7 01 32	− 4 33 42	
IRC 00146	7 05 59	+ 4 15 12	
IRC 00147	7 07 46	− 4 09 24	
IRC 00148	7 10 20	+ 2 43 00	
IRC 00149	7 11 16	− 3 52 00	
IRC 00150	7 11 45	− 3 48 36	
IRC 00151	7 11 45	+ 3 12 24	
IRC 00152	7 12 47	+ 0 43 06	
IRC 00153	7 14 58	+ 1 11 12	
IRC 00154	7 16 26	+ 3 37 36	
IRC 00155	7 26 46	− 1 48 06	
IRC 00156	7 26 52	− 4 10 42	
IRC 00157	7 27 47	+ 3 25 00	
IRC 00158	7 33 54	+ 2 11 12	
IRC 00159	7 36 22	− 0 08 54	
IRC 00160	7 38 11	+ 4 10 42	
IRC 00161	7 39 21	− 4 03 30	
IRC 00162	7 48 41	− 2 29 36	
IRC 00163	7 49 28	+ 3 24 30	
IRC 00164	7 50 02	− 2 29 36	
IRC 00165	7 57 14	− 3 32 42	
IRC 00166	7 58 41	− 1 15 24	
IRC 00167	7 59 42	+ 2 28 24	
IRC 00168	8 04 03	− 4 49 36	
IRC 00169	8 05 11	− 3 16 06	
IRC 00170	8 05 50	− 0 55 24	
IRC 00171	8 06 04	− 2 49 24	
IRC 00172	8 17 31	+ 2 55 36	
IRC 00173	8 22 29	+ 4 39 54	
IRC 00174	8 22 58	+ 2 16 00	
IRC 00175	8 23 36	− 4 44 24	
IRC 00176	8 36 08	+ 3 30 42	
IRC 00177	8 38 25	− 0 30 36	
IRC 00178	8 39 39	− 2 52 24	
IRC 00179	8 43 46	+ 1 48 54	
IRC 00180	8 49 34	− 3 13 12	
IRC 00181	8 50 06	+ 4 02 00	
IRC 00182	8 56 45	+ 1 59 12	
IRC 00183	9 04 23	+ 1 39 54	
IRC 00184	9 07 42	− 2 10 24	
IRC 00185	9 12 43	− 3 46 00	
IRC 00186	9 18 03	+ 0 23 36	
IRC 00187	9 22 54	− 4 54 42	
IRC 00188	9 32 55	− 1 34 12	
IRC 00189	9 35 53	+ 4 52 30	
IRC 00190	9 37 17	− 0 55 00	
IRC 00191	9 52 26	+ 0 03 12	
IRC 00192	10 04 58	+ 1 09 42	
IRC 00193	10 21 00	− 3 23 12	
IRC 00194	10 24 07	− 0 43 36	
IRC 00195	10 46 06	− 1 42 00	
IRC 00196	10 48 32	− 2 49 30	
IRC 00197	10 50 01	+ 0 03 06	
IRC 00198	10 50 11	+ 2 23 00	
IRC 00199	10 57 58	+ 3 53 00	

NAME	RA (1950)	DEC	POS REF
IRC 00200	10 59 19	− 2 12 54	
IRC 00201	11 01 08	− 2 56 06	
IRC 00202	11 03 30	+ 1 29 06	
IRC 00203	11 14 43	+ 2 17 00	
IRC 00204	11 20 43	+ 0 24 30	
IRC 00205	11 25 24	+ 3 07 00	
IRC 00206	11 27 44	− 2 43 30	
IRC 00207	11 28 48	− 4 00 36	
IRC 00208	11 31 03	+ 2 46 30	
IRC 00209	11 34 24	− 0 32 54	
IRC 00210	11 35 16	+ 4 35 42	
IRC 00211	11 46 44	− 3 02 06	
IRC 00212	11 48 07	+ 2 02 36	
IRC 00213	11 55 41	+ 3 45 06	
IRC 00214	12 02 03	+ 2 53 42	
IRC 00215	12 17 50	+ 3 34 42	
IRC 00216	12 22 00	− 4 45 36	
IRC 00217	12 22 40	+ 1 02 54	
IRC 00218	12 26 34	− 3 50 00	
IRC 00219	12 26 35	− 2 09 24	
IRC 00220	12 27 48	+ 4 41 00	
IRC 00221	12 35 50	+ 2 08 00	
IRC 00222	12 36 09	− 4 05 36	
IRC 00223	12 39 08	− 1 10 36	
IRC 00224	12 44 47	+ 4 24 42	
IRC 00225	12 45 19	+ 3 50 30	
IRC 00226	12 53 05	+ 3 40 00	
IRC 00227	12 57 30	+ 0 34 36	
IRC 00228	12 58 59	+ 1 47 24	
IRC 00229	13 10 14	− 1 29 24	
IRC 00230	13 11 30	− 2 32 30	
IRC 00231	13 12 29	+ 4 46 54	
IRC 00232	13 19 31	+ 3 00 36	
IRC 00233	13 19 53	− 3 30 24	
IRC 00234	13 20 43	− 4 39 54	
IRC 00235	13 32 58	− 4 08 06	
IRC 00236	13 40 31	+ 3 47 00	
IRC 00237	13 49 17	− 3 25 30	
IRC 00238	13 52 07	− 1 15 24	
IRC 00239	14 12 21	+ 3 33 54	
IRC 00240	14 16 59	− 2 02 06	
IRC 00241	14 19 01	− 2 09 36	
IRC 00242	14 22 02	− 2 07 06	
IRC 00243	14 24 50	+ 4 53 54	
IRC 00244	14 28 17	+ 4 59 42	
IRC 00245	14 29 43	+ 4 21 30	
IRC 00246	14 35 22	+ 3 44 00	
IRC 00247	14 35 53	− 3 23 42	
IRC 00248	14 39 22	− 3 18 42	
IRC 00249	14 42 38	− 1 12 42	
IRC 00250	14 45 11	− 3 10 00	
IRC 00251	14 48 26	− 2 05 36	
IRC 00252	14 48 28	− 0 02 54	
IRC 00253	14 51 09	+ 2 25 54	
IRC 00254	14 55 02	+ 0 02 06	
IRC 00255	14 56 11	− 0 21 06	
IRC 00256	14 56 53	+ 4 45 54	
IRC 00257	14 58 43	− 2 33 24	
IRC 00258	14 59 16	+ 0 03 36	
IRC 00259	15 00 23	+ 2 17 12	
IRC 00260	15 06 00	− 0 49 24	
IRC 00261	15 11 27	− 1 42 24	
IRC 00262	15 12 22	− 2 13 54	
IRC 00263	15 15 53	− 0 16 30	
IRC 00264	15 18 31	+ 0 53 54	
IRC 00265	15 22 21	− 2 03 30	
IRC 00266	15 26 17	+ 3 59 42	
IRC 00267	15 28 22	− 4 01 24	
IRC 00268	15 29 55	+ 3 48 36	
IRC 00269	15 41 02	− 1 33 00	
IRC 00270	15 41 34	+ 2 33 06	
IRC 00271	15 45 20	+ 0 50 24	
IRC 00272	15 46 16	− 0 51 24	
IRC 00273	15 47 43	+ 2 20 54	
IRC 00274	15 52 26	− 3 50 12	
IRC 00275	16 01 23	+ 3 51 36	
IRC 00276	16 04 23	− 3 44 30	
IRC 00277	16 06 02	− 1 24 24	
IRC 00278	16 06 29	+ 3 34 54	
IRC 00279	16 07 12	− 3 20 30	
IRC 00280	16 11 46	− 3 33 42	
IRC 00281	16 13 11	− 2 15 54	
IRC 00282	16 15 41	− 4 34 30	
IRC 00283	16 22 15	− 2 21 24	
IRC 00284	16 24 11	− 2 30 30	
IRC 00285	16 25 02	+ 2 59 00	
IRC 00286	16 26 02	+ 0 47 00	
IRC 00287	16 27 26	− 0 00 54	
IRC 00288	16 29 37	− 1 31 42	
IRC 00289	16 34 44	− 1 45 06	
IRC 00290	16 40 18	− 3 33 30	
IRC 00291	16 42 35	− 2 59 42	
IRC 00292	16 43 17	− 3 55 30	
IRC 00293	16 55 14	− 2 41 36	
IRC 00294	16 58 25	− 4 08 54	
IRC 00295	17 03 05	+ 3 49 54	
IRC 00296	17 11 45	− 4 41 06	
IRC 00297	17 12 03	− 0 44 12	
IRC 00298	17 13 57	+ 4 46 36	
IRC 00299	17 14 02	− 0 23 12	
IRC 00300	17 16 20	− 4 15 36	
IRC 00301	17 17 16	+ 2 11 24	
IRC 00302	17 20 25	+ 0 55 24	
IRC 00303	17 22 58	− 3 01 12	
IRC 00304	17 24 02	+ 4 10 54	
IRC 00305	17 30 43	+ 0 08 06	
IRC 00306	17 30 44	+ 2 28 06	
IRC 00307	17 31 23	− 1 57 00	
IRC 00308	17 32 49	− 1 19 00	
IRC 00309	17 35 32	+ 4 05 06	
IRC 00310	17 36 03	− 1 43 06	
IRC 00311	17 36 56	+ 1 37 54	
IRC 00312	17 37 00	+ 3 25 12	
IRC 00313	17 37 35	− 2 07 30	
IRC 00314	17 37 56	− 2 50 00	
IRC 00315	17 39 57	− 4 49 36	
IRC 00316	17 40 37	− 3 52 24	
IRC 00317	17 41 00	+ 4 35 00	
IRC 00318	17 42 10	− 1 30 54	
IRC 00319	17 43 52	+ 1 03 54	
IRC 00320	17 45 03	− 3 37 42	
IRC 00321	17 46 17	+ 3 36 06	
IRC 00322	17 46 56	− 2 13 06	
IRC 00323	17 47 00	+ 0 55 00	
IRC 00324	17 49 06	− 2 27 12	
IRC 00325	17 49 31	+ 4 29 42	
IRC 00326	17 50 03	+ 1 19 12	
IRC 00327	17 50 29	− 2 34 00	
IRC 00328	17 51 15	− 3 16 06	
IRC 00329	17 51 35	− 4 11 54	
IRC 00330	17 53 34	− 1 24 06	
IRC 00331	17 54 10	− 4 04 36	
IRC 00332	17 55 34	+ 2 43 12	
IRC 00333	17 56 59	− 4 49 30	
IRC 00334	17 58 32	+ 0 41 42	
IRC 00335	18 02 57	+ 2 30 06	
IRC 00336	18 03 45	+ 3 23 42	
IRC 00337	18 03 59	− 4 56 06	
IRC 00338	18 04 52	+ 2 28 30	
IRC 00339	18 08 11	+ 3 18 42	
IRC 00340	18 10 20	+ 4 07 54	
IRC 00341	18 11 22	+ 2 22 30	
IRC 00342	18 12 01	− 2 37 00	
IRC 00343	18 13 35	+ 2 21 24	
IRC 00344	18 14 08	+ 3 40 24	
IRC 00345	18 16 53	+ 0 49 36	
IRC 00346	18 18 22	+ 3 21 06	
IRC 00347	18 18 41	− 2 54 42	
IRC 00348	18 20 49	− 4 31 54	
IRC 00349	18 21 23	+ 3 35 30	
IRC 00350	18 24 25	+ 3 53 00	
IRC 00351	18 24 26	+ 1 07 06	
IRC 00352	18 25 21	+ 3 42 54	
IRC 00353	18 28 57	+ 4 20 36	
IRC 00354	18 30 10	+ 4 15 36	
IRC 00355	18 30 52	− 0 29 36	
IRC 00356	18 31 21	+ 3 40 24	
IRC 00357	18 31 40	− 1 01 30	
IRC 00358	18 34 02	− 3 00 36	
IRC 00359	18 34 44	− 2 42 12	
IRC 00360	18 36 32	− 2 01 30	
IRC 00361	18 36 34	+ 1 39 00	
IRC 00362	18 36 46	+ 3 06 12	
IRC 00363	18 38 48	− 4 23 30	
IRC 00364	18 39 32	− 2 48 00	
IRC 00365	18 39 51	− 2 21 12	
IRC 00366	18 39 56	+ 4 34 12	
IRC 00367	18 40 51	− 3 34 54	
IRC 00368	18 41 02	− 1 36 30	
IRC 00369	18 41 02	− 3 06 00	
IRC 00370	18 41 42	− 3 51 06	
IRC 00371	18 41 43	− 2 36 30	
IRC 00372	18 42 06	+ 1 49 42	
IRC 00373	18 42 59	+ 4 34 24	
IRC 00374	18 43 21	− 1 43 36	
IRC 00375	18 43 54	− 3 00 30	
IRC 00376	18 44 32	− 4 48 12	
IRC 00377	18 45 06	− 2 04 12	
IRC 00378	18 45 34	+ 4 11 00	
IRC 00379	18 45 35	− 2 01 00	
IRC 00380	18 46 21	+ 2 22 06	
IRC 00381	18 47 19	− 1 32 36	
IRC 00382	18 47 58	+ 4 32 30	
IRC 00383	18 48 05	− 3 37 54	
IRC 00384	18 48 49	− 0 06 42	
IRC 00385	18 49 48	− 3 47 12	
IRC 00386	18 49 57	− 3 15 54	
IRC 00387	18 50 19	− 2 51 24	
IRC 00388	18 51 01	+ 2 37 30	
IRC 00389	18 51 14	+ 0 34 42	
IRC 00390	18 51 18	− 0 36 06	
IRC 00391	18 51 23	+ 1 33 06	
IRC 00392	18 52 12	+ 0 21 30	
IRC 00393	18 53 06	+ 0 17 06	
IRC 00394	18 53 19	− 4 51 36	
IRC 00395	18 53 34	− 0 31 54	
IRC 00396	18 53 58	+ 0 28 12	
IRC 00397	18 54 01	+ 4 19 24	
IRC 00398	18 54 59	+ 0 23 06	
IRC 00399	18 55 06	+ 2 38 42	
IRC 00400	18 55 21	− 0 48 30	
IRC 00401	18 55 29	− 4 13 24	
IRC 00402	18 55 58	+ 4 35 42	
IRC 00403	18 56 20	− 3 08 00	
IRC 00404	18 57 31	− 1 38 30	
IRC 00405	18 58 31	− 4 30 36	
IRC 00406	18 59 19	+ 4 50 36	
IRC 00407	18 59 50	+ 1 26 06	
IRC 00408	19 00 04	+ 1 15 00	
IRC 00409	19 02 17	+ 2 54 24	
IRC 00410	19 02 20	− 4 06 12	
IRC 00411	19 02 33	+ 1 32 00	
IRC 00412	19 04 51	− 1 12 30	
IRC 00413	19 06 13	− 4 08 24	
IRC 00414	19 06 15	+ 3 11 12	
IRC 00415	19 10 45	+ 1 29 36	
IRC 00416	19 11 23	+ 2 32 24	
IRC 00417	19 12 20	+ 4 09 36	
IRC 00418	19 12 29	− 3 24 12	
IRC 00419	19 13 00	+ 3 13 00	
IRC 00420	19 15 46	+ 0 39 24	
IRC 00421	19 16 00	+ 0 59 54	
IRC 00422	19 16 27	+ 4 11 36	
IRC 00423	19 16 37	+ 3 18 42	
IRC 00424	19 16 52	+ 0 25 30	
IRC 00425	19 18 10	− 4 35 36	
IRC 00426	19 20 10	− 3 19 42	
IRC 00427	19 20 38	− 2 41 36	
IRC 00428	19 20 50	+ 1 34 00	
IRC 00429	19 22 58	+ 3 01 24	
IRC 00430	19 23 33	+ 3 24 36	
IRC 00431	19 23 58	+ 0 14 36	
IRC 00432	19 24 15	− 0 20 54	
IRC 00433	19 25 06	+ 1 56 30	
IRC 00434	19 26 19	+ 4 44 30	
IRC 00435	19 26 41	+ 0 07 30	
IRC 00436	19 26 43	+ 3 45 30	
IRC 00437	19 27 40	+ 2 47 54	
IRC 00438	19 27 44	− 0 55 42	
IRC 00439	19 28 01	− 2 53 12	
IRC 00440	19 28 13	+ 3 32 42	
IRC 00441	19 28 33	+ 1 54 12	
IRC 00442	19 29 51	− 4 27 54	
IRC 00443	19 30 37	+ 4 55 12	
IRC 00444	19 32 41	+ 1 58 24	
IRC 00445	19 32 52	+ 0 36 24	
IRC 00446	19 33 33	− 0 33 24	
IRC 00447	19 38 14	+ 2 22 12	
IRC 00448	19 38 28	− 4 02 00	
IRC 00449	19 39 54	+ 1 34 24	
IRC 00450	19 41 14	+ 3 37 24	
IRC 00451	19 43 46	+ 1 34 12	
IRC 00452	19 45 54	+ 1 45 36	
IRC 00453	19 46 05	+ 3 34 12	
IRC 00454	19 48 34	− 2 35 36	
IRC 00455	19 48 55	+ 3 57 24	
IRC 00456	19 49 39	− 0 30 00	
IRC 00457	19 49 59	+ 0 52 36	
IRC 00458	19 54 58	− 2 01 12	
IRC 00459	19 55 55	− 3 41 00	
IRC 00460	19 57 14	− 4 08 42	
IRC 00461	19 57 45	− 2 01 06	
IRC 00462	19 58 07	+ 1 13 36	
IRC 00463	20 00 43	+ 4 35 42	
IRC 00464	20 01 50	− 0 51 00	
IRC 00465	20 02 34	+ 4 26 12	
IRC 00466	20 05 08	− 1 45 06	
IRC 00467	20 07 55	− 1 46 36	
IRC 00468	20 10 29	− 0 29 06	
IRC 00469	20 10 37	− 1 09 36	
IRC 00470	20 11 49	− 0 09 30	
IRC 00471	20 12 11	+ 4 38 06	
IRC 00472	20 12 19	− 4 43 54	
IRC 00473	20 20 44	− 0 36 24	
IRC 00474	20 21 23	+ 0 47 12	
IRC 00475	20 22 11	+ 1 12 30	
IRC 00476	20 27 05	− 3 03 06	
IRC 00477	20 27 39	− 4 55 36	
IRC 00478	20 27 43	+ 1 42 42	
IRC 00479	20 29 18	− 1 56 42	
IRC 00480	20 29 48	+ 1 59 06	
IRC 00481	20 31 29	+ 2 10 00	
IRC 00482	20 34 05	+ 2 13 54	
IRC 00483	20 34 07	− 2 43 24	
IRC 00484	20 35 46	− 1 17 00	
IRC 00485	20 36 45	+ 1 57 42	
IRC 00486	20 36 49	+ 0 18 36	
IRC 00487	20 38 19	+ 1 00 12	
IRC 00488	20 42 40	+ 3 05 54	
IRC 00489	20 43 46	− 4 16 06	
IRC 00490	20 44 04	− 1 05 12	
IRC 00491	20 44 17	+ 2 15 06	
IRC 00492	20 44 27	− 2 40 00	
IRC 00493	20 46 10	+ 1 51 00	
IRC 00494	20 46 46	− 0 45 06	
IRC 00495	20 49 44	− 3 24 36	
IRC 00496	20 51 05	− 1 49 54	
IRC 00497	20 54 53	− 3 25 42	
IRC 00498	20 59 02	− 4 19 36	
IRC 00499	21 03 17	− 0 24 30	
IRC 00500	21 04 59	− 0 21 42	
IRC 00501	21 05 58	+ 3 01 00	
IRC 00502	21 12 04	− 0 07 00	
IRC 00503	21 22 43	− 3 46 36	
IRC 00504	21 32 08	+ 1 36 12	
IRC 00505	21 36 05	− 4 22 30	
IRC 00506	21 37 01	+ 2 00 42	
IRC 00507	21 37 42	− 2 00 54	
IRC 00508	21 39 37	+ 1 03 30	
IRC 00509	21 43 58	− 2 26 36	
IRC 00510	21 58 28	+ 0 22 36	
IRC 00511	22 00 22	− 0 10 24	
IRC 00512	22 03 10	+ 4 48 42	
IRC 00513	22 03 13	− 0 34 12	
IRC 00514	22 04 04	− 0 40 06	
IRC 00515	22 14 58	+ 4 53 54	
IRC 00516	22 15 38	+ 2 29 12	
IRC 00517	22 25 22	+ 4 27 00	
IRC 00518	22 26 15	− 0 16 54	
IRC 00519	22 31 08	+ 0 56 00	
IRC 00520	22 32 02	+ 0 20 42	
IRC 00521	22 35 09	− 4 29 24	
IRC 00522	22 35 59	+ 3 12 12	
IRC 00523	22 40 20	+ 4 42 12	
IRC 00524	22 51 19	+ 1 35 12	
IRC 00525	22 57 37	− 0 39 06	
IRC 00526	22 58 11	+ 2 45 00	
IRC 00527	23 08 40	+ 4 44 24	
IRC 00528	23 14 34	+ 3 00 54	
IRC 00529	23 20 59	+ 0 01 12	
IRC 00530	23 22 03	+ 3 26 30	
IRC 00531	23 41 29	+ 0 06 06	
IRC 00532	23 43 49	+ 3 12 42	
IRC 00533	23 49 23	+ 2 38 42	
IRC 00534	23 51 17	+ 0 19 00	
IRC 00535	23 52 07	− 0 09 54	
IRC 00536	23 56 02	− 3 50 24	
IRC 00537	23 57 13	− 0 33 24	
IRC+10001	0 14 10	+ 9 57 54	
IRC+10002	0 16 06	+12 25 12	
IRC+10003	0 18 01	+ 7 55 06	
IRC+10004	0 24 20	+ 9 52 36	
IRC+10005	0 29 26	+14 19 24	
IRC+10006	0 37 11	+13 55 24	
IRC+10007	0 46 05	+ 7 19 00	
IRC+10008	0 57 12	+ 6 12 54	
IRC+10009	1 00 20	+ 7 36 54	
IRC+10010	1 02 18	+ 5 23 36	
IRC+10011	1 03 48.0	+12 19 45	
IRC+10011	1 03 49	+12 18 42	
IRC+10012	1 05 46	+ 9 38 36	
IRC+10013	1 14 42	+13 39 06	
IRC+10014	1 14 58	+ 8 40 00	
IRC+10015	1 17 10	+ 5 54 06	

NAME	RA (1950)	DEC	POS REF
	h m s	° ′ ″	
IRC+10016	1 22 20	+14 35 06	
IRC+10017	1 27 34	+ 5 53 24	
IRC+10018	1 28 07	+14 46 06	
IRC+10019	1 34 06	+ 7 34 24	
IRC+10020	1 38 51	+ 5 14 12	
IRC+10021	1 42 46	+ 8 54 12	
IRC+10022	1 43 42	+10 07 00	
IRC+10023	1 51 41	+ 8 32 00	
IRC+10024	1 59 53	+13 14 06	
IRC+10025	1 59 59	+ 7 26 06	
IRC+10026	2 02 43	+ 9 49 54	
IRC+10027	2 03 33	+ 8 00 12	
IRC+10028	2 10 22	+ 8 36 30	
IRC+10029	2 23 41	+ 6 05 30	
IRC+10030	2 33 16	+ 5 22 36	
IRC+10031	2 38 28	+ 5 51 54	
IRC+10032	2 50 52	+14 28 12	
IRC+10033	2 51 04	+ 9 07 24	
IRC+10034	2 54 06	+14 24 30	
IRC+10035	2 58 03	+10 40 30	
IRC+10036	3 02 03	+ 8 53 42	
IRC+10037	3 03 34	+11 28 36	
IRC+10038	3 07 24	+13 15 42	
IRC+10039	3 08 07	+ 9 48 24	
IRC+10040	3 08 15	+14 36 24	
IRC+10041	3 09 47	+ 6 28 36	
IRC+10042	3 16 29	+12 17 12	
IRC+10043	3 21 28	+11 40 24	
IRC+10044	3 22 08	+ 8 50 54	
IRC+10045	3 28 07	+12 46 00	
IRC+10046	3 30 50	+14 30 42	
IRC+10047	3 40 31	+12 38 12	
IRC+10048	3 42 17	+ 9 47 00	
IRC+10049	3 42 34	+12 12 24	
IRC+10050	3 50 46	+11 15 42	
IRC+10051	3 55 55	+10 52 42	
IRC+10052	4 00 30	+ 8 44 36	
IRC+10053	4 01 34	+12 22 06	
IRC+10054	4 06 01	+ 9 57 42	
IRC+10055	4 08 37	+ 8 08 30	
IRC+10056	4 11 14	+ 9 08 12	
IRC+10057	4 11 30	+14 25 00	
IRC+10058	4 16 56	+10 00 24	
IRC+10059	4 23 46	+14 36 06	
IRC+10060	4 25 36	+10 03 30	
IRC+10061	4 26 29	+ 9 50 36	
IRC+10062	4 26 59	+ 5 03 30	
IRC+10063	4 28 16	+14 59 36	
IRC+10064	4 30 23	+12 45 00	
IRC+10065	4 32 47	+12 36 00	
IRC+10066	4 35 30	+ 8 13 36	
IRC+10067	4 36 05	+ 6 43 30	
IRC+10068	4 39 39	+ 6 47 06	
IRC+10069	4 41 37	+11 35 00	
IRC+10070	4 47 05	+13 36 42	
IRC+10071	4 47 10	+ 6 52 54	
IRC+10072	4 49 43	+14 09 36	
IRC+10073	4 51 40	+ 8 50 12	
IRC+10074	4 52 06	+ 7 41 42	
IRC+10075	4 53 32	+13 26 30	
IRC+10076	4 59 05	+ 6 35 36	
IRC+10077	5 06 31	+12 24 36	
IRC+10078	5 06 37	+14 17 42	
IRC+10079	5 12 04	+ 5 06 06	
IRC+10080	5 12 46	+ 9 21 12	
IRC+10081	5 13 11	+11 55 24	
IRC+10082	5 15 16	+13 22 00	
IRC+10083	5 18 32	+ 7 18 36	
IRC+10084	5 22 26	+ 6 18 36	
IRC+10085	5 25 04	+11 34 30	
IRC+10086	5 25 41	+ 8 39 24	
IRC+10087	5 29 14	+ 7 35 00	
IRC+10088	5 30 04	+13 00 42	
IRC+10089	5 30 32	+ 7 07 06	
IRC+10090	5 32 33	+ 8 40 30	
IRC+10091	5 34 10	+ 9 16 06	
IRC+10092	5 34 14	+10 25 54	
IRC+10093	5 34 19	+11 00 36	
IRC+10094	5 38 21	+12 16 00	
IRC+10095	5 39 02	+14 48 24	
IRC+10096	5 46 30	+13 11 12	
IRC+10097	5 49 38	+ 9 25 06	
IRC+10098	5 51 12	+ 8 26 24	
IRC+10099	5 51 28	+10 35 54	
IRC+10100	5 52 28	+ 7 24 00	
IRC+10101	5 54 41	+14 03 36	
IRC+10102	5 58 45	+10 40 42	
IRC+10103	5 58 53	+10 54 42	
IRC+10104	5 59 27	+ 8 27 06	
IRC+10105	5 59 41	+13 00 24	
IRC+10106	6 00 36	+13 43 54	
IRC+10107	6 03 41	+10 10 30	
IRC+10108	6 06 38	+ 5 17 42	
IRC+10109	6 08 41	+11 14 00	
IRC+10110	6 10 22	+ 6 01 30	
IRC+10111	6 12 20	+ 6 30 12	
IRC+10112	6 13 36	+11 29 12	
IRC+10113	6 15 01	+ 8 32 36	
IRC+10114	6 17 16	+14 40 24	
IRC+10115	6 17 32	+11 22 42	
IRC+10116	6 18 05	+ 5 45 30	
IRC+10117	6 18 53	+13 15 00	
IRC+10118	6 19 17	+ 7 22 36	
IRC+10119	6 21 09	+ 8 31 24	
IRC+10120	6 21 24	+14 15 12	
IRC+10121	6 22 37	+14 45 12	
IRC+10122	6 23 16	+13 39 36	
IRC+10123	6 24 04	+10 26 06	
IRC+10124	6 24 19	+ 5 25 00	
IRC+10125	6 27 41	+ 8 06 30	
IRC+10126	6 31 58	+ 5 00 42	
IRC+10127	6 32 36	+10 02 06	
IRC+10128	6 33 07	+14 15 24	
IRC+10129	6 34 38	+14 45 06	
IRC+10130	6 36 12	+ 5 14 06	
IRC+10131	6 36 40	+11 27 24	
IRC+10132	6 38 28	+11 03 36	
IRC+10133	6 39 34	+ 7 26 36	
IRC+10134	6 41 11	+13 16 24	
IRC+10135	6 42 18	+ 9 05 36	
IRC+10136	6 42 32	+12 56 30	
IRC+10137	6 42 52	+ 8 05 30	
IRC+10138	6 44 35	+ 8 05 30	
IRC+10139	6 45 41	+ 5 36 06	
IRC+10140	6 46 29	+12 14 06	
IRC+10141	6 47 14	+12 07 00	
IRC+10142	6 47 35	+13 28 30	
IRC+10143	6 49 59	+ 8 29 06	
IRC+10144	6 52 56	+ 6 26 24	
IRC+10145	6 54 37	+ 8 39 00	
IRC+10146	6 55 43	+ 6 14 12	
IRC+10147	6 58 13	+10 42 36	
IRC+10148	7 00 52	+11 02 06	
IRC+10149	7 01 02	+12 40 00	
IRC+10150	7 02 36	+10 38 12	
IRC+10151	7 02 52	+ 9 16 06	
IRC+10152	7 04 14	+ 8 40 00	
IRC+10153	7 04 17	+ 8 57 12	
IRC+10154	7 05 54	+10 06 00	
IRC+10155	7 07 16	+ 7 48 36	
IRC+10156	7 10 00	+14 40 42	
IRC+10157	7 12 32	+ 8 28 12	
IRC+10158	7 12 55	+ 5 09 00	
IRC+10159	7 12 57	+ 6 00 42	
IRC+10160	7 12 58	+ 8 04 06	
IRC+10161	7 21 01	+ 6 51 42	
IRC+10162	7 21 31	+ 8 59 42	
IRC+10163	7 22 58	+ 9 23 36	
IRC+10164	7 25 26	+ 9 01 30	
IRC+10165	7 26 59	+12 06 42	
IRC+10166	7 27 22	+10 09 54	
IRC+10167	7 30 01	+ 8 25 36	
IRC+10168	7 30 35	+11 08 00	
IRC+10169	7 32 24	+ 6 18 12	
IRC+10170	7 36 42	+ 5 21 06	
IRC+10171	7 38 36	+ 8 30 00	
IRC+10172	7 39 04	+13 36 06	
IRC+10173	7 39 14	+14 19 42	
IRC+10174	7 41 20	+14 18 00	
IRC+10175	7 42 56	+ 5 20 12	
IRC+10176	7 45 26	+ 5 32 36	
IRC+10177	7 46 14	+13 30 00	
IRC+10178	7 47 24	+14 51 24	
IRC+10179	7 53 50	+11 10 54	
IRC+10180	7 53 54	+ 6 32 06	
IRC+10181	7 56 46	+13 22 54	
IRC+10182	8 03 29	+ 5 43 30	
IRC+10183	8 09 55	+ 7 07 36	
IRC+10184	8 13 31	+10 48 06	
IRC+10185	8 13 49	+11 52 54	
IRC+10186	8 13 50	+ 9 20 54	
IRC+10187	8 18 55	+ 5 07 12	
IRC+10188	8 21 10	+10 47 24	
IRC+10189	8 24 01	+12 49 30	
IRC+10190	8 29 53	+ 8 39 36	
IRC+10191	8 31 55	+ 5 40 42	
IRC+10192	8 33 23	+13 23 24	
IRC+10193	8 44 09	+ 6 36 24	
IRC+10194	8 45 53	+12 44 00	
IRC+10195	8 45 55	+10 36 54	
IRC+10196	8 52 47	+ 6 08 30	
IRC+10197	8 53 12	+11 49 12	
IRC+10198	8 54 19	+11 02 12	
IRC+10199	8 55 34	+11 02 12	
IRC+10200	9 00 38	+ 8 24 54	
IRC+10201	9 03 21	+ 5 17 24	
IRC+10202	9 04 50	+ 6 32 00	
IRC+10203	9 05 38	+13 25 24	
IRC+10204	9 18 37	+12 27 36	
IRC+10205	9 20 49	+ 7 55 42	
IRC+10206	9 29 14	+11 31 12	
IRC+10207	9 29 20	+ 9 56 00	
IRC+10208	9 32 01	+ 8 24 54	
IRC+10209	9 34 35	+ 7 03 54	
IRC+10210	9 38 33	+10 07 06	
IRC+10211	9 41 01	+14 15 06	
IRC+10212	9 42 52	+10 27 12	
IRC+10213	9 43 32	+ 6 56 36	
IRC+10214	9 43 44	+12 02 36	
IRC+10215	9 44 52	+11 39 42	
IRC+10216	9 45 14.8	+13 30 41	
IRC+10216	9 45 18	+13 30 36	
IRC+10216	9 45 18	+13 31	
IRC+10217	9 48 19	+13 18 00	
IRC+10218	9 51 05	+ 6 11 42	
IRC+10219	9 51 19	+10 29 36	
IRC+10220	9 51 29	+ 5 10 42	
IRC+10221	9 52 17	+ 5 26 12	
IRC+10222	9 55 28	+ 8 33 00	
IRC+10223	9 56 12	+ 5 02 54	
IRC+10224	9 57 35	+ 8 16 54	
IRC+10225	10 05 14	+10 14 24	
IRC+10226	10 05 46	+12 12 24	
IRC+10227	10 06 52	+ 9 50 24	
IRC+10228	10 13 58	+13 58 30	
IRC+10229	10 19 37	+ 9 13 06	
IRC+10230	10 22 40	+ 9 02 12	
IRC+10231	10 29 29	+14 23 36	
IRC+10232	10 32 09	+ 7 12 36	
IRC+10233	10 46 08	+ 8 55 42	
IRC+10234	10 50 58	+13 59 06	
IRC+10235	10 53 26	+ 6 27 00	
IRC+10236	11 07 58	+11 34 06	
IRC+10237	11 13 13	+13 34 42	
IRC+10238	11 21 19	+10 47 12	
IRC+10239	11 22 21	+11 42 30	
IRC+10240	11 25 26	+12 14 42	
IRC+10241	11 28 53	+ 9 01 36	
IRC+10242	11 34 21	+ 9 48 12	
IRC+10243	11 35 52	+ 8 24 24	
IRC+10244	11 38 13	+13 21 36	
IRC+10245	11 43 17	+ 6 48 36	
IRC+10246	11 43 32	+ 7 27 30	
IRC+10247	11 46 31	+14 50 54	
IRC+10248	12 00 01	+ 8 20 12	
IRC+10249	12 01 44	+ 5 12 12	
IRC+10250	12 02 40	+ 9 00 54	
IRC+10251	12 17 17	+11 52 00	
IRC+10252	12 19 41	+ 5 07 54	
IRC+10253	12 21 37	+ 6 14 30	
IRC+10254	12 28 48	+ 7 52 36	
IRC+10255	12 30 36	+ 7 31 06	
IRC+10256	12 35 56	+ 7 15 24	
IRC+10257	12 36 22	+14 04 36	
IRC+10258	12 40 44	+10 22 36	
IRC+10259	12 53 01	+11 45 54	
IRC+10260	12 56 16	+ 8 28 42	
IRC+10261	12 59 41	+11 13 30	
IRC+10262	13 00 05	+ 5 27 06	
IRC+10263	13 00 53	+ 5 10 24	
IRC+10264	13 01 23	+ 7 19 36	
IRC+10265	13 01 32	+11 29 42	
IRC+10266	13 10 03	+11 49 24	
IRC+10267	13 12 00	+11 35 36	
IRC+10268	13 13 52	+ 6 45 42	
IRC+10269	13 14 46	+13 56 00	
IRC+10270	13 15 02	+ 5 43 54	
IRC+10271	13 16 08	+13 10 36	
IRC+10272	13 27 30	+ 7 26 12	
IRC+10273	13 33 20	+ 8 32 54	
IRC+10274	13 35 28	+13 42 00	
IRC+10275	13 54 28	+ 6 49 06	
IRC+10276	13 55 31	+ 7 42 36	
IRC+10277	13 56 17	+14 53 30	
IRC+10278	14 12 24	+10 19 36	
IRC+10279	14 15 43	+13 23 54	
IRC+10280	14 26 00	+ 5 54 06	
IRC+10281	14 39 10	+ 8 22 30	
IRC+10282	14 44 15	+ 7 29 06	
IRC+10283	14 44 37	+ 5 06 00	
IRC+10284	14 48 37	+12 22 24	
IRC+10285	14 52 55	+ 6 59 24	
IRC+10286	15 08 08	+11 51 30	
IRC+10287	15 09 47	+14 34 24	
IRC+10288	15 12 42	+ 5 07 06	
IRC+10289	15 17 47	+14 44 24	
IRC+10290	15 19 20	+14 29 12	
IRC+10291	15 24 05	+10 12 30	
IRC+10292	15 36 47	+10 44 06	
IRC+10293	15 41 46	+ 8 17 24	
IRC+10294	15 41 48	+ 6 35 06	
IRC+10295	15 44 01	+ 7 29 42	
IRC+10296	15 45 52	+13 57 06	
IRC+10297	15 46 19	+ 5 33 24	
IRC+10298	15 52 18	+ 5 44 06	
IRC+10299	15 54 55	+14 33 12	
IRC+10300	16 01 40	+10 08 00	
IRC+10301	16 02 12	+10 45 00	
IRC+10302	16 06 07	+ 8 40 00	
IRC+10303	16 06 10	+ 8 44 42	
IRC+10304	16 10 46	+ 5 08 42	
IRC+10305	16 24 22	+11 05 54	
IRC+10306	16 27 00	+10 37 42	
IRC+10307	16 30 16	+11 35 30	
IRC+10308	16 34 13	+ 5 06 54	
IRC+10309	16 36 37	+14 09 54	
IRC+10310	16 43 14	+12 13 36	
IRC+10311	16 43 26	+ 8 40 00	
IRC+10312	16 48 43	+ 9 57 54	
IRC+10313	16 48 44	+10 25 54	
IRC+10314	16 50 22	+ 5 28 54	
IRC+10315	16 55 19	+ 9 26 54	
IRC+10316	16 56 46	+11 35 12	
IRC+10317	16 59 20	+ 6 41 30	
IRC+10318	17 00 51	+14 09 42	
IRC+10319	17 03 50	+ 9 48 00	
IRC+10320	17 10 07	+10 38 42	
IRC+10321	17 11 17	+ 5 53 00	
IRC+10322	17 11 56	+ 8 59 12	
IRC+10323	17 12 19	+11 07 36	
IRC+10324	17 12 22	+14 26 36	
IRC+10325	17 16 16	+10 55 00	
IRC+10326	17 21 34	+ 8 54 30	
IRC+10327	17 22 54	+ 8 57 54	
IRC+10328	17 25 20	+ 8 28 42	
IRC+10329	17 25 40	+ 5 05 36	
IRC+10330	17 31 25	+14 52 30	
IRC+10331	17 32 39	+12 35 36	
IRC+10332	17 33 03	+ 5 03 12	
IRC+10333	17 33 32	+12 04 30	
IRC+10334	17 34 23	+11 52 42	
IRC+10335	17 36 00	+14 21 12	
IRC+10336	17 45 28	+ 6 25 36	
IRC+10337	17 49 56	+ 6 46 54	
IRC+10338	17 50 53	+10 45 36	
IRC+10339	17 53 56	+11 34 54	
IRC+10340	17 53 58	+10 37 36	
IRC+10341	17 54 01	+11 22 12	
IRC+10342	17 54 11	+11 10 30	
IRC+10343	17 57 33	+12 49 00	
IRC+10344	17 57 38	+ 6 08 30	
IRC+10345	17 58 02	+ 5 36 30	
IRC+10346	17 59 28	+ 8 26 36	
IRC+10347	18 00 55	+11 54 24	
IRC+10348	18 04 46	+ 8 22 30	
IRC+10349	18 04 55	+ 6 32 00	
IRC+10350	18 04 56	+ 8 43 30	
IRC+10351	18 06 08	+ 5 16 54	
IRC+10352	18 11 16	+12 26 42	
IRC+10353	18 11 37	+ 5 20 06	
IRC+10354	18 15 40	+ 6 55 06	
IRC+10355	18 16 44	+ 7 14 06	
IRC+10356	18 18 23	+ 5 54 42	
IRC+10357	18 24 45	+ 7 29 24	
IRC+10358	18 26 22	+ 6 15 54	
IRC+10359	18 26 50	+12 18 24	
IRC+10360	18 27 48	+ 6 16 00	
IRC+10361	18 28 29	+ 8 02 42	
IRC+10362	18 32 26	+ 7 02 00	
IRC+10363	18 32 58	+ 6 25 06	
IRC+10364	18 33 36	+ 7 38 30	
IRC+10365	18 34 59	+10 23 00	
IRC+10365	18 34 59.0	+10 23 00	
IRC+10366	18 35 56	+ 8 47 24	

NAME	RA (1950)	DEC	POS REF
	h m s	° ′ ″	
IRC+10367	18 37 10	+11 48 06	
IRC+10368	18 37 34	+ 9 55 30	
IRC+10369	18 39 18	+ 6 23 12	
IRC+10370	18 39 33	+ 6 46 30	
IRC+10371	18 40 10	+13 58 00	
IRC+10372	18 40 40	+ 6 43 36	
IRC+10373	18 40 50	+12 20 36	
IRC+10374	18 41 17	+13 54 30	
IRC+10375	18 41 32	+10 51 30	
IRC+10376	18 42 50	+12 53 24	
IRC+10377	18 43 17	+ 8 41 06	
IRC+10378	18 44 31	+ 9 22 00	
IRC+10379	18 44 53	+ 5 24 06	
IRC+10380	18 46 58	+ 8 32 30	
IRC+10381	18 48 26	+10 54 30	
IRC+10382	18 49 50	+14 02 42	
IRC+10383	18 51 04	+ 9 35 42	
IRC+10384	18 52 05	+10 34 24	
IRC+10385	18 52 34	+ 8 11 24	
IRC+10386	18 53 02	+ 6 33 12	
IRC+10387	18 54 51	+ 6 38 12	
IRC+10388	18 56 07	+12 54 42	
IRC+10389	18 56 14	+14 17 30	
IRC+10390	18 56 46	+10 19 24	
IRC+10391	18 56 59	+ 5 18 30	
IRC+10392	18 57 19	+14 59 54	
IRC+10393	18 57 47	+ 9 45 30	
IRC+10394	18 58 37	+12 39 36	
IRC+10395	18 58 59	+ 8 15 06	
IRC+10396	18 59 23	+ 7 44 36	
IRC+10397	18 59 50	+10 10 00	
IRC+10398	18 59 59	+ 8 16 06	
IRC+10399	19 00 15	+ 8 23 06	
IRC+10400	19 00 50	+12 10 12	
IRC+10401	19 00 53	+ 7 26 00	
IRC+10402	19 01 11	+ 8 17 36	
IRC+10403	19 01 43	+10 41 36	
IRC+10404	19 03 03	+13 46 24	
IRC+10405	19 03 28	+12 08 00	
IRC+10406	19 03 58	+ 8 09 06	
IRC+10407	19 04 33	+ 7 04 36	
IRC+10408	19 05 32	+ 6 13 06	
IRC+10409	19 07 52	+10 58 06	
IRC+10410	19 08 38	+ 5 06 06	
IRC+10411	19 10 12	+ 6 48 00	
IRC+10412	19 12 00	+11 37 36	
IRC+10413	19 12 41	+14 34 24	
IRC+10414	19 14 38	+ 9 58 54	
IRC+10415	19 15 22	+12 03 42	
IRC+10416	19 17 58	+ 9 07 42	
IRC+10417	19 18 35	+ 5 01 24	
IRC+10418	19 18 50	+ 9 43 30	
IRC+10419	19 23 29	+ 8 06 24	
IRC+10420	19 24 26	+11 15 12	
IRC+10420	19 24 27.0	+11 15 03	
IRC+10421	19 24 55	+11 23 42	
IRC+10422	19 25 47	+11 40 42	
IRC+10423	19 25 47	+ 5 25 54	
IRC+10424	19 26 04	+ 9 31 30	
IRC+10425	19 26 43	+10 31 36	
IRC+10426	19 30 01	+ 9 54 12	
IRC+10427	19 30 56	+ 6 09 24	
IRC+10428	19 31 17	+ 5 22 12	
IRC+10429	19 31 38	+11 39 24	
IRC+10430	19 31 41	+ 7 16 42	
IRC+10431	19 32 20	+ 7 01 30	
IRC+10432	19 35 10	+ 5 10 24	
IRC+10433	19 35 43	+11 36 30	
IRC+10434	19 36 16	+10 57 12	
IRC+10435	19 41 42	+14 09 42	
IRC+10436	19 41 56	+14 35 54	
IRC+10437	19 42 16	+13 06 54	
IRC+10438	19 43 05	+ 7 39 54	
IRC+10439	19 43 53	+10 29 06	
IRC+10440	19 45 44	+14 43 00	
IRC+10441	19 48 20	+ 8 44 24	
IRC+10442	19 51 51	+ 8 20 00	
IRC+10443	19 52 40	+11 28 30	
IRC+10444	19 52 53	+ 6 16 54	
IRC+10445	19 54 28	+11 58 06	
IRC+10446	19 57 26	+10 23 00	
IRC+10447	19 58 37	+ 8 25 00	
IRC+10448	20 01 43	+ 7 08 06	
IRC+10449	20 04 41	+13 10 36	
IRC+10450	20 04 45	+12 48 06	
IRC+10451	20 05 16	+ 5 54 12	
IRC+10452	20 05 44	+13 20 54	
IRC+10453	20 07 25	+14 35 12	
IRC+10454	20 08 44	+ 6 12 00	
IRC+10455	20 08 52	+14 39 24	
IRC+10456	20 08 55	+ 8 34 00	
IRC+10457	20 09 35	+ 7 32 06	
IRC+10458	20 10 24	+12 50 54	
IRC+10459	20 12 31	+ 8 56 30	
IRC+10460	20 13 05	+12 54 54	
IRC+10461	20 13 27	+ 7 31 06	
IRC+10462	20 14 32	+ 6 54 36	
IRC+10463	20 17 10	+13 03 30	
IRC+10464	20 20 40	+ 8 17 36	
IRC+10465	20 20 49	+ 7 47 54	
IRC+10466	20 22 08	+14 48 12	
IRC+10467	20 23 21	+ 9 53 36	
IRC+10468	20 23 41	+13 44 42	
IRC+10469	20 26 25	+11 54 42	
IRC+10470	20 27 00	+ 9 44 00	
IRC+10471	20 31 10	+ 9 20 54	
IRC+10472	20 32 17	+ 5 03 54	
IRC+10473	20 35 13	+14 25 06	
IRC+10474	20 36 20	+13 08 12	
IRC+10475	20 39 16	+11 41 54	
IRC+10476	20 39 31	+ 8 07 30	
IRC+10477	20 44 15	+ 6 16 42	
IRC+10478	20 47 25	+11 25 12	
IRC+10479	20 47 56	+ 5 54 24	
IRC+10480	20 53 11	+13 31 36	
IRC+10481	20 54 05	+ 8 38 42	
IRC+10482	20 56 25	+14 06 06	
IRC+10483	20 57 52	+13 22 36	
IRC+10484	21 00 40	+14 31 36	
IRC+10485	21 02 03	+ 5 18 00	
IRC+10486	21 03 38	+ 7 37 42	
IRC+10487	21 05 59	+ 6 47 00	
IRC+10488	21 09 48	+11 34 24	
IRC+10489	21 13 17	+ 5 02 54	
IRC+10490	21 13 17	+ 9 04 12	
IRC+10491	21 15 49	+ 7 32 30	
IRC+10492	21 16 26	+10 59 42	
IRC+10493	21 17 40	+12 45 06	
IRC+10494	21 18 35	+ 7 08 24	
IRC+10495	21 24 55	+13 53 54	
IRC+10496	21 25 55	+ 7 58 30	
IRC+10497	21 28 23	+12 45 06	
IRC+10498	21 28 38	+10 56 12	
IRC+10499	21 30 37	+ 6 55 36	
IRC+10500	21 36 44	+ 8 04 24	
IRC+10501	21 36 57	+ 9 02 30	
IRC+10502	21 39 43	+ 5 27 06	
IRC+10503	21 41 43	+ 9 38 54	
IRC+10504	21 42 40	+12 28 12	
IRC+10505	21 58 34	+ 5 52 12	
IRC+10506	21 58 39	+ 8 00 54	
IRC+10507	21 59 23	+ 6 02 30	
IRC+10508	22 02 38	+14 34 30	
IRC+10509	22 04 38	+11 31 36	
IRC+10510	22 04 52	+11 39 12	
IRC+10511	22 06 27	+12 17 36	
IRC+10512	22 06 50	+12 42 36	
IRC+10513	22 08 12	+11 22 42	
IRC+10514	22 09 50	+14 18 36	
IRC+10515	22 15 53	+13 21 30	
IRC+10516	22 22 13	+ 9 32 42	
IRC+10517	22 23 59	+11 07 12	
IRC+10518	22 26 39	+ 8 52 12	
IRC+10519	22 28 01	+12 50 54	
IRC+10520	22 34 35	+12 19 00	
IRC+10521	22 40 20	+ 6 24 06	
IRC+10522	22 44 13	+11 54 36	
IRC+10523	22 51 40	+ 8 37 54	
IRC+10524	22 54 32	+14 09 24	
IRC+10525	22 59 37	+10 20 00	
IRC+10526	23 02 17	+14 56 06	
IRC+10527	23 04 07	+10 16 24	
IRC+10528	23 04 29	+ 9 08 30	
IRC+10529	23 06 56	+ 8 24 36	
IRC+10530	23 10 30	+ 8 41 30	
IRC+10531	23 14 17	+10 19 06	
IRC+10532	23 17 44	+ 5 06 30	
IRC+10533	23 17 58	+ 8 39 24	
IRC+10534	23 20 33	+12 02 06	
IRC+10535	23 25 26	+ 6 06 24	
IRC+10536	23 26 37	+12 29 00	
IRC+10537	23 31 15	+ 6 01 24	
IRC+10538	23 32 54	+ 8 14 36	
IRC+10539	23 37 23	+ 5 21 24	
IRC+10540	23 40 52	+10 02 54	
IRC+10541	23 48 49	+ 9 02 06	
IRC+10542	23 49 13	+ 8 46 30	
IRC+10543	23 51 34	+14 12 06	
IRC+10544	23 53 22	+14 57 06	
IRC+10545	23 56 46	+ 6 35 24	
IRC+20001	0 03 20	+24 17 30	
IRC+20002	0 07 30	+24 54 42	
IRC+20003	0 09 38	+22 16 36	
IRC+20004	0 12 02	+19 55 54	
IRC+20005	0 14 40	+22 18 36	
IRC+20006	0 15 17	+19 57 12	
IRC+20007	0 25 28	+17 36 42	
IRC+20008	0 25 38	+16 10 24	
IRC+20009	0 29 20	+19 22 00	
IRC+20010	0 29 55	+18 31 00	
IRC+20011	0 37 16	+21 09 36	
IRC+20012	0 43 56	+15 12 42	
IRC+20013	0 44 37	+23 59 42	
IRC+20014	0 52 31	+24 17 24	
IRC+20015	0 54 30	+23 09 06	
IRC+20016	1 02 16	+15 58 54	
IRC+20017	1 02 35	+18 55 42	
IRC+20018	1 07 31	+15 25 00	
IRC+20019	1 07 59	+23 12 24	
IRC+20020	1 08 42	+20 45 36	
IRC+20021	1 11 01	+24 18 36	
IRC+20022	1 20 43	+20 12 12	
IRC+20023	1 21 47	+23 41 00	
IRC+20024	1 23 06	+22 50 54	
IRC+20025	1 25 08	+16 26 42	
IRC+20026	1 28 47	+15 05 12	
IRC+20027	1 29 07	+15 21 36	
IRC+20028	1 32 06	+18 12 12	
IRC+20029	1 43 52	+18 49 36	
IRC+20030	1 44 40	+21 09 36	
IRC+20031	1 51 54	+20 33 54	
IRC+20032	1 52 49	+16 57 00	
IRC+20033	1 53 02	+23 20 06	
IRC+20034	1 54 37	+17 34 30	
IRC+20035	1 58 46	+17 42 42	
IRC+20036	1 59 41	+16 02 30	
IRC+20037	2 00 59	+18 01 12	
IRC+20038	2 04 20	+23 14 06	
IRC+20039	2 05 17	+15 34 36	
IRC+20040	2 05 25	+24 34 36	
IRC+20041	2 07 51	+19 15 36	
IRC+20042	2 09 46	+23 56 06	
IRC+20043	2 10 19	+15 02 36	
IRC+20044	2 18 22	+23 12 12	
IRC+20045	2 27 02	+15 50 12	
IRC+20046	2 32 11	+22 15 00	
IRC+20047	2 37 43	+20 58 12	
IRC+20048	2 40 54	+17 20 30	
IRC+20049	2 45 33	+17 17 54	
IRC+20050	2 45 45	+18 04 24	
IRC+20051	2 53 01	+18 07 12	
IRC+20052	2 58 43	+21 36 06	
IRC+20053	3 05 31	+18 35 30	
IRC+20054	3 08 44	+19 32 06	
IRC+20055	3 11 05	+18 47 00	
IRC+20056	3 19 55	+20 34 06	
IRC+20057	3 20 02	+20 42 24	
IRC+20058	3 21 08	+19 43 30	
IRC+20059	3 21 20	+24 32 06	
IRC+20060	3 22 20	+21 01 54	
IRC+20061	3 24 00	+24 39 00	
IRC+20062	3 32 26	+18 44 12	
IRC+20063	3 44 35	+23 57 06	
IRC+20064	3 45 08	+24 50 24	
IRC+20065	3 50 08	+20 03 42	
IRC+20066	3 50 59	+22 58 12	
IRC+20067	3 51 06	+15 27 54	
IRC+20068	4 01 22	+23 57 42	
IRC+20069	4 01 24	+19 04 42	
IRC+20070	4 01 46	+21 56 54	
IRC+20071	4 05 08	+17 12 54	
IRC+20072	4 05 16	+21 25 30	
IRC+20073	4 12 24	+23 56 54	
IRC+20074	4 16 56	+15 30 12	
IRC+20075	4 19 29	+20 42 30	
IRC+20076	4 20 05	+17 26 00	
IRC+20077	4 20 44	+22 50 42	
IRC+20078	4 25 05	+15 55 12	
IRC+20079	4 25 35	+16 14 30	
IRC+20080	4 25 42	+19 04 12	
IRC+20081	4 25 43	+15 50 42	
IRC+20082	4 26 07	+24 37 36	
IRC+20083	4 27 15	+16 04 00	
IRC+20084	4 28 15	+23 14 24	
IRC+20085	4 29 50	+22 33 30	
IRC+20086	4 32 09	+17 06 24	
IRC+20087	4 33 04	+16 24 36	
IRC+20088	4 38 46	+24 33 30	
IRC+20089	4 40 59	+20 40 42	
IRC+20090	4 41 04	+17 52 42	
IRC+20091	4 42 10	+24 37 24	
IRC+20092	4 44 50	+22 03 30	
IRC+20093	4 46 52	+15 49 24	
IRC+20094	4 47 47	+15 42 30	
IRC+20095	4 50 28	+22 41 24	
IRC+20096	4 53 10	+18 20 42	
IRC+20097	4 54 28	+17 05 12	
IRC+20098	4 59 56	+15 14 42	
IRC+20099	5 05 23	+21 58 30	
IRC+20100	5 06 44	+22 58 00	
IRC+20101	5 08 17	+24 20 06	
IRC+20102	5 08 47	+15 59 24	
IRC+20103	5 10 59	+17 23 54	
IRC+20104	5 15 57	+24 41 54	
IRC+20105	5 16 17	+22 02 54	
IRC+20106	5 24 17	+23 04 00	
IRC+20107	5 25 08	+17 12 00	
IRC+20108	5 27 04	+16 06 12	
IRC+20109	5 27 16	+22 30 12	
IRC+20110	5 28 06	+20 09 06	
IRC+20111	5 28 08	+18 31 30	
IRC+20112	5 29 16	+18 33 42	
IRC+20113	5 34 38	+21 06 42	
IRC+20114	5 35 10	+21 52 12	
IRC+20115	5 35 12	+22 47 42	
IRC+20116	5 35 26	+24 58 06	
IRC+20117	5 35 56	+16 54 42	
IRC+20118	5 38 28	+17 29 54	
IRC+20119	5 39 02	+18 31 00	
IRC+20120	5 42 10	+24 24 24	
IRC+20121	5 42 40	+20 40 30	
IRC+20122	5 44 52	+24 40 54	
IRC+20123	5 45 59	+24 33 24	
IRC+20124	5 48 50	+23 22 54	
IRC+20125	5 50 11	+18 57 00	
IRC+20126	5 51 25	+20 16 12	
IRC+20127	5 52 51	+20 10 24	
IRC+20128	5 53 58	+20 17 06	
IRC+20129	5 54 05	+22 50 00	
IRC+20130	6 00 13	+16 24 30	
IRC+20131	6 01 05	+23 16 06	
IRC+20132	6 01 05	+21 14 00	
IRC+20133	6 06 32	+22 12 06	
IRC+20134	6 08 52	+21 53 12	
IRC+20135	6 08 55	+23 13 24	
IRC+20136	6 09 16	+22 55 00	
IRC+20137	6 10 06	+20 39 12	
IRC+20138	6 10 26	+18 33 42	
IRC+20139	6 11 50	+22 31 42	
IRC+20140	6 12 31	+17 46 06	
IRC+20141	6 12 46	+18 18 54	
IRC+20142	6 13 30	+17 11 42	
IRC+20143	6 13 32	+16 41 42	
IRC+20144	6 19 58	+22 32 42	
IRC+20145	6 23 17	+19 06 06	
IRC+20146	6 24 56	+20 35 24	
IRC+20147	6 26 07	+16 38 24	
IRC+20148	6 27 17	+15 00 36	
IRC+20149	6 27 54	+23 29 30	
IRC+20150	6 29 41	+23 08 42	
IRC+20151	6 30 20	+15 52 06	
IRC+20152	6 31 32	+16 07 12	
IRC+20153	6 34 08	+21 09 12	
IRC+20154	6 34 49	+16 26 42	
IRC+20155	6 36 02	+19 17 30	
IRC+20156	6 37 02	+20 31 42	
IRC+20157	6 38 38	+21 54 12	
IRC+20158	6 40 40	+22 59 00	
IRC+20159	6 44 46	+21 44 36	
IRC+20160	6 48 22	+15 08 30	
IRC+20161	6 48 58	+23 39 24	
IRC+20162	6 49 46	+18 41 30	
IRC+20163	6 57 23	+16 08 42	
IRC+20164	6 59 02	+19 25 30	
IRC+20165	6 59 23	+24 15 54	
IRC+20166	6 59 31	+17 49 30	
IRC+20167	6 59 38	+16 44 30	
IRC+20168	6 59 46	+17 33 42	
IRC+20169	7 01 10	+20 38 36	
IRC+20170	7 04 17	+24 14 54	
IRC+20171	7 04 19	+22 46 30	
IRC+20172	7 05 10	+24 10 54	
IRC+20173	7 08 12	+24 44 42	
IRC+20174	7 09 58	+17 43 54	

NAME	RA (1950)	DEC	POS REF	NAME	RA (1950)	DEC	POS REF	NAME	RA (1950)	DEC	POS REF
	h m s	° ′ ″			h m s	° ′ ″			h m s	° ′ ″	
IRC+20175	7 10 30	+16 14 30		IRC+20293	16 05 48	+17 11 30		IRC+20411	19 28 34	+18 37 06	
IRC+20176	7 11 38	+24 58 36		IRC+20294	16 09 29	+23 37 06		IRC+20412	19 29 02	+23 24 12	
IRC+20177	7 17 10	+22 04 36		IRC+20295	16 11 37	+16 33 42		IRC+20413	19 31 09	+23 32 36	
IRC+20178	7 18 57	+20 32 12		IRC+20296	16 19 43	+19 16 00		IRC+20414	19 31 35	+16 45 00	
IRC+20179	7 24 41	+22 14 36		IRC+20297	16 23 02	+19 21 24		IRC+20415	19 32 34	+23 46 42	
IRC+20180	7 26 20	+22 53 36		IRC+20298	16 23 35	+19 00 24		IRC+20416	19 32 56	+18 53 54	
IRC+20181	7 28 13	+20 39 00		IRC+20299	16 24 08	+23 08 54		IRC+20417	19 33 32	+22 12 36	
IRC+20182	7 28 58	+17 11 42		IRC+20300	16 28 04	+21 35 54		IRC+20418	19 34 13	+23 31 36	
IRC+20183	7 30 56	+18 26 30		IRC+20301	16 28 20	+20 34 42		IRC+20419	19 34 50	+21 36 54	
IRC+20184	7 31 59	+24 23 54		IRC+20302	16 29 06	+22 18 06		IRC+20420	19 36 13	+21 15 42	
IRC+20185	7 36 38	+17 47 36		IRC+20303	16 35 31	+22 32 42		IRC+20421	19 36 37	+15 37 12	
IRC+20186	7 37 59	+23 08 12		IRC+20304	16 38 56	+24 57 30		IRC+20422	19 37 05	+20 04 00	
IRC+20187	7 38 11	+20 32 42		IRC+20305	16 39 25	+16 03 06		IRC+20423	19 37 06	+17 03 42	
IRC+20188	7 41 26	+24 30 36		IRC+20306	16 43 05	+15 50 24		IRC+20424	19 37 10	+16 27 36	
IRC+20189	7 43 16	+18 37 54		IRC+20307	16 49 38	+15 01 30		IRC+20425	19 37 37	+21 54 42	
IRC+20190	7 51 18	+21 14 00		IRC+20308	16 49 40	+24 44 12		IRC+20426	19 37 52	+17 53 42	
IRC+20191	7 54 09	+15 55 30		IRC+20309	16 53 12	+18 30 42		IRC+20427	19 38 47	+17 21 36	
IRC+20192	7 54 14	+21 27 00		IRC+20310	16 58 51	+22 42 24		IRC+20428	19 40 55	+23 24 30	
IRC+20193	7 55 39	+16 39 06		IRC+20311	17 00 29	+20 47 36		IRC+20429	19 41 43	+23 04 24	
IRC+20194	7 57 56	+17 26 42		IRC+20312	17 01 43	+19 45 24		IRC+20430	19 42 19	+18 28 06	
IRC+20195	8 03 19	+22 46 42		IRC+20313	17 04 09	+22 08 54		IRC+20431	19 43 39	+20 27 30	
IRC+20196	8 07 10	+17 09 36		IRC+20314	17 07 18	+18 44 36		IRC+20432	19 45 09	+21 39 12	
IRC+20197	8 08 26	+19 17 54		IRC+20315	17 11 36	+18 04 12		IRC+20433	19 45 10	+18 24 36	
IRC+20198	8 11 44	+24 53 24		IRC+20316	17 12 57	+24 53 36		IRC+20434	19 46 04	+22 38 36	
IRC+20199	8 19 37	+15 09 36		IRC+20317	17 12 58	+17 52 00		IRC+20435	19 46 26	+21 33 06	
IRC+20200	8 28 45	+18 15 00		IRC+20318	17 13 38	+23 47 30		IRC+20436	19 47 18	+21 27 24	
IRC+20201	8 29 47	+20 36 42		IRC+20319	17 15 31	+23 08 30		IRC+20437	19 47 47	+21 45 00	
IRC+20202	8 35 52	+21 19 42		IRC+20320	17 18 07	+18 06 36		IRC+20438	19 48 05	+24 48 00	
IRC+20203	8 38 50	+16 30 42		IRC+20321	17 19 22	+16 46 54		IRC+20439	19 50 23	+22 19 42	
IRC+20204	8 40 22	+20 47 06		IRC+20322	17 19 36	+22 58 00		IRC+20440	19 50 49	+16 17 24	
IRC+20205	8 41 52	+18 18 54		IRC+20323	17 23 38	+16 57 24		IRC+20441	19 53 42	+15 29 36	
IRC+20206	8 52 36	+17 25 54		IRC+20324	17 26 12	+15 54 24		IRC+20442	19 54 52	+17 10 24	
IRC+20207	8 53 49	+20 02 30		IRC+20325	17 29 10	+19 33 42		IRC+20443	19 55 14	+24 07 42	
IRC+20208	8 56 25	+18 18 54		IRC+20326	17 29 42	+17 47 36		IRC+20444	19 56 16	+15 52 30	
IRC+20209	9 12 30	+15 09 06		IRC+20327	17 33 20	+20 44 36		IRC+20445	19 56 31	+19 21 30	
IRC+20210	9 24 53	+23 32 54		IRC+20328	17 33 26	+15 36 54		IRC+20446	19 57 49	+17 23 00	
IRC+20211	9 28 53	+23 11 00		IRC+20329	17 40 26	+24 35 12		IRC+20447	19 58 44	+18 14 42	
IRC+20212	9 31 08	+23 40 12		IRC+20330	17 40 53	+17 42 12		IRC+20448	19 58 55	+15 08 54	
IRC+20213	9 34 19	+16 40 06		IRC+20331	17 42 49	+21 31 06		IRC+20449	20 01 01	+18 21 30	
IRC+20214	9 38 44	+24 04 12		IRC+20332	17 43 32	+18 52 12		IRC+20450	20 01 30	+21 21 30	
IRC+20215	9 42 59	+24 00 06		IRC+20333	17 46 55	+22 33 24		IRC+20451	20 01 43	+20 55 00	
IRC+20216	10 03 11	+18 20 30		IRC+20334	17 47 26	+20 39 06		IRC+20452	20 02 53	+20 30 00	
IRC+20217	10 05 29	+17 36 06		IRC+20335	17 48 41	+24 00 42		IRC+20453	20 02 56	+19 50 54	
IRC+20218	10 13 55	+23 40 06		IRC+20336	17 49 20	+19 03 54		IRC+20454	20 03 11	+15 20 12	
IRC+20219	10 17 11	+20 05 36		IRC+20337	17 53 46	+22 28 06		IRC+20455	20 03 37	+19 06 00	
IRC+20220	10 26 37	+23 18 30		IRC+20338	17 55 07	+15 55 00		IRC+20456	20 04 27	+24 17 12	
IRC+20221	10 41 59	+19 41 12		IRC+20339	17 55 46	+15 24 36		IRC+20457	20 05 49	+16 31 06	
IRC+20222	10 43 44	+19 09 30		IRC+20340	17 57 47	+16 45 06		IRC+20458	20 09 01	+18 19 54	
IRC+20223	10 53 36	+22 36 54		IRC+20341	17 58 00	+23 35 24		IRC+20459	20 11 16	+16 06 12	
IRC+20224	11 04 04	+18 00 24		IRC+20342	17 58 17	+17 06 06		IRC+20460	20 11 59	+16 51 30	
IRC+20225	11 06 17	+20 31 36		IRC+20343	17 59 23	+21 35 36		IRC+20461	20 13 20	+23 21 06	
IRC+20226	11 11 28	+20 47 42		IRC+20344	18 00 33	+20 58 24		IRC+20462	20 18 05	+17 38 06	
IRC+20227	11 12 34	+23 22 12		IRC+20345	18 00 46	+15 00 12		IRC+20463	20 19 20	+22 42 00	
IRC+20228	11 21 03	+17 07 12		IRC+20346	18 01 09	+19 33 30		IRC+20464	20 20 08	+16 45 12	
IRC+20229	11 25 16	+15 24 42		IRC+20347	18 02 44	+16 54 24		IRC+20465	20 21 02	+18 12 12	
IRC+20230	11 27 06	+15 40 24		IRC+20348	18 03 56	+22 12 36		IRC+20466	20 22 18	+15 58 42	
IRC+20231	11 27 53	+18 40 54		IRC+20349	18 04 23	+20 15 42		IRC+20467	20 22 57	+16 49 42	
IRC+20232	11 29 28	+18 26 12		IRC+20350	18 05 07	+15 13 36		IRC+20468	20 23 07	+23 50 12	
IRC+20233	11 38 11	+21 37 42		IRC+20351	18 10 19	+21 43 42		IRC+20469	20 25 26	+22 04 36	
IRC+20234	11 45 25	+20 30 06		IRC+20352	18 10 44	+22 48 42		IRC+20470	20 26 53	+16 06 24	
IRC+20235	11 53 38	+15 59 42		IRC+20353	18 11 11	+21 52 06		IRC+20471	20 29 52	+18 27 36	
IRC+20236	11 57 31	+19 41 54		IRC+20354	18 12 42	+15 32 06		IRC+20472	20 31 35	+20 37 30	
IRC+20237	12 01 41	+19 03 24		IRC+20355	18 12 49	+16 15 12		IRC+20473	20 32 02	+19 21 36	
IRC+20238	12 06 38	+17 28 12		IRC+20356	18 15 43	+17 57 54		IRC+20474	20 35 38	+18 05 54	
IRC+20239	12 07 47	+19 47 30		IRC+20357	18 16 00	+21 23 30		IRC+20475	20 37 56	+19 17 42	
IRC+20240	12 13 49	+24 12 54		IRC+20358	18 16 03	+23 16 24		IRC+20476	20 40 44	+21 52 12	
IRC+20241	12 18 12	+18 04 12		IRC+20359	18 16 16	+24 20 24		IRC+20477	20 40 44	+16 54 30	
IRC+20242	12 27 38	+18 10 12		IRC+20360	18 17 10	+24 25 30		IRC+20478	20 41 41	+17 23 24	
IRC+20243	12 31 04	+24 42 54		IRC+20361	18 18 12	+21 56 06		IRC+20479	20 41 43	+19 03 30	
IRC+20244	12 32 38	+18 39 12		IRC+20362	18 20 03	+23 15 24		IRC+20480	20 43 01	+16 13 06	
IRC+20245	12 32 39	+22 09 30		IRC+20363	18 20 37	+17 48 00		IRC+20481	20 43 14	+17 54 24	
IRC+20246	12 34 28	+17 21 36		IRC+20364	18 21 33	+21 44 24		IRC+20482	20 44 17	+15 56 42	
IRC+20247	12 44 08	+16 50 54		IRC+20365	18 27 59	+16 36 00		IRC+20483	20 45 04	+15 36 36	
IRC+20248	12 45 49	+19 35 54		IRC+20366	18 30 43	+23 34 42		IRC+20484	20 45 31	+19 08 36	
IRC+20249	12 49 44	+17 20 36		IRC+20367	18 32 16	+15 11 24		IRC+20485	20 45 34	+22 04 54	
IRC+20250	12 50 51	+21 31 00		IRC+20368	18 36 01	+22 40 12		IRC+20486	20 46 37	+22 48 36	
IRC+20251	12 56 28	+17 40 36		IRC+20369	18 36 35	+18 22 36		IRC+20487	20 47 47	+16 48 00	
IRC+20252	13 00 44	+24 05 42		IRC+20370	18 39 41	+17 37 36		IRC+20488	20 49 37	+23 08 42	
IRC+20253	13 01 32	+19 58 24		IRC+20371	18 42 32	+17 27 12		IRC+20489	20 50 41	+24 43 24	
IRC+20254	13 03 56	+22 52 54		IRC+20372	18 43 31	+20 29 24		IRC+20490	20 50 48	+23 11 00	
IRC+20255	13 05 27	+23 53 00		IRC+20373	18 44 24	+22 29 06		IRC+20491	20 51 10	+20 44 24	
IRC+20256	13 07 20	+17 06 36		IRC+20374	18 44 31	+18 38 42		IRC+20492	20 52 36	+17 26 42	
IRC+20257	13 07 43	+24 51 54		IRC+20375	18 45 48	+24 44 12		IRC+20493	20 54 50	+16 03 12	
IRC+20258	13 12 43	+19 10 30		IRC+20376	18 46 07	+19 03 30		IRC+20494	20 56 02	+22 07 54	
IRC+20259	13 28 22	+19 55 06		IRC+20377	18 46 21	+15 46 24		IRC+20495	20 56 03	+23 42 00	
IRC+20260	13 34 37	+24 51 54		IRC+20378	18 48 20	+24 02 12		IRC+20496	20 56 50	+22 09 54	
IRC+20261	13 40 14	+23 33 54		IRC+20379	18 48 38	+23 43 36		IRC+20497	20 58 11	+19 08 12	
IRC+20262	13 41 24	+22 57 30		IRC+20380	18 52 38	+22 34 42		IRC+20498	20 59 34	+18 47 54	
IRC+20263	13 47 03	+16 02 30		IRC+20381	18 56 08	+16 42 42		IRC+20499	21 00 22	+15 46 00	
IRC+20264	13 47 21	+21 30 54		IRC+20382	18 57 52	+22 44 30		IRC+20500	21 00 58	+24 15 06	
IRC+20265	13 50 08	+16 58 30		IRC+20383	18 59 34	+22 48 54		IRC+20501	21 01 17	+23 47 42	
IRC+20266	13 51 34	+17 31 36		IRC+20384	19 00 40	+20 39 00		IRC+20502	21 01 57	+22 19 00	
IRC+20267	13 52 20	+18 38 36		IRC+20385	19 03 01	+17 43 12		IRC+20503	21 12 52	+18 24 36	
IRC+20268	13 54 46	+21 11 54		IRC+20386	19 03 19	+17 16 12		IRC+20504	21 17 01	+23 16 00	
IRC+20269	14 04 05	+17 12 36		IRC+20387	19 04 03	+24 16 06		IRC+20505	21 19 45	+19 35 42	
IRC+20270	14 13 23	+19 26 30		IRC+20388	19 06 31	+24 06 06		IRC+20506	21 20 14	+21 47 06	
IRC+20271	14 15 06	+15 29 30		IRC+20389	19 08 53	+21 54 42		IRC+20507	21 21 04	+23 15 42	
IRC+20272	14 17 23	+16 32 00		IRC+20390	19 12 50	+21 59 30		IRC+20508	21 21 09	+23 02 06	
IRC+20273	14 18 47	+19 24 24		IRC+20391	19 13 21	+18 25 12		IRC+20509	21 21 19	+24 05 24	
IRC+20274	14 42 55	+17 10 30		IRC+20392	19 13 47	+22 53 54		IRC+20510	21 26 05	+24 24 54	
IRC+20275	14 43 41	+15 20 24		IRC+20393	19 14 49	+21 50 00		IRC+20511	21 26 43	+21 57 36	
IRC+20276	14 49 05	+19 18 24		IRC+20394	19 16 15	+15 25 42		IRC+20512	21 27 40	+23 25 12	
IRC+20277	15 09 47	+19 09 54		IRC+20395	19 17 10	+16 46 00		IRC+20513	21 29 59	+24 15 30	
IRC+20278	15 09 50	+22 30 00		IRC+20396	19 17 19	+17 06 42		IRC+20514	21 36 06	+24 42 00	
IRC+20279	15 12 34	+21 31 00		IRC+20397	19 17 21	+22 57 06		IRC+20515	21 38 43	+21 58 12	
IRC+20280	15 23 30	+15 36 12		IRC+20398	19 17 24	+22 28 42		IRC+20516	21 40 19	+21 28 36	
IRC+20281	15 25 32	+19 44 06		IRC+20399	19 19 29	+17 34 30		IRC+20517	21 40 26	+22 15 24	
IRC+20282	15 34 09	+15 15 30		IRC+20400	19 22 25	+17 39 54		IRC+20518	21 42 08	+17 07 12	
IRC+20283	15 36 07	+24 41 06		IRC+20401	19 22 39	+21 23 06		IRC+20519	21 43 46	+22 43 12	
IRC+20284	15 46 31	+18 17 42		IRC+20402	19 23 17	+19 41 36		IRC+20520	21 44 53	+23 37 12	
IRC+20285	15 48 22	+15 17 00		IRC+20403	19 23 43	+21 23 30		IRC+20521	21 49 56	+21 02 06	
IRC+20286	15 49 05	+21 07 24		IRC+20404	19 24 02	+16 34 36		IRC+20522	21 51 18	+18 56 30	
IRC+20287	15 51 05	+17 25 42		IRC+20405	19 24 19	+19 47 42		IRC+20523	21 54 01	+22 37 42	
IRC+20288	15 52 23	+20 27 24		IRC+20406	19 24 52	+23 29 42		IRC+20524	21 54 04	+21 00 12	
IRC+20289	15 54 08	+15 48 54		IRC+20407	19 26 41	+24 33 42		IRC+20525	21 54 52	+17 31 30	
IRC+20290	15 58 58	+17 57 12		IRC+20408	19 26 56	+23 09 36		IRC+20526	21 57 30	+23 42 00	
IRC+20291	16 02 29	+22 46 36		IRC+20409	19 27 10	+15 04 54		IRC+20527	22 04 18	+24 43 36	
IRC+20292	16 05 13	+21 57 06		IRC+20410	19 27 46	+22 36 24		IRC+20528	22 05 05	+17 45 30	

NAME	RA (1950)	DEC	POS REF
	h m s	° ′ ″	
IRC+20529	22 09 34	+23 31 42	
IRC+20530	22 09 46	+24 42 06	
IRC+20531	22 16 58	+15 17 24	
IRC+20532	22 31 37	+24 18 36	
IRC+20533	22 36 33	+20 52 06	
IRC+20534	22 39 19	+20 54 24	
IRC+20535	22 41 17	+22 55 24	
IRC+20536	22 44 08	+23 18 06	
IRC+20537	22 47 33	+24 20 12	
IRC+20538	22 48 53	+17 51 12	
IRC+20539	22 52 08	+16 41 00	
IRC+20540	22 52 16	+24 06 54	
IRC+20541	22 52 34	+19 17 54	
IRC+20542	22 55 23	+17 45 30	
IRC+20543	22 55 37	+21 14 42	
IRC+20544	22 56 34	+24 38 06	
IRC+20545	22 58 02	+19 08 24	
IRC+20546	23 08 14	+17 20 24	
IRC+20547	23 19 19	+20 21 54	
IRC+20548	23 22 53	+23 07 30	
IRC+20549	23 29 57	+23 34 30	
IRC+20550	23 31 00	+22 13 30	
IRC+20551	23 31 23	+20 35 06	
IRC+20552	23 33 26	+24 17 30	
IRC+20553	23 39 13	+22 09 36	
IRC+20554	23 49 50	+21 23 30	
IRC+20555	23 49 56	+18 50 42	
IRC+20556	23 54 08	+22 22 12	
IRC+20557	23 55 11	+24 51 54	
IRC+20558	23 57 34	+19 58 00	
IRC+30001	0 02 23	+26 23 30	
IRC+30002	0 03 53	+26 48 42	
IRC+30003	0 04 34	+34 34 42	
IRC+30004	0 05 49	+28 49 00	
IRC+30005	0 07 52	+28 22 24	
IRC+30006	0 08 09	+31 58 00	
IRC+30007	0 12 27	+31 15 24	
IRC+30008	0 18 08	+32 38 06	
IRC+30009	0 19 47	+26 42 42	
IRC+30010	0 24 28	+30 53 36	
IRC+30011	0 28 21	+28 29 00	
IRC+30012	0 29 43	+25 45 00	
IRC+30013	0 35 50	+29 02 00	
IRC+30014	0 36 38	+30 35 12	
IRC+30015	0 44 34	+32 24 54	
IRC+30016	0 49 10	+32 05 42	
IRC+30017	0 54 04	+26 04 06	
IRC+30018	0 54 08	+31 37 30	
IRC+30019	0 55 05	+28 43 42	
IRC+30020	1 07 36	+25 11 24	
IRC+30021	1 08 30	+30 22 00	
IRC+30022	1 08 53	+29 50 00	
IRC+30023	1 11 08	+26 52 06	
IRC+30024	1 11 20	+28 16 00	
IRC+30025	1 13 18	+25 30 36	
IRC+30026	1 14 38	+26 01 54	
IRC+30027	1 18 20	+28 29 06	
IRC+30028	1 20 06	+31 35 00	
IRC+30029	1 42 18	+28 29 24	
IRC+30030	1 45 58	+33 53 12	
IRC+30031	1 50 14	+29 20 36	
IRC+30032	1 54 54	+27 34 00	
IRC+30033	1 55 12	+30 54 06	
IRC+30034	2 06 34	+34 45 30	
IRC+30035	2 08 19	+25 41 30	
IRC+30036	2 09 28	+30 05 42	
IRC+30037	2 15 02	+28 47 36	
IRC+30038	2 15 38	+31 54 24	
IRC+30039	2 17 04	+32 05 54	
IRC+30040	2 20 26	+28 30 06	
IRC+30041	2 22 07	+33 38 42	
IRC+30042	2 24 09	+26 48 00	
IRC+30043	2 32 43	+34 28 54	
IRC+30044	2 33 58	+34 03 06	
IRC+30045	2 35 33	+27 18 30	
IRC+30046	2 37 58	+30 59 30	
IRC+30047	2 38 24	+34 18 36	
IRC+30048	2 39 11	+32 12 30	
IRC+30049	2 40 04	+25 51 36	
IRC+30050	2 44 55	+29 02 30	
IRC+30051	2 48 27	+34 51 42	
IRC+30052	2 48 41	+32 55 06	
IRC+30053	2 52 40	+30 50 54	
IRC+30054	2 55 56	+34 59 36	
IRC+30055	2 56 39	+29 38 24	
IRC+30056	3 14 58	+32 44 24	
IRC+30057	3 15 04	+27 13 54	
IRC+30058	3 15 38	+34 02 30	
IRC+30059	3 16 45	+28 59 30	
IRC+30060	3 16 48	+32 58 00	
IRC+30061	3 16 59	+31 50 30	
IRC+30062	3 17 19	+28 52 00	
IRC+30063	3 19 25	+32 03 42	
IRC+30064	3 24 59	+33 18 12	
IRC+30065	3 28 07	+28 32 24	
IRC+30066	3 44 56	+33 37 06	
IRC+30067	3 45 11	+27 31 00	
IRC+30068	3 50 59	+31 44 06	
IRC+30069	3 56 41	+28 40 00	
IRC+30070	4 01 41	+26 04 06	
IRC+30071	4 05 29	+26 43 00	
IRC+30072	4 06 28	+33 21 42	
IRC+30073	4 07 47	+33 27 06	
IRC+30074	4 08 40	+29 15 36	
IRC+30075	4 09 50	+32 24 00	
IRC+30076	4 10 08	+33 19 30	
IRC+30077	4 10 16	+28 59 36	
IRC+30078	4 10 39	+26 17 36	
IRC+30079	4 12 22	+33 42 06	
IRC+30080	4 13 47	+31 14 30	
IRC+30081	4 15 32	+31 50 54	
IRC+30082	4 16 58	+31 49 36	
IRC+30083	4 17 11	+34 27 00	
IRC+30084	4 17 15	+27 13 12	
IRC+30085	4 18 08	+27 13 30	
IRC+30086	4 21 18	+28 54 42	
IRC+30087	4 28 01	+27 23 06	
IRC+30088	4 29 14	+31 00 30	
IRC+30089	4 32 06	+29 37 24	
IRC+30090	4 32 52	+28 24 42	
IRC+30091	4 34 28	+32 31 30	
IRC+30092	4 40 59	+25 14 42	
IRC+30093	4 42 03	+32 49 30	
IRC+30094	4 43 53	+25 32 00	
IRC+30095	4 45 53	+28 37 42	
IRC+30096	4 46 01	+31 21 36	
IRC+30097	4 47 15	+28 01 24	
IRC+30098	4 48 24	+28 26 36	
IRC+30099	4 48 52	+28 55 12	
IRC+30100	4 53 45	+33 05 24	
IRC+30101	4 56 53	+27 07 36	
IRC+30102	5 03 10	+34 47 30	
IRC+30103	5 04 10	+32 50 24	
IRC+30104	5 04 17	+30 43 00	
IRC+30105	5 08 28	+29 50 42	
IRC+30106	5 14 17	+31 46 06	
IRC+30107	5 14 53	+33 19 24	
IRC+30108	5 15 57	+30 25 00	
IRC+30109	5 18 16	+34 08 36	
IRC+30110	5 18 34	+32 27 42	
IRC+30111	5 18 59	+34 37 24	
IRC+30112	5 23 08	+28 33 42	
IRC+30113	5 23 37	+32 00 36	
IRC+30114	5 23 47	+34 06 54	
IRC+30115	5 23 58	+29 53 00	
IRC+30116	5 24 18	+34 26 24	
IRC+30117	5 25 37	+32 25 42	
IRC+30118	5 27 25	+31 28 00	
IRC+30119	5 27 29	+32 45 24	
IRC+30120	5 30 30	+32 43 00	
IRC+30121	5 32 48	+27 38 00	
IRC+30122	5 34 49	+30 51 30	
IRC+30123	5 36 52	+28 40 42	
IRC+30124	5 37 29	+31 53 30	
IRC+30125	5 37 53	+28 04 24	
IRC+30126	5 38 55	+32 01 06	
IRC+30127	5 44 59	+30 36 24	
IRC+30128	5 47 41	+27 39 36	
IRC+30129	5 48 13	+32 06 24	
IRC+30130	5 48 34	+28 18 00	
IRC+30131	5 49 23	+33 54 06	
IRC+30132	5 52 48	+32 07 54	
IRC+30133	5 55 31	+27 51 00	
IRC+30134	5 56 55	+28 07 36	
IRC+30135	5 58 18	+34 50 06	
IRC+30136	6 01 08	+28 29 24	
IRC+30137	6 03 10	+29 30 36	
IRC+30138	6 05 41	+25 40 00	
IRC+30139	6 05 44	+34 54 00	
IRC+30140	6 06 12	+26 32 30	
IRC+30141	6 06 44	+31 24 54	
IRC+30142	6 06 57	+33 36 36	
IRC+30143	6 07 47	+26 01 30	
IRC+30144	6 09 03	+32 42 24	
IRC+30145	6 10 41	+33 15 30	
IRC+30146	6 12 09	+29 30 30	
IRC+30147	6 12 19	+25 21 06	
IRC+30148	6 13 54	+33 13 30	
IRC+30149	6 14 32	+34 03 12	
IRC+30150	6 20 56	+25 02 42	
IRC+30151	6 23 27	+29 21 06	
IRC+30152	6 27 41	+32 50 24	
IRC+30153	6 27 52	+27 28 54	
IRC+30154	6 30 04	+31 37 30	
IRC+30155	6 30 38	+30 17 12	
IRC+30156	6 30 48	+28 19 54	
IRC+30157	6 31 31	+29 24 42	
IRC+30158	6 32 46	+31 30 54	
IRC+30159	6 34 35	+27 39 00	
IRC+30160	6 36 25	+26 11 24	
IRC+30161	6 37 53	+25 22 00	
IRC+30162	6 38 46	+28 00 24	
IRC+30163	6 38 54	+31 30 24	
IRC+30164	6 40 52	+25 10 54	
IRC+30165	6 41 37	+29 00 42	
IRC+30166	6 43 55	+30 20 12	
IRC+30167	6 46 29	+32 39 24	
IRC+30168	6 50 28	+34 50 24	
IRC+30169	6 52 56	+34 31 24	
IRC+30170	6 56 22	+26 07 06	
IRC+30171	6 58 27	+30 36 12	
IRC+30172	6 59 28	+31 25 06	
IRC+30173	7 02 34	+31 28 00	
IRC+30174	7 03 47	+31 40 12	
IRC+30175	7 04 07	+34 05 06	
IRC+30176	7 04 15	+28 22 30	
IRC+30177	7 04 47	+29 45 00	
IRC+30178	7 07 59	+30 19 30	
IRC+30179	7 12 51	+27 59 30	
IRC+30180	7 17 04	+31 27 06	
IRC+30181	7 17 36	+31 34 00	
IRC+30182	7 17 54	+25 05 36	
IRC+30183	7 22 37	+27 53 42	
IRC+30184	7 23 00	+33 28 12	
IRC+30185	7 23 16	+26 03 12	
IRC+30186	7 26 43	+28 01 24	
IRC+30187	7 30 44	+30 37 12	
IRC+30188	7 31 25	+32 00 00	
IRC+30189	7 31 41	+28 51 30	
IRC+30190	7 32 50	+27 00 12	
IRC+30191	7 40 15	+29 00 06	
IRC+30192	7 40 19	+32 34 12	
IRC+30193	7 41 03	+25 54 24	
IRC+30194	7 42 14	+28 08 42	
IRC+30195	7 42 19	+30 54 00	
IRC+30196	7 44 16	+33 32 00	
IRC+30197	7 56 11	+34 48 30	
IRC+30198	8 00 26	+27 56 24	
IRC+30199	8 23 27	+28 03 06	
IRC+30200	8 31 25	+26 24 24	
IRC+30201	8 43 41	+28 56 12	
IRC+30202	8 49 29	+28 27 00	
IRC+30203	8 51 13	+30 46 12	
IRC+30204	8 52 38	+28 07 30	
IRC+30205	8 55 16	+33 23 36	
IRC+30206	8 56 30	+32 36 42	
IRC+30207	9 01 21	+29 28 06	
IRC+30208	9 07 01	+25 27 00	
IRC+30209	9 07 38	+31 10 00	
IRC+30210	9 17 59	+34 36 24	
IRC+30211	9 21 46	+26 24 06	
IRC+30212	9 28 13	+25 16 06	
IRC+30213	9 33 46	+31 23 36	
IRC+30214	9 38 38	+31 30 24	
IRC+30215	9 42 35	+34 44 12	
IRC+30216	9 44 24	+33 00 42	
IRC+30217	9 47 52	+31 37 30	
IRC+30218	9 49 53	+26 14 54	
IRC+30219	10 13 12	+30 49 24	
IRC+30220	10 19 37	+25 45 24	
IRC+30221	10 21 17	+33 58 24	
IRC+30222	10 21 26	+34 25 42	
IRC+30223	10 35 53	+32 14 00	
IRC+30224	10 39 21	+31 57 00	
IRC+30225	10 43 57	+34 59 36	
IRC+30226	10 50 31	+34 29 00	
IRC+30227	10 50 51	+26 28 24	
IRC+30228	10 52 58	+33 46 30	
IRC+30229	11 15 29	+31 48 30	
IRC+30230	11 15 46	+33 22 06	
IRC+30231	11 28 18	+28 43 12	
IRC+30232	11 41 37	+25 30 06	
IRC+30233	11 44 24	+27 17 12	
IRC+30234	12 01 01	+29 56 54	
IRC+30235	12 09 17	+26 08 54	
IRC+30236	12 14 00	+33 20 30	
IRC+30237	12 14 26	+28 01 06	
IRC+30238	12 24 28	+28 32 30	
IRC+30239	12 27 44	+31 46 36	
IRC+30240	12 31 13	+33 31 00	
IRC+30241	12 34 26	+27 19 54	
IRC+30242	12 34 29	+32 52 06	
IRC+30243	12 56 38	+34 49 06	
IRC+30244	12 57 54	+31 02 54	
IRC+30245	13 04 49	+27 53 30	
IRC+30246	13 09 35	+28 08 00	
IRC+30247	13 16 10	+34 21 36	
IRC+30248	13 27 29	+27 55 42	
IRC+30249	13 42 10	+33 45 54	
IRC+30250	13 48 56	+34 54 36	
IRC+30251	13 49 34	+34 41 12	
IRC+30252	13 54 17	+27 44 30	
IRC+30253	13 57 25	+28 01 36	
IRC+30254	14 20 03	+29 35 42	
IRC+30255	14 21 41	+27 30 00	
IRC+30256	14 21 47	+27 38 12	
IRC+30257	14 21 58	+25 55 54	
IRC+30258	14 26 32	+26 04 30	
IRC+30259	14 29 41	+30 35 30	
IRC+30260	14 35 01	+26 57 30	
IRC+30261	14 37 08	+32 45 06	
IRC+30262	14 39 05	+31 47 24	
IRC+30263	14 41 14	+26 44 30	
IRC+30264	14 42 50	+27 16 54	
IRC+30265	14 43 08	+32 59 54	
IRC+30266	14 59 56	+25 12 12	
IRC+30267	15 00 26	+31 52 54	
IRC+30268	15 02 20	+27 08 30	
IRC+30269	15 06 14	+26 29 24	
IRC+30270	15 12 03	+31 58 24	
IRC+30271	15 13 28	+33 30 00	
IRC+30272	15 19 19	+31 32 36	
IRC+30273	15 24 20	+34 30 30	
IRC+30274	15 25 30	+25 16 30	
IRC+30275	15 32 32	+26 53 00	
IRC+30276	15 34 55	+32 44 54	
IRC+30277	15 42 26	+32 18 00	
IRC+30278	15 46 04	+31 53 30	
IRC+30279	15 47 31	+26 13 24	
IRC+30280	15 55 31	+27 01 06	
IRC+30281	16 03 42	+31 03 24	
IRC+30282	16 05 14	+32 30 36	
IRC+30283	16 08 07	+25 12 00	
IRC+30284	16 10 25	+25 01 30	
IRC+30285	16 11 06	+26 39 24	
IRC+30286	16 18 43	+34 44 30	
IRC+30287	16 20 09	+31 00 30	
IRC+30288	16 20 28	+33 55 00	
IRC+30289	16 20 35	+33 49 12	
IRC+30290	16 21 08	+30 58 06	
IRC+30291	16 23 07	+29 21 54	
IRC+30292	16 25 59	+34 54 36	
IRC+30292	16 25 59.0	+34 54 36	
IRC+30293	16 35 47	+27 08 30	
IRC+30294	16 39 23	+31 41 30	
IRC+30295	16 40 04	+33 01 06	
IRC+30296	16 41 01	+26 09 06	
IRC+30297	16 48 43	+29 53 42	
IRC+30298	16 57 52	+27 23 12	
IRC+30299	16 58 16	+26 19 00	
IRC+30300	17 02 49	+28 44 36	
IRC+30301	17 08 28	+29 13 54	
IRC+30302	17 08 38	+27 39 12	
IRC+30303	17 15 35	+28 57 54	
IRC+30304	17 16 25	+32 44 24	
IRC+30305	17 17 24	+27 20 06	
IRC+30306	17 21 03	+25 28 06	
IRC+30307	17 28 43	+26 09 00	
IRC+30308	17 34 18	+31 27 36	
IRC+30309	17 34 22	+27 35 54	
IRC+30310	17 38 03	+31 13 42	
IRC+30311	17 41 06	+29 40 36	
IRC+30312	17 44 29	+27 44 42	
IRC+30313	17 45 48	+28 24 12	
IRC+30314	17 45 49	+28 46 12	
IRC+30315	17 45 53	+30 22 30	
IRC+30316	17 46 49	+25 38 36	
IRC+30317	17 48 59	+30 06 30	
IRC+30318	17 50 14	+26 31 06	
IRC+30319	17 50 35	+30 45 12	
IRC+30320	17 54 27	+31 08 12	
IRC+30321	17 54 54	+26 59 12	
IRC+30322	17 55 26	+29 46 36	
IRC+30323	17 55 34	+33 48 12	

NAME	RA (1950)	DEC	POS REF
	h m s	° ′ ″	
IRC+30324	17 55 50	+29 15 06	
IRC+30325	17 58 47	+33 12 36	
IRC+30326	17 59 46	+33 18 12	
IRC+30327	18 05 23	+34 49 30	
IRC+30328	18 10 02	+31 24 00	
IRC+30329	18 10 46	+25 05 00	
IRC+30330	18 12 32	+30 11 00	
IRC+30331	18 15 49	+34 54 24	
IRC+30332	18 17 56	+29 39 00	
IRC+30333	18 18 09	+25 50 12	
IRC+30334	18 18 39	+31 44 12	
IRC+30335	18 25 56	+31 10 24	
IRC+30336	18 29 09	+25 07 54	
IRC+30337	18 36 43	+30 24 36	
IRC+30338	18 38 58	+31 38 36	
IRC+30339	18 39 31	+28 45 54	
IRC+30340	18 40 07	+28 54 30	
IRC+30341	18 41 06	+29 45 30	
IRC+30342	18 44 02	+26 36 12	
IRC+30343	18 48 12	+33 17 54	
IRC+30344	18 50 28	+33 27 06	
IRC+30345	18 51 11	+30 34 06	
IRC+30346	18 52 16	+27 50 36	
IRC+30347	18 53 59	+30 05 24	
IRC+30348	18 56 30	+25 10 36	
IRC+30349	18 57 44	+26 10 00	
IRC+30350	18 58 07	+32 04 30	
IRC+30351	19 01 28	+29 04 12	
IRC+30352	19 01 28	+34 20 24	
IRC+30353	19 03 02	+31 40 06	
IRC+30354	19 03 03	+30 39 36	
IRC+30355	19 03 14	+27 03 06	
IRC+30356	19 03 29	+31 29 54	
IRC+30357	19 03 50	+29 51 00	
IRC+30358	19 05 16	+30 06 54	
IRC+30359	19 06 08	+30 32 54	
IRC+30360	19 07 07	+29 34 54	
IRC+30361	19 08 08	+32 19 42	
IRC+30362	19 09 44	+32 31 42	
IRC+30363	19 12 01	+32 27 54	
IRC+30364	19 13 29	+30 26 12	
IRC+30365	19 14 15	+29 15 06	
IRC+30366	19 14 47	+31 03 00	
IRC+30367	19 17 05	+27 10 12	
IRC+30368	19 19 11	+27 56 30	
IRC+30369	19 22 29	+28 25 06	
IRC+30370	19 28 45	+27 51 12	
IRC+30371	19 29 53	+31 46 00	
IRC+30372	19 31 56	+30 01 42	
IRC+30373	19 32 10	+25 14 24	
IRC+30374	19 32 12	+27 57 00	
IRC+30375	19 32 49	+30 39 42	
IRC+30376	19 33 04	+33 41 00	
IRC+30377	19 34 48	+25 13 12	
IRC+30378	19 35 48	+34 54 24	
IRC+30379	19 36 59	+28 23 42	
IRC+30380	19 37 24	+30 02 12	
IRC+30381	19 38 53	+28 55 24	
IRC+30382	19 39 02	+32 29 54	
IRC+30383	19 39 46	+30 42 06	
IRC+30384	19 40 02	+26 30 42	
IRC+30385	19 41 42	+34 22 06	
IRC+30386	19 41 53	+27 00 42	
IRC+30387	19 42 00	+27 39 00	
IRC+30388	19 42 44	+34 17 42	
IRC+30389	19 42 46	+30 34 36	
IRC+30390	19 43 31	+31 21 12	
IRC+30391	19 43 46	+30 07 30	
IRC+30392	19 46 41	+26 00 30	
IRC+30393	19 47 13	+30 17 12	
IRC+30394	19 48 17	+26 13 42	
IRC+30395	19 48 37	+32 47 12	
IRC+30396	19 50 18	+25 51 30	
IRC+30397	19 51 05	+29 31 30	
IRC+30398	19 51 28	+33 49 06	
IRC+30399	19 52 14	+33 39 00	
IRC+30400	19 53 41	+32 37 54	
IRC+30401	19 54 28	+34 56 54	
IRC+30402	19 55 10	+25 35 06	
IRC+30403	19 56 22	+25 12 54	
IRC+30404	19 56 28	+31 20 54	
IRC+30405	19 57 21	+30 16 42	
IRC+30406	19 59 18	+33 47 24	
IRC+30407	19 59 55	+33 22 24	
IRC+30408	20 00 31	+30 38 06	
IRC+30409	20 01 38	+30 19 54	
IRC+30410	20 01 56	+29 00 54	
IRC+30411	20 02 09	+29 40 06	
IRC+30412	20 03 42	+25 27 30	
IRC+30413	20 03 44	+27 59 06	
IRC+30414	20 07 38	+28 10 12	
IRC+30415	20 08 01	+26 08 30	
IRC+30416	20 08 18	+29 11 30	
IRC+30417	20 08 39	+33 18 30	
IRC+30418	20 09 44	+26 40 06	
IRC+30419	20 10 31	+33 13 36	
IRC+30420	20 11 04	+32 05 00	
IRC+30421	20 11 08	+25 05 24	
IRC+30422	20 13 02	+29 36 36	
IRC+30423	20 13 33	+30 55 00	
IRC+30424	20 13 41	+27 39 24	
IRC+30425	20 15 59	+33 55 36	
IRC+30426	20 16 35	+34 13 24	
IRC+30427	20 16 43	+26 50 12	
IRC+30428	20 19 20	+30 42 06	
IRC+30429	20 20 35	+31 05 36	
IRC+30430	20 21 52	+32 02 00	
IRC+30431	20 22 18	+30 53 12	
IRC+30432	20 23 58	+26 04 42	
IRC+30433	20 25 53	+25 53 42	
IRC+30434	20 27 19	+30 11 54	
IRC+30435	20 27 38	+33 40 06	
IRC+30436	20 29 13	+29 33 12	
IRC+30437	20 29 38	+32 22 36	
IRC+30438	20 32 29	+28 06 06	
IRC+30439	20 32 49	+34 42 54	
IRC+30440	20 33 03	+28 23 54	
IRC+30441	20 34 16	+34 57 12	
IRC+30442	20 35 26	+30 50 42	
IRC+30443	20 35 53	+33 36 36	
IRC+30444	20 37 00	+30 08 06	
IRC+30445	20 40 15	+27 18 00	
IRC+30446	20 41 15	+27 04 30	
IRC+30447	20 41 32	+31 57 00	
IRC+30448	20 42 44	+25 06 00	
IRC+30449	20 43 32	+32 17 36	
IRC+30450	20 43 35	+30 32 00	
IRC+30451	20 44 12	+33 47 00	
IRC+30452	20 44 29	+29 58 42	
IRC+30453	20 45 13	+34 11 06	
IRC+30454	20 46 11	+28 03 54	
IRC+30455	20 46 59	+31 40 12	
IRC+30456	20 47 12	+33 02 24	
IRC+30457	20 48 12	+33 59 54	
IRC+30458	20 49 56	+26 53 42	
IRC+30459	20 50 21	+26 59 06	
IRC+30460	20 51 12	+25 23 36	
IRC+30461	20 51 51	+33 14 30	
IRC+30462	20 52 26	+27 52 12	
IRC+30463	20 52 55	+33 34 06	
IRC+30464	20 53 00	+30 13 24	
IRC+30465	20 57 56	+32 18 06	
IRC+30466	21 00 11	+34 34 30	
IRC+30467	21 00 34	+26 19 30	
IRC+30468	21 01 10	+27 07 54	
IRC+30469	21 02 47	+27 12 06	
IRC+30470	21 03 42	+30 01 06	
IRC+30471	21 03 52	+29 12 24	
IRC+30472	21 10 48	+30 01 24	
IRC+30473	21 32 36	+28 03 36	
IRC+30474	21 34 07	+34 47 06	
IRC+30475	21 34 08	+32 17 42	
IRC+30476	21 34 26	+31 53 06	
IRC+30477	21 40 16	+33 50 24	
IRC+30478	21 42 24	+25 25 00	
IRC+30479	21 45 01	+25 19 42	
IRC+30480	21 47 33	+34 01 12	
IRC+30481	22 01 41	+28 06 30	
IRC+30482	22 02 57	+26 26 24	
IRC+30483	22 03 31	+29 40 30	
IRC+30484	22 03 37	+33 15 42	
IRC+30485	22 04 41	+25 05 54	
IRC+30486	22 08 00	+32 02 36	
IRC+30487	22 10 35	+34 21 30	
IRC+30488	22 11 18	+25 10 36	
IRC+30489	22 15 29	+26 41 36	
IRC+30490	22 18 41	+26 41 42	
IRC+30491	22 21 37	+31 00 36	
IRC+30492	22 23 16	+30 13 12	
IRC+30493	22 25 28	+31 36 06	
IRC+30494	22 26 34	+27 34 12	
IRC+30495	22 30 04	+30 36 30	
IRC+30496	22 38 17	+26 29 00	
IRC+30497	22 39 07	+30 42 36	
IRC+30498	22 40 35	+27 53 36	
IRC+30499	22 40 43	+29 57 54	
IRC+30500	22 41 52	+29 20 42	
IRC+30501	22 44 22	+25 04 24	
IRC+30502	22 46 41	+27 05 42	
IRC+30503	22 59 07	+32 20 54	
IRC+30504	23 01 22	+27 48 36	
IRC+30505	23 03 04	+28 42 42	
IRC+30506	23 04 40	+25 11 42	
IRC+30507	23 07 45	+33 30 00	
IRC+30508	23 14 54	+29 35 36	
IRC+30509	23 17 22	+26 00 24	
IRC+30510	23 18 22	+30 08 54	
IRC+30511	23 19 58	+25 38 36	
IRC+30512	23 31 08	+30 44 42	
IRC+30513	23 31 28	+31 03 24	
IRC+30514	23 31 35	+29 36 00	
IRC+30515	23 36 53	+32 03 12	
IRC+30516	23 41 28	+29 05 00	
IRC+30517	23 44 22	+28 08 12	
IRC+30518	23 44 50	+25 51 06	
IRC+30519	23 45 56	+30 14 30	
IRC+30520	23 49 10	+29 28 30	
IRC+30521	23 54 25	+32 03 06	
IRC+30522	23 57 34	+25 36 36	
IRC+40001	0 01 44	+39 50 30	
IRC+40002	0 01 56	+41 50 42	
IRC+40003	0 02 01	+43 16 30	
IRC+40004	0 04 17	+42 47 54	
IRC+40005	0 09 41	+43 32 24	
IRC+40006	0 17 14	+44 25 54	
IRC+40007	0 19 25	+43 52 00	
IRC+40008	0 20 18	+38 28 36	
IRC+40009	0 21 23	+38 18 00	
IRC+40010	0 24 53	+35 19 12	
IRC+40011	0 33 58	+44 12 30	
IRC+40012	0 36 53	+37 56 36	
IRC+40013	0 39 59	+41 00 24	
IRC+40014	0 41 54	+40 24 54	
IRC+40015	0 49 53	+44 51 36	
IRC+40016	0 56 34	+42 35 00	
IRC+40017	0 56 40	+39 20 54	
IRC+40018	1 01 14	+38 24 54	
IRC+40019	1 06 53	+35 21 00	
IRC+40020	1 14 11	+44 38 30	
IRC+40021	1 14 46	+44 22 12	
IRC+40022	1 31 03	+35 21 00	
IRC+40023	1 32 13	+37 55 42	
IRC+40024	1 33 51	+41 08 42	
IRC+40025	1 36 22	+44 08 24	
IRC+40026	1 39 12	+39 07 36	
IRC+40027	1 47 58	+42 28 24	
IRC+40028	1 48 10	+37 46 12	
IRC+40029	1 48 40	+39 01 06	
IRC+40030	1 48 41	+38 53 54	
IRC+40031	1 50 17	+40 29 24	
IRC+40032	1 51 24	+36 53 06	
IRC+40033	1 53 01	+37 01 36	
IRC+40034	2 00 49	+42 05 24	
IRC+40035	2 02 52	+40 29 24	
IRC+40036	2 10 04	+44 00 00	
IRC+40037	2 14 21	+44 04 12	
IRC+40038	2 15 44	+36 51 36	
IRC+40039	2 22 47	+36 47 30	
IRC+40040	2 22 50	+37 53 24	
IRC+40041	2 24 11	+36 44 06	
IRC+40042	2 27 16	+37 58 12	
IRC+40043	2 29 01	+35 55 36	
IRC+40044	2 30 24	+41 34 24	
IRC+40045	2 32 31	+37 05 12	
IRC+40046	2 34 07	+38 45 42	
IRC+40047	2 36 51	+39 37 12	
IRC+40048	2 38 35	+44 47 12	
IRC+40049	2 40 44	+36 02 42	
IRC+40050	2 54 52	+38 24 42	
IRC+40051	2 56 26	+40 50 06	
IRC+40052	2 56 50	+43 56 36	
IRC+40053	3 01 18	+35 40 42	
IRC+40054	3 01 56	+38 39 12	
IRC+40055	3 04 54	+40 46 00	
IRC+40056	3 05 40	+36 50 30	
IRC+40057	3 06 08	+44 40 00	
IRC+40058	3 08 04	+39 25 06	
IRC+40059	3 08 13	+37 52 30	
IRC+40060	3 14 25	+39 22 36	
IRC+40061	3 24 52	+44 12 42	
IRC+40062	3 27 13	+39 29 00	
IRC+40063	3 29 28	+43 35 00	
IRC+40064	3 37 26	+38 52 36	
IRC+40065	3 38 49	+37 18 06	
IRC+40066	3 39 08	+36 21 00	
IRC+40067	3 41 36	+44 37 06	
IRC+40068	3 41 49	+42 24 36	
IRC+40069	3 47 01	+42 26 06	
IRC+40070	3 48 55	+39 43 42	
IRC+40071	3 49 05	+44 55 36	
IRC+40072	3 50 44	+36 23 30	
IRC+40073	4 04 29	+42 05 24	
IRC+40074	4 04 29	+42 54 00	
IRC+40075	4 04 43	+42 17 36	
IRC+40076	4 05 53	+36 17 54	
IRC+40077	4 06 56	+42 02 06	
IRC+40078	4 07 26	+42 05 36	
IRC+40079	4 11 28	+40 21 42	
IRC+40080	4 12 41	+41 32 30	
IRC+40081	4 14 32	+42 36 36	
IRC+40082	4 16 35	+40 56 54	
IRC+40083	4 16 51	+36 28 06	
IRC+40084	4 16 52	+37 05 06	
IRC+40085	4 19 20	+43 59 54	
IRC+40086	4 20 04	+36 06 12	
IRC+40087	4 21 05	+35 07 54	
IRC+40088	4 21 22	+39 11 24	
IRC+40089	4 26 19	+39 45 42	
IRC+40090	4 26 20	+38 42 00	
IRC+40091	4 26 59	+35 10 12	
IRC+40092	4 32 54	+44 53 00	
IRC+40093	4 33 14	+41 10 00	
IRC+40094	4 33 17	+36 57 12	
IRC+40095	4 38 01	+40 06 00	
IRC+40096	4 38 14	+40 24 12	
IRC+40097	4 41 46	+43 41 24	
IRC+40098	4 43 54	+35 45 00	
IRC+40099	4 46 32	+37 24 30	
IRC+40100	4 47 20	+39 20 24	
IRC+40101	4 49 11	+38 25 12	
IRC+40102	4 49 14	+36 37 30	
IRC+40103	4 51 38	+40 40 06	
IRC+40104	4 51 40	+43 20 36	
IRC+40105	4 52 29	+43 25 06	
IRC+40106	4 55 29	+44 37 24	
IRC+40107	4 56 56	+39 35 06	
IRC+40108	4 57 12	+40 09 36	
IRC+40109	4 58 22	+43 45 00	
IRC+40110	4 58 58	+41 01 00	
IRC+40111	5 02 39	+44 48 00	
IRC+40112	5 02 55	+38 39 54	
IRC+40113	5 03 10	+35 19 36	
IRC+40114	5 05 14	+42 31 00	
IRC+40115	5 05 38	+38 56 12	
IRC+40116	5 06 23	+44 16 54	
IRC+40117	5 06 54	+37 14 30	
IRC+40118	5 11 42	+40 04 42	
IRC+40119	5 14 41	+42 44 36	
IRC+40120	5 15 52	+35 45 12	
IRC+40121	5 16 49	+35 44 36	
IRC+40122	5 17 36	+35 02 42	
IRC+40123	5 19 13	+38 49 36	
IRC+40124	5 19 13	+36 30 06	
IRC+40125	5 21 16	+37 20 42	
IRC+40126	5 21 22	+36 10 00	
IRC+40127	5 23 31	+36 51 36	
IRC+40128	5 23 36	+35 25 24	
IRC+40129	5 24 42	+43 50 36	
IRC+40130	5 25 32	+39 00 00	
IRC+40131	5 28 00	+38 16 42	
IRC+40132	5 29 03	+41 26 00	
IRC+40133	5 30 46	+41 05 42	
IRC+40134	5 32 42	+37 59 54	
IRC+40135	5 36 44	+37 36 36	
IRC+40136	5 38 27	+38 54 42	
IRC+40137	5 40 49	+37 58 36	
IRC+40138	5 41 56	+35 41 00	
IRC+40139	5 42 22	+37 38 24	
IRC+40140	5 44 03	+43 11 36	
IRC+40141	5 45 05	+44 53 36	
IRC+40142	5 45 44	+39 10 06	
IRC+40143	5 47 40	+37 17 54	
IRC+40144	5 48 01	+39 08 00	
IRC+40145	5 50 53	+39 30 06	
IRC+40146	5 53 32	+35 34 30	
IRC+40147	5 54 58	+43 29 30	
IRC+40148	5 55 51	+44 56 42	
IRC+40149	5 55 58	+38 26 12	
IRC+40150	5 56 20	+37 12 42	
IRC+40151	5 57 38	+39 40 24	
IRC+40152	6 02 08	+44 41 42	
IRC+40153	6 11 48	+39 57 42	
IRC+40154	6 14 17	+39 29 12	
IRC+40155	6 14 43	+35 37 36	

NAME	RA (1950) h m s	DEC ° ' "	POS REF
IRC+40156	6 29 45	+40 44 54	
IRC+40157	6 31 08	+42 32 06	
IRC+40158	6 33 07	+38 28 42	
IRC+40159	6 35 11	+39 26 06	
IRC+40160	6 35 44	+42 32 12	
IRC+40161	6 39 27	+44 34 36	
IRC+40162	6 40 48	+40 40 24	
IRC+40163	6 41 31	+36 52 42	
IRC+40164	6 46 24	+37 34 00	
IRC+40165	6 47 17	+41 50 24	
IRC+40166	6 49 42	+35 51 00	
IRC+40167	6 53 58	+37 27 30	
IRC+40168	6 55 38	+38 06 42	
IRC+40169	6 59 55	+44 58 36	
IRC+40170	7 08 15	+39 24 00	
IRC+40171	7 14 32	+39 11 54	
IRC+40172	7 15 00	+38 08 30	
IRC+40173	7 17 03	+42 39 42	
IRC+40174	7 18 43	+36 50 54	
IRC+40175	7 20 40	+40 46 12	
IRC+40176	7 21 11	+37 41 36	
IRC+40177	7 25 05	+41 04 36	
IRC+40178	7 25 39	+40 47 00	
IRC+40179	7 28 46	+35 42 42	
IRC+40180	7 33 54	+40 08 12	
IRC+40181	7 34 45	+38 22 06	
IRC+40182	7 36 08	+36 54 42	
IRC+40183	7 36 55	+38 28 00	
IRC+40184	7 40 46	+38 57 00	
IRC+40185	7 42 04	+42 12 42	
IRC+40186	7 43 22	+37 38 24	
IRC+40187	7 46 47	+39 53 30	
IRC+40188	7 47 57	+37 13 12	
IRC+40189	7 48 52	+36 17 54	
IRC+40190	7 56 34	+36 13 12	
IRC+40191	7 58 40	+35 32 54	
IRC+40192	8 00 23	+36 29 00	
IRC+40193	8 11 34	+37 49 06	
IRC+40194	8 17 59	+35 29 42	
IRC+40195	8 19 26	+43 21 00	
IRC+40196	8 21 20	+42 09 54	
IRC+40197	8 48 37	+43 55 06	
IRC+40198	8 53 57	+41 31 54	
IRC+40199	8 57 21	+37 47 54	
IRC+40200	8 57 23	+41 58 06	
IRC+40201	9 00 37	+38 56 42	
IRC+40202	9 03 22	+38 39 30	
IRC+40203	9 06 38	+38 53 06	
IRC+40204	9 12 35	+44 54 30	
IRC+40205	9 25 30	+36 22 54	
IRC+40206	9 27 43	+44 54 00	
IRC+40207	9 28 30	+35 19 12	
IRC+40208	9 31 10	+36 37 12	
IRC+40209	9 31 58	+39 50 12	
IRC+40210	9 46 29	+36 58 54	
IRC+40211	9 47 11	+39 51 42	
IRC+40212	9 49 31	+35 45 42	
IRC+40213	9 51 40	+36 19 12	
IRC+40214	10 00 26	+41 32 30	
IRC+40215	10 02 29	+43 04 36	
IRC+40216	10 08 16	+37 38 24	
IRC+40217	10 14 20	+41 43 00	
IRC+40218	10 19 21	+41 45 06	
IRC+40219	10 24 59	+36 57 30	
IRC+40220	10 45 46	+36 33 36	
IRC+40221	10 56 46	+36 21 30	
IRC+40222	11 06 34	+36 35 00	
IRC+40223	11 06 50	+43 28 30	
IRC+40224	11 06 52	+44 46 00	
IRC+40225	11 20 06	+43 45 06	
IRC+40226	11 32 51	+35 08 24	
IRC+40227	11 43 02	+36 10 12	
IRC+40228	11 44 37	+43 44 42	
IRC+40229	11 52 03	+37 25 12	
IRC+40230	11 52 40	+37 01 36	
IRC+40231	12 12 07	+39 37 00	
IRC+40232	12 13 38	+40 56 24	
IRC+40233	12 21 25	+40 59 30	
IRC+40234	12 23 23	+39 17 06	
IRC+40235	12 29 32	+43 44 54	
IRC+40236	12 31 21	+41 37 42	
IRC+40237	12 41 10	+41 31 54	
IRC+40238	12 44 57	+38 38 24	
IRC+40239	12 53 41	+38 35 06	
IRC+40240	13 01 37	+43 16 36	
IRC+40241	13 11 19	+37 09 12	
IRC+40242	13 11 28	+40 25 06	
IRC+40243	13 12 58	+42 31 36	
IRC+40244	13 18 04	+40 24 54	
IRC+40245	13 21 38	+37 17 24	
IRC+40246	13 29 04	+36 44 42	
IRC+40247	13 35 30	+42 27 12	
IRC+40248	13 46 49	+39 47 36	
IRC+40249	13 49 39	+39 55 00	
IRC+40250	13 51 02	+40 35 12	
IRC+40251	13 57 25	+37 26 24	
IRC+40252	13 58 13	+38 06 12	
IRC+40253	14 05 55	+44 05 00	
IRC+40254	14 12 04	+35 50 00	
IRC+40255	14 15 52	+35 44 42	
IRC+40256	14 19 47	+44 13 06	
IRC+40257	14 27 44	+39 05 00	
IRC+40258	14 30 05	+38 31 42	
IRC+40259	14 32 37	+36 50 06	
IRC+40260	14 36 17	+43 51 00	
IRC+40261	14 41 48	+40 40 30	
IRC+40262	14 48 31	+37 28 42	
IRC+40263	15 00 04	+40 35 06	
IRC+40264	15 12 21	+42 21 06	
IRC+40265	15 15 19	+36 32 36	
IRC+40266	15 20 45	+39 45 30	
IRC+40267	15 29 06	+41 00 12	
IRC+40268	15 33 23	+39 10 30	
IRC+40269	15 34 34	+37 32 30	
IRC+40270	15 37 47	+42 51 12	
IRC+40271	15 39 35	+38 42 54	
IRC+40272	15 44 53	+38 28 24	
IRC+40273	15 47 43	+39 43 12	
IRC+40274	15 49 21	+35 48 30	
IRC+40275	15 52 56	+43 16 54	
IRC+40276	15 56 38	+36 09 30	
IRC+40277	15 57 07	+36 46 42	
IRC+40278	16 07 08	+36 37 06	
IRC+40279	16 09 56	+41 57 54	
IRC+40280	16 09 59	+36 33 00	
IRC+40281	16 10 08	+42 30 00	
IRC+40282	16 18 29	+37 05 54	
IRC+40283	16 27 01	+41 59 24	
IRC+40284	16 29 10	+35 19 30	
IRC+40285	16 33 29	+37 27 00	
IRC+40286	16 34 43	+36 08 00	
IRC+40287	16 41 12	+39 00 42	
IRC+40288	16 43 36	+43 18 30	
IRC+40289	16 45 44	+42 19 42	
IRC+40290	17 01 44	+35 28 54	
IRC+40291	17 07 55	+40 50 30	
IRC+40292	17 08 41	+40 45 06	
IRC+40293	17 12 40	+36 25 54	
IRC+40294	17 12 45	+39 10 36	
IRC+40295	17 13 17	+36 51 36	
IRC+40296	17 17 02	+41 35 36	
IRC+40297	17 17 11	+43 39 36	
IRC+40298	17 34 21	+35 25 12	
IRC+40299	17 40 07	+40 00 30	
IRC+40300	17 41 37	+44 06 42	
IRC+40301	17 45 07	+36 06 06	
IRC+40302	17 46 12	+36 34 24	
IRC+40303	17 50 27	+40 00 00	
IRC+40304	17 51 02	+38 49 42	
IRC+40305	17 51 40	+40 01 00	
IRC+40306	17 54 31	+37 15 12	
IRC+40307	18 02 17	+41 21 30	
IRC+40308	18 05 17	+43 26 42	
IRC+40309	18 06 01	+43 27 30	
IRC+40310	18 06 17	+41 42 36	
IRC+40311	18 06 18	+36 23 12	
IRC+40312	18 06 26	+42 13 00	
IRC+40313	18 18 05	+36 02 36	
IRC+40314	18 22 15	+38 42 00	
IRC+40315	18 22 16	+39 33 36	
IRC+40316	18 22 29	+43 52 54	
IRC+40317	18 23 46	+39 02 24	
IRC+40318	18 27 26	+41 01 42	
IRC+40319	18 28 50	+36 12 36	
IRC+40320	18 29 10	+38 36 06	
IRC+40321	18 30 35	+36 57 42	
IRC+40322	18 35 13	+38 44 12	
IRC+40323	18 36 28	+39 38 00	
IRC+40324	18 38 20	+40 17 12	
IRC+40325	18 41 06	+36 54 30	
IRC+40326	18 41 36	+39 14 54	
IRC+40327	18 42 24	+38 28 30	
IRC+40328	18 43 40	+43 34 54	
IRC+40329	18 51 40	+40 55 54	
IRC+40330	18 51 54	+42 50 12	
IRC+40331	18 52 44	+36 49 54	
IRC+40332	18 52 57	+42 27 36	
IRC+40333	18 53 17	+41 32 06	
IRC+40334	18 53 47	+43 52 54	
IRC+40335	18 57 45	+41 33 36	
IRC+40336	18 58 41	+40 37 06	
IRC+40337	19 02 23	+40 02 30	
IRC+40338	19 06 32	+39 04 36	
IRC+40339	19 10 40	+41 10 12	
IRC+40340	19 13 19	+40 17 30	
IRC+40341	19 14 36	+38 02 42	
IRC+40342	19 15 28	+38 56 12	
IRC+40343	19 15 50	+37 31 30	
IRC+40344	19 18 10	+40 41 42	
IRC+40345	19 18 22	+37 47 06	
IRC+40346	19 23 10	+35 55 36	
IRC+40347	19 24 10	+36 05 12	
IRC+40348	19 29 40	+43 31 42	
IRC+40349	19 31 07	+36 43 54	
IRC+40350	19 31 14	+43 19 12	
IRC+40351	19 31 32	+43 34 30	
IRC+40352	19 35 34	+43 07 06	
IRC+40353	19 37 03	+37 53 30	
IRC+40354	19 37 48	+43 08 30	
IRC+40355	19 38 29	+43 47 00	
IRC+40356	19 39 05	+42 57 30	
IRC+40357	19 39 10	+36 36 36	
IRC+40358	19 39 51	+40 02 36	
IRC+40359	19 40 05	+42 05 36	
IRC+40360	19 42 04	+41 38 42	
IRC+40361	19 42 28	+37 13 54	
IRC+40362	19 43 07	+40 36 06	
IRC+40363	19 43 46	+42 24 36	
IRC+40364	19 48 47	+38 35 42	
IRC+40365	19 48 59	+37 41 54	
IRC+40366	19 50 25	+36 18 30	
IRC+40367	19 54 52	+40 16 00	
IRC+40368	19 55 36	+44 07 54	
IRC+40369	19 56 29	+42 23 06	
IRC+40370	19 58 38	+36 59 24	
IRC+40371	19 58 39	+36 38 12	
IRC+40372	19 58 50	+40 02 42	
IRC+40373	19 59 43	+43 04 30	
IRC+40374	20 00 02	+44 35 42	
IRC+40375	20 00 08	+43 58 42	
IRC+40376	20 01 41	+35 48 30	
IRC+40377	20 01 52	+35 11 00	
IRC+40378	20 01 59	+44 34 24	
IRC+40379	20 02 37	+40 18 06	
IRC+40380	20 02 38	+36 40 12	
IRC+40381	20 03 20	+44 40 24	
IRC+40382	20 03 33	+41 25 00	
IRC+40383	20 05 37	+36 25 00	
IRC+40384	20 06 05	+41 30 42	
IRC+40385	20 06 19	+36 31 36	
IRC+40386	20 06 22	+41 45 30	
IRC+40387	20 06 53	+36 00 06	
IRC+40388	20 07 19	+36 47 00	
IRC+40389	20 08 01	+41 21 24	
IRC+40390	20 08 14	+36 07 24	
IRC+40391	20 08 31	+35 47 54	
IRC+40392	20 09 05	+36 25 30	
IRC+40393	20 09 14	+35 58 06	
IRC+40394	20 09 32	+35 33 42	
IRC+40395	20 11 29	+41 18 06	
IRC+40396	20 11 31	+37 35 36	
IRC+40397	20 11 34	+38 34 12	
IRC+40398	20 12 01	+43 13 24	
IRC+40399	20 12 03	+44 27 54	
IRC+40400	20 12 08	+39 14 42	
IRC+40401	20 15 08	+40 13 00	
IRC+40402	20 15 46	+42 33 36	
IRC+40403	20 16 44	+37 17 54	
IRC+40404	20 17 08	+38 50 36	
IRC+40405	20 17 29	+36 34 24	
IRC+40406	20 19 21	+35 27 36	
IRC+40407	20 19 26	+38 02 42	
IRC+40408	20 19 29	+36 46 36	
IRC+40409	20 19 47	+37 22 06	
IRC+40410	20 19 48	+40 17 30	
IRC+40411	20 20 28	+40 06 00	
IRC+40412	20 20 59	+40 52 00	
IRC+40413	20 21 14	+36 41 54	
IRC+40414	20 23 36	+40 42 36	
IRC+40415	20 24 07	+38 11 00	
IRC+40416	20 24 16	+40 58 24	
IRC+40417	20 24 53	+38 05 12	
IRC+40418	20 25 16	+36 23 12	
IRC+40419	20 25 35	+35 56 24	
IRC+40420	20 25 36	+40 55 00	
IRC+40421	20 25 40	+35 23 06	
IRC+40422	20 26 37	+37 37 06	
IRC+40423	20 26 43	+41 42 42	
IRC+40424	20 27 00	+39 49 12	
IRC+40425	20 28 35	+36 41 30	
IRC+40426	20 28 55	+44 45 30	
IRC+40427	20 29 41	+40 29 06	
IRC+40428	20 29 47	+39 42 36	
IRC+40429	20 30 14	+35 17 12	
IRC+40430	20 30 49	+41 04 42	
IRC+40431	20 31 07	+40 35 06	
IRC+40432	20 31 50	+38 30 00	
IRC+40433	20 31 57	+35 05 00	
IRC+40434	20 32 14	+42 15 12	
IRC+40435	20 35 03	+37 42 06	
IRC+40436	20 35 39	+36 40 12	
IRC+40437	20 36 58	+37 42 42	
IRC+40438	20 37 15	+44 55 06	
IRC+40439	20 37 43	+39 01 30	
IRC+40440	20 39 24	+40 55 42	
IRC+40441	20 40 39	+38 31 30	
IRC+40442	20 41 36	+43 01 00	
IRC+40443	20 41 46	+37 58 54	
IRC+40444	20 41 59	+44 17 36	
IRC+40445	20 43 07	+40 14 06	
IRC+40446	20 43 28	+42 09 00	
IRC+40447	20 44 20	+44 41 42	
IRC+40448	20 44 33	+39 56 06	
IRC+40448	20 44 33.0	+39 56 06	
IRC+40449	20 45 02	+39 41 30	
IRC+40450	20 45 35	+35 41 54	
IRC+40451	20 46 53	+40 49 00	
IRC+40452	20 47 14	+35 22 42	
IRC+40453	20 47 53	+38 21 54	
IRC+40454	20 48 10	+37 18 54	
IRC+40455	20 48 38	+36 52 42	
IRC+40456	20 48 49	+39 38 12	
IRC+40457	20 51 23	+39 15 12	
IRC+40458	20 56 06	+44 35 30	
IRC+40459	20 57 23	+36 33 30	
IRC+40460	21 00 02	+40 15 06	
IRC+40461	21 00 05	+35 07 06	
IRC+40462	21 00 21	+44 12 36	
IRC+40463	21 00 26	+39 18 30	
IRC+40464	21 00 35	+44 35 36	
IRC+40465	21 02 19	+37 38 42	
IRC+40466	21 02 43	+37 04 36	
IRC+40467	21 02 44	+42 14 24	
IRC+40468	21 03 05	+43 43 36	
IRC+40469	21 04 44	+38 31 06	
IRC+40470	21 05 01	+37 35 06	
IRC+40471	21 05 10	+38 22 00	
IRC+40472	21 08 24	+39 28 24	
IRC+40473	21 08 58	+43 59 12	
IRC+40474	21 09 41	+39 49 54	
IRC+40475	21 12 47	+37 49 54	
IRC+40476	21 14 49	+36 37 36	
IRC+40477	21 14 57	+40 50 54	
IRC+40478	21 20 35	+42 10 30	
IRC+40479	21 20 53	+40 43 12	
IRC+40480	21 21 06	+35 01 54	
IRC+40481	21 24 11	+39 58 30	
IRC+40482	21 24 12	+35 37 36	
IRC+40483	21 25 23	+36 29 00	
IRC+40484	21 31 20	+43 41 36	
IRC+40485	21 32 05	+38 51 00	
IRC+40486	21 32 45	+38 18 06	
IRC+40487	21 37 37	+44 57 24	
IRC+40488	21 38 13	+43 02 42	
IRC+40489	21 39 56	+35 17 12	
IRC+40490	21 41 06	+40 55 24	
IRC+40491	21 41 11	+37 46 54	
IRC+40492	21 42 46	+43 11 30	
IRC+40493	21 44 40	+37 25 24	
IRC+40494	21 45 59	+36 21 00	
IRC+40495	21 46 08	+42 06 24	
IRC+40496	21 46 41	+44 00 42	
IRC+40497	21 46 47	+39 42 54	
IRC+40498	21 55 09	+39 40 54	
IRC+40499	21 56 52	+35 22 30	
IRC+40500	22 00 03	+36 45 00	
IRC+40501	22 03 29	+35 06 00	
IRC+40502	22 03 59	+44 46 24	
IRC+40503	22 05 20	+37 29 54	
IRC+40504	22 09 37	+38 10 00	
IRC+40505	22 10 29	+38 18 42	
IRC+40506	22 11 43	+39 28 12	
IRC+40507	22 13 48	+37 30 06	
IRC+40508	22 22 13	+36 05 24	

NAME	RA (1950)	DEC	POS REF
	h m s	° ′ ″	
IRC+40509	22 24 48	+44 30 06	
IRC+40510	22 25 57	+43 51 54	
IRC+40511	22 26 01	+35 18 06	
IRC+40512	22 26 50	+40 04 24	
IRC+40513	22 28 10	+37 17 06	
IRC+40514	22 33 50	+36 30 30	
IRC+40515	22 37 53	+40 24 42	
IRC+40516	22 38 19	+44 00 42	
IRC+40517	22 38 46	+36 00 36	
IRC+40518	22 39 32	+42 17 00	
IRC+40519	22 41 49	+39 12 12	
IRC+40520	22 41 51	+41 33 30	
IRC+40521	22 42 38	+38 56 06	
IRC+40522	22 47 41	+40 47 42	
IRC+40523	22 49 46	+43 02 42	
IRC+40524	22 50 38	+38 21 12	
IRC+40525	22 51 04	+36 14 12	
IRC+40526	22 55 07	+42 44 42	
IRC+40527	22 57 56	+35 38 36	
IRC+40528	23 01 21	+37 34 54	
IRC+40529	23 03 49	+36 03 42	
IRC+40530	23 07 51	+39 55 42	
IRC+40531	23 12 23	+40 31 36	
IRC+40532	23 13 59	+36 47 36	
IRC+40533	23 15 28	+40 35 06	
IRC+40534	23 17 29	+41 48 36	
IRC+40535	23 18 13	+39 20 36	
IRC+40536	23 21 16	+39 27 24	
IRC+40537	23 21 46	+41 20 12	
IRC+40538	23 27 10	+38 22 12	
IRC+40539	23 28 50	+38 57 30	
IRC+40540	23 32 01	+43 16 30	
IRC+40541	23 32 18	+37 44 42	
IRC+40542	23 38 13	+44 31 36	
IRC+40543	23 39 45	+44 42 36	
IRC+40544	23 42 08	+41 47 12	
IRC+40545	23 42 34	+43 38 30	
IRC+40546	23 49 35	+37 34 00	
IRC+40547	23 50 29	+41 04 42	
IRC+40548	23 58 27	+38 13 30	
IRC+50001	0 07 31	+54 35 54	
IRC+50002	0 09 25	+47 53 06	
IRC+50003	0 13 28	+46 44 12	
IRC+50004	0 14 13	+49 11 00	
IRC+50005	0 18 45	+50 40 06	
IRC+50006	0 20 31	+51 29 42	
IRC+50007	0 26 14	+48 08 06	
IRC+50008	0 28 55	+52 33 42	
IRC+50009	0 30 02	+50 53 24	
IRC+50010	0 34 01	+48 40 36	
IRC+50011	0 34 34	+53 25 30	
IRC+50012	0 34 50	+45 19 54	
IRC+50013	0 36 22	+49 04 36	
IRC+50014	0 43 31	+47 58 24	
IRC+50015	0 45 19	+53 16 54	
IRC+50016	0 49 53	+47 08 36	
IRC+50017	0 50 01	+49 26 06	
IRC+50018	0 50 38	+52 25 00	
IRC+50019	0 50 40	+48 15 06	
IRC+50020	0 52 13	+48 24 06	
IRC+50021	0 54 10	+48 25 42	
IRC+50022	0 57 58	+46 39 36	
IRC+50023	1 00 13	+52 52 00	
IRC+50024	1 00 20	+45 36 06	
IRC+50025	1 01 08	+52 14 06	
IRC+50026	1 03 10	+49 35 06	
IRC+50027	1 04 07	+53 14 00	
IRC+50028	1 04 11	+49 08 36	
IRC+50029	1 04 32	+45 20 30	
IRC+50030	1 08 04	+53 28 00	
IRC+50031	1 08 16	+45 56 00	
IRC+50032	1 09 38	+45 04 00	
IRC+50033	1 19 20	+45 16 12	
IRC+50034	1 19 29	+51 31 24	
IRC+50035	1 23 30	+54 53 54	
IRC+50036	1 25 34	+51 25 42	
IRC+50037	1 26 35	+46 24 12	
IRC+50038	1 27 02	+46 45 12	
IRC+50039	1 30 14	+54 41 24	
IRC+50040	1 30 32	+46 15 54	
IRC+50041	1 34 55	+48 22 24	
IRC+50042	1 37 02	+53 36 30	
IRC+50043	1 40 03	+48 16 12	
IRC+50044	1 40 27	+51 16 30	
IRC+50045	1 41 24	+45 53 24	
IRC+50046	1 47 16	+53 29 42	
IRC+50047	1 50 33	+53 59 54	
IRC+50048	1 51 33	+50 03 00	
IRC+50049	1 55 35	+45 11 42	
IRC+50050	1 56 16	+54 34 24	
IRC+50051	1 56 24	+45 54 54	
IRC+50052	1 59 46	+54 59 36	
IRC+50053	2 00 54	+49 28 24	
IRC+50054	2 05 23	+51 34 12	
IRC+50055	2 07 46	+48 42 54	
IRC+50056	2 10 11	+52 49 30	
IRC+50057	2 14 04	+48 15 00	
IRC+50058	2 15 51	+51 02 06	
IRC+50059	2 21 04	+49 47 42	
IRC+50060	2 22 15	+50 03 42	
IRC+50061	2 23 28	+51 53 54	
IRC+50062	2 25 03	+51 03 24	
IRC+50063	2 25 21	+48 17 30	
IRC+50064	2 25 23	+47 39 24	
IRC+50065	2 27 07	+47 38 30	
IRC+50066	2 28 43	+49 58 06	
IRC+50067	2 28 59	+54 04 54	
IRC+50068	2 30 16	+45 26 06	
IRC+50069	2 32 38	+53 16 06	
IRC+50070	2 34 47	+50 17 24	
IRC+50071	2 36 49	+51 55 54	
IRC+50072	2 40 48	+49 01 24	
IRC+50073	2 43 55	+45 51 00	
IRC+50074	2 44 17	+52 06 54	
IRC+50075	2 47 19	+51 52 30	
IRC+50076	2 48 52	+53 48 24	
IRC+50077	2 50 41	+52 33 36	
IRC+50078	2 51 41	+46 35 12	
IRC+50079	2 53 17	+51 04 30	
IRC+50080	2 53 19	+54 26 24	
IRC+50081	2 57 02	+48 25 00	
IRC+50082	2 58 54	+47 54 24	
IRC+50083	3 00 13	+48 02 54	
IRC+50084	3 01 08	+53 18 54	
IRC+50085	3 01 31	+52 26 06	
IRC+50086	3 05 28	+49 25 12	
IRC+50087	3 08 59	+47 32 06	
IRC+50088	3 10 14	+47 39 00	
IRC+50089	3 11 25	+54 41 54	
IRC+50090	3 11 48	+46 24 00	
IRC+50091	3 12 38	+50 45 42	
IRC+50092	3 12 41	+45 09 42	
IRC+50093	3 15 40	+51 14 24	
IRC+50094	3 17 10	+46 30 24	
IRC+50095	3 20 44	+49 41 24	
IRC+50096	3 22 59	+47 21 30	
IRC+50097	3 25 38	+48 35 30	
IRC+50098	3 27 01	+47 49 54	
IRC+50099	3 32 39	+52 46 06	
IRC+50100	3 37 48	+51 20 54	
IRC+50101	3 40 31	+48 22 12	
IRC+50102	3 41 31	+48 51 00	
IRC+50103	3 42 19	+53 44 54	
IRC+50104	3 43 20	+52 54 42	
IRC+50105	3 43 22	+52 31 06	
IRC+50106	3 44 58	+50 42 06	
IRC+50107	3 45 14	+53 01 30	
IRC+50108	3 45 51	+50 55 36	
IRC+50109	3 46 37	+48 34 42	
IRC+50110	4 11 14	+48 16 54	
IRC+50111	4 11 18	+53 35 12	
IRC+50112	4 11 23	+52 50 12	
IRC+50113	4 11 27	+46 42 30	
IRC+50114	4 11 57	+48 03 06	
IRC+50115	4 12 48	+50 30 24	
IRC+50116	4 13 26	+50 45 12	
IRC+50117	4 14 45	+49 44 54	
IRC+50118	4 19 02	+47 32 54	
IRC+50119	4 26 32	+45 50 42	
IRC+50120	4 29 24	+52 42 06	
IRC+50121	4 29 47	+48 36 42	
IRC+50122	4 30 34	+47 08 06	
IRC+50123	4 32 07	+45 06 54	
IRC+50124	4 35 56	+52 58 54	
IRC+50125	4 40 26	+48 40 12	
IRC+50126	4 44 01	+45 54 00	
IRC+50127	4 44 25	+47 33 06	
IRC+50128	4 46 48	+50 19 36	
IRC+50129	4 47 11	+52 09 06	
IRC+50130	4 50 25	+49 49 06	
IRC+50131	4 52 04	+46 00 30	
IRC+50132	4 54 19	+48 29 06	
IRC+50133	4 55 46	+53 04 54	
IRC+50134	4 59 29	+47 05 24	
IRC+50135	4 59 30	+50 33 36	
IRC+50136	5 01 54	+53 48 42	
IRC+50137	5 07 19.7	+52 48 53	
IRC+50137	5 07 20	+52 48 42	
IRC+50138	5 12 07	+49 29 30	
IRC+50139	5 12 58	+45 56 24	
IRC+50140	5 13 11	+47 24 24	
IRC+50141	5 13 16	+53 31 30	
IRC+50142	5 19 27	+46 58 12	
IRC+50143	5 19 39	+50 11 00	
IRC+50144	5 23 10	+50 05 00	
IRC+50145	5 23 46	+48 40 36	
IRC+50146	5 24 04	+48 11 54	
IRC+50147	5 31 31	+54 52 54	
IRC+50148	5 32 29	+54 24 00	
IRC+50149	5 36 08	+46 43 42	
IRC+50150	5 37 40	+51 38 30	
IRC+50151	5 46 49	+47 26 30	
IRC+50152	5 51 32	+53 27 06	
IRC+50153	5 53 22	+45 30 36	
IRC+50154	5 53 35	+48 22 36	
IRC+50155	5 55 26	+54 17 06	
IRC+50156	5 56 14	+45 56 06	
IRC+50157	5 57 53	+48 57 36	
IRC+50158	5 59 47	+50 37 00	
IRC+50159	6 06 07	+46 34 36	
IRC+50160	6 06 34	+47 44 36	
IRC+50161	6 11 14	+53 35 30	
IRC+50162	6 17 34	+52 32 54	
IRC+50163	6 20 26	+51 05 30	
IRC+50164	6 21 02	+49 18 54	
IRC+50165	6 23 41	+46 18 00	
IRC+50166	6 23 43	+53 44 00	
IRC+50167	6 26 20	+46 43 00	
IRC+50168	6 29 05	+46 56 30	
IRC+50169	6 29 35	+47 14 36	
IRC+50170	6 31 55	+45 39 54	
IRC+50171	6 34 08	+51 14 54	
IRC+50172	6 43 50	+48 50 30	
IRC+50173	6 53 22	+47 39 54	
IRC+50174	7 08 08	+49 52 12	
IRC+50175	7 09 29	+51 30 42	
IRC+50176	7 10 43	+46 30 12	
IRC+50177	7 14 29	+48 36 42	
IRC+50178	7 20 45	+47 16 36	
IRC+50179	7 21 05	+51 58 54	
IRC+50180	7 24 34	+46 06 30	
IRC+50181	7 24 59	+48 01 24	
IRC+50182	7 27 19	+50 09 06	
IRC+50183	7 30 31	+46 15 42	
IRC+50184	7 32 56	+46 17 54	
IRC+50185	7 42 25	+51 08 54	
IRC+50186	7 51 03	+47 41 06	
IRC+50187	8 02 09	+51 49 54	
IRC+50188	8 09 57	+47 24 06	
IRC+50189	8 12 37	+46 56 54	
IRC+50190	8 14 27	+54 17 36	
IRC+50191	8 21 54	+52 26 30	
IRC+50192	8 33 07	+49 32 42	
IRC+50193	8 37 35	+46 00 12	
IRC+50194	8 55 49	+48 14 06	
IRC+50195	9 18 26	+53 51 00	
IRC+50196	9 23 32	+49 54 12	
IRC+50197	9 25 37	+50 15 30	
IRC+50198	9 29 29	+51 53 42	
IRC+50199	9 39 23	+51 29 24	
IRC+50200	9 40 42	+53 59 12	
IRC+50201	9 46 11	+53 47 00	
IRC+50202	9 53 01	+54 28 30	
IRC+50203	10 17 34	+49 21 12	
IRC+50204	10 35 59	+53 55 42	
IRC+50205	10 50 32	+54 51 00	
IRC+50206	10 57 23	+45 47 42	
IRC+50207	11 02 55	+54 06 54	
IRC+50208	11 04 45	+49 26 42	
IRC+50209	11 06 23	+51 39 00	
IRC+50210	11 21 50	+48 52 54	
IRC+50211	11 25 08	+45 27 30	
IRC+50212	11 26 00	+49 49 54	
IRC+50213	11 43 26	+48 03 00	
IRC+50214	11 48 13	+51 41 36	
IRC+50215	11 51 07	+53 57 54	
IRC+50216	12 14 58	+53 27 30	
IRC+50217	12 17 21	+49 15 30	
IRC+50218	12 21 37	+51 50 24	
IRC+50219	12 42 46	+45 42 42	
IRC+50220	12 44 18	+47 38 42	
IRC+50221	12 51 01	+46 55 30	
IRC+50222	12 52 39	+47 28 06	
IRC+50223	13 00 28	+45 39 00	
IRC+50224	13 03 37	+45 31 42	
IRC+50225	13 08 07	+47 18 12	
IRC+50226	13 17 14	+45 47 00	
IRC+50227	13 20 57	+47 15 42	
IRC+50228	13 28 03	+45 59 36	
IRC+50229	13 35 15	+52 50 24	
IRC+50230	13 35 41	+50 58 12	
IRC+50231	13 38 49	+54 55 54	
IRC+50232	13 45 10	+47 59 00	
IRC+50233	13 45 33	+49 33 36	
IRC+50234	13 51 27	+52 34 00	
IRC+50235	13 56 46	+46 50 12	
IRC+50236	13 57 08	+45 43 00	
IRC+50237	14 06 26	+49 41 36	
IRC+50238	14 23 30	+52 04 42	
IRC+50239	14 32 53	+49 35 06	
IRC+50240	15 04 53	+54 45 36	
IRC+50241	15 08 01	+53 30 24	
IRC+50242	15 09 59	+50 05 30	
IRC+50243	15 16 32	+45 48 00	
IRC+50244	15 26 32	+53 11 00	
IRC+50245	15 37 23	+47 05 06	
IRC+50246	15 49 18	+48 37 54	
IRC+50247	16 00 48	+53 03 12	
IRC+50248	16 01 08	+47 22 24	
IRC+50249	16 05 20	+48 50 06	
IRC+50250	16 11 37	+48 13 24	
IRC+50251	16 17 47	+49 09 06	
IRC+50252	16 24 46	+47 56 00	
IRC+50253	16 37 20	+49 00 24	
IRC+50254	16 41 19	+48 30 24	
IRC+50255	16 41 50	+54 59 42	
IRC+50256	16 51 55	+47 29 30	
IRC+50257	16 52 27	+49 02 24	
IRC+50258	16 53 33	+46 21 24	
IRC+50259	16 54 50	+50 06 42	
IRC+50260	16 54 59	+53 30 00	
IRC+50261	16 58 36	+52 23 30	
IRC+50262	17 10 13	+45 23 00	
IRC+50263	17 13 02	+45 14 42	
IRC+50264	17 18 56	+46 17 42	
IRC+50265	17 20 41	+53 28 06	
IRC+50266	17 29 15	+52 20 30	
IRC+50267	17 32 55	+53 59 30	
IRC+50268	17 34 17	+48 51 12	
IRC+50269	17 35 19	+48 36 30	
IRC+50270	17 35 58	+45 56 24	
IRC+50271	17 37 52	+46 11 06	
IRC+50272	17 47 22	+45 43 06	
IRC+50273	17 55 22	+45 21 36	
IRC+50274	17 55 25	+51 29 42	
IRC+50275	17 58 17	+51 50 42	
IRC+50276	17 58 29	+45 30 24	
IRC+50277	18 10 13	+47 38 36	
IRC+50278	18 19 43	+50 29 54	
IRC+50279	18 20 17	+49 05 36	
IRC+50280	18 26 25	+49 16 06	
IRC+50281	18 32 50	+52 19 24	
IRC+50282	18 33 23	+51 44 24	
IRC+50283	18 39 02	+46 02 42	
IRC+50284	18 47 45	+47 27 30	
IRC+50285	18 49 49	+46 40 42	
IRC+50286	18 51 59	+50 38 30	
IRC+50287	18 59 34	+46 25 24	
IRC+50288	19 07 17	+52 20 30	
IRC+50289	19 11 47	+46 53 54	
IRC+50290	19 14 45	+50 04 12	
IRC+50291	19 15 58	+53 16 42	
IRC+50292	19 16 16	+51 15 00	
IRC+50293	19 18 05	+48 52 42	
IRC+50294	19 23 14	+50 08 42	
IRC+50295	19 27 20	+45 56 12	
IRC+50296	19 28 35	+48 53 42	
IRC+50297	19 28 44	+46 02 42	
IRC+50298	19 29 10	+50 31 12	
IRC+50299	19 29 59	+50 11 54	
IRC+50300	19 32 19	+49 09 12	
IRC+50301	19 35 26	+50 05 06	
IRC+50302	19 36 09	+48 40 42	
IRC+50303	19 36 25	+54 50 06	
IRC+50304	19 39 28	+48 40 42	
IRC+50305	19 39 59	+47 12 42	
IRC+50306	19 42 12	+48 39 42	
IRC+50307	19 42 25	+50 56 36	
IRC+50308	19 43 21	+45 00 30	
IRC+50309	19 45 59	+47 46 42	
IRC+50310	19 49 22	+52 51 12	
IRC+50311	19 52 19	+49 27 42	
IRC+50312	19 58 34	+52 00 42	
IRC+50313	19 59 56	+49 57 54	

NAME	RA (1950) h m s	DEC ° ′ ″	POS REF
IRC+50314	20 00 01	+49 54 06	
IRC+50315	20 03 46	+51 41 36	
IRC+50316	20 07 58	+47 43 42	
IRC+50317	20 09 11	+52 13 30	
IRC+50318	20 11 20	+49 18 00	
IRC+50319	20 11 40	+48 41 36	
IRC+50320	20 12 02	+46 35 24	
IRC+50321	20 13 57	+54 00 00	
IRC+50322	20 13 57	+47 33 42	
IRC+50323	20 14 53	+51 02 36	
IRC+50324	20 18 01	+47 44 12	
IRC+50325	20 19 13	+53 25 36	
IRC+50326	20 21 13	+51 51 12	
IRC+50327	20 21 38	+48 40 00	
IRC+50328	20 22 15	+50 01 36	
IRC+50329	20 25 50	+53 40 12	
IRC+50330	20 26 59	+48 45 00	
IRC+50331	20 29 48	+49 03 06	
IRC+50332	20 31 17	+54 46 42	
IRC+50333	20 31 43	+54 17 24	
IRC+50334	20 32 03	+46 49 00	
IRC+50335	20 36 08	+51 24 36	
IRC+50336	20 37 38	+53 21 00	
IRC+50337	20 39 35	+45 06 12	
IRC+50338	20 39 41	+47 57 12	
IRC+50339	20 44 00	+46 01 00	
IRC+50340	20 45 06	+45 52 06	
IRC+50341	20 45 37	+45 23 24	
IRC+50342	20 46 10	+47 39 00	
IRC+50343	20 47 49	+50 20 36	
IRC+50344	20 47 58	+50 35 24	
IRC+50345	20 48 05	+49 56 24	
IRC+50346	20 48 34	+45 13 54	
IRC+50347	20 50 10	+47 10 06	
IRC+50348	20 50 28	+51 06 12	
IRC+50349	20 50 37	+46 35 00	
IRC+50350	20 51 08	+49 40 36	
IRC+50351	20 56 15	+46 16 36	
IRC+50352	20 56 46	+47 27 30	
IRC+50353	20 59 10	+45 11 24	
IRC+50354	20 59 31	+49 56 24	
IRC+50355	21 00 54	+47 49 42	
IRC+50356	21 01 16	+46 17 54	
IRC+50357	21 03 34	+51 36 42	
IRC+50358	21 03 50	+45 48 12	
IRC+50359	21 04 53	+47 27 00	
IRC+50360	21 05 45	+53 12 00	
IRC+50361	21 08 28	+48 30 54	
IRC+50362	21 08 39	+52 38 36	
IRC+50363	21 08 42	+47 26 54	
IRC+50364	21 11 21	+50 25 06	
IRC+50365	21 11 24	+50 13 30	
IRC+50366	21 13 37	+46 12 12	
IRC+50367	21 14 14	+53 49 12	
IRC+50368	21 15 14	+49 46 12	
IRC+50369	21 15 33	+45 29 54	
IRC+50370	21 15 47	+45 51 42	
IRC+50371	21 16 59	+49 52 24	
IRC+50372	21 17 43	+50 35 42	
IRC+50373	21 18 08	+48 55 12	
IRC+50374	21 18 36	+49 08 12	
IRC+50375	21 19 41	+47 57 00	
IRC+50376	21 21 52	+52 19 00	
IRC+50377	21 23 01	+48 48 30	
IRC+50378	21 24 42	+49 29 54	
IRC+50379	21 26 13	+45 34 00	
IRC+50380	21 27 42	+46 44 24	
IRC+50381	21 27 46	+47 08 24	
IRC+50382	21 28 58	+47 27 00	
IRC+50383	21 31 13	+54 05 42	
IRC+50384	21 31 25	+45 38 00	
IRC+50385	21 32 08	+45 22 12	
IRC+50386	21 34 10	+45 09 12	
IRC+50387	21 35 31	+50 50 36	
IRC+50388	21 38 22	+45 13 36	
IRC+50389	21 38 47	+51 31 36	
IRC+50390	21 38 58	+54 05 42	
IRC+50391	21 38 59	+49 36 00	
IRC+50392	21 40 13	+45 32 24	
IRC+50393	21 40 30	+54 35 42	
IRC+50394	21 40 30	+52 50 12	
IRC+50395	21 41 51	+45 24 12	
IRC+50396	21 42 44	+45 06 24	
IRC+50397	21 43 27	+52 02 24	
IRC+50398	21 44 10	+49 42 06	
IRC+50399	21 44 53	+52 19 36	
IRC+50400	21 46 55	+52 40 00	
IRC+50401	21 47 30	+52 11 12	
IRC+50402	21 49 10	+46 22 06	
IRC+50403	21 50 03	+54 51 42	
IRC+50404	21 50 03	+48 12 06	
IRC+50405	21 53 02	+51 14 30	
IRC+50406	21 53 05	+49 56 00	
IRC+50407	21 53 12	+47 59 30	
IRC+50408	21 53 21	+54 14 42	
IRC+50409	21 53 22	+50 15 30	
IRC+50410	21 53 55	+52 17 06	
IRC+50411	21 56 05	+52 38 36	
IRC+50412	21 56 35	+54 19 36	
IRC+50413	21 57 37	+48 17 42	
IRC+50414	21 59 14	+48 17 12	
IRC+50415	21 59 58	+48 29 06	
IRC+50416	22 00 30	+54 28 12	
IRC+50417	22 03 17	+46 30 12	
IRC+50418	22 04 44	+48 13 00	
IRC+50419	22 05 37	+47 29 42	
IRC+50420	22 05 42	+50 43 42	
IRC+50421	22 06 16	+49 32 30	
IRC+50422	22 10 59	+49 07 30	
IRC+50423	22 11 16	+53 22 42	
IRC+50424	22 14 57	+49 50 42	
IRC+50425	22 18 40	+49 08 12	
IRC+50426	22 19 14	+51 04 24	
IRC+50427	22 19 21	+45 23 54	
IRC+50428	22 21 36	+51 58 36	
IRC+50429	22 23 04	+51 00 54	
IRC+50430	22 24 53	+45 09 06	
IRC+50431	22 25 35	+52 59 36	
IRC+50432	22 26 43	+49 52 30	
IRC+50433	22 27 26	+47 27 12	
IRC+50434	22 27 44	+45 34 54	
IRC+50435	22 30 25	+52 57 54	
IRC+50436	22 32 27	+46 42 30	
IRC+50437	22 34 08	+47 59 54	
IRC+50438	22 34 50	+52 21 54	
IRC+50439	22 37 31	+46 48 24	
IRC+50440	22 38 35	+49 44 30	
IRC+50441	22 40 19	+53 38 30	
IRC+50442	22 42 07	+49 08 24	
IRC+50443	22 42 43	+52 15 30	
IRC+50444	22 43 05	+46 56 30	
IRC+50445	22 44 10	+45 57 24	
IRC+50446	22 45 39	+54 54 00	
IRC+50447	22 46 01	+49 19 00	
IRC+50448	22 49 26	+52 04 36	
IRC+50449	22 49 50	+50 42 24	
IRC+50450	22 50 28	+50 26 00	
IRC+50451	22 53 04	+54 55 12	
IRC+50452	22 54 14	+49 27 42	
IRC+50453	22 56 59	+52 22 54	
IRC+50454	22 58 38	+46 14 42	
IRC+50455	22 59 31	+45 37 12	
IRC+50456	22 59 37	+50 35 42	
IRC+50457	23 01 55	+49 47 06	
IRC+50458	23 05 19	+46 07 30	
IRC+50459	23 09 16	+52 36 54	
IRC+50460	23 09 21	+48 44 00	
IRC+50461	23 15 07	+50 33 24	
IRC+50462	23 15 28	+48 44 00	
IRC+50463	23 17 21	+48 23 00	
IRC+50464	23 23 16	+52 42 00	
IRC+50465	23 26 59	+50 57 00	
IRC+50466	23 27 11	+51 24 30	
IRC+50467	23 27 42	+48 51 24	
IRC+50468	23 30 32	+45 51 00	
IRC+50469	23 33 21	+50 59 00	
IRC+50470	23 34 56	+46 50 00	
IRC+50471	23 35 10	+46 11 00	
IRC+50472	23 35 13	+45 49 30	
IRC+50473	23 35 19	+51 57 42	
IRC+50474	23 36 37	+51 58 36	
IRC+50475	23 37 23	+45 09 36	
IRC+50476	23 37 54	+51 47 30	
IRC+50477	23 43 35	+46 08 36	
IRC+50478	23 43 55	+54 12 54	
IRC+50479	23 48 19	+47 13 42	
IRC+50480	23 48 42	+48 41 54	
IRC+50481	23 51 09	+53 18 24	
IRC+50482	23 51 49	+53 03 30	
IRC+50483	23 52 50	+48 21 12	
IRC+50484	23 55 53	+51 06 36	
IRC+60001	0 00 44	+55 24 24	
IRC+60002	0 01 40	+64 52 06	
IRC+60003	0 03 36	+60 47 06	
IRC+60004	0 06 32	+58 52 06	
IRC+60005	0 06 47	+63 40 12	
IRC+60006	0 09 25	+60 59 30	
IRC+60007	0 17 59	+61 35 54	
IRC+60008	0 18 37	+59 40 00	
IRC+60009	0 20 28	+55 30 12	
IRC+60010	0 22 59	+57 41 12	
IRC+60011	0 33 20	+62 24 54	
IRC+60012	0 34 05	+62 50 42	
IRC+60013	0 35 06	+63 36 54	
IRC+60014	0 35 42	+60 02 36	
IRC+60015	0 36 17	+59 24 00	
IRC+60016	0 37 32	+59 13 54	
IRC+60017	0 37 36	+56 15 30	
IRC+60018	0 42 56	+57 46 42	
IRC+60019	0 46 04	+57 33 06	
IRC+60020	0 46 12	+64 39 36	
IRC+60021	0 46 13	+56 48 24	
IRC+60022	0 48 15	+61 32 12	
IRC+60023	0 48 23	+62 39 06	
IRC+60024	0 49 25	+59 27 24	
IRC+60025	0 51 17	+63 17 00	
IRC+60026	0 51 48	+58 17 30	
IRC+60027	0 51 56	+58 42 12	
IRC+60028	0 52 14	+57 00 54	
IRC+60029	0 53 11	+57 43 30	
IRC+60030	0 53 38	+58 53 54	
IRC+60031	0 53 39	+60 27 12	
IRC+60032	0 54 43	+58 08 06	
IRC+60033	0 57 51	+56 20 54	
IRC+60034	0 59 35	+61 35 30	
IRC+60035	1 00 10	+62 48 54	
IRC+60036	1 00 31	+58 38 24	
IRC+60037	1 02 11	+62 06 00	
IRC+60038	1 04 43	+62 22 54	
IRC+60039	1 05 09	+63 18 06	
IRC+60040	1 07 08	+62 15 00	
IRC+60041	1 10 32	+62 41 30	
IRC+60042	1 14 32	+59 02 36	
IRC+60043	1 15 04	+57 32 36	
IRC+60044	1 16 18	+56 04 00	
IRC+60045	1 16 48	+57 15 42	
IRC+60046	1 16 48	+57 59 42	
IRC+60047	1 16 54	+63 45 42	
IRC+60048	1 21 47	+60 48 30	
IRC+60049	1 22 11	+57 22 54	
IRC+60050	1 22 33	+59 58 30	
IRC+60051	1 26 05	+61 30 06	
IRC+60052	1 26 07	+64 47 12	
IRC+60053	1 28 34	+62 04 24	
IRC+60054	1 30 09	+61 18 36	
IRC+60055	1 30 16	+58 03 42	
IRC+60056	1 30 16	+57 29 30	
IRC+60057	1 30 37	+58 58 36	
IRC+60058	1 34 25	+62 31 54	
IRC+60059	1 34 53	+57 43 42	
IRC+60060	1 36 32	+60 39 24	
IRC+60061	1 39 49	+56 15 24	
IRC+60062	1 40 17	+58 33 00	
IRC+60063	1 42 36	+60 45 00	
IRC+60064	1 43 37	+60 07 36	
IRC+60065	1 43 41	+62 19 06	
IRC+60066	1 47 40	+64 36 30	
IRC+60067	1 50 32	+59 54 36	
IRC+60068	1 52 49	+61 57 24	
IRC+60069	1 53 08	+59 01 06	
IRC+60070	1 54 56	+59 01 12	
IRC+60071	1 57 50	+63 54 00	
IRC+60072	1 58 25	+61 39 54	
IRC+60073	2 04 41	+59 01 30	
IRC+60074	2 06 49	+56 19 24	
IRC+60075	2 08 40	+63 56 06	
IRC+60076	2 12 08	+63 00 42	
IRC+60077	2 14 22	+63 38 36	
IRC+60078	2 15 22	+57 11 54	
IRC+60079	2 15 43	+58 43 36	
IRC+60080	2 15 43	+63 56 00	
IRC+60081	2 16 45	+59 26 42	
IRC+60082	2 16 57	+56 45 42	
IRC+60083	2 17 35	+56 56 12	
IRC+60084	2 18 01	+60 40 36	
IRC+60085	2 18 05	+57 38 00	
IRC+60086	2 18 35	+56 22 42	
IRC+60087	2 18 56	+56 52 24	
IRC+60088	2 19 16	+58 21 30	
IRC+60089	2 19 45	+56 59 00	
IRC+60090	2 21 46	+57 13 00	
IRC+60091	2 23 45	+60 27 54	
IRC+60092	2 31 43	+64 56 36	
IRC+60093	2 34 48	+56 49 36	
IRC+60094	2 36 03	+59 23 00	
IRC+60095	2 42 43	+62 48 06	
IRC+60096	2 46 08	+60 49 36	
IRC+60097	2 46 53	+56 46 54	
IRC+60098	2 47 00	+60 32 42	
IRC+60099	2 47 02	+55 41 12	
IRC+60100	2 47 19	+57 39 06	
IRC+60101	2 47 19	+59 01 24	
IRC+60102	2 47 22	+63 13 24	
IRC+60103	2 51 38	+60 01 54	
IRC+60104	2 52 19	+64 07 54	
IRC+60105	2 52 31	+62 24 24	
IRC+60106	2 53 07	+57 21 12	
IRC+60107	2 55 18	+62 54 06	
IRC+60108	2 56 01	+57 28 30	
IRC+60109	3 01 46	+56 31 36	
IRC+60110	3 03 07	+55 32 06	
IRC+60111	3 03 39	+60 18 24	
IRC+60112	3 04 11	+58 50 54	
IRC+60113	3 07 29	+57 43 06	
IRC+60114	3 08 43	+55 58 00	
IRC+60115	3 09 29	+55 31 00	
IRC+60116	3 12 32	+64 34 36	
IRC+60117	3 20 16	+64 24 30	
IRC+60118	3 20 24	+56 03 06	
IRC+60119	3 22 25	+55 57 54	
IRC+60120	3 25 54	+58 41 42	
IRC+60121	3 26 23	+55 12 24	
IRC+60122	3 31 43	+63 05 30	
IRC+60123	3 37 03	+61 40 12	
IRC+60124	3 37 31	+62 29 54	
IRC+60125	3 37 45	+63 03 36	
IRC+60126	3 38 29	+59 49 00	
IRC+60127	3 41 40	+63 11 12	
IRC+60128	3 43 59	+59 25 54	
IRC+60129	3 46 15	+63 33 42	
IRC+60130	3 47 51	+63 50 00	
IRC+60131	3 49 19	+63 14 36	
IRC+60132	3 51 00	+62 05 12	
IRC+60133	3 51 51	+57 31 30	
IRC+60134	3 52 56	+60 58 00	
IRC+60135	3 55 03	+61 37 06	
IRC+60136	3 57 14	+55 09 42	
IRC+60137	4 00 26	+55 47 36	
IRC+60138	4 01 28	+61 39 36	
IRC+60139	4 04 58	+55 01 12	
IRC+60140	4 13 15	+62 13 42	
IRC+60141	4 17 27	+60 36 54	
IRC+60142	4 26 09	+64 20 42	
IRC+60143	4 26 29	+57 18 12	
IRC+60144	4 30 49	+62 10 12	
IRC+60145	4 44 35	+61 25 42	
IRC+60146	4 45 05	+59 37 00	
IRC+60147	4 47 26	+63 25 06	
IRC+60148	4 52 43	+55 44 36	
IRC+60149	4 52 53	+59 02 24	
IRC+60150	4 56 44	+56 06 54	
IRC+60151	4 58 57	+60 22 12	
IRC+60152	5 01 56	+61 06 24	
IRC+60153	5 01 58	+56 34 30	
IRC+60154	5 15 05	+63 12 54	
IRC+60155	5 15 38	+62 36 06	
IRC+60156	5 19 12	+60 40 12	
IRC+60157	5 25 26	+63 01 30	
IRC+60158	5 41 19	+64 45 00	
IRC+60159	5 49 02	+63 00 06	
IRC+60160	5 50 09	+64 58 24	
IRC+60161	6 02 11	+60 30 24	
IRC+60162	6 05 37	+58 55 54	
IRC+60163	6 06 45	+60 27 42	
IRC+60164	6 11 16	+60 00 54	
IRC+60165	6 12 10	+56 45 24	
IRC+60166	6 13 19	+61 32 00	
IRC+60167	6 22 29	+58 26 06	
IRC+60168	6 25 02	+61 34 36	
IRC+60169	6 30 02	+60 58 54	
IRC+60170	6 30 24	+55 24 00	
IRC+60171	6 30 26	+64 07 54	
IRC+60172	6 36 21	+59 54 54	
IRC+60173	6 38 47	+55 32 06	
IRC+60174	6 40 12	+56 58 42	
IRC+60175	6 40 14	+57 58 12	
IRC+60176	6 49 11	+61 04 42	
IRC+60177	6 52 56	+57 37 30	
IRC+60178	6 53 03	+58 28 06	
IRC+60179	6 57 14	+55 24 24	
IRC+60180	7 03 49	+61 19 24	
IRC+60181	7 11 32	+59 43 06	
IRC+60182	7 18 09	+55 54 42	
IRC+60183	7 36 47	+57 11 54	

NAME	RA (1950)	DEC	POS REF
	h m s	° ′ ″	
IRC+60184	7 51 55	+57 20 54	
IRC+60185	8 03 20	+60 51 54	
IRC+60186	8 06 01	+58 24 06	
IRC+60187	8 26 10	+60 53 36	
IRC+60188	8 35 55	+64 29 54	
IRC+60189	8 57 03	+62 44 54	
IRC+60190	9 01 20	+60 29 06	
IRC+60191	9 01 55	+64 58 30	
IRC+60192	9 12 08	+56 57 12	
IRC+60193	9 18 04	+56 54 42	
IRC+60194	9 21 44	+64 09 00	
IRC+60195	9 27 38	+63 17 00	
IRC+60196	9 35 24	+58 45 00	
IRC+60197	9 42 56	+57 21 36	
IRC+60198	9 47 25	+59 15 24	
IRC+60199	9 56 26	+57 03 24	
IRC+60200	10 05 29	+64 11 36	
IRC+60201	10 10 58	+59 38 54	
IRC+60202	10 11 17	+56 36 00	
IRC+60203	10 11 41	+60 13 54	
IRC+60204	10 43 18	+57 37 54	
IRC+60205	10 48 13	+59 34 36	
IRC+60206	10 58 49	+56 38 42	
IRC+60207	10 59 13	+58 56 00	
IRC+60208	11 00 37	+62 01 12	
IRC+60209	11 18 08	+55 06 00	
IRC+60210	11 34 35	+62 27 24	
IRC+60211	11 38 59	+55 26 36	
IRC+60212	11 44 14	+55 54 24	
IRC+60213	11 53 55	+58 08 42	
IRC+60214	12 09 16	+57 20 00	
IRC+60215	12 18 08	+61 35 12	
IRC+60216	12 18 25	+58 08 12	
IRC+60217	12 22 40	+57 02 54	
IRC+60218	12 25 11	+55 59 06	
IRC+60219	12 34 07	+59 46 12	
IRC+60220	12 38 02	+56 07 24	
IRC+60221	12 49 11	+57 59 54	
IRC+60222	12 51 50	+56 13 42	
IRC+60223	13 09 57	+56 38 54	
IRC+60224	13 21 52	+55 11 06	
IRC+60225	13 48 11	+55 06 54	
IRC+60226	13 49 54	+64 57 42	
IRC+60227	14 12 07	+58 20 30	
IRC+60228	14 30 57	+55 37 00	
IRC+60229	14 40 50	+55 01 06	
IRC+60230	14 42 35	+56 18 42	
IRC+60231	14 50 11	+59 30 00	
IRC+60232	15 21 49	+63 30 30	
IRC+60233	15 23 48	+59 08 12	
IRC+60234	15 26 53	+60 50 30	
IRC+60235	15 37 44	+57 37 24	
IRC+60236	15 45 23	+55 37 42	
IRC+60237	15 47 49	+61 35 42	
IRC+60238	16 00 55	+58 42 12	
IRC+60239	16 02 16	+59 32 36	
IRC+60240	16 07 23	+62 22 06	
IRC+60241	16 16 24	+59 52 06	
IRC+60242	16 23 19	+61 37 30	
IRC+60243	16 34 17	+60 34 12	
IRC+60244	16 36 24	+63 10 30	
IRC+60245	16 36 59	+56 06 54	
IRC+60246	16 40 36	+64 40 30	
IRC+60247	16 46 45	+63 36 12	
IRC+60248	16 47 24	+57 54 24	
IRC+60249	17 08 05	+64 22 42	
IRC+60250	17 12 04	+57 55 06	
IRC+60251	17 36 13	+57 45 36	
IRC+60252	17 40 18	+62 34 12	
IRC+60253	17 52 44	+56 54 12	
IRC+60254	17 52 54	+57 05 30	
IRC+60255	17 55 39	+58 13 36	
IRC+60256	18 04 36	+62 38 42	
IRC+60257	18 26 46	+58 26 12	
IRC+60258	18 40 14	+56 44 12	
IRC+60259	18 50 26	+59 19 36	
IRC+60260	19 00 40	+57 45 12	
IRC+60261	19 01 17	+60 03 00	
IRC+60262	19 02 11	+63 01 42	
IRC+60263	19 10 41	+56 46 30	
IRC+60264	19 12 57	+57 37 12	
IRC+60265	19 19 17	+57 33 06	
IRC+60266	19 31 31	+58 48 24	
IRC+60267	19 31 32	+63 01 00	
IRC+60268	19 32 19	+60 02 42	
IRC+60269	19 40 56	+55 20 36	
IRC+60270	19 42 00	+55 45 12	
IRC+60271	19 43 11	+58 13 36	
IRC+60272	19 43 53	+55 43 00	
IRC+60273	19 54 01	+60 28 36	
IRC+60274	19 54 56	+58 42 24	
IRC+60275	19 55 25	+59 36 42	
IRC+60276	19 59 17	+55 39 36	
IRC+60277	20 00 26	+62 14 54	
IRC+60278	20 00 58	+64 40 24	
IRC+60279	20 04 44	+61 51 24	
IRC+60280	20 06 11	+56 50 24	
IRC+60281	20 06 52	+56 25 36	
IRC+60282	20 09 17	+63 03 12	
IRC+60283	20 09 25	+61 12 36	
IRC+60284	20 12 32	+60 29 12	
IRC+60285	20 13 31	+59 35 36	
IRC+60286	20 20 26	+63 49 12	
IRC+60287	20 20 36	+63 16 12	
IRC+60288	20 21 31	+62 43 42	
IRC+60289	20 22 45	+55 03 00	
IRC+60290	20 23 07	+58 39 36	
IRC+60291	20 25 25	+55 34 54	
IRC+60292	20 30 31	+62 46 36	
IRC+60293	20 30 34	+56 36 06	
IRC+60294	20 33 42	+61 09 30	
IRC+60295	20 34 12	+61 37 54	
IRC+60296	20 38 03	+59 21 30	
IRC+60297	20 43 09	+56 18 36	
IRC+60298	20 44 16	+61 39 00	
IRC+60299	20 45 46	+58 13 54	
IRC+60300	20 54 23	+59 49 30	
IRC+60301	20 58 08	+58 41 42	
IRC+60302	20 58 10	+59 14 24	
IRC+60303	21 00 56	+59 31 00	
IRC+60304	21 06 53	+58 33 42	
IRC+60305	21 11 30	+59 53 42	
IRC+60306	21 12 40	+61 39 24	
IRC+60307	21 13 08	+56 41 06	
IRC+60308	21 15 44	+55 35 12	
IRC+60309	21 16 47	+55 03 24	
IRC+60310	21 17 15	+62 22 54	
IRC+60311	21 17 19	+60 58 36	
IRC+60312	21 17 20	+63 20 54	
IRC+60313	21 17 53	+58 24 42	
IRC+60314	21 18 02	+62 12 06	
IRC+60315	21 18 10	+55 14 30	
IRC+60316	21 19 02	+56 09 54	
IRC+60317	21 24 25	+62 21 36	
IRC+60318	21 26 01	+59 31 54	
IRC+60319	21 28 53	+64 03 54	
IRC+60320	21 29 16	+61 29 42	
IRC+60321	21 33 50	+60 41 06	
IRC+60322	21 38 43	+59 22 12	
IRC+60323	21 40 57	+64 30 24	
IRC+60324	21 41 16	+61 31 42	
IRC+60325	21 41 56	+58 32 36	
IRC+60326	21 43 59	+60 53 12	
IRC+60327	21 44 41	+57 49 24	
IRC+60328	21 45 38	+64 22 00	
IRC+60329	21 45 55	+60 27 42	
IRC+60330	21 47 47	+61 02 24	
IRC+60331	21 50 52	+55 44 54	
IRC+60332	21 53 52	+61 18 36	
IRC+60333	21 55 11	+63 23 12	
IRC+60334	21 56 20	+56 30 54	
IRC+60335	21 57 20	+62 27 54	
IRC+60336	21 58 12	+57 07 36	
IRC+60337	22 00 08	+56 44 12	
IRC+60338	22 02 23	+62 52 30	
IRC+60339	22 03 28	+62 32 30	
IRC+60340	22 03 41	+62 49 54	
IRC+60341	22 03 52	+62 15 42	
IRC+60342	22 04 49	+59 14 42	
IRC+60343	22 06 53	+59 18 36	
IRC+60344	22 09 05	+57 57 12	
IRC+60345	22 09 43	+56 47 42	
IRC+60346	22 10 23	+60 30 30	
IRC+60347	22 10 49	+63 02 42	
IRC+60348	22 12 14	+57 45 42	
IRC+60349	22 16 30	+62 34 12	
IRC+60350	22 18 16	+55 47 24	
IRC+60351	22 18 25	+61 55 30	
IRC+60352	22 20 08	+55 03 30	
IRC+60353	22 21 14	+55 42 36	
IRC+60354	22 24 03	+63 04 30	
IRC+60355	22 26 26	+58 58 36	
IRC+60356	22 27 19	+58 08 54	
IRC+60357	22 28 17	+56 45 06	
IRC+60358	22 30 37	+58 21 36	
IRC+60359	22 30 40	+55 10 54	
IRC+60360	22 31 39	+56 22 42	
IRC+60361	22 31 43	+58 38 06	
IRC+60362	22 34 34	+58 09 36	
IRC+60363	22 36 41	+56 32 06	
IRC+60364	22 41 16	+59 29 30	
IRC+60365	22 42 18	+61 28 00	
IRC+60366	22 45 51	+61 00 24	
IRC+60367	22 47 14	+59 02 42	
IRC+60368	22 47 41	+55 38 30	
IRC+60369	22 47 55	+59 23 30	
IRC+60370	22 48 06	+60 01 42	
IRC+60371	22 48 58	+63 59 00	
IRC+60372	22 48 59	+61 30 36	
IRC+60373	22 51 04	+59 50 12	
IRC+60374	22 51 19	+61 01 12	
IRC+60375	22 52 31	+60 33 12	
IRC+60376	22 54 01	+62 09 54	
IRC+60377	22 54 37	+61 15 24	
IRC+60378	22 56 11	+56 42 36	
IRC+60379	22 58 00	+56 40 42	
IRC+60380	22 59 23	+56 50 00	
IRC+60381	22 59 25	+61 18 06	
IRC+60382	23 00 02	+59 33 06	
IRC+60383	23 02 17	+56 11 24	
IRC+60384	23 02 28	+58 18 00	
IRC+60385	23 02 33	+64 29 36	
IRC+60386	23 05 49	+60 03 24	
IRC+60387	23 05 51	+55 26 36	
IRC+60388	23 07 59	+60 58 24	
IRC+60389	23 09 31	+59 25 54	
IRC+60390	23 10 38	+63 40 06	
IRC+60391	23 11 34	+60 51 00	
IRC+60392	23 12 47	+63 55 54	
IRC+60393	23 13 52	+62 04 54	
IRC+60394	23 14 14	+60 41 36	
IRC+60395	23 14 44	+60 10 06	
IRC+60396	23 16 16	+58 16 06	
IRC+60397	23 17 13	+62 28 06	
IRC+60398	23 17 31	+56 58 12	
IRC+60399	23 18 04	+61 42 00	
IRC+60400	23 18 19	+61 56 06	
IRC+60401	23 20 13	+59 51 30	
IRC+60402	23 20 20	+59 02 06	
IRC+60403	23 21 13	+55 53 24	
IRC+60404	23 22 32	+62 00 42	
IRC+60405	23 25 49	+59 04 12	
IRC+60406	23 26 36	+59 28 00	
IRC+60407	23 26 54	+56 23 06	
IRC+60408	23 27 49	+59 08 36	
IRC+60409	23 27 53	+60 01 54	
IRC+60410	23 28 10	+57 42 06	
IRC+60411	23 28 25	+59 58 06	
IRC+60412	23 30 05	+61 50 00	
IRC+60413	23 32 38	+58 16 42	
IRC+60414	23 34 49	+55 36 12	
IRC+60415	23 36 01	+61 38 00	
IRC+60416	23 39 59	+64 13 42	
IRC+60417	23 41 41	+61 31 00	
IRC+60418	23 42 07	+56 18 00	
IRC+60419	23 42 14	+55 06 42	
IRC+60420	23 42 25	+56 11 00	
IRC+60421	23 43 44	+60 11 00	
IRC+60422	23 44 35	+57 10 12	
IRC+60423	23 44 38	+58 22 06	
IRC+60424	23 45 46	+60 45 42	
IRC+60425	23 47 43	+60 49 24	
IRC+60426	23 48 11	+61 36 06	
IRC+60427	23 49 39	+61 32 06	
IRC+60428	23 50 26	+60 43 36	
IRC+60429	23 51 52	+57 13 06	
IRC+60430	23 54 46	+60 45 06	
IRC+60431	23 55 26	+56 12 36	
IRC+60432	23 57 43	+60 04 36	
IRC+60433	23 58 43	+60 04 30	
IRC+60434	23 59 41	+60 25 42	
IRC+70001	0 00 01	+73 45 06	
IRC+70002	0 01 17	+66 26 12	
IRC+70003	0 03 34	+69 46 36	
IRC+70004	0 07 58	+71 01 12	
IRC+70005	0 11 21	+73 06 54	
IRC+70006	0 12 19	+66 20 54	
IRC+70007	0 15 05	+74 19 30	
IRC+70008	0 22 13	+69 51 54	
IRC+70009	0 32 29	+70 14 36	
IRC+70010	0 32 40	+67 39 06	
IRC+70011	0 35 25	+68 18 06	
IRC+70012	0 42 50	+68 54 36	
IRC+70013	0 50 02	+69 41 24	
IRC+70014	0 50 47	+73 52 06	
IRC+70015	0 54 46	+67 25 36	
IRC+70016	1 01 04	+74 34 30	
IRC+70017	1 03 14	+65 31 42	
IRC+70018	1 07 07	+65 51 00	
IRC+70019	1 10 02	+67 32 36	
IRC+70020	1 11 51	+66 24 12	
IRC+70021	1 12 24	+71 28 54	
IRC+70022	1 12 27	+69 59 54	
IRC+70023	1 13 01	+74 55 54	
IRC+70024	1 15 53	+72 21 24	
IRC+70025	1 17 38	+67 10 06	
IRC+70026	1 18 40	+66 35 00	
IRC+70027	1 22 25	+67 52 24	
IRC+70028	1 24 08	+65 49 12	
IRC+70029	1 31 15	+65 32 54	
IRC+70030	1 35 28	+65 15 42	
IRC+70031	1 50 23	+68 56 00	
IRC+70032	1 52 25	+69 57 30	
IRC+70033	1 58 23	+71 03 12	
IRC+70034	2 12 38	+67 04 24	
IRC+70035	2 25 35	+69 01 30	
IRC+70036	2 31 57	+67 44 54	
IRC+70037	2 33 28	+65 31 54	
IRC+70038	2 43 17	+71 45 36	
IRC+70039	2 50 16	+74 06 42	
IRC+70040	3 08 52	+74 03 24	
IRC+70041	3 09 50	+65 21 24	
IRC+70042	3 19 34	+74 50 06	
IRC+70043	3 25 05	+71 41 30	
IRC+70044	3 28 05	+70 40 12	
IRC+70045	3 34 42	+65 03 42	
IRC+70046	3 44 52	+65 22 24	
IRC+70047	3 46 13	+67 28 24	
IRC+70048	3 50 19	+69 24 42	
IRC+70049	4 01 05	+68 32 54	
IRC+70050	4 05 17	+68 34 00	
IRC+70051	4 08 40	+74 46 12	
IRC+70052	4 09 27	+66 25 30	
IRC+70053	4 24 40	+69 15 54	
IRC+70054	4 35 08	+66 03 12	
IRC+70055	4 45 59	+68 05 00	
IRC+70056	4 48 43	+74 13 00	
IRC+70057	4 56 02	+74 11 36	
IRC+70058	4 58 04	+73 41 42	
IRC+70059	5 05 25	+68 36 24	
IRC+70060	5 06 18	+66 59 12	
IRC+70061	5 18 43	+73 40 00	
IRC+70062	5 29 27	+72 26 12	
IRC+70063	5 29 29	+65 01 24	
IRC+70064	5 35 40	+68 46 00	
IRC+70065	5 37 23	+65 40 30	
IRC+70066	5 41 16	+69 56 54	
IRC+70067	5 55 59	+74 31 00	
IRC+70068	5 57 11	+66 54 24	
IRC+70069	6 07 47	+65 44 12	
IRC+70070	6 40 45	+71 24 36	
IRC+70071	6 55 44	+70 53 00	
IRC+70072	6 57 21	+69 16 00	
IRC+70073	7 00 14	+70 48 54	
IRC+70074	7 05 06	+66 01 24	
IRC+70075	7 09 35	+68 53 30	
IRC+70076	7 25 46	+68 34 36	
IRC+70077	7 30 41	+67 34 06	
IRC+70078	7 31 08	+66 35 06	
IRC+70079	7 54 07	+67 57 00	
IRC+70080	7 54 16	+74 03 12	
IRC+70081	8 01 59	+66 38 24	
IRC+70082	8 06 25	+65 22 24	
IRC+70083	8 15 11	+72 34 24	
IRC+70084	8 16 03	+67 41 12	
IRC+70085	8 29 49	+67 21 42	
IRC+70086	8 46 37	+70 29 12	
IRC+70087	8 58 03	+67 49 30	
IRC+70088	9 04 04	+67 04 42	
IRC+70089	9 04 30	+69 24 54	
IRC+70090	9 30 04	+70 02 36	
IRC+70091	9 35 26	+67 30 24	
IRC+70092	9 38 22	+72 29 12	
IRC+70093	9 42 07	+65 51 30	
IRC+70094	10 30 34	+69 48 42	
IRC+70095	10 30 35	+70 01 30	
IRC+70096	10 38 20	+68 42 12	
IRC+70097	10 38 31	+65 58 54	
IRC+70098	10 39 31	+69 20 06	
IRC+70099	10 41 10	+69 02 00	
IRC+70100	10 41 37	+67 40 24	
IRC+70101	10 44 14	+65 52 54	
IRC+70102	10 52 06	+72 08 30	
IRC+70103	10 53 51	+74 36 06	

NAME	RA (1950)	DEC	POS REF
	h m s	° ′ ″	
IRC+70104	10 55 38	+70 15 42	
IRC+70105	11 08 47	+71 52 00	
IRC+70106	11 17 57	+65 37 24	
IRC+70107	11 28 25	+69 36 24	
IRC+70108	11 33 08	+69 35 42	
IRC+70109	11 37 23	+68 30 00	
IRC+70110	11 39 44	+67 01 30	
IRC+70111	12 03 05	+69 02 06	
IRC+70112	12 12 40	+70 28 12	
IRC+70113	12 27 52	+69 28 30	
IRC+70114	12 32 34	+70 17 36	
IRC+70115	12 45 34	+67 04 06	
IRC+70116	12 54 33	+66 16 24	
IRC+70117	12 58 04	+66 53 00	
IRC+70118	13 24 47	+72 39 12	
IRC+70119	13 33 35	+73 41 06	
IRC+70120	13 35 58	+71 29 54	
IRC+70121	13 37 43	+74 33 12	
IRC+70122	14 00 42	+68 54 00	
IRC+70123	14 11 04	+69 39 42	
IRC+70124	14 16 12	+67 01 36	
IRC+70125	14 50 47	+74 21 54	
IRC+70126	14 56 47	+66 08 00	
IRC+70127	15 07 34	+65 58 42	
IRC+70128	15 17 02	+72 00 06	
IRC+70129	15 20 46	+72 00 30	
IRC+70130	15 29 53	+70 33 30	
IRC+70131	15 37 29	+69 26 30	
IRC+70132	15 42 16	+67 13 42	
IRC+70133	16 21 54	+69 13 30	
IRC+70134	16 28 13	+67 09 36	
IRC+70135	16 30 38	+72 23 12	
IRC+70136	16 32 32	+66 51 36	
IRC+70137	16 41 30	+72 46 24	
IRC+70138	17 19 24	+67 20 42	
IRC+70139	17 24 02	+71 54 54	
IRC+70140	17 32 14	+68 09 54	
IRC+70141	17 36 51	+68 30 36	
IRC+70142	18 09 35	+71 33 36	
IRC+70143	18 19 50	+67 24 36	
IRC+70144	18 21 55	+72 42 36	
IRC+70145	18 25 48	+65 32 00	
IRC+70146	18 38 55	+74 17 00	
IRC+70147	18 54 59	+71 13 54	
IRC+70148	19 09 53	+66 01 06	
IRC+70149	19 10 03	+67 11 54	
IRC+70150	19 12 32	+67 34 42	
IRC+70151	19 13 25	+73 48 54	
IRC+70152	19 13 45	+67 26 42	
IRC+70153	19 16 29	+73 16 24	
IRC+70154	19 23 40	+68 55 12	
IRC+70155	19 23 45	+65 32 42	
IRC+70156	19 24 20	+71 35 42	
IRC+70157	19 31 26	+70 52 12	
IRC+70158	19 32 31	+69 34 24	
IRC+70159	19 35 34	+69 41 30	
IRC+70160	19 48 20	+70 08 12	
IRC+70161	20 02 35	+67 44 00	
IRC+70162	20 04 39	+67 53 12	
IRC+70163	20 12 26	+66 05 36	
IRC+70164	20 15 15	+72 27 12	
IRC+70165	20 17 24	+66 51 12	
IRC+70166	20 19 51	+68 43 12	
IRC+70167	20 36 28	+68 23 00	
IRC+70168	21 08 52	+68 17 24	
IRC+70169	21 23 13	+65 21 30	
IRC+70170	21 26 13	+70 00 12	
IRC+70171	21 26 59	+71 36 06	
IRC+70172	21 38 10	+65 34 24	
IRC+70173	21 38 16	+68 11 36	
IRC+70174	21 40 08	+73 55 00	
IRC+70175	21 41 09	+71 04 36	
IRC+70176	21 42 26	+72 05 12	
IRC+70177	21 44 05	+73 24 36	
IRC+70178	21 45 15	+67 24 42	
IRC+70179	21 48 29	+65 00 06	
IRC+70180	21 56 06	+65 54 06	
IRC+70181	21 57 22	+74 45 54	
IRC+70182	21 58 43	+65 11 42	
IRC+70183	22 06 42	+74 29 24	
IRC+70184	22 07 28	+72 31 30	
IRC+70185	22 08 52	+72 05 36	
IRC+70186	22 18 08	+66 34 30	
IRC+70187	22 24 41	+70 30 42	
IRC+70188	22 31 31	+66 40 00	
IRC+70189	22 43 46	+65 28 00	
IRC+70190	22 47 57	+65 56 36	
IRC+70191	23 00 40	+70 48 36	
IRC+70192	23 01 40	+66 56 42	
IRC+70193	23 11 04	+66 48 36	
IRC+70194	23 16 36	+67 50 06	
IRC+70195	23 27 27	+65 16 54	
IRC+70196	23 31 25	+70 05 30	
IRC+70197	23 31 31	+68 12 24	
IRC+70198	23 32 50	+71 21 42	
IRC+70199	23 38 14	+70 09 30	
IRC+70200	23 40 52	+73 43 36	
IRC+70201	23 46 41	+68 23 12	
IRC+70202	23 49 41	+66 18 24	
IRC+80001	0 11 10	+75 44 54	
IRC+80002	0 29 01	+76 18 06	
IRC+80003	1 26 45	+79 23 54	
IRC+80004	1 55 50	+75 42 54	
IRC+80005	2 14 41	+78 32 06	
IRC+80006	2 29 09	+76 29 36	
IRC+80007	2 59 20	+79 13 24	
IRC+80008	3 01 52	+75 36 42	
IRC+80009	3 41 42	+80 10 00	
IRC+80010	4 18 23	+80 41 30	
IRC+80011	5 33 04	+75 01 12	
IRC+80012	5 58 19	+75 35 54	
IRC+80013	6 10 42	+76 42 06	
IRC+80014	6 32 48	+78 02 12	
IRC+80015	6 41 23	+77 02 30	
IRC+80016	6 52 52	+77 02 42	
IRC+80017	7 24 07	+75 10 00	
IRC+80018	8 44 01	+79 09 00	
IRC+80019	8 44 20	+78 20 36	

NAME	RA (1950)	DEC	POS REF
	h m s	° ′ ″	
IRC+80020	10 30 50	+75 58 00	
IRC+80021	10 51 12	+77 21 12	
IRC+80022	11 06 05	+78 03 24	
IRC+80023	11 12 38	+75 24 42	
IRC+80024	11 34 38	+77 52 00	
IRC+80025	13 33 53	+76 47 36	
IRC+80026	14 08 52	+77 46 54	
IRC+80027	14 18 49	+77 21 54	
IRC+80028	14 27 29	+75 55 00	
IRC+80029	14 55 20	+75 04 54	
IRC+80030	15 31 21	+78 48 12	
IRC+80031	15 32 50	+77 31 00	
IRC+80032	17 23 29	+80 11 00	
IRC+80033	17 52 59	+78 18 42	
IRC+80034	17 55 28	+80 38 54	
IRC+80035	18 32 01	+77 30 06	
IRC+80036	19 23 14	+76 28 00	
IRC+80037	19 53 20	+78 29 36	
IRC+80038	20 00 58	+76 20 42	
IRC+80039	20 14 08	+80 01 42	
IRC+80040	20 24 53	+75 05 00	
IRC+80041	20 42 11	+80 19 54	
IRC+80042	20 50 02	+80 22 06	
IRC+80043	21 10 07	+75 40 54	
IRC+80044	21 16 13	+76 48 12	
IRC+80045	21 20 45	+77 38 24	
IRC+80046	21 20 50	+75 58 24	
IRC+80047	21 21 45	+79 33 24	
IRC+80048	21 35 54	+78 24 06	
IRC+80049	21 41 34	+76 09 42	
IRC+80050	21 46 38	+78 47 06	
IRC+80051	21 52 55	+79 18 54	
IRC+80052	21 55 24	+80 04 24	
IRC+80053	21 57 18	+76 23 54	
IRC+80054	22 35 46	+77 20 42	
IRC+80055	22 36 11	+75 06 54	
IRC+80056	23 06 21	+75 06 36	
IRC+80057	23 37 19	+77 21 24	
IRC−10001	0 01 54	−10 47 24	
IRC−10002	0 02 41	− 5 59 24	
IRC−10003	0 03 43	−11 03 24	
IRC−10004	0 10 13	−11 18 00	
IRC−10005	0 11 55	− 8 03 30	
IRC−10006	0 16 55	− 9 06 00	
IRC−10007	0 21 32	− 9 37 24	
IRC−10008	0 22 01	−10 10 24	
IRC−10009	0 24 35	− 6 52 54	
IRC−10010	0 25 32	−11 56 24	
IRC−10011	0 39 28	− 9 55 06	
IRC−10012	0 41 43	−10 52 36	
IRC−10013	0 46 57	−13 50 30	
IRC−10014	0 53 11	− 7 37 12	
IRC−10015	0 53 29	−11 32 12	
IRC−10016	0 58 01	−12 27 30	
IRC−10017	1 00 32	− 5 06 30	
IRC−10018	1 06 05	−10 26 54	
IRC−10019	1 08 46	−13 46 12	
IRC−10020	1 19 59	− 5 12 06	
IRC−10021	1 21 30	− 8 26 30	
IRC−10022	1 23 12	−14 51 36	
IRC−10023	1 41 24	− 5 00 30	
IRC−10024	1 43 28	− 5 58 54	
IRC−10025	1 47 24	− 5 06 12	
IRC−10026	1 47 50	−13 08 00	
IRC−10027	1 49 01	−10 35 00	
IRC−10028	1 55 58	− 7 19 00	
IRC−10029	1 57 04	−14 07 00	
IRC−10030	1 57 57	− 8 45 54	
IRC−10031	2 01 46	−12 05 54	
IRC−10032	2 03 37	−10 27 00	
IRC−10033	2 15 44	−14 21 36	
IRC−10034	2 20 15	−10 25 42	
IRC−10035	2 31 18	−13 22 06	
IRC−10036	2 32 14	− 8 04 30	
IRC−10037	2 33 31	− 8 02 42	
IRC−10038	2 41 38	− 6 37 00	
IRC−10039	2 43 02	−14 11 54	
IRC−10040	2 45 32	−12 39 54	
IRC−10041	2 49 49	− 8 28 00	
IRC−10042	2 53 42	− 6 13 36	
IRC−10043	2 54 00	− 9 05 42	
IRC−10044	3 01 25	−14 24 36	
IRC−10045	3 04 01	− 6 16 30	
IRC−10046	3 13 48	− 5 55 24	
IRC−10047	3 22 47	−12 31 24	
IRC−10048	3 30 34	− 9 37 36	
IRC−10049	3 38 56	−10 55 00	
IRC−10050	3 40 52	− 9 55 24	
IRC−10051	3 43 47	−12 15 06	
IRC−10052	3 46 17	− 7 09 30	
IRC−10053	3 49 31	−12 06 30	
IRC−10054	3 54 07	−13 44 06	
IRC−10055	3 55 40	−13 38 30	
IRC−10056	3 57 07	−12 42 42	
IRC−10057	3 57 48	− 6 31 00	
IRC−10058	4 00 55	− 7 03 00	
IRC−10059	4 03 32	−10 26 00	
IRC−10060	4 04 26	− 7 48 36	
IRC−10061	4 06 29	− 8 14 06	
IRC−10062	4 11 08	−10 30 54	
IRC−10063	4 12 02	−10 23 06	
IRC−10064	4 12 55	− 7 44 36	
IRC−10065	4 15 23	−10 13 30	
IRC−10066	4 20 05	− 5 36 54	
IRC−10067	4 23 20	−10 02 12	
IRC−10068	4 31 00	−10 53 36	
IRC−10069	4 31 47	− 6 56 12	
IRC−10070	4 31 49	− 8 20 12	
IRC−10071	4 31 49	− 9 04 24	
IRC−10072	4 33 47	− 5 22 00	
IRC−10073	4 35 50	−14 24 00	
IRC−10074	4 36 57	−14 26 54	
IRC−10075	4 38 11	−14 17 24	
IRC−10076	4 39 25	− 8 02 54	
IRC−10077	4 42 01	−12 45 30	
IRC−10078	4 51 41	−12 32 06	
IRC−10079	4 56 01	− 6 08 54	
IRC−10080	4 57 22	−14 52 36	

NAME	RA (1950)	DEC	POS REF
	h m s	° ′ ″	
IRC−10081	5 05 20	− 5 08 42	
IRC−10082	5 05 30	−12 39 12	
IRC−10083	5 07 16	− 5 34 54	
IRC−10084	5 09 02	−11 54 30	
IRC−10085	5 12 07	− 8 15 30	
IRC−10086	5 19 53	− 8 43 06	
IRC−10087	5 20 43	− 7 04 06	
IRC−10088	5 20 54	− 9 21 42	
IRC−10089	5 21 32	− 7 51 12	
IRC−10090	5 22 00	−10 23 36	
IRC−10091	5 22 08	− 6 11 24	
IRC−10092	5 22 41	−10 22 24	
IRC−10093	5 32 50	− 5 24 42	
IRC−10094	5 36 34	−14 04 12	
IRC−10095	5 37 19	− 8 11 24	
IRC−10096	5 39 26	− 8 55 36	
IRC−10097	5 44 55	−12 49 24	
IRC−10098	5 45 23	− 9 40 30	
IRC−10099	5 49 09	−12 47 36	
IRC−10100	5 49 22	−10 32 30	
IRC−10101	5 52 23	−11 46 42	
IRC−10102	5 54 11	−14 10 24	
IRC−10103	5 55 15	− 6 05 36	
IRC−10104	5 56 43	−10 53 42	
IRC−10105	5 59 12	− 5 20 36	
IRC−10106	5 59 38	− 5 07 54	
IRC−10107	6 03 32	− 5 52 24	
IRC−10108	6 03 50	− 7 05 24	
IRC−10109	6 03 53	− 5 42 42	
IRC−10110	6 07 20	−14 34 54	
IRC−10111	6 08 58	− 7 14 00	
IRC−10112	6 10 25	− 7 17 12	
IRC−10113	6 12 25	− 6 15 30	
IRC−10114	6 16 29	− 9 22 24	
IRC−10115	6 16 32	−15 00 00	
IRC−10116	6 16 55	− 9 44 30	
IRC−10117	6 16 58	−12 35 24	
IRC−10118	6 18 44	−11 48 00	
IRC−10119	6 19 19	− 8 12 54	
IRC−10120	6 21 16	− 9 50 36	
IRC−10121	6 21 49	−11 30 36	
IRC−10122	6 22 41	− 9 06 06	
IRC−10123	6 24 23	− 7 53 06	
IRC−10124	6 26 53	− 8 03 54	
IRC−10125	6 26 58	− 9 53 00	
IRC−10126	6 27 50	−10 02 30	
IRC−10127	6 29 05	−12 21 24	
IRC−10128	6 29 28	− 8 07 30	
IRC−10129	6 29 29	−14 52 42	
IRC−10130	6 30 44	− 9 56 00	
IRC−10131	6 33 23	− 5 19 54	
IRC−10132	6 34 28	−13 16 30	
IRC−10133	6 34 42	−12 03 00	
IRC−10134	6 36 10	− 9 16 30	
IRC−10135	6 36 57	−14 06 06	
IRC−10136	6 37 53	− 6 17 54	
IRC−10137	6 39 34	− 9 07 00	
IRC−10138	6 40 18	−14 24 24	
IRC−10139	6 45 12	− 8 56 36	
IRC−10140	6 51 51	−11 58 24	
IRC−10141	6 53 52	−13 58 30	
IRC−10142	6 54 47	− 8 59 54	
IRC−10143	6 55 41	− 8 57 12	
IRC−10144	6 58 26	−14 16 42	
IRC−10145	6 59 26	− 5 38 54	
IRC−10146	7 01 38	− 5 15 24	
IRC−10147	7 02 04	− 8 52 36	
IRC−10148	7 02 05	− 9 53 00	
IRC−10149	7 04 31	− 7 28 30	
IRC−10150	7 04 54	−11 54 30	
IRC−10151	7 05 26	−10 39 30	
IRC−10152	7 05 42	−11 50 30	
IRC−10153	7 10 19	− 7 50 06	
IRC−10154	7 10 47	−11 09 42	
IRC−10155	7 11 02	−14 29 36	
IRC−10156	7 11 47	−14 31 00	
IRC−10157	7 11 58	− 9 51 54	
IRC−10158	7 15 07	− 6 35 42	
IRC−10159	7 16 54	−11 22 24	
IRC−10160	7 16 56	−10 48 42	
IRC−10161	7 16 57	− 8 41 12	
IRC−10162	7 18 37	−10 16 36	
IRC−10163	7 23 19	− 5 44 24	
IRC−10164	7 24 05	− 8 49 42	
IRC−10165	7 25 29	− 9 28 06	
IRC−10166	7 26 56	−10 13 24	
IRC−10167	7 27 46	− 9 16 12	
IRC−10168	7 28 37	−10 00 00	
IRC−10169	7 31 29	−14 24 54	
IRC−10170	7 33 56	− 8 12 00	
IRC−10171	7 34 47	−14 13 00	
IRC−10172	7 35 35	− 5 35 42	
IRC−10173	7 36 33	− 8 59 36	
IRC−10174	7 38 52	− 9 25 42	
IRC−10175	7 39 55	−10 45 54	
IRC−10176	7 43 32	− 6 39 12	
IRC−10177	7 45 19	−11 50 06	
IRC−10178	7 47 21	−13 57 24	
IRC−10179	7 47 25	− 8 27 12	
IRC−10180	7 47 43	− 9 03 00	
IRC−10181	7 50 44	−11 29 30	
IRC−10182	7 50 49	− 7 55 24	
IRC−10183	7 51 20	− 6 19 06	
IRC−10184	7 58 28	−12 41 54	
IRC−10185	7 59 50	−12 52 24	
IRC−10186	8 00 47	−12 04 54	
IRC−10187	8 08 07	− 9 27 12	
IRC−10188	8 08 58	−12 46 36	
IRC−10189	8 13 17	−13 28 00	
IRC−10190	8 16 47	− 7 23 54	
IRC−10191	8 16 52	−11 22 00	
IRC−10192	8 19 28	− 9 30 24	
IRC−10193	8 20 27	− 7 23 00	
IRC−10194	8 22 04	− 8 21 30	
IRC−10195	8 24 22	−12 22 06	
IRC−10196	8 27 13	− 6 09 00	
IRC−10197	8 31 22	− 9 49 24	
IRC−10198	8 33 28	−11 07 24	

NAME	RA (1950)	DEC	POS REF
	h m s	° ′ ″	
IRC−10199	8 37 18	− 9 24 30	
IRC−10200	8 37 41	−12 17 54	
IRC−10201	8 37 44	−14 51 36	
IRC−10202	8 38 04	−14 38 12	
IRC−10203	8 39 23	− 5 25 42	
IRC−10204	8 41 15	− 7 02 54	
IRC−10205	8 43 44	−10 49 36	
IRC−10206	8 43 46	−10 38 54	
IRC−10207	8 43 59	−13 21 42	
IRC−10208	8 51 07	−11 13 00	
IRC−10209	8 52 13	−11 11 36	
IRC−10210	8 53 12	− 8 57 00	
IRC−10211	9 01 20	−12 29 00	
IRC−10212	9 07 55	−11 24 30	
IRC−10213	9 14 16	− 6 09 06	
IRC−10214	9 17 23	−11 46 06	
IRC−10215	9 18 02	− 9 21 12	
IRC−10216	9 21 29	− 5 14 42	
IRC−10217	9 25 10	− 8 26 36	
IRC−10218	9 25 45	− 7 30 12	
IRC−10219	9 26 55	−13 31 06	
IRC−10220	9 30 31	−13 17 30	
IRC−10221	9 32 06	− 5 41 00	
IRC−10222	9 33 05	−14 28 00	
IRC−10223	9 40 15	− 7 52 12	
IRC−10224	9 43 56	− 5 48 00	
IRC−10225	9 45 37	− 7 55 36	
IRC−10226	9 49 09	−14 36 36	
IRC−10227	9 49 13	−11 06 42	
IRC−10228	10 01 14	− 9 20 00	
IRC−10229	10 03 07	−12 20 30	
IRC−10230	10 05 16	− 7 23 12	
IRC−10231	10 06 58	−13 07 00	
IRC−10232	10 07 17	−14 31 06	
IRC−10233	10 08 11	−12 06 24	
IRC−10234	10 08 22	− 8 09 36	
IRC−10235	10 09 50	−10 04 42	
IRC−10236	10 14 34	−14 24 30	
IRC−10237	10 18 37	− 5 11 06	
IRC−10238	10 20 13	− 9 08 54	
IRC−10239	10 23 15	− 6 48 54	
IRC−10240	10 28 08	−10 32 54	
IRC−10241	10 28 26	− 7 23 42	
IRC−10242	10 35 03	−13 07 12	
IRC−10243	10 35 22	−11 45 36	
IRC−10244	10 40 01	−13 43 06	
IRC−10245	10 42 31	− 6 34 24	
IRC−10246	10 46 19	− 8 44 12	
IRC−10247	10 57 46	−13 49 12	
IRC−10248	11 03 24	− 8 52 54	
IRC−10249	11 05 10	−12 19 06	
IRC−10250	11 11 39	− 8 03 30	
IRC−10251	11 12 51	−11 18 54	
IRC−10252	11 13 10	−12 19 30	
IRC−10253	11 16 46	−14 30 30	
IRC−10254	11 22 04	−10 35 06	
IRC−10255	11 23 25	−13 29 00	
IRC−10256	11 29 10	−12 06 30	
IRC−10257	11 30 17	− 7 33 06	
IRC−10258	11 48 33	−10 56 00	
IRC−10259	11 50 12	− 7 19 00	
IRC−10260	11 57 47	− 9 54 30	
IRC−10261	12 00 18	− 7 24 00	
IRC−10262	12 03 01	− 5 33 54	
IRC−10263	12 04 41	− 6 29 24	
IRC−10264	12 12 01	− 5 45 30	
IRC−10265	12 17 47	− 8 43 12	
IRC−10266	12 18 16	−12 34 30	
IRC−10267	12 18 20	−13 17 12	
IRC−10268	12 20 46	−11 31 54	
IRC−10269	12 36 42	− 7 43 06	
IRC−10270	12 38 33	− 8 58 12	
IRC−10271	12 39 22	− 7 13 30	
IRC−10272	12 47 08	−14 48 36	
IRC−10273	12 50 23	−14 20 30	
IRC−10274	12 51 44	− 9 15 54	
IRC−10275	12 54 34	−11 48 12	
IRC−10276	13 05 16	−10 28 06	
IRC−10277	13 05 58	− 8 43 00	
IRC−10278	13 06 53	− 9 27 06	
IRC−10279	13 07 07	−10 04 00	
IRC−10280	13 08 42	−10 14 36	
IRC−10281	13 10 08	− 8 42 54	
IRC−10282	13 12 05	−10 06 06	
IRC−10283	13 18 07	−11 11 24	
IRC−10284	13 19 29	−14 09 24	
IRC−10285	13 19 30	−12 19 24	
IRC−10286	13 22 31	−10 54 24	
IRC−10287	13 24 04	−12 26 42	
IRC−10288	13 29 21	− 5 59 54	
IRC−10289	13 30 19	− 9 54 42	
IRC−10290	13 30 24	− 6 56 06	
IRC−10291	13 36 04	−11 13 00	
IRC−10292	13 38 44	−10 12 06	
IRC−10293	13 38 58	− 8 27 12	
IRC−10294	13 44 32	− 9 27 24	
IRC−10295	13 53 10	− 9 19 00	
IRC−10296	13 56 17	−13 42 12	
IRC−10297	14 03 57	−13 57 42	
IRC−10298	14 05 58	− 8 37 12	
IRC−10299	14 08 38	−10 14 12	
IRC−10300	14 10 13	−10 02 12	
IRC−10301	14 10 25	−13 37 12	
IRC−10302	14 13 23	− 5 45 54	
IRC−10303	14 15 19	−14 28 12	
IRC−10304	14 16 27	−13 11 54	
IRC−10305	14 16 33	−14 10 24	
IRC−10306	14 26 04	− 6 40 36	
IRC−10307	14 54 05	−11 12 24	
IRC−10308	14 55 05	−12 13 30	
IRC−10309	14 57 49	−11 41 30	
IRC−10310	15 00 56	− 7 22 42	
IRC−10311	15 02 10	− 7 49 42	
IRC−10312	15 04 41	−14 28 54	
IRC−10313	15 11 35	−14 01 30	
IRC−10314	15 12 11	− 5 18 42	
IRC−10315	15 14 18	− 9 12 06	
IRC−10316	15 15 29	− 9 57 24	

NAME	RA (1950)	DEC	POS REF
	h m s	° ′ ″	
IRC−10317	15 16 39	− 8 58 00	
IRC−10318	15 16 59	−10 27 06	
IRC−10319	15 20 14	−14 57 30	
IRC−10320	15 22 32	− 5 44 42	
IRC−10321	15 24 55	−14 46 30	
IRC−10322	15 31 28	− 9 54 12	
IRC−10323	15 32 43	−14 37 36	
IRC−10324	15 38 19	−12 06 12	
IRC−10325	15 44 39	−10 08 30	
IRC−10326	15 51 44	−10 43 36	
IRC−10327	15 52 49	−12 43 00	
IRC−10328	15 55 41	−13 17 30	
IRC−10329	15 57 39	−12 12 12	
IRC−10330	16 01 39	−11 43 24	
IRC−10331	16 08 53	−13 51 12	
IRC−10332	16 10 23	−14 59 24	
IRC−10333	16 10 29	−10 12 30	
IRC−10334	16 11 05	−11 43 00	
IRC−10335	16 16 10	−14 45 12	
IRC−10336	16 17 02	−14 31 36	
IRC−10337	16 18 43	− 7 35 24	
IRC−10338	16 20 17	− 7 05 36	
IRC−10339	16 23 56	−12 19 06	
IRC−10340	16 25 02	− 7 29 00	
IRC−10341	16 30 43	−14 03 12	
IRC−10342	16 30 43	−12 27 30	
IRC−10343	16 34 25	−10 28 12	
IRC−10344	16 36 06	− 8 31 06	
IRC−10345	16 38 24	−11 44 24	
IRC−10346	16 41 52	−13 59 30	
IRC−10347	16 43 54	−11 33 06	
IRC−10348	16 49 26	−12 52 06	
IRC−10349	16 51 36	− 6 38 06	
IRC−10350	16 51 50	− 7 29 06	
IRC−10351	16 51 58	− 6 04 12	
IRC−10352	16 54 02	−10 19 24	
IRC−10353	16 55 09	− 9 28 00	
IRC−10354	16 56 53	− 7 32 00	
IRC−10355	16 57 29	−10 32 42	
IRC−10356	17 03 26	−10 25 00	
IRC−10357	17 08 02	−11 41 54	
IRC−10358	17 10 13	−14 46 30	
IRC−10359	17 10 17	−10 31 06	
IRC−10360	17 11 19	−14 56 30	
IRC−10361	17 12 20	− 9 53 36	
IRC−10362	17 15 01	−11 56 24	
IRC−10363	17 15 33	− 9 42 24	
IRC−10364	17 16 11	− 9 21 00	
IRC−10365	17 18 50	−14 33 30	
IRC−10366	17 19 14	−13 05 54	
IRC−10367	17 21 53	− 6 55 12	
IRC−10368	17 24 40	− 6 11 12	
IRC−10369	17 26 33	− 7 25 24	
IRC−10370	17 32 11	− 7 12 42	
IRC−10371	17 32 36	−11 30 24	
IRC−10372	17 32 49	−14 15 54	
IRC−10373	17 35 23	−10 54 00	
IRC−10374	17 35 37	−14 04 36	
IRC−10375	17 39 07	− 6 26 12	
IRC−10376	17 41 16	− 6 15 42	
IRC−10377	17 41 29	−12 11 12	
IRC−10378	17 41 51	− 7 49 54	
IRC−10379	17 43 01	−14 00 36	
IRC−10380	17 46 13	− 9 07 30	
IRC−10381	17 48 28	− 8 00 42	
IRC−10382	17 49 57	− 6 07 36	
IRC−10383	17 50 14	−13 16 54	
IRC−10384	17 51 49	−10 14 24	
IRC−10385	17 52 43	−13 37 06	
IRC−10386	17 53 14	−12 52 24	
IRC−10387	17 56 17	− 9 46 36	
IRC−10388	17 56 20	− 6 38 36	
IRC−10389	17 56 40	− 6 06 36	
IRC−10390	17 58 37	−12 54 06	
IRC−10391	17 59 31	−12 19 12	
IRC−10392	17 59 37	−14 30 00	
IRC−10393	18 00 45	−13 15 30	
IRC−10394	18 01 34	−12 44 36	
IRC−10395	18 03 59	− 8 13 24	
IRC−10396	18 04 05	− 9 42 12	
IRC−10397	18 04 10	−14 37 24	
IRC−10398	18 06 53	−13 56 54	
IRC−10399	18 06 59	−11 43 54	
IRC−10400	18 07 39	− 6 52 12	
IRC−10401	18 07 40	−10 34 54	
IRC−10402	18 07 42	− 7 19 42	
IRC−10403	18 08 00	− 6 06 24	
IRC−10404	18 09 03	− 7 27 00	
IRC−10405	18 09 06	−14 55 24	
IRC−10406	18 10 30	−10 29 54	
IRC−10407	18 11 37	− 6 57 36	
IRC−10408	18 12 21	− 6 48 00	
IRC−10409	18 15 31	−13 27 24	
IRC−10410	18 17 02	−12 19 36	
IRC−10411	18 17 34	−14 08 24	
IRC−10412	18 17 56	−13 46 54	
IRC−10413	18 19 31	−11 36 54	
IRC−10414	18 20 28	−13 44 06	
IRC−10415	18 20 35	−12 42 36	
IRC−10416	18 20 51	−12 53 42	
IRC−10417	18 20 55	− 8 57 06	
IRC−10418	18 22 19	− 6 53 00	
IRC−10419	18 22 47	−13 47 54	
IRC−10420	18 23 35	−10 04 54	
IRC−10421	18 23 52	− 7 48 24	
IRC−10422	18 24 48	−12 29 42	
IRC−10423	18 24 52	− 7 44 30	
IRC−10424	18 25 01	− 8 42 24	
IRC−10425	18 25 17	−13 05 00	
IRC−10426	18 26 16	−11 34 06	
IRC−10427	18 26 26	− 9 28 42	
IRC−10428	18 26 56	−11 11 54	
IRC−10429	18 27 29	− 8 14 06	
IRC−10430	18 28 22	− 8 27 12	
IRC−10431	18 28 26	− 9 24 36	
IRC−10432	18 29 36	− 9 57 36	
IRC−10433	18 29 49	−14 54 00	
IRC−10434	18 30 30	− 7 29 00	

NAME	RA (1950)	DEC	POS REF
	h m s	° ′ ″	
IRC−10435	18 30 31	−14 08 36	
IRC−10436	18 31 24	−13 06 54	
IRC−10437	18 32 08	− 7 43 24	
IRC−10438	18 32 28	− 8 16 54	
IRC−10439	18 32 49	− 8 44 12	
IRC−10440	18 33 35	− 8 55 24	
IRC−10441	18 34 23	− 7 39 00	
IRC−10442	18 35 13	− 6 54 54	
IRC−10442 A	18 35 12.5	− 6 55 10	
IRC−10442 A1	18 35 13	− 6 55 10	
IRC−10442 A2	18 35 16	− 6 55 29	
IRC−10442 A3	18 35 14	− 6 55 20	
IRC−10442 A4	18 35 12	− 6 55 25	
IRC−10442 B	18 35 16.5	− 6 56 24	
IRC−10443	18 35 18	−12 24 54	
IRC−10444	18 35 41	−14 53 06	
IRC−10445	18 35 43	−10 03 06	
IRC−10446	18 36 01	−13 49 00	
IRC−10447	18 36 41	− 6 03 24	
IRC−10448	18 36 49	−11 13 42	
IRC−10449	18 37 19	− 7 50 00	
IRC−10450	18 37 35	− 5 45 42	
IRC−10451	18 38 01	−14 33 12	
IRC−10452	18 38 20	− 5 42 36	
IRC−10453	18 38 38	− 6 24 42	
IRC−10454	18 39 26	− 5 04 42	
IRC−10455	18 39 38	− 7 23 30	
IRC−10456	18 40 45	−11 23 24	
IRC−10457	18 40 49	− 8 20 06	
IRC−10458	18 41 59	− 6 35 12	
IRC−10459	18 41 59	− 9 17 12	
IRC−10460	18 43 04	− 5 38 42	
IRC−10461	18 44 50	− 5 46 06	
IRC−10462	18 44 56	−12 23 00	
IRC−10463	18 45 30	−12 26 00	
IRC−10464	18 46 37	− 9 48 12	
IRC−10465	18 46 59	− 5 57 54	
IRC−10466	18 47 07	− 9 42 42	
IRC−10467	18 47 38	− 7 58 06	
IRC−10468	18 47 42	−13 37 42	
IRC−10469	18 48 11	− 6 48 24	
IRC−10470	18 48 37	−12 41 24	
IRC−10471	18 49 47	− 5 24 24	
IRC−10472	18 51 03	−12 41 30	
IRC−10473	18 52 01	− 5 07 24	
IRC−10474	18 52 25	−12 48 06	
IRC−10475	18 52 44	− 8 15 00	
IRC−10476	18 53 05	−10 26 12	
IRC−10477	18 53 12	−11 02 54	
IRC−10478	18 53 25	−14 19 54	
IRC−10479	18 53 49	−10 35 36	
IRC−10480	18 54 24	− 5 54 36	
IRC−10481	18 54 37	− 9 49 54	
IRC−10482	18 58 39	−12 49 54	
IRC−10483	18 59 01	− 5 48 36	
IRC−10484	18 59 17	− 6 48 36	
IRC−10485	19 01 14	−10 19 42	
IRC−10486	19 01 43	− 5 45 36	
IRC−10487	19 02 21	− 7 12 42	
IRC−10488	19 02 43	−12 46 24	
IRC−10489	19 06 14	−12 26 24	
IRC−10490	19 08 46	− 9 32 42	
IRC−10491	19 09 14	−11 47 24	
IRC−10492	19 10 23	−10 48 00	
IRC−10493	19 10 29	−12 21 36	
IRC−10494	19 11 04	−11 18 36	
IRC−10495	19 11 09	− 5 34 54	
IRC−10496	19 11 27	− 9 39 00	
IRC−10497	19 12 41	− 7 08 36	
IRC−10498	19 13 40	−11 39 36	
IRC−10499	19 14 33	− 7 56 42	
IRC−10500	19 15 27	− 5 30 12	
IRC−10501	19 17 25	− 6 43 36	
IRC−10502	19 17 37	− 8 07 36	
IRC−10503	19 17 38	−10 39 00	
IRC−10504	19 17 48	− 7 08 06	
IRC−10505	19 17 54	− 5 30 30	
IRC−10506	19 19 49	−10 22 00	
IRC−10507	19 20 23	− 7 29 36	
IRC−10508	19 20 50	−11 13 30	
IRC−10509	19 21 27	− 9 32 00	
IRC−10510	19 22 14	− 8 56 42	
IRC−10511	19 22 21	−13 32 36	
IRC−10512	19 22 33	−13 59 54	
IRC−10513	19 23 12	− 9 06 42	
IRC−10514	19 23 19	− 7 18 36	
IRC−10515	19 28 48	−10 54 00	
IRC−10516	19 32 20	−10 40 12	
IRC−10517	19 33 28	− 5 29 24	
IRC−10518	19 34 05	−10 15 36	
IRC−10519	19 41 21	−11 47 42	
IRC−10520	19 42 09	−10 41 30	
IRC−10521	19 44 08	−12 16 00	
IRC−10522	19 46 04	−12 26 12	
IRC−10523	19 46 50	−11 06 12	
IRC−10524	19 47 20	− 7 44 12	
IRC−10525	19 48 55	−13 09 06	
IRC−10526	19 51 25	− 8 42 06	
IRC−10527	19 56 19	− 8 01 00	
IRC−10528	20 07 23	−10 40 42	
IRC−10529	20 07 46	− 6 24 42	
IRC−10530	20 09 28	−11 22 06	
IRC−10531	20 14 01	−13 33 36	
IRC−10532	20 14 11	− 7 15 54	
IRC−10533	20 14 13	− 8 28 36	
IRC−10534	20 14 52	−12 39 06	
IRC−10535	20 15 18	−12 42 06	
IRC−10536	20 17 47	− 6 31 24	
IRC−10537	20 18 11	−14 56 24	
IRC−10538	20 23 09	− 8 46 36	
IRC−10539	20 25 08	− 5 49 30	
IRC−10540	20 30 48	− 6 23 36	
IRC−10541	20 32 19	− 7 37 06	
IRC−10542	20 36 01	− 9 51 24	
IRC−10543	20 36 28	− 9 33 42	
IRC−10544	20 37 24	−14 11 30	
IRC−10545	20 39 16	− 5 48 24	
IRC−10546	20 41 46	− 5 01 00	

NAME	RA (1950)	DEC	POS REF
	h m s	° ′ ″	
IRC−10547	20 41 49	−14 21 54	
IRC−10548	20 45 07	− 5 12 42	
IRC−10549	20 46 38	− 8 58 36	
IRC−10550	20 48 41	−11 17 00	
IRC−10551	20 49 20	− 6 29 12	
IRC−10552	20 50 03	− 7 56 06	
IRC−10553	20 54 14	− 9 53 06	
IRC−10554	20 56 43	−14 59 00	
IRC−10555	20 59 53	−10 11 36	
IRC−10556	21 06 22	− 5 17 00	
IRC−10557	21 06 51	−11 34 42	
IRC−10558	21 10 00	−14 35 54	
IRC−10559	21 13 37	− 9 25 24	
IRC−10560	21 19 58	− 5 50 42	
IRC−10561	21 20 13	− 9 31 42	
IRC−10562	21 20 20	− 6 27 00	
IRC−10563	21 20 26	− 7 19 00	
IRC−10564	21 27 55	−14 23 54	
IRC−10565	21 28 53	− 5 47 30	
IRC−10566	21 29 39	−12 29 36	
IRC−10567	21 33 29	−14 06 12	
IRC−10568	21 34 38	−11 41 00	
IRC−10569	21 42 19	− 9 17 54	
IRC−10570	21 43 37	− 9 30 12	
IRC−10571	21 53 22	−14 16 12	
IRC−10572	21 53 48	− 9 49 30	
IRC−10573	21 54 17	−14 20 54	
IRC−10574	21 56 35	− 9 12 36	
IRC−10575	22 04 40	−10 41 30	
IRC−10576	22 09 35	−11 18 54	
IRC−10577	22 14 06	−13 05 42	
IRC−10578	22 14 14	− 8 02 06	
IRC−10579	22 19 02	−12 48 12	
IRC−10580	22 19 07	− 7 51 42	
IRC−10581	22 19 11	− 6 26 00	
IRC−10582	22 33 43	− 5 24 30	
IRC−10583	22 34 38	−10 31 24	
IRC−10584	22 35 56	−14 17 30	
IRC−10585	22 39 31	− 5 21 42	
IRC−10586	22 43 37	−11 26 06	
IRC−10587	22 46 58	−13 51 36	
IRC−10588	22 50 00	− 7 50 42	
IRC−10589	22 52 20	− 9 38 42	
IRC−10590	22 57 00	−13 20 30	
IRC−10591	22 58 47	− 7 19 54	
IRC−10592	22 59 56	− 6 50 42	
IRC−10593	23 11 43	− 6 19 00	
IRC−10594	23 12 00	−10 57 36	
IRC−10595	23 12 14	− 7 58 24	
IRC−10596	23 13 17	− 9 21 42	
IRC−10597	23 14 17	− 8 00 00	
IRC−10598	23 20 09	−11 05 24	
IRC−10599	23 23 14	−11 26 00	
IRC−10600	23 24 50	−13 12 00	
IRC−10601	23 25 27	−12 28 54	
IRC−10602	23 26 25	− 9 32 24	
IRC−10603	23 29 40	−11 49 30	
IRC−10604	23 35 26	− 8 13 06	
IRC−10605	23 45 59	− 6 39 12	
IRC−10606	23 47 50	−14 42 54	
IRC−10607	23 50 14	−12 17 12	
IRC−10608	23 59 22	− 6 17 30	
IRC−10609	23 59 33	−14 57 24	
IRC−20001	0 05 55	−17 51 24	
IRC−20002	0 06 19	−22 27 12	
IRC−20003	0 08 26	−18 50 54	
IRC−20004	0 09 28	−24 50 30	
IRC−20005	0 09 41	−18 12 12	
IRC−20006	0 12 09	−19 12 24	
IRC−20007	0 19 12	−20 20 12	
IRC−20008	0 20 27	−16 12 30	
IRC−20009	0 23 50	−18 58 12	
IRC−20010	0 41 05	−18 15 36	
IRC−20011	0 45 13	−18 20 06	
IRC−20012	0 50 14	−24 16 12	
IRC−20013	0 56 19	−19 54 12	
IRC−20014	1 20 55	−18 11 30	
IRC−20015	1 31 59	−19 13 36	
IRC−20016	1 33 30	−15 39 24	
IRC−20017	1 37 37	−23 10 06	
IRC−20018	1 41 40	−16 11 00	
IRC−20019	1 48 09	−17 53 30	
IRC−20020	1 49 23	−15 53 54	
IRC−20021	1 54 21	−22 46 06	
IRC−20022	1 54 51	−17 54 36	
IRC−20023	1 57 23	−21 04 06	
IRC−20024	1 57 35	−21 19 12	
IRC−20025	2 01 28	−17 45 00	
IRC−20026	2 02 23	−17 31 42	
IRC−20027	2 06 25	−18 00 36	
IRC−20028	2 09 16	−17 58 00	
IRC−20029	2 09 27	−23 55 00	
IRC−20030	2 13 16	−23 35 54	
IRC−20031	2 13 39	−20 45 00	
IRC−20032	2 16 32	−19 45 54	
IRC−20033	2 28 14	−22 45 42	
IRC−20034	2 30 18	−16 56 06	
IRC−20035	2 36 13	−20 39 30	
IRC−20036	2 39 47	−22 48 42	
IRC−20037	2 48 40	−21 13 24	
IRC−20038	2 55 53	−23 48 00	
IRC−20039	3 09 03	−23 52 30	
IRC−20040	3 16 08	−22 42 00	
IRC−20041	3 17 18	−21 56 36	
IRC−20042	3 17 25	−24 18 06	
IRC−20043	3 31 55	−16 19 42	
IRC−20044	3 46 24	−21 03 24	
IRC−20045	3 51 14	−15 07 24	
IRC−20046	3 52 43	−15 02 42	
IRC−20047	3 53 01	−24 10 36	
IRC−20048	4 01 22	−24 35 30	
IRC−20049	4 02 02	−15 51 30	
IRC−20050	4 10 40	−23 57 06	
IRC−20051	4 11 45	−16 06 00	
IRC−20052	4 15 42	−18 37 24	
IRC−20053	4 16 04	−20 49 30	
IRC−20054	4 17 47	−18 51 54	
IRC−20055	4 18 29	−16 56 36	
IRC−20056	4 19 52	−22 48 00	
IRC−20057	4 21 01	−25 00 00	
IRC−20058	4 29 50	−20 48 42	
IRC−20059	4 38 12	−19 45 54	
IRC−20060	4 39 25	−24 04 06	
IRC−20061	4 42 57	−21 22 30	
IRC−20062	4 43 04	−23 57 00	
IRC−20063	4 47 59	−16 18 12	
IRC−20064	4 56 07	−16 47 24	
IRC−20065	5 00 41	−22 51 42	
IRC−20066	5 02 43	−21 58 24	
IRC−20067	5 03 22	−22 26 06	
IRC−20068	5 15 46	−18 39 12	
IRC−20069	5 17 42	−17 55 24	
IRC−20070	5 19 46	−24 48 42	
IRC−20071	5 26 10	−20 47 30	
IRC−20072	5 30 29	−16 21 00	
IRC−20073	5 30 31	−17 51 00	
IRC−20074	5 32 00	−18 49 54	
IRC−20075	5 38 59	−16 53 54	
IRC−20076	5 39 23	−20 48 00	
IRC−20077	5 40 31	−23 43 06	
IRC−20078	5 42 22	−22 27 42	
IRC−20079	5 44 11	−23 39 30	
IRC−20080	5 45 04	−21 33 12	
IRC−20081	5 49 11	−20 53 12	
IRC−20082	5 51 25	−23 07 36	
IRC−20083	5 59 41	−21 06 12	
IRC−20084	6 02 45	−16 28 54	
IRC−20085	6 03 42	−24 11 00	
IRC−20086	6 04 52	−21 48 30	
IRC−20087	6 05 32	−19 09 24	
IRC−20088	6 12 11	−19 30 12	
IRC−20089	6 12 58	−20 15 36	
IRC−20090	6 15 31	−16 47 54	
IRC−20091	6 17 35	−22 04 54	
IRC−20092	6 20 34	−17 56 00	
IRC−20093	6 21 28	−15 02 42	
IRC−20094	6 22 57	−23 26 42	
IRC−20095	6 28 01	−19 10 36	
IRC−20096	6 34 30	−19 12 42	
IRC−20097	6 34 50	−22 13 12	
IRC−20098	6 35 40	−18 11 24	
IRC−20099	6 36 19	−19 50 24	
IRC−20100	6 36 47	−18 08 06	
IRC−20101	6 39 08	−22 14 00	
IRC−20102	6 40 19	−18 57 36	
IRC−20103	6 40 53	−20 06 36	
IRC−20104	6 42 08	−22 25 06	
IRC−20105	6 42 57	−16 38 54	
IRC−20106	6 43 56	−21 50 06	
IRC−20107	6 45 10	−20 16 12	
IRC−20108	6 46 44	−20 22 00	
IRC−20109	6 48 07	−17 01 30	
IRC−20110	6 49 37	−18 58 24	
IRC−20111	6 51 05	−21 54 24	
IRC−20112	6 52 04	−24 07 12	
IRC−20113	6 53 27	−16 48 06	
IRC−20114	6 54 41	−23 53 42	
IRC−20115	6 59 33	−23 25 06	
IRC−20116	7 00 15	−15 34 24	
IRC−20117	7 01 56	−16 31 30	
IRC−20118	7 02 44	−20 45 12	
IRC−20119	7 04 15	−24 32 24	
IRC−20120	7 04 17	−23 00 42	
IRC−20121	7 06 16	−17 29 06	
IRC−20122	7 08 01	−16 11 06	
IRC−20123	7 11 15	−22 35 06	
IRC−20124	7 12 55	−22 41 00	
IRC−20125	7 14 29	−23 13 36	
IRC−20126	7 14 40	−19 17 12	
IRC−20127	7 16 11	−17 10 12	
IRC−20128	7 19 34	−24 07 42	
IRC−20129	7 20 11	−20 24 36	
IRC−20130	7 23 34	−20 53 12	
IRC−20131	7 27 01	−19 21 24	
IRC−20132	7 27 22	−17 28 36	
IRC−20133	7 30 26	−20 32 42	
IRC−20134	7 33 00	−23 52 24	
IRC−20135	7 33 47	−19 46 06	
IRC−20136	7 36 07	−15 56 00	
IRC−20137	7 37 10	−16 43 42	
IRC−20138	7 37 27	−15 43 24	
IRC−20139	7 38 08	−15 08 42	
IRC−20140	7 38 46	−23 58 12	
IRC−20141	7 39 14	−22 13 12	
IRC−20142	7 44 17	−21 25 24	
IRC−20143	7 45 02	−19 16 42	
IRC−20144	7 45 28	−15 52 36	
IRC−20145	7 47 08	−24 43 54	
IRC−20146	7 47 13	−22 26 00	
IRC−20147	7 47 25	−17 06 06	
IRC−20148	7 51 55	−18 11 54	
IRC−20149	7 54 36	−20 17 36	
IRC−20150	7 54 45	−22 44 54	
IRC−20151	7 55 22	−15 04 06	
IRC−20152	7 55 42	−20 17 24	
IRC−20153	7 56 58	−23 10 42	
IRC−20154	8 02 15	−17 31 12	
IRC−20155	8 03 08	−16 58 30	
IRC−20156	8 05 20	−22 46 00	
IRC−20157	8 05 28	−24 09 54	
IRC−20158	8 05 30	−20 32 12	
IRC−20159	8 08 25	−15 10 36	
IRC−20160	8 10 59	−15 37 54	
IRC−20161	8 12 50	−21 47 24	
IRC−20162	8 15 58	−23 04 24	
IRC−20163	8 17 16	−19 55 30	
IRC−20164	8 17 53	−23 17 54	
IRC−20165	8 20 25	−15 45 24	
IRC−20166	8 22 52	−23 53 06	
IRC−20167	8 27 56	−20 44 06	
IRC−20168	8 28 46	−15 49 12	
IRC−20169	8 30 52	−17 48 12	
IRC−20170	8 31 30	−18 36 42	
IRC−20171	8 34 36	−17 47 12	
IRC−20172	8 36 24	−19 33 42	
IRC−20173	8 37 37	−17 07 24	
IRC−20174	8 39 25	−15 45 42	
IRC−20175	8 52 59	−18 03 12	
IRC−20176	8 53 25	−19 01 42	
IRC−20177	8 53 26	−24 05 54	
IRC−20178	8 54 14	−16 31 00	
IRC−20179	8 56 16	−24 19 12	
IRC−20180	8 56 35	−15 47 36	
IRC−20181	8 56 48	−23 05 00	
IRC−20182	9 07 01	−24 38 24	
IRC−20183	9 08 04	−19 42 06	
IRC−20184	9 11 18	−23 10 42	
IRC−20185	9 13 30	−15 29 06	
IRC−20186	9 17 10	−15 37 36	
IRC−20187	9 20 55	−20 49 30	
IRC−20188	9 23 34	−23 48 00	
IRC−20189	9 23 38	−23 33 42	
IRC−20190	9 25 02	−22 07 36	
IRC−20191	9 26 53	−20 31 54	
IRC−20192	9 27 31	−23 07 30	
IRC−20193	9 30 55	−20 53 12	
IRC−20194	9 35 50	−16 29 30	
IRC−20195	9 37 56	−16 07 30	
IRC−20196	9 42 44	−23 46 54	
IRC−20197	9 42 56	−21 48 06	
IRC−20198	9 43 19	−23 39 30	
IRC−20199	9 48 46	−22 47 12	
IRC−20200	9 51 03	−17 41 24	
IRC−20201	9 52 31	−18 46 30	
IRC−20202	9 53 13	−17 14 30	
IRC−20203	9 53 39	−19 43 06	
IRC−20204	10 04 44	−16 54 00	
IRC−20205	10 05 11	−22 15 00	
IRC−20206	10 08 56	−18 42 36	
IRC−20207	10 11 49	−23 33 54	
IRC−20208	10 17 28	−22 42 30	
IRC−20209	10 23 13	−16 29 12	
IRC−20210	10 23 46	−16 35 00	
IRC−20211	10 25 32	−21 28 30	
IRC−20212	10 25 37	−21 08 54	
IRC−20213	10 31 37	−23 29 00	
IRC−20214	10 33 52	−16 05 00	
IRC−20215	10 34 45	−23 37 42	
IRC−20216	10 36 10	−16 37 12	
IRC−20217	10 47 11	−15 55 54	
IRC−20218	10 49 12	−20 59 12	
IRC−20219	10 49 34	−24 06 06	
IRC−20220	10 57 00	−16 05 06	
IRC−20221	10 57 22	−18 01 54	
IRC−20222	10 58 09	−18 03 36	
IRC−20223	11 10 35	−16 58 24	
IRC−20224	11 10 54	−21 45 54	
IRC−20225	11 15 18	−21 52 36	
IRC−20226	11 19 25	−24 43 42	
IRC−20227	11 21 23	−19 38 00	
IRC−20228	11 26 21	−16 19 24	
IRC−20229	11 27 27	−17 30 06	
IRC−20230	11 37 20	−16 20 30	
IRC−20231	11 42 10	−18 04 30	
IRC−20232	11 43 38	−24 35 36	
IRC−20233	12 07 34	−22 20 42	
IRC−20234	12 08 02	−24 49 24	
IRC−20235	12 13 14	−17 16 00	
IRC−20236	12 15 50	−20 31 54	
IRC−20237	12 17 08	−18 56 54	
IRC−20238	12 27 13	−16 14 06	
IRC−20239	12 27 42	−23 25 00	
IRC−20240	12 31 44	−23 07 06	
IRC−20241	12 32 19	−20 33 54	
IRC−20242	12 34 29	−17 15 24	
IRC−20243	12 34 59	−16 59 42	
IRC−20244	12 40 33	−24 43 00	
IRC−20245	12 46 03	−19 14 30	
IRC−20246	12 51 56	−19 50 12	
IRC−20247	13 06 23	−22 50 42	
IRC−20248	13 13 17	−19 40 30	
IRC−20249	13 16 13	−22 54 12	
IRC−20250	13 18 20	−24 12 06	
IRC−20251	13 20 29	−18 04 42	
IRC−20252	13 20 36	−24 23 24	
IRC−20253	13 24 43	−15 42 30	
IRC−20254	13 26 58	−23 01 24	
IRC−20255	13 30 08	−15 05 12	
IRC−20256	13 32 41	−22 21 42	
IRC−20257	13 39 40	−19 08 30	
IRC−20258	13 44 40	−17 36 54	
IRC−20259	13 45 00	−20 53 36	
IRC−20260	13 45 13	−18 19 36	
IRC−20261	13 47 08	−17 53 06	
IRC−20262	13 54 40	−22 46 12	
IRC−20263	14 05 23	−17 35 24	
IRC−20264	14 06 13	−19 00 24	
IRC−20265	14 08 04	−16 04 00	
IRC−20266	14 14 15	−16 12 42	
IRC−20267	14 27 32	−21 16 42	
IRC−20268	14 44 23	−21 07 00	
IRC−20269	14 45 31	−21 12 30	
IRC−20270	14 46 29	−24 02 12	
IRC−20271	14 48 07	−15 50 06	
IRC−20272	14 48 15	−24 41 30	
IRC−20273	14 51 28	−24 26 30	
IRC−20274	14 52 29	−21 47 42	
IRC−20275	14 54 32	−21 12 06	
IRC−20276	14 55 44	−19 31 12	
IRC−20277	14 57 37	−22 39 00	
IRC−20278	14 58 41	−18 36 30	
IRC−20279	15 03 51	−16 03 36	
IRC−20280	15 05 59	−22 52 06	
IRC−20281	15 07 01	−23 47 36	
IRC−20282	15 09 22	−18 56 06	
IRC−20283	15 13 27	−22 13 06	
IRC−20284	15 19 11	−23 52 36	
IRC−20285	15 19 29	−18 29 42	
IRC−20286	15 21 26	−22 44 06	
IRC−20287	15 25 27	−16 32 30	
IRC−20288	15 29 19	−23 42 42	
IRC−20289	15 30 26	−15 09 30	
IRC−20290	15 34 50	−16 09 06	
IRC−20291	15 37 19	−23 39 24	

NAME	RA (1950) h m s	DEC ° ′ ″	POS REF
IRC−20292	15 39 05	−19 31 30	
IRC−20293	15 40 47	−21 40 30	
IRC−20294	15 44 55	−19 33 00	
IRC−20295	15 45 58	−20 17 36	
IRC−20296	15 50 59	−16 34 42	
IRC−20297	15 51 03	−18 48 06	
IRC−20298	15 51 58	−20 40 42	
IRC−20299	15 52 42	−18 38 36	
IRC−20300	15 53 27	−18 09 24	
IRC−20301	15 54 14	−15 53 24	
IRC−20302	15 55 21	−15 18 30	
IRC−20303	15 57 21	−22 29 00	
IRC−20304	16 00 55	−24 35 24	
IRC−20305	16 02 32	−19 40 06	
IRC−20306	16 03 05	−21 36 12	
IRC−20307	16 03 59	−20 39 30	
IRC−20308	16 04 32	−20 44 54	
IRC−20309	16 05 19	−23 39 36	
IRC−20310	16 16 51	−22 10 06	
IRC−20311	16 17 38	−24 03 06	
IRC−20312	16 17 43	−21 43 42	
IRC−20313	16 17 46	−23 43 12	
IRC−20314	16 20 22	−23 21 36	
IRC−20315	16 20 53	−22 15 42	
IRC−20316	16 21 11	−19 55 24	
IRC−20317	16 26 32	−19 14 12	
IRC−20318	16 28 17	−16 30 24	
IRC−20319	16 30 50	−16 02 06	
IRC−20320	16 32 26	−24 51 06	
IRC−20321	16 36 16	−21 46 24	
IRC−20322	16 36 43	−20 46 54	
IRC−20323	16 37 35	−20 18 00	
IRC−20324	16 38 19	−19 52 06	
IRC−20325	16 38 42	−17 38 30	
IRC−20326	16 41 43	−22 59 30	
IRC−20327	16 42 35	−19 02 54	
IRC−20328	16 42 46	−19 46 12	
IRC−20329	16 43 13	−16 48 54	
IRC−20330	16 43 40	−16 29 42	
IRC−20331	16 45 12	−24 26 00	
IRC−20332	16 46 04	−20 22 12	
IRC−20333	16 46 06	−19 23 06	
IRC−20334	16 46 38	−21 46 30	
IRC−20335	16 50 18	−21 35 30	
IRC−20336	16 52 10	−21 53 30	
IRC−20337	16 53 37	−15 24 36	
IRC−20338	16 53 52	−15 51 42	
IRC−20339	16 54 31	−23 15 12	
IRC−20340	16 54 56	−19 42 30	
IRC−20341	17 00 13	−20 29 54	
IRC−20342	17 00 20	−20 04 00	
IRC−20343	17 00 25	−21 45 06	
IRC−20344	17 00 51	−24 46 30	
IRC−20345	17 03 31	−23 50 36	
IRC−20346	17 03 55	−16 42 42	
IRC−20347	17 04 54	−16 01 36	
IRC−20348	17 07 34	−15 39 54	
IRC−20349	17 07 46	−24 18 00	
IRC−20350	17 12 26	−21 23 00	
IRC−20351	17 13 27	−15 10 30	
IRC−20352	17 14 08	−17 37 30	
IRC−20353	17 14 55	−24 13 30	
IRC−20354	17 15 26	−16 15 54	
IRC−20355	17 16 34	−18 54 12	
IRC−20356	17 16 55	−21 40 42	
IRC−20357	17 18 20	−21 30 54	
IRC−20358	17 18 55	−20 31 36	
IRC−20359	17 21 23	−22 20 30	
IRC−20360	17 23 21	−20 41 12	
IRC−20361	17 23 40	−21 25 42	
IRC−20362	17 24 31	−18 54 54	
IRC−20363	17 25 52	−23 24 06	
IRC−20364	17 26 47	−19 25 36	
IRC−20365	17 26 53	−24 53 42	
IRC−20366	17 28 09	−23 37 06	
IRC−20367	17 28 13	−20 13 12	
IRC−20368	17 30 08	−22 23 42	
IRC−20369	17 31 08	−24 50 30	
IRC−20370	17 31 47	−23 41 54	
IRC−20371	17 33 18	−22 25 42	
IRC−20372	17 34 31	−16 19 12	
IRC−20373	17 34 40	−15 23 00	
IRC−20374	17 35 13	−20 50 24	
IRC−20375	17 35 58	−21 39 00	
IRC−20376	17 37 15	−24 40 06	
IRC−20377	17 38 52	−16 45 12	
IRC−20378	17 38 56	−20 46 06	
IRC−20379	17 39 08	−20 23 42	
IRC−20380	17 39 53	−17 27 12	
IRC−20381	17 41 34	−22 55 54	
IRC−20382	17 42 01	−18 38 12	
IRC−20383	17 42 59	−16 05 30	
IRC−20384	17 44 46	−22 27 12	
IRC−20385	17 45 01	−24 45 30	
IRC−20386	17 45 23	−22 01 06	
IRC−20387	17 45 34	−24 37 12	
IRC−20388	17 45 41	−19 45 54	
IRC−20389	17 45 46	−23 13 30	
IRC−20390	17 46 57	−23 19 54	
IRC−20391	17 47 01	−21 30 54	
IRC−20392	17 47 16	−22 23 24	
IRC−20393	17 47 52	−21 46 06	
IRC−20394	17 48 31	−22 10 00	
IRC−20395	17 49 56	−24 12 06	
IRC−20396	17 50 00	−18 08 06	
IRC−20397	17 51 23	−23 13 30	
IRC−20398	17 51 51	−23 29 12	
IRC−20399	17 51 53	−23 58 30	
IRC−20400	17 52 29	−24 06 12	
IRC−20401	17 53 02	−17 27 06	
IRC−20402	17 53 02	−21 07 00	
IRC−20403	17 54 02	−19 20 54	
IRC−20404	17 54 02	−19 31 30	
IRC−20405	17 54 05	−23 55 42	
IRC−20406	17 55 26	−22 32 42	
IRC−20407	17 55 49	−16 35 36	
IRC−20408	17 56 20	−21 25 36	
IRC−20409	17 56 53	−23 31 06	
IRC−20410	17 57 05	−20 21 42	
IRC−20411	17 57 13	−24 02 00	
IRC−20412	17 57 59	−22 54 30	
IRC−20413	17 58 11	−20 31 36	
IRC−20414	17 58 25	−15 21 42	
IRC−20415	17 58 28	−17 09 12	
IRC−20416	17 58 50	−22 44 54	
IRC−20417	17 59 01	−23 37 36	
IRC−20418	17 59 22	−23 28 06	
IRC−20419	17 59 26	−17 08 00	
IRC−20420	17 59 26	−19 10 42	
IRC−20421	17 59 28	−22 55 36	
IRC−20422	17 59 53	−22 00 54	
IRC−20423	18 00 28	−21 49 12	
IRC−20424	18 00 58.0	−20 19 12	
IRC−20424	18 00 59	−20 19 30	
IRC−20425	18 01 02	−16 56 06	
IRC−20426	18 01 56	−15 42 24	
IRC−20427	18 02 38	−21 14 00	
IRC−20428	18 03 47	−22 04 00	
IRC−20429	18 04 37	−19 18 12	
IRC−20430	18 04 52	−17 09 36	
IRC−20431	18 05 05	−22 14 00	
IRC−20432	18 05 20	−23 52 00	
IRC−20433	18 05 20	−20 03 00	
IRC−20434	18 05 25	−18 33 36	
IRC−20435	18 05 50	−21 24 42	
IRC−20436	18 06 22	−17 22 54	
IRC−20437	18 06 34	−23 07 42	
IRC−20438	18 06 52	−15 17 36	
IRC−20439	18 07 14	−24 00 54	
IRC−20440	18 07 37	−23 40 06	
IRC−20441	18 08 05	−18 53 06	
IRC−20442	18 08 43	−21 18 12	
IRC−20443	18 08 44	−23 42 36	
IRC−20444	18 09 06	−18 52 54	
IRC−20445	18 09 22	−21 07 36	
IRC−20446	18 09 51	−17 25 36	
IRC−20447	18 09 58	−16 19 24	
IRC−20448	18 09 58	−24 53 42	
IRC−20449	18 10 47	−19 15 06	
IRC−20450	18 10 50	−17 10 06	
IRC−20451	18 11 18	−21 44 00	
IRC−20452	18 11 31	−22 47 00	
IRC−20453	18 12 36	−18 56 30	
IRC−20454	18 13 31	−16 40 00	
IRC−20455	18 13 31	−17 40 24	
IRC−20456	18 14 17	−17 23 30	
IRC−20457	18 14 47	−15 18 24	
IRC−20458	18 14 59	−17 50 36	
IRC−20459	18 15 14	−24 19 54	
IRC−20460	18 15 32	−18 29 06	
IRC−20461	18 15 34	−15 20 36	
IRC−20462	18 15 51	−15 13 00	
IRC−20463	18 16 22	−15 46 36	
IRC−20464	18 16 29	−15 38 06	
IRC−20465	18 17 16	−15 51 24	
IRC−20466	18 17 35	−16 12 24	
IRC−20467	18 18 08	−15 15 54	
IRC−20468	18 18 22	−24 56 30	
IRC−20469	18 19 00	−23 34 30	
IRC−20470	18 19 42	−19 24 42	
IRC−20471	18 20 22	−20 40 42	
IRC−20472	18 20 34	−21 41 30	
IRC−20473	18 20 37	−23 03 54	
IRC−20474	18 21 07	−19 24 12	
IRC−20475	18 21 43	−19 45 30	
IRC−20476	18 21 59	−16 18 12	
IRC−20477	18 22 04	−18 33 54	
IRC−20478	18 22 23	−20 34 24	
IRC−20479	18 23 02	−19 43 06	
IRC−20480	18 23 12	−21 51 36	
IRC−20481	18 23 22	−18 08 36	
IRC−20482	18 23 31	−22 08 06	
IRC−20483	18 23 46	−21 08 42	
IRC−20484	18 25 08	−16 47 24	
IRC−20485	18 25 10	−21 16 06	
IRC−20486	18 25 38	−19 48 42	
IRC−20487	18 26 07	−17 49 06	
IRC−20488	18 27 31	−16 55 42	
IRC−20489	18 27 32	−20 05 24	
IRC−20490	18 28 28	−21 17 12	
IRC−20491	18 29 05	−24 59 24	
IRC−20492	18 29 37	−23 16 00	
IRC−20493	18 30 08	−19 48 36	
IRC−20494	18 30 14	−20 08 30	
IRC−20495	18 30 50	−24 03 54	
IRC−20496	18 31 55	−19 33 30	
IRC−20497	18 32 28	−19 18 42	
IRC−20498	18 33 22	−23 55 06	
IRC−20499	18 33 44	−23 48 12	
IRC−20500	18 33 47	−19 56 24	
IRC−20501	18 33 55	−15 59 12	
IRC−20502	18 34 10	−19 14 54	
IRC−20503	18 35 24	−24 40 24	
IRC−20504	18 35 29	−18 24 42	
IRC−20505	18 36 10	−15 05 00	
IRC−20506	18 37 23	−15 16 30	
IRC−20507	18 37 24	−18 35 42	
IRC−20508	18 38 25	−17 07 36	
IRC−20509	18 39 57	−15 58 36	
IRC−20510	18 39 58	−19 19 54	
IRC−20511	18 40 53	−15 19 30	
IRC−20512	18 41 04	−21 45 12	
IRC−20513	18 42 13	−20 30 30	
IRC−20514	18 42 59	−17 21 06	
IRC−20515	18 43 04	−19 39 36	
IRC−20516	18 43 19	−22 26 42	
IRC−20517	18 44 18	−20 25 36	
IRC−20518	18 44 33	−23 59 54	
IRC−20519	18 45 07	−16 50 00	
IRC−20520	18 45 16	−19 15 36	
IRC−20521	18 45 31	−22 33 12	
IRC−20522	18 45 35	−23 16 06	
IRC−20523	18 46 43	−20 23 12	
IRC−20524	18 50 13	−21 32 30	
IRC−20525	18 51 05	−21 25 12	
IRC−20526	18 51 10	−22 48 12	
IRC−20527	18 52 03	−16 35 36	
IRC−20528	18 52 07	−22 44 06	
IRC−20529	18 53 49	−18 23 24	
IRC−20530	18 54 46	−21 10 42	
IRC−20531	18 55 33	−19 14 36	
IRC−20532	18 56 29	−19 21 00	
IRC−20533	18 58 36	−22 46 00	
IRC−20534	19 00 43	−22 47 06	
IRC−20535	19 01 09	−19 28 24	
IRC−20536	19 01 41	−21 48 54	
IRC−20537	19 02 07	−21 01 42	
IRC−20538	19 04 46	−17 06 24	
IRC−20539	19 05 50	−19 01 42	
IRC−20540	19 05 56	−22 19 12	
IRC−20540	19 05 56.0	−22 19 12	
IRC−20541	19 06 28	−15 07 24	
IRC−20542	19 06 46	−21 06 24	
IRC−20543	19 08 00	−15 09 36	
IRC−20544	19 08 56	−20 23 00	
IRC−20545	19 10 37	−18 12 30	
IRC−20546	19 11 02	−18 56 30	
IRC−20547	19 11 39	−18 55 24	
IRC−20548	19 13 22	−17 03 36	
IRC−20549	19 13 50	−19 24 06	
IRC−20550	19 14 45	−19 01 00	
IRC−20551	19 15 28	−19 27 00	
IRC−20552	19 15 46	−16 26 24	
IRC−20553	19 16 09	−15 37 54	
IRC−20554	19 16 17	−16 00 24	
IRC−20555	19 16 43	−21 01 06	
IRC−20556	19 17 36	−17 08 24	
IRC−20557	19 17 56	−18 17 36	
IRC−20558	19 18 52	−16 03 12	
IRC−20559	19 22 30	−24 03 12	
IRC−20560	19 23 19	−21 52 12	
IRC−20561	19 23 28	−21 21 00	
IRC−20562	19 24 09	−18 36 42	
IRC−20563	19 24 49	−17 22 24	
IRC−20564	19 26 50	−16 15 24	
IRC−20565	19 27 16	−19 29 24	
IRC−20566	19 30 26	−16 42 30	
IRC−20567	19 31 07	−22 44 54	
IRC−20568	19 31 26	−16 29 00	
IRC−20569	19 31 31	−23 57 42	
IRC−20570	19 34 28	−22 04 06	
IRC−20571	19 37 51	−16 24 42	
IRC−20572	19 43 25	−19 53 06	
IRC−20573	19 43 41	−16 19 54	
IRC−20574	19 44 17	−17 11 24	
IRC−20575	19 45 45	−16 16 42	
IRC−20576	19 48 41	−19 20 12	
IRC−20577	19 53 09	−19 21 00	
IRC−20578	19 57 21	−16 40 54	
IRC−20579	19 58 28	−15 11 00	
IRC−20580	20 00 12	−22 15 36	
IRC−20581	20 00 22	−23 50 30	
IRC−20582	20 05 58	−15 34 12	
IRC−20583	20 11 23	−16 03 30	
IRC−20584	20 13 43	−18 34 06	
IRC−20585	20 14 05	−21 28 30	
IRC−20586	20 16 09	−16 01 06	
IRC−20587	20 16 31	−19 16 42	
IRC−20588	20 25 26	−15 52 00	
IRC−20589	20 26 37	−22 33 36	
IRC−20590	20 29 43	−21 51 42	
IRC−20591	20 31 11	−23 25 06	
IRC−20592	20 37 14	−18 19 24	
IRC−20593	20 41 43	−19 13 30	
IRC−20594	20 46 29	−18 13 06	
IRC−20595	20 52 01	−18 07 06	
IRC−20596	21 04 29	−16 37 30	
IRC−20597	21 12 48	−20 51 42	
IRC−20598	21 12 56	−15 22 24	
IRC−20599	21 19 26	−17 02 54	
IRC−20600	21 20 10	−22 52 54	
IRC−20601	21 21 17	−21 04 00	
IRC−20602	21 23 52	−22 37 54	
IRC−20603	21 24 25	−21 25 24	
IRC−20604	21 25 55	−22 01 36	
IRC−20605	21 37 21	−16 53 36	
IRC−20606	21 39 06	−23 29 36	
IRC−20607	21 39 51	−19 05 36	
IRC−20608	21 44 16	−16 21 42	
IRC−20609	21 48 13	−20 25 06	
IRC−20610	21 52 39	−23 31 42	
IRC−20611	21 52 48	−21 22 54	
IRC−20612	21 55 52	−21 25 36	
IRC−20613	21 56 04	−15 22 06	
IRC−20614	21 56 45	−18 14 00	
IRC−20615	21 59 08	−15 38 30	
IRC−20616	22 15 52	−21 04 36	
IRC−20617	22 18 49	−21 51 36	
IRC−20618	22 20 32	−22 18 30	
IRC−20619	22 25 07	−22 07 36	
IRC−20620	22 40 55	−19 05 36	
IRC−20621	22 42 47	−15 51 12	
IRC−20622	22 44 55	−19 51 12	
IRC−20623	22 51 26	−19 26 00	
IRC−20624	22 54 27	−20 36 12	
IRC−20625	23 01 37	−16 17 06	
IRC−20626	23 02 34	−17 21 00	
IRC−20627	23 02 44	−22 46 00	
IRC−20628	23 03 58	−24 01 00	
IRC−20629	23 06 47	−21 26 30	
IRC−20630	23 07 16	−22 43 54	
IRC−20631	23 15 51	−19 06 54	
IRC−20632	23 16 50	−18 21 36	
IRC−20633	23 20 19	−20 22 12	
IRC−20634	23 21 47	−17 35 30	
IRC−20635	23 23 26	−20 55 00	
IRC−20636	23 32 11	−15 31 42	
IRC−20637	23 38 33	−24 26 06	
IRC−20638	23 38 57	−18 18 06	
IRC−20639	23 39 09	−20 01 54	
IRC−20640	23 39 11	−18 06 24	
IRC−20641	23 39 49	−15 43 00	
IRC−20642	23 41 12	−15 34 06	
IRC−20643	23 50 11	−16 39 00	

NAME	RA (1950)	DEC	POS REF
	h m s	° ′ ″	
IRC−20644	23 53 32	−22 16 12	
IRC−30001	0 04 01	−32 52 30	
IRC−30002	0 05 01	−25 46 30	
IRC−30003	0 09 05	−28 04 24	
IRC−30004	0 11 11	−26 17 54	
IRC−30005	0 11 14	−26 33 42	
IRC−30006	0 12 49	−32 19 06	
IRC−30007	0 13 35	−31 43 24	
IRC−30008	0 20 53	−30 07 30	
IRC−30009	0 31 16	−29 49 36	
IRC−30010	0 33 19	−25 09 12	
IRC−30011	0 36 20	−25 23 00	
IRC−30012	0 53 30	−28 02 42	
IRC−30013	1 03 04	−31 57 42	
IRC−30014	1 21 11	−31 11 36	
IRC−30015	1 24 40	−32 48 00	
IRC−30016	1 27 59	−26 28 00	
IRC−30017	1 32 04	−28 29 24	
IRC−30018	1 39 52	−32 34 30	
IRC−30019	1 42 38	−28 58 06	
IRC−30020	2 00 10	−31 38 00	
IRC−30021	2 26 58	−26 19 06	
IRC−30022	2 28 27	−31 29 42	
IRC−30023	2 35 08	−27 11 24	
IRC−30024	2 40 47	−26 19 24	
IRC−30025	2 42 13	−29 24 36	
IRC−30026	2 47 01	−32 37 00	
IRC−30027	3 06 26	−26 38 06	
IRC−30028	3 09 53	−29 10 54	
IRC−30029	3 30 20	−25 49 12	
IRC−30030	3 41 09	−31 10 36	
IRC−30031	3 48 19	−32 25 12	
IRC−30032	4 01 31	−25 58 12	
IRC−30033	4 09 21	−25 15 54	
IRC−30034	4 21 37	−27 56 30	
IRC−30035	4 25 58	−29 19 24	
IRC−30036	4 31 30	−29 52 00	
IRC−30037	4 33 37	−30 39 30	
IRC−30038	4 34 32	−27 40 36	
IRC−30039	4 37 26	−30 33 12	
IRC−30040	4 41 12	−30 51 24	
IRC−30041	5 00 10	−26 20 30	
IRC−30042	5 10 56	−27 13 36	
IRC−30043	5 17 26	−25 10 30	
IRC−30044	5 27 29	−30 59 30	
IRC−30045	5 31 00	−25 23 36	
IRC−30046	5 33 50	−25 46 00	
IRC−30047	5 36 06	−27 14 24	
IRC−30048	5 39 02	−27 58 06	
IRC−30049	5 45 05	−31 42 54	
IRC−30050	5 47 14	−32 20 54	
IRC−30051	5 48 37	−29 12 36	
IRC−30052	5 53 38	−28 57 36	
IRC−30053	6 01 16	−26 16 36	
IRC−30054	6 08 26	−31 34 36	
IRC−30055	6 14 07	−27 29 30	
IRC−30056	6 15 16	−31 01 00	
IRC−30057	6 16 50	−26 08 36	
IRC−30058	6 18 54	−30 37 06	
IRC−30059	6 21 27	−26 21 00	
IRC−30060	6 21 40	−27 02 30	
IRC−30061	6 21 56	−25 32 54	
IRC−30062	6 27 11	−26 05 12	
IRC−30063	6 29 31	−32 49 54	
IRC−30064	6 30 07	−27 07 06	
IRC−30065	6 31 32	−29 36 00	
IRC−30066	6 31 50	−30 32 54	
IRC−30067	6 34 23	−30 32 06	
IRC−30068	6 35 56	−32 17 36	
IRC−30069	6 41 08	−26 04 24	
IRC−30070	6 50 56	−26 53 54	
IRC−30071	6 56 38	−28 53 54	
IRC−30072	6 59 46	−27 51 24	
IRC−30073	7 03 32	−25 01 54	
IRC−30074	7 03 58	−30 49 24	
IRC−30075	7 05 10	−29 27 42	
IRC−30076	7 06 18	−26 19 00	
IRC−30077	7 07 44	−27 47 54	
IRC−30078	7 09 07	−29 02 24	
IRC−30079	7 10 35	−31 53 24	
IRC−30080	7 10 51	−31 41 36	
IRC−30081	7 11 56	−26 01 00	
IRC−30082	7 12 49	−26 57 24	
IRC−30083	7 14 37	−27 47 42	
IRC−30084	7 16 50	−26 30 24	
IRC−30085	7 19 01	−25 48 00	
IRC−30086	7 19 18	−29 12 24	
IRC−30087	7 20 53	−25 40 24	
IRC−30088	7 20 59	−25 22 30	
IRC−30089	7 21 12	−29 16 42	
IRC−30090	7 21 28	−27 44 24	
IRC−30091	7 22 10	−29 12 30	
IRC−30092	7 22 50	−31 42 54	
IRC−30093	7 26 02	−26 43 42	
IRC−30094	7 28 51	−30 51 30	
IRC−30095	7 34 37	−31 12 54	
IRC−30096	7 35 40	−26 18 00	
IRC−30097	7 37 31	−27 35 12	
IRC−30098	7 41 34	−28 17 36	
IRC−30099	7 41 48	−28 50 06	
IRC−30100	7 44 38	−32 11 06	
IRC−30101	7 48 17	−27 50 42	
IRC−30102	7 49 46	−30 19 00	
IRC−30103	7 51 52	−26 13 00	
IRC−30104	7 52 35	−27 56 42	
IRC−30105	7 53 40	−28 31 06	
IRC−30106	7 53 47	−29 20 54	
IRC−30107	7 54 16	−30 08 42	
IRC−30108	7 56 52	−32 26 06	
IRC−30109	7 58 22	−32 34 42	
IRC−30110	7 58 24	−29 58 30	
IRC−30111	7 59 29	−31 39 24	
IRC−30112	8 00 13	−26 05 54	
IRC−30113	8 01 09	−32 20 00	
IRC−30114	8 01 47	−31 18 12	
IRC−30115	8 02 16	−32 31 54	
IRC−30116	8 02 26	−25 33 12	
IRC−30117	8 02 28	−27 44 24	
IRC−30118	8 02 36	−29 49 24	
IRC−30119	8 03 16	−26 37 24	
IRC−30120	8 09 50	−28 09 30	
IRC−30121	8 15 06	−31 16 54	
IRC−30122	8 17 56	−29 11 24	
IRC−30123	8 19 22	−32 54 06	
IRC−30124	8 20 02	−25 28 06	
IRC−30125	8 22 55	−30 13 06	
IRC−30126	8 26 56	−30 36 54	
IRC−30127	8 27 45	−30 23 24	
IRC−30128	8 28 29	−31 59 30	
IRC−30129	8 30 01	−31 48 24	
IRC−30130	8 32 23	−26 56 24	
IRC−30131	8 37 38	−29 22 42	
IRC−30132	8 41 47	−25 25 30	
IRC−30133	8 43 25	−28 01 06	
IRC−30134	8 44 32	−29 32 36	
IRC−30135	8 46 09	−28 27 30	
IRC−30136	8 48 26	−27 31 54	
IRC−30137	8 57 37	−27 59 00	
IRC−30138	8 58 59	−27 19 12	
IRC−30139	9 00 45	−27 59 54	
IRC−30140	9 02 31	−32 14 00	
IRC−30141	9 05 22	−26 02 06	
IRC−30142	9 05 52	−25 39 24	
IRC−30143	9 05 55	−27 06 36	
IRC−30144	9 07 36	−27 58 42	
IRC−30145	9 10 22	−26 17 42	
IRC−30146	9 11 13	−29 27 42	
IRC−30147	9 12 37	−29 57 12	
IRC−30148	9 15 01	−31 31 36	
IRC−30149	9 16 09	−32 49 06	
IRC−30150	9 19 17	−25 45 00	
IRC−30151	9 21 03	−28 36 12	
IRC−30152	9 25 16	−29 14 06	
IRC−30153	9 27 44	−26 22 12	
IRC−30154	9 33 51	−25 42 06	
IRC−30155	9 39 44	−32 16 42	
IRC−30156	9 48 54	−29 39 24	
IRC−30157	9 51 56	−25 41 30	
IRC−30158	9 52 47	−25 07 42	
IRC−30159	9 54 14	−32 00 00	
IRC−30160	10 09 50	−32 20 36	
IRC−30161	10 13 34	−26 14 12	
IRC−30162	10 13 38	−31 55 36	
IRC−30163	10 13 41	−30 43 00	
IRC−30164	10 24 52	−30 48 54	
IRC−30165	10 24 58	−25 17 30	
IRC−30166	10 27 12	−29 24 30	
IRC−30167	10 34 53	−27 09 24	
IRC−30168	10 45 12	−31 20 12	
IRC−30169	10 48 56	−28 21 30	
IRC−30170	11 00 50	−31 41 12	
IRC−30171	11 09 50	−32 09 54	
IRC−30172	11 09 52	−29 30 42	
IRC−30173	11 12 13	−25 48 30	
IRC−30174	11 16 25	−30 11 54	
IRC−30175	11 23 53	−25 29 12	
IRC−30176	11 29 54	−26 28 30	
IRC−30177	11 30 23	−30 48 36	
IRC−30178	11 30 34	−31 35 00	
IRC−30179	11 37 45	−28 13 00	
IRC−30180	11 37 46	−29 58 54	
IRC−30181	11 39 10	−32 13 24	
IRC−30182	11 46 13	−26 28 36	
IRC−30183	11 47 20	−27 18 36	
IRC−30184	11 51 40	−30 37 54	
IRC−30185	11 53 07	−28 11 36	
IRC−30186	11 56 47	−29 47 06	
IRC−30187	12 01 03	−32 07 42	
IRC−30188	12 08 56	−26 47 54	
IRC−30189	12 12 56	−31 24 54	
IRC−30190	12 17 18	−26 27 54	
IRC−30191	12 21 12	−30 03 12	
IRC−30192	12 34 44	−27 46 24	
IRC−30193	12 38 35	−27 38 00	
IRC−30194	12 41 22	−28 02 42	
IRC−30195	12 45 01	−29 31 12	
IRC−30196	12 48 11	−29 34 30	
IRC−30197	12 49 05	−30 48 42	
IRC−30198	12 50 06	−25 44 06	
IRC−30199	12 56 14	−29 43 24	
IRC−30200	13 02 52	−25 45 06	
IRC−30201	13 05 21	−32 08 06	
IRC−30202	13 05 48	−32 50 42	
IRC−30203	13 14 04	−31 14 54	
IRC−30204	13 25 13	−26 09 00	
IRC−30205	13 26 05	−31 44 12	
IRC−30206	13 38 37	−26 17 12	
IRC−30207	13 46 13	−28 07 06	
IRC−30208	13 52 30	−26 10 54	
IRC−30209	13 54 07	−26 54 42	
IRC−30210	13 54 51	−30 49 30	
IRC−30211	13 55 56	−32 33 00	
IRC−30212	13 59 32	−27 11 06	
IRC−30213	14 03 33	−26 26 12	
IRC−30214	14 06 58	−30 23 54	
IRC−30215	14 08 42	−28 38 24	
IRC−30216	14 09 50	−27 01 36	
IRC−30217	14 10 37	−29 40 30	
IRC−30218	14 16 13	−26 54 54	
IRC−30219	14 17 14	−31 16 30	
IRC−30220	14 20 13	−27 31 36	
IRC−30221	14 22 45	−27 17 54	
IRC−30222	14 27 59	−29 52 24	
IRC−30223	14 38 13	−25 04 12	
IRC−30224	14 39 02	−28 43 36	
IRC−30225	14 44 50	−32 02 36	
IRC−30226	14 47 20	−27 45 30	
IRC−30227	14 53 26	−32 26 30	
IRC−30228	15 01 08	−25 05 12	
IRC−30229	15 06 02	−26 18 30	
IRC−30230	15 07 38	−30 57 00	
IRC−30231	15 14 46	−29 57 42	
IRC−30232	15 15 21	−27 44 54	
IRC−30233	15 18 38	−28 30 06	
IRC−30234	15 19 04	−32 00 54	
IRC−30235	15 22 08	−26 34 30	
IRC−30236	15 30 21	−27 00 54	
IRC−30237	15 31 35	−27 52 42	
IRC−30238	15 33 09	−28 50 00	
IRC−30239	15 34 00	−27 58 00	
IRC−30240	15 38 26	−29 08 06	
IRC−30241	15 40 54	−30 42 36	
IRC−30242	15 42 47	−25 20 42	
IRC−30243	15 47 30	−29 23 30	
IRC−30244	15 47 32	−26 08 42	
IRC−30245	15 48 53	−30 02 54	
IRC−30246	15 49 44	−25 56 54	
IRC−30247	15 55 32	−30 35 24	
IRC−30248	15 58 11	−31 44 36	
IRC−30249	15 58 31	−25 03 00	
IRC−30250	15 59 00	−28 50 54	
IRC−30251	15 59 28	−26 00 36	
IRC−30252	16 00 20	−25 43 12	
IRC−30253	16 05 06	−26 11 36	
IRC−30254	16 05 38	−32 42 54	
IRC−30255	16 07 17	−29 09 30	
IRC−30256	16 07 57	−29 17 24	
IRC−30257	16 10 19	−32 13 00	
IRC−30258	16 11 33	−32 15 24	
IRC−30259	16 15 41	−28 37 12	
IRC−30260	16 18 08	−25 28 06	
IRC−30261	16 18 32	−27 48 06	
IRC−30262	16 19 13	−31 53 12	
IRC−30263	16 21 01	−28 08 00	
IRC−30264	16 24 14	−31 11 42	
IRC−30265	16 26 20	−26 19 24	
IRC−30266	16 33 28	−31 08 06	
IRC−30267	16 36 59	−28 51 24	
IRC−30268	16 37 25	−32 17 06	
IRC−30269	16 38 44	−27 00 36	
IRC−30270	16 49 23	−30 16 06	
IRC−30271	16 53 26	−30 29 36	
IRC−30272	16 53 32	−32 54 42	
IRC−30273	16 54 37	−32 30 24	
IRC−30274	16 56 55	−25 01 06	
IRC−30275	16 57 50	−29 36 06	
IRC−30276	16 59 07	−29 31 06	
IRC−30277	16 59 31	−32 39 24	
IRC−30278	17 02 40	−29 36 54	
IRC−30279	17 04 20	−31 46 06	
IRC−30280	17 05 07	−30 59 24	
IRC−30281	17 06 40	−31 18 54	
IRC−30282	17 08 02	−32 15 54	
IRC−30283	17 08 58	−29 15 12	
IRC−30284	17 09 43	−32 43 54	
IRC−30285	17 10 28	−31 47 24	
IRC−30286	17 10 47	−31 24 12	
IRC−30287	17 12 01	−30 29 12	
IRC−30288	17 12 14	−26 32 12	
IRC−30289	17 13 05	−31 25 24	
IRC−30290	17 14 58	−25 31 42	
IRC−30291	17 20 13	−28 05 42	
IRC−30292	17 20 38	−28 26 06	
IRC−30293	17 20 50	−29 16 54	
IRC−30294	17 22 27	−26 48 24	
IRC−30295	17 22 34	−25 20 36	
IRC−30296	17 23 06	−32 58 36	
IRC−30297	17 23 45	−31 03 12	
IRC−30298	17 24 22	−31 04 30	
IRC−30299	17 25 18	−29 01 30	
IRC−30300	17 26 53	−26 25 42	
IRC−30301	17 27 19	−26 43 06	
IRC−30302	17 27 47	−27 16 54	
IRC−30303	17 32 16.4	−31 59 17	
IRC−30303	17 32 17	−31 59 00	
IRC−30304	17 33 36	−32 14 00	
IRC−30304	17 33 36.5	−32 13 53	
IRC−30305	17 34 52.2	−32 07 40	
IRC−30305	17 34 55	−32 07 24	
IRC−30306	17 35 00	−30 39 30	
IRC−30307	17 35 04	−28 00 54	
IRC−30308	17 35 27	−31 55 42	
IRC−30309	17 36 02	−31 41 30	
IRC−30310	17 36 36.3	−31 26 58	
IRC−30310	17 36 38	−31 26 12	
IRC−30311	17 37 26	−29 12 12	
IRC−30312	17 37 29	−31 56 36	
IRC−30312	17 37 29.0	−31 56 51	
IRC−30313	17 37 43	−32 11 12	
IRC−30314	17 38 06	−30 17 42	
IRC−30315	17 39 26	−25 16 00	
IRC−30316	17 39 30	−30 04 54	
IRC−30317	17 40 18	−32 38 12	
IRC−30318	17 40 58	−30 24 06	
IRC−30319	17 42 02	−28 18 12	
IRC−30320	17 42 02	−28 09 30	
IRC−30321	17 42 31	−28 58 00	
IRC−30322	17 42 37	−28 38 00	
IRC−30323	17 43 56	−26 57 30	
IRC−30324	17 44 25	−27 49 12	
IRC−30325	17 46 50	−28 59 42	
IRC−30326	17 48 51	−28 00 42	
IRC−30327	17 48 58	−29 37 12	
IRC−30328	17 49 31	−28 38 24	
IRC−30329	17 50 04	−31 43 12	
IRC−30330	17 50 58	−28 19 54	
IRC−30331	17 52 02	−27 59 30	
IRC−30332	17 52 10	−29 06 42	
IRC−30333	17 52 47	−28 01 24	
IRC−30334	17 53 43	−25 16 36	
IRC−30335	17 53 49	−26 26 54	
IRC−30336	17 53 52	−27 19 06	
IRC−30337	17 53 55	−31 18 30	
IRC−30338	17 54 03	−25 48 30	
IRC−30339	17 54 26	−30 09 06	
IRC−30340	17 54 27	−29 51 54	
IRC−30341	17 55 54	−30 14 42	
IRC−30342	17 56 03	−26 38 06	
IRC−30343	17 56 35	−31 17 42	
IRC−30344	17 58 03	−25 00 42	
IRC−30345	17 59 07	−29 17 06	
IRC−30346	17 59 46	−27 49 36	
IRC−30347	18 00 08	−25 13 54	
IRC−30348	18 01 37	−26 02 24	

NAME	RA (1950) h m s	DEC ° ' "	POS REF
IRC−30349	18 01 47	−26 07 00	
IRC−30350	18 01 51	−28 02 54	
IRC−30351	18 01 51	−29 35 12	
IRC−30352	18 02 27	−27 04 54	
IRC−30353	18 02 35	−30 25 30	
IRC−30354	18 02 38	−25 14 54	
IRC−30355	18 02 55	−25 27 06	
IRC−30356	18 03 45	−27 51 00	
IRC−30357	18 04 19	−26 24 42	
IRC−30358	18 04 28	−29 26 42	
IRC−30359	18 04 56	−28 27 42	
IRC−30360	18 05 05	−31 00 36	
IRC−30361	18 05 27	−31 13 00	
IRC−30362	18 05 38	−30 37 12	
IRC−30363	18 05 49	−26 16 24	
IRC−30364	18 06 11	−27 40 54	
IRC−30365	18 07 21	−26 52 24	
IRC−30366	18 08 01	−25 46 12	
IRC−30367	18 08 59	−29 52 24	
IRC−30368	18 10 04	−29 26 12	
IRC−30369	18 11 47	−28 41 00	
IRC−30370	18 11 52	−29 50 30	
IRC−30371	18 12 06	−26 19 54	
IRC−30372	18 13 25	−30 01 42	
IRC−30373	18 14 43	−27 22 42	
IRC−30374	18 14 53	−27 03 42	
IRC−30375	18 15 50	−29 47 00	
IRC−30376	18 17 46	−29 50 54	
IRC−30377	18 18 35	−26 49 36	
IRC−30378	18 19 09	−32 14 00	
IRC−30379	18 20 20	−26 00 24	
IRC−30380	18 20 59	−29 07 36	
IRC−30381	18 21 49	−30 47 24	
IRC−30382	18 21 55	−25 58 06	
IRC−30383	18 22 18	−32 10 12	
IRC−30384	18 23 52	−25 42 54	
IRC−30385	18 24 49	−27 39 36	
IRC−30386	18 24 54	−25 27 00	
IRC−30387	18 29 49	−28 56 36	
IRC−30388	18 30 20	−28 08 30	
IRC−30389	18 32 25	−27 23 12	
IRC−30390	18 33 05	−32 22 00	
IRC−30391	18 33 06	−28 02 12	
IRC−30392	18 36 38	−28 41 54	
IRC−30393	18 37 49	−26 07 54	
IRC−30394	18 43 40	−29 41 12	
IRC−30395	18 51 04	−32 31 36	
IRC−30396	18 52 10	−26 21 30	
IRC−30397	18 53 22	−29 38 12	
IRC−30398	18 56 04	−29 54 30	
IRC−30399	18 59 23	−29 56 36	
IRC−30400	18 59 39	−25 10 36	
IRC−30401	19 03 48	−27 44 36	
IRC−30402	19 04 25	−28 42 54	
IRC−30403	19 04 26	−28 56 06	
IRC−30404	19 09 19	−32 56 12	
IRC−30405	19 10 12	−25 59 30	
IRC−30406	19 11 23	−29 54 54	
IRC−30407	19 12 29	−25 20 36	
IRC−30408	19 16 37	−31 48 30	
IRC−30409	19 17 14	−31 54 42	
IRC−30410	19 19 13	−32 01 42	
IRC−30411	19 19 48	−29 09 42	
IRC−30412	19 26 45	−27 05 24	
IRC−30413	19 29 19	−30 58 30	
IRC−30414	19 29 55	−30 28 06	
IRC−30415	19 37 53	−29 02 06	
IRC−30416	19 50 02	−32 13 06	
IRC−30417	19 50 44	−31 03 06	
IRC−30418	19 52 46	−26 25 54	
IRC−30419	19 52 50	−29 19 06	
IRC−30420	19 53 05	−28 10 06	
IRC−30421	19 53 53	−27 18 12	
IRC−30422	19 55 56	−26 19 54	
IRC−30423	19 59 34	−27 51 06	
IRC−30424	20 01 09	−32 12 00	
IRC−30425	20 03 51	−27 22 06	
IRC−30426	20 04 45	−30 52 42	
IRC−30427	20 06 52	−25 44 42	
IRC−30428	20 12 47	−30 08 06	
IRC−30429	20 22 17	−30 08 36	
IRC−30430	20 24 52	−28 25 36	
IRC−30431	20 27 29	−27 10 12	
IRC−30432	20 33 20	−30 53 12	
IRC−30433	20 35 43	−28 15 06	
IRC−30434	20 38 17	−31 46 42	
IRC−30435	20 43 41	−27 25 30	
IRC−30436	20 47 41	−32 14 54	
IRC−30437	20 48 52	−27 06 06	
IRC−30438	20 51 07	−28 06 24	
IRC−30439	20 58 13	−32 27 00	
IRC−30440	21 03 22	−32 32 36	
IRC−30441	21 04 11	−25 12 36	
IRC−30442	21 07 04	−29 55 42	
IRC−30443	21 10 18	−27 49 06	
IRC−30444	21 18 49	−30 21 54	
IRC−30445	21 26 36	−29 00 24	
IRC−30446	21 26 51	−32 41 12	
IRC−30447	21 36 22	−30 31 54	
IRC−30448	21 39 11	−26 05 12	
IRC−30449	22 00 27	−31 41 24	
IRC−30450	22 01 31	−30 09 24	
IRC−30451	22 05 59	−32 43 54	
IRC−30452	22 37 37	−30 55 30	
IRC−30453	22 39 35	−29 37 36	
IRC−30454	22 40 36	−30 45 06	
IRC−30455	22 49 26	−25 34 12	
IRC−30456	22 52 33	−29 52 54	
IRC−30457	22 53 11	−32 48 36	
IRC−30458	22 54 53	−29 53 30	
IRC−30459	22 55 05	−26 26 06	
IRC−30460	22 57 23	−25 25 54	
IRC−30461	22 58 35	−29 07 30	
IRC−30462	23 00 56	−27 05 30	
IRC−30463	23 04 10	−30 34 36	
IRC−30464	23 04 42	−25 52 00	
IRC−30465	23 06 25	−30 24 30	
IRC−30466	23 07 03	−28 21 30	

NAME	RA (1950) h m s	DEC ° ' "	POS REF
IRC−30467	23 14 24	−28 42 42	
IRC−30468	23 16 07	−32 48 12	
IRC−30469	23 16 21	−28 39 42	
IRC−30470	23 52 05	−31 03 06	
IRC−30471	23 54 38	−26 54 24	
IRC−30472	23 56 49	−29 46 00	
IRS2 3"N,3"E	17 42 29.2	−28 59 20	
IRS7 2.4"S,2E	17 42 29.4	−28 59 15	
IR12.9−0.3	18 11 44.3	−17 53 02	
IR34.3+0.2	18 50 46.3	+ 1 11 12	
IR35.2−1.7	18 59 13.6	+ 1 09 01	
IR35.6−0.0	18 53 51.7	+ 2 16 30	
IR40.6−0.1	19 03 35.5	+ 6 41 56	
ISS #1	12 56 45	−29 44	
ISS #2	14 28 01	−29 52	
ISS #3	7 54 23	−30 09	
ISS #4	8 27 40	−30 25	
ISS #5	16 53 16	−30 30	
ISS #6	11 51 30	−30 41	
ISS #7	11 30 25	−30 49	
ISS #8	13 54 40	−30 49	
ISS #9	10 25 00	−30 50	
ISS #10	12 49 10	−30 50	
ISS #11	12 14 05	−31 04	
ISS #12	7 58 30	−31 07	
ISS #13	16 33 28	−31 08	
ISS #14	10 44 30	−31 20	
ISS #15	14 36 28	−31 26	
ISS #16	9 30 50	−31 32	
ISS #17	12 12 45	−31 32	
ISS #18	11 30 32	−31 35	
ISS #19	12 33 30	−31 41	
ISS #20	18 13 00	−31 46	
ISS #21	19 17 20	−31 55	
ISS #22	15 19 12	−32 01	
ISS #23	17 34 25	−32 07	
ISS #24	12 01 20	−32 08	
ISS #25	11 09 50	−32 08	
ISS #26	17 37 35	−32 11	
ISS #27	11 39 14	−32 13	
ISS #28	17 07 55	−32 15	
ISS #29	16 37 20	−32 17	
ISS #30	18 33 15	−32 21	
ISS #31	7 57 00	−32 26	
ISS #32	10 09 55	−32 27	
ISS #33	14 16 35	−32 28	
ISS #34	14 53 28	−32 28	
ISS #35	8 02 19	−32 32	
ISS #36	11 32 00	−32 32	
ISS #37	7 58 18	−32 33	
ISS #38	14 56 05	−32 34	
ISS #39	13 20 20	−32 56	
ISS #40	9 16 20	−32 58	
ISS #41	8 19 52	−33 02	
ISS #42	17 40 00	−33 02	
ISS #43	12 48 10	−33 05	
ISS #44	18 33 05	−33 05	
ISS #45	19 17 50	−33 06	
ISS #46	16 53 55	−33 11	
ISS #47	17 54 50	−33 11	
ISS #48	19 51 45	−33 11	
ISS #49	18 24 30	−33 21	
ISS #50	17 11 32	−33 23	
ISS #51	17 32 40	−33 25	
ISS #52	17 22 30	−33 32	
ISS #53	17 31 55	−33 34	
ISS #54	18 59 45	−33 35	
ISS #55	18 22 50	−33 36	
ISS #56	16 32 12	−33 37	
ISS #57	17 28 30	−33 40	
ISS #58	12 10 36	−33 51	
ISS #59	19 29 15	−33 51	
ISS #60	12 48 15	−33 52	
ISS #61	15 27 45	−33 52	
ISS #62	17 29 33	−34 02	
ISS #63	16 38 00	−34 03	
ISS #64	17 28 00	−34 03	
ISS #65	17 47 53	−34 03	
ISS #66	14 34 15	−34 04	
ISS #67	19 37 00	−34 05	
ISS #68	16 46 55	−34 12	
ISS #69	13 46 32	−34 12	
ISS #70	15 54 15	−34 14	
ISS #71	10 49 12	−34 15	
ISS #72	12 30 50	−34 22	
ISS #73	18 20 50	−34 23	
ISS #74	18 46 30	−34 32	
ISS #75	17 50 00	−34 54	
ISS #76	10 02 30	−34 55	
ISS #77	14 40 36	−34 58	
ISS #78	19 06 55	−34 59	
ISS #79	18 04 05	−35 02	
ISS #80	14 53 08	−35 09	
ISS #81	16 33 05	−35 09	
ISS #82	20 20 05	−35 10	
ISS #83	12 21 25	−35 23	
ISS #84	18 03 05	−35 35	
ISS #85	17 44 20	−35 43	
ISS #86	11 46 17	−35 44	
ISS #87	11 23 04	−35 47	
ISS #88	11 08 30	−35 54	
ISS #89	11 13 32	−36 02	
ISS #90	15 18 38	−36 05	
ISS #91	14 03 44	−36 07	
ISS #92	17 32 10	−36 10	
ISS #93	12 46 40	−36 16	
ISS #94	23 04 50	−36 24	
ISS #95	13 17 47	−36 27	
ISS #96	14 45 31	−36 27	
ISS #97	14 16 56	−36 38	
ISS #98	20 18 16	−36 38	
ISS #99	20 13 06	−36 38	
ISS #100	18 14 15	−36 46	
ISS #101	18 17 16	−36 46	
ISS #102	17 00 50	−36 48	
ISS #103	17 39 27	−36 56	
ISS #104	14 54 30	−36 58	
ISS #105	18 05 42	−36 59	

NAME	RA (1950) h m s	DEC ° ' "	POS REF
ISS #106	15 40 19	−37 01	
ISS #107	17 46 27	−37 03	
ISS #108	17 30 13	−37 06	
ISS #109	13 04 00	−37 12	
ISS #110	20 23 15	−37 16	
ISS #111	18 37 51	−37 31	
ISS #112	22 22 42	−37 50	
ISS #113	17 18 40	−37 52	
ISS #114	15 48 25	−38 01	
ISS #115	20 00 04	−38 05	
ISS #116	20 35 40	−38 06	
ISS #117	14 30 46	−38 15	
ISS #118	21 36 50	−38 16	
ISS #119	20 29 30	−38 18	
ISS #120	19 15 20	−38 20	
ISS #121	18 59 12	−38 22	
ISS #122	12 49 55	−38 31	
ISS #123	17 16 50	−38 35	
ISS #124	17 33 06	−38 38	
ISS #125	13 37 12	−38 44	
ISS #126	14 26 00	−38 48	
ISS #127	17 22 20	−38 51	
ISS #128	17 00 20	−39 00	
ISS #129	17 39 02	−39 00	
ISS #130	16 20 07	−39 04	
ISS #131	16 01 35	−39 05	
ISS #132	13 28 08	−39 09	
ISS #133	20 14 25	−39 14	
ISS #134	19 20 30	−39 17	
ISS #135	14 25 10	−39 19	
ISS #136	19 06 36	−39 26	
ISS #137	22 48 12	−39 26	
ISS #138	13 23 14	−39 30	
ISS #139	13 36 44	−39 32	
ISS #140	12 54 41	−39 32	
ISS #141	17 11 30	−39 35	
ISS #142	17 10 56	−39 41	
ISS #143	23 56 20	−39 44	
ISS #144	18 58 40	−39 49	
ISS #145	22 03 40	−39 49	
ISS #146	13 36 50	−39 50	
ISS #147	15 30 40	−39 56	
ISS #148	15 34 27	−39 57	
ISS #149	18 04 12	−39 58	
ISS #150	20 50 25	−40 00	
ISS #151	17 44 05	−40 06	
ISS #152	0 25 59	−40 11	
ISS #153	14 27 18	−40 13	
ISS #154	15 07 35	−40 13	
ISS #155	15 36 17	−40 14	
ISS #156	17 32 30	−40 16	
ISS #157	12 44 25	−40 17	
ISS #158	18 25 40	−40 17	
ISS #159	17 06 35	−40 17	
ISS #160	17 17 40	−40 20	
ISS #161	22 40 30	−40 22	
ISS #162	15 24 10	−40 32	
ISS #163	15 33 28	−40 32	
ISS #164	19 04 52	−40 36	
ISS #165	15 01 30	−40 40	
ISS #166	20 26 00	−40 41	
ISS #167	15 04 05	−40 43	
ISS #168	17 48 02	−40 46	
ISS #169	22 08 55	−40 48	
ISS #170	15 02 32	−40 52	
ISS #171	23 07 28	−40 52	
ISS #172	14 56 24	−40 55	
ISS #173	20 18 30	−40 55	
ISS #174	21 20 35	−40 55	
ISS #175	13 01 59	−40 56	
ISS #176	15 53 32	−40 56	
ISS #177	20 22 27	−40 59	
ISS #178	15 02 47	−41 17	
ISS #179	12 27 17	−41 28	
ISS #180	14 41 40	−41 32	
ISS #181	17 36 59	−41 37	
ISS #182	19 03 20	−41 38	
ISS #183	21 26 03	−41 38	
ISS #184	17 18 55	−41 40	
ISS #185	22 40 36	−41 41	
ISS #186	17 54 14	−41 42	
ISS #187	12 18 50	−41 45	
ISS #188	13 13 00	−41 45	
ISS #189	17 17 35	−41 50	
ISS #190	20 07 15	−41 52	
ISS #191	21 22 25	−41 55	
ISS #192	14 32 19	−41 56	
ISS #193	19 55 15	−41 59	
ISS #194	19 51 49	−42 00	
ISS #195	18 05 25	−42 01	
ISS #196	14 37 30	−42 02	
ISS #197	18 09 10	−42 06	
ISS #198	16 51 08	−42 16	
ISS #199	21 20 00	−42 17	
ISS #200	20 38 00	−42 19	
ISS #201	18 29 56	−42 21	
ISS #202	15 34 41	−42 24	
ISS #203	0 23 49	−42 35	
ISS #204	12 43 00	−42 36	
ISS #205	21 29 15	−42 38	
ISS #206	12 52 38	−42 40	
ISS #207	12 27 10	−42 44	
ISS #208	16 50 09	−42 58	
ISS #209	17 33 43	−42 58	
ISS #210	19 56 58	−43 10	
ISS #211	18 36 00	−43 14	
ISS #212	17 39 00	−43 40	
ISS #213	18 44 40	−43 40	
ISS #214	17 40 00	−43 42	
ISS #215	15 54 35	−43 49	
ISS #216	20 53 31	−43 50	
ISS #217	19 20 18	−43 51	
ISS #218	22 26 46	−44 00	
ISS #219	15 38 20	−44 05	
ISS #220	20 52 35	−44 16	
ISS #221	15 32 16	−44 17	
ISS #222	17 22 00	−44 25	
ISS #223	17 07 05	−44 29	

NAME	RA (1950)	DEC	POS REF
ISS #224	20 12 00	−44 31	
ISS #225	17 16 00	−44 39	
ISS #226	20 03 30	−44 40	
ISS #227	20 30 29	−44 41	
ISS #228	17 16 30	−44 43	
ISS #229	16 28 40	−44 46	
ISS #230	16 55 21	−44 46	
ISS #231	21 05 35	−44 47	
ISS #232	16 45 11	−44 48	
ISS #233	22 39 00	−44 50	
ISS #234	18 47 25	−45 00	
ISS #235	16 52 00	−45 01	
ISS #236	21 30 10	−45 04	
ISS #237	21 16 40	−45 14	
ISS #238	17 33 15	−45 29	
ISS #239	18 12 45	−45 35	
ISS #240	18 33 20	−45 35	
ISS #241	18 28 10	−45 44	
ISS #242	16 43 05	−45 44	
ISS #243	16 43 05	−45 46	
ISS #244	16 43 05	−45 47	
ISS #245	16 43 00	−45 48	
ISS #246	18 39 35	−45 48	
ISS #247	17 20 10	−46 15	
ISS #248	17 15 15	−48 08	
ISS #249	16 36 46	−48 13	
ISS #250	19 31 31	−48 14	
ISS #251	0 44 40	−48 16	
ISS #252	22 06 16	−48 17	
ISS #253	22 16 15	−48 17	
ISS #254	0 17 35	−48 18	
ISS #255	23 19 35	−48 20	
ISS #256	18 33 25	−48 21	
ISS #257	18 51 25	−48 21	
ISS #258	18 35 20	−48 24	
ISS #259	16 17 42	−48 24	
ISS #260	17 30 35	−48 26	
ISS #261	17 00 40	−48 25	
ISS #262	19 48 20	−48 27	
ISS #263	2 35 40	−48 29	
ISS #264	12 39 49	−48 34	
ISS #265	22 33 50	−48 34	
ISS #266	17 06 10	−48 37	
ISS #267	9 22 50	−48 40	
ISS #268	12 50 16	−48 40	
ISS #269	12 38 45	−48 42	
ISS #270	13 11 46	−48 42	
ISS #271	17 07 50	−48 49	
ISS #272	7 34 50	−48 50	
ISS #273	7 09 27	−48 50	
ISS #274	11 32 33	−48 52	
ISS #275	9 11 50	−48 54	
ISS #276	15 03 50	−48 54	
ISS #277	8 26 45	−48 59	
ISS #278	3 46 00	−49 00	
ISS #279	12 44 00	−49 00	
ISS #280	10 37 51	−49 01	
ISS #281	23 16 00	−49 01	
ISS #282	13 55 24	−49 03	
ISS #283	15 48 02	−49 03	
ISS #284	15 59 32	−49 05	
ISS #285	19 04 24	−49 05	
ISS #286	14 44 00	−49 06	
ISS #287	18 24 59	−49 06	
ISS #288	8 06 14	−49 07	
ISS #289	12 22 20	−49 07	
ISS #290	16 06 06	−49 07	
ISS #291	10 25 59	−49 09	
ISS #292	23 58 31	−49 09	
ISS #293	10 44 37	−49 09	
ISS #294	15 26 20	−49 12	
ISS #295	16 20 13	−49 14	
ISS #296	1 29 10	−49 17	
ISS #297	9 18 38	−49 19	
ISS #298	15 32 12	−49 19	
ISS #299	15 38 59	−49 19	
ISS #300	11 24 50	−49 26	
ISS #301	16 10 10	−49 27	
ISS #302	19 50 20	−49 35	
ISS #303	14 19 05	−49 36	
ISS #304	15 14 45	−49 39	
ISS #305	13 36 54	−49 42	
ISS #306	19 56 58	−49 45	
ISS #307	8 33 12	−49 46	
ISS #308	17 53 05	−49 48	
ISS #309	11 29 10	−49 50	
ISS #310	7 54 56	−49 51	
ISS #311	17 28 02	−49 51	
ISS #312	7 12 18	−49 52	
ISS #313	16 25 30	−49 52	
ISS #314	16 50 05	−49 52	
ISS #315	20 24 00	−49 54	
ISS #316	23 04 16	−49 55	
ISS #317	16 13 16	−49 56	
ISS #318	12 10 49	−49 56	
ISS #319	0 57 15	−50 01	
ISS #320	15 32 12	−50 02	
ISS #321	20 21 40	−50 02	
ISS #322	8 12 07	−50 03	
ISS #323	16 35 27	−50 03	
ISS #324	16 16 05	−50 03	
ISS #325	17 33 34	−50 03	
ISS #326	20 21 03	−50 03	
ISS #327	2 52 10	−50 05	
ISS #328	22 22 50	−50 05	
ISS #329	23 53 50	−50 05	
ISS #330	21 17 51	−50 08	
ISS #331	19 57 21	−50 17	
ISS #332	12 53 30	−50 19	
ISS #333	18 49 26	−50 20	
ISS #334	11 58 50	−50 22	
ISS #335	16 46 15	−50 22	
ISS #336	19 06 57	−50 23	
ISS #337	19 19 25	−50 24	
ISS #338	14 49 05	−50 24	
ISS #339	13 35 20	−50 25	
ISS #340	11 45 20	−50 28	
ISS #341	12 05 32	−50 28	

NAME	RA (1950)	DEC	POS REF
ISS #342	12 51 11	−50 28	
ISS #343	20 38 30	−50 28	
ISS #344	13 36 46	−50 29	
ISS #345	14 49 10	−50 29	
ISS #346	17 38 10	−50 29	
ISS #347	11 13 40	−50 30	
ISS #348	15 49 09	−50 31	
ISS #349	19 14 25	−50 31	
ISS #350	17 22 10	−50 31	
ISS #351	13 39 46	−50 32	
ISS #352	14 19 59	−50 33	
ISS #353	6 48 42	−50 33	
ISS #354	12 53 50	−50 34	
ISS #355	13 43 29	−50 35	
ISS #356	19 08 54	−50 36	
ISS #357	23 58 46	−50 36	
ISS #358	10 25 35	−50 37	
ISS #359	17 22 10	−50 39	
ISS #360	11 04 14	−50 41	
ISS #361	15 28 40	−50 42	
ISS #362	15 30 45	−50 42	
ISS #363	18 13 50	−50 44	
ISS #364	11 25 12	−50 46	
ISS #365	20 16 20	−50 48	
ISS #366	7 25 05	−50 50	
ISS #367	13 53 30	−50 50	
ISS #368	14 17 50	−50 50	
ISS #369	20 18 00	−50 54	
ISS #370	11 02 24	−50 55	
ISS #371	16 15 45	−50 55	
ISS #372	7 33 33	−51 00	
ISS #373	10 14 37	−51 00	
ISS #374	10 26 00	−51 00	
ISS #375	17 28 11	−51 02	
ISS #376	16 12 00	−51 05	
ISS #377	19 00 03	−51 05	
ISS #378	18 53 30	−51 09	
ISS #379	6 45 41	−51 12	
ISS #380	19 21 15	−51 12	
ISS #381	12 11 15	−51 15	
ISS #382	14 53 30	−51 14	
ISS #383	8 38 37	−51 17	
ISS #384	13 43 29	−51 17	
ISS #385	18 45 20	−51 17	
ISS #386	22 43 41	−51 19	
ISS #387	6 59 29	−51 20	
ISS #388	12 25 15	−51 20	
ISS #389	20 38 55	−51 20	
ISS #390	17 18 30	−51 22	
ISS #391	21 01 45	−51 29	
ISS #392	23 11 15	−51 31	
ISS #393	20 02 00	−51 32	
ISS #394	22 45 32	−51 36	
ISS #395	3 05 40	−51 38	
ISS #396	17 49 25	−51 39	
ISS #397	6 22 51	−52 40	
ISS #398	5 48 55	−56 11	
ISS #399	9 29 42	−65 49	
ISS #400	12 28 23	−56 50	
ISS #401	9 14 47	−57 20	
ISS #402	8 21 30	−59 21	
ISS #403	12 18 39	−60 08	
ISS #404	10 15 25	−61 05	
ISS #405	9 30 59	−62 34	
ISS #406	9 12 40	−69 31	
ISS #407	23 59 03	−77 20	
ISS #408	0 42 09	−77 23	
ISS #409	6 39 40	−77 30	
ISS #410	9 28 00	−77 30	
ISS #411	7 38 00	−77 31	
ISS #412	0 23 09	−77 32	
ISS #413	10 38 15	−77 42	
ISS #414	0 33 49	−77 44	
IV ZW 67	21 00 16	+36 30 00	
JM1	5 39 26.2	− 1 51 44	780514
J320	5 02 48.6	+10 38 25	739909
J900	6 23 01.8	+17 49 15	"
KAPTEYNS STAR	5 09 41.4	−44 59 53	CSI 79
KE 56	17 45 31	−28 00 36	
KEPLER SN	17 27 40	−21 26	ED
KEPLER SNR	17 27 34	−21 25 30	
KEPLER SNR	17 27 37	−21 26 36	
KEPLER SNR	17 27 38	−21 26 24	
KEPLER SNR	17 27 40	−21 25 06	
KEPLER SNR	17 27 41	−21 27 18	
KEPLER SNR	17 27 43	−21 26 06	
KEPLER SNR	17 27 45	−21 28 30	
KEPLER SNR	17 27 46	−21 27 06	
KKH 21	18 06 20	+67 38	
KL	5 32 46.7	− 5 24 28	
KL NEB. IRC1	5 32 46.7	− 5 24 17	
KL NEB. IRC2	5 32 47.0	− 5 24 23	
KL NEB. IRC2	5 32 47.0	− 5 24 24	731102
KL NEB. IRC3	5 32 46.5	− 5 24 24	
KL NEB. IRC3	5 32 46.7	− 5 24 25	
KL NEB. IRC4	5 32 46.8	− 5 24 28	
KL NEB. IRC4	5 32 46.8	− 5 24 29	
KL NEB. IRC5	5 32 46.7	− 5 24 33	
KL NEB. IRC5	5 32 46.9	− 5 24 33	
KL NEB. IRC6	5 32 46.7	− 5 24 20	
KL NEB. IRC7	5 32 46.9	− 5 24 24	
KL NEB. IRC8	5 32 47.3	− 5 24 29	
KL NEB. IRC9	5 32 46.4	− 5 23 53	
KL NEB. IRE2	5 32 46.7	− 5 24 34	670701
KL NEBULA	5 32 46.3	− 5 24 28	
KL NEBULA	5 32 46.7	− 5 24 34	670701
KL NEBULA	5 32 46.8	− 5 24 28	
KL NEBULA	5 32 46.9	− 5 24 24	
KL NEBULA 1'N	5 32 46.7	− 5 23 34	ED
KL NEBULA10"S	5 32 46.7	− 5 24 44	"
KL NEBULA30"N	5 32 46.7	− 5 24 28	
KL REGION A	5 32 46.4	− 5 24 17	
KL REGION B	5 32 46.8	− 5 24 22	
KL REGION C	5 32 46.8	− 5 24 28	
KL REGION D	5 32 46.8	− 5 24 33	
KM 12	15 15 19.9	−17 48 46	779905
KS 15	18 59 09.1	−37 02 29	ED
KS 15E	18 59 10.7	−37 02 45	"

NAME	RA (1950)	DEC	POS REF
KUWANO OBJECT	20 19 01.1	+21 24 43	799905
K2−8	17 02 45.3	−10 01 40	819914
K3 NOM.	0 22 42	−73 04	
K3 W24	"	"	ED
K3 1	"	"	"
K3 2	"	"	"
K3 24	"	"	"
K3 50	"	"	"
K3 54	"	"	"
K3−1	18 20 52.7	+ 3 34 56	819914
K3−2	18 22 24.6	− 1 32 36	"
K3−6	18 30 43.8	+ 0 09 32	"
K3−7	18 31 37.0	− 2 29 59	769910
K3−8	18 32 25.5	+ 5 02 21	819914
K3−9	18 37 40.3	− 8 46 36	"
K3−10	18 37 49.5	+14 08 57	"
K3−12	18 42 18.7	+ 6 03 56	"
K3−14	18 46 11.4	+10 32 38	"
K3−15	18 46 10.6	+ 9 50 46	769910
K3−16	18 50 42.0	+12 12 17	"
K3−19	18 59 01.3	− 1 23 20	"
K3−20	18 59 34.1	− 1 53 03	819914
K3−22	19 07 06.3	+11 55 54	"
K3−23	19 07 22.2	+11 00 25	"
K3−25	19 11 02.0	+ 2 13 03	739909
K3−28	19 12 50.0	+ 2 27 48	769910
K3−29	19 13 12.4	+13 58 33	819914
K3−30	19 13 59.4	+ 5 07 58	769910
K3−31	19 16 50.6	+18 56 51	"
K3−32	19 17 29.0	+22 29 03	"
K3−33	19 20 04.2	+10 35 36	819914
K3−37	19 31 41.0	+24 25 54	769910
K3−39	19 33 49.0	+24 48 10	"
K3−40	19 34 14.7	+23 33 05	819914
K3−41	19 37 00.0	+16 13 49	739909
K3−44	19 38 41.0	+18 37 51	819914
K3−47	19 48 23.8	+28 03 41	"
K3−48	19 50 05.6	+27 10 49	"
K3−49	19 52 05.9	+33 14 20	"
K3−50	19 59 50.1	+33 24 19	
K3−50	19 59 50.1	+33 24 27	
K3−50	19 59 50.4	+33 24 27	
K3−50	20 00	+33 24	
K3−50 #1	19 59 50	+33 24 18	
K3−50 #2	19 59 54	+33 26 24	
K3−50 A	19 59 50.1	+33 24 19	
K3−50 C1	19 59 58.4	+33 25 49	
K3−50 C2	19 59 59.7	+33 25 52	
K3−50 IRS	19 59 50.1	+33 24 19	700802
K3−50 IRS1	"	"	ED
K3−51	20 00 20.6	+17 28 23	769910
K3−52	20 01 11.3	+30 24 09	819914
K3−53	20 01 18.0	+26 52 28	769910
K3−54	20 02 52.0	+25 18 04	"
K3−56	20 05 18	+44 06	P−K
K3−59	20 23 28.6	+43 42 54	819914
K3−60	21 25 57.9	+57 26 05	"
K3−62	21 30 08.8	+52 20 37	"
K3−66			
K3−67			
K3−69			
K3−81	21 20 16.2	+37 54 24	729903
K4−1	18 14 00.6	+ 1 52 02	819914
K4−2	18 29 49.4	+ 7 11 50	"
K4−3	18 31 22.7	+ 5 50 49	"
K4−4	18 41 44.6	+ 6 43 46	"
K4−5	18 42 54.1	− 6 21 42	"
K4−7	18 45 52.4	− 6 43 58	739909
K4−8	18 51 36.1	− 8 57 22	819914
K4−9	18 51 42.1	+28 28 27	819910
K4−10	18 56 53.7	+20 32 52	819914
K4−11	19 01 08.9	+ 8 39 35	"
K4−12	19 01 32.1	+16 21 49	"
K4−13	19 01 48.3	+10 06 18	"
K4−14	19 02 07.0	+ 1 17 48	769910
K4−15	19 02 20.4	+ 0 15 46	819914
K4−16	19 02 36.0	+15 43 03	769910
K4−17	19 06 49.4	− 1 13 52	819914
K4−18	19 09 38.0	+ 2 32 56	739909
K4−19	19 10 54	+ 3 20	P−K
K4−20	19 11 07.0	+ 7 21 19	819914
K4−21	19 21 06	+10 46	P−K
K4−22	19 15 17.0	+ 2 43 42	769910
K4−23	19 16 17.4	+14 54 17	819914
K4−24	19 18 56.2	+14 00 26	739909
K4−25	19 19 51.5	+ 0 06 56	769910
K4−26	19 21 01.2	+ 0 32 45	"
K4−27	19 27 57.5	+11 17 22	"
K4−28	19 27 58.7	+14 40 57	819914
K4−29	19 28 31.3	+22 57 16	"
K4−30	19 31 00.7	+22 52 02	"
K4−31	19 34 45.6	+13 34 42	769910
K4−32	19 40 01.6	+24 23 06	819914
K4−33	19 43 42.0	+28 30 53	"
K4−34	19 44 10.0	+16 53 43	769910
K4−35	19 46 41.5	+19 59 20	739909
K4−36	19 47 05.6	+ 5 11 08	"
K4−37	19 49 02.4	+30 54 48	819914
K4−38	19 49 08.0	+19 49 54	769910
K4−39	19 50 56.8	+23 05 55	"
K4−40	19 52 06	+24 50	P−K
K4−41	19 54 37.0	+32 14 13	819914
K4−42	20 04 34.0	+24 51 38	769910
K4−43	20 25 57.3	+22 41 26	"
K4−45	21 33 41.0	+53 33 46	819914
K4−46	23 07 07.3	+54 28 36	"
K4−47			
K4−48			
K4−49			
K4−50			
K4−51	20 10 33	+40 36	AS
K4−54	20 41 12.0	+45 45 42	729903
K4−56	20 54 06	+46 22	739905
K4−57	22 46 34.8	+58 13 12	729903
K4−58	22 47 16.2	+66 45 48	"
K4−59	1 27 14.4	+60 15 54	"
L 1517 #1	4 52 34.4	+30 28 22	
L 1517 #2	4 52 47.8	+30 29 19	

NAME	RA (1950)	DEC	POS REF
L 1517 #3	4 52 44.5	+30 31 38	
L 1517 #4	4 52 42.5	+30 33 48	
L 1517 #5	4 52 36.6	+30 35 49	
L 1517 #6	4 52 45.4	+30 36 37	
L 1517 #7	4 52 23.9	+30 29 55	
L 1517 #8	4 52 22.4	+30 28 39	
L 1517 #9	4 52 21.1	+30 33 56	
L 1517 #10	4 52 16.2	+30 28 38	
L 1517 #11	4 52 11.1	+30 33 24	
L 1517 #12	4 51 59.5	+30 35 44	
L 1517 #13	4 51 42.6	+30 27 41	
L 1551 #1	4 28 44.4	+18 07 37	
L 1551 #2	4 28 46.1	+18 07 36	
L 1551 #3	4 28 31.2	+18 09 55	
L 1551 #4	4 28 54.4	+18 02 42	
L 1551 #5	4 28 39.7	+18 01 52	
L 1551 #6	4 27 56.4	+17 59 02	
L 1630 #1	5 44 10.9	+ 0 04 17	
L 1630 #2	5 44 02.9	+ 0 05 17	
L 1630 #3	5 44 16.9	+ 0 03 32	
L 1630 #4	5 44 06.9	+ 0 03 52	
L 1630 #5	5 44 04.9	+ 0 04 40	
L 1630 #6	5 44 00.9	+ 0 05 47	
L 1630 #7	5 43 56.9	+ 0 05 47	
L 1630 #8	5 44 00.9	+ 0 03 17	
L 1630 #9	5 44 11.6	+ 0 01 37	
L 1630 #10	5 44 04.9	+ 0 00 47	
L 1630 #11	5 44 02.9	+ 0 00 12	
L 1630 #12	5 44 15.6	+ 0 01 17	
L 1630 #13	5 43 58.9	+ 0 01 47	
L 1630 #14	5 44 12.9	+ 0 08 12	
L 1630 #15	5 44 01.6	+ 0 07 47	
L 1630 #16	5 43 58.9	+ 0 07 47	
L 1630 #17	5 44 24.9	+ 0 04 37	
L 1630 #18	5 44 22.9	+ 0 04 17	
L 1630 #19	5 44 09.6	− 0 00 13	
L 1630 #20	5 44 30.9	+ 0 10 17	
L 1630 #21	5 44 33.2	+ 0 18 17	
L 1630 #22	5 44 31.2	+ 0 17 32	
L 1630 #23	5 44 40.2	+ 0 08 02	
L 1630 #24	5 44 35.6	+ 0 09 17	
L 1630 #25	5 44 33.9	+ 0 16 47	
L 1630 #26	5 44 37.6	+ 0 18 07	
L 1630 #27	5 44 37.2	+ 0 16 57	
L 1630 #28	5 44 41.2	+ 0 17 32	
L 1630 #29	5 44 45.6	+ 0 18 22	
L 1630 #30	5 44 43.6	+ 0 17 27	
L 1630 #31	5 44 40.9	+ 0 10 47	
L 1630 #32	5 44 55.2	+ 0 12 22	
L 1630 #33	5 44 08.6	+ 0 11 07	
L 1630 #34	5 44 11.6	+ 0 15 47	
L 1630 #35	5 44 10.6	+ 0 16 52	
L 1630 #36	5 44 53.9	+ 0 19 47	
L 1630 #37	5 44 36.9	+ 0 20 17	
L 1630 #38	5 44 23.6	+ 0 18 57	
L 1630 #39	5 44 08.6	+ 0 19 07	
L 1630 #40	5 44 30.6	+ 0 22 12	
L 1630 #41	5 44 31.4	+ 0 20 57	
L 1630 #42	5 44 38.9	+ 0 21 17	
L 1630 #43	5 44 39.0	+ 0 23 37	
L 1630 #44	5 43 40.6	+ 0 22 57	
L 1630 #45	5 44 46.6	+ 0 02 57	
L 1630 #46	5 44 32.9	− 0 00 13	
L 1630 #47	5 44 40.4	− 0 00 53	
L 1630 #48	5 43 44.9	− 0 01 23	
L 1630 #49	5 43 44.9	+ 0 02 22	
L 1630 #50	5 43 32.9	+ 0 01 07	
L 1630 #51	5 43 31.2	+ 0 03 42	
L 1630 #52	5 43 50.9	+ 0 04 37	
L 1630 #53	5 43 42.9	+ 0 06 07	
L 1630 #54	5 43 44.9	+ 0 05 57	
L 1630 #55	5 43 52.4	+ 0 08 17	
L 1630 #56	5 43 40.4	+ 0 07 47	
L 1630 #57	5 43 34.9	− 0 03 13	
L 1630 #58	5 43 22.6	− 0 01 23	
L 1630 #59	5 43 31.6	− 0 15 23	
L 1630 #60	5 43 34.2	− 0 15 23	
L 1630 #61	5 43 34.9	− 0 12 28	
L 1630 #62	5 43 34.2	− 0 17 33	
L 1630 #63	5 43 35.6	− 0 11 03	
L 1630 #64	5 43 45.6	− 0 06 33	
L 1630 #65	5 43 26.9	− 0 09 23	
L 1630 #66	5 43 15.3	− 0 13 45	
L 1630 #67	5 43 54.9	− 0 04 58	
L 1630 #68	5 43 48.9	− 0 10 03	
L 1630 #69	5 43 48.6	− 0 16 13	
L 1630 #70	5 44 16.6	− 0 04 48	
AR LAC	22 06 39.4	+45 29 46	779907
BET LAC	22 21 35.3	+51 58 40	CSI 79
BL LAC	22 00 39.4	+42 02 09	809908
CT LAC	22 04 40	+48 13 00	GCVS
EV LAC	22 44 38.5	+44 04 32	779907
EW LAC	22 54 51.5	+48 25 00	"
R LAC	22 41 02.1	+42 06 29	"
RT LAC	21 59 28.6	+43 38 56	"
RX LAC	22 47 40.8	+40 47 10	"
S LAC	22 26 49.2	+40 03 33	"
SW LAC	22 51 22.6	+37 40 19	"
U LAC	22 45 39.7	+54 53 40	"
4 LAC	22 22 28.9	+49 13 20	CSI 79
5 LAC	22 27 26.4	+47 27 00	"
10 LAC	22 37 00.7	+38 47 21	"
LALL 21185	11 00 36.5	+36 18 19	"
LB 8741	8 47 38.7	+19 05 03	
LB 8775	8 48 53.7	+16 23 40	809908
LB 9612	15 17 08.2	+23 56 53	
LB 9707	15 23 08.8	+21 24 36	
LB 9743	15 25 45.7	+22 43 25	809908
LB 9743	15 25 45.8	+22 43 24	
LDS 749B			
AB LEO	9 30 32.3	+20 04 47	CSI 79
AD LEO	10 16 53.9	+20 07 18	"
ALF LEO	10 05 42.6	+12 12 43	"
BET LEO	11 46 30.5	+14 51 04	"
CW LEO	9 45 15	+13 30 39	GCVS
EPS LEO	9 43 00.9	+24 00 18	CSI 79
ETA LEO	10 04 36.4	+17 00 24	"
GAM LEO A	10 17 13.0	+20 05 42	"
GAM LEO B	10 17 13.3	+20 05 38	"
GAM 1 LEO	10 17 13.0	+20 05 42	"
MUU LEO	9 49 55.3	+26 14 34	"
PI LEO	9 57 34.3	+ 8 17 05	"
R LEO	9 44 52.2	+11 39 40	"
RHO LEO	10 30 10.7	+ 9 33 51	"
RS LEO	9 40 38.9	+20 05 31	"
S LEO	11 07 58.7	+ 6 27 01	"
V LEO	9 57 17.4	+21 29 43	"
VY LEO	10 53 25.7	+ 6 27 08	"
W LEO	10 51 02.7	+13 59 05	"
6 LEO	9 29 16.7	+ 9 56 12	"
37 LEO	10 13 59.7	+13 58 41	"
39 LEO	10 14 29.7	+23 21 26	"
46 LEO	10 29 31.7	+14 23 39	"
54 LEO	10 52 54.5	+25 00 59	"
56 LEO	10 53 25.7	+ 6 27 08	"
72 LEO	11 12 32.7	+23 22 04	"
75 LEO	11 14 42.9	+ 2 17 07	"
87 LEO	11 27 45.4	− 2 43 37	"
ALF LEP	5 30 31.3	−17 51 22	"
ETA LEP	5 54 07.5	−14 10 30	"
GAM LEP	5 42 22.6	−22 27 46	"
R LEP	4 57 19.7	−14 52 46	"
RX LEP	5 09 02.7	−11 54 34	"
S LEP	6 03 41.7	−24 11 22	"
T LEP	5 02 43.1	−21 58 18	"
17 LEP	6 02 45.1	−16 28 45	"
LF 24	3 42 30.3	+32 17 04	"
LFT 526			
LFT 1081	13 12 06	− 3 03 18	
LFT 1086			
LFT 1427	18 39 03	+ 0 53 24	
LFT 1597			
LHA 483−41	19 24 34	+23 48 00	820108
LHA 61	6 38 28	+ 9 29 07	729902
LHA 70	6 38 36	+ 9 36 30	
LHA 79	6 38 59	+ 9 43 48	
LHS 69	22 51 09	− 7 02 18	799901
LHS 239	7 47 32	+ 7 20 54	"
LHS 240	7 47 33	+ 7 20 42	"
ALF 2 LIB	14 48 06.3	−15 50 05	CSI 79
AP LIB	15 14 45.3	−24 11 22	809908
BET LIB	15 14 18.7	− 9 11 57	CSI 79
DEL LIB	14 58 17.7	− 8 19 17	"
FS LIB	15 57 37	−12 12 35	GCVS
NUU LIB	15 03 49.9	−16 03 49	CSI 79
R LIB	15 50 45.7	−16 05 18	"
RR LIB	15 53 27.9	−18 09 54	"
RS LIB	15 21 24.6	−22 43 44	"
RT LIB	15 03 37.3	−18 32 44	"
RU LIB	15 30 29.6	−15 09 16	"
RW LIB	15 20 07.7	−23 52 51	"
S LIB	15 18 31.1	−20 12 31	"
SIG LIB	15 01 08.2	−25 05 10	"
T LIB	15 07 53.9	−19 49 55	"
U LIB	15 39 07.9	−21 01 10	"
UW LIB	14 28 08.3	−16 35 19	"
UZ LIB	15 29 41.2	− 8 21 58	"
V LIB	14 37 34.7	−17 26 34	"
X LIB	15 33 19.4	−21 00 18	"
Y LIB	15 09 02.3	− 5 49 27	"
18 LIB A	14 56 11.0	−10 56 37	"
42 LIB	15 37 19.1	−23 39 24	"
48 LIB	15 55 23.0	−14 08 10	"
LII 2.2	17 48	−27 02	ED
LII 32.3	18 48	− 0 37	"
LII 358.3	17 38	−30 22	"
LILLER 1	17 30 07.2	−33 21 54	
LKHA 21	6 37 56	+ 9 57 06	549902
LKHA 25	6 38 00	+ 9 51	
LKHA 79	6 38 59	+ 9 43 48	549902
LKHA 86	3 40 36.4	+31 58 51	
LKHA 87	3 40 50.0	+32 08 01	
LKHA 88	3 40 50.5	+32 02 01	
LKHA 89	3 40 50.6	+32 04 54	
LKHA 92	3 41 17.8	+31 55 06	
LKHA 93	3 41 21.3	+32 01 16	
LKHA 95	3 41 29.5	+31 58 39	
LKHA 97	3 41 36.4	+31 54 39	
LKHA 98	3 41 47.7	+31 59 53	
LKHA 101	4 26 57.3	+35 09 56	
LKHA 101	4 27 00	+35 10 42	740903
LKHA 101 40"E	4 27 03	+35 10 42	ED
LKHA 101 40"N	4 27 00	+35 11 22	"
LKHA 101 40"S	4 27 00	+35 10 02	"
LKHA 101 40"W	4 26 57	+35 10 42	"
LKHA 101 80"E	4 27 05	+35 10 42	"
LKHA 101 80"N	4 27 00	+35 12 02	"
LKHA 101 80"S	4 27 00	+35 09 22	"
LKHA 101 80"W	4 26 55	+35 10 42	"
LKHA 101 120E	4 27 08	+35 10 42	"
LKHA 108	18 00 48	−24 22	
LKHA 120	20 59 31	+50 10	729902
LKHA 123	17 59 24	−23 02	730001
LKHA 127	18 06 34	−23 26 06	
LKHA 131	20 44 51	+43 33 30	
LKHA 132	20 44 56	+43 35 48	
LKHA 133	20 44 59	+43 34 06	
LKHA 134	20 46 18	+43 36	
LKHA 135	20 46 36	+43 29	
LKHA 137	20 48 51	+44 07 12	
LKHA 138	20 48 51	+44 09 36	
LKHA 141	20 49 07	+44 05 30	
LKHA 142,3	20 49 08	+44 10 00	
LKHA 144	20 49 10	+44 06 36	
LKHA 145	20 49 13	+44 06 18	
LKHA 146	20 49 16	+44 04 24	
LKHA 147	20 49 16	+43 38 18	
LKHA 149	20 49 19	+44 12 30	729902
LKHA 150	20 49 29	+44 07 00	
LKHA 151	20 49 30	+44 03 21	
LKHA 152	20 49 31	+44 11 42	
LKHA 153	20 49 35	+44 15 00	
LKHA 154	20 49 37	+44 09 48	
LKHA 157	20 49 47	+44 12 30	
LKHA 161	20 49 56	+44 04 48	
LKHA 166	20 50 18	+44 26 12	
LKHA 167	20 50 19	+44 26 12	
LKHA 168	20 50 20	+44 05 54	
LKHA 169	20 50 21	+43 52 24	589902
LKHA 170	20 50 27	+44 10 04	729902
LKHA 172	20 50 41	+44 05 47	"
LKHA 174	20 50 45	+44 08 54	
LKHA 175	20 50 48	+44 06 18	
LKHA 183	20 53 25	+44 51 30	589902
LKHA 185	20 56 12	+43 41 48	
LKHA 186	20 56 32	+43 42 18	
LKHA 187	20 56 34	+43 42 06	
LKHA 188	20 56 37	+43 41 35	729902
LKHA 188 G1	20 56 33	+43 42 17	ED
LKHA 188 G2	20 56 32	+43 42 17	"
LKHA 188 G3	"	"	"
LKHA 188 G4	20 56 31	+43 42 17	"
LKHA 188 G5	20 56 30	+43 42 03	"
LKHA 188 IRS2	20 50 10.4	+44 12 16	
LKHA 188 IRS3	20 56 15.0	+43 39 02	
LKHA 188 IRS4	20 56 21.6	+43 43 21	
LKHA 188 IRS5	20 56 22.4	+43 41 04	
LKHA 188 IRS6	20 56 29.9	+43 40 05	
LKHA 189	20 56 36	+43 42 18	589902
LKHA 190	20 57 06	+44 03 49	GCVS
LKHA 191	20 57 18	+43 45 20	729902
LKHA 192	20 57 30	+44 06 06	589902
LKHA 197	0 07 57.3	+58 33 25	729902
LKHA 198	0 08 44	+58 33 08	
LKHA 198 40"E	0 08 47	+58 33 08	ED
LKHA 198 40"W	0 08 41	+58 33 08	"
LKHA 198−2	0 08 31	+58 31 14	
LKHA 198−3	0 08 57	+58 30 38	
LKHA 198−4	0 09 20	+58 31 26	
LKHA 202	0 41 00	+61 59	
LKHA 208	6 04 53.2	+18 39 55	729902
LKHA 209	6 05 12.1	+18 38 57	"
LKHA 215	6 29 54	+10 12	
LKHA 215	6 29 56	+10 11 24	
LKHA 218	7 00 24	−11 21	
LKHA 220	7 01 48	−11 21	
LKHA 224	20 18 43.6	+41 11 59	ED
LKHA 225	20 18 44.5	+41 11 56	"
LKHA 228	20 23 08	+42 19 43	729902
LKHA 230			
LKHA 231			
LKHA 232			
LKHA 233	22 32 30	+40 23	
LKHA 234	21 41 48	+65 54	
LKHA 234	21 41 57.5	+65 53 03	781207
LKHA 245	21 51 34	+46 58 43	729902
LKHA 257	21 52 23	+46 57 27	"
LKHA 257	21 52 24	+46 58	
LKHA 259	23 56 10	+66 09 30	729902
LKHA 262	2 53 17.4	+19 51 19	"
LKHA 263	2 53 17.8	+19 51 33	"
LKHA 264	2 53 46.9	+19 53 34	"
LKHA 266	4 29 03.6	+18 15 16	"
LKHA 270	3 26 11.9	+31 12 28	"
LKHA 271	3 26 16.2	+31 05 19	"
LKHA 272	3 45 43.2	+36 47 10	"
LKHA 273	3 45 56.9	+38 47 31	"
LKHA 274	6 28 24	+10 28 18	
LKHA 274	6 28 24.1	+10 28 14	729902
LKHA 295	5 43 18	− 0 13	730001
LKHA 298	5 43 31.2	+ 0 03 42	760501
LKHA 300	5 43 44.9	+ 0 02 22	"
LKHA 301	5 43 45.6	− 0 06 33	"
LKHA 302	5 43 49	− 0 09 42	639901
LKHA 303	5 43 54	+ 0 23 48	"
LKHA 308	5 44 33.2	+ 0 18 17	760501
LKHA 310	5 44 37.6	+ 0 18 07	"
LKHA 321	21 00 26	+49 40	729902
LKHA 324	21 02 20	+50 03	"
LKHA 325	3 25 46	+30 33	"
LKHA 326	3 27 52	+30 23	"
LKHA 327	3 30 29	+31 00	"
LKHA 328	3 30 53	+31 04	"
LKHA 329	3 42 27.9	+32 16 36	
LKHA 329	3 42 28.0	+32 16 39	729902
LKHA 330	3 42 39.4	+32 14 54	"
LKHA 330	3 42 39.5	+32 14 53	
LKHA 331	4 28 22.4	+24 04 30	729902
LKHA 332	4 39 04.2	+25 17 33	"
LKHA 332 G1	4 39 03.8	+25 17 26	ED
LKHA 332 G2	4 38 46.2	+25 17 19	"
LKHA 334	5 51 06	+ 1 37 39	729902
LKHA 335	5 51 23	+ 1 43 31	"
LKHA 337	5 52 01	+ 1 28 59	"
LKHA 338	6 08 20.6	− 6 12 06	"
LKHA 339	6 08 28.0	− 6 13 57	"
LKHA 340	6 27 34.5	+10 33 55	"
LKHA 341	6 28 04	+10 35 24	
LKHA 341	6 28 04.1	+10 35 19	729902
LKHA 342	6 28 44	+10 34 45	"
LKHA 343	6 29 19.4	+10 27 32	"
LKHA 344	6 29 20.0	+10 38 41	"
LKHA 349	21 35 45	+57 03 04	"
LKHA 349C	"	"	
LMC BW 1	5 06 47.5	−69 10 23	809910
LMC BW 2	5 06 56.0	−69 06 17	"
LMC BW 3	5 07 05.3	−69 11 41	"
LMC BW 4	5 07 16.1	−69 05 10	"
LMC BW 9	5 07 27.2	−69 07 11	"
LMC BW 10	5 07 29.1	−69 16 01	"
LMC BW 11	5 07 29.4	−69 15 36	"
LMC BW 19	5 07 58.5	−69 13 31	"
LMC BW 21	5 07 59.3	−69 12 06	"
LMC BW 24	5 08 03.7	−69 14 31	"
LMC BW 25	5 08 05.1	−69 13 43	"
LMC BW 34	5 08 22.6	−69 08 16	"
LMC BW 42	5 08 37.6	−69 19 32	"
LMC BW 44	5 08 40.3	−69 07 26	"
LMC BW 48	5 08 46.9	−69 20 38	"
LMC BW 50	5 08 49.8	−69 06 41	"
LMC BW 53	5 08 56.3	−69 08 30	"
LMC BW 54	5 08 58.5	−69 01 20	"
LMC BW 61	5 09 08.2	−68 59 09	"
LMC BW 68	5 09 21.0	−69 14 01	"

NAME	RA (1950)	DEC	POS REF
LMC BW 78	5 09 39.3	−69 08 40	"
LMC BW 83	5 09 47.5	−69 17 50	"
LMC BW 85	5 09 49.0	−69 19 18	"
LMC BW 104	5 10 46.6	−69 06 57	"
LMC BW 105	5 10 46.6	−69 08 45	"
LMC BW 108	5 10 52.5	−69 06 55	"
LMC C7			
LMC C11			
LMC C20			
LMC C38			
LMC C48			
LMC NOVA	5 05 37	−70 13	779903
LMC N159 K1	5 40 21.4	−69 46 52	
LMC N159 K2	5 40 26.4	−69 46 54	
LMC N159 K3	5 40 19.0	−69 47 57	
LMC N159 K4	5 40 23.0	−69 47 43	
LMC N159 K5	5 40 20.4	−69 47 03	
LMC N159 K6	5 40 16.8	−69 47 20	
LMC O 2	5 22 25.8	−69 48 06	809910
LMC O 3	5 22 26.8	−69 49 20	"
LMC O 7	5 22 46.4	−69 51 46	"
LMC O 13	5 23 03.2	−69 50 37	"
LMC O 16	5 23 14.1	−69 49 42	"
LMC O 17	5 23 14.6	−69 40 29	"
LMC O 26	5 23 34.2	−69 55 47	"
LMC O 33	5 23 48.7	−69 54 00	"
LMC O 40	5 24 00.7	−69 48 53	"
LMC O 42	5 24 02.3	−69 57 37	"
LMC O 43	5 24 02.6	−69 58 04	"
LMC O 47	5 24 10.1	−70 02 11	"
LMC O 57	5 24 31.9	−69 55 17	"
LMC O 75	5 24 58.2	−69 39 39	"
LMC O 86	5 25 20.4	−70 01 16	"
LMC O 97	5 25 47.5	−69 56 54	"
LMC O 110	5 26 17.9	−69 49 16	"
LMC O 114	5 26 36.7	−69 50 55	"
LMC RC 2	5 18 10.6	−68 54 29	"
LMC RC 12	5 18 50.2	−69 02 37	"
LMC RC 13	5 18 50.9	−68 48 06	"
LMC RC 38	5 20 23.6	−69 03 39	"
LMC RC 45	5 21 03.1	−68 56 26	"
LMC RC 48	5 21 11.1	−69 02 17	"
LMC RC 51	5 21 17.8	−69 04 12	"
LMC RC 53	5 21 25.8	−69 01 04	"
LMC RC 54	5 21 27.0	−69 00 30	"
LMC W 40	4 59 00	−65 57 42	789909
LMC W 46	5 00 24	−70 15 48	"
LMC W 47	5 00 26	−65 02 30	"
LMC W 56	5 02 04	−70 53 18	"
LMC W 64	5 02 43	−65 11 06	"
LMC W 65	5 02 47	−66 26 30	"
LMC W 67	5 03 11	−66 02 54	"
LMC W 78	5 05 06	−70 27 42	"
LMC W 84	5 07 05	−69 58 12	"
LMC W 105	5 11 42	−65 16 06	"
LMC W 106	5 11 44	−66 52 42	"
LMC W 107	5 11 50	−65 09 48	"
LMC W 108	5 12 06	−65 47 36	"
LMC W 112	5 12 55	−65 43 18	"
LMC W 131	5 17 10	−64 48 30	"
LMC W 137	5 19 45	−65 04 12	"
LMC W 157	5 26 04	−73 19 48	"
LMC W 186	5 35 10	−71 01 24	"
LMC W 190	5 38 00	−70 49 06	"
LMC W 196	5 39 19	−72 10 24	"
LMC W 214	5 51 45	−72 30 42	"
LMC W 231	6 07 09	−73 28 12	"
LMC W 239	6 09 14	−73 50 06	"
LMC W 256	6 13 44	−67 28 24	"
LMC W 272	6 17 07	−68 13 12	"
LMC W 300	6 29 34	−70 55 30	"
LMC 49			
LMC 110			
LMC 120			
LMC 141			
LMC 153			
LMC 430			
R LMI	9 42 34.6	+34 44 33	CSI 79
R LMI	9 42 35.0	+34 44 18	
RW LMI	10 13 19	+30 49 07	GCVS
S LMI	9 50 44.6	+35 09 41	779907
LP 44−113			
LP 101−48			
LP 131−66	12 47 56	+55 04 30	799901
LP 380−5	13 45 48	+23 49 36	"
LP 543−32	7 47 32	+ 7 20 54	"
LP 543−33	7 47 33	+ 7 20 42	"
LP 658−2	5 52 39.9	− 4 08 46	CSI 79
LP 701−29	22 51 09	− 7 02 18	799901
LS 9	14 02 01	−64 21	689903
LS 13	17 13 52	−45 28	"
LS 15	18 36 28	−10 09	"
LSV+20 16	6 06 01.4	+20 38 58	ED
LSV+20 17	6 06 20.8	+20 38 55	"
LSV+20 19	6 06 40.9	+20 29 51	"
LSV+20 20	6 06 51.3	+20 37 42	"
LSV+20 21	6 06 56.4	+20 39 09	"
EX LUP	15 59 41.9	−40 10 06	CSI 79
GI LUP	15 03 03	−41 16 44	GCVS
R LUP	15 50 13.1	−36 09 02	CSI 79
RS LUP	14 20 07.9	−47 17 47	"
RT LUP	14 27 24.4	−48 28 08	"
RU LUP	15 53 22.9	−37 40 57	
RW LUP	14 23 10.2	−43 55 39	CSI 79
RY LUP	15 56 04.9	−40 13 28	"
S LUP	14 50 07.9	−46 24 26	"
T LUP	14 18 59.0	−49 37 49	"
TAU 2 LUP	14 22 57.1	−45 09 15	"
U LUP	15 57 35.9	−29 46 57	"
UU LUP	14 46 52	−47 14 09	GCVS
V LUP	14 56 10.2	−53 12 10	CSI 79
Z LUP	14 32 41.3	−43 09 14	"
ALF LYN	9 18 00.7	+34 36 17	"
R LYN	6 57 10.8	+55 24 07	779907
S LYN	6 40 15.4	+57 57 44	"
ST LYN	8 25 32.3	+38 49 28	"
T LYN	8 19 32.9	+33 40 49	"
U LYN	6 36 19.2	+59 54 49	"

NAME	RA (1950)	DEC	POS REF
Y LYN	7 24 33.5	+46 05 35	"
15 LYN	6 52 57.1	+58 29 26	
LYNGA 8 IRS1	16 15 15.3	−50 13 06	
LYNGA 8 IRS2	16 15 16.3	−50 15 42	
LYNGA 8 IRS3	16 15 28.3	−50 17 11	
ALF LYR	18 35 14.6	+38 44 09	CSI 79
BET LYR	18 48 14.0	+33 18 12	779907
BET LYR A	"	"	"
DEL LYR	18 52 45.2	+36 50 02	"
DEL 2 LYR	"	"	"
EP LYR	19 16 19.0	+27 45 31	CSI 79
GAM LYR	18 57 04.3	+32 37 10	"
HK LYR	18 41 05.6	+36 54 29	779907
KP LYR	18 29 10.9	+38 36 15	"
MV LYR	19 05 44.3	+43 56 22	"
R LYR	18 53 48.7	+43 52 46	"
RR LYR	19 23 52.1	+42 41 10	"
RS LYR	19 11 06.9	+33 17 29	CSI 79
RT LYR	18 59 29.2	+37 26 35	"
RY LYR	18 43 03.6	+34 37 22	779907
S LYR	19 11 08.6	+25 55 15	CSI 79
T LYR	18 30 36.1	+36 57 37	"
THE LYR	19 14 37.7	+38 02 36	"
U LYR	19 18 19.0	+37 46 48	779907
V LYR	19 07 07.9	+29 34 00	CSI 79
W LYR	18 13 11.7	+36 39 12	779907
XY LYR	18 36 27.3	+39 37 23	"
Z LYR	18 57 48.1	+34 53 03	"
ZET 1 LYR	18 43 02.9	+37 33 04	CSI 79
L1 G64	0 01 32	−73 45	ED
L1 NOM.	"	"	"
L1 1	"	"	"
L1 2	"	"	"
L1 3	"	"	"
L1 4	"	"	"
L1 5	"	"	"
L1 64	"	"	"
L1 143	"	"	"
L11 1			
L11 2			
L11 3			
L27 1			
L27 2			
L63 #1	16 47 10	−18 02	ED
L63 #2	16 46 10	−17 40	"
L63 #3	16 44 50	−17 31	"
L63 #4	16 47 30	−17 55	"
L113 NOM.	1 48 40	−73 58 36	749907
L113 1	"	"	"
L113 2	"	"	"
L134N #1	15 51 20	− 2 54	ED
L134N #2	15 51 40	− 2 46	"
L134N #3	15 50 50	− 2 53	"
L134N #4	15 50 50	− 2 46	"
L134N #5	15 52 00	− 2 39	"
L183	15 51 30	− 2 43 31	
L183 2'N	15 51 30	− 2 43 29	ED
L183 2'S	15 51 30	− 2 43 33	"
L1014	21 22 22	+49 46 10	
L1147 #1	20 39 40	+67 07	ED
L1147 #2	20 40 20	+67 10	"
L1147 #3	20 40 20	+67 08	"
L1147 #4	20 39 40	+67 12	"
L1147 #5	20 39 20	+67 06	"
L1147 #6	20 39 10	+67 05	"
L1147 #7	20 39 00	+67 10	"
L1147 #8	20 40 30	+67 19	"
L1147 #9	20 40 40	+67 04	"
L1147 #10	20 41 10	+67 13	"
L1235 #1	22 13 10	+73 10	"
L1235 #2	22 12 40	+73 08	"
L1235 #3	22 11 50	+73 08	"
L1235 #4	22 14 10	+73 08	"
L1235 #5	22 09 10	+73 09	"
L1235 #6	22 11 50	+73 03	"
L1253 #1	23 54 50	+58 14	"
L1253 #2	23 54 30	+58 09	"
L1253 #3	23 54 50	+58 21	"
L1253 #4	23 54 50	+58 08	"
L1253 #5	23 54 10	+58 21	"
L1253 #6	23 54 10	+58 19	"
L1253 #7	23 54 30	+58 20	"
L1253 #8	23 54 40	+58 20	"
L1253 #9	23 54 30	+58 18	"
L1253 #10	23 54 10	+58 13	"
L1253 #11	23 53 50	+58 12	"
L1253 #12	23 54 10	+58 09	"
L1257 #1	23 55 10	+59 22	"
L1257 #2	23 55 20	+59 20	"
L1257 #3	23 55 00	+59 24	"
L1257 #4	23 54 30	+59 28	"
L1257 #5	23 54 20	+59 28	"
L1257 #6	23 55 10	+59 26	"
L1257 #7	23 54 40	+59 30	"
L1257 #8	23 54 20	+59 30	"
L1257 #9	23 54 40	+59 32	"
L1262	23 23 47	+74 01 30	
L1283−23	18 07 40	+17 35 30	
L1363−3			
L1407 #1	4 25 40	+54 07	ED
L1407 #2	4 25 30	+54 08	"
L1407 #3	4 26 10	+54 12	"
L1407 #4	4 25 30	+54 15	"
L1407 #5	4 26 00	+54 16	"
L1407 #6	4 26 10	+54 16	"
L1407 #7	4 26 50	+54 16	"
L1512−34B			
L1544 #1	5 01 00	+25 11	ED
L1544 #2	5 01 00	+25 13	"
L1544 #3	5 01 20	+25 10	"
L1544 #4	5 01 30	+25 10	"
L1551 IRS5	4 28 31.6	+17 59 52	
L1551 IRS5	4 28 40.2	+18 01 45	
L745−46A	7 38 00.4	−17 17 20	CSI 79
MACC H5	23 56 48	+66 06 30	729902
MACC H9	0 10 48	+65 19 38	"
MACC H10	0 10 13	+65 17 28	"
MACC H12	0 04 26	+65 21 55	"

NAME	RA (1950)	DEC	POS REF
MACC SH15	0 10 43	+65 19	
MAFFEI 1	2 32 36	+59 25 48	740903
MAFFEI 2	2 38 10.1	+59 23 32	729905
MARK 1	1 13 19.7	+32 49 36	789906
MARK 3	6 09 48.1	+71 03 00	739901
MARK 6	6 45 43.4	+74 29 07	"
MARK 9	7 32 42.0	+58 53 00	"
MARK 10	7 43 07.4	+61 03 23	"
MARK 11	7 43 17.0	+74 27 30	"
MARK 13	7 51 56.8	+60 26 17	"
MARK 14	8 05 21.7	+72 56 33	"
MARK 19	9 12 53.5	+59 58 53	"
MARK 25	10 00 22.2	+59 40 43	"
MARK 33	10 29 22.2	+54 39 23	"
MARK 34	10 30 52.2	+60 17 20	"
MARK 35	10 42 16.4	+56 13 20	"
MARK 36	11 02 15.6	+29 24 34	"
MARK 40	11 22 48.0	+54 39 26	"
MARK 42	11 51 05.3	+46 29 20	"
MARK 49	12 16 36.4	+ 4 08 07	"
MARK 50	12 20 50.9	+ 2 57 20	"
MARK 52	12 23 08.9	+ 0 51 00	"
MARK 54	12 54 32.0	+32 43 07	"
MARK 59	12 56 38.2	+35 06 50	"
MARK 67	13 39 39.4	+30 46 17	"
MARK 69	13 43 51.3	+29 53 03	"
MARK 78	7 37 55.9	+65 17 43	"
MARK 79	7 38 46.9	+49 55 47	"
MARK 86	8 09 43.1	+46 08 33	"
MARK 101	9 01 00.7	+51 48 46	"
MARK 102	9 08 18.1	+46 50 33	"
MARK 106	9 16 18.4	+55 34 21	"
MARK 110	9 21 44.4	+52 30 14	"
MARK 114	9 26 36.8	+56 04 20	"
MARK 124	9 45 24.3	+50 43 26	"
MARK 132	9 58 08.0	+55 09 10	"
MARK 133	9 57 52.0	+72 21 53	"
MARK 139	10 12 46.1	+44 02 10	"
MARK 141	10 15 38.7	+64 13 14	"
MARK 142	10 22 23.1	+51 55 40	"
MARK 151	10 39 15.3	+48 01 40	"
MARK 155	10 48 24.0	+44 50 07	"
MARK 158	10 56 01.6	+61 47 46	"
MARK 161	10 59 07.3	+45 29 47	"
MARK 171	11 25 44.2	+58 50 23	769909
MARK 171A	"	"	
MARK 171B	11 25 41.8	+58 50 00	"
MARK 176	11 29 54.0	+53 13 27	739901
MARK 188	11 44 53.9	+56 14 57	"
MARK 190	11 49 10.1	+48 57 34	"
MARK 198	12 06 43.2	+47 20 07	"
MARK 201	12 11 39.9	+54 48 20	"
MARK 205	12 19 31.8	+75 35 10	"
MARK 206	12 21 58.8	+67 43 01	"
MARK 207	12 22 48.0	+54 46 53	"
MARK 213	12 29 00.9	+58 14 20	"
MARK 231	12 54 05.0	+57 08 37	"
MARK 236	12 58 18.0	+61 55 27	"
MARK 266	13 36 14.7	+48 31 53	"
MARK 267	13 37 28.5	+43 18 17	"
MARK 268	13 38 54.2	+30 37 47	"
MARK 270	13 39 40.7	+67 55 33	"
MARK 273	13 42 51.2	+56 08 20	"
MARK 279	13 51 51.9	+69 33 13	"
MARK 281	13 55 00.6	+42 05 20	"
MARK 290	15 34 45.4	+58 04 00	"
MARK 291	15 52 54.1	+19 20 20	"
MARK 297	16 03 01.2	+20 40 43	"
MARK 298	16 03 21.7	+17 56 03	"
MARK 304	22 14 45.2	+13 59 27	"
MARK 307	22 33 31.4	+20 03 53	"
MARK 315	23 01 35.6	+22 21 10	"
MARK 316	23 11 09.9	+13 44 57	"
MARK 319	23 16 10.3	+24 57 27	"
MARK 321	23 17 37.0	+23 56 40	"
MARK 330	23 40 29.3	+19 08 47	"
MARK 332	23 56 52.1	+20 28 33	"
MARK 335	0 03 45.3	+19 55 30	789906
MARK 341	0 34 13.5	+23 42 34	739901
MARK 343	0 35 46.8	+14 45 53	"
MARK 347	0 45 17.0	+22 06 07	"
MARK 348	0 46 04.9	+31 41 04	789906
MARK 352	0 57 08.8	+31 33 30	"
MARK 353	1 00 35.0	+22 04 26	739901
MARK 358	1 23 45.3	+31 21 16	789906
MARK 359	1 24 50.1	+18 55 07	739901
MARK 360	1 41 13.9	+16 48 47	"
MARK 363	1 48 12.0	+21 45 00	"
MARK 372	2 46 31.1	+19 05 57	789906
MARK 373	6 50 42.7	+50 25 00	739901
MARK 374	6 55 33.9	+54 15 53	"
MARK 376	7 10 35.8	+45 47 07	"
MARK 382	7 52 03.2	+39 19 07	"
MARK 391	8 51 32.3	+39 43 40	"
MARK 401	9 27 19.5	+29 45 33	"
MARK 421	11 01 40.6	+38 28 43	809908
MARK 423	11 24 07.6	+35 31 17	739901
MARK 439	12 22 07.7	+39 39 33	"
MARK 463	13 53 39.8	+18 36 40	"
MARK 464	13 53 45.1	+38 48 54	"
MARK 465	13 59 14.8	+37 02 27	"
MARK 471	14 20 46.9	+33 04 37	"
MARK 474	14 33 06.0	+48 52 47	"
MARK 477	14 39 03.0	+53 42 53	"
MARK 478	14 40 04.6	+35 38 53	"
MARK 486	15 35 21.5	+54 43 04	"
MARK 489	15 42 36.0	+41 14 26	"
MARK 493	15 57 16.6	+35 10 13	"
MARK 501	16 52 12.3	+39 50 22	769909
MARK 504	16 59 10.4	+29 28 47	739901
MARK 506	17 20 45.6	+30 55 30	"
MARK 509	20 41 26.4	−10 54 16	789901
MARK 518	21 56 09.3	+11 47 53	"
MARK 529	23 11 47.8	− 3 00 00	"
MARK 531	23 21 22.2	+ 9 23 37	769909
MARK 533	23 25 24.8	+ 8 30 17	789901
MARK 534	23 26 13.6	+ 3 14 09	"
MARK 538	23 33 41.2	+ 1 52 42	"

NAME	RA (1950) DEC	POS REF
	h m s ° ′ ″	
MARK 541	23 53 28.2 + 7 14 36	"
MARK 543	23 59 52.9 + 3 04 26	"
MARK 545	0 07 18.6 +25 38 42	"
MARK 575	1 45 52.8 +12 21 51	"
MARK 609	3 22 57.9 − 6 18 58	"
MARK 612	3 28 09.9 − 3 18 35	"
MARK 617	4 31 35.5 − 8 40 42	"
MARK 618	4 34 00.0 −10 28 36	789906
MARK 632	10 41 07.9 +16 09 14	789901
MARK 668	14 04 45.9 +28 41 35	"
MARK 684	14 28 53.1 +28 30 29	"
MARK 691	15 44 43.2 +18 02 22	"
MARK 693	15 51 53.5 +23 16 41	"
MARK 699	16 22 05.0 +41 11 42	"
MARK 700	17 01 21.1 +31 31 26	"
MARK 704	9 15 39.5 +16 30 59	809902
MARK 710	9 52 10.2 + 9 30 32	"
MARK 716	10 07 27.5 +23 21 19	"
MARK 734	11 19 10.9 +12 00 47	"
MARK 744	11 37 04.7 +32 11 13	"
MARK 766	12 15 55.5 +30 05 27	"
MARK 769	12 22 53.9 +16 44 49	"
MARK 771	12 29 33.1 +20 26 02	"
MARK 783	13 00 30.4 +16 40 34	"
MARK 817	14 34 58.0 +59 00 40	819906
MARK 830	14 49 07.3 +58 52 04	"
MARK 841	15 01 36.4 +10 37 59	"
MARK 845	15 06 12.5 +51 38 41	"
MARK 849	15 17 50.9 +28 45 26	"
MARK 871	16 06 15.6 +12 27 41	"
MARK 876	16 13 36.2 +65 50 37	"
MARK 883	16 27 48 +24 32	769902
MARK 926	23 02 07.2 − 8 57 19	789906
MARK 1092	5 01 57.6 −10 08 40	819906
MARK 1095	5 13 38.0 − 0 12 17	819908
MARK 1239	9 49 46.3 − 1 22 35	819907
MARK 1298	11 26 43.6 − 4 07 34	"
MAYALL 44		
MC 1	0 04 21 +65 21	
MC 12.8+0.5	18 08 29.6 −17 32 04	
MC 4	0 13 58 +65 28	
MCG 2−58−22	22 47 48 +11 22	MCG
MCG 8−11−11	5 51 09.9 +46 25 55	789906
MCG−2−58−22	23 02 07.2 − 8 57 19	"
MCG−2−58−22	23 02 18 − 9 00	
MCG−5−23−16	9 45 28 −30 43 00	809909
MCG−5−23−16	9 45 28 −30 43 33	"
MCG−5−23−16	9 45 28 −30 43 36	"
MCG−6−30−15	13 33 02 −34 02 24	"
R MEN	5 44 20.9 −75 16 14	CSI 79
U MEN	4 14 01.4 −81 58 53	"
W MEN	5 27 07.9 −71 13 28	"
ME2−1	15 19 23.0 −23 27 05	739909
ME2−2	22 29 36 +47 32 46	709904
MHA 328−116	19 55 19.9 +39 41 38	CSI 79
S MIC	21 23 46.4 −30 04 08	"
T MIC	20 24 52.4 −28 25 37	"
U MIC	20 25 56.3 −40 35 14	"
V MIC	21 20 35.5 −40 55 18	"
W MIC	21 19 49.3 −42 11 20	"
Y MIC	21 04 01.1 −34 28 49	"
MIRA	2 16 49.0 − 3 12 12	"
MON #1	6 28 28.9 + 9 52 37	
MON #2	6 28 52.0 + 9 47 00	
MON #3	6 28 54.2 +11 08 20	
MON #4	6 28 56.2 +10 52 21	
MON #5	6 29 51.9 + 9 01 18	
MON #6	6 29 53.3 +10 27 40	
MON #7	6 30 15.2 + 9 34 47	
MON #8	6 30 19.7 + 9 29 42	
MON #9	6 30 46.3 +10 36 42	
MON #10	6 31 12.1 + 9 09 51	
MON #11	6 31 39.8 + 9 07 32	
MON #12	6 32 32.2 +10 01 45	
MON #13	6 32 33.7 + 9 40 15	
MON #14	6 32 41.1 +10 53 02	
MON #15	6 33 24.7 + 8 55 09	
MON #16	6 33 30.8 +10 48 18	
MON #17	6 33 48.0 + 9 28 12	
MON #18	6 34 01.1 + 9 34 16	
MON #19	6 34 51.7 +10 06 55	
MON #20	6 34 50.5 +10 53 50	
MON #21	6 34 51.5 + 9 50 29	
MON #22	6 35 10.0 +10 24 09	
MON #23	6 35 27.9 + 9 13 05	
MON #24	6 35 23.9 + 8 42 09	
MON #25	6 35 51.2 + 9 02 24	
MON #26	6 36 01.0 + 9 04 23	
MON #27	6 36 26.1 + 8 46 55	
MON #28	6 36 41.1 +11 27 05	
MON #29	6 37 04.7 +10 15 41	
MON #30	6 37 07.9 + 9 18 25	
MON #31	6 37 10.9 + 9 37 16	
MON #32	6 37 18.6 + 8 56 00	
MON #33	6 37 22.8 + 9 20 51	
MON #34	6 37 42.4 +10 20 15	
MON #35	6 37 50.2 +10 41 18	
MON #36	6 38 01.1 +11 23 37	
MON #37	6 38 13.4 + 9 56 37	
MON #38	6 38 25 + 9 32 30	
MON #39−1	6 38 25.0 + 9 02 05	
MON #40	6 38 30.6 +11 03 05	
MON #41	6 38 53.3 +10 56 29	
MON #42	6 39 14.0 + 9 41 04	
MON #43	6 39 55.8 +10 22 54	
MON #44	6 41 11.1 +10 19 10	
MON #45	6 42 11.9 + 9 53 58	
MON #46	6 42 21.4 + 9 05 30	
MON #47	6 42 23.4 +10 04 50	
MON #48	6 42 41.4 + 9 49 10	
MON #49	6 42 41.5 +10 08 50	
MON #50	6 42 40.5 +10 53 19	
MON #51	6 42 45.6 + 9 43 49	
MON #52	6 42 52.6 + 9 34 53	
MON #53	6 43 48.5 + 9 15 33	
MON #54	6 34 40.6 + 9 50 46	
MON #55	6 28 21.0 +10 28 14	
MON R1 #1	6 27 57 + 9 53 48	

NAME	RA (1950) DEC	POS REF
	h m s ° ′ ″	
MON R1 #5	6 28 31 +10 24 48	
MON R2	6 05 19 − 6 22 17	
MON R2	6 05 20 − 6 22	ED
MON R2 #1	6 05 20 − 6 22 30	
MON R2 #2	6 05 18 − 6 22 25	
MON R2 #3	6 05 40 − 6 20 50	
MON R2 #4	6 05 10 − 6 20 50	
MON R2 #5	6 05 07 − 6 23 20	
MON R2 IRS1	6 05 19.8 − 6 22 38	
MON R2 IRS1	6 05 20.0 − 6 22 38	ED
MON R2 IRS1	6 05 20.0 − 6 22 40	"
MON R2 IRS2	6 05 19.4 − 6 22 24	
MON R2 IRS2	6 05 19.5 − 6 22 24	ED
MON R2 IRS3	6 05 21.5 − 6 22 26	
MON R2 IRS3	6 05 21.8 − 6 22 25	ED
MON R2 IRS3	6 05 21.8 − 6 22 26	790510
MON R2 IRS3	6 05 21.9 − 6 22 26	ED
MON R2 IRS4	6 05 18.5 − 6 22 56	
MON R2 IRS4	6 05 18.8 − 6 22 57	ED
MON R2 IRS5	6 05 19.2 − 6 22 11	
MON R2 IRS5	6 05 19.5 − 6 22 10	ED
AX MON	6 27 52.3 + 5 54 06	CSI 79
BET MON	6 26 23.9 − 7 00 00	"
BET MON A	" "	"
BET MON ABC	" "	"
BN MON	6 19 12.2 + 7 21 47	"
BX MON	7 22 54 − 3 30 01	GCVS
CL MON	6 52 52.9 + 6 26 58	CSI 79
CZ MON	6 42 01.4 + 3 22 08	"
DF MON	6 45 04.4 + 0 43 55	"
DK MON	6 48 06 + 1 47 37	GCVS
FU MON	6 19 49.6 + 3 27 44	CSI 79
GY MON	6 50 42.7 − 4 30 46	"
HH MON	6 52 47.9 − 7 21 35	"
IO MON	6 38 14 + 9 33 44	GCVS
IP MON	6 38 16 + 9 35 32	"
KV MON	6 36 57 + 9 49 07	"
KW MON	6 37 33 + 9 31 58	"
KY MON	6 37 39 + 9 36 58	"
LL MON	6 37 41 + 9 53 46	"
LM MON	6 37 52 + 9 53 57	"
LR MON	6 38 02 + 9 52 26	"
LU MON	6 38 12 + 9 40 44	"
LX MON	6 38 20 + 9 51 13	"
MM MON	6 38 28 + 9 55 37	"
MO MON	6 38 47 + 9 29 53	"
MQ MON	6 39 24 + 9 44 20	"
NOVA MON 1976	6 20 11.2 − 0 19 10	769904
NW MON	6 37 55 + 9 37 57	GCVS
NX MON	6 37 56 + 9 36 51	"
OY MON	6 38 55 + 9 43 22	"
PT MON	6 37 47 + 9 52 28	"
PZ MON	6 45 45.9 + 1 16 31	CSI 79
R MON	6 36 25.3 + 8 48 00	"
R MON	6 36 26.4 + 8 47 12	
R MON 40"N	6 36 25.3 + 8 48 40	ED
R MON 40"S	6 36 25.3 + 8 47 20	"
RR MON	7 14 58.9 + 1 11 48	CSI 79
RV MON	6 55 40.7 + 6 14 07	"
RY MON	7 04 31.0 − 7 28 40	"
S MON	6 38 13.3 + 9 56 36	"
SS MON	6 38 21 +10 29 25	GCVS
SU MON	7 39 55.3 −10 45 37	CSI 79
T MON	6 22 30.9 + 7 06 51	"
U MON	7 28 24.2 − 9 40 14	"
V MON	6 20 12.3 − 2 10 08	"
VY MON	6 28 21 +10 28 18	820108
V360 MON	6 38 21 + 9 39 19	GCVS
V365 MON	6 38 29 + 9 29 00	"
V372 MON	6 39 08 + 4 27 27	"
V419 MON	6 38 09 + 9 36 20	"
V432 MON	6 38 34 + 9 36 48	"
WZ MON	6 47 43 − 7 38 40	"
X MON	6 54 48.3 − 8 59 47	CSI 79
XY MON	6 49 52 − 3 25 13	GCVS
Y MON	6 54 04.6 +11 18 16	CSI 79
12 MON	6 29 39.9 + 4 53 35	"
13 MON	6 30 11.9 + 7 22 15	"
15 MON	6 38 13.3 + 9 56 36	"
MR 62	16 37 37 −47 55	689903
MR 66	16 58 58 −45 55	"
MR 112	20 34 06 +41 10	629902
MR 114	22 09 19.9 +57 40 45	CSI 79
MR 119	22 58 08 +60 40	629902
MR 2251−178	22 51 25.9 −17 50 54	809908
MSB 57	9 11 15 −23 11	549905
MSH 03−19		
MSH 14−121	14 53 12.2 −10 56 40	809908
MT 41		
EPS MUS	12 14 50.9 −67 40 56	CSI 79
R MUS	12 39 00.3 −69 08 00	"
RR MUS	11 37 11.2 −72 16 35	"
RS MUS	12 20 21.3 −75 13 32	"
SY MUS	11 29 49.4 −65 08 30	"
T MUS	13 17 19.4 −74 10 47	"
MVP3	5 32 04 − 5 14 35	
MVP4	5 32 50 − 5 14 32	
MVP11	5 32 52 − 5 17 50	
MVP12	5 32 51 − 5 19 26	
MVP17	5 33 16 − 5 19 16	
MWC 17	1 44 12 +60 27	MWC
MWC 43	2 19 44.5 +57 17 50	CSI 79
MWC 56	2 38 51.0 +61 03 05	"
MWC 84	4 15 39.3 +55 52 45	"
MWC 137	6 15 54 +15 18	MWC
MWC 297	18 25 00.9 − 3 51 39	771005
MWC 300	18 26 41 − 6 07	MWC
MWC 342	20 21 14.6 +39 20 09	CSI 79
MWC 345	20 24 14.7 +54 31 10	"
MWC 349	20 31 00 +40 29	MWC
MWC 349A	" "	"
MWC 349B	" "	"
MWC 445	2 17 06.2 +57 04 58	CSI 79
MWC 448	2 19 50 +57 05	MWC
MWC 553	7 14 55 − 7 29	"
MWC 574	7 45 43 −13 59	"
MWC 623	19 54 33.2 +30 58 12	CSI 79
MWC 645	21 51 41 +52 46	MWC

NAME	RA (1950) DEC	POS REF
	h m s ° ′ ″	
MWC 674	0 39 28.3 +63 46 36	CSI 79
MWC 778	5 47 09 +23 53	MWC
MWC 790	6 04 12 +30 11	"
MWC 819	6 41 59 + 1 23	"
MWC 922	18 18 26.3 −13 03 06	740503
MWC 930	18 23 42 − 7 14	MWC
MWC 939	18 31 24 −17 38	"
MWC 957	18 43 32 −23 30 06	819916
MWC 1032	20 50 23.7 +44 14 42	CSI 79
MWC 1055	22 06 35.0 +53 58 40	"
MWC 1080	23 15 10 +60 35	MWC
MWC 1080 20"S	" "	ED
MWC 1080 40"N	23 15 10 +60 36	"
MWC 1080 40"S	23 15 10 +60 34	"
MXB 1730−335	17 30 07.2 −33 21 19	
MXB 1730−335	17 30 08 −33 21 16	
MY 129		
MYCN 18	13 35 54.4 −67 07 33	769910
MYCN 26	16 52 39.6 −26 47 03	"
MZ 3	16 13 23.3 −51 51 44	"
M1	5 31 30 +21 59	RNGC
M1−1	1 34 13 +50 12 57	709904
M1−2	1 55 33 +52 39 15	"
M1−4	3 37 59.1 +52 07 26	749905
M1−5	5 43 46.0 +24 20 59	739909
M1−6	6 33 11.0 + 0 03 11	769910
M1−7	6 34 17.8 +24 03 12	"
M1−8	6 50 56.5 + 3 12 11	"
M1−9	7 02 42.5 + 2 51 35	739909
M1−11	7 09 05.4 −19 45 55	"
M1−12	7 17 12.0 −21 38 17	"
M1−14	7 25 46.0 −20 06 58	"
M1−15	7 29 36.0 −19 21 00	"
M1−16	7 34 54.9 − 9 31 55	"
M1−17	7 38 01.0 −11 25 02	"
M1−19	17 00 30 −33 25 42	789908
M1−20	17 26 00.7 −19 13 31	819914
M1−21	17 31 20.5 −19 07 23	"
M1−26	17 42 45.0 −30 11 02	739909
M1−30	17 49 39 −34 37 48	819916
M1−31	17 49 40.2 −22 21 18	769910
M1−37	18 02 15 −28 22 18	789908
M1−38	18 02 55.6 −28 40 54	769910
M1−39	18 04 42 −13 29	P−K
M1−44	18 13 09.5 −27 05 37	769910
M1−45	18 20 11.0 −19 18 41	"
M1−55	18 33 34 −21 51 30	819917
M1−56	18 34 52.2 −17 08 25	769910
M1−59	18 40 36 − 9 08	P−K
M1−60	18 40 48.0 −13 47 51	769910
M1−61	18 43 03.6 −14 31 01	819914
M1−62	18 47 25 −22 37 54	819916
M1−64	18 48 12 +35 11	P−K
M1−65	18 54 11.9 +10 48 14	769910
M1−66	18 55 50.3 − 1 07 39	819914
M1−67	19 09 16.7 +16 46 29	739909
M1−69	19 11 24.0 + 3 32 33	769910
M1−72	19 39 19.3 +17 38 14	"
M1−74	19 40 01.3 +15 01 57	739909
M1−76	20 14 34 +36 56 48	709904
M1−77	21 17 18 +46 06	P−K
M1−78	21 19 05 +51 40 41	709904
M1−82 #1	5 37 31 +35 39 55	ED
M1−82 #2	5 37 47 +35 48 40	"
M1−82 #3	5 37 51 +35 49 30	"
M1−82 IRS2	5 37 36 +35 49	
M1−92	19 34 18 +29 26	730001
M1−99	20 25 33.0 +37 12 50	760902
M2−4	16 57 48 −34 45 18	789908
M2−6	17 01 06 −30 49 24	809909
M2−9	17 02 52.5 −10 04 31	739909
M2−9	17 02 52.6 −10 04 31	ED
M2−9	17 03 −10 04	
M2−9	17 02 52.6 −10 04 31	ED
M2−9 8"E	17 02 53.1 −10 04 31	"
M2−9 8"E,8"N	17 02 53.1 −10 04 24	"
M2−9 8"E,8"S	17 02 53.1 −10 04 39	"
M2−9 8"N	17 02 52.6 −10 04 23	"
M2−9 8"S	17 02 52.6 −10 04 39	"
M2−9 8"W	17 02 52.1 −10 04 31	"
M2−10	17 10 54 −31 16 18	789908
M2−11	17 17 23.1 −28 57 40	769910
M2−12	17 20 55.6 −25 56 40	"
M2−13	17 25 44.6 −13 23 49	819914
M2−14	17 38 54 −24 09 48	789908
M2−18	17 50 21 −32 58 18	819916
M2−21	17 54 57.8 −29 44 06	769910
M2−27	18 00 38.1 −31 17 55	"
M2−30	18 09 24.9 −27 59 01	"
M2−31	18 10 10 −25 31 00	819916
M2−32	18 11 34 −32 38 06	"
M2−35	18 14 22 −31 56 54	809909
M2−39	18 18 57.5 −24 12 09	769910
M2−43	18 24 03.0 − 2 44 47	739909
M2−49	21 41 29.9 +50 11 29	819914
M2−53	22 30 24 +55 55	P−K
M2−54	22 49 29.0 +51 34 44	819914
M2−56	23 54 06.6 +70 31 31	"
M3−3	7 24 06.3 − 5 16 00	739909
M3−10	17 24 11.0 −28 25 22	769910
M3−13	17 38 35 −22 11 36	819917
M3−17	17 53 12 −31 04 00	789908
M3−18	17 54 15.6 −21 41 09	769910
M3−20	17 56 09.7 −28 13 38	"
M3−21	17 59 08.0 −36 38 55	739909
M3−27	18 25 31.6 +14 27 11	769910
M3−28	18 29 55.6 −10 08 05	"
M3−31	18 41 04 −19 58 00	819917
M3−32	18 41 38 −25 24 42	819916
M3−38	17 17 54.0 −29 00 03	769910
M3−54	18 30 13.7 −13 46 34	819914
M4−3	17 07 35 −27 05 00	819916
M4−8	18 09 23.0 −10 43 38	769910
M4−10	18 31 24.1 −13 14 43	"
M4−18	4 21 31 +60 00 25	709904
M2 #11	21 30 55 − 1 03	RNGC
M2 NOM.	" "	
M3 AA	13 39 57 +28 38	RNGC

NAME	RA (1950)	DEC	POS REF
	h m s	° ' "	
M3 BI	"	"	"
M3 I−III−28	"	"	"
M3 I−21	"	"	"
M3 II−18	"	"	"
M3 II−46	"	"	"
M3 III−28	"	"	"
M3 III−77	"	"	"
M3 IV−25	"	"	"
M3 95	"	"	"
M3 193	"	"	"
M3 216	"	"	"
M3 297	"	"	"
M3 1397	"	"	"
M5 I−68	15 16 02	+ 2 16	"
M5 I−71	"	"	"
M5 IV−81	"	"	"
M5 1−68	"	"	"
M5 3−3	"	"	"
M5 3−78	"	"	"
M5 4−19	"	"	"
M5 4−47	"	"	"
M8	18 00 33	−24 23 24	
M8	18 00 35	−24 23 00	
M8	18 00 36.3	−24 22 49	
M8	18 00 37.7	−24 22 44	
M8	18 01 12	−24 19 30	819916
M8	18 01 15	−24 24	ED
M8 (PEAK)	18 00 35.6	−24 23 07	"
M8 #1	17 57 57	−23 51 00	
M8 #1	18 00 36	−24 23 48	
M8 #2	17 57 55	−23 50 24	
M8 #2	18 01 07	−24 28 18	
M8 #3	17 57 48	−23 49 42	
M8 #3	18 01 14	−24 25 12	
M8 #4	17 57 23	−23 18 06	
M8 #4	18 01 53	−24 27 54	
M8 IRS1	17 59 29.8	−24 15 16	
M8 IRS3	17 59 33.2	−24 10 24	
M8E	18 01 12	−24 19 30	819916
M8E #1	18 01 52.6	−24 27 50	
M8E #2	18 01 43.8	−24 29 04	
M8E #3	18 01 46.4	−24 27 22	
M8E #4	18 02 03.5	−24 30 18	
M8E #5	18 01 55.1	−24 25 06	
M8E IRS1	18 01 52.6	−24 27 50	770207
M10 II−24	16 54 29	− 4 02	RNGC
M10 II−50	"	"	"
M10 III−16	"	"	"
M13 I−2	16 39 54	+36 33	"
M13 I−13	"	"	"
M13 I−18	"	"	"
M13 I−23	"	"	"
M13 I−24	"	"	"
M13 I−48	"	"	"
M13 II−67	"	"	"
M13 II−76	"	"	"
M13 II−90	"	"	"
M13 III−18	"	"	"
M13 III−56	"	"	"
M13 III−63	"	"	"
M13 III−72	"	"	"
M13 III−73	"	"	"
M13 IV−25	"	"	"
M15	21 27 35	+11 57	"
M16	18 16 07	−13 50	"
M16 I	18 15 16	−13 47 04	
M16 II	18 16 04	−13 54 30	
M16 III	18 15 35	−13 44 24	
M16 IRS1	18 15 55.0	−13 53 58	
M16 IRS2	18 16 02.6	−13 52 49	
M16 IRS3	18 16 03.8	−13 49 50	
M16 IRS4	18 15 53.2	−13 52 29	
M17	18 17 29.0	−16 14 00	
M17	18 17 34	−16 13 24	740908
M17	18 17 34.5	−16 13 24	
M17	18 17 35	−16 11	
M17	18 17 35	−16 11 03	
M17	18 17 51	−16 12	RNGC
M17	18 18	−16 18	
M17 (1)	18 17 32.2	−16 13 21	
M17 (2)	18 17 32	−16 12 53	
M17 #1	18 17 32.7	−16 13 03	
M17 #2	18 17 37.4	−16 11 40	
M17 #3	18 17 42.1	−16 10 16	
M17 #4	18 17 46.9	−16 08 52	
M17 #5	18 17 28.0	−16 14 28	
M17 #6	18 17 23.3	−16 15 52	
M17 #7	18 17 48.0	−16 11 24	
M17 #8	18 17 53.8	−16 12 32	
M17 #9	18 17 59.6	−16 13 40	
M17 #10	18 17 36.3	−16 09 08	
M17 #11	18 17 30.5	−16 08 00	
M17 #12	18 17 26.9	−16 11 56	
M17 #13	18 17 38.5	−16 14 12	
M17 #14	18 17 44.4	−16 15 20	
M17 A	18 17 51	−16 12	RNGC
M17 A'	18 17 28.9	−16 14 00	
M17 ANON STAR	18 17 36.0	−16 12 06	ED
M17 B	18 17 57	−16 13	"
M17 B'	18 17 37.3	−16 09 48	
M17 C'	18 17 38.5	−16 03 12	
M17 CS	18 17 51	−16 12	RNGC
M17 C1	"	"	"
M17 C18	"	"	"
M17 C24	"	"	"
M17 C26	"	"	"
M17 C27	"	"	"
M17 C31	"	"	"
M17 C33	"	"	"
M17 C34	"	"	"
M17 C35	"	"	"
M17 C37	"	"	"
M17 C40	"	"	"
M17 C43	"	"	"
M17 C47	"	"	"
M17 C57	"	"	"
M17 C61	"	"	"
M17 C102	"	"	"

NAME	RA (1950)	DEC	POS REF
	h m s	° ' "	
M17 D'	18 18 18	−16 09 30	
M17 IR	18 17 26.5	−16 14 54	731101
M17 IRE1	18 17 34	−16 13 30	
M17 IRS	18 17 26.5	−16 14 54	
M17 IRS1	"	"	731101
M17 NE	18 17 51	−16 11 25	
M17 NORTHERN	18 17 37.5	−16 10 30	
M17 POS 1	18 17 30	−16 13	ED
M17 POS 1	18 17 34.4	−16 13 23	CSI 79
M17 POS 2	18 17 34.4	−16 14 53	ED
M17 POS 3	18 17 34.4	−16 16 23	"
M17 POS 4	18 17 28.4	−16 13 23	"
M17 POS 5	18 17 40.4	−16 13 23	"
M17 POS 6	18 17 30.4	−16 14 23	"
M17 POS 7	18 17 34.4	−16 11 53	"
M17 POS 8	18 17 52.5	−16 11 53	"
M17 POS 9	18 17 34.4	−16 10 23	"
M17 POS 10	18 17 40.4	−16 10 23	"
M17 POS 11	18 17 40.4	−16 11 53	"
M17 POS 12	18 17 46.4	−16 11 53	"
M17 POS 13	18 17 28.4	−16 11 53	"
M17 POS 14	18 17 34.4	−16 08 53	"
M17 SOURCE1	18 17 35	−16 13 30	
M17 SOURCE2	18 17 37	−16 12 00	
M17 SOURCE3	18 17 33	−16 12 30	
M17 SOURCE4	18 17 29	−16 10 30	
M17 SOURCE5	18 17 30	−16 09 30	
M17 SOURCE6	18 17 33	−16 10 30	
M17 SOURCE7	18 17 35	−16 15 00	
M17 SOURCE8	18 17 47	−16 11 00	
M17 SOURCE9	18 17 42	−16 11 30	
M17 SOURCE10	18 17 43	−16 12 00	
M17 SOUTHERN	18 17 34.2	−16 13 20	
M17 SW	18 17 26.5	−16 14 54	731101
M17 SW IRS1	"	"	"
M17 1'E	18 17 38	−16 13 24	ED
M17 1'E,1'N	18 17 38	−16 12 24	"
M17 1'E,1'S	18 17 38	−16 14 24	"
M17 1'N	18 17 34	−16 12 24	"
M17 1'S	18 17 34	−16 14 24	"
M17 1'W	18 17 30	−16 13 24	"
M17 1'W,1'N	18 17 30	−16 12 24	"
M17 2'E	18 17 42	−16 13 24	"
M17 2'N	18 17 34	−16 11 24	"
M17 2'S	18 17 34	−16 15 24	"
M17 2'W	18 17 26	−16 13 24	"
M17 4	18 16 47.0	−15 59 22	
M17 17	18 17 10.0	−16 03 25	
M17 165	18 17 29.5	−16 09 58	
M17 225	18 17 32.8	−16 09 55	
M17 229	18 17 32.8	−16 12 17	
M17 234	18 17 33.0	−16 11 39	
M17 286	18 17 36.7	−16 12 07	
M17 349	18 17 41.4	−16 11 34	
M17 360	18 17 42.5	−16 12 17	
M17 373	18 17 42.7	−16 17 17	
M17 483	18 17 53.0	−16 00 43	
M17/KW IRS	18 17 26.5	−16 14 54	731101
M17C	18 17 30	−16 01 30	
M17C	18 17 34	−16 01 30	
M17C	18 17 38	−16 00 00	
M17C	18 17 38	−16 01 00	
M17C	18 17 38	−16 02 00	
M17C	18 17 38	−16 03 00	
M17C	18 17 38	−16 04 00	
M17C	18 17 42	−16 01 30	
M17C	18 17 46	−16 01 30	
M17N	18 17 42.0	−16 09 44	
M17N	18 17 45	−16 10 16	
M17S	18 17 30.7	−16 14 34	
M17S	18 17 32.7	−16 13 03	
M17S	18 17 34	−16 13 18	721005
M17S #1	18 17 26.5	−16 13 25	
M17S #2	18 17 27.5	−16 13 25	
M17S #3	18 17 28.5	−16 13 25	
M17S #4	18 17 29.5	−16 13 25	
M17S #5	18 17 30.5	−16 13 25	
M17S #6	18 17 31.5	−16 13 25	
M17S #7	18 17 32.5	−16 13 25	
M17S #8	18 17 33.5	−16 13 25	
M17S #9	18 17 34.5	−16 13 25	
M17S #10	18 17 35.5	−16 13 25	
M17S #11	18 17 36.5	−16 13 25	
M17S #12	18 17 37.5	−16 13 25	
M17S #13	18 17 38.5	−16 13 25	
M17S #14	18 17 39.5	−16 13 25	
M17S IRS2	18 17 27.5	−16 13 25	760101
M20	17 59 18.5	−23 02 12	
M20 IRS2	17 59 27	−22 57 16	
M20 IRS4	17 59 33.9	−22 58 28	
M20 IRS5	17 59 32.9	−22 59 46	
M22 III−106	18 33 21	−23 56 54	819916
M31	0 40 00.3	+41 00 03	769909
M31 BA289	0 40 02	+41 00	RNGC
M31 BA519	"	"	"
M31 KOWAL 1	"	"	"
M31 KOWAL 33	"	"	"
M31 KOWAL 41	"	"	"
M31 KOWAL 58	"	"	"
M31 KOWAL 64	"	"	"
M31 KOWAL 72	"	"	"
M31 KOWAL 73	"	"	"
M31 KOWAL 76	"	"	"
M31 KOWAL 78	"	"	"
M31 KOWAL 87	"	"	"
M31 KOWAL 90	"	"	"
M31 KOWAL 96	"	"	"
M31 KOWAL 108	"	"	"
M31 KOWAL 114	"	"	"
M31 KOWAL 119	"	"	"
M31 KOWAL 127	"	"	"
M31 KOWAL 148	"	"	"
M31 KOWAL 150	"	"	"
M31 KOWAL 172	"	"	"
M31 KOWAL 199	"	"	"
M31 KOWAL 205	"	"	"
M31 KOWAL 208	"	"	"
M31 KOWAL 213	"	"	"

NAME	RA (1950)	DEC	POS REF
	h m s	° ' "	
M31 KOWAL 217	"	"	"
M31 KOWAL 219	"	"	"
M31 KOWAL 222	"	"	"
M31 KOWAL 230	"	"	"
M31 KOWAL 233	"	"	"
M31 KOWAL 234	"	"	"
M31 KOWAL 244	"	"	"
M31 KOWAL 256	"	"	"
M31 KOWAL 263	"	"	"
M31 KOWAL 272	"	"	"
M31 KOWAL 276	"	"	"
M31 KOWAL 279	"	"	"
M31 KOWAL 280	"	"	"
M31 KOWAL 301	"	"	"
M31 KOWAL 302	"	"	"
M31 KOWAL 315	"	"	"
M31 KOWAL 327	"	"	"
M31 VAR A−1	"	"	"
M31 VAR 15	"	"	"
M32	0 39 58.0	+40 35 33	769909
M33	1 31 04.6	+30 23 40	"
M33 D	1 31 06	+30 24	RNGC
M33 E	"	"	"
M33 NOM.	"	"	
M33 VAR A	"	"	RNGC
M33 VAR B	"	"	"
M33 VAR C	"	"	"
M33 VAR 83	"	"	"
M42	5 32 46.5	− 5 24 40	ED
M42	5 32 46.6	− 5 24 00	
M42	5 32 48	− 5 25	
M42	5 32 48.5	− 5 25 17	
M42	5 32 48.9	− 5 24 53	ED
M42	5 32 49.6	− 5 25 16	
M42	5 32 50	− 5 25	
M42	5 32 50	− 5 25 00	
M42	5 32 52	− 5 25	RNGC
M42 C	5 32 46.9	− 5 24 30	ED
M42 E	5 32 50.8	− 5 24 30	"
M42 IRE1	5 32 52	− 5 25	RNGC
M42 IRE2	5 33 46	− 5 24 45	
M42 IRE3	5 32 52	− 5 25	RNGC
M42 N	5 32 46.9	− 5 23 30	ED
M42 S	5 32 46.9	− 5 25 30	"
M42 W	5 32 42.5	− 5 24 30	"
M43	5 33 04	− 5 18	RNGC
M51	13 27 46.9	+47 27 16	769909
M51 S3	13 27 39	+47 21	ED
M51 S4	13 27 52	+47 21	"
M51 9MFU	13 27 46.9	+47 27 16	769909
M51 11MFU	"	"	"
M51 15"E	13 27 48.4	+47 27 16	ED
M51 15"W	13 27 45.4	+47 27 16	"
M51 120"N	13 27 46.9	+47 29 16	"
M67 I−17	8 48 20	+12 00	RNGC
M67 II−22	"	"	"
M67 III−34	"	"	"
M67 IV−20	"	"	"
M67 IV−68	"	"	"
M67 IV−77	"	"	"
M67 IV−81	"	"	"
M67 NOM.	"	"	"
M67 84	8 48 28.2	+12 03 54	CSI 79
M67 94	8 48 31.0	+12 01 27	"
M67 105	8 48 32.7	+11 59 28	"
M67 108	8 48 33.3	+11 56 35	"
M67 115	8 48 34.2	+12 00 34	"
M67 117	8 48 34.3	+11 58 15	"
M67 141	8 48 37.3	+11 59 21	"
M67 151	8 48 41.7	+12 05 04	"
M67 164	8 48 44.6	+12 01 47	"
M67 170	8 48 45.7	+11 58 34	"
M67 193	8 48 51.3	+12 04 19	"
M67 223	8 48 59.3	+12 07 56	"
M67 224	8 48 59.3	+11 55 41	"
M67 227	8 49 00.5	+11 58 00	"
M67 231	8 49 00.7	+11 59 01	"
M67 244	8 49 06.0	+11 57 22	"
M67 1465	8 48 20	+12 00	RNGC
M71 A2	19 51 29	+18 39	"
M71 A3	"	"	"
M71 A4	"	"	"
M71 A5	"	"	"
M71 A6	"	"	"
M71 A7	"	"	"
M71 A9	"	"	"
M71 B	"	"	"
M71 C	"	"	"
M71 N	"	"	"
M71 S	"	"	"
M71 T	"	"	"
M71 X	"	"	"
M71 18	"	"	"
M71 19	"	"	"
M71 21	"	"	"
M71 29	"	"	"
M71 30	"	"	"
M71 45	"	"	"
M71 46	"	"	"
M71 49	"	"	"
M71 75	"	"	"
M71 76	"	"	"
M71 77	"	"	"
M71 78	"	"	"
M71 79	"	"	"
M71 113	"	"	"
M78 #1	5 43 54.9	+ 0 01 47	
M78 #2	5 43 58.9	+ 0 01 47	
M78 #3	5 44 00.9	+ 0 03 17	
M78 #4	5 44 00.9	+ 0 05 47	
M78 #5	5 44 02.9	+ 0 05 17	
M78 #6	5 44 06.9	+ 0 03 47	
M78 #7	5 44 08.9	+ 0 01 17	
M78 #8	5 44 09.5	+ 0 03 33	
M78 #9	5 44 10.9	+ 0 04 17	
M78 #10	5 44 10.9	+ 0 00 17	
M78 #11	5 44 11.5	+ 0 01 38	
M78 #12	5 44 14.9	+ 0 02 57	

NAME	RA (1950) h m s	DEC ° ′ ″	POS REF
M78 #13	5 44 16.9	+ 0 03 32	
M78 H−H	5 43 34	− 0 11 17	
M78 NOM.	5 44 13	+ 0 02	
M78 104	"	"	RNGC
M78 106	"	"	"
M78 107	"	"	"
M78 108	"	"	"
M78 109	5 43 58.9	+ 0 01 47	
M78 111	5 43 51	− 0 03	ED
M78 121	5 44 13	+ 0 02	RNGC
M78 122	"	"	"
M78 125	"	"	"
M78 127	"	"	"
M78 128−9	"	"	"
M78 140	5 43 41	− 0 15	ED
M81	9 51 27.6	+69 18 13	769909
M81 NUCLEUS	9 51 32	+69 18	
M82	9 51 32.0	+69 55 00	ED
M82	9 51 32.4	+69 55 04	"
M82	9 51 42	+69 55 06	
M82	9 51 43.5	+69 55 03	
M82	9 51 43.8	+69 55 02	
M82	9 51 43.9	+69 55 01	
M82	9 51 44.0	+69 55 04	
M82	9 51 45.3	+69 55 11	769909
M82 #1	9 51 38.7	+69 54 53	ED
M82 #2	9 51 40.7	+69 54 57	"
M82 #3	9 51 45.8	+69 55 10	"
M82 #4	9 51 47.5	+69 55 15	"
M82 IR A	9 51 31.8	+69 55 01	"
M82 IR B	9 51 32.2	+69 55 05	"
M82 IR B	9 51 32.3	+69 55 05	"
M82 PERIPHERY	9 51 43	+69 55	RNGC
M83	12 22 31.5	+13 09 51	769909
M87	12 28 17.8	+12 39 58	"
M87 JET	12 28 16.9	+12 40 03	ED
M92 II−12	17 15 50	+43 16	"
M92 II−70	17 15 40	+43 15	"
M92 III−4	17 15 50	+43 18	"
M92 III−13	17 15 50	+43 17	"
M92 III−65	17 15 40	+43 15	"
M92 III−82	"	"	"
M92 IV−2	17 15 30	+43 05	"
M92 IV−10	17 15 30	+43 06	"
M92 IV−114	17 15 30	+43 08	"
M92 VII−18	17 15 20	+43 10	780507
M92 VIII−43	17 15 30	+43 09	ED
M92 X−49	17 15 40	+43 10	"
M92 XI−19	17 15 50	+43 09	"
M92 XII−8	17 15 50	+43 10	"
M100−CH 1	12 20 50	+16 05	
M100−CH 2	12 19 14	+16 01	
M100−CH 4	12 20 32	+16 11	
M101 S10	14 01 26.6	+54 35 25	769909
M101 S13	"	"	"
M101 1970G	"	"	"
NA 1	17 10 13.8	− 3 12 27	769910
NAB 0024+22	0 24 38.4	+22 25 23	809908
NAB 0024+224	0 24 38.5	+22 25 23	
NAB 0205+02	2 05 14.5	+ 2 28 43	809908
NAB 0205+024	"	"	"
NAB 0205+024	2 05 14.6	+ 2 28 43	
NEW SOURCE	18 45 45	− 4 45	
NEY−ALLEN	5 32 48.5	− 5 25 12	740903
NEY−ALLEN I	"	"	"
NGC 24	0 07 23.8	−25 14 33	
NGC 40	0 10 16	+72 14 39	709904
NGC 45	0 11 32.0	−23 27 34	
NGC 100	0 21 27.1	+16 12 34	
NGC 121 I−23	0 24 36	−71 48 48	749907
NGC 121 LE1	"	"	"
NGC 121 NOM.	"	"	"
NGC 121 T−V8	"	"	"
NGC 121 T1	"	"	"
NGC 121 T56	"	"	"
NGC 121 T64	"	"	"
NGC 121 T68	"	"	"
NGC 121 T73	"	"	"
NGC 121 V1	"	"	"
NGC 134	0 27 53.2	−33 31 16	
NGC 148	0 31 47.6	−32 03 40	759903
NGC 150	0 31 46.6	−28 04 46	821013
NGC 152 B11	0 30 55	−73 23 30	819916
NGC 152 C19	"	"	"
NGC 152 E18	"	"	"
NGC 152 F28	"	"	"
NGC 152 H−A33	"	"	"
NGC 152 H−A66	"	"	"
NGC 152 H23	"	"	"
NGC 152 NOM.	"	"	"
NGC 152 1	"	"	"
NGC 152 2	"	"	"
NGC 152 3	"	"	"
NGC 152 4	"	"	"
NGC 185	0 36 12.0	+48 03 50	769909
NGC 205	0 37 38.7	+41 24 44	"
NGC 221	0 39 58.0	+40 35 33	"
NGC 224	0 40 00.3	+41 00 03	"
NGC 224 NOM.	0 40 02	+41 00	
NGC 225	0 40 32	+61 31	RNGC
NGC 246	0 44 35.3	−12 09 03	739909
NGC 247	0 44 39.8	−21 01 58	759903
NGC 253	0 45 05.6	−25 33 38	
NGC 253	0 45 05.6	−25 33 39	
NGC 253	0 45 05.7	−25 33 40	ED
NGC 253	0 45 05.8	−25 33 39	
NGC 253	0 45 07.6	−25 33 39	759903
NGC 253	0 45 20.0	−25 22 15	
NGC 253 8"NE	0 45 06.0	−25 33 36	ED
NGC 254	0 45 02.2	−31 41 38	759903
NGC 281	0 49 26.2	+56 17 48	
NGC 339 G151	0 56 08	−74 44 36	819916
NGC 339 LE1	"	"	"
NGC 339 LE2	"	"	"
NGC 339 LE4	"	"	"
NGC 339 NOM.	"	"	"
NGC 339 87	"	"	"
NGC 339 151	"	"	"
NGC 361 A1−9	1 00 41	−71 51 30	ED
NGC 361 A1−16	1 00 34	−71 52 00	"
NGC 361 A1−40	1 00 37	−71 51 40	"
NGC 361 A1−45	1 00 32	−71 53 20	"
NGC 362	1 00 32	−71 07 00	749907
NGC 404	1 06 39.3	+35 27 10	769909
NGC 411 NOM.	1 06 21	−72 02 06	749907
NGC 411 1	"	"	"
NGC 411 2	"	"	"
NGC 416 LE1	1 06 41	−72 37	ED
NGC 416 LE2	1 06 37	−72 37	"
NGC 419 A4−13	1 06 59	−73 08	"
NGC 419 A5−15	1 06 53	−73 09	"
NGC 419 LE16	1 06 31	−73 09	"
NGC 419 LE18	1 06 53	−73 09	"
NGC 419 LE20	1 06 40	−73 09	"
NGC 419 LE21	1 06 41	−73 09	"
NGC 419 LE22	1 06 51	−73 09	"
NGC 419 LE23	"	"	"
NGC 419 LE25	1 06 45	−73 09	"
NGC 419 LE27	1 06 49	−73 09	"
NGC 419 LE29	1 06 50	−73 08	"
NGC 419 LE35	1 06 46	−73 09	"
NGC 419 LE37	1 06 55	−73 09	"
NGC 419 NOM.	1 06 47	−73 09	819916
NGC 419 W54	1 06 56	−73 10	ED
NGC 419 W71	1 06 51	−73 10	"
NGC 419 W72	1 06 47	−73 10	"
NGC 419 W82	"	"	"
NGC 419 W91	1 06 40	−73 09	"
NGC 419 W108	1 06 47	−73 08	"
NGC 419 W109	1 06 45	−73 08	"
NGC 419 W115	1 06 34	−73 08	"
NGC 419 W135	1 06 35	−73 08	"
NGC 419 135	1 06 47	−73 09	819916
NGC 419 4−133	1 07 05	−73 29	ED
NGC 419 5−3	1 06 44	−73 10	"
NGC 419 5−7	1 06 48	−73 10	"
NGC 419 5−8	1 06 50	−73 09	"
NGC 419 5−14	1 06 52	−73 09	"
NGC 419 5−15	1 06 53	−73 09	"
NGC 419 6−1	1 06 47	−73 09	"
NGC 434	1 10 13	−58 30 42	789907
NGC 474	1 17 31.7	+ 3 09 17	769909
NGC 488	1 19 11.2	+ 4 59 36	"
NGC 493	1 19 35.0	+ 0 41 04	
NGC 520	1 21 59.4	+ 3 32 13	769909
NGC 524	1 22 10.1	+ 9 16 45	"
NGC 526A	1 21 39	−35 19	RNGC
NGC 578	1 28 05.7	−22 55 29	
NGC 584	1 28 50.1	− 7 07 33	759903
NGC 595	1 30 42	+30 26	RNGC
NGC 596	1 30 21.6	− 7 17 20	759903
NGC 598	1 31 04.6	+30 23 40	769909
NGC 604	1 31 41	+30 32	RNGC
NGC 604 B/C	1 31 42.7	+30 31 40	ED
NGC 604 D	1 31 43.6	+30 31 40	"
NGC 604 E	1 31 44.0	+30 31 37	"
NGC 604 F	1 31 44.4	+30 31 30	"
NGC 604 G	1 31 44.0	+30 31 24	"
NGC 604 J	1 31 45.0	+30 31 24	"
NGC 604 K	1 31 45.7	+30 31 09	"
NGC 612	1 31 41	−36 45	"
NGC 613	1 31 58.7	−29 40 19	759903
NGC 628	1 34 00.7	+15 31 55	769909
NGC 662	1 41 39.4	+37 26 43	"
NGC 701	1 48 35.2	− 9 57 01	
NGC 755	1 53 54.0	− 9 18 20	
NGC 772	1 56 35.0	+18 45 58	
NGC 779	1 57 12.4	+ 6 12 28	
NGC 784	1 58 24.9	+28 35 46	
NGC 803	2 01 01.5	+15 47 30	
NGC 891	2 19 24.5	+42 07 13	
NGC 908	2 20 46.1	−21 27 35	
NGC 918	2 23 03.9	+18 16 16	
NGC 925	2 24 16.8	+33 21 16	
NGC 936	2 25 04.7	− 1 22 42	769909
NGC 949	2 27 44.5	+36 54 53	
NGC 959	2 29 21.1	+35 16 30	
NGC 984	2 31 51.2	+23 11 40	769909
NGC 986	2 31 34	−39 15 54	789907
NGC 1003	2 36 06.1	+40 39 29	
NGC 1023	2 37 15.5	+38 50 56	769906
NGC 1035	2 37 01.4	− 8 20 52	
NGC 1052	2 38 37.0	− 8 28 05	759903
NGC 1055	2 39 11.0	+ 0 13 44	
NGC 1058 SN	2 40 27	+37 08	RNGC
NGC 1068	2 40 06	− 0 01 42	
NGC 1068	2 40 06.5	− 0 13 32	769909
NGC 1073	2 41 05.6	+ 1 09 55	"
NGC 1084	2 43 31.8	− 7 47 08	759903
NGC 1090	2 44 00.6	− 0 27 22	
NGC 1097	2 44 11.5	−30 29 06	759903
NGC 1097POS1	"	"	"
NGC 1097POS2	2 44 11.7	−30 29 06	ED
NGC 1097POS3	2 44 11.9	−30 29 06	"
NGC 1097POS4	2 44 12.1	−30 29 06	"
NGC 1097POS5	2 44 12.3	−30 29 06	"
NGC 1097POS6	2 44 12.5	−30 29 06	"
NGC 1097POS7	2 44 11.3	−30 29 06	"
NGC 1097POS8	2 44 11.1	−30 29 06	"
NGC 1097POS9	2 44 10.9	−30 29 06	"
NGC 1097POS10	2 44 10.7	−30 29 06	"
NGC 1097POS11	2 44 10.5	−30 29 06	"
NGC 1097POS12	2 44 11.5	−30 29 03	"
NGC 1097POS13	2 44 11.5	−30 29 00	"
NGC 1097POS14	2 44 11.5	−30 28 57	"
NGC 1097POS15	2 44 11.5	−30 28 54	"
NGC 1097POS16	2 44 11.5	−30 28 51	"
NGC 1097POS17	2 44 11.5	−30 29 09	"
NGC 1097POS18	2 44 11.5	−30 29 12	"
NGC 1097POS19	2 44 11.5	−30 29 15	"
NGC 1097POS20	2 44 11.5	−30 29 18	"
NGC 1097POS21	2 44 11.5	−30 29 21	"
NGC 1097POS22	2 44 11.5	−30 29 24	"
NGC 1097POS23	2 44 11.7	−30 29 03	"
NGC 1097POS24	2 44 11.4	−30 29 03	"
NGC 1097POS25	2 44 11.3	−30 29 09	"
NGC 1097POS26	2 44 11.7	−30 29 09	"
NGC 1097POS27	2 44 11.3	−30 29 03	"
NGC 1097POS28	2 44 11.1	−30 29 12	"
NGC 1097POS29	2 44 12.1	−30 29 10	"
NGC 1097POS30	2 44 11.8	−30 28 58	"
NGC 1097POS31	2 44 12.1	−30 29 02	"
NGC 1097POS32	2 44 11.3	−30 29 16	"
NGC 1097POS33	2 44 10.9	−30 29 02	"
NGC 1097POS34	2 44 11.4	−30 29 12	"
NGC 1167	2 58 35.3	+35 00 31	769909
NGC 1169	3 00 10.9	+46 11 26	
NGC 1171	3 00 40.4	+43 12 11	
NGC 1187 SN	3 00 23	−23 04	RNGC
NGC 1232	3 07 30.0	−20 46 13	759903
NGC 1249	3 08 35.0	−53 31 24	
NGC 1253	3 11 38.0	− 3 00 28	
NGC 1255	3 11 22.5	−25 54 41	
NGC 1275	3 16 29.9	+41 19 55	769909
NGC 1291	3 15 28	−41 17 24	789907
NGC 1292	3 16 07.6	−27 47 34	759903
NGC 1297	3 16 58.6	−19 16 48	"
NGC 1300	3 17 25.3	−19 35 30	
NGC 1302	3 17 42.3	−26 14 25	759903
NGC 1313	3 17 39	−66 40 42	749906
NGC 1316	3 20 47	−37 23 12	789908
NGC 1316 SN	3 20 45	−37 24 52	ED
NGC 1316 SN	3 21 06	−37 23 32	"
NGC 1316 SN1	"	"	"
NGC 1316 SN2	3 20 45	−37 24 52	"
NGC 1325	3 22 12.3	−21 43 12	
NGC 1326	3 22 01.0	−36 38 27	821013
NGC 1332	3 24 03.6	−21 30 30	759903
NGC 1332 SN	3 24 30	−21 28	ED
NGC 1333	3 25 58.2	+31 05 47	
NGC 1333 #1	3 26 14.1	+31 14 33	
NGC 1333 #2	3 26 12.1	+31 12 13	
NGC 1333 #3	3 26 04.8	+31 11 33	
NGC 1333 #4	3 26 20.1	+31 16 12	
NGC 1333 #5	3 26 15.1	+31 08 03	
NGC 1333 #6	3 26 22.1	+31 16 33	
NGC 1333 #7	3 26 04.1	+31 12 33	
NGC 1333 #8	3 25 58.8	+31 12 03	
NGC 1333 #9	3 25 38.1	+31 07 03	
NGC 1333 #10	3 25 46.1	+31 08 03	
NGC 1333 #11	3 25 51.8	+31 08 03	
NGC 1333 #12	3 25 56.1	+31 09 48	
NGC 1333 #13	3 25 58.1	+31 05 33	
NGC 1333 #14	3 26 00.1	+31 06 18	
NGC 1333 #15	3 25 51.1	+31 06 03	
NGC 1333 #16	3 25 53.7	+31 05 26	
NGC 1333 #17	3 25 42.1	+31 06 43	
NGC 1333 #18	3 25 48.1	+31 06 33	
NGC 1333 #20	3 26 16.1	+31 05 03	
NGC 1333 #21	3 25 40.1	+31 06 03	
NGC 1333 #22	3 26 24.1	+30 58 28	
NGC 1333 #23	3 26 02.1	+31 00 23	
NGC 1333 #24	3 25 40.1	+30 59 08	
NGC 1333 #25	3 26 21.4	+30 57 33	
NGC 1333 HH11	3 25 58.5	+31 05 34	
NGC 1333 IRS	3 26 00.5	+31 06 21	
NGC 1333 IR14	3 26 00.1	+31 06 18	
NGC 1333 NH3	3 26 01.0	+31 04 45	
NGC 1333 VLA	3 24 35.7	+31 13 26	
NGC 1337	3 25 39.7	− 8 33 36	
NGC 1344	3 26 17.8	−31 14 27	759903
NGC 1350	3 29 10	−33 47 54	789908
NGC 1351A	3 26 52	−35 21 00	"
NGC 1358	3 31 10.5	− 5 15 30	759903
NGC 1365	3 31 41	−36 18 24	789908
NGC 1371	3 32 52.7	−25 05 54	759903
NGC 1379	3 34 08	−35 36 18	789908
NGC 1380	3 34 32	−35 08 24	"
NGC 1385	3 35 20.0	−24 39 50	
NGC 1386	3 34 52	−36 09 48	789908
NGC 1387	3 35 02	−35 40 12	"
NGC 1395	3 36 19.2	−23 11 25	759903
NGC 1398	3 36 45.0	−26 29 55	"
NGC 1399	3 36 34	−35 36 42	789908
NGC 1400	3 37 15.4	−18 50 56	759903
NGC 1404	3 36 57	−35 45 18	789908
NGC 1406	3 37 22.6	−31 28 59	759903
NGC 1407	3 37 56.2	−18 44 22	"
NGC 1415	3 38 46.0	−22 43 25	"
NGC 1421	3 40 08.8	−13 38 56	
NGC 1425	3 40 09.4	−30 03 11	759903
NGC 1433	3 40 27	−47 22 48	789907
NGC 1448	3 42 53.2	−44 48 04	
NGC 1487	3 54 05	−42 30 42	789907
NGC 1494	3 56 15.0	−49 03 00	
NGC 1497	3 59 08.6	+22 59 41	769909
NGC 1499	4 00 04	+36 17	RNGC
NGC 1501	4 02 42	+60 47 00	709904
NGC 1507	4 01 55.7	− 2 19 21	
NGC 1514	4 06 08	+30 38 42	709904
NGC 1527	4 06 56	−48 01 42	759905
NGC 1535	4 11 57.0	−12 51 42	739909
NGC 1543	4 11 44	−57 51 48	759905
NGC 1546	4 13 32	−56 11 06	749907
NGC 1549	4 14 39	−55 42 54	"
NGC 1553	4 15 05	−55 54 12	"
NGC 1559	4 17 01.0	−62 54 18	
NGC 1560	4 27 07.6	+71 46 34	
NGC 1566	4 18 53.3	−55 03 23	789906
NGC 1574	4 20 59	−57 05 24	749907
NGC 1587	4 28 05.2	+ 0 33 17	769909
NGC 1588	4 28 09.5	+ 0 33 30	"
NGC 1596	4 26 32	−55 08 12	749907
NGC 1600	4 29 12.0	− 5 11 27	759903
NGC 1614	4 31 35.7	− 8 40 56	"
NGC 1617	4 30 33	−54 42 24	749907
NGC 1637	4 38 57.5	− 2 57 11	759903
NGC 1651 2421	4 37 45	−70 40 40	ED
NGC 1651 3304	4 37 51	−70 41 10	"
NGC 1651 4325	4 38 04	−70 41 10	"
NGC 1651 4328	4 38 05	−70 41 10	"
NGC 1651H2421	4 37 45	−70 40 40	"
NGC 1651H3304	4 37 51	−70 41 10	"
NGC 1651H4325	4 38 04	−70 41 10	"

NAME	RA (1950)	DEC	POS REF
NGC 1651H4328	4 38 05	−70 41 10	"
NGC 1651H4402	4 37 58	−70 42 00	"
NGC 1652 NOM.	4 38 30	−68 46 12	819916
NGC 1652 1	"	"	"
NGC 1652 2	"	"	"
NGC 1652H2406	4 38 21	−68 45 40	ED
NGC 1652H3210	4 38 29	−68 46 30	"
NGC 1672	4 44 55	−59 20 18	759905
NGC 1685	4 50 03	− 3 01	RNGC
NGC 1700	4 54 28.1	− 4 56 30	759903
NGC 1718 NOM.	4 52 23	−67 07 54	749906
NGC 1718 1	"	"	"
NGC 1718 2	"	"	"
NGC 1718 3	"	"	"
NGC 1718 4	"	"	"
NGC 1718 5	"	"	"
NGC 1744	4 57 55.6	−26 05 42	
NGC 1751 LE1	4 54 33	−69 53 06	789907
NGC 1751 LE2	"	"	"
NGC 1751 LE3	"	"	"
NGC 1751 LE4	"	"	"
NGC 1751 LE5	"	"	"
NGC 1751 NOM.	"	"	"
NGC 1783 G6	4 59 00	−66 04 24	749906
NGC 1783 G7	4 59 07	−66 05 00	ED
NGC 1783 G12	4 59 13	−66 04 24	"
NGC 1783 G13	4 59 06	−66 04 33	"
NGC 1783 G14	4 59 08	−66 04 24	"
NGC 1783 G30	4 58 53	−66 03 49	"
NGC 1783 G32	4 58 47	−66 04 08	"
NGC 1783 G39	4 59 00	−66 04 24	749906
NGC 1783 G40	4 58 57	−66 05 37	ED
NGC 1783 G85	4 59 00	−66 04 24	749906
NGC 1783 G108	"	"	"
NGC 1783 LE1	"	"	"
NGC 1783 LE2	"	"	"
NGC 1783 LE4	"	"	"
NGC 1783 LE5	"	"	"
NGC 1783 LE7	"	"	"
NGC 1783 LE8	"	"	"
NGC 1783 LE9	"	"	"
NGC 1783 LE10	"	"	"
NGC 1783 LE11	"	"	"
NGC 1783 NOM.	"	"	"
NGC 1783 30	4 58 53	−66 03 49	ED
NGC 1784	5 03 06.8	−11 56 18	
NGC 1792	5 03 31.0	−38 02 49	
NGC 1795 NOM.	5 00 09	−69 52 24	789907
NGC 1795 1	"	"	"
NGC 1795 2	"	"	"
NGC 1806 LE1	5 02 18	−68 02 12	"
NGC 1806 LE2	"	"	"
NGC 1806 LE3	"	"	"
NGC 1806 LE4	"	"	"
NGC 1806 LE5	"	"	"
NGC 1806 NOM.	"	"	"
NGC 1806 9	"	"	"
NGC 1808	5 05 59	−37 34 36	"
NGC 1831 NOM.	5 06 12	−64 59 00	749906
NGC 1831 1	"	"	"
NGC 1831 2	"	"	"
NGC 1831 3	"	"	"
NGC 1841 G95	4 52 59	−84 04 54	819916
NGC 1841 G113	"	"	"
NGC 1841 G117	"	"	"
NGC 1841 G129	"	"	"
NGC 1841 G142	"	"	"
NGC 1841 LE1	"	"	"
NGC 1841 NOM.	"	"	"
NGC 1841 67	"	"	"
NGC 1841 142	"	"	"
NGC 1841H1301	4 53 23	−84 04 52	ED
NGC 1841H2413	4 52 29	−84 04 37	"
NGC 1846 H1	5 07 43	−67 31 00	"
NGC 1844 H12	5 07 30	−67 22 41	"
NGC 1844 H14	5 07 31	−67 22 54	"
NGC 1846 H21	5 07 38	−67 31 18	789907
NGC 1846 H38	5 07 35	−67 32 00	ED
NGC 1846 H39	5 07 38	−67 31 18	789907
NGC 1846 H58	5 07 31	−67 31 10	ED
NGC 1846 LE4	5 07 43	−67 31 20	"
NGC 1846 LE5	5 07 41	−67 31 20	"
NGC 1846 LE8	5 07 36	−67 31 40	"
NGC 1846 LE11	5 07 31	−67 31 20	"
NGC 1846 LE13	5 07 34	−67 31 00	"
NGC 1846 LE15	5 07 29	−67 29 50	"
NGC 1846 LE17	5 07 44	−67 30 50	"
NGC 1846 NOM.	5 07 38	−67 31 18	789907
NGC 1846 1302	"	"	"
NGC 1846 4403	"	"	"
NGC 1846 4508	"	"	"
NGC 1852 2	5 09 31	−67 50 00	ED
NGC 1852 3	5 09 30	−67 50 10	"
NGC 1852 4	5 09 29	−67 50 30	"
NGC 1852 5	5 09 27	−67 50 20	"
NGC 1852 6	5 09 25	−67 50 20	"
NGC 1872 1	5 13 19	−69 21 30	"
NGC 1872 2	5 13 23	−69 22 40	"
NGC 1872 3	5 13 30	−69 22 20	"
NGC 1872 4	5 13 36	−69 22 30	"
NGC 1892	5 16 55.0	−65 00 48	
NGC 1893 1	5 19 11.9	+33 27 59	CSI 79
NGC 1903 NOM.	5 17 43	−69 23 12	789907
NGC 1903 1	"	"	"
NGC 1903 2	"	"	"
NGC 1916 CORE	5 18 58	−69 27 20	"
NGC 1916 LE1	5 18 56	−69 27 20	ED
NGC 1916 4	5 18 58	−69 27 20	"
NGC 1917 LE1	5 19 19	−69 03 20	"
NGC 1917 LE2	5 19 18	−69 03 20	"
NGC 1917 LE3	5 19 22	−69 02 50	"
NGC 1917 LE4	5 19 15	−69 03 00	"
NGC 1947	5 26 28	−63 48 06	749906
NGC 1952	5 31 30	+21 59	RNGC
NGC 1953 LE1	5 25 46	−68 53 00	ED
NGC 1953 LE2	5 25 41	−68 52 20	"
NGC 1953 3	5 25 46	−68 52 50	"
NGC 1962 NOM.	5 26 35	−68 52 42	789907
NGC 1962 29	"	"	"
NGC 1964	5 31 14.8	−21 58 46	
NGC 1976	5 32 52	− 5 25	RNGC
NGC 1976 #1	5 32 49.0	− 5 27 14	ED
NGC 1976 #2	5 32 49.0	− 5 23 14	"
NGC 1976 #3	5 32 45.0	− 5 20 14	"
NGC 1978 H1−8	5 28 41	−66 17 00	"
NGC 1978 H2−7	5 28 36	−66 16 10	"
NGC 1978 I−18	5 28 45	−66 17 10	"
NGC 1978 I−25	5 28 42	−66 16 30	749906
NGC 1978 LE1	5 28 41	−66 16 50	ED
NGC 1978 LE3	5 28 40	−66 16 10	"
NGC 1978 LE4	5 28 39	−66 16 20	"
NGC 1978 LE6	5 28 41	−66 16 10	"
NGC 1978 LE7	5 28 43	−66 16 50	"
NGC 1978 LE8	"	"	"
NGC 1978 LE9	5 28 45	−66 16 50	"
NGC 1978 LE11	5 28 38	−66 16 00	"
NGC 1978 NOM.	5 28 42	−66 16 30	749906
NGC 1978H1−12	"	"	"
NGC 1978H1−14	"	"	"
NGC 1978H1−15	5 28 44	−66 17 10	ED
NGC 1978H1−18	5 28 45	−66 17 10	"
NGC 1978H1−25	5 28 42	−66 16 30	749906
NGC 1978H1−35	5 28 46	−66 16 30	ED
NGC 1978H2−10	5 28 38	−66 16 10	"
NGC 1978H2−13	5 28 36	−66 16 00	"
NGC 1978H2−15	5 28 38	−66 16 00	"
NGC 1978H2−16	5 28 37	−66 16 50	"
NGC 1978H2−18	5 28 38	−66 16 50	"
NGC 1984 NOM.	5 28 01	−69 10 24	789907
NGC 1984 16	"	"	"
NGC 1987LE1+2	5 27 53	−70 46 40	ED
NGC 1987 LE3	5 28 05	−70 47 20	"
NGC 1987 LE4	5 28 00	−70 47 30	"
NGC 1987 LE5	5 27 58	−70 46 40	"
NGC 1994 NOM.	5 28 42	−69 10 48	789907
NGC 1994 2	"	"	"
NGC 1994 4	"	"	"
NGC 1994 5	"	"	"
NGC 2019 2	5 32 31	−70 11 20	ED
NGC 2019 5	5 32 28	−70 11 30	"
NGC 2021 NOM.	5 33 37	−67 29 06	789907
NGC 2021 22	"	"	"
NGC 2022	5 39 20.0	+ 9 03 54	739909
NGC 2023	5 39 07	− 2 17 42	
NGC 2023 NOM.	5 39 14	− 2 15	
NGC 2023 101			RNGC
NGC 2023 102−4	"	"	"
NGC 2023 105	"	"	"
NGC 2023 106	"	"	"
NGC 2023 108	"	"	"
NGC 2023 110	"	"	"
NGC 2023 112			
NGC 2024	5 39	− 1 55	
NGC 2024	5 39 06.3	− 1 56 10	741007
NGC 2024	5 39 08	− 1 55 03	
NGC 2024	5 39 12	− 1 55 42	
NGC 2024	5 39 13	− 1 55 48	
NGC 2024	5 39 14	− 1 57 00	ED
NGC 2024	5 39 14.0	− 1 57 00	
NGC 2024	5 39 19	− 1 55 42	
NGC 2024	5 39 26	− 1 51	
NGC 2024 (1)	5 39 14.5	− 1 57 48	
NGC 2024 #1	5 39 06.3	− 1 56 10	
NGC 2024 #1	5 39 24	− 1 51 52	ED
NGC 2024 #2	5 39 14.3	− 1 55 59	
NGC 2024 #2	5 39 20	− 1 51 52	ED
NGC 2024 IRS1	5 39 06.3	− 1 56 10	741007
NGC 2024 IRS2	5 39 14.3	− 1 55 59	"
NGC 2024 SW	5 39 07.5	− 1 57 30	
NGC 2024 1	5 39 26.2	− 1 51 44	
NGC 2071	5 44 30.1	+ 0 20 40	
NGC 2071	5 44 30.2	+ 0 20 42	790114
NGC 2071	5 44 30.8	+ 0 20 43	
NGC 2071	5 44 31.2	+ 0 20 48	
NGC 2071	5 44 30	+ 0 16	ED
NGC 2071 IRS	5 44 30.1	+ 0 20 40	
NGC 2071 IRS	5 44 30.2	+ 0 20 42	
NGC 2071 IRS	5 44 31.2	+ 0 20 45	
NGC 2071 IRS1	5 44 30.6	+ 0 20 42	
NGC 2071 IRS2	5 44 31.2	+ 0 20 48	
NGC 2071 IRS3	5 44 30.6	+ 0 20 48	
NGC 2071 IRS4	5 44 31.2	+ 0 20 54	
NGC 2076	5 44 35	−16 47	RNGC
NGC 2090	5 46 34.0	−34 14 32	
NGC 2107 NOM.	5 43 49	−70 39 36	749907
NGC 2107 1	"	"	"
NGC 2110	5 49 47	− 7 18	RNGC
NGC 2121 LE1	5 48 56	−71 29 40	ED
NGC 2121 LE2	5 49 01	−71 29 50	"
NGC 2121 LE4	5 49 01	−71 29 40	"
NGC 2121 LE5	5 49 06	−71 28 40	"
NGC 2121 LE6	5 48 52	−71 30 10	"
NGC 2133 1	5 52 11	−71 10 50	"
NGC 2134 1	5 52 35	−71 07 10	"
NGC 2134 2	5 52 35	−71 06 20	"
NGC 2134 3	5 52 41	−71 05 20	"
NGC 2134 4	5 52 28	−71 05 20	"
NGC 2134 5	5 52 35	−71 06 20	"
NGC 2146A	6 15 52.6	+78 33 17	
NGC 2154 LE1	5 57 42	−67 16 10	ED
NGC 2154 LE2	5 57 44	−67 15 50	"
NGC 2154 LE3	5 57 44	−67 16 40	"
NGC 2162 1	6 00 12	−63 43 10	"
NGC 2162 2	6 00 13	−63 43 00	"
NGC 2170 IRS1	6 05 20.0	− 6 22 38	"
NGC 2170 IRS3	6 05 21.9	− 6 22 26	760905
NGC 2173 H45A	5 59 04	−72 59 51	ED
NGC 2173 LE1	5 59 04	−72 59 00	"
NGC 2173 LE4	5 59 00	−72 58 37	"
NGC 2173 LE5	5 59 01	−72 58 00	"
NGC 2173 1401	5 59 26	−72 58 36	"
NGC 2173 4306	5 59 09	−72 59 23	"
NGC 2173H1401	5 59 26	−72 58 36	"
NGC 2173H4306	5 59 09	−72 59 23	"
NGC 2173STARA	5 59 03	−72 58 48	"
NGC 2175	6 05 33.0	+20 39 06	
NGC 2190 LE3	6 02 27	−74 43 00	ED
NGC 2190 NOM.	6 02 35	−74 43 24	789907
NGC 2190 1417	"	"	"
NGC 2190 4324	"	"	"
NGC 2193H1307	6 06 11	−65 05 10	ED
NGC 2193H2201	6 06 07	−65 05 10	"
NGC 2193H4303	6 06 13	−65 05 40	"
NGC 2209 LE3	6 10 02	−73 49 40	"
NGC 2209 NOM.	6 09 50	−73 49 36	749907
NGC 2209 W9	"	"	"
NGC 2209 W46	6 09 55	−73 49 40	ED
NGC 2209 W50	6 09 43	−73 49 40	"
NGC 2209 5	6 09 51	−73 50 20	"
NGC 2209 46	6 09 55	−73 49 40	"
NGC 2209 50	6 09 43	−73 49 40	"
NGC 2213 LE1	6 11 21	−71 30 20	"
NGC 2213 LE2	6 11 30	−71 30 40	"
NGC 2213 LE3	6 11 29	−71 31 50	"
NGC 2213 11	6 11 24	−71 30 50	"
NGC 2213 12	6 11 31	−71 30 50	"
NGC 2217	6 19 40.3	−27 12 31	759903
NGC 2244 2	6 29 16.0	+ 4 58 46	CSI 79
NGC 2244 3	6 29 29.9	+ 4 51 37	"
NGC 2244 4	6 29 12.9	+ 5 04 10	"
NGC 2244 5	6 28 58.7	+ 5 03 46	"
NGC 2244 6	6 28 41.4	+ 4 52 13	"
NGC 2244 7	6 29 30.9	+ 5 00 13	"
NGC 2257 C27	6 29 57	−64 17 18	789907
NGC 2257 H23	"	"	"
NGC 2257 H62	"	"	"
NGC 2257 LE4	6 29 57	−64 17 20	ED
NGC 2257 LE7	6 29 57	−64 18 30	"
NGC 2257 LE8	6 30 03	−64 18 40	"
NGC 2257 LE11	6 30 07	−64 16 20	"
NGC 2257 NOM.	6 29 57	−64 17 18	789907
NGC 2257H4503	6 29 57	−64 18 30	ED
NGC 2257H4621	6 30 07	−64 18 10	"
NGC 2257H4709	6 30 03	−64 18 40	"
NGC 2261	6 36 26	+ 8 46	RNGC
NGC 2264	6 38 24.9	+ 9 32 29	720302
NGC 2264	6 38 25.3	+ 9 32 25	
NGC 2264 IR	6 38 24.9	+ 9 32 29	720302
NGC 2264 IRS	"	"	
NGC 2264 IRS4	6 38 24.1	+10 02 35	
NGC 2264 V1	6 36 58	+ 9 47	ED
NGC 2264 V2	6 36 58	+ 9 38	"
NGC 2264 V18	6 37 20	+ 9 35	"
NGC 2264 V20	6 37 21	+ 9 39	"
NGC 2264 V116	6 38 18	+ 9 26	"
NGC 2264 V193	6 38 56	+ 9 35	"
NGC 2264 W20	6 36 42.3	+ 9 44 49	CSI 79
NGC 2264 W30	6 37 08.3	+ 9 30 48	"
NGC 2264 W33	6 37 12	+ 9 37	ED
NGC 2264 W36	6 37 18.9	+ 9 37 19	CSI 79
NGC 2264 W43	6 37 36.4	+ 9 44 40	"
NGC 2264 W46	6 37 39.5	+ 9 48 57	"
NGC 2264 W50	6 37 43.3	+ 9 51 53	"
NGC 2264 W67	6 37 52	+ 9 50 36	740903
NGC 2264 W68	6 37 51.7	+ 9 57 42	CSI 79
NGC 2264 W73	6 37 53.0	+10 00 34	"
NGC 2264 W83	6 37 57.3	+ 9 42 12	"
NGC 2264 W84	6 37 57.1	+ 9 36 29	"
NGC 2264 W88	6 37 58.0	+ 9 48 51	"
NGC 2264 W90	6 37 59.0	+ 9 50 47	"
NGC 2264 W100	6 38 03.7	+ 9 54 13	"
NGC 2264 W104	6 38 04.1	+ 9 55 51	"
NGC 2264 W107	6 38 05.7	+10 04 34	"
NGC 2264 W108	6 38 06.3	+ 9 47 42	"
NGC 2264 W109	6 38 06.3	+ 9 54 41	"
NGC 2264 W110	6 38 07	+ 9 46	ED
NGC 2264 W112	6 38 06.7	+ 9 41 54	CSI 79
NGC 2264 W125	6 38 11.3	+ 9 51 20	"
NGC 2264 W131	6 38 13.3	+ 9 56 36	"
NGC 2264 W132	6 38 12.5	+ 9 36 50	"
NGC 2264 W137	6 38 15.9	+ 9 55 19	"
NGC 2264 W138	6 38 16.0	+ 9 27 02	"
NGC 2264 W139	6 38 16	+ 9 34	ED
NGC 2264 W145	6 38 16.0	+ 9 30 56	CSI 79
NGC 2264 W151	6 38 17.2	+ 9 50 27	"
NGC 2264 W154	6 38 17.2	+ 9 34 20	"
NGC 2264 W157	6 38 17.9	+ 9 36 00	"
NGC 2264 W158	6 38 18.9	+ 9 57 44	"
NGC 2264 W165	6 38 19.1	+ 9 25 48	"
NGC 2264 W177	6 38 23.1	+10 19 42	"
NGC 2264 W178	6 38 24.7	+ 9 30 48	"
NGC 2264 W179	6 38 24.7	+ 9 55 49	"
NGC 2264 W181	6 38 25.1	+ 9 55 45	"
NGC 2264 W187	6 38 28.0	+ 9 38 42	"
NGC 2264 W188	6 38 31	+ 9 39	ED
NGC 2264 W189	6 38 28.3	+ 9 30 12	CSI 79
NGC 2264 W190	6 38 34	+ 9 59	ED
NGC 2264 W192	6 38 34	+ 9 43	"
NGC 2264 W206	6 38 36.9	+ 9 46 45	CSI 79
NGC 2264 W209	6 38 38.7	+ 9 36 49	"
NGC 2264 W212	6 38 42.0	+ 9 54 09	"
NGC 2264 W215	6 38 44.9	+ 9 52 41	"
NGC 2264 W220	6 38 47.9	+ 9 21 44	"
NGC 2264 W222	6 38 48.9	+ 9 54 15	"
NGC 2264 W224	6 38 52.0	+ 9 23 48	"
NGC 2264 W226	6 38 55.9	+ 9 50 11	"
NGC 2264 W228	6 38 58.3	+ 9 46 15	"
NGC 2264 W229	6 38 57.9	+10 04 59	"
NGC 2264 W231	6 39 04.9	+ 9 33 24	"
NGC 2264 W237	6 39 29.7	+ 9 35 29	"
NGC 2264 W238	6 39 37	+10 16	ED
NGC 2264 W239	6 39 38	+10 16	"
NGC 2264 2	6 38 24.9	+ 9 32 29	720302
NGC 2264A	6 38 22	+ 9 25 42	
NGC 2264B	6 38 25	+ 9 32 30	
NGC 2264C	6 38 34	+ 9 27 42	
NGC 2268	7 00 47.6	+84 27 41	
NGC 2273B	6 42 02.8	+60 23 38	
NGC 2280	6 42 50.0	−27 35 12	
NGC 2300	7 15 45.1	+85 48 31	769909
NGC 2329	7 05 21.7	+48 41 48	"
NGC 2332	7 05 43.3	+50 15 48	"
NGC 2336	7 18 28.0	+80 16 35	
NGC 2346	7 06 49.2	− 0 43 24	739909

NAME	RA (1950) DEC	POS REF
	h m s ° ′ ″	
NGC 2357	7 14 39.9 +23 26 49	
NGC 2366	7 23 34.2 +69 18 42	769909
NGC 2366	7 23 38.0 +69 19 15	
NGC 2371/2	7 22 25.5 +29 35 23	749905
NGC 2392	7 26 13.2 +21 00 51	739909
NGC 2403	7 32 05.5 +65 42 40	769909
NGC 2419	7 34 48 +39 00	RNGC
NGC 2427	7 35 01.0 −47 31 18	
NGC 2434	7 34 59 −69 10 18	789907
NGC 2438	7 39 32.5 −14 36 56	739909
NGC 2440	7 39 41.5 −18 05 26	"
NGC 2440 6"NW	7 39 41.2 −18 05 22	ED
NGC 2452	7 45 24.7 −27 12 43	739909
NGC 2541	8 11 01.8 +49 12 53	
NGC 2549	8 14 56.6 +57 57 35	769909
NGC 2562	8 17 28.6 +21 17 27	"
NGC 2563	8 17 40.7 +21 13 40	"
NGC 2591	8 30 43.2 +78 11 54	
NGC 2610	8 31 05.0 −15 58 39	739909
NGC 2613	8 31 11.1 −22 48 01	
NGC 2634	8 42 56.0 +74 09 06	769909
NGC 2655	8 49 09.1 +78 24 53	"
NGC 2672	8 46 31.3 +19 15 40	"
NGC 2683	8 49 34.8 +33 36 23	
NGC 2701	8 55 26.0 +53 57 53	
NGC 2749	9 02 32.4 +18 30 53	769909
NGC 2768	9 07 45.2 +60 14 40	"
NGC 2770	9 06 30.3 +33 19 42	
NGC 2782	9 10 54.0 +40 19 18	769909
NGC 2784	9 10 05.7 −23 57 56	759903
NGC 2792	9 10 33.7 −42 13 08	739909
NGC 2808	9 11 04 −64 39 30	779907
NGC 2818	9 13 59.4 −36 24 58	739909
NGC 2831	9 16 43.3 +33 57 20	739910
NGC 2832	9 16 43.7 +33 57 45	769909
NGC 2835	9 15 36.6 −22 08 45	
NGC 2841	9 18 34.9 +51 11 19	769909
NGC 2867	9 20 00.8 −58 05 57	769910
NGC 2867 5"E	9 20 01.4 −58 05 57	ED
NGC 2883	9 23 09 −33 53	RNGC
NGC 2903	9 29 19.9 +21 43 19	769909
NGC 2907	9 29 14.8 −16 31 00	759903
NGC 2911	9 31 05.5 +10 22 30	769909
NGC 2968	9 39 22 − 8 23	ED
NGC 2974	9 40 01.8 − 3 28 08	759903
NGC 2976	9 43 10.0 +68 08 43	769909
NGC 2986	9 41 56.8 −21 02 53	759903
NGC 2992	9 43 17.6 −14 05 45	"
NGC 2993	9 43 24.2 −14 08 13	"
NGC 3003	9 45 37.9 +33 39 16	
NGC 3026	9 48 00.8 +28 47 07	
NGC 3027	9 51 16.8 +72 26 27	
NGC 3031	9 51 27.6 +69 18 13	769909
NGC 3034	9 51 45.3 +69 55 11	"
NGC 3034 NE	9 51 43 +69 55	RNGC
NGC 3034 NOM.	" "	
NGC 3077	9 59 21.9 +68 58 33	769909
NGC 3078	9 56 08.1 −26 41 13	759903
NGC 3079	9 58 35.4 +55 55 11	
NGC 3081	9 57 10.0 −22 35 09	759903
NGC 3115	10 02 44.4 − 7 28 32	"
NGC 3125	10 04 18.0 −29 41 30	"
NGC 3132	10 04 55.1 −40 11 29	739909
NGC 3136	10 04 27 −67 08	RNGC
NGC 3153	10 10 09.5 +12 55 00	
NGC 3158	10 10 52.6 +39 00 48	769909
NGC 3159	10 10 55.1 +38 54 05	739910
NGC 3190	10 15 20.7 +22 05 03	719904
NGC 3193	10 15 39.5 +22 08 45	769909
NGC 3198	10 16 51.7 +45 48 07	
NGC 3201 1117	10 15 24 +46 05	ED
NGC 3201 1309	10 15 12 +46 08	"
NGC 3201 1312	10 15 18 +46 07	"
NGC 3201 1314	" "	"
NGC 3201 1315		"
NGC 3201 1410	10 15 18 +46 08	"
NGC 3201 1501	10 15 18 +46 09	"
NGC 3201 1626	10 15 30 +46 08	"
NGC 3201 2321	10 15 24 +46 12	"
NGC 3201 2405	10 15 18 +46 09	"
NGC 3201 2608	10 15 24 +46 09	"
NGC 3201 3204	10 15 36 +46 13	"
NGC 3201 3217	10 15 42 +46 12	"
NGC 3201 3218	" "	"
NGC 3201 3304	10 15 36 +46 12	"
NGC 3201 3401	10 15 30 +46 11	"
NGC 3201 3405	10 15 36 +46 11	"
NGC 3201 3414	10 15 42 +46 10	"
NGC 3201 3504	10 15 30 +46 10	"
NGC 3201 3522	10 15 36 +46 10	"
NGC 3201 3616	" "	"
NGC 3201 4318	10 15 36 +46 06	"
NGC 3201 4319	10 15 30 +46 06	"
NGC 3201 4403	10 15 42 +46 09	"
NGC 3201 4507	10 15 36 +46 08	"
NGC 3201 4524	10 15 30 +46 07	"
NGC 3225	10 21 52.1 +58 24 15	
NGC 3226	10 20 43.5 +20 09 07	769909
NGC 3227	10 20 47.6 +20 07 00	"
NGC 3242	10 22 21.3 −18 23 23	739909
NGC 3247	10 22 10 −57 30 30	
NGC 3250	10 24 21 −39 41 18	789908
NGC 3254	10 26 31.3 +29 44 50	
NGC 3256	10 25 43 −43 39 00	779909
NGC 3264	10 29 08.1 +56 20 30	
NGC 3281	10 29 36 −34 35 48	789908
NGC 3294	10 33 23.7 +37 35 01	
NGC 3308	10 34 01.2 −27 10 43	759903
NGC 3309	10 34 14.5 −27 15 33	"
NGC 3310	10 35 40.3 +53 45 45	769909
NGC 3311	10 34 21.6 −27 16 08	759903
NGC 3319	10 36 14.7 +41 56 50	
NGC 3320	10 36 37.1 +47 39 31	
NGC 3320	10 36 37.4 +47 39 25	769909
NGC 3338	10 39 28.2 +14 00 34	
NGC 3351	10 41 19.6 +11 58 00	769909
NGC 3359	10 43 20.5 +63 29 14	
NGC 3365	10 43 38.2 + 2 04 38	

NAME	RA (1950) DEC	POS REF
	h m s ° ′ ″	
NGC 3368	10 44 06.9 +12 05 05	769909
NGC 3377	10 45 02.6 +14 14 51	"
NGC 3379	10 45 11.3 +12 50 48	"
NGC 3384	10 45 38.7 +12 53 41	"
NGC 3430	10 49 24.7 +33 13 00	
NGC 3432	10 49 42.0 +36 52 58	
NGC 3443	10 50 20.1 +17 50 24	
NGC 3486	10 57 40.0 +29 14 40	769909
NGC 3495	10 58 41.1 + 3 53 48	
NGC 3501	11 00 08.1 +18 15 36	
NGC 3504	11 00 28.1 +28 14 35	769909
NGC 3510	11 01 00.8 +29 09 12	
NGC 3516	11 03 22.6 +72 50 25	769909
NGC 3521	11 03 15.1 + 0 13 58	"
NGC 3521	11 03 15.5 + 0 14 12	
NGC 3528	11 04 50 −19 12 06	819917
NGC 3549	11 08 02.8 +53 39 30	
NGC 3556	11 08 36.8 +55 56 33	769909
NGC 3557	11 07 35 −37 16 00	789908
NGC 3568	11 08 26 −37 10 24	"
NGC 3576	11 09 46.3 −61 02 09	
NGC 3576	11 09 47 −61 02	
NGC 3576 1	11 09 46.0 −61 02 10	ED
NGC 3576 2	11 09 43.6 −61 02 15	"
NGC 3576 3	11 09 43.2 −61 02 48	"
NGC 3576 4	11 09 41.1 −61 02 50	"
NGC 3576 5	11 09 52.3 −61 02 10	"
NGC 3576 6	11 09 55 −61 02 24	"
NGC 3576 7	11 09 47 −61 02	
NGC 3585	11 10 50.0 −26 28 48	769909
NGC 3587	11 11 51 +55 18	RNGC
NGC 3600	11 13 06.5 +41 51 50	
NGC 3603	11 12 51.1 −60 59 38	
NGC 3603	11 12 55.7 −60 59 21	
NGC 3603	11 12 59 −61 00	ED
NGC 3603 E	11 12 58.5 −61 00 20	"
NGC 3603 IRS1	11 12 50.8 −60 59 37	
NGC 3603 IRS1	11 12 51.5 −60 59 38	ED
NGC 3603 IRS4	11 12 52.3 −60 58 08	
NGC 3603 IRS4	11 12 54.3 −60 57 58	
NGC 3603 IRS5	11 12 40.4 −60 57 38	
NGC 3603 IRS6	11 13 14.3 −60 57 26	
NGC 3603 IRS6	11 13 16.5 −60 57 19	
NGC 3603 IRS7	11 12 48.6 −61 03 07	
NGC 3603 IRS8	11 12 57.9 −60 59 43	
NGC 3603IRS8+9	11 13 05 −61 00 20	
NGC 3603IRS8A	11 13 01.8 −60 59 48	
NGC 3603IRS8B	" "	
NGC 3603 IRS9	11 12 59.4 −61 00 25	
NGC 3603 IRS9	11 13 02.8 −61 00 21	
NGC 3603IRS12	11 12 47.1 −61 00 58	
NGC 3603IRS13	11 12 42.8 −61 02 14	
NGC 3603IRS14	11 12 51.2 −60 59 22	
NGC 3603IRS15	11 13 13.7 −60 55 45	
NGC 3603IRS15	11 13 15.7 −60 55 41	
NGC 3603IRS16	11 13 08.1 −60 58 28	
NGC 3603 W	11 12 53.0 −60 59 30	ED
NGC 3607	11 14 16.1 +18 19 35	769909
NGC 3608	11 14 20.7 +18 25 20	"
NGC 3613	11 15 42.4 +58 16 29	"
NGC 3621	11 15 50.4 −32 32 25	
NGC 3623	11 16 18.6 +13 22 00	
NGC 3627	11 17 37.9 +13 16 08	769909
NGC 3628	11 17 39.6 +13 51 48	
NGC 3640	11 18 32.3 + 3 30 35	769909
NGC 3665	11 22 00.9 +39 02 16	"
NGC 3666	11 21 49.7 +11 37 03	
NGC 3675	11 23 24.2 +43 51 36	
NGC 3690	11 25 44.2 +58 50 23	769909
NGC 3699	11 25 40 −59 40 54	779909
NGC 3705	11 27 32.2 + 9 33 11	
NGC 3717	11 29 03.6 −30 01 52	
NGC 3726	11 30 38.3 +47 18 13	
NGC 3733	11 32 16.9 +55 07 39	
NGC 3735	11 33 04.8 +70 48 42	
NGC 3755	11 33 54.1 +36 41 15	
NGC 3756	11 34 04.7 +54 34 22	
NGC 3782	11 36 40.2 +46 47 26	
NGC 3783	11 36 33.0 −37 27 41	789906
NGC 3811 NOM.	11 38 36.5 +47 58 08	769909
NGC 3811 SN	" "	
NGC 3813	11 38 40.0 +36 49 28	
NGC 3842	11 41 26.4 +20 13 40	769909
NGC 3877	11 43 29.4 +47 46 18	"
NGC 3879	11 44 04.3 +69 39 40	
NGC 3893	11 46 01.1 +48 59 20	769909
NGC 3894	11 46 11.4 +59 41 41	"
NGC 3904	11 46 41.4 −28 59 54	759903
NGC 3917	11 48 07.7 +52 06 14	
NGC 3918	11 47 50.1 −56 54 10	769910
NGC 3923	11 48 29.7 −28 31 40	759903
NGC 3936	11 49 47.7 −26 37 40	
NGC 3949	11 51 05.2 +48 08 16	
NGC 3953	11 51 12.9 +52 36 20	
NGC 3956	11 51 28.0 −20 17 18	
NGC 3962	11 52 06.7 −13 41 48	759903
NGC 3972	11 53 10.0 +55 35 48	769909
NGC 3976	11 53 23.2 + 7 01 38	
NGC 3992	11 55 00.7 +53 39 15	
NGC 3992	11 55 01.0 +53 39 13	769909
NGC 3998	11 55 21.4 +55 43 57	"
NGC 4010	11 56 03.2 +47 32 20	"
NGC 4013	11 55 57.1 +44 13 30	"
NGC 4051	12 00 35.9 +44 48 48	76909
NGC 4062	12 01 30.6 +32 10 33	
NGC 4085	12 02 50.5 +50 37 56	769909
NGC 4088	12 03 03.1 +50 49 13	"
NGC 4094	12 03 19.7 −14 14 53	
NGC 4096	12 03 28.4 +47 45 20	
NGC 4100	12 03 36.4 +49 51 36	769909
NGC 4116	12 05 03.2 + 2 58 13	
NGC 4124	12 05 35.8 +10 39 27	769909
NGC 4125	12 05 37.7 +65 27 03	"
NGC 4127	12 06 01.3 +77 04 57	
NGC 4142	12 07 00.0 +53 22 37	
NGC 4144	12 07 28.3 +46 44 07	
NGC 4145	12 07 30.3 +40 09 41	
NGC 4147	12 07 38 +18 49	RNGC

NAME	RA (1950) DEC	POS REF
	h m s ° ′ ″	
NGC 4151	12 08 00.8 +39 41 11	769909
NGC 4157	12 08 34.6 +50 45 51	"
NGC 4168	12 09 43.5 +13 29 05	"
NGC 4178	12 10 13.1 +11 08 30	"
NGC 4179	12 10 18.5 + 1 34 41	"
NGC 4183	12 10 47.2 +43 58 35	"
NGC 4192	12 11 15.4 +15 10 23	"
NGC 4194	12 11 41.7 +54 48 21	"
NGC 4206	12 12 43.7 +13 18 10	"
NGC 4214	12 13 08.8 +36 36 19	"
NGC 4216	12 13 20.3 +13 25 38	"
NGC 4217	12 13 21.7 +47 22 12	
NGC 4235	12 14 35.7 + 7 28 11	769909
NGC 4236	12 14 23.8 +69 43 52	
NGC 4244	12 15 00.4 +38 05 12	
NGC 4254	12 16 16.9 +14 41 46	769909
NGC 4258	12 16 29.7 +47 34 55	"
NGC 4261	12 16 49.5 + 6 06 15	"
NGC 4264	12 17 02.4 + 6 07 30	"
NGC 4270	12 17 15.4 + 5 44 31	"
NGC 4272	12 17 17.5 +30 36 55	"
NGC 4278	12 17 36.5 +29 33 26	"
NGC 4283	12 17 50.3 +29 35 18	"
NGC 4294	12 18 44.8 +11 47 18	"
NGC 4303	12 19 21.4 + 4 44 58	"
NGC 4321	12 20 23.2 +16 06 00	"
NGC 4321 SN	12 20 41 +16 05	
NGC 4359	12 21 42.0 +31 47 56	
NGC 4361	12 21 54.7 −18 30 29	759903
NGC 4365	12 21 55.0 + 7 35 43	769909
NGC 4370	12 22 21.9 + 7 43 15	"
NGC 4371	12 22 22.8 +11 58 53	"
NGC 4374	12 22 31.5 +13 09 51	"
NGC 4377	12 22 40.6 +15 02 28	"
NGC 4380	12 22 49.6 +10 17 33	"
NGC 4382	12 22 53.2 +18 28 03	"
NGC 4385	12 23 09.2 + 0 50 53	"
NGC 4387	12 23 09.6 +13 05 18	"
NGC 4388	12 23 14.8 +12 56 18	"
NGC 4406	12 23 39.7 +13 13 25	"
NGC 4414	12 23 58.0 +31 29 54	
NGC 4435	12 25 08.6 +13 21 23	769909
NGC 4438	12 25 13.5 +13 17 11	"
NGC 4442	12 25 31.3 +10 04 53	"
NGC 4449	12 25 45.2 +44 22 15	"
NGC 4450	12 25 58.0 +17 21 40	"
NGC 4455	12 26 13.5 +23 05 53	
NGC 4458	12 26 25.9 +13 31 10	769909
NGC 4459	12 26 28.3 +14 15 20	"
NGC 4461	12 26 31.1 +13 27 43	"
NGC 4464	12 26 48.1 + 8 26 05	"
NGC 4468	12 26 59.6 +14 19 33	"
NGC 4472	12 27 13.9 + 8 16 32	"
NGC 4473	12 27 17.0 +13 42 23	"
NGC 4476	12 27 26.7 +12 37 27	"
NGC 4478	12 27 45.5 +12 36 18	"
NGC 4479	12 27 46.8 +13 51 15	"
NGC 4486	12 28 17.8 +12 39 58	"
NGC 4486A	12 28 26 +12 33	RNGC
NGC 4486B	12 28 00 +12 46 00	769914
NGC 4490	12 28 10.5 +41 54 56	769909
NGC 4494	12 28 54.8 +26 02 58	"
NGC 4498	12 29 08.8 +17 07 46	"
NGC 4501	12 29 28.1 +14 41 50	"
NGC 4507	12 32 54.5 −39 38 02	789906
NGC 4517A	12 29 54.5 + 0 39 56	
NGC 4519	12 30 58.1 + 8 55 48	769909
NGC 4522	12 31 07.8 + 9 27 02	"
NGC 4526	12 31 30.4 + 7 58 33	"
NGC 4532	12 31 46.7 + 6 44 43	"
NGC 4535	12 31 47.9 + 8 28 25	"
NGC 4536	12 31 53.5 + 2 27 50	
NGC 4536 SN	12 31 56.5 + 2 28 27	810308
NGC 4545	12 32 19.8 +63 48 01	
NGC 4546	12 32 54.9 − 3 31 04	759903
NGC 4550	12 32 59.3 +12 29 48	769909
NGC 4552	12 33 08.4 +12 49 56	
NGC 4559	12 33 28.9 +28 14 23	
NGC 4565	12 33 51.3 +26 15 35	
NGC 4565	12 33 51.8 +26 15 50	769909
NGC 4565	12 33 52.1 +26 15 44	
NGC 4566	12 33 41.1 +54 29 43	769909
NGC 4569	12 34 18.7 +13 26 18	"
NGC 4578	12 34 58.7 + 9 49 48	"
NGC 4583	12 35 35 +33 44	RNGC
NGC 4592	12 36 44.5 − 0 15 17	
NGC 4593	12 37 04.7 − 5 04 16	759903
NGC 4594	12 37 22.8 −11 21 00	"
NGC 4621	12 39 31.2 +11 55 15	769909
NGC 4631	12 39 41.5 +32 48 54	"
NGC 4631 A	12 39 44.7 +32 49 16	
NGC 4631 PEAK	12 39 40.9 +32 49 19	
NGC 4636	12 40 16.6 + 2 57 43	769909
NGC 4643	12 40 46.9 + 2 15 06	"
NGC 4649	12 41 09.0 +11 49 23	"
NGC 4651	12 41 12.5 +16 40 05	"
NGC 4654	12 41 25.7 +13 23 58	"
NGC 4660	12 42 01.1 +11 27 51	"
NGC 4670	12 42 49.8 +27 23 58	"
NGC 4697	12 46 00.7 − 5 31 39	759903
NGC 4698	12 45 51.8 + 8 45 37	769909
NGC 4705	12 46 50.2 − 4 55 26	759903
NGC 4713	12 47 25.3 + 5 34 59	
NGC 4725	12 47 59.9 +25 46 20	
NGC 4725 SN	" "	769909
NGC 4736	12 48 32.4 +41 23 28	"
NGC 4742	12 49 11.7 −10 11 01	759903
NGC 4754	12 49 46.9 +11 35 06	769909
NGC 4758	12 50 14.8 +16 07 10	"
NGC 4760	12 50 31.0 −10 13 25	759903
NGC 4762	12 50 25.5 +11 30 05	769909
NGC 4800	12 52 20.6 +46 48 06	"
NGC 4808	12 53 16.4 + 4 34 29	
NGC 4826	12 54 16.9 +21 57 18	769909
NGC 4874	12 57 10.5 +28 13 45	"
NGC 4881	12 57 33.0 +28 30 52	739910
NGC 4883	12 57 31 +28 18 06	769914
NGC 4886	12 57 39.5 +28 15 16	739910

NAME	RA (1950) DEC	POS REF
	h m s ° ′ ″	
NGC 4889	12 57 43.6 +28 14 48	769909
NGC 4906	12 58 15 +28 11 30	769914
NGC 4921	12 59 01.8 +28 09 20	769909
NGC 4923	12 59 07 +28 06 54	769914
NGC 4939	13 01 37.6 −10 04 22	
NGC 4951	13 02 31.8 − 6 13 38	
NGC 4958	13 03 11.9 − 7 45 04	759903
NGC 4976	13 05 42 −49 14 18	779909
NGC 5005	13 08 37.6 +37 19 25	769909
NGC 5018	13 10 19.9 −19 15 12	759903
NGC 5023	13 09 58.0 +44 18 13	
NGC 5024	13 10 29 +18 26	RNGC
NGC 5033	13 11 09.6 +36 51 27	
NGC 5033	13 11 09.7 +36 51 30	769909
NGC 5042	13 12 47.9 −23 43 10	
NGC 5055	13 13 34.9 +42 17 55	
NGC 5055 SN	" "	769909
NGC 5061	13 15 20.1 −26 34 23	759903
NGC 5102	13 19 07 −36 22 12	789908
NGC 5107	13 19 09.3 +38 47 57	
NGC 5128	13 22 31.8 −42 45 30	
NGC 5128	13 22 33 −42 45 24	779909
NGC 5128 #1	13 22 35.4 −42 45 57	
NGC 5128 #2	13 22 34.5 −42 45 50	
NGC 5128 #3	13 22 33.6 −42 45 44	
NGC 5128 #4	13 22 30.9 −42 45 23	
NGC 5128 #5	13 22 30.2 −42 45 21	
NGC 5128 #6	13 22 29.1 −42 45 10	
NGC 5128 #7	13 22 28.2 −42 45 03	
NGC 5128 #8	13 22 27.3 −42 44 56	
NGC 5128 #9	13 22 26.3 −42 44 49	
NGC 5161	13 26 24.0 −32 54 56	
NGC 5170	13 27 07.3 −17 42 24	
NGC 5189	13 29 59.5 −65 43 00	769910
NGC 5194	13 27 46.9 +47 27 16	769909
NGC 5195	13 27 52.4 +47 31 48	"
NGC 5204	13 27 44.5 +58 40 42	739910
NGC 5205	13 28 18.6 +62 46 12	
NGC 5236	13 34 10.2 −29 36 49	759903
NGC 5248	13 35 02.4 + 9 08 23	769909
NGC 5253	13 37 05.2 −31 23 21	759903
NGC 5253 SN	" "	"
NGC 5272	13 39 57 +28 38	RNGC
NGC 5272 AA	" "	"
NGC 5272 II46	" "	"
NGC 5272 297	" "	"
NGC 5272 1397	" "	"
NGC 5289	13 43 01.0 +41 45 13	
NGC 5290	13 43 11.6 +41 57 48	
NGC 5300	13 45 44.3 + 4 12 00	
NGC 5301	13 44 21.4 +46 21 28	769909
NGC 5307	13 47 51 −50 57 30	779909
NGC 5315	13 50 12.7 −66 16 06	769910
NGC 5320	13 48 13.7 +41 36 49	
NGC 5348	13 51 40.4 + 5 28 19	
NGC 5350	13 51 15.1 +40 36 35	769909
NGC 5353	13 51 19.8 +40 31 47	"
NGC 5354	13 51 19.6 +40 33 00	"
NGC 5363	13 53 36.3 + 5 29 58	"
NGC 5371	13 53 34.2 +40 42 23	
NGC 5408	14 00 18 −41 08 16	779909
NGC 5447	14 00 43 +54 31	RNGC
NGC 5448	14 00 56.1 +49 24 48	769909
NGC 5455	14 01 13 +54 26	RNGC
NGC 5457	14 01 26.6 +54 35 25	769909
NGC 5461	14 01 55 +54 33	RNGC
NGC 5462	14 02 07 +54 36	"
NGC 5471	14 02 49 +54 38	"
NGC 5485	14 05 27.9 +55 14 21	769909
NGC 5486	14 05 41.6 +55 20 23	
NGC 5496	14 09 03.6 − 0 55 24	
NGC 5506	14 10 38.7 − 2 58 27	759903
NGC 5506	14 10 38.7 − 2 58 29	ED
NGC 5523	14 23 35.0 +25 33 01	
NGC 5529	14 13 27.5 +36 27 30	
NGC 5548	14 15 44.0 +25 22 01	769909
NGC 5566	14 17 49.4 + 4 09 42	"
NGC 5577	14 18 41.5 + 3 39 48	
NGC 5585	14 18 12.9 +56 57 32	769909
NGC 5592	14 21 00.2 −28 27 41	759903
NGC 5626	14 26 44 −29 32	ED
NGC 5630	14 25 37.2 +41 28 51	
NGC 5634	14 26 59 − 5 45	RNGC
NGC 5673	14 29 45.9 +50 10 48	
NGC 5676	14 31 01.4 +49 40 37	
NGC 5690	14 35 09.4 + 2 30 23	
NGC 5701	14 36 41.5 + 5 34 50	769909
NGC 5705	14 37 15.4 − 0 30 15	
NGC 5713	14 37 37.6 − 0 04 35	769909
NGC 5728	14 39 36.8 −17 02 22	759903
NGC 5740	14 41 52.1 + 1 53 25	
NGC 5746	14 42 24.2 + 2 09 53	769909
NGC 5792	14 55 47.9 − 0 53 28	
NGC 5798	14 55 31.2 +30 10 07	
NGC 5806	14 57 28.1 + 2 05 22	
NGC 5813	14 58 38.9 + 1 53 57	769909
NGC 5824	15 00 54 −32 52 30	779909
NGC 5846	15 03 57.0 + 1 47 57	769909
NGC 5861	15 06 32.7 −11 07 54	
NGC 5866	15 05 07.8 +55 57 16	769909
NGC 5873	15 09 38 −37 56 12	789908
NGC 5879	15 08 29.2 +57 11 25	769909
NGC 5882	15 13 24.9 −45 27 56	769910
NGC 5894	15 10 32.3 +59 59 42	
NGC 5904	15 16 02 + 2 16	RNGC
NGC 5907	15 14 34.8 +56 30 33	
NGC 5921	15 19 27.2 + 5 14 53	769909
NGC 5949	15 27 18.6 +64 56 04	-
NGC 5951	15 31 23.6 +15 10 27	
NGC 5962	15 34 14.1 +16 46 23	769909
NGC 5970	15 36 08.1 +12 20 53	"
NGC 5979	15 43 26.0 −61 03 48	769910
NGC 5982	15 37 38.5 +59 31 03	769909
NGC 5984	15 40 33.1 +14 23 28	
NGC 5987	15 38 52.3 +58 14 33	769909
NGC 6012	15 51 54.5 +14 44 55	"
NGC 6015	15 50 40.1 +62 27 34	
NGC 6058	16 02 50 +40 49	RNGC

NAME	RA (1950) DEC	POS REF
	h m s ° ′ ″	
NGC 6070	16 07 25.7 + 0 50 22	
NGC 6093	16 14 04 −22 51 12	819916
NGC 6106	16 16 21.4 + 7 31 56	
NGC 6118	16 19 12.4 − 2 10 01	
NGC 6121 NOM.	16 20 31 −26 24 42	819916
NGC 6121 219	" "	"
NGC 6121 243	" "	"
NGC 6121 398	" "	"
NGC 6121 515	" "	"
NGC 6121 516	" "	"
NGC 6121 522	" "	"
NGC 6121 529	" "	"
NGC 6121 571	" "	"
NGC 6153	16 28 05.0 −40 08 58	739909
NGC 6171 E	16 29 42 −12 56	RNGC
NGC 6171 NOM.	" "	
NGC 6171 217	" "	RNGC
NGC 6171 273	" "	"
NGC 6181	16 30 09.4 +19 55 48	769909
NGC 6181	16 30 09.6 +19 55 50	
NGC 6193	16 36 14.6 −48 45 53	
NGC 6193 IRS1	16 37 23 −48 39 08	
NGC 6193 IRS3	16 37 26 −48 36 50	
NGC 6193 IRS4	16 37 53 −48 37 34	
NGC 6205	16 39 54 +36 33	RNGC
NGC 6205 SW	" "	"
NGC 6205 2	" "	"
NGC 6205 3	" "	"
NGC 6205 4	" "	"
NGC 6205 5	" "	"
NGC 6210	16 42 23.5 +23 53 17	739909
NGC 6217	16 35 05.1 +78 18 05	769909
NGC 6221	16 48 26 −59 09 00	759905
NGC 6229	16 45 36 +47 37	RNGC
NGC 6231 NOM.	16 50 40 −41 44 36	779909
NGC 6231 91	" "	"
NGC 6231 92	16 50 55 −41 51 17	ED
NGC 6240	16 50 27.8 + 2 29 03	719904
NGC 6254 I−2	16 54 29 − 4 02	RNGC
NGC 6254 II24	" "	"
NGC 6254 NOM.	" "	
NGC 6254III21	" "	RNGC
NGC 6255	16 53 00.8 +36 34 51	
NGC 6284	17 01 25 −24 41 42	809909
NGC 6302	17 10 21.1 −37 02 38	739909
NGC 6304 NOM.	17 11 21 −29 24 18	789908
NGC 6304 1208	" "	"
NGC 6304 1232	" "	"
NGC 6304 2236	" "	"
NGC 6304 3238	" "	"
NGC 6304 4203	" "	"
NGC 6304 4223	" "	"
NGC 6304 4238	" "	"
NGC 6304 9054	" "	"
NGC 6308	17 09 54.0 +23 26 23	769909
NGC 6309	17 11 14.9 −12 51 11	739909
NGC 6334	17 17 21.1 −35 46 29	
NGC 6334	17 17 28 −36 03 12	789908
NGC 6334 I	17 17 32.5 −35 44 00	
NGC 6334 I(N)	17 17 32.5 −35 42 30	
NGC 6334 V	17 16 36.0 −35 54 45	
NGC 6334(B)	17 17 28 −36 03 12	789908
NGC 6334/I	17 17 32.5 −35 42 00	791002
NGC 6334/I	17 17 32.5 −35 43 48	
NGC 6334/I	17 17 34 −35 44 30	
NGC 6334/I(N)	17 17 32.5 −35 42 00	
NGC 6334/II	17 17 21 −35 46 25	
NGC 6334/II	17 17 22.6 −35 48 00	
NGC 6334/III	17 17 07 −35 49 11	
NGC 6334/III	17 17 07.8 −35 48 12	
NGC 6334/IV	17 16 59 −35 51 49	
NGC 6334/V	17 16 37 −35 55 00	
NGC 6334/VI	17 16 39 −36 06 43	
NGC 6334AIRS1	17 16 59.8 −35 51 58	
NGC 6334AIRS2	17 16 58.2 −35 51 13	
NGC 6334AIRS3	17 16 57.5 −35 51 46	
NGC 6334B IR	17 16 36.7 −35 54 38	
NGC 6334C IR	17 16 56.6 −35 52 04	
NGC 6334C IRC	17 16 10.5 −35 48 21	
NGC 6334C 2.2	17 16 11.7 −35 48 26	
NGC 6334CSTAR	17 16 11.3 −35 48 06	
NGC 6334D IR	17 17 24.0 −35 45 56	
NGC 6334D 3.6	17 16 22.3 −35 46 13	
NGC 6334E IR	17 17 31.6 −35 42 36	
NGC 6334F IRC	17 16 32.9 −35 44 02	
NGC 6334IRSV−1	17 16 36.6 −35 54 46	
NGC 6334IRSV1E	17 16 39.2 −35 54 49	
NGC 6334IRS1	17 17 32.5 −35 44 07	
NGC 6334VIRS2	17 16 37.0 −35 54 37	
NGC 6339	17 15 29.6 +40 53 52	
NGC 6342	17 18 13 −19 32 18	809909
NGC 6357	17 21 24.1 −34 08 24	
NGC 6357	17 21 25 −34 09 24	789908
NGC 6357 (A)	17 21 26.9 −34 07 45	
NGC 6357 (B)	17 21 25.4 −34 06 29	
NGC 6357 A	17 21 21 −34 07	
NGC 6357 A	17 22 22 −34 17 36	
NGC 6357 B	17 21 29 −34 00 36	
NGC 6366 I−68	17 25 04 − 5 02	RNGC
NGC 6366 I−73	" "	"
NGC 6366 NOM.	" "	
NGC 6366II−70	" "	RNGC
NGC 6366III50	" "	"
NGC 6366IV−50	" "	"
NGC 6366IV−70	" "	"
NGC 6368	17 24 51.6 +11 35 06	
NGC 6369	17 26 17.9 −23 43 12	739909
NGC 6369 10"N	17 26 17.9 −23 43 02	ED
NGC 6383	17 31 27 −32 33 00	789908
NGC 6384	17 29 59.0 + 7 05 43	
NGC 6384 SN	" "	769909
NGC 6388	17 32 34 −44 43	RNGC
NGC 6395	17 27 10.6 +71 08 10	
NGC 6402 A	17 35 03 − 3 15	ED
NGC 6402 B	17 35 01 − 3 14	"
NGC 6402 C	" "	"
NGC 6402 D	17 35 07 − 3 14	"
NGC 6402 E	17 34 59 − 3 13	"

NAME	RA (1950) DEC	POS REF
	h m s ° ′ ″	
NGC 6402 F	17 34 57 − 3 14	"
NGC 6402 G	17 35 00 − 3 15	"
NGC 6402 H	" "	"
NGC 6402 I	17 34 55 − 3 14	"
NGC 6402 J	17 35 03 − 3 15	"
NGC 6402 K	17 35 05 − 3 16	"
NGC 6402 L	17 35 02 − 3 15	"
NGC 6402 M	17 35 02 − 3 16	"
NGC 6402 N	17 35 04 − 3 16	"
NGC 6402 O	17 35 05 − 3 16	"
NGC 6402 P	17 34 57 − 3 16	"
NGC 6402 Q	17 34 58 − 3 16	"
NGC 6412	17 31 22.9 +75 44 26	769909
NGC 6439	17 45 26.0 −16 27 44	739909
NGC 6440	17 45 54 −20 20 48	819917
NGC 6441	17 46 49 −37 02 12	789908
NGC 6445	17 46 17.2 −19 59 41	739909
NGC 6454	17 44 02 +55 43	RNGC
NGC 6503	17 49 58.7 +70 09 26	769909
NGC 6514 130	17 59 26.4 −22 55 58	
NGC 6522	18 00 23 −30 02 12	789908
NGC 6522 A3	" "	"
NGC 6522 A29	" "	"
NGC 6522 B74	" "	"
NGC 6522 B143	" "	"
NGC 6522 B159	" "	"
NGC 6522 D3	" "	"
NGC 6522 D9	" "	"
NGC 6522 D11	" "	"
NGC 6522 I202	" "	"
NGC 6522 31	" "	"
NGC 6522 32	" "	"
NGC 6522 51	18 00 19 −29 49 42	GCVS
NGC 6522 56	18 00 23 −30 02 12	789908
NGC 6522 64	" "	"
NGC 6522 86	" "	"
NGC 6522 103	18 01 30 −29 51 18	GCVS
NGC 6522 107	18 00 23 −30 02 12	789908
NGC 6522 120	18 01 22 −29 54 37	GCVS
NGC 6522 133	18 00 23 −30 02 12	789908
NGC 6522 138	" "	"
NGC 6522 142	" "	"
NGC 6522 179	" "	"
NGC 6522 181	17 59 28 −29 54 09	GCVS
NGC 6522 200	17 59 02 −29 56 53	"
NGC 6522 205	18 00 23 −30 02 12	789908
NGC 6522 207	" "	"
NGC 6522 228	17 59 51 −29 57 37	GCVS
NGC 6522 289	18 00 23 −30 02 12	789908
NGC 6522 313	18 01 32 −29 59 36	GCVS
NGC 6522 320	18 01 15 −30 01 31	"
NGC 6522 340	18 01 15 −30 05 07	"
NGC 6522 403	18 00 23 −30 02 12	789908
NGC 6522 426	" "	"
NGC 6522 434	" "	"
NGC 6522 435	" "	"
NGC 6522 574	18 01 24 −30 13 31	GCVS
NGC 6522 575	18 00 23 −30 02 12	789908
NGC 6522 590	" "	"
NGC 6522 644	" "	"
NGC 6522 652	17 59 50 −30 12 19	GCVS
NGC 6522 721	18 00 46 −29 52 46	"
NGC 6522 745	18 00 24 −29 53 53	"
NGC 6522 826	18 01 38 −29 54 00	"
NGC 6522 830	18 01 35 −30 04 12	"
NGC 6522III106	18 00 23 −30 02 12	789908
NGC 6522 4−41	" "	"
NGC 6522 5−24A	" "	"
NGC 6523	18 01 12 −24 19 30	819916
NGC 6528	18 01 37 −30 03 36	789908
NGC 6530 7	18 00 48.3 −24 21 47	CSI 79
NGC 6530 45	18 01 11.1 −24 11 08	"
NGC 6530 65	18 01 21.7 −24 23 21	"
NGC 6530 118	18 02 06.4 −24 24 09	"
NGC 6537	18 02 15.5 −19 50 30	739909
NGC 6541	18 04 25 −43 18	779909
NGC 6543	17 58 36 +66 38	RNGC
NGC 6567	18 10 48.2 −19 05 13	739909
NGC 6570	18 08 50.3 +14 04 52	
NGC 6572	18 09 40.6 + 6 50 25	
NGC 6572	18 09 41.7 + 6 50 37	739909
NGC 6574	18 09 34.7 +14 58 03	769909
NGC 6578	18 13 18.6 −20 28 04	739909
NGC 6611 1	18 15 46.2 −13 49 16	CSI 79
NGC 6618	18 17 51 −16 12	RNGC
NGC 6624	18 20 28 −30 23 14	
NGC 6626 A	18 21 23 −24 51	ED
NGC 6626 B	" "	"
NGC 6626 C	18 21 22 −24 51	"
NGC 6626 D	18 21 27 −24 52	"
NGC 6626 E	18 21 25 −24 52	"
NGC 6626 F	18 21 20 −24 52	"
NGC 6626 G	18 21 22 −24 53	"
NGC 6626 H	18 21 24 −24 53	"
NGC 6629	18 22 41.2 −23 13 45	739909
NGC 6637 I−12	18 28 03 −32 23	ED
NGC 6637 I−30	" "	"
NGC 6637 I−42	18 28 01 −32 23	"
NGC 6637I−40*	18 28 02 −32 24	"
NGC 6637I−43*	18 28 03 −32 25	"
NGC 6637II−14	18 28 01 −32 23	"
NGC 6637II−35	18 28 02 −32 22	"
NGC 6637II−53	18 28 03 −32 23	"
NGC 6637II19*	18 27 58 −32 22	"
NGC 6637II37*	18 28 03 −32 22	"
NGC 6637III−3	18 28 06 −32 23	"
NGC 6637III26	18 28 08 −32 22	"
NGC 6637III41	18 28 10 −32 23	"
NGC 6637III43	" "	"
NGC 6637IV−11	18 28 04 −32 24	"
NGC 6637IV−20	18 28 05 −32 23	"
NGC 6637IV−27	18 28 06 −32 23	"
NGC 6643	18 21 12.6 +74 32 40	
NGC 6643	18 21 13.3 +74 32 43	769909
NGC 6644	18 29 30 −25 10 00	819916
NGC 6652	18 32 29 −33 02 00	809909
NGC 6654	18 25 14.4 +73 09 11	769909
NGC 6656 NOM.	18 33 21 −23 56 54	819916

NAME	RA (1950) DEC	POS REF
	h m s ° ′ ″	
NGC 6656II−14	" "	"
NGC 6656II−15	" "	"
NGC 6656II−26	" "	"
NGC 665(II−67	" "	"
NGC 6656II−80	" "	"
NGC 6656III−3	" "	"
NGC 6656III12	" "	"
NGC 6656III26	" "	"
NGC 6656IV−17	" "	"
NGC 6656IV−97	" "	"
NGC 6656IV102	" "	"
NGC 6656 V−9	" "	"
NGC 6674	18 36 31.1 +25 19 55	769909
NGC 6681	18 39 57 −32 20 24	809909
NGC 6689	18 35 22.3 +70 28 57	
NGC 6702	18 45 30.9 +45 39 03	769909
NGC 6712 B−66	18 50 20 − 8 47	RNGC
NGC 6712 LM 5	" "	"
NGC 6712 LM 8	" "	"
NGC 6712 LM10	" "	"
NGC 6712 NOM.	" "	
NGC 6715	18 51 51 −30 32 42	809909
NGC 6720	18 51 40 +32 58	RNGC
NGC 6741	19 00 02.0 − 0 31 12	739909
NGC 6744	19 05 01 −63 56 12	759905
NGC 6751	19 03 15.0 − 6 04 07	739909
NGC 6752	19 06 27 −60 03 54	759905
NGC 6753	19 07 11 −57 07 54	779909
NGC 6764	19 07 01.3 +50 51 09	
NGC 6764	19 07 01.5 +50 51 03	769909
NGC 6769	19 13 57 −60 35 30	759905
NGC 6778	19 15 49.4 − 1 41 24	739909
NGC 6790	19 20 24.5 + 1 25 02	"
NGC 6803	19 28 53.5 + 9 57 00	"
NGC 6807	19 32 06.0 + 5 34 28	"
NGC 6808	19 38 28 −70 45 06	779909
NGC 6810	19 39 21 −58 46 30	"
NGC 6814	19 39 55.4 −10 26 37	759903
NGC 6818	19 41 09.0 −14 16 21	739909
NGC 6822	19 42 06.4 −14 55 23	759903
NGC 6823 NO.2	19 41 03.0 +23 10 32	CSI 79
NGC 6826	19 43 31 +50 24	RNGC
NGC 6833	19 48 17 +48 50	"
NGC 6838 A4	19 51 29 +18 39	"
NGC 6838 NOM.	" "	
NGC 6838 21	" "	RNGC
NGC 6838 45	" "	"
NGC 6838 46	" "	"
NGC 6838 113	" "	"
NGC 6857	19 59 56 +33 23	"
NGC 6864	20 03 08 −22 04 00	819917
NGC 6868	20 06 16 −48 31 36	779909
NGC 6871 IRS1	20 01 14.9 +35 51 43	
NGC 6871 IRS2	20 01 24.5 +35 57 07	
NGC 6871 IRS3	20 01 40.6 +35 48 23	
NGC 6871 IRS4	20 01 16 +35 48 01	
NGC 6879	20 08 09.9 +16 46 24	739909
NGC 6881	20 08 59 +37 16	RNGC
NGC 6884	20 08 49 +46 19	"
NGC 6886	20 10 29.6 +19 50 16	739909
NGC 6888	20 10 59 +38 10	RNGC
NGC 6890	20 14 49 −44 57 48	779909
NGC 6891	20 12 48.0 +12 32 54	739909
NGC 6905	20 20 08.5 +19 56 39	"
NGC 6910 3	20 21 23.9 +40 42 46	CSI 79
NGC 6923	20 28 33.7 −31 00 05	759903
NGC 6925	20 31 13.9 −32 09 11	
NGC 6934	20 31 40 + 7 14	RNGC
NGC 6935	20 34 39 −52 17 06	779907
NGC 6942	20 36 52 −54 28 54	779909
NGC 6946	20 33 48.8 +59 58 50	769909
NGC 6951	20 36 37.7 +65 55 48	"
NGC 6958	20 45 30 −38 10 54	789908
NGC 7000 ANON	20 52 06.5 +44 12 39	
NGC 7006	20 59 08 +16 00	RNGC
NGC 7006 I−1	20 59 09 +16 00	ED
NGC 7006II−46	20 59 07 +16 01	"
NGC 7006II103	20 59 12 +15 59	"
NGC 7006III40	20 59 11 +16 01	"
NGC 7006III46	20 59 12 +15 59	"
NGC 7006 V19	20 59 08 +16 00	RNGC
NGC 7006 V54	20 59 08 +15 59	ED
NGC 7009	21 01 27.6 −11 33 54	739909
NGC 7009 6"E	21 01 28.0 −11 33 54	ED
NGC 7009 6"W	21 01 27.2 −11 33 54	"
NGC 7009 7"E	21 01 28.1 −11 33 54	"
NGC 7009 7"W	21 01 27.1 −11 33 54	"
NGC 7020	21 07 13 −64 13 48	759905
NEAR NGC 7023	20 45 25.0 +67 46 44	
NGC 7026	21 04 38 +47 39	RNGC
NGC 7027	21 05 09 +42 02 03	
NGC 7027	21 05 09.4 +42 02 03	749905
NGC 7027	21 05 09.4 +42 02 05	"
NGC 7027	21 05 09.5 +42 02 03	ED
NGC 7027 CEN	21 05 09.3 +42 02 03	
NGC 7027 E	21 05 09.6 +42 02 03	
NGC 7027 S	21 05 09.3 +42 01 59	
NGC 7027 W	21 05 09.0 +42 02 03	
NGC 7027 4"E	21 05 09.8 +42 02 03	ED
NGC 70272"S2W	21 05 09.2 +42 02 01	"
NGC 70273"S2E	" "	"
NGC 70273"S2E	21 05 09.6 +42 02 00	"
NGC 70275"S2W		"
NGC 7029	21 08 26 −49 29 18	759905
NGC 7049	21 15 37 −48 46 30	"
NGC 7059	21 23 35.0 −60 13 54	
NGC 7070A	21 28 36 −43 04 00	779909
NGC 7078	21 27 35 +11 57	RNGC
NGC 7083	21 31 50.0 −64 07 42	
NGC 7090	21 32 59.0 −54 46 54	
NGC 7096	21 37 27 −64 08 24	759905
NGC 7098	21 39 16 −75 20 30	"
NGC 7099	21 37 32 −23 24 24	819917
NGC 7129	21 41 53.2 +65 50 02	
NGC 7129	21 41 57.2 +65 50 02	
NGC 7129	21 41 57.2 +65 50 32	
NGC 7129	21 41 57.8 +65 53 04	
NGC 7129	21 41 58 +65 52 50	
NGC 7129	21 42 01.2 +65 50 02	
NGC 7129 #1	21 41 14.9 +65 56 49	
NGC 7129 #2	21 41 31.6 +65 56 20	
NGC 7129 #3	21 41 29.5 +65 54 42	
NGC 7129 #4	21 41 18.2 +65 53 57	
NGC 7129 #5	21 41 36.2 +65 50 48	
NGC 7129 #6	21 41 50.4 +65 50 48	
NGC 7129 #7	21 41 41.1 +65 52 49	
NGC 7129 #8	21 41 49.4 +65 52 23	
NGC 7129 #9	21 41 34.2 +65 58 42	
NGC 7129 #10	21 41 38.3 +65 57 04	
NGC 7129 #11	21 41 46.4 +65 57 55	
NGC 7129 #12	21 41 57.5 +65 53 07	
NGC 7129 #13	21 41 52.5 +65 53 22	
NGC 7129 #14	21 42 21.9 +65 56 06	
NGC 7129 #15	21 42 27.0 +65 57 44	
NGC 7129 #16	21 42 19.7 +65 49 49	
NGC 7172	21 59 06.3 −32 06 27	759903
NGC 7177	21 58 18.5 +17 29 50	769909
NGC 7184	21 59 53.3 −21 03 18	
NGC 7205	22 05 10.0 −57 41 18	
NGC 7213	22 06 09 −47 24 42	759905
NGC 7225	22 10 19 −26 23 42	819916
NGC 7307	22 30 57 −41 11 30	759905
NGC 7307	22 30 57.0 −41 11 30	
NGC 7314	22 33 00.4 −26 18 31	
NGC 7320	22 33 45.8 +33 41 21	
NGC 7331	22 34 47.7 +34 09 35	769909
NGC 7331 4.8E	22 34 48.1 +34 09 35	ED
NGC 7331 4.8N	22 34 47.7 +34 09 40	"
NGC 7331 4.8S	22 34 47.7 +34 09 30	"
NGC 7331 4.8W	22 34 47.3 +34 09 35	"
NGC 7331 9.5E	22 34 48.5 +34 09 35	"
NGC 7331 9.5N	22 34 47.7 +34 09 45	"
NGC 7331 9.5S	22 34 47.7 +34 09 25	"
NGC 7331 9.5W	22 34 46.9 +34 09 35	"
NGC 7331 14.3E	22 34 48.9 +34 09 35	"
NGC 7331 14.3N	22 34 47.7 +34 09 49	"
NGC 7331 14.3S	22 34 47.7 +34 09 21	"
NGC 7331 14.3W	22 34 46.5 +34 09 35	"
NGC 7331 19.1E	22 34 49.2 +34 09 35	"
NGC 7331 19.1N	22 34 47.7 +34 09 54	"
NGC 7331 19.1S	22 34 47.7 +34 09 16	"
NGC 7331 19.1W	22 34 46.2 +34 09 35	"
NGC 7331 23.8E	22 34 49.6 +34 09 35	"
NGC 7331 23.8N	22 34 47.7 +34 09 59	"
NGC 7331 23.8S	22 34 47.7 +34 09 11	"
NGC 7331 23.8W	22 34 45.8 +34 09 35	"
NGC 7331 28.6E	22 34 50.1 +34 09 35	"
NGC 7331 28.6N	22 34 47.7 +34 10 04	"
NGC 7331 28.6S	22 34 47.7 +34 09 06	"
NGC 7331 28.6W	22 34 45.4 +34 09 35	"
NGC 7331 33.3E	22 34 50.4 +34 09 35	"
NGC 7331 33.3N	22 34 47.7 +34 10 08	"
NGC 7331 33.3S	22 34 47.7 +34 09 02	"
NGC 7331 33.3W	22 34 45.0 +34 09 35	"
NGC 7331 38.1E	22 34 50.8 +34 09 35	"
NGC 7331 38.1N	22 34 47.7 +34 10 13	"
NGC 7331 38.1S	22 34 47.7 +34 08 57	"
NGC 7331 38.1W	22 34 44.6 +34 09 35	"
NGC 7331 42.9N	22 34 47.7 +34 10 18	"
NGC 7331 42.9S	22 34 47.7 +34 08 52	"
NGC 7331 47.6N	22 34 47.7 +34 10 23	"
NGC 7331 47.6S	22 34 47.7 +34 08 47	"
NGC 7331 52.4N	22 34 47.7 +34 10 27	"
NGC 7331 52.4S	22 34 47.7 +34 08 43	"
NGC 7331 57.1N	22 34 47.7 +34 10 32	"
NGC 7331 57.1S	22 34 47.7 +34 08 38	"
NGC 7331 61.9S	22 34 47.7 +34 08 33	"
NGC 7331 66.7S	22 34 47.7 +34 08 28	"
NGC 7332	22 35 01.2 +23 32 16	769909
NGC 7354	22 38 28 +61 01	RNGC
NGC 7361	22 39 31.0 −30 19 14	759903
NGC 7368	22 42 40.3 −39 36 22	
NGC 7377	22 45 05.0 −22 34 34	759903
NGC 7380 2	22 44 54.2 +57 49 12	CSI 79
NGC 7410	22 52 11 −39 55 42	789908
NGC 7418	22 53 48 −37 17 48	"
NGC 7419 A	22 52 18 +60 34	RNGC
NGC 7419 C	" "	"
NGC 7419 D	" "	"
NGC 7419 E	" "	"
NGC 7419 G	" "	
NGC 7419 NOM.		
NGC 7432	22 55 33 +12 52	RNGC
NGC 7448	22 57 34.9 +15 42 50	769909
NGC 7456	22 59 22 −39 50 18	789908
NGC 7462	22 59 58 −41 06 12	"
NGC 7469	23 00 44.4 + 8 36 19	769909
NGC 7496	23 06 59 −43 42 00	819917
NGC 7497	23 06 34.6 +17 54 23	
NGC 7531	23 12 02 −43 52 18	819917
NGC 7538	23 11 22 +61 13 48	
NGC 7538	23 11 22.9 +61 13 50	
NGC 7538	23 11 36.8 +61 12 19	
NGC 7538	23 12 02 +61 13	RNGC
NGC 7538 (1)	23 11 21.8 +61 13 45	
NGC 7538 (2)	23 11 36.4 +61 12 01	
NGC 7538 (3)	23 11 26.0 +61 14 14	
NGC 7538 (4)	23 11 30.1 +61 14 43	
NGC 7538 #1	23 11 32.4 +61 12 36	ED
NGC 7538 #2	23 11 33.2 +61 12 15	"
NGC 7538 #3	23 11 33.6 +61 11 57	"
NGC 7538 #4	23 11 36.4 +61 13 15	"
NGC 7538 #5	23 11 36.5 +61 12 48	"
NGC 7538 #6	23 11 36.4 +61 12 21	"
NGC 7538 #7	23 11 36.4 +61 11 57	"
NGC 7538 #8	23 11 36.6 +61 11 30	"
NGC 7538 #9	23 11 36.4 +61 10 54	"
NGC 7538 #10	23 11 36.0 +61 10 35	"
NGC 7538 #11	23 11 36.6 +61 09 50	"
NGC 7538 #12	23 11 40.3 +61 12 54	"
NGC 7538 #13	23 11 40.3 +61 12 27	"
NGC 7538 #14	23 11 39.4 +61 11 57	"
NGC 7538 #15	23 11 44.2 +61 12 27	"
NGC 7538 #16	23 11 48.0 +61 10 35	"
NGC 7538 #17	23 11 51.6 +61 10 54	"
NGC 7538 A	23 10 36 +61 08 30	
NGC 7538 B	23 11 24.1 +61 12 43	
NGC 7538 C	23 11 36.6 +61 11 48	
NGC 7538 D	23 12 13 +61 13 54	
NGC 7538 E	23 11 52.8 +61 10 58	790511
NGC 7538 E	23 11 53 +61 10 40	
NGC 7538 E	23 12 53 +61 18 54	
NGC 7538 HII	23 11 23 +61 12 50	
NGC 7538 IRS1	23 11 36.5 +61 11 50	
NGC 7538 IRS1	23 11 36.7 +61 11 48	
NGC 7538 IRS1	23 11 36.7 +61 11 49	
NGC 7538 IRS1	23 11 36.8 +61 11 49	ED
NGC 7538 IRS1	23 11 36.8 +61 11 58	
NGC 7538 IRS2	23 11 36.8 +61 11 56	
NGC 7538 IRS2	23 11 37 +61 11 50	
NGC 7538 IRS2	23 11 37.0 +61 11 58	760603
NGC 7538 IRS3	23 11 34.9 +61 11 52	ED
NGC 7538 IRS3	23 11 35.0 +61 11 51	
NGC 7538 IRS4	23 11 24.1 +61 12 43	740203
NGC 7538 IRS5	23 11 21.7 +61 13 50	
NGC 7538 IRS6	23 11 25.8 +61 13 54	
NGC 7538 IRS7	23 11 28.2 +61 14 19	
NGC 7538 IRS8	23 11 18.8 +61 14 29	
NGC 7538 IRS9	23 11 52.8 +61 10 58	ED
NGC 7538 IRS9	23 11 52.8 +61 10 59	790803
NGC 7538IRS9B	23 11 53.0 +61 10 42	ED
NGC 7538IRS9P	23 11 48.8 +61 10 44	"
NGC 7538IRS9R	23 11 51.3 +61 10 53	"
NGC 7538IRS10	23 11 57.8 +61 11 37	
NGC 7538IRS11	23 11 35.2 +61 10 37	
NGC 7538 N	23 11 36 +61 11 55	
NGC 7538 N	23 11 36.9 +61 12 00	
NGC 7538 PTA	23 11 50.5 +61 10 50	
NGC 7538 PTB	23 11 52.8 +61 10 42	
NGC 7538 S	23 11 36 +61 10 30	
NGC 7538 S OH	23 11 34 +61 10 40	
NGC 7538 VES1	23 11 36.9 +61 11 52	
NGC 7538 VES2	23 11 36.9 +61 12 00	
NGC 7538 1'N	23 12 02 +61 14	ED
NGC 7538 1'W	23 11 58 +61 13	"
NGC 7552	23 13 24.9 −42 51 27	
NGC 7552	23 13 25 −42 51 24	819917
NGC 7557	23 13 08 + 6 25	RNGC
NGC 7562	23 13 25.1 + 6 24 53	769909
NGC 7582	23 15 38.3 −42 38 39	730018
NGC 7583	23 15 20 + 7 08	RNGC
NGC 7585	23 15 27.3 − 4 55 20	759903
NGC 7590	23 16 10 −42 30 42	819917
NGC 7603	23 16 22.6 − 0 01 39	769909
NGC 7611	23 17 04.9 + 7 47 24	"
NGC 7612	23 17 12.2 + 8 18 09	"
NGC 7619	23 17 42.6 + 7 55 57	"
NGC 7623	23 17 58.0 + 8 07 20	"
NGC 7625	23 18 00.6 +16 57 15	"
NGC 7626	23 18 10.3 + 7 56 35	
NGC 7635	23 18 26.9 +60 55 13	ED
NGC 7640	23 19 42.8 +40 34 11	
NGC 7648	23 21 22.2 + 9 23 37	769909
NGC 7662	23 23 30 +42 16	RNGC
NGC 7662 6"NE	" "	"
NGC 7662 6"NW	" "	"
NGC 7683	23 26 32 +11 10	
NGC 7702	23 32 44 −56 17 12	789908
NGC 7714	23 33 40.5 + 1 52 46	769909
NGC 7721	23 36 14.2 − 6 47 40	
NGC 7722	23 36 09.4 +15 40 38	769909
NGC 7727	23 37 19.1 −12 34 09	759903
NGC 7742	23 41 43.1 +10 29 25	769909
NGC 7743	23 41 48.6 + 9 39 25	"
NGC 7769	23 48 31.5 +19 52 25	"
NGC 7793	23 55 15.0 −32 52 06	821013
NGC 7814	0 00 41.1 +15 52 03	769909
NGC 7817	0 01 24.9 +20 28 18	
NIS #1	3 27 31 +22 28 43	
NIS #2	3 48 21 +15 36 29	
NIS #3	4 08 34 +51 02 46	
NIS #4	4 22 50 +16 27 21	
NIS #5	6 07 14 +17 33 10	
NIS #6	7 05 23 + 7 35 19	
NIS #7	7 27 40 +28 14 11	
NIS #8	20 33 51 +40 48 41	
NIS #9	20 43 21 +41 04 55	
NIS #10	20 43 26 +39 03 25	
NIS #11	20 45 33 +40 46 47	
NIS #12	23 07 37 +50 56 31	
NIS #13	23 10 32 +56 20 24	
GAM 1 NOR	16 13 15.6 −49 56 42	CSI 79
KT NOR	16 24 06 −56 14 55	GCVS
R NOR	15 32 20.9 −49 20 31	CSI 79
RT NOR	16 20 02.9 −59 14 01	"
RZ NOR	16 28 40 −53 09 37	GCVS
S NOR	16 14 42.4 −57 46 41	CSI 79
T NOR	15 40 11.6 −54 49 43	"
V NOR	16 06 19.6 −49 06 20	"
W NOR	16 12 50.9 −52 28 58	"
NORTHERN SPUR	23 30 +63 36	
NP 0532	5 31 31.7 +21 59 29	790808
N9	0 41 42 −73 19	569903
N13 A	0 43 36 −73 39	"
N25	0 46 24 −73 31	"
N46 NW	0 50 06 −73 07	"
N46 SE	" "	"
N64 A	0 56 48 −72 56	"
N81	1 07 48 −73 28	"
N159 FIELD	5 40 21.4 −69 46 52	
N159 PS	5 40 26.4 −69 46 54	
OA 129	4 20 43.5 − 1 27 28	809908
R OCT	5 41 09.7 −86 25 13	CSI 79
TW OCT	19 37 41.3 −77 22 33	"
U OCT	13 17 59.3 −83 57 51	"
X OCT	10 28 01.2 −84 05 32	"
OE 110	3 06 21.1 +10 17 48	809908
OH 471	6 42 53.1 +44 54 31	"
OH0739−14	7 39 58.9 −14 35 44	740203
OH0739−14	7 39 58.9 −14 35 45	ED
OH0739−14 N	7 39 58.9 −14 35 40	"
OH5.0+1.5	17 48 25 −23 50 36	
OH12.8−1.9	18 17 40 −18 48 37	
OH12.9−0.3	18 11 44.3 −17 53 02	790114

NAME	RA (1950)	DEC	POS REF
OH18.3+0.1	18 20 58	−12 51 48	
OH19.1−1.0	18 26 40	−12 39 54	
OH20.2−0.1	18 25 26.5	−11 18 00	
OH20.7+0.1	18 25 40	−10 52 06	
OH21.5+0.5	18 25 45.5	−10 00 14	
OH23.7+1.2	18 27 25	− 7 39 00	
OH26.2−0.6	18 38 32.5	− 6 18 06	
OH26.4−1.9	18 43 44	− 6 43 44	
OH26.4−2.0	18 43 45	− 6 43 54	
OH26.5+0.6	18 34 51	− 5 26 23	
OH26.5+0.6	18 34 51.6	− 5 27 24	749902
OH26.5+0.6	18 34 52.5	− 5 26 42	
OH26.5+0.6	18 34 52.6	− 5 26 37	771109
OH28.6−0.6	18 43 10	− 4 04 06	
OH30.1−0.2	18 44 33.0	− 2 38 56	771109
OH30.1−0.7	18 46 05.0	− 2 53 57	
OH30.7+0.4	18 43 16.5	− 1 50 00	
OH31.7−0.8	18 49 26	− 1 30 24	
OH32.8−0.3	18 49 48	− 0 18 00	
OH32.8−0.3	18 49 48.0	− 0 17 55	
OH45.07+0.13	19 11 00.4	+10 45 44	
OH45.10+0.12	19 11 07.0	+10 46 42	
OH45.4+0.0	19 12 04.4	+11 04 15	
OH45.47+0.05	"	"	
OH45.47+0.13	19 11 46.1	+11 07 06	
OH45.5+0.1	19 11 58.3	+11 05 20	
OH45.5−0.0	19 11 59.5	+11 05 30	
OH48.6+0.2	19 17 35	+13 54	ED
OH69.54−0.98	20 08 09.8	+31 22 41	
OH75.78+0.34	20 19 52.0	+37 17 04	
OH231.8+4.2	7 39 58.9	−14 35 44	740203
OH284.2−0.8	10 19 44.4	−57 50 40	
OH284.2−0.8	10 19 44.7	−57 50 42	
OH308.9+0.1IR	13 39 34.4	−61 53 45	
OH309.8+0.5I1	13 47 12.7	−61 20 17	
OH309.8+0.5I2	13 47 02.3	−61 20 14	
OH309.8+0.5I3	13 47 13.7	−61 20 05	
OH327.4−0.1	15 47 39.4	−54 00 01	
OH327.4−0.6	15 50 17.6	−54 24 33	
OH328.2+0.0	15 51 31.1	−53 23 24	
OH328.4−0.2	15 53 31.8	−53 28 53	
OH328.7−0.2	15 55 15.9	−53 16 31	
OH330.4+0.1	16 01 59.7	−51 57 44	
OH331.6−0.3	16 09 40.6	−51 22 45	
OH337.3−0.2	16 34 01.9	−47 17 33	
OH337.4−0.1	16 33 45.0	−47 13 12	
OH337.5+0.1	16 33 30.1	−46 54 19	
OH337.9+0.3	16 34 02.0	−46 34 40	
OH338.0−0.1	16 36 18.8	−46 44 44	
OH338.5+0.1	16 37 30.1	−46 13 10	
OH338.5+0.1IR	16 37 15.2	−46 14 20	
OH338.5−0.2	16 38 16.4	−46 26 51	
OH351.8−0.54A	17 23 20.5	−36 06 45	
OH351.8−0.54B	17 23 21.7	−36 06 44	ED
OI 061	7 36 42.5	+ 1 44 00	809908
OI 090.4	7 54 22.6	+10 04 39	"
OI 158	7 35 14.1	+17 49 11	"
OJ 287	8 51 57	+20 17 59	
OJ 287	8 51 57.3	+20 17 59	809908
OK 222	9 12 53.5	+29 45 55	"
OL 133	10 20 12.5	+19 08 37	"
OM 280	11 47 44.0	+24 34 35	"
OMC CENTRAL	5 32 46.5	− 5 24 15	
OMC NORTHERN	5 32 46.3	− 5 24 10	
OMC PEAK 2	5 32 48.3	− 5 24 33	
OMC POS 1	5 32 46.2	− 5 23 28	
OMC POS 1	5 32 46.2	− 5 24 01	ED
OMC POS 2	5 32 46.2	− 5 23 44	
OMC POS 2	5 32 48.2	− 5 24 33	ED
OMC POS 3	5 32 45.2	− 5 23 50	
OMC POS 3	5 32 47.2	− 5 24 29	ED
OMC POS 4	5 32 44.9	− 5 24 05	
OMC POS 4	5 32 46.2	− 5 24 28	ED
OMC POS 5	5 32 46.4	− 5 23 50	"
OMC POS 5	5 32 47.3	− 5 24 00	
OMC POS 6	5 32 46.3	− 5 23 56	
OMC POS 6	5 32 47.2	− 5 24 00	ED
OMC POS 7	5 32 45.8	− 5 24 05	
OMC POS 7	5 32 45.8	− 5 24 14	ED
OMC POS 8	5 32 45.8	− 5 23 50	"
OMC POS 8	5 32 45.8	− 5 24 13	
OMC POS 9	5 32 46.2	− 5 24 05	
OMC POS 9	5 32 46.8	− 5 24 45	ED
OMC POS 10	5 32 46.2	− 5 24 13	
OMC POS 10	5 32 46.7	− 5 24 18	ED
OMC POS 11	5 32 47.0	− 5 24 13	
OMC POS 11	5 32 47.1	− 5 24 23	ED
OMC POS 12	5 32 46.2	− 5 24 30	
OMC POS 13	5 32 47.3	− 5 24 29	
OMC POS 14	5 32 48.3	− 5 24 37	
OMC 46.3−2406	5 32 46.3	− 5 24 06	
OMC 48.3−2436	5 32 48.3	− 5 24 36	
OMC−1	5 32 46.7	− 5 24 19	
OMC−1	5 32 47	− 5 24 30	
OMC−1	5 32 47	− 5 24 50	ED
OMC−1 A	5 32 45.7	− 5 24 09	
OMC−1 B	5 32 45.8	− 5 24 15	
OMC−1 C	5 32 45.9	− 5 24 20	
OMC−1 D	5 32 46.1	− 5 24 32	
OMC−1 E	5 32 46.1	− 5 24 14	
OMC−1 F	5 32 46.3	− 5 24 27	
OMC−1 G	5 32 46.4	− 5 24 17	
OMC−1 H	5 32 46.4	− 5 24 01	
OMC−1 I	5 32 46.4	− 5 24 25	
OMC−1 IRS1	5 32 46.2	− 5 24 33	790607
OMC−1 IRS2	5 32 46.2	− 5 23 44	"
OMC−1 J	5 32 46.6	− 5 24 33	
OMC−1 K	5 32 46.6	− 5 24 30	
OMC−1 L	5 32 46.9	− 5 24 14	
OMC−1 M	5 32 46.9	− 5 23 58	
OMC−1 N	5 32 46.9	− 5 24 27	
OMC−1 N	5 32 47	− 5 24 20	ED
OMC−1 P	5 32 46.9	− 5 24 31	
OMC−1 Q	5 32 47.0	− 5 24 10	
OMC−1 R	5 32 47.0	− 5 24 25	
OMC−1 S	5 32 46	− 5 25 50	ED
OMC−1 S	5 32 47.2	− 5 24 01	
OMC−1 T	5 32 47.2	− 5 24 28	

NAME	RA (1950)	DEC	POS REF
OMC−1 U	5 32 47.4	− 5 24 26	
OMC−1 V	5 32 47.5	− 5 24 33	
OMC−1 W	5 32 47.8	− 5 24 25	
OMC−1 X	5 32 47.8	− 5 24 31	
OMC−1 Y	5 32 47.9	− 5 24 09	
OMC−1 Z	5 32 47.9	− 5 24 19	
OMC−2	5 32 59	− 5 11 37	
OMC−2	5 32 59	− 5 12 10	
OMC−2	5 32 59	− 5 12 11	ED
OMC−2	5 32 59.5	− 5 12 30	
OMC−2	5 33 00	− 5 12 18	
OMC−2 IRS1	5 32 57.0	− 5 12 15	ED
OMC−2 IRS3	5 32 59.1	− 5 12 10	
OMC−2 IRS3	5 32 59.5	− 5 12 10	740801
OMC−2 IRS3	5 32 59.5	− 5 12 30	"
OMC−2 IRS4	5 32 59.5	− 5 11 30	ED
OMC−2 IRS4	5 32 59.6	− 5 11 32	
OMC−3	5 32 42.3	− 4 56 55	
ON 1	20 08 10	+31 23	ED
ON 1−IRS1	20 08 09.3	+31 22 41	
ON 1−IRS2	20 08 09.8	+31 19 40	
ON 1−IRS3	20 08 13.5	+31 18 03	
ON 3	19 59 58.7	+33 26 01	
ON 3 C	20 00 00	+33 26 00	ED
ON 3 C1	19 59 59	+33 25 50	"
ON 3 C2	20 00 00	+33 25 50	"
ON 231	12 19 01.1	+28 30 36	809908
ON 231 I	12 19 01	+28 30 30	ED
ON 231 II	12 19 00	+28 30 20	"
ON 325	12 15 21.1	+30 23 40	809908
OO 2284	2 19	+57	ED
OP 313	13 08 07.6	+32 36 41	809908
OPH #1	16 14 12.9	−24 56 56	
OPH #1	16 23 30	−24 17 20	
OPH #2	16 15 29.0	−23 43 42	
OPH #3	16 18 10.7	−23 36 25	
OPH #4	16 18 12.9	−24 38 05	
OPH #5	16 20 40.0	−25 36 35	
OPH #6	16 22 17.8	−24 20 03	
OPH #7	16 22 18.6	−24 22 28	
OPH #8	16 22 20.6	−24 23 25	
OPH #9	16 22 22.8	−24 21 07	
OPH #10	16 22 31.4	−23 47 15	
OPH #11	16 22 33.9	−24 27 13	
OPH #12	16 22 36.7	−24 06 56	
OPH #13	16 22 54.8	−24 14 01	
OPH #14	16 23 01.7	−24 16 50	
OPH #15	16 23 04.0	−24 36 09	
OPH #16	16 23 07.7	−24 27 26	
OPH #17	16 23 11.6	−23 11 54	
OPH #18	16 23 15.5	−24 15 38	
OPH #19	16 23 15.8	−24 13 37	
OPH #20	16 23 17.5	−24 12 33	
OPH #21	16 23 19.9	−24 16 18	
OPH #22	16 23 22.0	−24 14 15	
OPH #23	16 23 22.6	−24 18 04	
OPH #24	16 23 22.9	−24 09 29	
OPH #25	16 23 32.8	−24 16 44	
OPH #26	16 23 41.5	−24 13 47	
OPH #27	16 23 43.3	−24 16 24	
OPH #28	16 23 56.5	−24 38 53	
OPH #29	16 24 07.7	−24 30 40	
OPH #30	16 24 08.9	−24 12 31	
OPH #31	16 24 25.4	−24 24 34	
OPH #32	16 24 26.9	−24 20 37	
OPH #33	16 24 28.6	−24 21 00	
OPH #34	16 24 38.8	−24 15 24	
OPH #35	16 24 45.2	−24 16 43	
OPH #36	16 24 48.3	−24 19 02	
OPH #37	16 25 02.2	−24 19 54	
OPH #38	16 25 07.8	−24 16 44	
OPH #39	16 25 46.9	−25 40 01	
OPH #40	16 26 21.8	−25 46 13	
OPH #41	16 27 01.5	−23 44 40	
OPH #42	16 28 17.4	−24 31 02	
OPH #43	16 29 44.1	−26 16 48	
OPH #44	16 30 00.8	−24 16 24	
OPH #45	16 30 20.5	−23 44 06	
OPH #46	16 34 46.5	−24 20 09	
OPH #47	16 35 53.0	−24 05 26	
OPH #48	16 36 48.9	−24 00 19	
OPH #49	16 37 16.4	−23 47 56	
OPH #50	16 38 04.6	−24 03 26	
OPH #51	16 14 14.0	−25 54 55	
OPH #52	16 14 49.8	−23 16 38	
OPH #53	16 15 12.1	−25 33 58	
OPH #54	16 15 25.4	−25 57 05	
OPH #55	16 16 39.5	−25 27 31	
OPH #56	16 16 41.7	−23 15 22	
OPH #57	16 16 52.1	−23 58 19	
OPH #58	16 17 37.4	−24 03 02	
OPH #59	16 17 44.0	−23 43 37	
OPH #60	16 17 45.4	−25 28 42	
OPH #61	16 18 08.7	−25 28 28	
OPH #62	16 19 23.2	−23 34 47	
OPH #63	16 19 27.5	−22 59 30	
OPH #64	16 20 12.4	−24 32 24	
OPH #65	16 20 22.0	−23 21 06	
OPH #66	16 21 55.4	−23 09 02	
OPH #67	16 22 35.0	−23 20 01	
OPH #68	16 24 28.5	−25 22 57	
OPH #69	16 25 17.5	−26 29 01	
OPH #70	16 25 20.3	−26 21 57	
OPH #71	16 25 27.7	−26 06 57	
OPH #72	16 25 32.0	−25 05 19	
OPH #73	16 25 47.4	−23 30 25	
OPH #74	16 26 20.2	−26 19 22	
OPH #75	16 26 36.7	−23 43 37	
OPH #76	16 27 09.9	−25 00 24	
OPH #77	16 28 09.3	−24 33 13	
OPH #78	16 28 18.4	−26 25 50	
OPH #79	16 28 43.8	−23 37 32	
OPH #80	16 30 16.7	−23 17 34	
OPH #81	16 31 39.4	−24 18 13	
OPH #82	16 32 07.5	−26 22 49	
OPH #83	16 32 26.1	−24 50 40	
OPH #84	16 33 06.7	−24 41 40	
OPH #85	16 36 25.3	−24 49 27	

NAME	RA (1950)	DEC	POS REF
OPH #86	16 37 53.1	−26 31 04	
OPH #87	16 38 27.0	−23 34 49	
OPH A	16 23 28.5	−24 18 55	
OPH DC #1	16 22 17.8	−24 20 03	
OPH DC #3	16 22 20.6	−24 23 25	
OPH DC #4	16 22 22.8	−24 21 07	
OPH DC #10	16 23 01.7	−24 16 50	
OPH DC #14	16 23 15.8	−24 13 37	
OPH DC #16	16 23 22.0	−24 14 15	
OPH DC #31	16 24 48.3	−24 19 02	
OPH DC #34	16 25 02.2	−24 19 54	
OPH FIR #1	16 23 09	−24 19	
OPH FIR #2	16 23 05	−24 17	
OPH FIR #3	16 23 31	−24 19	
OPH FIR #4	16 23 09	−24 22	
OPH FIR #5	16 22 48	−24 19	
OPH FIR #6	16 22 26	−24 19	
OPH S1	16 23 32.8	−24 16 44	
ALF OPH	17 32 36.6	+12 35 41	CSI 79
BET OPH	17 41 00.0	+ 4 35 11	"
BF OPH	17 02 59.3	−26 30 48	"
CHI OPH	16 24 07.2	−18 20 38	"
DEL OPH	16 11 43.3	− 3 34 00	"
DEL OPH	16 11 47	− 3 33 55	
IX OPH	17 06 40	−27 13 09	GCVS
KK OPH	17 07 01	−27 11 38	"
PHI OPH	16 28 16.3	−16 30 17	CSI 79
R OPH	17 04 53.3	−16 01 38	"
RHO OPH	16 23 30.8	−24 20 00	
RHO OPH #1	16 23 32.0	−24 16 53	
RHO OPH #2	16 23 29.0	−24 17 20	
RHO OPH #3	16 23 29.0	−24 16 40	
RHO OPH #4	16 18 39.0	−23 56 44	
RHO OPH #4	16 23 28.0	−24 16 53	
RHO OPH #5	16 23 28.0	−24 16 26	
RHO OPH #6	16 23 26.1	−24 16 53	
RHO OPH #7	16 19 09.2	−24 02 06	
RHO OPH #7	16 23 24.1	−24 17 20	
RHO OPH #8	16 19 26.8	−23 49 04	
RHO OPH #8	16 22 40.0	−24 19 30	
RHO OPH #9	16 22 40.0	−24 20 10	
RHO OPH #10	16 20 21.9	−23 21 05	
RHO OPH #11	16 19 51.0	−23 58 48	
RHO OPH #12	16 19 56.8	−24 11 55	
RHO OPH #13	16 19 49.7	−24 29 47	
RHO OPH #14	16 20 37.2	−24 30 32	
RHO OPH #15	16 20 25.7	−24 18 33	
RHO OPH #16	16 21 02.3	−23 41 24	
RHO OPH #17	16 21 14.8	−24 25 54	
RHO OPH #20	16 22 23.7	−23 48 22	
RHO OPH #21	16 22 28.1	−23 39 38	
RHO OPH #22	16 22 05.8	−24 25 37	
RHO OPH #23	16 22 48.8	−24 32 27	
RHO OPH #24	16 22 59.9	−23 54 06	
RHO OPH #25	16 23 21.8	−24 36 28	
RHO OPH #27	16 23 45.2	−24 05 16	
RHO OPH #29	16 24 07.7	−24 30 40	780902
RHO OPH #30	16 24 08.3	−24 38 50	
RHO OPH #31	16 24 08.9	−24 12 30	
RHO OPH #34	16 25 02.1	−24 19 54	
RHO OPH #35	16 25 08.9	−24 09 23	
RHO OPH #37	16 25 46.1	−23 57 30	
RHO OPH #38	16 25 43.9	−24 41 21	
RHO OPH #39	16 25 57.2	−24 42 35	
RHO OPH #40	16 26 52.9	−23 55 08	
RHO OPH #41	16 26 43.6	−24 13 20	
RHO OPH #42	16 26 11.2	−24 17 22	
RHO OPH #46	16 28 03.1	−23 58 07	
RHO OPH #47	16 27 57.8	−23 32 35	
RHO OPH #52	16 28 05.2	−24 44 27	
RHO OPH #53	16 28 10.0	−24 56 35	
RHO OPH #54	16 28 32.8	−24 59 38	
RHO OPH #55	16 28 32.5	−25 02 09	
RHO OPH #61	16 29 14.6	−24 44 34	
RHO OPH #65	16 29 34.6	−24 16 28	
RHO OPH #66	16 29 23.4	−23 53 53	
RHO OPH #73	16 30 06.7	−24 44 59	
RHO OPH #74	16 30 07.7	−24 11 01	
RHO OPH #76	16 31 01.4	−24 36 43	
RHO OPH #78	16 31 00.1	−23 36 11	
RHO OPH #79	16 30 57.4	−23 37 34	
RHO OPH #80	16 31 25.0	−24 07 32	
RHO OPH #81	16 31 47.0	−24 41 33	
RHO OPH #83	16 32 32.0	−24 37 41	
RHO OPH #85	16 31 49.5	−24 17 57	
RHO OPH #86	16 32 02.3	−23 15 38	
RHO OPH #87	16 33 06.7	−24 41 41	
RHO OPH #95	16 34 23.0	−24 26 43	
RHO OPH #96	16 36 36.2	−24 23 07	
RHO OPH #98	16 38 01.9	−24 09 38	
RHO OPH #100	16 40 37.0	−24 05 42	
RHO OPH #101	16 41 40.1	−24 02 42	
RHO OPH #102	16 42 45.7	−23 55 22	
RHO OPH #104	16 43 52.6	−23 46 15	
RHO OPH #105	16 43 17.2	−23 44 25	
RHO OPH #106	16 41 49.2	−23 50 50	
RHO OPH #107	16 40 49.7	−24 00 44	
RHO OPH #109	16 38 34.7	−23 50 58	
RHO OPH #111	16 34 47.3	−24 04 06	
RHO OPH #112	16 34 02.4	−24 17 10	
RHO OPH AB	16 22 34.9	−23 19 56	CSI 79
RHO OPH C	16 22 34.9	−23 17 29	"
RHO OPH D	16 22 24.0	−23 20 46	"
RR OPH	16 46 07.6	−19 22 28	"
RS OPH	17 47 29.3	− 6 41 04	"
RT OPH	17 54 11.3	+11 10 30	"
RU OPH	17 30 29.4	+ 9 27 23	"
RY OPH	18 14 07.3	+ 3 40 26	"
S OPH	16 31 22.3	−17 03 25	"
SIG OPH	17 24 01.9	+ 4 10 55	"
SS OPH	16 55 18.4	− 2 40 48	"
T OPH	16 30 52.0	−16 01 42	"
TT OPH	16 47 06.1	+ 3 43 03	"
TW OPH	17 26 44.7	−19 26 36	"
TX OPH	17 01 31.9	+ 5 03 08	"
TY OPH	18 28 52.5	+ 4 20 54	"
UZ OPH	17 19 31.5	+ 6 57 25	"
V OPH	16 23 56.5	−12 18 54	"

NAME	RA (1950) DEC	POS REF
	h m s ° ′ ″	
V426 OPH	18 05 25 + 5 51 25	GCVS
V446 OPH	16 43 53 −11 33 33	"
V453 OPH	17 24 12.6 − 2 21 48	CSI 79
V551 OPH	17 37 44.2 −27 22 12	"
V564 OPH	17 49 36.7 + 7 57 08	"
V679 OPH	18 39 31.1 + 6 46 09	"
V853 OPH	16 25 43 −24 19 47	GCVS
V1111 OPH	18 34 57 +10 22 27	"
V1121 OPH	16 46 26 −14 18 22	"
W OPH	16 18 42.5 − 7 35 03	CSI 79
X OPH	18 35 57.4 + 8 47 18	"
XX OPH	17 41 15.3 − 6 14 50	"
Y OPH	17 49 57.7 − 6 07 58	"
Z OPH	17 17 01.7 + 1 33 41	"
ZET OPH	16 34 24.1 −10 28 02	"
12 OPH	16 33 42.9 − 2 13 01	"
27 OPH	16 55 17.9 + 9 27 03	"
67 OPH	17 58 08.3 + 2 55 55	"
70 OPH	18 02 55.5 + 2 30 33	"
OQ 100	14 00 21.5 +16 14 22	809908
OQ 172	14 42 50.6 +10 11 13	"
OQ 530	14 18 00.0 +54 40 00	"
AA ORI	5 32 43 − 5 48 26	GCVS
AB ORI	5 32 47 − 5 45 14	"
AI ORI	5 33 00 − 5 13 03	"
AL ORI	5 33 03 − 4 57 09	"
ALF ORI	5 52 27.7 + 7 23 56	CSI 79
ALF ORI	5 52 32 + 7 23 44	"
AR ORI	5 33 27 − 5 06 05	GCVS
AV ORI	5 33 34 − 6 44 23	"
AZ ORI	5 33 26.9 − 5 13 29	CSI 79
BD ORI	5 34 06 − 6 21 08	GCVS
BE ORI	5 34 34 − 6 35 10	"
BET ORI	5 12 07.9 − 8 15 27	CSI 79
BF ORI	5 34 46.3 − 6 36 11	"
BL ORI	6 22 36.9 +14 45 03	"
BN ORI	5 33 47.7 + 6 48 10	"
BO ORI	5 33 14 − 4 26 46	GCVS
CE ORI	5 33 20 − 5 03 28	"
CHI 1 ORI	5 51 25.1 +20 16 06	CSI 79
CHI 2 ORI	6 00 56.9 +20 08 27	"
CO ORI	5 24 50.7 +11 23 15	"
CY ORI	6 12 02.9 + 9 35 52	"
DEL ORI	5 29 26.9 − 0 20 01	"
DEL ORI A	" "	"
DL ORI	5 39 01 − 8 07 23	GCVS
DL ORI/G1	5 38 29 − 8 05 42	
DL ORI/G2	5 38 27 − 8 04 22	
DL ORI/G3	5 38 26 − 8 07 10	
DL ORI/G4	5 38 27 − 8 05 11	
DL ORI/G5	5 38 28 − 8 04 44	
EPS ORI	5 33 40.4 − 1 13 54	CSI 79
ETA ORI	5 21 57.6 − 2 26 27	"
ETA ORI AB	" "	"
EZ ORI	5 31 48.9 − 5 06 52	"
FU ORI	5 42 38.9 + 9 02 57	"
FU ORI NNE	5 42 40.8 + 9 03 45	ED
FU ORI NNW	5 42 37.0 + 9 03 45	"
FU ORI SSE	5 42 40.8 + 9 02 09	"
FU ORI SSW	5 42 37.0 + 9 02 09	"
FU ORI 56"E	5 42 42.6 + 9 02 57	"
FU ORI 56"W	5 42 35.1 + 9 02 57	"
GAM ORI	5 22 26.7 + 6 18 21	CSI 79
GI ORI	6 10 25 +18 33 33	GCVS
GK ORI	6 14 58.3 + 8 32 28	CSI 79
GP ORI	4 59 59.1 +15 15 32	"
GW ORI	5 26 20.7 +11 49 51	"
GX ORI	5 27 14.0 +12 11 17	829902
HI ORI	5 28 35.7 +12 07 31	"
HK ORI	5 28 39.9 +12 06 54	CSI 79
HT ORI	5 30 33 − 6 09 04	GCVS
IOT ORI	5 32 59.1 − 5 56 27	CSI 79
IU ORI	5 32 08.9 − 5 43 45	"
IX ORI	5 32 13 − 5 24 36	GCVS
KAP ORI	5 45 22.9 − 9 41 07	CSI 79
KN ORI	5 32 30 − 5 13 31	GCVS
KP ORI	5 32 29 − 5 43 19	"
KX ORI	5 32 36.5 − 4 45 47	CSI 79
LAM ORI	5 32 22.9 + 9 54 10	"
LP ORI	5 32 42.4 − 5 29 45	"
LX ORI	5 32 46 − 5 41 26	GCVS
LZ ORI	5 32 48.9 − 4 43 34	CSI 79
MX ORI	5 32 53.5 − 5 11 01	"
NU ORI	5 33 03.7 − 5 17 53	"
NV ORI	5 33 04.1 − 5 34 53	"
OME ORI	5 36 32.5 + 4 05 38	"
OT ORI	5 33 23 − 5 18 23	GCVS
PHI 1 ORI	5 32 04.3 + 9 27 25	CSI 79
PI 1 ORI	4 52 08.3 +10 04 22	"
PI 3 ORI	4 47 07.3 + 6 52 31	"
PI 4 ORI	4 48 32.3 + 5 31 15	"
PQ ORI	5 33 50 − 2 12 49	GCVS
R ORI	4 56 18.5 + 8 03 45	CSI 79
RT ORI	5 30 31.6 + 7 07 09	"
RY ORI	5 29 44.3 − 2 51 46	"
S ORI	5 26 32.6 − 4 43 50	"
SIG ORI	5 36 13.9 − 2 37 36	"
SIG ORI E	5 36 16.3 − 2 37 16	"
SW ORI	5 31 49 − 6 38 10	GCVS
SY ORI	5 32 41 − 4 29 32	"
T ORI	5 33 23.1 − 5 30 17	CSI 79
THE 1 ORI	5 32 48.9 − 5 25 13	"
THE 1 ORI	5 32 48.5 − 5 25 12	740903
THE 1 ORI A	5 32 48.3 − 5 25 22	CSI 79
THE 1 ORI B	5 32 48.6 − 5 25 29	"
THE 1 ORI C	5 32 48.9 − 5 25 13	"
THE 1 ORI D	5 32 49.7 − 5 25 01	"
THE 2 ORI	5 32 55.3 − 5 26 49	"
THE 2 ORI A	" "	"
THE 2 ORI B	5 32 58.9 − 5 26 51	"
TT ORI	5 32 49 − 4 47 38	GCVS
TV ORI	5 33 08.6 − 5 03 02	CSI 79
TW ORI	5 33 05 − 6 47 15	GCVS
U ORI	5 52 50.9 +20 10 05	CSI 79
U ORI	5 52 51.0 +20 10 24	"
UPS ORI	5 29 30.5 − 7 20 11	CSI 79
UU ORI	5 38 22 − 8 06 02	GCVS
UX ORI	5 02 01 − 3 51 26	"
V ORI	5 03 25.0 + 4 02 12	CSI 79
VV ORI	5 30 59.0 − 1 11 21	"
VY ORI	5 31 08 − 5 03 31	GCVS
VZ ORI	5 31 18 − 5 32 49	"
V346 ORI	5 22 07.9 + 1 40 57	CSI 79
V350 ORI	5 37 49 − 9 43 42	GCVS
V359 ORI	5 33 05.2 − 4 52 06	CSI 79
V360 ORI	5 33 05 − 5 11 21	GCVS
V361 ORI	5 33 03.9 − 5 27 07	CSI 79
V370 ORI	5 27 3.9 +12 10 29	29902S
V372 ORI	5 32 19.6 − 5 36 09	CSI 79
V380 ORI	5 33 59.1 − 6 44 47	
V380 ORI	5 34 00.9 − 6 44 33	CSI 79
V384 ORI	5 30 43 − 5 44 17	GCVS
V386 ORI	5 31 18 − 5 33 07	"
V390 ORI	5 33 32 − 5 00 35	"
V442 ORI	5 26 45.5 +12 54 01	829902
V447 ORI	5 27 47.4 +12 34 42	"
V448 ORI	5 28 03.5 +12 06 20	"
V451 ORI	5 28 40.1 +10 59 12	"
V452 ORI	5 28 54.8 +12 28 21	"
V453 ORI	5 29 00.5 +12 29 50	"
V466 ORI	5 30 35 − 5 28 29	GCVS
V486 ORI	5 32 45 − 5 45 14	"
V573 ORI	5 33 17 − 6 36 40	"
V577 ORI	5 33 32 − 6 44 41	"
V586 ORI	5 34 32 − 6 11 04	"
V614 ORI	5 38 51.2 + 9 06 50	829902
V625 ORI	5 40 36.5 + 9 04 55	"
V630 ORI	5 41 32.6 + 9 09 43	"
V631 ORI	5 41 57.2 + 8 55 46	"
V649 ORI	5 26 36.4 +11 49 37	"
W ORI	5 02 48.5 + 1 06 37	CSI 79
WX ORI	5 31 40 − 5 15 45	GCVS
XX ORI	5 32 10 − 6 07 29	"
YY ORI	5 32 21 − 5 59 54	"
YZ ORI	5 32 26 − 5 05 24	"
ZET ORI	5 38 13.9 − 1 58 00	CSI 79
ZET 1 ORI	" "	"
16 ORI	5 06 34.3 + 9 45 59	"
25 ORI	5 22 08.7 + 1 48 08	"
29 ORI	5 21 32.1 − 7 51 07	"
40 ORI	5 34 09.3 + 9 15 53	"
42 ORI	5 32 55.0 − 4 52 09	"
ORI IRA+IRB	5 32 48 − 5 24	
ORION #1	5 32 46.2 − 5 24 02	
ORION #2	5 32 48.3 − 5 24 34	
ORION #3	5 32 47.3 − 5 24 26	
ORION #4	5 32 46.2 − 5 24 27	
ORION #5	5 32 46.4 − 5 23 50	
ORION A	5 32 49.7 − 5 25 12	
ORION A	5 32 50 − 5 25 00	ED
ORION A	5 32 50.8 − 5 25 40	"
ORION AREA II	5 32 38.2 − 5 25 08	"
ORION AREAIII	5 32 45.8 − 5 25 08	"
ORION AREA IV	5 32 49.0 − 5 26 00	"
ORION AREA V	5 32 52.2 − 5 25 08	"
ORION AREA VI	5 32 55.4 − 5 25 08	"
ORION AREAVII	5 32 59.0 − 5 24 30	"
ORION B + B'	5 32 48.5 − 5 24 12	"
ORION H2	5 32 46.2 − 5 24 02	
ORION H2 PK1	" "	780708
ORION H2 PK2	5 32 48.3 − 5 24 34	"
ORION H2 PK5	5 32 46.4 − 5 23 50	"
ORION IRC2	5 32 47.1 − 5 24 23	ED
ORION IRS2	5 32 46.5 − 5 23 55	"
ORION KL	5 32 46.7 − 5 24 15	
ORION NEB #1	5 32 55.0 − 5 26 50	ED
ORION NEB #2	5 32 56.5 − 5 26 17	"
ORION NEB #3	5 32 54.2 − 5 26 47	"
ORION NEB #4	5 32 52.2 − 5 27 02	"
ORION NEB. A	5 32 47.2 − 5 25 34	"
ORION NEB. B	5 32 49.0 − 5 25 10	
ORION NEB. C	5 32 48.0 − 5 24 37	
ORION NEB. 1	5 32 48.0 − 5 25 40	
ORION NEB. 2	5 32 45.0 − 5 25 10	
ORION NEB. 3	5 32 47.0 − 5 24 25	
ORION NEB. 4	5 32 49.0 − 5 25 16	
ORION NEB. 5	5 32 50.2 − 5 25 16	
ORION NEB. 6	5 32 52.4 − 5 26 46	
ORION NEB. 7	5 32 43.0 − 5 23 16	
ORION NEBULA	5 32 45.9 − 5 24 04	
ORION NEBULA	5 32 46 − 5 24 00	
ORION NEBULA	5 32 46 − 5 24 05	
ORION NEBULA	5 32 46.1 − 5 24 05	
ORION NEBULA	5 32 46.5 − 5 24 26	
ORION NEBULA	5 32 46.7 − 5 24 28	
ORION NEBULA	5 32 47 − 5 24 20	ED
ORION NEBULA	5 32 47.5 − 5 24 30	"
ORION NEBULA	5 32 48 − 5 24 35	"
ORION NEBULA	5 32 48 − 5 25 12	"
ORION NEBULA	5 32 48.0 − 5 25 26	
ORION NEBULA	5 32 48.5 − 5 25 17	
ORION NEBULA	5 32 48.5 − 5 25 31	ED
ORION NEBULA	5 32 49.0 − 5 25 46	"
ORION PEAK1	5 32 46.3 − 5 24 02	"
ORION PEAK3	5 32 47.4 − 5 24 27	"
ORION PEAK5	5 32 46.5 − 5 23 50	"
ORION PK1	5 32 46.3 − 5 24 01	"
ORION PK2	5 32 48.3 − 5 24 33	"
ORION PK3	5 32 47.4 − 5 24 28	"
ORION PK5	5 32 46.5 − 5 23 49	"
ORION POS A	5 32 53.3 − 5 26 04	
ORION POS 2	5 32 56.8 − 5 26 13	
ORION POS 3.5	5 32 53.5 − 5 26 52	
ORION POS 4	5 32 52.4 − 5 27 04	
ORION POS1	5 32 46.2 − 5 24 01	ED
ORION POS3.25	5 32 54.0 − 5 26 47	
ORION POS6	5 32 45.0 − 5 24 10	ED
ORION POS13	5 32 45.5 − 5 24 01	"
ORION POS14	5 32 46.7 − 5 24 07	"
ORION POS15	5 32 45.7 − 5 23 41	"
ORION POS16	5 32 45.6 − 5 23 52	"
ORION POS17	5 32 47.1 − 5 24 20	"
ORION POS19	5 32 47.7 − 5 23 55	"
ORION POS20	5 32 47.0 − 5 23 55	"
ORION POS21	5 32 46.2 − 5 24 05	"
ORION POS23	5 32 45.7 − 5 23 35	"
ORION POS25	5 32 47.8 − 5 24 26	"
ORION POS26	5 32 48.8 − 5 24 35	"
ORION POS28	5 32 45.0 − 5 23 55	"
ORION POS29	5 32 46.6 − 5 23 40	"
ORION POS30A	5 32 46.4 − 5 23 55	"
ORION POS30B	" "	"
ORION POS31	5 32 45.0 − 5 24 10	"
ORION POS33	5 32 45.6 − 5 24 05	"
ORION POS34	5 32 46.3 − 5 23 40	"
ORION POS35	5 32 45.2 − 5 24 15	"
ORION POS39	5 32 45.4 − 5 23 57	"
ORION POS44	5 32 47.6 − 5 24 30	"
OT 081	17 49 10.4 + 9 39 43	809908
OV−236	19 21 −29 18	ED
OX 169	21 41 13.8 +17 30 02	809908
OY 091	22 54 46.0 + 7 27 10	"
P 0735+178	7 35 14.1 +17 49 11	"
PAL 12 STAR13		
PAL 12 STAR14		
PAL 12 STAR15		
PAL 12 STAR20		
PARSAMYAN 1		
PARSAMYAN 3		
PARSAMYAN 4		
PARSAMYAN 5	6 03 37.0 −15 39 01	
PARSAMYAN 7		
PARSAMYAN 8		
PARSAMYAN 10		
PARSAMYAN 11		
PARSAMYAN 12		
PARSAMYAN 14		
PARSAMYAN 15	6 42 15.5 + 3 01 18	
PARSAMYAN 16		
PARSAMYAN 17	6 55 37.6 − 7 52 35	
PARSAMYAN 18	6 57 16.7 − 7 41 54	
PARSAMYAN 19		
PARSAMYAN 20		
PARSAMYAN 21	19 26 37.5 + 9 32 24	
PARSAMYAN 22	20 22 44.7 +42 04 16	
PARSAMYAN 23		
AR PAV	18 15 23.9 −66 05 57	CSI 79
DEL PAV	20 03 50.3 −66 18 42	"
R PAV	18 08 04.9 −63 37 42	"
RT PAV	18 30 55.5 −69 55 30	"
X PAV	20 07 37.7 −60 05 24	"
Y PAV	21 19 47.0 −69 56 55	"
Z PAV	19 30 54.4 −62 52 06	"
PB 2	8 19 03.3 −46 10 39	769910
PB 5	9 14 21.0 −45 16 12	739909
PB 8	11 30 57.5 −56 49 43	769910
PB 10	19 25 54.4 +12 13 35	"
PC 11	16 33 37.1 −55 36 25	"
PC 12	16 40 54 −18 51	P−K
PC 13	16 47 06 −30 14 48	809909
PC 18	17 37 20 −47 01 54	759905
PC 19	18 22 13.6 + 2 27 48	769910
PC 20	18 40 29.3 + 0 19 37	"
PC 23	19 49 57.2 +32 51 33	819914
PEAK1 4"NW	5 32 46.2 − 5 23 58	ED
PEAK1 4"SE	5 32 46.4 − 5 24 06	"
PEAK1 4"SW	5 32 46.3 − 5 24 04	"
PEAK1 8"SE	5 32 46.5 − 5 24 09	"
PEAK1 8"SW	5 32 46.1 − 5 24 09	"
PEAK2 3"W	5 32 48.1 − 5 24 33	"
AG PEG	21 48 36.1 +12 23 26	CSI 79
AK PEG	23 00 40.5 +11 05 21	"
ALF PEG	23 02 16.0 +14 56 08	"
BET PEG	23 01 20.7 +27 48 39	"
CHI PEG	0 12 00.6 +19 55 42	"
DS PEG	21 39 54.4 +35 16 53	779907
EI PEG	23 19 14.6 +12 19 16	CSI 79
EPS PEG	21 41 43.7 + 9 38 40	"
EPS PEG	21 41 47 + 9 38 34	
EQ PEG	23 29 18.9 +19 39 43	CSI 79
ETA PEG	22 40 39.2 +29 57 32	"
EZ PEG	23 14 26 +25 26 48	GCVS
GAM PEG	0 10 39.3 +14 54 19	CSI 79
IOT PEG	22 04 40.7 +25 06 00	"
NUU PEG	22 03 09.3 + 4 48 47	"
PHI PEG	23 49 56.3 +18 50 32	"
R PEG	23 04 08.0 +10 16 22	
R PEG	23 04 08.2 +10 16 20	CSI 79
RR PEG	21 42 15.9 +24 46 40	"
RS PEG	22 09 49.6 +14 18 43	"
RT PEG	22 01 59.3 +34 52 45	779907
RV PEG	22 23 17.3 +30 13 09	CSI 79
RW PEG	23 01 38.5 +15 05 44	"
RZ PEG	22 03 39.1 +33 15 41	779907
S PEG	23 18 00.9 + 8 38 40	CSI 79
SV PEG	22 14 31.0 +35 06 39	
SX PEG	22 47 57.9 +17 37 43	CSI 79
T PEG	22 06 27.3 +12 17 41	"
TU PEG	21 42 39.1 +12 28 05	
TW PEG	22 01 41.0 +28 06 30	
TW PEG	22 01 43.2 +28 06 19	CSI 79
UU PEG	21 28 39 +10 56 02	GCVS
V PEG	21 58 30.1 + 5 52 18	CSI 79
W PEG	23 17 15.2 +26 00 21	"
X PEG	21 17 39.4 +13 41 57	"
Y PEG	22 09 13.6 +14 06 41	"
Z PEG	23 57 32.7 +25 37 41	"
ZET PEG	22 38 57.9 +10 34 10	"
2 PEG	21 27 40.7 +23 25 06	"
9 PEG	21 42 08.4 +17 07 10	"
12 PEG	21 43 46.1 +22 43 02	"
25 PEG	22 05 29.2 +21 27 30	"
31 PEG	22 19 03.3 +11 57 08	"
51 PEG	22 55 00.3 +20 30 00	"
55 PEG	23 04 28.9 + 9 08 19	"
57 PEG	23 06 59.9 + 8 24 20	"
85 PEG	23 59 33.1 +26 49 02	"
PEG(A2326)	23 26 +14	ED
AC PER	3 41 36.9 +44 37 25	CSI 79
AD PER	2 16 57.0 +56 45 51	779907
ALF PER	3 20 44.3 +49 41 05	CSI 79
AX PER	1 33 05.3 +54 00 19	"
BET PER	3 04 54.4 +40 45 52	779907
BS PER	2 23 28.0 +51 53 41	CSI 79

NAME	RA (1950) DEC	POS REF
BU PER	2 15 20.9 +57 11 29	779907
CF PER	2 00 04 +57 27 32	GCVS
DEL PER	3 39 21.2 +47 37 45	CSI 79
EO PER	2 46 56 +57 07 45	GCVS
EPS PER	3 54 29.3 +39 52 01	CSI 79
ETA PER	2 47 01.9 +55 41 22	"
FZ PER	2 17 27.1 +56 55 47	779907
IO PER	3 03 03 +55 33 03	GCVS
IOT PER	3 05 26.7 +49 25 25	CSI 79
IP PER	3 37 38.4 +32 22 17	779907
IS PER	1 28 56 +53 59 30	GCVS
KAP PER	3 06 06.7 +44 40 08	CSI 79
KK PER	2 06 48.4 +56 19 24	779907
KS PER	4 45 19.9 +43 11 19	"
MUU PER	4 11 12.9 +48 17 02	CSI 79
OMI PER	3 41 10.5 +32 07 53	779907
PHI PER	1 40 30.7 +50 26 15	CSI 79
PP PER	2 13 34.1 +58 17 55	779907
PR PER	2 18 08.1 +57 38 06	"
PSI PER	3 32 55.4 +48 01 40	CSI 79
R PER	3 26 51.7 +35 30 02	779907
RHO PER	3 01 57.9 +38 38 52	"
RR PER	2 25 06.1 +51 02 55	"
RS PER	2 18 51.3 +56 52 55	"
RZ PER	1 26 37.3 +50 35 54	CSI 79
S PER	2 19 15.1 +58 21 34	779907
S PER	2 19 16.0 +58 21 30	
SU PER	2 18 35.2 +56 22 35	779907
SY PER	4 12 46.6 +50 30 11	CSI 79
T PER	2 15 45.7 +58 43 54	779907
TX PER	2 44 53.5 +36 45 32	"
TZ PER	2 10 20 +58 08 51	GCVS
U PER	1 56 14.7 +54 34 50	779907
W PER	2 46 55.4 +56 46 38	"
X PER	3 52 15.1 +30 53 59	CSI 79
XI PER	3 55 42.7 +35 38 55	"
XX PER	1 59 47.2 +54 59 33	779907
XY PER	3 46 17.4 +38 49 50	"
Y PER	3 24 18.0 +44 00 12	"
YZ PER	2 34 46.9 +56 49 49	"
ZET PER	3 50 58.9 +31 44 11	CSI 79
5 PER	2 07 58.9 +57 24 38	"
9 PER	2 18 51.1 +55 37 05	"
10 PER	2 21 43.0 +56 23 03	"
24 PER	2 55 57.2 +34 59 02	"
48 PER	4 05 01.3 +47 34 51	"
49 PER	4 04 56.5 +37 35 53	"
PE1-7	16 26 48.1 -45 56 22	769910
PE2-1	8 02 23 -44 21 00	789907
PE2-2	9 07 14 -44 05 30	"
PE2-3	9 08 27 -44 12 18	"
PE2-7	10 39 18 -55 54	P-K
PE2-9	16 21 14 -48 36 42	779909
PE2-15	18 42 45.4 - 7 00 01	819914
PE2-16	18 51 31.0 - 4 42 41	769910
PG 0026+12	0 26 38.1 +12 59 30	809908
PG 0026+129	" "	
PG 0906+48	9 06 45.3 +48 25 56	809908
PG 0906+484	9 06 45.1 +48 25 56	
PG 0906+484	9 06 45.3 +48 25 56	809908
PG 1001+05	10 01 43.3 + 5 27 35	"
PG 1001+054	" "	
PG 1211+14	12 11 +14	ED
PG 1307+08	13 07 + 8	"
PG 1351+64	13 51 46.3 +64 00 28	809908
PG 1351+640	13 51 46.2 +64 00 29	"
PG 1358+04	13 58 00.6 + 4 19 27	809908
PG 1413+01	14 13 03.6 + 1 31 13	"
PG 1519+22	15 19 +22	ED
PG 1550+191	15 50 33.1 +19 05 18	"
PSI PHE	1 51 38.5 -46 32 48	CSI 79
R PHE	23 53 51.9 -50 03 54	"
RT PHE	1 51 34 -49 14 54	GCVS
RU PHE	23 25 26 -47 43 30	"
S PHE	23 56 29.6 -56 51 12	CSI 79
ST PHE	0 33 45.9 -56 05 59	"
SY PHE	1 28 20.4 -42 57 51	"
SZ PHE	1 31 54.5 -43 29 50	"
T PHE	0 28 01.5 -46 41 22	"
TT PHE	1 43 24.4 -42 10 40	"
TU PHE	23 32 39 -55 19 26	GCVS
V PHE	23 29 43.6 -46 15 26	CSI 79
W PHE	1 17 52.2 -56 10 45	"
PHL 658		
PHL 909	0 54 31.9 +14 29 59	
PHL 938		
PHL 957	1 00 33.4 +13 00 11	809908
PHL 1027	1 30 31.6 + 3 23 41	"
PHL 1070		
PHL 1092	1 37 19.0 + 6 04 11	809908
PHL 1377	2 32 36.6 - 4 15 10	"
PIC A		
R PIC	4 44 49.2 -49 20 05	CSI 79
RR PIC	6 35 10.3 -62 35 48	"
S PIC	5 09 37.2 -48 34 00	"
T PIC	5 13 41.3 -46 58 30	"
V PIC	6 12 36.5 -59 53 51	"
W PIC	5 41 50.1 -46 28 30	"
Y PIC	5 09 44.3 -45 38 13	"
PICTOR A	5 18 24.1 -45 49 45	ED
PISMIS 17IRS1	10 59 14.8 -59 32 34	
PISMIS 17IRS2	" "	
PKS 0046-315	0 46 57.9 -31 32 48	809908
PKS 0106+01	1 06 04.5 + 1 19 01	"
PKS 0122-00	1 22 55.8 - 0 21 34	719903
PKS 0159-11	1 59 30.4 -11 47 00	809908
PKS 0237-23	2 37 52.7 -23 22 09	"
PKS 0312-77	3 12 55.7 -77 03 01	"
PKS 0349-27	3 49 -27	ED
PKS 0402-362	4 02 02.2 -36 13 16	809908
PKS 0405-12	4 05 27.5 -12 19 32	"
PKS 0414-06	4 14 49.2 - 6 01 04	"
PKS 0521-36	5 21 -36	ED
PKS 0537-441	5 37 -44 06	"
PKS 0548-322	5 48 -32 12	
PKS 0622-441	6 22 02.7 -44 11 24	809908
PKS 0637-75	6 37 23.4 -75 13 38	"
PKS 0735+178	7 35 14.1 +17 49 11	"
PKS 0736+01	7 36 42.5 + 1 44 00	"
PKS 0837-12	8 37 28.0 -12 03 54	"
PKS 0837-120	" "	"
PKS 0859-14	8 59 54.8 -14 03 38	"
PKS 0925-203	9 25 33.6 -20 21 45	"
PKS 1004+13	10 04 45.1 +13 03 38	"
PKS 1004-217	10 04 25.4 -21 44 44	"
PKS 1011-282	10 11 12.2 -28 16 32	"
PKS 1050-184	10 50 06.9 -18 29 21	"
PKS 1055+01	10 55 55.5 + 1 49 42	"
PKS 1101-325	11 01 08.2 -32 35 05	"
PKS 1103-006	11 03 58.1 - 0 36 38	"
PKS 1144-379	11 44 -37 54	ED
PKS 1217+02	12 17 38.4 + 2 20 21	809908
PKS 1302-102	13 02 55.8 -10 17 17	"
PKS 1308+32	13 08 07.6 +32 36 41	"
PKS 1327-21	13 27 23.4 -21 26 34	"
PKS 1354+19	13 54 42.1 +19 33 44	"
PKS 1355-41	13 55 57.3 -41 38 19	"
PKS 1424-11	14 24 56.0 -11 50 26	"
PKS 1448-232	14 48 09.2 -23 17 11	"
PKS 1451-375	14 51 18.3 -37 35 23	"
PKS 1508-05	15 08 15.0 - 5 31 49	"
PKS 1510-08	15 10 09.0 - 8 54 48	"
PKS 1656+053	16 56 05.7 + 5 19 47	"
PKS 1934-63	19 34 -63	ED
PKS 2115-30	21 15 11.2 -30 31 50	809908
PKS 2126-15	21 26 26.7 -15 51 52	"
PKS 2126-158	" "	"
PKS 2135-14	21 35 01.2 -14 46 27	"
PKS 2135-147	" "	"
PKS 2145+06	21 45 36.1 + 6 43 41	"
PKS 2154-18	21 54 -18	
PKS 2155-304	21 55 58.2 -30 27 52	809908
PKS 2158-380	21 58 17.2 -38 00 51	"
PKS 2204-573	22 04 30.4 -57 22 15	809908
PKS 2216-03	22 16 16.0 - 3 50 36	"
PKS 2251+11	22 51 40.6 +11 20 39	"
PKS 2300-683	23 00 28.5 -68 23 56	"
PKS 2310-322	23 10 27.5 -32 14 07	"
PKS 2344+09	23 44 03.7 + 9 14 05	"
PKS 2344+092	" "	
PKS 2349-01	23 49 22.3 - 1 25 54	789906
POINT SOURCE	5 32 46.8 - 5 24 17	"
ALF PSA	22 54 53.4 -29 53 14	CSI 79
R PSA	22 15 09.7 -29 51 15	"
RX PSA	22 10 21 -27 31 07	GCVS
S PSA	22 00 51.9 -28 17 34	CSI 79
V PSA	22 52 34.9 -29 52 42	"
BET PSC	23 01 19.7 + 3 33 01	"
NUU PSC	1 38 49.5 + 5 14 06	"
R PSC	1 28 03.3 + 2 37 26	"
RZ PSC	1 06 56.9 +27 41 30	"
S PSC	1 14 57.3 + 8 40 03	"
TV PSC	0 25 26.2 +17 36 58	"
TX PSC	23 43 50.0 + 3 12 32	"
U PSC	1 20 20 +12 36 25	GCVS
X PSC	1 09 29.2 +21 56 59	CSI 79
Z PSC	1 13 20.9 +25 30 18	"
19 PSC	23 43 50.0 + 3 12 32	"
29 PSC	23 59 15.5 - 3 18 19	"
30 PSC	23 59 23.7 - 6 17 30	"
54 PSC	0 36 45.3 +20 58 51	"
109 PSC	1 42 11.6 +19 50 01	"
AC PUP	8 20 25.7 -15 45 16	"
AR PUP	8 01 09.2 -36 26 46	"
FK PUP	8 07 20 -36 08 03	GCVS
FW PUP	7 30 26 -12 39 21	"
GO PUP	7 45 22 -11 48 20	"
GT PUP	7 12 44.2 -37 58 33	CSI 79
KQ PUP	7 31 30.0 -14 24 50	"
L2 PUP	7 12 00.6 -44 33 26	"
OMI PUP	7 46 00.3 -25 48 42	"
R PUP	7 38 56.2 -31 32 35	"
RHO PUP	8 05 24.7 -24 09 31	"
RS PUP	8 11 08.9 -34 25 35	"
RT PUP	8 03 32.0 -38 37 56	"
RU PUP	8 05 20.0 -22 45 59	"
RV PUP	6 40 57.7 -42 19 49	"
RW PUP	6 07 56.3 -50 11 47	"
RX PUP	8 12 25.9 -41 32 58	"
ST PUP	6 47 12.9 -37 12 58	"
SU PUP	7 54 35 -44 00 34	GCVS
VV PUP	8 12 51.9 -18 53 52	"
W PUP	7 44 17.7 -42 04 21	CSI 79
Z PUP	7 30 28.3 -20 33 12	"
Z PUP	7 30 29.0 -20 32 49	
ZET PUP	8 01 49.5 -39 51 40	CSI 79
3 PUP	7 41 47.9 -28 50 02	"
R PYX	8 43 23.7 -28 01 03	"
S PYX	9 02 53.9 -24 52 49	"
V PYX	8 51 25.6 -34 37 43	"
P0828+411	8 28 +41 06	ED
P1153+433	11 53 +43 18	"
P837	5 29 38.9 - 5 26 32	749908
P967	5 30 11.2 - 5 33 23	"
P972	5 30 13.4 - 5 06 29	"
P1139	5 30 49.0 - 6 08 30	CSI 79
P1196	5 31 02.5 - 6 05 40	"
P1207	5 31 05.0 - 5 35 34	729902
P1212	5 31 16 - 5 07	779904
P1241	5 31 16 - 5 03	"
P1270	5 31 19.7 - 5 59 13	729902
P1281	5 31 22.3 - 5 34 06	CSI 79
P1322		
P1372		
P1374	5 31 41.9 - 5 24 57	CSI 79
P1391	5 31 46.9 - 5 13 45	"
P1393	5 31 47 - 5 30 18	829909
P1394	5 31 46.9 - 5 38 45	CSI 79
P1397	5 31 47.7 - 5 48 44	729902
P1403	5 31 50 - 5 06 10	GCVS
P1404	5 31 49.3 - 5 38 44	729902
P1409	5 31 48.9 - 5 06 52	CSI 79
P1410		
P1423		
P1425	5 31 54.7 - 4 32 11	749908
P1429		
P1455	5 31 57 - 5 23	779904
P1469		
P1492		
P1507	5 32 06.6 - 5 04 56	CSI 79
P1511	5 32 02.9 - 5 44 45	"
P1538	5 32 13.6 - 4 26 50	749908
P1539	5 32 10 - 5 12	779904
P1540		
P1553		
P1562	5 32 15.5 - 5 09 46	CSI 79
P1575	5 32 15 - 6 01	779904
P1585	5 32 18 - 5 08 48	829909
P1586	5 32 18 - 5 12 42	GCVS
P1605	5 32 19.6 - 5 36 09	CSI 79
P1623	5 32 22.4 - 5 20 32	"
P1649	5 32 24.9 - 5 34 56	"
P1657	5 32 26 - 6 00	779904
P1659	5 32 28 - 5 25 07	GCVS
P1660	5 32 27.1 - 5 31 47	CSI 79
P1683	5 32 34 - 5 07	779904
P1684	5 32 32 - 5 24 55	GCVS
P1685	5 32 32 - 5 27 13	"
P1691	5 32 36 - 6 21	ED
P1693	5 32 34 - 5 11 25	GCVS
P1703		
P1712	5 32 34 - 5 08	779904
P1724		
P1736		
P1744	5 32 38.4 - 5 14 08	CSI 79
P1746	5 32 38 - 5 27 13	GCVS
P1750		
P1762	5 32 41 - 5 07 49	GCVS
P1764	5 32 42 - 5 08 43	"
P1768	5 32 40.6 - 5 54 01	CSI 79
P1772	5 32 42.4 - 5 29 45	"
P1784	5 32 43 - 5 25 38	GCVS
P1785	5 32 43 - 5 28 14	"
P1789	5 32 39 - 6 04	779904
P1795	5 32 44.7 - 4 37 33	CSI 79
P1799	5 32 44 - 5 18 50	GCVS
P1817	5 32 47.0 - 4 46 37	729902
P1828	5 32 46 - 5 41 26	GCVS
P1870	5 32 48 - 5 25 44	"
P1885	5 32 49 - 5 23 38	"
P1898	5 32 49 - 5 41 06	829909
P1902	5 32 48.9 - 6 10 09	749908
P1905	5 32 50.2 - 5 05 46	CSI 79
P1910	5 32 50 - 5 24 38	GCVS
P1922	5 32 51 - 5 22 26	"
P1931	5 32 50.9 - 6 00 20	729902
P1937	5 32 52 - 5 22 50	GCVS
P1946	5 32 54.3 - 4 30 44	729902
P1952	5 32 54 - 5 08 56	GCVS
P1953	5 32 53.5 - 5 11 01	CSI 79
P1955	5 32 51 - 5 14	779904
P1956	5 32 53.2 - 5 23 29	CSI 79
P1971		
P1988	5 32 55.7 - 5 12 45	740801
P1993	5 32 55.3 - 5 26 49	CSI 79
P2001	5 32 56 - 5 32 38	GCVS
P2006	5 32 57.9 - 5 11 45	740801
P2007	5 32 57.7 - 5 12 40	"
P2020	5 32 59 - 5 10 33	GCVS
P2021	5 32 58 - 5 17 03	"
P2029	5 33 00 - 5 13 03	"
P2030		
P2031	5 32 58.9 - 5 26 51	CSI 79
P2032	5 32 59 - 5 27 33	GCVS
P2033		
P2068	5 33 04 - 5 06 06	829909
P2074	5 33 03.7 - 5 17 53	CSI 79
P2084	5 33 05 - 5 11 21	GCVS
P2085	5 33 03.9 - 5 27 07	CSI 79
P2086	5 33 04.1 - 5 34 53	"
P2100		
P2118	5 33 08.2 - 5 14 04	CSI 79
P2119	5 33 09 - 5 14 16	GCVS
P2133	5 33 10 - 5 28 28	"
P2143		
P2164		
P2167	5 33 14 - 5 30 04	GCVS
P2171	5 33 16 - 5 07 34	
P2172	5 33 16 - 5 11 10	GCVS
P2173		
P2174		
P2181	5 33 17 - 5 09 10	GCVS
P2208		
P2216		
P2243	5 33 24 - 5 08 59	GCVS
P2244	5 33 24 - 5 10 00	829909
P2247	5 33 23.1 - 5 30 17	CSI 79
P2252		
P2257		
P2271	5 33 26.9 - 5 38 49	CSI 79
P2279	5 33 30 - 5 14 48	829909
P2284	5 33 30.9 - 5 24 20	CSI 79
P2292	5 33 32.0 - 5 41 50	749908
P2305	5 33 34.3 - 5 19 27	"
P2317	5 33 36.6 - 5 09 05	"
P2340		
P2346	5 33 44.5 - 4 23 26	749908
P2404	5 34 04.7 - 5 25 33	"
P2441	5 34 22.8 - 4 27 27	729902
P2445	5 34 22.9 - 5 01 20	749908
P2576	5 35 10.5 - 6 04 14	"
Q0122-379	1 22 02.2 -38 00 04	809908
Q0420-388	4 20 30.1 -38 51 50	
Q1101-264	11 00 59.9 -26 29 05	809908
Q1246-057	12 46 28.9 - 5 42 58	"
Q1309-056	13 09 00.7 - 5 36 43	"
R 15 IRS5	10 42 23 -58 58 56	
R 136	5 39 03.4 -69 07 34	CSI 79
R 627	11 21 39 +21 38 06	781106
RB 37	12 57 12 +28 16	679901
RB 38	12 57 12 +28 15	"
RB 40	12 57 18 +28 13	"
RB 42	12 57 18 +28 14	"
RB 45	12 57 18 +28 16	"

NAME	RA (1950)	DEC	POS REF
RB 46	12 57 18	+28 14	"
RB 74	12 57 42	+28 18	"
RB 85	12 57 48	+28 20	"
RCW 36 IR1	8 57 34.9	−43 32 16	
RCW 36 IR2	8 57 38.6	−43 33 47	
RCW 36 IR3	8 57 39.1	−43 33 08	
RCW 36 IR4	8 47 39.7	−43 34 17	
RCW 36 IR5	8 47 40.8	−43 32 34	
RCW 38	8 57 20.9	−47 18 50	
RCW 38	8 57 24.2	−47 18 50	
RCW 38 IRS1	8 57 23.5	−47 18 37	
RCW 38 IRS2	8 57 24.2	−47 18 50	
RCW 39 IR	9 01 43.5	−48 14 18	
RCW 42	9 22 45.5	−51 46 27	
RCW 57	11 09 43.9	−61 02 09	
RCW 57 IRS1	11 09 45.9	−61 02 06	
RCW 97	15 49 12.9	−54 26 27	
RCW 108	16 36 14.2	−48 45 54	
RCW 108	16 36 14.6	−48 45 53	
RCW 110B	16 50 40.3	−45 12 32	
RCW 113	16 53 24	−40 16 36	
RCW 117	17 05 36	−41 32 24	
RCW 117	17 06 01.5	−41 32 20	
RCW 121	17 14 57.3	−39 16 16	
RCW 121	17 14 58.0	−39 16 05	ED
RCW 121 IRS1	17 14 57.6	−39 16 16	
RCW 122	17 16 39.9	−38 54 15	
RCW 122	17 16 40.1	−38 54 18	
RCW 122	17 16 40.6	−38 54 18	
RED RECTANGLE	6 17 36.7	−10 36 42	ED
RED RECTANGLE	6 17 36.9	−10 36 51	CSI 79
RED RECTANGLE	6 17 37.0	−10 36 59	ED
RED RECTANGLE	6 17 37.0	−10 37 01	"
GAM RET	4 00 10.0	−62 17 54	CSI 79
R RET	4 33 01.0	−63 07 54	"
RX RET	3 47 16.2	−66 50 47	"
RG 0044−2958	0 44 26.2	−29 58 49	
RG 0050−2722	0 50 28.4	−27 22 17	
RGO 53	13 23 48	−47 13 36	779909
RGO 55	"	"	"
RGO 70	"	"	"
RGO 73	"	"	"
RGO 153	"	"	"
RGO 382	10 09 46.3	− 3 29 39	CSI 79
RGO 393	10 26 23.4	+ 1 06 28	"
RGO 402	10 48 18.9	+ 7 05 06	"
RGO 525	13 42 39	+18 03 42	709903
RGO 543	14 16 36	− 7 03 48	"
RGO 567	14 51 07	+19 21 12	"
RGO 581	15 16 52.2	− 7 32 20	CSI 79
RGO 625	16 24 13.9	+54 25 06	"
RGO 643	16 52 45.0	− 8 13 47	"
RGO 644AB	16 52 48.3	− 8 14 39	"
RGO 673	17 23 15.7	+ 2 10 12	"
RGO 699	17 55 22.9	+ 4 33 18	"
RGO 701	18 02 28.3	− 3 01 51	"
RGO 740	18 55 33.6	+ 5 51 23	"
RGO 745A	19 04 58.6	+20 48 56	"
RGO 745B	19 05 04.9	+20 48 05	"
RGO 820B	21 04 38.3	+38 29 29	"
RGO 9371	11 37 33	+67 36 24	709903
RGO 9653	19 17 50.9	− 7 45 16	CSI 79
RNO 54	5 39 18	+22 36	
RNO 90	16 31 00	−15 41	800101
RNO 91	16 31 36	−15 44	"
ROA 40	13 23 48	−47 13 36	779909
ROA 43	"	"	"
ROA 46	"	"	"
ROA 48	"	"	"
ROA 49	"	"	"
ROA 53	"	"	"
ROA 55	"	"	"
ROA 56	"	"	"
ROA 58	"	"	"
ROA 61	"	"	"
ROA 62	"	"	"
ROA 70	"	"	"
ROA 74	"	"	"
ROA 84	"	"	"
ROA 90	"	"	"
ROA 91	"	"	"
ROA 96	"	"	"
ROA 102	"	"	"
ROA 124	"	"	"
ROA 132	"	"	"
ROA 139	"	"	"
ROA 150	"	"	"
ROA 155	"	"	"
ROA 159	"	"	"
ROA 161	"	"	"
ROA 162	"	"	"
ROA 171	"	"	"
ROA 179	"	"	"
ROA 180	"	"	"
ROA 201	"	"	"
ROA 213	"	"	"
ROA 219	"	"	"
ROA 231	"	"	"
ROA 234	"	"	"
ROA 248	"	"	"
ROA 253	"	"	"
ROA 256	"	"	"
ROA 269	"	"	"
ROA 270	"	"	"
ROA 272	"	"	"
ROA 279	"	"	"
ROA 287	"	"	"
ROA 297	"	"	"
ROA 300	"	"	"
ROA 312	"	"	"
ROA 320	"	"	"
ROA 357	"	"	"
ROA 364	"	"	"
ROA 371	"	"	"
ROA 394	"	"	"
ROA 402	"	"	"
ROA 415	"	"	"
ROA 421	"	"	"

NAME	RA (1950)	DEC	POS REF
ROA 425	"	"	"
ROA 447	"	"	"
ROA 451	"	"	"
ROA 461	"	"	"
ROA 462	"	"	"
ROA 464	"	"	"
ROA 465	"	"	"
ROA 472	"	"	"
ROA 480	"	"	"
ROA 483	"	"	"
ROA 505	"	"	"
ROA 509	"	"	"
ROA 513	"	"	"
ROA 537	"	"	"
ROA 557	"	"	"
ROA 577	"	"	"
ROA 3598	"	"	"
ROA 5941	"	"	"
ROA 6113	"	"	"
ROB 29			
ROBERTS 22	10 19 44.6	−57 50 41	
ROBERTS 80	17 59 01	−23 37 36	IRC
ROBERTS 89	18 38 39	− 4 30	629902
ROBERTS 93	19 26 12	+19 29	"
ROSETTE IRS	6 31 59.0	+ 4 15 09	731003
ROSETTE NEB	6 31 58.7	+ 4 15 17	
ROSS 248	23 39 25.9	+43 55 12	CSI 79
ROSS 627	11 21 39	+21 38 06	
ROSS 640			
R20	0 58 58	−72 27	609903
R29	1 01 35	−72 23	"
R59	4 54 26.5	−69 17 13	CSI 79
R67	4 59 50.9	−70 15 40	"
R69	5 00 23	−68 31	609903
R71	5 02 50.1	−71 24 20	CSI 79
R76	5 06 01.9	−67 57 04	"
R92	5 20 54.6	−65 50 51	"
R94	5 21 38.6	−65 47 58	
R108	5 30 38	−67 19	609903
R117	5 32 41.9	−67 43 58	CSI 79
R143	5 39 12.7	−69 09 49	780108
R150	5 40 41.7	−69 41 05	CSI 79
S 27 #1	18 13 11.0	−19 53 39	
S 27 #2	18 13 46.8	−19 53 39	
S 27 #3	18 13 50.5	−19 53 08	
S 27 #4	18 14 08.9	−19 52 59	
S 27 #5	18 13 26.3	−19 49 00	
S 27 #5	18 14 27.4	−19 52 36	
S 27 #6	18 13 42.0	−19 52 05	
S 27 #7	18 14 20.4	−19 52 09	
S 27 #8	18 14 31.9	−19 52 00	
S 27 #8	18 14 39.7	−19 48 51	
S 27 #9	18 13 32.1	−19 51 47	
S 27 #10	18 14 18.7	−19 51 51	
S 27 #11	18 14 46.0	−19 51 24	
S 27 #12	18 13 20.3	−19 50 53	
S 27 #13	18 14 18.6	−19 50 57	
S 27 #14	18 14 39.2	−19 50 57	
S 27 #15	18 13 23.7	−19 50 21	
S 27 #16	18 13 24.7	−19 50 03	
S 27 #17	18 14 20.5	−19 50 21	
S 27 #18	18 13 50.7	−19 49 54	
S 27 #19	18 14 10.6	−19 49 54	
S 27 #20	18 14 26.6	−19 49 54	
S 27 #21	18 13 40.5	−19 49 41	
S 27 #22	18 14 14.7	−19 49 45	
S 27 #23	18 14 34.5	−19 49 45	
S 27 #24	18 14 18.7	−19 49 36	
S 27 #25	18 14 21.4	−19 49 36	
S 27 #26	18 13 22.1	−19 49 18	
S 27 #27	18 13 26.0	−19 49 18	
S 27 #28	18 14 10.4	−19 49 18	
S 27 #29	18 14 31.7	−19 49 18	
S 27 #30	18 13 53.4	−19 49 09	
S 27 #31	18 13 30.9	−19 49 00	
S 27 #32	18 14 30.3	−19 49 00	
S 27 #33	18 13 30.4	−19 49 09	
S 27 #34	18 13 21.7	−19 49 00	
S 27 #36	18 13 35.9	−19 48 51	
S 27 #37	18 14 21.5	−19 48 51	
S 27 #39	18 13 12.8	−19 48 47	
S 27 POS1	18 13 51	−19 45 00	ED
S 27 POS2	18 13 51	−19 46 00	"
S 27 POS3	18 13 51	−19 47 00	"
S 27 POS4	18 13 56	−19 45 30	"
S 27 POS5	18 13 56	−19 46 30	"
S 27 POS6	18 13 56	−19 47 30	"
S 27 POS7	18 13 58	−19 48 20	"
S 27 POS8	18 13 58	−19 54 20	"
S 27 POS9	18 14 00	−19 46 20	"
S 27 POS10	18 14 00	−19 47 20	"
S 27 POS11	18 14 00	−19 48 00	"
S 27 POS12	18 14 02	−19 48 20	"
S 27 POS13	18 14 02	−19 50 00	"
S 27 POS14	18 14 02	−19 53 20	"
S 27 POS15	18 14 02	−19 55 00	"
S 27 POS16	18 14 06	−19 47 20	"
S 27 POS17	18 14 06	−19 49 00	"
S 27 POS18	18 14 06	−19 50 40	"
S 27 POS19	18 14 06	−19 52 20	"
S 27 POS20	18 14 06	−19 54 00	"
S 27 POS21	18 14 06	−19 55 40	"
S 27 POS22	18 14 10	−19 48 00	"
S 27 POS23	18 14 10	−19 49 40	"
S 27 POS24	18 14 10	−19 53 00	"
S 27 POS25	18 14 10	−19 54 40	"
S 27 POS26	18 14 14	−19 48 40	"
S 27 POS27	18 14 14	−19 50 20	"
S 27 POS28	18 13 57	−19 48 10	"
S 27 POS29	18 14 00	−19 47 30	"
S 27 POS30	18 14 00	−19 48 10	"
S 27 POS31	18 14 00	−19 49 10	"
S 27 POS32	18 14 05	−19 48 10	"
S 71	18 59 28.0	+ 2 04 56	739909
S 88 P	19 44 41.0	+25 05 20	ED
S 88 S	19 44 42.5	+25 05 10	"
S 88 STAR 1	19 44 40.0	+25 05 40	"
S 88 STAR 5	19 44 38.5	+25 05 50	"

NAME	RA (1950)	DEC	POS REF
S 88B	19 44 40	+25 05 30	"
S 88B	19 44 41.8	+25 05 18	770711
S 93	19 52 56.5	+27 04 55	759901
S 104 #13			
S 106	20 25 34	+37 12 45	ED
S 106 #3 PEAK	20 25 33.0	+37 12 56	"
S106#3 15"N6E	20 25 33.5	+37 13 11	"
S106#3 2"S10W	20 25 32.2	+37 12 54	"
S106#3 7"N8E	20 25 33.7	+37 13 03	"
S106#3 7"S17W	20 25 31.6	+37 12 49	"
S106#3 7"S8E	20 25 33.7	+37 12 49	"
S106#3 7"S8W	20 25 32.3	+37 12 49	"
S 106 A	20 25 33.8	+37 12 54	"
S 106 B	20 25 33.8	+37 13 02	"
S 106 C	20 25 32.4	+37 13 04	"
S 106 C	20 25 34.3	+37 13 07	
S 106 FIELD 1	20 25 25	+37 12 30	
S 106 FIELD 2	20 25 42	+37 13 00	
S 106 FIELD 3	20 25 29	+37 07 30	
S 106 IR	20 25 35	+37 13 51	599901
S 106 IRS1	20 25 32.2	+37 12 36	
S 106 IRS2	20 25 32.5	+37 13 00	
S 106 IRS3	20 25 32.8	+37 12 45	
S 106 IRS4	20 25 32.8	+37 12 50	
S 106 IRS5	20 25 33.9	+37 12 59	
S 106 IRS6	20 25 34.1	+37 12 29	
S 106 IRS7	20 25 34.5	+37 12 41	
S 106 IRS8	20 25 34.6	+37 13 03	
S 106 IRS9	20 25 33.7	+37 11 14	
S 106 PS	20 25 33.8	+37 12 52	
S 106 SOURCE1	20 25 32.4	+37 12 40	ED
S 106 SOURCE1	20 25 33.0	+37 12 50	
S 106 SOURCE2	20 25 33.6	+37 12 50	ED
S 106 SOURCE2	20 25 34.3	+37 13 07	
S 106 SOURCE3	20 25 33.6	+37 13 10	ED
S 106 SOURCE3	20 25 33.8	+37 12 52	760902
S 106 S1	20 25 33.0	+37 12 45	ED
S 106 S2	20 25 34.5	+37 13 08	"
S 106A	20 25 30	+37 12 50	
S 130	20 42 27.8	+63 02 35	759901
S 138	22 30 47	+58 13	599901
S 140	22 17 40.6	+63 03 41	
S 140	22 17 41.3	+63 03 49	
S 140	22 17 41.6	+63 03 46	780202
S 140	22 17 42	+63 03 45	
S 140 #1	22 19 23.2	+62 56 15	
S 140 #2	22 19 30.4	+62 57 50	
S 140 #3	22 19 25.8	+63 00 05	
S 140 #4	22 17 25.1	+63 08 10	
S 140 #5	22 17 19	+63 04 40	
S 140 #6	22 17 27	+63 03 00	
S 140 IR	22 17 41.3	+63 03 49	
S 140 IR	22 17 42	+63 03 50	
S 140 IRS1	22 17 41.2	+63 03 44	
S 140 IRS1	22 17 41.3	+63 03 49	780203
S 140 IRS2	22 17 41.1	+63 04 02	
S 140 IRS3	22 17 42.7	+63 03 47	
S 146 IRS1	22 47 29.7	+59 38 55	
S 152	22 56 34	+58 31	599901
S 156	23 03 05.5	+59 58 13	759901
S 156A	23 03 04.6	+59 58 29	ED
S 157A	23 13 52	+59 46	599901
S 157B	"	"	"
S 158A	23 11 21.7	+61 13 50	740203
S 158G	23 11 34	+61 12	ED
S 159	23 13 23	+60 50 36	760601
S 159A	23 13 22.8	+60 50 24	739902
S 162A1	23 18 30	+60 53	599901
S 186	1 05 37.5	+62 51 40	759901
S 208	4 15 40.2	+52 51 39	"
S 228	5 10 00.4	+37 23 41	
S 228	5 10 11	+37 23 43	599901
S 235 IRS1	5 37 31	+35 39 55	ED
S 235 IRS1	5 37 45.1	+35 48 09	
S 235 IRS2	5 37 47	+35 48 40	ED
S 235 IRS2	5 37 48.9	+35 48 34	
S 235 IRS3	5 37 31.3	+35 40 49	
S 235 IRS3	5 37 51	+35 49 30	ED
S 235 IRS4	5 37 30.9	+35 40 01	
S 235 IRS5	5 37 18.7	+35 43 14	
S 235 IRS6	5 38 14.8	+35 49 50	
S 235 IRS7	5 38 24.4	+35 51 08	
S 235 IRS8	5 37 56.5	+35 42 41	
S 235 IRS9	5 37 29.7	+35 44 42	
S 235 IRS10	5 37 53.3	+35 57 01	
S 235 IRS11	5 37 38.7	+35 49 00	
S 235 IRS12	5 37 12.8	+35 49 00	
S 235A	5 37 21	+35 49	599901
S 235A	5 37 31.2	+35 40 44	
S 235B	5 37 31	+35 39 55	ED
S 235B	5 37 32	+35 40	
S 237	5 28 07	+34 14	599901
S 252 H−ALPHA	6 06 54.0	+20 30 50	ED
S 252A	"	"	"
S 252C			
S 255	6 09 58.5	+18 00 15	599901
S 255	6 09 58.6	+18 00 12	
S 255 #1	6 09 49.5	+17 59 56	
S 255 #2	6 09 54.5	+18 02 32	
S 255 #3	6 10 04.6	+18 03 20	
S 255 #4	6 10 28.3	+18 02 20	
S 255 #5	6 09 40.7	+17 56 55	
S 255 #6	6 09 30.5	+17 54 50	
S 255 IR	6 09 58.4	+18 00 12	
S 255 IRS1	"	"	771004
S 255/257	6 09 59.4	+17 59 48	
S 266	6 15 55.3	+15 18 00	759901
S 269 (1)	6 11 50.3	+13 50 33	
S 269 (2)	6 11 47.1	+13 50 33	
S 269 IRS1	6 11 46.0	+13 50 44	ED
S 269 IRS2	6 11 47.0	+13 50 32	740203
S 270	6 07 13	+12 50	599901
S 288	7 06 10.0	− 4 14 12	759901
S 307	7 33 16.6	−18 39 20	"
S−R 3	16 23 07.7	−24 27 26	
S−R 4	16 22 54.8	−24 14 01	729902
S−R 9	16 24 38.8	−24 15 24	"
S−R 10	16 24 53.9	−24 19 39	"

NAME	RA (1950) DEC	POS REF
	h m s ° ′ ″	
S−R 12	16 24 17.6 −24 34 59	"
S−R 13	16 25 43.6 −24 21 43	"
S−R 17	16 29 20 −24 34	599902
S−R 20		
S−R 22	16 22 22.8 −24 22 55	729902
S−R 24	16 23 56.5 −24 38 53	"
S−R 24 N	" "	"
S−R 24 S	" "	"
S−1	16 23 32.7 −24 16 44	730903
S−2	16 23 22.5 −24 18 13	"
S−3	16 22 18.8 −24 22 38	"
S−4	16 22 20.5 −24 23 39	"
S−16	16 22 35.4 −24 27 14	"
S−26	16 23 08.9 −24 14 13	"
S−28	16 23 19.7 −24 16 14	"
S−29	16 23 21.4 −24 14 13	"
SAN 1	5 29 42 − 3 08	729902
SAN 2	5 31 20 − 1 11	"
SAN 4	5 37 08 − 2 32 42	"
SAN 5	5 39 01 − 8 07 23	"
SANDULEAK	5 46 02.7 −71 17 13	"
SAO 062852	12 05 35.5 +39 56 01	CSI 79
SAO 062869	12 07 22.0 +39 42 41	"
SAO 76704	4 38 03.8 +25 53 50	SAO
SA29−130		
R SCL	1 24 39.9 −32 48 05	CSI 79
S SCL	0 12 51.0 −32 19 21	"
SY SCL	0 04 25 −29 53 30	GCVS
TT SCL	0 14 24 −30 30 31	"
U SCL	1 09 12.2 −30 22 46	CSI 79
X SCL	0 47 06 −35 11 25	GCVS
Y SCL	23 06 22.9 −30 24 17	CSI 79
SCO X−1	16 17 04 −15 31 15	GCVS
AH SCO	17 08 01.9 −32 15 51	CSI 79
AK SCO	16 51 23.0 −36 48 27	"
ALF SCO	16 26 20.1 −26 19 21	"
ALF SCO	16 26 21 −26 19 27	
BET SCO A	16 02 31.4 −19 40 10	CSI 79
BET SCO AB	" "	"
BET SCO C	" "	"
BM SCO	17 37 42.7 −32 11 20	"
DEL SCO	15 57 22.3 −22 28 49	"
LAM SCO	17 30 12.6 −37 04 08	"
NUU SCO	16 09 05.0 −19 19 54	"
OMI SCO	16 17 37.3 −24 03 00	"
PI SCO	15 55 49.3 −25 58 17	"
R SCO	16 14 40.3 −22 49 07	"
RR SCO	16 53 26.3 −30 30 06	"
RS SCO	16 51 59.7 −45 01 22	"
RT SCO	17 00 09.6 −36 51 30	"
RU SCO	17 38 42.9 −43 43 47	"
RW SCO	17 11 34.3 −33 22 43	"
RZ SCO	16 01 35.0 −23 58 25	"
S SCO	16 14 41.6 −22 46 06	"
SIG SCO	16 18 08.6 −25 28 27	"
ST SCO	16 33 22.7 −31 08 20	"
SU SCO	16 37 25.2 −32 17 00	"
SX SCO	17 44 06.4 −35 41 02	"
TAU SCO	16 32 45.9 −28 06 49	"
V381 SCO	17 43 40.9 −35 45 54	"
V407 SCO	17 49 07.9 −35 00 58	"
V450 SCO	17 39 02.4 −35 13 44	"
V635 SCO	17 18 50.3 −41 41 47	"
V636 SCO	17 19 05.3 −45 33 59	"
V644 SCO	17 24 11.9 −39 57 57	"
V861 SCO	16 53 06.7 −40 44 43	"
V861 SCO	16 53 07 −40 44 44	
V866 SCO	16 08 41 −18 31 00	GCVS
W SCO	16 08 49.7 −20 00 33	CSI 79
X SCO	16 05 35.2 −21 23 57	"
Y SCO	16 26 31 −19 14 19	GCVS
Z SCO	16 03 02.3 −21 36 19	CSI 79
22 SCO	16 27 09.9 −25 00 24	"
FR SCT	18 20 35 −12 42 36	GCVS
NOVA SCT 1970	18 43 00 − 8 36	
R SCT	18 44 48.7 − 5 45 35	CSI 79
RX SCT	18 34 24.4 − 7 38 40	"
RY SCT	18 22 42.6 −12 43 07	"
RZ SCT	18 23 48.9 − 9 13 55	"
S SCT	18 47 37.0 − 7 57 58	"
UY SCT	18 24 48.0 −12 30 02	"
SCULPTOR BM1	0 57 37 −34 11	ED
SCULPTOR BM3	0 58 04 −34 05	"
SCULPTOR BM4	0 58 03 −34 02	"
SCULPTOR BM5	0 58 14 −34 01	"
SCULPTOR BM6	0 58 25 −34 01	"
SCULPTOR BM7	0 57 40 −34 03	"
SCULPTOR BM8	0 57 30 −34 05	"
SCULPTOR BM9	0 57 29 −34 06	"
SCULPTOR BM10	0 57 36 −34 01	"
SCULPTOR BM11	0 57 37 −34 00	"
SCULPTOR BM12	0 57 51 −33 58	"
SCULPTOR BM13	0 57 55 −33 56	"
SCULPTOR BM14	0 57 58 −33 57	"
SCULPTOR BM15	0 57 25 −33 59	"
SCULPTOR BM16	0 57 20 −34 01	"
SCULPTOR BM17	0 56 55 −33 58	"
SCULPTOR BM18	0 57 04 −33 53	"
SCULPTOR BM19	0 57 23 −33 53	"
SCULPTOR BM20	0 57 45 −33 52	"
SCULPTOR BM21	0 57 44 −33 56	"
SCULPTOR BM22	0 57 14 −33 56	"
SCULPTOR BM23	0 57 40 −34 03	"
SCULPTOR BM24	0 57 09 −34 00	"
SCULPTOR BM25	0 58 07 −34 08	"
SCULPTOR V544	0 57 36 −33 46	"
ALF SER	15 41 48.1 + 6 34 52	CSI 79
BG SER	15 41 01 − 1 33 12	GCVS
BQ SER	18 33 47.1 + 4 21 20	CSI 79
CV SER	18 16 19.7 −11 39 14	"
DR SER	18 44 50.7 + 5 24 30	"
ETA SER	18 18 43.2 − 2 54 47	"
EU SER	18 16 19 −13 51 55	GCVS
GAM SER	15 54 08.3 +15 49 23	CSI 79
KAP SER	15 46 29.2 +18 17 39	"
LAM SER	15 44 00.7 + 7 30 29	"
NOVA SER 1970	18 28 17 + 2 34 40	GCVS
NOVA SER 1978	17 48 59.7 −14 43 08	ED

NAME	RA (1950) DEC	POS REF
	h m s ° ′ ″	
R SER	15 48 23.2 +15 17 01	CSI 79
RT SER	17 37 03.5 −11 55 09	"
S SER	15 19 18.9 +14 29 33	"
T SER	18 26 17.4 + 6 07 43	"
TAU 4 SER	15 34 09.0 +15 15 54	"
U SER	16 04 53.0 +10 03 47	"
VV SER	18 26 14 + 0 06 37	GCVS
W SER	18 06 58.3 −15 33 36	CSI 79
WX SER	15 25 31.7 +19 44 20	"
WX SER	15 25 32.0 +19 44 06	
ZET SER	17 57 50.3 − 3 41 18	CSI 79
16 SER	15 34 05.2 +10 10 32	"
SERPENS #1	18 27 29.3 + 1 13 10	
SERPENS #2	18 27 24.2 + 1 12 45	
SERPENS #3	18 27 17.0 + 1 09 27	
SERPENS #4	18 27 25.2 + 1 10 31	
SERPENS #5	18 27 19.5 + 1 08 27	
SERPENS #6	18 27 39.7 + 1 14 35	
SERPENS #7	18 27 37.2 + 1 12 31	
SERPENS #8	18 27 39.2 + 1 13 31	
SERPENS #9	18 27 13.2 + 1 16 31	
SERPENS #10	18 27 17.7 + 1 07 11	
SERPENS #11	18 27 23.2 + 1 07 01	
SERPENS #12	18 27 38.8 + 1 06 27	
SERPENS #13	18 27 28.2 + 1 17 34	
SERPENS #14	18 27 00.7 + 1 15 14	
SERPENS #15	18 27 27.5 + 1 19 52	
SERPENS #16	18 27 26.0 + 1 18 22	
SERPENS #17	18 27 16.5 + 1 20 36	
SERPENS #18	18 27 09.2 + 1 10 31	
SERPENS #19	18 27 25.2 + 1 08 49	
SERPENS #20	18 27 25.2 + 1 12 01	
SERPENS DC	18 27 25 + 1 12 40	
SERPENS OBJ.	18 27 24.5 + 1 12 40	
SEX A/A1009	10 09 − 4	ED
S SEX	10 32 22.3 − 0 04 59	CSI 79
Z SEX	10 08 24.1 + 2 48 17	"
ALF SGE	19 37 51.5 +17 53 49	"
FG SGE	20 09 42.9 +20 11 00	769910
HM SGE	19 39 41 +16 37 33	ED
GAM SGE	19 56 31.9 +19 21 17	CSI 79
R SGE	20 11 46.6 +16 34 25	"
S SGE	19 53 44.9 +16 30 03	"
U SGE	19 16 37.0 +19 31 03	"
X SGE	20 02 52.6 +20 30 16	"
SGR A	17 42 27 −29 03 00	ED
SGR A	17 42 29 −28 58 48	
SGR A	17 42 29 −28 59 20	
SGR A	17 42 29.7 −28 59 17	
SGR A	17 42 29.9 −28 59 15	
SGR A	17 42 30 −28 59 03	ED
SGR A	17 42 32 −28 59 42	
SGR A	17 42 32.5 −28 59 22	
SGR A	17 42 40 −29 02 00	
SGR A #1	17 42 28.4 −28 59 17	
SGR A #1	17 42 29.6 −28 59 17	750903
SGR A #2	17 42 28.4 −28 59 20	
SGR A #2	17 42 29.0 −28 59 21	750903
SGR A #3	17 42 28.6 −28 59 14	
SGR A #3	17 42 28.9 −28 59 14	750903
SGR A #4	17 42 28.6 −28 59 17	
SGR A #5	17 42 28.6 −28 59 20	
SGR A #5	17 42 29.9 −28 59 07	750903
SGR A #6	17 42 28.6 −28 59 23	
SGR A #7	17 42 28.8 −28 59 14	
SGR A #7	17 42 29.2 −28 59 12	750903
SGR A #8	17 42 28.8 −28 59 17	
SGR A #8	17 42 29.4 −28 58 48	750903
SGR A #9	17 42 28.8 −28 59 20	
SGR A #9	17 42 29.6 −28 59 23	750903
SGR A #10	17 42 28.8 −28 59 23	
SGR A #10	17 42 29.8 −28 59 12	750903
SGR A #11	17 42 28.4 −28 59 06	"
SGR A #11	17 42 28.8 −28 59 26	
SGR A #12	17 42 28.9 −28 59 25	750903
SGR A #12	17 42 29.0 −28 59 19	
SGR A #13	17 42 29.0 −28 59 22	
SGR A #14	17 42 29.1 −28 59 11	
SGR A #15	17 42 29.1 −28 59 14	
SGR A #16	17 42 29.1 −28 59 17	
SGR A #17	17 42 29.1 −28 59 20	
SGR A #18	17 42 29.1 −28 59 23	
SGR A #19	17 42 29.1 −28 59 26	
SGR A #20	17 42 29.1 −28 59 29	
SGR A #21	17 42 29.3 −28 59 19	
SGR A #22	17 42 29.3 −28 59 22	
SGR A #23	17 42 29.3 −28 59 25	
SGR A #24	17 42 29.4 −28 59 11	
SGR A #25	17 42 29.4 −28 59 14	
SGR A #26	17 42 29.4 −28 59 17	
SGR A #27	17 42 29.4 −28 59 20	
SGR A #28	17 42 29.4 −28 59 23	
SGR A #29	17 42 29.4 −28 59 26	
SGR A #30	17 42 29.4 −28 59 29	
SGR A #31	17 42 29.5 −28 59 19	
SGR A #32	17 42 29.5 −28 59 22	
SGR A #33	17 42 29.5 −28 59 25	
SGR A #34	17 42 29.6 −28 59 11	
SGR A #35	17 42 29.6 −28 59 14	
SGR A #36	17 42 29.6 −28 59 17	
SGR A #37	17 42 29.6 −28 59 20	
SGR A #38	17 42 29.6 −28 59 23	
SGR A #39	17 42 29.6 −28 59 26	
SGR A #40	17 42 29.6 −28 59 29	
SGR A #41	17 42 29.7 −28 59 19	
SGR A #42	17 42 29.7 −28 59 22	
SGR A #43	17 42 29.7 −28 59 25	
SGR A #44	17 42 29.9 −28 59 11	
SGR A #45	17 42 29.9 −28 59 14	
SGR A #46	17 42 29.9 −28 59 17	
SGR A #47	17 42 29.9 −28 59 20	
SGR A #48	17 42 29.9 −28 59 23	
SGR A #49	17 42 29.9 −28 59 26	
SGR A #50	17 42 30.1 −28 59 11	
SGR A #51	17 42 30.1 −28 59 14	
SGR A #52	17 42 30.1 −28 59 17	
SGR A #53	17 42 30.1 −28 59 20	
SGR A #54	17 42 30.1 −28 59 23	

NAME	RA (1950) DEC	POS REF
	h m s ° ′ ″	
SGR A #55	17 42 30.1 −28 59 26	
SGR A #56	17 42 30.3 −28 59 23	
SGR A #57	17 42 30.3 −28 59 26	
SGR A #58	17 42 30.6 −28 59 20	
SGR A #59	17 42 30.6 −28 59 23	
SGR A #60	17 42 30.6 −28 59 26	
SGR A #61	17 42 30.9 −28 59 20	
SGR A #62	17 42 30.9 −28 59 23	
SGR A #63	17 42 30.9 −28 59 26	
SGR A IRS 1	17 42 29.7 −28 59 18	
SGR A IRS 2	17 42 29.1 −28 59 23	
SGR A IRS 4	17 42 30.4 −28 59 24	
SGR A IRS 6	17 42 28.8 −28 59 17	
SGR A IRS 8	17 42 29.6 −28 58 50	
SGR A IRS 9	17 42 29.7 −28 59 25	
SGR A IRS 10	17 42 29.7 −28 59 14	
SGR A WEST	17 42 28.6 −28 59 30	ED
SGR A WEST	17 42 29.3 −28 59 17	
SGR A WEST	17 42 29.5 −28 59 17	730902
SGR A WEST	17 42 30.2 −28 59 16	
SGR A WEST NE	" "	
SGR A WEST SW	17 42 28.3 −28 59 39	
SGR A WEST SW	17 42 28.3 −28 59 49	
SGR A WEST(C)	17 42 29.8 −28 59 16	ED
SGR A WEST(E)	17 42 31.1 −28 59 16	"
SGR A WEST(N)	17 42 29.0 −28 59 20	780303
SGR A WEST(N)	17 42 29.8 −28 58 55	ED
SGR A WEST(S)	17 42 27.5 −29 00 04	
SGR A WEST(S)	17 42 29.8 −28 59 34	ED
SGR A WEST(W)	17 42 27.8 −28 59 16	"
SGR A WEST(1)	17 42 30.4 −28 59 16	"
SGR A WEST(2)	17 42 29.8 −28 59 09	"
SGR A WEST(3)	17 42 29.8 −28 59 16	"
SGR A WEST(4)	17 42 29.8 −28 59 24	"
SGR A WEST(5)	17 42 29.0 −28 59 14	"
SGR A WEST(6)	17 42 29.1 −28 59 21	"
SGR A WEST#1	17 42 30.1 −28 59 20	
SGR A WEST#2	17 42 31.3 −28 58 56	
SGR A WEST#3	17 42 30.8 −28 59 08	
SGR A WEST#4	17 42 30.2 −28 59 18	
SGR A WEST#5	17 42 29.6 −28 59 28	
SGR A WEST#6	17 42 28.9 −28 59 36	
SGR A WEST#7	17 42 28.1 −28 59 43	
SGR A WEST#8	17 42 27.4 −28 59 49	
SGR A WEST#9	17 42 26.6 −28 59 53	
SGR A WEST#10	17 42 31.7 −28 58 44	
SGR A WEST#12	17 42 28.7 −28 59 12	
SGR A WEST#13	17 42 29.4 −28 59 15	
SGR A WEST#14	17 42 30.2 −28 59 18	
SGR A WEST#15	17 42 30.9 −28 59 21	
SGR A WEST#16	17 42 31.7 −28 59 24	
SGR A WEST#17	17 42 27.8 −28 59 09	
SGR A 45"N	17 42 32 −28 58 57	ED
SGR A 45"S	17 42 32 −29 00 27	"
SGR B	17 44 13 −28 23 06	
SGR B2	17 44 10.0 −28 22 00	ED
SGR B2	17 44 10.7 −28 21 53	"
SGR B2	17 44 11 −28 21 30	
SGR B2	17 44 11 −28 22	
SGR B2	17 44 11 −28 22 00	
SGR B2	17 44 11 −28 22 30	
SGR B2	17 44 11.0 −28 22 00	
SGR B2	17 44 12 −28 21 44	
SGR B2	17 44 12 −28 22 12	ED
SGR B2	17 44 13 −28 22 00	
SGR B2	17 44 13.1 −28 22 49	ED
SGR B2	17 44 14.4 −28 22 34	
SGR B2	17 44 21 −28 21 54	
SGR B2 H2O	17 44 08 −28 22 06	
SGR B2 IRS 1	17 44 04.7 −28 21 18	
SGR B2 IRS 2	17 44 05.5 −28 21 02	
SGR B2 IRS 3	17 44 09.6 −28 22 35	
SGR B2 IRS 4	17 44 10.5 −28 20 34	
SGR B2 IRS 5	17 44 10.9 −28 23 56	
SGR B2 IRS 6	17 44 14.7 −28 21 30	
SGR B2 NIR 1	17 44 10 −28 21 00	
SGR B2 NIR 2	17 44 10 −28 22 24	
SGR B2 RADIO	17 44 09 −28 21 30	
SGR B2 1'N	17 44 14.4 −28 21 34	
SGR C		
SGR D		
SGR E		
SGR I #1	17 56 15 −29 03 36	
SGR I #2	17 56 31 −29 05 00	
SGR I #3	17 56 34 −29 04 46	
SGR I #4	17 56 45 −29 04 35	
SGR I #5	17 56 46 −29 04 43	
SGR I #6	17 56 50 −29 04 29	
SGR I #7	17 56 59 −29 04 24	
SGR I #8	17 56 59 −29 04 35	
SGR I #9	17 57 00 −29 03 42	
SGR I #10	17 57 11 −29 03 53	
SGR I #11	17 57 16 −29 04 35	
SGR I #12	17 57 16 −29 03 43	
SGR I #13	17 57 18 −29 03 30	
SGR I #14	17 57 18 −29 03 40	
SGR I #15	17 57 21 −29 03 57	
SGR I D6	17 55 15 −28 54 10	GCVS
SGR I D7		
SGR I D10		
SGR I D11		
SGR I D13	17 57 17 −28 53 13	GCVS
SGR I D14	17 57 33 −28 54 06	"
SGR I D16	17 56 52 −28 56 51	"
SGR I D17		
SGR I D18	17 56 35 −28 59 34	GCVS
SGR I D19	17 56 27 −28 57 34	"
SGR I D20	17 55 20 −28 57 45	"
SGR I D21	17 55 31 −29 01 15	"
SGR I D26	17 57 05 −29 00 26	"
SGR I D30	17 57 01 −29 04 20	"
SGR I D32	17 55 24 −29 03 33	"
SGR I D35	17 56 54 −29 07 03	"
SGR I D36	17 57 11 −29 08 43	"
SGR I D43	17 56 58 −29 13 26	"
SGR I D44	17 56 05 −29 15 06	"
SGR I D45		
SGR I D47		

NAME	RA (1950) DEC	POS REF
SGR I D49	17 56 53 −29 01 03	GCVS
SGR I D54	17 56 14 −29 02 11	"
SGR I D56	17 55 23 −29 03 00	"
SGR I D57	17 56 35 −29 03 16	"
SGR I D59	17 57 13 −29 03 55	"
SGR I D61		
SGR I D65		
SGR I D68	17 55 14 −29 11 22	GCVS
SGR I D71	17 57 42 −29 10 59	"
SGR I D74		
SGR I D77	17 55 22 −28 56 03	GCVS
SGR I D81		
SGR I D87		
SGR I D95		
SGR I D100		
SGR I D103	17 57 37 −28 49 53	GCVS
SGR I D106	17 57 09 −28 48 49	"
SGR I D117		
SGR I D133		
SGR I D139	17 57 36 −29 15 53	GCVS
SGR IRA	17 42 30 −28 59	
SGR IRB	17 44 24 −28 22	
SGR IRC	17 41 24 −29 26	
AO SGR	18 09 01.4 −29 52 20	CSI 79
AQ SGR	19 31 27.0 −16 29 01	"
AR SGR	18 56 39.7 −23 46 36	"
AX SGR	18 05 31.9 −18 33 47	"
EPS SGR	18 20 51.1 −34 24 35	"
ETA SGR	18 14 14.6 −36 46 40	"
FN SGR	18 50 57.2 −19 03 35	"
GAM SGR	18 02 35.6 −30 25 34	"
GU SGR	18 21 11.6 −24 16 51	"
KW SGR	17 48 50.9 −28 00 49	"
MUU SGR	18 10 46.3 −21 04 24	"
MV SGR	18 41 33 −21 00 24	GCVS
NOVA SGR 1977	18 35 11.8 −23 25 28	ED
NOVA SGR 1978	18 30 14.9 −20 08 11	780412
NUU 1 SGR	18 51 09.0 −22 48 28	CSI 79
PI SGR	19 06 47.3 −21 06 16	"
R SGR	19 13 45.7 −19 23 48	"
RR SGR	19 52 48.9 −29 19 16	"
RT SGR	20 14 25.6 −39 16 55	"
RV SGR	18 24 41.3 −33 21 25	"
RW SGR	19 10 59.0 −18 56 51	"
RX SGR	19 11 37.4 −18 54 02	"
RY SGR	19 13 16.9 −33 36 39	"
RZ SGR	20 11 59.5 −44 34 05	"
S SGR	19 16 31.5 −19 06 42	"
ST SGR	18 58 42.3 −12 49 56	"
SZ SGR	17 42 00.1 −18 38 13	"
T SGR	19 13 23.2 −17 03 54	"
U SGR	18 28 56.4 −19 09 41	"
UPS SGR	19 18 51.7 −16 03 01	"
UW SGR	19 43 32.5 −18 16 29	"
VV SGR	17 54 06 −19 19 56	GCVS
VX SGR	18 05 00.9 −22 13 50	CSI 79
VX SGR	18 05 03.0 −22 13 56	"
VX SGR	18 05 05.0 −22 14 00	"
V348 SGR	18 37 18.3 −22 57 29	CSI 79
V348 SGR	18 37 24 −23 03	
V350 SGR	18 42 19.0 −20 42 00	CSI 79
V540 SGR	17 56 42.0 −35 55 32	"
V585 SGR	18 01 12 −35 43 44	GCVS
V659 SGR	18 08 32 −36 25 06	"
V745 SGR	17 52 07 −29 07 29	"
V758 SGR	17 46 49 −29 00 04	"
V774 SGR	17 51 24 −23 13 38	"
V781 SGR	17 52 47.9 −28 01 24	CSI 79
V1017 SGR	18 28 53 −29 26 01	GCVS
V1921 SGR	18 35 44 −21 46 13	"
V1942 SGR	19 16 17.7 −16 00 02	CSI 79
V1943 SGR	20 03 51 −27 22 06	GCVS
V2464 SGR	17 56 35 −29 03 18	
V2467 SGR	17 56 36 −29 03 59	
V2478 SGR	17 57 01 −29 04 29	
V3876 SGR	18 30 14.9 −20 08 11	
W SGR	18 01 49.4 −29 35 01	CSI 79
X SGR	17 44 24.6 −27 48 48	"
Y SGR	18 18 26.4 −18 53 01	"
Z SGR	19 16 45.9 −21 01 41	"
9 SGR	18 00 48.3 −24 21 47	"
22 SGR	18 24 53.0 −25 27 03	"
SH 255	6 09 58.4 +18 00 12	771004
SH2−71	18 59 28.0 + 2 04 56	739909
SH2−106	20 25 34.1 +37 12 42	
SH2−106 #2	20 25 33.7 +37 12 47	ED
SH2−106 #3	20 25 33.7 +37 12 37	"
SH2−106 #4	20 25 34.5 +37 12 37	"
SH2−106 #5	20 25 34.5 +37 12 47	"
SH2−106 #6	20 25 34.1 +37 12 55	"
SH2−106 #7	20 25 33.0 +37 12 42	"
SH2−106 #8	20 25 34.1 +37 12 29	"
SH2−149 IR	22 54 20 +58 15	
SH2−149 IRS	" "	780711
SH2−149A		"
SH2−157.1	23 13 +59 13	729906
SH2−266	6 15 55.3 +15 18 00	759901
SIMEIS 130		
SIMEIS 188#2B	18 06 56 −24 07 36	
SIRIUS	6 42 56.7 −16 38 45	CSI 79
SK 14−67		
SK 52−68		
SK 107−68		
SK 108−69		
SK 116−69		
SK 120−69		
SK 152−69		
SK 213−69		
SK 228−67		
SK 256−69		
SK 280−69		
SK−65−9		
SK−65−10		
SK−65−11		
SK−65−40		
SK−66−12		
SK−66−137		
SK−67−2		

NAME	RA (1950) DEC	POS REF
SK−67−12		
SK−67−110		
SK−67−120		
SK−67−159		
SK−67−224		
SK−68−14		
SK−68−107		
SK−68−135		
SK−68−140		
SK−68−177		
SK−68−179		
SK−69−104		
SK−69−51		
SK−69−68		
SK−69−108		
SK−69−213		
SK−69−215		
SK−69−228		
SK−69−247		
SK−69−253		
SK−69−254		
SK−69−274		
SK−69−279		
SK−70−32		
SK−70−116		
SK−71−17		
SLS 1267	9 10 −50 15	ED
SLS 2778	12 50 −62 36	"
SLS 3981	17 10 −40 17	"
SMC B 2	0 46 02.4 −73 38 32	809910
SMC B 5	0 46 30.1 −73 37 32	"
SMC B 8	0 46 35.2 −73 29 30	"
SMC B 10	0 46 53.6 −73 29 01	"
SMC B 13	0 47 03.9 −73 30 21	"
SMC B 18	0 47 20.6 −73 24 18	"
SMC B 22	0 47 31.3 −73 38 46	"
SMC B 23	0 47 33.3 −73 24 42	"
SMC B 24	0 47 35.0 −73 38 05	"
SMC B 25	0 47 36.4 −73 31 13	"
SMC B 28	0 47 39.3 −73 28 23	"
SMC B 30	0 47 46.3 −73 34 10	"
SMC B 31	0 47 47.0 −73 24 59	"
SMC B 36	0 47 53.9 −73 24 38	"
SMC B 39	0 48 07.4 −73 29 03	"
SMC B 40	0 48 16.8 −73 29 49	"
SMC B 45	0 48 29.0 −73 29 03	"
SMC B 47	0 48 37.5 −73 39 06	"
SMC B 52	0 49 02.5 −73 44 01	"
SMC B 65	0 49 39.8 −73 39 24	"
SMC B 74	0 50 25.9 −73 30 50	"
SMC N76B K1	1 01 23.0 −72 22 04	
SMC N76B K2	1 01 29.7 −72 22 35	
SMC N76B K3	1 01 29.5 −72 22 26	
SN 1	16 18 30.2 − 0 09 13	819914
SN 1972E	13 37 05.2 −31 23 21	759903
SN 1975A	6 14 16 −21 19	ED
SOURCE Q	4 36 22.6 +25 47 22	
SOURCE 1	16 23 32.7 −24 16 44	
SOURCE 2	16 23 22.5 −24 18 13	
SOURCE 3	16 22 18.8 −24 22 38	
SOURCE 4	16 22 20.5 −24 23 39	
SOURCE 16	16 22 35.4 −24 27 14	730903
SS 7	7 31 00.5 −11 42 08	739903
SS 29	11 06 27.3 −65 31 02	"
SS 65	16 47 53.3 −37 12 59	"
SS 73	17 03 30.3 −45 20 08	"
SS 76	17 05 47.1 −27 08 44	"
SS 78	17 06 57.7 −32 55 05	"
SS 96	17 38 04.8 −36 46 14	"
SS 110	17 51 06.2 −34 26 28	"
SS 117	17 59 07.6 −31 59 14	"
SS 123	18 01 45.5 −21 51 43	"
SS 125	18 02 34.8 −24 30 57	"
SS 141	18 08 53.9 −33 11 27	"
SS 166 EAST	18 26 16.7 −17 29 14	"
SS 166 WEST	" "	"
SS 167	18 28 40.7 −18 17 40	"
SS 170	18 31 38.4 − 0 28 45	"
SS 433	19 09 18 + 4 53 54	
SS 433	19 09 21.3 + 4 53 54	809912
ST 3	20 19 46 +37 14	669904
STELLAR OBJ	13 50 40 −61 59 18	
STEPANIAN	15 35 44 +19 01 30	809911
STRAND 58		
SW 77	16 23 +26	ED
SWST 1	18 12 58.8 −30 53 10	769910
T ANON IRS1	10 36 50.4 −58 20 44	
T ANON IRS2	10 36 44.1 −58 20 47	
T ANON IRS3	10 36 44.2 −58 22 09	
T ANON IRS5	10 36 35.6 −58 25 06	
T 6B		
T 23		
T 29		
T 69		
T 90		
T 258		
TAU #1	4 15 34.6 +28 12 01	
TAU #2	4 18 50.8 +28 19 35	
TAU #3	4 20 22.6 +24 53 13	
TAU #4	4 22 37.4 +24 01 03	
TAU #5	4 24 00.9 +25 59 36	
TAU #6	4 26 05.7 +24 37 17	
TAU #7	4 26 22.0 +24 26 29	
TAU #8	4 27 40.4 +25 54 59	
TAU #9	4 29 09.6 +24 27 17	
TAU #10	4 29 37.7 +23 52 07	
TAU #11	4 29 39.2 +25 46 14	
TAU #12	4 30 05.2 +24 03 39	
TAU #13	4 30 21.7 +26 09 18	
TAU #14	4 35 53.4 +26 25 14	
TAU #15	4 36 22.8 +25 47 08	
TAU #16	4 36 34.4 +26 05 35	
TAU #17	4 36 40.6 +25 10 11	
TAU #18	4 36 51.8 +25 39 13	
TAU #19	4 41 14.3 +25 19 20	
TAU #20	4 44 01.9 +26 05 26	
TAU #21	4 45 44.1 +25 32 59	
TAU #22	4 15 40.9 +28 12 53	

NAME	RA (1950) DEC	POS REF
TAU #23	4 29 13.5 +24 22 40	
TAU #24	4 29 28.9 +24 13 38	
TAU #25	4 29 30.1 +24 13 44	
TAU #26	4 30 04.7 +24 03 18	
TAU #27	4 30 32.3 +24 15 04	
TAU #28	4 30 32.7 +24 14 54	
TAU #29	4 34 12.0 +25 11 30	
TAU #30	4 40 30.7 +25 06 03	
TAU A	5 31 30 +21 59	RNGC
TAU−AUR STAR4	4 38 13 +28 34 16	
AA TAU	4 31 54 +24 22 46	GCVS
ALF TAU	4 33 02.9 +16 24 36	CSI 79
ALF TAU	4 33 03 +16 24 41	
BET TAU	5 23 07.7 +28 34 00	CSI 79
BP TAU	4 16 08.9 +28 59 01	"
BW TAU	4 30 31 + 5 15 03	GCVS
CE TAU	5 29 16.7 +18 33 31	CSI 79
CI TAU	4 30 52 +22 43 50	GCVS
CQ TAU	5 32 54.1 +24 43 02	CSI 79
CT TAU	5 55 41.7 +27 04 38	"
CW TAU	4 11 11 +28 03 20	GCVS
CX TAU	4 11 44 +26 40 54	"
CY TAU	4 14 30 +28 13 31	"
CZ TAU	4 15 27 +28 09 45	"
DD TAU	4 15 27 +28 09 09	"
DD TAU IRS	4 15 35 +28 11	
DE TAU	4 18 49 +27 48 02	GCVS
DEL TAU	4 20 02.7 +17 25 35	CSI 79
DF TAU	4 24 00 +25 35 42	GCVS
DG TAU	4 24 00.9 +25 59 36	780909
DH TAU	4 26 37 +26 26 31	GCVS
DI TAU	4 26 38 +26 26 19	"
DK TAU	4 27 40.4 +25 54 59	780909
DL TAU	4 30 36 +25 14 22	GCVS
DM TAU	4 30 57 +18 03 37	"
DN TAU	4 32 25 +24 08 56	"
DO TAU	4 35 25 +26 04 56	"
DO TAU/EAST	" "	
DP TAU	4 39 34 +25 10 03	GCVS
DQ TAU	4 43 59 +16 54 38	"
DR TAU	4 44 12 +16 53 19	"
DS TAU	4 44 39 +29 20 00	"
DV TAU	5 28 10.3 +18 31 25	CSI 79
EPS TAU	4 25 41.5 +19 04 15	"
ETA TAU	3 44 30.3 +23 57 07	"
FM TAU	4 11 07 +28 05 14	GCVS
FN TAU	4 11 24 +28 21 43	"
FP TAU	4 11 43 +26 38 36	"
FX TAU	4 27 13 +24 19 41	"
GAM TAU	4 16 56.6 +15 30 29	CSI 79
GG TAU	4 29 37 +17 25 25	GCVS
GH TAU	4 30 04.7 +24 03 18	780909
GI TAU	4 30 32.3 +24 15 04	"
GK TAU	4 30 32.7 +24 14 54	"
GO TAU	4 40 00 +25 14 37	GCVS
HK TAU	4 28 31 +24 18 36	"
HK TAU G1	4 29 41 +24 12	ED
HK TAU G2	4 29 18 +24 16	"
HL TAU	4 28 44.4 +18 07 37	760504
HN TAU	4 30 41 +17 52 27	GCVS
HO TAU	4 32 05 +22 26 21	"
HP TAU	4 32 48 +22 48 18	"
HP TAU G1	4 32 52.4 +22 48 53	ED
HP TAU G2	4 32 54.2 +22 48 10	"
HP TAU G3	4 32 53.7 +22 48 06	"
IK TAU	3 50 39 +11 15 01	GCVS
IK TAU	3 50 46.0 +11 15 42	
IQ TAU	4 26 54 +26 00 42	GCVS
IS TAU	4 30 46 +26 00 27	"
KAP TAU	4 22 23.0 +22 10 50	CSI 79
NML TAU	3 50 40 +11 15	650701
R TAU	4 25 33.4 +10 03 07	CSI 79
R TAU	4 25 36.0 +10 03 30	
RR TAU	5 36 23.3 +26 20 56	CSI 79
RU TAU	5 49 44 +15 57 33	GCVS
RV TAU	4 44 01.9 +26 05 26	780909
RX TAU	4 35 30.4 + 8 14 12	CSI 79
RY TAU	4 18 50.8 +28 19 35	780909
RY TAU 40"E	4 18 51.9 +28 19 29	ED
RY TAU 40"N	4 18 50.8 +28 20 15	"
RY TAU 40"S	4 18 50.8 +28 18 55	"
RY TAU 40"W	4 18 50.1 +28 19 35	"
S TAU	4 26 27.9 + 9 49 56	CSI 79
ST TAU	5 42 13.3 +13 33 23	"
SU TAU	5 46 11.9 +19 03 00	"
SW TAU	4 21 54.7 + 4 00 32	"
SZ TAU	4 34 20.1 +18 26 33	"
T TAU	4 19 04.1 +19 25 05	"
T TAU N	" "	"
T TAU S	" "	"
T TAU 5"E	4 19 04.4 +19 25 06	ED
T TAU 5"N	4 19 04.1 +19 25 11	"
T TAU 5"S	4 19 04.1 +19 25 01	"
T TAU 5"W	4 19 03.8 +19 25 06	"
T TAU 40"E	4 19 06.7 +19 25 06	"
T TAU 40"N	4 19 04.1 +19 25 46	"
T TAU 40"S	4 19 04.1 +19 24 26	"
T TAU 40"W	4 19 01.6 +19 25 06	"
T TAU 70"W	4 18 59.4 +19 25 06	"
THE 1 TAU	4 25 42.9 +15 51 09	CSI 79
THE 2 TAU	4 25 48.2 +15 45 40	"
TT TAU	4 48 22.9 +28 26 34	"
TU TAU	5 42 09.7 +24 24 00	"
TX TAU	4 05 08.3 +26 28 08	"
UX TAU	4 27 09.9 +18 07 21	"
UX TAU A	" "	"
UX TAU B	" "	"
UZ TAU	4 29 39.0 +25 46 31	"
UZ TAU F,P	4 29 39.2 +25 46 14	780909
V TAU	4 49 08.3 +17 27 17	CSI 79
VY TAU	4 36 18 +22 42 04	GCVS
V410 TAU	4 15 23 +28 20 40	"
W TAU	4 25 02.7 +15 55 55	CSI 79
WW TAU	3 58 34.5 +30 06 56	"
XZ TAU	4 28 46.1 +18 07 36	760504
Y TAU	5 42 40.4 +20 40 32	CSI 79
Z TAU	5 49 32.1 +15 47 03	"
ZET TAU	5 34 39.2 +21 06 49	"

NAME	RA (1950) DEC	POS REF
	h m s ° ′ ″	
10 TAU	3 34 19.0 + 0 14 38	"
17 TAU	3 41 54.0 +23 57 26	"
20 TAU	3 42 50.7 +24 12 46	"
23 TAU	3 43 21.1 +23 47 38	"
27 TAU	3 46 10.9 +23 54 06	"
28 TAU	3 46 12.3 +23 59 07	"
45 TAU	4 08 40.3 + 5 23 38	"
46 TAU	4 10 51.3 + 7 35 22	"
57 TAU	4 17 08.4 +13 54 57	"
58 TAU	4 17 45.9 +14 58 36	"
63 TAU	4 20 32.6 +16 39 42	"
64 TAU	4 21 12.5 +17 19 46	"
68 TAU	4 22 35.5 +17 48 54	"
76 TAU	4 25 33.2 +14 37 51	"
90 TAU	4 35 21.5 +12 24 42	"
105 TAU	5 04 55.9 +21 38 24	"
111 TAU	5 21 30.2 +17 20 18	"
119 TAU	5 29 16.7 +18 33 31	"
139 TAU	5 54 53.3 +25 56 58	"
TC 1	17 41 52.6 −46 04 10	769910
BL TEL	19 02 43.9 −51 29 41	CSI 79
BR TEL	20 20 13.9 −53 01 53	
NT TEL	19 18 56 −50 29	
RR TEL	20 00 18.9 −55 51 30	CSI 79
RS TEL	18 15 06.9 −46 34 05	"
RX TEL	19 03 17.9 −46 02 53	"
SV TEL	18 52 27.9 −49 32 03	"
V TEL	19 14 21.1 −50 32 54	"
TERZAN 2	17 24 20.8 −30 45 36	
TERZAN 5	17 45 00.1 −25 45 52	719901
NEAR TERZAN 5	17 44 56.1 −25 44 52	ED
TH2−B	13 25 16 −63 33 48	759905
TH3−1	17 02 40 −25 21 00	809909
TH3−3	17 14 10 −28 56 18	789908
TH3−4	17 15 38 −31 36 00	"
TH3−5	17 15 51 −30 51 06	"
TH3−6	17 16 07 −31 09 45	"
TH3−7	17 17 51.7 −29 19 54	769910
TH3−8	17 19 37.4 −32 11 17	"
TH3−9	17 20 45 −30 59 06	789908
TH3−10	17 21 27 −30 49 12	"
TH3−11	17 21 05 −31 40 48	"
TH3−12	17 21 55 −29 42 42	"
TH3−13	17 22 06 −30 38 06	"
TH3−14	17 22 37 −26 55 12	819916
TH3−16	17 24 13 −29 18 48	789908
TH3−17	17 24 21 −29 00 36	"
TH3−18	17 25 17 −28 36 18	"
TH3−19	17 25 32 −28 25 06	"
TH3−20	17 25 55.0 −29 41 01	769910
TH3−24	17 27 39 −30 15 00	819916
TH3−25	17 27 39 −27 03 42	789908
TH3−27	17 32 54.6 −24 23 30	769910
TH3−30	17 30 34 −28 05 36	819916
TH3−31	17 31 06 −29 27 36	"
TH3−34	17 34 30 −32 13 42	"
TH3−55	17 27 45 −30 58 54	"
TH4−3	17 45 36.0 −22 15 53	769910
TH4−6	17 48 00.8 −18 46 00	"
TH4−7	17 49 22.0 −21 50 33	"
TH4−8	17 49 42.0 −21 14 00	"
TH4−10	17 54 11 −18 06 24	819917
TON 153	13 17 34.2 +27 43 52	
TON 155	13 18 53.7 +29 03 30	809908
TON 156	13 18 54.8 +29 03 01	
TON 157	13 21 00.0 +29 25 45	
TON 157	13 21 00.3 +29 25 45	809908
TON 202	14 25 21.9 +26 45 38	"
TON 256	16 12 08.7 +26 11 46	"
TON 490	10 11 05.6 +25 04 10	
TON 490	10 11 05.7 +25 04 11	809908
TR 14 IRS2	10 42 18.5 −59 18 45	
TR 15 IRS1	10 43 11.0 −59 07 07	
TR 15 IRS3	10 42 47.8 −59 00 05	
TR 15 IRS4	10 42 39.1 −59 08 29	
TR 16 IRS3	10 43 14.2 −59 24 18	
TR 16 IRS4	10 42 58.6 −59 22 14	
TR 16 IRS5	10 42 52.1 −59 21 06	
TR 16 IRS7	10 42 47.2 −59 22 29	
TR 16−100		
TR 24 IRS4	16 53 33.6 −40 24 25	
TR 24 IRS5	16 53 36.6 −40 21 09	
TR 24 IRS7	16 53 23.1 −40 19 56	
TR 24 IRS9	16 53 11.0 −40 26 29	
TR 24 IRS10	16 53 23.6 −40 17 14	
TR 27 1	17 32 54 −33 27	739904
TR 27−28	17 33 29 −33 24 10	
RV TRA	15 27 53.9 −62 22 56	CSI 79
V TRA	16 44 53.9 −67 41 42	"
X TRA	15 09 29.0 −69 53 34	"
TRAPEZIUM	5 32 48.5 − 5 25 12	740903
TRAPEZIUM	5 32 48.5 − 5 25 17	
TRAPEZIUM #1	5 32 47.0 − 5 24 20	ED
TRAPEZIUM #2	5 32 49.7 − 5 25 01	CSI 79
TRAPEZIUM #3	5 32 48.2 − 5 24 20	ED
TRAPEZIUM 1'S	5 32 48.5 − 5 24 12	"
R TRI	2 33 59.8 +34 02 52	779907
RW TRI	2 22 42 +27 52 20	GCVS
EPS TUC	23 57 19.9 −65 51 17	CSI 79
S TUC	0 20 47.3 −61 57 19	"
T TUC	22 37 16.7 −61 48 53	"
U TUC	0 55 44.9 −75 15 42	"
47 TUC	0 21 53 −72 21	RNGC
47 TUC #1406	0 19 40 −72 32	ED
47 TUC #1407	" "	"
47 TUC #1414	0 20 30 −72 34	"
47 TUC #1421	0 20 50 −72 38	"
47 TUC #1425	0 21 40 −72 37	"
47 TUC #1505	0 20 40 −72 29	"
47 TUC #1510	0 19 40 −72 32	"
47 TUC #1513	0 20 40 −72 30	"
47 TUC #1518	0 20 40 −72 32	"
47 TUC #1602	0 21 32 −72 32	"
47 TUC #1603	0 21 28 −72 32	"
47 TUC #1604	0 21 23 −72 33	"
47 TUC #2416	0 19 10 −72 28	"
47 TUC #2426	0 19 30 −72 29	"
47 TUC #2525	0 20 10 −72 28	"
47 TUC #2603	0 19 43 −72 27	"
47 TUC #2605	0 19 44 −72 25	"
47 TUC #3407	0 18 30 −72 18	"
47 TUC #3410	0 18 50 −72 19	"
47 TUC #3501	0 19 00 −72 21	"
47 TUC #3512	0 19 40 −72 17	"
47 TUC #4411	0 21 10 −72 07	"
47 TUC #4415	0 21 30 −72 07	"
47 TUC #4417	" "	"
47 TUC #4418	0 21 40 −72 06	"
47 TUC #4503	0 20 20 −72 12	"
47 TUC #4603	0 21 46 −72 11	"
47 TUC #5309	0 24 00 −72 06	"
47 TUC #5312	0 24 30 −72 07	"
47 TUC #5404	0 22 10 −72 07	"
47 TUC #5406	0 22 30 −72 06	"
47 TUC #5422	0 24 00 −72 08	"
47 TUC #5427	0 24 10 −72 11	"
47 TUC #5527	0 23 30 −72 10	"
47 TUC #5529	0 23 40 −72 11	"
47 TUC #5627	0 23 06 −72 11	"
47 TUC #5739	0 22 54 −72 15	"
47 TUC #6407	0 25 10 −72 14	"
47 TUC #6408	0 25 00 −72 15	"
47 TUC #6502	0 24 10 −72 13	"
47 TUC #6509	0 24 00 −72 14	"
47 TUC #7320	0 25 30 −72 23	"
47 TUC #7502	0 24 00 −72 29	"
47 TUC #7507	0 23 50 −72 27	"
47 TUC #7525	0 24 00 −72 31	"
47 TUC #8406	0 22 40 −72 35	"
47 TUC #8416	0 24 20 −72 33	"
47 TUC #8517	0 23 10 −72 33	"
47 TUC #8518	0 23 19 −72 33	"
47 TUC A8	0 21 53 −72 21	RNGC
47 TUC A19	" "	"
47 TUC R10	" "	"
47 TUC R17	" "	"
47 TUC R18	" "	"
47 TUC R23	" "	"
47 TUC R26	" "	"
47 TUC R32	" "	"
47 TUC R36	" "	"
47 TUC V1	" "	"
47 TUC V2	" "	"
47 TUC V3	" "	"
47 TUC V4	" "	"
47 TUC V5	" "	"
47 TUC V6	" "	"
47 TUC V7	" "	"
47 TUC V8	" "	"
47 TUC V11	" "	"
47 TUC V13	" "	"
47 TUC V15	" "	"
47 TUC V16	" "	"
47 TUC V17	" "	"
47 TUC V18	" "	"
47 TUC V19	" "	"
47 TUC V21	" "	"
47 TUC V25	" "	"
47 TUC V28	" "	"
47 TUC W3	" "	"
47 TUC W12	" "	"
47 TUC W12A	" "	"
47 TUC W76	" "	"
47 TUC W77	" "	"
47 TUC W78	" "	"
47 TUC W81	" "	"
47 TUC W300	" "	"
TYCHO SNR	0 23 03 +63 50 06	
T1032−283	10 32 −28 18	ED
T1038−290	10 38 −29 00	"
T1238−364	12 38 −36 24	"
T1350−383	13 50 −38 18	"
T1351−375	13 51 17.3 −37 31 51	789906
UCL 1	5 32 54 − 5 24 54	
UCL 2	5 39 00 − 1 55 00	ED
UCL 4	2 22 00 +61 52 30	
UCL 4	2 22 00 +61 52 54	
UCL 4A	2 23 18 +61 39 12	
UCL 4B	2 23 06 +62 02 30	
UCL 7	20 30 34 +40 04 24	
UCL 8	18 00 33 −24 23 24	
UCL 9	17 57 30 −24 04 18	
UCL 10	17 27 15 −34 39 42	
UCL 11 #1	17 21 29 −34 06 00	
UCL 11 #2	17 22 22 −34 17 36	
UCL 12	17 25 55 −36 39 06	
UCL 13	17 19 52 −35 51 42	
UCL 14 #1	17 17 26 −35 43 12	
UCL 14 #2	17 17 08 −35 47 42	
UCL 14 #3	17 16 50 −35 51 48	
UCL 15	17 14 02 −36 16 54	
UCL 16	17 16 42 −38 57 42	
UCL 17	17 05 48 −41 31 36	
UCL 18	16 56 02 −40 07 36	
UCL 18A	16 57 02 −40 32 06	
UCL 19	16 37 29 −46 26 54	
UCL 20	16 37 31 −47 03 48	
UCL 21	16 33 00 −47 22 42	
UCL 22	16 18 39 −49 55 54	
UCL 23	16 18 06 −50 15 06	
UCL 24	16 17 38 −50 28 12	
UCL 25	16 16 59 −50 30 42	
UCL 26	16 16 35 −50 45 48	
UCL 27	16 16 15 −50 54 06	
UCL 28	16 12 55 −51 09 48	
UCL 29	16 08 14 −51 20 00	
UCL 30	16 07 30 −51 22 06	
UCL 31	16 05 44 −51 49 24	
UCL 32	16 06 21 −52 01 00	
UCL 33	15 55 08 −53 37 36	
UCL 34	15 49 51 −54 26 48	
UCL 34A	15 49 00 −54 25 12	
UCL 35	9 00 05 −47 31 42	
UCL 36	8 57 21 −47 17 42	
UCL 37	8 57 42 −43 35 54	
UCL 39	19 08 27 + 9 01 30	
UCL 41	17 13 06 −37 54 54	
UCL 42	17 08 45 −38 31 30	
UCL 43	17 08 18 −39 06 24	
UCL 43A	17 07 54 −39 05 42	
UCL 44	17 02 54 −40 49 06	
UCL 45	17 01 00 −40 43 06	
UGC 94	0 07 51.3 +25 33 16	769909
UGC 98	0 08 05.9 +32 42 18	"
UGC 100	0 08 11.5 +33 04 24	"
UGC 238	0 22 25.6 +31 04 04	"
UGC 255	0 24 10.5 +31 25 35	"
UGC 279	0 25 36.6 +30 31 33	"
UGC 433	0 38 18 +31 27	UGC
UGC 562	0 52 24.6 +31 16 15	769909
UGC 711	1 06 03.3 + 1 22 27	
UGC 927	1 20 22.2 +33 16 04	769909
UGC 979	1 22 31.0 +33 45 55	"
UGC 1577	2 02 32.2 +30 56 20	"
UGC 1835	2 19 46.9 +28 01 50	"
UGC 2082	2 33 22.7 +25 12 24	
UGC 2134	2 35 56.1 +27 38 02	769909
UGC 2274	2 45 12.3 +34 12 41	"
UGC 3137	4 39 21.3 +76 19 36	
UGC 3580	6 50 02.4 +69 37 38	
UGC 3691	7 05 10.0 +15 15 30	
UGC 4238	8 05 08.4 +76 34 11	
UGC 4329	8 16 12 +21 20	UGC
UGC 4334	8 16 51.9 +22 11 18	769909
UGC 4354	8 18 30 +21 05	UGC
UGC 4386	8 21 06 +21 12	"
UGC 4399	8 23 12 +21 37	"
UGC 4514	8 35 54.3 +53 38 00	
UGC 4559	8 41 04.2 +30 18 01	
UGC 5459	10 04 53.8 +53 19 45	
UGC 6399	11 20 36 +51 12	
UGC 6667	11 39 45.1 +51 52 30	
UGC 6818	11 48 10.2 +46 05 08	
UGC 6923	11 54 14.0 +53 26 20	
UGC 6983	11 56 36 +52 59	
UGC 7089	12 03 24 +43 25	
UGC 7513	12 23 09.9 + 7 29 36	769909
UGC 7699	12 30 21.2 +37 53 47	
UGC 7737	12 32 06 +15 29	UGC
UGC 7774	12 33 58.3 +40 16 48	
UGC 7941	12 43 54.8 +64 50 31	
UGC 8146	13 00 03.3 +58 58 06	
UGC 8246	13 07 44.8 +34 26 48	
UGC 8918	13 57 42 + 9 13	UGC
UGC 8938	13 59 18.0 + 9 43 53	769909
UGC 8942	13 59 35.7 +10 10 08	"
UGC 8944	13 59 43.3 + 9 40 45	"
UGC 8948	14 00 06 + 9 19	UGC
UGC 8950	14 00 12 + 9 25	"
UGC 8951	14 00 18 + 9 01	"
UGC 8967	14 01 00 + 9 43	"
UGC 9023	14 04 24 + 9 34	"
UGC 9764	15 09 49.7 +65 05 10	
UGC 9858	15 24 52.0 +40 44 16	
UGC 9977	15 39 26.6 + 0 52 22	
UGC 10288	16 11 51.0 − 0 04 54	
UGC 11093	17 59 26.0 + 6 58 01	
UGC 11651	20 55 05.0 +25 46 29	
UGC 11707	21 12 20.2 +26 31 39	
UGC 12417	23 10 18 + 5 31	UGC
UGC 12423	23 10 36 + 6 08	"
UGC 12442	23 12 01.9 + 4 13 33	769909
UGC 12447	23 12 10.3 + 4 15 43	"
UGC 12454	23 12 36 + 9 24	UGC
UGC 12472	23 14 12 + 8 37	"
UGC 12486	23 15 43.7 + 6 18 45	769909
UGC 12494	23 16 24 + 6 35	UGC
UGC 12497	23 16 36 + 7 25	"
UGC 12498	23 16 36 + 7 50	"
UGC 12539	23 18 54.6 + 7 56 38	769909
UGC 12666	23 31 12.2 +32 06 26	"
UKS 1751−241	17 51 23.5 −24 08 12	
UMA #1	10 42 +48 15	
UMA #2	10 52 +45 10	
UMA #3	11 16 +43 01	
UMA #4	12 00 +46 12	
UMA #5	12 01 +51 08	
UMA II CL1		
ALF UMA	11 00 39.5 +62 01 15	CSI 79
AN UMA	11 01 33 +45 20 52	GCVS
AZ UMA	11 44 36.1 +43 44 57	779907
BET UMA	10 58 50.2 +56 39 02	CSI 79
CHI UMA	11 43 24.9 +48 03 22	"
DEL UMA	12 12 57.5 +57 18 35	"
EPS UMA	12 51 50.2 +56 13 51	779907
ETA UMA	13 45 34.3 +49 33 43	CSI 79
GAM UMA	11 51 12.5 +53 58 21	"
MUU UMA	10 19 21.4 +41 45 05	"
NUU UMA	11 15 46.9 +33 22 02	"
OMI UMA	8 26 07.6 +60 53 13	"
R UMA	10 41 07.5 +69 02 23	779907
RHO UMA	8 58 03.9 +67 49 34	CSI 79
RS UMA	12 36 41.2 +58 45 28	779907
RU UMA	11 39 02.0 +38 45 08	"
RY UMA	12 18 04.0 +61 35 14	"
S UMA	12 41 45.6 +61 22 01	"
ST UMA	11 25 06.8 +45 27 38	"
SU UMA	8 08 05 +62 45 28	GCVS
SV UMA	10 43 27.8 +55 17 57	779907
T UMA	12 34 07.3 +59 45 44	"
UX UMA	13 32 41.9 +52 22 49	CSI 79
VY UMA	10 41 37.2 +67 40 27	779907
W UMA	9 40 15.4 +56 10 56	"
X UMA	8 37 14.1 +50−18 54	"
XI UMA	11 15 31.1 +31 48 39	CSI 79
Y UMA	12 38 04.4 +56 07 15	779907
Z UMA	11 53 54.3 +58 08 59	"
15 UMA	9 05 21.3 +51 48 27	CSI 79
61 UMA	11 38 25.2 +34 29 01	"
83 UMA	13 38 50.5 +54 56 01	"
ALF UMI	1 48 48.7 +89 01 42	"
BET UMI	14 50 49.6 +74 21 35	"
R UMI	16 30 37.8 +72 23 10	779907
RR UMI	14 56 46.7 +66 07 52	"

NAME	RA (1950) DEC	POS REF
	h m s ° ′ ″	
S UMI	15 31 27.1 +78 48 08	"
T UMI	13 33 38.3 +73 40 38	CSI 79
THE UMI	15 32 51.2 +77 30 58	"
U UMI	14 16 14.2 +67 01 28	779907
U0052−326	0 52 −32 36	ED
U0147−270	1 47 −27 00	"
U0151−498	1 51 −49 48	"
U0219−345	2 19 −34 30	"
U0418−583	4 18 −58 18	"
U0532−527	5 32 −52 42	"
U0547−245	5 47 −24 30	"
U0632−629	6 32 −62 54	"
U1310−302	13 10 −30 12	"
U1352−336	13 52 −33 36	"
U28 130	12 51 41 +27 35	"
V 569		
VA 51	4 10 18.7 +16 38 26	CSI 79
VA 52	4 10 20 +14 36 42	699902
VA 60	4 11 39.9 +12 18 35	CSI 79
VA 68	4 12 04 +12 55 42	699902
VA 72	4 12 22 +14 16 18	"
VA 76	4 12 43 +16 38 06	"
VA 79	4 12 55.7 +15 16 36	CSI 79
VA 108	4 14 46.5 +16 49 33	"
VA 123	4 15 07.9 +18 08 07	"
VA 135	4 15 29 +17 17 54	699902
VA 146	4 15 59 +13 14 36	"
VA 156	4 16 14.9 +17 24 16	CSI 79
VA 179	4 17 02.9 +16 24 12	"
VA 182	4 17 08.4 +13 54 57	"
VA 201	4 18 03.7 +13 44 45	"
VA 208	4 18 33 +11 55 24	699902
VA 215	4 18 45.1 +14 17 32	CSI 79
VA 229	4 19 14.2 +13 57 36	"
VA 249	4 19 53.7 +14 56 24	"
VA 272	4 20 32.6 +16 39 42	"
VA 276	4 20 35 +15 38 42	699902
VA 279	4 20 42.3 +14 33 17	CSI 79
VA 282	4 20 52 +15 45 42	699902
VA 294	4 21 06 +13 56 00	"
VA 301	4 21 12.5 +17 19 46	CSI 79
VA 308	4 21 22.3 +14 38 36	"
VA 310	4 21 22.9 +17 53 22	"
VA 315	4 21 29.4 +16 57 52	"
VA 319	4 21 35.7 +16 46 18	"
VA 334	4 21 57 +15 45 30	699902
VA 351	4 22 21 +17 09 06	"
VA 354	4 22 32 +17 47 54	"
VA 355	4 22 35.5 +17 48 54	CSI 79
VA 360	4 22 45.7 +15 49 40	"
VA 363	4 22 54 +17 54 00	699902
VA 368	4 23 00 +14 53 12	"
VA 384	4 23 14.7 +15 24 42	CSI 79
VA 388	4 23 29.5 +15 30 22	"
VA 389	4 23 31.9 +16 44 28	"
VA 400	4 23 47.6 +16 38 06	"
VA 404	4 23 56 +12 34 18	699902
VA 407	4 24 07 +13 01 24	"
VA 435	4 24 36 +14 08 48	"
VA 444	4 24 42 +15 15 06	"
VA 446	4 24 44.7 +15 28 42	CSI 79
VA 459	4 24 52.3 +14 18 00	"
VA 472	4 25 15.1 +13 45 27	"
VA 485	4 25 33.2 +14 37 51	"
VA 491	4 25 48.2 +15 45 40	"
VA 495	4 25 55.0 +17 10 32	"
VA 500	4 25 59 +16 10 36	699902
VA 502	4 26 01 +15 52 12	"
VA 504	4 26 01.9 +12 56 17	CSI 79
VA 512	4 26 08 +16 14 00	699902
VA 544	4 26 36.5 +17 45 16	CSI 79
VA 547	4 26 37.6 +17 47 04	"
VA 548	4 26 39 +16 08 00	699902
VA 560	4 27 05.1 +16 33 54	CSI 79
VA 569	4 27 17.3 +15 31 48	"
VA 575	4 27 31 +17 23 18	699902
VA 584	4 27 41.7 +16 05 11	CSI 79
VA 587	4 27 43.3 +15 37 36	"
VA 589	4 27 47.4 +15 35 04	"
VA 591	4 27 48.2 +13 37 00	"
VA 597	4 27 54.7 +16 02 29	"
VA 622	4 28 36 +17 36 36	699902
VA 625	4 28 40.0 +13 47 49	CSI 79
VA 627	4 28 40.9 +17 35 39	"
VA 644	4 29 00.1 +15 44 43	"
VA 645	4 29 02 +15 23 24	699902
VA 677	4 29 38 +13 00 18	"
VA 684	4 29 58.3 +15 54 03	CSI 79
VA 692	4 30 07.7 +15 42 51	"
VA 712	4 30 45.2 +16 39 30	"
VA 725	4 31 00.3 +14 44 26	"
VA 727	4 31 07.7 +15 03 35	"
VA 747	4 31 40.4 +15 43 28	"
VA 748	4 31 43.9 +15 24 06	"
VA 751	4 31 48.3 +17 38 43	"
VA 771	4 32 46.7 +11 59 54	"
VA 778	4 33 13.7 +15 34 58	"
VB 8	16 52 55 − 8 18 06	709903
VB 17	4 11 35.9 +14 29 58	CSI 79
VB 49	4 21 20.9 +16 15 51	"
VB 96 IRS1	7 17 43.6 −23 51 04	
VBH 24	8 53 20.6 −43 16 28	CSI 79
VBH 25A	8 54 42 −42 54	759902
VBH 25C	8 55 18.9 −43 03 46	
VBH 25D	8 54 54 −43 05	759902
VBH 28	8 56 36 −43 14	"
VBH 46A	10 59 13.5 −59 34 24	
VBH 46BCD	" "	
VD1−1	16 39 09 −38 48 48	779909
VD1−2	16 43 21 −38 31 36	"
VD1−5	16 48 06 −39 57 54	"
VD1−6	16 51 02 −38 39 18	"
VD1−7	16 54 06 −37 01 18	789908
VD1−8	17 01 10 −37 49 06	779909
VE 2−45	17 59 01 −23 37 36	IRC
VE 2−57		
VE 22	8 57 30 −45 23 54	789907
VE 26	8 41 54 −45 55	P−K
VE 27	8 50 17 −46 06 48	789907
VEGA	18 35 14.6 +38 44 09	CSI 79
VEL X−1	9 00 −40	"
AI VEL	8 12 26.2 −44 25 21	CSI 79
BL VEL	8 07 04 −46 22 08	GCVS
BN VEL	8 11 37.3 −47 57 57	CSI 79
CM VEL	10 05 41.3 −53 00 54	"
FP VEL	9 51 39 −52 16 25	GCVS
GAM VEL	8 07 59.3 −47 11 17	CSI 79
GAM 2 VEL	" "	"
GS VEL	10 43 36 −56 19 46	GCVS
LAM VEL	9 06 09.3 −43 13 46	CSI 79
MUU VEL	10 44 36.7 −49 09 18	"
RS VEL	9 22 09.2 −48 38 47	"
RW VEL	9 18 37.2 −49 18 37	"
SS VEL	10 50 48.5 −53 09 52	"
T VEL	8 36 03.3 −47 11 09	"
TV VEL	10 32 28.9 −53 59 25	"
UU VEL	9 33 51 −53 50 23	GCVS
W VEL	10 13 22.6 −54 13 44	CSI 79
WY VEL	9 20 20.9 −52 20 59	"
WZ VEL	10 15 31.7 −47 41 47	"
X VEL	9 53 23.1 −41 20 58	"
XZ VEL	10 15 29 −49 50 46	GCVS
Y VEL	9 27 20.7 −51 57 38	CSI 79
Z VEL	9 51 09.4 −53 56 32	"
VII ZW 403	11 24 42 +79 17	MCG
AL VIR	14 08 26.7 −13 04 31	CSI 79
ALF VIR	13 22 33.3 −10 54 01	"
ALF VIR A+B	" "	"
BET VIR	11 48 05.3 + 2 02 46	"
BK VIR	12 27 48.0 + 4 41 33	"
DEL VIR	12 53 04.9 + 3 40 06	"
EPS VIR	12 59 41.2 +11 13 37	"
EQ VIR	13 32 06.5 − 8 05 05	"
GAM VIR AB	12 39 07.3 − 1 10 30	"
KAP VIR	14 10 13.3 −10 02 29	"
NUU VIR	11 43 17.3 + 6 48 34	"
OME VIR	11 35 52.9 + 8 24 38	"
PHI VIR	14 25 37.3 − 2 00 15	"
PSI VIR	12 51 44.9 − 9 16 02	"
R VIR	12 35 57.6 + 7 15 45	"
RR VIR	14 02 13.6 − 8 57 21	"
RS VIR	14 24 45.0 + 4 53 54	
RS VIR	14 24 46.5 + 4 54 26	CSI 79
RT VIR	13 00 05.0 + 5 27 06	
RT VIR	13 00 05.6 + 5 27 14	CSI 79
RU VIR	12 44 28.9 + 4 25 49	"
RV VIR	13 05 16.5 −12 53 51	"
S VIR	13 30 23.4 − 6 56 17	"
SS VIR	12 22 46.0 + 1 04 28	"
SU VIR	12 02 33.5 +12 39 17	"
SW VIR	13 11 29.7 − 2 32 31	"
T VIR	12 12 02.5 − 5 45 27	"
THE VIR	13 07 21.4 − 5 16 19	"
TY VIR	11 49 16.7 − 5 28 59	"
U VIR	12 48 33.4 + 5 49 29	"
V VIR	13 25 13.0 − 2 54 49	"
W VIR	13 23 26.9 − 3 07 07	"
Y VIR	12 31 18.1 − 4 08 45	"
Z VIR	14 07 39.3 −13 04 07	"
70 VIR	13 25 58.9 +14 02 42	"
74 VIR	13 29 21.7 − 5 59 52	"
82 VIR	13 38 59.0 − 8 27 04	"
109 VIR	14 43 43.0 + 2 06 07	"
VMA 2		
R VOL	7 06 32.3 −72 56 07	CSI 79
T VOL	6 57 49.2 −67 03 08	"
X VOL	7 57 29 −65 09 28	GCVS
VS 1	16 23 16.7 −24 21 29	
VS 1	16 23 17.5 −24 12 33	780902
VS 2	16 23 40.7 −24 13 44	
VS 3	16 23 47.0 −24 13 24	
VS 4	16 23 36.7 −24 16 22	
VS 5	16 23 52.0 −24 19 39	
VS 6	16 23 52.7 −24 15 44	
VS 7	16 23 53.4 −24 13 44	
VS 8	16 24 00.7 −24 14 54	
VS 9	16 24 00.7 −24 12 14	
VS 10	16 23 50.7 −24 08 04	
VS 11	16 23 42.7 −24 09 44	
VS 12	16 23 14.8 −24 15 21	
VS 13	16 24 44.8 −24 16 39	
VS 13	16 24 45.2 −24 16 43	780902
VS 14	16 24 48.3 −24 19 02	"
VS 14	16 24 48.8 −24 18 54	
VS 15	16 25 07.8 −24 16 46	
VS 16	16 25 02.8 −24 19 54	
VS 17	16 24 28.8 −24 20 54	750401
VS 18	16 24 26.8 −24 20 34	
VS 19	16 22 56.8 −24 11 01	
VS 20	16 23 06.8 −24 08 01	
VS 21	16 24 02.8 −24 13 24	
VS 22	16 24 20.8 −24 11 24	
VS 23	16 24 08.8 −24 12 24	
VS 24	16 24 12.8 −24 11 34	
VS 25	16 24 25.7 −24 24 36	
VS 26	16 24 17.0 −24 22 01	
VS 27	16 23 28.7 −24 16 14	
VS 28	16 23 44.7 −24 16 24	
VSB 67		
VSB 165		
VSB 205		
VUL R1 #2	19 44 20 +24 29 30	
VUL R1 #7	19 44 30 +24 04 18	
VUL R1 #8N	19 44 41 +24 05 54	
VUL R1 #8S	19 44 40 +24 05 36	
VUL R1 #16	19 44 40 +24 07 30	ED
VUL R2 #16	19 19 23 +21 09 18	
ALF VUL	19 26 37.3 +24 33 43	CSI 79
CG VUL	19 14 44.2 +21 49 11	"
CU VUL	19 46 25 +21 30 01	GCVS
EP VUL	19 31 11 +23 32 42	"
NOVA VUL 1976	19 27 06 +20 21	790115
NQ VUL	" "	"
R VUL	21 02 09.3 +23 37 18	CSI 79
SV VUL	19 49 27.7 +27 19 51	"
T VUL	20 49 20.7 +28 03 42	"
V VUL	20 34 24.1 +26 25 45	"
WW VUL	19 23 49.4 +21 06 25	"
VV 1−4	6 12 05.0 +12 22 22	739909
VV 1−7	7 39 00.9 −18 52 17	"
VV 8	1 55 33 +52 39 15	709904
VV 80	16 13 23.3 −51 51 44	769910
VV 144		
VY 1−1	0 16 02 +53 35 41	709904
VY 1−2	17 52 24 +28 00	P−K
VY 2−1	18 24 53.2 −26 08 36	769910
VY 2−2	19 21 59.0 + 9 47 59	739909
VY 2−3	23 20 24 +46 38	P−K
WALKER 67	6 37 52 + 9 50 36	740903
WOLF−LN/A2359	23 59 −15	ED
WRAY 813	11 26 40 −65 25 24	709901
WRAY 1763	17 39 58 −36 37 00	"
WU 0138−29.8	1 38 −29 48	
WU 1059+67.6	10 59 +67 36	ED
WU 1428+40.3	14 28 +40 18	"
WU 1506+01.2	15 06 + 1 12	"
WU 2035−29.3	20 35 −29 18	"
WU 2101−24.3	21 01 −24 18	"
WU 2143+01.0	21 43 + 1 00	"
WU 2225−30.7	22 25 −30 42	"
WU 2240−15.9	22 40 −15 54	"
WU 2314−08.9	23 14 − 8 54	"
WU 2338−15.4	23 38 −15 24	"
WU 2357+04.8	23 57 + 4 48	"
W3	2 21 53 +61 52 20	
W3	2 21 53.0 +61 52 21	ED
W3	2 22 00 +61 52 30	
W3	2 22 49 +61 51	ED
W3 A	2 21 +61 50	"
W3 A	2 21 55.0 +61 52 00	
W3 A	2 21 56.3 +61 52 55	
W3 A	2 22 00 +61 52	ED
W3 A	2 22 57 +61 52 40	"
W3 A IRS1	2 21 56.3 +61 52 55	740206
W3 A IRS1,2	2 21 57 +61 52 48	
W3 B	2 22 50.3 +61 52 17	ED
W3 B IRS3	2 21 50.7 +61 52 21	
W3 BS4	2 23 46.5 +61 42 30	791001
W3 C	2 23 14 +61 38 57	
W3 C IRS4	2 21 43.4 +61 52 49	740206
W3 C IRS4	2 21 44 +61 52 48	
W3 CONT OHIR	2 21 46.5 +61 52 22	
W3 H2O	2 21 53 +61 52 20	
W3 IRS1	2 21 55.4 +61 52 21	ED
W3 IRS1	2 21 56.0 +61 52 43	"
W3 IRS1	2 21 56.3 +61 52 55	
W3 IRS1 7"N	2 21 55.4 +61 52 28	ED
W3 IRS1 7"S	2 21 55.4 +61 52 14	"
W3 IRS1 14"N	2 21 55.4 +61 52 35	"
W3 IRS1 21"N	2 21 55.4 +61 52 42	"
W3 IRS1 28"N	2 21 55.4 +61 52 49	"
W3 IRS1 35"N	2 21 55.4 +61 52 56	"
W3 IRS1 42"N	2 21 55.4 +61 53 03	"
W3 IRS2	2 21 56.8 +61 52 42	"
W3 IRS2 13"E	2 21 58.6 +61 52 42	"
W3 IRS2 13"N	2 21 56.8 +61 52 55	"
W3 IRS2A	2 21 56.0 +61 52 45	
W3 IRS3	2 21 50.1 +61 52 22	740206
W3 IRS3	2 21 50.3 +61 52 21	ED
W3 IRS4	2 21 43.4 +61 52 49	740206
W3 IRS4	2 21 43.5 +61 52 49	
W3 IRS5	2 21 53.1 +61 52 20	740206
W3 IRS5	2 21 53.2 +61 52 21	
W3 IRS6	2 21 53.9 +61 52 16	ED
W3 IRS7	2 21 57.9 +61 52 11	"
W3 IRS8	2 21 46.5 +61 52 18	740206
W3 IRS8	2 23 16.7 +61 38 56	
W3 IRS9	2 22 +61 53	ED
W3 IRS10	2 21 42.4 +61 53 02	
W3 N	2 23 00 +62 02	ED
W3 N	2 23 01.8 +62 02 11	
W3 OH	2 23 16.7 +61 38 56	
W3 OH	2 23 16.8 +61 38 53	
W3 OH	2 23 17 +61 38 55	
W3 OH IRS8	2 21 46.5 +61 52 18	740206
W3 OH SOURCE1	2 21 46.4 +61 52 17	
W3 OH SOURCE2	2 21 54 +61 51 58	
W3 SOURCE 1	2 21 58 +61 52 24	
W3 SOURCE 2	2 23 24 +61 39 06	
W3 SOURCE 3	2 23 10 +62 02 54	
W3 SOURCE 4	2 23 50 +61 42 18	
W3 SOURCE 5	2 24 37 +61 14 42	
W3 SOURCE 6	2 22 17 +61 51 24	
W3(OH)	2 23 30 +61 40	ED
W5 EAST #1	2 57 23.9 +60 17 28	"
W5 EAST #2	2 57 27.5 +60 17 28	"
W5 EAST #3	2 57 31.1 +60 17 28	"
W5 EAST #4	2 57 34.7 +60 17 28	"
W5 EAST #5	2 57 38.3 +60 17 28	"
W5 EAST #6	2 57 41.9 +60 17 28	"
W5 EAST #7	2 57 34.7 +60 18 52	"
W5 EAST #8	2 57 34.7 +60 18 24	"
W5 EAST #9	2 57 34.7 +60 17 56	"
W5 EAST #10	2 57 34.7 +60 17 00	"
W5 EAST #11	2 57 34.7 +60 16 32	"
W5 EAST/IRS1	2 57 34.7 +60 17 28	
W28 A2 (1)	17 57 27 −24 03 55	
W28 A2 (2)	17 57 26.9 −24 03 23	
W28 C	17 57 46.4 −23 20 48	
W28 C SOURCE3	17 58 55.4 −23 13 00	
W30	18 02 36 −21 37	589903
W31	18 06 00 −20 11	"
W31	18 06 31.1 −20 20 10	
W31 #1	18 02 17 −20 04	
W31 #2	18 04 47 −20 20	
W31 #3	18 05 39 −19 52	
W31 #4	18 06 03 −20 05	
W31 #5	18 06 24 −20 20	
W31 #6	18 06 24 −20 08	
W31 #7	18 07 31 −19 58	
W33	18 10 24 −18 00	589903
W33	18 11 18.1 −17 56 28	
W33	18 11 18.1 −17 56 30	
W33	18 11 18.3 −17 57 30	

NAME	RA (1950) DEC	POS REF
	h m s ° ′ ″	
W33 A	18 11 43.7 −17 53 02	770104
W33 A	18 11 44.1 −17 52 57	
W33 A	18 11 44.2 −17 52 57	
W33 A IR	18 11 44.2 −17 52 59	
W33 B	18 10 57.4 −18 02 47	
W33 CONT (1)	18 11 17.6 −17 56 30	
W33 CONT (2)	18 11 19.3 −17 56 48	
W33 IRS1	18 11 19.6 −17 56 54	
W33 IRS2	18 11 19.0 −17 56 18	
W33 IRS3	18 11 18.1 −17 56 38	770104
W35	18 15 00 −11 55	589903
W35 #1	18 14 57 −11 40 04	
W35 #2	18 14 58 −11 43 34	
W35 #3	18 15 06 −11 42 14	
W35 #4	18 15 16 −11 41 29	
W35 #5	18 15 21 −11 44 31	
W35 #6	18 15 23 −11 44 18	
W35 #7	18 15 25 −11 46 29	
W39	18 23 24 −12 40	589903
W40	18 28 51.7 − 2 07 33	780607
W40	18 29 36 − 2 12	589903
W40 IRS1	18 28 51.7 − 2 07 33	
W40 IRS2	18 28 47.7 − 2 07 41	
W40 IRS3	18 28 47.6 − 2 06 19	
W41	18 31 48 − 8 49	589903
W42	18 33 36 − 7 30	"
W43	18 45 00.8 − 1 59 48	ED
W43	18 45 01 − 1 59 48	"
W43	18 45 02.8 − 2 00 45	
W43	18 45 24 − 2 02	589903
W43 MAIN	18 45 32.6 − 2 00 22	
W44	18 53 36 + 1 16	589903
W48	18 59 14.2 + 1 08 41	
W48 IRS1	18 59 14.7 + 1 08 53	
W48 IRS2	18 59 12.2 + 1 08 20	
W49	19 07 50 + 9 01 15	761003
W49	19 07 56 + 9 03	
W49 A	19 07 55.9 + 9 01 01	
W49 A (1)	19 07 50.8 + 9 01 14	
W49 A (2)	19 07 50.4 + 9 02 20	
W49 A−1 OH	19 07 49.9 + 9 01 18	
W49 A−2 OH	19 07 58.3 + 9 00 01	
W49 B	19 08 44 + 9 00 48	
W49 E	19 07 58.2 + 8 59 58	ED
W49 IRS1	19 07 49.8 + 9 01 11	770208
W49 NW	" "	"
W49 OH	19 07 50 + 9 01 10	ED
W49 OH(1)	19 07 49.8 + 9 01 16	
W49 OH(2)	19 07 58.2 + 9 00 03	
W49 W	19 07 49.9 + 9 01 18	760601
W49 1'E	19 07 54 + 9 01 15	ED
W51	19 21 21.7 +14 25 10	
W51	19 21 23.0 +14 24 54	
W51	19 21 23.3 +14 24 52	
W51	19 21 25 +14 24 40	780407
W51	19 21 27 +14 24 30	
W51	19 21 28.8 +14 24 41	
W51 #1	19 21 11 +14 25 12	
W51 #13	19 20 21 +14 01 54	
W51 #2	19 21 16 +14 24 36	
W51 #4	19 21 22 +14 25 06	
W51 #5	19 21 25 +14 24 48	
W51 #6	19 21 30 +14 27 18	
W51 #7	19 21 33 +14 26 54	
W51 #8	19 21 36 +14 29 54	
W51 #9	19 21 29 +14 25 06	
W51 #10	19 21 43 +14 23 42	
W51 #11	19 20 54 +14 21 06	
W51 #12	19 20 53 +14 10 24	
W51 A	19 21 23 +14 26	
W51 A	19 21 23.9 +14 25 40	
W51 A	19 21 24.5 +14 24 42	
W51 B	19 20 50 +14 20	
W51 B	19 20 56 +14 21 00	
W51 C CO	19 20 03 +14 00 54	
W51 D	19 20 23 +14 01 54	
W51 E	19 20 42.6 +14 10 00	
W51 IRS1	19 21 24.2 +14 24 42	ED
W51 IRS1N	19 21 24.5 +14 24 51	
W51 IRS1S	19 21 24.0 +14 24 40	
W51 IRS2	19 21 22.1 +14 25 12	
W51 IRS2	19 21 22.3 +14 25 15	
W51 IRS2	19 21 22.4 +14 25 12	
W51 IRS2	19 21 22.5 +14 25 16	ED
W51 IRS2 EAST	19 21 22.5 +14 25 13	820406
W51 IRS2 EAST	19 21 22.6 +14 25 14	
W51 IRS2 WEST	19 21 22.3 +14 25 17	
W51 IRS2N	19 21 22.3 +14 25 13	
W51 IRS2S	19 21 22.4 +14 25 12	
W51 1'E	19 21 29 +14 24 40	ED
W51 1'E,1'S	19 21 29 +14 23 40	"
W51 1'N	19 21 25 +14 25 40	"
W51 1'S	19 21 25 +14 23 40	"
W51 1'W	19 21 21 +14 24 40	"
W54	18 00 17.0 −24 23 40	
W58 C CO,OH	19 59 59 +33 26 00	
W75 IRS1	20 37 10 +42 12 05	
W75 IRS1	20 37 10.0 +42 12 09	800603
W75 IRS1	20 37 10.0 +42 12 10	ED
W75 IRS2	20 37 11.7 +42 09 14	740203
W75 IRS2	20 37 11.7 +42 09 45	ED
W75 IRS2	20 37 12 +42 09 40	
W75 N	20 36 50.6 +42 26 57	ED
W75 N	20 36 51.1 +42 27 19	
W75 N OH	" "	ED
W75 S	20 37 13.5 +42 12 00	"
W75 S	20 37 13.7 +42 12 00	
W75 S OH	20 37 14 +42 12 05	
W75 S OH	20 37 14.9 +42 12 10	ED
W75N	20 37 +42 20	"
W80 #1	20 53 54.0 +43 43 52	
W80 #2	20 49 05.3 +44 13 52	
W80 #3	20 49 14.4 +44 21 09	
W80 #4	20 48 49.0 +44 15 12	
W80 #5	20 56 40.4 +43 14 09	
W80 #6	20 58 52.8 +43 46 51	
W80 #7	20 52 57.5 +44 03 38	
W80 #8	20 53 54.5 +43 40 41	

NAME	RA (1950) DEC	POS REF
	h m s ° ′ ″	
W80 #9	20 53 54.8 +43 43 54	
W475 A	13 06 36 +10 01	LTT
W489	13 34 12.9 + 3 56 59	CSI 79
W1346		
W80 #10	20 54 03.3 +43 40 51	
W80 #11	20 54 08.4 +43 41 28	
X−RAY 1	4 29 21 +17 55 24	819918
X−RAY 2	4 29 23 +18 13 54	"
YALE 49A	0 15 30.9 +43 44 21	CSI 79
YALE 49B	0 15 33.9 +43 44 45	"
YALE 392	1 50 25.3 −22 40 50	"
YALE 422	2 00 09 + 5 28 24	709903
YALE 450	2 09 53.7 + 3 22 45	CSI 79
YALE 642	3 03 50.0 + 1 47 08	"
YALE 742	3 30 34.3 − 9 37 34	"
YALE 757	3 35 46 −11 35	639902
YALE 948.1	4 15 04 −26 11 30	709903
YALE 1121	4 55 13.9 −61 13 53	CSI 79
YALE 1181	5 09 41.4 −44 59 53	"
YALE 1255	5 28 55.3 − 3 41 03	"
YALE 1305	5 39 13.9 +12 29 18	"
YALE 1430	6 08 28.1 −21 50 34	"
YALE 1609	6 51 34.9 +33 20 18	"
YALE 1641.1	6 56 20.7 −44 13 17	"
YALE 1668	7 06 38.9 +38 37 23	"
YALE 1755	7 24 42.9 + 5 22 42	"
YALE 1785C	7 31 26.1 +31 58 49	779907
YALE 1809B	7 37 32.6 − 3 28 58	CSI 79
YALE 1827	7 42 03.9 + 3 40 42	"
YALE 2267	9 28 51.5 −13 16 01	"
YALE 2299.1	9 37 49 −40 50 42	709903
YALE 2336.1	9 49 37 + 3 27 24	"
YALE 2390	10 08 19.0 +49 42 27	CSI 79
YALE 2420	10 16 53.9 +20 07 18	"
YALE 2456	10 26 23.4 + 1 06 28	"
YALE 2512	10 43 19 −18 50 30	709903
YALE 2524	10 48 18.9 + 7 05 06	CSI 79
YALE 2576	11 00 36.5 +36 18 19	"
YALE 2582A	11 02 59.7 +43 47 01	"
YALE 2582B	11 03 01.9 +43 46 41	"
YALE 2631	11 17 28.5 +66 07 02	"
YALE 2654	11 25 53 + 7 49	639902
YALE 2730	11 45 08.9 + 1 06 00	CSI 79
YALE 2890AB	12 30 50.9 + 9 17 32	"
YALE 2951	12 48 10 − 0 29 24	709903
YALE 3079	13 27 26.6 +10 39 02	CSI 79
YALE 3135	13 43 11.7 +15 09 41	"
YALE 3278	14 26 18.9 −62 28 05	"
YALE 3296	14 31 34.9 −12 18 33	"
YALE 3375A	14 54 32.3 −21 11 27	"
YALE 3375B	14 54 31.0 −21 11 16	"
YALE 3458	15 16 52.2 − 7 32 20	"
YALE 3501	15 29 03.1 −41 04 38	"
YALE 3547	15 39 19.9 −19 18 34	"
YALE 3712A	16 16 36.9 +67 21 31	"
YALE 3712B	16 16 39.3 +67 22 34	"
YALE 3746	16 27 31.0 −12 31 50	"
YALE 3783.1	16 37 17.9 −45 53 58	"
YALE 3845	16 52 48.3 − 8 14 39	"
YALE 3845AB	" "	"
YALE 3878	17 02 27.9 − 4 58 39	"
YALE 3880	17 02 38.2 − 5 00 19	"
YALE 3924C	17 15 34.3 −34 56 29	"
YALE 3958	17 24 50.2 −46 49 51	"
YALE 3992	17 33 27.9 −44 16 33	"
YALE 4098	17 55 22.9 + 4 33 18	"
YALE 4133	18 02 28.3 − 3 01 51	"
YALE 4266	18 30 42.3 −11 40 16	"
YALE 4338	18 46 44.9 −23 53 28	"
YALE 4398	18 55 33.6 + 5 51 23	"
YALE 4472	19 09 35.2 + 2 48 42	"
YALE 4607	19 32 27.5 +69 34 33	"
YALE 4794	20 10 19.3 −45 18 46	"
YALE 4924	20 38 42.6 −52 50 31	"
YALE 5077A	21 04 39.9 +38 29 58	"
YALE 5077B	21 04 38.3 +38 29 29	"
YALE 5084	21 06 29.9 −13 28 40	"
YALE 5117	21 14 19.9 −39 03 41	"
YALE 5190	21 30 14.2 −49 12 34	"
YALE 5314	21 59 33.0 −56 59 32	"
YALE 5358	22 06 57.1 − 4 52 44	"
YALE 5475	22 35 44.9 −15 35 35	"
YALE 5546	22 50 31.3 −14 31 00	"
YALE 5572	22 57 38.1 −22 47 37	"
YALE 5584	23 02 38.6 −36 08 28	"
YALE 5616	23 10 51.7 +56 53 30	"
YALE 5817	0 02 27.9 −37 36 10	"
I ZW 1	0 51 00.0 +12 25 00	809908
I ZW 92	14 39 12 +53 44	ED
I ZW 186	17 27 +50 18	
I ZW 187	17 27 04.3 +50 15 31	809908
I ZW 1727+50	17 27 06 +50 15	ED
II ZW 23	4 47 00 + 3 15	740903
II ZW 40	5 53 06 + 3 24	"
II ZW 136	21 30 01.2 + 9 55 01	789906
II ZW 0553+03	5 53 06 + 3 24	740903
III ZW 2	0 07 56.7 +10 41 48	809908
III ZW 55	3 38 38.3 −10 17 30	789906
III ZW 55 N	" "	"
III ZW 77	16 22 06 +41 12	ED
IV ZW 67	21 00 16 +36 30 00	
ZW0039.5	0 39 32.3 +40 03 10	789906
ZW0039.5+4003	" "	"
ZW0934+013	9 34 26.5 + 1 19 14	"
Z119−053	8 16 30 +21 13	ZWICKY
Z406−086	23 19 06 + 8 42	"
Z1549+47	15 49 40.9 +47 24 15	769909
1E 1145.1−6141	11 45 06 −61 41	ED
1E 2259+586	22 59 02.8 +58 36 33	
2A 0311−227	3 12 00.0 −22 46 49	799906
2A 1822−371	18 22 −37 06	ED
2S0921−630	9 21 −63 00	"
2S1702−363	17 02 −36 18	"
2S1728−337 #1	17 28 41 −33 47 39	"
2S1728−337 #2	17 28 42 −33 47 46	"
2S1728−337 #3	17 28 39 −33 48 01	"
2S1728−337 #4	17 28 40 −33 47 58	"
2S1728−337 #5	17 28 40 −33 48 09	"

NAME	RA (1950) DEC	POS REF
	h m s ° ′ ″	
3C 6.1	0 13 35.0 +79 00 11	769906
3C 9	0 17 49.8 +15 24 17	809908
3C 13	0 31 32.7 +39 07 39	769906
3C 16	0 35 06 +12 50	ED
3C 17	0 35 47.2 − 2 24 11	769906
3C 19	0 38 13.8 +32 53 40	"
3C 22	0 48 06 +50 57	ED
3C 28	0 53 08.9 +26 08 23	769906
3C 31	1 04 39.2 +32 08 45	"
3C 33	1 06 14.5 +13 04 15	"
3C 34	1 07 32 +31 30	ED
3C 41	1 23 55 +32 56	"
3C 48	1 34 49.8 +32 54 20	809908
3C 49	1 38 28.4 +13 38 20	769906
3C 57	1 59 30.4 −11 47 00	809908
3C 65	2 20 38 +39 48	ED
3C 66A	2 19 30.0 +42 48 30	809908
3C 68.1	2 29 27.2 +34 10 34	"
3C 76.1	3 00 27.2 +16 14 37	769906
3C 78	3 05 49.1 + 3 55 13	"
3C 79	3 07 11.3 +16 54 37	"
3C 84	3 16 29.6 +41 19 52	"
3C 88	3 25 18.3 + 2 23 20	"
3C 94	3 50 04.0 − 7 19 56	809908
3C 95	3 49 09.5 −14 38 07	"
3C 98	3 56 10.2 +10 17 32	769906
3C 109	4 10 54.8 +11 04 41	"
3C 111	4 15 01.1 +37 54 37	729901
3C 120	4 30 31.5 + 5 15 01	789906
3C 133	4 59 55 +25 12	3CR
3C 135	5 11 33.8 + 0 53 08	769906
3C 138	5 18 16.7 +16 35 26	"
3C 147	5 38 43.6 +49 49 43	"
3C 171	6 51 11.0 +54 12 48	"
3C 175	7 10 15.3 +11 51 30	"
3C 184	7 34 34 +70 20	3CR
3C 192	8 02 35.5 +24 18 28	769906
3C 196	8 09 59.4 +48 22 08	"
3C 198	8 19 52.3 + 6 06 47	"
3C 200	8 24 21.7 +29 28 41	"
3C 206	8 37 28.0 −12 03 54	809908
3C 212	8 55 55.6 +14 21 24	769906
3C 217	9 05 55 +38 04	ED
3C 219	9 17 50.7 +45 51 44	769906
3C 227	9 45 06.6 + 7 39 17	"
3C 232	9 55 25.4 +32 38 23	809908
3C 234	9 58 57.4 +29 01 37	769906
3C 249.1	11 00 27.4 +77 15 08	809908
3C 264	11 42 29.6 +19 53 03	769906
3C 265	11 42 53.4 +31 50 25	"
3C 273	12 26 + 2	
3C 273	12 26 33.4 + 2 19 42	809908
3C 273B	" "	"
3C 274	12 28 17.6 +12 40 02	769906
3C 277.3	12 51 46.3 +27 53 50	"
3C 279	12 53 − 5	
3C 279	12 53 35.8 − 5 31 08	809908
3C 280	12 54 41.4 +47 36 30	769906
3C 286	13 28 49.7 +30 45 58	809908
3C 287	13 28 16.1 +25 24 37	"
3C 289	13 43 29 +50 01	ED
3C 293	13 50 03.4 +31 41 32	769906
3C 295	14 09 33.4 +52 26 14	"
3C 296	14 14 26.0 +11 02 15	"
3C 298	14 16 39.1 + 6 42 21	809908
3C 303	14 41 24.8 +52 14 19	769906
3C 305	14 48 17.6 +63 28 36	"
3C 309.1	14 58 56.7 +71 52 11	809908
3C 318	15 17 50.6 +20 26 53	769906
3C 323.1	15 45 31.1 +21 01 33	"
3C 324	15 47 37.3 +21 34 42	"
3C 330,G2	16 09 14.1 +66 04 24	"
3C 334	16 18 07.4 +17 43 31	"
3C 336	16 22 32.5 +23 52 01	"
3C 343.1	16 37 55.2 +62 46 35	"
3C 345	16 41 17.6 +39 54 11	809908
3C 348	16 48 40.0 + 5 04 35	769906
3C 351	17 04 03.5 +60 48 31	809908
3C 352	17 09 18.0 +46 05 06	769906
3C 356	17 23 06 +51 01	ED
3C 368	18 02 42 +10 57	"
3C 371	18 07 18.5 +69 48 59	769906
3C 380	18 28 13.4 +48 42 39	"
3C 381	18 32 24.4 +47 24 39	"
3C 382	18 33 12.1 +32 39 15	"
3C 390.3	18 45 37.8 +79 43 03	"
3C 401	19 39 38.8 +60 34 32	"
3C 405	19 57 44.4 +40 35 45	"
3C 427.1	21 04 44.8 +76 21 10	"
3C 432	21 20 25.4 +16 51 56	"
3C 438	21 53 45.5 +37 46 14	"
3C 445	22 21 14.7 − 2 21 27	"
3C 446	22 23 11.1 − 5 12 17	809908
3C 454.3	22 51 29.5 +15 52 55	"
3C 456	23 09 56.7 + 9 03 08	769906
3C 459	23 14 02.3 + 3 48 56	"
3C 460	23 18 59.8 +23 19 00	"
3CR 33	1 06 14.5 +13 04 15	"
3CR 34	1 23 55 +32 56	ED
3CR 46	1 32 34.5 +37 38 46	769906
3CR 65	2 20 38 +39 48	ED
3CR 68.1	2 29 27.2 +34 10 34	809908
3CR 68.2		
3CR 98	3 56 10.2 +10 17 32	769906
3CR 109	4 10 54.8 +11 04 41	"
3CR 123		
3CR 171	6 51 11.0 +54 12 48	769906
3CR 192	8 02 35.5 +24 18 28	"
3CR 200	8 24 21.7 +29 28 41	"
3CR 217	9 05 55 +38 04	ED
3CR 219	9 17 50.7 +45 51 44	769906
3CR 223	9 36 50.9 +36 07 35	"
3CR 234	9 58 57.4 +29 01 37	"
3CR 236	10 03 05.4 +35 08 49	"
3CR 239		
3CR 241		
3CR 265	11 42 53.4 +31 50 25	769906
3CR 274.1	12 32 57.1 +21 37 18	"

NAME	RA (1950)	DEC	POS REF
	h m s	° ′ ″	
3CR 277.3	12 51 46.3	+27 53 50	"
3CR 280	12 54 41.4	+47 36 30	"
3CR 284	13 08 41.4	+27 44 03	"
3CR 285	13 19 05.1	+42 50 57	"
3CR 288	13 36 38.7	+39 06 23	"
3CR 289	13 43 29	+50 01	ED
3CR 295	14 09 33.4	+52 26 14	769906
3CR 299	14 19 06.4	+41 58 30	"
3CR 318	15 17 50.6	+20 26 53	"
3CR 349	16 58 04.9	+47 07 16	"
3CR 352	17 09 18.0	+46 05 06	"
3CR 381	18 32 24.4	+47 24 39	"
3CR 382	18 33 12.1	+32 39 15	"
3CR 388	18 42 35.4	+45 30 22	"
3CR 441			
3U1636−53 H	16 36	−53	
3U1758−20 A	17 58	−20	
4C 06.41	10 38 40.9	+ 6 25 58	809908
4C 13.41	10 04 45.1	+13 03 38	"
4C 16.39	14 00 20.5	+16 14 21	
4C 25.40	12 23 09.1	+25 15 12	809908
4C 29.68	23 25 42.3	+29 20 38	"
4C 31.30	7 42 30.7	+31 50 16	"
4C 31.63	22 01 01.1	+31 31 10	"
4C 34.47	17 21 32.0	+34 20 42	"
4C 37.43	15 12 46.9	+37 01 56	"
4C 39.25	9 23 55.3	+39 15 23	"
4C 47.08	3 00 10.0	+47 04 33	"
4C−4.8	20 53 10.8	− 4 25 18	RA42
4U0115+634	1 15	+63 24	ED
4U0535+262	5 35 47.9	+26 17 17	CSI 79
4U1700−37	17 00 32.6	−37 46 28	"
0010+40	0 10	+40	ED
0015.9+1610	0 15 54	+16 10	"
0026+129	0 26 38.1	+12 59 30	809908
0026+34	0 26 34.8	+34 39 56	790910
0031−076	0 31	− 7 36	ED
0031−077	0 31	− 7 42	"
0032−073	0 32	− 7 18	"
0036−392	0 36 02.3	−39 16 13	809908
0037+061	0 37	+ 6 06	ED
0040+51	0 40	+51	
0044+030	0 44 31.2	+ 3 03 35	809908
0046−315	0 46 57.9	−31 32 48	"
0047−832	0 47 10.8	−83 13 10	"
0048−097	0 48 10.0	− 9 45 24	"
0100+020	1 00	+ 2 00	ED
0102+48	1 02	+48	
0108+38	1 08	+38	
0109+22	1 09 23.6	+22 28 45	809908
0109+224	"	"	"
0118−272	1 18	−27 12	ED
0120+092	1 20	+ 9 12	"
0121+034	1 21	+ 3 24	"
0122−380	1 22 02.2	−38 00 04	809908
0135−247	1 35 17.2	−24 46 09	"
0139−097	1 39	− 9 42	ED
0202+14	2 02	+14	"
0202−765	2 02 00.2	−76 34 29	809908
0205−010	2 05	− 1 00	ED
0215+015	2 15 13.5	+ 1 30 54	809908
0217−189	2 17	−18 54	ED
0223+34	2 23	+34	
0235+16	2 35 52.6	+16 24 05	809908
0235+164	"	"	"
0237−233	2 37 52.7	−23 22 09	"
0240+007	2 40	+ 0 42	ED
0241+622	2 41 01.3	+62 15 27	809908
0254−334/2	2 54 43.8	−33 27 29	"
0256+075	2 56	+ 7 30	ED
0300+47	3 00 10.0	+47 04 33	809908
0300+471	"	"	"
0301−243	3 01	−24 18	ED
0302−223	3 02	−22 18	"
0312−770	3 12 55.7	−77 03 01	809908
0318−196	3 18	−19 36	ED
0332+078	3 32	+ 7 48	
0337−21	3 37	−21	ED
0341−256	3 41	−25 36	"
0346−163	3 46	−16 18	"
0347−383	3 47 53.7	−38 19 30	809908
0348+049	3 48	+ 4 54	
0351+026	3 51	+ 2 36	ED
0355−483	3 55 52.6	−48 20 50	809908
0402−362	4 02 02.2	−36 13 16	"
0406+121	4 06	+12 06	
0406+121	4 06 35.6	+12 09 50	790910
0420−01	4 20 43.5	− 1 27 28	809908
0420−388	4 20 30.1	−38 51 50	780901
0422+004	4 22 12.5	+ 0 29 17	809908
0422−380	4 22 55.6	−38 03 02	"
0442−18	4 42	−18	ED
0454−220	4 54 02.2	−22 03 56	809908
0454−234	4 54	−23 24	ED
0458+138	4 58	+13 48	
0506+101	5 06	+10 06	ED
0521−36	5 21 13.7	−36 30 12	809908
0521−365	"	"	"
0528+134	5 28	+13 24	ED
0528−250	5 28 05.2	−25 05 43	809908
0537−286	5 37 56.9	−28 41 27	"
0537−441	5 37 20.5	−44 06 40	"
0539−057	5 39	− 5 42	
0548−322	5 48 50.3	−32 16 56	809908
0602+67	6 02	+67	
0622−441	6 22 02.7	−44 11 24	809908
0659+44	6 59	+44	ED
0727−11	7 27	−11	"
0735+17	7 35 14.1	+17 49 11	809908
0735+178	"	"	"
0736+01	7 36 42.5	+ 1 44 00	"
0739−14	7 39 59.3	−14 35 42	
0754+100	7 54 22.6	+10 04 39	809908
0818−128	8 18 36.2	−12 49 25	"
0822+67	8 22	+67	ED
0823+033	8 23	+ 3 18	"
0823−223	8 23	−22 18	"
0827+24	8 27 54.4	+24 21 07	689906
0829+046	8 29 10.9	+ 4 39 51	809908
0837−120	8 37 28.0	−12 03 54	"
0840+42	8 40	+42	ED
0844+377	8 44	+37 42	"
0919+515	9 19	+51 30	"
0919−260	9 19 16.7	−26 05 54	809908
0925−203	9 25 33.6	−20 21 45	"
0931−114	9 31	−11 24	
0948.9+4426	9 48 54	+44 26	ED
0949.9+4409	9 49 54	+44 09	"
0957+561	9 57 57.3	+56 08 23	809908
0957+561 A	"	"	"
0957+561 AB	9 57 57.3	+56 08 20	ED
0957+561 B	9 57 57.4	+56 08 17	809908
1011+250	10 11 05.7	+25 04 11	"
1028+313	10 28 09.8	+31 18 21	"
1032−199	10 32	−19 54	ED
1034−293	10 34	−29 18	"
1034−293	10 34 55.9	−29 18 27	809908
1049.4−0904	10 49 24	− 9 04	ED
1055+01	10 55 55.5	+ 1 49 42	809908
1059+730	10 59	+73 00	ED
1100+223	11 00	+22 18	
1101−325	11 01 08.2	−32 35 05	809908
1103−006	11 03 58.1	− 0 36 38	"
1104+167	11 04 35.2	+16 44 06	"
1107−187	11 07	−18 42	
1124−186	11 24	−18 36	ED
1128−047	11 28	− 4 42	"
1133+46	11 33	+46	"
1143−245	11 43 36.4	−24 30 53	809908
1144−379	11 44	−37 54	ED
1145−071	11 45	− 7 06	"
1145−61	11 45	−61	
1146−037	11 46 23.9	− 3 47 30	809908
1153+2341	11 53	+23 41	ED
1156−094	11 56	− 9 24	"
1157+46	11 57	+46	"
1203−261	12 03	−26 06	"
1218+304	12 18 51.8	+30 27 14	809908
1219+28	12 19 01.1	+28 30 36	"
1223−62	12 23	−62	
1225+317	12 25 55.9	+31 45 13	809908
1226+023	12 26 33.4	+ 2 19 42	"
1232−249	12 32 59.4	−24 55 46	"
1239+1852	12 39	+18 52	ED
1239−599 NOM.	12 39	−59 54	
1239−599 6	"	"	
1239−599 12	"	"	
1243−072	12 43 28.8	− 7 14 24	809908
1244−255	12 44 06.7	−25 31 26	"
1253+4422	12 53	+44 22	ED
1256−220	12 56	−22 00	"
1258−61	12 58	−61	
1302−102	13 02 55.8	−10 17 17	809908
1304+3110	13 04	+31 10	ED
1305+2952	13 05	+29 52	"
1308+32	13 08 07.6	+32 36 41	809908
1308+326	"	"	"
1309−216	13 09 49.6	−21 40 30	"
1318.1+3157	13 18 06	+31 57	ED
1327−214	13 27 23.4	−21 26 34	809908
1335−127	13 35	−12 42	ED
1339+053	13 39	+ 5 18	"
1346−03	13 46 08.3	− 3 38 31	809908
1349−439	13 49 51.4	−43 57 49	"
1352−104	13 52	−10 24	ED
1354−152	13 54	−15 12	"
1355−416	13 55 57.3	−41 38 19	809908
1402+044	14 02 30.0	+ 4 29 55	"
1403+546	14 03	+54 36	ED
1406−076	14 06 17.9	− 7 38 16	809908
1413+135	14 13	+13 30	ED
1418+54	14 18 00.0	+54 40 00	809908
1418+546	"	"	"
1424−419	14 24	−41 54	ED
1431+3146	14 31	+31 46	"
1432+42	14 32	+42	"
1442+101	14 42 50.6	+10 11 13	809908
1510−08	15 10 09.0	− 8 54 48	"
1510−089	"	"	"
1511−100	15 11	−10 00	ED
1514−241	15 14 45.3	−24 11 22	809908
1519+279	15 19	+27 54	ED
1519−273	15 19	−27 18	"
1526+286	15 26	+28 36	"
1532+016	15 32	+ 1 36	"
1534.4+3748	15 34 24	+37 48	"
1538+149	15 38 30.6	+14 57 25	809908
1538−522 G	15 38	−52 12	
1538−522 NOM.	"	"	
1538−522 12	"	"	
1543+46	15 43	+46	ED
1543−47	15 43	−47	"
1553−54 12	15 53	−54	"
1556−605 NOM.	15 56	−60 30	"
1556−605 24	"	"	
1556−605 41	"	"	
1557+272	15 57	+27 12	ED
1604.0+3935	16 04 00	+39 35	"
1607.6+3953	16 07 36	+39 53	"
1613+31	16 13	+31	"
1617−155	16 17	−15 30	
1620+103	16 20 12.3	+10 20 12	809908
1622−253	16 22	−25 18	ED
1623+26	16 23 44.8	+26 51 27	809908
1635+119	16 35 26.1	+11 55 41	"
1640+396	16 40	+39 36	ED
1640+401	16 40	+40 06	"
1641+399	16 41 17.6	+39 54 11	809908
1642−455 G1	16 42	−45 30	
1642−455 G2	"	"	
1642−455 NOM.	"	"	
1647+43	16 47	+43	ED
1653−40	16 53	−40	"
1700−37	17 00 32.6	−37 46 28	CSI 79
1701+610	17 01	+61 00	ED
1702−363 NOM.	17 02	−36 18	
1702−363 ZG	"	"	ED
1702−363 4	"	"	"
1704+607	17 04 03.5	+60 48 31	809908
1705−440 NOM.	17 05	−44 00	
1705−440 3	"	"	ED
1715−321 NOM.	17 15	−32 06	
1715−321 12	"	"	
1717+178	17 16 57.0	+17 45 00	809908
1722+119	17 22	+11 54	ED
1726+499	17 26	+49 54	"
1727+50	17 27 04.3	+50 15 31	809908
1727+502	"	"	"
1728−16 E	17 28	−16	ED
1728−16 NOM.	"	"	
1728−247 GF	17 28	−24 42	ED
1728−247 NOM.	"	"	
1742−294 G1	17 42	−29 24	
1742−294 G2	"	"	
1742−294 NOM.	"	"	
1749+096	17 49 10.4	+ 9 39 43	809908
1758−20 NOM.	17 58	−20	
1758−205 G	17 58	−20 30	
1758−205 NOM.	"	"	
1758−250 G	17 58	−25 00	
1758−250 G2	"	"	
1758−250 NOM.	"	"	
1758−250 4	"	"	
1758−250 8	"	"	
1758−250 9	"	"	
1811−171 G1	18 11	−17 06	
1811−171 NOM.	"	"	
1813−14	18 13	−14	ED
1845−024 G	18 45	− 2 24	
1845−024 NOM.	"	"	
1845−024 2	"	"	
1847+335	18 47	+33 30	ED
1921−293	19 21	−29 18	"
1953−325	19 53	−32 30	"
1954−388	19 54 39.0	−38 53 13	809908
2005+40	20 05 59.5	+40 21 02	"
2032+107	20 32 58.6	+10 45 42	"
2044−168	20 44 30.8	−16 50 09	"
2047+098	20 47	+ 9 48	
2058−425	20 58 42.3	−42 31 05	809908
2106−413	21 06	−41 18	ED
2115−305	21 15 11.2	−30 31 50	809908
2126−158	21 26 26.7	−15 51 52	"
2131−021	21 31 35.3	− 2 06 36	"
2134+00	21 34 05.3	+ 0 28 25	"
2134+004	"	"	"
2135−147	21 35 01.2	−14 46 27	"
2141+174	21 41	+17 24	ED
2155−152	21 55 23.1	−15 15 21	809908
2155−304	21 55 58.2	−30 27 52	"
2201+171	22 01 02.9	+17 11 19	"
2204−408	22 04 33.0	−40 51 35	"
2207+020	22 07 00.3	+ 2 03 56	"
2212−299	22 12 25.1	−29 59 20	"
2215−037	22 15	− 3 42	ED
2216−03	22 16 16.0	− 3 50 36	809908
2216−043	22 16	− 4 18	ED
2227−399	22 27 45.2	−39 58 24	809908
2233−148	22 33	−14 48	ED
2240−260	22 40	−26 00	"
2246−309	22 46 32.5	−30 55 00	809908
2251+15	22 51 29.5	+15 52 55	"
2251−178	22 51 25.9	−17 50 54	"
2254+074	22 54 46.0	+ 7 27 10	"
2254−204	22 54	−20 24	ED
2255+41	22 55 04.7	+41 38 14	790910
2255+416	"	"	"
2300−683	23 00 28.5	−68 23 56	809908
2310−322	23 10 27.5	−32 14 07	"
2329−384	23 29 18.9	−38 28 22	"
2335+031	23 35 34.5	+ 3 10 01	"
2344+184	23 44	+18 24	ED
2352−342	23 52 50.5	−34 14 20	809908
2358+40	23 58	+40	ED
0.0+0.0	17 42	−28 55	"
0.02−0.06	17 42 43.5	−28 55 58	
0.03−0.10	17 42 54.4	−28 56 28	
0.03−0.40	17 44 05.5	−29 06 00	
0.04−0.25	17 43 30.5	−29 00 58	
0.04−0.57	17 44 45.5	−29 11 02	
0.05−1.50	17 48 26.4	−29 39 15	
0.08−0.19	17 43 22.2	−28 56 29	
0.11−0.36	17 44 05.7	−29 00 30	
0.11−0.38	17 44 11.1	−29 01 00	
0.12−0.19	17 43 28.5	−28 54 59	
0.12−1.57	17 48 54.6	−29 37 46	
0.13−0.43	17 44 26.2	−29 02 01	
0.13−0.64	17 45 13.6	−29 08 32	
0.14−1.64	17 49 11.6	−29 38 47	
0.17−0.39	17 44 22.4	−28 58 31	
0.17−1.70	17 49 29.4	−29 39 17	
0.18−0.41	17 44 29.1	−28 58 31	
0.18−1.80	17 49 55.5	−29 41 48	
0.2+0.0	17 42 44.8	−28 44 08	
0.20−0.60	17 45 15.2	−29 03 32	
0.20−1.71	17 49 37.1	−29 37 48	
0.23−0.56	17 45 10.3	−29 01 02	
0.23−0.76	17 45 58.0	−29 07 04	
0.23−1.79	17 50 00.8	−29 39 18	
0.25−0.72	17 45 51.6	−29 04 33	
0.25−1.82	17 50 11.1	−29 38 49	
0.26−0.54	17 45 10.2	−28 58 33	
0.26−0.61	17 45 26.6	−29 01 03	
0.27−0.59	17 45 23.1	−28 59 36	
0.27−0.65	17 45 37.7	−29 01 33	
0.27−1.92	17 50 36.1	−29 40 50	
0.27−1.93	17 50 39.3	−29 41 20	
0.28−0.61	17 45 30.2	−29 00 03	
0.28−0.74	17 45 59.3	−29 03 34	
0.28−0.77	17 46 06.7	−29 05 04	
0.28−0.97	17 46 53.3	−29 11 07	
0.29−0.66	17 45 42.8	−29 01 03	
0.29−0.99	17 47 01.3	−29 11 07	
0.29−2.00	17 51 00.1	−29 42 21	

NAME	RA (1950) DEC	POS REF
	h m s ° ′ ″	
0.31−0.59	17 45 30.3 −28 57 34	
0.31−1.91	17 50 40.6 −29 38 50	
0.31−2.02	17 51 06.2 −29 41 51	
0.31−2.06	17 51 16.6 −29 43 21	
0.32−0.74	17 46 06.2 −29 01 34	
0.32−2.09	17 51 24.2 −29 43 21	
0.33−0.56	17 45 24.3 −28 55 33	
0.33−0.62	17 45 39.2 −28 57 34	
0.33−2.01	17 51 07.9 −29 40 21	
0.34−0.67	17 45 51.6 −28 58 34	
0.34−1.97	17 50 57.9 −29 38 51	
0.35−0.65	17 45 48.5 −28 57 34	
0.35−0.94	17 46 56.9 −29 06 37	
0.35−2.10	17 51 30.9 −29 42 22	
0.36−2.05	17 51 21.2 −29 40 21	
0.37−0.90	17 46 51.0 −29 04 07	
0.39−0.76	17 46 21.2 −28 59 05	
0.39−0.79	17 46 27.5 −28 59 35	
0.39−0.81	17 46 31.9 −29 00 05	
0.39−2.10	17 51 36.1 −29 40 22	
0.40−2.14	17 51 48.3 −29 40 52	
0.41−0.80	17 46 31.0 −28 59 06	
0.41−2.11	17 51 40.7 −29 39 22	
0.42−0.75	17 46 20.9 −28 57 05	
0.42−0.86	17 46 47.5 −29 00 05	
0.42−1.03	17 47 28.3 −29 06 07	
0.43−0.83	17 46 43.4 −28 59 06	
0.43−2.14	17 51 50.9 −29 39 22	
0.43−2.23	17 52 12.6 −29 41 53	
0.44−0.78	17 46 32.4 −28 56 36	
0.45−2.22	17 52 13.2 −29 40 23	
0.46−0.72	17 46 20.1 −28 54 06	
0.46−0.76	17 46 31.6 −28 55 06	
0.46−0.83	17 46 46.2 −28 57 06	
0.47−2.16	17 52 02.1 −29 37 53	
0.48−2.18	17 52 07.6 −29 37 53	
0.48−2.30	17 52 36.8 −29 41 24	
0.49−1.22	17 48 21.6 −29 08 10	
0.50−0.82	17 46 51.6 −28 55 07	
0.50−0.85	17 46 56.2 −28 56 07	
0.50−1.20	17 48 18.9 −29 07 09	
0.51−0.88	17 47 04.9 −28 56 07	
0.52−0.98	17 47 31.1 −28 59 08	
0.52−1.03	17 47 41.8 −29 00 37	
0.52−1.07	17 47 53.0 −29 01 38	
0.52−1.21	17 48 24.5 −29 06 09	
0.53−1.31	17 48 48.9 −29 08 40	
0.54−1.22	17 48 30.2 −29 05 39	
0.54−1.25	17 48 36.9 −29 06 09	
0.55−1.33	17 48 56.7 −29 08 11	
0.55−2.32	17 52 51.3 −29 38 55	
0.56−1.09	17 48 02.1 −29 00 38	
0.56−1.42	17 49 19.2 −29 10 11	
0.56−2.46	17 53 25.9 −29 42 26	
0.57−1.12	17 48 09.9 −29 00 38	
0.57−1.19	17 48 26.6 −29 02 40	
0.59−0.99	17 47 41.3 −28 55 38	
0.59−0.99	17 47 43.9 −28 55 38	
0.60−0.95	17 47 33.1 −28 54 08	
0.60−2.45	17 53 29.1 −29 39 56	
0.61−1.03	17 47 55.7 −28 56 09	
0.61−1.42	17 49 27.5 −29 08 12	
0.62−2.51	17 53 45.6 −29 40 27	
0.63−1.09	17 48 12.5 −28 56 40	
0.63−1.17	17 48 31.5 −28 59 10	
0.64−1.25	17 48 50.4 −29 01 10	
0.64−1.48	17 49 44.1 −29 08 13	
0.65−1.11	17 48 19.7 −28 56 10	
0.65−2.54	17 53 59.2 −29 39 57	
0.65−2.65	17 54 25.2 −29 43 28	
0.67−1.35	17 49 19.0 −29 02 42	
0.68−1.65	17 50 31.3 −29 11 15	
0.69−1.61	17 50 24.3 −29 09 44	
0.70−1.40	17 49 33.6 −29 02 43	
0.71−1.60	17 50 22.1 −29 08 14	
0.73−1.26	17 49 05.1 −28 56 41	
0.73−1.56	17 50 17.2 −29 06 13	
0.73−1.67	17 50 42.7 −29 09 14	
0.73−2.60	17 54 23.0 −29 37 58	
0.74−1.18	17 48 47.9 −28 54 11	
0.74−1.22	17 48 58.1 −28 55 11	
0.74−1.31	17 49 18.3 −28 58 12	
0.76−1.28	17 49 14.8 −28 55 42	
0.76−1.47	17 49 58.6 −29 01 42	
0.77−1.27	17 49 12.4 −28 55 12	
0.77−1.36	17 49 35.3 −28 58 13	
0.77−1.39	17 49 43.4 −28 58 43	
0.77−1.72	17 51 00.5 −29 09 15	
0.77−1.74	17 51 05.1 −29 09 15	
0.78−1.50	17 50 09.0 −29 01 43	
0.78−1.67	17 50 50.6 −29 06 45	
0.79−1.69	17 50 55.1 −29 06 46	
0.80−1.56	17 50 25.5 −29 02 44	
0.80−1.60	17 50 35.7 −29 03 44	
0.80−2.79	17 55 17.8 −29 40 00	
0.81−1.47	17 50 07.9 −28 59 14	
0.81−2.89	17 55 43.4 −29 42 31	
0.82−1.35	17 49 40.6 −28 55 13	
0.82−1.48	17 50 11.0 −28 59 14	
0.82−1.55	17 50 27.7 −29 01 13	
0.82−1.64	17 50 47.4 −29 03 44	
0.82−1.66	17 50 53.8 −29 04 44	
0.82−2.80	17 55 24.1 −29 39 00	
0.83−1.46	17 50 08.0 −28 57 44	
0.83−1.50	17 50 16.5 −28 59 14	
0.84−1.61	17 50 44.3 −29 01 44	
0.84−1.68	17 50 59.2 −29 04 16	
0.84−1.84	17 51 37.2 −29 08 46	
0.84−1.86	17 51 42.4 −29 09 47	
0.85−1.47	17 50 13.1 −28 57 14	
0.85−1.90	17 51 52.5 −29 10 17	
0.85−2.96	17 56 06.4 −29 42 32	
0.86−1.52	17 50 26.3 −28 58 14	
0.86−1.62	17 50 48.6 −29 01 14	
0.87−1.53	17 50 29.4 −28 57 45	
0.87−1.57	17 50 38.8 −28 59 15	
0.87−2.87	17 55 47.2 −29 39 01	
0.89−1.82	17 51 41.8 −29 05 46	

NAME	RA (1950) DEC	POS REF
	h m s ° ′ ″	
0.91−1.47	17 50 20.1 −28 54 14	
0.91−1.48	17 50 23.3 −28 54 44	
0.91−1.55	17 50 40.3 −28 56 45	
0.92−1.58	17 50 47.9 −28 57 15	
0.92−1.71	17 51 18.0 −29 00 45	
0.92−1.91	17 52 05.6 −29 06 48	
0.92−1.92	17 52 08.5 −29 07 17	
0.93−1.94	17 52 15.7 −29 07 17	
0.94−1.78	17 51 38.0 −29 02 17	
0.94−2.03	17 52 38.1 −29 09 49	
0.95−1.57	17 50 48.9 −28 55 15	
0.96−1.70	17 51 22.6 −28 58 16	
0.98−1.71	17 51 28.5 −28 57 47	
0.98−1.85	17 52 00.2 −29 02 18	
0.99−1.79	17 51 48.2 −28 59 46	
0.99−2.03	17 52 43.4 −29 07 18	
1.00−2.07	17 52 56.5 −29 07 49	
1.02−1.70	17 51 29.5 −28 55 17	
1.03−1.80	17 51 54.1 −28 57 48	
1.03−1.90	17 52 18.8 −29 01 17	
1.04−2.23	17 53 38.4 −29 10 20	
1.05−1.82	17 52 02.6 −28 57 48	
1.09−1.86	17 52 18.5 −28 56 48	
1.10−1.89	17 52 26.8 −28 56 49	
1.10−1.92	17 52 32.6 −28 57 49	
1.11−1.94	17 52 40.4 −28 58 19	
1.15−2.07	17 53 16.7 −28 59 50	
1.16−2.04	17 53 10.9 −28 58 20	
1.16−2.17	17 53 41.2 −29 02 21	
1.16−2.29	17 54 09.7 −29 05 52	
1.18−1.97	17 52 57.1 −28 55 20	
1.18−2.10	17 53 26.9 −28 59 21	
1.18−2.44	17 54 47.3 −29 09 54	
1.20−2.48	17 54 59.6 −29 09 54	
1.21−1.98	17 53 03.6 −28 54 20	
1.21−2.15	17 53 42.1 −28 59 22	
1.21−2.33	17 54 26.0 −29 04 52	
1.24−2.45	17 54 57.0 −29 06 54	
1.26−2.28	17 54 22.0 −29 00 52	
1.27−2.11	17 53 42.3 −28 54 52	
1.28−2.14	17 53 49.9 −28 55 22	
1.28−2.27	17 54 19.5 −28 59 23	
1.30−2.17	17 54 00.3 −28 55 22	
1.30−2.19	17 54 05.1 −28 55 52	
1.30−2.28	17 54 26.7 −28 58 53	
1.30−2.38	17 54 49.1 −29 01 23	
1.31−2.68	17 56 02.6 −29 10 26	
1.32−2.21	17 54 13.3 −28 55 23	
1.32−2.23	17 54 17.8 −28 55 53	
1.34−2.27	17 54 29.7 −28 56 23	
1.34−2.73	17 56 19.8 −29 09 57	
1.35−2.44	17 55 12.6 −29 00 54	
1.36−2.48	17 55 21.4 −29 01 24	
1.38−2.29	17 54 40.5 −28 54 54	
1.41−2.43	17 55 17.6 −28 57 25	
1.41−2.85	17 56 56.2 −29 09 59	
1.41−2.86	17 56 59.2 −29 10 28	
1.42−2.54	17 55 44.3 −29 00 25	
1.42−2.87	17 57 02.7 −29 09 59	
1.43−2.36	17 55 03.3 −28 54 24	
1.43−2.38	17 55 06.9 −28 54 55	
1.43−2.46	17 55 25.7 −28 57 25	
1.43−2.48	17 55 30.9 −28 57 55	
1.44−2.59	17 55 59.2 −29 00 56	
1.45−2.61	17 56 06.2 −29 00 56	
1.45−2.64	17 56 11.5 −29 01 26	
1.46−2.41	17 55 19.0 −28 54 25	
1.47−2.67	17 56 22.5 −29 01 56	
1.48−0.06	17 46 12.4 −27 41 01	
1.48−2.51	17 55 44.6 −28 56 26	
1.51−2.50	17 55 46.9 −28 54 26	
1.51−2.64	17 56 21.4 −28 58 27	
1.54−2.55	17 56 03.3 −28 54 27	
1.54−2.77	17 56 54.9 −29 00 58	
1.56−2.62	17 56 21.5 −28 55 27	
2.6−0.4	17 50 10.8 −26 55 58	
2.6−0.4	17 50 10.9 −26 56 00	
2.60−0.40	17 50 10.8 −26 55 58	
4.31+2.85	17 41 44.5 −23 45 29	
4.32+2.85	17 41 44.9 −23 44 29	
4.39+2.80	17 42 06.0 −23 42 29	
4.41+2.87	17 41 53.2 −23 39 29	
4.42+2.72	17 42 28.1 −23 43 30	
4.48+2.56	17 43 12.8 −23 45 32	
4.53+2.67	17 42 55.5 −23 39 31	
4.54+2.44	17 43 47.2 −23 46 03	
4.54+2.66	17 42 57.8 −23 39 31	
4.55+2.58	17 43 17.1 −23 41 32	
4.57+2.30	17 44 21.7 −23 49 04	
4.62+2.53	17 43 38.8 −23 39 33	
4.65+2.31	17 44 30.7 −23 44 35	
4.67+2.24	17 44 48.8 −23 46 05	
4.67+2.36	17 44 22.8 −23 42 04	
4.74+2.09	17 45 31.4 −23 47 07	
4.77+2.09	17 45 35.4 −23 45 37	
4.78+2.06	17 45 46.1 −23 46 07	
4.79+2.09	17 45 38.6 −23 44 37	
4.83+2.14	17 45 33.6 −23 40 37	
4.85+2.10	17 45 45.8 −23 41 07	
4.91+1.90	17 46 38.8 −23 44 09	
4.92+1.69	17 47 28.3 −23 50 11	
4.93+1.77	17 47 10.4 −23 47 10	
4.93+1.91	17 46 39.6 −23 43 09	
4.97+1.66	17 47 41.3 −23 48 42	
4.98+1.70	17 47 32.8 −23 46 41	
4.99+1.61	17 47 55.7 −23 49 12	
5.00+1.55	17 48 09.2 −23 50 13	
5.00+1.84	17 47 04.1 −23 41 10	
5.03+1.56	17 48 11.9 −23 48 43	
5.05+1.57	17 48 10.6 −23 47 13	
5.07+1.54	17 48 21.3 −23 47 13	
5.10+1.43	17 48 50.2 −23 48 44	
5.14+1.58	17 48 22.2 −23 42 13	
5.21+1.56	17 48 35.9 −23 39 44	
5.23+1.35	17 49 24.8 −23 44 45	
5.24+1.27	17 49 46.1 −23 46 46	
5.26+1.19	17 50 03.9 −23 48 17	
5.26+1.36	17 49 26.7 −23 42 45	

NAME	RA (1950) DEC	POS REF
	h m s ° ′ ″	
5.29+1.13	17 50 23.1 −23 48 17	
5.31+1.32	17 49 41.3 −23 41 46	
5.32+1.05	17 50 46.5 −23 49 18	
5.36+1.03	17 50 54.3 −23 47 48	
5.36+1.07	17 50 46.2 −23 46 48	
5.37+0.96	17 51 11.1 −23 49 19	
5.4+1.2	17 50 −23 41	ED
5.4−0.8	17 58 −24 41	"
5.40+1.12	17 50 39.9 −23 43 18	
5.40+1.20	17 50 21.1 −23 40 47	
5.41+1.05	17 50 56.0 −23 44 49	
5.41+1.10	17 50 47.2 −23 43 18	
5.43+1.15	17 50 37.4 −23 40 48	
5.44+0.89	17 51 36.3 −23 47 50	
5.49+1.05	17 51 08.3 −23 40 49	
5.51+0.94	17 51 35.0 −23 42 50	
5.53+0.96	17 51 33.1 −23 41 20	
5.56+0.80	17 52 13.2 −23 44 51	
5.57+0.74	17 52 29.6 −23 45 52	
5.59+0.81	17 52 15.0 −23 42 52	
5.60+0.69	17 52 42.4 −23 45 53	
5.63+0.75	17 52 33.5 −23 42 22	
5.65+0.60	17 53 11.0 −23 46 24	
5.68+0.76	17 52 39.1 −23 39 52	
5.74+0.39	17 54 10.3 −23 47 56	
5.77+0.35	17 54 24.3 −23 47 26	
5.78+0.37	17 54 20.0 −23 46 26	
5.81+0.37	17 54 23.8 −23 44 56	
5.82+0.23	17 54 58.4 −23 48 27	
5.82+0.26	17 54 51.6 −23 47 27	
5.83+0.40	17 54 18.8 −23 42 56	
5.85+0.30	17 54 46.1 −23 44 57	
5.86+0.33	17 54 39.0 −23 43 27	
5.88+0.41	17 54 24.8 −23 39 56	
05.89−0.40	17 57 27.2 −24 04 10	
5.9−0.4	17 57 26.8 −24 04 11	
5.9−0.8	17 59 −24 15	ED
5.90+0.38	17 54 33.9 −23 39 57	
5.91+0.24	17 55 08.4 −23 43 28	
5.91+0.30	17 54 54.3 −23 41 57	
5.91+0.33	17 54 47.3 −23 40 57	
5.92+0.05	17 55 50.6 −23 48 29	
5.92+0.15	17 55 27.8 −23 45 59	
5.96+0.07	17 44 50.7 −23 45 59	
5.97+0.11	17 55 43.6 −23 44 29	
5.98+0.01	17 56 07.2 −23 47 00	
6.01+0.02	17 56 10.1 −23 45 00	
6.03−0.13	17 56 45.2 −23 48 31	
6.04−0.15	17 56 51.7 −23 48 31	
6.05−0.19	17 57 02.2 −23 49 32	
6.07+0.0	17 56 21.9 −23 42 30	
6.07+0.05	17 56 10.5 −23 41 00	
6.08−0.29	17 57 28.9 −23 50 33	
6.11−0.15	17 57 00.2 −23 45 02	
6.13−0.09	17 56 50.9 −23 42 02	
6.24−0.30	17 57 52.6 −23 42 34	
6.28−0.31	17 57 58.7 −23 41 04	
6.34−0.44	17 58 36.2 −23 41 35	
6.37−0.49	17 58 53.5 −23 41 36	
6.38−0.68	17 59 36.2 −23 46 38	
6.39−0.72	17 59 48.4 −23 47 38	
6.39−0.74	17 59 51.4 −23 48 08	
6.43−0.75	17 59 59.6 −23 46 08	
6.44−0.72	17 59 54.1 −23 45 08	
6.44−0.79	18 00 09.9 −23 47 09	
6.47−0.61	17 59 33.9 −23 40 07	
6.48−0.71	17 59 58.0 −23 42 38	
6.49−0.76	18 00 08.6 −23 43 39	
6.55−1.10	18 01 35.9 −23 50 42	
6.58−0.91	18 00 55.4 −23 43 10	
6.60−1.09	18 01 39.3 −23 47 42	
6.61−1.08	18 01 37.3 −23 46 42	
6.64−0.96	18 01 15.6 −23 41 41	
6.67−1.33	18 02 42.9 −23 50 44	
6.69−1.26	18 02 30.6 −23 47 44	
6.69−1.36	18 02 53.0 −23 50 45	
6.70−1.09	18 01 51.7 −23 42 13	
6.71−1.07	18 01 49.9 −23 41 12	
6.73−1.19	18 02 17.7 −23 43 43	
6.74−1.31	18 02 48.4 −23 46 45	
6.84−1.32	18 03 03.0 −23 42 15	
6.86−1.30	18 03 01.1 −23 40 15	
6.86−1.46	18 03 38.0 −23 44 46	
6.94−1.59	18 04 16.5 −23 44 48	
6.96−1.48	18 03 55.7 −23 40 17	
6.97−1.49	18 03 58.8 −23 40 17	
6.98−1.52	18 04 05.3 −23 40 17	
7.00−1.75	18 05 02.3 −23 46 19	
7.01−1.56	18 04 18.3 −23 40 18	
7.01−1.64	18 04 39.1 −23 42 19	
7.02−1.88	18 05 34.6 −23 48 51	
7.07−1.72	18 05 04.0 −23 41 49	
7.09−1.74	18 05 09.4 −23 41 20	
7.10−1.83	18 05 31.7 −23 43 20	
7.12−1.77	18 05 21.4 −23 40 20	
7.15−2.07	18 06 33.6 −23 47 53	
7.16−1.87	18 05 48.7 −23 41 21	
7.16−2.16	18 06 57.2 −23 49 54	
7.24−2.15	18 07 04.3 −23 45 24	
7.5+0.06	17 59 11.9 −22 27 51	
8.74+2.99	17 51 05.0 −19 53 34	
8.76+2.95	17 51 15.7 −19 53 34	
8.79+2.70	17 52 15.0 −20 00 04	
8.83+2.78	17 52 02.5 −19 55 06	
8.84+2.75	17 52 09.9 −19 56 03	
8.86+2.57	17 52 53.8 −20 00 05	
8.88+2.66	17 52 34.2 −19 56 34	
8.90+2.72	17 52 23.4 −19 53 37	
8.98+2.38	17 53 50.4 −20 00 07	
8.98+2.43	17 53 38.9 −19 58 37	
8.98+2.51	17 53 21.5 −19 56 06	
8.98+2.56	17 53 10.4 −19 54 36	
9.09+2.28	17 54 25.0 −19 57 08	
9.16+2.27	17 54 37.3 −19 53 42	
9.19+2.23	17 54 49.3 −19 53 42	
9.23+1.94	17 55 58.4 −20 00 12	
9.26+2.10	17 55 28.4 −19 53 44	
9.37+1.81	17 56 45.4 −19 56 43	

NAME	RA (1950) DEC	POS REF
	h m s ° ′ ″	
9.49+1.66	17 57 34.4 −19 55 18	
9.49+1.68	17 57 30.0 −19 54 45	
9.52+1.52	17 58 07.8 −19 57 46	
9.68+1.20	17 59 40.1 −19 58 50	
9.7+0.7	18 02 −20 13	ED
9.81+0.92	18 00 58.9 −20 00 23	
9.82+1.10	18 00 19.8 −19 54 51	
9.83+1.11	18 00 19.1 −19 53 54	
9.89+0.90	18 01 13.8 −19 56 53	
10.03+0.67	18 02 23.2 −19 56 26	
10.04+0.59	18 02 41.2 −19 58 26	
10.08+0.52	18 03 01.1 −19 57 57	
10.1−0.1	18 05 18.2 −20 16 46	
10.15+0.54	18 03 07.5 −19 54 00	
10.16+0.47	18 03 22.8 −19 55 31	
10.19+0.51	18 03 17.0 −19 52 58	
10.20+0.39	18 03 45.1 −19 55 32	
10.22+0.28	18 04 13.5 −19 58 00	
10.22+0.46	18 03 33.0 −19 52 58	
10.24+0.39	18 03 51.3 −19 54 02	
10.24+0.42	18 03 42.9 −19 52 58	
10.27+0.25	18 04 25.8 −19 56 30	
10.28+0.23	18 04 31.5 −19 56 30	
10.31+0.17	18 04 50.1 −19 56 31	
10.33+0.06	18 05 15.0 −19 58 32	
10.34+0.13	18 05 01.5 −19 56 31	
10.35+0.14	18 05 00.3 −19 55 34	
10.36+0.08	18 05 15.0 −19 56 32	
10.36+0.20	18 04 47.2 −19 53 01	
10.4+0.0	18 05 38.2 −19 55 28	
10.4−0.2	18 06 −20 03	ED
10.40+0.01	18 05 35.0 −19 56 33	
10.40+0.14	18 05 05.9 −19 53 02	
10.48+0.0	18 05 47.3 −19 53 03	
10.52−0.27	18 06 51.7 −19 58 35	
10.61−0.32	18 07 14.5 −19 55 06	
10.77−0.67	18 08 51.6 −19 57 10	
10.80−0.72	18 09 07.9 −19 57 10	
10.81−0.73	18 09 12.0 −19 56 40	
10.84−0.66	18 08 58.7 −19 53 10	
10.88−0.80	18 09 34.5 −19 55 11	
10.90−0.84	18 09 47.4 −19 55 12	
10.90−0.87	18 09 52.7 −19 56 12	
10.92−0.91	18 10 05.8 −19 56 12	
10.93−1.00	18 10 27.4 −19 58 13	
10.96−1.07	18 10 44.7 −19 58 44	
11.01−1.13	18 11 05.6 −19 57 45	
11.02−1.15	18 11 11.3 −19 58 15	
11.09−1.27	18 11 47.3 −19 57 46	
11.09−1.34	18 12 02.7 −19 59 47	
11.10−1.22	18 11 36.7 −19 55 49	
11.18−1.46	18 12 39.5 −19 58 18	
11.26−1.65	18 13 32.2 −19 59 50	
11.29−1.55	18 13 13.0 −19 55 19	
11.31−1.61	18 13 29.4 −19 56 20	
11.33−1.77	18 14 08.4 −19 59 51	
11.40−1.83	18 14 30.8 −19 57 22	
11.57−2.26	18 16 27.1 −20 00 56	
11.59−2.07	18 15 47.7 −19 54 28	
11.6+0.1	18 07 41.7 −18 53 32	
11.60−2.11	18 15 56.7 −19 54 55	
11.63−2.18	18 16 17.1 −19 55 26	
12.21−0.11	18 09 44.9 −18 25 09	
12.91−0.26	18 11 44.2 −17 52 57	
14.17−0.06	18 13 32.6 −16 40 58	
14.17−0.06	18 13 32.9 −16 40 43	
15.1−0.7	18 18 −16 10	ED
16.4−0.6	18 20 −14 59	"
17.1+0.9	18 16 −13 39	"
17.4−0.6	18 22 −14 06	"
18.2−0.4	18 23 −13 18	"
18.3+0.4	18 19 53.1 −12 49 11	
18.3+0.4	18 19 54.1 −12 48 54	
18.4+1.8	18 15 −12 05	ED
19.2+0.4	18 22 −12 02	"
19.2−1.0	18 26 40.1 −12 39 57	
19.60−0.23	18 24 48.7 −11 59 25	
20.2−0.8	18 28 −11 43	ED
20.3−0.1	18 25 26.9 −11 18 08	
20.4−0.3	18 26 48.5 −11 17 56	
20.60+1.48	18 20 34.5 −10 17 26	
20.66+1.27	18 21 27.5 −10 20 28	
20.69+1.15	18 21 56.2 −10 22 29	
20.7+0.1	18 25 41.6 −10 52 22	
20.7+0.1	18 25 41.9 −10 52 33	
20.70+1.26	18 21 33.9 −10 18 29	
20.72+1.30	18 21 26.2 −10 16 28	
20.74+1.32	18 21 25.5 −10 14 28	
20.75+1.35	18 21 20.8 −10 13 28	
20.76+1.06	18 22 22.2 −10 21 00	
20.78+1.04	18 22 30.6 −10 20 31	
20.79+1.01	18 22 37.0 −10 21 01	
20.79+1.05	18 22 29.8 −10 19 31	
20.8+1.5	18 21 −10 06	ED
20.83+0.91	18 23 02.8 −10 21 32	
20.85+1.05	18 22 35.9 −10 16 31	
20.91+0.75	18 23 46.8 −10 21 33	
20.91+1.01	18 22 52.7 −10 14 31	
20.93+0.72	18 23 54.6 −10 21 45	
20.94+0.90	18 23 19.1 −10 15 58	
20.95+0.73	18 23 55.4 −10 20 34	
20.95+0.85	18 23 29.4 −10 16 59	
20.95+0.87	18 23 26.7 −10 16 33	
20.95+0.94	18 23 09.9 −10 14 32	
20.96+0.77	18 23 48.6 −10 18 34	
20.98+0.85	18 23 33.7 −10 15 33	
20.99+0.75	18 23 57.9 −10 17 34	
21.00+0.84	18 23 38.3 −10 14 33	
21.01+0.68	18 24 12.7 −10 18 34	
21.03+0.56	18 24 42.4 −10 21 05	
21.05+0.74	18 24 06.8 −10 14 34	
21.09+0.48	18 25 04.6 −10 20 06	
21.11+0.47	18 25 11.4 −10 19 07	
21.11+0.55	18 24 52.2 −10 17 02	
21.12+0.44	18 25 18.9 −10 19 37	
21.14+0.39	18 25 31.0 −10 19 37	
21.15+0.45	18 25 20.6 −10 17 37	
21.16+0.23	18 26 07.6 −10 23 20	
21.19+0.48	18 25 16.4 −10 14 37	
21.20+0.37	18 25 41.5 −10 17 04	
21.22+0.35	18 25 50.1 −10 16 38	
21.23+0.45	18 25 29.1 −10 13 37	
21.24+0.12	18 26 40.6 −10 21 51	
21.26+0.10	18 26 48.3 −10 21 40	
21.26+0.32	18 25 59.8 −10 15 38	
21.29+0.26	18 26 17.2 −10 15 39	
21.30+0.23	18 26 23.9 −10 16 05	
21.31+0.22	18 26 28.2 −10 15 39	
21.33+0.02	18 27 13.5 −10 20 11	
21.33+0.13	18 26 49.3 −10 17 06	
21.35−0.07	18 27 33.8 −10 21 42	
21.36−0.11	18 27 43.6 −10 21 53	
21.37−0.08	18 27 39.2 −10 20 42	
21.39−0.04	18 27 33.4 −10 18 42	
21.39−0.14	18 27 54.0 −10 21 12	
21.40−0.11	18 27 48.8 −10 20 12	
21.44−0.17	18 28 04.6 −10 19 43	
21.48−0.10	18 27 55.7 −10 15 42	
21.49−0.05	18 27 45.7 −10 13 42	
21.49−0.17	18 28 10.8 −10 17 09	
21.51−0.31	18 28 45.0 −10 19 44	
21.59−0.52	18 29 39.4 −10 21 46	
21.60−0.34	18 29 01.8 −10 15 45	
21.60−0.50	18 29 36.9 −10 20 16	
21.62−0.59	18 29 56.4 −10 21 58	
21.65−0.37	18 29 13.2 −10 13 45	
21.68−0.45	18 29 33.4 −10 14 46	
21.68−0.50	18 29 44.3 −10 16 12	
21.69−0.47	18 29 39.3 −10 14 46	
21.70−0.78	18 30 48.3 −10 22 49	
21.73−0.52	18 29 54.7 −10 13 47	
21.73−0.65	18 30 21.3 −10 17 48	
21.74−0.74	18 30 43.2 −10 19 19	
21.75−0.58	18 30 10.1 −10 14 47	
21.75−0.83	18 31 03.5 −10 21 19	
21.76−0.85	18 31 08.8 −10 21 19	
21.78−0.75	18 30 51.0 −10 17 49	
21.8−0.4	18 30 −10 07	ED
21.81−0.74	18 30 51.4 −10 15 49	
21.85−1.03	18 31 58.9 −10 22 02	
21.88−0.95	18 31 45.3 −10 18 21	
21.89−0.95	18 31 45.2 −10 17 17	
21.90−1.16	18 32 32.6 −10 22 52	
21.91−1.21	18 32 45.1 −10 23 34	
21.92−1.07	18 32 16.1 −10 19 22	
21.93−1.06	18 32 13.3 −10 18 22	
22.04−1.27	18 33 11.9 −10 18 54	
22.17−1.46	18 34 07.5 −10 16 56	
22.21−1.50	18 34 20.5 −10 15 56	
22.22−1.70	18 35 05.7 −10 20 58	
22.23−1.69	18 35 03.2 −10 19 58	
22.25−1.59	18 34 43.8 −10 15 57	
22.25−1.83	18 35 37.3 −10 22 59	
22.25−1.86	18 35 44.3 −10 23 40	
22.30−1.60	18 34 53.1 −10 13 58	
22.30−1.90	18 35 58.7 −10 22 11	
22.31−1.65	18 35 04.8 −10 14 58	
22.32−1.72	18 35 19.9 −10 15 58	
22.34−1.77	18 35 33.7 −10 16 25	
22.34−1.93	18 36 08.4 −10 21 00	
22.38−1.95	18 36 18.1 −10 19 31	
22.4+1.6	18 24 − 8 39	ED
22.40−1.99	18 36 27.2 −10 19 31	
22.71−2.63	18 39 21.8 −10 20 37	
22.74−2.81	18 40 04.5 −10 23 50	
22.94+1.63	18 24 30.8 − 8 09 29	
23.0+0.8	18 28 − 8 30	ED
23.0−0.4	18 32 − 9 03	"
23.02+1.59	18 24 49.0 − 8 06 30	
23.03+1.49	18 25 10.1 − 8 08 30	
23.15+1.23	18 26 21.1 − 8 09 33	
23.16+1.18	18 26 33.0 − 8 10 33	
23.17+1.16	18 26 37.1 − 8 10 34	
23.19+1.05	18 27 03.8 − 8 12 35	
23.20+1.22	18 26 28.4 − 8 07 33	
23.21+0.97	18 27 21.6 − 8 14 05	
23.21+1.20	18 26 32.7 − 8 07 33	
23.23+0.95	18 27 29.0 − 8 13 06	
23.25+1.03	18 27 14.5 − 8 10 05	
23.30+0.95	18 27 36.5 − 8 09 36	
23.31+1.10	18 27 04.9 − 8 04 35	
23.32+0.90	18 27 50.0 − 8 10 06	
23.34+0.87	18 27 59.1 − 8 09 37	
23.34+0.95	18 27 41.4 − 8 07 36	
23.36+0.93	18 27 47.2 − 8 07 06	
23.39+0.91	18 27 55.1 − 8 05 36	
23.40+0.80	18 28 18.8 − 8 08 37	
23.43+0.74	18 28 36.7 − 8 08 38	
23.43+0.88	18 28 05.2 − 8 04 37	
23.46+0.53	18 29 24.8 − 8 12 40	
23.48+0.79	18 28 31.9 − 8 04 38	
23.50+0.47	18 29 41.6 − 8 12 10	
23.52+0.37	18 30 06.2 − 8 14 11	
23.52+0.61	18 29 15.2 − 8 07 09	
23.54+0.59	18 29 20.1 − 8 07 10	
23.55+0.52	18 29 37.7 − 8 08 10	
23.56+0.32	18 30 20.7 − 8 13 12	
23.58+0.31	18 30 24.4 − 8 12 42	
23.60+0.41	18 30 06.8 − 8 08 41	
23.65+0.29	18 30 36.9 − 8 09 42	
23.65+0.31	18 30 33.2 − 8 09 12	
23.67+0.39	18 30 17.2 − 8 05 42	
23.67+0.42	18 30 11.8 − 8 04 41	
23.69+0.38	18 30 22.1 − 8 04 42	
23.7+1.2	18 27 24.2 − 7 38 57	
23.70+0.08	18 31 27.9 − 8 12 44	
23.71+0.27	18 30 49.5 − 8 06 43	
23.73+0.30	18 30 44.1 − 8 04 43	
23.75+0.27	18 30 53.6 − 8 04 43	
23.76+0.11	18 31 29.1 − 8 08 44	
23.78−0.07	18 32 10.2 − 8 12 46	
23.8+0.2	18 31 06.8 − 8 06 14	
23.82−0.13	18 32 28.1 − 8 12 16	
23.83−0.18	18 32 39.1 − 8 13 17	
23.84−0.24	18 32 53.0 − 8 14 17	
23.85−0.12	18 32 29.5 − 8 10 16	
23.91−0.14	18 32 40.5 − 8 07 47	
23.92−0.16	18 32 44.7 − 8 07 47	
23.93−0.42	18 33 42.9 − 8 14 19	
23.95−0.21	18 32 58.9 − 8 07 17	
23.96−0.43	18 33 48.1 − 8 12 49	
23.97−0.15	18 32 49.8 − 8 04 47	
23.98−0.40	18 33 43.0 − 8 11 19	
23.99−0.27	18 33 16.2 − 8 07 18	
24.01−0.40	18 33 46.4 − 8 09 19	
24.02−0.40	18 33 48.3 − 8 09 19	
24.04−0.49	18 34 09.0 − 8 10 20	
24.06−0.42	18 33 56.7 − 8 07 20	
24.06−0.49	18 34 11.9 − 8 09 20	
24.08−0.54	18 34 23.0 − 8 09 50	
24.12−0.54	18 34 29.5 − 8 07 51	
24.12−0.61	18 34 43.8 − 8 09 51	
24.13−0.58	18 34 38.3 − 8 08 21	
24.13−0.72	18 35 08.2 − 8 11 52	
24.14−0.68	18 35 00.3 − 8 10 22	
24.17−0.80	18 35 30.0 − 8 11 53	
24.18−0.87	18 35 46.1 − 8 13 23	
24.19−0.65	18 35 01.8 − 8 06 52	
24.21−0.91	18 35 58.4 − 8 12 54	
24.25−0.87	18 35 53.2 − 8 09 54	
24.34−1.00	18 36 31.3 − 8 08 55	
24.38−1.03	18 36 42.7 − 8 07 25	
24.38−1.15	18 37 10.2 − 8 10 56	
24.40−1.04	18 36 47.2 − 8 06 56	
24.44−1.37	18 38 03.4 − 8 13 28	
24.47−1.20	18 37 30.2 − 8 07 27	
24.48−1.21	18 37 33.2 − 8 07 27	
24.48−1.28	18 37 48.7 − 8 08 58	
24.48−1.29	18 37 50.7 − 8 09 28	
24.49−1.45	18 38 27.0 − 8 12 59	
24.53−1.26	18 37 49.4 − 8 05 58	
24.55−1.27	18 37 53.7 − 8 04 58	
24.55−1.54	18 38 51.3 − 8 12 30	
24.58−1.53	18 38 52.6 − 8 10 30	
24.62−1.54	18 38 59.4 − 8 09 00	
24.66−1.68	18 39 33.7 − 8 10 32	
24.67−1.59	18 39 17.0 − 8 07 31	
24.74−1.84	18 40 18.3 − 8 11 03	
24.75−1.76	18 40 02.5 − 8 08 03	
24.77−1.95	18 40 44.8 − 8 12 04	
24.79−1.73	18 39 59.9 − 8 05 03	
24.79−2.01	18 40 59.0 − 8 12 35	
24.80−2.01	18 41 01.9 − 8 12 05	
24.81−2.03	18 41 06.3 − 8 12 05	
24.85−2.17	18 41 41.3 − 8 13 36	
24.95−2.30	18 42 21.4 − 8 12 08	
25.0+0.4	18 33 − 6 55	ED
25.02+1.65	18 28 21.1 − 6 18 30	
25.07+1.61	18 28 36.1 − 6 17 00	
25.09+1.40	18 29 23.0 − 6 22 02	
25.09+1.64	18 28 30.1 − 6 15 30	
25.1−0.4	18 40 − 7 10	ED
25.10−2.59	18 43 39.7 − 8 12 10	
25.10−2.68	18 43 58.7 − 8 14 41	
25.13+1.33	18 29 42.1 − 6 21 33	
25.14+1.47	18 29 14.0 − 6 17 32	
25.19+1.43	18 29 27.0 − 6 16 02	
25.20+1.32	18 29 51.0 − 6 18 33	
25.24+1.27	18 30 07.1 − 6 17 34	
25.27+1.03	18 31 02.1 − 6 22 36	
25.30+1.26	18 30 16.3 − 6 15 04	
25.33+1.11	18 30 51.1 − 6 17 35	
25.34+0.97	18 31 23.2 − 6 20 36	
25.34+1.02	18 31 11.0 − 6 19 06	
25.35+0.94	18 31 29.2 − 6 21 07	
25.36+1.08	18 31 02.1 − 6 16 36	
25.36+1.15	18 30 45.3 − 6 14 35	
25.37+0.95	18 31 31.2 − 6 19 37	
25.39+0.85	18 31 53.2 − 6 21 37	
25.46+0.83	18 32 05.1 − 6 18 08	
25.52+0.67	18 32 46.1 − 6 19 39	
25.54+0.72	18 32 37.9 − 6 17 09	
25.56+0.55	18 33 16.1 − 6 20 40	
25.57+0.44	18 33 41.1 − 6 23 11	
25.57+0.58	18 33 11.1 − 6 19 10	
25.57+0.88	18 32 08.7 − 6 11 10	
25.58+0.53	18 33 24.1 − 6 20 11	
25.59+0.61	18 33 07.0 − 6 17 10	
25.59+0.80	18 32 28.3 − 6 12 11	
25.60+0.66	18 32 58.1 − 6 15 40	
25.63+0.32	18 34 14.1 − 6 23 12	
25.65+0.53	18 33 32.2 − 6 15 41	
25.69+0.41	18 34 01.1 − 6 17 42	
25.70+0.23	18 34 42.1 − 6 22 14	
25.70+0.37	18 34 11.1 − 6 18 42	
25.74+0.16	18 35 00.1 − 6 21 44	
25.74+0.25	18 34 41.1 − 6 19 13	
25.76+0.09	18 35 19.0 − 6 22 45	
25.76+0.26	18 34 42.1 − 6 18 14	
25.76+0.28	18 34 37.2 − 6 17 43	
25.79+0.10	18 35 18.1 − 6 21 15	
25.81+0.30	18 34 39.3 − 6 14 43	
25.81+0.36	18 34 25.6 − 6 12 45	
25.82+0.17	18 35 07.1 − 6 17 14	
25.84+0.04	18 35 37.2 − 6 20 15	
25.84+0.36	18 34 28.1 − 6 11 15	
25.87+0.06	18 35 37.1 − 6 17 45	
25.87+0.22	18 35 02.7 − 6 13 16	
25.88+0.02	18 35 46.1 − 6 18 46	
25.88−0.08	18 36 07.1 − 6 21 17	
25.90+0.12	18 35 27.2 − 6 14 45	
25.91−0.09	18 36 13.2 − 6 19 47	
25.92+0.09	18 35 35.9 − 6 14 17	
25.93−0.05	18 36 08.0 − 6 17 47	
25.95+0.02	18 35 53.3 − 6 14 46	
25.95−0.25	18 36 51.1 − 6 22 18	
25.96+0.13	18 35 32.8 − 6 11 17	
25.96+1.54	18 30 29.7 − 5 32 04	
25.97−0.12	18 36 26.1 − 6 17 47	
25.97−0.17	18 36 37.0 − 6 18 48	
25.98−0.02	18 36 06.9 − 6 14 18	
25.98−0.31	18 37 09.1 − 6 22 19	
25.98−0.34	18 37 15.1 − 6 23 19	
25.99−0.06	18 36 16.1 − 6 15 17	

NAME	RA (1950) DEC	POS REF
	h m s ° ′ ″	
25.99−0.12	18 36 28.1 − 6 16 17	
26.00−0.26	18 36 59.0 − 6 19 48	
26.01−0.11	18 36 28.2 − 6 15 17	
26.02−0.07	18 36 21.9 − 6 13 49	
26.02−0.26	18 37 01.1 − 6 18 49	
26.02−0.30	18 37 11.1 − 6 19 49	
26.04+1.54	18 30 39.6 − 5 28 05	
26.04−0.16	18 36 42.2 − 6 15 18	
26.07−0.12	18 36 36.0 − 6 12 20	
26.08+1.31	18 31 32.7 − 5 32 07	
26.10−0.56	18 38 14.2 − 6 22 51	
26.11+1.30	18 31 37.7 − 5 30 37	
26.12+1.47	18 31 03.7 − 5 25 36	
26.13+1.67	18 30 21.8 − 5 19 36	
26.14+1.53	18 30 53.1 − 5 22 37	
26.14+1.62	18 30 32.4 − 5 20 06	
26.15−0.40	18 37 46.2 − 6 15 50	
26.15−0.55	18 38 19.1 − 6 19 51	
26.15−0.64	18 38 38.2 − 6 22 52	
26.15−0.67	18 38 45.1 − 6 23 22	
26.17+1.48	18 31 06.5 − 5 22 38	
26.17−0.48	18 38 05.2 − 6 16 51	
26.17−0.58	18 38 27.1 − 6 19 52	
26.18−0.52	18 38 15.2 − 6 17 21	
26.19−0.31	18 37 32.5 − 6 11 22	
26.19−0.45	18 38 02.2 − 6 15 21	
26.19−0.66	18 38 47.2 − 6 20 52	
26.2−0.6	18 38 33.3 − 6 17 55	
26.20+1.48	18 31 09.2 − 5 20 38	
26.21−0.71	18 38 59.2 − 6 20 53	
26.21−0.78	18 39 14.2 − 6 23 23	
26.22−0.69	18 38 56.1 − 6 19 53	
26.24+1.01	18 32 55.6 − 5 31 40	
26.25−0.43	18 38 03.8 − 6 11 23	
26.25−0.60	18 38 41.4 − 6 15 52	
26.25−0.82	18 39 28.2 − 6 22 24	
26.26+1.22	18 32 11.6 − 5 25 08	
26.26+1.26	18 32 04.6 − 5 23 38	
26.26−0.58	18 38 37.2 − 6 14 52	
26.26−0.64	18 38 50.3 − 6 16 22	
26.27+1.29	18 31 58.8 − 5 22 38	
26.28−0.61	18 38 45.3 − 6 14 52	
26.30−0.57	18 38 39.3 − 6 12 24	
26.30−0.67	18 39 01.2 − 6 15 23	
26.31−0.60	18 38 47.2 − 6 12 54	
26.32−0.89	18 39 49.1 − 6 20 25	
26.33+1.33	18 31 55.5 − 5 18 09	
26.35−0.63	18 38 57.0 − 6 11 25	
26.35−0.69	18 39 09.9 − 6 12 55	
26.35−0.71	18 39 14.9 − 6 13 55	
26.35−0.72	18 39 18.5 − 6 13 55	
26.35−1.00	18 40 17.1 − 6 21 26	
26.37+0.73	18 34 10.7 − 5 32 42	
26.37+0.96	18 33 20.6 − 5 26 11	
26.37+1.19	18 32 31.7 − 5 20 11	
26.37−0.94	18 40 06.0 − 6 18 55	
26.38+0.85	18 33 45.5 − 5 28 41	
26.39+0.74	18 34 08.7 − 5 31 12	
26.4−1.9	18 43 45.2 − 6 43 50	
26.40+0.94	18 33 28.6 − 5 25 11	
26.40−0.85	18 39 49.3 − 6 14 55	
26.41+1.03	18 33 09.4 − 5 22 12	
26.41−1.00	18 40 24.0 − 6 18 26	
26.45+0.65	18 34 33.7 − 5 30 43	
26.45−1.00	18 40 27.2 − 6 16 26	
26.46−1.16	18 41 03.0 − 6 20 27	
26.46−1.23	18 41 19.0 − 6 22 28	
26.47+0.90	18 33 42.6 − 5 22 41	
26.48−1.11	18 40 55.1 − 6 17 57	
26.49+0.50	18 35 12.6 − 5 32 45	
26.49+0.60	18 34 49.7 − 5 30 14	
26.50+0.56	18 35 00.6 − 5 30 44	
26.50+0.83	18 34 02.7 − 5 23 12	
26.53+0.40	18 35 37.7 − 5 33 15	
26.54+0.44	18 35 30.7 − 5 31 45	
26.54−1.36	18 41 57.0 − 6 21 29	
26.55+0.74	18 34 28.8 − 5 22 43	
26.56+0.38	18 35 46.6 − 5 32 16	
26.56+0.79	18 34 17.2 − 5 20 45	
26.57+0.31	18 36 00.6 − 5 33 46	
26.57+0.34	18 35 55.6 − 5 32 46	
26.57+0.45	18 35 32.6 − 5 29 45	
26.57+0.55	18 35 08.7 − 5 27 14	
26.57−1.29	18 41 45.1 − 6 17 59	
26.59+0.46	18 35 31.8 − 5 28 17	
26.60+0.27	18 36 13.6 − 5 33 17	
26.60−1.23	18 41 34.1 − 6 14 58	
26.61+0.35	18 35 57.6 − 5 30 16	
26.62+0.43	18 35 41.6 − 5 27 46	
26.63+0.31	18 36 08.6 − 5 30 47	
26.63−1.37	18 42 08.2 − 6 17 00	
26.63−1.44	18 42 22.1 − 6 19 00	
26.64+0.72	18 34 41.9 − 5 18 45	
26.65+0.21	18 36 31.6 − 5 32 17	
26.65+0.56	18 35 16.8 − 5 22 45	
26.65+0.64	18 34 59.5 − 5 20 16	
26.66+0.35	18 36 02.6 − 5 27 46	
26.68−1.54	18 42 49.2 − 6 19 01	
26.69+0.13	18 36 54.6 − 5 32 18	
26.69+0.31	18 36 15.6 − 5 27 17	
26.69+0.37	18 36 00.6 − 5 25 46	
26.70+0.48	18 35 38.4 − 5 22 17	
26.70+0.54	18 35 27.1 − 5 20 17	
26.71+0.35	18 36 08.5 − 5 25 17	
26.72+0.02	18 37 20.6 − 5 33 49	
26.72+0.11	18 36 59.6 − 5 31 18	
26.73−1.50	18 42 45.1 − 6 15 31	
26.74−0.01	18 37 27.5 − 5 33 49	
26.74−1.54	18 42 56.3 − 6 16 01	
26.75+0.50	18 35 41.9 − 5 18 47	
26.76+0.16	18 36 54.6 − 5 27 48	
26.76−0.07	18 37 43.5 − 5 33 50	
26.77+0.23	18 36 40.6 − 5 25 18	
26.77+0.32	18 36 21.7 − 5 22 47	
26.77−1.67	18 43 26.1 − 6 18 02	
26.78+0.23	18 36 41.6 − 5 24 48	
26.78−1.61	18 43 16.1 − 6 15 32	
26.79+0.03	18 37 26.5 − 5 29 49	
26.79+0.26	18 36 35.6 − 5 23 18	
26.80+0.24	18 36 42.7 − 5 23 48	
26.80−0.06	18 37 45.6 − 5 31 50	
26.80−0.13	18 37 59.6 − 5 33 51	
26.81−0.02	18 37 39.5 − 5 30 20	
26.81−0.09	18 37 53.5 − 5 32 20	
26.81−0.13	18 38 01.6 − 5 32 51	
26.81−0.15	18 38 07.6 − 5 33 51	
26.82+0.03	18 37 27.6 − 5 28 19	
26.82−1.78	18 43 56.1 − 6 18 33	
26.84−0.14	18 38 07.6 − 5 31 51	
26.85+0.04	18 37 31.5 − 5 26 20	
26.85+0.15	18 37 05.6 − 5 23 19	
26.85+0.33	18 36 27.2 − 5 18 19	
26.85−0.24	18 38 30.6 − 5 33 52	
26.86−0.10	18 38 00.5 − 5 29 51	
26.86−1.80	18 44 04.2 − 6 16 34	
26.88−0.12	18 38 07.6 − 5 29 21	
26.88−0.15	18 38 14.5 − 5 29 51	
26.88−0.24	18 38 32.7 − 5 32 22	
26.89+0.15	18 37 10.7 − 5 21 21	
26.89+0.21	18 36 58.9 − 5 19 20	
26.89−1.88	18 44 25.2 − 6 17 34	
26.90+0.19	18 37 03.7 − 5 19 51	
26.90−0.21	18 38 29.5 − 5 30 22	
26.90−0.28	18 38 43.7 − 5 32 52	
26.90−1.96	18 44 44.1 − 6 19 05	
26.91+0.0	18 37 44.6 − 5 24 20	
26.91+0.14	18 37 15.5 − 5 20 21	
26.91−0.13	18 38 13.7 − 5 27 51	
26.92−0.33	18 38 56.6 − 5 32 53	
26.93−2.02	18 45 00.1 − 6 19 06	
26.95−0.10	18 38 11.6 − 5 24 51	
26.95−0.25	18 38 43.7 − 5 28 52	
26.95−0.42	18 39 18.7 − 5 33 53	
26.96+1.69	18 31 49.0 − 4 34 39	
26.96−0.37	18 39 08.7 − 5 31 53	
26.97+0.06	18 37 40.1 − 5 19 22	
26.97−0.10	18 38 12.7 − 5 23 51	
26.98+0.06	18 37 41.4 − 5 18 52	
26.98−0.14	18 38 22.7 − 5 24 21	
26.99−0.10	18 38 16.7 − 5 22 51	
26.99−0.29	18 38 56.6 − 5 28 23	
27.00+1.74	18 31 42.8 − 4 31 09	
27.00−0.16	18 38 30.8 − 5 23 52	
27.00−0.20	18 38 38.7 − 5 24 52	
27.01+0.02	18 37 52.5 − 5 18 22	
27.01+1.60	18 32 16.1 − 4 34 40	
27.01−0.38	18 39 17.7 − 5 29 23	
27.01−0.51	18 39 45.6 − 5 32 54	
27.02−0.08	18 38 15.4 − 5 20 23	
27.03−0.31	18 39 04.5 − 5 26 23	
27.04+1.53	18 32 32.8 − 4 34 40	
27.05−0.40	18 39 27.7 − 5 27 54	
27.06+1.43	18 32 55.6 − 4 36 41	
27.06−0.08	18 38 18.4 − 5 18 23	
27.06−0.38	18 39 24.6 − 5 26 54	
27.07−0.11	18 38 26.4 − 5 18 23	
27.07−0.25	18 38 55.7 − 5 22 53	
27.07−0.45	18 39 39.6 − 5 27 54	
27.08−0.24	18 38 54.6 − 5 21 54	
27.08−0.51	18 39 52.7 − 5 29 25	
27.08−0.53	18 39 57.7 − 5 29 55	
27.09−0.16	18 38 39.7 − 5 19 24	
27.09−0.28	18 39 05.1 − 5 22 25	
27.1−0.4	18 39 22.6 − 5 23 48	
27.10−0.51	18 39 56.6 − 5 28 25	
27.10−0.60	18 40 14.5 − 5 30 55	
27.11−0.18	18 38 46.1 − 5 18 24	
27.12−0.39	18 39 31.7 − 5 23 54	
27.12−0.56	18 40 08.6 − 5 28 55	
27.13−0.25	18 39 03.2 − 5 19 25	
27.13−0.27	18 39 07.9 − 5 19 55	
27.13−0.50	18 39 56.6 − 5 26 25	
27.14−0.80	18 41 01.6 − 5 33 57	
27.15+1.24	18 33 47.8 − 4 37 13	
27.15−0.69	18 40 39.5 − 5 30 56	
27.15−0.77	18 40 57.6 − 5 32 57	
27.16−0.44	18 39 47.7 − 5 22 54	
27.16−0.48	18 39 56.7 − 5 24 25	
27.16−0.60	18 40 22.7 − 5 27 26	
27.16−0.76	18 40 55.6 − 5 31 57	
27.17−0.30	18 39 18.2 − 5 18 25	
27.17−0.70	18 40 44.6 − 5 29 57	
27.17−0.74	18 40 52.6 − 5 30 57	
27.18−0.33	18 39 26.5 − 5 18 56	
27.19−0.37	18 39 35.4 − 5 19 26	
27.20−0.47	18 39 59.2 − 5 21 57	
27.20−0.86	18 41 20.6 − 5 32 28	
27.21−0.39	18 39 43.0 − 5 19 26	
27.22+1.24	18 33 54.0 − 4 33 13	
27.22−0.39	18 39 42.4 − 5 18 26	
27.22−0.69	18 40 46.6 − 5 26 57	
27.22−0.73	18 40 56.6 − 5 27 57	
27.23−0.50	18 40 07.9 − 5 21 27	
27.24−0.49	18 40 07.0 − 5 19 57	
27.24−0.52	18 40 12.7 − 5 20 57	
27.25−0.90	18 41 36.6 − 5 30 58	
27.26−0.77	18 41 08.6 − 5 26 57	
27.27−0.97	18 41 53.5 − 5 31 59	
27.28−0.53	18 40 19.9 − 5 19 28	
27.28−0.55	18 40 24.5 − 5 19 58	
27.29+1.03	18 34 47.8 − 4 35 15	
27.29−0.97	18 41 54.5 − 5 30 59	
27.30−0.67	18 40 53.3 − 5 21 59	
27.30−0.85	18 41 30.6 − 5 26 58	
27.30−0.94	18 41 50.6 − 5 29 29	
27.30−0.98	18 41 58.6 − 5 30 29	
27.31−0.57	18 40 31.6 − 5 18 28	
27.32−1.10	18 42 25.6 − 5 33 00	
27.33+0.98	18 35 02.9 − 4 34 46	
27.34−0.85	18 41 33.6 − 5 24 58	
27.35+1.00	18 34 59.9 − 4 33 16	
27.36−0.95	18 41 59.6 − 5 26 29	
27.37−1.18	18 42 49.6 − 5 32 31	
27.38+0.81	18 35 45.1 − 4 36 47	
27.38−0.87	18 41 43.1 − 5 23 01	
27.38−0.97	18 42 05.8 − 5 25 59	
27.38−1.13	18 42 40.6 − 5 30 31	
27.40+0.86	18 35 37.0 − 4 34 17	
27.40−1.02	18 42 16.6 − 5 26 30	
27.40−1.13	18 42 40.6 − 5 29 31	
27.42+0.90	18 35 28.9 − 4 32 17	
27.42−1.27	18 43 13.5 − 5 32 02	
27.43−1.10	18 42 37.6 − 5 27 01	
27.46−1.03	18 42 27.8 − 5 23 30	
27.46−1.42	18 43 50.6 − 5 34 03	
27.47+0.63	18 36 34.0 − 4 37 19	
27.47+0.73	18 36 12.2 − 4 34 18	
27.48−1.30	18 43 27.7 − 5 30 02	
27.49+0.72	18 36 15.7 − 4 33 18	
27.49−1.07	18 42 38.6 − 5 23 03	
27.51−1.11	18 42 48.8 − 5 23 01	
27.52+0.57	18 36 51.7 − 4 35 50	
27.52+0.75	18 36 13.3 − 4 31 18	
27.54+0.67	18 36 33.0 − 4 32 19	
27.56+0.47	18 37 17.1 − 4 36 51	
27.56−1.37	18 43 49.6 − 5 27 33	
27.57+0.43	18 37 28.2 − 4 37 21	
27.57+0.62	18 36 47.2 − 4 32 20	
27.58−1.16	18 43 08.7 − 5 21 04	
27.58−1.65	18 44 53.5 − 5 34 05	
27.59+0.44	18 37 27.9 − 4 35 51	
27.59+0.53	18 37 09.2 − 4 33 20	
27.6−0.9	18 42 01.4 − 5 12 23	
27.60+0.49	18 37 18.9 − 4 33 51	
27.60+0.59	18 36 56.7 − 4 31 20	
27.63+0.32	18 37 57.6 − 4 36 52	
27.63+0.33	18 37 53.7 − 4 36 52	
27.64+0.50	18 37 19.4 − 4 31 21	
27.64−1.73	18 45 16.6 − 5 33 06	
27.65+0.42	18 37 38.2 − 4 33 21	
27.66+0.48	18 37 27.0 − 4 30 51	
27.67−1.78	18 45 31.6 − 5 33 07	
27.68+0.43	18 37 39.1 − 4 31 22	
27.70+0.20	18 38 29.9 − 4 36 53	
27.70+0.29	18 38 12.4 − 4 34 23	
27.71−1.58	18 44 52.7 − 5 25 35	
27.71−1.75	18 45 29.7 − 5 30 07	
27.72+0.32	18 38 08.1 − 4 32 23	
27.73+0.41	18 37 48.6 − 4 29 22	
27.74−1.44	18 44 26.2 − 5 20 06	
27.76+0.13	18 38 51.7 − 4 35 24	
27.77−1.53	18 44 49.3 − 5 20 37	
27.78+0.25	18 38 30.0 − 4 30 53	
27.80−0.01	18 39 27.2 − 4 37 25	
27.82−0.02	18 39 31.1 − 4 36 26	
27.82−0.06	18 39 40.5 − 4 37 26	
27.83+0.16	18 38 53.1 − 4 30 54	
27.84+0.22	18 38 41.0 − 4 28 54	
27.84−1.65	18 45 21.0 − 5 20 08	
27.87+0.01	18 39 31.0 − 4 32 56	
27.87−0.11	18 39 56.2 − 4 36 26	
27.88+0.04	18 39 26.1 − 4 31 25	
27.88−0.15	18 40 05.0 − 4 36 57	
27.89−0.10	18 39 54.4 − 4 34 56	
27.89−0.17	18 40 10.2 − 4 36 27	
27.89−1.71	18 45 39.9 − 5 19 39	
27.91−0.15	18 40 08.9 − 4 35 27	
27.92−0.19	18 40 18.4 − 4 35 57	
27.96−0.12	18 40 07.7 − 4 31 27	
27.98−0.27	18 40 41.7 − 4 34 28	
27.99−0.17	18 40 20.6 − 4 31 27	
27.99−0.31	18 40 50.6 − 4 35 28	
27.99−0.40	18 41 10.7 − 4 37 29	
28.0+1.4	18 35 − 3 47	ED
28.01−0.33	18 40 58.6 − 4 34 59	
28.02−0.36	18 41 06.7 − 4 34 59	
28.02−0.44	18 41 21.7 − 4 37 29	
28.04−0.44	18 41 25.6 − 4 36 30	
28.05−0.22	18 40 39.6 − 4 29 58	
28.07−0.29	18 40 55.9 − 4 30 29	
28.07−0.47	18 41 34.3 − 4 35 30	
28.08−0.36	18 41 11.5 − 4 31 59	
28.10−0.38	18 41 19.6 − 4 31 29	
28.10−0.42	18 41 26.3 − 4 32 30	
28.10−0.45	18 41 33.4 − 4 33 30	
28.12−0.52	18 41 50.7 − 4 34 01	
28.13−0.34	18 41 13.5 − 4 28 59	
28.15−0.59	18 42 09.7 − 4 34 31	
28.18−0.67	18 42 30.3 − 4 35 02	
28.21−0.81	18 43 04.4 − 4 37 33	
28.22−0.63	18 42 26.7 − 4 32 02	
28.25−0.59	18 42 20.5 − 4 29 32	
28.27−0.89	18 43 27.1 − 4 36 34	
28.31−0.93	18 43 40.2 − 4 35 34	
28.31−0.97	18 43 48.4 − 4 36 35	
28.34−0.91	18 43 38.5 − 4 33 34	
28.38−1.13	18 44 30.6 − 4 37 06	
28.44−1.16	18 44 42.8 − 4 35 07	
28.46−1.02	18 44 16.2 − 4 30 06	
28.46−1.08	18 44 26.4 − 4 31 06	
28.49−1.05	18 44 24.8 − 4 29 06	
28.5−0.0	18 40 47.8 − 3 58 59	
28.53−1.33	18 45 30.0 − 4 35 08	
28.55−1.34	18 45 33.5 − 4 33 38	
28.58−1.53	18 46 16.8 − 4 37 40	
28.69−1.56	18 46 36.2 − 4 32 41	
28.7−0.2	18 42 − 3 55	ED
28.7−0.6	18 43 10.2 − 4 03 59	
28.70−1.71	18 47 09.6 − 4 36 12	
28.71−1.54	18 46 34.0 − 4 30 41	
28.71−1.58	18 46 43.1 − 4 32 11	
28.73−1.62	18 46 54.3 − 4 32 11	
28.73−1.76	18 47 23.5 − 4 35 42	
28.74−1.64	18 46 58.2 − 4 32 12	
28.75−1.60	18 46 50.7 − 4 30 41	
28.8+3.5	18 29 − 2 07	ED
28.80−1.67	18 47 11.5 − 4 29 42	
29.21+1.31	18 37 21.4 − 2 45 21	
29.22+1.45	18 36 52.0 − 2 41 20	
29.22+1.51	18 36 39.4 − 2 39 19	
29.27+1.31	18 37 28.8 − 2 42 21	
29.27+1.37	18 37 15.1 − 2 40 21	
29.27+1.52	18 36 43.3 − 2 36 49	
29.29+1.18	18 37 58.4 − 2 44 52	

NAME	RA (1950) DEC	POS REF
	h m s ° ′ ″	
29.35+1.37	18 37 25.4 − 2 36 21	
29.37+1.15	18 38 13.1 − 2 41 23	
29.38+1.04	18 38 37.8 − 2 43 54	
29.38+1.15	18 38 16.1 − 2 40 53	
29.4−0.8	18 45 12.3 − 3 32 55	
29.40+1.07	18 38 34.3 − 2 41 53	
29.43+1.09	18 38 32.1 − 2 39 53	
29.45+0.83	18 39 29.5 − 2 45 55	
29.53+0.76	18 39 53.8 − 2 43 56	
29.55+0.64	18 40 22.4 − 2 45 57	
29.55+0.99	18 39 06.7 − 2 36 25	
29.58+0.82	18 39 47.2 − 2 39 26	
29.59+0.57	18 40 40.9 − 2 45 58	
29.60+0.66	18 40 23.9 − 2 42 57	
29.62+0.54	18 40 51.8 − 2 45 28	
29.64+0.64	18 40 31.7 − 2 40 58	
29.67+0.50	18 41 04.8 − 2 43 29	
29.67+0.57	18 40 50.8 − 2 41 28	
29.71+0.44	18 41 23.8 − 2 43 00	
29.71+0.68	18 40 32.2 − 2 36 28	
29.72+0.33	18 41 46.3 − 2 45 30	
29.73+0.39	18 41 34.8 − 2 43 30	
29.78+0.27	18 42 05.4 − 2 44 01	
29.82+0.15	18 42 36.5 − 2 45 02	
29.82+0.26	18 42 13.6 − 2 42 01	
29.86+0.08	18 42 54.5 − 2 45 03	
29.88+0.0	18 43 15.4 − 2 46 04	
29.88+0.05	18 43 05.5 − 2 45 03	
29.89+0.33	18 42 05.8 − 2 36 31	
29.92+0.09	18 43 00.5 − 2 41 33	
29.92+0.23	18 42 31.1 − 2 38 02	
29.94+0.05	18 43 11.6 − 2 41 33	
29.97+0.08	18 43 08.2 − 2 39 03	
29.99+0.05	18 43 16.7 − 2 39 04	
29.99+0.11	18 43 03.9 − 2 37 33	
30.06+0.0	18 43 36.3 − 2 36 34	
30.07−0.35	18 44 50.6 − 2 45 37	
30.08−0.30	18 44 41.7 − 2 44 07	
30.1−0.4	18 45 − 2 46	ED
30.10−0.07	18 43 54.6 − 2 36 35	
30.14−0.34	18 44 57.5 − 2 41 37	
30.18−0.34	18 45 00.1 − 2 39 37	
30.20−0.27	18 44 49.5 − 2 36 37	
30.21−0.45	18 45 26.7 − 2 41 08	
30.24−0.44	18 45 30.3 − 2 39 08	
30.30−0.48	18 45 43.6 − 2 36 39	
30.33−0.60	18 46 13.2 − 2 38 40	
30.34−0.58	18 46 10.5 − 2 37 40	
30.37−0.60	18 46 16.4 − 2 36 40	
30.39−0.85	18 47 12.6 − 2 42 42	
30.44−1.05	18 48 01.2 − 2 45 14	
30.49−1.00	18 47 57.2 − 2 41 14	
30.53−1.06	18 48 13.7 − 2 40 44	
30.54−1.01	18 48 02.7 − 2 38 44	
30.56−1.23	18 48 53.2 − 2 43 46	
30.68−1.44	18 49 50.6 − 2 43 18	
30.69−1.24	18 49 08.8 − 2 37 16	
30.7+0.4	18 43 16.6 − 1 49 57	
30.71−1.30	18 49 25.5 − 2 37 47	
30.71−1.45	18 49 56.0 − 2 41 48	
30.72−1.56	18 50 21.2 − 2 44 19	
30.75−1.36	18 49 42.0 − 2 37 17	
30.77−1.38	18 49 48.2 − 2 36 48	
30.79−1.48	18 50 10.5 − 2 38 48	
30.81−0.06	18 45 17.5 − 1 59 14	
30.84−1.74	18 51 13.0 − 2 43 21	
30.87−1.68	18 51 03.3 − 2 39 50	
30.88−1.73	18 51 15.7 − 2 40 51	
30.89−1.61	18 50 50.5 − 2 36 50	
30.9+0.1	18 45 09.0 − 1 49 09	
31.0+0.2	18 45 − 1 41	ED
31.0−0.2	18 46 07.0 − 1 51 30	
31.0−0.2	18 46 07.1 − 1 51 27	
31.5−0.1	18 46 29.9 − 1 20 31	
31.7−0.8	18 49 26.5 − 1 30 24	
31.8−0.5	18 49 − 1 18	ED
32.0+1.6	18 41 − 0 09	"
32.8−0.3	18 49 48.2 − 0 17 54	
33.0+0.6	18 47 + 0 17	ED
34.05+1.73	18 44 47.8 + 1 43 22	
34.12+1.66	18 45 08.6 + 1 45 21	
34.15+1.54	18 45 39.2 + 1 43 50	
34.15+1.59	18 45 29.2 + 1 45 21	
34.20+1.49	18 45 54.9 + 1 44 50	
34.26+1.36	18 46 30.0 + 1 44 49	
34.29+1.36	18 46 32.0 + 1 46 19	
34.37+1.23	18 47 08.9 + 1 46 47	
34.39+1.05	18 47 49.5 + 1 43 16	
34.4−0.2	18 52 + 1 09	ED
34.56+0.89	18 48 43.4 + 1 47 44	
34.80+0.31	18 51 13.6 + 1 44 08	
34.81+0.35	18 51 06.1 + 1 46 09	
34.92+0.10	18 52 09.9 + 1 45 06	
34.98−0.08	18 52 55.7 + 1 43 05	
35.0+0.2	18 52 + 1 52	ED
35.05−0.09	18 53 05.7 + 1 47 05	
35.12−0.20	18 53 36.5 + 1 47 33	
35.20−0.33	18 54 14.9 + 1 48 02	
35.26−0.48	18 54 53.0 + 1 47 01	
35.53−1.05	18 57 23.7 + 1 45 55	
35.56−1.19	18 57 55.4 + 1 43 24	
35.71−1.44	18 59 06.1 + 1 44 22	
35.73−1.41	18 59 02.7 + 1 46 22	
35.82−1.72	19 00 18.8 + 1 42 49	
36.2−1.0	18 58 + 2 23	ED
37.1−0.9	19 00 + 3 10	"
37.6+2.2	18 50 + 5 06	"
38.65−1.55	18 46 28.9 − 4 34 40	
38.8−0.4	19 01 + 4 58	ED
39.09+1.79	18 53 51.6 + 6 14 03	
39.18+1.62	18 54 39.1 + 6 14 01	
39.28+1.31	18 55 55.1 + 6 10 29	
39.31+1.23	18 56 17.1 + 6 09 58	
39.32+1.51	18 55 17.2 + 6 18 00	
39.50+0.78	18 58 14.4 + 6 07 54	
39.51+0.94	18 57 39.5 + 6 12 25	
39.51+1.12	18 57 01.3 + 6 17 56	
39.54+0.84	18 58 05.5 + 6 11 24	
39.60+0.60	18 59 04.1 + 6 07 52	
39.67+0.79	18 58 30.0 + 6 16 53	
39.70+0.51	18 59 33.9 + 6 10 51	
39.74+0.54	18 59 32.3 + 6 13 51	
39.77+0.40	19 00 05.2 + 6 11 50	
39.80+0.29	19 00 32.7 + 6 10 19	
39.82+0.32	19 00 27.7 + 6 11 49	
39.84+0.45	19 00 01.6 + 6 16 50	
39.94+0.23	19 00 59.5 + 6 15 48	
39.95−0.08	19 02 08.6 + 6 07 45	
40.01+0.05	19 01 47.0 + 6 14 46	
40.01−0.02	19 02 03.2 + 6 12 46	
40.02−0.19	19 02 39.1 + 6 08 14	
40.04+0.01	19 01 58.3 + 6 14 46	
40.08−0.13	19 02 31.6 + 6 13 15	
40.09−0.24	19 02 57.9 + 6 10 44	
40.10−0.13	19 02 36.2 + 6 14 14	
40.16−0.23	19 03 02.9 + 6 14 43	
40.17−0.26	19 03 10.7 + 6 14 13	
40.19−0.30	19 03 21.2 + 6 14 43	
40.23−0.44	19 03 56.2 + 6 12 42	
40.24−0.48	19 04 06.4 + 6 12 11	
40.26−0.57	19 04 28.3 + 6 10 40	
40.27−0.67	19 04 49.5 + 6 08 40	
40.29−0.37	19 03 47.8 + 6 17 42	
40.30−0.49	19 04 15.2 + 6 14 41	
40.34−0.58	19 04 37.8 + 6 14 40	
40.36−0.50	19 04 23.1 + 6 17 41	
40.37−0.68	19 05 02.5 + 6 13 39	
40.39−0.71	19 05 11.0 + 6 13 39	
40.42−0.71	19 05 14.8 + 6 15 09	
40.43−0.79	19 05 34.0 + 6 13 38	
40.47−0.77	19 05 32.3 + 6 16 08	
40.48−0.98	19 06 19.4 + 6 10 37	
40.50−0.79	19 05 41.2 + 6 17 08	
40.50−1.10	19 06 46.9 + 6 08 36	
40.51−0.81	19 05 46.6 + 6 17 38	
40.54−0.92	19 06 14.0 + 6 15 37	
40.54−1.17	19 07 06.9 + 6 08 35	
40.59−1.13	19 07 05.0 + 6 12 35	
40.60−1.31	19 07 42.9 + 6 08 04	
40.62−1.23	19 07 29.2 + 6 11 04	
40.66−1.12	19 07 10.0 + 6 16 35	
40.68−1.31	19 07 53.1 + 6 12 33	
40.69−1.25	19 07 40.8 + 6 14 34	
40.71−1.21	19 07 35.3 + 6 16 34	
40.77−1.32	19 08 04.4 + 6 17 03	
40.88−1.70	19 09 37.3 + 6 12 00	
40.90−1.67	19 09 34.4 + 6 14 00	
42.3−0.1	19 06 43.8 + 8 11 40	
42.4−0.4	19 08 + 8 09	ED
42.6+0.0	19 06 34.8 + 8 32 53	
43.2+0.0	19 08 + 9 03	ED
44.17+1.65	19 03 49.1 +10 40 12	
44.20+1.40	19 04 46.6 +10 34 40	
44.22+1.48	19 04 31.9 +10 38 10	
44.29+1.35	19 05 08.1 +10 38 39	
44.29+1.45	19 04 47.8 +10 41 10	
44.39+1.07	19 06 20.8 +10 35 37	
44.44+1.18	19 06 03.0 +10 41 37	
44.45+1.02	19 06 38.3 +10 37 36	
44.63+0.69	19 08 10.0 +10 37 33	
44.64+0.53	19 08 45.1 +10 34 01	
44.68+0.64	19 08 26.7 +10 39 02	
44.70+0.72	19 08 11.3 +10 42 33	
44.71+0.64	19 08 28.8 +10 41 02	
44.72+0.58	19 08 42.8 +10 39 32	
44.74+0.62	19 08 38.3 +10 42 02	
44.82+0.19	19 10 18.4 +10 33 58	
44.83+0.28	19 10 02.1 +10 36 59	
44.87+0.27	19 10 08.8 +10 38 59	
44.93+0.17	19 10 36.3 +10 38 58	
44.97+0.13	19 10 49.0 +10 40 27	
45.00+0.07	19 11 05.8 +10 39 57	
45.03−0.04	19 11 32.1 +10 38 56	
45.04−0.11	19 11 50.6 +10 37 25	
45.08−0.27	19 12 28.9 +10 34 54	
45.15−0.15	19 12 10.2 +10 41 54	
45.23−0.52	19 13 38.9 +10 35 51	
45.23−0.56	19 13 47.7 +10 34 21	
45.24−0.42	19 13 18.0 +10 39 22	
45.26−0.42	19 13 21.8 +10 40 22	
45.29−0.54	19 13 49.6 +10 38 21	
45.4+0.2	19 11 +11 05	ED
45.45−0.84	19 15 12.5 +10 38 18	
45.57−0.89	19 15 38.8 +10 43 17	
45.61−0.96	19 15 58.3 +10 43 16	
45.62−1.09	19 16 26.7 +10 40 15	
45.65−1.11	19 16 34.2 +10 41 15	
45.72−1.43	19 17 51.8 +10 35 43	
45.78−1.64	19 18 42.8 +10 33 11	
45.98−1.67	19 19 14.2 +10 42 40	
45.99−1.81	19 19 45.4 +10 39 39	
46.6+0.8	19 12 +12 26	ED
49.5−0.3	19 21 +14 28	"
50.4+0.4	19 20 +15 35	"
55.2−0.8	19 35 +19 12	"
55.6+0.6	19 30 +20 15	"
59.4−0.2	19 41 +23 09	"
61.6+0.0	19 45 +25 09	"
64.8+1.4	19 47 +28 37	"
70.8+1.2	20 03 +33 37	"
71.4+2.2	20 00 +34 40	"
72.2+0.6	20 09 +34 28	"
72.926−0.894	20 16 51 +34 13 48	
73.4−2.0	20 23 +33 59	ED
74.900+0.500	20 16 42 +36 39 42	
75.242−1.772	20 26 52 +36 36 54	
75.358+0.113	20 19 36 +36 48 12	
75.406−2.500	20 30 13 +35 18 54	
75.860+0.407	20 19 51 +37 23 24	
76.074+1.951	20 14 00 +38 26 06	
76.218+0.117	20 22 04 +37 30 36	
76.327−1.887	20 30 30 +36 25 24	
76.413−0.582	20 25 30 +37 15 06	
77.00−0.60	20 27 18 +37 43 30	
77.041+0.177	20 24 14 +38 12 54	
77.05+2.10	20 16 11 +39 19 36	
77.25+2.00	20 17 12 +39 26 06	
77.40+1.30	20 20 36 +39 09 24	
77.45+1.80	20 18 38 +39 29 06	
77.969−1.853	20 35 19 +37 45 06	
77.989+0.0124	20 30 50 +39 40 24	
78.054+1.748	20 20 39 +39 57 00	
78.055+0.604	20 25 30 +39 17 12	
78.10+3.835	20 11 40 +41 12 24	
78.163−0.381	20 29 55 +38 47 30	
78.186+1.816	20 20 46 +40 05 48	
78.2−0.4	20 30 +38 49	ED
78.401+3.803	20 12 45 +41 23 54	
78.412+1.385	20 23 17 +40 01 54	
78.45+1.10	20 24 37 +39 54 00	
78.455+2.718	20 17 41 +40 50 00	
78.464−0.844	20 32 52 +38 45 18	
78.5+1.4	20 24 +40 07	ED
78.70+0.70	20 27 04 +39 51 54	
78.744−1.432	20 36 01 +38 37 24	
78.75−0.40	20 31 48 +39 15 00	
78.873+0.740	20 27 26 +40 01 42	
78.938+2.772	20 18 54 +41 15 36	
78.988+2.458	20 20 25 +41 07 18	
79.051+3.603	20 15 35 +41 49 24	
79.223+2.249	20 22 03 +41 11 36	
79.223+3.428	20 16 53 +41 52 12	
79.343+0.287	20 30 48 +40 08 12	
79.350+1.304	20 26 30 +40 44 42	
79.366+1.635	20 25 08 +40 57 12	
79.371−0.123	20 32 49 +39 58 12	
79.4+3.8	20 16 +42 13	ED
79.4−0.2	20 33 +39 53	"
79.442+0.995	20 28 07 +40 38 12	
79.55−1.35	20 38 13 +39 18 36	
79.737+1.170	20 28 17 +40 58 48	
79.747+0.486	20 31 13 +40 34 48	
79.920+2.339	20 23 49 +41 48 48	
79.935+3.270	20 19 45 +42 21 48	
80.078+0.105	20 33 52 +40 36 54	
80.120−2.554	20 44 54 +39 00 24	
80.223+1.436	20 28 41 +41 31 42	
80.323+2.637	20 23 46 +42 18 48	
80.381+0.425	20 33 30 +41 03 00	
80.4+2.0	20 26 +42 00	ED
80.405+0.712	20 32 21 +41 14 30	
80.595−0.879	20 39 39 +40 25 30	
80.65+1.45	20 29 59 +41 52 48	
80.869+0.501	20 34 45 +41 29 06	
80.883−1.889	20 44 49 +40 01 06	
81.000−0.142	20 37 54 +41 11 42	
81.039+2.892	20 24 54 +43 02 36	
81.046+4.413	20 18 03 +43 55 06	
81.20+1.55	20 31 19 +42 22 48	
81.337+1.884	20 30 18 +42 41 24	
81.360+1.211	20 33 18 +42 18 18	
81.472+0.554	20 36 29 +41 59 42	
81.591−0.003	20 38 02 +41 44 48	
81.639+2.179	20 30 00 +43 06 30	
81.677+4.586	20 19 15 +44 32 24	
81.725+0.544	20 37 22 +42 11 18	
81.763+1.555	20 33 08 +42 50 00	
81.8+0.3	20 39 +42 06	ED
81.871+0.816	20 36 41 +42 28 12	
82.014−0.857	20 44 03 +41 34 06	
82.191+2.281	20 31 21 +43 36 42	
82.484+2.315	20 32 10 +43 52 00	
82.55+1.15	20 37 30 +43 12 42	
82.609+0.412	20 40 53 +42 48 12	
82.941+0.323	20 42 23 +43 00 30	
83.050+2.690	20 32 23 +44 32 36	
83.364−0.020	20 45 18 +43 07 18	
83.662+0.066	20 45 58 +43 24 30	
83.813+3.282	20 32 18 +45 30 30	
83.940+0.794	20 43 49 +44 04 54	
84.292+0.885	20 44 39 +44 24 48	
84.567+0.446	20 47 32 +44 20 48	
84.60−1.800	20 57 06 +42 55 12	
84.897+3.809	20 33 37 +46 41 24	
85.0−1.0	20 47 +45 02	ED
85.012−0.245	20 52 05 +44 14 48	
85.073−3.428	20 05 03 +42 11 06	
86.067−2.061	21 03 33 +43 50 24	
86.279−1.165	21 00 38 +44 36 00	
86.567+3.744	20 39 55 +47 58 18	
86.987+0.585	20 55 49 +46 17 12	
87.076+1.870	20 50 27 +47 11 18	
93.8+2.8	21 14 +52 48	ED
94.2+1.6	21 22 +52 14	"
99.0+3.5	21 37 +56 54	"
267.94−1.06	8 57 22.3 −47 18 59	
285.05+0.07	10 28 43.3 −57 33 27	
285.26−0.05	10 29 36.6 −57 46 50	
286.50+0.06	10 39 59.7 −58 17 41	
291.27−0.71#1	11 09 44.2 −61 02 51	
291.27−0.71#2	11 09 46.0 −61 02 06	
291.27−0.71#3	11 09 48.3 −61 02 39	
291.57−0.43	11 12 55.7 −60 53 16	
300.93−0.03	12 31 03.7 −62 33 20	
305.2+0.21 #1	13 07 58.0 −62 18 37	
305.2+0.21 #2	13 08 03.4 −62 18 32	
305.36+0.15	13 09 25.3 −62 12 58	
305.36+0.21#1	13 09 21.8 −62 17 34	
305.36+0.21#2	13 09 22.7 −62 17 52	
305.4+0.2	13 09 22.0 −62 21 24	
305.91−1.91	13 15 46.6 −64 21 45	
309.9+0.5 #1	13 47 01.6 −61 20 18	
309.9+0.5 #2	13 47 11.2 −61 20 19	
309.9+0.5 #3	13 47 28.9 −61 19 06	
315.22+0.01	14 29 45.7 −60 10 23	
315.22+0.01I	14 29 42.0 −60 10 08	
315.22+0.01II	14 29 44.3 −60 09 58	
316.81−0.06#1	14 41 33.1 −59 36 59	
316.81−0.06#2	14 41 36.2 −59 37 44	
316.81−0.06#3	14 41 37.0 −59 36 41	
324.20+0.12	15 29 01.0 −55 46 08	
324.20+0.12	15 29 01.9 −55 46 09	
326.64+0.61	15 40 35.1 −53 56 27	
326.77−0.26IR	15 44 59.8 −54 32 51	

NAME	RA (1950) DEC	POS REF
	h m s ° ′ ″	
327.1−0.3	15 50 −54 20	ED
327.12+0.51	15 43 42.0 −53 43 27	
327.12+0.51	15 43 43.6 −53 43 36	
327.29−0.57	15 49 10.0 −54 28 10	
327.39+0.45	15 45 29.2 −53 36 06	
327.39+0.45#1	15 45 28.9 −53 36 11	
327.39+0.45#2	15 45 28.9 −53 35 35	
327.4−0.1	15 47 40.4 −54 00 01	
327.4−0.6	15 50 17.3 −54 24 34	
328.2+0.0	15 51 30.0 −53 23 58	
328.2+0.0	15 51 32.8 −53 23 38	
328.24−0.54IR	15 54 11.1 −53 50 49	
328.3+0.43	15 50 17.0 −53 02 52	
328.30+0.43	15 50 17.3 −53 03 06	
328.4−0.2	15 53 32.0 −53 28 54	
328.7−0.2	15 55 16.2 −53 16 34	
328.81+0.64IR	15 52 00.4 −52 34 16	
329.18−0.32IR	15 57 59.4 −53 03 46	
330.4+0.1	16 01 59.5 −51 57 36	
330.4+0.1	16 01 59.8 −51 57 40	
330.88−0.36I1	16 06 31.0 −51 58 06	
330.88−0.36I3	16 06 28.8 −51 58 16	
330.88−0.36I4	16 06 29.4 −51 58 30	
331.13−0.25	16 07 17.9 −51 43 31	
331.28−0.20IR	16 07 47.2 −51 34 26	
331.34−0.34IR	16 08 39.9 −51 38 54	
331.51−0.1 #1	16 08 19.9 −51 20 18	
331.51−0.1 #2	16 08 21.1 −51 20 51	
331.51−0.1 #3	16 08 22.7 −51 20 02	
331.51−0.1 #4	16 08 30.1 −51 21 51	
331.51−0.10	16 08 21.1 −51 20 21	
331.6−0.3	16 09 41.0 −51 22 23	
332.65−0.63	16 15 52.4 −50 56 47	
332.65−0.63	16 16 00.1 −50 58 49	
333.13−0.43	16 17 15.4 −50 28 55	
333.13−0.43#1	16 17 11.4 −50 27 49	
333.13−0.43#2	16 17 13.0 −50 28 03	
333.13−0.43#3	16 17 15.3 −50 28 52	
333.23−0.05IR	16 16 00.6 −50 07 53	
335.61−0.31IR	16 27 26.3 −48 37 04	
335.78+0.17	16 26 04.6 −48 09 52	
336.36−0.15IR	16 29 49.4 −47 57 35	
336.99−0.03	16 31 50.3 −47 24 47	
337.3−0.2	16 34 02.1 −47 17 25	
337.4−0.1	16 30 −47 10	ED
337.4−0.4 #1	16 35 05.1 −47 22 32	
337.4−0.4 #2	16 35 08.8 −47 22 59	
337.40−0.40IR	16 35 06.4 −47 22 18	
337.5+0.1A	16 30 −47 00	ED
337.5+0.1B	" "	"
337.5+0.1C	" "	"
337.5+0.1D	" "	"
337.5+0.1NOM.		
337.61−0.06	16 34 24.3 −46 59 01	
337.71−0.05	16 34 46.1 −46 54 59	
337.86+0.26	16 34 02.2 −46 34 39	
337.86+0.26#1	16 34 01.1 −46 34 42	
337.86+0.26#2	16 34 02.4 −46 35 04	
337.9+0.3	16 34 01.9 −46 34 45	
337.91−0.47	16 37 21.3 −47 02 24	
337.91−0.47#1	16 37 26.1 −47 02 11	
337.91−0.47#2	16 37 26.6 −47 01 05	
337.99+0.14	16 35 06.0 −46 34 37	
337.99+0.14#1	16 35 04.5 −46 34 33	
337.99+0.14#2	16 35 07.9 −46 33 46	
338.0−0.1	16 36 13.7 −46 44 32	
338.0−0.1	16 36 14.9 −46 44 46	
338.08+0.02IR	16 35 58.0 −46 34 45	
338.47+0.29IR	16 36 20.6 −46 07 08	
338.5+0.1	16 37 27.0 −46 13 26	
338.5+0.1	16 37 27.9 −46 13 34	
338.5−0.2	16 38 16.2 −46 27 00	
338.5−0.2	16 38 19.1 −46 26 38	
338.68−0.08IR	16 38 45.6 −46 11 49	
338.88−0.08IR	16 39 29.1 −46 03 44	
338.92+0.56	16 36 55.2 −45 36 19	
339.62−0.12	16 42 27.3 −45 31 20	
339.62−0.12	16 42 27.8 −45 31 18	
339.93+0.37	16 41 32.5 −44 57 50	
339.98−0.19	16 44 04.4 −45 17 53	
340.00−0.51	16 45 32.4 −45 29 09	
340.00−0.51	16 45 33.2 −45 29 46	
340.14−0.45	16 45 49.8 −45 19 35	
340.24−0.06	16 44 30.5 −45 01 17	
340.42−0.01	16 44 55.2 −44 51 10	
340.42−0.01	16 44 55.5 −44 51 23	
341.12−0.00	16 47 26.4 −44 18 23	
341.12−0.00	16 47 26.5 −44 18 31	
342.01+0.25	16 49 31.1 −43 27 44	
343.38+0.25	16 54 14.3 −42 23 26	
344.83−1.67	17 07 21.3 −42 25 06	
344.93+0.01	17 00 28 −41 20	ED
345.05−1.86	17 08 49.0 −42 21 58	
345.41−0.94	17 06 05.1 −41 31 55	
345.51+0.35	17 00 53.8 −40 40 15	
345.69−0.09#1	17 03 18.1 −40 47 52	
345.69−0.09#1	17 03 24.3 −40 47 35	
345.69−0.09#2	17 03 23.0 −40 47 21	
345.69−0.09#2	17 03 23.9 −40 47 34	
345.69−0.09#3	17 03 23.9 −40 47 16	
346.01+0.04	17 03 49.6 −40 26 57	
346.18+0.02	17 04 17.9 −40 19 56	
346.86−0.81	17 07 24.9 −39 55 03	
347.4+0.4	17 06 36.6 −39 08 18	820308
347.40+0.40	"	
347.40+0.40	17 06 40.7 −39 08 20	
347.57+0.11	17 08 24.7 −39 10 12	
347.57+0.11	17 08 27.8 −39 09 50	
347.61+1.82	17 01 30.7 −38 06 32	
347.63+0.15IR	17 08 24.6 −39 05 45	
347.66+1.73	17 02 03.4 −38 07 03	
347.67+1.71	17 02 06.9 −38 07 33	
347.83+1.55	17 03 19.6 −38 05 36	
347.89+1.42	17 03 58.6 −38 07 37	
347.94+1.44	17 04 05.3 −38 04 37	
347.97+1.34	17 04 32.6 −38 06 38	
348.13+1.09	17 06 04.5 −38 07 42	
348.25+0.94	17 07 02.6 −38 07 44	

NAME	RA (1950) DEC	POS REF
	h m s ° ′ ″	
348.57+0.50	17 09 47.5 −38 07 49	
348.57+0.54	17 09 38.1 −38 06 19	
348.67+0.39	17 10 35.8 −38 06 51	
348.73−1.04	17 16 40.6 −38 54 18	
348.73−1.04#1	17 16 40.6 −38 54 15	
348.74+0.27	17 11 17.2 −38 07 53	
348.78+0.23	17 11 32.3 −38 07 23	
348.85+0.16	17 12 02.4 −38 06 24	
348.96+0.01	17 12 58.6 −38 06 26	
348.97−0.06	17 13 19.5 −38 07 57	
348.98−0.02	17 13 12.2 −38 06 27	
349.03−0.05	17 13 28.4 −38 04 57	
349.06−0.09	17 13 42.5 −38 04 58	
349.09+0.11	17 12 54.1 −37 56 37	
349.09+0.11#1	17 12 59.3 −37 55 34	
349.09+0.11#2	17 13 02.7 −37 56 55	
349.09−0.13	17 13 57.4 −38 04 58	
349.09−0.18	17 14 10.9 −38 06 29	
349.09−0.19	17 14 13.8 −38 06 59	
349.09−0.21	17 14 17.1 −38 07 29	
349.11−0.17	17 14 10.7 −38 04 59	
349.13−0.22	17 14 26.1 −38 05 59	
349.15−0.26	17 14 39.6 −38 06 30	
349.18+0.20	17 12 51.6 −37 48 47	
349.18+0.20	17 12 52.2 −37 48 53	
349.21−0.38	17 15 19.8 −38 07 31	
349.27−0.39	17 15 35.2 −38 05 02	
349.32−0.55	17 16 23.3 −38 08 04	
349.36−0.20	17 15 01.8 −37 54 21	
349.39−0.01	17 14 28.5 −37 45 57	
349.39−0.58	17 16 42.1 −38 06 04	
349.47−0.69	17 17 24.7 −38 05 36	
349.50−0.52	17 16 50.9 −37 58 59	
349.50−0.75	17 17 44.5 −38 06 36	
349.52+0.25	17 13 40.8 −37 30 12	
349.54−0.82	17 18 07.5 −38 06 37	
349.70−1.09	17 19 42.7 −38 08 11	
349.71−1.05	17 19 36.0 −38 06 10	
349.81−0.32	17 16 46.2 −37 36 13	
349.88−1.29	17 21 04.5 −38 06 14	
349.88−1.35	17 21 22.0 −38 08 14	
349.93−1.41	17 21 43.6 −38 07 45	
349.96−0.03	17 16 05.2 −37 18 38	
349.97−1.41	17 21 51.1 −38 05 45	
350.07−1.61	17 22 59.5 −38 07 48	
350.22−1.80	17 24 11.7 −38 06 20	
350.55+0.06	17 17 23.6 −36 46 43	
350.85+0.19	17 17 46.8 −36 27 59	
350.85+0.19A	17 17 47.2 −36 27 49	
350.85+0.19B	17 17 47.2 −36 27 36	
350.97+0.43	17 17 11.9 −36 12 26	
351.14+0.08	17 19 04.4 −36 15 55	
351.16+0.70	17 16 34.5 −35 54 44	
351.16+0.70#1	17 16 34.3 −35 53 52	
351.16+0.70#2	17 16 36.8 −35 54 47	
351.16+0.70#3	17 16 38.8 −35 54 11	
351.22+0.25	17 18 37.6 −36 06 13	
351.41+0.64	17 17 32.0 −35 44 05	
351.41+0.64	17 17 32.4 −35 44 02	
351.60+0.32	17 19 20.1 −35 46 25	
351.78−0.54IR	17 23 21.2 −36 06 42	
352.52+2.77	17 12 15.0 −33 35 57	
352.60+2.76	17 12 30.6 −33 32 57	
352.61−0.19	17 24 13.9 −25 13 10	
352.68+2.63	17 13 12.7 −33 33 29	
352.74+2.75	17 12 55.4 −33 25 58	
352.80+2.45	17 14 16.6 −33 33 31	
352.80+2.61	17 13 38.9 −33 28 00	
352.86+2.43	17 14 32.0 −33 31 32	
352.93+2.24	17 15 26.3 −33 34 33	
352.96+2.16	17 15 51.9 −33 36 04	
352.99+2.16	17 15 54.5 −33 34 34	
353.03+2.25	17 15 40.3 −33 29 34	
353.05+2.04	17 16 34.0 −33 35 36	
353.05+2.10	17 16 20.0 −33 33 35	
353.06+2.29	17 15 35.5 −33 26 34	
353.11+2.15	17 16 16.6 −33 29 05	
353.15+0.09	17 24 36.9 −34 37 22	
353.23−0.24	17 26 09.5 −34 44 42	
353.31+1.35	17 20 00.1 −33 46 38	
353.32+1.64	17 18 52.6 −33 36 11	
353.38+1.72	17 18 45.3 −33 30 41	
353.39+1.84	17 18 17.8 −33 26 10	
353.41−0.36IR	17 27 09.2 −34 39 18	
353.43+1.73	17 18 50.5 −33 27 41	
353.43+1.75	17 18 44.1 −33 27 11	
353.45+0.99	17 21 47.8 −33 52 12	
353.45+1.53	17 19 39.8 −33 33 43	
353.48+1.04	17 21 41.4 −33 49 12	
353.51+1.05	17 21 44.3 −33 47 12	
353.52+1.57	17 19 43.7 −33 28 43	
353.55+1.60	17 19 42.0 −33 26 13	
353.59+0.81	17 22 54.5 −33 51 15	
353.59+0.91	17 22 32.3 −33 47 44	
353.60+1.23	17 21 16.0 −33 36 16	
353.60−0.23	17 27 08.1 −34 25 31	
353.60−0.23	17 27 08.5 −34 25 31	
353.60−0.23A	17 27 04.6 −34 25 46	
353.60−0.23B	17 27 08.3 −34 25 31	
353.64+1.15	17 21 41.7 −33 37 17	
353.64+1.25	17 21 16.8 −33 33 46	
353.67+0.72	17 23 27.6 −33 50 16	
353.67+0.86	17 22 55.0 −33 45 15	
353.70+1.43	17 20 46.7 −33 24 45	
353.72+0.59	17 24 06.7 −33 52 17	
353.73+0.52	17 24 25.9 −33 53 48	
353.77+1.33	17 21 19.4 −33 24 46	
353.79+1.16	17 22 03.0 −33 29 18	
353.81+0.69	17 23 58.9 −33 44 17	
353.81+1.10	17 22 20.9 −33 30 48	
353.83+1.10	17 22 24.2 −33 29 18	
353.83+1.14	17 22 15.8 −33 28 18	
353.86+0.51	17 24 50.0 −33 47 49	
353.88+0.40	17 25 19.5 −33 50 50	
353.89+0.40	17 25 21.0 −33 50 20	
353.90+0.30	17 25 46.8 −33 52 51	
353.90+0.87	17 23 31.4 −33 33 51	
353.91+0.86	17 23 34.8 −33 33 51	

NAME	RA (1950) DEC	POS REF
	h m s ° ′ ″	
353.93+0.40	17 25 27.2 −33 47 50	
353.93+0.45	17 25 15.0 −33 46 20	
353.93+0.80	17 23 50.3 −33 34 52	
353.94+0.46	17 25 14.8 −33 45 20	
353.94+1.06	17 22 50.2 −33 25 19	
353.95+0.89	17 23 34.7 −33 30 51	
353.96+0.91	17 23 30.9 −33 29 21	
353.97+0.71	17 24 18.9 −33 35 53	
353.97+1.03	17 23 04.2 −33 24 50	
353.99+0.85	17 23 50.0 −33 30 22	
354.00+0.29	17 26 06.7 −33 48 22	
354.00+0.88	17 23 44.2 −33 28 21	
354.01+0.65	17 24 40.0 −33 35 53	
354.04+0.23	17 26 27.3 −33 48 22	
354.06+0.26	17 26 20.2 −33 46 22	
354.07+0.56	17 25 11.6 −33 35 24	
354.07+0.88	17 23 56.1 −33 24 52	
354.08+0.01	17 27 25.8 −33 53 55	
354.09+0.51	17 25 27.2 −33 36 25	
354.10+0.00	17 27 29.8 −33 52 55	
354.10+0.06	17 27 17.2 −33 50 54	
354.10+0.66	17 24 51.7 −33 30 54	
354.13+0.13	17 27 04.9 −33 47 24	
354.13+0.43	17 25 53.6 −33 37 26	
354.15+0.03	17 27 32.1 −33 49 25	
354.15+0.16	17 26 59.9 −33 45 24	
354.15+0.73	17 24 43.4 −33 26 23	
354.15−0.04	17 27 48.8 −33 51 55	
354.17+0.05	17 27 31.6 −33 47 55	
354.17−0.10	17 28 04.6 −33 52 56	
354.18−0.06	17 27 59.3 −33 50 56	
354.19+0.09	17 27 24.7 −33 45 25	
354.22+0.55	17 25 38.4 −33 28 25	
354.23+0.32	17 26 35.8 −33 35 57	
354.23−0.10	17 28 14.5 −33 49 56	
354.24−0.21	17 28 44.0 −33 52 57	
354.24−0.24	17 28 50.5 −33 53 57	
354.26+0.49	17 25 59.5 −33 28 56	
354.27+0.58	17 25 39.7 −33 24 55	
354.29+0.19	17 27 16.5 −33 37 29	
354.29−0.10	17 28 24.6 −33 46 57	
354.29−0.26	17 29 03.4 −33 51 58	
354.33+0.36	17 26 40.7 −33 29 28	
354.34−0.39	17 29 44.8 −33 54 00	
354.35+0.34	17 26 50.3 −33 28 58	
354.35−0.21	17 29 02.7 −33 47 28	
354.36+0.18	17 27 30.0 −33 34 00	
354.36−0.29	17 29 23.7 −33 49 29	
354.36−0.34	17 29 33.7 −33 51 29	
354.38+0.28	17 27 08.4 −33 29 29	
354.40−0.34	17 29 39.4 −33 49 29	
354.40−0.45	17 30 05.9 −33 53 00	
354.41+0.22	17 27 27.9 −33 30 29	
354.41−0.24	17 29 19.0 −33 45 29	
354.41−0.32	17 29 36.7 −33 47 59	
354.42+0.24	17 27 23.3 −33 28 59	
354.42+0.31	17 27 06.6 −33 26 59	
354.42−0.38	17 29 54.0 −33 49 30	
354.44−0.36	17 29 52.1 −33 48 00	
354.46+0.04	17 28 19.1 −33 34 01	
354.46+0.19	17 27 41.8 −33 28 30	
354.46+0.20	17 27 38.9 −33 28 30	
354.46−0.03	17 28 36.7 −33 36 02	
354.46−0.03	17 28 35.0 −33 36 02	
354.47+0.0	17 28 28.3 −33 34 32	
354.49+0.15	17 27 58.8 −33 28 31	
354.50+0.07	17 28 16.9 −33 30 31	
354.50−0.39	17 30 09.2 −33 46 00	
354.51−0.51	17 30 39.3 −33 49 32	
354.52−0.59	17 31 00.8 −33 51 32	
354.53+0.03	17 28 29.9 −33 30 21	
354.53+0.03	17 28 33.4 −33 30 05	
354.53+0.17	17 27 59.9 −33 26 00	
354.56−0.11	17 29 10.0 −33 33 33	
354.56−0.44	17 30 31.3 −33 44 31	
354.58−0.07	17 29 04.6 −33 31 03	
354.59+0.05	17 28 38.3 −33 27 02	
354.59−0.25	17 29 49.0 −33 36 34	
354.60+0.03	17 28 44.0 −33 27 02	
354.60+0.07	17 28 33.6 −33 25 32	
354.60+0.26	17 27 48.4 −33 19 19	
354.60−0.59	17 31 12.6 −33 47 33	
354.61−0.18	17 29 35.1 −33 33 34	
354.61−0.72	17 31 45.9 −33 51 04	
354.62+0.47IR	17 27 03.7 −33 11 31	
354.62−0.28	17 30 01.9 −33 36 05	
354.63−0.83	17 32 16.2 −33 54 05	
354.64−0.09	17 29 18.3 −33 29 03	
354.64−0.35	17 30 22.4 −33 37 36	
354.67−0.40	17 30 39.1 −33 37 36	
354.68−0.06	17 29 19.4 −33 26 03	
354.69−0.23	17 29 59.5 −33 31 05	
354.69−0.31	17 30 19.1 −33 33 36	
354.69−0.36	17 30 30.6 −33 35 06	
354.70−0.17	17 29 48.4 −33 28 34	
354.70−0.44	17 30 52.8 −33 37 37	
354.71−0.08	17 29 26.3 −33 25 04	
354.72−0.27	17 30 13.1 −33 31 05	
354.72−0.86	17 32 37.0 −33 50 36	
354.73−0.85	17 32 35.3 −33 49 36	
354.73−0.93	17 32 55.6 −33 52 06	
354.74−0.30	17 30 25.5 −33 31 06	
354.75−0.06	17 29 28.5 −33 22 17	
354.75−0.20	17 30 03.0 −33 27 05	
354.75−0.24	17 30 11.4 −33 28 05	
354.75−0.45	17 31 03.0 −33 35 07	
354.76−0.37	17 30 43.5 −33 32 06	
354.77−0.38	17 30 48.9 −33 32 07	
354.78−0.22	17 30 12.2 −33 26 35	
354.79−0.30	17 30 32.5 −33 28 36	
354.81−0.31	17 30 40.2 −33 27 36	
354.82−1.05	17 33 39.3 −33 51 08	
354.83−0.38	17 30 56.9 −33 29 07	
354.83−0.92	17 33 09.9 −33 46 37	
354.85−0.60	17 31 53.3 −33 35 09	
354.85−0.65	17 32 07.7 −33 36 39	
354.85−1.12	17 34 01.5 −33 52 09	
354.86−0.61	17 31 59.5 −33 35 09	

NAME	RA (1950)	DEC	POS REF
	h m s	° ′ ″	
354.87−0.99	17 33 31.0	−33 47 08	
354.88−0.54	17 31 44.8	−33 31 38	
354.88−0.54	17 31 45.1	−33 31 47	
354.88−1.17	17 34 17.4	−33 52 09	
354.89−0.36	17 31 02.5	−33 25 07	
354.89−0.48	17 31 32.2	−33 29 08	
354.9−0.6	17 32 07.5	−33 36 40	
354.93−0.51	17 31 46.0	−33 28 39	
354.93−1.13	17 34 15.9	−33 48 39	
354.93−1.15	17 34 22.0	−33 49 09	
354.94−0.59	17 32 06.8	−33 30 10	
354.94−0.68	17 32 26.7	−33 33 10	
354.94−0.72	17 32 36.1	−33 34 41	
354.95−0.75	17 32 47.5	−33 35 11	
354.95−1.23	17 34 44.7	−33 50 40	
354.97−1.23	17 34 45.4	−33 49 40	
355.00−0.88	17 33 27.0	−33 36 42	
355.01−0.56	17 32 10.5	−33 25 40	
355.01−0.64	17 32 29.7	−33 28 40	
355.01−0.80	17 33 06.9	−33 33 42	
355.01−1.33	17 35 16.0	−33 50 41	
355.02−0.71	17 32 47.3	−33 30 11	
355.02−0.84	17 33 18.9	−33 34 12	
355.02−1.45	17 35 46.3	−33 54 12	
355.03+0.17	17 29 17.4	−33 01 06	
355.03−1.42	17 35 41.6	−33 52 42	
355.04−0.69	17 32 47.3	−33 28 41	
355.04−1.48	17 35 59.0	−33 54 13	
355.05−0.78	17 33 08.9	−33 31 12	
355.05−0.81	17 33 15.5	−33 32 12	
355.05−1.20	17 34 51.0	−33 44 41	
355.06−0.70	17 32 51.3	−33 27 41	
355.06−1.01	17 34 07.2	−33 37 44	
355.06−1.41	17 35 44.3	−33 51 12	
355.07−0.71	17 32 55.1	−33 27 41	
355.07−0.79	17 33 16.5	−33 30 12	
355.08−1.31	17 35 22.6	−33 46 42	
355.08−1.48	17 36 04.1	−33 52 13	
355.09−0.75	17 33 08.0	−33 27 42	
355.09−0.82	17 33 26.9	−33 30 12	
355.09−0.96	17 34 00.1	−33 34 44	
355.1−0.7	17 32 51.2	−33 27 42	
355.10−0.97	17 34 03.0	−33 34 44	
355.10−1.45	17 36 00.4	−33 50 13	
355.10−1.58	17 36 30.8	−33 54 14	
355.12−1.09	17 34 34.5	−33 37 45	
355.13−1.50	17 36 16.3	−33 50 14	
355.14−0.85	17 33 40.9	−33 28 43	
355.14−1.02	17 34 22.6	−33 34 14	
355.15−1.01	17 34 19.8	−33 33 44	
355.16+1.65	17 23 49.0	−32 04 52	
355.17−0.84	17 33 42.6	−33 26 43	
355.17−0.87	17 33 48.8	−33 27 43	
355.17−0.94	17 34 08.5	−33 30 14	
355.18−0.90	17 33 58.3	−33 28 13	
355.18−0.98	17 34 16.9	−33 31 14	
355.18−1.47	17 36 17.1	−33 46 44	
355.19−1.49	17 36 23.9	−33 47 14	
355.21−0.88	17 33 56.9	−33 26 13	
355.21−0.96	17 34 19.2	−33 28 44	
355.23+1.44	17 24 49.5	−32 08 54	
355.23−0.98	17 34 26.3	−33 28 45	
355.23−1.02	17 34 37.2	−33 29 45	
355.26−1.00	17 34 35.6	−33 27 45	
355.27−1.01	17 34 38.4	−33 27 15	
355.28−1.28	17 35 45.8	−33 35 47	
355.28−1.64	17 37 12.8	−33 47 16	
355.28−1.67	17 37 21.3	−33 48 16	
355.30−1.01	17 34 45.4	−33 25 45	
355.30−1.14	17 35 14.9	−33 30 16	
355.30−1.59	17 37 03.7	−33 44 45	
355.31−1.15	17 35 19.9	−33 30 17	
355.31−1.88	17 38 17.7	−33 53 18	
355.32−1.28	17 35 52.2	−33 33 18	
355.32−1.36	17 36 11.2	−33 36 18	
355.32−1.73	17 37 43.4	−33 48 17	
355.32−1.92	17 38 29.4	−33 54 18	
355.33−1.25	17 35 46.9	−33 32 17	
355.35+1.55	17 24 42.1	−31 58 54	
355.36−1.82	17 38 10.5	−33 49 18	
355.37+1.51	17 24 53.4	−31 59 24	
355.38+0.08	17 30 32.1	−32 46 28	
355.38−1.15	17 35 30.5	−33 26 17	
355.38−1.51	17 36 56.8	−33 37 50	
355.39+1.54	17 24 49.3	−31 57 24	
355.40+1.29	17 25 50.1	−32 04 56	
355.40+1.45	17 25 12.3	−31 59 55	
355.40−1.37	17 36 27.8	−33 32 19	
355.40−1.80	17 38 11.3	−33 46 18	
355.41−1.40	17 36 35.1	−33 32 49	
355.42−1.30	17 36 13.8	−33 29 18	
355.42−1.89	17 38 57.0	−33 48 19	
355.43−1.84	17 38 24.8	−33 45 48	
355.43−2.10	17 39 30.4	−33 54 21	
355.44−1.21	17 35 54.5	−33 25 18	
355.44−1.27	17 36 09.6	−33 27 18	
355.44−1.99	17 39 05.6	−33 50 20	
355.45−1.95	17 38 56.2	−33 48 50	
355.47−1.50	17 37 09.0	−33 32 50	
355.48−1.32	17 36 28.3	−33 26 49	
355.48−2.10	17 39 36.5	−33 51 51	
355.48−2.13	17 39 42.6	−33 52 51	
355.49−1.44	17 36 56.5	−33 30 20	
355.50−1.33	17 36 31.7	−33 26 19	
355.51+1.12	17 26 49.2	−32 05 28	
355.51−2.05	17 39 29.3	−33 48 51	
355.52−1.34	17 36 39.6	−33 25 19	
355.53+1.23	17 26 25.2	−32 00 57	
355.54+1.09	17 27 01.0	−32 04 59	
355.54−1.59	17 37 42.8	−33 32 22	
355.55−2.17	17 40 04.3	−33 50 22	
355.56−2.27	17 40 32.0	−33 52 53	
355.57−2.18	17 40 11.3	−33 49 52	
355.57−2.20	17 40 16.5	−33 50 22	
355.59+1.19	17 26 45.8	−31 58 58	
355.61+1.00	17 27 33.3	−32 04 30	
355.62−1.51	17 37 34.5	−33 25 51	
355.63−1.59	17 37 55.4	−33 27 52	
355.64+1.05	17 27 24.9	−32 01 29	
355.64−1.91	17 39 15.9	−33 37 55	
355.65+0.93	17 27 54.4	−32 04 30	
355.65−2.40	17 41 16.1	−33 52 55	
355.67+0.87	17 28 12.2	−32 06 01	
355.67+1.01	17 27 39.5	−32 01 00	
355.67−2.46	17 41 36.2	−33 53 25	
355.68+0.90	17 28 06.2	−32 04 31	
355.68−1.65	17 38 17.1	−33 27 23	
355.68−1.85	17 39 06.5	−33 33 55	
355.69+0.92	17 28 03.7	−32 03 01	
355.69−1.71	17 38 32.7	−33 28 53	
355.70+0.96	17 27 56.0	−32 01 31	
355.70−1.73	17 38 40.0	−33 28 54	
355.71−1.79	17 38 56.5	−33 30 24	
355.72−1.93	17 39 31.7	−33 34 26	
355.72−1.94	17 39 36.1	−33 34 26	
355.73−2.53	17 42 00.8	−33 52 26	
355.74−1.70	17 38 40.4	−33 25 54	
355.75+0.96	17 28 02.8	−31 58 31	
355.75−2.09	17 40 16.6	−33 37 57	
355.76−1.77	17 39 00.1	−33 26 54	
355.77+0.62	17 29 27.2	−32 09 04	
355.78−2.04	17 40 09.4	−33 34 27	
355.78−2.46	17 41 51.0	−33 47 56	
355.78−2.62	17 42 29.8	−33 52 57	
355.83+0.61	17 29 38.5	−32 06 04	
355.83−2.44	17 41 54.4	−33 44 56	
355.84+0.79	17 28 58.0	−32 00 03	
355.84−2.57	17 42 27.1	−33 48 27	
355.85+0.55	17 29 55.8	−32 07 05	
355.85+0.69	17 29 24.1	−32 02 34	
355.86−1.89	17 39 43.0	−33 25 56	
355.86−2.00	17 40 10.2	−33 28 57	
355.89+0.44	17 30 27.1	−32 09 06	
355.90+0.69	17 29 31.1	−32 00 04	
355.91−2.11	17 40 44.5	−33 30 28	
355.91−2.61	17 42 49.2	−33 45 58	
355.94+0.52	17 30 16.0	−32 03 35	
355.94−2.15	17 40 58.2	−33 29 59	
355.94−2.37	17 41 54.3	−33 37 01	
355.95+0.51	17 30 19.4	−32 03 36	
355.95−0.05	17 32 33.4	−32 21 49	
355.95−2.05	17 40 35.9	−33 25 58	
355.98−2.75	17 43 32.6	−33 46 30	
356.00−2.43	17 42 16.6	−33 35 32	
356.01+0.55	17 30 21.5	−31 59 06	
356.01−2.20	17 41 23.1	−33 28 00	
356.01−2.26	17 41 36.6	−33 29 30	
356.01−2.43	17 42 19.4	−33 35 02	
356.02+0.42	17 30 54.2	−32 03 07	
356.02+0.50	17 30 33.3	−32 00 06	
356.04+0.31	17 31 21.1	−32 05 38	
356.04−2.18	17 41 21.5	−33 26 00	
356.06−2.21	17 41 31.7	−33 25 30	
356.07+0.24	17 31 44.4	−32 06 39	
356.07−2.58	17 43 04.9	−33 36 33	
356.08−2.46	17 42 37.8	−33 32 32	
356.09−2.30	17 41 59.5	−33 27 01	
356.10−2.59	17 43 11.6	−33 35 34	
356.12+0.16	17 32 09.3	−32 06 40	
356.13+0.42	17 31 10.8	−31 57 38	
356.13−2.33	17 42 11.1	−33 26 01	
356.13−2.47	17 42 45.7	−33 30 33	
356.17−2.52	17 43 04.4	−33 30 03	
356.20+0.13	17 32 29.2	−32 03 10	
356.22−0.01	17 33 06.1	−32 06 42	
356.22−0.03	17 33 09.6	−32 07 42	
356.23+0.07	17 32 49.0	−32 04 11	
356.23+0.21	17 32 15.1	−31 59 10	
356.24−0.11	17 33 33.9	−32 09 13	
356.24−2.49	17 43 07.0	−33 25 33	
356.25+0.24	17 32 12.3	−31 57 40	
356.26−0.14	17 33 43.5	−32 09 13	
356.26−2.62	17 43 42.3	−33 28 35	
356.28+0.19	17 32 28.5	−31 57 40	
356.28−0.04	17 33 22.8	−32 05 12	
356.33−0.19	17 34 07.2	−32 07 14	
356.36−0.27	17 34 30.4	−32 08 15	
356.37−0.28	17 34 33.1	−32 08 15	
356.38−0.16	17 34 08.0	−32 03 44	
356.38−0.22	17 34 21.3	−32 05 44	
356.40−0.07	17 33 47.8	−32 00 13	
356.41−0.33	17 34 52.1	−32 07 45	
356.43−0.20	17 34 24.4	−32 02 45	
356.45−0.27	17 34 43.4	−32 04 15	
356.46−0.33	17 35 01.0	−32 05 16	
356.46−0.38	17 35 09.9	−32 07 18	
356.47−0.11	17 34 07.1	−31 57 44	
356.50−0.40	17 35 22.2	−32 05 17	
356.50−0.44	17 35 30.0	−32 06 47	
356.50−0.55	17 35 58.7	−32 10 07	
356.53−0.42	17 35 32.0	−32 04 47	
356.53−0.45	17 35 38.2	−32 05 47	
356.55−0.38	17 35 25.5	−32 02 17	
356.56−0.47	17 35 47.3	−32 04 48	
356.57−0.40	17 35 32.6	−32 02 17	
356.58−0.29	17 35 07.5	−31 57 46	
356.59−0.41	17 35 38.4	−32 01 17	
356.59−0.61	17 36 27.2	−32 07 49	
356.61−0.45	17 35 51.7	−32 01 48	
356.62−0.65	17 36 40.2	−32 07 50	
356.64−0.33	17 35 23.9	−31 55 57	
356.64−0.51	17 36 09.9	−32 01 48	
356.66−0.69	17 36 55.8	−32 06 50	
356.72−0.58	17 36 36.9	−32 00 19	
356.72−0.61	17 36 45.0	−32 00 50	
356.72−0.67	17 36 58.9	−32 03 20	
356.73−0.78	17 37 27.3	−32 05 51	
356.75−0.59	17 36 45.1	−31 59 20	
356.76−0.57	17 36 40.9	−31 57 50	
356.76−0.77	17 37 29.1	−32 04 21	
356.79−0.88	17 37 59.2	−32 06 22	
356.79−0.93	17 38 12.8	−32 07 53	
356.80−0.80	17 37 42.6	−32 03 22	
356.82−0.75	17 37 34.1	−32 00 22	
356.86−0.94	17 38 25.0	−32 04 23	
356.95−0.98	17 38 47.6	−32 01 24	
356.97−1.06	17 39 10.0	−32 02 55	
356.98−1.15	17 39 34.5	−32 05 26	
356.98−1.21	17 39 47.8	−32 07 26	
357.04−1.17	17 39 46.7	−32 02 56	
357.07−1.16	17 39 49.5	−32 00 56	
357.07−1.28	17 40 18.3	−32 04 57	
357.08−1.14	17 39 47.8	−31 59 56	
357.12−1.24	17 40 18.9	−32 00 57	
357.12−1.36	17 40 44.5	−32 04 58	
357.17−1.22	17 40 20.2	−31 57 57	
357.18−0.52	17 37 34.1	−31 34 07	
357.18−0.52	17 37 35.0	−31 34 52	
357.19−1.29	17 40 39.0	−31 58 58	
357.19−1.52	17 41 34.7	−32 06 30	
357.22−1.36	17 41 00.9	−31 59 59	
357.26−1.71	17 42 32.2	−32 08 32	
357.29−1.49	17 41 42.9	−32 00 31	
357.31−1.51	17 41 48.9	−32 00 01	
357.32−1.73	17 42 45.6	−32 06 33	
357.33+2.69	17 25 25.2	−29 42 25	
357.33+2.78	17 25 05.5	−29 39 24	
357.36+2.71	17 25 26.6	−29 39 55	
357.37−1.75	17 42 56.8	−32 04 33	
357.38−1.70	17 42 46.2	−32 02 33	
357.39+2.73	17 25 28.3	−29 37 55	
357.39−1.58	17 42 18.1	−31 58 02	
357.42+2.68	17 25 43.0	−29 38 26	
357.46+2.61	17 26 05.2	−29 38 26	
357.47−2.05	17 44 25.3	−32 08 36	
357.48+0.37	17 34 49.1	−30 51 41	
357.49+2.49	17 26 37.8	−29 40 58	
357.54+2.54	17 26 33.5	−29 36 58	
357.57+2.42	17 27 05.3	−29 39 29	
357.59−2.15	17 45 05.7	−32 05 38	
357.63−1.97	17 44 29.6	−31 58 07	
357.64+2.29	17 27 45.3	−29 40 00	
357.64−2.23	17 45 33.3	−32 05 39	
357.68+2.16	17 28 21.7	−29 42 31	
357.68−0.06	17 37 00.9	−30 54 29	
357.68−0.06	17 37 01.2	−30 54 20	
357.69−2.16	17 45 23.8	−32 00 39	
357.71−0.27	17 37 53.4	−31 00 11	
357.72+2.26	17 28 04.0	−29 37 01	
357.73+2.25	17 28 07.2	−29 37 01	
357.73−2.34	17 46 12.8	−32 04 10	
357.73−2.38	17 46 21.5	−32 05 41	
357.75+0.34	17 35 37.9	−30 38 35	
357.77−0.15	17 37 32.3	−30 53 18	
357.78+2.07	17 28 57.4	−29 40 03	
357.78+2.09	17 28 52.8	−29 39 32	
357.78−2.56	17 47 11.9	−32 08 42	
357.79−2.49	17 46 57.7	−32 06 12	
357.80+2.03	17 29 08.9	−29 40 33	
357.81+2.13	17 28 47.2	−29 37 02	
357.82−2.54	17 47 14.4	−32 05 43	
357.83+2.92	17 25 50.1	−29 09 20	
357.84+3.03	17 25 26.4	−29 05 19	
357.86−2.41	17 46 49.8	−31 59 42	
357.87+2.91	17 25 57.7	−29 07 50	
357.90+1.94	17 29 45.9	−29 38 34	
357.90+3.07	17 25 27.3	−29 01 20	
357.92+1.88	17 30 01.9	−29 39 35	
357.93−2.47	17 47 13.2	−31 58 12	
357.94+1.94	17 29 52.0	−29 37 05	
357.96+1.83	17 30 19.9	−29 39 36	
357.97+2.77	17 26 46.3	−29 07 52	
357.98+1.70	17 30 53.4	−29 42 37	
357.98+3.03	17 25 48.6	−28 58 21	
357.99+1.81	17 30 27.9	−29 38 36	
357.99+2.67	17 27 12.3	−29 10 24	
357.99+3.14	17 25 24.3	−28 54 20	
358.01+2.63	17 27 25.0	−29 10 24	
358.01+2.90	17 26 21.8	−29 01 22	
358.01+2.98	17 26 03.5	−28 58 21	
358.02+1.73	17 30 54.3	−29 39 37	
358.02+1.74	17 30 50.6	−29 39 07	
358.03+2.74	17 27 01.8	−29 05 54	
358.05+2.97	17 26 12.7	−28 56 52	
358.05+3.05	17 25 54.2	−28 54 21	
358.06+1.66	17 31 14.5	−29 40 08	
358.06+2.60	17 27 38.1	−29 08 55	
358.06+2.75	17 27 04.9	−29 03 53	
358.08+1.66	17 31 18.3	−29 38 38	
358.08+3.00	17 26 09.5	−28 54 22	
358.11+1.63	17 31 30.0	−29 38 08	
358.12+2.86	17 26 49.2	−28 57 23	
358.13+2.93	17 26 35.0	−28 54 22	
358.14+1.49	17 32 06.2	−29 41 39	
358.14+2.52	17 28 09.0	−29 07 55	
358.14+2.54	17 28 04.1	−29 06 55	
358.15+1.51	17 32 03.3	−29 40 09	
358.15+1.58	17 31 46.7	−29 38 09	
358.15+2.86	17 26 52.6	−28 55 53	
358.16+0.50	17 36 01.9	−30 12 54	
358.16+0.50	17 36 02.2	−30 12 54	
358.16+2.68	17 27 35.1	−29 00 54	
358.17+1.45	17 32 18.8	−29 41 10	
358.17+1.54	17 31 59.4	−29 38 09	
358.17+2.78	17 27 13.4	−28 57 24	
358.19+1.38	17 32 38.1	−29 42 41	
358.19+1.52	17 32 06.2	−29 38 10	
358.21+1.41	17 32 35.5	−29 40 40	
358.21+1.48	17 32 18.4	−29 38 10	
358.21+2.84	17 27 07.8	−28 53 24	
358.22+2.35	17 29 00.1	−29 09 27	
358.23+2.77	17 27 26.3	−28 54 54	
358.24+2.39	17 28 54.4	−29 06 57	
358.25+1.38	17 32 48.6	−29 39 41	
358.27+1.42	17 32 41.8	−29 37 11	
358.27+2.72	17 27 43.9	−28 54 25	
358.29+1.22	17 33 31.8	−29 42 43	
358.29+1.39	17 32 52.3	−29 37 11	
358.32+2.19	17 29 52.0	−29 09 29	
358.33+1.27	17 33 26.6	−29 39 12	
358.35+1.13	17 34 02.5	−29 42 44	
358.35+1.15	17 33 57.3	−29 41 43	
358.36+1.24	17 33 37.6	−29 38 13	
358.37+2.36	17 29 20.3	−29 01 28	

NAME	RA (1950) DEC	POS REF
	h m s ° ′ ″	
358.38+1.13	17 34 05.2 −29 41 14	
358.38+2.55	17 28 37.5 −28 54 27	
358.39+2.23	17 29 53.8 −29 04 59	
358.39+2.47	17 28 57.4 −28 56 28	
358.40+1.04	17 34 29.2 −29 42 45	
358.41+1.11	17 34 14.8 −29 40 14	
358.42+1.01	17 34 38.9 −29 42 45	
358.42+1.19	17 33 58.3 −29 37 14	
358.42+2.29	17 29 45.2 −29 00 58	
358.43+1.04	17 34 33.7 −29 41 45	
358.43+1.10	17 34 19.3 −29 39 44	
358.44+1.15	17 34 09.4 −29 37 14	
358.44+2.38	17 29 26.9 −28 57 29	
358.45+2.10	17 30 31.8 −29 05 30	
358.45+2.27	17 29 52.5 −29 00 29	
358.46+1.99	17 30 59.4 −29 09 02	
358.48+2.06	17 30 45.8 −29 05 31	
358.49+0.99	17 34 55.3 −29 40 16	
358.49+2.25	17 30 03.6 −28 58 59	
358.51+0.96	17 35 04.7 −29 40 16	
358.51+1.99	17 31 07.0 −29 06 31	
358.51+2.28	17 29 59.7 −28 57 00	
358.52+2.25	17 30 08.1 −28 57 30	
358.53+0.93	17 35 15.5 −29 39 46	
358.53+2.01	17 31 04.7 −29 04 31	
358.54+1.96	17 31 18.3 −29 06 03	
358.55+1.89	17 31 34.8 −29 07 33	
358.56+2.20	17 30 26.0 −28 57 01	
358.57+0.89	17 35 29.5 −29 39 17	
358.61+2.15	17 30 45.8 −28 56 02	
358.62+2.02	17 31 15.8 −28 59 32	
358.63+0.74	17 36 13.8 −29 40 48	
358.63+2.00	17 31 23.7 −29 00 02	
358.64+1.66	17 32 41.9 −29 10 36	
358.65+1.97	17 31 32.2 −29 00 02	
358.65+2.08	17 31 07.7 −28 56 32	
358.67+1.69	17 32 40.4 −29 08 05	
358.69+1.63	17 32 55.6 −29 09 06	
358.70+0.71	17 36 31.4 −29 38 19	
358.70+1.86	17 32 05.0 −29 01 03	
358.71+0.74	17 36 25.5 −29 37 19	
358.72+0.63	17 36 51.9 −29 39 50	
358.73+0.52	17 37 19.1 −29 42 51	
358.73+0.58	17 37 05.2 −29 40 50	
358.73+1.56	17 33 17.9 −29 09 07	
358.73+1.83	17 32 46.7 −29 00 34	
358.74+1.88	17 32 06.1 −28 58 34	
358.74+2.02	17 31 33.1 −28 54 03	
358.75+0.67	17 36 46.7 −29 37 20	
358.75+1.77	17 32 34.6 −29 01 35	
358.75+1.97	17 31 47.1 −28 55 04	
358.76+1.93	17 31 57.1 −28 55 34	
358.77+1.63	17 33 09.6 −29 05 06	
358.78+1.72	17 32 49.6 −29 01 36	
358.78+1.76	17 32 39.7 −29 00 35	
358.80+0.50	17 37 35.0 −29 39 51	
358.80+1.86	17 32 21.1 −28 56 05	
358.80+1.90	17 32 10.0 −28 54 35	
358.81+0.48	17 37 41.4 −29 40 22	
358.81+1.92	17 32 07.7 −28 53 35	
358.82+1.41	17 34 05.7 −29 09 38	
358.82+1.84	17 32 28.7 −28 55 35	
358.83+1.39	17 34 12.4 −29 09 38	
358.83+1.59	17 33 27.6 −29 03 37	
358.83+1.77	17 32 46.1 −28 57 36	
358.83+1.86	17 32 23.2 −28 54 35	
358.84+1.71	17 33 00.3 −28 59 05	
358.85+1.81	17 32 39.0 −28 55 06	
358.87+1.61	17 33 27.9 −29 00 37	
358.87+1.83	17 32 37.0 −28 53 36	
358.88+0.46	17 37 55.3 −29 37 22	
358.89+0.41	17 38 09.6 −29 38 23	
358.89+1.57	17 33 41.2 −29 01 07	
358.90+0.32	17 38 32.6 −29 40 53	
358.90+1.62	17 33 29.9 −28 58 37	
358.91+0.35	17 38 27.0 −29 39 23	
358.92+1.56	17 33 46.9 −28 59 37	
358.93+1.59	17 33 40.7 −28 58 38	
358.93+1.66	17 33 24.1 −28 56 07	
358.93+1.74	17 33 05.0 −28 53 37	
358.95+1.29	17 34 54.0 −29 07 09	
358.97+1.60	17 33 43.5 −28 56 08	
358.98+0.17	17 39 17.8 −29 41 25	
358.98+0.31	17 38 45.6 −29 37 24	
358.99+1.18	17 35 25.4 −29 08 41	
359.00+0.10	17 39 36.5 −29 42 56	
359.00+1.47	17 34 19.6 −28 58 39	
359.00+1.55	17 34 01.0 −28 56 09	
359.02+0.20	17 39 17.1 −29 38 25	
359.02+1.57	17 33 59.1 −28 54 39	
359.03+1.33	17 34 55.3 −29 01 41	
359.05+0.11	17 39 42.7 −29 39 56	
359.05+1.02	17 36 10.6 −29 10 43	
359.06+1.06	17 36 04.1 −29 08 42	
359.06−0.01	17 40 12.2 −29 42 57	
359.07+1.46	17 34 31.1 −28 55 40	
359.08+0.14	17 39 39.4 −29 37 26	
359.10+1.01	17 36 20.2 −29 08 13	
359.10+1.37	17 34 56.9 −28 57 11	
359.10+1.41	17 34 48.2 −28 55 40	
359.11+1.08	17 36 06.3 −29 05 42	
359.12+0.99	17 36 29.1 −29 08 13	
359.12−0.06	17 40 32.6 −29 41 58	
359.14+1.19	17 35 46.4 −29 00 42	
359.14+1.33	17 35 13.2 −28 56 11	
359.14+1.41	17 34 53.3 −28 53 41	
359.15+0.91	17 36 51.4 −29 09 15	
359.15−0.05	17 40 33.1 −29 39 58	
359.19+1.22	17 35 44.4 −28 57 12	
359.19−0.11	17 40 55.0 −29 39 59	
359.20+0.86	17 37 09.2 −29 08 14	
359.20−0.15	17 41 05.0 −29 40 29	
359.22+0.26	17 39 32.7 −29 26 37	
359.22+1.18	17 35 59.6 −28 57 13	
359.23−0.20	17 41 21.2 −29 40 30	
359.25+1.20	17 35 57.9 −28 54 43	
359.25−0.13	17 41 08.9 −29 37 29	
359.27−0.35	17 42 03.4 −29 43 01	

NAME	RA (1950) DEC	POS REF
	h m s ° ′ ″	
359.28+1.01	17 36 47.9 −28 59 14	
359.30+1.12	17 36 25.6 −28 54 44	
359.30+1.16	17 36 14.3 −28 53 43	
359.31−0.32	17 42 02.1 −29 40 31	
359.32+0.99	17 36 57.3 −28 58 15	
359.32+1.09	17 36 36.0 −28 54 44	
359.34+0.77	17 37 52.1 −29 04 16	
359.34−0.45	17 42 36.8 −29 43 02	
359.35+0.54	17 38 47.7 −29 10 49	
359.35+0.55	17 38 43.4 −29 10 49	
359.35+0.91	17 37 20.2 −28 59 15	
359.36+0.58	17 38 38.9 −29 09 19	
359.36+0.67	17 38 18.5 −29 06 18	
359.36−0.35	17 42 17.5 −29 38 32	
359.37+0.88	17 37 31.5 −28 59 15	
359.37+1.03	17 36 54.2 −28 54 15	
359.38+0.78	17 37 54.9 −29 01 47	
359.39+1.00	17 37 04.5 −28 54 15	
359.40+0.83	17 37 45.9 −28 59 16	
359.40−0.37	17 42 26.1 −29 37 32	
359.41+0.98	17 37 13.2 −28 53 46	
359.41−0.44	17 42 44.3 −29 39 03	
359.42−0.51	17 43 02.8 −29 40 33	
359.43+0.56	17 38 55.0 −29 06 19	
359.46+0.64	17 38 40.1 −29 02 19	
359.46+0.78	17 38 06.3 −28 57 47	
359.46−0.57	17 43 22.7 −29 40 34	
359.47+0.86	17 37 49.4 −28 54 47	
359.48+0.54	17 39 04.4 −29 04 19	
359.48−0.58	17 43 27.1 −29 40 04	
359.49−0.52	17 43 13.9 −29 37 34	
359.52+0.45	17 39 31.2 −29 05 20	
359.54+0.72	17 38 32.7 −28 55 48	
359.55+0.37	17 39 55.2 −29 06 22	
359.56+0.74	17 38 32.6 −28 53 48	
359.57−0.76	17 44 23.3 −29 40 36	
359.58+0.49	17 39 30.3 −29 00 50	
359.58+0.69	17 38 45.2 −28 54 19	
359.60−0.70	17 44 12.1 −29 37 36	
359.60−0.73	17 44 20.0 −29 38 36	
359.62+0.15	17 40 55.8 −29 09 24	
359.62+0.22	17 40 41.0 −29 07 22	
359.65+0.48	17 39 45.0 −28 57 51	
359.65−0.92	17 45 12.6 −29 41 38	
359.69+0.51	17 39 42.2 −28 54 51	
359.69−0.85	17 45 00.0 −29 37 38	
359.69−0.89	17 45 10.9 −29 38 38	
359.70−0.90	17 45 14.0 −29 38 38	
359.70−0.96	17 45 29.3 −29 40 39	
359.71−0.97	17 45 33.6 −29 40 09	
359.72+0.40	17 40 12.6 −28 56 52	
359.72−1.08	17 45 59.2 −29 43 10	
359.73+0.18	17 41 06.5 −29 03 23	
359.73−0.02	17 41 52.8 −29 09 26	
359.74+0.19	17 41 03.9 −29 02 24	
359.74+0.32	17 40 34.3 −28 58 23	
359.76+0.17	17 41 12.5 −29 01 54	
359.76−0.98	17 45 42.1 −29 37 39	
359.77−0.02	17 41 56.7 −29 07 25	
359.78+0.01	17 41 52.8 −29 05 55	
359.78+0.36	17 40 29.6 −28 54 53	
359.78−0.11	17 42 20.6 −29 09 56	
359.81−1.06	17 46 07.7 −29 37 40	
359.81−1.09	17 46 15.5 −29 39 10	
359.82+0.10	17 41 36.4 −29 00 54	
359.85−1.20	17 46 45.9 −29 40 11	
359.86+0.01	17 42 05.0 −29 01 56	
359.86−1.28	17 47 08.5 −29 42 12	
359.87+0.06	17 41 54.4 −28 59 55	
359.87+0.08	17 41 49.8 −28 59 25	
359.87−1.23	17 46 55.4 −29 40 12	
359.88+0.0	17 42 09.0 −29 00 55	
359.88−1.19	17 46 49.3 −29 38 42	
359.89+0.07	17 41 55.2 −28 58 26	
359.90+0.06	17 41 58.6 −28 57 56	
359.90+0.09	17 41 51.0 −28 57 26	
359.92−0.02	17 42 19.8 −28 59 56	
359.92−0.09	17 42 36.8 −29 01 57	
359.92−0.14	17 42 46.6 −29 03 27	
359.93−0.15	17 42 50.3 −29 03 27	
359.95+0.0	17 42 20.1 −28 57 27	
359.95−0.02	17 42 23.5 −28 57 57	
359.95−0.04	17 42 28.8 −28 58 57	
359.95−1.47	17 48 05.2 −29 43 14	
359.96−0.05	17 42 33.4 −28 58 27	
359.97−0.03	17 42 29.0 −28 57 27	
359.97−0.10	17 42 46.2 −28 59 57	
359.97−0.12	17 42 50.6 −29 00 27	
359.97−0.43	17 44 03.7 −29 09 59	
359.98−0.19	17 43 07.7 −29 01 58	
359.98−0.30	17 43 33.4 −29 05 28	
359.98−1.37	17 47 46.1 −29 38 44	
359.98−1.41	17 47 55.5 −29 40 14	
359.99−0.04	17 42 33.3 −28 56 57	
359.99−0.21	17 43 13.5 −29 01 59	
359.99−0.32	17 43 41.3 −29 05 29	
359.99−1.34	17 47 39.6 −29 37 43	
360.00+0.01	17 42 23.6 −28 54 57	
360.00−0.01	17 42 29.5 −28 55 27	
360.00−0.09	17 42 46.8 −28 57 58	
360.00−0.11	17 42 51.5 −28 58 28	
78−0−103	20 33 36 +40 48	
78−0−120	20 41 12 +41 11	
78−0−127	20 43 24 +39 04	
78−0−133	20 44 36 +39 55	
78−0−136	20 45 24 +40 48	
110+10	22 20 +68 40	ED
222+0	7 00 − 8 00	"
230+0	7 20 −15 00	"
233+0	7 30 −17 40	"
284−G53	20 14 44 −45 59 54	779909

NAME	RA (1950) DEC	POS REF
	h m s ° ′ ″	

C. BIBLIOGRAPHY - CHRONOLOGICAL LISTING

The *Bibliography of Infrared Astronomy* identifies each observation in the Catalog with the original article published in the scientific literature. Over 1,700 infrared journal articles and other references are listed in this appendix. Each entry contains the year and month of publication, authors' names, journal name or document number, volume, page, and full title of the reference.

The Bibliography is arranged chronologically by bibliographic reference number. The reference number in the catalog (BIBLIO) indicates the original journal reference for each observation and is keyed to the Bibliography. The number is made up of the year and month of publication, and a sequential number assigned to the article (for example "790104" is broken down into 79-01-04, where 79 = 1979, 01 = January, and 04 = article #4 in that month).

A version of the Bibliography sorted alphabetically by first author follows the chronological Bibliography listings in this volume. The alphabetical listing is useful for quickly locating familiar articles in the literature, which are often identified by the name of the first author.

598901 ARGELANDER, F. W. A. <ASTRON. BEOB. STERNWARTE KONIGL. RHEIN, 3-5, BONN>
BONNER STERNVERZEICHNIS, SECTIONS 1-3.

928901 THOME, J. M. <RESULTADOS OBS. NACIONAL ARGENTINA, 16-19>
CORDOBA DURCHMUSTERUNG, PARTS I-IV.

958901 DREYER, J. L. E. <MEM. R. A. S., L1>
INDEX CATALOGUE.

968901 GILL, D., KAPTEYN, J. C. <ANN. CAPE OBS., 3-5>
CAPE PHOTOGRAPHIC DURCHMUSTERUNG, PARTS I-III.

189901 CANNON, A. J., PICKERING, E. C. <HARVARD ANNALS, 91-100>
THE HENRY DRAPER CATALOG.

229901 GINGRICH, C. H. <AP. J., 56, 139>
PARALLAXES OF STARS IN THE REGION OF B. D. +31 643.

339901 MERRILL, P. W., BURWELL, C. G. <AP. J., 78, 87>
CATALOGUE AND BIBLIOGRAPHY OF STARS OF CLASSES B AND A WHOSE SPECTRA HAVE BRIGHT HYDROGEN LINES.

379901 HETZLER, C. <AP. J., 86, 509>
INFRARED STELLAR SURVEYS AND INDEX SEQUENCES.

419901 LUYTEN, W. J. <LUNDPRESS, MINNEAPOLIS, MN>
BRUCE PROPER MOTION SURVEY.

439901 MERRILL, P. W., BURWELL, C. G. <AP. J., 98, 153>
SUPPLEMENT TO THE MOUNT WILSON CATALOGUE AND BIBLIOGRAPHY OF STARS OF CLASSES B AND A WHOSE SPECTRA HAVE BRIGHT HYDROGEN LINES.

470901 STEBBINS, J., WHITFORD, A. E. <AP. J., 106, 235>
SIX-COLOR PHOTOMETRY OF STARS. V. INFRARED RADIATION FROM THE REGION OF THE GALACTIC CENTER.

470902 KUIPER, G. P., WILSON, W., CASHMAN, R. J. <AP. J., 106, 243>
AN INFRARED STELLAR SPECTROMETER.

499901 MERRILL, P. W., BURWELL, C. G. <AP. J., 110, 387>
SECOND SUPPLEMENT TO THE MOUNT WILSON CATALOGUE AND BIBLIOGRAPHY OF STARS OF CLASSES B AND A WHOSE SPECTRA HAVE BRIGHT HYDROGEN LINES.

509901 MERRILL, P. W., BURWELL, C. G. <AP. J., 112, 72>
ADDITIONAL STARS WHOSE SPECTRA HAVE A BRIGHT H-ALPHA LINE.

519901 KUKARKIN, B. V., PARENAGO, P. P., EFREMOV, YU. N., KHOLOPOV, P. N. <PUBL. OFFICE NAUKA, MOSCOW>
CATALOGUE OF STARS SUSPECTED TO BE VARIABLE.

529901 JENKINS, L. F. <YALE UNIV. OBS. >
GENERAL CATALOGUE OF TRIGONOMETRIC STELLAR PARALLAXES.

529902 VAN BUEREN, H. G. <B. A. N., 11, 385>
ON THE STRUCTURE OF THE HYADES CLUSTER.

539901 SANDAGE, A. R. <A. J., 58, 61>
THE COLOR-MAGNITUDE DIAGRAM FOR THE GLOBULAR CLUSTER M3.

539902 MUNCH, L., MORGAN, W. W. <AP. J., 118, 161>
A PROBABLE CLUSTERING OF BLUE GIANTS IN CYGNUS.

549901 NASSAU, J. J., BLANCO, V. M., MORGAN, W. W. <AP. J., 120, 478>
REDDENED EARLY M- AND S-TYPE STARS NEAR THE GALACTIC EQUATOR.

549902 HERBIG, G. H. <AP. J., 119, 483>
EMISSION-LINE STARS ASSOCIATED WITH THE NEBULOUS CLUSTER NGC 2264.

549903 HERBIG, G. H. <P. A. S. P., 66, 19>
BRIGHT H-ALPHA STARS IN IC 348.

549904 MORGAN, W. W., JOHNSON, H. L., ROMAN, N. G. <P. A. S. P., 66, 85>
A VERY RED STAR OF EARLY TYPE IN CYGNUS.

549905 MERRILL, P. W., SANFORD, R. F., BURWELL, C. G. <P. A. S. P., 66, 107>
ADDITIONAL STARS OF CLASSES N AND S - SECOND LIST.

549906 MORGAN, W. W., MEINEL, A. B., JOHNSON, H. M. <AP. J., 120, 506>
SPECTRAL CLASSIFICATION WITH EXCEEDINGLY LOW DISPERSION.

569901 WALKER, M. F. <AP. J. SUPPL., 2, 365>
STUDIES OF EXTREMELY YOUNG CLUSTERS. I. NGC 2264.

569902 HERBIG, G. H. <P. A. S. P., 68, 353>
THE SOURCE OF ILLUMINATION OF NGC 1579.

569903 HENIZE, K. G. <AP. J. SUPPL., 2, 315>
CATALOGUES OF H-ALPHA EMISSION STARS AND NEBULAE IN THE MAGELLANIC CLOUDS.

569904 FREDERICK, L. W. <A. J., 61, 437>
PROPER MOTIONS IN THE NUCLEUS OF THE ZETA PERSEI ASSOCIATION.

569905 SCHULTE, D. H. <AP. J., 123, 250>
SOME RECENT RESULTS OF LOW-DISPERSION SPECTRAL CLASSIFICATION.

569906 SCHULTE, D. H. <AP. J., 124, 530>
NEW MEMBERS OF THE ASSOCIATION VI CYGNI.

579901 BLANCO, V. M., NASSAU, J. J. <AP. J., 125, 408>
REDDENED EARLY M- AND S-TYPE STARS IN TWO GALACTIC ZONES.

579902 VELGHE, A. G. <AP. J., 126, 302>
H-ALPHA EMISSION STARS AND PLANETARY NEBULAE IN THE VICINITY OF M8 AND M20 AND IN VELA FROM L-230 TO L-241 ALONG THE GALACTIC EQUATOR.

579903 HERBIG, G. H. <AP. J., 125, 654>
EMISSION-LINE STARS IN THE VICINITY OF MESSIER 8, MESSIER 20, AND SIMEIS 188.

579904 LUYTEN, W. J. <LUNDPRESS, MINNEAPOLIS, MN>
A CATALOGUE OF 9867 STARS IN THE SOUTHERN HEMISPHERE WITH PROPER MOTIONS EXCEEDING 0.2 ARC SECONDS ANNUALLY.

589901 SCHULTE, D. H. <AP. J., 128, 41>
NEW MEMBERS OF THE ASSOCIATION VI CYGNI. II.

589902 HERBIG, G. H. <AP. J., 128, 259>
NGC 7000, IC 5070, AND THE ASSOCIATED EMISSION-LINE STARS.

589903 WESTERHOUT, G. <B. A. N., 14, 215>
A SURVEY OF THE CONTINUOUS RADIATION FROM THE GALACTIC SYSTEM AT A FREQUENCY OF 1390 MC/S.

589904 ARP, H. C. <A. J., 63, 273>
SOUTHERN HEMISPHERE PHOTOMETRY. III. THE COLOR-MAGNITUDE DIAGRAM OF NGC 419 AND THE ADJOINING FIELD IN THE SMALL MAGELLANIC CLOUD.

589905 ARP, H. C. <A. J., 63, 487>
SOUTHERN HEMISPHERE PHOTOMETRY. V. THE COLOR-MAGNITUDE DIAGRAM OF NGC 361 AND THE ADJOINING FIELD IN THE SMALL MAGELLANIC CLOUD.

599901 SHARPLESS, S. <AP. J. SUPPL., 4, 257>
A CATALOGUE OF HII REGIONS.

599902 DOLIDZE, M. V., ARAKELYAN, M. A. <SOV. AST., 3, 434>
THE T-ASSOCIATION NEAR RHO OPHIUCHI.

600301 MOROZ, V. I. <SOV. AST., 4, 250>
THE RADIATION FLUX FROM THE CRAB NEBULA AT 2 MICRONS AND SOME CONCLUSIONS ON THE SPECTRUM AND MAGNETIC FIELD.

609901 HERBIG, G. H. <AP. J., 131, 516>
EMISSION-LINE STARS IN IC 5146.

609902 RODGERS, A. W., CAMPBELL, C. T., WHITEOAK, J. B. <M. N. R. A. S., 121, 103>
A CATALOGUE OF H-ALPHA EMISSION REGIONS IN THE SOUTHERN MILKY WAY.

609903 FEAST, M. W., THACKERAY, A. D., WESSELINK, A. J. <M. N. R. A. S., 121, 25>
THE BRIGHTEST STARS IN THE MAGELLANIC CLOUDS.

609904 HODGE, P. W. <AP. J., 132, 341>
STUDIES OF THE LARGE MAGELLANIC CLOUD. II. THE GLOBULAR CLUSTER NGC 1846.

609905 HODGE, P. W. <AP. J., 132, 346>
STUDIES OF THE LARGE MAGELLANIC CLOUD. III. THE GLOBULAR CLUSTER NGC 1978.

619901 HODGE, P. W. <A. J., 66, 83>
THE FORNAX DWARF GALAXY. I. THE GLOBULAR CLUSTERS.

619902 HODGE, P. W. <AP. J., 134, 226>
STUDIES OF THE LARGE MAGELLANIC CLOUD. VII. THE OPEN CLUSTER NGC 1844.

620001 KUIPER, G. P., GORANSON, R., BINDER, A., JOHNSON, H. L. <COMM. LUNAR AND PLANETARY LAB., 1, 119>
AN INFRARED STELLAR SPECTROMETER.

620002 KUIPER, G. P. <COMM. LUNAR AND PLANETARY LAB., 1, 179>
INFRARED SPECTRA OF STARS AND PLANETS. II. WATER VAPOR IN OMICRON CETI.

629901 UPGREN JR., A. R. <A. J., 67, 37>
THE SPACE DISTRIBUTION OF LATE-TYPE STARS IN A NORTH GALACTIC POLE REGION.

629902 ROBERTS, M. S. <A. J., 67, 79>
THE GALACTIC DISTRIBUTION OF THE WOLF-RAYET STARS.

629903 GASCOIGNE, S. C. B. <M. N. R. A. S., 124, 201>
NGC 1783, A CLUSTER IN THE LARGE MAGELLANIC CLOUD.

630001 KUIPER, G. P. <COMM. LUNAR AND PLANETARY LAB., 2, 17>
INFRARED SPECTRA OF STARS AND PLANETS. III. RECONNAISSANCE OF A0-B8 STARS, 1-2.5 MICRONS.

631001 JOHNSON, H. L., BORGMAN, J. <B. A. N., 17, 115>
THE LAW OF INTERSTELLAR EXTINCTION.

639901 HERBIG, G. H., KUHI, L. V. <AP. J., 137, 398>
EMISSION-LINE STARS IN THE REGION OF NGC 2068.

639902 JENKINS, L. F. <YALE UNIV. OBS. >
GENERAL CATALOGUE OF TRIGONOMETRIC STELLAR PARALLAXES WITH 1963 SUPPLEMENT.

639903 HODGE, P. W. <AP. J., 137, 1033>
STUDIES OF THE LARGE MAGELLANIC CLOUD. VIII. THE CLUSTER NGC 1831.

639904 TIFFT, W. G. <M. N. R. A. S., 125, 199>
MAGELLANIC CLOUD INVESTIGATIONS. I. THE REGION OF NGC 121.

640201 WILDEY, R. L., MURRAY, B. C. <AP. J., 139, 435>
10-MICRON PHOTOMETRY OF 25 STARS FROM B8 TO M7.

640301 MOROZ, V. I. <SOV. AST., 7, 601>
RADIATION EMISSION FROM THE ORION NEBULA IN THE 0.85-1.7 MICRON WAVELENGTH REGION.

640401 JOHNSON, H. L. <AP. J., 139, 1022>
THE BRIGHTNESS OF 3C 273 AT 2.2 MICRONS.

640501 LOW, F. J., JOHNSON, H. L. <AP. J., 139, 1130>
STELLAR PHOTOMETRY AT 10 MICRONS.

640502 MOROZ, V. I. <SOV. AST., 7, 755>
INFRARED OBSERVATIONS OF THE CRAB NEBULA.

641001 WOOLF, N. J., SCHWARZSCHILD, M., ROSE, W. K. <AP. J., 140, 833>
INFRARED SPECTRA OF RED-GIANT STARS.

641101 MITCHELL, R. I. <AP. J., 140, 1607>
NINE-COLOR PHOTOMETRY OF EPSILON AUR, 0.35-9.5 MICRONS.

649901 HOFFLEIT, D. <YALE UNIV. OBS. >
CATALOGUE OF BRIGHT STARS.

650001 JOHNSON, H. L. <COMM. LUNAR AND PLANETARY LAB., 3, 73>
THE ABSOLUTE CALIBRATION OF THE ARIZONA PHOTOMETRY.

650002 JOHNSON, H. L. <COMM. LUNAR AND PLANETARY LAB., 3, 79>
INTERSTELLAR EXTINCTION IN THE GALAXY.

650003 JOHNSON, H. L., LOW, F. J., STEINMETZ, D. L. <COMM. LUNAR AND PLANETARY LAB., 3, 95>
INFRARED OBSERVATIONS OF THE NEUGEBAUER-MARTZ-LEIGHTON "INFRARED STAR" IN CYGNUS.

650004 JOHNSON, H. L., MENDOZA V, E. E., WISNIEWSKI, W. Z. <COMM. LUNAR AND PLANETARY LAB., 3, 97>
OBSERVATIONS OF "INFRARED STARS".

650101 MENDOZA V, E. E., JOHNSON, H. L. <AP. J., 141, 161>
MULTICOLOR PHOTOMETRY OF CARBON STARS.

650102 JOHNSON, H. L. <AP. J., 141, 170>
INFRARED PHOTOMETRY OF M-DWARF STARS.

650103 OKE, J. B. <AP. J., 141, 6>
THE OPTICAL SPECTRUM OF 3C 273.

650104 LOW, F. J., MITCHELL, R. I. <AP. J., 141, 327>
NEW INFRARED PHOTOMETRY OF EPSILON AURIGAE.

650105 LOW, F. J., JOHNSON, H. L. <AP. J., 141, 336>
THE SPECTRUM OF 3C 273.

650106 DANIELSON, R. E., WOOLF, N. J., GAUSTAD, J. E. <AP. J., 141, 116>
A SEARCH FOR INTERSTELLAR ICE ABSORPTION IN THE INFRARED SPECTRUM OF MU CEPHEI.

650107 BELTON, M. J. S., WOOLF, N. J. <AP. J., 141, 145>
THE PROBLEM OF BETA LYRAE. I. SIX-COLOR PHOTOMETRY.

650108 LOW, F. J. <AP. J., 141, 326>
THE INFRARED BRIGHTNESS OF ALPHA LEONIS AND GAMMA ORIONIS.

650401 JOHNSON, H. L. <AP. J., 141, 923>
INTERSTELLAR EXTINCTION IN THE GALAXY.

650701 NEUGEBAUER, G., MARTZ, D. E., LEIGHTON, R. B. <AP. J., 142, 399>
OBSERVATIONS OF EXTREMELY COOL STARS.

650702 MUENCH, G., SCARGLE, J. D. <AP. J., 142, 401>
THE SPECTRA OF TWO EXTREMELY RED OBJECTS.

651001 MENDOZA V, E. E. <AP. J., 142, 1270>
MULTICOLOR PHOTOMETRY OF AN EARLY-TYPE FLARE STAR.

651002 MERTZ, L. <A. J., 70, 548>
ASTRONOMICAL INFRARED SPECTROMETER.

659901 KUKARKIN, B. V., KHOLOPOV, P. N., EFREMOV, YU. N., KUROCHKIN, N. E. <PUBL. OFFICE NAUKA, MOSCOW>
SECOND CATALOGUE OF SUSPECTED VARIABLE STARS.

660001 JOHNSON, H. L., MENDOZA V, E. E. <ANN. D'AST., 29, 525>
THE LAW OF INTERSTELLAR EXTINCTION IN PERSEUS.

660101 MENDOZA V, E. E. <COMM. LUNAR AND PLANETARY LAB., 6, 59>
INFRARED PHOTOMETRY OF T TAURI STARS AND RELATED OBJECTS.

660102 OKE, J. B., CONTI, P. S. <AP. J., 143, 134>
ABSOLUTE PHOTOELECTRIC SPECTROPHOTOMETRY OF STARS IN THE HYADES.

660103 JOHNSON, H. L. <AP. J., 143, 187>
INFRARED PHOTOMETRY OF GALAXIES.

660201 GOULD, R. J. <AP. J., 143, 603>
12. 8-MICRON EMISSION FROM PLANETARY NEBULAE.

660202 SPINRAD, H., YOUNKIN, R. L. <P. A. S. P., 78, 65>
INFRARED BANDS OF VANADIUM OXIDE IN THREE MIRA STARS.

660301 MENDOZA V, E. E. <AP. J., 143, 1010>
INFRARED PHOTOMETRY OF T TAURI STARS AND RELATED OBJECTS.

660302 JOHNSON, H. L., MITCHELL, R. I., IRIARTE, B., WISNIEWSKI, W. Z. <COMM. LUNAR AND PLANETARY LAB., 4, 99>
UBVRIJKL PHOTOMETRY OF THE BRIGHT STARS.

660303 KUHI, L. V. <AP. J., 143, 753>
WOLF-RAYET STARS. I. THE CONTINUOUS ENERGY DISTRIBUTION

660304 MERTZ, L., COLEMAN, I. <AP. J., 143, 1000>
INFRARED SPECTRUM OF THE TAURUS RED OBJECT.

660401 WHITEOAK, J. B. <AP. J., 144, 305>
THE WAVELENGTH DEPENDENCE OF INTERSTELLAR EXTINCTION.

660402 JOHNSON, H. L., MENDOZA V, E. E., WISNIEWSKI, W. Z. <AP. J., 144, 458>
ERRATUM TO "OBSERVATIONS OF 'INFRARED STARS' ".

660403 BOYCE, P. B., FORD JR., W. K. <P. A. S. P., 78, 163>
INTERSTELLAR HELIUM AT 10, 830 IN THE ORION NEBULA.

660501 WILDEY, R. L. <ZEIT. FUR AP., 64, 32>
TEN MICRON STELLAR FLUX MEASUREMENTS-SYNOPSIS AND DIAGNOSIS.

660502 CHEN, K., REUNING, E. G. <A. J., 71, 283>
INFRARED PHOTOMETRY OF BETA PERSEI.

660701 SPINRAD, H. <AP. J., 145, 195>
OBSERVATIONS OF STELLAR MOLECULAR HYDROGEN.

660702 MOROZ, V. I. <SOV. AST., 10, 47>
INFRARED SPECTRA OF STARS (1-2.5 MICRONS).

660801 MENDOZA V, E. E. <AP. J., 145, 660>
ERRATUM TO "INFRARED PHOTOMETRY OF T TAURI STARS AND RELATED OBJECTS. "

660901 KUHI, L. V. <AP. J., 145, 715>
WOLF-RAYET STARS. II. THE INFRARED SPECTRUM.

660902 BOYARCHUK, A. A., ESIPOV, V. F., MOROZ, V. I. <SOV. AST., 10, 331>
THE CONTINUOUS SPECTRUM OF AG PEGASI.

661001 ULRICH, B. T., NEUGEBAUER, G., MCCAMMON, D., LEIGHTON, R. B., HUGHES, E. E., BECKLIN, E. E. <AP. J., 146, 288>
FURTHER OBSERVATIONS OF EXTREMELY COOL STARS.

661101 JOHNSON, H. L. <AP. J., 146, 613>
THE BOLOMETRIC CORRECTIONS AND EFFECTIVE TEMPERATURES OF TWO GIANT STARS IN THE GLOBULAR CLUSTER M3.

661201 HARWIT, M., MCNUTT, D. P., SHIVANANDAN, K., ZAJAC, B. J. <A. J., 71, 1026>
RESULTS OF THE FIRST INFRARED ASTRONOMICAL ROCKET FLIGHT.

669901 VAN DEN BERGH, S. <A. J., 71, 990>
A STUDY OF REFLECTION NEBULAE.

669902 ABELL, G. O. <AP. J., 144, 259>
PROPERTIES OF SOME OLD PLANETARY NEBULAE.

669903 HARAMUNDANIS, K. L. <SMITHSONIAN INST. >
SMITHSONIAN ASTROPHYSICAL OBSERVATORY STAR CATALOG.

669904 GASCOIGNE, S. C. B. <M. N. R. A. S., 134, 59>
COLOUR-MAGNITUDE DIAGRAMS FOR NINE GLOBULAR-LIKE CLUSTERS IN THE MAGELLANIC CLOUDS.

669905 STEPHENSON, C. B. <A. J., 71, 477>
SEARCH FOR NEW NORTHERN WOLF-RAYET STARS.

670101 WING, R. F., SPINRAD, H., KUHI, L. V. <AP. J., 147, 117>
INFRARED STARS.

670102 PACHOLCZYK, A. G., WISNIEWSKI, W. Z. <AP. J., 147, 394>
INFRARED RADIATION FROM THE SEYFERT GALAXY NGC 1068.

670103 ARGUE, A. N. <M. N. R. A. S., 135, 23>
RED AND INFRA-RED MAGNITUDES AND COLOURS FOR 300 F, G, AND K TYPE STARS.

670201 MCCAMMON, D., MUENCH, G., NEUGEBAUER, G. <AP. J., 147, 575>
INFRARED SPECTRA OF LOW-TEMPERATURE STARS.

670202 BECKLIN, E. E., NEUGEBAUER, G. <AP. J., 147, 799>
OBSERVATIONS OF AN INFRARED STAR IN THE ORION NEBULA.

670203 MAFFEI, P. <AP. J., 147, 802>
VARIABILITY OF INFRARED STARS. I. LONG-PERIOD VARIABLES

670204 ULRICH, B. T., NEUGEBAUER, G., MCCAMMON, D., LEIGHTON, R. B., HUGHES, E. E., BECKLIN, E. E. <AP. J., 147, 858>
ERRATUM TO "FURTHER OBSERVATIONS OF EXTREMELY COOL STARS".

670301 JOHNSON, H. L. <AP. J., 147, 912>
THE LAW OF INTERSTELLAR EXTINCTION FOR EMISSION NEBULAE ASSOCIATED WITH O-TYPE STARS.

670302 FORBES, F. F. <AP. J., 147, 1226>
THE INFRARED POLARIZATION OF THE INFRARED STAR IN CYGNUS.

670401 STEIN, W. A. <AP. J., 148, 295>
INFRARED CONTINUUM FROM HII REGIONS.

670402 WISNIEWSKI, W. Z., WING, R. F., SPINRAD, H., JOHNSON, H. L. <AP. J. (LETTERS), 148, L29>
ADDITIONAL OBSERVATIONS OF "INFRARED STARS".

670701 KLEINMANN, D. E., LOW, F. J. <AP. J. (LETTERS), 149, L1>
DISCOVERY OF AN INFRARED NEBULA IN ORION.

670801 JOHNSON, H. L. <AP. J., 149, 345>
THE COLORS OF M SUPERGIANTS.

670802 BESSELL, M. S. <AP. J. (LETTERS), 149, L67>
A DIFFERENT INTERPRETATION OF RHO PUPPIS.

670901 EGGEN, O. J. <AP. J. SUPPL., 14, 307>
NARROW- AND BROAD-BAND PHOTOMETRY OF RED STARS. I. NORTHERN GIANTS.

670902 LEE, T. A., NARIAI, K. <AP. J. (LETTERS), 149, L93>
INFRARED RADIATION FROM UPSILON SAGITARII.

670903 GILLETT, F. C., LOW, F. J., STEIN, W. A. <AP. J. (LETTERS), 149, L97>
INFRARED OBSERVATIONS OF THE PLANETARY NEBULA NGC 7027.

671001 JOHNSON, H. L. <AP. J. (LETTERS), 150, L39>
INFRARED EMISSION FROM CIRCUMSTELLAR SHELLS.

671101 OKE, J. B. <AP. J., 150, 513>
EFFECTIVE TEMPERATURES AND GRAVITIES OF LAMBDA BOOTIS STARS.

671102 WHITEOAK, J. B. <AP. J., 150, 521>
ENERGY DISTRIBUTIONS OF G AND K DWARFS AT RED WAVELENGTHS.

671103 FITCH, W. S., PACHOLCZYK, A. G., WEYMANN, R. J. <AP. J. (LETTERS), 150, L67>
LIGHT VARIATIONS OF THE SEYFERT GALAXY NGC 4151.

671201 OKE, J. B., SARGENT, W. L. W., NEUGEBAUER, G., BECKLIN, E. E. <AP. J. (LETTERS), 150, L173>
A VARIABLE RADIO-QUIET COMPACT GALAXY I ZW 1727+50.

679901 ROOD, H. J., BAUM, W. A. <A. J., 72, 398>
PHOTOGRAPHIC BRIGHTNESS PROFILES OF COMA CLUSTER GALAXIES. I. CATALOGUE OR PROGRAM GALAXIES.

679902 PEREK, L., KOHOUTEK, L. <PUBL. HOUSE CZECH. ACADEMY OF SCIENCE>
CATALOGUE OF GALACTIC PLANETARY NEBULAE.

679903 EGGEN, O. J., GREENSTEIN, J. L. <AP. J., 150, 927>
OBSERVATIONS OF PROPER-MOTION STARS. III.

679904 OLSEN, E. T. <A. J., 72, 738>
ACCURATE POSITIONS OF SELECTED 4C SOURCES.

679905 OOSTERHOFF, P. TH., PONSEN, J., SCHUURMAN, M. C. <B. A. N. SUPPL., 1, 397>
VARIABLE STARS IN THE GALACTIC WINDOW SAGITTARIUS II AT ALPHA - 18H 09M, DELTA - -27 55 (1900).

679906 SANDAGE, A., WILDEY, R. <AP. J., 150, 469>
THE ANOMALOUS COLOR-MAGNITUDE DIAGRAM OF THE REMOTE GLOBULAR CLUSTER NGC 7006.

679907 HENIZE, K. G. <AP. J. SUPPL., 14, 125>
OBSERVATIONS OF SOUTHERN PLANETARY NEBULAE.

680101 BECKLIN, E. E., NEUGEBAUER, G. <AP. J., 151, 145>
INFRARED OBSERVATIONS OF THE GALACTIC CENTER.

680201 GARRISON, R. F. <P. A. S. P., 80, 20>
THE SPECTRUM OF STAR NO. 1 IN NGC 2024.

680202 KNAPPENBERGER, P. H., FREDERICK, L. W. <P. A. S. P., 80, 96>
THE HE I 10,830 LINE IN THE SPECTRUM OF BETA LYRAE.

680301 OKE, J. B., SARGENT, W. L. W. <AP. J., 151, 807>
THE NUCLEUS OF THE SEYFERT GALAXY NGC 4151.

680302 MENDOZA V, E. E. <AP. J., 151, 977>
INFRARED EXCESSES IN T TAURI STARS AND RELATED OBJECTS.

680303 JONES, D. H. P. <M. N. R. A. S., 139, 189>
NARROW BAND PHOTOMETRY OF K AND M STARS.

680304 GLUSHNEVA, I. N., ESIPOV, V. F. <SOV. AST., 11, 828>
THE INFRARED SPECTRUM OF ALGOL.

680401 WISNIEWSKI, W. Z., JOHNSON, H. L. <COMM. LUNAR AND PLANETARY LAB., 7, 57>
UBVRIJKL LIGHT CURVES OF CLASSICAL CEPHEIDS.

680402 VAUGHAN JR., A. H., ZIRIN, H. <AP. J., 152, 123>
THE HELIUM LINE 10830A IN LATE-TYPE STARS.

680403 FAY JR., T. D., FREDERICK, L. W., JOHNSON, H. R. <AP. J., 152, 151>
COMPARISON OF SELECTED CARBON STARS AND M STARS AT 1 MICRON.

680404 NEY, E. P., STEIN, W. A. <AP. J. (LETTERS), 152, L21>
OBSERVATIONS OF THE CRAB NEBULA AT 5800A, 2.2 MICRONS, AND 3.5 MICRONS WITH A 4-MINUTE BEAM.

680405 BECKLIN, E. E., KLEINMANN, D. E. <AP. J. (LETTERS), 152, L25>
INFRARED OBSERVATIONS OF THE CRAB NEBULA.

680501 JOHNSON, H. L., MACARTHUR, J. W., MITCHELL, R. I. <AP. J., 152, 465>
THE SPECTRAL-ENERGY CURVES OF SUBDWARFS. I.

680502 NEUGEBAUER, G., WESTPHAL, J. A. <AP. J. (LETTERS), 152, L89>
INFRARED OBSERVATIONS OF ETA CARINAE.

680503 IRVINE, W. M., SIMON, T., MENZEL, D. H., CHARON, J., LECOMTE, G., GRIBOVAL, P., YOUNG, A. T. <A. J., 73, 251>
MULTICOLOR PHOTOELECTRIC PHOTOMETRY OF THE BRIGHTER PLANETS. II. OBSERVATIONS FROM LE HOUGA OBSERVATORY.

680601 LEE, T. A. <AP. J., 152, 913>
INTERSTELLAR EXTINCTION IN THE ORION ASSOCIATION.

680602 VISVANATHAN, N., OKE, J. B. <AP. J. (LETTERS), 152, L165>
NON-THERMAL COMPONENT IN THE CONTINUUM OF NGC 1068.

680603 ZIRIN, H. <AP. J. (LETTERS), 152, L177>
HE-3 IN SEVERAL MAGNETIC STARS.

680701 FORD JR., W. K., PURGATHOFER, A. T., RUBIN, V. C. <AP. J. (LETTERS), 153, L39>
OPTICAL SPECTRA NEAR 1 MICRON: THE SEYFERT GALAXY NGC 4151 AND THE PLANETARY NEBULA NGC 6543.

680702 KOMAROV, N. S., POZIGUN, V. A. <SOV. AST., 12, 105>
STELLAR ENERGY DISTRIBUTION AT INFRARED WAVELENGTHS.

680703 MOROZ, V. I., VASIL'CHENKO, N. V., DANILYANTS, L. B., KAUFMAN, S. A. <SOV. AST., 12, 150>
EXPERIMENTAL OBSERVATIONS AT 8-14 MICRONS WITH A PHOTOCONDUCTIVE CELL COOLED BY LIQUID HELIUM.

680801 EGGEN, O. J. <AP. J. SUPPL., 16, 49>
NARROW- AND BROAD-BAND PHOTOMETRY OF RED STARS. II. DWARFS.

680802 PRICE, S. D. <A. J., 73, 431>
RESULTS OF AN INFRARED STELLAR SURVEY.

680803 JOHNSON, H. L., COLEMAN, I., MITCHELL, R. I., STEINMETZ, D. L. <COMM. LUNAR AND PLANETARY LAB., 7, 83>
STELLAR SPECTROSCOPY, 1.2 TO 2.6 MICRONS.

680901 GILLETT, F. C., STEIN, W. A., LOW, F. J. <AP. J. (LETTERS), 153, L185>
THE SPECTRUM OF NML CYGNUS FROM 2.8 TO 5.6 MICRONS.

680902 MOROZ, V. I., DIBAI, E. A. <SOV. AST., 12, 184>
PHOTOMETRIC OBSERVATIONS OF SOME PECULIAR OBJECTS IN THE WAVELENGTH RANGE 1-2.5 MICRONS.

680903 ACKERMANN, G., FUGMANN, G., HERMANN, W., VOELCKER, K. <ZEIT. FUR AP., 69, 130>
NEUE INFRAROT-STERNE.

681001 OKE, J. B., SANDAGE, A. R. <AP. J., 154, 21>
ENERGY DISTRIBUTIONS, K CORRECTIONS, AND THE STEBBINS-WHITFORD EFFECT FOR GIANT ELLIPTICAL GALAXIES.

681002 VAUGHAN JR., A. H. <AP. J., 154, 87>
THE HE I 10830A LINE IN PLANETARY NEBULAE AND THE ORION NEBULA.

681003 CARLETON, N. P., LILLER, W., ROESLER, F. L. <AP. J., 154, 385>
A SEARCH FOR STELLAR CARBON DIOXIDE.

681101 GILLETT, F. C., LOW, F. J., STEIN, W. A. <AP. J., 154, 677>
STELLAR SPECTRA FROM 2.8 TO 14 MICRONS.

681102 WESTERLUND, B. E. <AP. J. (LETTERS), 154, L67>
ON THE EXTENDED INFRARED SOURCE IN ARA.

681103 IRVINE, W. M., SIMON, T., MENZEL, D. H., PIKOOS, C., YOUNG, A. T. <A. J., 73, 807>
MULTICOLOR PHOTOELECTRIC PHOTOMETRY OF THE BRIGHTER PLANETS. III. OBSERVATIONS FROM BOYDEN OBSERVATORY.

681104 WISNIEWSKI, W. Z., KLEINMANN, D. E. <A. J., 73, 866>
MULTICOLOR PHOTOMETRY OF SEYFERT GALAXIES AND MEASUREMENT AT 1.55 MICRONS OF THE JET IN M87.

681105 LOW, F. J., KLEINMANN, D. E. <A. J., 73, 868>
INFRARED OBSERVATIONS OF SEYFERT GALAXIES, QUASISTELLAR SOURCES, AND PLANETARY NEBULAE.

681106 PACHOLCZYK, A. G., WEYMANN, R. J. <A. J., 73, 870>
INFRARED RADIATION FROM THE NUCLEI OF SEYFERT GALAXIES.

681201 WERNER, M. W., HARWIT, M. <AP. J., 154, 881>
OBSERVATIONAL EVIDENCE FOR THE EXISTENCE OF DENSE CLOUDS OF INTERSTELLAR MOLECULAR HYDROGEN.

681202 JOHNSON, H. L. <AP. J. (LETTERS), 154, L125>
THE INFRARED SPECTRUM OF THE NML CYGNUS OBJECT.

681203 FELDMAN, P. D., MCNUTT, D. P., SHIVANANDAN, K. <AP. J. (LETTERS), 154, L131>
ROCKET OBSERVATIONS OF BRIGHT CELESTIAL INFRARED SOURCES IN URSA MAJOR.

689901 MAFFEI, P. <P. A. S. P., 80, 618>
INFRARED OBJECT IN THE REGION OF IC 1805.

689902 MACCONNELL, D. J. <AP. J. SUPPL., 16, 275>
A STUDY OF THE CEPHEUS IV ASSOCIATION.

689903 SMITH, L. F. <M. N. R. A. S., 138, 109>
A REVISED SPECTRAL CLASSIFICATION SYSTEM AND A NEW CATALOGUE FOR GALACTIC WOLF-RAYET STARS.

689904 BRACCESI, A., LYNDS, R., SANDAGE, A. <AP. J. (LETTERS), 152, L105>
SPECTROSCOPIC AND PHOTOMETRIC DATA FOR A SAMPLE OF QUASI-STELLAR OBJECTS IDENTIFIED BY THEIR INFRARED EXCESS.

689905 DIBAI, E. A., ESIPOV, V. F. <SOV. AST., 12, 448>
SPECTRA OF H-ALPHA EMISSION OBJECTS IN THE DIFFUSE NEBULAE IC 1396 AND SIMEIZ 130.

689906 HAZARD, C., GULKIS, S., SUTTON, J. <AP. J., 154, 413>
OCCULTATION STUDIES OF WEAK RADIO SOURCES: LIST 2.

690001 NEUGEBAUER, G., LEIGHTON, R. B. <NASA SP-3047>
TWO-MICRON SKY SURVEY-A PRELIMINARY CATALOG.

690002 LEE, T. A., NARIAI, K. <P. A. S. J., 21, 67>
INFRARED PHOTOMETRY OF A HELIUM STAR, HD 30353.

690101 STEIN, W. A., GAUSTAD, J. E., GILLETT, F. C., KNACKE, R. F. <AP. J. (LETTERS), 155, L3>
CIRCUMSTELLAR INFRARED EMISSION FROM TWO PECULIAR OBJECTS-R AQUARII AND R CORONAE BOREALIS.

690102 HOFFMANN, W. F., FREDERICK, C. L. <AP. J. (LETTERS), 155, L9>
FAR-INFRARED OBSERVATION OF THE GALACTIC-CENTER REGION AT 100 MICRONS.

690201 MITCHELL, R. I., JOHNSON, H. L. <COMM. LUNAR AND PLANETARY LAB., 8, 1>
THIRTEEN-COLOR NARROW-BAND PHOTOMETRY OF ONE THOUSAND BRIGHT STARS.

690202 KODAIRA, K., GREENSTEIN, J. L., OKE, J. B. <AP. J., 155, 525>
ABUNDANCES IN TWO HORIZONTAL-BRANCH A STARS.

690203 GILLETT, F. C., STEIN, W. A. <AP. J. (LETTERS), 155, L97>
DETECTION OF THE 12.8-MICRON NE+ EMISSION LINE FROM THE PLANETARY NEBULA IC 418.

690301 VISVANATHAN, N. <AP. J. (LETTERS), 155, L133>
THE CONTINUUM OF BL LAC.

690302 STEIN, W. A., GAUSTAD, J. E., GILLETT, F. C., KNACKE, R. F. <AP. J. (LETTERS), 155, L177>
THE SPECTRUM OF NML CYGNUS FROM 7.5 TO 14 MICRONS.

690303 WOOLF, N. J., NEY, E. P. <AP. J. (LETTERS), 155, L181>
CIRCUMSTELLAR INFRARED EMISSION FROM COOL STARS.

690304 KNACKE, R. F., GAUSTAD, J. E., GILLETT, F. C., STEIN, W. A. <AP. J. (LETTERS), 155, L189>
A POSSIBLE IDENTIFICATION OF INTERSTELLAR SILICATE ABSORPTION IN THE INFRARED SPECTRUM OF 119 TAURI.

690305 NEY, E. P., ALLEN, D. A. <AP. J. (LETTERS), 155, L193>
THE INFRARED SOURCES IN THE TRAPEZIUM REGION OF M42.

690306 STEIN, W. A., GILLETT, F. C. <AP. J. (LETTERS), 155, L197>
SPECTRAL DISTRIBUTION OF INFRARED RADIATION FROM THE TRAPEZIUM REGION OF THE ORION NEBULA.

690307 THACKERAY, A. D. <M. N. A. S. S. A., 28, 37>
THE SPECTRUM OF ETA CARINAE IN THE 10, 000A REGION.

690308 BECKMAN, J. E., BASTIN, J. A., CLEGG, P. E. <NATURE, 221, 944>
CONTINUOUS SPECTRUM OF TAURUS A AT 1.2 MM WAVELENGTH.

690401 LOW, F. J., SMITH, B. J. <COMM. LUNAR AND PLANETARY LAB., 8, 87>
INFRARED OBSERVATIONS OF A PREPLANETARY SYSTEM.

690402 JOHNSON, H. L. <COMM. LUNAR AND PLANETARY LAB., 8, 91>
THE INFRARED SPECTRUM OF THE NML CYGNUS OBJECT.

690403 OKE, J. B., NEUGEBAUER, G., BECKLIN, E. E. <AP. J. (LETTERS), 156, L41>
SPECTROPHOTOMETRY AND INFRARED PHOTOMETRY OF BL LACERTAE.

690404 WESTPHAL, J. A., NEUGEBAUER, G. <AP. J. (LETTERS), 156, L45>
INFRARED OBSERVATIONS OF ETA CARINAE TO 20 MICRONS.

690405 BAHNG, J. <M. N. R. A. S., 143, 73>
INFRA-RED COLOURS OF G, K, AND M STARS.

690501 NOSKOVA, R. I. <SOV. AST., 12, 1039>
ABSOLUTE SPECTROPHOMETRY OF SOME INFRARED LINES IN PLANETARY-NEBULA SPECTRA.

690601 NEUGEBAUER, G., BECKLIN, E. E., KRISTIAN, J., LEIGHTON, R. B., SNELLEN, G., WESTPHAL, J. A. <AP. J. (LETTERS), 156, L115>
INFRARED AND OPTICAL MEASUREMENTS OF THE CRAB PULSAR NP 0532.

690701 SANDAGE, A. R., BECKLIN, E. E., NEUGEBAUER, G. <AP. J., 157, 55>
UBVRIHKL PHOTOMETRY OF THE CENTRAL REGION OF M31.

690702 LOCKWOOD, G. W. <AP. J., 157, 275>
IDENTIFICATION, STRUCTURE, AND VARIATIONS OF NEW TIO BANDS IN THE ONE-MICRON SPECTRA OF MIRA VARIABLES.

690703 BERTOLA, F., D'ODORICO, S., FORD JR., W. K., RUBIN, V. C. <AP. J. (LETTERS), 157, L27>
OBSERVATIONS OF M82 IN THE OPTICAL INFRARED.

690704 BECKLIN, E. E., NEUGEBAUER, G. <AP. J. (LETTERS), 157, L31>
1.65-19.5 MICRON OBSERVATIONS OF THE GALACTIC CENTER.

690705 WOOLF, N. J. <AP. J. (LETTERS), 157, L37>
INFRARED EMISSION FROM PLANETARY NEBULAE.

690706 ALDUSEVA, V. YA., ESIPOV, V. F. <SOV. AST., 13, 83>
THE 10830A HE I LINE IN THE ENVELOPE OF BETA LYRAE.

690801 LOW, F. J., KLEINMANN, D. E., FORBES, F. F., AUMANN, H. H. <AP. J. (LETTERS), 157, L97>
THE INFRARED SPECTRUM, DIAMETER, AND POLARIZATION OF THE GALACTIC NUCLEUS.

690802 MONTGOMERY, E. F., CONNES, P., CONNES, J., EDMONDS JR., F. N. <AP. J. SUPPL., 19, 1>
THE INFRARED SPECTRUM OF ARCTURUS.

690901 SPINRAD, H., TAYLOR, B. J. <AP. J., 157, 1279>
SCANNER ABUNDANCE STUDIES. I. AN INVESTIGATION OF SUPERMETALLICITY IN LATE-TYPE EVOLVED STARS.

690902 LEE, T. A., FEAST, M. W. <AP. J. (LETTERS), 157, L173>
INFRARED EXCESS OF RY SGR.

691001 KNACKE, R. F., CUDABACK, D. D., GAUSTAD, J. E. <AP. J., 158, 151>
INFRARED SPECTRA OF HIGHLY REDDENED STARS: A SEARCH FOR INTERSTELLAR ICE GRAINS.

691002 EGGEN, O. J. <AP. J., 158, 225>
NARROW- AND BROAD-BAND PHOTOMETRY OF RED STARS. IV. POPULATION SEPARATION IN GIANT STARS.

691003 SOLINGER, A. B. <AP. J. (LETTERS), 158, L21>
ON THE NUCLEAR REGION OF M82.

691004 THOMPSON, R. I., SCHNOPPER, H. W., MITCHELL, R. I., JOHNSON, H. L. <AP. J. (LETTERS), 158, L55>
1-4 MICRON SPECTRA OF FOUR CARBON STARS AND SIRIUS.

691005 EGGEN, O. J. <P. A. S. P., 81, 553>
STELLAR GROUPS IN THE OLD DISK POPULATION.

691101 GAUSTAD, J. E., GILLETT, F. C., KNACKE, R. F., STEIN, W. A. <AP. J., 158, 613>
SPECTRA OF "INFRARED STARS" FROM 2.8 TO 5.1 MICRONS.

691102 HYLAND, A. R., BECKLIN, E. E., NEUGEBAUER, G., WALLERSTEIN, G. <AP. J., 158, 619>
OBSERVATIONS OF THE INFRARED OBJECT, VY CANIS MAJORIS.

691103 SERKOWSKI, K., ROBERTSON, J. W. <AP. J., 158, 441>
REGIONAL VARIATIONS IN THE WAVELENGTH DEPENDENCE OF INTERSTELLAR POLARIZATION.

691104 THOMPSON, R. I., SCHNOPPER, H. W., MITCHELL, R. I., JOHNSON, H. L. <AP. J. (LETTERS), 158, L117>
1-4 MICRON SPECTRA OF FOUR M STARS AND ALPHA TAURI.

691105 STEIN, W. A., GILLETT, F. C. <NATURE, 224, 675>
POSSIBLE VARIATIONS OF LAMBDA - 10 MICRONS RADIATION FROM NGC 4151.

691201 BECKLIN, E. E., FROGEL, J. A., HYLAND, A. R., KRISTIAN, J., NEUGEBAUER, G. <AP. J. (LETTERS), 158, L133>
THE UNUSUAL INFRARED OBJECT IRC+10216.

691202 BAHNG, J. <P. A. S. P., 81, 863>
INFRARED COLOR INDICES OF CARBON STARS.

691203 LEE, T. A. <P. A. S. P., 81, 878>
OBSERVATIONS OF THE 5 MICRON SOURCE IN ORION.

699901 KUKARKIN, B. V., KHOLOPOV, P. N., EFREMOV, YU. N., KUKARKINA, N. P., KUROCHKIN, N. E., MEDVEDEVA, G. I., PEROVA, N. B., FEDOROVITCH, V. P., FROLOV, M. S. <PUBL. OFFICE NAUKA, MOSCOW>
GENERAL CATALOG OF VARIABLE STARS. VOLUMES I AND II.

699902 VAN ALTENA, W. F. <A. J., 74, 2>
LOW-LUMINOSITY MEMBERS OF THE HYADES CLUSTER. II.

700001 HASHIMOTO, J., MAIHARA, T., OKUDA, H., SATO, S. <P. A. S. J., 22, 335>
INFRARED POLARIZATION OF THE PECULIAR M-TYPE VARIABLE VY CANIS MAJORIS.

700101 OKE, J. B., NEUGEBAUER, G., BECKLIN, E. E. <AP. J., 159, 341>
ABSOLUTE SPECTRAL ENERGY DISTRIBUTION OF QUASI-STELLAR OBJECTS FROM 0.3 TO 2.2 MICRONS.

700102 HAYES, D. S. <AP. J., 159, 165>
AN ABSOLUTE SPECTROPHOTOMETRIC CALIBRATION OF THE ENERGY DISTRIBUTION OF TWELVE STANDARD STARS.

700103 BORGMAN, J., KOORNNEEF, J., SLINGERLAND, J. <ASTR. AP., 4, 248>
INFRA-RED PHOTOMETRY OF A HEAVILY REDDENED CLUSTER IN ARA.

700201 KODAIRA, K., GREENSTEIN, J. L., OKE, J. B. <AP. J., 159, 485>
THE UNUSUAL COMPOSITION OF +39 4926.

700202 ZWICKY, F., OKE, J. B., NEUGEBAUER, G., SARGENT, W. L. W., FAIRALL, A. P. <P. A. S. P., 82, 93>
THE VARIABLE COMPACT GALAXY ZW 0039.5+4003.

700301 FORBES, F. F., STONAKER, W. F., JOHNSON, H. L. <A. J., 75, 158>
STELLAR AND PLANETARY SPECTRA IN THE INFRARED FROM 1.35 TO 4.10 MICRONS.

700302 LOW, F. J. <AFCRL-70-0179>
SKY SURVEY.

700303 GILLETT, F. C., STEIN, W. A. <AP. J., 159, 817>
INFRARED STUDIES OF GALACTIC NEBULAE. I. NGC 6523, NGC 6572, AND BD 30 3639.

700304 WING, R. F., SPINRAD, H. <AP. J., 159, 973>
INFRARED CN BANDS IN M SUPERGIANTS AND CARBON STARS.

700305 AUMANN, H. H., LOW, F. J. <AP. J. (LETTERS), 159, L159>
FAR-INFRARED OBSERVATIONS OF THE GALACTIC CENTER.

700306 KLEINMANN, D. E., LOW, F. J. <AP. J. (LETTERS), 159, L165>
OBSERVATIONS OF INFRARED GALAXIES.

700307 LOW, F. J. <AP. J. (LETTERS), 159, L173>
THE INFRARED-GALAXY PHENOMENON.

700308 PARK, W. M., VICKERS, D. G., CLEGG, P. E. <ASTR. AP., 5, 325>
SUBMILLIMETER RADIATION FROM THE ORION NEBULA.

700401 HYLAND, A. R., BECKLIN, E. E., NEUGEBAUER, G., WALLERSTEIN, G. <AP. J., 160, 381>
ERRATUM TO "OBSERVATIONS OF THE INFRARED OBJECT, VY CANIS MAJORIS".

700402 LOCKWOOD, G. W. <AP. J. (LETTERS), 160, L47>
NEAR-INFRARED PHOTOMETRY OF TWO EXTREMELY RED OBJECTS.

700403 DOMBROVSKII, V. A. <ASTROFIZIKA, 6, 207>
POLARIZATION OF THE LIGHT FROM RED VARIABLE STARS OF HIGH LUMINOSITY.

700501 PEIMBERT, M., SPINRAD, H. <AP. J., 160, 429>
PHYSICAL CONDITIONS IN THE NUCLEUS OF M82.

700502 LOW, F. J., JOHNSON, H. L., KLEINMANN, D. E., LATHAM, A. S., GEISEL, S. L. <AP. J., 160, 531>
PHOTOMETRIC AND SPECTROSCOPIC OBSERVATIONS OF INFRARED STARS.

700503 THOMPSON, R. I., SCHNOPPER, H. W. <AP. J. (LETTERS), 160, L97>
IDENTIFICATION OF INFRARED CN BANDS IN THE SPECTRA OF SEVERAL CARBON STARS.

700504 SHAROV, A. S. <SOV. AST., 13, 947>
THE INFRARED BRIGHTNESS OF THE MILKY WAY.

700601 BREGER, M., KUHI, L. V. <AP. J., 160, 1129>
EFFECTIVE TEMPERATURES, GRAVITIES, AND THE MASS DETERMINATION OF A AND F STARS.

700602 SPINRAD, H., LUEBKE JR., W. R. <AP. J., 160, 1141>
A CURVE-OF-GROWTH ANALYSIS OF THE SUPER-METAL-RICH G DWARF HR 72.

700603 GILLETT, F. C., STEIN, W. A., SOLOMON, P. M. <AP. J. (LETTERS), 160, L173>
THE SPECTRUM OF VY CANIS MAJORIS FROM 2.9 TO 14 MICRONS.

700604 HYLAND, A. R., NEUGEBAUER, G. <AP. J. (LETTERS), 160, L177>
INFRARED OBSERVATIONS OF NOVA SERPENTIS 1970.

700701 EGGEN, O. J., STOKES, N. R. <AP. J., 161, 199>
NARROW-BAND AND BROAD-BAND PHOTOMETRY OF RED STARS. III. SOUTHERN GIANTS.

700801 GREENSTEIN, J. L., NEUGEBAUER, G., BECKLIN, E. E. <AP. J., 161, 519>
THE FAINT END OF THE MAIN SEQUENCE.

700802 NEUGEBAUER, G., GARMIRE, G. <AP. J. (LETTERS), 161, L91>
INFRARED OBSERVATIONS OF THE NEBULA K3-50.

700803 MILLER, J. S. <AP. J. (LETTERS), 161, L95>
SCANNER OBSERVATIONS OF THE LEO INFRARED OBJECT IRC+10216.

700804 GEISEL, S. L., KLEINMANN, D. E., LOW, F. J. <AP. J. (LETTERS), 161, L101>
INFRARED EMISSION OF NOVAE.

700805 HACKWELL, J. A., GEHRZ, R. D., WOOLF, N. J. <NATURE, 227, 822>
INTERSTELLAR SILICATE ABSORPTION BANDS.

700806 GEISEL, S. L. <AP. J. (LETTERS), 161, L105>
INFRARED EXCESSES, LOW EXCITATION EMISSION LINES, AND MASS LOSS.

700901 JOHNSON, H. L., MENDEZ, M. E. <A. J., 75, 785>
INFRARED SPECTRA FOR 32 STARS.

700902 OKE, J. B., SCHILD, R. E. <AP. J., 161, 1015>
THE ABSOLUTE SPECTRAL ENERGY DISTRIBUTION OF ALPHA LYRAE.

700903 RANK, D. M., HOLTZ, J. Z., GEBALLE, T. R., TOWNES, C. H. <AP. J. (LETTERS), 161, L185>
DETECTION OF 10.5-MICRON LINE EMISSION FROM THE PLANETARY NEBULA NGC 7027.

700904 KLEINMANN, D. E., LOW, F. J. <AP. J. (LETTERS), 161, L203>
INFRARED OBSERVATIONS OF GALAXIES AND OF THE EXTENDED NUCLEUS IN M82.

700905 PACHOLCZYK, A. G. <AP. J. (LETTERS), 161, L207>
INFRARED VARIABILITY OF THE SEYFERT GALAXY NGC 1068.

700906 GEHRZ, R. D., WOOLF, N. J. <AP. J. (LETTERS), 161, L213>
RV TAURI STARS: A NEW CLASS OF INFRARED OBJECT.

700907 GEHRZ, R. D., NEY, E. P., STRECKER, D. W. <AP. J. (LETTERS), 161, L219>
OBSERVATIONS OF ANOMALOUS RADIATION AT LONG WAVELENGTHS FROM IC CLASS VARIABLES.

700908 LOW, F. J., KRISHNA SWAMY, K. S. <NATURE, 227, 1333>
NARROW-BAND INFRARED PHOTOMETRY OF ALPHA ORI.

701001 LEE, T. A. <AP. J., 162, 217>
PHOTOMETRY OF HIGH-LUMINOSITY M-TYPE STARS.

701002 FROGEL, J. A. <AP. J. (LETTERS), 162, L5>
WATER ABSORPTION IN THE INFRARED SPECTRUM OF LONG-PERIOD VARIABLE STARS AND ASSOCIATED MICROWAVE EMISSION.

701003 GILLETT, F. C., HYLAND, A. R., STEIN, W. A. <AP. J. (LETTERS), 162, L21>
89 HERCULIS: AN F2 SUPERGIANT WITH LARGE CIRCUMSTELLAR INFRARED EMISSION.

701004 KEMP, J. C., SWEDLUND, J. B. <AP. J. (LETTERS), 162, L67>
LARGE INFRARED CIRCULAR POLARIZATION OF GRW+70 8247.

701005 ACKERMANN, G. <ASTR. AP., 8, 315>
EXTREME RED STARS IN CYGNUS.

701101 ROBBINS, R. R. <AP. J., 162, 507>
THE PROFILE OF HE I 10830A IN NGC 7027 AND THE ORION NEBULA.

701102 SMITH, L. F., KUHI, L. V. <AP. J., 162, 535>
WOLF-RAYET STARS. IV. LINE INTENSITIES IN THE SPECTRA OF TWO WN6 STARS.

701103 LOW, F. J., AUMANN, H. H. <AP. J. (LETTERS), 162, L79>
OBSERVATIONS OF GALACTIC AND EXTRAGALACTIC SOURCES BETWEEN 50 AND 300 MICRONS.

701104 FRIEDLANDER, M. W., JOSEPH, R. D. <AP. J. (LETTERS), 162, L87>
DETECTION OF CELESTIAL SOURCES AT FAR-INFRARED WAVELENGTHS.

701105 WOOLF, N. J., STEIN, W. A., STRITTMATTER, P. A. <ASTR. AP., 9, 252>
INFRARED EMISSION FROM BE STARS.

701201 SARGENT, W. L. W., SEARLE, L. <AP. J. (LETTERS), 162, L155>
ISOLATED EXTRAGALACTIC HII REGIONS.

709901 WACKERLING, L. R. <MEM. R. A. S., 73, 153>
A CATALOGUE OF EARLY-TYPE STARS WHOSE SPECTRA HAVE SHOWN EMISSION LINES.

709902 CRAWFORD, D. L., GLASPEY, J. W., PERRY, C. L. <A. J., 75, 822>
FOUR-COLOR AND H-BETA PHOTOMETRY OF OPEN CLUSTERS. IV. H AND CHI PERSEI.

709903 WOOLLEY, R., EPPS, E. A., PENSTON, M. J., POCOCK, S. B. <ROYAL OBS. ANNALS, 5>
CATALOGUE OF STARS WITHIN TWENTY-FIVE PARSECS OF THE SUN.

709904 RUBIN, R. H. <ASTR. AP., 8, 171>
RADIO OBSERVATIONS OF PLANETARY NEBULAE AND POSSIBLE PLANETARY NEBULAE.

710001 COHEN, M. <AP. LETTERS, 9, 95>
OPTICAL IDENTIFICATIONS OF INFRARED SOURCES.

710101 SPINRAD, H., SARGENT, W. L. W., OKE, J. B., NEUGEBAUER, G., LANDAU, R., KING, I. R., GUNN, J. E., GARMIRE, G., DIETER, N. H. <AP. J. (LETTERS), 163, L25>
MAFFEI 1: A NEW MASSIVE MEMBER OF THE LOCAL GROUP?

710102 GILLETT, F. C., KNACKE, R. F., STEIN, W. A. <AP. J. (LETTERS), 163, L57>
INFRARED STUDIES OF GALACTIC NEBULAE. II. THE COMPACT NEBULAE IC 4997, VV 8, AND FG SAGITTAE.

710201 WAMPLER, E. J. <AP. J., 164, 1>
PHOTOELECTRIC SPECTROPHOTOMETRY OF SEYFERT GALAXIES.

710202 GILLETT, F. C., STEIN, W. A. <AP. J., 164, 77>
INFRARED STUDIES OF GALACTIC NEBULAE. II. B STARS ASSOCIATED WITH NEBULOSITY.

710203 GILLETT, F. C., MERRILL, K. M., STEIN, W. A. <AP. J., 164, 83>
OBSERVATIONS OF INFRARED RADIATION FROM COOL STARS.

710204 LOW, F. J. <AFCRL-71-0387>
PRELIMINARY RESULTS OF AN INFRARED SKY SURVEY.

710205 PACHOLCZYK, A. G. <AP. J., 163, 449>
LIGHT VARIATIONS OF THE SEYFERT GALAXY NGC 4151. III. LONG-TERM PHOTOGRAPHIC B-VARIATIONS AND INFRARED K-DATA.

710206 HOFFMANN, W. F., FREDERICK, C. L., EMERY, R. J. <AP. J. (LETTERS), 164, L23>
100-MICRON MAP OF THE GALACTIC-CENTER REGION.

710207 HOLTZ, J. Z., GEBALLE, T. R., RANK, D. M. <AP. J. (LETTERS), 164, L29>
INFRARED LINE EMISSION FROM PLANETARY NEBULAE.

710208 MEISEL, D. D. <P. A. S. P., 83, 49>
1-MICRON IMAGE-TUBE SPECTRA OF GAMMA CASSIOPEIAE AND ZETA TAURI.

710401 GRASDALEN, G. L., GAUSTAD, J. E. <A. J., 76, 231>
A COMPARISON OF THE TWO-MICRON SKY SURVEY WITH THE DEARBORN CATALOG OF FAINT RED STARS.

710402 SCHILD, R. E., NEUGEBAUER, G., WESTPHAL, J. A. <A. J., 76, 237>
INTERSTELLAR ABSORPTION AND COLOR EXCESSES IN SCO OB-1.

710403 GEHRZ, R. D., WOOLF, N. J. <AP. J., 165, 285>
MASS LOSS FROM M STARS.

710404 HARPER JR., D. A., LOW, F. J. <AP. J. (LETTERS), 165, L9>
FAR-INFRARED EMISSION FROM HII REGIONS.

710405 DYCK, H. M., FORREST, W. J., GILLETT, F. C., STEIN, W. A., GEHRZ, R. D., WOOLF, N. J., SHAWL, S. J. <AP. J., 165, 57>
VISUAL INTRINSIC POLARIZATION AND INFRARED EXCESS OF COOL STARS.

710406 SPINRAD, H., LIEBERT, J., SMITH, H. E., SCHWEIZER, F., KUHI, L. V. <AP. J., 165, 17>
THE DETECTION OF THE GALACTIC NUCLEUS AT ONE MICRON.

710407 SCHMIDT, E. G. <AP. J., 165, 335>
A PHOTOMETRIC STUDY OF FOUR CLASSICAL CEPHEIDS.

710501 FORBES, F. F. <AP. J. (LETTERS), 165, L83>
THE INFRARED POLARIZATION OF ETA CARINAE AND VY CANIS MAJORIS.

710502 RODGERS, A. W. <AP. J., 165, 665>
THE REDDENING OF ETA CARINAE.

710503 STEIN, W. A., GILLETT, F. C., KNACKE, R. F. <NATURE, 231, 254>
POSSIBLE UPPER LIMIT TO THE DISTANCE OF BL LACERTAE.

710504 SMYTH, M. J., CORK, G. M. W., HARRIS, J., WALLACE, T. <NAT. PHYS. SCI., 231, 104>
INFRARED SPECTRA OF STARS, 1-2.5 MICRONS.

710601 WALLERSTEIN, G. <AP. J., 166, 725>
ON THE INFRARED EXCESS OF W CEPHEI AND SIMILAR STARS.

710602 NEUGEBAUER, G., GARMIRE, G., RIEKE, G. H., LOW, F. J. <AP. J. (LETTERS), 166, L45>
INFRARED OBSERVATIONS ON THE SIZE OF NGC 1068.

710603 CUDABACK, D. D., GAUSTAD, J. E., KNACKE, R. F. <AP. J. (LETTERS), 166, L49>
SILICON MONOXIDE IN THE INFRARED SPECTRUM OF ALPHA ORIONIS.

710604 WING, R. F. <P. A. S. P., 83, 301>
THE SPECTRAL TYPE AND INFRARED BRIGHTNESS OF R DORADUS.

710605 NEUGEBAUER, G., SARGENT, W. L. W., WESTPHAL, J. A., PORTER, F. C. <P. A. S. P., 83, 305>
1.6-10 MICRON OBSERVATIONS OF R DORADUS AND W HYDRAE.

710701 HUMPHREYS, R. M., STRECKER, D. W., NEY, E. P. <AP. J. (LETTERS), 167, L35>
HIGH-LUMINOSITY G SUPERGIANTS.

710702 SWINGS, J. P., ALLEN, D. A. <AP. J. (LETTERS), 167, L41>
THE INFRARED OBJECT HD 45677.

710703 HYLAND, A. R. <PROC. A. S. A., 1, 14>
GALACTIC INFRARED ASTRONOMY.

710704 PENSTON, M. V., PENSTON, M. J., NEUGEBAUER, G., TRITTON, K. P., BECKLIN, E. E., VISVANATHAN, N. <M. N. R. A. S., 153, 29>
OBSERVATIONS OF NGC 4151 DURING 1970 IN THE OPTICAL AND AND INFRA-RED.

710801 FAY JR., T. D. <AP. J., 168, 99>
COMPUTED AND OBSERVED CYANIDE-RADICAL SPECTRA OF THREE N STARS IN THE INFRARED.

710901 RIEKE, G. H., LOW, F. J. <COMM. LUNAR AND PLANETARY LAB., 9, 181>
MAP OF THE GALACTIC NUCLEUS AT 10 MICRONS.

710902 RIEKE, G. H., LOW, F. J. <NATURE, 233, 53>
MAP OF THE GALACTIC NUCLEUS AT 10 MICRONS.

710903 STEIN, W. A., GILLETT, F. C. <NAT. PHYS. SCI., 233, 16>
PHOTOMETRIC MEASUREMENTS AT 11 MICRONS OF NGC 4151.

710904 AITKEN, D. K., POLDEN, P. G. <NAT. PHYS. SCI., 233, 45>
MEASUREMENT OF THE 10 MICRON FLUX FROM THE CRAB NEBULA.

710905 STEIN, W. A., GILLETT, F. C. <NAT. PHYS. SCI., 233, 72>
SEARCH FOR INTERSTELLAR SILICATE ABSORPTION IN SPECTRUM OF VI CYG NO. 12.

710906 LOW, F. J., RIEKE, G. H. <NAT. PHYS. SCI., 233, 256>
VARIATIONS IN THE 10-MICRON FLUX FROM NGC 1068.

711001 HOUCK, J. R., SOIFER, B. T., PIPHER, J. L., HARWIT, M. <AP. J. (LETTERS), 169, L31>
ROCKET-INFRARED FOUR-COLOR PHOTOMETRY OF THE GALAXY'S CENTRAL REGIONS.

711002 LOCKWOOD, G. W., WING, R. F. <AP. J., 169, 63>
LIGHT CURVES OF MIRA VARIABLES AT 1.04 MICRONS.

711101 DYCK, H. M., FORBES, F. F., SHAWL, S. J. <A. J., 76, 901>
POLARIMETRY OF RED AND INFRARED STARS AT 1 TO 4 MICRONS.

711102 BECKLIN, E. E., FROGEL, J. A., KLEINMANN, D. E., NEUGEBAUER, G., NEY, E. P., STRECKER, D. W. <AP. J. (LETTERS), 170, L15>
INFRARED OBSERVATIONS OF THE CORE OF CENTAURUS A, NGC 5128.

711103 FORREST, W. J., GILLETT, F. C., STEIN, W. A. <AP. J. (LETTERS), 170, L29>
VARIABILITY OF RADIATION FROM CIRCUMSTELLAR GRAINS SURROUNDING R CORONAE BOREALIS.

711104 PENSTON, M. V., ALLEN, D. A., HYLAND, A. R. <AP. J. (LETTERS), 170, L33>
THE NATURE OF BECKLIN'S STAR.

711105 COHEN, M., WOOLF, N. J. <AP. J., 169, 543>
TWO YOUNG BRIGHT INFRARED OBJECTS.

711106 JOHNSON, T. V., MCCORD, T. B. <AP. J., 169, 589>
SPECTRAL GEOMETRIC ALBEDO OF THE GALILEAN SATELLITES, 0.3 TO 2.5 MICRONS.

711107 DYCK, H. M., KINMAN, T. D., LOCKWOOD, G. W., LANDOLT, A. U. <NAT. PHYS. SCI., 234, 71>
OBSERVATIONS OF OJ 287 BETWEEN 0.36 AND 3.4 MICRONS.

711201 HOFFMANN, W. F., FREDERICK, C. L., EMERY, R. J. <AP. J. (LETTERS), 170, L89>
100-MICRON SURVEY OF THE GALACTIC PLANE.

711202 KOVAR, R. P., POTTER, A. E., KOVAR, N. S., TRAFTON, L. <AP. J., 170, 449>
THE INFRARED SPECTRUM OF IC 418.

719901 TERZAN, A. <ASTR. AP., 12, 477>
FOUR NEW STAR CLUSTERS IN THE DIRECTION OF THE CENTRAL AREA OF THE GALAXY.

719902 JUNG, J., BISCHOFF, M. <STRASBOURG INF. BULL., 2, 8>
CATALOGUE OF STELLAR IDENTIFICATIONS.

719903 DE VENY, J. B., OSBORN, W. H., JANES, K. <P. A. S. P., 83, 611>
A CATALOGUE OF QUASARS.

719904 GALLOUET, L., HEIDMANN, N. <ASTR. AP. SUPPL., 3, 325>
OPTICAL POSITIONS OF BRIGHT GALAXIES.

719905 HAZARD, C., SUTTON, J., ARGUE, A. N., KENWORTHY, C. M., MORRISON, L. V., MURRAY, C. A. <NAT. PHYS. SCI., 233, 89>
ACCURATE RADIO AND OPTICAL POSITIONS OF 3C273B.

719906 WALKER, M. F. <AP. J., 167, 1>
ELECTRONOGRAPHIC PHOTOMETRY OF STAR CLUSTERS IN THE MAGELLANIC CLOUDS. II. THE COLOR-MAGNITUDE DIAGRAM OF NGC 2209.

719907 KUKARKIN, B. V., KHOLOPOV, P. N., EFREMOV, YU. N., KUKARKINA, N. P., KUROCHKIN, N. E., MEDVEDEVA, G. I., PEROVA, N. B., PSKOVSKY, YU. P., FEDOROVICH, V. P., FROLOV, M. S. <PUBL. OFFICE NAUKA, MOSCOW>
GENERAL CATALOG OF VARIABLE STARS. FIRST SUPPLEMENT.

720001 HYLAND, A. R., BECKLIN, E. E., FROGEL, J. A., NEUGEBAUER, G. <ASTR. AP., 16, 204>
INFRARED OBSERVATIONS OF 1612 MHZ IR/OH SOURCES.

720002 LOCKWOOD, G. W. <AP. J. SUPPL., 24, 375>
NEAR-INFRARED PHOTOMETRY OF MIRA VARIABLES.

720003 ROARK, T. P., BAUMERT, J. H., WHITE, N. M. <AP. LETTERS, 10, 55>
NEAR INFRARED PHOTOMETRY OF THE THETA CORONAE BOREALIS SYSTEM.

720004 ALLEN, D. A., SWINGS, J. P. <AP. LETTERS, 10, 83>
INFRARED EXCESSES AND FORBIDDEN EMISSION LINES IN EARLY-TYPE STARS.

720005 FROGEL, J. A., PERSSON, S. E., KLEINMANN, D. E. <AP. LETTERS, 11, 227>
ERRATUM TO "INFRARED PHOTOMETRY OF THE H II REGION SHARPLESS 266"

720006 KNACKE, R. F. <AP. LETTERS, 11, 201>
INFRARED PHOTOMETRY OF HBV 475 AND MHA 328-116.

720101 STROM, S. E., STROM, K. M., BROOKE, A. L., BREGMAN, J., YOST, J. <AP. J., 171, 267>
CIRCUMSTELLAR SHELLS IN THE YOUNG CLUSTER NGC 2264. II. INFRARED AND FURTHER OPTICAL OBSERVATIONS.

720102 ANGEL, J. R. P., LANDSTREET, J. D., OKE, J. B. <AP. J. (LETTERS), 171, L11>
THE SPECTRAL DEPENDENCE OF CIRCULAR POLARIZATION IN GRW+70 8247.

720103 JOYCE, R. R., GEZARI, D. Y., SIMON, M. <AP. J. (LETTERS), 171, L67>
345-MICRON GROUND-BASED OBSERVATIONS OF M17, M82, AND VENUS.

720104 DOMBROVSKII, V. A., KHOZOV, G. V. <ASTROFIZIKA, 8, 5>
PHOTOMETRIC AND POLARIMETRIC STUDY OF INFRARED STARS IN THE VISIBLE AND INFRARED SPECTRAL REGIONS.

720201 FAY JR., T. D., HONEYCUTT, R. K. <A. J., 77, 29>
SCANNER OBSERVATIONS OF COOL STARS FROM 3400 TO 11000A.

720202 HUMPHREYS, R. M., STRECKER, D. W., NEY, E. P. <AP. J., 172, 75>
SPECTROSCOPIC AND PHOTOMETRIC OBSERVATIONS OF M SUPERGIANTS IN CARINA.

720203 BEER, R., HUTCHISON, R. B., NORTON, R. H., LAMBERT, D. L. <AP. J., 172, 89>
ASTRONOMICAL INFRARED SPECTROSCOPY WITH A CONNES-TYPE INTERFEROMETER. III. ALPHA ORIONIS, 2600–3450 INVERSE CM.

720204 RIEKE, G., LEE, T., COYNE S. J., G. V. <P. A. S. P., 84, 37>
PHOTOMETRY AND POLARIMETRY OF V1057 CYGNI.

720205 KOVAR, R. P., POTTER, A. E., KOVAR, N. S., TRAFTON, L. <P. A. S. P., 84, 46>
PASCHEN BETA EMISSION IN THE SPECTRUM OF OMICRON CETI.

720301 GILLETT, F. C., MERRILL, K. M., STEIN, W. A. <AP. J., 172, 367>
INFRARED STUDIES OF GALACTIC NEBULAE. IV. CONTINUUM AND LINE RADIATION FROM PLANETARY NEBULAE.

720302 ALLEN, D. A. <AP. J. (LETTERS), 172, L55>
INFRARED OBJECTS IN HII REGIONS.

720303 HUMPHREYS, R. M., LOCKWOOD, G. W. <AP. J. (LETTERS), 172, L59>
SPECTROSCOPIC AND PHOTOMETRIC CHANGES IN THE PECULIAR INFRARED STAR VX SAGITTARIUS.

720304 FURNISS, I., JENNINGS, R. E., MOORWOOD, A. F. M. <NAT. PHYS. SCI., 236, 6>
FAR INFRARED OBSERVATIONS OF M42, NGC 2024 AND M1.

720401 COHEN, M. <AP. J. (LETTERS), 173, L61>
BD+40 4124 AND TWO NEARBY STARS.

720402 STROM, K. M., STROM, S. E., BREGER, M., BROOKE, A. L., YOST, J., GRASDALEN, G. L., CARRASCO, L. <AP. J. (LETTERS), 173, L65>
INFRARED AND OPTICAL OBSERVATIONS OF A YOUNG STELLAR GROUP SURROUNDING BD+40 4124.

720403 TOOMBS, R. I., BECKLIN, E. E., FROGEL, J. A., LAW, S. K., PORTER, F. C., WESTPHAL, J. A. <AP. J. (LETTERS), 173, L71>
INFRARED DIAMETER OF IRC+10216 DETERMINED FROM LUNAR OCCULTATIONS.

720404 STROM, S. E., STROM, K. M., YOST, J., CARRASCO, L., GRASDALEN, G. L. <AP. J., 173, 353>
THE NATURE OF THE HERBIG AE- AND BE-TYPE STARS ASSOCIATED WITH NEBULOSITY.

720501 HYLAND, A. R., HIRST, R. A., ROBINSON, G., THOMAS, J. A. <AP. LETTERS, 11, 7>
INFRARED OBSERVATIONS OF SOME SOUTHERN IR-OH SOURCES.

720502 KHROMOV, G. S., MOROZ, V. I. <SOV. AST., 15, 892>
INFRARED RADIATION OF PLANETARY NEBULAE. I. OBSERVATIONS AT 1.0 – 2.5 MICRONS AND THE CONTINUOUS SPECTRUM.

720503 GLASS, I. S. <NAT. PHYS. SCI., 237, 7>
OBSERVATIONS OF 30 DORADUS IN THE INFRARED.

720504 DYCK, H. M., KINMAN, T. D., LOCKWOOD, G. W. <NAT. PHYS. SCI., 237, 48>
ERRATUM TO "OBSERVATIONS OF OJ 287 BETWEEN 0.36 AND 3.4 MICRONS."

720601 LEE, T. A. <A. J., 77, 374>
ON THE NATURE OF SOME FAINT INFRARED STARS.

720602 ALLEN, D. A., SWINGS, J. P. <AP. J., 174, 583>
THE PECULIAR NEBULA M2-9.

720603 FROGEL, J. A., PERSSON, S. E., KLEINMANN, D. E. <AP. LETTERS, 11, 95>
INFRARED PHOTOMETRY OF THE HII REGION SHARPLESS 266.

720701 STRITTMATTER, P. A., SERKOWSKI, K., CARSWELL, R., STEIN, W. A., MERRILL, K. M., BURBIDGE, E. M. <AP. J. (LETTERS), 175, L7>
COMPACT EXTRAGALACTIC NONTHERMAL SOURCES.

720801 LOW, F. J. <AFCRL-72-0016>
GROUNDBASED INFRARED OBSERVATIONS OF CELESTIAL SOURCES.

720802 GAMMON, R. H., GAUSTAD, J. E., TREFFERS, R. R. <AP. J., 175, 687>
TEN-MICRON SPECTROSCOPY OF CIRCUMSTELLAR SHELLS.

720803 CAPPS, R. W., DYCK, H. M. <AP. J., 175, 693>
THE MEASUREMENT OF POLARIZED 10-MICRON RADIATION FROM COOL STARS WITH CIRCUMSTELLAR SHELLS.

720804 WILLNER, S. P., BECKLIN, E. E., VISVANATHAN, N. <AP. J., 175, 699>
OBSERVATIONS OF PLANETARY NEBULAE AT 1.65 TO 3.4 MICRON

720805 YOUNG, E. T., KNACKE, R. F., JOYCE, R. R. <NATURE, 238, 263>
INFRARED PHOTOMETRY OF MARKARIAN 231.

720806 SIMON, T., MORRISON, N. D., WOLFF, S. C., MORRISON, D. <ASTR. AP., 20, 99>
FAR-INFRARED AND UVBY PHOTOMETRY OF V1057 CYGNI.

720807 SWINGS, J. P., ALLEN, D. A. <P. A. S. P., 84, 523>
PHOTOMETRY OF SYMBIOTIC AND VV CEPHEI STARS IN THE NEAR INFRARED (WITH A NOTE ON MWC 56).

720808 FROGEL, J. A., KLEINMANN, D. E., KUNKEL, W., NEY, E. P., STRECKER, D. W. <P. A. S. P., 84, 581>
MULTICOLOR PHOTOMETRY OF THE M DWARF PROXIMA CENTAURI.

720901 RIEKE, G. H., LOW, F. J. <AP. J. (LETTERS), 176, L95>
INFRARED PHOTOMETRY OF EXTRAGALACTIC SOURCES.

720902 FURNISS, I., JENNINGS, R. E., MOORWOOD, A. F. M. <AP. J. (LETTERS), 176, L105>
DETECTION OF FAR-INFRARED ASTRONOMICAL SOURCES.

720903 RIEKE, G. H. <AP. J. (LETTERS), 176, L61>
INFRARED OBSERVATIONS OF VARIABLE RADIO OBJECTS.

720904 STROM, K. M., STROM, S. E., BREGER, M., BROOKE, A. L., YOST, J., GRASDALEN, G. L., CARRASCO, L. <AP. J. (LETTERS), 176, L93>
ERRATUM TO "INFRARED AND OPTICAL OBSERVATIONS OF A YOUNG STELLAR GROUP SURROUNDING BD+40 4124".

720905 STROM, S. E., STROM, K. M., YOST, J., CARRASCO, L., GRASDALEN, G. L. <AP. J., 176, 845>
ERRATUM TO "THE NATURE OF THE HERBIG AE- AND BE-TYPE STARS ASSOCIATED WITH NEBULOSITY".

720906 SCHULTZ, G. V., WIEMER, W. <ASTR. AP., 20, 317>
IDENTIFICATIONS OF IRC-OBJECTS.

720907 ALLEN, D. A., SWINGS, J. P., HARVEY, P. M. <ASTR. AP., 20, 333>
INFRARED PHOTOMETRY OF NORTHERN WOLF-RAYET STARS.

721001 WILSON, W. J., SCHWARTZ, P. R., NEUGEBAUER, G., HARVEY, P. M., BECKLIN, E. E. <AP. J., 177, 523>
INFRARED STARS WITH STRONG 1665/1667-MHZ OH MICROWAVE EMISSION.

721002 SIMON, T., MORRISON, D., CRUIKSHANK, D. P. <AP. J. (LETTERS), 177, L17>
20-MICRON FLUXES OF BRIGHT STELLAR STANDARDS.

721003 HARPER JR., D. A., LOW, F. J., RIEKE, G. H., ARMSTRONG, K. R. <AP. J. (LETTERS), 177, L21>
OBSERVATIONS OF PLANETS, NEBULAE, AND GALAXIES AT 350 MICRONS.

721004 GEBALLE, T. R., WOLLMAN, E. R., RANK, D. M. <AP. J. (LETTERS), 177, L27>
OBSERVATIONS OF CARBON MONOXIDE IN COOL STARS AT 4.7 MICRONS.

721005 LEMKE, D., LOW, F. J. <AP. J. (LETTERS), 177, L53>
21-MICRON OBSERVATIONS OF HII REGIONS.

721006 LEE, T. A., WAMSTEKER, W., WISNIEWSKI, W. Z., WDOWIAK, T. J. <AP. J. (LETTERS), 177, L59>
PHOTOMETRY OF SUPERNOVA 1972 IN NGC 5253.

721007 SOIFER, B. T., PIPHER, J. L., HOUCK, J. R. <AP. J., 177, 315>
ROCKET INFRARED OBSERVATIONS OF HII REGIONS.

721008 BECKLIN, E. E., KRISTIAN, J., NEUGEBAUER, G., WYNN-WILLIAMS, C. G. <NAT. PHYS. SCI., 239, 130>
DISCOVERY OF INFRARED EMISSION FROM THE RADIO SOURCE NEAR CYGNUS X-3.

721009 DYCK, H. M., MILKEY, R. W. <P. A. S. P., 84, 597>
INFRARED EXCESSES IN EARLY-TYPE STARS: FREE-FREE EMISSION.

721010 NEY, E. P. <P. A. S. P., 84, 613>
INFRARED EXCESSES IN SUPERGIANT STARS: EVIDENCE FOR SILICTAES.

721101 HOUCK, J. R., SOIFER, B. T., HARWIT, M., PIPHER, J. L. <AP. J. (LETTERS), 178, L29>
THE FAR-INFRARED AND SUBMILLIMETER BACKGROUND.

721102 RIEKE, G. H., LOW, F. J. <AP. J. (LETTERS), 177, L115>
VARIABILITY OF EXTRAGALACTIC SOURCES AT 10 MICRONS.

721103 HACKWELL, J. A. <ASTR. AP., 21, 239>
LONG WAVELENGTH SPECTROMETRY AND PHOTOMETRY OF M, S AND C-STARS.

721201 EPSTEIN, E. E., FOGARTY, W. G., HACKNEY, K. R., HACKNEY,R.L.,LEACOCK, R. J., POMPHREY, R. B., SCOTT, R. L.,SMITH,A.G., HAWKINS, R. W., ROEDER, R. C., GARY, B. L., PENSTON,M.V., TRITTON, K. P., BERTAUD, CH., VERON, M. P., WLERICK, G., BERNARD, A., BIGAY, J. H., MERLIN, P., DURAND, A., SAUSE, G., BECKLIN, E. E., NEUGEBAUER, G., WYNN-WILLIAMS, C. G. <AP. J. (LETTERS), 178, L51>
3C 120, BL LACERTAE, AND OJ 287: COORDINATED OPTICAL, INFRARED, AND RADIO OBSERVATIONS OF INTRADAY VARIABILITY.

721202 FROGEL, J. A., PERSSON, S. E. <AP. J., 178, 667>
STUDIES OF SMALL HII REGIONS. I. INFRARED PHOTOMETRY OF SHARPLESS 138, 152, AND 270.

721203 GEHRZ, R. D. <AP. J., 178, 715>
INFRARED RADIATION FROM RV TAURI STARS. I. AN INFRARED SURVEY OF RV TAURI STARS AND RELATED OBJECTS.

721204 FORREST, W. J., GILLETT, F. C., STEIN, W. A. <AP. J. (LETTERS), 178, L129>
INFRARED MEASUREMENTS OF R CORONAE BOREALIS THROUGH ITS 1972 MARCH-JUNE MINIMUM.

721205 GEHRZ, R. D., NEY, E. P. <P. A. S. P., 84, 768>
INFRARED OBSERVATIONS OF SOUTHERN RV TAURI STARS.

721206 JOHNSON, H. L., THOMPSON, R. I., FORBES, F. F., STEINMETZ, D. L. <P. A. S. P., 84, 775>
THE INFRARED SPECTRUM OF ALPHA HERCULIS FROM 4000 TO 4800 CM-1.

721207 THOMPSON, R. I., JOHNSON, H. L., FORBES, F. F., STEINMETZ, D. L. <P. A. S. P., 84, 779>
THE INFRARED SPECTRUM OF ALPHA HERCULIS FROM 5700 TO 6700 CM-1.

729901 GEARHART, M. R., LUND, J. M., FRANTZ, D. J., KRAUS, J. D. <A. J., 77, 557>
OPTICAL IDENTIFICATIONS OF OHIO SURVEY RADIO SOURCES.

729902 HERGIG, G. H., RAO, N. K. <AP. J., 174, 401>
SECOND CATALOG OF EMISSION-LINE STARS OF THE ORION POPULATION.

729903 KOHOUTEK, L. <ASTR. AP., 16, 291>
HAMBURG SCHMIDT-CAMERA SURVEY OF FAINT PLANETARY NEBULAE. CYGNUS-PERSEUS REGION.

729904 CHOPINET, M., LORTET-ZUCKERMANN, M. C. <ASTR. AP., 18, 166>
A NOTE TO DESIGNATIONS OF PLANETARY NEBULAE.

729905 ALLEN, R. J., RAIMOND, E. <ASTR. AP., 18, 317>
A RADIO MAP OF THE SPIRAL GALAXY MAFFEI 2 AT 1415 MHZ.

729906 CHOPINET, M., LORTET-ZUCKERMANN, M. C. <ASTR. AP., 18, 373>
INTERACTION OF HOT STARS AND OF THE INTERSTELLAR MEDIUM. II. EXCITING STAR AND SPECTRA OF THE BRIGHT KNOT INSIDE THE DIFFUSE NEBULA SHARPLESS 157.

729907 WALKER, M. F. <M. N. R. A. S., 159, 379>
ELECTRONOGRAPHIC PHOTOMETRY OF STAR CLUSTERS IN THE MAGELLANIC CLOUDS. IV. THE COLOUR-MAGNITUDE DIAGRAM OF NGC 419.

730001 ALLEN, D. A. <M. N. R. A. S., 161, 145>
NEAR INFRA-RED MAGNITUDES OF 248 EARLY-TYPE EMISSION-LINE STARS AND RELATED OBJECTS.

730002 THOMAS, J. A., HYLAND, A. R., ROBINSON, G. <M. N. R. A. S., 165, 201>
SOUTHERN INFRA-RED STANDARDS AND THE ABSOLUTE CALIBRATION OF INFRA-RED PHOTOMETRY.

730003 GLASS, I. S. <M. N. R. A. S., 164, 155>
THE JHKL COLOURS OF GALAXIES.

730004 COHEN, M. <M. N. R. A. S., 161, 85>
INFRA-RED OBSERVATIONS OF YOUNG STARS-I. STARS IN YOUNG CLUSTERS.

730005 COHEN, M. <M. N. R. A. S., 161, 97>
INFRA-RED OBSERVATIONS OF YOUNG STARS-II. T TAURI STARS AND THE ORION POPULATION.

730006 COHEN, M. <M. N. R. A. S., 161, 105>
INFRA-RED OBSERVATIONS OF YOUNG STARS-III. NEBULOUS EMISSION-LINE STARS.

730007 ROBINSON, G., HYLAND, A. R., THOMAS, J. A. <M. N. R. A. S., 161, 281>
OBSERVATION AND INTERPRETATION OF THE INFRA-RED SPECTRUM OF ETA CARINAE.

730008 FEAST, M. W., GLASS, I. S. <M. N. R. A. S., 161, 293>
INFRA-RED PHOTOMETRY OF R CORONAE BOREALIS TYPE VARIABLES AND RELATED OBJECTS.

730009 WISNIEWSKI, W. Z. <M. N. R. A. S., 161, 331>
MULTICOLOUR OBSERVATIONS OF UZ LIBRAE.

730010 COHEN, M. <M. N. R. A. S., 164, 395>
INFRA-RED OBSERVATIONS OF YOUNG STARS-IV. RADIATIVE MECHANISMS AND INTERPRETATIONS.

730011 MACGREGOR, A. D., PHILLIPS, J. P., SELBY, M. J. <M. N. R. A. S., 164, 31P>
THE DETECTION OF M15 AT 10.2 MICRONS.

730012 FEAST, M. W., GLASS, I. S. <M. N. R. A. S., 164, 35P>
THE NATURE OF A NEBULOUS OBJECT IN THE CHAMAELEON T ASSOCIATION.

730013 GLASS, I. S., WEBSTER, B. L. <M. N. R. A. S., 165, 77>
INFRA-RED PHOTOMETRY OF RR TELESCOPII AND OTHER EMISSION-LINE OBJECTS.

730014 AITKEN, D. K., JONES, B. <M. N. R. A. S., 165, 363>
SOME FEATURES OF THE INFRA-RED SPECTRUM OF NGC 7027 AND AN ESTIMATE OF ITS SULPHUR ABUNDANCE.

730015 SWINGS, J. P. <AP. LETTERS, 15, 71>
SPECTRA OF SOUTHERN STELLAR PLANETARY NEBULAE AND PECULIAR EMISSION-LINE STARS WITH INFRARED EXCESSES.

730016 BECKLIN, E. E., NEUGEBAUER, G., WYNN-WILLIAMS, C. G. <AP. LETTERS, 15, 87>
THE SPATIAL DISTRIBUTION OF THE INFRARED EMISSION FROM NGC 7027.

730017 PENSTON, M. V. <M. N. R. A. S., 162, 359>
THE V-K COLOURS OF THE NUCLEI OF BRIGHHT GALAXIES.

730018 GLASS, I. S. <M. N. R. A. S., 162, 35P>
INFRA-RED OBSERVATIONS OF NGC 7552 AND NGC 7582 AND THEIR IDENTIFICATION WITH PKS RADIO SOURCES.

730019 GLASS, I. S., FEAST, M. W. <M. N. R. A. S., 163, 245>
INFRA-RED PHOTOMETRY OF RED GIANTS IN THE GLOBULAR CLUSTERS 47 TUC AND OMEGA CEN.

730020 PENSTON, M. V., PENSTON, M. J. <M. N. R. A. S., 162, 109>
NEW OBSERVATIONS OF TWO COMPACT GALAXIES.

730021 SATO, S., MAIHARA, T., OKUDA, H. <P. A. S. J., 25, 571>
NEAR-INFRARED OBSERVATIONS OF NOVA CEPHEI 1971.

730022 KLEINMANN, D. E. <AP. LETTERS, 13, 49>
BRIGHT INFRARED SOURCES IN M17.

730023 GLASS, I. S., FEAST, M. W. <AP. LETTERS, 13, 81>
AN INFRARED OBJECT PROBABLY ASSOCIATED WITH OH 338.5+0.1.

730024 GEHRZ, R. D., NEY, E. P., BECKLIN, E. E., NEUGEBAUER, G. <AP. LETTERS, 13, 89>
THE INFRARED SPECTRUM AND ANGULAR SIZE OF ETA CARINAE.

730025 BECKLIN, E. E., NEUGEBAUER, G., WYNN-WILLIAMS, C. G. <AP. LETTERS, 13, 147>
INFRARED EMISSION FROM THE OH/H2O SOURCES IN W49.

730026 SCHWARTZ, R. D., PEIMBERT, M. <AP. LETTERS, 13, 157>
PHOTOELECTRIC PHOTOMETRY OF NGC 7027.

730101 HUMPHREYS, R. M., STRECKER, D. W., MURDOCK, T. L., LOW, F. J. <AP. J. (LETTERS), 179, L49>
IRC+10420 - ANOTHER ETA CARINAE?

730102 GEZARI, D. Y., JOYCE, R. R., SIMON, M. <AP. J. (LETTERS), 179, L67>
OBSERVATIONS OF THE GALACTIC NUCLEUS AT 350 MICRONS.

730103 SERKOWSKI, K. <AP. J. (LETTERS), 179, L101>
INFRARED CIRCULAR POLARIZATION OF NML CYGNI AND VY CANIS MAJORIS.

730104 WING, R. F., WARNER, J. W., SMITH, M. G. <AP. J., 179, 135>
ON THE NATURE OF THE SAGITTARIUS OBJECT IRC-20385.

730105 SCHILD, R. E. <AP. J., 179, 221>
A SPECTROSCOPICALLY DISTINGUISHED CLASS OF BE STARS.

730106 GILLETT, F. C., FORREST, W. J. <AP. J., 179, 483>
SPECTRA OF THE BECKLIN-NEUGEBAUER POINT SOURCE AND THE KLEINMANN-LOW NEBULA FROM 2.8 TO 13.5 MICRONS.

730107 KNACKE, R. F., STROM, K. M., STROM, S. E. <AP. J., 179, 493>
INFRARED OBSERVATIONS OF A HIGHLY REDDENED STAR NEAR NGC 6231.

730201 WOOLF, N. J., STEIN, W. A., GILLETT, F. C., MERRILL, K. M., BECKLIN, E. E., NEUGEBAUER, G., PEPIN, T. J. <AP. J. (LETTERS), 179, L111>
THE INFRARED SOURCES IN M8.

730202 JOHNSON, H. M. <AP. J. (LETTERS), 180, L7>
COMPARISON OF FAR-INFRARED, OPTICAL, AND RADIOFREQUENCY DATA OF DIFFUSE NEBULAE.

730203 KNACKE, R. F., STROM, K. M., STROM, S. E., YOUNG, E., KUNKEL, W. <AP. J., 179, 847>
A YOUNG STELLAR GROUP IN THE VICINITY OF R CORONAE AUSTRINAE.

730204 CHALDU, R., HONEYCUTT, R. K., PENSTON, M. V. <P. A. S. P., 85, 87>
THE EXTINCTION CURVE FOR CYGNUS OB2 NO. 12.

730205 KNACKE, R. F., DRESSLER, A. M. <P. A. S. P., 85, 100>
THE SPATIAL DISTRIBUTION OF THE 11.7 MICRON RADIATION OF NGC 7027.

730206 CIATTI, F. <ASTR. AP., 22, 465>
THE INFRARED SPECTRUM OF THE SUPERNOVA IN NGC 5253.

730207 EMERSON, J. P., JENNINGS, R. E., MOORWOOD, A. F. M. <NAT. PHYS. SCI., 241, 108>
RCW 117 AND DR 15 OBSERVED IN THE FAR INFRARED.

730301 KIRSHNER, R. P., WILLNER, S. P., BECKLIN, E. E., NEUGEBAUER, G., OKE, J. B. <AP. J. (LETTERS), 180, L97>
SPECTROPHOTOMETRY OF THE SUPERNOVA IN NGC 5253 FROM 0.33 TO 2.2 MICRONS.

730302 SPINRAD, H., BAHCALL, J., BECKLIN, E. E., GUNN, J. E., KRISTIAN, J., NEUGEBAUER, G., SARGENT, W. L. W., SMITH, H. <AP. J., 180, 351>
OPTICAL AND NEAR-INFRARED OBSERVATIONS OF THE NEARBY SPIRAL GALAXY MAFFEI 2.

730303 NEY, E. P., STRECKER, D. W., GEHRZ, R. D. <AP. J., 180, 809>
DUST EMISSION NEBULAE AROUND ORION O AND B STARS.

730304 LOCKWOOD, G. W. <AP. J., 180, 845>
SCANNER PHOTOMETRY OF WEAK TIO BANDS NEAR 1 MICRON IN COOL M STARS.

730305 GLUSHNEVA, I. N. <SOV. AST., 16, 846>
SPECTRAL ENERGY DISTRIBUTION IN SEVERAL BINARIES AT 3300-7300A AND 0.88-1.53 MICRONS.

730306 JAMESON, R. F., LONGMORE, A. J., CRAWFORD, B. <NATURE, 242, 107>
5-MICRON INFRARED EMISSION FROM ALGOL.

730307 BAUMERT, J. H. <P. A. S. P., 85, 205>
ON THE VARIABILITY OF CASE 621 AND MSB 57.

730401 BECKLIN, E. E., FOMALONT, E. B., NEUGEBAUER, G. <AP. J. (LETTERS), 181, L27>
INFRARED AND RADIO OBSERVATIONS OF THE NUCLEUS OF NGC 253.

730402 JOHNSON, H. L. <P. A. S. P., 85, 179>
THE INFRARED SPECTRUM OF CHI CYGNI FROM 4000 TO 6700 CM-1.

730501 DICKINSON, D. F., CHAISSON, E. J. <AP. J. (LETTERS), 181, L135>
LONG-PERIOD VARIABLES: CORRELATION OF STELLAR PERIOD WITH OH RADIAL-VELOCITY PATTERN.

730502 BECKLIN, E. E., NEUGEBAUER, G., WYNN-WILLIAMS, C. G. <AP. J. (LETTERS), 182, L7>
ON THE NATURE OF THE INFRARED POINT SOURCE IN THE ORION NEBULA.

730503 MILKEY, R. W., DYCK, H. M. <AP. J., 181, 833>
LOW-TEMPERATURE FREE-FREE EMISSION: INFRARED EXCESSES IN BE STARS.

730601 VOGT, S. S. <A. J., 78, 389>
LOW-DISPERSION SPECTROSCOPIC CLASSIFICATION OF THE UNIDENTIFIED SOURCES IN THE TWO-MICRON SKY SURVEY.

730602 HARPER JR., D. A., LOW, F. J. <AP. J. (LETTERS), 182, L89>
FAR-INFRARED OBSERVATIONS OF GALACTIC NUCLEI.

730603 GEBALLE, T. R., RANK, D. M. <AP. J. (LETTERS), 182, L113>
OBSERVATION OF 9.0-MICRON LINE EMISSION FROM AR III IN NGC 7027 AND NGC 6572.

730604 BECKLIN, E. E., FROGEL, J. A., NEUGEBAUER, G., PERSSON, S. E., WYNN-WILLIAMS, C. G. <AP. J. (LETTERS), 182, L125>
THE HII REGION G333.6-0.2, A VERY POWERFUL 1-20 MICRON SOURCE.

730605 SPINRAD, H. <AP. J., 182, 381>
A NOTE ON THE STELLAR CONTENT OF NGC 5195.

730606 PERSSON, S. E., FROGEL, J. A. <AP. J., 182, 503>
INFRARED PHOTOMETRY OF PLANETARY NEBULAE.

730607 GRASDALEN, G. L. <AP. J., 182, 781>
V1057 CYGNI AND PRE-MAIN-SEQUENCE EVOLUTION.

730701 STRECKER, D. W., NEY, E. P., MURDOCK, T. L. <AP. J. (LETTERS), 183, L13>
CYGNIDS AND TAURIDS-TWO CLASSES OF INFRARED OBJECTS.

730702 GEBALLE, T. R., WOLLMAN, E. R., RANK, D. M. <AP. J., 183, 499>
OBSERVATIONS OF CARBON MONOXIDE AT 4.7 MICRONS IN IRC+10216, VY CANIS MAJORIS, AND NML CYGNI.

730703 RIEKE, G. H., HARPER JR., D. A., LOW, F. J., ARMSTRONG, K. R. <AP. J. (LETTERS), 183, L67>
350-MICRON OBSERVATIONS OF SOURCES IN HII REGIONS, THE GALACTIC CENTER, AND NGC 253.

730704 BREGER, M., HARDORP, J. <AP. J. (LETTERS), 183, L77>
INFRARED POLARIMETRY OF VERY YOUNG OBJECTS INCLUDING THE BECKLIN-NEUGEBAUER SOURCE.

730705 PENSTON, M. V. <AP. J., 183, 505>
MULTICOLOR OBSERVATIONS OF STARS IN THE VICINITY OF THE ORION NEBULA.

730706 GILLETT, F. C., FORREST, W. J., MERRILL, K. M. <AP. J., 183, 87>
8-13 MICRON SPECTRA OF NGC 7027, BD+30 3639, AND NGC 6572.

730707 ERICKSON, E. F., SWIFT, C. D., WITTEBORN, F. C., MORD, A. J.,AUGASON, G. C., CAROFF, L. J., KUNZ, L. W., GIVER, L. P. <AP. J., 183, 535>
INFRARED SPECTRUM OF THE ORION NEBULA BETWEEN 55 AND 200 MICRONS.

730708 GUSEV, E. B., KOMAROV, N. S., MEDVEDEV, YU. A. <SOV. AST., 17, 150>
SPECTRAL ENERGY DISTRIBUTION OF SIX STARS.

730801 LOCKWOOD, G. W., ZINTER, T. A. <A. J., 78, 471>
A LIST OF ADDITIONAL VARIABLE STARS IN THE TWO-MICRON SKY SURVEY.

730802 LOER, S. J., ALLEN, D. A., DYCK, H. M. <AP. J. (LETTERS), 183, L97>
2.2- AND 3.5-MICRON POLARIZATION MEASUREMENTS OF THE BECKLIN-NEUGEBAUER OBJECT IN THE ORION NEBULA.

730803 DYCK, H. M., CAPPS, R. W., FORREST, W. J., GILLETT, F. C. <AP. J. (LETTERS), 183, L99>
DISCOVERY OF LARGE 10-MICRON LINEAR POLARIZATION OF THE BECKLIN-NEUGEBAUER SOURCE IN THE ORION NEBULA

730804 SERKOWSKI, K., RIEKE, G. H. <AP. J. (LETTERS), 183, L103>
CIRCULAR POLARIZATION OF THE BECKLIN-NEUGEBAUER INFRARED SOURCES IN THE ORION NEBULA.

730805 LOW, F. J., RIEKE, G. H., ARMSTRONG, K. R. <AP. J. (LETTERS), 183, L105>
GROUND-BASED OBSERVATIONS AT 34 MICRONS.

730806 GREENSTEIN, J. L. <AP. J. (LETTERS), 184, L23>
MWC 349, AN OPTICAL, RADIO, AND INFRARED SOURCE.

730807 DANZIGER, I. J., FROGEL, J. A., PERSSON, S. E. <AP. J. (LETTERS), 184, L29>
OBSERVATIONS OF NGC 6302 FROM 0.35 TO 20 MICRONS.

730808 AITKEN, D. K., JONES, B. <AP. J., 184, 127>
OBSERVATIONS OF THE INFRARED EXTINCTION OF IRS 5 IN W3 COMPARED WITH THE GALACTIC CENTER AND THE BECKLIN- NEUGEBAUER OBJECT.

730809 ROBINSON, G., THOMAS, J. A., HIRST, R. A., HYLAND, A. R. <P. A. S. P., 85, 436>
THE NATURE OF NGC 6231-92.

730901 EMERSON, J. P., JENNINGS, R. E., MOORWOOD, A. F. M. <AP. J., 184, 401>
FAR-INFRARED OBSERVATIONS OF HII REGIONS FROM BALLOON ALTITUDES.

730902 RIEKE, G. H., LOW, F. J. <AP. J., 184, 415>
INFRARED MAPS OF THE GALACTIC NUCLEUS.

730903 GRASDALEN, G. L., STROM, K. M., STROM, S. E. <AP. J. (LETTERS), 184, L53>
A 2-MICRON MAP OF THE OPHIUCHUS DARK-CLOUD REGION.

730904 WOLLMAN, E. R., GEBALLE, T. R., GREENBERG, L. T., HOLTZ, J. Z., RANK, D. M. <AP. J. (LETTERS), 184, L85>
OBSERVATIONS OF SILICON MONOXIDE IN COOL STARS AT 4.05 MICRONS.

730905 BALDWIN, J. R., FROGEL, J. A., PERSSON, S. E. <AP. J., 184, 427>
THE STRENGTHS OF INFRARED CO AND H2O BANDS IN LATE-TYPE STARS.

730906 WING, R. F., LOCKWOOD, G. W. <AP. J., 184, 873>
THE PERIOD AND SPECTRAL RANGE OF IK TAURI.

730907 GLASS, I. S., FEAST, M. W. <NAT. PHYS. SCI., 245, 39>
PECULIAR OBJECT NEAR X2+5

731001 HANSEN, O. L., BLANCO, V. M. <A. J., 78, 669>
CLASSIFICATION OF UNIDENTIFIED, SOUTHERN IRC SOURCES NEAR THE GALACTIC PLANE.

731002 COHEN, M., BARLOW, M. J. <AP. J. (LETTERS), 185, L37>
INFRARED OBSERVATIONS OF TWO SYMMETRIC NEBULAE.

731003 COHEN, M. <AP. J. (LETTERS), 185, L75>
AN UNUSUAL INFRARED SOURCE NEAR THE ROSETTE NEBULA.

731004 WOOLF, N. J. <AP. J., 185, 229>
INFRARED EMISSION FROM UNUSUAL BINARY STARS.

731005 KIRSHNER, R. P., OKE, J. B., PENSTON, M. V., SEARLE, L. <AP. J., 185, 303>
THE SPECTRA OF SUPERNOVAE.

731006 LEE, T. A. <P. A. S. P., 85, 637>
VISUAL AND INFRARED PHOTOMETRY OF RY SAGITTARII NEAR THE PHASE OF DEEP MINIMUM.

731007 FROGEL, J. A., PERSSON, S. E. <P. A. S. P., 85, 641>
INFRARED PHOTOMETRY OF THE X-RAY SOURCES 2U 0900-40 AND 2U 1700-37.

731008 THOMPSON, R. I., JOHNSON, H. L., FORBES, F. F., STEINMETZ, D. L. <P. A. S. P., 85, 643>
THE INFRARED SPECTRUM OF TWO CARBON STARS FROM 4000 TO 6700 CM-1.

731009 BECKLIN, E. E., NEUGEBAUER, G., HAWKINS, F. J., MASON, K. O.,SANFORD, P. W., MATTHEWS, K., WYNN-WILLIAMS, C. G. <NATURE, 245, 302>
INFRARED AND X-RAY VARIABILITY OF CYG X-3.

731101 KLEINMANN, D. E., WRIGHT, E. L. <AP. J. (LETTERS), 185, L131>
A NEW INFRARED SOURCE IN M17.

731102 RIEKE, G. H., LOW, F. J., KLEINMANN, D. E. <AP. J. (LETTERS), 186, L7>
HIGH-RESOLUTION MAPS OF THE KLEINMANN-LOW NEBULA IN ORION.

731103 SOIFER, B. T., HOUCK, J. R. <AP. J., 186, 169>
ROCKET-INFRARED OBSERVATIONS OF THE GALACTIC CENTER.

731104 MORRISON, D., SIMON, T. <AP. J., 186, 193>
BROAD-BAND 20-MICRON PHOTOMETRY OF 76 STARS.

731105 FROGEL, J. A., PERSSON, S. E. <AP. J., 186, 207>
INFRARED SOURCES IN SHARPLESS 228.

731106 MERRILL, K. M., STEIN, W. A. <ASTR. AP., 29, 163>
A SEARCH FOR VARIABILITY OF FREE-FREE EMISSION FROM CIRCUMSTELLAR GAS SURROUNDING BE STARS.

731201 BECKLIN, E. E., MATTHEWS, K., NEUGEBAUER, G., WYNN-WILLIAMS, C. G. <AP. J. (LETTERS), 186, L69>
THE SIZE OF NGC 1068 AT 10 MICRONS.

731202 SIMON, M., RIGHINI, G., JOYCE, R. R., GEZARI, D. Y. <AP. J. (LETTERS), 186, L127>
A STRONG 350-MICRON SOURCE IN THE OPHIUCHUS DARK CLOUD.

731203 COHEN, M., GAUSTAD, J. E. <AP. J. (LETTERS), 186, L131>
INFRARED EXCESSES IN THE M SUPERGIANTS OF H AND CHI PERSEI.

731204 BECKLIN, E. E., KRISTIAN, J., MATTHEWS, K., NEUGEBAUER, G. <AP. J. (LETTERS), 186, L137>
MEASUREMENTS OF THE CRAB PULSAR AT 2.2 AND 3.5 MICRONS.

731205 WING, R. F., STOCK, J. <AP. J., 186, 979>
CARBON STARS IN OMEGA CENTAURI.

731206 HYLAND, A. R., MOULD, J. R. <AP. J., 186, 993>
INFRARED VARIABILITY AND THE INTERSTELLAR REDDENING OF THE X-RAY SOURCE HD 77581.

731207 LAMBERT, D. L., BROOKE, A. L., BARNES, T. G. <AP. J., 186, 573>
H2 QUADRUPOLE ROTATION-VIBRATION LINES IN INFRARED SPECTRA OF COOL STARS.

731208 GIGUERE, P. T. <AP. J., 186, 585>
ONE-MICRON REGION SEARCH FOR HCN IN TWO CARBON STARS.

731209 WOOLF, N. J. <P. A. S. P., 85, 730>
THE 10-MICRON EXCESS OF ALPHA HERCULIS.

731210 OLTHOF, H., VAN DUINEN, R. J. <ASTR. AP., 29, 315>
TWO COLOUR FAR INFRARED PHOTOMETRY OF SOME GALACTIC H II REGIONS.

731211 BORGMAN, J. <ASTR. AP., 29, 443>
THE 9.7 MICRON ABSORPTION FEATURE IN THE GALACTIC CENTER.

731212 BECKLIN, E. E., HANSEN, O., KIEFFER, H., NEUGEBAUER, G. <A. J., 78, 1063>
STELLAR FLUX CALIBRATION AT 10 AND 20 MICRONS USING MARINER 6, 7, AND 9 RESULTS.

739901 PETERSON, S. D. <A. J., 78, 811>
OPTICAL POSITIONS OF THE MARKARIAN GALAXIES.

739902 MARKARIAN, B. E., LIPOVETSKY, V. A. <ASTROFIZIKA, 9, 487>
GALAXIES WITH ULTRAVIOLET CONTINUUM. VI.

739903 SANDULEAK, N., STEPHENSON, C. B. <AP. J., 185, 899>
LOW-DISPERSION SPECTRA AND GALACTIC DISTRIBUTION OF VARIOUS INTERESTING STRONG-EMISSION-LINE OBJECTS IN THE SOUTHERN MILKY WAY.

739904 ALBERS, H. <AP. J., 182, 817>
THE RED STAR IN THE OPEN CLUSTER TRUMPLER 27.

739905 WELIN, G. <ASTR. AP. SUPPL., 9, 183>
H-ALPHA EMISSION STARS IN AND NEAR NGC 7000.

739906 SULENTIC, J. W., TIFFT, W. G. <UNIV. OF ARIZONA PRESS>
THE REVISED NEW GENERAL CATALOG OF NONSTELLAR ASTRONOMICAL OBJECTS.

739907 STEPHENSON, C. B. <PUBL. WARNER AND SWASEY OBS., 1, 4>
A GENERAL CATALOGUE OF COOL CARBON STARS.

739908 NILSON, P. <UPPSALA AST. OBS. ANNALER, 6>
UPPSALA GENERAL CATALOGUE OF GALAXIES.

739909 MILNE, D. K. <A. J., 78, 239>
IMPROVED OPTICAL POSITIONS FOR 153 PLANETARY NEBULAE.

739910 GALLOUET, L., HEIDMANN, N., DAMPIERRE, F. <ASTR. AP. SUPPL., 12, 89>
OPTICAL POSITIONS OF BRIGHT GALAXIES. II.

739911 EKERS, R. D. <ASTR. AP., 22, 309>
UPPER LIMITS TO THE 21 CM CONTINUUM RADIATION FROM TWO MAGNETIC WHITE DWARFS.

739912 HAWKINS, F. J., MASON, K. O., SANFORD, P. W. <NAT. PHYS. SCI., 241, 109>
DETERMINATION OF THE POSITION OF GX2+5 WITH COPERNICUS.

739913 HENIZE, K. G., MENDOZA V., E. E. <AP. J., 180, 115>
EMISSION-LINE STARS IN THE CHAMAELEON T ASSOCIATION.

740001 BECKLIN, E. E., NEUGEBAUER, G. <HII REGIONS AND THE GALACTIC CENTER, ESRO, 39>
INFRARED OBSERVATION OF NGC 6334.

740002 HIRAI, M. <P. A. S. J., 26, 163>
SPECTROSCOPIC OBSERVATION OF THE CARBON STARS Y CANUM VENATICORUM AND U HYDRAE IN THE ONE-MICRON REGION.

740101 HUMPHREYS, R. M., NEY, E. P. <AP. J. (LETTERS), 187, L75>
SUPERGIANT BINARY STARS.

740102 BARNES, T. G., LAMBERT, D. L., POTTER, A. E. <AP. J., 187, 73>
INFRARED SPECTRA OF GAMMA 2 VELORUM AND ZETA PUPPIS.

740103 STROM, K. M., STROM, S. E., GRASDALEN, G. L. <AP. J., 187, 83>
AN INFRARED SOURCE ASSOCIATED WITH A HERBIG-HARO OBJECT.

740104 STEIN, W. A., GILLETT, F. C., MERRILL, K. M. <AP. J., 187, 213>
OBSERVATIONS OF THE INFRARED RADIATION FROM THE NUCLEI OF NGC 1068 AND NGC 4151.

740105 ZAPPALA, R. R. <AP. J., 187, 257>
ON THE NATURE OF BD-10 4462.

740106 BRUECK, M. T. <M. N. R. A. S., 166, 123>
PHOTOGRAPHIC SURFACE PHOTOMETRY OF THE NEBULAE SURROUNDING V380 ORI AND R MON.

740107 HUMPHREYS, R. M., NEY, E. P. <ASTR. AP., 30, 159>
INFRARED OBSERVATIONS OF HD 65750, A RED GIANT IN A REFLECTION NEBULA.

740108 SIBILLE, F., BERGEAT, J., LUNEL, M. <ASTR. AP., 30, 181>
INFRARED OBSERVATION OF DR 21 AT 2.2 MICRONS.

740201 RANK, D. M., GEBALLE, T. R., WOLLMAN, E. R. <AP. J. (LETTERS), 187, L111>
DETECTION OF OXYGEN-17 IN IRC+10216.

740202 JAMESON, R. F., LONGMORE, A. J., MCLINN, J. A., WOOLF, N. J. <AP. J. (LETTERS), 187, L109>
INFRARED SPECTRUM OF NGC 1068.

740203 WYNN-WILLIAMS, C. G., BECKLIN, E. E., NEUGEBAUER, G. <AP. J., 187, 473>
INFRARED STUDIES OF HII REGIONS AND OH SOURCES.

740204 BECKLIN, E. E., FROGEL, J. A., KLEINMANN, D. E., NEUGEBAUER, G., PERSSON, S. E., WYNN-WILLIAMS, C. G. <AP. J., 187, 487>
INFRARED EMISSION FROM THE SOUTHERN HII REGION H2-3.

740205 SCHWARTZ, P. R., HARVEY, P. M., BARRETT, A. H. <AP. J., 187, 491>
TIME VARIATION OF THE H_2O MASER AND INFRARED CONTINUUM IN LATE-TYPE STARS.

740206 WYNN-WILLIAMS, C. G., BECKLIN, E. E. <P. A. S. P., 86, 5>
INFRARED EMISSION FROM HII REGIONS.

740207 SCHILD, R. E., OKE, J. B., SEARLE, L. <AP. J., 188, 71>
THE ENERGY DISTRIBUTION OF THE VERY RED STAR IN NGC 6231.

740208 HARVEY, P. M. <AP. J., 188, 95>
INFRARED VARIABILITY OF V1016 CYGNI.

740209 WEBSTER, B. L., GLASS, I. S. <M. N. R. A. S., 166, 491>
THE COOLEST WOLF-RAYET STARS.

740210 OKE, J. B. <AP. J. SUPPL., 27, 21>
ABSOLUTE SPECTRAL ENERGY DISTRIBUTIONS FOR WHITE DWARFS.

740211 PERINOTTO, M. <ASTR. AP., 35, 293>
PHOTOELECTRIC SPECTROPHOTOMETRY OF PLANETARY NEBULAE.

740212 ANDRILLAT, Y., DUCHESNE, M. <ASTR. AP., 35, 467>
MORPHOLOGIE DE LA REGION CENTRALE DE LA NEBULEUSE D'ORION DANS LE PROCHE INFRAROUGE.

740301 DYCK, H. M., CAPPS, R. W., BEICHMAN, C. A. <AP. J. (LETTERS), 188, L103>
INFRARED POLARIZATION OF THE GALACTIC NUCLEUS.

740302 PERSSON, S. E., FROGEL, J. A. <AP. J., 188, 523>
SPECTROPHOTOMETRIC OBSERVATIONS OF THE COMPACT HII REGION K3-50 AND OF NGC 6857.

740303 TREFFERS, R. R., COHEN, M. <AP. J., 188, 545>
HIGH-RESOLUTION SPECTRA OF COOL STARS IN THE 10- AND 20-MICRON REGIONS.

740304 KOLOTILOV, E. A., NOSKOVA, R. I. <SOV. AST., 17, 611>
ABSOLUTE SPECTROPHOTOMETRY OF THE PLANETARY NEBULA NGC 7027 IN THE WAVELENGTH RANGE 7000-10, 400A.

740305 NORDH, H. L., OLOFSSON, S. G. <ASTR. AP., 31, 343>
ANALYSIS OF THE ENERGY DISTRIBUTION OF THE BE STAR PI AQR.

740401 DYCK, H. M., LOCKWOOD, G. W., CAPPS, R. W. <AP. J., 189, 89>
INFRARED FLUXES, SPECTRAL TYPES, AND TEMPERATURES FOR VERY COOL STARS.

740402 ADE, P. A. R., CLEGG, P. E., RATHER, J. D. G. <AP. J. (LETTERS), 189, L23>
1-MILLIMETER OBSERVATIONS OF THE GALACTIC HII REGIONS M42 AND DR 21.

740403 MERRILL, K. M., SOIFER, B. T. <AP. J. (LETTERS), 189, L27>
SPECTROPHOTOMETRIC OBSERVATIONS OF A HIGHLY ABSORBED OBJECT IN CYGNUS.

740404 HARVEY, P. M., GATLEY, I., WERNER, M. W., ELIAS, J. H., EVANS II, N. J., ZUCKERMAN, B., MORRIS, G., SATO, T., LITVAK, M. M. <AP. J. (LETTERS), 189, L87>
DUST AND GAS IN THE ORION MOLECULAR CLOUD: OBSERVATIONS OF 1-MM CONTINUUM AND 2-CM H_2CO EMISSION.

740405 GLASS, I. S. <M. N. A. S. S. A., 33, 53>
JHKL PHOTOMETRY OF 145 SOUTHERN STARS.

740406 FEAST, M. W., GLASS, I. S. <M. N. R. A. S., 167, 81>
INFRA-RED PHOTOMETRY OF SOME OLD NOVAE.

740407 AITKEN, D. K., JONES, B. <M. N. R. A. S., 167, 11P>
OBSERVATIONS OF NE II IN THE COMPACT HII REGION G333.6-0.2.

740408 HARVEY, P. M., BECHIS, K. P., WILSON, W. J., BALL, J. A. <AP. J. SUPPL., 27, 331>
TIME VARIATIONS IN THE OH MICROWAVE AND INFRARED EMISSION FROM LATE-TYPE STARS.

740409 KUHI, L. V. <ASTR. AP. SUPPL., 15, 47>
SPECTRAL ENERGY DISTRIBUTIONS OF T TAURI STARS.

740501 GEHRELS, T. <A. J., 79, 590>
WAVELENGTH DEPENDENCE OF POLARIZATION. XXVII. INTERSTELLAR POLARIZATION FROM 0.22 TO 2.2 MICRONS.

740502 GLASS, I. S., PENSTON, M. V. <M. N. R. A. S., 167, 237>
AN INFRARED SURVEY OF RW AURIGAE STARS.

740503 ALLEN, D. A., GLASS, I. S. <M. N. R. A. S., 167, 337>
INFRARED PHOTOMETRY OF SOUTHERN EMISSION-LINE STARS.

740504 CONNES, P., MICHEL, G. <AP. J. (LETTERS), 190, L29>
HIGH-RESOLUTION FOURIER SPECTRA OF STARS AND PLANETS.

740505 SCHILD, R. E., CHAFFEE, F., FROGEL, J. A., PERSSON, S. E. <AP. J., 190, 73>
THE NATURE OF INFRARED EXCESSES IN EXTREME BE STARS.

740506 BAUMERT, J. H. <AP. J., 190, 85>
MEAN ABSOLUTE MAGNITUDES OF CARBON STARS AND RELATED OBJECTS.

740507 VANGENDEREN, A. M., GLASS, I. S., FEAST, M. W. <M. N. R. A. S., 167, 283>
THE LONG PERIOD, HIGH LATITUDE, ECLIPSING SYSTEMS V748 CEN (-CEN X-4?) AND BL TEL.

740508 OINAS, V. <AP. J. SUPPL., 27, 391>
STRONG-LINE K STARS. I. PHOTOMETRY.

740509 LEMKE, D., LOW, F. J., THUM, C. <ASTR. AP., 32, 231>
INFRARED MAP OF THE ORION NEBULA.

740601 VEEDER, G. J. <A. J., 79, 702>
OLD DISK FLARE STARS.

740602 SUTTON, E. C., BECKLIN, E. E., NEUGEBAUER, G. <AP. J. (LETTERS), 190, L69>
34-MICRON OBSERVATIONS OF ETA CARINAE, G333.6-0.2, AND THE GALACTIC CENTER.

740603 HUMPHREYS, R. M., NEY, E. P. <AP. J., 190, 339>
INFRARED STARS IN BINARY SYSTEMS.

740604 MORGAN, T. H., POTTER, A. E., KONDO, Y. <AP. J., 190, 349>
COMPLEX INFRARED EMISSION FEATURES IN THE SPECTRUM OF BETA LYRAE.

740605 JAMESON, R. F., LONGMORE, A. J., MCLINN, J. A., WOOLF, N. J. <AP. J., 190, 353>
INFRARED EMISSION BY DUST IN NGC 1068 AND THREE PLANETARY NEBULAE.

740606 NEY, E. P., HUMPHREYS, R. M. <P. A. S. P., 86, 304>
BM SCORPII AND A POSSIBLE CLUSTER OF INFRARED SOURCES.

740701 KLEINMANN, D. E., WRIGHT, E. L. <AP. J. (LETTERS), 191, L19>
10-MICRON OBSERVATIONS OF SOUTHERN-HEMISPHERE GALAXIES.

740702 GEZARI, D. Y., JOYCE, R. R., RIGHINI, G., SIMON, M. <AP. J. (LETTERS), 191, L33>
350-MICRON MAPPING OF THE ORION MOLECULAR CLOUD.

740703 SOIFER, B. T., HUDSON, H. S. <AP. J. (LETTERS), 191, L83>
SUBMILLIMETER OBSERVATIONS OF THE ORION NEBULA AND NGC 2024.

740704 STROM, K. M., STROM, S. E., KINMAN, T. D. <AP. J. (LETTERS), 191, L93>
OPTICAL POLARIZATION OF SELECTED HERBIG-HARO OBJECTS.

740705 STRECKER, D. W., NEY, E. P. <A. J., 79, 797>
INFRARED OBSERVATIONS OF ANONYMOUS IRC SOURCES.

740706 STROM, S. E., GRASDALEN, G. L., STROM, K. M. <AP. J., 191, 111>
INFRARED AND OPTICAL OBSERVATIONS OF HERBIG-HARO OBJECTS.

740707 SCHWARTZ, R. D. <AP. J., 191, 419>
THE T TAURI EMISSION NEBULA.

740708 ALLEN, D. A. <M. N. R. A. S., 168, 1>
INFRARED OBSERVATIONS OF NORTHERN EMISSION-LINE STARS.

740709 ANDREWS, P. J., GLASS, I. S., HAWARDEN, T. G. <M. N. R. A. S., 168, 7P>
PHOTOMETRY OF AP LIB AND PKS 0521-36.

740710 GAHM, G. F., NORDH, H. L., OLOFSSON, S. G., CARLBORG, N. C. J. <ASTR. AP., 33, 399>
SIMULTANEOUS SPECTROSCOPIC AND PHOTOELECTRIC OBSERVATIONS OF THE T TAURI STAR RU LUPI.

740711 OLTHOF, H. <ASTR. AP., 33, 471>
MULTICOLOUR FAR INFRARED PHOTOMETRY OF GALACTIC H II REGIONS.

740801 GATLEY, I., BECKLIN, E. E., MATTHEWS, K., NEUGEBAUER, G., PENSTON, M. V., SCOVILLE, N. Z. <AP. J. (LETTERS), 191, L121>
A NEW INFRARED COMPLEX AND MOLECULAR CLOUD IN ORION.

740802 KNACKE, R. F., CAPPS, R. W. <AP. J. (LETTERS), 192, L19>
INFRARED POLARIZATION OF NGC 1068.

740803 FAZIO, G. G., KLEINMANN, D. E., NOYES, R. W., WRIGHT, E. L., ZEILIK II, M., LOW, F. J. <AP. J. (LETTERS), 192, L23>
A HIGH-RESOLUTION MAP OF THE ORION NEBULA REGION AT FAR-INFRARED WAVELENGTHS.

740804 WERNER, M. W., ELIAS, J. H., GEZARI, D. Y., WESTBROOK, W. E. <AP. J. (LETTERS), 192, L31>
1-MILLIMETER CONTINUUM RADIATION FROM ORION MOLECULAR CLOUD 2.

740805 ZAPPALA, R. R., BECKLIN, E. E., MATTHEWS, K., NEUGEBAUER, G. <AP. J., 192, 109>
ANGULAR DIAMETER OF IRC +10011 AT 2.2, 10, AND 20 MICRONS

740806 LOCKWOOD, G. W. <AP. J., 192, 113>
NEAR-INFRARED PHOTOMETRY OF UNIDENTIFIED IRC STARS. II.

740807 GEHRZ, R. D., HACKWELL, J. A., JONES, T. W. <AP. J., 191, 675>
INFRARED OBSERVATIONS OF BE STARS FROM 2.3 TO 19.5 MICRONS.

740808 GLASS, I. S. <M. N. R. A. S., 168, 249>
JHKL PHOTOMETRY OF LMC STARS.

740809 HUMPHREYS, R. M., NEY, E. P. <P. A. S. P., 86, 444>
IRC+60370 AND THE INFRARED RADIATION FROM LUMINOUS G AND K SUPERGIANTS.

740810 CIATTI, F., D'ODORICO, S., MAMMANO, A. <ASTR. AP., 34, 181>
PROPERTIES AND EVOLUTION OF BQ() STARS.

740811 LUNEL, M., BERGEAT, J., SIBILLE, F., LORTET-ZUCKERMAN, M. C. <ASTR. AP., 34, 299>
INFRARED SOURCES IN SHARPLESS 157.

740812 SWINGS, J. P. <ASTR. AP., 34, 333>
SIMILARITIES IN THE SPECTRA OF THREE SOUTHERN PECULIAR EMISSION LINE STARS WITH INFRARED EXCESS: HD 45677, HD 87643 AND GG CARINAE (HD 94878).

740813 CIATTI, F., ROSINO, L. <ASTR. AP. SUPPL., 16, 305>
PHOTOGRAPHIC AND SPECTROSCOPIC OBSERVATIONS OF N AQL 1970, N CYG 1970 AND N SCT 1970.

740901 SZKODY, P. <AP. J. (LETTERS), 192, L75>
INFRARED PHOTOMETRY OF SS CYGNI AND RX ANDROMEDAE NEAR MAXIMUM.

740902 HACKWELL, J. A., BOPP, B. W., GEHRZ, R. D. <AP. J. (LETTERS), 192, L79>
INFRARED OBSERVATIONS OF BD -10 4662.

740903 HALL, R. T. <SAMSO-TR-74-212>
A CATALOG OF 10-MICRON CELESTIAL OBJECTS.

740904 RIEKE, G. H., KINMAN, T. D. <AP. J. (LETTERS), 192, L115>
CORRELATED OPTICAL AND INFRARED BEHAVIOR OF OJ 287 AND SIMILAR RADIO SOURCES.

740905 BECKLIN, E. E., HAWKINS, F. J., MASON, K. O., MATTHEWS, K., NEUGEBAUER, G., PACKMAN, D., SANFORD, P. W., SCHUPLER, B. R., STARK, A., WYNN-WILLIAMS, C. G. <AP. J. (LETTERS), 192, L119>
INFRARED, RADIO, AND X-RAY OBSERVATIONS OF CYGNUS X-3.

740906 FROGEL, J. A., PERSSON, S. E. <AP. J., 192, 351>
COMPACT INFRARED SOURCES ASSOCIATED WITH SOUTHERN HII REGIONS.

740907 HACKWELL, J. A., GEHRZ, R. D., SMITH, J. R. <AP. J., 192, 383>
INFRARED PHOTOMETRY OF WOLF-RAYET STARS FROM 2.3 TO 23 MICRONS.

740908 HARPER JR., D. A. <AP. J., 192, 557>
FAR-INFRARED EMISSION FROM HII REGIONS. II. MULTICOLOR PHOTOMETRY OF SELECTED SOURCES AND 2.2 ARC MINUTE RESOLUTION MAPS OF M42 AND NGC 2024.

740909 VAN BREDA, I. G., GLASS, I. S., WHITTET, D. C. B. <M. N. R. A. S., 168, 551>
THE EXTINCTION CURVES OF HD 92964 AND HD 147889.

740910 KHROMOV, G. S. <SOV. AST., 18, 195>
INFRARED RADIATION OF PLANETARY NEBULAE. II. NEW AND REVISED OBSERVATIONS AT 1.0-2.5 MICRONS.

741001 GRASDALEN, G. L. <A. J., 79, 1047>
NEAR-INFRARED MAGNITUDES AND (V-K) COLORS OF GLOBULAR CLUSTERS.

741002 SIMON, T. <A. J., 79, 1054>
BROAD-BAND 20-MICRON PHOTOMETRY OF 63 STARS.

741003 BLANCO, V. M., HANSEN, O. L. <A. J., 79, 1052>
CLASSIFICATION OF UNIDENTIFIED SOURCES FROM A 2-MICRON SOUTHERN SKY SURVEY.

741004 VEEDER, G. J. <A. J., 79, 1056>
LUMINOSITIES AND TEMPERATURES OF M DWARF STARS FROM INFRARED PHOTOMETRY.

741005 STROM, S. E., STROM, K. M., GRASDALEN, G. L., CAPPS, R. W. <AP. J. (LETTERS), 193, L7>
INFRARED OBSERVATIONS OF HII REGIONS IN EXTERNAL GALAXIES.

741006 FAWLEY, W. M., COHEN, M. <AP. J., 193, 367>
THE OPEN CLUSTER NGC 7419 AND ITS M7 SUPERGIANT IRC+60375.

741007 GRASDALEN, G. L. <AP. J., 193, 373>
AN INFRARED STUDY OF NGC 2024.

741008 GEHRZ, R. D., HACKWELL, J. A. <AP. J., 193, 385>
NEW INFRARED MEASUREMENTS OF W VIRGINIS STARS.

741009 COHEN, M., BARLOW, M. J. <AP. J., 193, 401>
AN INFRARED PHOTOMETRIC SURVEY OF PLANETARY NEBULAE.

741010 RIEKE, G. H. <AP. J. (LETTERS), 193, L81>
THE SPECTRUM OF VI CYGNI NO. 12 NEAR 10 MICRONS.

741011 LOCKWOOD, G. W. <AP. J., 193, 103>
STELLAR ENERGY DISTRIBUTIONS IN AN INFRARED CLUSTER IN ARA.

741012 THOMPSON, R. I., JOHNSON, H. L. <AP. J., 193, 147>
A LOWER LIMIT ON THE CARBON-12/CARBON-13 RATIO IN ALPHA HERCULIS.

741013 PIPHER, J. L., GRASDALEN, G. L., SOIFER, B. T. <AP. J., 193, 283>
INFRARED OBSERVATIONS OF THE RADIO SOURCE G30.8-0.0 IN THE W43 COMPLEX.

741014 MURDIN, P., PENSTON, M. J., PENSTON, M. V., GLASS, I. S., SANFORD, P. W., HAWKINS, F. J., MASON, K. O., WILLMORE, A. P. <M. N. R. A. S., 169, 25>
OPTICAL OBSERVATIONS OF STARS NEAR COPERNICUS X-RAY POSITIONS.

741015 STROM, S. E., STROM, K. M., CARRASCO, L. <P. A. S. P., 86, 798>
A STUDY OF THE YOUNG CLUSTER IC 348.

741016 BEER, R., LAMBERT, D. L., SNEDEN, C. <P. A. S. P., 86, 806>
THE SILICON MONOXIDE RADICAL AND THE ATMOSPHERE OF ALPHA ORIONIS.

741017 COHEN, M. <P. A. S. P., 86, 813>
INFRARED OBSERVATIONS OF NEW COMETARY NEBULAE.

741101 BAUMERT, J. H. <A. J., 79, 1287>
COMPARISON OF A GENERAL CATALOGUE OF COOL CARBON STARS AND THE TWO-MICRON SKY SURVEY.

741102 HOUCK, J. R., SCHAACK, D. F., REED, R. A. <AP. J. (LETTERS), 193, L139>
20 TO 40 MICRON SPECTROSCOPY OF THE ORION NEBULA.

741103 KINMAN, T. D., GRASDALEN, G. L., RIEKE, G. H. <AP. J. (LETTERS), 194, L1>
OPTICAL AND INFRARED OBSERVATIONS OF THE JET OF M87.

741104 FRIEDLANDER, M. W., GOEBEL, J. H., JOSEPH, R. D. <AP. J. (LETTERS), 194, L5>
DETECTION OF NEW CELESTIAL OBJECTS AT FAR-INFRARED WAVELENGTHS.

741105 HACKWELL, J. A., GEHRZ, R. D. <AP. J., 194, 49>
INFRARED PHOTOMETRY OF HIGH-LUMINOSITY SUPERGIANTS EARLIER THAN M AND THE INTERSTELLAR EXTINCTION LAW.

741106 DYCK, H. M., BEICHMAN, C. A. <AP. J., 194, 57>
OBSERVATIONS OF INFRARED POLARIZATION IN THE ORION NEBULA.

741107 MORRISON, D. <AP. J., 194, 203>
RADIOMETRIC DIAMETERS AND ALBEDOS OF 40 ASTEROIDS.

741108 COHEN, M. <M. N. R. A. S., 169, 257>
INFRARED OBSERVATIONS OF YOUNG STARS-V. THE FAINT MEMBERS OF THE ORION POPULATION.

741109 PENSTON, M. V., PENSTON, M. J., SELMES, R. A., BECKLIN, E. E., NEUGEBAUER, G. <M. N. R. A. S., 169, 357>
BROADBAND OPTICAL AND INFRARED OBSERVATIONS OF SEYFERT GALAXIES.

741110 COHEN, M., FAWLEY, W. M. <M. N. R. A. S., 169, 31P>
TEN MICRON OBSERVATIONS OF GLOBULAR CLUSTERS.

741111 AITKEN, D. K., JONES, B., PENMAN, J. M. <M. N. R. A. S., 169, 35P>
DETECTION OF IONIZED NEON IN THE GALACTIC CENTRE.

741112 CHURMS, J., FEAST, M. W., GLASS, I. S., HARDING, G. A., LLOYD EVANS, T., MARTIN, W. L. <M. N. R. A. S., 169, 39P>
NEBULOSITY ASSOCIATED WITH THE POWERFUL INFRARED AND RADIO SOURCE G333.6-0.2.

741113 WARD, D. B., HARWIT, M. <NATURE, 252, 27>
OBSERVATIONS OF THE ORION NEBULA AT 100 MICRONS.

741201 STRECKER, D. W., NEY, E. P. <A. J., 79, 1410>
0.9-18-MICRON PHOTOMETRY OF THE 14 CIT OBJECTS.

741202 GEHRZ, R. D., HACKWELL, J. A. <AP. J., 194, 619>
CIRCUMSTELLAR DUST EMISSION FROM WC9 STARS.

741203 HUMPHREYS, R. M., NEY, E. P. <AP. J., 194, 623>
VISUAL AND INFRARED OBSERVATIONS OF LATE-TYPE SUPERGIANTS IN THE SOUTHERN SKY.

741204 PERSSON, S. E., FROGEL, J. A. <P. A. S. P., 86, 985>
1.2 MICRON TO 3.5 MICRON PHOTOMETRY OF EIGHT OPTICAL H II REGIONS.

741205 BOPP, B. W., GEHRZ, R. D., HACKWELL, J. A. <P. A. S. P., 86, 989>
INFRARED OBSERVATIONS OF LATE-TYPE DWARF STARS.

749901 MARKARIAN, B. E., LIPOVETSKY, V. A. <ASTROFIZIKA, 10, 302>
GALAXIES WITH ULTRAVIOLET CONTINUUM. VII.

749902 ANDERSSON, C., JOHANSSON, L. E. B., GOSS, W. M., WINNBERG, A., NGUYEN-QUANG-RIEU <ASTR. AP., 30, 475>
OH 26.5+0.6 - A STRONG OH SOURCE AT 1612 MHZ.

749903 STIENON, F. M., CHARTRAN III, M. R., SHAO, C. Y. <A. J., 79, 47>
THE EMISSION-LINE VARIABLE HBV 475.

749904 HERBIG, G. H. <LICK OBS. BULL., 658>
DRAFT CATALOG OF HERBIG-HARO OBJECTS.

749905 CAHN, J. H., RUBIN, R. H. <A. J., 79, 128>
INTERFEROMETRIC SURVEY OF PLANETARY NEBULAE.

749906 HOLMBERG, E. B., LAUBERTS, A., SCHUSTER, H. -E., WEST, R. M. <ASTR. AP. SUPPL., 18, 463>
THE ESO/UPPSALA SURVEY OF THE ESO(B) ATLAS OF THE SOUTHERN SKY. I.

749907 HOLMBERG, E. B., LAUBERTS, A., SCHUSTER, H. -E., WEST, R. M. <ASTR. AP. SUPPL., 18, 491>
THE ESO/UPPSALA SURVEY OF THE ESO(B) ATLAS OF THE SOUTHERN SKY. II.

749908 ANDREWS, A. D. <CONTR. ARMAGH OBS., 1, 101>
CATALOGUE OF PHOTOMETRIC AND ASTROMETRIC DATA FOR 4117 STARS IN THE ORION NEBULA AGGREGATE.

749909 KUKARKIN, B. V., KHOLOPOV, P. N., EFREMOV, YU. N., KUKARKINA, N. P., KUROCHKIN, N. E., MEDVEDEVA, G. I., PEROVA, N. B., PSKOVSKY, YU. P., FEDOROVICH, V. P., FROLOV, M. S. <PUBL. OFFICE NAUKA, MOSCOW>
GENERAL CATALOGUE OF VARIABLE STARS. SECOND SUPPLEMENT.

750001 MILONE, E. F. <MULT. PER. VAR. STARS, IAU COLL. NO. 29>
INFRARED PHOTOMETRY OF ECLIPSING BINARIES WITH CHANGING LIGHT CURVES.

750101 FROGEL, J. A., PERSSON, S. E., AARONSON, M., BECKLIN, E. E., MATTHEWS, K., NEUGEBAUER, G. <AP. J. (LETTERS), 195, L15>
STELLAR CONTENT OF THE NUCLEI OF ELLIPTICAL GALAXIES DETERMINED FROM 2.3-MICRON CO BAND STRENGTHS.

750102 RIGHINI, G., SIMON, M., JOYCE, R. R., GEZARI, D. Y. <AP. J. (LETTERS), 195, L77>
350-MICRON MAPPING OF SAGITTARIUS B2.

750103 LOCKWOOD, G. W., DYCK, H. M., RIDGWAY, S. T. <AP. J., 195, 385>
THE COMPOSITE SPECTRUM AND ENERGY DISTRIBUTION OF XX OPHIUCHI.

750104 FORREST, W. J., GILLETT, F. C., STEIN, W. A. <AP. J., 195, 423>
CIRCUMSTELLAR GRAINS AND THE INTRINSIC POLARIZATION OF STARLIGHT.

750105 VITRICHENKO, E. A., VOLKOV, I. V., SHANIN, G. I., SHEVCHENKO, V. S., SHCHERBAKOV, A. G. <SOV. AST., 18, 513>
INFRARED SPECTROSCOPY WITH A CONTACT IMAGE CONVERTER. 1.EXPERIMENTAL PROCEDURE.

750106 SIMON, T., DYCK, H. M. <NATURE, 253, 101>
SILICATE ABSORPTION AT 18 MICRONS IN TWO PECULIAR INFRARED SOURCES.

750201 GRASDALEN, G. L., JOYCE, R. R., KNACKE, R. F., STROM, S. E., STROM, K. M. <A. J., 80, 117>
PHOTOMETRIC STUDY OF THE CHAMAELEON T-ASSOCIATION.

750202 BREGMAN, J. D., RANK, D. M. <AP. J. (LETTERS), 195, L125>
IDENTIFICATION OF THE 890 CM-1 CARBONATE SIGNATURE IN NGC 7027.

750203 HARVEY, P. M., HOFFMANN, W. F., CAMPBELL, M. F. <AP. J. (LETTERS), 196, L31>
FAR-INFRARED OBSERVATIONS OF W51 WITH HIGH SPATIAL RESOLUTION.

750204 GRASDALEN, G. L. <AP. J., 195, 605>
(V-K) COLORS OF GALAXIES: STATISTICAL DIFFERENCES BETWEEN SPIRALS AND ELLIPTICALS AND THE COLOR-DIAMETER RELATION FOR ELLIPTICAL GALAXIES.

750205 COHEN, M., ANDERSON, C. M., COWLEY, A., COYNE S. J., G. V., FAWLEY, W. M., GULL, T. R., HARLAN, E. A., HERBIG, G. H.,HOLDEN, F., HUDSON, H. S., JAKOUBEK, R. O., JOHNSON, H. M., SCHIFFER III, F. H., SOIFER, B. T., ZUCKERMAN, B. <AP. J., 196, 179>
THE PECULIAR OBJECT HD 44179 ("THE RED RECTANGLE").

750206 SERKOWSKI, K., MATHEWSON, D. S., FORD, V. L. <AP. J., 196, 261>
WAVELENGTH DEPENDENCE OF INTERSTELLAR POLARIZATION AND RATIO OF TOTAL TO SELECTIVE EXTINCTION.

750207 STEIN, W. A. <P. A. S. P., 87, 5>
RECENT REVELATIONS OF INFRARED ASTRONOMY.

750208 MCNAMARA, B. J. <P. A. S. P., 87, 97>
PRE-MAIN-SEQUENCE MASSES AND EVOLUTION IN NGC 2264.

750209 MIHALAS, D., FROST, S. A., LOCKWOOD, G. W. <P. A. S. P., 87, 153>
OBSERVATIONS OF THE C III 8500(3S1S-3P1P) LINE IN O AND OF STARS.

750210 TREFFERS, R. R. <ASTR. AP., 38, 345>
A FOURIER TRANSFORM SPECTROMETER FOR OBSERVATIONS OF STARS IN THE INTERMEDIATE INFRARED.

750211 CIATTI, F., MAMMANO, A. <ASTR. AP., 38, 435>
EJECTION OF NEBULAE BY BQ RADIOSTARS WITH INFRARED EXCESS.

750212 DANZIGER, I. J. <ASTR. AP., 38, 475>
THE INFRARED CONTINUUM OF THE COMPACT PLANETARY NEBULA NGC 6210.

750213 MAMMANO, A., CIATTI, F. <ASTR. AP., 39, 405>
THE SYMBIOTIC BINARY V1016 CYGNI, EARLY STAGE OF A PLANETARY NEBULA.

750214 GLASS, I. S., ALLEN, D. A. <OBSERVATORY, 95, 27>
INFRA-RED SOURCES NEAR COD-42 11721.

750301 STROM, K. M., STROM, S. E., CARRASCO, L., VRBA, F. J. <AP. J., 196, 489>
M78: AN ACTIVE REGION OF STAR FORMATION IN THE DARK CLOUD LYNDS 1630.

750302 ALLEN, D. A., GLASS, I. S. <M. N. R. A. S., 170, 579>
EMISSION-LINE STARS WITH INFRARED DUST EMISSION: IMPLICATIONS OF THE GALACTIC DISTRIBUTION.

750401 VRBA, F. J., STROM, K. M., STROM, S. E., GRASDALEN, G. L. <AP. J., 197, 77>
FURTHER STUDY OF THE STELLAR CLUSTER EMBEDDED IN THE OPHIUCHUS DARK CLOUD COMPLEX.

750402 SHIELDS, G. A., OKE, J. B. <AP. J., 197, 5>
THE EMISSION-LINE SPECTRUM OF NGC 1068.

750403 RIEKE, G. H., LOW, F. J. <AP. J., 197, 17>
THE NUCLEUS OF NGC 253.

750404 FROGEL, J. A., PERSSON, S. E. <AP. J., 197, 351>
INFRARED EMISSION FROM OH 284.2-0.8.

750405 PENSTON, M. V., HUNTER, J. K. <M. N. R. A. S., 171, 219>
FURTHER OBSERVATIONS OF THE ORION NEBULA CLUSTER.

750406 NOSKOVA, R. I. <ASTROFIZIKA, 11, 169>
SPECTRUM OF PLANETARY NEBULA IC 4997 IN THE NEAR INFRARED REGION.

750407 SIMON, T. <P. A. S. P., 87, 317>
INFRARED LIGHT CURVES FOR V1057 CYGNI (1971-74).

750501 STEPHENSON, C. B. <A. J., 80, 404>
SPECTRAL TYPES FOR FOUR SUSPECTED CARBON STARS OF THE TWO-MICRON SKY SURVEY.

750502 RUSSELL, R. W., SOIFER, B. T., FORREST, W. J. <AP. J. (LETTERS), 198, L41>
SPECTROPHOTOMETRIC OBSERVATIONS OF MU CEPHEI AND THE MOON FROM 4 TO 8 MICRONS.

750503 HAYES, D. S., LATHAM, D. W., HAYES, S. H. <AP. J., 197, 587>
MEASUREMENTS OF THE MONOCHROMATIC FLUX FROM VEGA IN THE NEAR-INFRARED.

750504 OKE, J. B., SCHWARZSCHILD, M. <AP. J., 198, 63>
ABSOLUTE SPECTROPHOTOMETRY IN M31 AND M32.

750505 COHEN, M., BARLOW, M. J., KUHI, L. V. <ASTR. AP., 40, 291>
WOLF-RAYET STARS. VI. THE NATURE OF THE OPTICAL AND INFRARED CONTINUA.

750506 BERGEAT, J., SIBILLE, F., LUNEL, M. <ASTR. AP., 40, 347>
AN INFRARED POINT-SOURCE IN SHARPLESS 149.

750507 SIBILLE, F., BERGEAT, J., LUNEL, M., KANDEL, R. <ASTR. AP., 40, 441>
INFRARED OBSERVATIONS OF SHARPLESS 2-106, A POSSIBLE LOCATION FOR STAR FORMATION.

750601 STRECKER, D. W. <A. J., 80, 451>
VARIABILITY OF R CRB AND NML CYG AT 3.5 MICRONS.

750602 GILLETT, F. C., KLEINMANN, D. E., WRIGHT, E. L., CAPPS, R. W. <AP. J. (LETTERS), 198, L65>
OBSERVATIONS OF M82 AND NGC 253 AT 8-13 MICRONS.

750603 NEY, E. P., MERRILL, K. M., BECKLIN, E. E., NEUGEBAUER, G., WYNN-WILLIAMS, C. G. <AP. J. (LETTERS), 198, L129>
STUDIES OF THE INFRARED SOURCE CRL 2688.

750604 MEISEL, D. D., BERG, R. A. <AP. J., 198, 551>
HELIUM 10830A IN ALPHA VIRGINIS A AND B.

750605 CHIU, B. C., MORRISON, P., SARTORI, L. <AP. J., 198, 617>
THE LIGHT OF THE SUPERNOVA OUTBURST. II. THE CASE OF SUPERNOVA 1972E.

750606 ULRICH, M. -H., KINMAN, T. D., LYNDS, C. R., RIEKE, G. H., EKERS, R. D. <AP. J., 198, 261>
NONTHERMAL CONTINUUM RADIATION IN THREE ELLIPTICAL GALAXIES.

750607 GLASS, I. S. <M. N. R. A. S., 171, 19P>
INTERMEDIATE INFRARED COLOURS OF M-DWARF STARS.

750608 COHEN, M. <P. A. S. P., 87, 421>
INFRARED OBSERVATIONS OF LATE-TYPE STARS IN NEBULAE.

750609 HYLAND, A. R., MOULD, J. R., ROBINSON, G., THOMAS, J. A. <P. A. S. P., 87, 439>
INFRARED OBSERVATIONS AND THE EFFECTIVE TEMPERATURE OF THE PECULIAR STAR HD 101065.

750610 ANDRILLAT, Y., BARANNE, A., HOUZIAUX, L. <ASTR. AP., 41, 99>
SPECTRES DE QUELQUES NEBULEUSES PLANETAIRES ENTRE 8000 ET 11000 A.

750611 ANDRILLAT, Y., VREUX, J. M. <ASTR. AP., 41, 133>
SPECTRES D'ETOILES DE TYPE O ET DE TYPE WOLF-RAYET ENTRE 0, 8 ET 1, 1 MICRONS.

750701 RIEKE, G. H., LOW, F. J. <AP. J. (LETTERS), 199, L13>
THE INFRARED SPECTRUM OF NGC 1068.

750702 BRANDSHAFT, D., MCLAREN, R. A., WERNER, M. W. <AP. J. (LETTERS), 199, L115>
SPECTROSCOPY OF THE ORION NEBULA FROM 80 TO 135 MICRONS.

750703 GLASS, I. S., PENSTON, M. V. <M. N. R. A. S., 172, 227>
INFRARED PHOTOMETRY IN THE R CRA ASSOCIATION.

750704 SMYTH, M. J., DOW, M. J., NAPIER, W. MCD. <M. N. R. A. S., 172, 235>
INFRARED LIGHT CURVES OF ALGOL.

750705 ALLEN, D. A., PENSTON, M. V. <M. N. R. A. S., 172, 245>
INFRARED SOURCES IN OBSCURED REGIONS.

750706 ZEILIK II, M., KLEINMANN, D. E., WRIGHT, E. L. <AP. J., 199, 401>
G45.5+0.1 AND G45.1+0.1: COMPACT INFRARED SOURCES.

750707 AITKEN, D. K., JONES, B. <M. N. R. A. S., 172, 141>
THE INFRARED SPECTRUM AND STRUCTURE OF ETA CARINAE.

750708 THUM, C., LEMKE, D. <ASTR. AP., 41, 467>
INFRARED MEASUREMENTS ON SEVERAL SOURCES IN THE DR-21 REGION.

750801 FAZIO, G. G., KLEINMANN, D. E., NOYES, R. W., WRIGHT, E. L., ZEILIK II, M., LOW, F. J. <AP. J. (LETTERS), 199, L177>
A HIGH-RESOLUTION MAP OF THE W3 REGION AT FAR-INFRARED WAVELENGTHS.

750802 FORREST, W. J., MERRILL, K. M., RUSSELL, R. W., SOIFER, B. T. <AP. J. (LETTERS), 199, L181>
SPECTROPHOTOMETRY OF CRL 2688 FROM 2 TO 24 MICRONS.

750803 MERRILL, K. M., SOIFER, B. T., RUSSELL, R. W. <AP. J. (LETTERS), 200, L37>
THE 2-4 MICRON SPECTRUM OF NGC 7027.

750804 WARD, D. B. <AP. J. (LETTERS), 200, L41>
FAR-INFRARED SPECTROSCOPY OF THE ORION NEBULA.

750805 EMERSON, J. P., FURNISS, I., JENNINGS, R. E. <M. N. R. A. S., 172, 411>
40-350 MICRON EMISSION FROM NGC 2023.

750806 SIMON, T., DYCK, H. M. <M. N. R. A. S., 172, 19P>
INFRARED PHOTOMETRY OF NGC 1068 AT 25 AND 33 MICRONS.

750807 SOIFER, B. T., PIPHER, J. L. <AP. J., 199, 663>
INFRARED PHOTOMETRIC AND SPECTROPHOTOMETRIC OBSERVATIONS OF THE GALACTIC HII REGION G29.9-0.0.

750901 COYNE S. J., G. V., MCLEAN, I. S. <A. J., 80, 702>
WAVELENGTH DEPENDENCE OF POLARIZATION XXX. INTRINSIC POLARIZATION IN PHI PERSEI.

750902 RIEKE, G. H., LOW, F. J. <AP. J. (LETTERS), 200, L67>
MEASUREMENTS OF GALACTIC NUCLEI AT 34 MICRONS.

750903 BECKLIN, E. E., NEUGEBAUER, G. <AP. J. (LETTERS), 200, L71>
HIGH-RESOLUTION MAPS OF THE GALACTIC CENTER AT 2.2 AND 10-MICRONS.

750904 FROGEL, J. A., PERSSON, S. E., AARONSON, M., BECKLIN, E. E., MATTHEWS, K., NEUGEBAUER, G. <AP. J. (LETTERS), 200, L123>
THE V-(2.2 MICRON) COLORS OF ELLIPTICAL GALAXIES.

750905 GILLETT, F. C., FORREST, W. J., MERRILL, K. M., CAPPS, R. W.,SOIFER, B. T. <AP. J., 200, 609>
THE 8-13 MICRON SPECTRA OF COMPACT HII REGIONS.

750906 GREENE, A. E., WING, R. F. <AP. J., 200, 688>
THE TEMPERATURE AND SPECTRUM OF VX AQUILAE.

750907 QUERCI, M., QUERCI, F. <ASTR. AP., 42, 329>
THE INFRARED SPECTRUM OF THE CARBON STARS UU AUR AND Y CVN FROM 4000 TO 6800 CM-1.

751001 SCHMIDT, G. D., VRBA, F. J. <AP. J. (LETTERS), 201, L33>
THE NATURE OF HERBIG-HARO OBJECTS 1 AND 2: COMPACT EMISSION NEBULAE.

751002 HAGEN, W., SIMON, T., DYCK, H. M. <AP. J. (LETTERS), 201, L81>
POSSIBLE IDENTIFICATION OF A CIRCUMSTELLAR 33-MICRON SILICATE EMISSION BAND IN COOL-STAR SPECTRA.

751003 KLEINMANN, S. G., LEBOFSKY, M. J. <AP. J. (LETTERS), 201, L91>
AN UNUSUAL NEBULA NEAR UOA 27.

751004 VOELKER, K. <ASTR. AP. SUPPL., 22, 1>
INFRARED OBSERVATIONS OF THE ASSOCIATION *CYG OB* 2.

751005 THUAN, T. X., OKE, J. B., GUNN, J. E. <AP. J., 201, 45>
FURTHER OBSERVATIONS OF BL LACERTAE.

751006 FROGEL, J. A., DICKINSON, D. F., HYLAND, A. R. <AP. J., 201, 392>
CO IN THE INFRARED AND RADIO SPECTRA OF CARBON STARS.

751007 ALLEN, D. A., STROM, K. M., GRASDALEN, G. L., STROM, S. E., MERRILL, K. M. <M. N. R. A. S., 173, 47P>
HARO 13A: A LUMINOUS, HEAVILY OBSCURED STAR IN ORION.

751008 JOYCE, R. R., KNACKE, R. F., SIMON, M., YOUNG, E. <P. A. S. P., 87, 683>
FURTHER INFRARED AND MILLIMETER OBSERVATIONS OF MARKARIAN 231.

751009 GRASDALEN, G. L., CARRASCO, L. <ASTR. AP., 43, 259>
NGC 2175: THE CLUSTER AGE AND THE NATURE OF THE NEBULOSITY SURROUNDING S 252A.

751010 ANDRILLAT, Y., COLLIN-SOUFFRIN, S. <ASTR. AP., 43, 419>
SPECTRES DE NOYAUX DE GALAXIES DE SEYFERT ENTRE 8000 ET 11000 A.

751011 HANSEN, O. L., HESSER, J. E. <NATURE, 257, 568>
OBSERVATIONS OF EIGHT GLOBULAR CLUSTERS AT 2.3 AND 4.7 MICRONS.

751101 WARD, D. B., DENNISON, B., GULL, G. E., HARWIT, M. <AP. J. (LETTERS), 202, L31>
DETECTION OF THE (0 III) 88.16 MICRON LINE IN M17.

751102 GEHRZ, R. D., HACKWELL, J. A., SMITH, J. R. <AP. J. (LETTERS), 202, L33>
8-13 MICRON MAPS OF THE TRAPEZIUM REGION OF THE ORION NEBULA.

751103 MCCARTHY, D. W., LOW, F. J. <AP. J. (LETTERS), 202, L37>
INITIAL RESULTS OF SPATIAL INTERFEROMETRY AT 5 MICRONS.

751104 COHEN, M., BARLOW, M. J. <AP. LETTERS, 16, 165>
INFRARED OBSERVATIONS OF THREE UNUSUAL NEBULAE.

751105 ADAMS, T. F. <AP. J., 202, 114>
A STUDY OF THE COMPACT NEBULAE VV 8 AND M3-27.

751106 LONGMORE, A. J., JAMESON, R. F. <M. N. R. A. S., 173, 271>
INFRARED OBSERVATIONS AND A MODEL OF BETA PER.

751107 COHEN, M. <M. N. R. A. S., 173, 279>
INFRARED OBSERVATIONS OF YOUNG STARS-VI. A 2- TO 4-MICRON SEARCH FOR MOLECULAR FEATURES.

751108 BOKSENBERG, A., SHORTRIDGE, K., ALLEN, D. A., FOSBURY, R. A. E., PENSTON, M. V., SAVAGE, A. <M. N. R. A. S., 173, 381>
NEW OBSERVATIONS OF THE OPTICAL SPECTRUM OF THE SEYFERT GALAXY NGC 4151.

751109 GNEDIN, YU. N., MITROFANOV, I. G. <SOV. AST., 19, 673>
THE NATURE OF THE KLEINMANN-LOW AND BECKLIN-NEUGEBAUER INFRARED SOURCES.

751110 MUSTEL, E. R. <SOV. AST., 19, 685>
HELIUM IN TYPE 1 SUPERNOVA ENVELOPES.

751201 HANSEN, O. L., BLANCO, V. M. <A. J., 80, 1011>
CLASSIFICATION OF 831 TWO-MICRON SKY SURVEY SOURCES SOUTH OF +5 DEGREES.

751202 FURNISS, I., JENNINGS, R. E., MOORWOOD, A. F. M. <AP. J., 202, 400>
40-350 MICRON OBSERVATIONS OF GALACTIC SOURCES.

751203 WESTBROOK, W. E., BECKLIN, E. E., MERRILL, K. M., NEUGEBAUER, G., SCHMIDT, M., WILLNER, S. P., WYNN-WILLIAMS, C. G. <AP. J., 202, 407>
OBSERVATIONS OF AN ISOLATED COMPACT INFRARED SOURCE IN PERSEUS.

751204 COHEN, M. <M. N. R. A. S., 173, 489>
INFRARED OBSERVATIONS OF SOUTHERN WC9 STARS AND HE 2-113.

751205 JOYCE, R. R. <P. A. S. P., 87, 917>
THE INFRARED SPECTRUM OF ETA CARINAE: 3-14 MICRONS.

751206 THOMPSON, R. I., REED, M. A. <P. A. S. P., 87, 929>
A MOTOR-MICROMETER-DRIVEN INFRARED FOURIER-TRANSFORM SPECTROMETER.

751207 DANKS, A. C. <P. A. S. P., 87, 941>
INFRARED STAR IN RCW 113.

751208 THUM, C., LEMKE, D. <ASTR. AP., 45, 83>
NEAR INFRARED SOURCES IN SGR B2.

759901 KAZES, I., LE SQUEREN, A. M., GADEA, F. <ASTR. AP., 42, 9>
RADIO OBSERVATIONS OF SMALL GALACTIC NEBULAE.

759902 VAN DEN BERGH, S., HERBST, W. <A. J., 80, 208>
CATALOGUE OF SOUTHERN STARS EMBEDDED IN NEBULOSITY.

759903 GALLOUET, L., HEIDMANN, N., DAMPIERRE, F. <ASTR. AP. SUPPL., 19, 1>
OPTICAL POSITIONS OF BRIGHT GALAXIES. III.

759904 MILNE, D. K., ALLER, L. H. <ASTR. AP., 38, 183>
RADIO OBSERVATIONS AT 5 GHZ OF SOUTHERN PLANETARY NEBULAE.

759905 HOLMBERG, E. B., LAUBERTS, A., SCHUSTER, H. -E., WEST, R. M. <ASTR. AP. SUPPL., 22, 327>
THE ESO/UPPSALA SURVEY OF THE ESO(B) ATLAS OF THE SOUTHERN SKY. III.

759906 GLUSHKOV, YU., I., DENISYUK, E. K., KARYAGINA, Z. V. <ASTR. AP., 39, 481>
YOUNG STELLAR CLUSTERS IN DIFFUSE NEBULAE.

760001 ANDRILLAT, Y. <MEM. SOC. ROY. DES SCI. DE LIEGE, 9, 355>
SPECTRES DES ETOILES CHAUDES ET DES NEBULEUSES PLANETAIRES DANS LE PROCHE INFRAROUGE (82000-11000A).

760002 IIJIMA, T., ITO, K., MATSUMOTO, T., UYAMA, K. <P. A. S. J., 28, 27>
NEAR-INFRARED PROFILE OF M31.

760003 KAWARA, K., MAIHARA, T., NOGUCHI, K., ODA, N., SATO, S., OISHI, M., IIJIMA, T. <P. A. S. J., 28, 163>
MULTI-BAND PHOTOMETRY OF NOVA CYGNI 1975.

760004 OISHI, M., MAIHARA, T., NOGUCHI, K., OKUDA, H., SATO, S. <P. A. S. J., 28, 175>
INFRARED POLARIZATION OF CRL 2591.

760005 SATO, S., KOBAYASHI, Y., KAWARA, K., MAIHARA, T., OKUDA, H. <P. A. S. J., 28, 391>
INFRARED PHOTOMETRY OF CRL 877 ASSOCIATED WITH THE RADIO COMPLEX IN THE MONOCEROS R2 REGION.

760006 ITO, K., MATSUMOTO, T., UYAMA, K. <P. A. S. J., 28, 427>
OBSERVATION OF THE DIFFUSE INFRARED RADIATION FROM OUR GALAXY AT 2.4 MICRONS.

760101 ANDRIESSE, C. D., DE VRIES, J. S. <ASTR. AP., 46, 143>
INFRARED OBSERVATIONS OF M17S AT MEDIUM SPATIAL AND SPECTRAL RESOLUTION.

760102 PIPHER, J. L., SOIFER, B. T. <ASTR. AP., 46, 153>
INFRARED OBSERVATIONS OF THE H2O MASER ASSOCIATED WITH THE HII REGIONS S 255 (IC 2162) AND S 257.

760103 ZEILIK II, M. <ASTR. AP., 46, 319>
INFRARED EMISSION FROM S 157 A AND S 252 A.

760104 TELESCO, C. M., HARPER JR., D. A., LOEWENSTEIN, R. F. <AP. J. (LETTERS), 203, L53>
FAR-INFRARED PHOTOMETRY OF NGC 1068.

760105 COHEN, M. <AP. J., 203, 169>
DEEP ICE ABSORPTION IN A PECULIAR INFRARED SOURCE.

760106 BOEHM, K. H., SIEGMUND, W. A., SCHWARTZ, R. D. <AP. J., 203, 399>
EMISSION-LINE SPECTRA OF INDIVIDUAL CONDENSATIONS OF HERBIG-HARO OBJECTS.

760107 COHEN, M., SCHWARTZ, R. D. <M. N. R. A. S., 174, 137>
INFRARED OBSERVATIONS OF YOUNG STARS-VII. SIMULTANEOUS OPTICAL AND INFRARED MONITORING FOR VARIABILITY.

760108 JAMESON, R. F., LONGMORE, A. J. <M. N. R. A. S., 174, 217>
INFRARED OBSERVATIONS AND A MODEL OF BETA LYR.

760109 JORDEN, P. R., MACGREGOR, A. D., SELBY, M. J., WHITELOCK, P. A. <M. N. R. A. S., 174, 1P>
INFRARED PHOTOMETRY OF A HEAVILY REDDENED ASSOCIATION IN W35.

760110 NOSKOVA, R. I. <ASTROFIZIKA, 12, 31>
SPECTRUM OF THE PLANETARY NEBULA BD+30 3639 IN THE NEAR-INFRARED REGION.

760111 GRASDALEN, G. L., JOYCE, R. R. <NATURE, 259, 187>
CORONAL LINES IN NEAR INFRARED SPECTRUM OF NOVA CYGNI 1975.

760201 SIBILLE, F., LUNEL, M., BERGEAT, J. <ASTR. AP., 47, 161>
INFRARED STUDY OF SEVEN POSSIBLE COMPACT HII REGIONS.

760202 BELL, R. A., GUSTAFSSON, B., NORDH, H. L., OLOFSSON, S. G. <ASTR. AP., 46, 391>
THE LUMINOSITY DEPENDENCE OF THE 1.65 MICRON FLUX FROM K AND EARLY M STARS. OBSERVATIONS AND INTERPRETATION.

760203 KEMP, J. C., RUDY, R. J. <AP. J. (LETTERS), 203, L131>
NOVA CYGNI 1975: NARROW-BAND POLARIMETRY AND PHOTOMETRY 0.36-1.7 MICRONS.

760204 GALLAGHER, J. S., NEY, E. P. <AP. J. (LETTERS), 204, L35>
THE EARLY INFRARED DEVELOPMENT OF NOVA CYGNI 1975.

760205 FAY JR., T. D., RIDGWAY, S. T. <AP. J., 203, 600>
CARBON STAR PHOTOMETRY: CO AND 3.2 MICRON BANDS.

760206 AITKEN, D. K., GRIFFITHS, J., JONES, B., PENMAN, J. M. <M. N. R. A. S., 174, 41P>
FURTHER OBSERVATIONS OF IONIZED NEON IN THE GALACTIC CENTRE.

760207 SHENAVRIN, V. I., MOROZ, V. I., LIBERMAN, A. A. <SOV. AST. (LETTERS), 2, 36>
INFRARED OBSERVATIONS OF NOVA CYGNI 1975. I. J, K, L PHOTOMETRY.

760208 KOLOTILOV, E. A., LIBERMAN, A. A. <SOV. AST. (LETTERS), 2, 37>
INFRARED OBSERVATIONS OF NOVA CYGNI 1975. II. SPECTRA IN THE 0.6-1.1 MICRON RANGE.

760209 SHENAVRIN, V. I., MOROZ, V. I. <SOV. AST. (LETTERS), 2, 39>
INFRARED OBSERVATIONS OF NOVA CYGNI 1975. III. SPECTRA IN THE 0.6-2.5 MICRON RANGE.

760210 LIBERMAN, A. A., MOROZ, V. I., SHENAVRIN, V. I. <SOV. AST. (LETTERS), 2, 39>
INFRARED OBSERVATIONS OF NOVA CYGNI 1975. IV. PHOTOMETRY WITH A GERMANIUM BOLOMETER COOLED BY LIQUID HELIUM.

760211 GLASS, I. S. <IAUC NO. 2911>
VY CANIS MAJORIS.

760212 PENSTON, M. V., ALLEN, D. A., LLOYD, C. <OBSERVATORY, 96, 22>
AN INTERESTING STAR IN THE LAMBDA ORIONIS ASSOCIATION.

760213 MAIHARA, T., NOGUCHI, K., OISHI, M., OKUDA, H., SATO, S. <NATURE, 259, 465>
VARIATIONS OF THE INFRARED POLARISATION OF VY CANIS MAJORIS.

760214 ZIRIN, H. <NATURE, 259, 466>
FE XIII LINE IN R AQUARII.

760301 ALLEN, D. A., SWINGS, J. P. <ASTR. AP., 47, 293>
THE SPECTRA OF PECULIAR BE STARS WITH INFRARED EXCESSES.

760302 DICKINSON, D. F. <AP. J. SUPPL., 30, 259>
WATER EMISSION FROM INFRARED STARS.

760303 WERNER, M. W., GATLEY, I., HARPER JR., D. A., BECKLIN, E. E.,LOEWENSTEIN, R. F., TELESCO, C. M., THRONSON JR., H. A. <AP. J., 204, 420>
ONE ARC-MINUTE RESOLUTION MAPS OF THE ORION NEBULA AT 20, 50, AND 100 MICRONS.

760304 STROM, S. E., STROM, K. M., GOAD, J. W., VRBA, F. J., RICE, W. <AP. J., 204, 684>
COLOR AND METALLICITY GRADIENTS IN E AND S0 GALAXIES.

760305 ANDRILLAT, Y., SWINGS, J. P. <AP. J. (LETTERS), 204, L123>
8200 TO 11200A SPECTRA OF PECULIAR EMISSION-LINE OBJECTS WITH INFRARED EXCESS.

760306 RYDGREN, A. E., STROM, S. E., STROM, K. M. <AP. J. SUPPL., 30, 307>
THE NATURE OF THE OBJECTS OF JOY: A STUDY OF THE T TAURI PHENOMENON.

760307 THOMAS, J. A., ROBINSON, G., HYLAND, A. R. <M. N. R. A. S., 174, 711>
INTERMEDIATE BANDWIDTH SPECTROMETRY IN THE 10-MICRON REGION AND ITS INTERPRETATION.

760308 FEAST, M. W., CATCHPOLE, R. M., GLASS, I. S. <M. N. R. A. S., 174, 81P>
THE BOLOMETRIC ABSOLUTE MAGNITUDE OF S TYPE STARS WITH LITHIUM PRODUCTION.

760309 NOSKOVA, R. I. <SOV. AST., 20, 170>
ABSOLUTE SPECTROPHOTOMETRY OF THE PLANETARY NEBULAE IC 2149, IC 4593, AND NGC 6210 IN THE NEAR INFRARED.

760401 NEUGEBAUER, G., BECKLIN, E. E., OKE, J. B., SEARLE, L. <AP. J., 205, 29>
OPTICAL AND INFRARED SPECTROPHOTOMETRY OF 18 MARKARIAN GALAXIES.

760402 STEIN, W. A., WEEDMAN, D. W. <AP. J., 205, 44>
THE ORIGIN OF ULTRAVIOLET AND INFRARED CONTINUUM RADIATION FROM SEYFERT GALAXIES.

760403 HARPER JR., D. A., LOW, F. J., RIEKE, G. H., THRONSON JR., H. A. <AP. J., 205, 136>
THE INFRARED EMISSION OF M17.

760404 WING, R. F., DEAN, C. A., MACCONNELL, D. J. <AP. J., 205, 186>
THE TEMPERATURE, LUMINOSITY, AND SPECTRUM OF KAPTEYN'S STAR.

760405 WOLLMAN, E. R., GEBALLE, T. R., LACY, J. H., TOWNES, C. H., RANK, D. M. <AP. J. (LETTERS), 205, L5>
SPECTRAL AND SPATIAL RESOLUTION OF THE 12.8 MICRON NE II EMISSION FROM THE GALACTIC CENTER.

760406 GRASDALEN, G. L., JOYCE, R. R. <AP. J. (LETTERS), 205, L11>
ADDITIONAL OBSERVATIONS OF THE UNIDENTIFIED INFRARED FEATURES AT 3.28 AND 3.4 MICRONS.

760407 THUAN, T. X., OKE, J. B. <AP. J., 205, 360>
COLOR GRADIENTS IN THE NUCLEAR REGION OF M31.

760408 HARVEY, P. M., CAMPBELL, M. F., HOFFMANN, W. F. <AP. J. (LETTERS), 205, L69>
HIGH-RESOLUTION FAR-INFRARED OBSERVATIONS OF THE GALACTIC CENTER.

760409 WARD, D. B., DENNISON, B., GULL, G. E., HARWIT, M. <AP. J. (LETTERS), 205, L75>
FAR-INFRARED SPECTRAL OBSERVATIONS OF M42 AND M17.

760410 GRASDALEN, G. L. <AP. J. (LETTERS), 205, L83>
BRACKETT-ALPHA EMISSION IN THE BECKLIN-NEUGEBAUER OBJECT.

760411 RIEKE, G. H., GRASDALEN, G. L., KINMAN, T. D., HINTZEN, P., WILLS, B. J., WILLS, D. <NATURE, 260, 754>
PHOTOMETRIC AND SPECTROSCOPIC OBSERVATIONS OF THE BL LACERTAE OBJECT AO 0235+164.

760412 GLASS, I. S. <M. N. R. A. S., 175, 191>
MORE JHKL COLOURS OF GALAXIES.

760413 RYDGREN, A. E. <P. A. S. P., 88, 111>
T TAURI STARS AND THE (J-H), (H-K) DIAGRAM.

760501 STROM, K. M., STROM, S. E., VRBA, F. J. <A. J., 81, 308>
INFRARED SURVEYS OF DARK-CLOUD COMPLEXES. I. THE LYNDS 1630 DARK CLOUD.

760502 STROM, S. E., VRBA, F. J., STROM, K. M. <A. J., 81, 314>
INFRARED SURVEYS OF DARK CLOUD COMPLEXES. II. THE NGC 1333 REGION.

760503 VRBA, F. J., STROM, S. E., STROM, K. M. <A. J., 81, 317>
INFRARED SURVEYS OF DARK-CLOUD COMPLEXES. III. THE R CORONA AUSTRINA DARK CLOUD.

760504 STROM, K. M., STROM, S. E., VRBA, F. J. <A. J., 81, 320>
INFRARED SURVEYS OF DARK-CLOUD COMPLEXES. IV. THE LYNDS 1517 AND LYNDS 1551 CLOUDS.

760505 CRAINE, E. R., SCHUSTER, W. J., TAPIA, S., VRBA, F. J. <AP. J., 205, 802>
ON THE NATURE OF IRC +10420.

760506 GAUTIER III, T. N., THOMPSON, R. I., FINK, U., LARSON, H. P. <AP. J., 205, 841>
A LOWER LIMIT ON THE SURFACE CARBON-12/CARBON-13 RATIO IN ALPHA ORIONIS.

760507 NEUGEBAUER, G., BECKLIN, E. E., BECKWITH, S., MATTHEWS, K., WYNN-WILLIAMS, C. G. <AP. J. (LETTERS), 205, L139>
LATE-TYPE GIANTS AND SUPERGIANTS IN THE GALACTIC CENTER.

760508 THOMPSON, R. I., REED, M. A. <AP. J. (LETTERS), 205, L159>
1.3 TO 2.5 MICRON SPECTRA OF MWC 349 AND LKHA 101.

760509 HUDSON, H. S., SOIFER, B. T. <AP. J., 206, 100>
SUBMILLIMETER OBSERVATIONS OF NGC 2024, OMC-2, AND MON R-2.

760510 RIEKE, G. H. <AP. J. (LETTERS), 206, L15>
THE SIZES OF THE NUCLEI OF GALAXIES AT 10 MICRONS.

760511 CITTERIO, O., CONTI, G., DI BENEDETTO, P., TANZI, E. G. <M. N. R. A. S., 175, 35P>
INFRARED AND X-RAY OBSERVATIONS OF THE DECLINE OF A0620-00.

760512 ALLEN, D. A., HYLAND, A. R., LONGMORE, A. J. <M. N. R. A. S., 175, 61P>
A FIRST LOOK AT THE AFCRL INFRARED SKY SURVEY CATALOGUE.

760513 WAMSTEKER, W. <IAUC NO. 2954>
POSSIBLE INFRARED COUNTERPART OF MXB1730-335.

760514 MILONE, E. F. <AP. J. SUPPL., 31, 93>
INFRARED PHOTOMETRY OF RT LACERTAE.

760515 BLACK, J. H., GALLAGHER, J. S. <NATURE, 261, 296>
THE INFRARED SPECTRUM OF NOVA CYGNI 1975.

760516 HAYAKAWA, S., ITO, K., MATSUMOTO, T., ONO, T., UYAMA, K. <NATURE, 261, 29>
INFRARED PROFILE OF THE MILKEY WAY AT 2.4 MICRONS.

760601 CLEGG, P. E., ROWAN-ROBINSON, M., ADE, P. A. R. <A. J., 81, 399>
MILLIMETER OBSERVATIONS OF GALACTIC SOURCES.

760602 O'CONNELL, R. W. <AP. J., 206, 370>
GALAXY SPECTRAL SYNTHESIS. I. STELLAR POPULATIONS IN THE NUCLEI OF GIANT ELLIPTICALS.

760603 WILLNER, S. P. <AP. J., 206, 728>
8 TO 13 MICRON SPECTROPHOTOMETRY OF COMPACT SOURCES IN NGC 7538.

760604 LOW, F. J., KURTZ, R. F., VRBA, F. J., RIEKE, G. H. <AP. J. (LETTERS), 206, L153>
AN OBSERVATIONAL STUDY OF THE AFCRL INFRARED SKY SURVEY. I. LIMITED GROUND-BASED SURVEY AND RESULTS FROM PRELIMINARY CATALOG.

760605 LEBOFSKY, M. J., KLEINMANN, S. G., RIEKE, G. H., LOW, F. J. <AP. J. (LETTERS), 206, L157>
AN OBSERVATIONAL STUDY OF THE AFCRL INFRARED SKY SURVEY. II. PRESENT RESULTS OF A NEW PROGRAM TO STUDY THE FINAL CATALOG.

760606 GEHRZ, R. D., HACKWELL, J. A. <AP. J. (LETTERS), 206, L161>
A SEARCH FOR ANONYMOUS AFCRL INFRARED SOURCES.

760607 FAZIO, G. G., WRIGHT, E. L., ZEILIK II, M., LOW, F. J. <AP. J. (LETTERS), 206, L165>
A FAR-INFRARED MAP OF THE OPHIUCHUS DARK CLOUD REGION.

760608 CAPPS, R. W., KNACKE, R. F. <P. A. S. P., 88, 224>
INFRARED POLARIZATION OF IRC+10216.

760609 MERRILL, K. M., STEIN, W. A. <P. A. S. P., 88, 285>
2-14 MICRON STELLAR SPECTROPHOTOMETRY I. STARS OF THE CONVENTIONAL SPECTRAL SEQUENCE.

760610 MERRILL, K. M., STEIN, W. A. <P. A. S. P., 88, 294>
2-14 MICRON STELLAR SPECTROPHOTOMETRY II. STARS FROM THE 2 MICRON INFRARED SKY SURVEY.

760611 KLEINMANN, D. E. <IAUC NO. 2959>
POSSIBLE INFRARED COUNTERPART OF MXB1730-335.

760701 SCHULTZ, G. V., KREYSA, E., SHERWOOD, W. A. <ASTR. AP., 50, 171>
THE DISCOVERY OF SOME INFRARED COUNTERPARTS OF TYPE II OH/IR SOURCES.

760702 GRASDALEN, G. L., JOYCE, R. R. <ASTR. AP., 50, 297>
NEAR-INFRARED OBSERVATIONS OF SMALL HII REGIONS IN THE SMALL MAGELLANIC CLOUD.

760703 KIRSHNER, R. P., ARP, H. C., DUNLAP, J. R. <AP. J., 207, 44>
OBSERVATIONS OF SUPERNOVAE: 1975A IN NGC 2207 AND 1975B IN THE PERSEUS CLUSTER.

760704 LADA, C. J., DICKINSON, D. F., GOTTLIEB, C. A., WRIGHT, E. L. <AP. J., 207, 113>
H20 AND 22 GHZ CONTINUUM OBSERVATIONS OF M17.

760705 RIGHINI, G., SIMON, M., JOYCE, R. R. <AP. J., 207, 119>
3 MILLIMETER AND 350 MICRON CONTINUUM OBSERVATIONS OF THE DR-21 AND SGR B2 REGIONS.

760706 ALLEN, D. A. <AP. J., 207, 367>
THE NEAR-INFRARED CONTINUA OF EMISSION-LINE GALAXIES.

760707 KLEINMANN, S. G., BRECHER, K., INGHAM, W. H. <AP. J., 207, 532>
INFRARED EMISSION FROM A0620-00.

760708 TREFFERS, R. R., WOOLF, N. J., FINK, U., LARSON, H. P. <AP. J., 207, 680>
THE INFRARED EMISSION OF UPSILON SAGITTARII, 89 HERCULIS, AND R CORONAE BOREALIS.

760709 SOIFER, B. T., RUSSELL, R. W., MERRILL, K. M. <AP. J. (LETTERS), 207, L83>
2-4 MICRON SPECTROPHOTOMETRIC OBSERVATIONS OF THE GALACTIC CENTER.

760710 GAUTIER III, T. N., FINK, U., TREFFERS, R. R., LARSON, H. P. <AP. J. (LETTERS), 207, L129>
DETECTION OF MOLECULAR HYDROGEN QUADRUPOLE EMISSION IN THE ORION NEBULA.

760711 FRANKSTON, M., SCHILD, R. E. <A. J., 81, 500>
NEAR-INFRARED OBSERVATIONS OF THE EDGE-ON SPIRAL GALAXY NGC 4565.

760712 COX, L. J., HOUGH, J. H., ADAMS, D. J., JAMESON, R. F. <M. N. R. A. S., 176, 131>
LINEAR POLARIZATION MEASUREMENTS OF OMI SCO IN THE NEAR INFRARED.

760713 GLASS, I. S. <IAUC NO. 2974>
CIRCINUS X-1.

760801 BOEHM, K. H., SIEGMUND, W. A., SCHWARTZ, R. D. <ASTR. AP., 50, 361>
SPECTROPHOTOMETRY OF R MONOCEROTIS.

760802 MACGREGOR, A. D., SANCHEZ MAGRO, C., SELBY, M. J., WHITELOCK, P. A. <ASTR. AP., 50, 389>
THE SPATIAL DISTRIBUTION OF DUST IN THE PLANETARY NEBULAE NGC 6537, IC 418, BD +30 3639 AND NGC 6572.

760803 STROM, S. E., VRBA, F. J., STROM, K. M. <A. J., 81, 638>
INFRARED SURVEYS OF DARK CLOUD COMPLEXES. V. THE NGC 7129 REGION AND THE SERPENS DARK CLOUD.

760804 MERRILL, K. M., RUSSELL, R. W., SOIFER, B. T. <AP. J., 207, 763>
INFRARED OBSERVATIONS OF ICES AND SILICATES IN MOLECULAR CLOUDS.

760805 BECKLIN, E. E., BECKWITH, S., GATLEY, I., MATTHEWS, K., NEUGEBAUER, G., SARAZIN, C., WERNER, M. W. <AP. J., 207, 770>
INFRARED STUDIES OF AN IONIZATION FRONT REGION IN THE ORION NEBULA.

760806 GILLETT, F. C., SOIFER, B. T. <AP. J., 207, 780>
INFRARED SPECTROPHOTOMETRY OF OH 231.8+4.2-OH 0739-14.

760807 SZKODY, P. <AP. J., 207, 824>
THE MINIMUM STATE OF DWARF NOVAE.

760808 GORDON, C. <AP. J., 207, 860>
TYPE I SUPERNOVAE. II. THE SPECTRUM OF SN 1972E IN NGC 5253, 250 DAYS AFTER THE EXPLOSION.

760809 GIGUERE, P. T., WOOLF, N. J., WEBBER, J. C. <AP. J. (LETTERS), 207, L195>
IRC+10420: A HOT SUPERGIANT MASER.

760810 KLEINMANN, D. E., GILLETT, F. C., WRIGHT, E. L. <AP. J., 208, 42>
8-13 MICRON SPECTROPHOTOMETRY OF NGC 1068.

760811 CATO, B. T., RONNANG, B. O., RYDBECK, O. E. H., LEWIN, P. T.,YNGVESSON, K. S., CARDIASMENOS, A. G., SHANLEY, J. F. <AP. J., 208, 87>
WATER VAPOR EMISSION FROM HII REGIONS AND INFRARED STARS.

760812 GRASDALEN, G. L. <AP. J. (LETTERS), 208, L11>
PASCHEN-ALPHA IN 3C 273.

760813 HUMPHREYS, R. M., WARNER, J. W., GALLAGHER, J. S. <P. A. S. P., 88, 380>
CRL 2688 - "THE EGG NEBULA" - PREPLANETARY NEBULA OR PROTOSTELLAR SYSTEM?

760814 CAPPS, R. W., KNACKE, R. F. <P. A. S. P., 88, 564>
ERRATUM TO "INFRARED POLARIZATION OF IRC+10216."

760901 SIMON, T. <A. J., 81, 764>
BROAD-BAND 20-MICRON PHOTOMETRY OF 50 STARS.

760902 PIPHER, J. L., SHARPLESS, S., SAVEDOFF, M. P., KERRIDGE, S. J., KRASSNER, J., SCHURMANN, S., SOIFER, B. T., MERRILL, K. M. <ASTR. AP., 51, 255>
OPTICAL, INFRARED AND RADIO STUDIES OF COMPACT HII REGIONS. I. THE COMPLEX IN S 106.

760903 LONGMORE, A. J., HYLAND, A. R., ALLEN, D. A. <PROC. A. S. A., 3, 47>
THE AFCRL CATALOGUE: SOME SOUTHERN SOURCES STUDIED.

760904 GRASDALEN, G. L., JOYCE, R. R. <AP. J., 208, 317>
INFRARED OBSERVATIONS OF NGC 5128.

760905 BECKWITH, S., EVANS II, N. J., BECKLIN, E. E., NEUGEBAUER, G. <AP. J., 208, 390>
INFRARED OBSERVATIONS OF MONOCEROS R2.

760906 CAMPBELL, M. F., ELIAS, J. H., GEZARI, D. Y., HARVEY, P. M., HOFFMANN, W. F., HUDSON, H. S., NEUGEBAUER, G., SOIFER, B. T., WERNER, M. W., WESTBROOK, W. E. <AP. J., 208, 396>
FAR-INFRARED OBSERVATIONS OF IRC +10216.

760907 MOULD, J. R., HYLAND, A. R. <AP. J., 208, 399>
INFRARED OBSERVATIONS AND THE STRUCTURE OF THE LOWER MAIN SEQUENCE.

760908 ZIRIN, H. <AP. J., 208, 414>
FURTHER OBSERVATIONS OF THE 10830A HELIUM LINE IN STARS AND THEIR SIGNIFICANCE AS A MEASURE OF STELLAR ACTIVITY.

760909 WRIGHT, E. L., FAZIO, G. G., LOW, F. J. <AP. J. (LETTERS), 208, L87>
FAR-INFRARED OBSERVATIONS OF M20 (NGC 6514).

760910 PERSSON, S. E., FROGEL, J. A., AARONSON, M. <AP. J., 208, 753>
THE 10 MICRON SILICATE FEATURE IN SOUTHERN HII REGIONS.

760911 FORREST, W. J., SOIFER, B. T. <AP. J. (LETTERS), 208, L129>
16-25 MICRON SPECTROSCOPY OF THE TRAPEZIUM AND BN-KL SOURCE IN ORION.

760912 FORREST, W. J., HOUCK, J. R., REED, R. A. <AP. J. (LETTERS), 208, L133>
16-40 MICRON SPECTROSCOPY OF THE TRAPEZIUM AND THE KLEINMANN-LOW NEBULA IN ORION.

760913 PRICE, S. D., WALKER, R. G. <AFGL-TR-76-0208>
THE AFGL FOUR COLOR INFRARED SKY SURVEY:CATALOG OF OBSERVATIONS AT 4.2, 11.0, 19.8, AND 27.4 MICRONS.

761001 ANDRILLAT, Y., HOUZIAUX, L. <ASTR. AP., 52, 119>
SPECTRAL VARIATIONS OF HBV 475 IN THE NEAR INFRARED.

761002 MCNAMARA, B. J. <A. J., 81, 845>
PRE-MAIN-SEQUENCE MASSES AND THE AGE SPREAD IN THE ORION CLUSTER.

761003 WESTBROOK, W. E., WERNER, M. W., ELIAS, J. H., GEZARI, D. Y.,HAUSER, M. G., LO, K. Y., NEUGEBAUER, G. <AP. J., 209, 94>
ONE-MILLIMETER CONTINUUM EMISSION STUDIES OF FOUR MOLECULAR CLOUDS.

761004 JONES, T. W., MERRILL, K. M. <AP. J., 209, 509>
MODEL DUST ENVELOPES AROUND LATE-TYPE STARS.

761005 BERGEAT, J., SIBILLE, F., LUNEL, M., LEFEVRE, J. <ASTR. AP., 52, 227>
CARBON STARS AND CIRCUMSTELLAR SHELLS.

761006 WILLIAMS, P. M., BEATTIE, D. H., STEWART, J. M. <OBSERVATORY, 96, 184>
OBSERVATIONS OF SOUTHERN STARS WITH A NEW INFRARED PHOTOMETER.

761007 WEGNER, G. <M. N. R. A. S., 177, 3>
ON ELEMENT ABUNDANCES IN STARS BELONGING TO THE GAM PUPPIS GROUP.

761008 ALLEN, D. A., WRIGHT, A. E., GOSS, W. M. <M. N. R. A. S., 177, 91>
THE DWARF EMISSION GALAXY HE 2-10.

761009 WEGNER, G. <M. N. R. A. S., 177, 99>
ON THE REDDENING AND THE EFFECTIVE TEMPERATURE OF HD 101065.

761010 KHOZOV, G. V. <ASTROFIZIKA, 12, 468>
INFRARED STARS: A REVIEW OF THE OBSERVATIONAL DATA.

761011 DYCK, H. M., SIMON, T. <P. A. S. P., 88, 738>
THE INFRARED SPECTRA OF NGC 7027 AND BD+30 3639.

761101 VRBA, F. J., STROM, S. E., STROM, K. M. <A. J., 81, 958>
MAGNETIC FIELD STRUCTURE IN THE VICINITY OF FIVE DARK CLOUD COMPLEXES.

761102 TREFFERS, R. R., FINK, U., LARSON, H. P., GAUTIER III, T. N. <AP. J., 209, 793>
THE SPECTRUM OF THE PLANETARY NEBULA NGC 7027 FROM 0.9 TO 2.7 MICRONS.

761103 TREFFERS, R. R., FINK, U., LARSON, H. P., GAUTIER III, T. N. <AP. J. (LETTERS), 209, L115>
THE 1.4-2.7 MICRON SPECTRUM OF THE POINT SOURCE AT THE GALACTIC CENTER.

761104 RIEKE, G. H. <AP. J. (LETTERS), 210, L5>
THE INFRARED EMISSION OF MARKARIAN 231.

761105 THOMPSON, R. I., ERICKSON, E. F., WITTEBORN, F. C., STRECKER, D. W. <AP. J. (LETTERS), 210, L31>
COMBINED GROUND AND AIRCRAFT BASED 1-4 MICRON SPECTRA OF LKHA 101.

761106 BALUTEAU, J. -P., BUSSOLETTI, E., ANDEREGG, M., MOORWOOD, A. F. M., CORON, N. <AP. J. (LETTERS), 210, L45>
INFRARED LINE EMISSION FROM THE ORION NEBULA: DETECTION OF (S III) (18.71 MICRONS) AND (O III) (88.35 MICRONS).

761107 TURNROSE, B. E. <AP. J., 210, 33>
THE STELLAR CONTENT OF THE NUCLEAR REGIONS OF SC GALAXIES.

761108 CAPPS, R. W., KNACKE, R. F. <AP. J., 210, 76>
INFRARED POLARIZATION OF THE GALACTIC CENTER.

761109 HACKWELL, J. A., GEHRZ, R. D., SMITH, J. R., STRECKER, D. W. <AP. J., 210, 137>
INFRARED LIGHT VARIATIONS OF WOLF-RAYET STARS.

761110 MERRILL, K. M., STEIN, W. A. <P. A. S. P., 88, 808>
ERRATUM TO "2-14 MICRON STELLAR SPECTROPHOTOMETRY I. STARS OF THE CONVENTIONAL SPECTRAL SEQUENCE. "

761111 NOSKOVA, R. I. <SOV. AST., 20, 684>
DETAILED NEAR-INFRARED SPECTROPHOTOMETRY OF THE PLANETARY NEBULAE NGC 6572, 6891, AND 7662.

761112 RIDGWAY, S., HALL, D. N. B., KLEINMANN, S. G., WEINBERGER, D. A., WOJSLAW, R. S. <NATURE, 264, 345>
CIRCUMSTELLAR ACETYLENE IN THE INFRARED SPECTRUM OF IRC+10216.

761201 ADE, P. A. R., ROWAN-ROBINSON, M., CLEGG, P. E. <ASTR. AP., 53, 403>
MILLIMETRE EMISSION FROM EXTRAGALACTIC OBJECTS. II. LUMINOSITIES, SPECTRA, AND CONTRIBUTION TO THE MICROWAVE BACKGROUND.

761202 SOIFER, B. T., RUSSELL, R. W., MERRILL, K. M. <AP. J., 210, 334>
2-4 MICRON SPECTROPHOTOMETRIC OBSERVATIONS OF COMPACT HII REGIONS.

761203 COHEN, M., KUHI, L. V. <AP. J., 210, 365>
SPECTROPHOTOMETRIC STUDIES OF YOUNG STARS. I. THE CEPHEUS IV ASSOCIATION.

761204 KNACKE, R. F., CAPPS, R. W., JOHNS, M. <AP. J. (LETTERS), 210, L69>
THE POLARIZATION OF BL LACERTAE AT VISIBLE AND INFRARED WAVELENGTHS.

761205 KLEINMANN, D. E., KLEINMANN, S. G., WRIGHT, E. L. <AP. J. (LETTERS), 210, L83>
THE INFRARED SOURCE NEAR THE RAPID-BURST X-RAY SOURCE MXB 1730-335.

761206 ALLEN, D. A., GLASS, I. S. <AP. J., 210, 666>
EMISSION-LINE STARS IN THE LARGE MAGELLANIC CLOUD: SPECTROSCOPY AND INFRARED PHOTOMETRY.

761207 HINKLE, K. H., LAMBERT, D. L., SNELL, R. L. <AP. J., 210, 684>
THE CARBON-12/CARBON-13 RATIO IN STELLAR ATMOSPHERES. VI. FIVE LUMINOUS COOL STARS.

761208 HINKLE, K. H., BARNES, T. G., LAMBERT, D. L., BEER, R. <AP. J. (LETTERS), 210, L141>
SILICON MONOXIDE IN THE 4 MICRON INFRARED SPECTRUM OF LONG-PERIOD VARIABLES.

761209 JOYCE, R. R., SIMON, M. <P. A. S. P., 88, 870>
3-MILLIMETER AND INFRARED CONTINUUM OBSERVATIONS OF MARKARIAN GALAXIES.

761210 MERRILL, K. M., STEIN, W. A. <P. A. S. P., 88, 874>
2-14 MICRON STELLAR SPECTROPHOTOMETRY III. AFCRL SKY SURVEY OBJECTS.

761211 WHITTET, D. C. B., VAN BREDA, I. G., GLASS, I. S. <M. N. R. A. S., 177, 625>
INFRARED PHOTOMETRY, EXTINCTION CURVES AND R VALUES FOR STARS IN THE SOUTHERN MILKY WAY.

761212 EMERSON, J. P. <M. N. R. A. S., 177, 113P>
IDENTIFICATION OF THE 100-MICRON SOURCES IN CYG X.

761213 NEY, E. P., STODDART, J., HUBBARD, R. <IAUC NO. 3023>
NOVA VULPECULAE 1976.

769901 MARKARIAN, B. E., LIBOVETSKY, V. A. <ASTROFIZIKA, 12, 389>
GALAXIES WITH ULTRAVIOLET CONTINUUM. VIII.

769902 MARKARIAN, B. E., LIBOVETSKY, V. A. <ASTROFIZIKA, 12, 657>
GALAXIES WITH ULTRAVIOLET CONTINUUM. IX.

769903 MAYO, S. K., WHELAN, J. A. J., WICKRAMASINGHE, D. T. <IAUC NO. 2957>
NEW OPTICAL CANDIDATE FOR CIRCINUS X-1.

769904 BOLEY, F., WOLFSON, R., BRADT, H., DOXSEY, R., JERNIGAN, G., HILTNER, W. A. <AP. J. (LETTERS), 203, L13>
OPTICAL IDENTIFICATION OF A0620-00.

769905 DIXON, R. S. <OHIO STATE UNIVERSITY, RA42>
MASTER LIST OF RADIO SOURCES.

769906 SMITH, H. E., SPINRAD, H., SMITH, E. O. <P. A. S. P., 88, 621>
THE REVISED 3C CATALOG OF RADIO SOURCES: A REVIEW OF IDENTIFICATIONS AND SPECTROSCOPY.

769907 STEPHENSON, C. B. <PUBL. WARNER AND SWASEY OBS., 2, 2>
A GENERAL CATALOGUE OF S STARS.

769908 CATCHPOLE, R. M., FEAST, M. W. <M. N. R. A. S., 175, 501>
LITHIUM AND S-TYPE STARS.

769909 DRESSEL, L. L., CONDON, J. J. <AP. J. SUPPL., 31, 187>
ACCURATE OPTICAL POSITIONS OF BRIGHT GALAXIES.

769910 MILNE, D. K. <A. J., 81, 753>
OPTICAL POSITIONS FOR PLANETARY NEBULAE. II.

769911 HESSER, J. E., HARTWICK, F. D. A., UGARTE, P. <AP. J. SUPPL., 32, 283>
INSTRUMENTAL COLOR-MAGNITUDE DIAGRAMS FOR 24 LARGE MAGELLANIC CLOUD STAR CLUSTERS.

769912 LLOYD EVANS, T. <M. N. R. A. S., 174, 169>
RED VARIABLES IN THE CENTRAL BULGE OF THE GALAXY. I.

769913 KUKARKIN, B. V., KHOLOPOV, P. N., KUKARKINA, N. P., KUROCHKIN, N. P., MEDVEDEVA, G. I., PEROVA, N. B., PSOVSKY, YU. P., FEDOROVITCH, V. P., FROLOV, M. S. <PUBL. OFFICE NAUKA, MOSCOW>
GENERAL CATALOGUE OF VARIABLE STARS. THIRD SUPPLEMENT.

769914 DE VAUCOULEURS, G., DE VAUCOULEURS, A., CORWIN JR., H. G. <UNIV. TEXAS PRESS>
SECOND REFERENCE CATALOGUE OF BRIGHT GALAXIES.

769915 KUKARKIN, B. V., KHOLOPOV, P. N., FEDOROVICH, V. P., KIREYEVA, N. N., KUKARKINA, N. P., MEDVEDEVA, G. I., PEROVA, N. B. <IBVS NO. 1248>
62ND NAME-LIST OF VARIABLE STARS.

770001 KOLOTILOV, E. A., ZAJTSEVA, G. V., SHENAVRIN, V. I. <ASTROFIZIKA, 13, 449>
SPECTRAL AND PHOTOMETRIC OBSERVATIONS OF FAST IRREGULAR VARIABLES. III. VX CAS, UX ORI, BN ORI, AND WW VUL - RESULTS OF U, B, V, J, H, K, L PHOTOMETRY.

770002 ANDRILLAT, Y., SWINGS, J. P. <AP. LETTERS, 18, 151>
8000-11000A SPECTRA OF EMISSION-LINE GALAXIES WITH INFRARED EXCESSES.

770003 CAPPS, R. W., KNACKE, R. F. <AP. LETTERS, 19, 113>
POLARIZATION OF 3C 371 AND AP LIBRAE AT 2.2 MICRONS.

770004 MAIHARA, T., NOGUCHI, K., OKUDA, H., SATO, S., OISHI, M. <P. A. S. J., 29, 415>
INFRARED POLARIZATION OF THE GALACTIC CENTER.

770005 NOGUCHI, K., MAIHARA, T., OKUDA, H., SATO, S., MUKAI, T. <P. A. S. J., 29, 511>
THREE-MICRON ABSORPTION BAND OF CARBON STARS.

770006 MATSUMOTO, T., MURAKAMI, H., HAMAJIMA, K. <P. A. S. J., 29, 583>
NEAR-INFRARED SURFACE PHOTOMETRY OF THE CENTRAL REGION OF M31.

770101 BRIOT, D. <ASTR. AP., 54, 599>
PASCHEN LINES IN BE STARS-CORRELATION BETWEEN THE PRESENCE OF PASCHEN EMISSION LINES AND THE INFRARED EXCESS.

770102 DENNISON, B., WARD, D. B., GULL, G. E., HARWIT, M. <A. J., 82, 39>
FAR-INFRARED POLARIZATION OF M42.

770103 FAY JR., T. D., MUFSON, S. L., DUNCAN, B. J., HOOVER, R. B., SANFORD, P. W., CHARLES, P. A., WHITE, N. E., WISNIEWSKI, W. Z., WAMSTEKER, W. <AP. J., 211, 152>
OPTICAL, INFRARED, AND X-RAY OBSERVATIONS OF NGC 6624.

770104 DYCK, H. M., SIMON, T. <AP. J., 211, 421>
INFRARED OBSERVATIONS OF COMPACT HII REGIONS IN THE SPECTRAL RANGE 3.4-33 MICROMETERS.

770105 TELESCO, C. M., HARPER JR., D. A. <AP. J., 211, 475>
FAR-INFRARED OBSERVATIONS OF NGC 7027.

770106 VRBA, F. J., SCHMIDT, G. D., BURKE JR., E. W. <AP. J., 211, 480>
THE INFRARED DEVELOPMENT OF NOVA AQUILAE 1975.

770107 WYNN-WILLIAMS, C. G., BECKLIN, E. E., FORSTER, J. R., MATTHEWS, K., NEUGEBAUER, G., WELCH, W. J., WRIGHT, M. C. H. <AP. J. (LETTERS), 211, L89>
ON THE RELATIONSHIP BETWEEN THE INFRARED SOURCE CRL 2591 (UOA-27) AND ITS RADIO AND H2O COUNTERPARTS.

770201 RUSSELL, R. W., SOIFER, B. T., PUETTER, R. C. <ASTR. AP., 54, 959>
THE 4-8 MICRON SPECTRUM OF THE BNKL SOURCE IN ORION.

770202 BECKLIN, E. E., MATTHEWS, K., NEUGEBAUER, G., WYNN-WILLIAMS, C. G. <ASTR. AP., 55, 19>
ON THE INFRARED EMISSION FROM SGR B2.

770203 WING, R. F., YORKA, S. B. <M. N. R. A. S., 178, 383>
THE BRIGHTEST S-TYPE STARS IN THE INFRARED.

770204 FEAST, M. W., CATCHPOLE, R. M., LLOYD EVANS, T., ROBERTSON, B. S. C., DEAN, J. F., BYWATER, R. A. <M. N. R. A. S., 178, 415>
THE RCB VARIABLES-VII. THE INFRARED VARIABILITY OF RY SGR.

770205 JOHANSSON, S. <M. N. R. A. S., 178, 17P>
NEW FE II IDENTIFICATIONS IN THE INFRARED SPECTRUM OF ETA CARINAE.

770206 DYCK, H. M. <A. J., 82, 129>
INFRARED MAP OF M8.

770207 WRIGHT, E. L., LADA, C. J., FAZIO, G. G., KLEINMANN, D. E., LOW, F. J. <A. J., 82, 132>
NEW INFRARED-CO SOURCE IN M8.

770208 HARVEY, P. M., CAMPBELL, M. F., HOFFMANN, W. F. <AP. J., 211, 786>
HIGH-RESOLUTION FAR-INFRARED OBSERVATIONS OF HII REGIONS: SAGITTARIUS B2, W49, DR 21-W75.

770209 LANDSTREET, J. D., ANGEL, J. R. P. <AP. J., 211, 825>
DETECTION OF POLARIZATION VARIATION ACROSS ABSORPTION FEATURES OF MIRA VARIABLES.

770210 SIMON, M., JOYCE, R. R., RIGHINI-COHEN, G., SIMON, M. N. <AP. J., 212, 84>
RADIO AND INFRARED STUDIES OF THE 100 MICROMETER SOURCES HFE 2 AND FJM 3.

770211 SHIVANANDAN, K., MCNUTT, D. P., DAEHLER, M., MOORE, W. J. <NATURE, 265, 513>
FAR INFRARED OBSERVATIONS OF IRC+10216.

770212 OKUDA, H., MAIHARA, T., ODA, N., SUGIYAMA, T. <NATURE, 265, 515>
2.4 MICRON MAPPING OF THE GALACTIC CENTRAL REGION.

770213 ITO, K., MATSUMOTO, T., UYAMA, K. <NATURE, 265, 517>
INFRARED PROFILE OF CENTRAL REGION OF OUR GALAXY AT 2.47 MICRONS.

770214 SANDFORD II, M. T., GOW, C. E., HONEYCUTT, R. K., JEKOWSKI, J. P., OLIVAS, P. N. <P. A. S. P., 89, 31>
NEAR-INFRARED VIDICON IMAGES OF CIT FIELDS.

770301 WILLIAMS, P. M., BEATTIE, D. H., STEWART, J. M. <M. N. R. A. S., 178, 619>
INFRARED PHOTOMETRY OF R ASSOCIATIONS - I. EARLY-TYPE STARS IN CMA R1 AND VEL R2.

770302 KOORNNEEF, J. <ASTR. AP., 55, 469>
HIGHLY REDDENED ARA CLUSTER REVISITED.

770303 ERICKSON, E. F., STRECKER, D. W., SIMPSON, J. P., GOORVITCH, D., AUGASON, G. C., SCARGLE, J. D., CAROFF, L. J., WITTEBORN, F. C. <AP. J., 212, 696>
SPECTRUM OF THE KLEINMANN-LOW NEBULA FROM 29 TO 125 MICROMETERS.

770401 HEFELE, H., WACKER, W., WEINBERGER, R. <ASTR. AP., 56, 407>
INFRARED OBSERVATIONS OF COMPACT HII REGIONS NEAR CLASS I OH MASER SOURCES.

770402 FLORKOWSKI, D. R., GOTTESMAN, S. T. <M. N. R. A. S., 179, 105>
HD 193793, A RADIO-EMITTING WOLF-RAYET BINARY STAR.

770403 AITKEN, D. K., GRIFFITHS, J., JONES, B. <M. N. R. A. S., 179, 179>
INFRARED LINE AND CONTINUUM SPATIAL STUDIES OF THE SOUTHERN HII REGION G333.6–0.2.

770404 RUSSELL, R. W., SOIFER, B. T., MERRILL, K. M. <AP. J., 213, 66>
OBSERVATIONS OF THE UNIDENTIFIED 3.3 MICROMETER EMISSION FEATURE IN NEBULAE.

770405 BARNES, T. G., BEER, R., HINKLE, K. H., LAMBERT, D. L. <AP. J., 213, 71>
A HIGH-RESOLUTION INFRARED SPECTRUM OF IRC +10216.

770406 O'DELL, S. L., PUSCHELL, J. J., STEIN, W. A. <AP. J., 213, 351>
THE 0.36-3.5 MICROMETER SPECTRAL-FLUX DISTRIBUTION OF SEVERAL BL LACERTAE OBJECTS.

770407 RIGHINI-COHEN, G., SIMON, M. <AP. J., 213, 390>
THE RELATIONSHIP OF SUBMILLIMETER OPTICAL DEPTH TO 13-CO COLUMN DENSITY IN MOLECULAR CLOUDS.

770408 WARNER, J. W., STROM, S. E., STROM, K. M. <AP. J., 213, 427>
CIRCUMSTELLAR SHELLS IN NGC 2264: A REEVALUATION.

770409 CHINI, R., ELSAESSER, H., HEFELE, H., WEINBERGER, R. <ASTR. AP., 56, 323>
ON THE INFRARED SOURCES IN THE OPHIUCHUS DARK CLOUD REGION.

770410 ROUAN, D., LENA, P. J., PUGET, J. L., DE BOER, K. S., WIJNBERGEN, J. J. <AP. J. (LETTERS), 213, L35>
FAR-INFRARED OBSERVATIONS OF THE GALACTIC PLANE AND MOLECULAR CLOUD S140.

770411 GREENBERG, L. T., DYAL, P., GEBALLE, T. R. <AP. J. (LETTERS), 213, L71>
DETECTION OF (S III) FINE-STRUCTURE EMISSION IN IONIZED NEBULAE.

770412 WILLIAMS, P. M., BEATTIE, D. H., STEWART, J. M. <OBSERVATORY, 97, 76>
INFRARED PHOTOMETRY OF CV SERPENTIS WITH A NOTE ON CRL 2120.

770413 GREENSTEIN, J. L., OKE, J. B. <P. A. S. P., 89, 131>
AN INTERPRETATION OF THE SPECTRUM OF THE RED RECTANGLE.

770414 JOHNSON, H. M., SNOW JR., T. P., GEHRZ, R. D., HACKWELL, J. A. <P. A. S. P., 89, 165>
COPERNICUS SPECTRA AND INFRARED PHOTOMETRY OF 42 ORIONIS.

770415 FEAST, M. W. <IAUC NO. 3056>
NOVA IN LARGE MAGELLANIC CLOUD.

770501 WYNN-WILLIAMS, C. G., BECKLIN, E. E., MATTHEWS, K., NEUGEBAUER, G., WERNER, M. W. <M. N. R. A. S., 179, 255>
INFRARED STUDIES OF HII REGIONS AND DUST CLOUDS NEAR K3-50.

770502 JOYCE, R. R., CAPPS, R. W., GILLETT, F. C., GRASDALEN, G. L.,KLEINMANN, S. G., SARGENT, D. G. <AP. J. (LETTERS), 213, L125>
ACCURATE PHOTOMETRIC POSITIONS FOR 60 SOURCES FROM THE AFCRL SKY SURVEY.

770503 FROGEL, J. A., PERSSON, S. E., AARONSON, M. <AP. J., 213, 723>
COMPACT INFRARED SOURCES ASSOCIATED WITH SOUTHERN HII REGIONS. II.

770504 BARLOW, M. J., COHEN, M. <AP. J., 213, 737>
INFRARED PHOTOMETRY AND MASS LOSS RATES FOR OBA SUPERGIANTS AND OF STARS.

770505 LUTZ, B. L., SOUZA, S. P. <AP. J. (LETTERS), 213, L129>
A SEARCH FOR C2 IN THE INTERSTELLAR SPECTRUM OF ZETA OPHIUCHI.

770506 FERLAND, G. J., WOOTTEN, H. A. <AP. J. (LETTERS), 214, L27>
THE SHELL PHASE IN NOVA CYGNI (1975).

770507 MALANUSHENKO, V. M., SHANIN, G. I., SHCHERBAKOV, A. G. <SOV. AST., 21, 267>
STUDIES OF NOVA CYGNI 1975 AT THE CRIMEAN ASTROPHYSICAL OBSERVATORY. II. SPECTROSCOPY IN THE NEAR INFRARED RANGE.

770508 KOLOTILOV, E. A., LIBERMAN, A. A. <SOV. AST., 21, 327>
NEAR-INFRARED SPECTRUM OF NOVA CYGNI 1975.

770509 SHENAVRIN, V. I., MOROZ, V. I., LIBERMAN, A. A. <SOV. AST., 21, 358>
WIDE-BAND INFRARED PHOTOMETRY OF NOVA CYGNI 1975 – V1500 CYG.

770510 HOFMANN, W., LEMKE, D., THUM, C. <ASTR. AP., 57, 111>
SURFACE BRIGHTNESS OF THE CENTRAL REGION OF THE MILKY WAY AT 2.4 AND 3.4 MICRONS.

770601 ULVESTAD, J. S. <NASA X-693-77-165>
IRC+10216: AN EVOLVING INFRARED SOURCE.

770602 ADAMS, D. J., HOUGH, J. H. <M. N. R. A. S., 179, 73P>
THE POLARIZATION OF THE GALACTIC CENTRE AT 2.2 MICRON.

770603 BREGMAN, J. D. <P. A. S. P., 89, 335>
OBSERVATIONS AND INTERPRETATION OF THE INFRARED SPECTRUM OF HD 44179.

770604 WARD, D. B., GULL, G. E., HARWIT, M. <AP. J. (LETTERS), 214, L63>
FAR-INFRARED SPECTROMETRY OF HII REGIONS AND THE GALACTIC CENTER.

770605 RIDGWAY, S. T., WELLS, D. C., JOYCE, R. R. <A. J., 82, 414>
ANGULAR DIAMETERS FOR 11 LATE-TYPE STARS BY THE LUNAR OCCULTATION TECHNIQUE.

770606 ENNIS, D. J., BECKLIN, E. E., BECKWITH, S., ELIAS, J. H., GATLEY, I., MATTHEWS, K., NEUGEBAUER, G., WILLNER, S. P. <AP. J., 214, 478>
INFRARED OBSERVATIONS OF NOVA CYGNI 1975.

770607 STECKER, F. W., PUGET, J. L., FAZIO, G. G. <AP. J. (LETTERS), 214, L51>
THE COSMIC FAR-INFRARED BACKGROUND AT HIGH GALACTIC LATITUDES.

770608 MCCARTHY, D. W., LOW, F. J., HOWELL, R. <AP. J. (LETTERS), 214, L85>
ANGULAR DIAMETER MEASUREMENTS OF ALPHA ORIONIS, VY CANIS MAJORIS, AND IRC+10216 AT 8.3, 10.2, AND 11.1 MICROMETERS.

770609 WILLNER, S. P. <AP. J., 214, 706>
8 TO 13 MICROMETER SPECTROPHOTOMETRY OF COMPACT SOURCES IN W3.

770610 LOWE, R. P., MOORHEAD, J. M., WEHLAU, W. H. <AP. J., 214, 712>
NEAR-INFRARED FOURIER SPECTROSCOPY OF THE ORION NEBULA.

770611 O'DELL, S. L., PUSCHELL, J. J., STEIN, W. A., WARNER, J. W. <AP. J. (LETTERS), 214, L105>
DEVELOPMENT OF A SPECTRAL BREAK IN THE NONTHERMAL EMISSION OF AO 0235+164.

770612 LOW, F. J., KURTZ, R. F., POTEET, W. M., NISHIMURA, T. <AP. J. (LETTERS), 214, L115>
FAR-INFRARED SCANS OF THE GALACTIC PLANE.

770613 PUETTER, R. C., RUSSELL, R. W., SELLGREN, K., SOIFER, B. T. <P. A. S. P., 89, 320>
SPECTRA OF LATE-TYPE STARS FROM 4-8 MICRONS.

770614 BASCHEK, B., WEHRSE, R. <P. A. S. P., 89, 345>
COMMENTS ON THE PAPER BY A. E. RYDGREN "T TAURI STARS AND THE (J-H), (H-K) DIAGRAM".

770615 HAYAKAWA, S., ITO, K., MATSUMOTO, T., UYAMA, K. <ASTR. AP., 58, 325>
OVERALL DISTRIBUTION OF INFRARED SOURCES IN OUR GALAXY.

770616 HATFIELD, B. F., BRODZIK, D. <IAUC NO. 3082>
NOVA SAGITTARII 1977.

770701 ULVESTAD, J. S. <NASA X-693-77-186>
CIT 6: A STRONG INFRARED SOURCE.

770702 BLACKWELL, D. E., SHALLIS, M. J. <M. N. R. A. S., 180, 177>
STELLAR ANGULAR DIAMETERS FROM INFRARED PHOTOMETRY. APPLICATION TO ARCTURUS AND OTHER STARS; WITH EFFECTIVE TEMPERATURES.

770703 HARVEY, P. M., CAMPBELL, M. F., HOFFMANN, W. F. <AP. J., 215, 151>
FAR-INFRARED EMISSION FROM COMPACT SOURCES IN NGC 2264 AND THE ROSETTE NEBULA.

770704 DENNISON, B. <AP. J., 215, 529>
ON THE INFRARED POLARIZATION OF THE ORION NEBULA.

770705 KLEINMANN, S. G., SARGENT, D. G., GILLETT, F. C., GRASDALEN, G. L., JOYCE, R. R. <AP. J. (LETTERS), 215, L79>
SPECTRAL AND SPATIAL OBSERVATIONS OF THE UNUSUAL OBJECT AFGL 437.

770706 PRICE, S. D. <AFGL-TR-77-0160>
THE AFGL FOUR COLOR INFRARED SKY SURVEY: SUPPLEMENTAL CATALOG.

770707 LOREN, R. B. <AP. J., 215, 129>
THE MONOCEROS R2 CLOUD: NEAR-INFRARED AND MOLECULAR OBSERVATIONS OF A ROTATING COLLAPSING CLOUD.

770708 HARTMANN, L., ANDERSON, C. M. <AP. J., 215, 188>
ABUNDANCES IN LATE-TYPE DWARFS.

770709 BALDWIN, J. A., WAMPLER, E. J., BURBIDGE, E. M., O'DELL, S. L., SMITH, H. E., HAZARD, C., NORDSIECK, K.H.,POOLEY, G., STEIN, W. A. <AP. J., 215, 408>
1400+162—AN EXTENDED RADIO SOURCE IDENTIFIED WITH A BL LACERTAE OBJECT IN A GROUP OF GALAXIES.

770710 HONEYCUTT, R. K., RAMSEY, L. W., WARREN JR., W. H., RIDGWAY, S. T. <AP. J., 215, 584>
SPECTROPHOTOMETRY OF COOL ANGULAR-DIAMETER STARS.

770711 PIPHER, J. L., SHARPLESS, S., SAVEDOFF, M. P., KRASSNER, J., VARLESE, S., SOIFER, B. T., ZEILIK II, M. <ASTR. AP., 59, 215>
OPTICAL, INFRARED, AND RADIO STUDIES OF COMPACT HII REGIONS.

770712 MERRILL, K. M. <IAUC NO. 3088>
HM SAGITTAE.

770801 GUETTER, H. H. <A. J., 82, 598>
SPECTROSCOPIC STUDIES OF STARS IN PER OB2.

770802 LEBOFSKY, M. J., RIEKE, G. H. <A. J., 82, 646>
CRL 3068—A DUST-ENSHROUDED CARBON STAR.

770803 RYTER, C. E., PUGET, J. L. <AP. J., 215, 775>
FAR-INFRARED EMISSION OF MOLECULAR CLOUDS.

770804 KEMP, J. C., RIEKE, G. H., LEBOFSKY, M. J., COYNE S. J., G. V. <AP. J. (LETTERS), 215, L107>
THE INFRARED POLARIZATION OF NGC 1275, NGC 4151, MARKARIAN 231, AND 3C 273.

770805 KNACKE, R. F., CAPPS, R. W. <AP. J., 216, 271>
INFRARED POLARIZATION OF THE GALACTIC CENTER. II.

770806 GATLEY, I., BECKLIN, E. E., WERNER, M. W., WYNN-WILLIAMS, C. G. <AP. J., 216, 277>
AIRBORNE FAR-INFRARED OBSERVATIONS OF THE GALACTIC CENTER REGION.

770807 MCMILLAN, R. S. <AP. J. (LETTERS), 216, L41>
WALKER NO. 67 IN NGC 2264: A CANDIDATE FOR STRONG INTERSTELLAR CIRCULAR POLARIZATION.

770808 SOUZA, S. P., LUTZ, B. L. <AP. J. (LETTERS), 216, L49>
DETECTION OF C2 IN THE INTERSTELLAR SPECTRUM OF CYGNUS OB2 NUMBER 12 (VI CYGNI NUMBER 12).

770809 BERNAT, A. P., BARNES, T. G., SCHUPLER, B. R., POTTER, A. E. <P. A. S. P., 89, 541>
INFRARED SPECTRA OF THE WN STARS HD 50896 AND HD 151932.

770810 JAMESON, R. F. <IAUC NO. 3095>
AM HERCULIS.

770901 HILDEBRAND, R. H., WHITCOMB, S. E., WINSTON, R., STIENING, R. F., HARPER JR., D. A., MOSELEY, S. H. <AP. J., 216, 698>
SUBMILLIMETER PHOTOMETRY OF EXTRAGALACTIC OBJECTS.

770902 SIMON, T., DYCK, H. M. <A. J., 82, 725>
BROAD-BAND 20-33-MICRON PHOTOMETRY OF YOUNG STARS.

770903 PERSSON, S. E., AARONSON, M., FROGEL, J. A. <A. J., 82, 729>
BROAD-BAND INFRARED COLORS AND CO AND H2O ABSORPTION INDICES FOR LATE-TYPE DWARF STARS.

770904 THOMPSON, R. I., BOROSON, T. A. <AP. J. (LETTERS), 216, L75>
INFRARED EMISSION LINES FROM IRC +10420.

770905 ERICKSON, E. F., CAROFF, L. J., SIMPSON, J. P., STRECKER, D. W., GOORVITCH, D. <AP. J., 216, 404>
THE FAR-INFRARED SPECTRUM OF THE CORE OF SAGITTARIUS B2.

770906 WING, R. F., COHEN, J. G., BRAULT, J. W. <AP. J., 216, 659>
CONFIRMATION OF THE PRESENCE OF IRON HYDRIDE IN SUNSPOTS AND COOL STARS.

770907 SHCHERBAKOV, A. G. <SOV. AST. (LETTERS), 3, 244>
THE INFRARED SPECTRUM OF NOVA VULPECULAE 1976.

770908 HARRIS, S., ROWAN-ROBINSON, M. <ASTR. AP., 60, 405>
THE BRIGHTEST SOURCES IN THE AFCRL SURVEY.

770909 HYLAND, A. R., SCHWARZ, M. P. <PROC. A. S. A., 3, 137>
INTERPRETATION OF QUASAR COLOURS IN THE NEAR IR.

770910 WILLIAMS, P. M., STEWART, M. J., BEATTIE, D. H., LEE, T. J. <IAUC NO. 3107>
HD 193793.

771001 COHEN, M., HUDSON, H. S., O'DELL, S. L., STEIN, W. A. <M. N. R. A. S., 181, 233>
A STUDY OF THE PLANETARY NEBULAE ABELL 30 AND ABELL 78.

771002 HARTOOG, M. R., PERSSON, S. E., AARONSON, M. <P. A. S. P., 89, 660>
THE STRENGTH OF THE 2.3-MICRON CO BAND IN WEAK-G-BAND STARS.

771003 AITKEN, D. K., JONES, B., BREGMAN, J. D., LESTER, D. F., RANK, D. M. <AP. J., 217, 103>
SPECTRAL OBSERVATIONS OF ETA CARINAE AT 4 MICRONS.

771004 EVANS II, N. J., BLAIR, G. N., BECKWITH, S. <AP. J., 217, 448>
THE ENERGETICS OF MOLECULAR CLOUDS. I. METHODS OF ANALYSIS AND APPLICATION TO THE S255 MOLECULAR CLOUD.

771005 ALLEN, D. A., HYLAND, A. R., LONGMORE, A. J., CASWELL, J. L.,GOSS, W. M., HAYNES, R. F. <AP. J., 217, 108>
OPTICAL, INFRARED, AND RADIO STUDIES OF AFCRL SOURCES.

771006 SZKODY, P. <AP. J., 217, 140>
INFRARED PHOTOMETRY OF DWARF NOVAE AND POSSIBLY RELATED OBJECTS.

771007 HAWLEY, S. A., GRANDI, S. A. <AP. J., 217, 420>
OBSERVATIONS OF (S III) IN NGC 604 AND N/S ABUNDANCE GRADIENTS.

771008 SUTTON, E. C., STOREY, J. W. V., BETZ, A. L., TOWNES, C. H., SPEARS, D. L. <AP. J. (LETTERS), 217, L97>
SPATIAL HETERODYNE INTERFEROMETRY OF VY CANIS MAJORIS, ALPHA ORIONIS, ALPHA SCORPII, AND R LEONIS AT 11 MICRONS.

771009 ZEILIK II, M., HECKERT, P. A. <A. J., 82, 824>
LARGE-BEAM INFRARED OBSERVATIONS OF COMPACT HII REGIONS.

771010 JORDEN, P. R., MACGREGOR, A. D., SELBY, M. J., WHITELOCK, P. A., SANCHEZ MAGRO, C. <M. N. R. A. S., 181, 157>
INFRARED SOURCES IN THE COMPACT HII REGION G45.5+0.1.

771101 HOYLE, F., WICKRAMASINGHE, N. C. <M. N. R. A. S., 181, 51P>
POLYSACCHARIDES AND THE INFRARED SPECTRUM OF OH 26.5+0.6.

771102 WYNN-WILLIAMS, C. G. <M. N. R. A. S., 181, 61P>
RADIO EMISSION FROM THE INFRARED SOURCE CRL 618: AN EXTREMELY YOUNG PLANETARY NEBULA.

771103 HERBIG, G. H. <AP. J., 217, 693>
ERUPTIVE PHENOMENA IN EARLY STELLAR EVOLUTION.

771104 WILLNER, S. P., SOIFER, B. T., RUSSELL, R. W., JOYCE, R. R., GILLETT, F. C. <AP. J. (LETTERS), 217, L121>
2 TO 8 MICRON SPECTROPHOTOMETRY OF M82.

771105 RUSSELL, R. W., SOIFER, B. T., WILLNER, S. P. <AP. J. (LETTERS), 217, L149>
THE 4 TO 8 MICRON SPECTRUM OF NGC 7027.

771106 PHILLIPS, T. G., HUGGINS, P. J., NEUGEBAUER, G., WERNER, M. W. <AP. J. (LETTERS), 217, L161>
DETECTION OF SUBMILLIMETER (870 MICRON) CO EMISSION FROM THE ORION MOLECULAR CLOUD.

771107 WARNER, J. W., WING, R. F. <AP. J., 218, 105>
SUPERGIANTS IN THE FIELD OF THE CLUSTER M6, AND THE DISTRIBUTION OF INTERSTELLAR MATTER IN THE DIRECTION OF THE GALACTIC CENTER.

771108 WRIGHT, E. L., FAZIO, G. G., LOW, F. J. <AP. J., 217, 724>
A HIGH-RESOLUTION FAR-INFRARED SURVEY OF THE W31 REGION.

771109 EVANS II, N. J., BECKWITH, S. <AP. J., 217, 729>
NEW INFRARED OBJECTS ASSOCIATED WITH OH MASERS.

771110 CRUIKSHANK, D. P., PILCHER, C. B., MORRISON, D. <AP. J., 217, 1006>
IDENTIFICATION OF A NEW CLASS OF SATELLITES IN THE OUTER SOLAR SYSTEM.

771111 THOMPSON, R. I., STRITTMATTER, P. A., ERICKSON, E. F., WITTEBORN, F. C., STRECKER, D. W. <AP. J., 218, 170>
OBSERVATION OF PREPLANETARY DISKS AROUND MWC 349 AND LKHA 101.

771112 FAWLEY, W. M. <AP. J., 218, 181>
ON THE NEAR-INFRARED EXCESSES OF VERY COOL SUPERGIANTS.

771201 KODAIRA, K., TANAKA, W., ONAKA, T., WATANABE, T., YOSHIDA, H. <TOKYO AST. BULL., 2, 2889>
NEAR-INFRARED PHOTOMETRY OF LATE-TYPE STARS WITH BALLOON-BORNE TELESCOPE.

771202 LACY, C. H. <AP. J., 218, 444>
ABSOLUTE DIMENSIONS AND MASSES OF THE REMARKABLE SPOTTED DM4E ECLIPSING BINARY FLARE STAR CM DRACONIS.

771203 RIEKE, G. H., LEBOFSKY, M. J., KEMP, J. C., COYNE S. J., G. V., TAPIA, S. <AP. J. (LETTERS), 218, L37>
INFRARED AND VISIBLE POLARIMETRY AND PHOTOMETRY OF HIGHLY VARIABLE QUASI-STELLAR SOURCES.

771204 LOREN, R. B. <AP. J., 218, 716>
THE STAR-FORMATION PROCESS IN MOLECULAR CLOUDS ASSOCIATED WITH HERBIG BE/AE STARS. I. LKHA 198, BD +40 4124, AND NGC 7129.

771205 WOLLMAN, E. R., GEBALLE, T. R., LACY, J. H., TOWNES, C. H., RANK, D. M. <AP. J. (LETTERS), 218, L103>
NE II 12.8 MICRON EMISSION FROM THE GALACTIC CENTER. II.

771206 GEBALLE, T. R., WOLLMAN, E. R., LACY, J. H., RANK, D. M. <P. A. S. P., 89, 840>
OBSERVATIONS AND ANALYSIS OF CARBON MONOXIDE IN COOL STARS AT FIVE MICRONS.

779901 MARKARIAN, B. E., LIBOVETSKY, V. A., STEPANIAN, J. A. <ASTROFIZIKA, 13, 225>
GALAXIES WITH ULTRAVIOLET CONTINUUM. X.

779902 MARKARIAN, B. E., LIBOVETSKY, V. A., STEPANIAN, J. A. <ASTROFIZIKA, 13, 397>
GALAXIES WITH ULTRAVIOLET CONTINUUM. XI.

779903 GRAHAM, J. A. <IAUC NO. 3049>
NOVA IN LARGE MAGELLANIC CLOUD.

779904 WARREN JR., W. H., HESSER, J. E. <AP. J. SUPPL., 34, 115>
A PHOTOMETRIC STUDY OF THE ORION OB1 ASSOCIATION. I. OBSERVATIONAL DATA.

779905 KLEMOLA, A. R., MARSDEN, B. G. <A. J., 82, 849>
PREDICTED OCCULTATIONS BY THE RINGS OF URANUS, 1977-1980.

779906 FANTI, C., FANTI, R., PADRIELLI, L., VAN DER LAAN, H., DE RUITER, H. <ASTR. AP., 61, 487>
A SEARCH FOR RADIO EMISSION FROM A SAMPLE OF OPTICALLY SELECTED QUASARS.

779907 PLAUT, L. <ASTR. AP. SUPPL., 28, 169>
POSITIONS OF VARIABLE STARS AS DERIVED FROM THE ASTROGRAPHIC (CARTE DU CIEL) CATALOGUES.

779908 ADAM, G. <ASTR. AP. SUPPL., 29, 293>
ACCURATE POSITIONS OF QUASARS AND QUASAR CANDIDATES SOUTH OF DECLINATION -45 DEGREES.

779909 HOLMBERG, E. B., LAUBERTS, A., SCHUSTER, H. -E., WEST, R. M. <ASTR. AP. SUPPL., 27, 295>
THE ESO/UPPSALA SURVEY OF THE ESO(B) ATLAS OF THE SOUTHERN SKY. IV.

779910 LEE, S. -W. <ASTR. AP. SUPPL., 28, 409>
UBV PHOTOMETRY OF BRIGHT STARS IN NGC 3201.

779911 LEE, S. -W. <ASTR. AP. SUPPL., 27, 381>
UBV PHOTOMETRY OF BRIGHT STARS IN 47 TUC.

780001 SATO, S., KAWARA, K., KOBAYASHI, Y., MAIHARA, T., ODA, N., OKUDA, H. <P. A. S. J., 30, 419>
INFRARED OBSERVATIONS OF NOVA VULPECULAE 1976 (NQ VUL).

780002 TANAKA, W. <P. A. S. J., 30, 637>
BALLOON-BORNE NEAR-INFRARED MULTICOLOR PHOTOMETRY OF LATE-TYPE STARS.

780003 IIJIMA, T., ISHIDA, K. <P. A. S. J., 30, 657>
TWO-MICRON OBJECTS IN THE NORTHERN MONOCEROS REGION.

780004 DOROSHENKO, V. T., EFIMOV, YU. S., ROSENBUSH, A. E., TEREBIZH, V. Y., SHENAVRIN, V. I. <ASTROFIZIKA, 14, 5>
THE OPTICAL AND INFRARED OBSERVATIONS OF SU TAU.

780005 MAIHARA, T., ODA, N., SUGIYAMA, T., OKUDA, H. <P. A. S. J., 30, 1>
2.4-MICRON OBSERVATION OF THE GALAXY AND THE GALACTIC STRUCTURE.

780006 HAYAKAWA, S., ITO, K., MATSUMOTO, T., MURAKAMI, H., UYAMA, K. <P. A. S. J., 30, 369>
NEAR-INFRARED OBSERVATION OF THE GALAXY IN THE GALACTIC ANTICENTER DIRECTION.

780007 KOBAYASHI, Y., KAWARA, K., MAIHARA, T., OKUDA, H., SATO, S., NOGUCHI, K. <P. A. S. J., 30, 377>
INFRARED POLARIZATIONS OF CRL OBJECTS AND OH 0739-14.

780101 BEICHMAN, C. A., DYCK, H. M., SIMON, T. <ASTR. AP., 62, 261>
A HIGH SPATIAL RESOLUTION MAP OF THE ORION NEBULA AT 33 MICRONS.

780102 GLASS, I. S. <M. N. R. A. S., 182, 93>
AN INFRARED SEARCH FOR OH/IR STARS.

780103 JAMESON, R. F., HOUGH, J. H. <M. N. R. A. S., 182, 179>
NEAR-INFRARED POLARIZATION OF THE NUCLEUS OF M31.

780104 STRECKER, D. W., ERICKSON, E. F., WITTEBORN, F. C. <A. J., 83, 26>
AIRBORNE INFRARED SPECTROPHOTOMETRY OF MIRA VARIABLES.

780105 FORREST, W. J., GILLETT, F. C., HOUCK, J. R., MCCARTHY, J. F., MERRILL, K. M., PIPHER, J. L., PUETTER, R. C., RUSSELL, R. W., SOIFER, B. T., WILLNER, S. P. <AP. J., 219, 114>
SPECTROPHOTOMETRY OF OH 26.5+0.6 FROM 2 TO 40 MICRONS.

780106 LEBOFSKY, M. J., SARGENT, D. G., KLEINMANN, S. G., RIEKE, G. H. <AP. J., 219, 487>
AN OBSERVATIONAL STUDY OF THE AFCRL INFRARED SKY SURVEY. III. FURTHER SEARCHES FOR AFCRL/AFGL SOURCES AND AN EVALUATION OF THE CONTENTS OF THE MID-INFRARED SKY.

780107 PIPHER, J. L., DUTHIE, J. G., SAVEDOFF, M. P. <AP. J., 219, 494>
LAMELLAR GRATING OBSERVATIONS OF THE ORION NEBULA FROM 100 TO 500 MICRONS.

780108 HYLAND, A. R., THOMAS, J. A., ROBINSON, G. <A. J., 83, 20>
INFRARED STUDIES OF 30 DORADUS. I. THE 2-MICRON SOURCES OF THE INNER REGION.

780109 BECKLIN, E. E., MATTHEWS, K., NEUGEBAUER, G., WILLNER, S. P. <AP. J., 219, 121>
INFRARED OBSERVATIONS OF THE GALACTIC CENTER. I. NATURE OF THE COMPACT SOURCES.

780110 JOYCE, R. R., GEZARI, D. Y., SCOVILLE, N. Z., FURENLID, I. <AP. J. (LETTERS), 219, L29>
2.1 MICRON H2 EMISSION: HIGH-SPECTRAL-RESOLUTION OBSERVATIONS OF THE ORION NEBULA.

780111 BECKWITH, S., PERSSON, S. E., GATLEY, I. <AP. J. (LETTERS), 219, L33>
DETECTION OF MOLECULAR HYDROGEN EMISSION FROM FIVE PLANETARY NEBULAE.

780112 HUMPHREYS, R. M. <AP. J., 219, 445>
LUMINOUS VARIABLE STARS IN M31 AND M33.

780113 SHIELDS, G. A. <AP. J., 219, 565>
IONIZATION STRUCTURE AND COMPOSITION OF THE PLANETARY NEBULA NGC 7027.

780114 JAMESON, R. F., AKINCI, R., ADAMS, D. J., GILES, A. B., MCCALL, A. <NATURE, 271, 334>
INFRARED LIGHT CURVES OF AM HERCULIS.

780115 LUUD, L., VENNIK, J., PEHK, M. <SOV. AST. (LETTERS), 4, 46>
A NEW ACTIVE STATE IN CH CYGNI, AND A POSSIBLE MODEL.

780116 VIOTTI, R., FERRARI-TONIOLO, M., MARCOCCI, M., NATALI, G., PERSI, P., SPADA, G., SARACENO, P. <ASTR. AP., 62, 287>
OPTICAL AND INFRARED OBSERVATIONS OF BETA LYRAE.

780201 THACKERAY, A. D. <M. N. R. A. S., 182, 11P>
INFRARED FE II LINES IN ETA CARINAE AND A POSSIBLE INTERPRETATION OF INFRARED EXCESSES.

780202 HARVEY, P. M., CAMPBELL, M. F., HOFFMANN, W. F. <AP. J., 219, 891>
STRONG FAR-INFRARED EMISSION FROM A COMPACT SOURCE IN SHARPLESS 140.

780203 BLAIR, G. N., EVANS II, N. J., VANDEN BOUT, P. A., PETERS III, W. L. <AP. J., 219, 896>
THE ENERGETICS OF MOLECULAR CLOUDS. II. THE S140 MOLECULAR CLOUD.

780204 HILDEBRAND, R. H., WHITCOMB, S. E., WINSTON, R., STIENING, R. F., HARPER JR., D. A., MOSELEY, S. H. <AP. J. (LETTERS), 219, L101>
SUBMILLIMETER OBSERVATIONS OF THE GALACTIC CENTER.

780205 NORDH, H. L., OLOFSSON, S. G., AUGASON, G. C. <A. J., 83, 188>
AIRBORNE PHOTOMETRIC OBSERVATIONS BETWEEN 1.25 AND 3.25 MICRONS OF LATE-TYPE STARS.

780206 O'DELL, S. L., PUSCHELL, J. J., STEIN, W. A., WARNER, J. W., ULRICH, M. -H. <AP. J., 219, 818>
THE SPECTRAL-FLUX DISTRIBUTION (0.36-3.5 MICRON) OF NONSTELLAR LIGHT FROM THE BROAD-LINE RADIO GALAXIES 3C 227 AND 3C 382.

780207 NETZER, H. <AP. J., 219, 822>
HE I LINES IN THE SPECTRA OF QSOS AND SEYFERT GALAXIES.

780208 WILLNER, S. P. <AP. J., 219, 870>
INFRARED OBSERVATIONS OF THE GALACTIC CENTER. II. (NE II) EMISSION.

780209 NEY, E. P., HATFIELD, B. F. <AP. J. (LETTERS), 219, L111>
THE ISOTHERMAL DUST CONDENSATION OF NOVA VULPECULAE 1976.

780210 ELIAS, J. H., ENNIS, D. J., GEZARI, D. Y., HAUSER, M. G., HOUCK, J. R., LO, K. Y., MATTHEWS, K., NADEAU, D., NEUGEBAUER, G., WERNER, M. W., WESTBROOK, W. E. <AP. J., 220, 25>
1 MILLIMETER CONTINUUM OBSERVATIONS OF EXTRAGALACTIC OBJECTS.

780211 STROM, K. M., STROM, S. E., WELLS, D. C., ROMANISHIN, W. <AP. J., 220, 62>
AN OPTICAL AND INFRARED STUDY OF NGC 2768 AND NGC 3115.

780212 FROGEL, J. A., PERSSON, S. E., AARONSON, M., MATTHEWS, K. <AP. J., 220, 75>
PHOTOMETRIC STUDIES OF COMPOSITE STELLAR SYSTEMS. I. CO AND JHK OBSERVATIONS OF E AND S0 GALAXIES.

780213 NEUGEBAUER, G., BECKLIN, E. E., MATTHEWS, K., WYNN-WILLIAMS, C. G. <AP. J., 220, 149>
INFRARED OBSERVATIONS OF THE GALACTIC CENTER. III. 2.2 MICRON SPECTROSCOPY.

780214 JOYCE, R. R., SIMON, M., SIMON, T. <AP. J., 220, 156>
OBSERVATIONS OF BRACKETT-ALPHA EMISSION IN THE REGION OF THE BN OBJECT.

780215 JONES, T. J., DYCK, H. M. <AP. J., 220, 159>
INFRARED POLARIMETRY OF THREE BIPOLAR NEBULAE.

780216 HINKLE, K. H. <AP. J., 220, 210>
INFRARED SPECTROSCOPY OF MIRA VARIABLES. I. R LEONIS: THE CO AND OH VIBRATION-ROTATION OVERTONE BANDS.

780217 DAVIDSON, K., HUMPHREYS, R. M., MERRILL, K. M. <AP. J., 220, 239>
OPTICAL AND INFRARED OBSERVATIONS OF THE NEW EMISSION-LINE OBJECT HM SAGITTAE.

780218 NORDH, H. L., OLOFSSON, S. G., AUGASON, G. C. <A. J., 83, 188>
AIRBORNE PHOTOMETRIC OBSERVATIONS BETWEEN 1.25 AND 3.25 MICRONS OF LATE-TYPE STARS.

780219 AARONSON, M. <P. A. S. P., 90, 28>
IDENTIFICATION OF THE NUCLEUS IN THE SPIRAL GALAXY NGC 4631.

780301 CHRISTENSEN, C. G. <A. J., 83, 244>
ABSOLUTE SPECTRAL ENERGY DISTRIBUTIONS AND (FE/H) VALUES OF METAL-POOR STARS AND GLOBULAR CLUSTERS.

780302 GATLEY, I., BECKLIN, E. E., WERNER, M. W., HARPER JR., D. A. <AP. J., 220, 822>
FAR-INFRARED OBSERVATIONS OF HII REGIONS NEAR THE GALACTIC CENTER.

780303 RIEKE, G. H., TELESCO, C. M., HARPER JR., D. A. <AP. J., 220, 556>
THE INFRARED EMISSION OF THE GALACTIC CENTER.

780304 RUSSELL, R. W., SOIFER, B. T., WILLNER, S. P. <AP. J., 220, 568>
THE INFRARED SPECTRA OF CRL 618 AND HD 44179 (CRL 915).

780305 RIEKE, G. H., LEBOFSKY, M. J. <AP. J. (LETTERS), 220, L37>
10 MICRON OBSERVATIONS OF BRIGHT GALAXIES.

780306 DYCK, H. M., CAPPS, R. W. <AP. J. (LETTERS), 220, L49>
NEAR-INFRARED POLARIMETRY OF COMPACT INFRARED SOURCES ASSOCIATED WITH HII REGIONS AND MOLECULAR CLOUDS.

780307 BECKLIN, E. E., MATTHEWS, K., NEUGEBAUER, G., WILLNER, S. P. <AP. J., 220, 831>
INFRARED OBSERVATIONS OF THE GALACTIC CENTER. IV. THE INTERSTELLAR EXTINCTION.

780308 MITCHELL, R. M., ROBINSON, G. <AP. J., 220, 841>
THE SPECTRAL AND SPATIAL DISTRIBUTION OF RADIATION FROM ETA CARINAE. I. A SPHERICAL DUST SHELL MODEL APPROACH.

780309 MOULD, J. R., MCELROY, D. B. <AP. J., 220, 935>
OLD DISK SUBDWARFS.

780310 HYLAND, A. R., BECKLIN, E. E., NEUGEBAUER, G. <AP. J. (LETTERS), 220, L73>
THE L-ALPHA/H-ALPHA INTENSITY RATIO IN PKS 0237-23.

780311 SHANIN, G. I. <SOV. AST. (LETTERS), 4, 100>
THE NEAR-INFRARED SPECTRUM OF HM SAGITTAE.

780401 WYNN-WILLIAMS, C. G., BECKLIN, E. E., MATTHEWS, K., NEUGEBAUER, G. <M. N. R. A. S., 183, 237>
TWO-MICRON LINE EMISSION FROM THE HII REGION G333.6-0.2.

780402 SMYTH, M. J., NANDY, K. <M. N. R. A. S., 183, 215>
INFRARED PHOTOMETRY OF EARLY-TYPE STARS-I.

780403 KLEINMANN, S. G., HALL, D. N. B., RIDGWAY, S. T., WRIGHT, E. L. <A. J., 83, 373>
HIGH-RESOLUTION 2-MICRON SPECTROSCOPY OF CYG OB II NO. 12.

780404 COHEN, M., FITZGERALD, M. P., KUNKEL, W., LASKER, B. M., OSMER, P. S. <AP. J., 221, 151>
STUDIES OF BIPOLAR NEBULAE. IV. MZ 3(-PK 331-1 1).

780405 HARTMANN, L. <AP. J., 221, 193>
THE INFRARED ECLIPSE OF V444 CYGNI AND THE STRUCTURE OF WOLF-RAYET WINDS.

780406 MOULD, J. R., MCELROY, D. B. <AP. J., 221, 580>
TIO BAND STRENGTHS IN METAL-RICH GLOBULAR CLUSTERS.

780407 DAIN, F. W., GULL, G. E., MELNICK, G., HARWIT, M., WARD, D. B. <AP. J. (LETTERS), 221, L17>
OBSERVATIONS OF (O III) 88 MICRON LINE EMISSION FROM HII REGIONS AND THE GALACTIC CENTER.

780408 GEHRZ, R. D., HACKWELL, J. A., BRIOTTA, D. A. <AP. J. (LETTERS), 221, L23>
OBSERVATIONS OF THE HIGHLY EVOLVED CARBON STAR CRL 3099.

780409 HUMPHREYS, R. M., WARNER, J. W. <AP. J. (LETTERS), 221, L73>
INFRARED DETECTION OF LUMINOUS STARS IN M31 AND M33.

780410 FAZIO, G. G., LADA, C. J., KLEINMANN, D. E., WRIGHT, E. L., HO, P. T. P., LOW, F. J. <AP. J. (LETTERS), 221, L77>
A NEW, COMPACT FAR-INFRARED SOURCE IN THE W31 REGION.

780411 KLEINMANN, S. G., SARGENT, D. G., MOSELEY, S. H., HARPER JR., D. A., LOEWENSTEIN, R. F., TELESCO, C. M., THRONSON JR., H. A. <ASTR. AP., 65, 139>
FAR-INFRARED OBSERVATIONS OF SOURCES ASSOCIATED WITH DOUBLE-LOBED REFLECTION NEBULAE.

780412 GEHRZ, R. D., GRASDALEN, G. L., HACKWELL, J. A., MCCLAIN, D. <IAUC NO. 3213>
NOVA SAGITTARII 1978 - IRC-20494 -V3876 SAGITTARII.

780501 GLASS, I. S. <M. N. R. A. S., 183, 335>
VARIATIONS OF CIRCINUS X-1 IN THE INFRARED.

780502 THRONSON JR., H. A., HARPER JR., D. A., KEENE, J., LOEWENSTEIN, R. F., MOSELEY, S. H., TELESCO, C. M. <A. J., 83, 492>
OBSERVATIONS OF FIVE MODERATE-LUMINOSITY FAR-INFRARED SOURCES IN ORION AND MONOCEROS.

780503 HACKWELL, J. A., GEHRZ, R. D., SMITH, J. R., BRIOTTA, D. A. <AP. J., 221, 797>
INFRARED MAPS OF W3 FROM 4.9 MICRONS TO 20 MICRONS.

780504 RODRIGUEZ, L. F., CHAISSON, E. J. <AP. J., 221, 816>
A COMPARATIVE STUDY OF HIGH-RADIOFREQUENCY AND FAR-INFRARED OBSERVATIONS OF GALACTIC HII REGIONS.

780505 AARONSON, M. <AP. J. (LETTERS), 221, L103>
THE MORPHOLOGICAL DISTRIBUTION OF BRIGHT GALAXIES IN THE UVK COLOR PLANE.

780506 LEBOFSKY, M. J., RIEKE, G. H., KEMP, J. C. <AP. J., 222, 95>
INFRARED PHOTOMETRY AND POLARIMETRY OF NGC 1068.

780507 COHEN, J. G., FROGEL, J. A., PERSSON, S. E. <AP. J., 222, 165>
INFRARED PHOTOMETRY, BOLOMETRIC MAGNITUDES, AND EFFECTIVE TEMPERATURES FOR GIANTS IN M3, M13, M92, AND M67.

780508 EGGEN, O. J. <AP. J., 222, 191>
INTERMEDIATE-BAND PHOTOMETRY OF LATE-TYPE STARS. VI. MAIN-SEQUENCE STARS NEAR THE SUN.

780509 WHITE, N. M., WING, R. F. <AP. J., 222, 209>
PHOTOELECTRIC TWO-DIMENSIONAL SPECTRAL CLASSIFICATION OF M SUPERGIANTS.

780510 SERRA, G., PUGET, J. L., RYTER, C. E., WIJNBERGEN, J. J. <AP. J. (LETTERS), 222, L21>
THE FAR-INFRARED EMISSION OF INTERSTELLAR MATTER BETWEEN GALACTIC LONGITUDES L-36 AND L-55 DEGREES.

780511 HAGEN, W. <AP. J. (LETTERS), 222, L37>
THE CIRCUMSTELLAR ENVELOPES OF M GIANTS AND SUPERGIANTS.

780512 GLASS, I. S. <NATURE, 273, 35>
INFRARED SOURCES IN THE VICINITY OF 2S1728-337.

780513 HALL, D. N. B., RIDGWAY, S. T. <NATURE, 273, 281>
CIRCUMSTELLAR METHANE IN THE INFRARED SPECTRUM OF IRC+10216.

780514 WHITTET, D. C. B., VAN BREDA, I. G. <ASTR. AP., 66, 57>
THE CORRELATION OF THE INTERSTELLAR EXTINCTION LAW WITH THE WAVELENGTH OF MAXIMUM POLARIZATION.

780515 SHAVER, P. A., DANKS, A. C. <ASTR. AP., 65, 323>
RADIO AND INFRARED OBSERVATIONS OF THE OH/H20 SOURCE G12.2-0.1.

780601 WARNER, J. W., BLACK, J. H. <A. J., 83, 586>
A 5 GHZ SURVEY OF INFRARED SOURCES.

780602 DYCK, H. M., JONES, T. J. <A. J., 83, 594>
NEAR-INFRARED OBSERVATIONS OF INTERSTELLAR POLARIZATION.

780603 VEEDER, G. J., MATSON, D. L., SMITH, J. C. <A. J., 83, 651>
VISUAL AND INFRARED PHOTOMETRY OF ASTEROIDS.

780604 SWEENEY, L. H., HEINSHEIMER, T. F., YATES, F. F., MARAN, S. P., LESH, J. R., NAGY, T. A. <AEROSPACE TR-0078(3409-20)-1>
INTERIM EQUATORIAL INFRARED CATALOGUE, NUMBER 1.

780605 SNEDEN, C., LAMBERT, D. L., TOMKIN, J., PETERSON, R. C. <AP. J., 222, 585>
LIGHT-ELEMENT ABUNDANCES IN THE WEAK G-BAND STAR HR 6766.

780606 THOMPSON, R. I., LEBOFSKY, M. J., RIEKE, G. H. <AP. J. (LETTERS), 222, L49>
THE 2-2.5 MICRON SPECTRUM OF NGC 1068: A DETECTION OF EXTRAGALACTIC MOLECULAR HYDROGEN.

780607 ZEILIK II, M., LADA, C. J. <AP. J., 222, 896>
NEAR-INFRARED AND CO OBSERVATIONS OF W40 AND W48.

780608 MOULD, J. R., HALL, D. N. B., RIDGWAY, S. T., HINTZEN, P., AARONSON, M. <AP. J. (LETTERS), 222, L123>
THE COMPOSITE SPECTRA OF FU ORIONIS STARS.

780609 GOEBEL, J. H., BREGMAN, J. D., STRECKER, D. W., WITTEBORN, F. C., ERICKSON, E. F. <AP. J. (LETTERS), 222, L129>
C3 AND INFRARED SPECTROPHOTOMETRY OF Y CANUM VENATICORUM.

780610 GATLEY, I., HARVEY, P. M., THRONSON JR., H. A. <AP. J. (LETTERS), 222, L133>
FAR-INFRARED OBSERVATIONS OF HII REGIONS IN M33.

780611 MELNICK, G., GULL, G. E., HARWIT, M., WARD, D. B. <AP. J. (LETTERS), 222, L137>
OBSERVATIONS OF THE 51.8 MICRON (O III) EMISSION LINE IN ORION.

780612 HEFELE, H., SCHULTE IN DEN BAUMEN, J. <ASTR. AP., 66, 465>
8-13 MICRON SPECTROPHOTOMETRY OF THE COMPACT H II REGION G45.1+0.1.

780613 SCRIMGER, J. N., LOWE, R. P., MOORHEAD, J. M., WEHLAU, W. H. <P. A. S. P., 90, 257>
OBSERVATIONS OF NGC 7027 IN THE NEAR INFRARED.

780614 GLASS, I. S., FEAST, M. W. <IAUC NO. 3226>
2S1702-363.

780615 GEHRZ, R. D., GRASDALEN, G., HACKWELL, J. A., MCCLAIN, D., MCLAUGHLIN, S. F., SNEDEN, C. <IAUC NO. 3235>
NOVA SERPENTIS 1978.

780701 MARTIN, W. L., PENFOLD, J. E., GLASS, I. S. <M. N. R. A. S., 184, 15P>
SPECTROSCOPIC AND PHOTOMETRIC OBSERVATIONS OF THREE COMPACT GALAXIES.

780702 ELIAS, J. H. <A. J., 83, 791>
2.2-MICRON FIELD STARS AT THE NORTH GALACTIC POLE.

780703 TRAUB, W. A., CARLETON, N. P., BLACK, J. H. <AP. J., 223, 140>
A SEARCH FOR EMISSION FROM VIBRATIONALLY EXCITED H2.

780704 SNEDEN, C., GEHRZ, R. D., HACKWELL, J. A., YORK, D. G., SNOW JR, T. P. <AP. J., 223, 168>
INFRARED COLORS AND THE DIFFUSE INTERSTELLAR BANDS.

780705 BECKWITH, S., GATLEY, I., MATTHEWS, K., NEUGEBAUER, G. <AP. J. (LETTERS), 223, L41>
MOLECULAR HYDROGEN EMISSION FROM T TAURI STARS.

780706 BREGMAN, J. D., GOEBEL, J. H., STRECKER, D. W. <AP. J. (LETTERS), 223, L45>
IDENTIFICATION OF THE 3.9 MICRON ABSORPTION BAND IN CARBON STARS.

780707 HALL, D. N. B., KLEINMANN, S. G., RIDGWAY, S. T., GILLETT, F. C. <AP. J. (LETTERS), 223, L47>
HIGH-RESOLUTION 1.5-5 MICRON SPECTROSCOPY OF THE BECKLIN-NEUGEBAUER SOURCE IN ORION.

780708 BECKWITH, S., PERSSON, S. E., NEUGEBAUER, G., BECKLIN, E. E. <AP. J., 223, 464>
OBSERVATIONS OF THE MOLECULAR HYDROGEN EMISSION FROM THE ORION NEBULA.

780709 HERBST, W., RACINE, R., WARNER, J. W. <AP. J., 223, 471>
OPTICAL AND INFRARED PROPERTIES OF THE NEWLY FORMED STARS IN CANIS MAJOR R1.

780710 PUETTER, R. C., RUSSELL, R. W., SOIFER, B. T., WILLNER, S. P. <AP. J. (LETTERS), 223, L93>
INFRARED SPECTRA OF HM SAGITTAE AND V1016 CYGNI.

780711 RUSSELL, R. W. <ASTR. AP., 67, 273>
THE INFRARED SOURCE ASSOCIATED WITH SH 2-149.

780712 GOW, C. E., SANDFORD II, M. T., HONEYCUTT, R. K. <ASTR. AP., 67, 435>
PHOTOGRAPHS OF THE ORION NEBULA IN H-ALPHA, H-BETA AND HE I 10830.

780801 WERNER, M. W., BECKLIN, E. E., GATLEY, I., ELLIS, M. J., HYLAND, A. R., ROBINSON, G., THOMAS, J. A. <M. N. R. A. S., 184, 365>
FAR-INFRARED OBSERVATIONS OF LARGE MAGELLANIC CLOUD HII REGIONS.

780802 KOORNNEEF, J. <M. N. R. A. S., 184, 477>
THE INFRARED ANGULAR DIAMETER OF ETA CARINAE.

780803 NADEAU, D., NEUGEBAUER, G., BECKLIN, E. E., ELIAS, J. H., ENNIS, D. J., MATTHEWS, K., SELLGREN, K. <M. N. R. A. S., 184, 523>
THE LIGHT CURVE AT 10 MICRONS OF ALGOL NEAR SECONDARY MINIMUM.

780804 ELIAS, J. H. <AP. J., 223, 859>
A STUDY OF THE IC 5146 DARK CLOUD COMPLEX.

780805 MCCARTHY, D. W., HOWELL, R., LOW, F. J. <AP. J. (LETTERS), 223, L113>
APPARENT VARIATION IN THE DIAMETER OF OMICRON CETI AT 10.2 MICRONS.

780806 O'DELL, S. L., PUSCHELL, J. J., STEIN, W. A., OWEN, F. N., PORCAS, R. W., MUFSON, S. L., MOFFETT, T. J., ULRICH, M. -H. <AP. J., 224, 22>
COORDINATED PHOTOMETRIC AND SPECTROSCOPIC OBSERVATIONS OF STRONG EXTRAGALACTIC 90 GHZ SOURCES.

780807 MOORWOOD, A. F. M., BALUTEAU, J. -P., ANDEREGG, M., CORON, N., BIRAUD, Y. <AP. J., 224, 101>
INFRARED LINE EMISSION FROM HII REGIONS. II. AIRBORNE OBSERVATIONS OF THE ORION NEBULA, W3, AND NGC 7538.

780808 MCCARTHY, J. F., FORREST, W. J., HOUCK, J. R. <AP. J., 244, 109>
16-38 MICRON SPECTROSCOPY OF NGC 7027.

780809 FERLAND, G. J., SHIELDS, G. A. <AP. J. (LETTERS), 224, L15>
FINE-STRUCTURE LINES AND THE 10 MICRON EXCESS OF NOVA CYGNI 1975.

780810 TOKUNAGA, A. T., ERICKSON, E. F., CAROFF, L. J., DANA, R. A. <AP. J. (LETTERS), 224, L19>
THE FAR-INFRARED SPECTRUM OF S140 IR.

780811 DANKS, A. C., HOUZIAUX, L. <P. A. S. P., 90, 453>
SPECTROSCOPIC OBSERVATIONS OF 27 CANIS MAJORIS FROM 0.14 TO 4.7 MICRONS.

780812 TSUJI, T. <ASTR. AP., 68, L23>
POSSIBLE IDENTIFICATION OF H2O THERMAL EMISSION IN THE INFRARED SPECTRA OF LATE-TYPE STARS.

780901 WRIGHT, E. L., KLEINMANN, D. E. <NATURE, 275, 298>
INFRARED OBSERVATIONS OF THE MOST LUMINOUS QUASAR.

780902 ELIAS, J. H. <AP. J., 224, 453>
AN INFRARED STUDY OF THE OPHIUCHUS DARK CLOUD.

780903 PILACHOWSKI, C. A. <AP. J., 224, 412>
OBSERVATIONS OF CO IN GLOBULAR CLUSTER STARS.

780904 HAWLEY, S. A. <AP. J., 224, 417>
THE CHEMICAL COMPOSITION OF GALACTIC AND EXTRAGALACTIC HII REGIONS.

780905 HARTMANN, L. <AP. J., 224, 520>
DISK STRUCTURE IN EARLY-TYPE STELLAR ENVELOPES.

780906 SCARGLE, J. D., ERICKSON, E. F., WITTEBORN, F. C., STRECKER, D. W. <AP. J., 224, 527>
INFRARED EXCESSES IN EARLY-TYPE STARS: GAMMA CASSIOPEIAE.

780907 SUTTON, E. C., STOREY, J. W. V., TOWNES, C. H., SPEARS, D. L. <AP. J. (LETTERS), 224, L123>
VARIATIONS IN THE SPATIAL DISTRIBUTION OF 11 MICRON RADIATION FROM OMICRON CETI.

780908 YOUNG, E. T., KNACKE, R. F. <AP. J., 224, 848>
A SEARCH FOR THE GROUND STATE S(2) LINE OF MOLECULAR HYDROGEN IN THE ORION NEBULA.

780909 ELIAS, J. H. <AP. J., 224, 857>
A STUDY OF THE TAURUS DARK CLOUD COMPLEX.

780910 GREEN, R. F., RICHSTONE, D. O., SCHMIDT, M. <AP. J., 224, 892>
PG 1413+01: A WHITE DWARF-RED DWARF ECLIPSING BINARY.

780911 JONES, B., MERRILL, K. M. <IAUC NO. 3268>
NOVA CYGNI 1978.

780912 ALLEN, D. A., SMITH, M. G., WRIGHT, A. E. <IAUC NO. 3274>
NGC 7213.

781001 GLASS, I. S. <M. N. R. A. S., 185, 23>
THE LONG-TERM INFRARED BEHAVIOUR OF RCB STARS.

781002 KLEINMANN, S. G., DICKINSON, D. F., SARGENT, D. G. <A. J., 83, 1206>
STELLAR H2O MASERS.

781003 RIDGWAY, S. T., CARBON, D. F., HALL, D. N. B. <AP. J., 225, 138>
POLYATOMIC SPECIES CONTRIBUTING TO THE CARBON-STAR 3 MICRON BAND.

781004 RUDNICK, L., OWEN, F. N., JONES, T. W., PUSCHELL, J. J., STEIN, W. A. <AP. J. (LETTERS), 225, L5>
COORDINATED CENTIMETER, MILLIMETER, INFRARED, AND VISUAL POLARIMETRY OF COMPACT NONTHERMAL SOURCES.

781005 LOREN, R. B., WOOTTEN, H. A. <AP. J. (LETTERS), 225, L81>
STAR FORMATION IN THE BRIGHT-RIMMED MOLECULAR CLOUD IC 1848 A.

781006 MCMILLAN, R. S. <AP. J., 225, 417>
ARE LONG WAVELENGTHS OF MAXIMUM INTERSTELLAR POLARIZATION DUE TO WATER ICE MANTLES ON GRAINS?

781007 COHEN, M., VOGEL, S. N. <M. N. R. A. S., 185, 47>
WOLF-RAYET STARS--VIII. 2- TO 4-MICRON SPECTROPHOTOMETRY OF LATE WC STARS.

781008 RANK, D. M., DINERSTEIN, H. L., LESTER, D. F., BREGMAN, J. D., AITKEN, D. K., JONES, B. <M. N. R. A. S., 185, 179>
OBSERVATIONS OF INFRARED EMISSION LINES IN THE SOUTHERN COMPACT HII REGIONS G333.6-0.2 AND G298.2-0.3.

781009 COX, L. J., HOUGH, J. H., MCCALL, A. <M. N. R. A. S., 185, 199>
THE HATFIELD NEAR-INFRARED POLARIMETER.

781010 ARNOLD, E. M., KREYSA, E., SCHULTZ, G. V., SHERWOOD, W. A. <ASTR. AP., 70, L1>
1MM CONTINUUM OBSERVATIONS OF SOUTHERN HII REGIONS.

781011 HOUGH, J. H., MCCALL, A., ADAMS, D. J., JAMESON, R. F. <ASTR. AP., 69, 431>
LINEAR POLARIZATION OF THE GALACTIC CENTRE IN THE NEAR INFRARED.

781012 HARVEY, P. M., HOFFMANN, W. F., CAMPBELL, M. F. <ASTR. AP., 70, 165>
HIGH ANGULAR RESOLUTION OBSERVATIONS OF ETA CARINAE FROM 35-175 MICRONS.

781013 TANZI, E. G., TREVES, E. A., SALINARI, P., TARENGHI, M. <IAUC NO. 3281>
V861 SCORPII.

781014 GEHRZ, R. D., GRASDALEN, G., HACKWELL, J. A., NEY, E. P. <IAUC NO. 3296>
NOVA CYGNI 1978.

781101 DE BRUYN, A. G., SARGENT, W. L. W. <A. J., 83, 1257>
ABSOLUTE SPECTROPHOTOMETRY OF 68 SEYFERT GALAXY NUCLEI.

781102 TAYLOR, B. J. <A. J., 83, 1377>
NEAR-INFRARED ENERGY DISTRIBUTIONS OF M31.

781103 JONES, B., MERRILL, K. M., PUETTER, R. C., WILLNER, S. P. <A. J., 83, 1437>
THE INFRARED SPECTRUM OF GL 3068.

781104 GULL, G. E., HOUCK, J. R., MCCARTHY, J. F., FORREST, W. J., HARWIT, M. <A. J., 83, 1440>
FAR-INFRARED POLARIZATION OF THE KLEINMANN-LOW NEBULA IN ORION.

781105 O'DELL, S. L., PUSCHELL, J. J., STEIN, W. A., WARNER, J. W. <AP. J. SUPPL., 38, 267>
THE CHANGES IN SPECTRAL-FLUX DISTRIBUTION DURING VARIABILITY OF EXTRAGALACTIC NONTHERMAL SOURCES, 0.36 TO 3.5 MICRONS.

781106 MOULD, J. R., LIEBERT, J. <AP. J. (LETTERS), 226, L29>
INFRARED PHOTOMETRY AND THE ATMOSPHERIC COMPOSITION OF COOL WHITE DWARFS.

781107 THOMPSON, R. I., TOKUNAGA, A. T. <AP. J., 226, 119>
ANALYSIS OF OBSCURED INFRARED OBJECTS. II. ALLEN'S INFRARED SOURCE IN NGC 2264.

781108 WILLIAMS, P. M., BEATTIE, D. H., LEE, T. J., STEWART, J. M., ANTONOPOULOU, E. <M. N. R. A. S., 185, 467>
CONDENSATION OF A SHELL AROUND HD 193793.

781109 HOFMANN, W., LEMKE, D., FREY, A. <ASTR. AP., 70, 427>
MAPPING OF THE GALACTIC CENTER AND THE AQUILA REGION IN THE NEAR INFRARED FROM BALLOON ALTITUDES.

781110 BENSAMMAR, S., KANDEL, R., ASSUS, P., JOURNET, A. <ASTR. AP., 70, 585>
UPPER LIMITS TO THE DIAMETER OF VY CANIS MAJORIS.

781111 SCHMITZ, M., BROWN, L. W., MEAD, J. M., NAGY, T. A. <NASA TM-79683>
MERGED INFRARED CATALOGUE.

781201 SOLF, J. <ASTR. AP. SUPPL., 34, 409>
SPECTRAL TYPE AND LUMINOSITY CLASSIFICATION OF LATE-TYPE M STARS FROM NEAR-INFRARED IMAGE TUBE COUDE SPECTROGRAMS.

781202 MOREL, M., MAGNENAT, P. <ASTR. AP. SUPPL., 34, 477>
UBVRIJKLMNH PHOTOELECTRIC PHOTOMETRIC CATALOGUE (MAGNETIC TAPE).

781203 WARNER, J. W., HUBBARD, R. P., GALLAGHER, J. S. <A. J., 83, 1614>
PHOTOMETRIC AND SPECTRAL PROPERTIES OF SOME T TAURI STARS.

781204 PUETTER, R. C., SMITH, H. E., SOIFER, B. T., WILLNER, S. P., PIPHER, J. L. <AP. J. (LETTERS), 226, L53>
SPECTROPHOTOMETRY OF QUASI-STELLAR OBJECTS AT OPTICAL AND INFRARED WAVELENGTHS: PG 0026+129 AND 3C 273.

781205 OGDEN, P. M., ROESLER, F. L., REYNOLDS, R. J., SCHERB, F., LARSON, H. P., SMITH, H. A., DAEHLER, M. <AP. J. (LETTERS), 226, L91>
MEASUREMENTS OF THE VELOCITY AND WIDTH OF THE H2 2.1 MICRON EMISSION LINE FROM THE ORION NEBULA.

781206 PRIEDHORSKY, W., MATTHEWS, K., NEUGEBAUER, G., WERNER, M. W.,KRZEMINSKI, W. <AP. J., 226, 397>
JOINT INFRARED AND VISUAL MONITORING OF AM HERCULIS.

781207 BECHIS, K. P., HARVEY, P. M., CAMPBELL, M. F., HOFFMANN, W. F. <AP. J., 226, 439>
STAR FORMATION IN THE NGC 7129 REGION: A CO MOLECULAR-LINE AND FAR-INFRARED CONTINUUM STUDY.

781208 BECK, S. C., LACY, J. H., BAAS, F., TOWNES, C. H. <AP. J., 226, 545>
NE II 12.8 MICRON EMISSION AND GALACTIC DYNAMICS IN M82.

781209 RIEKE, G. H. <AP. J., 226, 550>
THE INFRARED EMISSION OF SEYFERT GALAXIES.

781210 TELESCO, C. M. <AP. J. (LETTERS), 226, L125>
EXTENDED 10 MICRON EMISSION FROM THE DARK LANE IN NGC 5128 (CENTAURUS A).

781211 CHEUNG, L., FROGEL, J. A., GEZARI, D. Y., HAUSER, M. G. <AP. J. (LETTERS), 226, L149>
1.0 MILLIMETER CONTINUUM MAP OF COOL SOURCES IN THE NGC 6334 COMPLEX.

781212 YEE, H. K. C., OKE, J. B. <AP. J., 226, 753>
PHOTOELECTRIC SPECTROPHOTOMETRY OF RADIO GALAXIES.

781213 HARRIS, D. H., WOOLF, N. J., RIEKE, G. H. <AP. J., 226, 829>
ICE MANTLES AND ABNORMAL EXTINCTION IN THE RHO OPHIUCHI CLOUD.

781214 CAPPS, R. W., GILLETT, F. C., KNACKE, R. F. <AP. J., 226, 863>
INFRARED OBSERVATIONS OF THE OH SOURCE W33 A.

781215 MOULD, J. R. <AP. J., 226, 923>
INFRARED SPECTROSCOPY OF M DWARFS.

781216 SLOVAK, M. H. <ASTR. AP., 70, L75>
THE INFRARED VARIABILITY OF THE ERUPTIVE VARIABLE HM SAGITTAE.

781217 FERRARI-TONIOLO, M., PERSI, P., VIOTTI, R. <M. N. R. A. S., 185, 841>
COORDINATED INFRARED AND OPTICAL OBSERVATIONS OF GAMMA CAS AND X PER IN LATE 1976.

781218 PAPOULAR, R., LENA, P. J., MARTEN, A., ROUAN, D., WIJNBERGEN, J. J. <NATURE, 276, 593>
POSSIBLE IDENTIFICATION OF THE 45 MICRON ICE SIGNATURE IN ORION.

781219 PUSCHELL, J. J. <P. A. S. P., 90, 652>
OPTICAL AND INFRARED PHOTOMETRY OF ARAKELIAN 120.

781220 HARVEY, P. M., GATLEY, I., THRONSON JR., H. A. <P. A. S. P., 90, 655>
AN UPPER LIMIT TO FAR INFRARED EMISSION FROM THE CRAB NEBULA.

781221 BECKLIN, E. E., NEUGEBAUER, G. <P. A. S. P., 90, 657>
2.2-MICRON MAP OF THE CENTRAL 1 DEGREE OF THE GALACTIC CENTER.

781222 PILACHOWSKI, C. A. <P. A. S. P., 90, 675>
OBSERVATIONS OF CARBON MONOXIDE IN METAL-DEFICIENT STARS.

781223 ELIAS, J. H., LANNING, H., NEUGEBAUER, G. <P. A. S. P., 90, 697>
INFRARED AND OPTICAL VARIATIONS IN OMICRON CASSIOPEIAE (HD 4180).

789901 KOJOIAN, G., ELLIOTT, R., TOVMASSIAN, H. M. <A. J., 83, 1545>
ACCURATE OPTICAL POSITIONS FOR MARKARIAN GALAXIES 508-700.

789902 WADE, R. A., SZKODY, P., CORDOVA, F. <IAUC NO. 3279>
H 2155-304.

789903 MIKAMI, T. <ANNALS TOKYO AST. OBS., XVII, 1>
COMPILED DATA OF C- AND M- TYPE STARS IN THE SOLAR NEIGHBORHOOD.

789904 NAGY, T. A., MEAD, J. M. <NASA TM-79564>
HD-SAO-DM CROSS INDEX.

789905 SRAMEK, R. A., WEEDMAN, D. W. <AP. J., 221, 468>
AN OPTICAL AND RADIO STUDY OF QUASARS.

789906 WILSON, A. S., MEURS, E. J. A. <ASTR. AP. SUPPL., 33, 407>
ACCURATE OPTICAL POSITIONS OF SEYFERT GALAXIES.

789907 HOLMBERG, E. B., LAUBERTS, A., SCHUSTER, H. -E., WEST, R. M. <ASTR. AP. SUPPL., 31, 15>
THE ESO/UPPSALA SURVEY OF THE ESO(B) ATLAS OF THE SOUTHERN SKY. V.

789908 HOLMBERG, E. B., LAUBERTS, A., SCHUSTER, H. -E., WEST, R. M. <ASTR. AP. SUPPL., 34, 285>
THE ESO/UPPSALA SURVEY OF THE ESO(B) ATLAS OF THE SOUTHERN SKY. VI.

789909 WESTERLUND, B. E., OLANDER, N., RICHER, H. B., CRABTREE, D. R. <ASTR. AP. SUPPL., 31, 61>
A CATALOGUE OF CARBON STARS IN THE LARGE MAGELLANIC CLOUD.

789910 KHOLOPOV, P. N., KUKARKINA, N. P., PEROVA, N. B. <IBVS NO. 1414>
63RD NAME-LIST OF VARIABLE STARS.

790001 ENGELS, D. <ASTR. AP. SUPPL., 36, 337>
CATALOGUE OF LATE-TYPE STARS WITH OH, H2O OR SIO MASER EMISSION.

790002 KLEINMANN, S. G., PAYNE-GAPOSCHKIN, C. <EARTH AND EXT. SCI., 3, 161>
THE REDDEST STARS IN THE TWO MICRON SKY SURVEY.

790003 KODAIRA, K., TANAKA, W., ONAKA, T., WATANABE, T. <P. A. S. J., 31, 667>
BALLOON-BORNE NEAR-INFRARED MULTICOLOR PHOTOMETRY OF LATE-TYPE STARS. II. DATA ANALYSIS.

790004 CATCHPOLE, R. M., ROBERTSON, B. S. C., LLOYD EVANS, T. H. H.,FEAST, M. W., GLASS, I. S., CARTER, B. S. <S. A. A. O. CIRC., 1, 61>
J, H, K, L, INFRARED PHOTOMETRY OF MIRA VARIABLES AND OF OTHER LATE TYPE STARS.

790101 COX, G. G., PARKER, E. A. <M. N. R. A. S., 186, 197>
TIME VARIATIONS OF STELLAR WATER MASERS.

790102 TAYLOR, B. J. <A. J., 84, 96>
OBSERVATIONS OF SECONDARY SPECTROPHOTOMETRIC STANDARDS IN THE WAVELENGTH RANGE BETWEEN 5840 AND 10800A.

790103 PERSSON, S. E., FROGEL, J. A., AARONSON, M. <AP. J. SUPPL., 39, 61>
PHOTOMETRIC STUDIES OF COMPOSITE STELLAR SYSTEMS. III. UBVR AND JHK OBSERVATIONS OF E AND S0 GALAXIES.

790104 SIMON, M., SIMON, T., JOYCE, R. R. <AP. J., 227, 64>
BRACKETT-LINE OBSERVATIONS OF M82.

790105 HARVEY, P. M., HOFFMANN, W. F., CAMPBELL, M. F. <AP. J., 227, 114>
FAR-INFRARED OBSERVATIONS OF THE CARINA I AND II HII REGIONS.

790106 KLEINMANN, S. G., JOYCE, R. R., SARGENT, D. G., GILLETT, F. C., TELESCO, C. M. <AP. J., 227, 126>
AN OBSERVATIONAL STUDY OF THE AFGL INFRARED SKY SURVEY. IV. FURTHER RESULTS FROM THE REVISED CATALOG.

790107 SOIFER, B. T., OKE, J. B., MATTHEWS, K., NEUGEBAUER, G. <AP. J. (LETTERS), 227, L1>
THE HYDROGEN LINES IN THE HIGH-LUMINOSITY QUASAR B2 1225+31.

790108 PUETTER, R. C., SMITH, H. E., WILLNER, S. P. <AP. J. (LETTERS), 227, L5>
SPECTROPHOTOMETRY OF QUASI-STELLAR OBJECTS AT OPTICAL AND INFRARED WAVELENGTHS: THE H-ALPHA/L-ALPHA RATIO IN

790109 PUSCHELL, J. J., STEIN, W. A., JONES, T. W., WARNER, J. W., OWEN, F. N., RUDNICK, L., ALLER, H., HODGE, P. <AP. J. (LETTERS), 227, L11>
B2 1308+326: PHOTOMETRY AND POLARIZATION DURING THE OUTBURST OF 1978 SPRING.

790110 LACY, J. H., BAAS, F., TOWNES, C. H., GEBALLE, T. R. <AP. J. (LETTERS), 227, L17>
OBSERVATIONS OF THE MOTION AND DISTRIBUTION OF THE IONIZED GAS IN THE CENTRAL PARSEC OF THE GALAXY.

790111 MELNICK, G., GULL, G. E., HARWIT, M. <AP. J. (LETTERS), 227, L29>
OBSERVATIONS OF THE 63 MICRON (O I) EMISSION LINE IN THE ORION AND OMEGA NEBULAE.

790112 MELNICK, G., GULL, G. E., HARWIT, M. <AP. J. (LETTERS), 227, L35>
51.8 MICRON (O III) LINE EMISSION OBSERVED IN FOUR GALACTIC H II REGIONS.

790113 DINERSTEIN, H. L., LESTER, D. F., RANK, D. M. <AP. J. (LETTERS), 227, L39>
DETECTION OF A NEAR-INFRARED COMPLEX ASSOCIATED WITH S140 IRS.

790114 EVANS II, N. J., BECKWITH, S., BROWN, R. L., GILMORE, W. <AP. J., 227, 450>
TYPE I OH MASERS: A STUDY OF POSITIONS, POLARIZATION, NEARBY WATER MASERS, AND RADIO CONTINUUM AND INFRARED PROPERTIES.

790115 FERLAND, G. J., LAMBERT, D. L., NETZER, H., HALL, D. N. B., RIDGWAY, S. T. <AP. J., 227, 489>
CARBON MONOXIDE EMISSION AND THE ETA CARINAE STAGE OF NOVA NQ VULPECULAE.

790116 FROGEL, J. A., PERSSON, S. E., COHEN, J. G. <AP. J., 227, 499>
INFRARED COLORS, CO BAND STRENGTHS, AND PHYSICAL PARAMETERS FOR GIANTS IN M71.

790117 DANKS, A. C., WAMSTEKER, W., VOGT, N., SALINARI, P., TARENGHI, M., DUERBECK, H. W. <AP. J. (LETTERS), 227, L59>
INFRARED AND VISIBLE PHOTOMETRY OF FAIRALL-9 (ESO 113-IG 45).

790118 MENDOZA V, E. E. <ASTR. AP., 71, 147>
H-ALPHA AND O I PHOTOMETRY OF THE PLEIADES.

790119 ZAJTSEVA, G. V., LYUTYI, V. M. <ASTROFIZIKA, 15, 48>
PHOTOMETRIC INVESTIGATION AND RAPID PERIODICITY OF RR TAU.

790201 GLASS, I. S. <M. N. R. A. S., 186, 317>
INFRARED OBSERVATIONS OF LATE-TYPE SUPERGIANTS IN THE MAGELLANIC CLOUDS.

790202 WILKING, B. A., LEBOFSKY, M. J., RIEKE, G. H., KEMP, J. C. <A. J., 84, 199>
INFRARED POLARIMETRY IN THE RHO OPHIUCHUS DARK CLOUD.

790203 RIDGWAY, S. T., WELLS, D. C., JOYCE, R. R., ALLEN, R. G. <A. J., 84, 247>
TWENTY-EIGHT ANGULAR DIAMETERS FOR LATE-TYPE STARS BY THE LUNAR OCCULTATION TECHNIQUE.

790204 KLEINMANN, S. G., DICKINSON, D. F., SARGENT, D. G. <A. J., 84, 279>
ERRATUM:"STELLAR H2O MASERS" (A. J. 83, 1206(1978))

790205 HARVEY, P. M. <P. A. S. P., 91, 143>
A FAR-INFRARED PHOTOMETER FOR THE KUIPER AIRBORNE OBSERVATORY.

790206 RIEKE, G. H., LEBOFSKY, M. J. <AP. J., 227, 710>
ON THE INFRARED VARIABILITY OF 3C 120, NGC 1275, AND III ZW 2.

790207 CRABTREE, D. R., MARTIN, P. G. <AP. J., 227, 900>
CIRCUMSTELLAR DUST ENVELOPES: CALCULATION OF ECLIPSE LIGHT CURVES AND FRINGE VISIBILITIES.

790208 HINKLE, K. H., BARNES, T. G. <AP. J., 227, 923>
INFRARED SPECTROSCOPY OF MIRA VARIABLES. II. R LEONIS, THE H2O VIBRATION-ROTATION BANDS.

790209 MAIHARA, T., ODA, N., OKUDA, H. <AP. J. (LETTERS), 227, L129>
A BALLOON OBSERVATION OF DIFFUSE FAR-INFRARED EMISSION FROM THE GALACTIC PLANE.

790210 PUETTER, R. C., RUSSELL, R. W., SOIFER, B. T., WILLNER, S. P. <AP. J., 228, 118>
SPECTROPHOTOMETRY OF COMPACT HII REGIONS FROM 4 TO 8 MICRONS.

790211 LOWE, R. P., MOORHEAD, J. M., WEHLAU, W. H. <AP. J., 228, 191>
NEAR-INFRARED FOURIER SPECTROSCOPY OF THE ORION NEBULA. II. THE WEAK LINES.

790212 EPCHTEIN, N., TURON, P. <ASTR. AP., 72, L4>
10 MICRON OBSERVATION OF H II REGIONS WITH THE ESO 3.6 METER TELESCOPE.

790213 ODA, N., MAIHARA, T., SUGIYAMA, T., OKUDA, H. <ASTR. AP., 72, 309>
COSMIC DUST IN THE CENTRAL REGION OF THE GALAXY AND ANOMALOUS INFRARED SOURCE AT L-355, B--1.

790214 PERSSON, S. E. <IAUC NO. 3324>
H2155-304.

790215 PERSSON, S. E. <IAUC NO. 3324>
H 2155-304.

790301 JONES, T. J. <AP. J., 228, 787>
POLARIMETRY OF BE STARS AT 1.25 AND 2.2 MICRONS.

790302 SOIFER, B. T., NEUGEBAUER, G., MATTHEWS, K. <NATURE, 278, 231>
INFRARED OBSERVATIONS OF THE X-RAY QUASARS 0241+622 AND MR2251-178.

790303 JAMESON, R. F., SHERRINGTON, M. R., KING, A. R., GILES, A. B. <NATURE, 278, 233>
INFRARED OBSERVATIONS OF THE BLACK-HOLE CANDIDATE V861 SCO.

790304 PERSI, P., FERRARI-TONIOLO, M., SPADA, G., CONTI, G., DI BENEDETTO, P., TANZI, E. G., TARENGHI, M. <M. N. R. A. S., 187, 293>
NEAR-INFRARED PHOTOMETRY OF HDE 245770 (A 0535+26).

790305 SMYTH, M. J., DEAN, J. F., ROBERTSON, B. S. C. <M. N. R. A. S., 187, 29P>
MULTICOLOUR PHOTOMETRY AND THE DUST SHELL OF HR 5999.

790306 ABOLINS, J. A., ADAMS, D. J., JAMESON, R. F., HOUGH, J. H., AXON, D. J. <M. N. R. A. S., 186, 23P>
DETECTION OF A BRIGHT RIDGE IN THE 2.2-MICRON EMISSION OF M82.

790307 GLASS, I. S. <M. N. R. A. S., 186, 29P>
INFRARED OBSERVATIONS OF ACTIVE SOUTHERN GALAXIES AND QSOS.

790308 LEBOFSKY, M. J. <A. J., 84, 324>
VARIABLE EXTINCTION AT THE GALACTIC CENTER.

790309 ZEILIK II, M. <A. J., 84, 341>
LARGE-BEAM NEAR-INFRARED AND 24-GHZ OBSERVATIONS OF M8.

790310 MOULD, J. R., STUTMAN, D., MCELROY, D. B. <AP. J., 228, 423>
TIO BAND STRENGTHS IN METAL-RICH GLOBULAR CLUSTERS. II.

790311 WRIGHT, E. L., DECAMPLI, W., FAZIO, G. G., KLEINMANN, D. E., LADA, C. J., LOW, F. J. <AP. J., 228, 439>
DISCOVERY OF A COMPACT FAR-INFRARED SOURCE, IR 12.4+0.5.

790312 HARVEY, P. M., CAMPBELL, M. F., HOFFMANN, W. F. <AP. J., 228, 445>
HIGH-ANGULAR-RESOLUTION FAR-INFRARED OBSERVATIONS OF THE RHO OPHIUCHI DARK CLOUD.

790313 SCARGLE, J. D., STRECKER, D. W. <AP. J., 228, 838>
COOL STARS: EFFECTIVE TEMPERATURES, ANGULAR DIAMETERS, AND REDDENING DETERMINED FROM 1-5 MICRON FLUX CURVES AND MODEL ATMOSPHERES.

790314 SHANIN, G. I. <SOV. AST., 23, 158>
INFRARED SPECTROSCOPY WITH A CONTACT-TYPE IMAGE TUBE: FU ORIONIS STARS.

790401 GOSNELL, T. R., HUDSON, H. S., PUETTER, R. C. <A. J., 84, 538>
GROUND-BASED OBSERVATIONS OF SOURCES IN THE AFGL INFRARED SKY SURVEY.

790402 HAGEN, W. <P. A. S. P., 91, 165>
SIMULTANEOUS MICROWAVE AND INFRARED OBSERVATIONS OF STELLAR WATER MASER SOURCES.

790403 WILLIAMS, P. M., ANTONOPOULOU, E. <M. N. R. A. S., 187, 183>
COOLING OF THE NEWLY CONDENSED SHELL AROUND HD 193793.

790404 AARONSON, M., HUCHRA, J., MOULD, J. R. <AP. J., 229, 1>
THE INFRARED LUMINOSITY/H I VELOCITY-WIDTH RELATION AND ITS APPLICATION TO THE DISTANCE SCALE.

790405 LEBOFSKY, M. J., RIEKE, G. H. <AP. J., 229, 111>
EXTINCTION IN INFRARED-EMITTING GALACTIC NUCLEI.

790406 THOMPSON, R. I., TOKUNAGA, A. T. <AP. J., 229, 153>
INFRARED SPECTROSCOPY OF LINELESS OBJECTS ASSOCIATED WITH STAR FORMATION REGIONS.

790407 O'BRIEN, G., LAMBERT, D. L. <AP. J. (LETTERS), 229, L33>
HE I 10830A EMISSION FROM ALPHA BOOTIS AND ALPHA 1 HERCULIS.

790408 TOKUNAGA, A. T., THOMPSON, R. I. <AP. J., 229, 583>
ANALYSIS OF OBSCURED INFRARED OBJECTS. III. THE INFRARED POINT SOURCE IN M17 SW.

790409 GRASDALEN, G. L. <AP. J., 229, 587>
THE 10 MICRON PROPERTIES OF PLANETARY NEBULAE.

790410 WILLNER, S. P., RUSSELL, R. W., PUETTER, R. C., SOIFER, B. T., HARVEY, P. M. <AP. J. (LETTERS), 229, L65>
THE 4 TO 8 MICRON SPECTRUM OF THE GALACTIC CENTER.

790411 SWINGS, J. P., ANDRILLAT, Y. <ASTR. AP., 74, 85>
THE BUTTERFLY NEBULA M 2-9: ITS POSSIBLE RELATION TO B(E) STARS AND/OR TO PROTOPLANETARY NEBULAE.

790412 FREY, A., LEMKE, D., THUM, C., FAHRBACH, U. <ASTR. AP., 74, 133>
NEAR INFRARED OBSERVATIONS OF NGC 2024.

790413 AVETISYAN, V. Z., KIR'YAN, V. V., POGODIN, M. A., SHAKHBAZYAN, YU. L. <ASTROFIZIKA, 15, 229>
SPECTRAL ENERGY DISTRIBUTION OF SOME STARS OF EARLY SPECTRAL CLASSES WITH GAS-DUST ENVELOPES.

790501 THRONSON JR., H. A., HARVEY, P. M., GATLEY, I. <AP. J. (LETTERS), 229, L133>
STAR FORMATION AT A FRONT: FAR-INFRARED OBSERVATIONS OF AFGL 333.

790503 GLASS, I. S. <M. N. R. A. S., 187, 305>
INFRARED PHOTOMETRY OF STARS IN THE CHAMAELEON T ASSOCIATION.

790504 SELBY, M. J., WADE, R., SANCHEZ MAGRO, C. <M. N. R. A. S., 187, 553>
SPECKLE INTERFEROMETRY IN THE NEAR-INFRARED.

790505 PHILLIPS, J. P., WADE, R., SELBY, M. J., SANCHEZ MAGRO, C. <M. N. R. A. S., 187, 45P>
JHKLM PHOTOMETRY OF NOVA CYGNI 1978.

790506 BALLY, J., JOYCE, R. R., SCOVILLE, N. Z. <AP. J., 229, 917>
NEAR-INFRARED OBSERVATIONS OF IONIZED HYDROGEN AT THE CORE OF THE GALAXY.

790507 LESTER, D. F., DINERSTEIN, H. L., RANK, D. M. <AP. J., 229, 981>
INFRARED AND OPTICAL MEASUREMENTS OF THE IONIZED GAS IN K3-50.

790508 HARVEY, P. M., CAMPBELL, M. F., HOFFMANN, W. F., THRONSON JR., H. A., GATLEY, I. <AP. J., 229, 990>
INFRARED OBSERVATIONS OF NGC 2071(IRS) AND AFGL 490: TWO LOW-LUMINOSITY YOUNG STARS.

790509 NEUGEBAUER, G., OKE, J. B., BECKLIN, E. E., MATTHEWS, K. <AP. J., 230, 79>
ABSOLUTE SPECTRAL ENERGY DISTRIBUTION OF QUASI-STELLAR OBJECTS FROM 0.3 TO 10 MICRONS.

790510 SIMON, T., SIMON, M., JOYCE, R. R. <AP. J., 230, 127>
B-ALPHA LINE SURVEY OF COMPACT INFRARED SOURCES.

790511 THRONSON JR., H. A., HARPER JR., D. A. <AP. J., 230, 133>
COMPACT HII REGIONS IN THE FAR-INFRARED.

790512 GEBALLE, T. R., LACY, J. H., BECK, S. C. <AP. J. (LETTERS), 230, L47>
THE 8 MICRON BAND OF SILICON MONOXIDE IN THE EXPANDING CLOUD AROUND VY CANIS MAJORIS.

790513 PIPHER, J. L., SOIFER, B. T., KRASSNER, J. <ASTR. AP., 74, 302>
INFRARED PHOTOMETRY AND SPECTROPHOTOMETRY OF G75.84+0.4.

790514 KOPPENAAL, K., SARGENT, A. I., NORDH, H. L., VAN DUINEN, R. J., AALDERS, J. W. G. <ASTR. AP., 75, L1>
OBSERVATIONS OF NEW FAR INFRARED SOURCES IN THE CEPHEUS OB3 MOLECULAR CLOUD.

790515 VREUX, J. M., ANDRILLAT, Y. <ASTR. AP., 75, 93>
O STARS HE II AND H LINES IN THE 1 MICRON REGION.

790516 NOSKOVA, R. I. <SOV. AST., 23, 297>
PHYSICAL PARAMETERS OF NINE PLANETARY NEBULAE.

790517 GLASS, I. S. <IAUC NO. 3363>
SS433.

790601 GLASS, I. S. <M. N. R. A. S., 187, 807>
INFRARED OBSERVATIONS OF GALACTIC X-RAY SOURCES.

790602 BARTON, J. R., PHILLIPS, B. A., ALLEN, D. A. <M. N. R. A. S., 187, 813>
STEAM IN RX PUPPIS.

790603 CARNEY, B. W., AARONSON, M. <A. J., 84, 867>
SUBDWARF BOLOMETRIC CORRECTIONS.

790604 GRASDALEN, G. L., SNEDEN, C. <P. A. S. P., 91, 337>
HIGHLY REDDENED M-TYPE SUPERGIANTS FROM THE IRC CATALOG.

790605 WOLFF, S. C., BEICHMAN, C. A. <AP. J., 230, 519>
THE PHYSICAL PROPERTIES AND ORBITAL PARAMETERS OF THE B0 IA STAR HD 152667 -V861 SCORPII: A SUPERGIANT WITH A BLACK HOLE COMPANION?

790606 SUTTON, E. C., BETZ, A. L., STOREY, J. W. V., SPEARS, D. L. <AP. J. (LETTERS), 230, L105>
THE BRIGHTNESS DISTRIBUTION OF IRC+10216 AT 11 MICRONS.

790607 NADEAU, D., GEBALLE, T. R. <AP. J. (LETTERS), 230, L169>
VELOCITY PROFILES OF THE 2.1 MICRON H2 EMISSION LINE IN THE ORION MOLECULAR CLOUD.

790608 SIMON, M., RIGHINI-COHEN, G., JOYCE, R. R., SIMON, T. <AP. J. (LETTERS), 230, L175>
A DETERMINATION OF THE REDDENING OF THE H2 EMISSION FROM THE ORION MOLECULAR CLOUD.

790609 HAYAKAWA, S., MATSUMOTO, T., MURAKAMI, H., UYAMA, K., YAMAGAMI, T., THOMAS, J. A. <NATURE, 279, 510>
NEAR IR SURFACE BRIGHTNESS OF SOUTHERN GALACTIC PLANE.

790610 WRIGHT, E. L., HARPER JR., D. A., HILDEBRAND, R. H., KEENE, J., WHITCOMB, S. E. <NATURE, 279, 703>
MILLIMETRE AND SUBMILLIMETRE MEASUREMENTS OF THE CRAB NEBULA.

790611 AITKEN, D. K., ROCHE, P. F., SPENSER, P. M., JONES, B. <ASTR. AP., 76, 60>
INFRARED SPATIAL AND SPECTRAL STUDIES OF AN IONIZATION FRONT REGION IN THE ORION NEBULA.

790612 WILSON, T. L., FAZIO, G. G., JAFFE, D., KLEINMANN, D. E., WRIGHT, E. L., LOW, F. J. <ASTR. AP., 76, 86>
A COMPARISON OF HIGH RESOLUTION RADIO AND FAR-INFRARED MAPS OF M17.

790701 BECK, S. C., LACY, J. H., GEBALLE, T. R. <AP. J., 231, 28>
NE II EMISSION AND GALACTIC DYNAMICS IN NGC 253.

790702 HARVEY, P. M., THRONSON JR., H. A., GATLEY, I. <AP. J., 231, 115>
FAR-INFRARED OBSERVATIONS OF OPTICAL EMISSION-LINE STARS: EVIDENCE FOR EXTENSIVE COOL DUST CLOUDS.

790703 KRASSNER, J., SMITH, L. L., HILGEMAN, T. <AP. J. (LETTERS), 231, L31>
NEAR-INFRARED OBSERVATIONS OF A NEW MOLECULAR FEATURE IN IRC+10216.

790704 ANDRILLAT, Y., VREUX, J. M. <ASTR. AP., 76, 221>
THE HE 10830A EMISSION LINE IN O STAR SPECTRA.

790705 WAMSTEKER, W. <ASTR. AP., 76, 226>
THE CONTINUOUS ENERGY DISTRIBUTION OF NOVA CYGNI 1975.

790706 PHILLIPS, M. M., FELDMAN, F. R., MARSHALL, F. E., WAMSTEKER, W. <ASTR. AP., 76, L14>
ESO 103-G35: A NEW SEYFERT GALAXY AND POSSIBLE X-RAY SOURCE.

790707 SERRA, G., BOISSE, P., GISPERT, R., WIJNBERGEN, J. J., RYTER, C. E., PUGET, J. L. <ASTR. AP., 76, 259>
FAR INFRARED DIFFUSE EMISSION FROM THE GALACTIC PLANE. II. THE LONGITUDE PROFILE.

790708 KNACKE, R. F., CAPPS, R. W., JOHNS, M. <NATURE, 280, 215>
OBSERVATION OF LARGE 2.2 MICRON POLARISATION IN 3C 345.

790709 IMPEY, C. D. <IAUC NO. 3379>
SS433.

790801 WEGNER, G., GLASS, I. S. <M. N. R. A. S., 188, 327>
A NEW BIPOLAR NEBULA IN CENTAURUS.

790802 JAMESON, R. F., AKINCI, R. <M. N. R. A. S., 188, 421>
1.2 AND 2.2 MICRON LIGHT CURVES OF W UMA TYPE STARS.

790803 WERNER, M. W., BECKLIN, E. E., GATLEY, I., MATTHEWS, K., NEUGEBAUER, G., WYNN-WILLIAMS, C. G. <M. N. R. A. S., 188, 463>
AN INFRARED STUDY OF THE NGC 7538 REGION.

790804 HAGEN, W. <A. J., 84, 1189>
BROAD-BAND 10 MICRON AND 20 MICRON PHOTOMETRY OF SOUTHERN SOURCES FROM THE AFGL INFRARED SKY SURVEY.

790805 WING, R. F., RINSLAND, C. P. <A. J., 84, 1235>
ATMOSPHERIC EXTINCTION IN THE FOUR-MICRON REGION.

790806 MCCORD, T. B., CLARK, R. N. <P. A. S. P., 91, 571>
ATMOSPHERIC EXTINCTION 0.65-2.50 MICRONS ABOVE MAUNA KEA.

790807 BROCKA, B. <P. A. S. P., 91, 519>
A SURVEY OF SYMBIOTIC STARS AT 1612 MHZ.

790808 GRASDALEN, G. L. <P. A. S. P., 91, 436>
NEAR INFRARED OBSERVATIONS OF THE CRAB NEBULA.

790809 OWENS, D. K., MUEHLNER, D. J., WEISS, R. <AP. J., 231, 702>
A LARGE-BEAM SKY SURVEY AT MILLIMETER AND SUBMILLIMETER WAVELENGTHS MADE FROM BALLOON ALTITUDES.

790810 MCCARTHY, J. F., FORREST, W. J., HOUCK, J. R. <AP. J., 231, 711>
OBSERVATIONS OF (S III) 18.71 MICRON EMISSION IN GALACTIC H II REGIONS.

790811 THOMPSON, R. I., TOKUNAGA, A. T. <AP. J., 231, 736>
ANALYSIS OF OBSCURED INFRARED OBJECTS. IV. GL 490 AND GL 2591.

790812 LESTER, D. F., DINERSTEIN, H. L., RANK, D. M. <AP. J., 232, 139>
FINE-STRUCTURE LINES AND ELEMENTAL ABUNDANCES IN THE ORION NEBULA.

790813 SOIFER, B. T., PUETTER, R. C., RUSSELL, R. W., WILLNER, S. P., HARVEY, P. M., GILLETT, F. C. <AP. J. (LETTERS), 232, L53>
THE 4-8 MICRON SPECTRUM OF THE INFRARED SOURCE W33A.

790814 LAMY, PH. L., NGUYEN-TRONG, T., ADJABSCHIRZADEH, A., KOUTCHMY, S. <ASTR. AP., 77, 257>
ASTRONOMICAL APPLICATIONS OF INFRA-RED TELEVISION IMAGING.

790815 KRASSNER, J., PIPHER, J. L., SHARPLESS, S. <ASTR. AP., 77, 302>
OPTICAL, RADIO, AND INFRARED OBSERVATIONS OF COMPACT H II REGIONS. III. THE NEBULA S235A.

790816 KULKARNI, P. V., ASHOK, N. M., APPARAO, K. M. V., CHITRE, S. M. <NATURE, 280, 819>
DISCOVERY OF IR BURSTS FROM LILLER 1/MXB1730-333.

790901 GILES, A. B., KING, A. R., COOKE, B. A., MCHARDY, I. M., LAWRENCE, A. <NATURE, 281, 282>
INFRARED OBSERVATIONS OF SS433.

790902 ALLEN, D. A. <NATURE, 281, 284>
INFRARED OBSERVATIONS OF SS433.

790903 BLACKWELL, D. E., SHALLIS, M. J., SELBY, M. J. <M. N. R. A. S., 188, 847>
THE INFRARED FLUX METHOD FOR DETERMINING STELLAR ANGULAR DIAMETERS AND EFFECTIVE TEMPERATURES.

790904 ZEILIK II, M., HECKERT, P. A., COHEN, N. L. <A. J., 84, 1323>
NEAR-INFRARED AND RADIO OBSERVATIONS OF IRC-10442 (GL5268S).

790905 THRONSON JR., H. A., LOEWENSTEIN, R. F., STOKES, G. M. <A. J., 84, 1328>
FAR-INFRARED OBSERVATIONS OF THE LAGOON NEBULA (M8).

790906 DYCK, H. M., LONSDALE, C. J. <A. J., 84, 1339>
THE RELATIONSHIP BETWEEN THE INFRARED POLARIZATION OF PROTOSTELLAR SOURCES AND NEARBY INTERSTELLAR POLARIZATION.

790907 SZKODY, P., DYCK, H. M., CAPPS, R. W., BECKLIN, E. E., CRUIKSHANK, D. P. <A. J., 84, 1359>
INFRARED PHOTOMETRY OF NOVA SERPENTIS 1978.

790908 SCOVILLE, N. Z., HALL, D. N. B., KLEINMANN, S. G., RIDGWAY, S. T. <AP. J. (LETTERS), 232, L121>
DETECTION OF CO BAND EMISSION IN THE BECKLIN-NEUGEBAUER OBJECT.

790909 RIGHINI-COHEN, G., SIMON, M., YOUNG, E. T. <AP. J., 232, 782>
INFRARED LINE OBSERVATIONS OF DR 21, W75N, AND K3-50.

790910 RIEKE, G. H., LEBOFSKY, M. J., KINMAN, T. D. <AP. J. (LETTERS), 232, L151>
A POSSIBLY NEW TYPE OF QSO IDENTIFIED THROUGH INFRARED MEASUREMENTS.

790911 MCBREEN, B., FAZIO, G. G., STIER, M., WRIGHT, E. L. <AP. J. (LETTERS), 232, L183>
EVIDENCE FOR A VARIABLE FAR-INFRARED SOURCE IN NGC 6334.

790912 SHENAVRIN, V. I., TARANOVA, O. G., MOROZ, V. I., GRIGOR'EV, A. V. <SOV. AST., 23, 567>
OPTICAL AND INFRARED PHOTOMETRY OF R CORONAE BOREALIS AT THE 1977 MINIMUM.

790913 TANZI, E. G., TREVES, A., SALINARI, P., TARENGHI, M. <ASTR. AP., 78, 226>
ON THE SYSTEM V861 SCO - OAO1653-40.

791001 ZEILIK II, M. <A. J., 84, 1566>
NEAR-INFRARED OBSERVATIONS OF TWO FAR-INFRARED SOURCES IN THE W3 REGION: G133.8+1.4 (W3N) AND G133.982+1.14 (BS4).

791002 SCOVILLE, N. Z., GEZARI, D. Y., CHIN, G., JOYCE, R. R. <A. J., 84, 1571>
SEARCH FOR H2 EMISSION AT 2.1 MICRONS IN TEN SOUTHERN HEMISPHERE SOURCES.

791003 FISCHER, J., RIGHINI-COHEN, G., SIMON, M., CASSAR, L. <A. J., 84, 1574>
FAR INFRARED, NEAR INFRARED, AND RADIO MOLECULAR LINE STUDIES OF HFE 2, HFE 3, AND FJM 6.

791004 WYNN-WILLIAMS, C. G., BECKLIN, E. E., MATTHEWS, K., NEUGEBAUER, G. <M. N. R. A. S., 189, 163>
TWO-MICRON SPECTROPHOTOMETRY OF THE GALAXY NGC 253.

791005 NICOLSON, G. D., GLASS, I. S., FEAST, M. W., ANDREWS, P. J. <M. N. R. A. S., 189, 29P>
THE BL LAC OBJECT PKS 1144-379.

791006 TREFFERS, R. R. <AP. J. (LETTERS), 233, L17>
DETECTION OF MOLECULAR HYDROGEN IN THE SUPERNOVA REMNANT IC 443.

791007 OGDEN, P. M., ROESLER, F. L., LARSON, H. P., SMITH, H. A., REYNOLDS, R. J., SCHERB, F. <AP. J. (LETTERS), 233, L21>
EVIDENCE FOR TEMPORAL VARIATIONS IN THE H2 2.1 MICRON EMISSION FROM THE ORION NEBULA.

791008 STOREY, J. W. V., WATSON, D. M., TOWNES, C. H. <AP. J., 233, 109>
OBSERVATIONS OF FAR-INFRARED FINE STRUCTURE LINES: (O III) 88.35 MICRONS AND (O I) 63.2 MICRONS.

791009 TOKUNAGA, A. T., THOMPSON, R. I. <AP. J., 233, 127>
ANALYSIS OF OBSCURED INFRARED POINT SOURCES. V. S106 IR AND S235 B.

791010 SMITH, H. A., LARSON, H. P., FINK, U. <AP. J., 233, 132>
THE SPECTRUM OF THE BECKLIN-NEUGEBAUER SOURCE IN ORION FROM 3.3 TO 5.5 MICRONS.

791011 HYLAND, A. R., ROBINSON, G., MITCHELL, R. M., THOMAS, J. A., BECKLIN, E. E. <AP. J., 233, 145>
THE SPECTRAL AND SPATIAL DISTRIBUTION OF RADIATION FROM ETA CARINAE. II. HIGH-RESOLUTION INFRARED MAPS OF THE HOMUNCULUS.

791012 COHEN, M., SCHWARTZ, R. D. <AP. J. (LETTERS), 233, L77>
THE EXCITING STAR OF HERBIG-HARO OBJECT 1.

791013 WEISTROP, D., SMITH, B. A., REITSEMA, H. J. <AP. J., 233, 504>
FAR-RED SURFACE PHOTOMETRY OF THE X-RAY EMITTING BL LACERTAE OBJECT PKS 0548-322.

791014 GATLEY, I., BECKLIN, E. E., SELLGREN, K., WERNER, M. W. <AP. J., 233, 575>
FAR-INFRARED OBSERVATIONS OF M17: THE INTERACTION OF AN HII REGION WITH A MOLECULAR CLOUD.

791015 FORREST, W. J., MCCARTHY, J. F., HOUCK, J. R. <AP. J., 233, 611>
16-39 MICRON SPECTROSCOPY OF OXYGEN-RICH STARS.

791016 FOY, R., CHELLI, A., SIBILLE, F., LENA, P. <ASTR. AP., 79, L5>
ANGULAR DIAMETER OF IRC+10216, MIRA, R CAS, AND GL 2591 IN THE NEAR INFRARED.

791017 SHALLIS, M. J., BLACKWELL, D. E. <ASTR. AP., 79, 48>
ANGULAR DIAMETERS, RADII, AND EFFECTIVE TEMPERATURES OF AP STARS.

791018 LEGER, A., KLEIN, J., DE CHEVEIGNE, S., GUINET, C., DEFOURNEAU, D., BELIN, M. <ASTR. AP., 79, 256>
THE 3.1 MICRON ABSORPTION IN MOLECULAR CLOUDS IS PROBABLY DUE TO AMORPHOUS H2O ICE.

791019 SIBILLE, F., CHELLI, A., LENA, P. <ASTR. AP., 79, 315>
INFRARED SPECKLE INTERFEROMETRY.

791020 SHCHERBAKOV, A. G. <SOV. AST. (LETTERS), 5, 290>
THE 10830 HE I LINE IN THE COOL GIANT HR 1105.

791101 WALKER, A. R., WILD, P. A. T., BYRNE, P. B. <M. N. R. A. S., 189, 455>
THE ANGULAR DIAMETER OF THE CARBON STAR AQ SAGITTARII.

791102 KNACKE, R. F., CAPPS, R. W. <A. J., 84, 1705>
OBSERVATION OF TWENTY MICRON POLARIZATION IN THE ORION NEBULA.

791103 BERNAT, A. P., HALL, D. N. B., HINKLE, K. H., RIDGWAY, S. T. <AP. J. (LETTERS), 233, L135>
OBSERVATIONS OF CO CIRCUMSTELLAR ABSORPTION IN THE 4.6 MICRON SPECTRUM OF ALPHA ORIONIS.

791104 AITKEN, D. K., ROCHE, P. F., SPENSER, P. M., JONES, B. <AP. J., 233, 925>
8-13 MICRON SPECTROPHOTOMETRY OF PLANETARY NEBULAE.

791105 SCHNEIDER, D. P., GREENSTEIN, J. L. <AP. J., 233, 935>
HIGH TIME RESOLUTION SPECTROPHOTOMETRY OF NOVA DQ HERCULIS (1934).

791106 FINK, U., LARSON, H. P. <AP. J., 233, 1021>
THE INFRARED SPECTRA OF URANUS, NEPTUNE, AND TITAN FROM 0.8 TO 2.5 MICRONS.

791107 HACKWELL, J. A., GEHRZ, R. D., GRASDALEN, G. L. <AP. J., 234, 133>
DUST FORMATION AROUND HD 193793.

791108 SHENAVRIN, V. I. <SOV. AST., 23, 696>
PHOTOMETRY OF XX CAM, UV CAS, AND SU TAU IN THE OPTICAL AND INFRARED RANGES.

791109 STRECKER, D. W., ERICKSON, E. F., WITTEBORN, F. C. <AP. J. SUPPL., 41, 501>
AIRBORNE STELAR SPECTROPHOTOMETRY FROM 1.2 TO 5.5 MICRONS: ABSOLUTE CALIBRATION AND SPECTRA OF STARS EARLIER THAN M3.

791110 RUDY, R. J., GOSNELL, T. R., WILLNER, S. P. <AFGL-TR-79-0172>
GROUND-BASED MEASUREMENTS OF SOURCES IN THE AFGL INFRARED SKY SURVEY.

791201 GUETTER, H. H. <A. J., 84, 1846>
PHOTOMETRIC STUDIES OF STARS IN ORI OB1 (BELT).

791202 GRASDALEN, G. L., HACKWELL, J. A., GEHRZ, R. D., MCCLAIN, D. <AP. J. (LETTERS), 234, L129>
RY SCUTI: SILICATES AROUND AN EARLY-TYPE SUPERGIANT BINARY SYSTEM.

791203 THOMPSON, R. I., RIEKE, G. H., TOKUNAGA, A. T., LEBOFSKY, M. J. <AP. J. (LETTERS), 234, L135>
1.2-2.5 MICRON SPECTROSCOPY, PHOTOMETRY, AND POLARIMETRY OF SS 433.

791204 MCALARY, C. W., MCLAREN, R. A., CRABTREE, D. R. <AP. J., 234, 471>
BROAD-BAND NEAR-INFRARED OBSERVATIONS OF SEYFERT GALAXIES.

791205 WILLNER, S. P., JONES, B., PUETTER, R. C., RUSSELL, R. W., SOIFER, B. T. <AP. J., 234, 496>
INFRARED SPECTRA OF IC 418 AND NGC 6572.

791206 HINKLE, K. H., BARNES, T. G. <AP. J., 234, 548>
INFRARED SPECTROSCOPY OF MIRA VARIABLES. III. R LEONIS, THE ATOMIC LINES.

791207 BECK, S. C., LACY, J. H., GEBALLE, T. R. <AP. J. (LETTERS), 234, L213>
DETECTION OF THE 12.28 MICRON ROTATIONAL LINE OF MOLECULAR HYDROGEN IN THE ORION MOLECULAR CLOUD.

791208 HERTER, T., DUTHIE, J. G., PIPHER, J. L., SAVEDOFF, M. P. <AP. J., 234, 897>
AIRBORNE FAR-INFRARED SPECTROSCOPIC OBSERVATIONS OF W51 AND W49.

791209 SMITH, J., LYNCH, D. K., CUDABACK, D. D., WERNER, M. W. <AP. J., 234, 902>
SUBMILLIMETER EMISSION FROM L1641 AND THE ORION NEBULA.

791210 KIPLINGER, A. L. <AP. J., 234, 997>
SS CYGNI: THE ACCRETION DISK IN ERUPTION AND AT MINIMUM LIGHT.

791211 COHEN, M., KUHI, L. V. <AP. J. SUPPL., 41, 743>
OBSERVATIONAL STUDIES OF PRE-MAIN-SEQUENCE EVOLUTION.

791212 WYNN-WILLIAMS, C. G., BECKLIN, E. E. <NATURE, 282, 810>
THE IR ENERGY DISTRIBUTION OF SS433.

799901 LIEBERT, J., DAHN, C. C., GRESHAM, M., STRITTMATTER, P. A. <AP. J., 233, 226>
NEW RESULTS FROM A SURVEY OF FAINT PROPER-MOTION STARS: A PROBABLE DEFICIENCY OF VERY LOW LUMINOSITY DEGENERATES.

799902 DEMERS, S., KUNKEL, W. E. <P. A. S. P., 91, 761>
DISCOVERY OF VERY RED GIANTS IN THE FORNAX GALAXY.

799903 DEMERS, S., KUNKEL, W. E., HARDY, E. <AP. J., 232, 84>
THE GIANT BRANCH OF FORNAX.

799904 CRAINE, E. R., DUERR, R. E., HORNER, V. M., IMHOFF, C. L., ROUTSIS, D. E., SWIHART, D. L., TURNSHEK, D. A. <STEWARD OBS., A, 3>
NEAR INFRARED PHOTOGRAPHIC SKY SURVEY.

799905 ARGYLE, R. W. <IAUC NO. 3348>
NOVALIKE OBJECT IN VULPECULA (NOVA VULPECULAE 1979?).

799906 GRIFFITHS, R. E., WARD, M. J., BLADES, J. C., WILSON, A. S. <IAUC NO. 3326>
2A 0311-227.

799907 KHOLOPOV, P. N., KUKARKINA, N. P., PEROVA, N. B. <IBVS NO. 1581>
64TH NAME-LIST OF VARIABLE STARS.

800001 ALLEN, D. A. <AP. LETTERS, 20, 131>
CANDIDATE SYMBIOTIC STARS IN THE LARGE MAGELLANIC CLOUD.

800002 KOBAYASHI, Y., KAWARA, K., KOZASA, T., SATO, S., OKUDA, H. <P. A. S. J., 32, 291>
2.2 MICRON POLARIZATION MAPPING OF THE GALACTIC CENTER.

800003 KOBAYASHI, Y., KAWARA, K., SATO, S., OKUDA, H. <P. A. S. J., 32, 295>
NARROW-BAND POLARIMETRY OF THE BN OBJECT AND AFGL 2591 BETWEEN 2 AND 4 MICRONS.

800004 **SHAHAM, J.** **<COMM. ON AP., 9, 1>**
SS433 - AN OCTOBER 1979 VIEW.

800005 **LLOYD EVANS, T.** **<S. A. A. O. CIRC., 1, 163>**
INFRARED PHOTOMETRY OF CLASSICAL CEPHEIDS.

800101 **COHEN, M.** **<A. J., 85, 29>**
RED AND NEBULOUS OBJECTS IN DARK CLOUDS: A SURVEY.

800102 **MERRILL, K. M.** **<IAUC NO. 3444>**
SUPERNOVA IN NGC 4321.

800103 **MCCARTHY, D. W., HOWELL, R., LOW, F. J.** **<AP. J. (LETTERS), 235, L27>**
SPATIAL SPECTRA OF IRC+10216 FROM 2.2 TO 20 MICRONS. DEVIATIONS FROM SPHERICAL SYMMETRY.

800104 **AUGASON, G. C., TAYLOR, B. J., STRECKER, D. W., ERICKSON, E. F., WITTEBORN, F. C.** **<AP. J., 235, 138>**
COMPARISON OF PREDICTED AND OBSERVED SPECTRAL ENERGY DISTRIBUTION OF K AND M STARS. I. ALPHA BOOTIS.

800105 **RIDGWAY, S. T., JOYCE, R. R., WHITE, N. M., WING, R. F.** **<AP. J., 235, 126>**
EFFECTIVE TEMPERATURES OF LATE-TYPE STARS: THE FIELD GIANTS FROM K0 TO M6.

800106 **GOEBEL, J. H., BREGMAN, J. D., GOORVITCH, D., STRECKER, D. W., PUETTER, R. C., RUSSELL, R. W., SOIFER, B. T., WILLNER, S. P., FORREST, W. J., HOUCK, J. R., MCCARTHY, J. F.** **<AP. J., 235, 104>**
THE INFRARED SPECTRUM OF THE CARBON STAR Y CANUM VENATICORUM BETWEEN 1.2 AND 30 MICRONS.

800107 **PERSSON, S. E., FROGEL, J. A., COHEN, J. G., AARONSON, M., MATTHEWS, K.** **<AP. J., 235, 452>**
THE SPREAD IN CO ABSORPTION AND EFFECTIVE TEMPERATURE AMONG THE GIANTS IN OMEGA CENTAURI.

800108 **TELESCO, C. M., HARPER, D. A.** **<AP. J., 235, 392>**
GALAXIES AND FAR-INFRARED EMISSION.

800109 **SMYTH, M. J., SIM, M. E.** **<NATURE, 283, 457>**
IR SOURCES IN THE SOUTHERN COALSACK.

800201 **RUDY, R. J., WILLNER, S. P.** **<P. A. S. P., 92, 75>**
CARBON MONOXIDE IN A CH STAR IN M22.

800202 **JONES, T. J., WOLFF, S. C.** **<P. A. S. P., 92, 84>**
OBSERVATIONS OF PASCHEN ALPHA IN P CYGNI AND OTHER OB STARS.

800203 **BOEHM, K. H., BRUGEL, E. W., MANNERY, E.** **<AP. J. (LETTERS), 235, L137>**
VERY LOW-EXCITATION HERBIG-HARO OBJECTS.

800204 **WILKING, B. A., LEBOFSKY, M. J., MARTIN, P. G., RIEKE, G. H.,KEMP, J. C.** **<AP. J., 235, 905>**
THE WAVELENGTH DEPENDENCE OF INTERSTELLAR LINEAR POLARIZATION.

800205 **HARVEY, P. M., THRONSON JR., H. A., GATLEY, I.** **<AP. J., 235, 894>**
A FAR-INFRARED STUDY OF THE REFLECTION NEBULA NGC 2023.

800206 **THOMPSON, R. I., TOKUNAGA, A. T.** **<AP. J., 235, 889>**
ANALYSIS OF OBSCURED INFRARED OBJECTS. VI. H AND HE LINES IN W51 AND K3-50.

800207 **PHILLIPS, M. M., FROGEL, J. A.** **<AP. J., 235, 761>**
INFRARED AND OPTICAL PROPERTIES OF THE EMISSION-LINE GALAXIES NGC 1386 AND NGC 1365.

800208 **MOORE, R. L., ANGEL, J. R. P., RIEKE, G. H., LEBOFSKY, M. J.,WISNIEWSKI, W. Z., MUFSON, S. L., VRBA, F. J., MILLER, H. R., MCGIMSEY, B. Q., WILLIAMON, R. M.** **<AP. J., 235, 717>**
OPTICAL AND INFRARED VARIABILITY OF B2 1308+326.

800209 **HERZOG, A. D., GEHRZ, R. D., HACKWELL, J. A.** **<AP. J., 236, 189>**
THE OPTICAL IDENTIFICATION OF THE INFRARED SOURCE IN MWC 349.

800210 **PHILLIPS, J. P., SELBY, M. J., WADE, R., SANCHEZ MAGRO, C.** **<M. N. R. A. S., 190, 337>**
INFRARED OBSERVATIONS OF BINARY STARS - I.

800211 **ALLEN, D. A., BARTON, J. R., GILLINGHAM, P. R., PHILLIPS, B. A.** **<M. N. R. A. S., 190, 531>**
THE NATURE OF OH 0739-14.

800212 **WALKER, A. R.** **<M. N. R. A. S., 190, 543>**
INFRARED PHOTOMETRY OF GALACTIC CARBON STARS.

800213 **NEY, E. P., MERRILL, K. M.** **<AFGL-TR-80-0050>**
STUDY OF SOURCES IN AFGL ROCKET INFRARED STUDY.

800214 **JONES, A. W., SELBY, M. J., MOUNTAIN, C. M., WADE, R., SANCHEZ MAGRO, C., MUNOZ, M. P.** **<NATURE, 283, 550>**
IR FLASHES FROM THE X-RAY RAPID BURSTER.

800301 **SZKODY, P., DYCK, H. M., CAPPS, R. W., BECKLIN, E. E., CRUIKSHANK, D. P.** **<A. J., 85, 348>**
ERRATUM: "INFRARED PHOTOMETRY OF NOVA SERPENTIS 1978".

800302 **BECKLIN, E. E., GATLEY, I., MATTHEWS, K., NEUGEBAUER, G., SELLGREN, K., WERNER, M. W., WYNN-WILLIAMS, C. G.** **<AP. J., 236, 441>**
INFRARED EMISSION AND STAR FORMATION IN THE CENTRAL REGIONS OF THE GALAXY IC 342.

800303 **O'CONNELL, R. W.** **<AP. J., 236, 430>**
GALAXY SPECTRAL SYNTHESIS. II. M32 AND THE AGES OF GALAXIES.

800304 **SMITH, H. E., SPINRAD, H.** **<AP. J., 236, 419>**
SPECTROPHOTOMETRY OF FAINT, RED 3C QSO CANDIDATES.

800305 **VIALLEFOND, F., LENA, P., DE MUIZON, M., NICOLLIER, C., ROUAN, D., WIJNBERGEN, J. J.** **<ASTR. AP., 83, 22>**
FAR INFRARED EMISSION FROM THE GALACTIC PLANE. I. OBSERVATIONS AT THE GALACTIC LONGITUDE LII - 27.5 DEGREES.

800306 **DE MUIZON, M., ROUAN, D., LENA, P., NICOLLIER, C., WIJNBERGEN, J.** **<ASTR. AP., 83, 140>**
FAR INFRARED STUDY OF MOLECULAR CLOUDS: DUST TEMPERATURE PROFILES IN S 140, IC 1396, R CRA.

800307 **BENSAMMAR, S., FRIEDJUNG, M., ASSUS, P.** **<ASTR. AP., 83, 261>**
INFRARED OBSERVATIONS OF KUWANO'S NOVALIKE OBJECT.

800308 **GROOTE, D., HUNGER, K., SCHULTZ, G. V.** **<ASTR. AP., 83, L5>**
THE IR-EXCESS OF HELIUM-VARIABLE STARS.

800309 **NEEDHAM, J. D., PHILLIPS, J. P., SELBY, M. J., SANCHEZ MAGRO, C.** **<ASTR. AP., 83, 370>**
INFRARED OBSERVATIONS OF BINARY STARS - II.

800310 **ALLEN, D. A.** **<NATURE, 284, 323>**
EMISSION AT 3.3 MICRONS AND EVIDENCE FOR DUST IN 3C273.

800401 **MUFSON, S. L., WISNIEWSKI, W. Z., MCMILLAN, R. S.** **<IAUC NO. 3471>**
KR AURIGAE.

800402 **HUMPHREYS, R. M., MERRILL, K. M., BLACK, J. H.** **<AP. J. (LETTERS), 237, L17>**
THE PERPLEXING SPECTRUM OF AFGL 2789 (V645 CYGNI).

800403 **FAZIO, G. G., MCBREEN, B., STIER, M. T., WRIGHT, E. L.** **<AP. J. (LETTERS), 237, L39>**
THE FAR-INFRARED SIZE OF IRC+10216.

800404 **HARVEY, P. M., LADA, C. J.** **<AP. J., 237, 61>**
TWO MICRON SPECTROSCOPY AND 2.7MM CO LINE OBSERVATIONS OF V645 CYGNI.

800405 **THRONSON JR., H. A., GATLEY, I., HARVEY, P. M., SELLGREN, K.,WERNER, M. W.** **<AP. J., 237, 66>**
MONOCEROS R2: FAR-INFRARED OBSERVATIONS OF A VERY YOUNG CLUSTER.

800406 **SITKO, M. L., SAVAGE, B. D.** **<AP. J., 237, 82>**
ULTRAVIOLET, VISUAL, AND INFRARED OBSERVATIONS OF THE PECULIAR BE STAR HD 45677.

800407 **PUSCHELL, J. J., STEIN, W. A.** **<AP. J., 237, 331>**
OBSERVATIONS OF STRONGLY POLARIZED EXTRAGALACTIC SOURCES.

800408 **MALKAN, M., KLEINMANN, D. E., APT, J.** **<AP. J., 237, 432>**
INFRARED STUDIES OF GLOBULAR CLUSTERS NEAR THE GALACTIC CENTER.

800409 **DINERSTEIN, H. L.** **<AP. J., 237, 486>**
INFRARED LINE MEASUREMENTS AND THE ABUNDANCE OF SULFUR IN PLANETARY NEBULAE.

800410 WILLIS, A. J., WILSON, R., VANDEN BOUT, P., SANNER, F., BLACK, J., DAVIS, R. J., DUPREE, A. K., GURSKY, H., HARTMANN, L., RAYMOND, J., MATILSKY, T., BURGER, M., DE LOORE, C., VAN DESSEL, E. L., WHITELOCK, P., MENZIES, J., MEIKLE, W. P. S., JOSEPH, R.D., SANFORD, P.,POLLARD, G., SANDFORD, M. C. W. <AP. J., 237, 596>
ULTRAVIOLET, VISIBLE, INFRARED, AND X-RAY OBSERVATIONS OF SCORPIUS X-1.

800411 COHEN, M., SCHWARTZ, R. D. <M. N. R. A. S., 191, 165>
A SEARCH FOR THE EXCITING STARS OF HERBIG-HARO OBJECTS.

800412 SHERRINGTON, M. R., LAWSON, P. A., KING, A. R., JAMESON, R. F. <M. N. R. A. S., 191, 185>
INFRARED AND OPTICAL LIGHT CURVES OF EX HYDRAE AND VW HYDRI.

800413 NICOLSON, G. D., FEAST, M. W., GLASS, I. S. <M. N. R. A. S., 191, 293>
RECENT CHANGES IN THE OPTICAL, INFRARED AND RADIO EMISSION FROM CIRCINUS X-1.

800414 WHITTET, D. C. B., BLADES, J. C. <M. N. R. A. S., 191, 309>
GRAIN GROWTH IN INTERSTELLAR CLOUDS.

800415 THE, P. S., TJIN A DJIE, H. R. E., WAMSTEKER, W. <ASTR. AP., 84, 263>
TR 27-28: A WC9-TYPE STAR WITH LARGE INFRARED EXCESS.

800416 LEBOFSKY, M. J., RIEKE, G. H. <NATURE, 284, 410>
VARIATIONS IN THE THERMAL EMISSION OF SEYFERT GALAXIES.

800501 TOKUNAGA, A. T., YOUNG, E. T. <AP. J. (LETTERS), 237, L93>
HIGH-RESOLUTION SPECTRA OF THE 3.3 MICROMETER UNIDENTIFIED EMISSION FEATURE IN NGC 7027 AND HD 44179.

800502 LONSDALE, C. J., DYCK, H. M., CAPPS, R. W., WOLSTENCROFT, R. D. <AP. J. (LETTERS), 238, L31>
NEAR-INFRARED CIRCULAR POLARIZATION OBSERVATIONS OF MOLECULAR CLOUD SOURCES.

800503 CAMPBELL, M. F., HOFFMANN, W. F., THRONSON JR., H. A., HARVEY, P. M. <AP. J., 238, 122>
FAR-INFRARED SURVEY OF CYGNUS X.

800504 RIEKE, G. H., LEBOFSKY, M. J., THOMPSON, R. I., LOW, F. J., TOKUNAGA, A. T. <AP. J., 238, 24>
THE NATURE OF THE NUCLEAR SOURCES IN M82 AND NGC 253.

800505 DWEK, E., SELLGREN, K., SOIFER, B. T., WERNER, M. W. <AP. J., 238, 140>
EXCITATION MECHANISMS FOR THE UNIDENTIFIED INFRARED EMISSION FEATURES.

800506 AARONSON, M., MOULD, J., HUCHRA, J. <AP. J., 237, 655>
A DISTANCE SCALE FROM THE INFRARED MAGNITUDE/H I VELOCITY WIDTH RELATION. I. THE CALIBRATION.

800507 GEHRZ, R. D., GRASDALEN, G. L., HACKWELL, J. A., NEY, E. P. <AP. J., 237, 855>
THE EVOLUTION OF THE DUST SHELL OF NOVA SERPENTIS 1978.

800508 LAMBERT, D. L., CLEGG, R. E. S. <M. N. R. A. S., 191, 367>
THE KEENAN AND WING BANDS IN S STARS.

800509 COHEN, M. <M. N. R. A. S., 191, 499>
INFRARED OBSERVATIONS OF YOUNG STARS - VIII. SPECTRA IN TEN-MICRON REGION.

800510 EPCHTEIN, N., GUIBERT, J., NGUYEN-QUANG-RIEU,., TURON, P., WAMSTEKER, W. <ASTR. AP., 85, L1>
INFRARED PHOTOMETRY OF MIRA VARIABLES. OH MASER PUMPING EFFICIENCY.

800511 MAMMANO, A., CIATTI, F., VITTONE, A. <ASTR. AP., 85, 14>
THE UNIQUE SPECTRUM OF SS 433, A STAR INSIDE A SUPERNOVA REMNANT.

800512 FOY, R. <ASTR. AP., 85, 287>
DETAILED ANALYSIS OF HIGH VELOCITY STARS.

800513 SOIFER, B. T., NEUGEBAUER, G., MATTHEWS, K., BECKLIN, E. E., WYNN-WILLIAMS, C. G., CAPPS, R. <NATURE, 285, 91>
IR OBSERVATIONS OF THE DOUBLE QUASAR 0957+561 A, B AND THE INTERVENING GALAXY.

800514 BAILEY, J., HOUGH, J. H., AXON, D. J. <NATURE, 285, 306>
IR PHOTOMETRY AND POLARIMETRY OF 2A0311-227.

800601 ROSSANO, G. S., RUSSELL, R. W., CORNETT, R. H. <P. A. S. P., 92, 357>
NEAR INFRARED PHOTOGRAPHY WITH A VACUUM-COLD CAMERA.

800602 PHILLIPS, T. G., HUGGINS, P. J., KUIPER, T. B. H., MILLER, R. E. <AP. J. (LETTERS), 238, L103>
DETECTION OF THE 610 MICRON (492 GHZ) LINE OF INTERSTELLAR ATOMIC CARBON.

800603 FISCHER, J., RIGHINI-COHEN, G., SIMON, M. <AP. J. (LETTERS), 238, L155>
DETECTION OF H2 EMISSION IN THE DR 21/W75 COMPLEX, OMC-2, AND HERBIG-HARO OBJECT NO. 2.

800604 MOSELEY, H. <AP. J., 238, 892>
OBSERVATIONS OF COOL DUST IN PLANETARY NEBULAE.

800605 BLADES, J. C., WHITTET, D. C. B. <M. N. R. A. S., 191, 701>
OBSERVATIONS OF UNIDENTIFIED INFRARED FEATURES IN THE PRE-MAIN SEQUENCE STAR HD 97048.

800606 MOULD, J., AARONSON, M., HUCHRA, J. <AP. J., 238, 458>
A DISTANCE SCALE FROM THE INFRARED MAGNITUDE/H I VELOCITY-WIDTH RELATION. II. THE VIRGO CLUSTER.

800607 NEUGEBAUER, G., MORTON, D., OKE, J. B., BECKLIN, E. E., DALTABUIT, E., MATTHEWS, K., PERSSON, S. E., SMITH, A. M., SOIFER, B. T., TORRES-PEIMBERT, S., WYNN-WILLIAMS, C. G. <AP. J., 238, 502>
RECOMBINATION SPECTRUM AND REDDENING IN NGC 1068.

800608 MOORWOOD, A. F. M., BALUTEAU, J. -P., ANDEREGG, M., CORON, N., BIRAUD, Y., FITTON, B. <AP. J., 238, 565>
INFRARED LINE EMISSION FROM H II REGIONS. III. AIRBORNE OBSERVATIONS OF (S III) (18 AND 33 MICRONS), (O III) (52 AND 88 MICRONS), AND (N III) (57 MICRONS) ON M17.

800609 WITTEBORN, F. C., STRECKER, D. W., ERICKSON, E. F., SMITH, S. M., GOEBEL, J. H., TAYLOR, B. J. <AP. J., 238, 577>
THE SPECTRUM OF IRC+10216 FORM 2.0 TO 8.5 MICRONS.

800610 COHEN, M., BARLOW, M. J. <AP. J., 238, 585>
INFRARED PHOTOMETRY OF SOUTHERN PLANETARY NEBULAE AND EMISSION-LINE OBJECTS.

800611 ERICKSON, E. F., TOKUNAGA, A. T. <AP. J., 238, 596>
FAR-INFRARED SPECTRA OF W51-IRS2 AND W49 NW.

800612 DE VRIES, J. S., VAN DER WAAL, P. B., ANDRIESSE, C. D. <ASTR. AP., 86, 248>
HIGH-RESOLUTION (NE II) OBSERVATIONS IN G333.6-0.2.

800613 ARDEBERG, A., VIRDEFORS, B. <ASTR. AP. SUPPL., 40, 307>
A CATALOGUE OF STELLAR SPECTROPHOTOMETRIC DATA.

800614 LEBOFSKY, M. J., RIEKE, G. H., WALSH, D., WEYMANN, R. J. <NATURE, 285, 385>
THE IR SPECTRUM OF THE DOUBLE QSO.

800701 SZKODY, P., CAPPS, R. W. <A. J., 85, 882>
INFRARED OBSERVATIONS OF POLARS: AM HER, VV PUP, AND AN UMA.

800702 BECKWITH, S., NEUGEBAUER, G., BECKLIN, E. E., MATTHEWS, K. <A. J., 85, 886>
MOLECULAR HYDROGEN EMISSION IN NGC 7027.

800703 DYCK, H. M. <A. J., 85, 891>
NEAR-INFRARED SLIT SCANS OF MOLECULAR CLOUD SOURCES.

800704 AARONSON, M., MOULD, J., HUCHRA, J., SULLIVAN III, W. T., SCHOMMER, R. A., BOTHUN, G. D. <AP. J., 239, 12>
A DISTANCE SCALE FROM THE INFRARED MAGNITUDE/H I VELOCITY-WIDTH RELATION. III. THE EXPANSION RATE OUTSIDE THE LOCAL SUPERCLUSTER.

800705 COHEN, J. G., FROGEL, J. A., PERSSON, S. E., ZINN, R. <AP. J., 239, 74>
PAL 12 - A METAL-RICH GLOBULAR CLUSTER IN THE OUTER HALO.

800706 BALLY, J., SCOVILLE, N. Z. <AP. J., 239, 121>
STRUCTURE AND EVOLUTION OF MOLECULAR CLOUDS NEAR H II REGIONS. I. CO OBSERVATIONS OF AN EXPANDING MOLECULAR SHELL SURROUNDING THE PELICAN NEBULA.

800707 FROGEL, J. A., PERSSON, S. E., COHEN, J. G. <AP. J., 239, 495>
LUMINOSITIES AND TEMPERATURES OF THE REDDEST STARS IN THREE LMC CLUSTERS.

800708 THRONSON JR., H. A., CAMPBELL, M. F., HOFFMANN, W. F. <AP. J., 239, 533>
THE LARGE-SCALE FAR-INFRARED STRUCTURE OF W3 AND W4.

800709 WERNER, M. W., BECKWITH, S., GATLEY, I., SELLGREN, K., BERRIMAN, G., WHITING, D. L. <AP. J., 239, 540>
SIMULTANEOUS FAR-INFRARED, NEAR-INFRARED, AND RADIO OBSERVATIONS OF OH/IR STARS.

800710 GEHRZ, R. D., HACKWELL, J. A., GRASDALEN, G. L., NEY, E. P., NEUGEBAUER, G., SELLGREN, K. <AP. J., 239, 570>
THE OPTICALLY THIN DUST SHELL OF NOVA CYGNI 1978.

800711 JONES, T. J., HYLAND, A. R. <M. N. R. A. S., 192, 359>
NEW RESULTS ON INTERSTELLAR REDDENING IN THE NEAR INFRARED.

800712 BERGEAT, J., LUNEL, M. <ASTR. AP., 87, 139>
IJHKL PHOTOMETRY OF CARBON STARS.

800801 GEHRZ, R. D., HACKWELL, J. A., GRASDALEN, G. L., MERRILL, K. M., HUMPHREYS, R. M., WILLIAMSON, F. O., PUETTER, R. C., RUSSELL, R. W., WILLNER, S. P. <A. J., 85, 1071>
ON THE NATURE OF THE PECULIAR INFRARED SOURCE AFGL 2636.

800802 DYCK, H. M., LONSDALE, C. J. <A. J., 85, 1077>
ICE-BAND POLARIMETRY OF GL 2591.

800803 NISHIMURA, T., LOW, F. J., KURTZ, R. F. <AP. J. (LETTERS), 239, L101>
FAR-INFRARED SURVEY OF THE GALACTIC PLANE.

800804 WATSON, D. M., STOREY, J. W. V., TOWNES, C. H., HALLER, E. E., HANSEN, W. L. <AP. J. (LETTERS), 239, L129>
DETECTION OF CO J-21-20(124.2 MICRONS) AND J-22-21(118.6 MICRONS) EMISSION FROM THE ORION NEBULA.

800805 FORREST, W. J., MCCARTHY, J. F., HOUCK, J. R. <AP. J. (LETTERS), 240, L37>
DETECTION OF (O IV) AND (NE V) INFRARED EMISSION LINES FROM NGC 7027.

800806 KEENE, J., HARPER, D. A., HILDEBRAND, R. H., WHITCOMB, S. E. <AP. J. (LETTERS), 240, L43>
FAR-INFRARED OBSERVATIONS OF THE GLOBULE B335.

800807 CHEUNG, L. H., FROGEL, J. A., GEZARI, D. Y., HAUSER, M. G. <AP. J., 240, 74>
1.0 MILLIMETER MAPS AND RADIAL DENSITY DISTRIBUTIONS OF SOUTHERN H II/MOLECULAR CLOUD COMPLEXES.

800808 PETERSON, R. C., WILLMARTH, D. W., CARNEY, B. W., CHAFFEE JR., F. H. <AP. J., 239, 928>
BD-0 4234: A HIGH-VELOCITY, METAL-POOR, DOUBLE-LINED SPECTROSCOPIC BINARY.

800809 WHITTET, D. C. B., VAN BREDA, I. G. <M. N. R. A. S., 192, 467>
INFRARED PHOTOMETRY OF SOUTHERN EARLY-TYPE STARS.

800810 ALLEN, D. A., HYLAND, A. R., CASWELL, J. L. <M. N. R. A. S., 192, 505>
ROBERTS 22: A BIPOLAR NEBULA WITH OH EMISSION.

800811 WILLIAMS, P. M., ADAMS, D. J., ARAKAKI, S., BEATTIE, D. H., BORN, J., LEE, T. J., ROBERTSON, D. J., STEWART, J. M. <M. N. R. A. S., 192, 25P>
NEAR INFRARED SPECTROMETRY OF WC STARS.

800812 GLASS, I. S. <M. N. R. A. S., 192, 37P>
JHK OBSERVATIONS OF TWO Z - 3 QSOS.

800813 HEFELE, H., HOLZLE, E. <ASTR. AP., 88, 145>
8-13 MICRON SPECTROPHOTOMETRY OF S 106.

800814 AKINCI, R., JAMESON, R. F. <ASTR. AP., 88, 320>
J, K, L, INFRARED OBSERVATIONS OF RZ SCUTUM.

800815 TARANOVA, O. G., YUDIN, B. F. <SOV. AST. (LETTERS), 6, 273>
INFRARED VARIABILITY OF HM SAGITTAE AND V1016 CYGNI.

800816 SATO, S., KAWARA, K., KOBAYASHI, Y., MAIHARA, T., OKUDA, H. <NATURE, 286, 688>
NO IR BURST FROM THE X-RAY RAPID BURSTER MXB1730-335.

800817 GILES, A. B., KING, A. R., JAMESON, R. F., SHERRINGTON, M. R., HOUGH, J. H., BAILEY, J. A., CUNNINGHAM, E. C. <NATURE, 286, 689>
THE IR VARIABILITY OF SS433.

800818 KREYSA, E., PAULINY-TOTH, I. I. K., SCHULTZ, G. V., SHERWOOD, W. A., WITZEL, A. <AP. J. (LETTERS), 240, L17>
MILLIMETER CONTINUUM OBSERVATIONS OF FLAT SPECTRA RADIO SOURCES.

800901 FISCHER, J., RIGHINI-COHEN, G., SIMON, M., JOYCE, R. R., SIMON, T. <AP. J. (LETTERS), 240, L95>
OBSERVATIONS OF H2 EMISSION FROM NGC 7538.

800902 RUSSELL, R. W., MELNICK, G., GULL, G. E., HARWIT, M. <AP. J. (LETTERS), 240, L99>
DETECTION OF THE 157 MICRON (1910GHZ) (C II) EMISSION LINE FROM THE INTERSTELLAR GAS COMPLEXES NGC 2024 AND M42.

800903 WRIGHT, E. L., HARPER, D. A., LOEWENSTEIN, R. F., KEENE, J., WHITCOMB, S. E. <AP. J. (LETTERS), 240, L157>
SEARCH FOR FAR-INFRARED EMISSION FROM YOUNG SUPERNOVA REMNANTS.

800904 MCLAREN, R. A., BETZ, A. L. <AP. J. (LETTERS), 240, L159>
INFRARED OBSERVATIONS OF CIRCUMSTELLAR AMMONIA IN OH/IR SUPERGIANTS.

800905 PERSSON, S. E., COHEN, J. G., SELLGREN, K., MOULD, J., FROGEL, J. A. <AP. J., 240, 779>
INFRARED PHOTOMETRY OF THE SEMISTELLAR NUCLEUS OF M31.

800906 FROGEL, J. A., PERSSON, S. E., COHEN, J. G. <AP. J., 240, 785>
PHOTOMETRIC STUDIES OF COMPOSITE STELLAR SYSTEMS. IV. INFRARED PHOTOMETRY OF GLOBULAR CLUSTERS IN M31 AND A COMPARISON WITH EARLY-TYPE GALAXIES.

800907 AARONSON, M., MOULD, J. <AP. J., 240, 804>
CARBON STARS IN THE FORNAX DWARF SPHEROIDAL GALAXY.

800908 MCALARY, C. W., MCLAREN, R. A. <AP. J., 240, 853>
INFRARED SPECTROPHOTOMETRY OF SS 433.

800909 GOORVITCH, D., GOEBEL, J. H., AUGASON, G. C. <AP. J., 240, 588>
THEORETICAL PROFILES FOR THE 1-0 S(I) H2 LINE IN CARBON STARS.

800910 MOULD, J., AARONSON, M. <AP. J., 240, 464>
THE EXTENDED GIANT BRANCHES OF INTERMEDIATE AGE GLOBULAR CLUSTERS IN THE MAGELLANIC CLOUDS.

800911 AITKEN, D. K., BARLOW, M. J., ROCHE, P. F., SPENSER, P. M. <M. N. R. A. S., 192, 679>
8-13 MICRON SPECTRA OF VERY LATE TYPE WOLF-RAYET STARS.

800912 MURDIN, P., ALLEN, D. A., MORTON, D. C., WHELAN, J. A. J., THOMAS, R. M. <M. N. R. A. S., 192, 709>
THE K DWARFS ASSOCIATED WITH THE X-RAY TRANSIENTS A0620-00 AND A1742-28.

800913 ALLEN, D. A., BARTON, J. R., GILLINGHAM, P. R. <M. N. R. A. S., 192, 805>
AN INFRARED CANDIDATE FOR OH 205.1-14.1.

800914 THE, P. S., BAKKER, R., TJIN A DJIE, H. R. E. <ASTR. AP., 89, 209>
STUDIES OF THE CARINA NEBULA. II. THE EXTINCTION LAW IN THE DIRECTION OF 14 O-TYPE STARS.

800915 VOLOSHINA, I. B., GLUSHNEVA, I. N., SHENAVRIN, V. I. <SOV. AST., 24, 576>
ENERGY DISTRIBUTIONS IN THE NEAR-IR REGION IN THE SPECTRA OF STARS USED AS SPECTROPHOTOMETRIC STANDARDS.

800916 LEWIN, W. H. G., COMINSKY, L. R., WALKER, A. R., ROBERTSON, B. S. C. <NATURE, 287, 27>
SIMULTANEOUS IR AND X-RAY BURST OBSERVATION OF SER X-1.

801001 STAUFFER, J. R. <A. J., 85, 1341>
OBSERVATIONS OF PRE-MAIN-SEQUENCE STARS IN THE PLEIADES.

801002 GULL, G. E., RUSSELL, R. W., MELNICK, G., HARWIT, M. <A. J., 85, 1379>
FAR-INFRARED POLARIZATION OF THE KLEINMANN-LOW NEBULA.

801003 FROGEL, J. A. <AP. J. (LETTERS), 241, L41>
INFRARED PHOTOMETRY OF THE GLOBULAR CLUSTER ASSOCIATED WITH NGC 5128.

801004 WATSON, D. M., STOREY, J. W. V., TOWNES, C. H., HALLER, E. E. <AP. J. (LETTERS), 241, L43>
FAR-INFRARED (O III) LINE EMISSION FROM THE GALACTIC CENTER.

801005 TELESCO, C. M., BECKLIN, E. E., WYNN-WILLIAMS, C. G. <AP. J. (LETTERS), 241, L69>
EXTENDED 20 MICRON EMISSION FROM THE CENTER OF NGC 1068.

801006 HYLAND, A. R., MCGREGOR, P. J., ROBINSON, G., THOMAS, J. A., BECKLIN, E. E., GATLEY, I., WERNER, M. W. <AP. J., 241, 709>
THE INFRARED EMISSION OF G333.6-0.2, AN EXTREMELY NONSPHERICAL H II REGION.

801007 ELIAS, J. H. <AP. J., 241, 728>
H2 EMISSION FROM HERBIG-HARO OBJECTS.

801008 LACY, J. H., TOWNES, C. H., GEBALLE, T. R., HOLLENBACH, D. J. <AP. J., 241, 132>
OBSERVATIONS OF THE MOTION AND DISTRIBUTION OF THE IONIZED GAS IN THE CENTRAL PARSEC OF THE GALAXY. II.

801009 SELBY, M. J., BLACKWELL, D. E., PETFORD, A. D., SHALLIS, M. J. <M. N. R. A. S., 193, 111>
MEASUREMENT OF THE ABSOLUTE FLUX FROM VEGA IN THE K BAND (2.2 MICRONS).

801010 AITKEN, D. K., ROCHE, P. F., SPENSER, P. M. <M. N. R. A. S., 193, 207>
8-13 MICRON SPECTROPHOTOMETRY OF V1016 CYG AND THE SHAPE OF THE 'SILICATE' FEATURE.

801011 ALTAMORE, A., BARATTA, G. B., CASSATELLA, A., GRASDALEN, G. L., PERSI, P., VIOTTI, R. <ASTR. AP., 90, 290>
ULTRAVIOLET, OPTICAL, AND INFRARED OBSERVATIONS OF THE HERBIG BE STAR HD 200775.

801012 MOORWOOD, A. F. M., SALINARI, P., FURNISS, I., JENNINGS, R. E., KING, K. J. <ASTR. AP., 90, 304>
INFRARED SPECTROSCOPY WITH A BALLOON BORNE MICHELSON INTERFEROMETER. II. OBSERVATION OF O III, O I, AND N III FINE STRUCTURE LINES IN H II REGIONS.

801013 WICKRAMASINGHE, D. T., ALLEN, D. A. <NATURE, 287, 518>
THE 3.4 MICRON INTERSTELLAR ABSORPTION FEATURE.

801101 CUTRI, R. M., RUDY, R. J. <AP. J. (LETTERS), 241, L141>
DETECTION OF THE 3.3 MICRON FEATURE IN THE SEYFERT GALAXY NGC 4151.

801102 HARVEY, P. M., CAMPBELL, M. F., HOFFMANN, W. F. <AP. J. (LETTERS), 241, L183>
ERRATUM TO "HIGH-RESOLUTION FAR-INFRARED OBSERVATIONS OF THE GALACTIC CENTER".

801103 RICHER, H. B., FROGEL, J. A. <AP. J. (LETTERS), 242, L9>
DISCOVERY OF THE FIRST SC STAR IN THE MAGELLANIC CLOUDS.

801104 ELIAS, J. H., FROGEL, J. A., HUMPHREYS, R. M. <AP. J. (LETTERS), 242, L13>
HV 11417: A PECULIAR M SUPERGIANT IN THE SMALL MAGELLANIC CLOUD.

801105 JONES, T. J., HYLAND, A. R., ROBINSON, G., SMITH, R., THOMAS, J. <AP. J., 242, 132>
INFRARED OBSERVATIONS OF A BOK GLOBULE IN THE SOUTHERN COALSACK.

801106 JONES, B., MERRILL, K. M., STEIN, W., WILLNER, S. P. <AP. J., 242, 141>
THE DEPENDENCE OF THE 8-13 MICRON SPECTRUM OF NGC 7027 ON POSITION IN THE NEBULA.

801107 FEAST, M. W., CATCHPOLE, R. M., CARTER, B. S., ROBERTS, G. <M. N. R. A. S., 193, 377>
A PERIOD-LUMINOSITY RELATION FOR SUPERGIANT RED VARIABLES IN THE LARGE MAGELLANIC CLOUD.

801108 FRIDLUND, C. V. M., NORDH, H. L., VAN DUINEN, R. J., AALDERS, J. W. G., SARGENT, A. I. <ASTR. AP., 91, L1>
A LOW-LUMINOSITY FAR INFRARED SOURCE IN THE L1551 MOLECULAR CLOUD.

801109 AKOPIAN, A. A., KIR'YAN, V. V., MELIK-ALAVERDIAN, YU. K., TOVMASSIAN, H. M. <ASTROFIZIKA, 16, 669>
INFRARED PHOTOMETRY OF S STARS.

801110 TOVMASSIAN, H. M., MELIK-ALAVERDIAN, YU. K., AVETISIAN, V. S. <ASTROFIZIKA, 16, 791>
ON THE VARIATION IR-EMISSION OF V915 AQL.

801111 MCCALL, A., HOUGH, J. H. <ASTR. AP. SUPPL., 42, 141>
NEAR INFRARED POLARIMETRY OF COOL STARS.

801201 GEHRZ, R. D., HACKWELL, J. A., GRASDALEN, G. L., MERRILL, K. M., HUMPHREYS, R. M., WILLIAMSON, F. O., PUETTER, R. C., RUSSELL, R. W., WILLNER, S. P. <A. J., 85, 1676>
ERRATUM TO "ON THE NATURE OF THE PECULIAR INFRARED SOURCE AFGL 2636".

801202 HOUCK, J. R., FORREST, W. J., MCCARTHY, J. F. <AP. J. (LETTERS), 242, L65>
MEDIUM-RESOLUTION SPECTRA OF M82 AND NGC 1068 FROM 16 TO 30 MICRONS.

801203 KNACKE, R. F., YOUNG, E. T. <AP. J. (LETTERS), 242, L183>
DETECTION OF THE S(9), V-0-0 ROTATION LINE OF THE HYDROGEN MOLECULE IN ORION.

801204 WERNER, M. W., BECKLIN, E. E., GATLEY, I., NEUGEBAUER, G., SELLGREN, K., THRONSON JR., H. A., HARPER, D. A., LOEWENSTEIN, R., MOSELEY, S. H. <AP. J., 242, 601>
HIGH ANGULAR RESOLUTION FAR-INFRARED OBSERVATIONS OF THE W3 REGION.

801205 THRONSON JR., H. A., THOMPSON, R. I., HARVEY, P. M., RICKARD, L. J., TOKUNAGA, A. T. <AP. J., 242, 609>
STAR FORMATION IN IC 1848A.

801206 WHITE, N. M. <AP. J., 242, 646>
THE OCCULTATION OF 119 TAU AND THE EFFECTIVE TEMPERATURES OF THREE M SUPERGIANTS.

801207 MCCARTHY, J. F., FORREST, W. J., BRIOTTA JR., D. A., HOUCK, J. R. <AP. J., 242, 965>
THE GALACTIC CENTER: 16-30 MICRON OBSERVATIONS AND THE 18 MICRON EXTINCTION.

801208 LADA, C. J., WILKING, B. A. <AP. J., 242, 1056>
INFRARED OBSERVATIONS OF BARNARD 35: HEAT SOURCES FOR BRIGHT-RIMMED MOLECULAR CLOUDS.

801209 TREVES, A., CHIAPPETTI, L., TANZI, E. G., TARENGHI, M., GURSKY, H., DUPREE, A. K., HARTMANN, L. W., RAYMOND, J., DAVIS, R. J., BLACK, J., MATILSKY, T.A., VANDEN BOUT, P.,SANNER, F., POLLARD, G., SANFORD, P. W., JOSEPH, R. D., MEIKLE, W. P. S. <AP. J., 242, 1114>
ULTRAVIOLET, X-RAY, AND INFRARED OBSERVATIONS OF HDE 226868 - CYGNUS X-1.

801210 GRASDALEN, G. L., CASTELAZ, M., GEHRZ, R. D. <IAUC NO. 3551>
NOVA CYGNI 1980.

801211 NEY, E. <IAUC NO. 3553>
HONDA'S VARIABLE IN CYGNUS (NOVA CYGNI 1980).

801212 KOORNNEEF, J., LUB, J., BARBIER, R. <IAUC NO. 3556>
SUPERNOVA IN NGC 1316.

801213 NECKEL, TH., HARRIS, A. W., EIROA, C. <ASTR. AP., 92, L9>
DISCOVERY OF THE EXCITING STAR IN THE NORTH AMERICA - PELICAN NEBULA COMPLEX?

801214 PERSI, P., FERRARI-TONIOLO, M., GRASDALEN, G. L., SPADA, G. <ASTR. AP., 92, 238>
INFRARED PHOTOMETRY OF HDE 226868 (CYG X-1) FROM 2.3 TO 10 MICRONS: MASS LOSS RATE.

801215 WILLIAMS, P. M., ALLEN, D. A. <OBSERVATORY, 100, 202>
INFRARED OBSERVATIONS OF THE WC5 WOLF-RAYET STAR HD 115473.

801216 FEAST, M. W., GLASS, I. S. <OBSERVATORY, 100, 208>
THE SYMBIOTIC-NOVA SYSTEM AS 239.

809901 ST. CLAIR DINGER, A., DICKINSON, D. F. <A. J., 85, 1247>
A CATALOG OF NONSTELLAR WATER MASER SOURCES.

809902 FOLTZ, C. B., PETERSON, B. M., BOROSON, T. A. <A. J., 85, 1328>
ACCURATE OPTICAL POSITIONS FOR MARKARIAN OBJECTS 701-797.

809903 ALTAMORE, A., SMRIGLIO, F., BUSSOLETTI, E., CORSI, C. E., ROSSI, L. <AP. AND SP. SCI., 72, 159>
A SEARCH FOR CARBON STARS IN THE AFGL CATALOGUE.

809904 RODRIGUEZ, L. F., MORAN, J. M., HO, P. T. P., GOTTLIEB, E. W. <AP. J., 235, 845>
RADIO OBSERVATIONS OF WATER VAPOR, HYDROXYL, SILICON MONOXIDE, AMMONIA, CARBON MONOXIDE, AND COMPACT H II REGIONS IN THE VICINITIES OF SUSPECTED HERBIG-HARO OBJECTS.

809905 KUTNER, M. L., MACHNIK, D. E., TUCKER, K. D., DICKMAN, R. L. <AP. J., 237, 734>
MOLECULAR CLOUDS ASSOCIATED WITH REFLECTION NEBULAE. I. A SURVEY OF CARBON MONOXIDE EMISSION.

809906 GRAHAM, J. A., PHILIPS, M. M. <AP. J. (LETTERS), 239, L97>
THE FIRST BRIGHT GLOBULAR CLUSTER IN NGC 5128.

809907 MAZA, J <IAUC NO. 3548>
SUPERNOVA IN NGC 1316.

809908 HEWITT, A., BURBIDGE, G. <AP. J. SUPPL., 43, 57>
A REVISED OPTICAL CATALOG OF QUASI-STELLAR OBJECTS.

809909 HOLMBERG, E. B., LAUBERTS, A., SCHUSTER, H. -E., WEST, R. M. <ASTR. AP. SUPPL., 39, 173>
THE ESO/UPPSALA SURVEY OF THE ESO(B) ATLAS OF THE SOUTHERN SKY. VII.

809910 BLANCO, V. M., MCCARTHY S. J., M. F., BLANCO, B. M. <AP. J., 242, 938>
CARBON AND LATE M-TYPE STARS IN THE MAGELLANIC CLOUDS.

809911 MARGON, B., DOWNES, R. A, SZKODY, P. <IAUC NO. 3465>
STEPANYAN'S STAR.

809912 KAPLAN, G. H., KALLARAKAL, V. V., HARRINGTON, R. S., JOHNSTON, K. J., SPENCER, J. H. <A. J., 85, 64>
THE COINCIDENCE OF THE RADIO AND OPTICAL EMISSION FROM SS433.

809913 GILMORE, W. <A. J., 85, 894>
RADIO CONTINUUM INTERFEROMETRY OF DARK CLOUDS. I. A SEARCH FOR NEWLY FORMED H II REGIONS.

809914 LLOYD EVANS, T. <M. N. R. A. S., 193, 87>
RED STARS IN MAGELLANIC CLOUD GLOBULAR CLUSTERS.

809915 BIDELMAN, W. P. <PUBL. WARNER AND SWASEY OBS., 2, 185>
SPECTRAL CLASSIFICATIONS FOR THE STARS OF THE CALTECH TWO-MICRON SURVEY.

810001 NOGUCHI, K., KAWARA, K., KOBAYASHI, Y., OKUDA, H., SATO, S., OISHI, M. <P. A. S. J., 33, 373>
NEAR-INFRARED PHOTOMETRY OF CARBON STARS.

810002 NOGUCHI, K., HAYAKAWA, S., MATSUMOTO, T., UYAMA, K. <P. A. S. J., 33, 583>
NEAR-INFRARED MULTICOLOR OBSERVATION OF THE DIFFUSE GALACTIC EMISSION.

810003 HAMAJIMA, K., ICHIKAWA, T., ISHIDA, K., HIDAYAT, B., RAHARTO, M. <P. A. S. J., 33, 591>
ON THE 2.4 MICRON ENHANCEMENT CENTERED AT ABOUT L-355 DEGREES, B--1 DEGREE.

810004 ENNIS, D. J., SOIFER, B. T., NEUGEBAUER, G., WERNER, M. <AP. LETTERS, 22, 13>
ONE MILLIMETER CONTINUUM OBSERVATIONS OF HIGH REDSHIFT QUASARS.

810101 PUSCHELL, J. J. <A. J., 86, 16>
VISUAL-INFRARED VARIATIONS IN THE BROAD-LINE RADIO GALAXY 3C382.

810102 LEDDEN, J. E., O'DELL, S. L., STEIN, W. A., WISNIEWSKI, W. Z. <AP. J., 243, 47>
THE SPECTRAL FLUX DISTRIBUTION OF THE CANDIDATE BL LACERTAE OBJECT 1218+304 (-2A1219+305).

810103 JONES, T. W., RUDNICK, L., OWEN, F. N., PUSCHELL, J. J., ENNIS, D. J., WERNER, M. W. <AP. J., 243, 97>
THE BROAD-BAND SPECTRA AND VARIABILITY OF COMPACT NONTHERMAL SOURCES.

810104 MELNICK, G., RUSSELL, R. W., GULL, G. E., HARWIT, M. <AP. J., 243, 170>
FAR-INFRARED EMISSION-LINE ABD CONTINUUM OBSERVATIONS OF NGC 7027.

810105 PUETTER, R. C., SMITH, H. E., WILLNER, S. P., PIPHER, J. L. <AP. J., 243, 345>
OPTICAL AND INFRARED SPECTROPHOTOMETRY OF QUASI-STELLAR OBJECTS: THE SPECTRA OF 14 QSOS.

810106 SOIFER, B. T., NEUGEBAUER, G., OKE, J. B., MATTHEWS, K. <AP. J., 243, 369>
INFRARED AND OPTICAL OBSERVATIONS OF THE HYDROGEN LINES IN QUASARS.

810107 VRBA, F. J., COYNE, G. V., TAPIA, S. <AP. J., 243, 489>
OBSERVATIONS OF GRAIN AND MAGNETIC FIELD PROPERTIES OF THE R CORONAE AUSTRALIS DARK CLOUD.

810108 COCHRAN, A. L. <AP. J. SUPPL., 45, 83>
SPECTROPHOTOMETRY WITH A SELF-SCANNED SILICON PHOTODIODE ARRAY. II. SECONDARY STANDARD STARS.

810109 SNELL, R. L. <AP. J. SUPPL., 45, 121>
A STUDY OF NINE INTERSTELLAR DARK CLOUDS.

810110 HOWARTH, I. D., WILSON, R., CARTER, B. S., MENZIES, J. W., ROBERTS, G., WHITELOCK, P. A., VAN DESSEL, E. L., DE LOORE, C., BURGER, M., SANDFORD, M. C. W. <ASTR. AP., 93, 219>
IUE AND OPTICAL OBSERVATIONS OF V861 SCORPII.

810201 MOULD, J. R. <P. A. S. P., 93, 25>
THE INFRARED COLOR-MAGNITUDE RELATION FOR EARLY-TYPE GALAXIES IN THE PEGASUS I CLUSTER.

810202 TANZI, E. G., CHINCARINI, G., TARENGHI, M. <P. A. S. P., 93, 68>
INFRARED OBSERVATIONS OF AE AQUARII.

810203 WILLIAMS, T. B., MORTON, D. C., GREEN, R. F. <A. J., 86, 178>
A SPECTROPHOTOMETRIC SEARCH FOR THE HALO OF MARKARIAN 10.

810204 PRICE, S. D. <A. J., 86, 193>
INFRARED MAPPING OF THE GALACTIC PLANE. I. LOW-RESOLUTION MAPS BETWEEN 0 AND 320 DEGREES LONGITUDE.

810205 NORDH, H. L., VAN DUINEN, R. J., SARGENT, A. I., FRIDLUND, M., AALDERS, J. W. G. <A. J., 86, 276>
HFE 2 AND L43 - TWO COLD FAR-INFRARED SOURCES.

810206 KONDO, Y., WORRALL, D. M., MUSHOTZKY, R. F., HACKNEY, R. L., HACKNEY, K. R. H., OKE, J. B., YEE, H. K. C., NEUGEBAUER, G., MATTHEWS, K., FELDMAN, P. A., BROWN, R. L. <AP. J., 243, 690>
QUASI-SIMULTANEOUS OBSERVATIONS OF BL LAC OBJECT MRK 501 IN X-RAY, UV, VISIBLE, IR, AND RADIO FREQUENCIES.

810207 BALZANO, V. A., WEEDMAN, D. W. <AP. J., 243, 756>
THE NEAR-INFRARED PROPERTIES OF GALACTIC NUCLEI.

810208 BALUTEAU, J. -P., MOORWOOD, A. F. M., BIRAUD, Y., CORON, N., ANDEREGG, M., FITTON, B. <AP. J., 244, 66>
INFRARED LINE EMISSION FROM H II REGIONS. IV. AIRBORNE OBSERVATIONS OF NGC 7538, W49, AND M8.

810209 EVANS II, N. J., BECKLIN, E. E., BEICHMAN, C., GATLEY, I., HIDERBRAND, R. H., KEENE, J., SLOVAK, M. H., WERNER, M. W., WHITCOMB, S. E. <AP. J., 244, 115>
FAR-INFRARED OBSERVATIONS OF THE CEPHEUS OB3 MOLECULAR CLOUD.

810210 ULRICH, R. K., WOOD, B. C. <AP. J., 244, 147>
OBSERVATIONS AND ANALYSIS OF THE HELIUM I RECOMBINATION LINES 5876 AND 10830 IN EIGHT T TAURI STARS.

810211 PENNYPACKER, C. R. <AP. J., 244, 286>
INFRARED STUDIES OF PULSARS.

810212 STOREY, J. W. V., WATSON, D. M., TOWNES, C. H. <AP. J. (LETTERS), 244, L27>
DETECTION OF INTERSTELLAR OH IN THE FAR-INFRARED.

810213 HARRIS, A. W., LEMKE, D. <M. N. R. A. S., 194, 593>
A NEAR INFRARED SURVEY OF W51.

810214 BOISSE, P., GISPERT, R., CORON, N., WIJNBERGEN, J. J., SERRA, G., RYTER, C., PUGET, J. L. <ASTR. AP., 94, 265>
A FAR-INFRARED SURVEY OF THE MILKY WAY FROM SAGITTARIUS TO CYGNUS: EVIDENCE FOR LARGE SCALE VARIATIONS OF THE STAR FORMATION RATE AND INITIAL MASS FUNCTION.

810215 SCHULTE IN DEN BAUMEN, J., HEFELE, H., HOLZLE, E., ORTLIEB, N. <ASTR. AP., 94, 280>
OBSERVATIONS OF LATE TYPE OBJECTS WITH A NEW SPECTROPHOTOMETER IN THE 8-13 MICRON RANGE.

810216 MOORWOOD, A. F. M., SALINARI, P. <ASTR. AP., 94, 299>
INFRARED OBJECTS NEAR TO H2O MASERS IN REGIONS OF ACTIVE STAR FORMATION.

810217 BERGEAT, J., VAN'T VEER, F., LUNEL, M., GARNIER, R., SIBILLE, F., ROUX, S. <ASTR. AP., 94, 350>
INFRARED LIGHT CURVES OF THE CONTACT BINARY 44 I BOOTIS.

810218 SARGENT, A. I., VAN DUINEN, R. J., NORDH, H. L., AALDERS, J. W. G. <ASTR. AP., 94, 377>
FAR INFRARED OBSERVATIONS OF S 255 AND S 187.

810219 SCHULZ, A., LENZEN, R., SCHMIDT, TH., PROETEL, K. <ASTR. AP., 95, 94>
POLARIZATION OF STARLIGHT IN M17.

810220 EIROA, C., NECKEL, TH., SANCHEZ MAGRO, C., SELBY, M. J. <ASTR. AP., 95, 206>
NEAR INFRARED OBSERVATIONS OF THE H II REGION S 146.

810221 BERGEAT, J., VAN'T VEER, F., LUNEL, M., GARNIER, R., SIBILLE, F., ROUX, S. <ASTR. AP. SUPPL., 43, 257>
INFRARED LIGHT CURVES OF THE CONTACT BINARY 44 I BOOTIS.

810301 ELLIOT, J. L., FRENCH, R. G., FROGEL, J. A., ELIAS, J. H., MINK, D. J., LILLER, W. <A. J., 86, 444>
ORBITS OF NINE URANIAN RINGS.

810302 **HOHLFELD, R. G., KRUMM, N.** <AP. J., 244, 476>
AN INFRARED SEARCH FOR MASSIVE GALACTIC ENVELOPES.

810303 **HERTER, T., PIPHER, J. L., HELFER, H. L., WILLNER, S. P., PUETTER, R. C., RUDY, R. J., SOIFER, B. T.** <AP. J., 244, 511>
MEASUREMENTS OF FORBIDDEN LINE RADIATION OF AR II (6.99 MICRONS) IN W3 IRS1.

810304 **SMITH, H. A., LARSON, H. P., FINK, U.** <AP. J., 244, 835>
MOLECULAR HYDROGEN AND THE 2 MICRON SPECTRUM OF NGC 7027.

810305 **DOWNES, D., GENZEL, R., BECKLIN, E. E., WYNN-WILLIAMS, C. G.** <AP. J., 244, 869>
OUTFLOW OF MATTER IN THE KL NEBULA: THE ROLE OF IRC2.

810306 **RAFANELLI, P., BIRKLE, K., HEFELE, H.** <IAUC NO. 3584>
SUPERNOVA IN NGC 4536.

810307 **SALINARI, P.** <IAUC NO. 3586>
SUPERNOVA IN NGC 1316.

810308 **WILLIAMS, P. M., ZEALEY, W. J., SALINARI, P., MOORWOOD, A. F. M.** <IAUC NO. 3587>
SUPERNOVA IN NGC 4536.

810309 **TANZI, E. G., TARENGHI, M.** <IAUC NO. 3589>
SUPERNOVA (EVANS) IN NGC 1316.

810310 **TANZI, E. G., TARENGHI, M.** <IAUC NO. 3589>
SUPERNOVA IN IN NGC 4536.

810311 **GLASS, I. S.** <M. N. R. A. S., 194, 795>
JHK OBSERVATIONS OF QUASARS AND BL LAC OBJECTS.

810312 **VOGT, N., WAMSTEKER, W., BREYSACHER, J., SCHUSTER, H. -E.** <ASTR. AP., 96, 120>
DISCOVERY OF A STELLAR OBJECT WITH SURROUNDING NEBULOSITY.

810313 **MELIK-ALAVERDYAN, YU. K., MOVSESYAN, T. A., TOVMASYAN, G. M.,KIR'YAN, V. V.** <SOV. AST. (LETTERS), 7, 98>
THE INFRARED EMISSION OF RHO CASSIOPEIAE AND R CORONAE BOREALIS.

810401 **NADEAU, D., NEUGEBAUER, G., MATTHEWS, K., GEBALLE, T. R.** <A. J., 86, 561>
SPECTROSCOPY OF THE B-GAMMA LINE IN THE GALACTIC CENTER.

810402 **BEICHMAN, C., HARRIS, S.** <AP. J., 245, 589>
THE FORMATION OF A T TAURI STAR: OBSERVATIONS OF THE INFRARED SOURCE IN L1551.

810403 **ALTAMORE, A., BARATTA, G. B., CASSATELLA, A., FRIEDJUNG, M.** <AP. J., 245, 630>
ULTRAVIOLET AND COORDINATED GROUND-BASED OBSERVATIONS OF Z ANDROMEDAE.

810404 **SCHNEIDER, D. P., YOUNG, P., SHECTMAN, S. A.** <AP. J., 245, 644>
MV LYRAE: A SPECTROSCOPIC STUDY OF THE LOW STATE.

810405 **LEBOFSKY, M. J.** <AP. J. (LETTERS), 245, L59>
EVOLUTION OF HIGH-REDSHIFT GALAXIES.

810406 **DEGIOIA-EASTWOOD, K., HACKWELL, J. A., GRASDALEN, G. L., GEHRZ, R. D.** <AP. J. (LETTERS), 245, L75>
A CORRELATION BETWEEN INFRARED EXCESS AND PERIOD FOR MIRA VARIABLES.

810407 **AARONSON, M., PERSSON, S. E., FROGEL, J. A.** <AP. J., 245, 18>
THE INFRARED COLOR-MAGNITUDE RELATION FOR EARLY-TYPE GALAXIES IN VIRGO AND COMA.

810408 **KEENE, J.** <AP. J., 245, 115>
FAR-INFRARED OBSERVATIONS OF GLOBULES.

810409 **SELLGREN, K.** <AP. J., 245, 138>
SPATIAL OBSERVATIONS OF THE ORION NEBULA IN THE UNIDENTIFIED 3.28 MICRON FEATURE.

810410 **ERICKSON, E. F., KNACKE, R. F., TOKUNAGA, A. T., HAAS, M. R.** <AP. J., 245, 148>
THE 45 MICRON H2O ICE BAND IN THE KLEINMANN-LOW NEBULA.

810411 **CARNEY, B. W., PETERSON, R. C.** <AP. J., 245, 238>
ABUNDANCE ANALYSES OF SUBDWARFS OF THE REMOTE HALO.

810412 **GILES, A. B., ADAMS, D. J.** <IAUC NO. 3594>
GX 339-4 - 4U1658-48.

810413 **LAWRENCE, A., GILES, A. B., MCHARDY, I. M., COOKE, B. A.** <M. N. R. A. S., 195, 149>
FAST SIMULTANEOUS INFRARED AND OPTICAL PHOTOMETRY OF NGC 4151.

810414 **ALLEN, D. A., WARD, M. J., WRIGHT, A. E.** <M. N. R. A. S., 195, 155>
THE ECLIPSING AM HERCULIS STAR 2A0311-227.

810415 **JAMESON, R. F., KING, A. R., SHERRINGTON, M. R.** <M. N. R. A. S., 195, 235>
INFRARED AND OPTICAL LIGHT CURVES OF THE DWARF NOVA EM CYGNI.

810416 **AARONSON, M., DAWE, J. A., DICKENS, R. J., MOULD, J. R., MURRAY, J. B.** <M. N. R. A. S., 195, 1P>
THE FORNAX AND GRUS CLUSTERS AND THE LOCAL INFALL VELOCITY.

810417 **EPCHTEIN, N., GUIBERT, J., NGUYEN-QUANG-RIEU,., TURON, P., WAMSTEKER, W.** <ASTR. AP., 97, 1>
NEW COMPACT INFRARED OBJECTS ASSOCIATED WITH TWO SOUTHERN TYPE - I. OH MASERS.

810418 **MAIHARA, T., ODA, N., SHIBAI, H., OKUDA, H.** <ASTR. AP., 97, 139>
OBSERVATIONS OF DIFFUSE FAR INFRARED EMISSION AND DISTRIBUTION OF INTERSTELLAR DUST.

810419 **WAMSTEKER, W.** <ASTR. AP., 97, 329>
STANDARD STARS AND CALIBRATION FOR JHKLM PHOTOMETRY.

810501 **CUTRI, R. M., AITKEN, D. K., JONES, B., MERRILL, K. M., PUETTER, R. C., ROCHE, P. F., RUDY, R. J., RUSSELL, R. W., SOIFER, B. T., WILLNER, S. P.** <AP. J., 245, 818>
INFRARED SPECTROPHOTOMETRY OF THREE SEYFERT GALAXIES AND 3C273.

810502 **JOHNSON, P. E., RIEKE, G. H., LEBOFSKY, M. J., KEMP, J. C.** <AP. J., 245, 871>
SHOCK-INDUCED GRAIN ALIGNMENT IN THE ORION NEBULA.

810503 **YOUNG, P., SCHNEIDER, D. P., SHECTMAN, S. A.** <AP. J., 245, 1035>
THE VORACIOUS VORTEX IN HT CASSIOPEIAE.

810504 **TULLY, R. B., BOESGAARD, A. M., DYCK, H. M., SCHEMPP, W. V.** <AP. J., 246, 38>
STAR FORMATION AND ABUNDANCES IN THE NEARBY IRREGULAR GALAXY VII ZW 403.

810505 **FEAST, M. W.** <IAUC NO. 3599>
NOVA CORONAE AUSTRINAE 1981.

810506 **VRBA, F. J., RYDGREN, A. E.** <IAUC NO. 3604>
NOVA CORONAE AUSTRINAE 1981.

810507 **HOUGH, J. H., BAILEY, J., CUNNINGHAM, E. C., MCCALL, A., AXON, D. J.** <M. N. R. A. S., 195, 429>
LINEAR POLARIZATION OF T TAURI STARS.

810508 **FRANK, J., KING, A. R., SHERRINGTON, M. R., JAMESON, R. F., AXON, D. J.** <M. N. R. A. S., 195, 505>
INFRARED AND OPTICAL LIGHT CURVES OF UX URSAE MAJORIS AND U GEMINORUM.

810509 **SWINGS, J. P.** <ASTR. AP., 98, 112>
THE STRONGLY POLARIZED P CYGNI STAR WITH INFRARED EXCESS CPD-52 9243.

810510 **GILMORE, G., REID, I. N.** <NATURE, 291, 208>
RG0044-2958:A PECULIAR M SUPERGIANT AT A DISTANCE OF 2.5 MPC.

810511 **SHERWOOD, W. A., SCHULTZ, G. V., KREYSA, E.** <NATURE, 291, 301>
MILLIMETRE OBSERVATIONS OF QUASAR Q0420-388.

810601 **CLARK, T. A., MILONE, E. F.** <P. A. S. P., 93, 338>
INFRARED VARIABILITY AND SPECTRUM OF SS 433.

810602 **HERBST, W., WARNER, J. W.** <A. J., 86, 885>
TWO YOUNG STARS IN L 43.

810603 **EVANS II, N. J., BLAIR, G. N.** <AP. J., 246, 394>
THE ENERGETICS OF MOLECULAR CLOUDS. III. THE S235 MOLECULAR CLOUD.

810604 EVANS II, N. J., BEICHMAN, C., GATLEY, I., HARVEY, P., NADEAU, D., SELLGREN, K. <AP. J., 246, 409>
INFRARED STUDIES OF THE S235 MOLECULAR CLOUD.

810605 WHITCOMB, S. E., GATLEY, I., HILDEBRAND, R. H., KEENE, J., SELLGREN, K., WERNER, M. W. <AP. J., 246, 416>
FAR-INFRARED PROPERTIES OF DUST IN THE REFLECTION NEBULA NGC 7023.

810606 WRIGHT, E. L., HARPER, D. A., LOEWENSTEIN, R. F., MOSELEY, H. <AP. J., 246, 426>
FAR-INFRARED OBSERVATIONS OF THE H2O MASERS IN NGC 281, NGC 2175, AND S255/257.

810607 GOEBEL, J. H., BREGMAN, J. D., WITTEBORN, F. C., TAYLOR, B. J., WILLNER, S. P. <AP. J., 246, 455>
IDENTIFICATION OF NEW INFRARED BANDS IN A CARBON-RICH MIRA VARIABLE.

810608 LIEBERT, J., LEBOFSKY, M. J., RIEKE, G. H. <AP. J. (LETTERS), 246, L73>
INFRARED PHOTOMETRY AND THE ATMOSPHERIC COMPOSITION OF COOL WHITE DWARFS: THE LOWEST LUMINOSITY CANDIDATES.

810609 CONDON, J. J., O'DELL, S. L., PUSCHELL, J. J., STEIN, W. A. <AP. J., 246, 624>
RADIO EMISSION FROM BRIGHT, OPTICALLY SELECTED QUASARS.

810610 WYNN-WILLIAMS, C. G., BECKLIN, E. E., BEICHMAN, C. A., CAPPS, R., SHAKESHAFT, J. R. <AP. J., 246, 801>
THE MULTIPLE INFRARED SOURCE GL 437.

810611 FROGEL, J. A., PERSSON, S. E., COHEN, J. G. <AP. J., 246, 842>
INFRARED PHOTOMETRY OF RED GIANTS IN THE GLOBULAR CLUSTER 47 TUCANAE.

810612 MOTCH, C., ILOVAISKY, S. A., CHEVALIER, C. <IAUC NO. 3609>
GX 339-4 - 4U1658-48.

810613 TELESCO, C., KOEHLER, R., GATLEY, I. <IAUC NO. 3613>
SUPERNOVA IN NGC 6946.

810614 LUNEL, M., BERGEAT, J., SIBILLE, F., GARNIER, R. <M. N. R. A. S., 195, 765>
OBSERVATIONS OF INFRARED SOURCES ASSOCIATED WITH ON 1 AND G110.25+0.01.

810615 LONGMORE, A. J., LEE, T. J., ALLEN, D. A., ADAMS, D. J. <M. N. R. A. S., 195, 825>
INFRARED OBSERVATIONS OF THE CATACLYSMIC VARIABLE RW TRI.

810616 AITKEN, D. K., ROCHE, P. F., SPENSER, P. M., JONES, B. <M. N. R. A. S., 195, 921>
INFRARED SPECTRAL OBSERVATIONS OF THE BNKL COMPLEX IN ORION.

810617 TOKUNAGA, A. T., LEBOFSKY, M. J., RIEKE, G. H. <ASTR. AP., 99, 108>
INFRARED REFLECTION NEBULAE IN S106 AND NGC 7538E.

810618 EPCHTEIN, N., LEPINE, J. R. D. <ASTR. AP., 99, 210>
INFRARED SURVEY OF SOUTHERN GALACTIC MASER SOURCES IN THE LONGITUDE RANGE 320 TO 30 DEGREES.

810619 LEMKE, D., HARRIS, A. W. <ASTR. AP., 99, 285>
A NEAR INFRARED MAP OF M17.

810620 CHINI, R. <ASTR. AP., 99, 346>
MULTICOLOUR PHOTOMETRY OF STARS IN THE OPHIUCHUS DARK CLOUD REGION.

810621 REIPURTH, B. <ASTR. AP. SUPPL., 44, 379>
SMALL NEBULAE AND HERBIG-HARO OBJECTS. I. A SURVEY OF SOUTHERN DARK CLOUDS.

810622 THE, P. S., TJIN A DJIE, H. R. E., BAKKER, R., BASTIAANSEN, P. A., BURGER, M., CASSATELLA, A., FREDGA,K., GAHM,G., LISEAU, R., SMYTH, M. J., VIOTTI, R.,WAMSTEKER, W., ZEUGE, W. <ASTR. AP. SUPPL., 44, 451>
THE VARIABLE SHELL STAR HR 5999: V. THE SPECTRAL ENERGY DISTRIBUTION.

810623 CATCHPOLE, R. M., GLASS, I. S., CARTER, B. S., ROBERTS, G. <NATURE, 291, 392>
IR VARIABILITY OF SS433.

810701 RYDGREN, A. E., VRBA, F. J. <A. J., 86, 1069>
NEARLY SIMULTANEOUS OPTICAL AND INFRARED PHOTOMETRY OF T TAURI STARS.

810702 HECKERT, P. A., ZEILIK II, M. <A. J., 86, 1076>
POLARIMETRY FROM 1 TO 5 MICRONS OF COMPACT INFRARED SOURCES.

810703 PUSCHELL, J. J. <AP. J., 247, 48>
NONSTELLAR 10 MICRON EMISSION FROM E/S0 GALAXIES WITH COMPACT RADIO SOURCES.

810704 GEBALLE, T. R., WAMSTEKER, W., DANKS, A. C., LACY, J. H., BECK, S. C. <AP. J., 247, 130>
INFRARED LINE AND CONTINUUM VIEWS OF G333.6-0.2.

810705 STOREY, J. W. V., WATSON, D. M., TOWNES, C. H., HALLER, E. E., HANSEN, W. L. <AP. J., 247, 136>
FAR-INFRARED OBSERVATIONS OF SHOCKED CO IN ORION.

810706 TELESCO, C. M., GATLEY, I. <AP. J. (LETTERS), 247, L11>
NGC 1097: THE STRUCTURE OF THE CENTRAL 3 KILOPARSECS AT 10 MICRONS.

810707 GRINDLEY, J. E., HERTZ, P. <AP. J. (LETTERS), 247, L17>
DISCOVERY OF AN OBSCURED GLOBULAR CLUSTER ASSOCIATED WITH GX 354+0 (-4U/MXB 1728-34).

810708 BEALL, J. H., ROSE, W. K., DENNIS, B. R., CRANNELL, C. J., DOLAN, J. F., FROST, K. J., ORWIG, L. E. <AP. J., 247, 458>
CONCURRENT RADIO, INFRARED, OPTICAL, AND X-RAY OBSERVATIONS OF THE NUCLEUS OF THE SEYFERT GALAXY NGC 4151.

810709 CAMPBELL, M. F., HOFFMANN, W. F., THRONSON JR., H. A. <AP. J., 247, 530>
AN EXTENDED FAR-INFRARED EMISSION COMPLEX AT IC 1318B AND IC 1318C.

810710 SZKODY, P. <AP. J., 247, 577>
IUE OBSERVATIONS OF EIGHT DWARF NOVAE: A STUDY OF THE OUTBURST CYCLE FROM 0.12 TO 3.5 MICRONS.

810711 BARLOW, M. J., SMITH, L. J., WILLIS, A. J. <M. N. R. A. S., 196, 101>
MASS-LOSS FOR 21 WOLF-RAYET STARS.

810712 ROBERTSON, B. S. C., FEAST, M. W. <M. N. R. A. S., 196, 111>
THE BOLOMETRIC, INFRARED, AND VISUAL ABSOLUTE MAGNITUDES OF MIRA VARIABLES.

810713 BAILEY, J., SHERRINGTON, M. R., GILES, A. B., JAMESON, R. F. <M. N. R. A. S., 196, 121>
INFRARED LIGHT CURVES OF THE DWARF NOVA Z CHAMAELEONTIS.

810714 REID, I. N., GILMORE, G. <M. N. R. A. S., 196, 15P>
A STAR OF VERY LOW LUMINOSITY.

810715 AITKEN, D. K., ROCHE, P. F. <M. N. R. A. S., 196, 39P>
FURTHER INFRARED STUDIES OF THE PRE-MAIN-SEQUENCE OBJECT HD 97048.

810716 POGODIN, M. A. <SOV. AST., 25, 454>
PHOTOMETRY OF SOME HERBIG EMISSION STARS IN THE NEAR-IR REGION OF THE SPECTRUM.

810717 TANZI, E. G., MARASCHI, L., TREVES, A., TARENGHI, M. <ASTR. AP., 100, 68>
INFRARED AND X-RAY OBSERVATIONS OF THE BINARY SYSTEM V861 SCO.

810718 HAYAKAWA, S., MATSUMOTO, T., MURAKAMI, H., UYAMA, K., THOMAS, J. A., YAMAGAMI, T. <ASTR. AP., 100, 116>
DISTRIBUTION OF NEAR INFRARED SOURCES IN THE GALACTIC DISK.

810719 MOORWOOD, A. F. M., SALINARI, P. <ASTR. AP., 100, L16>
DETECTION OF THE 3.3 MICRON EMISSION FEATURE IN THE NUCLEII OF IC 4329A AND NGC 5506.

810720 ENGELS, D., SHERWOOD, W. A., WAMSTEKER, W., SCHULTZ, G. V. <ASTR. AP. SUPPL., 45, 5>
INFRARED OBSERVATIONS OF SOUTHERN BRIGHT STARS.

810801 SZKODY, P. <P. A. S. P., 93, 456>
STEPANIAN'S STAR: THE ENERGY DISTRIBUTION REVEALS A NONTYPICAL CATACLYSMIC VARIABLE.

810802 AARONSON, M. <P. A. S. P., 93, 535>
ERRATUM TO "IDENTIFICATION OF THE NUCLEUS IN THE SPIRAL GALAXY NGC 4631".

810803 BEICHMAN, C. A., PRAVDO, S.H., NEUGEBAUER, G., SOIFER, B. T.,MATTHEWS, K., WOOTEN, H. A. <AP. J., 247, 780>
EXTREMELY RED COMPACT RADIO SOURCES: THE EMPTY FIELD OBJECTS.

810804 ZINN, R., PERSSON, S. E. <AP. J., 247, 849>
THE AGES AND METALLICITIES OF THE GLOBULAR CLUSTERS IN THE FORNAX DWARF SPHEROIDAL GALAXY.

810805 SITKO, M. L. <AP. J., 247, 1024>
SPECTRAL ENERGY DISTRIBUTIONS OF HOT STARS WITH CIRCUMSTELLAR DUST.

810806 FORREST, W. J., HOUCK, J. R., MCCARTHY, J. F. <AP. J., 248, 195>
A FAR-INFRARED EMISSION FEATURE IN CARBON-RICH STARS AND PLANETARY NEBULAE.

810807 GNEDIN, YU. N., KHOZOV, G. V., LARIONOV, V. M. <SOV. AST. (LETTERS), 7, 256>
INFRARED PHOTOMETRY OF GALACTIC X-RAY SOURCES.

810808 IMPEY, C. D., BRAND, P. W. J. L. <NATURE, 292, 814>
IR PHOTOMETRY OF FLAT RADIO SOURCES.

810901 LESTER, D. F., BREGMAN, J. D., WITTEBORN, F. C., RANK, D. M.,DINERSTEIN, H. L. <AP. J., 248, 524>
THE ABUNDANCE OF ARGON AT THE GALACTIC CENTER.

810902 THRONSON JR., H. A., HARVEY, P. M. <AP. J., 248, 584>
NEAR-INFRARED SPECTROSCOPY OF POSSIBLE PRECURSORS TO PLANETARY NEBULAE: HM SAGITTAE.

810903 DA COSTA, G. S., FROGEL, J. A., COHEN, J. G. <AP. J., 248, 612>
THE GIANT BRANCH OF THE GLOBULAR CLUSTER NGC 3201.

810904 LAMBERT, D. L., HINKLE, K. H., HALL, D. N. B. <AP. J., 248, 638>
CIRCUMSTELLAR SHELLS OF LUMINOUS SUPERGIANTS. I. CARBON MONOXIDE IN RHO CASSIOPEIAE AND HR 8752.

810905 HALL, D. N. B., KLEINMANN, S. G., SCOVILLE, N. Z., RIDGWAY, S. T. <AP. J., 248, 898>
2 MICRON SPECTROSCOPY OF THE NUCLEUS OF NGC 1068.

810906 BREGER, M., GEHRZ, R. D., HACKWELL, J. A. <AP. J., 248, 963>
INTERSTELLAR GRAIN SIZE. II. INFRARED PHOTOMETRY AND POLARIZATION IN ORION.

810907 THRONSON JR., H. A. <AP. J., 248, 984>
NEAR-INFRARED SPECTROSCOPY OF POSSIBLE PRECURSORS TO PLANETARY NEBULAE: AFGL 618.

810908 LESTER, D. F., WERNER, M. W., STOREY, J. W. V., WATSON, D. M., TOWNES, C. H. <AP. J. (LETTERS), 248, L109>
DETECTION OF (O I) 63 MICRON EMISSION FROM THE GALACTIC CENTER.

810909 ALLEN, D. A., BARTON, J. R., WALLACE, P. T. <M. N. R. A. S., 196, 797>
THE SIZE OF A WOLF-RAYET STAR'S DUST SHELL MEASURED BY SPECKKLE INTERFEROMETRY.

810910 WILLIAMS, P. M., ANTONOPOULOU, E. <M. N. R. A. S., 196, 915>
INFRARED PHOTOMETRY OF SOUTHERN WOLF-RAYET STARS.

810911 FRANK, J., KING, A. R., SHERRINGTON, M. R., GILES, A. B., JAMESON, R. F. <M. N. R. A. S., 196, 921>
THE INFRARED SPECTRUM OF THE DWARF NOVA EX HYDRAE.

810912 AITKEN, D. K., ROCHE, P. F., PHILLIPS, M. M. <M. N. R. A. S., 196, 101P>
THE QUESTION OF EXTINCTION IN ACTIVE GALACTIC NUCLEI: INFRARED SPECTRAL OBSERVATIONS OF NGC 1614, NGC 7469, AND NGC 1275.

810913 TARANOVA, O. G., YUDIN, B. F. <SOV. AST., 25, 598>
PHOTOMETRY OF SYMBIOTIC STARS IN THE UBVRJHKLMN SYSTEM. CI CYGNI.

810914 IPATOV, A. P., YUDIN, B. F. <SOV. AST. (LETTERS), 7, 309>
SPECTROPHOTOMETRY OF HM SAGITTAE.

811001 RUDY, R. J., LEVAN, P. D., RODRIGUEZ-ESPINOSA, J. M. <P. A. S. P., 93, 558>
FURTHER OBSERVATIONS OF 3C 273 FOR THE 3.3 MICRON DUST FEATURE.

811002 HAGEN, W., HUMPHREYS, R. M., STENCEL, R. E. <P. A. S. P., 93, 567>
HIGH-DISPERSION SPECTROSCOPY OF THE MOST LUMINOUS F- AND G-TYPE SUPERGIANTS IN THE LARGE MAGELLANIC CLOUD AND THE MILKY WAY.

811003 FERRARI-TONIOLO, M., PERSI, P., GRASDALEN, G. L. <P. A. S. P., 93, 633>
INFRARED EXCESS AND MASS-LOSS RATE OF THE EXTREME OF STAR HD 108.

811004 WEISTROP, D., SHAFFER, B. D., MUSHOTZKY, R. F., REITSEMA, H. J., SMITH, B. A. <AP. J., 249, 3>
CCD PHOTOMETRY OF THE BL LACERTAE OBJECTS 1218+304, 1219+28, AND 1727+50: POINT SOURCES, ASSOCIATED NEBULOSITY, AND BROAD-BAND SPECTRA.

811005 BLITZ, L., ISRAEL, F. P., NEUGEBAUER, G., GATLEY, I., LEE, T. J., BEATTIE, D. H. <AP. J., 249, 76>
THE LARGEST H II REGIONS IN M101.

811006 SCHNEPS, M. H., LANE, A. P., DOWNES, D., MORAN, J. M., GENZEL, R., REID, M. J. <AP. J., 249, 124>
PROPER MOTIONS AND DISTANCES OF H2O MASER SOURCES. III. W51 NORTH.

811007 COHEN, J. G., FROGEL, J. A., PERSSON, S. E., ELIAS, J. H. <AP. J., 249, 481>
BOLOMETRIC LUMINOSITIES AND INFRARED PROPERTIES OF CARBON STARS IN THE MAGELLANIC CLOUDS AND THE GALAXY.

811008 BECK, S. C., LACY, J. H., TOWNES, C. H., ALLER, L. H., GEBALLE, T. R., BAAS, F. <AP. J., 249, 592>
THE ABUNDANCES OF NEON, SULFUR, AND ARGON IN PLANETARY NEBULAE.

811009 SARGENT, A. I., VAN DUINEN, R. J., FRIDLUND, C. V. M., NORDH, H. L., AALDERS, J. W. G. <AP. J., 249, 607>
FAR-INFRARED OBSERVATIONS OF STAR-FORMING REGIONS.

811010 THOMPSON, R. I., THRONSON JR., H. A., CAMPBELL, B. G. <AP. J., 249, 622>
THE NATURE OF NGC 2024: NEAR-INFRARED SPECTROSCOPY OF IRS 1 AND IRS 2.

811011 ELIAS, J. H., FROGEL, J. A., HUMPHREYS, R. M., PERSSON, S. E. <AP. J. (LETTERS), 249, L55>
INFRARED LUMINOSITIES OF M SUPERGIANTS AND THEIR USE AS DISTANCE INDICATORS.

811012 BRUGEL, E. W., BOEHM, K. H., MANNERY, E. <AP. J. SUPPL., 47, 117>
EMISSION LINE SPECTRA OF HERBIG-HARO OBJECTS.

811013 HASSALL, B. J. M., PRINGLE, J. E., WARD, M. J., WHELAN, J. A., MAYO, S. K., ECHEVARRIA, J., JONES, D. H. P., WALLIS, R. E., ALLEN, D. A., HYLAND, A. R. <M. N. R. A. S., 197, 275>
OBSERVATIONS AND MODELS OF H2252-035.

811014 MOORWOOD, A. F. M., SALINARI, P. <ASTR. AP., 102, 197>
INFRARED OBJECTS NEAR TO H2O MASERS IN REGIONS OF ACTIVE STAR FORMATION. II. SURVEY AND 1-20 MICRON OBSERVATIONS OF SOUTHERN SOURCES.

811015 SHAVER, P. A., RETALLACK, D. S., WAMSTEKER, W., DANKS, A. C. <ASTR. AP., 102, 225>
THE DISTANCE TO G316.8-0.1.

811016 BEICHMAN, C. A., NEUGEBAUER, G., SOIFER, B. T., WOOTTEN, H. A., ROELLIG, T., HARVEY, P. M. <NATURE, 293, 711>
COMPACT RADIO SOURCE 1413+135 IS A FAR-IR EXTRAGALACTIC OBJECT.

811017 BREGMAN, J. N., LEBOFSKY, M. J., ALLER, M. F., RIEKE, G. H., ALLER, H. D., HODGE, P. E., GLASSGOLD, A. E., HUGGINS, P. J. <NATURE, 293, 714>
MUTIFREQUENCY OBSERVATIONS OF THE RED QSO 1413+135.

811101 RIEKE, G. H., LEBOFSKY, M. J. <AP. J., 250, 87>
SPECTRAL COMPONENTS OF NGC 4151.

811102 MCALARY, C. W., MCLAREN, R. A. <AP. J., 250, 98>
NEAR-INFRARED SPECTROPHOTOMETRY OF NGC 4151.

811103 MCGREGOR, P. J., HYLAND, A. R. <AP. J., 250, 116>
INFRARED STUDIES OF THE TWO STELLAR POPULATIONS IN 30 DORADUS.

811104 HERTER, T., HELFER, H. L., PIPHER, J. L., FORREST, W. J., MCCARTHY, J., HOUCK, J. R., WILLNER, S. P., PUETTER, R. C., RUDY, R. J., SOIFER, B. T. <AP. J., 250, 186>
ABUNDANCES OF ARGON, SULFUR, AND NEON IN SIX GALACTIC H II REGIONS FROM INFRARED FORBIDDEN LINES.

811105 EVANS II, N. J., BLAIR, G. N., HARVEY, P., ISRAEL, F., PETERS III, W. L., SCHOLTES, M., DE GRAAUW, T., VANDEN BOUT, P. <AP. J., 250, 200>
THE ENERGETICS OF MOLECULAR CLOUDS. IV. THE S88 MOLECULAR CLOUD.

811106 RUSSELL, R. W., MELNICK, G., SMYERS, S. D., KURTZ, N. T., GOSNELL, T. R., HARWIT, M., WERNER, M. W. <AP. J. (LETTERS), 250, L35>
GIANT (C II) HALOS AROUND H II REGIONS.

811107 WATSON, D. M., STOREY, J. W. V., TOWNES, C. H., HALLER, E. E. <AP. J., 250, 605>
FAR-INFRARED (O III) AND (N III) LINE EMISSION FROM GALACTIC H II REGIONS AND PLANETARY NEBULAE.

811108 SOIFER, B. T., WILLNER, S. P., CAPPS, R. W., RUDY, R. J. <AP. J., 250, 631>
4-8 MICRON SPECTROPHOTOMETRY OF OH 0739-14.

811109 CATCHPOLE, R. M., FEAST, M. W. <M. N. R. A. S., 197, 385>
THE LUMINOSITIES OF RED SUPERGIANT VARIABLES IN THE SMALL MAGELLANIC CLOUD.

811110 BAILEY, J., CUNNINGHAM, E. C., HOUGH, J. H., AXON, D. J. <M. N. R. A. S., 197, 627>
INFRARED AND OPTICAL POLARIZATION OF MARKARIAN 421.

811111 TARANOVA, O. G., YUDIN, B. F. <SOV. AST., 25, 710>
PHOTOMETRY OF SYMBIOTIC STARS IN THE UBVRJHKLMN SYSTEM. 2.Z ANDROMEDAE.

811112 DENNEFELD, M., ANDRILLAT, Y. <ASTR. AP., 103, 44>
NEAR-INFRARED SPECTROSCOPY OF NORTHERN SUPERNOVA-REMNANTS.

811113 ALLEN, D. A., WICKRAMASINGHE, D. T. <NATURE, 294, 239>
DIFFUSE INTERSTELLAR ABSORPTION BANDS BETWEEN 2.9 AND 4.0 MICRONS.

811114 STOCKE, J. T., RIEKE, G. H., LEBOFSKY, M. J. <NATURE, 294, 319>
NEW OBSERVATIONAL CONSTRAINTS ON THE M87 JET.

811201 LEVAN, P. D., PUETTER, R. C., RUDY, R. J., SMITH, H. E., WILLNER, S. P. <AP. J., 251, 10>
HE I 10830 OBSERVATIONS OF FIVE SEYFERT GALAXIES.

811202 CARNEY, B. W., PETERSON, R. C. <AP. J., 251, 190>
FIELD POPULATION II BLUE STRAGGLERS.

811203 ELIAS, J. H., FROGEL, J. A., HACKWELL, J. A., PERSSON, S. E. <AP. J. (LETTERS), 251, L13>
INFRARED LIGHT CURVES OF TYPE I SUPERNOVAE.

811204 HOWELL, R. R., MCCARTHY, D. W., LOW, F. J. <AP. J. (LETTERS), 251, L21>
ONE-DIMENSIONAL INFRARED SPECKEL INTERFEROMETRY.

811205 PRAVDO, S. H., NUGENT, J. J., NOUSEK, J. A., JENSEN, K., WILSON, A. S., BECKER, R. H. <AP. J., 251, 501>
DISCOVERY OF A SEYFERT 1 GALAXY WITH AN UNUSUALLY SOFT X-RAY SPECTRUM.

811206 HARDING, P., JONES, T. J., RODGERS, A. W. <AP. J., 251, 530>
MAPPING OF NGC 5128 (-CENTAURUS A) AT J, H, AND K.

811207 PERSSON, S. E., GEBALLE, T. R., SIMON, T., LONSDALE, C. J., BAAS, F. <AP. J. (LETTERS), 251, L85>
HIGH VELOCITY H2 LINE EMISSION IN THE NGC 2071 REGION.

811208 LADA, C. J., THRONSON JR., H. A., SMITH, H. A., HARPER, D. A., KEENE, J., LOEWENSTEIN, R. F., SMITH, J. <AP. J. (LETTERS), 251, L91>
FAR-INFRARED AND SUBMILLIMETER OBSERVATIONS OF BARNARD 35: HEAT SOURCES FOR BRIGHT-RIMMED MOLECULAR CLOUDS.

811209 TAPIA, M. <M. N. R. A. S., 197, 949>
NEAR-INFRARED OBSERVATIONS OF TRAPEZIUM-TYPE MULTIPLE SYSTEMS. CATALOGUE OF OBSERVATIONS AND A NEW DETERMINATION OF THE REDDENING LAW.

811210 GLASS, I. S. <M. N. R. A. S., 197, 1067>
THE INFRARED CONTINUA OF ACTIVE GALAXIES.

811211 GATLEY, I., BECKLIN, E. E., HYLAND, A. R., JONES, T. J. <M. N. R. A. S., 197, 17P>
DISCOVERY OF A PROTOSTAR IN THE LARGE MAGELLANIC CLOUD.

811212 LACASSE, M. G., BOYLE, D., LEVREAULT, R., PIPHER, J. L., SHARPLESS, S. <ASTR. AP., 104, 57>
POLARIMETRIC OBSERVATIONS OF S106.

819901 DOWNES, R. A., MARGON, B. <A. J., 86, 19>
B 272: QUASAR OR H II REGION?

819902 LOREN, R. B. <A. J., 86, 69>
THE DENSITIES OF THE MOLECULAR CLOUDS ASSOCIATED WITH HERBIG BE/AE AND OTHER YOUNG STARS.

819903 MILLER, H. R. <A. J., 86, 87>
PHOTOELECTRIC COMPARISON SEQUENCES IN THE FIELDS OF FIVE SEYFERT GALAXIES.

819904 KLEMOLA, A. R., HARLAN, E. A., WIRTANEN, C. A. <A. J., 86, 583>
TRIGONOMETRIC PARALLAXES MEASURED AT LICK OBSERVATORY. LIST III.

819905 FOLTZ, C. B., PETERSON, B. M., BOROSON, T. A. <A. J., 86, 802>
ERRATUM TO "ACCURATE OPTICAL POSITIONS FOR MARKARIAN GALAXIES 701-797. "

819906 KOJOIAN, G., ELLIOTT, R., TOVMASSIAN, H. M. <A. J., 86, 811>
ACCURATE OPTICAL POSITIONS FOR MARKARIAN GALAXIES 798-1095.

819907 KOJOIAN, G., ELLIOTT, R., BICAY, M. D. <A. J., 86, 816>
ACCURATE OPTICAL POSITIONS FOR MARKARIAN GALAXIES 1096-1302.

819908 KOJOIAN, G., ELLIOTT, R., BICAY, M. D., ARAKELIAN, M. A. <A. J., 86, 820>
ACCURATE OPTICAL POSITIONS OF ARAKELIAN GALAXIES.

819909 HERBIG, G. H., JONES, B. F. <A. J., 86, 1232>
LARGE PROPER MOTIONS OF THE HERBIG-HARO OBJECTS HH 1 AND HH 2.

819910 ABBOTT, D. C., BIEGING, J. H., CHURCHWELL, E. <AP. J., 250, 645>
MASS LOSS FROM VERY LUMINOUS OB STARS AND THE CYGNUS SUPERBUBBLE.

819912 CRAGG, T., EVANS, R. <IAUC NO. 3583>
SUPERNOVA IN NGC 1316.

819913 FELLI, M., HARTEN, R. H. <ASTR. AP., 100, 28>
A HIGH-RESOLUTION SEARCH FOR SMALL-SCALE STRUCTURE IN SHARPLESS H II REGIONS AT 4.995 GHZ. II. GENERAL PROPERTIES OF THE ENTIRE SAMPLE.

819914 BLACKWELL, S. R., PURTON, C. R. <ASTR. AP. SUPPL., 46, 181>
OPTICAL POSITIONS FOR NORTHERN STELLAR PLANETARY NEBULAE.

819915 GILMORE, A. C. <IAUC NO. 3591>
NOVA CORONAE AUSTRINAE 1981.

819916 LAUBERTS, A., HOLMBERG, E. B., SCHUSTER, H. -E., WEST, R. M. <ASTR. AP. SUPPL., 43, 307>
THE ESO/UPPSALA SURVEY OF THE ESO(B) ATLAS OF THE SOUTHERN SKY. VIII.

819917 LAUBERTS, A., HOLMBERG, E. B., SCHUSTER, H. -E., WEST, R. M. <ASTR. AP. SUPPL., 46, 311>
THE ESO/UPPSALA SURVEY OF THE ESO(B) ATLAS OF THE SOUTHERN SKY. IX.

819918 FEIGELSON, E. D., KRISS, G. A. <AP. J. (LETTERS), 248, L35>
DISCOVERY OF THREE X-RAY LUMINOUS PRE-MAIN-SEQUENCE STARS.

819919 KHOLOPOV, P. N., SAMUS, N. N., KUKARKINA, N. P., MEDVEDEVA, G. I., PEROVA, N. B. <IBVS NO. 1921>
65TH NAME-LIST OF VARIABLE STARS.

819920 KHOLOPOV, P. N., SAMUS, N. N., KUKARKINA, N. P., MEDVEDEVA, G. I., PEROVA, N. B. <IBVS NO. 2042>
66TH NAME-LIST OF VARIABLE STARS.

819921 OCHSENBEIN, F., BISCHOFF, M., EGRET, D. <ASTR. AP. SUPPL., 43, 259>
MICROFICHE EDITION OF CSI.

820001 MIKAMI, T., ISHIDA, K., HAMAJIMA, K., KAWARA, K. <P. A. S. J., 34, 223>
STELLAR CONTENTS CONTRIBUTING TO THE NEAR-INFRARED RADIATION OF THE GALAXY.

820002 KAWARA, K., KOZASA, T., SATO, S., KOBAYASHI, Y., OKUDA, H., JUGAKU, J. <P. A. S. J., 34, 389>
NEAR-INFRARED SOURCE COUNTS IN THE GALACTIC PLANE.

820003 THE, P. S., ARENS, M., VAN DER HUCHT, K. A. <AP. LETTERS, 22, 109>
AN INVESTIGATION OF THE SCORPIUS OPEN CLUSTER C1715-387, CONTAINING TWO WN7, TWO OF AND ONE RED SUPERGIANT MEMBERS.

820004 LACASSE, M. G. <AP. LETTERS, 23, 61>
NEAR INFRARED POLARIZATION IN TWO PECULIAR NEBULAE: M2-9 AND THE PV CEPHEI NEBULA.

820101 FROGEL, J. A., BLANCO, V. M., MCCARTHY, M. F., COHEN, J. G. <AP. J., 252, 133>
THE LATE-TYPE STELLAR CONTENT OF THE FORNAX AND SCULPTOR DWARF GALAXIES.

820102 HACKWELL, J. A., GRASDALEN, G. L., GEHRZ, R. D. <AP. J., 252, 250>
10 AND 20 MICRON IMAGES OF REGIONS OF STAR FORMATION.

820103 KEENE, J., HILDEBRAND, R. H., WHITCOMB, S. E. <AP. J. (LETTERS), 252, L11>
A HIGH RESOLUTION SUBMILLIMETER MAP OF OMC-1.

820104 JAFFE, D. T., STIER, M. T., FAZIO, G. G. <AP. J., 252, 609>
A HIGH RESOLUTION FAR-INFRARED SURVEY OF A SECTION OF THE GALACTIC PLANE. I. THE NATURE OF THE SOURCES.

820105 HINKLE, K. H., HALL, D. N. B., RIDGWAY, S. T. <AP. J., 252, 697>
TIME SERIES INFRARED SPECTROSCOPY OF THE MIRA VARIABLE CHI CYGNI.

820106 RIEKE, G. H., LEBOFSKY, M. J., KEMP, J. C. <AP. J. (LETTERS), 252, L53>
NONTHERMAL OPTICAL-INFRARED EMISSION FROM NGC 1052.

820107 PROBST, R. G., O'CONNELL, R. W. <AP. J. (LETTERS), 252, L69>
THE LUMINOSITY FUNCTION OF VERY LOW MASS STARS.

820108 HERBST, W., MILLER, D. P., WARNER, J. W., HERZOG, A. <A. J., 87, 98>
R ASSOCIATIONS. VI. THE REDDENING LAW IN DUST CLOUDS AND THE NATURE OF EARLY-TYPE EMISSION STARS IN NEBULOSITY FROM A STUDY OF FIVE ASSOCIATIONS.

820109 PRICE, S. D., MARCOTTE, L. P., MURDOCK, T. L. <A. J., 87, 131>
INFRARED MAPPING OF THE GALACTIC PLANE. II. MEDIUM-RESOLUTION MAPS OF THE CYGNUS X REGION.

820110 ISRAEL, F. P., GATLEY, I., MATTHEWS, K., NEUGEBAUER, G. <ASTR. AP., 105, 229>
OBSERVATIONS OF NGC 604 OVER SIX DECADES IN FREQUENCY.

820111 IMPEY, C. D., BRAND, P. W. J. L., TAPIA, S. <M. N. R. A. S., 198, 1>
A POLARIZATION BURST IN THE BL LAC OBJECT AO 0235+164.

820112 GLASS, I. S., FEAST, M. W. <M. N. R. A. S., 198, 199>
INFRARED PHOTOMETRY OF MIRA VARIABLES IN THE BAADE WINDOWS AND THE DISTANCE TO THE GALACTIC CENTRE.

820113 STIER, M. T., JAFFE, D. T., FAZIO, G. G., ROBERGE, W. G., THUM, C., WILSON, T. L. <AP. J. SUPPL., 48, 127>
A HIGH RESOLUTION FAR-INFRARED SURVEY OF A SECTION OF THE GALACTIC PLANE. II. FAR-INFRARED, CO, AND RADIO CONTINUUM RESULTS.

820114 BUSOLETTI, E., GUIDI, I., MELCHIORRI, F., NATALE, V. <ASTR. AP., 105, 184>
FAR IR EMISSION OF THE GALACTIC PLANE AT HIGH LONGITUDES.

820115 TARANOVA, O. G., YUDIN, B. F. <SOV. AST. (LETTERS), 8, 46>
INFRARED PHOTOMETRY OF HM SAGITTAE.

820116 BELYAKINA, T. S., EFIMOV, YU. S., PAVLENKO, E. P., SHENAVRIN, V. I. <SOV. AST., 26, 1>
OBJECT KUWANO, A NOVALIKE (SYMBIOTIC?) BINARY WITH A RED GIANT: PHOTOMETRY AND POLARIMETRY.

820117 TARANOVA, O. G., YUDIN, B. F. <SOV. AST., 26, 57>
PHOTOMETRY OF SYMBIOTIC STARS IN THE UBVRJHKLMN SYSTEM. 3.AX PER, AG DRA, BF CYG, V443 HER, AND YY HER.

820118 CARTER, D., ALLEN, D. A., MALIN, D. F. <NATURE, 295, 126>
NATURE OF THE SHELLS OF NGC 1344.

820119 LEE, T. J., BEATTIE, D. H., GATLEY, I., BRAND, P. W. J. L., JONES, T., HYLAND, A. R. <NATURE, 295, 214>
OCCURRENCE OF THE 3.3-MICRON FEATURE IN GALAXIES.

820201 BREGMAN, J. N., GLASSGOLD, A. E., HUGGINS, P. J., POLLACK, J. T., PICA, A. J., SMITH, A. G., WEBB, J. R., KU, W. H. -M., RUDY, R. J., LEVAN, P.D., WILLIAMS, P. M.,BRAND, P. W. J. L., NEUGEBAUER, G., BALONEK, T. J., DENT, W. A., ALLER, H. D., ALLER, M. F., HODGE, P. E. <AP. J., 253, 19>
SIMULTANEOUS OBSERVATIONS OF THE BL LACERTAE OBJECT I ZW 187.

820202 RUDY, R. J., LEVAN, P. D., PUETTER, R. C., SMITH, H. E., WILNER, S. P. <AP. J., 253, 53>
INFRARED POLARIMETRY OF NINE SEYFERT GALAXIES.

820203 EVANS II, N. J., BLAIR, G. N., NADEAU, D., VANDEN BOUT, P. <AP. J., 253, 115>
THE ENERGETICS OF MOLECULAR CLOUDS. V. THE S37 MOLECULAR CLOUD.

820204 SCOVILLE, N. Z., HALL, D. N. B., KLEINMANN, S. G., RIDGWAY, S. T. <AP. J., 253, 136>
VELOCITY, REDDENING, AND TEMPERATURE STRUCTURE OF THE H2 EMISSION IN ORION.

820205 NADEAU, D., GEBALLE, T. R., NEUGEBAUER, G. <AP. J., 253, 154>
THE MOTION AND DISTRIBUTION OF THE VIBRATIONALLY EXCITED H2 IN THE ORION MOLECULAR CLOUD.

820206 WILLNER, S. P., GILLETT, F. C., HERTER, T. L., JONES, B., KRASSNER, J., MERRILL, K. M., PIPHER, J. L., PUETTER, R. C., RUDY, R. J., RUSSELL, R. W., SOIFER, B. T. <AP. J., 253, 174>
INFRARED SPECTRA OF PROTOSTARS: COMPOSITION OF THE DUST SHELLS.

820207 JONES, T. J., HYLAND, A. R., CASWELL, J. L., GATLEY, I. <AP. J., 253, 208>
A SEARCH FOR THE INFRARED COUNTERPART OF TYPE II OH MASERS. II. STATISTICAL ANALYSIS.

820208 FROGEL, J. A., COHEN, J. G. <AP. J., 253, 580>
THE LATE-TYPE STELLAR CONTENT OF MAGELLANIC CLOUD CLUSTERS.

820209 BECK, S. C., BLOEMHOF, E. E., SERABYN, E., TOWNES, C. H., TOKUNAGA, A. T., LACY, J. H., SMITH, H. A. <AP. J. (LETTERS), 253, L83>
HIGH SPECTRAL AND SPATIAL RESOLUTION OBSERVATIONS OF THE 12.28 MICRON EMISSION FROM H2 IN THE ORION MOLECULAR CLOUD.

820210 RUSSELL, R. W., GULL, G., BECKWITH, S., EVANS II, N. J. <P. A. S. P., 94, 97>
HIGH-SPECTRAL-RESOLUTION OBSERVATIONS OF THE 7.7 MICRON FEATURE IN HD 44179.

820211 NEUGEBAUER, G., BECKLIN, E. E., MATTHEWS, K. <A. J., 87, 395>
THE DOUBLE STRUCTURE OF W3-IRS 5 AS DETERMINED FROM HIGH-RESOLUTION SPATIAL SCANS.

820212 DYCK, H. M., HOWELL, R. R. <A. J., 87, 400>
SPECKLE INTERFEROMETRY OF MOLECULAR CLOUD SOURCES AT 4.8 MICRONS.

820213 GISPERT, R., PUGET, J. L., SERRA, G. <ASTR. AP., 106, 293>
FAR INFRARED SURVEY OF EXTENDED MOLECULAR CLOUDS H II REGIONS COMPLEXES ALONG THE GALACTIC PLANE.

820214 LOCKWOOD, G. W., WING, R. F. <M. N. R. A. S., 198, 385>
THE LIGHT AND SPECTRUM VARIATIONS OF VX SAGITTARII, AN EXTREMELY COOL SUPERGIANT.

820215 WICKRAMASINGHE, D. T., ALLEN, D. A., BESSELL, M. S. <M. N. R. A. S., 198, 473>
INFRARED PHOTOMETRY OF COOL WHITE DWARFS.

820216 NETO, A. D., PACHECO, J. A. DE FREITAS <M. N. R. A. S., 198, 659>
INFRARED EXCESS AND LINE EMISSION IN BE STARS.

820217 AARONSON, M., MOULD, J. <AP. J. SUPPL., 48, 161>
THE EXTENDED GIANT BRANCHES OF INTERMEDIATE AGE GLOBULAR CLUSTERS IN THE MAGELLANIC CLOUDS. II.

820301 MCBREEN, B., FAZIO, G. G., JAFFE, D. T. <AP. J., 254, 126>
HIGH RESOLUTION FAR-INFRARED OBSERVATIONS OF THE EVOLVED H II REGION M16.

820302 MOULD, J. R., CANNON, R. D., AARONSON, M., FROGEL, J. A. <AP. J., 254, 500>
CARBON STARS IN THE CARINA DWARF SPHEROIDAL GALAXY.

820303 THRONSON JR., H. A., THOMPSON, R. I. <AP. J., 254, 543>
NEAR-INFRARED SPECTROSCOPY OF MODERATE LUMINOSITY SOURCES: OMC-2 IRS3 AND IRS4.

820304 GEHRZ, R. D., GRASDALEN, G. L., CASTELAZ, M., GULLIXSON, C., MOZURKEWICH, D., HACKWELL, J. A. <AP. J., 254, 550>
ANATOMY OF A REGION OF STAR FORMATION: INFRARED IMAGES OF S106 (AFGL 2584).

820305 HARVEY, P. M., WILKING, B. A., JOY, M. <AP. J. (LETTERS), 254, L29>
FAR-INFRARED PHOTOMETRY OF COMPACT EXTRAGALACTIC OBJECTS: DETECTION OF 3C 345.

820306 WILLIAMS, P. M., LONGMORE, A. J. <IAUC NO. 3676>
NOVA AQUILAE 1982.

820307 APPARAO, K. M. V., ALLEN, D. <ASTR. AP., 107, L5>
INFRARED SCANS OF GAMMA RAY BURST SOURCE REGIONS.

820308 EPCHTEIN, N., NGUYEN-QUANG-RIEU <ASTR. AP., 107, 229>
NEW INFRARED COUNTERPARTS OF SOUTHERN TYPE II OH MASER SOURCES.

820309 DACHS, J., WAMSTEKER, W. <ASTR. AP., 107, 240>
INFRARED PHOTMETRY OF SOUTHERN BE STARS.

820310 KOORNNEEF, J. <ASTR. AP., 107, 247>
THE GAS TO DUST RATIO AND THE NEAR-INFRARED EXTINCTION LAW IN THE LARGE MAGELLANIC CLOUD.

820311 GLASS, I. S., MOORWOOD, A. F. M., EICHENDORF, W. <ASTR. AP., 107, 276>
MID-INFRARED OBSERVATIONS OF SEYFERT 1 AND NARROW-LINE X-RAY GALAXIES.

820312 PENNY, A. J. <M. N. R. A. S., 198, 773>
CRAB PULSAR INFRARED FLUXES AND PULSE SHAPES.

820313 YUDIN, B. F. <SOV. AST., 26, 187>
INFRARED OBSERVATIONS OF V1016 CYGNI.

820401 STAUDE, H. J., LENZEN, R., DYCK, H. M., SCHMIDT, G. D. <AP. J., 255, 95>
THE BIPOLAR NEBULA S106: PHOTOMETRIC, POLARIMETRIC, AND SPECTROPOLARIMETRIC OBSERVATIONS.

820402 COHEN, J. G., FROGEL, J. A. <AP. J. (LETTERS), 255, L39>
WHAT IS THE SECOND PARAMETER?: THE ANOMOLOUS GLOBULAR CLUSTER NGC 7006.

820403 HARVEY, P. M. <AP. J. (LETTERS), 255, L55>
INFRARED PHOTOMETRY OF THE ULTRACOMPACT RADIO SOURCE IN NGC 6334.

820404 CAPPS, R. W., SITKO, M. L., STEIN, W. A. <AP. J., 255, 413>
THE SPECTRAL FLUX DISTRIBUTIONS OF SOURCES IN AN OPTICALLY SELECTED SAMPLE OF QSOS: 1E13-1E15 HZ.

820405 LACY, J. H., BECK, S. C., GEBALLE, T. R. <AP. J., 255, 510>
INFRARED EMISSION LINE STUDIES OF THE STRUCTURE AND EXCITATION OF H II REGIONS.

820406 GENZEL, R., BECKLIN, E. E., WYNN-WILLIAMS, C. G., MORAN, J. M., REID, M. J., JAFFE, D. T., DOWNES, D. <AP. J., 255, 527>
INFRARED AND RADIO OBSERVATIONS OF W51: ANOTHER ORION-KL AT A DISTANCE OF 7 KILOPARSECS?

820407 BECKWITH, S., ZUCKERMAN, B. <AP. J., 255, 536>
MOLECULAR HYDROGEN EMISSION FROM W51.

820408 DINERSTEIN, H. L., WERNER, M. W., CAPPS, R. W., DWEK, E. <AP. J., 255, 552>
A SEARCH FOR HOT DUST IN THE FAST MOVING KNOTS IN CASSIOPEIA A.

820409 DYCK, H. M., SIMON, T., ZUCKERMAN, B. <AP. J. (LETTERS), 255, L103>
DISCOVERY OF AN INFRARED COMPANION TO T TAURI.

820410 HARVEY, P. M., WILKING, B. A. <P. A. S. P., 94, 285>
FAR-INFRARED PHOTMETRY OF OPTICAL EMISSION-LINE STARS. II.

820411 WHITELOCK, P. <IAUC NO. 3687>
SY MUSCAE.

820412 WHITTET, D. C. B., BODE, M. F., KILKENNY, D. <IAUC NO. 3689>
NOVA AQUILAE 1982.

820413 RUDY, R. J., LEVAN, P. D., RODRIGUEZ-ESPINOSA, J. M. <A. J., 87, 598>
INFRARED PHOTOMETRY OF 30 SEYFERT GALAXIES.

820414 ADELMAN, S. J., SHORE, S. N. <A. J., 87, 665>
SPECTROPHOTOMETRY OF THE RS CVN STARS. I. THE F, G, AND K STANDARDS.

820415 RIDGWAY, S. T., JACOBY, G. H., JOYCE, R. R., SIEGEL, M. J., WELLS, D. C. <A. J., 87, 680>
ANGULAR DIAMETERS BY THE LUNAR OCCULTATION TECHNIQUE. IV. ALPHA LEO AND THE CEPHEID ZETA GEM.

820416 WILKING, B. A., LEBOFSKY, M. J., RIEKE, G. H. <A. J., 87, 695>
THE WAVELENGTH DEPENDENCE OF INTERSTELLAR LINEAR POLARIZATION: STARS WITH EXTREME VALUES OF LAMBDA MAX.

820417 LEITHERER, C., HEFELE, H., STAHL, O., WOLF, B. <ASTR. AP., 108, 102>
SPECTROSCOPY AND INFRARED PHOTOMETRY OF CYG OB 2 STARS: VELOCITY LAW AND MASS-LOSS RATES.

820418 ELSAESSER, H., BIRLE, K., EIROA, C., LENZEN, R. <ASTR. AP., 108, 274>
ON THE INFRARED SOURCES 1 AND 2 IN NGC 7538.

820419 WILLIAMS, P. M. <M. N. R. A. S., 199, 93>
THE STRONG 3.3 MICRON EMISSION LINE IN WOLF-RAYET STARS.

820420 GLASS, I. S., FEAST, M. W. <M. N. R. A. S., 199, 245>
INFRARED PHOTOMETRY OF MIRA VARIABLES IN THE LMC AND THE PULSATIONAL PROPERTIES OF MIRAS.

820421 WALSH, J. R., WHITE, N. J. <M. N. R. A. S., 199, 9P>
A CLUSTER OF NEAR-INFRARED SOURCES IN THE NEUTRAL INTRUSIONS WITHIN M16 (NGC 6611).

820422 GEZARI, D. Y., SCHMITZ, M., MEAD, J. M. <NASA TM-83819>
CATALOG OF INFRARED OBSERVATIONS.

820501 LACY, J. H., SOIFER, B. T., NEUGEBAUER, G., MATTHEW, S., MALKAN, M., BECKLIN, E. E., WU, C. -C., BOGGESS, A., GULL, T. R. <AP. J., 256, 75>
INFRARED, OPTICAL, AND ULTRAVIOLET OBSERVATIONS OF HYDROGEN LINE EMISSION FROM SEYFERT GALAXIES.

820502 RYDGREN, A. E., SCHMELZ, J. T., VRBA, F. J. <AP. J., 256, 168>
EVIDENCE FOR A CHARACTERISTIC MAXIMUM TEMPERATURE IN THE CIRCUMSTELLAR DUST ASSOCIATED WITH T TAURI STARS.

820503 RUDY, R. J., TOKUNAGA, A. T. <AP. J. (LETTERS), 256, L1>
OBSERVATIONS OF PASCHEN-ALPHA IN THE BROAD-LINE RADIO GALAXY 3C 445.

820504 JENNINGS, D. E., BRAULT, J. W. <AP. J. (LETTERS), 256, L29>
LABORATORY MEASUREMENTS OF THE PURE ROTATION S(2) AND S(3) TRANSITIONS IN H2.

820505 FITZPATRICK, E. L., SAVAGE, B. D., SITKO, M. L. <AP. J., 256, 578>
ULTRAVIOLET, VISUAL, AND INFRARED OBSERVATIONS OF THE WC7 VARIABLE HD 193793.

820506 LIEBERT, J., STOCKMAN, H. S., WILLIAMS, R. E., TAPIA, S., GREEN, R. F., RAUTENKRANZ, D., FERGUSON, D. H. <AP. J., 256, 594>
PG 1550+191: A NEW AM HERCULIS TYPE BINARY SYSTEM.

820507 RIDGWAY, S. T., JACOBY, G. H., JOYCE, R. R., SIEGEL, M. J., WELLS, D. C. <A. J., 87, 808>
ANGULAR DIAMETERS BY THE LUNAR OCCULTATION TECHNIQUE. V. 26 LATE-TYPE STARS.

820508 KRASSNER, J., PIPHER, J. L., SHARPLESS, S., HERTER, T. <ASTR. AP., 109, 223>
RADIO, INFRARED, AND OPTICAL OBSERVATIONS OF COMPACT H II REGIONS.

820509 EICHENDORF, W., HECK, A., CACCIN, B., RUSSO, G., SOLLAZZO, C. <ASTR. AP., 109, 274>
UV, OPTICAL AND IR OBSERVATIONS OF THE CEPHEID R MUSCAE.

820510 DYCK, H. M., STAUDE, H. J. <ASTR. AP., 109, 320>
NEAR-INFRARED SLIT SCANS OF MOLECULAR CLOUD SOURCES. II.

820511 FRISK, U., BELL, R. A., GUSTAFSSON, B., NORDH, H. L., OLOFFSON, S. G. <M. N. R. A. S., 199, 471>
THE TEMPERATURE OF ARCTURUS.

820512 GILES, A. B. <M. N. R. A. S., 199, 483>
A POWERFUL METHOD FOR STAR COUNTING IN THE INFRARED.

820513 FOX, M. W. <M. N. R. A. S., 199, 715>
PHOTOMETRY OF RED VARIABLES IN 47 TUCANAE.

820514 AITKEN, D. K., ROCHE, P. F., ALLEN, M. C., PHILLIPS, M. M. <M. N. R. A. S., 199, 31P>
A HIGH-EXCITATION OPTICALLY OBSCURED H II REGION IN THE NUCLEUS OF NGC 5253.

820515 EVANS, A., BODE, M. F., WHITTET, D. C. B., DAVIES, J. K., KILKENNY, D., BAINES, D. W. T. <M. N. R. A. S., 199, 37P>
THE VARIABILITY OF RY LUPI.

820516 MELIK-ALAVERDIAN, YU., MOVSESYAN, T. A. <ASTROFIZIKA, 18, 275>
INFRARED EXCESS OF STARS WITH PROPER POLARIZATION.

820601 MCCARTHY, D. W., LOW, F. J., KLEINMANN, S. G., GILLETT, F. C. <AP. J. (LETTERS), 257, L7>
INFRARED SPECKLE INTERFEROMETRY OF THE NUCLEUS OF NGC 1068.

820602 MCGONEGAL, R., MCLAREN, R. A., MCALARY, C. W., MADORE, B. F. <AP. J. (LETTERS), 257, L33>
THE CEPHEID DISTANCE SCALE: A NEW APPLICATION FOR INFRARED PHOTOMETRY.

820603 STACEY, G. J., KURTZ, N. T., SMYERS, S. D., HARWIT, M., RUSSELL, R. W., MELNICK, G. <AP. J. (LETTERS), 257, L37>
THE MASS OF HOT, SHOCKED CO IN ORION: FIRST OBSERVATIONS OF THE J - 17 - J - 16 TRANSITION AT 153 MICTONS.

820604 RUDY, R. J., JONES, B., LEVAN, P. D., PUETTER, R. C., SMITH, H. E., WILLNER, S. P., TOKUNAGA, A. T. <AP. J., 257, 570>
NEAR-INFRARED SPECTROPHOTOMETRY OF FOUR SEYFERT 1 GALAXIES AND NGC 1275.

820605 BALLY, J., LANE, A. P. <AP. J., 257, 612>
OBSERVATIONS OF 2 MICRON MOLECULAR HYDROGEN EMISSION FROM NGC 2071, CEPHEUS A, AND GL 961.

820606 SZKODY, P., RAYMOND, J. C., CAPPS, R. W. <AP. J., 257, 686>
THE LOW STATE OF AM HERCULIS: OBSERVATIONS FROM 0.12 TO 10 MICRONS.

820607 PUSCHELL, J. J., OWEN, F. N., LAING, R. A. <AP. J. (LETTERS), 257, L57>
NEAR-INFRARED PHOTOMETRY OF DISTANT RADIO GALAXIES: SPECTRAL FLUX DISTRIBUTIONS AND REDSHIFT ESTIMATES.

820608 PRZBYLSKI, A. <AP. J. (LETTERS), 257, L83>
A NOTE ON THE TEMPERATURE OF HD 101065.

820609 MCCARTHY, D. W. <AP. J. (LETTERS), 257, L93>
TRIPLE STRUCTURE OF INFRARED SOURCE 3 IN THE MONOCEROS R2 MOLECULAR CLOUD.

820610 BAILEY, J., HOUGH, J. H. <P. A. S. P., 94, 618>
A SIMULTANEOUS INFRARED/OPTICAL POLARIMETER.

820611 MIDDLEDITCH, J., PENNYPACKER, C., BURNS, S. <IAUC NO. 3701>
1E 2259+586.

820612 STAUFFER, J. <A. J., 87, 899>
THE FAINT END OF THE HYADES MAIN SEQUENCE.

820613 SUTTON, E. C., SUBRAMANIAN, S., TOWNES, C. H. <ASTR. AP., 110, 324>
INTERFEROMETRIC MEASUREMENTS OF STELLAR POSITIONS IN THE INFRARED.

820614 CHINI, R. <ASTR. AP., 110, 332>
CIRCUMSTELLAR SHELLS IN M17.

820615 BAILEY, J., HOUGH, J. H., AXON, D. J., GATLEY, I., LEE, T. J., SZKODY, P., STOKES, G., BERRIMAN, G. <M. N. R. A. S., 199, 801>
A MULTIWAVELENGTH STUDY OF THE AM HERCULIS TYPE BINARY 2A 0311-227.

820616 HYLAND, A. R., ALLEN, D. A. <M. N. R. A. S., 199, 943>
AN INFRARED STUDY OF QUASARS.

820617 WARD, M., ALLEN, D. A., WILSON, A. S., SMITH, M. G., WRIGHT, A. E. <M. N. R. A. S., 199, 953>
THE NEAR INFRARED PROPERTIES OF SEYFERT AND RELATED ACTIVE GALAXIES.

820618 ALLEN, D. A., WARD, M. J., HYLAND, A. R. <M. N. R. A. S., 199, 969>
THE NEAR-INFRARED CONTINUA OF BL LACERTAE OBJECTS.

820619 MORGAN, D. H., NANDY, K. <M. N. R. A. S., 199, 979>
INFRARED INTERSTELLAR EXTINCTION IN THE LMC.

820620 ALLEN, D. A., BAINES, D. W. T., BLADES, J. C., WHITTET, D. C. B. <M. N. R. A. S., 199, 1017>
A SURVEY OF 3 MICRON EMISSION FEATURES IN STELLAR SPECTRA.

820621 LILLY, S. J., LONGAIR, M. S. <M. N. R. A. S., 199, 1053>
INFRARED STUDIES OF A SAMPLE OF 3C RADIO GALAXIES.

820622 WALSH, J. R., WHITE, N. J. <OBSERVATORY, 102, 78>
2.2-MICRON MAPPING OF THE NUCLEAR REGION OF NGC 5128 (CENTAURUS A).

820623 CHEN, P., GAO, H., HAO, Y., CHU, Q., ZHOU, K. <CHIN. AST. AP., 6, 153>
CONSTRUCTION OF A 1-3 MICRON INFRARED PHOTOMETER AND ITS TEST OBSERVATIONS.

820701 BECKLIN, E. E., GATLEY, I., WERNER, M. W. <AP. J., 258, 135>
FAR-INFRARED OBSERVATIONS OF SAGITTARIUS A: THE LUMINOSITY AND DUST DENSITY IN THE CENTRAL PARSEC OF THE GALAXY.

820702 FISCHER, J., JOYCE, R. R., SIMON, M., SIMON, T. <AP. J., 258, 165>
NEAR-INFRARED OBSERVATIONS OF THE FAR-INFRARED SOURCE V REGION IN NGC 6334.

820703 SMITH, H. A., THRONSON JR., H. A., LADA, C. J., HARPER, D. A., LOEWENSTEIN, R. F., SMITH, J. <AP. J., 258, 170>
FAR-INFRARED OBSERVATIONS OF FU ORIONIS.

820704 WOLLMAN, E. R., SMITH, H. A., LARSON, H. P. <AP. J., 258, 506>
INFRARED SPECTRA OF GALACTIC CENTER SOURCES.

820705 HARVEY, P. M., GATLEY, I., THRONSON JR., H. A., WERNER, M. W. <AP. J., 258, 568>
FAR-INFRARED MAPPING OF THE DOUBLE-LOBED H II REGION S106.

820706 PANEK, R. J., EATON, J. A. <AP. J., 258, 572>
THE INFRARED LIGHT CURVE OF U GEMINORUM.

820707 ELIAS, J. H., FROGEL, J. A., MATTHEWS, K., NEUGEBAUER, G. <A. J., 87, 1029>
INFRARED STANDARD STARS.

820708 RIDGWAY, S. T., JACOBY, G. H., JOYCE, R. R., SIEGEL, M. J., WELLS, D. C. <A. J., 87, 1044>
ANGULAR DIAMETERS BY THE LUNAR OCCULTATION TECHNIQUE. VI. LIMB DARKENING OF ALPHA TAURI.

820709 GEHRZ, R. D., HACKWELL, J. A., GRASDALEN, G. L. <IAUC NO. 3711>
NOVA AQUILAE 1982.

820710 BAILEY, J., HANES, D. A., WATTS, D. J., GILES, A. B., GREENHILL, J. G. <IAUC NO. 3712>
CW 1103+254.

820711 AITKEN, D., ROCHE, P., WHITMORE, B. <IAUC NO. 3717>
NOVA AQUILAE 1982.

820712 PERSI, P., FERRARI-TONIOLO, M. <ASTR. AP., 111, L7>
INFRARED ENERGY DISTRIBUTION OF CYG. OB2 NO. 12.

820713 BRAZ, M. A., EPCHTEIN, N. <ASTR. AP., 111, 91>
NEW INFRARED OBJECTS TOWARDS SOUTHERN TYPE I OH AND H2O MASERS.

820714 IMPEY, C. D., BRAND, P. W. J. L., WOLSTENCROFT, R. D., WILLIAMS, P. M. <M. N. R. A. S., 200, 19>
INFRARED POLARIMETRY AND PHOTOMETRY OF BL LAC OBJECTS.

820715 AITKEN, D. K., ROCHE, P. F. <M. N. R. A. S., 200, 217>
8-13 MICRON SPECTROPHOTOMETRY OF COMPACT PLANETARY NEBULAE AND EMISSION LINE OBJECTS.

820716 AXON, D. J., ALLEN, D. A., BAILEY, J., HOUGH, J. H., WARD, M. J., JAMESON, R. F. <M. N. R. A. S., 200, 239>
THE VARIABLE INFRARED SOURCE NEAR HH100.

820801 DAVIS, D. S., LARSON, H. P., SMITH, H. A. <AP. J., 259, 166>
AIRBORNE OBSERVATIONS OF THE ORION MOLECULAR HYDROGEN EMISSON SPECTRUM.

820802 FROGEL, J. A., WHITFORD, A. E. <AP. J. (LETTERS), 259, L7>
LUMINOSITY OF M GIANTS IN THE NUCLEAR BULGE OF THE GALAXY.

820803 HERTER, T., BRIOTTA JR., D. A., GULL, G. E., HOUCK, J. R. <AP. J. (LETTERS), 259, L25>
OBSERVATIONS OF THE 30 MICRON FEATURE IN IRC+10216.

820804 GEZARI, D. Y. <AP. J. (LETTERS), 259, L29>
THE REMARKABLE 400 MICRON SOURCE NGC 6334/I(NORTH).

820805 GEBALLE, T. R., RUSSELL, R. W., NADEAU, D. <AP. J. (LETTERS), 259, L47>
DETERMINATION OF THE INTRINSIC Q(3)/S(1) LINE INTENSITY RATIO OF MOLECULAR HYDROGEN.

820806 SITKO, M. L., STEIN, W. A., ZHANG, Y. -X., WISNIEWSKI, W. Z. <AP. J., 259, 486>
0.35-3.5 MICRON PHOTOMETRY OF X-RAY EMITTING QSOS.

820807 FIX, J. D., MUTEL, R. L., GAUME, R. A., CLAUSSEN, M. J. <AP. J., 259, 657>
RADIO AND INFRARED OBSERVATIONS OF THE OH MASER SOURCE OH 351.78-0.54.

820808 ZIRIN, H., LIGGETT, M. A. <AP. J., 259, 719>
THE VARIABLE HE 10830A LINE OF ALGOL.

820809 MCCARTHY, D. W., LOW, F. J., KLEINMANN, S. G., ARGANBRIGHT, D. V. <AP. J. (LETTERS), 257, L75>
INFRARED DETECTION OF THE LOW-MASS COMPANION TO ZETA AQUARII B.

820810 DRAINE, B. T., ROBERGE, W. G. <AP. J. (LETTERS), 259, L91>
A MODEL FOR THE INTENSE MOLECULAR LINE EMISSION FROM OMC-1.

820811 HERTER, T., BRIOTTA JR., D. A., GULL, G. E., SHURE, M. A., HOUCK, J. R. <AP. J. (LETTERS), 259, L109>
DETECTION OF THE (S III) 33.47 MICRON LINE IN THE ORION NEBULA.

820812 TAPIA, M. <P. A. S. P., 94, 669>
A DUST SHELL AROUND THE YELLOW SUPERGIANT COD-61 3326.

820813 GRIERSMITH, D., HYLAND, A. R., JONES, T. J. <A. J., 87, 1106>
PHOTOMETRIC PROPERTIES OF BRIGHT EARLY-TYPE SPIRAL GALAXIES. IV. MULTIAPERTURE UBVJHK PHOTOMETRY FOR THE INNER (BULGE) REGIONS OF 65 GALAXIES.

820814 THRONSON JR., H. A. <A. J., 87, 1207>
NEAR-INFRARED SPECTROSCOPY OF POSSIBLE PRECURSORS TO PLANETARY NEBULAE: THE CYGNUS EGG AND THE RED RECTANGLE.

820815 BAILEY, J., GILES, A. B., WATTS, D. J., GREENHILL, J. G. <IAUC NO. 3720>
H 0139-68.

820816 CHEVALIER, C., ILOVAISKY, S. A. <ASTR. AP., 112, 68>
COLOR VARIABILITY AND OPTICAL LIGHT CURVE OF 2S0921-630.

820817 CONDAL, A. R. <ASTR. AP., 112, 124>
NGC 2440: IONIZATION STRUCTURE, EXTINCTION, AND NEAR INFRARED SPECTRUM.

820818 DENNEFELD, M. <ASTR. AP., 112, 215>
A SPECTROPHOTOMETRIC STUDY OF KEPLER SUPERNOVA REMNANT.

820819 PERSI, P., FERRARI-TONIOLO, M. <ASTR. AP., 112, 292>
NEAR-INFRARED SOURCES IN THE NGC 6334 MOLECULAR CLOUD.

820820 JAMESON, R. F., KING, A. R., SHERRINGTON, M. R. <M. N. R. A. S., 200, 455>
INFRARED, OPTICAL AND ULTRAVIOLET OBSERVATIONS OF TT ARI.

820821 JONES, T. J., HYLAND, A. R. <M. N. R. A. S., 200, 509>
MULTIAPERTURE JHK PHOTOMETRY OF THE GLOBULAR CLUSTERS IN FORNAX DWARF SPHEROIDAL GALAXY.

820822 GATLEY, I., HYLAND, A. R., JONES, T. J. <M. N. R. A. S., 200, 521>
STAR FORMATION IN THE MAGELLANIC CLOUDS. II. DICOVERY OF A PROTOSTAR IN THE SMALL MAGELLANIC CLOUD.

820823 CATCHPOLE, R. M. <M. N. R. A. S., 200, 33P>
FAINT RED STARS AT THE GALACTIC CENTRE.

820824 JOYCE, R. R., SIMON, T. <M. N. R. A. S., 200, 39P>
POLARIMETRY OF THE H2 EMISSION FROM THE ORION MOLECULAR CLOUD.

820825 AVETISSIAN, V. Z., MELIK-ALAVERDIAN, YU. K. <ASTROFIZIKA, 18, 386>
MOLECULAR ABSORPTION BANDS IN IR SPECTRA OF M GIANTS.

820901 FROGEL, J. A., ELIAS, J. H., PHILLIPS, M. M. <AP. J., 260, 70>
8-13 MICRON OBSERVATIONS OF NINE EMISSION-LINE GALAXIES.

820902 KNACKE, R. F., MCCORKLE, S., PUETTER, R. C., ERICKSON, E. F.,KRATSCHMER, W. <AP. J., 260, 141>
OBSERVATION OF INTERSTELLAR AMMONIA ICE.

820903 MOORE, R. L., MCGRAW, J. T., ANGEL, J. R. P., DUERR, R., LEBOFSKY, M. J., RIEKE, M. J., WISNIEWSKI, W. Z., AXON, D. J., BAILEY, J., HOUGH, J. M., THOMPSON, I., BREGER, M., SCHULZ, H., CLAYTON, G. C., MARTIN, P. G., MILLER, J. S., SCHMIDT, G. D., AFRICANO, J., MILLER, H. R. <AP. J., 260, 415>
THE NOISE OF BL LACERTAE.

820904 JOYCE, R. R., SIMON, T. <AP. J., 260, 604>
NEAR-INFRARED SPECTROPHOTOMETRY OF POLARIZED COMPACT INFRARED SOURCES.

820905 ZIRIN, H. <AP. J., 260, 655>
10830 HE I OBSERVATIONS OF 455 STARS.

820906 HALL, D. N. B., KLEINMANN, S. G., SCOVILLE, N. Z. <AP. J. (LETTERS), 260, L53>
BROAD HELIUM EMISSION IN THE GALACTIC CENTER.

820907 THRONSON JR., H. A., PRICE, S. D. <A. J., 87, 1288>
INFRARED MAPPING OF THE GALACTIC PLANE. III. THE LARGE-SCALE MID-INFRARED STRUCTURE OF W3, W4, AND W5.

820908 ZEILIK, M., HECKERT, P., HENSON, G., SMITH, P. <A. J., 87, 1304>
INFRARED PHOTOMETRY OF BETA LYRAE: 1977-1982.

820909 ALLEN, D. A. <IAUC NO. 3727>
SUPERNOVA IN NGC 1332.

820910 VREUX, J. M., DENNEFELD, M., ANDRILLAT, Y. <ASTR. AP., 113, L10>
R136: WN OR O SPECTRAL CHARACTERISTICS?

820911 BROSCH, N., ISAACMAN, R. <ASTR. AP., 113, 231>
MULTIAPERATURE PHOTOMETRY OF GALAXIES. II. NEAR-INFRARED OBSERVATIONS OF SIX ISOLATED OBJECTS.

820912 SHERRINGTON, M. R., JAMESON, R. F., BAILEY, J., GILES, A. B. <M. N. R. A. S., 200, 861>
INFRARED LIGHT CURVES OF THE DWARF NOVA OY CARINAE.

820913 CUDLIP, W., FURNISS, I., KING, K. J., JENNINGS, R. E. <M. N. R. A. S., 200, 1169>
FAR INFRARED POLARIMETRY OF W51A AND M42.

820914 AITKEN, D. K., ROCHE, P. F., ALLEN, D. A. <M. N. R. A. S., 200, 69P>
THE INFRARED SPECTRUM OF GAMMA VELORUM.

820915 AXON, D. J., BAILEY, J., HOUGH, J. H. <NATURE, 299, 234>
DISCOVERY OF A VERY RED NUCLEUS IN THE RADIO ELLIPTICAL IC 5063 (PKS2048-57).

821001 LADA, C. J., GAUTIER III, T. N. <AP. J., 261, 161>
THE ENERGETIC MOLECULAR OUTFLOW NEAR AFGL 961: MILLIMETER-WAVE AND INFRARED OBSERVATIONS.

821002 WORRALL, D. M., PUSCHELL, J. J., JONES, B., BRUHWEILER, F. C., ALLER, M. F., ALLER, H. D., HODGE, P. D., SITKO, M. L., STEIN, W. A., ZHANG, Y. -X., KU, W. H. -M. <AP. J., 261, 403>
TWO MULTIFREQUENCY OBSERVATIONS OF THE BL LACERTAE OBJECT OJ 287.

821003 SMITH, J. <AP. J., 261, 463>
THE FAR-INFRARED DISK OF M51.

821004 CAMPBELL, M. F., HOFFMANN, W. F., THRONSON JR., H. A., NILES, D., NAWFEL, R., HAWRYLYCZ, M. <AP. J., 261, 550>
FAR-INFRARED SOURCES IN CYGNUS X: AN EXTENDED EMISSION COMPLEX AT DR 21 AND UNRESOLVED SOURCES AT S106 AND ON 2.

821005 HAGEN, W. <P. A. S. P., 94, 835>
OBSERVATIONS OF COOL STARS AT 20, 25, AND 33 MICRONS.

821006 KOORNNEEF, J. <IAUC NO. 3740>
SUPERNOVA IN NGC 1187.

821007 ILOVAISKY, S. A., CHEVALIER, C., MOTCH, C. <ASTR. AP., 114, L7>
THE NATURE OF THE 1E1145.1-6141 OPTICAL COUNTERPART.

821008 KRASSNER, J. <ASTR. AP., 114, 19>
2-4 MICRON SPECTROSCOPY OF THE COMPACT H II REGION G45.13+0.14A.

821009 **CLEGG, R. E. S., HINKLE, K. H., LAMBERT, D. L. <M. N. R. A. S., 201, 95>**
HIGH-RESOLUTION 3 MICRON SPECTROSCOPY OF IRC+10216.

821010 **LONGMORE, A. J., SHARPLES, R. M. <M. N. R. A. S., 201, 111>**
INFRARED OBSERVATIONS OF EARLY-TYPE GALAXIES WITH DUST-LANES.

821011 **ELLIS, R. S., GONDHALEKAR, P. M., EFSTATHIOU, G. <M. N. R. A. S., 201, 223>**
THE ULTRAVIOLET SPECTRA OF THE NUCLEI OF SPIRAL GALAXIES. I. NGC 4594, 3031, 5194 AND 4258.

821012 **THRONSON JR., H. A., LADA, C. J., HARVEY, P. M., WERNER, M. W. <M. N. R. A. S., 201, 429>**
THE BUBBLE NEBULA: FAR-INFRARED AND RADIO MOLECULAR OBSERVATIONS OF NGC 7635.

821013 **AARONSON, M., HUCHRA, J., MOULD, J. R., TULLY, R. B., FISHER, J. R., VAN WOERDEN, H., GOSS, W. M., CHAMARAUX, P., MEBOLD, U., SIEGMAN, B., BERRIMAN, G., PERSSON, S. E. <AP. J. SUPPL., 50, 241>**
A CATALOG OF INFRARED MAGNITUDES AND H I VELOCITY WIDTHS FOR NEARBY GALAXIES.

821014 ***GEZARI, D. Y., SCHMITZ, M., MEAD, J. M. <NASA TM-84001>***
FAR INFRARED SUPPLEMENT: CATALOG OF INFRARED OBSERVATIONS.

821101 **HERTER, T., HELFER, H. L., PIPHER, J. L., BRIOTTA JR., D. A.,FORREST, W. J., HOUCK, J. R., RUDY, R. J., WILLNER, S. P. <AP. J., 262, 153>**
ABUNDANCES IN FIVE NEARBY GALACTIC H II REGIONS FROM INFRARED FORBIDDEN LINES.

821102 **HERTER, T., BRIOTTA JR., D. A., GULL, G. E., SHURE, M. A., HOUCK, J. R. <AP. J., 262, 164>**
OBSERVATIONS OF THE INFRARED FINE-STRUCTURE LINES OF S III AT 18.71 AND 33.47 MICRONS IN FOUR H II REGIONS.

821103 **RINSLAND, C. P., WING, R. F. <AP. J., 262, 201>**
OBSERVATIONS OF THE FIRST-OVERTONE SILICON MONOXIDE BANDS IN LATE-TYPE STARS.

821104 **MASON, K. O., CORDOVA, F. A. <AP. J., 262, 253>**
INFRARED PHOTMETRY OF THE X-RAY BINARY 2A 1822-371: A MODEL FOR THE ULTRAVIOLET, OTICAL, AND INFRARED LIGHT CURVE.

821105 **ENNIS, D. J., NEUGEBAUER, G., WERNER, M. <AP. J., 262, 451>**
VARIABILITY OF COMPACT RADIO SOURCES AT A WAVELENGTH OF 1 MILLIMETER.

821106 **ENNIS, D. J., NEUGEBAUER, G., WERNER, M. <AP. J., 262, 460>**
1 MILLIMETER CONTINUUM OBSERVATIONS OF QUASARS.

821107 **FELLI, M., PANAGIA, N. <AP. J., 262, 650>**
MASS LOSS FROM WOLF-RAYET STARS: AN ANALYSIS OF RADIO AND INFRARED OBSERVATIONS OF MR 111 - AS 422.

821108 **STAUFFER, J. R. <A. J., 87, 1507>**
OBSERVATIONS OF LOW-MASS STARS IN THE PLEIADES: HAS A PRE-MAIN SEQUENCE BEEN DETECTED?

821109 **CARNEY, B. W. <A. J., 87, 1527>**
INFRARED PHOTOMETRY OF HYADES DWARFS.

821110 **MOORWOOD, A. F. M., GLASS, I. S. <ASTR. AP., 115, 84>**
INFRARED EMISSION AND STAR FORMATION IN NGC 5253.

821111 **WILLEMS, F., DE JONG, T. <ASTR. AP., 115, 213>**
INFRARED OBSERVATIONS OF OH/IR STARS.

821112 **NORDH, H. L., VAN DUINEN, R. J., SARGENT, A. I., FRIDLUND, C. V. M., AALDERS, J. W. G., BEINTEMA, D. <ASTR. AP., 115, 308>**
FAR INFRARED OBSERVATIONS OF A STAR FORMING REGION IN SERPENS.

821113 **WOLSTENCROFT, R. D., GILMORE, G., WILLIAMS, P. M. <M. N. R. A. S., 201, 479>**
RAPID VARIABILITY OF OJ 287 AT 1.25 MICRONS.

821114 **ALLEN, D. A., CHEREPASHCHUK, A. M. <M. N. R. A. S., 201, 521>**
THE ELLIPSOIDAL LIGHT CURVE OF VV PUPPIS.

821201 **RIEKE, G. H., LEBOFSKY, M. J., WISNIEWSKI, W. Z. <AP. J., 263, 73>**
ABRUPT CUTOFFS IN THE OPTICAL-INFRARED SPECTRA OF NONTHERMAL SOURCES.

821202 **GALLAGHER, J. S., GOAD, J. W., MOULD, J. <AP. J., 263, 101>**
STRUCTURE OF THE M33 NUCLEUS.

821203 **TELESCO, C. M., GATLEY, I., STEWART, J. M. <AP. J. (LETTERS), 263, L13>**
THE DISTRIBUTION OF INFRARED OBSCURATION IN NGC 7331: EVIDENCE FOR A MASSIVE MOLECULAR RING.

821204 **BECKLIN, E. E., TOKUNAGA, A. T., WYNN-WILLIAMS, C. G. <AP. J., 263, 624>**
THE INFRARED EMISSION FROM THE ELLIPTICAL GALAXY NGC 1052.

821205 **MOULD, J., AARONSON, M. <AP. J., 263, 629>**
THE EXTENDED GIANT BRANCHES OF INTERMEDIATE AGE GLOBULAR CLUSTERS IN THE MAGELLANIC CLOUDS. III.

821206 **LEBOFSKY, M. J., RIEKE, G. H., DESHPANDE, M. R., KEMP, J. C. <AP. J., 263, 672>**
POLARIZATION OF COMPACT SOURCES IN THE GALACTIC CENTER.

821207 **LEBOFSKY, M. J., RIEKE, G. H., TOKUNAGA, A. T. <AP. J., 263, 736>**
M SUPERGIANTS AND STAR FORMATION AT THE GALACTIC CENTER.

821208 **MEISEL, D. D., SAUNDERS, B. A., FRANK, Z. A., PACKARD, M. L. <AP. J., 263, 759>**
THE HELIUM 10830A LINE IN EARLY-TYPE STARS: AN ATLAS OF FABRY-PEROT SCANS.

821209 **NEUGEBAUER, G., SOIFER, B. T., MATTHEWS, K., MARGON, B., CHANAN, G. A. <A. J., 87, 1639>**
INFRARED PROPERTIES OF SERENDIPITOUS X-RAY QUASARS.

821210 **PALMER, L. G., WING, R. F. <A. J., 87, 1739>**
A NEW SEARCH FOR M AND C STARS.

821211 **BENTLEY, A. F. <A. J., 87, 1810>**
SPATIAL OBSERVATIONS OF DUST EMISSION IN NGC 7027.

821212 **LONSDALE, C. J., BECKLIN, E. E., LEE, T. J., STEWART, J. M. <A. J., 87, 1819>**
NEW MEMBERS OF THE INFRARED CLUSTER IN THE ORION MOLECULAR CLOUD.

821213 **ELIAS, J. H., FROGEL, J. A., MATTHEWS, K., NEUGEBAUER, G. <A. J., 87, 1893>**
ERRATUM TO "INFRARED STANDARD STARS".

821214 **GROOTE, D., HUNGER, K. <ASTR. AP., 116, 64>**
SHELL AND PHOTOSPHERE OF SIGMA ORI E: NEW OBSERVATIONS AND IMPROVED MODEL.

821215 **PHILLIPS, J. P., WHITE, G. J., ADE, P. A. R., CUNNINGHAM, C. T., RICHARDSON, K. J., ROBSON, E. I., WATT, G. D. <ASTR. AP., 116, 130>**
CO J-3-2 AND SUBMILLIMETRE CONTINUUM OBSERVATIONS OF TWO MOLECULAR OUTFLOW SOURCES.

821216 **HOFMANN, R. G. <ASTR. AP., 116, 179>**
A NEW NEAR-INFRARED SOURCE IN THE MOLECULAR CLOUD ASSOCIATED WITH S 106.

821217 **WHITE, G. J., PHILLIPS, J. P., WILLIAMS, P. M., WATT, G. D., RICHARDSON, K. J. <ASTR. AP., 116, 293>**
NEAR INFRARED SPECTROSCOPY OF W51 IRS-2.

821218 **FOSBURY, R. A. E., BOKSENBERG, A., SNIJDERS, M. A. J., DANZIGER, I. J., DISNEY, M. J., GOSS, W. M., PENSTON, M. V., WAMSTEKER, W., WELLINGTON, K. J., WILSON, A. S. <M. N. R. A. S., 201, 991>**
VERY EXTENDED IONIZED GAS IN RADIO GALAXIES. I. A RADIO, OPTICAL AND ULTRAVIOLET STUDY OF PKS 2158-380.

821219 **HYLAND, A. R., JONES, T. J., MITCHELL, R. M. <M. N. R. A. S., 201, 1095>**
A STUDY OF THE CHAMAELEON DARK CLOUD COMPLEX: SURVEY, STRUCTURE AND EMBEDDED SOURCES.

829901 **ARGYLE, R. <IAUC NO. 3673>**
NOVA AQUILAE 1982.

829902 **DUERR, R., IMHOFF, C. L., LADA, C. J. <AP. J., 261, 135>**
STAR FORMATION IN THE LAMBDA ORIONIS REGION. I. THE DISTRIBUTION OF YOUNG OBJECTS.

829903 **KAPLAN, G. H., JOSTIES, F. J., ANGERHOFER, P. E., JOHNSTON, K. J., SPENCER, J. H. <A. J., 87, 570>**
PRECISE RADIO SOURCE POSITIONS FROM INTERFEROMETRIC OBSERVATIONS.

829904 **ANANTH, A. G., NAGARAJA, B. V. <AP. J., 259, 664>**
IDENTIFICATION OF ACTIVE STAR FORMATION REGIONS IN THE GALACTIC PLANE.

829905 KOJOIAN, G., ELLIOTT, R., BICAY, M. D. <A. J., 87, 1364>
ACCURATE OPTICAL POSITIONS FOR MARKARIAN GALAXIES 1303-1399.

829906 DE VEGT, C. <ASTR. AP., 109, 282>
COMPARISON OF PRECISE OPTICAL AND RADIO POSITIONS FOR CYG OB2 MEMBERS AND P CYG.

829907 KOJOIAN, G., ELLIOTT, R., BICAY, M. D. <AP. J. SUPPL., 50, 161>
ACCURATE OPTICAL POSITIONS OF EXTRAGALACTIC EMISSION-LINE OBJECTS: UNIVERSITY OF MICHIGAN LISTS I-IV.

829908 CLINE, T. L. <NASA TM-83967>
DEVELOPMENTS IN HIGH-PRECISION GAMMA-RAY BURST SOURCE STUDIES.

829909 KUKARKIN, B. V., KHOLOPOV, P. N., ARTIUKHINA, N. M., FEDOROVICH, V. P., FROLOV, M. S., GORANSKIJ, V. P., GORYNYA, N. A., KARITSKAYA, E. A., KIREEVA, N. N., KUKARKINA, N. P., KUROCHKIN, N. E., MEDVEDEVA, G. I., PEROVA, N. B., PONOMAREVA, G. A., SAMUS', N. N., SHUGAROV, S. YU. <PUBL. OFFICE NAUKA, MOSCOW>
NEW CATALOGUE OF SUSPECTED VARIABLE STARS.

830001 KAWARA, K., KOZASA, T., SATO, S., OKUDA, H., KOBAYASHI, Y., JUGAKU, J. <MEM. FAC. SCI., KYOTO UNIV., XXXVI, 353>
NEAR-INFRARED SOURCE COUNTS IN THE GALACTIC PLANE. II. A LIST OF NEAR-INFRARED SOURCES.

830002 KOBAYASHI, Y., OKUDA, H., SATO, S., JUGAKU, J., DYCK, H. M. <P. A. S. J., 35, 101>
INFRARED POLARIZATION IN THE DIRECTION TO THE GALACTIC CENTER.

830201 PRICE, S. D., MURDOCK, T. L., SHIVANANDAN, K. <AFGL-TR-83-0055>
FAR INFRARED SKY SURVEY EXPERIMENT. FINAL REPORT.

D. BIBLIOGRAPHY - FIRST AUTHOR ALPHABETICAL LISTING

This version of the Bibliography is sorted alphabetically by first author. It is useful for quickly locating familiar articles in the literature, which are often identified by the name of the first author.

The *Bibliography of Infrared Astronomy* identifies each observation in the Catalog with the original article published in the scientific literature. Over 1,700 infrared journal articles and other references are listed in this appendix. Each entry contains the year and month of publication, authors' names, journal name or document number, volume, page, and full title of the reference.

AARONSON, M. <AP. J. (LETTERS), 221, L103> 780505
THE MORPHOLOGICAL DISTRIBUTION OF BRIGHT GALAXIES IN THE UVK COLOR PLANE.

AARONSON, M. <P. A. S. P., 90, 28> 780219
IDENTIFICATION OF THE NUCLEUS IN THE SPIRAL GALAXY NGC 4631.

AARONSON, M. <P. A. S. P., 93, 535> 810802
ERRATUM TO "IDENTIFICATION OF THE NUCLEUS IN THE SPIRAL GALAXY NGC 4631".

AARONSON, M., DAWE, J. A., DICKENS, R. J., MOULD, J. R., MURRAY, J. B. <M. N. R. A. S., 195, 1P> 810416
THE FORNAX AND GRUS CLUSTERS AND THE LOCAL INFALL VELOCITY.

AARONSON, M., HUCHRA, J., MOULD, J. R. <AP. J., 229, 1> 790404
THE INFRARED LUMINOSITY/H I VELOCITY-WIDTH RELATION AND ITS APPLICATION TO THE DISTANCE SCALE.

AARONSON, M., HUCHRA, J., MOULD, J. R., TULLY, R. B., FISHER, J. R., VAN WOERDEN, H., GOSS, W. M., CHAMARAUX, P., MEBOLD, U., SIEGMAN, B., BERRIMAN, G., PERSSON, S. E. <AP. J. SUPPL., 50, 241> 821013
A CATALOG OF INFRARED MAGNITUDES AND H I VELOCITY WIDTHS FOR NEARBY GALAXIES.

AARONSON, M., MOULD, J. <AP. J. SUPPL., 48, 161> 820217
THE EXTENDED GIANT BRANCHES OF INTERMEDIATE AGE GLOBULAR CLUSTERS IN THE MAGELLANIC CLOUDS. II.

AARONSON, M., MOULD, J. <AP. J., 240, 804> 800907
CARBON STARS IN THE FORNAX DWARF SPHEROIDAL GALAXY.

AARONSON, M., MOULD, J., HUCHRA, J. <AP. J., 237, 655> 800506
A DISTANCE SCALE FROM THE INFRARED MAGNITUDE/H I VELOCITY WIDTH RELATION. I. THE CALIBRATION.

AARONSON, M., MOULD, J., HUCHRA, J., SULLIVAN III, W. T., SCHOMMER, R. A., BOTHUN, G. D. <AP. J., 239, 12> 800704
A DISTANCE SCALE FROM THE INFRARED MAGNITUDE/H I VELOCITY-WIDTH RELATION. III. THE EXPANSION RATE OUTSIDE THE LOCAL SUPERCLUSTER.

AARONSON, M., PERSSON, S. E., FROGEL, J. A. <AP. J., 245, 18> 810407
THE INFRARED COLOR-MAGNITUDE RELATION FOR EARLY-TYPE GALAXIES IN VIRGO AND COMA.

ABBOTT, D. C., BIEGING, J. H., CHURCHWELL, E. <AP. J., 250, 645> 819910
MASS LOSS FROM VERY LUMINOUS OB STARS AND THE CYGNUS SUPERBUBBLE.

ABELL, G. O. <AP. J., 144, 259> 669902
PROPERTIES OF SOME OLD PLANETARY NEBULAE.

ABOLINS, J. A., ADAMS, D. J., JAMESON, R. F., HOUGH, J. H., AXON, D. J. <M. N. R. A. S., 186, 23P> 790306
DETECTION OF A BRIGHT RIDGE IN THE 2.2-MICRON EMISSION OF M82.

ACKERMANN, G. <ASTR. AP., 8, 315> 701005
EXTREME RED STARS IN CYGNUS.

ACKERMANN, G., FUGMANN, G., HERMANN, W., VOELCKER, K. <ZEIT. FUR AP., 69, 130> 680903
NEUE INFRAROT-STERNE.

ADAM, G. <ASTR. AP. SUPPL., 29, 293> 779908
ACCURATE POSITIONS OF QUASARS AND QUASAR CANDIDATES SOUTH OF DECLINATION -45 DEGREES.

ADAMS, D. J., HOUGH, J. H. <M. N. R. A. S., 179, 73P> 770602
THE POLARIZATION OF THE GALACTIC CENTRE AT 2.2 MICRON.

ADAMS, T. F. <AP. J., 202, 114> 751105
A STUDY OF THE COMPACT NEBULAE VV 8 AND M3-27.

ADE, P. A. R., CLEGG, P. E., RATHER, J. D. G. <AP. J. (LETTERS), 189, L23> 740402
1-MILLIMETER OBSERVATIONS OF THE GALACTIC HII REGIONS M42 AND DR 21.

ADE, P. A. R., ROWAN-ROBINSON, M., CLEGG, P. E. <ASTR. AP., 53, 403> 761201
MILLIMETRE EMISSION FROM EXTRAGALACTIC OBJECTS. II. LUMINOSITIES, SPECTRA, AND CONTRIBUTION TO THE MICROWAVE BACKGROUND.

ADELMAN, S. J., SHORE, S. N. <A. J., 87, 665> 820414
SPECTROPHOTOMETRY OF THE RS CVN STARS. I. THE F, G, AND K STANDARDS.

AITKEN, D. K., BARLOW, M. J., ROCHE, P. F., SPENSER, P. M. <M. N. R. A. S., 192, 679> 800911
8-13 MICRON SPECTRA OF VERY LATE TYPE WOLF-RAYET STARS.

AITKEN, D. K., GRIFFITHS, J., JONES, B. <M. N. R. A. S., 179, 179> 770403
INFRARED LINE AND CONTINUUM SPATIAL STUDIES OF THE SOUTHERN HII REGION G333.6-0.2.

AITKEN, D. K., GRIFFITHS, J., JONES, B., PENMAN, J. M. <M. N. R. A. S., 174, 41P> 760206
FURTHER OBSERVATIONS OF IONIZED NEON IN THE GALACTIC CENTRE.

AITKEN, D. K., JONES, B. <AP. J., 184, 127> 730808
OBSERVATIONS OF THE INFRARED EXTINCTION OF IRS 5 IN W3 COMPARED WITH THE GALACTIC CENTER AND THE BECKLIN- NEUGEBAUER OBJECT.

AITKEN, D. K., JONES, B. <M. N. R. A. S., 165, 363> 730014
SOME FEATURES OF THE INFRA-RED SPECTRUM OF NGC 7027 AND AN ESTIMATE OF ITS SULPHUR ABUNDANCE.

AITKEN, D. K., JONES, B. <M. N. R. A. S., 167, 11P> 740407
OBSERVATIONS OF NE II IN THE COMPACT HII REGION G333.6-0.2.

AITKEN, D. K., JONES, B. <M. N. R. A. S., 172, 141> 750707
THE INFRARED SPECTRUM AND STRUCTURE OF ETA CARINAE.

AITKEN, D. K., JONES, B., BREGMAN, J. D., LESTER, D. F., RANK, D. M. <AP. J., 217, 103> 771003
SPECTRAL OBSERVATIONS OF ETA CARINAE AT 4 MICRONS.

AITKEN, D. K., JONES, B., PENMAN, J. M. <M. N. R. A. S., 169, 35P> 741111
DETECTION OF IONIZED NEON IN THE GALACTIC CENTRE.

AITKEN, D. K., POLDEN, P. G. <NAT. PHYS. SCI., 233, 45> 710904
MEASUREMENT OF THE 10 MICRON FLUX FROM THE CRAB NEBULA.

AITKEN, D. K., ROCHE, P. F. <M. N. R. A. S., 196, 39P> 810715
FURTHER INFRARED STUDIES OF THE PRE-MAIN-SEQUENCE OBJECT HD 97048.

AITKEN, D. K., ROCHE, P. F. <M. N. R. A. S., 200, 217> 820715
8-13 MICRON SPECTROPHOTOMETRY OF COMPACT PLANETARY NEBULAE AND EMISSION LINE OBJECTS.

AITKEN, D. K., ROCHE, P. F., ALLEN, D. A. <M. N. R. A. S., 200, 69P> 820914
THE INFRARED SPECTRUM OF GAMMA VELORUM.

AITKEN, D. K., ROCHE, P. F., ALLEN, M. C., PHILLIPS, M. M. <M. N. R. A. S., 199, 31P> 820514
A HIGH-EXCITATION OPTICALLY OBSCURED H II REGION IN THE NUCLEUS OF NGC 5253.

AITKEN, D. K., ROCHE, P. F., PHILLIPS, M. M. <M. N. R. A. S., 196, 101P> 810912
THE QUESTION OF EXTINCTION IN ACTIVE GALACTIC NUCLEI: INFRARED SPECTRAL OBSERVATIONS OF NGC 1614, NGC 7469, AND NGC 1275.

AITKEN, D. K., ROCHE, P. F., SPENSER, P. M. <M. N. R. A. S., 193, 207> 801010
8-13 MICRON SPECTROPHOTOMETRY OF V1016 CYG AND THE SHAPE OF THE 'SILICATE' FEATURE.

AITKEN, D. K., ROCHE, P. F., SPENSER, P. M., JONES, B. <AP. J., 233, 925> 791104
8-13 MICRON SPECTROPHOTOMETRY OF PLANETARY NEBULAE.

AITKEN, D. K., ROCHE, P. F., SPENSER, P. M., JONES, B. <ASTR. AP., 76, 60> 790611
INFRARED SPATIAL AND SPECTRAL STUDIES OF AN IONIZATION FRONT REGION IN THE ORION NEBULA.

AITKEN, D. K., ROCHE, P. F., SPENSER, P. M., JONES, B. <M. N. R. A. S., 195, 921> 810616
INFRARED SPECTRAL OBSERVATIONS OF THE BNKL COMPLEX IN ORION.

AITKEN, D., ROCHE, P., WHITMORE, B. <IAUC NO. 3717> 820711
NOVA AQUILAE 1982.

AKINCI, R., JAMESON, R. F. <ASTR. AP., 88, 320> 800814
J, K, L, INFRARED OBSERVATIONS OF RZ SCUTUM.

AKOPIAN, A. A., KIR'YAN, V. V., MELIK-ALAVERDIAN, YU. K., TOVMASSIAN, H. M. <ASTROFIZIKA, 16, 669> 801109
INFRARED PHOTOMETRY OF S STARS.

ALBERS, H. <AP. J., 182, 817> 739904
THE RED STAR IN THE OPEN CLUSTER TRUMPLER 27.

ALDUSEVA, V. YA., ESIPOV, V. F. <SOV. AST., 13, 83> 690706
THE 10830A HE I LINE IN THE ENVELOPE OF BETA LYRAE.

ALLEN, D. A. <AP. J. (LETTERS), 172, L55> 720302
INFRARED OBJECTS IN HII REGIONS.

ALLEN, D. A. <AP. J., 207, 367> 760706
THE NEAR-INFRARED CONTINUA OF EMISSION-LINE GALAXIES.

ALLEN, D. A. <AP. LETTERS, 20, 131> 800001
CANDIDATE SYMBIOTIC STARS IN THE LARGE MAGELLANIC CLOUD.

ALLEN, D. A. <IAUC NO. 3727> 820909
SUPERNOVA IN NGC 1332.

ALLEN, D. A. <M. N. R. A. S., 161, 145> 730001
NEAR INFRA-RED MAGNITUDES OF 248 EARLY-TYPE EMISSION-LINE STARS AND RELATED OBJECTS.

ALLEN, D. A. <M. N. R. A. S., 168, 1> 740708
INFRARED OBSERVATIONS OF NORTHERN EMISSION-LINE STARS.

ALLEN, D. A. <NATURE, 281, 284> 790902
INFRARED OBSERVATIONS OF SS433.

ALLEN, D. A. <NATURE, 284, 323> 800310
EMISSION AT 3.3 MICRONS AND EVIDENCE FOR DUST IN 3C273.

ALLEN, D. A., BAINES, D. W. T., BLADES, J. C., WHITTET, D. C. B. <M. N. R. A. S., 199, 1017> 820620
A SURVEY OF 3 MICRON EMISSION FEATURES IN STELLAR SPECTRA.

ALLEN, D. A., BARTON, J. R., GILLINGHAM, P. R. <M. N. R. A. S., 192, 805> 800913
AN INFRARED CANDIDATE FOR OH 205.1-14.1.

ALLEN, D. A., BARTON, J. R., GILLINGHAM, P. R., PHILLIPS, B. A. <M. N. R. A. S., 190, 531> 800211
THE NATURE OF OH 0739-14.

ALLEN, D. A., BARTON, J. R., WALLACE, P. T. <M. N. R. A. S., 196, 797> 810909
THE SIZE OF A WOLF-RAYET STAR'S DUST SHELL MEASURED BY SPECKKLE INTERFEROMETRY.

ALLEN, D. A., CHEREPASHCHUK, A. M. <M. N. R. A. S., 201, 521> 821114
THE ELLIPSOIDAL LIGHT CURVE OF VV PUPPIS.

ALLEN, D. A., GLASS, I. S. <AP. J., 210, 666> 761206
EMISSION-LINE STARS IN THE LARGE MAGELLANIC CLOUD: SPECTROSCOPY AND INFRARED PHOTOMETRY.

ALLEN, D. A., GLASS, I. S. <M. N. R. A. S., 167, 337> 740503
INFRARED PHOTOMETRY OF SOUTHERN EMISSION-LINE STARS.

ALLEN, D. A., GLASS, I. S. <M. N. R. A. S., 170, 579> 750302
EMISSION-LINE STARS WITH INFRARED DUST EMISSION: IMPLICATIONS OF THE GALACTIC DISTRIBUTION.

ALLEN, D. A., HYLAND, A. R., CASWELL, J. L. <M. N. R. A. S., 192, 505> 800810
ROBERTS 22: A BIPOLAR NEBULA WITH OH EMISSION.

ALLEN, D. A., HYLAND, A. R., LONGMORE, A. J. <M. N. R. A. S., 175, 61P> 760512
A FIRST LOOK AT THE AFCRL INFRARED SKY SURVEY CATALOGUE.

ALLEN, D. A., HYLAND, A. R., LONGMORE, A. J., CASWELL, J. L.,GOSS, W. M., HAYNES, R. F. <AP. J., 217, 108> 771005
OPTICAL, INFRARED, AND RADIO STUDIES OF AFCRL SOURCES.

ALLEN, D. A., PENSTON, M. V. <M. N. R. A. S., 172, 245> 750705
INFRARED SOURCES IN OBSCURED REGIONS.

ALLEN, D. A., SMITH, M. G., WRIGHT, A. E. <IAUC NO. 3274> 780912
NGC 7213.

ALLEN, D. A., STROM, K. M., GRASDALEN, G. L., STROM, S. E., MERRILL, K. M. <M. N. R. A. S., 173, 47P> 751007
HARO 13A: A LUMINOUS, HEAVILY OBSCURED STAR IN ORION.

ALLEN, D. A., SWINGS, J. P. <AP. J., 174, 583> 720602
THE PECULIAR NEBULA M2-9.

ALLEN, D. A., SWINGS, J. P. <AP. LETTERS, 10, 83> 720004
INFRARED EXCESSES AND FORBIDDEN EMISSION LINES IN EARLY-TYPE STARS.

ALLEN, D. A., SWINGS, J. P. <ASTR. AP., 47, 293> 760301
THE SPECTRA OF PECULIAR BE STARS WITH INFRARED EXCESSES.

ALLEN, D. A., SWINGS, J. P., HARVEY, P. M. <ASTR. AP., 20, 333> 720907
INFRARED PHOTOMETRY OF NORTHERN WOLF-RAYET STARS.

ALLEN, D. A., WARD, M. J., HYLAND, A. R. <M. N. R. A. S., 199, 969> 820618
THE NEAR-INFRARED CONTINUA OF BL LACERTAE OBJECTS.

ALLEN, D. A., WARD, M. J., WRIGHT, A. E. <M. N. R. A. S., 195, 155> 810414
THE ECLIPSING AM HERCULIS STAR 2A0311-227.

ALLEN, D. A., WICKRAMASINGHE, D. T. <NATURE, 294, 239> 811113
DIFFUSE INTERSTELLAR ABSORPTION BANDS BETWEEN 2.9 AND 4.0 MICRONS.

ALLEN, D. A., WRIGHT, A. E., GOSS, W. M. <M. N. R. A. S., 177, 91> 761008
THE DWARF EMISSION GALAXY HE 2-10.

ALLEN, R. J., RAIMOND, E. <ASTR. AP., 18, 317> 729905
A RADIO MAP OF THE SPIRAL GALAXY MAFFEI 2 AT 1415 MHZ.

ALTAMORE, A., BARATTA, G. B., CASSATELLA, A., FRIEDJUNG, M. <AP. J., 245, 630> 810403
ULTRAVIOLET AND COORDINATED GROUND-BASED OBSERVATIONS OF Z ANDROMEDAE.

ALTAMORE, A., BARATTA, G. B., CASSATELLA, A., GRASDALEN, G. L., PERSI, P., VIOTTI, R. <ASTR. AP., 90, 290> 801011
ULTRAVIOLET, OPTICAL, AND INFRARED OBSERVATIONS OF THE HERBIG BE STAR HD 200775.

ALTAMORE, A., SMRIGLIO, F., BUSSOLETTI, E., CORSI, C. E., ROSSI, L. <AP. AND SP. SCI., 72, 159> 809903
A SEARCH FOR CARBON STARS IN THE AFGL CATALOGUE.

ANANTH, A. G., NAGARAJA, B. V. <AP. J., 259, 664> 829904
IDENTIFICATION OF ACTIVE STAR FORMATION REGIONS IN THE GALACTIC PLANE.

ANDERSSON, C., JOHANSSON, L. E. B., GOSS, W. M., WINNBERG, A., NGUYEN-QUANG-RIEU <ASTR. AP., 30, 475> 749902
OH 26.5+0.6 - A STRONG OH SOURCE AT 1612 MHZ.

ANDREWS, A. D. <CONTR. ARMAGH OBS., 1, 101> 749908
CATALOGUE OF PHOTOMETRIC AND ASTROMETRIC DATA FOR 4117 STARS IN THE ORION NEBULA AGGREGATE.

ANDREWS, P. J., GLASS, I. S., HAWARDEN, T. G. <M. N. R. A. S., 168, 7P> 740709
PHOTOMETRY OF AP LIB AND PKS 0521-36.

ANDRIESSE, C. D., DE VRIES, J. S. <ASTR. AP., 46, 143> 760101
INFRARED OBSERVATIONS OF M17S AT MEDIUM SPATIAL AND SPECTRAL RESOLUTION.

ANDRILLAT, Y. <MEM. SOC. ROY. DES SCI. DE LIEGE, 9, 355> 760001
SPECTRES DES ETOILES CHAUDES ET DES NEBULEUSES PLANETAIRES DANS LE PROCHE INFRAROUGE (82000-11000A).

ANDRILLAT, Y., BARANNE, A., HOUZIAUX, L. <ASTR. AP., 41, 99> 750610
SPECTRES DE QUELQUES NEBULEUSES PLANETAIRES ENTRE 8000 ET 11000 A.

ANDRILLAT, Y., COLLIN-SOUFFRIN, S. <ASTR. AP., 43, 419> 751010
SPECTRES DE NOYAUX DE GALAXIES DE SEYFERT ENTRE 8000 ET 11000 A.

ANDRILLAT, Y., DUCHESNE, M. <ASTR. AP., 35, 467> 740212
MORPHOLOGIE DE LA REGION CENTRALE DE LA NEBULEUSE D'ORION DANS LE PROCHE INFRAROUGE.

ANDRILLAT, Y., HOUZIAUX, L. <ASTR. AP., 52, 119> 761001
SPECTRAL VARIATIONS OF HBV 475 IN THE NEAR INFRARED.

ANDRILLAT, Y., SWINGS, J. P. <AP. J. (LETTERS), 204, L123> 760305
8200 TO 11200A SPECTRA OF PECULIAR EMISSION-LINE OBJECTS WITH INFRARED EXCESS.

ANDRILLAT, Y., SWINGS, J. P. <AP. LETTERS, 18, 151> 770002
8000-11000A SPECTRA OF EMISSION-LINE GALAXIES WITH INFRARED EXCESSES.

ANDRILLAT, Y., VREUX, J. M. <ASTR. AP., 41, 133> 750611
SPECTRES D'ETOILES DE TYPE O ET DE TYPE WOLF-RAYET ENTRE 0, 8 ET 1, 1 MICRONS.

ANDRILLAT, Y., VREUX, J. M. <ASTR. AP., 76, 221> 790704
THE HE 10830A EMISSION LINE IN O STAR SPECTRA.

ANGEL, J. R. P., LANDSTREET, J. D., OKE, J. B. <AP. J. (LETTERS), 171, L11> 720102
THE SPECTRAL DEPENDENCE OF CIRCULAR POLARIZATION IN GRW+70 8247.

APPARAO, K. M. V., ALLEN, D. <ASTR. AP., 107, L5> 820307
INFRARED SCANS OF GAMMA RAY BURST SOURCE REGIONS.

ARDEBERG, A., VIRDEFORS, B. <ASTR. AP. SUPPL., 40, 307> 800613
A CATALOGUE OF STELLAR SPECTROPHOTOMETRIC DATA.

ARGELANDER, F. W. A. <ASTRON. BEOB. STERNWARTE KONIGL. RHEIN, 3-5, BONN> 598901
BONNER STERNVERZEICHNIS, SECTIONS 1-3.

ARGUE, A. N. <M. N. R. A. S., 135, 23> 670103
RED AND INFRA-RED MAGNITUDES AND COLOURS FOR 300 F, G, AND K TYPE STARS.

ARGYLE, R. <IAUC NO. 3673> 829901
NOVA AQUILAE 1982.

ARGYLE, R. W. <IAUC NO. 3348> 799905
NOVALIKE OBJECT IN VULPECULA (NOVA VULPECULAE 1979?).

ARNOLD, E. M., KREYSA, E., SCHULTZ, G. V., SHERWOOD, W. A. <ASTR. AP., 70, L1> 781010
1MM CONTINUUM OBSERVATIONS OF SOUTHERN HII REGIONS.

ARP, H. C. <A. J., 63, 273> 589904
SOUTHERN HEMISPHERE PHOTOMETRY. III. THE COLOR-MAGNITUDE DIAGRAM OF NGC 419 AND THE ADJOINING FIELD IN THE SMALL MAGELLANIC CLOUD.

ARP, H. C. <A. J., 63, 487> 589905
SOUTHERN HEMISPHERE PHOTOMETRY. V. THE COLOR-MAGNITUDE DIAGRAM OF NGC 361 AND THE ADJOINING FIELD IN THE SMALL MAGELLANIC CLOUD.

AUGASON, G. C., TAYLOR, B. J., STRECKER, D. W., ERICKSON, E. F., WITTEBORN, F. C. <AP. J., 235, 138> 800104
COMPARISON OF PREDICTED AND OBSERVED SPECTRAL ENERGY DISTRIBUTION OF K AND M STARS. I. ALPHA BOOTIS.

AUMANN, H. H., LOW, F. J. <AP. J. (LETTERS), 159, L159> 700305
FAR-INFRARED OBSERVATIONS OF THE GALACTIC CENTER.

AVETISSIAN, V. Z., MELIK-ALAVERDIAN, YU. K. <ASTROFIZIKA, 18, 386> 820825
MOLECULAR ABSORPTION BANDS IN IR SPECTRA OF M GIANTS.

AVETISYAN, V. Z., KIR'YAN, V. V., POGODIN, M. A., SHAKHBAZYAN, YU. L. <ASTROFIZIKA, 15, 229> 790413
SPECTRAL ENERGY DISTRIBUTION OF SOME STARS OF EARLY SPECTRAL CLASSES WITH GAS-DUST ENVELOPES.

AXON, D. J., ALLEN, D. A., BAILEY, J., HOUGH, J. H., WARD, M. J., JAMESON, R. F. <M. N. R. A. S., 200, 239> 820716
THE VARIABLE INFRARED SOURCE NEAR HH100.

AXON, D. J., BAILEY, J., HOUGH, J. H. <NATURE, 299, 234> 820915
DISCOVERY OF A VERY RED NUCLEUS IN THE RADIO ELLIPTICAL IC 5063 (PKS2048-57).

BAHNG, J. <M. N. R. A. S., 143, 73> 690405
INFRA-RED COLOURS OF G, K, AND M STARS.

BAHNG, J. <P. A. S. P., 81, 863> 691202
INFRARED COLOR INDICES OF CARBON STARS.

BAILEY, J., CUNNINGHAM, E. C., HOUGH, J. H., AXON, D. J. <M. N. R. A. S., 197, 627> 811110
INFRARED AND OPTICAL POLARIZATION OF MARKARIAN 421.

BAILEY, J., GILES, A. B., WATTS, D. J., GREENHILL, J. G. <IAUC NO. 3720> 820815
H 0139-68.

BAILEY, J., HANES, D. A., WATTS, D. J., GILES, A. B., GREENHILL, J. G. <IAUC NO. 3712> 820710
CW 1103+254.

BAILEY, J., HOUGH, J. H. <P. A. S. P., 94, 618> 820610
A SIMULTANEOUS INFRARED/OPTICAL POLARIMETER.

BAILEY, J., HOUGH, J. H., AXON, D. J. <NATURE, 285, 306> 800514
IR PHOTOMETRY AND POLARIMETRY OF 2A0311-227.

BAILEY, J., HOUGH, J. H., AXON, D. J., GATLEY, I., LEE, T. J., SZKODY, P., STOKES, G., BERRIMAN, G. <M. N. R. A. S., 199, 801> 820615
A MULTIWAVELENGTH STUDY OF THE AM HERCULIS TYPE BINARY 2A 0311-227.

BAILEY, J., SHERRINGTON, M. R., GILES, A. B., JAMESON, R. F. <M. N. R. A. S., 196, 121> 810713
INFRARED LIGHT CURVES OF THE DWARF NOVA Z CHAMAELEONTIS.

BALDWIN, J. A., WAMPLER, E. J., BURBIDGE, E. M., O'DELL, S. L., SMITH, H. E., HAZARD, C., NORDSIECK, K.H.,POOLEY, G., STEIN, W. A. <AP. J., 215, 408> 770709
1400+162—AN EXTENDED RADIO SOURCE IDENTIFIED WITH A BL LACERTAE OBJECT IN A GROUP OF GALAXIES.

BALDWIN, J. R., FROGEL, J. A., PERSSON, S. E. <AP. J., 184, 427> 730905
THE STRENGTHS OF INFRARED CO AND H2O BANDS IN LATE-TYPE STARS.

BALLY, J., JOYCE, R. R., SCOVILLE, N. Z. <AP. J., 229, 917> 790506
NEAR-INFRARED OBSERVATIONS OF IONIZED HYDROGEN AT THE CORE OF THE GALAXY.

BALLY, J., LANE, A. P. <AP. J., 257, 612> 820605
OBSERVATIONS OF 2 MICRON MOLECULAR HYDROGEN EMISSION FROM NGC 2071, CEPHEUS A, AND GL 961.

BALLY, J., SCOVILLE, N. Z. <AP. J., 239, 121> 800706
STRUCTURE AND EVOLUTION OF MOLECULAR CLOUDS NEAR H II REGIONS. I. CO OBSERVATIONS OF AN EXPANDING MOLECULAR SHELL SURROUNDING THE PELICAN NEBULA.

BALUTEAU, J. -P., BUSSOLETTI, E., ANDEREGG, M., MOORWOOD, A. F. M., CORON, N. <AP. J. (LETTERS), 210, L45> 761106
INFRARED LINE EMISSION FROM THE ORION NEBULA: DETECTION OF (S III) (18.71 MICRONS) AND (O III) (88.35 MICRONS).

BALUTEAU, J. -P., MOORWOOD, A. F. M., BIRAUD, Y., CORON, N., ANDEREGG, M., FITTON, B. <AP. J., 244, 66> 810208
INFRARED LINE EMISSION FROM H II REGIONS. IV. AIRBORNE OBSERVATIONS OF NGC 7538, W49, AND M8.

BALZANO, V. A., WEEDMAN, D. W. <AP. J., 243, 756> 810207
THE NEAR-INFRARED PROPERTIES OF GALACTIC NUCLEI.

BARLOW, M. J., COHEN, M. <AP. J., 213, 737> 770504
INFRARED PHOTOMETRY AND MASS LOSS RATES FOR OBA SUPERGIANTS AND OF STARS.

BARLOW, M. J., SMITH, L. J., WILLIS, A. J. <M. N. R. A. S., 196, 101> 810711
MASS-LOSS FOR 21 WOLF-RAYET STARS.

BARNES, T. G., BEER, R., HINKLE, K. H., LAMBERT, D. L. <AP. J., 213, 71> 770405
A HIGH-RESOLUTION INFRARED SPECTRUM OF IRC +10216.

BARNES, T. G., LAMBERT, D. L., POTTER, A. E. <AP. J., 187, 73> 740102
INFRARED SPECTRA OF GAMMA 2 VELORUM AND ZETA PUPPIS.

BARTON, J. R., PHILLIPS, B. A., ALLEN, D. A. <M. N. R. A. S., 187, 813> 790602
STEAM IN RX PUPPIS.

BASCHEK, B., WEHRSE, R. <P. A. S. P., 89, 345> 770614
COMMENTS ON THE PAPER BY A. E. RYDGREN "T TAURI STARS AND THE (J-H), (H-K) DIAGRAM".

BAUMERT, J. H. <A. J., 79, 1287> 741101
COMPARISON OF A GENERAL CATALOGUE OF COOL CARBON STARS AND THE TWO-MICRON SKY SURVEY.

BAUMERT, J. H. <AP. J., 190, 85> 740506
MEAN ABSOLUTE MAGNITUDES OF CARBON STARS AND RELATED OBJECTS.

BAUMERT, J. H. <P. A. S. P., 85, 205> 730307
ON THE VARIABILITY OF CASE 621 AND MSB 57.

BEALL, J. H., ROSE, W. K., DENNIS, B. R., CRANNELL, C. J., DOLAN, J. F., FROST, K. J., ORWIG, L. E. <AP. J., 247, 458> 810708
CONCURRENT RADIO, INFRARED, OPTICAL, AND X-RAY OBSERVATIONS OF THE NUCLEUS OF THE SEYFERT GALAXY NGC 4151.

BECHIS, K. P., HARVEY, P. M., CAMPBELL, M. F., HOFFMANN, W. F. <AP. J., 226, 439> 781207
STAR FORMATION IN THE NGC 7129 REGION: A CO MOLECULAR-LINE AND FAR-INFRARED CONTINUUM STUDY.

BECK, S. C., BLOEMHOF, E. E., SERABYN, E., TOWNES, C. H., TOKUNAGA, A. T., LACY, J. H., SMITH, H. A. <AP. J. (LETTERS), 253, L83> 820209
HIGH SPECTRAL AND SPATIAL RESOLUTION OBSERVATIONS OF THE 12.28 MICRON EMISSION FROM H2 IN THE ORION MOLECULAR CLOUD.

BECK, S. C., LACY, J. H., BAAS, F., TOWNES, C. H. <AP. J., 226, 545> 781208
NE II 12.8 MICRON EMISSION AND GALACTIC DYNAMICS IN M82.

BECK, S. C., LACY, J. H., GEBALLE, T. R. <AP. J., 231, 28> 790701
NE II EMISSION AND GALACTIC DYNAMICS IN NGC 253.

BECK, S. C., LACY, J. H., GEBALLE, T. R. <AP. J. (LETTERS), 234, L213> 791207
DETECTION OF THE 12.28 MICRON ROTATIONAL LINE OF MOLECULAR HYDROGEN IN THE ORION MOLECULAR CLOUD.

BECK, S. C., LACY, J. H., TOWNES, C. H., ALLER, L. H., GEBALLE, T. R., BAAS, F. <AP. J., 249, 592> 811008
THE ABUNDANCES OF NEON, SULFUR, AND ARGON IN PLANETARY NEBULAE.

BECKLIN, E. E., BECKWITH, S., GATLEY, I., MATTHEWS, K., NEUGEBAUER, G., SARAZIN, C., WERNER, M. W. <AP. J., 207, 770> 760805
INFRARED STUDIES OF AN IONIZATION FRONT REGION IN THE ORION NEBULA.

BECKLIN, E. E., FOMALONT, E. B., NEUGEBAUER, G. <AP. J. (LETTERS), 181, L27> 730401
INFRARED AND RADIO OBSERVATIONS OF THE NUCLEUS OF NGC 253.

BECKLIN, E. E., FROGEL, J. A., HYLAND, A. R., KRISTIAN, J., NEUGEBAUER, G. <AP. J. (LETTERS), 158, L133> 691201
THE UNUSUAL INFRARED OBJECT IRC+10216.

BECKLIN, E. E., FROGEL, J. A., KLEINMANN, D. E., NEUGEBAUER, G., NEY, E. P., STRECKER, D. W. <AP. J. (LETTERS), 170, L15> 711102
INFRARED OBSERVATIONS OF THE CORE OF CENTAURUS A, NGC 5128.

BECKLIN, E. E., FROGEL, J. A., KLEINMANN, D. E., NEUGEBAUER, G., PERSSON, S. E., WYNN-WILLIAMS, C. G. <AP. J., 187, 487> 740204
INFRARED EMISSION FROM THE SOUTHERN HII REGION H2-3.

BECKLIN, E. E., FROGEL, J. A., NEUGEBAUER, G., PERSSON, S. E., WYNN-WILLIAMS, C. G. <AP. J. (LETTERS), 182, L125> 730604
THE HII REGION G333.6-0.2, A VERY POWERFUL 1-20 MICRON SOURCE.

BECKLIN, E. E., GATLEY, I., MATTHEWS, K., NEUGEBAUER, G., SELLGREN, K., WERNER, M. W., WYNN-WILLIAMS, C. G. <AP. J., 236, 441> 800302
INFRARED EMISSION AND STAR FORMATION IN THE CENTRAL REGIONS OF THE GALAXY IC 342.

BECKLIN, E. E., GATLEY, I., WERNER, M. W. <AP. J., 258, 135> 820701
FAR-INFRARED OBSERVATIONS OF SAGITTARIUS A: THE LUMINOSITY AND DUST DENSITY IN THE CENTRAL PARSEC OF THE GALAXY.

BECKLIN, E. E., HANSEN, O., KIEFFER, H., NEUGEBAUER, G. <A. J., 78, 1063> 731212
STELLAR FLUX CALIBRATION AT 10 AND 20 MICRONS USING MARINER 6, 7, AND 9 RESULTS.

BECKLIN, E. E., HAWKINS, F. J., MASON, K. O., MATTHEWS, K., NEUGEBAUER, G., PACKMAN, D., SANFORD, P. W., SCHUPLER, B. R., STARK, A., WYNN-WILLIAMS, C. G. <AP. J. (LETTERS), 192, L119> 740905
INFRARED, RADIO, AND X-RAY OBSERVATIONS OF CYGNUS X-3.

BECKLIN, E. E., KLEINMANN, D. E. <AP. J. (LETTERS), 152, L25> 680405
INFRARED OBSERVATIONS OF THE CRAB NEBULA.

BECKLIN, E. E., KRISTIAN, J., MATTHEWS, K., NEUGEBAUER, G. <AP. J. (LETTERS), 186, L137> 731204
MEASUREMENTS OF THE CRAB PULSAR AT 2.2 AND 3.5 MICRONS.

BECKLIN, E. E., KRISTIAN, J., NEUGEBAUER, G., WYNN-WILLIAMS, C. G. <NAT. PHYS. SCI., 239, 130> 721008
DISCOVERY OF INFRARED EMISSION FROM THE RADIO SOURCE NEAR CYGNUS X-3.

BECKLIN, E. E., MATTHEWS, K., NEUGEBAUER, G., WILLNER, S. P. <AP. J., 219, 121> 780109
INFRARED OBSERVATIONS OF THE GALACTIC CENTER. I. NATURE OF THE COMPACT SOURCES.

BECKLIN, E. E., MATTHEWS, K., NEUGEBAUER, G., WILLNER, S. P. <AP. J., 220, 831> 780307
INFRARED OBSERVATIONS OF THE GALACTIC CENTER. IV. THE INTERSTELLAR EXTINCTION.

BECKLIN, E. E., MATTHEWS, K., NEUGEBAUER, G., WYNN-WILLIAMS, C. G. <AP. J. (LETTERS), 186, L69> 731201
THE SIZE OF NGC 1068 AT 10 MICRONS.

BECKLIN, E. E., MATTHEWS, K., NEUGEBAUER, G., WYNN-WILLIAMS, C. G. <ASTR. AP., 55, 19> 770202
ON THE INFRARED EMISSION FROM SGR B2.

BECKLIN, E. E., NEUGEBAUER, G. <AP. J. (LETTERS), 157, L31> 690704
1.65-19.5 MICRON OBSERVATIONS OF THE GALACTIC CENTER.

BECKLIN, E. E., NEUGEBAUER, G. <AP. J. (LETTERS), 200, L71> 750903
HIGH-RESOLUTION MAPS OF THE GALACTIC CENTER AT 2.2 AND 10-MICRONS.

BECKLIN, E. E., NEUGEBAUER, G. <AP. J., 147, 799> 670202
OBSERVATIONS OF AN INFRARED STAR IN THE ORION NEBULA.

BECKLIN, E. E., NEUGEBAUER, G. <AP. J., 151, 145> 680101
INFRARED OBSERVATIONS OF THE GALACTIC CENTER.

BECKLIN, E. E., NEUGEBAUER, G. <P. A. S. P., 90, 657> 781221
2.2-MICRON MAP OF THE CENTRAL 1 DEGREE OF THE GALACTIC CENTER.

BECKLIN, E. E., NEUGEBAUER, G. <HII REGIONS AND THE GALACTIC CENTER, ESRO, 39> 740001
INFRARED OBSERVATION OF NGC 6334.

BECKLIN, E. E., NEUGEBAUER, G., HAWKINS, F. J., MASON, K. O.,SANFORD, P. W., MATTHEWS, K., WYNN-WILLIAMS, C. G. <NATURE, 245, 302> 731009
INFRARED AND X-RAY VARIABILITY OF CYG X-3.

BECKLIN, E. E., NEUGEBAUER, G., WYNN-WILLIAMS, C. G. <AP. J. (LETTERS), 182, L7> 730502
ON THE NATURE OF THE INFRARED POINT SOURCE IN THE ORION NEBULA.

BECKLIN, E. E., NEUGEBAUER, G., WYNN-WILLIAMS, C. G. <AP. LETTERS, 13, 147> 730025
INFRARED EMISSION FROM THE OH/H2O SOURCES IN W49.

BECKLIN, E. E., NEUGEBAUER, G., WYNN-WILLIAMS, C. G. <AP. LETTERS, 15, 87> 730016
THE SPATIAL DISTRIBUTION OF THE INFRARED EMISSION FROM NGC 7027.

BECKLIN, E. E., TOKUNAGA, A. T., WYNN-WILLIAMS, C. G. <AP. J., 263, 624> 821204
THE INFRARED EMISSION FROM THE ELLIPTICAL GALAXY NGC 1052.

BECKMAN, J. E., BASTIN, J. A., CLEGG, P. E. <NATURE, 221, 944> 690308
CONTINUOUS SPECTRUM OF TAURUS A AT 1.2 MM WAVELENGTH.

BECKWITH, S., EVANS II, N. J., BECKLIN, E. E., NEUGEBAUER, G. <AP. J., 208, 390> 760905
INFRARED OBSERVATIONS OF MONOCEROS R2.

BECKWITH, S., GATLEY, I., MATTHEWS, K., NEUGEBAUER, G. <AP. J. (LETTERS), 223, L41> 780705
MOLECULAR HYDROGEN EMISSION FROM T TAURI STARS.

BECKWITH, S., NEUGEBAUER, G., BECKLIN, E. E., MATTHEWS, K. <A. J., 85, 886> 800702
MOLECULAR HYDROGEN EMISSION IN NGC 7027.

BECKWITH, S., PERSSON, S. E., GATLEY, I. <AP. J. (LETTERS), 219, L33> 780111
DETECTION OF MOLECULAR HYDROGEN EMISSION FROM FIVE PLANETARY NEBULAE.

BECKWITH, S., PERSSON, S. E., NEUGEBAUER, G., BECKLIN, E. E. <AP. J., 223, 464> 780708
OBSERVATIONS OF THE MOLECULAR HYDROGEN EMISSION FROM THE ORION NEBULA.

BECKWITH, S., ZUCKERMAN, B. <AP. J., 255, 536> 820407
MOLECULAR HYDROGEN EMISSION FROM W51.

BEER, R., HUTCHISON, R. B., NORTON, R. H., LAMBERT, D. L. <AP. J., 172, 89> 720203
ASTRONOMICAL INFRARED SPECTROSCOPY WITH A CONNES-TYPE INTERFEROMETER. III. ALPHA ORIONIS, 2600-3450 INVERSE CM.

BEER, R., LAMBERT, D. L., SNEDEN, C. <P. A. S. P., 86, 806> 741016
THE SILICON MONOXIDE RADICAL AND THE ATMOSPHERE OF ALPHA ORIONIS.

BEICHMAN, C. A., DYCK, H. M., SIMON, T. <ASTR. AP., 62, 261> 780101
A HIGH SPATIAL RESOLUTION MAP OF THE ORION NEBULA AT 33 MICRONS.

BEICHMAN, C. A., NEUGEBAUER, G., SOIFER, B. T., WOOTTEN, H. A., ROELLIG, T., HARVEY, P. M. <NATURE, 293, 711> 811016
COMPACT RADIO SOURCE 1413+135 IS A FAR-IR EXTRAGALACTIC OBJECT.

BEICHMAN, C. A., PRAVDO, S.H., NEUGEBAUER, G., SOIFER, B. T.,MATTHEWS, K., WOOTEN, H. A. <AP. J., 247, 780> 810803
EXTREMELY RED COMPACT RADIO SOURCES: THE EMPTY FIELD OBJECTS.

BEICHMAN, C., HARRIS, S. <AP. J., 245, 589> 810402
THE FORMATION OF A T TAURI STAR: OBSERVATIONS OF THE INFRARED SOURCE IN L1551.

BELL, R. A., GUSTAFSSON, B., NORDH, H. L., OLOFSSON, S. G. <ASTR. AP., 46, 391> 760202
THE LUMINOSITY DEPENDENCE OF THE 1.65 MICRON FLUX FROM K AND EARLY M STARS. OBSERVATIONS AND INTERPRETATION.

BELTON, M. J. S., WOOLF, N. J. <AP. J., 141, 145> 650107
THE PROBLEM OF BETA LYRAE. I. SIX-COLOR PHOTOMETRY.

BELYAKINA, T. S., EFIMOV, YU. S., PAVLENKO, E. P., SHENAVRIN, V. I. <SOV. AST., 26, 1> 820116
OBJECT KUWANO, A NOVALIKE (SYMBIOTIC?) BINARY WITH A RED GIANT: PHOTOMETRY AND POLARIMETRY.

BENSAMMAR, S., FRIEDJUNG, M., ASSUS, P. <ASTR. AP., 83, 261> 800307
INFRARED OBSERVATIONS OF KUWANO'S NOVALIKE OBJECT.

BENSAMMAR, S., KANDEL, R., ASSUS, P., JOURNET, A. <ASTR. AP., 70, 585> 781110
UPPER LIMITS TO THE DIAMETER OF VY CANIS MAJORIS.

BENTLEY, A. F. <A. J., 87, 1810> 821211
SPATIAL OBSERVATIONS OF DUST EMISSION IN NGC 7027.

BERGEAT, J., LUNEL, M. <ASTR. AP., 87, 139> 800712
IJHKL PHOTOMETRY OF CARBON STARS.

BERGEAT, J., SIBILLE, F., LUNEL, M. <ASTR. AP., 40, 347> 750506
AN INFRARED POINT-SOURCE IN SHARPLESS 149.

BERGEAT, J., SIBILLE, F., LUNEL, M., LEFEVRE, J. <ASTR. AP., 52, 227> 761005
CARBON STARS AND CIRCUMSTELLAR SHELLS.

BERGEAT, J., VAN'T VEER, F., LUNEL, M., GARNIER, R., SIBILLE, F., ROUX, S. <ASTR. AP., 94, 350> 810217
INFRARED LIGHT CURVES OF THE CONTACT BINARY 44 I BOOTIS.

BERGEAT, J., VAN'T VEER, F., LUNEL, M., GARNIER, R., SIBILLE, F., ROUX, S. <ASTR. AP. SUPPL., 43, 257> 810221
INFRARED LIGHT CURVES OF THE CONTACT BINARY 44 I BOOTIS.

BERNAT, A. P., BARNES, T. G., SCHUPLER, B. R., POTTER, A. E. <P. A. S. P., 89, 541> 770809
INFRARED SPECTRA OF THE WN STARS HD 50896 AND HD 151932.

BERNAT, A. P., HALL, D. N. B., HINKLE, K. H., RIDGWAY, S. T. <AP. J. (LETTERS), 233, L135> 791103
OBSERVATIONS OF CO CIRCUMSTELLAR ABSORPTION IN THE 4.6 MICRON SPECTRUM OF ALPHA ORIONIS.

BERTOLA, F., D'ODORICO, S., FORD JR., W. K., RUBIN, V. C. <AP. J. (LETTERS), 157, L27> 690703
OBSERVATIONS OF M82 IN THE OPTICAL INFRARED.

BESSELL, M. S. <AP. J. (LETTERS), 149, L67> 670802
A DIFFERENT INTERPRETATION OF RHO PUPPIS.

BIDELMAN, W. P. <PUBL. WARNER AND SWASEY OBS., 2, 185> 809915
SPECTRAL CLASSIFICATIONS FOR THE STARS OF THE CALTECH TWO-MICRON SURVEY.

BLACK, J. H., GALLAGHER, J. S. <NATURE, 261, 296> 760515
THE INFRARED SPECTRUM OF NOVA CYGNI 1975.

BLACKWELL, D. E., SHALLIS, M. J. <M. N. R. A. S., 180, 177> 770702
STELLAR ANGULAR DIAMETERS FROM INFRARED PHOTOMETRY. APPLICATION TO ARCTURUS AND OTHER STARS; WITH EFFECTIVE TEMPERATURES.

BLACKWELL, D. E., SHALLIS, M. J., SELBY, M. J. <M. N. R. A. S., 188, 847> 790903
THE INFRARED FLUX METHOD FOR DETERMINING STELLAR ANGULAR DIAMETERS AND EFFECTIVE TEMPERATURES.

BLACKWELL, S. R., PURTON, C. R. <ASTR. AP. SUPPL., 46, 181> 819914
OPTICAL POSITIONS FOR NORTHERN STELLAR PLANETARY NEBULAE.

BLADES, J. C., WHITTET, D. C. B. <M. N. R. A. S., 191, 701> 800605
OBSERVATIONS OF UNIDENTIFIED INFRARED FEATURES IN THE PRE-MAIN SEQUENCE STAR HD 97048.

BLAIR, G. N., EVANS II, N. J., VANDEN BOUT, P. A., PETERS III, W. L. <AP. J., 219, 896> 780203
THE ENERGETICS OF MOLECULAR CLOUDS. II. THE S140 MOLECULAR CLOUD.

BLANCO, V. M., HANSEN, O. L. <A. J., 79, 1052> 741003
CLASSIFICATION OF UNIDENTIFIED SOURCES FROM A 2-MICRON SOUTHERN SKY SURVEY.

BLANCO, V. M., MCCARTHY S. J., M. F., BLANCO, B. M. <AP. J., 242, 938> 809910
CARBON AND LATE M-TYPE STARS IN THE MAGELLANIC CLOUDS.

BLANCO, V. M., NASSAU, J. J. <AP. J., 125, 408> 579901
REDDENED EARLY M- AND S-TYPE STARS IN TWO GALACTIC ZONES.

BLITZ, L., ISRAEL, F. P., NEUGEBAUER, G., GATLEY, I., LEE, T. J., BEATTIE, D. H. <AP. J., 249, 76> 811005
THE LARGEST H II REGIONS IN M101.

BOEHM, K. H., BRUGEL, E. W., MANNERY, E. <AP. J. (LETTERS), 235, L137> 800203
VERY LOW-EXCITATION HERBIG-HARO OBJECTS.

BOEHM, K. H., SIEGMUND, W. A., SCHWARTZ, R. D. <AP. J., 203, 399> 760106
EMISSION-LINE SPECTRA OF INDIVIDUAL CONDENSATIONS OF HERBIG-HARO OBJECTS.

BOEHM, K. H., SIEGMUND, W. A., SCHWARTZ, R. D. <ASTR. AP., 50, 361> 760801
SPECTROPHOTOMETRY OF R MONOCEROTIS.

BOISSE, P., GISPERT, R., CORON, N., WIJNBERGEN, J. J., SERRA, G., RYTER, C., PUGET, J. L. <ASTR. AP., 94, 265> 810214
A FAR-INFRARED SURVEY OF THE MILKY WAY FROM SAGITTARIUS TO CYGNUS: EVIDENCE FOR LARGE SCALE VARIATIONS OF THE STAR FORMATION RATE AND INITIAL MASS FUNCTION.

BOKSENBERG, A., SHORTRIDGE, K., ALLEN, D. A., FOSBURY, R. A. E., PENSTON, M. V., SAVAGE, A. <M. N. R. A. S., 173, 381> 751108
NEW OBSERVATIONS OF THE OPTICAL SPECTRUM OF THE SEYFERT GALAXY NGC 4151.

BOLEY, F., WOLFSON, R., BRADT, H., DOXSEY, R., JERNIGAN, G., HILTNER, W. A. <AP. J. (LETTERS), 203, L13> 769904
OPTICAL IDENTIFICATION OF A0620-00.

BOPP, B. W., GEHRZ, R. D., HACKWELL, J. A. <P. A. S. P., 86, 989> 741205
INFRARED OBSERVATIONS OF LATE-TYPE DWARF STARS.

BORGMAN, J. <ASTR. AP., 29, 443> 731211
THE 9.7 MICRON ABSORPTION FEATURE IN THE GALACTIC CENTER.

BORGMAN, J., KOORNNEEF, J., SLINGERLAND, J. <ASTR. AP., 4, 248> 700103
INFRA-RED PHOTOMETRY OF A HEAVILY REDDENED CLUSTER IN ARA.

BOYARCHUK, A. A., ESIPOV, V. F., MOROZ, V. I. <SOV. AST., 10, 331> 660902
THE CONTINUOUS SPECTRUM OF AG PEGASI.

BOYCE, P. B., FORD JR., W. K. <P. A. S. P., 78, 163> 660403
INTERSTELLAR HELIUM AT 10, 830 IN THE ORION NEBULA.

BRACCESI, A., LYNDS, R., SANDAGE, A. <AP. J. (LETTERS), 152, L105> 689904
SPECTROSCOPIC AND PHOTOMETRIC DATA FOR A SAMPLE OF QUASI-STELLAR OBJECTS IDENTIFIED BY THEIR INFRARED EXCESS.

BRANDSHAFT, D., MCLAREN, R. A., WERNER, M. W. <AP. J. (LETTERS), 199, L115> 750702
SPECTROSCOPY OF THE ORION NEBULA FROM 80 TO 135 MICRONS.

BRAZ, M. A., EPCHTEIN, N. <ASTR. AP., 111, 91> 820713
NEW INFRARED OBJECTS TOWARDS SOUTHERN TYPE I OH AND H2O MASERS.

BREGER, M., GEHRZ, R. D., HACKWELL, J. A. <AP. J., 248, 963> 810906
INTERSTELLAR GRAIN SIZE. II. INFRARED PHOTOMETRY AND POLARIZATION IN ORION.

BREGER, M., HARDORP, J. <AP. J. (LETTERS), 183, L77> 730704
INFRARED POLARIMETRY OF VERY YOUNG OBJECTS INCLUDING THE BECKLIN-NEUGEBAUER SOURCE.

BREGER, M., KUHI, L. V. <AP. J., 160, 1129> 700601
EFFECTIVE TEMPERATURES, GRAVITIES, AND THE MASS DETERMINATION OF A AND F STARS.

BREGMAN, J. D. <P. A. S. P., 89, 335> 770603
OBSERVATIONS AND INTERPRETATION OF THE INFRARED SPECTRUM OF HD 44179.

BREGMAN, J. D., GOEBEL, J. H., STRECKER, D. W. <AP. J. (LETTERS), 223, L45> 780706
IDENTIFICATION OF THE 3.9 MICRON ABSORPTION BAND IN CARBON STARS.

BREGMAN, J. D., RANK, D. M. <AP. J. (LETTERS), 195, L125> 750202
IDENTIFICATION OF THE 890 CM-1 CARBONATE SIGNATURE IN NGC 7027.

BREGMAN, J. N., GLASSGOLD, A. E., HUGGINS, P. J., POLLACK, J. T., PICA, A. J., SMITH, A. G., WEBB, J. R., KU, W. H. -M., RUDY, R. J., LEVAN, P.D., WILLIAMS, P. M.,BRAND, P. W. J. L., NEUGEBAUER, G., BALONEK, T. J., DENT, W. A., ALLER, H. D., ALLER, M. F., HODGE, P. E. <AP. J., 253, 19> 820201
SIMULTANEOUS OBSERVATIONS OF THE BL LACERTAE OBJECT I ZW 187.

BREGMAN, J. N., LEBOFSKY, M. J., ALLER, M. F., RIEKE, G. H., ALLER, H. D., HODGE, P. E., GLASSGOLD, A. E., HUGGINS, P. J. <NATURE, 293, 714> 811017
MUTIFREQUENCY OBSERVATIONS OF THE RED QSO 1413+135.

BRIOT, D. <ASTR. AP., 54, 599> 770101
PASCHEN LINES IN BE STARS-CORRELATION BETWEEN THE PRESENCE OF PASCHEN EMISSION LINES AND THE INFRARED EXCESS.

BROCKA, B. <P. A. S. P., 91, 519> 790807
A SURVEY OF SYMBIOTIC STARS AT 1612 MHZ.

BROSCH, N., ISAACMAN, R. <ASTR. AP., 113, 231> 820911
MULTIAPERATURE PHOTOMETRY OF GALAXIES. II. NEAR-INFRARED OBSERVATIONS OF SIX ISOLATED OBJECTS.

BRUECK, M. T. <M. N. R. A. S., 166, 123> 740106
PHOTOGRAPHIC SURFACE PHOTOMETRY OF THE NEBULAE SURROUNDING V380 ORI AND R MON.

BRUGEL, E. W., BOEHM, K. H., MANNERY, E. <AP. J. SUPPL., 47, 117> 811012
EMISSION LINE SPECTRA OF HERBIG-HARO OBJECTS.

BUSOLETTI, E., GUIDI, I., MELCHIORRI, F., NATALE, V. <ASTR. AP., 105, 184> 820114
FAR IR EMISSION OF THE GALACTIC PLANE AT HIGH LONGITUDES.

CAHN, J. H., RUBIN, R. H. <A. J., 79, 128> 749905
INTERFEROMETRIC SURVEY OF PLANETARY NEBULAE.

CAMPBELL, M. F., ELIAS, J. H., GEZARI, D. Y., HARVEY, P. M., HOFFMANN, W. F., HUDSON, H. S., NEUGEBAUER, G., SOIFER, B. T., WERNER, M. W., WESTBROOK, W. E. <AP. J., 208, 396> 760906
FAR-INFRARED OBSERVATIONS OF IRC +10216.

CAMPBELL, M. F., HOFFMANN, W. F., THRONSON JR., H. A. <AP. J., 247, 530> 810709
AN EXTENDED FAR-INFRARED EMISSION COMPLEX AT IC 1318B AND IC 1318C.

CAMPBELL, M. F., HOFFMANN, W. F., THRONSON JR., H. A., HARVEY, P. M. <AP. J., 238, 122> 800503
FAR-INFRARED SURVEY OF CYGNUS X.

CAMPBELL, M. F., HOFFMANN, W. F., THRONSON JR., H. A., NILES, D., NAWFEL, R., HAWRYLYCZ, M. <AP. J., 261, 550> 821004
FAR-INFRARED SOURCES IN CYGNUS X: AN EXTENDED EMISSION COMPLEX AT DR 21 AND UNRESOLVED SOURCES AT S106 AND ON 2.

CANNON, A. J., PICKERING, E. C. <HARVARD ANNALS, 91-100> 189901
THE HENRY DRAPER CATALOG.

CAPPS, R. W., DYCK, H. M. <AP. J., 175, 693> 720803
THE MEASUREMENT OF POLARIZED 10-MICRON RADIATION FROM COOL STARS WITH CIRCUMSTELLAR SHELLS.

CAPPS, R. W., GILLETT, F. C., KNACKE, R. F. <AP. J., 226, 863> 781214
INFRARED OBSERVATIONS OF THE OH SOURCE W33 A.

CAPPS, R. W., KNACKE, R. F. <AP. J., 210, 76> 761108
INFRARED POLARIZATION OF THE GALACTIC CENTER.

CAPPS, R. W., KNACKE, R. F. <AP. LETTERS, 19, 113> 770003
POLARIZATION OF 3C 371 AND AP LIBRAE AT 2.2 MICRONS.

CAPPS, R. W., KNACKE, R. F. <P. A. S. P., 88, 224> 760608
INFRARED POLARIZATION OF IRC+10216.

CAPPS, R. W., KNACKE, R. F. <P. A. S. P., 88, 564> 760814
ERRATUM TO "INFRARED POLARIZATION OF IRC+10216."

CAPPS, R. W., SITKO, M. L., STEIN, W. A. <AP. J., 255, 413> 820404
THE SPECTRAL FLUX DISTRIBUTIONS OF SOURCES IN AN OPTICALLY SELECTED SAMPLE OF QSOS: 1E13-1E15 HZ.

CARLETON, N. P., LILLER, W., ROESLER, F. L. <AP. J., 154, 385> 681003
A SEARCH FOR STELLAR CARBON DIOXIDE.

CARNEY, B. W. <A. J., 87, 1527> 821109
INFRARED PHOTOMETRY OF HYADES DWARFS.

CARNEY, B. W., AARONSON, M. <A. J., 84, 867> 790603
SUBDWARF BOLOMETRIC CORRECTIONS.

CARNEY, B. W., PETERSON, R. C. <AP. J., 245, 238> 810411
ABUNDANCE ANALYSES OF SUBDWARFS OF THE REMOTE HALO.

CARNEY, B. W., PETERSON, R. C. <AP. J., 251, 190> 811202
FIELD POPULATION II BLUE STRAGGLERS.

CARTER, D., ALLEN, D. A., MALIN, D. F. <NATURE, 295, 126> 820118
NATURE OF THE SHELLS OF NGC 1344.

CATCHPOLE, R. M. <M. N. R. A. S., 200, 33P> 820823
FAINT RED STARS AT THE GALACTIC CENTRE.

CATCHPOLE, R. M., FEAST, M. W. <M. N. R. A. S., 175, 501> 769908
LITHIUM AND S-TYPE STARS.

CATCHPOLE, R. M., FEAST, M. W. <M. N. R. A. S., 197, 385> 811109
THE LUMINOSITIES OF RED SUPERGIANT VARIABLES IN THE SMALL MAGELLANIC CLOUD.

CATCHPOLE, R. M., GLASS, I. S., CARTER, B. S., ROBERTS, G. <NATURE, 291, 392> 810623
IR VARIABILITY OF SS433.

CATCHPOLE, R. M., ROBERTSON, B. S. C., LLOYD EVANS, T. H. H.,FEAST, M. W., GLASS, I. S., CARTER, B. S. <S. A. A. O. CIRC., 1, 61> 790004
J, H, K, L, INFRARED PHOTOMETRY OF MIRA VARIABLES AND OF OTHER LATE TYPE STARS.

CATO, B. T., RONNANG, B. O., RYDBECK, O. E. H., LEWIN, P. T.,YNGVESSON, K. S., CARDIASMENOS, A. G., SHANLEY, J. F. <AP. J., 208, 87> 760811
WATER VAPOR EMISSION FROM HII REGIONS AND INFRARED STARS.

CHALDU, R., HONEYCUTT, R. K., PENSTON, M. V. <P. A. S. P., 85, 87> 730204
THE EXTINCTION CURVE FOR CYGNUS OB2 NO. 12.

CHEN, K., REUNING, E. G. <A. J., 71, 283> 660502
INFRARED PHOTOMETRY OF BETA PERSEI.

CHEN, P., GAO, H., HAO, Y., CHU, Q., ZHOU, K. <CHIN. AST. AP., 6, 153> 820623
CONSTRUCTION OF A 1-3 MICRON INFRARED PHOTOMETER AND ITS TEST OBSERVATIONS.

CHEUNG, L. H., FROGEL, J. A., GEZARI, D. Y., HAUSER, M. G. <AP. J., 240, 74> 800807
1.0 MILLIMETER MAPS AND RADIAL DENSITY DISTRIBUTIONS OF SOUTHERN H II/MOLECULAR CLOUD COMPLEXES.

CHEUNG, L., FROGEL, J. A., GEZARI, D. Y., HAUSER, M. G. <AP. J. (LETTERS), 226, L149> 781211
1.0 MILLIMETER CONTINUUM MAP OF COOL SOURCES IN THE NGC 6334 COMPLEX.

CHEVALIER, C., ILOVAISKY, S. A. <ASTR. AP., 112, 68> 820816
COLOR VARIABILITY AND OPTICAL LIGHT CURVE OF 2S0921-630.

CHINI, R. <ASTR. AP., 110, 332> 820614
CIRCUMSTELLAR SHELLS IN M17.

CHINI, R. <ASTR. AP., 99, 346> 810620
MULTICOLOUR PHOTOMETRY OF STARS IN THE OPHIUCHUS DARK CLOUD REGION.

CHINI, R., ELSAESSER, H., HEFELE, H., WEINBERGER, R. <ASTR. AP., 56, 323> 770409
ON THE INFRARED SOURCES IN THE OPHIUCHUS DARK CLOUD REGION.

CHIU, B. C., MORRISON, P., SARTORI, L. <AP. J., 198, 617> 750605
THE LIGHT OF THE SUPERNOVA OUTBURST. II. THE CASE OF SUPERNOVA 1972E.

CHOPINET, M., LORTET-ZUCKERMANN, M. C. <ASTR. AP., 18, 166> 729904
A NOTE TO DESIGNATIONS OF PLANETARY NEBULAE.

CHOPINET, M., LORTET-ZUCKERMANN, M. C. <ASTR. AP., 18, 373> 729906
INTERACTION OF HOT STARS AND OF THE INTERSTELLAR MEDIUM. II. EXCITING STAR AND SPECTRA OF THE BRIGHT KNOT INSIDE THE DIFFUSE NEBULA SHARPLESS 157.

CHRISTENSEN, C. G. <A. J., 83, 244> 780301
ABSOLUTE SPECTRAL ENERGY DISTRIBUTIONS AND (FE/H) VALUES OF METAL-POOR STARS AND GLOBULAR CLUSTERS.

CHURMS, J., FEAST, M. W., GLASS, I. S., HARDING, G. A., LLOYD EVANS, T., MARTIN, W. L. <M. N. R. A. S., 169, 39P> 741112
NEBULOSITY ASSOCIATED WITH THE POWERFUL INFRARED AND RADIO SOURCE G333.6–0.2.

CIATTI, F. <ASTR. AP., 22, 465> 730206
THE INFRARED SPECTRUM OF THE SUPERNOVA IN NGC 5253.

CIATTI, F., D'ODORICO, S., MAMMANO, A. <ASTR. AP., 34, 181> 740810
PROPERTIES AND EVOLUTION OF BQ() STARS.

CIATTI, F., MAMMANO, A. <ASTR. AP., 38, 435> 750211
EJECTION OF NEBULAE BY BQ RADIOSTARS WITH INFRARED EXCESS.

CIATTI, F., ROSINO, L. <ASTR. AP. SUPPL., 16, 305> 740813
PHOTOGRAPHIC AND SPECTROSCOPIC OBSERVATIONS OF N AQL 1970, N CYG 1970 AND N SCT 1970.

CITTERIO, O., CONTI, G., DI BENEDETTO, P., TANZI, E. G. <M. N. R. A. S., 175, 35P> 760511
INFRARED AND X-RAY OBSERVATIONS OF THE DECLINE OF A0620–00.

CLARK, T. A., MILONE, E. F. <P. A. S. P., 93, 338> 810601
INFRARED VARIABILITY AND SPECTRUM OF SS 433.

CLEGG, P. E., ROWAN-ROBINSON, M., ADE, P. A. R. <A. J., 81, 399> 760601
MILLIMETER OBSERVATIONS OF GALACTIC SOURCES.

CLEGG, R. E. S., HINKLE, K. H., LAMBERT, D. L. <M. N. R. A. S., 201, 95> 821009
HIGH-RESOLUTION 3 MICRON SPECTROSCOPY OF IRC+10216.

CLINE, T. L. <NASA TM-83967> 829908
DEVELOPMENTS IN HIGH-PRECISION GAMMA-RAY BURST SOURCE STUDIES.

COCHRAN, A. L. <AP. J. SUPPL., 45, 83> 810108
SPECTROPHOTOMETRY WITH A SELF-SCANNED SILICON PHOTODIODE ARRAY. II. SECONDARY STANDARD STARS.

COHEN, J. G., FROGEL, J. A. <AP. J. (LETTERS), 255, L39> 820402
WHAT IS THE SECOND PARAMETER?: THE ANOMOLOUS GLOBULAR CLUSTER NGC 7006.

COHEN, J. G., FROGEL, J. A., PERSSON, S. E. <AP. J., 222, 165> 780507
INFRARED PHOTOMETRY, BOLOMETRIC MAGNITUDES, AND EFFECTIVE TEMPERATURES FOR GIANTS IN M3, M13, M92, AND M67.

COHEN, J. G., FROGEL, J. A., PERSSON, S. E., ELIAS, J. H. <AP. J., 249, 481> 811007
BOLOMETRIC LUMINOSITIES AND INFRARED PROPERTIES OF CARBON STARS IN THE MAGELLANIC CLOUDS AND THE GALAXY.

COHEN, J. G., FROGEL, J. A., PERSSON, S. E., ZINN, R. <AP. J., 239, 74> 800705
PAL 12 - A METAL-RICH GLOBULAR CLUSTER IN THE OUTER HALO.

COHEN, M. <A. J., 85, 29> 800101
RED AND NEBULOUS OBJECTS IN DARK CLOUDS: A SURVEY.

COHEN, M. <AP. J. (LETTERS), 173, L61> 720401
BD+40 4124 AND TWO NEARBY STARS.

COHEN, M. <AP. J. (LETTERS), 185, L75> 731003
AN UNUSUAL INFRARED SOURCE NEAR THE ROSETTE NEBULA.

COHEN, M. <AP. J., 203, 169> 760105
DEEP ICE ABSORPTION IN A PECULIAR INFRARED SOURCE.

COHEN, M. <AP. LETTERS, 9, 95> 710001
OPTICAL IDENTIFICATIONS OF INFRARED SOURCES.

COHEN, M. <M. N. R. A. S., 161, 105> 730006
INFRA-RED OBSERVATIONS OF YOUNG STARS-III. NEBULOUS EMISSION-LINE STARS.

COHEN, M. <M. N. R. A. S., 161, 85> 730004
INFRA-RED OBSERVATIONS OF YOUNG STARS-I. STARS IN YOUNG CLUSTERS.

COHEN, M. <M. N. R. A. S., 161, 97> 730005
INFRA-RED OBSERVATIONS OF YOUNG STARS-II. T TAURI STARS AND THE ORION POPULATION.

COHEN, M. <M. N. R. A. S., 164, 395> 730010
INFRA-RED OBSERVATIONS OF YOUNG STARS-IV. RADIATIVE MECHANISMS AND INTERPRETATIONS.

COHEN, M. <M. N. R. A. S., 169, 257> 741108
INFRARED OBSERVATIONS OF YOUNG STARS-V. THE FAINT MEMBERS OF THE ORION POPULATION.

COHEN, M. <M. N. R. A. S., 173, 279> 751107
INFRARED OBSERVATIONS OF YOUNG STARS-VI. A 2- TO 4-MICRON SEARCH FOR MOLECULAR FEATURES.

COHEN, M. <M. N. R. A. S., 173, 489> 751204
INFRARED OBSERVATIONS OF SOUTHERN WC9 STARS AND HE 2-113.

COHEN, M. <M. N. R. A. S., 191, 499> 800509
INFRARED OBSERVATIONS OF YOUNG STARS - VIII. SPECTRA IN TEN-MICRON REGION.

COHEN, M. <P. A. S. P., 86, 813> 741017
INFRARED OBSERVATIONS OF NEW COMETARY NEBULAE.

COHEN, M. <P. A. S. P., 87, 421> 750608
INFRARED OBSERVATIONS OF LATE-TYPE STARS IN NEBULAE.

COHEN, M., ANDERSON, C. M., COWLEY, A., COYNE S. J., G. V., FAWLEY, W. M., GULL, T. R., HARLAN, E. A., HERBIG, G. H., HOLDEN, F., HUDSON, H. S., JAKOUBEK, R. O., JOHNSON, H. M., SCHIFFER III, F. H., SOIFER, B. T., ZUCKERMAN, B. <AP. J., 196, 179> 750205
THE PECULIAR OBJECT HD 44179 ("THE RED RECTANGLE").

COHEN, M., BARLOW, M. J. <AP. J. (LETTERS), 185, L37> 731002
INFRARED OBSERVATIONS OF TWO SYMMETRIC NEBULAE.

COHEN, M., BARLOW, M. J. <AP. J., 193, 401> 741009
AN INFRARED PHOTOMETRIC SURVEY OF PLANETARY NEBULAE.

COHEN, M., BARLOW, M. J. <AP. J., 238, 585> 800610
INFRARED PHOTOMETRY OF SOUTHERN PLANETARY NEBULAE AND EMISSION-LINE OBJECTS.

COHEN, M., BARLOW, M. J. <AP. LETTERS, 16, 165> 751104
INFRARED OBSERVATIONS OF THREE UNUSUAL NEBULAE.

COHEN, M., BARLOW, M. J., KUHI, L. V. <ASTR. AP., 40, 291> 750505
WOLF-RAYET STARS. VI. THE NATURE OF THE OPTICAL AND INFRARED CONTINUA.

COHEN, M., FAWLEY, W. M. <M. N. R. A. S., 169, 31P> 741110
TEN MICRON OBSERVATIONS OF GLOBULAR CLUSTERS.

COHEN, M., FITZGERALD, M. P., KUNKEL, W., LASKER, B. M., OSMER, P. S. <AP. J., 221, 151> 780404
STUDIES OF BIPOLAR NEBULAE. IV. MZ 3(-PK 331-1 1).

COHEN, M., GAUSTAD, J. E. <AP. J. (LETTERS), 186, L131> 731203
INFRARED EXCESSES IN THE M SUPERGIANTS OF H AND CHI PERSEI.

COHEN, M., HUDSON, H. S., O'DELL, S. L., STEIN, W. A. <M. N. R. A. S., 181, 233> 771001
A STUDY OF THE PLANETARY NEBULAE ABELL 30 AND ABELL 78.

COHEN, M., KUHI, L. V. <AP. J. SUPPL., 41, 743> 791211
OBSERVATIONAL STUDIES OF PRE-MAIN-SEQUENCE EVOLUTION.

COHEN, M., KUHI, L. V. <AP. J., 210, 365> 761203
SPECTROPHOTOMETRIC STUDIES OF YOUNG STARS. I. THE CEPHEUS IV ASSOCIATION.

COHEN, M., SCHWARTZ, R. D. <AP. J. (LETTERS), 233, L77> 791012
THE EXCITING STAR OF HERBIG-HARO OBJECT 1.

COHEN, M., SCHWARTZ, R. D. <M. N. R. A. S., 174, 137> 760107
INFRARED OBSERVATIONS OF YOUNG STARS-VII. SIMULTANEOUS OPTICAL AND INFRARED MONITORING FOR VARIABILITY.

COHEN, M., SCHWARTZ, R. D. <M. N. R. A. S., 191, 165> 800411
A SEARCH FOR THE EXCITING STARS OF HERBIG-HARO OBJECTS.

COHEN, M., VOGEL, S. N. <M. N. R. A. S., 185, 47> 781007
WOLF-RAYET STARS--VIII. 2- TO 4-MICRON SPECTROPHOTOMETRY OF LATE WC STARS.

COHEN, M., WOOLF, N. J. <AP. J., 169, 543> 711105
TWO YOUNG BRIGHT INFRARED OBJECTS.

CONDAL, A. R. <ASTR. AP., 112, 124> 820817
NGC 2440: IONIZATION STRUCTURE, EXTINCTION, AND NEAR INFRARED SPECTRUM.

CONDON, J. J., O'DELL, S. L., PUSCHELL, J. J., STEIN, W. A. <AP. J., 246, 624> 810609
RADIO EMISSION FROM BRIGHT, OPTICALLY SELECTED QUASARS.

CONNES, P., MICHEL, G. <AP. J. (LETTERS), 190, L29> 740504
HIGH-RESOLUTION FOURIER SPECTRA OF STARS AND PLANETS.

COX, G. G., PARKER, E. A. <M. N. R. A. S., 186, 197> 790101
TIME VARIATIONS OF STELLAR WATER MASERS.

COX, L. J., HOUGH, J. H., ADAMS, D. J., JAMESON, R. F. <M. N. R. A. S., 176, 131> 760712
LINEAR POLARIZATION MEASUREMENTS OF OMI SCO IN THE NEAR INFRARED.

COX, L. J., HOUGH, J. H., MCCALL, A. <M. N. R. A. S., 185, 199> 781009
THE HATFIELD NEAR-INFRARED POLARIMETER.

COYNE S. J., G. V., MCLEAN, I. S. <A. J., 80, 702> 750901
WAVELENGTH DEPENDENCE OF POLARIZATION XXX. INTRINSIC POLARIZATION IN PHI PERSEI.

CRABTREE, D. R., MARTIN, P. G. <AP. J., 227, 900> 790207
CIRCUMSTELLAR DUST ENVELOPES: CALCULATION OF ECLIPSE LIGHT CURVES AND FRINGE VISIBILITIES.

CRAGG, T., EVANS, R. <IAUC NO. 3583> 819912
SUPERNOVA IN NGC 1316.

CRAINE, E. R., DUERR, R. E., HORNER, V. M., IMHOFF, C. L., ROUTSIS, D. E., SWIHART, D. L., TURNSHEK, D. A. <STEWARD OBS., A, 3> 799904
NEAR INFRARED PHOTOGRAPHIC SKY SURVEY.

CRAINE, E. R., SCHUSTER, W. J., TAPIA, S., VRBA, F. J. <AP. J., 205, 802> 760505
ON THE NATURE OF IRC +10420.

CRAWFORD, D. L., GLASPEY, J. W., PERRY, C. L. <A. J., 75, 822> 709902
FOUR-COLOR AND H-BETA PHOTOMETRY OF OPEN CLUSTERS. IV. H AND CHI PERSEI.

CRUIKSHANK, D. P., PILCHER, C. B., MORRISON, D. <AP. J., 217, 1006> 771110
IDENTIFICATION OF A NEW CLASS OF SATELLITES IN THE OUTER SOLAR SYSTEM.

CUDABACK, D. D., GAUSTAD, J. E., KNACKE, R. F. <AP. J. (LETTERS), 166, L49> 710603
SILICON MONOXIDE IN THE INFRARED SPECTRUM OF ALPHA ORIONIS.

CUDLIP, W., FURNISS, I., KING, K. J., JENNINGS, R. E. <M. N. R. A. S., 200, 1169> 820913
FAR INFRARED POLARIMETRY OF W51A AND M42.

CUTRI, R. M., AITKEN, D. K., JONES, B., MERRILL, K. M., PUETTER, R. C., ROCHE, P. F., RUDY, R. J., RUSSELL, R. W., SOIFER, B. T., WILLNER, S. P. <AP. J., 245, 818> 810501
INFRARED SPECTROPHOTOMETRY OF THREE SEYFERT GALAXIES AND 3C273.

CUTRI, R. M., RUDY, R. J. <AP. J. (LETTERS), 241, L141> 801101
DETECTION OF THE 3.3 MICRON FEATURE IN THE SEYFERT GALAXY NGC 4151.

DA COSTA, G. S., FROGEL, J. A., COHEN, J. G. <AP. J., 248, 612> 810903
THE GIANT BRANCH OF THE GLOBULAR CLUSTER NGC 3201.

DACHS, J., WAMSTEKER, W. <ASTR. AP., 107, 240> 820309
INFRARED PHOTMETRY OF SOUTHERN BE STARS.

DAIN, F. W., GULL, G. E., MELNICK, G., HARWIT, M., WARD, D. B. <AP. J. (LETTERS), 221, L17> 780407
OBSERVATIONS OF (O III) 88 MICRON LINE EMISSION FROM HII REGIONS AND THE GALACTIC CENTER.

DANIELSON, R. E., WOOLF, N. J., GAUSTAD, J. E. <AP. J., 141, 116> 650106
A SEARCH FOR INTERSTELLAR ICE ABSORPTION IN THE INFRARED SPECTRUM OF MU CEPHEI.

DANKS, A. C. <P. A. S. P., 87, 941> 751207
INFRARED STAR IN RCW 113.

DANKS, A. C., HOUZIAUX, L. <P. A. S. P., 90, 453> 780811
SPECTROSCOPIC OBSERVATIONS OF 27 CANIS MAJORIS FROM 0.14 TO 4.7 MICRONS.

DANKS, A. C., WAMSTEKER, W., VOGT, N., SALINARI, P., TARENGHI, M., DUERBECK, H. W. <AP. J. (LETTERS), 227, L59> 790117
INFRARED AND VISIBLE PHOTOMETRY OF FAIRALL-9 (ESO 113-IG 45).

DANZIGER, I. J. <ASTR. AP., 38, 475> 750212
THE INFRARED CONTINUUM OF THE COMPACT PLANETARY NEBULA NGC 6210.

DANZIGER, I. J., FROGEL, J. A., PERSSON, S. E. <AP. J. (LETTERS), 184, L29> 730807
OBSERVATIONS OF NGC 6302 FROM 0.35 TO 20 MICRONS.

DAVIDSON, K., HUMPHREYS, R. M., MERRILL, K. M. <AP. J., 220, 239> 780217
OPTICAL AND INFRARED OBSERVATIONS OF THE NEW EMISSION-LINE OBJECT HM SAGITTAE.

DAVIS, D. S., LARSON, H. P., SMITH, H. A. <AP. J., 259, 166> 820801
AIRBORNE OBSERVATIONS OF THE ORION MOLECULAR HYDROGEN EMISSON SPECTRUM.

DE BRUYN, A. G., SARGENT, W. L. W. <A. J., 83, 1257> 781101
ABSOLUTE SPECTROPHOTOMETRY OF 68 SEYFERT GALAXY NUCLEI.

DE MUIZON, M., ROUAN, D., LENA, P., NICOLLIER, C., WIJNBERGEN, J. <ASTR. AP., 83, 140> 800306
FAR INFRARED STUDY OF MOLECULAR CLOUDS: DUST TEMPERATURE PROFILES IN S 140, IC 1396, R CRA.

DE VAUCOULEURS, G., DE VAUCOULEURS, A., CORWIN JR., H. G. <UNIV. TEXAS PRESS> 769914
SECOND REFERENCE CATALOGUE OF BRIGHT GALAXIES.

DE VEGT, C. <ASTR. AP., 109, 282> 829906
COMPARISON OF PRECISE OPTICAL AND RADIO POSITIONS FOR CYG OB2 MEMBERS AND P CYG.

DE VENY, J. B., OSBORN, W. H., JANES, K. <P. A. S. P., 83, 611> 719903
A CATALOGUE OF GUASARS.

DE VRIES, J. S., VAN DER WAAL, P. B., ANDRIESSE, C. D. <ASTR. AP., 86, 248> 800612
HIGH-RESOLUTION (NE II) OBSERVATIONS IN G333.6-0.2.

DEGIOIA-EASTWOOD, K., HACKWELL, J. A., GRASDALEN, G. L., GEHRZ, R. D. <AP. J. (LETTERS), 245, L75> 810406
A CORRELATION BETWEEN INFRARED EXCESS AND PERIOD FOR MIRA VARIABLES.

DEMERS, S., KUNKEL, W. E. <P. A. S. P., 91, 761> 799902
DISCOVERY OF VERY RED GIANTS IN THE FORNAX GALAXY.

DEMERS, S., KUNKEL, W. E., HARDY, E. <AP. J., 232, 84> 799903
THE GIANT BRANCH OF FORNAX.

DENNEFELD, M. <ASTR. AP., 112, 215> 820818
A SPECTROPHOTOMETRIC STUDY OF KEPLER SUPERNOVA REMNANT.

DENNEFELD, M., ANDRILLAT, Y. <ASTR. AP., 103, 44> 811112
NEAR-INFRARED SPECTROSCOPY OF NORTHERN SUPERNOVA-REMNANTS.

DENNISON, B. <AP. J., 215, 529> 770704
ON THE INFRARED POLARIZATION OF THE ORION NEBULA.

DENNISON, B., WARD, D. B., GULL, G. E., HARWIT, M. <A. J., 82, 39> 770102
FAR-INFRARED POLARIZATION OF M42.

DIBAI, E. A., ESIPOV, V. F. <SOV. AST., 12, 448> 689905
SPECTRA OF H-ALPHA EMISSION OBJECTS IN THE DIFFUSE NEBULAE IC 1396 AND SIMEIZ 130.

DICKINSON, D. F. <AP. J. SUPPL., 30, 259> 760302
WATER EMISSION FROM INFRARED STARS.

DICKINSON, D. F., CHAISSON, E. J. <AP. J. (LETTERS), 181, L135> 730501
LONG-PERIOD VARIABLES: CORRELATION OF STELLAR PERIOD WITH OH RADIAL-VELOCITY PATTERN.

DINERSTEIN, H. L. <AP. J., 237, 486> 800409
INFRARED LINE MEASUREMENTS AND THE ABUNDANCE OF SULFUR IN PLANETARY NEBULAE.

DINERSTEIN, H. L., LESTER, D. F., RANK, D. M. <AP. J. (LETTERS), 227, L39> 790113
DETECTION OF A NEAR-INFRARED COMPLEX ASSOCIATED WITH S140 IRS.

DINERSTEIN, H. L., WERNER, M. W., CAPPS, R. W., DWEK, E. <AP. J., 255, 552> 820408
A SEARCH FOR HOT DUST IN THE FAST MOVING KNOTS IN CASSIOPEIA A.

DIXON, R. S. <OHIO STATE UNIVERSITY, RA42> 769905
MASTER LIST OF RADIO SOURCES.

DOLIDZE, M. V., ARAKELYAN, M. A. <SOV. AST., 3, 434> 599902
THE T-ASSOCIATION NEAR RHO OPHIUCHI.

DOMBROVSKII, V. A. <ASTROFIZIKA, 6, 207> 700403
POLARIZATION OF THE LIGHT FROM RED VARIABLE STARS OF HIGH LUMINOSITY.

DOMBROVSKII, V. A., KHOZOV, G. V. <ASTROFIZIKA, 8, 5> 720104
PHOTOMETRIC AND POLARIMETRIC STUDY OF INFRARED STARS IN THE VISIBLE AND INFRARED SPECTRAL REGIONS.

DOROSHENKO, V. T., EFIMOV, YU. S., ROSENBUSH, A. E., TEREBIZH, V. Y., SHENAVRIN, V. I. <ASTROFIZIKA, 14, 5> 780004
THE OPTICAL AND INFRARED OBSERVATIONS OF SU TAU.

DOWNES, D., GENZEL, R., BECKLIN, E. E., WYNN-WILLIAMS, C. G. <AP. J., 244, 869> 810305
OUTFLOW OF MATTER IN THE KL NEBULA: THE ROLE OF IRC2.

DOWNES, R. A., MARGON, B. <A. J., 86, 19> 819901
B 272: QUASAR OR H II REGION?

DRAINE, B. T., ROBERGE, W. G. <AP. J. (LETTERS), 259, L91> 820810
A MODEL FOR THE INTENSE MOLECULAR LINE EMISSION FROM OMC-1.

DRESSEL, L. L., CONDON, J. J. <AP. J. SUPPL., 31, 187> 769909
ACCURATE OPTICAL POSITIONS OF BRIGHT GALAXIES.

DREYER, J. L. E. <MEM. R. A. S., L1> 958901
INDEX CATALOGUE.

DUERR, R., IMHOFF, C. L., LADA, C. J. <AP. J., 261, 135> 829902
STAR FORMATION IN THE LAMBDA ORIONIS REGION. I. THE DISTRIBUTION OF YOUNG OBJECTS.

DWEK, E., SELLGREN, K., SOIFER, B. T., WERNER, M. W. <AP. J., 238, 140> 800505
EXCITATION MECHANISMS FOR THE UNIDENTIFIED INFRARED EMISSION FEATURES.

DYCK, H. M. <A. J., 82, 129> 770206
INFRARED MAP OF M8.

DYCK, H. M. <A. J., 85, 891> 800703
NEAR-INFRARED SLIT SCANS OF MOLECULAR CLOUD SOURCES.

DYCK, H. M., BEICHMAN, C. A. <AP. J., 194, 57> 741106
OBSERVATIONS OF INFRARED POLARIZATION IN THE ORION NEBULA.

DYCK, H. M., CAPPS, R. W. <AP. J. (LETTERS), 220, L49> 780306
NEAR-INFRARED POLARIMETRY OF COMPACT INFRARED SOURCES ASSOCIATED WITH HII REGIONS AND MOLECULAR CLOUDS.

DYCK, H. M., CAPPS, R. W., BEICHMAN, C. A. <AP. J. (LETTERS), 188, L103> 740301
INFRARED POLARIZATION OF THE GALACTIC NUCLEUS.

DYCK, H. M., CAPPS, R. W., FORREST, W. J., GILLETT, F. C. <AP. J. (LETTERS), 183, L99> 730803
DISCOVERY OF LARGE 10-MICRON LINEAR POLARIZATION OF THE BECKLIN-NEUGEBAUER SOURCE IN THE ORION NEBULA.

DYCK, H. M., FORBES, F. F., SHAWL, S. J. <A. J., 76, 901> 711101
POLARIMETRY OF RED AND INFRARED STARS AT 1 TO 4 MICRONS.

DYCK, H. M., FORREST, W. J., GILLETT, F. C., STEIN, W. A., GEHRZ, R. D., WOOLF, N. J., SHAWL, S. J. <AP. J., 165, 57> 710405
VISUAL INTRINSIC POLARIZATION AND INFRARED EXCESS OF COOL STARS.

DYCK, H. M., HOWELL, R. R. <A. J., 87, 400> 820212
SPECKLE INTERFEROMETRY OF MOLECULAR CLOUD SOURCES AT 4.8 MICRONS.

DYCK, H. M., JONES, T. J. <A. J., 83, 594> 780602
NEAR-INFRARED OBSERVATIONS OF INTERSTELLAR POLARIZATION.

DYCK, H. M., KINMAN, T. D., LOCKWOOD, G. W. <NAT. PHYS. SCI., 237, 48> 720504
ERRATUM TO "OBSERVATIONS OF OJ 287 BETWEEN 0.36 AND 3.4 MICRONS."

DYCK, H. M., KINMAN, T. D., LOCKWOOD, G. W., LANDOLT, A. U. <NAT. PHYS. SCI., 234, 71> 711107
OBSERVATIONS OF OJ 287 BETWEEN 0.36 AND 3.4 MICRONS.

DYCK, H. M., LOCKWOOD, G. W., CAPPS, R. W. <AP. J., 189, 89> 740401
INFRARED FLUXES, SPECTRAL TYPES, AND TEMPERATURES FOR VERY COOL STARS.

DYCK, H. M., LONSDALE, C. J. <A. J., 84, 1339> 790906
THE RELATIONSHIP BETWEEN THE INFRARED POLARIZATION OF PROTOSTELLAR SOURCES AND NEARBY INTERSTELLAR POLARIZATION.

DYCK, H. M., LONSDALE, C. J. <A. J., 85, 1077> 800802
ICE-BAND POLARIMETRY OF GL 2591.

DYCK, H. M., MILKEY, R. W. <P. A. S. P., 84, 597> 721009
INFRARED EXCESSES IN EARLY-TYPE STARS: FREE-FREE EMISSION.

DYCK, H. M., SIMON, T. <AP. J., 211, 421> 770104
INFRARED OBSERVATIONS OF COMPACT HII REGIONS IN THE SPECTRAL RANGE 3.4-33 MICROMETERS.

DYCK, H. M., SIMON, T. <P. A. S. P., 88, 738> 761011
THE INFRARED SPECTRA OF NGC 7027 AND BD+30 3639.

DYCK, H. M., SIMON, T., ZUCKERMAN, B. <AP. J. (LETTERS), 255, L103> 820409
DISCOVERY OF AN INFRARED COMPANION TO T TAURI.

DYCK, H. M., STAUDE, H. J. <ASTR. AP., 109, 320> 820510
NEAR-INFRARED SLIT SCANS OF MOLECULAR CLOUD SOURCES. II.

EGGEN, O. J. <AP. J. SUPPL., 14, 307> 670901
NARROW- AND BROAD-BAND PHOTOMETRY OF RED STARS. I. NORTHERN GIANTS.

EGGEN, O. J. <AP. J. SUPPL., 16, 49> 680801
NARROW- AND BROAD-BAND PHOTOMETRY OF RED STARS. II. DWARFS.

EGGEN, O. J. <AP. J., 158, 225> 691002
NARROW- AND BROAD-BAND PHOTOMETRY OF RED STARS. IV. POPULATION SEPARATION IN GIANT STARS.

EGGEN, O. J. <AP. J., 222, 191> 780508
INTERMEDIATE-BAND PHOTOMETRY OF LATE-TYPE STARS. VI. MAIN-SEQUENCE STARS NEAR THE SUN.

EGGEN, O. J. <P. A. S. P., 81, 553> 691005
STELLAR GROUPS IN THE OLD DISK POPULATION.

EGGEN, O. J., GREENSTEIN, J. L. <AP. J., 150, 927> 679903
OBSERVATIONS OF PROPER-MOTION STARS. III.

EGGEN, O. J., STOKES, N. R. <AP. J., 161, 199> 700701
NARROW-BAND AND BROAD-BAND PHOTOMETRY OF RED STARS. III. SOUTHERN GIANTS.

EICHENDORF, W., HECK, A., CACCIN, B., RUSSO, G., SOLLAZZO, C. <ASTR. AP., 109, 274> 820509
UV, OPTICAL AND IR OBSERVATIONS OF THE CEPHEID R MUSCAE.

EIROA, C., NECKEL, TH., SANCHEZ MAGRO, C., SELBY, M. J. <ASTR. AP., 95, 206> 810220
NEAR INFRARED OBSERVATIONS OF THE H II REGION S 146.

EKERS, R. D. <ASTR. AP., 22, 309> 739911
UPPER LIMITS TO THE 21 CM CONTINUUM RADIATION FROM TWO MAGNETIC WHITE DWARFS.

ELIAS, J. H. <A. J., 83, 791> 780702
2.2-MICRON FIELD STARS AT THE NORTH GALACTIC POLE.

ELIAS, J. H. <AP. J., 223, 859> 780804
A STUDY OF THE IC 5146 DARK CLOUD COMPLEX.

ELIAS, J. H. <AP. J., 224, 453> 780902
AN INFRARED STUDY OF THE OPHIUCHUS DARK CLOUD.

ELIAS, J. H. <AP. J., 224, 857> 780909
A STUDY OF THE TAURUS DARK CLOUD COMPLEX.

ELIAS, J. H. <AP. J., 241, 728> 801007
H2 EMISSION FROM HERBIG-HARO OBJECTS.

ELIAS, J. H., ENNIS, D. J., GEZARI, D. Y., HAUSER, M. G., HOUCK, J. R., LO, K. Y., MATTHEWS, K., NADEAU, D., 780210
NEUGEBAUER, G., WERNER, M. W., WESTBROOK, W. E. <AP. J., 220, 25>
1 MILLIMETER CONTINUUM OBSERVATIONS OF EXTRAGALACTIC OBJECTS.

ELIAS, J. H., FROGEL, J. A., HACKWELL, J. A., PERSSON, S. E. <AP. J. (LETTERS), 251, L13> 811203
INFRARED LIGHT CURVES OF TYPE I SUPERNOVAE.

ELIAS, J. H., FROGEL, J. A., HUMPHREYS, R. M. <AP. J. (LETTERS), 242, L13> 801104
HV 11417: A PECULIAR M SUPERGIANT IN THE SMALL MAGELLANIC CLOUD.

ELIAS, J. H., FROGEL, J. A., HUMPHREYS, R. M., PERSSON, S. E. <AP. J. (LETTERS), 249, L55> 811011
INFRARED LUMINOSITIES OF M SUPERGIANTS AND THEIR USE AS DISTANCE INDICATORS.

ELIAS, J. H., FROGEL, J. A., MATTHEWS, K., NEUGEBAUER, G. <A. J., 87, 1029> 820707
INFRARED STANDARD STARS.

ELIAS, J. H., FROGEL, J. A., MATTHEWS, K., NEUGEBAUER, G. <A. J., 87, 1893> 821213
ERRATUM TO "INFRARED STANDARD STARS".

ELIAS, J. H., LANNING, H., NEUGEBAUER, G. <P. A. S. P., 90, 697> 781223
INFRARED AND OPTICAL VARIATIONS IN OMICRON CASSIOPEIAE (HD 4180).

ELLIOT, J. L., FRENCH, R. G., FROGEL, J. A., ELIAS, J. H., MINK, D. J., LILLER, W. <A. J., 86, 444> 810301
ORBITS OF NINE URANIAN RINGS.

ELLIS, R. S., GONDHALEKAR, P. M., EFSTATHIOU, G. <M. N. R. A. S., 201, 223> 821011
THE ULTRAVIOLET SPECTRA OF THE NUCLEI OF SPIRAL GALAXIES. I. NGC 4594, 3031, 5194 AND 4258.

ELSAESSER, H., BIRLE, K., EIROA, C., LENZEN, R. <ASTR. AP., 108, 274> 820418
ON THE INFRARED SOURCES 1 AND 2 IN NGC 7538.

EMERSON, J. P. <M. N. R. A. S., 177, 113P> 761212
IDENTIFICATION OF THE 100-MICRON SOURCES IN CYG X.

EMERSON, J. P., FURNISS, I., JENNINGS, R. E. <M. N. R. A. S., 172, 411> 750805
40-350 MICRON EMISSION FROM NGC 2023.

EMERSON, J. P., JENNINGS, R. E., MOORWOOD, A. F. M. <AP. J., 184, 401> 730901
FAR-INFRARED OBSERVATIONS OF HII REGIONS FROM BALLOON ALTITUDES.

EMERSON, J. P., JENNINGS, R. E., MOORWOOD, A. F. M. <NAT. PHYS. SCI., 241, 108> 730207
RCW 117 AND DR 15 OBSERVED IN THE FAR INFRARED.

ENGELS, D. <ASTR. AP. SUPPL., 36, 337> 790001
CATALOGUE OF LATE-TYPE STARS WITH OH, H2O OR SIO MASER EMISSION.

ENGELS, D., SHERWOOD, W. A., WAMSTEKER, W., SCHULTZ, G. V. <ASTR. AP. SUPPL., 45, 5> 810720
INFRARED OBSERVATIONS OF SOUTHERN BRIGHT STARS.

ENNIS, D. J., BECKLIN, E. E., BECKWITH, S., ELIAS, J. H., GATLEY, I., MATTHEWS, K., NEUGEBAUER, G., WILLNER, S. P. <AP. J., 214, 478> 770606
INFRARED OBSERVATIONS OF NOVA CYGNI 1975.

ENNIS, D. J., NEUGEBAUER, G., WERNER, M. <AP. J., 262, 451> 821105
VARIABILITY OF COMPACT RADIO SOURCES AT A WAVELENGTH OF 1 MILLIMETER.

ENNIS, D. J., NEUGEBAUER, G., WERNER, M. <AP. J., 262, 460> 821106
1 MILLIMETER CONTINUUM OBSERVATIONS OF QUASARS.

ENNIS, D. J., SOIFER, B. T., NEUGEBAUER, G., WERNER, M. <AP. LETTERS, 22, 13> 810004
ONE MILLIMETER CONTINUUM OBSERVATIONS OF HIGH REDSHIFT QUASARS.

EPCHTEIN, N., GUIBERT, J., NGUYEN-QUANG-RIEU,., TURON, P., WAMSTEKER, W. <ASTR. AP., 97, 1> 810417
NEW COMPACT INFRARED OBJECTS ASSOCIATED WITH TWO SOUTHERN TYPE - I. OH MASERS.

EPCHTEIN, N., GUIBERT, J., NGUYEN-QUANG-RIEU,., TURON, P., WAMSTEKER, W. <ASTR. AP., 85, L1> 800510
INFRARED PHOTOMETRY OF MIRA VARIABLES. OH MASER PUMPING EFFICIENCY.

EPCHTEIN, N., LEPINE, J. R. D. <ASTR. AP., 99, 210> 810618
INFRARED SURVEY OF SOUTHERN GALACTIC MASER SOURCES IN THE LONGITUDE RANGE 320 TO 30 DEGREES.

EPCHTEIN, N., NGUYEN-QUANG-RIEU <ASTR. AP., 107, 229> 820308
NEW INFRARED COUNTERPARTS OF SOUTHERN TYPE II OH MASER SOURCES.

EPCHTEIN, N., TURON, P. <ASTR. AP., 72, L4> 790212
10 MICRON OBSERVATION OF H II REGIONS WITH THE ESO 3.6 METER TELESCOPE.

EPSTEIN, E. E., FOGARTY, W. G., HACKNEY, K. R., HACKNEY,R.L.,LEACOCK, R. J., POMPHREY, R. B., SCOTT, R. L.,SMITH,A.G., HAWKINS, R. W., ROEDER, R. C., GARY, B. L., PENSTON,M.V., TRITTON, K. P., BERTAUD, CH., VERON, M. P., WLERICK, G., BERNARD, A., BIGAY, J. H., MERLIN, P., DURAND, A., SAUSE, G., BECKLIN, E. E., NEUGEBAUER, G., WYNN-WILLIAMS, C. G. <AP. J. (LETTERS), 178, L51> 721201
3C 120, BL LACERTAE, AND OJ 287: COORDINATED OPTICAL, INFRARED, AND RADIO OBSERVATIONS OF INTRADAY VARIABILITY.

ERICKSON, E. F., CAROFF, L. J., SIMPSON, J. P., STRECKER, D. W., GOORVITCH, D. <AP. J., 216, 404> 770905
THE FAR-INFRARED SPECTRUM OF THE CORE OF SAGITTARIUS B2.

ERICKSON, E. F., KNACKE, R. F., TOKUNAGA, A. T., HAAS, M. R. <AP. J., 245, 148> 810410
THE 45 MICRON H2O ICE BAND IN THE KLEINMANN-LOW NEBULA.

ERICKSON, E. F., STRECKER, D. W., SIMPSON, J. P., GOORVITCH, D., AUGASON, G. C., SCARGLE, J. D., CAROFF, L. J., WITTEBORN, F. C. <AP. J., 212, 696> 770303
SPECTRUM OF THE KLEINMANN-LOW NEBULA FROM 29 TO 125 MICROMETERS.

ERICKSON, E. F., SWIFT, C. D., WITTEBORN, F. C., MORD, A. J.,AUGASON, G. C., CAROFF, L. J., KUNZ, L. W., GIVER, L. P. <AP. J., 183, 535> 730707
INFRARED SPECTRUM OF THE ORION NEBULA BETWEEN 55 AND 200 MICRONS.

ERICKSON, E. F., TOKUNAGA, A. T. <AP. J., 238, 596> 800611
FAR-INFRARED SPECTRA OF W51-IRS2 AND W49 NW.

EVANS II, N. J., BECKLIN, E. E., BEICHMAN, C., GATLEY, I., HIDERBRAND, R. H., KEENE, J., SLOVAK, M. H., WERNER, M. W., WHITCOMB, S. E. <AP. J., 244, 115> 810209
FAR-INFRARED OBSERVATIONS OF THE CEPHEUS OB3 MOLECULAR CLOUD.

EVANS II, N. J., BECKWITH, S. <AP. J., 217, 729> 771109
NEW INFRARED OBJECTS ASSOCIATED WITH OH MASERS.

EVANS II, N. J., BECKWITH, S., BROWN, R. L., GILMORE, W. <AP. J., 227, 450> 790114
TYPE I OH MASERS: A STUDY OF POSITIONS, POLARIZATION, NEARBY WATER MASERS, AND RADIO CONTINUUM AND INFRARED PROPERTIES.

EVANS II, N. J., BEICHMAN, C., GATLEY, I., HARVEY, P., NADEAU, D., SELLGREN, K. <AP. J., 246, 409> 810604
INFRARED STUDIES OF THE S235 MOLECULAR CLOUD.

EVANS II, N. J., BLAIR, G. N. <AP. J., 246, 394> 810603
THE ENERGETICS OF MOLECULAR CLOUDS. III. THE S235 MOLECULAR CLOUD.

EVANS II, N. J., BLAIR, G. N., BECKWITH, S. <AP. J., 217, 448> 771004
THE ENERGETICS OF MOLECULAR CLOUDS. I. METHODS OF ANALYSIS AND APPLICATION TO THE S255 MOLECULAR CLOUD.

EVANS II, N. J., BLAIR, G. N., HARVEY, P., ISRAEL, F., PETERS III, W. L., SCHOLTES, M., DE GRAAUW, T., VANDEN BOUT, P. <AP. J., 250, 200> 811105
THE ENERGETICS OF MOLECULAR CLOUDS. IV. THE S88 MOLECULAR CLOUD.

EVANS II, N. J., BLAIR, G. N., NADEAU, D., VANDEN BOUT, P. <AP. J., 253, 115> 820203
THE ENERGETICS OF MOLECULAR CLOUDS. V. THE S37 MOLECULAR CLOUD.

EVANS, A., BODE, M. F., WHITTET, D. C. B., DAVIES, J. K., KILKENNY, D., BAINES, D. W. T. <M. N. R. A. S., 199, 37P> 820515
THE VARIABILITY OF RY LUPI.

FANTI, C., FANTI, R., PADRIELLI, L., VAN DER LAAN, H., DE RUITER, H. <ASTR. AP., 61, 487> 779906
A SEARCH FOR RADIO EMISSION FROM A SAMPLE OF OPTICALLY SELECTED QUASARS.

FAWLEY, W. M. <AP. J., 218, 181> 771112
ON THE NEAR-INFRARED EXCESSES OF VERY COOL SUPERGIANTS.

FAWLEY, W. M., COHEN, M. <AP. J., 193, 367> 741006
THE OPEN CLUSTER NGC 7419 AND ITS M7 SUPERGIANT IRC+60375.

FAY JR., T. D. <AP. J., 168, 99> 710801
COMPUTED AND OBSERVED CYANIDE-RADICAL SPECTRA OF THREE N STARS IN THE INFRARED.

FAY JR., T. D., FREDERICK, L. W., JOHNSON, H. R. <AP. J., 152, 151> 680403
COMPARISON OF SELECTED CARBON STARS AND M STARS AT 1 MICRON.

FAY JR., T. D., HONEYCUTT, R. K. <A. J., 77, 29> 720201
SCANNER OBSERVATIONS OF COOL STARS FROM 3400 TO 11000A.

FAY JR., T. D., MUFSON, S. L., DUNCAN, B. J., HOOVER, R. B., SANFORD, P. W., CHARLES, P. A., WHITE, N. E., WISNIEWSKI, W. Z., WAMSTEKER, W. <AP. J., 211, 152> 770103
OPTICAL, INFRARED, AND X-RAY OBSERVATIONS OF NGC 6624.

FAY JR., T. D., RIDGWAY, S. T. <AP. J., 203, 600> 760205
CARBON STAR PHOTOMETRY: CO AND 3.2 MICRON BANDS.

FAZIO, G. G., KLEINMANN, D. E., NOYES, R. W., WRIGHT, E. L., ZEILIK II, M., LOW, F. J. <AP. J. (LETTERS), 192, L23> 740803
A HIGH-RESOLUTION MAP OF THE ORION NEBULA REGION AT FAR-INFRARED WAVELENGTHS.

FAZIO, G. G., KLEINMANN, D. E., NOYES, R. W., WRIGHT, E. L., ZEILIK II, M., LOW, F. J. <AP. J. (LETTERS), 199, L177> 750801
A HIGH-RESOLUTION MAP OF THE W3 REGION AT FAR-INFRARED WAVELENGTHS.

FAZIO, G. G., LADA, C. J., KLEINMANN, D. E., WRIGHT, E. L., HO, P. T. P., LOW, F. J. <AP. J. (LETTERS), 221, L77> 780410
A NEW, COMPACT FAR-INFRARED SOURCE IN THE W31 REGION.

FAZIO, G. G., MCBREEN, B., STIER, M. T., WRIGHT, E. L. <AP. J. (LETTERS), 237, L39> 800403
THE FAR-INFRARED SIZE OF IRC+10216.

FAZIO, G. G., WRIGHT, E. L., ZEILIK II, M., LOW, F. J. <AP. J. (LETTERS), 206, L165> 760607
A FAR-INFRARED MAP OF THE OPHIUCHUS DARK CLOUD REGION.

FEAST, M. W. <IAUC NO. 3056> 770415
NOVA IN LARGE MAGELLANIC CLOUD.

FEAST, M. W. <IAUC NO. 3599> 810505
NOVA CORONAE AUSTRINAE 1981.

FEAST, M. W., CATCHPOLE, R. M., CARTER, B. S., ROBERTS, G. <M. N. R. A. S., 193, 377> 801107
A PERIOD-LUMINOSITY RELATION FOR SUPERGIANT RED VARIABLES IN THE LARGE MAGELLANIC CLOUD.

FEAST, M. W., CATCHPOLE, R. M., GLASS, I. S. <M. N. R. A. S., 174, 81P> 760308
THE BOLOMETRIC ABSOLUTE MAGNITUDE OF S TYPE STARS WITH LITHIUM PRODUCTION.

FEAST, M. W., CATCHPOLE, R. M., LLOYD EVANS, T., ROBERTSON, B. S. C., DEAN, J. F., BYWATER, R. A. <M. N. R. A. S., 178, 415> 770204
THE RCB VARIABLES-VII. THE INFRARED VARIABILITY OF RY SGR.

FEAST, M. W., GLASS, I. S. <M. N. R. A. S., 161, 293> 730008
INFRA-RED PHOTOMETRY OF R CORONAE BOREALIS TYPE VARIABLES AND RELATED OBJECTS.

FEAST, M. W., GLASS, I. S. <M. N. R. A. S., 164, 35P> 730012
THE NATURE OF A NEBULOUS OBJECT IN THE CHAMAELEON T ASSOCIATION.

FEAST, M. W., GLASS, I. S. <M. N. R. A. S., 167, 81> 740406
INFRA-RED PHOTOMETRY OF SOME OLD NOVAE.

FEAST, M. W., GLASS, I. S. <OBSERVATORY, 100, 208> 801216
THE SYMBIOTIC-NOVA SYSTEM AS 239.

FEAST, M. W., THACKERAY, A. D., WESSELINK, A. J. <M. N. R. A. S., 121, 25> 609903
THE BRIGHTEST STARS IN THE MAGELLANIC CLOUDS.

FEIGELSON, E. D., KRISS, G. A. <AP. J. (LETTERS), 248, L35> 819918
DISCOVERY OF THREE X-RAY LUMINOUS PRE-MAIN-SEQUENCE STARS.

FELDMAN, P. D., MCNUTT, D. P., SHIVANANDAN, K. <AP. J. (LETTERS), 154, L131> 681203
ROCKET OBSERVATIONS OF BRIGHT CELESTIAL INFRARED SOURCES IN URSA MAJOR.

FELLI, M., HARTEN, R. H. <ASTR. AP., 100, 28> 819913
A HIGH-RESOLUTION SEARCH FOR SMALL-SCALE STRUCTURE IN SHARPLESS H II REGIONS AT 4.995 GHZ. II. GENERAL PROPERTIES OF THE ENTIRE SAMPLE.

FELLI, M., PANAGIA, N. <AP. J., 262, 650> 821107
MASS LOSS FROM WOLF-RAYET STARS: AN ANALYSIS OF RADIO AND INFRARED OBSERVATIONS OF MR 111 - AS 422.

FERLAND, G. J., LAMBERT, D. L., NETZER, H., HALL, D. N. B., RIDGWAY, S. T. <AP. J., 227, 489> 790115
CARBON MONOXIDE EMISSION AND THE ETA CARINAE STAGE OF NOVA NQ VULPECULAE.

FERLAND, G. J., SHIELDS, G. A. <AP. J. (LETTERS), 224, L15> 780809
FINE-STRUCTURE LINES AND THE 10 MICRON EXCESS OF NOVA CYGNI 1975.

FERLAND, G. J., WOOTTEN, H. A. <AP. J. (LETTERS), 214, L27> 770506
THE SHELL PHASE IN NOVA CYGNI (1975).

FERRARI-TONIOLO, M., PERSI, P., GRASDALEN, G. L. <P. A. S. P., 93, 633> 811003
INFRARED EXCESS AND MASS-LOSS RATE OF THE EXTREME OF STAR HD 108.

FERRARI-TONIOLO, M., PERSI, P., VIOTTI, R. <M. N. R. A. S., 185, 841> 781217
COORDINATED INFRARED AND OPTICAL OBSERVATIONS OF GAMMA CAS AND X PER IN LATE 1976.

FINK, U., LARSON, H. P. <AP. J., 233, 1021> 791106
THE INFRARED SPECTRA OF URANUS, NEPTUNE, AND TITAN FROM 0.8 TO 2.5 MICRONS.

FISCHER, J., JOYCE, R. R., SIMON, M., SIMON, T. <AP. J., 258, 165> 820702
NEAR-INFRARED OBSERVATIONS OF THE FAR-INFRARED SOURCE V REGION IN NGC 6334.

FISCHER, J., RIGHINI-COHEN, G., SIMON, M. <AP. J. (LETTERS), 238, L155> 800603
DETECTION OF H2 EMISSION IN THE DR 21/W75 COMPLEX, OMC-2, AND HERBIG-HARO OBJECT NO. 2.

FISCHER, J., RIGHINI-COHEN, G., SIMON, M., CASSAR, L. <A. J., 84, 1574> 791003
FAR INFRARED, NEAR INFRARED, AND RADIO MOLECULAR LINE STUDIES OF HFE 2, HFE 3, AND FJM 6.

FISCHER, J., RIGHINI-COHEN, G., SIMON, M., JOYCE, R. R., SIMON, T. <AP. J. (LETTERS), 240, L95> 800901
OBSERVATIONS OF H2 EMISSION FROM NGC 7538.

FITCH, W. S., PACHOLCZYK, A. G., WEYMANN, R. J. <AP. J. (LETTERS), 150, L67> 671103
LIGHT VARIATIONS OF THE SEYFERT GALAXY NGC 4151.

FITZPATRICK, E. L., SAVAGE, B. D., SITKO, M. L. <AP. J., 256, 578> 820505
ULTRAVIOLET, VISUAL, AND INFRARED OBSERVATIONS OF THE WC7 VARIABLE HD 193793.

FIX, J. D., MUTEL, R. L., GAUME, R. A., CLAUSSEN, M. J. <AP. J., 259, 657> 820807
RADIO AND INFRARED OBSERVATIONS OF THE OH MASER SOURCE OH 351.78-0.54.

FLORKOWSKI, D. R., GOTTESMAN, S. T. <M. N. R. A. S., 179, 105> 770402
HD 193793, A RADIO-EMITTING WOLF-RAYET BINARY STAR.

FOLTZ, C. B., PETERSON, B. M., BOROSON, T. A. <A. J., 85, 1328> 809902
ACCURATE OPTICAL POSITIONS FOR MARKARIAN OBJECTS 701-797.

FOLTZ, C. B., PETERSON, B. M., BOROSON, T. A. <A. J., 86, 802> 819905
ERRATUM TO "ACCURATE OPTICAL POSITIONS FOR MARKARIAN GALAXIES 701-797. "

FORBES, F. F. <AP. J. (LETTERS), 165, L83> 710501
THE INFRARED POLARIZATION OF ETA CARINAE AND VY CANIS MAJORIS.

FORBES, F. F. <AP. J., 147, 1226> 670302
THE INFRARED POLARIZATION OF THE INFRARED STAR IN CYGNUS.

FORBES, F. F., STONAKER, W. F., JOHNSON, H. L. <A. J., 75, 158> 700301
STELLAR AND PLANETARY SPECTRA IN THE INFRARED FROM 1.35 TO 4.10 MICRONS.

FORD JR., W. K., PURGATHOFER, A. T., RUBIN, V. C. <AP. J. (LETTERS), 153, L39> 680701
OPTICAL SPECTRA NEAR 1 MICRON: THE SEYFERT GALAXY NGC 4151 AND THE PLANETARY NEBULA NGC 6543.

FORREST, W. J., GILLETT, F. C., HOUCK, J. R., MCCARTHY, J. F., MERRILL, K. M., PIPHER, J. L., PUETTER, R. C., RUSSELL, R. W., SOIFER, B. T., WILLNER, S. P. <AP. J., 219, 114> 780105
SPECTROPHOTOMETRY OF OH 26.5+0.6 FROM 2 TO 40 MICRONS.

FORREST, W. J., GILLETT, F. C., STEIN, W. A. <AP. J. (LETTERS), 170, L29> 711103
VARIABILITY OF RADIATION FROM CIRCUMSTELLAR GRAINS SURROUNDING R CORONAE BOREALIS.

FORREST, W. J., GILLETT, F. C., STEIN, W. A. <AP. J. (LETTERS), 178, L129> 721204
INFRARED MEASUREMENTS OF R CORONAE BOREALIS THROUGH ITS 1972 MARCH-JUNE MINIMUM.

FORREST, W. J., GILLETT, F. C., STEIN, W. A. <AP. J., 195, 423> 750104
CIRCUMSTELLAR GRAINS AND THE INTRINSIC POLARIZATION OF STARLIGHT.

FORREST, W. J., HOUCK, J. R., MCCARTHY, J. F. <AP. J., 248, 195> 810806
A FAR-INFRARED EMISSION FEATURE IN CARBON-RICH STARS AND PLANETARY NEBULAE.

FORREST, W. J., HOUCK, J. R., REED, R. A. <AP. J. (LETTERS), 208, L133> 760912
16-40 MICRON SPECTROSCOPY OF THE TRAPEZIUM AND THE KLEINMANN-LOW NEBULA IN ORION.

FORREST, W. J., MCCARTHY, J. F., HOUCK, J. R. <AP. J. (LETTERS), 240, L37> 800805
DETECTION OF (O IV) AND (NE V) INFRARED EMISSION LINES FROM NGC 7027.

FORREST, W. J., MCCARTHY, J. F., HOUCK, J. R. <AP. J., 233, 611> 791015
16-39 MICRON SPECTROSCOPY OF OXYGEN-RICH STARS.

FORREST, W. J., MERRILL, K. M., RUSSELL, R. W., SOIFER, B. T. <AP. J. (LETTERS), 199, L181> 750802
SPECTROPHOTOMETRY OF CRL 2688 FROM 2 TO 24 MICRONS.

FORREST, W. J., SOIFER, B. T. <AP. J. (LETTERS), 208, L129> 760911
16-25 MICRON SPECTROSCOPY OF THE TRAPEZIUM AND BN-KL SOURCE IN ORION.

FOSBURY, R. A. E., BOKSENBERG, A., SNIJDERS, M. A. J., DANZIGER, I. J., DISNEY, M. J., GOSS, W. M., PENSTON, M. V., WAMSTEKER, W., WELLINGTON, K. J., WILSON, A. S. <M. N. R. A. S., 201, 991> 821218
VERY EXTENDED IONIZED GAS IN RADIO GALAXIES. I. A RADIO, OPTICAL AND ULTRAVIOLET STUDY OF PKS 2158-380.

FOX, M. W. <M. N. R. A. S., 199, 715> 820513
PHOTOMETRY OF RED VARIABLES IN 47 TUCANAE.

FOY, R. <ASTR. AP., 85, 287> 800512
DETAILED ANALYSIS OF HIGH VELOCITY STARS.

FOY, R., CHELLI, A., SIBILLE, F., LENA, P. <ASTR. AP., 79, L5> 791016
ANGULAR DIAMETER OF IRC+10216, MIRA, R CAS, AND GL 2591 IN THE NEAR INFRARED.

FRANK, J., KING, A. R., SHERRINGTON, M. R., GILES, A. B., JAMESON, R. F. <M. N. R. A. S., 196, 921> 810911
THE INFRARED SPECTRUM OF THE DWARF NOVA EX HYDRAE.

FRANK, J., KING, A. R., SHERRINGTON, M. R., JAMESON, R. F., AXON, D. J. <M. N. R. A. S., 195, 505> 810508
INFRARED AND OPTICAL LIGHT CURVES OF UX URSAE MAJORIS AND U GEMINORUM.

FRANKSTON, M., SCHILD, R. E. <A. J., 81, 500> 760711
NEAR-INFRARED OBSERVATIONS OF THE EDGE-ON SPIRAL GALAXY NGC 4565.

FREDERICK, L. W. <A. J., 61, 437> 569904
PROPER MOTIONS IN THE NUCLEUS OF THE ZETA PERSEI ASSOCIATION.

FREY, A., LEMKE, D., THUM, C., FAHRBACH, U. <ASTR. AP., 74, 133> 790412
NEAR INFRARED OBSERVATIONS OF NGC 2024.

FRIDLUND, C. V. M., NORDH, H. L., VAN DUINEN, R. J., AALDERS, J. W. G., SARGENT, A. I. <ASTR. AP., 91, L1> 801108
A LOW-LUMINOSITY FAR INFRARED SOURCE IN THE L1551 MOLECULAR CLOUD.

FRIEDLANDER, M. W., GOEBEL, J. H., JOSEPH, R. D. <AP. J. (LETTERS), 194, L5> 741104
DETECTION OF NEW CELESTIAL OBJECTS AT FAR-INFRARED WAVELENGTHS.

FRIEDLANDER, M. W., JOSEPH, R. D. <AP. J. (LETTERS), 162, L87> 701104
DETECTION OF CELESTIAL SOURCES AT FAR-INFRARED WAVELENGTHS.

FRISK, U., BELL, R. A., GUSTAFSSON, B., NORDH, H. L., OLOFFSON, S. G. <M. N. R. A. S., 199, 471> 820511
THE TEMPERATURE OF ARCTURUS.

FROGEL, J. A. <AP. J. (LETTERS), 162, L5> 701002
WATER ABSORPTION IN THE INFRARED SPECTRUM OF LONG-PERIOD VARIABLE STARS AND ASSOCIATED MICROWAVE EMISSION.

FROGEL, J. A. <AP. J. (LETTERS), 241, L41> 801003
INFRARED PHOTOMETRY OF THE GLOBULAR CLUSTER ASSOCIATED WITH NGC 5128.

FROGEL, J. A., BLANCO, V. M., MCCARTHY, M. F., COHEN, J. G. <AP. J., 252, 133> 820101
THE LATE-TYPE STELLAR CONTENT OF THE FORNAX AND SCULPTOR DWARF GALAXIES.

FROGEL, J. A., COHEN, J. G. <AP. J., 253, 580> 820208
THE LATE-TYPE STELLAR CONTENT OF MAGELLANIC CLOUD CLUSTERS.

FROGEL, J. A., DICKINSON, D. F., HYLAND, A. R. <AP. J., 201, 392> 751006
CO IN THE INFRARED AND RADIO SPECTRA OF CARBON STARS.

FROGEL, J. A., ELIAS, J. H., PHILLIPS, M. M. <AP. J., 260, 70> 820901
8-13 MICRON OBSERVATIONS OF NINE EMISSION-LINE GALAXIES.

FROGEL, J. A., KLEINMANN, D. E., KUNKEL, W., NEY, E. P., STRECKER, D. W. <P. A. S. P., 84, 581> 720808
MULTICOLOR PHOTOMETRY OF THE M DWARF PROXIMA CENTAURI.

FROGEL, J. A., PERSSON, S. E. <AP. J., 178, 667> 721202
STUDIES OF SMALL HII REGIONS. I. INFRARED PHOTOMETRY OF SHARPLESS 138, 152, AND 270.

FROGEL, J. A., PERSSON, S. E. <AP. J., 186, 207> 731105
INFRARED SOURCES IN SHARPLESS 228.

FROGEL, J. A., PERSSON, S. E. <AP. J., 192, 351> 740906
COMPACT INFRARED SOURCES ASSOCIATED WITH SOUTHERN HII REGIONS.

FROGEL, J. A., PERSSON, S. E. <AP. J., 197, 351> 750404
INFRARED EMISSION FROM OH 284.2-0.8.

FROGEL, J. A., PERSSON, S. E. <P. A. S. P., 85, 641> 731007
INFRARED PHOTOMETRY OF THE X-RAY SOURCES 2U 0900-40 AND 2U 1700-37.

FROGEL, J. A., PERSSON, S. E., AARONSON, M. <AP. J., 213, 723> 770503
COMPACT INFRARED SOURCES ASSOCIATED WITH SOUTHERN HII REGIONS. II.

FROGEL, J. A., PERSSON, S. E., AARONSON, M., BECKLIN, E. E., MATTHEWS, K., NEUGEBAUER, G. <AP. J. (LETTERS), 200, L123> 750904
THE V-(2.2 MICRON) COLORS OF ELLIPTICAL GALAXIES.

FROGEL, J. A., PERSSON, S. E., AARONSON, M., BECKLIN, E. E., MATTHEWS, K., NEUGEBAUER, G. <AP. J. (LETTERS), 195, L15> 750101
STELLAR CONTENT OF THE NUCLEI OF ELLIPTICAL GALAXIES DETERMINED FROM 2.3-MICRON CO BAND STRENGTHS.

FROGEL, J. A., PERSSON, S. E., AARONSON, M., MATTHEWS, K. <AP. J., 220, 75> 780212
PHOTOMETRIC STUDIES OF COMPOSITE STELLAR SYSTEMS. I. CO AND JHK OBSERVATIONS OF E AND S0 GALAXIES.

FROGEL, J. A., PERSSON, S. E., COHEN, J. G. <AP. J., 227, 499> 790116
INFRARED COLORS, CO BAND STRENGTHS, AND PHYSICAL PARAMETERS FOR GIANTS IN M71.

FROGEL, J. A., PERSSON, S. E., COHEN, J. G. <AP. J., 239, 495> 800707
LUMINOSITIES AND TEMPERATURES OF THE REDDEST STARS IN THREE LMC CLUSTERS.

FROGEL, J. A., PERSSON, S. E., COHEN, J. G. <AP. J., 240, 785> 800906
PHOTOMETRIC STUDIES OF COMPOSITE STELLAR SYSTEMS. IV. INFRARED PHOTOMETRY OF GLOBULAR CLUSTERS IN M31 AND A COMPARISON WITH EARLY-TYPE GALAXIES.

FROGEL, J. A., PERSSON, S. E., COHEN, J. G. <AP. J., 246, 842> 810611
INFRARED PHOTOMETRY OF RED GIANTS IN THE GLOBULAR CLUSTER 47 TUCANAE.

FROGEL, J. A., PERSSON, S. E., KLEINMANN, D. E. <AP. LETTERS, 11, 227> 720005
ERRATUM TO "INFRARED PHOTOMETRY OF THE H II REGION SHARPLESS 266"

FROGEL, J. A., PERSSON, S. E., KLEINMANN, D. E. <AP. LETTERS, 11, 95> 720603
INFRARED PHOTOMETRY OF THE HII REGION SHARPLESS 266.

FROGEL, J. A., WHITFORD, A. E. <AP. J. (LETTERS), 259, L7> 820802
LUMINOSITY OF M GIANTS IN THE NUCLEAR BULGE OF THE GALAXY.

FURNISS, I., JENNINGS, R. E., MOORWOOD, A. F. M. <AP. J. (LETTERS), 176, L105> 720902
DETECTION OF FAR-INFRARED ASTRONOMICAL SOURCES.

FURNISS, I., JENNINGS, R. E., MOORWOOD, A. F. M. <AP. J., 202, 400> 751202
40-350 MICRON OBSERVATIONS OF GALACTIC SOURCES.

FURNISS, I., JENNINGS, R. E., MOORWOOD, A. F. M. <NAT. PHYS. SCI., 236, 6> 720304
FAR INFRARED OBSERVATIONS OF M42, NGC 2024 AND M1.

GAHM, G. F., NORDH, H. L., OLOFSSON, S. G., CARLBORG, N. C. J. <ASTR. AP., 33, 399> 740710
SIMULTANEOUS SPECTROSCOPIC AND PHOTOELECTRIC OBSERVATIONS OF THE T TAURI STAR RU LUPI.

GALLAGHER, J. S., GOAD, J. W., MOULD, J. <AP. J., 263, 101> 821202
STRUCTURE OF THE M33 NUCLEUS.

GALLAGHER, J. S., NEY, E. P. <AP. J. (LETTERS), 204, L35> 760204
THE EARLY INFRARED DEVELOPMENT OF NOVA CYGNI 1975.

GALLOUET, L., HEIDMANN, N. <ASTR. AP. SUPPL., 3, 325> 719904
OPTICAL POSITIONS OF BRIGHT GALAXIES.

GALLOUET, L., HEIDMANN, N., DAMPIERRE, F. <ASTR. AP. SUPPL., 12, 89> 739910
OPTICAL POSITIONS OF BRIGHT GALAXIES. II.

GALLOUET, L., HEIDMANN, N., DAMPIERRE, F. <ASTR. AP. SUPPL., 19, 1> 759903
OPTICAL POSITIONS OF BRIGHT GALAXIES. III.

GAMMON, R. H., GAUSTAD, J. E., TREFFERS, R. R. <AP. J., 175, 687> 720802
TEN-MICRON SPECTROSCOPY OF CIRCUMSTELLAR SHELLS.

GARRISON, R. F. <P. A. S. P., 80, 20> 680201
THE SPECTRUM OF STAR NO. 1 IN NGC 2024.

GASCOIGNE, S. C. B. <M. N. R. A. S., 124, 201> 629903
NGC 1783, A CLUSTER IN THE LARGE MAGELLANIC CLOUD.

GASCOIGNE, S. C. B. <M. N. R. A. S., 134, 59> 669904
COLOUR-MAGNITUDE DIAGRAMS FOR NINE GLOBULAR-LIKE CLUSTERS IN THE MAGELLANIC CLOUDS.

GATLEY, I., BECKLIN, E. E., HYLAND, A. R., JONES, T. J. <M. N. R. A. S., 197, 17P> 811211
DISCOVERY OF A PROTOSTAR IN THE LARGE MAGELLANIC CLOUD.

GATLEY, I., BECKLIN, E. E., MATTHEWS, K., NEUGEBAUER, G., PENSTON, M. V., SCOVILLE, N. Z. <AP. J. (LETTERS), 191, L121> 740801
A NEW INFRARED COMPLEX AND MOLECULAR CLOUD IN ORION.

GATLEY, I., BECKLIN, E. E., SELLGREN, K., WERNER, M. W. <AP. J., 233, 575> 791014
FAR-INFRARED OBSERVATIONS OF M17: THE INTERACTION OF AN HII REGION WITH A MOLECULAR CLOUD.

GATLEY, I., BECKLIN, E. E., WERNER, M. W., HARPER JR., D. A. <AP. J., 220, 822> 780302
FAR-INFRARED OBSERVATIONS OF HII REGIONS NEAR THE GALACTIC CENTER.

GATLEY, I., BECKLIN, E. E., WERNER, M. W., WYNN-WILLIAMS, C. G. <AP. J., 216, 277> 770806
AIRBORNE FAR-INFRARED OBSERVATIONS OF THE GALACTIC CENTER REGION.

GATLEY, I., HARVEY, P. M., THRONSON JR., H. A. <AP. J. (LETTERS), 222, L133> 780610
FAR-INFRARED OBSERVATIONS OF HII REGIONS IN M33.

GATLEY, I., HYLAND, A. R., JONES, T. J. <M. N. R. A. S., 200, 521> 820822
STAR FORMATION IN THE MAGELLANIC CLOUDS. II. DICOVERY OF A PROTOSTAR IN THE SMALL MAGELLANIC CLOUD.

GAUSTAD, J. E., GILLETT, F. C., KNACKE, R. F., STEIN, W. A. <AP. J., 158, 613> 691101
SPECTRA OF "INFRARED STARS" FROM 2.8 TO 5.1 MICRONS.

GAUTIER III, T. N., FINK, U., TREFFERS, R. R., LARSON, H. P. <AP. J. (LETTERS), 207, L129> 760710
DETECTION OF MOLECULAR HYDROGEN QUADRUPOLE EMISSION IN THE ORION NEBULA.

GAUTIER III, T. N., THOMPSON, R. I., FINK, U., LARSON, H. P. <AP. J., 205, 841> 760506
A LOWER LIMIT ON THE SURFACE CARBON-12/CARBON-13 RATIO IN ALPHA ORIONIS.

GEARHART, M. R., LUND, J. M., FRANTZ, D. J., KRAUS, J. D. <A. J., 77, 557> 729901
OPTICAL IDENTIFICATIONS OF OHIO SURVEY RADIO SOURCES.

GEBALLE, T. R., LACY, J. H., BECK, S. C. <AP. J. (LETTERS), 230, L47> 790512
THE 8 MICRON BAND OF SILICON MONOXIDE IN THE EXPANDING CLOUD AROUND VY CANIS MAJORIS.

GEBALLE, T. R., RANK, D. M. <AP. J. (LETTERS), 182, L113> 730603
OBSERVATION OF 9.0-MICRON LINE EMISSION FROM AR III IN NGC 7027 AND NGC 6572.

GEBALLE, T. R., RUSSELL, R. W., NADEAU, D. <AP. J. (LETTERS), 259, L47> 820805
DETERMINATION OF THE INTRINSIC Q(3)/S(1) LINE INTENSITY RATIO OF MOLECULAR HYDROGEN.

GEBALLE, T. R., WAMSTEKER, W., DANKS, A. C., LACY, J. H., BECK, S. C. <AP. J., 247, 130> 810704
INFRARED LINE AND CONTINUUM VIEWS OF G333.6–0.2.

GEBALLE, T. R., WOLLMAN, E. R., LACY, J. H., RANK, D. M. <P. A. S. P., 89, 840> 771206
OBSERVATIONS AND ANALYSIS OF CARBON MONOXIDE IN COOL STARS AT FIVE MICRONS.

GEBALLE, T. R., WOLLMAN, E. R., RANK, D. M. <AP. J. (LETTERS), 177, L27> 721004
OBSERVATIONS OF CARBON MONOXIDE IN COOL STARS AT 4.7 MICRONS.

GEBALLE, T. R., WOLLMAN, E. R., RANK, D. M. <AP. J., 183, 499> 730702
OBSERVATIONS OF CARBON MONOXIDE AT 4.7 MICRONS IN IRC+10216, VY CANIS MAJORIS, AND NML CYGNI.

GEHRELS, T. <A. J., 79, 590> 740501
WAVELENGTH DEPENDENCE OF POLARIZATION. XXVII. INTERSTELLAR POLARIZATION FROM 0.22 TO 2.2 MICRONS.

GEHRZ, R. D. <AP. J., 178, 715> 721203
INFRARED RADIATION FROM RV TAURI STARS. I. AN INFRARED SURVEY OF RV TAURI STARS AND RELATED OBJECTS.

GEHRZ, R. D., GRASDALEN, G. L., CASTELAZ, M., GULLIXSON, C., MOZURKEWICH, D., HACKWELL, J. A. <AP. J., 254, 550> 820304
ANATOMY OF A REGION OF STAR FORMATION: INFRARED IMAGES OF S106 (AFGL 2584).

GEHRZ, R. D., GRASDALEN, G. L., HACKWELL, J. A., MCCLAIN, D. <IAUC NO. 3213> 780412
NOVA SAGITTARII 1978 - IRC-20494 -V3876 SAGITTARII.

GEHRZ, R. D., GRASDALEN, G. L., HACKWELL, J. A., NEY, E. P. <AP. J., 237, 855> 800507
THE EVOLUTION OF THE DUST SHELL OF NOVA SERPENTIS 1978.

GEHRZ, R. D., GRASDALEN, G., HACKWELL, J. A., MCCLAIN, D., MCLAUGHLIN, S. F., SNEDEN, C. <IAUC NO. 3235> 780615
NOVA SERPENTIS 1978.

GEHRZ, R. D., GRASDALEN, G., HACKWELL, J. A., NEY, E. P. <IAUC NO. 3296> 781014
NOVA CYGNI 1978.

GEHRZ, R. D., HACKWELL, J. A. <AP. J. (LETTERS), 206, L161> 760606
A SEARCH FOR ANONYMOUS AFCRL INFRARED SOURCES.

GEHRZ, R. D., HACKWELL, J. A. <AP. J., 193, 385> 741008
NEW INFRARED MEASUREMENTS OF W VIRGINIS STARS.

GEHRZ, R. D., HACKWELL, J. A. <AP. J., 194, 619> 741202
CIRCUMSTELLAR DUST EMISSION FROM WC9 STARS.

GEHRZ, R. D., HACKWELL, J. A., BRIOTTA, D. A. <AP. J. (LETTERS), 221, L23> 780408
OBSERVATIONS OF THE HIGHLY EVOLVED CARBON STAR CRL 3099.

GEHRZ, R. D., HACKWELL, J. A., GRASDALEN, G. L. <IAUC NO. 3711> 820709
NOVA AQUILAE 1982.

GEHRZ, R. D., HACKWELL, J. A., GRASDALEN, G. L., MERRILL, K. M., HUMPHREYS, R. M., WILLIAMSON, F. O., PUETTER, R. C., RUSSELL, R. W., WILLNER, S. P. <A. J., 85, 1071> 800801
ON THE NATURE OF THE PECULIAR INFRARED SOURCE AFGL 2636.

GEHRZ, R. D., HACKWELL, J. A., GRASDALEN, G. L., MERRILL, K. M., HUMPHREYS, R. M., WILLIAMSON, F. O., PUETTER, R. C., RUSSELL, R. W., WILLNER, S. P. <A. J., 85, 1676> 801201
ERRATUM TO "ON THE NATURE OF THE PECULIAR INFRARED SOURCE AFGL 2636".

GEHRZ, R. D., HACKWELL, J. A., GRASDALEN, G. L., NEY, E. P., NEUGEBAUER, G., SELLGREN, K. <AP. J., 239, 570> 800710
THE OPTICALLY THIN DUST SHELL OF NOVA CYGNI 1978.

GEHRZ, R. D., HACKWELL, J. A., JONES, T. W. <AP. J., 191, 675> 740807
INFRARED OBSERVATIONS OF BE STARS FROM 2.3 TO 19.5 MICRONS.

GEHRZ, R. D., HACKWELL, J. A., SMITH, J. R. <AP. J. (LETTERS), 202, L33> 751102
8-13 MICRON MAPS OF THE TRAPEZIUM REGION OF THE ORION NEBULA.

GEHRZ, R. D., NEY, E. P. <P. A. S. P., 84, 768> 721205
INFRARED OBSERVATIONS OF SOUTHERN RV TAURI STARS.

GEHRZ, R. D., NEY, E. P., BECKLIN, E. E., NEUGEBAUER, G. <AP. LETTERS, 13, 89> 730024
THE INFRARED SPECTRUM AND ANGULAR SIZE OF ETA CARINAE.

GEHRZ, R. D., NEY, E. P., STRECKER, D. W. <AP. J. (LETTERS), 161, L219> 700907
OBSERVATIONS OF ANOMALOUS RADIATION AT LONG WAVELENGTHS FROM IC CLASS VARIABLES.

GEHRZ, R. D., WOOLF, N. J. <AP. J. (LETTERS), 161, L213> 700906
RV TAURI STARS: A NEW CLASS OF INFRARED OBJECT.

GEHRZ, R. D., WOOLF, N. J. <AP. J., 165, 285> 710403
MASS LOSS FROM M STARS.

GEISEL, S. L. <AP. J. (LETTERS), 161, L105> 700806
INFRARED EXCESSES, LOW EXCITATION EMISSION LINES, AND MASS LOSS.

GEISEL, S. L., KLEINMANN, D. E., LOW, F. J. <AP. J. (LETTERS), 161, L101> 700804
INFRARED EMISSION OF NOVAE.

GENZEL, R., BECKLIN, E. E., WYNN-WILLIAMS, C. G., MORAN, J. M., REID, M. J., JAFFE, D. T., DOWNES, D. <AP. J., 255, 527> 820406
INFRARED AND RADIO OBSERVATIONS OF W51: ANOTHER ORION-KL AT A DISTANCE OF 7 KILOPARSECS?

GEZARI, D. Y. <AP. J. (LETTERS), 259, L29> 820804
THE REMARKABLE 400 MICRON SOURCE NGC 6334/I(NORTH).

GEZARI, D. Y., JOYCE, R. R., RIGHINI, G., SIMON, M. <AP. J. (LETTERS), 191, L33> 740702
350-MICRON MAPPING OF THE ORION MOLECULAR CLOUD.

GEZARI, D. Y., JOYCE, R. R., SIMON, M. <AP. J. (LETTERS), 179, L67> 730102
OBSERVATIONS OF THE GALACTIC NUCLEUS AT 350 MICRONS.

GEZARI, D. Y., SCHMITZ, M., MEAD, J. M. <NASA TM-83819> 820422
CATALOG OF INFRARED OBSERVATIONS.

GEZARI, D. Y., SCHMITZ, M., MEAD, J. M. <NASA TM-84001> 821014
FAR INFRARED SUPPLEMENT: CATALOG OF INFRARED OBSERVATIONS.

GIGUERE, P. T. <AP. J., 186, 585> 731208
ONE-MICRON REGION SEARCH FOR HCN IN TWO CARBON STARS.

GIGUERE, P. T., WOOLF, N. J., WEBBER, J. C. <AP. J. (LETTERS), 207, L195> 760809
IRC+10420: A HOT SUPERGIANT MASER.

GILES, A. B. <M. N. R. A. S., 199, 483> 820512
A POWERFUL METHOD FOR STAR COUNTING IN THE INFRARED.

GILES, A. B., ADAMS, D. J. <IAUC NO. 3594> 810412
GX 339-4 - 4U1658-48.

GILES, A. B., KING, A. R., COOKE, B. A., MCHARDY, I. M., LAWRENCE, A. <NATURE, 281, 282> 790901
INFRARED OBSERVATIONS OF SS433.

GILES, A. B., KING, A. R., JAMESON, R. F., SHERRINGTON, M. R., HOUGH, J. H., BAILEY, J. A., CUNNINGHAM, E. C. <NATURE, 286, 689> 800817
THE IR VARIABILITY OF SS433.

GILL, D., KAPTEYN, J. C. <ANN. CAPE OBS., 3-5> 968901
CAPE PHOTOGRAPHIC DURCHMUSTERUNG, PARTS I-III.

GILLETT, F. C., FORREST, W. J. <AP. J., 179, 483> 730106
SPECTRA OF THE BECKLIN-NEUGEBAUER POINT SOURCE AND THE KLEINMANN-LOW NEBULA FROM 2.8 TO 13.5 MICRONS.

GILLETT, F. C., FORREST, W. J., MERRILL, K. M. <AP. J., 183, 87> 730706
8-13 MICRON SPECTRA OF NGC 7027, BD+30 3639, AND NGC 6572.

GILLETT, F. C., FORREST, W. J., MERRILL, K. M., CAPPS, R. W.,SOIFER, B. T. <AP. J., 200, 609> 750905
THE 8-13 MICRON SPECTRA OF COMPACT HII REGIONS.

GILLETT, F. C., HYLAND, A. R., STEIN, W. A. <AP. J. (LETTERS), 162, L21> 701003
89 HERCULIS: AN F2 SUPERGIANT WITH LARGE CIRCUMSTELLAR INFRARED EMISSION.

GILLETT, F. C., KLEINMANN, D. E., WRIGHT, E. L., CAPPS, R. W. <AP. J. (LETTERS), 198, L65> 750602
OBSERVATIONS OF M82 AND NGC 253 AT 8-13 MICRONS.

GILLETT, F. C., KNACKE, R. F., STEIN, W. A. <AP. J. (LETTERS), 163, L57> 710102
INFRARED STUDIES OF GALACTIC NEBULAE. II. THE COMPACT NEBULAE IC 4997, VV 8, AND FG SAGITTAE.

GILLETT, F. C., LOW, F. J., STEIN, W. A. <AP. J., 154, 677> 681101
STELLAR SPECTRA FROM 2.8 TO 14 MICRONS.

GILLETT, F. C., LOW, F. J., STEIN, W. A. <AP. J. (LETTERS), 149, L97> 670903
INFRARED OBSERVATIONS OF THE PLANETARY NEBULA NGC 7027.

GILLETT, F. C., MERRILL, K. M., STEIN, W. A. <AP. J., 164, 83> 710203
OBSERVATIONS OF INFRARED RADIATION FROM COOL STARS.

GILLETT, F. C., MERRILL, K. M., STEIN, W. A. <AP. J., 172, 367> 720301
INFRARED STUDIES OF GALACTIC NEBULAE. IV. CONTINUUM AND LINE RADIATION FROM PLANETARY NEBULAE.

GILLETT, F. C., SOIFER, B. T. <AP. J., 207, 780> 760806
INFRARED SPECTROPHOTOMETRY OF OH 231.8+4.2-OH 0739-14.

GILLETT, F. C., STEIN, W. A. <AP. J. (LETTERS), 155, L97> 690203
DETECTION OF THE 12.8-MICRON NE+ EMISSION LINE FROM THE PLANETARY NEBULA IC 418.

GILLETT, F. C., STEIN, W. A. <AP. J., 159, 817> 700303
INFRARED STUDIES OF GALACTIC NEBULAE. I. NGC 6523, NGC 6572, AND BD 30 3639.

GILLETT, F. C., STEIN, W. A. <AP. J., 164, 77> 710202
INFRARED STUDIES OF GALACTIC NEBULAE. II. B STARS ASSOCIATED WITH NEBULOSITY.

GILLETT, F. C., STEIN, W. A., LOW, F. J. <AP. J. (LETTERS), 153, L185> 680901
THE SPECTRUM OF NML CYGNUS FROM 2.8 TO 5.6 MICRONS.

GILLETT, F. C., STEIN, W. A., SOLOMON, P. M. <AP. J. (LETTERS), 160, L173> 700605
THE SPECTRUM OF VY CANIS MAJORIS FROM 2.9 TO 14 MICRONS.

GILMORE, A. C. <IAUC NO. 3591> 819915
NOVA CORONAE AUSTRINAE 1981.

GILMORE, G., REID, I. N. <NATURE, 291, 208> 810510
RG0044-2958:A PECULIAR M SUPERGIANT AT A DISTANCE OF 2.5 MPC.

GILMORE, W. <A. J., 85, 894> 809913
RADIO CONTINUUM INTERFEROMETRY OF DARK CLOUDS. I. A SEARCH FOR NEWLY FORMED H II REGIONS.

GINGRICH, C. H. <AP. J., 56, 139> 229901
PARALLAXES OF STARS IN THE REGION OF B. D. +31 643.

GISPERT, R., PUGET, J. L., SERRA, G. <ASTR. AP., 106, 293> 820213
FAR INFRARED SURVEY OF EXTENDED MOLECULAR CLOUDS H II REGIONS COMPLEXES ALONG THE GALACTIC PLANE.

GLASS, I. S. <IAUC NO. 2911> 760211
VY CANIS MAJORIS.

GLASS, I. S. <IAUC NO. 2974> 760713
CIRCINUS X-1.

GLASS, I. S. <IAUC NO. 3363> 790517
SS433.

GLASS, I. S. <M. N. A. S. S. A., 33, 53> 740405
JHKL PHOTOMETRY OF 145 SOUTHERN STARS.

GLASS, I. S. <M. N. R. A. S., 162, 35P> 730018
INFRA-RED OBSERVATIONS OF NGC 7552 AND NGC 7582 AND THEIR IDENTIFICATION WITH PKS RADIO SOURCES.

GLASS, I. S. <M. N. R. A. S., 164, 155> 730003
THE JHKL COLOURS OF GALAXIES.

GLASS, I. S. <M. N. R. A. S., 168, 249> 740808
JHKL PHOTOMETRY OF LMC STARS.

GLASS, I. S. <M. N. R. A. S., 171, 19P> 750607
INTERMEDIATE INFRARED COLOURS OF M-DWARF STARS.

GLASS, I. S. <M. N. R. A. S., 175, 191> 760412
MORE JHKL COLOURS OF GALAXIES.

GLASS, I. S. <M. N. R. A. S., 182, 93> 780102
AN INFRARED SEARCH FOR OH/IR STARS.

GLASS, I. S. <M. N. R. A. S., 183, 335> 780501
VARIATIONS OF CIRCINUS X-1 IN THE INFRARED.

GLASS, I. S. <M. N. R. A. S., 185, 23> 781001
THE LONG-TERM INFRARED BEHAVIOUR OF RCB STARS.

GLASS, I. S. <M. N. R. A. S., 186, 29P> 790307
INFRARED OBSERVATIONS OF ACTIVE SOUTHERN GALAXIES AND QSOS.

GLASS, I. S. <M. N. R. A. S., 186, 317> 790201
INFRARED OBSERVATIONS OF LATE-TYPE SUPERGIANTS IN THE MAGELLANIC CLOUDS.

GLASS, I. S. <M. N. R. A. S., 187, 305> 790503
INFRARED PHOTOMETRY OF STARS IN THE CHAMAELEON T ASSOCIATION.

GLASS, I. S. <M. N. R. A. S., 187, 807> 790601
INFRARED OBSERVATIONS OF GALACTIC X-RAY SOURCES.

GLASS, I. S. <M. N. R. A. S., 192, 37P> 800812
JHK OBSERVATIONS OF TWO Z - 3 QSOS.

GLASS, I. S. <M. N. R. A. S., 194, 795> 810311
JHK OBSERVATIONS OF QUASARS AND BL LAC OBJECTS.

GLASS, I. S. <M. N. R. A. S., 197, 1067> 811210
THE INFRARED CONTINUA OF ACTIVE GALAXIES.

GLASS, I. S. <NAT. PHYS. SCI., 237, 7> 720503
OBSERVATIONS OF 30 DORADUS IN THE INFRARED.

GLASS, I. S. <NATURE, 273, 35> 780512
INFRARED SOURCES IN THE VICINITY OF 2S1728-337.

GLASS, I. S., ALLEN, D. A. <OBSERVATORY, 95, 27> 750214
INFRA-RED SOURCES NEAR COD-42 11721.

GLASS, I. S., FEAST, M. W. <AP. LETTERS, 13, 81> 730023
AN INFRARED OBJECT PROBABLY ASSOCIATED WITH OH 338.5+0.1.

GLASS, I. S., FEAST, M. W. <IAUC NO. 3226> 780614
2S1702-363.

GLASS, I. S., FEAST, M. W. <M. N. R. A. S., 163, 245> 730019
INFRA-RED PHOTOMETRY OF RED GIANTS IN THE GLOBULAR CLUSTERS 47 TUC AND OMEGA CEN.

GLASS, I. S., FEAST, M. W. <M. N. R. A. S., 198, 199> 820112
INFRARED PHOTOMETRY OF MIRA VARIABLES IN THE BAADE WINDOWS AND THE DISTANCE TO THE GALACTIC CENTRE.

GLASS, I. S., FEAST, M. W. <M. N. R. A. S., 199, 245> 820420
INFRARED PHOTOMETRY OF MIRA VARIABLES IN THE LMC AND THE PULSATIONAL PROPERTIES OF MIRAS.

GLASS, I. S., FEAST, M. W. <NAT. PHYS. SCI., 245, 39> 730907
PECULIAR OBJECT NEAR X2+5

GLASS, I. S., MOORWOOD, A. F. M., EICHENDORF, W. <ASTR. AP., 107, 276> 820311
MID-INFRARED OBSERVATIONS OF SEYFERT 1 AND NARROW-LINE X-RAY GALAXIES.

GLASS, I. S., PENSTON, M. V. <M. N. R. A. S., 167, 237> 740502
AN INFRARED SURVEY OF RW AURIGAE STARS.

GLASS, I. S., PENSTON, M. V. <M. N. R. A. S., 172, 227> 750703
INFRARED PHOTOMETRY IN THE R CRA ASSOCIATION.

GLASS, I. S., WEBSTER, B. L. <M. N. R. A. S., 165, 77> 730013
INFRA-RED PHOTOMETRY OF RR TELESCOPII AND OTHER EMISSION-LINE OBJECTS.

GLUSHKOV, YU., I., DENISYUK, E. K., KARYAGINA, Z. V. <ASTR. AP., 39, 481> 759906
YOUNG STELLAR CLUSTERS IN DIFFUSE NEBULAE.

GLUSHNEVA, I. N. <SOV. AST., 16, 846> 730305
SPECTRAL ENERGY DISTRIBUTION IN SEVERAL BINARIES AT 3300-7300A AND 0.88-1.53 MICRONS.

GLUSHNEVA, I. N., ESIPOV, V. F. <SOV. AST., 11, 828> 680304
THE INFRARED SPECTRUM OF ALGOL.

GNEDIN, YU. N., KHOZOV, G. V., LARIONOV, V. M. <SOV. AST. (LETTERS), 7, 256> 810807
INFRARED PHOTOMETRY OF GALACTIC X-RAY SOURCES.

GNEDIN, YU. N., MITROFANOV, I. G. <SOV. AST., 19, 673> 751109
THE NATURE OF THE KLEINMANN-LOW AND BECKLIN-NEUGEBAUER INFRARED SOURCES.

GOEBEL, J. H., BREGMAN, J. D., GOORVITCH, D., STRECKER, D. W., PUETTER, R. C., RUSSELL, R. W., SOIFER, B. T., WILLNER, S. P., FORREST, W. J., HOUCK, J. R., MCCARTHY, J. F. <AP. J., 235, 104> 800106
THE INFRARED SPECTRUM OF THE CARBON STAR Y CANUM VENATICORUM BETWEEN 1.2 AND 30 MICRONS.

GOEBEL, J. H., BREGMAN, J. D., STRECKER, D. W., WITTEBORN, F. C., ERICKSON, E. F. <AP. J. (LETTERS), 222, L129> 780609
C3 AND INFRARED SPECTROPHOTOMETRY OF Y CANUM VENATICORUM.

GOEBEL, J. H., BREGMAN, J. D., WITTEBORN, F. C., TAYLOR, B. J., WILLNER, S. P. <AP. J., 246, 455> 810607
IDENTIFICATION OF NEW INFRARED BANDS IN A CARBON-RICH MIRA VARIABLE.

GOORVITCH, D., GOEBEL, J. H., AUGASON, G. C. <AP. J., 240, 588> 800909
THEORETICAL PROFILES FOR THE 1-0 S(1) H2 LINE IN CARBON STARS.

GORDON, C. <AP. J., 207, 860> 760808
TYPE I SUPERNOVAE. II. THE SPECTRUM OF SN 1972E IN NGC 5253, 250 DAYS AFTER THE EXPLOSION.

GOSNELL, T. R., HUDSON, H. S., PUETTER, R. C. <A. J., 84, 538> 790401
GROUND-BASED OBSERVATIONS OF SOURCES IN THE AFGL INFRARED SKY SURVEY.

GOULD, R. J. <AP. J., 143, 603> 660201
12. 8-MICRON EMISSION FROM PLANETARY NEBULAE.

GOW, C. E., SANDFORD II, M. T., HONEYCUTT, R. K. <ASTR. AP., 67, 435> 780712
PHOTOGRAPHS OF THE ORION NEBULA IN H-ALPHA, H-BETA AND HE I 10830.

GRAHAM, J. A. <IAUC NO. 3049> 779903
NOVA IN LARGE MAGELLANIC CLOUD.

GRAHAM, J. A., PHILIPS, M. M. <AP. J. (LETTERS), 239, L97> 809906
THE FIRST BRIGHT GLOBULAR CLUSTER IN NGC 5128.

GRASDALEN, G. L. <A. J., 79, 1047> 741001
NEAR-INFRARED MAGNITUDES AND (V-K) COLORS OF GLOBULAR CLUSTERS.

GRASDALEN, G. L. <AP. J. (LETTERS), 205, L83> 760410
BRACKETT-ALPHA EMISSION IN THE BECKLIN-NEUGEBAUER OBJECT.

GRASDALEN, G. L. <AP. J. (LETTERS), 208, L11> 760812
PASCHEN-ALPHA IN 3C 273.

GRASDALEN, G. L. <AP. J., 182, 781> 730607
V1057 CYGNI AND PRE-MAIN-SEQUENCE EVOLUTION.

GRASDALEN, G. L. <AP. J., 193, 373> 741007
AN INFRARED STUDY OF NGC 2024.

GRASDALEN, G. L. <AP. J., 195, 605> 750204
(V-K) COLORS OF GALAXIES: STATISTICAL DIFFERENCES BETWEEN SPIRALS AND ELLIPTICALS AND THE COLOR-DIAMETER RELATION FOR ELLIPTICAL GALAXIES.

GRASDALEN, G. L. <AP. J., 229, 587> 790409
THE 10 MICRON PROPERTIES OF PLANETARY NEBULAE.

GRASDALEN, G. L. <P. A. S. P., 91, 436> 790808
NEAR INFRARED OBSERVATIONS OF THE CRAB NEBULA.

GRASDALEN, G. L., CARRASCO, L. <ASTR. AP., 43, 259> 751009
NGC 2175: THE CLUSTER AGE AND THE NATURE OF THE NEBULOSITY SURROUNDING S 252A.

GRASDALEN, G. L., CASTELAZ, M., GEHRZ, R. D. <IAUC NO. 3551> 801210
NOVA CYGNI 1980.

GRASDALEN, G. L., GAUSTAD, J. E. <A. J., 76, 231> 710401
A COMPARISON OF THE TWO-MICRON SKY SURVEY WITH THE DEARBORN CATALOG OF FAINT RED STARS.

GRASDALEN, G. L., HACKWELL, J. A., GEHRZ, R. D., MCCLAIN, D. <AP. J. (LETTERS), 234, L129> 791202
RY SCUTI: SILICATES AROUND AN EARLY-TYPE SUPERGIANT BINARY SYSTEM.

GRASDALEN, G. L., JOYCE, R. R. <AP. J. (LETTERS), 205, L11> 760406
ADDITIONAL OBSERVATIONS OF THE UNIDENTIFIED INFRARED FEATURES AT 3.28 AND 3.4 MICRONS.

GRASDALEN, G. L., JOYCE, R. R. <AP. J., 208, 317> 760904
INFRARED OBSERVATIONS OF NGC 5128.

GRASDALEN, G. L., JOYCE, R. R. <ASTR. AP., 50, 297> 760702
NEAR-INFRARED OBSERVATIONS OF SMALL HII REGIONS IN THE SMALL MAGELLANIC CLOUD.

GRASDALEN, G. L., JOYCE, R. R. <NATURE, 259, 187> 760111
CORONAL LINES IN NEAR INFRARED SPECTRUM OF NOVA CYGNI 1975.

GRASDALEN, G. L., JOYCE, R. R., KNACKE, R. F., STROM, S. E., STROM, K. M. <A. J., 80, 117> 750201
PHOTOMETRIC STUDY OF THE CHAMAELEON T-ASSOCIATION.

GRASDALEN, G. L., SNEDEN, C. <P. A. S. P., 91, 337> 790604
HIGHLY REDDENED M-TYPE SUPERGIANTS FROM THE IRC CATALOG.

GRASDALEN, G. L., STROM, K. M., STROM, S. E. <AP. J. (LETTERS), 184, L53> 730903
A 2-MICRON MAP OF THE OPHIUCHUS DARK-CLOUD REGION.

GREEN, R. F., RICHSTONE, D. O., SCHMIDT, M. <AP. J., 224, 892> 780910
PG 1413+01: A WHITE DWARF-RED DWARF ECLIPSING BINARY.

GREENBERG, L. T., DYAL, P., GEBALLE, T. R. <AP. J. (LETTERS), 213, L71> 770411
DETECTION OF (S III) FINE-STRUCTURE EMISSION IN IONIZED NEBULAE.

GREENE, A. E., WING, R. F. <AP. J., 200, 688> 750906
THE TEMPERATURE AND SPECTRUM OF VX AQUILAE.

GREENSTEIN, J. L. <AP. J. (LETTERS), 184, L23> 730806
MWC 349, AN OPTICAL, RADIO, AND INFRARED SOURCE.

GREENSTEIN, J. L., NEUGEBAUER, G., BECKLIN, E. E. <AP. J., 161, 519> 700801
THE FAINT END OF THE MAIN SEQUENCE.

GREENSTEIN, J. L., OKE, J. B. <P. A. S. P., 89, 131> 770413
AN INTERPRETATION OF THE SPECTRUM OF THE RED RECTANGLE.

GRIERSMITH, D., HYLAND, A. R., JONES, T. J. <A. J., 87, 1106> 820813
PHOTOMETRIC PROPERTIES OF BRIGHT EARLY-TYPE SPIRAL GALAXIES. IV. MULTIAPERTURE UBVJHK PHOTOMETRY FOR THE INNER (BULGE) REGIONS OF 65 GALAXIES.

GRIFFITHS, R. E., WARD, M. J., BLADES, J. C., WILSON, A. S. <IAUC NO. 3326> 799906
2A 0311-227.

GRINDLEY, J. E., HERTZ, P. <AP. J. (LETTERS), 247, L17> 810707
DISCOVERY OF AN OBSCURED GLOBULAR CLUSTER ASSOCIATED WITH GX 354+0 (-4U/MXB 1728-34).

GROOTE, D., HUNGER, K. <ASTR. AP., 116, 64> 821214
SHELL AND PHOTOSPHERE OF SIGMA ORI E: NEW OBSERVATIONS AND IMPROVED MODEL.

GROOTE, D., HUNGER, K., SCHULTZ, G. V. <ASTR. AP., 83, L5> 800308
THE IR-EXCESS OF HELIUM-VARIABLE STARS.

GUETTER, H. H. <A. J., 82, 598> 770801
SPECTROSCOPIC STUDIES OF STARS IN PER OB2.

GUETTER, H. H. <A. J., 84, 1846> 791201
PHOTOMETRIC STUDIES OF STARS IN ORI OB1 (BELT).

GULL, G. E., HOUCK, J. R., MCCARTHY, J. F., FORREST, W. J., HARWIT, M. <A. J., 83, 1440> 781104
FAR-INFRARED POLARIZATION OF THE KLEINMANN-LOW NEBULA IN ORION.

GULL, G. E., RUSSELL, R. W., MELNICK, G., HARWIT, M. <A. J., 85, 1379> 801002
FAR-INFRARED POLARIZATION OF THE KLEINMANN-LOW NEBULA.

GUSEV, E. B., KOMAROV, N. S., MEDVEDEV, YU. A. <SOV. AST., 17, 150> 730708
SPECTRAL ENERGY DISTRIBUTION OF SIX STARS.

HACKWELL, J. A. <ASTR. AP., 21, 239> 721103
LONG WAVELENGTH SPECTROMETRY AND PHOTOMETRY OF M, S AND C-STARS.

HACKWELL, J. A., BOPP, B. W., GEHRZ, R. D. <AP. J. (LETTERS), 192, L79> 740902
INFRARED OBSERVATIONS OF BD -10 4662.

HACKWELL, J. A., GEHRZ, R. D. <AP. J., 194, 49> 741105
INFRARED PHOTOMETRY OF HIGH-LUMINOSITY SUPERGIANTS EARLIER THAN M AND THE INTERSTELLAR EXTINCTION LAW.

HACKWELL, J. A., GEHRZ, R. D., GRASDALEN, G. L. <AP. J., 234, 133> 791107
DUST FORMATION AROUND HD 193793.

HACKWELL, J. A., GEHRZ, R. D., SMITH, J. R. <AP. J., 192, 383> 740907
INFRARED PHOTOMETRY OF WOLF-RAYET STARS FROM 2.3 TO 23 MICRONS.

HACKWELL, J. A., GEHRZ, R. D., SMITH, J. R., BRIOTTA, D. A. <AP. J., 221, 797> 780503
INFRARED MAPS OF W3 FROM 4.9 MICRONS TO 20 MICRONS.

HACKWELL, J. A., GEHRZ, R. D., SMITH, J. R., STRECKER, D. W. <AP. J., 210, 137> 761109
INFRARED LIGHT VARIATIONS OF WOLF-RAYET STARS.

HACKWELL, J. A., GEHRZ, R. D., WOOLF, N. J. <NATURE, 227, 822> 700805
INTERSTELLAR SILICATE ABSORPTION BANDS.

HACKWELL, J. A., GRASDALEN, G. L., GEHRZ, R. D. <AP. J., 252, 250> 820102
10 AND 20 MICRON IMAGES OF REGIONS OF STAR FORMATION.

HAGEN, W. <A. J., 84, 1189> 790804
BROAD-BAND 10 MICRON AND 20 MICRON PHOTOMETRY OF SOUTHERN SOURCES FROM THE AFGL INFRARED SKY SURVEY.

HAGEN, W. <AP. J. (LETTERS), 222, L37> 780511
THE CIRCUMSTELLAR ENVELOPES OF M GIANTS AND SUPERGIANTS.

HAGEN, W. <P. A. S. P., 91, 165> 790402
SIMULTANEOUS MICROWAVE AND INFRARED OBSERVATIONS OF STELLAR WATER MASER SOURCES.

HAGEN, W. <P. A. S. P., 94, 835> 821005
OBSERVATIONS OF COOL STARS AT 20, 25, AND 33 MICRONS.

HAGEN, W., HUMPHREYS, R. M., STENCEL, R. E. <P. A. S. P., 93, 567> 811002
HIGH-DISPERSION SPECTROSCOPY OF THE MOST LUMINOUS F- AND G-TYPE SUPERGIANTS IN THE LARGE MAGELLANIC CLOUD AND THE MILKY WAY.

HAGEN, W., SIMON, T., DYCK, H. M. <AP. J. (LETTERS), 201, L81> 751002
POSSIBLE IDENTIFICATION OF A CIRCUMSTELLAR 33-MICRON SILICATE EMISSION BAND IN COOL-STAR SPECTRA.

HALL, D. N. B., KLEINMANN, S. G., RIDGWAY, S. T., GILLETT, F. C. <AP. J. (LETTERS), 223, L47> 780707
HIGH-RESOLUTION 1.5-5 MICRON SPECTROSCOPY OF THE BECKLIN-NEUGEBAUER SOURCE IN ORION.

HALL, D. N. B., KLEINMANN, S. G., SCOVILLE, N. Z. <AP. J. (LETTERS), 260, L53> 820906
BROAD HELIUM EMISSION IN THE GALACTIC CENTER.

HALL, D. N. B., KLEINMANN, S. G., SCOVILLE, N. Z., RIDGWAY, S. T. <AP. J., 248, 898> 810905
2 MICRON SPECTROSCOPY OF THE NUCLEUS OF NGC 1068.

HALL, D. N. B., RIDGWAY, S. T. <NATURE, 273, 281> 780513
CIRCUMSTELLAR METHANE IN THE INFRARED SPECTRUM OF IRC+10216.

HALL, R. T. <SAMSO-TR-74-212> 740903
A CATALOG OF 10-MICRON CELESTIAL OBJECTS.

HAMAJIMA, K., ICHIKAWA, T., ISHIDA, K., HIDAYAT, B., RAHARTO, M. <P. A. S. J., 33, 591> 810003
ON THE 2.4 MICRON ENHANCEMENT CENTERED AT ABOUT L-355 DEGREES, B--1 DEGREE.

HANSEN, O. L., BLANCO, V. M. <A. J., 78, 669> 731001
CLASSIFICATION OF UNIDENTIFIED, SOUTHERN IRC SOURCES NEAR THE GALACTIC PLANE.

HANSEN, O. L., BLANCO, V. M. <A. J., 80, 1011> 751201
CLASSIFICATION OF 831 TWO-MICRON SKY SURVEY SOURCES SOUTH OF +5 DEGREES.

HANSEN, O. L., HESSER, J. E. <NATURE, 257, 568> 751011
OBSERVATIONS OF EIGHT GLOBULAR CLUSTERS AT 2.3 AND 4.7 MICRONS.

HARAMUNDANIS, K. L. <SMITHSONIAN INST. > 669903
SMITHSONIAN ASTROPHYSICAL OBSERVATORY STAR CATALOG.

HARDING, P., JONES, T. J., RODGERS, A. W. <AP. J., 251, 530> 811206
MAPPING OF NGC 5128 (-CENTAURUS A) AT J, H, AND K.

HARPER JR., D. A. <AP. J., 192, 557> 740908
FAR-INFRARED EMISSION FROM HII REGIONS. II. MULTICOLOR PHOTOMETRY OF SELECTED SOURCES AND 2.2 ARC MINUTE RESOLUTION MAPS OF M42 AND NGC 2024.

HARPER JR., D. A., LOW, F. J. <AP. J. (LETTERS), 165, L9> 710404
FAR-INFRARED EMISSION FROM HII REGIONS.

HARPER JR., D. A., LOW, F. J. <AP. J. (LETTERS), 182, L89> 730602
FAR-INFRARED OBSERVATIONS OF GALACTIC NUCLEI.

HARPER JR., D. A., LOW, F. J., RIEKE, G. H., ARMSTRONG, K. R. <AP. J. (LETTERS), 177, L21> 721003
OBSERVATIONS OF PLANETS, NEBULAE, AND GALAXIES AT 350 MICRONS.

HARPER JR., D. A., LOW, F. J., RIEKE, G. H., THRONSON JR., H. A. <AP. J., 205, 136> 760403
THE INFRARED EMISSION OF M17.

HARRIS, A. W., LEMKE, D. <M. N. R. A. S., 194, 593> 810213
A NEAR INFRARED SURVEY OF W51.

HARRIS, D. H., WOOLF, N. J., RIEKE, G. H. <AP. J., 226, 829> 781213
ICE MANTLES AND ABNORMAL EXTINCTION IN THE RHO OPHIUCHI CLOUD.

HARRIS, S., ROWAN-ROBINSON, M. <ASTR. AP., 60, 405> 770908
THE BRIGHTEST SOURCES IN THE AFCRL SURVEY.

HARTMANN, L. <AP. J., 221, 193> 780405
THE INFRARED ECLIPSE OF V444 CYGNI AND THE STRUCTURE OF WOLF-RAYET WINDS.

HARTMANN, L. <AP. J., 224, 520> 780905
DISK STRUCTURE IN EARLY-TYPE STELLAR ENVELOPES.

HARTMANN, L., ANDERSON, C. M. <AP. J., 215, 188> 770708
ABUNDANCES IN LATE-TYPE DWARFS.

HARTOOG, M. R., PERSSON, S. E., AARONSON, M. <P. A. S. P., 89, 660> 771002
THE STRENGTH OF THE 2.3-MICRON CO BAND IN WEAK-G-BAND STARS.

HARVEY, P. M. <AP. J. (LETTERS), 255, L55> 820403
INFRARED PHOTOMETRY OF THE ULTRACOMPACT RADIO SOURCE IN NGC 6334.

HARVEY, P. M. <AP. J., 188, 95> 740208
INFRARED VARIABILITY OF V1016 CYGNI.

HARVEY, P. M. <P. A. S. P., 91, 143> 790205
A FAR-INFRARED PHOTOMETER FOR THE KUIPER AIRBORNE OBSERVATORY.

HARVEY, P. M., BECHIS, K. P., WILSON, W. J., BALL, J. A. <AP. J. SUPPL., 27, 331> 740408
TIME VARIATIONS IN THE OH MICROWAVE AND INFRARED EMISSION FROM LATE-TYPE STARS.

HARVEY, P. M., CAMPBELL, M. F., HOFFMANN, W. F. <AP. J. (LETTERS), 205, L69> 760408
HIGH-RESOLUTION FAR-INFRARED OBSERVATIONS OF THE GALACTIC CENTER.

HARVEY, P. M., CAMPBELL, M. F., HOFFMANN, W. F. <AP. J. (LETTERS), 241, L183> 801102
ERRATUM TO "HIGH-RESOLUTION FAR-INFRARED OBSERVATIONS OF THE GALACTIC CENTER".

HARVEY, P. M., CAMPBELL, M. F., HOFFMANN, W. F. <AP. J., 211, 786> 770208
HIGH-RESOLUTION FAR-INFRARED OBSERVATIONS OF HII REGIONS: SAGITTARIUS B2, W49, DR 21-W75.

HARVEY, P. M., CAMPBELL, M. F., HOFFMANN, W. F. <AP. J., 215, 151> 770703
FAR-INFRARED EMISSION FROM COMPACT SOURCES IN NGC 2264 AND THE ROSETTE NEBULA.

HARVEY, P. M., CAMPBELL, M. F., HOFFMANN, W. F. <AP. J., 219, 891> 780202
STRONG FAR-INFRARED EMISSION FROM A COMPACT SOURCE IN SHARPLESS 140.

HARVEY, P. M., CAMPBELL, M. F., HOFFMANN, W. F. <AP. J., 228, 445> 790312
HIGH-ANGULAR-RESOLUTION FAR-INFRARED OBSERVATIONS OF THE RHO OPHIUCHI DARK CLOUD.

HARVEY, P. M., CAMPBELL, M. F., HOFFMANN, W. F., THRONSON JR., H. A., GATLEY, I. <AP. J., 229, 990> 790508
INFRARED OBSERVATIONS OF NGC 2071(IRS) AND AFGL 490: TWO LOW-LUMINOSITY YOUNG STARS.

HARVEY, P. M., GATLEY, I., THRONSON JR., H. A. <P. A. S. P., 90, 655> 781220
AN UPPER LIMIT TO FAR INFRARED EMISSION FROM THE CRAB NEBULA.

HARVEY, P. M., GATLEY, I., THRONSON JR., H. A., WERNER, M. W. <AP. J., 258, 568> 820705
FAR-INFRARED MAPPING OF THE DOUBLE-LOBED H II REGION S106.

HARVEY, P. M., GATLEY, I., WERNER, M. W., ELIAS, J. H., EVANS II, N. J., ZUCKERMAN, B., MORRIS, G., SATO, T., LITVAK, M. M. <AP. J. (LETTERS), 189, L87> 740404
DUST AND GAS IN THE ORION MOLECULAR CLOUD: OBSERVATIONS OF 1-MM CONTINUUM AND 2-CM H2CO EMISSION.

HARVEY, P. M., HOFFMANN, W. F., CAMPBELL, M. F. <AP. J. (LETTERS), 196, L31> 750203
FAR-INFRARED OBSERVATIONS OF W51 WITH HIGH SPATIAL RESOLUTION.

HARVEY, P. M., HOFFMANN, W. F., CAMPBELL, M. F. <AP. J., 227, 114> 790105
FAR-INFRARED OBSERVATIONS OF THE CARINA I AND II HII REGIONS.

HARVEY, P. M., HOFFMANN, W. F., CAMPBELL, M. F. <ASTR. AP., 70, 165> 781012
HIGH ANGULAR RESOLUTION OBSERVATIONS OF ETA CARINAE FROM 35-175 MICRONS.

HARVEY, P. M., LADA, C. J. <AP. J., 237, 61> 800404
TWO MICRON SPECTROSCOPY AND 2.7MM CO LINE OBSERVATIONS OF V645 CYGNI.

HARVEY, P. M., THRONSON JR., H. A., GATLEY, I. <AP. J., 231, 115> 790702
FAR-INFRARED OBSERVATIONS OF OPTICAL EMISSION-LINE STARS: EVIDENCE FOR EXTENSIVE COOL DUST CLOUDS.

HARVEY, P. M., THRONSON JR., H. A., GATLEY, I. <AP. J., 235, 894> 800205
A FAR-INFRARED STUDY OF THE REFLECTION NEBULA NGC 2023.

HARVEY, P. M., WILKING, B. A. <P. A. S. P., 94, 285> 820410
FAR-INFRARED PHOTMETRY OF OPTICAL EMISSION-LINE STARS. II.

HARVEY, P. M., WILKING, B. A., JOY, M. <AP. J. (LETTERS), 254, L29> 820305
FAR-INFRARED PHOTOMETRY OF COMPACT EXTRAGALACTIC OBJECTS: DETECTION OF 3C 345.

HARWIT, M., MCNUTT, D. P., SHIVANANDAN, K., ZAJAC, B. J. <A. J., 71, 1026> 661201
RESULTS OF THE FIRST INFRARED ASTRONOMICAL ROCKET FLIGHT.

HASHIMOTO, J., MAIHARA, T., OKUDA, H., SATO, S. <P. A. S. J., 22, 335> 700001
INFRARED POLARIZATION OF THE PECULIAR M-TYPE VARIABLE VY CANIS MAJORIS.

HASSALL, B. J. M., PRINGLE, J. E., WARD, M. J., WHELAN, J. A., MAYO, S. K., ECHEVARRIA, J., JONES, D. H. P., WALLIS, R. E., ALLEN, D. A., HYLAND, A. R. <M. N. R. A. S., 197, 275> 811013
OBSERVATIONS AND MODELS OF H2252-035.

HATFIELD, B. F., BRODZIK, D. <IAUC NO. 3082> 770616
NOVA SAGITTARII 1977.

HAWKINS, F. J., MASON, K. O., SANFORD, P. W. <NAT. PHYS. SCI., 241, 109> 739912
DETERMINATION OF THE POSITION OF GX2+5 WITH COPERNICUS.

HAWLEY, S. A. <AP. J., 224, 417> 780904
THE CHEMICAL COMPOSITION OF GALACTIC AND EXTRAGALACTIC HII REGIONS.

HAWLEY, S. A., GRANDI, S. A. <AP. J., 217, 420> 771007
OBSERVATIONS OF (S III) IN NGC 604 AND N/S ABUNDANCE GRADIENTS.

HAYAKAWA, S., ITO, K., MATSUMOTO, T., MURAKAMI, H., UYAMA, K. <P. A. S. J., 30, 369> 780006
NEAR-INFRARED OBSERVATION OF THE GALAXY IN THE GALACTIC ANTICENTER DIRECTION.

HAYAKAWA, S., ITO, K., MATSUMOTO, T., ONO, T., UYAMA, K. <NATURE, 261, 29> 760516
INFRARED PROFILE OF THE MILKEY WAY AT 2.4 MICRONS.

HAYAKAWA, S., ITO, K., MATSUMOTO, T., UYAMA, K. <ASTR. AP., 58, 325> 770615
OVERALL DISTRIBUTION OF INFRARED SOURCES IN OUR GALAXY.

HAYAKAWA, S., MATSUMOTO, T., MURAKAMI, H., UYAMA, K., THOMAS, J. A., YAMAGAMI, T. <ASTR. AP., 100, 116> 810718
DISTRIBUTION OF NEAR INFRARED SOURCES IN THE GALACTIC DISK.

HAYAKAWA, S., MATSUMOTO, T., MURAKAMI, H., UYAMA, K., YAMAGAMI, T., THOMAS, J. A. <NATURE, 279, 510> 790609
NEAR IR SURFACE BRIGHTNESS OF SOUTHERN GALACTIC PLANE.

HAYES, D. S. <AP. J., 159, 165> 700102
AN ABSOLUTE SPECTROPHOTOMETRIC CALIBRATION OF THE ENERGY DISTRIBUTION OF TWELVE STANDARD STARS.

HAYES, D. S., LATHAM, D. W., HAYES, S. H. <AP. J., 197, 587> 750503
MEASUREMENTS OF THE MONOCHROMATIC FLUX FROM VEGA IN THE NEAR-INFRARED.

HAZARD, C., GULKIS, S., SUTTON, J. <AP. J., 154, 413> 689906
OCCULTATION STUDIES OF WEAK RADIO SOURCES: LIST 2.

HAZARD, C., SUTTON, J., ARGUE, A. N., KENWORTHY, C. M., MORRISON, L. V., MURRAY, C. A. <NAT. PHYS. SCI., 233, 89> 719905
ACCURATE RADIO AND OPTICAL POSITIONS OF 3C273B.

HECKERT, P. A., ZEILIK II, M. <A. J., 86, 1076> 810702
POLARIMETRY FROM 1 TO 5 MICRONS OF COMPACT INFRARED SOURCES.

HEFELE, H., HOLZLE, E. <ASTR. AP., 88, 145> 800813
8-13 MICRON SPECTROPHOTOMETRY OF S 106.

HEFELE, H., SCHULTE IN DEN BAUMEN, J. <ASTR. AP., 66, 465> 780612
8-13 MICRON SPECTROPHOTOMETRY OF THE COMPACT H II REGION G45.1+0.1.

HEFELE, H., WACKER, W., WEINBERGER, R. <ASTR. AP., 56, 407> 770401
INFRARED OBSERVATIONS OF COMPACT HII REGIONS NEAR CLASS I OH MASER SOURCES.

HENIZE, K. G. <AP. J. SUPPL., 14, 125> 679907
OBSERVATIONS OF SOUTHERN PLANETARY NEBULAE.

HENIZE, K. G. <AP. J. SUPPL., 2, 315> 569903
CATALOGUES OF H-ALPHA EMISSION STARS AND NEBULAE IN THE MAGELLANIC CLOUDS.

HENIZE, K. G., MENDOZA V., E. E. <AP. J., 180, 115> 739913
EMISSION-LINE STARS IN THE CHAMAELEON T ASSOCIATION.

HERBIG, G. H. <AP. J., 119, 483> 549902
EMISSION-LINE STARS ASSOCIATED WITH THE NEBULOUS CLUSTER NGC 2264.

HERBIG, G. H. <AP. J., 125, 654> 579903
EMISSION-LINE STARS IN THE VICINITY OF MESSIER 8, MESSIER 20, AND SIMEIS 188.

HERBIG, G. H. <AP. J., 128, 259> 589902
NGC 7000, IC 5070, AND THE ASSOCIATED EMISSION-LINE STARS.

HERBIG, G. H. <AP. J., 131, 516> 609901
EMISSION-LINE STARS IN IC 5146.

HERBIG, G. H. <AP. J., 217, 693> 771103
ERUPTIVE PHENOMENA IN EARLY STELLAR EVOLUTION.

HERBIG, G. H. <LICK OBS. BULL., 658> 749904
DRAFT CATALOG OF HERBIG-HARO OBJECTS.

HERBIG, G. H. <P. A. S. P., 66, 19> 549903
BRIGHT H-ALPHA STARS IN IC 348.

HERBIG, G. H. <P. A. S. P., 68, 353> 569902
THE SOURCE OF ILLUMINATION OF NGC 1579.

HERBIG, G. H., JONES, B. F. <A. J., 86, 1232> 819909
LARGE PROPER MOTIONS OF THE HERBIG-HARO OBJECTS HH 1 AND HH 2.

HERBIG, G. H., KUHI, L. V. <AP. J., 137, 398> 639901
EMISSION-LINE STARS IN THE REGION OF NGC 2068.

HERBST, W., MILLER, D. P., WARNER, J. W., HERZOG, A. <A. J., 87, 98> 820108
R ASSOCIATIONS. VI. THE REDDENING LAW IN DUST CLOUDS AND THE NATURE OF EARLY-TYPE EMISSION STARS IN NEBULOSITY FROM A STUDY OF FIVE ASSOCIATIONS.

HERBST, W., RACINE, R., WARNER, J. W. <AP. J., 223, 471> 780709
OPTICAL AND INFRARED PROPERTIES OF THE NEWLY FORMED STARS IN CANIS MAJOR R1.

HERBST, W., WARNER, J. W. <A. J., 86, 885> 810602
TWO YOUNG STARS IN L 43.

HERGIG, G. H., RAO, N. K. <AP. J., 174, 401> 729902
SECOND CATALOG OF EMISSION-LINE STARS OF THE ORION POPULATION.

HERTER, T., BRIOTTA JR., D. A., GULL, G. E., HOUCK, J. R. <AP. J. (LETTERS), 259, L25> 820803
OBSERVATIONS OF THE 30 MICRON FEATURE IN IRC+10216.

HERTER, T., BRIOTTA JR., D. A., GULL, G. E., SHURE, M. A., HOUCK, J. R. <AP. J. (LETTERS), 259, L109> 820811
DETECTION OF THE (S III) 33.47 MICRON LINE IN THE ORION NEBULA.

HERTER, T., BRIOTTA JR., D. A., GULL, G. E., SHURE, M. A., HOUCK, J. R. <AP. J., 262, 164> 821102
OBSERVATIONS OF THE INFRARED FINE-STRUCTURE LINES OF S III AT 18.71 AND 33.47 MICRONS IN FOUR H II REGIONS.

HERTER, T., DUTHIE, J. G., PIPHER, J. L., SAVEDOFF, M. P. <AP. J., 234, 897> 791208
AIRBORNE FAR-INFRARED SPECTROSCOPIC OBSERVATIONS OF W51 AND W49.

HERTER, T., HELFER, H. L., PIPHER, J. L., BRIOTTA JR., D. A.,FORREST, W. J., HOUCK, J. R., RUDY, R. J., WILLNER, S. P. <AP. J., 262, 153> 821101
ABUNDANCES IN FIVE NEARBY GALACTIC H II REGIONS FROM INFRARED FORBIDDEN LINES.

HERTER, T., HELFER, H. L., PIPHER, J. L., FORREST, W. J., MCCARTHY, J., HOUCK, J. R., WILLNER, S. P., PUETTER, R. C., RUDY, R. J., SOIFER, B. T. <AP. J., 250, 186> 811104
ABUNDANCES OF ARGON, SULFUR, AND NEON IN SIX GALACTIC H II REGIONS FROM INFRARED FORBIDDEN LINES.

HERTER, T., PIPHER, J. L., HELFER, H. L., WILLNER, S. P., PUETTER, R. C., RUDY, R. J., SOIFER, B. T. <AP. J., 244, 511> 810303
MEASUREMENTS OF FORBIDDEN LINE RADIATION OF AR II (6.99 MICRONS) IN W3 IRS1.

HERZOG, A. D., GEHRZ, R. D., HACKWELL, J. A. <AP. J., 236, 189> 800209
THE OPTICAL IDENTIFICATION OF THE INFRARED SOURCE IN MWC 349.

HESSER, J. E., HARTWICK, F. D. A., UGARTE, P. <AP. J. SUPPL., 32, 283> 769911
INSTRUMENTAL COLOR-MAGNITUDE DIAGRAMS FOR 24 LARGE MAGELLANIC CLOUD STAR CLUSTERS.

HETZLER, C. <AP. J., 86, 509> 379901
INFRARED STELLAR SURVEYS AND INDEX SEQUENCES.

HEWITT, A., BURBIDGE, G. <AP. J. SUPPL., 43, 57> 809908
A REVISED OPTICAL CATALOG OF QUASI-STELLAR OBJECTS.

HILDEBRAND, R. H., WHITCOMB, S. E., WINSTON, R., STIENING, R. F., HARPER JR., D. A., MOSELEY, S. H. <AP. J., 216, 698> 770901
SUBMILLIMETER PHOTOMETRY OF EXTRAGALACTIC OBJECTS.

HILDEBRAND, R. H., WHITCOMB, S. E., WINSTON, R., STIENING, R. F., HARPER JR., D. A., MOSELEY, S. H. <AP. J. (LETTERS), 219, L101> 780204
SUBMILLIMETER OBSERVATIONS OF THE GALACTIC CENTER.

HINKLE, K. H. <AP. J., 220, 210> 780216
INFRARED SPECTROSCOPY OF MIRA VARIABLES. I. R LEONIS: THE CO AND OH VIBRATION-ROTATION OVERTONE BANDS.

HINKLE, K. H., BARNES, T. G. <AP. J., 227, 923> 790208
INFRARED SPECTROSCOPY OF MIRA VARIABLES. II. R LEONIS, THE H2O VIBRATION-ROTATION BANDS.

HINKLE, K. H., BARNES, T. G. <AP. J., 234, 548> 791206
INFRARED SPECTROSCOPY OF MIRA VARIABLES. III. R LEONIS, THE ATOMIC LINES.

HINKLE, K. H., BARNES, T. G., LAMBERT, D. L., BEER, R. <AP. J. (LETTERS), 210, L141> 761208
SILICON MONOXIDE IN THE 4 MICRON INFRARED SPECTRUM OF LONG-PERIOD VARIABLES.

HINKLE, K. H., HALL, D. N. B., RIDGWAY, S. T. <AP. J., 252, 697> 820105
TIME SERIES INFRARED SPECTROSCOPY OF THE MIRA VARIABLE CHI CYGNI.

HINKLE, K. H., LAMBERT, D. L., SNELL, R. L. <AP. J., 210, 684> 761207
THE CARBON-12/CARBON-13 RATIO IN STELLAR ATMOSPHERES. VI. FIVE LUMINOUS COOL STARS.

HIRAI, M. <P. A. S. J., 26, 163> 740002
SPECTROSCOPIC OBSERVATION OF THE CARBON STARS Y CANUM VENATICORUM AND U HYDRAE IN THE ONE-MICRON REGION.

HODGE, P. W. <A. J., 66, 83> 619901
THE FORNAX DWARF GALAXY. I. THE GLOBULAR CLUSTERS.

HODGE, P. W. <AP. J., 132, 341> 609904
STUDIES OF THE LARGE MAGELLANIC CLOUD. II. THE GLOBULAR CLUSTER NGC 1846.

HODGE, P. W. <AP. J., 132, 346> 609905
STUDIES OF THE LARGE MAGELLANIC CLOUD. III. THE GLOBULAR CLUSTER NGC 1978.

HODGE, P. W. <AP. J., 134, 226> 619902
STUDIES OF THE LARGE MAGELLANIC CLOUD. VII. THE OPEN CLUSTER NGC 1844.

HODGE, P. W. <AP. J., 137, 1033> 639903
STUDIES OF THE LARGE MAGELLANIC CLOUD. VIII. THE CLUSTER NGC 1831.

HOFFLEIT, D. <YALE UNIV. OBS. > 649901
CATALOGUE OF BRIGHT STARS.

HOFFMANN, W. F., FREDERICK, C. L. <AP. J. (LETTERS), 155, L9> 690102
FAR-INFRARED OBSERVATION OF THE GALACTIC-CENTER REGION AT 100 MICRONS.

HOFFMANN, W. F., FREDERICK, C. L., EMERY, R. J. <AP. J. (LETTERS), 164, L23> 710206
100-MICRON MAP OF THE GALACTIC-CENTER REGION.

HOFFMANN, W. F., FREDERICK, C. L., EMERY, R. J. <AP. J. (LETTERS), 170, L89> 711201
100-MICRON SURVEY OF THE GALACTIC PLANE.

HOFMANN, R. G. <ASTR. AP., 116, 179> 821216
A NEW NEAR-INFRARED SOURCE IN THE MOLECULAR CLOUD ASSOCIATED WITH S 106.

HOFMANN, W., LEMKE, D., FREY, A. <ASTR. AP., 70, 427> 781109
MAPPING OF THE GALACTIC CENTER AND THE AQUILA REGION IN THE NEAR INFRARED FROM BALLOON ALTITUDES.

HOFMANN, W., LEMKE, D., THUM, C. <ASTR. AP., 57, 111> 770510
SURFACE BRIGHTNESS OF THE CENTRAL REGION OF THE MILKY WAY AT 2.4 AND 3.4 MICRONS.

HOHLFELD, R. G., KRUMM, N. <AP. J., 244, 476> 810302
AN INFRARED SEARCH FOR MASSIVE GALACTIC ENVELOPES.

HOLMBERG, E. B., LAUBERTS, A., SCHUSTER, H. -E., WEST, R. M. <ASTR. AP. SUPPL., 18, 463> 749906
THE ESO/UPPSALA SURVEY OF THE ESO(B) ATLAS OF THE SOUTHERN SKY. I.

HOLMBERG, E. B., LAUBERTS, A., SCHUSTER, H. -E., WEST, R. M. <ASTR. AP. SUPPL., 18, 491> 749907
THE ESO/UPPSALA SURVEY OF THE ESO(B) ATLAS OF THE SOUTHERN SKY. II.

HOLMBERG, E. B., LAUBERTS, A., SCHUSTER, H. -E., WEST, R. M. <ASTR. AP. SUPPL., 22, 327> 759905
THE ESO/UPPSALA SURVEY OF THE ESO(B) ATLAS OF THE SOUTHERN SKY. III.

HOLMBERG, E. B., LAUBERTS, A., SCHUSTER, H. -E., WEST, R. M. <ASTR. AP. SUPPL., 27, 295> 779909
THE ESO/UPPSALA SURVEY OF THE ESO(B) ATLAS OF THE SOUTHERN SKY. IV.

HOLMBERG, E. B., LAUBERTS, A., SCHUSTER, H. -E., WEST, R. M. <ASTR. AP. SUPPL., 39, 173> 809909
THE ESO/UPPSALA SURVEY OF THE ESO(B) ATLAS OF THE SOUTHERN SKY. VII.

HOLMBERG, E. B., LAUBERTS, A., SCHUSTER, H. -E., WEST, R. M. <ASTR. AP. SUPPL., 34, 285> 789908
THE ESO/UPPSALA SURVEY OF THE ESO(B) ATLAS OF THE SOUTHERN SKY. VI.

HOLMBERG, E. B., LAUBERTS, A., SCHUSTER, H. -E., WEST, R. M. <ASTR. AP. SUPPL., 31, 15> 789907
THE ESO/UPPSALA SURVEY OF THE ESO(B) ATLAS OF THE SOUTHERN SKY. V.

HOLTZ, J. Z., GEBALLE, T. R., RANK, D. M. <AP. J. (LETTERS), 164, L29> 710207
INFRARED LINE EMISSION FROM PLANETARY NEBULAE.

HONEYCUTT, R. K., RAMSEY, L. W., WARREN JR., W. H., RIDGWAY, S. T. <AP. J., 215, 584> 770710
SPECTROPHOTOMETRY OF COOL ANGULAR-DIAMETER STARS.

HOUCK, J. R., FORREST, W. J., MCCARTHY, J. F. <AP. J. (LETTERS), 242, L65> 801202
MEDIUM-RESOLUTION SPECTRA OF M82 AND NGC 1068 FROM 16 TO 30 MICRONS.

HOUCK, J. R., SCHAACK, D. F., REED, R. A. <AP. J. (LETTERS), 193, L139> 741102
20 TO 40 MICRON SPECTROSCOPY OF THE ORION NEBULA.

HOUCK, J. R., SOIFER, B. T., HARWIT, M., PIPHER, J. L. <AP. J. (LETTERS), 178, L29> 721101
THE FAR-INFRARED AND SUBMILLIMETER BACKGROUND.

HOUCK, J. R., SOIFER, B. T., PIPHER, J. L., HARWIT, M. <AP. J. (LETTERS), 169, L31> 711001
ROCKET-INFRARED FOUR-COLOR PHOTOMETRY OF THE GALAXY'S CENTRAL REGIONS.

HOUGH, J. H., BAILEY, J., CUNNINGHAM, E. C., MCCALL, A., AXON, D. J. <M. N. R. A. S., 195, 429> 810507
LINEAR POLARIZATION OF T TAURI STARS.

HOUGH, J. H., MCCALL, A., ADAMS, D. J., JAMESON, R. F. <ASTR. AP., 69, 431> 781011
LINEAR POLARIZATION OF THE GALACTIC CENTRE IN THE NEAR INFRARED.

HOWARTH, I. D., WILSON, R., CARTER, B. S., MENZIES, J. W., ROBERTS, G., WHITELOCK, P. A., VAN DESSEL, E. L., DE LOORE, C., BURGER, M., SANDFORD, M. C. W. <ASTR. AP., 93, 219> 810110
IUE AND OPTICAL OBSERVATIONS OF V861 SCORPII.

HOWELL, R. R., MCCARTHY, D. W., LOW, F. J. <AP. J. (LETTERS), 251, L21> 811204
ONE-DIMENSIONAL INFRARED SPECKEL INTERFEROMETRY.

HOYLE, F., WICKRAMASINGHE, N. C. <M. N. R. A. S., 181, 51P> 771101
POLYSACCHARIDES AND THE INFRARED SPECTRUM OF OH 26.5+0.6.

HUDSON, H. S., SOIFER, B. T. <AP. J., 206, 100> 760509
SUBMILLIMETER OBSERVATIONS OF NGC 2024, OMC-2, AND MON R-2.

HUMPHREYS, R. M. <AP. J., 219, 445> 780112
LUMINOUS VARIABLE STARS IN M31 AND M33.

HUMPHREYS, R. M., LOCKWOOD, G. W. <AP. J. (LETTERS), 172, L59> 720303
SPECTROSCOPIC AND PHOTOMETRIC CHANGES IN THE PECULIAR INFRARED STAR VX SAGITTARIUS.

HUMPHREYS, R. M., MERRILL, K. M., BLACK, J. H. <AP. J. (LETTERS), 237, L17> 800402
THE PERPLEXING SPECTRUM OF AFGL 2789 (V645 CYGNI).

HUMPHREYS, R. M., NEY, E. P. <AP. J. (LETTERS), 187, L75> 740101
SUPERGIANT BINARY STARS.

HUMPHREYS, R. M., NEY, E. P. <AP. J., 190, 339> 740603
INFRARED STARS IN BINARY SYSTEMS.

HUMPHREYS, R. M., NEY, E. P. <AP. J., 194, 623> 741203
VISUAL AND INFRARED OBSERVATIONS OF LATE-TYPE SUPERGIANTS IN THE SOUTHERN SKY.

HUMPHREYS, R. M., NEY, E. P. <ASTR. AP., 30, 159> 740107
INFRARED OBSERVATIONS OF HD 65750, A RED GIANT IN A REFLECTION NEBULA.

HUMPHREYS, R. M., NEY, E. P. <P. A. S. P., 86, 444> 740809
IRC+60370 AND THE INFRARED RADIATION FROM LUMINOUS G AND K SUPERGIANTS.

HUMPHREYS, R. M., STRECKER, D. W., MURDOCK, T. L., LOW, F. J. <AP. J. (LETTERS), 179, L49> 730101
IRC+10420 - ANOTHER ETA CARINAE?

HUMPHREYS, R. M., STRECKER, D. W., NEY, E. P. <AP. J. (LETTERS), 167, L35> 710701
HIGH-LUMINOSITY G SUPERGIANTS.

HUMPHREYS, R. M., STRECKER, D. W., NEY, E. P. <AP. J., 172, 75> 720202
SPECTROSCOPIC AND PHOTOMETRIC OBSERVATIONS OF M SUPERGIANTS IN CARINA.

HUMPHREYS, R. M., WARNER, J. W. <AP. J. (LETTERS), 221, L73> 780409
INFRARED DETECTION OF LUMINOUS STARS IN M31 AND M33.

HUMPHREYS, R. M., WARNER, J. W., GALLAGHER, J. S. <P. A. S. P., 88, 380> 760813
CRL 2688 - "THE EGG NEBULA" - PREPLANETARY NEBULA OR PROTOSTELLAR SYSTEM?

HYLAND, A. R. <PROC. A. S. A., 1, 14> 710703
GALACTIC INFRARED ASTRONOMY.

HYLAND, A. R., ALLEN, D. A. <M. N. R. A. S., 199, 943> 820616
AN INFRARED STUDY OF QUASARS.

HYLAND, A. R., BECKLIN, E. E., FROGEL, J. A., NEUGEBAUER, G. <ASTR. AP., 16, 204> 720001
INFRARED OBSERVATIONS OF 1612 MHZ IR/OH SOURCES.

HYLAND, A. R., BECKLIN, E. E., NEUGEBAUER, G. <AP. J. (LETTERS), 220, L73> 780310
THE L-ALPHA/H-ALPHA INTENSITY RATIO IN PKS 0237-23.

HYLAND, A. R., BECKLIN, E. E., NEUGEBAUER, G., WALLERSTEIN, G. <AP. J., 158, 619> 691102
OBSERVATIONS OF THE INFRARED OBJECT, VY CANIS MAJORIS.

HYLAND, A. R., BECKLIN, E. E., NEUGEBAUER, G., WALLERSTEIN, G. <AP. J., 160, 381> 700401
ERRATUM TO "OBSERVATIONS OF THE INFRARED OBJECT, VY CANIS MAJORIS".

HYLAND, A. R., HIRST, R. A., ROBINSON, G., THOMAS, J. A. <AP. LETTERS, 11, 7> 720501
INFRARED OBSERVATIONS OF SOME SOUTHERN IR-OH SOURCES.

HYLAND, A. R., JONES, T. J., MITCHELL, R. M. <M. N. R. A. S., 201, 1095> 821219
A STUDY OF THE CHAMAELEON DARK CLOUD COMPLEX: SURVEY, STRUCTURE AND EMBEDDED SOURCES.

HYLAND, A. R., MCGREGOR, P. J., ROBINSON, G., THOMAS, J. A., BECKLIN, E. E., GATLEY, I., WERNER, M. W. <AP. J., 241, 709> 801006
THE INFRARED EMISSION OF G333.6-0.2, AN EXTREMELY NONSPHERICAL H II REGION.

HYLAND, A. R., MOULD, J. R. <AP. J., 186, 993> 731206
INFRARED VARIABILITY AND THE INTERSTELLAR REDDENING OF THE X-RAY SOURCE HD 77581.

HYLAND, A. R., MOULD, J. R., ROBINSON, G., THOMAS, J. A. <P. A. S. P., 87, 439> 750609
INFRARED OBSERVATIONS AND THE EFFECTIVE TEMPERATURE OF THE PECULIAR STAR HD 101065.

HYLAND, A. R., NEUGEBAUER, G. <AP. J. (LETTERS), 160, L177> 700604
INFRARED OBSERVATIONS OF NOVA SERPENTIS 1970.

HYLAND, A. R., ROBINSON, G., MITCHELL, R. M., THOMAS, J. A., BECKLIN, E. E. <AP. J., 233, 145> 791011
THE SPECTRAL AND SPATIAL DISTRIBUTION OF RADIATION FROM ETA CARINAE. II. HIGH-RESOLUTION INFRARED MAPS OF THE HOMUNCULUS.

HYLAND, A. R., SCHWARZ, M. P. <PROC. A. S. A., 3, 137> 770909
INTERPRETATION OF QUASAR COLOURS IN THE NEAR IR.

HYLAND, A. R., THOMAS, J. A., ROBINSON, G. <A. J., 83, 20> 780108
INFRARED STUDIES OF 30 DORADUS. I. THE 2-MICRON SOURCES OF THE INNER REGION.

IIJIMA, T., ISHIDA, K. <P. A. S. J., 30, 657> 780003
TWO-MICRON OBJECTS IN THE NORTHERN MONOCEROS REGION.

IIJIMA, T., ITO, K., MATSUMOTO, T., UYAMA, K. <P. A. S. J., 28, 27> 760002
NEAR-INFRARED PROFILE OF M31.

ILOVAISKY, S. A., CHEVALIER, C., MOTCH, C. <ASTR. AP., 114, L7> 821007
THE NATURE OF THE 1E1145.1-6141 OPTICAL COUNTERPART.

IMPEY, C. D. <IAUC NO. 3379> 790709
SS433.

IMPEY, C. D., BRAND, P. W. J. L. <NATURE, 292, 814> 810808
IR PHOTOMETRY OF FLAT RADIO SOURCES.

IMPEY, C. D., BRAND, P. W. J. L., TAPIA, S. <M. N. R. A. S., 198, 1> 820111
A POLARIZATION BURST IN THE BL LAC OBJECT AO 0235+164.

IMPEY, C. D., BRAND, P. W. J. L., WOLSTENCROFT, R. D., WILLIAMS, P. M. <M. N. R. A. S., 200, 19> 820714
INFRARED POLARIMETRY AND PHOTOMETRY OF BL LAC OBJECTS.

IPATOV, A. P., YUDIN, B. F. <SOV. AST. (LETTERS), 7, 309> 810914
SPECTROPHOTOMETRY OF HM SAGITTAE.

IRVINE, W. M., SIMON, T., MENZEL, D. H., CHARON, J., LECOMTE, G., GRIBOVAL, P., YOUNG, A. T. <A. J., 73, 251> 680503
MULTICOLOR PHOTOELECTRIC PHOTOMETRY OF THE BRIGHTER PLANETS. II. OBSERVATIONS FROM LE HOUGA OBSERVATORY.

IRVINE, W. M., SIMON, T., MENZEL, D. H., PIKOOS, C., YOUNG, A. T. <A. J., 73, 807> 681103
MULTICOLOR PHOTOELECTRIC PHOTOMETRY OF THE BRIGHTER PLANETS. III. OBSERVATIONS FROM BOYDEN OBSERVATORY.

ISRAEL, F. P., GATLEY, I., MATTHEWS, K., NEUGEBAUER, G. <ASTR. AP., 105, 229> 820110
OBSERVATIONS OF NGC 604 OVER SIX DECADES IN FREQUENCY.

ITO, K., MATSUMOTO, T., UYAMA, K. <NATURE, 265, 517> 770213
INFRARED PROFILE OF CENTRAL REGION OF OUR GALAXY AT 2.47 MICRONS.

ITO, K., MATSUMOTO, T., UYAMA, K. <P. A. S. J., 28, 427> 760006
OBSERVATION OF THE DIFFUSE INFRARED RADIATION FROM OUR GALAXY AT 2.4 MICRONS.

JAFFE, D. T., STIER, M. T., FAZIO, G. G. <AP. J., 252, 609> 820104
A HIGH RESOLUTION FAR-INFRARED SURVEY OF A SECTION OF THE GALACTIC PLANE. I. THE NATURE OF THE SOURCES.

JAMESON, R. F. <IAUC NO. 3095> 770810
AM HERCULIS.

JAMESON, R. F., AKINCI, R. <M. N. R. A. S., 188, 421> 790802
1.2 AND 2.2 MICRON LIGHT CURVES OF W UMA TYPE STARS.

JAMESON, R. F., AKINCI, R., ADAMS, D. J., GILES, A. B., MCCALL, A. <NATURE, 271, 334> 780114
INFRARED LIGHT CURVES OF AM HERCULIS.

JAMESON, R. F., HOUGH, J. H. <M. N. R. A. S., 182, 179> 780103
NEAR-INFRARED POLARIZATION OF THE NUCLEUS OF M31.

JAMESON, R. F., KING, A. R., SHERRINGTON, M. R. <M. N. R. A. S., 195, 235> 810415
INFRARED AND OPTICAL LIGHT CURVES OF THE DWARF NOVA EM CYGNI.

JAMESON, R. F., KING, A. R., SHERRINGTON, M. R. <M. N. R. A. S., 200, 455> 820820
INFRARED, OPTICAL AND ULTRAVIOLET OBSERVATIONS OF TT ARI.

JAMESON, R. F., LONGMORE, A. J. <M. N. R. A. S., 174, 217> 760108
INFRARED OBSERVATIONS AND A MODEL OF BETA LYR.

JAMESON, R. F., LONGMORE, A. J., CRAWFORD, B. <NATURE, 242, 107> 730306
5-MICRON INFRARED EMISSION FROM ALGOL.

JAMESON, R. F., LONGMORE, A. J., MCLINN, J. A., WOOLF, N. J. <AP. J. (LETTERS), 187, L109> 740202
INFRARED SPECTRUM OF NGC 1068.

JAMESON, R. F., LONGMORE, A. J., MCLINN, J. A., WOOLF, N. J. <AP. J., 190, 353> 740605
INFRARED EMISSION BY DUST IN NGC 1068 AND THREE PLANETARY NEBULAE.

JAMESON, R. F., SHERRINGTON, M. R., KING, A. R., GILES, A. B. <NATURE, 278, 233> 790303
INFRARED OBSERVATIONS OF THE BLACK-HOLE CANDIDATE V861 SCO.

JENKINS, L. F. <YALE UNIV. OBS. > 639902
GENERAL CATALOGUE OF TRIGONOMETRIC STELLAR PARALLAXES WITH 1963 SUPPLEMENT.

JENKINS, L. F. <YALE UNIV. OBS. > 529901
GENERAL CATALOGUE OF TRIGONOMETRIC STELLAR PARALLAXES.

JENNINGS, D. E., BRAULT, J. W. <AP. J. (LETTERS), 256, L29> 820504
LABORATORY MEASUREMENTS OF THE PURE ROTATION S(2) AND S(3) TRANSITIONS IN H2.

JOHANSSON, S. <M. N. R. A. S., 178, 17P> 770205
NEW FE II IDENTIFICATIONS IN THE INFRARED SPECTRUM OF ETA CARINAE.

JOHNSON, H. L. <AP. J. (LETTERS), 150, L39> 671001
INFRARED EMISSION FROM CIRCUMSTELLAR SHELLS.

JOHNSON, H. L. <AP. J. (LETTERS), 154, L125> 681202
THE INFRARED SPECTRUM OF THE NML CYGNUS OBJECT.

JOHNSON, H. L. <AP. J., 139, 1022> 640401
THE BRIGHTNESS OF 3C 273 AT 2.2 MICRONS.

JOHNSON, H. L. <AP. J., 141, 170> 650102
INFRARED PHOTOMETRY OF M-DWARF STARS.

JOHNSON, H. L. <AP. J., 141, 923> 650401
INTERSTELLAR EXTINCTION IN THE GALAXY.

JOHNSON, H. L. <AP. J., 143, 187> 660103
INFRARED PHOTOMETRY OF GALAXIES.

JOHNSON, H. L. <AP. J., 146, 613> 661101
THE BOLOMETRIC CORRECTIONS AND EFFECTIVE TEMPERATURES OF TWO GIANT STARS IN THE GLOBULAR CLUSTER M3.

JOHNSON, H. L. <AP. J., 147, 912> 670301
THE LAW OF INTERSTELLAR EXTINCTION FOR EMISSION NEBULAE ASSOCIATED WITH O-TYPE STARS.

JOHNSON, H. L. <AP. J., 149, 345> 670801
THE COLORS OF M SUPERGIANTS.

JOHNSON, H. L. <COMM. LUNAR AND PLANETARY LAB., 3, 73> 650001
THE ABSOLUTE CALIBRATION OF THE ARIZONA PHOTOMETRY.

JOHNSON, H. L. <COMM. LUNAR AND PLANETARY LAB., 3, 79> 650002
INTERSTELLAR EXTINCTION IN THE GALAXY.

JOHNSON, H. L. <COMM. LUNAR AND PLANETARY LAB., 8, 91> 690402
THE INFRARED SPECTRUM OF THE NML CYGNUS OBJECT.

JOHNSON, H. L. <P. A. S. P., 85, 179> 730402
THE INFRARED SPECTRUM OF CHI CYGNI FROM 4000 TO 6700 CM-1.

JOHNSON, H. L., BORGMAN, J. <B. A. N., 17, 115> 631001
THE LAW OF INTERSTELLAR EXTINCTION.

JOHNSON, H. L., COLEMAN, I., MITCHELL, R. I., STEINMETZ, D. L. <COMM. LUNAR AND PLANETARY LAB., 7, 83> 680803
STELLAR SPECTROSCOPY, 1.2 TO 2.6 MICRONS.

JOHNSON, H. L., LOW, F. J., STEINMETZ, D. L. <COMM. LUNAR AND PLANETARY LAB., 3, 95> 650003
INFRARED OBSERVATIONS OF THE NEUGEBAUER-MARTZ-LEIGHTON "INFRARED STAR" IN CYGNUS.

JOHNSON, H. L., MACARTHUR, J. W., MITCHELL, R. I. <AP. J., 152, 465> 680501
THE SPECTRAL-ENERGY CURVES OF SUBDWARFS. I.

JOHNSON, H. L., MENDEZ, M. E. <A. J., 75, 785> 700901
INFRARED SPECTRA FOR 32 STARS.

JOHNSON, H. L., MENDOZA V, E. E. <ANN. D'AST., 29, 525> 660001
THE LAW OF INTERSTELLAR EXTINCTION IN PERSEUS.

JOHNSON, H. L., MENDOZA V, E. E., WISNIEWSKI, W. Z. <AP. J., 144, 458> 660402
ERRATUM TO "OBSERVATIONS OF 'INFRARED STARS' ".

JOHNSON, H. L., MENDOZA V, E. E., WISNIEWSKI, W. Z. <COMM. LUNAR AND PLANETARY LAB., 3, 97> 650004
OBSERVATIONS OF "INFRARED STARS".

JOHNSON, H. L., MITCHELL, R. I., IRIARTE, B., WISNIEWSKI, W. Z. <COMM. LUNAR AND PLANETARY LAB., 4, 99> 660302
UBVRIJKL PHOTOMETRY OF THE BRIGHT STARS.

JOHNSON, H. L., THOMPSON, R. I., FORBES, F. F., STEINMETZ, D. L. <P. A. S. P., 84, 775> 721206
THE INFRARED SPECTRUM OF ALPHA HERCULIS FROM 4000 TO 4800 CM-1.

JOHNSON, H. M. <AP. J. (LETTERS), 180, L7> 730202
COMPARISON OF FAR-INFRARED, OPTICAL, AND RADIOFREQUENCY DATA OF DIFFUSE NEBULAE.

JOHNSON, H. M., SNOW JR., T. P., GEHRZ, R. D., HACKWELL, J. A. <P. A. S. P., 89, 165> 770414
COPERNICUS SPECTRA AND INFRARED PHOTOMETRY OF 42 ORIONIS.

JOHNSON, P. E., RIEKE, G. H., LEBOFSKY, M. J., KEMP, J. C. <AP. J., 245, 871> 810502
SHOCK-INDUCED GRAIN ALIGNMENT IN THE ORION NEBULA.

JOHNSON, T. V., MCCORD, T. B. <AP. J., 169, 589> 711106
SPECTRAL GEOMETRIC ALBEDO OF THE GALILEAN SATELLITES, 0.3 TO 2.5 MICRONS.

JONES, A. W., SELBY, M. J., MOUNTAIN, C. M., WADE, R., SANCHEZ MAGRO, C., MUNOZ, M. P. <NATURE, 283, 550> 800214
IR FLASHES FROM THE X-RAY RAPID BURSTER.

JONES, B., MERRILL, K. M. <IAUC NO. 3268> 780911
NOVA CYGNI 1978.

JONES, B., MERRILL, K. M., PUETTER, R. C., WILLNER, S. P. <A. J., 83, 1437> 781103
THE INFRARED SPECTRUM OF GL 3068.

JONES, B., MERRILL, K. M., STEIN, W., WILLNER, S. P. <AP. J., 242, 141> 801106
THE DEPENDENCE OF THE 8-13 MICRON SPECTRUM OF NGC 7027 ON POSITION IN THE NEBULA.

JONES, D. H. P. <M. N. R. A. S., 139, 189> 680303
NARROW BAND PHOTOMETRY OF K AND M STARS.

JONES, T. J. <AP. J., 228, 787> 790301
POLARIMETRY OF BE STARS AT 1.25 AND 2.2 MICRONS.

JONES, T. J., DYCK, H. M. <AP. J., 220, 159> 780215
INFRARED POLARIMETRY OF THREE BIPOLAR NEBULAE.

JONES, T. J., HYLAND, A. R. <M. N. R. A. S., 192, 359> 800711
NEW RESULTS ON INTERSTELLAR REDDENING IN THE NEAR INFRARED.

JONES, T. J., HYLAND, A. R. <M. N. R. A. S., 200, 509> 820821
MULTIAPERTURE JHK PHOTOMETRY OF THE GLOBULAR CLUSTERS IN FORNAX DWARF SPHEROIDAL GALAXY.

JONES, T. J., HYLAND, A. R., CASWELL, J. L., GATLEY, I. <AP. J., 253, 208> 820207
A SEARCH FOR THE INFRARED COUNTERPART OF TYPE II OH MASERS. II. STATISTICAL ANALYSIS.

JONES, T. J., HYLAND, A. R., ROBINSON, G., SMITH, R., THOMAS, J. <AP. J., 242, 132> 801105
INFRARED OBSERVATIONS OF A BOK GLOBULE IN THE SOUTHERN COALSACK.

JONES, T. J., WOLFF, S. C. <P. A. S. P., 92, 84> 800202
OBSERVATIONS OF PASCHEN ALPHA IN P CYGNI AND OTHER OB STARS.

JONES, T. W., MERRILL, K. M. <AP. J., 209, 509> 761004
MODEL DUST ENVELOPES AROUND LATE-TYPE STARS.

JONES, T. W., RUDNICK, L., OWEN, F. N., PUSCHELL, J. J., ENNIS, D. J., WERNER, M. W. <AP. J., 243, 97> 810103
THE BROAD-BAND SPECTRA AND VARIABILITY OF COMPACT NONTHERMAL SOURCES.

JORDEN, P. R., MACGREGOR, A. D., SELBY, M. J., WHITELOCK, P. A. <M. N. R. A. S., 174, 1P> 760109
INFRARED PHOTOMETRY OF A HEAVILY REDDENED ASSOCIATION IN W35.

JORDEN, P. R., MACGREGOR, A. D., SELBY, M. J., WHITELOCK, P. A., SANCHEZ MAGRO, C. <M. N. R. A. S., 181, 157> 771010
INFRARED SOURCES IN THE COMPACT HII REGION G45.5+0.1.

JOYCE, R. R. <P. A. S. P., 87, 917> 751205
THE INFRARED SPECTRUM OF ETA CARINAE: 3-14 MICRONS.

JOYCE, R. R., CAPPS, R. W., GILLETT, F. C., GRASDALEN, G. L.,KLEINMANN, S. G., SARGENT, D. G. <AP. J. (LETTERS), 213, L125> 770502
ACCURATE PHOTOMETRIC POSITIONS FOR 60 SOURCES FROM THE AFCRL SKY SURVEY.

JOYCE, R. R., GEZARI, D. Y., SCOVILLE, N. Z., FURENLID, I. <AP. J. (LETTERS), 219, L29> 780110
2.1 MICRON H2 EMISSION: HIGH-SPECTRAL-RESOLUTION OBSERVATIONS OF THE ORION NEBULA.

JOYCE, R. R., GEZARI, D. Y., SIMON, M. <AP. J. (LETTERS), 171, L67> 720103
345-MICRON GROUND-BASED OBSERVATIONS OF M17, M82, AND VENUS.

JOYCE, R. R., KNACKE, R. F., SIMON, M., YOUNG, E. <P. A. S. P., 87, 683> 751008
FURTHER INFRARED AND MILLIMETER OBSERVATIONS OF MARKARIAN 231.

JOYCE, R. R., SIMON, M. <P. A. S. P., 88, 870> 761209
3-MILLIMETER AND INFRARED CONTINUUM OBSERVATIONS OF MARKARIAN GALAXIES.

JOYCE, R. R., SIMON, M., SIMON, T. <AP. J., 220, 156> 780214
OBSERVATIONS OF BRACKETT-ALPHA EMISSION IN THE REGION OF THE BN OBJECT.

JOYCE, R. R., SIMON, T. <AP. J., 260, 604> 820904
NEAR-INFRARED SPECTROPHOTOMETRY OF POLARIZED COMPACT INFRARED SOURCES.

JOYCE, R. R., SIMON, T. <M. N. R. A. S., 200, 39P> 820824
POLARIMETRY OF THE H2 EMISSION FROM THE ORION MOLECULAR CLOUD.

JUNG, J., BISCHOFF, M. <STRASBOURG INF. BULL., 2, 8> 719902
CATALOGUE OF STELLAR IDENTIFICATIONS.

KAPLAN, G. H., JOSTIES, F. J., ANGERHOFER, P. E., JOHNSTON, K. J., SPENCER, J. H. <A. J., 87, 570> 829903
PRECISE RADIO SOURCE POSITIONS FROM INTERFEROMETRIC OBSERVATIONS.

KAPLAN, G. H., KALLARAKAL, V. V., HARRINGTON, R. S., JOHNSTON, K. J., SPENCER, J. H. <A. J., 85, 64> 809912
THE COINCIDENCE OF THE RADIO AND OPTICAL EMISSION FROM SS433.

KAWARA, K., KOZASA, T., SATO, S., KOBAYASHI, Y., OKUDA, H., JUGAKU, J. <P. A. S. J., 34, 389> 820002
NEAR-INFRARED SOURCE COUNTS IN THE GALACTIC PLANE.

KAWARA, K., KOZASA, T., SATO, S., OKUDA, H., KOBAYASHI, Y., JUGAKU, J. <MEM. FAC. SCI., KYOTO UNIV., XXXVI, 353> 830001
NEAR-INFRARED SOURCE COUNTS IN THE GALACTIC PLANE. II. A LIST OF NEAR-INFRARED SOURCES.

KAWARA, K., MAIHARA, T., NOGUCHI, K., ODA, N., SATO, S., OISHI, M., IIJIMA, T. <P. A. S. J., 28, 163> 760003
MULTI-BAND PHOTOMETRY OF NOVA CYGNI 1975.

KAZES, I., LE SQUEREN, A. M., GADEA, F. <ASTR. AP., 42, 9> 759901
RADIO OBSERVATIONS OF SMALL GALACTIC NEBULAE.

KEENE, J. <AP. J., 245, 115> 810408
FAR-INFRARED OBSERVATIONS OF GLOBULES.

KEENE, J., HARPER, D. A., HILDEBRAND, R. H., WHITCOMB, S. E. <AP. J. (LETTERS), 240, L43> 800806
FAR-INFRARED OBSERVATIONS OF THE GLOBULE B335.

KEENE, J., HILDEBRAND, R. H., WHITCOMB, S. E. <AP. J. (LETTERS), 252, L11> 820103
A HIGH RESOLUTION SUBMILLIMETER MAP OF OMC-1.

KEMP, J. C., RIEKE, G. H., LEBOFSKY, M. J., COYNE S. J., G. V. <AP. J. (LETTERS), 215, L107> 770804
THE INFRARED POLARIZATION OF NGC 1275, NGC 4151, MARKARIAN 231, AND 3C 273.

KEMP, J. C., RUDY, R. J. <AP. J. (LETTERS), 203, L131> 760203
NOVA CYGNI 1975: NARROW-BAND POLARIMETRY AND PHOTOMETRY 0.36-1.7 MICRONS.

KEMP, J. C., SWEDLUND, J. B. <AP. J. (LETTERS), 162, L67> 701004
LARGE INFRARED CIRCULAR POLARIZATION OF GRW+70 8247.

KHOLOPOV, P. N., KUKARKINA, N. P., PEROVA, N. B. <IBVS NO. 1414> 789910
63RD NAME-LIST OF VARIABLE STARS.

KHOLOPOV, P. N., KUKARKINA, N. P., PEROVA, N. B. <IBVS NO. 1581> 799907
64TH NAME-LIST OF VARIABLE STARS.

KHOLOPOV, P. N., SAMUS, N. N., KUKARKINA, N. P., MEDVEDEVA, G. I., PEROVA, N. B. <IBVS NO. 2042> 819920
66TH NAME-LIST OF VARIABLE STARS.

KHOLOPOV, P. N., SAMUS, N. N., KUKARKINA, N. P., MEDVEDEVA, G. I., PEROVA, N. B. <IBVS NO. 1921> 819919
65TH NAME-LIST OF VARIABLE STARS.

KHOZOV, G. V. <ASTROFIZIKA, 12, 468> 761010
INFRARED STARS: A REVIEW OF THE OBSERVATIONAL DATA.

KHROMOV, G. S. <SOV. AST., 18, 195> 740910
INFRARED RADIATION OF PLANETARY NEBULAE. II. NEW AND REVISED OBSERVATIONS AT 1.0-2.5 MICRONS.

KHROMOV, G. S., MOROZ, V. I. <SOV. AST., 15, 892> 720502
INFRARED RADIATION OF PLANETARY NEBULAE. I. OBSERVATIONS AT 1.0 - 2.5 MICRONS AND THE CONTINUOUS SPECTRUM.

KINMAN, T. D., GRASDALEN, G. L., RIEKE, G. H. <AP. J. (LETTERS), 194, L1> 741103
OPTICAL AND INFRARED OBSERVATIONS OF THE JET OF M87.

KIPLINGER, A. L. <AP. J., 234, 997> 791210
SS CYGNI: THE ACCRETION DISK IN ERUPTION AND AT MINIMUM LIGHT.

KIRSHNER, R. P., ARP, H. C., DUNLAP, J. R. <AP. J., 207, 44> 760703
OBSERVATIONS OF SUPERNOVAE: 1975A IN NGC 2207 AND 1975B IN THE PERSEUS CLUSTER.

KIRSHNER, R. P., OKE, J. B., PENSTON, M. V., SEARLE, L. <AP. J., 185, 303> 731005
THE SPECTRA OF SUPERNOVAE.

KIRSHNER, R. P., WILLNER, S. P., BECKLIN, E. E., NEUGEBAUER, G., OKE, J. B. <AP. J. (LETTERS), 180, L97> 730301
SPECTROPHOTOMETRY OF THE SUPERNOVA IN NGC 5253 FROM 0.33 TO 2.2 MICRONS.

KLEINMANN, D. E. <AP. LETTERS, 13, 49> 730022
BRIGHT INFRARED SOURCES IN M17.

KLEINMANN, D. E. <IAUC NO. 2959> 760611
POSSIBLE INFRARED COUNTERPART OF MXB1730-335.

KLEINMANN, D. E., GILLETT, F. C., WRIGHT, E. L. <AP. J., 208, 42> 760810
8-13 MICRON SPECTROPHOTOMETRY OF NGC 1068.

KLEINMANN, D. E., KLEINMANN, S. G., WRIGHT, E. L. <AP. J. (LETTERS), 210, L83> 761205
THE INFRARED SOURCE NEAR THE RAPID-BURST X-RAY SOURCE MXB 1730-335.

KLEINMANN, D. E., LOW, F. J. <AP. J. (LETTERS), 149, L1> 670701
DISCOVERY OF AN INFRARED NEBULA IN ORION.

KLEINMANN, D. E., LOW, F. J. <AP. J. (LETTERS), 159, L165> 700306
OBSERVATIONS OF INFRARED GALAXIES.

KLEINMANN, D. E., LOW, F. J. <AP. J. (LETTERS), 161, L203> 700904
INFRARED OBSERVATIONS OF GALAXIES AND OF THE EXTENDED NUCLEUS IN M82.

KLEINMANN, D. E., WRIGHT, E. L. <AP. J. (LETTERS), 185, L131> 731101
A NEW INFRARED SOURCE IN M17.

KLEINMANN, D. E., WRIGHT, E. L. <AP. J. (LETTERS), 191, L19> 740701
10-MICRON OBSERVATIONS OF SOUTHERN-HEMISPHERE GALAXIES.

KLEINMANN, S. G., BRECHER, K., INGHAM, W. H. <AP. J., 207, 532> 760707
INFRARED EMISSION FROM A0620-00.

KLEINMANN, S. G., DICKINSON, D. F., SARGENT, D. G. <A. J., 83, 1206> 781002
STELLAR H2O MASERS.

KLEINMANN, S. G., DICKINSON, D. F., SARGENT, D. G. <A. J., 84, 279> 790204
ERRATUM:"STELLAR H2O MASERS" (A. J. 83, 1206(1978))

KLEINMANN, S. G., HALL, D. N. B., RIDGWAY, S. T., WRIGHT, E. L. <A. J., 83, 373> 780403
HIGH-RESOLUTION 2-MICRON SPECTROSCOPY OF CYG OB II NO. 12.

KLEINMANN, S. G., JOYCE, R. R., SARGENT, D. G., GILLETT, F. C., TELESCO, C. M. <AP. J., 227, 126> 790106
AN OBSERVATIONAL STUDY OF THE AFGL INFRARED SKY SURVEY. IV. FURTHER RESULTS FROM THE REVISED CATALOG.

KLEINMANN, S. G., LEBOFSKY, M. J. <AP. J. (LETTERS), 201, L91> 751003
AN UNUSUAL NEBULA NEAR UOA 27.

KLEINMANN, S. G., PAYNE-GAPOSCHKIN, C. <EARTH AND EXT. SCI., 3, 161> 790002
THE REDDEST STARS IN THE TWO MICRON SKY SURVEY.

KLEINMANN, S. G., SARGENT, D. G., GILLETT, F. C., GRASDALEN, G. L., JOYCE, R. R. <AP. J. (LETTERS), 215, L79> 770705
SPECTRAL AND SPATIAL OBSERVATIONS OF THE UNUSUAL OBJECT AFGL 437.

KLEINMANN, S. G., SARGENT, D. G., MOSELEY, S. H., HARPER JR., D. A., LOEWENSTEIN, R. F., TELESCO, C. M., THRONSON JR., H. A. <ASTR. AP., 65, 139> 780411
FAR-INFRARED OBSERVATIONS OF SOURCES ASSOCIATED WITH DOUBLE-LOBED REFLECTION NEBULAE.

KLEMOLA, A. R., HARLAN, E. A., WIRTANEN, C. A. <A. J., 86, 583> 819904
TRIGONOMETRIC PARALLAXES MEASURED AT LICK OBSERVATORY. LIST III.

KLEMOLA, A. R., MARSDEN, B. G. <A. J., 82, 849> 779905
PREDICTED OCCULTATIONS BY THE RINGS OF URANUS, 1977-1980.

KNACKE, R. F. <AP. LETTERS, 11, 201> 720006
INFRARED PHOTOMETRY OF HBV 475 AND MHA 328-116.

KNACKE, R. F., CAPPS, R. W. <A. J., 84, 1705> 791102
OBSERVATION OF TWENTY MICRON POLARIZATION IN THE ORION NEBULA.

KNACKE, R. F., CAPPS, R. W. <AP. J. (LETTERS), 192, L19> 740802
INFRARED POLARIZATION OF NGC 1068.

KNACKE, R. F., CAPPS, R. W. <AP. J., 216, 271> 770805
INFRARED POLARIZATION OF THE GALACTIC CENTER. II.

KNACKE, R. F., CAPPS, R. W., JOHNS, M. <NATURE, 280, 215> 790708
OBSERVATION OF LARGE 2.2 MICRON POLARISATION IN 3C 345.

KNACKE, R. F., CAPPS, R. W., JOHNS, M. <AP. J. (LETTERS), 210, L69> 761204
THE POLARIZATION OF BL LACERTAE AT VISIBLE AND INFRARED WAVELENGTHS.

KNACKE, R. F., CUDABACK, D. D., GAUSTAD, J. E. <AP. J., 158, 151> 691001
INFRARED SPECTRA OF HIGHLY REDDENED STARS: A SEARCH FOR INTERSTELLAR ICE GRAINS.

KNACKE, R. F., DRESSLER, A. M. <P. A. S. P., 85, 100> 730205
THE SPATIAL DISTRIBUTION OF THE 11.7 MICRON RADIATION OF NGC 7027.

KNACKE, R. F., GAUSTAD, J. E., GILLETT, F. C., STEIN, W. A. <AP. J. (LETTERS), 155, L189> 690304
A POSSIBLE IDENTIFICATION OF INTERSTELLAR SILICATE ABSORPTION IN THE INFRARED SPECTRUM OF 119 TAURI.

KNACKE, R. F., MCCORKLE, S., PUETTER, R. C., ERICKSON, E. F.,KRATSCHMER, W. <AP. J., 260, 141> 820902
OBSERVATION OF INTERSTELLAR AMMONIA ICE.

KNACKE, R. F., STROM, K. M., STROM, S. E. <AP. J., 179, 493> 730107
INFRARED OBSERVATIONS OF A HIGHLY REDDENED STAR NEAR NGC 6231.

KNACKE, R. F., STROM, K. M., STROM, S. E., YOUNG, E., KUNKEL, W. <AP. J., 179, 847> 730203
A YOUNG STELLAR GROUP IN THE VICINITY OF R CORONAE AUSTRINAE.

KNACKE, R. F., YOUNG, E. T. <AP. J. (LETTERS), 242, L183> 801203
DETECTION OF THE S(9), V-0-0 ROTATION LINE OF THE HYDROGEN MOLECULE IN ORION.

KNAPPENBERGER, P. H., FREDERICK, L. W. <P. A. S. P., 80, 96> 680202
THE HE I 10,830 LINE IN THE SPECTRUM OF BETA LYRAE.

KOBAYASHI, Y., KAWARA, K., KOZASA, T., SATO, S., OKUDA, H. <P. A. S. J., 32, 291> 800002
2.2 MICRON POLARIZATION MAPPING OF THE GALACTIC CENTER.

KOBAYASHI, Y., KAWARA, K., MAIHARA, T., OKUDA, H., SATO, S., NOGUCHI, K. <P. A. S. J., 30, 377> 780007
INFRARED POLARIZATIONS OF CRL OBJECTS AND OH 0739-14.

KOBAYASHI, Y., KAWARA, K., SATO, S., OKUDA, H. <P. A. S. J., 32, 295> 800003
NARROW-BAND POLARIMETRY OF THE BN OBJECT AND AFGL 2591 BETWEEN 2 AND 4 MICRONS.

KOBAYASHI, Y., OKUDA, H., SATO, S., JUGAKU, J., DYCK, H. M. <P. A. S. J., 35, 101> 830002
INFRARED POLARIZATION IN THE DIRECTION TO THE GALACTIC CENTER.

KODAIRA, K., GREENSTEIN, J. L., OKE, J. B. <AP. J., 155, 525> 690202
ABUNDANCES IN TWO HORIZONTAL-BRANCH A STARS.

KODAIRA, K., GREENSTEIN, J. L., OKE, J. B. <AP. J., 159, 485> 700201
THE UNUSUAL COMPOSITION OF +39 4926.

KODAIRA, K., TANAKA, W., ONAKA, T., WATANABE, T. <P. A. S. J., 31, 667> 790003
BALLOON-BORNE NEAR-INFRARED MULTICOLOR PHOTOMETRY OF LATE-TYPE STARS. II. DATA ANALYSIS.

KODAIRA, K., TANAKA, W., ONAKA, T., WATANABE, T., YOSHIDA, H. <TOKYO AST. BULL., 2, 2889> 771201
NEAR-INFRARED PHOTOMETRY OF LATE-TYPE STARS WITH BALLOON-BORNE TELESCOPE.

KOHOUTEK, L. <ASTR. AP., 16, 291> 729903
HAMBURG SCHMIDT-CAMERA SURVEY OF FAINT PLANETARY NEBULAE. CYGNUS-PERSEUS REGION.

KOJOIAN, G., ELLIOTT, R., BICAY, M. D. <A. J., 86, 816> 819907
ACCURATE OPTICAL POSITIONS FOR MARKARIAN GALAXIES 1096–1302.

KOJOIAN, G., ELLIOTT, R., BICAY, M. D. <A. J., 87, 1364> 829905
ACCURATE OPTICAL POSITIONS FOR MARKARIAN GALAXIES 1303-1399.

KOJOIAN, G., ELLIOTT, R., BICAY, M. D. <AP. J. SUPPL., 50, 161> 829907
ACCURATE OPTICAL POSITIONS OF EXTRAGALACTIC EMISSION-LINE OBJECTS: UNIVERSITY OF MICHIGAN LISTS I-IV.

KOJOIAN, G., ELLIOTT, R., BICAY, M. D., ARAKELIAN, M. A. <A. J., 86, 820> 819908
ACCURATE OPTICAL POSITIONS OF ARAKELIAN GALAXIES.

KOJOIAN, G., ELLIOTT, R., TOVMASSIAN, H. M. <A. J., 83, 1545> 789901
ACCURATE OPTICAL POSITIONS FOR MARKARIAN GALAXIES 508–700.

KOJOIAN, G., ELLIOTT, R., TOVMASSIAN, H. M. <A. J., 86, 811> 819906
ACCURATE OPTICAL POSITIONS FOR MARKARIAN GALAXIES 798-1095.

KOLOTILOV, E. A., LIBERMAN, A. A. <SOV. AST., 21, 327> 770508
NEAR-INFRARED SPECTRUM OF NOVA CYGNI 1975.

KOLOTILOV, E. A., LIBERMAN, A. A. <SOV. AST. (LETTERS), 2, 37> 760208
INFRARED OBSERVATIONS OF NOVA CYGNI 1975. II. SPECTRA IN THE 0.6–1.1 MICRON RANGE.

KOLOTILOV, E. A., NOSKOVA, R. I. <SOV. AST., 17, 611> 740304
ABSOLUTE SPECTROPHOTOMETRY OF THE PLANETARY NEBULA NGC 7027 IN THE WAVELENGTH RANGE 7000–10, 400A.

KOLOTILOV, E. A., ZAJTSEVA, G. V., SHENAVRIN, V. I. <ASTROFIZIKA, 13, 449> 770001
SPECTRAL AND PHOTOMETRIC OBSERVATIONS OF FAST IRREGULAR VARIABLES. III. VX CAS, UX ORI, BN ORI, AND WW VUL - RESULTS OF U, B, V, J, H, K, L PHOTOMETRY.

KOMAROV, N. S., POZIGUN, V. A. <SOV. AST., 12, 105> 680702
STELLAR ENERGY DISTRIBUTION AT INFRARED WAVELENGTHS.

KONDO, Y., WORRALL, D. M., MUSHOTZKY, R. F., HACKNEY, R. L., HACKNEY, K. R. H., OKE, J. B., YEE, H. K. C., NEUGEBAUER, G., MATTHEWS, K., FELDMAN, P. A., BROWN, R. L. <AP. J., 243, 690> 810206
QUASI-SIMULTANEOUS OBSERVATIONS OF BL LAC OBJECT MRK 501 IN X-RAY, UV, VISIBLE, IR, AND RADIO FREQUENCIES.

KOORNNEEF, J. <ASTR. AP., 107, 247> 820310
THE GAS TO DUST RATIO AND THE NEAR-INFRARED EXTINCTION LAW IN THE LARGE MAGELLANIC CLOUD.

KOORNNEEF, J. <ASTR. AP., 55, 469> 770302
HIGHLY REDDENED ARA CLUSTER REVISITED.

KOORNNEEF, J. <IAUC NO. 3740> 821006
SUPERNOVA IN NGC 1187.

KOORNNEEF, J. <M. N. R. A. S., 184, 477> 780802
THE INFRARED ANGULAR DIAMETER OF ETA CARINAE.

KOORNNEEF, J., LUB, J., BARBIER, R. <IAUC NO. 3556> 801212
SUPERNOVA IN NGC 1316.

KOPPENAAL, K., SARGENT, A. I., NORDH, H. L., VAN DUINEN, R. J., AALDERS, J. W. G. <ASTR. AP., 75, L1> 790514
OBSERVATIONS OF NEW FAR INFRARED SOURCES IN THE CEPHEUS OB3 MOLECULAR CLOUD.

KOVAR, R. P., POTTER, A. E., KOVAR, N. S., TRAFTON, L. <AP. J., 170, 449> 711202
THE INFRARED SPECTRUM OF IC 418.

KOVAR, R. P., POTTER, A. E., KOVAR, N. S., TRAFTON, L. <P. A. S. P., 84, 46> 720205
PASCHEN BETA EMISSION IN THE SPECTRUM OF OMICRON CETI.

KRASSNER, J. <ASTR. AP., 114, 19> 821008
2–4 MICRON SPECTROSCOPY OF THE COMPACT H II REGION G45.13+0.14A.

KRASSNER, J., PIPHER, J. L., SHARPLESS, S. <ASTR. AP., 77, 302> 790815
OPTICAL, RADIO, AND INFRARED OBSERVATIONS OF COMPACT H II REGIONS. III. THE NEBULA S235A.

KRASSNER, J., PIPHER, J. L., SHARPLESS, S., HERTER, T. <ASTR. AP., 109, 223> 820508
RADIO, INFRARED, AND OPTICAL OBSERVATIONS OF COMPACT H II REGIONS.

KRASSNER, J., SMITH, L. L., HILGEMAN, T. <AP. J. (LETTERS), 231, L31> 790703
NEAR-INFRARED OBSERVATIONS OF A NEW MOLECULAR FEATURE IN IRC+10216.

KREYSA, E., PAULINY-TOTH, I. I. K., SCHULTZ, G. V., SHERWOOD, W. A., WITZEL, A. <AP. J. (LETTERS), 240, L17> 800818
MILLIMETER CONTINUUM OBSERVATIONS OF FLAT SPECTRA RADIO SOURCES.

KUHI, L. V. <AP. J., 143, 753> 660303
WOLF-RAYET STARS. I. THE CONTINUOUS ENERGY DISTRIBUTION

KUHI, L. V. <AP. J., 145, 715> 660901
WOLF-RAYET STARS. II. THE INFRARED SPECTRUM.

KUHI, L. V. <ASTR. AP. SUPPL., 15, 47> 740409
SPECTRAL ENERGY DISTRIBUTIONS OF T TAURI STARS.

KUIPER, G. P. <COMM. LUNAR AND PLANETARY LAB., 1, 179> 620002
INFRARED SPECTRA OF STARS AND PLANETS. II. WATER VAPOR IN OMICRON CETI.

KUIPER, G. P. <COMM. LUNAR AND PLANETARY LAB., 2, 17> 630001
INFRARED SPECTRA OF STARS AND PLANETS. III. RECONNAISSANCE OF A0–B8 STARS, 1-2.5 MICRONS.

KUIPER, G. P., GORANSON, R., BINDER, A., JOHNSON, H. L. <COMM. LUNAR AND PLANETARY LAB., 1, 119> 620001
AN INFRARED STELLAR SPECTROMETER.

KUIPER, G. P., WILSON, W., CASHMAN, R. J. <AP. J., 106, 243> 470902
AN INFRARED STELLAR SPECTROMETER.

KUKARKIN, B. V., KHOLOPOV, P. N., ARTIUKHINA, N. M., FEDOROVICH, V. P., FROLOV, M. S., GORANSKIJ, V. P., GORYNYA, N. A., KARITSKAYA, E. A., KIREEVA, N. N., KUKARKINA, N. P., KUROCHKIN, N. E., MEDVEDEVA, G. I., PEROVA, N. B., PONOMAREVA, G. A., SAMUS', N. N., SHUGAROV, S. YU. <PUBL. OFFICE NAUKA, MOSCOW> 829909
NEW CATALOGUE OF SUSPECTED VARIABLE STARS.

KUKARKIN, B. V., KHOLOPOV, P. N., EFREMOV, YU. N., KUKARKINA, N. P., KUROCHKIN, N. E., MEDVEDEVA, G. I., PEROVA, N. B., FEDOROVITCH, V. P., FROLOV, M. S. <PUBL. OFFICE NAUKA, MOSCOW> 699901
GENERAL CATALOG OF VARIABLE STARS. VOLUMES I AND II.

KUKARKIN, B. V., KHOLOPOV, P. N., EFREMOV, YU. N., KUKARKINA, N. P., KUROCHKIN, N. E., MEDVEDEVA, G. I., PEROVA, N. B., PSKOVSKY, YU. P., FEDOROVICH, V. P., FROLOV, M. S. <PUBL. OFFICE NAUKA, MOSCOW> 719907
GENERAL CATALOG OF VARIABLE STARS. FIRST SUPPLEMENT.

KUKARKIN, B. V., KHOLOPOV, P. N., EFREMOV, YU. N., KUKARKINA, N. P., KUROCHKIN, N. E., MEDVEDEVA, G. I., PEROVA, N. B., PSKOVSKY, YU. P., FEDOROVICH, V. P., FROLOV, M. S. <PUBL. OFFICE NAUKA, MOSCOW> 749909
GENERAL CATALOGUE OF VARIABLE STARS. SECOND SUPPLEMENT.

KUKARKIN, B. V., KHOLOPOV, P. N., EFREMOV, YU. N., KUROCHKIN, N. E. <PUBL. OFFICE NAUKA, MOSCOW> 659901
SECOND CATALOGUE OF SUSPECTED VARIABLE STARS.

KUKARKIN, B. V., KHOLOPOV, P. N., FEDOROVICH, V. P., KIREYEVA, N. N., KUKARKINA, N. P., MEDVEDEVA, G. I., PEROVA, N. B. <IBVS NO. 1248> 769915
62ND NAME-LIST OF VARIABLE STARS.

KUKARKIN, B. V., KHOLOPOV, P. N., KUKARKINA, N. P., KUROCHKIN, N. P., MEDVEDEVA, G. I., PEROVA, N. B., PSOVSKY, YU. P., FEDOROVITCH, V. P., FROLOV, M. S. <PUBL. OFFICE NAUKA, MOSCOW> 769913
GENERAL CATALOGUE OF VARIABLE STARS. THIRD SUPPLEMENT.

KUKARKIN, B. V., PARENAGO, P. P., EFREMOV, YU. N., KHOLOPOV, P. N. <PUBL. OFFICE NAUKA, MOSCOW> 519901
CATALOGUE OF STARS SUSPECTED TO BE VARIABLE.

KULKARNI, P. V., ASHOK, N. M., APPARAO, K. M. V., CHITRE, S. M. <NATURE, 280, 819> 790816
DISCOVERY OF IR BURSTS FROM LILLER 1/MXB1730-333.

KUTNER, M. L., MACHNIK, D. E., TUCKER, K. D., DICKMAN, R. L. <AP. J., 237, 734> 809905
MOLECULAR CLOUDS ASSOCIATED WITH REFLECTION NEBULAE. I. A SURVEY OF CARBON MONOXIDE EMISSION.

LACASSE, M. G. <AP. LETTERS, 23, 61> 820004
NEAR INFRARED POLARIZATION IN TWO PECULIAR NEBULAE: M2-9 AND THE PV CEPHEI NEBULA.

LACASSE, M. G., BOYLE, D., LEVREAULT, R., PIPHER, J. L., SHARPLESS, S. <ASTR. AP., 104, 57> 811212
POLARIMETRIC OBSERVATIONS OF S106.

LACY, C. H. <AP. J., 218, 444> 771202
ABSOLUTE DIMENSIONS AND MASSES OF THE REMARKABLE SPOTTED DM4E ECLIPSING BINARY FLARE STAR CM DRACONIS.

LACY, J. H., BAAS, F., TOWNES, C. H., GEBALLE, T. R. <AP. J. (LETTERS), 227, L17> 790110
OBSERVATIONS OF THE MOTION AND DISTRIBUTION OF THE IONIZED GAS IN THE CENTRAL PARSEC OF THE GALAXY.

LACY, J. H., BECK, S. C., GEBALLE, T. R. <AP. J., 255, 510> 820405
INFRARED EMISSION LINE STUDIES OF THE STRUCTURE AND EXCITATION OF H II REGIONS.

LACY, J. H., SOIFER, B. T., NEUGEBAUER, G., MATTHEW, S., MALKAN, M., BECKLIN, E. E., WU, C. -C., BOGGESS, A., GULL, T. R. <AP. J., 256, 75> 820501
INFRARED, OPTICAL, AND ULTRAVIOLET OBSERVATIONS OF HYDROGEN LINE EMISSION FROM SEYFERT GALAXIES.

LACY, J. H., TOWNES, C. H., GEBALLE, T. R., HOLLENBACH, D. J. <AP. J., 241, 132> 801008
OBSERVATIONS OF THE MOTION AND DISTRIBUTION OF THE IONIZED GAS IN THE CENTRAL PARSEC OF THE GALAXY. II.

LADA, C. J., DICKINSON, D. F., GOTTLIEB, C. A., WRIGHT, E. L. <AP. J., 207, 113> 760704
H20 AND 22 GHZ CONTINUUM OBSERVATIONS OF M17.

LADA, C. J., GAUTIER III, T. N. <AP. J., 261, 161> 821001
THE ENERGETIC MOLECULAR OUTFLOW NEAR AFGL 961: MILLIMETER-WAVE AND INFRARED OBSERVATIONS.

LADA, C. J., THRONSON JR., H. A., SMITH, H. A., HARPER, D. A., KEENE, J., LOEWENSTEIN, R. F., SMITH, J. <AP. J. (LETTERS), 251, L91> 811208
FAR-INFRARED AND SUBMILLIMETER OBSERVATIONS OF BARNARD 35: HEAT SOURCES FOR BRIGHT-RIMMED MOLECULAR CLOUDS.

LADA, C. J., WILKING, B. A. <AP. J., 242, 1056> 801208
INFRARED OBSERVATIONS OF BARNARD 35: HEAT SOURCES FOR BRIGHT-RIMMED MOLECULAR CLOUDS.

LAMBERT, D. L., BROOKE, A. L., BARNES, T. G. <AP. J., 186, 573> 731207
H2 QUADRUPOLE ROTATION-VIBRATION LINES IN INFRARED SPECTRA OF COOL STARS.

LAMBERT, D. L., CLEGG, R. E. S. <M. N. R. A. S., 191, 367> 800508
THE KEENAN AND WING BANDS IN S STARS.

LAMBERT, D. L., HINKLE, K. H., HALL, D. N. B. <AP. J., 248, 638> 810904
CIRCUMSTELLAR SHELLS OF LUMINOUS SUPERGIANTS. I. CARBON MONOXIDE IN RHO CASSIOPEIAE AND HR 8752.

LAMY, PH. L., NGUYEN-TRONG, T., ADJABSCHIRZADEH, A., KOUTCHMY, S. <ASTR. AP., 77, 257> 790814
ASTRONOMICAL APPLICATIONS OF INFRA-RED TELEVISION IMAGING.

LANDSTREET, J. D., ANGEL, J. R. P. <AP. J., 211, 825> 770209
DETECTION OF POLARIZATION VARIATION ACROSS ABSORPTION FEATURES OF MIRA VARIABLES.

LAUBERTS, A., HOLMBERG, E. B., SCHUSTER, H. -E., WEST, R. M. <ASTR. AP. SUPPL., 43, 307> 819916
THE ESO/UPPSALA SURVEY OF THE ESO(B) ATLAS OF THE SOUTHERN SKY. VIII.

LAUBERTS, A., HOLMBERG, E. B., SCHUSTER, H. -E., WEST, R. M. <ASTR. AP. SUPPL., 46, 311> 819917
THE ESO/UPPSALA SURVEY OF THE ESO(B) ATLAS OF THE SOUTHERN SKY. IX.

LAWRENCE, A., GILES, A. B., MCHARDY, I. M., COOKE, B. A. <M. N. R. A. S., 195, 149> 810413
FAST SIMULTANEOUS INFRARED AND OPTICAL PHOTOMETRY OF NGC 4151.

LEBOFSKY, M. J. <A. J., 84, 324> 790308
VARIABLE EXTINCTION AT THE GALACTIC CENTER.

LEBOFSKY, M. J. <AP. J. (LETTERS), 245, L59> 810405
EVOLUTION OF HIGH-REDSHIFT GALAXIES.

LEBOFSKY, M. J., KLEINMANN, S. G., RIEKE, G. H., LOW, F. J. <AP. J. (LETTERS), 206, L157> 760605
AN OBSERVATIONAL STUDY OF THE AFCRL INFRARED SKY SURVEY. II. PRESENT RESULTS OF A NEW PROGRAM TO STUDY THE FINAL CATALOG.

LEBOFSKY, M. J., RIEKE, G. H. <A. J., 82, 646> 770802
CRL 3068--A DUST-ENSHROUDED CARBON STAR.

LEBOFSKY, M. J., RIEKE, G. H. <AP. J., 229, 111> 790405
EXTINCTION IN INFRARED-EMITTING GALACTIC NUCLEI.

LEBOFSKY, M. J., RIEKE, G. H. <NATURE, 284, 410> 800416
VARIATIONS IN THE THERMAL EMISSION OF SEYFERT GALAXIES.

LEBOFSKY, M. J., RIEKE, G. H., DESHPANDE, M. R., KEMP, J. C. <AP. J., 263, 672> 821206
POLARIZATION OF COMPACT SOURCES IN THE GALACTIC CENTER.

LEBOFSKY, M. J., RIEKE, G. H., KEMP, J. C. <AP. J., 222, 95> 780506
INFRARED PHOTOMETRY AND POLARIMETRY OF NGC 1068.

LEBOFSKY, M. J., RIEKE, G. H., TOKUNAGA, A. T. <AP. J., 263, 736> 821207
M SUPERGIANTS AND STAR FORMATION AT THE GALACTIC CENTER.

LEBOFSKY, M. J., RIEKE, G. H., WALSH, D., WEYMANN, R. J. <NATURE, 285, 385> 800614
THE IR SPECTRUM OF THE DOUBLE QSO.

LEBOFSKY, M. J., SARGENT, D. G., KLEINMANN, S. G., RIEKE, G. H. <AP. J., 219, 487> 780106
AN OBSERVATIONAL STUDY OF THE AFCRL INFRARED SKY SURVEY. III. FURTHER SEARCHES FOR AFCRL/AFGL SOURCES AND AN EVALUATION OF THE CONTENTS OF THE MID-INFRARED SKY.

LEDDEN, J. E., O'DELL, S. L., STEIN, W. A., WISNIEWSKI, W. Z. <AP. J., 243, 47> 810102
THE SPECTRAL FLUX DISTRIBUTION OF THE CANDIDATE BL LACERTAE OBJECT 1218+304 (-2A1219+305).

LEE, S. -W. <ASTR. AP. SUPPL., 27, 381> 779911
UBV PHOTOMETRY OF BRIGHT STARS IN 47 TUC.

LEE, S. -W. <ASTR. AP. SUPPL., 28, 409> 779910
UBV PHOTOMETRY OF BRIGHT STARS IN NGC 3201.

LEE, T. A. <A. J., 77, 374> 720601
ON THE NATURE OF SOME FAINT INFRARED STARS.

LEE, T. A. <AP. J., 152, 913> 680601
INTERSTELLAR EXTINCTION IN THE ORION ASSOCIATION.

LEE, T. A. <AP. J., 162, 217> 701001
PHOTOMETRY OF HIGH-LUMINOSITY M-TYPE STARS.

LEE, T. A. <P. A. S. P., 81, 878> 691203
OBSERVATIONS OF THE 5 MICRON SOURCE IN ORION.

LEE, T. A. <P. A. S. P., 85, 637> 731006
VISUAL AND INFRARED PHOTOMETRY OF RY SAGITTARII NEAR THE PHASE OF DEEP MINIMUM.

LEE, T. A., FEAST, M. W. <AP. J. (LETTERS), 157, L173> 690902
INFRARED EXCESS OF RY SGR.

LEE, T. A., NARIAI, K. <AP. J. (LETTERS), 149, L93> 670902
INFRARED RADIATION FROM UPSILON SAGITARII.

LEE, T. A., NARIAI, K. <P. A. S. J., 21, 67> 690002
INFRARED PHOTOMETRY OF A HELIUM STAR, HD 30353.

LEE, T. A., WAMSTEKER, W., WISNIEWSKI, W. Z., WDOWIAK, T. J. <AP. J. (LETTERS), 177, L59> 721006
PHOTOMETRY OF SUPERNOVA 1972 IN NGC 5253.

LEE, T. J., BEATTIE, D. H., GATLEY, I., BRAND, P. W. J. L., JONES, T., HYLAND, A. R. <NATURE, 295, 214> 820119
OCCURRENCE OF THE 3.3-MICRON FEATURE IN GALAXIES.

LEGER, A., KLEIN, J., DE CHEVEIGNE, S., GUINET, C., DEFOURNEAU, D., BELIN, M. <ASTR. AP., 79, 256> 791018
THE 3.1 MICRON ABSORPTION IN MOLECULAR CLOUDS IS PROBABLY DUE TO AMORPHOUS H2O ICE.

LEITHERER, C., HEFELE, H., STAHL, O., WOLF, B. <ASTR. AP., 108, 102> 820417
SPECTROSCOPY AND INFRARED PHOTOMETRY OF CYG OB 2 STARS: VELOCITY LAW AND MASS-LOSS RATES.

LEMKE, D., HARRIS, A. W. <ASTR. AP., 99, 285> 810619
A NEAR INFRARED MAP OF M17.

LEMKE, D., LOW, F. J. <AP. J. (LETTERS), 177, L53> 721005
21-MICRON OBSERVATIONS OF HII REGIONS.

LEMKE, D., LOW, F. J., THUM, C. <ASTR. AP., 32, 231> 740509
INFRARED MAP OF THE ORION NEBULA.

LESTER, D. F., BREGMAN, J. D., WITTEBORN, F. C., RANK, D. M.,DINERSTEIN, H. L. <AP. J., 248, 524> 810901
THE ABUNDANCE OF ARGON AT THE GALACTIC CENTER.

LESTER, D. F., DINERSTEIN, H. L., RANK, D. M. <AP. J., 229, 981> 790507
INFRARED AND OPTICAL MEASUREMENTS OF THE IONIZED GAS IN K3-50.

LESTER, D. F., DINERSTEIN, H. L., RANK, D. M. <AP. J., 232, 139> 790812
FINE-STRUCTURE LINES AND ELEMENTAL ABUNDANCES IN THE ORION NEBULA.

LESTER, D. F., WERNER, M. W., STOREY, J. W. V., WATSON, D. M., TOWNES, C. H. <AP. J. (LETTERS), 248, L109> 810908
DETECTION OF (O I) 63 MICRON EMISSION FROM THE GALACTIC CENTER.

LEVAN, P. D., PUETTER, R. C., RUDY, R. J., SMITH, H. E., WILLNER, S. P. <AP. J., 251, 10> 811201
HE I 10830 OBSERVATIONS OF FIVE SEYFERT GALAXIES.

LEWIN, W. H. G., COMINSKY, L. R., WALKER, A. R., ROBERTSON, B. S. C. <NATURE, 287, 27> 800916
SIMULTANEOUS IR AND X-RAY BURST OBSERVATION OF SER X-1.

LIBERMAN, A. A., MOROZ, V. I., SHENAVRIN, V. I. <SOV. AST. (LETTERS), 2, 39> 760210
INFRARED OBSERVATIONS OF NOVA CYGNI 1975. IV. PHOTOMETRY WITH A GERMANIUM BOLOMETER COOLED BY LIQUID HELIUM.

LIEBERT, J., DAHN, C. C., GRESHAM, M., STRITTMATTER, P. A. <AP. J., 233, 226> 799901
NEW RESULTS FROM A SURVEY OF FAINT PROPER-MOTION STARS: A PROBABLE DEFICIENCY OF VERY LOW LUMINOSITY DEGENERATES.

LIEBERT, J., LEBOFSKY, M. J., RIEKE, G. H. <AP. J. (LETTERS), 246, L73> 810608
INFRARED PHOTOMETRY AND THE ATMOSPHERIC COMPOSITION OF COOL WHITE DWARFS: THE LOWEST LUMINOSITY CANDIDATES.

LIEBERT, J., STOCKMAN, H. S., WILLIAMS, R. E., TAPIA, S., GREEN, R. F., RAUTENKRANZ, D., FERGUSON, D. H. <AP. J., 256, 594> 820506
PG 1550+191: A NEW AM HERCULIS TYPE BINARY SYSTEM.

LILLY, S. J., LONGAIR, M. S. <M. N. R. A. S., 199, 1053> 820621
INFRARED STUDIES OF A SAMPLE OF 3C RADIO GALAXIES.

LLOYD EVANS, T. <M. N. R. A. S., 174, 169> 769912
RED VARIABLES IN THE CENTRAL BULGE OF THE GALAXY. I.

LLOYD EVANS, T. <M. N. R. A. S., 193, 87> 809914
RED STARS IN MAGELLANIC CLOUD GLOBULAR CLUSTERS.

LLOYD EVANS, T. <S. A. A. O. CIRC., 1, 163> 800005
INFRARED PHOTOMETRY OF CLASSICAL CEPHEIDS.

LOCKWOOD, G. W. <AP. J. (LETTERS), 160, L47> 700402
NEAR-INFRARED PHOTOMETRY OF TWO EXTREMELY RED OBJECTS.

LOCKWOOD, G. W. <AP. J. SUPPL., 24, 375> 720002
NEAR-INFRARED PHOTOMETRY OF MIRA VARIABLES.

LOCKWOOD, G. W. <AP. J., 157, 275> 690702
IDENTIFICATION, STRUCTURE, AND VARIATIONS OF NEW TIO BANDS IN THE ONE-MICRON SPECTRA OF MIRA VARIABLES.

LOCKWOOD, G. W. <AP. J., 180, 845> 730304
SCANNER PHOTOMETRY OF WEAK TIO BANDS NEAR 1 MICRON IN COOL M STARS.

LOCKWOOD, G. W. <AP. J., 192, 113> 740806
NEAR-INFRARED PHOTOMETRY OF UNIDENTIFIED IRC STARS. II.

LOCKWOOD, G. W. <AP. J., 193, 103> 741011
STELLAR ENERGY DISTRIBUTIONS IN AN INFRARED CLUSTER IN ARA.

LOCKWOOD, G. W., DYCK, H. M., RIDGWAY, S. T. <AP. J., 195, 385> 750103
THE COMPOSITE SPECTRUM AND ENERGY DISTRIBUTION OF XX OPHIUCHI.

LOCKWOOD, G. W., WING, R. F. <AP. J., 169, 63> 711002
LIGHT CURVES OF MIRA VARIABLES AT 1.04 MICRONS.

LOCKWOOD, G. W., WING, R. F. <M. N. R. A. S., 198, 385> 820214
THE LIGHT AND SPECTRUM VARIATIONS OF VX SAGITTARII, AN EXTREMELY COOL SUPERGIANT.

LOCKWOOD, G. W., ZINTER, T. A. <A. J., 78, 471> 730801
A LIST OF ADDITIONAL VARIABLE STARS IN THE TWO-MICRON SKY SURVEY.

LOER, S. J., ALLEN, D. A., DYCK, H. M. <AP. J. (LETTERS), 183, L97> 730802
2.2- AND 3.5-MICRON POLARIZATION MEASUREMENTS OF THE BECKLIN-NEUGEBAUER OBJECT IN THE ORION NEBULA.

LONGMORE, A. J., HYLAND, A. R., ALLEN, D. A. <PROC. A. S. A., 3, 47> 760903
THE AFCRL CATALOGUE: SOME SOUTHERN SOURCES STUDIED.

LONGMORE, A. J., JAMESON, R. F. <M. N. R. A. S., 173, 271> 751106
INFRARED OBSERVATIONS AND A MODEL OF BETA PER.

LONGMORE, A. J., LEE, T. J., ALLEN, D. A., ADAMS, D. J. <M. N. R. A. S., 195, 825> 810615
INFRARED OBSERVATIONS OF THE CATACLYSMIC VARIABLE RW TRI.

LONGMORE, A. J., SHARPLES, R. M. <M. N. R. A. S., 201, 111> 821010
INFRARED OBSERVATIONS OF EARLY-TYPE GALAXIES WITH DUST-LANES.

LONSDALE, C. J., BECKLIN, E. E., LEE, T. J., STEWART, J. M. <A. J., 87, 1819> 821212
NEW MEMBERS OF THE INFRARED CLUSTER IN THE ORION MOLECULAR CLOUD.

LONSDALE, C. J., DYCK, H. M., CAPPS, R. W., WOLSTENCROFT, R. D. <AP. J. (LETTERS), 238, L31> 800502
NEAR-INFRARED CIRCULAR POLARIZATION OBSERVATIONS OF MOLECULAR CLOUD SOURCES.

LOREN, R. B. <A. J., 86, 69> 819902
THE DENSITIES OF THE MOLECULAR CLOUDS ASSOCIATED WITH HERBIG BE/AE AND OTHER YOUNG STARS.

LOREN, R. B. <AP. J., 215, 129> 770707
THE MONOCEROS R2 CLOUD: NEAR-INFRARED AND MOLECULAR OBSERVATIONS OF A ROTATING COLLAPSING CLOUD.

LOREN, R. B. <AP. J., 218, 716> 771204
THE STAR-FORMATION PROCESS IN MOLECULAR CLOUDS ASSOCIATED WITH HERBIG BE/AE STARS. I. LKHA 198, BD +40 4124, AND NGC 7129.

LOREN, R. B., WOOTTEN, H. A. <AP. J. (LETTERS), 225, L81> 781005
STAR FORMATION IN THE BRIGHT-RIMMED MOLECULAR CLOUD IC 1848 A.

LOW, F. J. <AFCRL-70-0179> 700302
SKY SURVEY.

LOW, F. J. <AFCRL-71-0387> 710204
PRELIMINARY RESULTS OF AN INFRARED SKY SURVEY.

LOW, F. J. <AFCRL-72-0016> 720801
GROUNDBASED INFRARED OBSERVATIONS OF CELESTIAL SOURCES.

LOW, F. J. <AP. J. (LETTERS), 159, L173> 700307
THE INFRARED-GALAXY PHENOMENON.

LOW, F. J. <AP. J., 141, 326> 650108
THE INFRARED BRIGHTNESS OF ALPHA LEONIS AND GAMMA ORIONIS.

LOW, F. J., AUMANN, H. H. <AP. J. (LETTERS), 162, L79> 701103
OBSERVATIONS OF GALACTIC AND EXTRAGALACTIC SOURCES BETWEEN 50 AND 300 MICRONS.

LOW, F. J., JOHNSON, H. L. <AP. J., 139, 1130> 640501
STELLAR PHOTOMETRY AT 10 MICRONS.

LOW, F. J., JOHNSON, H. L. <AP. J., 141, 336> 650105
THE SPECTRUM OF 3C 273.

LOW, F. J., JOHNSON, H. L., KLEINMANN, D. E., LATHAM, A. S., GEISEL, S. L. <AP. J., 160, 531> 700502
PHOTOMETRIC AND SPECTROSCOPIC OBSERVATIONS OF INFRARED STARS.

LOW, F. J., KLEINMANN, D. E. <A. J., 73, 868> 681105
INFRARED OBSERVATIONS OF SEYFERT GALAXIES, QUASISTELLAR SOURCES, AND PLANETARY NEBULAE.

LOW, F. J., KLEINMANN, D. E., FORBES, F. F., AUMANN, H. H. <AP. J. (LETTERS), 157, L97> 690801
THE INFRARED SPECTRUM, DIAMETER, AND POLARIZATION OF THE GALACTIC NUCLEUS.

LOW, F. J., KRISHNA SWAMY, K. S. <NATURE, 227, 1333> 700908
NARROW-BAND INFRARED PHOTOMETRY OF ALPHA ORI.

LOW, F. J., KURTZ, R. F., POTEET, W. M., NISHIMURA, T. <AP. J. (LETTERS), 214, L115> 770612
FAR-INFRARED SCANS OF THE GALACTIC PLANE.

LOW, F. J., KURTZ, R. F., VRBA, F. J., RIEKE, G. H. <AP. J. (LETTERS), 206, L153> 760604
AN OBSERVATIONAL STUDY OF THE AFCRL INFRARED SKY SURVEY. I. LIMITED GROUND-BASED SURVEY AND RESULTS FROM PRELIMINARY CATALOG.

LOW, F. J., MITCHELL, R. I. <AP. J., 141, 327> 650104
NEW INFRARED PHOTOMETRY OF EPSILON AURIGAE.

LOW, F. J., RIEKE, G. H. <NAT. PHYS. SCI., 233, 256> 710906
VARIATIONS IN THE 10-MICRON FLUX FROM NGC 1068.

LOW, F. J., RIEKE, G. H., ARMSTRONG, K. R. <AP. J. (LETTERS), 183, L105> 730805
GROUND-BASED OBSERVATIONS AT 34 MICRONS.

LOW, F. J., SMITH, B. J. <COMM. LUNAR AND PLANETARY LAB., 8, 87> 690401
INFRARED OBSERVATIONS OF A PREPLANETARY SYSTEM.

LOWE, R. P., MOORHEAD, J. M., WEHLAU, W. H. <AP. J., 214, 712> 770610
NEAR-INFRARED FOURIER SPECTROSCOPY OF THE ORION NEBULA.

LOWE, R. P., MOORHEAD, J. M., WEHLAU, W. H. <AP. J., 228, 191> 790211
NEAR-INFRARED FOURIER SPECTROSCOPY OF THE ORION NEBULA. II. THE WEAK LINES.

LUNEL, M., BERGEAT, J., SIBILLE, F., GARNIER, R. <M. N. R. A. S., 195, 765> 810614
OBSERVATIONS OF INFRARED SOURCES ASSOCIATED WITH ON 1 AND G110.25+0.01.

LUNEL, M., BERGEAT, J., SIBILLE, F., LORTET-ZUCKERMAN, M. C. <ASTR. AP., 34, 299> 740811
INFRARED SOURCES IN SHARPLESS 157.

LUTZ, B. L., SOUZA, S. P. <AP. J. (LETTERS), 213, L129> 770505
A SEARCH FOR C2 IN THE INTERSTELLAR SPECTRUM OF ZETA OPHIUCHI.

LUUD, L., VENNIK, J., PEHK, M. <SOV. AST. (LETTERS), 4, 46> 780115
A NEW ACTIVE STATE IN CH CYGNI, AND A POSSIBLE MODEL.

LUYTEN, W. J. <LUNDPRESS, MINNEAPOLIS, MN> 579904
A CATALOGUE OF 9867 STARS IN THE SOUTHERN HEMISPHERE WITH PROPER MOTIONS EXCEEDING 0.2 ARC SECONDS ANNUALLY.

LUYTEN, W. J. <LUNDPRESS, MINNEAPOLIS, MN> 419901
BRUCE PROPER MOTION SURVEY.

MACCONNELL, D. J. <AP. J. SUPPL., 16, 275> 689902
A STUDY OF THE CEPHEUS IV ASSOCIATION.

MACGREGOR, A. D., PHILLIPS, J. P., SELBY, M. J. <M. N. R. A. S., 164, 31P> 730011
THE DETECTION OF M15 AT 10.2 MICRONS.

MACGREGOR, A. D., SANCHEZ MAGRO, C., SELBY, M. J., WHITELOCK, P. A. <ASTR. AP., 50, 389> 760802
THE SPATIAL DISTRIBUTION OF DUST IN THE PLANETARY NEBULAE NGC 6537, IC 418, BD +30 3639 AND NGC 6572.

MAFFEI, P. <AP. J., 147, 802> 670203
VARIABILITY OF INFRARED STARS. I. LONG-PERIOD VARIABLES

MAFFEI, P. <P. A. S. P., 80, 618> 689901
INFRARED OBJECT IN THE REGION OF IC 1805.

MAIHARA, T., NOGUCHI, K., OISHI, M., OKUDA, H., SATO, S. <NATURE, 259, 465> 760213
VARIATIONS OF THE INFRARED POLARISATION OF VY CANIS MAJORIS.

MAIHARA, T., NOGUCHI, K., OKUDA, H., SATO, S., OISHI, M. <P. A. S. J., 29, 415> 770004
INFRARED POLARIZATION OF THE GALACTIC CENTER.

MAIHARA, T., ODA, N., OKUDA, H. <AP. J. (LETTERS), 227, L129> 790209
A BALLOON OBSERVATION OF DIFFUSE FAR-INFRARED EMISSION FROM THE GALACTIC PLANE.

MAIHARA, T., ODA, N., SHIBAI, H., OKUDA, H. <ASTR. AP., 97, 139> 810418
OBSERVATIONS OF DIFFUSE FAR INFRARED EMISSION AND DISTRIBUTION OF INTERSTELLAR DUST.

MAIHARA, T., ODA, N., SUGIYAMA, T., OKUDA, H. <P. A. S. J., 30, 1> 780005
2.4-MICRON OBSERVATION OF THE GALAXY AND THE GALACTIC STRUCTURE.

MALANUSHENKO, V. M., SHANIN, G. I., SHCHERBAKOV, A. G. <SOV. AST., 21, 267> 770507
STUDIES OF NOVA CYGNI 1975 AT THE CRIMEAN ASTROPHYSICAL OBSERVATORY. II. SPECTROSCOPY IN THE NEAR INFRARED RANGE.

MALKAN, M., KLEINMANN, D. E., APT, J. <AP. J., 237, 432> 800408
INFRARED STUDIES OF GLOBULAR CLUSTERS NEAR THE GALACTIC CENTER.

MAMMANO, A., CIATTI, F. <ASTR. AP., 39, 405> 750213
THE SYMBIOTIC BINARY V1016 CYGNI, EARLY STAGE OF A PLANETARY NEBULA.

MAMMANO, A., CIATTI, F., VITTONE, A. <ASTR. AP., 85, 14> 800511
THE UNIQUE SPECTRUM OF SS 433, A STAR INSIDE A SUPERNOVA REMNANT.

MARGON, B., DOWNES, R. A, SZKODY, P. <IAUC NO. 3465> 809911
STEPANYAN'S STAR.

MARKARIAN, B. E., LIBOVETSKY, V. A. <ASTROFIZIKA, 12, 389> 769901
GALAXIES WITH ULTRAVIOLET CONTINUUM. VIII.

MARKARIAN, B. E., LIBOVETSKY, V. A. <ASTROFIZIKA, 12, 657> 769902
GALAXIES WITH ULTRAVIOLET CONTINUUM. IX.

MARKARIAN, B. E., LIBOVETSKY, V. A., STEPANIAN, J. A. <ASTROFIZIKA, 13, 225> 779901
GALAXIES WITH ULTRAVIOLET CONTINUUM. X.

MARKARIAN, B. E., LIBOVETSKY, V. A., STEPANIAN, J. A. <ASTROFIZIKA, 13, 397> 779902
GALAXIES WITH ULTRAVIOLET CONTINUUM. XI.

MARKARIAN, B. E., LIPOVETSKY, V. A. <ASTROFIZIKA, 10, 302> 749901
GALAXIES WITH ULTRAVIOLET CONTINUUM. VII.

MARKARIAN, B. E., LIPOVETSKY, V. A. <ASTROFIZIKA, 9, 487> 739902
GALAXIES WITH ULTRAVIOLET CONTINUUM. VI.

MARTIN, W. L., PENFOLD, J. E., GLASS, I. S. <M. N. R. A. S., 184, 15P> 780701
SPECTROSCOPIC AND PHOTOMETRIC OBSERVATIONS OF THREE COMPACT GALAXIES.

MASON, K. O., CORDOVA, F. A. <AP. J., 262, 253> 821104
INFRARED PHOTMETRY OF THE X-RAY BINARY 2A 1822-371: A MODEL FOR THE ULTRAVIOLET, OTICAL, AND INFRARED LIGHT CURVE.

MATSUMOTO, T., MURAKAMI, H., HAMAJIMA, K. <P. A. S. J., 29, 583> 770006
NEAR-INFRARED SURFACE PHOTOMETRY OF THE CENTRAL REGION OF M31.

MAYO, S. K., WHELAN, J. A. J., WICKRAMASINGHE, D. T. <IAUC NO. 2957> 769903
NEW OPTICAL CANDIDATE FOR CIRCINUS X-1.

MAZA, J <IAUC NO. 3548> 809907
SUPERNOVA IN NGC 1316.

MCALARY, C. W., MCLAREN, R. A. <AP. J., 240, 853> 800908
INFRARED SPECTROPHOTOMETRY OF SS 433.

MCALARY, C. W., MCLAREN, R. A. <AP. J., 250, 98> 811102
NEAR-INFRARED SPECTROPHOTOMETRY OF NGC 4151.

MCALARY, C. W., MCLAREN, R. A., CRABTREE, D. R. <AP. J., 234, 471> 791204
BROAD-BAND NEAR-INFRARED OBSERVATIONS OF SEYFERT GALAXIES.

MCBREEN, B., FAZIO, G. G., JAFFE, D. T. <AP. J., 254, 126> 820301
HIGH RESOLUTION FAR-INFRARED OBSERVATIONS OF THE EVOLVED H II REGION M16.

MCBREEN, B., FAZIO, G. G., STIER, M., WRIGHT, E. L. <AP. J. (LETTERS), 232, L183> 790911
EVIDENCE FOR A VARIABLE FAR-INFRARED SOURCE IN NGC 6334.

MCCALL, A., HOUGH, J. H. <ASTR. AP. SUPPL., 42, 141> 801111
NEAR INFRARED POLARIMETRY OF COOL STARS.

MCCAMMON, D., MUENCH, G., NEUGEBAUER, G. <AP. J., 147, 575> 670201
INFRARED SPECTRA OF LOW-TEMPERATURE STARS.

MCCARTHY, D. W. <AP. J. (LETTERS), 257, L93> 820609
TRIPLE STRUCTURE OF INFRARED SOURCE 3 IN THE MONOCEROS R2 MOLECULAR CLOUD.

MCCARTHY, D. W., HOWELL, R., LOW, F. J. <AP. J. (LETTERS), 223, L113> 780805
APPARENT VARIATION IN THE DIAMETER OF OMICRON CETI AT 10.2 MICRONS.

MCCARTHY, D. W., HOWELL, R., LOW, F. J. <AP. J. (LETTERS), 235, L27> 800103
SPATIAL SPECTRA OF IRC+10216 FROM 2.2 TO 20 MICRONS. DEVIATIONS FROM SPHERICAL SYMMETRY.

MCCARTHY, D. W., LOW, F. J. <AP. J. (LETTERS), 202, L37> 751103
INITIAL RESULTS OF SPATIAL INTERFEROMETRY AT 5 MICRONS.

MCCARTHY, D. W., LOW, F. J., HOWELL, R. <AP. J. (LETTERS), 214, L85> 770608
ANGULAR DIAMETER MEASUREMENTS OF ALPHA ORIONIS, VY CANIS MAJORIS, AND IRC+10216 AT 8.3, 10.2, AND 11.1 MICROMETERS.

MCCARTHY, D. W., LOW, F. J., KLEINMANN, S. G., ARGANBRIGHT, D. V. <AP. J. (LETTERS), 257, L75> 820809
INFRARED DETECTION OF THE LOW-MASS COMPANION TO ZETA AQUARII B.

MCCARTHY, D. W., LOW, F. J., KLEINMANN, S. G., GILLETT, F. C. <AP. J. (LETTERS), 257, L7> 820601
INFRARED SPECKLE INTERFEROMETRY OF THE NUCLEUS OF NGC 1068.

MCCARTHY, J. F., FORREST, W. J., BRIOTTA JR., D. A., HOUCK, J. R. <AP. J., 242, 965> 801207
THE GALACTIC CENTER: 16-30 MICRON OBSERVATIONS AND THE 18 MICRON EXTINCTION.

MCCARTHY, J. F., FORREST, W. J., HOUCK, J. R. <AP. J., 231, 711> 790810
OBSERVATIONS OF (S III) 18.71 MICRON EMISSION IN GALACTIC H II REGIONS.

MCCARTHY, J. F., FORREST, W. J., HOUCK, J. R. <AP. J., 244, 109> 780808
16-38 MICRON SPECTROSCOPY OF NGC 7027.

MCCORD, T. B., CLARK, R. N. <P. A. S. P., 91, 571> 790806
ATMOSPHERIC EXTINCTION 0.65-2.50 MICRONS ABOVE MAUNA KEA.

MCGONEGAL, R., MCLAREN, R. A., MCALARY, C. W., MADORE, B. F. <AP. J. (LETTERS), 257, L33> 820602
THE CEPHEID DISTANCE SCALE: A NEW APPLICATION FOR INFRARED PHOTOMETRY.

MCGREGOR, P. J., HYLAND, A. R. <AP. J., 250, 116> 811103
INFRARED STUDIES OF THE TWO STELLAR POPULATIONS IN 30 DORADUS.

MCLAREN, R. A., BETZ, A. L. <AP. J. (LETTERS), 240, L159> 800904
INFRARED OBSERVATIONS OF CIRCUMSTELLAR AMMONIA IN OH/IR SUPERGIANTS.

MCMILLAN, R. S. <AP. J. (LETTERS), 216, L41> 770807
WALKER NO. 67 IN NGC 2264: A CANDIDATE FOR STRONG INTERSTELLAR CIRCULAR POLARIZATION.

MCMILLAN, R. S. <AP. J., 225, 417> 781006
ARE LONG WAVELENGTHS OF MAXIMUM INTERSTELLAR POLARIZATION DUE TO WATER ICE MANTLES ON GRAINS?

MCNAMARA, B. J. <A. J., 81, 845> 761002
PRE-MAIN-SEQUENCE MASSES AND THE AGE SPREAD IN THE ORION CLUSTER.

MCNAMARA, B. J. <P. A. S. P., 87, 97> 750208
PRE-MAIN-SEQUENCE MASSES AND EVOLUTION IN NGC 2264.

MEISEL, D. D. <P. A. S. P., 83, 49> 710208
1-MICRON IMAGE-TUBE SPECTRA OF GAMMA CASSIOPEIAE AND ZETA TAURI.

MEISEL, D. D., BERG, R. A. <AP. J., 198, 551> 750604
HELIUM 10830A IN ALPHA VIRGINIS A AND B.

MEISEL, D. D., SAUNDERS, B. A., FRANK, Z. A., PACKARD, M. L. <AP. J., 263, 759> 821208
THE HELIUM 10830A LINE IN EARLY-TYPE STARS: AN ATLAS OF FABRY-PEROT SCANS.

MELIK-ALAVERDIAN, YU., MOVSESYAN, T. A. <ASTROFIZIKA, 18, 275> 820516
INFRARED EXCESS OF STARS WITH PROPER POLARIZATION.

MELIK-ALAVERDYAN, YU. K., MOVSESYAN, T. A., TOVMASYAN, G. M.,KIR'YAN, V. V. <SOV. AST. (LETTERS), 7, 98> 810313
THE INFRARED EMISSION OF RHO CASSIOPEIAE AND R CORONAE BOREALIS.

MELNICK, G., GULL, G. E., HARWIT, M. <AP. J. (LETTERS), 227, L29> 790111
OBSERVATIONS OF THE 63 MICRON (O I) EMISSION LINE IN THE ORION AND OMEGA NEBULAE.

MELNICK, G., GULL, G. E., HARWIT, M. <AP. J. (LETTERS), 227, L35> 790112
51.8 MICRON (O III) LINE EMISSION OBSERVED IN FOUR GALACTIC H II REGIONS.

MELNICK, G., GULL, G. E., HARWIT, M., WARD, D. B. <AP. J. (LETTERS), 222, L137> 780611
OBSERVATIONS OF THE 51.8 MICRON (O III) EMISSION LINE IN ORION.

MELNICK, G., RUSSELL, R. W., GULL, G. E., HARWIT, M. <AP. J., 243, 170> 810104
FAR-INFRARED EMISSION-LINE ABD CONTINUUM OBSERVATIONS OF NGC 7027.

MENDOZA V, E. E. <AP. J., 142, 1270> 651001
MULTICOLOR PHOTOMETRY OF AN EARLY-TYPE FLARE STAR.

MENDOZA V, E. E. <AP. J., 143, 1010> 660301
INFRARED PHOTOMETRY OF T TAURI STARS AND RELATED OBJECTS.

MENDOZA V, E. E. <AP. J., 145, 660> 660801
ERRATUM TO "INFRARED PHOTOMETRY OF T TAURI STARS AND RELATED OBJECTS."

MENDOZA V, E. E. <AP. J., 151, 977> 680302
INFRARED EXCESSES IN T TAURI STARS AND RELATED OBJECTS.

MENDOZA V, E. E. <ASTR. AP., 71, 147> 790118
H-ALPHA AND O I PHOTOMETRY OF THE PLEIADES.

MENDOZA V, E. E. <COMM. LUNAR AND PLANETARY LAB., 6, 59> 660101
INFRARED PHOTOMETRY OF T TAURI STARS AND RELATED OBJECTS.

MENDOZA V, E. E., JOHNSON, H. L. <AP. J., 141, 161> 650101
MULTICOLOR PHOTOMETRY OF CARBON STARS.

MERRILL, K. M. <IAUC NO. 3088> 770712
HM SAGITTAE.

MERRILL, K. M. <IAUC NO. 3444> 800102
SUPERNOVA IN NGC 4321.

MERRILL, K. M., RUSSELL, R. W., SOIFER, B. T. <AP. J., 207, 763> 760804
INFRARED OBSERVATIONS OF ICES AND SILICATES IN MOLECULAR CLOUDS.

MERRILL, K. M., SOIFER, B. T. <AP. J. (LETTERS), 189, L27> 740403
SPECTROPHOTOMETRIC OBSERVATIONS OF A HIGHLY ABSORBED OBJECT IN CYGNUS.

MERRILL, K. M., SOIFER, B. T., RUSSELL, R. W. <AP. J. (LETTERS), 200, L37> 750803
THE 2-4 MICRON SPECTRUM OF NGC 7027.

MERRILL, K. M., STEIN, W. A. <ASTR. AP., 29, 163> 731106
A SEARCH FOR VARIABILITY OF FREE-FREE EMISSION FROM CIRCUMSTELLAR GAS SURROUNDING BE STARS.

MERRILL, K. M., STEIN, W. A. <P. A. S. P., 88, 285> 760609
2-14 MICRON STELLAR SPECTROPHOTOMETRY I. STARS OF THE CONVENTIONAL SPECTRAL SEQUENCE.

MERRILL, K. M., STEIN, W. A. <P. A. S. P., 88, 294> 760610
2-14 MICRON STELLAR SPECTROPHOTOMETRY II. STARS FROM THE 2 MICRON INFRARED SKY SURVEY.

MERRILL, K. M., STEIN, W. A. <P. A. S. P., 88, 808> 761110
ERRATUM TO "2-14 MICRON STELLAR SPECTROPHOTOMETRY I. STARS OF THE CONVENTIONAL SPECTRAL SEQUENCE."

MERRILL, K. M., STEIN, W. A. <P. A. S. P., 88, 874> 761210
2-14 MICRON STELLAR SPECTROPHOTOMETRY III. AFCRL SKY SURVEY OBJECTS.

MERRILL, P. W., BURWELL, C. G. <AP. J., 110, 387> 499901
SECOND SUPPLEMENT TO THE MOUNT WILSON CATALOGUE AND BIBLIOGRAPHY OF STARS OF CLASSES B AND A WHOSE SPECTRA HAVE BRIGHT HYDROGEN LINES.

MERRILL, P. W., BURWELL, C. G. <AP. J., 112, 72> 509901
ADDITIONAL STARS WHOSE SPECTRA HAVE A BRIGHT H-ALPHA LINE.

MERRILL, P. W., BURWELL, C. G. <AP. J., 78, 87> 339901
CATALOGUE AND BIBLIOGRAPHY OF STARS OF CLASSES B AND A WHOSE SPECTRA HAVE BRIGHT HYDROGEN LINES.

MERRILL, P. W., BURWELL, C. G. <AP. J., 98, 153> 439901
SUPPLEMENT TO THE MOUNT WILSON CATALOGUE AND BIBLIOGRAPHY OF STARS OF CLASSES B AND A WHOSE SPECTRA HAVE BRIGHT HYDROGEN LINES.

MERRILL, P. W., SANFORD, R. F., BURWELL, C. G. <P. A. S. P., 66, 107> 549905
ADDITIONAL STARS OF CLASSES N AND S - SECOND LIST.

MERTZ, L. <A. J., 70, 548> 651002
ASTRONOMICAL INFRARED SPECTROMETER.

MERTZ, L., COLEMAN, I. <AP. J., 143, 1000> 660304
INFRARED SPECTRUM OF THE TAURUS RED OBJECT.

MIDDLEDITCH, J., PENNYPACKER, C., BURNS, S. <IAUC NO. 3701> 820611
1E 2259+586.

MIHALAS, D., FROST, S. A., LOCKWOOD, G. W. <P. A. S. P., 87, 153> 750209
OBSERVATIONS OF THE C III 8500(3S1S-3P1P) LINE IN O AND OF STARS.

MIKAMI, T. <ANNALS TOKYO AST. OBS., XVII, 1> 789903
COMPILED DATA OF C- AND M- TYPE STARS IN THE SOLAR NEIGHBORHOOD.

MIKAMI, T., ISHIDA, K., HAMAJIMA, K., KAWARA, K. <P. A. S. J., 34, 223> 820001
STELLAR CONTENTS CONTRIBUTING TO THE NEAR-INFRARED RADIATION OF THE GALAXY.

MILKEY, R. W., DYCK, H. M. <AP. J., 181, 833> 730503
LOW-TEMPERATURE FREE-FREE EMISSION: INFRARED EXCESSES IN BE STARS.

MILLER, H. R. <A. J., 86, 87> 819903
PHOTOELECTRIC COMPARISON SEQUENCES IN THE FIELDS OF FIVE SEYFERT GALAXIES.

MILLER, J. S. <AP. J. (LETTERS), 161, L95> 700803
SCANNER OBSERVATIONS OF THE LEO INFRARED OBJECT IRC+10216.

MILNE, D. K. <A. J., 78, 239> 739909
IMPROVED OPTICAL POSITIONS FOR 153 PLANETARY NEBULAE.

MILNE, D. K. <A. J., 81, 753> 769910
OPTICAL POSITIONS FOR PLANETARY NEBULAE. II.

MILNE, D. K., ALLER, L. H. <ASTR. AP., 38, 183> 759904
RADIO OBSERVATIONS AT 5 GHZ OF SOUTHERN PLANETARY NEBULAE.

MILONE, E. F. <AP. J. SUPPL., 31, 93> 760514
INFRARED PHOTOMETRY OF RT LACERTAE.

MILONE, E. F. <MULT. PER. VAR. STARS, IAU COLL. NO. 29> 750001
INFRARED PHOTOMETRY OF ECLIPSING BINARIES WITH CHANGING LIGHT CURVES.

MITCHELL, R. I. <AP. J., 140, 1607> 641101
NINE-COLOR PHOTOMETRY OF EPSILON AUR, 0.35-9.5 MICRONS.

MITCHELL, R. I., JOHNSON, H. L. <COMM. LUNAR AND PLANETARY LAB., 8, 1> 690201
THIRTEEN-COLOR NARROW-BAND PHOTOMETRY OF ONE THOUSAND BRIGHT STARS.

MITCHELL, R. M., ROBINSON, G. <AP. J., 220, 841> 780308
THE SPECTRAL AND SPATIAL DISTRIBUTION OF RADIATION FROM ETA CARINAE. I. A SPHERICAL DUST SHELL MODEL APPROACH.

MONTGOMERY, E. F., CONNES, P., CONNES, J., EDMONDS JR., F. N. <AP. J. SUPPL., 19, 1> 690802
THE INFRARED SPECTRUM OF ARCTURUS.

MOORE, R. L., ANGEL, J. R. P., RIEKE, G. H., LEBOFSKY, M. J.,WISNIEWSKI, W. Z., MUFSON, S. L., VRBA, F. J., MILLER, H. R., MCGIMSEY, B. Q., WILLIAMON, R. M. <AP. J., 235, 717> 800208
OPTICAL AND INFRARED VARIABILITY OF B2 1308+326.

MOORE, R. L., MCGRAW, J. T., ANGEL, J. R. P., DUERR, R., LEBOFSKY, M. J., RIEKE, M. J., WISNIEWSKI, W. Z., AXON, D. J., BAILEY, J., HOUGH, J. M., THOMPSON, I., BREGER, M., SCHULZ, H., CLAYTON, G. C., MARTIN, P. G., MILLER, J. S., SCHMIDT, G. D., AFRICANO, J., MILLER, H. R. <AP. J., 260, 415> 820903
THE NOISE OF BL LACERTAE.

MOORWOOD, A. F. M., BALUTEAU, J. -P., ANDEREGG, M., CORON, N., BIRAUD, Y. <AP. J., 224, 101> 780807
INFRARED LINE EMISSION FROM HII REGIONS. II. AIRBORNE OBSERVATIONS OF THE ORION NEBULA, W3, AND NGC 7538.

MOORWOOD, A. F. M., BALUTEAU, J. -P., ANDEREGG, M., CORON, N., BIRAUD, Y., FITTON, B. <AP. J., 238, 565> 800608
INFRARED LINE EMISSION FROM H II REGIONS. III. AIRBORNE OBSERVATIONS OF (S III) (18 AND 33 MICRONS), (O III) (52 AND 88 MICRONS), AND (N III) (57 MICRONS) ON M17.

MOORWOOD, A. F. M., GLASS, I. S. <ASTR. AP., 115, 84> 821110
INFRARED EMISSION AND STAR FORMATION IN NGC 5253.

MOORWOOD, A. F. M., SALINARI, P. <ASTR. AP., 100, L16> 810719
DETECTION OF THE 3.3 MICRON EMISSION FEATURE IN THE NUCLEII OF IC 4329A AND NGC 5506.

MOORWOOD, A. F. M., SALINARI, P. <ASTR. AP., 102, 197> 811014
INFRARED OBJECTS NEAR TO H2O MASERS IN REGIONS OF ACTIVE STAR FORMATION. II. SURVEY AND 1-20 MICRON OBSERVATIONS OF SOUTHERN SOURCES.

MOORWOOD, A. F. M., SALINARI, P. <ASTR. AP., 94, 299> 810216
INFRARED OBJECTS NEAR TO H2O MASERS IN REGIONS OF ACTIVE STAR FORMATION.

MOORWOOD, A. F. M., SALINARI, P., FURNISS, I., JENNINGS, R. E., KING, K. J. <ASTR. AP., 90, 304> 801012
INFRARED SPECTROSCOPY WITH A BALLOON BORNE MICHELSON INTERFEROMETER. II. OBSERVATION OF O III, O I, AND N III FINE STRUCTURE LINES IN H II REGIONS.

MOREL, M., MAGNENAT, P. <ASTR. AP. SUPPL., 34, 477> 781202
UBVRIJKLMNH PHOTOELECTRIC PHOTOMETRIC CATALOGUE (MAGNETIC TAPE).

MORGAN, D. H., NANDY, K. <M. N. R. A. S., 199, 979> 820619
INFRARED INTERSTELLAR EXTINCTION IN THE LMC.

MORGAN, T. H., POTTER, A. E., KONDO, Y. <AP. J., 190, 349> 740604
COMPLEX INFRARED EMISSION FEATURES IN THE SPECTRUM OF BETA LYRAE.

MORGAN, W. W., JOHNSON, H. L., ROMAN, N. G. <P. A. S. P., 66, 85> 549904
A VERY RED STAR OF EARLY TYPE IN CYGNUS.

MORGAN, W. W., MEINEL, A. B., JOHNSON, H. M. <AP. J., 120, 506> 549906
SPECTRAL CLASSIFICATION WITH EXCEEDINGLY LOW DISPERSION.

MOROZ, V. I. <SOV. AST., 10, 47> 660702
INFRARED SPECTRA OF STARS (1-2.5 MICRONS).

MOROZ, V. I. <SOV. AST., 4, 250> 600301
THE RADIATION FLUX FROM THE CRAB NEBULA AT 2 MICRONS AND SOME CONCLUSIONS ON THE SPECTRUM AND MAGNETIC FIELD.

MOROZ, V. I. <SOV. AST., 7, 601> 640301
RADIATION EMISSION FROM THE ORION NEBULA IN THE 0.85-1.7 MICRON WAVELENGTH REGION.

MOROZ, V. I. <SOV. AST., 7, 755> 640502
INFRARED OBSERVATIONS OF THE CRAB NEBULA.

MOROZ, V. I., DIBAI, E. A. <SOV. AST., 12, 184> 680902
PHOTOMETRIC OBSERVATIONS OF SOME PECULIAR OBJECTS IN THE WAVELENGTH RANGE 1-2.5 MICRONS.

MOROZ, V. I., VASIL'CHENKO, N. V., DANILYANTS, L. B., KAUFMAN, S. A. <SOV. AST., 12, 150> 680703
EXPERIMENTAL OBSERVATIONS AT 8-14 MICRONS WITH A PHOTOCONDUCTIVE CELL COOLED BY LIQUID HELIUM.

MORRISON, D. <AP. J., 194, 203> 741107
RADIOMETRIC DIAMETERS AND ALBEDOS OF 40 ASTEROIDS.

MORRISON, D., SIMON, T. <AP. J., 186, 193> 731104
BROAD-BAND 20-MICRON PHOTOMETRY OF 76 STARS.

MOSELEY, H. <AP. J., 238, 892> 800604
OBSERVATIONS OF COOL DUST IN PLANETARY NEBULAE.

MOTCH, C., ILOVAISKY, S. A., CHEVALIER, C. <IAUC NO. 3609> 810612
GX 339-4 - 4U1658-48.

MOULD, J. R. <AP. J., 226, 923> 781215
INFRARED SPECTROSCOPY OF M DWARFS.

MOULD, J. R. <P. A. S. P., 93, 25> 810201
THE INFRARED COLOR-MAGNITUDE RELATION FOR EARLY-TYPE GALAXIES IN THE PEGASUS I CLUSTER.

MOULD, J. R., CANNON, R. D., AARONSON, M., FROGEL, J. A. <AP. J., 254, 500> 820302
CARBON STARS IN THE CARINA DWARF SPHEROIDAL GALAXY.

MOULD, J. R., HALL, D. N. B., RIDGWAY, S. T., HINTZEN, P., AARONSON, M. <AP. J. (LETTERS), 222, L123> 780608
THE COMPOSITE SPECTRA OF FU ORIONIS STARS.

MOULD, J. R., HYLAND, A. R. <AP. J., 208, 399> 760907
INFRARED OBSERVATIONS AND THE STRUCTURE OF THE LOWER MAIN SEQUENCE.

MOULD, J. R., LIEBERT, J. <AP. J. (LETTERS), 226, L29> 781106
INFRARED PHOTOMETRY AND THE ATMOSPHERIC COMPOSITION OF COOL WHITE DWARFS.

MOULD, J. R., MCELROY, D. B. <AP. J., 220, 935> 780309
OLD DISK SUBDWARFS.

MOULD, J. R., MCELROY, D. B. <AP. J., 221, 580> 780406
TIO BAND STRENGTHS IN METAL-RICH GLOBULAR CLUSTERS.

MOULD, J. R., STUTMAN, D., MCELROY, D. B. <AP. J., 228, 423> 790310
TIO BAND STRENGTHS IN METAL-RICH GLOBULAR CLUSTERS. II.

MOULD, J., AARONSON, M. <AP. J., 240, 464> 800910
THE EXTENDED GIANT BRANCHES OF INTERMEDIATE AGE GLOBULAR CLUSTERS IN THE MAGELLANIC CLOUDS.

MOULD, J., AARONSON, M. <AP. J., 263, 629> 821205
THE EXTENDED GIANT BRANCHES OF INTERMEDIATE AGE GLOBULAR CLUSTERS IN THE MAGELLANIC CLOUDS. III.

MOULD, J., AARONSON, M., HUCHRA, J. <AP. J., 238, 458> 800606
A DISTANCE SCALE FROM THE INFRARED MAGNITUDE/H I VELOCITY-WIDTH RELATION. II. THE VIRGO CLUSTER.

MUENCH, G., SCARGLE, J. D. <AP. J., 142, 401> 650702
THE SPECTRA OF TWO EXTREMELY RED OBJECTS.

MUFSON, S. L., WISNIEWSKI, W. Z., MCMILLAN, R. S. <IAUC NO. 3471> 800401
KR AURIGAE.

MUNCH, L., MORGAN, W. W. <AP. J., 118, 161> 539902
A PROBABLE CLUSTERING OF BLUE GIANTS IN CYGNUS.

MURDIN, P., ALLEN, D. A., MORTON, D. C., WHELAN, J. A. J., THOMAS, R. M. <M. N. R. A. S., 192, 709> 800912
THE K DWARFS ASSOCIATED WITH THE X-RAY TRANSIENTS A0620-00 AND A1742-28.

MURDIN, P., PENSTON, M. J., PENSTON, M. V., GLASS, I. S., SANFORD, P. W., HAWKINS, F. J., MASON, K. O., WILLMORE, A. P. <M. N. R. A. S., 169, 25> 741014
OPTICAL OBSERVATIONS OF STARS NEAR COPERNICUS X-RAY POSITIONS.

MUSTEL, E. R. <SOV. AST., 19, 685> 751110
HELIUM IN TYPE 1 SUPERNOVA ENVELOPES.

NADEAU, D., GEBALLE, T. R. <AP. J. (LETTERS), 230, L169> 790607
VELOCITY PROFILES OF THE 2.1 MICRON H2 EMISSION LINE IN THE ORION MOLECULAR CLOUD.

NADEAU, D., GEBALLE, T. R., NEUGEBAUER, G. <AP. J., 253, 154> 820205
THE MOTION AND DISTRIBUTION OF THE VIBRATIONALLY EXCITED H2 IN THE ORION MOLECULAR CLOUD.

NADEAU, D., NEUGEBAUER, G., BECKLIN, E. E., ELIAS, J. H., ENNIS, D. J., MATTHEWS, K., SELLGREN, K. <M. N. R. A. S., 184, 523> 780803
THE LIGHT CURVE AT 10 MICRONS OF ALGOL NEAR SECONDARY MINIMUM.

NADEAU, D., NEUGEBAUER, G., MATTHEWS, K., GEBALLE, T. R. <A. J., 86, 561> 810401
SPECTROSCOPY OF THE B-GAMMA LINE IN THE GALACTIC CENTER.

NAGY, T. A., MEAD, J. M. <NASA TM-79564> 789904
HD-SAO-DM CROSS INDEX.

NASSAU, J. J., BLANCO, V. M., MORGAN, W. W. <AP. J., 120, 478> 549901
REDDENED EARLY M- AND S-TYPE STARS NEAR THE GALACTIC EQUATOR.

NECKEL, TH., HARRIS, A. W., EIROA, C. <ASTR. AP., 92, L9> 801213
DISCOVERY OF THE EXCITING STAR IN THE NORTH AMERICA - PELICAN NEBULA COMPLEX?

NEEDHAM, J. D., PHILLIPS, J. P., SELBY, M. J., SANCHEZ MAGRO, C. <ASTR. AP., 83, 370> 800309
INFRARED OBSERVATIONS OF BINARY STARS - II.

NETO, A. D., PACHECO, J. A. DE FREITAS <M. N. R. A. S., 198, 659> 820216
INFRARED EXCESS AND LINE EMISSION IN BE STARS.

NETZER, H. <AP. J., 219, 822> 780207
HE I LINES IN THE SPECTRA OF QSOS AND SEYFERT GALAXIES.

NEUGEBAUER, G., BECKLIN, E. E., BECKWITH, S., MATTHEWS, K., WYNN-WILLIAMS, C. G. <AP. J. (LETTERS), 205, L139> 760507
LATE-TYPE GIANTS AND SUPERGIANTS IN THE GALACTIC CENTER.

NEUGEBAUER, G., BECKLIN, E. E., KRISTIAN, J., LEIGHTON, R. B., SNELLEN, G., WESTPHAL, J. A. <AP. J. (LETTERS), 156, L115> 690601
INFRARED AND OPTICAL MEASUREMENTS OF THE CRAB PULSAR NP 0532.

NEUGEBAUER, G., BECKLIN, E. E., MATTHEWS, K. <A. J., 87, 395> 820211
THE DOUBLE STRUCTURE OF W3-IRS 5 AS DETERMINED FROM HIGH-RESOLUTION SPATIAL SCANS.

NEUGEBAUER, G., BECKLIN, E. E., MATTHEWS, K., WYNN-WILLIAMS, C. G. <AP. J., 220, 149> 780213
INFRARED OBSERVATIONS OF THE GALACTIC CENTER. III. 2.2 MICRON SPECTROSCOPY.

NEUGEBAUER, G., BECKLIN, E. E., OKE, J. B., SEARLE, L. <AP. J., 205, 29> 760401
OPTICAL AND INFRARED SPECTROPHOTOMETRY OF 18 MARKARIAN GALAXIES.

NEUGEBAUER, G., GARMIRE, G. <AP. J. (LETTERS), 161, L91> 700802
INFRARED OBSERVATIONS OF THE NEBULA K3-50.

NEUGEBAUER, G., GARMIRE, G., RIEKE, G. H., LOW, F. J. <AP. J. (LETTERS), 166, L45> 710602
INFRARED OBSERVATIONS ON THE SIZE OF NGC 1068.

NEUGEBAUER, G., LEIGHTON, R. B. <NASA SP-3047> 690001
TWO-MICRON SKY SURVEY-A PRELIMINARY CATALOG.

NEUGEBAUER, G., MARTZ, D. E., LEIGHTON, R. B. <AP. J., 142, 399> 650701
OBSERVATIONS OF EXTREMELY COOL STARS.

NEUGEBAUER, G., MORTON, D., OKE, J. B., BECKLIN, E. E., DALTABUIT, E., MATTHEWS, K., PERSSON, S. E., SMITH, A. M., SOIFER, B. T., TORRES-PEIMBERT, S., WYNN-WILLIAMS, C. G. <AP. J., 238, 502> 800607
RECOMBINATION SPECTRUM AND REDDENING IN NGC 1068.

NEUGEBAUER, G., OKE, J. B., BECKLIN, E. E., MATTHEWS, K. <AP. J., 230, 79> 790509
ABSOLUTE SPECTRAL ENERGY DISTRIBUTION OF QUASI-STELLAR OBJECTS FROM 0.3 TO 10 MICRONS.

NEUGEBAUER, G., SARGENT, W. L. W., WESTPHAL, J. A., PORTER, F. C. <P. A. S. P., 83, 305> 710605
1.6-10 MICRON OBSERVATIONS OF R DORADUS AND W HYDRAE.

NEUGEBAUER, G., SOIFER, B. T., MATTHEWS, K., MARGON, B., CHANAN, G. A. <A. J., 87, 1639> 821209
INFRARED PROPERTIES OF SERENDIPITOUS X-RAY QUASARS.

NEUGEBAUER, G., WESTPHAL, J. A. <AP. J. (LETTERS), 152, L89> 680502
INFRARED OBSERVATIONS OF ETA CARINAE.

NEY, E. <IAUC NO. 3553> 801211
HONDA'S VARIABLE IN CYGNUS (NOVA CYGNI 1980).

NEY, E. P. <P. A. S. P., 84, 613> 721010
INFRARED EXCESSES IN SUPERGIANT STARS: EVIDENCE FOR SILICTAES.

NEY, E. P., ALLEN, D. A. <AP. J. (LETTERS), 155, L193> 690305
THE INFRARED SOURCES IN THE TRAPEZIUM REGION OF M42.

NEY, E. P., HATFIELD, B. F. <AP. J. (LETTERS), 219, L111> 780209
THE ISOTHERMAL DUST CONDENSATION OF NOVA VULPECULAE 1976.

NEY, E. P., HUMPHREYS, R. M. <P. A. S. P., 86, 304> 740606
BM SCORPII AND A POSSIBLE CLUSTER OF INFRARED SOURCES.

NEY, E. P., MERRILL, K. M. <AFGL-TR-80-0050> 800213
STUDY OF SOURCES IN AFGL ROCKET INFRARED STUDY.

NEY, E. P., MERRILL, K. M., BECKLIN, E. E., NEUGEBAUER, G., WYNN-WILLIAMS, C. G. <AP. J. (LETTERS), 198, L129> 750603
STUDIES OF THE INFRARED SOURCE CRL 2688.

NEY, E. P., STEIN, W. A. <AP. J. (LETTERS), 152, L21> 680404
OBSERVATIONS OF THE CRAB NEBULA AT 5800A, 2.2 MICRONS, AND 3.5 MICRONS WITH A 4-MINUTE BEAM.

NEY, E. P., STODDART, J., HUBBARD, R. <IAUC NO. 3023> 761213
NOVA VULPECULAE 1976.

NEY, E. P., STRECKER, D. W., GEHRZ, R. D. <AP. J., 180, 809> 730303
DUST EMISSION NEBULAE AROUND ORION O AND B STARS.

NICOLSON, G. D., FEAST, M. W., GLASS, I. S. <M. N. R. A. S., 191, 293> 800413
RECENT CHANGES IN THE OPTICAL, INFRARED AND RADIO EMISSION FROM CIRCINUS X-1.

NICOLSON, G. D., GLASS, I. S., FEAST, M. W., ANDREWS, P. J. <M. N. R. A. S., 189, 29P> 791005
THE BL LAC OBJECT PKS 1144-379.

NILSON, P. <UPPSALA AST. OBS. ANNALER, 6> 739908
UPPSALA GENERAL CATALOGUE OF GALAXIES.

NISHIMURA, T., LOW, F. J., KURTZ, R. F. <AP. J. (LETTERS), 239, L101> 800803
FAR-INFRARED SURVEY OF THE GALACTIC PLANE.

NOGUCHI, K., HAYAKAWA, S., MATSUMOTO, T., UYAMA, K. <P. A. S. J., 33, 583> 810002
NEAR-INFRARED MULTICOLOR OBSERVATION OF THE DIFFUSE GALACTIC EMISSION.

NOGUCHI, K., KAWARA, K., KOBAYASHI, Y., OKUDA, H., SATO, S., OISHI, M. <P. A. S. J., 33, 373> 810001
NEAR-INFRARED PHOTOMETRY OF CARBON STARS.

NOGUCHI, K., MAIHARA, T., OKUDA, H., SATO, S., MUKAI, T. <P. A. S. J., 29, 511> 770005
THREE-MICRON ABSORPTION BAND OF CARBON STARS.

NORDH, H. L., OLOFSSON, S. G. <ASTR. AP., 31, 343> 740305
ANALYSIS OF THE ENERGY DISTRIBUTION OF THE BE STAR PI AQR.

NORDH, H. L., OLOFSSON, S. G., AUGASON, G. C. <A. J., 83, 188> 780205
AIRBORNE PHOTOMETRIC OBSERVATIONS BETWEEN 1.25 AND 3.25 MICRONS OF LATE-TYPE STARS.

NORDH, H. L., OLOFSSON, S. G., AUGASON, G. C. <A. J., 83, 188> 780218
AIRBORNE PHOTOMETRIC OBSERVATIONS BETWEEN 1.25 AND 3.25 MICRONS OF LATE-TYPE STARS.

NORDH, H. L., VAN DUINEN, R. J., SARGENT, A. I., FRIDLUND, C. V. M., AALDERS, J. W. G., BEINTEMA, D. <ASTR. AP., 115, 308> 821112
FAR INFRARED OBSERVATIONS OF A STAR FORMING REGION IN SERPENS.

NORDH, H. L., VAN DUINEN, R. J., SARGENT, A. I., FRIDLUND, M., AALDERS, J. W. G. <A. J., 86, 276> 810205
HFE 2 AND L43 - TWO COLD FAR-INFRARED SOURCES.

NOSKOVA, R. I. <ASTROFIZIKA, 11, 169> 750406
SPECTRUM OF PLANETARY NEBULA IC 4997 IN THE NEAR INFRARED REGION.

NOSKOVA, R. I. <ASTROFIZIKA, 12, 31> 760110
SPECTRUM OF THE PLANETARY NEBULA BD+30 3639 IN THE NEAR-INFRARED REGION.

NOSKOVA, R. I. <SOV. AST., 12, 1039> 690501
ABSOLUTE SPECTROPHOMETRY OF SOME INFRARED LINES IN PLANETARY-NEBULA SPECTRA.

NOSKOVA, R. I. <SOV. AST., 20, 170> 760309
ABSOLUTE SPECTROPHOTOMETRY OF THE PLANETARY NEBULAE IC 2149, IC 4593, AND NGC 6210 IN THE NEAR INFRARED.

NOSKOVA, R. I. <SOV. AST., 20, 684> 761111
DETAILED NEAR-INFRARED SPECTROPHOTOMETRY OF THE PLANETARY NEBULAE NGC 6572, 6891, AND 7662.

NOSKOVA, R. I. <SOV. AST., 23, 297> 790516
PHYSICAL PARAMETERS OF NINE PLANETARY NEBULAE.

O'BRIEN, G., LAMBERT, D. L. <AP. J. (LETTERS), 229, L33> 790407
HE I 10830A EMISSION FROM ALPHA BOOTIS AND ALPHA 1 HERCULIS.

O'CONNELL, R. W. <AP. J., 206, 370> 760602
GALAXY SPECTRAL SYNTHESIS. I. STELLAR POPULATIONS IN THE NUCLEI OF GIANT ELLIPTICALS.

O'CONNELL, R. W. <AP. J., 236, 430> 800303
GALAXY SPECTRAL SYNTHESIS. II. M32 AND THE AGES OF GALAXIES.

O'DELL, S. L., PUSCHELL, J. J., STEIN, W. A. <AP. J., 213, 351> 770406
THE 0.36-3.5 MICROMETER SPECTRAL-FLUX DISTRIBUTION OF SEVERAL BL LACERTAE OBJECTS.

O'DELL, S. L., PUSCHELL, J. J., STEIN, W. A., OWEN, F. N., PORCAS, R. W., MUFSON, S. L., MOFFETT, T. J., ULRICH, M. -H. 780806
<AP. J., 224, 22>
COORDINATED PHOTOMETRIC AND SPECTROSCOPIC OBSERVATIONS OF STRONG EXTRAGALACTIC 90 GHZ SOURCES.

O'DELL, S. L., PUSCHELL, J. J., STEIN, W. A., WARNER, J. W. <AP. J. (LETTERS), 214, L105> 770611
DEVELOPMENT OF A SPECTRAL BREAK IN THE NONTHERMAL EMISSION OF AO 0235+164.

O'DELL, S. L., PUSCHELL, J. J., STEIN, W. A., WARNER, J. W. <AP. J. SUPPL., 38, 267> 781105
THE CHANGES IN SPECTRAL-FLUX DISTRIBUTION DURING VARIABILITY OF EXTRAGALACTIC NONTHERMAL SOURCES, 0.36 TO 3.5 MICRONS.

O'DELL, S. L., PUSCHELL, J. J., STEIN, W. A., WARNER, J. W., ULRICH, M. -H. <AP. J., 219, 818> 780206
THE SPECTRAL-FLUX DISTRIBUTION (0.36-3.5 MICRON) OF NONSTELLAR LIGHT FROM THE BROAD-LINE RADIO GALAXIES 3C 227 AND 3C 382.

OCHSENBEIN, F., BISCHOFF, M., EGRET, D. <ASTR. AP. SUPPL., 43, 259> 819921
MICROFICHE EDITION OF CSI.

ODA, N., MAIHARA, T., SUGIYAMA, T., OKUDA, H. <ASTR. AP., 72, 309> 790213
COSMIC DUST IN THE CENTRAL REGION OF THE GALAXY AND ANOMALOUS INFRARED SOURCE AT L-355, B--1.

OGDEN, P. M., ROESLER, F. L., LARSON, H. P., SMITH, H. A., REYNOLDS, R. J., SCHERB, F. <AP. J. (LETTERS), 233, L21> 791007
EVIDENCE FOR TEMPORAL VARIATIONS IN THE H2 2.1 MICRON EMISSION FROM THE ORION NEBULA.

OGDEN, P. M., ROESLER, F. L., REYNOLDS, R. J., SCHERB, F., LARSON, H. P., SMITH, H. A., DAEHLER, M. <AP. J. (LETTERS), 226, L91> 781205
MEASUREMENTS OF THE VELOCITY AND WIDTH OF THE H2 2.1 MICRON EMISSION LINE FROM THE ORION NEBULA.

OINAS, V. <AP. J. SUPPL., 27, 391> 740508
STRONG-LINE K STARS. I. PHOTOMETRY.

OISHI, M., MAIHARA, T., NOGUCHI, K., OKUDA, H., SATO, S. <P. A. S. J., 28, 175> 760004
INFRARED POLARIZATION OF CRL 2591.

OKE, J. B. <AP. J. SUPPL., 27, 21> 740210
ABSOLUTE SPECTRAL ENERGY DISTRIBUTIONS FOR WHITE DWARFS.

OKE, J. B. <AP. J., 141, 6> 650103
THE OPTICAL SPECTRUM OF 3C 273.

OKE, J. B. <AP. J., 150, 513> 671101
EFFECTIVE TEMPERATURES AND GRAVITIES OF LAMBDA BOOTIS STARS.

OKE, J. B., CONTI, P. S. <AP. J., 143, 134> 660102
ABSOLUTE PHOTOELECTRIC SPECTROPHOTOMETRY OF STARS IN THE HYADES.

OKE, J. B., NEUGEBAUER, G., BECKLIN, E. E. <AP. J., 159, 341> 700101
ABSOLUTE SPECTRAL ENERGY DISTRIBUTION OF QUASI-STELLAR OBJECTS FROM 0.3 TO 2.2 MICRONS.

OKE, J. B., NEUGEBAUER, G., BECKLIN, E. E. <AP. J. (LETTERS), 156, L41> 690403
SPECTROPHOTOMETRY AND INFRARED PHOTOMETRY OF BL LACERTAE.

OKE, J. B., SANDAGE, A. R. <AP. J., 154, 21> 681001
ENERGY DISTRIBUTIONS, K CORRECTIONS, AND THE STEBBINS-WHITFORD EFFECT FOR GIANT ELLIPTICAL GALAXIES.

OKE, J. B., SARGENT, W. L. W. <AP. J., 151, 807> 680301
THE NUCLEUS OF THE SEYFERT GALAXY NGC 4151.

OKE, J. B., SARGENT, W. L. W., NEUGEBAUER, G., BECKLIN, E. E. <AP. J. (LETTERS), 150, L173> 671201
A VARIABLE RADIO-QUIET COMPACT GALAXY I ZW 1727+50.

OKE, J. B., SCHILD, R. E. <AP. J., 161, 1015> 700902
THE ABSOLUTE SPECTRAL ENERGY DISTRIBUTION OF ALPHA LYRAE.

OKE, J. B., SCHWARZSCHILD, M. <AP. J., 198, 63> 750504
ABSOLUTE SPECTROPHOTOMETRY IN M31 AND M32.

OKUDA, H., MAIHARA, T., ODA, N., SUGIYAMA, T. <NATURE, 265, 515> 770212
2.4 MICRON MAPPING OF THE GALACTIC CENTRAL REGION.

OLSEN, E. T. <A. J., 72, 738> 679904
ACCURATE POSITIONS OF SELECTED 4C SOURCES.

OLTHOF, H. <ASTR. AP., 33, 471> 740711
MULTICOLOUR FAR INFRARED PHOTOMETRY OF GALACTIC H II REGIONS.

OLTHOF, H., VAN DUINEN, R. J. <ASTR. AP., 29, 315> 731210
TWO COLOUR FAR INFRARED PHOTOMETRY OF SOME GALACTIC H II REGIONS.

OOSTERHOFF, P. TH., PONSEN, J., SCHUURMAN, M. C. <B. A. N. SUPPL., 1, 397> 679905
VARIABLE STARS IN THE GALACTIC WINDOW SAGITTARIUS II AT ALPHA - 18H 09M, DELTA - -27 55 (1900).

OWENS, D. K., MUEHLNER, D. J., WEISS, R. <AP. J., 231, 702> 790809
A LARGE-BEAM SKY SURVEY AT MILLIMETER AND SUBMILLIMETER WAVELENGTHS MADE FROM BALLOON ALTITUDES.

PACHOLCZYK, A. G. <AP. J. (LETTERS), 161, L207> 700905
INFRARED VARIABILITY OF THE SEYFERT GALAXY NGC 1068.

PACHOLCZYK, A. G. <AP. J., 163, 449> 710205
LIGHT VARIATIONS OF THE SEYFERT GALAXY NGC 4151. III. LONG-TERM PHOTOGRAPHIC B-VARIATIONS AND INFRARED K-DATA.

PACHOLCZYK, A. G., WEYMANN, R. J. <A. J., 73, 870> 681106
INFRARED RADIATION FROM THE NUCLEI OF SEYFERT GALAXIES.

PACHOLCZYK, A. G., WISNIEWSKI, W. Z. <AP. J., 147, 394> 670102
INFRARED RADIATION FROM THE SEYFERT GALAXY NGC 1068.

PALMER, L. G., WING, R. F. <A. J., 87, 1739> 821210
A NEW SEARCH FOR M AND C STARS.

PANEK, R. J., EATON, J. A. <AP. J., 258, 572> 820706
THE INFRARED LIGHT CURVE OF U GEMINORUM.

PAPOULAR, R., LENA, P. J., MARTEN, A., ROUAN, D., WIJNBERGEN, J. J. <NATURE, 276, 593> 781218
POSSIBLE IDENTIFICATION OF THE 45 MICRON ICE SIGNATURE IN ORION.

PARK, W. M., VICKERS, D. G., CLEGG, P. E. <ASTR. AP., 5, 325> 700308
SUBMILLIMETER RADIATION FROM THE ORION NEBULA.

PEIMBERT, M., SPINRAD, H. <AP. J., 160, 429> 700501
PHYSICAL CONDITIONS IN THE NUCLEUS OF M82.

PENNY, A. J. <M. N. R. A. S., 198, 773> 820312
CRAB PULSAR INFRARED FLUXES AND PULSE SHAPES.

PENNYPACKER, C. R. <AP. J., 244, 286> 810211
INFRARED STUDIES OF PULSARS.

PENSTON, M. V. <AP. J., 183, 505> 730705
MULTICOLOR OBSERVATIONS OF STARS IN THE VICINITY OF THE ORION NEBULA.

PENSTON, M. V. <M. N. R. A. S., 162, 359> 730017
THE V-K COLOURS OF THE NUCLEI OF BRIGHHT GALAXIES.

PENSTON, M. V., ALLEN, D. A., HYLAND, A. R. <AP. J. (LETTERS), 170, L33> 711104
THE NATURE OF BECKLIN'S STAR.

PENSTON, M. V., ALLEN, D. A., LLOYD, C. <OBSERVATORY, 96, 22> 760212
AN INTERESTING STAR IN THE LAMBDA ORIONIS ASSOCIATION.

PENSTON, M. V., HUNTER, J. K. <M. N. R. A. S., 171, 219> 750405
FURTHER OBSERVATIONS OF THE ORION NEBULA CLUSTER.

PENSTON, M. V., PENSTON, M. J. <M. N. R. A. S., 162, 109> 730020
NEW OBSERVATIONS OF TWO COMPACT GALAXIES.

PENSTON, M. V., PENSTON, M. J., NEUGEBAUER, G., TRITTON, K. P., BECKLIN, E. E., VISVANATHAN, N. <M. N. R. A. S., 153, 29> 710704
OBSERVATIONS OF NGC 4151 DURING 1970 IN THE OPTICAL AND AND INFRA-RED.

PENSTON, M. V., PENSTON, M. J., SELMES, R. A., BECKLIN, E. E., NEUGEBAUER, G. <M. N. R. A. S., 169, 357> 741109
BROADBAND OPTICAL AND INFRARED OBSERVATIONS OF SEYFERT GALAXIES.

PEREK, L., KOHOUTEK, L. <PUBL. HOUSE CZECH. ACADEMY OF SCIENCE> 679902
CATALOGUE OF GALACTIC PLANETARY NEBULAE.

PERINOTTO, M. <ASTR. AP., 35, 293> 740211
PHOTOELECTRIC SPECTROPHOTOMETRY OF PLANETARY NEBULAE.

PERSI, P., FERRARI-TONIOLO, M. <ASTR. AP., 111, L7> 820712
INFRARED ENERGY DISTRIBUTION OF CYG. OB2 NO. 12.

PERSI, P., FERRARI-TONIOLO, M. <ASTR. AP., 112, 292> 820819
NEAR-INFRARED SOURCES IN THE NGC 6334 MOLECULAR CLOUD.

PERSI, P., FERRARI-TONIOLO, M., GRASDALEN, G. L., SPADA, G. <ASTR. AP., 92, 238> 801214
INFRARED PHOTOMETRY OF HDE 226868 (CYG X-1) FROM 2.3 TO 10 MICRONS: MASS LOSS RATE.

PERSI, P., FERRARI-TONIOLO, M., SPADA, G., CONTI, G., DI BENEDETTO, P., TANZI, E. G., TARENGHI, M. <M. N. R. A. S., 187, 293> 790304
NEAR-INFRARED PHOTOMETRY OF HDE 245770 (A 0535+26).

PERSSON, S. E. <IAUC NO. 3324> 790215
H 2155-304.

PERSSON, S. E. <IAUC NO. 3324> 790214
H2155-304.

PERSSON, S. E., AARONSON, M., FROGEL, J. A. <A. J., 82, 729> 770903
BROAD-BAND INFRARED COLORS AND CO AND H2O ABSORPTION INDICES FOR LATE-TYPE DWARF STARS.

PERSSON, S. E., COHEN, J. G., SELLGREN, K., MOULD, J., FROGEL, J. A. <AP. J., 240, 779> 800905
INFRARED PHOTOMETRY OF THE SEMISTELLAR NUCLEUS OF M31.

PERSSON, S. E., FROGEL, J. A. <AP. J., 182, 503> 730606
INFRARED PHOTOMETRY OF PLANETARY NEBULAE.

PERSSON, S. E., FROGEL, J. A. <AP. J., 188, 523> 740302
SPECTROPHOTOMETRIC OBSERVATIONS OF THE COMPACT HII REGION K3-50 AND OF NGC 6857.

PERSSON, S. E., FROGEL, J. A. <P. A. S. P., 86, 985> 741204
1.2 MICRON TO 3.5 MICRON PHOTOMETRY OF EIGHT OPTICAL H II REGIONS.

PERSSON, S. E., FROGEL, J. A., AARONSON, M. <AP. J. SUPPL., 39, 61> 790103
PHOTOMETRIC STUDIES OF COMPOSITE STELLAR SYSTEMS. III. UBVR AND JHK OBSERVATIONS OF E AND S0 GALAXIES.

PERSSON, S. E., FROGEL, J. A., AARONSON, M. <AP. J., 208, 753> 760910
THE 10 MICRON SILICATE FEATURE IN SOUTHERN HII REGIONS.

PERSSON, S. E., FROGEL, J. A., COHEN, J. G., AARONSON, M., MATTHEWS, K. <AP. J., 235, 452> 800107
THE SPREAD IN CO ABSORPTION AND EFFECTIVE TEMPERATURE AMONG THE GIANTS IN OMEGA CENTAURI.

PERSSON, S. E., GEBALLE, T. R., SIMON, T., LONSDALE, C. J., BAAS, F. <AP. J. (LETTERS), 251, L85> 811207
HIGH VELOCITY H2 LINE EMISSION IN THE NGC 2071 REGION.

PETERSON, R. C., WILLMARTH, D. W., CARNEY, B. W., CHAFFEE JR., F. H. <AP. J., 239, 928> 800808
BD-0 4234: A HIGH-VELOCITY, METAL-POOR, DOUBLE-LINED SPECTROSCOPIC BINARY.

PETERSON, S. D. <A. J., 78, 811> 739901
OPTICAL POSITIONS OF THE MARKARIAN GALAXIES.

PHILLIPS, J. P., SELBY, M. J., WADE, R., SANCHEZ MAGRO, C. <M. N. R. A. S., 190, 337> 800210
INFRARED OBSERVATIONS OF BINARY STARS - I.

PHILLIPS, J. P., WADE, R., SELBY, M. J., SANCHEZ MAGRO, C. <M. N. R. A. S., 187, 45P> 790505
JHKLM PHOTOMETRY OF NOVA CYGNI 1978.

PHILLIPS, J. P., WHITE, G. J., ADE, P. A. R., CUNNINGHAM, C. T., RICHARDSON, K. J., ROBSON, E. I., WATT, G. D. <ASTR. AP., 116, 130> 821215
CO J-3-2 AND SUBMILLIMETRE CONTINUUM OBSERVATIONS OF TWO MOLECULAR OUTFLOW SOURCES.

PHILLIPS, M. M., FELDMAN, F. R., MARSHALL, F. E., WAMSTEKER, W. <ASTR. AP., 76, L14> 790706
ESO 103-G35: A NEW SEYFERT GALAXY AND POSSIBLE X-RAY SOURCE.

PHILLIPS, M. M., FROGEL, J. A. <AP. J., 235, 761> 800207
INFRARED AND OPTICAL PROPERTIES OF THE EMISSION-LINE GALAXIES NGC 1386 AND NGC 1365.

PHILLIPS, T. G., HUGGINS, P. J., KUIPER, T. B. H., MILLER, R. E. <AP. J. (LETTERS), 238, L103> 800602
DETECTION OF THE 610 MICRON (492 GHZ) LINE OF INTERSTELLAR ATOMIC CARBON.

PHILLIPS, T. G., HUGGINS, P. J., NEUGEBAUER, G., WERNER, M. W. <AP. J. (LETTERS), 217, L161> 771106
DETECTION OF SUBMILLIMETER (870 MICRON) CO EMISSION FROM THE ORION MOLECULAR CLOUD.

PILACHOWSKI, C. A. <AP. J., 224, 412> 780903
OBSERVATIONS OF CO IN GLOBULAR CLUSTER STARS.

PILACHOWSKI, C. A. <P. A. S. P., 90, 675> 781222
OBSERVATIONS OF CARBON MONOXIDE IN METAL-DEFICIENT STARS.

PIPHER, J. L., DUTHIE, J. G., SAVEDOFF, M. P. <AP. J., 219, 494> 780107
LAMELLAR GRATING OBSERVATIONS OF THE ORION NEBULA FROM 100 TO 500 MICRONS.

PIPHER, J. L., GRASDALEN, G. L., SOIFER, B. T. <AP. J., 193, 283> 741013
INFRARED OBSERVATIONS OF THE RADIO SOURCE G30.8-0.0 IN THE W43 COMPLEX.

PIPHER, J. L., SHARPLESS, S., SAVEDOFF, M. P., KERRIDGE, S. J., KRASSNER, J., SCHURMANN, S., SOIFER, B. T., MERRILL, K. M. <ASTR. AP., 51, 255> 760902
OPTICAL, INFRARED AND RADIO STUDIES OF COMPACT HII REGIONS. I. THE COMPLEX IN S 106.

PIPHER, J. L., SHARPLESS, S., SAVEDOFF, M. P., KRASSNER, J., VARLESE, S., SOIFER, B. T., ZEILIK II, M. <ASTR. AP., 59, 215> 770711
OPTICAL, INFRARED, AND RADIO STUDIES OF COMPACT HII REGIONS.

PIPHER, J. L., SOIFER, B. T. <ASTR. AP., 46, 153> 760102
INFRARED OBSERVATIONS OF THE H2O MASER ASSOCIATED WITH THE HII REGIONS S 255 (IC 2162) AND S 257.

PIPHER, J. L., SOIFER, B. T., KRASSNER, J. <ASTR. AP., 74, 302> 790513
INFRARED PHOTOMETRY AND SPECTROPHOTOMETRY OF G75.84+0.4.

PLAUT, L. <ASTR. AP. SUPPL., 28, 169> 779907
POSITIONS OF VARIABLE STARS AS DERIVED FROM THE ASTROGRAPHIC (CARTE DU CIEL) CATALOGUES.

POGODIN, M. A. <SOV. AST., 25, 454> 810716
PHOTOMETRY OF SOME HERBIG EMISSION STARS IN THE NEAR-IR REGION OF THE SPECTRUM.

PRAVDO, S. H., NUGENT, J. J., NOUSEK, J. A., JENSEN, K., WILSON, A. S., BECKER, R. H. <AP. J., 251, 501> 811205
DISCOVERY OF A SEYFERT 1 GALAXY WITH AN UNUSUALLY SOFT X-RAY SPECTRUM.

PRICE, S. D. <A. J., 73, 431> 680802
RESULTS OF AN INFRARED STELLAR SURVEY.

PRICE, S. D. <A. J., 86, 193> 810204
INFRARED MAPPING OF THE GALACTIC PLANE. I. LOW-RESOLUTION MAPS BETWEEN 0 AND 320 DEGREES LONGITUDE.

PRICE, S. D. <AFGL-TR-77-0160> 770706
THE AFGL FOUR COLOR INFRARED SKY SURVEY: SUPPLEMENTAL CATALOG.

PRICE, S. D., MARCOTTE, L. P., MURDOCK, T. L. <A. J., 87, 131> 820109
INFRARED MAPPING OF THE GALACTIC PLANE. II. MEDIUM-RESOLUTION MAPS OF THE CYGNUS X REGION.

PRICE, S. D., MURDOCK, T. L., SHIVANANDAN, K. <AFGL-TR-83-0055> 830201
FAR INFRARED SKY SURVEY EXPERIMENT. FINAL REPORT.

PRICE, S. D., WALKER, R. G. <AFGL-TR-76-0208> 760913
THE AFGL FOUR COLOR INFRARED SKY SURVEY:CATALOG OF OBSERVATIONS AT 4.2, 11.0, 19.8, AND 27.4 MICRONS.

PRIEDHORSKY, W., MATTHEWS, K., NEUGEBAUER, G., WERNER, M. W.,KRZEMINSKI, W. <AP. J., 226, 397> 781206
JOINT INFRARED AND VISUAL MONITORING OF AM HERCULIS.

PROBST, R. G., O'CONNELL, R. W. <AP. J. (LETTERS), 252, L69> 820107
THE LUMINOSITY FUNCTION OF VERY LOW MASS STARS.

PRZBYLSKI, A. <AP. J. (LETTERS), 257, L83> 820608
A NOTE ON THE TEMPERATURE OF HD 101065.

PUETTER, R. C., RUSSELL, R. W., SELLGREN, K., SOIFER, B. T. <P. A. S. P., 89, 320> 770613
SPECTRA OF LATE-TYPE STARS FROM 4-8 MICRONS.

PUETTER, R. C., RUSSELL, R. W., SOIFER, B. T., WILLNER, S. P. <AP. J. (LETTERS), 223, L93> 780710
INFRARED SPECTRA OF HM SAGITTAE AND V1016 CYGNI.

PUETTER, R. C., RUSSELL, R. W., SOIFER, B. T., WILLNER, S. P. <AP. J., 228, 118> 790210
SPECTROPHOTOMETRY OF COMPACT HII REGIONS FROM 4 TO 8 MICRONS.

PUETTER, R. C., SMITH, H. E., SOIFER, B. T., WILLNER, S. P., PIPHER, J. L. <AP. J. (LETTERS), 226, L53> 781204
SPECTROPHOTOMETRY OF QUASI-STELLAR OBJECTS AT OPTICAL AND INFRARED WAVELENGTHS: PG 0026+129 AND 3C 273.

PUETTER, R. C., SMITH, H. E., WILLNER, S. P. <AP. J. (LETTERS), 227, L5> 790108
SPECTROPHOTOMETRY OF QUASI-STELLAR OBJECTS AT OPTICAL AND INFRARED WAVELENGTHS: THE H-ALPHA/ L-ALPHA RATIO IN

PUETTER, R. C., SMITH, H. E., WILLNER, S. P., PIPHER, J. L. <AP. J., 243, 345> 810105
OPTICAL AND INFRARED SPECTROPHOTOMETRY OF QUASI-STELLAR OBJECTS: THE SPECTRA OF 14 QSOS.

PUSCHELL, J. J. <A. J., 86, 16> 810101
VISUAL-INFRARED VARIATIONS IN THE BROAD-LINE RADIO GALAXY 3C382.

PUSCHELL, J. J. <AP. J., 247, 48> 810703
NONSTELLAR 10 MICRON EMISSION FROM E/S0 GALAXIES WITH COMPACT RADIO SOURCES.

PUSCHELL, J. J. <P. A. S. P., 90, 652> 781219
OPTICAL AND INFRARED PHOTOMETRY OF ARAKELIAN 120.

PUSCHELL, J. J., OWEN, F. N., LAING, R. A. <AP. J. (LETTERS), 257, L57> 820607
NEAR-INFRARED PHOTOMETRY OF DISTANT RADIO GALAXIES: SPECTRAL FLUX DISTRIBUTIONS AND REDSHIFT ESTIMATES.

PUSCHELL, J. J., STEIN, W. A. <AP. J., 237, 331> 800407
OBSERVATIONS OF STRONGLY POLARIZED EXTRAGALACTIC SOURCES.

PUSCHELL, J. J., STEIN, W. A., JONES, T. W., WARNER, J. W., OWEN, F. N., RUDNICK, L., ALLER, H., HODGE, P. <AP. J. (LETTERS), 227, L11> 790109
B2 1308+326: PHOTOMETRY AND POLARIZATION DURING THE OUTBURST OF 1978 SPRING.

QUERCI, M., QUERCI, F. <ASTR. AP., 42, 329> 750907
THE INFRARED SPECTRUM OF THE CARBON STARS UU AUR AND Y CVN FROM 4000 TO 6800 CM-1.

RAFANELLI, P., BIRKLE, K., HEFELE, H. <IAUC NO. 3584> 810306
SUPERNOVA IN NGC 4536.

RANK, D. M., DINERSTEIN, H. L., LESTER, D. F., BREGMAN, J. D., AITKEN, D. K., JONES, B. <M. N. R. A. S., 185, 179> 781008
OBSERVATIONS OF INFRARED EMISSION LINES IN THE SOUTHERN COMPACT HII REGIONS G333.6-0.2 AND G298.2-0.3.

RANK, D. M., GEBALLE, T. R., WOLLMAN, E. R. <AP. J. (LETTERS), 187, L111> 740201
DETECTION OF OXYGEN-17 IN IRC+10216.

RANK, D. M., HOLTZ, J. Z., GEBALLE, T. R., TOWNES, C. H. <AP. J. (LETTERS), 161, L185> 700903
DETECTION OF 10.5-MICRON LINE EMISSION FROM THE PLANETARY NEBULA NGC 7027.

REID, I. N., GILMORE, G. <M. N. R. A. S., 196, 15P> 810714
A STAR OF VERY LOW LUMINOSITY.

REIPURTH, B. <ASTR. AP. SUPPL., 44, 379> 810621
SMALL NEBULAE AND HERBIG-HARO OBJECTS. I. A SURVEY OF SOUTHERN DARK CLOUDS.

RICHER, H. B., FROGEL, J. A. <AP. J. (LETTERS), 242, L9> 801103
DISCOVERY OF THE FIRST SC STAR IN THE MAGELLANIC CLOUDS.

RIDGWAY, S. T., CARBON, D. F., HALL, D. N. B. <AP. J., 225, 138> 781003
POLYATOMIC SPECIES CONTRIBUTING TO THE CARBON-STAR 3 MICRON BAND.

RIDGWAY, S. T., JACOBY, G. H., JOYCE, R. R., SIEGEL, M. J., WELLS, D. C. <A. J., 87, 1044> 820708
ANGULAR DIAMETERS BY THE LUNAR OCCULTATION TECHNIQUE. VI. LIMB DARKENING OF ALPHA TAURI.

RIDGWAY, S. T., JACOBY, G. H., JOYCE, R. R., SIEGEL, M. J., WELLS, D. C. <A. J., 87, 808> 820507
ANGULAR DIAMETERS BY THE LUNAR OCCULTATION TECHNIQUE. V. 26 LATE-TYPE STARS.

RIDGWAY, S. T., JACOBY, G. H., JOYCE, R. R., SIEGEL, M. J., WELLS, D. C. <A. J., 87, 680> 820415
ANGULAR DIAMETERS BY THE LUNAR OCCULTATION TECHNIQUE. IV. ALPHA LEO AND THE CEPHEID ZETA GEM.

RIDGWAY, S. T., JOYCE, R. R., WHITE, N. M., WING, R. F. <AP. J., 235, 126> 800105
EFFECTIVE TEMPERATURES OF LATE-TYPE STARS: THE FIELD GIANTS FROM K0 TO M6.

RIDGWAY, S. T., WELLS, D. C., JOYCE, R. R. <A. J., 82, 414> 770605
ANGULAR DIAMETERS FOR 11 LATE-TYPE STARS BY THE LUNAR OCCULTATION TECHNIQUE.

RIDGWAY, S. T., WELLS, D. C., JOYCE, R. R., ALLEN, R. G. <A. J., 84, 247> 790203
TWENTY-EIGHT ANGULAR DIAMETERS FOR LATE-TYPE STARS BY THE LUNAR OCCULTATION TECHNIQUE.

RIDGWAY, S., HALL, D. N. B., KLEINMANN, S. G., WEINBERGER, D. A., WOJSLAW, R. S. <NATURE, 264, 345> 761112
CIRCUMSTELLAR ACETYLENE IN THE INFRARED SPECTRUM OF IRC+10216.

RIEKE, G. H. <AP. J. (LETTERS), 176, L61> 720903
INFRARED OBSERVATIONS OF VARIABLE RADIO OBJECTS.

RIEKE, G. H. <AP. J. (LETTERS), 193, L81> 741010
THE SPECTRUM OF VI CYGNI NO. 12 NEAR 10 MICRONS.

RIEKE, G. H. <AP. J. (LETTERS), 206, L15> 760510
THE SIZES OF THE NUCLEI OF GALAXIES AT 10 MICRONS.

RIEKE, G. H. <AP. J. (LETTERS), 210, L5> 761104
THE INFRARED EMISSION OF MARKARIAN 231.

RIEKE, G. H. <AP. J., 226, 550> 781209
THE INFRARED EMISSION OF SEYFERT GALAXIES.

RIEKE, G. H., GRASDALEN, G. L., KINMAN, T. D., HINTZEN, P., WILLS, B. J., WILLS, D. <NATURE, 260, 754> 760411
PHOTOMETRIC AND SPECTROSCOPIC OBSERVATIONS OF THE BL LACERTAE OBJECT AO 0235+164.

RIEKE, G. H., HARPER JR., D. A., LOW, F. J., ARMSTRONG, K. R. <AP. J. (LETTERS), 183, L67> 730703
350-MICRON OBSERVATIONS OF SOURCES IN HII REGIONS, THE GALACTIC CENTER, AND NGC 253.

RIEKE, G. H., KINMAN, T. D. <AP. J. (LETTERS), 192, L115> 740904
CORRELATED OPTICAL AND INFRARED BEHAVIOR OF OJ 287 AND SIMILAR RADIO SOURCES.

RIEKE, G. H., LEBOFSKY, M. J. <AP. J. (LETTERS), 220, L37> 780305
10 MICRON OBSERVATIONS OF BRIGHT GALAXIES.

RIEKE, G. H., LEBOFSKY, M. J. <AP. J., 227, 710> 790206
ON THE INFRARED VARIABILITY OF 3C 120, NGC 1275, AND III ZW 2.

RIEKE, G. H., LEBOFSKY, M. J. <AP. J., 250, 87> 811101
SPECTRAL COMPONENTS OF NGC 4151.

RIEKE, G. H., LEBOFSKY, M. J., KEMP, J. C. <AP. J. (LETTERS), 252, L53> 820106
NONTHERMAL OPTICAL-INFRARED EMISSION FROM NGC 1052.

RIEKE, G. H., LEBOFSKY, M. J., KEMP, J. C., COYNE S. J., G. V., TAPIA, S. <AP. J. (LETTERS), 218, L37> 771203
INFRARED AND VISIBLE POLARIMETRY AND PHOTOMETRY OF HIGHLY VARIABLE QUASI-STELLAR SOURCES.

RIEKE, G. H., LEBOFSKY, M. J., KINMAN, T. D. <AP. J. (LETTERS), 232, L151> 790910
A POSSIBLY NEW TYPE OF QSO IDENTIFIED THROUGH INFRARED MEASUREMENTS.

RIEKE, G. H., LEBOFSKY, M. J., THOMPSON, R. I., LOW, F. J., TOKUNAGA, A. T. <AP. J., 238, 24> 800504
THE NATURE OF THE NUCLEAR SOURCES IN M82 AND NGC 253.

RIEKE, G. H., LEBOFSKY, M. J., WISNIEWSKI, W. Z. <AP. J., 263, 73> 821201
ABRUPT CUTOFFS IN THE OPTICAL-INFRARED SPECTRA OF NONTHERMAL SOURCES.

RIEKE, G. H., LOW, F. J. <AP. J. (LETTERS), 176, L95> 720901
INFRARED PHOTOMETRY OF EXTRAGALACTIC SOURCES.

RIEKE, G. H., LOW, F. J. <AP. J. (LETTERS), 177, L115> 721102
VARIABILITY OF EXTRAGALACTIC SOURCES AT 10 MICRONS.

RIEKE, G. H., LOW, F. J. <AP. J. (LETTERS), 199, L13> 750701
THE INFRARED SPECTRUM OF NGC 1068.

RIEKE, G. H., LOW, F. J. <AP. J. (LETTERS), 200, L67> 750902
MEASUREMENTS OF GALACTIC NUCLEI AT 34 MICRONS.

RIEKE, G. H., LOW, F. J. <AP. J., 184, 415> 730902
INFRARED MAPS OF THE GALACTIC NUCLEUS.

RIEKE, G. H., LOW, F. J. <AP. J., 197, 17> 750403
THE NUCLEUS OF NGC 253.

RIEKE, G. H., LOW, F. J. <NATURE, 233, 53> 710902
MAP OF THE GALACTIC NUCLEUS AT 10 MICRONS.

RIEKE, G. H., LOW, F. J. <COMM. LUNAR AND PLANETARY LAB., 9, 181> 710901
MAP OF THE GALACTIC NUCLEUS AT 10 MICRONS.

RIEKE, G. H., LOW, F. J., KLEINMANN, D. E. <AP. J. (LETTERS), 186, L7> 731102
HIGH-RESOLUTION MAPS OF THE KLEINMANN-LOW NEBULA IN ORION.

RIEKE, G. H., TELESCO, C. M., HARPER JR., D. A. <AP. J., 220, 556> 780303
THE INFRARED EMISSION OF THE GALACTIC CENTER.

RIEKE, G., LEE, T., COYNE S. J., G. V. <P. A. S. P., 84, 37> 720204
PHOTOMETRY AND POLARIMETRY OF V1057 CYGNI.

RIGHINI-COHEN, G., SIMON, M. <AP. J., 213, 390> 770407
THE RELATIONSHIP OF SUBMILLIMETER OPTICAL DEPTH TO 13-CO COLUMN DENSITY IN MOLECULAR CLOUDS.

RIGHINI-COHEN, G., SIMON, M., YOUNG, E. T. <AP. J., 232, 782> 790909
INFRARED LINE OBSERVATIONS OF DR 21, W75N, AND K3-50.

RIGHINI, G., SIMON, M., JOYCE, R. R. <AP. J., 207, 119> 760705
3 MILLIMETER AND 350 MICRON CONTINUUM OBSERVATIONS OF THE DR-21 AND SGR B2 REGIONS.

RIGHINI, G., SIMON, M., JOYCE, R. R., GEZARI, D. Y. <AP. J. (LETTERS), 195, L77> 750102
350-MICRON MAPPING OF SAGITTARIUS B2.

RINSLAND, C. P., WING, R. F. <AP. J., 262, 201> 821103
OBSERVATIONS OF THE FIRST-OVERTONE SILICON MONOXIDE BANDS IN LATE-TYPE STARS.

ROARK, T. P., BAUMERT, J. H., WHITE, N. M. <AP. LETTERS, 10, 55> 720003
NEAR INFRARED PHOTOMETRY OF THE THETA CORONAE BOREALIS SYSTEM.

ROBBINS, R. R. <AP. J., 162, 507> 701101
THE PROFILE OF HE I 10830A IN NGC 7027 AND THE ORION NEBULA.

ROBERTS, M. S. <A. J., 67, 79> 629902
THE GALACTIC DISTRIBUTION OF THE WOLF-RAYET STARS.

ROBERTSON, B. S. C., FEAST, M. W. <M. N. R. A. S., 196, 111> 810712
THE BOLOMETRIC, INFRARED, AND VISUAL ABSOLUTE MAGNITUDES OF MIRA VARIABLES.

ROBINSON, G., HYLAND, A. R., THOMAS, J. A. <M. N. R. A. S., 161, 281> 730007
OBSERVATION AND INTERPRETATION OF THE INFRA-RED SPECTRUM OF ETA CARINAE.

ROBINSON, G., THOMAS, J. A., HIRST, R. A., HYLAND, A. R. <P. A. S. P., 85, 436> 730809
THE NATURE OF NGC 6231-92.

RODGERS, A. W. <AP. J., 165, 665> 710502
THE REDDENING OF ETA CARINAE.

RODGERS, A. W., CAMPBELL, C. T., WHITEOAK, J. B. <M. N. R. A. S., 121, 103> 609902
A CATALOGUE OF H-ALPHA EMISSION REGIONS IN THE SOUTHERN MILKY WAY.

RODRIGUEZ, L. F., CHAISSON, E. J. <AP. J., 221, 816> 780504
A COMPARATIVE STUDY OF HIGH-RADIOFREQUENCY AND FAR-INFRARED OBSERVATIONS OF GALACTIC HII REGIONS.

RODRIGUEZ, L. F., MORAN, J. M., HO, P. T. P., GOTTLIEB, E. W. <AP. J., 235, 845> 809904
RADIO OBSERVATIONS OF WATER VAPOR, HYDROXYL, SILICON MONOXIDE, AMMONIA, CARBON MONOXIDE, AND COMPACT H II REGIONS IN THE VICINITIES OF SUSPECTED HERBIG-HARO OBJECTS.

ROOD, H. J., BAUM, W. A. <A. J., 72, 398> 679901
PHOTOGRAPHIC BRIGHTNESS PROFILES OF COMA CLUSTER GALAXIES. I. CATALOGUE OR PROGRAM GALAXIES.

ROSSANO, G. S., RUSSELL, R. W., CORNETT, R. H. <P. A. S. P., 92, 357> 800601
NEAR INFRARED PHOTOGRAPHY WITH A VACUUM-COLD CAMERA.

ROUAN, D., LENA, P. J., PUGET, J. L., DE BOER, K. S., WIJNBERGEN, J. J. <AP. J. (LETTERS), 213, L35> 770410
FAR-INFRARED OBSERVATIONS OF THE GALACTIC PLANE AND MOLECULAR CLOUD S140.

RUBIN, R. H. <ASTR. AP., 8, 171> 709904
RADIO OBSERVATIONS OF PLANETARY NEBULAE AND POSSIBLE PLANETARY NEBULAE.

RUDNICK, L., OWEN, F. N., JONES, T. W., PUSCHELL, J. J., STEIN, W. A. <AP. J. (LETTERS), 225, L5> 781004
COORDINATED CENTIMETER, MILLIMETER, INFRARED, AND VISUAL POLARIMETRY OF COMPACT NONTHERMAL SOURCES.

RUDY, R. J., GOSNELL, T. R., WILLNER, S. P. <AFGL-TR-79-0172> 791110
GROUND-BASED MEASUREMENTS OF SOURCES IN THE AFGL INFRARED SKY SURVEY.

RUDY, R. J., JONES, B., LEVAN, P. D., PUETTER, R. C., SMITH, H. E., WILLNER, S. P., TOKUNAGA, A. T. <AP. J., 257, 570> 820604
NEAR-INFRARED SPECTROPHOTOMETRY OF FOUR SEYFERT 1 GALAXIES AND NGC 1275.

RUDY, R. J., LEVAN, P. D., PUETTER, R. C., SMITH, H. E., WILNER, S. P. <AP. J., 253, 53> 820202
INFRARED POLARIMETRY OF NINE SEYFERT GALAXIES.

RUDY, R. J., LEVAN, P. D., RODRIGUEZ-ESPINOSA, J. M. <A. J., 87, 598> 820413
INFRARED PHOTOMETRY OF 30 SEYFERT GALAXIES.

RUDY, R. J., LEVAN, P. D., RODRIGUEZ-ESPINOSA, J. M. <P. A. S. P., 93, 558> 811001
FURTHER OBSERVATIONS OF 3C 273 FOR THE 3.3 MICRON DUST FEATURE.

RUDY, R. J., TOKUNAGA, A. T. <AP. J. (LETTERS), 256, L1> 820503
OBSERVATIONS OF PASCHEN-ALPHA IN THE BROAD-LINE RADIO GALAXY 3C 445.

RUDY, R. J., WILLNER, S. P. <P. A. S. P., 92, 75> 800201
CARBON MONOXIDE IN A CH STAR IN M22.

RUSSELL, R. W. <ASTR. AP., 67, 273> 780711
THE INFRARED SOURCE ASSOCIATED WITH SH 2-149.

RUSSELL, R. W., GULL, G., BECKWITH, S., EVANS II, N. J. <P. A. S. P., 94, 97> 820210
HIGH-SPECTRAL-RESOLUTION OBSERVATIONS OF THE 7.7 MICRON FEATURE IN HD 44179.

RUSSELL, R. W., MELNICK, G., GULL, G. E., HARWIT, M. <AP. J. (LETTERS), 240, L99> 800902
DETECTION OF THE 157 MICRON (1910GHZ) (C II) EMISSION LINE FROM THE INTERSTELLAR GAS COMPLEXES NGC 2024 AND M42.

RUSSELL, R. W., MELNICK, G., SMYERS, S. D., KURTZ, N. T., GOSNELL, T. R., HARWIT, M., WERNER, M. W. <AP. J. (LETTERS), 250, L35> 811106
GIANT (C II) HALOS AROUND H II REGIONS.

RUSSELL, R. W., SOIFER, B. T., FORREST, W. J. <AP. J. (LETTERS), 198, L41> 750502
SPECTROPHOTOMETRIC OBSERVATIONS OF MU CEPHEI AND THE MOON FROM 4 TO 8 MICRONS.

RUSSELL, R. W., SOIFER, B. T., MERRILL, K. M. <AP. J., 213, 66> 770404
OBSERVATIONS OF THE UNIDENTIFIED 3.3 MICROMETER EMISSION FEATURE IN NEBULAE.

RUSSELL, R. W., SOIFER, B. T., PUETTER, R. C. <ASTR. AP., 54, 959> 770201
THE 4-8 MICRON SPECTRUM OF THE BNKL SOURCE IN ORION.

RUSSELL, R. W., SOIFER, B. T., WILLNER, S. P. <AP. J. (LETTERS), 217, L149> 771105
THE 4 TO 8 MICRON SPECTRUM OF NGC 7027.

RUSSELL, R. W., SOIFER, B. T., WILLNER, S. P. <AP. J., 220, 568> 780304
THE INFRARED SPECTRA OF CRL 618 AND HD 44179 (CRL 915).

RYDGREN, A. E. <P. A. S. P., 88, 111> 760413
T TAURI STARS AND THE (J-H), (H-K) DIAGRAM.

RYDGREN, A. E., SCHMELZ, J. T., VRBA, F. J. <AP. J., 256, 168> 820502
EVIDENCE FOR A CHARACTERISTIC MAXIMUM TEMPERATURE IN THE CIRCUMSTELLAR DUST ASSOCIATED WITH T TAURI STARS.

RYDGREN, A. E., STROM, S. E., STROM, K. M. <AP. J. SUPPL., 30, 307> 760306
THE NATURE OF THE OBJECTS OF JOY: A STUDY OF THE T TAURI PHENOMENON.

RYDGREN, A. E., VRBA, F. J. <A. J., 86, 1069> 810701
NEARLY SIMULTANEOUS OPTICAL AND INFRARED PHOTOMETRY OF T TAURI STARS.

RYTER, C. E., PUGET, J. L. <AP. J., 215, 775> 770803
FAR-INFRARED EMISSION OF MOLECULAR CLOUDS.

SALINARI, P. <IAUC NO. 3586> 810307
SUPERNOVA IN NGC 1316.

SANDAGE, A. R. <A. J., 58, 61> 539901
THE COLOR-MAGNITUDE DIAGRAM FOR THE GLOBULAR CLUSTER M3.

SANDAGE, A. R., BECKLIN, E. E., NEUGEBAUER, G. <AP. J., 157, 55> 690701
UBVRIHKL PHOTOMETRY OF THE CENTRAL REGION OF M31.

SANDAGE, A., WILDEY, R. <AP. J., 150, 469> 679906
THE ANOMALOUS COLOR-MAGNITUDE DIAGRAM OF THE REMOTE GLOBULAR CLUSTER NGC 7006.

SANDFORD II, M. T., GOW, C. E., HONEYCUTT, R. K., JEKOWSKI, J. P., OLIVAS, P. N. <P. A. S. P., 89, 31> 770214
NEAR-INFRARED VIDICON IMAGES OF CIT FIELDS.

SANDULEAK, N., STEPHENSON, C. B. <AP. J., 185, 899> 739903
LOW-DISPERSION SPECTRA AND GALACTIC DISTRIBUTION OF VARIOUS INTERESTING STRONG-EMISSION-LINE OBJECTS IN THE SOUTHERN MILKY WAY.

SARGENT, A. I., VAN DUINEN, R. J., FRIDLUND, C. V. M., NORDH, H. L., AALDERS, J. W. G. <AP. J., 249, 607> 811009
FAR-INFRARED OBSERVATIONS OF STAR-FORMING REGIONS.

SARGENT, A. I., VAN DUINEN, R. J., NORDH, H. L., AALDERS, J. W. G. <ASTR. AP., 94, 377> 810218
FAR INFRARED OBSERVATIONS OF S 255 AND S 187.

SARGENT, W. L. W., SEARLE, L. <AP. J. (LETTERS), 162, L155> 701201
ISOLATED EXTRAGALACTIC HII REGIONS.

SATO, S., KAWARA, K., KOBAYASHI, Y., MAIHARA, T., ODA, N., OKUDA, H. <P. A. S. J., 30, 419> 780001
INFRARED OBSERVATIONS OF NOVA VULPECULAE 1976 (NQ VUL).

SATO, S., KAWARA, K., KOBAYASHI, Y., MAIHARA, T., OKUDA, H. <NATURE, 286, 688> 800816
NO IR BURST FROM THE X-RAY RAPID BURSTER MXB1730-335.

SATO, S., KOBAYASHI, Y., KAWARA, K., MAIHARA, T., OKUDA, H. <P. A. S. J., 28, 391> 760005
INFRARED PHOTOMETRY OF CRL 877 ASSOCIATED WITH THE RADIO COMPLEX IN THE MONOCEROS R2 REGION.

SATO, S., MAIHARA, T., OKUDA, H. <P. A. S. J., 25, 571> 730021
NEAR-INFRARED OBSERVATIONS OF NOVA CEPHEI 1971.

SCARGLE, J. D., ERICKSON, E. F., WITTEBORN, F. C., STRECKER, D. W. <AP. J., 224, 527> 780906
INFRARED EXCESSES IN EARLY-TYPE STARS: GAMMA CASSIOPEIAE.

SCARGLE, J. D., STRECKER, D. W. <AP. J., 228, 838> 790313
COOL STARS: EFFECTIVE TEMPERATURES, ANGULAR DIAMETERS, AND REDDENING DETERMINED FROM 1-5 MICRON FLUX CURVES AND MODEL ATMOSPHERES.

SCHILD, R. E. <AP. J., 179, 221> 730105
A SPECTROSCOPICALLY DISTINGUISHED CLASS OF BE STARS.

SCHILD, R. E., CHAFFEE, F., FROGEL, J. A., PERSSON, S. E. <AP. J., 190, 73> 740505
THE NATURE OF INFRARED EXCESSES IN EXTREME BE STARS.

SCHILD, R. E., NEUGEBAUER, G., WESTPHAL, J. A. <A. J., 76, 237> 710402
INTERSTELLAR ABSORPTION AND COLOR EXCESSES IN SCO OB-1.

SCHILD, R. E., OKE, J. B., SEARLE, L. <AP. J., 188, 71> 740207
THE ENERGY DISTRIBUTION OF THE VERY RED STAR IN NGC 6231.

SCHMIDT, E. G. <AP. J., 165, 335> 710407
A PHOTOMETRIC STUDY OF FOUR CLASSICAL CEPHEIDS.

SCHMIDT, G. D., VRBA, F. J. <AP. J. (LETTERS), 201, L33> 751001
THE NATURE OF HERBIG-HARO OBJECTS 1 AND 2: COMPACT EMISSION NEBULAE.

SCHMITZ, M., BROWN, L. W., MEAD, J. M., NAGY, T. A. <NASA TM-79683> 781111
MERGED INFRARED CATALOGUE.

SCHNEIDER, D. P., GREENSTEIN, J. L. <AP. J., 233, 935> 791105
HIGH TIME RESOLUTION SPECTROPHOTOMETRY OF NOVA DQ HERCULIS (1934).

SCHNEIDER, D. P., YOUNG, P., SHECTMAN, S. A. <AP. J., 245, 644> 810404
MV LYRAE: A SPECTROSCOPIC STUDY OF THE LOW STATE.

SCHNEPS, M. H., LANE, A. P., DOWNES, D., MORAN, J. M., GENZEL, R., REID, M. J. <AP. J., 249, 124> 811006
PROPER MOTIONS AND DISTANCES OF H2O MASER SOURCES. III. W51 NORTH.

SCHULTE IN DEN BAUMEN, J., HEFELE, H., HOLZLE, E., ORTLIEB, N. <ASTR. AP., 94, 280> 810215
OBSERVATIONS OF LATE TYPE OBJECTS WITH A NEW SPECTROPHOTOMETER IN THE 8-13 MICRON RANGE.

SCHULTE, D. H. <AP. J., 123, 250> 569905
SOME RECENT RESULTS OF LOW-DISPERSION SPECTRAL CLASSIFICATION.

SCHULTE, D. H. <AP. J., 124, 530> 569906
NEW MEMBERS OF THE ASSOCIATION VI CYGNI.

SCHULTE, D. H. <AP. J., 128, 41> 589901
NEW MEMBERS OF THE ASSOCIATION VI CYGNI. II.

SCHULTZ, G. V., KREYSA, E., SHERWOOD, W. A. <ASTR. AP., 50, 171> 760701
THE DISCOVERY OF SOME INFRARED COUNTERPARTS OF TYPE II OH/IR SOURCES.

SCHULTZ, G. V., WIEMER, W. <ASTR. AP., 20, 317> 720906
IDENTIFICATIONS OF IRC-OBJECTS.

SCHULZ, A., LENZEN, R., SCHMIDT, TH., PROETEL, K. <ASTR. AP., 95, 94> 810219
POLARIZATION OF STARLIGHT IN M17.

SCHWARTZ, P. R., HARVEY, P. M., BARRETT, A. H. <AP. J., 187, 491> 740205
TIME VARIATION OF THE H2O MASER AND INFRARED CONTINUUM IN LATE-TYPE STARS.

SCHWARTZ, R. D. <AP. J., 191, 419> 740707
THE T TAURI EMISSION NEBULA.

SCHWARTZ, R. D., PEIMBERT, M. <AP. LETTERS, 13, 157> 730026
PHOTOELECTRIC PHOTOMETRY OF NGC 7027.

SCOVILLE, N. Z., GEZARI, D. Y., CHIN, G., JOYCE, R. R. <A. J., 84, 1571> 791002
SEARCH FOR H2 EMISSION AT 2.1 MICRONS IN TEN SOUTHERN HEMISPHERE SOURCES.

SCOVILLE, N. Z., HALL, D. N. B., KLEINMANN, S. G., RIDGWAY, S. T. <AP. J. (LETTERS), 232, L121> 790908
DETECTION OF CO BAND EMISSION IN THE BECKLIN-NEUGEBAUER OBJECT.

SCOVILLE, N. Z., HALL, D. N. B., KLEINMANN, S. G., RIDGWAY, S. T. <AP. J., 253, 136> 820204
VELOCITY, REDDENING, AND TEMPERATURE STRUCTURE OF THE H2 EMISSION IN ORION.

SCRIMGER, J. N., LOWE, R. P., MOORHEAD, J. M., WEHLAU, W. H. <P. A. S. P., 90, 257> 780613
OBSERVATIONS OF NGC 7027 IN THE NEAR INFRARED.

SELBY, M. J., BLACKWELL, D. E., PETFORD, A. D., SHALLIS, M. J. <M. N. R. A. S., 193, 111> 801009
MEASUREMENT OF THE ABSOLUTE FLUX FROM VEGA IN THE K BAND (2.2 MICRONS).

SELBY, M. J., WADE, R., SANCHEZ MAGRO, C. <M. N. R. A. S., 187, 553> 790504
SPECKLE INTERFEROMETRY IN THE NEAR-INFRARED.

SELLGREN, K. <AP. J., 245, 138> 810409
SPATIAL OBSERVATIONS OF THE ORION NEBULA IN THE UNIDENTIFIED 3.28 MICRON FEATURE.

SERKOWSKI, K. <AP. J. (LETTERS), 179, L101> 730103
INFRARED CIRCULAR POLARIZATION OF NML CYGNI AND VY CANIS MAJORIS.

SERKOWSKI, K., MATHEWSON, D. S., FORD, V. L. <AP. J., 196, 261> 750206
WAVELENGTH DEPENDENCE OF INTERSTELLAR POLARIZATION AND RATIO OF TOTAL TO SELECTIVE EXTINCTION.

SERKOWSKI, K., RIEKE, G. H. <AP. J. (LETTERS), 183, L103> 730804
CIRCULAR POLARIZATION OF THE BECKLIN-NEUGEBAUER INFRARED SOURCES IN THE ORION NEBULA.

SERKOWSKI, K., ROBERTSON, J. W. <AP. J., 158, 441> 691103
REGIONAL VARIATIONS IN THE WAVELENGTH DEPENDENCE OF INTERSTELLAR POLARIZATION.

SERRA, G., BOISSE, P., GISPERT, R., WIJNBERGEN, J. J., RYTER, C. E., PUGET, J. L. <ASTR. AP., 76, 259> 790707
FAR INFRARED DIFFUSE EMISSION FROM THE GALACTIC PLANE. II. THE LONGITUDE PROFILE.

SERRA, G., PUGET, J. L., RYTER, C. E., WIJNBERGEN, J. J. <AP. J. (LETTERS), 222, L21> 780510
THE FAR-INFRARED EMISSION OF INTERSTELLAR MATTER BETWEEN GALACTIC LONGITUDES L-36 AND L-55 DEGREES.

SHAHAM, J. <COMM. ON AP., 9, 1> 800004
SS433 - AN OCTOBER 1979 VIEW.

SHALLIS, M. J., BLACKWELL, D. E. <ASTR. AP., 79, 48> 791017
ANGULAR DIAMETERS, RADII, AND EFFECTIVE TEMPERATURES OF AP STARS.

SHANIN, G. I. <SOV. AST. (LETTERS), 4, 100> 780311
THE NEAR-INFRARED SPECTRUM OF HM SAGITTAE.

SHANIN, G. I. <SOV. AST., 23, 158> 790314
INFRARED SPECTROSCOPY WITH A CONTACT-TYPE IMAGE TUBE: FU ORIONIS STARS.

SHAROV, A. S. <SOV. AST., 13, 947> 700504
THE INFRARED BRIGHTNESS OF THE MILKY WAY.

SHARPLESS, S. <AP. J. SUPPL., 4, 257> 599901
A CATALOGUE OF HII REGIONS.

SHAVER, P. A., DANKS, A. C. <ASTR. AP., 65, 323> 780515
RADIO AND INFRARED OBSERVATIONS OF THE OH/H20 SOURCE G12.2-0.1.

SHAVER, P. A., RETALLACK, D. S., WAMSTEKER, W., DANKS, A. C. <ASTR. AP., 102, 225> 811015
THE DISTANCE TO G316.8-0.1.

SHCHERBAKOV, A. G. <SOV. AST. (LETTERS), 3, 244> 770907
THE INFRARED SPECTRUM OF NOVA VULPECULAE 1976.

SHCHERBAKOV, A. G. <SOV. AST. (LETTERS), 5, 290> 791020
THE 10830 HE I LINE IN THE COOL GIANT HR 1105.

SHENAVRIN, V. I. <SOV. AST., 23, 696> 791108
PHOTOMETRY OF XX CAM, UV CAS, AND SU TAU IN THE OPTICAL AND INFRARED RANGES.

SHENAVRIN, V. I., MOROZ, V. I. <SOV. AST. (LETTERS), 2, 39> 760209
INFRARED OBSERVATIONS OF NOVA CYGNI 1975. III. SPECTRA IN THE 0.6-2.5 MICRON RANGE.

SHENAVRIN, V. I., MOROZ, V. I., LIBERMAN, A. A. <SOV. AST. (LETTERS), 2, 36> 760207
INFRARED OBSERVATIONS OF NOVA CYGNI 1975. I. J, K, L PHOTOMETRY.

SHENAVRIN, V. I., MOROZ, V. I., LIBERMAN, A. A. <SOV. AST., 21, 358> 770509
WIDE-BAND INFRARED PHOTOMETRY OF NOVA CYGNI 1975 - V1500 CYG.

SHENAVRIN, V. I., TARANOVA, O. G., MOROZ, V. I., GRIGOR'EV, A. V. <SOV. AST., 23, 567> 790912
OPTICAL AND INFRARED PHOTOMETRY OF R CORONAE BOREALIS AT THE 1977 MINIMUM.

SHERRINGTON, M. R., JAMESON, R. F., BAILEY, J., GILES, A. B. <M. N. R. A. S., 200, 861> 820912
INFRARED LIGHT CURVES OF THE DWARF NOVA OY CARINAE.

SHERRINGTON, M. R., LAWSON, P. A., KING, A. R., JAMESON, R. F. <M. N. R. A. S., 191, 185> 800412
INFRARED AND OPTICAL LIGHT CURVES OF EX HYDRAE AND VW HYDRI.

SHERWOOD, W. A., SCHULTZ, G. V., KREYSA, E. <NATURE, 291, 301> 810511
MILLIMETRE OBSERVATIONS OF QUASAR Q0420-388.

SHIELDS, G. A. <AP. J., 219, 565> 780113
IONIZATION STRUCTURE AND COMPOSITION OF THE PLANETARY NEBULA NGC 7027.

SHIELDS, G. A., OKE, J. B. <AP. J., 197, 5> 750402
THE EMISSION-LINE SPECTRUM OF NGC 1068.

SHIVANANDAN, K., MCNUTT, D. P., DAEHLER, M., MOORE, W. J. <NATURE, 265, 513> 770211
FAR INFRARED OBSERVATIONS OF IRC+10216.

SIBILLE, F., BERGEAT, J., LUNEL, M. <ASTR. AP., 30, 181> 740108
INFRARED OBSERVATION OF DR 21 AT 2.2 MICRONS.

SIBILLE, F., BERGEAT, J., LUNEL, M., KANDEL, R. <ASTR. AP., 40, 441> 750507
INFRARED OBSERVATIONS OF SHARPLESS 2-106, A POSSIBLE LOCATION FOR STAR FORMATION.

SIBILLE, F., CHELLI, A., LENA, P. <ASTR. AP., 79, 315> 791019
INFRARED SPECKLE INTERFEROMETRY.

SIBILLE, F., LUNEL, M., BERGEAT, J. <ASTR. AP., 47, 161> 760201
INFRARED STUDY OF SEVEN POSSIBLE COMPACT HII REGIONS.

SIMON, M., JOYCE, R. R., RIGHINI-COHEN, G., SIMON, M. N. <AP. J., 212, 84> 770210
RADIO AND INFRARED STUDIES OF THE 100 MICROMETER SOURCES HFE 2 AND FJM 3.

SIMON, M., RIGHINI-COHEN, G., JOYCE, R. R., SIMON, T. <AP. J. (LETTERS), 230, L175> 790608
A DETERMINATION OF THE REDDENING OF THE H2 EMISSION FROM THE ORION MOLECULAR CLOUD.

SIMON, M., RIGHINI, G., JOYCE, R. R., GEZARI, D. Y. <AP. J. (LETTERS), 186, L127> 731202
A STRONG 350-MICRON SOURCE IN THE OPHIUCHUS DARK CLOUD.

SIMON, M., SIMON, T., JOYCE, R. R. <AP. J., 227, 64> 790104
BRACKETT-LINE OBSERVATIONS OF M82.

SIMON, T. <A. J., 79, 1054> 741002
BROAD-BAND 20-MICRON PHOTOMETRY OF 63 STARS.

SIMON, T. <A. J., 81, 764> 760901
BROAD-BAND 20-MICRON PHOTOMETRY OF 50 STARS.

SIMON, T. <P. A. S. P., 87, 317> 750407
INFRARED LIGHT CURVES FOR V1057 CYGNI (1971-74).

SIMON, T., DYCK, H. M. <A. J., 82, 725> 770902
BROAD-BAND 20-33-MICRON PHOTOMETRY OF YOUNG STARS.

SIMON, T., DYCK, H. M. <M. N. R. A. S., 172, 19P> 750806
INFRARED PHOTOMETRY OF NGC 1068 AT 25 AND 33 MICRONS.

SIMON, T., DYCK, H. M. <NATURE, 253, 101> 750106
SILICATE ABSORPTION AT 18 MICRONS IN TWO PECULIAR INFRARED SOURCES.

SIMON, T., MORRISON, D., CRUIKSHANK, D. P. <AP. J. (LETTERS), 177, L17> 721002
20-MICRON FLUXES OF BRIGHT STELLAR STANDARDS.

SIMON, T., MORRISON, N. D., WOLFF, S. C., MORRISON, D. <ASTR. AP., 20, 99> 720806
FAR-INFRARED AND UVBY PHOTOMETRY OF V1057 CYGNI.

SIMON, T., SIMON, M., JOYCE, R. R. <AP. J., 230, 127> 790510
B-ALPHA LINE SURVEY OF COMPACT INFRARED SOURCES.

SITKO, M. L. <AP. J., 247, 1024> 810805
SPECTRAL ENERGY DISTRIBUTIONS OF HOT STARS WITH CIRCUMSTELLAR DUST.

SITKO, M. L., SAVAGE, B. D. <AP. J., 237, 82> 800406
ULTRAVIOLET, VISUAL, AND INFRARED OBSERVATIONS OF THE PECULIAR BE STAR HD 45677.

SITKO, M. L., STEIN, W. A., ZHANG, Y. -X., WISNIEWSKI, W. Z. <AP. J., 259, 486> 820806
0.35-3.5 MICRON PHOTOMETRY OF X-RAY EMITTING QSOS.

SLOVAK, M. H. <ASTR. AP., 70, L75> 781216
THE INFRARED VARIABILITY OF THE ERUPTIVE VARIABLE HM SAGITTAE.

SMITH, H. A., LARSON, H. P., FINK, U. <AP. J., 233, 132> 791010
THE SPECTRUM OF THE BECKLIN-NEUGEBAUER SOURCE IN ORION FROM 3.3 TO 5.5 MICRONS.

SMITH, H. A., LARSON, H. P., FINK, U. <AP. J., 244, 835> 810304
MOLECULAR HYDROGEN AND THE 2 MICRON SPECTRUM OF NGC 7027.

SMITH, H. A., THRONSON JR., H. A., LADA, C. J., HARPER, D. A., LOEWENSTEIN, R. F., SMITH, J. <AP. J., 258, 170> 820703
FAR-INFRARED OBSERVATIONS OF FU ORIONIS.

SMITH, H. E., SPINRAD, H. <AP. J., 236, 419> 800304
SPECTROPHOTOMETRY OF FAINT, RED 3C QSO CANDIDATES.

SMITH, H. E., SPINRAD, H., SMITH, E. O. <P. A. S. P., 88, 621> 769906
THE REVISED 3C CATALOG OF RADIO SOURCES: A REVIEW OF IDENTIFICATIONS AND SPECTROSCOPY.

SMITH, J. <AP. J., 261, 463> 821003
THE FAR-INFRARED DISK OF M51.

SMITH, J., LYNCH, D. K., CUDABACK, D. D., WERNER, M. W. <AP. J., 234, 902> 791209
SUBMILLIMETER EMISSION FROM L1641 AND THE ORION NEBULA.

SMITH, L. F. <M. N. R. A. S., 138, 109> 689903
A REVISED SPECTRAL CLASSIFICATION SYSTEM AND A NEW CATALOGUE FOR GALACTIC WOLF-RAYET STARS.

SMITH, L. F., KUHI, L. V. <AP. J., 162, 535> 701102
WOLF-RAYET STARS. IV. LINE INTENSITIES IN THE SPECTRA OF TWO WN6 STARS.

SMYTH, M. J., CORK, G. M. W., HARRIS, J., WALLACE, T. <NAT. PHYS. SCI., 231, 104> 710504
INFRARED SPECTRA OF STARS, 1-2.5 MICRONS.

SMYTH, M. J., DEAN, J. F., ROBERTSON, B. S. C. <M. N. R. A. S., 187, 29P> 790305
MULTICOLOUR PHOTOMETRY AND THE DUST SHELL OF HR 5999.

SMYTH, M. J., DOW, M. J., NAPIER, W. MCD. <M. N. R. A. S., 172, 235> 750704
INFRARED LIGHT CURVES OF ALGOL.

SMYTH, M. J., NANDY, K. <M. N. R. A. S., 183, 215> 780402
INFRARED PHOTOMETRY OF EARLY-TYPE STARS-I.

SMYTH, M. J., SIM, M. E. <NATURE, 283, 457> 800109
IR SOURCES IN THE SOUTHERN COALSACK.

SNEDEN, C., GEHRZ, R. D., HACKWELL, J. A., YORK, D. G., SNOW JR, T. P. <AP. J., 223, 168> 780704
INFRARED COLORS AND THE DIFFUSE INTERSTELLAR BANDS.

SNEDEN, C., LAMBERT, D. L., TOMKIN, J., PETERSON, R. C. <AP. J., 222, 585> 780605
LIGHT-ELEMENT ABUNDANCES IN THE WEAK G-BAND STAR HR 6766.

SNELL, R. L. <AP. J. SUPPL., 45, 121> 810109
A STUDY OF NINE INTERSTELLAR DARK CLOUDS.

SOIFER, B. T., HOUCK, J. R. <AP. J., 186, 169> 731103
ROCKET-INFRARED OBSERVATIONS OF THE GALACTIC CENTER.

SOIFER, B. T., HUDSON, H. S. <AP. J. (LETTERS), 191, L83> 740703
SUBMILLIMETER OBSERVATIONS OF THE ORION NEBULA AND NGC 2024.

SOIFER, B. T., NEUGEBAUER, G., MATTHEWS, K. <NATURE, 278, 231> 790302
INFRARED OBSERVATIONS OF THE X-RAY QUASARS 0241+622 AND MR2251-178.

SOIFER, B. T., NEUGEBAUER, G., MATTHEWS, K., BECKLIN, E. E., WYNN-WILLIAMS, C. G., CAPPS, R. <NATURE, 285, 91> 800513
IR OBSERVATIONS OF THE DOUBLE QUASAR 0957+561 A, B AND THE INTERVENING GALAXY.

SOIFER, B. T., NEUGEBAUER, G., OKE, J. B., MATTHEWS, K. <AP. J., 243, 369> 810106
INFRARED AND OPTICAL OBSERVATIONS OF THE HYDROGEN LINES IN QUASARS.

SOIFER, B. T., OKE, J. B., MATTHEWS, K., NEUGEBAUER, G. <AP. J. (LETTERS), 227, L1> 790107
THE HYDROGEN LINES IN THE HIGH-LUMINOSITY QUASAR B2 1225+31.

SOIFER, B. T., PIPHER, J. L. <AP. J., 199, 663> 750807
INFRARED PHOTOMETRIC AND SPECTROPHOTOMETRIC OBSERVATIONS OF THE GALACTIC HII REGION G29.9-0.0.

SOIFER, B. T., PIPHER, J. L., HOUCK, J. R. <AP. J., 177, 315> 721007
ROCKET INFRARED OBSERVATIONS OF HII REGIONS.

SOIFER, B. T., PUETTER, R. C., RUSSELL, R. W., WILLNER, S. P., HARVEY, P. M., GILLETT, F. C. <AP. J. (LETTERS), 232, L53> 790813
THE 4-8 MICRON SPECTRUM OF THE INFRARED SOURCE W33A.

SOIFER, B. T., RUSSELL, R. W., MERRILL, K. M. <AP. J. (LETTERS), 207, L83> 760709
2-4 MICRON SPECTROPHOTOMETRIC OBSERVATIONS OF THE GALACTIC CENTER.

SOIFER, B. T., RUSSELL, R. W., MERRILL, K. M. <AP. J., 210, 334> 761202
2-4 MICRON SPECTROPHOTOMETRIC OBSERVATIONS OF COMPACT HII REGIONS.

SOIFER, B. T., WILLNER, S. P., CAPPS, R. W., RUDY, R. J. <AP. J., 250, 631> 811108
4-8 MICRON SPECTROPHOTOMETRY OF OH 0739-14.

SOLF, J. <ASTR. AP. SUPPL., 34, 409> 781201
SPECTRAL TYPE AND LUMINOSITY CLASSIFICATION OF LATE-TYPE M STARS FROM NEAR-INFRARED IMAGE TUBE COUDE SPECTROGRAMS.

SOLINGER, A. B. <AP. J. (LETTERS), 158, L21> 691003
ON THE NUCLEAR REGION OF M82.

SOUZA, S. P., LUTZ, B. L. <AP. J. (LETTERS), 216, L49> 770808
DETECTION OF C2 IN THE INTERSTELLAR SPECTRUM OF CYGNUS OB2 NUMBER 12 (VI CYGNI NUMBER 12).

SPINRAD, H. <AP. J., 145, 195> 660701
OBSERVATIONS OF STELLAR MOLECULAR HYDROGEN.

SPINRAD, H. <AP. J., 182, 381> 730605
A NOTE ON THE STELLAR CONTENT OF NGC 5195.

SPINRAD, H., BAHCALL, J., BECKLIN, E. E., GUNN, J. E., KRISTIAN, J., NEUGEBAUER, G., SARGENT, W. L. W., SMITH, H. <AP. J., 180, 351> 730302
OPTICAL AND NEAR-INFRARED OBSERVATIONS OF THE NEARBY SPIRAL GALAXY MAFFEI 2.

SPINRAD, H., LIEBERT, J., SMITH, H. E., SCHWEIZER, F., KUHI, L. V. <AP. J., 165, 17> 710406
THE DETECTION OF THE GALACTIC NUCLEUS AT ONE MICRON.

SPINRAD, H., LUEBKE JR., W. R. <AP. J., 160, 1141> 700602
A CURVE-OF-GROWTH ANALYSIS OF THE SUPER-METAL-RICH G DWARF HR 72.

SPINRAD, H., SARGENT, W. L. W., OKE, J. B., NEUGEBAUER, G., LANDAU, R., KING, I. R., GUNN, J. E., GARMIRE, G., DIETER, N. H. <AP. J. (LETTERS), 163, L25> 710101
MAFFEI 1: A NEW MASSIVE MEMBER OF THE LOCAL GROUP?

SPINRAD, H., TAYLOR, B. J. <AP. J., 157, 1279> 690901
SCANNER ABUNDANCE STUDIES. I. AN INVESTIGATION OF SUPERMETALLICITY IN LATE-TYPE EVOLVED STARS.

SPINRAD, H., YOUNKIN, R. L. <P. A. S. P., 78, 65> 660202
INFRARED BANDS OF VANADIUM OXIDE IN THREE MIRA STARS.

SRAMEK, R. A., WEEDMAN, D. W. <AP. J., 221, 468> 789905
AN OPTICAL AND RADIO STUDY OF QUASARS.

ST. CLAIR DINGER, A., DICKINSON, D. F. <A. J., 85, 1247> 809901
A CATALOG OF NONSTELLAR WATER MASER SOURCES.

STACEY, G. J., KURTZ, N. T., SMYERS, S. D., HARWIT, M., RUSSELL, R. W., MELNICK, G. <AP. J. (LETTERS), 257, L37> 820603
THE MASS OF HOT, SHOCKED CO IN ORION: FIRST OBSERVATIONS OF THE J - 17 - J - 16 TRANSITION AT 153 MICTONS.

STAUDE, H. J., LENZEN, R., DYCK, H. M., SCHMIDT, G. D. <AP. J., 255, 95> 820401
THE BIPOLAR NEBULA S106: PHOTOMETRIC, POLARIMETRIC, AND SPECTROPOLARIMETRIC OBSERVATIONS.

STAUFFER, J. <A. J., 87, 899> 820612
THE FAINT END OF THE HYADES MAIN SEQUENCE.

STAUFFER, J. R. <A. J., 85, 1341> 801001
OBSERVATIONS OF PRE-MAIN-SEQUENCE STARS IN THE PLEIADES.

STAUFFER, J. R. <A. J., 87, 1507> 821108
OBSERVATIONS OF LOW-MASS STARS IN THE PLEIADES: HAS A PRE-MAIN SEQUENCE BEEN DETECTED?

STEBBINS, J., WHITFORD, A. E. <AP. J., 106, 235> 470901
SIX-COLOR PHOTOMETRY OF STARS. V. INFRARED RADIATION FROM THE REGION OF THE GALACTIC CENTER.

STECKER, F. W., PUGET, J. L., FAZIO, G. G. <AP. J. (LETTERS), 214, L51> 770607
THE COSMIC FAR-INFRARED BACKGROUND AT HIGH GALACTIC LATITUDES.

STEIN, W. A. <AP. J., 148, 295> 670401
INFRARED CONTINUUM FROM HII REGIONS.

STEIN, W. A. <P. A. S. P., 87, 5> 750207
RECENT REVELATIONS OF INFRARED ASTRONOMY.

STEIN, W. A., GAUSTAD, J. E., GILLETT, F. C., KNACKE, R. F. <AP. J. (LETTERS), 155, L177> 690302
THE SPECTRUM OF NML CYGNUS FROM 7.5 TO 14 MICRONS.

STEIN, W. A., GAUSTAD, J. E., GILLETT, F. C., KNACKE, R. F. <AP. J. (LETTERS), 155, L3> 690101
CIRCUMSTELLAR INFRARED EMISSION FROM TWO PECULIAR OBJECTS-R AQUARII AND R CORONAE BOREALIS.

STEIN, W. A., GILLETT, F. C. <AP. J. (LETTERS), 155, L197> 690306
SPECTRAL DISTRIBUTION OF INFRARED RADIATION FROM THE TRAPEZIUM REGION OF THE ORION NEBULA.

STEIN, W. A., GILLETT, F. C. <NAT. PHYS. SCI., 233, 16> 710903
PHOTOMETRIC MEASUREMENTS AT 11 MICRONS OF NGC 4151.

STEIN, W. A., GILLETT, F. C. <NAT. PHYS. SCI., 233, 72> 710905
SEARCH FOR INTERSTELLAR SILICATE ABSORPTION IN SPECTRUM OF VI CYG NO. 12.

STEIN, W. A., GILLETT, F. C. <NATURE, 224, 675> 691105
POSSIBLE VARIATIONS OF LAMBDA - 10 MICRONS RADIATION FROM NGC 4151.

STEIN, W. A., GILLETT, F. C., KNACKE, R. F. <NATURE, 231, 254> 710503
POSSIBLE UPPER LIMIT TO THE DISTANCE OF BL LACERTAE.

STEIN, W. A., GILLETT, F. C., MERRILL, K. M. <AP. J., 187, 213> 740104
OBSERVATIONS OF THE INFRARED RADIATION FROM THE NUCLEI OF NGC 1068 AND NGC 4151.

STEIN, W. A., WEEDMAN, D. W. <AP. J., 205, 44> 760402
THE ORIGIN OF ULTRAVIOLET AND INFRARED CONTINUUM RADIATION FROM SEYFERT GALAXIES.

STEPHENSON, C. B. <A. J., 71, 477> 669905
SEARCH FOR NEW NORTHERN WOLF-RAYET STARS.

STEPHENSON, C. B. <A. J., 80, 404> 750501
SPECTRAL TYPES FOR FOUR SUSPECTED CARBON STARS OF THE TWO-MICRON SKY SURVEY.

STEPHENSON, C. B. <PUBL. WARNER AND SWASEY OBS., 1, 4> 739907
A GENERAL CATALOGUE OF COOL CARBON STARS.

STEPHENSON, C. B. <PUBL. WARNER AND SWASEY OBS., 2, 2> 769907
A GENERAL CATALOGUE OF S STARS.

STIENON, F. M., CHARTRAN III, M. R., SHAO, C. Y. <A. J., 79, 47> 749903
THE EMISSION-LINE VARIABLE HBV 475.

STIER, M. T., JAFFE, D. T., FAZIO, G. G., ROBERGE, W. G., THUM, C., WILSON, T. L. <AP. J. SUPPL., 48, 127> 820113
A HIGH RESOLUTION FAR-INFRARED SURVEY OF A SECTION OF THE GALACTIC PLANE. II. FAR-INFRARED, CO, AND RADIO CONTINUUM RESULTS.

STOCKE, J. T., RIEKE, G. H., LEBOFSKY, M. J. <NATURE, 294, 319> 811114
NEW OBSERVATIONAL CONSTRAINTS ON THE M87 JET.

STOREY, J. W. V., WATSON, D. M., TOWNES, C. H. <AP. J. (LETTERS), 244, L27> 810212
DETECTION OF INTERSTELLAR OH IN THE FAR-INFRARED.

STOREY, J. W. V., WATSON, D. M., TOWNES, C. H. <AP. J., 233, 109> 791008
OBSERVATIONS OF FAR-INFRARED FINE STRUCTURE LINES: (O III) 88.35 MICRONS AND (O I) 63.2 MICRONS.

STOREY, J. W. V., WATSON, D. M., TOWNES, C. H., HALLER, E. E., HANSEN, W. L. <AP. J., 247, 136> 810705
FAR-INFRARED OBSERVATIONS OF SHOCKED CO IN ORION.

STRECKER, D. W. <A. J., 80, 451> 750601
VARIABILITY OF R CRB AND NML CYG AT 3.5 MICRONS.

STRECKER, D. W., ERICKSON, E. F., WITTEBORN, F. C. <A. J., 83, 26> 780104
AIRBORNE INFRARED SPECTROPHOTOMETRY OF MIRA VARIABLES.

STRECKER, D. W., ERICKSON, E. F., WITTEEBORN, F. C. <AP. J. SUPPL., 41, 501> 791109
AIRBORNE STELAR SPECTROPHOTOMETRY FROM 1.2 TO 5.5 MICRONS: ABSOLUTE CALIBRATION AND SPECTRA OF STARS EARLIER THAN M3.

STRECKER, D. W., NEY, E. P. <A. J., 79, 1410> 741201
0.9-18-MICRON PHOTOMETRY OF THE 14 CIT OBJECTS.

STRECKER, D. W., NEY, E. P. <A. J., 79, 797> 740705
INFRARED OBSERVATIONS OF ANONYMOUS IRC SOURCES.

STRECKER, D. W., NEY, E. P., MURDOCK, T. L. <AP. J. (LETTERS), 183, L13> 730701
CYGNIDS AND TAURIDS-TWO CLASSES OF INFRARED OBJECTS.

STRITTMATTER, P. A., SERKOWSKI, K., CARSWELL, R., STEIN, W. A., MERRILL, K. M., BURBIDGE, E. M. <AP. J. (LETTERS), 175, L7> 720701
COMPACT EXTRAGALACTIC NONTHERMAL SOURCES.

STROM, K. M., STROM, S. E., BREGER, M., BROOKE, A. L., YOST, J., GRASDALEN, G. L., CARRASCO, L. <AP. J. (LETTERS), 176, L93> 720904
ERRATUM TO "INFRARED AND OPTICAL OBSERVATIONS OF A YOUNG STELLAR GROUP SURROUNDING BD+40 4124".

STROM, K. M., STROM, S. E., BREGER, M., BROOKE, A. L., YOST, J., GRASDALEN, G. L., CARRASCO, L. <AP. J. (LETTERS), 173, L65> 720402
INFRARED AND OPTICAL OBSERVATIONS OF A YOUNG STELLAR GROUP SURROUNDING BD+40 4124.

STROM, K. M., STROM, S. E., CARRASCO, L., VRBA, F. J. <AP. J., 196, 489> 750301
M78: AN ACTIVE REGION OF STAR FORMATION IN THE DARK CLOUD LYNDS 1630.

STROM, K. M., STROM, S. E., GRASDALEN, G. L. <AP. J., 187, 83> 740103
AN INFRARED SOURCE ASSOCIATED WITH A HERBIG-HARO OBJECT.

STROM, K. M., STROM, S. E., KINMAN, T. D. <AP. J. (LETTERS), 191, L93> 740704
OPTICAL POLARIZATION OF SELECTED HERBIG-HARO OBJECTS.

STROM, K. M., STROM, S. E., VRBA, F. J. <A. J., 81, 308> 760501
INFRARED SURVEYS OF DARK-CLOUD COMPLEXES. I. THE LYNDS 1630 DARK CLOUD.

STROM, K. M., STROM, S. E., VRBA, F. J. <A. J., 81, 320> 760504
INFRARED SURVEYS OF DARK-CLOUD COMPLEXES. IV. THE LYNDS 1517 AND LYNDS 1551 CLOUDS.

STROM, K. M., STROM, S. E., WELLS, D. C., ROMANISHIN, W. <AP. J., 220, 62> 780211
AN OPTICAL AND INFRARED STUDY OF NGC 2768 AND NGC 3115.

STROM, S. E., GRASDALEN, G. L., STROM, K. M. <AP. J., 191, 111> 740706
INFRARED AND OPTICAL OBSERVATIONS OF HERBIG-HARO OBJECTS.

STROM, S. E., STROM, K. M., BROOKE, A. L., BREGMAN, J., YOST, J. <AP. J., 171, 267> 720101
CIRCUMSTELLAR SHELLS IN THE YOUNG CLUSTER NGC 2264. II. INFRARED AND FURTHER OPTICAL OBSERVATIONS.

STROM, S. E., STROM, K. M., CARRASCO, L. <P. A. S. P., 86, 798> 741015
A STUDY OF THE YOUNG CLUSTER IC 348.

STROM, S. E., STROM, K. M., GOAD, J. W., VRBA, F. J., RICE, W. <AP. J., 204, 684> 760304
COLOR AND METALLICITY GRADIENTS IN E AND S0 GALAXIES.

STROM, S. E., STROM, K. M., GRASDALEN, G. L., CAPPS, R. W. <AP. J. (LETTERS), 193, L7> 741005
INFRARED OBSERVATIONS OF HII REGIONS IN EXTERNAL GALAXIES.

STROM, S. E., STROM, K. M., YOST, J., CARRASCO, L., GRASDALEN, G. L. <AP. J., 176, 845> 720905
ERRATUM TO "THE NATURE OF THE HERBIG AE- AND BE-TYPE STARS ASSOCIATED WITH NEBULOSITY".

STROM, S. E., STROM, K. M., YOST, J., CARRASCO, L., GRASDALEN, G. L. <AP. J., 173, 353> 720404
THE NATURE OF THE HERBIG AE- AND BE-TYPE STARS ASSOCIATED WITH NEBULOSITY.

STROM, S. E., VRBA, F. J., STROM, K. M. <A. J., 81, 314> 760502
INFRARED SURVEYS OF DARK CLOUD COMPLEXES. II. THE NGC 1333 REGION.

STROM, S. E., VRBA, F. J., STROM, K. M. <A. J., 81, 638> 760803
INFRARED SURVEYS OF DARK CLOUD COMPLEXES. V. THE NGC 7129 REGION AND THE SERPENS DARK CLOUD.

SULENTIC, J. W., TIFFT, W. G. <UNIV. OF ARIZONA PRESS> 739906
THE REVISED NEW GENERAL CATALOG OF NONSTELLAR ASTRONOMICAL OBJECTS.

SUTTON, E. C., BECKLIN, E. E., NEUGEBAUER, G. <AP. J. (LETTERS), 190, L69> 740602
34-MICRON OBSERVATIONS OF ETA CARINAE, G333.6-0.2, AND THE GALACTIC CENTER.

SUTTON, E. C., BETZ, A. L., STOREY, J. W. V., SPEARS, D. L. <AP. J. (LETTERS), 230, L105> 790606
THE BRIGHTNESS DISTRIBUTION OF IRC+10216 AT 11 MICRONS.

SUTTON, E. C., STOREY, J. W. V., BETZ, A. L., TOWNES, C. H., SPEARS, D. L. <AP. J. (LETTERS), 217, L97> 771008
SPATIAL HETERODYNE INTERFEROMETRY OF VY CANIS MAJORIS, ALPHA ORIONIS, ALPHA SCORPII, AND R LEONIS AT 11 MICRONS.

SUTTON, E. C., STOREY, J. W. V., TOWNES, C. H., SPEARS, D. L. <AP. J. (LETTERS), 224, L123> 780907
VARIATIONS IN THE SPATIAL DISTRIBUTION OF 11 MICRON RADIATION FROM OMICRON CETI.

SUTTON, E. C., SUBRAMANIAN, S., TOWNES, C. H. <ASTR. AP., 110, 324> 820613
INTERFEROMETRIC MEASUREMENTS OF STELLAR POSITIONS IN THE INFRARED.

SWEENEY, L. H., HEINSHEIMER, T. F., YATES, F. F., MARAN, S. P., LESH, J. R., NAGY, T. A. <AEROSPACE TR-0078(3409-20)-1> 780604
INTERIM EQUATORIAL INFRARED CATALOGUE, NUMBER 1.

SWINGS, J. P. <AP. LETTERS, 15, 71> 730015
SPECTRA OF SOUTHERN STELLAR PLANETARY NEBULAE AND PECULIAR EMISSION-LINE STARS WITH INFRARED EXCESSES.

SWINGS, J. P. <ASTR. AP., 34, 333> 740812
SIMILARITIES IN THE SPECTRA OF THREE SOUTHERN PECULIAR EMISSION LINE STARS WITH INFRARED EXCESS: HD 45677, HD 87643 AND GG CARINAE (HD 94878).

SWINGS, J. P. <ASTR. AP., 98, 112> 810509
THE STRONGLY POLARIZED P CYGNI STAR WITH INFRARED EXCESS CPD-52 9243.

SWINGS, J. P., ALLEN, D. A. <AP. J. (LETTERS), 167, L41> 710702
THE INFRARED OBJECT HD 45677.

SWINGS, J. P., ALLEN, D. A. <P. A. S. P., 84, 523> 720807
PHOTOMETRY OF SYMBIOTIC AND VV CEPHEI STARS IN THE NEAR INFRARED (WITH A NOTE ON MWC 56).

SWINGS, J. P., ANDRILLAT, Y. <ASTR. AP., 74, 85> 790411
THE BUTTERFLY NEBULA M 2-9: ITS POSSIBLE RELATION TO B(E) STARS AND/OR TO PROTOPLANETARY NEBULAE.

SZKODY, P. <AP. J. (LETTERS), 192, L75> 740901
INFRARED PHOTOMETRY OF SS CYGNI AND RX ANDROMEDAE NEAR MAXIMUM.

SZKODY, P. <AP. J., 207, 824> 760807
THE MINIMUM STATE OF DWARF NOVAE.

SZKODY, P. <AP. J., 217, 140> 771006
INFRARED PHOTOMETRY OF DWARF NOVAE AND POSSIBLY RELATED OBJECTS.

SZKODY, P. <AP. J., 247, 577> 810710
IUE OBSERVATIONS OF EIGHT DWARF NOVAE: A STUDY OF THE OUTBURST CYCLE FROM 0.12 TO 3.5 MICRONS.

SZKODY, P. <P. A. S. P., 93, 456> 810801
STEPANIAN'S STAR: THE ENERGY DISTRIBUTION REVEALS A NONTYPICAL CATACLYSMIC VARIABLE.

SZKODY, P., CAPPS, R. W. <A. J., 85, 882> 800701
INFRARED OBSERVATIONS OF POLARS: AM HER, VV PUP, AND AN UMA.

SZKODY, P., DYCK, H. M., CAPPS, R. W., BECKLIN, E. E., CRUIKSHANK, D. P. <A. J., 85, 348> 800301
ERRATUM: "INFRARED PHOTOMETRY OF NOVA SERPENTIS 1978".

SZKODY, P., DYCK, H. M., CAPPS, R. W., BECKLIN, E. E., CRUIKSHANK, D. P. <A. J., 84, 1359> 790907
INFRARED PHOTOMETRY OF NOVA SERPENTIS 1978.

SZKODY, P., RAYMOND, J. C., CAPPS, R. W. <AP. J., 257, 686> 820606
THE LOW STATE OF AM HERCULIS: OBSERVATIONS FROM 0.12 TO 10 MICRONS.

TANAKA, W. <P. A. S. J., 30, 637> 780002
BALLOON-BORNE NEAR-INFRARED MULTICOLOR PHOTOMETRY OF LATE-TYPE STARS.

TANZI, E. G., CHINCARINI, G., TARENGHI, M. <P. A. S. P., 93, 68> 810202
INFRARED OBSERVATIONS OF AE AQUARII.

TANZI, E. G., MARASCHI, L., TREVES, A., TARENGHI, M. <ASTR. AP., 100, 68> 810717
INFRARED AND X-RAY OBSERVATIONS OF THE BINARY SYSTEM V861 SCO.

TANZI, E. G., TARENGHI, M. <IAUC NO. 3589> 810309
SUPERNOVA (EVANS) IN NGC 1316.

TANZI, E. G., TARENGHI, M. <IAUC NO. 3589> 810310
SUPERNOVA IN IN NGC 4536.

TANZI, E. G., TREVES, A., SALINARI, P., TARENGHI, M. <ASTR. AP., 78, 226> 790913
ON THE SYSTEM V861 SCO - OAO1653-40.

TANZI, E. G., TREVES, E. A., SALINARI, P., TARENGHI, M. <IAUC NO. 3281> 781013
V861 SCORPII.

TAPIA, M. <M. N. R. A. S., 197, 949> 811209
NEAR-INFRARED OBSERVATIONS OF TRAPEZIUM-TYPE MULTIPLE SYSTEMS. CATALOGUE OF OBSERVATIONS AND A NEW DETERMINATION OF THE REDDENING LAW.

TAPIA, M. <P. A. S. P., 94, 669> 820812
A DUST SHELL AROUND THE YELLOW SUPERGIANT COD-61 3326.

TARANOVA, O. G., YUDIN, B. F. <SOV. AST. (LETTERS), 6, 273> 800815
INFRARED VARIABILITY OF HM SAGITTAE AND V1016 CYGNI.

TARANOVA, O. G., YUDIN, B. F. <SOV. AST. (LETTERS), 8, 46> 820115
INFRARED PHOTOMETRY OF HM SAGITTAE.

TARANOVA, O. G., YUDIN, B. F. <SOV. AST., 25, 598> 810913
PHOTOMETRY OF SYMBIOTIC STARS IN THE UBVRJHKLMN SYSTEM. CI CYGNI.

TARANOVA, O. G., YUDIN, B. F. <SOV. AST., 25, 710> 811111
PHOTOMETRY OF SYMBIOTIC STARS IN THE UBVRJHKLMN SYSTEM. 2.Z ANDROMEDAE.

TARANOVA, O. G., YUDIN, B. F. <SOV. AST., 26, 57> 820117
PHOTOMETRY OF SYMBIOTIC STARS IN THE UBVRJHKLMN SYSTEM. 3.AX PER, AG DRA, BF CYG, V443 HER, AND YY HER.

TAYLOR, B. J. <A. J., 83, 1377> 781102
NEAR-INFRARED ENERGY DISTRIBUTIONS OF M31.

TAYLOR, B. J. <A. J., 84, 96> 790102
OBSERVATIONS OF SECONDARY SPECTROPHOTOMETRIC STANDARDS IN THE WAVELENGTH RANGE BETWEEN 5840 AND 10800A.

TELESCO, C. M. <AP. J. (LETTERS), 226, L125> 781210
EXTENDED 10 MICRON EMISSION FROM THE DARK LANE IN NGC 5128 (CENTAURUS A).

TELESCO, C. M., BECKLIN, E. E., WYNN-WILLIAMS, C. G. <AP. J. (LETTERS), 241, L69> 801005
EXTENDED 20 MICRON EMISSION FROM THE CENTER OF NGC 1068.

TELESCO, C. M., GATLEY, I. <AP. J. (LETTERS), 247, L11> 810706
NGC 1097: THE STRUCTURE OF THE CENTRAL 3 KILOPARSECS AT 10 MICRONS.

TELESCO, C. M., GATLEY, I., STEWART, J. M. <AP. J. (LETTERS), 263, L13> 821203
THE DISTRIBUTION OF INFRARED OBSCURATION IN NGC 7331: EVIDENCE FOR A MASSIVE MOLECULAR RING.

TELESCO, C. M., HARPER JR., D. A. <AP. J., 211, 475> 770105
FAR-INFRARED OBSERVATIONS OF NGC 7027.

TELESCO, C. M., HARPER JR., D. A., LOEWENSTEIN, R. F. <AP. J. (LETTERS), 203, L53> 760104
FAR-INFRARED PHOTOMETRY OF NGC 1068.

TELESCO, C. M., HARPER, D. A. <AP. J., 235, 392> 800108
GALAXIES AND FAR-INFRARED EMISSION.

TELESCO, C., KOEHLER, R., GATLEY, I. <IAUC NO. 3613> 810613
SUPERNOVA IN NGC 6946.

TERZAN, A. <ASTR. AP., 12, 477> 719901
FOUR NEW STAR CLUSTERS IN THE DIRECTION OF THE CENTRAL AREA OF THE GALAXY.

THACKERAY, A. D. <M. N. A. S. S. A., 28, 37> 690307
THE SPECTRUM OF ETA CARINAE IN THE 10, 000A REGION.

THACKERAY, A. D. <M. N. R. A. S., 182, 11P> 780201
INFRARED FE II LINES IN ETA CARINAE AND A POSSIBLE INTERPRETATION OF INFRARED EXCESSES.

THE, P. S., ARENS, M., VAN DER HUCHT, K. A. <AP. LETTERS, 22, 109> 820003
AN INVESTIGATION OF THE SCORPIUS OPEN CLUSTER C1715-387, CONTAINING TWO WN7, TWO OF AND ONE RED SUPERGIANT MEMBERS.

THE, P. S., BAKKER, R., TJIN A DJIE, H. R. E. <ASTR. AP., 89, 209> 800914
STUDIES OF THE CARINA NEBULA. II. THE EXTINCTION LAW IN THE DIRECTION OF 14 O-TYPE STARS.

THE, P. S., TJIN A DJIE, H. R. E., BAKKER, R., BASTIAANSEN, P. A., BURGER, M., CASSATELLA, A., FREDGA,K., GAHM,G., LISEAU, R., SMYTH, M. J., VIOTTI, R.,WAMSTEKER, W., ZEUGE, W. <ASTR. AP. SUPPL., 44, 451> 810622
THE VARIABLE SHELL STAR HR 5999: V. THE SPECTRAL ENERGY DISTRIBUTION.

THE, P. S., TJIN A DJIE, H. R. E., WAMSTEKER, W. <ASTR. AP., 84, 263> 800415
TR 27-28: A WC9-TYPE STAR WITH LARGE INFRARED EXCESS.

THOMAS, J. A., HYLAND, A. R., ROBINSON, G. <M. N. R. A. S., 165, 201> 730002
SOUTHERN INFRA-RED STANDARDS AND THE ABSOLUTE CALIBRATION OF INFRA-RED PHOTOMETRY.

THOMAS, J. A., ROBINSON, G., HYLAND, A. R. <M. N. R. A. S., 174, 711> 760307
INTERMEDIATE BANDWIDTH SPECTROMETRY IN THE 10-MICRON REGION AND ITS INTERPRETATION.

THOME, J. M. <RESULTADOS OBS. NACIONAL ARGENTINA, 16-19> 928901
CORDOBA DURCHMUSTERUNG, PARTS I-IV.

THOMPSON, R. I., BOROSON, T. A. <AP. J. (LETTERS), 216, L75> 770904
INFRARED EMISSION LINES FROM IRC +10420.

THOMPSON, R. I., ERICKSON, E. F., WITTEBORN, F. C., STRECKER, D. W. <AP. J. (LETTERS), 210, L31> 761105
COMBINED GROUND AND AIRCRAFT BASED 1-4 MICRON SPECTRA OF LKHA 101.

THOMPSON, R. I., JOHNSON, H. L. <AP. J., 193, 147> 741012
A LOWER LIMIT ON THE CARBON-12/CARBON-13 RATIO IN ALPHA HERCULIS.

THOMPSON, R. I., JOHNSON, H. L., FORBES, F. F., STEINMETZ, D. L. <P. A. S. P., 85, 643> 731008
THE INFRARED SPECTRUM OF TWO CARBON STARS FROM 4000 TO 6700 CM-1.

THOMPSON, R. I., JOHNSON, H. L., FORBES, F. F., STEINMETZ, D. L. <P. A. S. P., 84, 779> 721207
THE INFRARED SPECTRUM OF ALPHA HERCULIS FROM 5700 TO 6700 CM-1.

THOMPSON, R. I., LEBOFSKY, M. J., RIEKE, G. H. <AP. J. (LETTERS), 222, L49> 780606
THE 2-2.5 MICRON SPECTRUM OF NGC 1068: A DETECTION OF EXTRAGALACTIC MOLECULAR HYDROGEN.

THOMPSON, R. I., REED, M. A. <AP. J. (LETTERS), 205, L159> 760508
1.3 TO 2.5 MICRON SPECTRA OF MWC 349 AND LKHA 101.

THOMPSON, R. I., REED, M. A. <P. A. S. P., 87, 929> 751206
A MOTOR-MICROMETER-DRIVEN INFRARED FOURIER-TRANSFORM SPECTROMETER.

THOMPSON, R. I., RIEKE, G. H., TOKUNAGA, A. T., LEBOFSKY, M. J. <AP. J. (LETTERS), 234, L135> 791203
1.2-2.5 MICRON SPECTROSCOPY, PHOTOMETRY, AND POLARIMETRY OF SS 433.

THOMPSON, R. I., SCHNOPPER, H. W. <AP. J. (LETTERS), 160, L97> 700503
IDENTIFICATION OF INFRARED CN BANDS IN THE SPECTRA OF SEVERAL CARBON STARS.

THOMPSON, R. I., SCHNOPPER, H. W., MITCHELL, R. I., JOHNSON, H. L. <AP. J. (LETTERS), 158, L117> 691104
1-4 MICRON SPECTRA OF FOUR M STARS AND ALPHA TAURI.

THOMPSON, R. I., SCHNOPPER, H. W., MITCHELL, R. I., JOHNSON, H. L. <AP. J. (LETTERS), 158, L55> 691004
1-4 MICRON SPECTRA OF FOUR CARBON STARS AND SIRIUS.

THOMPSON, R. I., STRITTMATTER, P. A., ERICKSON, E. F., WITTEBORN, F. C., STRECKER, D. W. <AP. J., 218, 170> 771111
OBSERVATION OF PREPLANETARY DISKS AROUND MWC 349 AND LKHA 101.

THOMPSON, R. I., THRONSON JR., H. A., CAMPBELL, B. G. <AP. J., 249, 622> 811010
THE NATURE OF NGC 2024: NEAR-INFRARED SPECTROSCOPY OF IRS 1 AND IRS 2.

THOMPSON, R. I., TOKUNAGA, A. T. <AP. J., 226, 119> 781107
ANALYSIS OF OBSCURED INFRARED OBJECTS. II. ALLEN'S INFRARED SOURCE IN NGC 2264.

THOMPSON, R. I., TOKUNAGA, A. T. <AP. J., 229, 153> 790406
INFRARED SPECTROSCOPY OF LINELESS OBJECTS ASSOCIATED WITH STAR FORMATION REGIONS.

THOMPSON, R. I., TOKUNAGA, A. T. <AP. J., 231, 736> 790811
ANALYSIS OF OBSCURED INFRARED OBJECTS. IV. GL 490 AND GL 2591.

THOMPSON, R. I., TOKUNAGA, A. T. <AP. J., 235, 889> 800206
ANALYSIS OF OBSCURED INFRARED OBJECTS. VI. H AND HE LINES IN W51 AND K3-50.

THRONSON JR., H. A. <A. J., 87, 1207> 820814
NEAR-INFRARED SPECTROSCOPY OF POSSIBLE PRECURSORS TO PLANETARY NEBULAE: THE CYGNUS EGG AND THE RED RECTANGLE.

THRONSON JR., H. A. <AP. J., 248, 984> 810907
NEAR-INFRARED SPECTROSCOPY OF POSSIBLE PRECURSORS TO PLANETARY NEBULAE: AFGL 618.

THRONSON JR., H. A., CAMPBELL, M. F., HOFFMANN, W. F. <AP. J., 239, 533> 800708
THE LARGE-SCALE FAR-INFRARED STRUCTURE OF W3 AND W4.

THRONSON JR., H. A., GATLEY, I., HARVEY, P. M., SELLGREN, K.,WERNER, M. W. <AP. J., 237, 66> 800405
MONOCEROS R2: FAR-INFRARED OBSERVATIONS OF A VERY YOUNG CLUSTER.

THRONSON JR., H. A., HARPER JR., D. A. <AP. J., 230, 133> 790511
COMPACT HII REGIONS IN THE FAR-INFRARED.

THRONSON JR., H. A., HARPER JR., D. A., KEENE, J., LOEWENSTEIN, R. F., MOSELEY, S. H., TELESCO, C. M. <A. J., 83, 492> 780502
OBSERVATIONS OF FIVE MODERATE-LUMINOSITY FAR-INFRARED SOURCES IN ORION AND MONOCEROS.

THRONSON JR., H. A., HARVEY, P. M. <AP. J., 248, 584> 810902
NEAR-INFRARED SPECTROSCOPY OF POSSIBLE PRECURSORS TO PLANETARY NEBULAE: HM SAGITTAE.

THRONSON JR., H. A., HARVEY, P. M., GATLEY, I. <AP. J. (LETTERS), 229, L133> 790501
STAR FORMATION AT A FRONT: FAR-INFRARED OBSERVATIONS OF AFGL 333.

THRONSON JR., H. A., LADA, C. J., HARVEY, P. M., WERNER, M. W. <M. N. R. A. S., 201, 429> 821012
THE BUBBLE NEBULA: FAR-INFRARED AND RADIO MOLECULAR OBSERVATIONS OF NGC 7635.

THRONSON JR., H. A., LOEWENSTEIN, R. F., STOKES, G. M. <A. J., 84, 1328> 790905
FAR-INFRARED OBSERVATIONS OF THE LAGOON NEBULA (M8).

THRONSON JR., H. A., PRICE, S. D. <A. J., 87, 1288> 820907
INFRARED MAPPING OF THE GALACTIC PLANE. III. THE LARGE-SCALE MID-INFRARED STRUCTURE OF W3, W4, AND W5.

THRONSON JR., H. A., THOMPSON, R. I. <AP. J., 254, 543> 820303
NEAR-INFRARED SPECTROSCOPY OF MODERATE LUMINOSITY SOURCES: OMC-2 IRS3 AND IRS4.

THRONSON JR., H. A., THOMPSON, R. I., HARVEY, P. M., RICKARD, L. J., TOKUNAGA, A. T. <AP. J., 242, 609> 801205
STAR FORMATION IN IC 1848A.

THUAN, T. X., OKE, J. B. <AP. J., 205, 360> 760407
COLOR GRADIENTS IN THE NUCLEAR REGION OF M31.

THUAN, T. X., OKE, J. B., GUNN, J. E. <AP. J., 201, 45> 751005
FURTHER OBSERVATIONS OF BL LACERTAE.

THUM, C., LEMKE, D. <ASTR. AP., 41, 467> 750708
INFRARED MEASUREMENTS ON SEVERAL SOURCES IN THE DR-21 REGION.

THUM, C., LEMKE, D. <ASTR. AP., 45, 83> 751208
NEAR INFRARED SOURCES IN SGR B2.

TIFFT, W. G. <M. N. R. A. S., 125, 199> 639904
MAGELLANIC CLOUD INVESTIGATIONS. I. THE REGION OF NGC 121.

TOKUNAGA, A. T., ERICKSON, E. F., CAROFF, L. J., DANA, R. A. <AP. J. (LETTERS), 224, L19> 780810
THE FAR-INFRARED SPECTRUM OF S140 IR.

TOKUNAGA, A. T., LEBOFSKY, M. J., RIEKE, G. H. <ASTR. AP., 99, 108> 810617
INFRARED REFLECTION NEBULAE IN S106 AND NGC 7538E.

TOKUNAGA, A. T., THOMPSON, R. I. <AP. J., 229, 583> 790408
ANALYSIS OF OBSCURED INFRARED OBJECTS. III. THE INFRARED POINT SOURCE IN M17 SW.

TOKUNAGA, A. T., THOMPSON, R. I. <AP. J., 233, 127> 791009
ANALYSIS OF OBSCURED INFRARED POINT SOURCES. V. S106 IR AND S235 B.

TOKUNAGA, A. T., YOUNG, E. T. <AP. J. (LETTERS), 237, L93> 800501
HIGH-RESOLUTION SPECTRA OF THE 3.3 MICROMETER UNIDENTIFIED EMISSION FEATURE IN NGC 7027 AND HD 44179.

TOOMBS, R. I., BECKLIN, E. E., FROGEL, J. A., LAW, S. K., PORTER, F. C., WESTPHAL, J. A. <AP. J. (LETTERS), 173, L71> 720403
INFRARED DIAMETER OF IRC+10216 DETERMINED FROM LUNAR OCCULTATIONS.

TOVMASSIAN, H. M., MELIK-ALAVERDIAN, YU. K., AVETISIAN, V. S. <ASTROFIZIKA, 16, 791> 801110
ON THE VARIATION IR-EMISSION OF V915 AQL.

TRAUB, W. A., CARLETON, N. P., BLACK, J. H. <AP. J., 223, 140> 780703
A SEARCH FOR EMISSION FROM VIBRATIONALLY EXCITED H2.

TREFFERS, R. R. <AP. J. (LETTERS), 233, L17> 791006
DETECTION OF MOLECULAR HYDROGEN IN THE SUPERNOVA REMNANT IC 443.

TREFFERS, R. R. <ASTR. AP., 38, 345> 750210
A FOURIER TRANSFORM SPECTROMETER FOR OBSERVATIONS OF STARS IN THE INTERMEDIATE INFRARED.

TREFFERS, R. R., COHEN, M. <AP. J., 188, 545> 740303
HIGH-RESOLUTION SPECTRA OF COOL STARS IN THE 10- AND 20-MICRON REGIONS.

TREFFERS, R. R., FINK, U., LARSON, H. P., GAUTIER III, T. N. <AP. J. (LETTERS), 209, L115> 761103
THE 1.4-2.7 MICRON SPECTRUM OF THE POINT SOURCE AT THE GALACTIC CENTER.

TREFFERS, R. R., FINK, U., LARSON, H. P., GAUTIER III, T. N. <AP. J., 209, 793> 761102
THE SPECTRUM OF THE PLANETARY NEBULA NGC 7027 FROM 0.9 TO 2.7 MICRONS.

TREFFERS, R. R., WOOLF, N. J., FINK, U., LARSON, H. P. <AP. J., 207, 680> 760708
THE INFRARED EMISSION OF UPSILON SAGITTARII, 89 HERCULIS, AND R CORONAE BOREALIS.

TREVES, A., CHIAPPETTI, L., TANZI, E. G., TARENGHI, M., GURSKY, H., DUPREE, A. K., HARTMANN, L. W., RAYMOND, J., DAVIS, R. J., BLACK, J., MATILSKY, T.A., VANDEN BOUT, P.,SANNER, F., POLLARD, G., SANFORD, P. W., JOSEPH, R. D., MEIKLE, W. P. S. <AP. J., 242, 1114> 801209
ULTRAVIOLET, X-RAY, AND INFRARED OBSERVATIONS OF HDE 226868 - CYGNUS X-1.

TSUJI, T. <ASTR. AP., 68, L23> 780812
POSSIBLE IDENTIFICATION OF H2O THERMAL EMISSION IN THE INFRARED SPECTRA OF LATE-TYPE STARS.

TULLY, R. B., BOESGAARD, A. M., DYCK, H. M., SCHEMPP, W. V. <AP. J., 246, 38> 810504
STAR FORMATION AND ABUNDANCES IN THE NEARBY IRREGULAR GALAXY VII ZW 403.

TURNROSE, B. E. <AP. J., 210, 33> 761107
THE STELLAR CONTENT OF THE NUCLEAR REGIONS OF SC GALAXIES.

ULRICH, B. T., NEUGEBAUER, G., MCCAMMON, D., LEIGHTON, R. B., HUGHES, E. E., BECKLIN, E. E. <AP. J., 147, 858> 670204
ERRATUM TO "FURTHER OBSERVATIONS OF EXTREMELY COOL STARS".

ULRICH, B. T., NEUGEBAUER, G., MCCAMMON, D., LEIGHTON, R. B., HUGHES, E. E., BECKLIN, E. E. <AP. J., 146, 288> 661001
FURTHER OBSERVATIONS OF EXTREMELY COOL STARS.

ULRICH, M. -H., KINMAN, T. D., LYNDS, C. R., RIEKE, G. H., EKERS, R. D. <AP. J., 198, 261> 750606
NONTHERMAL CONTINUUM RADIATION IN THREE ELLIPTICAL GALAXIES.

ULRICH, R. K., WOOD, B. C. <AP. J., 244, 147> 810210
OBSERVATIONS AND ANALYSIS OF THE HELIUM I RECOMBINATION LINES 5876 AND 10830 IN EIGHT T TAURI STARS.

ULVESTAD, J. S. <NASA X-693-77-165> 770601
IRC+10216: AN EVOLVING INFRARED SOURCE.

ULVESTAD, J. S. <NASA X-693-77-186> 770701
CIT 6: A STRONG INFRARED SOURCE.

UPGREN JR., A. R. <A. J., 67, 37> 629901
THE SPACE DISTRIBUTION OF LATE-TYPE STARS IN A NORTH GALACTIC POLE REGION.

VAN ALTENA, W. F. <A. J., 74, 2> 699902
LOW-LUMINOSITY MEMBERS OF THE HYADES CLUSTER. II.

VAN BREDA, I. G., GLASS, I. S., WHITTET, D. C. B. <M. N. R. A. S., 168, 551> 740909
THE EXTINCTION CURVES OF HD 92964 AND HD 147889.

VAN BUEREN, H. G. <B. A. N., 11, 385> 529902
ON THE STRUCTURE OF THE HYADES CLUSTER.

VAN DEN BERGH, S. <A. J., 71, 990> 669901
A STUDY OF REFLECTION NEBULAE.

VAN DEN BERGH, S., HERBST, W. <A. J., 80, 208> 759902
CATALOGUE OF SOUTHERN STARS EMBEDDED IN NEBULOSITY.

VANGENDEREN, A. M., GLASS, I. S., FEAST, M. W. <M. N. R. A. S., 167, 283> 740507
THE LONG PERIOD, HIGH LATITUDE, ECLIPSING SYSTEMS V748 CEN (-CEN X-4?) AND BL TEL.

VAUGHAN JR., A. H. <AP. J., 154, 87> 681002
THE HE I 10830A LINE IN PLANETARY NEBULAE AND THE ORION NEBULA.

VAUGHAN JR., A. H., ZIRIN, H. <AP. J., 152, 123> 680402
THE HELIUM LINE 10830A IN LATE-TYPE STARS.

VEEDER, G. J. <A. J., 79, 1056> 741004
LUMINOSITIES AND TEMPERATURES OF M DWARF STARS FROM INFRARED PHOTOMETRY.

VEEDER, G. J. <A. J., 79, 702> 740601
OLD DISK FLARE STARS.

VEEDER, G. J., MATSON, D. L., SMITH, J. C. <A. J., 83, 651> 780603
VISUAL AND INFRARED PHOTOMETRY OF ASTEROIDS.

VELGHE, A. G. <AP. J., 126, 302> 579902
H-ALPHA EMISSION STARS AND PLANETARY NEBULAE IN THE VICINITY OF M8 AND M20 AND IN VELA FROM L-230 TO L-241 ALONG THE GALACTIC EQUATOR.

VIALLEFOND, F., LENA, P., DE MUIZON, M., NICOLLIER, C., ROUAN, D., WIJNBERGEN, J. J. <ASTR. AP., 83, 22> 800305
FAR INFRARED EMISSION FROM THE GALACTIC PLANE. I. OBSERVATIONS AT THE GALACTIC LONGITUDE LII - 27.5 DEGREES.

VIOTTI, R., FERRARI-TONIOLO, M., MARCOCCI, M., NATALI, G., PERSI, P., SPADA, G., SARACENO, P. <ASTR. AP., 62, 287> 780116
OPTICAL AND INFRARED OBSERVATIONS OF BETA LYRAE.

VISVANATHAN, N. <AP. J. (LETTERS), 155, L133> 690301
THE CONTINUUM OF BL LAC.

VISVANATHAN, N., OKE, J. B. <AP. J. (LETTERS), 152, L165> 680602
NON-THERMAL COMPONENT IN THE CONTINUUM OF NGC 1068.

VITRICHENKO, E. A., VOLKOV, I. V., SHANIN, G. I., SHEVCHENKO, V. S., SHCHERBAKOV, A. G. <SOV. AST., 18, 513> 750105
INFRARED SPECTROSCOPY WITH A CONTACT IMAGE CONVERTER. 1.EXPERIMENTAL PROCEDURE.

VOELKER, K. <ASTR. AP. SUPPL., 22, 1> 751004
INFRARED OBSERVATIONS OF THE ASSOCIATION CYG OB 2.

VOGT, N., WAMSTEKER, W., BREYSACHER, J., SCHUSTER, H. -E. <ASTR. AP., 96, 120> 810312
DISCOVERY OF A STELLAR OBJECT WITH SURROUNDING NEBULOSITY.

VOGT, S. S. <A. J., 78, 389> 730601
LOW-DISPERSION SPECTROSCOPIC CLASSIFICATION OF THE UNIDENTIFIED SOURCES IN THE TWO-MICRON SKY SURVEY.

VOLOSHINA, I. B., GLUSHNEVA, I. N., SHENAVRIN, V. I. <SOV. AST., 24, 576> 800915
ENERGY DISTRIBUTIONS IN THE NEAR-IR REGION IN THE SPECTRA OF STARS USED AS SPECTROPHOTOMETRIC STANDARDS.

VRBA, F. J., COYNE, G. V., TAPIA, S. <AP. J., 243, 489> 810107
OBSERVATIONS OF GRAIN AND MAGNETIC FIELD PROPERTIES OF THE R CORONAE AUSTRALIS DARK CLOUD.

VRBA, F. J., RYDGREN, A. E. <IAUC NO. 3604> 810506
NOVA CORONAE AUSTRINAE 1981.

VRBA, F. J., SCHMIDT, G. D., BURKE JR., E. W. <AP. J., 211, 480> 770106
THE INFRARED DEVELOPMENT OF NOVA AQUILAE 1975.

VRBA, F. J., STROM, K. M., STROM, S. E., GRASDALEN, G. L. <AP. J., 197, 77> 750401
FURTHER STUDY OF THE STELLAR CLUSTER EMBEDDED IN THE OPHIUCHUS DARK CLOUD COMPLEX.

VRBA, F. J., STROM, S. E., STROM, K. M. <A. J., 81, 317> 760503
INFRARED SURVEYS OF DARK-CLOUD COMPLEXES. III. THE R CORONA AUSTRINA DARK CLOUD.

VRBA, F. J., STROM, S. E., STROM, K. M. <A. J., 81, 958> 761101
MAGNETIC FIELD STRUCTURE IN THE VICINITY OF FIVE DARK CLOUD COMPLEXES.

VREUX, J. M., ANDRILLAT, Y. <ASTR. AP., 75, 93> 790515
O STARS HE II AND H LINES IN THE 1 MICRON REGION.

VREUX, J. M., DENNEFELD, M., ANDRILLAT, Y. <ASTR. AP., 113, L10> 820910
R136: WN OR O SPECTRAL CHARACTERISTICS?

WACKERLING, L. R. <MEM. R. A. S., 73, 153> 709901
A CATALOGUE OF EARLY-TYPE STARS WHOSE SPECTRA HAVE SHOWN EMISSION LINES.

WADE, R. A., SZKODY, P., CORDOVA, F. <IAUC NO. 3279> 789902
H 2155-304.

WALKER, A. R. <M. N. R. A. S., 190, 543> 800212
INFRARED PHOTOMETRY OF GALACTIC CARBON STARS.

WALKER, A. R., WILD, P. A. T., BYRNE, P. B. <M. N. R. A. S., 189, 455> 791101
THE ANGULAR DIAMETER OF THE CARBON STAR AQ SAGITTARII.

WALKER, M. F. <AP. J. SUPPL., 2, 365> 569901
STUDIES OF EXTREMELY YOUNG CLUSTERS. I. NGC 2264.

WALKER, M. F. <AP. J., 167, 1> 719906
ELECTRONOGRAPHIC PHOTOMETRY OF STAR CLUSTERS IN THE MAGELLANIC CLOUDS. II. THE COLOR-MAGNITUDE DIAGRAM OF NGC 2209.

WALKER, M. F. <M. N. R. A. S., 159, 379> 729907
ELECTRONOGRAPHIC PHOTOMETRY OF STAR CLUSTERS IN THE MAGELLANIC CLOUDS. IV. THE COLOUR-MAGNITUDE DIAGRAM OF NGC 419.

WALLERSTEIN, G. <AP. J., 166, 725> 710601
ON THE INFRARED EXCESS OF W CEPHEI AND SIMILAR STARS.

WALSH, J. R., WHITE, N. J. <M. N. R. A. S., 199, 9P> 820421
A CLUSTER OF NEAR-INFRARED SOURCES IN THE NEUTRAL INTRUSIONS WITHIN M16 (NGC 6611).

WALSH, J. R., WHITE, N. J. <OBSERVATORY, 102, 78> 820622
2.2-MICRON MAPPING OF THE NUCLEAR REGION OF NGC 5128 (CENTAURUS A).

WAMPLER, E. J. <AP. J., 164, 1> 710201
PHOTOELECTRIC SPECTROPHOTOMETRY OF SEYFERT GALAXIES.

WAMSTEKER, W. <ASTR. AP., 76, 226> 790705
THE CONTINUOUS ENERGY DISTRIBUTION OF NOVA CYGNI 1975.

WAMSTEKER, W. <ASTR. AP., 97, 329> 810419
STANDARD STARS AND CALIBRATION FOR JHKLM PHOTOMETRY.

WAMSTEKER, W. <IAUC NO. 2954> 760513
POSSIBLE INFRARED COUNTERPART OF MXB1730-335.

WARD, D. B. <AP. J. (LETTERS), 200, L41> 750804
FAR-INFRARED SPECTROSCOPY OF THE ORION NEBULA.

WARD, D. B., DENNISON, B., GULL, G. E., HARWIT, M. <AP. J. (LETTERS), 202, L31> 751101
DETECTION OF THE (0 III) 88.16 MICRON LINE IN M17.

WARD, D. B., DENNISON, B., GULL, G. E., HARWIT, M. <AP. J. (LETTERS), 205, L75> 760409
FAR-INFRARED SPECTRAL OBSERVATIONS OF M42 AND M17.

WARD, D. B., GULL, G. E., HARWIT, M. <AP. J. (LETTERS), 214, L63> 770604
FAR-INFRARED SPECTROMETRY OF HII REGIONS AND THE GALACTIC CENTER.

WARD, D. B., HARWIT, M. <NATURE, 252, 27> 741113
OBSERVATIONS OF THE ORION NEBULA AT 100 MICRONS.

WARD, M., ALLEN, D. A., WILSON, A. S., SMITH, M. G., WRIGHT, A. E. <M. N. R. A. S., 199, 953> 820617
THE NEAR INFRARED PROPERTIES OF SEYFERT AND RELATED ACTIVE GALAXIES.

WARNER, J. W., BLACK, J. H. <A. J., 83, 586> 780601
A 5 GHZ SURVEY OF INFRARED SOURCES.

WARNER, J. W., HUBBARD, R. P., GALLAGHER, J. S. <A. J., 83, 1614> 781203
PHOTOMETRIC AND SPECTRAL PROPERTIES OF SOME T TAURI STARS.

WARNER, J. W., STROM, S. E., STROM, K. M. <AP. J., 213, 427> 770408
CIRCUMSTELLAR SHELLS IN NGC 2264: A REEVALUATION.

WARNER, J. W., WING, R. F. <AP. J., 218, 105> 771107
SUPERGIANTS IN THE FIELD OF THE CLUSTER M6, AND THE DISTRIBUTION OF INTERSTELLAR MATTER IN THE DIRECTION OF THE GALACTIC CENTER.

WARREN JR., W. H., HESSER, J. E. <AP. J. SUPPL., 34, 115> 779904
A PHOTOMETRIC STUDY OF THE ORION OB1 ASSOCIATION. I. OBSERVATIONAL DATA.

WATSON, D. M., STOREY, J. W. V., TOWNES, C. H., HALLER, E. E. <AP. J., 250, 605> 811107
FAR-INFRARED (O III) AND (N III) LINE EMISSION FROM GALACTIC H II REGIONS AND PLANETARY NEBULAE.

WATSON, D. M., STOREY, J. W. V., TOWNES, C. H., HALLER, E. E. <AP. J. (LETTERS), 241, L43> 801004
FAR-INFRARED (O III) LINE EMISSION FROM THE GALACTIC CENTER.

WATSON, D. M., STOREY, J. W. V., TOWNES, C. H., HALLER, E. E., HANSEN, W. L. <AP. J. (LETTERS), 239, L129> 800804
DETECTION OF CO J-21-20(124.2 MICRONS) AND J-22-21(118.6 MICRONS) EMISSION FROM THE ORION NEBULA.

WEBSTER, B. L., GLASS, I. S. <M. N. R. A. S., 166, 491> 740209
THE COOLEST WOLF-RAYET STARS.

WEGNER, G. <M. N. R. A. S., 177, 3> 761007
ON ELEMENT ABUNDANCES IN STARS BELONGING TO THE GAM PUPPIS GROUP.

WEGNER, G. <M. N. R. A. S., 177, 99> 761009
ON THE REDDENING AND THE EFFECTIVE TEMPERATURE OF HD 101065.

WEGNER, G., GLASS, I. S. <M. N. R. A. S., 188, 327> 790801
A NEW BIPOLAR NEBULA IN CENTAURUS.

WEISTROP, D., SHAFFER, B. D., MUSHOTZKY, R. F., REITSEMA, H. J., SMITH, B. A. <AP. J., 249, 3> 811004
CCD PHOTOMETRY OF THE BL LACERTAE OBJECTS 1218+304, 1219+28, AND 1727+50: POINT SOURCES, ASSOCIATED NEBULOSITY, AND BROAD-BAND SPECTRA.

WEISTROP, D., SMITH, B. A., REITSEMA, H. J. <AP. J., 233, 504> 791013
FAR-RED SURFACE PHOTOMETRY OF THE X-RAY EMITTING BL LACERTAE OBJECT PKS 0548-322.

WELIN, G. <ASTR. AP. SUPPL., 9, 183> 739905
H-ALPHA EMISSION STARS IN AND NEAR NGC 7000.

WERNER, M. W., BECKLIN, E. E., GATLEY, I., ELLIS, M. J., HYLAND, A. R., ROBINSON, G., THOMAS, J. A. <M. N. R. A. S., 184, 365> 780801
FAR-INFRARED OBSERVATIONS OF LARGE MAGELLANIC CLOUD HII REGIONS.

WERNER, M. W., BECKLIN, E. E., GATLEY, I., MATTHEWS, K., NEUGEBAUER, G., WYNN-WILLIAMS, C. G. <M. N. R. A. S., 188, 463> 790803
AN INFRARED STUDY OF THE NGC 7538 REGION.

WERNER, M. W., BECKLIN, E. E., GATLEY, I., NEUGEBAUER, G., SELLGREN, K., THRONSON JR., H. A., HARPER, D. A., LOEWENSTEIN, R., MOSELEY, S. H. <AP. J., 242, 601> 801204
HIGH ANGULAR RESOLUTION FAR-INFRARED OBSERVATIONS OF THE W3 REGION.

WERNER, M. W., BECKWITH, S., GATLEY, I., SELLGREN, K., BERRIMAN, G., WHITING, D. L. <AP. J., 239, 540> 800709
SIMULTANEOUS FAR-INFRARED, NEAR-INFRARED, AND RADIO OBSERVATIONS OF OH/IR STARS.

WERNER, M. W., ELIAS, J. H., GEZARI, D. Y., WESTBROOK, W. E. <AP. J. (LETTERS), 192, L31> 740804
1-MILLIMETER CONTINUUM RADIATION FROM ORION MOLECULAR CLOUD 2.

WERNER, M. W., GATLEY, I., HARPER JR., D. A., BECKLIN, E. E.,LOEWENSTEIN, R. F., TELESCO, C. M., THRONSON JR., H. A. <AP. J., 204, 420> 760303
ONE ARC-MINUTE RESOLUTION MAPS OF THE ORION NEBULA AT 20, 50, AND 100 MICRONS.

WERNER, M. W., HARWIT, M. <AP. J., 154, 881> 681201
OBSERVATIONAL EVIDENCE FOR THE EXISTENCE OF DENSE CLOUDS OF INTERSTELLAR MOLECULAR HYDROGEN.

WESTBROOK, W. E., BECKLIN, E. E., MERRILL, K. M., NEUGEBAUER, G., SCHMIDT, M., WILLNER, S. P., WYNN-WILLIAMS, C. G. <AP. J., 202, 407> 751203
OBSERVATIONS OF AN ISOLATED COMPACT INFRARED SOURCE IN PERSEUS.

WESTBROOK, W. E., WERNER, M. W., ELIAS, J. H., GEZARI, D. Y.,HAUSER, M. G., LO, K. Y., NEUGEBAUER, G. <AP. J., 209, 94> 761003
ONE-MILLIMETER CONTINUUM EMISSION STUDIES OF FOUR MOLECULAR CLOUDS.

WESTERHOUT, G. <B. A. N., 14, 215> 589903
A SURVEY OF THE CONTINUOUS RADIATION FROM THE GALACTIC SYSTEM AT A FREQUENCY OF 1390 MC/S.

WESTERLUND, B. E. <AP. J. (LETTERS), 154, L67> 681102
ON THE EXTENDED INFRARED SOURCE IN ARA.

WESTERLUND, B. E., OLANDER, N., RICHER, H. B., CRABTREE, D. R. <ASTR. AP. SUPPL., 31, 61> 789909
A CATALOGUE OF CARBON STARS IN THE LARGE MAGELLANIC CLOUD.

WESTPHAL, J. A., NEUGEBAUER, G. <AP. J. (LETTERS), 156, L45> 690404
INFRARED OBSERVATIONS OF ETA CARINAE TO 20 MICRONS.

WHITCOMB, S. E., GATLEY, I., HILDEBRAND, R. H., KEENE, J., SELLGREN, K., WERNER, M. W. <AP. J., 246, 416> 810605
FAR-INFRARED PROPERTIES OF DUST IN THE REFLECTION NEBULA NGC 7023.

WHITE, G. J., PHILLIPS, J. P., WILLIAMS, P. M., WATT, G. D., RICHARDSON, K. J. <ASTR. AP., 116, 293> 821217
NEAR INFRARED SPECTROSCOPY OF W51 IRS-2.

WHITE, N. M. <AP. J., 242, 646> 801206
THE OCCULTATION OF 119 TAU AND THE EFFECTIVE TEMPERATURES OF THREE M SUPERGIANTS.

WHITE, N. M., WING, R. F. <AP. J., 222, 209> 780509
PHOTOELECTRIC TWO-DIMENSIONAL SPECTRAL CLASSIFICATION OF M SUPERGIANTS.

WHITELOCK, P. <IAUC NO. 3687> 820411
SY MUSCAE.

WHITEOAK, J. B. <AP. J., 144, 305> 660401
THE WAVELENGTH DEPENDENCE OF INTERSTELLAR EXTINCTION.

WHITEOAK, J. B. <AP. J., 150, 521> 671102
ENERGY DISTRIBUTIONS OF G AND K DWARFS AT RED WAVELENGTHS.

WHITTET, D. C. B., BLADES, J. C. <M. N. R. A. S., 191, 309> 800414
GRAIN GROWTH IN INTERSTELLAR CLOUDS.

WHITTET, D. C. B., BODE, M. F., KILKENNY, D. <IAUC NO. 3689> 820412
NOVA AQUILAE 1982.

WHITTET, D. C. B., VAN BREDA, I. G. <ASTR. AP., 66, 57> 780514
THE CORRELATION OF THE INTERSTELLAR EXTINCTION LAW WITH THE WAVELENGTH OF MAXIMUM POLARIZATION.

WHITTET, D. C. B., VAN BREDA, I. G. <M. N. R. A. S., 192, 467> 800809
INFRARED PHOTOMETRY OF SOUTHERN EARLY-TYPE STARS.

WHITTET, D. C. B., VAN BREDA, I. G., GLASS, I. S. <M. N. R. A. S., 177, 625> 761211
INFRARED PHOTOMETRY, EXTINCTION CURVES AND R VALUES FOR STARS IN THE SOUTHERN MILKY WAY.

WICKRAMASINGHE, D. T., ALLEN, D. A. <NATURE, 287, 518> 801013
THE 3.4 MICRON INTERSTELLAR ABSORPTION FEATURE.

WICKRAMASINGHE, D. T., ALLEN, D. A., BESSELL, M. S. <M. N. R. A. S., 198, 473> 820215
INFRARED PHOTOMETRY OF COOL WHITE DWARFS.

WILDEY, R. L. <ZEIT. FUR AP., 64, 32> 660501
TEN MICRON STELLAR FLUX MEASUREMENTS-SYNOPSIS AND DIAGNOSIS.

WILDEY, R. L., MURRAY, B. C. <AP. J., 139, 435> 640201
10-MICRON PHOTOMETRY OF 25 STARS FROM B8 TO M7.

WILKING, B. A., LEBOFSKY, M. J., MARTIN, P. G., RIEKE, G. H.,KEMP, J. C. <AP. J., 235, 905> 800204
THE WAVELENGTH DEPENDENCE OF INTERSTELLAR LINEAR POLARIZATION.

WILKING, B. A., LEBOFSKY, M. J., RIEKE, G. H. <A. J., 87, 695> 820416
THE WAVELENGTH DEPENDENCE OF INTERSTELLAR LINEAR POLARIZATION: STARS WITH EXTREME VALUES OF LAMBDA MAX.

WILKING, B. A., LEBOFSKY, M. J., RIEKE, G. H., KEMP, J. C. <A. J., 34, 199> 790202
INFRARED POLARIMETRY IN THE RHO OPHIUCHUS DARK CLOUD.

WILLEMS, F., DE JONG, T. <ASTR. AP., 115, 213> 821111
INFRARED OBSERVATIONS OF OH/IR STARS.

WILLIAMS, P. M. <M. N. R. A. S., 199, 93> 820419
THE STRONG 3.3 MICRON EMISSION LINE IN WOLF-RAYET STARS.

WILLIAMS, P. M., ADAMS, D. J., ARAKAKI, S., BEATTIE, D. H., BORN, J., LEE, T. J., ROBERTSON, D. J., STEWART, J. M. <M. N. R. A. S., 192, 25P> 800811
NEAR INFRARED SPECTROMETRY OF WC STARS.

WILLIAMS, P. M., ALLEN, D. A. <OBSERVATORY, 100, 202> 801215
INFRARED OBSERVATIONS OF THE WC5 WOLF-RAYET STAR HD 115473.

WILLIAMS, P. M., ANTONOPOULOU, E. <M. N. R. A. S., 187, 183> 790403
COOLING OF THE NEWLY CONDENSED SHELL AROUND HD 193793.

WILLIAMS, P. M., ANTONOPOULOU, E. <M. N. R. A. S., 196, 915> 810910
INFRARED PHOTOMETRY OF SOUTHERN WOLF-RAYET STARS.

WILLIAMS, P. M., BEATTIE, D. H., LEE, T. J., STEWART, J. M., ANTONOPOULOU, E. <M. N. R. A. S., 185, 467> 781108
CONDENSATION OF A SHELL AROUND HD 193793.

WILLIAMS, P. M., BEATTIE, D. H., STEWART, J. M. <M. N. R. A. S., 178, 619> 770301
INFRARED PHOTOMETRY OF R ASSOCIATIONS - I. EARLY-TYPE STARS IN CMA R1 AND VEL R2.

WILLIAMS, P. M., BEATTIE, D. H., STEWART, J. M. <OBSERVATORY, 96, 184> 761006
OBSERVATIONS OF SOUTHERN STARS WITH A NEW INFRARED PHOTOMETER.

WILLIAMS, P. M., BEATTIE, D. H., STEWART, J. M. <OBSERVATORY, 97, 76> 770412
INFRARED PHOTOMETRY OF CV SERPENTIS WITH A NOTE ON CRL 2120.

WILLIAMS, P. M., LONGMORE, A. J. <IAUC NO. 3676> 820306
NOVA AQUILAE 1982.

WILLIAMS, P. M., STEWART, M. J., BEATTIE, D. H., LEE, T. J. <IAUC NO. 3107> 770910
HD 193793.

WILLIAMS, P. M., ZEALEY, W. J., SALINARI, P., MOORWOOD, A. F. M. <IAUC NO. 3587> 810308
SUPERNOVA IN NGC 4536.

WILLIAMS, T. B., MORTON, D. C., GREEN, R. F. <A. J., 86, 178> 810203
A SPECTROPHOTOMETRIC SEARCH FOR THE HALO OF MARKARIAN 10.

WILLIS, A. J., WILSON, R., VANDEN BOUT, P., SANNER, F., BLACK, J., DAVIS, R. J., DUPREE, A. K., GURSKY, H., HARTMANN, L., RAYMOND, J., MATILSKY, T., BURGER, M., DE LOORE, C., VAN DESSEL, E. L., WHITELOCK, P., MENZIES, J., MEIKLE, W. P. S., JOSEPH, R.D., SANFORD, P.,POLLARD, G., SANDFORD, M. C. W. <AP. J., 237, 596> 800410
ULTRAVIOLET, VISIBLE, INFRARED, AND X-RAY OBSERVATIONS OF SCORPIUS X-1.

WILLNER, S. P. <AP. J., 206, 728> 760603
8 TO 13 MICRON SPECTROPHOTOMETRY OF COMPACT SOURCES IN NGC 7538.

WILLNER, S. P. <AP. J., 214, 706> 770609
8 TO 13 MICROMETER SPECTROPHOTOMETRY OF COMPACT SOURCES IN W3.

WILLNER, S. P. <AP. J., 219, 870> 780208
INFRARED OBSERVATIONS OF THE GALACTIC CENTER. II. (NE II) EMISSION.

WILLNER, S. P., BECKLIN, E. E., VISVANATHAN, N. <AP. J., 175, 699> 720804
OBSERVATIONS OF PLANETARY NEBULAE AT 1.65 TO 3.4 MICRON

WILLNER, S. P., GILLETT, F. C., HERTER, T. L., JONES, B., KRASSNER, J., MERRILL, K. M., PIPHER, J. L., PUETTER, R. C., RUDY, R. J., RUSSELL, R. W., SOIFER, B. T. <AP. J., 253, 174> 820206
INFRARED SPECTRA OF PROTOSTARS: COMPOSITION OF THE DUST SHELLS.

WILLNER, S. P., JONES, B., PUETTER, R. C., RUSSELL, R. W., SOIFER, B. T. <AP. J., 234, 496> 791205
INFRARED SPECTRA OF IC 418 AND NGC 6572.

WILLNER, S. P., RUSSELL, R. W., PUETTER, R. C., SOIFER, B. T., HARVEY, P. M. <AP. J. (LETTERS), 229, L65> 790410
THE 4 TO 8 MICRON SPECTRUM OF THE GALACTIC CENTER.

WILLNER, S. P., SOIFER, B. T., RUSSELL, R. W., JOYCE, R. R., GILLETT, F. C. <AP. J. (LETTERS), 217, L121> 771104
2 TO 8 MICRON SPECTROPHOTOMETRY OF M82.

WILSON, A. S., MEURS, E. J. A. <ASTR. AP. SUPPL., 33, 407> 789906
ACCURATE OPTICAL POSITIONS OF SEYFERT GALAXIES.

WILSON, T. L., FAZIO, G. G., JAFFE, D., KLEINMANN, D. E., WRIGHT, E. L., LOW, F. J. <ASTR. AP., 76, 86> 790612
A COMPARISON OF HIGH RESOLUTION RADIO AND FAR-INFRARED MAPS OF M17.

WILSON, W. J., SCHWARTZ, P. R., NEUGEBAUER, G., HARVEY, P. M., BECKLIN, E. E. <AP. J., 177, 523> 721001
INFRARED STARS WITH STRONG 1665/1667-MHZ OH MICROWAVE EMISSION.

WING, R. F. <P. A. S. P., 83, 301> 710604
THE SPECTRAL TYPE AND INFRARED BRIGHTNESS OF R DORADUS.

WING, R. F., COHEN, J. G., BRAULT, J. W. <AP. J., 216, 659> 770906
CONFIRMATION OF THE PRESENCE OF IRON HYDRIDE IN SUNSPOTS AND COOL STARS.

WING, R. F., DEAN, C. A., MACCONNELL, D. J. <AP. J., 205, 186> 760404
THE TEMPERATURE, LUMINOSITY, AND SPECTRUM OF KAPTEYN'S STAR.

WING, R. F., LOCKWOOD, G. W. <AP. J., 184, 873> 730906
THE PERIOD AND SPECTRAL RANGE OF IK TAURI.

WING, R. F., RINSLAND, C. P. <A. J., 84, 1235> 790805
ATMOSPHERIC EXTINCTION IN THE FOUR-MICRON REGION.

WING, R. F., SPINRAD, H. <AP. J., 159, 973> 700304
INFRARED CN BANDS IN M SUPERGIANTS AND CARBON STARS.

WING, R. F., SPINRAD, H., KUHI, L. V. <AP. J., 147, 117> 670101
INFRARED STARS.

WING, R. F., STOCK, J. <AP. J., 186, 979> 731205
CARBON STARS IN OMEGA CENTAURI.

WING, R. F., WARNER, J. W., SMITH, M. G. <AP. J., 179, 135> 730104
ON THE NATURE OF THE SAGITTARIUS OBJECT IRC-20385.

WING, R. F., YORKA, S. B. <M. N. R. A. S., 178, 383> 770203
THE BRIGHTEST S-TYPE STARS IN THE INFRARED.

WISNIEWSKI, W. Z. <M. N. R. A. S., 161, 331> 730009
MULTICOLOUR OBSERVATIONS OF UZ LIBRAE.

WISNIEWSKI, W. Z., JOHNSON, H. L. <COMM. LUNAR AND PLANETARY LAB., 7, 57> 680401
UBVRIJKL LIGHT CURVES OF CLASSICAL CEPHEIDS.

WISNIEWSKI, W. Z., KLEINMANN, D. E. <A. J., 73, 866> 681104
MULTICOLOR PHOTOMETRY OF SEYFERT GALAXIES AND MEASUREMENT AT 1.55 MICRONS OF THE JET IN M87.

WISNIEWSKI, W. Z., WING, R. F., SPINRAD, H., JOHNSON, H. L. <AP. J. (LETTERS), 148, L29> 670402
ADDITIONAL OBSERVATIONS OF "INFRARED STARS".

WITTEBORN, F. C., STRECKER, D. W., ERICKSON, E. F., SMITH, S. M., GOEBEL, J. H., TAYLOR, B. J. <AP. J., 238, 577> 800609
THE SPECTRUM OF IRC+10216 FORM 2.0 TO 8.5 MICRONS.

WOLFF, S. C., BEICHMAN, C. A. <AP. J., 230, 519> 790605
THE PHYSICAL PROPERTIES AND ORBITAL PARAMETERS OF THE B0 IA STAR HD 152667 -V861 SCORPII: A SUPERGIANT WITH A BLACK HOLE COMPANION?

WOLLMAN, E. R., GEBALLE, T. R., GREENBERG, L. T., HOLTZ, J. Z., RANK, D. M. <AP. J. (LETTERS), 184, L85> 730904
OBSERVATIONS OF SILICON MONOXIDE IN COOL STARS AT 4.05 MICRONS.

WOLLMAN, E. R., GEBALLE, T. R., LACY, J. H., TOWNES, C. H., RANK, D. M. <AP. J. (LETTERS), 218, L103> 771205
NE II 12.8 MICRON EMISSION FROM THE GALACTIC CENTER. II.

WOLLMAN, E. R., GEBALLE, T. R., LACY, J. H., TOWNES, C. H., RANK, D. M. <AP. J. (LETTERS), 205, L5> 760405
SPECTRAL AND SPATIAL RESOLUTION OF THE 12.8 MICRON NE II EMISSION FROM THE GALACTIC CENTER.

WOLLMAN, E. R., SMITH, H. A., LARSON, H. P. <AP. J., 258, 506> 820704
INFRARED SPECTRA OF GALACTIC CENTER SOURCES.

WOLSTENCROFT, R. D., GILMORE, G., WILLIAMS, P. M. <M. N. R. A. S., 201, 479> 821113
RAPID VARIABILITY OF OJ 287 AT 1.25 MICRONS.

WOOLF, N. J. <AP. J. (LETTERS), 157, L37> 690705
INFRARED EMISSION FROM PLANETARY NEBULAE.

WOOLF, N. J. <AP. J., 185, 229> 731004
INFRARED EMISSION FROM UNUSUAL BINARY STARS.

WOOLF, N. J. <P. A. S. P., 85, 730> 731209
THE 10-MICRON EXCESS OF ALPHA HERCULIS.

WOOLF, N. J., NEY, E. P. <AP. J. (LETTERS), 155, L181> 690303
CIRCUMSTELLAR INFRARED EMISSION FROM COOL STARS.

WOOLF, N. J., SCHWARZSCHILD, M., ROSE, W. K. <AP. J., 140, 833> 641001
INFRARED SPECTRA OF RED-GIANT STARS.

WOOLF, N. J., STEIN, W. A., GILLETT, F. C., MERRILL, K. M., BECKLIN, E. E., NEUGEBAUER, G., PEPIN, T. J. <AP. J. (LETTERS), 179, L111> 730201
THE INFRARED SOURCES IN M8.

WOOLF, N. J., STEIN, W. A., STRITTMATTER, P. A. <ASTR. AP., 9, 252> 701105
INFRARED EMISSION FROM BE STARS.

WOOLLEY, R., EPPS, E. A., PENSTON, M. J., POCOCK, S. B. <ROYAL OBS. ANNALS, 5> 709903
CATALOGUE OF STARS WITHIN TWENTY-FIVE PARSECS OF THE SUN.

WORRALL, D. M., PUSCHELL, J. J., JONES, B., BRUHWEILER, F. C., ALLER, M. F., ALLER, H. D., HODGE, P. D., SITKO, M. L., STEIN, W. A., ZHANG, Y. -X., KU, W. H. -M. <AP. J., 261, 403> 821002
TWO MULTIFREQUENCY OBSERVATIONS OF THE BL LACERTAE OBJECT OJ 287.

WRIGHT, E. L., DECAMPLI, W., FAZIO, G. G., KLEINMANN, D. E., LADA, C. J., LOW, F. J. <AP. J., 228, 439> 790311
DISCOVERY OF A COMPACT FAR-INFRARED SOURCE, IR 12.4+0.5.

WRIGHT, E. L., FAZIO, G. G., LOW, F. J. <AP. J., 217, 724> 771108
A HIGH-RESOLUTION FAR-INFRARED SURVEY OF THE W31 REGION.

WRIGHT, E. L., FAZIO, G. G., LOW, F. J. <AP. J. (LETTERS), 208, L87> 760909
FAR-INFRARED OBSERVATIONS OF M20 (NGC 6514).

WRIGHT, E. L., HARPER JR., D. A., HILDEBRAND, R. H., KEENE, J., WHITCOMB, S. E. <NATURE, 279, 703> 790610
MILLIMETRE AND SUBMILLIMETRE MEASUREMENTS OF THE CRAB NEBULA.

WRIGHT, E. L., HARPER, D. A., LOEWENSTEIN, R. F., KEENE, J., WHITCOMB, S. E. <AP. J. (LETTERS), 240, L157> 800903
SEARCH FOR FAR-INFRARED EMISSION FROM YOUNG SUPERNOVA REMNANTS.

WRIGHT, E. L., HARPER, D. A., LOEWENSTEIN, R. F., MOSELEY, H. <AP. J., 246, 426> 810606
FAR-INFRARED OBSERVATIONS OF THE H2O MASERS IN NGC 281, NGC 2175, AND S255/257.

WRIGHT, E. L., KLEINMANN, D. E. <NATURE, 275, 298> 780901
INFRARED OBSERVATIONS OF THE MOST LUMINOUS QUASAR.

WRIGHT, E. L., LADA, C. J., FAZIO, G. G., KLEINMANN, D. E., LOW, F. J. <A. J., 82, 132> 770207
NEW INFRARED-CO SOURCE IN M8.

WYNN-WILLIAMS, C. G. <M. N. R. A. S., 181, 61P> 771102
RADIO EMISSION FROM THE INFRARED SOURCE CRL 618: AN EXTREMELY YOUNG PLANETARY NEBULA.

WYNN-WILLIAMS, C. G., BECKLIN, E. E. <NATURE, 282, 810> 791212
THE IR ENERGY DISTRIBUTION OF SS433.

WYNN-WILLIAMS, C. G., BECKLIN, E. E. <P. A. S. P., 86, 5> 740206
INFRARED EMISSION FROM HII REGIONS.

WYNN-WILLIAMS, C. G., BECKLIN, E. E., BEICHMAN, C. A., CAPPS, R., SHAKESHAFT, J. R. <AP. J., 246, 801> 810610
THE MULTIPLE INFRARED SOURCE GL 437.

WYNN-WILLIAMS, C. G., BECKLIN, E. E., FORSTER, J. R., MATTHEWS, K., NEUGEBAUER, G., WELCH, W. J., WRIGHT, M. C. H. <AP. J. (LETTERS), 211, L89> 770107
ON THE RELATIONSHIP BETWEEN THE INFRARED SOURCE CRL 2591 (UOA-27) AND ITS RADIO AND H2O COUNTERPARTS.

WYNN-WILLIAMS, C. G., BECKLIN, E. E., MATTHEWS, K., NEUGEBAUER, G. <M. N. R. A. S., 183, 237> 780401
TWO-MICRON LINE EMISSION FROM THE HII REGION G333.6-0.2.

WYNN-WILLIAMS, C. G., BECKLIN, E. E., MATTHEWS, K., NEUGEBAUER, G. <M. N. R. A. S., 189, 163> 791004
TWO-MICRON SPECTROPHOTOMETRY OF THE GALAXY NGC 253.

WYNN-WILLIAMS, C. G., BECKLIN, E. E., MATTHEWS, K., NEUGEBAUER, G., WERNER, M. W. <M. N. R. A. S., 179, 255> 770501
INFRARED STUDIES OF HII REGIONS AND DUST CLOUDS NEAR K3-50.

WYNN-WILLIAMS, C. G., BECKLIN, E. E., NEUGEBAUER, G. <AP. J., 187, 473> 740203
INFRARED STUDIES OF HII REGIONS AND OH SOURCES.

YEE, H. K. C., OKE, J. B. <AP. J., 226, 753> 781212
PHOTOELECTRIC SPECTROPHOTOMETRY OF RADIO GALAXIES.

YOUNG, E. T., KNACKE, R. F. <AP. J., 224, 848> 780908
A SEARCH FOR THE GROUND STATE S(2) LINE OF MOLECULAR HYDROGEN IN THE ORION NEBULA.

YOUNG, E. T., KNACKE, R. F., JOYCE, R. R. <NATURE, 238, 263> 720805
INFRARED PHOTOMETRY OF MARKARIAN 231.

YOUNG, P., SCHNEIDER, D. P., SHECTMAN, S. A. <AP. J., 245, 1035> 810503
THE VORACIOUS VORTEX IN HT CASSIOPEIAE.

YUDIN, B. F. <SOV. AST., 26, 187> 820313
INFRARED OBSERVATIONS OF V1016 CYGNI.

ZAJTSEVA, G. V., LYUTYI, V. M. <ASTROFIZIKA, 15, 48> 790119
PHOTOMETRIC INVESTIGATION AND RAPID PERIODICITY OF RR TAU.

ZAPPALA, R. R. <AP. J., 187, 257> 740105
ON THE NATURE OF BD-10 4462.

ZAPPALA, R. R., BECKLIN, E. E., MATTHEWS, K., NEUGEBAUER, G. <AP. J., 192, 109> 740805
ANGULAR DIAMETER OF IRC +10011 AT 2.2, 10, AND 20 MICRONS

ZEILIK II, M. <A. J., 84, 1566> 791001
NEAR-INFRARED OBSERVATIONS OF TWO FAR-INFRARED SOURCES IN THE W3 REGION: G133.8+1.4 (W3N) AND G133.982+1.14 (BS4).

ZEILIK II, M. <A. J., 84, 341> 790309
LARGE-BEAM NEAR-INFRARED AND 24-GHZ OBSERVATIONS OF M8.

ZEILIK II, M. <ASTR. AP., 46, 319> 760103
INFRARED EMISSION FROM S 157 A AND S 252 A.

ZEILIK II, M., HECKERT, P. A. <A. J., 82, 824> 771009
LARGE-BEAM INFRARED OBSERVATIONS OF COMPACT HII REGIONS.

ZEILIK II, M., HECKERT, P. A., COHEN, N. L. <A. J., 84, 1323> 790904
NEAR-INFRARED AND RADIO OBSERVATIONS OF IRC-10442 (GL5268S).

ZEILIK II, M., KLEINMANN, D. E., WRIGHT, E. L. <AP. J., 199, 401> 750706
G45.5+0.1 AND G45.1+0.1: COMPACT INFRARED SOURCES.

ZEILIK II, M., LADA, C. J. <AP. J., 222, 896> 780607
NEAR-INFRARED AND CO OBSERVATIONS OF W40 AND W48.

ZEILIK, M., HECKERT, P., HENSON, G., SMITH, P. <A. J., 87, 1304> 820908
INFRARED PHOTOMETRY OF BETA LYRAE: 1977-1982.

ZINN, R., PERSSON, S. E. <AP. J., 247, 849> 810804
THE AGES AND METALLICITIES OF THE GLOBULAR CLUSTERS IN THE FORNAX DWARF SPHEROIDAL GALAXY.

ZIRIN, H. <AP. J. (LETTERS), 152, L177> 680603
HE-3 IN SEVERAL MAGNETIC STARS.

ZIRIN, H. <AP. J., 208, 414> 760908
FURTHER OBSERVATIONS OF THE 10830A HELIUM LINE IN STARS AND THEIR SIGNIFICANCE AS A MEASURE OF STELLAR ACTIVITY.

ZIRIN, H. <AP. J., 260, 655> 820905
10830 HE I OBSERVATIONS OF 455 STARS.

ZIRIN, H. <NATURE, 259, 466> 760214
FE XIII LINE IN R AQUARII.

ZIRIN, H., LIGGETT, M. A. <AP. J., 259, 719> 820808
THE VARIABLE HE 10830A LINE OF ALGOL.

ZWICKY, F., OKE, J. B., NEUGEBAUER, G., SARGENT, W. L. W., FAIRALL, A. P. <P. A. S. P., 82, 93> 700202
THE VARIABLE COMPACT GALAXY ZW 0039.5+4003.

☆U.S. GOVERNMENT PRINTING OFFICE:1984 -739 -010/ 4 REGION NO. 4

BIBLIOGRAPHIC DATA SHEET

1. Report No.	2. Government Accession No.	3. Recipient's Catalog No.
NASA RP-1118		
4. Title and Subtitle Catalog of Infrared Observations Including: Bibliography of Infrared Astronomy and Index of Infrared Source Positions		5. Report Date May 1984
		6. Performing Organization Code 693.2
7. Author(s) Daniel Y. Gezari, Marion Schmitz, and Jaylee M. Mead		8. Performing Organization Report No.
9. Performing Organization Name and Address NASA Goddard Space Flight Center Greenbelt, MD 20771		10. Work Unit No.
		11. Contract or Grant No.
12. Sponsoring Agency Name and Address National Aeronautics and Space Administration Washington, DC 20546		13. Type of Report and Period Covered Reference Publication
		14. Sponsoring Agency Code

15. Supplementary Notes

Marion Schmitz: Computer Sciences Corporation, Silver Spring, Maryland.

The companion paper is NASA RP-1119.

16. Abstract

The Catalog of Infrared Observations and its Far Infrared Supplement summarize all infrared astronomical observations at infrared wavelengths (1 - 1000 microns) published in the scientific literature between 1965 and 1982. The Catalog includes as appendices the Bibliography of Infrared Astronomy which keys observations in the Catalog with the original journal references, and the Index of Infrared source positions which gives source positions for alphabetically listed sources in the Catalog. The Catalog data base contains over 85,000 observations of about 10,000 infrared sources, of which about 2,000 have no known visible counterpart.

17. Key Words (Selected by Author(s))	18. Distribution Statement
Infrared Catalog Infrared Sources Infrared Astronomy Astronomy data base	Unclassified - Unlimited Subject Category 89

19. Security Classif. (of this report)	20. Security Classif. (of this page)	21. No. of Pages	22. Price*
Unclassified	Unclassified	557	A24

*For sale by the National Technical Information Service, Springfield, Virginia 22161

GSFC 25-44 (10/77)

National Aeronautics and
Space Administration

Washington, D.C.
20546

Official Business
Penalty for Private Use, $300

SPECIAL FOURTH CLASS MAIL
BOOK

Postage and Fees Paid
National Aeronautics and
Space Administration
NASA-451

U.S. MAIL

NASA

POSTMASTER: If Undeliverable (Section 158
Postal Manual) Do Not Return